

## CMEs (general)

---

---

### Space Weather Live

<https://www.spaceweatherlive.com/en.html>

---

#### CAMEL. II. A 3D Coronal Mass Ejection **Catalog** Based on Coronal Mass Ejection Automatic Detection with Deep Learning

Jiahui **Shan**<sup>1,2</sup>, Huapeng Zhang<sup>3,4</sup>, Lei Lu<sup>1,2</sup>, Yan Zhang<sup>3,4</sup>, Li Feng<sup>1,2</sup>, Yunyi Ge<sup>1</sup>, Jianchao Xue<sup>1,2</sup>, and Shuting Li<sup>1,2</sup>

2024 ApJS 272 18

<https://iopscience.iop.org/article/10.3847/1538-4365/ad37bc/pdf>

The **catalog** websites written at <http://github.com/h1astro/CAMEL-II>

---

We perform hindcasts Мы делаем ретроспективные прогнозы

Coronal mass ejections (CMEs) and coronal jets are two types of common solar eruptive phenomena, which often independently happen at different spatial scales. Chen+, 2021

---

#### Collection, Collation, and Comparison of 3D Coronal CME Reconstructions

**Catalogs**

[C. Kay](#), [E. Palmerio](#)

Space Weather. [Volume22, Issue1](#) e2023SW003796 2024

<https://arxiv.org/pdf/2311.10712.pdf>

<https://agupubs.onlinelibrary.wiley.com/doi/epdf/10.1029/2023SW003796>

---

#### A CME Source Region **Catalogue** and their Associated Properties

[Satabdwa Majumdar](#), [Ritesh Patel](#), [Vaibhav Pant](#), [Dipankar Banerjee](#), [Aarushi Rawat](#), [Abhas Pradhan](#), [Paritosh Singh](#)

ApJS 268 38 2023

<https://arxiv.org/pdf/2307.13208.pdf>

See <https://allssc.aries.res.in/catalogs>

<https://iopscience.iop.org/article/10.3847/1538-4365/aceb62/pdf>

---

#### SMM CME CATALOG 1980, 1985-1989

<https://www2.hao.ucar.edu/mlso/solar-maximum-mission/smm-cme-catalog>

---

### RESEARCH TOPIC

#### The Magnetic Structures and Their Role in The Evolution of Coronal Mass Ejections

Front. Phys. 2021 <https://www.frontiersin.org/research-topics/17314/the-magnetic-structures-and-their-role-in-the-evolution-of-coronal-mass-ejections#articles>

---

Solar Orbiter First Results (Cruise Phase): many papers on <sup>3</sup>He-rich SEPs, near-relativistic electrons, stealth CME, ICMEs, GCR flux, Forbush

The first spacecraft coronagraph observations of CMEs were made by the OSO-7 coronagraph in the early 1970s (Tousey, [1973](#)). These were followed by better quality and longer periods of CME observations using **Skylab** (1973 – 1974; MacQueen *et al.*, [1980](#)), **P78-1 (Solwind)** (1979 – 1985; Sheeley Jr *et al.*, [1980](#)), and **SMM** (1980; 1984 – 1989; Hundhausen, [1999](#)). In late 1995, **SOHO** was launched and two of its three **LASCO** coronagraphs still operate today (Brueckner *et al.*, [1995](#)). Finally late in 2006, LASCO was joined by the **STEREO CORs** (Howard *et al.*, 2008a).

---

## **SDO JSOC Data-Product FITS File Changes**

<http://jsoc.stanford.edu/>

## **Space Weather Database Of Notifications, Knowledge, Information (DONKI)**

One-stop on-line **tool for space weather** researchers and forecasters.

<https://ccmc.gsfc.nasa.gov/donki/>

**The GOES, PAMELA and STEREO data are available at**

<https://www.ngdc.noaa.gov/stp/satellite/goes/>

<https://www.ssdsc.asi.it/pamela/> and

<http://www.srl.caltech.edu/STEREO/>, respectively.

---

## **Earth-affecting Solar Transients: A **Review** of Progresses in Solar Cycle 24**

Jie **Zhang**, [Manuela Temmer](#), [Nat Gopalswamy](#), +

<https://arxiv.org/ftp/arxiv/papers/2012/2012.06116.pdf> File 2021

2020 <https://arxiv.org/abs/2012.06116>

|          |         |   |  |
|----------|---------|---|--|
| CMEs     | CDAW    | SOHO CME catalog<br><a href="https://cdaw.gsfc.nasa.gov/CME_list/">https://cdaw.gsfc.nasa.gov/CME_list/</a>   | (S. Yashiro et al. 2004)                       |
| CMEs     | SEEDS   | SOHO and STEREO CME catalogs based on automated method.<br><a href="http://spaceweather.gmu.edu/seeds/">http://spaceweather.gmu.edu/seeds/</a>  | (O. Olmedo et al. 2008)                        |
| CMEs     | CACTUS  | SOHO and STEREO CME catalogs based on automated method<br><a href="http://sidc.oma.be/cactus/">http://sidc.oma.be/cactus/</a>   | (E. Robbrecht and Berghmans 2004)              |
| CMEs     | ARTEMIS | SOHO CME catalog based on automated method<br><a href="http://cesam.lam.fr/lascomission/ARTEMIS/index.html">http://cesam.lam.fr/lascomission/ARTEMIS/index.html</a>                             | (Boursier et al. 2005)                         |
| CMEs     | CORIMP  | SOHO CME catalog based on automated method<br><a href="http://alshamess.ifa.hawaii.edu/CORIMP/">http://alshamess.ifa.hawaii.edu/CORIMP/</a>   | (Byrne et al. 2012)                            |
| CMEs     | --      | STEREO COR1 catalog, including CMEs and other events<br><a href="https://cor1.gsfc.nasa.gov/catalog/">https://cor1.gsfc.nasa.gov/catalog/</a>   | --   |
| CMEs     | MVCC    | STEREO Dual-viewpoint CME catalog<br><a href="http://solar.jhuapl.edu/Data-Products/COR-CME-Catalog.php">http://solar.jhuapl.edu/Data-Products/COR-CME-Catalog.php</a>                          | (Angelos Vourlidas et al. 2017)                |
| CMEs     | KINCAT  | STEREO COR2 CMEs (2007-2013) with GCS model results<br><a href="http://www.affects-fp7.eu/cme-database/index.php">http://www.affects-fp7.eu/cme-database/index.php</a>                          | (Bosman et al. 2012)                           |
| ICMEs-IH | HELCAST | STEREO HI event catalogs including HICAT, HIJoinCAT, HIgeoCAT <a href="http://www.helcats-fp7.eu/">http://www.helcats-fp7.eu/</a>   | (Harrison et al. 2018)                         |
| ICMEs-IS | --      | ACE ICMEs since 1996 compiled by Richardson & Cane<br><a href="http://www.srl.caltech.edu/ACE/ASC/DATA/level3/icmetable2.htm">http://www.srl.caltech.edu/ACE/ASC/DATA/level3/icmetable2.htm</a> | (I. G. Richardson and Cane 2010)               |
| ICMEs-IS | --      | WIND ICME catalog (1995-2015)<br><a href="https://wind.nasa.gov/ICME_catalog/ICME_catalog_viewer.php">https://wind.nasa.gov/ICME_catalog/ICME_catalog_viewer.php</a>                            | (T. Nieves-Chinchilla, Vourlidas, et al. 2018) |
| CMEs     | CDAW    | SOHO CME catalog<br><a href="https://cdaw.gsfc.nasa.gov/CME_list/">https://cdaw.gsfc.nasa.gov/CME_list/</a>   | (S. Yashiro et al. 2004)                       |
| CMEs     | SEEDS   | SOHO and STEREO CME catalogs based on automated method.<br><a href="http://spaceweather.gmu.edu/seeds/">http://spaceweather.gmu.edu/seeds/</a>  | (O. Olmedo et al. 2008)                        |
| CMEs     | CACTUS  | SOHO and STEREO CME catalogs based on automated method<br><a href="http://sidc.oma.be/cactus/">http://sidc.oma.be/cactus/</a>   | (E. Robbrecht and Berghmans 2004)              |
| CMEs     | ARTEMIS | SOHO CME catalog based on automated method<br><a href="http://cesam.lam.fr/lascomission/ARTEMIS/index.html">http://cesam.lam.fr/lascomission/ARTEMIS/index.html</a>                             | (Boursier et al. 2005)                         |
| CMEs     | CORIMP  | SOHO CME catalog based on automated method<br><a href="http://alshamess.ifa.hawaii.edu/CORIMP/">http://alshamess.ifa.hawaii.edu/CORIMP/</a>   | (Byrne et al. 2012)                            |
| CMEs     | --      | STEREO COR1 catalog, including CMEs and other events<br><a href="https://cor1.gsfc.nasa.gov/catalog/">https://cor1.gsfc.nasa.gov/catalog/</a>   | --   |
| CMEs     | MVCC    | STEREO Dual-viewpoint CME catalog<br><a href="http://solar.jhuapl.edu/Data-Products/COR-CME-Catalog.php">http://solar.jhuapl.edu/Data-Products/COR-CME-Catalog.php</a>                          | (Angelos Vourlidas et al. 2017)                |
| CMEs     | KINCAT  | STEREO COR2 CMEs (2007-2013) with GCS model results<br><a href="http://www.affects-fp7.eu/cme-database/index.php">http://www.affects-fp7.eu/cme-database/index.php</a>                          | (Bosman et al. 2012)                           |
| ICMEs-IH | HELCAST | STEREO HI event catalogs including HICAT, HIJoinCAT, HIgeoCAT <a href="http://www.helcats-fp7.eu/">http://www.helcats-fp7.eu/</a>   | (Harrison et al. 2018)                         |
| ICMEs-IS | --      | ACE ICMEs since 1996 compiled by Richardson & Cane<br><a href="http://www.srl.caltech.edu/ACE/ASC/DATA/level3/icmetable2.htm">http://www.srl.caltech.edu/ACE/ASC/DATA/level3/icmetable2.htm</a> | (I. G. Richardson and Cane 2010)               |
| ICMEs-IS | --      | WIND ICME catalog (1995-2015)<br><a href="https://wind.nasa.gov/ICME_catalog/ICME_catalog_viewer.php">https://wind.nasa.gov/ICME_catalog/ICME_catalog_viewer.php</a>                            | (T. Nieves-Chinchilla, Vourlidas, et al. 2018) |
| ICMEs-IS | --      | WIND Magnetic Cloud list (1995-2006)<br><a href="https://wind.nasa.gov/mfi/mag_cloud_pub1.html">https://wind.nasa.gov/mfi/mag_cloud_pub1.html</a>   | (Lepping and Wu 2007)                          |
| ICMEs-IS | --      | WIND ICME catalog (1995-2015)<br><a href="http://space.ustc.edu.cn/dreams/wind_icmes/">http://space.ustc.edu.cn/dreams/wind_icmes/</a>  | (Chi et al. 2016)                              |
| ICMEs-IS | --      | ICMEs and other large scale structures in solar wind<br><a href="ftp://www.iki.rssi.ru/pub/omni/">ftp://www.iki.rssi.ru/pub/omni/</a>   | (Yu. I. Yermolaev et al. 2009)                 |

---

**Catalog of Solar Failed Eruptions and Other Dynamic Features Registered by SDO/AIA**Tomasz **Mrozek**<sup>1,2</sup>, Sylwester Kołomański<sup>1</sup>, Marek Stęśliński<sup>2</sup>, and Dominik Gronkiewicz<sup>3</sup>

2020 ApJS 249 21

<https://iopscience.iop.org/article/10.3847/1538-4365/ab9e00/pdf><http://eruptivesun.com>, <http://eruptivesun.com/help>

---

**The CME catalogue** <http://nldr.library.ucar.edu/repository/collections/TECH-NOTE000-000-000-180> from the Coronagraph/Polarimeter (C/P) onboard the **Solar Maximum Mission (SMM) spacecraft (time span: 1980–1989)** <https://umbra.nascom.nasa.gov/smm/> and the white light observations of the solar corona from the **Mauna Loa Solar Observatory (MLSO) (time span: 1980–today)**, which employs three corona meters: MK3, MK4 and recently with the COSMO K-cor. <https://www2.hao.ucar.edu/mlso/mlso-data-and-movies>

Sadykov et al.

**Table 1.** Event catalogs currently implemented in the Interactive Multi-Instrument Database of Solar Flares (<https://solarflare.njit.edu/>).

| Source Name               | Dates presented          | Source web link   |
|---------------------------|--------------------------|---|
| Primary flare lists       |                          |   |
| GOES flare list           | Jan, 2002 — current time | <a href="ftp://ftp.swpc.noaa.gov/pub/warehouse/">ftp://ftp.swpc.noaa.gov/pub/warehouse/</a>                   |
| RHESSI flare list         | Feb, 2002 — current time | <a href="http://hesperia.gsfc.nasa.gov/hessidata/dbase/">http://hesperia.gsfc.nasa.gov/hessidata/dbase/</a>   |
| HEK flare list            | Feb, 2010 — current time | <a href="https://www.lmsal.com/isolsearch">https://www.lmsal.com/isolsearch</a>                               |
| Secondary event catalogs  |                          |   |
| IRIS observing logs       | Jul, 2013 — current time | <a href="http://iris.lmsal.com/search/">http://iris.lmsal.com/search/</a>                                     |
| Hinode flare catalog      | Nov, 2006 — July, 2016   | <a href="http://st4a.stelab.nagoya-u.ac.jp/hinode_flare/">http://st4a.stelab.nagoya-u.ac.jp/hinode_flare/</a> |
| Fermi GBM flare catalog   | Nov, 2008 — current time | <a href="https://hesperia.gsfc.nasa.gov/fermi/gbm/qlook/">https://hesperia.gsfc.nasa.gov/fermi/gbm/qlook/</a> |
| Nobeyama coverage check   | Jan, 2010 — current time | <a href="ftp://solar-pub.nao.ac.jp/pub/nsro/norp/xdr/">ftp://solar-pub.nao.ac.jp/pub/nsro/norp/xdr/</a>       |
| OVSA flare catalog        | Jan, 2002 — Dec, 2003    | <a href="http://www.ovsa.njit.edu/data/">http://www.ovsa.njit.edu/data/</a>                                   |
| CACTus CME catalog        | Jan, 2002 — current time | <a href="http://sidc.oma.be/cactus/">http://sidc.oma.be/cactus/</a>   |
| Filament eruption catalog | Apr, 2010 — Oct, 2014    | <a href="http://aia.cfa.harvard.edu/filament/">http://aia.cfa.harvard.edu/filament/</a>                       |
| Konus-Wind flare catalog  | Jan, 2002 — Jul, 2016    | <a href="http://www.ioffe.ru/LEA/Solar/index.html">http://www.ioffe.ru/LEA/Solar/index.html</a>               |

---

**SMART/SDDI Filament Disappearance Catalogue (2016–2019)**Daikichi **Seki**, **Kenichi Otsuji**, **Takako T. Ishii**, **Kumi Hirose**, **Tomoya Iju**, **Satoru UeNo**, **Denis P. Cabezas**, **Ayumi Asai**, **Hiroaki Isobe**, **Kiyoshi Ichimoto**, **Kazunari Shibata**

Sun and Geosphere

2020

<https://arxiv.org/ftp/arxiv/papers/2003/2003.03454.pdf>See <https://www.kwasan.kyoto-u.ac.jp/observation/event/sddi-catalogue/>

---

**Filament eruption catalog** 2010 Apr–2014 Oct<http://aia.cfa.harvard.edu/filament/>

---

The theme issue '**Solar eruptions and their space weather impact**'. **Reviews**  
Philosophical Transactions of the Royal Society A: Mathematical, Physical and Engineering Sciences  
v. 377 [Issue 2148](#) **2019**  
<https://royalsocietypublishing.org/toc/rsta/377/2148>

-----  
Topical collections: [Earth-affecting Solar Transients](#) **CMEs/ICMEs**  
Solar Phys. **2017**  
[https://link.springer.com/journal/11207/topicalCollection/AC\\_74be62d9d035e23ca163bf5434bd2877](https://link.springer.com/journal/11207/topicalCollection/AC_74be62d9d035e23ca163bf5434bd2877)

-----  
**A Catalog of Prominence Eruptions Detected Automatically in the SDO/AIA 304 Å Images**  
2010-2016 [https://cdaw.gsfc.nasa.gov/CME\\_list/autope/](https://cdaw.gsfc.nasa.gov/CME_list/autope/)

-----  
**Solar Prominences** **Book**  
Vial, J.-C. • Engvold, O. Editors  
Springer **2015** **File**  
<https://link.springer.com/content/pdf/10.1007%2F978-3-319-10416-4.pdf>

-----  
**A catalog of Earth-directed coronal mass ejections (CMEs) observed by STEREO**  
[http://sprg.ssl.berkeley.edu/~liuxying/CME\\_catalog.htm](http://sprg.ssl.berkeley.edu/~liuxying/CME_catalog.htm)

-----  
**Recent results from Hinode:**  
PASJ special issue, Volume 66 Issue SP1 December **2014**  
<http://pasj.oxfordjournals.org/content/66/SP1.toc>

-----  
**Solar Eruptions and Energetic Particles: An Introduction** **Book**  
N. **Gopalswamy**<sup>1</sup>, R. Mewaldt<sup>2</sup>, and J. Torsti<sup>3</sup>  
Book Series: [Geophysical Monograph Series](#) Volume 165, **2013**  
<https://agupubs.onlinelibrary.wiley.com/doi/book/10.1029/GM165>

-----  
**Space Weather and Coronal Mass Ejections** **Book**  
Timothy A. **Howard**  
Springer, **2013**  
[http://books.google.ru/books?id=ihO4BAAAQBAJ&pg=PA97&lpg=PA97&dq=DeForest,+C.+E.&source=bl&ots=XIvsgYLfFB&sig=525J\\_9PFZBGda9BsysLsvRRQh34&hl=ru&sa=X&ei=HxlfVOr7HoG6PdDNgegL&ved=0CC4Q6AEwBQ#v=onepage&q=DeForest%2C%20C.%20E.&f=false](http://books.google.ru/books?id=ihO4BAAAQBAJ&pg=PA97&lpg=PA97&dq=DeForest,+C.+E.&source=bl&ots=XIvsgYLfFB&sig=525J_9PFZBGda9BsysLsvRRQh34&hl=ru&sa=X&ei=HxlfVOr7HoG6PdDNgegL&ved=0CC4Q6AEwBQ#v=onepage&q=DeForest%2C%20C.%20E.&f=false)

-----  
Solar Phys. Volume 284, Issue 1, May **2013**  
**Topical Issue**  
**Flux-Rope Structure of Coronal Mass Ejections** / Guest Editors: N. Gopalswamy, T. Nieves-Chinchilla, M. Hidalgo, J. Zhang, and P. Riley

-----  
Timothy **Howard**  
**Coronal Mass Ejections. An introduction** **Book** **File**  
Springer **2011**

-----  
[Journal of Atmospheric and Solar-Terrestrial Physics](#)  
[Volume 73, Issue 10](#), Pages 1077-1292 (20 June **2011**)

## Three dimensional aspects of CMEs, their source regions and interplanetary manifestations

Edited by Marilena Mierla, Nandita Srivastava and Luciano Rodriguez

-----  
Solar Phys.

[Numbers 1-2 / Май 2009 г.](#)

**STEREO Science Results at Solar Minimum** | Guest Editors: E. R. Christian, M. L. Kaiser, T. A. Kucera, O. C. St. Cyr

-----  
**Coronal Mass Ejections**

Kunow, H., Crooker, N.U., Linker, J.A. (et al.) (Eds.)

[H. Kunow](#), [N. U. Crooker](#), [J. A. Linker](#), [R. Schwenn](#) and [R. Von Steiger](#)

Space Sciences Series of ISSI, Vol. 21, 2006

Издатель: Springer New York

DOI: 10.1007/978-0-387-45088-9

Reprinted from Space Science Reviews Journal, Vol. 123/1-4

**Title:** Coronal Mass Ejections

**Authors:** [Kunow, H.](#); [Crooker, N. U.](#); [Linker, J. A.](#); [Schwenn, R.](#); [von Steiger, R.](#)

**Publication:** Coronal Mass Ejections, Edited by H. Kunow, N.U. Crooker, J.A. Linker, R. Schwenn, and R. Von Steiger. Berlin: Springer, 2007.

-----  
**Space Science Reviews (2006), v. 123**

**This volume is the result of a series of workshops during the years 2000–2004 to study in detail origin, development, and effects of coronal mass ejections (CMEs).**

Special Issue: Coronal Mass Ejections

Guest Editors: N. U. Crooker, J. A. Linker and R. Schwenn

1-2

Foreword

H. Kunow, N. U. Crooker, J. A. Linker, R. Schwenn and R. von Steiger

Show Summary

Download PDF (69.4 KB)

3-11

A Brief History of CME Science

David Alexander, Ian G. Richardson and Thomas H. Zurbuchen

Show Summary

Download PDF (148.8 KB)

13-30

Coronal Mass Ejections: Overview of Observations

H. S. Hudson, J.-L. Bougeret and J. Burkepile

Show Summary

Download PDF (518.9 KB)

31-43

In-Situ Solar Wind and Magnetic Field Signatures of Interplanetary Coronal Mass Ejections

Thomas H. Zurbuchen and Ian G. Richardson

Show Summary

Download PDF (348.7 KB)

45-56

An Introduction to CMEs and Energetic Particles

H. V. Cane and D. Lario

[Show Summary](#)

[Download PDF \(745.2 KB\)](#)

57-80

An Introduction to Theory and Models of CMEs, Shocks, and Solar Energetic Particles

Z. Mikić and M. A. Lee

[Show Summary](#)

[Download PDF \(289.3 KB\)](#)

81-92

An Introduction to the Pre-CME Corona

David Alexander

[Show Summary](#)

[Download PDF \(155.0 KB\)](#)

93-109

Solar Imprint on ICMEs, Their Magnetic Connectivity, and Heliospheric Evolution

N. U. Crooker and T. S. Horbury

[Show Summary](#)

[Download PDF \(291.2 KB\)](#)

111-126

ICMEs in the Outer Heliosphere and at High Latitudes: An Introduction

R. von Steiger and J. D. Richardson

[Show Summary](#)

[Download PDF \(572.5 KB\)](#)

127-176

Coronal Observations of CMEs

Report of Working Group A

R. Schwenn, J. C. Raymond, D. Alexander, A. Ciaravella and N. Gopalswamy, et al.

[Show Summary](#)

[Download PDF \(1.3 MB\)](#)

177-216

Understanding Interplanetary Coronal Mass Ejection Signatures

Report of Working Group B

R. F. Wimmer-Schweingruber, N. U. Crooker, A. Balogh, V. Bothmer and R. J. Forsyth, et al.

[Show Summary](#)

[Download PDF \(1.0 MB\)](#)

217-250

Energetic Particle Observations

Report of Working Group C

B. Klecker, H. Kunow, H. V. Cane, S. Dalla and B. Heber, et al.

[Show Summary](#)

[Download PDF \(529.3 KB\)](#)

251-302

CME Theory and Models

Report of Working Group D

T. G. Forbes, J. A. Linker, J. Chen, C. Cid and J. Kóta, et al.

[Show Summary](#)

[Download PDF \(1.5 MB\)](#)

303-339

The Pre-CME Sun

Report of Working Group E

N. Gopalswamy, Z. Mikić, D. Maia, D. Alexander and H. Cremades, et al.

[Show Summary](#)

[Download PDF \(1.1 MB\)](#)

341-382

Multi-Wavelength Observations of CMEs and Associated Phenomena

Report of Working Group F

M. Pick, T. G. Forbes, G. Mann, H. V. Cane and J. Chen, et al.

[Show Summary](#)

[Download PDF \(934.5 KB\)](#)

383-416

ICMEs in the Inner Heliosphere: Origin, Evolution and Propagation Effects

Report of Working Group G

R. J. Forsyth, V. Bothmer, C. Cid, N. U. Crooker and T. S. Horbury, et al.

[Show Summary](#)

[Download PDF \(1.1 MB\)](#)

417-451

ICMEs at High Latitudes and in the Outer Heliosphere

Report of Working Group H

P. R. Gazis, A. Balogh, S. Dalla, R. Decker and B. Heber, et al.

[Show Summary](#)

[Download PDF \(1.4 MB\)](#)

453-470

CME Disturbance Forecasting

G. Siscoe and R. Schwenn

[Show Summary](#)

[Download PDF \(345.2 KB\)](#)

471-480

Coronal Mass Ejections

A Personal Workshop Summary

R. F. Wimmer-Schweingruber

[Show Summary](#)

[Download PDF \(382.5 KB\)](#)

481-484

Glossary

[Show Summary](#)

[Download PDF \(72.4 KB\)](#)

-----

**[Adv.Space Res. Vol. 40, Issue 12, 2007](#)**

Many papers on **Coronal Mass Ejections**



-----  
[Advances in Space Research, Volume 38, Issue 3](#), pp. 389-560 (2006)

**Many papers on** Coronal Mass Ejections and Solar Particle Events in Solar Cycle 23

-----  
**Solar Eruptions and Energetic Particles**

AGU Monograph, Vol. 165, 2006, ed. N. Gopalswamy, R. Mewaldt, & Torsti, J. (Washington DC: American Geophysical Union)

<http://onlinelibrary.wiley.com/book/10.1029/GM165>

-----  
**CMEs on young, solar-type stars**

Alicia [Aarnio](#):

RHESSI Science Nuggets, No. 214, Dec 2013

[http://sprg.ssl.berkeley.edu/~tohban/wiki/index.php/CMEs\\_on\\_young\\_solar-type\\_stars](http://sprg.ssl.berkeley.edu/~tohban/wiki/index.php/CMEs_on_young_solar-type_stars)

stellar flares and CMEs behave like solar ones.

We find that the relationship between solar flare energy and associated CME mass follows a log-linear relationship over several orders of magnitude in both quantities. Further, we suggest this relationship holds to even higher flare energies and CME masses for young, solar-type stars. We use the relationship to estimate mass loss rates from 10<sup>-12</sup> to 10<sup>-9</sup> MSun yr<sup>-1</sup>. We have also found a set of conditions (frequent eruptions, >10<sup>-10</sup> MSun yr<sup>-1</sup>) in which CMEs can indeed slow stellar rotation toward the end of the TTS phase.

**Solar Flares and Coronal Mass Ejections: A Statistically Determined Flare Flux –CME Mass Correlation**

A.N. [Aarnio](#) · K.G. Stassun · W.J. Hughes · S.L. McGregor

Solar Phys (2011) 268: 195–212, **File**

In an effort to examine the relationship between flare flux and corresponding CME mass, we temporally and spatially correlate all X-ray flares and CMEs in the LASCO and GOES archives from 1996 to 2006. We cross-reference 6733 CMEs having wellmeasured masses against 12 050 X-ray flares having position information as determined from their optical counterparts. For a given flare, we search in time for CMEs which occur 10 – 80 minutes afterward, and we further require the flare and CME to occur within ±45° in position angle on the solar disk. There are 826 CME/flare pairs which fit these criteria. Comparing the flare fluxes with CME masses of these paired events, we find CME mass increases with flare flux, following an approximately log-linear, broken relationship: in the limit of lower flare fluxes,  $\log(\text{CME mass}) \propto 0.68 \log(\text{flare flux})$ , and in the limit of higher flare fluxes,  $\log(\text{CME mass}) \propto 0.33 \log(\text{flare flux})$ . We show that this broken power-law, and in particular the flatter slope at higher flare fluxes, may be due to an observational bias against CMEs associated with the most energetic flares: halo CMEs. Correcting for this bias yields a single power-law relationship of the form  $\log(\text{CME mass}) \propto 0.70 \log(\text{flare flux})$ . This function describes the relationship between CME mass and flare flux over at least 3 dex in flare flux, from  $\approx 10^{-7} - 10^{-4} \text{ Wm}^{-2}$ .

**Serendipitous observation of a coronal mass ejection during the total solar eclipse of 14 December 2020**

[Guillermo Abramson](#)

2021

<https://arxiv.org/pdf/2106.00784.pdf>

We report observations of the total solar eclipse of 14 December 2020, during which a coronal mass ejection can be seen propagating. A comprehensive set of photographs covering a high dynamic range of exposure allow to characterize its dimensions. The displacement of the front can be seen occurring during the few minutes of totality.

**A Small-scale Eruption Leading to a Blowout Macrospicule Jet in an On-disk Coronal Hole**

Mitzi [Adams](#), Alphonse C. Sterling, Ronald L. Moore, and G. Allen Gary

2014 ApJ 783 11

We examine the three-dimensional magnetic structure and dynamics of a solar EUV-macroscopic jet that occurred on **2011 February 27** in an on-disk coronal hole. The observations are from the Solar Dynamics Observatory (SDO) Atmospheric Imaging Assembly (AIA) and the SDO Helioseismic and Magnetic Imager (HMI). The observations reveal that in this event, closed-field-carrying cool absorbing plasma, as in an erupting mini-filament, erupted and opened, forming a blowout jet. Contrary to some jet models, there was no substantial recently emerged, closed, bipolar-magnetic field in the base of the jet. Instead, over several hours, flux convergence and cancellation at the polarity inversion line inside an evolved arcade in the base apparently destabilized the entire arcade, including its cool-plasma-carrying core field, to undergo a blowout eruption in the manner of many standard-sized, arcade-blowout eruptions that produce a flare and coronal mass ejection. Internal reconnection made bright "flare" loops over the polarity inversion line inside the blowing-out arcade field, and external reconnection of the blowing-out arcade field with an ambient open field made longer and dimmer EUV loops on the outside of the blowing-out arcade. That the loops made by the external reconnection were much larger than the loops made by the internal reconnection makes this event a new variety of blowout jet, a variety not recognized in previous observations and models of blowout jets.

## **Effects of Initial Conditions on Magnetic Reconnection in a Solar Transient**

[Satyam Agarwal](#), [Ramit Bhattacharyya](#) & [Thomas Wiegmann](#)

[Solar Physics](#) volume 297, Article number: 91 (2022)

<https://doi.org/10.1007/s11207-022-02016-2>

Coronal magnetic field extrapolations are necessary to understand the magnetic field morphology of the source region in solar coronal transients. The extrapolation models are broadly classified into nonforce-free and force-free, depending on whether the model allows for a Lorentz force or not. Presently, these models are employed to carry out state-of-the-art data-driven and data-constrained magnetohydrodynamics (MHD) simulations to explore magnetic reconnection (MR)—the underlying cause of the transients. It is then imperative to study the influence of different extrapolation models on simulated evolution. For this purpose, the numerical model EULAG-MHD is employed to carry out simulations with different initial magnetic and velocity fields obtained through nonforce-free and force-free extrapolations. The selected active region is NOAA 11977, hosting a C6.6 class eruptive flare. Both extrapolations are found to be in good agreement with the observed line-of-sight and transverse magnetic fields. Further, a morphological comparison on the global scale and particularly for selected topologies, such as a magnetic null point and a hyperbolic flux tube (HFT), suggests that similar magnetic field line structures are reproducible in both models, although the extent of agreement between the two varies. Astoundingly, generation of a three-dimensional null near the HFT is observed in all the simulations, inferring the evolution to be independent of the particular initial field configuration. Moreover, the magnetic field lines (MFLs) undergoing MRs at the null point and HFT evolve similarly, further confirming the near independence of reconnection details on the chosen initial conditions. Consequently, both the extrapolation techniques can be suitable for initiating data-driven and data-constrained simulations.

## **Prediction of Solar Eruptions Using Filament Metadata**

Ashna [Aggarwal](#)<sup>1,2</sup>, Nicole Schanche<sup>2,3</sup>, Katharine K. Reeves<sup>2</sup>, Dustin Kempton<sup>4</sup>, and Rafal Angryk

2018 ApJS 236 15

<https://sci-hub.do/10.3847/1538-4365/aab77f>

<https://iopscience.iop.org/article/10.3847/1538-4365/aab77f/pdf>

We perform a statistical analysis of erupting and non-erupting solar filaments to determine the properties related to the eruption potential. In order to perform this study, we correlate filament eruptions documented in the Heliophysics Event Knowledgebase (HEK) with HEK filaments that have been grouped together using a spatiotemporal tracking algorithm. The HEK provides metadata about each filament instance, including values for length, area, tilt, and chirality. We add additional metadata properties such as the distance from the nearest active region and the magnetic field decay index. We compare trends in the metadata from erupting and non-erupting filament tracks to discover which properties present signs of an eruption. We find that a change in filament length over time is the most important factor in discriminating between erupting and non-erupting filament tracks, with erupting tracks being more likely to have decreasing length. We attempt to find an ensemble of predictive filament metadata using a Random Forest Classifier approach, but find the probability of correctly predicting an eruption with the current metadata is only slightly better than chance. **2012/01/09-13**

## **Automatic method for detection of solar coronal width using extreme ultra-violet (EUV) radiation**

Najmeh [Ahmadi](#), [Sherwin Parsi](#)

2019

<https://arxiv.org/pdf/1904.00104.pdf>

Solar corona, the last main layer of the atmosphere of the Sun, is detectable in the EUV and X-ray. The corona is expanding into space up to millions of kilometers and is observable during the eclipse. The temperature is increasing about millions of Kelvin. The investigation of this layer is significant for solar physicists because it is dynamic and features. Active regions (AR) and solar mass ejections (CMEs) are the important features in the solar corona. In this research, the solar limb and coronal width is studied from full-disk images at 284 Å taken by SOHO/EIT during eleven-year period (2000-2010). Next, using image processing methods and by applying region growing function, the corona is segmented and extracted from images in different angles. The radial velocities of CMEs are extracted.

## **Magnetic Interaction of a Super-CME with the Earth's Magnetosphere: Scenario for Young Earth**

Vladimir S. [Airapetian](#), Alex Gloer, William Danchi

Proceedings of 18th Cambridge Workshop on Cool Stars, Stellar Systems, and the Sun  
Proceedings of Lowell Observatory (9-13 June 2014) Edited by G. van Belle & H. Harris  
<http://arxiv.org/pdf/1410.7355v2.pdf>

Solar eruptions, known as Coronal Mass Ejections (CMEs), are frequently observed on our Sun. Recent Kepler observations of superflares on G-type stars have implied that so called super-CMEs, possessing kinetic energies 10 times of the most powerful CME event ever observed on the Sun, could be produced with a frequency of 1 event per 800-2000 yr on solar-like slowly rotating stars. We have performed a 3D time-dependent global magnetohydrodynamic simulation of the magnetic interaction of such a CME cloud with the Earth's magnetosphere. We calculated the global structure of the perturbed magnetosphere and derive the latitude of the open-closed magnetic field boundary. We also estimated energy fluxes penetrating the Earth's ionosphere and discuss the consequences of energetic particle fluxes on biological systems on early Earth.

## **The CME-productivity associated with flares from two active regions**

Adv. Space Res., 39(9), Pages 1469-1472, 2007

S. [Akiyama](#), S. Yashiro and N. Gopalswamy

We report on two flare-productive adjacent active regions (ARs), with different levels of coronal mass ejection (CME) association. AR 10039 and AR 10044 produced strong X-ray flares during their disk passages. We suggest that different pre-eruption evolution and magnetic configuration in the two regions might have contributed to the difference between the two ARs.

## **Evolution of CME Properties in the Inner Heliosphere: Prediction for Solar Orbiter and Parker Solar Probe**

Nada [Al-Haddad](#), [Noe Lugaz](#), [Stefaan Poedts](#), [Charles J. Farrugia](#) and, [Teresa Nieves-Chinchilla](#)  
ApJ **884** 179 **2019**

<https://arxiv.org/pdf/1910.04811.pdf>  
<https://sci-hub.se/10.3847/1538-4357/ab4126>

The evolution of the magnetic field and plasma quantities inside a coronal mass ejection (CME) with distance are known from statistical studies using data from 1 au monitors, planetary missions, Helios, and Ulysses. This does not cover the innermost heliosphere, below 0.29 au, where no data are yet publicly available. Here, we describe the evolution of the properties of simulated CMEs in the inner heliosphere using two different initiation mechanisms. We compare the radial evolution of these properties with that found from statistical studies based on observations in the inner heliosphere by Helios and MESSENGER. We find that the evolution of the radial size and magnetic field strength is nearly indistinguishable for twisted flux rope from that of writhed CMEs. The evolution of these properties is also consistent with past studies, primarily with recent statistical studies using in situ measurements and with studies using remote observations of CMEs.

## **Fitting and Reconstruction of Thirteen Simple Coronal Mass Ejections**

[Nada Al-Haddad](#), [Teresa Nieves-Chinchilla](#), [Neel P. Savani](#), [Noe Lugaz](#), [Ilija I. Roussev](#)  
Solar Phys. May 2018, 293:73

<https://arxiv.org/pdf/1804.02359.pdf>  
<https://link.springer.com/content/pdf/10.1007%2Fs11207-018-1288-3.pdf>

Coronal mass ejections (CMEs) are the main drivers of geomagnetic disturbances, but the effects of their interaction with Earth's magnetic field depend on their magnetic configuration and orientation. Fitting and reconstruction techniques have been developed to determine the important geometrical and physical CME properties. In many instances, there is disagreement between such different methods but also between fitting from in situ measurements and reconstruction based on remote imaging. Here, we compare three methods based on different assumptions for measurements of thirteen CMEs by the Wind spacecraft from 1997 to 2015. These CMEs are selected from the interplanetary coronal mass ejections catalog on [this https URL](#) due to their simplicity in terms of 1) small expansion speed throughout the CME and 2) little asymmetry in the magnetic field profile. This makes these thirteen events ideal candidates to compare codes that do not include expansion nor distortion. We find that, for these simple events, the codes are in relatively good agreement in terms of the CME axis orientation for six out of the 13 events. Using the Grad-Shafranov technique, we can determine the shape of the cross-section, which is assumed to be circular for the other two models, a force-free fitting and a circular-cylindrical non-force-free fitting. Five of the events are found to have a clear circular cross-section, even when this is not a pre-condition of the reconstruction. We make an initial attempt at evaluating the adequacy of the different assumptions for these simple CMEs. The conclusion of this work strongly suggests that attempts at reconciling in situ and remote-sensing views of CMEs must take in consideration the compatibility of the different models with specific CME structures to better reproduce flux ropes. **1997-01-10, 1998-08-**

19, 2000-07-01, 2001-04-21, 2002-09-29, 2008-05-23, 2009-09-30, 2012-05-16, 2012-11-12, 2013-06-27, 2013-12-24, 2014-04-11, 2015-05-06

**Table 1.** List of 13 CMEs used in this study

### **Formation of Radio Type II Bursts During a Multiple Coronal Mass Ejection Event**

Firas [Al-Hamadani](#), Silja Pohjolainen, Eino Valtonen

[Solar Physics](#) December 2017, 292:183

<https://link.springer.com/content/pdf/10.1007%2Fs11207-017-1208-y.pdf>

We study the solar event on **27 September 2001** that consisted of three consecutive coronal mass ejections (CMEs) originating from the same active region, which were associated with several periods of radio type II burst emission at decameter–hectometer (DH) wavelengths. Our analysis shows that the first radio burst originated from a low-density environment, formed in the wake of the first, slow CME. The frequency-drift of the burst suggests a low-speed burst driver, or that the shock was not propagating along the large density gradient. There is also evidence of band-splitting within this emission lane. The origin of the first shock remains unclear, as several alternative scenarios exist. The second shock showed separate periods of enhanced radio emission. This shock could have originated from a CME bow shock, caused by the fast and accelerating second or third CME. However, a shock at CME flanks is also possible, as the density depletion caused by the three CMEs would have affected the emission frequencies and hence the radio source heights could have been lower than usual. The last type II burst period showed enhanced emission in a wider bandwidth, which was most probably due to the CME–CME interaction. Only one shock that could reliably be associated with the investigated CMEs was observed to arrive near Earth.





### **Microwave and EUV Observations of an Erupting Filament and Associated Flare and Coronal Mass Ejections**

C. E. [Alissandrakis](#), A. A. Kochanov, S. Patsourakos, A. T. Altyntsev, S. V. Lesovoi, N. N. Lesovoya  
Publ. Astron. Soc. Japan 65, No SP1, S8 [10 pages] (2013)

<http://pasj.asj.or.jp/v65/sp1/65S008/65S008.pdf>

A filament eruption was observed with the Siberian Solar Radio Telescope (SSRT) on **2012 June 23**, starting at around 06:40 UT, beyond the west limb. The filament could be followed in SSRT images to heights above  $1R_{\odot}$ , and coincided with the core of the CME, seen in LASCO C2 images. We briefly discuss the dynamics of the eruption: the top of the filament showed a smooth acceleration up to an apparent velocity of  $\sim 1100$  km s $^{-1}$ . Images behind the limb from STEREO-A show a two-ribbon flare and the interaction of the main filament, located along the primary neutral line, with an arch-like structure, oriented in the perpendicular direction. The interaction was accompanied by strong emission and twisting motions. The microwave images show a low-temperature component, a high-temperature component associated with the interaction of the two filaments and another high-temperature component apparently associated with the top of flare loops. We computed the differential emission measure from the high-temperature AIA bands and from this the expected microwave brightness temperature; for emission associated with the top of the flare loops, the computed brightness was 35% lower than the observed value.

### **Machine Learning-Based Investigation of the Associations between CMEs and Filaments**

M. [Al-Omari](#) , R. Qahwaji , T. Colak  and S. Ipson 

[Solar Phys.](#) 262(2), 511–539, 2010

In this work we study the association between eruptive filaments/prominences and coronal mass ejections (CMEs) using machine learning-based algorithms that analyse the solar data available between January 1996 and December 2001. The support vector machine (SVM) learning algorithm is used for the purpose of knowledge extraction from the association results. The aim is to identify patterns of associations that can be represented using SVM learning rules for the subsequent use in near real-time and reliable CME prediction systems. Timing and location data in the US National Geophysical Data Center (NGDC) filament catalogue and the Solar and Heliospheric Observatory/Large Angle and Spectrometric Coronagraph (SOHO/LASCO) CME catalogue are processed to associate filaments with CMEs. In the previous studies, which classified CMEs into gradual and impulsive CMEs, the associations were refined based on the CME speed and acceleration. Then the associated pairs were refined manually to increase the accuracy of the training dataset. In the current study, a data-mining system is created to process and associate filament and CME data, which are arranged in numerical training vectors. Then the data are fed to SVMs to extract the embedded knowledge and provide the learning rules that can have the potential, in the future, to provide automated predictions of CMEs. The features representing the event time (average of the start and end times), duration, type, and extent of the filaments are extracted from all the associated and not-associated filaments and converted to a numerical format that is suitable for SVM use. Several validation and verification methods are used on the extracted dataset to determine if CMEs can be predicted solely and efficiently based on the associated filaments. More than 14 000 experiments are carried out to optimise the SVM and determine the input features that provide the best performance.

**Erratum:** [Solar Physics](#), January 2013, Volume 282, Issue 1, p 319

The online version of the original article can be found under doi:10.1007/s11207-010-9516-5.

The online version of the original article can be found at <http://dx.doi.org/10.1007/s11207-010-9516-5>

Erratum to: [Solar Phys](#) (2010) 262:511–539 DOI 10.1007/s11207-010-9516-5

This article was published with an erroneous version of the title and running title. Please find the correct version of the article title on this page, which should be regarded as the final version by the reader.

## **A BRIEF HISTORY OF CME SCIENCE**

DAVID [ALEXANDER](#)<sup>1,\*</sup>, IAN G. RICHARDSON<sup>2</sup> and THOMAS H. ZURBUCHEN<sup>3</sup>

Space Science Reviews (2006) 123: 3–11

## **AN INTRODUCTION TO THE PRE-CME CORONA**

DAVID [ALEXANDER](#)

Space Science Reviews (2006) 123: 81–92

## **Microwave and EUV Observations of an Erupting Filament and Associated Flare and CME**

[Alissandrakis](#), C. E.; Kochanov, A. A.; Patsourakos, S.; Altyntsev, A. T.; Lesovoi, S. V.; Lesovoya, N. N. E-print, Sept, 2013; PASJ

<http://arxiv.org/pdf/1309.1703v1.pdf>

A filament eruption was observed with the Siberian Solar Radio Telescope (SSRT) on **June 23 2012**, starting around 06:40 UT, beyond the West limb. The filament could be followed in SSRT images to heights above 1 Rs, and coincided with the core of the CME, seen in LASCO C2 images. We discuss briefly the dynamics of the eruption: the top of the filament showed a smooth acceleration up to an apparent velocity of 1100 km/s. Images behind the limb from STEREO-A show a two ribbon flare and the interaction of the main filament, located along the primary neutral line, with an arch-like structure, oriented in the perpendicular direction. The interaction was accompanied by strong emission and twisting motions. The microwave images show a low temperature component, a high temperature component associated with the interaction of the two filaments and another high temperature component apparently associated with the top of flare loops. We computed the differential emission measure from the high temperature AIA bands and from this the expected microwave brightness temperature; for the emission associated with the top of flare loops the computed brightness was 35% lower than the observed.

## **Next-Generation Comprehensive Data-Driven Models of Solar Eruptive Events**

[Joel C. Allred](#), [Graham S. Kerr](#), [Meriem Alaoui](#), [Juan Camilo Buitrago-Casas](#), +++

White paper submitted to the Decadal Survey for Solar and Space Physics (Heliophysics) 2024-2033  
**2023**

<https://arxiv.org/pdf/2307.14946.pdf>

Solar flares and coronal mass ejections are interrelated phenomena that together are known as solar eruptive events. These are the main drivers of space weather and understanding their origins is a primary goal of Heliophysics. In this white paper, we advocate for the allocation of sufficient resources to bring together experts in observations and modeling to construct and test next generation data-driven models of solar eruptive events. We identify the key components necessary for constructing comprehensive end-to-end models including global scale 3D MHD resolving magnetic field evolution and reconnection, small scale simulations of particle acceleration in reconnection exhausts, kinetic scale transport of flare-accelerated particles into the lower solar atmosphere, and the radiative and hydrodynamics responses of the solar atmosphere to flare heating. Using this modeling framework, long-standing questions regarding how solar eruptive events release energy, accelerate particles, and heat plasma can be explored. To address open questions in solar flare physics, we recommend that NASA and NSF provide sufficient research and analysis funds to bring together a large body of researchers and numerical tools to tackle the end-to-end modeling framework that we outline. Current dedicated theory and modeling funding programs are relatively small scale and infrequent; funding agencies must recognize that modern space physics demands the use of both observations and modeling to make rapid progress. **2013-05-13**

## **Prediction of Geoeffective CMEs Using SOHO Images and Deep Learning.**

[Alobaid](#), K.A., Wang, J.T.L., Wang, H. et al.

Sol Phys 299, 159 (2024)

<https://doi.org/10.1007/s11207-024-02385-w>

<https://link.springer.com/content/pdf/10.1007/s11207-024-02385-w.pdf>

The application of machine learning to the study of coronal mass ejections (CMEs) and their impacts on Earth has seen significant growth recently. Understanding and forecasting CME geoeffectiveness are crucial for protecting infrastructure in space and ensuring the resilience of technological systems on Earth. Here we present GeoCME, a deep-learning framework designed to predict, deterministically or probabilistically, whether a CME event that arrives at Earth will cause a geomagnetic storm. A geomagnetic storm is defined as a disturbance of the Earth's magnetosphere during which the minimum Dst index value is less than  $-50$  nT. GeoCME is trained on observations from the instruments including LASCO C2, EIT, and MDI on board the Solar and Heliospheric Observatory (SOHO), focusing on a dataset that includes 136 halo/partial halo CMEs in Solar Cycle 23. Using ensemble and transfer learning techniques, GeoCME is capable of extracting features hidden in the SOHO observations and making predictions based on the learned features. Our experimental results demonstrate the good performance of GeoCME, achieving a Matthew's correlation

coefficient of 0.807 and a true skill statistics score of 0.714 when the tool is used as a deterministic prediction model. When the tool is used as a probabilistic forecasting model, it achieves a Brier score of 0.094 and a Brier skill score of 0.493. These results are promising, showing that the proposed GeoCME can help enhance our understanding of CME-triggered solar-terrestrial interactions. **17 September 2002**

## **Estimating Coronal Mass Ejection Mass and Kinetic Energy by Fusion of Multiple Deep-learning Models**

Khalid A. **Alobaid**<sup>1,2,3</sup>, Yasser Abdullallah<sup>1,2</sup>, Jason T. L. Wang<sup>1,2</sup>, Haimin Wang<sup>1,4,5</sup>, Shen Fan<sup>1,2</sup>, Jialiang Li<sup>1,2</sup>, Huseyin Cavus<sup>6,7</sup>, and Vasyli Yurchyshyn<sup>5</sup>

**2023** ApJL 958 L34

<https://iopscience.iop.org/article/10.3847/2041-8213/ad0c4a/pdf>

<https://arxiv.org/abs/2312.01691>

Coronal mass ejections (CMEs) are massive solar eruptions, which have a significant impact on Earth. In this paper, we propose a new method, called DeepCME, to estimate two properties of CMEs, namely, CME mass and kinetic energy. Being able to estimate these properties helps better understand CME dynamics. Our study is based on the CME catalog maintained at the Coordinated Data Analysis Workshops Data Center, which contains all CMEs manually identified since 1996 using the Large Angle and Spectrometric Coronagraph (LASCO) on board the Solar and Heliospheric Observatory. We use LASCO C2 data in the period between 1996 January and 2020 December to train, validate, and test DeepCME through 10-fold cross validation. The DeepCME method is a fusion of three deep-learning models, namely ResNet, InceptionNet, and InceptionResNet. Our fusion model extracts features from LASCO C2 images, effectively combining the learning capabilities of the three component models to jointly estimate the mass and kinetic energy of CMEs. Experimental results show that the fusion model yields a mean relative error (MRE) of 0.013 (0.009, respectively) compared to the MRE of 0.019 (0.017, respectively) of the best component model InceptionResNet (InceptionNet, respectively) in estimating the CME mass (kinetic energy, respectively). To our knowledge, this is the first time that deep learning has been used for CME mass and kinetic energy estimations.

## **Detection of Coronal Mass Ejections Using Unsupervised Deep Clustering**

[Rasha Alshehhi](#) & [Prashanth R. Marpu](#)

[Solar Physics](#) volume 296, Article number: 104 (2021)

<https://link.springer.com/content/pdf/10.1007/s11207-021-01854-w.pdf>

<https://doi.org/10.1007/s11207-021-01854-w>

Coronal mass ejection (CME) is a highly energetic solar phenomenon. It has a significant impact on the space weather in the near-Earth environment. With the accumulation of CME observations, it becomes more challenging to handle them manually. Therefore, we need an automatic method for identifying CMEs. We propose an unsupervised method for classifying and detecting changes in CMEs. The method consists of four main steps: (i) feature extraction: features derived from difference-image and features derived from pretrained convolutional neural networks (CNN), (ii) dimensional reduction using Principal Component Analysis (PCA), (iii) unsupervised classification using K-mean clustering based on PCA components and (iv) morphological post-processing to improve the clustering output. We compare the results with manual catalog (e.g., coordinated data analysis workshops (CDWA) data center) and automatic detection catalogs (e.g., solar eruption detection system (SEEDS), computer-aided CME tracking (CACTus) and coronal image processing (CORIMP)). The comparison is based on CME characteristics (e.g., time of first appearance, position angle, angular width and velocity). We demonstrate the benefit of this unsupervised method, which produces comparable results to classical methods. **2011 November 22, 2014 February 9, 2016 January 8, 2017 September 6**

## **Laboratory study of the torus instability threshold in solar-relevant, line-tied magnetic flux ropes**

[Andrew Alt](#), [Clayton E. Myers](#), [Hantao Ji](#), [Jonathan Jara-Almonte](#), [Jongsoo Yoo](#), [Sayak Bose](#), [Aaron Goodman](#), [Masaaki Yamada](#), [Bernhard Kliem](#), [Antonia Savcheva](#)

ApJ **908** 41 **2021**

<https://arxiv.org/pdf/2010.10607.pdf>

<https://doi.org/10.3847/1538-4357/abda4b>

Coronal mass ejections (CME) occur when long-lived magnetic flux ropes (MFR) anchored to the solar surface destabilize and erupt away from the Sun. This destabilization is often described in terms of an ideal magnetohydrodynamic (MHD) instability called the torus instability. It occurs when the external magnetic field decreases sufficiently fast such that its decay index,  $n = -z \partial(\ln B) / \partial z$  is larger than a critical value,  $n > n_{cr}$ , where  $n_{cr} = 1.5$  for a full, large aspect ratio torus. However, when this is applied to solar MFRs, a range of conflicting values for  $n_{cr}$  is found in the literature. To investigate this discrepancy, we have conducted laboratory experiments on arched, line-tied flux ropes and have applied a theoretical model of the torus instability. Our model describes an MFR as a partial torus with footpoints anchored in a conducting surface and numerically calculates various magnetic forces on it. This calculation yields a better prediction of  $n_{cr}$  which takes into account the specific parameters of the MFR. We describe a systematic methodology to properly translate laboratory results to their solar counterparts, provided that the MFRs have sufficiently small edge safety factor, or equivalently, large enough twist. After this translation, our model predicts that  $n_{cr}$  in solar conditions often falls near  $n_{Solcr} \sim 0.9$  and within a larger range of  $n_{Solcr} \sim (0.7, 1.2)$  depending

on the parameters. The methodology of translating laboratory MFRs to their solar counterparts enables quantitative investigations of the initiation of CMEs through laboratory experiments. These experiments allow for new physics insights that are required for better predictions of space weather events but are difficult to obtain otherwise.

### **Coronal Mass Ejections and Exoplanets: A Numerical Perspective**

[Julián D. Alvarado-Gómez](#) (1), [Jeremy J. Drake](#) (2), [Ofer Cohen](#) (3), [Federico Fraschetti](#) (2 and 4), [Cecilia Garraffo](#) (2 and 5), [Katja Poppenhäger](#) (1 and 6)

Astronomical Notes (Astronomische Nachrichten) 2021

<https://arxiv.org/pdf/2111.09704.pdf>

Coronal mass ejections (CMEs) are more energetic than any other class of solar phenomena. They arise from the rapid release of up to 10<sup>33</sup> erg of magnetic energy mainly in the form of particle acceleration and bulk plasma motion. Their stellar counterparts, presumably involving much larger energies, are expected to play a fundamental role in shaping the environmental conditions around low-mass stars, in some cases perhaps with catastrophic consequences for planetary systems due to processes such as atmospheric erosion and depletion. Despite their importance, the direct observational evidence for stellar CMEs is almost non-existent. In this way, numerical simulations constitute extremely valuable tools to shed some light on eruptive behavior in the stellar regime. Here we review recent results obtained from realistic modeling of CMEs in active stars, highlighting their key role in the interpretation of currently available observational constraints. We include studies performed on M-dwarf stars, focusing on how emerging signatures in different wavelengths related to these events vary as a function of the magnetic properties of the star. Finally, the implications and relevance of these numerical results are discussed in the context of future characterization of host star-exoplanet systems.

### **Tuning the Exo-Space Weather Radio for Stellar Coronal Mass Ejections**

[Julián D. Alvarado-Gómez](#) (1 and 2), [Jeremy J. Drake](#) (2), [Federico Fraschetti](#) (2 and 3), [Cecilia Garraffo](#) (2 and 4), [Ofer Cohen](#) (5), [Christian Vocks](#) (1), [Katja Poppenhäger](#) (1), [Sofia P. Moschou](#) (2), [Rakesh K. Yadav](#) (6), [Ward B. Manchester IV](#) (7)

ApJ 2020

<https://arxiv.org/pdf/2004.05379.pdf>

Coronal mass ejections (CMEs) on stars other than the Sun have proven very difficult to detect. One promising pathway lies in the detection of type II radio bursts. Their appearance and distinctive properties are associated with the development of an outward propagating CME-driven shock. However, dedicated radio searches have not been able to identify these transient features in other stars. Large Alfvén speeds and the magnetic suppression of CMEs in active stars have been proposed to render stellar eruptions "radio-quiet". Employing 3D magnetohydrodynamic simulations, we study here the distribution of the coronal Alfvén speed, focusing on two cases representative of a young Sun-like star and a mid-activity M-dwarf (Proxima Centauri). These results are compared with a standard solar simulation and used to characterize the shock-prone regions in the stellar corona and wind. Furthermore, using a flux-rope eruption model, we drive realistic CME events within our M-dwarf simulation. We consider eruptions with different energies to probe the regimes of weak and partial CME magnetic confinement. While these CMEs are able to generate shocks in the corona, those are pushed much farther out compared to their solar counterparts. This drastically reduces the resulting type II radio burst frequencies down to the ionospheric cutoff, which impedes their detection with ground-based instrumentation. **Feb-March 2011 (CR 2107)**

### **(Simulating) Coronal Mass Ejections in Active Stars**

[Julián D. Alvarado-Gómez](#) (1 and 2), [Jeremy J. Drake](#) (2), [Cecilia Garraffo](#) (3), [Sofia P. Moschou](#) (2), [Ofer Cohen](#) (4), [Rakesh K. Yadav](#) (3), [Federico Fraschetti](#)

Proceedings of the IAU Symposium 354, Solar and Stellar Magnetic Fields: Origins and Manifestations.

Eds: A. Kosovichev, K. Strassmeier, M. Jardine 2020

<https://arxiv.org/pdf/1912.12314.pdf>

The stellar magnetic field completely dominates the environment around late-type stars. It is responsible for driving the coronal high-energy radiation (e.g. EUV/X-rays), the development of stellar winds, and the generation of transient events such as flares and coronal mass ejections (CMEs). While progress has been made for the first two processes, our understanding of the eruptive behavior in late-type stars is still very limited. One example of this is the fact that despite the frequent and highly energetic flaring observed in active stars, direct evidence for stellar CMEs is almost non-existent. Here we discuss realistic 3D simulations of stellar CMEs, analyzing their resulting properties in contrast with solar eruptions, and use them to provide a common framework to interpret the available stellar observations. Additionally, we present results from the first 3D CME simulations in M-dwarf stars, with emphasis on possible observable signatures imprinted in the stellar corona.

### **Coronal response to magnetically-suppressed CME events in M-dwarf stars**

[Julián D. Alvarado-Gómez](#) (1), [Jeremy J. Drake](#) (1), [Sofia P. Moschou](#) (1), [Cecilia Garraffo](#) (2,1), [Ofer Cohen](#) (3), [Rakesh K. Yadav](#) (2), [Federico Fraschetti](#)

ApJL 2019

<https://arxiv.org/pdf/1909.04092.pdf>

We report the results of the first state-of-the-art numerical simulations of Coronal Mass Ejections (CMEs) taking place in realistic magnetic field configurations of moderately active M-dwarf stars. Our analysis indicates that a clear, novel, and observable, coronal response is generated due to the collapse of the eruption and its eventual release into the stellar wind. Escaping CME events, weakly suppressed by the large-scale field, induce a flare-like signature in the emission from coronal material at different temperatures due to compression and associated heating. Such flare-like profiles display a distinctive temporal evolution in their Doppler shift signal (from red to blue), as the eruption first collapses towards the star and then perturbs the ambient magnetized plasma on its way outwards. For stellar fields providing partial confinement, CME fragmentation takes place, leading to rise and fall flow patterns which resemble the solar coronal rain cycle. In strongly suppressed events, the response is better described as a gradual brightening, in which the failed CME is deposited in the form of a coronal rain cloud leading to a much slower rise in the ambient high-energy flux by relatively small factors ( $\sim 2-3$ ). In all the considered cases (escaping/confined) a fractional decrease in the emission from mid-range coronal temperature plasma occurs, similar to the coronal dimming events observed on the Sun. Detection of the observational signatures of these CME-induced features requires a sensitive next generation X-ray space telescope.

## Suppression of **Coronal Mass Ejections in active stars** by an overlying large-scale magnetic field: A numerical study

[Julián D. Alvarado-Gómez](#), [Jeremy J. Drake](#), [Ofar Cohen](#), [Sofia P. Moschou](#), [Cecilia Garraffo](#)

ApJ 862, Issue 2, article id. 93 2018

<https://arxiv.org/pdf/1806.02828.pdf>

We present results from a set of numerical simulations aimed at exploring the mechanism of coronal mass ejection (CME) suppression in active stars by an overlying large-scale magnetic field. We use a state-of-the-art 3D magnetohydrodynamic (MHD) code which considers a self-consistent coupling between an Alfvén wave-driven stellar wind solution, and a first-principles CME model based on the eruption of a flux-rope anchored to a mixed polarity region. By replicating the driving conditions used in simulations of strong solar CMEs, we show that a large-scale dipolar magnetic field of 75 G is able to fully confine eruptions within the stellar corona. Our simulations also consider CMEs exceeding the magnetic energy used in solar studies, which are able to escape the large-scale magnetic field confinement. The analysis includes a qualitative and quantitative description of the simulated CMEs and their dynamics, which reveals a drastic reduction of the radial speed caused by the overlying magnetic field. With the aid of recent observational studies, we place our numerical results in the context of solar and stellar flaring events. In this way, we find that this particular large-scale magnetic field configuration establishes a suppression threshold around  $\sim 3 \times 10^{32}$  erg in the CME kinetic energy. Extending the solar flare-CME relations to other stars, such CME kinetic energies could be typically achieved during erupting flaring events with total energies larger than  $6 \times 10^{32}$  erg (GOES class  $\sim X70$ ). See <https://phys.org/news/2018-08-coronal-mass-ejection-star-sun.html>

See **1. Introduction**

## Identification of Low Coronal Sources of "Stealth" Coronal Mass Ejections Using New Image Processing Techniques

Nathalia [Alzate](#) and Huw Morgan

2017 ApJ 840 103

<https://sci-hub.ru/10.3847/1538-4357/aa6caa>

Coronal mass ejections (CMEs) are generally associated with low coronal signatures (LCSs), such as flares, filament eruptions, extreme ultraviolet (EUV) waves, or jets. A number of recent studies have reported the existence of stealth CMEs as events without LCSs, possibly due to observational limitations. Our study focuses on a set of **40 stealth CMEs** identified from a study by D'Huys et al. New image processing techniques are applied to high-cadence, multi-instrument sets of images spanning the onset and propagation time of each of these CMEs to search for possible LCSs. Twenty-three of these events are identified as small, low-mass, unstructured blobs or puffs, often occurring in the aftermath of a large CME, but associated with LCSs such as small flares, jets, or filament eruptions. Of the larger CMEs, seven are associated with jets and eight with filament eruptions. Several of these filament eruptions are different from the standard model of an erupting filament/flux tube in that they are eruptions of large, faint flux tubes that seem to exist at large heights for a long time prior to their slow eruption. For two of these events, we see an eruption in Large Angle Spectrometric Coronagraph C2 images and the consequent changes at the bottom edge of the eruption in EUV images. All 40 events in our study are associated with some form of LCS. We conclude that stealth CMEs arise from observational and processing limitations. **2012-01-07, 2012-02-22, 2012-02-29, 2012-04-22, June 02 2012, 2012-07-07, Aug 12 2012, Oct 20 2012, Nov 25 2012**

**Table 1** Description of the 2012 Events

## Low-Coronal Sources of "Stealth" Coronal Mass Ejections

Nathalia [Alzate](#) & Huw Morgan

UKSP Nuggets of 2016 #69

<http://www.uksolphys.org/uksp-nugget/69-low-coronal-sources-of-stealth-coronal-mass-ejections/>

Coronal mass ejections (CMEs) are generally associated with eruptive phenomena in the lower corona such as flares, filament eruptions, EUV waves or jets, collectively known as low-coronal signatures (LCSs). CMEs lacking these



signatures are identified as “stealth” events. In this nugget we report on our application of new image processing techniques [1,2] to events previously classified as stealth CMEs [3]. The processed EUV images reveal LCSs for all the listed “stealth” CMEs ranging from flares and jets to filament eruptions. Many events identified as CMEs are small blobs or puffs [4], often occurring in the aftermath of a large CME. Several of the larger, structured “stealth” CMEs arise from the slow eruption of sizeable, faint flux tubes situated at high latitude and large heights, therefore in regions of low density and weak magnetic field. A “stealth” CME is therefore a misconception arising from observational and processing limitations. **23 February 2012**

## **JETS, CORONAL "PUFFS," AND A SLOW CORONAL MASS EJECTION CAUSED BY AN OPPOSITE-POLARITY REGION WITHIN AN ACTIVE REGION FOOTPOINT**

N. [Alzate](#) and H. Morgan

**2016 ApJ 823 129**

During a period of three days beginning 2013 January 17, twelve recurrent reconnection events occur within a small region of opposing flux embedded within one footpoint of an active region, accompanied by flares and jets observed in EUV and fast and faint structureless "puffs" observed by coronagraphs. During the same period a slow structured CME gradually erupts, with one end anchored close to, or within, the jetting region. Four of the jet events occur in pairs—a narrow, primary jet followed within a few tens of minutes by a wider, more massive, jet. All the jets are slow, with an apparent speed of  $\sim 100 \text{ km s}^{-1}$ . The speed of the wide puffs in the coronagraph data is  $\sim 300 \text{ km s}^{-1}$ , and the timing of their appearance rules out a direct association with the EUV jetting material. The jet material propagates along large-scale closed-field loops and does not escape to the extended corona. The rapid reconfiguration of the closed loops following reconnection causes an outwardly propagating disturbance, or wave front, which manifests as puffs in coronagraph data. Furthermore, the newly expanded closed flux tube forms a pressure imbalance, which can result in a secondary jet. The reconnection events, through recurrent field reconfiguration, also leads to the gradual eruption of the structured flux tube appearing as the slow CME. Faint propagating coronal disturbances resulting from flares/jets may be common, but are usually obscured by associated ejections. Occasionally, the associated material ejections are absent, and coronal puffs may be clearly observed. **17-19 January 2013.**

## **Coronal “Puffs”: fast and slow ejections caused by active region jets**

Nathalia [Alzate](#) & Huw Morgan

UKSP Nugget #52, Oct **2014**

<http://www.uksolphys.org/uksp-nugget/52-coronal-puffs-fast-and-slow-ejections-caused-by-active-region-jets/>

An eruption loses its moorings among a series of small puffs. **17-19 January 2013.**

## **Magnetic cage and rope as the key for solar eruptions.**

[Amari](#) T, Canou A, Aly JJ, Delyon F, Alauzet F.

**2018 Nature 554, Issue 7691, 211–215. doi: 10.1038/nature24671**

<https://sci-hub.ru/10.1038/nature24671>

<https://www.nature.com/articles/nature24671>

Solar flares are spectacular coronal events that release large amounts of energy. They are classified as either eruptive or confined, depending on whether they are associated with a coronal mass ejection. Two types of model have been developed to identify the mechanism that triggers confined flares, although it has hitherto not been possible to decide between them because the magnetic field at the origin of the flares could not be determined with the required accuracy. In the first type of model, the triggering is related to the topological complexity of the flaring structure, which implies the presence of magnetically singular surfaces. This picture is observationally supported by the fact that radiative emission occurs near these features in many flaring regions. The second type of model attributes a key role to the formation of a twisted flux rope, which becomes unstable. Its plausibility is supported by simulations, by interpretations of some observations and by laboratory experiments. Here we report modelling of a confined event that uses the measured photospheric magnetic field as input. We first use a static model to compute the slowly evolving magnetic state of the corona before the eruption, and then use a dynamical model to determine the evolution during the eruption itself. We find that a magnetic flux rope must be present throughout the entire event to match the field measurements. This rope evolves slowly before saturating and suddenly erupting. Its energy is insufficient to break through the overlying field, whose lines form a confining cage, but its twist is large enough to trigger a kink instability, leading to the confined flare, as previously suggested. Topology is not the main cause of the flare, but it traces out the locations of the X-ray emission. We show that a weaker magnetic cage would have produced a more energetic eruption with a coronal mass ejection, associated with a predicted energy upper bound for a given region.

## **CORONAL MASS EJECTION INITIATION BY CONVERGING PHOTOSPHERIC FLOWS: TOWARD A REALISTIC MODEL**

T. [Amari](#)<sup>1</sup>, J.-J. Aly<sup>2</sup>, J.-F. Luciani<sup>1</sup>, Z. Mikic<sup>3</sup> and J. Linker

**2011 ApJ 742 L27**

In the context of coronal mass ejections triggering, we reconsider the class of models in which the evolution of an active region (AR) is driven by imposed boundary motions converging toward the polarity inversion line (PIL). We introduce a new model problem in which there is a large-scale flow with a diverging structure on the photosphere. This flow is reminiscent of that of the well-known moat flow around each of the two spots of a bipolar AR and transports only part of the magnetic flux toward the PIL. It is thus more compatible with observations than the one used in our previous study, which forced the whole positive and negative polarity parts of the AR approaching each other. We also include a diffusion term associated with small-scale turbulent photospheric motions, but keep the associated diffusivity at a low value in the particular study described here. We show that the evolution of an initial sheared force-free field first leads to the formation of a twisted flux rope which stays in equilibrium for some time. Eventually, however, the configuration suffers a global disruption whose underlying mechanism is found by energetic considerations to be nonequilibrium. It begins indeed when the magnetic energy becomes of the order of the energy of an accessible partially open field. For triggering an eruption by converging flows, it is thus not necessary to advect the whole AR toward the PIL, but only its central part.

## **CORONAL MASS EJECTION INITIATION: ON THE NATURE OF THE FLUX CANCELLATION MODEL**

T. [Amari](#)<sup>1,2,3,4</sup>, J.-J. Aly<sup>2</sup>, Z. Mikic<sup>3</sup>, and J. Linker<sup>3</sup>

Astrophysical Journal Letters, 717:L26–L30, 2010 July, [File](#)

We consider a three-dimensional bipolar force-free magnetic field with a nonzero magnetic helicity, occupying a half-space, and study the problem of its evolution driven by an imposed photospheric flux decrease. For this specific setting of the Flux Cancellation Model describing coronal mass ejections occurring in active regions, we address the issues of the physical meaning of flux decrease, of the influence on field evolution of the size of the domain over which this decrease is imposed, and of the existence of an energetic criterion characterizing the possible onset of disruption of the configuration. We show that (1) the imposed flux disappearance can be interpreted in terms of transport of positive and negative fluxes toward the inversion line, where they get annihilated. (2) For the particular case actually computed, in which the initial state is quite sheared, the formation of a twisted flux rope and the subsequent global disruption of the configuration are obtained when the flux has decreased by only a modest amount over a limited part of the whole active region. (3) The disruption is produced when the magnetic energy becomes of the order of the decreasing energy of a semi-open field, and then before reaching the energy of the associated fully open field. This suggests that the mechanism leading to the disruption is nonequilibrium as in the case where flux is imposed to decrease over the whole region.

## **Magnetic flux ropes: Fundamental structures for eruptive phenomena**

Tahar [Amari](#) and Jean-Jacques Aly<sup>2</sup>

Proceedings of the International Astronomical Union / Volume 4 / Symposium S257, pp 211 - 222 ,

Published online: 16 Mar 2009, [File](#)

<http://journals.cambridge.org/action/displayIssue?iid=4866212>

We consider some general aspects of twisted magnetic flux ropes (TFR), which are thought to play a fundamental role in the structure and dynamics of large scale eruptive events. We first discuss the possibility to show the presence of a TFR in a pre-eruptive configuration by using a model along with observational informations provided by a vector magnetograph. Then we present, in the framework of a generic model in which the coronal field is driven into an evolution by changes imposed at the photospheric level, several mechanisms which may lead to the formation and the disruption of a TFR, including the development of a MHD instability, and we discuss the issues of the energy and helicity contents of an erupting configuration. Finally we report some results of a recent and more ambitious approach to the physics of TFRs in which one tries to describe in a consistent way their rising through the convection zone, their emergence through the photosphere, and their subsequent evolution in the corona. [Review](#)

## **CORONAL MASS EJECTION INITIATION AND COMPLEX TOPOLOGY CONFIGURATIONS IN THE FLUX CANCELLATION AND BREAKOUT MODELS**

T. [Amari](#), J. J. Aly, Z. Mikic and J. Linker

The Astrophysical Journal, 671: L189–L192, 2007

<http://www.journals.uchicago.edu/doi/pdf/10.1086/524942>

We present some new results showing that the flux cancellation model for coronal mass ejections (CMEs) works well also in a complex-topology magnetic field. We consider as a model problem the case of the flux cancellation-driven evolution of a quadrupolar configuration.

## **STABILITY AND DYNAMICS OF A FLUX ROPE FORMED VIA FLUX EMERGENCE INTO THE SOLAR ATMOSPHERE**

J. M. [An](#)<sup>1</sup> and T. Magara

2013 ApJ 773 21

We study the stability and dynamics of a flux rope formed through the emergence of a twisted magnetic flux tube into the solar atmosphere. A three-dimensional magnetohydrodynamic simulation has been performed to investigate several

key factors affecting the dynamics of the flux rope. The stability of the flux rope is examined by deriving the decay index of the coronal magnetic field surrounding the flux rope. We investigate a transition between the quasi-static and dynamic states of the flux rope through an analysis of the curvature and scale height of emerging magnetic field. A practical application of this analysis for global eruptions is also considered.

## **Diagnosis of Magnetic and Electric Fields of Chromospheric Jets through spectropolarimetric Observations of H I Paschen Lines**

Tetsu [Anan](#), Roberto Casini, Kiyoshi Ichimoto

E-print, Feb 2014

Magnetic fields govern the plasma dynamics in the outer layers of the solar atmosphere, and electric fields acting on neutral atoms that move across the magnetic field enable us to study the dynamical coupling between neutrals and ions in the plasma. In order to measure the magnetic and electric fields of chromospheric jets, the full Stokes spectra of the Paschen series of neutral hydrogen in a surge and in some active region jets that took place at the solar limb were observed on **May 5, 2012**, using the spectropolarimeter of the Domeless Solar Telescope at Hida observatory, Japan. First, we inverted the Stokes spectra taking into account only the effect of magnetic fields on the energy structure and polarization of the hydrogen levels. Having found no definitive evidence of the effects of electric fields in the observed Stokes profiles, we then estimated an upper bound for these fields by calculating the polarization degree under the magnetic field configuration derived in the first step, with the additional presence of a perpendicular (Lorentz type) electric field of varying strength. The inferred direction of the magnetic field on the plane of the sky (POS) approximately aligns to the active region jets and the surge, with magnetic field strengths in the range  $10 \text{ G} < B < 640 \text{ G}$  for the surge. Using magnetic field strengths of 70, 200, and 600 G, we obtained upper limits for possible electric fields of 0.04, 0.3, and 0.8 V/cm, respectively. This upper bound is conservative, since in our modeling we neglected the possible contribution of collisional depolarization. Because the velocity of neutral atoms of hydrogen moving across the magnetic field derived from these upper limits of the Lorentz electric field is far below the bulk velocity of the plasma perpendicular to the magnetic field as measured by the Doppler shift, we conclude that the neutral atoms must be highly frozen to the magnetic field in the surge.

## **Predicting Flares and Solar Energetic Particle Events: The FORSPEF Tool**

A. [Anastasiadis](#), A. Papaioannou, I. Sandberg, M. Georgoulis, K. Tziotziou, A. Kouloumvakos, P. Jiggins  
[Solar Physics](#) September 2017, 292:134

A novel integrated prediction system for solar flares (SFs) and solar energetic particle (SEP) events is presented here. The tool called forecasting solar particle events and flares (FORSPEF) provides forecasts of solar eruptive events, such as SFs with a projection to occurrence and velocity of coronal mass ejections (CMEs), and the likelihood of occurrence of an SEP event. In addition, the tool provides nowcasting of SEP events based on actual SF and CME near real-time data, as well as the SEP characteristics (e.g. peak flux, fluence, rise time, and duration) per parent solar event. The prediction of SFs relies on the effective connected magnetic field strength (BeffBeff) metric, which is based on an assessment of potentially flaring active-region (AR) magnetic configurations, and it uses a sophisticated statistical analysis of a large number of AR magnetograms. For the prediction of SEP events, new statistical methods have been developed for the likelihood of the SEP occurrence and the expected SEP characteristics. The prediction window in the forecasting scheme is 24 hours with a refresh rate of 3 hours, while the respective prediction time for the nowcasting scheme depends on the availability of the near real-time data and ranges between 15 – 20 minutes for solar flares and 6 hours for CMEs. We present the modules of the FORSPEF system, their interconnection, and the operational setup. Finally, we demonstrate the validation of the modules of the FORSPEF tool using categorical scores constructed on archived data, and we also discuss independent case studies. **26 Oct-8 Nov 2003, 20 Jan 2005, 7 March 2012, 2014-12-18** <http://tromos.space.noa.gr/forspef/>  
**CESRA Highlight #1551, Oct 2017** <http://www.astro.gla.ac.uk/users/eduard/cesra/?p=1551>

## **Internal structure of a coronal mass ejection revealed by Akatsuki radio occultation observations**

H. [Ando](#), D. Shiota, T. Imamura, M. Tokumaru, A. Asai, H. Isobe, M. Pätzold, B. Häusler, M. Nakamura

JGR Volume 120, Issue 7 July 2015 Pages 5318–5328

A coronal mass ejection (CME) was observed at the heliocentric distance of 12.7  $R_{\odot}$  by radio occultation measurements using the Akatsuki spacecraft. The temporal developments of the bulk velocity and the electron column density along the raypath traversing the CME were obtained, and under the assumption that the irregularities are transported across the raypath, the internal structure of the CME covering the region from the core to the tail was retrieved. The suggested internal structure was compared with Large Angle Spectroscopic Coronagraph images, a numerical study and previous radio occultation observations of CMEs to propose a CME model; the bulk velocity and the electron density have relatively large values in the core, decrease behind the core, and increase again in the tail region where the fast plasma flow associated with the magnetic reconnection converges. *This implies that the magnetic reconnection behind the CMEs might continue up to at least the heliocentric distance of  $\sim 13 R_{\odot}$ .* **13 June 2011**

## **A two-Type Classification of Lasco Coronal Mass Ejection,**

**Andrews**, M. D. and R.A. Howard.

*Space Science Reviews*, **95**, Numbers 1-2, p. 147-163 (2001); **File**

The causes and origins of Coronal Mass Ejections (CMEs) remain among the outstanding questions in Space Physics. The observations of CMEs by the LASCO coronagraphs on SOHO suggest that there are two distinct types of CMEs. The two types of events can be most easily distinguished by examining height-time plots. The Type A (Acceleration) events produce curved plots that often indicate a constant acceleration. These events are usually associated with pre-existing helmet-streamers, and are often associated with prominence eruptions or filament disappearance. The Type C (Constant speed) events show a constant speed. These events are usually brighter, larger, and faster than Type A events and may be associated with X-ray flares. While the two types of events can be distinguished in other ways, the height-time plots are a simple and unambiguous way to make this identification.

## **Observations and Simulations of Reconnecting Current Sheets in the Solar Corona**

Spiro **Antiochos**, Pankaj Kumar, Judy Jarpen, and Joel Dahlin

EGU2020-5597 May 2020

<https://meetingorganizer.copernicus.org/EGU2020/displays/36057>

Jets and mass ejections are ubiquitous features of the Sun's corona. These explosive dynamics are all believed to be driven by magnetic reconnection at two types of current sheets that form in the solar atmosphere: those that form at magnetic null points and separatrix surfaces, and those, such as the heliospheric current sheet, that form as a result of a large expansion of a bipolar magnetic field. In our breakout model, both types of current sheets are essential for the explosive release of magnetic energy. We report on the first direct observations of reconnection and island formation in a null-point current sheet associated with a large coronal jet. The topology and velocities of the islands are in excellent agreement with our numerical simulations of coronal jets. We discuss the implications of the observations and our models for understanding the energetic particles produced by these events and their release into interplanetary space, as well as the implications for observations by Solar Orbiter and the Parker Solar Probe. **20-21 Apr 2019**

**Presentaton #5597** <https://presentations.copernicus.org/EGU2020/presentations-ST1.7.zip> **File**

## **Reconnection nanojets in the solar corona**

**Antolin, Patrick**; **Pagano, Paolo**; **Testa, Paola**; **Petralia, Antonino**; **Reale, Fabio**

*Nature Astronomy*, Volume 5, p. 54-62, 2021

<https://www.nature.com/articles/s41550-020-1199-8#citeas>

<https://doi.org/10.1038/s41550-020-1199-8>

The solar corona is shaped and mysteriously heated to millions of degrees by the Sun's magnetic field. It has long been hypothesized that the heating results from a myriad of tiny magnetic energy outbursts called nanoflares, driven by the fundamental process of magnetic reconnection. Misaligned magnetic field lines can break and reconnect, producing nanoflares in avalanche-like processes. However, no direct and unique observations of such nanoflares exist to date, and the lack of a smoking gun has cast doubt on the possibility of solving the coronal heating problem. From coordinated multi-band high-resolution observations, we report on the discovery of very fast and bursty nanojets, the telltale signature of reconnection-based nanoflares resulting in coronal heating. Using state-of-the-art numerical simulations, we demonstrate that the nanojet is a consequence of the slingshot effect from the magnetically tensed, curved magnetic field lines reconnecting at small angles. Nanojets are therefore the key signature of reconnection-based coronal heating in action.

**IRIS Nugget**, May 2021, <https://iris.lmsal.com/nugget>

## **Hybrid Reconstruction to Derive 3D Height –Time Evolution for Coronal Mass Ejections**

A. **Antunes** · A. Thernisien · A. Yahil

*Solar Phys* (2009) 259: 199–212; **File**

We present a hybrid combination of forward and inverse reconstruction methods using multiple observations of a coronal mass ejection (CME) to derive the three-dimensional (3D) “true” height – time plots for individual CME components. We apply this hybrid method to the components of the **31 December 2007** CME. This CME, observed clearly in both the STEREO A and STEREO B COR2 white-light coronagraphs, evolves asymmetrically across the 15-solar-radius field of view within a span of three hours. The method has two reconstruction steps. We fit a boundary envelope for the potential 3D CME shape using a flux-rope-type model oriented to best match the observations. Using this forward model as a constraining envelope, we then run an inverse reconstruction, solving for the simplest underlying 3D electron density distribution that can, when rendered, reproduce the observed coronagraph data frames. We produce plots for each segment to establish the 3D or “true” height – time plots for each center of mass as well as for the bulk CME motion, and we use these plots along with our derived density profiles to estimate the CME's asymmetric expansion rate.

## **Magnetic Helicity Signs and Flaring Propensity: Comparing Force-free Parameter with the Helicity signs of H $\alpha$ Filaments and X-ray Sigmoids**

V. [Aparna](#), [Manolis K. Georgoulis](#), [Petrus C. Martens](#)

ApJ 967 134 2024

<https://arxiv.org/ftp/arxiv/papers/2403/2403.17075.pdf>

<https://iopscience.iop.org/article/10.3847/1538-4357/ad38c1/pdf>

Sigmoids produce strong eruptive events. Earlier studies have shown that the ICME axial magnetic field  $B_z$  can be predicted with some credibility by observing the corresponding filament or the polarity inversion line in the region of eruption and deriving the magnetic field direction from that. Sigmoids are coronal structures often associated with filaments in the sigmoidal region. In this study, firstly we compare filament chirality with sigmoid handedness to observe their correlation. Secondly, we perform non-linear force-free approximations of the coronal magnetic connectivity using photospheric vector magnetograms underneath sigmoids to obtain a weighted-average value of the force-free parameter and to correlate it with filament chirality and the observed coronal sigmoid handedness. Importantly, we find that the sigmoids and their filament counterparts do not always have the same helicity signs. Production of eruptive events by regions that do not have the same signs of helicities is  $\sim 3.5$  times higher than when they do. A case study of magnetic energy/ helicity evolution in NOAA AR 12473 is also presented. **2011-11-24, 2012-05-05, 2012-06-15, Dec 23, 2015 - Jan 01, 2016.**

## **Solar Filaments and Interplanetary Magnetic Field $B_z$**

V. [Aparna](#) and Petrus C. Martens

2020 ApJ 897 68

<https://doi.org/10.3847/1538-4357/ab908b>

The direction of the axis of an interplanetary coronal mass ejection (ICME) plays an important role in determining if it will cause a geomagnetic disturbance in the Earth's magnetosphere upon impact. Long period southward-pointing ICME fields are known to cause significant space weather impacts and thus geomagnetic storms. We present an extensive analysis of CME-ICME directionality using 86 halo-CMEs observed between 2007 and 2017 to compare the direction of the source filament axial magnetic field on the Sun and the direction of the interplanetary magnetic field near the Earth at the L1 Lagrangian point. Excluding 12 cases that were too ambiguous to determine, for the remaining 74 ICMEs, we find an agreement in terms of the northward/southward orientation of  $B_z$  between ICMEs and their CME source regions in 85% of cases. Some of the previous studies discussed here have obtained an agreement of 77% and 55%. We therefore suggest that our method can be meaningful as a first step in efficiently predicting geoeffective ICMEs by observing and analyzing the source regions of CMEs on the Sun.

## **A HOT FLUX ROPE OBSERVED BY SDO/AIA**

**(A 7~MK hot Flux Rope Observed by SDO/AIA)**

V. [Aparna](#), Durgesh Tripathi

2016 ApJ 819 71

<http://arxiv.org/pdf/1601.01620v1.pdf>

A filament eruption was observed on **October 31, 2010** in the images recorded by the Atmospheric Imaging Assembly (AIA) on board the Solar Dynamic Observatory (SDO) in its Extreme Ultra-Violet (EUV) channels. The filament showed a slow rise phase followed by a fast rise and was classified to be an asymmetric eruption. In addition, multiple localized brightening which was spatially and temporally associated with the slow rise phase were identified leading us to believe that the tether-cutting mechanism to be the cause of the initiation of the eruption. An associated flux rope was detected in high temperature channels of AIA namely 94Å and 131Å corresponding to 7 MK and 11 MK plasma respectively. In addition, these channels are also sensitive to cooler plasma corresponding to  $\sim 1-2$  MK. In this study we have applied the algorithm devised by Warren et al. (2012) to remove cooler emission from the 94Å channel to deduce only the high temperature structure of the flux rope and to study its temporal evolution. We found that the flux rope was very clearly seen in clean 94Å channel image corresponding to Fe XVIII emission which corresponds to a plasma at a temperature of 7 MK. This temperature matched well with that obtained using DEM analysis. This study provides important constraints in the modelling of the thermodynamic structure of the flux ropes in CMEs.

## **SOLARIS: Solar Sail Investigation of the Sun**

Thierry [Appourchaux](#), [Frédéric Auchère](#), [Ester Antonucci](#), [Laurent Gizon](#), [Malcolm MacDonald](#), [Hirohisa Hara](#), [Takashi Sekii](#), [Daniel Moses](#), [Angelos Vourlidas](#)

Advances in Solar Sailing, pp 259-268, Feb 2014 2017

<https://arxiv.org/ftp/arxiv/papers/1707/1707.08193.pdf>

In this paper, we detail the scientific objectives and outline a strawman payload of the SOLAR sail Investigation of the Sun (SOLARIS). The science objectives are to study the 3D structure of the solar magnetic and velocity field, the variation of total solar irradiance with latitude, and the structure of the corona. We show how we can meet these science objective using solar-sail technologies currently under development. We provide a tentative mission profile considering several trade-off approaches. We also provide a tentative mass budget breakdown and a perspective for a programmatic implementation.

## **Introduction to the physics of solar eruptions and their space weather impact** **Introduction**

Vasilis [Archontis](#), [Loukas Vlahos](#)

Philosophical Transactions of the Royal Society A: Mathematical, Physical and Engineering Sciences v. 377  
[Issue 2148](#) Article ID:20190152 **2019**

<https://arxiv.org/pdf/1905.08361.pdf>

<https://royalsocietypublishing.org/doi/pdf/10.1098/rsta.2019.0152>

The physical processes, which drive powerful solar eruptions, play an important role in our understanding of the Sun-Earth connection. In this Special Issue, we firstly discuss how magnetic fields emerge from the solar interior to the solar surface, to build up active regions, which commonly host large-scale coronal disturbances, such as coronal mass ejections (CMEs). Then, we discuss the physical processes associated with the driving and triggering of these eruptions, the propagation of the large-scale magnetic disturbances through interplanetary space and the interaction of CMEs with Earth's magnetic field. The acceleration mechanisms for the solar energetic particles related to explosive phenomena (e.g. flares and/or CMEs) in the solar corona are also discussed. The main aim of this Issue, therefore, is to encapsulate the present state-of-the-art in research related to the genesis of solar eruptions and their space-weather implications. This article is part of the theme issue 'Solar eruptions and their space weather impact'.

## **The emergence of magnetic flux and its role on the onset of solar dynamic events** **Review**

V. [Archontis](#), [P. Syntelis](#)

Philosophical Transactions A v. 377 [Issue 2148](#) Article ID:20180387 **2019**

<https://arxiv.org/pdf/1904.06274.pdf>

<https://royalsocietypublishing.org/doi/pdf/10.1098/rsta.2018.0387>

A plethora of solar dynamic events, such as the formation of active regions, the emission of jets and the occurrence of eruptions is often associated to the emergence of magnetic flux from the interior of the Sun to the surface and above. Here, we present a short review on the onset, driving and/or triggering of such events by magnetic flux emergence. We briefly describe some key observational examples, theoretical aspects and numerical simulations, towards revealing the mechanisms that govern solar dynamics and activity related to flux emergence. We show that the combination of important physical processes like shearing and reconnection of magnetic fieldlines in emerging flux regions or at their vicinity, can power some of the most dynamic phenomena in the Sun on various temporal and spatial scales. Based on previous and recent observational and numerical studies, we highlight that, in most cases, none of these processes alone can drive and also trigger explosive phenomena releasing considerable amount of energy towards the outer solar atmosphere and space, such as flares, jets and large-scale eruptions (e.g. CMEs). In addition, one has to take into account the physical properties of the emerging field (e.g. strength, amount of flux, relative orientation to neighbouring and pre-existing magnetic fields, etc.) in order to better understand the exact role of magnetic flux emergence on the onset of solar dynamic events.

## **Helical Blowout Jets in the Sun**

V. [Archontis](#), A. W. Hood

New UKSP Nugget: 53, Nov **2014**

<http://www.uksolphys.org/uksp-nugget/53-helical-blowout-jets-in-the-sun/>

Numerical simulations demonstrate untwisting and Alfvén wave propagation as a jet erupts

This “blowout” jet is a broad, curtain-like structure, as opposed to the “standard” jets which are more elongated and not commonly associated with the eruption of cool material. In this nugget, we report on the emission of a “blowout” jet in an EFR with a sea-serpent configuration. We show that the “blowout” jet is untwisting during its ejection and, for the first time, we provide direct evidence of propagating torsional Alfvén waves during the emission of the “blowout” jets.

## **Recurrent Explosive Eruptions and the "Sigmoid-to-arcade" Transformation in the Sun Driven by Dynamical Magnetic Flux Emergence**

V. [Archontis](#)<sup>1,2</sup>, A. W. Hood<sup>2</sup>, and K. Tsinganos

**2014** ApJ 786 L21

<http://arxiv.org/pdf/1405.6955v1.pdf>

We report on three-dimensional MHD simulations of recurrent mini coronal mass ejection (CME)-like eruptions in a small active region (AR), which is formed by the dynamical emergence of a twisted (not kink unstable) flux tube from the solar interior. The eruptions develop as a result of the repeated formation and expulsion of new flux ropes due to continuous emergence and reconnection of sheared field lines along the polarity inversion line of the AR. The acceleration of the eruptions is triggered by tether-cutting reconnection at the current sheet underneath the erupting field. We find that each explosive eruption is followed by reformation of a sigmoidal structure and a subsequent "sigmoid-to-flare arcade" transformation in the AR. These results might have implications for recurrent CMEs and eruptive sigmoids/flares observations and theoretical studies.

## **The Emergence of Weakly Twisted Magnetic Fields in the Sun**

V. [Archontis](#)<sup>1,2</sup>, A. W. Hood<sup>2</sup>, and K. Tsinganos

2013 ApJ 778 42

We have studied the emergence of a weakly twisted magnetic flux tube from the upper convection zone into the solar atmosphere. It is found that the rising magnetized plasma does not undergo the classical, single  $\Omega$ -shaped loop emergence, but it becomes unstable in two places, forming two magnetic lobes that are anchored in small-scale bipolar structures at the photosphere, between the two main flux concentrations. The two magnetic lobes rise and expand into the corona, forming an overall undulating magnetic flux system. The dynamical interaction of the lobes results in the triggering of high-speed and hot jets and the formation of successive cool and hot loops that coexist in the emerging flux region. Although the initial emerging field is weakly twisted, a highly twisted magnetic flux rope is formed at the low atmosphere, due to shearing and reconnection. The new flux rope (hereafter post-emergence flux rope) does not erupt. It remains confined by the overlying field. Although there is no ejective eruption of the post-emergence rope, it is found that a considerable amount of axial and azimuthal flux is transferred into the solar atmosphere during the emergence of the magnetic field.

## A NUMERICAL MODEL OF STANDARD TO BLOWOUT JETS

V. [Archontis](#) and A. W. Hood

2013 ApJ 769 L21

We report on three-dimensional (3D) MHD simulations of the formation of jets produced during the emergence and eruption of solar magnetic fields. The interaction between an emerging and an ambient magnetic field in the solar atmosphere leads to (external) reconnection and the formation of "standard" jets with an inverse Y-shaped configuration. Eventually, low-atmosphere (internal) reconnection of sheared fieldlines in the emerging flux region produces an erupting magnetic flux rope and a reconnection jet underneath it. The erupting plasma blows out the ambient field and, moreover, it unwinds as it is ejected into the outer solar atmosphere. The fast emission of the cool material that erupts together with the hot outflows due to external/internal reconnection form a wider "blowout" jet. We show the transition from "standard" to "blowout" jets and report on their 3D structure. The physical plasma properties of the jets are consistent with observational studies.

## Magnetic flux emergence: a precursor of solar plasma expulsion

V. [Archontis](#) and A. W. Hood

A&A 537, A62 (2012)

**Aims.** We model the emergence of magnetized plasma from the top of the convection zone to the lower corona. We investigate the eruption of coronal flux ropes above emerging flux regions.

**Methods.** We performed three-dimensional numerical experiments in which the time-dependent and resistive equations of MHD are solved self-consistently, using the Lare3D code.

**Results.** A subphotospheric magnetic flux tube rises from the convectively unstable layer into the solar surface, followed by the formation and eruption of a new flux rope into the corona. Firstly, we examined the case where the corona is field-free. The expansion of the emerging field forms an envelope sheath that surrounds the newly formed flux rope. The erupting ropes are confined by the envelope field. The eruptions are driven by the gradient of the gas pressure and the tension of fieldlines that reconnect within the emerging flux region. The amount of the initial twist of the emerging field and the dense plasma that is lifted up, determine the height-time profile of the erupting ropes. Secondly, we examined the case of emergence into a pre-existing magnetic field in the upper solar atmosphere. A variety of different ambient field configurations was used in the experiments. External reconnection between the emerging and the pre-existing field may result in the removal of sufficient flux from the interacting fields and the full ejection of the flux ropes.

**Conclusions.** The results indicate that the relative contact angle of the interacting flux systems and their field strengths are crucial parameters that ultimately affect the evolution of the eruption of the rope into the higher solar atmosphere. One important result is that for any contact angle that favors reconnection, ejective eruptions occur earlier when the ambient field is relatively strong. In many cases, the erupting plasma adopts an S-like configuration. The sigmoidal structure accelerates during the fast eruption of the rope. The acceleration is enhanced by the external and internal reconnection of fieldlines during the rising motion of the rope. A key result is that in the reconnection-favored cases, the flux ropes experience ejective eruptions when the envelope flux is reduced (owing to removal by external reconnection) below that of the erupting flux rope. If the envelope flux stays higher than the erupting flux, the magnetic flux rope remains confined by the envelope field.

## Flux emergence and coronal eruption

V. [Archontis](#) and A. W. Hood

A&A 514, A56 (2010)

**Aims.** Our aim is to study the photospheric flux distribution of a twisted flux tube that emerges from the solar interior. We also report on the eruption of a new flux rope when the emerging tube rises into a pre-existing magnetic field in the corona.

Methods. To study the evolution, we use 3D numerical simulations by solving the time-dependent and resistive MHD equations. We qualitatively compare our numerical results with MDI magnetograms of emerging flux at the solar surface.

Results. We find that the photospheric magnetic flux distribution consists of two regions of opposite polarities and elongated magnetic tails on the two sides of the polarity inversion line (PIL), depending on the azimuthal nature of the emerging field lines and the initial field strength of the rising tube. Their shape is progressively deformed due to plasma motions towards the PIL. Our results are in qualitative agreement with observational studies of magnetic flux emergence in active regions (ARs). Moreover, if the initial twist of the emerging tube is small, the photospheric magnetic field develops an undulating shape and does not possess tails. In all cases, we find that a new flux rope is formed above the original axis of the emerging tube that may erupt into the corona, depending on the strength of the ambient field.

### **A stellar flare-coronal mass ejection event revealed by X-ray plasma motions**

C. [Argiroffi](#) (1 and 2), [F. Reale](#) (1 and 2), [J. J. Drake](#) (3), [A. Ciaravella](#) (2), [P. Testa](#) (3), [R. Bonito](#) (2), [M. Miceli](#) (1 and 2), [S. Orlando](#) (2), [G. Peres](#) (1 and 2)

Nature Astronomy **2019** See <https://rdcu.be/bEAta>

<https://arxiv.org/pdf/1905.11325.pdf>

Coronal mass ejections (CMEs), often associated with flares, are the most powerful magnetic phenomena occurring on the Sun. Stars show magnetic activity levels up to  $10^4$  times higher, and CME effects on stellar physics and circumstellar environments are predicted to be significant. However, stellar CMEs remain observationally unexplored. Using time-resolved high-resolution X-ray spectroscopy of a stellar flare on the active star HR 9024 observed with Chandra/HETGS, we distinctly detected Doppler shifts in S XVI, Si XIV, and Mg XII lines that indicate upward and downward motions of hot plasmas ( $\sim 10$ –25 MK) within the flaring loop, with velocity  $v \sim 100$ –400 km/s, in agreement with a model of flaring magnetic tube. Most notably, we also detected a later blueshift in the O VIII line which reveals an upward motion, with  $v = 90 \pm 30$  km/s, of cool plasma ( $\sim 4$  MK), that we ascribe to a CME coupled to the flare. From this evidence we were able to derive a CME mass of  $1 \times 10^{21}$  g and a CME kinetic energy of  $5 \times 10^{34}$  erg. These values provide clues in the extrapolation of the solar case to higher activity levels, suggesting that CMEs could indeed be a major cause of mass and angular momentum loss.

### **Global energetics of solar flares. XIII. The Neupert effect and acceleration of coronal mass ejections**

[Markus J. Aschwanden](#)

ApJ **2021**

<https://arxiv.org/pdf/2112.07759.pdf> **File**

Our major aim is a height-time model  $r(t)$  of the propagation of  $\{ \text{Coronal Mass Ejections (CMEs)} \}$ , where the lower corona is self-consistently connected to the heliospheric path. We accomplish this task by using the Neupert effect to derive the peak time, duration, and rate of the CME acceleration phase, as obtained from the time derivative of the  $\{ \text{soft X-ray (SXR)} \}$  light curve. This novel approach offers the advantage to obtain the kinematics of the CME height-time profile  $r(t)$ , the CME velocity profile  $v(t) = dr(t)/dt$ , and the CME acceleration profile  $a(t) = dv(t)/dt$  from  $\{ \text{Geostationary Orbiting Earth Satellite (GOES)} \}$  and white-light data, without the need of  $\{ \text{hard X-ray (HXR)} \}$  data. We apply this technique to a data set of 576 (GOES X and M-class) flare events observed with GOES and the  $\{ \text{Large Angle Solar Coronagraph (LASCO)} \}$ . Our analysis yields acceleration rates in the range of  $a_A = 0.1$ –13  $\text{km s}^{-2}$ , acceleration durations of  $\tau_A = 1.2$ –45 min, and acceleration distances in the range of  $d_A = 3$ –1063 Mm, with a median of  $d_A = 39$  Mm, which corresponds to the hydrostatic scale height of a corona with a temperature of  $T_e \approx 0.8$  MK. The results are consistent with standard flare/CME models that predict magnetic reconnection and synchronized (primary) acceleration of CMEs in the low corona (at a height of  $\sim 0.1 R_{\text{sun}}$ ), while secondary (weaker) acceleration may occur further out at heliospheric distances. **2011-03-09, 2011-03-12, 2011-08-09, 2011-09-05, 2011-11-15, 2011-12-30, 2012-01-23, 2012-03-06, 2012-03-07, 2012-07-06, 2012-07-09, 2012-07-14, 2013-05-14, 2013-05-31, 2013-10-15, 2013-11-05, 2014-02-02, 2014-02-13, 2014-02-25, 2014-05-06, 2014-10-20**

**Table 1.** Measurements of timing [ $t_A$ ,  $t_B$ ,  $t_1$ ,  $t_n$ ], distances from Sun center [ $r_A$ ,  $r_B$ ,  $r_1$ ,  $r_n$ ], velocity [ $v_B$ ], and acceleration rate [ $a_A$ ] of CMEs and solar flares based on predictions by the Neupert effect, for 24 selected flares (Table 1 and Figures 1–6).

**Table 2.** Measurements of timing [ $t_A$ ,  $t_B$ ,  $t_1$ ,  $t_n$ ], altitudes [ $r_A$ ,  $r_B$ ,  $r_1$ ,  $r_n$ ], velocity [ $v_B$ ], and acceleration rate [ $a_A$ ] of CME kinematics. The full table of 576 events is available as a machine-readable file.

**RHESSI Science Nuggets #422 2021 Bridging solar flares to coronal mass ejections**

[https://sprg.ssl.berkeley.edu/~tohban/wiki/index.php/Bridging\\_solar\\_flares\\_to\\_coronal\\_mass\\_ejections](https://sprg.ssl.berkeley.edu/~tohban/wiki/index.php/Bridging_solar_flares_to_coronal_mass_ejections)

**23 Dec 1996**

### **Correlation of the sunspot number and the waiting time distribution of solar flares, coronal mass ejections, and solar wind switchback events observed with the Parker Solar Probe**

[Markus J. Aschwanden](#), [Thierry Dudok de Wit](#)

ApJ **912** 94 **2021**

<https://arxiv.org/pdf/2102.02305.pdf>

<https://doi.org/10.3847/1538-4357/abef69>



Waiting time distributions of solar flares and coronal mass ejections (CMEs) exhibit power law-like distribution functions with slopes in the range of  $\alpha\tau \approx 1.4-3.2$ , as observed in annual data sets during 4 solar cycles (1974-2012). We find a close correlation between the waiting time power law slope  $\alpha\tau$  and the sunspot number (SN), i.e.,  $\alpha\tau = 1.38 + 0.01 \times \text{SN}$ . The waiting time distribution can be fitted with a Pareto-type function of the form  $N(\tau) = N_0 (\tau_0 + \tau)^{-\alpha\tau}$ , where the offset  $\tau_0$  depends on the instrumental sensitivity, the detection threshold of events, and pulse pile-up effects. The time-dependent power law slope  $\alpha\tau(t)$  of waiting time distributions depends only on the global solar magnetic flux (quantified by the sunspot number) or flaring rate, independent of other physical parameters of self-organized criticality (SOC) or magneto-hydrodynamic (MHD) turbulence models. Power law slopes of  $\alpha\tau \approx 1.2-1.6$  were also found in solar wind switchback events, as observed with the Parker Solar Probe (PSP). We conclude that the annual variability of switchback events in the heliospheric solar wind is modulated by flare and CME rates originating in the photosphere and lower corona.

## Global Energetics of Solar Flares. VII. Aerodynamic Drag in Coronal Mass Ejections

Markus J. [Aschwanden](#)<sup>1</sup> and Nat Gopalswamy

2019 ApJ 877 149

<https://sci-hub.ru/10.3847/1538-4357/ab1b39>

The free energy that is dissipated in a magnetic reconnection process of a solar flare, generally accompanied by a coronal mass ejection (CME), has been considered as the ultimate energy source of the global energy budget of solar flares in previous statistical studies. Here we explore the effects of the aerodynamic drag force on CMEs, which supplies additional energy from the slow solar wind to a CME event, besides the magnetic energy supply. For this purpose, we fit the analytical aerodynamic drag model of Cargill and Vršnak et al. to the height-time profiles  $r(t)$  of LASCO/SOHO data in 14,316 CME events observed during the first 8 yr (2010–2017) of the Solar Dynamics Observatory era (ensuring EUV coverage with AIA). Our main findings are (1) a mean solar wind speed of  $w = 472 \pm 414 \text{ km s}^{-1}$ , (2) a maximum drag-accelerated CME energy of  $E_{\text{drag}} \lesssim 2 \times 10^{32} \text{ erg}$ , (3) a maximum flare-accelerated CME energy of  $E_{\text{flare}} \lesssim 1.5 \times 10^{33} \text{ erg}$ , (4) the ratio of the summed kinetic energies of all flare-accelerated CMEs to the drag-accelerated CMEs amounts to a factor of 4, (5) the inclusion of the drag force slightly lowers the overall energy budget of CME kinetic energies in flares from  $\approx 7\%$  to  $\approx 4\%$ , and (6) the arrival times of CMEs at Earth can be predicted with an accuracy of  $\approx 23\%$ .

**Table 1** Statistics of CME Parameters for 14,316 Eruptive CME Events Detected with LASCO/SOHO during 2010–2017

## Global Energetics of Solar Flares: VI. Refined Energetics of Coronal Mass Ejections

Markus J. [Aschwanden](#)

ApJ 847 27 2017

<https://arxiv.org/pdf/1704.01993.pdf>

<https://iopscience.iop.org/article/10.3847/1538-4357/aa8952/pdf>

In this study we refine a CME model presented in an earlier study on the global energetics of solar flares and associated CMEs, and apply it to all (860) GOES M- and X-class flare events observed during the first 7 years (2010-2016) of the Solar Dynamics Observatory (SDO) mission, which doubles the statistics of the earlier study. The model refinements include: (1) the CME geometry in terms of a 3D sphere undergoing self-similar adiabatic expansion; (2) the inclusion of solar gravitational deceleration during the acceleration and propagation of the CME, which discriminates eruptive and confined CMEs; (4) a self-consistent relationship between the CME center-of-mass motion detected during EUV dimming and the leading-edge motion observed in white-light coronagraphs; (5) the equi-partition of the CME kinetic and thermal energy; and (6) the Rosner-Tucker-Vaiana (RTV) scaling law. The refined CME model is entirely based on EUV dimming observations (using AIA/SDO data) and complements the traditional white-light scattering model (using LASCO/SOHO data), and both models are independently capable to determine fundamental CME parameters such as the CME mass, speed, and energy. Comparing the two methods we find that: (1) LASCO is less sensitive than AIA in detecting CMEs (in 24% of the cases); (2) CME masses below  $m_{\text{CME}} \sim 10^{14} \text{ g}$  are under-estimated by LASCO; (3) AIA and LASCO masses, speeds, and energy agree closely in the statistical mean after elimination of outliers; (4) the CMEs parameters of the speed  $v$ , emission measure-weighted flare peak temperature  $T_e$ , and length scale  $L$  are consistent with the following scaling laws (derived from first principles):  $v \propto T_e^{1/2}$ ,  $v \propto (m_{\text{CME}})^{1/4}$ , and  $m_{\text{CME}} \propto L^2$ .

## Global Energetics of Solar Flares: V. Energy Closure in Flares and Coronal Mass Ejections

Markus J. [Aschwanden](#), Amir Campi, Christina M.S. Cohen, [Gordon Holman](#), [Ju Jing](#), [Matthieu Kretzschmar](#), [Eduard P. Kontar](#), [James McTiernan](#), [Richard A. Mewaldt](#), [Aidan O'Flanagan](#), [Ian G. Richardson](#), [Daniel Ryan](#), [Harry P. Warren](#), [Yan Xu](#)

ApJ 836 17 2017

<https://arxiv.org/pdf/1701.01176v1.pdf>

In this study we synthesize the results of four previous studies on the global energetics of solar flares and associated coronal mass ejections (CMEs), which include magnetic, thermal, nonthermal, and CME energies in 399 solar M and X-class flare events observed during the first 3.5 years of the Solar Dynamics Observatory (SDO) mission. Our findings are: (1) The sum of the mean nonthermal energy of flare-accelerated particles ( $E_{\text{nt}}$ ), the energy of direct heating ( $E_{\text{dir}}$ ), and the energy in coronal mass ejections (ECME), which are the primary energy dissipation processes in a flare, is found to have a ratio of  $(E_{\text{nt}} + E_{\text{dir}} + E_{\text{CME}}) / E_{\text{mag}} = 0.87 \pm 0.18$ , compared with the dissipated magnetic free

energy  $E_{\text{mag}}$ , which confirms energy closure within the measurement uncertainties and corroborates the magnetic origin of flares and CMEs; (2) The energy partition of the dissipated magnetic free energy is:  $0.51 \pm 0.17$  in nonthermal energy of  $\geq 6$  keV electrons,  $0.17 \pm 0.17$  in nonthermal  $\geq 1$  MeV ions,  $0.07 \pm 0.14$  in CMEs, and  $0.07 \pm 0.17$  in direct heating; (3) The thermal energy is almost always less than the nonthermal energy, which is consistent with the thick-target model; (4) The bolometric luminosity in white-light flares is comparable with the thermal energy in soft X-rays (SXR); (5) Solar Energetic Particle (SEP) events carry a fraction  $\approx 0.03$  of the CME energy, which is consistent with CME-driven shock acceleration; and (6) The warm-target model predicts a lower limit of the low-energy cutoff at  $e \approx 6$  keV, based on the mean differential emission measure (DEM) peak temperature of  $T_e = 8.6$  MK during flares. This work represents the first statistical study that establishes energy closure in solar flare/CME events.

**2011-Feb-15, 2011-Aug-04, 2011-Sep-22, 2012-Jan-23, 2012-Jan-27, 2012-Mar-07, 2012-May-17, 2013-May-13, 2013-Jun-21**

**Table 1. SEP kinetic energies for selected 3-spacecraft events from 2011-2013.** The higher value of the two lower limits of CME/LASCO (column 6) and CME/AIA energies (column 7) is used in the SEP/CME ratio (column 8).

## Global Energetics of Solar Flares: IV. Coronal Mass Ejection Energetics

Markus J. [Aschwanden](#)

ApJ 831 105 2016

<http://arxiv.org/pdf/1605.04952v1.pdf> File

[http://www.lmsal.com/~aschwand/eprints/2016\\_global4.pdf](http://www.lmsal.com/~aschwand/eprints/2016_global4.pdf)

This study entails the fourth part of a global flare energetics project, in which the mass  $m_{\text{CME}}$ , kinetic energy  $E_{\text{kin}}$ , and the gravitational potential energy  $E_{\text{grav}}$  of coronal mass ejections (CMEs) is measured in 399 M and X-class flare events observed during the first 3.5 yrs of the Solar Dynamics Observatory (SDO) mission, *using a new method based on the EUV dimming effect*. The EUV dimming is modeled in terms of a radial adiabatic expansion process, which is fitted to the observed evolution of the total emission measure of the CME source region. The model derives the evolution of the mean electron density, the emission measure, the bulk plasma expansion velocity, the mass, and the energy in the CME source region. The EUV dimming method is truly complementary to the Thomson scattering method in white light, which probes the CME evolution in the heliosphere at  $r > 2R_{\odot}$ , while the EUV dimming method tracks the CME launch in the corona. We compare the CME parameters obtained in white light with the LASCO/C2 coronagraph with those obtained from EUV dimming with the Atmospheric Imaging Assembly (AIA) onboard SDO for all identical events in both data sets. We investigate correlations between CME parameters, the relative timing with flare parameters, frequency occurrence distributions, and the energy partition between magnetic, thermal, nonthermal, and CME energies. CME energies are found to be systematically lower than the dissipated magnetic energies, which is consistent with a magnetic origin of CMEs. **2010-10-16, 2010-06-12, 2011-05-29, 2011-08-02, 2011-09-24, 2011-09-28, 2011-11-09, 2012-01-27, 2012-03-10, 2012-03-13, 2012-06-06, 2012-07-05, 2012-07-19, 2012-08-11, 2012-09-09, 2012-11-13, 2013-05-22, 2013-08-17, 2013-10-24, 2013-11-01, 2013-11-03, 2013-11-06, 2013-11-19, 2014-01-07**

**Table 3. Temporal and spatial parameters of the first 10 entries** (out of the 399 events) listed in the complete machine-readable data file.

**Table 4. CME parameters** of the first 10 entries (out of the 399 events) listed in the complete machine-readable data file.

## 3D Reconstruction of Active Regions with STEREO (Invited **Review**)

Markus J. [Aschwanden](#) and Jean-Pierre Wuelser

E-print, Feb 2010, J. Atmos. Solar-Terr. Physics,

We review data analysis and physical modeling related to the 3D reconstruction of active regions in the solar corona, using stereoscopic image pairs from the STEREO/EUVI instrument. This includes the 3D geometry of coronal loops (with measurements of the loop inclination plane, coplanarity, circularity, and hydrostaticity), the 3D electron density and temperature distribution (which enables diagnostics of hydrostatic, hydrodynamic, and heating processes), the 3D magnetic field (independent of any theoretical model based on photospheric extrapolations), as well as the 3D reconstruction of CME phenomena, such as EUV dimming, CME acceleration, CME bubble expansion, and associated Lorentz forces that excite MHD kink-mode oscillations in the surroundings of a CME launch site. The mass of CMEs, usually measured from white-light coronagraphs, can be determined independently from the EUV dimming in the CME source region. The full 3D density and temperature structure of an active region can be reconstructed in unprecedented detail with instant stereoscopic tomography.

2. 3D Geometry of Active Regions
3. 3D Density Reconstruction of Active Regions
4. 3D Temperature Diagnostics of Active Regions
5. 3D Magnetic Field Modeling of Active Regions
6. **3D Reconstruction of EUV Dimming and CME mass**
7. 3D Motion of Loop Oscillations and Waves

## 4D-Modeling of CME Expansion and EUV Dimming with Fitting to STEREO/EUVI Observations

Markus J. [Aschwanden](#)

E-print, June 2009; *Annales Geophysicae*, 27, 3275-3286, 2009, [File](#)

This is the first attempt to model the kinematics of a CME launch and the resulting EUV dimming quantitatively with a self-consistent model. Our 4D-model assumes self-similar expansion of a spherical CME geometry that consists of a CME front with density compression and a cavity with density rarefaction, satisfying mass conservation of the total CME and swept-up corona. The model contains 12 free parameters and is fitted to the **2008 March 25**, 18:30 UT, CME event observed with STEREO/A and B. Our model is able reproduce the observed CME expansion and related EUV dimming during the initial phase from 18:30 UT to 19:00 UT. The CME kinematics can be characterized by a constant acceleration (i.e., a constant magnetic driving force). While the observations of EUVI/A are consistent with a spherical bubble geometry, we detect significant asymmetries and density inhomogeneities with EUVI/B. This new forward-modeling method demonstrates how the observed EUV dimming can be used to model physical parameters of the CME source region, the CME geometry, and CME kinematics.

### **First Measurements of the Mass of Coronal Mass Ejections from the EUV Dimming Observed with STEREO EUVI A+B Spacecraft**

Markus J. [Aschwanden](#), Nariaki V. Nitta, Jean-Pierre Wuelser, James R. Lemen, Anne Sandman, Angelos Vourlidas, Robin C. Colaninno

E-print, April 2009, *ApJ*, 706:376–392, 2009 November, [File](#),

The masses of Coronal Mass Ejections (CMEs) have traditionally been determined from whitelight coronagraphs, based on the Thomson scattering of electrons, which depends on the (generally unknown) angle of the CME propagation direction. Here we develop a new method of measuring CME masses from the EUV dimming seen with EUV imaging telescopes in multiple temperature filters. As a test we investigate 8 CME events with previous mass determinations from STEREO/COR2, of which 5 cases are fully detected with EUVI, 2 partially, and 1 not, using an automated multi-wavelength detection code. We find CME masses in the range of  $m_{\text{CME}} = (2 - 7) \times 10^{15} \text{ g}$ . The agreement between the two EUVI/A and B spacecraft is  $m_{\text{A}}/m_{\text{B}} = 1.3 \pm 0.6$  and the consistency with white-light measurements by COR2 is  $m_{\text{EUV}}/m_{\text{COR2}} = 1.1 \pm 0.3$ . The consistency between EUVI and COR2 implies no significant mass backflows (or inflows) at  $r < 4R_{\odot}$  and adequate temperature coverage for the bulk of the CME mass in the range of  $T \approx 0.5 - 3.0 \text{ MK}$ . The temporal evolution of the EUV dimming allows us also to model the evolution of the CME density  $n_e(t)$ , volume  $V(t)$ , height-time  $h(t)$ , and propagation speed  $v(t)$  in terms of an adiabatically expanding self-similar geometry. We determine e-folding EUV dimming times of  $\tau_{\text{dim}} = 1.3 \pm 1.4 \text{ hr}$ . We test the adiabatic expansion model in terms of the predicted detection delay ( $\tau_{\text{t}} \approx 0.7 \text{ hr}$ ) between EUVI and COR2 for the fastest CME event (2008-Mar-25) and find good agreement with the observed delay ( $\tau_{\text{t}} \approx 0.8 \text{ hr}$ ).

### **Solar Flare and CME Observations with STEREO/EUVI**

M.J. [Aschwanden](#), · J.P. Wuelser, N.V. Nitta, · J.R. Lemen

E-print, Dec 2008; *Solar Phys.* (2009) **256**: 3-40 DOI 10.1007/s11207-009-9347-4, 2009, [File](#)

STEREO/EUVI observed 185 flare events (detected above the GOES class C1 level or at  $>25 \text{ keV}$  with RHESSI) during the first two years of the mission (Dec 2006 - Nov 2008), while coronal mass ejections (CME) were reported in about a third of these events. We compile a **comprehensive catalog of these EUVI-observed events**, containing the peak fluxes in soft X-rays, hard X-rays, and EUV, as well as a classification and statistics of prominent EUV features: 79% show impulsive EUV emission (coincident with hard X-rays), 73% show delayed EUV emission from postflare loops and arcades, 24% represent occulted flares, 17% exhibit EUV dimming, 5% show loop oscillations or propagating waves, and at least 3% show erupting filaments. We analyze an example of each EUV feature by stereoscopic modeling of their 3D geometry. We find that impulsive EUV emission indicates compression of cold coronal plasma during the flare energy release, in contrast to the delayed postflare EUV emission that results from cooling of the soft X-ray emitting flare loops. Occulted flares allow us to determine CME-related coronal dimming uncontaminated from flare-related EUV emission. From modeling the time evolution of EUV dimming we can accurately quantify the initial expansion of CMEs and determine their masses. Further we find evidence that coronal loop oscillations are excited by the rapid initial expansion of CMEs. These examples demonstrate that stereoscopic EUV data provide powerful new methods to model the 3D aspects in the hydrodynamics of flares and kinematics of CMEs.

### **Photospheric signatures of CME onset**

O P M [Aslam](#), D MacTaggart, T Williams, L Fletcher, P Romano

*MNRAS*, Volume 534, Issue 1, October 2024, Pages 444–454,

<https://doi.org/10.1093/mnras/stae2110>

<https://watermark.silverchair.com/stae2110.pdf>

Coronal mass ejections (CMEs) are solar eruptions that involve large-scale changes to the magnetic topology of an active region. There exists a range of models for CME onset which are based on twisted or sheared magnetic field above a polarity inversion line (PIL). We present observational evidence that topological changes at PILs, in the photosphere, form a key part of CME onset, as implied by many models. In particular, we study the onset of 30 CMEs

and investigate topological changes in the photosphere by calculating the magnetic winding flux, using the artop code. By matching the times and locations of winding signatures with CME observations produced by the almanac code, we confirm that these signatures are indeed associated with CMEs. Therefore, as well as presenting evidence that changes in magnetic topology at the photosphere are a common signature of CME onset, our approach also allows for the finding of the source location of a CME within an active region. **2011.02.15, 2011.10.15**

**Table 1.** A table of 30 CME events with winding signatures related to CME onset. 2010-2015

### **Powerful non-geoeffective interplanetary disturbance of July 2012 observed by muon hodoscope URAGAN**

I.I. [Astapov](#), , , N.S. Barbashinaa, A.A. Petrukhina, V.V. Shutenko, I.S. Veselovsky  
Advances in Space Research Volume 56, Issue 12, 15 December **2015**, Pages 2833–2838  
<http://www.sciencedirect.com/science/article/pii/S0273117715001854>

The most powerful coronal mass ejection of the 24th solar cycle took place on the opposite side of the Sun on **July 23, 2012** and had no geomagnetic consequences. Nevertheless, as a result of passing of the ejection through the heliosphere, variations of galactic cosmic rays flux were observed on the Earth. These variations were registered by the muon hodoscope URAGAN (MEPhI, Moscow). Muon flux angular distributions on the Earth's surface are reported and analyzed.

### **The spheromak tilting and how it affects modelling coronal mass ejections**

Eleanna [Asvestari](#), [Tobias Rindlisbacher](#), [Jens Pomoell](#), [Emilia Kilpua](#)

ApJ **926** 87 **2022**

<https://arxiv.org/pdf/2111.08770.pdf>

<https://iopscience.iop.org/article/10.3847/1538-4357/ac3a73/pdf>

Spheromak type flux ropes are increasingly used for modelling coronal mass ejections (CMEs). Many models aim in accurately reconstructing the magnetic field topology of CMEs, considering its importance in assessing their impact on modern technology and human activities in space and on ground. However, so far there is little discussion about how the details of the magnetic structure of a spheromak affect its evolution through the ambient field in the modelling domain, and what impact this has on the accuracy of magnetic field topology predictions. If the spheromak has its axis of symmetry (geometric axis) at an angle with respect to the direction of the ambient field, then the spheromak starts rotating so that its symmetry axis finally aligns with the ambient field. When using the spheromak in space weather forecasting models this tilting can happen already during insertion and significantly affects the results. In this paper we highlight this issue previously not examined in the field of space weather and we estimate the angle by which the spheromak rotates under different conditions. To do this we generated simple purely radial ambient magnetic field topologies (weak/strong positive/negative) and inserted spheromaks with varying initial speed and tilt, and magnetic helicity sign. We employ different physical and geometric criteria to locate the magnetic centre of mass and axis of symmetry of the spheromak. We confirm that spheromaks rotate in all investigated conditions and their direction and angle of rotation depend on the spheromak's initial properties and ambient magnetic field strength and orientation.

### **Modelling a multi-spacecraft coronal mass ejection encounter with EUHFORIA**

[E. Asvestari](#), [J. Pomoell](#), [E. Kilpua](#), [S. Good](#), [T. Chatzistergos](#), [M. Temmer](#), [E. Palmerio](#), [S. Poedts](#), [J. Magdalenic](#)

A&A **652**, A27 **2021**

<https://arxiv.org/pdf/2105.11831.pdf>

<https://www.aanda.org/articles/aa/pdf/2021/08/aa40315-21.pdf>

<https://doi.org/10.1051/0004-6361/202140315>

Coronal mass ejections (CMEs) are a manifestation of the Sun's eruptive nature. They can have a great impact on Earth, but also on human activity in space and on the ground. Therefore, modelling their evolution as they propagate through interplanetary space is essential. EUropean Heliospheric FOrecasting Information Asset (EUHFORIA) is a data-driven, physics-based model, tracing the evolution of CMEs through background solar wind conditions. It employs a spheromak flux rope, which provides it with the advantage of reconstructing the internal magnetic field configuration of CMEs. This is something that is not included in the simpler cone CME model used so far for space weather forecasting. This work aims at assessing the spheromak CME model included in EUHFORIA. We employed the spheromak CME model to reconstruct a well observed CME and compare model output to in situ observations. We focus on an eruption from **6 January 2013** encountered by two radially aligned spacecraft, Venus Express and STEREO-A. We first analysed the observed properties of the source of this CME eruption and we extracted the CME properties as it lifted off from the Sun. Using this information, we set up EUHFORIA runs to model the event. The model predicts arrival times from half to a full day ahead of the in situ observed ones, but within errors established from similar studies. In the modelling domain, the CME appears to be propagating primarily southward, which is in accordance with white-light images of the CME eruption close to the Sun. In order to get the observed magnetic field topology, we aimed at selecting a spheromak rotation angle for which the axis of symmetry of the spheromak is perpendicular to the direction of the polarity inversion line (PIL). The modelled magnetic field profiles, their amplitude, arrival times, and sheath region length are all affected by the choice of radius of the modelled spheromak.

## **FESTIVAL: A Multiscale Visualization Tool for Solar Imaging Data**

F. [Auchère](#) · E. Soubrié · K. Bocchialini · F. LeGall

Solar Phys (2008) 248: 213–224

<http://www.springerlink.com/content/g42h84170449n7mq/fulltext.pdf>

**Abstract** Since 4 December 2006, the SECCHI instrument suites onboard the two STEREO A and B probes have been imaging the solar corona and the heliosphere on a wide range of angular scales. The EUVI telescopes have a plate scale of 1.7 arcseconds pixel<sup>-1</sup>, while that of the HI2 wide-angle cameras is 2.15 arcminutes pixel<sup>-1</sup>, *i.e.* 75 times larger, with the COR1 and COR2 coronagraphs having intermediate plate scales. These very different instruments, aimed at studying Coronal Mass Ejections and their propagation in the heliosphere, create a data visualization challenge. This paper presents FESTIVAL, a SolarSoftware package originally developed to be able to map the SECCHI data into dynamic composite images of the sky as seen by the STEREO and SOHO probes. Data from other imaging instruments can also be displayed. Using the mouse, the user can quickly and easily zoom in and out and pan through these composite images to explore all spatial scales from EUVI to HI2 while keeping the native resolution of the original data. A large variety of numerical filters can be applied, and additional data (*i.e.* coordinate grids, stars catalogs, *etc.*) can be overlaid on the images. The architecture of FESTIVAL is such that it is easy to add support for other instruments and these new data immediately benefit from the already existing capabilities. Also, because its mapping engine is fully 3D, FESTIVAL provides a convenient environment to display images from future out-of-the-Ecliptic solar missions, such as *Solar Orbiter* or *Solar Probe*.

## **The return of the jet**

[Guillaume Aulanier](#)

[Nature Astronomy](#) (2021)

<https://doi.org/10.1038/s41550-021-01416-x>

Turmoil has engulfed the solar community for decades about which physical mechanisms are sufficient to trigger and drive solar eruptions. New high-resolution numerical magnetohydrodynamic simulations bring an old idea back into the light: the reconnection jet from the tether-cutting model.

## **Drifting of the line-tied footpoints of CME flux-ropes**

Guillaume [Aulanier](#), [Jaroslav Dudik](#)

A&A 621, A72 (2019)

<https://arxiv.org/pdf/1811.04253.pdf>

[http://www.lesia.obspm.fr/perso/guillaume-aulanier/Aulanier\\_Dudik\\_2018\\_AeA.pdf](http://www.lesia.obspm.fr/perso/guillaume-aulanier/Aulanier_Dudik_2018_AeA.pdf)

<https://sci-hub.ru/10.1051/0004-6361/201834221>

**Context.** Bridging the gap between heliospheric and solar observations of eruptions requires to map ICME footpoints down to the Sun's surface. But this not straightforward. Improving the understanding of the spatio-temporal evolutions of eruptive flares requires a comprehensive standard model. But the current one is two-dimensional only and it cannot address the question of CME footpoints.

**Aims.** Existing 3D extensions to the standard model show that flux-rope footpoints are surrounded by curved-shaped QSL-footprints that can be related with hook-shaped flare-ribbons. We build upon this finding and further address the joint questions of their timeevolution, and of the formation of flare loops at the ends of flaring PILs of the erupting bipole, which are both relevant for flare understanding in general and for ICME studies in particular.

**Methods.** We calculate QSLs and relevant field lines in an MHD simulation of a torus-unstable flux-rope. The evolving QSL footprints are used to define the outer edge of the flux rope at different times, and to identify and characterize new 3D reconnection geometries and sequences that occur above the ends of the flaring PIL. We also analyse flare-ribbons as observed in EUV by SDO/AIA and IRIS during two X-class flares.

**Results.** The flux-rope footpoints are drifting during the eruption, which is unexpected due to line-tying. This drifting is due to a series of coronal reconnections that erode the flux rope on one side and enlarge it on the other side. Other changes in the flux-rope footpoint-area are due to multiple reconnections of individual field lines whose topology can evolve sequentially from arcade to flux rope and finally to flare loop. These are associated with deformations and displacements of QSL footprints, which resemble those of the studied flare ribbons.

**Conclusions.** Our model predicts continuous deformations and a drifting of ICME flux-rope footpoints whose areas are surrounded by equally-evolving hooked-shaped flare-ribbons, as well as the formation of flare loops at the ends of flaring PILs which originate from the flux-rope itself, both of which being due to purely three-dimensional reconnection geometries. The observed evolution of flare-ribbons in two events supports the model, but more observations are required to test all its predictions. **July 12, 2012, September 10, 2014**

## **The physical mechanisms that initiate and drive solar eruptions**

**Review**

[G. Aulanier](#)

E-print, Sept 2013; 2014, IAU Symposium, 300, 184

[http://www.lesia.obspm.fr/perso/guillaume-aulanier/Review\\_2014\\_InitiatingDriving\\_Eruptions.pdf](http://www.lesia.obspm.fr/perso/guillaume-aulanier/Review_2014_InitiatingDriving_Eruptions.pdf)

Solar eruptions are due to a sudden destabilization of force-free coronal magnetic fields. But the detailed mechanisms which can bring the corona towards an eruptive stage, then trigger and drive the eruption, and finally make it explosive, are not fully understood. A large variety of storage-and-release models have been developed and opposed to each other since 40 years. For example, photospheric flux emergence vs. flux cancellation, localized coronal reconnection vs. large-scale ideal instabilities and loss of equilibria, tether-cutting vs. breakout reconnection, and so on. The competition

between all these approaches has led to a tremendous drive in developing and testing all these concepts, by coupling state-of-the-art models and observations. Thanks to these developments, it now becomes possible to compare all these models with one another, and to revisit their interpretation in light of their common and their different behaviors. This approach leads me to argue that no more than two distinct physical mechanisms can actually initiate and drive prominence eruptions: the magnetic breakout and the torus instability. In this view, all other processes (including flux emergence, flux cancellation, flare reconnection and long-range couplings) should be considered as various ways that lead to, or than strengthen, one of the aforementioned driving mechanisms.

## **The standard flare model in three dimensions**

### **I. Strong-to-weak shear transition in post-flare loops**

G. [Aulanier](#), M. Janvier, and B. Schmieder

E-print, 20 May, 2012, **File**; A&A

The standard CSHKP model for eruptive flares is two-dimensional. Yet observational interpretations of photospheric currents in pre-eruptive sigmoids, shear in post-flare loops, and relative positioning and shapes flare ribbons, all together require three-dimensional extensions to the model. The paper focuses on the strong-to-weak shear transition in post-flare loop, and on the time-evolution of the geometry of photospheric electric currents, which occur during the development of eruptive flares. The objective is to understand the three-dimensional physical processes which cause them, and to know how much the post-flare and the pre-eruptive distributions of shear depend on each other. The strong-to-weak shear transition in post-flare loops is identified and quantified in a flare observed by STEREO, as well as in a magnetohydrodynamic simulation of CME initiation performed with the OHM code. In both approaches, the magnetic shear is evaluated with field line footpoints. In the simulation, the shear is also estimated from ratios between magnetic field components. The modeled strong-to-weak shear transition in post-flare loops comes from two effects. Firstly, a reconnection-driven transfer of the differential magnetic shear, from the pre- to the post-eruptive configuration. Secondly, a vertical straightening of the inner legs of the CME, which induces an outer shear weakening. The model also predicts the occurrence of narrow electric current layers inside J-shaped flare ribbons, which are dominated by direct currents. Finally, the simulation naturally accounts for energetics and time-scales for weak and strong flares, when typical scalings for young and decaying solar active regions are applied. The results provide three-dimensional extensions to the standard flare model. These extensions involve MHD processes that should be tested with observations. **May 9, 2011**

## **FORMATION OF TORUS-UNSTABLE FLUX ROPES AND ELECTRIC CURRENTS IN ERUPTING SIGMOIDS**

G. [Aulanier](#), T. Török, P. Démoulin, E. E. DeLuca

ApJ, 708:314–333, 2010 January, **File**

We analyze the physical mechanisms that form a three-dimensional coronal flux rope and later cause its eruption. This is achieved by a zero- $\beta$  MHD simulation of an initially potential, asymmetric bipolar field, which evolves by means of simultaneous slow magnetic field diffusion and sub-Alfvénic, line-tied shearing motions in the photosphere. As in similar models, flux-cancellation driven photospheric reconnection in a bald-patch separatrix transforms the sheared arcades into a slowly rising and stable flux rope. A bifurcation from a bald-patch to a quasi-separatrix layer (QSL) topology occurs later on in the evolution, while the flux rope keeps growing and slowly rising, now due to shear-driven coronal slip-running reconnection, which is of tether-cutting type and takes place in the QSL. As the flux rope reaches the altitude at which the decay index  $-\partial \ln B / \partial \ln z$  of the potential field exceeds  $\sim 3/2$ , it rapidly accelerates upward while the overlying arcade eventually develops an inverse tear-drop shape, as observed in coronal mass ejections (CMEs). This transition to eruption is in accordance with the onset criterion of the torus instability. Thus we find that photospheric flux-cancellation and tether-cutting coronal reconnection do not trigger CMEs in bipolar magnetic fields, but are key pre-eruptive mechanisms for flux ropes to build up and to rise to the critical height above the photosphere at which the torus instability causes the eruption. In order to interpret recent Hinode X-Ray Telescope observations of an erupting sigmoid, we produce simplified synthetic soft X-ray images from the distribution of the electric currents in the simulation. We find that a bright sigmoidal envelope is formed by pairs of J-shaped field lines in the pre-eruptive stage. These field lines form through the bald-patch reconnection, and merge later on into S-shaped loops through the tethercutting reconnection. During the eruption, the central part of the sigmoid brightens due to the formation of a vertical current layer in the wake of the erupting flux rope. Slip-running reconnection in this layer yields the formation of flare loops. A rapid decrease of currents due to field line expansion, together with the increase of narrow currents in the reconnecting QSL, yields the sigmoid hooks to thin in the early stages of the eruption. Finally, a slightly rotating erupting loop-like feature (ELLF) detaches from the center of the sigmoid. Most of this ELLF is not associated with the erupting flux rope, but with a current shell which develops within expanding field lines above the rope. Only the short, curved end of the ELLF corresponds to a part of the flux rope. We argue that the features found in the simulation are generic for the formation and eruption of soft X-ray sigmoids.

## Radio evidence for breakout reconnection in solar eruptive events

H. Aurass, G. Holman, S. Braune, G. Mann, P. Zlobec

E-print, May 2013, File; A&A

Magnetic reconnection is understood to be fundamental to energy release in solar eruptive events (SEEs). In these events reconnection produces a magnetic flux rope above an arcade of hot flare loops. Breakout reconnection, a secondary reconnection high in the corona between this flux rope and the overlying magnetic field, has been hypothesized. Direct observational evidence for breakout reconnection has been elusive, however. The aim of this study is to establish a plausible interpretation of the combined radio and hard X-ray (HXR) emissions observed during the impulsive phase of the near-limb X3.9-class SEE on **2003 November 03**. We study radio spectra (AIP), simultaneous radio images (Nancay Multi-frequency Radio Heliograph, NRH), and single-frequency polarimeter data (OAT). The radio emission is nonthermal plasma radiation with a complex structure in frequency and time. Emphasis is on the time interval when the HXR flare loop height was observed by the Ramaty High Energy Solar Spectroscopic Imager (RHESSI) to be at its minimum and an X-ray source was observed above the top of the arcade loops. Two stationary, meter-wavelength sources are observed radially aligned at 0.18 and 0.41Rs above the active region and hard X-ray sources. The lower source is apparently associated with the upper reconnection jet of the flare current sheet (CS), and the upper source is apparently associated with breakout reconnection. Sources observed at lower radio frequencies surround the upper source at the expected locations of the breakout reconnection jets. We believe the upper radio source is the most compelling evidence to date for the onset of breakout reconnection during a SEE. The height stationarity of the breakout sources and their dynamic radio spectrum discriminate them from propagating disturbances. Timing and location arguments reveal for the first time that both the earlier described "above the flare loop top" HXR source and the lower radio source are emission from the upper reconnection jet above the vertical flare CS.

## RADIO EVIDENCE OF BREAK-OUT RECONNECTION?

H. Aurass<sup>1</sup>, G. Mann<sup>1</sup>, P. Zlobec<sup>2</sup> and M. Karlický<sup>3</sup>

2011 ApJ 730 57, File

We reconsider the **2003 October 28** X17 flare/coronal mass ejection (CME), studying the five minutes immediately before the impulsive flare phase (not discussed in previous work). To this aim we examine complementary dynamic radio spectrograms, single frequency polarimeter records, radio images, space-based longitudinal field magnetograms, and ultraviolet images. We find widely distributed faint and narrowband meter wave radio sources located outside active regions but associated with the boundaries of magnetic flux connectivity cells, inferred from the potential extrapolation of the observed photospheric longitudinal field as a model for coronal magnetic field structures. The meter wave radio sources occur during the initial decimeter wave effects, which are well known to be associated with filament destabilization in the flaring active region (here NOAA 10486). Antiochos et al. predict in their break-out model for CME initiation that "... huge phenomena ... may be controlled by detailed plasma processes that occur in relatively tiny regions." They suggest that the expected faint energy release "... on long field lines far away from any neutral line ... may be detectable in radio/microwave emission from nonthermal particles..." In this paper, we describe meter wave sources whose properties correctly coincide with the quoted predictions of the break-out reconnection model of the CME initiation.

## Observational evidence for breakout reconnection

Henry Aurass and Gordon Holman:

RHESSI Science Nugget No. 196, March 2013

[http://sprg.ssl.berkeley.edu/~tohban/wiki/index.php/Observational\\_evidence\\_for\\_breakout\\_reconnection](http://sprg.ssl.berkeley.edu/~tohban/wiki/index.php/Observational_evidence_for_breakout_reconnection)

Coronal particle acceleration marks the eruption of a solar eruptive event (SEE).

2003-11-03

## Coronal current sheet signatures during the 17 May 2002 CME-flare

H. Aurass<sup>1</sup>, F. Landini<sup>2</sup>, G. Poletto

E-print, Aug 2009, File; A&A

Context. The relation between current sheets (CSs) associated with flares, revealed by characteristic radio signatures, and current sheets associated with coronal mass ejections (CMEs), detected in coronal ultraviolet (UV) and white light data, has not been analyzed, yet.

Aims. We aim at establishing the relationship between CSs associated with a limb flare and CSs associated with the CME that apparently develops after the flare. We use a unique data set, acquired on May 17, 2002, which includes radio and extreme ultraviolet (XUV) observations.

Methods. Spectral radio diagnostics, UV spectroscopic techniques, white light coronagraph imaging, and (partly) radio imaging are used to illustrate the relation between the CSs and to infer the physical parameters of the radially aligned features that develop in the aftermath of the CME.

Results. During the flare, several phenomena are interpreted in accordance with earlier work and with reference to the common eruptive flare scenario as evidence of flare CSs in the low corona. These are drifting pulsating structures in dynamic radio spectra, an erupting filament, expanding coronal loops morphologically recalling the later white light CME, and associated with earlier reported hard X-ray source sites. In the aftermath of the CME, UV spectra allowed us to estimate the CS temperature and density, over the 1.5 - 2.1  $R_{\odot}$  interval of heliocentric altitudes. The UV detected CS, however, appears to be only one of many current sheets that exist underneath the erupting flux rope. A type II burst following the CME radio continuum in time at lower frequencies is considered as the radio signature of a coronal shock excited at the flank of the CME.

Conclusions. *The results show that we can build an overall scenario where the CME is interpreted in terms of an erupting arcade crossing the limb of the Sun and connected to underlying structures via multiple CSs. Eventually, the observed limb flare seems to be a consequence of the ongoing CME.*

## **Electric Current Neutralization in Solar Active Regions and Its Relation to Eruptive Activity**

Ellis A. [Avallone](#), [Xudong Sun](#)

ApJ **893** 123 **2020**

<https://arxiv.org/pdf/2003.02814.pdf>

<https://doi.org/10.3847/1538-4357/ab7afa>

It is well established that magnetic free energy associated with electric currents powers solar flares and coronal mass ejections (CMEs) from solar active regions (ARs). However, the conditions that determine whether an AR will produce an eruption are not well understood. Previous work suggests that the degree to which the driving electric currents, or the sum of all currents within a single magnetic polarity, are neutralized may serve as a good proxy for assessing the ability of ARs to produce eruptions. Here, we investigate the relationship between current neutralization and flare/CME production using a sample of 15 flare-active and 15 flare-quiet ARs. All flare-quiet and 4 flare-active ARs are also CME-quiet. We additionally test the relation of current neutralization to the degree of shear along polarity inversion lines (PILs) in an AR. We find that flare-productive ARs are more likely to exhibit non-neutralized currents, specifically those that also produce a CME. We find that flare/CME-active ARs also exhibit higher degrees of PIL shear than flare/CME-quiet ARs. We additionally observe that currents become more neutralized during magnetic flux emergence in flare-quiet ARs. Our investigation suggests that current neutralization in ARs is indicative of their eruptive potential. **2011.02.15, 2013.06.19-20, 2017.09.4-7**

**HMI Science Nuggets** #138 March 2020 <http://hmi.stanford.edu/hminuggets/?p=3224>

**RHESSI NUGGETS** #391 Oct 2020 <https://iopscience.iop.org/article/10.3847/1538-4357/ab7afa/pdf>

## **Mass motion in a prominence bubble revealing a kinked flux rope configuration**

Arun Kumar [Awasthi](#), [Rui Liu](#)

Frontiers in Physics - Stellar and Solar Physics

**2019**

<https://arxiv.org/pdf/1911.12100.pdf>

Prominence bubbles are cavities rising into quiescent prominences from below. The bubble-prominence interface is often the active location for the formation of plumes, which flow turbulently into quiescent prominences. Not only the origin of prominence bubbles is poorly understood, but most of their physical characteristics are still largely unknown. Here, we investigate the dynamical properties of a bubble, which is observed since its early emergence beneath the spine of a quiescent prominence on **20 October 2017** in the  $H\alpha$  line-center and in  $\pm 0.4$  angstrom line-wing wavelengths by the 1-m New Vacuum Solar Telescope. We report the prominence bubble to be exhibiting a disparate morphology in the  $H\alpha$  line-center compared to its line-wings' images, indicating a complex pattern of mass motion along the line-of-sight. Combining Doppler maps with flow maps in the plane of sky derived from a Nonlinear Affine Velocity Estimator, we obtained a comprehensive picture of mass motions revealing a counter-clockwise rotation inside the bubble; with blue-shifted material flowing upward and red-shifted material flowing downward. This sequence of mass motions is interpreted to be either outlining a kinked flux rope configuration of the prominence bubble or providing observational evidence of the internal kink instability in the prominence plasma.

## **Pre-Eruptive Magnetic Reconnection within a Multi-Flux-Rope System in the Solar Corona**

Arun Kumar [Awasthi](#), [Rui Liu](#), [Haimin Wang](#), [Yuming Wang](#), [Chenglong Shen](#)

ApJ **857** 124 **2018**

<https://arxiv.org/pdf/1803.04088.pdf>

[sci-hub.se/10.3847/1538-4357/aab7fb](https://doi.org/10.3847/1538-4357/aab7fb)

The solar corona is frequently disrupted by coronal mass ejections (CMEs), whose core structure is believed to be a flux rope made of helical magnetic field. This has become a "standard" picture although it remains elusive how the flux rope forms and evolves toward eruption. While 1/3 of the ejecta passing through spacecrafts demonstrate a flux-rope structure, the rest have complex magnetic fields. Are they originating from a coherent flux rope, too? Here we investigate the source region of a complex ejecta, focusing on a flare precursor with definitive signatures of magnetic reconnection, i.e., nonthermal electrons, flaring plasma, and bi-directional outflowing blobs. Aided by nonlinear force-free field modeling, we conclude that the reconnection occurs within a system of



multiple braided flux ropes with different degree of coherency. The observation signifies the importance of internal structure and dynamics in understanding CMEs and in predicting their impacts on Earth. **22 June 2015**

## **Coronal Mass Ejections from the Sun - Propagation and Near Earth Effects**

Arun **Babu**

THESIS, 2014

<http://arxiv.org/pdf/1407.4258v1.pdf>

Owing to our dependence on spaceborne technology, an awareness of disturbances in the near-Earth space environment is proving to be increasingly crucial. Earth-directed Coronal mass ejections (CMEs) emanating from the Sun are the primary drivers of space weather disturbances. Studies of CMEs, their kinematics, and their near-Earth effects are therefore gaining in importance.

The effect of CMEs near the Earth is often manifested as transient decreases in galactic cosmic ray intensity, which are called **Forbush decreases (FDs)**. In this thesis we probe the structure of CMEs and their associated shocks using FD observations by the GRAPES-3 muon telescope at Ooty. We have established that the cumulative diffusion of galactic cosmic rays into the CME is the dominant mechanism for causing FDs (Chapter 3).

This diffusion takes place through a turbulent sheath region between the CME and the shock. One of our main results concerns the turbulence level in this region. We have quantitatively established that cross-field diffusion aided by magnetic field turbulence accounts for the observed lag between the FD and the magnetic field enhancement of the sheath region (Chapter 4).

We have also investigated the nature of the driving forces acting on CMEs in this thesis. Using CME data from the SECCHI coronagraphs aboard STEREO spacecraft, we have found evidence for the non-force-free nature of the magnetic field configuration inside these CMEs, which is the basis for the (often-invoked) Lorentz self-force driving (Chapter 5).

Taken together the work presented in this thesis is a comprehensive attempt to characterise CME propagation from typical coronagraph fields of view to the Earth.

## **Plasma Physical Parameters along CME-driven Shocks. II. Observation–Simulation Comparison**

F. **Bacchini**<sup>1</sup>, R. Susino<sup>2</sup>, A. Bemporad<sup>2</sup>, and G. Lapenta<sup>1</sup>

2015 ApJ 809 58

In this work, we compare the spatial distribution of the plasma parameters along the **1999 June 11** coronal mass ejection (CME)-driven shock front with the results obtained from a CME-like event simulated with the FLIPMHD3D code, based on the FLIP-MHD particle-in-cell method. The observational data are retrieved from the combination of white-light coronagraphic data (for the upstream values) and the application of the Rankine–Hugoniot equations (for the downstream values). The comparison shows a higher compression ratio  $X$  and Alfvénic Mach number  $MA$  at the shock nose, and a stronger magnetic field deflection  $d$  toward the flanks, in agreement with observations. Then, we compare the spatial distribution of  $MA$  with the profiles obtained from the solutions of the shock adiabatic equation relating  $MA$ ,  $X$ , and  $\theta_{Bn}$  (the angle between the upstream magnetic field and the shock front normal) for the special cases of parallel and perpendicular shock, and with a semi-empirical expression for a generically oblique shock. The semi-empirical curve approximates the actual values of  $MA$  very well, if the effects of a non-negligible shock thickness  $\delta_{sh}$  and plasma-to magnetic pressure ratio  $\beta_u$  are taken into account throughout the computation. Moreover, the simulated shock turns out to be supercritical at the nose and sub-critical at the flanks. Finally, we develop a new one-dimensional Lagrangian ideal MHD method based on the GrAALe code, to simulate the ion-electron temperature decoupling due to the shock transit. Two models are used, a simple solar wind model and a variable- $\gamma$  model. Both produce results in agreement with observations, the second one being capable of introducing the physics responsible for the additional electron heating due to secondary effects (collisions, Alfvén waves, etc.).

## **Evidence for precursors of the coronal hole jets in solar bright points**

Salome R. **Bagashvili**, **Bidzina M. Shergelashvili**, **Darejan R. Japaridze**, **Vasil Kukhianidze**, **Stefaan Poedts**, **Teimuraz V. Zaqarashvili**, **Maxim L. Khodachenko**, **Patrick De Causmaecker**

ApJL 2018

<https://arxiv.org/pdf/1803.00551.pdf>

A set of 23 observations of coronal jet events that occurred in coronal bright points has been analyzed. The focus was on the temporal evolution of the mean brightness before and during coronal jet events. In the absolute majority of the cases either single or recurrent coronal jets were preceded by slight precursor disturbances observed in the mean intensity curves. The key conclusion is that we were able to detect quasi-periodical oscillations with characteristic periods from sub-minute up to 3-4 min values in the bright point brightness which precede the jets. Our basic claim is that along with the conventionally accepted scenario of bright point evolution through new magnetic flux emergence and its reconnection with the initial structure of the bright point and the coronal hole, certain MHD oscillatory and wave-like motions can be excited and these can take an important place in the observed dynamics. These quasi-oscillatory phenomena might play the role of links between different epochs of the coronal jet ignition and evolution. They can be an indication of the MHD wave excitation processes due to the system entropy variations, density

variations or shear flows. It is very likely a sharp outflow velocity transverse gradients at the edges between the open and closed field line regions. We suppose that magnetic reconnections can be the source of MHD waves due to impulsive generation or rapid temperature variations, and shear flow driven nonmodel MHD wave evolution (self-heating and/or overreflection mechanisms). **9 Dec 2015 Table 23 events (2015-2016)**

## **Shock and Discontinuity Formation in the Front of an Expanding Coronal Magnetic Arcade in Two-fluid Simulations**

T. E. **Bagwell** and Z. W. Ma

2020 ApJ 898 167

<https://doi.org/10.3847/1538-4357/aba2d4>

The dynamic evolution of a magnetic arcade associated with footpoint shearing motions is investigated by an ideal two-fluid (electron-ion) code. The two-fluid numerical simulations produce conspicuous differences compared to earlier MHD simulations beyond the inner arcade region. The decoupling motion between electrons and heavier ions during the arcade expansion induces a growing charge separation and strong electric field in the front of the expanding arcade. The presence of this electric field provides an additional force, along with the magnetic and thermal pressures, that drives the growth of an outwardly expanding wave that steepens into a propagating discontinuity in the plasma and magnetic field. The propagation speed of the discontinuity eventually exceeds the local phase velocity of the MHD fast mode and becomes a perpendicular fast-like shock. There is significant heating at the shock due to adiabatic compression, with preferential heating of the ion fluid also being observed. In addition, parameter tests indicate that (1) the propagation speed of the shock before exiting the inner arcade is independent of the maximum shear speed; (2) slower shearing speeds produce weaker shocks with weaker adiabatic heating; (3) the ion-to-electron mass ratio,  $m_i/m_e$ , impacts the strength of the charge separation linearly but has a moderate effect on the propagation speed; and (4) the normalized value of the ion inertial length does not affect the formation and speed of the shock as a whole.

## **Signatures of Magnetic Reconnection at the Footpoints of Fan-shaped Jets on a Light Bridge Driven by Photospheric Convective Motions**

Xianyong **Bai**<sup>1,2</sup>, Hector Socas-Navarro<sup>3,4</sup>, Daniel Nóbrega-Siverio<sup>5,6</sup>, Jiangtao Su<sup>1,2</sup>, Yuanyong Deng<sup>1,2</sup>, Dong Li<sup>7,8</sup>, Wenda Cao<sup>9</sup>, and Kaifan Ji<sup>1</sup>

2019 ApJ 870 90

<https://arxiv.org/pdf/1811.03723.pdf>

<http://iopscience.iop.org/article/10.3847/1538-4357/aaf1d1/pdf>

Dynamical jets are generally found on light bridges (LBs), which are key to studying sunspot decay. So far, their formation mechanism is not fully understood. In this paper, we used state-of-the-art observations from the Goode Solar Telescope, the Interface Region Imaging Spectrograph, the Spectro-polarimeter on board Hinode, and the Atmospheric Imaging Assembly (AIA) on board the Solar Dynamics Observatory to analyze the fan-shaped jets on LBs in detail. A continuous upward motion of the jets in the ascending phase is found from the H $\alpha$  velocity that lasts for 12 minutes and is associated with the H $\alpha$  line wing enhancements. Two mini jets appear on the bright fronts of the fan-shaped jets visible in the AIA 171 and 193 Å channels, with a time interval as short as 1 minute. Two kinds of small-scale convective motions are identified in the photospheric images, along with the H $\alpha$  line wing enhancements. One seems to be associated with the formation of a new convection cell, and the other manifests as the motion of a dark lane passing through the convection cell. The finding of three-lobe Stokes V profiles and their inversion with the NICOLE code indicate that there are magnetic field lines with opposite polarities in LBs. From the H $\alpha$  -0.8 Å images, we found ribbon-like brightenings propagating along the LBs, possibly indicating slipping reconnection. Our observation supports the idea that the fan-shaped jets under study are caused by magnetic reconnection, and photospheric convective motions play an important role in triggering the magnetic reconnection. **2014 August 1**

## **Further Evidence for the Minifilament-Eruption Scenario for Solar Polar Coronal Jets**

[Tomi K. Baikie](#), [Alphonse C. Sterling](#), [Ronald L. Moore](#), [Amanda M. Alexander](#), [David A. Falconer](#), [Antonia Savcheva](#), [Sabrina L. Savage](#)

ApJ 927 79 2022

<https://arxiv.org/pdf/2201.08882.pdf>

<https://iopscience.iop.org/article/10.3847/1538-4357/ac473e/pdf>

We examine a sampling of 23 polar-coronal-hole jets. We first identified the jets in soft X-ray (SXR) images from the X-ray telescope (XRT) on the Hinode spacecraft, over 2014-2016. During this period, frequently the polar holes were small or largely obscured by foreground coronal haze, often making jets difficult to see. We selected 23 jets among those adequately visible during this period, and examined them further using Solar Dynamics Observatory (SDO) Atmospheric Imaging Assembly (AIA) 171, 193, 211, and 304 Å images. In SXRs we track the lateral drift of the jet spire relative to the jet base's jet bright point (JBP). In 22 of 23 jets the spire either moves away from (18 cases) or is stationary relative to (4 cases) the JBP. The one exception where the spire moved toward the JBP may be a consequence of line-of-sight projection effects at the limb. From the AIA images, we clearly identify an erupting minifilament in 20 of the 23 jets, while the remainder are consistent with such an eruption having taken place. We also confirm that some jets can trigger onset of nearby "sympathetic" jets, likely because eruption of the minifilament field of the first jet

removes magnetic constraints on the base-field region of the second jet. The propensity for spire drift away from the JBP, the identification of the erupting minifilament in the majority of jets, and the magnetic-field topological changes that lead to sympathetic jets, all support or are consistent with the minifilament-eruption model for jets. **13 Aug 2014, 27 Feb 2015, 2015 March 19, 8 Apr 2015, 2015 June 5, 2016 March 17, 2016 March 23, 2016 April 01**  
**Table 1.** Jets selected for further analysis 2014-2016

### **RADIO IMAGING OF SHOCK-ACCELERATED ELECTRONS ASSOCIATED WITH AN ERUPTING PLASMOID ON 2010 NOVEMBER 3**

H. M. [Bain](#), Säm Krucker<sup>1</sup>, L. Glesener, and R. P. Lin  
**2012 ApJ 750 44**

We present observations of a metric type II solar radio burst that occurred on the **3rd of November 2010** in association with an erupting plasmoid. The eruption was well observed by the Atmospheric Imaging Assembly (AIA) on board the Solar Dynamics Observatory and the Reuven Ramaty High Energy Solar Spectroscopic Imager, while the burst occurred in the frequency range of the Nançay Radioheliograph (NRH). Such events, where the type II emission occurs in the NRH frequency range, allowing us to image the burst, are infrequent. Combining these data sets, we find that the type II is located ahead of the hot ( $\sim 11$  MK) core of the plasmoid, which is surrounded by a well-defined envelope of cool (few MK) plasma. Using two methods, we determine the propagation velocity of the shock: (1) fitting the type II emission observed in PHOENIX and HUMAIN radio spectrogram data; (2) direct imaging of the type II source location using NRH observations. We use LASCO C2 polarized brightness images to normalize our coronal density model. However, we find that information from imaging is required in order to fine-tune this normalization. We determine a shock propagation velocity between  $1900 \text{ km s}^{-1}$  and  $2000 \text{ km s}^{-1}$ . This is faster than the plasmoid observed at extreme-ultraviolet wavelengths by AIA ( $v = 670\text{-}1440 \text{ km s}^{-1}$ , where the cooler plasma propagates faster than the hot core). The positioning of the type II, ahead of the plasmoid, suggests that the electrons are accelerated in a piston-driven shock.

### **Coronal Mass Ejections Associated with Slow Long Duration Flares**

U. [Bağ-Steślicka](#), S. Kołomański, T. Mrozek  
**Solar Phys. 2013, File**

It is well known that there is a temporal relationship between coronal mass ejections (CMEs) and associated flares. The duration of the acceleration phase is related to the duration of the rise phase of a flare. We investigate CMEs associated with slow long duration events (LDEs), i.e. flares with the long rising phase. We determined the relationships between flares and CMEs and analyzed the CME kinematics in detail. The parameters of the flares (GOES flux, duration of the rising phase) show strong correlations with the CME parameters (velocity, acceleration during main acceleration phase, and duration of the CME acceleration phase). These correlations confirm the strong relation between slow LDEs and CMEs. We also analyzed the relation between the parameters of the CMEs, i.e. a velocity, an acceleration during the main acceleration phase, a duration of the acceleration phase, and a height of a CME at the end of the acceleration phase. The CMEs associated with the slow LDEs are characterized by high velocity during the propagation phase, with the median equal to  $1423 \text{ km s}^{-1}$ . In half of the analyzed cases, the main acceleration was low ( $a < 300 \text{ m s}^{-2}$ ), which suggests that the high velocity is caused by the prolonged acceleration phase (the median for the duration of the acceleration phase is equal 90 minutes). The CMEs were accelerated up to several solar radii (with the median  $\approx 7 R_{\odot}$ ), which is much higher than in typical impulsive CMEs. Therefore, slow LDEs may potentially precede extremely strong geomagnetic storms. The analysis of slow LDEs and associated CMEs may give important information for developing more accurate space-weather forecasts, especially for extreme events.

### **Tables**

### **Evolution of Plasma Composition in an Eruptive Flux Rope**

[Deborah Baker](#) (1), [Lucie M. Green](#) (1), [David H. Brooks](#) (2), [Pascal Démoulin](#) (3), [Lidia van-Driel-Gesztelyi](#) (1, 3, 4), [Teodora Mihalescu](#) (1), [Andy S. H. To](#) (1), [David M. Long](#) (1), [Stephanie L. Yardley](#) (1), [Miho Janvier](#) (5), [Gherardo Valori](#) (6)

**ApJ 924:17 2022**

<https://arxiv.org/pdf/2110.11714.pdf>

<https://iopscience.iop.org/article/10.3847/1538-4357/ac32d2/pdf>

Magnetic flux ropes are bundles of twisted magnetic field enveloping a central axis. They harbor free magnetic energy and can be progenitors of coronal mass ejections (CMEs), but identifying flux ropes on the Sun can be challenging. One of the key coronal observables that has been shown to indicate the presence of a flux rope is a peculiar bright coronal structure called a sigmoid. In this work, we show Hinode EUV Imaging Spectrometer (EIS) observations of sigmoidal active region 10977. We analyze the coronal plasma composition in the active region and its evolution as the sigmoid (flux rope) forms and erupts as a CME. Plasma with photospheric composition was observed in coronal loops close to the main polarity inversion line during episodes of significant flux cancellation, suggestive of the injection of photospheric plasma into these loops driven by photospheric flux cancellation. Concurrently, the increasingly sheared core field contained plasma with coronal composition. As flux cancellation decreased and the sigmoid/flux rope formed, the plasma evolved to an intermediate composition in between photospheric and typical active region coronal compositions. Finally, the flux rope contained predominantly photospheric plasma during and after a failed eruption preceding the CME. Hence, plasma composition observations of active region 10977 strongly support models of

flux rope formation by photospheric flux cancellation forcing magnetic reconnection first at the photospheric level then at the coronal level. **2007 December 4–7**

### **Plasma Upflows Induced by Magnetic Reconnection Above an Eruptive Flux Rope**

[Deborah Baker](#), [Teodora Mihailescu](#), [Pascal Démoulin](#), [Lucie M. Green](#), [Lidia van Driel-Gesztelyi](#), [Gherardo Valori](#), [David H. Brooks](#), [David M. Long](#) & [Miho Janvier](#)

*Solar Physics* volume 296, Article number: 103 (2021)

<https://link.springer.com/content/pdf/10.1007/s11207-021-01849-7.pdf>

<https://doi.org/10.1007/s11207-021-01849-7>

One of the major discoveries of Hinode's Extreme-ultraviolet Imaging Spectrometer (EIS) is the presence of upflows at the edges of active regions. As active regions are magnetically connected to the large-scale field of the corona, these upflows are a likely contributor to the global mass cycle in the corona. Here we examine the driving mechanism(s) of the very strong upflows with velocities in excess of  $70 \text{ km s}^{-1}$ , known as blue-wing asymmetries, observed during the eruption of a flux rope in AR 10977 (eruptive flare SOL2007-12-07T04:50). We use Hinode/EIS spectroscopic observations combined with magnetic-field modeling to investigate the possible link between the magnetic topology of the active region and the strong upflows. A Potential Field Source Surface (PFSS) extrapolation of the large-scale field shows a quadrupolar configuration with a separator lying above the flux rope. Field lines formed by induced reconnection along the separator before and during the flux-rope eruption are spatially linked to the strongest blue-wing asymmetries in the upflow regions. The flows are driven by the pressure gradient created when the dense and hot arcade loops of the active region reconnect with the extended and tenuous loops overlying it. In view of the fact that separator reconnection is a specific form of the more general quasi-separatrix (QSL) reconnection, we conclude that the mechanism driving the strongest upflows is, in fact, the same as the one driving the persistent upflows of  $\approx 10 - 20 \text{ km s}^{-1}$  observed in all active regions.

### **A major solar eruptive event in July 2012: Defining extreme space weather scenarios.**

[Baker](#) DN, Li X, Pulkkinen A, Ngwira CM, Mays LL, Galvin AB, Simunac KDC

(2013) *Space Weather* 11:585–591

### **Forecasting a CME by Spectroscopic Precursor?**

D. [Baker](#), L. van Driel-Gesztelyi and L. M. Green

*Solar Physics*, Volume 276, Numbers 1-2, 219-239, 2012, [File](#)

Multi-temperature plasma flows resulting from the interaction between a mature active region (AR) inside an equatorial coronal hole (CH) are investigated. Outflow velocities observed by Hinode EIS ranged from a few to  $13 \text{ km s}^{-1}$  for three days at the AR's eastern and western edges. However, on the fourth day, velocities intensified up to  $20 \text{ km s}^{-1}$  at the AR's western footpoint about six hours prior to a CME. 3D MHD numerical simulations of the observed magnetic configuration of the AR-CH complex showed that the expansion of the mature AR's loops drives persistent outflows along the neighboring CH field (Murray et al. in *Solar Phys.* 261, 253, 2010). Based on these simulations, intensification of outflows observed pre-eruption on the AR's western side where same-polarity AR and CH field interface, is interpreted to be the result of the expansion of a sigmoidal AR, in particular, a flux rope containing a filament that provides stronger compression of the neighboring CH field on this side of the AR. Intensification of outflows in the AR is proposed as a new type of CME precursor.

### **Forecasting a CME by Spectroscopic Precursor?**

D. [Baker](#), L. van Driel-Gesztelyi and L. M. Green

2012, *Sol. Phys.*, DOI 10.1007/s11207-011-9893-4

### **Spectroscopic Precursor to a CME**

Deb [Baker](#), Lidia van Driel-Gesztelyi and Lucie Green

Hinode/EIS Nugget, Jan 2012

[http://msslxr.mssl.ucl.ac.uk:8080/SolarB/nuggets/nugget\\_2012jan.jsp](http://msslxr.mssl.ucl.ac.uk:8080/SolarB/nuggets/nugget_2012jan.jsp)

Coronal mass ejections are eruptions of plasma and magnetic field from low in the Sun's atmosphere. They act as a valve to release magnetic energy from the Sun's atmosphere and are the major driver of space weather events. Theoretical and observational developments since their discovery in the early 1970's have shown that coronal mass ejections are driven by changes in the magnetic field which occur over a wide range of time scales from hours to weeks. Since it is not currently possible to directly observe the magnetic field in this region of the Sun to understand these changes, other observational signatures must be used as a proxy for the magnetic field evolution. In the past this has included the slow rise of filaments or coronal loops which indicate an overall rise or expansion of the magnetic structure which can in many cases be interpreted as being that of a twisted rope of magnetic field. This nugget discusses how plasma outflows from an active region which erupts to produce a coronal mass ejection can be used to understand when important changes in the magnetic field start to occur.

**17-18 Oct 2007**

## Signatures of Interchange Reconnection: STEREO, ACE and Hinode Observations Combined

D. Baker<sup>1</sup>, A. P. Rouillard<sup>2,3</sup>, L. van Driel-Gesztelyi<sup>1,4,5</sup>, P. D'émoulin<sup>4</sup>, L. K. Harra<sup>1</sup>, B. Lavraud<sup>6,7</sup>, J.A. Davies<sup>3</sup>, A. Opitz<sup>6,7</sup>, J. G. Luhmann<sup>8</sup>, J.-A. Sauvaud<sup>6,7</sup>, and A. B. Galvin<sup>9</sup>

E-print, Sept **2009**; Ann. Geophys., 27, 3883-3897, **2009**

[Abstract](#) [Full Article](#) (PDF, 4868 KB)

Combining STEREO, ACE and Hinode observations has presented an opportunity to follow a filament eruption and coronal mass ejection (CME) on the **17th of October 2007** from an active region (AR) inside a coronal hole (CH) into the heliosphere. This particular combination of 'open' and closed magnetic topologies provides an ideal scenario for interchange reconnection to take place. With Hinode and STEREO data we were able to identify the emergence time and type of structure seen in the in-situ data four days later. On the 21st, ACE observed in-situ the passage of an ICME with 'open' magnetic topology. The magnetic field configuration of the source, a mature AR located inside an equatorial CH, has important implications for the solar and interplanetary signatures of the eruption. We interpret the formation of an 'anemone' structure of the erupting AR and the passage in-situ of the ICME being disconnected at one leg, as manifested by uni-directional suprathermal electron flux in the ICME, to be a direct result of interchange reconnection between closed loops of the CME originating from the AR and 'open' field lines of the surrounding CH.

## Coronal Mass Ejections Associated with Slow Long Duration Flares

U. Bak-Steslicka, S. Kolomanski, T. Mrozek

E-print, Feb **2013**; Solar Phys., April **2013**, Volume 283, Issue 2, pp 505-517, **File**

It is well known that there is temporal relationship between coronal mass ejections (CMEs) and associated flares. The duration of the acceleration phase is related to the duration of the rise phase of a flare. We investigate CMEs associated with slow long duration events (LDEs), i.e. flares with the long rising phase. We determined the relationships between flares and CMEs and analyzed the CME kinematics in detail. The parameters of the flares (GOES flux, duration of the rising phase) show strong correlations with the CME parameters (velocity, acceleration during main acceleration phase and duration of the CME acceleration phase). These correlations confirm the strong relation between slow LDEs and CMEs. We also analyzed the relation between the parameters of the CMEs, i.e. a velocity, an acceleration during the main acceleration phase, a duration of the acceleration phase, and a height of a CME at the end of the acceleration phase. The CMEs associated with the slow LDEs are characterized by high velocity during the propagation phase, with the median equal 1423 km/s. In half of the analyzed cases, the main acceleration was low ( $a < 300 \text{ m/s}^2$ ), which suggests that the high velocity is caused by the prolonged acceleration phase (the median for the duration of the acceleration phase is equal 90 minutes). The CMEs were accelerated up to several solar radii (with the median 7  $R_{\text{sun}}$ ), which is much higher than in typical impulsive CMEs. Therefore, slow LDEs may potentially precede extremely strong geomagnetic storms. The analysis of slow LDEs and associated CMEs may give important information for developing more accurate space weather forecasts, especially for extreme events.

**Table:** 23 Feb 1997, 14 Nov 1997, 20 Apr 1998, 16 June 1998, 5 May 2000, 16 Oct 2000, 2 Feb 2001, 1 Apr 2001, 3 Apr 2001, 5 Apr 2001, 15 May 2001, 28 Dec 2001, 10 March 2002, 21 May 2002, 24 Oct 2003, 18 Nov 2003, 28 July 2004, 29 July 2004, 31 July 2004, 14 July 2005, 27 July 2005, 6 Sept 2005, 16 March 2011

## Investigation of Slow Rising LDE Flares and Associated CMEs

Bak-Steslicka, U.; Kolomanski, S.; Jakimiec, J

Freiburg ESP Meeting **2008**, **Poster**

We investigated limb long duration flares with slow rising phases (slow LDE) accompanied with CMEs.

It was shown by other authors that acceleration phase of CME lasts as long as the rising phase of associated flare. Thus, slow evolution of slow rising flares allows to study earliest stages of CME evolution in details.

Using LASCO data we examined statistical properties of these CME while SXT, EIT and TRACE data were utilized to analyse structure and evolution of associated slow LDE flares. The SXT, EIT and TRACE data allow us to identify CME related structures visible in EUV and SXR.

## The Hyper-inflation Stage in the Coronal Mass Ejection Formation: A Missing Link That Connects Flares, Coronal Mass Ejections, and Shocks in the Low Corona

Laura A. Balmaceda<sup>1,2</sup>, Angelos Vourlidis<sup>3</sup>, Guillermo Stenborg<sup>3</sup>, and Ryun-Young Kwon<sup>4</sup>

**2022** ApJ 931 141

<https://iopscience.iop.org/article/10.3847/1538-4357/ac695c/pdf>

We analyze the formation and three-dimensional (3D) evolution of two coronal mass ejections (CMEs) and their associated waves in the low corona via a detailed multi-viewpoint analysis of extreme-ultraviolet observations. We analyze the kinematics in the radial and lateral directions and identify three stages in the early evolution of the CME: (1) a hyper-inflation stage, when the CME laterally expands at speeds of  $\sim 1000 \text{ km s}^{-1}$ , followed by (2) a shorter and slower expansion stage of a few minutes and ending with (3) a self-similar phase that carries the CME into the middle corona. The first two stages coincide with the impulsive phase of the accompanying flare, the formation and separation of an EUV wave from the CME, and the start of the metric type II radio burst. Our 3D analysis suggests that the hyper-

inflation phase may be a crucial stage in the CME formation with wide-ranging implications for solar eruption research. It likely represents the formation stage of the magnetic structure that is eventually ejected into the corona, as the white-light CME. It appears to be driven by the injection of poloidal flux into the ejecting magnetic structure, which leads to the lateral (primarily) growth of the magnetic flux rope. The rapid growth results in the creation of EUV waves and eventually shocks at the CME flanks that are detected as metric type II radio bursts. In other words, the hyper-inflation stage in the early CME evolution may be the "missing" link between CMEs, flares, and coronal shocks. **2011 March 7, 2011 June 7**

### **On the Expansion Speed of Coronal Mass Ejections: Implications for Self-Similar Evolution**

[L. A. Balmaceda](#), [A. Vourlidas](#), [G. Stenborg](#) & [O. C. St. Cyr](#)

[Solar Physics](#) volume 295, Article number: 107 (2020)

<https://link.springer.com/content/pdf/10.1007/s11207-020-01672-6.pdf>

A proper characterization of the kinematics of coronal mass ejections (CMEs) is important not only for practical purposes, i.e. space weather forecasting, but also to improve our current understanding of the physics behind their evolution in the middle corona and into the heliosphere. The first and core step toward this goal is the estimation of the three main components of the CME speeds, namely the expansion speed relative to the center of motion in both, the radial and lateral directions, and the propagation speed (i.e.  $V_{\text{front}}$ ,  $V_{\text{lat}}$ ,  $V_{\text{bulk}}$ , respectively). To this aim, we exploit the observations obtained with COR2 onboard the Solar Terrestrial Relations Observatory (STEREO) from 2007 to 2014 to investigate the relationships among the different components as a function of the heliocentric distance of the CME events. Here, we analyze a sample of 475 CMEs. The selected events exhibit clear flux rope signatures as seen either edge on (i.e. F-CMEs: three-part structure, presence of a cavity) or face on (i.e. L- or loop CMEs) in white light images. Our main findings are: i) L-CMEs show almost twice as large expansion speeds compared to F-CMEs ( $V_{\text{front,L}}=367 \text{ kms}^{-1}$ ,  $V_{\text{lat,L}}=365 \text{ kms}^{-1}$  vs.  $V_{\text{front,F}}=215 \text{ kms}^{-1}$ ,  $V_{\text{lat,F}}=182 \text{ kms}^{-1}$ ); ii) the relationship between the two components of the expansion speeds is linear and does not change with height; iii) the ratio of the propagation speed to the lateral expansion speed is a function of the angular width that describes the self-similarity evolution of a CME; and iv) 65% of the CMEs exhibit a self-similar evolution at 10 solar radii, reaching 70% at 15 solar radii. **2008-02-23**

### **How Reliable Are the Properties of Coronal Mass Ejections Measured from a Single Viewpoint?**

Laura A. [Balmaceda](#)<sup>1,5</sup>, Angelos [Vourlidas](#)<sup>2,6</sup>, Guillermo [Stenborg](#)<sup>3</sup>, and Alisson Dal Lago<sup>4</sup>

**2018 ApJ 863 57**

<https://sci-hub.ru/10.3847/1538-4357/aacff8>

We present an analysis of widths and kinematic properties of coronal mass ejections (CMEs) obtained via a supervised image segmentation algorithm, the CORonal SEGmentation Technique (CORSET), on simultaneous observations from the two COR2 telescopes on the Solar Terrestrial Relations Observatory (STEREO) mission, from 2007 May to 2014 September. The sample of 460 events with measurements from two vantage points offers the opportunity to test the accuracy and constraints of single-viewpoint properties that underlie the bulk of CME research to date. In addition, we examine the dependence of the properties on the morphology of the events. The main findings are as follows. (1) The radial speeds derived from different perspectives are in good agreement with a relatively low intrinsic uncertainty of 39%. (2) Projection effects are more important for determination of CME width rather than for speed. (3) The expansion speeds depend on CME morphology, with loop-type CMEs expanding twice as fast as flux-rope CMEs, possibly underpinning the more explosive nature. (4) Triangulations of CME speed and propagation direction are optimal from viewpoints separated by  $60^\circ$ – $90^\circ$ ; e.g., between the Lagrangian points L1 and L5 (or L4). (5) The projected speeds are underestimated, on average, by at least 20% when compared to their deprojected (triangulated) values. We also discuss in detail the lessons learned from the application of the CORSET algorithm to event tracking. Our findings should hopefully be a useful guide in the use of (semi)automated algorithms for extraction of CME physical parameters and in the interpretation of single-viewpoint observations (likely to be the norm after the end of the STEREO mission).

### **The Role of a Tiny Brightening in a Huge Geo-effective Solar Eruption Leading to the St Patrick's Day Storm**

Yumi [Bamba](#), [Satoshi Inoue](#), [Keiji Hayashi](#)

**ApJ 2019**

<https://arxiv.org/pdf/1902.04871.pdf>

The largest magnetic storm in solar cycle 24 was caused by a fast coronal mass ejection (CME) that was related to a small C9.1 flare that occurred on **15 March 2015** in solar active region (AR) NOAA 12297. The purpose of this study is to understand the onset mechanism of the geo-effective huge solar eruption. We focused on the C2.4 flare that occurred prior to the C9.1 flare of the filament eruption. The magnetic field structure in the AR was complicated: there were several filaments including the one that erupted and caused the CME. We hence carefully investigated the photospheric magnetic field, brightenings observed in the solar atmosphere, and the three-dimensional coronal magnetic field extrapolated from nonlinear force-free field modeling, using data from Hinode and Solar Dynamics Observatory. We found three intriguing points: (1) There was a compact but noticeably highly twisted magnetic field structure that is represented by a small filament in the C2.4 flaring region, where a tiny precursor brightening was observed before the

C2.4 flare. (2) The C2.4 flaring region is located in the vicinity of a foot point of the closed field that prohibits the filament from erupting. (3) The filament shows a sudden eruption after the C2.4 flare and accompanying small filament eruption. From our analysis, we suggest that a small magnetic disturbance that was represented by the tiny precursor brightening at the time of the C2.4 flare is related to the trigger of the huge filament eruption.

## **Transverse Oscillation of Coronal Loops Induced by Eruptions of a Magnetic Flux Tube and a Plasmoid**

[K. Safna Banu](#), [Ram Ajor Maurya](#) & [P. T. Jain Jacob](#)

[Solar Physics](#) volume 297, Article number: 134 (2022)

<https://doi.org/10.1007/s11207-022-02065-7>

We studied transverse oscillations in hot coronal loops of active region NOAA 12673 located at the west limb. Loop oscillations were associated with a plasmoid ejection from the same location. During the rising phase of the plasmoid, a magnetic flux tube was seen to be rising and bending towards the loop system that erupted before the plasmoid ejection. In addition to the plasmoid ejection, a large coronal mass ejection (CME) and an X8.2 flare were observed in the same active region for several hours ( $\approx 7$  hours). After the plasmoid ejection, a follow-up shock wave from the flare site was triggered by a sudden momentum transfer towards the solar disk. It was found to be propagating across the entire solar disk with an average speed of  $\approx 1290$  km s<sup>-1</sup>. By analyzing the time sequence of these events, we found that a plasmoid ejection perturbed the loops from their equilibrium and set them in oscillation. We found different oscillations of the fundamental mode in two loops, fast decaying (with a period of 7.93 minutes and an average damping time of  $\approx 19$  minutes) and slow decaying (with a period of 6.31 minutes and an average damping time of  $\approx 34$  minutes). The two different oscillations could be due to their lengths, magnetic fields, and plasma densities. Using the methods of coronal seismology, we estimated the average magnetic field in the coronal loops to be 29 G and 36 G, which is consistent with the order of the coronal magnetic fields found in other studies. **10 Sep 2017**

## **Evolution of coronal mass ejections in the early stage**

Xingming [Bao](#), Hongqi Zhang, Jun Lin, Yunchun Jiang and Leping Li

*Adv. Space Res.*, 39(12), p. 1847-1852, 2007, *File*

This work reports the investigation of two coronal mass ejections (CME) observed in white light, Ha, EUV and X-ray by various

instruments both in space and on ground on **February 18, 2003 and January 19, 2005**, respectively. The white light coronal images show that the first CME began with the rarefaction of a region above the solar limb and was followed by the formation of its leading edge at the boundary of the rarefying region at altitude of 0.46 Rx from the solar surface. The rarefaction coincided the slow rising phase of the filament eruption, and the CME leading edge was observed to form as the filament eruption started to accelerate apparently. In the early stage of the second CME, a bright loop was first observed above the solar limb with height of 0.37 Rx in EUV images. We found that the more gradual CMEs initial process, the larger the timing difference between CMEs and their associated flares. The lower part of the filament brightened in Ha images as the filament rose to a certain height. These brightenings imply that the filament may be heated by magnetic reconnection below the filament in the early stage of the eruption. We suggest that the possible mechanism which led to the formation of the CME leading edge and cavity is magnetic reconnection which occurred under the filament when it reached a certain height.

## **Coronal mass ejections and the associated activities on the solar disk observed on October 26, 2003**

X. [Bao](#), H. Zhang<sup>1</sup>, J. Lin<sup>2,3</sup>, and G. A. Stenborg<sup>4</sup>

*A&A* 463, 321-331 (2007)

We analyzed four CMEs that happen to take off near the west limb of the Sun on October 26, 2003.

We have explored more explicitly than in previous studies the relationship between different types of CMEs and the associated on-disk activities.

## **Improving CME evolution and arrival predictions with AMR and grid stretching in Icarus**

T. [Baratashvili](#)<sup>1</sup>, C. Verbeke<sup>1,2</sup>, N. Wijsen<sup>1</sup> and S. Poedts<sup>1,3</sup>

*A&A* 667, A133 (2022)

<https://www.aanda.org/articles/aa/pdf/2022/11/aa44111-22.pdf>

Context. Coronal mass ejections (CMEs) are one of the main drivers of disturbances in interplanetary space. Strong CMEs, when directed towards the Earth, cause geomagnetic storms upon interacting with the Earth's magnetic field, and can cause significant damage to our planet and affect everyday life. As such, efficient space weather prediction tools are necessary to forecast the arrival and impact of CME eruptions. Recently, a new heliospheric model called Icarus was developed based on MPI-AMRVAC, which is a 3D ideal magnetohydrodynamics model for the solar wind and CME propagation, and it introduces advanced numerical techniques to make the simulations more efficient. In this model the reference frame is chosen to be co-rotating with the Sun, and radial grid stretching together with adaptive mesh refinement (AMR) can be applied to the numerical domain.

Aims. Grid stretching and AMR speed up simulation results and performance. Our aim is to combine the advanced techniques available in the Icarus model in order to obtain better results with fewer computational resources than with the equidistant grid. Different AMR strategies are suggested, depending on the purpose of the simulation.

Methods. In this study, we model the CME event that occurred on July 12, 2012. A cone model was used to study the CME's evolution through the background solar wind, and its arrival at and impact with the Earth. Grid stretching and AMR were combined in the simulations by using multiple refinement criteria, to assess its influence on the simulations' accuracy and the required computational resources. We compare simulation results to the EUHFORIA model. Results. We applied different refinement criteria to investigate the potential of solution AMR for different applications. As a result, the simulations were sped up by a factor of  $\sim 17$  for the most optimal configuration in Icarus. For the cone CME model, we found that limiting the AMR to the region around the CME-driven shock yields the best results. The results modelled by the simulations with radial grid stretching and AMR level 4 are similar to the results provided by the original EUHFORIA and Icarus simulations with the 'standard' resolution and equidistant grids. The simulations with 5 AMR levels yielded better results than the simulations with an equidistant grid and standard resolution. Conclusions. Solution AMR is flexible and provides the user the freedom to modify and locally increase the grid resolution according to the purpose of the simulation. We find that simulations with a combination of grid stretching and AMR can reproduce the simulations performed on equidistant grids significantly faster. The advanced techniques implemented in Icarus can be further used to improve the forecasting procedures, since the reduced simulation time is essential to make physics-based forecasts less computationally expensive. **July 12-15, 2012**

### **Spectro-imagery of an active tornado-like prominence: formation and evolution**

[Krzysztof Barczynski](#), [Brigitte Schmieder](#), [Aaron W. Peat](#), [Nicolas Labrosse](#), [Pierre Mein](#), [Nicole Mein](#)  
A&A 653, A94 2021

<https://arxiv.org/pdf/2106.04259.pdf>

<https://www.aanda.org/articles/aa/pdf/2021/09/aa40976-21.pdf>

The nature of flows in tornado-prominences is an open issue. While the AIA imager aboard the Solar Dynamics Observatory (SDO) allowed us to follow the global structure of a tornado-like prominence during five hours, the Interface Region Imaging Spectrograph (IRIS), and the Multi subtractive Double pass spectrograph (MSDP) permitted to obtain plasma diagnostics of its fine structures. We aim to address two questions. Is the observed plasma rotation conceptually acceptable in a flux rope magnetic support configuration with dips? How is the plasma density distributed in the tornado-like prominence? We calculated line-of-sight velocities and non-thermal line widths using Gaussian fitting for Mg II lines and bisector method for H-alpha line. We determined the electron density from Mg II line integrated intensities and profile fitting methods using 1D NLTE radiative transfer theory models. The global structure of the prominence observed in H-alpha, and Mg II h and k lines fits with a magnetic field structure configuration with dips. Coherent Dopplershifts in red- and blue-shifted areas observed in both lines were detected along rapidly-changing vertical and horizontal structures. However, the tornado at the top of the prominence consists of multiple-fine threads with opposite flows suggesting counter streaming flows rather than rotation. Surprisingly we found that the electron density at the top of the prominence could be larger ( $10^{11} \text{ cm}^{-3}$ ) than in the inner part of the prominence. We suggest that the tornado is in a formation state with cooling of hot plasma in a first phase, and following that, a phase of leakage of the formed blobs with large transverse flows of material along long loops extended away of the UV prominence top. The existence of such long magnetic field lines on both sides of the prominence would avoid the tornado-like prominence to really turn around its axis. **2018 April 19**

### **Electric current evolution at the footpoints of solar eruptions**

Krzysztof [Barczynski](#), [Guillaume Aulanier](#), [Miho Janvier](#), [Brigitte Schmieder](#), [Sophie Masson](#)

ApJ 2020

<https://arxiv.org/pdf/2004.07990.pdf>

Electric currents play a critical role in the triggering of solar flares and their evolution. The aim of the present paper is to test whether the surface electric current has a surface or subsurface fixed source as predicts the circuit approach of flare physics, or is the response of the surface magnetic field to the evolution of the coronal magnetic field as the MHD approach proposes. Out of all 19 X-class flares as observed by SDO from 2011 to 2016 near the disk center, we analyzed the only 9 eruptive flares for which clear ribbon-hooks were identifiable. Flare ribbons with hooks are considered to be the footprints of eruptive flux ropes in MHD flare models. For the first time, fine measurements of time-evolution of electric currents inside the hooks in the observations as well as in the OHM 3D MHD simulation are performed. Our analysis shows a decrease of the electric current in the area surrounded by the ribbon hooks during and after the eruption. We interpret the decrease of the electric currents as due to the expansion of the flux rope in the corona during the eruption. Our analysis brings a new contribution to the standard flare model in 3D. **15 February 2011, 7 September 2011, 29th March 2014, 10th September 2014, 7 November 2014, 11 March 2015**

Table 1. Properties of flares, ribbon and ribbon hooks visibility for 19 flares (2011-2015).

### **Periodic behaviour of coronal mass ejections, eruptive events, and solar activity proxies during solar cycles 23 and 24**

Tatiana [Barlyaeva](#) [JulienWojakabPhilippeLamyabBriceBocletabImreToth](#)

[Journal of Atmospheric and Solar-Terrestrial Physics](#)

Volume 177, October 2018, Pages 12-28

[sci-hub.ru/10.1016/j.jastp.2018.05.012](https://doi.org/10.1016/j.jastp.2018.05.012)

<https://arxiv.org/pdf/1704.02336.pdf> File



We report on the parallel analysis of the periodic behaviour of [coronal mass ejections](#) (CMEs) based on 21 years [1996–2016] of observations with the SOHO/LASCO–C2 coronagraph, [solar flares](#), prominences, and several proxies of [solar activity](#). We consider values of the rates globally and whenever possible, distinguish solar hemispheres and [solar cycles](#) 23 and 24. Periodicities are investigated using both frequency (periodogram) and time-frequency (wavelet) analysis. We find that these different processes, in addition to following the  $\approx 11$ -year Solar Cycle, exhibit diverse statistically significant oscillations with [properties common](#) to all solar, coronal, and heliospheric processes: variable periodicity, intermittence, asymmetric development in the northern and southern solar hemispheres, and largest amplitudes during the maximum phase of solar cycles, being more pronounced during solar cycle 23 than the weaker cycle 24. However, our analysis reveals an extremely complex and diverse situation. For instance, there exists very limited commonality for periods of less than one year. The few exceptions are the periods of 3.1–3.2 months found in the global occurrence rates of CMEs and in the [sunspot](#) area (SSA) and those of 5.9–6.1 months found in the northern hemisphere. Mid-range periods of  $\approx 1$  and  $\approx 2$  years are more wide spread among the studied processes, but exhibit a very distinct behaviour with the first one being present only in the northern hemisphere and the second one only in the [southern hemisphere](#). These periodic behaviours likely results from the complexity of the underlying physical processes, prominently the emergence of [magnetic flux](#).

### **The State of the Corona During the Weak Solar Cycle 24: the View from LASCO Images**

[Barlyaeva](#), T.; Lamy, P.; Llebaria, A.; Boclet, B.

Ground-based Solar Observations in the Space Instrumentation Era

ASP Conference Series, Vol. 504, p. 287, 2016

<http://aspbooks.org/publications/504/287.pdf>

The LASCO-C2 coronagraph onboard SOHO continues its white-light imaging of the corona from 1.5 to 6.0 solar radii, thus allowing investigating the consequences of the weak Solar Cycle 24 on the corona and comparing it to the previous cycle (23). Temporal variations of the global radiance of the corona are presented. We pay particular attention to the mid-term variations which are distinctly different between the two cycles and highlight the similarities and differences. Finally, we rely on our ARTEMIS II catalog of coronal mass ejections (CMEs) to compare their global rates during these two cycles.

### **The Solar Stormwatch CME catalogue: Results from the first space weather citizen science project,**

[Barnard](#), L., et al.

(2014), *Space Weather*, 12, 657–674, doi:10.1002/2014SW001119. **File (2015)**

<http://onlinelibrary.wiley.com/doi/10.1002/2014SW001119/pdf>

Solar Stormwatch was the first space weather citizen science project, the aim of which is to identify and track coronal mass ejections (CMEs) observed by the Heliospheric Imagers aboard the STEREO satellites. The project has now been running for approximately 4 years, with input from >16,000 citizen scientists, resulting in a data set of >38,000 time-elongation profiles of CME trajectories, observed over 18 preselected position angles. We present our method for reducing this data set into a CME catalogue. The resulting catalogue consists of 144 CMEs over the period January 2007 to February 2010, of which 110 were observed by STEREO-A and 77 were observed by STEREO-B. For each CME, the time-elongation profiles generated by the citizen scientists are averaged into a consensus profile along each position angle that the event was tracked. We consider this catalogue to be unique, being at present the only citizen science-generated CME catalogue, tracking CMEs over an elongation range of  $4^\circ$  out to a maximum of approximately  $70^\circ$ . Using single spacecraft fitting techniques, we estimate the speed, direction, solar source region, and latitudinal width of each CME. This shows that at present, the Solar Stormwatch catalogue (which covers only solar minimum years) contains almost exclusively slow CMEs, with a mean speed of approximately 350 km s<sup>-1</sup>. The full catalogue is available for public access at [www.met.reading.ac.uk/~spate/solarstormwatch](http://www.met.reading.ac.uk/~spate/solarstormwatch). This includes, for each event, the unprocessed time-elongation profiles generated by Solar Stormwatch, the consensus time-elongation profiles, and a set of summary plots, as well as the estimated CME properties.

### **The Coronal Mass Ejection of 1998 April 20: Direct Imaging at Radio Wavelengths**

T. S. [Bastian](#)<sup>1</sup>, M. Pick<sup>2</sup>, A. Kerdraon<sup>2</sup>, D. Maia<sup>2,4</sup>, and A. Vourlidas<sup>3</sup>

2001 ApJ 558 L65

<https://iopscience.iop.org/article/10.1086/323421/pdf>

Spectroscopic data were obtained between 40 and 800 MHz by the spectrometer at Trensdorf, Germany, and between 20 kHz and 14 MHz with the WAVES instrument on board the Wind spacecraft. Energetic particle data were obtained from the Wind 3D Plasma and Energetic Particle experiment. The CME was observed in white light by the Large-Angle Spectrometric COronagraph experiment on board the Solar and Heliospheric Observatory spacecraft. For the first time, the expanding CME loops are imaged directly at radio wavelengths. We show that the radio-emitting CME loops are the result of nonthermal synchrotron emission from electrons with energies of  $\sim 0.5$ –5 MeV interacting with magnetic fields of  $\sim 0.1$  to a few gauss. They appear nearly simultaneously with the onset of an associated type II radio burst, shock-accelerated type III radio bursts, and the initiation of a solar energetic particle event. We suggest possible sources of the energetic electrons responsible for this "radio CME" and point out diagnostic uses for synchrotron emission from CME loops. **20 Apr 1998**

## Identifying the energy release site in a Solar microflare with a jet

[Andrea Francesco Battaglia](#), [Wen Wang](#), [Jonas Saqri](#), [Tatiana Podladchikova](#), [Astrid M. Veronig](#), [Hannah Collier](#), [Ewan C. M. Dickson](#), [Olena Podladchikova](#), [Christian Monstein](#), [Alexander Warmuth](#), [Frédéric Schuller](#), [Louise Harra](#), [Säm Krucker](#)

A&A 2022

<https://arxiv.org/pdf/2212.11098.pdf>

One of the main science questions of the Solar Orbiter and Parker Solar Probe missions deals with understanding how electrons in the lower solar corona are accelerated and how they subsequently access interplanetary space. We aim to investigate the electron acceleration and energy release sites as well as the manner in which accelerated electrons access the interplanetary space in the case of the **SOL2021-02-18T18:05** event, a GOES A8 class microflare associated with a coronal jet. This study takes advantage of three different vantage points, Solar Orbiter, STEREO-A, and Earth, with observations ranging from radio to X-ray. Multi-wavelength timing analysis combined with UV/EUV imagery and X-ray spectroscopy by Solar Orbiter/STIX (Spectrometer/Telescope for Imaging X-rays) is used to investigate the origin of the observed emission during different flare phases. The event under investigation satisfies the classical picture of the onset time of the acceleration of electrons coinciding with the jet and the radio type III bursts. This microflare features prominent hard X-ray nonthermal emission down to at least 10 keV and a spectrum that is much harder than usual for a microflare with a spectral index of 2.9. From Earth's vantage point, the microflare is seen near the limb, revealing the coronal energy release site above the flare loop in EUV, which, from STIX spectroscopic analysis, turns out to be hot (at roughly the same temperature of the flare). Moreover, this region is moving toward higher altitudes over time (about 30 km/s). During the flare, the same region spatially coincides with the origin of the coronal jet. We conclude that the energy release site observed above-the-loop corresponds to the electron acceleration site, corroborating that interchange reconnection is a viable candidate for particle acceleration in the low corona on field lines open to interplanetary space.

## The LASCO Coronal Brightness Index

Karl [Battams](#), [Russell A. Howard](#), [Hillary A. Dennison](#), [Robert S. Weigel](#), [Judith L. Lean](#)

Solar Phys. 2020

<https://arxiv.org/pdf/2001.07596.pdf>

We present the construction of a new white-light coronal brightness index (CBI) from the entire archive of observations recorded by the Large Angle Spectrometric Coronagraph (LASCO) C2 camera between 1996 and 2017, comprising two full solar cycles. We reduce all fully calibrated daily C2 observations of the white light corona into a single daily coronal brightness observation for every day of observation recorded by the instrument, with mean daily brightness values binned into 0.1 R<sub>sun</sub> radial x 1 degree angular regions from 2.4 -- 6.2 R<sub>sun</sub> for a full 360-degrees. As a demonstration of the utility of the CBI, we construct a new solar irradiance proxy that correlates well with a variety of direct solar irradiance observations, with correlations shown to be in the range of 0.77-0.89. We also present a correlation mapping technique to show how irradiance correlations depend on, and relate to, coronal structure/locations, and to demonstrate how the LASCO CBI can be used to perform long-term "spatial correlation" studies to investigate relationships between the solar corona and any arbitrary concurrent geophysical index. Using this technique we find possible relationships between coronal brightness and plasma temperature, interplanetary magnetic field magnitude and (very weakly) proton density.

## FINMHD: An Adaptive Finite-element Code for Magnetic Reconnection and Formation of Plasmoid Chains in Magnetohydrodynamics

Hubert [Baty](#)

2019 ApJS 243 23

<https://sci-hub.ru/10.3847/1538-4365/ab2cd2>

Solving the problem of fast eruptive events in magnetically dominated astrophysical plasmas requires the use of particularly well adapted numerical tools. Indeed, the central mechanism based on magnetic reconnection is determined by a complex behavior with quasi-singular forming current layers enriched by their associated small-scale magnetic islands called plasmoids. A new code is thus presented for the solution of two-dimensional dissipative magnetohydrodynamics (MHD) equations in cartesian geometry specifically developed to this end. A current-vorticity formulation representative of an incompressible model is chosen in order to follow the formation of the current sheets and the ensuing magnetic reconnection process. A finite-element discretization using triangles with quadratic basis functions on an unstructured grid is employed, and implemented via a highly adaptive characteristic-Galerkin scheme. The adaptivity of the code is illustrated on simplified test equations and finally for magnetic reconnection associated with the nonlinear development of the tilt instability between two repelling current channels. Varying the Lundquist number  $S$  has allowed us to study the transition between the steady-state Sweet-Parker reconnection regime (for  $S \lesssim 104$ ) and the plasmoid-dominated reconnection regime (for  $S \gtrsim 105$ ). The implications for the understanding of the mechanism explaining the fast conversion of free magnetic energy in astrophysical environments such as the solar corona are briefly discussed.

## On the factors determining the eruptive character of solar flares

Christian [Baumgartner](#), [Julia K. Thalmann](#), [Astrid M. Veronig](#)

ApJ 853 105 2017

<https://arxiv.org/pdf/1712.05106.pdf>

We investigated how the magnetic field in solar active regions (ARs) controls flare activity, i.e., whether a confined or eruptive flare occurs. We analyzed 44 flares of GOES class M5.0 and larger that occurred during 2011–2015. We used 3D potential magnetic field models to study their location (using the flare distance from **the flux-weighted AR center** dFC) and the strength of the magnetic field in the corona above (via decay index  $n$  and flux ratio). We also present a first systematic study of the orientation of the coronal magnetic field, using the orientation  $\phi$  of the flare-relevant polarity inversion line as a measure. We analyzed all quantities with respect to the size of the underlying dipole field, characterized by the distance between the opposite-polarity centers, dPC. Flares originating from underneath the AR dipole (dFC/dPC < 0.5) tend to be eruptive if launched from compact ARs (dPC  $\leq$  60 Mm) and confined if launched from extended ARs. Flares ejected from the periphery of ARs (dFC/dPC > 0.5) are predominantly eruptive. In confined events the flare-relevant field adjusts its orientation quickly to that of the underlying dipole with height ( $\Delta\phi$  & 40° until the apex of the dipole field), in contrast to eruptive events where it changes more slowly with height. The critical height for torus instability,  $h_{crit} = h(n = 1.5)$ , discriminates best between confined ( $h_{crit}$  & 40 Mm) and eruptive flares ( $h_{crit}$  . 40 Mm). It discriminates better than  $\Delta\phi$ , implying that the decay of the confining field plays a stronger role than its orientation at different heights. **2014-10-25**

**Table 1.** Event list (**Flares  $\geq$ M5.0** that occurred between January 2011 and December 2015.)

## **A Precursor to Solar Prominence Eruptions: Detection and Analysis of EUV Prominence Oscillations**

William **Beckwith-Chandler**<sup>3</sup>, Claire Foullon, and Erwin Verwichte

**2024** ApJ 977 253

<https://iopscience.iop.org/article/10.3847/1538-4357/ad8e3c/pdf>

The eruption of prominences can have a significant influence on the solar–terrestrial environment. However, accurately predicting these eruptions remains a challenge. We apply automated detection methods for extreme ultraviolet (EUV) prominences observed by the twin spacecraft from the Solar Terrestrial Relations Observatory (STEREO) mission and the Solar Dynamics Observatory near Earth. We study an event, during 2011 March, when each STEREO spacecraft is in quadrature with respect to the Earth. For two time ranges, we obtain longitudinal height profiles as a function of time. We also track the corresponding EUV filaments across the solar disk, which reveal the emergence of ultra-long-period oscillations in the EUV filament channels. Our analysis shows a correlation between the prominence's increasing height and the oscillation periods, suggesting a potential link to the subsequent eruption observed by the STEREO spacecraft off-limb. These findings offer new insights into prominence dynamics and may pave the way for improved eruption prediction. **2011.03.18-22-26**

## **THE HEIGHT EVOLUTION OF THE "TRUE" CORONAL MASS EJECTION MASS DERIVED FROM STEREO COR1 AND COR2 OBSERVATIONS**

B. M. **Bein**<sup>1</sup>, M. Temmer<sup>1</sup>, A. Vourlidas<sup>2</sup>, A. M. Veronig<sup>1</sup>, and D. Utz

**2013** ApJ 768 31; **File**

<http://arxiv.org/pdf/1303.3372v1.pdf>

Using combined STEREO-A and STEREO-B EUVI, COR1, and COR2 data, we derive deprojected coronal mass ejection (CME) kinematics and CME "true" mass evolutions for a sample of 25 events that occurred during 2007 December to 2011 April. We develop a fitting function to describe the CME mass evolution with height. The function considers both the effect of the coronagraph occulter, at the beginning of the CME evolution, and an actual mass increase. The latter becomes important at about 10-15  $R_{\odot}$  and is assumed to mostly contribute up to 20  $R_{\odot}$ . The mass increase ranges from 2% to 6% per  $R_{\odot}$  and is positively correlated to the total CME mass. Due to the combination of COR1 and COR2 mass measurements, we are able to estimate the "true" mass value for very low coronal heights (<3  $R_{\odot}$ ). Based on the deprojected CME kinematics and initial ejected masses, we derive the kinetic energies and propelling forces acting on the CME in the low corona (<3  $R_{\odot}$ ). The derived CME kinetic energies range between  $1.0\text{--}66 \times 10^{23}$  J, and the forces range between  $2.2\text{--}510 \times 10^{14}$  N.

## **IMPULSIVE ACCELERATION OF CORONAL MASS EJECTIONS. II. RELATION TO SOFT X-RAY FLARES AND FILAMENT ERUPTIONS**

B. M. **Bein**<sup>1</sup>, S. Berkebile-Stoiser<sup>1</sup>, A. M. Veronig<sup>1</sup>, M. Temmer<sup>1</sup>, and B. Vršnak

**2012** ApJ 755 44, **File**

<http://arxiv.org/pdf/1206.2144v1.pdf>

Using high time cadence images from the STEREO EUVI, COR1, and COR2 instruments, we derived detailed kinematics of the main acceleration stage for a sample of 95 coronal mass ejections (CMEs) in comparison with associated flares and filament eruptions. We found that CMEs associated with flares reveal on average significantly higher peak accelerations and lower acceleration phase durations, initiation heights, and heights, at which they reach their peak velocities and peak accelerations. This means that CMEs that are associated with flares are characterized by higher and more impulsive accelerations and originate from lower in the corona where the magnetic field is stronger. For CMEs that are associated with filament eruptions we found only for the CME peak acceleration significantly lower

values than for events that were not associated with filament eruptions. The flare rise time was found to be positively correlated with the CME acceleration duration and negatively correlated with the CME peak acceleration. For the majority of the events the CME acceleration starts before the flare onset (for 75% of the events) and the CME acceleration ends after the soft X-ray (SXR) peak time (for 77% of the events). In ~60% of the events, the time difference between the peak time of the flare SXR flux derivative and the peak time of the CME acceleration is smaller than  $\pm 5$  minutes, which hints at a feedback relationship between the CME acceleration and the energy release in the associated flare due to magnetic reconnection.

### **Impulsive acceleration of coronal mass ejections: I. Statistics and CME source region characteristics**

B. M. [Bein](#), S. Berkebile-Stoiser, A. M. Veronig, M. Temmer, N. Muhr, I. Kienreich, D. Utz  
E-print, 5 Aug, 2011, [File](#); 2011 ApJ 738 191, [File](#)?

We use high time cadence images acquired by the STEREO EUVI and COR instruments to study the evolution of coronal mass ejections (CMEs), from their initiation, through the impulsive acceleration to the propagation phase. For a set of 95 CMEs we derived detailed height, velocity and acceleration profiles and statistically analysed characteristic CME parameters: peak acceleration, peak velocity, acceleration duration, initiation height, height at peak velocity, height at peak acceleration and size of the CME source region. The CME peak accelerations derived range from 20 to 6800  $\text{m s}^{-2}$  and are inversely correlated to the acceleration duration and to the height at peak acceleration. 74% of the events reach their peak acceleration at heights below 0.5  $R_{\text{sun}}$ . CMEs which originate from compact sources low in the corona are more impulsive and reach higher peak accelerations at smaller heights. These findings can be explained by the Lorentz force, which drives the CME accelerations and decreases with height and CME size.

8 May 2007, 23 May 2007, 5 April 2008, 6 November 2008, 13 February 2009, 5 May 2010

### **Caltech Lab Experiments and the Insights They Provide Into Solar Corona Phenomena**

[Paul M. Bellan](#)

JGR [Volume 125, Issue 8](#) August 2020 e2020JA028139

<https://agupubs.onlinelibrary.wiley.com/doi/10.1029/2020JA028139>

A comprehensive overview of two decades of Caltech experiments relevant to solar corona physics is presented. The extent to which the experiments scale to the solar corona, the basic configurations and operation, and the importance of the magnetic force  $\mathbf{J} \times \mathbf{B}$  common to all the experiments is discussed. Summaries are given of the various configurations used, the main observations, and interpretations of these observations, including new models developed to provide these interpretations. Topics include observations and explanations for flux rope self-collimation, axial flows along flux ropes, eruption of arched flux ropes, strapping magnetic fields that inhibit eruption, the torus instability, and effects such as X-ray emission of a kink-driven secondary Rayleigh-Taylor instability.

### **First Determination in the Extended Corona of the 2D Thermal Evolution of a Current Sheet after a Solar Eruption**

Alessandro [Bemporad](#)<sup>1,2</sup>, Guanglu Shi<sup>2,3</sup>, Shuting Li<sup>2,3</sup>, Beili Ying<sup>2,3</sup>, Li Feng<sup>2,3</sup>, Jun Lin<sup>4</sup>, Lucia Abbo<sup>1</sup>, Vincenzo Andretta<sup>5</sup>, Aleksandr Burtovoi<sup>6</sup>, Vania Da Deppo<sup>7</sup>Show full author list  
2024 ApJ 964 92

<https://iopscience.iop.org/article/10.3847/1538-4357/ad2516/pdf>

For the first time the evolution of the coronal reconfiguration after a coronal mass ejection (CME) was observed by the multichannel Metis Coronagraph on board the ESA–Solar Orbiter mission. The images acquired in visible light (VL) between 3.0 and 5.4  $R_{\text{e}}$  show the formation after a CME of a bright elongated radial feature interpreted as a post-CME current sheet (CS). The unique combination of VL and UV images allowed the time evolution of multiple plasma physical parameters inside and outside the CS region to be mapped in 2D for the first time. The CS electron temperature reached peak values higher than 1 MK, more than twice as high as the surrounding corona. An elongated vertical diffusion region, characterized as a region of much higher thermal pressure and lower magnetic pressure, is observed to slowly propagate outward during 13 hr of observations. Inside this region the Alfvénic Mach number is of the order of  $MA \approx 0.02\text{--}0.11$ , the plasma  $\beta$  is close to unity, and the level of turbulence is higher than in the surrounding corona, but decreases slowly with time. All these results provide one of the most complete pictures of these features, and support the idea of a magnetic reconnection coupled with turbulence, thus allowing significant heating of the local plasma, despite the weakness of involved coronal magnetic fields in the considered altitude range. **2021 February 12–13**

### **Analysis of the first coronagraphic multi-band observations of a sungrazing comet**

A. [Bemporad](#)<sup>1</sup>, S. Pennella<sup>2</sup>, K. Battams<sup>3</sup>, S. Giordano<sup>1</sup>, B. Gray<sup>4</sup>, M. M. Knight, + + +  
A&A 680, A90 (2023)

<https://www.aanda.org/articles/aa/pdf/2023/12/aa46881-23.pdf>

Context. Between **24 and 25 December 2021** a sungrazing comet (SOHO-4341) approached the Sun, being observed by “classical” visible light (VL) coronagraphs on board the SOHO and STEREO missions, and also by the innovative Metis coronagraph on board the ESA-NASA Solar Orbiter mission in the VL and ultraviolet (UV H I Lyman- $\alpha$ ) band.

**Aims.** We show how VL data acquired by the Metis coronagraph can be combined with those provided by other space-based coronagraphs to reconstruct the comet orbit, but also to provide information on the dust composition from the polarized VL emission. Moreover, we show how the UV emission can be employed to measure local plasma parameters of the ambient solar wind.

**Methods.** By using the comet positions tracked with VL Metis images (with spatial resolution that is four times better than UV), the UV images (with a time cadence that is five times faster than VL) have been coaligned to maximize the signal-to-noise ratio in the UV band. The local electron density  $n_e$  was measured from the observed exponential decay of the UV Lyman- $\alpha$  intensity along the tail, while the solar wind speed  $v_{\text{wind}}$  was measured from the UV Lyman- $\alpha$  tail inclination with respect to the cometary orbital path deprojected in 3D. Moreover, the proton kinetic temperature  $T_k$  was also obtained by the aperture angle of the UV Lyman- $\alpha$  tail.

**Results.** When the comet was at an average heliocentric distance of  $14.3 R_{\odot}$ , the comet had a radial speed of  $155 \text{ km s}^{-1}$  and a tangential speed of  $59 \text{ km s}^{-1}$ . The comet had a UV Lyman- $\alpha$  tail extending in the anti-solar direction over more than  $1.5 R_{\odot}$ . From the analysis of the tail shape in UV we obtained the local solar wind speed ( $v_{\text{wind}} = 190 \text{ km s}^{-1}$ ), electron density ( $n_e = 1.5 \times 10^4 \text{ cm}^{-3}$ ), and proton temperature ( $T_k = 1.2 \times 10^6 \text{ K}$ ). Moreover, theoretical analysis of the measured UV Lyman- $\alpha$  intensity allowed us to estimate the radius of the cometary nucleus ( $R_{\text{com}} = 65 \text{ m}$ ) and the water outgassing rate ( $\text{QH}_2\text{O} = 4.8 \times 10^{28} \text{ molec s}^{-1}$ ).

**Conclusions.** These results show that sungrazing comets are unique “local probes” for the ambient coronal plasma, providing measurements that are not as affected by the line-of-sight integration effects as those provided by remote sensing instruments, in regions of the Heliosphere that are not explored in situ by the ongoing space missions.

## **A Coronal Mass Ejection followed by a prominence eruption and a plasma blob as observed by Solar Orbiter**

[A. Bemporad](#), [V. Andretta](#), [R. Susino](#), [S. Mancuso](#), [D. Spadaro](#), [M. Mierla](#), [D. Berghmans](#), [E. D’Huys](#), [A. N. Zhukov](#), [D.-C. Talpeanu](#), [R. Colaninno](#), [P. Hess](#), [J. Koza](#), [S. Jejcic](#), [P. Heinzel](#), [E. Antonucci](#), [V. Da Deppo](#), [S. Fineschi](#), [F. Frassati](#), [G. Jerse](#), [F. Landini](#), [G. Naletto](#), [G. Nicolini](#), [M. Pancrazzi](#), [M. Romoli](#), [C. Sasso](#), [A. Slemer](#), [M. Stangalini](#), [L. Teriaca](#)

A&A 665, A7 2022

<https://arxiv.org/pdf/2202.10294.pdf>

<https://www.aanda.org/articles/aa/pdf/2022/09/aa43162-22.pdf>

On **February 12, 2021** two subsequent eruptions occurred above the West limb, as seen along the Sun-Earth line. The first event was a typical slow Coronal Mass Ejection (CME), followed  $\sim 7$  hours later by a smaller and collimated prominence eruption, originating Southward with respect to the CME, followed by a plasma blob. These events were observed not only by SOHO and STEREO-A missions, but also by the suite of remote sensing instruments on-board Solar Orbiter (SolO). This work shows how data acquired by the Full Sun Imager (FSI), Metis coronagraph, and Heliospheric Imager (SoloHI) from the SolO perspective can be combined to study the eruptions and the different source regions. Moreover, we show how Metis data can be analyzed to provide new information about solar eruptions. Different 3D reconstruction methods were applied to the data acquired by different spacecraft including remote sensing instruments on-board SolO. Images acquired by both Metis channels in the Visible Light (VL) and H I Lyman- $\alpha$  line (UV) were combined to derive physical information on the expanding plasma. The polarization ratio technique was also applied for the first time to the Metis images acquired in the VL channel. The two eruptions were followed in 3D from their source region to their expansion in the intermediate corona. Thanks to the combination of VL and UV Metis data, the formation of a post-CME Current Sheet (CS) was followed for the first time in the intermediate corona. The plasma temperature gradient across a post-CME blob propagating along the CS was also measured for the first time. Application of the polarization ratio technique to Metis data shows that, thanks to the combination of four different polarization measurements, the errors are reduced by  $\sim 5\text{--}7\%$ , thus better constraining the 3D distribution of plasma.

## **Measuring the electron temperatures of coronal mass ejections with future space-based multi-channel coronagraphs: a numerical test**

A. [Bemporad](#)<sup>1</sup>, P. Pagano<sup>2</sup> and S. Giordano

A&A 619, A25 (2018)

<https://sci-hub.ru/10.1051/0004-6361/201833058>

**Context.** The determination from coronagraphic observations of physical parameters of the plasma embedded in coronal mass ejections (CMEs) is of crucial importance for our understanding of the origin and evolution of these phenomena. **Aims.** The aim of this work is to perform the first ever numerical simulations of a CME as it will be observed by future two-channel (visible light VL and UV Ly- $\alpha$ ) coronagraphs, such as the Metis instrument on-board ESA-Solar Orbiter mission, or any other future coronagraphs with the same spectral band-passes. These simulations are then used to test and optimize the plasma diagnostic techniques to be applied to future observations of CMEs.

**Methods.** The CME diagnostic techniques are tested here by analyzing synthetic coronagraphic observations. First, a numerical three-dimensional (3D) magnetohydrodynamic (MHD) simulation of a CME is performed, and the plasma parameters in the simulation are used to generate synthetic visible light (VL) and ultraviolet (UV) coronagraphic two-dimensional (2D) images of the eruption (i.e., integrated along the line-of-sight). Second, synthetic data are analyzed with different assumptions (as will be done with real data), to infer the kinematic properties of the CME (such as the extension along the line-of-sight of the emitting region, the expansion speed, and the CME propagation direction), as

well as physical parameters of the CME plasma (the plasma electron density and temperature). A comparison between input parameters from the simulation and output parameters from the synthetic data analysis is then performed. Results. The inversion of VL polarized data allows to successfully determine the CME speed and 3D propagation direction (with the polarization ratio technique), as well as to derive information on the extension along the line-of-sight of the emitting plasma, a crucial parameter needed to convert the plasma electron column densities into number densities. These parameters are used to analyze UV Ly- $\alpha$  images and to estimate the CME plasma temperature, also taking into account Doppler dimming effect. Output plasma temperatures are in general underestimated, both in the CME body and core regions. By neglecting the UV Ly- $\alpha$  radiative excitation of H atoms, reliable temperatures can be more easily derived in the CME core (within  $\sim 60\%$ ). On the other hand, we show that a determination of temperatures (within  $\sim 20\text{--}30\%$ ) in the CME body requires 2D maps of CME radial speeds and Doppler dimming coefficients to be derived.

## Measuring coronal magnetic fields with remote sensing observations of shock waves **Review**

Alessandro **Bemporad**, Roberto Susino, Federica Frassati, Silvano Fineschi

Frontiers in Astronomy and Space Sciences, Volume 3, id.17 2016

<https://arxiv.org/ftp/arxiv/papers/1608/1608.05536.pdf>

Recent works demonstrated that remote sensing observations of shock waves propagating into the corona and associated with major solar eruptions can be used to derive the strength of coronal magnetic fields met by the shock over a very large interval of heliocentric distances and latitudes. This opinion article will summarize most recent results obtained on this topic and will discuss the weaknesses and strengths of these techniques to open a constructive discussion with the scientific community.

## Physical Conditions of Coronal Plasma at the transit of a Shock driven by a Coronal Mass Ejection

A. **Bemporad**, R. Susino, S. Mancuso

ApJ 2015

<http://arxiv.org/pdf/1509.09131v1.pdf>

We report here on the determination of plasma physical parameters across a shock driven by a Coronal Mass Ejection using White Light (WL) coronagraphic images and Radio Dynamic Spectra (RDS). The event analyzed here is the spectacular eruption that occurred on **June 7th 2011**, a fast CME followed by the ejection of columns of chromospheric plasma, part of them falling back to the solar surface, associated with a M2.5 flare and a type-II radio burst. Images acquired by the SOHO/LASCO coronagraphs (C2 and C3) were employed to track the CME-driven shock in the corona between  $2\text{--}12 R_{\odot}$  in an angular interval of about  $110^{\circ}$ . In these intervals we derived 2-Dimensional (2D) maps of electron density, shock velocity and shock compression ratio, and we measured the shock inclination angle with respect to the radial direction. Under plausible assumptions, these quantities were used to infer 2D maps of shock Mach number MA and strength of coronal magnetic fields at the shock's heights. We found that in the early phases ( $2\text{--}4 R_{\odot}$ ) the whole shock surface is super-Alfvénic, while later on (i.e. higher up) it becomes super-Alfvénic only at the nose. This is in agreement with the location for the source of the observed type-II burst, as inferred from RDS combined with the shock kinematic and coronal densities derived from WL. For the first time, a coronal shock is used to derive a 2D map of the coronal magnetic field strength over a  $10 R_{\odot}$  altitude and  $\sim 110^{\circ}$  latitude intervals.

## Uncertainties in polarimetric 3D reconstructions of coronal mass ejections

Alessandro **Bemporad**, Paolo Pagano

A&A 576, A93 2015

<http://arxiv.org/pdf/1503.00314v1.pdf>

This work is aimed at quantifying the uncertainties in the 3D reconstruction of the location of coronal mass ejections (CMEs) obtained with the polarization ratio technique. The method takes advantage of the different distributions along the line of sight (LOS) of total (tB) and polarized (pB) brightnesses to estimate the average location of the emitting plasma. To this end, we assumed two simple electron density distributions along the LOS (a constant density and Gaussian density profiles) for a plasma blob and synthesized the expected tB and pB for different distances  $z$  of the blob from the plane of the sky (POS) and different projected altitudes  $\rho$ . Reconstructed locations of the blob along the LOS were thus compared with the real ones, allowing a precise determination of uncertainties in the method. Independently of the analytical density profile, when the blob is centered at a small distance from the POS (i.e. for limb CMEs) the distance from the POS starts to be significantly overestimated. Polarization ratio technique provides the LOS position of the center of mass of what we call folded density distribution, given by reflecting and summing in front of the POS the fraction of density profile located behind that plane. On the other hand, when the blob is far from the POS, but with very small projected altitudes (i.e. for halo CMEs,  $\rho < 1.4 R_{\odot}$ ), the inferred distance from that plane is significantly underestimated. Better determination of the real blob position along the LOS is given for intermediate locations, and in particular when the blob is centered at an angle of  $20^{\circ}$  from the POS. These results have important consequences not only for future 3D reconstruction of CMEs with polarization ratio technique, but also for the design of future coronagraphs aimed at providing a continuous monitoring of halo-CMEs for space weather prediction purposes.

## Plasma Physical Parameters along Coronal-mass-ejection-driven Shocks. I. Ultraviolet and White-light Observations

A. [Bemporad](#)<sup>1</sup>, R. Susino<sup>1</sup>, and G. Lapenta

2014 ApJ 784 102

<http://arxiv.org/pdf/1403.0870v1.pdf>

In this work, UV and white-light (WL) coronagraphic data are combined to derive the full set of plasma physical parameters along the front of a shock driven by a coronal mass ejection. Pre-shock plasma density, shock compression ratio, speed, and inclination angle are estimated from WL data, while pre-shock plasma temperature and outflow velocity are derived from UV data. The Rankine-Hugoniot (RH) equations for the general case of an oblique shock are then applied at three points along the front located between 2.2 and 2.6  $R_{\odot}$  at the shock nose and at the two flanks. Stronger field deflection (by  $\sim 46^{\circ}$ ), plasma compression (factor  $\sim 2.7$ ), and heating (factor  $\sim 12$ ) occur at the nose, while heating at the flanks is more moderate (factor 1.5-3.0). Starting from a pre-shock corona where protons and electrons have about the same temperature ( $T_p \sim T_e \sim 1.5 \times 10^6$  K), temperature increases derived with RH equations could better represent the proton heating (by dissipation across the shock), while the temperature increase implied by adiabatic compression (factor  $\sim 2$  at the nose,  $\sim 1.2$ -1.5 at the flanks) could be more representative of electron heating: the transit of the shock causes a decoupling between electron and proton temperatures. Derived magnetic field vector rotations imply a draping of field lines around the expanding flux rope. The shock turns out to be super-critical (sub-critical) at the nose (at the flanks), where derived post-shock plasma parameters can be very well approximated with those derived by assuming a parallel (perpendicular) shock.

## Super- and sub-critical regions in shocks driven by radio-loud and radio-quiet CMEs.

[Bemporad](#) A and Mancuso S

(2013) JAdR 4: 287-291

## Study of Multiple Coronal Mass Ejections at Solar Minimum Conditions

A. [Bemporad](#), F. P. Zuccarello, C. Jacobs, M. Mierla and S. Poedts

Solar Physics, 2012, DOI: 10.1007/s11207-012-9999-3

The aim of this work is to provide a physical explanation for the genesis of multiple coronal mass ejections (CMEs) in an asymmetric coronal field configuration. We analyze STEREO observations of a multiple eruption and compare the results from the data analysis with predictions provided by magnetohydrodynamic (MHD) simulations. To this end, the multiple CMEs (MCMEs) observed on **21 – 22 September 2009** were selected. Both eruptions originated from the same source region and showed approximately the same latitudinal deflection, by more than 15 degrees, toward the heliospheric current sheet (HCS) during their propagation in the COR1 field of view. Numerical MHD simulations of the MCMEs have been performed, starting from an asymmetric coronal field configuration that mimics the potential field source surface extrapolation for 21 September 2009. The results demonstrate that, by shearing the footpoints at the base of the southern arcade, we were able to reproduce the observed dynamics of the MCMEs. Both CMEs are deflected toward the HCS due to an imbalance in the magnetic pressure and tension forces; the global field strength turns out to be a crucial parameter in order to release two subsequent eruptions, and hence to reproduce the observed evolution.

## IDENTIFICATION OF SUPER- AND SUBCRITICAL REGIONS IN SHOCKS DRIVEN BY CORONAL MASS EJECTIONS

A. [Bemporad](#) and S. Mancuso

2011 ApJ 739 L64, [File](#)

In this work, we focus on the analysis of a coronal mass ejection (CME) driven shock observed by the Solar and Heliospheric Observatory/Large Angle and Spectrometric Coronagraph Experiment. We show that white-light coronagraphic images can be employed to estimate the compression ratio  $X = \rho_d / \rho_u$  all along the front of CME-driven shocks.  $X$  increases from the shock flanks (where  $X \sim 1.2$ ) to the shock center (where  $X \sim 3.0$  is maximum). From the estimated  $X$  values, we infer the Alfvén Mach number for the general case of an oblique shock. It turns out that only a small region around the shock center is supercritical at earlier times, while higher up in the corona the whole shock becomes subcritical. This suggests that CME-driven shocks could be efficient particle accelerators at the initiation phases of the event, while at later times they progressively lose energy, also losing their capability to accelerate high-energy particles. This result has important implications on the localization of particle acceleration sites and in the context of predictive space weather studies.

## FIRST COMPLETE DETERMINATION OF PLASMA PHYSICAL PARAMETERS ACROSS A CORONAL MASS EJECTION-DRIVEN SHOCK

A. [Bemporad](#) and S. Mancuso

Astrophysical Journal, 720:130–143, 2010

We report on the study of a fast coronal mass ejection (CME)-driven shock associated with the solar eruption of **2002 March 22**. This event was observed in the intermediate corona both in white light and the extreme ultraviolet (EUV) by the LASCO and UVCS instruments on board the *Solar and Heliospheric Observatory*, as well as in metric and decametric wavelengths through space- and ground-based radio observatories. Clear signatures of shock transit are (1) strong type II emission lanes observed after the CME initiation, (2) strong Ovi  $\lambda\lambda 1032, 1037$  line profile broadenings (up to  $\sim 2 \times 10^7$  K) associated with the shock transit across the UVCS slit field of view, and (3) a density enhancement located in LASCO images above the CME front. Since the UVCS slit was centered at  $4.1R_{\odot}$ , in correspondence with the flank of the expanding CME, this observation represents the highest UV detection of a shock obtained so far with the UVCS instrument. White-light and EUV data have been combined in order to estimate not only the shock compression ratio and the plasma temperature, but also the strength of the involved coronal magnetic fields, by applying the Rankine–Hugoniot equations for the general case of oblique shocks.

Results show that, for a compression ratio  $X = 2.06$  as derived from LASCO data, the coronal plasma is heated across the shock from an initial temperature of  $2.3 \times 10^5$  K up to  $1.9 \times 10^6$  K, while at the same time the magnetic field undergoes a compression from a pre-shock value of  $\sim 0.02$  G up to a post-shock field of  $\sim 0.04$  G. Magnetic and kinetic energy density increases at the shock are comparable (in agreement with the idea of equipartition of energy), and both are more than two times larger than the thermal energy density increase. This is the first time that a complete characterization of pre- and post-shock plasma physical parameters has been derived in the solar corona.

## **SIDE MAGNETIC RECONNECTIONS INDUCED BY CORONAL MASS EJECTIONS: OBSERVATIONS AND SIMULATIONS**

A. [Bemporad](#)<sup>1</sup>, A. Soenen<sup>2</sup>, C. Jacobs<sup>2</sup>, F. Landini<sup>3</sup>, and S. Poedts<sup>2</sup>

Astrophysical Journal, 718:251–265, 2010 July; **File**

Over the last few years coronagraphic and spectroscopic observations have demonstrated that small-scale eruptions, such as “jets,” “narrow coronal mass ejections (CMEs),” “mini CMEs,” “streamer puffs,” “streamer detachments,” and others, occur ubiquitously on the Sun. Nevertheless, the origin of small-scale eruptive events and how these are interrelated with larger scale CMEs have been poorly investigated so far. In this work, we study a series of small-scale side eruptions that occurred during and after a large-scale CME. Observations show that a CME can be associated not only with a single reconnection process, leading to the large-scale phenomenon, but also with many other side reconnections occurring at different locations and times around the main flux rope, possibly induced by the CME expansion in the surrounding corona. White light and EUV observations of a slow CME acquired by the *SOHO/LASCO* and *SOHO/UVCS* instruments are analyzed here to characterize the locations of side reconnections induced by the CME. The magnetic reconnection rate  $M$  has been estimated from the UVCS data from the ratio between the inflows and outflows observed around the reconnection region, and from the LASCO data from the observed aperture angles between the slow mode shocks (SMSs) associated with the reconnection. It turns out that  $M \sim 0.05$  at the heliocentric distance of  $1.8R_{\odot}$ , while between  $\sim 2.5$  and  $5.5R_{\odot}$ ,

$M$  values progressively decrease with time/altitude from  $M \sim 1$  down to  $M \sim 0.3$ . Such large values of  $M$  are theoretically acceptable only if flux pile-up reconnection is envisaged. The observed occurrence of multiple reconnections associated with a CME is verified by numerical simulations of an eruption occurring within multiple helmet streamers. The simulations confirm that small side reconnections are a consequence of CME expansion against the surrounding coronal streamers. The simulated and observed evolution of aperture angles between the SMSs are in good agreement as well. These results demonstrate the effect of the global coronal magnetic field in the occurrence of small-scale eruptions due to lateral reconnection in a preceding CME event.

**2005 December 10,**

([See The role of lateral magnetic reconnection in solar eruptive events](#))

A. [Soenen](#)<sup>1,2</sup>, A. [Bemporad](#)<sup>3</sup>, C. [Jacobs](#)<sup>1,2</sup>, and S. [Poedts](#)

Ann. Geophys., 27, 3941–3948, 2009, **File**)

## **STEREOSCOPIC RECONSTRUCTION FROM STEREO/EUV IMAGERS DATA OF THE THREE-DIMENSIONAL SHAPE AND EXPANSION OF AN ERUPTING PROMINENCE**

A. [Bemporad](#)

Astrophysical Journal, 701:298–305, 2009; **File**

On **2007 May 9**, a prominence eruption was observed in the He II  $\lambda 304$  filter by the two EUV Imagers (EUVI) telescopes aboard the *STEREO A* and *B* spacecrafts. The high spatial resolution ( $\sim 1.5$  pixel<sup>-1</sup>) EUVI images have been used to infer via triangulation the three-dimensional (3D) shape and orientation of the prominence  $\sim 12$  minutes after the beginning (13:40 UT) of the eruption. At this time, the prominence has the shape of a “hook” with the base anchored at the Sun. The “hook” prominence is highly inclined southward with



respect to the radial direction, has an average thickness of  $0.061R_{\odot}$ , a length of  $0.43R_{\odot}$ , and lies in first approximation on a plane inclined by  $\sim 54.5^{\circ}$  with respect to the line of sight. Thanks to the very high temporal cadence ( $\sim 37$  s) of EUVI observations it has been possible also to infer the 3D early eruption trajectory. In the following  $\sim 20$  minutes the prominence rotates westward, undergoing a strong latitudinal acceleration,  $\sim 3$  times larger than the radial acceleration. In this time interval, the prominence expands in a direction mainly parallel to the plane of the sky; the total volume occupied by the plasma increases by a factor of  $\sim 8$ , while the prominence thickness increases only by  $\sim 12\%$ . This is related to the fact that the early prominence expansion is anisotropic and occurs mainly on a plane parallel to the plane of the sky. Even if the small-scale spatial distribution of the erupting material observed in the He II EUVI images is quite complex, both the approximately planar shape and the successive planar expansion suggest that on larger spatial scales the prominence can be globally approximated as a two-dimensional “ribbon-like” feature, instead of a 3D twisted flux tube.

## **SPECTROSCOPIC DETECTION OF TURBULENCE IN *POST-CME CURRENT SHEETS***

A. [Bemporad](#)

*Astrophysical Journal*, 689:572Y584, 2008, [File](#)

Plasma in **post-CME current sheets** (CSs) is expected to be highly turbulent because of the tearing and coalescence instability and/or local microscopic instabilities. For this reason, in the last decade the inconsistency between the observed ( $\sim 10^4$ – $10^5$  km) and the expected ( $\sim 10$  m) CS thickness has been tentatively explained in many MHD models as a consequence of plasma turbulence that should be able to significantly broaden the CS. However, from the observational point of view, little is known about this subject. A few post-CME CSs have been observed in UVCS spectra as a strong emission in the high-temperature [Fe XVIII] line, usually unobservable in the solar corona. In this work, published data on post-CME CSs observed by UVCS are reanalyzed, concentrating for the first time on the evolution of turbulence derived from the nonthermal broadening of the [Fe XVIII] line profiles. Derived turbulent speeds are on the order of  $\sim 60$  km s $^{-1}$  a few hours after the CME and slowly decay down to  $\sim 30$  km s $^{-1}$  in the following 2 days. From this evolution the anomalous diffusivity due to microinstabilities has been estimated, and the scenario of multiple small-scale reconnections is tested. Results show that the existence of many ( $\sim 10^{11}$  to  $10^{17}$  cm $^{-3}$ ) microscopic CSs (CSs) of small sizes ( $\sim 10$ – $10^4$  m) could explain not only the high CS temperatures but also the much larger observed thickness of macroscopic CSs, thanks to turbulent broadening.

## **A Comprehensive Study of the Initiation and Early Evolution of a Coronal Mass Ejection from Ultraviolet and White-Light Data**

A. [Bemporad](#), J. Raymond, G. Poletto, and M. Romoli

*The Astrophysical Journal*, 655:576–590, 2007, [File](#)

2000 January 31. Based on vector magnetograph data and magnetic field models, we find that field disruption in an active region (AR) was driven by flux emergence and shearing motions, leading to the CME and to post-CME arcades seen in the EUV.

## **CURRENT SHEET EVOLUTION IN THE AFTERMATH OF A CME EVENT**

A. [Bemporad](#), G. Poletto, S. T. Suess, Y.-K. Ko, N. A. Schwadron, H. A. Elliott, and J. C. Raymond

*The Astrophysical Journal*, 638:1110–1128, 2006, [File](#)

We report on SOHO UVCS observations of the coronal restructuring following a coronal mass ejection (CME) on 2002 November 26, at the time of a SOHO-Ulysses quadrature campaign.

## **A NEW VARIETY OF CORONAL MASS EJECTION: STREAMER PUFFS FROM COMPACT EJECTIVE FLARES**

A. [Bemporad](#), Alphonse C. Sterling, Ronald L. Moore, and G. Poletto

*The Astrophysical Journal*, 635:L189–L192, 2005

These streamer puffs differ from “streamer blowout” CMEs in that (1) while the streamer is transiently inflated by the puff, it is not disrupted, and (2) each puff comes from a compact explosion in the outskirts of the streamer arcade, not from an extensive eruption along the main neutral line of the streamer arcade.

## **Deflection of Coronal Mass Ejections in Unipolar Ambient Magnetic Fields**

[Michal Ben-Nun](#), [Tibor Török](#), [Erika Palmerio](#), [Cooper Downs](#), [Viacheslav S. Titov](#), [Mark G. Linton](#), [Ronald M. Caplan](#), [Roberto Lionello](#)

*ApJ* 957 74 2023

<https://arxiv.org/pdf/2310.02412.pdf>

<https://iopscience.iop.org/article/10.3847/1538-4357/acfe6c/pdf>

The trajectories of coronal mass ejections (CMEs) are often seen to substantially deviate from a purely radial propagation direction. Such deviations occur predominantly in the corona and have been attributed to "channeling" or deflection of the eruptive flux by asymmetric ambient magnetic fields. Here, we investigate an additional mechanism that does not require any asymmetry of the pre-eruptive ambient field. Using magnetohydrodynamic numerical simulations, we show that the trajectory of CMEs through the solar corona can significantly deviate from a radial direction when propagation takes place in a unipolar radial field. We demonstrate that the deviation is most prominent below  $\sim 15$  solar radii and can be attributed to an "effective  $I \times B$  force" that arises from the intrusion of a magnetic flux rope with a net axial electric current into a unipolar background field. These results are important for predictions of CME trajectories in the context of space weather forecasts, as well as for reaching a deeper understanding of the fundamental physics underlying CME interactions with the ambient fields in the extended solar corona.

## **On Fields and Mass Constraints for the Uniform Propagation of Magnetic-Flux Ropes Undergoing Isotropic Expansion**

Daniel Benjamín [Berdichevsky](#)

[Solar Physics](#) May 2013, Volume 284, [Issue 1](#), pp 245–259

<https://link.springer.com/content/pdf/10.1007%2Fs11207-012-0176-5.pdf>

An analytical 3-D magnetohydrodynamic (MHD) solution of a magnetic-flux rope (FR) is presented. This FR solution may explain the uniform propagation, beyond  $\sim 0.05$  AU, of coronal mass ejections (CMEs) commonly observed by today's missions like The Solar Mass Ejection Imager (SMEI), Solar and Heliospheric Observatory (SOHO) and Solar Terrestrial Relations Observatory (STEREO), tracked to tens of times the radius of the Sun, and in some cases up to 1 AU, and/or beyond. Once a CME occurs, we present arguments regarding its evolution based on its mass and linear momentum conservation. Here, we require that the gravitational and magnetic forces balance each other in the framework of the MHD theory for a simple model of the evolution of a CME, assuming it interacts weakly with the steady solar wind. When satisfying these ansätze we identify a relation between the transported mechanical mass of the interplanetary CME with its geometrical parameters and the intensity of the magnetic field carried by the structure. In this way we are able to estimate the mass of the interplanetary CME (ICME) for a list of cases, from the Wind mission records of ICME encountered near Earth, at 1 AU. We obtain a range for masses of  $\sim 109$  to 1013 kg, or assuming a uniform distribution, of  $\sim 0.5$  to 500  $\text{cm}^{-3}$  for the hadron density of these structures, a result that appears to be consistent with observations.

Correction: [Solar Physics](#) November 2019, 294:167 <https://link.springer.com/content/pdf/10.1007%2Fs11207-019-1557-9.pdf>

## **Solar Filament Eruptions in $H\alpha$ Doppler Velocity**

I. A. [Berezin](#)<sup>1</sup>, A. G. Tlatov<sup>1</sup>, and A. A. Pevtsov<sup>2</sup>

2023 ApJ 950 100

<https://iopscience.iop.org/article/10.3847/1538-4357/acd113/pdf>

We use observations taken with a novel solar telescope spectroheliograph to investigate the association between the early filament rise and coronal mass ejections (CMEs). The instrument allows the  $H\alpha$  full line profile to be registered in each pixel of the solar disk with a time cadence of about 1 minute. We analyze observations of three eruptive filaments in 2021 and show that patrol telescope measurements of the  $H\alpha$  line profile with a spectral resolution  $R = 40,000$  can be used to detect precursors of filament eruptions with an advance of several hours and to estimate the initial acceleration of CMEs. Our limited case study also suggests that while detecting an early filament rise may serve as an indicator of a possible eruption, the filament ascent alone is not a definite sign of a CME. **2021 February 20, 2021 August 28 and 2021 November 6**

## **RELATION BETWEEN THE CORONAL MASS EJECTION ACCELERATION AND THE NON-THERMAL FLARE CHARACTERISTICS**

S. [Berkebile-Stoiser](#), A. M. Veronig, B. M. Bein, and M. Temmer

2012 ApJ 753 88, [File](#)

We investigate the relationship between the main acceleration phase of coronal mass ejections (CMEs) and the particle acceleration in the associated flares as evidenced in Reuven Ramaty High Energy Solar Spectroscopic Imager non-thermal X-rays for a set of 37 impulsive flare-CME events. Both the CME peak velocity and peak acceleration yield distinct correlations with various parameters characterizing the flare-accelerated electron spectra. The highest correlation coefficient is obtained for the relation of the CME peak velocity and the total energy in accelerated electrons ( $c = 0.85$ ), supporting the idea that the acceleration of the CME and the particle acceleration in the associated flare draw their energy from a common source, probably magnetic reconnection in the current sheet behind the erupting structure. In general, the CME peak velocity shows somewhat higher correlations with the non-thermal flare parameters than the CME peak acceleration, except for the spectral index of the accelerated electron spectrum, which yields a higher correlation with the CME peak acceleration ( $c = -0.6$ ), indicating that the hardness of the flare-accelerated electron spectrum is tightly coupled to the impulsive acceleration process of the rising CME structure. We also obtained high correlations between the CME initiation height  $h_0$  and the non-thermal flare parameters, with the highest correlation of  $h_0$  to the spectral index  $\delta$  of flare-accelerated electrons ( $c = 0.8$ ). This means that CMEs erupting at low coronal heights, i.e., in regions of stronger magnetic fields, are accompanied by flares that are more efficient at accelerating electrons to high energies. In the majority of events ( $\sim 80\%$ ), the non-thermal flare emission starts after the CME acceleration, on

average delayed by 6 minutes, in line with the standard flare model where the rising flux rope stretches the field lines underneath until magnetic reconnection sets in. We find that the current sheet length at the onset of magnetic reconnection is  $21 \pm 7$  Mm. The flare hard X-ray peaks are well synchronized with the peak of the CME acceleration profile, and in 75% of the cases they occur within  $\pm 5$  minutes. Our findings provide strong evidence for the tight coupling between the CME dynamics and the particle acceleration in the associated flare in impulsive events, with the total energy in accelerated electrons being closely correlated with the peak velocity (and thus the kinetic energy) of the CME, whereas the number of electrons accelerated to high energies is decisively related to the CME peak acceleration and the height of the pre-eruptive structure.

### **Geoeffectiveness Prediction of CMEs**

[Diana Besliu-Ionescu](#) and [Marilena Mierla](#)

Front. Astron. Space Sci., 8:672203 2021 |

<https://www.frontiersin.org/articles/10.3389/fspas.2021.672203/full>

<https://doi.org/10.3389/fspas.2021.672203>

Coronal mass ejections (CMEs), the most important pieces of the puzzle that drive space weather, are continuously studied for their geomagnetic impact. We present here an update of a logistic regression method model, that attempts to forecast if a CME will arrive at the Earth and it will be associated with a geomagnetic storm defined by a minimum Dst value smaller than  $-30$  nT. The model is run for a selection of CMEs listed in the LASCO catalogue during the solar cycle 24. It is trained on three fourths of these events and validated for the remaining one fourth. Based on five CME properties (the speed at 20 solar radii, the angular width, the acceleration, the measured position angle and the source position – binary variable) the model successfully predicted 98% of the events from the training set, and 98% of the events from the validation one.

### **Small-Scale Activity Above the Penumbra of a Fast-Rotating Sunspot**

L. [Bharti](#), C. Quintero Noda, S. Rakesh, B. Sobha, A. Pandya, C. Joshi

[Solar Physics](#) March 2018, 293:46

High-resolution observations of small-scale activity above the filamentary structure of a fast-rotating sunspot of NOAA Active Region 10930 are presented. The penumbral filament that intrudes into the umbra shows a central dark core and substructures. It almost approached another end of the umbra, like a light bridge. The chromospheric Ca II H images show many jet-like structures with a bright leading edge above it. These bright jets move across the filament tips and show coordinated up and down motions. Transition region images also show brightening at the same location above the intrusion. Coronal 195 Å images suggest that one end of the bright coronal loop footpoints resides in this structure. The intrusion has opposite polarity with respect to the umbra. Strong downflows are observed at the edges along the length of the intrusion where the opposite-polarity field is enhanced. We also observe a counter-Evershed flow in the filamentary structure that also displays brightening and energy dissipation in the upper atmosphere. This scenario suggests that the jets and brightenings are caused by low-altitude reconnection driven by opposite-polarity fields and convective downflows above such structures.

### **Lambda-shaped jets from a penumbral intrusion into a sunspot umbra: a possibility for magnetic reconnection\***

L. [Bharti](#)<sup>1,2</sup>, S. K. Solanki<sup>1,3</sup> and J. Hirzberger

A&A 597, A127 (2017)

[http://www.aanda.org/articles/aa/full\\_html/2017/01/aa29656-16/aa29656-16.html](http://www.aanda.org/articles/aa/full_html/2017/01/aa29656-16/aa29656-16.html)

We present the results of high resolution co-temporal and co-spatial photospheric and chromospheric observations of sunspot penumbral intrusions. The data were taken with the Swedish Solar Telescope (SST) on the Canary Islands. Time series of Ca II H images show a series of transient jets extending roughly 3000 km above a penumbral intrusion into the umbra. For most of the time series, jets were seen along the whole length of the intruding bright filament. Some of these jets develop a clear  $\lambda$ -shaped structure, with a small loop appearing at their footpoint and lasting for around a minute. In the framework of earlier studies, the observed transient  $\lambda$  shape of these jets suggests that they could be caused by magnetic reconnection between a curved arcade-like or flux rope-like field in the lower part of the penumbral intrusion and the more vertical umbral magnetic field forming a cusp-shaped structure above the penumbral intrusion.  
**2006 August 13**

### **Fine structure above a light bridge in the transition region and corona**

Lokesh [Bharti](#)

MNRAS Letters 2015

<http://arxiv.org/pdf/1505.02412v1.pdf>

We present the results of multi wavelength, co-spatial and near co-temporal observations of jets above a sunspot light bridge. The data were obtained with the Solar Optical Telescope (SOT) on board Hinode, the Interface Region Spectrograph (IRIS) and the Atmospheric Imaging Assembly (AIA) on board the Solar Dynamic Observatory (SDO). Most of the jets in the Ca II H images show decreasing brightness with height while in the IRIS slit jaw images at 1330 Å jets show a bright leading edge. These jets show rising and falling motion as evident from the parabolic profile obtained from the time-distance diagram. The rising and falling speeds of the jets are similar. These jets show a coordinated behaviour between neighbouring jets moving jointly up and down. Some of the jets show a plasma ejection

from the leading edge which is also hotter at the transition region (TR) and coronal temperatures. A similar behaviour is seen in the AIA wave bands that suggests that jets above the LB reach up to the lower corona and the leading edges are heated up to coronal temperatures. Such jets are important means of transfer mass and energy to the transition region and corona above sunspots. **October 25, 2014.**

### **Solar flares associated coronal mass ejections in case of type II radio bursts**

Beena [Bhatt](#), Lalan Prasad, Harish Chandra, Suman Garia

Astrophysics and Space Science August 2016, 361:265

We have statistically studied 220 events from 1996 to 2008 (i.e. solar cycle 23). Two sets of flare-CME are examined: one with Deca-hectometric (DH) type II and other without DH type II radio burst. Out of 220 events 135 (flare-halo CME) are accompanied with DH type II radio burst and 85 are without DH type II radio burst. Statistical analysis is performed to examine the distribution of solar flare-halo CME around the solar disk and to investigate the relationship between solar flare and halo CME parameters in case of with and without DH type II radio burst. In our analysis we have observed that: (i) 10–20° latitudinal belt is more effective than the other belts for DH type II and without DH type II radio burst. In this belt, the southern region is more effective in case of DH type II radio burst, whereas in case of without DH type II radio burst dominance exists in the northern region. (ii) 0–10° longitudinal belt is more effective than the other belts for DH type II radio burst and without DH type II radio burst. In this belt, the western region is more effective in case of DH type II radio burst, while in case of without DH type II radio burst dominance exists in the eastern region. (iii) Mean speed of halo CMEs (1382 km/s) with DH type II radio burst is more than the mean speed of halo CMEs (775 km/s) without DH type II radio burst. (iv) Maximum number of M-class flares is found in both the cases. (v) Average speed of halo CMEs in each class accompanied with DH type II radio burst is higher than the average speed of halo CMEs in each class without DH type II radio burst. (vi) Average speed of halo CMEs, associated with X-class flares, is greater than the other class of solar flares in both the cases.

### **The energetic relationship among geoeffective solar flares, associated CMEs and SEPs**

Nipa J [Bhatt](#)<sup>1</sup>, Rajmal Jain<sup>2</sup> and Arun Kumar Awasthi<sup>2</sup>

Res. Astron. Astrophys. 13 978, 2013

<https://iopscience.iop.org/article/10.1088/1674-4527/13/8/009/pdf>

Major solar eruptions (flares, coronal mass ejections (CMEs) and solar energetic particles (SEPs)) strongly influence geospace and space weather. Currently, the mechanism of their influence on space weather is not well understood and requires a detailed study of the energetic relationship among these eruptive phenomena. From this perspective, we investigate 30 flares (observed by RHESSI), followed by weak to strong geomagnetic storms. Spectral analysis of these flares suggests a new power-law relationship ( $r \sim 0.79$ ) between the hard X-ray (HXR) spectral index (before flare-peak) and linear speed of the associated CME observed by LASCO/SOHO. For 12 flares which were followed by SEP enhancement near Earth, HXR and SEP spectral analysis reveals a new scaling law ( $r \sim 0.9$ ) **between the hardest X-ray flare spectrum and the hardest SEP spectrum. Furthermore, a strong correlation is obtained between the linear speed of the CME and the hardest spectrum of the corresponding SEP event ( $r \sim 0.96$ ). We propose that the potentially geoeffective flare and associated CME and SEP are well-connected** through a possible feedback mechanism, and should be regarded within the framework of a solar eruption. Owing to their space weather effects, these new results will help improve our current understanding of the Sun-Earth relationship, which is a major goal of research programs in heliophysics. **28-29 Oct 2003**

**Table 1** Characteristics of X-ray Flares, associated CMEs and SEPs (2002-2006)

### **Exploring the Origin of Stealth Coronal Mass Ejections with Magnetofrictional Simulations**

[P. Bhowmik](#), [A. R. Yeates](#) & [O. E. K. Rice](#)

[Solar Physics](#) volume 297, Article number: 41 (2022)

<https://link.springer.com/content/pdf/10.1007/s11207-022-01974-x.pdf>

Coronal mass ejections (CMEs) – among the most energetic events originating from the Sun – can cause significant and sudden disruption to the magnetic and particulate environment of the heliosphere. Thus, in the current era of space-based technologies, early warning that a CME has left the Sun is crucial. Some CMEs exhibit signatures at the solar surface and in the lower corona as the eruption occurs, thus enabling their prediction before arriving at near-Earth satellites. However, a significant fraction of CMEs exhibit no such detectable signatures and are known as “stealth CMEs”. Theoretical and observational studies aiming to understand the physical mechanism behind stealth CMEs have identified coronal streamers as potential sources. In this paper, we show that such streamer-blowout eruptions – which do not involve the lift-off of a low-coronal magnetic flux rope – are naturally produced even in the quasi-static magnetofrictional model for the coronal magnetic field. Firstly, we show that magnetofriction can reproduce in this way a particular stealth CME event observed during **1 – 2 June 2008**. Secondly, we show that the magnetofrictional model predicts the occurrence of repeated eruptions without clear low-coronal signatures from such arcades, provided that the high, overlying magnetic field lines are sufficiently sheared by differential rotation. A two-dimensional parameter study shows that such eruptions are robust under variation of the parameters, and that the eruption frequency is primarily determined by the footpoint shearing. This suggests that magnetofrictional models could, in principle, provide early indication – even pre-onset – of stealth eruptions, whether or not they originate from the eruption of a low-coronal flux rope.

### **Two Classes of Eruptive Events During Solar Minimum**

[P. Bhowmik](#) & [A. R. Yeates](#)

*Solar Physics* volume 296, Article number: 109 (2021)

<https://arxiv.org/pdf/2107.01941>

<https://link.springer.com/content/pdf/10.1007/s11207-021-01845-x.pdf>

<https://doi.org/10.1007/s11207-021-01845-x>

During solar minimum, the Sun is relatively inactive with few sunspots observed on the solar surface. Consequently, we observe a smaller number of highly energetic events such as solar flares or coronal mass ejections (CMEs), which are often associated with active regions on the photosphere. Nonetheless, our magnetofrictional simulations during the minimum period suggest that the solar corona is still dynamically evolving in response to the large-scale shearing velocities on the solar surface. The non-potential evolution of the corona leads to the accumulation of magnetic free energy and helicity, which is periodically shed in eruptive events. We find that these events fall into two distinct classes: One set of events are caused by eruption and ejection of low-lying coronal flux ropes, and they could explain the origin of occasional CMEs during solar minimum. The other set of events are not driven by destabilisation of low-lying structures but rather by eruption of overlying sheared arcades. These could be associated with streamer blowouts or stealth CMEs. The two classes differ significantly in the amount of magnetic flux and helicity shed through the outer coronal boundary. We additionally explore how other measurables such as current, open magnetic flux, free energy, coronal holes, and the horizontal component of the magnetic field on the outer model boundary vary during the two classes of event. This study emphasises the importance and necessity of understanding the dynamics of the coronal magnetic field during solar minimum. **2018 11 08-13, 2019 01 24**

### **Partial eruption of a filament with twisting nonuniform fields**

Yi Bi, [Yunchun Jiang](#), [Jiayan Yang](#), [Yongyuan Xiang](#), [Yunfang Cai](#), [Weiwei Liu](#)

ApJ **805** 48 **2015**

<http://arxiv.org/pdf/1504.03090v1.pdf>

The eruption of the filament with the kink fashion is often regarded as a signature of the kink instability. However, the kink instability threshold for the filament magnetic structure has been not widely understood. Using the H-alpha observation from the New Vacuum Solar Telescope (NVST), we present a partial eruptive filament. In the eruption, a filament thread appeared to split from the middle portion of the filament and to break out in a kinklike fashion. During this period, the left filament material remained below, which erupted without the kinking motion later on. The coronal magnetic field lines associated with the filament are obtained from the nonlinear force-free field (NLFFF) extrapolations using the 12 minutes cadence vector magnetograms of the Helioseismic and Magnetic Imager (HMI) on board the Solar Dynamic Observatory (SDO). We studied the extrapolated field lines passing through the magnetic dips that are in good agreement with the observed filament. The field lines are non-uniformly twisted and appear to be made up by two twisted flux ropes winding about each other. One of them has higher twist than the other, and the highly twisted one has its dips aligned with the kinking eruptive thread at the beginning of its eruption. Before the eruption, moreover, the highly twisted flux rope was found to expand with the approximately constant field twist. In addition, the helicity flux maps deduced from the HMI magnetograms show that some helicity is injected into the overlying magnetic arcade, but no significant helicity is injected into the flux ropes. Accordingly, we suggest that the highly twisted flux rope became kink unstable when the instability threshold declined with the expansion of the flux rope. **2014 Nov 4**

### **Solar Filament Material Oscillations and Drainage before Eruption**

Yi Bi<sup>1,3</sup>, [Yunchun Jiang](#)<sup>1</sup>, [Jiayan Yang](#)<sup>1</sup>, [Junchao Hong](#)<sup>1,2</sup>, [Haidong Li](#)<sup>1</sup>, [Dan Yang](#)<sup>1,2</sup>, and [Bo Yang](#)  
**2014 ApJ 790 100**

Both large-amplitude longitudinal (LAL) oscillations and material drainage in a solar filament are associated with the flow of material along the filament axis, often followed by an eruption. However, the relationship between these two motions and a subsequent eruption event is poorly understood. We analyze a filament eruption using EUV imaging data captured by the Atmospheric Imaging Array on board the Solar Dynamics Observatory and the H $\alpha$  images from the Global Oscillation Network Group. Hours before the eruption, the filament was activated, with one of its legs undergoing a slow rising motion. The asymmetric activation inclined the filament relative to the solar surface. After the active phase, LAL oscillations were observed in the inclined filament. The oscillation period increased slightly over time, which may suggest that the magnetic fields supporting the filament evolve to be flatter during the slow rising phase. After the oscillations, a significant amount of filament material was drained toward one filament endpoint, followed immediately by the violent eruption of the filament. The material drainage may further support the change in magnetic topology prior to the eruption. Moreover, we suggest that the filament material drainage could play a role in the transition from a slow to a fast rise of the erupting filament.

### **ERUPTION OF A SOLAR FILAMENT CONSISTING OF TWO THREADS**

Yi Bi (毕以), [Yunchun Jiang](#) (姜云春), [Haidong Li](#) (李海东), [Junchao Hong](#) (洪俊超), and [Ruisheng Zheng](#)  
**2012 ApJ 758 42**

The trigger and driving mechanism for the eruption of a filament consisting of two dark threads was studied with unprecedented high cadence and resolution of He II 304 Å observations made by the Atmospheric Imaging Assembly (AIA) on board the Solar Dynamics Observatory (SDO) and the observations made by the Solar Magnetic Activity Research Telescope and the Extreme Ultraviolet Imager (EUVI) telescope on board the Solar Terrestrial Relations

Observatory Ahead (STEREO-A). The filament was located at the periphery of the active region NOAA 11228 and erupted on **2011 June 6**. At the onset of the eruption, a turbulent filament thread was found to be heated and to elongate in stride over a second one. After it rose slowly, most interestingly, the elongating thread was driven to contact and interact with the second one, and it then erupted with its southern leg being wrapped by a newly formed thread produced by the magnetic reconnection between fields carried by the two threads. Combining the observations from STEREO-A/EUVI and SDO/AIA 304 Å images, the three-dimensional shape of the axis of the filament was obtained and it was found that only the southern leg of the eruptive filament underwent rotation. We suggest that the eruption was triggered by the reconnection of the turbulent filament thread and the surrounding magnetic field, and that it was mainly driven by the kink instability of the southern leg of the eruptive filament that possessed a more twisted field introduced by the reconnection-produced thread.

## **A fundamental mechanism of solar eruption initiation in multipolar magnetic field**

[Xinkai Bian](#), [Chaowei Jiang](#), [Xueshang Feng](#), [Pingbing Zuo](#), [Yi Wang](#)

ApJ **956** 73 **2023**

<https://arxiv.org/pdf/2308.04924.pdf>

<https://iopscience.iop.org/article/10.3847/1538-4357/acf5dc/pdf>

Recently we established a fundamental mechanism of solar eruption initiation, in which an eruption can be initiated from a bipolar field through magnetic reconnection in the current sheet (CS) that is formed slowly in the core field as driven by photospheric shearing motion. Here using a series of fully 3D MHD simulations with a range of different photospheric magnetic flux distributions, we extended this fundamental mechanism to the quadrupolar magnetic field containing a null point above the core field, which is the basic configuration of the classical breakout model. As is commonly believed, in such multipolar configuration, the reconnection triggered in the CS originated at the null point (namely, the breakout reconnection) plays the key role in eruption initiation by establishing a positive feedback-loop between the breakout reconnection and the expansion of the core field. However, our simulation showed that the key of eruption initiation in such multipolar configuration remains to be the slow formation of the CS in the sheared core rather than the onset of fast breakout reconnection. The breakout reconnection only helps the formation of the core CS by letting the core field expand faster, but the eruption cannot occur when the bottom surface driving is stopped well before the core CS is formed, even though the fast reconnection has already been triggered in the breakout CS. This study clarified the role of breakout reconnection and confirmed formation of the core CS as the key to the eruption initiation in a multipolar magnetic field.

## **MHD simulation of rapid change of photospheric magnetic field during solar eruption caused by magnetic reconnection**

[Xinkai Bian](#)<sup>1</sup> and [Chaowei Jiang](#)<sup>1</sup>

Front. Astron. Space Sci. **10**: 1097672. **2023**

doi: 10.3389/fspas.2023.1097672

<https://www.frontiersin.org/articles/10.3389/fspas.2023.1097672/pdf>

It has been well observed that the horizontal component of the magnetic field at photosphere changes rapidly and irreversibly after solar eruptions. Specifically, the horizontal magnetic field near the polarity inversion line increases substantially, while that near the center of the magnetic polarity decreases. Such a phenomenon is considered as the dynamic feedback from the corona to the photosphere, but the underlying mechanism remains in debate. Here based on a recent magnetohydrodynamics (MHD) simulation of homologous eruptions initiated by magnetic reconnection, we analyzed the rapid changes of the horizontal magnetic field, the magnetic inclination angle, the Lorentz force and as well as the derivative variation of the horizontal magnetic field. The simulation reproduces a pattern of rapid evolution of the horizontal field during the eruptions in agreement with typical observations. Our analysis suggests the physical reasons for this phenomenon: 1) The magnetic field near the polarity inversion line becomes more horizontal after flares due to the compression of the downward outflow of flare reconnection, and accordingly the magnetic inclination angle decreases and the downward Lorentz force increases; 2) The magnetic field near the center of the magnetic polarities become more vertical mainly due to the expansion effect of the velocity divergence term, and as a result the magnetic inclination angle and the upward Lorentz force increase.

## **The role of photospheric converging motion in initiation of solar eruptions**

[Xinkai Bian](#), [Chaowei Jiang](#), [Xueshang Feng](#)

Front. Astron. Space Sci. **9**: 982108 **2022**

<https://arxiv.org/pdf/2209.06561.pdf>

<https://doi.org/10.3389/fspas.2022.982108>

<https://www.frontiersin.org/articles/10.3389/fspas.2022.982108/pdf>

It is well known that major solar eruptions are often produced by active regions with continual photospheric shearing and converging motions. Here, through high accuracy magnetohydrodynamics simulation, we show how solar eruption is initiated in a single bipolar configuration as driven by first shearing and then converging motions at the bottom surface. Different from many previous simulations, we applied the converging motion without magnetic diffusion, thus it only increases the magnetic gradient across the polarity inversion line but without magnetic flux cancellation. The converging motion at the footpoints of the sheared arcade creates a current sheet in a quasi-static way, and the eruption is triggered by magnetic reconnection of the current sheet, which supports the same scenario as shown in our previous

simulation with only shearing motion. With the converging motion, the current sheet is formed at a lower height and has a higher current density than with shearing motion alone, which makes reconnection more effective and eruption stronger. Moreover, the converging motion renders a fast decay rate of the overlying field with height and thus favorable for an eruption. This demonstrates that the converging flow is more efficient to create the current sheet and more favorable for eruption than by solely the shearing flow.

## **Homologous Coronal Mass Ejections Caused by Recurring Formation and Disruption of Current Sheet within a Sheared Magnetic Arcade**

[Xinkai Bian](#), [Chaowei Jiang](#), [Xueshang Feng](#), [Pingbing Zuo](#), [Yi Wang](#)

ApJ 2022

<https://arxiv.org/pdf/2201.02909.pdf>

The Sun often produces coronal mass ejections with similar structure repeatedly from the same source region, and how these homologous eruptions are initiated remains an open question. Here, by using a new magnetohydrodynamic simulation, we show that homologous solar eruptions can be efficiently produced by recurring formation and disruption of coronal current sheet as driven by continuously shearing of the same polarity inversion line within a single bipolar configuration. These eruptions are initiated by the same mechanism, in which an internal current sheet forms slowly in a gradually sheared bipolar field and reconnection of the current sheet triggers and drives the eruption. Each of the eruptions does not release all the free energy but with a large amount left in the post-flare arcade below the erupting flux rope. Thus, a new current sheet can be more easily formed by further shearing of the post-flare arcade than by shearing a potential field arcade, and this is favorable for producing the next eruption. Furthermore, it is found that the new eruption is stronger since the newly formed current sheet has a larger current density and a lower height. In addition, our results also indicate the existence of a magnetic energy threshold for a given flux distribution, and eruption occurs once this threshold is approached.

## **Numerical Simulation of a Fundamental Mechanism of Solar Eruption with Different Magnetic Flux Distributions**

[Xinkai Bian](#), [Chaowei Jiang](#), [Xueshang Feng](#), [Pingbing Zuo](#), [Yi Wang](#), [Xinyi Wang](#)

A&A 658, A174 2022

<https://arxiv.org/pdf/2111.04984.pdf>

<https://doi.org/10.1051/0004-6361/202141996>

<https://www.aanda.org/articles/aa/pdf/2022/02/aa41996-21.pdf>

Solar eruptions are explosive release of coronal magnetic field energy as manifested in solar flares and coronal mass ejection. Observations have shown that the core of eruption-productive regions are often a sheared magnetic arcade, i.e., a single bipolar configuration, and, particularly, the corresponding magnetic polarities at the photosphere are elongated along a strong-gradient polarity inversion line (PIL). It remains unclear what mechanism triggers the eruption in a single bipolar field and why the one with a strong PIL is eruption-productive. Recently, using high accuracy simulations, we have established a fundamental mechanism of solar eruption initiation that a bipolar field as driven by quasi-static shearing motion at the photosphere can form an internal current sheet, and then fast magnetic reconnection triggers and drives the eruption. Here we investigate the behavior of the fundamental mechanism with different photospheric magnetic flux distributions, i.e., magnetograms, by combining theoretical analysis and numerical simulation. Our study shows that the bipolar fields of different magnetograms, as sheared continually, all exhibit similar evolutions from the slow storage to fast release of magnetic energy in accordance with the fundamental mechanism, which demonstrates the robustness of the mechanism. We further found that the magnetograms with stronger PIL produce larger eruptions, and the key reason is that the sheared bipolar fields with stronger PIL can achieve more non-potentiality, and their internal current sheet can form at a lower height and with a larger current density, by which the reconnection can be more efficient. This also provides a viable trigger mechanism for the observed eruptions in active region with strong PIL.

## **Relations between Coronal Mass Ejections and the Photospheric Magnetic Field in Cycles 23 and 24**

Irina A. [Bilenko](#)

2020 ApJ 889 1

<https://orcid.org/0000-0002-9543-0542>

The number of coronal mass ejections (CMEs) and their parameters and cycle variations were investigated and compared to the photospheric magnetic field evolution in cycles 23 and 24. The Coordinated Data Analysis Workshops (CDAW) catalog of white-light CMEs detected by the Solar and Heliospheric Observatory/Large Angle and Spectrometric Coronagraph coronagraphs and the data on the photospheric magnetic fields from the Kitt Peak Vacuum Telescope Spectromagnetograph (KPVT/Spectromagnetograph) and the Synoptic Optical Long-term Investigations of the Sun Vector-Spectromagnetograph (SOLIS/VSM) were used. The results suggest that not only did the number of CMEs increase in cycle 24, but that their parameters, cycle variations, distributions, and dependencies on the photospheric magnetic fields were also different. Various CME categories behave in different ways during solar cycles. The differences in the number and parameters of CMEs and their cycle variations may be related to the differences in the photospheric magnetic fields during the cycles. The strong photospheric magnetic fields maintained approximately the same strength from cycle 23 to cycle 24, whereas the weak fields became weaker and the area they occupied

increased. Taking into account that the global magnetic field diminished from cycle 23 to cycle 24, the increase in the number of CMEs in cycle 24 can be understood. A detailed analysis of the similarities and differences in CME parameters and their cycle evolution indicates that, along with the influence of changes in the CME detection mode in 2004 and 2010, the changes in CME rate and parameters were also associated with real differences in the behavior of strong and weak photospheric magnetic fields in cycles 23 and 24.

## **Influence of the Solar Global Magnetic-Field Structure Evolution on CMEs**

Irina A. **Bilenko**

Solar Physics, Volume 289, Issue 11, pp 4209-4237 **2014**

<https://arxiv.org/pdf/1804.08354.pdf>

We consider the influence of the solar global magnetic-field structure (GMFS) cycle evolution on the occurrence rate and parameters of coronal mass ejections (CMEs) in Solar Cycles 23–24. It has been shown that, over solar cycles, CMEs are not distributed randomly, but they are regulated by evolutionary changes in the GMFS. It is proposed that the generation of magnetic Rossby waves in the solar tachocline results in the GMFS cycle changes. Each Rossby wave period favors a particular GMFS. It is proposed that the changes in wave periods result in GMFS reorganization and consequently in CME location, occurrence rate, and parameter changes. The CME rate and parameters depend on the sharpness of the GMFS changes, the strength of the global magnetic field, and the phase of a cycle

## **From the Sun to the Earth: The 13 May 2005 Coronal Mass Ejection**

M.M. **Bisi** · A.R. Breen · B.V. Jackson · R.A. Fallows · A.P. Walsh · Z. Mikić · P. Riley · C.J. Owen · A.

Gonzalez-Esparza · E. Aguilar-Rodriguez · H. Morgan · E.A. Jensen · A.G. Wood · M.J. Owens · M.

Tokumaru · P.K. Manoharan · I.V. Chashei · A.S. Giunta · J.A. Linker · V.I. Shishov · S.A. Tyul'bashev · G.

Agalya · S.K. Glubokova · M.S. Hamilton · K. Fujiki · P.P. Hick · J.M. Clover · B. Pintér

Solar Phys (**2010**) 265: 49–127

We report the results of a multi-instrument, multi-technique, coordinated study of the solar eruptive event of 13 May 2005. We discuss the resultant Earth-directed (halo) coronal mass ejection (CME), and the effects on the terrestrial space environment and upper Earth atmosphere. The interplanetary CME (ICME) impacted the Earth's magnetosphere and caused the most-intense geomagnetic storm of 2005 with a Disturbed Storm Time (*Dst*) index reaching  $-263$  nT at its peak. The terrestrial environment responded to the storm on a global scale. We have combined observations and measurements from coronal and interplanetary remote-sensing instruments, interplanetary and near-Earth *in-situ* measurements, remote-sensing observations and *in-situ* measurements of the terrestrial magnetosphere and ionosphere, along with coronal and heliospheric modelling. These analyses are used to trace the origin, development, propagation, terrestrial impact, and subsequent consequences of this event to obtain the most comprehensive view of a geo-effective solar eruption to date. This particular event is also part of a NASA-sponsored Living With a Star (LWS) study and an on-going US NSF-sponsored Solar, Heliospheric, and Interplanetary Environment (SHINE) community investigation.

## **Mysteries of Flare/CME Initiation**

**Interesting**

Shaun **Bloomfield** and Hugh Hudson

RHESSI Science Nugget, No. 228, June **2014**

[http://sprg.ssl.berkeley.edu/~tohban/wiki/index.php/RHESSI\\_Science\\_Nuggets](http://sprg.ssl.berkeley.edu/~tohban/wiki/index.php/RHESSI_Science_Nuggets)

nearby major flares can occur in pairs - but how? **10 June 2014**

## **Predicting Coronal Mass Ejections Using Machine Learning Methods**

Monica G. **Bobra**, Stathis Itonidis

ApJ 821 127 **2016**

<http://arxiv.org/pdf/1603.03775v1.pdf> **File**

Of all the activity observed on the Sun, two of the most energetic events are flares and Coronal Mass Ejections (CMEs). Usually, solar active regions that produce large flares will also produce a CME, but this is not always true (Yashiro et al., 2005). Despite advances in numerical modeling, it is still unclear which circumstances will produce a CME (Webb & Howard, 2012). Therefore, it is worthwhile to empirically determine which features distinguish flares associated with CMEs from flares that are not. At this time, no extensive study has used physically meaningful features of active regions to distinguish between these two populations. As such, we attempt to do so by using features derived from [1] photospheric vector magnetic field data taken by the Solar Dynamics Observatory's Helioseismic and Magnetic Imager instrument and [2] X-ray flux data from the Geostationary Operational Environmental Satellite's X-ray Flux instrument. We build a catalog of active regions that either produced both a flare and a CME (the positive class) or simply a flare (the negative class). We then use machine-learning algorithms to [1] determine which features distinguish these two



populations, and [2] forecast whether an active region that produces an M- or X-class flare will also produce a CME. We compute the True Skill Statistic, a forecast verification metric, and find that it is a relatively high value of approximately 0.8 plus or minus 0.2. We conclude that a combination of six parameters, which are all intensive in nature, will capture most of the relevant information contained in the photospheric magnetic field.

## **The Double-Bubble CME of the 2020 December 14 Total Solar Eclipse**

[Benjamin Boe](#), [Bryan Yamashiro](#), [Miloslav Druckmuller](#), [Shadia Habbal](#)

ApJL **914** L39 **2021**

<https://arxiv.org/pdf/2106.04027.pdf>

<https://doi.org/10.3847/2041-8213/ac05ca>

Total solar eclipses (TSEs) continue to provide an invaluable platform for exploring the magnetic topology of the solar corona and for studying dynamic events such as Coronal Mass Ejections (CMEs) -- with a higher spatial resolution over a larger spatially continuous extent than is possible to achieve with any other method at present. In this Letter, we present observations of the full extent of a 'double-bubble' CME structure from the solar surface out to over 5 solar radii, as captured during the **2020 December 14** TSE. Its evolution through the corona was recorded from two observing sites separated by 13 minutes in their times of totality. The eclipse observations are complemented by a plethora of space-based observations including: Extreme Ultraviolet observations of the solar disk and low corona from SDO/AIA and STEREO-A/EUVI, white-light coronagraph observations from SOHO/LASCO-C2, radio from STEREO-A/WAVES and WIND/WAVES, and X-ray from GOES-16. We also characterize the magnetic field with a potential field source surface model. This CME event itself is of particular interest, as it demonstrates interactions between a prominence channel and an active region that led to the double-bubble structure. Despite the plethora of space-based observations, only the eclipse data are able to provide the proper context to connect these observations and yield a detailed study of this unique CME.

## **CME Induced Thermodynamic Changes in the Corona as Inferred from Fe XI and Fe XIV Emission Observations during the 2017 August 21 Total Solar Eclipse**

[Benjamin Boe](#), [Shadia Habbal](#), [Miloslav Druckmuller](#), [Adalbert Ding](#), [Jana Hoderova](#), [Pavel Starha](#)

**2020 ApJ 888** 100

<https://arxiv.org/pdf/1911.11222.pdf>

<https://doi.org/10.3847/1538-4357/ab5e34>

We present the first remote sensing observations of the impact from a Coronal Mass Ejection (CME) on the thermodynamic properties of the solar corona between 1 and 3 Rs. Measurements of the Fe XI (789.2 nm) and Fe XIV (530.3 nm) emission were acquired with identical narrow-bandpass imagers at three observing sites during the 2017 August 21 Total Solar Eclipse. Additional continuum imagers were used to observe K+F corona scattering, which is critical for the diagnostics presented here. The total distance between sites along the path of totality was 1400 km, corresponding to a difference of 28 minutes between the times of totality at the first and last site. These observations were used to measure the Fe XI and Fe XIV emission relative to continuum scattering, as well as the relative abundance of Fe 10+ and Fe 13+ from the line ratio. The electron temperature ( $T_e$ ) was then computed via theoretical ionization abundance values. We find that the range of  $T_e$  is  $1.1\text{--}1.2 \times 10^6$  K in coronal holes and  $1.2\text{--}1.4 \times 10^6$  K in streamers. Statistically significant changes of  $T_e$  occurred throughout much of the corona between the sites as a result of serendipitous CME activity prior to the eclipse. These results underscore the unique advantage of multi-site and multi-wavelength total solar eclipse observations for probing the dynamic and thermodynamic properties of the corona over an uninterrupted distance range from 1 to 3 Rs.

## **Solar Jet on 2014 April 16 Modeled by Kelvin--Helmholtz Instability**

[M. Bogdanova](#), [I. Zhelyazkov](#), [R. Joshi](#), [R. Chandra](#)

**2017**

<https://arxiv.org/pdf/1711.10734.pdf>

We study here the arising of Kelvin--Helmholtz Instability (KHI) in one fast jet of **2014 April 16** observed by the Atmospheric Imaging Assembly (AIA) on board Solar Dynamics Observatory (SDO) in different UV and EUV wavelengths. The evolution of jet indicates the blob like structure at its boundary which could be the observational evidence of the KHI. We model the jet as a moving cylindrical magnetic flux tube of radius  $a$  embedded in a magnetic field  $B_i$  and surrounded by rest magnetized plasma with magnetic field  $B_e$ . We explore the propagation of the kink MHD mode along the jet that can become unstable against the KHI if its speed exceeds a critical value. Concerning magnetic fields topology we consider three different configurations, notably of (i) spatially homogeneous magnetic fields (untwisted magnetic flux tube), (ii) internal (label 'i') twisted magnetic field and external homogeneous one (label 'e') (single-twisted flux tube), and (iii) both internal and external twisted magnetic fields (double-twisted magnetic flux tube). Plasma densities in the two media  $\rho_i$  and  $\rho_e$  are assumed to be homogeneous. The density contrast is defined in two ways: first as  $\rho_e/\rho_i$  and second as  $\rho_e/(\rho_i + \rho_e)$ . Computations show that the KHI can occur at accessible flow velocities in all the cases of untwisted and single-twisted flux tubes. It turns out, however, that in the case of a double-twisted flux tube the KHI can merge at an accessible jet speed only when the density contrast is calculated from the ratio  $\rho_e/(\rho_i + \rho_e)$ . Evaluated KHI developing times and kink mode wave phase velocities at wavelength of 4 Mm lie in the ranges of 1--6.2 min and 202--271 km/s, respectively---all being reasonable for the modeled jet.

## **Validation of CME Detection Software (CACTus) by Means of Simulated Data, and Analysis of Projection Effects on CME Velocity Measurements**

K. **Bonte**, C. Jacobs, E. Robbrecht, A. De Groof, D. Berghmans and S. Poedts

Solar Physics, Volume 270, Number 1, 253-272, **2011**, **File**

In the context of space weather forecasting, an automated detection of coronal mass ejections (CMEs) becomes more and more important for efficiently handling a large data flow which is expected from recently-launched and future solar missions. In this paper we validate the detection software package “CACTus” by applying the program to synthetic data from our 3D time-dependent CME simulations instead of observational data. The main strength of this study is that we know in advance what should be detected. We describe the sensitivities and strengths of automated detection, more specific for the CACTus program, resulting in a better understanding of CME detection on one hand and the calibration of the CACTus software on the other hand, suggesting possible improvements of the package. In addition, the simulation is an ideal tool to investigate projection effects on CME velocity measurements

## **Eruptive Event Generator Based on the Gibson-Low Magnetic Configuration†**

D. **Borovikov**, I. V. Sokolov, W. B. Manchester, M. Jin, T. I. Gombosi

JGR Volume 122, Issue 8 Pages 7979–7984 **2017**

<http://onlinelibrary.wiley.com/doi/10.1002/2017JA024304/pdf>

Coronal Mass Ejections (CMEs), a kind of energetic solar eruptions, are an integral subject of space weather research. Numerical magnetohydrodynamic (MHD) modeling, which requires powerful computational resources, is one of the primary means of studying the phenomenon. With increasing accessibility of such resources, grows the demand for user-friendly tools that would facilitate the process of simulating CMEs for scientific and operational purposes. The Eruptive Event Generator based on Gibson-Low flux rope (EEGGL), a new publicly available computational model presented in this paper, is an effort to meet this demand. EEGGL allows one to compute the parameters of a model flux rope driving a CME via an intuitive graphical user interface (GUI). We provide a brief overview of the physical principles behind EEGGL and its functionality. Ways towards future improvements of the tool are outlined.

## **Three-Dimensional Properties of Coronal Mass Ejections from STEREO/SECCHI Observations**

E. **Bosman**, V. Bothmer, G. Nisticò, A. Vourlidas, R. A. Howard, J. A. Davies

Solar Physics, November **2012**, Volume 281, Issue 1, pp 167-185, **File**

We identify 565 coronal mass ejections (CMEs) between **January 2007 and December 2010** in observations from the twin STEREO/SECCHI/COR2 coronagraphs aboard the STEREO mission. Our list is in full agreement with the corresponding SOHO/LASCO CME Catalog ( [http://cdaw.gsfc.nasa.gov/CME\\_list/](http://cdaw.gsfc.nasa.gov/CME_list/) ) for events with angular widths of 45° and up. The monthly event rates behave similarly to sunspot rates showing a three- to fourfold rise between September 2009 and March 2010. We select 51 events with well-defined white-light structure and model them as three-dimensional (3D) flux ropes using a forward-modeling technique developed by Thernisien, Howard and Vourlidas (Astrophys. J. 652, 763–773, 2006). We derive their 3D properties and identify their source regions. We find that the majority of the CME flux ropes (82 %) lie within 30° of the solar equator. Also, 82 % of the events are displaced from their source region, to a lower latitude, by 25° or less. These findings provide strong support for the deflection of CMEs towards the solar equator reported in earlier observations, e.g. by Cremades and Bothmer (Astron. Astrophys. 422, 307–322, 2004). **Tables.**

## **Comparison of CME and ICME Structures Derived from Remote-Sensing and In Situ Observations**

V. **Bothmer**, N. Mrotzek

*Solar Physics* November **2017**, 292:157

<https://link.springer.com/article/10.1007/s11207-017-1171-7>

We present results from the comparison of the near-Sun and in situ analysis of two Earth-directed coronal mass ejections (CMEs) with different 3D orientations and solar source region characteristics. The CME on **14 July 2000**, the so-called Bastille Day storm, a well-studied event, was observed from a single-point perspective by the Large Angle and Spectrometric Coronagraph (LASCO) onboard the Solar and Heliospheric Observatory (SOHO). It caused a major geomagnetic storm with a peak Kp of 9. The CME originated from a magnetic bipolar photospheric source region with the polarity inversion line being oriented rather parallel to the heliographic equator. In contrast, the CME on **29 September 2013**, which caused a geomagnetic storm with a peak Kp intensity of 8-, originated from a magnetic quadrupolar photospheric source region with the polarity inversion line between the two bipoles almost vertically oriented with respect to the heliographic equator. The results of a graduated cylindrical shell (GCS) analysis of the CMEs near the Sun are compared with the minimum variance analysis (MVA) of the magnetic field structure of the interplanetary CME (ICME) measured in situ near Earth’s orbit. The results are in good agreement for the September 2013 CME and ICME, whereas the July 2000 ICME appears substantially inclined near Earth’s orbit. The discrepancy can likely be explained taking into account kinks in the CME’s near-Sun structure of the CME that expands into the interplanetary medium.

## **Photospheric Field Evolution in the Source Regions of Coronal Mass Ejections**

**Bothmer**, V.; Tripathi, D.

SOHO-17. 10 Years of SOHO and Beyond, Proceedings of the conference held 7-12 May, **2006** at Giardini Naxos, Sicily, Italy. Edited by H. Lacoste and L. Ouwehand. ESA SP-617. European Space Agency, 2006. Published on CDROM, p.20.1

Six coronal mass ejections associated with erupting quiescent filaments on the visible solar disk were identified in data from SoHO (Solar and Heliospheric Observatory) LASCO (Large Angle and Spectrometric Coronagraph), EIT (Extreme ultraviolet Imaging Telescope) and MDI (Michelson Doppler Imager) data and ground-based H $\alpha$  observations from Big Bear and Meudon observatories. These events were analysed to investigate whether their initiations could be related to changes of the underlying photospheric field. The results show that in five out of the six events, substantial changes in the photospheric magnetic field occurred in the source regions prior and around the CME's lift-off times as identified from emerging/diminishing flux detected by MDI. In one event large magnetic flux changes could be identified not in the source region itself, but in a neighbouring active region. The results demonstrate that new missions, such as STEREO and Hinode (Solar-B) in conjunction with SoHO and ground-based measurements, will provide joint data sets that have the potential to provide new insight into the physical causes of CMEs.

(see p. 257 in **Modern Solar Facilities – Advanced Solar Science**

Proceedings of a Workshop held at Göttingen September 27-29, 2006

Franz **Kneer**, Klaus G. Puschmann, Axel D. Wittmann (Eds.); **File 2007**)

## **The ARTEMIS Catalog of LASCO Coronal Mass Ejections**

### **Automatic Recognition of Transient Events and Marseille Inventory from Synoptic maps**

Y. **Boursier** · P. Lamy · A. Llebaria · F. Goudail · S. Robelus

Solar Phys., **2009**, 257(1), Page: 125 – 147, DOI: 10.1007/s11207-009-9370-5, **File**

The LASCO-C2 coronagraph aboard the SOHO solar observatory has been providing a continuous flow of coronal images since 1996. Synoptic maps for each Carrington rotation have been built from these images, and offer a global view of the temporal evolution of the solar corona, particularly the occurrence of transient events. Coronal Mass Ejections (CMEs) present distinct signatures thus offering a novel approach to the problem of their identification and characterization. We present in this article an automated method of detection based on their morphological appearance on synoptic maps. It is based on adaptive filtering and segmentation, followed by merging with high-level knowledge. The program builds a catalog which lists the CMEs detected for each Carrington Rotation, together with their main estimated parameters: time of appearance, position angle, angular extent, average velocity and intensity. Our final catalog LASCO-ARTEMIS (Automatic Recognition of Transient Events and Marseille Inventory from Synoptic maps) is compared with existing catalogs, CDAW, CACTUS and SEEDS. We find that, likewise the automated CACTUS and SEEDS catalogs, we detect many more events than the CDAW catalog which is based on visual detection. The total number of detected CMEs strongly depends upon the sensitivity to small, faint and numerous events.

## **Three-Dimensional Kinematics of Coronal Mass Ejections from STEREO/SECCHI-COR2 Observations in 2007 – 2008**

Y. **Boursier** · P. Lamy · A. Llebaria

Solar Phys (2009) 256: 131–147, DOI 10.1007/s11207-009-9358-1, **2009**, **File**

### **STEREO SCIENCE RESULTS AT SOLAR MINIMUM**

We present a new method to perform the three dimensional characterization of coronal mass ejections (CMEs) using stereoscopic images obtained with the STEREO/SECCHI-COR2 coronagraphs. Two approaches are proposed, and each associated algorithm gives the trajectory of the CME and its kinematical properties (velocity and acceleration profiles) intended for space weather forecast. The first approach is based on forward modeling appropriate to the reconstruction of surfaces in an optically thin medium, and performs a local approximation of the observed CME by a hemispherical shell, thus tracking the leading edge of the event. The second approach is based on tracking the center of gravity of the radiance of the CME in the images. More than 16 000 blind tests have been performed to assess the performance of each algorithm. For that purpose, we used three distinct libraries of simulated images of CMEs that correspond to three CME models: hemispherical shell, flux rope, and cloud-like. The two methods are applied to a set of CMEs observed in 2007 and 2008 by the SECCHI-COR2 coronagraphs, and when possible, our results are compared to those already published. The determinations of the direction of propagation and of the velocity are generally found in good agreement.

## **A Coronal Mass Ejection Impacting Parker Solar Probe at 14 Solar Radii**

Carlos R. **Braga**<sup>1</sup>, Vamsee Krishna Jagarlamudi<sup>1</sup>, Angelos Vourlidas<sup>1</sup>, Guillermo Stenborg<sup>1</sup>, and Teresa Nieves-Chinchilla<sup>2</sup>

**2024** ApJ 965 185

<https://iopscience.iop.org/article/10.3847/1538-4357/ad2b4e/pdf>

The relationship between CME properties in the corona and their interplanetary counterparts is not well understood. Until recently, a wide spatial gap existed between the two regions, which prevented us from disentangling the spatial and temporal evolution of CMEs. NASA's Parker Solar Probe (PSP) has imaged multiple CMEs since its launch in 2018, but these events either intercepted the spacecraft far from the corona or completely missed it. Here we describe one of the first CMEs observed simultaneously by remote sensing and in situ instruments, and compare the corresponding measured properties, such as orientation, cross section diameter, density, and speed. The CME encounter occurred on **2022 June 2**, while PSP was around 14 solar radii from the Sun center. We reconstruct the CME with forward modeling and determine its morphology and kinematics. The reconstruction suggests that PSP misses the CME apex but encounters its flank. The encounter time matches the period when the PSP in situ measurements indicate the passage of a CME. We also reconstruct the flux rope diameter and orientation using the in situ magnetic field measurements. The results are consistent with the CME reconstruction from imaging data. The close agreement between remote sensing and in situ analyses suggests that discrepancies found in past studies are more likely associated with the CME temporal evolution. We also find that the magnetic field of the CME flank extrapolated to 1 au is well below the average solar wind background and likely indistinguishable from it. This point could explain past events where the CMEs' interplanetary counterparts were not identified.

## **Coronal mass ejections observed by heliospheric imagers at 0.2 and 1 au The events on April 1 and 2, 2019**

Carlos R. **Braga**<sup>1,2</sup> and Angelos Vourlidas

A&A 650, A31 (2021)

<https://arxiv.org/pdf/2011.05229.pdf>

<https://www.aanda.org/articles/aa/pdf/2021/06/aa39490-20.pdf>

<https://doi.org/10.1051/0004-6361/202039490>

**Context.** We study two coronal mass ejections (CMEs) observed between **April 1 to 2, 2019** by both the inner Wide-Field Imager for Parker Solar Probe (WISPR-I) onboard the Parker Solar Probe (PSP) spacecraft (located between about 46 and 38 solar radii during this period) and the inner heliospheric imager (HI-1) onboard the Solar Terrestrial Relations Observatory Ahead (STEREO-A) spacecraft, orbiting the Sun at about 0.96 au. This is the first study of CME observations from two viewpoints in similar directions but at considerably different solar distances.

**Aims.** Our objective is to derive CME kinematics from WISPR-I observations and to compare them with results from HI-1. This allows us to understand how the PSP observations affect the CME kinematics, especially due to its proximity to the Sun.

**Methods.** We estimated the CME positions, speeds, accelerations, propagation directions, and longitudinal deflections using imaging observations from two spacecrafts and a set of analytical expressions that consider the CME as a point structure and take the rapid change in spacecraft position into account. We derived the kinematics using each viewpoint independently and both viewpoints as a constraint.

**Results.** We found that both CMEs are slow ( $<400 \text{ km s}^{-1}$ ), propagating eastward of the Sun-Earth line (westward of PSP and STEREO-A). The second CME seems to accelerate between  $\sim 0.1$  and  $\sim 0.2$  au and deflect westward with an angular speed consistent with the solar rotation speed. We found some discrepancies in the CME solar distance (up to 0.05 au, particularly for CME #1), latitude (up to  $\sim 10^\circ$ ), and longitude (up to  $24^\circ$ ) when comparing results from different fit cases (different observations or set of free parameters).

**Conclusions.** Discrepancies in longitude are likely due to the feature that is tracked visually, rather than instrumental biases or fit assumptions. For similar reasons, the CME #1 solar distance, as derived from WISPR-I observations, is larger than the HI-1 result, regardless of the fit parameters considered. Error estimates for CME kinematics do not show any clear trend associated with the observing instrument. The source region location and the lack of any clear in situ counterparts (both at near-Earth and at PSP) support our estimate of the propagation direction for both events.

## **Very narrow coronal mass ejections producing solar energetic particles**

K. **Bronarska**<sup>1</sup>, M. S. Wheatland<sup>2</sup>, N. Gopalswamy<sup>3</sup> and G. Michalek<sup>1</sup>

A&A 619, A34 (2018)

<https://sci-hub.ru/10.1051/0004-6361/201833237>

**Aims.** Our main aim is to study the relationship between low-energy solar particles (energies below 1 MeV) and very narrow coronal mass ejections (“jets” with angular width  $\leq 20^\circ$ ).

**Methods.** For this purpose, we considered 125 very narrow coronal mass ejections (CMEs) from 1999 to 2003 that are potentially associated with low-energy solar particles (LESPs). These events were chosen on the basis of their source location. We studied only very narrow CMEs at the western limb, which are expected to have good magnetic connectivity with Earth.

**Results.** We found 24 very narrow CMEs associated with energetic particles such as ions (protons and  $3\text{He}$ ), electrons, or both. We show that arrival times at Earth of energetic particles are consistent with onset times of the respective CMEs, and that in the same time intervals, there are no other potential sources of energetic particles. We also demonstrate statistical differences for the angular width distributions using the Kolmogorov–Smirnov test for angular widths for these 24 events. We consider a coherent sample of jets (mostly originating from boundaries of coronal holes) to identify properties of events that produce solar energetic particles (velocities, widths, and position angles). Our study presents a new approach and result: very narrow CMEs can generate low-energy particles in the vicinity of Earth without other activity on the Sun. The results could be very useful for space weather forecasting. **2000/07/10, 14 December 2001**

**Table 2.** Properties of 24 very narrow CMEs generating low-energy SEPs

## **Determination of projection effects of CMEs using quadrature observations with the two STEREO spacecraft**

**K.Bronarska, G.Michalek**

[Advances in Space Research](#) Volume 62, Issue 2, 15 July 2018, Pages 408-416

<https://sci-hub.ru/10.1016/j.asr.2018.04.031>

<https://doi.org/10.1016/j.asr.2018.04.031>

Since 1995 [coronal mass ejections](#) (CMEs) have been routinely observed thanks to the sensitive Large Angle and Spectrometric Coronagraphs (LASCO) on board the Solar and Heliospheric Observatory (SOHO) mission. Their observed characteristics are stored, among other, in the SOHO/LASCO catalog. These parameters are commonly used in scientific studies. Unfortunately, coronagraphic observations of CMEs are subject to projection effects. This makes it practically impossible to determine the true properties of CMEs and therefore makes it more difficult to forecast their geoeffectiveness. In this study, using [quadrature](#) observations with the two Solar Terrestrial Relations Observatory (STEREO) spacecrafts, we estimate the projection effect affecting velocity of CMEs included in the SOHO/LASCO catalog. It was demonstrated that this effect depends significantly on width and source location of CMEs. It can be very significant for narrow events and originating from the disk center. The effect diminishes with increasing width and absolute longitude of source location of CMEs. For very wide (width  $\geq 250^\circ$ ) or limb events (longitude  $\geq 70^\circ$ ) projection effects completely disappears.

## **Visibility of coronal mass ejections in SOHO/LASCO coronagraphs**★

**K.Bronarska, G.Michalek, S.Yashiro, S.Akiyama**

[Advances in Space Research](#) Volume 60, Issue 9, 1 November 2017, Pages 2108-2115

<http://sci-hub.ru/10.1016/j.asr.2017.07.033>

We studied the detection efficiency of coronal mass ejections (CMEs) of the Large Angle Spectrometric Coronagraph (LASCO) on board the Solar and Heliospheric Observatory (SOHO). For this purpose LASCO/SOHO observations are compared with these obtained by the two Solar Terrestrial Relations Observatory (STEREO) satellites in quadrature in the period of time **June-November 2011**. These unprecedented observations enable us to the direct detection of CMEs that are not visible in LASCO coronagraphs (invisible events). Determination of these events allowed us to evaluate the detection efficiency of LASCO coronagraphs. We found that the total visibility function is  $\approx 0.80$ . Having source location, from associated flares or other signatures observed in the corona, longitudinal variation of the visibility function was also found. It was demonstrated that invisible-to-LASCO CMEs are narrow (average width is only  $20^\circ$ ), slow (average velocity is  $328 \text{ km s}^{-1}$ ) and originate from the disk center. We have shown that the detection efficiency of the LASCO coronagraphs with typical data availability is sufficient to detect all potentially geoeffective CMEs.

## **Helicity-conserving relaxation in unstable and merging magnetic flux ropes**

**Philippa Browning, Mykola Gordovskyy, Alan Hood**

**2023**

<https://arxiv.org/pdf/2308.08277.pdf>

Twisted magnetic flux ropes are reservoirs of free magnetic energy. In a highly-conducting plasma such as the solar corona, energy release through multiple magnetic reconnections can be modelled as a helicity-conserving relaxation to a minimum energy state. One possible trigger for this relaxation is the ideal kink instability in a twisted flux rope. We show that this provides a good description for confined solar flares, and develop from idealised cylindrical models to realistic models of coronal loops. Using 3D magnetohydrodynamic simulations combined with test-particle simulations of non-thermal electrons and ions, we predict multiple observational signatures of such flares. We then show how interactions and mergers of flux ropes can release free magnetic energy, using relaxation theory to complement simulations of merging-compression formation in spherical tokamaks and heating avalanches in the solar corona.

## **Empirical Model of 10-130 MeV Solar Energetic Particle Spectra at 1 AU Based on Coronal Mass Ejection Speed and Direction**

Alessandro **Bruno**, **Ian G. Richardson**

Solar Phys. **2021**

<https://arxiv.org/pdf/2101.04234.pdf> **File**

We present a new empirical model to predict solar energetic particle (SEP) event-integrated and peak intensity spectra between 10 and 130 MeV at 1 AU, based on multi-point spacecraft measurements from the Solar Terrestrial Relations Observatory (STEREO), the Geostationary Operational Environmental Satellites (GOES) and the Payload for Antimatter Matter Exploration and Light-nuclei Astrophysics (PAMELA) satellite experiment. The analyzed data sample includes 32 SEP events occurring between 2010 and 2014, with a statistically significant proton signal at energies in excess of a few tens of MeV, unambiguously recorded at three spacecraft locations. The spatial distributions of SEP intensities are reconstructed by assuming an energy-dependent 2D Gaussian functional form, and accounting for the correlation between the intensity and the speed of the parent coronal mass ejection (CME), and the magnetic field line connection angle. The CME measurements used are from the SpaceWeather Database Of Notifications, Knowledge, Information (DONKI). The model performance, including its extrapolations to lower/higher energies, is

tested by comparing with the spectra of 20 SEP events not used to derive the model parameters. Despite the simplicity of the model, the observed and predicted event-integrated and peak intensities at Earth and at the STEREO spacecraft for these events show remarkable agreement, both in the spectral shapes and their absolute values.

**Table 1.** List of CMEs associated with the SEP events analyzed in this work. (2010-2014)

**Table 4.** List of CMEs associated with the SEP events used for testing the empirical model (2011-2017)

### **Recurrent 3He-rich solar energetic particle injections observed by Solar Orbiter at ~0.5 au\***

R. Bučik<sup>1</sup>, G. M. Mason<sup>2</sup>, N. V. Nitta<sup>3</sup>, V. Krupar<sup>4,5</sup>, L. Rodriguez<sup>6</sup>, G. C. Ho<sup>2</sup>, S. T. Hart<sup>7,1</sup>, M. A. Dayeh<sup>1</sup>, J. Rodríguez-Pacheco<sup>8</sup>, R. Gómez-Herrero<sup>8</sup> and R. F. Wimmer-Schweingruber<sup>9</sup>  
A&A 673, L5 (2023)

<https://www.aanda.org/articles/aa/pdf/2023/05/aa45875-23.pdf>

We report Solar Orbiter observations of six recurrent solar energetic particle injections in **2022 March 3–6** at ~0.5 au. All but one were associated with jets emanating from a plage near a large sunspot in active region 12 957. We saw large jets in injections with high 3He and Fe enrichments and minor jets in injections with no or lower enrichments.

Furthermore, the event with the highest enrichment showed a more compact configuration of the underlying photospheric magnetic field. The higher fluences as well as harder spectra were seen in the event with a simultaneous jet and wider eruption. However, in this case, the energy buildup time in the source might be required to produce such spectra. Extreme-ultraviolet images from Solar Orbiter revealed a number of intersecting loops at the base of jets not seen from 1 au that might be a precondition for the recurrent events.

### **Impulsive Solar Energetic Particle Events: EUV Waves and Jets** MINI **REVIEW**

R. Bucik

Front. Astron. Space Sci. 8 807961 2022 File

<https://www.frontiersin.org/articles/10.3389/fspas.2021.807961/full>

<https://doi.org/10.3389/fspas.2021.807961>

<https://arxiv.org/abs/2112.14282>

Impulsive solar energetic particle (ISEP) events show peculiar elemental composition, with enhanced 3He and heavy-ion abundances, markedly different from our solar system composition. Furthermore, the events are characterized by a wide variety of energy spectral shapes from power laws to rounded spectra toward the low energies. Solar sources of the events have been firmly associated with coronal jets. Surprisingly, new observations have shown that events are often accompanied by so-called extreme-ultraviolet (EUV) coronal waves – a large-scale phenomenon compared to jets.

This paper outlines the current understanding of the linkage of EUV waves with jets and energetic ions in ISEP events.

**2007 May 23, 2008 Nov 4, 2009 Dec 22, 2010 January 26, 2010 Feb 2, 2010 Jun 12, 2011 Jan 27, 2011 Feb 18, 2014 May 16**

**Table 1.** The ISEP events with reported EUV wave speed.

### **3He-rich Solar Energetic Particles from Sunspot Jets**

Radoslav Bučik<sup>1,2</sup>, Mark E. Wiedenbeck<sup>3</sup>, Glenn M. Mason<sup>4</sup>, Raúl Gómez-Herrero<sup>5</sup>, Nariaki V. Nitta<sup>6</sup>, and Linghua Wang<sup>7</sup>

2018 ApJL 869 L21

[sci-hub.ru/10.3847/2041-8213/aaf37f](https://sci-hub.ru/10.3847/2041-8213/aaf37f)

<https://arxiv.org/pdf/1812.07735.pdf>

Solar sources of suprathermal (<1 MeV nucleon<sup>-1</sup>) 3He-rich solar energetic particles (SEPs) have been commonly associated with jets originating in small, compact active regions at the periphery of near-equatorial coronal holes. Sources of relatively rare, high-energy (>10 MeV nucleon<sup>-1</sup>) 3He-rich SEPs remain unexplored. Here we present two of the most intense 3He-rich (3He/4He > 1) SEP events of the current solar cycle 24 measured on the Advanced Composition Explorer at energy >10 MeV nucleon<sup>-1</sup>. Although 3He shows high intensities, Z > 2 ions are below the detection threshold. The events are accompanied by type-III radio bursts, but no type-II emission as typically seen for suprathermal 3He-rich SEPs. The corresponding solar sources were analyzed using high-resolution, extreme-ultraviolet imaging and photospheric magnetic field observations on the Solar Dynamics Observatory. We find the sources of these events associated with jets originating at the boundary of large sunspots with complex βγδ magnetic configuration. Thus, details of the underlying photospheric field apparently are important to produce 3He to high energies in the examined events. **2011 February 18, 2015 August 24**

### **3He-Rich Solar Energetic Particles in Helical Jets on the Sun**

Radoslav Bucik, Davina E. Innes, Glenn M. Mason, Mark E. Wiedenbeck, Raul Gomez-Herrero, Nariaki V. Nitta

2018 ApJ 852 76

<https://arxiv.org/pdf/1711.09394.pdf>

Particle acceleration in stellar flares is ubiquitous in the Universe, however, our Sun is the only astrophysical object where energetic particles and their source flares can both be observed. The acceleration mechanism in solar flares,

tremendously enhancing (up to a factor of ten thousand) rare elements like  $^3\text{He}$  and ultra-heavy nuclei, has been puzzling for almost 50 years. Here we present some of the most intense  $^3\text{He}$ - and Fe-rich solar energetic particle events ever reported. The events were accompanied by non-relativistic electron events and type III radio bursts. The corresponding high-resolution, extreme-ultraviolet imaging observations have revealed for the first time a helical structure in the source flare with a jet-like shape. The helical jets originated in relatively small, compact active regions, located at the coronal hole boundary. A mini-filament at the base of the jet appears to trigger these events. The events were observed with the two Solar Terrestrial Relations Observatories STEREO on the backside of the Sun, during the period of increased solar activity in 2014. The helical jets may be a distinct feature of these intense events that is related to the production of high  $^3\text{He}$  and Fe enrichments. **2014 Apr 30, 17 July 2014, 2014 Jul 19, 2014 Jul 20**

## **Magnetohydrodynamic Modeling Investigations of Kelvin–Helmholtz Instability and Associated Magnetosonic Wave Emission along Coronal Mass Ejections**

Sara **Butler**<sup>1,2,3</sup>, Weiru Chen<sup>1,4</sup>, and Hava Turkakin<sup>1,5</sup>

**2022** ApJ 935 164

<https://iopscience.iop.org/article/10.3847/1538-4357/ac7b92/pdf>

Previous studies have suggested that the Kelvin–Helmholtz instability (KHI) and magnetohydrodynamic (MHD) wave emissions via the KHI along various shear flow boundaries in a solar–terrestrial environment may be possible. We expand upon these previous studies to investigate the linear and nonlinear evolution of the KHI and emission of MHD waves along the boundaries of coronal mass ejections (CMEs). Our results demonstrate that the KHI and MHD wave emission due to the KHI are possible along the CME boundaries during the KHI development. We found that magnetic field orientation in the region outside of the CME has strong effects on the strength of MHD wave emission. While a smaller parallel component of the magnetic field resulted in larger growth rates in the KHI development, a larger parallel component of the magnetic field resulted in stronger MHD wave emissions. For all cases we investigated, we identified emitted waves to be fast MHD waves. We suggest that these emitted MHD waves may be able to carry available kinetic energy from the CME flow to the outside of the CME, thereby contributing to solar coronal heating via energy dissipation.

## **Investigating the Kinematics of Coronal Mass Ejections with the Automated CORIMP Catalog**

Jason P. **Byrne**

J. Space Weather Space Clim., 5, A19 **2015**

<http://arxiv.org/pdf/1506.04046v1.pdf>

Studying coronal mass ejections (CMEs) in coronagraph data can be challenging due to their diffuse structure and transient nature, compounded by the variations in their dynamics, morphology, and frequency of occurrence. The large amounts of data available from missions like the Solar and Heliospheric Observatory (SOHO) make manual cataloging of CMEs tedious and prone to human error, and so a robust method of detection and analysis is required and often preferred. A new coronal image processing catalog called CORIMP has been developed in an effort to achieve this, through the implementation of a dynamic background separation technique and multiscale edge detection. These algorithms together isolate and characterise CME structure in the field-of-view of the Large Angle Spectrometric Coronagraph (LASCO) onboard SOHO. CORIMP also applies a Savitzky-Golay filter, along with quadratic and linear fits, to the height-time measurements for better revealing the true CME speed and acceleration profiles across the plane-of-sky. Here we present a sample of new results from the CORIMP CME catalog, and directly compare them with the other automated catalogs of Computer Aided CME Tracking (CACTus) and Solar Eruptive Events Detection System (SEEDS), as well as the manual CME catalog at the Coordinated Data Analysis Workshop (CDAW) Data Center and a previously published study of the sample events. We further investigate a form of unsupervised machine learning by using a k-means clustering algorithm to distinguish detections of multiple CMEs that occur close together in space and time. While challenges still exist, this investigation and comparison of results demonstrates the reliability and robustness of the **CORIMP catalog** (<http://alshamess.ifa.hawaii.edu/CORIMP/>), proving its effectiveness at detecting and tracking CMEs throughout the LASCO dataset. **2000 Jan. 02, 2000 Apr. 18, 2000 Apr. 23, 2001 Apr. 23, 2002 Apr. 21, 2004 Apr. 1**

## **Bridging EUV and white-light observations to inspect the initiation phase of a "two-stage" solar eruptive event**

**Byrne**, J. P., Morgan, H., Seaton, D. B., Bain, H. M., Habbal, S. R.

E-print, June **2014**; Solar Phys.

<http://arxiv.org/pdf/1406.4919v1.pdf>

The initiation phase of CMEs is a very important aspect of solar physics, as these phenomena ultimately drive space weather in the heliosphere. This phase is known to occur between the photosphere and low corona, where many models introduce an instability and/or magnetic reconnection that triggers a CME, often with associated flaring activity. To this end, it is important to obtain a variety of observations of the low corona in order to build as clear a picture as possible of the dynamics that occur therein. Here, we combine the EUV imagery of the SWAP instrument on board PROBA2 with the white-light imagery of the ground-based Mk4 coronameter at MLSO in order to bridge the observational gap that exists between the disk imagery of AIA on board SDO and the coronal imagery of LASCO on board SOHO. Methods of multiscale image analysis were applied to the observations to better reveal the coronal signal while suppressing noise

and other features. This allowed an investigation into the initiation phase of a CME that was driven by a rising flux rope structure from a "two-stage" flaring active region underlying an extended helmet streamer. It was found that the initial outward motion of the erupting loop system in the EUV observations coincided with the first X-ray flare peak, and led to a plasma pile-up of the white-light CME core material. The characterized CME core then underwent a strong jerk in its motion, as the early acceleration increased abruptly, simultaneous with the second X-ray flare peak. The overall system expanded into the helmet streamer to become the larger CME structure observed in the LASCO coronagraph images, which later became concave-outward in shape. Theoretical models for the event are discussed in light of these unique observations, and it is concluded that the formation of either a kink-unstable or torus-unstable flux rope may be the likeliest scenario. **8 March 2011**

## **Improved methods for determining the kinematics of coronal mass ejections and coronal waves**

J. P. **Byrne**, D. M. Long, P. T. Gallagher, D. S. Bloomfield, S. A. Maloney, R. T. J. McAteer, H. Morgan, S. R. Habbal

E-print, July **2013**; A&A 557, A102 (2013)

<http://arxiv.org/pdf/1307.8155v1.pdf>

**Context:** The study of solar eruptive events and associated phenomena is of great importance in the context of solar and heliophysics. Coronal mass ejections (CMEs) and coronal waves are energetic manifestations of the restructuring of the solar magnetic field and mass motion of the plasma. Characterising this motion is vital for deriving the dynamics of these events and thus understanding the physics driving their initiation and propagation. The development and use of appropriate methods for measuring event kinematics is therefore imperative.

**Aims:** Traditional approaches to the study of CME and coronal wave kinematics do not return wholly accurate nor robust estimates of the true event kinematics and associated uncertainties. We highlight the drawbacks of these approaches, and demonstrate improved methods for accurate and reliable determination of the kinematics.

**Methods:** The Savitzky-Golay filter is demonstrated as a more appropriate fitting technique for CME and coronal wave studies, and a residual resampling bootstrap technique is demonstrated as a statistically rigorous method for the determination of kinematic error estimates and goodness-of-fit tests.

**Results:** It is shown that the scatter on distance-time measurements of small sample size can significantly limit the ability to derive accurate and reliable kinematics. This may be overcome by (i) increasing measurement precision and sampling cadence, and (ii) applying robust methods for deriving the kinematics and reliably determining their associated uncertainties. If a priori knowledge exists and a pre-determined model form for the kinematics is available (or indeed any justified fitting-form to be tested against the data), then its precision can be examined using a bootstrapping technique to determine the confidence interval associated with the model/fitting parameters.

**Conclusions:** Improved methods for determining the kinematics of CMEs and coronal waves are demonstrated to great effect, overcoming many issues highlighted in traditional numerical differencing and error propagation techniques.

**2000 January 2, 2007 December 7, 2010 August 14. 2011 January 12**

## **AUTOMATIC DETECTION AND TRACKING OF CORONAL MASS EJECTIONS. II. MULTISCALE FILTERING OF CORONAGRAPH IMAGES**

Jason P. **Byrne**<sup>1</sup>, Huw Morgan<sup>1,2</sup>, Shadia R. Habbal<sup>1</sup>, and Peter T. Gallagher

**2012 ApJ 752 145, File**

Studying coronal mass ejections (CMEs) in coronagraph data can be challenging due to their diffuse structure and transient nature, and user-specific biases may be introduced through visual inspection of the images. The large amount of data available from the Solar and Heliospheric Observatory (SOHO), Solar TERrestrial RELations Observatory (STEREO), and future coronagraph missions also makes manual cataloging of CMEs tedious, and so a robust method of detection and analysis is required. This has led to the development of automated CME detection and cataloging packages such as CACTus, SEEDS, and ARTEMIS. Here, we present the development of a new CORIMP (coronal image processing) CME detection and tracking technique that overcomes many of the drawbacks of current catalogs. It works by first employing the dynamic CME separation technique outlined in a companion paper, and then characterizing CME structure via a multiscale edge-detection algorithm. The detections are chained through time to determine the CME kinematics and morphological changes as it propagates across the plane of sky. The effectiveness of the method is demonstrated by its application to a selection of SOHO/LASCO and STEREO/SECCHI images, as well as to synthetic coronagraph images created from a model corona with a variety of CMEs. The algorithms described in this article are being applied to the whole LASCO and SECCHI data sets, and a catalog of results will soon be available to the public.

## **The Kinematics and Morphology of Solar Coronal Mass Ejections**

**Review**

J. P. **Byrne**

A thesis, **2012, File**

In this thesis the implementation of multiscale image processing techniques to identify and track the CME front through coronagraph images is detailed. An ellipse characterisation of the CME front is used to determine the CME kinematics and morphology with increased precision as compared to techniques used in current CME catalogues, and e\_orts are underway to automate this procedure for applying to a large number of CME observations for future analysis. It was found that CMEs do not simply undergo constant acceleration, but rather tend to show a higher acceleration early in



their propagation. The angular width of CMEs was also found to change as they propagate, normally increasing with height from the Sun. However these results were derived from plane-of-sky measurements with no correction for how the true CME geometry and direction affect the kinematics and morphology observed. With the advent of the unique dual perspectives of the STEREO spacecraft, the multiscale methods were extended to an elliptical tiepointing technique in order to reconstruct the front of a CME in three dimensions. Applying this technique to the Earth-directed CME of 12 December 2008 allowed an accurate determination of its true kinematics and morphology, and the CME was found to undergo early acceleration, non-radial motion, angular width expansion, and aerodynamic drag in the solar wind as it propagated towards Earth. This study and its conclusions are of vital importance to the fields of space weather monitoring and forecasting.

## The kinematics of coronal mass ejections using multiscale methods

J. P. **Byrne**, P. T. Gallagher<sup>1</sup>, R. T. J. McAteer<sup>1</sup>, and C. A. Young<sup>2</sup>

A&A 495, 325–334 (2009), DOI: [10.1051/0004-6361:200809811](https://doi.org/10.1051/0004-6361:200809811); **File**

<https://sci-hub.ru/10.1051/0004-6361:200809811>

**Aims.** The diffuse morphology and transient nature of coronal mass ejections (CMEs) make them difficult to identify and track using traditional image processing techniques. We apply multiscale methods to enhance the visibility of the faint CME front. This enables an ellipse characterisation to objectively study the changing morphology and kinematics of a sample of events imaged by the Large Angle Spectrometric Coronagraph (LASCO) onboard the Solar and Heliospheric Observatory (SOHO) and the Sun Earth Connection Coronal and Heliospheric Investigation (SECCHI) onboard the Solar Terrestrial Relations Observatory (STEREO). The accuracy of these methods allows us to test the CMEs for non-constant acceleration and expansion.

**Methods.** We exploit the multiscale nature of CMEs to extract structure with a multiscale decomposition, akin to a Canny edge detector. Spatio-temporal filtering highlights the CME front as it propagates in time. We apply an ellipse parameterisation of the front to extract the kinematics (height, velocity, acceleration) and changing morphology (width, orientation).

**Results.** The kinematic evolution of the CMEs discussed in this paper have been shown to differ from existing catalogues. These catalogues are based upon running-difference techniques that can lead to over-estimating CME heights. Our resulting kinematic curves are not well-fitted with the constant acceleration model. It is shown that some events have high acceleration below  $\sim 5 R_{\odot}$ . Furthermore, we find that the CME angular widths measured by these catalogues are over-estimated, and indeed for some events our analysis shows non-constant CME expansion across the plane-of-sky.

## First Simultaneous Views of the Axial and Lateral Perspectives of a Coronal Mass Ejection

I. **Cabello**, H. Cremades, L. Balmaceda, I. Dohmen

Solar Phys. Volume 291, [Issue 6](#), pp 1799-1817 **2016**

**File**

<http://arxiv.org/pdf/1607.07001v1.pdf>

The different appearances exhibited by coronal mass ejections (CMEs) are believed to be in part the result of different orientations of their main axis of symmetry, consistent with a flux-rope configuration. There are observational reports of CMEs seen along their main axis (axial perspective) and perpendicular to it (lateral perspective), but no simultaneous observations of both perspectives from the same CME have been reported to date. The stereoscopic views of the telescopes onboard the Solar-Terrestrial Relations Observatory (STEREO) twin spacecraft, in combination with the views from the Solar and Heliospheric Observatory (SOHO) and the Solar Dynamics Observatory (SDO), allow us to study the axial and lateral perspectives of a CME simultaneously for the first time. In addition, this study shows that the lateral angular extent ( $L$ ) increases linearly with time, while the angular extent of the axial perspective ( $D$ ) presents this behavior only from the low corona to  $\approx 5 R_{\odot}$ , where it slows down. The ratio  $L/D \approx 1.6$  obtained here as the average over several points in time is consistent with measurements of  $L$  and  $D$  previously performed on events exhibiting only one of the perspectives from the single vantage point provided by SOHO. **15 February 2011, 8 March 2011, 5 March 2013, 28 March 2013**

## A fast-filament eruption observed in the $H\alpha$ spectral line. I. Imaging spectroscopy diagnostic

**Denis P. Cabezas**, [Kiyoshi Ichimoto](#), [Ayumi Asai](#), [Satoru UeNo](#), [Satoshi Morita](#), [Ken-ichi Otsuji](#), [Kazunari Shibata](#)

A&A 690, A172 **2024**

<https://arxiv.org/pdf/2406.20020>

**Context.** Solar filament eruptions usually appear to occur in association with the sudden explosive release of magnetic energy accumulated in long-lived arched magnetic structures. It is the released energy that occasionally drives fast-filament eruptions that can be source regions of coronal mass ejections. **Aim.** The goal of this paper is to investigate the dynamic processes of a fast-filament eruption by using unprecedented high-resolution full-disk  $H\alpha$  imaging spectroscopy observations. **Methods.** The whole process of the eruption was captured in a wide spectral window of the  $H\alpha$  line ( $\pm 9.0 \text{ \AA}$ ). Applying the "cloud model" and obtaining two dimensional optical thickness spectra we derive the Doppler velocity, the true eruption profiles (height, velocity, and acceleration), and the trajectory of the filament eruption in 3D space. **Results.** The Doppler velocity maps show that the filament was predominantly blue-shifted. During the main and final process of the eruption, strongly blue-shifted materials are manifested traveling with velocities exceeding 250 km/s. The spectral analysis further revealed that the erupting filament is made of multiple components, some of which were Doppler-shifted approximately to  $-300 \text{ km/s}$ . It is found that the filament eruption attains a maximum true velocity and acceleration of about 600 km/s and  $2.5 \text{ km/s}^2$ , respectively, and its propagation direction deviates from the radial direction. On the other hand, downflows manifested as red-shifted plasma close to the

footpoints of the erupting filament move with velocities 45–125 km/s. We interpret these red-shifted signatures as draining material, and therefore mass loss of the filament that has implications for the dynamic and the acceleration process of the eruption. Furthermore, we have estimated the total mass of the H $\alpha$  filament resulting in  $\sim 5.4 \times 10^{15}$ g.  
**2017 April 23**

### **"Dandelion" Filament Eruption and Coronal Waves Associated with a Solar Flare on 2011 February 16**

Denis P. [Cabezas](#), Lurdes M. Martínez, Yovanny J. Buleje, [Mutsumi Ishitsuka](#), [José K. Ishitsuka](#), [Satoshi Morita](#), [Ayumi Asai](#), [Satoru UeNo](#), [Takako T. Ishii](#), [Reizaburo Kitai](#), [Shinsuke Takasao](#), [Yusuke Yoshinaga](#), [Kenichi Otsuji](#), [Kazunari Shibata](#)

ApJ **2017**

<https://arxiv.org/pdf/1701.00308v1.pdf>

Coronal disturbances associated with solar flares, such as H $\alpha$  Moreton waves, X-ray waves, and extreme ultraviolet (EUV) coronal waves are discussed herein in relation to magnetohydrodynamics fast-mode waves or shocks in the corona. To understand the mechanism of coronal disturbances, full-disk solar observations with high spatial and temporal resolution over multiple wavelengths are of crucial importance. We observed a filament eruption, whose shape is like a "dandelion", associated with the M1.6 flare that occurred on **2011 February 16** in the H $\alpha$  images taken by the Flare Monitoring Telescope at Ica University, Peru. We derive the three-dimensional velocity field of the erupting filament. We also identify winking filaments that are located far from the flare site in the H $\alpha$  images, whereas no Moreton wave is observed. By comparing the temporal evolution of the winking filaments with those of the coronal wave seen in the extreme ultraviolet images data taken by the Atmospheric Imaging Assembly on board the *Solar Dynamics Observatory* and by the Extreme Ultraviolet Imager on board the *Solar Terrestrial Relations Observatory-Ahead*, we confirm that the winking filaments were activated by the EUV coronal wave.

### **Observational study of intermittent solar jets: p-mode modulation**

[Qiuzhuo Cai](#), [Guiping Ruan](#), [Chenxi Zheng](#), [Brigitte Schmieder](#), [Jinhan Guo](#), [Yao Chen](#), [Jiangtao Su](#), [Yang Liu](#), [Jihong Liu](#), [Wenda Cao](#)

A&A 682, A183 (2024)

<https://arxiv.org/pdf/2312.03571.pdf>

<https://www.aanda.org/articles/aa/pdf/2024/02/aa48053-23.pdf>

Aims. Recurring jets are observed in the solar atmosphere, which can erupt intermittently. By the observation of intermittent jets, we want to understand the causes of periodic eruption characteristics. Methods. We report intermittent jets observed by the GST. The analysis was aided by 1400 Å and 2796 Å data from IRIS. These observational instruments allowed us to analyze the temporal characteristics of jet events. Results. The jet continued for up to 4 hours. The time distance diagram shows that the peak of the jet has obviously periodic eruption characteristics (5 minutes) during 18:00 UT–18:50 UT. We also found periodic brightening phenomenon (5 minutes) during jets bursts in the observed bands in the Transition Region (1400 Å and 2796 Å), which may be a response to intermittent jets in the upper solar atmosphere. The time lag is 3 minutes. Evolutionary images in the TiO band revealed the horizontal movement of granulation at the location of jet. Compared to the quiet region of the Sun, we found that the footpoint of the jet is enhanced at the center of the H  $\alpha$  spectral line profile, with no significant changes in the line wings. This suggests the presence of prolonged heating at the footpoint of the jet. In the mixed-polarity magnetic field region of the jet, we observed magnetic flux emergence, cancellation, and shear indicating possible intermittent magnetic reconnection. That is confirmed by the NLFFF model reconstructed using the magneto-friction method. Conclusions. The multi-wavelength analysis indicates that the events we studied were triggered by magnetic reconnection caused by mixed-polarity magnetic fields. We suggest that the horizontal motion of the granulation in the photosphere drives the magnetic reconnection, which is modulated by p-mode oscillations. **August 6, 2016,**

### **Multiband Study of a Bidirectional Jet Occurred in the Upper Chromosphere**

Qiangwei Cai, [Chengcai Shen](#), [Lei Ni](#), [Katharine K. Reeves](#), [Kaifeng Kang](#), [Jun Lin](#)

JGR Volume 124, Issue 12 December 2019 Pages 9824–9846

<https://agupubs.onlinelibrary.wiley.com/doi/pdf/10.1029/2019JA027017>

<https://sci-hub.ru/10.1029/2019JA027017>

We present a study of a jet observed by the Solar Dynamics Observatory (SDO) and the Interface Region Imaging Spectrograph (IRIS), which provide high spatial-temporal resolution observational data of (extreme) ultraviolet images, spectra, and magnetograms. The jet was observed in multiple bands of AIA and manifested clear bidirectional flows in IRIS observations. The emission profiles of the Si IV 1402 Å line of the jet exhibited non-Gaussian features and double-peaked spectra, with the Doppler velocity and the nonthermal velocity up to 100 and 160 km s<sup>-1</sup>, respectively. The plasma flows of the jet projected on the sky plane and in the line of sight (LOS) are the typical observational evidence of magnetic reconnection. The EM loci curves indicated that the plasma contains multi-temperature components. The result deduced from the DEM method and changes in intensity of several spectral lines imply that the temperature of the plasma in the jet is heated to at least 10<sup>5.6</sup> K. The electron density is about 10<sup>11</sup> cm<sup>-3</sup> according to the intensity ratios of the O IV 1399.77/1401.16 Å doublet and Si IV 1402.77/O IV 1401.16 Å lines. Via different approaches, we reached the conclusion that the jet occurred in the upper chromosphere. Investigating the magnetograms

in the period when the jet appeared, we suggest that the jet results from the magnetic reconnection between the moving magnetic structure and the magnetic field nearby. **12 August 2014**

### **Comprehensive Characterization of Solar Eruptions With Remote and In-Situ Observations, and Modeling: The Major Solar Events on 4 November 2015**

Iver H. [Cairns](#), [Kamen A. Kozarev](#), [Nariaki V. Nitta](#), [Neus Agueda](#), [Markus Battarbee](#), [Eoin P. Carley](#), [Nina Dresing](#), [Raul Gomez-Herrero](#), [Karl-Ludwig Klein](#), [David Lario](#), [Jens Pomoell](#), [Carolina Salas-Matamoros](#), [Astrid M. Veronig](#), [Bo Li](#), [Patrick McCauley](#)

Solar Phys. **295**, Article number: 32 **2020** **File**

<https://arxiv.org/pdf/1910.03319.pdf>

<https://link.springer.com/content/pdf/10.1007/s11207-020-1591-7.pdf>

Solar energetic particles (SEPs) are an important product of solar activity. They are connected to solar active regions and flares, coronal mass ejections (CMEs), EUV waves, shocks, Type II and III radio emissions, and X-ray bursts. These phenomena are major probes of the partition of energy in solar eruptions, as well as for the organization, dynamics, and relaxation of coronal and interplanetary magnetic fields. Many of these phenomena cause terrestrial space weather, posing multiple hazards for humans and their technology from space to the ground. Since particular flares, shocks, CMEs, and EUV waves produce SEP events but others do not, since propagation effects from the low corona to 1 AU appear important for some events but not others, and since Type II and III radio emissions and X-ray bursts are sometimes produced by energetic particles leaving these acceleration sites, it is necessary to study the whole system with a multi-frequency and multi-instrument perspective that combines both in-situ and remote observations with detailed modelling of phenomena. This article demonstrates this comprehensive approach, and shows its necessity, by analysing a trio of unusual and striking solar eruptions, radio and X-ray bursts, and SEP events that occurred on **4 November 2015**. These events show both strong similarities and differences from standard events and each other, despite having very similar interplanetary conditions and only two are sites and CME genesis regions. They are therefore major targets for further in-depth observational studies, and for testing both existing and new theories and models. Based on the very limited modelling available we identify the aspects that are and are not understood, and we discuss ideas that may lead to improved understanding of the SEP, radio, and space-weather events.

### **YOHKOH SXT FULL-RESOLUTION OBSERVATIONS OF SIGMOIDS: STRUCTURE, FORMATION, AND ERUPTION**

Richard C. [Canfield](#),<sup>1</sup> Maria D. Kazachenko,<sup>1</sup> Loren W. Acton,<sup>1</sup> D. H. Mackay,<sup>2</sup> Ji Son,<sup>3</sup> and Tanya L. Freeman<sup>4</sup>

The Astrophysical Journal, 671: L81–L84, 2007

<http://www.journals.uchicago.edu/doi/pdf/10.1086/524729>

We study the structure of 107 bright sigmoids using full-resolution (2.5\_ pixels) images from the *Yohkoh* Soft X-Ray Telescope (SXT) obtained between 1991 December and 2001 December. We find that none of these sigmoids are made of single loops of S or inverse-S shape; all comprise a pattern of multiple loops. We also find that all S-shaped sigmoids are made of right-bearing loops and all inverse-S-shaped sigmoids of left-bearing loops, without exception. We co-align the SXT images with Kitt Peak magnetograms to determine the magnetic field directions in each sigmoid. We use a potential-field source surface model to determine the direction of the overlying magnetic field. We find that sigmoids for which the relative orientation of these two fields has a parallel component outnumber antiparallel ones by more than an order of magnitude. We find that the number of sigmoids per active region varies with the solar cycle in a manner that is consistent with this finding. Finally, those few sigmoids that are antiparallel erupt roughly twice as often as those that are parallel. We briefly discuss the implications of these results in terms of formation and eruption mechanisms of flux tubes and sigmoids.

### **EVIDENCE FOR A PRE-ERUPTIVE TWISTED FLUX ROPE USING THE THEMIS VECTOR MAGNETOGRAPH**

A. [Canou](#), T. Amari, V. Bommier, B. Schmieder, G. Aulanier, and H. Li

ApJ 693 L27-L30, **2009**

<http://www.iop.org/EJ/abstract/1538-4357/693/1/L27>

Although there is evidence that twisted structures form during large-scale eruptive events, it is not yet clear whether these exist in the pre-eruptive phase as twisted flux ropes (TFRs) in equilibrium. This question has become a major issue since several theoretical mechanisms can lead to the formation of TFRs. These models consider either the evolution of a coronal configuration driven by photospheric changes or the emergence of TFR from the convection zone. We consider as a target for addressing this issue the active region NOAA AR 10808 known at the origin of several large-scale eruptive phenomena, and associated with the emergence of a  $\delta$ -spot. Using the THEMIS vector magnetogram as photospheric boundary conditions for our nonlinear force-free reconstruction model of the low corona and without any other assumption, we show that the resulting pre-eruptive configuration exhibits a TFR above the neutral line of the emerging  $\delta$ -spot. In addition, the free magnetic energy of this configuration could even be large enough to explain such resulting large-scale eruptive events. **2005 September 13**

## The Deflection of the Cartwheel CME: ForeCAT Results

Luisa [Capannolo](#)<sup>1</sup>, Merav Opher<sup>1</sup>, Christina Kay<sup>2</sup>, and Enrico Landi<sup>3</sup>

2017 ApJ 839 37 DOI 10.3847/1538-4357/aa6a16

<http://iopscience.iop.org/sci-hub.cc/0004-637X/839/1/37/>

[sci-hub.ru/10.3847/1538-4357/aa6a16](http://sci-hub.ru/10.3847/1538-4357/aa6a16)

We analyze the Cartwheel coronal mass ejection's (CME; **2008 April 9**) trajectory in the low corona with the ForeCAT model. This complex event presented a significant rotation in the low corona and a reversal in its original latitude direction. We successfully reproduce the observed CME's trajectory (latitude and longitude deflection) and speed. Through a test, we are able to constrain the CME's mass to  $(2.3-3.0) \times 10^{14}$  g and the CME's initial shape. We are able to constrain the expansion of the CME as well: the angular width linearly increases until  $2.1^\circ$ , and is constant afterward. In order to match the observed latitude, we include a non-radial initial speed of  $-42 \text{ km s}^{-1}$ . Despite allowing the CME to rotate in the model, the magnetic forces of the solar background are not able to reproduce the observed rotation. We suggest that the complex reversal in latitude and the significant rotation of the Cartwheel CME can be justified with an asymmetrical reconnection event that ejected the CME non-radially and also initiated its rotation.

## Internal magnetic field structures observed by PSP/WISPR in a filament related coronal mass ejection

[G.M. Cappello](#), [M. Temmer](#), [A. Vourlidis](#), [C. Braga](#), [P.C. Liewer](#), [J. Qiu](#), [G. Stenborg](#), [A. Kouloumvakos](#), [A.M. Veronig](#), [V. Bothmer](#)

A&A 688, A162 2024

<https://arxiv.org/pdf/2402.14682.pdf>

<https://www.aanda.org/articles/aa/pdf/2024/08/aa49613-24.pdf>

We track and investigate from white-light data taken with the Wide-field Instrument for Solar PRobe (WISPR) aboard Parker Solar Probe (PSP), localized density enhancements, reflecting small-scale magnetic structures belonging to a filament-related coronal mass ejection (CME). We aim to investigate the 3D location, morphology, and evolution of the internal magnetic fine structures of CMEs. Specifically, we ask: what is their relationship with the filament/source region and the flux rope? The fast tangential motion of the PSP spacecraft during its perihelion permits viewing the same event from multiple angles in short times relative to the event's evolution. Hence, we can derive the three-dimensional information of selected CME features from a single spacecraft using triangulation techniques. We group small-scale structures with roughly similar speeds, longitude and latitude, into three distinct morphological groups. We find twisted magnetic field patterns close to the eastern leg of the CME that may be related to 'horns' outlining the edges of the flux-rope cavity. Aligned thread-like bundles are identified close to the western leg. They may be related to confined density enhancements evolving during the filament eruption. High density blob-like features (magnetic islands) are widely spread in longitude ( $\sim 40^\circ$ ) close to the flanks and rear part of the CME. We demonstrate that CME flux ropes may comprise different morphological groups with a cluster behavior, apart from the blobs which instead span a wide range of longitudes. This may hint either to the three-dimensionality of the post-CME current sheet (CS) or to the influence of the ambient corona in the evolutionary behavior of the CS. Importantly, we show that the global appearance of the CME can be very different in WISPR (0.11--0.16 AU) and instruments near 1 AU because of shorter line-of-sight integration of WISPR. **8 Dec 2022**

## Unveiling the journey of a highly inclined CME

### Insights from the **March 13, 2012**, event with $110^\circ$ longitudinal separation

F. [Carcaboso](#)<sup>1,2,3</sup>, M. [Dumbović](#)<sup>4</sup>, C. [Kay](#)<sup>2,3</sup>, D. [Lario](#)<sup>2</sup>, L. K. [Jian](#)<sup>2</sup>, L. B. [Wilson III](#)<sup>2</sup>, R. [Gómez-Herrero](#)<sup>5</sup>, M. [Temmer](#)<sup>6</sup>, S. G. [Heinemann](#)<sup>7</sup>, T. [Nieves-Chinchilla](#)<sup>2</sup> and A. M. [Veronig](#)<sup>6,8</sup>

A&A, 684, A90 (2024)

<https://doi.org/10.1051/0004-6361/202347083>

<https://arxiv.org/pdf/2401.17501.pdf>

<https://www.aanda.org/articles/aa/pdf/2024/04/aa47083-23.pdf>

Context. A fast ( $\sim 2000 \text{ km s}^{-1}$ ) and wide ( $> 110^\circ$ ) coronal mass ejection (CME) erupted from the Sun on **March 13, 2012**. Its interplanetary counterpart was detected in situ two days later by STEREO-A and near-Earth spacecraft, such as ACE, Wind, and Cluster. We suggest that at 1 au the CME extended at least  $110^\circ$  in longitude, with Earth crossing its east flank and STEREO-A crossing its west flank. Despite their separation, measurements from both positions showed very similar in situ CME signatures. The solar source region where the CME erupted was surrounded by three coronal holes (CHs). Their locations with respect to the CME launch site were east (negative polarity), southwest (positive polarity) and west (positive polarity). The solar magnetic field polarity of the area covered by each CH matches that observed at 1 au in situ. Suprathermal electrons at each location showed mixed signatures with only some intervals presenting clear counterstreaming flows as the CME transits both locations. The strahl population coming from the shortest magnetic connection of the structure to the Sun showed more intensity.

Aims. The aim of this work is to understand the propagation and evolution of the CME and its interaction with the surrounding CHs, to explain the similarities and differences between the observations at each spacecraft, and report what one of the most longitudinal expanded CME structures measured in situ would be.

Methods. Known properties of the large-scale structures from a variety of catalogues and previous studies were used to have a better overview of this particular event. In addition, multipoint observations were used to reconstruct the 3D geometry of the CME and determine the context of the solar and heliospheric conditions before the CME eruption and

during its propagation. The graduated cylindrical shell model (GCS) was used to reproduce the orientation, size and speed of the structure with a simple geometry. Also, the Drag-Based Model (DBM) was utilised to understand the conditions of the interplanetary medium better in terms of the drag undergone by the structure while propagating in different directions. Finally, a comparative analysis of the different regions of the structure through the different observatories was carried out in order to directly compare the in situ plasma and magnetic field properties at each location.

Results. The study presents important findings regarding the in situ measured CME on March 15, 2012, detected at a longitudinal separation of  $110^\circ$  in the ecliptic plane despite its initial inclination being around  $45^\circ$  when erupted (March 13). This suggests that the CME may have deformed and/or rotated, allowing it to be observed near its legs with spacecraft at a separation angle greater than  $100^\circ$ . The CME structure interacted with high-speed streams generated by the surrounding CHs. The piled-up plasma in the sheath region exhibited an unexpected correlation in magnetic field strength despite the large separation in longitude. In situ observations reveal that at both locations there was a flank encounter – where the spacecraft crossed the first part of the CME – then encountered ambient solar wind, and finally passed near the legs of the structure.

Conclusions. A scenario covering all evidence is proposed for both locations with a general view of the whole structure and solar wind conditions. Also, the study shows the necessity of having multipoint observations of large-scale structures in the heliosphere.

## Radio Observations of Coronal Mass Ejection Initiation and Development in the Low Solar Corona Review

[Eoin P. Carley](#), [Nicole Vilmer](#) and [Angelos Vourlidas](#)

Front. Astron. Space Sci. 7:551558. 2020 File

<https://www.frontiersin.org/articles/10.3389/fspas.2020.551558/full>

<https://sci-hub.ru/https://www.frontiersin.org/articles/10.3389/fspas.2020.551558/full>

Coronal mass ejections (CMEs) are large eruptions of plasma and magnetic field from the low solar corona into the heliosphere. These eruptions are often associated with energetic electrons that produce various kinds of radio emission. However, there is ongoing investigation into exactly where, when, and how the electron acceleration occurs during flaring and eruption, and how the associated radio emission can be exploited as a diagnostic of both particle acceleration and CME eruptive physics. Here, we review past and present developments in radio observations of flaring and eruption, from the destabilization of flux ropes to the development of a CME and the eventual driving of shocks in the corona. We concentrate primarily on the progress made in CME radio physics in the past two decades and show how radio imaging spectroscopy provides the ability to diagnose the locations and kinds of electron acceleration during eruption, which provides insight into CME eruptive models in the early stages of their evolution ( $\ll 10 R_\odot$ ). We finally discuss how new instrumentation in the radio domain will pave the way for a deeper understanding of CME physics in the near future. 20 Apr 1998, 2011-01-27, 2014-03-18, 2014-09-01, 2015 May 9, 2017 September 10

## Estimation of a Coronal Mass Ejection Magnetic Field Strength using Radio Observations of Gyrosynchrotron Radiation

[Eoin P. Carley](#), [Nicole Vilmer](#), [Paulo J. A. Simões](#), [Brían Ó Ferraigh](#)

A&A 608, A137 2017

<https://arxiv.org/pdf/1709.05184.pdf>

Coronal mass ejections (CMEs) are large eruptions of plasma and magnetic field from the low solar corona into interplanetary space. These eruptions are often associated with the acceleration of energetic electrons which produce various sources of high intensity plasma emission. In relatively rare cases, the energetic electrons may also produce gyrosynchrotron emission from within the CME itself, allowing for a diagnostic of the CME magnetic field strength. Such a magnetic field diagnostic is important for evaluating the total magnetic energy content of the CME, which is ultimately what drives the eruption. Here we report on an unusually large source of gyrosynchrotron radiation in the form of a type IV radio burst associated with a CME occurring on **2014-September-01**, observed using instrumentation from the Nan\c{c}ay Radio Astronomy Facility. A combination of spectral flux density measurements from the Nan\c{c}ay instruments and the Radio Solar Telescope Network (RSTN) from 300MHz to 5 GHz reveals a gyrosynchrotron spectrum with a peak flux density at  $>1$  GHz. Using this radio analysis, a model for gyrosynchrotron radiation, a non-thermal electron density diagnostic using the Fermi Gamma Ray Burst Monitor (GBM) and images of the eruption from the GOES Soft X-ray Imager (SXI), we are able to calculate both the magnetic field strength and the properties of the X-ray and radio emitting energetic electrons within the CME. We find the radio emission is produced by non-thermal electrons of energies  $>1$ MeV with a spectral index of  $\delta \sim 3$  in a CME magnetic field of 4.4 G at a height of  $1.3 R_\odot$ , while the X-ray emission is produced from a similar distribution of electrons but with much lower energies on the order of 10 keV. We conclude by comparing X-ray and radio-emitting electron distributions and how such an analysis can be used to define the plasma properties of a CME.

CESRA Highlight #1701 Jan 2018

<http://cesra.net/?p=1701>

## Radio Diagnostics of electron acceleration sites during the eruption of a flux rope in the solar corona

[Eoin Carley](#)\*<sup>1,2</sup>, [Nicole Vilmer](#)<sup>3</sup>, and [Peter Gallagher](#)<sup>2</sup>

2016

<http://arxiv.org/pdf/1609.01463v1.pdf>

Electron acceleration in the solar corona is often associated with flares and the eruption of twisted magnetic structures known as flux ropes. However, the locations and mechanisms of such particle acceleration during the flare and eruption are still subject to much investigation. Observing the exact sites of particle acceleration can help confirm how the flare and eruption are initiated and how they evolve. Here we use the Atmospheric Imaging Assembly to analyse a flare and erupting flux rope on **2014-April-18**, while observations from the Nancay Radio Astronomy Facility allows us to diagnose the sites of electron acceleration during the eruption. Our analysis shows evidence for a pre-formed flux rope which slowly rises and becomes destabilised at the time of a C-class flare, plasma jet and the escape of  $>75$  keV electrons from rope center into the corona. As the eruption proceeds, continued acceleration of electrons with energies of  $\sim 5$  keV occurs above the flux rope for a period over 5 minutes. At flare peak, one site of electron acceleration is located close to the flare site while another is driven by the erupting flux rope into the corona at speeds of up to 400 km/s. Energetic electrons then fill the erupting volume, eventually allowing the flux rope legs to be clearly imaged from radio sources at 150-445MHz. Following the analysis of Joshi et al. (2015), we conclude that the sites of energetic electrons are consistent with flux rope eruption via a tether-cutting or flux cancellation scenario inside a magnetic fan-spine structure. In total, our radio observations allow us to better understand the evolution of a flux rope eruption and its associated electron acceleration sites, from eruption initiation to propagation into the corona.

See CESRA 2016 p.39

[http://cesra2016.sciencesconf.org/conference/cesra2016/pages/CESRA2016\\_prog\\_abs\\_book\\_v3.pdf](http://cesra2016.sciencesconf.org/conference/cesra2016/pages/CESRA2016_prog_abs_book_v3.pdf)

### **Quasiperiodic acceleration of electrons by a plasmoid-driven shock in the solar atmosphere**

Eoin P. **Carley**, David M. Long, Jason P. Byrne, Pietro Zucca, D. Shaun Bloomfield, Joseph McCauley and Peter T. Gallagher

E-print, Oct **2013**; Nature Physics (**2013**) doi:10.1038/nphys2767

<https://sci-hub.ru/10.1038/nphys2767>

Cosmic rays and solar energetic particles may be accelerated to relativistic energies by shock waves in astrophysical plasmas. On the Sun, shocks and particle acceleration are often associated with the eruption of magnetized plasmoids, called coronal mass ejections (CMEs). However, the physical relationship between CMEs and shock particle acceleration is not well understood. Here, we use extreme ultraviolet, radio and white-light imaging of a solar eruptive event on **22 September 2011** to show that a CME-induced shock (Alfvén Mach number  $2.4^{+0.7}_{-0.8}$ ) was coincident with a coronal wave and an intense metric radio burst generated by intermittent acceleration of electrons to kinetic energies of  $2\text{--}46$  keV ( $0.1\text{--}0.4c$ ). Our observations show that plasmoid-driven quasiperpendicular shocks are capable of producing quasiperiodic acceleration of electrons, an effect consistent with a turbulent or rippled plasma shock surface.

### **Coronal Mass Ejection Mass, Energy, and Force Estimates Using STEREO**

Eoin P. **Carley**, R.T. James McAteer, Peter T. Gallagher

E-print, Apr **2012**, **2012 ApJ** 752 36, **File**

Understanding coronal mass ejection (CME) energetics and dynamics has been a long-standing problem, and although previous observational estimates have been made, such studies have been hindered by large uncertainties in CME mass. Here, the two vantage points of the Solar Terrestrial Relations Observatory (STEREO) COR1 and COR2 coronagraphs were used to accurately estimate the mass of the **2008 December 12** CME. Acceleration estimates derived from the position of the CME front in 3-D were combined with the mass estimates to calculate the magnitude of the kinetic energy and driving force at different stages of the CME evolution. The CME asymptotically approaches a mass of  $3.4^{+1.0}_{-1.0} \times 10^{15}$  g beyond  $\sim 10 R_{\text{sun}}$ . The kinetic energy shows an initial rise towards  $6.3^{+3.7}_{-3.7} \times 10^{29}$  erg at  $\sim 3 R_{\text{sun}}$ , beyond which it rises steadily to  $4.2^{+2.5}_{-2.5} \times 10^{30}$  erg at  $\sim 18 R_{\text{sun}}$ . The dynamics are described by an early phase of strong acceleration, dominated by a force of peak magnitude of  $3.4^{+2.2}_{-2.2} \times 10^{14}$  N at  $\sim 3 R_{\text{sun}}$ , after which a force of  $3.8^{+5.4}_{-5.4} \times 10^{13}$  N takes affect between  $\sim 7\text{--}18 R_{\text{sun}}$ . These results are consistent with magnetic (Lorentz) forces acting at heliocentric distances of  $<7 R_{\text{sun}}$ , while solar wind drag forces dominate at larger distances ( $>7 R_{\text{sun}}$ ).

### **Investigating the Dynamics and Density Evolution of Returning Plasma Blobs from the **2011 June 7** Eruption**

Jack **Carlyle**<sup>1,2</sup>, David R. Williams<sup>1</sup>, Lidia van Driel-Gesztelyi<sup>1,3,4</sup>, Davina Innes<sup>2</sup>, Andrew Hillier<sup>5</sup>, and Sarah Matthew

**2014 ApJ** 782 87

This work examines in-falling matter following an enormous coronal mass ejection on **2011 June 7**. The material formed discrete concentrations, or blobs, in the corona and fell back to the surface, appearing as dark clouds against the bright corona. In this work we examined the density and dynamic evolution of these blobs in order to formally assess the intriguing morphology displayed throughout their descent. The blobs were studied in five wavelengths (94, 131, 171, 193, and 211 Å) using the Solar Dynamics Observatory Atmospheric Imaging Assembly, comparing background emission to attenuated emission as a function of wavelength to calculate column densities across the descent of four separate blobs. We found the material to have a column density of hydrogen of approximately  $2 \times 10^{19} \text{ cm}^{-2}$ , which is comparable with typical pre-eruption filament column densities. Repeated splitting of the returning material is seen in a

manner consistent with the Rayleigh-Taylor instability. Furthermore, the observed distribution of density and its evolution is also a signature of this instability. By approximating the three-dimensional geometry (with data from STEREO-A), volumetric densities were found to be approximately  $2 \times 10^{-14}$  g cm<sup>-3</sup>, and this, along with observed dominant length scales of the instability, was used to infer a magnetic field of the order 1 G associated with the descending blobs.

### **Magnetic Energy Powers the Corona: How We Can Understand its 3D Storage & Release**

[Amir Caspi](#), [Daniel B. Seaton](#), [Roberto Casini](#), [Cooper Downs](#), [Sarah E. Gibson](#), [Holly Gilbert](#), [Lindsay Glesener](#), [Silvina E. Guidoni](#), [J. Marcus Hughes](#), [David McKenzie](#), [Joseph Plowman](#), [Katharine K. Reeves](#), [Pascal Saint-Hilaire](#), [Albert Y. Shih](#), [Matthew J. West](#)

White paper to the Decadal Survey for Solar and Space Physics (Heliophysics) 2024-2033 **2023**

<https://arxiv.org/pdf/2305.17146.pdf>

The coronal magnetic field is the prime driver behind many as-yet unsolved mysteries: solar eruptions, coronal heating, and the solar wind, to name a few. It is, however, still poorly observed and understood. We highlight key questions related to magnetic energy storage, release, and transport in the solar corona, and their relationship to these important problems. We advocate for new and multi-point co-optimized measurements, sensitive to magnetic field and other plasma parameters, spanning from optical to  $\gamma$ -ray wavelengths, to bring closure to these long-standing and fundamental questions. We discuss how our approach can fully describe the 3D magnetic field, embedded plasma, particle energization, and their joint evolution to achieve these objectives.

### **Radio emission observed in decimetric waves associated with the onset of CMEs**

J.R. [Cecatto](#), A.C. Soares, F.C.R. Fernandes, F.R.H. Madsen, M.C. Andrade, H.S. Sawant

Journal of Atmospheric and Solar-Terrestrial Physics, Volume 67, Issues 17-18, December **2005**, Pages 1674-1679

Since the first observations by Skylab and SMM satellites coronal mass ejections (CME) have been more and more investigated. However, until now their origin and trigger mechanism remain an open question no matter if they are associated to flares or not. Recent observations over a broad spectrum suggest that flare energy is released in regions from where the decimetric emission is coming. Then, investigations of decimetric radio emission observed in association with CME phenomena may give clues to solve the previously mentioned questions. Using the Brazilian solar spectroscope (BSS), observations of solar bursts dynamic spectra with high time (100, 50, 20 ms) and frequency (50–100 channels) resolutions have been carried out daily ( $\sim$ 11–19 UT) within the range of 1000–2500 MHz. A sample of 274 CMEs were recorded by the large angle spectroscopic coronagraph (LASCO) instrument, on board the solar and heliospheric observatory (SOHO) satellite, within 11–19 UT, during the period of 1999–2002. From those, 42 CMEs are associated to BSS data and selected for analysis. It is interesting to note that in about half of the cases only one type of burst radio emission was recorded while in the remaining cases either two or more types were observed. There is a dominance of either continuum and/or pulsations. Here, we describe the association of burst radio emission with the starting time of CME phenomena.

### **Recent insights on CME deflections at low heights**

**Review**

Mariana [Cécere](#), Andrea Costa, Hebe Cremades, and Guillermo Stenborg

Front. Astron. Space Sci. 10 :1260432. **2023**

<https://www.frontiersin.org/articles/10.3389/fspas.2023.1260432/pdf>

It has been shown that the magnetic structures surrounding coronal mass ejection (CME) events play a crucial role in their development and evolution along the first few solar radii. In particular, active regions, coronal holes, pseudostreamers, and helmet streamers are among the main coronal structures involved in the deviation of the trajectory of CMEs from their radial direction. Therefore, comprehensive observational studies along with their theoretical interpretation, aided by numerical simulations of the early evolution of CMEs, are the key ingredients to help determine their 3D trajectory in the interplanetary medium to narrow down the error in the estimation of the time of arrival of geoeffective events. In this mini-review, we compile the last decade of theoretical, numerical, and observational research that has shed light on the causes influencing the early deflection of CMEs away from their otherwise radial trajectory.

### **Evidence for a Magnetic Reconnection Origin of Plasma Outflows along Post-CME Rays**

Jongchul [Chae](#)<sup>1</sup>, Kyuhyoun Cho<sup>1</sup>, Ryun-Young Kwon<sup>2,3</sup>, and Eun-Kyung Lim

**2017** ApJ 841 49

<http://sci-hub.ru/10.3847/1538-4357/aa6d7a>

Bright rays are often observed after coronal mass ejections (CMEs) erupt. These rays are dynamical structures along which plasmas move outward. We investigated the outflows along the post-CME rays observed by the COR2 on board STEREO Behind on **2013 September 21 and 22**. We tracked two CMEs, two ray tips, and seven blobs using the NAVÉ optical flow technique. As a result, we found that the departure times of blobs and ray tips from the optimally chosen starting height coincided with the occurrence times of the corresponding recurrent small flares within 10 minutes. These small flares took place many hours after the major flares. This result supports a magnetic reconnection origin of the outward flows along the post-CME ray and the importance of magnetic islands for understanding the process of magnetic reconnection. The total energy of magnetic reconnection maintaining the outflows for 40 hr is

estimated at  $10^{22}$  erg. Further investigations of plasma outflows along post-CME rays will shed much light on the physical properties of magnetic reconnection occurring in the solar corona.

## **Measuring Solar Doppler Velocities in the He ii 30.38 nm Emission Using the EUV Variability Experiment (EVE)**

P. C. [Chamberlin](#)

Solar Phys. 2016

The EUV Variability Experiment (EVE) onboard the Solar Dynamics Observatory has provided unprecedented measurements of the solar EUV irradiance at high temporal cadence with good spectral resolution and range since May 2010. The main purpose of EVE was to connect the Sun to the Earth by providing measurements of the EUV irradiance as a driver for space weather and Living With a Star studies, but after launch the instrument has demonstrated the significance of its measurements in contributing to studies looking at the sources of solar variability for pure solar physics purposes. This paper expands upon previous findings that EVE can in fact measure wavelength shifts during solar eruptive events and therefore provide Doppler velocities for plasma at all temperatures throughout the solar atmosphere from the chromosphere to hot flaring temperatures. This process is not straightforward as EVE was not designed or optimized for these types of measurements. In this paper we describe the many detailed instrumental characterizations needed to eliminate the optical effects in order to provide an absolute baseline for the Doppler shift studies. An example is given of a solar eruption on **7 September 2011** (SOL2011-09-07), associated with an X1.2 flare, where EVE Doppler analysis shows plasma ejected from the Sun in the He ii 30.38 nm emission at a velocity of almost 120 kms<sup>-1</sup> along the line-of-sight.

## **Filament Eruption Driving EUV Loop Contraction then Expansion above a Stable Filament**

[Ramesh Chandra](#), [Pascal Demoulin](#), [Pooja Devi](#), [Reetika Joshi](#), [Brigitte Schmieder](#)

ApJ 922 227 2021

<https://arxiv.org/pdf/2109.07821.pdf>

<https://doi.org/10.3847/1538-4357/ac2837>

We analyze the observations of EUV loop evolution associated with the filament eruption located at the border of an active region. The event SOL**2013-03-16T14:00** was observed with a large difference of view point by the Solar Dynamics Observatory and Solar Terrestrial Relations Observatory --A spacecraft. The filament height is fitted with the sum of a linear and exponential function. These two phases point to different physical mechanisms such as: tether-cutting reconnection and a magnetic instability. While no X-ray emission is reported, this event presents the classical eruption features like: separation of double ribbons and the growth of flare loops. We report the migration of the southern foot of the erupting filament flux rope due to the interchange reconnection with encountered magnetic loops of a neighbouring AR. Parallel to the erupting filament, a stable filament remains in the core of active region. The specificity of this eruption is that coronal loops, located above the nearly joining ends of the two filaments, first contract in phase, then expand and reach a new stable configuration close to the one present at the eruption onset. Both contraction and expansion phases last around 20 min. The main difference with previous cases is that the PIL bent about 180 deg around the end of the erupting filament because the magnetic configuration is at least tri-polar. These observations are challenging for models which interpreted previous cases of loop contraction within a bipolar configuration. New simulations are required to broaden the complexity of the configurations studied.

## **Solar flares associated coronal mass ejection accompanied with DH type II radio burst in relation with interplanetary magnetic field, geomagnetic storms and cosmic ray intensity**

Harish [Chandra](#), [Beena Bhatt](#)

[New Astronomy Volume 60](#), April 2018, Pages 22-32

[sci-hub.ru/10.1016/j.newast.2017.10.001](http://sci-hub.ru/10.1016/j.newast.2017.10.001)

In this paper, we have selected 114 flare-CME events accompanied with Deca-hectometric (DH) type II radio burst chosen from 1996 to 2008 (i.e., solar cycle 23). Statistical analyses are performed to examine the relationship of flare-CME events accompanied with DH type II radio burst with Interplanetary Magnetic field (IMF), Geomagnetic storms (GSs) and Cosmic Ray Intensity (CRI). The collected sample events are divided into two groups. In the first group, we considered 43 events which lie under the CME span and the second group consists of 71 events which are outside the CME span. Our analysis indicates that flare-CME accompanied with DH type II radio burst is inconsistent with CSHKP flare-CME model. We apply the Chree analysis by the superposed epoch method to both set of data to find the geo-effectiveness. We observed different fluctuations in IMF for arising and decay phase of solar cycle in both the cases. Maximum decrease in Dst during arising and decay phase of solar cycle is different for both the cases. It is noted that when flare lie outside the CME span CRI shows comparatively more variation than the flare lie under the CME span. Furthermore, we found that flare lying under the CME span is more geo effective than the flare outside of CME span. We noticed that the time lag between IMF Peak value and GSs, IMF and CRI is on average one day for both the cases. Also, the time lag between CRI and GSs is on average 0 to 1 day for both the cases. In case flare lie under the CME span we observed high correlation (0.64) between CRI and Dst whereas when flare lie outside the CME span a weak correlation (0.47) exists. Thus, flare position with respect to CME span play a key role for geo-effectiveness of CME.



## **A Study of a long duration B9 flare-CME event and associated piston-driven shock**

R. **Chandra**, P. F. Chen, A. Fulara, A. K. Srivastava, W. Uddin

Adv. Space Research [Volume 61, Issue 2](#), 15 January 2018, Pages 705-714

<https://arxiv.org/pdf/1710.08734.pdf>

We present and discuss here the observations of a small long duration GOES B- class flare associated with a quiescent filament eruption, a global EUV wave and a CME on **2011 May 11**. The event was well observed by the Solar Dynamics Observatory (SDO), GONG H $\{\alpha\}$ , STEREO and HiRAS spectrograph. As the filament erupted, ahead of the filament we observed the propagation of EIT wave fronts, as well as two flare ribbons on both sides of the polarity inversion line (PIL) on the solar surface. The observations show the co-existence of two types of EUV waves, i.e., a fast and a slow one. A type II radio burst with up to the third harmonic component was also associated with this event. The evolution of photospheric magnetic field showed flux emergence and cancellation at the filament site before its eruption.

## **Investigation of recurrent EUV jets from highly dynamic magnetic field region**

Navin **Chandra**, Ramesh Chandra, Yang Guo, Tetsuya Magara, Ivan Zhelyazkov, Young-Jae Moon, Wahab Uddin

Astrophysics and Space Science January 2017, 362:10

<https://link.springer.com/content/pdf/10.1007/s10509-016-2983-x.pdf>

In this work, we present observations and interpretations of recurrent extreme ultraviolet (EUV) jets that occurred between **2012 July 1 21:00 UT and 2012 July 2 10:00 UT** from the western edge of the NOAA active region 11513. *Solar Dynamics Observatory/Atmospheric Imaging Assembly (SDO/AIA)*, *SDO/Helioseismic and Magnetic Imager (SDO/HMI)* and *Reuven Ramaty High Energy Solar Spectroscopic Imager (RHESSI)* observations have been used for the present study. Observations as well as potential-field source-surface (PFSS) extrapolation suggest an open field configuration in the vicinity of the jet activity area. 18 EUV jets were observed from the western edge of the active region along the open field channel. All the jet events appeared to be non-homologous and show different morphological properties and evolution. Some of the jets were small and narrow in size while the others were huge and wide. The average speed of these jets ranges from  $\sim 47$  to  $\sim 308$   $\text{kms}^{-1}$ . *SDO/AIA* 171 Å intensity profiles at the base of these jets show bumps corresponding to each jet, which is an evidence of recurrent magnetic reconnections. The magnetic field observation at the foot points of the jets revealed a very complex and dynamic magnetic activity which includes flux emergence, flux cancellation, dynamic motions, merging, separation, etc. We suggest that the recurrent jets are the result of recurrent magnetic reconnections among the various emerging bipolar fields themselves as well as with the open fields.

## **Two Step Filament Eruption During 14-15 March 2015**

R. **Chandra**, B. Filippov, R. Joshi, B. Schmieder

Solar Phys. 292:81 2017 DOI: 10.1007/s11207-017-1104-5

<https://arxiv.org/pdf/1704.08860.pdf>

<http://sci-hub.ru/10.1007/s11207-017-1104-5>

We present here an interesting two-step filament eruption during 14-15 March 2015. The filament was located in NOAA AR 12297 and associated with a halo Coronal Mass Ejection (CME). We use observations from the Atmospheric Imaging Assembly (AIA) and Heliospheric Magnetic Imager (HMI) instruments onboard the Solar Dynamics Observatory (SDO), and from the Solar and Heliospheric Observatory (SOHO) Large Angle and Spectrometric Coronagraph (LASCO). We also use H-alpha data from the Global Oscillation Network Group (GONG) telescope and the Kanzelhöhe Solar Observatory. The filament shows a first step eruption on **14 March 2015** and it stops its rise at a projected altitude  $\sim 125$  Mm on the solar disk. It remains at this height for  $\sim 12$  hrs. Finally it erupts on **15 March 2015** and produced a halo CME. We also find jet activity in the active region during both days, which could help the filament de-stabilization and eruption. The decay index is calculated to understand this two-step eruption. The eruption could be due to the presence of successive instability-stability-instability zones as the filament is rising.

## **Blowout Jets and Impulsive Eruptive Flare in a Bald-Patch Topology**

R. **Chandra**, C.H. Mandrini, B. Schmieder, B. Joshi, G.D. Cristiani, H. Cremades, E. Pariat, F.A. Nuevo, A.K. Srivastava, W. Uddin

A&A 598, A41 (2017)

<https://arxiv.org/pdf/1610.01918v1.pdf> File

Context: A subclass of broad EUV and X-ray jets, called blowout jets, have become a topic of research since they could be the link between standard collimated jets and CMEs. }

Aim: Our aim is to understand the origin of a series of broad jets, some accompanied by flares and associated with narrow and jet-like CMEs.

Methods: We analyze observations of a series of recurrent broad jets observed in AR 10484 on **21-24 October 2003**. In particular, one of them occurred simultaneously with an M2.4 flare on 23 October at 02:41 UT (SOLA2003-10-23). Both events were observed by ARIES H-alpha Solar Tower-Telescope, TRACE, SOHO, and RHESSI instruments. The flare was very impulsive and followed by a narrow CME. A local force-free model of AR 10484 is the basis to compute its topology. We find bald patches (BPs) at the flare site. This BP topology is present for at least two days before. Large-scale field lines, associated with the BPs, represent open loops. This is confirmed by a global PFSS model.

Following the brightest leading edge of the H-alpha and EUV jet emission, we can temporarily associate it with a narrow CME.

Results: Considering their characteristics, the observed broad jets appear to be of the blowout class. As the most plausible scenario, we propose that magnetic reconnection could occur at the BP separatrices forced by the destabilization of a continuously reformed flux rope underlying them. The reconnection process could bring the cool flux-rope material into the reconnected open field lines driving the series of recurrent blowout jets and accompanying CMEs.

Conclusions: Based on a model of the coronal field, we compute the AR 10484 topology at the location where flaring and blowout jets occurred from 21 to 24 October 2003. This topology can consistently explain the origin of these events.

**Хорошее Введение про CMEs and jets**

### **Peculiar Stationary EUV Wave Fronts in the eruption on 2011 May 11**

R. **Chandra**, P. F. Chen, A. Fulara, A. K. Srivastava, W. Uddin

ApJ **2016 File**

<http://arxiv.org/pdf/1602.08693v1.pdf>

<https://iopscience.iop.org/article/10.3847/0004-637X/822/2/106/pdf>

We present and interpret the observations of extreme ultraviolet (EUV) waves associated with a filament eruption on **2011 May 11**. The filament eruption also produces a small B-class two ribbon flare and a coronal mass ejection (CME). The event is observed by the Solar Dynamic Observatory (SDO) with high spatio-temporal resolution data recorded by Atmospheric Imaging Assembly (AIA). As the filament erupts, we observe two types of EUV waves (slow and fast) propagating outwards. The faster EUV wave has a propagation velocity of  $\sim 500$  km/s and the slower EUV wave has an initial velocity of  $\sim 120$  km/s. We report for the first time that not only the slower EUV wave stops at a magnetic separatrix to form bright stationary fronts, but also the faster EUV wave transits a magnetic separatrix, leaving another stationary EUV front behind.

### **Sunspot Waves and Triggering of Homologous Active Region Jets**

Ramesh **Chandra**, G.R. Gupta, Sargam Mulay, Durgesh Tripathi

MNRAS, Volume 446, Issue 4, p.3741-3748 **2015**

<http://arxiv.org/pdf/1410.8315v1.pdf>

<https://watermark.silverchair.com/stu2305.pdf>

We present and discuss multi-wavelength observations of five homologous recurrent solar jets that occurred in active region NOAA 11133 on **11 December, 2010**. These jets were well observed by the Solar Dynamic observatory (SDO) with high spatial and temporal resolution. The speed of the jets ranged between 86 and 267 km/s. A type III radio burst was observed in association with all the five jets. The investigation of the over all evolution of magnetic field in the source regions suggested that the flux was continuously emerging on longer term. However, all the jets but J5 were triggered during a local dip in the magnetic flux, suggesting the launch of the jets during localised submergence of magnetic flux. Additionally, using the PFSS modelling of the photospheric magnetic field, we found that all the jets were ejected in the direction of open field lines. We also traced sunspot oscillations from the sunspot interior to foot-point of jets and found presence of  $\sim 3$  minute oscillations in all the SDO/AIA passbands. The wavelet analysis revealed an increase in amplitude of the oscillations just before the trigger of the jets, that decreased after the jets were triggered. The observations of increased amplitude of the oscillation and its subsequent decrease provides evidence of wave-induced reconnection triggering the jets.

### **Solar Energetic Particle Events during the Rise Phases of Solar Cycles 23 and 24**

R. **Chandra**, N. Gopalswamy, P. Mäkelä, H. Xie, S. Yashiro, S. Akiyama, W. Uddin, A.K. Srivastava, N.C. Joshi, R. Jain, A.K. Awasthi, P.K. Manoharan, K. Mahalakshmi, V.C. Dwivedi, D.P. Choudhary, N.V. Nitta  
Advances in Space Research, **Volume 52, Issue 12**, Pages 2102-2111 **2013, File**

<https://sci-hub.ru/10.1016/j.asr.2013.09.006>

<https://doi.org/10.1016/j.asr.2013.09.006>

We present a comparative study of the properties of coronal mass ejections (CMEs) and flares associated with the solar energetic particle (SEP) events in the rising phases of solar cycles (SC) 23 (1996-1998) (22 events) and 24 (2009-2011) (20 events), which are associated with type II radio bursts. Based on the SEP intensity, we divided the events into three categories, i.e. weak (intensity  $< 1$  pfu), minor ( $1 \text{ pfu} < \text{intensity} < 10$  pfu) and major (intensity  $> 10$  pfu). We examine the correlation of SEP intensity with flare size and CME properties. We find that most of the major SEP events are associated with halo or partial halo CMEs originating close to the sun center and western-hemisphere. The fraction of halo CMEs in SC 24 is larger than the SC 23. For the minor SEP events one event in SC23 and one event in SC24 have widths  $< 120^\circ$  and all other events are associated with halo or partial halo CMEs as in the case of major SEP events. In case of weak SEP events, majority (more than 60%) of events are associated with CME width  $< 120^\circ$ . For both the SC the average CMEs speeds are similar. For major SEP events, average CME speeds are higher in comparison to minor and weak events. The SEP event intensity and GOES X-ray flare size are poorly correlated. During the rise phase of solar cycle 23 and 24, we find north-south asymmetry in the SEP event source locations: in cycle 23 most sources are

located in the south, whereas during cycle 24 most sources are located in the north. This result is consistent with the asymmetry found with sunspot area and intense flares. **Tables**

## **Simulation of Homologous and Cannibalistic Coronal Mass Ejections produced by the Emergence of a Twisted Flux Rope into the Solar Corona**

Piyali [Chatterjee](#) and Yuhong Fan

2013 ApJ 778 L8

We report the first results of a magnetohydrodynamic simulation of the development of a homologous sequence of three coronal mass ejections (CMEs) and demonstrate their so-called cannibalistic behavior. These CMEs originate from the repeated formations and partial eruptions of kink unstable flux ropes as a result of continued emergence of a twisted flux rope across the lower boundary into a pre-existing coronal potential arcade field. The simulation shows that a CME erupting into the open magnetic field created by a preceding CME has a higher speed. The second of the three successive CMEs is cannibalistic, catching up and merging with the first into a single fast CME before exiting the domain. All the CMEs including the leading merged CME, attained speeds of about  $1000 \text{ km s}^{-1}$  as they exit the domain. The reformation of a twisted flux rope after each CME eruption during the sustained flux emergence can naturally explain the X-ray observations of repeated reformations of sigmoids and "sigmoid-under-cusp" configurations at a low-coronal source of homologous CMEs.

**ERRATUM:** 2014 ApJ 792 L24

We have found that the magnetic and kinetic energies were erroneously over-estimated by a factor of  $4\pi$  in making the plot in Figure 2 of the published paper. A corrected version of Figure 2 is included below.

## **Stationarity and periodicities of linear speed of coronal mass ejection: a statistical signal processing approach**

Anirban [Chattopadhyay](#), Mofazzal Hossain Khondekar & Anup Kumar Bhattacharjee

[Astrophysics and Space Science](#) September 2017, 362:179

In this paper initiative has been taken to search the periodicities of linear speed of Coronal Mass Ejection in solar cycle 23. Double exponential smoothing and Discrete Wavelet Transform are being used for detrending and filtering of the CME linear speed time series. To choose the appropriate statistical methodology for the said purpose, Smoothed Pseudo Wigner-Ville distribution (SPWVD) has been used beforehand to confirm the non-stationarity of the time series. The Time-Frequency representation tool like Hilbert Huang Transform and Empirical Mode decomposition has been implemented to unearth the underneath periodicities in the non-stationary time series of the linear speed of CME. Of all the periodicities having more than 95% Confidence Level, the relevant periodicities have been segregated out using Integral peak detection algorithm. The periodicities observed are of low scale ranging from 2–159 days with some relevant periods like 4 days, 10 days, 11 days, 12 days, 13.7 days, 14.5 and 21.6 days. These short range periodicities indicate the probable origin of the CME is the active longitude and the magnetic flux network of the sun. The results also insinuate about the probable mutual influence and causality with other solar activities (like solar radio emission, ApAp index, solar wind speed, etc.) owing to the similitude between their periods and CME linear speed periods. The periodicities of 4 days and 10 days indicate the possible existence of the Rossby-type waves or planetary waves in Sun.

## **Simultaneous Eruption and Shrinkage of Preexisting Flare Loops during a Subsequent Solar Eruption**

[Huadong Chen](#), [Lyndsay Fletcher](#), [Guiping Zhou](#), [Xin Cheng](#), [Ya Wang](#), [Sargam Mulay](#), [Ruisheng Zheng](#), [Suli Ma](#), [Xiaofan Zhang](#)

2024 ApJ 976 207

<https://iopscience.iop.org/article/10.3847/1538-4357/ad8c25/pdf>

<https://arxiv.org/pdf/2410.12202>

We investigated two consecutive solar eruption events in the solar active region 12994 at the solar eastern limb on **2022 April 15**. We found that the flare loops formed by the first eruption were involved in the second eruption. During the initial stage of the second flare, the middle part of these flare loops (E-loops) erupted outward along with the flux ropes below, while the parts of the flare loops (I-loops1 and I-loops2) on either side of the E-loops first rose and then contracted. Approximately 1 hr after the eruption, the heights of I-loops1 and I-loops2 decreased by 9 Mm and 45 Mm, respectively, compared to before the eruption. Their maximum descent velocities were  $30 \text{ km s}^{-1}$  and  $130 \text{ km s}^{-1}$ , respectively. The differential emission measure results indicate that the plasma above I-loops1 and I-loops2 began to be heated about 23 minutes and 44 minutes after the start of the second flare, respectively. Within  $\sim 20$  minutes, the plasma temperature in these regions increased from  $\sim 3 \text{ MK}$  to  $\sim 6 \text{ MK}$ . We proposed an adiabatic heating mechanism where magnetic energy would be converted into thermal and kinetic energy when the prestretched loops contract. Our calculations show that the magnetic energy required to heat the two high-temperature regions are 1029–1030 erg, which correspond to a loss of field strength of 2–3 G.

## **Theoretical Studies on the Evolution of Solar Filaments in Response to New Emerging Flux**

[Yuhao Chen](#), [Jialiang Hu](#), [Guanchong Cheng](#), [Jing Ye](#), [Zhixing Mei](#), [Chengcai Shen](#), [Jun Lin](#)

ApJL 977 L26 2024

<https://arxiv.org/pdf/2411.13839>

<https://iopscience.iop.org/article/10.3847/2041-8213/ad94ea/pdf>

New emerging flux (NEF) has long been considered a mechanism for solar eruptions, but detailed process remains an open question. In this work, we explore how NEF drives a coronal magnetic configuration to erupt. This configuration is created by two magnetic sources of strengths  $M$  and  $S$  embedded in the photosphere, one electric-current-carrying flux rope (FR) floating in the corona, and an electric current induced on the photospheric surface by the FR. The source  $M$  is fixed accounting for the initial background field, and  $S$  changes playing the role of NEF. We introduce the channel function  $C$  to forecast the overall evolutionary behavior of the configuration. Location, polarity, and strength of NEF governs the evolutionary behavior of FR before eruption. In the case of  $|S/M| < 1$  with reconnection occur between new and old fields, the configuration in equilibrium evolves to the critical state, invoking the catastrophe. In this case, if polarities of the new and old fields are opposite, reconnection occurs as NEF is close to FR; and if polarities are the same, reconnection happens as NEF appears far from FR. With different combinations of the relative polarity and the location, the evolutionary behavior of the system gets complex, and the catastrophe may not occur. If  $|S/M| > 1$  and the two fields have opposite polarity, the catastrophe always takes place; but if the polarities are the same, catastrophe occurs only as NEF is located far from FR; otherwise, the evolution ends up either with failed eruption or without catastrophe at all.

## **An Introduction on Solar Imaging Data Analytic Challenges and Opportunities for Statisticians**

**Review**

[Yang Chen](#), [Ward Manchester](#), [Meng Jin](#), [Alexei Pevtsov](#)

2024

<https://arxiv.org/pdf/2405.12331>

We give a gentle introduction to solar imaging data, focusing on challenges and opportunities of data-driven approaches for solar eruptions. The various solar phenomena prediction problems that might benefit from statistical methods are presented. Available data and software will be described. State-of-art solar eruption forecasting with data driven approaches are summarized and discussed. Based on the characteristics of the datasets and state-of-art approaches, we point out several promising directions to explore from statistical modeling and computational perspectives.

## **Observations of a Failed Solar Filament Eruption Involving External Reconnection**

[Yuehong Chen](#), [Xin Cheng](#), [Jun Chen](#), [Yu Dai](#), [Mingde Ding](#)

ApJ 959 67 2023

<https://arxiv.org/pdf/2311.17637.pdf>

<https://iopscience.iop.org/article/10.3847/1538-4357/ad09d8/pdf>

We report a failed solar filament eruption that involves external magnetic reconnection in a quadrupolar magnetic configuration. The evolution exhibits three kinematic evolution phases: a slow-rise phase, an acceleration phase, and a deceleration phase. In the early slow rise, extreme-ultraviolet (EUV) brightenings appear at the expected null point above the filament and are connected to the outer polarities by the hot loops, indicating the occurrence of a breakout reconnection. Subsequently, the filament is accelerated outward, accompanied by the formation of low-lying high-temperature post-flare loops ( $> 15$  MK), complying with the standard flare model. However, after 2--3 minutes, the erupting filament starts to decelerate and is finally confined in the corona. The important finding is that the confinement is closely related to an external reconnection as evidenced by the formation of high-lying large-scale hot loops ( $> 10$  MK) with their brightened footpoints at the outer polarities, the filament fragmentation and subsequent falling along the newly formed large-scale loops, as well as a hard X-ray source close to one of the outer footpoint brightenings. We propose that, even though the initial breakout reconnection and subsequent flare reconnection commence and accelerate the filament eruption, the following external reconnection between the erupting flux rope and overlying field, as driven by the upward filament eruption, makes the eruption finally failed, as validated by the numerical simulation of a failed flux rope eruption. 2022 May 3

## **Can the Parker Solar Probe Detect a CME-flare Current Sheet?**

[Yuhao Chen](#), [Zhong Liu](#), [Pengfei Chen](#), [David F. Webb](#), [Qi Hao](#), [Jialiang Hu](#), [Guanchong Cheng](#), [Zhixing Mei](#), [Jing Ye](#), [Qian Wang](#), [Jun Lin](#)

ApJS 269 22 2023

<https://arxiv.org/pdf/2309.06432.pdf>

<https://iopscience.iop.org/article/10.3847/1538-4365/acf8c7/pdf>

A current sheet (CS) is the central structure in the disrupting magnetic configuration during solar eruptions. More than 90% of the free magnetic energy (the difference between the energy in the non-potential magnetic field and that in the potential one) stored in the coronal magnetic field beforehand is converted into heating and kinetic energy of the plasma, as well as accelerating charged particles, by magnetic reconnection occurring in the CS. However, the detailed physical properties and fine structures of the CS are still unknown since there is no relevant information obtained via in situ detections. The Parker Solar Probe (PSP) may provide us such information should it traverse a CS in the eruption. The perihelion of PSP's final orbit is located at about 10 solar radii from the center of the Sun, so it can observe the CS at a very close distance, or even traverses the CS, which provides us a unique opportunity to look into fine properties and structures of the CS, helping reveal the detailed physics of large-scale reconnection that was impossible before. We evaluate the probability that PSP can traverse a CS, and examine the orbit of a PSP-like spacecraft that has the highest probability to traverse a CS.

### **1. INTRODUCTION**

## **An Atypical Plateau-like Extreme-ultraviolet Late-phase Solar Flare Driven by the Non-radial Eruption of a Magnetic Flux Rope**

[Yuehong Chen](#), [Yu Dai](#), [Mingde Ding](#)

A&A 675, A147 2023

<https://arxiv.org/pdf/2305.14980.pdf>

<https://www.aanda.org/articles/aa/pdf/2023/07/aa45914-23.pdf>

Recent observations in extreme-ultraviolet (EUV) wavelengths reveal an EUV late phase in some solar flares, which is characterized by a second peak in the warm coronal emissions (about 3 MK) occurring several tens of minutes to a few hours after the corresponding main flare peak. We aim to clarify the physical origin of an atypical plateau-like EUV late phase in an X1.8-class solar flare occurring on **2011 September 7** from active region (AR) 11283. We first characterize the plateau-like late phase using EUV Variability Experiment (EVE) full-disk integrated irradiance observations and Atmospheric Imaging Assembly (AIA) spatially-resolved imaging observations on board the Solar Dynamics Observatory (SDO). Then we perform a nonlinear force-free-field (NLFFF) extrapolation, from which a filament-hosting magnetic flux rope (MFR) is revealed. The eruption of the MFR is tracked both in the plane of the sky (POS) and along the line of sight (LOS) through visual inspection and spectral fitting, respectively. Finally, we carry out differential emission measure (DEM) analysis to explore the thermodynamics of the late-phase loops. The MFR shows a non-radial eruption from a fan-spine magnetic structure. The eruption of the MFR and its interaction with overlying arcades invoke multiple magnetic reconnections, which are responsible for the production of different groups of late-phase loops. Afterwards, the late-phase loops enter a long-lasting cooling stage, appearing sequentially in AIA passbands of decreasing response temperatures. Due to their different lengths, the different groups of late-phase loops cool down at different cooling rates, which makes their warm coronal emission peaks temporally separated from each other. Combining the emissions from all late-phase loops together, an elongated plateau-like late phase is formed.

## **A Model for Confined Solar Eruptions Including External Reconnection**

[Jun Chen](#), [Xin Cheng](#), [Bernhard Kliem](#), [Mingde Ding](#)

ApJL 951 L35 2023

<https://arxiv.org/pdf/2306.04993.pdf>

<https://iopscience.iop.org/article/10.3847/2041-8213/acdef5/pdf>

The violent disruption of the coronal magnetic field is often observed to be restricted to the low corona, appearing as a confined eruption. The possible causes of the confinement remain elusive. Here, we model the eruption of a magnetic flux rope in a quadrupolar active region, with the parameters set such that magnetic X-lines exist both below and above the rope. This facilitates the onset of magnetic reconnection in either place but with partly opposing effects on the eruption. The lower reconnection initially adds poloidal flux to the rope, increasing the upward hoop force and supporting the rise of the rope. However, when the flux of the magnetic side lobes enters the lower reconnection, the flux rope is found to separate from the reconnection site and the flux accumulation ceases. At the same time, the upper reconnection begins to reduce the poloidal flux of the rope, decreasing its hoop force; eventually this cuts the rope completely. The relative weight of the two reconnection processes is varied in the model, and it is found that their combined effect and the tension force of the overlying field confine the eruption if the flux ratio of the outer to the inner polarities exceeds a threshold, which is about 1.3 for our Cartesian box and chosen parameters. We hence propose that external reconnection between an erupting flux rope and overlying flux can play a vital role in confining eruptions.

## **Eruption of a Magnetic Flux Rope in a Comprehensive Radiative Magnetohydrodynamic Simulation of flare-productive active regions**

[Feng Chen](#), [Matthias Rempel](#), [Yuhong Fan](#)

ApJ 2023

<https://arxiv.org/pdf/2303.05405.pdf>

Radiative magnetohydrodynamic simulation includes sufficiently realistic physics to allow for the synthesis of remote sensing observables that can be quantitatively compared with observations. We analyze the largest flare in a simulation of the emergence of large flare-productive active regions described by Chen et al. The flare is accompanied by a spectacular coronal mass ejection and reaches M2 class, as measured from synthetic soft X-ray flux. The eruption reproduces many key features of observed solar eruptions. A pre-existing magnetic flux rope is formed along the highly sheared polarity inversion line between a sunspot pair and is covered by an overlying multi-pole magnetic field. During the eruption, the progenitor flux rope actively reconnects with the canopy field and evolves to the large-scale multi-thermal flux rope that is observed in the corona. Meanwhile, the magnetic energy released via reconnection is channeled down to the lower atmosphere and gives rise to bright soft X-ray post-flare loops and flare ribbons that reproduce the morphology and dynamic evolution of observed flares. The model helps to shed light on questions of where and when the a flux rope may form and how the magnetic structures in an eruption are related to observable emission properties.

## **Radio Imaging Spectropolarimetry of CMEs and CME Progenitors**

Bin Chen (1), [Timothy S. Bastian](#) (2), [Sarah Gibson](#) (3), [Yuhong Fan](#) (3), [Stephen M. White](#) (4), [Dale E. Gary](#) (1), [Angelos Vourlidas](#) (5), [Sijie Yu](#) (1), [Surajit Mondal](#) (1), [Gregory D. Fleishman](#) (1), [Pascal Saint-Hilaire](#) (6)

Science white paper submitted to the 2024 Solar and Space Physics Decadal Survey. **2023**

All submitted white papers (including this one) are available at [this https URL](https://arxiv.org/pdf/2301.12188.pdf)  
<https://arxiv.org/pdf/2301.12188.pdf>

Coronal mass ejections (CMEs) are the most important drivers of space weather. Central to most CMEs is thought to be the eruption of a bundle of highly twisted magnetic field lines known as magnetic flux ropes. A comprehensive understanding of CMEs and their impacts hence requires detailed observations of physical parameters that lead to the formation, destabilization, and eventual eruption of the magnetic flux ropes. Recent advances in remote-sensing observations of coronal cavities, filament channels, sigmoids, EUV "hot channels," white light CMEs, and in situ observations of magnetic clouds points to the possibility of significant progress in understanding CMEs. In this white paper, we provide a brief overview of the potential of radio diagnostics for CMEs and CME progenitors, with a particular focus on the unique means for constraining their magnetic field and energetic electron population. Using synthetic observations based on realistic 3D MHD models, we also demonstrate the transformative potential of advancing such diagnostics by using broadband radio imaging spectropolarimetry with a high image dynamic range and high image fidelity. To achieve this goal, a solar-dedicated radio facility with such capabilities is recommended for implementation in the coming decade.

### **Quantifying Energy Release in Solar Flares and Solar Eruptive Events: New Frontiers with a Next-Generation Solar Radio Facility**

Bin [Chen](#) (1), [Dale E. Gary](#) (1), [Sijie Yu](#) (1), [Surajit Mondal](#) (1), [Gregory D. Fleishman](#) (1), [Xiaocan Li](#) (2), [Chengcai Shen](#) (3), [Fan Guo](#) (4), [Stephen M. White](#) (5), [Timothy S. Bastian](#) (6), [Pascal Saint-Hilaire](#) (7), [James F. Drake](#) (8), [Joel Dahlin](#) (9), [Lindsay Glesener](#) (10), [Hantao Ji](#) (11), [Astrid Veronig](#) (12), [Mitsuo Oka](#) (7), [Katharine K. Reeves](#) (3), [Judith Karpen](#) (9)

Science white paper to the 2024 Solar and Space Physics Decadal Survey **2023**

<https://arxiv.org/pdf/2301.12192.pdf>

Solar flares and the often associated solar eruptive events serve as an outstanding laboratory to study the magnetic reconnection and the associated energy release and conversion processes under plasma conditions difficult to reproduce in the laboratory, and with considerable spatiotemporal details not possible elsewhere in the universe. In the past decade, thanks to advances in multi-wavelength imaging spectroscopy, as well as developments in theories and numerical modeling, significant progress has been made in improving our understanding of solar flare/eruption energy release. In particular, broadband imaging spectroscopy at microwave wavelengths offered by the Expanded Owens Valley Solar Array (EOVSA) has enabled the revolutionary capability of measuring the time-evolving coronal magnetic fields at or near the flare reconnection region. However, owing to EOVSA's limited dynamic range, imaging fidelity, and angular resolution, such measurements can only be done in a region around the brightest source(s) where the signal-to-noise is sufficiently large. In this white paper, after a brief introduction to the outstanding questions and challenges pertinent to magnetic energy release in solar flares and eruptions, we will demonstrate how a next-generation radio facility with many (~100-200) antenna elements can bring the next revolution by enabling high dynamic range, high fidelity broadband imaging spectropolarimetry along with a sub-second time resolution and arcsecond-level angular resolution. We recommend to prioritize the implementation of such a ground-based instrument within this decade. We also call for facilitating multi-wavelength, multi-messenger observations and advanced numerical modeling in order to achieve a comprehensive understanding of the "system science" of solar flares and eruptions. **2017 Sept. 10**

### **Similarities and Differences of SARs in Solar Cycle 24**

Anqin [Chen](#), [Ting Li](#) & [Jingxiu Wang](#)

[Solar Physics](#) volume 297, Article number: 142 (2022)

<https://doi.org/10.1007/s11207-022-02076-4>

Solar Cycle 24 is a particularly weak cycle and there are only six super active regions (SARs). Except for NOAA active region (AR) 12192, all other SARs are coronal mass ejection rich (CME-rich) and produced CMEs faster than 1000 kms<sup>-1</sup>–11000 kms<sup>-1</sup>. By studying the similarities and differences between CME-poor SARs and CME-rich SARs in Solar Cycle 24, we aim to improve our understanding of the cause of major explosive solar activity events. Using the magnetograms of the Helioseismic and Magnetic Imager (HMI) and the images of the Atmospheric Imaging Assembly (AIA) on board the Solar Dynamics Observatory (SDO), the magnetic-field characteristics of the six SARs and their established overall or even global magnetic connectivity are studied. It is found that the area of strong magnetic shear ( $A\psi A\psi$ ) of all the six SARs is larger than 100 Mm<sup>2</sup>100 Mm<sup>2</sup>, and the composite magnetic-field index (IcomIcom: Chen and Wang in *Astron. Astrophys.* 543, A49, 2012) of them is higher than 1. However, the total free magnetic-energy density (EfreeEfree) and the IcomIcom for the majority of them are relatively low compared to the SARs in Solar Cycles 22 and 23. Compared with their very high total unsigned magnetic flux, the CME-poor AR 12192 has a lower EfreeEfree, a shorter magnetic-neutral line with steep horizontal gradient, a smaller  $A\psi A\psi$ , and a lower IcomIcom. It is also revealed that the current helicity proxy, in terms of either the twist parameter or the best force-free parameter, has a good correlation with the fastest CME velocities of the SARs and serves as a good criterion to distinguish the CME-poor SARs from the CME-rich SARs. Except for NOAA AR 12192, all other SARs are found to connect closely with other ARs, and the AR cluster is a common feature of CME-rich SARs.

### **Multispacecraft Remote Sensing and In Situ Observations of the 2020 November 29 Coronal Mass Ejection and Associated Shock: From Solar Source to Heliospheric Impacts**

[Chong Chen](#), [Ying D. Liu](#), [Bei Zhu](#)

ApJ 937 44 2022

<https://arxiv.org/pdf/2207.07534.pdf>

<https://iopscience.iop.org/article/10.3847/1538-4357/ac7ff6/pdf>

We investigate the source eruption, propagation and expansion characteristics, and heliospheric impacts of the **2020 November 29** coronal mass ejection (CME) and associated shock, using remote sensing and in situ observations from multiple spacecraft. A potential--field source--surface model is employed to examine the coronal magnetic fields surrounding the source region. The CME and associated shock are tracked from the early stage to the outer corona using extreme ultraviolet and white light observations. Forward models are applied to determine the structures and kinematics of the CME and the shock near the Sun. The shock shows an ellipsoidal structure, expands in all directions, and encloses the whole Sun as viewed from both SOHO and STEREO A, which results from the large expansion of the CME flux rope and its fast acceleration. The structure and potential impacts of the shock are mainly determined by its radial and lateral expansions. The CME and shock arrive at Parker Solar Probe and STEREO A. Only based on the remote sensing observations, it is difficult to predict whether and when the CME/shock would arrive at the Earth. Combining Wind in situ measurements and WSA-ENLIL simulation results, we confirm that the far flank of the CME (or the CME leg) arrives at the Earth with no shock signature. These results highlight the importance of multipoint remote sensing and in situ observations for determining the heliospheric impacts of CMEs.

### **Numerical Investigations of Catastrophe in Coronal Magnetic Configuration Triggered by Newly Emerging Flux**

Yuhao [Chen](#)<sup>1,2</sup>, Jing Ye<sup>1,3</sup>, Zhixing Mei<sup>1,3</sup>, Chengcai Shen<sup>4</sup>, Ilia I. Roussev<sup>5</sup>, Terry G. Forbes<sup>6</sup>, Jun Lin<sup>1,2,3</sup>, and Udo Ziegler<sup>7</sup>

2022 ApJ 933 148

<https://iopscience.iop.org/article/10.3847/1538-4357/ac73ef/pdf>

We performed 2D magnetohydrodynamical numerical experiments to study the response of the coronal magnetic configuration to the newly emerging magnetic flux. The configuration includes an electric-current-carrying flux rope modeling the prominence floating in the corona and the background magnetic field produced by two separated magnetic dipoles embedded in the photosphere. Parameters for one dipole are fixed in space and time to model the quiet background, and those for another one are time dependent to model the new flux. These numerical experiments duplicate important results of the analytic solution but also reveal new results. Unlike previous works, the configuration here possesses no symmetry, and the flux rope could move in any direction. The non-force-free environment causes the deviation of the flux rope equilibrium in the experiments from that determined in the analytic solution. As the flux rope radius decreases, the equilibrium could be found, and it evolves quasi-statically until the flux rope reaches the critical location at which the catastrophe occurs. As the radius increases, no equilibrium exists at all. During the catastrophe, two current sheets form in different ways. One forms as the surrounding closed magnetic field is stretched by the catastrophe, and another one forms as the flux rope squeezes the magnetic field nearby. Although reconnection happens in both the current sheets, it erases the first one quickly and enhances the second simultaneously. These results indicate the occurrence of the catastrophe in asymmetric and non-force-free environment, and the non-radial motion of the flux rope following the catastrophe.

### **Blobs in a Solar EUV Jet**

Jie [Chen](#), Robertus Erdelyi, Jiajia Liu, Yuanyong Deng, Fionnlagh Dover, Qingmin Zhang, Mei Zhang, Jiangtao Su, and Leping Li

Front. Astron. Space Sci. 8:786856. doi: 10.3389/fspas.2021.786856, 2022

<https://www.frontiersin.org/articles/10.3389/fspas.2021.786856/pdf>

<https://doi.org/10.3389/fspas.2021.786856>

An Extreme Ultraviolet (EUV) jet that occurred around 22:30 on **July 2, 2012** was observed by the Atmospheric Imaging Assembly (AIA) on-board the Solar Dynamics Observatory (SDO). There were two phases of the jet. In Phase 1, two blobs were observed. In Phase 2, the intensity of the jet was almost coherent initially. One minute later, three blobs were formed at the same time in the jet, and the width of the jet changed after the formation of these blobs. The formation and evolution processes of the blobs in these two phases are analyzed in this paper. The physical parameters of the blobs are determined. The measured width of the blobs is 0.8 – 2.3 Mm, and the apparent velocities of the blobs are from 59 km s<sup>-1</sup> to 185 km s<sup>-1</sup>. The formation mechanism of the blobs is likely to be tear-mode instability. **2012 July 2**

### **Solar Prominence Bubble and Plumes Caused By an Eruptive Magnetic Flux Rope**

Changxue [Chen](#)<sup>1,2</sup>, Yang Su<sup>1,2</sup>, Jianchao Xue<sup>1</sup>, Weiqun Gan<sup>1</sup>, and Yu Huang<sup>1</sup>

ApJL 923 L10 2021

<https://iopscience.iop.org/article/10.3847/2041-8213/ac3bd0/pdf>

<https://doi.org/10.3847/2041-8213/ac3bd0>

Prominence bubbles and plumes often form near the lower prominence--corona boundary. They are believed to play an important role in mass supply and evolution of solar prominences. However, how they form is still an open question. In this Letter we present a unique high-resolution H $\alpha$  observation of a quiescent prominence by the New Vacuum Solar Telescope. Two noteworthy bubble--plume events are studied in detail. The two events are almost identical, except that

an erupting mini filament appeared below the prominence–bubble interface in the second event, unlike the first one or any of the reported bubble observations. Analysis of the H $\alpha$  and extreme-ultraviolet data indicates that the rising magnetic flux rope (MFR) in the mini filament is the cause of bubble expansion and that the interaction between the prominence and MFR results in plume formation. These observations provided clear evidence that emerging MFR may be a common trigger of bubbles and suggested a new mechanism of plumes in addition to Rayleigh–Taylor instability and reconnection. **14 April 2021**

### **Partial Eruption, Confinement, and Twist Buildup and Release of a Double-decker Filament**

[Jialin Chen](#), [Yingna Su](#), [Rui Liu](#), [Bernhard Kliem](#), [Qingmin Zhang](#), [Haisheng Ji](#), [Tie Liu](#)

ApJ **923** 142 **2021**

<https://arxiv.org/pdf/2111.13174.pdf>

<https://doi.org/10.3847/1538-4357/ac2ba1>

We investigate the failed partial eruption of a filament system in NOAA AR 12104 on **2014 July 5**, using multiwavelength EUV, magnetogram, and H $\alpha$  observations, as well as magnetic field modeling. The filament system consists of two almost co-spatial segments with different end points, both resembling a C shape. Following an ejection and a precursor flare related to flux cancellation, only the upper segment rises and then displays a prominent twisted structure, while rolling over toward its footpoints. The lower segment remains undisturbed, indicating that the system possesses a double-decker structure. The erupted segment ends up with a reverse-C shape, with material draining toward its footpoints, while losing its twist. Using the flux rope insertion method, we construct a model of the source region that qualitatively reproduces key elements of the observed evolution. At the eruption onset, the model consists of a flux rope atop a flux bundle with negligible twist, which is consistent with the observational interpretation that the filament possesses a double-decker structure. The flux rope reaches the critical height of the torus instability during its initial relaxation, while the lower flux bundle remains in stable equilibrium. The eruption terminates when the flux rope reaches a dome-shaped quasi-separatrix layer that is reminiscent of a magnetic fan surface, although no magnetic null is found. The flux rope is destroyed by reconnection with the confining overlying flux above the dome, transferring its twist in the process.

### **Direct Observation of A Large-scale CME Flux Rope Event Arising from an Unwinding Coronal Jet**

[Hechao Chen](#), [Jiayan Yang](#), [Junchao Hong](#), [Haidong Li](#), [Yadan Duan](#)

ApJ **911** 33 **2021**

<https://arxiv.org/pdf/2102.13336.pdf> [File](#)

<https://doi.org/10.3847/1538-4357/abe6a8>

Coronal mass ejections (CMEs) and coronal jets are two types of common solar eruptive phenomena, which often independently happen at different spatial scales. In this work, we present a stereoscopic observation of a large-scale CME flux rope arising from an unwinding blowout jet in a multipolar complex magnetic system. Based on a multi-band observational analysis, we find that this whole event starts with a small filament whose eruption occurs at a coronal geyser site after a series of homologous jets. Aided by magnetic field extrapolations, it reveals that the coronal geyser site forms above an elongate opposite-polarity interface, where the emergence-driven photospheric flux cancellation and repetitive reconnection are responsible for those preceding recurrent jets and also contribute to the ultimate filament destabilization. By interacting with overlying fields, the erupting filament breaks one of its legs and results in an unwinding blowout jet. Our estimation suggests that around 1.4–2.0 turns of twist release in its jet spire. This prominent twist transport in jet spire rapidly creates a newborn larger-scale flux rope from the jet base to a remote site. Soon after its formation, this large-scale flux rope erupts towards the outer corona causing an Earth-directed CME. In its source region, two sets of distinct post-flare loops form in succession, indicating this eruption involves two-stage of flare magnetic reconnection. This work not only reveals a real magnetic coupling process between different eruptive activities but provides a new hint for understanding the creation of large-scale CME flux ropes during the solar eruption. **2 Jul 2012**

### **High-resolution Chromospheric Observations of a Solar Minifilament: Formation and Destabilization**

Hechao [Chen](#)<sup>1,2,3</sup>, Junchao Hong<sup>1,3,4</sup>, Bo Yang<sup>1,3</sup>, Zhe Xu<sup>5,3</sup>, and Jiayan Yang

**2020** ApJ 902 8

<https://doi.org/10.3847/1538-4357/abb1c1>

Using H $\alpha$  line core and off-band imaging data from the New Vacuum Solar Telescope in China, we present a high-resolution observation on the entire life cycle of a solar minifilament from its birth to its final eruption. We find that the minifilament originates from a series of cascade-like reconfigurations of chromospheric fine structures. During which, owing to strong photospheric shearing and converging flows near its polarity inversion line, basic short chromospheric fibrils first slowly coalesce to elongated dark threads, and then further create a longer filament channel in a "head-to-tail" linkage scenario. In this course, obvious magnetic flux cancellation simultaneously proceeds below it, and further facilitates its destabilization. In its onset phase, clear clues indicate that the minifilament first starts to rise without brightening signals; instead, after a slow-to-fast acceleration, obvious runaway reconnection soon takes over its final jet-like eruption. Besides, off-band observations further reveal that the formed minifilament has a possible flux-rope configuration, and chromospheric upflows that detected in its early forming phase persistently supplies cool plasma into



its channel. This observation is consistent with earlier observations and supports the view that both miniature and large-scale filaments may share analogous formation and destabilization mechanisms.

### **Coronal Mini-jets in an Activated Solar Tornado-like Prominence**

[Huadong Chen](#), [Jun Zhang](#), [Bart De Pontieu](#), [Suli Ma](#), [Bernhard Kliem](#), [Eric Priest](#)

ApJ 899 19 2020

<https://arxiv.org/pdf/2006.08252.pdf>

<https://iopscience.iop.org/article/10.3847/1538-4357/ab9cad/pdf>

High-resolution observations from the Interface Region Imaging Spectrometer (IRIS) reveal the existence of a particular type of small solar jets, which arose singly or in clusters from a tornado-like prominence suspended in the corona. In this study, we perform a detailed statistical analysis of 43 selected mini-jets in the tornado event. Our results show that the mini-jets typically have: (1) a projected length of 1.0-6.0 Mm, (2) a width of 0.2-1.0 Mm, (3) a lifetime of 10-50 s, (4) a velocity of 100-350 km s<sup>-1</sup>, and (5) an acceleration of 3-20 km s<sup>-2</sup>. Based on spectral diagnostics and EM-Loci analysis, these jets seem to be multi-thermal small-scale plasma ejections with an estimated average electron density of  $\sim 2.4 \times 10^{10}$  cm<sup>-3</sup> and an approximate mean temperature of  $\sim 2.6 \times 10^5$  K. Their mean kinetic energy density, thermal energy density and dissipated magnetic field strength are roughly estimated to be  $\sim 9$  erg cm<sup>-3</sup>, 3 erg cm<sup>-3</sup>, and 16 G, respectively. The accelerations of the mini-jets, the UV and EUV brightenings at the footpoints of some mini-jets, and the activation of the host prominence suggest that the tornado mini-jets are probably created by fine-scale external or internal magnetic reconnections (a) between the prominence field and the enveloping or background field or (b) between twisted or braided flux tubes within the prominence. The observations provide insight into the geometry of such reconnection events in the corona and have implications for the structure of the prominence magnetic field and the instability that is responsible for the eruption of prominences and coronal mass ejections. **2015 March 19-20**

### **Observational Analysis on the Early Evolution of a CME Flux-rope: Pre-flare reconnection and Flux-rope's Footpoint Drift**

Hechao [Chen](#), [Jiayan Yang](#), [Kaifan Ji](#), [Yadan Duan](#)

ApJ 887 118 2019

<https://arxiv.org/pdf/1911.00257.pdf>

<https://doi.org/10.3847/1538-4357/ab527e>

We study the early evolution of a hot-channel-like magnetic flux rope (MFR) toward eruption. Combining with imaging observation and magnetic field extrapolation, we find that the hot channel possibly originated from a pre-existing seed MFR with a hyperbolic flux tube (HFT). In the precursor phase, three-dimensional tether-cutting reconnection at the HFT is most likely resulting in the heating and buildup of the hot channel. In this process, the forming hot channel was rapidly enlarged at its spatial size and slipped its feet to two remote positions. Afterward, it instantly erupted outwards with an exponential acceleration, leaving two core dimmings near its feet. We suggest that pre-flare reconnection at the HFT played a crucial role in enlarging the seed MFR and facilitating the onset of its final solar eruption. Moreover, a recently predicted drifting of MFR's footpoints was detected at both core dimmings. In particular, we find that MFR's west footpoint drift was induced by a new reconnection geometry among the erupting MFR's leg and thereby inclined arcades. As MFR's west footpoints gradually drifted to a new position, a set of newborn atypical flare loops connected into the west core dimming, causing a rapid decrease of dimmed area inside this core dimming and also generating a secondary flare ribbon at their remote feet. This reveals that core dimmings may suffer a pronounced diminishment due to the eruptive MFR's footpoint drift, implying that mapping the real footpoints of the erupting MFR down to the Sun's surface is more difficult than previously thought. **2014 March 20**

### **Characteristics of a Gradual Filament Eruption and Subsequent CME Propagation in Relation to a Strong Geomagnetic Storm**

Chong [Chen](#), [Ying D. Liu](#), [Rui Wang](#), [Xiaowei Zhao](#), [Huidong Hu](#), [Bei Zhu](#)

ApJ 884:90 2019

<https://arxiv.org/pdf/1908.11100.pdf>

<https://sci-hub.se/10.3847/1538-4357/ab3f36>

An unexpected strong geomagnetic storm occurred on **2018 August 26**, which was caused by a slow coronal mass ejection (CME) from a gradual eruption of a large quiet-region filament. We investigate the eruption and propagation characteristics of this CME in relation to the strong geomagnetic storm with remote sensing and in situ observations. Coronal magnetic fields around the filament are extrapolated and compared with EUV observations. We determine the propagation direction and tilt angle of the CME flux rope near the Sun using a graduated cylindrical shell (GCS) model and the Sun-to-Earth kinematics of the CME with wide-angle imaging observations from STEREO A. We reconstruct the flux-rope structure using a Grad-Shafranov technique based on the in situ measurements at the Earth and compare it with those from solar observations and the GCS results. Our conclusions are as follows: (1) the eruption of the filament was unusually slow and occurred in the regions with relatively low critical heights of the coronal field decay index; (2) the axis of the CME flux rope rotated in the corona as well as in interplanetary space, which tended to be aligned with the local heliospheric current sheet; (3) the CME was bracketed between slow and fast solar winds, which enhanced the magnetic field inside the CME at 1 AU; (4) the geomagnetic storm was caused by the enhanced magnetic field and a southward orientation of the flux rope at 1 AU from the rotation of the flux rope.

## Observing Current Sheet Formation Forced by Non-radial Rotating Motion of Mini-filaments

Hechao [Chen](#)<sup>1,2,3</sup>, Jiayan Yang<sup>1,3</sup>, Yadan Duan<sup>4</sup>, and Kaifan Ji<sup>1,3</sup>

2019 *ApJ* 879 74

[sci-hub.se/10.3847/1538-4357/ab24ce](https://doi.org/10.3847/1538-4357/ab24ce)

In this paper, we study two externally forced magnetic reconnection events near NOAA active region 12494 for their current sheet (CS) formation. In both events, small-scale reconnection happened between mini-filaments and other preexisting magnetic fields. Initially, mini-filaments underwent obvious non-radial rotating motion due to their loss of equilibrium. With their clockwise/anti-clockwise rotation, the axial fluxes of the mini-filaments slowly came to squeeze the anti-parallel ambient fields, leading to an X-shaped structure. As the squeezing effect strengthened, CS regions gradually formed and grew in length, with a temperature around 1.8 MK. Afterward, clear cusp regions, plasma heating (~5 MK), and newborn magnetic structures came to be in sequence. Finally, mini-filaments erupted in a complex fashion due to the involvement of external reconnection. Based on the multiwavelength imaging observations, the apparent thickness/length, temperature/emission of the CS regions and their related plasma flows are carefully analyzed. Their reconnection rates are roughly estimated as 0.01–0.06 and 0.01–0.02. In particular, a chain of high-speed plasmoid ejections was detected along with a set of the reconnected field lines in Event1, implying the onset of tearing-mode instability inside its CS region. These observations indicate that non-radial rotating motion of filaments can serve as external flows to drive reconnection, and also provide a basic scenario of CS formation within small-scale magnetic reconnection processes. **2016 February 6**

(~S10E05)

## Untwisting and Disintegration of a Solar Filament Associated with Photospheric Flux Cancellation

Huadong [Chen](#), [Ruisheng Zheng](#), [Leping Li](#), [Suli Ma](#), [Yi Bi](#), [Shuhong Yang](#)

*ApJ* 871 229 2019

<https://arxiv.org/pdf/1812.07139.pdf>

Using the high-resolution observations from New Vacuum Solar Telescope (NVST) jointly with the Solar Dynamics Observatory data, we investigate two successive confined eruptions (Erup1 and Erup2) of a small filament in a decaying active region on **2017 November 10**. During the process of Erup1, the overlying magnetic arcade is observed to inflate with the rising filament at beginning and then stop the ongoing of the explosion. In the hot EUV channel, a coronal sigmoidal structure appears during the first eruption and fade away after the second one. The untwisting rotation and disintegration of the filament in Erup2 are clearly revealed by the NVST H<sub>α</sub> intensity data, hinting at a pre-existing twisted configuration of the filament. By tracking two rotating features in the filament, the average rotational angular velocity of the unwinding filament is found to be ~10.5 degree/min. A total twist of ~1.3 pi is estimated to be stored in the filament before the eruption, which is far below the criteria for kink instability. In the course of several hours prior to the event, some photospheric flux activities, including the flux convergence and cancellation, are detected around the northern end of the filament, where some small-scale EUV brightenings are also captured. Moreover, strongly-sheared transverse fields are found in the cancelling magnetic features from the vector magnetograms. Our observational results support the flux cancellation model, in which the interaction between the converging and sheared opposite-polarity fluxes destabilizes the filament and triggers the ensuing ejection.

## Witnessing tether-cutting reconnection at the onset of a partial eruption

Hechao [Chen](#), [Yadan Duan](#), [Jiayan Yang](#), [Bo Yang](#), [Jun Dai](#)

2018 *ApJ* 869 78

<https://arxiv.org/pdf/1811.01606.pdf>

[sci-hub.tw/10.3847/1538-4357/aaead1](https://doi.org/10.3847/1538-4357/aaead1)

In this paper, we study the onset process of a solar eruption on **21 February 2015**, focusing on its unambiguous precursor phase. With multi-wavelength imaging observations from the Atmospheric Imaging Assembly (AIA), definitive tether-cutting (TC) reconnection signatures, i.e., flux convergence and cancellation, bidirectional jets, as well as topology change of hot loops, were clearly observed below the pre-eruption filament. As TC reconnection progressed between the sheared arcades that enveloped the filament, a channel-like magnetic flux rope (MFR) arose in multi-wavelength AIA passbands wrapping around the main axis of the filament. With the subsequent ascent of the newborn MFR, the filament surprisingly split into three branches. After a 7-hour slow rise phase, the high-lying branch containing by the MFR abruptly accelerated causing a two-ribbon flare; while the two low-lying branches remained stable forming a partial eruption. Complemented by kinematic analysis and decay index calculation, we conclude that TC reconnection played a key role in building up the eruptive MFR and triggering its slow rise. The onset of the torus instability may have led the high-lying branch into the standard eruption scenario in the fashion of a catastrophe.

## Magnetic Reconnection Null Points as the Origin of Semi-relativistic Electron Beams in a Solar Jet

Bin [Chen](#), [Sijie Yu](#), [Marina Battaglia](#), [Samaiyah Farid](#), [Antonia Savcheva](#), [Katharine K. Reeves](#), [Säm Krucker](#), [T. S. Bastian](#), [Fan Guo](#), [Svetlin Tassev](#)

*ApJ* 866(1), 62 2018

<https://arxiv.org/pdf/1808.05951.pdf>

<https://iopscience.iop.org/article/10.3847/1538-4357/aadb89/pdf>

[https://web.njit.edu/~binchen/download/publications/Chen+2018\\_TP3/Chen\\_et\\_al\\_2018\\_type3\\_apj.pdf](https://web.njit.edu/~binchen/download/publications/Chen+2018_TP3/Chen_et_al_2018_type3_apj.pdf)

Magnetic reconnection, the central engine that powers explosive phenomena throughout the Universe, is also perceived as one of the principal mechanisms for accelerating particles to high energies. Although various signatures of magnetic reconnection have been frequently reported, observational evidence that links particle acceleration directly to the reconnection site has been rare, especially for space plasma environments currently inaccessible to in situ measurements. Here we utilize broadband radio dynamic imaging spectroscopy available from the Karl G. Jansky Very Large Array to observe decimetric type III radio bursts in a solar jet with high angular ( $\sim 20''$ ), spectral ( $\sim 1\%$ ), and temporal resolution (50 milliseconds). These observations allow us to derive detailed trajectories of semi-relativistic (tens of keV) electron beams in the low solar corona with unprecedentedly high angular precision ( $< 0''.65$ ). We found that each group of electron beams, which corresponds to a cluster of type III bursts with 1-2-second duration, diverges from an extremely compact region ( $\sim 600\text{ km}^2$ ) in the low solar corona. The beam-diverging sites are located behind the erupting jet spire and above the closed arcades, coinciding with the presumed location of magnetic reconnection in the jet eruption picture supported by extreme ultraviolet/X-ray data and magnetic modeling. We interpret each beam-diverging site as a reconnection null point where multitudes of magnetic flux tubes join and reconnect. Our data suggest that the null points likely consist of a high level of density inhomogeneities possibly down to 10-km scales. These results, at least in the present case, strongly favor a reconnection-driven electron acceleration scenario. **2014 November 1**

## Diagnosing the magnetic field structure of a coronal cavity observed during the 2017 total solar eclipse

Yajie [Chen](#), [Hui Tian](#), [Yingna Su](#), [Zhongquan Qu](#), [Linhua Deng](#), [Patricia R. Jibben](#), [Zihao Yang](#), [Jingwen Zhang](#), [Tanmoy Samanta](#), [Jiansen He](#), [Linghua Wang](#), [Yingjie Zhu](#), [Yue Zhong](#), [Yu Liang](#)

ApJ **856** 21 **2018**

<https://arxiv.org/pdf/1802.04432.pdf>

We present an investigation of a coronal cavity observed above the western limb in the coronal red line Fe X 6374  $\{\AA\}$  using a telescope of Peking University and in the green line Fe XIV 5303  $\{\AA\}$  using a telescope of Yunnan Observatories, Chinese Academy of Sciences during the total solar eclipse on **2017 August 21**. A series of magnetic field models are constructed based on the magnetograms taken by the Helioseismic and Magnetic Imager onboard the Solar Dynamics Observatory (SDO) one week before the eclipse. The model field lines are then compared with coronal structures seen in images taken by the Atmospheric Imaging Assembly on board SDO and in our coronal red line images. The best-fit model consists of a flux rope with a twist angle of  $3.1\pi$ , which is consistent with the most probable value of the total twist angle of interplanetary flux ropes observed at 1 AU. Linear polarization of the Fe XIII 10747  $\{\AA\}$  line calculated from this model shows a "lagomorphic" signature that is also observed by the Coronal Multichannel Polarimeter of the High Altitude Observatory. We also find a ring-shaped structure in the line-of-sight velocity of Fe XIII 10747  $\{\AA\}$ , which implies hot plasma flows along a helical magnetic field structure, in the cavity. These results suggest that the magnetic structure of the cavity is a highly twisted flux rope, which may erupt eventually. The temperature structure of the cavity has also been investigated using the intensity ratio of Fe XIII 10747  $\{\AA\}$  and Fe X 6374  $\{\AA\}$ .

## Solar Tornadoes Triggered by Interaction between Filaments and EUV Jets

Huadong [Chen](#)<sup>1</sup>, Jun Zhang<sup>1</sup>, Suli Ma<sup>1,2</sup>, Xiaoli Yan<sup>3</sup>, and Jianchao Xue

**2017** ApJL **841** L13

<http://sci-hub.cc/10.3847/2041-8213/aa71a2>

We investigate the formations and evolutions of two successive solar tornadoes in/near AR 12297 during **2015 March 19–20**. Recurrent EUV jets close to two filaments were detected along a large-scale coronal loop prior to the appearances of the tornadoes. Under the disturbances from the activities, the filaments continually ascended and finally interacted with the loops tracked by the jets. Subsequently, the structures of the filaments and the loop were merged together, probably via magnetic reconnections, and formed tornado-like structures with a long spiral arm. Our observations suggest that solar tornadoes can be triggered by the interaction between filaments and nearby coronal jets, which has rarely been reported before. At the earlier development phase of the first tornado, about 30 small-scale sub-jets appeared in the tornado's arm, accompanied by local EUV brightenings. They have an ejection direction approximately vertical to the axis of the arm and a typical maximum speed of  $\sim 280\text{ km s}^{-1}$ . During the ruinations of the two tornadoes, fast plasma outflows from the strong EUV brightenings inside tornadoes are observed, in company with the unangling or unwinding of the highly twisted tornado structures. These observational features indicate that self reconnections probably occurred between the tangled magnetic fields of the tornadoes and resulted in the rapid disintegrations and disappearances of the tornadoes. According to the reconnection theory, we also derive the field strength of the tornado core to be  $\sim 8\text{ G}$ .

## Double Coronal X-ray and Microwave Sources Associated With A Magnetic Breakout Solar Eruption

Yao [Chen](#), Zhao Wu, Wei Liu, Richard A. Schwartz, Di Zhao, Bing Wang, Guohui Du

**2017**

<https://arxiv.org/pdf/1705.06074.pdf>

Double coronal hard X-ray (HXR) sources are believed to be critical observational evidence of bi-directional energy release through magnetic reconnection in a large-scale current sheet in solar ares. Here we present a study on double coronal sources observed in both HXR and microwave regimes, revealing new characteristics distinct from earlier reports. This event is associated with a footpoint-occulted X1.3-class flare (**25 April 2014**, starting at 00:17 UT) and a coronal mass ejection that are likely triggered by the magnetic breakout process, with the lower source extending upward from the top of the partially-occulted flare loops and the upper source co-incident with rapidly squeezing-in side lobes (at a speed of  $\sim 250$  km/s on both sides). The upper source can be identified at energies as high as 70-100 keV. The X-ray upper source is characterized by flux curves different from the lower source, a weak energy dependence of projected centroid altitude above 20 keV, a shorter duration and a HXR photon spectrum slightly-harder than those of the lower source. In addition, the microwave emission at 34 GHz also exhibits a similar double source structure and the microwave spectra at both sources are in line with gyro-synchrotron emission given by non-thermal energetic electrons. These observations, especially the co-occurrence of the very-fast squeezing-in motion of side lobes and the upper source, indicate that the upper source is associated with (possibly caused by) this fast motion of arcades. This sheds new lights on the origin of the corona double-source structure observed in both HXRs and microwaves.

### **A Complex Solar Coronal Jet with Two Phases**

Jie **Chen**, Jiangtao Su, Yuanyong Deng, E. R. Priest

ApJ **840** 54 **2017**

<https://arxiv.org/pdf/1704.02072.pdf>

<https://iopscience.iop.org/article/10.3847/1538-4357/aa6c59/pdf>

Jets often occur repeatedly from almost the same location. In this paper, a complex solar jet was observed with two phases to the west of NOAA AR 11513 on **July 2nd, 2012**. If it had been observed at only moderate resolution, the two phases and their points of origin would have been regarded as identical. However, at high resolution we find the two phases merge into one another and the accompanying footpoint brightenings occur at different locations. The phases originate from different magnetic patches rather than being one phase originating from the same patch. Photospheric line of sight (LOS) magnetograms show that the bases of the two phases lie in two different patches of magnetic flux which decrease in size during the occurrence of the two phases. Based on these observations, we suggest the driving mechanism of the two successive phases is magnetic cancellation of two separate magnetic fragments with an opposite polarity fragment between them.

### **Undercover EUV Solar Jets Observed by the Interface Region Imaging Spectrograph**

N.-H. **Chen**, D. E. Innes

ApJ **833** 22 **2016**

<https://arxiv.org/pdf/1610.08149v1.pdf>

It is well-known that extreme ultraviolet emission emitted at the solar surface is absorbed by overlying cool plasma. Especially in active regions dark lanes in EUV images suggest that much of the surface activity is obscured. Simultaneous observations from IRIS, consisting of UV spectra and slit-jaw images give vital information with sub-arcsecond spatial resolution on the dynamics of jets not seen in EUV images. We studied a series of small jets from recently formed bipole pairs beside the trailing spot of active region 11991, which occurred on **2014 March 5** from 15:02:21 UT to 17:04:07 UT. There were collimated outflows with bright roots in the SJI 1400  $\{\AA\}$  (transition region) and 2796  $\{\AA\}$  (upper chromosphere) that were mostly not seen in AIA 304  $\{\AA\}$  (transition region) and AIA 171  $\{\AA\}$  (lower corona) images. The Si IV spectra show strong blue-wing but no red-wing enhancements in the line profiles of the ejecta for all recurrent jets indicating outward flows without twists. We see two types of Mg II line profiles produced by the jets spires: reversed and non-reversed. Mg II lines remain optically thick but turn into optically thin in the highly Doppler shifted wings. The energy flux contained in each recurrent jet is estimated using a velocity differential emission measure technique which measures the emitting power of the plasma as a function of line-of-sight velocity. We found that all the recurrent jets release similar energy ( $108 \text{ erg cm}^{-2} \text{ s}^{-1}$ ) toward the corona and the downward component is less than 3%.

### **IMAGING A MAGNETIC-BREAKOUT SOLAR ERUPTION**

Yao **Chen**<sup>1</sup>, Guohui Du<sup>1</sup>, Di Zhao<sup>1</sup>, Zhao Wu<sup>1</sup>, Wei Liu<sup>2</sup>, Bing Wang<sup>1</sup>, Guiping Ruan<sup>1</sup>, Shiwei Feng<sup>1</sup>, and Hongqiang Song

**2016** ApJ **820** L37

The fundamental mechanism initiating coronal mass ejections (CMEs) remains controversial. One of the leading theories is magnetic breakout, in which magnetic reconnection occurring high in the corona removes the confinement on an energized low-corona structure from the overlying magnetic field, thus allowing it to erupt. Here, we report critical observational evidence of this elusive breakout reconnection in a multi-polar magnetic configuration that leads to a CME and an X-class, long-duration flare. Its occurrence is supported by the presence of pairs of heated cusp-shaped loops around an X-type null point and signatures of reconnection inflows. Other peculiar features new to the breakout picture include sequential loop brightening, coronal hard X-rays at energies up to  $\sim 100$  keV, and extended high-corona X-rays above the later restored multi-polar structure. These observations, from a novel perspective with clarity never achieved before, present crucial clues to understanding the initiation mechanism of solar eruptions.

## **Tether-cutting Reconnection between Two Solar Filaments Triggering Outflows and a Coronal Mass Ejection**

Huadong **Chen**, Jun Zhang, Leping Li, Suli Ma

ApJLetter **818** L27 **2016**

<http://arxiv.org/pdf/1602.00378v1.pdf>

Triggering mechanisms of solar eruptions have long been a challenge. A few previous case studies have indicated that preceding gentle filament merging via magnetic reconnection may launch following intense eruption, according with the tether-cutting (TC) model. However, detailed process of TC reconnection between filaments has not been exhibited yet. In this work, we report the high resolution observations from the Interface Region Imaging Spectrometer (IRIS) of TC reconnection between two sheared filaments in NOAA active region 12146. The TC reconnection commenced since 15:35 UT on **2014 August 29** and triggered an eruptive GOES C4.3-class flare 8 minutes later. An associated coronal mass ejection appeared in the field of view of SOHO/LASCO C2 about 40 minutes later. Thanks to the high spatial resolution of IRIS data, bright plasma outflows generated by the TC reconnection are clearly observed, which moved along the subarcsecond fine-scale flux tube structures in the erupting filament. Based on the imaging and spectral observations, the mean plane-of-sky and line-of-sight velocities of the TC reconnection outflows are separately measured to be 79 and 86 km/s, which derives an average real speed of 120 km/s. In addition, it is found that spectral features, such as peak intensities, Doppler shifts, and line widths in the TC reconnection region evidently enhanced compared with those in the nearby region just before the flare.

## **RECURRENT SOLAR JETS INDUCED BY A SATELLITE SPOT AND MOVING MAGNETIC FEATURES**

Jie **Chen**<sup>1</sup>, Jiangtao Su<sup>1</sup>, Zhiqiang Yin<sup>1</sup>, T. G. Priya<sup>1,2</sup>, Hongqi Zhang<sup>1</sup>, Jihong Liu<sup>3</sup>, Haiqing Xu<sup>1</sup>, and Sijie Yu<sup>1</sup>

**2015** ApJ 815 71

Recurrent and homologous jets were observed to the west edge of active region NOAA 11513 at the boundary of a coronal hole. We find two kinds of cancellations between opposite polarity magnetic fluxes, inducing the generation of recurrent jets. First, a satellite spot continuously collides with a pre-existing opposite polarity magnetic field and causes recurrent solar jets. Second, moving magnetic features, which emerge near the sunspot penumbra, pass through the ambient plasma and eventually collide with the opposite polarity magnetic field. Among these recurrent jets, a blowout jet that occurred around 21:10 UT is investigated. The rotation of the pre-existing magnetic field and the shear motion of the satellite spot accumulate magnetic energy, which creates the possibility for the jet to experience blowout right from the standard.

## **Confined Flares in Solar Active Region 12192 from 2014 October 18 to 29**

Huadong **Chen**, Jun Zhang, Suli Ma, Shuhong Yang, Leping Li, Xin Huang, Junmin Xiao

ApJL **2015**

<http://arxiv.org/pdf/1507.00651v1.pdf>

Using the observations from the Atmospheric Imaging Assembly (AIA) and Helioseismic and Magnetic Imager (HMI) aboard the Solar Dynamics Observatory (SDO), we investigate six X-class and twenty-nine M-class flares occurring in solar active region (AR) 12192 from October 18 to 29. Among them, thirty (including six X- and twenty-four M-class) flares originated from the AR core and the other five M-flares appeared at the AR periphery. Four of the X-flares exhibited similar flaring structures, indicating they were homologous flares with analogous triggering mechanism. The possible scenario is: photospheric motions of emerged magnetic fluxes lead to shearing of the associated coronal magnetic field, which then yields a tether-cutting favorable configuration. Among the five periphery M-flares, four were associated with jet activities. The HMI vertical magnetic field data show that the photospheric fluxes of opposite magnetic polarities emerged, converged and canceled with each other at the footpoints of the jets before the flares. Only one M-flare from the AR periphery was followed by a coronal mass ejection (CME). From October 20 to 26, the mean decay index of the horizontal background field within the height range of 40?105 Mm is below the typical threshold for torus instability onset. This suggests that a strong confinement from the overlying magnetic field might be responsible for the poor CME production of AR 12192.

**Table 1.** X- and M-class flares in Solar AR 12192

## **Direct Observations of Tether-cutting Reconnection During a Major Solar Event From 2014 February 24 to 25**

Huadong **Chen**, Jun Zhang, Xin Cheng, Suli Ma, Shuhong Yang, Ting Li

ApJL, **797** L15 **2014**

<http://arxiv.org/pdf/1411.4454v1.pdf>

Using the multi-wavelength data from Atmospheric Imaging Assembly on board the Solar Dynamic Observatory, we investigated two successive solar flares, a C5.1 confined flare and an X4.9 ejective flare with a halo coronal mass

ejection, in NOAA AR 11990 from **2014 Feb 24 to 25**. Before the confined are onset, EUV brightening beneath the filament was detected. As the are began, a twisted helical flux rope (FR) wrapping around the filament moved upward and then stopped, and in the meantime an obvious X-ray source below it was observed. Prior to the ejective X4.9 flare, some pre-existing loop structures in the active region interacted with each other, which produced a brightening region beneath the filament. Meanwhile, a small flaring loop appeared below the interaction region and some new helical lines connecting the far ends of the loop structures was gradually formed and continually added into the former twisted FR. Then, due to the resulting imbalance between the magnetic pressure and tension, the new FR together with the filament erupted outward. Our observations coincide well with tether-cutting model, suggesting that the two flares probably have the same triggering mechanism, i.e., tether-cutting reconnection. To our knowledge, this is the first direct observation of tether-cutting reconnection occurring between the pre-existing loops in active region. In the ejective flare case, the erupting filament exhibited an omega-like kinked structure and underwent an exponential rise after a slow-rise phase, indicating the kink instability might be also responsible for the eruption initiation.

## **Direct Evidence of an Eruptive, Filament-Hosting Magnetic Flux Rope Leading to a Fast Solar Coronal Mass Ejection**

Bin **Chen**, Timothy S. Bastian, Dale E. Gary

ApJ, 794, 149 **2014**

<http://arxiv.org/pdf/1408.6473v1.pdf>

<https://iopscience.iop.org/article/10.1088/0004-637X/794/2/149/pdf>

[https://web.njit.edu/~binchen/download/publications/Chen+2014\\_MFR/Chen+2014\\_MFR.pdf](https://web.njit.edu/~binchen/download/publications/Chen+2014_MFR/Chen+2014_MFR.pdf)

Magnetic flux ropes (MFRs) are believed to be at the heart of solar coronal mass ejections (CMEs). A well-known example is the prominence cavity in the low corona that sometimes makes up a three-part white-light CME upon its eruption. Such a system, which is usually observed in quiet-Sun regions, has long been suggested to be the manifestation of an MFR with relatively cool filament material collecting near its bottom. However, observational evidence of eruptive, filament-hosting MFR systems has been elusive for those originating in active regions. By utilizing multi-passband extreme-ultra-violet (EUV) observations from SDO/AIA, we present direct evidence of an eruptive MFR in the low corona that exhibits a hot envelope and a cooler core; the latter is likely the upper part of a filament that undergoes a partial eruption, which is later observed in the upper corona as the coiled kernel of a fast, white-light CME. This MFR-like structure exists more than one hour prior to its eruption, and displays successive stages of dynamical evolution, in which both ideal and non-ideal physical processes may be involved. The timing of the MFR kinematics is found to be well correlated with the energy release of the associated long-duration C1.9 flare. **We suggest that the long-duration flare is the result of prolonged energy release associated with the vertical current sheet induced by the erupting MFR.** **2012 March 3**

[https://www.cfa.harvard.edu/~bchen/publications/Chen+2014\\_MFR/](https://www.cfa.harvard.edu/~bchen/publications/Chen+2014_MFR/) - accompanying animations

## **Overlying Extreme-ultraviolet Arcades Preventing Eruption of a Filament Observed by AIA/SDO**

Huadong **Chen**<sup>1,2</sup>, Suli Ma<sup>1</sup>, and Jun Zhang

**2013** ApJ 778 70

Using the multi-wavelength data from the Atmospheric Imaging Assembly/Solar Dynamic Observatory (AIA/SDO) and the Sun Earth Connection Coronal and Heliospheric Investigation/Solar Terrestrial Relations Observatory (SECCHI/STEREO), we report a failed filament eruption in NOAA AR 11339 on **2011 November 3**. The eruption was associated with an X1.9 flare, but without any coronal mass ejection (CME), coronal dimming, or extreme ultraviolet (EUV) waves. Some magnetic arcades above the filament were observed distinctly in EUV channels, especially in the AIA 94 Å and 131 Å wavebands, before and during the filament eruption process. Our results show that the overlying arcades expanded along with the ascent of the filament at first until they reached a projected height of about 49 Mm above the Sun's surface, where they stopped. The following filament material was observed to be confined by the stopped EUV arcades and not to escape from the Sun. After the flare, a new filament formed at the low corona where part of the former filament remained before its eruption. These results support that the overlying arcades play an important role in preventing the filament from successfully erupting outward. We also discuss in this paper the EUV emission of the overlying arcades during the flare. It is rare for a failed filament eruption to be associated with an X1.9 class flare, but not with a CME or EUV waves. Therefore, this study also provides valuable insight into the triggering mechanism of the initiation of CMEs and EUV waves.

## **Statistical study of coronal mass ejection source locations: 2. Role of active regions in CME production**

**Chen**, Caixia; Wang, Yuming; Shen, Chenglong; Ye, Pinzhong; Zhang, Jie; Wang, S.

J. Geophys. Res., Vol. 116, No. A12, A12108, **2011**

<http://dx.doi.org/10.1029/2011JA016844>

<http://onlinelibrary.wiley.com/doi/10.1029/2011JA016844/pdf>

This is the second paper of the statistical study of coronal mass ejection (CME) source locations, in which the relationship between CMEs and active regions (ARs) is statistically studied on the basis of the information of CME source locations and the ARs automatically extracted from magnetic synoptic charts of Michelson Doppler Imager (MDI) during 1997–1998. Totally, 224 CMEs with a known location and 108 MDI ARs are included in our sample. It is found that about 63% of the CMEs are related with ARs, at least about 53% of the ARs produced one or more CMEs, and particularly about 14% of ARs are CME-rich (3 or more CMEs were generated) during one transit across the visible disk. Several issues are then tried to clarify: whether or not the CMEs originating from ARs are distinct from others, whether or not the CME kinematics depend on AR properties, and whether or not the CME productivity depends on AR properties. The statistical results suggest that (1) there is no evident difference between AR-related and non-AR-related CMEs in terms of CME speed, acceleration and width, (2) the size, strength and complexity of ARs do little with the kinematic properties of CMEs, but have significant effects on the CME productivity, and (3) the sunspots in all the most productive ARs at least belong to  $\beta\gamma$  type, whereas 90% of those in CME-less ARs are  $\alpha$  or  $\beta$  type only. A detailed analysis on CME-rich ARs further reveals that (1) the distribution of the waiting time of same-AR CMEs, consists of two parts with a separation at about 15 hours, which implies that the CMEs with a waiting time shorter than 15 hours are probably truly physical related, and (2) an AR tends to produce such related same-AR CMEs at a pace of 8 hours, but cannot produce two or more fast CMEs ( $>800 \text{ km s}^{-1}$ ) within a time interval of 15 hours. This interesting phenomenon is particularly discussed.

**Table 4. Most Productive ARs and Corresponding CMEs**

## Coronal Mass Ejections: Models and Their Observational Basis

Peng-Fei **Chen**

Living Rev. Solar Phys., 8, (2011), 1, File

**Review**

<http://solarphysics.livingreviews.org/Articles/lrsp-2011-1/> - best files and two movies

Coronal mass ejections (CMEs) are the largest-scale eruptive phenomenon in the solar system, expanding from active region-sized nonpotential magnetic structure to a much larger size. The bulk of plasma with a mass of  $\sim 10^{11} - 10^{13} \text{ kg}$  is hauled up all the way out to the interplanetary space with a typical velocity of several hundred or even more than  $1000 \text{ km s}^{-1}$ , with a chance to impact our Earth, resulting in hazardous space weather conditions. They involve many other much smaller-sized solar eruptive phenomena, such as X-ray sigmoids, filament/prominence eruptions, solar flares, plasma heating and radiation, particle acceleration, EIT waves, EUV dimmings, Moreton waves, solar radio bursts, and so on. It is believed that, by shedding the accumulating magnetic energy and helicity, they complete the last link in the chain of the cycling of the solar magnetic field. In this review, I try to explicate our understanding on each stage of the fantastic phenomenon, including their pre-eruption structure, their triggering mechanisms and the precursors indicating the initiation process, their acceleration and propagation. Particular attention is paid to clarify some hot debates, e.g., whether magnetic reconnection is necessary for the eruption, whether there are two types of CMEs, how the CME frontal loop is formed, and whether halo CMEs are special.

## A CORONAL SEISMOLOGICAL STUDY WITH STREAMER WAVES

Y. **Chen**<sup>1</sup>, S. W. Feng<sup>1</sup>, B. Li<sup>1</sup>, H. Q. Song<sup>1</sup>, L. D. Xia<sup>1</sup>, X. L. Kong<sup>1</sup>, and Xing Li<sup>2</sup>

Astrophysical Journal, 728:147 (6pp), 2011, File

We present a novel method to evaluate the Alfvén speed and the magnetic field strength along the streamer plasma sheet in the outer corona. The method is based on recent observations of streamer waves, which are regarded as the fast kink body mode carried by the plasma sheet structure and generated upon the impact of a fast coronal mass ejection (CME) on a nearby streamer. The mode propagates outward with a phase speed consisting of two components. One is the phase speed of the mode in the plasma rest frame and the other is the speed of the solar wind streaming along the plasma sheet. The former can be well represented by the Alfvén speed outside the plasma sheet, according to a linear wave dispersion analysis with a simplified slab model of magnetized plasmas. The radial profiles of the Alfvén speed can be deduced with constraints put on the speed of the solar wind, which is done by making use of the measurements of streamer blobs flowing passively in the wind. The radial profiles of the strength of the coronal magnetic field can be depicted once the electron density distribution is specified, this is done by inverting the observed polarized brightness data. Comparing the diagnostic results corresponding to the first wave trough and the following crest, we find that both the Alfvén speed and magnetic field strength at a fixed distance decline with time. This is suggestive of the recovering process of the CME-disturbed corona.

## STREAMER WAVES DRIVEN BY CORONAL MASS EJECTIONS

Y. **Chen**, H. Q. Song, B. Li, L. D. Xia, Z. Wu, H. Fu, and Xing Li<sup>1</sup>

Astrophysical Journal, 714:644–651, 2010 May; File

Between **2004 July 5 and July 7**, two intriguing fast coronal mass ejection (CME)–streamer interaction events were recorded by the Large Angle and Spectrometric Coronagraph. At the beginning of the events, the streamer was pushed aside from its equilibrium position upon the impact of the rapidly outgoing and expanding ejecta; then, the

streamer structure, mainly the bright streamer belt, exhibited elegant large-scale sinusoidal wavelike motions. The motions were apparently driven by the restoring magnetic forces resulting from the CME impingement, suggestive of magnetohydrodynamic kink mode propagating outward along the plasma sheet of the streamer. The mode is supported collectively by the streamer-plasma sheet structure and is therefore named “streamer wave” in the present study. With the white light coronagraph data, we show that the streamer wave has a period of about 1 hr, a wavelength varying from 2 to 4 solar radii, an amplitude of about a few tens of solar radii, and a propagating phase speed in the range 300–500 km s<sup>-1</sup>. We also find that there is a tendency for the phase speed to decline with increasing heliocentric distance. These observations provide good examples of large-scale wave phenomena carried by coronal structures and have significance in developing seismological techniques for diagnosing plasma and magnetic parameters in the outer corona.

## **Initiation and propagation of coronal mass ejections**

P. F. **Chen**

E-print, Feb 2008, **File**; J. Astron. & Astrophys.,

This paper reviews recent progress in the research on the initiation and propagation of CMEs. In the initiation part, several trigger mechanisms are discussed; In the propagation part, the **observations and modelings of EIT waves/dimmings**, as the EUV counterparts of CMEs, are described.

## **SOHO/SUMER Observations of Prominence Oscillation Before Eruption**

P. F. **Chen**, D. E. Innes, & S. K. Solanki

E-print, Feb 2008; A&A

[http://lanl.arxiv.org/PS\\_cache/arxiv/pdf/0802/0802.1961v1.pdf](http://lanl.arxiv.org/PS_cache/arxiv/pdf/0802/0802.1961v1.pdf)

Coronal mass ejections (CMEs), as a large-scale eruptive phenomenon, often reveal some precursors in the initiation phase, e.g., X-ray brightening, filament darkening, etc, which are useful for CME modeling and space weather forecast. With the SOHO/SUMER spectroscopic observations of the **2000 September 26** event, we propose another precursor for CME eruptions, namely, long-time prominence oscillations. The prominence oscillation-and-eruption event was observed by ground-based H $\alpha$  telescopes and space-borne white-light, EUV imaging and spectroscopic instruments. In particular, the SUMER slit was observing the prominence in a sit-and-stare mode. The observations indicate that a siphon flow was moving from the proximity of the prominence to a site at a projected distance of 270", which was followed by repetitive H $\alpha$  surges and continual prominence oscillations. The oscillation lasted 4 hours before the prominence erupted as a blob-like CME. The analysis of the multiwavelength data indicates that the whole series of processes fits well into the **emerging flux trigger mechanism for CMEs**. In this mechanism, emerging magnetic flux drives a siphon flow due to increased gas pressure where the background polarity emerges. It also drives H $\alpha$  surges through magnetic reconnection where the opposite polarity emerges. The magnetic reconnection triggers the prominence oscillations, as well as its loss of equilibrium, which finally leads to the eruption of the prominence. It is also found that the reconnection between the emerging flux and the pre-existing magnetic loop proceeds in an intermittent, probably quasi-periodic, way.

## **Two energy release processes for CMEs: MHD catastrophe and magnetic reconnection**

Y. **Chen**, Y.Q. Hu and L.D. Xia

[Advances in Space Research](#)

[Volume 40, Issue 12, 2007](#), Pages 1780-1786

It remains an open question how magnetic energy is rapidly released in the solar corona so as to create solar explosions such as solar flares and coronal mass ejections (CMEs). Recent studies have confirmed that a system consisting of a flux rope embedded in a background field exhibits a catastrophic behavior, and the energy threshold at the catastrophic point may exceed the associated open field energy. The accumulated free energy in the corona is abruptly released when the catastrophe takes place, and it probably serves as the main means of energy release for CMEs at least in the initial phase. Such a release proceeds via an ideal MHD process in contrast with nonideal ones such as magnetic reconnection. The catastrophe results in a sudden formation of electric current sheets, which naturally provide proper sites for fast magnetic reconnection. The reconnection may be identified with a solar flare associated with the CME on one hand, and produces a further acceleration of the CME on the other. On this basis, several preliminary suggestions are made for future observational investigations, especially with the proposed Kuafu satellites, on the roles of the MHD catastrophe and magnetic reconnection in the magnetic energy release associated with CMEs and flares.

[The Astrophysical Journal](#), 649:1093-1099, **2006 October 1**

## **Force Balance Analysis of a Coronal Magnetic Flux Rope in Equilibrium or Eruption**

Y. **Chen**, <sup>1</sup>G. Q. Li, <sup>2</sup>and Y. Q. Hu <sup>1</sup>



Based on a **flux rope catastrophe model** for coronal mass ejections (CMEs), we calculate the Lorentz forces acting on the rope in equilibrium or eruption in the background field, which is taken to be either a partially open bipolar field or a closed quadrupolar field.

### **The Flux-Rope Scaling of the Acceleration of Coronal Mass Ejections and Eruptive Prominences**

J. **Chen**, C. Marque, A. Vourlidas, J. Krall, and P. W. Schuck

*The Astrophysical Journal*, 649:452-463, 2006

The new flux-rope scaling law of the acceleration of coronal mass ejections (CMEs) derived by Chen and Krall (2003) (Paper 1) is quantitatively tested by comparing the theoretical prediction with the near-Sun acceleration profiles of 13 eruptive prominences (EPs) and four CMEs.

### **On the CME velocity distribution**

**Chen** A.O., Chen P.F., Fang C.

*A&A*, 456 (3), 1153-1158, 2006, file

### **Magnetic Geometry and Dynamics of the Fast Coronal Mass Ejection of 1997 September 9.**

**Chen**, J., Santoro, R.A., Krall, J., Howard, R.A., Duffin, R., Moses, J.D.,

Brueckner, G.E., Darnell, J.A., Burkepile, J.T.,

2000. *Astrophys. J.* 533, 481–500.

### **Deciphering The Slow-rise Precursor of a Major Coronal Mass Ejection**

**X. Cheng**, **C. Xing**, **G. Aulanier**, **S. K. Solanki**, **H. Peter**, **M. D. Ding**

*ApJL* 954 L47 2023

<https://arxiv.org/pdf/2308.13136.pdf>

<https://iopscience.iop.org/article/10.3847/2041-8213/acf3e4/pdf>

Coronal mass ejections (CMEs) are explosive plasma phenomena prevalently occurring on the Sun and probably on other magnetically active stars. However, how their pre-eruptive configuration evolves toward the main explosion remains elusive. Here, based on comprehensive observations of a long-duration precursor in an event on **2012 March 13**, we determine that the heating and slow rise of the pre-eruptive hot magnetic flux rope (MFR) are achieved through a precursor reconnection located above cusp-shaped high-temperature precursor loops. It is observed that the hot MFR threads are built up continually with their middle initially showing an "M" shape and then being separated from the cusp of precursor loops, causing the slow rise of the entire MFR. The slow rise in combination with thermal-dominated hard X-ray source concentrated at the top of the precursor loops shows that the precursor reconnection is much weaker than the flare reconnection of the main eruption. We also perform a three-dimensional magnetohydrodynamics simulation that reproduces the early evolution of the MFR transiting from the slow to fast rise. It is also disclosed that it is the magnetic tension force pertinent to "M"-shaped threads that drives the slow rise, which, however, evolves into a magnetic pressure gradient dominated regime responsible for the rapid-acceleration eruption.

### **Ultra-high-resolution Observations of Persistent Null-point Reconnection in the Solar Corona**

**X. Cheng**, **E. R. Priest**, **H. T. Li**, **J. Chen**, **G. Aulanier**, **L. P. Chitta**, **Y. L. Wang**, **H. Peter**, **X. S. Zhu**, **C. Xing**, **M. D. Ding**, **S. K. Solanki**, **D. Berghmans**, **L. Teriaca**, **R. Aznar Cuadrado**, **A. N. Zhukov**, **Y. Guo**, **D. Long**, **L. Harra**, **P. J. Smith**, **L. Rodriguez**, **C. Verbeec**, **K. Barczynski**, **S. Parenti**

*Nature Communications* volume 14, Article number: 2107 2023

<https://arxiv.org/pdf/2304.08725.pdf>

<https://www.nature.com/articles/s41467-023-37888-w.pdf>

Magnetic reconnection is a key mechanism involved in solar eruptions and is also a prime possibility to heat the low corona to millions of degrees. Here, we present ultra-high-resolution extreme ultraviolet observations of persistent null-point reconnection in the corona at a scale of about 390 km over one hour observations of the Extreme-Ultraviolet Imager on board **Solar Orbiter** spacecraft. The observations show formation of a null-point configuration above a minor positive polarity embedded within a region of dominant negative polarity near a sunspot. The gentle phase of the persistent null-point reconnection is evidenced by sustained point-like high-temperature plasma (about 10 MK) near the null-point and constant outflow blobs not only along the outer spine but also along the fan surface. The blobs appear at a higher frequency than previously observed with an average velocity of about 80 km/s and life-times of about 40 s. The null-point reconnection also occurs explosively but only for 4 minutes, its coupling with a mini-filament eruption generates a spiral jet. These results suggest that magnetic reconnection, at previously unresolved scales, proceeds continually in a gentle and/or explosive way to persistently transfer mass and energy to the overlying corona. **2022 March 3**

### **Initiation and Early Kinematic Evolution of Solar Eruptions**

**X. Cheng**, **J. Zhang**, **B. Kliem**, **T. {Török}**, **C. Xing**, **Z. J. Zhou**, **B. Inhester**, **M. D. Ding**

*ApJ* 894:85 2020

<https://arxiv.org/pdf/2004.03790.pdf>

<https://iopscience.iop.org/article/10.3847/1538-4357/ab886a/pdf>

We investigate the initiation and early evolution of 12 solar eruptions, including six active region hot channel and six quiescent filament eruptions, which were well observed by the \textsl{Solar Dynamics Observatory}, as well as by the \textsl{Solar TERrestrial RELations Observatory} for the latter. The sample includes one failed eruption and 11 coronal mass ejections, with velocities ranging from 493 to 2140~km~s<sup>-1</sup>. A detailed analysis of the eruption kinematics yields the following main results. (1) The early evolution of all events consists of a slow-rise phase followed by a main-acceleration phase, the height-time profiles of which differ markedly and can be best fit, respectively, by a linear and an exponential function. This indicates that different physical processes dominate in these phases, which is at variance with models that involve a single process. (2) The kinematic evolution of the eruptions tends to be synchronized with the flare light curve in both phases. The synchronization is often but not always close. A delayed onset of the impulsive flare phase is found in the majority of the filament eruptions (5 out of 6). This delay, and its trend to be larger for slower eruptions, favor ideal MHD instability models. (3) The average decay index at the onset heights of the main acceleration is close to the threshold of the torus instability for both groups of events (although based on a tentative coronal field model for the hot channels), suggesting that this instability initiates and possibly drives the main acceleration. **2011-03-08, 2011-09-12, 2011-09-22, 2012-01-23, 2012-08-31, 2012-11-23, 2013-03-16, 2013-05-22, 2013-08-20, 2013-09-29, 2014-02-25, 2014-09-02**

**Table 1.** CME/flare properties of 12 eruption events

## Unambiguous Evidence of Filament Splitting-Induced Partial Eruptions

X. Cheng, B. Kliem, M. D. Ding

ApJ 856:48 2018

<https://arxiv.org/pdf/1802.04932.pdf>

<http://iopscience.iop.org/article/10.3847/1538-4357/aab08d/pdf>

Coronal mass ejections are often considered to result from the full eruption of a magnetic flux rope (MFR). However, it is recognized that, in some events, the MFR may release only part of its flux, with the details of the implied splitting not completely established due to limitations in observations. Here, we investigate two partial eruption events including a confined and a successful one. Both partial eruptions are a consequence of the vertical splitting of a filament-hosting MFR involving internal reconnection. A loss of equilibrium in the rising part of the magnetic flux is suggested by the impulsive onset of both events and by the delayed onset of reconnection in the confined event. The remaining part of the flux might be line-tied to the photosphere in a bald patch separatrix surface, and we confirm the existence of extended bald-patch sections for the successful eruption. The internal reconnection is signified by brightenings in the body of one filament and between the rising and remaining parts of both filaments. It evolves quickly into the standard current sheet reconnection in the wake of the eruption. As a result, regardless of being confined or successful, both eruptions produce hard X-ray sources and flare loops below the erupting but above the surviving flux, as well as a pair of flare ribbons enclosing the latter. **2014-12-24, 2015-11-04**

## Origin and Structures of Solar Eruptions I: Magnetic Flux Rope

(Invited **Review**)

Cheng, Xin; Guo, Yang; Ding, MingDe

Science China Earth Sciences, Volume 60, p. 1383-1407, 2017

<https://link.springer.com/content/pdf/10.1007%2Fs11430-017-9074-6.pdf>

<https://arxiv.org/pdf/1705.08198.pdf>

Coronal mass ejections (CMEs) and solar flares are the large-scale and most energetic eruptive phenomena in our solar system and able to release a large quantity of plasma and magnetic flux from the solar atmosphere into the solar wind. When these high-speed magnetized plasmas along with the energetic particles arrive at the Earth, they may interact with the magnetosphere and ionosphere, and seriously affect the safety of human high-tech activities in outer space. The travel time of a CME to 1 AU is about 1-3 days, while energetic particles from the eruptions arrive even earlier. An efficient forecast of these phenomena therefore requires a clear detection of CMEs/flares at the stage as early as possible. To estimate the possibility of an eruption leading to a CME/flare, we need to elucidate some fundamental but elusive processes including in particular the origin and structures of CMEs/flares. Understanding these processes can not only improve the prediction of the occurrence of CMEs/flares and their effects on geospace and the heliosphere but also help understand the mass ejections and flares on other solar-type stars. The main purpose of this review is to address the origin and early structures of CMEs/flares, from multi-wavelength observational perspective. First of all, we start with the ongoing debate of whether the pre-eruptive configuration, i.e., a helical magnetic flux rope (MFR), of CMEs/flares exists before the eruption and then emphatically introduce observational manifestations of the MFR. Secondly, we elaborate on the possible formation mechanisms of the MFR through distinct ways. Thirdly, we discuss the initiation of the MFR and associated dynamics during its evolution toward the CME/flare. Finally, we come to some conclusions and put forward some prospects in the future. **2011-07-03, 2012-07-07, 2012-07-14, 2013-05-22**

Cheng, X., Guo, Y., & Ding, M. D.

2017, SCIENCE CHINA Earth Sciences, submitted **Review**

The multi-wavelength observations of the origin and structures of CMEs, ares, and magnetic flux ropes are presented.

## On the Characteristics of Footpoints of Solar Magnetic Flux Ropes during the Eruption

X. **Cheng**, M. D. Ding

ApJ Supplement Series **2016**

<http://arxiv.org/pdf/1605.04047v1.pdf>

We investigate the footpoints of four erupted magnetic flux ropes (MFRs) that appear as sigmoidal hot channels prior to the eruptions in the Atmospheric Imaging Assembly high temperature passbands. The simultaneous Helioseismic and Magnetic Imager observations disclose that one footpoint of the MFRs originates in the penumbra or penumbra edge with a stronger magnetic field, while the other in the moss region with a weaker magnetic field. The significant deviation of the axis of the MFRs from the main polarity inversion lines and associated filaments suggests that the MFRs have ascended to a high altitude, thus being distinguishable from the source sigmoidal ARs. The more interesting thing is that, with the eruption of the MFRs, the average inclination angle and direct current at the footpoints with stronger magnetic field tend to decrease, which is suggestive of a straightening and untwisting of the magnetic field in the MFR legs. Moreover, the associated flare ribbons also display an interesting evolution. They initially appear as sporadic brightenings at the two footpoints of and in the regions below the MFRs and then quickly extend to two slender sheared J-shaped ribbons with the two hooks corresponding to the two ends of the MFRs. Finally, the straight parts of the two ribbons separate from each other, evolving into two widened parallel ones. These features mostly conform to and support the recently proposed three-dimensional standard CME/flare model, i.e., the twisted MFR eruption stretches and leads to the reconnection of the overlying field that transits from a strong to weak shear with the increasing height. **2012-07-12, 2013-04-11, 2014-04-18, 2014-09-10**

### **Spectroscopic Diagnostics of Solar Magnetic Flux Ropes Using Iron Forbidden Line**

X. **Cheng**, M. D. Ding

ApJL 823 L4 **2016**

<http://arxiv.org/pdf/1605.00195v1.pdf>

In this Letter, we present Interface Region Imaging Spectrograph Fe XXI 1354.08 Å forbidden line emission of two magnetic flux ropes (MFRs) that caused two fast coronal mass ejections with velocities of  $\geq 1000$  km s<sup>-1</sup> and strong flares (X1.6 and M6.5) on 2014 September 10 and **2015 June 22**, respectively. The EUV images at the 131 Å and 94 Å passbands provided by the Atmospheric Imaging Assembly on board Solar Dynamics Observatory reveal that both MFRs initially appear as suspended hot channel-like structures. Interestingly, part of the MFRs is also visible in the Fe XXI 1354.08 forbidden line, even prior to the eruption, e.g., for the **SOL2014-09-10** event. However, the line emission is very weak and that only appears at a few locations but not the whole structure of the MFRs. This implies that the MFRs could be comprised of different threads with different temperatures and densities, based on the fact that the formation of the Fe XXI forbidden line requires a critical temperature ( $\sim 11.5$  MK) and density. Moreover, the line shows a non-thermal broadening and a blueshift in the early phase. It suggests that magnetic reconnection at that time has initiated; it not only heats the MFR and, at the same time, produces a non-thermal broadening of the Fe XXI line but also produces the poloidal flux, leading to the ascending of the MFRs.

### **A Two-ribbon White-light Flare Associated with a Failed Solar Eruption Observed by ONSET, SDO, and IRIS**

X. **Cheng**, [Q. Hao](#), [M. D. Ding](#), [K. Liu](#), [P. F. Chen](#), [C. Fang](#), [Y. D. Liu](#)

ApJ 809 46 **2015**

<http://arxiv.org/pdf/1507.02109v1.pdf>

Two-ribbon brightenings are one of the most remarkable characteristics of an eruptive solar flare and are often used for predicting the occurrence of coronal mass ejections (CMEs). Nevertheless, it was called in question recently whether all two-ribbon flares are eruptive. In this paper, we investigate a two ribbon-like white-light (WL) flare that is associated with a failed magnetic flux rope (MFR) eruption on **2015 January 13**, which has no accompanying CME in the WL coronagraph. Observations by *Optical and Near-infrared Solar Eruption Tracer* and *Solar Dynamics Observatory* reveal that, with the increase of the flare emission and the acceleration of the unsuccessfully erupting MFR, two isolated kernels appear at the WL 3600 Å passband and quickly develop into two elongated ribbon-like structures. The evolution of the WL continuum enhancement is completely coincident in time with the variation of *Fermi* hard X-ray 26–50 keV flux. Increase of continuum emission is also clearly visible at the whole FUV and NUV passbands observed by *Interface Region Imaging Spectrograph*. Moreover, in one WL kernel, the  $\text{Si IV}$ ,  $\text{C II}$ , and  $\text{Mg II}$  h/k lines display significant enhancement and non-thermal broadening. However, their Doppler velocity pattern is location-dependent. At the strongly bright pixels, these lines exhibit a blueshift; while at moderately bright ones, the lines are generally redshifted. These results show that the failed MFR eruption is also able to produce a two-ribbon flare and high-energy electrons that heat the lower atmosphere, causing the enhancement of the WL and FUV/NUV continuum emissions and chromospheric evaporation.

See RHESSI Science Nugget No 257, July **2015**

[http://sprg.ssl.berkeley.edu/~tohban/wiki/index.php/A\\_Two-ribbon\\_White-light\\_Flare\\_Associated\\_with\\_a\\_Failed\\_Solar\\_Eruption](http://sprg.ssl.berkeley.edu/~tohban/wiki/index.php/A_Two-ribbon_White-light_Flare_Associated_with_a_Failed_Solar_Eruption)

### **Imaging and Spectroscopic Diagnostics on the Formation of Two Magnetic Flux Ropes Revealed by SDO/AIA and IRIS**

X. Cheng, M. D. Ding, C. Fang

ApJ 804 82 2015

<http://arxiv.org/pdf/1502.07801v1.pdf>

Helical magnetic flux rope (MFR) is a fundamental structure of corona mass ejections (CMEs) and has been discovered recently to exist as a sigmoidal channel structure prior to its eruption in the extreme ultraviolet (EUV) high temperature passbands of the Atmospheric Imaging Assembly (AIA). However, when and where the MFR is built up are still elusive. In this paper, we investigate two MFRs (MFR1 and MFR2) in detail, whose eruptions produced two energetic solar flares and CMEs on **2014 April 18** and **2014 September 10**, respectively. The AIA EUV images reveal that for a long time prior to their eruption, both MFR1 and MFR2 are under formation, which is probably through magnetic reconnection between two groups of sheared arcades driven by the shearing and converging flows in the photosphere near the polarity inversion line. At the footpoints of the MFR1, the Interface Region Imaging Spectrograph Si IV, C II, and Mg II lines exhibit weak to moderate redshifts and a non-thermal broadening in the pre-flare phase. However, a relatively large blueshift and an extremely strong non-thermal broadening are found at the formation site of the MFR2. These spectral features consolidate the proposition that the reconnection plays an important role in the formation of MFRs. For the MFR1, the reconnection outflow may propagate along its legs, penetrating into the transition region and the chromosphere at the footpoints. For the MFR2, the reconnection probably takes place in the lower atmosphere and results in the strong blueshift and non-thermal broadening for the Mg II, C II, and Si IV lines.

### **On the Relationship Between a Hot-channel-like Solar Magnetic Flux Rope and its embedded Prominence**

X. Cheng, M. D. Ding, J. Zhang, A. K. Srivastava, Y. Guo, P. F. Chen, J. Q. Sun

2014, ApJ Letters, 789 L35

<http://arxiv.org/pdf/1406.4196v1.pdf>

Magnetic flux rope (MFR) is a coherent and helical magnetic field structure that is recently found probably to appear as an elongated hot-channel prior to a solar eruption. In this paper, we investigate the relationship between the hot-channel and associated prominence through analyzing a limb event on **2011 September 12**. In the early rise phase, the hot-channel was cospatial with the prominence initially. It then quickly expanded, resulting in a separation of the top of the hot-channel from that of the prominence. Meanwhile, both of them experienced an instantaneous morphology transformation from a  $\Lambda$  shape to a reversed-Y shape and the top of these two structures showed an exponential increase in height. These features are a good indication for the occurrence of the kink instability. Moreover, the onset of the kink instability is found to coincide in time with the impulsive enhancement of the flare emission underneath the hot-channel, suggesting that the ideal kink instability likely also plays an important role in triggering the fast flare reconnection besides initiating the impulsive acceleration of the hot-channel and distorting its morphology. We conclude that the hot-channel is most likely the MFR system and the prominence only corresponds to the cool materials that are collected in the bottom of the helical field lines of the MFR against the gravity.

### **Formation of a Double-decker Magnetic Flux Rope in the Sigmoidal Solar Active Region 11520**

X. Cheng, M. D. Ding, J. Zhang, X. D. Sun, Y. Guo, Y. M. Wang, B. Kliem, Y. Y. Deng

E-print, May 2014; ApJ 2014 789 93

<http://arxiv.org/pdf/1405.4923v1.pdf>

In this paper, we address the formation of a magnetic flux rope (MFR) that erupted on **2012 July 12** and caused a strong geomagnetic storm event on July 15. Through analyzing the long-term evolution of the associated active region observed by the Atmospheric Imaging Assembly and the Helioseismic and Magnetic Imager on board the Solar Dynamics Observatory, it is found that the twisted field of an MFR, indicated by a continuous S-shaped sigmoid, is built up from two groups of sheared arcades near the main polarity inversion line half day before the eruption. The temperature within the twisted field and sheared arcades is higher than that of the ambient volume, suggesting that magnetic reconnection most likely works there. The driver behind the reconnection is attributed to shearing and converging motions at magnetic footpoints with velocities in the range of 0.1--0.6 km s<sup>-1</sup>. The rotation of the preceding sunspot also contributes to the MFR buildup. Extrapolated three-dimensional non-linear force-free field structures further reveal the locations of the reconnection to be in a bald-patch region and in a hyperbolic flux tube. About two hours before the eruption, indications for a second MFR in the form of an S-shaped hot channel are seen. It lies above the original MFR that continuously exists and includes a filament. The whole structure thus makes up a stable double-decker MFR system for hours prior to the eruption. Eventually, after entering the domain of instability, the high-lying MFR impulsively erupts to generate a fast coronal mass ejection and X-class flare; while the low-lying MFR remains behind and continuously maintains the sigmoidicity of the active region.

### **Tracking the Evolution of A Coherent Magnetic Flux Rope Continuously from the Inner to the Outer Corona**

X. **Cheng**, M. D. Ding, Y. Guo, J. Zhang, A. Vourlidas, Y. D. Liu, O. Olmedo, J. Q. Sun, and C. Li  
E-print, Oct 2013, **File**; 2014 ApJ 780 28

[http://sprg.ssl.berkeley.edu/~liuxying/pubs/2014\\_apj\\_cheng.pdf](http://sprg.ssl.berkeley.edu/~liuxying/pubs/2014_apj_cheng.pdf)

The magnetic flux rope (MFR) is believed to be the underlying magnetic structure of coronal mass ejections (CMEs). However, it remains unclear how an MFR evolves into and forms the multi-component structure of a CME. In this paper, we perform a comprehensive study of an extreme-ultraviolet (EUV) MFR eruption on **2013 May 22** by tracking its morphological evolution, studying its kinematics, and quantifying its thermal property. As EUV brightenings begin, the MFR starts to rise slowly and shows helical threads winding around an axis. Meanwhile, cool filamentary materials descend spirally down to the chromosphere. These features provide direct observational evidence of intrinsically helical structure of the MFR. Through detailed kinematical analysis, we find that the MFR evolution experiences two distinct phases: a slow rise phase and an impulsive acceleration phase. We attribute the first phase to the magnetic reconnection within the quasi-separatrix-layers surrounding the MFR, and the much more energetic second phase to the fast magnetic reconnection underneath the MFR. We suggest that the transition between these two phases be caused by the torus instability. Moreover, we identify that the MFR evolves smoothly into the outer corona and appears as a coherent structure within the white light CME volume. The MFR in the outer corona was enveloped by bright fronts that originated from plasma pile-up in front of the expanding MFR. The fronts are also associated with the preceding sheath region followed the outmost MFR-driven shock.

### **Investigating Two Successive Flux Rope Eruptions In A Solar Active Region**

X. **Cheng**, J. Zhang, M. D. Ding, O. Olmedo, X. D. Sun, Y. Guo & Y. Liu

E-print, April 2013; ApJL 2013 ApJ 769 L25

[http://sprg.ssl.berkeley.edu/~liuxying/pubs/2013\\_apj\\_cheng2.pdf](http://sprg.ssl.berkeley.edu/~liuxying/pubs/2013_apj_cheng2.pdf)

We investigate two successive flux rope (FR1 and FR2) eruptions resulting in two coronal mass ejections (CMEs) on **2012 January 23**. Both FRs appeared as an EUV channel structure in the images of high temperature passbands of the Atmospheric Imaging Assembly prior to the CME eruption. Through fitting their height evolution with a function consisting of linear and exponential components, we determine the onset time of the FR impulsive acceleration with high temporal accuracy for the first time. Using this onset time, we divide the evolution of the FRs in the low corona into two phases: a slow rise phase and an impulsive acceleration phase. In the slow rise phase of the FR1, the appearance of sporadic EUV and UV brightening and the strong shearing along the polarity inverse line indicates that the quasi-separatrix-layer reconnection likely initiates the slow rise. On the other hand for the FR2, we mainly contribute its slow rise to the FR1 eruption, which partially opened the overlying field and thus decreased the magnetic restriction. At the onset of the impulsive acceleration phase, the FR1 (FR2) reaches the critical height of 84.4pm11.2 Mm (86.2pm13.0 Mm) where the decline of the overlying field with height is fast enough to trigger the torus instability. After a very short interval (~2 minutes), the flare emission began to enhance. These results reveal the compound activity involving multiple magnetic FRs and further suggest that the ideal torus instability probably plays the essential role of initiating the impulsive acceleration of CMEs.

### **THE DRIVER OF CORONAL MASS EJECTIONS IN THE LOW CORONA: A FLUX ROPE**

X. **Cheng**<sup>1,2,3</sup>, J. Zhang<sup>2</sup>, M. D. Ding<sup>1,3</sup>, Y. Liu<sup>4,5</sup>, and W. Poomvises

2013 ApJ 763 43, **File**

[http://sprg.ssl.berkeley.edu/~liuxying/pubs/2013\\_apj\\_cheng.pdf](http://sprg.ssl.berkeley.edu/~liuxying/pubs/2013_apj_cheng.pdf)

Recent Solar Dynamic Observatory observations reveal that coronal mass ejections (CMEs) consist of a multi-temperature structure: a hot flux rope and a cool leading front (LF). The flux rope first appears as a twisted hot channel in the Atmospheric Imaging Assembly (AIA) 94 Å and 131 Å passbands. The twisted hot channel initially lies along the polarity inversion line and then rises and develops into a semi-circular flux-rope-like structure during the impulsive acceleration phase of CMEs. In the meantime, the rising hot channel compresses the surrounding magnetic field and plasma, which successively stack into the CME LF. In this paper, we study in detail two well-observed CMEs that occurred on **2011 March 7 and 2011 March 8**, respectively. Each of them is associated with an M-class flare. Through a kinematic analysis we find that (1) the hot channel rises earlier than the first appearance of the CME LF and the onset of the associated flare and (2) the speed of the hot channel is always faster than that of the LF, at least in the field of view of AIA. Thus, the hot channel acts as a continuous driver of the CME formation and eruption in the early acceleration phase. Subsequently, the two CMEs in white-light images can be well reproduced by the graduated cylindrical shell flux rope model. These results suggest that the pre-existing flux rope plays a key role in CME initiation and formation.

### **DIFFERENTIAL EMISSION MEASURE ANALYSIS OF MULTIPLE STRUCTURAL COMPONENTS OF CORONAL MASS EJECTIONS IN THE INNER CORONA**

X. **Cheng**<sup>1,2,3</sup>, J. Zhang<sup>2</sup>, S. H. Saar<sup>4</sup>, and M. D. Ding

2012 ApJ 761 62

In this paper, we study the temperature and density properties of multiple structural components of coronal mass ejections (CMEs) using differential emission measure (DEM) analysis. The DEM analysis is based on the six-passband EUV observations of solar corona from the Atmospheric Imaging Assembly on board the Solar Dynamic Observatory. The structural components studied include the hot channel in the core region (presumably the magnetic flux rope of the CME), the bright loop-like leading front (LF), and coronal dimming in the wake of the CME. We find that the presumed flux rope has the highest average temperature (>8 MK) and density ( $\sim 1.0 \times 10^9 \text{ cm}^{-3}$ ), resulting in an enhanced

emission measure over a broad temperature range ( $3 \leq T(\text{MK}) \leq 20$ ). On the other hand, the CME LF has a relatively cool temperature ( $\sim 2$  MK) and a narrow temperature distribution similar to the pre-eruption coronal temperature ( $1 \leq T(\text{MK}) \leq 3$ ). The density in the LF, however, is increased by 2%-32% compared with that of the pre-eruption corona, depending on the event and location. In coronal dimmings, the temperature is more broadly distributed ( $1 \leq T(\text{MK}) \leq 4$ ), but the density decreases by  $\sim 35\% \sim 40\%$ . These observational results show that: (1) CME core regions are significantly heated, presumably through magnetic reconnection; (2) CME LFs are a consequence of compression of ambient plasma caused by the expansion of the CME core region; and (3) the dimmings are largely caused by the plasma rarefaction associated with the eruption.

## **INVESTIGATION OF THE FORMATION AND SEPARATION OF AN EXTREME-ULTRAVIOLET WAVE FROM THE EXPANSION OF A CORONAL MASS EJECTION**

X. Cheng<sup>1,2,3</sup>, J. Zhang<sup>2</sup>, O. Olmedo<sup>4</sup>, A. Vourlidas<sup>5</sup>, M. D. Ding<sup>1,3</sup>, and Y. Liu

2012 ApJ 745 L5, [File](#)

We address the nature of EUV waves through direct observations of the formation of a diffuse wave driven by the expansion of a coronal mass ejection (CME) and its subsequent separation from the CME front. The wave and the CME on **2011 June 7** were well observed by the Atmospheric Imaging Assembly on board the Solar Dynamics Observatory. Following the solar eruption onset, marked by the beginning of the rapid increasing of the CME velocity and the X-ray flux of accompanying flare, the CME exhibits a strong lateral expansion. During this impulsive expansion phase, the expansion speed of the CME bubble increases from  $100 \text{ km s}^{-1}$  to  $450 \text{ km s}^{-1}$  in only six minutes. An important finding is that a diffuse wave front starts to separate from the front of the expanding bubble shortly after the lateral expansion slows down. Also a type II burst is formed near the time of the separation. After the separation, two distinct fronts propagate with different kinematic properties. The diffuse front travels across the entire solar disk, while the sharp front rises up, forming the CME ejecta with the diffuse front ahead of it. These observations suggest that the previously termed EUV wave is a composite phenomenon and driven by the CME expansion. While the CME expansion is accelerating, the wave front is cospatial with the CME front, thus the two fronts are indiscernible. Following the end of the acceleration phase, the wave moves away from the CME front with a gradually increasing distance between them.

## **Observing Flux Rope Formation During the Impulsive Phase of a Solar Eruption**

X. Cheng, J. Zhang, Y. Liu, M. D. Ding

E-print, March 2011; ApJ Letters 2011 732 L25, [File](#)

Magnetic flux rope is believed to be an important structural component of coronal mass ejections (CMEs). While there exist much observational evidence of the flux rope after the eruption, e.g., as seen in remote-sensing coronagraph images or in-situ solar wind data, the direct observation of flux ropes during CME impulsive phase has been rare. In this Letter, we present an unambiguous observation of a flux rope still in the formation phase in the low corona. The CME of interest occurred above the east limb on **2010 November 03** with footpoints partially blocked. The flux rope was seen as a bright blob of hot plasma in AIA 131Å passband (peak temperature  $\sim 11$  MK) rising from the core of the source active region, rapidly moving outward and stretching upward the surrounding background magnetic field. The stretched magnetic field seemed to curve-in behind the core, similar to the classical magnetic reconnection scenario in eruptive flares. On the other hand, the flux rope appeared as a dark cavity in AIA 211Å passband (2.0 MK) and 171Å passband (0.6 MK); in these relatively cool temperature bands, a bright rim clearly enclosed the dark cavity. The bright rim likely represents the pile-up of the surrounding coronal plasma compressed by the expanding flux rope. The composite structure seen in AIA multiple temperature bands is very similar to that in the corresponding coronagraph images, which consists of a bright leading edge and a dark cavity, commonly believed to be a flux rope.

## **A Comparative Study of Confined and Eruptive Flares in NOAA AR 10720**

X. Cheng, J. Zhang, M. D. Ding, Y. Guo, and J. T. Su

E-print March 2011, ApJ

We investigate the distinct properties of two types of flares: eruptive flares associated with CMEs and confined flares without CMEs. Our sample of study includes nine M and X-class flares, all from the same active region (AR), six of which are confined and three others are eruptive. The confined flares tend to be more impulsive in the soft X-ray time profiles and show more slender shapes in the EIT 195 Å images, while the eruptive ones are of long-duration events and show much more extended brightening regions. The location of the confined flares are closer to the center of the AR, while the eruptive flares are at the outskirts. This difference is quantified by the displacement parameter, the distance between the AR center and the flare location: the average displacement of the six confined flares is 16 Mm, while that of eruptive ones is as large as 39 Mm. Further, through nonlinear force-free field extrapolation, we find that the decay index of the transverse magnetic field in the low corona ( $\sim 10$  Mm) have a larger value for eruptive flares than that for confined one. In addition, the strength of the transverse magnetic field over the eruptive flare sites is weaker than that over the confined ones. These results demonstrate that the strength and the decay index of background magnetic field may determine whether or not a flare be eruptive or confined. The implication of these results on CME models is discussed in the context of torus instability of flux rope.

14-17Jan 2005

## **Re-flaring of a Post-Flare Loop System Driven by Flux Rope Emergence and Twisting**

X. [Cheng](#), M. D. Ding, Y. Guo, J. Zhang, J. Jing, T. Wiegelmann

E-print, 11 May 2010, *ApJL*

In this letter, we study in detail the evolution of the post-flare loops on **2005 January 15** that occurred between two consecutive solar eruption events, both of which generated a fast halo CME and a major flare. The post-flare loop system, formed after the first CME/flare eruption, evolved rapidly, as manifested by the unusual accelerating rise motion of the loops. Through nonlinear force-free field (NLFFF) models, we obtain the magnetic structure over the active region. It clearly shows that the flux rope below the loops also kept rising accompanied with increasing twist and length. Finally, the post-flare magnetic configuration evolved to a state that resulted in the second CME/flare eruption. This is an event in which the post-flare loops can re-flare in a short period of  $\sim 16$  hr following the first CME/flare eruption. The observed re-flaring at the same location is likely driven by the rapid evolution of the flux rope caused by the magnetic flux emergence and the rotation of the sunspot. This observation provides valuable information on CME/flare models and their prediction.

## **A STATISTICAL STUDY OF THE POST-IMPULSIVE-PHASE ACCELERATION OF FLARE-ASSOCIATED CORONAL MASS EJECTIONS**

X. [Cheng](#)<sup>1</sup>, J. Zhang<sup>1,2</sup>, M. D. Ding<sup>1</sup>, and W. Poomvises<sup>2</sup>

*Astrophysical Journal*, 712:752–760, 2010 March, **File**

It is now generally accepted that the impulsive acceleration of a coronal mass ejection (CME) in the inner corona is closely correlated in time with the main energy release of the associated solar flare. In this paper, we examine in detail the post-impulsive-phase acceleration of a CME in the outer corona, which is the phase of evolution immediately following the main impulsive acceleration of the CME; this phase is believed to correspond to the decay phase of the associated flare. This observational study is based on a statistical sample of 247 CMEs that are associated with M- and X-class *GOES* soft X-ray flares from 1996 to 2006. We find that, from many examples of events, the CMEs associated with flares with long-decay time (or so-called long-duration flares) tend to have positive post-impulsive-phase acceleration, even though some of them have already obtained a high speed at the end of the impulsive acceleration but do not show a deceleration expected from the aerodynamic dragging of the background solar wind. On the other hand, the CMEs associated with flares of short-decay time tend to have significant deceleration. In the scattering plot of all events, there is a weak correlation between CME post-impulsive-phase acceleration and flare decay time. The CMEs deviated from the general trend are mostly slow or weak ones associated with flares of short-decay time; the deviation is caused by the relatively stronger solar wind dragging force for these events. The implications of our results on CME dynamics and CME–flare relations are discussed.

## **Two candidate homologous CMEs on 2002 May 22**

J.X. [Cheng](#), C. Fang and P.F. Chen

[Advances in Space Research](#), Volume 38, Issue 3, Pages 470-474, 2006, *file*

## **Large-Scale Activity Initiated BY Halo CMEs**

I. [Chertok](#)<sup>1</sup> and V. Grechnev<sup>2</sup>

*Coronal and Stellar Mass Ejections, Proceedings IAU Symposium No. 226, 2005, K. P. Dere, J. Wang & Y. Yan, eds, 2006.*

We summarize results of our recent studies of CME-associated EUV dimmings and coronal waves by ‘derotated’ fixed-difference SOHO/EIT heliograms at  $195^\circ\text{A}$  with 12-min intervals and at  $171, 195, 284, 304^\circ\text{A}$  with 6-h intervals. Correctness of the derotated fixed-difference technique is confirmed by the consideration of the Bastille Day 2000 event. We also demonstrate that long narrow channeled dimmings and anisotropic coronal waves are typical of the complex global solar magnetosphere near the solar cycle maximum. Homology of large-scale dimmings and coronal waves takes place in a series of recurrent eruptive events. Along with dimmings coinciding entirely or partially in all four EIT bands, there exist dimmings that appear different, mainly in the transition-region line of  $304^\circ\text{A}$  and high-temperature coronal line of  $284^\circ\text{A}$ .

## **Yohkoh data on CME-flare relationships and post-eruption magnetic reconnection in the corona.**

[Chertok](#), I.M.

*Astron. Soc. Pac. Conf. Ser.*, Vol. 111, p. 369 – 374, 1996

The consideration of various observations, in particular of microwave and Yohkoh X-ray data, brings us to the conclusion that, generally speaking, CMEs and flares are independent phenomena in the sense that they may occur one without the other. At the same time CMEs and flares may take place jointly, initiating each other in different cause-and-effect combinations. In any case, a CME, irrespective of its origin, is accompanied by some post-eruption magnetic reconnection and energy release high in the corona. The intensity and character of these processes may be different depending on magnetic structures (either above active regions, outside them, or in the vicinity of coronal holes) which are affected by a CME.

## **Post-Eruption Energy Release in the Solar Corona as an Indicator of CMEs and Associated Disturbances**

**Chertok**, Ilia M.

Solar drivers of the interplanetary and terrestrial disturbances. *Astronomical Society of the Pacific Conference Series, Proceedings of the 16th (sixteenth) international workshop National Solar Observatory/Sacramento Peak, Sunspot, New Mexico, USA, 16-20 October 1995, San Francisco: Astronomical Society of the Pacific (ASP), 1996*, edited by K. S. Balasubramaniam, Stephen L. Keil, and Raymond N. Smartt, p.200

## **Probing the Physics of the Solar Atmosphere with the Multi-slit Solar Explorer (MUSE): II. Flares and Eruptions**

**Mark C. M. Cheung**, **Juan Martínez-Sykora**, **Paola Testa**, **Bart De Pontieu**, .....

*ApJ* **926** 53 **2021**

<https://arxiv.org/pdf/2106.15591.pdf>

<https://iopscience.iop.org/article/10.3847/1538-4357/ac4223/pdf>

Current state-of-the-art spectrographs cannot resolve the fundamental spatial (sub-arcseconds) and temporal scales (less than a few tens of seconds) of the coronal dynamics of solar flares and eruptive phenomena. The highest resolution coronal data to date are based on imaging, which is blind to many of the processes that drive coronal energetics and dynamics. As shown by IRIS for the low solar atmosphere, we need high-resolution spectroscopic measurements with simultaneous imaging to understand the dominant processes. In this paper: (1) we introduce the Multi-slit Solar Explorer (MUSE), a spaceborne observatory to fill this observational gap by providing high-cadence (<20 s), sub-arcsecond resolution spectroscopic rasters over an active region size of the solar transition region and corona; (2) using advanced numerical models, we demonstrate the unique diagnostic capabilities of MUSE for exploring solar coronal dynamics, and for constraining and discriminating models of solar flares and eruptions; (3) we discuss the key contributions MUSE would make in addressing the science objectives of the Next Generation Solar Physics Mission (NGSPM), and how MUSE, the high-throughput EUV Solar Telescope (EUVST) and the Daniel K Inouye Solar Telescope (and other ground-based observatories) can operate as a distributed implementation of the NGSPM. This is a companion paper to De Pontieu et al. (2021a), which focuses on investigating coronal heating with MUSE. **2014 05 01**

## **Homologous Helical Jets: Observations by IRIS, SDO and Hinode and Magnetic Modeling with Data-Driven Simulations**

Mark C. M. **Cheung**, B. De Pontieu, **T. D. Tarbell**, **Y. Fu**, **H. Tian**, **P. Testa**, **K. K. Reeves**, **J. Martinez-Sykora**, **P. Boerner**, **J. P. Wuelser**, **J. Lemen**, **A. M. Title**, **N. Hurlburt**, **L. Kleint**, **C. Kankelborg**, **S. Jaeggli**, **L. Golub**, **S. McKillop**, **S. Saar**, **M. Carlsson**, **V. Hansteen**

*ApJ*, **801** 83 **2015**

<http://arxiv.org/pdf/1501.01593v1.pdf>

We report on observations of recurrent jets by instruments onboard the Interface Region Imaging Spectrograph (IRIS), Solar Dynamics Observatory (SDO) and Hinode spacecrafts. Over a 4-hour period on **July 21st 2013**, recurrent coronal jets were observed to emanate from NOAA Active Region 11793. FUV spectra probing plasma at transition region temperatures show evidence of oppositely directed flows with components reaching Doppler velocities of +/- 100 km/s. Raster Doppler maps using a Si IV transition region line show all four jets to have helical motion of the same sense. Simultaneous observations of the region by SDO and Hinode show that the jets emanate from a source region comprising a pore embedded in the interior of a supergranule. The parasitic pore has opposite polarity flux compared to the surrounding network field. This leads to a spine-fan magnetic topology in the coronal field that is amenable to jet formation. Time-dependent data-driven simulations are used to investigate the underlying drivers for the jets. These numerical experiments show that the emergence of current-carrying magnetic field in the vicinity of the pore supplies the magnetic twist needed for recurrent helical jet formation.

## **Imaging Spectroscopy of CME-Associated Solar Radio Bursts**

**Sherry Chhabra**, **Dale E. Gary**, **Gregg Hallinan**, **Marin M. Anderso**, **Bin Chen**, **Lincoln J. Greenhill**, **Danny C. Price**

**2021** *ApJ* **906** 132

<https://arxiv.org/pdf/2011.06073.pdf>



<https://doi.org/10.3847/1538-4357/abc94b>

We present first results of a solar radio event observed with the Owens Valley Radio Observatory Long Wavelength Array (OVRO-LWA) at metric wavelengths. We examine a complex event consisting of multiple radio sources/bursts associated with a fast coronal mass ejection (CME) and an M2.1 GOES soft X-ray flare from **2015 September 20**. Images of 9--s cadence are used to analyze the event over a 120-minute period, and solar emission is observed out to a distance of  $\approx 3.5R_{\odot}$ , with an instantaneous bandwidth covering 22~MHz within the frequency range of 40--70~MHz. We present our results from the investigation of the radio event, focusing particularly on one burst source that exhibits outward motion, which we classify as a moving type IV burst. We image the event at multiple frequencies and use the source centroids to obtain the velocity for the outward motion. Spatial and temporal comparison with observations of the CME in white light from the LASCO(C2) coronagraph, indicates an association of the outward motion with the core of the CME. By performing graduated-cylindrical-shell (GCS) reconstruction of the CME, we constrain the density in the volume. The electron plasma frequency obtained from the density estimates do not allow us to completely dismiss plasma emission as the underlying mechanism. However, based on source height and smoothness of the emission in frequency and time, we argue that gyrosynchrotron is the more plausible mechanism. We use gyrosynchrotron spectral fitting techniques to estimate the evolving physical conditions during the outward motion of this burst source.

## **Observational Study of an Earth-affecting Problematic ICME from STEREO**

Yutian **Chi**<sup>1</sup>, Jie Zhang<sup>2,3</sup>, Chenglong Shen<sup>1,4</sup>, Phillip Hess<sup>5</sup>, Lijuan Liu<sup>6</sup>, Wageesh Mishra<sup>1</sup>, and Yuming Wang<sup>1,7</sup>

**2018 ApJ** 863 108

<http://sci-hub.tw/http://iopscience.iop.org/article/10.3847/1538-4357/aacf44/meta>

We present a study of the origin of one interplanetary coronal mass ejection (ICME) that lacked an easily identifiable signature of an associated progenitor coronal mass ejection (CME) near the Sun in the observations of SOHO/LASCO at the L1 point. We consider these kinds of ICMEs as problematic, as they pose the difficulty of understanding the Sun–Earth connection and providing space weather warnings; understanding the causes of problematic ICMEs is important for space weather forecasting. This study presents the first detailed analysis of a geoeffective problematic ICME that occurred on **2011 May 28**, whose progenitor CMEs are difficult to identify in LASCO images, but fortunately they were captured by SECCHI on board the STEREO spacecraft in the quadrature configuration. There are two progenitor CMEs launching from the Sun in succession of 8 hours. We apply the graduated cylindrical shell model to reconstruct the 3D geometry, propagating direction, velocity, and brightness of the two CMEs. The main cause of the first CME (CME-1) invisible in SOHO/LASCO is due to its low mass; that is, when the CME emerges above the occulter, its brightness is as faint as the noise. The second CME (CME-2) is small, including a narrow angular width and a small cross-section of the magnetic flux rope. Even though propagating toward the Earth, CME-2 appeared as a narrow CME instead of as a halo or partial halo CME in the LASCO field of view. We also show that CME-2 propagates faster than CME-1, and that they might have interacted in the interplanetary space. **2011-05-25**

## **First 4D Reconstruction of an Eruptive Prominence Using Three Simultaneous View Directions**

I. **Chifu**, B. Inhester, M. Mierla, V. Chifu, T. Wiegmann

*Solar Physics*, November **2012**, Volume 281, Issue 1, pp 121-135

Data from the STEREO (Solar Terrestrial Relations Observatory) mission are intensively used for 3D reconstruction of solar coronal structures. After the launch of the SDO (Solar Dynamic Observatory) satellite, its additional observations give the possibility to have a third eye for more accurate 3D reconstruction in the very low corona ( $< 1.5 R_{\odot}$ ). With our reconstruction code MBSR (Multi-view B-spline Stereoscopic Reconstruction), we use three view directions (STEREO A, B, and SDO) to perform the 3D reconstruction and evolution of a prominence which triggered a CME on **1 August 2010**. In the paper we present the reconstruction of this prominence from the moment it starts to erupt until it leaves the field of view of the coronagraph. We also determine the evolution of the leading edge of the CME. Based on the temporal evolution, we analyze some of its properties, such as velocity, acceleration, opening and rotation angles and evolution of the cavity.

## **On the three-dimensional relation between the coronal dimming, erupting filament and CME. Case study of the 28 October 2021 X1.0 event**

[Galina Chikunova](#), [Tatiana Podladchikova](#), [Karin Dissauer](#), [Astrid M. Veronig](#), [Mateja Dumbović](#), [Manuela Temmer](#), [Ewan C.M. Dickson](#)

*A&A* 678, A166 **2023**

<https://arxiv.org/pdf/2308.09815.pdf>

<https://www.aanda.org/articles/aa/pdf/2023/10/aa47011-23.pdf>

We investigate the relation between the spatiotemporal evolution of the dimming region and the dominant direction of the filament eruption and CME propagation for the **28 October 2021** X1.0 flare/CME event observed from multiple viewpoints by Solar Orbiter, STEREO-A, SDO, and SOHO. We propose a method to estimate the dominant dimming direction by tracking its area evolution and emphasize its accurate estimation by calculating the surface area of a sphere for each pixel. To determine the early flux rope propagation direction, we perform 3D reconstruction of the CME via graduated cylindrical shell modeling (GCS) and tie-pointing of the filament. The dimming initially expands radially and

later shifts southeast. The orthogonal projections of the reconstructed height evolution of the erupting filament onto the solar surface are located in the sector of the dominant dimming growth, while the orthogonal projections of the inner part of GCS reconstruction align with the total dimming area. The filament reaches a maximum speed of  $\approx 250$  km/s at a height of about  $\approx 180$  Mm. The direction of its motion is strongly inclined from the radial ( $64^\circ$  to the East,  $32^\circ$  to the South). The  $50^\circ$  difference in the 3D direction between the CME and the filament leg closely corresponds to the CME half-width determined from reconstruction, suggesting a potential relation of the reconstructed filament to the associated leg of the CME body. Our findings highlight that the dominant propagation of the dimming growth reflects the direction of the erupting magnetic structure (filament) low in the solar atmosphere, though the filament evolution is not related directly to the direction of the global CME expansion. The overall dimming morphology closely resembles the inner part of the CME reconstruction, validating the use of dimming observations to obtain insight into the CME direction.

## **Magnetic Flux Rope Shredding by a Hyperbolic Flux Tube: The Detrimental Effects of Magnetic Topology on Solar Eruptions**

Georgios [Chintzoglou](#), Angelos Vourlidas, Antonia Savcheva, [Svetlin Tassev](#), [Samuel Tun Beltran](#), [Guillermo Stenborg](#)

ApJ **843** 93 **2017**

<https://arxiv.org/pdf/1706.00057.pdf>

<http://sci-hub.cc/10.3847/1538-4357/aa77b2>

We present the analysis of an unusual failed eruption captured in high cadence and in many wavelengths during the observing campaign in support of the VAULT2.0 sounding rocket launch. The refurbished Very high Angular resolution Ultraviolet Telescope (VAULT2.0) is a  $\text{Ly}\alpha$  ( $\lambda$  1216 Å) spectroheliograph launched on **September 30, 2014**. The campaign targeted active region NOAA AR 12172 and was closely coordinated with the Hinode and IRIS missions and several ground-based observatories (NSO/IBIS, SOLIS, and BBSO). A filament eruption accompanied by a low level flaring event (at the GOES C-class level) occurred around the VAULT2.0 launch. No Coronal Mass Ejection (CME) was observed. The eruption and its source region, however, were recorded by the campaign instruments in many atmospheric heights ranging from the photosphere to the corona in high cadence and spatial resolution. This is a rare occasion which enables us to perform a comprehensive investigation on a failed eruption. We find that a rising Magnetic Flux Rope-like (MFR) structure was destroyed during its interaction with the ambient magnetic field creating downflows of cool plasma and diffuse hot coronal structures reminiscent of "cusps". We employ magnetofrictional simulations to show that the magnetic topology of the ambient field is responsible for the destruction of the MFR. Our unique observations suggest that the magnetic topology of the corona is a key ingredient for a successful eruption.

## **Formation of Magnetic Flux Ropes during Confined Flaring Well Before the Onset of a Pair of Major Coronal Mass Ejections**

Georgios [Chintzoglou](#), Spiros Patsourakos, Angelos Vourlidas

ApJ **809** 34 **2015**

<http://arxiv.org/pdf/1507.01165v1.pdf>

NOAA Active Region (AR) 11429 was the source of twin super-fast Coronal Mass Ejections (CMEs). The CMEs took place within a hour from each other, with the onset of the first taking place in the beginning of **March 7, 2012**. This AR fulfills all the requirements for a "super active region"; namely, Hale's law incompatibility and a  $\delta$ -spot magnetic configuration. One of the biggest storms of Solar Cycle 24 to date ( $\text{Dst} = -143$  nT) was associated with one of these events. Magnetic Flux Ropes (MFRs) are twisted magnetic structures in the corona, best seen in  $\sim 10$  MK hot plasma emission and are often considered the core of erupting structures. However, their "dormant" existence in the solar atmosphere (i.e. prior to eruptions), is an open question. Aided by multi-wavelength observations (SDO/HMI/AIA and STEREO EUVI B) and a Non-Linear Force-Free (NLFFF) model for the coronal magnetic field, our work uncovers two separate, weakly-twisted magnetic flux systems which suggest the existence of pre-eruption MFRs that eventually became the seeds of the two CMEs. The MFRs could have been formed during confined (i.e. not leading to major CMEs) flaring and sub-flaring events which took place the day before the two CMEs in the host AR 11429.

## **Capturing transient plasma flows and jets in the solar corona**

[L. P. Chitta](#), [S. K. Solanki](#), [H. Peter](#), [R. Aznar Cuadrado](#), [L. Teriaca](#), [U. Schühle](#), [F. Auchère](#), [D. Berghmans](#), [E. Kraaikamp](#), [S. Gissot](#), [C. Verbeecq](#)

A&A Letters **2021**

<https://arxiv.org/pdf/2109.15106.pdf>

Intensity bursts in ultraviolet (UV) to X-ray wavelengths, and plasma jets are typical signatures of magnetic reconnection and the associated impulsive heating of the solar atmospheric plasma. To gain new insights into the process, high-cadence observations are required to capture the rapid response of plasma to magnetic reconnection as well as the highly dynamic evolution of jets. Here we report 200 ms cadence extreme-UV observations recorded by the 174 Å High Resolution Imager of the Extreme Ultraviolet Imager onboard the **Solar Orbiter** mission. These observations, covering a quiet-Sun coronal region, reveal the onset signatures of magnetic reconnection as localized heating events. These localized sources then exhibit repeated plasma eruptions or jet activity. Our observations show that this spatial morphological change from localized sources to jet activity could occur rapidly on timescales of about 200 ms. The jets themselves are intermittent and are produced from the source region on timescales of about 200 ms. In the

initial phases of these events, plasma jets are observed to exhibit speeds, as inferred from propagating intensity disturbances, in the range of  $100\text{ km s}^{-1}$  to  $150\text{ km s}^{-1}$ . These jets then propagate to lengths of about  $5\text{ Mm}$ . We discuss examples of bidirectional and unidirectional jet activity observed to be initiated from the initially localized bursts in the corona. The transient nature of coronal bursts and plasma jets/flows and their dynamics could provide a benchmark for magnetic reconnection models of coronal bursts and jets. **2021 February 23**

### **A New Type of Jet in a Polar Limb of the Solar Coronal Hole**

Il-Hyun **Cho**<sup>1</sup>, Yong-Jae Moon<sup>1,2</sup>, Kyung-Suk Cho<sup>3,4</sup>, Valery M. Nakariakov<sup>2,5,6</sup>, Jin-Yi Lee<sup>1</sup>, and Yeon-Han Kim<sup>3</sup>

2019 ApJL 884 L38

<https://doi.org/10.3847/2041-8213/ab4799>

<https://arxiv.org/pdf/1910.09737.pdf>

A new type of chromospheric jet in a polar limb of a coronal hole is discovered in the Ca II filtergram of the Solar Optical Telescope on board the Hinode. We identify 30 jets in a filtered Ca II movie with a duration of 53 minutes. The average speed at their maximum heights is found to be  $132 \pm 44\text{ km s}^{-1}$  ranging from  $57$  to  $264\text{ km s}^{-1}$  along the propagation direction. The average lifetime is  $20 \pm 6$  ranging from 11 to 36 s. The speed and lifetime of the jets are located at end-tails of those parameters determined for type II spicules, hence implying a new type of jets. To confirm whether these jets are different from conventional spicules, we construct a time–height image averaged over a horizontal region of  $1''$ , and calculate lagged cross-correlations of intensity profiles at each height with the intensity at  $2\text{ Mm}$ . From this, we obtain a cross-correlation map as a function of lag and height. We find that the correlation curve as a function of lag time is well fitted into three different Gaussian functions whose standard deviations of the lag time are 193, 42, and 17 s. The corresponding propagation speeds are calculated to be  $9\text{ km s}^{-1}$ ,  $67\text{ km s}^{-1}$ , and  $121\text{ km s}^{-1}$ , respectively. The kinematic properties of the former two components seem to correspond to the 3-minute oscillations and type II spicules, while the latter component to the jets is addressed in this study.

### **A New Method to Determine the Temperature of CMEs Using a Coronagraph Filter System**

Kyuhyun **Cho**, Jongchul Chae, Eun-kyung Lim, Kyung-suk Cho, Su-Chan Bong, Heesu Yang

J. of Korean Astronomical Society (JKAS) 2016

<http://arxiv.org/pdf/1603.07047v1.pdf>

The coronagraph is an instrument enables the investigation of faint features in the vicinity of the Sun, particularly coronal mass ejections (CMEs). So far coronagraphic observations have been mainly used to determine the geometric and kinematic parameters of CMEs. Here, we introduce a new method for the determination of CME temperature using a two filter (4025 Å and 3934 Å) coronagraph system. The thermal motion of free electrons in CMEs broadens the absorption lines in the optical spectra that are produced by the Thomson scattering of visible light originating in the photosphere, which affects the intensity ratio at two different wavelengths. Thus the CME temperature can be inferred from the intensity ratio measured by the two filter coronagraph system. We demonstrate the method by invoking the graduated cylindrical shell (GCS) model for the 3 dimensional CME density distribution and discuss its significance. **2002 January 4**

### **Comparison of Helicity Signs in Interplanetary CMEs and Their Solar Source Regions**

K.-S. **Cho**, S.-H. Park, K. Marubashi, N. Gopalswamy, S. Akiyama, S. Yashiro, R.-S. Kim, E.-K. Lim

Solar Physics, May 2013, Volume 284, Issue 1, pp 105-127; **File**

If all coronal mass ejections (CMEs) have flux ropes, then the CMEs should keep their helicity signs from the Sun to the Earth according to the helicity conservation principle. This study presents an attempt to answer the question from the Coordinated Data Analysis Workshop (CDAW), “Do all CMEs have flux ropes?”, by using a qualitative helicity sign comparison between interplanetary CMEs (ICMEs) and their CME source regions. For this, we select 34 CME–ICME pairs whose source active regions (ARs) have continuous SOHO/MDI magnetogram data covering more than 24 hr without data gap during the passage of the ARs near the solar disk center. The helicity signs in the ARs are determined by estimation of cumulative magnetic helicity injected through the photosphere in the entire source ARs. The helicity signs in the ICMEs are estimated by applying the cylinder model developed by Marubashi (Adv. Space. Res., 26, 55, 2000) to 16 second resolution magnetic field data from the MAG instrument onboard the ACE spacecraft. It is found that 30 out of 34 events (88 %) are helicity sign-consistent events, while four events (12 %) are sign-inconsistent. Through a detailed investigation of the source ARs of the four sign-inconsistent events, we find that those events can be explained by the local helicity sign opposite to that of the entire AR helicity (**28 July 2000 ICME**), incorrectly reported solar source region in the CDAW list (**20 May 2005 ICME**), or the helicity sign of the pre-existing coronal magnetic field (**13 October 2000** and **20 November 2003 ICMEs**). We conclude that the helicity signs of the ICMEs are quite consistent with those of the injected helicities in the AR regions from where the CMEs erupted. **Table.**

### **A HIGH-FREQUENCY TYPE II SOLAR RADIO BURST ASSOCIATED WITH THE 2011 FEBRUARY 13 CORONAL MASS EJECTION**

K.-S. **Cho**<sup>1,2,3</sup>, N. Gopalswamy<sup>2</sup>, R.-Y. Kwon<sup>2,3</sup>, R.-S. Kim<sup>1,2,3</sup>, and S. Yashiro

2013 ApJ 765 148

We examine the relationship between the high-frequency (425 MHz) type II radio burst and the associated white-light coronal mass ejection (CME) that occurred on **2011 February 13**. The radio burst had a drift rate of 2.5 MHz s<sup>-1</sup>, indicating a relatively high shock speed. From SDO/AIA observations we find that a loop-like erupting front sweeps across high-density coronal loops near the start time of the burst (17:34:17 UT). The deduced distance of shock formation (0.06 Rs) from the flare center and speed of the shock (1100 km s<sup>-1</sup>) using the measured density from SDO/AIA observations are comparable to the height (0.05 Rs, from the solar surface) and speed (700 km s<sup>-1</sup>) of the CME leading edge observed by STEREO/EUVI. We conclude that the type II burst originates even in the low corona (<59 Mm or 0.08 Rs, above the solar surface) due to the fast CME shock passing through high-density loops.

### **Relationship between multiple type II solar radio bursts and CME observed by STEREO/SECCHI**

K.-S. **Cho**, S.-C. Bong, Y.-J. Moon, A. Shanmugaraju, R.-Y. Kwon and Y. D. Park  
A&A 530, A16 (2011), **File**

*Aims.* Two or more type II bursts are occasionally observed in close time sequence during solar eruptions, which are known as multiple type II bursts. The origin of the successive burst has been interpreted in terms of coronal mass ejections (CMEs) and/or flares. Detailed investigations of the relationship between CMEs and the bursts enable us to understand the nature of the multiple type II bursts. In this study, we examine multiple type II bursts and compare their kinematics with those of a CME occurring near the time of the bursts.

*Methods.* To do this, we selected multiple type II bursts observed by the Culgoora radiospectrographs and a limb CME detected in the low corona field of view (1.4–4 Rs) of a STEREO/SECCHI instrument on **December 31, 2007**. To determine the 3D kinematics of the CME, we applied the stereoscopic technique to the STEREO/SECCHI data.

*Results.* Our main results are as follows: (1) the multiple type II bursts occurred successively at ten minute intervals and displayed various emission structures and frequency drifting rates; (2) near the time of the bursts, the CME was observed by STEREO and SOHO simultaneously, but no evidence of other CMEs was detected; (3) inspection of the 3D kinematics of the CME using the stereoscopic observation by STEREO/SECCHI revealed that the CME propagated along the eastward radial direction as viewed from the Earth; (4) very close time and height associations were found between the CME nose and the first type II burst, and between CME-streamer interaction and the second type II burst.

*Conclusions.* On the basis of these results, we suggest that a single shock in the leading edge of the CME could be the source of the multiple type II bursts and support the notion that the CME nose and the CME-streamer interaction are the two main mechanisms able to generate the bursts.

### **A Coronal Mass Ejection and Hard X-Ray Emissions Associated with the Kink Instability**

Kyung-Suk **Cho**, Jeongwoo Lee, Su-Chan Bong, Yeon-Han Kim, Bhuwan Joshi and Young-Deuk Park  
BBSO preprint #1400, June 2009; ApJ, Volume 703, Number 1, p. 1-7, **2009**, **File**

We present a morphological study of the 2004 August 18 solar eruption that occurred in the active region NOAA 10656 near the west limb using (E)UV data from the Transition Region and Coronal Explorer (TRACE), H $\alpha$  filtergram of Big Bear Solar Observatory (BBSO), white light (WL) images of Mauna Loa Solar Observatory (MLSO), hard X-ray data of the Reuven Ramaty High Energy Solar Spectroscopic Imager (RHESSI), and microwave data of the Owens Valley Solar Array (OVSA). In this event, we have an excellent set of observations for tracing the early evolution of the coronal mass ejection (CME) from a flux rope emergence to its propagation into space as a well connected series of events thanks to the coronameter's field of view down to 1.1 solar radius in overlap with that of TRACE. This dataset reveals continuously evolving (E)UV, H $\alpha$ , and WL features that suggest the rise of a small, low-lying loop, its writhing motion, break of the kinked loop at its crossing point, and transformation of the ejecta to the CME. The hard X-ray and microwave sources are found in varying locations with a complicated temporal dependence, which, we interpret, is due to two successive flares in the event. The first flare appears to be associated with the rise of the small loop, which then triggers the second flare. During the second flare a hard X-ray coronal source is detected at the crossing point of the kinked loop, and more intriguingly, the kinked loop apparently breaks at the crossing point of the two legs, which indicates a magnetic reconnection at the X-point configuration. After the break of the kinked UV loop, a CME structure shows up in the MLSO field of view, and propagates away from the sun. It is concluded that this CME occurred due to the kink instability.

### **Low coronal observations of metric type II associated CMEs by MLSO coronameters:**

K.-S. **Cho**, S.-C. Bong, Y.-H. Kim, Y.-J. Moon, M. Dryer, A. Shanmugaraju, J. Lee and Y. D. Park  
A&A 491 (2008) 873-882, **File**

<http://www.aanda.org/10.1051/0004-6361:20079013>

*Aims.* We have investigated the relationship between coronal mass ejections (CMEs) and coronal type II radio bursts by using type II associated CMEs whose low coronal observations by MLSO MK coronameters (1.08-2.85 solar radii for MK4) were available.

*Methods.* For this we considered all type II burst data at 17:00 UT to 22:00 UT from 1996 to 2003, and then compared them with CME images that were obtained during the same MLSO (Mauna Loa Solar Observatory) observing periods. As a result, we selected 19 type II associated CMEs whose kinematics are well identified. A relationship between CMEs and type IIs has been examined in terms of spatial and temporal closeness without any extrapolation of

CME kinematics as well as in terms of CME-streamer interaction.

*Results.* We found that: (1) except one event, all the metric type II events occur simultaneously or after the CME appearance in MK field of view within 30 min, mostly within 10 min after; (2) the distribution of height difference between the CME front and type II formation shows that there are double peaks, one at the CME fronts and the other at about 1 solar radius behind the front; (3) about half of the events (9/19) are identified to have CME-streamer interaction (seven streamer deflection and two overlapping), and the interaction heights are very similar to those of type II formation as well as their interaction times are nearly coincident with those of type II starting; (4) for the other events (10/19), the CME front heights at the starting time of type IIs are comparable to the heights of type II formation. *Conclusions.* Our low coronal observations of type II associated CMEs suggest that CME front and/or CME-streamer interaction at CME flank are two main mechanisms to generate type II bursts.

## **Series of Small-scale Low Plasma $\beta$ Magnetic Flux Ropes Originating from the Same Longitudinal Region: Parker Solar Probe Observations**

Kyung-Eun **Choi**<sup>1</sup>, Dae-Young Lee<sup>2</sup>, Sung-Jun Noh<sup>3</sup>, and Oleksiy Agapitov

2024 ApJ 961 3

<https://iopscience.iop.org/article/10.3847/1538-4357/ad02f6/pdf>

In this study, we report on small-scale magnetic flux ropes (SMFRs) observed as a compact series in a narrow Carrington longitudinal range during three Parker Solar Probe (PSP) encounters. First, during  $\sim 1.5$  days of PSP's inbound part of Encounter 4, we identified a series of 11 SMFRs within  $1^{\circ}4$  in longitude over the radial distance of  $\sim 8.4 R_{\odot}$  (from  $\sim 44$  to  $35 R_{\odot}$ ). The identified SMFRs lasted from  $\sim 0.5$  to 1.8 hr, and adjacent events were separated mostly by a few hours and up to  $\sim 6.5$  hr at the longest, but some events were very closely spaced with intervals of a few  $\sim$  tens of minutes or less apart. Most of the identified SMFRs are successfully fitted to the force-free model. The SMFRs are clearly distinguished from the surroundings by a notable reduction in plasma  $\beta$ , which itself was comparably low (less than unity) in the background plasma. Furthermore, the magnetic field and plasma flow within the SMFRs fluctuated significantly less than the more turbulent surroundings. The fluctuations in the surrounding medium exhibited occasional Br polarity reversal (possibly switchbacks) and were Alfvénic to a large extent with far weaker compressional components. The majority of these key features with some differences have also been found in the series of SMFRs and their surroundings identified within  $1^{\circ}3$  or less in longitude during Encounters 1 and 5. We speculate that these SMFRs were repetitively generated by successive reconnection within a very narrow angular zone located close to the Sun but not necessarily at the same radial position. **2-3 Nov 2018, 3-4 Jun 2020, 2020-01-25-26**

## **Different Periodicities in the Sunspot Area and the Occurrence of Solar Flares and Coronal Mass Ejections in Solar Cycle 23 – 24**

D. P. **Choudhary**, J. K. Lawrence, M. Norris, A. C. Cadavid

Solar Physics, February 2014, Volume 289, Issue 2, pp 649-656

In order to investigate the relationship between magnetic-flux emergence, solar flares, and coronal mass ejections (CMEs), we study the periodicity in the time series of these quantities. It has been known that solar flares, sunspot area, and photospheric magnetic flux have a dominant periodicity of about 155 days, which is confined to a part of the phase of the solar cycle. These periodicities occur at different phases of the solar cycle during successive phases. We present a time-series analysis of sunspot area, flare and CME occurrence during Cycle 23 and the rising phase of Cycle 24 from 1996 to 2011. We find that the flux emergence, represented by sunspot area, has multiple periodicities. Flares and CMEs, however, do not occur with the same period as the flux emergence. Using the results of this study, we discuss the possible activity sources producing emerging flux.

## **Magnetic flux emergence and solar eruptions in partially ionized plasmas**

**Georgios Chouliaras, V. Archontis**

ApJ 2024

<https://arxiv.org/pdf/2412.10633>

We have performed 3D MHD simulations to study the effect of partial ionization in the process of magnetic flux emergence in the Sun. In fact, we continue previous work and we now focus: 1) on the emergence of the magnetic fields above the solar photosphere and 2) on the eruptive activity, which follows the emergence into the corona. We find that in the simulations with partial ionization (PI), the structure of the emerging field consists of arch-like fieldlines with very little twist since the axis of the initial rising field remains below the photosphere. The plasma inside the emerging volume is less dense and it is moving faster compared to the fully ionized (FI) simulation. In both cases, new flux ropes (FR) are formed due to reconnection between emerging fieldlines, and they eventually erupt in an ejective manner towards the outer solar atmosphere. We are witnessing three major eruptions in both simulations. At least for the first eruption, the formation of the eruptive FR occurs in the low atmosphere in the FI case and at coronal heights in the PI case. Also, in the first PI eruption, part of the eruptive FR carries neutrals in the high atmosphere, for a short period of time. Overall, the eruptions are relatively faster in the PI case, while a considerable amount of axial flux is found above the photosphere during the eruptions in both simulations.

## **H $\alpha$ and EUV observations of a partial CME**

Damian J. **Christian**, David B. Jess, Patrick Antolin, Mihalis Mathioudakis

ApJ, 804 147 2015

We have obtained H $\alpha$  high spatial and time resolution observations of the upper solar chromosphere and supplemented these with multi-wavelength observations from the Solar Dynamic Observatory (SDO) and the *Hinode* Extreme Ultraviolet Imaging Spectrometer (EIS). The H $\alpha$  observations were conducted on **11 February 2012** with the Hydrogen-Alpha Rapid Dynamics Camera (HARDcam) instrument at the National Solar Observatory's Dunn Solar Telescope. Our H $\alpha$  observations found large downflows of chromospheric material returning from coronal heights following a failed prominence eruption. We have detected several large condensations ("blobs") returning to the solar surface at velocities of  $\approx 200$  km s $^{-1}$  in both H $\alpha$  and several SDO AIA band passes. The average derived size of these "blobs" in H $\alpha$  is 500 by 3000 km $^2$  in the directions perpendicular and parallel to the direction of travel, respectively. A comparison of our "blob" widths to those found from coronal rain, indicate there are additional smaller, unresolved "blobs" in agreement with previous studies and recent numerical simulations. Our observed velocities and decelerations of the "blobs" in both H $\alpha$  and SDO bands are less than those expected for gravitational free-fall and imply additional magnetic or gas pressure impeding the flow. We derived a kinetic energy  $\approx 2$  orders of magnitude lower for the main eruption than a typical CME, which may explain its partial nature.

### **BRIGHT RAY-LIKE FEATURES IN THE AFTERMATH OF CORONAL MASS EJECTIONS: WHITE LIGHT VERSUS ULTRAVIOLET SPECTRA**

A. Ciaravella<sup>1</sup>, D. F. Webb<sup>2</sup>, S. Giordano<sup>3</sup>, and J. C. Raymond

2013 ApJ 766 65

Current sheets (CSs) are important signatures of magnetic reconnection in the eruption of confined solar magnetic structures. Models of coronal mass ejections (CMEs) involve formation of a CS connecting the ejected flux rope with the post-eruption magnetic loops. CSs have been identified in white light (WL) images of CMEs as narrow rays trailing the outward moving CME core, and in ultraviolet spectra as narrow bright features emitting the [Fe XVIII] line. In this work, samples of rays detected in WL images or in ultraviolet spectra have been analyzed. Temperatures, widths, and line intensities of the rays have been measured, and their correlation to the CME properties has been studied. The samples show a wide range of temperatures with hot, coronal, and cool rays. In some cases, the UV spectra support the identification of rays as CSs, but they show that some WL rays are cool material from the CME core. In many cases, both hot and cool material are present, but offset from each other along the Ultraviolet Coronagraph Spectrometer slit. We find that about 18% of the WL rays show very hot gas consistent with the CS interpretation, while about 23% show cold gas that we attribute to cool prominence material draining back from the CME core. The remaining events have ordinary coronal temperatures, perhaps because they have relaxed back to a quiescent state.

### **THE CURRENT SHEET ASSOCIATED WITH THE 2003 NOVEMBER 4 CORONAL MASS EJECTION: DENSITY, TEMPERATURE, THICKNESS, AND LINE WIDTH**

A. Ciaravella<sup>1, 2</sup> and J. C. Raymond<sup>2</sup>

Astrophysical Journal, 686:1372Y1382, 2008

<http://www.journals.uchicago.edu/doi/pdf/10.1086/590655>

In the wake of the **2003 November 4** coronal mass ejection associated with the largest solar flare of the last sunspot cycle, a current sheet (CS) was observed by the Ultraviolet Coronagraph Spectrometer (UVCS) as a narrow bright feature in the [Fe xviii] (106.8 K) line. This is the first UV observation in which the CS evolution is followed from its onset. UV spectra provide diagnostics of electron temperature, emission measure, Doppler shift, line width, and size of the CS as function of time. Since the UVCS slit was inside the Mark IV K-coronameter (MK4) field of view, the combination of UV spectra and MK4 white light data provides estimates of the electron density and depth along the line of sight of the CS. The thickness of the CS in the [Fe xviii] line is far larger than classical or anomalous resistivity would predict, and it might indicate an effective resistivity much larger than anomalous resistivity, such as that due to hyperdiffusion. The broad [Fe xviii] line profiles in the CS cannot be explained as thermal widths. They result from a combination of bulk motions and turbulence. The Petschek reconnection mechanism and turbulent reconnection may be consistent with the observations.

### **Ultraviolet Properties of Halo Coronal Mass Ejections: Doppler Shifts, Angles, Shocks, and Bulk Morphology**

A. Ciaravella, J. C. Raymond, and S. W. Kahler

The Astrophysical Journal, 652:774-792, 2006 (File)

<http://www.journals.uchicago.edu/cgi-bin/resolve?ApJ62290>

### **Extreme solar events**

**Review**

[Edward W. Cliver](#), [Carolus J. Schrijver](#), [Kazunari Shibata](#) & [Ilya G. Usoskin](#)

[Living Reviews in Solar Physics](#) volume 19, Article number: 2 (2022)

<https://arxiv.org/ftp/arxiv/papers/2205/2205.09265.pdf>

<https://link.springer.com/content/pdf/10.1007/s41116-022-00033-8.pdf>

We trace the evolution of research on extreme solar and solar-terrestrial events from the 1859 Carrington event to the rapid development of the last twenty years. Our focus is on the largest observed/inferred/theoretical cases of sunspot groups, flares on the Sun and Sun-like stars, coronal mass ejections, solar proton events, and geomagnetic storms. The

reviewed studies are based on modern observations, historical or long-term data including the auroral and cosmogenic radionuclide record, and Kepler observations of Sun-like stars. We compile a table of 100- and 1000-year events based on occurrence frequency distributions for the space weather phenomena listed above. Questions considered include the Sun-like nature of superflare stars and the existence of impactful but unpredictable solar "black swans" and extreme "dragon king" solar phenomena that can involve different physics from that operating in events which are merely large. **774 AD, 17 Sep 1770, 1 September 1859, 4 Feb 1872, 14-15 May 1921, 28 Feb 1942, 5 April 1947, 23 May 1967, 2-11 August 1972, 29 Apr 1973, 21 Apr 2002, 28 October 2003; 6, 13, 14 Dec 2006, 9 Nov 2011, 28 Oct 2013, 4 Nov 2015**

**Table 5** Historical fast transit ICME events

### **Numerical simulation of the 12 May 1997 CME Event: The role of magnetic reconnection**

**Cohen**, O.; Attrill, G. D. R.; Schwadron, N. A.; Crooker, N. U.; Owens, M. J.; Downs, C.; Gombosi, T. I. *J. Geophys. Res.*, Vol. 115, No. A10, A10104, **2010**

We perform a numerical study of the evolution of a Coronal Mass Ejection (CME) and its interaction with the coronal magnetic field based on the **12 May 1997**, CME event using a global MagnetoHydroDynamic (MHD) model for the solar corona. The ambient solar wind steady-state solution is driven by photospheric magnetic field data, while the solar eruption is obtained by superimposing an unstable flux rope onto the steady-state solution. During the initial stage of CME expansion, the core flux rope reconnects with the neighboring field, which facilitates lateral expansion of the CME footprint in the low corona. The flux rope field also reconnects with the oppositely orientated overlying magnetic field in the manner of the breakout model. During this stage of the eruption, the simulated CME rotates counter-clockwise to achieve an orientation that is in agreement with the interplanetary flux rope observed at 1 AU. A significant component of the CME that expands into interplanetary space comprises one of the side lobes created mainly as a result of reconnection with the overlying field. Within 3 hours, reconnection effectively modifies the CME connectivity from the initial condition where both footpoints are rooted in the active region to a situation where one footpoint is displaced into the quiet Sun, at a significant distance ( $\approx 1R_{\odot}$ ) from the original source region. The expansion and rotation due to interaction with the overlying magnetic field stops when the CME reaches the outer edge of the helmet streamer belt, where the field is organized on a global scale. The simulation thus offers a new view of the role reconnection plays in rotating a CME flux rope and transporting its footpoints while preserving its core structure.

### **USING MULTIPLE-VIEWPOINT OBSERVATIONS TO DETERMINE THE INTERACTION OF THREE CORONAL MASS EJECTIONS OBSERVED ON 2012 MARCH 5**

Robin C. **Colaninno**<sup>1</sup> and Angelos Vourlidas

**2015** ApJ 815 70

We examine the interaction of three coronal mass ejections (CMEs) that took place on 2012 March 5 at heights less than  $20 R_{\odot}$  in the corona. We used a forward fitting model to reconstruct the three-dimensional trajectories and kinematics of the CMEs and determine their interaction in the observations from three viewpoints: Solar and Heliospheric Observatory (SOHO), STEREO-A, and STEREO-B. The first CME (CME-1), a slow-rising eruption near disk center, is already in progress at 02:45 UT when the second CME (CME-2) erupts from AR 11429 on the east limb. These two CMEs are present in the corona not interacting when a third CME (CME-3) erupts from AR 11429 at 03:34 UT. CME-3 has a constant velocity of  $1456[\pm 31]$  km s<sup>-1</sup> and drives a shock that is observed as a halo from all viewpoints. We find that the shock driven by CME-3 passed through CME-1 with no observable change in the geometry, trajectory, or velocity of CME-1. However, the elevated temperatures detected in situ when CME-1 reached Earth indicate that the plasma inside CME-1 may have been heated by the passage of the shock. CME-2 is accelerated by CME-3 to more than twice its initial velocity and remains a separate structure ahead of the CME-3 front. CME-2 is deflected 24° northward by CME-3 for a total deflection of 40° from its source region. These results suggest that the collision of CME-2 and CME-3 is superelastic. This work demonstrates the capability and utility of fitting forward models to complex and interacting CMEs observed in the corona from multiple viewpoints.

### **Update of the Photometric Calibration of the LASCO-C2 Coronagraph Using Stars**

R. C. **Colaninno**, R. A. Howard

*Solar Phys.* Volume 290, [Issue 3](#), pp 997-1009, **2015**

<http://link.springer.com/article/10.1007/s11207-014-0635-2/fulltext.html>

We present an update to the photometric calibration of the LASCO-C2 coronagraph onboard the [SOHO](#) spacecraft. We obtained the new calibration using data from the beginning of the mission in 1996 until 2013. We re-examined the LASCO-C2 photometric calibration by comparing the past three calibrations and the present calibration with the goal of validating an in-flight calibration. We find a photometric calibration factor (PCF) that is very similar to the factor recently published in Gardès, Lamy, and Llebaria (*Solar Phys.* 283, 667, 2013), which calculated a calibration between 1996 and 2009. The average of our PCF between 1999 and 2009 is the same, within our margin of error, as the average given by Gardès, Lamy, and Llebaria (*Solar Phys.* 283, 667, 2013) during the same time period. However, we find a different evolution of the calibration over the lifetime of the LASCO-C2 instrument compared with past results. We find that the sensitivity of the instrument is decreasing by a constant  $0.20 [\pm 0.03]$  % per year. We also find no significant difference in the signal degradation before and after the [SOHO](#) interruption. We discuss the effects of this new PCF on the calibrated data set and the potential impact on scientific results derived from the previous calibration.

21 March 2007

## **FIRST DETERMINATION OF THE TRUE MASS OF CORONAL MASS EJECTIONS: A NOVEL APPROACH TO USING THE TWO *STEREO* VIEWPOINTS**

Robin C. [Colaninno](#)<sup>1</sup> and Angelos Vourlidas<sup>2</sup>

*Astrophysical Journal*, 698:852–858, **2009**, [File](#)

The twin Sun Earth Connection Coronal and Heliospheric Investigation (SECCHI) COR2 coronagraphs of the *Solar Terrestrial Relations Observatory (STEREO)* provide images of the solar corona from two viewpoints in the solar system. Since their launch in late 2006, the *STEREO* Ahead (A) and Behind (B) spacecraft have been slowly separating from Earth at a rate of 22.5 per year. By the end of 2007, the two spacecraft were separated by more than 40° from each other. At that time, we began to see large-scale differences in the morphology and total intensity between coronal mass ejections (CMEs) observed with SECCHI-COR2 on *STEREO*-A and B. Due to the effects of the Thomson scattering geometry, the intensity of an observed CME is dependent on the angle it makes with the observed plane of the sky. From the intensity images, we can calculate the integrated line-of-sight electron density and mass. We demonstrate that it is possible to simultaneously derive the direction and true total mass of the CME if we make the simple assumption that the same mass should be observed in COR2-A and B.

## **Analysis of the Velocity Field of CMEs Using Optical Flow Methods**

Robin C. [Colaninno](#) and Angelos Vourlidas,

*The Astrophysical Journal*, 652:1747-1754, **2006**, [File](#)

we introduce an image-processing algorithm from the field of computer vision and demonstrate that the velocity field of a CME can be obtained reliably over most of the area, with certain assumptions and restrictions.

## **A statistical study of CME properties and of the correlation between flares and CMEs over the solar cycles 23 and 24**

A. [Compagnino](#), P. Romano, F. Zuccarello

*Solar Phys.* January **2017**, 292:5

<http://arxiv.org/pdf/1609.08943v1.pdf>

We investigated some properties of coronal mass ejections (CMEs), such as speed, acceleration, polar angle, angular width and mass, using data acquired by LASCO aboard of SOHO from July 31, 1997, to March 31, 2014, i.e., during the solar cycles 23 and 24. We used two CME catalogs: one provided by the CDAW Data Center and one obtained by the CACTus detection algorithm. For both dataset, we found that the number of CMEs observed during the peak of cycle 24 was higher or comparable to the one during cycle 23, although the photospheric activity during cycle 24 was weaker than during cycle 23. More precisely, using the CMEs detected by CACTus we noted that the number of events  $N$  is of the same order of magnitude during the peaks of the two cycles, but the peak of CME distribution during the cycle 24 is more extended in time ( $N > 1500$  during 2012 and 2013). We ascribe the discrepancy between CDAW and CACTus results to the observer bias for CME definition in the CDAW catalog (Robbrecht et al., 2009; Webb and Howard, 2012; Yashiro et al., 2008). We also used a dataset containing 19811 flares of C, M, and X class, observed by GOES during the same period. Using both dataset, we studied the relationship between the mass ejected by the CMEs and the flux emitted during the corresponding flares: we found 11441 flares that were temporally-correlated with CMEs for CDAW and 9120 for CACTus. Moreover, we found a log-linear relationship between the flux of the flares integrated from the start to end in the 0.1-0.8 nm range and the CME mass:  $\log(\text{CME mass})$  proportional to  $0.23 \times \log(\text{flare flux})$ . We also found some differences in the mean CMEs velocity and acceleration between the events associated with flares and those that were not. In particular, the CMEs associated with flares are on average 100 km/s faster than the ones not associated with flares.

## **Excitation Sources of Oscillations in Solar Coronal Loops: A Multi-wavelength Analysis**

Sandra M. [Conde](#)<sup>1,2</sup>, Rekha Jain<sup>3</sup>, and Vera Jatenco-Pereira<sup>1</sup>

**2020** *ApJL* 890 L21

<https://doi.org/10.3847/2041-8213/ab7348>

An investigation into the excitation sources of oscillations detected in a coronal loop structure is carried out using the images obtained with Interface Region Imaging Spectrometer (IRIS) and the Atmospheric Imaging Assembly (AIA) instrument on board the Solar Dynamics Observatory (SDO). A loop structure in the active region AR 11967 on **2014 January 28**, oscillating in the vicinity of a strong eruption and an M3.6 class flare site, is clearly noticeable in SDO/AIA 171 Å images. We study in detail, the oscillations with detected periods between 4 and 13 minutes and their connection in IRIS SJI 1330 Å and SDO/AIA 1700 Å images; both of these wavelengths sample the lower parts of the solar atmosphere. The simultaneous presence of many oscillations in the region of interest in all three wavelength passbands suggest that these oscillations were excited in the lower-chromosphere–photosphere plasma connected to the loop structure and then propagated at higher heights. We further investigate the Doppler velocity measurements from the spectrograph snapshots in IRIS C ii 1336 Å, Si iv 1403 Å and Mg ii k 2796 Å. These show signatures of upflows in



the vicinity of the loop structure's endpoints estimated from 171 Å images. We suggest that some of the oscillations observed in AIA 171 Å have been triggered by plasma ejections and perturbations seen in the lower layers of the solar atmosphere. Based on the estimated phase speeds, the oscillations are likely to be slow magnetoacoustic in nature.

## **SOLAR CYCLE VARIATIONS OF CORONAL NULL POINTS: IMPLICATIONS FOR THE MAGNETIC BREAKOUT MODEL OF CORONAL MASS EJECTIONS**

G. R. [Cook](#)<sup>1</sup>, D. H. [Mackay](#)<sup>1</sup>, and [Dibyendu Nandy](#)<sup>2</sup>

*Astrophysical Journal*, 704:1021–1035, **2009** October

In this paper, we investigate the solar cycle variation of coronal null points and magnetic breakout configurations in spherical geometry, using a combination of magnetic flux transport and potential field source surface models. Within the simulations, a total of 2843 coronal null points and breakout configurations are found over two solar cycles. It is found that the number of coronal nulls present at any time varies cyclically throughout the solar cycle, in phase with the flux emergence rate. At cycle maximum, peak values of 15–17 coronal nulls per day are found. No significant variation in the number of nulls is found from the rising to the declining phase. This indicates that the magnetic breakout model is applicable throughout both phases of the solar cycle. In addition, it is shown that when the simulations are used to construct synoptic data sets, such as those produced by Kitt Peak, the number of coronal nulls drops by a factor of 1/6. The vast majority of the coronal nulls are found to lie above the active latitudes and are the result of the complex nature of the underlying active region fields. Only 8% of the coronal nulls are found to be connected to the global dipole. Another interesting feature is that 18% of coronal nulls are found to lie above the equator due to cross-equatorial interactions between bipoles lying in the northern and southern hemispheres. As the majority of coronal nulls form above active latitudes, their average radial extent is found to be in the lowcorona below  $1.25 R_{\odot}$  (175,000 km above the photosphere). Through considering the underlying photospheric flux, it is found that 71% of coronal nulls are produced through quadrupolar flux distributions resulting from bipoles in the same hemisphere interacting. When the number of coronal nulls present in each rotation is compared to the number of bipoles emerging, a wide scatter is found. The ratio of coronal nulls to emerging bipoles is found to be approximately 1/3. Overall, the spatio-temporal evolution of coronal nulls is found to follow the typical solar butterfly diagram and is in qualitative agreement with the observed time dependence of coronal mass ejection source-region locations.

## **Designing a New Coronal Magnetic Field Energy Diagnostic**

Marcel F. [Corchado-Albelo](#)<sup>1</sup>, [Kévin Dalmasse](#)<sup>2</sup>, [Sarah Gibson](#)<sup>3</sup>, [Yuhong Fan](#)<sup>3</sup>, and [Anna Malanushenko](#)  
**2021** *ApJ* 907 23

<https://doi.org/10.3847/1538-4357/abc8f0>

In the solar corona, the free energy, i.e., the excess in magnetic energy over a ground-state potential field, forms the reservoir of energy that can be released during solar flares and coronal mass ejections. Such free energy provides a measure of the magnetic field nonpotentiality. Recent theoretical and observational studies indicate that the presence of nonpotential magnetic fields is imprinted into the structures of infrared, off-limb, coronal polarization. In this paper, we investigate the possibility of exploiting such observations for mapping and studying the accumulation and release of coronal free magnetic energy, with the goal of developing a new tool for identifying "hot spots" of coronal free energy such as those associated with twisted and/or sheared coronal magnetic fields. We applied forward modeling of infrared coronal polarimetry to three-dimensional models of nonpotential and potential magnetic fields. From these we defined a quantitative diagnostic of nonpotentiality that in the future could be calculated from a comparison of infrared, off-limb, coronal polarization observations from, e.g., the Coronal Multi-channel Polarimeter or the Daniel K. Inouye Solar Telescope, and the corresponding polarization signal forward-modeled from a potential field extrapolated from photospheric magnetograms. We considered the relative diagnostic potential of linear and circular polarization, and the sensitivities of these diagnostics to coronal density distributions and assumed boundary conditions of the potential field. Our work confirms the capacity of polarization measurements for diagnosing nonpotentiality and free energy in the solar corona.

## **A MODEL OF CORONAL STREAMERS WITH UNDERLYING FLUX ROPES**

M. [Cottaar](#)<sup>1</sup> and Y. Fan

*Astrophysical Journal*, 704:576–590, **2009** October

We present global two-dimensional axisymmetric isothermal MHD simulations of the dynamic evolution of a coronal helmet streamer, driven at the lower boundary by the emergence of a twisted flux rope. By varying both the detached toroidal and poloidal fluxes emerged into the corona, but fixing the normal flux distribution at the surface at the end of the emergence, we obtain solutions that either settle to a new steady state of a stable helmet streamer containing a flux rope, or result in a disruption of the helmet with the underlying flux rope being expelled in a coronal mass ejection (CME)-like eruption. In all of the cases studied, we find that the transition from a stable to an eruptive state takes place at a magnetic energy that is very close to the Aly open field energy. Furthermore, we find that the transition from a stable to an eruptive end state does not occur at a single critical value of the total relative magnetic helicity, but depends on the profile of the underlying flux rope. Cases where the detached flux rope contains a higher amount of self-helicity, i.e., higher internal twist or detached poloidal flux, are found to become eruptive at a significantly lower total helicity. For the eruptive cases, the detached flux rope after emergence first rises quasi-statically due to a gradual opening of the field lines at the edge of the streamer and a slow reconnection below the flux rope, which continues to slowly increase the amount of the detached flux. This decreases the downward magnetic tension on the flux rope. The dynamic eruption is initiated when the magnetic

pressure gradient no longer decreases fast enough to balance the decrease in the magnetic tension. Later rapid reconnections below the flux rope are important for accelerating the flux rope. For the stable helmets, we find that no cavities are formed due to the simplifying assumption of isothermal energetics and the uniform density lower boundary condition. However during the eruption we see the development of the 3-part structure of a CME.

### **Inward Propagating Plasma Parcels in the Solar Corona: Models with Aerodynamic Drag, Ablation, and Snowplow Accretion**

Steven R. **Cranmer** (CU Boulder), [Craig E. DeForest](#) (SwRI), [Sarah E. Gibson](#) (HAO/NCAR)

ApJ 2021

<https://arxiv.org/pdf/2103.12039.pdf>

Although the solar wind flows primarily outward from the Sun to interplanetary space, there are times when small-scale plasma inflows are observed. Inward-propagating density fluctuations in polar coronal holes were detected by the COR2 coronagraph on board the STEREO-A spacecraft at heliocentric distances of 7 to 12 solar radii, and these fluctuations appear to undergo substantial deceleration as they move closer to the Sun. Models of linear magnetohydrodynamic waves have not been able to explain these deceleration patterns, so they have been interpreted more recently as jets from coronal sites of magnetic reconnection. In this paper, we develop a range of dynamical models of discrete plasma parcels with the goal of better understanding the observed deceleration trend. We found that parcels with a constant mass do not behave like the observed flows, and neither do parcels undergoing ablative mass loss. However, parcels that accrete mass in a snowplow-like fashion can become decelerated as observed. We also extrapolated OMNI in situ data down to the so-called Alfvén surface and found that the initial launch-point for the observed parcels may often be above this critical radius. In other words, in order for the parcels to flow back down to the Sun, their initial speeds are probably somewhat nonlinear (i.e., supra-Alfvénic) and thus the parcels may be associated with structures such as shocks, jets, or shear instabilities.

### **Asymmetric expansion of coronal mass ejections in the low corona**

H. **Cremades**<sup>1,2</sup>, F. A. Iglesias<sup>1,2</sup> and L. A. Merenda

A&A 635, A100 (2020)

<https://doi.org/10.1051/0004-6361/201936664>

**Aims.** Understanding how magnetic fields are structured within coronal mass ejections (CMEs), and how they evolve from the low corona into the heliosphere, is a major challenge for space weather forecasting and for solar physics. The study of CME morphology is a particularly auspicious approach to this problem, given that it holds a close relationship with the CME magnetic field configuration. Although earlier studies have suggested an asymmetry in the width of CMEs in orthogonal directions, this has not been inspected using multi-viewpoint observations.

**Methods.** The improved spatial, temporal, and spectral resolution, added to the multiple vantage points offered by missions of the Heliophysics System Observatory, constitute a unique opportunity to gain insight into this regard. We inspect the early evolution (below ten solar radii) of the morphology of a dozen CMEs occurring under specific conditions of observing spacecraft location and CME trajectory, favorable to reduce uncertainties typically involved in the 3D reconstruction used here. These events are carefully reconstructed by means of a forward modeling tool using simultaneous observations of the Solar-Terrestrial Relations Observatory (STEREO) Extreme Ultraviolet Imager and the Solar Dynamics Observatory Atmospheric Imaging Assembly as input when originating low in the corona, and followed up in the outer fields of view of the STEREO and the Solar and Heliospheric Observatory coronagraphs. We then examine the height evolution of the morphological parameters arising from the reconstructions.

**Results.** The multi-viewpoint analysis of this set of CMEs revealed that their initial expansion – below three solar radii – is considerably asymmetric and non-self-similar. Both angular widths, namely along the main axes of CMEs (AWL) and in the orthogonal direction (AWD, representative of the flux rope diameter), exhibit much steeper change rates below this height, with the growth rate of AWL found to be larger than that of AWD, also below that height. Angular widths along the main axes of CMEs are on average  $\approx 1.8$  times larger than widths in the orthogonal direction AWD. The ratios of the two expansion speeds, namely in the directions of CMEs main axes and in their orthogonal, are nearly constant in time after  $\sim 4$  solar radii, with an average ratio  $\approx 1.6$ . Heights at which the width change rate is defined to stabilize are greater for AWL than for AWD.

### **Coronal mass ejections associated to a super-active region**

H. **Cremades** et al.

CESRA nugget #2080 2018

<http://www.astro.gla.ac.uk/users/eduard/cesra/?p=2080>

During its transit through central meridian, and along four consecutive days, from **13 to 16 February 2011**, NOAA active region (AR) 11158 generated coronal mass ejections (CMEs) in association with waves observed in the extreme ultraviolet (EUV) low corona, and even with a Moreton wave. On those dates, the spacecraft of the **STEREO** mission were located in quadrature with **SOHO** and **SDO**, enabling the exceptional observation of this series of Earth-directed events. Moreover, low-frequency radio emissions registered by the **WAVES** experiment aboard the **Wind** spacecraft allows tracking of the events in the interplanetary medium. These circumstances motivate a joint analysis of the four coronal wave events, their associated CMEs, and interplanetary radio counterparts, by means of observations from multiple viewpoints and at various wavelengths.

## Mass Loss Rates from Coronal Mass Ejections: A Predictive Theoretical Model for Solar-Type Stars

Steven R. [Cranmer](#) (CU Boulder)

ApJ 2017

<https://arxiv.org/pdf/1704.06689.pdf>

Coronal mass ejections (CMEs) are eruptive events that cause a solar-type star to shed mass and magnetic flux. CMEs tend to occur together with flares, radio storms, and bursts of energetic particles. On the Sun, CME-related mass loss is roughly an order of magnitude less intense than that of the background solar wind. However, on other types of stars, CMEs have been proposed to carry away much more mass and energy than the time-steady wind. Earlier papers have used observed correlations between solar CMEs and flare energies, in combination with stellar flare observations, to estimate stellar CME rates. This paper sidesteps flares and attempts to calibrate a more fundamental correlation between surface-averaged magnetic fluxes and CME properties. For the Sun, there exists a power-law relationship between the magnetic filling factor and the CME kinetic energy flux, and it is generalized for use on other stars. An example prediction of the time evolution of wind/CME mass-loss rates for a solar-mass star is given. A key result is that for ages younger than about 1 Gyr (i.e., activity levels only slightly higher than the present-day Sun), the CME mass loss exceeds that of the time-steady wind. At younger ages, CMEs carry 10 to 100 times more mass than the wind, and such high rates may be powerful enough to disperse circumstellar disks and affect the habitability of nearby planets. The cumulative CME mass lost by the young Sun may have been as much as 1% of a solar mass.

## Asymmetric expansion of coronal mass ejections in the low corona

Hebe [Cremades](#), [Francisco A. Iglesias](#), [Luciano A. Merenda](#)

A&A 2020

<https://arxiv.org/pdf/2001.10085.pdf>

**Aims.** The study of the morphology of coronal mass ejections (CMEs) is an auspicious approach to understanding how magnetic fields are structured within CMEs. Although earlier studies have suggested an asymmetry in the width of CMEs in orthogonal directions, this has not been inspected using multi-viewpoint observations.

**Methods.** We inspect the early evolution (below ten solar radii) of the morphology of a dozen CMEs occurring under specific conditions of observing spacecraft location and CME trajectory, favorable to reduce uncertainties typically involved in the 3D reconstruction used here. These events are carefully reconstructed by means of a forward modeling tool using simultaneous observations of STEREO EUVI and SDO/AIA as input when originating low in the corona, and followed up in the outer fields of view of the STEREO and the SOHO coronagraphs. We then examine the height evolution of the morphological parameters arising from the reconstructions.

**Results.** The multi-viewpoint analysis of this set of CMEs revealed that their initial expansion --below three solar radii-- is considerably asymmetric and non-self-similar. Both angular widths, namely along the main axes of CMEs (AWL) and in the orthogonal direction (AWD, representative of the flux rope diameter), exhibit much steeper change rates below this height, with the growth rate of AWL found to be larger than that of AWD, also below that height. Angular widths along the main axes of CMEs are on average  $\approx 1.8$  times larger than widths in the orthogonal direction AWD. The ratios of the two expansion speeds, namely in the directions of CMEs main axes and in their orthogonal, are nearly constant in time after  $\sim 4$  solar radii, with an average ratio  $\approx 1.6$ . Heights at which the width change rate is defined to stabilize are greater for AWL than for AWD. **14 December 2010**

**Table 1:** Analyzed events and main attributes. (2010-2013)

## Coronal mass ejections from the same active region cluster: Two different perspectives

Hebe [Cremades](#), Cristina Hemilse Mandrini, Brigitte Schmieder, Alberto Maximiliano Crescitelli

Solar Phys Volume 290, Issue 6, pp 1671-1686 2015

<http://arxiv.org/pdf/1505.01384v1.pdf>

The cluster formed by active regions (ARs) NOAA 11121 and 11123, approximately located on the solar central meridian on **11 November 2010**, is of great scientific interest. This complex was the site of violent flux emergence and the source of a series of Earth-directed events on the same day. The onset of the events was nearly simultaneously observed by the Atmospheric Imaging Assembly (AIA) telescope aboard the Solar Dynamics Observatory (SDO) and the Extreme-Ultraviolet Imagers (EUVI) on the Sun-Earth Connection Coronal and Heliospheric Investigation (SECCHI) suite of telescopes onboard the Solar-Terrestrial Relations Observatory (STEREO) twin spacecraft. The progression of these events in the low corona was tracked by the Large Angle Spectroscopic Coronagraphs (LASCO) onboard the Solar and Heliospheric Observatory (SOHO) and the SECCHI/COR coronagraphs on STEREO. SDO and SOHO imagers provided data from the Earth's perspective, whilst the STEREO twin instruments procured images from the orthogonal directions. This spatial configuration of spacecraft allowed optimum simultaneous observations of the AR cluster and the coronal mass ejections that originated in it. Quadrature coronal observations provided by STEREO revealed a notably large amount of ejective events compared to those detected from Earth's perspective. Furthermore, joint observations by SDO/AIA and STEREO/SECCHI EUVI of the source region indicate that all events classified by GOES as X-ray flares had an ejective coronal counterpart in quadrature observations. These results have direct impact on current space weather forecasting because of the probable missing alarms when there is a lack of solar observations in a view direction perpendicular to the Sun-Earth line.

## Coronal Transient Events During Two Solar Minima: Their Solar Source Regions and Interplanetary Counterparts

H. [Cremades](#), C. H. Mandrini und S. Dasso

Solar Physics, Volume 274, Numbers 1-2, 233-249, **2011**, [File](#)

In the frame of two coordinated observational and research efforts, two full solar rotations were investigated in the times of two distinct solar minima. These two campaigns were dubbed Whole Sun Month (WSM; **10 August – 8 September 1996**) and Whole Heliosphere Interval (WHI; **20 March – 16 April 2008**). The nearly uninterrupted gathering of solar coronal data since the beginning of the Solar and Heliospheric Observatory (SOHO) era offers the exceptional possibility of comparing two solar minima for the first time, with regard to the coronal transient aspect. This study characterizes the variety of outward-traveling transients observed in the solar corona during both time intervals, from very narrow jet-like events to coronal mass ejections (CMEs). Their solar source regions and ensuing interplanetary structures were identified and characterized as well, toward a global-scale description of their role in determining the heliosphere's conditions. Multi-wavelength images provided by the space missions SOHO, Yokohoh (only WSM), and Solar-Terrestrial Relations Observatory (STEREO; only WHI) and ground-based observatories were analyzed for coronal ejecta and their solar sources, while data registered by the Advanced Composition Explorer (ACE) spacecraft were inspected for interplanetary CMEs and magnetic clouds. Notable differences arise from the analysis of the detailed survey of events: more (fewer) ejecta during WHI (WSM), 12% (40%) were produced by active regions during WHI (WSM), and nearly no (high) deflection from the radial direction was observed during WHI (WSM). Instrumental aspects such as dissimilar resolution, cadence, and fields of view are considered in order to discern instrumentally driven disparities from inherent differences between solar minima.

### **Coronal mass ejections: Solar cycle aspects**

Hebe [Cremades](#) and O.C. St. Cyr

[Advances in Space Research](#)

[Volume 40, Issue 7](#), Pages 1042-1048, **2007**, [File](#)

Research in the area of coronal mass ejections (CMEs) is now mature, since their discovery coincided with the first coronagraph that was flown in space in 1971. However, the continuity of space coronagraphs and similar instruments has allowed the detection and measurement of CMEs over almost three consecutive solar cycles. Their importance in the space weather field is well established, and some researchers believe the phenomenon may also be important for the longer-term space climate studies. In this review, we summarize the solar cycle variation of the main properties of CMEs detected by previous and ongoing missions. These include rate of detection, apparent angular width, detected mass, apparent speed, and apparent latitude. Their behavior in time is presented and discussed.

### **Cremades, H., Three-dimensional configuration and evolution of coronal mass ejections,**

Ph. D. thesis, Copernicus GmbH, Katlenburg-Lindau, Germany, ISBN: 3-936586-40-3, **2005**.

**Cremades, H. and V. Bothmer, Geometrical properties of coronal mass ejections,** in Proc. IAL symp. 226 on Coronal and Stellar Mass Ejections, eds. K. P. Dere, J. Wang, and Y. Yan, 48, **2005**.

### **On the three-dimensional configuration of coronal mass ejections**

H. [Cremades](#) and V. Bothmer

A&A 422, 307–322 (**2004**); [File](#)

Coronal mass ejections (CMEs) are a direct consequence of the dynamic nature of the solar atmosphere. They represent fundamental processes in which energy is transferred from the Sun into interplanetary space, including geospace. Their origin, 3D structure and internal magnetic field configuration are to date not well understood. The SOHO spacecraft, launched by the end of 1995, has provided unprecedented data on CMEs since instruments switched on in 1996. From a detailed investigation of the full set of LASCO (Large Angle Spectroscopic Coronagraph) observations from 1996 to the end of 2002, a set of structured CME events has been identified, which exhibits white-light fine structures likely indicative of their internal magnetic field configuration and possible 3D structure. Their source regions in the low corona and photosphere have been inferred by means of complementary analyses of data from the Extreme-Ultraviolet Imaging Telescope (EIT) and Michelson Doppler Imager (MDI) on board SOHO, and ground-based H $\alpha$  measurements. According to the results of this study, structured CMEs arise in a self-similar manner from pre-existing small scale loop systems, overlying regions of opposite magnetic polarities. From the characteristic pattern of the CMEs' source regions in both solar hemispheres, a generic scheme is presented in which the projected white-light topology of a CME depends primarily on the orientation and position of the source region's neutral line on the solar disk. The paper also provides information about the white-light characteristics of the analysed CMEs, such as angular width and position angle, with respect to their source region properties, such as heliographic location, inclination and length, including the frequency and variation of these parameters over the investigated time period.

## Remote sensing of the solar site of interchange reconnection associated with the May 1997 magnetic cloud

Crooker N.U., Webb D.F.

Journal of Geophysical Research, Volume 111, Issue A8, CiteID A08108, 2006.

The direction of suprathermal electron flux on open magnetic field lines in the **15 May 1997** magnetic cloud is used to predict the solar location of the interchange reconnection that released one end of what presumably were doubly connected field lines in the coronal mass ejection (CME) of origin on **12 May**.

## Constraining Stellar Coronal Mass Ejections Through Multi-Wavelength Analysis of the Active M Dwarf EQ Peg

M. K. Crosley, R. A. Osten

2018 *ApJ* 856 39

<https://arxiv.org/pdf/1802.03440.pdf>

Stellar coronal mass ejections remain experimentally unconstrained, unlike their stellar flare counterparts which are observed ubiquitously across the electromagnetic spectrum. Low frequency radio bursts in the form of a type II burst offer the best means of identifying and constraining the rate and properties of stellar CMEs. CME properties can be further improved through the use of proposed solar-stellar scaling relations and multi-wavelength observations of CMEs through the use of type II bursts and the associated flare expected to occur alongside. We report on 20 hours of observation of the nearby, magnetically active, and well characterized M dwarf star EQ Peg. The observations are simultaneously observed with the Jansky Very Large Array at their P-band (230-470 MHz) and at the Apache Point observatory in the SDSS u' filter ( $\lambda = 3557 \text{ \AA}$ ). Dynamic spectra of the P band data, constructed to search for signals in the frequency-time domains, did not reveal evidence for drifting radio bursts that could be ascribed to type II bursts. Given the sensitivity of our observations, we are able to place limits on the brightness temperature and source size of any bursts which may have occurred. Using solar scaling relations on four observed stellar flares, we predict CME parameters. Given the constraints on coronal density and photospheric field strength, our models suggest that the observed flares would have been insufficient to produce detectable type II bursts at our observed frequencies. We consider the implications of these results, and other recent findings, on stellar mass loss.

## Transient Mass Loss Analysis of Solar Observations using Stellar Methods

M. K. Crosley, R. A. Osten, C. Norman

2017 *ApJ*, 845, 67

<https://arxiv.org/pdf/1707.01928.pdf>

Low frequency dynamic spectra of radio bursts from nearby stars offer the best chance to directly detect the stellar signature of transient mass loss on low mass stars. Crosley et al. (2016) proposes a multi-wavelength methodology to determine coronal mass ejection parameters, such as Coronal Mass Ejection (CME) speed, mass, and kinetic energy. We test the validity and accuracy of the results derived from the methodology by using Geostationary Operational Environmental Satellite X-ray observations and Bruny Island Radio Spectrometer radio observations. These are analogous observations to those which would be found in the stellar studies. Derived results from these observations are compared to direct white light measurements of the Large Angle and Spectrometric Coronagraph.

We find that, when a pre-event temperature can be determined, that the accuracy of CME speeds are within a few hundred km/s, and are reliable when specific criteria has been met. CME mass and kinetic energies are only useful in determining approximate order of magnitude measurements when considering the large errors associated to them. These results will be directly applicable to interpretation of any detected stellar events and derivation of stellar CME properties. **2011-01-28, 2011-02-13, 2012-03-17, 2012-06-03, 2012-07-06, 2013-05-02, 2013-10-24, 2013-11-08, 2014-01-08, 2014-02-20, 2014-03-20, 2014-04-25, 2014-11-03, 2014-12-17,**

**Table 2.** SOHO/LASCO Measurements

**Table 4.** Parameters from GOES Measurements

## A Solar Energetic Particle Removal Algorithm for the Compact Coronagraph

Nicholas A. Crump, Dennis G. Socker, and Dennis Wang

2019 *Res. Notes AAS* 3 183

<https://iopscience.iop.org/article/10.3847/2515-5172/ab5f14>

2011 June 5, 2012 January 27, 2012-07-23

## Statistical Study of Magnetic Topology for Eruptive and Confined Solar Flares

Yanmei Cui, Haimin Wang, Yan Xu, Siqing Liu

*JGR* 2018

<http://sci-hub.tw/http://onlinelibrary.wiley.com/doi/10.1002/2017JA024710/abstract;jsessionid=1B28DD312655626B6C73EE27929AA447.f03t01>

Large flares and halo CMEs can often cause strong space environment disturbances and sequentially a series of space environment effects. The X-class flares associated with halo CMEs are particularly prone to these effects. In this paper, 58 X-class flares were collected and studied with the source locations in 30 degrees from the disk center, which were observed from 1996 to 2015. Among these events, 48 flares were associated with CMEs and defined as “eruptive” events. The other 10 flares without CMEs were defined as “confined” flares. By comparing the properties of flares and associated magnetic fields for the two sets of samples, we found: (1) Magnetic free energy and overlying transverse fields play important roles in producing solar eruptions. Eruptive flares with high-speed CMEs tend to occur in active regions with more free energy and larger decay index. (2) CME speeds are affected by magnetic free energy, which are described by parameters of the unsigned magnetic flux, the area of polarity inversion region, and the strength of transverse fields in the low altitude. These parameters have moderate positive correlations with CME speeds.

**Table 1:** Selected X-Class Flares and the associated CMEs from 1996 to 2015

### **Shock wave driven by CME evidenced by metric type II burst and EUV wave**

R.D. **Cunha-Silva**, F.C.R. Fernandes, C.L. Selhorst

Advances in Space Research Volume 56, Issue 12, 15 December 2015, Pages 2804–2810

<http://www.sciencedirect.com/science/article/pii/S0273117715005311>

Solar type II radio bursts are produced by plasma oscillations in the solar corona as a result of shock waves. The relationship between type II bursts and coronal shocks is well evidenced by observations since the 1960s. However, the drivers of the shocks associated with type II events at metric wavelengths remain as a controversial issue among solar physicists. The flares and the coronal mass ejections (CMEs) are considered as potential drivers of these shocks. In this article, we present an analysis of a metric type II burst observed on **May 17, 2013**, using data provided by spectrometers from e-CALLISTO (extended-Compound Astronomical Low-cost Low-frequency Instrument for Spectroscopy and Transportable Observatories) and EUV images from the Extreme Ultraviolet Imager (EUVI), aboard the Solar Terrestrial Relations Observatory (STEREO). The event was associated with an M3.2 SXR flare and a halo CME. The EUV wave produced by the expansion of the CME was clear from the EUV images. The heights of the EUV wave fronts proved to be consistent with the heights of the radio source obtained with the  $2-4 \times$  Newkirk density model, which provided a clue to an oblique propagation of the type-II-emitting shock segment. The results for the magnetic field in the regions of the shock also revealed to be consistent with the heights of the radio source obtained using the  $2-4 \times$  Newkirk density model. Exponential fit on the intensity maxima of the harmonic emission provided a shock speed of  $\sim 580-990 \text{ km s}^{-1}$ , consistent with the average speed of the associated EUV wave front of  $626 \text{ km s}^{-1}$ .

### **Explosive Events: Swirling Transition Region Jets**

W. **Curdt**, H. Tian, S. Kamio

Solar Physics, October 2012, Volume 280, Issue 2, pp 417-424

In this paper, we extend our earlier work to provide additional evidence for an alternative scenario to explain the nature of events called ‘explosive events’. The bidirectional, fast Doppler motion of explosive events observed spectroscopically in the transition region emission is classically interpreted as a pair of bidirectional jets moving upward and downward from a reconnection site. We discuss the problems of this model. In our previous work, we focused basically on the discrepancy of fast Doppler motion without detectable motion in the image plane. We now suggest an alternative scenario for the explosive events, based on our observations of spectral line tilts and bifurcated structure in some events. Both features are indicative of rotational motion in narrow structures. We explain the bifurcation as the result of rotation of hollow cylindrical structures and demonstrate that this kind of sheath model can also be applied to explain the nature of the puzzling ‘explosive events’. We find that the spectral tilt, the lack of apparent motion, the bifurcation, and a rapidly growing number of direct observations support an alternative scenario of linear, spicular-sized jets with a strong spinning motion.

### **MLSO Mark III K-Coronameter Observations of the CME Rate from 1989 – 1996**

O. C. St. **Cyr**, Q. A. Flint, H. Xie, D. F. Webb, J. T. Burkepile, A. R. Lecinski, C. Quirk, A. L. Stanger

Solar Phys. Volume 290, Issue 10, pp 2951-2962 2015

We report here an attempt to fill the 1990 – 1995 gap in the CME rate using the Mauna Loa Solar Observatory’s Mark III (Mk3) K-coronameter. The Mk3 instrument observed routinely several hours most days beginning in 1980 until it was upgraded to Mk4 in 1999. We describe the statistical properties of the CMEs detected during 1989 – 1996, and we determine a CME rate for each of those years. Since spaceborne coronagraphs have more complete duty cycles than a

ground-based instrument at a single location, we compare the Mk3-derived CME rate from 1989 with the rate from the SMM C/P coronagraph, and from 1996 with the rate from the SOHO LASCO coronagraphs.

### **Nanodust dynamics during a coronal mass ejection**

Andrzej [Czechowski](#) and Jens Kleimann

Ann. Geophys., 35, 1033-1049, 2017

<https://www.ann-geophys.net/35/1033/2017/angeo-35-1033-2017.pdf>

Short Summary: Interplanetary dust also includes very small (nanometer-sized) particles. The dynamics of nanodust is determined by electromagnetic forces, which accelerate the dust to velocities on the order of 500 km/s or, in the vicinity of the Sun, trap them in bound orbits. We investigate the behavior of nanodust during a coronal mass ejection. We find a new population of extremely fast (1000 km/s) nanodust. We also study the effect of the ion drag force.

### **Centre-to-limb properties of small, photospheric quiet Sun jets**

F. Rubio [da Costa](#), S. K. Solanki, S. Danilovic, J. Hizberger, V. Martínez-Pillet

A&A 574, A95 (2015)

<http://arxiv.org/pdf/1412.1620v1.pdf>

Strongly Doppler-shifted Stokes V profiles have been detected in the quiet Sun with the IMAx instrument on-board the SUNRISE stratospheric balloon-borne telescope. High velocities are required in order to produce such signals, hence these events have been interpreted as jets, although other sources are also possible. We aim to characterize the variation of the main properties of these events (occurrence rate, lifetime, size and velocities) with their position on the solar disk between disk centre and the solar limb. These events have been identified in Sunrise/IMaX data according to the same objective criteria at all available positions on the solar disk. Their properties were determined using standard techniques. Our study yielded a number of new insights into this phenomenon. Most importantly, the number density of these events is independent of the heliocentric angle, i.e. the investigated supersonic flows are nearly isotropically distributed. Size and lifetime are also nearly independent of the heliocentric angle, while their intensity contrast increases towards the solar limb. The Stokes V jets are associated with upflow velocities deduced from Stokes I, which are stronger towards the limb. Their intensity decreases with time, while their line-of-sight (LOS) velocity does not display a clear temporal evolution. Their association with linear polarization signals decreases towards the limb. The density of events appears to be independent of heliocentric angle, establishing that they are directed nearly randomly. If these events are jets triggered by magnetic reconnection between emerging magnetic flux and the ambient field, then our results suggest that there is no preferred geometry for the reconnection process. **10th and**

**13th June 2009**

### **The role of filament activation in a solar eruption**

F. Rubio [da Costa](#)<sup>1,2</sup>, F. Zuccarello<sup>1</sup>, L. Fletcher<sup>2</sup>, P. Romano<sup>3</sup> and N. Labrosse

A&A 539, A27 (2012), **File**

<http://arxiv.org/pdf/1412.1858v1.pdf>

Context. Observations show that the mutual relationship between filament eruptions and solar flares cannot be described in terms of a unique scenario. In some cases, the eruption of a filament appears to trigger a flare, while in others the observations are more consistent with magnetic reconnection that produces both the flare observational signatures (e.g., ribbons, plasma jets, post-flare loops, etc.) and later the destabilization and eruption of a filament. Aims. Contributing to a better comprehension of the role played by filament eruptions in solar flares, we study an event which occurred in NOAA 8471, where a flare and the activation of (at least) two filaments were observed on **28**

**February 1999.**

Methods. By using imaging data acquired in the 1216, 1600, 171 and 195 Å TRACE channels and by BBSO in the continuum and in the H $\alpha$  line, a morphological study of the event is carried out. Moreover, using TRACE 1216 and 1600 Å data, an estimate of the “pure” Ly $\alpha$  power is obtained. The extrapolation of the magnetic field lines is done using the SOHO/MDI magnetograms and assuming a potential field.

Results. Initially an area hosting a filament located over a  $\delta$  spot becomes brighter than the surroundings, both in the chromosphere and in the corona. This area increases in brightness and extension, eventually assuming a two-ribbon morphology, until it reaches the eastern part of the active region. Here a second filament becomes activated and the brightening propagates to the south, passing over a large supergranular cell. The potential magnetic field extrapolation indicates that the field line connectivity changes after the flare.

Conclusions. The event is triggered by the destabilization of a filament located between the two polarities of a  $\delta$  spot. This destabilization involves the magnetic arcades of the active region and causes the eruption of a second filament, that gives rise to a CME and to plasma motions over a supergranular cell. We conclude that in this event the two filaments play an active and decisive role, albeit in different stages of the phenomenon, in fact the destabilization of one filament causes brightenings, reconnection and ribbons, while the second one, whose eruption is caused by the field reconfiguration resulting from the previous reconnection, undergoes the greatest changes and causes the CME.

### **Sequential eruptions triggered by flux emergence - observations and modeling**

Sally [Dacie](#), [Tibor Torok](#), [Pascal Demoulin](#), [Mark Linton](#), [Cooper Downs](#), [Lidia van Driel-Gesztelyi](#), [David Long](#), [James Leake](#)

ApJ **862** 117 **2018**

<https://arxiv.org/pdf/1807.00020.pdf>

<http://sci-hub.tw/http://iopscience.iop.org/article/10.3847/1538-4357/aacce3/meta>

We describe and analyze observations by the Solar Dynamics Observatory of the emergence of a small, bipolar active region within an area of unipolar magnetic flux that was surrounded by a circular, quiescent filament. Within only eight hours of the start of the emergence, a partial splitting of the filament and two consecutive coronal mass ejections took place. We argue that all three dynamic events occurred as a result of particular magnetic-reconnection episodes between the emerging bipole and the pre-existing coronal magnetic field. In order to substantiate our interpretation, we consider three-dimensional magnetohydrodynamic simulations that model the emergence of magnetic flux in the vicinity of a large-scale coronal flux rope. The simulations qualitatively reproduce most of the reconnection episodes suggested by the observations; as well as the filament-splitting, the first eruption, and the formation of sheared/twisted fields that may have played a role in the second eruption. Our results suggest that the position of emerging flux with respect to the background magnetic configuration is a crucial factor for the resulting evolution, while previous results suggest that parameters such as the orientation or the amount of emerging flux are important as well. This poses a challenge for predicting the onset of eruptions that are triggered by flux emergence, and it calls for a detailed survey of the relevant parameter space by means of numerical simulations. **18 July 2014**

### **Modeling the formation and eruption of coronal structures by linking data-driven magnetofrictional and MHD simulations for AR 12673★**

F. Daei<sup>1</sup>, J. Pomoell<sup>1</sup>, D. J. Price<sup>1</sup>, A. Kumari<sup>1,2</sup>, S. Good<sup>1</sup> and E. K. J. Kilpua<sup>1</sup>

A&A 676, A141 (2023)

<https://www.aanda.org/articles/aa/pdf/2023/08/aa46183-23.pdf>

**Context.** The data-driven and time-dependent modeling of coronal magnetic fields is crucial for understanding solar eruptions. These efforts are complicated by the challenges of finding a balance between physical realism and computing efficiency. One possible technique is to couple two modeling approaches.

**Aims.** Our aim here is to showcase our progress in using time-dependent magnetofrictional model (TMFM) results as input to dynamical magnetohydrodynamic (MHD) simulations. However, due to the different evolution processes in these two models, using TMFM snapshots in an MHD simulation is nontrivial. We address these issues, both physically and numerically, discuss the incompatibility of the TMFM output to serve as the initial condition in MHD simulations, and show our methods of mitigating this. The evolution of the flux systems and the cause of the eruption are investigated.

**Methods.** TMFM is a prevalent approach that has proven to be a very useful tool in the study of the formation of unstable structures in the solar corona. In particular, it is capable of incorporating observational data as initial and boundary conditions and requires shorter computational time compared to MHD simulations. To leverage the efficiency of data-driven TMFM and also to simulate eruptive events in the MHD framework, one can apply TMFM up to a certain time before the expected eruption(s) and then proceed with the simulation in the full or ideal MHD regime in order to more accurately capture the eruption process.

**Results.** We show the results of a benchmark test case with a linked TMFM and MHD simulation to study the evolution of NOAA active region 12673. A rise of a twisted flux bundle through the MHD simulation domain is observed, but we find that the rate of the rise and the altitude reached depends on the time of the TMFM snapshot that was used to initialize the MHD simulation and the helicity injected into the system. The analysis suggested that torus instability and slip-running reconnection could play an important role in the eruption.

**Conclusions.** The results show that the linkage of TMFM and zero- $\beta$  MHD models can be successfully used to model the eruptive coronal magnetic fields. **3-6 Sep 2017**

### **Effect of the Heliospheric State on CME Evolution**

[Fithanegest Kassa Dagnev](#), [Nat Gopalswamy](#), [Solomon Belay Tessema](#), [Sachiko Akiyama](#), [Seiji Yashiro](#)  
2022 ApJ 936 122

<https://arxiv.org/ftp/arxiv/papers/2208/2208.03536.pdf>

<https://iopscience.iop.org/article/10.3847/1538-4357/ac8744/pdf>

The culmination of solar cycle 24 by the end of 2019 has created the opportunity to compare the differing properties of coronal mass ejections (CMEs) between two whole solar cycles: Solar cycle 23 (SC 23) and Solar cycle 24 (SC 24). We report on the width evolution of limb CMEs in SC 23 and 24 in order to test the suggestion by Gopalswamy et al.

(2015a) that CME flux ropes attain pressure balance at larger heliocentric distances in SC 24. We measure CME width as a function of heliocentric distance for a significantly large number of limb CMEs (~1000) and determine the distances where the CMEs reach constant width in each cycle. We introduced a new parameter: the transition height ( $h_c$ ) of a CME defined as the critical heliocentric distance beyond which the CME width stabilizes to a quasi-constant value. Cycle and phase-to-phase comparisons are based on this new parameter. We find that the average value of  $h_c$  in SC 24 is 62% higher than in SC 23. SC 24 CMEs attain their peak width at larger distances from the Sun as compared to SC 23 CMEs. The enhanced transition height in SC 24 is new observational ratification of the anomalous expansion. The anomalous expansion of SC 24 CMEs which is caused by the weak state of the heliosphere, accounts for the larger heliocentric distance where the pressure balance between CME flux rope and the ambient medium is attained. **2014**

**May 6**



## Intercycle and intracycle variation of halo CME rate obtained from SOHO/LASCO observations

Fithanegest Kassa [Dagnev](#), [Nat Gopalswamy](#), [Solomon Belay Tessema](#), [Sachiko Akiyama](#), [Seiji Yashiro](#), [Tesfay Yemane Tesfu](#)

ApJ **903** 118 **2020**

<https://arxiv.org/ftp/arxiv/papers/2009/2009.06033.pdf>

<https://doi.org/10.3847/1538-4357/abb887>

We report on the properties of halo coronal mass ejections (HCMEs) in solar cycles 23 and 24. We compare the HCMEs properties between the corresponding phases (rise, maximum, and declining) in cycles 23 and 24 in addition to comparing those between the whole cycles. Despite the significant decline in the sunspot number (SSN) in cycle 24, which dropped by 46% with respect to cycle 23, the abundance of HCMEs is similar in the two cycles. The HCME rate per SSN is 44% higher in cycle 24. In the maximum phase, cycle-24 rate normalized to SSN increased by 127% while the SSN dropped by 43%. The source longitudes of cycle-24 HCMEs are more uniformly distributed than those in cycle 23. We found that the average sky-plane speed in cycle 23 is ~16% higher than that in cycle 24. The size distributions of the associated flares between the two cycles and the corresponding phases are similar. The average speed at a central meridian distance (CMD) = 600 for cycle 23 is ~28% higher than that of cycle 24. We discuss the unusual bump in HCME activity in the declining phase of cycle 23 as due to exceptional active regions that produced many CMEs during October 2003 to October 2005. The differing HCME properties in the two cycles can be attributed to the anomalous expansion of cycle-24 CMEs. Considering the HCMEs in the rise, maximum and declining phases, we find that the maximum phase shows the highest contrast between the two cycles.

## A comparison of CME expansion speeds between solar cycles 23 and 24

Fithanegest Kassa [Dagnev](#), [Nat Gopalswamy](#), [Solomon Belay Tessema](#)

Journal of Physics Conference Series, to appear in the Proc. 19th International Astrophysics Conference held in Santa Fe, New Mexico, March 9 - 13, **2020**

<https://arxiv.org/ftp/arxiv/papers/2007/2007.13204.pdf>

We report on a comparison of the expansion speeds of limb coronal mass ejections (CMEs) between solar cycles 23 and 24. We selected a large number of limb CME events associated with soft X-ray flare size greater than or equal to M1.0 from both cycles. We used data and measurement tools available at the online CME catalog ([this https URL](#)) that consists of the properties of all CMEs detected by the Solar and Heliospheric Observatory's (SOHO) Large Angle and Spectrometric Coronagraph (LASCO). We found that the expansion speeds in cycle 24 are higher than those in cycle 23. We also found that the relation between radial and expansion speeds has different slopes in cycles 23 and 24. The cycle 24 slope is 45% higher than that in cycle 23. The expansion speed is also higher for a given radial speed. The difference increases with speed. For a 2000 km/s radial speed, the expansion speed in cycle 24 is ~48% higher. These results present additional evidence for the anomalous expansion of cycle 24-CMEs, which is due to the reduced total pressure in the heliosphere. **2001 April 02**

## The shock driving capability of a CME inferred from multiwavelength observations

Fithanegest Kassa [Dagnev](#), [Nat Gopalswamy](#), [Solomon Belay Tessema](#), [Ange Cynthia Umuhire](#), [Seiji Yashiro](#), [Pertti Mäkelä](#), [Hong Xie](#)

Sun and Geosphere, **Vol.14, No. 2, 2019** p. 105-110

<https://arxiv.org/ftp/arxiv/papers/2002/2002.04056.pdf>

[http://newserver.stil.bas.bg/SUNGEO/00SGArhiv/SG\\_v14\\_No2\\_2019-pp105-110.pdf](http://newserver.stil.bas.bg/SUNGEO/00SGArhiv/SG_v14_No2_2019-pp105-110.pdf)

The radial speed of a coronal mass ejection (CME) determines the shock-driving capability of a CME as indicated by the presence of a type II radio burst. Here we report on the **April 18, 2014** CME that was associated with a type II radio burst in the metric and interplanetary domains. We used the radio-burst data provided by the San Vito Solar Observatory of the Radio Solar Telescope Network and data from the Wind spacecraft. The CME is a full halo in the field of view of the coronagraphs on board the Solar and Heliospheric Observatory (SOHO). The CME was also observed by the coronagraphs on board the Solar Terrestrial Relations Observatory (STEREO). We computed the CME shock and flux rope speeds based on the multi-view observations by the different coronagraphs and by EUV instruments. We determined the shock speed from metric and interplanetary radio observations and found them to be consistent with white-light observations, provided the metric type II burst and its continuation into the decameter-hectometric domain are produced at the shock flanks, where the speed is still high enough to accelerate electrons that produce the type II bursts. Interestingly, there was an interplanetary type II burst segment consistent with an origin at the shock nose suggesting that the curved shock was crossing plasma levels separated by a few solar radii. We conclude that the CME speed is high enough to produce the interplanetary Type II burst and a solar energetic particle (SEP) event. However, the speed is not high enough to produce a ground level enhancement (GLE) event, which requires the shock to form at a height of ~1.5 Rs.

## STITCH: A Subgrid-Scale Model for Energy Buildup in the Solar Corona

[Joel T. Dahlin](#), [C. Richard DeVore](#), [Spiro K. Antiochos](#)

ApJ **941** 79 **2022**

<https://arxiv.org/pdf/2112.00641.pdf>

<https://iopscience.iop.org/article/10.3847/1538-4357/ac9e5a/pdf>

The solar corona routinely exhibits explosive activity, in particular coronal mass ejections and their accompanying eruptive flares, that have global-scale consequences. These events and their smaller counterparts, coronal jets, originate in narrow, sinuous filament channels. The key processes that form and evolve the channels operate on still smaller spatial scales and much longer time scales, culminating in a vast separation of characteristic lengths and times that govern these explosive phenomena. In this article, we describe implementation and tests of an efficient subgrid-scale model for generating eruptive structures in magnetohydrodynamics (MHD) coronal simulations. *STITCH -- Statistical Injection of Condensed Helicity* -- is a physics-based, reduced representation of helicity condensation: a process wherein small-scale vortical surface convection forms ubiquitous current sheets, and pervasive reconnection across the sheets mediates an inverse cascade of magnetic helicity and free energy, thereby forming the filament channels. STITCH abstracts these complex processes into a single new term, in the MHD Ohm's law and induction equation, which directly injects tangential magnetic flux into the low corona. We show that this approach is in very good agreement with a full helicity-condensation calculation that treats all of the dynamics explicitly, while enabling substantial reductions in temporal duration especially, but also in spatial resolution. In addition, we illustrate the flexibility of STITCH at forming localized filament channels and at energizing complex surface flux distributions that have sinuous boundaries. STITCH is simple to implement and computationally efficient, making it a powerful new technique for event-based, data-driven modeling of solar eruptions.

## **A Model for Energy Buildup and Eruption Onset in Coronal Mass Ejections**

Joel T. [Dahlin](#), [Spiro K. Antiochos](#), [C. Richard DeVore](#)

ApJ **879** 96 **2019**

<https://arxiv.org/pdf/1905.13218.pdf>

[sci-hub.se/10.3847/1538-4357/ab262a](https://sci-hub.se/10.3847/1538-4357/ab262a)

Coronal mass ejections (CMEs) and eruptive flares (EFs) are the most energetic explosions in the solar system. Their underlying origin is the free energy that builds up slowly in the sheared magnetic field of a filament channel. We report the first end-to-end numerical simulation of a CME/EF, from zero-free-energy initial state through filament-channel formation to violent eruption, driven solely by the magnetic-helicity condensation process. Helicity is the topological measure of linkages between magnetic flux systems, and is conserved in the corona, building up inexorably until it is ejected into interplanetary space. Numerous investigations have demonstrated that helicity injected by small-scale vortical motions, such as those observed in the photosphere, undergoes an inverse cascade from small scales to large, 'condensing' at magnetic-polarity boundaries. Our new results verify that this process forms a filament channel within a compact bipolar region embedded in a background dipole field, and show for the first time that a fast CME eventually occurs via the magnetic-breakout mechanism. We further show that the trigger for explosive eruption is reconnection onset in the flare current sheet that develops above the polarity inversion line: this reconnection forms flare loops below the sheet and a CME flux rope above, and initiates high-speed outward flow of the CME. Our findings have important implications for magnetic self-organization and explosive behavior in solar and other astrophysical plasmas, and for understanding and predicting explosive solar activity.

## **A partial filament eruption in three steps induced by external magnetic reconnection**

[Jun Dai](#), [Zhentong Li](#), [Ya Wang](#), [Zhe Xu](#), [Yanjie Zhang](#), [Leping Li](#), [Qingmin Zhang](#), [Yingna Su](#), [Haisheng Ji](#)

**2022** ApJ **929** 85

<https://arxiv.org/ftp/arxiv/papers/2201/2201.11314.pdf>

<https://iopscience.iop.org/article/10.3847/1538-4357/ac4fbc/pdf>

We present an investigation of partial filament eruption on **2012 June 17** in the active region NOAA 11504. For the first time, we observed the vertical splitting process during the partial eruption with high resolution narrow band images at 10830 Å. The active filament was rooted in a small sunspot of the active region. Particularly, it underwent the partial eruption in three steps, i.e. the precursor, the first eruption, and the second eruption, while the later two were associated with a C1.0 flare and a C3.9 flare, respectively. During the precursor, slow magnetic reconnection took place between the filament and the adjoining loops that also rooted in the sunspot. The continuous reconnection not only caused the filament to split into three groups of threads vertically but also formed a new filament, which was growing and accompanied brightening took place around the site. Subsequently, the growing filament erupted together with one group splitted threads, resulted in the first eruption. At the beginning of the first eruption, a subsequent magnetic reconnection occurred between the erupting splitted threads and another ambient magnetic loop. After about three minutes, the second eruption occurred as a result of the eruption of two larger unstable filaments induced by the magnetic reconnection. The high-resolution observation provides a direct evidence that magnetic reconnection between filament and its ambient magnetic fields could induce the vertical splitting of the filament, resulting in partial eruption.

## **A Time-dependent Self-similar Reconstruction of Solar Coronal Mass Ejections Based on the Gibson–Low Model**

Xinghua [Dai](#)

**2022** ApJ **925** 24

<https://iopscience.iop.org/article/10.3847/1538-4357/ac3eda/pdf>

The analytic Gibson–Low (GL) model, a time-dependent self-similar solution of the magnetohydrodynamics, is first used to directly reconstruct a coronal mass ejection (CME) through the method of forward modeling in this study. A systematic description of the GL model is presented at the beginning, and a set of parameters is introduced to define the

model. Then a CME on **2011 March 7** is reconstructed by fitting of GL (FGL) of the multi-viewpoint and time series observations. The first step of FGL is the initialization of the location and orientation of the GL using the information of the CME source region. The second step is to fit the parameters of size, shape, velocity, and strength of the magnetic field of the GL to the observations of coronagraphs at 20:24 and 20:39. The GL at 20:54 and 3 R<sub>☉</sub> is generated through the theory of self-similar expansion respectively. Comparisons between the synthetic images of the GL and the real observations of the CME prove the performance of FGL that the reconstructions well match the observations.

### **Oscillations and mass-draining that lead to a sympathetic eruption of a quiescent filament**

[Jun Dai](#), [Qingmin Zhang](#), [Yanjie Zhang](#), [Zhe Xu](#), [Yingna Su](#), [Haisheng Ji](#)

ApJ **923** 74 **2021**

<https://arxiv.org/pdf/2110.04695.pdf>

<https://doi.org/10.3847/1538-4357/ac2d97>

In this paper, we present a multi-wavelength analysis to mass-draining and oscillations in a large quiescent filament prior to its successful eruption on **2015 April 28**. The eruption of a smaller filament that was parallel and in close, 350 proximity was observed to induce longitudinal oscillations and enhance mass-draining within the filament of interest. The longitudinal oscillation with an amplitude of 25 Mm and 23 km underwent no damping during its observable cycle. Subsequently the slightly enhanced draining may have excited a eruption behind the limb, leading to a feedback that further enhanced the draining and induced simultaneous oscillations within the filament of interest. We find significant damping for these simultaneous oscillations, where the transverse oscillations proceeded with the amplitudes of 15 Mm and 14 km, while the longitudinal oscillations involved a larger displacement and velocity amplitude (57 Mm, 43 km). The second grouping of oscillation lasted for 2 cycles and had the similar period of 2 hours. From this, the curvature radius and transverse magnetic field strength of the magnetic dips supporting the filaments can be estimated to be 355 Mm and 34 G. The mass-draining within the filament of interest lasted for 14 hours. The apparent velocity grew from 35 km to 85 km, with the transition being coincident with the occurrence of the oscillations. We conclude that two filament eruptions are sympathetic, i.e. the eruption of the quiescent filament was triggered by the eruption of the nearby smaller filament.

### **The Formation and Eruption of A Sigmoidal Filament Driven by Rotating Network Magnetic Fields**

[Jun Dai](#), [Haisheng Ji](#), [Leping Li](#), [Jun Zhang](#), [Huadong Chen](#)

**2021** ApJ **906** 66

<https://arxiv.org/pdf/2012.06775.pdf>

<https://doi.org/10.3847/1538-4357/abcaf4>

We present the formation and eruption of a sigmoidal filament driven by rotating network magnetic fields (RNFs) near the center of the solar disk, which was observed by the one-meter aperture New Vacuum Solar Telescope (NVST) at Fuxian Solar Observatory (FSO) on **2018 July 12**. Counterclockwise RNFs twist two small-scale filaments at their northeastern foot-point region, giving a rotation of nearly 200 degree within about 140 minutes. The motion of the RNF has a tendency to accelerate at first and then decelerate obviously, as the average rotation speed increased from 10 to 150 ,and then slowed down to 50 . Coalescence then occurs between filaments F1 and F2. Meanwhile the fine structures in the southwestern region of the filament was involved in another interaction of coalescence. The subsequent EUV brightening due to plasma heating is observed in the two interaction regions. These interacting structures, including F1, F2 and the fine structures in the southwestern region, eventually evolve into a larger-scale sigmoidal filament twisted in the same direction as the RNFs gave. The twist of the sigmoidal filament has exceeded  $4\{\pi\}$  and the filament erupted finally. The motion of the sigmoidal filament keeps uniform until a nearby jet collides, causing the filament to erupt faster. These results provide evidence that RNF plays an important role in the formation and eruption of the sigmoidal filament. The phenomena also suggests that the kink instability is the trigger mechanism for the filament eruption.

### **Electron Density Reconstruction of Solar Coronal Mass Ejections Based on Genetic Algorithm: Method and Application**

Xinghua [Dai](#), [Huaning Wang](#)

**2020** ApJ **896** 155

<https://arxiv.org/pdf/1902.06953.pdf>

<https://doi.org/10.3847/1538-4357/ab963a>

We present a new method to reconstruct three dimensional density of Coronal Mass Ejection (CME) based on genetic algorithm (GA), namely genetic reconstruction method (GRM). At first, a model "CME" is constructed to produce synthetic CME images for the genetic reconstruction. Then the method is applied to coronagraph data from SOHO, STEREO-A and B on **September 30th, 2013**. In comparison with the existing methods for density reconstruction, GRM obtain global optimization of CME electron distribution. On the other hand, GRM decreases the difficulty of reconstruction by calculating electron number of every CME pixel in one of the view angles. Then the electrons are randomly redistributed along each line of sight (LOS) of CME pixel. Genetic operators named "crossover" and "mutation" are employed to optimize the electron distribution. Brightness of each pixel are recalculated through mechanism of Thomson scattering in multiple view angles. Genetic operator named "selection" is then employed to hold better distributions and eliminate the worse distributions according to fitness of recalculated brightness to the observed brightness. Such process may iterate through hundreds of times to obtain globally optimized electron

distributions. We compare the reconstructed brightness with observation to show the availability of GRM. Results of GRM are also compared with those of polarimetric reconstruction and forward modeling for the method availability. We further apply the reconstructed CME into Space Weather Modeling Framework (SWMF) to obtain evolution of interplanetary CME and its geo-effectiveness. Time difference of the CME arrival between ACE measurement and SWMF simulation is less than 5 hours.

### **Current sheets in the wake of an eruption of two crossing filaments**

Jun [Dai](#), [Jiayan Yang](#), [Leping Li](#), [Jun Zhang](#)

ApJ **869** 118 **2018**

<https://arxiv.org/pdf/1811.08563.pdf>

[sci-hub.tw/10.3847/1538-4357/aaedbb](http://sci-hub.tw/10.3847/1538-4357/aaedbb)

Employing Solar Dynamic Observatory/Atmospheric Imaging Assembly (AIA) multi-wavelength images, we study an eruption of two crossing filaments, and firstly report the current sheets (CSs) connecting the lower flare ribbons and the upper erupting filaments. On **July 8, 2014**, two crossing filaments are observed in the NOAA active region (AR) 12113. The lower-lying filament rises first, and then meets the higher-lying one. Thereafter, both of them erupt together. The filament eruption draws the overlying magnetic field lines upward, leading to the approach of two legs, with opposite magnetic polarities, of the overlying field lines. Two sets of bright CSs form at the interface of these two legs, and magnetic reconnection takes place in the CSs producing the underneath flare ribbons and post-flare loops. Several bright plasmoids appear in the CSs, and propagate along the CSs bi-directionally. The CSs and plasmoids are observed in AIA multi-wavelength channels, indicating that both of them have been heated during the reconnection process, with hot and warm components. Employing the differential emission measure (EM) analysis, we find that both the temperature and EM of the CSs decrease from the flare arcades outward to the erupting filaments, and those of the plasmoids are significantly larger than the regions where no plasmoid is detected.

### **Improvement on Mass Calculations of Solar CMEs**

Xinghua [Dai](#)<sup>1,2</sup>, Huaning Wang<sup>1</sup>, Xin Huang<sup>1</sup>, Zhanle Du<sup>1</sup>, and Han He

**2015** ApJ 801 39

The mass of a coronal mass ejection (CME) is calculated from the measured brightness and assumed geometry of Thomson scattering. The simplest geometry for mass calculations is to assume that all of the electrons are in the plane of the sky (POS). With additional information like source region or multiviewpoint observations, the mass can be calculated more precisely under the assumption that the entire CME is in a plane defined by its trajectory. Polarization measurements provide information on the average angle of the CME electrons along the line of sight of each CCD pixel from the POS, and this can further improve the mass calculations as discussed here. A CME event initiating on **2012 July 23** at 2:20 UT observed by the Solar Terrestrial Relations Observatory is employed to validate our method.

### **The Classification of Ambiguity in Polarimetric Reconstruction of Coronal Mass Ejection**

Xinghua [Dai](#)<sup>1,2</sup>, Huaning Wang<sup>1</sup>, Xin Huang<sup>1</sup>, Zhanle Du<sup>1</sup>, and Han He

**2014** ApJ 780 141

The Thomson scattering theory indicates that there exist explicit and implicit ambiguities in polarimetric analyses of coronal mass ejection (CME) observations. We suggest a classification for these ambiguities in CME reconstruction. Three samples, including double explicit, mixed, and double implicit ambiguity, are shown with the polarimetric analyses of STEREO CME observations. These samples demonstrate that this classification is helpful for improving polarimetric reconstruction.

### **EVOLUTION OF PILED-UP COMPRESSIONS IN MODELED CORONAL MASS EJECTION SHEATHS AND THE RESULTING SHEATH STRUCTURES**

Indrajit [Das](#)<sup>1</sup>, Merav Opher<sup>1,2</sup>, Rebekah Evans<sup>1</sup>, Cristiane Loesch<sup>3</sup>, and Tamas I. Gombosi<sup>4</sup>

Astrophysical Journal, 729:112 (7pp), **2011** March, **File**

We study coronal mass ejection (CME)-driven shocks and the resulting post-shock structures in the lower corona (2–7R<sub>⊙</sub>). Two CMEs are erupted by modified Titov–D’emoulin (TD) and Gibson–Low (GL) type flux ropes (FRs) with the Space Weather Modeling Framework. We observe a substantial pile-up of density compression and a narrow region of plasma depletion layer (PDL) in the simulations. As the CME/FR moves and expands in the solar wind medium, it pushes the magnetized material lying ahead of it. Hence, the magnetic field lines draping around the CME front are compressed in the sheath just ahead of the CME. These compressed field lines squeeze out the plasma sideways, forming PDL in the region. Solar plasma being pushed and displaced from behind forms a strong piled-up compression (PUC) of density downstream of the PDL. Both CMEs have comparable propagation speeds, while GL has larger expansion speed than TD due to its higher initial magnetic pressure. We argue that high CME expansion speed along with high solar wind density in the region is responsible for the large PUC found in the lower corona. In case of GL, the PUC is much wider, although the density compression ratio for both the cases is comparable. Although these simulations artificially initiate out-of-equilibrium CMEs and drive them in an artificial solar wind solution, we predict that PUCs, in general, will be large in the lower corona. This should affect the ion profiles of the accelerated solar energetic particles.

## Study of Interplanetary and Geomagnetic Response of Filament Associated CMEs

Kunjai Dave, Wageesh Mishra, Nandita Srivastava, R. M. Jadhav

Proceedings IAU Symposium No. 340, 2018

<https://arxiv.org/pdf/1807.00809.pdf>

It has been established that Coronal Mass Ejections (CMEs) may have significant impact on terrestrial magnetic field and lead to space weather events. In the present study, we selected several CMEs which are associated with filament eruptions on the Sun. We attempt to identify the presence of filament material within ICME at 1AU. We discuss how different ICMEs associated with filaments lead to moderate or major geomagnetic activity on their arrival at the Earth. Our study also highlights the difficulties in identifying the filament material at 1AU within isolated and in interacting CMEs. 23 May 2010, 6 Oct 2010, 23 Sep 2012

## A SELF-SIMILAR EXPANSION MODEL FOR USE IN SOLAR WIND TRANSIENT PROPAGATION STUDIES

J. A. Davies<sup>1</sup>, R. A. Harrison<sup>1</sup>, C. H. Perry<sup>1</sup>, C. Möstl<sup>2,3,4</sup>, N. Lugaz<sup>5</sup>, T. Rollett<sup>2</sup>, C. J. Davis<sup>1,6</sup>, S. R. Crothers<sup>1</sup>, M. Temmer<sup>2</sup>, C. J. Eyles<sup>1,7</sup>, and N. P. Savani

2012 ApJ 750 23

Since the advent of wide-angle imaging of the inner heliosphere, a plethora of techniques have been developed to investigate the three-dimensional structure and kinematics of solar wind transients, such as coronal mass ejections, from their signatures in single- and multi-spacecraft imaging observations. These techniques, which range from the highly complex and computationally intensive to methods based on simple curve fitting, all have their inherent advantages and limitations. In the analysis of single-spacecraft imaging observations, much use has been made of the fixed fitting (FPF) and harmonic mean fitting (HMF) techniques, in which the solar wind transient is considered to be a radially propagating point source (fixed, FP, model) and a radially expanding circle anchored at Sun centre (harmonic mean, HM, model), respectively. Initially, we compare the radial speeds and propagation directions derived from application of the FPF and HMF techniques to a large set of STEREO/Heliospheric Imager (HI) observations. As the geometries on which these two techniques are founded constitute extreme descriptions of solar wind transients in terms of their extent along the line of sight, we describe a single-spacecraft fitting technique based on a more generalized model for which the FP and HM geometries form the limiting cases. In addition to providing estimates of a transient's speed and propagation direction, the self-similar expansion fitting (SSEF) technique provides, in theory, the capability to estimate the transient's angular extent in the plane orthogonal to the field of view. Using the HI observations, and also by performing a Monte Carlo simulation, we assess the potential of the SSEF technique.

## Assessing the Accuracy of CME Speed and Trajectory Estimates from STEREO Observations Through a Comparison of Independent Methods

C.J. Davis · J. Kennedy · J.A. Davies

Solar Phys (2010) 263: 209–222, DOI 10.1007/s11207-010-9535-2; File

We have estimated the speed and direction of propagation of a number of Coronal Mass Ejections (CMEs) using single-spacecraft data from the STEREO Heliospheric Imager (HI) wide-field cameras. In general, these values are in good agreement with those predicted by Thernisien, Vourlidas, and Howard in *Solar Phys.* **256**, 111 – 130 (2009) using a forward modelling method to fit CMEs imaged by the STEREO COR2 coronagraphs. The directions of the CMEs predicted by both techniques are in good agreement despite the fact that many of the CMEs under study travel in directions that cause them to fade rapidly in the HI images. The velocities estimated from both techniques are in general agreement although there are some interesting differences that may provide evidence for the influence of the ambient solar wind on the speed of CMEs. The majority of CMEs with a velocity estimated to be below 400 km s<sup>-1</sup> in the COR2 field of view have higher estimated velocities in the HI field of view, while, conversely, those with COR2 velocities estimated to be above 400 km s<sup>-1</sup> have lower estimated HI velocities. We interpret this as evidence for the deceleration of fast CMEs and the acceleration of slower CMEs by interaction with the ambient solar wind beyond the COR2 field of view. We also show that the uncertainties in our derived parameters are influenced by the range of elongations over which each CME can be tracked. In order to reduce the uncertainty in the predicted arrival time of a CME at 1 Astronomical Unit (AU) to within six hours, the CME needs to be tracked out to at least 30 degrees elongation. This is in good agreement with predictions of the accuracy of our technique based on Monte Carlo simulations.

Within the set of studied CMEs, there are two clear events that were predicted from the HI data to travel over another spacecraft; *in-situ* measurements at these other spacecraft confirm the accuracy of these predictions. The ability of the HI cameras to image Corotating Interaction Region (CIR)-entrained transients as well as CMEs can result in some ambiguity

when trying to distinguishing individual signatures.

## **How a Strong Solar Coronal Mass Ejection can Eject Dust from the Moon's Surface to the Earth's Atmosphere**

Fran [De Aquino](#)

2014?

<https://hal.archives-ouvertes.fr/hal-01081735>

A solar coronal mass ejection (CME) is a massive ejection of plasma from the Sun to the space. In this article it is shown how a strong solar coronal mass ejection can eject dust from the Moon's Surface to the space. If this ejection occurs when the Moon is in specific regions of its trajectory around the Earth, then this lunar dust can be gravitationally attracted to the Earth, forming a dust shell at the Earth's atmosphere, which can block the sunlight for some days.

## **Properties of Streamer Wave Events Observed During the STEREO Era**

Bieke [Decraemer](#), [Andrei N. Zhukov](#), [Tom Van Doorselaere](#)

ApJ **893** 78 **2020**

<https://arxiv.org/pdf/2003.12350.pdf>

<https://doi.org/10.3847/1538-4357/ab8194>

Transverse waves are sometimes observed in solar helmet streamers, typically after the passage of a coronal mass ejection (CME). The CME-driven shock wave moves the streamer sideways, and a decaying oscillation of the streamer is observed after the CME passage. Previous works generally reported observations of streamer oscillations taken from a single vantage point (typically the SOHO spacecraft). We conduct a data survey searching for streamer wave events observed by the COR2 coronagraphs onboard the STEREO spacecraft. For the first time, we report observations of streamer wave events from multiple vantage points, by using the COR2 instrument on both STEREO A and B, as well as the SOHO/LASCO C2+C3 coronagraphs. We investigate the properties of streamer waves by comparing the different events and performing a statistical analysis. Common observational features give us additional insight on the physical nature of streamer wave events. The most important conclusion is that there appears to be no relation between the speed of the CME and the phase speed of the resulting streamer wave, indicating that the streamer wave speed is determined by the physical properties of the streamer rather than the properties of the CME. This result makes streamer waves events excellent candidates for coronal seismology studies. From a comparison between the measured phase speeds and the phase speeds calculated from the measured periods and wavelengths, we could determine that the speed of the post-shock solar wind flow in our streamers is around  $300 \text{ km s}^{-1}$ . **2013-02-06**

**Table 1.** Summary of the physical parameters measured for the 22 streamer wave events identified with STEREO/COR2.

## **3D Polarized Imaging of Coronal Mass Ejections: Chirality of a CME**

C. E. [DeForest](#)<sup>1</sup>, C. A. de Koning<sup>2</sup>, and H. A. Elliott<sup>1</sup>

2017 ApJ 850 130

<http://iopscience.iop.org/article/10.3847/1538-4357/aa94ca/pdf>

We report on a direct polarimetric determination of the chirality of a coronal mass ejection (CME), using the physics of Thomson scattering applied to synoptic polarized images from the Solar Terrestrial Relations Observatories/COR2 coronagraph. We confirmed the determination using in situ magnetic field measurements of the same CME with the ACE spacecraft. CME chirality is related to the helicity ejected from the solar corona along with the mass and field entrained in the CME. It is also important to prediction of the space-weather-relevant Z component of the CME magnetic field. Hence, remote measurement of CME chirality is an important step toward both understanding CME physics and predicting geoeffectiveness of individual CMEs. The polarimetric properties of Thomson scattering are well known and can, in principle, be used to measure the 3D structure of imaged objects in the solar corona and inner heliosphere. However, reduction of that principle to practice has been limited by the twin difficulties of background subtraction and the signal-to-noise ratio in coronagraph data. Useful measurements of the 3D structure require relative photometry at a few percent precision level in each linear polarization component of the K corona. This corresponds to a relative photometric precision of order  $10^{-4}$  in direct images of the sky before subtraction of the F corona and related signal. Our measurement was enabled by recent developments in signal processing, which enable a better separation of the photometric signal from noise in the synoptic COR2 data. We discuss the relevance of this demonstration measurement to future instrument requirements, and to the future measurements of 3D structures in CMEs and other solar wind features. **2010 Apr 3**

## **ERRATUM: "FEASIBILITY OF HELIOSPHERIC IMAGING FROM NEAR EARTH"**

(2015, ApJ, 804, 126)

C. E. [DeForest](#) and T. A. Howard

2015 ApJ 813 139

## **TRACKING CORONAL FEATURES FROM THE LOW CORONA TO EARTH: A QUANTITATIVE ANALYSIS OF THE 2008 DECEMBER 12 CORONAL MASS EJECTION**

C. E. [DeForest](#)<sup>1</sup>, T. A. Howard<sup>1</sup>, and D. J. McComas

2013 ApJ 769 43

We have tracked a slow magnetic cloud associated coronal mass ejection (CME) continuously from its origin as a flux rope structure in the low solar corona over a four-day passage to impact with spacecraft located near Earth. Combining measurements from the STEREO, ACE, and Wind space missions, we are able to follow major elements with enough specificity to relate pre-CME coronal structure in the low corona to the corresponding elements seen in the near-Earth in situ data. Combining extreme ultraviolet imaging, quantitative Thomson scattering data throughout the flight of the CME, and "ground-truth" in situ measurements, we: (1) identify the plasma observed by ACE and Wind with specific features in the solar corona (a segment of a long flux rope); (2) determine the onset mechanism of the CME (destabilization of a filament channel following flare reconnection, coupled with the mass draining instability) and demonstrate that it is consistent with the in situ measurements; (3) identify the origin of different layers of the sheath material around the central magnetic cloud (closed field lifted from the base of the corona, closed field entrained during passage through the corona, and solar wind entrained by the front of the CME); (4) measure mass accretion of the system via snowplow effects in the solar wind as the CME crossed the solar system; and (5) quantify the kinetic energy budget of the system in interplanetary space, and determine that it is consistent with no long-term driving force on the CME.

### DISCONNECTING OPEN SOLAR MAGNETIC FLUX

C. E. DeForest<sup>1</sup>, T. A. Howard<sup>1</sup>, and D. J. McComas<sup>1,2</sup>

Astrophysical Journal, 745:36 (9pp), 2012

[http://www.boulder.swri.edu/~howard/Papers/2012\\_Disconnection.pdf](http://www.boulder.swri.edu/~howard/Papers/2012_Disconnection.pdf) - File

Disconnection of open magnetic flux by reconnection is required to balance the injection of open flux by coronal mass ejections and other eruptive events. Making use of recent advances in heliospheric background subtraction, we have imaged many abrupt disconnection events. These events produce dense plasma clouds whose distinctive shape can now be traced from the corona across the inner solar system via heliospheric imaging. The morphology of each initial event is characteristic of magnetic reconnection across a current sheet, and the newly disconnected flux takes the form of a "U"-shaped loop that moves outward, accreting coronal and solar wind material. We analyzed one such event on 2008 December 18 as it formed and accelerated at  $20 \text{ m s}^{-2}$  to  $320 \text{ km s}^{-1}$ , thereafter expanding self-similarly until it exited our field of view 1.2 AU from the Sun. From acceleration and photometric mass estimates we derive the coronal magnetic field strength to be  $8 \mu\text{T}$ ,  $6R_{\odot}$  above the photosphere, and the entrained flux to be  $1.6 \times 10^{11} \text{ Wb}$  ( $1.6 \times 10^{19} \text{ Mx}$ ). We model the feature's propagation by balancing inferred magnetic tension force against accretion drag. This model is consistent with the feature's behavior and accepted solar wind parameters. By counting events over a 36 day window, we estimate a global event rate of  $1 \text{ day}^{-1}$  and a global solar minimum unsigned flux disconnection rate of  $6 \times 10^{13} \text{ Wbyr}^{-1}$  ( $6 \times 10^{21} \text{ Mxyr}^{-1}$ ) by this mechanism. That rate corresponds to  $\sim -0.2 \text{ nTyr}^{-1}$  change in the radial heliospheric field at 1 AU, indicating that the mechanism is important to the heliospheric flux balance.

### Lessons Learned from the Three-view Determination of CME Mass

Curt A. de Koning

2017 ApJ 844 61

<http://sci-hub.cc/10.3847/1538-4357/aa7a09>

If two viewpoints are available, it has been suggested that total-brightness images might be used to simultaneously derive the CME deprojected mass and propagation direction. Exploiting all available data provided by SOHO, STEREO-A, and STEREO-B supplies three combinations of spacecraft pairs for double-viewpoint analysis. We show that, if only aleatory variation is reckoned, then the CME deprojected mass can vary by as much as 100% between different pairs of spacecraft. Going beyond multiple double-viewpoint analyses, we also utilize these spacecraft to simultaneously estimate the CME deprojected mass and propagation direction with triple-viewpoint analysis. However, once again, if only aleatory variation is reckoned, then, for many events, there is no common mass value estimated by the three viewpoints. This indicates that epistemic uncertainty is significant and must be reckoned also. We consider in detail the mass in the coronagraph field of view, from one, two, and three viewpoints, for the CME observed on **2007 December 31**, focusing especially on the approximations used and uncertainties in this process. Altogether, we use triple-viewpoint analysis to estimate the mass of eight CMEs. When simultaneously estimating the CME deprojected mass and propagation direction using total-brightness images, the single degree of freedom provided by a third, independent viewpoint clarifies the calculation of, and reduces ambiguity in, the deprojected mass; however, the deprojected mass should not be confused with the true mass.

### Geometric Localization of CMEs in 3D Space Using STEREO Beacon Data: First Results

Curt A. de Koning · V.J. Pizzo · D.A. Biesecker

Solar Phys (2009) 256: 167–181, DOI 10.1007/s11207-009-9344-7, 2009, File

#### STEREO SCIENCE RESULTS AT SOLAR MINIMUM

The geometric localization technique (Pizzo and Biesecker, *Geophys. Res. Lett.* **31**, 21802, 2004) can readily be used with *Solar Terrestrial Relations Observatory* (STEREO) Space Weather Beacon data to observe coronal mass ejection (CME) propagation within three-dimensional space in near-real time. This technique is based upon simple triangulation concepts and utilizes a series of lines of sight from two space-based observatories to determine gross characteristics of CMEs, such as location and velocity. Since this work is aimed at space weather applications, the emphasis is on use of COR2 coronagraph

data, which has a field of view from  $2.5R_{\odot}$  to  $15R_{\odot}$ ; this spatial coverage allows us to observe the early temporal development of a CME, and hence to calculate its velocity, even for very fast CMEs. We apply this technique to highly-compressed COR2 beacon images for several CMEs at various spacecraft separation angles: 21 August 2007, when the separation angle between the two spacecraft was  $26^{\circ}$ ; 31 December 2007 and 2 January 2008, when the separation angle was  $44^{\circ}$ ; and 17 October 2008, when the spacecraft separation was  $79^{\circ}$ . We present results on the speed and direction of propagation for these events and discuss the error associated with this technique. We also compare our results to the two-dimensional plane-of-sky speeds calculated from STEREO and SOHO.

### **In-flight radiometric calibration of the Metis Visible Light channel using stars and comparison with STEREO-A/COR2 data**

Y. De Leo<sup>1,2</sup>, A. Burtovoi<sup>3</sup>, L. Teriaca<sup>1</sup>, M. Romoli<sup>3,4</sup>, + + +  
A&A 676, A45 (2023)

<https://www.aanda.org/articles/aa/pdf/2023/08/aa45979-23.pdf>

Context. We present the results for the in-flight radiometric calibration performed for the Visible Light (VL) channel of the Metis coronagraph on board Solar Orbiter.

Aims. The radiometric calibration is a fundamental step in building the official pipeline of the instrument, devoted to producing the calibrated data in physical units (L2 data).

Methods. To obtain the radiometric calibration factor ( $\epsilon_{VL}$ ), we used stellar targets transiting the Metis field of view. We derived  $\epsilon_{VL}$  by determining the signal of each calibration star by means of the aperture photometry and calculating its expected flux in the Metis band pass. The analyzed data set covers the time range from the beginning of the Cruise Phase of the mission (June 2020) until March 2021.

Results. Considering the uncertainties, the estimated factor  $\epsilon_{VL}$  is in a good agreement with that obtained during the on-ground calibration campaign. This implies that up to March 2021 there was no measurable reduction in the VL channel throughput. Finally, we compared the total and polarized brightness visible light images of the solar corona acquired with Metis and STEREO-A/COR2 during the November 2020 superior conjunction of these instruments. A general good agreement was obtained between the images of these instruments for both the total and polarized brightness. **18 November 2020**

### **Observation of the origin of CMEs in the low corona.**

Delannée, C., Delaboudinière, J.P., Lamy, P.,  
2000. Astron. Astrophys. 355, 725–742.

### **Initiation and Development of the white-light and radio CME on 15 April 2001**

P. Demoulin, A. Vourlidas, M. Pick, A. Bouteille

E-print, 9 March 2012, File; 2012 ApJ 750 147

The 2001 April 15 event was one of the largest of the last solar cycle. A former study (Maia et al., 2007) established that this event was associated with a coronal mass ejection (CME) observed both at white light and radio frequencies. This radio CME is illuminated by synchrotron emission from relativistic electrons. In this paper, we investigate the relation of the radio CME to its extreme ultraviolet (EUV) and white light counterpart and reach four main conclusions. i) The radio CME corresponds to the white light flux rope cavity. ii) The presence of a reconnecting current sheet behind the erupting flux rope is framed, both from below and above, by bursty radio sources. This reconnection is the source of relativistic radiating electrons which are injected down along the reconnected coronal arches and up along the flux rope border forming the radio CME. iii) Radio imaging reveals an important lateral over expansion in the low corona; this over expansion is at the origin of compression regions where type II and III bursts are imaged. iv) Already in the initiation phase, radio images reveal large scale interactions of the source active region with its surroundings, including another active region and open magnetic fields. Thus, these complementary radio, EUV, white light data validate the flux rope eruption model of CMEs.

ERRATUM: 2012 ApJ 754 156

### **Criteria for Flux Rope Eruption: Non Equilibrium versus Torus Instability**

P. Demoulin and G. Aulanier

E-print, June 2010, ApJ, 718(2), 1388-1399; File

The coronal magnetic configuration of an active region typically evolves quietly during few days before becoming suddenly eruptive and launching a coronal mass ejection (CME). The precise origin of the eruption is still debated. Among several mechanisms, it has been proposed that a loss of equilibrium, or an ideal magneto-hydrodynamic (MHD) instability such as the torus instability, could be responsible for the sudden eruptivity. Distinct approaches have also been formulated for limit cases having circular or translation symmetry. We revisit the previous theoretical approaches, setting them in the same analytical framework. The coronal field results from the contribution of a non-neutralized current channel added to a background magnetic field, which in our model is the potential field generated by two photospheric flux concentrations. The evolution on short Alfvénic time scale is governed by ideal MHD. We show analytically first that the loss of equilibrium and the stability analysis are two different views of the same physical mechanism. Second, we identify that the same physics is involved in the instability of circular and straight current



channels. Indeed, they are just two particular limiting case of more general current paths. A global instability of the magnetic configuration is present when the current channel is located at a coronal height,  $h$ , large enough so that the decay index of the potential field,  $(d \ln |B_p|) / (d \ln h)$  is larger than a critical value. At the limit of very thin current channels, previous analysis found a critical decay index of 1.5 and 1 for circular and straight current channels, respectively. However, with current channels being deformable and as thick as expected in the corona, we show that this critical index has similar values for circular and straight current channels, typically in the range [1.1,1.3].

## **Interaction of ICMEs with the Solar Wind (Review)**

**Demoulin P.**

E-print, Sept 2009, SW12 proceedings; **File**

Interplanetary Coronal Mass Ejections (ICMEs) are formed of plasma and magnetic field launched from the Sun into the Solar Wind (SW). These coherent magnetic structures, frequently formed by a flux rope, interact strongly with the SW. Such interaction is reviewed by comparing the results obtained from in situ observations and with numerical simulations. Like fast ships in the ocean, fast ICMEs drive an extended shock in front. However, their interaction with the SW is much more complex than that of the ship analogy. For example, as they expand in all directions while traveling away from the Sun, a sheath of SW plasma and magnetic field accumulates in front, which partially reconnects with the ICME magnetic field. Furthermore, not only ICMEs have a profound impact on the heliosphere, but the type of SW encountered by an ICME has an important impact on its evolution (e.g. increase of mass, global deceleration, lost of magnetic flux and helicity, distortion of the configuration).

## **Quantitative links between CMEs and magnetic clouds**

**P. Démoulin**

E-print, Sept. 2007, Ann. Geophys., 2008, 26, 3113, **File**

Magnetic clouds (MCs), and more generally interplanetary coronal mass ejections (ICMEs), are believed to be the interplanetary counterparts of CMEs. The link has usually been shown by taking into account the CME launch position on the Sun, the expected time delay and by comparing the orientation of the coronal and interplanetary magnetic field. Making such a link more quantitative is challenging since it requires the relation of very different kinds of magnetic field measurements: (i) photospheric magnetic maps, which are observed from a distant vantage point (remote sensing) and (ii) in situ measurements of MCs, which provide precise, directly measured, magnetic field data merely from one-dimensional linear samples. The association between events in these different domains can be made using adequate coronal and MC models. Then, global quantities like magnetic fluxes and helicity can be derived and compared. All the associations criteria are reviewed, with a description of the general trends found. A special focus is given on the cases which do not follow the earlier derived mean laws since interesting physics is usually associated to them.

## **Recent theoretical and observational developments in magnetic helicity studies**

Adv. Space Res. 39(11), Pages 1674-1693, 2007 **Обзор**

**P. Démoulin**

Magnetic helicity quantifies how the magnetic field is sheared and twisted compared to its lowest energy state (potential field). Such stressed magnetic fields are usually observed in association with flares, eruptive filaments, and coronal mass ejections (CMEs). Magnetic helicity plays a key role in magnetohydrodynamics because it is almost preserved on a timescale less than the global diffusion time scale. Its conservation defines a constraint to the magnetic field evolution.

Only relatively recently, scientists have realized that magnetic helicity can be computed from observations, and methods have been derived to bridge the gap between theory and observations. At the photospheric level, the rate (or flux) of magnetic helicity can be computed from the evolution of longitudinal magnetograms. The coronal helicity is estimated from magnetic extrapolation, while the helicity ejected in magnetic clouds (interplanetary counter-part of CMEs) is derived through modelling of in situ magnetic field measurements. Using its conserved property, a quantitative link between phenomena observed in the corona and then in the interplanetary medium has been achieved.

## **The Roles of Reconnected Flux and Overlying Fields in CME Speeds**

**Minda Deng**, Brian T. Welsch

Solar Phys. January 2017, 292:17

<http://arxiv.org/pdf/1504.02905v1.pdf>

The standard model of eruptive, two-ribbon flares involves reconnection of over-lying magnetic fields beneath a rising ejection. Numerous observers have reported evidence linking this reconnection, indicated by photospheric flux swept out by flare ribbons, to coronal mass ejection (CME) acceleration. This acceleration might be caused by reconnected fields that wrap around the ejection producing an increased outward hoop force. Other observations have linked stronger over-lying fields, measured by the power-law index of the fitted decay rate of field strength overlying eruption sites, to slower CME speeds. This might be caused by greater downward magnetic tension in stronger overlying fields. So overlying fields might both help and hinder the acceleration of CMEs: reconnection that converts overlying fields into flux winding about the ejection might help, but unreconnected overlying fields might hurt. Here, we investigate the roles of both ribbon fluxes and the decay rates of overlying fields in a set of 16 eruptive events. We confirm previous

results that higher CME speeds are associated with both larger ribbon fluxes and more rapidly decaying overlying fields. We find the association with ribbon fluxes to be weaker than a previous report, but stronger than the dependence on the decay rate of overlying fields. **1998 Apr 29, 1998 Nov 05, 2000 Jan 18, 2000 Jul 25, 2000 Aug 09, 2000 Nov 24, 2001 Apr 10, 2001 Apr 26, 2001 Sep 28, 2002 Mar 20, 2002 July 26, 2003 Oct 28, 2003 Oct 29, 2003 Nov 18, 2004 Nov 07, 2005 May 13**

## LASCO AND EIT OBSERVATIONS OF HELICAL STRUCTURE IN CORONAL MASS EJECTIONS

K. P. **DERE**,<sup>1</sup> G. E. BRUECKNER,<sup>2</sup> R. A. HOWARD, D. J. MICHELS, AND J. P. DELABOUDINIÈRE  
ASTROPHYSICAL JOURNAL, 516:465-474, **1999**; **File**

Observations of coronal mass ejections (CMEs) by the Large Angle Spectrometric Coronagraph (LASCO) on the Solar and Heliospheric Observatory (SOHO) show a significant fraction with circular intensity patterns. In the past, these would have been called .. disconnection II events, but we suggest that these are evidence of CMEs containing helical magnetic flux ropes that are often central to many theoretical models of CMEs and have been observed in magnetic clouds near 1 AU. Three examples are examined in detail with the LASCO and Extreme-Ultraviolet Imaging Telescope (EIT) data sets, which provide observations from their initiation through 30 R<sub>☉</sub>.

## EIT and LASCO Observations of the Initiation of a Coronal Mass Ejection. Solar

**Dere**, K.P., Brueckner, G.E., Howard, R.A., Koomen, M.J., Korendyke, C.M., Kreplin, R.W., Michels, D.J., Moses, J.D., Moulton, N.E., Socker, D.G., St. Cyr, O.C., Delaboudinière, J.P., Artzner, G.E., Brunaud, J., Gabriel, A.H., Hochedez, J.F., Millier, F., Song, X.Y., Chauvineau, J.P., Marioge, J.P., Defise, J.M., Jamar, C., Rochus, P., Catura, R.C., Lemen, J.R., Gurman, J.B., Neupert, W., Clette, F., Cugnon, P., van Dessel, E.L., Lamy, P.L., Llebaria, A., Schwenn, R., Simnett, G.M.,  
**1997**. Solar Phys. 175, 601–612.

<https://link.springer.com/content/pdf/10.1023/A:1004907307376.pdf>

We present the first observations of the initiation of a coronal mass ejection (CME) seen on the disk of the Sun. Observations with the EIT experiment on SOHO show that the CME began in a small volume and was initially associated with slow motions of prominence material and a small brightening at one end of the prominence. Shortly afterward, the prominence was accelerated to about 100 km s<sup>-1</sup> and was preceded by a bright loop-like structure, which surrounded an emission void, that traveled out into the corona at a velocity of 200–400 km s<sup>-1</sup>. These three components, the prominence, the dark void, and the bright loops are typical of CMEs when seen at distance in the corona and here are shown to be present at the earliest stages of the CME. The event was later observed to traverse the LASCO coronagraphs fields of view from 1.1 to 30 R<sub>☉</sub>. Of particular interest is the fact that this large-scale event, spanning as much as 70 deg in latitude, originated in a volume with dimensions of roughly 35" (2.5 x 104 km). Further, a disturbance that propagated across the disk and a chain of activity near the limb may also be associated with this event as well as a considerable degree of activity near the west limb. **23 December 1996**

## Does Nearby Open Flux Affect the Eruptivity of Solar Active Regions?

Marc L. **DeRosa**, [Graham Barnes](#)

ApJ **861** 131 **2018** DOI [10.3847/1538-4357/aac77a](https://doi.org/10.3847/1538-4357/aac77a)

<https://arxiv.org/pdf/1802.01199.pdf>

The most energetic solar flares are typically associated with the ejection of a cloud of coronal material into the heliosphere in the form of a coronal mass ejection (CME). However, there exist large flares which are not accompanied by a CME. The existence of these non-eruptive flares raises the question of whether such flares suffer from a lack of access to nearby open fields in the vicinity above the flare (reconnection) site. In this study, we use a sample of 56 flares from Sunspot Cycles 23 and 24 to test whether active regions that produce eruptive X-class flares are preferentially located near coronal magnetic field domains that are open to the heliosphere, as inferred from a potential field source surface model. The study shows that X-class flares having access to open fields are eruptive at a higher rate than those for which access is lacking. The significance of this result should be moderated due to the small number of non-eruptive X-class flares in the sample, based on the associated Bayes factor. **2001-04-15, 2002-08-21, 2013-11-10, 2014-12-20, 2017-09-06**

**Table 1.** Sample of flaring active regions

## Leveraging the Mathematics of Shape for Solar Magnetic Eruption Prediction

V. **Deshmukh**, [T. E. Berger](#), [E. Bradley](#), [J. D. Meiss](#)

Journal of Space Weather and Space Climate

**10**, 13

**2020**

<https://arxiv.org/pdf/2003.05827.pdf>

<https://www.swsc-journal.org/articles/swsc/pdf/2020/01/swsc190060.pdf>

Current operational forecasts of solar eruptions are made by human experts using a combination of qualitative shape-based classification systems and historical data about flaring frequencies. In the past decade, there has been a great deal of interest in crafting machine-learning (ML) flare-prediction methods to extract underlying patterns from a training set --e.g., a set of solar magnetogram images, each characterized by features derived from the magnetic field and labeled as to whether it was an eruption precursor. These patterns, captured by various methods (neural nets, support vector machines, etc.), can then be used to classify new images. A major challenge with any ML method is the featurization of the data: pre-processing the raw images to extract higher-level properties, such as characteristics of the magnetic field, that can streamline the training and use of these methods. It is key to choose features that are informative, from the standpoint of the task at hand. To date, the majority of ML-based solar eruption methods have used physics-based magnetic and electric field features such as the total unsigned magnetic flux, the gradients of the fields, the vertical current density, etc. In this paper, we extend the relevant feature set to include characteristics of the magnetic field that are based purely on the geometry and topology of 2D magnetogram images and show that this improves the prediction accuracy of a neural-net based flare-prediction method. **2017 Sept 1-7**

### **Observations of a prominence eruption and loop contraction**

[Pooja Devi](#), [Pascal Démoulin](#), [Ramesh Chandra](#), [Reetika Joshi](#), [Brigitte Schmieder](#), [Bhuwan Joshi](#)

A&A 647, A85 2021

<https://arxiv.org/pdf/2101.07682.pdf>

<https://www.aanda.org/articles/aa/pdf/2021/03/aa40042-20.pdf>

Context. Prominence eruptions provide key observations to understand the launch of coronal mass ejections as their cold plasma traces a part of the unstable magnetic configuration.

Aims. We select a well observed case to derive observational constraints for eruption models.

Methods. We analyze the prominence eruption and loop expansion and contraction observed on **02 March 2015** associated with a GOES M3.7 class flare (SOL2015-03-02T15:27) using the data from Atmospheric Imaging Assembly (AIA) and the Reuven Ramaty High Energy Solar Spectroscopic Imager (RHESSI). We study the prominence eruption and the evolution of loops using the time-distance techniques.

Results. The source region is a decaying bipolar active region where magnetic flux cancellation is present for several days before the eruption. AIA observations locate the erupting prominence within a flux rope viewed along its local axis direction. We identify and quantify the motion of loops in contraction and expansion located on the side of the erupting flux rope. Finally, RHESSI hard X-ray observations identify the loop top and two foot-point sources.

Conclusions. Both AIA and RHESSI observations support the standard model of eruptive flares. The contraction occurs 19 minutes after the start of the prominence eruption indicating that this contraction is not associated with the eruption driver. Rather, this prominence eruption is compatible with an unstable flux rope where the contraction and expansion of the lateral loop is the consequence of a side vortex developing after the flux rope is launched.

### **Spinning solar jets explained through the interplay between plasma sheets and vortex columns**

[Sahel Dey](#), [Piyali Chatterjee](#), [Robertus Erdelyi](#)

2024

<https://arxiv.org/pdf/2404.16096>

Bunches of swaying and spinning plasma jets in the solar atmosphere - the spicules - exhibit a variety of complex dynamics that are clearly observed in the images of the solar limb. Utilizing three-dimensional radiative magnetohydrodynamics (rMHD) simulation data, we uncover another facet of a forest of spicules that turns out to be a manifestation of the two-dimensional plasma drapery, instead of one-dimensional conical spikes. This fluted morphology is observed in other contexts like molecular clouds, auroras, and coronal loops. Further, using a sequence of high-cadence line-of-sight integrated images, generated from our simulation, we obtain multiple episodes of spinning amongst clusters of synthetic spicules, also reported in observations near the solar limb. This perception of rotation, according to our findings, is associated with hot swirling plasma columns, extending to coronal heights - that we label as coronal swirling conduits (CoSCo).

### **Recurring Homologous Solar Eruptions in NOAA AR 11429**

[Suman K. Dhakal](#), [Jie Zhang](#), [Panditi Vemareddy](#), [Nishu Karna](#)

ApJ 901 40 2020

<https://arxiv.org/pdf/2008.03447.pdf>

<https://doi.org/10.3847/1538-4357/abacbc>

[https://ui.adsabs.harvard.edu/link\\_gateway/2020ApJ...901...40D/PUB\\_PDF](https://ui.adsabs.harvard.edu/link_gateway/2020ApJ...901...40D/PUB_PDF)

We present the study of three homologous solar eruptions from NOAA active region (AR) 11429 over four days. This large and complex AR divided into two relatively simple sub-regions: northeast (NE) and southwest (SW). Recurrent eruptions occurred from the SW sub-region over different evolutionary phases, which provided a unique opportunity to isolate the physical processes responsible for solar eruptions. Persistent shearing and convergence of opposite magnetic polarities led to continuous flux cancellation along the SW polarity inversion line (PIL). A filament persistently lying along the SW-PIL was observed to survive each eruption, which suggests the partial eruption of the magnetic system. Further, following the first and second eruptions, a sigmoidal magnetic structure of similar morphology was reformed

along the SW-PIL. The photospheric motion of magnetic flux continuously injected and stored the negative helicity in the partially erupted magnetic system and built up the magnetic free energy for the successive eruptions. These results suggest that the shearing motion and magnetic flux cancellation of opposite fluxes were: (1) the dominant factor, irrespective of the evolutionary phase, that contributed to the recurrent homologous eruption, and (2) the key processes of forming the erupting structure, likely a magnetic flux rope, and its long-lasting continuation results in reformation of identical erupting structure. The study also finds that similar magnetic topology could result in the magnetic reconnection at the same location, and such flares during the precursor phase would help in the eruption by decreasing the constraint of overlying magnetic field. **2012/03/07, 2012/03/09, 2012/03/10**

[HMI Science Nuggets](http://hmi.stanford.edu/hminuggets/?p=3392) # 147 Oct 2020 <http://hmi.stanford.edu/hminuggets/?p=3392>

## **A Study of a Compound Solar Eruption with Two Consecutive Erupting Magnetic Structures**

Suman K. [Dhakal](#)<sup>1</sup>, Georgios Chintzoglou<sup>2,3</sup>, and Jie Zhang<sup>1</sup>

2018 ApJ 860 35 DOI [10.3847/1538-4357/aac028](https://doi.org/10.3847/1538-4357/aac028)

<https://arxiv.org/pdf/1807.00206.pdf>

<http://sci-hub.tw/http://iopscience.iop.org/0004-637X/860/1/35/>

We report a study of a compound solar eruption that was associated with two consecutively erupting magnetic structures and correspondingly two distinct peaks, during impulsive phase, of an M-class flare (M8.5). Simultaneous multi-viewpoint observations from SDO, GOES and STEREO-A show that this compound eruption originated from two pre-existing sigmoidal magnetic structures lying along the same polarity inversion line. Observations of the associated pre-existing filaments further show that these magnetic structures are lying one on top of the other, separated by 12 Mm in height, in a so-called "double-decker" configuration. The high-lying magnetic structure became unstable and erupted first, appearing as an expanding hot channel seen at extreme ultraviolet wavelengths. About 12 minutes later, the low-lying structure also started to erupt and moved at an even faster speed compared to the high-lying one. As a result, the two erupting structures interacted and merged with each other, appearing as a single coronal mass ejection in the outer corona. We find that the double-decker configuration is likely caused by the persistent shearing motion and flux cancellation along the source active region's strong-gradient polarity inversion line. The successive destabilization of these two separate but closely spaced magnetic structures, possibly in the form of magnetic flux ropes, led to a compound solar eruption. The study of the compound eruption provides a unique opportunity to reveal the formation process, initiation, and evolution of complex eruptive structures in solar active regions. **March 10, 2012**

## **Trigger of successive filament eruptions observed by SDO and STEREO**

Sajal Kumar [Dhara](#), Ravindra B., Pankaj Kumar, [Ravinder Kumar Banyal](#), [Shibu K. Mathew](#), [Bhuwan Joshi](#)

Solar Physics 292:145 **2017**

<https://arxiv.org/pdf/1706.07385.pdf>

Using multi-wavelength observation from SDO and STEREO, we investigated the mechanism of two successive eruptions (F1 & F2) of a filament in active region NOAA 11444 on 27 March, 2012. The filament was inverse 'J' shaped and lying along a quasi-circular polarity inversion line (PIL). The first part of the filament (F1) erupted at ~2:30UT on **27 March 2012**, the second part of the filament (F2) erupted at around 4:20 UT on the same day. A precursor/pre-flare brightening was observed below filament's main axis about 30 min prior to F1. The brightening was followed by a jet-like ejection below filament, which triggered the eruption. Before the eruption of F2, the filament seems to be trapped within the overlying arcade loops almost for ~1.5-hr before its successful eruption. Interestingly, we observed simultaneously contraction (~12km/s) and expansion (~20km/s) of arcade loops in the active region before F2. HMI magnetograms show the converging motion of the opposite polarities resulting in flux cancellation near PIL. We suggest that flux cancellation at PIL resulted jet-like ejection below filament's main axis, which triggered the eruption F1 similar to tether-cutting process. The eruption F2 was triggered by removal of the overlying arcade loops via reconnection process. Both filament eruptions produced high speed (~1000km/s) CMEs.

## **Observations of Photospheric Vortical Motions During the Early Stage of Filament Eruption**

Sajal Kumar [Dhara](#), B. Ravindra, Ravinder Kumar Banyal

Solar Phys. **2014**

<http://arxiv.org/pdf/1410.3592v1.pdf>

Solar filaments/prominences exhibit rotational motion during different phases of their evolution from their formation to eruption. We have observed the rotational/vortical motion in the photosphere near the ends of ten filaments during their initial phase of eruption, at the onset of the fast rise phase. All the filaments were associated with active regions. The photospheric vortical motions we observed lasted for 4–20 minutes. In the vicinity of the conjugate ends of the filament the direction of rotation was opposite, except for two cases, where rotational motion was observed at only one end point. The sudden onset of a large photospheric vortex motion could have played a role in destabilizing the filament by transporting axial flux into the activated filament thereby increasing the outward magnetic pressure in it. The outward magnetic pressure may have pushed the filament/flux rope to the height where the torus instability criterion was satisfied, and hence it could have caused the filament instability and eruption. **07–Jun–2011, 07–Sep–2011, 02–Jul–2012, 02–Sep–2012, 07–Apr–2012, 31–Dec–2013, 01–Jan–2014, 01–Jan–2014, 04–Apr–2014, 15–Apr–2014**

## **Solar signatures and eruption mechanism of the 2010 August 14 CME**

Elke **D'Huys**, Daniel B. Seaton, Anik De Groof, David Berghmans, Stefaan Poedts

Journal of Space Weather and Space Climate 7 A7 2017

<https://arxiv.org/pdf/1701.08814v1.pdf>

<http://www.swsc-journal.org/articles/swsc/pdf/2017/01/swsc160031.pdf>

On **2010 August 14**, a wide-angled coronal mass ejection (CME) was observed. This solar eruption originated from a destabilized filament that connected two active regions and the unwinding of this filament gave the eruption an untwisting motion that drew the attention of many observers. In addition to the erupting filament and the associated CME, several other low-coronal signatures that typically indicate the occurrence of a solar eruption were associated to this event. However, contrary to what is expected, the fast CME ( $v > 900 \text{ km s}^{-1}$ ) was accompanied by only a weak C4.4 flare.

We investigate the various eruption signatures that were observed for this event and focus on the kinematic evolution of the filament in order to determine its eruption mechanism. Had this solar eruption occurred just a few days earlier, it could have been a significant event for space weather. The risk to underestimate the strength of this eruption based solely on the C4.4 flare illustrates the need to include all eruption signatures in event analyses in order to obtain a complete picture of a solar eruption and assess its possible space weather impact.

## **The Effect of Limited Sample Sizes on the Accuracy of the Estimated Scaling Parameter for Power-Law-Distributed Solar Data**

Elke **D'Huys**, David Berghmans, Daniel B. Seaton, Stefaan Poedts

Solar Phys. 2016

<http://arxiv.org/pdf/1605.06972v1.pdf>

Many natural processes exhibit power-law behavior. The power-law exponent is linked to the underlying physical process and therefore its precise value is of interest. With respect to the energy content of nanoflares, for example, a power-law exponent steeper than 2 is believed to be a necessary condition to solve the enigmatic coronal heating problem. Studying power-law distributions over several orders of magnitudes requires sufficient data and appropriate methodology. In this paper we demonstrate the shortcomings of some popular methods in solar physics that are applied to data of typical sample sizes. We use synthetic data to study the effect of the sample size on the performance of different estimation methods and show that vast amounts of data are needed to obtain a reliable result with graphical methods (where the power-law exponent is estimated by a linear fit on a log-transformed histogram of the data). We **revisit published results on power laws for the angular width of solar coronal mass ejections and the radiative losses of nanoflares**. We demonstrate the benefits of the maximum likelihood estimator and advocate its use.

## **Observational Characteristics of CMEs without Low Coronal Signatures**

E. **D'Huys**, D.B. Seaton, S. Poedts, D. Berghmans

2014 ApJ 795 49

<http://arxiv.org/pdf/1409.1422v1.pdf>, File

Solar eruptions are usually associated with a variety of phenomena occurring in the low corona before, during, and after onset of eruption. Though easily visible in coronagraph observations, so-called stealth coronal mass ejections (CMEs) do not obviously exhibit any of these low-coronal signatures. The presence or absence of distinct low coronal signatures can be linked to different theoretical models to establish the mechanisms by which the eruption is initiated and driven. In this study, **40 CMEs without low coronal signatures, occurring in 2012**, are identified. Their observational and kinematic properties are analyzed and compared to those of regular CMEs. Solar eruptions without clear on-disk or low coronal signatures can lead to unexpected space weather impacts, since many early warning signs for significant space weather activity are not present in these events. A better understanding of their initiation mechanism(s) will considerably improve the ability to predict such space weather events.

**Table 3. CACTus detection parameters for the CMEs without low coronal signatures observed in 2012.**

**07 Jan 2012, 19 Jan 2012, 26 Jan 2012, 28 Jan 2012, 04 Feb 2012, 2012-02-23, 2012-04-16**

## **Influence of the magnetic field topology in the evolution of small-scale two-fluid jets in the solar atmosphere**

E. E. **Díaz-Figueroa**, [G. Ares de Parga](#), [J. J. González-Avilés](#)

2023

<https://arxiv.org/pdf/2302.00147.pdf>

We perform a series of numerical simulations to recreate small-scale two-fluid jets using the JOANNA code, considering the magnetohydrodynamics of two fluids (ions + electrons and neutral particles). We first excite the jets in a uniform magnetic field by using velocity pulse perturbations located at  $y_0 = 1.3, 1.5, \text{ and } 1.8 \text{ Mm}$ , considering the base of the photosphere at  $y = 0 \text{ Mm}$ . Then, we repeat the excitation of the jets in a magnetic field that mimics a flux tube. Mainly, the jets excited at the upper chromosphere ( $y \sim 1.8 \text{ Mm}$ ) reach lower heights than those excited at the lower chromosphere ( $y \sim 1.3 \text{ Mm}$ ); this is due to the higher initial vertical location because of the lesser amount of plasma dragging. In both scenarios, the dynamics of the neutral particles and ions show similar behavior; however, we can still identify some differences in the velocity drift, which in our simulations is of the order of  $10\text{--}3 \text{ km s}^{-1}$  at the tips of the jets once they reached their maximum heights. Also, we estimate the heat generation due to the friction between ions

and neutrals (Qini,n), which is of the order of  $0.002\text{--}0.06\text{ W m}^{-3}$ ; however it is small to contribute to the heating of the surroundings of the solar corona. The jets in the two magnetic environments do not show substantial differences other than a slight variation in the maximum heights reached, particularly in the uniform magnetic field scenario. Finally, the maximum heights reached by the three different jets are in the range of some morphological parameters corresponding to macrospicules, Type I spicules, and Type II spicules.

### **Comparative analysis of solar radio bursts before and during CME propagation**

G.**Dididze**, [B.M. Shergelashvili](#), [V.N. Melnik](#), [V.V. Dorovskyy](#), [A.I. Brazhenko](#), [S. Poedts](#), [T.V.](#)

[Zaqarashvili](#), [M. Khodachenko](#)

A&A **2019**

<https://arxiv.org/pdf/1903.12279.pdf>

Context. As is well known, CME propagation often results in the fragmentation of the solar atmosphere on smaller regions of density (magnetic field) enhancement (depletion). It is expected that this type of fragmentation may have radio signatures.

Aims. The general aim of the present paper is to perform a comparative analysis of type III solar and narrow-band type-III-like radio burst properties before and during CME events, respectively. The main goal is to analyze radio observational signatures of the dynamical processes in solar corona. In particular, we aim to perform a comparison of local plasma parameters without and with CME propagation, based on the analysis of decameter radio emission data. Methods. In order to examine this intuitive expectation, we performed a comparison of usual type III bursts before the CME with narrow-band type-III-like bursts, which are observationally detectable on top of the background type IV radio bursts associated with CME propagation. We focused on the analysis of in total 429 type III and 129 narrow-band type-III-like bursts. We studied their main characteristic parameters such as frequency drift rate, duration, and instantaneous frequency bandwidth using standard statistical methods. Furthermore, we inferred local plasma parameters (e.g., density scale height, emission source radial sizes) using known definitions of frequency drift, duration, and instantaneous frequency bandwidth.

Results. The analysis reveals that the physical parameters of coronal plasma before CMEs considerably differ from those during the propagation of CMEs (the observational periods 2 and 4 with type IV radio bursts associated with CMEs). Local density radial profiles and the characteristic spatial scales of radio emission sources vary with radial distance more drastically during the CME propagation compared to the cases of quasistatic solar atmosphere without CME(s) (observational periods 1 and 3).

Conclusions. The results of the work enable us to distinguish different regimes of plasma state in the solar corona. Our results create a solid perspective from which to develop novel tools for coronal plasma studies using radio dynamic spectra. **2014-06-13**

### **Are the Magnetic Field Directions of Surrounding Loops a Key Parameter for Confining a Solar Filament Eruption?**

Tao **Ding**<sup>1</sup>, Jun Zhang<sup>1</sup>, and Junchao Hong<sup>2</sup>

**2022** ApJL 933 L38

<https://iopscience.iop.org/article/10.3847/2041-8213/ac7c73/pdf>

Using high-resolution H $\alpha$  data from the 1 m New Vacuum Solar Telescope, combined with multiband Atmospheric Imaging Assembly extreme ultraviolet observations and Helioseismic and Magnetic Imager light-of-sight magnetograms from the Solar Dynamical Observatory, we study a quiet-Sun filament eruption on **2019 November 1**. During the erupting process, the filament was blocked by at least three sets of surrounding loops (L1–L3). The magnetic field direction of L2 is opposite to that of the top segment of the erupting filament. While the top segment contacted L2, a current sheet formed between L2 and the top segment. Then, magnetic reconnection took place, resulting in the destruction of L2 and the filament. On the other hand, the magnetic field direction of L1 is the same as that of the left leg of the erupting filament, and that of L3 is the same as that of the right leg. The left leg expanded eastward and met L1, then it stopped. The right leg expanded westward and collided with L3. It rebounded and finally stopped at the interaction region. These observations imply that the magnetic field directions of the surrounding magnetic structures are a key parameter for confining a filament eruption. While the field direction of a surrounding structure is the same as that of an eruptive filament, the filament is confined.

### **First Detection of Prominence Material Embedded within a $2 \times 10^6$ K CME Front Streaming away at $100\text{--}1500\text{ km s}^{-1}$ in the Solar Corona**

Adalbert **Ding**<sup>1,2</sup> and Shadia Rifai Habbal

**2017** ApJL 842 L7

<http://iopscience.iop.org/sci-hub.cc/2041-8205/842/1/L7/>

Coronal mass ejections (CMEs) are the largest and most dynamic explosions detected in the million degree solar corona, with speeds reaching up to  $3000\text{ km s}^{-1}$  at Earth's orbit. Triggered by the eruption of prominences, in most cases, one of the outstanding questions pertaining to the dynamic CME-prominence system is the fate of the cool  $10^4\text{--}10^5\text{ K}$  ejected filaments. We present spectroscopic observations acquired during the **2015 March 20** total solar eclipse, which captured a plethora of redshifted plasmoids from Fe xiv emission at  $2 \times 10^6\text{ K}$ . Approximately 10% of these plasmoids enshrouded the same neutral and singly ionized plasma below  $2 \times 10^5\text{ K}$ , observed in prominences anchored at the Sun at that time. This discovery was enabled by the novel design of a dual-channel spectrometer and the

exceptionally clear sky conditions on the island of Svalbard during totality. The Doppler redshifts corresponded to speeds ranging from under 100 to over 1500 km s<sup>-1</sup>. These are the first comprehensive spectroscopic observations to unambiguously detect a  $2 \times 10^6$  K filamentary CME front with inclusions of cool prominence material. The CME front covered a projected area of  $2.5 \times 1.5 R_s^2$  starting from the solar surface. These observations imply that cool prominence inclusions within a CME front maintain their ionic composition during expansion away from the Sun.

## Interaction between Two Coronal Mass Ejections in the 2013 May 22 Large Solar Energetic Particle Event

Liu-Guan [Ding](#)<sup>1,2</sup>, Gang Li<sup>2</sup>, Yong Jiang<sup>3</sup>, Gui-Ming Le<sup>4</sup>, Cheng-Long Shen<sup>5</sup>, Yu-Ming Wang<sup>5</sup>, Yao Chen<sup>6</sup>, Fei Xu<sup>1</sup>, Bin Gu<sup>1</sup>, and Ya-Nan Zhang  
2014 ApJ 793 L35.

We investigate the eruption and interaction of two coronal mass ejections (CMEs) during the large **2013 May 22** solar energetic particle event using multiple spacecraft observations. Two CMEs, having similar propagation directions, were found to erupt from two nearby active regions (ARs), AR11748 and AR11745, at ~08:48 UT and ~13:25 UT, respectively. The second CME was faster than the first CME. Using the graduated cylindrical shell model, we reconstructed the propagation of these two CMEs and found that the leading edge of the second CME caught up with the trailing edge of the first CME at a height of ~6 solar radii. After about two hours, the leading edges of the two CMEs merged at a height of ~20 solar radii. Type II solar radio bursts showed strong enhancement during this two hour period. Using the velocity dispersion method, we obtained the solar particle release (SPR) time and the path length for energetic electrons. Further assuming that energetic protons propagated along the same interplanetary magnetic field, we also obtained the SPR time for energetic protons, which were close to that of electrons. These release times agreed with the time when the second CME caught up with the trailing edge of the first CME, indicating that the CME-CME interaction (and shock-CME interaction) plays an important role in the process of particle acceleration in this event.

## THE "TWIN-CME" SCENARIO AND LARGE SOLAR ENERGETIC PARTICLE EVENTS IN SOLAR CYCLE 23

Liuguan [Ding](#)<sup>1,2</sup>, Yong Jiang<sup>1</sup>, Lulu Zhao<sup>2</sup>, and Gang Li  
2013 ApJ 763 30, [File](#)

Energetic particles in large solar energetic particle (SEP) events are a major concern for space weather. Recently, Li et al. proposed a "twin-CME" scenario for ground-level events. Here we extend that study to large SEP events in solar cycle 23. Depending on whether preceding coronal mass ejections (CMEs) within 9 hr exist and whether ions >10 MeV nucleon<sup>-1</sup> exceed 10 pfu, we categorize fast CMEs with speed >900 km s<sup>-1</sup> and width >60° from the western hemisphere source regions into four groups: groups I and II are "twin" and single CMEs that lead to large SEPs; groups III and IV are "twin" and single CMEs that do not lead to large SEPs. The major findings of this paper are: first, large SEP events tend to be "twin-CME" events. Of 59 western large SEP events in solar cycle 23, 43 are "twin-CME" (group I) events and 16 are single-CME (group II) events. Second, not all "twin CMEs" produced large SEPs: 28 twin CMEs did not produce large SEPs (group III events). Some of them produced excesses of particles up to a few MeV nucleon<sup>-1</sup>. Third, there were 39 single fast CMEs that did not produce SEPs (group IV events). Some of these also showed an excess of particles up to a few MeV nucleon<sup>-1</sup>. For all four groups of events, we perform statistical analyses on properties such as the angular width, the speed, the existence of accompanying metric type II radio bursts, and the associated flare class for the main CMEs and the preceding CMEs.

### [Tables](#)

## Statistics of coronal dimmings associated with coronal mass ejections.

### II. Relationship between coronal dimmings and their associated CMEs

Karin [Dissauer](#), [Astrid M. Veronig](#), [Manuela Temmer](#), [Tatiana Podladchikova](#)

ApJ 874 123 2018

<https://arxiv.org/pdf/1810.01589.pdf>

[sci-hub.se/10.3847/1538-4357/ab0962](https://sci-hub.se/10.3847/1538-4357/ab0962)

We present a statistical study of 62 coronal dimming events associated with Earth-directed CMEs during the quasi-quadrature period of STEREO and SDO. This unique setting allows us to study both phenomena in great detail and compare characteristic quantities statistically. Coronal dimmings are observed on-disk by SDO/AIA and HMI, while the CME kinematics during the impulsive acceleration phase is studied close to the limb with STEREO/EUVI and COR, minimizing projection effects. The dimming area, its total unsigned magnetic flux and its total brightness, reflecting properties of the total dimming region at its final extent, show the highest correlations with the CME mass ( $c \sim 0.6-0.7$ ). Their corresponding time derivatives, describing the dynamics of the dimming evolution, show the strongest correlations with the CME peak velocity ( $c \sim 0.6$ ). The highest correlation of  $c = 0.68 \pm 0.08$  is found with the mean intensity of dimmings, indicating that the lower the CME starts in the corona, the faster it propagates. No significant correlation between dimming parameters and the CME acceleration was found. However, for events where high-cadence STEREO observations were available, the mean unsigned magnetic field density in the dimming regions tends to be positively correlated with the CME peak acceleration ( $c = 0.42 \pm 0.20$ ). This suggests that stronger magnetic fields result in higher Lorentz forces providing stronger driving force for the CME acceleration. Specific coronal dimming parameters correlate with both, CME and flare quantities providing further evidence for the flare-CME feedback

relationship. For events in which the CME occurs together with a flare, coronal dimmings statistically reflect the properties of both phenomena. **2011 February 13, 2011-06-02, 2011 October 2, 2012-06-14, 2012-09-28**  
**Table 1.** Results of characteristic dimming parameters together with basic flare and CME quantities (2010-2012)  
See VarSITI Newsletter · Vol. 20 p.8-9, **2018** <http://www.varsiti.org>

## Statistics of coronal dimmings associated with coronal mass ejections.

### I. Characteristic dimming properties and flare association

Karin [Dissauer](#), [Astrid M. Veronig](#), [Manuela Temmer](#), [Tatiana Podladchikova](#), [Kamalam Vanninathan](#)  
ApJ **863** 169 **2018**

<https://arxiv.org/pdf/1807.05056.pdf>

<http://iopscience.iop.org/article/10.3847/1538-4357/aad3c6/pdf>

Coronal dimmings, localized regions of reduced emission in the EUV and soft X-rays, are interpreted as density depletions due to mass loss during the CME expansion. They contain crucial information on the early evolution of CMEs low in the corona. For 62 dimming events, characteristic parameters are derived, statistically analyzed and compared with basic flare quantities. On average, coronal dimmings have a size of  $2.15 \times 10^{10}$  km<sup>2</sup>, contain a total unsigned magnetic flux of  $1.75 \times 10^{21}$  Mx, and show a total brightness decrease of  $-1.91 \times 10^6$  DN, which results in a relative decrease of  $\sim 60\%$  compared to the pre-eruption intensity level. Their main evacuation phase lasts for  $\sim 50$  minutes. The dimming area, the total dimming brightness, and the total unsigned magnetic flux show the highest correlation with the flare SXR fluence ( $c \geq 0.7$ ). Their corresponding time derivatives, describing the dimming dynamics, strongly correlate with the GOES flare class ( $c \geq 0.6$ ). For 60% of the events we identified core dimmings, i.e. signatures of an erupting flux rope. They contain 20% of the magnetic flux covering only 5% of the total dimming area. Secondary dimmings map overlying fields that are stretched during the eruption and closed down by magnetic reconnection, thus adding flux to the erupting flux rope via magnetic reconnection. This interpretation is supported by the strong correlation between the magnetic fluxes of secondary dimmings and flare reconnection fluxes ( $c = 0.63 \pm 0.08$ ), the balance between positive and negative magnetic fluxes ( $c = 0.83 \pm 0.04$ ) within the total dimmings and the fact that for strong flares ( $> M1.0$ ) the reconnection and secondary dimming fluxes are roughly equal. **2011 June 21, 13 Dec 2011, 9 March 2012, 10 March 2012, 11 May 2012, 2012 June 6**

**Table 1.** Overview of the events under study 2010-2012

### On the detection of coronal dimmings and the extraction of their characteristic properties

Karin [Dissauer](#), [Astrid M. Veronig](#), [Manuela Temmer](#), [Tatiana Podladchikova](#), [Kamalam Vanninathan](#)  
ApJ **2018**

<https://arxiv.org/pdf/1802.03185.pdf>

Coronal dimmings are distinct phenomena associated to coronal mass ejections (CMEs). The study of coronal dimmings and the extraction of their characteristic parameters helps us to obtain additional information of CMEs, especially on the initiation and early evolution of Earth-directed CMEs. We present a new approach to detect coronal dimming regions based on a thresholding technique applied on logarithmic base-ratio images. Characteristic dimming parameters describing the dynamics, morphology, magnetic properties and the brightness of coronal dimming regions are extracted by cumulatively summing newly dimmed pixels over time. It is also demonstrated how core dimming regions are identified as a subset of the overall identified dimming region. We successfully apply our method to two well-observed coronal dimming events. For both events the core dimming regions are identified and the spatial evolution of the dimming area reveals the expansion of the dimming region around these footpoints. We also show that in the early impulsive phase of the dimming expansion the total unsigned magnetic flux involved in the dimming regions is balanced and that up to 30% of this flux results from the localized core dimming regions. Furthermore, the onset in the profile of the area growth rate is co-temporal with the start of the associated flares and in one case also with the fast rise of the CME, indicating a strong relationship of coronal dimmings with both flare and CMEs. **6 September, 2011, October 1, 2011, 26 December 2011**

### Stereoscopic observations of the effects of a halo CME on the solar coronal structure\*

S. [Dolei](#), P. Romano, D. Spadaro and R. Ventura

A&A 567, A9 (2014)

We investigated the substantial restructuring of the outer solar corona in the aftermath of the halo CME that occurred on **9 March 2012**. To perform our analysis, we used SOHO/LASCO, STEREO/COR1 and SDO/AIA data, which provide observations from different viewpoints. In particular, we applied the polarization ratio technique to the COR1 calibrated images to derive the three-dimensional structure of the CME and determine its direction and speed of propagation. We also estimated the CME mass from a sequence of four observations of the event and obtained values of up to  $2.2 \times 10^{16}$  g. The COR1 images show a brightness decrease in the coronal sector where the CME propagates. We verified that this intensity reduction is due to a plasma depletion. Moreover, the combined analysis performed by the two STEREO satellites allowed us to deduce that a preexisting streamer is located along the propagation direction of the CME and disappears after the passage of the event. The coronal mass loss associated with the plasma depletion is much lower than the mass expelled from the Sun in the COR1-B data. Conversely, the COR1-A observations allowed us to infer that the mass of the streamer carried away from the outer corona corresponds to about half of the CME mass. The results



highlight the importance of stereoscopic observations in the study of corona restructuring in the aftermath of a CME event.

### **Measurements with STEREO/COR1 data of drag forces acting on small-scale blobs falling in the intermediate corona**

S. [Dolei](#)<sup>1</sup>, A. Bemporad<sup>2</sup> and D. Spadaro  
A&A 562, A74 (2014)

In this work we study the kinematics of three small-scale ( $0.01 R_{\odot}$ ) blobs of chromospheric plasma falling back to the Sun after the huge eruptive event of **June 7, 2011**. From a study of 3D trajectories of blobs made with the Solar TERrestrial RELations Observatory (STEREO) data, we demonstrate the existence of a significant drag force acting on the blobs and calculate two drag coefficients, in the radial and tangential directions. The resulting drag coefficients  $CD$  are between 0 and 5, comparable in the two directions, making the drag force only a factor of 0.45–0.75 smaller than the gravitational force. To obtain a correct determination of electron densities in the blobs, we also demonstrate how, by combining measurements of total and polarized brightness, the  $H\alpha$  contribution to the white-light emission observed by the COR1 telescopes can be estimated. This component is significant for chromospheric plasma, being between 95 and 98% of the total white-light emission. Moreover, we demonstrate that the COR1 data can be employed even to estimate the  $H\alpha$  polarized component, which turns out to be in the order of a few percent of  $H\alpha$  total emission from the blobs. If the drag forces acting on small-scale blobs reported here are similar to those that play a role during the CME propagation, our results suggest that the magnetic drag should be considered even in the CME initiation modelling.

### **A ring of polarized light: evidence for twisted coronal magnetism in cavities.**

[Dove](#), J.B., Gibson, S.E., Rachmeler, L.A., Tomczyk, S., Judge, P.:  
2011, *Astrophys. J. Lett.* **731**, L1

Coronal prominence cavities may be manifestations of twisted or sheared magnetic fields capable of storing the energy required to drive solar eruptions. The Coronal Multi-Channel Polarimeter (CoMP), recently installed at Mauna Loa Solar Observatory, can measure polarimetric signatures of current-carrying magnetohydrodynamic (MHD) systems. For the first time, this instrument offers the capability of daily full-Sun observations of the forbidden lines of Fe XIII with high enough spatial resolution and throughput to measure polarimetric signatures of current-carrying MHD systems. By forward-calculating CoMP observables from analytic MHD models of **spheromak**-type magnetic flux ropes, we show that a predicted observable for such flux ropes oriented along the line of sight is a bright ring of linear polarization surrounding a region where the linear polarization strength is relatively depleted. We present CoMP observations of a coronal cavity possessing such a polarization ring.

### **Magnetohydrodynamic Simulations of Spicular Jet Propagation Applied to Lower Solar Atmosphere Model. II. Case Studies with Tilted Jets**

Fionnlagh Mackenzie [Dover](#)<sup>1</sup>, Rahul Sharma<sup>2</sup>, and Robertus Erdélyi<sup>1,3,4</sup>  
2022 ApJ 929 88

<https://iopscience.iop.org/article/10.3847/1538-4357/ac5aa9/pdf>

We report on numerical simulations of a propagating momentum pulse, representing an inclined jet structure in a stratified lower solar atmosphere model. Here, the numerical jets were generated via injection of a momentum pulse misaligned with the radial magnetic field, which resulted in a collimated structure that mimicked the observed inclined jet features in the chromosphere. The influence of inclination angle was examined for a variety of initial driver conditions (amplitude, period) and magnetic field magnitudes to identify their potential role in determining the morphological and dynamical characteristics of chromospheric jets. The numerical jets in our computational domain were consistent with the observed magnitudes of apex height and cross-sectional width for average inclination of chromospheric features. Furthermore, with an increasing misalignment between the momentum pulse and ambient magnetic field, the simulated structures showed a drop in the maximum apex height and length, while an increase in cross-sectional width magnitudes. Our numerical experiments also revealed the development of a pulse-like transverse motions in jets along with high density edges/nodes in the direction of jet displacement. It is postulated that dynamic kink instability might be responsible for the observed kinematic behavior of the inclined jet structures in the solar chromosphere.

### **Are switchbacks signatures of magnetic flux ropes generated by interchange reconnection in the corona?**

J. F. [Drake](#), [O. Agapitov](#), [M. Swisdak](#), [S. T. Badman](#), [S. D. Bale](#), [T. S. Horbury](#), [Justin C. Kasper](#), [R. J. MacDowall](#), [F. S. Mozer](#), [T. D. Phan](#), [M. Pulupa](#), [A. Szabo](#), [M. Velli](#)

A&A 2020

<https://arxiv.org/pdf/2009.05645.pdf>

The structure of magnetic flux ropes injected into the solar wind during reconnection in the coronal atmosphere is explored with particle-in-cell simulations and compared with  $\{it\}$  in situ measurements of magnetic "switchbacks" from the Parker Solar Probe. We suggest that multi-x-line reconnection between open and closed flux in the corona will inject flux ropes into the solar wind and that these flux ropes can convect outward over long distances before disintegrating. Simulations that explore the magnetic structure of flux ropes in the solar wind reproduce key features of the "switchback" observations: a rapid rotation of the radial magnetic field into the transverse direction (a consequence

of reconnection with a strong guide field); and the potential to reverse the radial field component. The potential implication of the injection of large numbers of flux ropes in the coronal atmosphere for understanding the generation of the solar wind is discussed. **Nov. 5, 2018**

## **Magnetohydrodynamic Simulations of Spicular Jet Propagation Applied to Lower Solar Atmosphere Model**

Fionnlagh Mackenzie [Dover](#)<sup>1</sup>, Rahul Sharma<sup>2</sup>, and Robertus Erdélyi<sup>1,3,4</sup>  
**2021 ApJ 913 19**

<https://doi.org/10.3847/1538-4357/abefd1>

We report a series of numerical experiments for the propagation of a momentum pulse representing a chromospheric jet, simulated using an idealized magnetohydrodynamic model. The jet in a stratified lower solar atmosphere is subjected to a varied initial driver (amplitude, period) and magnetic field conditions to examine the parameter influence over jet morphology and kinematics. The simulated jet captured key observed spicule characteristics including maximum heights, field-aligned mass motions/trajectories, and cross-sectional width deformations. Next, the jet features also show a prominent bright, bulb-like apex, similar to reported observed chromospheric jets, formed due to the higher density of plasma and/or waves. Furthermore, the simulations highlight the presence of not yet observed internal crisscross/knots substructures generated by shock waves reflected within the jet structure. Therefore we suggest verifying these predicted fine-scale structures in highly localized lower solar atmospheric jets, e.g., in spicules or fibrils by high-resolution observations, offered by the Daniel K. Inoyue Solar Telescope or otherwise.

## **Observations and 3D MHD Modeling of a Confined Helical Jet Launched by a Filament Eruption**

Lauren [Doyle](#), [Peter F. Wyper](#), [Eamon Scullion](#), [James A. McLaughlin](#), [Gavin Ramsay](#), [J. Gerard Doyle](#)  
**ApJ 887 246 2019**

<https://arxiv.org/pdf/1912.02133.pdf>

<https://iopscience.iop.org/article/10.3847/1538-4357/ab5d39/pdf>

We present a detailed analysis of a confined filament eruption and jet associated with a C1.5 class solar flare. Multi-wavelength observations from GONG and SDO reveal the filament forming over several days following the emergence and then partial cancellation of a minority polarity spot within a decaying bipolar active region. The emergence is also associated with the formation of a 3D null point separatrix that surrounds the minority polarity. The filament eruption occurs concurrent with brightenings adjacent to and below the filament, suggestive of breakout and flare reconnection, respectively. The erupting filament material becomes partially transferred into a strong outflow jet (~ 60 km/s) along coronal loops, becoming guided back towards the surface. Utilising high resolution H $\alpha$  observations from SST/CRISP, we construct velocity maps of the outflows demonstrating their highly structured but broadly helical nature. We contrast the observations with a 3D MHD simulation of a breakout jet in a closed-field background and find close qualitative agreement. We conclude that the suggested model provides an intuitive mechanism for transferring twist/helicity in confined filament eruptions, thus validating the applicability of the breakout model not only to jets and coronal mass ejections but also to confined eruptions and flares. **30 June 2013**

## **IMPLICATIONS OF MASS AND ENERGY LOSS DUE TO CORONAL MASS EJECTIONS ON MAGNETICALLY ACTIVE STARS**

Jeremy J. [Drake](#)<sup>1</sup>, Ofer Cohen<sup>1</sup>, Seiji Yashiro<sup>2,3</sup>, and Nat Gopalswamy  
**2013 ApJ 764 170**

<http://arxiv.org/pdf/1302.1136.pdf>

Analysis of a database of solar coronal mass ejections (CMEs) and associated flares over the period 1996-2007 finds well-behaved power-law relationships between the 1-8 Å flare X-ray fluence and CME mass and kinetic energy. We extrapolate these relationships to lower and higher flare energies to estimate the mass and energy loss due to CMEs from stellar coronae, assuming that the observed X-ray emission of the latter is dominated by flares with a frequency as a function of energy  $dn/dE = kE^{-\alpha}$ . For solar-like stars at saturated levels of X-ray activity, the implied losses depend fairly weakly on the assumed value of  $\alpha$  and are very large:  $\text{yr}^{-1}$  and . In order to avoid such large energy requirements, either the relationships between CME mass and speed and flare energy must flatten for X-ray fluence 1031 erg, or the flare-CME association must drop significantly below 1 for more energetic events. If active coronae are dominated by flares, then the total coronal energy budget is likely to be up to an order of magnitude larger than the canonical 10–3 L bol X-ray saturation threshold. This raises the question of what is the maximum energy a magnetic dynamo can extract from a star? For an energy budget of 1% of L bol, the CME mass loss rate is about  $5 \times 10^{-11} M_{\odot} \text{yr}^{-1}$ .

## **Tethered Prominence-CME Systems Captured during the 2012 November 13 and 2013 November 3 Total Solar Eclipses**

Miloslav [Druckmüller](#)<sup>1</sup>, Shadia R. Habbal<sup>2</sup>, Nathalia Alzate<sup>3</sup>, and Constantinos Emmanouilidis<sup>4</sup>  
**2017 ApJL 851 L41**

<http://sci-hub.tw/10.3847/2041-8213/aa9ed5>

We report on white light observations of high latitude tethered prominences acquired during the total solar eclipses of **2012 November 13 and 2013 November 3**, at solar maximum, with a field of view spanning several solar radii. Distinguished by their pinkish hue, characteristic of emission from neutral hydrogen and helium, the four tethered prominences were akin to twisted flux ropes, stretching out to the limit of the field of view, while remaining anchored at the Sun. Cotemporal observations in the extreme ultraviolet from the Solar Dynamics Observatory (SDO/AIA) clearly showed that the pinkish emission from the cool ( $\approx 10^4 - 10^5$  K) filamentary prominences was cospatial with the 30.4 nm He II emission, and was directly linked to filamentary structures emitting at coronal temperatures  $\geq 10^6$  K in 17.1 and 19.3 nm. The tethered prominences evolved from typical tornado types. Each one formed the core of different types of coronal mass ejections (CMEs), as inferred from coordinated LASCO C2, C3, and STEREO A and B coronagraph observations. Two of them evolved into a series of faint, unstructured puffs. One was a normal CME. The most striking one was a "light-bulb" type CME, whose three-dimensional structure was confirmed from all four coronagraphs. These first uninterrupted detections of prominence-CME systems anchored at the Sun, and stretching out to at least the edge of the field of view of LASCO C3, provide the first observational confirmation for the source of counter-streaming electron fluxes measured in interplanetary CMEs, or ICMEs.

### **Coronal transient phenomena.**

**Dryer, M.,**

**1982.** Space Sci. Rev. 33, 233–275.

### **Variations in the Correlations of Acceleration and Force of Slow and Fast CMEs with Solar Activity during Solar Cycles 23 – 24**

**Zhanle Du**

**Solar Physics** volume 296, Article number: 34 (2021)

<https://link.springer.com/content/pdf/10.1007/s11207-021-01778-5.pdf>

Studying the behavior of coronal mass ejections (CMEs) is important for both solar physics and space weather. The correlations of smoothed monthly mean daily integrated CME acceleration [a], mass [M], and the force [Ma] to drive CMEs with sunspot activity [RI] are analyzed for both slow and fast CMEs and for both Solar Cycles 23 and 24 separately. It is found that aa is inversely related to both RI and M. The correlation between Ma and RI for both slow and fast CMEs is negative at the rising phase of Solar Cycle 23 and positive otherwise. There is a sharp peak in  $\gamma = Ma/RI$  near the solar minimum (December 2008) for both slow and fast CMEs. However, for fast CMEs, there is a sharp negative peak near the previous solar minimum (August 1996) and another positive peak near the current solar minimum (2019). The positive (negative) peak tends to be related to the solar minimum from a stronger (weaker) to a weaker (stronger) solar cycle. These results suggest that the CME acceleration depends more on the strength of solar activity than on the CME's speed. Stronger magnetic activity may slow down the CMEs that are too massive or too fast and weaker activity may speed up the CMEs that are less massive or too slow. During a few years' period of magnetic-field polarity reversal around the solar minimum, the force provided by large-scale magnetic-field structures may not be strong enough to constrain CME motions, leading to the "escape" of CMEs with large  $|\gamma|$ .

### **Plasma Energization in Colliding Magnetic Flux Ropes**

Senbei **Du**<sup>1,2</sup>, Fan Guo<sup>2,3</sup>, Gary P. Zank<sup>1,4</sup>, Xiaocan Li<sup>3</sup>, and Adam Stanier

**2018** ApJ 867 16

[sci-hub.tw/10.3847/1538-4357/aae30e](https://arxiv.org/abs/1808.03301)

Magnetic flux ropes are commonly observed throughout the heliosphere, and recent studies suggest that interacting flux ropes are associated with some energetic particle events. In this work, we carry out 2D particle-in-cell (PIC) simulations to study the coalescence of two magnetic flux ropes (or magnetic islands), and the subsequent plasma energization processes. The simulations are initialized with two magnetic islands embedded in a reconnecting current sheet. The two islands collide and eventually merge into a single island. Particles are accelerated during this process as the magnetic energy is released and converted to the plasma energy, including bulk kinetic energy increase by the ideal electric field, and thermal energy increase by the fluid compression and the nonideal electric field. We find that contributions from these different energization mechanisms are all important and comparable with each other. Fluid shear and a nongyrotropic pressure tensor also contribute to the energy conversion process. For simulations with different box sizes ranging from  $L_x \sim 25-100d_i$  and ion-to-electron mass ratios  $m_i/m_e = 25, 100, \text{ and } 400$ , we find that the general evolution is qualitatively the same for all runs, and the energization depends only weakly on either the system size or the mass ratio. The results may help us understand plasma energization in solar and heliospheric environments.

### **Correlations Between CME Parameters and Sunspot Activity**

**Zhanle Du**

**Solar Physics**, Volume 278, Number 1 (2012), 203-215

<http://arxiv.org/abs/1112.5560v1>

Smoothed monthly mean coronal mass ejection (CME) parameters (speed, acceleration, central position angle, angular width, mass, and kinetic energy) for Cycle 23 are cross-analyzed, showing that there is a high correlation between most of them. The CME acceleration (a) is highly correlated with the reciprocal of its mass (M), with a correlation coefficient  $r=0.899$ . The force (Ma) to drive a CME is found to be well anti-correlated with the sunspot number (Rz),  $r=-0.750$ .

The relationships between CME parameters and  $R_z$  can be well described by an integral response model with a decay time scale of about 11 months. The correlation coefficients of CME parameters with the reconstructed series based on this model ( $r_1=0.886$ ) are higher than the linear correlation coefficients of the parameters with  $R_z$  ( $r_0=0.830$ ). If a double decay integral response model is used (with two decay time scales of about 6 and 60 months), the correlations between CME parameters and  $R_z$  improve ( $r_2=0.906$ ). The time delays between CME parameters with respect to  $R_z$  are also well predicted by this model ( $19/22=86\%$ ); the average time delays are 19 months for the reconstructed and 22 months for the original time series. The model implies that CMEs are related to the accumulation of solar magnetic energy. These relationships can help in understanding the mechanisms at work during the solar cycle.

## **On the Determining Physical Factor of Jet-Related Coronal Mass Ejection's Morphology in the High Corona**

[Yadan Duan](#), [Yuandeng Shen](#), [Zehao Tang](#), [Chenrui Zhou](#), [Song Tan](#)

ApJ 968 110 2024

<https://arxiv.org/pdf/2404.19179>

<https://iopscience.iop.org/article/10.3847/1538-4357/ad445c/pdf>

A solar jet can often cause coronal mass ejections (CMEs) with different morphologies in the high corona, for example, jet-like CMEs, bubble-like CMEs, and so-called twin CMEs that include a pair of simultaneous jet-like and bubble-like CMEs. However, what determines the morphology of a jet-related CME is still an open question. Using high spatiotemporal resolution stereoscopic observations taken by the Solar Dynamics Observatory (SDO) and the Solar Terrestrial Relations Observatory (STEREO) from October 2010 to December 2012, we performed a statistical study of jet-related CMEs to study the potential physical factors that determine the morphology of CMEs in the outer corona. Our statistical sample includes 16 jet-related CME events of which 7 are twin CME events and 9 are jet-like narrow CMEs. We find that all CMEs in our sample were accompanied by filament-driven blowout jets and Type III radio bursts during their initial formation and involved magnetic reconnection between filament channels and the surrounding magnetic fields. Most of our cases occurred in a fan-spine magnetic configuration. Our study suggests that the bubble-like components of twin CMEs lacking an obvious core are related to the expansion of the closed-loop systems next to the fan-spine topology, while the jet-like component is from the coronal extension of the jet plasma along open fields. Based on the statistical results, we conclude that the morphology of jet-related CMEs in the high corona may be related to the filament length and the initial magnetic null point height of the fan-spine structures. **2011 August 28, 2012 January 20, 2012 August 9, 2012 August 31**

**Table 1-2.** Information about all Events

## **The Initiation Mechanism of the First On-disk X-Class Flare of Solar Cycle 25**

[Aiyang Duan](#), [Chaowei Jiang](#), [ZhenJun Zhou](#), [Xueshang Feng](#)

A&A 674, A192 2023

<https://arxiv.org/pdf/2304.13241.pdf>

<https://www.aanda.org/articles/aa/pdf/2023/06/aa45583-22.pdf>

In this paper we study the initiation mechanism of the first on-disk X-class eruptive flare in solar cycle 25. Coronal magnetic field reconstructions reveal a magnetic flux rope (MFR) with configuration highly consistent with a filament existing for a long period before the flare, and the eruption of the whole filament indicates that the MFR erupted during the flare. However, quantitative analysis shows that the pre-flare MFR resides in a height too low to trigger a torus instability (TI). The filament experienced a slow rise before the flare onset, for which we estimate evolution of the filament height using a triangulation method by combining the SDO and STEREO observations, and find it is also much lower than the critical height for triggering TI. On the other hand, the pre-flare evolution of the current density shows progressive thinning of a vertical current layer on top of the flare PIL, which suggests that a vertical current sheet forms before the eruption. Meanwhile, there is continuously shearing motion along the PIL under the main branch of the filament, which can drive the coronal field to form such a current sheet. As such, we suggest that the event follows a reconnection-based initiation mechanism as recently established using a high-accuracy MHD simulation, in which an eruption is initiated by reconnection in a current sheet that forms gradually within continuously-sheared magnetic arcade. The eruption should be further driven by TI as the filament quickly rises into the TI domain during the eruption. **28 Oct 2021**

## **Macrospicules and Their Connection to Magnetic Reconnection in the Lower Atmosphere**

[Yadan Duan](#), [Yuandeng Shen](#), [Hechao Chen](#), [Zehao Tang](#), [Chenrui Zhou](#), [Xinping Zhou](#), [Song Tan](#)

ApJL 942 L22 2022

<https://arxiv.org/pdf/2212.03425.pdf>

<https://iopscience.iop.org/article/10.3847/2041-8213/acac2b/pdf>

Solar macrospicules are beam-like cool plasma ejections of size in-between spicules and coronal jets, which can elucidate potential connections between plasma jetting activity at different scales. With high-resolution observations from the *New Vacuum Solar Telescope* and Solar Dynamic Observatory, we investigate the origin of five groups of recurrent active-region macrospicules. Before the launch of each macrospicule, we detect a compact bright patch (BP) at its base where a newly emerging dipole contacts and cancel with the pre-existing ambient field. The spectral diagnosis from the *Interface Region Imaging Spectrograph* at one of BPs reveals signatures of reconnection at

the lower atmosphere. Multiwavelength imaging of these BPs show that they mainly occur at the rising phase of the flux emergence and slowly ascend from the lower to the upper chromosphere. Remarkable macrospicules occur and fade out once the BPs appear and decay from the AIA 304 Å images, respectively. We suggest that these macrospicules and related BPs form in a common reconnection process, in which the increasing reconnection height between the emerging dipole and the ambient field results in the observed variations from BPs to macrospicules. Interestingly, most macrospicules show similar characteristics to larger-scale coronal jets and/or smaller-scale spicules, i.e., the rotating motions, the presence of minifilaments and BPs before the eruptions, and magnetic flux emergence and cancellation. We conclude that the formation mechanism of macrospicules should be the same as spicules and coronal jets, i.e., solar jetting phenomena at different scales share the same physical mechanism in association with magnetic reconnection. **November 11, 2020**

## **Homologous Accelerated Electron Beams, Quasi-periodic fast-propagating Wave and CME Observed in one Fan-spine Jet**

[Yadan Duan](#), [Yuandeng Shen](#), [Xinping Zhou](#), [Zehao Tang](#), [Chengrui Zhou](#), [Song Tan](#)

ApJ **926** L39 **2022**

<https://arxiv.org/pdf/2201.08982.pdf>

<https://iopscience.iop.org/article/10.3847/2041-8213/ac4df2/pdf>

Using imaging and radio multi-wavelength observations, we studied the origin of two homologous accelerated electron beams and a quasi-periodic fast-propagating (QFP) wave train associated with a solar jet on **2012 July 14**. The jet occurred in a small-scale fan-spine magnetic system embedding in a large-scale pseudostreamer, which associated with a GOES C1.4 flare, a jet-like coronal mass ejection (CME), a type II radio burst, and a type III radio burst. During the initial stage, a QFP wave train and a fast moving on-disk radio source were detected in succession ahead of the jet along the outer spine of the fan-spine system. When the jet reached a height of about 1.3 solar radii, it underwent a bifurcation into two branches. Based on our analysis results, all the observed phenomena in association with the jet can be explained by using a fan-spine magnetic system. We propose that both the type III radio burst and the on-disk fast moving radio source were caused by the same physical process, i.e., the energetic electrons accelerated by the magnetic reconnection at the null point, and they were along the open field lines of the pseudostreamer and the closed outer spine of the fan-spine structure, respectively. Due to the bifurcation of the jet body, the lower branch along the closed outer spine of the fan-spine structure fell back to the solar surface, while the upper branch along the open field lines of the pseudostreamer caused the jet-like CME in the outer corona.

## **Structural evolution of a magnetic flux rope associated with a major flare in the solar active region 12205**

A. Y. [Duan](#), C. W. Jiang, Y. Guo, X. S. Feng, J. Cui

A&A, **659**, A25 **2022**

<https://doi.org/10.1051/0004-6361/202142061>

<https://www.aanda.org/articles/aa/pdf/2022/03/aa42061-21.pdf>

Solar eruptions are often generated as a result of the complex magnetic environment in solar active regions (ARs). Unravelling the relevant structure and evolution is vital to disclosing the underlying mechanisms that initiate such eruptions. In this work, we conduct a comprehensive study of the magnetic field structure and evolution responsible for a major flare eruption in a complex AR: NOAA 12205. The study is based on a detailed analysis of observations from the SDO and a time sequence of coronal magnetic field extrapolations. The AR is characterized by a long sequence of sunspots, harboring two groups of  $\delta$  type that evolved dynamically via continual rotation, shearing, colliding, and flux cancellation. Our study suggests that the joint effect of the sunspot motions along a large-scale magnetic flux rope (MFR) supporting a filament was gradually built up along the main polarity inversion line. A quantitative analysis of the coronal magnetic evolution strongly indicates that an ideal instability of the MFR finally led to the major eruption of the X1.6 flare, although it was preceded by episodes of localized reconnections. These localized reconnections should play a key role in building up the unstable MFR by, for example, tether-cutting reconnection low near the photosphere, as driven by the shearing and flux cancellation. Through these reconnections, the MF gains a significant amount of twisted flux and is lifted up to a height above the torus unstable threshold, at which the background restraining force decreases fast enough with the height. **7 Nov 2014**

## **Structure and Evolution of an Inter-Active Region Large-scale Magnetic Flux Rope**

Aiying [Duan](#)<sup>1</sup>, Chaowei Jiang<sup>2</sup>, Peng Zou<sup>2</sup>, Xueshang Feng<sup>2</sup>, and Jun Cui<sup>1</sup>

**2021** ApJ **906** 45

<https://doi.org/10.3847/1538-4357/abc701>

Magnetic flux rope (MFR) has been recognized as the key magnetic configuration of solar eruptions. While pre-eruption MFRs within the core of solar active regions (ARs) have been widely studied, those existing between two ARs, i.e., the intermediate ones in weak-field regions, were rarely studied. There are also major eruptions that occurred in such intermediate regions and study of the MFR there will help us understand the physics mechanism underlying the eruptions. Here, with a nonlinear force-free field reconstruction of solar coronal magnetic fields, we tracked the five-day evolution covering the full life of a large-scale inter-AR MFR forming between ARs NOAA 11943 and 11944, which is closely cospatial with a long sigmoidal filament channel and an eruptive X1.2 flare occurring on **2014 January 7**. Through topological analysis of the reconstructed 3D magnetic field, it is found that the MFR begins to

form early on **2014 January 6**; then with its magnetic twist degree continuously increasing for over 30 hr, it becomes highly twisted with field lines winding numbers approaching six turns, which might be the highest twisting degree in extrapolated MFRs that have been reported in the literature. The formation and strength of the MFR are attributed to a continuous sunspot rotation of AR 11944 and flux cancellation between the two ARs. The MFR and its associated filaments exhibit no significant change across the flare time, indicating it is not responsible for the flare eruption. After the flare, the MFR slowly disappears, possibly due to the disturbance by the eruption.

## Variation of Magnetic Flux Ropes Through Major Solar Flares

Aiying Duan, Chaowei Jiang, Zhenjun Zhou, Xueshang Feng, Jun Cui

ApJL **907** L23 **2021**

<https://arxiv.org/pdf/2012.14588.pdf>

<https://doi.org/10.3847/2041-8213/abd638>

It remains unclear how solar flares are triggered and in what conditions they can be eruptive with coronal mass ejections. Magnetic flux ropes (MFRs) has been suggested as the central magnetic structure of solar eruptions, and their ideal instabilities including mainly the kink instability (KI) and torus instability (TI) provide important candidates for triggering mechanisms. Here using magnetic field extrapolations from observed photospheric magnetograms, we systematically studied the variation of coronal magnetic fields, focusing on MFRs, through major flares including 29 eruptive and 16 confined events. We found that nearly 90% events possess MFR before flare and 70% have MFR even after flare. We calculated the controlling parameters of KI and TI, including the MFR's maximum twist number and the decay index of its strapping field. Using the KI and TI thresholds empirically derived from solely the pre-flare MFRs, two distinct different regimes are shown in the variation of the MFR controlling parameters through flares. For the events with both parameters below their thresholds before flare, we found no systematic change of the parameters after the flares, in either the eruptive or confined events. In contrast, for the events with any of the two parameters exceeding their threshold before flare (most of them are eruptive), there is systematic decrease in the parameters to below their thresholds after flares. These results provide a strong constraint for the values of the instability thresholds and also stress the necessity of exploring other eruption mechanisms in addition to the ideal instabilities. **2014 February 4, 2017 September 6**

**Table 1.** List of events and parameters of their pre- and post-flare MFRs. (2011-2017)

## A Study of Pre-Flare Solar Coronal Magnetic Fields: Magnetic Flux Ropes

Aiying Duan, Chaowei Jiang, Wen He, Xueshang Feng, Peng Zou, Jun Cui

ApJ **884** 73 **2019**

<https://arxiv.org/pdf/1908.08643.pdf>

<https://doi.org/10.3847/1538-4357/ab3e33>

Magnetic flux ropes (MFRs) are thought to be the central structure of solar eruptions, and their ideal MHD instabilities can trigger the eruption. Here we performed a study of all the MFR configurations that lead to major solar flares, either eruptive or confined, from 2011 to 2017 near the solar disk center. The coronal magnetic field is reconstructed from observed magnetograms, and based on magnetic twist distribution, we identified the MFR, which is defined as a coherent group of magnetic field lines winding an axis with more than one turn. It is found that 90% of the events possess pre-flare MFRs, and their three-dimensional structures are much more complex in details than theoretical MFR models. We further constructed a diagram based on two parameters, the magnetic twist number which controls the kink instability (KI), and the decay index which controls the torus instability (TI). It clearly shows lower limits for TI and KI thresholds, which are  $n_{crit}=1.3$  and  $|Tw|_{crit}=2$ , respectively, as all the events above  $n_{crit}$  and nearly 90% of the events above  $|Tw|_{crit}$  erupted. Furthermore, by such criterion, over 70% of the events can be discriminated between eruptive and confined flares, and KI seems to play a nearly equally important role as TI in discriminating between the two types of flare. There are more than half of events with both parameters below the lower limits, and 29% are eruptive. These events might be triggered by magnetic reconnection rather than MHD instabilities. **2011-02-15, 2011-03-09, 2011-08-03, 2012-01-23, 2012-03-06, 2012-05-10, 2012-07-02, 2012-07-05, 2012-07-12, 2013-04-11, 2013-10-24, 2013-11-01, 2013-11-03, 2013-11-05, 2013-11-08, 2013-12-31, 2014-01-07, 2014-02-02, 2014-02-04, 2014-03-29, 2014-04-18, 2014-09-28, 2014-10-22, 2014-10-24, 2014-11-07, 2014-12-04, 2014-12-18, 2014-12-20, 2015-03-11/12, 2013-06-22, 2015-06-25, 2015-08-24, 2015-09-04, 2015-09-28, 2017-09-06**

**Table 1.** List of events and properties of their MFRs (2011-2017)

## The Birth of a Jet-driven Twin CME and Its Deflection from Remote Magnetic Fields

Yadan Duan, Yuandeng Shen, Hechao Chen, Hongfei Liang

ApJ **881** 132 **2019**

<https://arxiv.org/pdf/1907.07310.pdf>

<https://doi.org/10.3847/1538-4357/ab32e9>

We report the formation of a complicated coronal mass ejection (CME) on **2015 August 23** by using the high temporal and high spatial resolution multi-wavelength observations taken by the Solar Dynamic Observatory and the Solar and Heliospheric Observatory. The CME exhibited both jet-like and bubble-like components simultaneously, and therefore we call it a twin CME. Detailed imaging and kinematic analysis results indicate that the twin CME were evolved from the eruption of a mini-filament driven blowout jet at the east edge of an equatorial coronal hole, in which the activation of the mini-filament was tightly associated with the continuous flux cancellation and quasi-periodic jet-like activities in the filament channel. Due to the magnetic reconnection between the filament and the ambient open field lines, the

filament broke partially at the northern part and resulted in an intriguing blowout jet in the south direction. It is interesting that the ejecting jet was deflected by a group of remote open field lines, which resulted in the significant direction change of the jet from southward to eastward. Based on the close temporal and spatial relationships among the jet, filament eruption, and the twin CME, we conclude that the jet-like CME should be the coronal extension of the jet plasma, while the bubble-like one should be originated from the eruption of the mini-filament confined by the closed magnetic fields at the jet-base.

### **Initiation of CMEs by Magnetic Flux Emergence**

Govind [Dubey](#), Bart van der Holst & Stefaan Poedts

J. Astrophys. Astr. (2006) 27, 159–166

### **Homologous prominence non-radial eruptions: A case study**

P. [Duchlev](#), K. Kolevaa, M. S. Madjarska, M. Dechev

New Astronomy 2016

<http://arxiv.org/pdf/1605.02299v1.pdf>

The present study provides important details on homologous eruptions of a solar prominence that occurred in active region NOAA 10904 on **2006 August 22**. We report on the preeruptive phase of the homologous feature as well as the kinematics and the morphology of a forth from a series of prominence eruptions that is critical in defining the nature of the previous consecutive eruptions. The evolution of the overlying coronal field during homologous eruptions is discussed and a new observational criterion for homologous eruptions is provided. We find a distinctive sequence of three activation periods each of them containing preeruptive precursors such as a brightening and enlarging of the prominence body followed by small surge- like ejections from its southern end observed in the radio 17 GHz. We analyse a fourth eruption that clearly indicates a full reformation of the prominence after the third eruption. The fourth eruption although occurring 11 hrs later has an identical morphology, the same angle of propagation with respect to the radial direction, as well as similar kinematic evolution as the previous three eruptions. We find an important feature of the homologous eruptive prominence sequence that is the maximum height increase of each consecutive eruption. The present analysis establishes that all four eruptions observed in H $\{\alpha\}$  are of confined type with the third eruption undergoing a thermal disappearance during its eruptive phase. We suggest that the observation of the same direction of the magnetic flux rope (MFR) ejections can be consider as an additional observational criterion for MFR homology. This observational indication for homologous eruptions is important, especially in the case of events of typical or poorly distinguishable morphology of eruptive solar phenomena.

### **Filament Leg--Leg Reconnection as a Source of Prominent Supra-Arcade Downflows**

[Jaroslav Dudik](#), [Guillaume Aulanier](#), [Jana Kasparova](#), [Marian Karlicky](#), [Alena Zemanova](#), [Juraj Lorincik](#), [Miloslav Druckmuller](#)

ApJL 937 L10 2022

<https://arxiv.org/pdf/2209.00306.pdf>

<https://iopscience.iop.org/article/10.3847/2041-8213/ac8eaf/pdf>

We report on interaction of the legs of the erupting filament of **2012 August 31** and associated prominent supra-arcade downflows (P-SADs) as observed by the Atmospheric Imaging Assembly onboard the Solar Dynamics Observatory. We employ a number of image processing techniques to enhance weak interacting features. As the filament erupts, both legs stretch outwards. The positive-polarity leg also untwists and splits into two parts. The first part runs into the conjugate (negative-polarity) leg, tearing it apart. The second part then converges into the remnant of the conjugate leg, after which both weaken and finally disappear. All these episodes of interaction of oppositely-oriented filament legs are followed by appearance of P-SADs, seen in the on-disk projection to be shaped as loop-tops, along with many weaker SADs. All SADs are preceded by hot supra-arcade downflowing loops. This observed evolution is consistent with the three-dimensional rr-rf (leg-leg) reconnection, where the erupting flux rope reconnects with itself. In our observations, as well as in some models, the reconnection in this geometry is found to be long-lasting. It plays a substantial role in the evolution of the flux rope of the erupting filament and leads to prominent supra-arcade downflows.

### **Observation of all pre- and post-reconnection structures involved in three-dimensional reconnection geometries in solar eruptions**

Jaroslav [Dudik](#), [Juraj Lorincik](#), [Guillaume Aulanier](#), [Alena Zemanova](#), [Brigitte Schmieder](#)

ApJ 887 71 2019

<https://arxiv.org/pdf/1910.08620.pdf>

[sci-hub.se/10.3847/1538-4357/ab4f86](https://sci-hub.se/10.3847/1538-4357/ab4f86)

We report on observations of the two newly-identified reconnection geometries involving erupting flux ropes. In 3D, a flux rope can reconnect either with a surrounding coronal arcade (recently named "ar-rf" reconnection) or with itself ("rr-rf" reconnection), and both kinds of reconnection create a new flux rope field line and a flare loop. For the first time, we identify all four constituents of both reconnections in a solar eruptive event, the filament eruption of **2011 June 07** observed by SDO/AIA. The ar-rf reconnection manifests itself as shift of one leg of the filament by more than 25" northward. At its previous location, a flare arcade is formed, while the new location of the filament leg previously

corresponded to a footpoint of a coronal loop in 171 Å. In addition, the evolution of the flare ribbon hooks is also consistent with the occurrence of ar-rf reconnection as predicted by MHD simulations. Specifically, the growing hook sweeps footpoints of preeruptive coronal arcades, and these locations become inside the hook. Furthermore, the rr-rf reconnection occurs during the peak phase above the flare arcade, in an apparently X-type geometry involving a pair of converging bright filament strands in the erupting filament. A new flare loop forms near the leg of one of the strands, while a bright blob, representing a remnant of the same strand, is seen ascending into the erupting filament. All together, these observations vindicate recent predictions of the 3D standard solar flare model.

## **Expanding and Contracting Coronal Loops as Evidence of Vortex Flows Induced by Solar Eruptions**

J. Dudík, F. P. Zuccarello, G. Aulanier, [B. Schmieder](#), [P. Démoulin](#)

ApJ **844** 54 2017

<https://arxiv.org/pdf/1706.04783.pdf>

Eruptive solar flares were predicted to generate large-scale vortex flows at both sides of the erupting magnetic flux rope. This process is analogous to a well-known hydrodynamic process creating vortex rings. The vortices lead to advection of closed coronal loops located at peripheries of the flaring active region. Outward flows are expected in the upper part and returning flows in the lower part of the vortex. Here, we examine two eruptive solar flares, an X1.1-class flare SOL2012-03-05T03:20 and a C3.5-class SOL2013-06-19T07:29. In both flares, we find that the coronal loops observed by the Atmospheric Imaging Assembly in its 171 Å, 193 Å, or 211 Å-passbands show coexistence of expanding and contracting motions, in accordance with the model prediction. In the X-class flare, multiple expanding/contracting loops coexist for more than 35 minutes, while in the C-class flare, an expanding loop in 193 Å appears to be close-by and co-temporal with an apparently imploding loop arcade seen in 171 Å. Later, the 193 Å-loop also switches to contraction. These observations are naturally explained by vortex flows present in a model of eruptive solar flares.

## **CME Deflection and East-West Asymmetry of Energetic Storm Particle Intensity during Solar Cycles 23 and 24**

A. Santa Fe Duenas<sup>1,2</sup>, R. W. Ebert<sup>1,2</sup>, Gang Li<sup>3</sup>, Zheyi Ding<sup>4</sup>, M. A. Dayeh<sup>1,2</sup>, M. I. Desai<sup>1,2</sup> and L. K. Jian<sup>5</sup>

ApJ **2024**

<https://arxiv.org/pdf/2404.01993.pdf>

We investigate the East-West asymmetry in energetic storm particle (ESP) heavy ion intensities at interplanetary shocks driven by coronal mass ejections (CMEs) during solar cycles (SCs) 23 and 24. We use observations from NASA's ACE and STEREO missions of helium (He), oxygen (O), and iron (Fe) intensities from ~0.13 to 3 MeV/nucleon. We examine the longitudinal distribution of ESP intensities and the correlation of ESP intensities with the near-Sun CME speed and the average transit CME speed for eastern and western events. We observed an East-West asymmetry reversal of ESP heavy ion intensities from SC 23 to 24. We have determined that this change in asymmetry is caused by a shift in the heliolongitude distribution of the CME speed ratio (the ratio of CME near-Sun speed to CME average transit speed) from west to east. **November 10 and 11, 2012**

## **The catalog of Hvar Observatory solar observations**

[Mateja Dumbovic](#), [Luci Karbonini](#), [Jasa Calogovic](#), [Filip Matkovic](#), [Karmen Martinic](#), [Akshay Kumar Remeshan](#), [Roman Brajsa](#), [Bojan Vrsnak](#)

Solar Phys. **2024**

<https://arxiv.org/pdf/2404.18576>

We compile the catalog of Hvar Observatory solar observations in the time period corresponding to regular digitally stored chromospheric and photospheric observations 2010-2019. We make basic characterisation of observed phenomena and compare them to catalogs which are based on full disc solar images. We compile a catalog of observed ARs consisting of 1100 entries, where each AR is classified according to McIntosh and Mt Wilson classifications. We find that HVAR observations are biased towards more frequently observing more complex ARs and observing them in longer time periods, likely related to the small FOV not encompassing the whole solar disc. In H $\alpha$  observations we catalog conspicuous filaments/prominences and flares. We characterise filaments according to their location, chirality (if possible) and eruptive signatures. Analysis of the eruptive filaments reveals a slight bias in HVAR catalog towards observation of partial eruptions, possibly related to the observers tendency to observe filament which already showed some activity. In the flare catalog we focus on their observed eruptive signatures (loops or ribbons) and their shape. In addition, we associate them to GOES soft X-ray flares to determine their corresponding class. We find that HVAR observations seem biased towards more frequently observing stronger flares and observing them in longer time periods. We demonstrate the feasibility of the catalog on a case study of the flare detected on **2 August 2011** in HVAR H $\alpha$  observations and related Sun-to-Earth phenomena. Through flare-CME-ICME association we demonstrate the agreement of remote and in situ properties. The data used for this study, as well as the catalog, are made publicly available.



## **The 2019 International Women's Day event: A two-step solar flare with multiple eruptive signatures and low Earth impact**

**Dumbovic**, M., **Veronig**, A. M., **Podladchikova**, T., **Thalmann**, J. K., **Chikunova**, G., **Dissauer**, K., **Magdalenic**, J., **Temmer**, M., Guo, J., **Samara**, E

A&A **2021**

<https://arxiv.org/pdf/2106.15417.pdf>

We present a detailed analysis of an eruptive event that occurred on early **2019 March 8** in active region AR 12734, to which we refer as the International Women's day event. The event under study is intriguing in several aspects: 1) low-coronal eruptive signatures come in "pairs" (a double-peak flare, two coronal dimmings, and two EUV waves); 2) although the event is characterized by a complete chain of eruptive signatures, the corresponding coronagraphic signatures are weak; 3) although the source region of the eruption is located close to the center of the solar disc and the eruption is thus presumably Earth-directed, heliospheric signatures are very weak with little Earth-impact. We analyze a number of multi-spacecraft and multi-instrument (both remote-sensing and in situ) observations, including Soft X-ray, (extreme-) ultraviolet (E)UV), radio and white-light emission, as well as plasma, magnetic field and particle measurements. We employ 3D NLFF modeling to investigate the coronal magnetic field configuration in and around the active region, the GCS model to make a 3D reconstruction of the CME geometry and the 3D MHD numerical model EUHFORIA to model the background state of the heliosphere. Our results indicate two subsequent eruptions of two systems of sheared and twisted magnetic fields, which merge already in the upper corona and start to evolve further out as a single entity. The large-scale magnetic field significantly influences both, the early and the interplanetary evolution of the structure. During the first eruption the stability of the overlying field was disrupted which enabled the second eruption. We find that during the propagation in the interplanetary space the large-scale magnetic field, i.e. , the location of heliospheric current sheet between the AR and the Earth likely influences propagation and the evolution of the erupted structure(s).

## **Validation of the CME Geomagnetic Forecast Alerts Under the COMESEP Alert System**

Mateja **Dumbović**, Nandita Srivastava, Yamini K. Rao, Bojan Vršnak, Andy Devos, Luciano Rodriguez

**Solar Physics** August **2017**, 292:96 **File**

<https://link.springer.com/content/pdf/10.1007%2Fs11207-017-1120-5.pdf>

Under the European Union 7th Framework Programme (EU FP7) project Coronal Mass Ejections and Solar Energetic Particles (COMESEP, <http://comesep.aeronomy.be>), an automated space weather alert system has been developed to forecast solar energetic particles (SEP) and coronal mass ejection (CME) risk levels at Earth. The COMESEP alert system uses the automated detection tool called Computer Aided CME Tracking (CACTus) to detect potentially threatening CMEs, a drag-based model (DBM) to predict their arrival, and a CME geoeffectiveness tool (CGFT) to predict their geomagnetic impact. Whenever CACTus detects a halo or partial halo CME and issues an alert, the DBM calculates its arrival time at Earth and the CGFT calculates its geomagnetic risk level. The geomagnetic risk level is calculated based on an estimation of the CME arrival probability and its likely geoeffectiveness, as well as an estimate of the geomagnetic storm duration. We present the evaluation of the CME risk level forecast with the COMESEP alert system based on a study of geoeffective CMEs observed during 2014. The validation of the forecast tool is made by comparing the forecasts with observations. In addition, we test the success rate of the automatic forecasts (without human intervention) against the forecasts with human intervention using advanced versions of the DBM and CGFT (independent tools available at the Hvar Observatory website, <http://oh.geof.unizg.hr>). The results indicate that the success rate of the forecast in its current form is unacceptably low for a realistic operation system. Human intervention improves the forecast, but the false-alarm rate remains unacceptably high. We discuss these results and their implications for possible improvement of the COMESEP alert system.

## **Anticorrelated temperature-density profiles in the quiet solar corona and coronal mass ejections: Approach based on the spine-type Hamiltonians**

Yu.V. **Dumin**

A&A **2020**

<https://arxiv.org/pdf/2002.08624.pdf>

Context: The mechanism of the solar corona heating remains one of key problems in astrophysics for a few decades; but none of the proposed mechanisms can give a definitive answer to this question. As a result, the novel scenarios are still suggested. Aims: Here, we perform a critical consideration of the recently-proposed mechanism for the formation of the anticorrelated temperature and density profiles due to specific features of relaxation in the strongly non-equilibrium plasmas described by the so-called spin-type Hamiltonians [L. Casetti and S. Gupta, 2014, Eur. Phys. J. B 87, 91; T.N. Teles et al., 2015, Phys. Rev. E 92, 020101(R)]. Methods: We employ the universal property of the above-mentioned systems to produce the long-lived anticorrelated temperature-density distributions and analyse their most important qualitative features that should be expected in the context of the coronal plasmas. Results: As follows from our consideration, the anticorrelated profiles predicted by the spine-type Hamiltonians can be hardly relevant to explanation of the temperature distribution in the quiet solar corona. However, they might be interesting for the interpretation of the large-scale inhomogeneity of the powerful coronal mass ejections, possessing the filament-type structure. **4 Jan 2002**

## **Tracking a *Ulysses* High-latitude ICME Event Back to Its Solar Origins**

C. **Dumitrache** · N.A. Popescu · A. Oncica

Solar Phys (2011) 272:137–157, **File**

High-latitude interplanetary mass ejections (ICMEs) observed beyond 1 AU are not studied very often. They are useful for improving our understanding of the 3D heliosphere. As there are only few such events registered by the Ulysses spacecraft, the task of detecting their solar counterparts is a challenge, especially during high solar activity periods, because there are dozens coronal mass ejections (CMEs) registered by SOHO that might be chosen as candidates. We analyzed a high-latitude ICME registered by the Ulysses spacecraft on 18 January 2002. Our investigation focused on the correlation between various plasma parameters that allow the identification to be made of the ICME and its components such as the forward shock, the magnetic cloud and the reverse shock.

Using a linear approach and a graphical method we have been able to track the ICME event back to the Sun and to compute the day of the occurrence of the solar CME. In order to decide among several CME candidates which one is the right solar counterpart of our event, we have performed a follow-up computation of these CMEs from the Sun to Ulysses, by using two different speed formulas. First, the computation was simply based on the initial CME velocity, while the other was based on the ICME velocity estimated from the CME initial speed (Lindsay et al. 1999).

Differences of hours have been obtained between the arrival time predicted in these two ways, but the second one gave the best results. Both methods indicated the same two CMEs as the solar counterparts. We have found the solar source of these CMEs as being a huge polar filament that erupted in several steps.

This ICME event displayed a double magnetic cloud configuration. A minimum variance analysis helped us to detect the smooth rotation of the clouds and their helicity. Both magnetic clouds show the same helicity as the filament that erupted and released them. A cylinder-shape model of both clouds gives the same helicity sign.

### **CMEs ‘en rafale’ observations and simulations**

Cristiana **Dumitrache**

Proceedings of the International Astronomical Union / Volume 4 / Symposium S257, pp 251 - 255 ,

Published online: 16 May 2009, **File**

A CME is triggered by the disappearance of a stable equilibrium as a result of the slow evolution of the photospheric magnetic field. This disappearance may be due to a loss of ideal-MHD equilibrium or stability as in the kink mode, or to a loss of resistive-MHD equilibrium as a result of magnetic reconnection. We have obtained CMEs in sequence by a time dependent magnetohydrodynamic computation performed on three solar radii. These successive CMEs resulted from a prominence eruption. Velocities of these CMEs decrease in time, from a CME to another. We present observational evidences for large-scale magnetic reconnections that caused the destabilization of a sigmoid filament. These reconnections covered half of the solar disk and produced CMEs in squall (sequential CMEs).

### **CMEs' speed, travel time and temperature: A Thermodynamic approach**

Héctor J. **Durand-Manterola**, Alberto Flandes, Ana Leonor Rivera, Alejandro Lara and Tatiana Niembro  
JGR 2017

<http://onlinelibrary.wiley.com/doi/10.1002/2017JA024369/epdf>

<http://sci-hub.cc/10.1002/2017JA024369>

Due to their important role in Space weather, Coronal Mass Ejections or CMEs have been thoroughly studied in order to forecast their speed and transit time from the Sun to the Earth. We present a Thermodynamic analytical model that describes the dynamics of CMEs. The thermodynamic approach has some advantages with respect to the hydrodynamic approach. First, it deals with the energy involved, which is a scalar quantity. Second, one may calculate the work done by the different forces separately and sum all contributions to determine the changes in speed, which simplifies the problem and allows us to obtain fully rigorous results. Our model considers the drag force, which dominates the dynamics of CMEs and the solar gravitational force, which has a much smaller effect, but it is, still, relevant enough to be considered.

We derive an explicit analytical expression for the speed of CMEs in terms of its most relevant parameters and obtain an analytical expression for the CME temperature. The model is tested with a CME observed at three different heliocentric distances with three different spacecraft (SOHO, ACE and Ulysses); also, with a set of 11 CMEs observed with the SOHO, Wind and ACE spacecraft and, finally, with two events observed with the STEREO spacecraft. In all cases, we have a consistent agreement between the theoretical and the observed speeds and transit times. Additionally, for the set of 11 events, we estimate their temperatures at their departure position from their temperatures measured near the orbit of the Earth.

**Table 2.** CMEs data parameters for the 11 selected CMEs. 2001-2007

### **A multiwavelength study of an M-class flare and the origin of an associated eruption from NOAA AR 11045**

**Dwivedi**, B. N.; Srivastava, Abhishek K.; Kumar, Mukul; Kumar, Pankaj

E-print, March 2012, New Astr.

In this paper, we study multiwavelength observations of an M6.4 flare in Active Region NOAA 11045 on **7 February 2010**. The space- and ground-based observations from STEREO, SoHO/MDI, EIT, and Nobeyama Radioheliograph were used for the study. This active region rapidly appeared at the north-eastern limb with an unusual emergence of a magnetic field. We find a unique observational signature of the magnetic field configuration at the flare site. Our observations show a change from dipolar to quadrupolar topology. This change in the magnetic field configuration

results in its complexity and a build-up of the flare energy. We did not find any signature of magnetic flux cancellation during this process. We interpret the change in the magnetic field configuration as a consequence of the flux emergence and photospheric flows that have opposite vortices around the pair of opposite polarity spots. The negative-polarity spot rotating counterclockwise breaks the positive-polarity spot into two parts. The STEREO-A 195 ° and STEREO-B 171 ° coronal images during the flare reveal that a twisted flux tube expands and erupts resulting in a coronal mass ejection (CME). The formation of co-spatial bipolar radio contours at the same location also reveals the ongoing reconnection process above the flare site and thus the acceleration of non-thermal particles. The reconnection may also be responsible for the detachment of a ring-shaped twisted flux tube that further causes a CME eruption with a maximum speed of 446 km/s in the outer corona.

### **Coronal radio-sounding detection of a CME during the 1997 Galileo solar conjunction**

A.I. **Efimov**, V.K. Rudash, L.N. Samoznaev, M.K. Bird, I.V. Chashei and D. Plettemeier

[Advances in Space Research](#), [Volume 42, Issue 1](#), 1 July 2008, Pages 110-116

Frequency fluctuations of the Galileo S-band radio signal were recorded nearly continuously during the spacecraft's solar conjunction from December 1996 to February 1997. A strong propagating disturbance, most probably associated with a coronal mass ejection (CME), was detected on **7 February** when the radio ray path proximate point was on the west solar limb at about 54 solar radii from the Sun. The CME passage through the line of sight is characterized by a significant increase in the fluctuation intensity of the recorded frequency and by an increase in the plasma speed from about  $234 \text{ km s}^{-1}$  up to about  $755 \text{ km s}^{-1}$ . These velocity estimates are obtained from a correlation analysis of frequency fluctuations recorded simultaneously at two widely-separated ground stations. The density turbulence power spectrum is found to steepen behind the CME front. The Galileo radio-sounding data are compared with SOHO/LASCO observations of the CME in the corona and with WIND spacecraft data near the Earth's orbit.

### **A Simple Technique for Identifying the Propagation Direction of CMEs in 3D Space**

Y. I. **Egorov** & [V. G. Fainshtein](#)

[Solar Physics](#) volume 296, Article number: 161 (2021)

<https://link.springer.com/content/pdf/10.1007/s11207-021-01904-3.pdf>

<https://doi.org/10.1007/s11207-021-01904-3>

By now several methods have been proposed enabling to determine the kinematic characteristics of coronal mass ejections (CMEs) in 3D space. Many of these methods are based on using the triangulation technique and stereoscopic observations of the CMEs with two and more spacecraft. As a rule, these methods involve relatively complicated procedures. Nevertheless, there is a need for a simple technique to find 3D characteristics of a CME motion fairly quickly. Such a technique, in particular, will enable to estimate on which side of the Sun (front side or back side for an observer on the Earth) the CME emerged, as well as to efficiently solve a problem relevant for solar-terrestrial physics: to determine the time of the CME arrival into Earth's orbit. Such a simple technique is proposed in this article. The technique comprises two stages. First, one identifies the CME motion direction in the solar equatorial plane by using the data from any pair of the COR2 and LASCO (Large Angle and Spectrometric Coronagraph) C3 coronagraphs on board the Solar Terrestrial Relations Observatory (STEREO) A, B and the Solar and Heliospheric Observatory (SOHO), respectively. Next, one measures the angle between the CME motion direction in 3D space and the equatorial plane. We illustrate the technique for five CMEs that emerged either on the front side or back side of the Sun. An important advantage of the proposed technique is the possibility to quickly filter the events, that emerged on the front or back side of the Sun, by using only the information of the CME central position angle from a CME catalog. For the investigated CMEs, we obtained the time dependencies of the motion direction in the equatorial plane (angle  $\varphi\varphi$ ), the angle between the CME motion direction in 3D space and the equatorial plane ( $\lambda\lambda$ ), the distance from Sun's center to the CME leading edge in 3D space (R3DR3D). For some investigated events, we compared our values for angle  $\varphi\varphi$  and distance R3DR3D with those obtained in other articles. **5 Apr 2008, 17 May 2008, 12 Dec 2008, 3 Nov 2011, 29 Mar 2014**

### **Studying Magnetic Field Variations Accompanying the 2011 June 7 Eruptive Event, by Using Nonlinear Force-Free Field Modeling**

Y. I. **Egorov**, [V. G. Fainshtein](#), [I. I. Myshyakov](#), [S. A. Anfinogentov](#)...

[Solar Physics](#) volume 295, Article number: 52 (2020)

<https://link.springer.com/content/pdf/10.1007/s11207-020-01613-3.pdf>

We study the features of the magnetic field variations within the **2011 June 7** eruptive event that includes a large filament eruption, a flare, and a CME formation. The magnetic field characteristics were obtained by using vector measurements of the magnetic field with the SDO/HMI and 3D magnetic field calculations based on nonlinear force-free field (NLFFF) modeling. Strong and relatively fast variations in the photospheric field characteristics after the flare onset are shown to be observed only within a small site ( $20'' \times 20'' \times 20''$ ) of the eruption region in the neighborhood of the polarity inversion line (PIL).

We found that the magnetic field strength, the electric current density, current helicity density and free magnetic energy density above this region are growing with height reaching their maximums at the level of  $\sim 15 \text{ Mm}$ . After 2011 July 7 00:00 UT, this height started gradually reducing.

The NLFFF extrapolation revealed the presence of a magnetic flux rope elongated approximately along the main PIL and an arcade of magnetic field lines over it. The flux-rope axis is located at height of  $\sim 15 \text{ Mm}$ . The flux-rope

footpoints approximately coincide with the eruptive filament footpoints. Thus, we concluded that the detected flux rope is associated with the magnetic structure of the observed filament. The detected strong variation of the magnetic field within the eruption region are most probably associated with the magnetic field reconfiguration after the filament eruption. The  $T_n$  parameter, which is the average magnetic field twist within the flux rope, was found to increase up to 2.5 rotations before the flare onset, and to dramatically decrease afterward. This may reflect the developing of kink instability that presumably triggered this eruption.

### **Ensemble forecasting of coronal mass ejections using the WSA-ENLIL with CONED Model**

D. **Emmons**<sup>1,2,\*</sup>, A. Acebal, A. Pulkkinen, <sup>3,4</sup>, A. Taktakishvili, P. MacNeice<sup>3</sup>, D. Odstrcil  
Space Weather, Volume 11, Issue 3, pages 95–106, March 2013

The combination of the Wang-Sheeley-Arge (WSA) coronal model, ENLIL heliospherical model version 2.7, and CONED Model version 1.3 (WSA-ENLIL with CONED Model) was employed to form ensemble forecasts for 15 halo coronal mass ejections (halo CMEs). The input parameter distributions were formed from 100 sets of CME cone parameters derived from the CONED Model. The CONED Model used image processing along with the bootstrap approach to automatically calculate cone parameter distributions from SOHO/LASCO imagery based on techniques described by Pulkkinen et al. (2010). The input parameter distributions were used as input to WSA-ENLIL to calculate the temporal evolution of the CMEs, which were analyzed to determine the propagation times to the L1 Lagrangian point and the maximum Kp indices due to the impact of the CMEs on the Earth's magnetosphere. The Newell et al. (2007) Kp index formula was employed to calculate the maximum Kp indices based on the predicted solar wind parameters near Earth assuming two magnetic field orientations: a completely southward magnetic field and a uniformly distributed clock-angle in the Newell et al. (2007) Kp index formula. The forecasts for 5 of the 15 events had accuracy such that the actual propagation time was within the ensemble average plus or minus one standard deviation. Using the completely southward magnetic field assumption, 10 of the 15 events contained the actual maximum Kp index within the range of the ensemble forecast, compared to 9 of the 15 events when using a uniformly distributed clock angle.

### **Global Energetics of Thirty-eight Large Solar Eruptive Events**

**Emslie**, A. G.; Dennis, B. R.; Shih, A. Y.; Chamberlin, P. C.; Mewaldt, R. A.; Moore, C. S.; Share, G. H.; Vourlidas, A.; Welsch, B. T.

Astrophysical Journal, Volume 759, Issue 1, article id. 71, 18 pp. (2012)

<http://arxiv.org/abs/1209.2654>

[http://www.astro.umd.edu/~share/publications/emslie\\_12.pdf](http://www.astro.umd.edu/~share/publications/emslie_12.pdf)

We have evaluated the energetics of 38 solar eruptive events observed by a variety of spacecraft instruments between 2002 February and 2006 December, as accurately as the observations allow. The measured energetic components include: (1) the radiated energy in the Geostationary Operational Environmental Satellite 1-8 Å band, (2) the total energy radiated from the soft X-ray (SXR) emitting plasma, (3) the peak energy in the SXR-emitting plasma, (4) the bolometric radiated energy over the full duration of the event, (5) the energy in flare-accelerated electrons above 20 keV and in flare-accelerated ions above 1 MeV, (6) the kinetic and potential energies of the coronal mass ejection (CME), (7) the energy in solar energetic particles (SEPs) observed in interplanetary space, and (8) the amount of free (non-potential) magnetic energy estimated to be available in the pertinent active region. Major conclusions include: (1) the energy radiated by the SXR-emitting plasma exceeds, by about half an order of magnitude, the peak energy content of the thermal plasma that produces this radiation; (2) the energy content in flare-accelerated electrons and ions is sufficient to supply the bolometric energy radiated across all wavelengths throughout the event; (3) the energy contents of flare-accelerated electrons and ions are comparable; (4) the energy in SEPs is typically a few percent of the CME kinetic energy (measured in the rest frame of the solar wind); and (5) the available magnetic energy is sufficient to power the CME, the flare-accelerated particles, and the hot thermal plasma. **2002 February 20, 2002 May 22, 2002 November 9, 2003 May 27, 2003 October 28, 2004 July 15, 2004 July 25, 2005 January 20,**  
**Table 1.** Event List with Component Energies ( $\times 10^{30}$  ergs)

### **Energy Partition in Large Solar Eruptive Events,**

Gordon **Emslie** and Brian Dennis

RHESSI Science Nugget, No. 185, Oct 2012

Where flare energy comes from, and where it goes to.

The paper also concludes that the energy radiated by the SXR-emitting plasma exceeds, by about half an order of magnitude, the peak energy content of the thermal plasma that produces this radiation, a situation that requires continuous re-energization of the hot plasma throughout the flare. Also, the energy contents in flare-accelerated electrons and ions are comparable, and together they are sufficient to supply the bolometric energy radiated across all wavelengths throughout the event. Finally, the paper finds that, in general, the available magnetic energy is sufficient to power the CME, the flare-accelerated particles, and the hot thermal plasma. This reaffirms the generally-held belief that the fundamental power source for SEEs lies in stressed active-region magnetic fields.

## Energy partition in two solar flare/CME events

**Emslie**, A. G., Kucharek, H.; Dennis, B. R.; Gopalswamy, N.; Holman, G. D.; Share, G. H.; Vourlidas, A.; Forbes, T. G.; Gallagher, P. T.; Mason, G. M.; and 5 coauthors

Journal of Geophysical Research, Volume 109, Issue A10, CiteID A10104, **2004**

Using coordinated observations from instruments on the Advanced Composition Explorer (ACE), the Solar and Heliospheric Observatory (SOHO), and the Ramaty High Energy Solar Spectroscopic Imager (RHESSI), we have evaluated the energetics of two well-observed flare/CME events on 21 April 2002 and **23 July 2002**. For each event, we have estimated the energy contents (and the likely uncertainties) of (1) the coronal mass ejection, (2) the thermal plasma at the Sun, (3) the hard X-ray producing accelerated electrons, (4) the gamma-ray producing ions, and (5) the solar energetic particles. The results are assimilated and discussed relative to the probable amount of nonpotential magnetic energy available in a large active region.

## Observations of a Flare-Generated Blast Wave in a Pseudo Coronal Mass Ejection Event

V. G. **Eselevich**, M. V. Eselevich, I. V. Zimovets,

*Solar Physics* June **2019**, 294:73

[sci-hub.se/10.1007/s11207-019-1467-x](https://doi.org/10.1007/s11207-019-1467-x)

We present an analysis of the event near the east limb, **SOL2014-03-06T09:23**, in which a pseudo coronal mass ejection (CME) was detected by the Large Angle and Spectrometric Coronagraph (LASCO) C2 instrument and indicated as “Poor Event; Only C2” in the Solar and Heliospheric Observatory (SOHO) LASCO CME Catalog. The analysis was performed based on two main methods: 1) investigation of the difference brightness profiles along specific directions in the solar corona using the EUV observations by the Atmospheric Imaging Assembly (AIA) instrument onboard the Solar Dynamics Observatory (SDO); 2) investigation of the spatially-resolved observations of the type II radio bursts made with the Nançay Radioheliograph. Based on the analysis performed we argue that the observed pseudo-CME could be a blast wave caused by impulsive flare energy release in the low corona. We also argue that, in the limited height range of  $\approx 0.2R_{\odot}$ – $0.5R_{\odot}$ , the front of this blast wave could steepen into a shock front.

## Evidence for shock generation in the solar corona in the absence of coronal mass ejections.

**Eselevich**, V.G., Eselevich, M.V., Zimovets, I.V., Sharykin, I.N.:

**2017**, Astron. Rep. 61, 805. DOI. ADS.

[sci-hub.se/10.1134/S1063772917080030](https://doi.org/10.1134/S1063772917080030)

The solar event **SOL2012-10-23T03:13**, which was associated with a X1.8 flare without an accompanying coronal mass ejection (CME) and with a Type II radio burst, is analyzed. A method for constructing the spatial and temporal profiles of the difference brightness detected in the AIA/SDO EUV and EUV channels is used together with the analysis of the Type II radio burst. The formation and propagation of a region of compression preceded by a collisional shock detected at distances  $R < 1.3 R_{\odot}$  from the center of the Sun is observed in this event ( $R_{\odot}$  is the solar radius). Comparison with a similar event studied earlier, SOL2011-02-28T07:34 [1], suggests that the region of compression and shock could be due to a transient (impulsive) action exerted on the surrounding plasma by an eruptive, high-temperature magnetic rope. The initial instability and eruption of this rope could be initiated by emerging magnetic flux, and its heating from magnetic reconnection. The cessation of the eruption of the rope could result from its interaction with surrounding magnetic structures (coronal loops).

## Initial formation of an “impulsive” coronal mass ejection

V. G. **Eselevich**, M. V. Eselevich, I. V. Zimovets, G. V. Rudenko

Astronomy Reports November **2016**, Volume 60, Issue 11, pp 1016–1027 **File**

Astronomicheskii Zhurnal, **2016**, Vol. 93, No. 11, pp. 990–1002.

An “impulsive” coronal mass ejection (CME) observed on **August 24, 2014** is analyzed using ultraviolet images obtained in the SDO/AIA 193, 304, 1600, and 1700 Å channels and H $\alpha$  (6562.8 Å) data obtained with the EI Teide and Big Bear telescopes. The formation of this impulsive CME was related to a magnetic tube (rope) moving with a velocity of  $\approx 35$  km/s and containing plasma that was cooler than the photospheric material. Moving in the corona, the magnetic tube collides with a quasi-stationary coronal magnetic rope, with its two bases rooted in the photosphere. This interaction results in the formation of the CME, with the surface of the coronal magnetic rope becoming the CME frontal structure. According to SDO/HMI data, no enhancements or changes in magnetic flux were detected in the vicinity of the CME bases during its formation. This may support the hypothesis that the magnetic tube starts its motion from layers in the vicinity of the temperature minimum.

## Evidence of a blast shock wave formation in a “CME–streamer” interaction

V.G. **Eselevich**, M.V. Eselevich, V.M. Sadykov, I.V. Zimovets

Advances in Space Research Volume 56, Issue 12, 15 December **2015**, Pages 2793–2803

<http://www.sciencedirect.com/science/article/pii/S0273117715002434>

Analysis of the solar event on **16 February 2011** (SOL2011-02-16T14:19) allows to classify it as an “impulsive” coronal mass ejection (CME) event. It is argued that the observed deviation of a streamer ray from its pre-event state and generation of a metric type II radio burst in this event was a result of a “CME–streamer” interaction in the lower corona ( $r \lesssim 1.5R_{\odot}$ ). Most probably, it was a consequence of an impulsive action of a compressed magnetic field to the

streamer. This compression of the coronal magnetic field was due to a moving and expanding magnetic flux rope, which was a core of the CME. The estimated radial speed of the type II burst sources was significantly ( $\approx 2\text{--}8$  times) larger than the radial speed of the erupting flux rope, and it decreased rapidly with time. This indicates that during the “CME–streamer” interaction a blast shock wave could be excited and propagated along the streamer.

### **Differences in the development of the initial phase of the formation of two types of coronal mass ejections**

V. G. [Eselevich](#), M. V. Eselevich

Cosmic Research, January **2015**, Volume 53, Issue 1, pp 21-30

Kosmicheskie Issledovaniya, **2015**, Vol. 53, No. 1, pp. 24–34.

Based on the results of an analysis of AIA/SDO and EUVI/STEREO data it was confirmed that the initial phase of the “gradual” coronal mass ejection (CME) begins as a motion from the rest of the outer shell of a coronal magnetic rope, which then becomes the basis of the frontal structure of a CME. It is shown by an example of an analysis of an event on **January 5, 2013** that a different type of CME, “impulsive,” can occur as a result of the ejection of a “cavity” from the lower solar corona (the 193 Å channel), which then becomes the basis for future CME. An analysis of the three-dimensional structure of the cavity, its dynamics and kinematics, as well as a comparison of the results of an analysis with numerical calculations allow us to interpret observations as a manifestation of the rapid rise of the magnetic tube (rope) filled with cold plasma. The appearance of the rope in the lower corona probably is a result of its rapid floating (with supersonic velocity) from the solar convective zone. Theoretical estimates show that the cause of the ejection of the magnetic tube from the convective zone can be the development of a Parker’s instability (“slow” wave).

### **Physical differences between the initial phase of the formation of two types of coronal mass ejections**

V. G. [Eselevich](#), M. V. Eselevich

Astronomy Reports, April **2014**, Volume 58, Issue 4, pp 260-271

Astronomicheskii Zhurnal, **2014**, Vol. 91, No. 4, pp. 320–331.

Physical differences in the formation of “gradual” and “impulsive” coronal mass ejections (CMEs) at heights of  $h < 0.2 R_{\odot}$  just before and during the initial phase of their motion are studied using AIA/SDO ultraviolet data ( $h$  is the altitude above the solar surface and  $R_{\odot}$  is the solar radius). The basic structure of a gradual CME is a magnetic rope located in the corona. During an hour or more preceding the initial phase, the magnetic rope demonstrates an increase in brightness and transverse size, first of the low, inner elements of the rope and then of elements in its outer envelope most distant from the Sun. The rope remains motionless during this time. The initial phase of a gradual CME begins from the motion of the magnetic rope’s outer envelope, which further becomes the basis for the CME frontal structure. At this stage, the inner low elements of the rope remain almost motionless. The initial phase of an impulsive CME begins with the appearance near the photosphere of a cavity moving away from the Sun; the dynamics of this cavity probably correspond to a magnetic tube filled with cool plasma rising from beneath the photosphere. This magnetic tube collides with and drags arch structures, which initially block the tube’s motion. These arch structures contribute to the CME formation, although the magnetic tube itself forms the basis of the CME.

### **Blast-wave and piston shocks connected with the formation and propagation of a coronal mass ejection**

V. G. [Eselevich](#), M. V. Eselevich, I. V. Zimovets

Astronomy Reports, February **2013**, Volume 57, Issue 2, pp 142-151

Astronomicheskii Zhurnal, **2013**, Vol. 90, No. 2, pp. 166–176. [Файл](#)

The solar coronal mass ejection observed on **November 3, 2010** is analyzed using AIA/SDO data (images in the 193 and 211 Å channels) and white-corona images obtained with the SOHO LASCO C2 and C3 coronagraphs. We have succeeded in revealing both piston and blast-wave shocks attributed to the formation and propagation of a coronal mass ejection. Both of these types of shocks could be responsible for type II radio bursts propagating in front of each shock.

### **DISTURBED ZONE AND PISTON SHOCK AHEAD OF CORONAL MASS EJECTION**

V. [Eselevich](#) and M. Eselevich

**2012** ApJ 761 68

The **2010 June 13** coronal mass ejection (CME) propagating toward the position angle P.A.  $245^{\circ}$  (measured counterclockwise from the Sun's north pole) was studied from the SDO/AIA and SOHO/LASCO C2, C3 data. We show that ahead of the CME frontal structure, as a result of its interaction with the undisturbed solar wind, a disturbed region (with an increased and disturbed plasma density), whose size increases as the CME travels away from the Sun, emerges gradually. Discontinuity formation at the disturbed zone front is observed in the narrow P.A.  $245^{\circ}\text{--}250^{\circ}$  range. Its characteristics satisfy the properties of a piston collision shock. In the other directions relative to the CME motion axis (P.A.  $> 250^{\circ}$  and P.A.  $< 245^{\circ}$ ), there exists only the disturbed zone, whose density gradually decreases with distance. The discontinuity that was always observed at all distances where measurements were made is absent. The analysis of this CME and several other limb CMEs with different velocities from the MK4, LASCO C2, C3, and STEREO/COR2 data confirmed the previously established laws of piston shock formation ahead of a CME, which are as follows: (1) Shock formation ahead of a CME in a vicinity along its propagation axis may occur at various distances  $R = R_u$  from

the Sun's center. Its formation is determined by fulfilling a local inequality  $u(R) > V_A(R)$ , where  $u(R)$  is a CME velocity relative to the surrounding solar wind and  $V_A(R)$  is a local Alfvén velocity that is approximately equal to the velocity of fast magnetic sound in the solar corona. (2) At  $R < 6 R_\odot$ , the shock front width  $\delta F$  is on the order of the proton mean free path  $\lambda_p$ , and the mechanism for energy dissipation at the front is, apparently, collisional. (3) At  $R = 10-15 R_\odot$ , one observes the formation of a new discontinuity  $\delta F \sim \lambda_p$  wide at the head of the collision front. Within limits of error,  $\delta F$  does not depend on  $R$  and is determined to be  $\delta F \approx 0.1-0.2 R_\odot$  by the LASCO C3 spatial resolution and  $\delta F \approx 0.03 R_\odot$  for COR2. This discontinuity is identified with a collisionless shock.

### Some properties of the development of the perturbed zone and shock preceding a coronal mass ejection

M. V. [Eselevich](#) & V. G. Eselevich

Astronomy Reports, Volume 55, Number 11, 1038-1050, 2011, File

*Astronomicheskii Zhurnal*, 2011, Vol. 88, No. 11, pp. 1124–1136.

SOHO/LASCO C2 and C3 data have been used to carry out a detailed study of the perturbed zone and shock that form as a coronal mass ejection (CME) moves away from the Sun, as a result of its interaction with the ambient solar wind. The event of **January 4, 2002** is used as an example. The perturbed zone is most extensive along the direction of propagation of the CME, decreases away from this direction, and reaches its minimum values perpendicular to this direction. The mass of the perturbed zone is  $\geq 0.1$  of the total mass of the CME. The condition for the formation of a shock preceding the CME (in the direction of propagation of the CME) is  $V - V_{SW} > V_A$ , where  $V$ ,  $V_{SW}$ , and  $V_A$  are the CME, solar wind, and Alfvén velocities, respectively. Perpendicular to the CME axis, at distances of  $\approx 4-6 R_\odot$  from the center of the Sun, the condition for the formation of shock is  $V/2 > V_A$ .

### Relations estimated at shock discontinuities excited by coronal mass ejections

M. V. [Eselevich](#) and V. G. Eselevich

Astronomy Reports, Volume 55, Number 4, 359-373, 2011

*Astronomicheskii Zhurnal*, 2011, Vol. 88, No. 4, pp. 393–408

An analysis of SOHO/LASCO C3 data shows that there are discontinuities in the radial profiles of the plasma density within limited regions in front of each of ten coronal mass ejections, which represent shocks. The shock velocities in various events reach  $V \approx 800-2500$  km/s. A comparison of the dependence of the Alfvén Mach number  $M_A$  on the shock strength  $\rho_2/\rho_1$  detected at distances  $R > 10 R_\odot$  from the center of the Sun with calculations carried out using ideal magnetic hydrodynamics shows that the effective ratio of specific heats  $\gamma$  describing processes inside the shock front varies from 2 to  $5/3$  ( $\rho_1$  and  $\rho_2$  are the densities in front of and behind the shock, and  $R_\odot$  is the solar radius). This corresponds to an effective number of degrees of freedom between two and three. A similar dependence  $M_A(\rho_2/\rho_1)$  was found for near-Earth bow shocks and interplanetary collisionless shocks. These features support the hypothesis that the studied discontinuities preceding coronal mass ejections are collisionless shocks.

### Detecting the widths of shock fronts preceding coronal mass ejections

M. V. [Eselevich](#)

Astronomy Reports, Volume 54, Number 2, 173-183, 2010, File

*Astronomicheskii Zhurnal*, 2010, Vol. 87, No. 2, pp. 197–208.

The perturbed zones and shocks preceding coronal mass ejections (CMEs) are studied using the data of the Mark 4, LASCO C2, and LASCO C3 coronagraphs. Detection of the perturbed zone indicating the presence or absence of the shock is most reliable in a frame moving with the frontal structure of the CME. The ability to correctly measure the width  $\delta F$  of the shock front using the Mark 4 and LASCO C2 data is established. The front width  $\delta F$  observed along the streamer belt at distances  $R < 5 R_\odot$  from the center of the Sun is of the order of the mean free path of protons. This means that the energy dissipation in the shock front is collisional at such distances. At distances  $R \geq (10 - 15) R_\odot$ , a new discontinuity with a front  $\delta^* F$  is formed. In the errors,  $\delta^* F \approx (0.1 - 0.2) R_\odot$  is independent of the distance  $R$  and is determined by the LASCO C3 spatial resolution. Initially, the discontinuity on the scale  $\delta^* F$  is weak and coexists with the front with width  $\delta F$ . The relative amplitude of this discontinuity increases and the brightness profile behind it flattens as long as the distance  $R$  increases. This transformation of the brightness profile from a front of width  $\delta F$  to a discontinuity of width  $\delta^* F \ll \delta F$  is explained as a transition from a collisional to a collisionless shock.

May 7, 1997, September 20, 1997, June 2, 1998, June 28, 2000

### On formation of a shock wave in front of a coronal mass ejection with velocity exceeding the critical one.

[Eselevich](#), M.V., Eselevich, V.G.,

2008. *Geophys. Res. Lett.* 35, L22105.

### **The SCORE Scale: A Coronal Mass Ejection Typification System Based On Speed**

**Evans**, Rebekah M.; Pulkkinen, Antti A.; Zheng, Yihua; Leila Mays, M.; Taktakishvili, Aleksandre; Kuznetsova, Maria M.; Hesse, Michael

*Space Weather*, Volume 11, Issue 6, pp. 333-334, 2013

<http://onlinelibrary.wiley.com/doi/10.1002/swe.20058/pdf>

### **LEARNING FROM THE OUTER HELIOSPHERE: INTERPLANETARY CORONAL MASS EJECTION SHEATH FLOWS AND THE EJECTA ORIENTATION IN THE LOWER CORONA**

R. M. **Evans**<sup>1</sup>, M. Opher<sup>1,2</sup>, and T. I. Gombosi<sup>3</sup>

*Astrophysical Journal*, 728:41 (7pp), 2011 February

The magnetic field structure of the ejecta of a coronal mass ejection (CME) is not known well near the Sun. Here we demonstrate, with a numerical simulation, a relationship between the subsonic plasma flows in the CME-sheath and the ejecta magnetic field direction. We draw an analogy to the outer heliosphere, where Opher et al. used *Voyager 2* measurements of the solar wind in the heliosheath to constrain the strength and direction of the local interstellar magnetic field. We simulate three ejections with the same initial free energy, but different ejecta magnetic field orientations in relation to the global coronal field. Each ejection is launched into the same background solar wind using the Space Weather Modeling Framework. The different ejecta magnetic field orientations cause the CME-pause (the location of pressure balance between solar wind and ejecta material) to evolve differently in the lower corona. As a result, the CME-sheath flow deflections around the CME-pauses are different. To characterize this non-radial deflection, we use  $\theta_F = \tan^{-1} v_N/v_T$ , where  $v_N$  and  $v_T$  are the normal and tangential plasma flow as measured in a spacecraft-centered coordinate system. Near the CME-pause, we found that  $\theta_F$  is very sensitive to the ejecta magnetic field, varying from  $45^\circ$  to  $98^\circ$  between the cases when the CME-driven shock is located at  $4.5R_\odot$ . The deflection angle for each case is found to evolve due to rotation of the ejecta magnetic field. We find that this rotation should slow or stop by  $10R_\odot$  (also suggested by observational studies). These results indicate that an observational study of CME-sheath flow deflection angles from several events (to account for the interaction with the solar wind), combined with numerical simulations (to estimate the ejecta magnetic field rotation between eruption and  $10R_\odot$ ) can be used to constrain the ejecta magnetic field in the lower corona.

### **Alfvén Profile in the Lower Corona: Implications for Shock Formation.**

**Evans**, R.M., Opher, M., Manchester, IV, W.B., Gombosi, T.I.,

2008. *Astrophys. J.* 687, 1355–1362.

### **The heliospheric imagers onboard the STEREO mission.**

**Eyles**, C. J., Harrison, R. A., Davis, C. J., Waltham, N. R., Shaughnessy, B. M., Mapson-Menard, H. C. A., ... & Howard, R. A.

(2009). *Solar Physics*, 254(2), 387-445

<http://sci-hub.tw/10.1007/s11207-008-9299-0>

Mounted on the sides of two widely separated spacecraft, the two Heliospheric Imager (HI) instruments onboard NASA's STEREO mission view, for the first time, the space between the Sun and Earth. These instruments are wide-angle visible-light imagers that incorporate sufficient baffling to eliminate scattered light to the extent that the passage of solar coronal mass ejections (CMEs) through the heliosphere can be detected. Each HI instrument comprises two cameras, HI-1 and HI-2, which have  $20^\circ$  and  $70^\circ$  fields of view and are off-pointed from the Sun direction by  $14.0^\circ$  and  $53.7^\circ$ , respectively, with their optical axes aligned in the ecliptic plane. This arrangement provides coverage over solar elongation angles from  $4.0^\circ$  to  $88.7^\circ$  at the viewpoints of the two spacecraft, thereby allowing the observation of Earth-directed CMEs along the Sun – Earth line to the vicinity of the Earth and beyond. Given the two separated platforms, this also presents the first opportunity to view the structure and evolution of CMEs in three dimensions. The STEREO spacecraft were launched from Cape Canaveral Air Force Base in late October 2006, and the HI instruments have been performing scientific observations since early 2007. The design, development, manufacture, and calibration of these unique instruments are reviewed in this paper. Mission operations, including the initial commissioning phase and the science operations phase, are described. Data processing and analysis procedures are briefly discussed, and groundtest results and in-orbit observations are used to demonstrate that the performance of the instruments meets the original scientific requirements.

### **Velocity Oscillations in CME and Related Shock: A Comparative Analysis.**

**Fainshtein**, V.G., Egorov, Y.I.

*Sol Phys* 299, 9 (2024).

<https://doi.org/10.1007/s11207-024-02250-w>

A number of studies have concluded that the velocity of coronal mass ejections (CME) does not change monotonically with time, but exhibits oscillations. They analyzed moving CMEs with oscillation-averaged velocities varying within a wide range. Investigations in the past several years have identified the CME boundary positions relying on data in



various CME catalogs providing the positions of the most remote and generally fastest part of the CME boundary. Unlike the previous investigations, we examined the velocity oscillations of both the CME (i.e., its body) and the CME-related shock for relatively fast CMEs. The characteristics of the two structures have been found to differ noticeably. In all cases considered, it was found that the amplitude of velocity oscillations was higher for a shock than for a CME body. In 7 out of 16 cases, the period of shock velocity oscillations is longer than the period of CME velocity oscillations; in 6 cases it is shorter.

### **Onset of a CME-Related Shock Within the Large-Angle Spectrometric Coronagraph (LASCO) Field of View**

V.G.[Fainshtein](#), [Ya.I.Egorov](#)

[Solar Physics](#) September 2019, 294:126

<https://link.springer.com/content/pdf/10.1007%2Fs11207-019-1519-2.pdf>

<https://doi.org/10.1007/s11207-019-1519-2>

We investigated the onset of a CME-related shock within the Large-Angle Spectrometric Coronagraph (LASCO) field of view (FOV). To detect the first moment of the shock onset, we found a CME on **17 July 2012** that formed at a relatively high altitude and moved with slow acceleration. We examined the possible mechanisms of shock generation. It was shown that bow-shock and piston-shock mechanisms can participate in shock generation, either at different stages of CME movement, or simultaneously. This event has been found to be accompanied by generation of solar energetic particles (SEP). We concluded that, at their initial stage, the source of SEP fluxes may be a solar flare, while the later dramatic increase in the flux of fast protons may be due to their generation in a CME-driven shock.

### **Coronal magnetic field value radial distributions obtained by using the information on fast halo coronal mass ejections**

V.G.[Fainshtein](#), [Ya.I.Egorov](#)

[Solar Phys.](#) 2017

<https://arxiv.org/pdf/1712.09046.pdf>

Based on the method of finding coronal magnetic field value radial profiles  $B(R)$  described in (Gopalswamy and Yashiro, 2011), and applied for the directions close to the sky plane, we determined magnetic field value radial distributions along the directions close to the Sun-Earth axis. For this purpose, by using the method in (Xue, Wang, and Dou, 2005), from the SOHO/LASCO data, we found 3D characteristics for fast halo coronal mass ejections (HCMEs) and for the HCME-related shocks. Through these data, we managed to obtain the  $B(R)$  distributions as far as 43 solar radii from the Sun center, which is approximately by a factor of 2 farther, than those in (Gopalswamy and Yashiro, 2011). We drew a conclusion that, to improve the accuracy of the Gopalswamy-Yashiro method to find the coronal magnetic field, one should develop a technique to detect the CME sites that move in the slow and in the fast solar wind. We propose a technique to select the CMEs, whose central (paraxial) part moves, indeed, in the slow wind. **2003-11-18, 2011-03-08**

### **Origin of a CME-related shock within the LASCO C3 field-of-view**

V.G.[Fainshtein](#), [Ya.I.Egorov](#)

[Solar Phys.](#) 2017

<https://arxiv.org/pdf/1712.09051.pdf>

We study the origin of a CME-related shock within the LASCO C3 field-of-view (FOV). A shock originates, when a CME body velocity on its axis surpasses the total velocity  $V_A + V_{SW}$ , where  $V_A$  is the Alfvén velocity,  $V_{SW}$  is the slow solar wind velocity. The formed shock appears collisionless, because its front width is manifold less, than the free path of coronal plasma charged particles. The Alfvén velocity dependence on the distance was found by using characteristic values of the magnetic induction radial component and of the proton concentration in the Earth orbit, and by using the known regularities of the variations in these solar wind characteristics with distance. A peculiarity of the analyzed CME is its formation at a relatively large height, and the CME body slow acceleration with distance. We arrived at a conclusion that the formed shock is a bow one relative to the CME body moving at a super Alfvén velocity. At the same time, the shock formation involves a steeping of the front edge of the coronal plasma disturbed region ahead of the CME body, which is characteristic of a piston shock. **2012 July 17**

### **Kinematics of CMEs and associated shock waves as deduced from LASCO data: comparative analysis**

V.G. [Fainshtein](#), [Ya.I. Egorov](#), [Yu.S. Zagainova](#)

2017

<https://arxiv.org/pdf/1712.09218.pdf>

From data by LASCO C2 and C3 coronagraphs, depending on time (distance), we have determined positions and velocities of the front for fast limb CMEs' body with their sources near the limb, and for the body of halo-type CME with the sources near the solar disk center. These characteristics of CME body are compared to similar kinematic characteristics obtained for CME body-associated shock waves (shocks). For the body of halo-type CME with the sources near the solar disk center and associated shocks, we determined and compared their kinematic characteristics in

3D space. It has been shown that for all the considered CME groups, the shock velocity is higher than the CME body velocity, both velocities decrease as the mass ejection moves. As this takes place, the distance between CME body and shock grows. On average, distance from CME body to shock, and velocity difference of these structures is greater for a halo CME, and even greater for a model CME in 3D. **2003-11-18, 2004-11-07, 2005-09-05, 2005-09-13**

**Table 1:** left column: CMEs with their sources within 30° related to the limb; right column: halo CMEs) with their sources within 30° as related to the solar disk center

### **On the occurrence and the motion of fast impulsive coronal mass ejections associated with powerful flares and unassociated with eruptive filaments**

V. G. **Fainshtein**, Yu. S. Zagainova

Cosmic Research, January **2015**, Volume 53, Issue 1, pp 31-46

Kosmicheskie Issledovaniya, **2015**, Vol. 53, No. 1, pp. 35–50.

The formation and initial stage of the motion of several rapid, impulsive coronal mass ejections of the “halo” type (HCME) associated with flares of M and X class, but unassociated with the eruption of solar filaments, was studied using GOES-12/SXI, SOHO/EIT, and SDO/AIA data. The HCMEs considered can be divided into three groups according to the features of their formation: (i) some HCMEs arise due to an imbalance of single emission looped structures observed in the 195 Å channel of an EIT instrument for several hours before the first recording of mass ejection in the field of view of an SXI X-ray telescope, and after the eruption, these loops become structural elements of HCMEs; (ii) HCMEs can be formed as a result of an imbalance of several loops in the process of combining these loops into a single structure; and (iii) HCME formation begins with the upward motion of the group of coronal loops observed using the AIA data first in the “hot” 131 Å channel, a few minutes later in the “cold” 211 Å channel, later in the 193 Å channel, and, finally, in the 171 Å channel. The action of moving looped structures on the overlying regions of the corona leads to the formation and the motion of the frontal structure of HCMEs with increased brightness. In this case, these eruptive loops do not become structural elements of HCMEs. All investigated HCMEs began their translational motion before the occurrence of the associated flares. According to the results of studying the kinematics of the considered HCMEs we concluded that there are two types of coronal mass ejections differing according to the time profile of the velocity, which is determined by the area and the magnetic configuration of the active region where the mass ejection was formed. It is shown that HCMEs occurring at different times in the same active region have the same type of velocity profile.

### **Initiation of CMEs associated with filament eruption, and the nature of CME related shocks**

V.G. **Fainshtein**, , Ya.I. Egorov

Advances in Space Research, Volume 55, Issue 3, 1 February **2015**, Pages 798–807

<http://www.sciencedirect.com/science/article/pii/S027311771400310X>

Using data from SDO, PROBA2 and other spacecraft, Fainshtein and Egorov (2013) have discovered processes accompanying initiation of six limb CMEs and have studied features of their motion. The said CMEs occurred after eruption of prominence or hot emission loop and were associated with X-ray flares. The follow-up study of the CMEs, associated with the prominence eruption, showed that the formation of such mass ejections and the initial stage of their motion may be characterised by special features. In this work, we give examples of CMEs with such features. We have revealed a positive correlation between the height of the CME-related eruptive prominence and the height of the frontal structure of CMEs measured before they began to move. By analysing two of the CMEs, using SDO data, we found out that the kinematics of CME body and its related shock differs considerably. We have established that the time dependence of shock position and velocity obtained from SDO data is in agreement with theoretical dependencies of variation in these motion parameters with time in the context of self-similar motion of an explosion shock. We have concluded that the shock are not piston-like with the CME body acting as a piston. **13 October 2010, 8 March 2011, 7 June 2011, 29 June 2011**

### **Investigation of CME properties using the data of SDO and PROBA2 spacecraft**

V.G. **Fainshtein**, Y.I. Egorov

Cosmic Res., 51 (**2013**), pp. 1–12

Formation and motion (at the initial stage) of six limb CMEs detected in the period June 2010 to June 2011 are investigated using the high-resolution data of the PROBA2 and SDO spacecraft combined with the data of SOHO/LASCO coronagraphs. It is demonstrated that several loop-like structures of enhanced brightness originate in the region of CME formation, and they move one after another with, as a rule, different velocities. These loop-like structures in the final analysis form the frontal structure of CME. Time dependences of the velocity and acceleration of the ejection’s front are obtained for all CMEs under consideration. A conclusion is drawn about possible existence of two classes of CMEs depending on their velocity time profiles. Ejections, whose velocity after reaching its maximum sharply drops by a value of more than 100 km/s and then goes over into a regime of slow change, belong to the first class. Another class of CMEs is formed by ejections whose velocity changes slowly immediately after reaching the maximum. It is demonstrated that the CME’s angular dimension increases at the initial stage of ejection motion up to a factor of 3 with a time scale of doubling the angular size value within the limits 3.5–11 min since the moment of the first measurement of this parameter of an ejection. For three CMEs it is shown that at the initial stage of their motion for a certain time interval they are stronger expanded than grow in the longitude direction.

## **Determining the Full Halo Coronal Mass Ejection Characteristics**

V.G. [Fainshtein](#)

Sun and Geosphere, **2010**; 5(1): 23 – 27, [File](#)

Observing halo coronal mass ejections (HCMEs) in the coronagraph field of view allows one to only determine the apparent parameters in the plane of the sky. Recently, several methods have been proposed allowing one to find some true geometrical and kinematical parameters of HCMEs. In most cases, a simple cone model was used to describe the CME shape. Observations show that various modifications of the cone model ("ice cream models") are most appropriate for describing the shapes of individual CMEs. This paper uses the method of determining full HCME parameters proposed by the author earlier, for determining the parameters of 45 full HCMEs, with various modifications of their shapes. I show that the determined CME characteristics depend significantly on the chosen CME shape. I conclude that the absence of criteria for a preliminary evaluation of the CME shape is a major source of error in determining the true parameters of a full HCME with any of the known methods. I show that, regardless of the chosen CME form, the trajectory of practically all the HCMEs in question deviate from the radial direction towards the Sun-Earth axis at the initial stage of their movement, and their angular size, on average, significantly exceeds that of all the observable CMEs.

## **Relationship between CME Parameters and Large-Scale Structure of Solar Magnetic Fields**

V.G. [Fainshtein](#)<sup>1</sup>, E.V. Ivanov<sup>2</sup>

Sun and Geosphere, **2010**; 5(1): 28 – 33, [File](#)

In this work, we explore how the parameters of coronal mass ejections (CME) associated with eruptive prominences (EP) depend on their position relative to the coronal streamer belt (CSB) and coronal streamer chains (CSCs). We show that the CMEs whose axes are close to CSB propagate at lower mean speed than the CMEs observed in the vicinity of CSCs. The CMEs concentrated at CSCs have larger mean kinetic energy than those associated with CSB. The mean mass is maximum for the events associated with CSB and minimum for events observed near the base of open magnetic field configurations (OMF) - counterparts of coronal holes. The mean angular size is virtually the same for the CMEs of both types. The CME deviation from the radial trajectory has been studied. It is shown that CMEs may deviate noticeably from the radial propagation both on their way from the origin site (prominence eruption site) up to about 2.5 solar radii ( $R_o$ ) and farther, from  $\sim 2.5$  up to  $20 R_o$ . In the epoch of solar minimum and at the rise of the cycle, the deviation in the first part of the trajectory (up to  $2.5 R_o$ ) is mainly towards the equator. In the other phases, no preferable direction has been revealed. As the EP latitude increases up to  $\pm 45^\circ$ , the CME deviation, on the average, increases, too. It is shown that about 50% of all CMEs change the sense of deviation when passing from the near-solar part of the trajectory to its far part so that, as the CME moves away from the Sun, its propagation becomes more radial. The results obtained show that large-scale solar magnetic fields have a significant effect on the characteristics and propagation of coronal mass ejections.

## **Determining the full halo coronal mass ejection characteristics**

V.G. [Fainshtein](#)

Proceedings of the International Astronomical Union / Volume 4 / Symposium S257, pp 279 – 281,

Published online: 16 May **2009**, [File](#)

In this paper we determined the parameters of 45 full halo coronal mass ejections (HCMEs) for various modifications of their cone forms ("ice cream cone models"). We show that the CME determined characteristics depend significantly on the CME chosen form. We show that, regardless of the CME chosen form, the trajectory of practically all the considered HCMEs deviate from the radial direction to the Sun-to-Earth axis at the initial stage of their movement.

## **The expansion of a coronal mass ejection within LASCO field of view: some regularities**

V.G. [Fainshtein](#)

Proceedings of the International Astronomical Union / Volume 4 / Symposium S257, pp 257 – 263,

Published online: 16 May **2009**, [File](#)

Forty five limb CMEs related with eruptive prominences and/or near-to-limb post-eruptive arcades have been tested. It is shown that CMEs can be divided into two groups. The first group includes coronal mass ejections whose " $2\alpha$ " latitude angular sizes apparent in the plane of the sky remain unchanged within measurement accuracy of several degrees. The second one is formed by CMEs that expand "non-radially", namely, their angular sizes increase by the relative value (10-30)% up to the position of the ejection front  $RF = R_{\text{em}}$  and run to the maximal value  $2\alpha_m$  at this distance. It has been found that CMEs of the second type are, on the average, wider, faster and have an outer shell brighter and with higher plasma density for long distances. It is shown that on average  $R_{\text{em}}$  increases as  $2\alpha_m$  rises.

## **A tool for empirical forecasting of major flares, coronal mass ejections, and solar particle events from a proxy of active-region free magnetic energy**

**Falconer**, David; Barghouty, Abdunnasser F.; Khazanov, Igor; Moore, Ron  
Space Weather, Vol. 9, No. 4, S04003, 2011, [File](#)

This paper describes a new forecasting tool developed for and currently being tested by NASA's Space Radiation Analysis Group (SRAG) at Johnson Space Center, which is responsible for the monitoring and forecasting of radiation exposure levels of astronauts. The new software tool is designed for the empirical forecasting of M- and X-class flares, coronal mass ejections, and solar energetic particle events. For each type of event, the algorithm is based on the empirical relationship between the event rate and a proxy of the active region's free magnetic energy. Each empirical relationship is determined from a data set of ~40,000 active-region magnetograms from ~1300 active regions observed by SOHO/Michelson Doppler Imager (MDI) that have known histories of flare, coronal mass ejection, and solar energetic particle event production. The new tool automatically extracts each strong-field magnetic area from an MDI full-disk magnetogram, identifies each as a NOAA active region, and measures the proxy of the active region's free magnetic energy from the extracted magnetogram. For each active region, the empirical relationship is then used to convert the free-magnetic-energy proxy into an expected event rate. The expected event rate in turn can be readily converted into the probability that the active region will produce such an event in a given forward time window. Descriptions of the data sets, algorithm, and software in addition to sample applications and a validation test are presented. Further development and transition of the new tool in anticipation of SDO/HMI are briefly discussed.

## **THE "MAIN SEQUENCE" OF EXPLOSIVE SOLAR ACTIVE REGIONS: DISCOVERY AND INTERPRETATION**

**David A. Falconer**<sup>1,2,3</sup>, [Ronald L. Moore](#)<sup>1</sup>, [G. Allen Gary](#)<sup>3</sup> and [Mitzi Adams](#)<sup>1</sup>  
ApJ 700 L166-L169, 2009

We examine the location and distribution of the production of coronal mass ejections (CMEs) and major flares by sunspot active regions in the phase space of two whole-active-region magnetic quantities measured from 1897 SOHO/MDI magnetograms. These magnetograms track the evolution of 44 active regions across the central disk of radius 0.5 R<sub>Sun</sub>. The two quantities are LWLSG, a gauge of the total free energy in an active region's magnetic field, and LΦ, a measure of the active region's total magnetic flux. From these data and each active region's history of production of CMEs, X flares, and M flares, we find (1) that CME/flare-productive active regions are concentrated in a straight-line "main sequence" in (log LWLSG, log LΦ) space, (2) that main-sequence active regions have nearly their maximum attainable free magnetic energy, and (3) evidence that this arrangement plausibly results from equilibrium between input of free energy to an explosive active region's magnetic field in the chromosphere and corona by contortion of the field via convection in and below the photosphere and loss of free energy via CMEs, flares, and coronal heating, an equilibrium between energy gain and loss that is analogous to that of the main sequence of hydrogen-burning stars in (mass, luminosity) space.

## **MAGNETOGRAM MEASURES OF TOTAL NONPOTENTIALITY FOR PREDICTION OF SOLAR CORONAL MASS EJECTIONS FROM ACTIVE REGIONS OF ANY DEGREE OF MAGNETIC COMPLEXITY**

D. A. **Falconer**,<sup>1</sup> R. L. Moore, and G. A. Gary  
Astrophysical Journal, 689:1433–1442, 2008

For investigating the magnetic causes of coronal mass ejections (CMEs) and for forecasting the CME productivity of active regions, in previous work we have gauged the total nonpotentiality of a whole active region by either of two measures, LSSM and LSGM, two measures of the magnetic field along the main neutral line in a vector magnetogram of the active region. This previous work was therefore restricted to nominally bipolar active regions, active regions that have a clearly identifiable main neutral line. In the present paper, we show that our work can be extended to include multipolar active regions of any degree of magnetic complexity by replacing LSSM and LSGM with their generalized counterparts, WLSS and WLSG, which are corresponding integral measures covering all neutral lines in an active region instead of only the main neutral line. In addition, we show that for active regions within 30 heliocentric degrees of disk center, WLSG can be adequately measured from line-of-sight magnetograms instead of vector magnetograms. This approximate measure of active-region total nonpotentiality, LWLSG, with the extensive set of 96 minute cadence full-disk line-of-sight magnetograms from SOHO MDI, can be used to study the evolution of active-region total nonpotentiality leading to the production of CMEs.

## **MAGNETIC CAUSES OF SOLAR CORONAL MASS EJECTIONS: DOMINANCE OF THE FREE MAGNETIC ENERGY OVER THE MAGNETIC TWIST ALONE**

D. A. **Falconer**, R. L. Moore, and G. A. Gary  
The Astrophysical Journal, 644:1258–1272, 2006, [File](#)

We examine the magnetic causes of coronal mass ejections (CMEs) by examining, along with the correlations of active-region magnetic measures with each other, the correlations of these measures with active-region CME productivity observed in time windows of a few days, either centered on or extending forward from the day of the magnetic measurement.

From the deprojected magnetograms, we find evidence that (1) magnetic twist and magnetic size are separate but comparably strong causes of active-region CME productivity, and (2) the total free magnetic energy in an active region's magnetic field is a stronger determinant of the active region's CME productivity than is the field's overall twist (or helicity) alone.

## **A data-driven MHD simulation of the 2011-02-15 coronal mass ejection from Active Region NOAA 11158**

[Yuhong Fan](#), [Maria D. Kazachenko](#), [Andrey N. Afanasyev](#), [George H. Fisher](#)

ApJ **975** 206 2024

<https://arxiv.org/pdf/2409.17507>

<https://iopscience.iop.org/article/10.3847/1538-4357/ad7f53/pdf>

We present a boundary data-driven magneto-hydrodynamic (MHD) simulation of the **2011-02-15** coronal mass ejection (CME) event of Active Region (AR) NOAA 11158. The simulation is driven at the lower boundary with an electric field derived from the normal magnetic field and the vertical electric current measured from the Solar Dynamics Observatory (SDO) Helioseismic Magnetic Imager (HMI) vector magnetograms. The simulation shows the build up of a pre-eruption coronal magnetic field that is close to the nonlinear force-free field (NLFFF) extrapolation, and it subsequently develops multiple eruptions. The sheared/twisted field lines of the pre-eruption magnetic field show qualitative agreement with the brightening loops in the SDO Atmospheric Imaging Assembly (AIA) hot passband images. We find that the eruption is initiated by the tether-cutting reconnection in a highly sheared field above the central polarity inversion line (PIL) and a magnetic flux rope with dipped field lines forms during the eruption. The modeled erupting magnetic field evolves to develop a complex structure containing two distinct flux ropes and produces an outgoing double-shell feature consistent with the Solar TERrestrial RELations Observatory B / Extreme UltraViolet Imager (STEREO-B/EUVI) observation of the CME. The foot points of the erupting field lines are found to correspond well with the dimming regions seen in the SDO/AIA observation of the event. These agreements suggest that the derived electric field is a promising way to drive MHD simulations to establish the realistic pre-eruption coronal field based on the observed vertical electric current and model its subsequent dynamic eruption.

## **An improved MHD simulation of the 2006 December 13 coronal mass ejection of active region NOAA 10930**

[Yuhong Fan](#)

ApJ **941** 61 2022

<https://arxiv.org/pdf/2211.03736.pdf>

<https://iopscience.iop.org/article/10.3847/1538-4357/aca0ec/pdf>

We present a magnetohydrodynamic (MHD) simulation of the coronal mass ejection (CME) on **13 December 2006** in the emerging delta-sunspot active region 10930, improving upon a previous simulation by Fan (2016) as follows. (1) Incorporate an ambient solar wind instead of using a static potential magnetic field extrapolation as the initial state. (2) In addition to imposing the emergence of a twisted flux rope, also impose at the lower boundary a random electric field that represents the effect of turbulent convection, which drives field-line braiding and produces resistive and viscous heating in the corona. With the inclusion of this heating, which depends on the magnetic field topology, we are able to model the synthetic soft X-ray images that would be observed by the X-Ray Telescope (XRT) of the Hinode satellite, produced by the simulated coronal magnetic field. We find that the simulated pre-eruption magnetic field with the build up of a twisted magnetic flux rope, produces synthetic soft X-ray emission that shows qualitatively similar morphology as that observed by the Hinode/XRT for both the ambient coronal loops of the active region and the central inverse-S shaped "sigmoid" that sharpens just before the onset of the eruption. The synthetic post-flare loop brightening also shows similar morphology as that seen in the Hinode/XRT image during the impulsive phase of the eruption. It is found that the kinematics of the erupting flux rope is significantly affected by the open magnetic fields and fast solar wind streams adjacent to the active region.

## **Simulations of prominence eruption preceded with large amplitude longitudinal oscillations and draining**

[Yuhong Fan](#)

ApJ **898** 34 2020

<https://arxiv.org/pdf/2006.11619.pdf>

<https://doi.org/10.3847/1538-4357/ab9d7f>

We present magnetohydrodynamic (MHD) simulations of the evolution from quasi-equilibrium to eruption of a prominence-forming twisted coronal flux rope under a coronal streamer. We have compared the cases with and without the formation of prominence condensations, and the case where prominence condensations form but we artificially initiate the draining of the prominence. We find that the prominence weight has a significant effect on the stability of the flux rope, and can significantly increase the loss-of-equilibrium height. The flux rope can be made to erupt earlier

by initiating draining of the prominence mass. We have also performed a simulation where large amplitude longitudinal oscillations of the prominence are excited during the quasi-static phase. We find that the gravity force along the magnetic field lines is the major restoring force for the oscillations, in accordance with the "pendulum model", although the oscillation periods are higher (by about 10% to 40%) than estimated from the model because of the dynamic deformation of the field line dips during the oscillations. The oscillation period is also found to be slightly smaller for the lower part of the prominence in the deeper dips compared to the upper part in the shallower dips. The oscillations are quickly damped out after about 2-3 periods and are followed by prominence draining and the eventual eruption of the prominence. However we do not find a significant enhancement of the prominence draining and earlier onset of eruption with the excitation of the prominence oscillations compared to the case without.

## **MHD simulation of prominence-cavity system**

Yuhong [Fan](#), [Tie Liu](#)

Frontiers in Astronomy and Space Sciences                      2019

<https://arxiv.org/pdf/1905.08226.pdf>

<https://www.frontiersin.org/articles/10.3389/fspas.2019.00027/full>

[sci-hub.se/10.3389/fspas.2019.00027](http://sci-hub.se/10.3389/fspas.2019.00027)

We present magnetohydrodynamic simulation of the evolution from quasi-equilibrium to onset of eruption of a twisted, prominence-forming coronal magnetic flux rope underlying a corona streamer. The flux rope is built up by an imposed flux emergence at the lower boundary. During the quasi-static phase of the evolution, we find the formation of a prominence-cavity system with qualitative features resembling observations, as shown by the synthetic SDO/AIA EUV images with the flux rope observed above the limb viewed nearly along its axis. The cavity contains substructures including "U"-shaped or horn-like features extending from the prominence enclosing a central "cavity" on top of the prominence. The prominence condensations form in the dips of the highly twisted field lines due to runaway radiative cooling and the cavity is formed by the density depleted portions of the prominence-carrying field lines extending up from the dips. The prominence "horns" are threaded by twisted field lines containing shallow dips, where the prominence condensations have evaporated to coronal temperatures. The central "cavity" enclosed by the horns is found to correspond to a central hot and dense core containing twisted field lines that do not have dips. The flux rope eventually erupts as its central part rises quasi-statically to a critical height consistent with the onset of the torus instability. The erupting flux rope accelerates to a fast speed of nearly 900 km/s and the associated prominence eruption shows significant rotational motion and a kinked morphology.

## **The eruption of a prominence carrying coronal flux rope: forward synthesis of the magnetic field strength measurement by the COronal Solar Magnetism Observatory Large Coronagraph**

Yuhong [Fan](#), [Sarah Gibson](#), [Steve Tomczyk](#)

ApJ            866 57            2018

<https://arxiv.org/pdf/1808.06142.pdf>

[sci-hub.tw/10.3847/1538-4357/aadd0e](http://sci-hub.tw/10.3847/1538-4357/aadd0e)

From a magnetohydrodynamic (MHD) simulation of the eruption of a prominence hosting coronal flux rope, we carry out forward synthesis of the circular polarization signal (Stokes V signal) of the FeXIII emission line at 1074.7 nm produced by the MHD model as measured by the proposed COronal Solar Magnetism Observatory (COSMO) Large Coronagraph (LC) and infer the line-of-sight magnetic field  $B_{LOS}$  above the limb. With an aperture of 150 cm, integration time of 12 min, and a resolution of 12 arcsec, the LC can measure a significant  $B_{LOS}$  with sufficient signal to noise level, from the simulated flux rope viewed nearly along its axis with a peak axial field strength of about 10 G. The measured  $B_{LOS}$  is found to relate well with the axial field strength of the flux rope for the height range of the prominence, and can discern the increase with height of the magnetic field strength in that height range that is a definitive signature of the concave upturning dipped field supporting the prominence. The measurement can also detect an outward moving  $B_{LOS}$  due to the slow rise of the flux rope as it develops the kink instability, during the phase when its rise speed is still below about 41 km/s and up to a height of about 1.3 solar radii. These results suggest that the COSMO LC has great potential in providing quantitative information about the magnetic field structure of CME precursors (e.g. the prominence cavities) and their early evolution for the onset of eruption.

## **MHD simulation of prominence eruption**

[Yuhong Fan](#)

ApJ            862 54            2018

<https://arxiv.org/pdf/1806.06305.pdf>

<http://sci-hub.tw/http://iopscience.iop.org/article/10.3847/1538-4357/aaccee/meta>

We carry out magnetohydrodynamic (MHD) simulations of the quasi-static evolution and eruption of a twisted coronal flux rope under a coronal streamer built up by an imposed flux emergence at the lower boundary. The MHD model incorporates a simple empirical coronal heating, optically thin radiative cooling, and field aligned thermal conduction, and thus allows the formation of prominence condensations. We find that during the quasi-static evolution, prominence/filament condensations of an elongated, sigmoid morphology form in the dips of the significantly twisted field lines of the emerged flux rope due to run-away radiative cooling. A prominence cavity also forms surrounding the prominence, which is best observed above the limb with the line-of-sight nearly along the length of the flux rope, as

shown by synthetic SDO/AIA EUV images. The magnetic field supporting the prominence is significantly non-force-free despite the low plasma-beta. By comparing with a simulation that suppresses prominence formation, we find that the prominence weight is dynamically important and can suppress the onset of the kink instability and hold the flux rope in equilibrium for a significantly long time, until draining of the prominence plasma develops and lightens the prominence weight. The flux rope eventually develops the kink instability and erupts, producing a prominence eruption. The synthetic AIA 304 angstrom images show that the prominence is lifted up into an erupting loop, exhibiting helical features along the loop and substantial draining along the loop legs, as often seen in observations.

## **Turbulence and Heating in the Flank and Wake Regions of a Coronal Mass Ejection**

Siteng [Fan](#), [Jiansen He](#), [Limei Yan](#), [Steven Tomczyk](#), [Hui Tian](#)...

[Solar Physics](#) January 2018, 293:6

As a coronal mass ejection (CME) passes, the flank and wake regions are typically strongly disturbed. Various instruments, including the Large Angle and Spectroscopic Coronagraph (LASCO), the Atmospheric Imaging Assembly (AIA), and the Coronal Multi-channel Polarimeter (CoMP), observed a CME close to the east limb on **26 October 2013**. A hot ( $\approx 10$  MK) rising blob was detected on the east limb, with an initial ejection flow speed of  $\approx 330$  km s<sup>-1</sup>. The magnetic structures on both sides and in the wake of the CME were strongly distorted, showing initiation of turbulent motions with Doppler-shift oscillations enhanced from  $\approx \pm 3$  km s<sup>-1</sup> to  $\approx \pm 15$  km s<sup>-1</sup> and effective thermal velocities from  $\approx 30$  km s<sup>-1</sup> to  $\approx 60$  km s<sup>-1</sup>, according to the CoMP observations at the Fe xiii line. The CoMP Doppler-shift maps suggest that the turbulence behaved differently at various heights; it showed clear wave-like torsional oscillations at lower altitudes, which are interpreted as the antiphase oscillation of an alternating red/blue Doppler shift across the strands at the flank. The turbulence seems to appear differently in the channels of different temperatures. Its turnover time was  $\approx 1000$  seconds for the Fe 171 Å channel, while it was  $\approx 500$  seconds for the Fe 193 Å channel. Mainly horizontal swaying rotations were observed in the Fe 171 Å channel, while more vertical vortices were seen in the Fe 193 Å channel. The differential-emission-measure profiles in the flank and wake regions have two components that evolve differently: the cool component decreased over time, evidently indicating a drop-out of cool materials due to ejection, while the hot component increased dramatically, probably because of the heating process, which is suspected to be a result of magnetic reconnection and turbulence dissipation. These results suggest a new turbulence-heating scenario of the solar corona and solar wind.

## **MHD simulations of the eruption of coronal flux ropes under coronal streamers**

Yuhong [Fan](#)

ApJ **844** 26 **2017**

<https://arxiv.org/pdf/1706.06076.pdf>

<http://sci-hub.cc/10.3847/1538-4357/aa7a56>

Using three-dimensional magnetohydrodynamic (MHD) simulations, we investigate the eruption of coronal flux ropes underlying coronal streamers and the development of a prominence eruption. We initialize a quasi-steady solution of a coronal helmet streamer, into which we impose at the lower boundary the slow emergence of a part of a twisted magnetic torus. As a result a quasi-equilibrium flux rope is built up under the streamer. With varying sizes of the streamer and the different length and total twist of the emerged flux rope, we found different scenarios for the evolution from quasi-equilibrium to eruption. In the cases with a broad streamer, the flux rope remains well confined until there is sufficient twist such that it first develops the kink instability and evolves through a sequence of kinked, confined states with increasing height until it eventually develops a "hernia-like" ejective eruption. For the significantly twisted flux ropes, prominence condensations form in the dips of the twisted field lines due to run-away radiative cooling. Once formed, the prominence carrying field becomes significantly non-force-free due to the prominence weight despite being low plasma  $\beta$ . As the flux rope erupts, we obtain the eruption of the prominence, which shows substantial draining along the legs of the erupting flux rope. The prominence may not show a kinked morphology even though the flux rope becomes kinked. On the other hand, in the case with a narrow streamer, the flux rope with less than 1 wind of twist can erupt via the onset of the torus instability.

## **Modeling the initiation of the 2006 December 13 coronal mass ejection in AR 10930: the structure and dynamics of the erupting flux rope**

Yuhong [Fan](#)

ApJ **824** 93 **2016**

<http://arxiv.org/pdf/1604.05687v1.pdf>

We carry out a three-dimensional magneto-hydrodynamic (MHD) simulation to model the initiation of the coronal mass ejection (CME) on **13 December 2006** in the emerging  $\delta$ -sunspot active region NOAA 10930. The setup of the simulation is similar to a previous simulation by Fan (2011), but with a significantly widened simulation domain to accommodate the wide CME. The simulation shows that the CME can result from the emergence of a east-west oriented twisted flux rope whose positive, following emerging pole corresponds to the observed positive rotating sunspot emerging against the southern edge of the dominant pre-existing negative sunspot. The erupting flux rope in the simulation accelerates to a terminal speed that exceeds 1500 km/s and undergoes a counter-clockwise rotation of nearly

180 degrees such that its front and flanks all exhibit southward directed magnetic fields, explaining the observed southward magnetic field in the magnetic cloud impacting the Earth. With continued driving of flux emergence, the source region coronal magnetic field also shows the reformation of a coronal flux rope underlying the flare current sheet of the erupting flux rope, ready for a second eruption. This may explain the build up for another X-class eruptive flare that occurred the following day from the same region.

## **MHD Equilibria and Triggers for Prominence Eruption**

Yuhong [Fan](#)

Chapter 12 of Solar Prominences, Astrophysics and Space Science Library, Volume 415. ISBN 978-3-319-10415-7. Springer International Publishing Switzerland, **2015**, p. 297

<http://arxiv.org/pdf/1512.08044v1.pdf>

Magneto-hydrodynamic (MHD) simulations of the emergence of twisted magnetic flux tubes from the solar interior into the corona are discussed to illustrate how twisted and sheared coronal magnetic structures (with free magnetic energy), capable of driving filament eruptions, can form in the corona in emerging active regions. Several basic mechanisms that can disrupt the quasi-equilibrium coronal structures and trigger the release of the stored free magnetic energy are discussed. These include both ideal processes such as the onset of the helical kink instability and the torus instability of a twisted coronal flux rope structure and the non-ideal process of the onset of fast magnetic reconnections in current sheets. Representative MHD simulations of the non-linear evolution involving these mechanisms are presented.

**2002 May 27**

## **THERMAL SIGNATURES OF TETHER-CUTTING RECONNECTIONS IN PRE-ERUPTION CORONAL FLUX ROPES: HOT CENTRAL VOIDS IN CORONAL CAVITIES**

Y. [Fan](#)

**2012 ApJ 758 60**

Using a three-dimensional MHD simulation, we model the quasi-static evolution and the onset of eruption of a coronal flux rope. The simulation begins with a twisted flux rope emerging at the lower boundary and pushing into a pre-existing coronal potential arcade field. At a chosen time the emergence is stopped with the lower boundary taken to be rigid. Then the coronal flux rope settles into a quasi-static rise phase during which an underlying, central sigmoid-shaped current layer forms along the so-called hyperbolic flux tube (HFT), a generalization of the X-line configuration. Reconnections in the dissipating current layer effectively add twisted flux to the flux rope and thus allow it to rise quasi-statically, even though the magnetic energy is decreasing as the system relaxes. We examine the thermal features produced by the current layer formation and the associated "tether-cutting" reconnections as a result of heating and field aligned thermal conduction. It is found that a central hot, low-density channel containing reconnected, twisted flux threading under the flux rope axis forms on top of the central current layer. When viewed in the line of sight roughly aligned with the hot channel (which is roughly along the neutral line), the central current layer appears as a high-density vertical column with upward extensions as a "U"-shaped dense shell enclosing a central hot, low-density void. Such thermal features have been observed within coronal prominence cavities. Our MHD simulation suggests that they are the signatures of the development of the HFT topology and the associated tether-cutting reconnections, and that the central void grows and rises with the reconnections, until the flux rope reaches the critical height for the onset of the torus instability and dynamic eruption ensues.

## **ON THE ERUPTION OF CORONAL FLUX ROPES**

Y. [Fan](#)

**2010 ApJ 719 728; File**

We present three-dimensional MHD simulations of the evolution of the magnetic field in the corona where the emergence of a twisted magnetic flux tube is driven at the lower boundary into a pre-existing coronal potential arcade field. Through a sequence of simulations in which we vary the amount of twisted flux transported into the corona before the emergence is stopped, we investigate the conditions that lead to a dynamic eruption of the resulting coronal flux rope. It is found that the critical condition for the onset of eruption is for the center of the flux rope to reach a critical height at which the corresponding potential field declines with height at a sufficiently steep rate, consistent with the onset of the torus instability of the flux rope. In some cases, immediately after the emergence is stopped, the coronal flux rope first settles into a quasi-static rise with an underlying sigmoid-shaped current layer developing. Preferential heating of field lines going through this current layer may give rise to the observed quiescent X-ray sigmoid loops before eruption. Reconnections in the current layer during the initial quasi-static stage is found to add detached flux to the coronal flux rope, allowing it to rise quasi-statically to the critical height and dynamic eruption of the flux rope then ensues. By identifying field lines whose tops are in the most intense part of the current layer during the eruption, we deduce the evolution and morphology of the post-flare X-ray loops and the flare ribbons at their footpoints.

## **THE EMERGENCE OF A TWISTED FLUX TUBE INTO THE SOLAR ATMOSPHERE: SUNSPOT ROTATIONS AND THE FORMATION OF A CORONAL FLUX ROPE**

Y. [Fan](#)



2009 ApJ 697 1529-1542

We present a three-dimensional simulation of the dynamic emergence of a twisted magnetic flux tube from the top layer of the solar convection zone into the solar atmosphere and corona. It is found that after a brief initial stage of flux emergence during which the two polarities of the bipolar region become separated and the tubes intersecting the photosphere become vertical, significant rotational motion sets in within each polarity. The rotational motions of the two polarities are found to twist up the inner field lines of the emerged fields such that they change their orientation into an inverse configuration (i.e., pointing from the negative polarity to the positive polarity over the neutral line). As a result, a flux rope with sigmoid-shaped, dipped core fields forms in the corona, and the center of the flux rope rises in the corona with increasing velocity as the twisting of the flux rope footpoints continues. The rotational motion in the two polarities is a result of propagation of nonlinear torsional Alfvén waves along the flux tube, which transports significant twist from the tube's interior portion toward its expanded coronal portion. This is a basic process whereby twisted flux ropes are developed in the corona with increasing twist and magnetic energy, leading up to solar eruptions.

### **ONSET OF CORONAL MASS EJECTIONS DUE TO LOSS OF CONFINEMENT OF CORONAL FLUX ROPES**

Y. **Fan** and S. E. Gibson

The Astrophysical Journal, 668:1232Y1245, 2007

Using MHD numerical simulations in a three-dimensional spherical geometry, we model the loss of confinement and eruption of a flux rope emerging quasi-statically into a preexisting coronal arcade field. Our numerical experiments investigated two distinct mechanisms that led to the eruption of the flux rope.

### **Dynamics of Threads Wrapping a Filament's Leg Prior to the Eruption on 2021 October 28**

Yue **Fang**<sup>1</sup>, Jun Zhang<sup>1</sup>, Yi Bi<sup>2</sup>, and Zhiping Song<sup>1</sup>

2023 ApJ 955 87

<https://iopscience.iop.org/article/10.3847/1538-4357/acf19e/pdf>

Although the magnetic field structures of solar filaments have been studied for several decades, the detailed evolution of the structure around a filament prior to its eruption is rarely observed. On **2021 October 28** in AR 12887, a major solar flare (X1.0 class) occurred at 15:35 UT. Based on the Solar Dynamics Observatory high-spatial-resolution observations, we find this flare is associated with the eruption of two filaments, namely F1 and F2. The two filaments are initially independent. The western leg (WLEG) of F1 approaches the northern leg of F2, due to the continuous movement and rotation of the magnetic field in which the WLEG roots in. We find first that there are some threads wrapping the WLEG. Brightening and bidirectionally plasmoid flows that originate from a brightening are detected in these threads, then the threads disappear, and the two filaments connect. NLFFF extrapolation reveals that there is a toroidal magnetic structure enveloping the WLEG and corresponding spatially to the threads. It is expected that a filament is enveloped by toroidal magnetic fields. According to the observations and extrapolation, we suggest that these threads represent the toroidal magnetic fields wrapping the WLEG. This paper provides new details about the dynamics of the toroidal magnetic fields. Magnetic reconnection takes place in the toroidal fields and thus destroys the fields, then F1 and F2 connect, and subsequently, the two filaments erupt and the flare occurs.

### **Coronal rain in magnetic arcades: Rebound shocks, Limit cycles, and Shear flows**

X. **Fang**, C. Xia, **R. Keppens**, **T. Van Doorselaere**

2015

<http://arxiv.org/pdf/1507.00882v1.pdf>

We extend our earlier multidimensional, magnetohydrodynamic simulations of coronal rain occurring in magnetic arcades with higher resolution, grid-adaptive computations covering a much longer (>6 hour) timespan. We quantify how in-situ forming blob-like condensations grow along and across field lines and show that rain showers can occur in limit cycles, here demonstrated for the first time in 2.5D setups. We discuss dynamical, multi-dimensional aspects of the rebound shocks generated by the siphon inflows and quantify the thermodynamics of a prominence-corona-transition-region like structure surrounding the blobs. We point out the correlation between condensation rates and the cross-sectional size of loop systems where catastrophic cooling takes place. We also study the variations of the typical number density, kinetic energy and temperature while blobs descend, impact and sink into the transition region. In addition, we explain the mechanisms leading to concurrent upflows while the blobs descend. As a result, there are plenty of shear flows generated with relative velocity difference around 80 km s<sup>-1</sup> in our simulations. These shear flows are siphon flows set up by multiple blob dynamics and they in turn affect the deformation of the falling blobs. In particular, we show how shear flows can break apart blobs into smaller fragments, within minutes.

### **Rotating Solar Jets in Simulations of Flux Emergence with Thermal Conduction**

Fang **Fang**, Yuhong Fan, Scott W. McIntosh

ApJL, 2014 789 L19

<http://arxiv.org/pdf/1406.2220v1.pdf>

We study the formation of coronal jets through numerical simulation of the emergence of a twisted magnetic flux rope into a pre-existing open magnetic field. Reconnection inside the emerging flux rope in addition to that between the

emerging and pre-existing fields give rise to the violent eruption studied. The simulated event closely resembles the coronal jets ubiquitously observed by Hinode/XRT and demonstrates that heated plasma is driven into the extended atmosphere above. Thermal conduction implemented in the model allows us to qualitatively compare simulated and observed emission from such events. We find that untwisting field lines after the reconnection drive spinning outflows of plasma in the jet column. The Poynting flux in the simulated jet is dominated by the untwisting motions of the magnetic fields loaded with high-density plasma. The simulated jet is comprised of spires of untwisting field that are loaded with a mixture of cold and hot plasma and exhibit rotational motion of order 20 km/s and match contemporary observations.

### **A new multi-wavelength solar telescope: Optical and Near-infrared Solar Eruption Tracer (ONSET)**

[Fang, Cheng](#); [Chen, Peng-Fei](#); [Li, Zhen](#); [Ding, Ming-De](#); [Dai, Yu](#); [Zhang, Xiao-Yu](#); [Mao, Wei-Jun](#); [Zhang, Jun-Ping](#); [Li, Ting](#); [Liang, Yong-Jun](#); [Lu, Hai-Tian](#)

Research in Astronomy and Astrophysics, Volume 13, Issue 12, article id. 1509-1517 (2013).

<https://arxiv.org/pdf/1307.4533.pdf>

A new multi-wavelength solar telescope, the Optical and Near-infrared Solar Eruption Tracer (ONSET) of Nanjing University, has been constructed. It was fabricated at the Nanjing Institute of Astronomical Optics & Technology, and the operation is jointly administered with Yunnan Astronomical Observatory. ONSET is able to observe the Sun in three wavelength windows: He I 10830 Å, H $\alpha$  and white-light at 3600 Å and 4250 Å, which are selected in order to simultaneously record the dynamics of the corona, chromosphere and photosphere respectively. Full-disk or partial-disk solar images with a field of 10' at three wavelengths can be obtained nearly simultaneously. It is designed to trace solar eruptions with high spatial and temporal resolutions. This telescope was installed at a new solar observing site near Fuxian Lake in Yunnan Province, southwest China. The site is located at E102N24, with an altitude of 1722 m. The seeing is stable and has high quality. We give a brief description of the scientific objectives and the basic structure of ONSET. Some preliminary results are also presented. **21 April 2011, 2012 March 9, 2013 March 13, 2013 April 30**

### **BUILDUP OF MAGNETIC SHEAR AND FREE ENERGY DURING FLUX EMERGENCE AND CANCELLATION**

Fang [Fang](#)<sup>1</sup>, Ward Manchester IV<sup>1</sup>, William P. Abbett<sup>2</sup>, and Bart van der Holst

**2012** ApJ 754 15

We examine a simulation of flux emergence and cancellation, which shows a complex sequence of processes that accumulate free magnetic energy in the solar corona essential for the eruptive events such as coronal mass ejections, filament eruptions, and flares. The flow velocity at the surface and in the corona shows a consistent shearing pattern along the polarity inversion line (PIL), which together with the rotation of the magnetic polarities, builds up the magnetic shear. Tether-cutting reconnection above the PIL then produces longer sheared magnetic field lines that extend higher into the corona, where a sigmoidal structure forms. Most significantly, reconnection and upward-energy-flux transfer are found to occur even as magnetic flux is submerging and appears to cancel at the photosphere. A comparison of the simulated coronal field with the corresponding coronal potential field graphically shows the development of non-potential fields during the emergence of the magnetic flux and formation of sunspots.

### **Torsional Alfvén Wave Cascade and Shocks Evolving in Solar Jets**

S. Vasheghani [Farahani](#)<sup>1</sup>, S. M. Hejazi<sup>1</sup>, and M. R. Boroomand<sup>2</sup>

**2021** ApJ 906 70

<https://doi.org/10.3847/1538-4357/abca8c>

The aim of this study is to model the nature of nonlinear torsional magnetohydrodynamic waves propagating in solar jets as they are elevated to the outer solar atmosphere. The contribution of sequential processes to the transfer of energy is taken under consideration: the nonlinear cascade and shock formation. Thus a straight magnetic cylinder embedded in a plasma with an initial magnetic field and parallel flow to the cylinder axis is implemented. To resemble a jet where the oscillation wavelength highly exceeds the radius, the second-order thin flux tube approximation proves adequate. A Cohen–Kulsrud type equation is presented, and its solution highly depends on the parameter presented in this study, which itself is constituted of various environmental and equilibrium conditions that affect the perturbations of the variables as well as the nonlinear forces connected to Alfvén wave propagation. The shock formation time of torsional waves is inversely proportional to the density contrast of the jet, while the efficiency of energy transfer to shorter scales is directly proportional to the density contrast. While the parallel flow with a shear at the boundary expedites shock formation, its efficiency regarding energy transfer is dramatically enhanced by the plasma- $\beta$ , significantly contributing to coronal heating. The observational and seismological aspect of the present study is that faster jets are less probable for observations at higher altitudes, as they experience energy transfer mostly at the base of the corona, while slow speed jets may be observed at higher altitudes contributing to solar wind acceleration.

### **Coronal Jet Collimation by Nonlinear Induced Flows**

S. Vasheghani [Farahani](#) and S. M. Hejazi

**2017** ApJ 844 148

<http://sci-hub.cc/10.3847/1538-4357/aa7da5>

We consider a straight, initially non-rotating, untwisted magnetic cylinder embedded in a plasma with a straight magnetic field, where a shear between the internal and external flows exists. By implementing magnetohydrodynamic theory and taking into account the second-order thin flux tube approximation, the balance between the internal nonlinear forces is visualized. The nonlinear differential equation containing the ponderomotive, magnetic tension, and centrifugal forces in the presence of the shear flow is obtained. The solution presents the scale of influence of the propagating torsional Alfvén wave on compressive perturbations. Explicit expressions for the compressive perturbations caused by the forces connected to the torsional Alfvén wave show that, in the presence of a shear flow, the magnetic tension and centrifugal forces do not cancel each other's effects as they did in its absence. This shear flow plays in favor of the magnetic tension force, resulting in a more efficient collimation. Regarding the ponderomotive force, the shear flow has no effect. The phase relations highlight the interplay of the shear flow and the plasma- $\beta$ . As the shear flow and plasma- $\beta$  increase, compressive perturbation amplitudes emerge. We conclude that the jet collimation due to the torsional Alfvén wave highly depends on the location of the jet. The shear flow tightens the collimation as the jet elevates up to the solar corona.

### **Torsional wave propagation in solar tornadoes**

S. Vasheghani [Farahani](#)<sup>1</sup>, E. Ghanbari<sup>2</sup>, G. Ghaffari<sup>1</sup> and H. Safari

A&A 599, A19 (2017) 10.1051/0004-6361/201629563

**Aims.** We investigate the propagation of torsional waves in coronal structures together with their collimation effects in the context of magnetohydrodynamic (MHD) theory. The interplay of the equilibrium twist and rotation of the structure, e.g. jet or tornado, together with the density contrast of its internal and external media is studied to shed light on the nature of torsional waves.

**Methods.** We consider a rotating magnetic cylinder embedded in a plasma with a straight magnetic field. This resembles a solar tornado. In order to express the dispersion relations and phase speeds of the axisymmetric magnetohydrodynamic waves, the second-order thin flux tube approximation is implemented for the internal medium and the ideal MHD equations are implemented for the external medium.

**Results.** The explicit expressions for the phase speed of the torsional wave show the modification of the torsional wave speed due to the equilibrium twist, rotation, and density contrast of the tornado. The speeds could be either sub-Alfvénic or ultra-Alfvénic depending on whether the equilibrium twist or rotation is dominant. The equilibrium twist increases the phase speed while the equilibrium rotation decreases it. The good agreement between the explicit versions for the phase speed and that obtained numerically proves adequate for the robustness of the model and method. The density ratio of the internal and external media also play a significant role in the speed and dispersion.

### **Editorial: The Magnetic Structures and Their Role in The Evolution of Coronal Mass Ejections.**

To the [THE RESEARCH TOPIC](#)

**Feng H, Hu Q and Song H**

(2021) Front. Phys. 9:820476. doi: 10.3389/fphy.2021.820476

<https://www.frontiersin.org/articles/10.3389/fphy.2021.820476/full>

<https://doi.org/10.3389/fphy.2021.820476>

The aim of this research topic is to present multi-faceted research, from distinctive perspectives involving the forefront of Heliophysics—the science about the Sun, the Earth, and what's in-between, on the magnetic structures and other key ingredients of CMEs at different evolution stages. Multiple analysis tools, including theoretical, numerical, and observational ones, are employed, making use of a variety of ground-based and space-borne remote-sensing and in-situ measurements.

### **Observations of magnetic flux ropes opened or disconnected from the Sun by magnetic reconnection in interplanetary space**

HengQiang [Feng](#), Yan Zhao, Jiemin Wang, Qiang Liu, and Guoqing Zhao

Front. Phys., 12 May 2021 |

<https://doi.org/10.3389/fphy.2021.679780>

<https://www.frontiersin.org/articles/10.3389/fphy.2021.679780/full>

During solar eruptions, many closed magnetic flux ropes are ejected into interplanetary space, which contribute to the heliospheric magnetic field and have important space weather effect because of their coherent magnetic field. Therefore, understanding the evolution of these closed flux ropes in the interplanetary space is important. In this paper, we examined all the magnetic and plasma data measured in 1997 by the Wind spacecraft and identified 621 reconnection exhausts. Of the 621 reconnection events, 31 were observed at the boundaries of magnetic flux ropes and were thought to cause the opening or disconnection magnetic field lines of the adjacent ropes. Of the 31 magnetic reconnection events, 29 were interchange reconnections and the closed field lines of these related flux ropes were opened by them. Only 2 of the 31 magnetic reconnection events disconnected the opened field lines of the original flux ropes. These observations indicate that interchange reconnection and disconnection may be two important mechanisms changing the magnetic topology of the magnetic flux ropes during their propagation during the interplanetary space.

**Nov 9, 1997, Nov 16, 1997**

**Table 1.** The magnetic reconnection exhausts and their related flux ropes. (1997)

Li [Feng](#)<sup>1,2\*</sup>, Weiqun Gan<sup>1,2</sup>, Siqing Liu<sup>3</sup>, Huaning Wang<sup>4</sup>, Hui Li<sup>1,2</sup>, et al.  
Front. Phys., 11 March 2020 | <https://doi.org/10.3389/fphy.2020.00045> **File**  
<https://www.frontiersin.org/articles/10.3389/fphy.2020.00045/full>

**THIS ARTICLE IS PART OF THE RESEARCH TOPIC**  
**Space Weather with Small Satellites [View all Articles](#)**

The **Advanced Space-based Solar Observatory (ASO-S)** is a mission aiming at exploring solar flares, coronal mass ejections (CMEs), solar magnetic field and their relationships. To fulfill its major scientific objectives, ASO-S has three elaborately-designed payloads onboard: the Full-disk vector MagnetoGraph (FMG), the Lyman-alpha Solar Telescope (LST), and the Hard X-ray Imager (HXI) dedicated to observe vector magnetic fields, CMEs, and flares, respectively. Beside the scientific objectives, we have an operational objective to observe solar eruptions and magnetic field for making related space weather forecasts. More specifically, we have set a priority for the downlink of CME data observed by LST, and will distribute those data to different space weather prediction centers in China within 2 h once the Science Operation and Data Center (SODC) of ASO-S receive the data. After data downlink and archiving, different automatic detection, tracking, and cataloging procedures are planned to run for the most critical solar eruptive features. On the other hand, based on the distributed and downloaded data, different space weather prediction centers are to activate their forecast systems for the ASO-S observed solar eruption events. Our particular interests are currently focused on nowcast of different eruption events, prediction of CME arrivals, forecast of solar flares and the onset of solar eruptions. We are also working on further forecast potentials using the ASO-S data to make contributions to other possible important issues of space weather.

## **On the error analyses of polarization measurements of the white-light coronagraph aboard ASO-S**

Li [Feng](#), [Hui Li](#), [Bernd Inhester](#), [Bo Chen](#), [Beili Ying](#), [Lei Lu](#), [Weiqun Gan](#)

Research in Astron. Astrophys. **2018**

<https://arxiv.org/pdf/1810.13003.pdf>

The Advanced Space-based Solar Observatory (ASO-S) mission aims to explore two most spectacular eruptions in the Sun: solar flares and coronal mass ejections (CMEs), and their magnetism. For the studies of CMEs, the payload Lyman-alpha Solar Telescope (LST) has been proposed. It includes a traditional white-light coronagraph and a Lyman-alpha coronagraph which opens a new window to CME observations. Polarization measurements taken by white-light coronagraphs are crucial to derive fundamental physical parameters of CMEs. To make such measurements, there are two options of Stokes polarimeter which have been used by existing white-light coronagraphs for space missions. One uses a single or triple linear polarizers, the other involves both a half-wave plate and a linear polarizer. We find that the former option subjects to less uncertainty in the derived Stokes vector propagated from detector noise. The latter option involves two plates which are prone to internal reflections and may have a reduced transmission factor. Therefore, the former option is adopted as our Stokes polarimeter scheme for LST. Based on the parameters of the intended linear polarizer(s) colorPol provided by CODIXX and the half-wave plate 2-APW-L2-012C by Altechna, it is further shown that the imperfect maximum transmittance of the polarizer significantly increases the variance amplification of Stokes vector by at least about 50% when compared with the ideal case. The relative errors of Stokes vector caused by the imperfection of colorPol polarizer and the uncertainty due to the polarizer assembling in the telescope are estimated to be about 5%. Among the considered parameters, we find that the dominant error comes from the uncertainty in the maximum transmittance of the polarizer.

## **Why does the apparent mass of a coronal mass ejection increase?**

Li [Feng](#), Yuming Wang, [Fang Shen](#), [Chenglong Shen](#), [Bernd Inhester](#), [Lei Lu](#), [Weiqun Gan](#)

ApJ **812** 70 **2015**

<http://arxiv.org/pdf/1509.02246v1.pdf>

Mass is one of the most fundamental parameters characterizing the dynamics of a coronal mass ejection (CME). It has been found that CME apparent mass measured from the brightness enhancement in coronagraph images shows an increasing trend during its evolution in the corona. However, the physics behind it is not clear. Does the apparent mass gain come from the mass outflow from the dimming regions in the low corona, or from the pileup of the solar wind plasma around the CME when it propagates outwards from the Sun? We analyzed the mass evolution of six CME events. Their mass can increase by a factor of 1.6 to 3.2 from 4 to 15 Rs in the field of view (FOV) of the coronagraph on board the Solar Terrestrial Relations Observatory (STEREO). Over the distance about 7 to 15 Rs, where the coronagraph occulting effect can be negligible, the mass can increase by a factor of 1.3 to 1.7. We adopted the 'snow-plough' model to calculate the mass contribution of the piled-up solar wind in the height range from about 7 to 15 Rs. For 2/3 of the events, the solar wind pileup is not sufficient to explain the measured mass increase. In the height range from about 7 to 15 Rs, the ratio of the modeled to the measured mass increase is roughly larger than 0.55. Although the ratios are believed to be overestimated, the result gives evidence that the solar wind pileup probably makes a non-negligible contribution to the mass increase. It is not clear yet whether the solar wind pileup is a major contributor to the final mass derived from coronagraph observations. However, our study suggests that the solar wind pileup plays increasingly important role in the mass increase as a CME moves further away from the Sun.

**2010-02-12, 2010-04-03, 2011-04-17, 2011-06-21, 2011-08-03, 2012-02-23**

## Radial Flow Pattern of a Slow CME

Li **Feng**, Bernd Inhester, Weiqun Gan

ApJ **805** 113 **2015**

<http://arxiv.org/pdf/1503.08502v1.pdf>

Height-time plots of the leading edge of coronal mass ejections (CME) have often been used to study CME kinematics. We propose a new method to analyze the CME kinematics in more detail by determining the radial mass transport process throughout the entire CME. Thus our method is able to estimate not only the speed of the CME front but also the radial flow speed inside the CME. We have applied the method to a slow CME with an average leading edge speed about  $480 \text{ km s}^{-1}$ . In the Lagrangian frame, the speed of the individual CME mass elements stay almost constant within 2 and 15 RS, the range over which we analyzed the CME. Hence we have no evidence of net radial forces acting on parts of the CME in this range nor of a pile-up of mass ahead of the CME. We find evidence that the leading edge trajectory obtained by tie-pointing may gradually lag behind the Lagrangian front-side trajectories derived from our analysis. Our results also allow a much more precise estimate of the CME energy. Compared with conventional estimates using the CME total mass and leading-edge motion, we find that the latter may overestimate the kinetic energy and the gravitational potential energy. **November 10 2010**

## MAGNETIC ENERGY PARTITION BETWEEN THE CORONAL MASS EJECTION AND FLARE FROM AR 11283

L. **Feng**<sup>1,2</sup>, T. Wiegmann<sup>2</sup>, Y. Su<sup>3</sup>, B. Inhester<sup>2</sup>, Y. P. Li<sup>1</sup>, X. D. Sun<sup>4</sup>, and W. Q. Gan

**2013** ApJ **765** 37

On **2011 September 6**, an X-class flare and a halo coronal mass ejection (CME) were observed from Earth erupting from the same active region AR 11283. The magnetic energy partition between them has been investigated. SDO/HMI vector magnetograms were used to obtain the coronal magnetic field using the nonlinear force-free field (NLFFF) extrapolation method. The free magnetic energies before and after the flare were calculated to estimate the released energy available to power the flare and the CME. For the flare energetics, thermal and nonthermal energies were derived using the RHESSI and GOES data. To obtain the radiative output, SDO/EVE data in the 0.1-37 nm waveband were utilized. We have reconstructed the three-dimensional (3D) periphery of the CME from the coronagraph images observed by STEREO-A, B, and SOHO. The mass calculations were then based on a more precise Thomson-scattering geometry. The subsequent estimate of the kinetic and potential energies of the CME took advantage of the more accurate mass, and the height and speed in a 3D frame. The released free magnetic energy resulting from the NLFFF model is about  $6.4 \times 10^{31}$  erg, which has a possible upper limit of  $1.8 \times 10^{32}$  erg. The thermal and nonthermal energies are lower than the radiative output of  $2.2 \times 10^{31}$  erg from SDO/EVE for this event. The total radiation covering the whole solar spectrum is probably a few times larger. The sum of the kinetic and potential energy of the CME could go up to  $6.5 \times 10^{31}$  erg. Therefore, the free energy is able to power the flare and the CME in AR 11283. Within the uncertainty, the flare and the CME may consume a similar amount of free energy.

## Comparisons of CME Morphological Characteristics Derived from Five 3D Reconstruction Methods

L. **Feng**<sup>1, 2</sup>, B. Inhester<sup>2</sup> and M. Mierla

Solar Phys., January **2013**, Volume 282, Issue 1, pp 221-238; **File**

We compare different methods to reconstruct three-dimensional (3D) coronal mass ejection (CME) morphology. The explored methods include geometric localisation, mask fitting, forward modelling, polarisation ratio, and local correlation tracking plus triangulation. These five methods are applied to the same CME event that occurred on **7 August 2010**. Their corresponding results are presented and compared, especially in their propagation direction and spatial extent in 3D. We find that the mask fitting and geometric localisation methods produce consistent results. Reconstructions including three-view observations are more precise than reconstructions done with only two views. Compared to the forward modelling method, in which an a priori shape of the CME geometry is assumed, the mask fitting has more flexibility. The polarisation ratio method makes use of the Thomson scattering geometry. We find that spatially the 3D CME derived from the mask fitting lies mostly in the overlap region obtained with the polarisation method using data from STEREO. In addition, the mask fitting can help resolve the front/back ambiguity inherent in the polarisation ratio method. However, the local correlation tracking plus triangulation did not show consistent results with the other four methods. This method performed poorly, primarily because the two STEREO spacecraft had a large angular separation. Under these circumstances, it is difficult to identify points taken from independent images that correspond to the same physical feature. Excluding the local correlation tracking method, the latitude of the CME's centre of gravity derived from the other methods deviates within  $1^\circ$ , and the longitude differs within  $19^\circ$ .

## RADIO SIGNATURES OF CORONAL-MASS-EJECTION-STREAMER INTERACTION AND SOURCE DIAGNOSTICS OF TYPE II RADIO BURST

S. W. **Feng**, Y. Chen, X. L. Kong, G. Li, H. Q. Song, X. S. Feng, and Ying Liu

**2012** ApJ **753** 21, **File**

It has been suggested that type II radio bursts are due to energetic electrons accelerated at coronal shocks. Radio observations, however, have poor or no spatial resolutions to pinpoint the exact acceleration locations of these electrons.

In this paper, we discuss a promising approach to infer the electron acceleration location by combining radio and white light observations. The key assumption is to relate specific morphological features (e.g., spectral bumps) of the dynamic spectra of type II radio bursts to imaging features (e.g., coronal mass ejection (CME) going into a streamer) along the CME (and its driven shock) propagation. In this study, we examine the CME-streamer interaction for the solar eruption dated on **2003 November 1**. The presence of spectral bump in the relevant type II radio burst is identified, which is interpreted as a natural result of the shock-radio-emitting region entering the dense streamer structure. The study is useful for further determinations of the location of type II radio burst and the associated electron acceleration by CME-driven shock.

## **MORPHOLOGICAL EVOLUTION OF A THREE-DIMENSIONAL CORONAL MASS EJECTION CLOUD RECONSTRUCTED FROM THREE VIEWPOINTS**

L. Feng<sup>1,2</sup>, B. Inhester<sup>2</sup>, Y. Wei<sup>2</sup>, W. Q. Gan<sup>1</sup>, T. L. Zhang<sup>3</sup>, and M. Y. Wang

**2012 ApJ 751 18**

The propagation properties of coronal mass ejections (CMEs) are crucial to predict its geomagnetic effect. A newly developed three-dimensional (3D) mask fitting reconstruction method using coronagraph images from three viewpoints has been described and applied to the CME ejected on **2010 August 7**. The CME's 3D localization, real shape, and morphological evolution are presented. Due to its interaction with the ambient solar wind, the morphology of this CME changed significantly in the early phase of evolution. Two hours after its initiation, it was expanding almost self-similarly. The CME's 3D localization is quite helpful to link remote sensing observations to in situ measurements. The investigated CME was propagating to Venus with its flank just touching STEREO B. Its corresponding interplanetary CME in the interplanetary space shows a possible signature of a magnetic cloud with a preceding shock in Venus Express (VEX) observations, while from STEREO B only a shock is observed. We have calculated three principal axes for the reconstructed 3D CME cloud. The orientation of the major axis is, in general, consistent with the orientation of a filament (polarity inversion line) observed by SDO/AIA and SDO/HMI. The flux rope axis derived by the Minimal Variance Analysis from VEX indicates a radial-directed axis orientation. It might be that locally only the leg of the flux rope passed through VEX. The height and speed profiles from the Sun to Venus are obtained. We find that the CME speed possibly had been adjusted to the speed of the ambient solar wind flow after leaving the COR2 field of view and before arriving at Venus. A southward deflection of the CME from the source region is found from the trajectory of the CME geometric center. We attribute it to the influence of the coronal hole where the fast solar wind emanated from.

## **Streamer Wave Events Observed in Solar Cycle 23**

S. W. Feng, Y. Chen, B. Li, H. Q. Song, X. L. Kong, L. D. Xia and X. S. Feng

*Solar Phys* (2011) 272:119–136, **File**

In this paper we conduct a data survey searching for well-defined streamer wave events observed by the Large Angle and Spectrometric Coronagraph (LASCO) on-board the Solar and Heliospheric Observatory (SOHO) throughout Solar Cycle 23. As a result, eight candidate events are found and presented here. We compare different events and find that in most of them the driving CMEs' ejecta are characterized by a high speed and a wide angular span, and the CME-streamer interactions occur generally along the flank of the streamer structure at an altitude no higher than the bottom of the field of view of LASCO C2. In addition, all front-side CMEs have accompanying flares. These common observational features shed light on the excitation conditions of streamer wave events.

We also conduct a further analysis on one specific streamer wave event on 5 June 2003. The heliocentric distances of four wave troughs/crests at various exposure times are determined; they are then used to deduce the wave properties like period, wavelength, and phase speeds. It is found that both the period and wavelength increase gradually with the wave propagation along the streamer plasma sheet, and the phase speed of the preceding wave is generally faster than that of the trailing ones. The associated coronal seismological study yields the radial profiles of the Alfvén speed and magnetic field strength in the region surrounding the streamer plasma sheet. Both quantities show a general declining trend with time. This is interpreted as an observational manifestation of the recovery process of the CME-disturbed corona. It is also found that the Alfvénic critical point is at about  $10 R_{\odot}$ , where the flow speed, which equals the Alfvén speed, is  $\sim 200 \text{ km s}^{-1}$ .

## **Evolution of a Halo Coronal Mass Ejection of **March 09, 2012** Associated with EUV Waves**

**Fernandes**, F. C. R.; Sampaio, L. S.; Cunha-Silva, R. D.

Ground-based Solar Observations in the Space Instrumentation Era

ASP Conference Series, Vol. 504, p. 67, **2016**

<http://aspbooks.org/publications/504/067.pdf>

In this work we analyse the evolution of a halo coronal mass ejection (CME) observed on **March 09, 2012**, exhibiting a velocity of  $950 \text{ ms}^{-1}$ . The EUV images recorded by the Extreme Ultraviolet Imager (EUVI), aboard STEREO show evidence of a shockwave produced by the expansion of the CME. The event was also associated with an M.6 class X-ray solar flare, starting at 03:22 UT, peaking at 03:53 UT and ending at 04:18 UT. Type II radio emission was also recorded in the metric wavelength (100–250 MHz) by e-Callisto spectrographs. The following spectrum-temporal

parameters of type II burst were estimated: starting frequency of  $(220 \pm 5)$  MHz, ending frequency of  $(170 \pm 5)$  MHz, frequency bandwidth of 34.3 MHz and starting and ending time of about 03:41:51 UT and 03:46:49 UT, respectively.

## **Development of Torus and Kink Instabilities in Eruptive Prominences**

Boris **Filippov**

2024 ApJ 977 259

<https://iopscience.iop.org/article/10.3847/1538-4357/ad95fe/pdf>

Several filament eruptions with pronounced writhing of the axis of the structure are analyzed. Initially, smooth arches of eruptive filaments are transformed into large-scale helical structures with at least one complete turn due to the development of kink instability. However, the initiation of the eruptions seems to be caused not by the kink instability but by catastrophic loss of equilibrium or torus instability. Calculations of the decay index of the coronal potential magnetic field indicate that the studied filaments began to rise rapidly at heights where the decay index was close to unity, the threshold for the catastrophic loss of equilibrium of straight flux ropes. Although it is often assumed that the kink instability precedes the subsequent torus instability leading to a full eruption, these examples testify to the possibility of the reverse order of the eruption development. **2012 May 22. 2014 June 19, 2021 May 9**

## **Influence of the Geometrical Shape of a Prominence and Structure of the Coronal Magnetic Field on the Probability of Eruption, Flare Development, and Coronal Mass Ejection.**

**Filippov**, B.P.

*Geomagn. Aeron.* **64**, 11–18 (2024).

<https://doi.org/10.1134/S0016793223600777>

The equilibrium conditions of a magnetic flux rope containing a prominence depend on the properties of the surrounding magnetic field of the corona and geometry of the flux rope itself. The eruption of a prominence is usually associated with a loss of stability in the external field upon reaching a height above which the field decay index exceeds the critical value for eruptive instability development. For flux ropes with an axis in the form of a straight line or a circle, the critical value of the field decay index is 1–1.5. By extrapolating the magnetic field in the corona from field measurements in the photosphere, it would be possible to predict the probability of eruption of a particular prominence. However, taking into account the fact that the ends of the magnetic flux rope are rooted in the photosphere and remain fixed because they are frozen in the photospheric plasma, significantly affects the critical value of the index and complicates the forecasting problem. If the magnetic flux rope retains the shape of a torus segment in its evolution, then the critical value of the field decay index for its vertex depends on what part of the torus it constitutes, being minimal for approximately half the torus and having a value significantly less than unity. How the eruption of a flux rope will develop after loss of equilibrium also depends on what part of the complete torus it constitutes at the time of onset of eruption. Shorter flux ropes are accelerated very energetically, but briefly, generating stronger electric induction fields that trigger flare processes. However, the terminal velocity that a short flux rope can achieve during acceleration is less than that of longer ropes that accelerate less intensely but for a longer time. The induction effects of the latter are less pronounced, so that they are capable of producing only weak flarelike manifestations. Thus, the eruption of a short prominence, which has gained a relatively low velocity, can be stopped at a certain height in the corona without generating a coronal mass ejection, but such a “failed eruption” contributes to the development of flare phenomena. Conversely, eruptions of long prominences more often lead to coronal mass ejections and weak flare manifestations.

## **High-altitude Spider-type Prominence above the Magnetic Null Point**

Boris **Filippov**<sup>1</sup>

2023 ApJ 958 184

<https://iopscience.iop.org/article/10.3847/1538-4357/ad02f9/pdf>

Rather unique observations of a high-altitude spider-type prominence in 2023 February are presented. The prominence or corresponding filament on the disk was not visible all the time but could appear and disappear in the course of a particular day. However, it persisted during the whole half of a solar rotation, being observable from day to day starting from the east limb of the Sun to the west limb. We show that the prominence was located in sagged coronal field lines just above a coronal magnetic null point. The presence of the null point and magnetic dips above it is confirmed by calculations of the potential magnetic field. The mass of the prominence apparently was appearing due to the condensation of hot coronal plasma after several eruptions that occurred in an active-region complex where the prominence was located. The prominence material flowed down along widely spread large coronal loops as coronal rain and was sometimes swept away by subsequent eruptions. **2023 February 7-21, 15**

## **Rising of a magnetic null point in the wake of an erupting flux rope**

**Filippov**

Monthly Notices of the Royal Astronomical Society, Volume 512, Issue 1, May 2022, Pages 1357–1364,

<https://doi.org/10.1093/mnras/stac575>

Arcades of flare loops rise, slowing down in the wake of eruptive prominences. They lag significantly from the top of prominences and do not reach too great heights in the corona. It is widely accepted that their evolution is governed by the limited reconnection rate in the current sheet developed below the eruptive prominence. We suggest that the shape

of eruptive prominences may be the determining factor in the ascension of the arcade. Arcade deceleration and their limited heights are analysed in the frame of a simple rectangular circuit model representing prominence eruption. A null point that appears below the rising electric current does not follow it to a great height but is detained by the influence of the field created by currents flowing along the vertical segments, 'legs', of the rectangular contour. As a result, the flare loops are able to reach only limited heights even with fast reconnection in a small current sheet.

## Dependence of the eruptive filaments dynamics on their length

**B. Filippov**

MNRAS, Volume 509, Issue 4, February 2022, Pages 5713–5720,

<https://doi.org/10.1093/mnras/stab3403>

We analyse numerically a model of eruption of a thin flux rope with the endpoints frozen in the photosphere. The flux rope is assumed to maintain a shape of partial current-carrying torus staying initially in equilibrium in the external dipolar magnetic field. There is an unstable equilibrium point, which can be reached by slow evolution of the system, and then a catastrophic loss of equilibrium and flux-rope eruption follow. Parameters of eruption, such as acceleration, velocity, electric field generated at the null point, depend in particular on the initial length of the flux rope or in other words on the endpoints separation. Analysis of the sample of 30 eruptive events observed on the Sun in the period from 2012 to 2016 showed that the eruptions of shorter filaments are more often associated with flaring phenomena and not followed by coronal mass ejections (CMEs). Eruptions of most lengthy filaments are followed as a rule by CMEs but are much rarely associated with flares.

## Critical decay index for eruptions of 'short' filaments

**Boris Filippov**

MNRAS Volume 503, Issue 3, May 2021, Pages 3926–3930,

<https://doi.org/10.1093/mnras/stab756>

<https://arxiv.org/ftp/arxiv/papers/2103/2103.07231.pdf>

<https://academic.oup.com/mnras/article-pdf/503/3/3926/36900760/stab756.pdf>

Model of a partial current-carrying torus loop anchored to the photosphere is analyzed. Conditions of the catastrophic loss of equilibrium are considered and corresponding value of the critical decay index of external magnetic field is found. Taking into account line-tying conditions leads to non-monotonous dependence of the critical decay index on the height of the apex and length of the flux rope (its endpoints separation). For relatively short flux ropes, the critical decay index is significantly lower than unity, which is in contrast to widespread models with the typical critical decay index above unity. The steep decrease of the critical index with height at low heights is due to the sharp increase of the curvature of the flux-rope axis that transforms from a nearly straight line to a crescent.

## Mass of prominences experiencing failed eruptions

**B. Filippov**

PASAustralia 2021

<https://arxiv.org/pdf/2103.03634.pdf>

A number of solar filaments/prominences demonstrate failed eruptions, when a filament at first suddenly starts to ascend and then decelerates and stops at some greater height in the corona. The mechanism of the termination of eruptions is not clear yet. One of the confining forces able to stop the eruption is the gravity force. Using a simple model of a partial current-carrying torus loop anchored to the photosphere and photospheric magnetic field measurements as the boundary condition for the potential magnetic field extrapolation into the corona, we estimated masses of 15 eruptive filaments. The values of the filament mass show rather wide distribution in the range of  $4 \times 10^{15}$  -  $270 \times 10^{16}$ g. Masses of the most of filaments, laying in the middle of the range, are in accordance with estimations made earlier on the basis of spectroscopic and white-light observations. **2014 March 20**  
Table 1 and 2 Failed filament eruptions (2012-2016)

## Failed prominence eruptions near 24 cycle maximum

**B. Filippov**

MNRAS Volume 494, Issue 2, Pages 2166–2177, 2020

<https://arxiv.org/pdf/2003.12988.pdf>

<https://doi.org/10.1093/mnras/staa896>

We analyze 16 failed filament eruptions observed near 24 solar cycle maximum from May 2013 to July 2014. No significant rotation of filament spines is observed during the ascent in all studied failed eruptions, which does not support kink-instability mechanism of triggering the eruptions. We calculate potential magnetic field distributions in the corona above the initial locations of the filaments to study their height dependence. In seven events, the vertical profiles of the decay index  $n$  are monotonic. The other nine events occur in the regions with the switchback or saddle-like  $n$ -profiles. The direction of the horizontal field near the saddle bottom is turned through more than  $100^\circ$  relative its direction at the initial filament position, which reveals the quadrupolar magnetic configuration with null points in these regions. The eruptive filaments stop above the null points where the total Lorenz force is directed upward. The most reasonable force that can terminate filament ascending and balance the Lorenz force seems the gravity. **2014 March 22, 2014 March 28**

**Table 1.** Failed filament eruptions in the quadrupolar magnetic configuration

**Table 2.** Failed filament eruptions in the dipolar magnetic configuration



## **Solar Total Eclipse of 21 August 2017: Study of the Inner Corona Dynamical Events Leading to a CME**

Boris [Filippov](#), [Serge Koutchmy](#), [Nicolas Lefaudeux](#)

Solar Phys. 295:24 2020

<https://arxiv.org/pdf/2001.10203.pdf>

[sci-hub.si/10.1007/s11207-020-1586-4](https://sci-hub.si/10.1007/s11207-020-1586-4)

Total solar eclipse (TSE) coronal large and small scale events were reported in the historical literature but a definite synoptic coverage was missing for studying a relationship with the more general magnetic context of the solar-disk. We here analyze temporal changes in the solar corona before, during, and after the total solar eclipse on 21 August 2017 from a set of ground-based and of space-borne observations. High-quality ground-based white-light (W-L) observations and a deep image processing allow us to reveal these changes for the first time with a fraction of a one-minute time resolution. Displacements of a number of fine coronal features were measured for the first time at these small radial distances, using a diffraction limited instrument at a single site. The comparison with space-based observations, including observations from the *Solar Terrestrial Relations Observatory* (STEREO) mission, showed that the features belong to a slow coronal mass ejection (CME) propagating through the corona with the nearly constant speed of 250 km/s. Our TSE images provide the same typical velocity as measured at a distance of one solar radius from the surface. The event was initiated by coronal dynamics manifested by a prominence eruption that started just before the eclipse observations and an ascent of a U-shaped structure visible in the AIA 171 Å channel, which we assume as the lower part of a coronal cavity. The prominence material was observed draining down towards the chromosphere along the prominence arch. While the prominence disappears in the STEREO-A field-of-view at the height of about 6' above the limb, the corresponding flux rope seems to continue towards the outer corona and produces the slow CME with turbulent motion. The overall mass of the moving features is evaluated based on absolute photometrical data extracted from our best W-L eclipse image.

## **Mass ejections from the solar atmosphere**

**Review**

B P [Filippov](#)1

[Physics-Uspekhi](#), Volume 62, 847-864 2019

Uspekhi Fizicheskikh Nauk 189 (9) 905 - 924 (2019)

<https://doi.org/10.3367/UFNr.2018.10.038467>

<https://sci-hub.ru/10.3367/UFNe.2018.10.038467>

Coronal mass ejections are the largest-scale eruptive phenomenon in the solar system. Their drastic effect on space weather is a reason for the significant interest in observing, simulating, and forecasting these events. We describe the main features of mass ejections from the solar atmosphere, their physical parameters and frequency, and its dependence on the solar cycle phase. We consider potential sources of ejections in the solar atmosphere and magnetic field configurations wherein the energy needed for sudden explosive acceleration of large masses of matter can be stored. The main instabilities of coronal structures that lead to the triggering and development of eruptive processes are analyzed. We show that coronal mass ejections are related to other manifestations of solar activity, while the eruptive processes observed using various techniques in various layer of the solar atmosphere and interplanetary space are the same phenomenon. We discuss indicators of the Sun's pre-eruptive regions approaching a catastrophe and the options to use them to forecast eruptions and space weather disturbances.

## **Difference of source regions between fast and slow coronal mass ejections**

B. [Filippov](#)

PASAustralia 2019

<https://arxiv.org/pdf/1904.04060.pdf>

Coronal mass ejections (CMEs) are tightly related to filament eruptions and usually are their continuation in the upper solar corona. It is common practice to divide all observed CMEs into fast and slow ones. Fast CMEs usually follow eruptive events in active regions near big sunspot groups and associated with major solar flares. Slow CMEs are more related to eruptions of quiescent prominences located far from active regions. We analyze ten eruptive events with particular attention to the events on **2013 September 29** and on **2016 January 26**, one of which was associated with a fast CME, while another was followed by a slow CME. We estimated the initial store of free magnetic energy in the two regions and show the resemblance of pre-eruptive situations. The difference of late behaviour of the two eruptive prominences is a consequence of the different structure of magnetic field above the filaments. We estimated this structure on the basis of potential magnetic field calculations. Analysis of other eight events confirmed that all fast CMEs originate in regions with rapidly changing with height value and direction of coronal magnetic field.

## **Two Scenarios for the Eruption of Magnetic Flux Ropes in the Solar Atmosphere**

[Filippov](#), B.P., [Den, O.E.](#)

[Astronomy Reports](#) 62(5), c. 359-365 2018

<https://link.springer.com/content/pdf/10.1134%2FS1063772918050037.pdf>

Eruptions of material from lower to upper layers of the solar atmosphere can be divided into two classes. The first class of eruptions maintain their (usually loop-like) shapes as they increase in size (eruptive prominences), or display a sudden expansion of fairly shapeless clumps of plasma in all directions (flare sprays). The second class refers to narrow, collimated flows of plasma on various scales (spicules, surges, jets). It is obvious that the magnetic configurations in

which these phenomena develop differ: for the first class they form closed structures that confine the plasma, and in the second class open structures directing flows of plasma in a particular direction, as a rule, upward. At the same time, the mechanisms initiating eruptions of both classes could be similar, or even practically identical. This mechanism could be instability of twisted magnetic tubes (flux ropes), leading to different consequences under different conditions. It is shown that the results of eruptive instability are determined by the ratio of the scales of the magnetic flux rope and the confining coronal field, and also by the configuration of the ambient magnetic field in the corona. Observations of both types of eruptions are analyzed, the conditions for their development are examined, and phenomenological models are proposed. **April 13, 2010, January 27, 2012, April 10–11, 2013**

## Two-step solar filament eruptions

Boris **Filippov**

MNRAS **2017**

<https://arxiv.org/pdf/1712.08173.pdf>

Coronal mass ejections (CMEs) are closely related to eruptive filaments and usually are the continuation of the same eruptive process into the upper corona. There are failed filament eruptions when a filament decelerates and stops at some greater height in the corona. Sometimes the filament after several hours starts to rise again and develops into the successful eruption with a CME formation. We propose a simple model for the interpretation of such two-step eruptions in terms of equilibrium of a flux rope in a two-scale ambient magnetic field. The eruption is caused by a slow decrease of the holding magnetic field. The presence of two critical heights for the initiation of the flux-rope vertical instability allows the flux rope to stay after the first jump some time in a metastable equilibrium near the second critical height. If the decrease of the ambient field continues, the next eruption step follows. **2011 October 18**

## Formation of a rotating jet during the filament eruption on 10-11 April 2013

B. **Filippov**, A. K. Srivastava, B. N. Dwivedi, S. Masson, G. Aulanier, N. C. Joshi, W. Uddin

MNRAS **2015**

<http://arxiv.org/pdf/1505.01615v1.pdf>

We analyze multi-wavelength and multi-viewpoint observations of a helically twisted plasma jet formed during a confined filament eruption on **10-11 April 2013**. Given a rather large scale event with its high spatial and temporal resolution observations, it allows us to clearly understand some new physical details about the formation and triggering mechanism of twisting jet. We identify a pre-existing flux rope associated with a sinistral filament, which was observed several days before the event. The confined eruption of the filament within a null point topology, also known as an Eiffel tower (or inverted-Y) magnetic field configuration results in the formation of a twisted jet after the magnetic reconnection near a null point. The sign of helicity in the jet is found to be the same as that of the sign of helicity in the filament. Untwisting motion of the reconnected magnetic field lines gives rise to the accelerating plasma along the jet axis. The event clearly shows the twist injection from the pre-eruptive magnetic field to the jet.

## Solar Magnetic Flux Ropes

**Review**

Boris **Filippov**, Olesya Martsenyuk, Abhishek K. Srivastava, and Wahab Uddin

Journal of Astrophysics & Astronomy, **2015**

<http://arxiv.org/ftp/arxiv/papers/1501/1501.02562.pdf>

The most probable initial magnetic configuration of a CME is a flux rope consisting of twisted field lines which fill the whole volume of a dark coronal cavity. The flux ropes can be in stable equilibrium in the coronal magnetic field for weeks and even months, but suddenly they lose their stability and erupt with high speed. Their transition to the unstable phase depends on the parameters of the flux rope (i.e., total electric current, twist, mass loading etc.), as well as on the properties of the ambient coronal magnetic field. One of the major governing factors is the vertical gradient of the coronal magnetic field which is estimated as decay index ( $n$ ). Cold dense prominence material can be collected in the lower parts of the helical flux tubes. Filaments are therefore good tracers of the flux ropes in the corona, which become visible long before the beginning of the eruption. The perspectives of the filament eruptions and following CMEs can be estimated by the comparison of observed filament heights with calculated decay index distributions. The present paper reviews the formation of magnetic flux ropes, their stable and unstable phases, eruption conditions, and also discusses their physical implications in the solar corona. **18.08.1995, June 17, 1998, 23.12.1998, 08.10.1999, 19.12.2000, 26.05.2001, 30.05.2001, 24.07.2001, August 1, 2001, 18.08.2001, 31.08.2001, 21.09.2001, 02.11.2002, 04.08.2004, 28.02.2005, 25 September 2011, 10-12 November 2001, 3-4 Aug 2012**

## Effects of coronal mass ejections on distant coronal streamers

B. P. **Filippov**, P. Kayshap, A. K. Srivastava, O. V. Martsenyuk

Astronomy Reports, August **2014**, Volume 58, Issue 8, pp 578-586

Astronomicheskii Zhurnal, **2014**, Vol. 91, No. 8, pp. 668–676.

<http://arxiv.org/pdf/1408.4324v1.pdf>

The effects of a large coronal mass ejection (CME) on a solar coronal streamer located roughly  $90^\circ$  from the main direction of the CME propagation observed on **January 2, 2012** by the SOHO/LASCO coronagraph are analyzed. Radial coronal streamers undergo some bending when CMEs pass through the corona, even at large angular distances from the streamers. The phenomenon resembles a bending wave traveling along the streamer. Some researchers interpret these phenomena as the effects of traveling shocks generated by rapid CMEs, while others suggest they are waves excited inside the streamers by external impacts. The analysis presented here did not find convincing arguments

in favor of either of these interpretations. It is concluded that the streamer behavior results from the effect of the magnetic field of a moving magnetic flux rope associated with the coronal ejection. The motion of the large-scale magnetic flux rope away from the Sun changes the surrounding magnetic field lines in the corona, and these changes resemble the half-period of a wave running along the streamer.

## **Filament eruption with apparent reshuffle of endpoints**

Boris [Filippov](#)

MNRAS, 2014

<http://arxiv.org/pdf/1405.5784v1.pdf>

Filament eruption on **30 April - 1 May 2010**, which shows the reconnection of one filament leg with a region far away from its initial position, is analyzed. Observations from three viewpoints are used for as precise as possible measurements of endpoint coordinates. The northern leg of the erupting prominence loop 'jumps' laterally to the latitude lower than the latitude of the originally southern endpoint. Thus, the endpoints reshuffled their positions in the limb view. Although this behaviour could be interpreted as the asymmetric zipping-like eruption, it does not look very likely. It seems more likely to be reconnection of the flux-rope field lines in its northern leg with ambient coronal magnetic field lines rooted in a quiet region far from the filament. From calculations of coronal potential magnetic field, we found that the filament before the eruption was stable for vertical displacements, but was liable to violation of the horizontal equilibrium. This is unusual initiation of an eruption with combination of initial horizontal and vertical flux-rope displacements showing a new unexpected possibility for the start of an eruptive event.

## **Filament eruption on 2010 October 21 from three viewpoints**

Boris [Filippov](#)

E-print, June 2013, [File](#); ApJ

A filament eruption on **2010 October 21** observed from three different viewpoints by the Solar Terrestrial Relations Observatory (STEREO) and the Solar Dynamic Observatory (SDO) is analyzed with invoking also data from the Solar and Heliospheric Observatory (SOHO) and the Kanzelhöhe Solar Observatory. The position of the filament just before the eruption at the central meridian not far from the center of the solar disk was favorable for photospheric magnetic field measurements in the area below the filament. Because of this, we were able to calculate with high precision the distribution of the coronal potential magnetic field near the filament. We found that the filament began to erupt when it approached the height in the corona where the magnetic field decay index was greater than one. We determined also that during the initial stage of the eruption the filament moved along the magnetic neutral surface

## **Formation of a White-Light Jet Within a Quadrupolar Magnetic Configuration**

Boris [Filippov](#) · Serge Koutchmy · Ehsan Tavabi

Solar Phys (2013) 286:143–156

We analyze multi-wavelength and multi-viewpoint observations of a large-scale event viewed on **7 April 2011**, originating from an active-region complex. The activity leads to a white-light jet being formed in the outer corona. The topology and evolution of the coronal structures were imaged in high resolution using the Atmospheric Imaging Assembly (AIA) onboard the Solar Dynamics Observatory (SDO). In addition, large field-of-view images of the corona were obtained using the Sun Watcher using Active Pixel System detector and Image Processing (SWAP) telescope onboard the PROject for Onboard Autonomy (PROBA2) microsatellite, providing evidence for the connectivity of the coronal structures with outer coronal features that were imaged with the Large Angle Spectrometric Coronagraph (LASCO) C2 on the Solar and Heliospheric Observatory (SOHO). The data sets reveal an Eiffel-tower type jet configuration extending into a narrow jet in the outer corona. The event starts from the growth of a dark area in the central part of the structure. The darkening was also observed in projection on the disk by the Solar TERrestrial RELations Observatory-Ahead (STEREO-A) spacecraft from a different point of view. We assume that the dark volume in the corona descends from a coronal cavity of a flux rope that moved up higher in the corona but still failed to erupt. The quadrupolar magnetic configuration corresponds to a saddle-like shape of the dark volume and provides a possibility for the plasma to escape along the open field lines into the outer corona, forming the white-light jet.

## **Electric Current Equilibrium in the Corona**

Boris [Filippov](#)

Solar Physics, April 2013, Volume 283, Issue 2, pp 401-411

A hyperbolic flux-tube configuration containing a null point below the flux rope is considered as a pre-eruptive state of coronal mass ejections that start simultaneously with flares. We demonstrate that this configuration is unstable and cannot exist for a long time in the solar corona. The inference follows from general equilibrium conditions and from analyzing simple models of the flux-rope equilibrium. A direct consequence of the stable flux-rope equilibrium in the corona are separatrices in the horizontal-field distribution in the chromosphere. They can be recognized as specific "herring-bone structures" in a chromospheric fibril pattern.

## Deflection of coronal rays by remote CMEs: shock wave or magnetic pressure?

Boris [Filippov](#)<sup>1</sup> and A.K. Srivastava<sup>2</sup>

E-print, June 2009, [File](#), Solar Phys.

We analyze five events of the interaction of coronal mass ejections (CMEs) with the remote coronal rays located up to 90° away from the CME as observed by the SOHO/LASCO C2 coronagraph. Using sequences of SOHO/LASCO C2 images, we estimate the kink propagation in the coronal rays during their interaction with the corresponding CMEs ranging from 180 to 920 km s<sup>-1</sup> within the interval of radial distances from 3 R<sub>☉</sub> to 6 R<sub>☉</sub>. We conclude that all studied events do not correspond to the expected pattern of shock wave propagation in the corona. Coronal ray deflection can be interpreted as the influence of the magnetic field of a moving flux rope related to a CME. The motion of a large-scale flux rope away from the Sun creates changes in the structure of surrounding field lines, which are similar to the kink propagation along coronal rays. The retardation of the potential should be taken into account since the flux rope moves at high speed comparable with the Alfvén speed.

## (Stellar) Coronal mass ejections and type II radio emission variability during a magnetic cycle on the solar-type star ε Eridani

[Dúalta Ó Fionnagáin](#), [Robert D. Kavanagh](#), [Aline A. Vidotto](#), [Sandra V. Jeffers](#), [Pascal Petit](#), [Stephen Marsden](#), [Julien Morin](#), [Aaron A Golden](#)

ApJ 2021

<https://arxiv.org/pdf/2111.02284.pdf>

We simulate possible stellar coronal mass ejection (CME) scenarios over the magnetic cycle of ε Eridani (18 Eridani; HD 22049). We use three separate epochs from 2008, 2011, and 2013, and estimate the radio emission frequencies associated with these events. These stellar eruptions have proven to be elusive, although a promising approach to detect and characterise these phenomena are low-frequency radio observations of potential type II bursts as CME induced shocks propagate through the stellar corona. **Stellar type II radio bursts** are expected to emit below 450 MHz, similarly to their solar counterparts. We show that the length of time these events remain above the ionospheric cutoff is not necessarily dependent on the stellar magnetic cycle, but more on the eruption location relative to the stellar magnetic field. We find that these type II bursts would remain within the frequency range of LOFAR for a maximum of 20-30 minutes post-eruption for the polar CMEs, (50 minutes for 2nd harmonics). We find evidence of slower equatorial CMEs, which result in slightly longer observable windows for the 2008 and 2013 simulations. Stellar magnetic geometry and strength has a significant effect on the detectability of these events. We place the CMEs in the context of the stellar mass-loss rate (27-48 × solar mass-loss rate), showing that they can amount to 3-50% of the stellar wind mass-loss rate for ε Eridani. Continuous monitoring of likely stellar CME candidates with low-frequency radio telescopes will be required to detect these transient events.

## Global Forces in Eruptive Solar Flares: The Lorentz Force Acting on the Solar Atmosphere and the Solar Interior

G. H. [Fisher](#), D. J. Bercik, B. T. Welsch and H. S. Hudson

Solar Physics, Volume 277, Number 1, 59-76, 2012

We compute the change in the Lorentz force integrated over the outer solar atmosphere implied by observed changes in vector magnetograms that occur during large, eruptive solar flares. This force perturbation should be balanced by an equal and opposite force perturbation acting on the solar photosphere and solar interior. The resulting expression for the estimated force change in the solar interior generalizes the earlier expression presented by Hudson, Fisher, and Welsch (Astron. Soc. Pac. CS-383, 221, 2008), providing horizontal as well as vertical force components, and provides a more accurate result for the vertical component of the perturbed force. We show that magnetic eruptions should result in the magnetic field at the photosphere becoming more horizontal, and hence should result in a downward (toward the solar interior) force change acting on the photosphere and solar interior, as recently argued from an analysis of magnetogram data by Wang and Liu (Astrophys. J. Lett. 716, L195, 2010). We suggest the existence of an observational relationship between the force change computed from changes in the vector magnetograms, the outward momentum carried by the ejecta from the flare, and the properties of the helioseismic disturbance driven by the downward force change. We use the impulse driven by the Lorentz-force change in the outer solar atmosphere to derive an upper limit to the mass of erupting plasma that can escape from the Sun. Finally, we compare the expected Lorentz-force change at the photosphere with simple estimates from flare-driven gasdynamic disturbances and from an estimate of the perturbed pressure from radiative backwarming of the photosphere in flaring conditions.

## Analysis of the helical kink stability of differently twisted magnetic flux ropes

[Marta Florido-Llinas](#), [Teresa Nieves-Chinchilla](#), [Mark G. Linton](#)

Solar Phys. 295, Article number: 118 2020

<https://arxiv.org/pdf/2007.06345.pdf>

<https://link.springer.com/content/pdf/10.1007/s11207-020-01687-z.pdf>

Magnetic flux ropes (MFRs) are usually considered to be the magnetic structure that dominates the transport of helicity from the Sun into the heliosphere. They entrain a confined plasma within a helically organized magnetic structure and are able to cause geomagnetic activity. The formation, evolution and twist distribution of MFRs are issues subject to strong debate. Although different twist profiles have been suggested so far, none of them has been thoroughly explored yet. The aim of this paper is to present a theoretical study of the conditions under which MFRs with different twist profiles are kink stable and thereby shed some light on the aforementioned discussions. The magnetic field is modeled according to the circular-cylindrical analytical flux rope model in Nieves-Chinchilla et al. (2016) as well as the Lundquist and Gold-Hoyle models, and the kink stability is analyzed with a numerical method that has been developed based on Linton, Longcope, and Fisher (1996). The results are discussed in relation to MFR rotations, magnetic forces, the reversed chirality scenario and the expansion throughout the heliosphere, among others, providing a theoretical background to improve the current understanding of the internal magnetic configuration of CMEs. The data obtained by new missions like Parker Solar Probe or Solar Orbiter will give the opportunity to explore these results and ideas by observing MFRs closer than ever to the Sun.

## **Polarimetric Reconstruction of Coronal Mass Ejections from LASCO-C2 Observations**

O. **Floyd**, P. Lamy

[Solar Physics](#) November 2019, 294:168

<https://link.springer.com/content/pdf/10.1007%2Fs11207-019-1553-0.pdf>

The three-dimensional morphology and direction of propagation of coronal mass ejections (CMEs) are essential information for identifying their source on the solar disk, for understanding the processes of their ejection and propagation in the corona, and for forecasting their possible impact with the Earth or any other objects in the solar system. The polarization of the Thomson scattering by an electron is known to provide information on its position with respect to the plane of the sky. This polarimetric technique is applied to reconstruct 15 CMEs on the basis of white-light polarized images obtained with the Large Angle Spectrometric Coronagraph (LASCO) C2, which have been extensively corrected for instrumental effects. It does provide valuable results in spite of the time delays between the three observations required to build the polarization maps. Most of these CMEs exhibit complex structures making a classification in terms of simple shapes such as arcade of loops or flux rope difficult or even questionable. Three of these CMEs benefited from multiple observations allowing us to follow their three-dimensional development as they propagated outward. All CMEs are tracked back to the solar surface and in several instances, active regions are identified as the probable sources. Finally, the projected speeds and masses derived from white-light unpolarized observations have been corrected for the projection angle to produce unbiased values. **4 November 1998, 4 January 2002, 9 July 2002, 18 July 2002, 1 August 2002, 2 August 2002, 3 August 2002, 7 August 2002, 3 June 2005, 17 January 2010, 8 March 2011, 25 October 2011, 8 December 2011, 12 January 2012, 17 September 2013, 11 May 2014**

Table 1 Parameters and properties of the 15 selected CMEs

## **The Interaction Between Coronal Mass Ejections and Streamers: A Statistical View over 15 Years (1996 – 2010)**

O. **Floyd**, P. Lamy, A. Llebaria

[Solar Physics](#), April 2014, Volume 289, Issue 4, pp 1313-1339; **File**

We report on the statistical analysis of the interaction between coronal mass ejections (CMEs) and streamers based on 15 years (from 1996 to 2010 inclusive) of observation of the solar corona with the LASCO-C2 coronagraph. We used synoptic maps and improved the method of analysis of past investigations by implementing an automatic detection of both CMEs and streamers. We identified five categories of interaction based on photometric and geometric variations between the pre- and post-CME streamers: “brightening”, “dimming”, “emergence”, “disappearance”, and “deviation”. A sixth category, “no change”, included all cases where none of the above variations is observed. A “global set” of 21 242 CMEs was considered as well as a subset of the 10 % brightest CMEs (denoted “top-ten”) and three typical periods of solar activity: minimum, intermediate, and maximum. We found that about half of the global population of CMEs are not associated with streamers, whereas 93 % of the 10 % brightest CMEs are associated. When there is a CME-streamer association, approximately 95 % of the streamers experience a change, either geometric or radiometric. The “no change” category therefore amounts to approximately 5 %, but this percentage varies from 1 – 2 % during minimum to 7 – 8 % during intermediate periods of activity; values of 3 – 5 % are recorded during maximum. Emergences and disappearances of streamers are not dominant processes; they constitute 16 – 17 % of the global set and 23 % (emergence) and 28 % (disappearance) of the “top-ten” set. Streamer deviations are observed for 57 % and 70 % of, respectively, the global set and “top-ten” CMEs. The cases of dimming and brightening are roughly equally present and each case constitutes approximately 30 – 35 % of either set, global or “top-ten”.

## **ARTEMIS II: A Second-Generation Catalog of LASCO Coronal Mass Ejections Including Mass and Kinetic Energy**

O. **Floyd**, P. Lamy, Y. Boursier, A. Llebaria

E-print, May 2013; [Solar Physics](#), November 2013, Volume 288, Issue 1, pp 269-289; **File**

The ARTEMIS-I catalog of coronal mass ejections (CMEs) was initially developed on a first generation of low-resolution synoptic maps constructed from the SOHO/LASCO-C2 images of the K-corona and resulted in an online database listing all events detected since January 1996 (Boursier et al., [Solar Phys.](#) 257, 125, 2009). A new generation

of synoptic maps with higher temporal (a factor of 1.5) and angular (a factor of 2.5) resolutions allowed us to reconsider the question of CME detection and resulted in the production of a new catalog: ARTEMIS-II. The parameters estimated for each detected CME are still the date and time of appearance, the position angle, the angular width, and (when detected at several solar distances) the global and median velocities. The new synoptic maps correct for the limited number of velocity determinations reported in the ARTEMIS-I catalog. We now determine the propagation velocity of 79 % of detected CMEs instead of 30 % in the previous version. A final major improvement is the estimation of the mass and kinetic energy of all CMEs for which we could determine the velocity, that is  $\approx 13\,000$  CMEs until December 2010. Individual comparisons of velocity determination of 23 CMEs for which a full three-dimensional kinematical solution has been published indicate that ARTEMIS-II performs extremely well except at the highest velocities, an intrinsic limitation of our method. Finally, individual comparisons of mass determination of seven CMEs for which a robust solution has been obtained from stereographic observations demonstrate the quality of the ARTEMIS-II results.

**Table**

## **X-ray Flare Associated with a Quiescent Filament Eruption and Coronal Mass Ejection**

**Foord**, Adi; Holman, Gordon D.

American Astronomical Society, AAS Meeting #225, #137.08, **2015**

To date, solar active regions are where most flares are found to occur. We present an analysis of multi-waveband observations of the large eruption of a 'quiescent' (outside of an active region) solar filament contemporaneous with X-ray emission. The eruption covers a 2-day time span, from **2013 September 29 to 2013 September 30**. The event was observed using the Reuven Ramaty High Energy Solar Spectroscopic Imager (RHESSI), the Solar Dynamics Observatory (SDO), and the Fermi Gamma-ray Space Telescope. Though not classified as a flare, the GOES class of the event was C1 and the X-ray light curves include a small impulsive-phase peak followed by a gradual-phase rise. The eruption produced a coronal mass ejection (CME) with a velocity of 1179 km/s. SDO Atmospheric Imaging Assembly (AIA) movies during the time span show that the filament lies outside any active region on the sun, and spans a length on the order of 600 arcseconds. Spatially resolved RHESSI emission during the gradual phase is found to come from an area along the post-eruption arcade, close to the westward expanding ribbon but confined to a length of only 150 arcseconds. No RHESSI emission is found along the eastward expanding ribbon. We infer the strength and geometry of the magnetic field during the eruption with the SDO Helioseismic and Magnetic Imager (HMI) and find a small ( $\sim 100$  arcseconds long) dipolar element within the filament channel that appears to be spatially correlated with the RHESSI emission. The dipolar element is observed to have magnetic field strengths as high as 1000 Gauss. The evolution of both the X-ray emission and AIA data support the notion that the flare was a consequence of magnetic reconnection between the dipole's magnetic field and the magnetic field supporting the filament. We conclude that solar eruptive events, which consist of both a flare and a CME, can occur outside active regions in association with a quiescent filament eruption if new, sufficiently strong magnetic flux emerges in the immediate area and reconnects with the filament's magnetic field.

## **CME THEORY AND MODELS**

**Review**

*Report of Working Group D*

T. G. **FORBES**<sup>1,\*</sup>, J. A. LINKER<sup>2</sup>, J. CHEN<sup>3</sup>, C. CID<sup>4</sup>, J. K. 'OTA<sup>5</sup>, M. A. LEE<sup>2</sup>, G. MANN<sup>6</sup>, Z. MIKI 'C<sup>1</sup>, M. S. POTGIETER<sup>7</sup>, J. M. SCHMIDT<sup>8</sup>, G. L. SISCOE<sup>9</sup>, R. VAINIO<sup>10</sup>, S. K. ANTIOCHOS<sup>3</sup> and P. RILEY  
Space Science Reviews (2006) 123: 251–302

<https://link.springer.com/content/pdf/10.1007/s11214-006-9019-8.pdf>

This chapter provides an overview of current efforts in the theory and modeling of CMEs. Five key areas are discussed: (1) CME initiation; (2) CME evolution and propagation; (3) the structure of interplanetary CMEs derived from flux rope modeling; (4) CME shock formation in the inner corona; and (5) particle acceleration and transport at CME driven shocks. In the section on CME initiation three contemporary models are highlighted. Two of these focus on how energy stored in the coronal magnetic field can be released violently to drive CMEs. The third model assumes that CMEs can be directly driven by currents from below the photosphere. CMEs evolve considerably as they expand from the magnetically dominated lower corona into the advectively dominated solar wind. The section on evolution and propagation presents two approaches to the problem. One is primarily analytical and focuses on the key physical processes involved. The other is primarily numerical and illustrates the complexity of possible interactions between the CME and the ambient medium. The section on flux rope fitting reviews the accuracy and reliability of various methods. The section on shock formation considers the effect of the rapid decrease in the magnetic field and plasma density with height. Finally, in the section on particle acceleration and transport, some recent developments in the theory of diffusive particle acceleration at CME shocks are discussed. These include efforts to combine self-consistently the process of particle acceleration in the vicinity of the shock with the subsequent escape and transport of particles to distant regions.

## **A review on the genesis of coronal mass ejections**

**Review**

T. G. **FORBES**

Journal of Geophysical Research, Volume 105, Issue A10, p. 23153-23166, **2000**

<https://agupubs.onlinelibrary.wiley.com/doi/epdf/10.1029/2000JA000005>

This paper provides a short review of some of the basic concepts related to the origin of coronal mass ejections (CMEs). The various ideas which have been put forward to explain the initiation of CMEs are categorized in terms of whether they are force-free or non-force-free and ideal or nonideal. A few representative models of each category are examined to illustrate the principles involved. At the present time there is no model which is sufficiently developed to aid forecasters in their efforts to predict CMEs, but given the current pace of research, this situation could improve dramatically in the near future.

### **Coronal Cavity Survey: Morphological Clues to Eruptive Magnetic Topologies**

B. C. [Forland](#), S. E. Gibson, J. B. Dove, L. A. Rachmeler, Y. Fan

*Solar Phys* (2013) 288:603–615

We present a survey on coronal prominence cavities conducted using 19 months of data from the Atmospheric Imaging Assembly (AIA) instrument aboard the Solar Dynamics Observatory (SDO) satellite. Coronal cavities are elliptical regions of rarefied density lying above and around prominences. They can be long-lived (weeks to months) but are often observed to eventually erupt as part of a coronal mass ejection (CME). We determine morphological properties of the cavities both by qualitatively assessing their shape, and quantitatively fitting them with ellipses. We demonstrate consistency between these two approaches, and find that fitted ellipses are taller than they are wide for almost all cavities studied, in agreement with an earlier analysis of white-light cavities. We examine correlations between cavity shape, aspect ratio, and propensity for eruption. We find that cavities with a teardrop-shaped morphology are more likely to erupt, and we discuss the implications of this morphology for magnetic topologies associated with CME models. We provide the full details of the survey for broad scientific use as supplemental material.

### **KELVIN-HELMHOLTZ INSTABILITY OF THE CME RECONNECTION OUTFLOW LAYER IN THE LOW CORONA**

Claire [Foullon](#)<sup>1</sup>, Erwin Verwichte<sup>1</sup>, Katariina Nykyri<sup>2</sup>, Markus J. Aschwanden<sup>3</sup>, and Iain G. Hannah

E-print, Sept 2013; 2013 *ApJ* 767 170

New capabilities for studying the Sun allow us to image for the first time the magnetic Kelvin-Helmholtz (KH) instability developing at the surface of a fast coronal mass ejection (CME) less than 150 Mm above the solar surface. We conduct a detailed observational investigation of this phenomenon, observed off the east solar limb on **2010 November 3**, in the EUV with SDO/AIA. In conjunction with STEREO-B/EUVI, we derive the CME source surface position. We ascertain the timing and early evolution of the CME outflow leading to the instability onset. We perform image and spectral analysis, exploring the CME plasma structuring and its parabolic flow pattern. As we evaluate and validate the consistency of the observations with theoretical considerations and predictions, we take the view that the ejection layer corresponds to a reconnection outflow layer surrounding the erupting flux rope, accounting for the timing, high temperature (~11.6 MK), and high flow shear (~680 km s<sup>-1</sup>) on the unstable CME northern flank and for the observed asymmetry between the CME flanks. From the irregular evolution of the CME flow pattern, we infer a shear gradient consistent with expected spatial flow variations across the KH-unstable flank. The KH phenomenon observed is tied to the first stage of a linked flare-CME event.

### **MAGNETIC KELVIN-HELMHOLTZ INSTABILITY AT THE SUN**

Claire [Foullon](#)<sup>1</sup>, Erwin Verwichte<sup>1</sup>, Valery M. Nakariakov<sup>1,2</sup>, Katariina Nykyri<sup>3</sup>, and Charles J. Farrugia<sup>4</sup>

*Astrophysical Journal Letters*, 729:L8 (4pp), 2011 March

Flows and instabilities play a major role in the dynamics of magnetized plasmas including the solar corona, magnetospheric and heliospheric boundaries, cometary tails, and astrophysical jets. The nonlinear effects, multiscale and microphysical interactions inherent to the flow-driven instabilities, are believed to play a role, e.g., in plasma entry across a discontinuity, generation of turbulence, and enhanced drag. However, in order to clarify the efficiency of macroscopic instabilities in these processes, we lack proper knowledge of their overall morphological features. Here we show the first observations of the temporally and spatially resolved evolution of the magnetic Kelvin-Helmholtz instability in the solar corona. Unprecedented high-resolution imaging observations of vortices developing at the surface of a fast coronal mass ejection are taken by the new *Solar Dynamics Observatory*, validating theories of the nonlinear dynamics involved. The new findings are a cornerstone for developing a unifying theory on flow-driven instabilities in rarefied magnetized plasmas, which is important for understanding the fundamental processes at work in key regions of the Sun-Earth system.

*New capabilities for studying the Sun allow us to detect and image KH waves for the first time, in a fast coronal mass ejection (CME) event where the instability develops at the flank of the CME ejection. 2010 November 3.*

### **Study of Plasma Heating Processes in a Coronal Mass Ejection-driven Shock Sheath Region Observed with the Metis Coronagraph**

Federica [Frassati](#)<sup>1</sup>, Alessandro Bemporad<sup>1</sup>, Salvatore Mancuso<sup>1</sup>, Silvio Giordano<sup>1</sup>, Vincenzo Andretta<sup>2</sup>, Aleksandr Burtovoi<sup>3,4</sup>, Vania Da Deppo<sup>5</sup>, Silvano Fineschi<sup>1</sup>, Catia Grimani<sup>6</sup>, Salvo Guglielmino<sup>7</sup>Show full author list

2024 *ApJ* 964 15

<https://iopscience.iop.org/article/10.3847/1538-4357/ad26fb/pdf>

On **2021 September 28**, a C1.6 class flare occurred in active region NOAA 12871, located approximately at 27°S and 51°W on the solar disk with respect to Earth's point of view. This event was followed by a partial halo coronal mass ejection (CME) that caused the deflection of preexisting coronal streamer structures, as observed in visible-light coronagraphic images. An associated type II radio burst was also detected by both space- and ground-based instruments, indicating the presence of a coronal shock propagating into interplanetary space. By using H  $\alpha$  and Ly $\alpha$  (121.6 nm) observations from the Metis coronagraph on board the Solar Orbiter mission, we demonstrate for the first time the capability of UV imaging to provide, via a Doppler dimming technique, an upper limit estimate of the evolution of the 2D proton kinetic temperature in the CME-driven shock sheath as it passes through the field of view of the instrument. Our results suggest that over the 22 minutes of observations, the shock propagated with a speed decreasing from about  $740 \pm 110$  km s<sup>-1</sup> to  $400 \pm 60$  km s<sup>-1</sup>. At the same time, the postshock proton temperatures peaked at latitudes around the shock nose and decreased with time from about  $6.8 \pm 1.01$  MK to  $3.1 \pm 0.47$  MK. The application of the Rankine–Hugoniot jump conditions demonstrates that these temperatures are higher by a factor of about 2–5 than those expected from simple adiabatic compression, implying that significant shock heating is still going on at these distances.

## Estimate of Plasma Temperatures Across a CME-Driven Shock from a Comparison Between EUV and Radio Data

Federica [Frassati](#), [Salvatore Mancuso](#) & [Alessandro Bemporad](#)

[Solar Physics](#) volume 295, Article number: 124 (2020)

<https://link.springer.com/content/pdf/10.1007/s11207-020-01686-0.pdf>

In this work, we analyze the evolution of an EUV wave front associated with a solar eruption that occurred on **30 October 2014**, with the aim of investigating, through differential emission measure (DEM) analysis, the physical properties of the plasma compressed and heated by the accompanying shock wave. The EUV wave was observed by the Atmospheric Imaging Assembly (AIA) onboard the Solar Dynamics Observatory (SDO) and was accompanied by the detection of a metric Type II burst observed by ground-based radio spectrographs. The EUV signature of the shock wave was also detected in two of the AIA channels centered at 193 Å and 211 Å as an EUV intensity enhancement propagating ahead of the associated CME. The density compression ratio  $X$  of the shock as inferred from the analysis of the EUV data is  $X \approx 1.23$ , in agreement with independent estimates obtained from the analysis of the Type II band-splitting of the radio data and inferred by adopting the upstream–downstream interpretation. By applying the Rankine–Hugoniot jump conditions under the hypothesis of a perpendicular shock, we also estimate the temperature ratio as  $T_D/T_U \approx 1.55$  and the post-shock temperature as  $T_D \approx 2.75$  MK. The modest compression ratio and temperature jump derived from the EUV analysis at the shock passage are typical of weak coronal shocks. **CESRA #2735 Dec 2020** <http://www.astro.gla.ac.uk/users/eduard/cesra/?p=2735>

## Comprehensive Analysis of the Formation of a Shock Wave Associated with a Coronal Mass Ejection

Federica [Frassati](#)<sup>1,2</sup>, Roberto Susino<sup>1</sup>, Salvatore Mancuso<sup>1</sup>, and Alessandro Bemporad

**2019** ApJ 871 212

<http://sci-hub.tw/10.3847/1538-4357/aaf9af>

On **2014 November 1**, a solar prominence eruption associated with a C2.7 class flare and a type II radio burst resulted in a fast partial halo coronal mass ejection (CME). Images acquired in the extreme ultraviolet (EUV) by the Solar Dynamics Observatory/Atmospheric Imaging Assembly (AIA) and PROBA2/SWAP and in white light (WL) by Solar and Heliospheric Observatory/Large Angle and Spectrometric Coronagraph show the expansion of a bright compression front ahead of the CME. In this work, we present a detailed investigation of the CME-driven shock associated with this event following the early evolution of the compression front observed near the Sun up to the extended corona. Our aim is to shed light on the long-debated issue concerning the location and timing of shock formation in the corona. Through differential emission measure analysis, we derived, for the first time, the compression ratio across the expanding EUV front observed by AIA at different temperature ranges: higher compression ratios corresponded to higher plasma temperature ranges, as expected. Moreover, comparison between up- and downstream temperatures and those expected via adiabatic compression shows that no additional heating mechanisms occurred in the early front expansion phase, implying that the shock formed beyond the AIA field of view. Finally, the analysis of the associated type II radio burst, in combination with the inferred coronal density distribution, allowed us to identify a well-defined region located northward of the CME source region as the site for shock formation and to outline its kinematics in accordance with the evolution of the expanding front as obtained from the EUV and WL data.

## Study of the early phase of a Coronal Mass Ejection driven shock in EUV images

Federica [Frassati](#), Roberto Susino, Salvatore Mancuso & Alessandro Bemporad

Astrophysics and Space Science October **2017**, 362:194

<https://link.springer.com/content/pdf/10.1007%2Fs10509-017-3173-1.pdf>

The **November 1st, 2014** prominence eruption (associated with a C2.7 class flare) resulted in a fast, partial-halo Coronal Mass Ejection (CME). During its early propagation, the CME produced a type II radio burst (seen by the Bruny Island Radio Spectrometer) starting around 04:57 UT when the front entered into the LASCO/C2 field of view (FOV) and the top of the CME front was at the heliocentric distance of about  $2.5 R_{\odot}$ . In order to identify the source of the type II radio burst, we studied the kinematic of the eruption with EUV images acquired by SDO/AIA. Profiles of the observed EUV front speed have been compared with the Alfvén speed profiles derived by combining the plasma electron densities obtained from Emission Measure analysis and model magnetic fields extrapolated on the plane of the



sky. Our results show that the northern half of the front became super-Alfvénic at approximately the same time when the type-II radio burst started. A comparison between the starting frequency of the type II emission and the frequencies corresponding to the coronal densities of the locations where the EUV front became super-Alfvénic suggests that the radio sources should be located in the northern flank of the front.

## **CORONAL MASS EJECTION RECONSTRUCTION FROM THREE VIEWPOINTS VIA SIMULATION MORPHING. I. THEORY AND EXAMPLES**

Richard A. [Frazin](#)

2012 ApJ 761 24

The problem of reconstructing the three-dimensional (3D) density distribution of a coronal mass ejection (CME) from three simultaneous coronagraph observations is timely in that the COR1 and COR2 coronagraphs on the dual-spacecraft STEREO mission complement the LASCO coronagraphs on the SOHO satellite and the Mk4 on Mauna Loa. While the separation angle between the STEREO spacecraft and the Earth depends on the time since the launch in 2006, the reconstruction problem is always severely underinformed. So far, all 3D reconstruction efforts have made use of relatively simple parameterized models in order to determine the 3D structure of the CME. Such approaches do not utilize the power of 3D MHD simulation to inform the reconstruction. This paper considers the situation in which a specific CME event observed in coronagraphs from three viewpoints is later simulated by solving MHD equations. The reconstruction is then subjected to an invertible morphological operator chosen so that morphed MHD simulation is most consistent with the three-viewpoint coronagraph data. The morphological operations are explained mathematically and synthetic examples are given. The practical application to reconstructing CMEs from STEREO and SOHO data is discussed.

## **Intercomparison of the LASCO-C2, SECCHI-COR1, SECCHI-COR2, and Mk4 Coronagraphs**

Richard A. [Frazin](#), Alberto M. Vásquez, William T. Thompson, Russell J. Hewett, Philippe Lamy, Antoine Llebaria, Angelos Vourlidis and Joan Burkepile

Solar Physics, Volume 280, Number 1 (2012), 273-293, **2012**, DOI: 10.1007/s11207-012-0028-3

In order to assess the reliability and consistency of white-light coronagraph measurements, we report on quantitative comparisons between polarized brightness [pB] and total brightness [B] images taken by the following white-light coronagraphs: LASCO-C2 on SOHO, SECCHI-COR1 and -COR2 on STEREO, and the ground-based MLSO-Mk4. The data for this comparison were taken on **16 April 2007**, when both STEREO spacecraft were within  $3.1^\circ$  of Earth's heliographic longitude, affording essentially the same view of the Sun for all of the instruments. Due to the difficulties of estimating stray-light backgrounds in COR1 and COR2, only Mk4 and C2 produce reliable coronal-hole values (but not at overlapping heights), and these cannot be validated without rocket flights or ground-based eclipse measurements. Generally, the agreement between all of the instruments' pB values is within the uncertainties in bright streamer structures, implying that measurements of bright CMEs also should be trustworthy. Dominant sources of uncertainty and stray light are discussed, as is the design of future coronagraphs from the perspective of the experiences with these instruments.

## **TOWARD RECONSTRUCTION OF CORONAL MASS EJECTION DENSITY FROM ONLY THREE POINTS OF VIEW**

R. A. [Frazin](#)<sup>1</sup>, M. Jacob<sup>2</sup>, W. B. Manchester IV<sup>1</sup>, H. Morgan<sup>3,4</sup>, and M. B. Wakin<sup>5</sup>

Astrophysical Journal, 695:636–641, **2009** April

<http://www.iop.org/EJ/toc/-alert=43190/0004-637X/695/1>

Understanding the structure of coronal mass ejections (CMEs) is one of the primary challenges in solar astrophysics. White-light coronagraphs make images of line-of-sight projections of the CME electron density ( $N_e$ ). The combination of the coronagraphs on the STEREO and *SOHO* spacecraft provides three simultaneous viewpoints that vary in angle with time, according to the spacecraft orbits. Three viewpoints are not enough to permit tomographic reconstruction via classical methods, but we argue here that recent advances in image processing methods that take into account prior information about the CME geometry may allow one to determine the CME density structure with only three viewpoints. The prior information considered here is that the CME is separated from a known (or simple) background by a closed surface, which may be described by a level set. We propose an alternating iterative procedure in which the surface is evolved via geometric partial differential equations in one step and the interior (and exterior)  $N_e$  values are determined in the next step.

## **Predicting relationships between solar jet variables**

Leonard A [Freeman](#)

2019

<https://arxiv.org/ftp/arxiv/papers/1904/1904.08289.pdf>

Studies of spicules and similar solar jets have revealed a strong correlation between some of the kinematic variables, particularly between the initial velocity  $V$ , and the subsequent deceleration,  $a$ . It has been proposed that this is caused by, and offers proof for a shock wave mechanism acting on the spicules. However it is shown here that these correlations arise simply from the statistics of the sample of spicules being studied, for example in the range of spicule heights. The relationship between two kinematic variables has been expressed as a linear equation but there is no general agreement on the actual linear equation, which shows wide variations. The reason for these variations is analysed and it is shown how the different linear equations can be derived from the co-ordinates of a single point: the mean spicule height and deceleration of the group of spicules being studied. Another method sometimes used is to determine the correlation coefficient of two of the kinematic variables from their scatter plots. It is shown how this too can be calculated from the sample statistics. The problems of the linear equations for the  $(a, V)$  correlation disappear if a square law relationship is used instead, which also provides a simple physical interpretation of the results. The implications of these results and the possibility that spicule behaviour is partly due to magnetic fields are discussed.

## **The high helium abundance and charge states of the interplanetary CME and its material source on the Sun**

[Hui Fu](#), [R.A. Harrison](#), [J.A. Davies](#), [LiDong Xia](#), [XiaoShuai Zhu](#), [Bo Li](#), [ZhengHua Huang](#), [D. Barnes](#)

ApJL 2020

<https://arxiv.org/pdf/2008.08816.pdf>

Identifying the source of the material within coronal mass ejections (CMEs) and understanding CME onset mechanisms are fundamental issues in solar and space physics. Parameters relating to plasma composition, such as charge states and He abundance ( $\lambda_{\text{He}}$ ), may be different for plasmas originating from differing processes or regions on the Sun. Thus, it is crucial to examine the relationship between in-situ measurements of CME composition and activity on the Sun. We study the CME that erupted on **2014 September 10**, in association with an X1.6 flare, by analyzing AIA imaging and IRIS spectroscopic observations and its in-situ signatures detected by Wind and ACE. We find that during the slow expansion and intensity increase of the sigmoid, plasma temperatures of 9 MK, and higher, first appear at the footpoints of the sigmoid, associated with chromospheric brightening. Then the high-temperature region extends along the sigmoid. IRIS observations confirm that this extension is caused by transportation of hot plasma upflow. Our results show that chromospheric material can be heated to 9 MK, and above, by chromospheric evaporation at the sigmoid footpoints before flare onset. The heated chromospheric material can transport into the sigmoidal structure and supply mass to the CME. The aforementioned CME mass supply scenario provides a reasonable explanation for the detection of high charge states and elevated  $\lambda_{\text{He}}$  in the associated ICME. The observations also demonstrate that the quasi-steady evolution in the precursor phase is dominated by magnetic reconnection between the rising flux rope and the overlying magnetic field structure.

## **Physical processes involved in the EUV "Surge" Event of 09 May 2012**

Marcelo López [Fuentes](#), [Cristina H. Mandrini](#), [Mariano Poisson](#), [Pascal Démoulin](#), [Germán](#)

[Cristiani](#), [Fernando M. López](#), [Maria Luisa Luoni](#)

Solar Phys. 293:166 2018

<https://arxiv.org/pdf/1810.12403.pdf>

<https://link.springer.com/content/pdf/10.1007%2Fs11207-018-1384-4.pdf>

We study an EUV confined ejection observed on **09 May 2012** in active region (AR) NOAA 11476. For the analysis we use observations in multiple wavelengths (EUV, X-rays,  $H\alpha$ , and magnetograms) from a variety of ground-based and space instruments. The magnetic configuration showed the presence of two rotating bipoles, with decreasing magnetic flux, within the following polarity of the AR. This evolution was present along some tens of hours before the studied event and continued even later. A minifilament with a length of  $\approx 30$  arcsec lay along the photospheric inversion line of the largest bipole. The minifilament was observed to erupt accompanied by an M4.7 flare (SOL20120509T12:23:00). Consequently, dense material, as well as twist, was injected along closed loops in the form of a very broad ejection whose morphology resembles that of typical  $H\alpha$  surges. We conclude that the flare and eruption can be explained as due to two reconnection processes, one occurring below the erupting minifilament and another one above it. This second process injects the minifilament plasma within the reconnected closed loops linking the main AR polarities. Analyzing the magnetic topology using a force-free model of the coronal field, we identify the location of quasi-separatrix layers (QSLs), where reconnection is prone to occur, and present a detailed interpretation of the chromospheric and coronal eruption observations. In particular, this event, contrary to what has been proposed in several models explaining surges and/or jets, is not originated by magnetic flux emergence but by magnetic flux cancellation accompanied by the rotation of the bipoles. In fact, the conjunction of these two processes, flux cancellation and bipole rotations, is at the origin of a series of events, homologous to the one we analyze in this article, that occurred in AR 11476 from **08 to 10 May 2012**.

## **Global Nature of Solar Coronal Shock Waves shown by Inconsistency between EUV Waves and Type II Radio Bursts**

Aarti [Fulara](#), [Ryun-Young Kwon](#)

ApJLetters 2021

<https://arxiv.org/pdf/2109.01509.pdf>

We re-examine the physical relationship between Extreme-Ultraviolet (EUV) waves and type II radio bursts. It has been often thought that they are two observational aspects of a single coronal shock wave. However, a lack of their speed correlation hampers the understanding of their respective (or common) natures in a single phenomenon. Knowing the uncertainties in identifying true wave components from observations and measuring their speeds, we re-examine the speeds of EUV waves reported in previous literature and compare these with type II radio bursts and Coronal Mass Ejections (CMEs). This confirms the inconsistency between the speeds of EUV waves and their associated type II radio bursts. Second, CME speeds are found to have a better correlation with type II radio bursts than EUV waves. Finally, there exists a tendency for type II speeds and their range to be much greater than those of EUV waves. We demonstrate that the speed inconsistency is in fact an intrinsic tendency and elucidate the nature of a coronal shock wave consisting of both driven and non-driven parts. This suggests that the speed inconsistency would remain even if all other uncertainties were removed. **2013 April 11**

### **Precursors of the Forbush Decrease on 2006 December 14 Observed with the Global Muon Detector Network (GMDN).**

**Fushishita** A, Kuwabara T, Kato C, Yasue S, Bieber JW, Evenson P, Da Silva MR, Dal Lago A, Schuch NJ, Tokumaru M, Duldig ML, Humble JE, Sabbah I, Al Jassar HK, Sharma MM, Munakata K (2010) *Astrophys. J.* 715:1239-1247

### **Coronal Mass Ejection Detection using Wavelets, Curvelets and Ridgelets: Applications for Space Weather Monitoring**

P.T. **Gallagher**, C.A. Young <sup>1, b</sup>, J.P. Byrnea, R.T.J. McAteera

E-print, Apr 2010, *Adv. Space Res.* Volume 47, Issue 12, 15 June 2011, Pages 2118-2126

Coronal mass ejections (CMEs) are large-scale eruptions of plasma and magnetic field that can produce adverse space weather at Earth and other locations in the Heliosphere. Due to the intrinsic multiscale nature of features in coronagraph images, wavelet and multiscale image processing techniques are well suited to enhancing the visibility of CMEs and suppressing noise. However, wavelets are better suited to identifying point-like features, such as noise or background stars, than to enhancing the visibility of the curved form of a typical CME front. Higher order multiscale techniques, such as ridgelets and curvelets, were therefore explored to characterise the morphology (width, curvature) and kinematics (position, velocity, acceleration) of CMEs. Curvelets in particular were found to be well suited to characterizing CME properties in a self-consistent manner. Curvelets are thus likely to be of benefit to autonomous monitoring of CME properties for space weather applications.

### **Rapid acceleration of a coronal mass ejection in the low corona and implications for propagation**

**Gallagher**, P. T., G. R. Lawrence, and B. R. Dennis,  
*ApJL*, 588(1), L53–L56. (2003), **File**

A high-velocity coronal mass ejection (CME) associated with the **2002 April 21 X1.5** flare is studied using a unique set of observations from the *Transition Region and Coronal Explorer (TRACE)*, the Ultraviolet Coronagraph Spectrometer (UVCS), and the Large Angle and Spectroscopic Coronagraph (LASCO). The event is first observed as a rapid rise in *GOES* X-rays, followed by two simultaneous brightenings that appear to be connected by an ascending looplike feature. While expanding, the appearance of the feature remains remarkably constant as it passes through the *TRACE* 195 Å passband and LASCO fields of view, allowing its height-time behavior to be accurately determined. The acceleration is consistent with an exponential rise with an *e*-folding time of ~138 s and peaks at ~1500 m s<sup>-2</sup> when the leading edge is at ~1.7 R<sub>sun</sub> from Sun center. The acceleration subsequently falls off with an *e*-folding time of over 1000 s. At distances beyond ~3.4 R<sub>sun</sub>, the height-time profile is approximately linear with a constant velocity of ~2500 km s<sup>-1</sup>. These results are briefly discussed in light of recent kinematic models of CMEs.

**See also**

### **RHESSI AND TRACE OBSERVATIONS OF THE 21 APRIL 2002 X1.5 FLARE**

PETER T. **GALLAGHER**<sup>1,2</sup>, BRIAN R. DENNIS<sup>1</sup>, SÄM KRUCKER<sup>3</sup>,  
RICHARD A. SCHWARTZ<sup>1,4</sup> and A. KIMBERLEY TOLBERT<sup>1,4</sup>  
*Solar Physics* **210**: 341–356, **2002**, **File**.

### **Eruptions from Quiet Sun Coronal Bright Points. II. Non-Potential Modeling**

Klaus **Galsgaard**, [Maria S. Madjarska](#), [Duncan H. Mackay](#), [Chaozhou Mou](#)

A&A 623, A78

2019

<https://arxiv.org/pdf/1901.09875.pdf>

Our recent observational study shows that the majority of coronal bright points (CBPs) in the quiet Sun are sources of one or more eruptions during their lifetime. Here, we investigate the non-potential time dependent structure of the magnetic field of the CBP regions with special emphasis on the time evolving magnetic structure at the spatial locations where the eruptions are initiated. The magnetic structure is evolved in time using a Non-Linear Force Free Field (NLFFF) relaxation approach, based on a time series of Helioseismic and Magnetic Imager (HMI) longitudinal magnetograms. This results in a continuous time series of NLFFFs. The time series is initiated with a potential field extrapolation based on a magnetogram taken well before the time of the eruptions. This initial field is then evolved in time in response to the observed changes in the magnetic field distribution at the photosphere. The local and global magnetic field structures from the time series of NLFFF field solutions are analysed in the vicinity of the eruption sites at the approximate times of the eruptions. The analysis shows that many of the CBP eruptions reported in Mou et al. (2018) contain twisted flux tube located at the sites of eruptions. The presence of flux ropes at these locations provides in many cases a direct link between the magnetic field structure, their eruption and the observation of mini coronal mass ejections (mini-CMEs). It is found that all repetitive eruptions are homologous. The NLFFF simulations show that twisted magnetic field structures are created at the locations hosting eruptions in CBPs. These twisted structures are produced by footpoint motions imposed by changes in the photospheric magnetic field observations. The true nature of the micro-flares remains unknown. Further 3D data-driven MHD modelling is required to show how these twisted regions become unstable and erupt. **01-03 Jan 2011**

## Correcting Projection Effects in CMEs using GCS-based Large Statistics of Multi-viewpoint Observations

[Harshita Gandhi](#), [Ritesh Patel](#), [Vaibhav Pant](#), [Satabdwa Majumdar](#), [Sanchita Pal](#), [Dipankar Banerjee](#), [Huw Morgan](#)

Space weather **Volume22, Issue2** e2023SW003805 **2024**

<https://arxiv.org/pdf/2402.07961.pdf>

<https://doi.org/10.1029/2023SW003805>

<https://agupubs.onlinelibrary.wiley.com/doi/epdf/10.1029/2023SW003805>

This study addresses the limitations of single-viewpoint observations of Coronal Mass Ejections (CMEs) by presenting results from a 3D catalog of 360 CMEs during solar cycle 24, fitted using the GCS model. The dataset combines 326 previously analyzed CMEs and 34 newly examined events, categorized by their source regions into active region (AR) eruptions, active prominence (AP) eruptions, and prominence eruptions (PE). Estimates of errors are made using a bootstrapping approach. The findings highlight that the average 3D speed of CMEs is  $\sim 1.3$  times greater than the 2D speed. PE CMEs tend to be slow, with an average speed of  $432 \text{ km s}^{-1}$ . AR and AP speeds are higher, at  $723 \text{ km s}^{-1}$  and  $813 \text{ km s}^{-1}$ , respectively, with the latter having fewer slow CMEs. The distinctive behavior of AP CMEs is attributed to factors like overlying magnetic field distribution or geometric complexities leading to less accurate GCS fits. A linear fit of projected speed to width gives a gradient of  $2 \text{ km s}^{-1} \text{ deg}^{-1}$ , which increases to  $5 \text{ km s}^{-1} \text{ deg}^{-1}$  when the GCS-fitted 'true' parameters are used. Notably, AR CMEs exhibit a high gradient of  $7 \text{ km s}^{-1} \text{ deg}^{-1}$ , while AP CMEs show a gradient of  $4 \text{ km s}^{-1} \text{ deg}^{-1}$ . PE CMEs, however, lack a significant speed-width relationship. We show that fitting multi-viewpoint CME images to a geometrical model such as GCS is important to study the statistical properties of CMEs, and can lead to a deeper insight into CME behavior that is essential for improving future space weather forecasting. **2013/04/05**, **2016/04/04**, **2017/09/04**

**Table 2** summarises the parameters for the 34 CMEs fitted during this study 2013-2021

## The Broken Lane of a Type II Radio Burst Caused by Collision of a Coronal Shock with a Flare Current Sheet

Guannan [Gao](#), Min Wang, Ning Wu, Jun Lin, E. Ebenezer, Baolin Tan

Solar Phys. Volume 291, **Issue 11**, pp 3369–3384 **2016**

<https://arxiv.org/pdf/1612.01784v1.pdf>

We investigated a peculiar metric type II solar radio burst with a broken lane structure, which was observed on **November 13, 2012**. In addition to the radio data, we also studied the data in the other wavelengths. The bursts were associated with two CMEs and two flares that originated from active region AR 11613. A long current sheet was developed in the first CME, and the second CME collided with the current sheet first and then merged with the first one. Combining information revealed by the multi-wavelength data indicated that a coronal shock accounting for the type II radio burst, and that the collision of this shock with the current sheet resulted in the broken lane of the type II radio burst. The type II burst lane resumed after the shock passed through the current sheet. We further estimated the thickness of the current sheet according to the gap on the lane of the type II burst, and found that the result is consistent with previous ones obtained for various events observed in different wavelengths by different instruments. In addition, the regular type II burst associated with the first CME/flare was also studied, and the magnetic field in each source region of the two type II bursts was further deduced in different way.

## Phase Relationships Between the CME-Energy Cycle, the Sunspot-Area Cycle and the Flare-Index Cycle

P. X. [Gao](#), J. L. Xie, J. Zhong

Solar Phys., Volume 289, Issue 5, pp 1831-1841. **2014**

We study the phase relationships between the coronal-mass-ejection (CME) energy cycle, the sunspot-area cycle, and the flare-index cycle from 1996 to 2010. The results show the following: i) The activity cycle of the flare index significantly leads the activity cycle of the sunspot area. ii) The activity cycle of the CME energy is inferred to be almost in phase with the activity cycle of the sunspot area; the activity cycle of the CME energy at low latitudes slightly leads the activity cycle of the sunspot area; the CME energy at high latitudes is shown to significantly lag behind the sunspot area. iii) The CME energy is shown to significantly lag behind the flare index; the CME energy at low latitudes is shown to slightly lag behind the flare index; the CME energy at high latitudes is shown to significantly lag behind the flare index.

### **Radio observations of the fine structure inside a post-CME current sheet**

Guan-Nan **Gao**<sup>1,2,3</sup>, Min Wang<sup>1,3,4</sup>, Jun Lin<sup>1</sup>, Ning Wu<sup>5</sup>, Cheng-Ming Tan<sup>4</sup>, Bernhard Kliem<sup>1,6</sup> and Yang Su<sup>7</sup>

Research in Astronomy and Astrophysics, Volume 14, Number 7, 843-854, **2014**

A solar radio burst was observed in a coronal mass ejection/flare event by the Solar Broadband Radio Spectrometer at the Huairou Solar Observing Station on **2004 December 1**. The data exhibited various patterns of plasma motions, suggestive of the interaction between sunward moving plasmoids and the flare loop system during the impulsive phase of the event. In addition to the radio data, the associated white-light, H $\alpha$ , extreme ultraviolet light, and soft and hard X-rays were also studied.

### **Distributions of Energy and Mass of Coronal Mass Ejections**

P. X. **Gao**, K. J. Li and J. C. Xu

Solar Physics, Volume 273, Number 1, 117-123, **2011**, File

The present study investigates the energy and mass distributions of all (11 322) coronal mass ejections (CMEs), 1406 CMEs associated solely with flares (FL CMEs), and 325 CMEs associated solely with filament eruptions (FE CMEs), all of which were observed by the Large Angle and Spectrometric Coronagraph on board the Solar and Heliospheric Observatory (SOHO/LASCO) from January 1996 to December 2009. The results show the following. i) The mean energy of FL CMEs is significantly lower than that of all CMEs. The mean energy of FE CMEs is significantly higher than those of FL CMEs and all CMEs. ii) The mean mass of FL CMEs is slightly larger than that of all CMEs. The mean mass of FE CMEs is significantly larger than those of FL CMEs and all CMEs. Our results suggest that CMEs should shed excess helicity stored in the corona and that the magnetic complexity determines the likelihood of CMEs.

### **Speed Distributions of CMEs in Cycle 23 at Low and High Latitudes \***

Peng-Xin **Gao** and Ke-Jun Li

Chin. J. Astron. Astrophys. Vol. 8 (**2008**), No. 2, 146–152

<http://www.chjaa.org>

**Abstract** We analyzed the speed ( $v$ ) distributions of 11584 coronal mass ejections (CMEs) observed by the Large Angle and Spectrometric Coronagraph Experiment on board the Solar and Heliospheric Observatory (SOHO/LASCO) in cycle 23 from 1996 to 2006. We find that the speed distributions for high-latitude (HL) and low-latitude (LL) CME events are nearly identical and to a good approximation they can be fitted with a lognormal distribution. This finding implies that statistically the same driving mechanism of a nonlinear nature is acting in both HL and LL CME events, and CMEs are intrinsically associated with the source's magnetic structure on large spatial scales. Statistically, the HL CMEs are slightly slower than the LL CMEs. For HL and LL CME events respectively, the speed distributions for accelerating and decelerating events are nearly identical and also to a good approximation they can be both fitted with a lognormal distribution, thus supplementing the results obtained by Yurchyshyn et al.

### **Photometric Calibration of the LASCO-C2 Coronagraph over 14 Years (1996 – 2009)**

B. **Gardès**, P. Lamy, A. Llebaria

Solar Physics, April **2013**, Volume 283, Issue 2, pp 667-690

We present a photometric calibration of the SOHO/LASCO-C2 coronagraph based on the analysis of all stars down to magnitude  $V=8$  that transited its field of view during the past 14 years of operation (1996–2009), extending the previous work of Llebaria, Lamy, and Danjard (Icarus 182, 281, 2006). The pre-processing of the images incorporates the most recent determination of the evolution of the LASCO-C2 performances. The automatic procedure then analyzes some 260 000 images to detect, locate, and measure those stars. Aperture photometry is performed using four different aperture sizes, and the zero points (ZPs) of the photometric transformations between the LASCO-C2 magnitudes for its orange filter and the standard  $V$  magnitudes are determined after introducing a correction for the color of the stars. A new statistical method (“bootstrap”) is introduced to assess the confidence intervals of the mean yearly value of the ZPs. The correction for finite aperture required to derive the calibration coefficient for the surface photometry of extended sources is based on the reconstructed image of bright saturated stars and a robust model for the growth curve. The

global temporal evolution of the sensitivity of LASCO-C2 is compatible with a continuous decrease at a rate of  $\approx 0.56$  % per year. However, it is better described by two separate linear variations with a discontinuity at the time of the loss of SOHO. After the resumption of normal operations in 1999, the linear decrease of the sensitivity amounts to  $\approx 0.35$  % per year.

## Nonlocal Ohms Law, Plasma Resistivity, and Reconnection During Collisions of Magnetic Flux Ropes

W. [Gekelman](#)<sup>1</sup>, T. DeHaas<sup>1</sup>, P. Pribyl<sup>1</sup>, S. Vincena<sup>1</sup>, B. Van Compernelle<sup>1</sup>, R. Sydora<sup>2</sup>, and S. K. P. Tripathi<sup>1</sup>

2018 ApJ 853 33

<http://sci-hub.tw/http://iopscience.iop.org/0004-637X/853/1/33/>

The plasma resistivity was evaluated in an experiment on the collision of two magnetic flux ropes. Whenever the ropes collide, some magnetic energy is lost as a result of reconnection. Volumetric data, in which all the relevant time-varying quantities were recorded in detail, are presented. Ohm's law is shown to be nonlocal and cannot be used to evaluate the plasma resistivity. The resistivity was instead calculated using the AC Kubo resistivity and shown to be anomalously high in certain regions of space.

## The Flare Likelihood and Region Eruption Forecasting (FLARECAST) Project: Flare forecasting in the big data & machine learning era Review

[M. K. Georgoulis](#), [D. S. Bloomfield](#), [M. Piana](#), [A. M. Massone](#), [M. Soldati](#), [P. T. Gallagher](#), [E. Pariat](#), [N. Vilmer](#), [E. Buchlin](#), [F. Baudin](#), [A. Csillaghy](#), [H. Sathiapal](#), [D. R. Jackson](#), [P. Alingery](#), [F. Benvenuto](#), [C. Campi](#), [K. Florios](#), [C. Gontikakis](#), [C. Guennou](#), [J. A. Guerra](#), [I. Kontogiannis](#), [V. Latorre](#), [S. A. Murray](#), [S.-H. Park](#), [S. von Stachelski](#), [A. Torbica](#), [D. Vischi](#), [M. Worsfold](#)

Journal of Space Weather and Space Climate, 11, 39 2021

<https://arxiv.org/pdf/2105.05993.pdf>

<https://www.swsc-journal.org/articles/swsc/pdf/2021/01/swsc200032.pdf>

<https://doi.org/10.1051/swsc/2021023>

The EU funded the FLARECAST project, that ran from Jan 2015 until Feb 2018. FLARECAST had a R2O focus, and introduced several innovations into the discipline of solar flare forecasting. FLARECAST innovations were: first, the treatment of hundreds of physical properties viewed as promising flare predictors on equal footing, extending multiple previous works; second, the use of fourteen (14) different ML techniques, also on equal footing, to optimize the immense Big Data parameter space created by these many predictors; third, the establishment of a robust, three-pronged communication effort oriented toward policy makers, space-weather stakeholders and the wider public. FLARECAST pledged to make all its data, codes and infrastructure openly available worldwide. The combined use of 170+ properties (a total of 209 predictors are now available) in multiple ML algorithms, some of which were designed exclusively for the project, gave rise to changing sets of best-performing predictors for the forecasting of different flaring levels. At the same time, FLARECAST reaffirmed the importance of rigorous training and testing practices to avoid overly optimistic pre-operational prediction performance. In addition, the project has (a) tested new and revisited physically intuitive flare predictors and (b) provided meaningful clues toward the transition from flares to eruptive flares, namely, events associated with coronal mass ejections (CMEs). These leads, along with the FLARECAST data, algorithms and infrastructure, could help facilitate integrated space-weather forecasting efforts that take steps to avoid effort duplication. In spite of being one of the most intensive and systematic flare forecasting efforts to-date, FLARECAST has not managed to convincingly lift the barrier of stochasticity in solar flare occurrence and forecasting: solar flare prediction thus remains inherently probabilistic. **12 Nov 2012, 2 January 2015, 5 Sep 2017**

## The source and engine of coronal mass ejections Review

Manolis K. [Georgoulis](#), [Alexander Nindos](#), and [Hongqi Zhang](#)

Philosophical Transactions of the Royal Society A: Mathematical, Physical and Engineering Sciences v. 377 Issue 2148 Article ID: 20180094 2019

<https://royalsocietypublishing.org/doi/pdf/10.1098/rsta.2018.0094>

Coronal mass ejections (CMEs) are large-scale expulsions of coronal plasma and magnetic field propagating through the heliosphere. Because CMEs are observed by white-light coronagraphs which, by design, occult the solar disc, supporting disc observations (e.g. in EUV, soft X-rays, Halpha and radio) must be employed for the study of their source regions and early development phases. We review the key properties of CME sources and highlight a certain causal sequence of effects that may occur whenever a strong (flux-massive and sheared) magnetic polarity inversion line develops in the coronal base of eruptive active regions (ARs). Storing non-potential magnetic energy and helicity in a much more efficient way than ARs lacking strong polarity inversion lines, eruptive regions engage in an irreversible course, making eruptions inevitable and triggered when certain thresholds of free energy and helicity are crossed. This evolution favours the formation of pre-eruption magnetic flux ropes. We describe the steps of this plausible path to sketch a picture of the pre-eruptive phase of CMEs that may apply to most events, particularly the ones populating the high end of the energy/helicity distribution, that also tend to have the strongest space-weather implications. **2007/12/05-07, 2012/03/05-06, 2012/07/18, 2015/02/09-10**

## Magnetic Complexity in Eruptive Solar Active Regions and Associated Eruption Parameters

Manolis K. **Georgoulis**

E-print Dec 2007, GRL

Using an efficient magnetic complexity index in the active-region solar photosphere, we quantify the preflare strength of the photospheric magnetic polarity inversion lines in 23 eruptive active regions with flare/CME/ICME events tracked all the way from the Sun to the Earth. We find that active regions with more intense polarity inversion lines host statistically stronger flares and faster, more impulsively accelerated, CMEs. No significant correlation is found between the strength of the inversion lines and the flare soft X-ray rise times, the ICME transit times, and the peak *Dst* indices of the induced geomagnetic storms. Corroborating these and previous results, we speculate on a possible interpretation for the connection between source active regions, flares, and CMEs. Further work is needed to validate this concept and uncover its physical details.

### **Interaction of a coronal mass ejection and a stream interaction region: A case study**

Paul **Geyer**<sup>1</sup>, Mateja Dumbović<sup>1</sup>, Manuela Temmer<sup>2</sup>, Astrid Veronig<sup>2</sup>, Karin Dissauer<sup>3</sup> and Bojan Vršnak<sup>1</sup>  
*A&A* 672, A168 (2023)

<https://doi.org/10.1051/0004-6361/202245433>

<https://www.aanda.org/articles/aa/pdf/2023/04/aa45433-22.pdf>

We investigated the interaction of a coronal mass ejection (CME) and a coronal hole (CH) in its vicinity using remote-sensing and 1 AU in situ data. We used extreme-ultraviolet images and magnetograms to identify coronal structures and coronagraph images to analyze the early CME propagation. The Wind spacecraft and the Advanced Composition Explorer (ACE) provide plasma and magnetic field data of near-Earth interplanetary space. We applied various diagnostic tools to the images and to the time-series data. We find that the CME erupts under a streamer and causes the evacuation of material at its far end, which is observable as dimming and subsequent CH formation. The CME is likely deflected in its early propagation and travels southwest of the Sun-Earth line. In situ data lack signatures of a large magnetic cloud, but show a small flux rope at the trailing edge of the interplanetary CME (ICME), followed by an Alfvénic wave. This wave is identified as exhaust from a Petschek-type reconnection region following the successful application of a Walén test. We infer that the two spacecraft at 1 AU most likely traverse the ICME leg that is in the process of reconnection along the heliospheric current sheet that separates the ICME and the high-speed stream outflowing from the CH. **2014: January 25, February 4-10, February 17**

### **Simulating the Formation of a Sigmoidal Flux Rope in AR10977 from SOHO/MDI**

#### **Magnetograms**

G. P. S. **Gibb**<sup>1</sup>, D. H. Mackay<sup>1</sup>, L. M. Green<sup>2</sup>, and K. A. Meyer

**2014** ApJ 782 71

The modeling technique of Mackay et al. is applied to simulate the coronal magnetic field of NOAA active region AR10977 over a seven day period (**2007 December 2-10**). The simulation is driven with a sequence of line-of-sight component magnetograms from SOHO/MDI and evolves the coronal magnetic field through a continuous series of non-linear force-free states. Upon comparison with Hinode/XRT observations, results show that the simulation reproduces many features of the active region's evolution. In particular, it describes the formation of a flux rope across the polarity inversion line during flux cancellation. The flux rope forms at the same location as an observed X-ray sigmoid. After five days of evolution, the free magnetic energy contained within the flux rope was found to be  $3.9 \times 10^{30}$  erg. This value is more than sufficient to account for the B1.4 GOES flare observed from the active region on **2007 December 7**. At the time of the observed eruption, the flux rope was found to contain 20% of the active region flux. We conclude that the modeling technique proposed in Mackay et al.—which directly uses observed magnetograms to energize the coronal field—is a viable method to simulate the evolution of the coronal magnetic field.

### **Magnetism and the Invisible Man: The mysteries of coronal cavities**

**Review**

Sarah **Gibson**

IAU 300, eds. Schmieder, Malherbe, and Wu, 2014

(2017)

<https://arxiv.org/pdf/1711.09254.pdf>

Magnetism defines the complex and dynamic solar corona. Twists and tangles in coronal magnetic fields build up energy and ultimately erupt, hurling plasma into interplanetary space. These coronal mass ejections (CMEs) are transient riders on the ever-outflowing solar wind, which itself possesses a three-dimensional morphology shaped by the global coronal magnetic field. Coronal magnetism is thus at the heart of any understanding of the origins of space weather at the Earth. However, we have historically been limited by the difficulty of directly measuring the magnetic fields of the corona, and have turned to observations of coronal plasma to trace out magnetic structure. This approach is complicated by the fact that plasma temperatures and densities vary among coronal magnetic structures, so that looking at any one wavelength of light only shows part of the picture. In fact, in some regimes it is the lack of plasma that is a significant indicator of the magnetic field. Such a case is the coronal cavity: a dark, elliptical region in which strong and twisted magnetism dwells. I will elucidate these enigmatic features by presenting observations of coronal cavities in multiple wavelengths and from a variety of observing vantages, including unprecedented coronal magnetic field measurements now being obtained by the Coronal Multichannel Polarimeter (CoMP). These observations demonstrate the presence of twisted magnetic fields within cavities, and also provide clues to how and why cavities ultimately erupt as CMEs. **5/25/11; 6/14/11; 6/24/11; 7/9/11; 7/14/11; 7/26/11; 7/27/11. Next row: 7/28/11; 7/29/11; 8/1/11; 8/10/11; 8/11/11; 8/12/11; Next row: 8/14/11; 8/24/11; 8/30/11; 11/11/11; 1/2/12. 2012-01-02-04, July 14, 2013**

## Coronal cavities: observations and implications for the magnetic environment of prominences

**Review**

Sarah E. **Gibson**

Solar Prominences, Astrophysics and Space Science Library, Volume 415. ISBN 978-3-319-10415-7. Springer International Publishing Switzerland, **2015**, p. 323

<https://arxiv.org/pdf/1702.02214.pdf>

<https://arxiv.org/pdf/1702.02214.pdf>

Dark and elliptical, coronal cavities yield important clues to the magnetic structures that cradle prominences, and to the forces that ultimately lead to their eruption. We review observational analyses of cavity morphology, thermal properties (density and temperature), line-of-sight and plane-of-sky flows, substructure including hot cores and central voids, linear polarization signatures, and observational precursors and predictors of eruption. We discuss a magnetohydrodynamic interpretation of these observations which argues that the cavity is a magnetic flux rope, and pose a set of open questions for further study. **July 22 2002, 16 June 2011, March 11-12, 2012, 16 May 2012, 23 July 2012,**

### THREE-DIMENSIONAL MORPHOLOGY OF A CORONAL PROMINENCE CAVITY

S. E. **Gibson**<sup>1</sup>, T. A. Kucera<sup>2</sup>, D. Rastawicki<sup>3</sup>, J. Dove<sup>4</sup>, G. de Toma<sup>1</sup>, J. Hao<sup>5</sup>, S. Hill<sup>6</sup>, H. S. Hudson<sup>7</sup>, C. Marqu´e<sup>8</sup>, P. S. McIntosh<sup>9</sup>, L. Rachmeler<sup>1</sup>, K. K. Reeves<sup>10</sup>, B. Schmieder<sup>11</sup>, D. J. Schmit<sup>12</sup>, D. B. Seaton<sup>8</sup>, A. C. Sterling<sup>13,16</sup>, D. Tripathi<sup>14</sup>, D. R. Williams<sup>15</sup>, and M. Zhang<sup>5</sup>

*Astrophysical Journal*, 724:1133–1146, **2010**

We present a three-dimensional density model of coronal prominence cavities, and a morphological fit that has been tightly constrained by a uniquely well-observed cavity. Observations were obtained as part of an International Heliophysical Year campaign by instruments from a variety of space- and ground-based observatories, spanning wavelengths from radio to soft X-ray to integrated white light. From these data it is clear that the prominence cavity is the limb manifestation of a longitudinally extended polar-crown filament channel, and that the cavity is a region of low density relative to the surrounding corona. As a first step toward quantifying density and temperature from campaign spectroscopic data, we establish the three-dimensional morphology of the cavity. This is critical for taking line-of-sight projection effects into account, since cavities are not localized in the plane of the sky and the corona is optically thin. We have augmented a global coronal streamer model to include a tunnel-like cavity with elliptical cross-section and a Gaussian variation of height along the tunnel length. We have developed a semi-automated routine that fits ellipses to cross-sections of the cavity as it rotates past the solar limb, and have applied it to Extreme Ultraviolet Imager observations from the two *Solar Terrestrial Relations Observatory* spacecraft. This defines the morphological parameters of our model, from which we reproduce forward modeled cavity observables. We find that cavity morphology and orientation, in combination with the viewpoints of the observing spacecraft, explain the observed variation in cavity visibility for the east versus west limbs.

### Partially ejected flux ropes: Implications for interplanetary coronal mass ejections,

**Gibson**, S. E., and Y. Fan,

E-print, March 2007; *J. Geophys. Res.*, 113, A09103 (**2008**); **File**

<http://dx.doi.org/10.1029/2008JA013151>

Connecting interplanetary coronal mass ejections (ICMEs) to their solar pre-eruption source requires a clear understanding of how that source may have evolved during eruption. Gibson and Fan (2006a) have presented a three-dimensional numerical magnetohydrodynamic simulation of a CME, which showed how, in the course of eruption, a coronal flux rope may writhe and reconnect both internally and with surrounding fields in a manner that leads to a partial ejection of only part of the rope as a CME. In this paper, we will explicitly describe how the evolution during eruption found in that simulation leads to alterations of the magnetic connectivity, helicity, orientation, and topology of the ejected portion of the rope so that it differs significantly from that of the pre-eruption rope. Moreover, because a significant part of the magnetic helicity remains behind in the lower portion of the rope that survives the eruption, the region is likely to experience further eruptions. These changes would complicate how ICMEs embedded in the solar wind relate to their solar source. In particular, the location and evolution of transient coronal holes, topology of magnetic clouds (“tethered spheromak”), and likelihood of interacting ICMEs would differ significantly from what would be predicted for a CME which did not undergo writhing and partial ejection during eruption.

### Partially-ejected flux ropes: implications for space weather

Sarah E. **Gibson**<sup>1</sup> and Yuhong Fan

Solar Activity and its Magnetic Origin, Proc. IAU Symposium No. 233, **2006**, Volker Bothmer, ed., **File**

The structure and evolution of the sources of solar activity directly affects the nature of space weather disturbances that reach the Earth. We have previously demonstrated that the loss of equilibrium and partial ejection of a coronal magnetic flux rope matches observations of coronal mass ejections (CMEs) and their precursors. In this paper we discuss the significance



of such a partially-ejected rope for space weather. We will consider how the evolution and bifurcation of the rope modifies it from its initial, source configuration. In particular, we will consider how reconnections and writhing motions lead to an escaping rope which has an axis rotated counterclockwise from the original rope axis orientation, and which is rooted in transient coronal holes external to the original source region.

### **THE CALM BEFORE THE STORM: THE LINK BETWEEN QUIESCENT CAVITIES AND CORONAL MASS EJECTIONS**

S. E. [Gibson](#),<sup>1</sup> D. Foster,<sup>2</sup> J. Burkepile,<sup>1</sup> G. de Toma,<sup>1</sup> and A. Stanger  
The Astrophysical Journal, 641:590–605, 2006, File

### **The Evolving Sigmoid: Evidence for Magnetic Flux Ropes in the Corona Before, During, and After CMES**

S. E. [Gibson](#), Y. Fan, T. Török, B. Kliem,  
Space Science Reviews (2006) 124: 131–144, File

### **Energy release from impacting prominence material following the 2011 June 7 eruption**

H. R. [Gilbert](#), A. R. Inglis, M. L. Mays, L. Ofman, B. J. Thompson, C. A. Young  
E-print, Sept 2013; 2013 ApJL 776 L12

Solar filaments exhibit a range of eruptive-like dynamic activity, ranging from the full or partial eruption of the filament mass and surrounding magnetic structure as a coronal mass ejection (CME), to a fully confined or 'failed' eruption. On **2011 June 7**, a dramatic partial eruption of a filament was observed by multiple instruments on SDO and STEREO. One of the interesting aspects of this event is the response of the solar atmosphere as non-escaping material falls inward under the influence of gravity. The impact sites show clear evidence of brightening in the observed EUV wavelengths due to energy release. Two plausible physical mechanisms explaining the brightening are considered: heating of the plasma due to the kinetic energy of impacting material compressing the plasma, or reconnection between the magnetic field of low-lying loops and the field carried by the impacting material. By analyzing the emission of the brightenings in several SDO/AIA wavelengths, and comparing the kinetic energy of the impacting material ( $7.6 \times 10^{26}$  -  $5.8 \times 10^{27}$  ergs) to the radiative energy ( $1.9 \times 10^{25}$  -  $2.5 \times 10^{26}$  ergs) we find the dominant mechanism of energy release involved in the observed brightening is plasma compression.

### **UVCS/SoHO Catalog of Coronal Mass Ejections from 1996 to 2005: Spectroscopic Proprieties**

S. [Giordano](#), A. Ciaravella, J. Raymond, Y.-K. Ko and R. Suleiman  
E-print, Feb 2013; JGR, 118, Issue 3, pages 967–981, March 2013  
<http://arxiv.org/pdf/1302.1998v2.pdf>

Ultraviolet spectra of the extended solar corona have been routinely obtained by SoHO/UVCS since 1996. Sudden variations of spectral parameters are mainly due to the detection of Coronal Mass Ejections (CMEs) crossing the instrumental slit. We present a catalog of CME ultraviolet spectra based upon a systematic search of events in the LASCO CME catalog, and we discuss their statistical properties. Our catalog includes 1059 events through the end of 2005, covering nearly a full solar cycle. It is online available at the URL [http://solarweb.oato.inaf.it/UVCS\\_CME](http://solarweb.oato.inaf.it/UVCS_CME) and embedded in the online LASCO CME catalog ([http://cdaw.gsfc.nasa.gov/CME\\_list](http://cdaw.gsfc.nasa.gov/CME_list)). The emission lines observed provide diagnostics of CME plasma parameters, such as the light-of-sight velocity, density and temperature and allow to link the CME onset data to the extended corona white-light images. The catalog indicates whether there are clear signatures of features such as shock waves, current sheets, O VI flares, helical motions and which part of the CME structures (front, cavity or prominence material) are detected. The most common detected structure is the cool prominence material (in about 70% of the events). For each event, the catalog also contains movie, images, plots and information relevant to address detailed scientific investigations. The number of events detected in UV is about 1/10 of the LASCO CMEs, and about 1/4 of the halo events. We find that UVCS tends to detect faster, more massive and energetic CME than LASCO and for about 40% of the events it has been possible to determine the plasma light-of-sight velocity. [http://solarweb.oato.inaf.it/UVCS\\_CME](http://solarweb.oato.inaf.it/UVCS_CME)  
**1999-05-17, 2000-06-28, 2003-11-04**

### **Observation of Heating by Flare-accelerated Electrons in a Solar Coronal Mass Ejection**

Lindsay [Glesener](#), S?m Krucker, Hazel Bain, Robert Lin  
E-print, Dec 2013; 2013 ApJ 779 L29.

We report a Reuven Ramaty High Energy Solar Spectroscopic Imager (RHESSI) observation of flare-accelerated electrons in the core of a coronal mass ejection (CME) and examine their role in heating the CME. Previous CME observations have revealed remarkably high thermal energies that can far surpass the CME's kinetic energy. A joint observation by RHESSI and the Atmospheric Imaging Assembly of a partly occulted flare on **2010 November 3** allows

us to test the hypothesis that this excess energy is collisionally deposited by flare-accelerated electrons. Extreme ultraviolet (EUV) images show an ejection forming the CME core and sheath, with isothermal multifilter analysis revealing temperatures of  $\sim 11$  MK in the core. RHESSI images reveal a large ( $\sim 100 \times 50$  arcsec<sup>2</sup>) hard X-ray (HXR) source matching the location, shape, and evolution of the EUV plasma, indicating that the emerging CME is filled with flare-accelerated electrons. The time derivative of the EUV emission matches the HXR light curve (similar to the Neupert effect observed in soft and HXR time profiles), directly linking the CME temperature increase with the nonthermal electron energy loss, while HXR spectroscopy demonstrates that the **nonthermal electrons contain enough energy to heat the CME**. This is the most direct observation to date of flare-accelerated electrons heating a CME, emphasizing the close relationship of the two in solar eruptive events.

### **The association of transequatorial loops in the solar corona with coronal mass ejection onset,**

Astron. Astrophys., 400, 759–767, doi: 10.1051/0004-6361:20021886, 2003.

**Glover**, A., Harra, L. K., Matthews, S. A., and Foley, C. A.:

### **A Multiple flare scenario where the classic long duration flare was not the source of a CME,**

**Goff**, C.P., van Driel-Gesztelyi, L., D'Amoulin, P., Culhane, J.L., Matthews, S.A., Harra, L.K., Mandrini, C.H., Klein, K.L., Kurokawa, H.

Solar Phys (2007) 240: 283–299

<https://link.springer.com/content/pdf/10.1007%2Fs11207-007-0260-4.pdf>

A series of flares (GOES class M, M and C) and a CME were observed in close succession on **20 January 2004** in NOAA 10540. Radio observations, which took the form of types II, III and N bursts, were associated with these events. We use the combined observations from TRACE, EIT, H $\alpha$  images from Kwasan, MDI magnetograms and GOES to understand the complex development of this event. Contrary to a standard interpretation, we conclude that the first two impulsive flares are part of the CME launch process while the following long-duration event flare represents simply the recovery phase. Observations show that the flare ribbons not only separate but also shift along the magnetic inversion line so that magnetic reconnection progresses stepwise to neighboring flux tubes. We conclude that “tether cutting” reconnection in the sheared arcade progressively transforms it to a twisted flux tube, which becomes unstable, leading to a CME. We interpret the third flare, a long-duration event, as a combination of the classical two-ribbon flare with the relaxation process following forced reconnection between the expanding CME structure and neighboring magnetic fields.

### **ERUPTING FLUX ROPE, RISING X-RAY SOURCE AND A SLOW CME ON 16 APRIL 2002**

C.P. **Goff**, L. van Driel-Gesztelyi<sup>1,2,3</sup>, L.K. Harra<sup>1</sup>, S.A. Matthews<sup>1</sup> & C.H. Mandrini<sup>4</sup>

Proceedings of the 11th European Solar Physics Meeting - The Dynamic Sun: Challenges for Theory and Observations, 11-16 September 2005 (ESA SP-596 or 600, December 2005)

### **Clustering of fast Coronal Mass Ejections during the solar cycles 23 and 24 and implications for CME-CME interactions**

[Jenny M. Rodríguez Gómez](#), [Tatiana Podladchikova](#), [Astrid Veronig](#), [Alexander Ruzmaikin](#), [Joan Feynman](#), [Anatoly Petrukovich](#)

ApJ 899 47 2020

<https://arxiv.org/pdf/2006.10404.pdf>

<https://doi.org/10.3847/1538-4357/ab9e72>

We study the clustering properties of fast Coronal Mass Ejections (CMEs) that occurred during solar cycles 23 and 24. We apply two methods: the Max spectrum method can detect the predominant clusters and the de-clustering threshold time method provides details on the typical clustering properties and time scales. Our analysis shows that during the different phases of solar cycles 23 and 24, CMEs with speed  $\geq 1000$  km/s preferentially occur as isolated events and in clusters with on average two members. However, clusters with more members appear particularly during the maximum phases of the solar cycles. Over the total period and in the maximum phases of solar cycles 23 and 24, about 50% are isolated events, 18% (12%) occur in clusters with 2 (3) members, and another 20% in larger clusters  $\geq 4$ , whereas in solar minimum fast CMEs tend to occur more frequently as isolated events (62%). During different solar cycle phases, the typical de-clustering time scales of fast CMEs are  $\tau_c = 28\text{--}32$  hrs, irrespective of the very different occurrence frequencies of CMEs during solar minimum and maximum. These findings suggest that  $\tau_c$  for extreme events may reflect the characteristic energy build-up time for large flare and CME-prolific active ARs. Associating statistically the clustering properties of fast CMEs with the Disturbance storm index  $\{Dst\}$  at Earth suggests that fast CMEs occurring in clusters tend to produce larger geomagnetic storms than isolated fast CMEs. This may be related to CME-CME interaction producing a more complex and stronger interaction with the Earth magnetosphere. **2000-11-23-25, 2005-08-22-23, 2017-09-09-10**

5. GEO-EFFECTIVENESS OF CME CLUSTERS

## SIMULATIONS OF THE

### **Kelvin-Helmholtz instability driven by coronal mass ejections in the turbulent corona**

Daniel O. [Gomez](#), Edward E. DeLuca, Pablo D. Mininni

2016 *ApJ* **818** 126

Recent high-resolution Atmospheric Imaging Assembly/*Solar Dynamics Observatory* images show evidence of the development of the Kelvin–Helmholtz (KH) instability, as coronal mass ejections (CMEs) expand in the ambient corona. A large-scale magnetic field mostly tangential to the interface is inferred, both on the CME and on the background sides. However, the magnetic field component along the shear flow is not strong enough to quench the instability. There is also observational evidence that the ambient corona is in a turbulent regime, and therefore the criteria for the development of the instability are a priori expected to differ from the laminar case. To study the evolution of the KH instability with a turbulent background, we perform three-dimensional simulations of the incompressible magnetohydrodynamic equations. The instability is driven by a velocity profile tangential to the CME–corona interface, which we simulate through a hyperbolic tangent profile. The turbulent background is generated by the application of a stationary stirring force. We compute the instability growth rate for different values of the turbulence intensity, and find that the role of turbulence is to attenuate the growth. The fact that KH instability is observed sets an upper limit on the correlation length of the coronal background turbulence.

See <http://arxiv.org/pdf/1408.2598v1.pdf>

### **Numerical simulations of a two-fluid jet at a magnetic null point in a solar arcade**

[J. J. González-Avilés](#), [K. Murawski](#), [T. V. Zaqarashvili](#)

*MNRAS* Volume 515, Issue 4, October 2022, Pages 5094–5105,

<https://doi.org/10.1093/mnras/stac2032>

<https://arxiv.org/pdf/2207.07610.pdf>

We study the formation and evolution of jets in the solar atmosphere using numerical simulations of partially ionized plasma. The two-fluid magnetohydrodynamic equations with ion+electron and neutral hydrogen components are used in two-dimensional (2D) Cartesian geometry. Numerical simulations show that a localized nonlinear Gaussian pulse of ion and neutral pressures initially launched from the magnetic null point of a potential arcade located below the transition region quickly develops into a shock due to the decrease of density with height. The shock propagates upwards into the solar corona and lifts the cold and dense chromospheric plasma behind in the form of a collimated jet with an inverted-Y shape. The inverted-Y shape of jets is connected with the topology of a magnetic null point. The pulse also excites a nonlinear wake in the chromosphere, which leads to quasi-periodic secondary shocks. The secondary shocks lift the chromospheric plasma upwards and create quasi-periodic jets in the lower corona. Ion and neutral fluids show generally similar behavior, but their relative velocity is higher near the upper part of jets, which leads to enhanced temperature or heating due to ion-neutral collisions. Simulations of jets with inverted-Y shape and their heating may explain the properties of some jets observed in the solar atmosphere.

### **Numerical simulations of macrospicule jets under energy imbalance conditions in the solar atmosphere**

[J J González-Avilés](#), [K Murawski](#), [A K Srivastava](#), [T V Zaqarashvili](#), [J A González-Esparza](#)

*MNRAS* , Volume 505, Issue 1, July 2021, Pages 50–64,

<https://doi.org/10.1093/mnras/stab1261>

Using numerical simulations, we study the effects of thermal conduction and radiative cooling on the formation and evolution of solar jets with some macrospicules features. We initially assume that the solar atmosphere is rarely in equilibrium through energy imbalance. Therefore, we test whether the background flows resulting from an imbalance between thermal conduction and radiative cooling influence the jets' behaviour. In this particular scenario, we trigger the formation of the jets by launching a vertical velocity pulse localized at the upper chromosphere for the following test cases: (i) adiabatic case; (ii) thermal conduction case; (iii) radiative cooling case; and (iv) thermal conduction + radiative cooling case. According to the test results, the addition of the thermal conduction results in smaller and hotter jets than in the adiabatic case. On the other hand, the radiative cooling dissipates the jet after reaching the maximum height ( $\approx 5.5$  Mm), making it shorter and colder than in the adiabatic and thermal conduction cases. Besides, the flow generated by the radiative cooling is more substantial than that caused by the thermal conduction. Despite the energy imbalance of the solar atmosphere background, the simulated jet shows morphological features of macrospicules. Furthermore, the velocity pulse steepens into a shock that propagates upward into a solar corona that maintains its initial temperature. The shocks generate the jets with a quasi-periodical behaviour that follows a parabolic path on time–distance plots consistent with macrospicule jets' observed dynamics.

## **II. Analysis of 3D plasma motions in a chromospheric jet formed due to magnetic reconnection**

[J. J. González-Avilés](#), [F. S. Guzmán](#), [V. Fedun](#), [G. Verth](#), [R. Sharma](#), [S. Shelyag](#), [S. Regnier](#)

*ApJ*

2018

<https://arxiv.org/pdf/1807.04224.pdf>

Within the framework of resistive MHD, implementing the C7 equilibrium atmosphere model and a 3D potential magnetic field realistic configuration, we simulate the formation of a plasma jet with the morphology, upward velocity up to 130 km/s and timescale formation between 60 and 90 s after beginning of simulation, similar to those expected for

Type II spicules. Initial results of this simulation were published in Paper I e.g. \cite{Gonzalez-Aviles\_et\_al\_2018} and present paper is devoted to the analysis of transverse displacements and rotational type motion of the jet. Our results suggest that 3D magnetic reconnection may be responsible for the formation of the jet in Paper I. In this paper, by calculating times series of the velocity components  $v_x$  and  $v_y$  in different points near to the jet for various heights we find transverse oscillations in agreement with spicule observations. We also obtain a time-distance plot of the temperature in a cross-cut at the plane  $x=0.1$  Mm and find significant transverse displacements of the jet. By analyzing temperature isosurfaces of 104 K with the distribution of  $v_x$ , we find that if the line-of-sight (LOS) is approximately perpendicular to the jet axis then there is both motion towards and away from the observer across the width of the jet. This red-blue shift pattern of the jet is caused by rotational motion, initially clockwise and anti-clockwise afterwards, which could be interpreted as torsional motion. From a nearly vertical perspective of the jet the LOS velocity component shows a central blue-shift region surrounded by red-shifted plasma.

## I. Jet Formation and Evolution Due to 3D Magnetic Reconnection

J. J. **González-Avilés**<sup>1</sup>, F. S. Guzmán<sup>1</sup>, V. Fedun<sup>2</sup>, G. Verth<sup>3</sup>, S. Shelyag<sup>4</sup>, and S. Regnier<sup>4</sup>  
2018 ApJ 856 176

<http://sci-hub.tw/http://iopscience.iop.org/0004-637X/856/2/176/>

<http://iopscience.iop.org/article/10.3847/1538-4357/aab36f/pdf>

Using simulated data-driven, 3D resistive MHD simulations of the solar atmosphere, we show that 3D magnetic reconnection may be responsible for the formation of jets with the characteristics of Type II spicules. We numerically model the photosphere-corona region using the C7 equilibrium atmosphere model. The initial magnetic configuration is a 3D potential magnetic field, extrapolated up to the solar corona region from a dynamic realistic simulation of the solar photospheric magnetoconvection model that mimics the quiet-Sun. In this case, we consider a uniform and constant value of the magnetic resistivity of  $12.56 \Omega \text{ m}$ . We have found that the formation of the jet depends on the Lorentz force, which helps to accelerate the plasma upward. Analyzing various properties of the jet dynamics, we found that the jet structure shows a Doppler shift close to regions with high vorticity. The morphology, the upward velocity covering a range up to  $130 \text{ km s}^{-1}$ , and the timescale formation of the structure between 60 and 90 s, are similar to those expected for Type II spicules.

**UKSP Nugget:** #97 June 2019

<http://www.uksolphys.org/uksp-nugget/97-jet-formation-and-evolution-due-to-3d-magnetic-reconnection/>

## Jet formation in solar atmosphere due to magnetic reconnection

J.J. **González-Avilés**, F.S. Guzmán, V. Fedun

ApJ 836 24 2017

<https://arxiv.org/pdf/1609.09422v1.pdf>

Using numerical simulations, we show that jets with features of type II spicules and cold coronal jets corresponding to temperatures 104 K can be formed due to magnetic reconnection in a scenario in presence of magnetic resistivity. For this we model the low chromosphere-corona region using the C7 equilibrium solar atmosphere model and assuming Resistive MHD rules the dynamics of the plasma. The magnetic field configurations we analyze correspond to two neighboring loops with opposite polarity. The separation of the loops' feet determines the thickness of a current sheet that triggers a magnetic reconnection process, and the further formation of a high speed and sharp structure. We analyze the cases where the magnetic field strength of the two loops is equal and different. In the first case, with a symmetric configuration the spicules raise vertically whereas in an asymmetric configuration the structure shows an inclination. With a number of simulations carried out under a 2.5D approach, we explore various properties of excited jets, namely, the morphology, inclination and velocity. The parameter space involves magnetic field strength between 20 and 40 G, and the resistivity is assumed to be uniform with a constant value of the order  $10^{-2} \Omega \text{ m}$

## Speed Evolution of Fast CME/Shocks: Analysis of Kilometric Type II Emissions

J. A. **Gonzalez-Esparza** and E. Aguilar-Rodriguez

Ann. Geophys., 27, 3957-3966, 2009, **File**

Fast CME/shocks propagating in the interplanetary medium can generate kilometric Type II (km-TII) radio emissions at the local plasma frequency and/or its harmonic, so these radio emissions provide a means of remotely tracking CME/shocks. We apply a new analysis technique, using the frequency drift of km-TII spectrum obtained by the Thermal Noise Receiver (TNR) of the WIND/WAVES experiment, to infer, at some adequate intervals, the propagation speed of six CME/shocks. We combine these results with previously reported speeds from coronagraph white light and interplanetary scintillation observations, and in-situ measurements, to study the temporal speed evolution of the six events. The speed values obtained by the km-TII analysis are in a reasonable agreement with the speed measurements obtained by other techniques at different heliocentric distance ranges. The combination of all the speed measurements show a gradual deceleration of the CME/shocks as they propagate to 1 AU. This new technique can be useful in studying the evolution of fast CME/shocks when adequate intervals of km-TII emissions are available.

## CME Classification Based on Wavelet Spectra

D.I. **González-Gómez** · X. Blanco-Cano · A.C. Raga

Solar Phys (2010) 266: 337–347

We study the internal structure of coronal mass ejections (CMEs) using wavelet analysis. We derive wavelet spectra, spatially integrated over regions of interest within LASCO C2 white-light coronagraphic images. These spectra show an inflection point, which we use to characterize each spectrum. In a diagram of flux vs. spatial scale of the inflection point, we find that the analyzed structures fall into two, distinct groups: a low-flux, small-spatial-scale group (which we call the “homogeneous” type), and a high-flux, larger-spatial-scale group (the “collimated” type). Interestingly, if we study different regions of a given image, all of the structures fall into one of the two groups described above. From a qualitative comparison with the images, it is clear that the two groups identified by the wavelet analysis correspond to two types of morphologies, which are seen as either more-homogeneous or more-collimated structures.

### **A morphological study of CMEs using wavelet analysis**

D.I. [González-Gómez](#), , X. Blanco-Cano, and A.C. Raga,

Advances in Space Research

Volume 46, Issue 1, 1 July 2010, Pages 22-30; **File**

The principal objective of this study is to analyze structures of Coronal Mass Ejections (CMEs) using a wavelet technique. We use data measured with the SOHO/LASCO coronagraphs C2–C3, EIT and STEREO COR1A–B, COR2A–B. We have found that different structures show up in a CME at different spatial scales of wavelets. We also study the orientation of the most intense flux and find the orientation of the structures in the CME.

**2 Jan 2008**

### **Acceleration of Type 2 Spicules in the Solar Chromosphere - 2: Viscous Braking and Upper Bounds on Coronal Energy Input**

Michael L. [Goodman](#)

**2014**

<http://arxiv.org/pdf/1403.2694v1.pdf>

A magnetohydrodynamic model is used to determine conditions under which the Lorentz force accelerates plasma to type 2 spicule speeds in the chromosphere. The model generalizes a previous model to include a more realistic pre-spicule state, and the vertical viscous force. Two cases of acceleration under upper chromospheric conditions are considered. The magnetic field strength for these cases is  $\leq 12.5$  and 25 G. Plasma is accelerated to terminal vertical speeds of 66 and 78 km/s in 100 s, compared with 124 and 397 km/s for the case of zero viscosity. The flows are localized within horizontal diameters  $\sim 80$  and 50 km. The total thermal energy generated by viscous dissipation is  $\sim 10$  times larger than that due to Joule dissipation, but the magnitude of the total cooling due to rarefaction is  $\gg$  this energy. Compressive heating dominates during the early phase of acceleration. The maximum energy injected into the corona by type 2 spicules, defined as the energy flux in the upper chromosphere, may largely balance total coronal energy losses in quiet regions, possibly also in coronal holes, but not in active regions. It is proposed that magnetic flux emergence in inter-granular regions drives type 2 spicules.

### **The multiview observatory for solar terrestrial science (MOST)**

N. [Gopalswamy](#)<sup>1\*</sup>, S. Christel<sup>1</sup>, S. F. Fung<sup>1</sup>, Q. Gong<sup>1</sup>, J. R. Gruesbeck<sup>1</sup>, + + +

Journal of Atmospheric and Solar-Terrestrial Physics, Volume 254, article id. 106165. **2024**

<https://arxiv.org/pdf/2303.02895>

[https://ntrs.nasa.gov/api/citations/20220013621/downloads/GopalswamyNat\\_MOST\\_WP.pdf](https://ntrs.nasa.gov/api/citations/20220013621/downloads/GopalswamyNat_MOST_WP.pdf)

### **The SOHO LASCO CME Catalog -- Version 2**

[Nat Gopalswamy](#), [Grzegorz Michalek](#), [Seiji Yashiro](#), [Pertti Mäkelä](#), [Sachiko Akiyama](#), [Hong Xie](#), [Angelos Vourlidas](#)

Proceedings of IAU Symposium 388 **2024**

<https://arxiv.org/pdf/2407.04165>

This paper provides an update on the coronal mass ejection (CME) catalog maintained at the CDAW Data Center, NASA Goddard Space Flight Center ([this https URL](https://cdaw.gsfc.nasa.gov/)). This is version 2 (v2) of the Catalog that has been made as the default version as of May 1, 2024. The new features of the Catalog v2 are (i) online measurement tool, (ii) combination JavaScript movies from the STEREO and Solar Dynamics Observatory (SDO) missions, and (iii) insertion of newly identified CMEs for the period 1996 to 2004. The CME identification was revisited resulting in a set of  $\sim 3000$  new CMEs added to the Catalog. A vast majority of these CMEs are weak and narrow. The resulting statistical properties of CMEs are not significantly different from those reported using version 1. **2003-01-20, 2012-01-02**

### **Implications of the abundance of halo coronal mass ejections for the strength of solar cycle 25**

[Nat Gopalswamy](#), [Grzegorz Michalek](#), [Seiji Yashiro](#), [Pertti Makela](#), [Sachiko Akiyama](#), [Hong Xie](#)

<https://arxiv.org/pdf/2407.04548>

We assess the relative strength of solar cycle (SC) 25 with respect to SCs 23 and 24 based on the abundance of halo coronal mass ejections (CMEs). We make use of the halo CME database ([this https URL](#)) to compare the halo CME abundance during the first four years in each of SCs 23 to 25. The main result is that in several aspects such as the abundance, occurrence rate, source locations, and halo heights, halo CMEs are similar between SCs 24 and 25 but different from SC 23. This result follows from the fact that weaker cycles have low heliospheric total pressure, whose backreaction on CMEs allows them to expand more and hence enhancing the chance of becoming a halo. The solar cycle variation of halo CME properties is consistent with the precursor-based cycle prediction methods that indicate SC 25 is similar to or only slightly stronger than SC 24.

### What do halo CMEs tell us about solar cycle 25?

[Nat Gopalswamy](#), [Grzegorz Michalek](#), [Seiji Yashiro](#), [Pertti Mäkelä](#), [Sachiko Akiyama](#), [Hong Xie](#)

ApJL 952 L13 2023

<https://arxiv.org/ftp/arxiv/papers/2306/2306.06633.pdf>

<https://iopscience.iop.org/article/10.3847/2041-8213/acdde2/pdf>

It is known that the weak state of the heliosphere due to diminished solar activity in cycle 24 back-reacted on coronal mass ejections (CMEs) to make them appear wider for a given speed. One of the consequences of the weak state of the heliosphere is that more CMEs appear as halo CMEs (HCMEs), and halos are formed at shorter heliocentric distances. Current predictions for the strength of solar cycle (SC) 25 range from half to twice the strength of SC 24. We compare the HCME occurrence rate and other properties during the rise phase of cycles 23, 24, and 25 to weigh in on the strength of SC 25. We find that HCME and solar wind properties in SC 25 are intermediate between SCs 23 and 24, but closer to SC 24. The HCME occurrence rate, normalized to the sunspot number, is higher in SCs 24 and 25 than in SC 23. The solar wind total pressure in SC 25 is ~35% smaller than that in SC 23. Furthermore, the occurrence rates of high-energy solar energetic particle events and intense geomagnetic storms are well below the corresponding values in SC 23, but similar to those in SC 24. We conclude that cycle 25 is likely to be similar to or slightly stronger than cycle 24, in agreement with polar-field precursor methods for cycle 25 prediction.

### What is Unusual about the Third Largest Geomagnetic Storm of Solar Cycle 24?

[N. Gopalswamy](#), [S. Yashiro](#), [S. Akiyama](#), [H. Xie](#), [P. Mäkelä](#), [M.-C. Fok](#), [C. P. Ferradas](#)

JGR Volume 127, Issue 8, article id. e30404 2022

<https://arxiv.org/ftp/arxiv/papers/2207/2207.11630.pdf>

<https://agupubs.onlinelibrary.wiley.com/doi/epdf/10.1029/2022JA030404>

We report on the solar and interplanetary (IP) causes of the third largest geomagnetic storm (2018 August 26) in solar cycle 24. The underlying coronal mass ejection (CME) originating from a quiescent filament region becomes a 440 km/s magnetic cloud (MC) at 1 au after ~5 days. The prolonged CME acceleration (for about 24 hrs) coincides with the time profiles of the post-eruption arcade intensity and reconnected flux. Chen et al. (2019) obtain lower speed since they assumed that the CME does not accelerate after about 12 hrs. The presence of multiple coronal holes near the filament channel and the high-speed wind from them seem to have the combined effect of producing complex rotation in the corona and IP medium resulting in a high-inclination MC. The Dst time profile in the main phase steepens significantly (rapid increase in storm intensity) coincident with the density increase (prominence material) in the second half of the MC. Simulations using the Comprehensive Inner Magnetosphere-Ionosphere (CIMI) model shows that a higher ring current energy results from larger dynamic pressure in MCs. Furthermore, the Dst index is highly correlated with the main-phase time integral of the ring current injection that includes density, consistent with the simulations. A complex temporal structure develops in the storm main phase if the underlying MC has a complex density structure during intervals of southward interplanetary magnetic field. We conclude that the high intensity of the storm results from the prolonged CME acceleration, complex rotation, and the high density in the 1-au MC.

### Effect of the Weakened Heliosphere in Solar Cycle 24 on the Properties of Coronal Mass Ejections

[N. Gopalswamy](#), [S. Akiyama](#), [S. Yashiro](#), [G. Michalek](#), [H. Xie](#), [P. Mäkelä](#)

Proc. 19th International Astrophysics Conference held in Santa Fe, New Mexico, March 9 - 13, 2020

<https://arxiv.org/ftp/arxiv/papers/2007/2007.08291.pdf>

Solar cycle (SC) 24 has come to an end by the end of 2019, providing information on two full cycles to understand the manifestations of SC 24, the smallest cycle in the Space Age that has resulted in a weak heliospheric state indicated by the reduced pressure. The backreaction of the heliospheric state is to make the coronal mass ejections (CMEs) appear physically bigger than in SC 23, but their magnetic content has been diluted resulting in a lower geoeffectiveness. The heliospheric magnetic field is also lower in SC 24, leading to the dearth of high-energy solar energetic particle (SEP) events. These space weather events closely follow fast and wide (FW) CMEs. All but FW CMEs are higher in number in SC 24. The CME rate vs. sunspot number (SSN) correlation is high in both cycles but the rate increases faster in SC 24. We revisit the study of limb CMEs (those with source regions within 30 degrees from the limb) previously studied over partial cycles. We find that limb CMEs are slower in SC 24 as in the general population but wider. Limb halo CMEs follow the same trend of slower SC-24 CMEs. However, the SC-24 CMEs become halos at a shorter distance from the Sun. Thus, slower CMEs becoming halos sooner is a clear indication of the backreaction of the weaker

heliospheric state on CMEs. We can further pin down the heliospheric state as the reason for the altered CME properties because the associated flares have similar distributions in the two cycles, unaffected by the heliospheric state. **2002-09-06**

**Table 3.** Halo CMEs originating within  $30^\circ$  from the limb in solar cycles 23 and 24

## The State of the Heliosphere Revealed by Limb Halo Coronal Mass Ejections in Solar Cycles 23 and 24

Nat **Gopalswamy**, [Sachiko Akiyama](#), [Seiji Yashiro](#)

ApJL 897:L1 **2020**

<https://arxiv.org/ftp/arxiv/papers/2006/2006.05844.pdf>

<https://iopscience.iop.org/article/10.3847/2041-8213/ab9b7b/pdf>

We compare the properties of halo coronal mass ejections (CMEs) that originate close to the limb (within a central meridian distance range of 60 to 90 deg) during solar cycles 23 and 24 to quantify the effect of the heliospheric state on CME properties. There are 44 and 38 limb halos in the cycles 23 and 24, respectively. Normalized to the cycle-averaged total sunspot number, there are 42 percent more limb halos in cycle 24. Although the limb halos as a population is very fast (average speed 1464 km s<sup>-1</sup>), cycle-24 halos are slower by 26 percent than the cycle-23 halos. We introduce a new parameter, the heliocentric distance of the CME leading edge at the time a CME becomes a full halo; this height is significantly shorter in cycle 24 (by 20 percent) and has a lower cutoff at 6 Rs. These results show that cycle-24 CMEs become halos sooner and at a lower speed than the cycle-23 ones. On the other hand, the flare sizes are very similar in the two cycles, ruling out the possibility of eruption characteristics contributing to the differing CME properties. In summary, this study reveals the effect of the reduced total pressure in the heliosphere that allows cycle-24 CMEs expand more and become halos sooner than in cycle 23. Our findings have important implications for the space-weather consequences of CMEs in cycle 25 (predicted to be similar to cycle 24) and for understanding the disparity in halo counts reported by automatic and manual catalogs. **2011 September 22**

**Table 1.** List of Limb Halo CMEs from Solar Cycles 23 and 24

## A Catalog of Type II Radio Bursts Observed by Wind/WAVES and their Statistical Properties

Nat **Gopalswamy**, [Pertti Mäkelä](#), [Seiji Yashiro](#)

Sun and Geosphere vol.14, no.2, p.111-121 **2019**

<https://arxiv.org/ftp/arxiv/papers/1912/1912.07370.pdf> **File**

Solar type II radio bursts are the signature of particle acceleration by shock waves in the solar corona and interplanetary medium. The shocks originate in solar eruptions involving coronal mass ejections (CMEs) moving at super-Alfvénic speeds. Type II bursts occur at frequencies ranging from hundreds of MHz to tens of kHz, which correspond to plasma frequencies prevailing in the inner heliosphere from the base of the solar corona to the vicinity of Earth. Type II radio bursts occurring at frequencies below the ionospheric cutoff are of particular importance, because they are due to very energetic CMEs that can disturb a large volume of the heliosphere. The underlying shocks accelerate not only electrons that produce the type II bursts, but also protons and heavy ions that have serious implications for space weather. The type II radio burst catalog ([this https URL](#)) presented here provides detailed information on the bursts observed by the Radio and Plasma Wave Experiment (WAVES) on board the Wind Spacecraft. The catalog is enhanced by compiling the associated flares, CMEs, solar energetic particle (SEP) events including their basic properties. We also present the statistical properties of the radio bursts and the associated phenomena, including solar-cycle variation of the occurrence rate of the type II bursts. **2000.11.09, 2005.01.15-16, 2012.07.04**

See [https://cdaw.gsfc.nasa.gov/CME\\_list/radio/waves\\_type2.html](https://cdaw.gsfc.nasa.gov/CME_list/radio/waves_type2.html)

## Coronal Flux Ropes and their Interplanetary Counterparts

N. **Gopalswamy**, S. Akiyama, S. Yashiro, H. Xie

J. Atmos. Solar-Terr. Phys. Volume 180, Pages 35-45, November **2018** **File (2017)**

<https://arxiv.org/pdf/1705.08912.pdf>

[sci-hub.tw/10.1016/j.jastp.2017.06.004](https://sci-hub.tw/10.1016/j.jastp.2017.06.004)

We report on a study comparing coronal flux ropes inferred from eruption data with their interplanetary counterparts constructed from in situ data. The eruption data include the source-region magnetic field, post-eruption arcades, and coronal mass ejections (CMEs). Flux ropes were fit to the interplanetary CMEs (ICMEs) considered for the 2011 and 2012 Coordinated Data Analysis Workshops (CDAWs). We computed the total reconnected flux involved in each of the associated solar eruptions and found it to be closely related to flare properties, CME kinematics, and ICME properties. By fitting flux ropes to the white-light coronagraph data, we obtained the geometric properties of the flux ropes and added magnetic properties derived from the reconnected flux. We found that the CME magnetic field in the corona is significantly higher than the ambient magnetic field at a given heliocentric distance. The radial dependence of the flux-rope magnetic field strength is faster than that of the ambient magnetic field. The magnetic field strength of the coronal flux rope is also correlated with that in interplanetary flux ropes constructed from in situ data, and with the observed peak magnetic field strength in ICMEs. The physical reason for the observed correlation between the peak field strength in MCs is the higher magnetic field content in faster coronal flux ropes and ultimately the higher reconnected flux in the eruption region. The magnetic flux ropes constructed from the eruption data and coronagraph observations provide a

realistic input that can be used by various models to predict the magnetic properties of ICMEs at Earth and other destination in the heliosphere. **1999 June 24**

**Table** ICMEs during solar cycle 23 with solar sources near Disk Center ( $E15^\circ \leq \text{source longitude} \leq W15^\circ$ ) (from Gopalswamy et al. 2010; 2013).

## **Sun-to-Earth Propagation of the 2015 June 21 Coronal Mass Ejection Revealed by Optical, EUV, and Radio Observations**

N. [Gopalswamy](#), [P. Makela](#), [S. Akiyama](#), [S. Yashiro](#), [H. Xie](#), [N. Thakur](#)

JASTP Volume 179, p. 225-238. **2018**

<https://arxiv.org/ftp/arxiv/papers/1807/1807.10979.pdf>

<https://pdf.sciencedirectassets.com/271871/1-s2.0-S1364682618X00145/1-s2.0-S13646826183025>

We investigate the propagation of the **2015 June 21** CME-driven shock as revealed by the type II bursts at metric and longer wavelengths and coronagraph observations. The CME was associated with the second largest geomagnetic storm of solar cycle 24 and a large solar energetic particle (SEP) event. The eruption consisted of two M-class flares, with the first one being confined, with no metric or interplanetary radio bursts. However, there was intense microwave burst, indicating accelerated particles injected toward the Sun. The second flare was eruptive that resulted in a halo CME. The CME was deflected primarily by an equatorial coronal hole that resulted in the modification of the intensity profile of the associated SEP event and the duration of the CME at Earth. The interplanetary type II burst was particularly intense and was visible from the corona all the way to the vicinity of the Wind spacecraft with fundamental-harmonic structure. We computed the shock speed using the type II drift rates at various heliocentric distances and obtained information on the evolution of the shock that matched coronagraph observations near the Sun and in-situ observations near Earth. The depth of the geomagnetic storm is consistent with the 1-AU speed of the CME and the magnitude of the southward component.

## **Extreme Kinematics of the 2017 September 10 Solar Eruption and the Spectral Characteristics of the Associated Energetic Particles**

N. [Gopalswamy](#), [S. Yashiro](#), [P. Makela](#), [H. Xie](#), [S. Akiyama](#), [C. Monstein](#)

ApJL **863** L39 **2018**

<https://arxiv.org/ftp/arxiv/papers/1807/1807.09906.pdf>

<http://sci-hub.tw/http://iopscience.iop.org/article/10.3847/2041-8213/aad86c/meta>

We report on the **2017 September 10** ground level enhancement (GLE) event associated with a coronal mass ejection (CME) whose initial acceleration ( $\sim 9.1 \text{ km s}^{-2}$ ) and initial speed ( $\sim 4300 \text{ km/s}$ ) were among the highest observed in the SOHO era. The GLE event was of low intensity ( $\sim 4.4\%$  above background) and softer-than-average fluence spectrum. We suggest that poor connectivity (longitudinal and latitudinal) of the source to Earth compounded by the weaker ambient magnetic field contributed to these GLE properties. Events with similar high initial speed either lacked GLE association or had softer fluence spectra. The shock-formation height inferred from the metric type II burst was  $\sim 1.4 R_s$ , consistent with other GLE events. The shock height at solar particle release (SPR) was  $\sim 4.4 \pm 0.38 R_s$ , consistent with the parabolic relationship between the shock height at SPR and source longitude. **2012 July 7, 2014 January 7**

## **Coronal mass ejections as a new indicator of the active Sun**

Nat [Gopalswamy](#)

Proc. IAU Symposium 340 on Long-term datasets for the understanding of solar and stellar magnetic cycles, February 19-24, 2018 Jaipur, India. **2018**

<https://arxiv.org/pdf/1804.11112.pdf>

Coronal mass ejections (CMEs) have become one of the key indicators of solar activity, especially in terms of the consequences of the transient events in the heliosphere. Although CMEs are closely related to the sunspot number (SSN), they are also related to other closed magnetic regions on the Sun such as quiescent filament regions. This makes CMEs a better indicator of solar activity. While sunspots mainly represent the toroidal component of solar magnetism, quiescent filaments (and hence CMEs associated with them) connect the toroidal and poloidal components via the rush-to-the-pole (RTTP) phenomenon. Taking the end of RTTP in each hemisphere as an indicator of solar polarity reversal, it is shown that the north-south reversal asymmetry has a quasi-periodicity of 3-5 solar cycles. Focusing on the geospace consequences of CMEs, it is shown that the maximum CME speeds averaged over Carrington rotation period show good correlation with geomagnetic activity indices such as Dst and aa.

## **A new technique to provide realistic input to CME forecasting models**

Nat [Gopalswamy](#), [Sachiko Akiyama](#), [Seiji Yashiro](#), [Hong Xie](#)

IAU Symposium 335: Space Weather of the Heliosphere: Processes and Forecasts **2017**

<https://arxiv.org/pdf/1709.03160.pdf>

We report on a technique to construct a flux rope (FR) from eruption data at the Sun. The technique involves line-of-sight magnetic fields, post-eruption arcades in the corona, and white-light coronal mass ejections (CMEs) so that the FR geometric and magnetic properties can be fully defined in addition to the kinematic properties. We refer to this FR as FRED (Flux Rope from Eruption Data). We illustrate the FRED construction using the **2012 July 12** eruption and



compare the coronal and interplanetary properties of the FR. The results indicate that the FRED input should help make realistic predictions of the components of the FR magnetic field in the heliosphere.

## Extreme Solar Eruptions and their Space Weather Consequences Review

Nat **Gopalswamy**

2017, be published by Elsevier as a chapter in the book, "Extreme Events in the Geospace: Origins, Predictability and Consequences", Ed. Natalia Buzulukova

<https://arxiv.org/ftp/arxiv/papers/1709/1709.03165.pdf> **File**

Solar eruptions generally refer to coronal mass ejections (CMEs) and flares. Both are important sources of space weather. Solar flares cause sudden change in the ionization level in the ionosphere. CMEs cause solar energetic particle (SEP) events and geomagnetic storms. A flare with unusually high intensity and/or a CME with extremely high energy can be thought of examples of extreme events on the Sun. These events can also lead to extreme SEP events and/or geomagnetic storms. Ultimately, the energy that powers CMEs and flares are stored in magnetic regions on the Sun, known as active regions. Active regions with extraordinary size and magnetic field have the potential to produce extreme events. Based on current data sets, we estimate the sizes of one-in-hundred and one-in-thousand year events as an indicator of the extremeness of the events. We consider both the extremeness in the source of eruptions and in the consequences. We then compare the estimated 100-year and 1000-year sizes with the sizes of historical extreme events measured or inferred.

**Carrington flare , 2003 October 28, 2004 November 10, October 2014**

**Table 1.** Integral fluence values for different models in units of  $10^{10}$  p cm<sup>-2</sup>

**Table 2.** Expected 100-year and 1000-year event sizes estimated from the tail of observed distributions fitted to various functions.

## A Hierarchical Relationship between the Fluence Spectra and CME Kinematics in Large Solar Energetic Particle Events: A Radio Perspective

N **Gopalswamy**, P Mäkelä, S Yashiro, [N Thakur](#), [S Akiyama](#), [H Xie](#)

Journal of Physics: Conference Series (JPCS), Proceedings of the 16th Annual International Astrophysics Conference held in Santa Fe, NM, 2017

<https://arxiv.org/ftp/arxiv/papers/1707/1707.00209.pdf>

We report on further evidence that solar energetic particles are organized by the kinematic properties of coronal mass ejections (CMEs)[1]. In particular, we focus on the starting frequency of type II bursts, which is related to the distance from the Sun where the radio emission starts. We find that the three groups of solar energetic particle (SEP) events known to have distinct values of CME initial acceleration, also have distinct average starting frequencies of the associated type II bursts. SEP events with ground level enhancement (GLE) have the highest starting frequency (107 MHz), while those associated with filament eruption (FE) in quiescent regions have the lowest starting frequency (22 MHz); regular SEP events have intermediate starting frequency (81 MHz). Taking the onset time of type II bursts as the time of shock formation, we determine the shock formation heights measured from the Sun center. We find that the shocks form on average closest to the Sun (1.51 Rs) in GLE events, farthest from the Sun in FE SEP events (5.38 Rs), and at intermediate distances in regular SEP events (1.72 Rs). Finally, we present the results of a case study of a CME with high initial acceleration ( $\sim 3$  km s<sup>-2</sup>) and a type II radio burst with high starting frequency ( $\sim 200$  MHz) but associated with a minor SEP event. We find that the relation between the fluence spectral index and CME initial acceleration continues to hold even for this minor SEP event. **2010 June 12, 2011 November 26, 2012 May 17**

## Estimation of Reconnection Flux using Post-eruption Arcades and Its Relevance to 1-au Magnetic Clouds

N. **Gopalswamy**, S. Yashiro, S. Akiyama, H. Xie

Solar Phys. 292, 65 2017

<https://arxiv.org/pdf/1701.01943v1.pdf> **File**

We report on a new method to compute the flare reconnection (RC) flux from post-eruption arcades (PEAs) and the underlying photospheric magnetic fields. In previous work, the RC flux has been computed using cumulative flare ribbon area. Here we obtain the RC flux as half of that underlying the PEA associated with the eruption using an image in EUV taken after the flare maximum. We apply this method to a set of 21 eruptions that originated near the solar disk center in solar cycle 23. We find that the RC flux from the arcade method ( $\{\Phi\}_rA$ ) has excellent agreement with that from the ribbon method ( $\{\Phi\}_rR$ ) according to:  $\{\Phi\}_rA = 1.24(\{\Phi\}_rR)^{0.99}$ . We also find  $\{\Phi\}_rA$  to be correlated with the poloidal flux ( $\{\Phi\}_P$ ) of the associated magnetic cloud at 1 au:  $\{\Phi\}_P = 1.20(\{\Phi\}_rA)^{0.85}$ . This relation is nearly identical to that obtained by Qiu et al. (2007) using a set of only 9 eruptions. Our result supports the idea that flare reconnection results in the formation of flux rope and PEA as a common process.

**1997 May 12, 2000 July 14, 2001 April 26, 2003 October 29, 2004 April 11**

**Table 1.** List of solar eruptions that were associated with magnetic clouds at Earth

**Table 2.** List of Events with RC flux Computed from H-alpha or TRACE 1600 A Ribbons

## **The 2012 July 23 Backside Eruption: An Extreme Energetic Particle Event?**

Nat **Gopalswamy**, Seiji Yashiro, Neeharika Thakur, Pertti Mäkelä, Hong Xie, Sachiko Akiyama  
ApJ **2016**

<https://arxiv.org/pdf/1610.05790v1.pdf> **File**

The backside coronal mass ejection (CME) of **2012 July 23** had a short Sun to Earth shock transit time (18.5 hours). The associated solar energetic particle (SEP) event had a  $>10$  MeV proton flux peaking at  $\sim 5000$  pfu, and the energetic storm particle (ESP) event was an order of magnitude larger, making it the most intense event in the space era at these energies. By a detailed analysis of the CME, shock, and SEP characteristics, we find that the July 23 event is consistent with a high-energy SEP event (accelerating particles to GeV energies). The time of maximum and fluence spectra in the range 10-100 MeV were very hard, similar to those of ground level enhancement (GLE) events. We found a hierarchical relationship between the CME initial speeds and the fluence spectral indices: CMEs with low initial speeds had SEP events with the softest spectra, while those with highest initial speeds had SEP events with the hardest spectra. CMEs attaining intermediate speeds result in moderately hard spectra. The July 23 event was in the group of hard-spectrum events. During the July 23 event, the shock speed ( $>2000$  km s $^{-1}$ ), the initial acceleration ( $\sim 1.70$  km s $^{-2}$ ), and the shock formation height ( $\sim 1.5$  solar radii) were all typical of GLE events. The associated type II burst had emission components from metric to kilometric wavelengths suggesting a strong shock. These observations confirm that the 2012 July 23 event is likely to be an extreme event in terms of the energetic particles it accelerated.

## **History and Development of Coronal Mass Ejections as a Key Player in Solar Terrestrial Relationship**

**Review**

N. **Gopalswamy**

Geoscience Letters Volume 3, article id.8, 18 pp. **2016** **File**

<http://arxiv.org/pdf/1602.03665v1.pdf>

Coronal mass ejections (CMEs) are relatively a recently-discovered phenomenon, in 1971, some fifteen years into the Space Era. It took another two decades to realize that CMEs are the most important players in solar terrestrial relationship as the root cause of severe weather in Earth's space environment. CMEs are now counted among the major natural hazards because they cause large solar energetic particle (SEP) events and major geomagnetic storms, both of which pose danger to humans and their technology in space and ground. Geomagnetic storms discovered in the 1700s, solar flares discovered in the 1800s, and SEP events discovered in the 1900s are all now found to be closely related to CMEs via various physical processes occurring at various locations in and around CMEs, when they interact with the ambient medium. This article identifies a number of key developments that preceded the discovery of white-light CMEs suggesting that CMEs were waiting to be discovered. The last two decades witnessed an explosion of CME research following the launch of the Solar and Heliospheric Observatory mission in 1995, resulting in the establishment of a full picture of CMEs.

## **Interaction between Coronal Mass Ejections: Limited Spatial Extent Revealed by SOHO Observations**

**Gopalswamy**, Nat; Reiner, Mike J.; Makela, Pertti; Yashiro, Seiji

41st COSPAR Scientific Assembly, abstracts from the meeting that was to be held 30 July - 7 August **2016** at the Istanbul Congress Center (ICC), Turkey, but was cancelled. Abstract D2.1-9-16

A spectacular CME interaction event was observed on **2013 May 22** by the Large Angle and Spectrometric Coronagraph (LASCO) on board the Solar and Heliospheric Observatory (SOHO) mission as confirmed by the radio signature detected by the Radio and Plasma Wave experiment (WAVES) on board the Wind spacecraft. The interaction event was also associated with an intense solar energetic particle event, typical of such events in solar cycles 23 and 24. Detailed height-time plots of the interacting CMEs at various position angles revealed a surprising result: only a limited spatial extent of the primary CME was affected by the interaction. The speed of the primary CME showed a sharp decline in the position angle range where it interacted with the preceding CME. At these position angles, the speed of the preceding CME increased. At position angles away from the interaction region, the speed of the primary CME remained roughly the same except for the usual drag deceleration. This result has important implications to theories on CME collision: treating the interacting CMEs to be rigid bodies and using the whole mass of the CMEs may not be correct.

## **CMEs during the Two Activity Peaks in Cycle 24 and their Space Weather Consequences**

N. **Gopalswamy**, P. Mäkelä, S. Akiyama, S. Yashiro, N. Thakur

Sun and Geosphere, **2015**

<http://arxiv.org/pdf/1509.04216v1.pdf> **File**

We report on a comparison between space weather events that occurred around the two peaks in the sunspot number (SSN) during solar cycle 24. The two SSN peaks occurred in the years 2012 and 2014. Even though SSN was larger during the second peak, we find that there were more space weather events during the first peak. The space weather events we considered are large solar energetic particle (SEP) events and major geomagnetic storms associated with coronal mass ejections (CMEs). We also considered interplanetary type II radio bursts, which are indicative of energetic CMEs driving shocks. When we compared the CME properties between the two SSN peaks, we find that more energetic CMEs occurred during the 2012 peak. In particular, we find that CMEs accompanying IP type II bursts had an average speed of 1543 km/s during the 2012 peak compared to 1201 km/s during the 2014 peak. This result is consistent

with the reduction in the average speed of the general population of CMEs during the second peak. All SEP events were associated with the interplanetary type II bursts, which are better than halo CMEs as indicators of space weather. The comparison between the two peaks also revealed the discordant behavior CME rate and SSN is more pronounced during the second peak. None of the 14 disk-center halo CMEs was associated with a major storm in 2014. The lone major storm in 2014 was due to the intensification of the (southward) magnetic field in the associated magnetic cloud by a shock that caught up and propagated into the magnetic cloud. **23-24 Apr 2012; 18-19 Feb 2014**

## **Short-term variability of the Sun-Earth system: an overview of progress made during the CAWSES-II period**

**Review**

**Gopalswamy**, Nat; Tsurutani, Bruce; Yan, Yihua

Progress in Earth and Planetary Science, Volume 2, article id. #13, 41 pp., **2015**

<http://arxiv.org/pdf/1504.06332v1.pdf> **File**

This paper presents an overview of results obtained during the CAWSES-II period on the short-term variability of the Sun and how it affects the near-Earth space environment. CAWSES-II was planned to examine the behavior of the solar-terrestrial system as the solar activity climbed to its maximum phase in solar cycle 24. After a deep minimum following cycle 23, the Sun climbed to a very weak maximum in terms of the sunspot number in cycle 24 (MiniMax24), so many of the results presented here refer to this weak activity in comparison with cycle 23. The short-term variability that has immediate consequence to Earth and geospace manifests as solar eruptions from closed-field regions and high-speed streams from coronal holes. Both electromagnetic (flares) and mass emissions (coronal mass ejections - CMEs) are involved in solar eruptions, while coronal holes result in high-speed streams that collide with slow wind forming the so-called corotating interaction regions (CIRs). Fast CMEs affect Earth via leading shocks accelerating energetic particles and creating large geomagnetic storms. CIRs and their trailing high-speed streams (HSSs), on the other hand, are responsible for recurrent small geomagnetic storms and extended days of auroral zone activity, respectively. The latter leads to the acceleration of relativistic magnetospheric 'killer' electrons. One of the major consequences of the weak solar activity is the altered physical state of the heliosphere that has serious implications for the shock-driving and storm-causing properties of CMEs. Finally, a discussion is presented on extreme space weather events prompted by the **23 July 2012** super storm event that occurred on the backside of the Sun. Many of these studies were enabled by the simultaneous availability of remote sensing and in situ observations from multiple vantage points with respect to the Sun-Earth line.

**TABLE 2** Major geomagnetic storms of cycle 24 ( $Dst < -100$  nT)

## **Kinematic and Energetic Properties of the 2012 March 12 Polar Coronal Mass Ejection**

N. **Gopalswamy**<sup>1</sup>, S. Yashiro<sup>1,2</sup>, and S. Akiyama

**2015** ApJ 809 106

<http://arxiv.org/ftp/arxiv/papers/1507/1507.04057.pdf>

We report on the energetics of the **2012 March 12** polar coronal mass ejection (CME) originating from a southern latitude of  $\sim 60^\circ$ . The polar CME is similar to low-latitude (LL) CMEs in almost all respects: three-part morphology; post-eruption arcade (PEA), CME, and filament kinematics; CME mass and kinetic energy; and the relative thermal energy content of the PEA. From polarized brightness images, we estimate the CME mass, which is close to the average mass of LL CMEs. The CME kinetic energy ( $3.3 \times 10^{30}$  erg) is also typical of the general population of CMEs. From photospheric magnetograms, we estimate the free energy ( $1.8 \times 10^{31}$  erg) in the polar crown source region, which we find is sufficient to power the CME and the PEA. About 19% of the free energy went into the CME kinetic energy. We compute the thermal energy content of the PEA ( $2.3 \times 10^{29}$  erg) and find it to be a small fraction (6.8%) of the CME kinetic energy. This fraction is remarkably similar to that in active region CMEs associated with major flares. We also show that the 2012 March 12 is one among scores of polar CMEs observed during the maximum phase of cycle 24. The cycle 24 polar crown prominence eruptions have the same rate of association with CMEs as those from LLs. This investigation supports the view that all CMEs are magnetically propelled from closed field regions, irrespective of their location on the Sun (polar crown filament regions, quiescent filament regions, or active regions).

## **CMEs during the Two Activity Peaks in Cycle 24 and their Space Weather Consequences**

N. **Gopalswamy**, P. Mäkelä, S. Akiyama, S. Yashiro, N. Thakur

Sun and Geosphere, **2015**

<http://arxiv.org/pdf/1509.04216v1.pdf> **File**

We report on a comparison between space weather events that occurred around the two peaks in the sunspot number (SSN) during solar cycle 24. The two SSN peaks occurred in the years 2012 and 2014. Even though SSN was larger during the second peak, we find that there were more space weather events during the first peak. The space weather events we considered are large solar energetic particle (SEP) events and major geomagnetic storms associated with coronal mass ejections (CMEs). We also considered interplanetary type II radio bursts, which are indicative of energetic CMEs driving shocks. When we compared the CME properties between the two SSN peaks, we find that more energetic CMEs occurred during the 2012 peak. In particular, we find that CMEs accompanying IP type II bursts had an

average speed of 1543 km/s during the 2012 peak compared to 1201 km/s during the 2014 peak. This result is consistent with the reduction in the average speed of the general population of CMEs during the second peak. All SEP events were associated with the interplanetary type II bursts, which are better than halo CMEs as indicators of space weather. The comparison between the two peaks also revealed the discordant behavior CME rate and SSN is more pronounced during the second peak. None of the 14 disk-center halo CMEs was associated with a major storm in 2014. The lone major storm in 2014 was due to the intensification of the (southward) magnetic field in the associated magnetic cloud by a shock that caught up and propagated into the magnetic cloud. **23-24 Apr 2012; 18-19 Feb 2014**

**Table 2. List of DH-km type II bursts in 2012, the associated CMEs and SEP events**

**Table 3. List of DH-km type II bursts in 2014, the associated CMEs and SEP events**

### High-energy solar particle events in cycle 24

Nat **Gopalswamy**, [Pertti Makela](#), [Seiji Yashiro](#), [Hong Xie](#), [Sachiko Akiyama](#), [Neeharika Thakur](#)

The 14th International Astrophysics Conference held in Tampa, FL during April 24-29, 2015. Accepted for publication in Journal of Physics: Conference Series (JPCS). edited by G. Zank, **2015**

<http://arxiv.org/ftp/arxiv/papers/1507/1507.06162.pdf>; **File**

The Sun is already in the declining phase of cycle 24, but the paucity of high-energy solar energetic particle (SEP) events continues with only two ground level enhancement (GLE) events as of March 31, 2015. In an attempt to understand this, we considered all the large SEP events of cycle 24 that occurred until the end of 2014. We compared the properties of the associated CMEs with those in cycle 23. We found that the CME speeds in the sky plane were similar, but almost all those cycle-24 CMEs were halos. A significant fraction of (16%) of the frontside SEP events were associated with eruptive prominence events. CMEs associated with filament eruption events accelerate slowly and attain peak speeds beyond the typical GLE release heights. When we considered only western hemispheric events that had good connectivity to the CME nose, there were only 8 events that could be considered as GLE candidates. One turned out to be the first GLE event of cycle 24 (2012 May 17). In two events, the CMEs were very fast (>2000 km/s) but they were launched into a tenuous medium (high Alfvén speed). In the remaining five events, the speeds were well below the typical GLE CME speed (~2000 km/s). Furthermore, the CMEs attained their peak speeds beyond the typical heights where GLE particles are released. We conclude that several factors contribute to the low rate of high-energy SEP events in cycle 24: (i) reduced efficiency of shock acceleration (weak heliospheric magnetic field), (ii) poor latitudinal and longitudinal connectivity), and (iii) variation in local ambient conditions (e.g., high Alfvén speed).

**Table 1. List of large SEP events from cycle 24**

**Table 2. List of candidate GLE events**

**Table 2. List of candidate GLE events**

| #          | CME   | Date | UT     | Imp.   | Flr  | Loc.   | FR   | Loc     | B0   | Final | Loc | Vsp | Max | E | Ip | 4 |
|------------|-------|------|--------|--------|------|--------|------|---------|------|-------|-----|-----|-----|---|----|---|
| 2011/06/07 | 06:16 | M2.5 | S21W54 | S08W51 | +0.1 | S08W51 | 1680 | 330-420 | 72   | 5     |     |     |     |   |    |   |
| 2011/08/04 | 03:41 | M9.3 | N19W36 | N19W30 | +6.0 | N13W30 | 2450 | 165-500 | 96   | 6     |     |     |     |   |    |   |
| 2011/08/09 | 07:48 | X6.9 | N17W69 | N08W68 | +6.3 | N02W68 | 2496 | 330-420 | 26   | 8     |     |     |     |   |    |   |
| 2011/11/26 | 06:09 | C1.2 | N08W49 | N10W47 | +1.5 | N08W47 | 1187 | 40-80   | 80   | 13    |     |     |     |   |    |   |
| 2012/05/17 | 01:25 | M5.1 | N11W76 | S07W76 | -2.4 | S05W76 | 1997 | >700    | 255  | 23    |     |     |     |   |    |   |
| 2012/09/27 | 23:24 | C3.7 | N06W34 | N16W29 | +6.9 | N09W29 | 1479 | 80-165  | 28   | 27    |     |     |     |   |    |   |
| 2013/05/22 | 13:08 | M5.0 | N15W70 | N02W59 | -1.8 | N04W59 | 1881 | 330-420 | 1660 | 33    |     |     |     |   |    |   |
| 2014/02/20 | 07:26 | M3.0 | S15W73 | S14W70 | -7.0 | S07W70 | 1281 | 330-420 | 22   |       |     |     |     |   |    |   |

**27 January 2012, 2012 May 27, 2014 January 6,**

### The dynamics of eruptive prominences

**Review**

Nat **Gopalswamy**

Solar Prominences, edited by J.-C. Vial & O. Engvold, Springer, in press (**2014**), Chapter 15, **File** Astrophysics and Space Science Library Volume 415, **2015**, pp 381-410

<http://arxiv.org/pdf/1407.2594v1.pdf>

[http://link.springer.com/chapter/10.1007/978-3-319-10416-4\\_15](http://link.springer.com/chapter/10.1007/978-3-319-10416-4_15)

This chapter discusses the dynamical properties of eruptive prominences in relation to coronal mass ejections (CMEs). The fact that eruptive prominences are a part of CMEs is emphasized in terms of their physical association and kinematics. The continued propagation of prominence material into the heliosphere is illustrated using in-situ observations. The solar-cycle variation of eruptive prominence locations is discussed with a particular emphasis on the rush-to-the-pole (RTTP) phenomenon. One of the consequences of the RTTP phenomenon is polar CMEs, which are shown to be similar to the low-latitude CMEs. This similarity is important because it provides important clues to the mechanism by which CMEs erupt. The nonradial motion of CMEs is discussed, including the deflection by coronal holes that have important space weather consequences. Finally, the implications of the presented observations for the modeling CME modeling are outlined. **1998-01-25, 24-11-2000, 2001-12-20, 2003-02-18, 2003-08-16-19, 2009-05-05, 2009-11-08, 2013-09-29-30, 2012-03-12,**

### The Peculiar Behavior of Halo Coronal Mass Ejections in Solar Cycle 24

N. **Gopalswamy**, H. Xie, S. Akiyama, P. Mäkelä, S. Yashiro, G. Michalek

ApJL 804 L23 2015

<http://arxiv.org/ftp/arxiv/papers/1504/1504.01797.pdf>

<https://iopscience.iop.org/article/10.1088/2041-8205/804/1/L23/pdf>

We report on a remarkable finding that the halo coronal mass ejections (CMEs) in cycle 24 are more abundant than in cycle 23, although the sunspot number in cycle 24 has dropped by about 40%. We also find that the distribution of halo-CME source locations is different in cycle 24: the longitude distribution of halos is much flatter with the number of halos originating at central meridian distance  $\geq 60$  degrees twice as large as that in cycle 23. On the other hand, the average speed and the associated soft X-ray flare size are the same in the two cycles, suggesting that the ambient medium into which the CMEs are ejected is significantly different. We suggest that both the higher abundance and larger central meridian longitudes of halo CMEs can be explained as a consequence of the diminished total pressure in the heliosphere in cycle 24 (Gopalswamy et al. 2014). The reduced total pressure allows CMEs expand more than usual making them appear as halos.

## **Anomalous Expansion of Coronal Mass Ejections during Solar Cycle 24 and its Space Weather Implications**

Nat **Gopalswamy**, Sachiko Akiyama, Seiji Yashiro, Hong Xie, and Pertti Mäkelä, Grzegorz Michalek  
E-print, April 2014; Geophysical Research Letters, Volume 41, Issue 8, pp. 2673-2680, 2014

<http://arxiv.org/pdf/1404.0252v1.pdf>

The familiar correlation between the speed and angular width of coronal mass ejections (CMEs) is also found in solar cycle 24, but the regression line has a larger slope: for a given CME speed, cycle 24 CMEs are significantly wider than those in cycle 23. The slope change indicates a significant change in the physical state of the heliosphere, due to the weak solar activity. The total pressure in the heliosphere (magnetic + plasma) is reduced by ~40%, which leads to the anomalous expansion of CMEs explaining the increased slope. The excess CME expansion contributes to the diminished effectiveness of CMEs in producing magnetic storms during cycle 24, both because the magnetic content of the CMEs is diluted and also because of the weaker ambient fields. The reduced magnetic field in the heliosphere may contribute to the lack of solar energetic particles accelerated to very high energies during this cycle.

## **Solar Eruptions and Energetic Particles: An Introduction**

**Review**

N. **Gopalswamy**<sup>1</sup>, R. Mewaldt<sup>2</sup>, and J. Torsti<sup>3</sup>

Book Series: [Geophysical Monograph Series](#) Volume 165, 2013

<https://agupubs.onlinelibrary.wiley.com/doi/book/10.1029/GM165>

<http://sci-hub.tw/10.1029/165GM02>

This introductory article highlights current issues concerning two related phenomena involving mass emission from the Sun: solar eruptions and solar energetic particles. A brief outline of the chapters is provided indicating how the current issues are addressed in the monograph. The sections in this introduction roughly group the chapters dealing with coronal mass ejections (CMEs), solar energetic particles (SEPs), shocks, and space weather. The concluding remarks include a brief summary of outstanding issues that drive current and future research on CMEs and SEPs.

## **Testing the empirical shock arrival model using quadrature observations**

N. **Gopalswamy**<sup>1,\*</sup>, P. Mäkelä<sup>1,2</sup>, H. Xie<sup>1,2</sup>, S. Yashiro

Space Weather, Volume 11, Issue 11, pages 661–669, November 2013

[http://cdaw.gsfc.nasa.gov/publications/gopal/gopal2013SW\\_testESA.pdf](http://cdaw.gsfc.nasa.gov/publications/gopal/gopal2013SW_testESA.pdf)

The empirical shock arrival (ESA) model was developed based on quadrature data from Helios (in situ) and P-78 (remote sensing) to predict the Sun-Earth travel time of coronal mass ejections (CMEs). The ESA model requires earthward CME speed as input, which is not directly measurable from coronagraphs along the Sun-Earth line. The Solar Terrestrial Relations Observatory (STEREO) and the Solar and Heliospheric Observatory (SOHO) were in quadrature during 2010–2012, so the speeds of Earth-directed CMEs were observed with minimal projection effects. We identified a set of 20 full halo CMEs in the field of view of SOHO that were also observed in quadrature by STEREO. We used the earthward speed from STEREO measurements as input to the ESA model and compared the resulting travel times with the observed ones from L1 monitors. We find that the model predicts the CME travel time within about 7.3 h, which is similar to the predictions by the ENLIL model. We also find that CME-CME and CME-coronal hole interaction can lead to large deviations from model predictions. **2011 February 15, 2012 July 12**

*Table 1. List of shocks detected at L1 and the corresponding halo CMEs observed by SOHO*

*Table 2. List of events with coronal holes visible on the disk.*

*Table 3. The number of preceding CMEs within a 24 h interval preceding the CMEs in Table 1*

## **Latitudinal Connectivity of Ground Level Enhancement Events**

N. **Gopalswamy** and P. Mäkelä

Proceedings of: 12th Annual International Astrophysical Conference, ASP Conference Series, ed. Q. Hu and G. Zank, in press, **2013**; **File**

We examined the source regions and coronal environment of the historical ground level enhancement (GLE) events in search of evidence for non-radial motion of the associated coronal mass ejection (CME). For the 13 GLE events that had source latitudes  $>30^\circ$  we found evidence for possible non-radial CME motion due to deflection by large-scale magnetic structures in nearby coronal holes, streamers, or pseudo streamers. Polar coronal holes are the main source of deflection in the rise and declining phases of solar cycles. In the maximum phase, deflection by large-scale streamers or pseudo streamers overlying high-latitude filaments seems to be important. The B0 angle reduced the ecliptic distance of some GLE source regions and increased in others with the net result that the average latitude of GLE events did not change significantly. The non-radial CME motion is the dominant factor that reduces the ecliptic distance of GLE source regions, thereby improving the latitudinal connectivity to Earth. We further infer that the GLE particles must be accelerated at the nose part of the CME-driven shocks, where the shock is likely to be quasi-parallel.

**Table 1. Historical GLE events with flare latitudes  $>30^\circ$**

## **Obscuration of Flare Emission by an Eruptive Prominence**

Nat **Gopalswamy** and Seiji Yashiro

E-print, Sept **2013**, **File**, PASJ

<http://cdaw.gsfc.nasa.gov/publications/gopal/gopal2013PASJ.pdf>

We report on the eclipsing of microwave flare emission by an eruptive prominence from a neighboring region as observed by the Nobeyama Radioheliograph at 17 GHz. The obscuration of the flare emission appears as a dimming feature in the microwave flare light curve. We use the dimming feature to derive the temperature of the prominence and the distribution of heating along the length of the filament. We find that the prominence is heated to a temperature above the quiet Sun temperature at 17 GHz. The duration of the dimming is the time taken by the eruptive prominence in passing over the flaring region. We also find evidence for the obscuration in EUV images obtained by the Solar and Heliospheric Observatory (SOHO) mission. **2002/05/21-22**

## **Height of Shock Formation in the Solar Corona Inferred from Observations of Type II Radio Bursts and Coronal Mass Ejections**

N. **Gopalswamy**, H. Xie, P. Makela, S. Yashiro, S. Akiyama, W. Uddin., A. K. Srivastava, N. C. Joshi, R. Chandra, P. K. Manoharan, K. Mahalakshmi, V. C. Dwivedi, R. Jain and A. K. Awasthi, N. V. Nitta, M. J. Aschwanden, D. P. Choudhary

E-print, Jan **2013**; Adv. Space Res., v. 51, No. 11, p. 1981-1989, **File**

Employing coronagraphic and EUV observations close to the solar surface made by the Solar Terrestrial Relations Observatory (STEREO) mission, we determined the heliocentric distance of coronal mass ejections (CMEs) at the starting time of associated metric type II bursts. We used the wave diameter and leading edge methods and measured the CME heights for a set of 32 metric type II bursts from solar cycle 24. We minimized the projection effects by making the measurements from a view that is roughly orthogonal to the direction of the ejection. We also chose image frames close to the onset times of the type II bursts, so no extrapolation was necessary. We found that the CMEs were located in the heliocentric distance range from 1.20 to 1.93 solar radii (Rs), with mean and median values of 1.43 and 1.38 Rs, respectively. We conclusively find that the shock formation can occur at heights substantially below 1.5 Rs. In a few cases, the CME height at type II onset was close to 2 Rs. In these cases, the starting frequency of the type II bursts was very low, in the range 25–40 MHz, which confirms that the shock can also form at larger heights. The starting frequencies of metric type II bursts have a weak correlation with the measured CME/shock heights and are consistent with the rapid decline of density with height in the inner corona.

**Table 2010-2012; 20100612, 20100613; 20100807; 20101016; 20101103; 20101103; 20101112; 20101215; 20101231; 20110127; 20110128; 20110211; 20110213; 20110214; 20110215; 20110216; 20110307; 20110308; 20110325; 20110511; 20110530; 20110802; 20110810; 20110828; 20110906; 20110930; 20111119; 20120105; 20120118; 20120120; 20120324; 20120424**

## **The Solar Connection of Enhanced Heavy Ion Charge States in the Interplanetary Medium: Implications for the Flux-rope Structure of CMEs**

N. **Gopalswamy**, P. Mäkelä, S. Akiyama, H. Xie, S. Yashiro, and A. A. Reinard

Solar Physics, Volume 284, Issue 1, pp 17-46, **2013**, **File**

We investigated a set of 54 interplanetary coronal mass ejection (ICME) events whose solar sources are very close to the disk center (within  $\pm 15$  degrees from the central meridian). The ICMEs consisted of 23 magnetic cloud (MC) events and 31 non-MC events. Our analyses suggest that the MC and non-MC ICMEs have more or less the same eruption characteristics at the Sun in terms of soft X-ray flares and CMEs. Both types have significant enhancements in charge states, although the non-MC structures have slightly lower levels of enhancement. The overall duration of charge state enhancement is also considerably smaller than that in MCs as derived from solar wind plasma and magnetic signatures. We find very good correlation between the Fe and O charge state measurements and the flare properties such as soft X-ray flare intensity and flare temperature for both MCs and non-MCs. These observations suggest that both MC and non-MC ICMEs are likely to have a flux-rope structure and the unfavorable observational geometry may be

responsible for the appearance of non-MC structures at 1 AU. We do not find any evidence for active region expansion resulting in ICMEs lacking a flux rope structure because the mechanism of producing high charge states and the flux rope structure at the Sun is the same for MC and non-MC events.

**Table:** [http://iopscience.iop.org/0004-637X/710/2/1111/fulltext/apj\\_710\\_2\\_1111.tables.html](http://iopscience.iop.org/0004-637X/710/2/1111/fulltext/apj_710_2_1111.tables.html)

**1999 September 19, 2001-03-19, 2002 May 27**

## **Observations of CMEs and Models of the Eruptive Corona** Review

N. **Gopalswamy**

E-print, Jan **2013**, **File**; Solar wind 13

[http://arxiv.org/pdf/0903.2776.pdf?origin=publication\\_detail](http://arxiv.org/pdf/0903.2776.pdf?origin=publication_detail)

<http://arxiv.org/pdf/1304.0087v1.pdf>

Current theoretical ideas on the internal structure of CMEs suggest that a flux rope is central to the CME structure, which has considerable observational support both from remote-sensing and in-situ observations. The flux-rope nature is also consistent with the post-eruption arcades with high-temperature plasma and the charge states observed within CMEs arriving at Earth. The model involving magnetic loop expansion to explain CMEs without flux ropes is not viable because it contradicts CME kinematics and flare properties near the Sun. The global picture of CMEs becomes complete if one includes the shock sheath to the CSHKP model.

**1999.09.20-24, 2000.10.10-14, 2006.12.14, 2012.03.12-14**

## **Radio-loud CMEs from the disk center lacking shocks at 1 AU**

N. **Gopalswamy**, P. Makela, S. Akiyama, S. Yashiro, H. Xie, R. J. MacDowall, M. L. Kaiser

E-print, June **2012**, JGR

A coronal mass ejection (CME) associated with a type II burst and originating close to the center of the solar disk typically results in a shock at Earth in 2-3 days and hence can be used to predict shock arrival at Earth. However, a significant fraction (about 28%) of such CMEs producing type II bursts were not associated with shocks at Earth. We examined a set of 21 type II bursts observed by the Wind/WAVES experiment at decameter-hectometric (DH) wavelengths that had CME sources very close to the disk center (within a central meridian distance of 30 degrees), but did not have a shock at Earth. We find that the near-Sun speeds of these CMEs average to ~644 km/s, only slightly higher than the average speed of CMEs associated with radio-quiet shocks. However, the fraction of halo CMEs is only ~30%, compared to 54% for the radio-quiet shocks and 91% for all radio-loud shocks. We conclude that the disk-center radio-loud CMEs with no shocks at 1 AU are generally of lower energy and they drive shocks only close to the Sun and dissipate before arriving at Earth. There is also evidence for other possible processes that lead to the lack of shock at 1 AU: (i) overtaking CME shocks merge and one observes a single shock at Earth, and (ii) deflection by nearby coronal holes can push the shocks away from the Sun-Earth line, such that Earth misses these shocks. The probability of observing a shock at 1 AU increases rapidly above 60% when the CME speed exceeds 1000 km/s and when the type II bursts propagate to frequencies below 1 MHz.

## **Properties of Ground level enhancement events and the associated solar eruptions during solar cycle 23.**

N. **Gopalswamy**, H. Xie, S. Yashiro, S. Akiyama, P. Mäkelä, I.G. Usoskin,

E-print, May **2012**, **File**; Space Sci. Rev., **2012**

Solar cycle 23 witnessed the most complete set of observations of coronal mass ejections (CMEs) associated with the Ground Level Enhancement (GLE) events. We present an overview of the observed properties of the GLEs and those of the two associated phenomena, viz., flares and CMEs, both being potential sources of particle acceleration. Although we do not find a striking correlation between the GLE intensity and the parameters of flares and CMEs, the solar eruptions are very intense involving X-class flares and extreme CME speeds (average ~2000 km/s). An M7.1 flare and a 1200 km/s CME are the weakest events in the list of 16 GLE events. Most (80%) of the CMEs are full halos with the three non-halos having widths in the range 167 to 212 degrees. The active regions in which the GLE events originate are generally large: 1290 msh (median 1010 msh) compared to 934 msh (median: 790 msh) for SEP-producing active regions. For accurate estimation of the CME height at the time of metric type II onset and GLE particle release, we estimated the initial acceleration of the CMEs using flare and CME observations. The initial acceleration of GLE-associated CMEs is much larger (by a factor of 2) than that of ordinary CMEs (2.3 km/s<sup>2</sup> vs. 1 km/s<sup>2</sup>). We confirmed the initial acceleration for two events for which CME measurements are available in the inner corona. The GLE particle release is delayed with respect to the onset of all electromagnetic signatures of the eruptions: type II bursts, low frequency type III bursts, soft X-ray flares and CMEs. The presence of metric type II radio bursts some 17 min (median: 16 min; range: 3 to 48 min) before the GLE onset indicates shock formation well before the particle release. The release of GLE particles occurs when the CMEs reach an average height of ~3.09 Rs (median: 3.18 Rs; range: 1.71 to 4.01 Rs) for well-connected events (source longitude in the range W20 ? W90). For poorly connected events, the average CME height at GLE particle release is ~66% larger (mean: 5.18 Rs; median: 4.61 Rs; range: 2.75 ? 8.49 Rs). The longitudinal dependence is consistent with shock accelerations because the shocks from poorly connected events need to expand more to cross the field lines connecting to an Earth observer. On the other hand, the CME height at metric type II burst onset has no longitudinal dependence because electromagnetic signals do not require magnetic connectivity to the observer. For several events, the GLE particle release is very close to the time of first appearance of the CME in the

coronagraphic field of view, so we independently confirmed the CME height at particle release. The CME height at metric type II burst onset is in the narrow range 1.29 to 1.8 Rs, with mean and median values of 1.53 and 1.47 Rs. The CME heights at metric type II burst onset and GLE particle release correspond to the minimum and maximum in the Alfvén speed profile. The increase in CME speed between these two heights suggests an increase in Alfvénic Mach number from 2 to 3. The CME heights at GLE particle release are in good agreement with those obtained from the velocity dispersion analysis (Reames, 2009a,b) including the source longitude dependence. We also discuss the implications of the delay of GLE particle release with respect to complex type III bursts by ~18 min (median: 16 in; range: 2 to 44 min) for the flare acceleration mechanism. A similar analysis is also performed on the delay of particle release relative to the hard X-ray emission. **6 Nov 1997 , 1998 August 24, 02-Nov-03, 17-Jan-05, 14-Jul-05**

## **The Relationship Between the Expansion Speed and Radial Speed of CMEs Confirmed Using Quadrature Observations of the 2011 February 15 CME**

Nat [Gopalswamy](#)<sup>1</sup>, Pertti Makela<sup>2</sup>, Seiji Yashiro<sup>2</sup>, and Joseph M. Davila<sup>1</sup>

Sun and Geosphere, **2012, File**

It is difficult to measure the true speed of Earth-directed CMEs from a coronagraph located along the Sun-Earth line because of the occulting disk. However, the expansion speed (the speed with which the CME appears to spread in the sky plane) can be measured by such a coronagraph. In order to convert the expansion speed to radial speed (which is important for space weather applications) one can use an empirical relationship between the two that assumes an average width for all CMEs. If we have the width information from quadrature observations, we can confirm the relationship between expansion and radial speeds derived by Gopalswamy et al. (2009a). The STEREO spacecraft were in quadrature with SOHO (STEREO-A ahead of Earth by 87° and STEREO-B 94° behind Earth) on **2011 February 15**, when a fast Earth-directed CME occurred. The CME was observed as a halo by the Large-Angle and Spectrometric Coronagraph (LASCO) on board SOHO. The sky-plane speed was measured by SOHO/LASCO as the expansion speed, while the radial speed was measured by STEREO-A and STEREO-B. In addition, STEREO-A and STEREO-B images provided the width of the CME, which is unknown from Earth view. From the SOHO and STEREO measurements, we confirm the relationship between the expansion speed ( $V_{exp}$ ) and radial speed ( $V_{rad}$ ) derived previously from geometrical considerations (Gopalswamy et al. 2009a):  $V_{rad} = \frac{V_{exp}}{1 + \cot w}$ , where  $w$  is the half width of the CME. STEREO-B images of the CME, we found that CME had a full width of 76°, so  $w = 38°$ . This gives the relation as  $V_{rad} = 1.14 V_{exp}$ . From LASCO observations, we measured  $V_{exp} = 897$  km/s, so we get the radial speed as 1023 km/s. Direct measurement of radial speed yields 945 km/s (STEREO-A) and 1058 km/s (STEREO-B). These numbers are different only by 7.6% and 3.4% (for STEREO-A and STEREO-B, respectively) from the computed value.

## **CORONAL MAGNETIC FIELD MEASUREMENT FROM EUV IMAGES MADE BY THE SOLAR DYNAMICS OBSERVATORY**

Nat [Gopalswamy](#)<sup>1</sup>, Nariaki Nitta<sup>2</sup>, Sachiko Akiyama<sup>1,3</sup>, Pertti Mäkelä<sup>1,3</sup> and Seiji Yashiro

**2012 ApJ 744 72, File**

By measuring the geometrical properties of the coronal mass ejection (CME) flux rope and the leading shock observed on **2010 June 13** by the Solar Dynamics Observatory (SDO) mission's Atmospheric Imaging Assembly we determine the Alfvén speed and the magnetic field strength in the inner corona at a heliocentric distance of ~1.4 Rs. The basic measurements are the shock standoff distance ( $\Delta R$ ) ahead of the CME flux rope, the radius of curvature of the flux rope ( $R_c$ ), and the shock speed. We first derive the Alfvénic Mach number ( $M$ ) using the relationship,  $\Delta R/R_c = 0.81[(\gamma - 1)M^2 + 2]/[(\gamma + 1)(M^2 - 1)]$ , where  $\gamma$  is the only parameter that needed to be assumed. For  $\gamma = 4/3$ , the Mach number declined from 3.7 to 1.5 indicating shock weakening within the field of view of the imager. The shock formation coincided with the appearance of a type II radio burst at a frequency of ~300 MHz (harmonic component), providing an independent confirmation of the shock. The shock compression ratio derived from the radio dynamic spectrum was found to be consistent with that derived from the theory of fast-mode MHD shocks. From the measured shock speed and the derived Mach number, we found the Alfvén speed to increase from ~140 km s<sup>-1</sup> to 460 km s<sup>-1</sup> over the distance range 1.2-1.5 Rs. By deriving the upstream plasma density from the emission frequency of the associated type II radio burst, we determined the coronal magnetic field to be in the range 1.3-1.5 G. The derived magnetic field values are consistent with other estimates in a similar distance range. This work demonstrates that the EUV imagers, in the presence of radio dynamic spectra, can be used as coronal magnetometers.

## **Universal Heliophysical Processes**

[Gopalswamy](#), N.

In: The Sun, the Solar Wind, and the Heliosphere, ed. M. P. Miralles and J. Sanchez Almeida, IAGA Special Sopron Book Series, Vol 4, Chapter 2, Springer, pp 9-20, **2011, File**, DOI: 10.1007/978/90-481-9787-3\_2  
The physical processes in the heliospace are a direct consequence of the influenced by Sun's mass and electromagnetic emissions. There has been enormous progress in studying these processes since the dawn of the space age half a century ago. The heliospace serves as a great laboratory to study numerous physical processes, using the vast array of ground and space-based measurements of various physical quantities. The observational capabilities collectively form the Great Observatory to make scientific investigations not envisioned by individual instrument teams. The International



Heliophysical Year (IHY) program has been promoting scientific investigations on the universality of physical processes such as shocks, particle acceleration, dynamo, magnetic reconnection, magnetic flux ropes, plasma-neutral matter interactions, turbulence, and so on. This paper highlights scientific deliberations on these and related topics that took place during the IAGA sessionon "Universal Heliophysical Processes" in Sopron, Hungary. The session featured several invited and contributed papers that focused on observations, theory and modeling of the universal heliophysical processes.

## **Coronal Mass Ejections and Solar Radio Emissions**

N. [Gopalswamy](#)

Accepted for Publication in the book **Planetary Radio Emissions VII**, Eds. Rucker, H. O., W. S. Kurth, P. Louarn, G. Fischer, Austrian Academy of Sciences Press, Vienna, in press (2011), **File**

Three types of low-frequency nonthermal radio bursts are associated with coronal mass ejections (CMEs): Type III bursts due to accelerated electrons propagating along open magnetic field lines, type II bursts due to electrons accelerated in shocks, and type IV bursts due to electrons trapped in post-eruption arcades behind CMEs. This paper presents a summary of results obtained during solar cycle 23 primarily using the white-light coronagraphic observations from the Solar Heliospheric Observatory (SOHO) and the WAVES experiment on board Wind.

[A review.](#)

## **The Strength and Radial Profile of Coronal Magnetic Field from the Standoff Distance of a CME-driven Shock**

Nat [Gopalswamy](#) and Seiji Yashiro<sup>2</sup>

E-print, July 2011, **File**

We determine the coronal magnetic field strength in the heliocentric distance range 6 to 23 solar radii ( $R_s$ ) by measuring the shock standoff distance and the radius of curvature of the flux rope during the **2008 March 25** coronal mass ejection (CME) imaged by white-light coronagraphs.

Assuming the adiabatic index, we determine the Alfvén Mach number, and hence the Alfvén speed in the ambient medium using the measured shock speed. By measuring the upstream plasma density using polarization brightness images, we finally get the magnetic field strength upstream of the shock. The estimated magnetic field decreases from ~48 mG around 6  $R_s$  to 8 mG at 23  $R_s$ . The radial profile of the magnetic field can be described by a power law in agreement with other estimates at similar heliocentric distances.

## **Coronal Mass Ejections: a Summary of Recent Results**

N. [Gopalswamy](#), [nat.gopalswamy@nasa.gov](mailto:nat.gopalswamy@nasa.gov)

Proceedings of the 20th Slovak National Solar Physics Workshop, ed. I. Dorotovic, Slovak Central Observatory, pp. 108 - 130, **2010**, **File** [A review](#)

Coronal mass ejections (CMEs) have been recognized as the most energetic phenomenon in the heliosphere, deriving their energy from the stressed magnetic fields on the Sun. This paper summarizes the properties of CMEs and highlights some of the recent results on CMEs. In particular, the morphological, physical, and kinematic properties of CMEs are summarized. The CME consequences in the heliosphere such as interplanetary shocks, type II radio bursts, energetic particles, geomagnetic storms, and cosmic ray modulation are discussed.

## **A Catalog of Halo Coronal Mass Ejections from SOHO**

N. [Gopalswamy](#)<sup>1</sup>, S. Yashiro<sup>2</sup>, G. Michalek<sup>3</sup>, H. Xie<sup>3</sup>, P. Mäkelä<sup>3</sup>, A. Vourlidas<sup>4</sup>, R. A. Howard<sup>4</sup>  
Sun and Geosphere, **2010**; 5(1): 7 – 16, **File**

[http://newserver.stil.bas.bg/SUNGEO/00SGArhiv/SG\\_v5\\_No1\\_2010-pp-7-16.pdf](http://newserver.stil.bas.bg/SUNGEO/00SGArhiv/SG_v5_No1_2010-pp-7-16.pdf)

Coronal mass ejections (CMEs) that appear to surround the occulting disk of the observing coronagraph are known as halo CMEs. Halos constitute a subset of energetic CMEs that have important heliospheric consequences. Here we describe an on-line catalog that contains all the halo CMEs that were identified in the images obtained by the Solar and Heliospheric Observatory (SOHO) mission's Large Angle and Spectrometric Coronagraph (LASCO) since 1996. Until the end of 2007, some 396 halo CMEs were recorded. For each halo CME, we identify the solar source (heliographic coordinates), the soft X-ray flare importance, and the flare onset time. From the sky-plane speed measurements and the solar source information we obtain the space speed of CMEs using a cone model. In addition to the description of the catalog ([http://cdaw.gsfc.nasa.gov/CME\\_list/HALO/halo.html](http://cdaw.gsfc.nasa.gov/CME_list/HALO/halo.html)), we summarize the statistical properties of the halo CMEs. We confirm that halo CMEs are twice faster than ordinary CMEs and are associated with major flares on the average. We also compared the annual rate of halo CMEs with that obtained by automatic detection methods and found that most of these methods have difficulty in identifying full halo CMEs.

## **Large-scale solar eruptions.**

**Gopalswamy, N.:**

2010, In: Gopalswamy, N., Hasan, S.S., Ambastha, A. (eds.)

*Heliophysical Processes, Astrophysics and Space Science Proceedings*, Springer, Berlin, 53, Chap. 4.

doi:10.1007/978-3-642-11341-3\_4., **File** (pp. 53-71)

This chapter provides an **over view** of coronal mass ejections (CMEs) and the associated flares including statistical properties, associated phenomena (solar energetic particles, interplanetary shocks, geomagnetic storms), and their heliospheric consequences.

### **Coronal Mass Ejections from Sunspot and Non-Sunspot Regions.**

**Gopalswamy** N, Akiyama S, Yashiro S, Mäkelä P

(2010b) In Magnetic Coupling between the Interior and Atmosphere of the Sun,

*Astrophysics and Space Science Proceedings*, eds. by S. S. Hasan and R. J. Rutten, p. 289

### **THE SOHO/LASCO CME CATALOG**

N. **Gopalswamy**, S. Yashiro, G. Michalek, G. Stenborg, A. Vourlidas, S. Freeland, and R. Howard  
Earth, Moon, and Planets, Volume 104, Issue 1, Page 295, 2009

Coronal mass ejections (CMEs) are routinely identified in the images of the solar corona obtained by the Solar and Heliospheric Observatory (SOHO) mission's Large Angle and Spectrometric Coronagraph (LASCO) since 1996. The identified CMEs are measured and their basic attributes are cataloged in a data base known as the SOHO/LASCO CME Catalog. The Catalog also contains digital data, movies, and plots for each CME, so detailed scientific investigations can be performed on CMEs and the related phenomena such as flares, radio bursts, solar energetic particle events, and geomagnetic storms. This paper provides a brief description of the Catalog and summarizes the statistical properties of CMEs obtained using the Catalog. Data products relevant to space weather research and some CME issues that can be addressed using the Catalog are discussed. The URL of the Catalog is: [http://cdaw.gsfc.nasa.gov/CME\\_list](http://cdaw.gsfc.nasa.gov/CME_list).

### **CME link to the geomagnetic storms**

Nat **Gopalswamy**

Solar and Stellar Variability: Impact on Earth and Planets, Proceedings IAU Symposium No. 264, 2009, p. 326-335, A.G. Kosovichev, A.H. Andrei & J.-P. Rozelot, eds.; **File**

Y:\obridko\otchet09

The coronal mass ejection (CME) link to geomagnetic storms stems from the southward component of the interplanetary magnetic field contained in the CME flux ropes and in the sheath between the flux rope and the CME-driven shock. A typical storm-causing CME is characterized by (i) high speed, (ii) large angular width (mostly halos and partial halos), and (iii) solar source location close to the central meridian. For CMEs originating at larger central meridian distances, the storms are mainly caused by the sheath field. Both the magnetic and energy contents of the storm-producing CMEs can be traced to the magnetic structure of active regions and the free energy stored in them.

### **Relation Between Type II Bursts and CMEs Inferred from STEREO Observations**

**Gopalswamy**, N.; Thompson, W. T.; Davila, J. M.; Kaiser, M. L.; Yashiro, S.; Mäkelä, P.; Michalek, G.; Bougeret, J.-L.; Howard, R. A.

E-print, July 2009; *Solar Phys.* (2009) 259: 227–254; **File**

The inner coronagraph (COR1) of the Solar Terrestrial Relations Observatory (STEREO) mission has made it possible to observe CMEs in the spatial domain overlapping with that of the metric type II radio bursts. The type II bursts were associated with generally weak flares (mostly B and C class soft X-ray flares), but the CMEs were quite energetic.

Using CME data for a set of type II bursts during the declining phase of solar cycle 23, we determine the CME height when the type II bursts start, thus giving an estimate of the heliocentric distance at which CME-driven shocks form. This distance has been determined to be  $\sim 1.5R_s$  (solar radii), which coincides with the distance at which the Alfvén speed profile has a minimum value. We also use type II radio observations from STEREO/WAVES and Wind/WAVES observations to show that CMEs with moderate speed drive either weak shocks or no shock at all when they attain a height where the Alfvén speed peaks ( $\sim 3R_s$ – $4R_s$ ). Thus the shocks seem to be most efficient in accelerating electrons in the heliocentric distance range of  $1.5R_s$  to  $4R_s$ . By combining the radial variation of the CME speed in the inner corona (CME speed increase) and interplanetary medium (speed decrease) we were able to correctly account for the deviations from the universal drift-rate spectrum of type II bursts, thus confirming the close physical connection between type II bursts and CMEs. The average height ( $\sim 1.5R_s$ ) of STEREO CMEs at the time of type II bursts is smaller than that ( $\sim 2.2R_s$ ) obtained for SOHO (Solar and Heliospheric Observatory) CMEs. We suggest that this may indicate, at least partly, the density reduction in the corona between the maximum and declining phases, so a given plasma level occurs closer to the Sun in the latter phase. In two cases, there was a diffuse shock-like feature ahead of the main body of the CME, indicating a standoff distance of  $1R_s$ – $2R_s$  by the time the CME left the LASCO field of view.

## **Erratum to: Relation Between Type II Bursts and CMEs Inferred from STEREO Observations, Solar Physics, Volume 277, Number 2, 459, 2012**

### **LARGE GEOMAGNETIC STORMS ASSOCIATED WITH LIMB HALO CORONAL MASS EJECTIONS**

NAT [GOPALSWAMY](#), SEJI YASHIRO†, HONG XIE, SACHIKO AKIYAMA, and PERTTI MÄKELÄ  
Advances in Geosciences, 2009, File

Solar cycle 23 witnessed the observation of hundreds of halo coronal mass ejections (CMEs), thanks to the high dynamic range and extended field of view of the Large Angle and Spectrometric Coronagraph (LASCO) on board the Solar and Heliospheric Observatory (SOHO) mission. More than two thirds of halo CMEs originating on the front side of the Sun have been found to be geoeffective ( $Dst \leq -50$  nT). The delay time between the onset of halo CMEs and the peak of ensuing geomagnetic storms has been found to depend on the solar source location (Gopalswamy et al., 2007). In particular, limb halo CMEs (source longitude  $> 45^\circ$ ) have a 20% shorter delay time on the average. It was suggested that the geomagnetic storms due to limb halos must be due to the sheath portion of the interplanetary CMEs (ICMEs) so that the shorter delay time can be accounted for. We confirm this suggestion by examining the sheath and ejecta portions of ICMEs from Wind and ACE data that correspond to the limb halos. Detailed examination showed that three pairs of limb halos were interacting events. Geomagnetic storms following five limb halos were actually produced by other disk halos. The storms followed by four isolated limb halos and the ones associated with interacting limb halos, were all due to the sheath portions of ICMEs.

### **Coronal Mass Ejections from Sunspot and non-Sunspot Regions**

N. [Gopalswamy](#)<sup>1</sup>, S. Akiyama<sup>1, 2</sup>, S. Yashiro, and P. Mäkelä<sup>1</sup>

To appear in “Magnetic Coupling between the Interior and the Atmosphere of the Sun”, eds. S. S. Hasan and R. J. Rutten, Astrophysics and Space Science Proceedings, Springer-Verlag, Heidelberg, Berlin, 2009; File. Summary. Coronal mass ejections (CMEs) originate from closed magnetic field regions on the Sun, which are active regions and quiescent filament regions. The energetic populations such as halo CMEs, CMEs associated with magnetic clouds, geoeffective CMEs, CMEs associated with solar energetic particles and interplanetary type II radio bursts, and shock-driving CMEs have been found to originate from sunspot regions. The CME and flare occurrence rates are found to be correlated with the sunspot number, but the correlations are significantly weaker during the maximum phase compared to the rise and declining phases. We suggest that the weaker correlation results from high-latitude CMEs from the polar crown filament regions that are not related to sunspots.

### **Coronal mass ejections and space weather**

Nat [Gopalswamy](#)

Climate and Weather of the Sun-Earth System (CAWSES): Selected Papers from the 2007 Kyoto Symposium, Edited by T. Tsuda, R. Fujii, K. Shibata, and M. A. Geller, pp. 77–120.  
c\_TERRAPUB, Tokyo, 2009, File.

Solar energetic particles (SEPs) and geomagnetic storms are the two primary space weather consequences of coronal mass ejections (CMEs) and their interplanetary counterparts (ICMEs). I summarize the observed properties of CMEs and ICMEs, paying particular attention to those properties that determine the ability of CMEs in causing space weather. Then I provide observational details of two the central issues: (i) for producing geomagnetic storms, the solar source location and kinematics along with the magnetic field structure and intensity are important, and (ii) for SEPs, the shock-driving ability of CMEs, the Alfvén speed in the ambient medium, and the connectivity to Earth are crucial parameters.

### **CME Interaction with Coronal Holes and their Interplanetary Consequences**

N. [Gopalswamy](#)<sup>1</sup>, P. Mäkelä<sup>1,2</sup>, H. Xie<sup>1,2</sup>, S. Akiyama<sup>1,2</sup>, and S. Yashiro<sup>1,2</sup>

JGR, 2009; File; J. Geophys. Res., Vol. 114, No. A3, A00A22

A significant number of interplanetary (IP) shocks (~17%) during cycle 23 were not followed by drivers. The number of such “driverless” shocks steadily increased with the solar cycle with 15%, 33%, and 52% occurring in the rise, maximum, and declining phase of the solar cycle. The solar sources of 15% of the driverless shocks were very close to the central meridian of the Sun (within  $\sim 15^\circ$ ), which is quite unexpected. More interestingly, all the driverless shocks with their solar sources near the solar disk center occurred during the declining phase of solar cycle 23. When we investigated the coronal environment of the source regions of driverless shocks, we found that in each case there was at least one coronal hole nearby suggesting that the coronal holes might have deflected the associated coronal mass ejections (CMEs) away from the Sun-Earth line. The presence of abundant low-latitude coronal holes during the declining phase further explains why CMEs originating close to the disk center mimic the limb CMEs, which normally lead to driverless shocks due to purely geometrical reasons. We also examined the solar source regions of shocks with drivers. For these, the coronal holes were located such that they either had no influence on the CME trajectories, or they deflected the CMEs towards the Sun-Earth line. We also obtained the open magnetic field distribution on the Sun by performing a potential field source surface extrapolation to the corona. It was found that the CMEs generally move

away from the open magnetic field regions. The CME-coronal hole interaction must be widespread in the declining phase, and may have a significant impact on the geoeffectiveness of CMEs.

### **Solar connections of geoeffective magnetic structures.**

**Gopalswamy N (2008) JASTP 70:2078-2100**

### **THE EXPANSION AND RADIAL SPEEDS OF CORONAL MASS EJECTIONS**

N. **Gopalswamy**<sup>1</sup>, A. Dal Lago<sup>2</sup>, S. Yashiro<sup>3</sup> and S. Akiyama

Cent. Eur. Astrophys. Bull. vol (2008) 1, 1, **File**

We show the relation between radial ( $V_{rad}$ ) and expansion ( $V_{exp}$ ) speeds of coronal mass ejections (CMEs) depends on the CME width. As CME width increases,  $V_{rad}=V_{exp}$  decreases from a value  $>1$  to  $<1$ . For widths approaching  $180^\circ$ , the ratio approaches 0 if the cone has a flat base, while it approaches 0.5 if the base has a bulge (ice cream cone). The speed difference between the limb and disk halos and the spherical expansion of superfast CMEs can be explained by the width dependence.

### **Major Solar Flares without Coronal Mass Ejections**

N. **Gopalswamy**<sup>1</sup>, S. Akiyama<sup>1,2</sup> and S. Yashiro<sup>1,2,3</sup>

Proceedings IAU Symposium No. 257, 2008, N. Gopalswamy, & D. Webb, eds.; **File**

We examine the source properties of X-class soft X-ray flares that were not associated with coronal mass ejections (CMEs). All the flares were associated with intense microwave bursts implying the production of high energy electrons. However, most (85%) of the flares were not associated with metric type III bursts, even though open field lines existed in all but two of the active regions. The X-class flares seem to be truly confined because there was no material ejection (thermal or nonthermal) away from the flaring region.

### **Coronal Mass Ejections, Type II Radio Bursts, and Solar Energetic Particle Events in the SOHO Era**

N. **Gopalswamy**<sup>1</sup>, S. Yashiro<sup>2</sup>, S. Akiyama<sup>2</sup>, P. Makela<sup>2</sup>, H. Xie<sup>2</sup>, M. L. Kaiser<sup>1</sup>, R. A. Howard<sup>3</sup> and J. L. Bougeret<sup>4</sup>

E-print, Feb 2008, **File**; Annales Geophysicae

Using the extensive and uniform data on coronal mass ejections (CMEs), solar energetic particle (SEP) events, and type II radio bursts during the SOHO era, we discuss how the CME properties such as speed, width and solar-source longitude decide whether CMEs are associated with type II radio bursts and SEP events. We discuss why some radio-quiet CMEs are associated with small SEP events while some radio-loud CMEs are not associated with SEP events. We conclude that either some fast and wide CMEs do not drive shocks or they drive weak shocks that do not produce significant levels of particle acceleration. We also infer that the Alfvén speed in the corona and near-Sun interplanetary medium ranges from  $<200$  km/s to  $\sim 1600$  km/s. Radio-quiet fast and wide CMEs are also poor SEP producers and the association rate of type II bursts and SEP events steadily increases with CME speed and width (i.e., energy). If we consider western hemispheric CMEs, the SEP association rate increases linearly from  $\sim 30\%$  for 800 km/s CMEs to 100% for  $\geq 1800$  km/s. Essentially all type II bursts in the decametre-hectometric (DH) wavelength range are associated with SEP events once the source location on the Sun is taken into account. This is a significant result for space weather applications, because if a CME originating from the western hemisphere is accompanied by a DH type II burst, there is a high probability that it will produce an SEP event.

### **Energetic Phenomena on the Sun**

Nat **Gopalswamy**

E-print, Nov. 2007

AIP Conf. Proc. , Kodai School on Solar Physics, edited by S. S. Hasan and D. Banerjee, V. 919, pp. 275-313, 2007; **File**

Solar flares, coronal mass ejections (CMEs), solar energetic particles (SEPs), and fast solar wind represent the energetic phenomena on the Sun.

This paper provides an **overview** of the energetic phenomena on the Sun including their origin interplanetary propagation and space weather consequences.

### **Radio Quiet Fast and Wide Coronal Mass Ejections**

N. **Gopalswamy**<sup>1</sup>, S. Yashiro<sup>2</sup>, H. Xie<sup>2</sup>, S. Akiyama<sup>2</sup>, E. Aguilar-Rodriguez<sup>2</sup>, M. L. Kaiser<sup>1</sup>, R. A., Howard<sup>3</sup> and J.-L. Bougeret<sup>4</sup>

E-print, Nov. 2007; Ap. J.

We report on the properties of radio-quiet (RQ) and radio-loud (RL) coronal mass ejections (CMEs) that are fast and wide (FW). RQ CMEs lack of type II radio bursts in the metric and decameterhectometric (DH) wavelengths. RL CMEs are associated with metric or DH type II bursts.

The RQ FW CMEs suggest that the Alfvén speed in the low-latitude outer corona can often exceed 1000 km/s and can vary over a factor of  $\geq 3$ . None of the RQ CMEs was associated with large solar energetic particles, which is

useful information for space weather applications.

## **Coronal Mass Ejections of Solar Cycle 23**

Nat [Gopalswamy](#)

J. Astrophys. Astr. , 2006, File

I summarize the statistical, physical, and morphological properties of coronal mass ejections (CMEs) of solar cycle 23, as observed by the Solar and Heliospheric Observatory (SOHO) mission. The SOHO data is by far the most extensive data, which made it possible to fully establish the properties of CMEs as a phenomenon of utmost importance to Sun-Earth connection as well as to the heliosphere. I also discuss various subsets of CMEs that are of primary importance for impact on Earth.

### **THE PRE-CME SUN**

*Report of Working Group E*

N. [GOPALSWAMY](#)<sup>1</sup>, Z. MIKI<sup>2</sup>, D. MAIA<sup>3</sup>, D. ALEXANDER<sup>4</sup>, H. CREMADES<sup>5</sup>,

P. KAUFMANN<sup>6</sup>, D. TRIPATHI<sup>5</sup> and Y.-M. WANG<sup>7</sup>

Space Science Reviews (2006) 123: 303–339

<https://link.springer.com/content/pdf/10.1007%2Fs11214-006-9020-2.pdf>

The coronal mass ejection (CME) phenomenon occurs in closed magnetic field regions on the Sun such as active regions, filament regions, transequatorial interconnection regions, and complexes involving a combination of these. This chapter describes the current knowledge on these closed field structures and how they lead to CMEs. After describing the specific magnetic structures observed in the CME source region, we compare the substructures of CMEs to what is observed before eruption. Evolution of the closed magnetic structures in response to various photospheric motions over different time scales (convection, differential rotation, meridional circulation) somehow leads to the eruption. We describe this pre-eruption evolution and attempt to link them to the observed features of CMEs. Small-scale energetic signatures in the form of electron acceleration (signified by nonthermal radio bursts at metric wavelengths) and plasma heating (observed as compact soft X-ray brightening) may be indicative of impending CMEs. We survey these pre-eruptive energy releases using observations taken before and during the eruption of several CMEs. Finally, we discuss how the observations can be converted into useful inputs to numerical models that can describe the CME initiation.

## **Coronal Mass Ejections and Type II Radio Bursts**

Nat [Gopalswamy](#)

In “Solar Eruptions and Energetic Particles”, AGU, Geophysical Monograph Series, Volume 165 p. 207 2006, File

### **Coronal mass ejections and space weather due to extreme events**

N. [Gopalswamy](#), S. Yashiro and S. Akiyama

in "Solar Influence on the Heliosphere and Earth's Environment: Recent Progress and Prospects", ed. N. Gopalswamy and A. Battacharyya, Quest Publications, Mumbai, p. 79, 2006. File

Abstract

This paper summarizes the extreme solar activity and its space weather implications during the declining phase of the solar cycle 23: October–November 2003 (AR 486), November 2004 (AR 696), January 2005 (AR 720), and September 2005 (AR 808). We have compiled and compared the properties of eruptions and the underlying active regions. All these are super active regions, but the flare and CME productivity varied significantly. While the CMEs from all the regions kept the level of solar energetic particles (SEPs) at storm level for several days, their geoeffectiveness (the ability to produce geomagnetic storms) was significantly different, probably due to the location of the eruptions on the Sun.

### **Coronal mass ejections and other extreme characteristics of the 2003 October–November solar eruptions.**

[Gopalswamy](#) N, Yashiro S, Liu Y, Michalek G, Vourlidas A, Kaiser ML, Howard RA (2005c) JGRA 110:A09S15

### **Workshop Highlights Progress in Solar–Heliospheric Physics**

Nat [Gopalswamy](#)

EOS, 80, No. 50, 525, 2005, File

### **Major Scientific Results from SOHO on Coronal Mass Ejections**

N. [Gopalswamy](#), B. Fleck and J. B. Gurman, File

## Type II radio bursts and energetic solar eruptions.

**Gopalswamy** N, Aguilar-Rodriguez E, Yashiro S, Nunes S, Kaiser ML, Howard RA (2005a) JGRA 110:A12S07

## Spectroscopic observation of a transition region network jet

**J. Gorman**, **L. P. Chitta**, **H. Peter**

A&A 660, A116 2022

<https://arxiv.org/pdf/2202.11375.pdf>

<https://www.aanda.org/articles/aa/pdf/2022/04/aa42995-21.pdf>

Ubiquitous transition region (TR) network jets are considered to be substantial sources of mass and energy to the corona and solar wind. We conduct a case study of a network jet to better understand the nature of mass flows along its length and the energetics involved in its launch. We present an observation of a jet with the Interface Region Imaging Spectrograph (IRIS), while also using data from the Solar Dynamics Observatory (SDO) to provide further context. The jet was located within a coronal hole close to the disk center. We find that a blueshifted secondary component of TR emission is associated with the jet and is persistent along its spire. This component exhibits upward speeds of approximately 20–70 km s<sup>-1</sup> and shows enhanced line broadening. However, plasma associated with the jet in the upper chromosphere shows downflows of 5–10 km s<sup>-1</sup>. Finally, the jet emanates from a seemingly unipolar magnetic footpoint. While a definitive magnetic driver is not discernible for this event, we infer that the energy driving the network jet is deposited at the top of the chromosphere, indicating that TR network jets are driven from the mid-atmospheric layers of the Sun. The energy flux associated with the line broadening indicates that the jet could be powered all the way into the solar wind. **November 23, 2016**

## Brightening and Darkening of the Extended Solar Corona during the Superflares of September 2017

Farid F. **Goryaev**<sup>1</sup>, Vladimir A. Slemzin<sup>1</sup>, Denis G. Rodkin<sup>1</sup>, Elke D'Huys<sup>2</sup>, O. Podladchikova<sup>2</sup>, and Matthew J. West<sup>2</sup>

2018 ApJL 856 L38

<http://sci-hub.tw/http://iopscience.iop.org/2041-8205/856/2/L38/>

On **2017 September 6 and 10**, the strongest X9.3 and X8.2 flares of the decade occurred in the active region NOAA Active Region 12673. During these flares, the Sun Watcher with Active Pixels and Image Processing (SWAP) telescope on board the Project for Onboard Autonomy 2 (PROBA2) satellite registered the unusual alternate brightening and darkening of the western corona at the heliocentric distances  $\approx 1.2$ – $1.7 R_{\odot}$ . The X9.3 flare on 2017 September 6 was accompanied by coronal brightening up to 30%–45% at distances  $\approx 1.35$ – $1.7 R_{\odot}$ . Numerical simulations showed that this brightening might be produced by resonant scattering of the flare radiation by the Fe ix–Fexi ions in the coronal plasma at the temperature  $T \sim 0.8$ – $1$  MK, and the densities seriously reduced in comparison with the typical values for the quiet background corona probably moving outward with velocities of 30–40 km s<sup>-1</sup>. At the maximum of the flare and one hour later, two coronal mass ejections (CMEs) originated, which dimmed the coronal emission in the SWAP 174 Å passband above the western limb by 20%–30%. The X8.2 flare on September 10 was accompanied by a CME, which rose up and progressively dimmed the western part of the corona up to 60%. An hour later the darkening, produced by a global rearrangement of the magnetic field structure and an evacuation of a significant part of the coronal plasma, extended over the complete western limb. A differential emission measure (DEM) analysis showed a decrease in the electron density of the background plasma with  $T \sim 1$ – $2$  MK at distances  $1.24$ – $1.33 R_{\odot}$  by 2–3.5 times after the CME. At the same time, an additional DEM peak at  $T \approx 0.8$  MK appeared, which may be associated with an additional emission in the SWAP passband produced by the flare radiation resonantly scattered by the coronal plasma.

## INTERRUPTED ERUPTION OF LARGE QUIESCENT FILAMENT ASSOCIATED WITH A HALO CME

S. **Gosain**<sup>1</sup>, Boris Filippov<sup>2</sup>, Ram Ajor Maurya<sup>3,4</sup>, and Ramesh Chandra

2016 ApJ 821 85 DOI: 10.3847/0004-637X/821/2/85

We analyze the observations of an eruptive quiescent filament associated with a halo Coronal Mass Ejection (CME). We use observations from the Atmospheric Imaging Assembly (AIA) instrument onboard the Solar Dynamics Observatory (SDO), Solar and Heliospheric Observatory (SOHO)/Large Angle and Spectrometric Coronagraph (LASCO), and the Solar Terrestrial Relations Observatory (STEREO A/B) satellites. The filament exhibits a slow-rise phase followed by a gradual acceleration and then completely disappears. The filament could be traced in STEREO observations up to an altitude of about  $1.44 R_{\odot}$ , where its rise speed reached  $\sim 14$  km s<sup>-1</sup> and disappeared completely at about 10:32 UT on **2011 October 21**. The CME associated with the filament eruption and two bright ribbons in the chromosphere both appeared at about 01:30 UT on **October 22**, i.e., 15 hr after the filament eruption was seen in He ii 304 Å filtergrams. We show that this delay is abnormally large even if the slow rise speed and slow acceleration of the filament are taken into account. To understand the cause of this delay, we compute the decay index ( $n$ ) of the overlying coronal magnetic field. The height distribution of the decay index,  $n$ , suggests that the zone of instability ( $n > 1$ ) at a lower altitude, 144–480 Mm, is followed by a zone of stability ( $n < 1$ ) between 540 and 660

Mm. We interpret the observed delay to be due to the presence of the latter zone, i.e., the zone of stability, which could provide a second quasi-equilibrium state to the filament until it finally erupts.

### **The solar flare myth.**

[Gosling](#), J.T.,

1993. *J. Geophys. Res.* 98, 18937–18950.

### **High-resolution Observation of Blowout Jets Regulated by Sunspot Rotation**

[Tingyu Gou](#), [Rui Liu](#), [Yang Su](#), [Astrid M. Veronig](#), [Hanya Pan](#), [Runbin Luo](#), [Weiqun Gan](#)

*Solar Phys.* **299**, 99 (2024).

<https://doi.org/10.1007/s11207-024-02333-8>

<https://arxiv.org/pdf/2406.02783>

Coronal jets are believed to be the miniature version of large-scale solar eruptions. In particular, the eruption of a mini-filament inside the base arch is suggested to be the trigger and even driver of blowout jets. Here we propose an alternative triggering mechanism, based on high-resolution H-alpha observations of a blowout jet associated with a mini-filament and an M1.2-class flare. The mini-filament remains largely stationary during the blowout jet, except that it is straddled by flare loops connecting two flare ribbons, indicating that the magnetic arcade embedding the mini-filament has been torn into two parts, with the upper part escaping with the blowout jet. In the wake of the flare, the southern end of the mini-filament fans out like neighboring fibrils, indicative of mass and field exchanges between the mini-filament and the fibrils. The blowout jet is preceded by a standard jet. With H-alpha fibrils moving toward the single-strand spire in a sweeping fashion, the standard jet transitions to the blowout jet. The similar pattern of standard-to-blowout jet transition occurs in an earlier C-class flare before the mini-filament forms. The spiraling morphology and sweeping direction of these fibrils are suggestive of their footpoints being dragged by the leading sunspot that undergoes clockwise rotation for over two days. Soon after the sunspot rotation reaches a peak angular speed as fast as 10 deg/hr, the dormant active region becomes flare-productive, and the mini-filament forms through the interaction of moving magnetic features from the rotating sunspot with satellite spots/pores. Hence, we suggest that the sunspot rotation plays a key role in building up free energy for flares and jets and in triggering blowout jets by inducing sweeping motions of fibrils. **2022 November 11**

### **Complete replacement of magnetic flux in a flux rope during a coronal mass ejection**

[Tingyu Gou](#), [Rui Liu](#), [Astrid M. Veronig](#), [Bin Zhuang](#), [Ting Li](#), [Wensi Wang](#), [Mengjiao Xu](#), [Yuming Wang](#)

*Nature Astronomy* **2023**

<https://arxiv.org/pdf/2305.03217.pdf>

<https://www.nature.com/articles/s41550-023-01966-2.pdf>

Solar coronal mass ejections are the most energetic events in the Solar System. In their standard formation model, a magnetic flux rope builds up into a coronal mass ejection through magnetic reconnection that continually converts overlying, untwisted magnetic flux into twisted flux enveloping the pre-existing rope. However, only a minority of coronal mass ejections carry a coherent magnetic flux rope as their core structure, which casts doubt on the universality of this orderly wrapping process. Here we provide observational evidence of a different formation and eruption mechanism of a magnetic flux rope from an S-shaped thread, where its magnetic flux is fully replaced via flare reconnections. One of the footpoints of the sigmoidal feature slipped and expanded during the formation, and then moved to a completely new place, associated with the highly dynamical evolution of flare ribbons and a twofold increase in magnetic flux through the footpoint, during the eruption. Such a configuration is not predicted by standard formation models or numerical simulations and highlights the three-dimensional nature of magnetic reconnections between the flux rope and the surrounding magnetic field. **2014 Sep 10, 12**

### **Solar Flare-CME Coupling Throughout Two Acceleration Phases of a Fast CME**

[Tingyu Gou](#), [Astrid M. Veronig](#), [Rui Liu](#), [Bin Zhuang](#), [Mateja Dumbovic](#), [Tatiana Podladchikova](#), [Hamish](#)

[A. S. Reid](#), [Manuela Temmer](#), [Karin Dissauer](#), [Bojan Vrsnak](#), [Yuming Wang](#)

*ApJL* **897** L36 **2020**

<https://arxiv.org/pdf/2006.11707.pdf>

<https://doi.org/10.3847/2041-8213/ab9ec5>

Solar flares and coronal mass ejections (CMEs) are closely coupled through magnetic reconnection. CMEs are usually accelerated impulsively within the low solar corona, synchronized with the impulsive flare energy release. We investigate the dynamic evolution of a fast CME and its associated X2.8 flare occurring on **2013 May 13**. The CME experiences two distinct phases of enhanced acceleration, an impulsive one with a peak value of  $\sim 5 \text{ km s}^{-2}$  followed by an extended phase with accelerations up to  $0.7 \text{ km s}^{-2}$ . The two-phase CME dynamics is associated with a two-episode flare energy release. While the first episode is consistent with the "standard" eruption of a magnetic flux rope, the second episode of flare energy release is initiated by the reconnection of a large-scale loop in the aftermath of the eruption and produces stronger nonthermal emission up to  $\gamma$ -rays. In addition, this long-duration flare reveals clear signs of ongoing magnetic reconnection during the decay phase, evidenced by extended HXR bursts with energies up to 100--300 keV and intermittent downflows of reconnected loops for  $>4$  hours. The observations reveal that the two-step flare reconnection substantially contributes to the two-phase CME acceleration, and the impulsive CME acceleration

precedes the most intense flare energy release. The implications of this non-standard flare/CME observation are discussed.

### The Birth of A Coronal Mass Ejection

Tingyu [Gou](#), [Rui Liu](#), [Bernhard Kliem](#), [Yuming Wang](#), [Astrid M. Veronig](#)

Science Advances Vol. 5, no. 3, eaau7004 2019 DOI: 10.1126/sciadv.aau7004 **File**

<https://arxiv.org/pdf/1811.04707.pdf>

<http://advances.sciencemag.org/content/advances/5/3/eaau7004.full.pdf>

[https://scholar.google.com/scholar\\_url?url=https://advances.sciencemag.org/content/advances/5/3/eaau7004.full.pdf&hl=ru&sa=T&oi=ucasa&ct=ufr&ei=sAT3Xt2ONcuAy9YP39-H6Ao&scisig=AAGBfm1bseYEHRB5IxI1ikfslPoFGSLZ6w](https://scholar.google.com/scholar_url?url=https://advances.sciencemag.org/content/advances/5/3/eaau7004.full.pdf&hl=ru&sa=T&oi=ucasa&ct=ufr&ei=sAT3Xt2ONcuAy9YP39-H6Ao&scisig=AAGBfm1bseYEHRB5IxI1ikfslPoFGSLZ6w)

The Sun's atmosphere is frequently disrupted by coronal mass ejections (CMEs), coupled with flares and energetic particles. In the standard picture, the coupling is explained by magnetic reconnection at a vertical current sheet connecting the flare loops and the CME, with the latter embedding a helical magnetic structure known as flux rope. As it jumps upward due to instabilities or loss of equilibrium, the flux rope stretches the overlying coronal loops so that oppositely directed field is brought together underneath, creating the current sheet. However, both the origin of flux ropes and their nascent paths toward eruption remain elusive. Here we present an observation of how a stellar-sized CME bubble evolves continuously from plasmoids, mini flux ropes that are barely resolved, within half an hour. The eruption initiates when plasmoids springing from a vertical current sheet merge into a leading plasmoid occupying the upper tip of the current sheet. Rising at increasing speed to stretch the overlying loops, this leading plasmoid then expands impulsively into the CME bubble, in tandem with hard X-ray bursts. This observation illuminates for the first time a complete CME evolutionary path that has the capacity to accommodate a wide variety of plasma phenomena by bridging the gap between micro-scale dynamics and macro-scale activities. **2013 May 13**

### Direct Observation of Two-Step Magnetic Reconnection in a Solar Flare

Tingyu [Gou](#), [Astrid M. Veronig](#), [Ewan Dickson](#), [Aaron Hernandez-Perez](#), [Rui Liu](#)

ApJ 845: L1 2017

<https://arxiv.org/pdf/1707.06198.pdf>

We report observations of an eruptive X2.8 flare on **2013 May 13**, which shows two distinct episodes of energy release in the impulsive phase. The first episode is characterized by the eruption of a magnetic flux rope, similar to the energy-release process in most standard eruptive flares. While the second episode, which is stronger than the first normal one and shows enhanced high-energy X-ray and even  $\gamma$ -ray emissions, is closely associated with magnetic reconnection of a large-scale loop in the aftermath of the eruption. The reconnection inflow of the loop leg is observed in the Solar Dynamics Observatory (SDO)/Atmospheric Imaging Assembly (AIA) 304 Å passband and accelerates towards the reconnection region to a speed as high as  $\sim 130$  km/s. Simultaneously the corresponding outflow jets are observed in the AIA hot passbands with a speed of  $\sim 740$  km/s and mean temperature of  $\sim 14$  MK. RHESSI observations show a strong burst of hard X-ray (HXR) and  $\gamma$ -ray emissions with hard electron spectra of  $\delta \approx 3$ , exhibiting a soft-hard-harder behavior. A distinct altitude decrease of the HXR loop-top source coincides with the inward swing of the loop leg observed in the AIA 304 Å passband, which is suggested to be related to the coronal implosion. This fast inflow of magnetic flux contained in the loop leg greatly enhances the reconnection rate and results in very efficient particle acceleration in the second-step reconnection, which also helps to achieve a second higher temperature peak up to  $T \approx 30$  MK.

### Tracking of Coronal White-Light Events by Texture

N. [Goussis](#)<sup>1,2</sup>, G. [Stenborg](#)<sup>3</sup>, A. [Vourlidis](#)<sup>4</sup> and R. [Howard](#)<sup>4</sup>

Solar Phys. 262(2), 481-494, **2010**

The extraction of the kinematic properties of coronal mass ejections (CMEs) from white-light coronagraph images involves a significant degree of user interaction: defining the edge of the event, separating the core from the front or from nearby unrelated structures, *etc.* To contribute towards a less subjective and more quantitative definition, and therefore better kinematic characterization of such events, we have developed a novel image-processing technique based on the concept of “texture of the event”. The texture is defined by the so-called gray-level co-occurrence matrix, and the technique consists of a supervised segmentation algorithm to isolate a particular region of interest based upon its similarity with a pre-specified model. Once the event is visually defined early in its evolution, it is possible to automatically track the event by applying the segmentation algorithm to the corresponding time series of coronagraph images. In this paper we describe the technique, present some examples, and show how the coronal background, the core of the event, and even the associated shock (if one exists) can be identified for different kind of CMEs detected by the LASCO and SECCHI coronagraphs.

### Eruptive Flare, CME, and Shock Wave in the 25 August 2001 High-Energy Solar Event

[V. V. Grechnev](#), [A. A. Kochanov](#) & [A. M. Uralov](#)

Solar Physics volume 298, Article number: 49 (2023)

<https://doi.org/10.1007/s11207-023-02144-3>

<https://link.springer.com/content/pdf/10.1007/s11207-023-02144-3.pdf> **File**



The major SOL2001-08-25 event produced a fast coronal mass ejection (CME: 1430 km s<sup>-1</sup>), strong flare emissions in hard X-rays and  $\gamma$ -rays extending to high energies, and neutrons detected both on spacecraft and by a low-latitude neutron monitor. To supplement the probable picture of this outstanding event, we reconstruct kinematic plots of the eruption and the shock-wave history. The hard X-ray and  $\gamma$ -ray emissions exhibited soft-hard-soft evolution. The emissions were strongest and hardest during a two-minute interval soon after the highest change rate of the magnetic flux within the flare ribbons of  $2.6 \times 10^{19}$  Mx s<sup>-1</sup>, which was simultaneous with the reconstructed acceleration of the erupting flux rope. We reveal an indication of accelerated electrons injected into the erupting flux rope that then precipitated far from the main flare site, producing a hard X-ray source that moved along the footprint of a stretching flux-rope leg. These results suggest that the particle acceleration was governed by magnetic reconnection during the eruption. As in a typical situation, a piston shock was excited early in the impulsive phase and gradually transformed into a bow shock later. The frequency drift of a Type-II burst is shown to be proportional to a power of frequency  $f$ ,  $df/dt \propto f^\epsilon$ , with a typical range of  $\epsilon$  being between 5/3 and 2. Overall, the SOL2011-08-25 event was a typical eruptive two-ribbon flare. Its strength was determined mainly by the intensity of the reconnection processes.

## **Reconciliation of Observational Challenges to the Impulsive-Piston Shock-Excitation Scenario.**

### **II. Shock Waves Produced in CME-less Events with a Null-Point Topology.**

**Grechnev, V.V., Kiselev, V.I., Uralov, A.M., Myshyakov, I.I.:**

*Solar Phys.*, **297**, Article number: 123 **2022**, **File** **See movies of 16 Apr 2014**

Continuing Article [I](#), we revisit challenging events previously identified by different authors, whose analysis led to conclusions about various mechanisms of the shock-wave excitation. Here, we reconsider four events that involved fan-spine coronal configurations with a null-point topology (NPT). The presence of Type-II radio bursts in all events as well as extreme-ultraviolet disturbances (EUV waves) observed in three events evidence the presence of shock waves, whereas no coronal mass ejections (CMEs) were detected in most events. One idea proposed to explain the observations was the shock-wave excitation by the straightening of a postreconnection kinked loop. The Type-II burst in another event appeared in association with a compact flare with a high thermal pressure that looked to be in favor of a flare-generated blast wave. One event was associated with a possible pseudo-CME. All of these challenging events have been reconciled in terms of an impulsively excited piston shock. CME-less filament eruptions in NPT configurations appear to represent a distinct category of events responsible for some of the observed shock waves. **14 November 2005** , **28 February 2011** , **6 March 2014** , **16 April 2014**

## **Reconciliation of Observational Challenges to the Impulsive-Piston Shock-Excitation Scenario.**

### **I. Kinematic Challenges**

**V.V. Grechnev · V.I. Kiselev · A.M. Uralov**

*Solar Phys.* **297**, Article number: 106 **2022** **File** **See movies of 8 December 2007**

Until now, there is no consensus on the origin of coronal shock waves.

Questions also remain about the patterns that govern the propagation of the presumably related disturbances observed in the extreme ultraviolet (EUV waves).

We present arguments in favor of the initial excitation of the waves by the impulsive acceleration of erupting structures. We consider two puzzling events that have been known thanks to the efforts of different research teams. Using recent findings and our methods, we aim to figure out what might actually have happened in these challenging events. In the first event, the expansion of the coronal mass ejection (CME) was determined by gravity starting from the low corona. The previous analysis led the authors to a conclusion about the flare-related origin of the associated shock wave. We also consider another event, in which an EUV wave had a strange kinematics. This was one of the weakest flares accompanied by EUV waves. Both of these challenging events have been reconciled in terms of an impulsively-excited piston shock. **24 December 1996**, **8 December 2007**

## **A Geoeffective CME Caused by the Eruption of a Quiescent Prominence on 29 September 2013**

**V. V. Grechnev & I. V. Kuzmenko**

*Solar Physics* volume 295, Article number: 55 (2020) **File**

<https://link.springer.com/content/pdf/10.1007/s11207-020-01619-x.pdf>

The eruption of a large prominence that occurred away of active regions in the SOL2013-09-29 event produced a fast coronal mass ejection (CME) and a shock wave. The event caused considerable geospace disturbances, including a proton enhancement that have been addressed in previous studies. Continuing with the analysis of this event, we focus on the development of the CME and shock wave, assess an expected geospace impact using simplest considerations, and compare the expectations with in situ measurements near Earth. The high CME speed in this non-flare-associated event was determined by a considerable reconnected flux that corresponds to a pattern established by different authors. Estimations based on a few approaches showed the reconnection flux in this event to be comparable with a typical value in flare-associated eruptions. The shock wave was most likely impulsively excited by the erupting prominence in the

same way as in flare-associated events and changed to the bow-shock regime later. The trajectory calculated for this scenario reproduces the Type II emission observed from 30 MHz to 70 kHz; its interruptions were probably caused by propagation effects. Properties of the near-Earth proton enhancement are discussed considering the results of recent studies

CESRA #2584 June 2020 <http://www.astro.gla.ac.uk/users/eduard/cesra/?p=2584>

## Development of a Fast CME and Properties of a Related Interplanetary Transient

V. V. [Grechnev](#), A. A. Kochanov, A. M. Uralov, V. A. Slemzin, D. G. Rodkin, F. F. Goryaev, V. I. Kiselev, I. I. Myshyakov

[Solar Physics](#) October 2019, 294:139

<https://link.springer.com/content/pdf/10.1007%2Fs11207-019-1529-0.pdf>

We study the development of a coronal mass ejection (CME) caused by a prominence eruption on **24 February 2011** and properties of a related interplanetary CME (ICME). The prominence destabilized, accelerated, and produced an M3.5 flare, a fast CME, and a shock wave. The eruption at the east limb was observed in quadrature by the Atmospheric Imaging Assembly (AIA) on board the Solar Dynamics Observatory (SDO) and by the Sun Earth Connection Coronal and Heliospheric Investigation (SECCHI) instrument suite on board the Solar-Terrestrial Relations Observatory (STEREO). The ICME produced by the SOL2011-02-24 event was measured in situ on STEREO-B two days later. The diagnostics made from multi-wavelength SDO/AIA images reveals a pre-eruptive heating of the prominence to about 7 MK and its subsequent heating during the eruption by flare-accelerated particles to about 10 MK. The hot plasma was detected in the related ICME as an enhancement in the ionic charge state of Fe, whose evolution was reproduced in the modeling. The analysis of the solar source region allows for predicting the variations of magnetic components in the ICME, while the flux-rope rotation by about  $40^\circ$  was indicated by observations. The magnetic-cloud propagation appears to be ballistic.

## Multi-instrument view on solar eruptive events observed with the Siberian Radioheliograph: From detection of small jets up to development of a shock wave and CME

V. V. [Grechnev](#), S. V. [Lesovoi](#), A. A. [Kochanov](#), A. M. [Uralov](#), A. T. [Altyntsev](#), A. V. [Gubin](#), D. A. [Zhdanov](#), E. F. [Ivanov](#), G. Ya. [Smolkov](#), L. K. [Kashapova](#) (Institute of Solar-Terrestrial Physics, Irkutsk, Russia)

Journal of Atmospheric and Solar-Terrestrial Physics [Volume 174](#), September 2018, Pages 46-65

<https://arxiv.org/pdf/1805.02564.pdf> **File**

<https://reader.elsevier.com/reader/sd/BC56B481FA5E7EABF46801D90BBABAAD2160ED3E82A6BDA7FD48FE34ED0563AA3022B96BD2AD0E382C8D3A86F96D2BAB>

The first 48-antenna stage of the Siberian Radioheliograph (SRH) started single-frequency test observations early in 2016, and since August 2016 it routinely observes the Sun at several frequencies in the 4-8 GHz range with an angular resolution of 1-2 arc minutes and an imaging interval of about 12 seconds. With limited opportunities of the incomplete antenna configuration, a high sensitivity of about 100 Jy allows the SRH to contribute to the studies of eruptive phenomena along three lines. First, some eruptions are directly visible in SRH images. Second, some small eruptions are detectable even without a detailed imaging information from microwave depressions caused by screening the background emission by cool erupted plasma. Third, SRH observations reveal new aspects of some events to be studied with different instruments. We focus on an eruptive C2.2 flare on **16 March 2016** around 06:40, one of the first flares observed by the SRH. Proceeding from SRH observations, we analyze this event using extreme-ultraviolet, hard X-ray, white-light, and metric radio data. An eruptive prominence expanded, brightened, and twisted, which indicates a time-extended process of the flux-rope formation together with the development of a large coronal mass ejection (CME). The observations rule out a passive role of the prominence in the CME formation. The abrupt prominence eruption impulsively excited a blast-wave-like shock, which appeared during the microwave burst and was manifested in an "EUV wave" and Type II radio burst. The shock wave decayed and did not transform into a bow shock because of the low speed of the CME. Nevertheless, this event produced a clear proton enhancement near Earth. Comparison with our previous studies of several events confirms that the impulsive-piston shock-excitation scenario is typical of various events. **16 March 2016, 1 May 2017, 3 August 2017, 9 September 2017,**

**Table 1:** Summary of shock waves studied

## The 26 December 2001 Solar Eruptive Event Responsible for GLE63.

### II. Multi-Loop Structure of Microwave Sources in a Major Long-Duration Flare

V.V. [Grechnev](#) . A. M. Uralov, V. I. Kiselev, A.A. Kochanov

[Solar Phys.](#) January 2017, 292:3 **File**

<https://arxiv.org/pdf/1611.08349v1.pdf>

Our analysis of the observations of the SOL2001-12-26 event, which was related to ground-level enhancement of cosmic-ray intensity GLE63, including microwave spectra and images from the *Nobeyama Radioheliograph* at 17 and 34 GHz, from the *Siberian Solar Radio Telescope* at 5.7 GHz, and from the *Transition Region and Coronal Explorer* in 1600 Å, has led to the following results: A flare ribbon overlapped with the sunspot umbra, which is typical of large particle events. Atypical were i) the long duration of the flare, which lasted more than one hour; ii) the moderate intensity of the microwave burst, which was about 104 sfu; iii) the low peak frequency of the gyrosynchrotron spectrum, which was about 6 GHz; and its insensitivity to the flux increase by more than one order of magnitude.

This was accompanied by a nearly constant ratio of the flux emitted by the volume in the high-frequency part of the spectrum to its elevated low-frequency part determined by the area of the source. With the self-similarity of the spectrum, a similarity was observed between the moving microwave sources and the brightest parts of the flare ribbons in 1600 Å images. We compared the 17 GHz and 1600 Å images and confirm that the microwave sources were associated with multiple flare loops, whose footpoints appeared in the ultraviolet as intermittent bright kernels. To understand the properties of the event, we simulated its microwave emission using a system of several homogeneous gyrosynchrotron sources above the ribbons. The scatter between the spectra and the sizes of the individual sources is determined by the inhomogeneity of the magnetic field within the ribbons. The microwave flux is mainly governed by the magnetic flux passing through the ribbons and the sources. The apparent simplicity of the microwave structures is caused by a poorer spatial resolution and dynamic range of the microwave imaging. The results indicate that microwave manifestations of accelerated electrons correspond to the structures observed in thermal emissions, as well-known models predict.

See CESRA Highlight # 1375, May 2017 <http://www.astro.gla.ac.uk/users/eduard/cesra/?p=1375>

## **A Tiny Eruptive Filament as a Flux-Rope Progenitor and Driver of a Large-Scale CME and Wave**

V.V. [Grechnev](#) (1), A.M. Uralov (1), A.A. Kochanov (1), I.V. Kuzmenko (2), D.V. Prosovetsky (1), Ya.I. Egorov (1), V.G. Fainshtein (1), L.K. Kashapova

Solar Phys., Volume 291, Issue 4, pp 1173-1208 2016

<http://arxiv.org/pdf/1604.00800v1.pdf> File

A solar eruptive event SOL2010-06-13 observed with SDO/AIA has been discussed in the contexts of the CME genesis and an associated EUV transient in terms of a shock driven by the apparent CME rim. We have revealed in this event an erupting flux rope, studied its properties, and detected wave signatures inside the developing CME. These findings have allowed us to establish new features in the genesis of the CME and associated EUV wave and to reconcile all of the episodes into a causally-related sequence. (1) A hot 11 MK flux rope developed from a compact filament, accelerated up to 3 km/s<sup>2</sup> 1 min before a hard X-ray burst and earlier than other structures, reached 420 km/s, and decelerated to 50 km/s. (2) The CME development was driven by the flux rope. Closed structures above the rope got sequentially involved in the expansion from below upwards, came closer together, and disappeared to reveal their envelope, the rim, which became the outer boundary of the cavity. The rim was associated with the separatrix surface of a magnetic domain, which contained the pre-eruptive filament. (3) The rim formation was associated with a successive compression of the upper active-region structures into the CME frontal structure (FS). When the rim was formed, it resembled a piston. (4) The disturbance responsible for the CME formation was excited by the flux rope inside the rim, and then propagated outward. EUV structures at different heights started to accelerate, when their trajectories in the distance-time diagram were crossed by the front of this disturbance. (5) Outside the rim and FS, the disturbance propagated like a blast wave, manifesting in a type II radio burst and a leading part of the EUV transient. Its main, trailing part was the FS, which consisted of swept-up 2 MK loops enveloping the rim. The wave decelerated and decayed soon, being not driven by the trailing piston, which slowed down.

## **Responsibility of a Filament Eruption for the Initiation of a Flare, CME, and Blast Wave, and its Possible Transformation into a Bow Shock**

V. V. [Grechnev](#) (1), A. M. Uralov (1), I. V. Kuzmenko (2), A. A. Kochanov (1), I. M. Chertok (3), S. S. Kalashnikov

Solar Phys., 2015, Volume 290, Issue 1, pp 129-158

<http://arxiv.org/pdf/1410.8696v1.pdf>

Multi-instrument observations of two filament eruptions on **24 February and 11 May 2011** suggest the following updated scenario for eruptive flare, CME and shock wave evolution. An initial destabilization of a filament results in stretching out of magnetic threads belonging to its body and rooted in the photosphere along the inversion line. Their reconnection leads to i) heating of parts of the filament or its environment, ii) initial development of the flare arcade cusp and ribbons, and iii) increasing similarity of the filament to a curved flux rope and its acceleration. Then the pre-eruption arcade enveloping the filament gets involved in reconnection according to the standard model and continues to form the flare arcade and ribbons. The poloidal magnetic flux in the curved rope developing from the filament progressively increases and forces its toroidal expansion. This flux rope impulsively expands and produces an MHD disturbance, which rapidly steepens into a shock. The shock passes through the arcade expanding above the filament and then freely propagates ahead of the CME like a decelerating blast wave for some time. If the CME is slow, then the shock eventually decays. Otherwise, the frontal part of the shock changes into the bow-shock regime. This was observed for the first time in the 24 February 2011 event. When reconnection ceases, the flux rope relaxes and constitutes the CME core-cavity system. The expanding arcade develops into the CME frontal structure. We also found that reconnection in the current sheet of a remote streamer forced by the shock's passage results in a running flare-like process within the streamer responsible for a type II burst. The development of dimming and various associated phenomena are discussed.

## **An Updated View of Solar Eruptive Flares and Development of Shocks and CMEs: History of the 2006 December 13 GLE-Productive Extreme Event**

V. **Grechnev**, V. Kiselev, A. Uralov, N. Meshalkina, A. Kochanov

E-print, Aug **2013**; Publ. Astron. Soc. Japan 65, No SP1, S9 [18 pages] (2013) ), **File**

An extreme **2006 December 13** event marked the onset of the Hinode era being the last major flare in the solar cycle 23 observed with NoRH and NoRP. The event produced a fast CME, strong shock, and big particle event responsible for GLE70. We endeavor to clarify relations between eruptions, shock wave, and the flare, and to shed light on a debate over the origin of energetic protons. One concept relates it with flare processes. Another one associates acceleration of ions with a bow shock driven by a CME at (2-4) $R_{\text{sun}}$ . The latter scenario is favored by a delayed particle release time after the flare. However, our previous studies have established that a shock wave is typically excited by an impulsively erupting magnetic rope (future CME core) during the flare rise, while the outer CME surface evolves from an arcade whose expansion is driven from inside. Observations of the 2006 December 13 event reveal two shocks following each other, whose excitation scenario contradicts the delayed CME-driven bow-shock hypothesis. Actually, the shocks developed much earlier, and could accelerate protons still before the flare peak. Then, the two shocks merged into a single stronger one and only decelerated and dampened long afterwards.

## **Microwave Negative Bursts as Indications of Reconnection between Eruptive Filaments and Large-Scale Coronal Magnetic Environment**

V. **Grechnev**, I. Kuzmenko, A. Uralov, I. Chertok, A. Kochanov

E-print, Aug **2013**, Publ. Astron. Soc. Japan 65, No. SP1, S10 [9 pages] (**2013**)

Low-temperature plasma ejected in solar eruptions can screen active regions as well as quiet solar areas. Absorption phenomena can be observed in microwaves as 'negative bursts' and in different spectral domains. We analyze two very different recent events with such phenomena and present an updated systematic view of solar events associated with negative bursts. Related filament eruptions can be normal, without essential changes of shape and magnetic configuration, and 'anomalous'. The latter are characterized by disintegration of an eruptive filament and dispersal of its remnants as a cloud over a large part of solar disk. Such phenomena can be observed as giant depressions in the He II 304 A line. One of possible scenarios for an anomalous eruption is proposed in terms of reconnection of filament's internal magnetic fields with external large-scale coronal surrounding. **2004 July 13., 2011 June 7, 2011 December 13.**

## **The 26 December 2001 Solar Eruptive Event Responsible for GLE63.**

### **III. CME, Shock Waves, and Energetic Particles**

V.V. **Grechnev** (1), V.I. Kiselev (1), A.M. Uralov (1), K.-L. Klein (2), A.A. Kochanov (1)

Solar Phys. 292:102 **2017**

<https://arxiv.org/pdf/1612.04092v1.pdf>

**File**

The **26 December 2001** moderate solar eruptive event (GOES importance M7.1, microwaves up to 4000 sfu at 9.4 GHz, CME speed 1446 km/s) produced strong fluxes of solar energetic particles (SEPs) and ground-level enhancement of cosmic-ray intensity (GLE63). To find a possible reason for the atypically high proton outcome of this event, we study its multi-wavelength images and dynamic radio spectra, and quantitatively reconcile the findings with each other. An additional eruption probably occurred in the same active region about half an hour before the main eruption, which produced two blast-wave-like shocks during the impulsive phase. Later on, the two shock waves merged around the frontal direction into a single shock, which is traced up to  $25R_{\odot}$  as a halo ahead of the expanding CME body, in agreement with an interplanetary type II event recorded by Wind/WAVES. The shape and kinematics of the halo indicate that the shock wave was in an intermediate regime between the blast wave and bow shock at these distances. The results show that i) the shock wave appeared during the flare rise and could accelerate particles earlier than usually assumed; ii) the particle event could be amplified by the preceding eruption, which stretched closed structures above the developing CME, facilitating its lift-off and escape of flare-accelerated particles, enabling a higher CME speed and a stronger shock ahead; iii) escape of flare-accelerated particles could be additionally facilitated by reconnection of the flux rope, where they were trapped, with a large coronal hole; iv) a rich seed population was provided by the first eruption for the acceleration by a trailing shock wave.

## **A Challenging Solar Eruptive Event of 18 November 2003 and the Causes of the 20 November Geomagnetic Superstorm.**

### **II. CMEs, Shock Waves, and Drifting Radio Bursts**

V.V. **Grechnev**, A.M. Uralov, I.M. Chertok, V.A. Slemzin, B.P. Filippov, Ya.I. Egorov, V.G. Fainshtein, A.N. Afanasyev, N.P. Prestage, M. Temmer

E-print, Aug **2013**; Solar Phys.

We continue our study (Grechnev et al. (2013), doi:10.1007/s11207-013-0316-6; Paper I) on the 18 November 2003 geoeffective event. To understand possible impact on geospace of coronal transients observed on that day, we investigated their properties from solar near-surface manifestations in extreme ultraviolet, LASCO white-light images, and dynamic radio spectra. We reconcile near-surface activity with the expansion of coronal mass ejections (CMEs) and determine their orientation relative to the earthward direction. The kinematic measurements, dynamic radio spectra, and

microwave and X-ray light curves all contribute to the overall picture of the complex event and confirm an additional eruption at 08:07-08:20 UT close to the solar disk center presumed in Paper I. Unusual characteristics of the ejection appear to match those expected for a source of the 20 November superstorm but make its detection in LASCO images hopeless. On the other hand, none of the CMEs observed by LASCO seem to be a promising candidate for a source of the superstorm being able to produce, at most, a glancing blow on the Earth's magnetosphere. Our analysis confirms free propagation of shock waves revealed in the event and reconciles their kinematics with "EUV waves" and dynamic radio spectra up to decameters.

## **A Challenging Solar Eruptive Event of 18 November 2003 and the Causes of the 20 November Geomagnetic Superstorm.**

### **I. Unusual History of an Eruptive Filament**

V. V. **Grechnev**, A. M. Uralov, V. A. Slemzin, I. M. Chertok, B. P. Filippov, G. V. Rudenko, M. Temmer  
E-print, May 2013; Solar Phys.

This is the first of four companion papers, which analyze a complex eruptive event of 18 November 2003 in AR 10501 and the causes of the largest Solar Cycle 23 geomagnetic storm on 20 November 2003. Analysis of a complete data set, not considered before, reveals a chain of eruptions to which hard X-ray and microwave bursts responded. A filament in AR 10501 was not a passive part of a larger flux rope, as usually considered. The filament erupted and gave origin to a CME. The chain of events was as follows: i) an eruption at 07:29 accompanied by a not reported M1.2 class flare associated with the onset of a first southeastern CME1, which is not responsible for the superstorm; ii) a confined eruption at 07:41 (M3.2 flare) that destabilized the filament; iii) the filament acceleration (07:56); iv) the bifurcation of the eruptive filament that transformed into a large cloud; v) an M3.9 flare in AR 10501 associated to this transformation. The transformation of the filament could be due to its interaction with the magnetic field in the neighborhood of a null point, located at a height of about 100 Mm above the complex formed by ARs 10501, 10503, and their environment. The CORONAS-F/SPIRIT telescope observed the cloud in 304 Å as a large Y-shaped darkening, which moved from the bifurcation region to the limb. The masses and kinematics of the cloud and the filament were similar. Remnants of the filament were not observed in the second southwestern CME2, previously regarded as a source of the 20 November superstorm. These facts do not support a simple scenario, in which the interplanetary magnetic cloud is considered as a flux rope formed from a structure initially associated with the pre-eruption filament in AR 10501. Observations suggest a possible additional eruption above the bifurcation region close to solar disk center between 08:07 and 08:17 that could be the source of the superstorm.

### **Coronal Shock Waves, EUV Waves, and Their Relation to CMEs.**

#### **III. Shock-Associated CME/EUV Wave in an Event with a Two-Component EUV Transient**

V. V. **Grechnev**, A. N. Afanasyev, A. M. Uralov, I. M. Chertok, M. V. Eselevich, V. G. Eselevich, G. V. Rudenko and Y. Kubo

Solar Physics, Volume 273, Number 2, 461-477, 2011, **File in Chertok's papers**

On 17 January 2010, STEREO-B observed in extreme ultraviolet (EUV) and white light a large-scale dome-shaped expanding coronal transient with perfectly connected off-limb and on-disk signatures. Veronig et al. (Astrophys. J. Lett. 716, L57, 2010) concluded that the dome was formed by a weak shock wave. We have revealed two EUV components, one of which corresponded to this transient. All of its properties found from EUV, white light, and a metric type II burst match expectations for a freely expanding coronal shock wave, including correspondence with the fast-mode speed distribution, while the transient sweeping over the solar surface had a speed typical of EUV waves. The shock wave was presumably excited by an abrupt filament eruption. Both a weak shock approximation and a power-law fit match kinematics of the transient near the Sun. Moreover, the power-law fit matches the expansion of the CME leading edge up to 24 solar radii. The second, quasi-stationary EUV component near the dimming was presumably associated with a stretched CME structure; no indications of opening magnetic fields have been detected far from the eruption region.

### **Coronal Shock Waves, EUV Waves, and Their Relation to CMEs.**

#### **I. Reconciliation of "EIT Waves", Type II Radio Bursts, and Leading Edges of CMEs**

V. V. **Grechnev**, A. M. Uralov, I. M. Chertok, I. V. Kuzmenko, A. N. Afanasyev, N. S. Meshalkina, S. S. Kalashnikov and Y. Kubo

Solar Physics, Volume 273, Number 2, 433-460, 2011, **File in Chertok's papers**

We show examples of the excitation of coronal waves by flare-related abrupt eruptions of magnetic rope structures. The waves presumably rapidly steepened into shocks and freely propagated afterwards like decelerating blast waves that showed up as Moreton waves and EUV waves. We propose a simple quantitative description for such shock waves to reconcile their observed propagation with drift rates of metric type II bursts and kinematics of leading edges of coronal mass ejections (CMEs). Taking account of different plasma density falloffs for propagation of a wave up and along the solar surface, we demonstrate a close correspondence between drift rates of type II bursts and speeds of EUV waves, Moreton waves, and CMEs observed in a few previously studied events.

24 September 1997, 1 June 2002, 13 July 2004, 19 May 2007

## Magnetic Helicity Evolution and Eruptive Activity in NOAA Active Region 11158

L. M. **Green**<sup>1</sup>, J. K. Thalmann<sup>2</sup>, G. Valori<sup>3</sup>, E. Pariat<sup>4</sup>, L. Linan<sup>5</sup>, and K. Moraitis<sup>6</sup>

2022 ApJ 937 59

<https://iopscience.iop.org/article/10.3847/1538-4357/ac88cb/pdf>

Coronal mass ejections are among the Sun's most energetic activity events yet the physical mechanisms that lead to their occurrence are not yet fully understood. They can drive major space weather impacts at Earth, so knowing why and when these ejections will occur is required for accurate space weather forecasts. In this study we use a 4 day time series of a quantity known as the helicity ratio,  $|HJ|/|HV|$  (helicity of the current-carrying part of the active region field to the total relative magnetic helicity within the volume), which has been computed from nonlinear force-free field extrapolations of NOAA active region 11158. We compare the evolution of  $|HJ|/|HV|$  with the activity produced in the corona of the active region and show this ratio can be used to indicate when the active region is prone to eruption. This occurs when  $|HJ|/|HV|$  exceeds a value of 0.1, as suggested by previous studies. We find the helicity ratio variations to be more pronounced during times of strong flux emergence, collision and reconnection between fields of different bipoles, shearing motions, and reconfiguration of the corona through failed and successful eruptions. When flux emergence, collision, and shearing motions have lessened, the changes in helicity ratio are somewhat subtle despite the occurrence of significant eruptive activity during this time. **2011 February 12–15**

## The origin, early evolution and predictability of solar eruptions

**Review**

Lucie **Green**, [Tibor Torok](#), [Bojan Vrsnak](#), [Ward Manchester IV](#), [Astrid Veronig](#)

Space Science Reviews 214: 46 **2018**

<https://arxiv.org/pdf/1801.04608.pdf>

<https://link.springer.com/content/pdf/10.1007%2Fs11214-017-0462-5.pdf> **File**

Coronal mass ejections (CMEs) were discovered in the early 1970s when space-borne coronagraphs revealed that eruptions of plasma are ejected from the Sun. Today, it is known that the Sun produces eruptive flares, filament eruptions, coronal mass ejections and failed eruptions; all thought to be due to a release of energy stored in the coronal magnetic field during its drastic reconfiguration. This review discusses the observations and physical mechanisms behind this eruptive activity, with a view to making an assessment of the current capability of forecasting these events for space weather risk and impact mitigation. Whilst a wealth of observations exist, and detailed models have been developed, there still exists a need to draw these approaches together. In particular more realistic models are encouraged in order to assess the full range of complexity of the solar atmosphere and the criteria for which an eruption is formed. From the observational side, a more detailed understanding of the role of photospheric flows and reconnection is needed in order to identify the evolutionary path that ultimately means a magnetic structure will erupt. **19 Oct 1994, 19 July 2000, 4th January 2002, 13 Feb 2009**

## Observations of flux rope formation prior to coronal mass ejections

L. M. **Green**, B. Kliem

Proc. IAU Symp. 300, 209, **2013**

<http://arxiv.org/pdf/1312.4388v1.pdf>

Understanding the magnetic configuration of the source regions of coronal mass ejections (CMEs) is vital in order to determine the trigger and driver of these events. Observations of four CME productive active regions are presented here, which indicate that the pre-eruption magnetic configuration is that of a magnetic flux rope. The flux ropes are formed in the solar atmosphere by the process known as flux cancellation and are stable for several hours before the eruption. The observations also indicate that the magnetic structure that erupts is not the entire flux rope as initially formed, raising the question of whether the flux rope is able to undergo a partial eruption or whether it undergoes a transition in specific flux rope configuration shortly before the CME. **19 December 1996, 5-13 December 2006, 11-12 February 2007, 3-7 December 2007**

## Photospheric flux cancellation and associated flux rope formation and eruption

L. M. **Green**<sup>1</sup>, B. Kliem<sup>1,2,3</sup>, and A. J. Wallace<sup>1</sup>

E-print, Nov. **2010**; A&A 526, A2 (**2011**)

**Aims.** We study an evolving bipolar active region that exhibits flux cancellation at the internal polarity inversion line, the formation of a soft X-ray sigmoid along the inversion line and a coronal mass ejection. The aim is to investigate the quantity of flux cancellation that is involved in flux rope formation in the time period leading up to the eruption.  
**Methods.** The active region is studied using its extreme ultraviolet and soft X-ray emissions as it evolves from a sheared arcade to flux rope configuration. The evolution of the photospheric magnetic field is described and used to estimate how much flux is reconnected into the flux rope.

**Results.** About one third of the active region flux cancels at the internal polarity inversion line in the 2.5 days leading up to the eruption. In this period, the coronal structure evolves from a weakly to a highly sheared arcade and then to a sigmoid that crosses the inversion line in the inverse direction. These properties suggest that a flux rope has formed

prior to the eruption. The amount of cancellation implies that up to 60% of the active region flux could be in the body of the flux rope. We point out that only part of the cancellation contributes to the flux in the rope if the arcade is only weakly sheared, as in the first part of the evolution. This reduces the estimated flux in the rope to ~ 30% or less of the active region flux. We suggest that the remaining discrepancy between our estimate and the limiting value of ~10% of the active region flux, obtained previously by the flux rope insertion method, results from the incomplete coherence of the flux rope, due to nonuniform cancellation along the polarity inversion line. A hot linear feature is observed in the active region which rises as part of the eruption and then likely traces out field lines close to the axis of the flux rope. The flux cancellation and changing magnetic connections at one end of this feature suggest that the flux rope reaches coherence by reconnection shortly before and early in the impulsive phase of the associated flare. The sigmoid is destroyed in the eruption but reforms quickly, with the amount of cancellation involved being much smaller than in the course of its original formation.

## **FLUX ROPE FORMATION PRECEDING CORONAL MASS EJECTION ONSET**

L. M. [GREEN](#)<sup>1</sup> AND B. KLIEM<sup>1,2,3</sup>

E-print, June **2009**, *File*; ApJL, 700, Number 2, L83-L87, **2009**.

We analyse the evolution of a sigmoidal (S shaped) active region toward eruption, which includes a coronal mass ejection (CME) but leaves part of the filament in place. The X-ray sigmoid is found to trace out three different magnetic topologies in succession: a highly sheared arcade of coronal loops in its long-lived phase, a bald-patch separatrix surface (BPSS) in the hours before the CME, and the first flare loops in its major transient intensity enhancement. The coronal evolution is driven by photospheric changes which involve the convergence and cancellation of flux elements under the sigmoid and filament. The data yield unambiguous evidence for the existence of a BPSS, and hence a flux rope, in the corona prior to the onset of the CME.

## **HOW ARE EMERGING FLUX, FLARES AND CMES RELATED TO MAGNETIC POLARITY IMBALANCE IN MDI DATA?**

L.M. [GREEN](#)<sup>1</sup>, P. D'EMOULIN<sup>2</sup>, C.H. MANDRINI<sup>3</sup>, L. VAN DRIEL-GESZTELYI<sup>1,2,4,5</sup>

*Solar Physics*, v. 215, Issue 2, p. 307-325 (**2003**), *File*

In order to understand whether major flares or coronal mass ejections (CMEs) can be related to changes in the longitudinal photospheric magnetic field, we study 4 young active regions during seven days of their disc passage. This time period precludes any biases which may be introduced in studies that look at the field evolution during the short-term flare or CME period only. Data from the Michelson Doppler Imager (MDI) with a time cadence of 96 minutes are used. Corrections are made to the data to account for area foreshortening and angle between line of sight and field direction, and also the underestimation of the flux densities. We make a systematic study of the evolution of the longitudinal magnetic field, and analyze flare and CME occurrence in the magnetic evolution. We find that the majority of CMEs and flares occur during or after new flux emergence. The flux in all four active regions is observed to have deviations from polarity balance both on the long-term (solar rotation) and on the short term (few hours). The long-term imbalance is not due to linkage outside the active region; it is primarily related to the east-west distance from central meridian, with the sign of polarity closer to the limb dominating. The sequence of short term imbalances are not closely linked to CMEs and flares and no permanent imbalance remains after them. We propose that both kinds of imbalance are due to the presence of a horizontal field component (parallel to the photospheric surface) in the emerging flux.

## **MULTI-WAVELENGTH OBSERVATIONS OF AN X-CLASS FLARE WITHOUT A CORONAL MASS EJECTION.**

L. M. [GREEN](#)<sup>1</sup>, S. A. MATTHEWS<sup>1</sup>, L. VAN DRIEL-GESZTELYI<sup>2</sup>, L. K. HARRA, and J. L. CULHANE<sup>1</sup>

*Solar Physics* **205**: 325–339, **2002**.

<http://springerlink.metapress.com/content/hrltnbwxv269/?p=9ff1e04d313d47d990bfce2e22135f3c&pi=96>

Developments in our knowledge of coronal mass ejections (CMEs) have shown that many of these transients occur in association with solar flares. On the occasions when there is a common occurrence of the eruption and the flare, it is most likely that the flare is of high intensity and/or long-duration (Burkepile, Hundhausen, and Webb, 1994; Munro *et al.*, 1979; Webb and Hundhausen, 1987). A model for the relationship between the long-duration event and eruption has been developed (Carmichael, 1964; Sturrock, 1966; Hirayama, 1974; Kopp and Pneuman, 1976), but not so for the high-intensity flares and eruptions. This work investigates the magnetic topology changes that occur for a X1.2 GOES classification flare which has no associated CME. It is found that the flare is likely to result from the interaction between two pre-existing loops low in the corona, producing a confined flare. Slightly higher in the corona, a loop is observed which exhibits an outward motion as a result of the reconfiguration during reconnection. The objective of this work is to gain insight on the magnetic topology of the event which is critical in order to determine whether a high-intensity flare is likely to be related to a CME or not. **30 Sept 2000**.

## **Erratum to: The Magnetic Helicity Budget of a CME-Prolific Active Region**

L.M. [Green](#)<sup>1</sup> · M. Lopez Fuentes<sup>2</sup> · C.H. Mandrini<sup>2,3</sup> · P. Demoulin<sup>4</sup> · L. van Driel-Gesztelyi<sup>1,4,5</sup> · J.L. Culhane<sup>1</sup>

### **The Post-Eruptive Arcade Formation in The Limb Event on July 31, 2004 From Microwave Solar Observations with the RATAN-600 Radio Telescope.**

Irina Yu. [Grigoryeva](#)<sup>1</sup>, Larisa K. Kashapova<sup>2</sup>, Valery N. Borovik<sup>1</sup>, Moisey A. Livshits<sup>3</sup>  
Sun and Geosphere, 2010; 5(2): 58-60

[http://www.shao.az/SG/v5n2/SG\\_v5\\_No2\\_2010-pp-58-60.pdf](http://www.shao.az/SG/v5n2/SG_v5_No2_2010-pp-58-60.pdf)

A CME/flare event occurred at the western limb on 31 July 2004. Five successive multi-wavelength scans in centimeter range were obtained with the RATAN-600 radio telescope starting at the early stage of post-eruptive arcade formation (24 min after a C8.3 flare peak) and lasting for 4 hours. Microwave radio emission of the arcade was rather intense at initial stage indicating a predominant contribution of thermal emission and then considerably decreased during the decay phase. Its maximum was co-spatial with the 195 E Fe XII loop tops. At the end of microwave observations the contribution of the emission from accelerated particles became significant. The similarity of microwave characteristics of two eruptive events (on 31 July 2004 at the western limb and on 25 January 2007 at the eastern limb) is shown.

### **CONSTRAINTS ON CORONAL MASS EJECTION EVOLUTION FROM IN SITU OBSERVATIONS OF IONIC CHARGE STATES**

Jacob R. [Gruesbeck](#)<sup>1</sup>, Susan T. Lepri<sup>1</sup>, Thomas H. Zurbuchen<sup>1</sup>, and Spiro K. Antiochos<sup>2</sup>

Astrophysical Journal, 730:103 (9pp), 2011 April; **File**

We present a novel procedure for deriving the physical properties of coronal mass ejections (CMEs) in the corona. Our methodology uses in situ measurements of ionic charge states of C, O, Si, and Fe in the heliosphere and interprets them in the context of a model for the early evolution of interplanetary CME (ICME) plasma, between 2 and 5R<sub>⊙</sub>. We find that the data are best fit by an evolution that consists of an initial heating of the plasma, followed by an expansion that ultimately results in cooling. The heating profile is consistent with a compression of coronal plasma due to flare reconnection jets and an expansion cooling due to the ejection, as expected from the standard CME/flare model. The observed frozen-in ionic charge states reflect this time history and, therefore, provide important constraints for the heating and expansion timescales, as well as the maximum temperature the CME plasma is heated to during its eruption. Furthermore, our analysis places severe limits on the possible density of CME plasma in the corona. We discuss the implications of our results for CME models and for future analysis of ICME plasma composition.

### **Testing predictors of eruptivity using parametric flux emergence simulations**

Chloé [Guennou](#), Etienne Pariat, Nicole Vilmer, [James E. Leake](#)

2017 J. Space Weather Space Clim., 7, A17

<https://arxiv.org/pdf/1706.04915.pdf>

<https://www.swsc-journal.org/articles/swsc/pdf/2017/01/swsc160047.pdf>

Solar flares and coronal mass ejections (CMEs) are among the most energetic events in the solar system, impacting the near-Earth environment. Flare productivity is empirically known to be correlated with the size and complexity of active regions. Several indicators, based on magnetic-field data from active regions, have been tested for forecasting in recent years. None of these indicators, or combinations thereof, have yet demonstrated an unambiguous eruption or are criterion. Furthermore, numerical simulations have been only barely used to test the predictability of these parameters. In this context, we used the 3D parametric MHD numerical simulations of the self-consistent formation of the flux emergence of a twisted ux tube, inducing the formation of stable and unstable magnetic flux ropes of Leake (2013, 2014). We use these numerical simulations to investigate the eruptive signatures observable in various magnetic scalar parameters and provide highlights on data analysis processing. Time series of 2D photospheric-like magnetograms are used from parametric simulations of stable and unstable flux emergence, to compute a list of about 100 different indicators. This list includes parameters previously used for operational forecasting, physical parameters used for the first time, as well as new quantities specifically developed for this purpose. Our results indicate that only parameters measuring the total non-potentiality of active regions associated with magnetic inversion line properties, such as the Falconer parameters Lss, WLss, Lsg and WLsg, as well as the new current integral WLsc and length Lsc parameters, present a significant ability to distinguish the eruptive cases of the model from the non-eruptive cases, possibly indicating that they are promising are and eruption predictors. A preliminary study about the effect of noise on the detection of the eruptive signatures is also proposed.

### **FLARES OF M-STARS IN UPPER SCORPIUS REGION AND FLARES AND CMES OF THE ACTIVE M-STAR AD LEO**

E. W. [Guenther](#)<sup>1</sup>, D. Wöckel<sup>1</sup> and P. Muheki<sup>2</sup>

Stars and their variability observed from space 2019

<https://arxiv.org/pdf/1911.09922.pdf>



Using the Kepler K2 data, we studied the flare-activity of young K- and M-stars in the Upper Sco region and found that they have 10000 to 80000 times as many super-flares with ( $E \geq 5 \times 10^{34}$  erg) than solar like stars. The power-law index for flares is  $N/dE \sim E^{-1.2}$  for K-stars,  $N/dE \sim E^{-1.4}$  for early M-star and  $dN/dE \sim E^{-1.3}$  for late M-stars, which is about the same as that of the Sun. We also observed the active M-star AD Leo spectroscopy for 222 hours, detected 22 flares but no coronal mass ejections.

### **IRIS observations of magnetic interactions in the solar atmosphere between pre-existing and emerging magnetic fields. I. Overall evolution**

Salvo L. [Guglielmino](#), [Francesca Zuccarello](#), [Peter R. Young](#), [Mariariata Murabito](#), [Paolo Romano](#)  
ApJ 2018

<https://arxiv.org/pdf/1802.05657.pdf>

We report multi-wavelength ultraviolet observations taken with the IRIS satellite, concerning the emergence phase in the upper chromosphere and transition region of an emerging flux region (EFR) embedded in the pre-existing field of active region NOAA 12529. IRIS data are complemented by full-disk observations of the Solar Dynamics Observatory satellite, relevant to the photosphere and the corona. The photospheric configuration of the EFR is also analyzed by measurements taken with the spectropolarimeter aboard the Hinode satellite, when the EFR was fully developed. Recurrent intense brightenings that resemble UV bursts, with counterparts in all coronal passbands, are identified at the edges of the EFR. Jet activity is also observed at chromospheric and coronal levels, near the observed brightenings. The analysis of the IRIS line profiles reveals the heating of dense plasma in the low solar atmosphere and the driving of bi-directional high-velocity flows with speed up to 100 km/s at the same locations. Compared with previous observations and numerical models, these signatures suggest evidence of several long-lasting, small-scale magnetic reconnection episodes between the emerging bipole and the ambient field. This process leads to the cancellation of a pre-existing photospheric flux concentration and appears to occur higher in the atmosphere than usually found in UV bursts, explaining the observed coronal counterparts. **April 13 and 14 2016**

### **Penumbral-like Filaments in the Solar Photosphere as a Manifestation of Flux Emergence**

Salvo L. [Guglielmino](#)<sup>1</sup>, [Francesca Zuccarello](#)<sup>1</sup>, and [Paolo Romano](#)  
**2014** ApJ 786 L22.

Rare observations of the solar photosphere show the appearance of orphan penumbrae, filamentary structures very similar to a bundle of sunspot penumbral filaments not connected to any umbra. Lim et al. found an orphan penumbra in active region NOAA 11391 near a mature sunspot. We analyze a different data set to study the same structure using the Solar Optical Telescope on board the Hinode satellite. Spectropolarimetric measurements along the Fe I 630.2 nm pair, complemented by G-band and Ca II H filtergrams, show the evolution of this penumbral-like structure and reveal that an emerging flux region is its ancestor. We find new evidence for the interaction between the emerging flux and the pre-existing field that leads to a brightening observed near the base of the chromosphere. Our analysis suggests that as a result of the combination of photospheric flux emergence and magneto-convection in inclined fields the horizontal component of the emerging field can be trapped in the photosphere by the overlying fields and form a structure resembling penumbral filaments.

### **Quantitative Analysis of CME Deflections in the Corona**

Bin [Gui](#), Chenglong Shen, Yuming Wang, Pinzhong Ye and Jijia Liu, Shui Wang and Xuepu Zhao  
Solar Physics, Volume 271, Numbers 1-2, 111-139, **2011**

In this paper, ten CME events viewed by the STEREO twin spacecraft are analyzed to study the deflections of CMEs during their propagation in the corona. Based on the three-dimensional information of the CMEs derived by the graduated cylindrical shell (GCS) model (Thernisien, Howard, and Vourlidas in *Astrophys. J.* 652, 1305, 2006), it is found that the propagation directions of eight CMEs had changed. By applying the theoretical method proposed by Shen et al. (*Solar Phys.* 269, 389, 2011) to all the CMEs, we found that the deflections are consistent, in strength and direction, with the gradient of the magnetic energy density. There is a positive correlation between the deflection rate and the strength of the magnetic energy density gradient and a weak anti-correlation between the deflection rate and the CME speed. Our results suggest that the deflections of CMEs are mainly controlled by the background magnetic field and can be quantitatively described by the magnetic energy density gradient (MEDG) model.

### **Characterizing Coronal Mass Ejections in Solar Cycle Analysis**

[Ryan Manuel D. Guido](#)

**2018**

<https://arxiv.org/ftp/arxiv/papers/1804/1804.10870.pdf>

The Sun is the major source of heat and light in our solar system. The solar cycle is the 11-year cycle of solar activity that can be determined by the rise and fall in the numbers and surface area of sunspots. Solar activity is associated with several factors including radio flux, solar irradiance, magnetic field, solar flares, coronal mass ejections, and solar cycles. This study attempts to determine the Sun's activity specifically for the coronal mass ejection, its trend during solar cycle 23, and its apparent difference. A time series analysis was used to measure the CME data for larger cases

and to see the apparent difference and trends of the CMEs. The result shows that a decreasing trend of coronal mass ejection from the year 1996 to 2016. It is therefore concluded that the coronal mass ejection data are normally distributed while coronal mass ejections are distributed and curved normally as fluctuation was found in the intensity of the disturbed storm time index as the number of great geomagnetic storms undeniably increased in the ascending and descending phases of the cycle. This reveals that eventhough the Sun has cycles and trends, it shows its inherent characteristics. The Sun still possess getting more dynamic through time which showcases through the limited parameters involved in this study.

## **Coronal Mass Ejections during Geomagnetic Storms on Earth.**

**Guido**, R.M.D.

(2016). International Journal of Astronomy. (5) 2. DOI: 10.5923/j.astronomy/20160502.02

## **Magnetic-Island Contraction and Particle Acceleration in Simulated Eruptive Solar Flares**

S. E. **Guidoni**, C. R. DeVore, J. T. Karpen, B. J. Lynch

ApJ 2016

<http://arxiv.org/pdf/1603.01309v1.pdf>

The mechanism that accelerates particles to the energies required to produce the observed high-energy impulsive emission in solar flares is not well understood. Drake et al. (2006) proposed a mechanism for accelerating electrons in contracting magnetic islands formed by kinetic reconnection in multi-layered current sheets. We apply these ideas to sunward-moving flux ropes (2.5D magnetic islands) formed during fast reconnection in a simulated eruptive flare. A simple analytic model is used to calculate the energy gain of particles orbiting the field lines of the contracting magnetic islands in our ultrahigh-resolution 2.5D numerical simulation. We find that the estimated energy gains in a single island range up to a factor of five. This is higher than that found by Drake et al. for islands in the terrestrial magnetosphere and at the heliopause, due to strong plasma compression that occurs at the flare current sheet. In order to increase their energy by two orders of magnitude and plausibly account for the observed high-energy flare emission, the electrons must visit multiple contracting islands. This mechanism should produce sporadic emission because island formation is intermittent. Moreover, a large number of particles could be accelerated in each magnetohydrodynamic-scale island, which may explain the inferred rates of energetic-electron production in flares. We conclude that island contraction in the flare current sheet is a promising candidate for electron acceleration in solar eruptions.

## **Dependence of coronal mass ejections on the morphology and toroidal flux of their source magnetic flux ropes**

**J. H. Guo**, **L. Linan**, **S. Poedts**, **Y. Guo**, **B. Schmieder**, **A. Lani**, **Y. W. Ni**, **M. Brchneleva**, **B. Perri**, **T. Baratashvili**, **S. T. Li**, **P. F. Chen**

A&A 690, A189 2024

<https://arxiv.org/pdf/2407.09457>

<https://www.aanda.org/articles/aa/pdf/2024/10/aa49731-24.pdf>

Context. Coronal mass ejections (CMEs) stand as intense eruptions of magnetized plasma from the Sun, playing a pivotal role in driving significant changes of the heliospheric environment. Deducing the properties of CMEs from their progenitors in solar source regions is crucial for space weather forecasting.

Aims. The primary objective of this paper is to establish a connection between CMEs and their progenitors in solar source regions, enabling us to infer the magnetic structures of CMEs before their full development.

Methods. We create a dataset comprising a magnetic flux rope series with varying projection shapes (S-, Z- and toroid-shaped), sizes and toroidal fluxes, using the Regularized Biot-Savart Laws (RBSL). These flux ropes are inserted into solar quiet regions, aimed at imitating the eruptions of quiescent filaments. Thereafter, we simulate the propagation of these flux ropes from the solar surface to a distance of  $25R_{\odot}$  with our global coronal magnetohydrodynamic (MHD) model which is named COCONUT.

Results. Our parametric survey reveals significant impacts of source flux ropes on the consequent CMEs. Regarding the flux-rope morphology, we find that the projection shape (e.g., sigmoid or torus) can influence the magnetic structures of CMEs at  $20R_{\odot}$ , albeit with minimal impacts on the propagation speed. However, these impacts diminish as source flux ropes become fat. In terms of toroidal flux, our simulation results demonstrate a pronounced correlation with the propagation speed of CMEs, as well as the successfulness in erupting.

Conclusions. This work builds the bridge between the CMEs in the outer corona and their progenitors in solar source regions. Our parametric survey suggests that the projection shape, cross-section radius and toroidal flux of source flux ropes are crucial parameters in predicting magnetic structures and propagation speed of CMEs, providing valuable insights for space weather prediction. On the one hand, the conclusion drawn here could be instructive in identifying the high-risk eruptions with the potential to induce stronger geomagnetic effects ( $B_z$  and propagation speed). On the other hand, our findings hold practical significance for refining the parameter settings of launched CMEs at  $21.5R_{\odot}$  in heliospheric simulations, such as with EUHFORIA, based on observations for their progenitors in solar source regions.

## **Formation and Evolution of Transient Prominence Bubbles Driven by Erupting Mini-filaments**

**Yilin Guo**, **Yijun Hou**, **Ting Li**, **Yuandeng Shen**, **Jincheng Wang**, **Jun Zhang**, **Jianchuan Zheng**, **Dong Wang**, **Lin Mei**

ApJ 970 110 2024

<https://arxiv.org/pdf/2405.04725>

<https://iopscience.iop.org/article/10.3847/1538-4357/ad54b8/pdf>

Prominence bubbles, the dark arch-shaped "voids" below quiescent prominences, are generally believed to be caused by the interaction between the prominences and the slowly-emerging or quasi-stable underlying magnetic loops. However, this scenario could not explain some short-lived bubbles with extremely dynamic properties of evolution. Based on high-resolution H $\alpha$  observations, here we propose that bubbles should be classified into two categories according to their dynamic properties: quasi-steady (Type-I) bubbles and transient (Type-II) bubbles. Type-I bubbles could remain relatively stable and last for several hours, indicating the existence of a quasi-stable magnetic topology, while Type-II bubbles grow and collapse quickly within one hour without stability duration, which are usually associated with erupting mini-filaments. Analysis of several typical Type-II bubbles from different views, especially including an on-disk event, reveals that Type-II bubbles quickly appear and expand at a velocity of  $\sim 5\text{--}25$  km s $^{-1}$  accompanied by an erupting mini-filament below. The mini-filament's rising velocity is slightly larger than that of the Type-II bubbles' boundary, which will lead to the collision with each other in a short time, subsequent collapse of Type-II bubbles, and formation of a large plume into the above prominence. We also speculate that only if the angle between the axis of the erupting mini-filament and the line-of-sight is large enough, the interaction between the erupting mini-filament and the overlying prominence could trigger a Type-II bubble with a typical arch-shaped but quickly-expanding bright boundary. 7-Nov-2018, 10-Nov-2018, 19-May-2019, 9-Mar-2023

### **Modelling the propagation of coronal mass ejections with COCONUT: implementation of the Regularized Biot-Savart Laws flux rope model**

[Jinhan Guo](#), [L. Linan](#), [S. Poedts](#), [Y. Guo](#), [A. Lani](#), [B. Schmieder](#), [M. Brchneleva](#), [B. Perri](#), [T. Baratashvili](#), [Y. W. Ni](#), [P. F. Chen](#)

A&A 2023

<https://arxiv.org/pdf/2311.13432.pdf>

Context: Coronal mass ejections (CMEs) are rapid eruptions of magnetized plasma that occur on the Sun, which are known as the main drivers of adverse space weather. Accurately tracking their evolution in the heliosphere in numerical models is of utmost importance for space weather forecasting. Aims: The main objective of this paper is to implement the Regularized Biot-Savart Laws (RBSL) method in a new global corona model COCONUT. This approach has the capability to construct the magnetic flux rope with an axis of arbitrary shape. Methods: We present the implementation process of the RBSL flux rope model in COCONUT, which is superposed onto a realistic solar wind reconstructed from the observed magnetogram around the minimum of solar activity. Based on this, we simulate the propagation of an S-shaped flux rope from the solar surface to a distance of 25 solar radii. Results: Our simulation successfully reproduces the birth process of a CME originating from a sigmoid in a self-consistent way. The model effectively captures various physical processes and retrieves the prominent features of the CMEs in observations. In addition, the simulation results indicate that the magnetic topology of the CME flux rope at around 20 solar radii deviates from a coherent structure, and manifests as a mix of open and closed field lines with diverse footpoints. Conclusions: This work demonstrates the potential of the RBSL flux rope model in reproducing CME events that are more consistent with observations. Moreover, our findings strongly suggest that magnetic reconnection during the CME propagation plays a critical role in destroying the coherent characteristic of a CME flux rope. 2007-02-11, 2011-03-08

### **Data-driven Modeling of a Coronal Magnetic Flux Rope: from Birth to Death**

[J. H. Guo](#), [Y. W. Ni](#), [Y. Guo](#), [C. Xia](#), [B. Schmieder](#), [S. Poedts](#), [Z. Zhong](#), [Y. H. Zhou](#), [F. Yu](#), [P. F. Chen](#)

ApJ 961 140 2024

<https://arxiv.org/pdf/2310.19617.pdf>

<https://iopscience.iop.org/article/10.3847/1538-4357/ad088d/pdf>

Magnetic flux ropes are a bundle of twisted magnetic field lines produced by internal electric currents, which are responsible for solar eruptions and are the major drivers of geomagnetic storms. As such, it is crucial to develop a numerical model that can capture the entire evolution of a flux rope, from its birth to death, in order to predict whether adverse space weather events might occur or not. In this paper, we develop a data-driven modeling that combines a time-dependent magneto-frictional approach with a thermodynamic magnetohydrodynamic model. Our numerical modeling successfully reproduces the formation and confined eruption of an observed flux rope, and unveils the physical details behind the observations. Regarding the long-term evolution of the active region, our simulation results indicate that the flux cancellation due to collisional shearing plays a critical role in the formation of the flux rope, corresponding to a substantial increase in magnetic free energy and helicity. Regarding the eruption stage, the deformation of the flux rope during its eruption can cause an increase in the downward tension force, which suppresses it from further rising. This finding may shed light on why some torus-unstable flux ropes lead to failed eruptions after large-angle rotations. Moreover, we find that twisted fluxes can accumulate during the confined eruptions, which would breed the subsequent eruptive flares. 2017 September 4-10

### **Data-constrained Magnetohydrodynamic Simulation of an Intermediate Solar Filament Eruption**

Yang [Guo](#)<sup>1</sup>, [Jinhan Guo](#)<sup>1,2</sup>, [Yiwei Ni](#)<sup>1</sup>, [M. D. Ding](#)<sup>1</sup>, [P. F. Chen](#)<sup>1</sup>, [Chun Xia](#)<sup>3</sup>, [Rony Keppens](#)<sup>2</sup>, and [Kai E. Yang](#)<sup>4</sup>

2023 ApJ 958 25

<https://iopscience.iop.org/article/10.3847/1538-4357/acf75b/pdf>

Solar eruptive activities could occur in weak magnetic field environments and over large spatial scales, which are especially relevant to eruptions involving intermediate or quiescent solar filaments. To handle the large scales, we implement and apply a flux rope embedding method using regularized Biot–Savart laws in the spherical coordinate system. Combined with a potential field source surface model and a magneto–frictional method, a nonlinear force-free field comprising a flux rope embedded in a potential field is constructed. Using the combined nonlinear force-free field as the initial condition, we then perform a zero- $\beta$  data-constrained magnetohydrodynamic (MHD) simulation for an M8.7 flare at 03:38 UT on **2012 January 23**. The MHD model reproduces the eruption process, flare ribbon evolution (represented by the quasi-separatrix layer evolution), and kinematics of the flux rope. This approach could potentially model global-scale eruptions from weak field regions.

## Understanding the Lateral Drifting of an Erupting Filament with a Data-constrained Magnetohydrodynamic Simulation

[Jinhan Guo](#), [Ye Qiu](#), [Yiwei Ni](#), [Yang Guo](#), [Chuan Li](#), [Yuhang Gao](#), [Brigitte Schmieder](#), [Stefaan Poedts](#), [Pengfei Chen](#)

ApJ **956** 119 **2023**

<https://arxiv.org/pdf/2308.08831.pdf>

<https://iopscience.iop.org/article/10.3847/1538-4357/acf198/pdf>

Solar filaments often exhibit rotation and deflection during eruptions, which would significantly affect the geoeffectiveness of the corresponding coronal mass ejections (CMEs). Therefore, understanding the mechanisms that lead to such rotation and lateral displacement of filaments is a great concern to space weather forecasting. In this paper, we examine an intriguing filament eruption event observed by the Chinese H $\alpha$  Solar Explorer (CHASE) and the Solar Dynamics Observatory (SDO). The filament, which eventually evolves into a CME, exhibits significant lateral drifting during its rising. Moreover, the orientation of the CME flux rope axis deviates from that of the pre-eruptive filament observed in the source region. To investigate the physical processes behind these observations, we perform a data-constrained magnetohydrodynamic (MHD) simulation. Many prominent observational features in the eruption are reproduced by our numerical model, including the morphology of the eruptive filament, eruption path, and flare ribbons. The simulation results reveal that the magnetic reconnection between the flux-rope leg and neighboring low-lying sheared arcades may be the primary mechanism responsible for the lateral drifting of the filament material. Such a reconnection geometry leads to flux-rope footpoint migration and a reconfiguration of its morphology. As a consequence, the filament material hosted in the flux rope drifts laterally, and the CME flux rope deviates from the pre-eruptive filament. This finding underscores the importance of external magnetic reconnection in influencing the orientation of a flux rope axis during eruption. **2022 August 18**

## Dynamical Evolution of an Active-region Filament Driven by Magnetic Reconnection

Yilin [Guo](#)<sup>1,2</sup>, Yijun Hou<sup>4,1,2</sup>, Ting Li<sup>1,2</sup>, and Jun Zhang<sup>4,3</sup>

2021 ApJ 920 77

<https://doi.org/10.3847/1538-4357/ac1ac6>

Studying solar filament dynamical evolutions is an important approach to reveal the driving mechanism of solar eruptions, which seriously impact on the Sun–Earth system and could cause disastrous space weather. To better understand the evolution process of solar filaments, here we investigate an active-region filament by employing observations from the New Vacuum Solar Telescope (NVST), Solar Dynamics Observatory, and Interface Region Imaging Spectrograph. The high-resolution NVST H $\alpha$  images show that the northern footpoint of the filament gradually moved northward. Near the northern footpoint, there is an arch filament system (AFS). Between adjacent footpoints of the filament and the AFS, transient brightening, underlying magnetic cancellation, and bidirectional flows were detected, which jointly imply that it could be the magnetic reconnection between the filament and the AFS that changes the connection of filament threads and drives its footpoint to move northward. In addition, during the footpoint evolution, the filament with highly twisted structure underwent several untwisting motions. Meanwhile, transient brightenings were also observed and appeared as bright knots around several positions where filament threads might braid with each other. And some bright blobs were also detected to propagate outward from the brightening region. These observations suggest that magnetic reconnection might be responsible for the untwisting motion. This work exposes us to a dynamical scenario of the filament evolution driven by magnetic reconnection, which will promote our understanding of the formation and eruption of the filaments.

## Data-constrained Magnetohydrodynamic Simulation of a Long Duration Eruptive Flare

[Yang Guo](#), [Ze Zhong](#), [M. D. Ding](#), [P. F. Chen](#), [Chun Xia](#), [Rony Keppens](#)

ApJ **919** 39 **2021**

<https://arxiv.org/pdf/2106.15080.pdf>

<https://doi.org/10.3847/1538-4357/ac10c8>

We perform a zero- $\beta$  magnetohydrodynamic simulation for the C7.7 class flare initiated at 01:18 UT on **2011 June 21** using the Message Passing Interface Adaptive Mesh Refinement Versatile Advection Code (MPI-AMRVAC). The initial condition for the simulation involves a flux rope which we realize through the regularized Biot-Savart laws, whose parameters are constrained by observations from the Atmospheric Imaging Assembly (AIA) on the Solar

Dynamics Observatory (SDO) and the Extreme Ultraviolet Imager (EUVI) on the twin Solar Terrestrial Relations Observatory (STEREO). This data-constrained initial state is then relaxed to a force-free state by the magneto-frictional module in MPI-AMRVAC. The further time-evolving simulation results reproduce the eruption characteristics obtained by SDO/AIA 94 Å, 304 Å, and STEREO/EUVI 304 Å observations fairly well. The simulated flux rope possesses similar eruption direction, height range, and velocities to the observations. Especially, the two phases of slow evolution and fast eruption are reproduced by varying the density distribution in light of the filament material draining process. Our data-constrained simulations also show other advantages, such as a large field of view (about 0.76 solar radii). We study the twist of the magnetic flux rope and the decay index of the overlying field, and find that in this event, both the magnetic strapping force and the magnetic tension force are sufficiently weaker than the magnetic hoop force, thus allowing the successful eruption of the flux rope. We also find that the anomalous resistivity is necessary in keeping the correct morphology of the erupting flux rope.

## **Observations and modeling of the onset of fast reconnection in the solar transition region**

[L.-J. Guo](#), [B. De Pontieu](#), [Y.-M. Huang](#), [H. Peter](#), [A. Bhattacharjee](#)

ApJ 2020

<https://arxiv.org/pdf/2009.11475.pdf>

Magnetic reconnection is a fundamental plasma process that plays a critical role not only in energy release in the solar atmosphere, but also in fusion, astrophysical, and other space plasma environments. One of the challenges in explaining solar observations in which reconnection is thought to play a critical role is to account for the transition of the dynamics from a slow quasi-continuous phase to a fast and impulsive energetic burst of much shorter duration. Despite the theoretical progress in identifying mechanisms that might lead to rapid onset, a lack of observations of this transition has left models poorly constrained. High-resolution spectroscopic observations from NASA's Interface Region Imaging Spectrograph (IRIS) now reveal tell-tale signatures of the abrupt transition of reconnection from a slow phase to a fast, impulsive phase during UV bursts or explosive events in the Sun's atmosphere. Our observations are consistent with numerical simulations of the plasmoid instability, and provide evidence for the onset of fast reconnection mediated by plasmoids and new opportunities for remote-sensing diagnostics of reconnection mechanisms on the Sun. **13-Aug-2013, 4-Feb-2014, 15-Apr-2014, 2014 May 04-05**

## **The Magnetic Flux Rope Structure of a Triangulated Solar Filament**

Yang [Guo](#)<sup>1</sup>, Yu Xu<sup>1</sup>, M. D. Ding<sup>1</sup>, P. F. Chen<sup>1</sup>, Chun Xia<sup>2</sup>, and Rony Keppens

2019 ApJL 884 L1

<https://doi.org/10.3847/2041-8213/ab4514>

Solar magnetic flux ropes are core structures driving solar activities. We construct a magnetic flux rope for a filament/prominence observed at 01:11 UT on **2011 June 21** in AR 11236 with a combination of state-of-the-art methods, including triangulation from multiperspective observations, the flux rope embedding method, the regularized Biot–Savart laws, and the magnetofrictional method. First, the path of the filament is reconstructed via the triangulation with 304 Å images observed by the Atmospheric Imaging Assembly on board Solar Dynamics Observatory (SDO) and by the Extreme Ultraviolet Imager on board the twin Solar Terrestrial Relations Observatory. Then, a flux rope is constructed with the regularized Biot–Savart laws using the information of its axis. Next, it is embedded into a potential magnetic field computed from the photospheric radial magnetic field observed by the Helioseismic and Magnetic Imager on board SDO. The combined magnetic field is finally relaxed by the magnetofrictional method to reach a nonlinear force-free state. It is found that both models constructed by the regularized Biot–Savart laws and after the magnetofrictional relaxation coincide with the 304 Å images. The distribution of magnetic dips coincides with part of the filament/prominence material, and the quasi-separatrix layers wrap the magnetic flux ropes, displaying hyperbolic flux tube structures. These models have the advantages of constructing magnetic flux ropes in the higher atmosphere and weak magnetic field regions, which could be used as initial conditions for magnetohydrodynamic simulations of coronal mass ejections.

## **The Role of a Magnetic Topology Skeleton in a Solar Active Region**

Juan [Guo](#)<sup>1,2</sup>, Huaning Wang<sup>1,3</sup>, Jingxiu Wang<sup>3</sup>, Xiaoshuai Zhu<sup>1,4</sup>, Xinghua Dai<sup>1</sup>, Xin Huang<sup>1</sup>, Han He<sup>1</sup>, Yan Yan<sup>1</sup>, and Hui Zhao

2019 ApJ 874 181

[sci-hub.se/10.3847/1538-4357/ab0aed](https://doi.org/10.3847/1538-4357/ab0aed)

We investigate the 3D magnetic topology in the active region NOAA 11719 nine hours before and after a flare–coronal mass ejection (CME) event on **2013 April 11**. The extrapolated 3D coronal magnetic field is computed employing a boundary integrated model, and a complex magnetic topology skeleton comprising five fairly robust null points and their relevant structures are revealed with a mathematical method based on a Poincaré index of isolated 3D null points. Comparative analyses show that the magnetic topology skeleton in this active region determines geometries of post-flare loops and flare ribbons, and characterizes the initial stage of the CME. The present work demonstrates that the magnetic topology skeleton plays an important role in the process of the flare–CME eruption.

## **Solar Magnetic Flux Rope Eruption Simulated by a Data-Driven Magnetohydrodynamic Model**

Yang [Guo](#), [Chun Xia](#), [Rony Keppens](#), [M. D. Ding](#), [P. F. Chen](#)

2019 ApJL 870 L21

<https://arxiv.org/pdf/1812.10030.pdf>

[sci-hub.tw/10.3847/2041-8213/aafabf](https://sci-hub.tw/10.3847/2041-8213/aafabf)

The combination of magnetohydrodynamic (MHD) simulation and multi-wavelength observations is an effective way to study mechanisms of magnetic flux rope eruption. We develop a data-driven MHD model using the zero- $\beta$  approximation. The initial condition is provided by nonlinear force-free field derived by the magneto-frictional method based on vector magnetic field observed by the Helioseismic and Magnetic Imager (HMI) aboard the Solar Dynamics Observatory (SDO). The bottom boundary uses observed time series of the vector magnetic field and the vector velocity derived by the Differential Affine Velocity Estimator for Vector Magnetograms (DAVE4VM). We apply the data-driven model to active region 11123 observed from 06:00 UT on **2011 November 11** to about 2 hours later. The evolution of the magnetic field topology coincides with the flare ribbons observed in the 304 and 1600 Å wavebands by the Atmospheric Imaging Assembly. The morphology, propagation path, and propagation range of the flux rope are comparable with the observations in 304 Å. We also find that a data-constrained boundary condition, where the bottom boundary is fixed to the initial values, reproduces a similar simulation result. This model can reproduce the evolution of a magnetic flux rope in its dynamic eruptive phase.

## Origin and Structures of Solar Eruptions II: Magnetic Modeling (Invited Review)

Yang [Guo](#), Xin Cheng, M. D. Ding

SCIENCE CHINA Earth Sciences

Volume 60, Issue 8, pp 1408-1439

2017

<https://arxiv.org/pdf/1706.05769.pdf>

<https://link.springer.com/content/pdf/10.1007%2Fs11430-017-9081-x.pdf>

The topology and dynamics of the three-dimensional magnetic field in the solar atmosphere govern various solar eruptive phenomena and activities, such as flares, coronal mass ejections, and filaments/prominences. We have to observe and model the vector magnetic field to understand the structures and physical mechanisms of these solar activities. Vector magnetic fields on the photosphere are routinely observed via the polarized light, and inferred with the inversion of Stokes profiles. To analyze these vector magnetic fields, we need first to remove the 180° ambiguity of the transverse components and correct the projection effect. Then, the vector magnetic field can be served as the boundary conditions for a force-free field modeling after a proper preprocessing. The photospheric velocity field can also be derived from a time sequence of vector magnetic fields. Three-dimensional magnetic field could be derived and studied with theoretical force-free field models, numerical nonlinear force-free field models, magnetohydrostatic models, and magnetohydrodynamic models. Magnetic energy can be computed with three-dimensional magnetic field models or a time series of vector magnetic field. The magnetic topology is analyzed by pinpointing the positions of magnetic null points, bald patches, and quasi-separatrix layers. As a well conserved physical quantity, magnetic helicity can be computed with various methods, such as the finite volume method, discrete flux tube method, and helicity flux integration method. This quantity serves as a promising parameter characterizing the activity level of solar active regions.

## Slow Patchy Extreme-ultraviolet Propagating Fronts Associated With Fast Coronal Magneto-acoustic Waves In Solar Eruptions

Y. [Guo](#), M. D. Ding, P. F. Chen

Astrophysical Journal Supplement Series 219(2) 36 2015

Using the high spatiotemporal resolution extreme ultraviolet (EUV) observations of the Atmospheric Imaging Assembly on board the Solar Dynamics Observatory, we conduct a statistical study of the observational properties of the coronal EUV propagating fronts. We find that it might be a universal phenomenon for two types of fronts to coexist in a large solar eruptive event. It is consistent with the hybrid model of EUV propagating fronts, which predicts that coronal EUV propagating fronts consist of both a fast magneto-acoustic wave and a nonwave component. We find that the morphologies, propagation behaviors, and kinematic features of the two EUV propagating fronts are completely different from each other. The fast magneto-acoustic wave fronts are almost isotropic. They travel continuously from the flaring region across multiple magnetic polarities to global distances. On the other hand, the slow nonwave fronts appear as anisotropic and sequential patches of EUV brightening. Each patch propagates locally in the magnetic domains where the magnetic field lines connect to the bottom boundary and stops at the magnetic domain boundaries. Within each magnetic domain, the velocities of the slow patchy nonwave component are an order of magnitude lower than that of the fast-wave component. However, the patches of the slow EUV propagating front can jump from one magnetic domain to a remote one. The velocities of such a transit between different magnetic domains are about one-third to one-half of those of the fast-wave component. The results show that the velocities of the nonwave component, both within one magnetic domain and between different magnetic domains, are highly nonuniform due to the inhomogeneity of the magnetic field in the lower atmosphere.

## Rayleigh-Taylor Type Instabilities in the Reconnection Exhaust Jet as a Mechanism for Supra-arcade Downflows in the Sun

L.-J. [Guo](#)<sup>1,2,3,4</sup>, Y.-M. Huang<sup>1,2,3</sup>, A. Bhattacharjee<sup>1,2,3</sup>, and D. E.

2014 ApJ 796 L29

<http://arxiv.org/pdf/1406.3305v1.pdf>

Supra-arcade downflows (hereafter referred to as SADs) are low-emission, elongated, finger-like features usually observed in active-region coronae above post-eruption flare arcades. Observations exhibit downward moving SADs intertwined with bright upward moving spikes. Whereas SADs are dark voids, spikes are brighter, denser structures. Although SADs have been observed for decades, the mechanism of formation of SADs remains an open issue. In our three-dimensional resistive magnetohydrodynamic simulations, we demonstrate that secondary Rayleigh-Taylor type instabilities develop in the downstream region of a reconnecting current sheet. The instability results in the formation of low-density coherent structures that resemble SADs, and high-density structures that appear to be spike-like. Comparison between the simulation results and observations suggests that secondary Rayleigh-Taylor type instabilities in the exhaust of reconnecting current sheets provide a plausible mechanism for observed SADs and spikes.

## **Twist Accumulation and Topology Structure of a Solar Magnetic Flux Rope**

Y. **Guo**, M. D. Ding, X. Cheng, J. Zhao, E. Pariat

E-print, Nov **2013**; **2013 ApJ** 779 157

To study the build up of a magnetic flux rope before a major flare and coronal mass ejection (CME), we compute the magnetic helicity injection, twist accumulation, and the topology structure of the three dimensional magnetic field, which is derived by the nonlinear force-free field model. The Extreme-ultraviolet Imaging Telescope on board the Solar and Heliospheric Observatory observed a series of confined flares without any CME before a major flare with a CME at 23:02 UT on **2005 January 15** in active region NOAA 10720. We derive the vector velocity at eight time points from 18:27 UT to 22:20 UT with the differential affine velocity estimator for vector magnetic fields, which were observed by the Digital Vector Magnetograph at Big Bear Solar Observatory. The injected magnetic helicity is computed with the vector magnetic and velocity fields. The helicity injection rate was  $(-16.47 \text{ pm } 3.52) \times 1040 \text{ Mx}^2/\text{hr}$ . We find that only about 1.8% of the injected magnetic helicity became finally the internal helicity of the magnetic flux rope, whose twist increasing rate was  $-0.18 \text{ pm } 0.08 \text{ Turns/hr}$ . The quasi-separatrix layers (QSLs) of the three dimensional magnetic field are computed by evaluating the squashing degree,  $Q$ . We find that the flux rope was wrapped by QSLs with large  $Q$  values, where the magnetic reconnection induced by the continuously injected magnetic helicity further produced the confined flares. We suggest that the flux rope was built up and heated by the magnetic reconnection in the QSLs.

## **DISTRIBUTION OF PLASMOIDS IN POST-CORONAL MASS EJECTION CURRENT SHEETS**

L.-J. **Guo**<sup>1,2,3,4</sup>, A. Bhattacharjee<sup>1,2,3,4</sup>, and Y.-M. Huang

**2013 ApJ** 771 L14

Recently, the fragmentation of a current sheet in the high-Lundquist-number regime caused by the plasmoid instability has been proposed as a possible mechanism for fast reconnection. In this work, we investigate this scenario by comparing the distribution of plasmoids obtained from Large Angle and Spectrometric Coronagraph (LASCO) observational data of a coronal mass ejection event with a resistive magnetohydrodynamic simulation of a similar event. The LASCO/C2 data are analyzed using visual inspection, whereas the numerical data are analyzed using both visual inspection and a more precise topological method. Contrasting the observational data with numerical data analyzed with both methods, we identify a major limitation of the visual inspection method, due to the difficulty in resolving smaller plasmoids. This result raises questions about reports of log-normal distributions of plasmoids and other coherent features in the recent literature. Based on nonlinear scaling relations of the plasmoid instability, we infer a lower bound on the current sheet width, assuming the underlying mechanism of current sheet broadening is resistive diffusion.

## **Recurrent coronal jets induced by repetitively accumulated electric currents\***

Y. **Guo**<sup>1,2</sup>, P. Démoulin<sup>3</sup>, B. Schmieder<sup>3</sup>, M. D. Ding<sup>1,2</sup>, S. Vargas Domínguez<sup>4</sup> and Y. Liu

*A&A* 555, A19 (**2013**)

Context. Jets of plasma are frequently observed in the solar corona. A self-similar recurrent behavior is observed in a fraction of them.

Aims. Jets are thought to be a consequence of magnetic reconnection; however, the physics involved is not fully understood. Therefore, we study some jet observations with unprecedented temporal and spatial resolutions.

Methods. The extreme-ultraviolet (EUV) jets were observed by the Atmospheric Imaging Assembly on board the Solar Dynamics Observatory (SDO). The Helioseismic and Magnetic Imager (HMI) on board SDO measured the vector magnetic field, from which we derive the magnetic flux evolution, the photospheric velocity field, and the vertical electric current evolution. The magnetic configuration before the jets is derived by the nonlinear force-free field extrapolation.

Results. Three EUV jets recurred in about one hour on **17 September 2010** in the following magnetic polarity of active region 11106. We derive that the jets are above a pair of parasitic magnetic bipoles that are continuously driven by photospheric diverging flows. The interaction drove the buildup of electric currents, which we observed as elongated patterns at the photospheric level. For the first time, the high temporal cadence of the HMI allows the evolution of such small currents to be followed. In the jet region, we found that the integrated absolute current peaks repetitively in phase with the 171 Å flux evolution. The current buildup and its decay are both fast, about ten minutes each, and the current maximum precedes the 171 Å also by about ten minutes. Then, the HMI temporal cadence is marginally fast enough to detect such changes.

Conclusions. The photospheric current pattern of the jets is found to be associated with the quasi-separatrix layers deduced from the magnetic extrapolation. From previous theoretical results, the observed diverging flows are expected to continuously build such currents. We conclude that the magnetic reconnection occurs periodically, in the current layer created between the emerging bipoles and the large-scale active region field. The periodic magnetic reconnection induced the observed recurrent coronal jets and the decrease of the vertical electric current magnitude.

### **Driving Mechanism and Onset Condition of a Confined Eruption**

Y. [Guo](#)<sup>1,2,3</sup>, M. D. Ding<sup>1,2</sup>, B. Schmieder<sup>3</sup>, H. Li<sup>4</sup>, T. Torok<sup>3,5</sup>, T. Wiegelmann<sup>6</sup>  
E-print, Nov **2010**, ApJL

We study a confined eruption accompanied by an M1.1 flare in solar active region (AR) NOAA 10767 on **2005 May 27**, where a pre-eruptive magnetic flux rope was reported in a nonlinear force-free field (NLFFF) extrapolation. The observations show a strong writhing motion of the erupting structure, suggesting that a flux rope was indeed present and converted some of its twist into writhe in the course of the eruption. Using the NLFFF extrapolation, we calculate the twist of the pre-eruptive flux rope and find that it is in very good agreement with thresholds of the helical kink instability found in numerical simulations. We conclude that the activation and rise of the flux rope were triggered and driven by the instability. Using a potential field extrapolation, we also estimate the height distribution of the decay index of the external magnetic field in the AR one hour prior to the eruption. We find that the decay index stays below the threshold for the torus instability for a significant height range above the erupting flux rope. This provides a possible explanation for the confinement of the eruption to the low corona.

### **A FLUX ROPE ERUPTION TRIGGERED BY JETS**

Juan [Guo](#)<sup>1</sup>, Yu Liu<sup>2</sup>, Hongqi Zhang<sup>1</sup>, Yuanyong Deng<sup>1</sup>, Jiaben Lin<sup>1</sup>, and Jiangtao Su<sup>1</sup>  
Astrophysical Journal, 711:1057–1061, **2010** March, [File](#)

We present an observation of a filament eruption caused by recurrent chromospheric plasma injections (surges/jets) on **2006 July 6**. The filament eruption was associated with an M2.5 two-ribbon flare and a coronal mass ejection (CME). There was a light bridge in the umbra of the main sunspot of NOAA 10898; one end of the filament was terminated at the region close to the light bridge, and recurrent surges were observed to be ejected from the light bridge. The surges occurred intermittently for about 8 hr before the filament eruption, and finally a clear jet was found at the light bridge to trigger the filament eruption. We analyzed the evolutions of the relative darkness of the filament and the loaded mass by the continuous surges quantitatively. It was found that as the occurrence of the surges, the relative darkness of the filament body continued growing for about 3–4 hr, reached its maximum, and kept stable for more than 2 hr until it erupted. If suppose 50% of the ejected mass by the surges could be trapped by the filament channel, then the total loaded mass into the filament channel will be about  $0.574 \times 10^{16}$  g with a momentum of  $0.574 \times 10^{22}$  g cm s<sup>-1</sup> by 08:08 UT, which is a non-negligible effect on the stability of the filament. Based on the observations, we present a model showing the important role that recurrent chromospheric mass injection play in the evolution and eruption of a flux rope. Our study confirms that the surge activities can efficiently supply the necessary material for some filament formation. Furthermore, our study indicates that the continuous mass with momentum loaded by the surge activities to the filament channel could make the filament unstable and cause it to erupt.

### **Magnetic properties of flare-CME productive active regions and CME speed:**

J. [Guo](#), H. Q. Zhang and O. V. Chumak  
A&A 462 (2007) 1121-1126 (Section 'The Sun')  
<http://www.aanda.org/10.1051/0004-6361:20065888>

Four measures, including the tilt angle (Tilt), total flux (Ft), length of the strong-field and strong-gradient main neutral line (Lsg) and effective distance (dE), are used to quantify the properties of the magnetic field of flare-CME productive active regions.

### **Stability of the coronal magnetic field around large confined and eruptive solar flares**

[Manu Gupta](#), [J. K. Thalmann](#), [A. M. Veronig](#)  
A&A **2024**

<https://arxiv.org/pdf/2402.12254.pdf>

Context. The coronal magnetic field, which overlies the current-carrying field of solar active regions, straps the magnetic configuration below. The characteristics of this overlying field are crucial in determining if a flare will be eruptive and accompanied by a coronal mass ejection (CME), or if it will remain confined without a CME.

Aims. In order to improve our understanding on the pre-requisites of eruptive solar flares, we study and compare different measures that characterize the eruptive potential of solar active regions — the critical height for torus instability as a local measure and the helicity ratio as a global measure — with the structural properties of the underlying magnetic field, namely the altitude of the center of the current-carrying magnetic structure.

Methods. Using time series of 3D optimization-based nonlinear force-free magnetic field models for 10 different active regions (ARs) around the time of large solar flares, we determine the altitudes of the current-weighted centers of the



non-potential model structures. Based on the potential magnetic field, we inspect the decay index,  $n$ , in multiple vertical planes oriented along of or perpendicular to the flare-relevant polarity inversion line, and estimate the critical height ( $h_{crit}$ ) for torus instability (TI) using different thresholds of  $n$ . The critical heights are interpreted with respect to the altitudes of the current-weighted centers of the associated non-potential structures, as well as the eruptive character of the associated flares, and the eruptive potential of the host AR, as characterized by the helicity ratio.

Results. Our most important findings are that (i)  $h_{crit}$  is more segregated in terms of flare type than the helicity ratio, and that (ii) coronal field configurations with a higher eruptive potential (in terms of the helicity ratio) also appear to be more prone to TI. Furthermore, we find no pronounced differences in the altitudes of the non-potential structures prior to confined and eruptive flares. An aspect which requires further investigation is that, quite generally, the modeled non-potential structures hardly reside in a torus-unstable regime, requiring further assessment regarding the applicability of the chosen NLFF modeling approach when targeted at the structural properties of the coronal magnetic field. **2011-02-15, 2011-03-09, 2011-09-26, 2011-11-05, 2012-03-07, 2014-10-24, 2015-01-30, 2015-03-11, 2017-09-06**

## **Magnetic helicity and energy budget around large confined and eruptive solar flares**

[Manu Gupta](#), [J. K. Thalmann](#), [A. M. Veronig](#)

A&A 653, A69 2021

<https://arxiv.org/pdf/2106.08781.pdf>

<https://www.aanda.org/articles/aa/pdf/2021/09/aa40591-21.pdf>

<https://doi.org/10.1051/0004-6361/202140591>

We investigate the coronal magnetic energy and helicity budgets of ten solar ARs, around the times of large flares. In particular, we are interested in a possible relation of the derived quantities to the particular type of the flares that the AR produces, i.e., whether they are associated with a CME or they are confined. Using an optimization approach, we employ time series of 3D nonlinear force-free magnetic field models of ten ARs, covering a time span of several hours around the time of occurrence of large solar flares (GOES class M1.0 and larger). We subsequently compute the 3D magnetic vector potentials associated to the model 3D coronal magnetic field using a finite-volume method. This allows us to correspondingly compute the coronal magnetic energy and helicity budgets, as well as related (intensive) quantities such as the relative contribution of free magnetic energy,  $EF/E$  (energy ratio), the fraction of non-potential (current-carrying) helicity,  $|HJ|/|HV|$  (helicity ratio), and the normalized current-carrying helicity,  $|HJ|/\phi^2$ . The total energy and helicity budgets of flare-productive ARs (extensive parameters) cover a broad range of magnitudes, with no obvious relation to the eruptive potential of the individual ARs, i.e., whether or not a CME is produced in association with the flare. The intensive eruptivity proxies,  $EF/E$  and  $|HJ|/|HV|$ , and  $|HJ|/\phi^2$ , however, seem to be distinctly different for ARs that produced CME-associated large flares compared to those which produced confined flares. For the majority of ARs in our sample, we are able to identify characteristic pre-flare magnitudes of the intensive quantities, clearly associated to subsequent CME-productivity. **2011-02-15, 2011-03-09, 2011-09-26, 2011-11-05, 2012-03-07, 2013-11-08, 2014-10-24, 2015-01-30, 2015-03-11, 2017-09-06**

Table. 1 List of flares under study

## **A Three-Dimensional Velocity of an Erupting Prominence Prior to a Coronal Mass Ejection**

[Maria V. Gutiérrez](#), [Kenichi Otsuji](#), [Ayumi Asai](#), [Raul Terrazas](#), [Mutsumi Ishitsuka](#), [Jose Ishitsuka](#), [Naoki Nakamura](#), [Yusuke Yoshinaga](#), [Satoshi Morita](#), [Takako T. Ishii](#), [Satoru UeNo](#), [Reizaburo Kitai](#), [Kazunari Shibata](#)

PASJ 2021

<https://arxiv.org/pdf/2101.08575.pdf>

We present a detailed three-dimensional (3D) view of a prominence eruption, coronal loop expansion, and coronal mass ejections (CMEs) associated with an M4.4 flare that occurred on **2011 March 8** in the active region NOAA 11165. Full-disk  $H\alpha$  images of the flare and filament ejection were successfully obtained by the Flare Monitoring Telescope (FMT) following its relocation to Ica University, Peru. Multiwavelength observation around the  $H\alpha$  line enabled us to derive the 3D velocity field of the  $H\alpha$  prominence eruption. Features in extreme ultraviolet were also obtained by the Atmospheric Imager Assembly onboard the *Solar Dynamic Observatory* and the Extreme Ultraviolet Imager on board the *Solar Terrestrial Relations Observatory - Ahead* satellite. We found that, following collision of the erupted filament with the coronal magnetic field, some coronal loops began to expand, leading to the growth of a clear CME. We also discuss the succeeding activities of CME driven by multiple interactions between the expanding loops and the surrounding coronal magnetic field.

## **Short term topological changes of coronal holes associated with prominence eruptions and subsequent CMEs**

H. [Gutiérrez](#), L. Taliashvili, Z. Mouradian

Advances in Space Research, Volume 51, Issue 10, 2013, pp. 1824-1833

[sci-hub.se/10.1016/j.asr.2012.03.008](https://doi.org/10.1016/j.asr.2012.03.008)

We study the short-term topological changes of equatorial and polar coronal hole (CH) boundaries, such as a variation of their area and disintegration, associated to reconnection with nearby (within  $15^\circ$  distance) quiescent prominence magnetic fields leading to eruptions and subsequent Coronal Mass Ejections (CMEs). The examples presented here correspond to the recent solar minimum years 2008 and 2009. We consider a temporal window of one day between the CH topological changes and the start and end times of prominence eruptions and onset of CMEs. To establish this

association we took into account observational conditions related to the instability of prominence/filaments, the occurrence of a CME, as well as the subsequent evolution after the CME. We found an association between short-term local topological changes in CH boundaries and the formation/disappearance of bright points near them, as well as, between short-term topological changes within the whole CH and eruptions of nearby quiescent prominences followed by the appearance of one or more CMEs. **2008/08/29, 2008/12/12, 2009/05/29**

## **Predicting the Loci of Solar Eruptions**

N. Gyenge, R. Erdélyi

**2017** Space Weather of the Heliosphere: Processes and Forecasts Proceedings IAU Symposium No. 335

<https://arxiv.org/pdf/1710.06196.pdf>

The longitudinal distribution of solar active regions shows non-homogeneous spatial behaviour, which is often referred to as Active Longitude (AL). Evidence for a significant statistical relationships between the AL and the longitudinal distribution of flare and coronal mass ejections (CME) occurrences is found in Gyenge et al, 2017 (ApJ, 838, 18). The present work forecasts the spatial position of AL, hence the most flare/CME capable active regions are also predictable. Our forecast method applies Autoregressive Integrated Moving Average model for the next 2 years time period. We estimated the dates when the solar flare/CME capable longitudinal belts face towards Earth.

## **Active longitude and CME occurrences**

N. Gyenge, T. Singh, T. S. Kiss, A. K. Srivastava, R. Erdélyi

**2017**

<https://arxiv.org/pdf/1702.06664.pdf>

The spatial inhomogeneity of the distribution of coronal mass ejection (CME) occurrences in the solar atmosphere could provide a tool to estimate the longitudinal position of the most probable CME-capable active regions in the Sun. The anomaly in the longitudinal distribution of active regions themselves is often referred to as active longitude (AL). In order to reveal the connection between the AL and CME spatial occurrences, here we investigate the morphological properties of active regions. The first morphological property studied is the separateness parameter, which is able to characterise the probability of the occurrence of an energetic event, such as solar flare or CME. The second morphological property is the sunspot tilt angle. The tilt angle of sunspot groups allows us to estimate the helicity of active regions. The increased helicity leads to a more complex built-up of the magnetic structure and also can cause CME eruption. We found that the most complex active regions appear near to the AL and the AL itself is associated with the most tilted active regions. Therefore, the number of CME occurrences is higher within the AL. The origin of the fast CMEs is also found to be associated with this region. We concluded that the source of the most probably CME-capable active regions is at the AL. By applying this method we can potentially forecast a flare and/or CME source several Carrington rotations in advance. This finding also provides new information for solar dynamo modelling.

**0/03/2011, 25/06/2011, 07/03/2012**

## **Laboratory demonstration of slow rise to fast acceleration of arched magnetic flux ropes**

Bao N. Ha\* and Paul M. Bellan

Geophysical Research Letters **2016**

<http://sci-hub.cc/10.1002/2016GL069744>

We demonstrate the slow rise to fast acceleration of an arched plasma-filled magnetic flux rope. The flux rope expansion is inhibited by an externally applied customizable strapping field. When the strapping field is not too strong and not too weak, expansion forces build up while the flux rope is in the strapping field region. When the flux rope moves to a critical height beyond the peak strapping field region, the plasma accelerates quickly corresponding to the observed slow rise to fast acceleration of solar eruptions. This behavior is in agreement with the predictions of the torus instability.

See Stanley, S. (2016), Lab experiment tests what triggers massive solar eruptions, Eos, 97, doi:10.1029/2016E0060487. Published on 07 October 2016.

## **Probability of Solar Flares Turn Out to Form a Coronal Mass Ejections Events Due to the Characterization of Solar Radio Burst Type II and III**

**Book**

Zety Sharizat Hamidi

International Letters of Chemistry, Physics and Astronomy 16 (2014) 1-85

[https://ui.adsabs.harvard.edu/search/filter\\_database\\_fq\\_database=OR&filter\\_database\\_fq\\_database=database%3A"astromy"&filter\\_database\\_fq\\_database=database%3A"physics"&fq=%7B!type%3D%20v%3D%24fq\\_database%7D&fq\\_database=\(database%3A"astronomy"%20OR%20database%3A"physics"\)&q=author%3A\("Hamidi"\)%20AND%20update%3A%5B2014-01%20TO%202014-12%5D&sort=date%20desc%2C%20bibcode%20desc&p=0](https://ui.adsabs.harvard.edu/search/filter_database_fq_database=OR&filter_database_fq_database=database%3A)  
[https://www.academia.edu/10330915/Probability\\_of\\_Solar\\_Flares\\_Turn\\_Out\\_to\\_Form\\_a\\_Coronal\\_Mass\\_Ejections\\_Events\\_Due\\_to\\_the\\_Characterization\\_of\\_Solar\\_Radio\\_Burst\\_Type\\_II\\_and\\_III?email\\_work\\_card=view-paper](https://www.academia.edu/10330915/Probability_of_Solar_Flares_Turn_Out_to_Form_a_Coronal_Mass_Ejections_Events_Due_to_the_Characterization_of_Solar_Radio_Burst_Type_II_and_III?email_work_card=view-paper)

The solar flare and Coronal Mass Ejections (CMEs) are well known as one of the most massive eruptions which potentially create major disturbances in the interplanetary medium and initiate severe magnetic storms when they collide with the Earth's magnetosphere. However, how far the solar flare can contribute to the formation of the CMEs is still not easy to be understood. These phenomena are associated with II and III burst it also divided by sub-type of burst depending on the physical characteristics and different mechanisms. In this work, we used a Compound Astronomical

Low-cost Low-frequency Instrument for Spectroscopy in Transportable Observatories (CALLISTO) system. The aim of the present study is to reveal dynamical properties of solar burst type II and III due to several mechanisms. Most of the cases of both solar radio bursts can be found in the range less than 400 MHz. Based on solar flare monitoring within 24 hours, the CMEs that have the potential to explode will dominantly be a class of M1 solar flare. Overall, the tendencies of SRBT III burst form the solar radio burst type III at 187 MHz to 449 MHz. Based on solar observations, it is evident that the explosive, short time-scale energy release during flares and the long term, gradual energy release expressed by CMEs can be reasonably understood only if both processes are taken as common and probably not independent signatures of a destabilization of pre-existing coronal magnetic field structures. The configurations of several active regions can be sourced regions of CMEs formation. The study of the formation, acceleration and propagation of CMEs requires advanced and powerful observational tools in different spectral ranges as many „stages“ as possible between the photosphere of the Sun and magnetosphere of the Sun and magnetosphere of the Earth. In conclusion, this range is a current regime of solar radio bursts during CMEs events. **9th March 2012, 13th November 2012, 23rd October 2012, 30th March 2013,**

## **Solar Coronal Jets Extending to High Altitudes Observed During the 2017 August 21 Total Eclipse**

[Yoichiro Hanaoka](#), [Ryuichi Hasuo](#), [Tsukasa Hirose](#), [Akiko C. Ikeda](#), [Tsutomu Ishibashi](#), [Norihiro Manago](#), [Yukio Masuda](#), [Sakuhiro Morita](#), [Jun Nakazawa](#), [Osamu Ohgoe](#), [Yoshiaki Sakai](#), [Kazuhiro Sasaki](#), [Koichi Takahashi](#), [Toshiyuki Toi](#)

ApJ **860** 142 **2018**

<https://arxiv.org/pdf/1805.04251.pdf>

Coronal jets, which extend from the solar surface to beyond  $2 R_{\odot}$ , were observed in the polar coronal hole regions during the total solar eclipse on **2017 August 21**. In a time-series of white-light images of the corona spanning 70 minutes taken with our multi-site observations of this eclipse, six jets were found as narrow structures upwardly ejected with the apparent speed of about  $450 \text{ km s}^{-1}$  in polar plumes. On the other hand, extreme-ultraviolet (EUV) images taken with the Atmospheric Image Assembly of the Solar Dynamics Observatory show that all of the eclipse jets were preceded by EUV jets. Conversely, all the EUV jets whose brightness is comparable to ordinary soft X-ray jets and which occurred in the polar regions near the eclipse period were observed as eclipse jets. These results suggest that ordinary polar jets generally reach high altitudes and escape from the Sun as part of the solar wind.

## **Coronal Mass Ejections Observed at the Total Solar Eclipse on 13 November 2012**

Yoichiro [Hanaoka](#), Jun Nakazawa, Osamu Ohgoe, Yoshiaki Sakai, Kazuo Shiota

Solar Physics, **2014**, Volume 289, Issue 7, pp 2587-2599

<http://arxiv.org/pdf/1309.3718v1.pdf>

<http://sci-hub.cc/10.1007/s11207-014-0476-z>

White-light observations of the total solar eclipse on **13 November 2012** were made at two sites, where the totality occurred 35 min apart. The structure of the corona from the solar limb to a couple of solar radii was observed with a wide dynamic range and a high signal-to-noise ratio. An ongoing coronal mass ejection (CME) and a pre-CME loop structure just before the eruption were observed in the height range between  $1 - 2 R_{\odot}$ . The source region of CMEs was revealed to be in this height range, where the material and the magnetic field of CMEs were located before the eruption. This height range includes the gap between the extreme ultraviolet observations of the low corona and the spaceborne white-light observations of the high corona, but the eclipse observation shows that this height range is essential for the study of CME initiation. The eclipse observation is basically just a snapshot of CMEs, but it indicates the importance of a continuous coverage of CME observations in this height range in the future.

## **Multi-thermal dynamics and energetics of a coronal mass ejection in the low solar atmosphere\***

I. G. [Hannah](#) and E. P. Kontar

A&A 553, A10 (**2013**); **File**

<http://arxiv.org/pdf/1212.5529v1.pdf>

**Aims.** The aim of this work is to determine the multi-thermal characteristics and plasma energetics of an eruptive plasmoid and occulted flare observed by the Solar Dynamics Observatory's Atmospheric Imaging Assembly (SDO/AIA).

**Methods.** We study a **2010 Nov. 3** event (peaking at 12:20 UT in GOES soft X-rays) of a coronal mass ejection and occulted flare that demonstrates the morphology of a classic erupting flux rope. The high spatial and time resolution and six coronal channels of the SDO/AIA images allows the dynamics of the multi-thermal emission during the initial phases of eruption to be studied in detail. The differential emission measure is calculated, using an optimized version of a regularized inversion method, for each pixel across the six channels at different times, resulting in emission measure maps and movies in a variety of temperature ranges.

**Results.** We find that the core of the erupting plasmoid is hot (8–11, 11–14 MK) with a similarly hot filamentary “stem” structure connecting it to the lower atmosphere, which could be interpreted as the current sheet in the flux rope model, though is wider than these models suggest. The velocity of the leading edge of the eruption is  $597\text{--}664 \text{ km s}^{-1}$  in the

temperature range  $\geq 3\text{--}4$  MK and between  $1029\text{--}1246$  km s<sup>-1</sup> for  $\leq 2\text{--}3$  MK. We estimate the density (in  $11\text{--}14$  MK) of the erupting core and stem during the impulsive phase to be about  $3 \times 10^9$  cm<sup>-3</sup>,  $6 \times 10^9$  cm<sup>-3</sup>,  $9 \times 10^8$  cm<sup>-3</sup> in the plasmoid core, stem, and surrounding envelope of material. This gives thermal energy estimates of  $5 \times 10^{29}$  erg,  $1 \times 10^{29}$  erg, and  $2 \times 10^{30}$  erg. The kinetic energy for the core and envelope is slightly lower. The thermal energy of the core and current sheet grows during the eruption, suggesting continuous influx of energy presumably via reconnection. Conclusions. The combination of the optimized regularized inversion method and SDO/AIA data allows the multi-thermal characteristics (i.e. velocity, density, and thermal energies) of the plasmoid eruption to be determined.

### **Emission measure maps of a CME seen by SDO/AIA**

Iain **Hannah** and Eduard Kontar

UKSP nugget: 31, 2013

<http://www.uksolphys.org/?p=5790>

Mapping dynamical heating in a CME.

The spectacular images from the Atmospheric Imaging Assembly on the Solar Dynamics Observatory (SDO/AIA) show a range of highly energetic phenomena in the solar corona like flares and coronal mass ejections (CMEs). These observations not only permit the dynamics to be studied but the different wavelength filters, particularly the six sensitive to coronal temperatures, also allow the heated plasma parameters to be investigated. In this nugget we demonstrate a regularized approach to recovering the underlying temperature distribution of the emitting material from a CME low in the solar corona. The SDO/AIA images show the CME formation which broadly matches the classic CSHKP model of an erupting plasmoid, stretching the magnetic field to produce a current sheet behind it. However in reality this event is considerably more complicated: this CME featured in a earlier nugget. **03-Nov-2010**

### **Simultaneous Near-Sun Observations of a Moving Type IV Radio Burst and the Associated White-Light Coronal Mass Ejection**

K. **Hariharan**, R. Ramesh, C. Kathiravan, T. J. Wang

Solar Phys. Volume 291, Issue 5, pp 1405-1416 **2016** DOI: 10.1007/s11207-016-0918-x

<http://sci-hub.cc/10.1007/s11207-016-0918-x>

We present rare contemporaneous low-frequency ( $< 100$  MHz) imaging, spectral, and polarimetric observations of a moving type IV radio burst that had close spatio-temporal association with a white-light coronal mass ejection (CME) near the Sun. We estimate the electron density near the burst region from white-light coronagraph polarized brightness (pB) images of the CME as well as the two-dimensional radio imaging observations of the thermal free-free emission at a typical radio frequency such as 80 MHz. We analyze the burst properties such as the degree of circular polarization, the spectral index, and fine structures using the radio polarimeter and the radio spectral observations. The obtained results suggest that second harmonic plasma emission from the enhanced electron density in the leading edge of the CME is the cause of the radio burst. We determine the strength of the coronal magnetic field ( $B$ ) for the first time based on this interpretation. The estimated value ( $B \approx 1$  gauss) in the CME leading edge at a heliocentric distance of ( $\approx 2.2 R_{\odot}$ ) agrees well with the similar  $B$  values reported earlier based on other types of observations. **31 March 2014**

See CESRA science highlight #1169, Jan 2017 <http://www.astro.gla.ac.uk/users/eduard/cesra/?p=1169>

### **Measuring Velocities in the Early Stage of an Eruption: Using "Overlappogram" Data from Hinode EIS**

Louise K. **Harra**<sup>1</sup>, Hirohisa Hara<sup>2</sup>, George A. Doschek<sup>3</sup>, Sarah Matthews<sup>1</sup>, Harry Warren<sup>3</sup>, J. Leonard Culhane<sup>1</sup>, and Magnus M. Woods<sup>1</sup>

**2017** ApJ 842 58

<http://sci-hub.cc/10.3847/1538-4357/aa7411>

In order to understand the onset phase of a solar eruption, plasma parameter measurements in the early phases are key to constraining models. There are two current instrument types that allow us to make such measurements: narrow-band imagers and spectrometers. In the former case, even narrow-band filters contain multiple emission lines, creating some temperature confusion. With imagers, however, rapid cadences are achievable and the field of view can be large. Velocities of the erupting structures can be measured by feature tracking. In the spectrometer case, slit spectrometers can provide spectrally pure images by "rastering" the slit to build up an image. This method provides limited temporal resolution, but the plasma parameters can be accurately measured, including velocities along the line of sight. Both methods have benefits and are often used in tandem. In this paper we demonstrate for the first time that data from the wide slot on the Hinode EUV Imaging Spectrometer, along with imaging data from AIA, can be used to deconvolve velocity information at the start of an eruption, providing line-of-sight velocities across an extended field of view. Using He ii 256 Å slot data at flare onset, we observe broadening or shift(s) of the emission line of up to  $\pm 280$  km s<sup>-1</sup>. These are seen at different locations—the redshifted plasma is seen where the hard X-ray source is later seen (energy deposition site). In addition, blueshifted plasma shows the very early onset of the fast rise of the filament. **2011-07-15, 2012-03-09, 2013-12-31**

Hinode/ EIS Nugget Jan 2018 [http://solarb.mssl.ucl.ac.uk/SolarB/nuggets/nugget\\_2018jan.jsp](http://solarb.mssl.ucl.ac.uk/SolarB/nuggets/nugget_2018jan.jsp)

### **The Characteristics of Solar X-Class Flares and CMEs: A Paradigm for Stellar Superflares and Eruptions?**

Louise K. [Harra](#), Carolus J. Schrijver, Miho Janvier, Shin Toriumi, Hugh Hudson, Sarah Matthews, Magnus M. Woods, Hirohisa Hara, Manuel Guedel, Adam Kowalski, Rachel Osten, Kanya Kusano, Theresa Lueftinger

Solar Phys. Volume 291, [Issue 6](#), pp 1761–1782 **2016** [Open Access File](#)

This paper explores the characteristics of 42 solar X-class flares that were observed between February 2011 and November 2014, with data from the Solar Dynamics Observatory (SDO) and other sources. This flare list includes nine X-class flares that had no associated CMEs. In particular our aim was to determine whether a clear signature could be identified to differentiate powerful flares that have coronal mass ejections (CMEs) from those that do not. Part of the motivation for this study is the characterization of the solar paradigm for flare/CME occurrence as a possible guide to the stellar observations; hence we emphasize spectroscopic signatures. To do this we ask the following questions: Do all eruptive flares have long durations? Do CME-related flares stand out in terms of active-region size vs. flare duration? Do flare magnitudes correlate with sunspot areas, and, if so, are eruptive events distinguished? Is the occurrence of CMEs related to the fraction of the active-region area involved? Do X-class flares with no eruptions have weaker non-thermal signatures? Is the temperature dependence of evaporation different in eruptive and non-eruptive flares? Is EUV dimming only seen in eruptive flares? We find only one feature consistently associated with CME-related flares specifically: coronal dimming in lines characteristic of the quiet-Sun corona, i.e. 1–2 MK. We do not find a correlation between flare magnitude and sunspot areas. Although challenging, it will be of importance to model dimming for stellar cases and make suitable future plans for observations in the appropriate wavelength range in order to identify stellar CMEs consistently. **19-03-2011, 24-Sept-2011, 03-11-2011, 07-03-2012, 12-07-2012, 23-10-2012, 08-11-2013, 24-02-2014, 22-10-2014**

**Table 1 The X-class flare sample.**

### **The Impact of a Filament Eruption on Nearby High-lying Cool Loops**

L. K. [Harra](#)<sup>1</sup>, S. A. Matthews<sup>1</sup>, D. M. Long<sup>1</sup>, G. A. Doschek<sup>2</sup>, and B. De Pontieu

**2014** ApJ 792 93

<http://fr.arxiv.org/pdf/1409.0377v1>

<http://arxiv.org/pdf/1409.0377v1.pdf>

The first spectroscopic observations of cool Mg II loops above the solar limb observed by NASA's Interface Region Imaging Spectrograph (IRIS) are presented. During the observation period, IRIS is pointed off-limb, allowing the observation of high-lying loops, which reach over 70 Mm in height. Low-lying cool loops were observed by the IRIS slit-jaw camera for the entire four-hour observing window. There is no evidence of a central reversal in the line profiles, and the Mg II h/k ratio is approximately two. The Mg II spectral lines show evidence of complex dynamics in the loops with Doppler velocities reaching  $\pm 40$  km s<sup>-1</sup>. The complex motions seen indicate the presence of multiple threads in the loops and separate blobs. Toward the end of the observing period, a filament eruption occurs that forms the core of a coronal mass ejection. As the filament erupts, it impacts these high-lying loops, temporarily impeding these complex flows, most likely due to compression. This causes the plasma motions in the loops to become blueshifted and then redshifted. The plasma motions are seen before the loops themselves start to oscillate as they reach equilibrium following the impact. The ratio of the Mg h/k lines also increases following the impact of the filament.

### **The Solar Source of a Magnetic Cloud Using a Velocity Difference Technique**

L.K. [Harra](#), · C.H. Mandrini, · S. Dasso, A.M. Gulisano, · K. Steed, · S. Imada

E-print, Nov 2010; Solar Phys. (**2011**) 268: 213–230, **File**

For large eruptions on the Sun, it is often a problem that the core dimming region cannot be observed due to the bright emission from the flare itself. However, spectroscopic data can provide the missing information through the measurement of Doppler velocities. In this paper we analyse the well-studied flare and coronal mass ejection that erupted on the Sun on **13 December 2006** and reached the Earth on 14 December 2006. In this example, although the imaging data were saturated at the flare site itself, we could extract information on the core dimming region through velocity measurements, as well as on the remote dimmings. The purpose of this paper is to determine more accurately the magnetic flux of the solar source region, potentially involved in the ejection, through a new technique. The results of its application are compared to the flux in the magnetic cloud observed at 1AU, as a way to check the reliability of this technique. We analysed data from the {it Hinode} EUV Imaging Spectrometer to estimate the Doppler velocity in the active region and its surroundings before and after the event. This allowed us to determine a Doppler velocity 'difference' image. We used the velocity difference image overlaid on a Michelson Doppler Imager magnetogram to identify the regions in which the blue-shifts were more prominent after the event; the magnetic flux in these regions was used as a proxy for the ejected flux and compared to the magnetic cloud flux. This new method provides a more accurate flux determination in the solar source region.

### **Spectroscopic observations of coronal waves and coronal mass ejections**

L.K. [Harra](#)

[Advances in Space Research](#)

[Volume 41, Issue 1](#), **2008**, Pages 138-143, **File**

It is common to use imaging instruments such as EUV and X-ray imagers and coronagraphs to study large-scale phenomena such as coronal mass ejections and coronal waves. Although high resolution spectroscopy is generally

limited to a small field of view, its importance in understanding global phenomena should not be under-estimated. I will review current spectroscopic observations of large-scale dynamic phenomena such as global coronal waves and coronal mass ejections. The aim is to determine plasma parameters such as flows, temperatures and densities to obtain a physical understanding of these phenomena.

### **How Does Large Flaring Activity from the Same Active Region Produce Oppositely Directed Magnetic Clouds?**

Louise K. [Harra](#) · Nancy U. Crooker · Cristina H. Mandrini · Lidia van Driel-Gesztelyi · Sergio Dasso · Jingxiu Wang · Heather Elliott · Gemma Attrill · Bernard V. Jackson · Mario M. Bisi  
Solar Phys, DOI 10.1007/s11207-007-9002-x, **2007**

We describe the interplanetary coronal mass ejections (ICMEs) that occurred as a result of a series of solar flares and eruptions from 4 to 8 November 2004. Two ICMEs/magnetic clouds occurring from these events had opposite magnetic orientations. This was despite the fact that the major flares related to these events occurred within the same active region that maintained the same magnetic configuration.

### **MATERIAL OUTFLOWS FROM CORONAL INTENSITY “DIMMING REGIONS” DURING CORONAL MASS EJECTION ONSET**

Louise K. [Harra](#), Alphonse C. Sterling  
Astrophysical Journal, 561:L215–L218, **2001**

<https://iopscience.iop.org/article/10.1086/324767/pdf>

One signature of expulsion of coronal mass ejections (CMEs) from the solar corona is the appearance of transient intensity dimmings in coronal images. These dimmings have generally been assumed to be due to discharge of CME material from the corona, and thus the “dimming regions” are thought of as an important signature of the sources of CMEs. We present spectral observations of two dimming regions at the time of expulsion of CMEs, using the Coronal Diagnostic Spectrometer (CDS) on the SOHO satellite. One of the dimming regions is at the solar limb and associated with a CME traveling in the plane of the sky, while the other region is on the solar disk and associated with an Earth-directed “halo” CME. From the limb event, we see Doppler signatures of  $\sim 30$  km s<sup>-1</sup> in coronal (Fe XVI and Mg IX) emission lines, where the enhanced velocities coincide with the locations of coronal dimming. This provides direct evidence that the dimmings are associated with outflowing material. We also see larger ( $\sim 100$  km s<sup>-1</sup>) Doppler velocities in transition region (O V and He I) emission lines, which are likely to be associated with motions of a prominence and loops at transition region temperatures. An “EIT wave” accompanies the disk event, and a dimming region behind the wave shows strong blueshifted Doppler signatures of  $\sim 100$  km s<sup>-1</sup> in O V, suggesting that material from the dimming regions behind the wave may be feeding the CME.

### **CMEs in the Heliosphere: I. A Statistical Analysis of the Observational Properties of CMEs Detected in the Heliosphere from 2007 to 2017 by STEREO/HI-1**

[R. A. Harrison](#), [J. A. Davies](#), [D. Barnes](#), [J. P. Byrne](#), [C. H. Perry](#), [V. Bothmer](#), [J. P. Eastwood](#), [P. T. Gallagher](#), [E. K. J. Kilpua](#), [C. Möstl](#), [L. Rodriguez](#), [A. P. Rouillard](#), [D. Odstrcil](#)

Solar Phys. 293:77 **2018**

<https://arxiv.org/ftp/arxiv/papers/1804/1804.02320.pdf>

<https://link.springer.com/content/pdf/10.1007%2Fs11207-018-1297-2.pdf>

We present a statistical analysis of coronal mass ejections (CMEs) imaged by the Heliospheric Imager (HI) instruments aboard NASAs twin-spacecraft STEREO mission between April 2007 and August 2017 for STEREO-A and between April 2007 and September 2014 for STEREO-B. The analysis exploits a catalogue that was generated within the FP7 HELCATS project. Here, we focus on the observational characteristics of CMEs imaged in the heliosphere by the inner (HI-1) cameras. More specifically, in this paper we present distributions of the basic observational parameters - namely occurrence frequency, central position angle (PA) and PA span - derived from nearly 2000 detections of CMEs in the heliosphere by HI-1 on STEREO-A or STEREO-B from the minimum between Solar Cycles 23 and 24 to the maximum of Cycle 24; STEREO-A analysis includes a further 158 CME detections from the descending phase of Cycle 24, by which time communication with STEREO-B had been lost. We compare heliospheric CME characteristics with properties of CMEs observed at coronal altitudes, and with sunspot number. As expected, heliospheric CME rates correlate with sunspot number, and are not inconsistent with coronal rates once instrumental factors/differences in cataloguing philosophy are considered. As well as being more abundant, heliospheric CMEs, like their coronal counterparts, tend to be wider during solar maximum. Our results confirm previous coronagraph analyses suggesting that CME launch sites don't simply migrate to higher latitudes with increasing solar activity. At solar minimum, CMEs tend to be launched from equatorial latitudes while, at maximum, CMEs appear to be launched over a much wider latitude range; this has implications for understanding the CME/solar source association. Our analysis provides some supporting evidence for the systematic dragging of CMEs to lower latitude as they propagate outwards. **2008-12-13, 2009-09-01, 2010-06-02, 2011-07-03, 2011-12-01, 2013-12-15**

HELIOSPHERIC IMAGER CME CATALOGUE [HTTPS://WWW.HELCATS-FP7.EU/CATALOGUES/WP2\\_CAT.HTML](https://www.helcats-fp7.eu/catalogues/wp2_cat.html)

## AN ANALYSIS OF THE ORIGIN AND PROPAGATION OF THE MULTIPLE CORONAL MASS EJECTIONS OF 2010 AUGUST 1

R. A. [Harrison](#)<sup>1</sup>, J. A. Davies<sup>1</sup>, C. Möstl<sup>2,3,4</sup>, Y. Liu<sup>4,5</sup>, M. Temmer<sup>2,3</sup>, M. M. Bisi<sup>6,7</sup>, J. P. Eastwood<sup>8</sup>, C. A. de Koning<sup>9</sup>, N. Nitta<sup>10</sup>, T. Rollett<sup>2,3</sup>, C. J. Farrugia<sup>11</sup>, R. J. Forsyth<sup>8</sup>, B. V. Jackson<sup>7</sup>, E. A. Jensen<sup>12</sup>, E. K. J. Kilpua<sup>13</sup>, D. Odstrcil<sup>14</sup>, and D. F. Webb

2012 ApJ 750 45, [File](#)

On 2010 August 1, the northern solar hemisphere underwent significant activity that involved a complex set of active regions near central meridian with, nearby, two large prominences and other more distant active regions. This activity culminated in the eruption of four major coronal mass ejections (CMEs), effects of which were detected at Earth and other solar system bodies. Recognizing the unprecedented wealth of data from the wide range of spacecraft that were available—providing the potential for us to explore methods for CME identification and tracking, and to assess issues regarding onset and planetary impact—we present a comprehensive analysis of this sequence of CMEs. We show that, for three of the four major CMEs, onset is associated with prominence eruption, while the remaining CME appears to be closely associated with a flare. Using instrumentation on board the Solar Terrestrial Relations Observatory spacecraft, three of the CMEs could be tracked out to elongations beyond 50°; their directions and speeds have been determined by various methods, not least to assess their potential for Earth impact. The analysis techniques that can be applied to the other CME, the first to erupt, are more limited since that CME was obscured by the subsequent, much faster event before it had propagated far from the Sun; we discuss the speculation that these two CMEs interact. The consistency of the results, derived from the wide variety of methods applied to such an extraordinarily complete data set, has allowed us to converge on robust interpretations of the CME onsets and their arrivals at 1 AU.

### Coronal mass ejection: key issues

[Review](#)

Richard [Harrison](#)

Proceedings of the International Astronomical Union (2008), *N. Gopalswamy & D.F. Webb, eds*, .  
4: 191-200, 2009, [File](#)

Coronal Mass Ejections (CMEs) have been addressed by a particularly active research community in recent years. With the advent of the International Heliophysical Year and the new STEREO and Hinode missions, in addition to the on-going SOHO mission, CME research has taken centre stage in a renewed international effort. This [review](#) aims to touch on some key observational areas, and their interpretation. First, we consider coronal dimming, which has become synonymous with CME onsets, and stress that recent advances have heralded a move from a perceived association between the two phenomena to a firm, well-defined physical link. What this means for our understanding of CME modeling is discussed. Second, with the new STEREO observations, and noting the on-going SMEI observations, it is important to review the opening field of CME studies in the heliosphere. Finally, we discuss some specific points with regard to EIT-waves and the flare-CME relationship. In the opinion of the author, these issues cover key hot topics which need consideration for significant progress in the field.

### Pre-CME Onset Fuses – Do the STEREO Heliospheric Imagers Hold the Clues to the CME Onset Process?

Richard A. [Harrison](#) · Christopher J. Davis · Jackie A. Davies

Solar Phys (2009) 259: 277–296, [File](#)

Understanding the onset of coronal mass ejections (CMEs) is surely one of the holy grails of solar physics today. Inspection of data from the Heliospheric Imagers (HI), which are part of the SECCHI instrument suite aboard the two NASA STEREO spacecraft, appears to have revealed pre-eruption signatures which may provide valuable evidence for identifying the CME onset mechanism. Specifically, an examination of the HI images has revealed narrow rays comprised of a series of outward-propagating plasma blobs apparently forming near the edge of the streamer belt prior to many CME eruptions. In this pilot study, we inspect a limited dataset to explore the significance of this phenomenon, which we have termed a pre-CME ‘fuse’. Although, the enhanced expulsion of blobs may be consistent with an increase in the release of outward-propagating blobs from the streamers themselves, it could also be interpreted as evidence for interchange reconnection in the period leading to a CME onset. Indeed, it is argued that the latter could even have implications for the end-of-life of CMEs. Thus, the presence of these pre-CME fuses provides evidence that the CME onset mechanism is either related to streamer reconnection processes or the reconnection between closed field lines in the streamer belt and adjacent, open field lines. We investigate the nature of these fuses, including their timing and location with respect to CME launch sites, as well as their speed and topology.

### First Imaging of Coronal Mass Ejections in the Heliosphere Viewed from Outside the Sun – Earth Line

Richard A. **Harrison** · Christopher J. Davis · Christopher J. Eyles · Danielle Bewsher · Steve R. Crothers · Jackie A. Davies · Russell A. Howard · Daniel J. Moses · Dennis G. Socker · Jeffrey S. Newmark · Jean-Philippe Halain · Jean-Marc Defise · Emmanuel Mazy · Pierre Rochus · David F. Webb · George M. Simnett

Solar Phys (2008) 247: 171–193, **File**

<http://www.springerlink.com/content/a3281715574015j4/fulltext.pdf>

**25 Jan 2007** We show for the first time images of solar coronal mass ejections (CMEs) viewed using the **Heliospheric Imager (HI)** instrument aboard the NASA **STEREO** spacecraft. The HI instruments are wide-angle imaging systems designed to detect CMEs in the heliosphere, in particular, for the first time, observing the propagation of such events along the Sun–Earth line, that is, those directed towards Earth. At the time of writing the STEREO spacecraft are still close to the Earth and the full advantage of the HI dual-imaging has yet to be realised. However, even these early results show that despite severe technical challenges in their design and implementation, the HI instruments can successfully detect CMEs in the heliosphere, and this is an extremely important milestone for CME research. For the principal event being analysed here we demonstrate an ability to track a CME from the corona to over 40 degrees. The time–altitude history shows a constant speed of ascent over at least the first 50 solar radii and some evidence for deceleration at distances of over 20 degrees.

### **Coronal dimming and the coronal mass ejection onset.**

**Harrison**, R.A., Bryans, P., Simnett, G.M., Lyons, M.,

**2003**. Astron. Astrophys. 400, 1071–1083.

### **A spectroscopic study of coronal dimming associated with a coronal mass ejection.**

**Harrison**, R.A., Lyons, M.,

**2000**. Astron. Astrophys. 358, 1097–1108.

### **Coronal Magnetic Storms: a New Perspective on Flares and the ‘Solar Flare Myth’ Debate.**

**Harrison**, R.A.,

**1996**. Solar Phys. 166, 441–444.

### **The nature of solar flares associated with coronal mass ejection.**

**Harrison**, R.A.,

**1995**. Astron. Astrophys. 304, 585–594.

<https://articles.adsabs.harvard.edu/pdf/1995a&a...304..585h>

An analysis is presented of solar X-ray flares associated with coronal mass ejections through the period 1986–1987. The nature of the flares apparently associated with mass ejection is explored. In particular the relationships between flare duration and intensity and the association with mass ejection are investigated. We believe that this study tackles the flare–CME analysis in a way that is uniquely unbiased. Past studies of a similar nature are discussed and a criticism of their approach is given. In particular, the author believes that the continual bias toward the so-called Long Duration Events and the brightest flares is misleading. The analysis supports the view that the flare and CME are signatures of the same magnetic "disease", that is, they represent the responses in different parts of the magnetic structure, to a particular activity; they do not drive one another but are closely related. The present statistical analysis allows a chance association to be given for a mass ejection event when an X-ray flare is observed. The use of such information in the prediction of geomagnetic activity generated when mass ejecta interact with the Earth is discussed.

### **Recurrent Coronal Mass Ejections and Their Geomagnetic Storms Association on 2012**

#### **January 19: Solar Surface to Upper Earth's Atmosphere Analyses**

A. **Hassanin**<sup>1</sup>, Amira Shimeis<sup>2</sup>, Hadeer F. Sabeha<sup>1</sup>, and F. N. Minta<sup>3</sup>

**2024** ApJ 974 301

<https://iopscience.iop.org/article/10.3847/1538-4357/ad77d4/pdf>

In this study, we have conducted an analysis of space weather disruptions that occurred on **19 January 2012**. Our analysis identified three coronal mass ejections (CMEs), CME1, CME2, and CME3—which were ejected at 09:48:05 universal time (UT), 14:36:05 UT, and 16:12:06 UT, respectively. Nonrecurrent disturbances in space weather, such as geomagnetic storms, result from CMEs originating from the Sun and traveling toward Earth. We assess the contribution of CME–CME interactions on 2012 January 19 and the volume emission rate of nitric oxide (NO) near the Earth's upper atmosphere in prolonging the geomagnetic disturbances observed on 2012 January 23. The findings suggest an increase in intensity at the interacting boundaries of CME1 and CME2, indicating an increase in pressure and density, leading to the compression of the magnetosphere. The 3D reconstructions of the CMEs provide evidence of unequal expansion and rotations within coronagraphic frames attributed to structural variability in the background solar wind during the eruptions. Furthermore, highlights from the in situ observations suggest that the impact of the recurrent CMEs on the geomagnetic disturbance was more pronounced within the auroral region synchronizing with a significant increase in NO volume emission rate on 2012 January 23, near the upper Earth's atmosphere. Our



focus is on exploring the interactions between these CMEs to understand their potential contribution to the extended duration of the observed geomagnetic disturbance.

## **A Model of Homologous Confined and Ejective Eruptions Involving Kink Instability and Flux Cancellation**

Alshaimaa **Hassanin**<sup>1</sup>, Bernhard Kliem<sup>2</sup>, Norbert Seehafer<sup>2</sup>, and Tibor Török<sup>3</sup>

2022 ApJL 929 L23

<https://iopscience.iop.org/article/10.3847/2041-8213/ac64a9/pdf>

<https://arxiv.org/pdf/2204.11767>

In this study, we model a sequence of a confined and a full eruption, employing the relaxed end state of the confined eruption of a kink-unstable flux rope as the initial condition for the ejective one. The full eruption, a model of a coronal mass ejection, develops as a result of converging motions imposed at the photospheric boundary, which drive flux cancellation. In this process, parts of the positive and negative external flux converge toward the polarity inversion line, reconnect, and cancel each other. Flux of the same amount as the canceled flux transfers to a flux rope, increasing the free magnetic energy of the coronal field. With sustained flux cancellation and the associated progressive weakening of the magnetic tension of the overlying flux, we find that a flux reduction of  $\approx 11\%$  initiates the torus instability of the flux rope, which leads to a full eruption. These results demonstrate that a homologous full eruption, following a confined one, can be driven by flux cancellation.

## **Helical Kink Instability in the confined Solar Eruption on 2002 May 27**

Alshaimaa **Hassanin**, Bernhard Kliem, Norbert Seehafer

Astron. Nachr. (Astron. News; AN) 337, 1082, 2016

<https://arxiv.org/pdf/1611.01008v1.pdf>

This paper presents an improved MHD modeling of the confined filament eruption in solar active region NOAA-9957 on **2002 May-27** by extending the parametric studies of the event in Torok & Kliem 2005 and Hassanin & Kliem 2016. Here the initial flux rope equilibrium is chosen to possess a small apex height identical to the observed initial filament height, which implies a more realistic inclusion of the photospheric line tying. The model matches the observations as closely as in the preceding studies, with the closest agreement again being obtained for an initial average flux rope twist of about  $4\pi$ . Thus, the model for strongly writhing confined solar eruptions, which assumes that a kink-unstable flux rope in the stability domain of the torus instability exists at the onset of the eruption's main acceleration phase, is further substantiated.

## **Helical Kink Instability in a Confined Solar Eruption**

Alshaimaa **Hassanin**, Bernhard Kliem

ApJ 832 106 2016

<http://arxiv.org/pdf/1609.00673v1.pdf>

A model for strongly writhing confined solar eruptions suggests an origin in the helical kink instability of a coronal flux rope which remains stable against the torus instability. This model is tested against the well observed filament eruption on **2002 May 27** in a parametric MHD simulation study which comprises all phases of the event. Good agreement with the essential observed properties is obtained. These include the confinement, terminal height, writhing, distortion, and dissolution of the filament, and the flare loops. The agreement is robust against variations in a representative range of parameter space. Careful comparisons with the observation data constrain the ratio of the external toroidal and poloidal field components to  $B_{\theta}/B_{\phi} \approx 1$  and the initial flux rope twist to  $\Phi \approx 4\pi$ . Different from ejective eruptions, two distinct phases of strong magnetic reconnection can occur. First, the erupting flux is cut by reconnection with overlying flux in the helical current sheet formed by the instability. If the resulting flux bundles are linked as a consequence of the erupting rope's strong writhing, they subsequently reconnect in the vertical current sheet between them. This reforms the overlying flux and a far less twisted flux rope, offering a pathway to homologous eruptions.

## **Reverse Current Model for Coronal Mass Ejection Cavity Formation**

Magnus A. **Haw**<sup>1</sup>, Pakorn Wongwaitayakornkul<sup>1</sup>, Hui Li<sup>2</sup>, and Paul M. Bellan<sup>1</sup>

2018 ApJL 862 L15

<http://sci-hub.tw/http://iopscience.iop.org/article/10.3847/2041-8213/aad33c/meta>

We report here a new model for explaining the three-part structure of coronal mass ejections (CMEs). The model proposes that the cavity in a CME forms because a rising electric current in the core prominence induces an oppositely directed electric current in the background plasma; this eddy current is required to satisfy the frozen-in magnetic flux condition in the background plasma. The magnetic force between the inner-core electric current and the oppositely directed induced eddy current propels the background plasma away from the core, creating a cavity and a density pileup at the cavity edge. The cavity radius saturates when an inward restoring force from magnetic and hydrodynamic pressure in the region outside the cavity edge balances the outward magnetic force. The model is supported by (i) laboratory experiments showing the development of a cavity as a result of the repulsion of an induced reverse current by a rising inner-core flux-rope current, (ii) 3D numerical magnetohydrodynamic (MHD) simulations that reproduce the laboratory experiments in quantitative detail, and (iii) an analytic model that describes cavity formation as a result of the plasma containing the induced reverse current being repelled from the inner core. This analytic model has broad

applicability because the predicted cavity widths are relatively independent of both the current injection mechanism and the injection timescale. **2011 October 4**

## **MHD simulations of the global solar corona around the Halloween event in 2003 using the synchronic frame format of the solar photospheric magnetic field**

Keiji [Hayashi](#), Xue Pu Zhao, Yang Liu

JOURNAL OF GEOPHYSICAL RESEARCH, VOL. 113, A07104, doi:10.1029/2007JA012814, **2008**

<http://dx.doi.org/10.1029/2007JA012814>

We performed two time-relaxation magnetohydrodynamics (MHD) simulations of the solar corona: one uses the boundary map representing the solar surface magnetic field distribution before the **Halloween event in 2003**, and the other uses map representing the postevent distribution. The aims of this study are to test a new concept of a solar surface magnetic field map capable of representing a particular time of interest and to examine the coronal responses to the solar photospheric magnetic field changes occurring over a few days. We used a new mapping scheme named “synchronic frame” that can include the longitudinal shift caused by the solar differential rotation and the solar surface variations occurring at the time of interest. These two time-relaxation MHD simulations using the two maps are separately performed to numerically obtain the quasi steady states of the solar corona before and after the Halloween event. Comparisons of the simulated coronal magnetic field structures to the SOHO/EIT measurements show that the combinations of our mapping method and simulation model reproduce the changes of the coronal structures well. We also find that the consequences of solar surface variations can be seen in the plasma quantities in the solar corona. These results show the capability and importance of the solar surface magnetic field mapping scheme for better reconstruction of global coronal structures, parts of which are sensitive to the solar surface magnetic field variations.

## **High-Energy Insights from an Escaping Coronal Mass Ejection with Solar Orbiter/STIX Observations**

[Laura A. Hayes](#), [Säm Krucker](#), [Hannah Collier](#), [Daniel Ryan](#)

A&A 691, A190 **2024**

<https://arxiv.org/pdf/2408.14194>

<https://www.aanda.org/articles/aa/pdf/2024/11/aa50882-24.pdf>

Solar eruptive events, including solar flares and coronal mass ejections (CMEs), are typically characterised by energetically significant X-ray emissions from flare-accelerated electrons and hot thermal plasmas. Occulted events, where the main flare is blocked by the solar limb, provide an opportunity to observe and analyse the X-ray emissions specifically associated with CMEs. This study investigates the X-ray and extreme ultraviolet (EUV) emissions associated with a large filament eruption and CME that occurred on **February 15, 2022**. This event was highly occulted from the three vantage points of Solar Orbiter, STEREO-A, and Earth. We utilised X-ray observations from the Spectrometer/Telescope for Imaging X-rays (STIX) and EUV observations from the Full Sun Imager (FSI) of the Extreme Ultraviolet Imager (EUI) on-board Solar Orbiter, supplemented by multi-viewpoint observations from STEREO-A/EUVI. This enabled a comprehensive analysis of the X-ray emissions in relation to the filament structure observed in EUV. We used STIX's imaging and spectroscopy capabilities to characterise the X-ray source associated with the eruption. Our analysis reveals that the X-ray emissions associated with the occulted eruption originated from an altitude exceeding 0.3R<sub>sun</sub> above the main flare site. The X-ray time-profile showed a sharp increase and exponential decay, and consisted of both a hot thermal component at 17 MK and non-thermal emissions (>11.4 keV) characterised by an electron spectral index of 3.9. Imaging analysis showed an extended X-ray source that coincided with the EUV emission as observed from EUI, and was imaged until the source grew to a size larger than the imaging limit of STIX (180 arcsec). The findings demonstrate that STIX combined with EUI provides a unique and powerful tool for examining the energetic properties of the CME component of solar energetic eruptions.

## **Quantitative Characterization of Magnetic Flux Rope Properties for Two Solar Eruption Events**

[Wen He](#), [Qiang Hu](#), [Chaowei Jiang](#), [Jiong Qiu](#), [Avijeet Prasad](#)

ApJ 934 103 **2022**

<https://arxiv.org/pdf/2201.03149.pdf>

<https://iopscience.iop.org/article/10.3847/1538-4357/ac78df/pdf>

In order to bridge the gap between heliospheric and solar observations of coronal mass ejections (CMEs), one of the key steps is to improve the understanding of their corresponding magnetic structures like the magnetic flux ropes (MFRs). But it remains a challenge to confirm the existence of a coherent MFR before or upon the CME eruption on the Sun and to quantitatively characterize the CME-MFR due to the lack of direct magnetic field measurement in the corona. In this study, we investigate the MFR structures, originating from two active regions (ARs), AR 11719 and AR 12158, and estimate their magnetic properties quantitatively. We perform the nonlinear force-free field extrapolations with preprocessed photospheric vector magnetograms. In addition, remote-sensing observations are employed to find indirect evidence of MFRs on the Sun and to analyze the time evolution of magnetic reconnection flux associated with the flare ribbons during the eruption. A coherent “pre-existing” MFR structure prior to the flare eruption is identified quantitatively for one event from the combined analysis of the extrapolation and observation. Then the characteristics of MFRs for two events on the Sun before and during the eruption, forming the CME-MFR, including the axial magnetic flux, field-line twist, and reconnection flux, are estimated and compared with the corresponding in situ modeling

results. We find that the magnetic reconnection associated with the accompanying flares for both events injects significant amount of flux into the erupted CME-MFRs. **2013 April 11, 2014 September 10**

### **Electric Currents through J-shaped and Non-J-shaped Flare Ribbons**

[Yuwei He](#), [Rui Liu](#), [Lijuan Liu](#), [Jun Chen](#), [Wensi Wang](#), [Yuming Wang](#)

ApJ **2020**

<https://arxiv.org/pdf/2007.05693.pdf>

Recently solar flares exhibiting a double J-shaped ribbons in the lower solar atmosphere have been paid increasing attention in the context of extending the two-dimensional standard flare model to three dimensions, as motivated by the spatial correlation between photospheric current channels and flare ribbons. Here we study the electric currents through the photospheric area swept by flare ribbons (termed synthesized ribbon area or SRA), with a sample of 71 two-ribbon flares, of which 36 are J-shaped. Electric currents flowing through one ribbon are highly correlated with those through the other, therefore belonging to the same current system. The non-neutrality factor of this current system is independent of the flare magnitude, implying that both direct and return currents participate in flares. J-shaped flares are distinct from non-J-shaped flares in the following aspects: 1) Electric current densities within J-shaped SRA are significantly smaller than those within non-J-shaped SRA, but J-shaped SRA and its associated magnetic flux are also significantly larger. 2) Electric currents through SRA are positively correlated with the flare magnitude, but J-shaped flares show stronger correlation than non-J-shaped flares. 3) The majority (75%) of J-shaped flares are eruptive, while the majority (86%) of non-J-shaped flares are confined; accordingly, hosting active regions of J-shaped flares are more likely to be sigmoidal than non-J-shaped flares. Thus, J-shaped flares constitute a distinct subset of two-ribbon flares, probably the representative of eruptive ones. Further, we found that combining SRA and its associated magnetic flux has the potential to differentiate eruptive from confined flares. **2013 April 12, 2013 August 12**

### **Data-driven MHD Simulation of the Formation and Initiation of a Large-scale Pre-flare Magnetic Flux Rope in Solar Active Region 12371**

Wen [He](#), [Chaowei Jiang](#), [Peng Zou](#), [Aiyang Duan](#), [Xueshang Feng](#), [Pingbing Zuo](#), [Yi Wang](#)

ApJ **892 9 2020**

<https://arxiv.org/pdf/2002.04837.pdf>

Solar eruptions are the most powerful drivers of space weather. To understand their cause and nature, it is crucial to know how the coronal magnetic field evolves before eruption. Here we study the formation process of a relatively large-scale magnetic flux rope (MFR) in active region NOAA~12371 that erupts with a major flare and coronal mass ejection on **2015 June 21**. A data-driven numerical magnetohydrodynamic model is employed to simulate three-dimensional coronal magnetic field evolution of one-day duration before the eruption. Comparison between the observed features and our modeled magnetic field discloses how the pre-eruption MFR forms. Initially, the magnetic field lines were weakly twisted as being simple sheared arcades. Then a long MFR was formed along the polarity inversion line due to the complex photospheric motion, which is mainly shearing rather than twisting. The presence of the MFR is evidenced by a coherent set of magnetic field lines with twist number above unity. Below the MFR a current sheet is shown in the model, suggesting that tether-cutting reconnection plays a key role in the MFR formation. The MFR's flux grows as more and more field lines are twisted due to continuous injection of magnetic helicity by the photospheric motions. Meanwhile, the height of the MFR's axis increases monotonely from its formation. By an analysis of the decay index of its overlying field, we suggest that it is because the MFR runs into the torus instability regime and becomes unstable that finally triggers the eruption.

### **A Stealth CME Bracketed between Slow and Fast Wind Producing Unexpected Geoeffectiveness**

Wen [He](#), [Ying D.Liu](#), [Huidong Hu](#), [Rui Wang](#), [Xiaowei Zhao](#)

ApJ **860 78 2018**

<https://arxiv.org/pdf/1805.03128.pdf>

<https://iopscience.iop.org/article/10.3847/1538-4357/aac381/pdf>

We investigate how a weak coronal mass ejection (CME) launched on **2016 October 8** without obvious signatures in the low corona produced a relatively intense geomagnetic storm. Remote sensing observations from SDO, STEREO and SOHO and in situ measurements from WIND are employed to track the CME from the Sun to the Earth. Using a graduated cylindrical shell (GCS) model, we estimate the propagation direction and the morphology of the CME near the Sun. CME kinematics are determined from the wide-angle imaging observations of STEREO A and are used to predict the CME arrival time and speed at the Earth. We compare ENLIL MHD simulation results with in situ measurements to illustrate the background solar wind where the CME was propagating. We also apply a Grad-Shafranov technique to reconstruct the flux rope structure from in situ measurements in order to understand the geoeffectiveness associated with the CME magnetic field structure. Key results are obtained concerning how a weak CME can generate a relatively intense geomagnetic storm: (1) there were coronal holes at low latitudes, which could produce high speed streams (HSSs) to interact with the CME in interplanetary space; (2) the CME was bracketed between a slow wind ahead and a HSS behind, which enhanced the southward magnetic field inside the CME and gave rise to the unexpected geomagnetic storm.

### **Tracking the Source of Solar Type II Bursts through Comparisons of Simulations and Radio Data**

[Alexander M. Hegedus](#) (1), [Ward B. Manchester IV](#) (1), [Justin C. Kasper](#) (1)

ApJ **2021**

<https://arxiv.org/pdf/2102.07875.pdf>

The most intense solar energetic particle events are produced by coronal mass ejections (CMEs) accompanied by intense type II radio bursts below 15 MHz. Understanding where these type II bursts are generated relative to an erupting CME would reveal important details of particle acceleration near the Sun, but the emission cannot be imaged on Earth due to distortion from its ionosphere. Here, a technique is introduced to identify the likely source location of the emission by comparing the observed dynamic spectrum observed from a single spacecraft against synthetic spectra made from hypothesized emitting regions within a magnetohydrodynamic (MHD) numerical simulation of the recreated CME. The radio-loud **2005 May 13** CME was chosen as a test case, with Wind/WAVES radio data used to frame the inverse problem of finding the most likely progression of burst locations. An MHD recreation is used to create synthetic spectra for various hypothesized burst locations. A framework is developed to score these synthetic spectra by their similarity to the type II frequency profile derived from Wind/WAVES data. Simulated areas with 4x enhanced entropy and elevated de Hoffmann Teller velocities are found to produce synthetic spectra similar to spacecraft observations. A geometrical analysis suggests that the eastern edge of the entropy derived shock around (-30, 0) degrees in heliocentric coordinates was emitting in the first hour of the event before ceasing emission, and that the western/southwestern edge of the shock centered around (6, -12) degrees was a dominant area of radio emission for the 2 hours of simulation data out to 20 solar radii. **2012-01-19**

### **CME–HSS Interaction and Characteristics Tracked from Sun to Earth**

Stephan G. [Heinemann](#), Manuela Temmer, Charles J. Farrugia, Karin Dissauer, Christina Kay, Thomas Wiegelmann, Mateja Dumbović, Astrid M. Veronig, Tatiana Podladchikova, Stefan J. Hofmeister, Noé Lugaz, Fernando Carcaboso

[Solar Physics](#) September **2019**, 294:121

[sci-hub.se/10.1007/s11207-019-1515-6](https://arxiv.org/pdf/1908.10161.pdf)

<https://arxiv.org/pdf/1908.10161.pdf>

In a thorough study, we investigate the origin of a remarkable plasma and magnetic field configuration observed in situ on **June 22, 2011**, near L1, which appears to be a magnetic ejecta (ME) and a shock signature engulfed by a solar wind high-speed stream (HSS). We identify the signatures as an Earth-directed coronal mass ejection (CME), associated with a C7.7 flare on **June 21, 2011**, and its interaction with a HSS, which emanates from a coronal hole (CH) close to the launch site of the CME. The results indicate that the major interaction between the CME and the HSS starts at a height of 1.3  $R_{\odot}$  up to 3  $R_{\odot}$ . Over that distance range, the CME undergoes a strong north-eastward deflection of at least 30° due to the open magnetic field configuration of the CH. We perform a comprehensive analysis for the CME–HSS event using multi-viewpoint data (from the Solar TERrestrial RELations Observatories, the Solar and Heliospheric Observatory and the Solar Dynamics Observatory), and combined modeling efforts (nonlinear force-free field modeling, Graduated Cylindrical Shell CME modeling, and the Forecasting a CME’s Altered Trajectory – ForeCAT model). We aim at better understanding its early evolution and interaction process as well as its interplanetary propagation and related in situ signatures, and finally the resulting impact on the Earth’s magnetosphere.

### **Hot prominence detected in the core of a coronal mass ejection: Analysis of SOHO/UVCS $L\alpha$ and SOHO/LASCO visible-light observations**

P. [Heinzel](#)<sup>1,4</sup>, R. Susino<sup>2</sup>, S. Jejić<sup>3,1</sup>, A. Bemporad<sup>2</sup> and U. Anzer<sup>4</sup>

A&A 589, A128 (**2016**)

Context. The paper deals with the physics of erupting prominences in the core of coronal mass ejections (CME).

Aims. We determine the physical parameters of an erupting prominence embedded in the core of a CME using SOHO/UVCS hydrogen  $L\alpha$  and  $L\beta$  lines and SOHO/LASCO visible light observations. In particular we analyze the CME event observed on **August 2, 2000**. We develop the non-LTE (NLTE; i.e. considering departures from the local thermodynamic equilibrium – LTE) spectral diagnostics based on  $L\alpha$  and visible light observations.

Methods. Our method is based on 1D NLTE modeling of eruptive prominences and takes into account the effect of large flow velocities, which reach up to 300 km s<sup>-1</sup> for the studied event (the so-called Doppler dimming). The NLTE radiative-transfer method can be used for both optically thin and thick prominence structures. We combine spectroscopic UVCS observations of an erupting prominence in the core of a CME with visible light images from LASCO-C2 in order to derive the geometrical parameters like projected thickness and velocity, together with the effective temperature and column density of electrons. These are then used to constrain our NLTE radiative transfer modeling which provides the kinetic temperature, microturbulent velocity, gas pressure, ionization degree, the line opacities, and the prominence effective thickness (geometrical filling factor).

Results. Analysis was made for 69 observational points (spatial pixels) inside the whole erupting prominence. Roughly one-half of them show a non-negligible  $L\alpha$  optical thickness for flow velocity 300 km s<sup>-1</sup> and about one-third for flow velocity 150 km s<sup>-1</sup>. All pixels with  $L\alpha\tau_0 \leq 0.3$  have been considered for further analysis, which is presented in the form of statistical distributions (histograms) of various physical quantities such as the kinetic temperature, gas pressure, and electron density for two representative flow velocities (150 and 300 km s<sup>-1</sup>) and non-zero microturbulence. For two pixels co-temporal LASCO visible-light data are also available, which further constrains the diagnostics of the electron density and effective thickness. Detailed NLTE modeling is presented for various sets of input parameters.

Conclusions. The studied CME event shows that the erupting prominence expands to large volumes, meaning that it is a low-pressure structure with low electron densities and high temperatures. This analysis provides a basis for future diagnostics using the METIS coronagraph on board the Solar Orbiter mission.

## From Starspots to Stellar Coronal Mass Ejections—Revisiting Empirical Stellar Relations

Konstantin [Herbst](#)<sup>1</sup>, Athanasios Papaioannou<sup>2</sup>, Vladimir S. Airapetian<sup>3,4</sup>, and Dimitra Atri<sup>5</sup>

2021 ApJ 907 89

<https://doi.org/10.3847/1538-4357/abcc04>

Upcoming missions, including the James Webb Space Telescope, will soon characterize the atmospheres of terrestrial-type exoplanets in habitable zones around cool K- and M-type stars by searching for atmospheric biosignatures. Recent observations suggest that the ionizing radiation and particle environment from active cool planet hosts may be detrimental to exoplanetary habitability. Since no direct information on the radiation field is available, empirical relations between signatures of stellar activity, including the sizes and magnetic fields of starspots, are often used. Here, we revisit the empirical relation between the starspot size and the effective stellar temperature and evaluate its impact on estimates of stellar flare energies, coronal mass ejections, and fluxes of the associated stellar energetic particle events.

## Pre-eruption processes: heating, particle acceleration and the formation of a hot channel before the 2012 October 20 M9.0 limb flare

Aaron [Hernandez-Perez](#), [Yang Su](#), [Astrid M. Veronig](#), [Julia K. Thalmann](#), [Peter Gömöry](#), [Bhuwan Joshi](#)

ApJ 2019

<https://arxiv.org/pdf/1902.08436.pdf>

We report a detailed study of the pre-eruption activities that led to the occurrence of an M9.0 flare/CME event on **2012 October 20** in NOAA AR 11598. This includes the study of the preceding confined C2.4 flare that occurred on the same AR ~25 minutes earlier. We observed that the M9.0 flare occurred as a consequence of two distinct triggering events well separated in time. The first triggering episode occurred as early as ~20 minutes before the onset of the M9.0 flare, evidenced by the destabilization and rise of a pre-existing filament to a new position of equilibrium at a higher coronal altitude during the decay phase of the C2.4 flare. This brought the system to a magnetic configuration where the establishment of the second triggering event was favorable. The second triggering episode occurred ~17 minutes later, during the early phase of the M9.0 flare, evidenced by the further rise of the filament and successful ejection. The second trigger is followed by a flare precursor phase, characterized by non-thermal emission and the sequential formation of a hot channel as shown by the SDO/AIA DEM (differential emission measure) maps, the RHESSI X-ray images and spectra. These observations are suggestive of magnetic reconnection and particle acceleration that can explain the precursor phase and can be directly related to the formation of the hot channel. We discuss on the triggering mechanisms, their implications during the early and precursor phases and highlight the importance of early activities and preceding small confined flares to understand the initiation of large eruptive flares.

## SoloHI observations of coronal mass ejections observed by multiple spacecraft★

P. [Hess](#)<sup>1</sup>, R. C. Colaninno<sup>1</sup>, A. Vourlidis<sup>2</sup>, R. A. Howard<sup>2</sup> and G. Stenborg<sup>2</sup>

A&A 679, A149 (2023)

<https://www.aanda.org/articles/aa/pdf/2023/11/aa46907-23.pdf>

Context. The Solar Orbiter Heliospheric Imager (SoloHI) instrument of the Solar Orbiter mission is a next-generation heliospheric imager. New observations from SoloHI demonstrate the improved spatial and temporal resolution compared to previous observations of the heliosphere and corona. At perihelion, the field of view (FoV) of SoloHI covers the transition between the coronagraph (COR2) and heliospheric imager (HI1) Sun-Earth Connection Coronal and Heliospheric Investigation (SECCHI) suite. In this paper, we focus on an active solar period following the first Solar Orbiter science perihelion that resulted in a number of well-observed large coronal mass ejections (CMEs) in SoloHI data in **March and April 2022**. Specifically, we highlight a series of events produced by AR12795 between **28 March and 2 April** and show overlapping observations with SECCHI/COR2 and HI1 and LASCO/C3.

Aims. We compare the performance of the SoloHI instrument against similar observations from 1 au imagers. We describe CME observations, highlighting the unique structural features captured within the SoloHI FoV. These observations demonstrate that SoloHI will provide new insights into CME morphology and evolution from a unique vantage point.

Methods. To provide a direct and relevant comparison, images from all the telescopes we used in the paper are presented in FoVs common to each and with minimal processing applied. The J-maps we used to highlight outflowing features are also presented to show that the CME kinematics can be tracked through the SoloHI FoV, and also to report how the rest of the Heliophysics Systems Observatory (HSO) can be used to support the SoloHI data.

Results. The high-resolution SoloHI images of these eruptions, taken from ~0.3 au, reveal a number of detailed structural CME features, including internal cavities or cores of the CME flux rope(s). They also show the surrounding material and associated sheath region of the compressed upstream solar wind plasma. Many features that could not have been observed by other instruments are highlighted and discussed.

Conclusions. The SoloHI instrument is performing well and has already provided detailed observations of CMEs that can help us understand the details of the internal structure and magnetic field of CMEs. These new observations in combination with synoptic observations from 1 au offer new opportunities for CME propagation from the corona to the heliosphere.

## HIGH-RESOLUTION IMAGING OF CORONAL MASS EJECTIONS FROM SOLOHI

Phil Hess<sup>1</sup>, R.C. Colaninno<sup>1</sup>, A. Vourlidis<sup>2</sup>, R.A. Howard<sup>2</sup>, G. Stenborg<sup>2</sup> and the Solo/Hi team)  
Solar Orbiter nugget #8 2023

<https://www.cosmos.esa.int/web/solar-orbiter/solar-nuggets/high-resolution-imaging-from-solohi>

2 Apr 2022

## WISPR Imaging of a Pristine CME

Phillip Hess, Alexis Rouillard, Athanasios Kouloumvakos, Paulett C. Liewer, Jie Zhang, Suman Dhakal, Guillermo Stenborg, Robin C. Colaninno, Russell A. Howard

ApJ 2019

<https://arxiv.org/pdf/1912.02255.pdf>

The Wide-field Imager for Solar Probe (WISPR) on board the Parker Solar Probe (PSP) observed a CME on **2018 November 01**, the first day of the initial PSP encounter. The speed of the CME, approximately 200-300 km s<sup>-1</sup> in the WISPR field of view, is typical of slow, streamer blowout CMEs. This event was also observed by the LASCO coronagraphs. WISPR and LASCO view remarkably similar structures that enable useful cross-comparison between the two data sets as well as stereoscopic imaging of the CME. Analysis is extended to lower heights by linking the white-light observations to EUV data from AIA, which reveal a structure that erupts more than a full day earlier before the CME finally gathers enough velocity to propagate outward. This EUV feature appears as a brightness enhancement in cooler temperatures such as 171 Å, but as a cavity in nominal coronal temperatures such as 193 Å. By comparing this circular, dark feature in 193 Å to the dark, white-light cavity at the center of the eruption in WISPR and LASCO, it can be seen that this is one coherent structure that exists prior to the eruption in the low corona before entering the heliosphere and likely corresponds to the core of the magnetic flux rope. It is also believed that the relative weakness of the event contributed to the clarity of the flux rope in WISPR, as the CME did not experience impulsive forces or strong interaction with external structures that can lead to more complex structural evolution.

## Inflows in the Inner White-light Corona: The Closing-down of Flux after Coronal Mass Ejections

P. Hess and Y.-M. Wang

2017 ApJ 850 6

<http://sci-hub.cc/10.3847/1538-4357/aa921d>

During times of high solar activity, the Solar and Heliospheric Observatory/Large Angle and Spectrometric Coronagraph C2 coronagraph has recorded multitudes of small features moving inward through its 2–6 R<sub>☉</sub> field of view. These outer-coronal inflows, which are concentrated around the heliospheric current sheet, tend to be poorly correlated with individual coronal mass ejection (CME) events. Using running-difference movies constructed from Solar Terrestrial Relations Observatory/COR1 coronagraph images taken during 2008–2014, we have identified large numbers of inward-moving features at heliocentric distances below 2 R<sub>☉</sub>, with the rate increasing with sunspot and CME activity. Most of these inner-coronal inflows are closely associated with CMEs, being observed during and in the days immediately following the eruptions. Here, we describe several examples of the pinching-off of tapered streamer structures in the wake of CMEs. This type of inflow event is characterized by a separation of the flow into incoming and outgoing components connected by a thin spike, which is interpreted as a continually elongating current sheet viewed edge-on; by the prior convergence of narrow rays toward the current sheet; and by a succession of collapsing loops that form a cusp-shaped structure at the base of the current sheet. The re-forming streamer overlies a growing post-eruption arcade that is visible in EUV images. These observations provide support for standard reconnection models for the formation/evolution of flux ropes during solar eruptive events. We suggest that inflow streams that occur over a relatively wide range of position angles result from the pinching-off of loop arcades whose axes are oriented parallel rather than perpendicular to the sky plane. **28 Feb 2010, 2011 March 1–2, 2011 Apr 7–10, 2012 June 2, 2013 February 14–15, 2013 May 23–24, 2013 July 1–2**

## A Study of the Earth-Affecting CMEs of Solar Cycle 24

Phillip Hess, Jie Zhang

[Solar Physics](#) June 2017, 292:80 **File**

Using in situ observations from the Advanced Composition Explorer (ACE), we have identified 70 Earth-affecting interplanetary coronal mass ejections (ICMEs) in Solar Cycle 24. Because of the unprecedented extent of heliospheric observations in Cycle 24 that has been achieved thanks to the Sun Earth Connection Coronal and Heliospheric Investigation (SECCHI) instruments onboard the Solar Terrestrial Relations Observatory (STEREO), we observe these events throughout the heliosphere from the Sun to the Earth, and we can relate these in situ signatures to remote sensing data. This allows us to completely track the event back to the source of the eruption in the low corona. We present a summary of the Earth-affecting CMEs in Solar Cycle 24 and a statistical study of the properties of these events including the source region. We examine the characteristics of CMEs that are more likely to be strongly geoeffective and examine the effect of the flare strength on in situ properties. We find that Earth-affecting CMEs in the first half of Cycle 24 are more likely to come from the northern hemisphere, but after April 2012, this reverses, and these events are more likely to originate in the southern hemisphere, following the observed magnetic asymmetry in the two

hemispheres. We also find that as in past solar cycles, CMEs from the western hemisphere are more likely to reach Earth. We find that Cycle 24 lacks in events driving extreme geomagnetic storms compared to past solar cycles. **Table 1** The catalog of Earth-affecting ICME events from 2007 to 2015.

## Comparing Automatic CME Detections in Multiple LASCO and SECCHI Catalogs

Phillip [Hess](#)<sup>1</sup> and Robin C. Colaninno

2017 ApJ 836 134

<http://iopscience.iop.org/sci-hub.cc/0004-637X/836/1/134/>

With the creation of numerous automatic detection algorithms, a number of different catalogs of coronal mass ejections (CMEs) spanning the entirety of the Solar and Heliospheric Observatory (SOHO) Large Angle Spectrometric Coronagraph (LASCO) mission have been created. Some of these catalogs have been further expanded for use on data from the Solar Terrestrial Earth Observatory (STEREO) Sun Earth Connection Coronal and Heliospheric Investigation (SECCHI) as well. We compare the results from different automatic detection catalogs (Solar Eruption Event Detection System (SEEDS), Computer Aided CME Tracking (CACTus), and Coronal Image Processing (CORIMP)) to ensure the consistency of detections in each. Over the entire span of the LASCO catalogs, the automatic catalogs are well correlated with one another, to a level greater than 0.88. Focusing on just periods of higher activity, these correlations remain above 0.7. We establish the difficulty in comparing detections over the course of LASCO observations due to the change in the instrument image cadence in 2010. Without adjusting catalogs for the cadence, CME detection rates show a large spike in cycle 24, despite a notable drop in other indices of solar activity. The output from SEEDS, using a consistent image cadence, shows that the CME rate has not significantly changed relative to sunspot number in cycle 24. These data, and mass calculations from CORIMP, lead us to conclude that any apparent increase in CME rate is a result of the change in cadence. We study detection characteristics of CMEs, discussing potential physical changes in events between cycles 23 and 24. We establish that, for detected CMEs, physical parameters can also be sensitive to the cadence.

## The 17 January 2005 Complex Solar Radio Event Associated with Interacting Fast Coronal Mass Ejections

A. [Hillar](#), O. Malandraki, K.-L. Klein, P. Preka-Papadema, X. Moussas, C. Bouratzis, E. Mitsakou, P. Tsitsipis and A. Kontogeorgos

Solar Physics, Volume 273, Number 2, 493-509, 2011

<http://arxiv.org/pdf/1101.5759v7.pdf>

On 17 January 2005 two fast coronal mass ejections were recorded in close succession during two distinct episodes of a 3B/X3.8 flare. Both were accompanied by metre-to-kilometre type-III groups tracing energetic electrons that escape into the interplanetary space and by decametre-to-hectometre type-II bursts attributed to CME-driven shock waves. A peculiar type-III burst group was observed below 600 kHz 1.5 hours after the second type-III group. It occurred without any simultaneous activity at higher frequencies, around the time when the two CMEs were expected to interact. We associate this emission with the interaction of the CMEs at heliocentric distances of about 25 R<sub>☉</sub>. <sup>Relative</sup> Relativistic electrons observed by the EPAM experiment onboard ACE near 1 AU revealed successive particle releases that can be associated with the two flare/CME events and the low-frequency type-III burst at the time of CME interaction. We compare the pros and cons of shock acceleration and acceleration in the course of magnetic reconnection for the escaping electron beams revealed by the type-III bursts and for the electrons measured in situ.

## Solar flares with and without SOHO/LASCO coronal mass ejections and type II shocks

[Hillar](#), A.; Petousis, V.; Mitsakou, E.; Vassiliou, C.; Moussas, X.; Polygiannakis, J.; Preka-Papadema, P.; Caroubalos, C.; Alissandrakis, C.; Tsitsipis, P.; Kontogeorgos, A.; Bougeret, J.-L.; Dumas, G.

Advances in Space Research, Volume 38, Issue 5, p. 1007-1010, 2006.

<http://arxiv.org/pdf/1009.3636v1.pdf>

We analyse of a set of radio rich (accompanied by type IV or II bursts) solar flares and their association with SOHO/LASCO Coronal Mass Ejections in the period 1998-2000. The intensity, impulsiveness and energetics of these events are investigated. We find that, on the average, flares associated both with type II's and CMEs are more impulsive and more energetic than flares associated with type II's only (without CME reported), as well as flares accompanied by type IV continua but not type II shocks. From the last two classes, flares with type II bursts (without CMEs reported) are the shortest in duration and the most impulsive.

## Observation of bi-directional jets in a prominence

[Hillier](#), A. ; [Polito](#), V.

Astronomy & Astrophysics, Volume 651, id.A60, 10 pp. 2021

<https://www.aanda.org/articles/aa/pdf/2021/07/aa35774-19.pdf>

Quiescent prominences host a large range of flows, many driven by buoyancy, which lead to velocity shear. The presence of these shear flows could bend and stretch the magnetic field resulting in the formation of current sheets which can lead to magnetic reconnection. Though this has been hypothesised to occur in prominences, with some observations that are suggestive of this process, clear evidence has been lacking. In this paper we present observations performed on June 30, 2015 using the Interface Region Imaging Spectrograph Si IV and Mg II slit-jaw imagers of two

bi-directional jets that occur inside the body of the prominence. Such jets are highly consistent with what would be expected from magnetic reconnection theory. Using this observation, we estimate that the prominence under study has an ambient field strength in the range of 4.5–9.2 G with 'turbulent' field strengths of 1 G. Our results highlight the ability of gravity-driven flows to stretch and fold the magnetic field of the prominence, implying that locally, the quiescent prominence field can be far from a static, force-free magnetic field. Movies are available at <https://www.aanda.org> 30 June 2015  
IRIS nugget 14 Jun 2022 <https://iris.lmsal.com/nugget>

## On Kelvin-Helmholtz and parametric instabilities driven by coronal waves

Andrew Hillier, Adrian Barker, Inigo Arregui, Henrik Latter

MNRAS 2018

<https://arxiv.org/pdf/1810.02773.pdf>

The Kelvin-Helmholtz instability has been proposed as a mechanism to extract energy from magnetohydrodynamic (MHD) kink waves in flux tubes, and to drive dissipation of this wave energy through turbulence. It is therefore a potentially important process in heating the solar corona. However, it is unclear how the instability is influenced by the oscillatory shear flow associated with an MHD wave. We investigate the linear stability of a discontinuous oscillatory shear flow in the presence of a horizontal magnetic field within a Cartesian framework that captures the essential features of MHD oscillations in flux tubes. We derive a Mathieu equation for the Lagrangian displacement of the interface and analyse its properties, identifying two different instabilities: a Kelvin-Helmholtz instability and a parametric instability involving resonance between the oscillatory shear flow and two surface Alfvén waves. The latter occurs when the system is Kelvin-Helmholtz stable, thus favouring modes that vary along the flux tube, and as a consequence provides an important and additional mechanism to extract energy. When applied to flows with the characteristic properties of kink waves in the solar corona, both instabilities can grow, with the parametric instability capable of generating smaller scale disturbances along the magnetic field than possible via the Kelvin-Helmholtz instability. The characteristic time-scale for these instabilities is  $\sim 100$  s, for wavelengths of 200 km. The parametric instability is more likely to occur for smaller density contrasts and larger velocity shears, making its development more likely on coronal loops than on prominence threads.

## Analysis of signal to noise ratio in coronagraph observations of coronal mass ejections

Johannes Hinrichs, Jackie A. Davies, Matthew J. West, Volker Bothmer, Bram Bourgoignie, Chris J. Eyles, Philipp Huke, Piers Jiggins, Bogdan Nicula and James Tappin

J. Space Weather Space Clim. 2021, 11, 11

<https://doi.org/10.1051/swsc/2020070>

<https://www.swsc-journal.org/articles/swsc/pdf/2021/01/swsc200025.pdf>

We establish a baseline signal-to-noise ratio (SNR) requirement for the European Space Agency (ESA)-funded Solar Coronagraph for OPERations (SCOPE) instrument in its field of view of 2.5–30 solar radii based on existing observations by the Solar and Heliospheric Observatory (SOHO). Using automatic detection of coronal mass ejections (CMEs), we analyse the impacts when SNR deviates significantly from our previously established baseline. For our analysis, SNR values are estimated from observations made by the C3 coronagraph on the Solar and Heliospheric Observatory (SOHO) spacecraft for a number of different CMEs. Additionally, we generate a series of artificial coronagraph images, each consisting of a modelled coronal background and a CME, the latter simulated using the graduated cylindrical shell (GCS) model together with the SCRaytrace code available in the Interactive Data Language (IDL) SolarSoft library. Images are created with CME SNR levels between 0.5 and 10 at the outer edge of the field of view (FOV), generated by adding Poisson noise, and velocities between 700 km s<sup>-1</sup> and 2800 km s<sup>-1</sup>. The images are analysed for the detectability of the CME above the noise with the automatic CME detection tool CACTus. We find in the analysed C3 images that CMEs near the outer edge of the field of view are typically 2% of the total brightness and have an SNR between 1 and 4 at their leading edge. An SNR of 4 is defined as the baseline SNR for SCOPE. The automated detection of CMEs in our simulated images by CACTus succeeded well down to SNR = 1 and for CME velocities up to 1400 km s<sup>-1</sup>. At lower SNR and higher velocity of  $\geq 2100$  km s<sup>-1</sup> the detection started to break down. For SCOPE, the results from the two approaches confirm that the initial design goal of SNR = 4 would, if achieved, deliver a comparable performance to established data used in operations today, with a more compact instrument design, and a margin in SNR before existing automatic detection produces significant false positives. 2012-Jan-21, 25-27 Jan 2012, 2012-Jul-23

## Scientific considerations for future spectroscopic measurements from space of activity on the Sun

Review

Gordon D. Holman

JGR 2016

<http://sci-hub.cc/10.1002/2016JA022651>

High-resolution UV and X-ray spectroscopy are important to understanding the origin and evolution of magnetic energy release in the solar atmosphere, as well as the subsequent evolution of heated plasma and accelerated particles. Electromagnetic radiation is observed from plasma heated to temperatures ranging from about 10 kK to above 10 MK, from accelerated electrons emitting photons primarily at X-ray energies, and from ions emitting in  $\gamma$  rays. These observations require space-based instruments sensitive to emissions at wavelengths shorter than the near UV. This article reviews some recent observations with emphasis on solar eruptive events, the models that describe them, and the



measurements they indicate are needed for substantial progress in the future. Specific examples are discussed demonstrating that imaging spectroscopy with a cadence of seconds or better is needed to follow, understand, and predict the evolution of solar activity. Critical to substantial progress is the combination of a judicious choice of UV, EUV, and soft X-ray imaging spectroscopy sensitive to the evolution of this thermal plasma combined with hard X-ray imaging spectroscopy sensitive to suprathermal electrons. The major challenge will be to conceive instruments that, within the bounds of possible technologies and funding, have the flexibility and field of view to obtain spectroscopic observations where and when events occur while providing an optimum balance of dynamic range, spectral resolution and range, and spatial resolution.

## **Direct Spatial Association of an X-Ray Flare with the Eruption of a Solar Quiescent Filament**

Gordon D. **Holman** & Adi Foord

ApJ 804 108 **2015**

[http://hesperia.gsfc.nasa.gov/~kim/Holman\\_Foord\\_2015\\_quiescent\\_filament\\_flare.pdf](http://hesperia.gsfc.nasa.gov/~kim/Holman_Foord_2015_quiescent_filament_flare.pdf)

Solar flares primarily occur in active regions. Hard X-ray flares have been found to occur only in active regions. They are often associated with the eruption of active region filaments and coronal mass ejections (CMEs). CMEs can also be associated with the eruption of quiescent filaments, not located in active regions. Here we report the first identification of a solar X-ray flare outside an active region observed by the Ramaty High Energy Solar Spectroscopic Imager (RHESSI). The X-ray emission was directly associated with the eruption of a long, quiescent filament and fast CME. Images from RHESSI show this flare emission to be located along a section of the western ribbon of the expanding, post-eruption arcade. EUV images from the Solar Dynamics Observatory (SDO) Atmospheric Imaging Assembly (AIA) show no connection between this location and nearby active regions. Therefore the flare emission is found to not be located in or associated with an active region. However, a nearby, small, magnetically strong dipolar region provides a likely explanation for the existence and location of the flare X-ray emission. This emerging dipolar region may have also triggered the filament eruption. **September 29, 2013**

## **RHESSI Detection of X-ray Emission from a Quiet-Sun Filament Eruption**

Gordon **Holman** and Adi Foord

RHESSI Science Nugget No. 250, April **2015**

[http://sprg.ssl.berkeley.edu/~tohban/wiki/index.php/RHESSI\\_Science\\_Nuggets](http://sprg.ssl.berkeley.edu/~tohban/wiki/index.php/RHESSI_Science_Nuggets)

The event described in this Nugget reveals the presence of intense energy release even in the quiet Sun, in the form of an otherwise innocuous-looking quiescent filament. The power of the the CME that resulted, and its interplanetary development, do not have the same kind of associations with a solar flare as in an active-region event. Nevertheless high temperatures and non-thermal effects result, and hard X-ray observations such as those of RHESSI (or more sensitive ones) can diagnose them. **September 29, 2013**

## **Solar eruptive events**

**Review**

Gordon D. **Holman**

Physics Today 65, 4, 56 (**2012**);

<https://sci-hub.tw/10.1063/PT.3.1520>

It's long been known that the Sun plays host to the most energetic explosions in the solar system. But key insights into how they work have only recently become available

## **CME volume calculation from 3D GCS reconstruction**

L. **Holzkecht**, **M. Temmer**, **M. Dumbovic**, **S. Wellenzohn**, **K. Krikova**, **S.G.Heinemann**, **M. Rodari**, **B. Vrsnak**, **A.M. Veronig**

Central European Astrophysical Bulletin (CEAB)

**2019**

<https://arxiv.org/pdf/1904.11418.pdf>

The mass evolution of a coronal mass ejection (CME) is an important parameter characterizing the drag force acting on a CME as it propagates through interplanetary space. Spacecraft measure in-situ plasma densities of CMEs during crossing events, but for investigating the mass evolution, we also need to know the CME geometry, more specific, its volume. Having derived the CME volume and mass from remote sensing data using 3D reconstructed CME geometry, we can calculate the CME density and compare it with in-situ proton density measurements near Earth. From that we may draw important conclusions on a possible mass increase as the CME interacts with the ambient solar wind in the heliosphere. In this paper we will describe in detail the method for deriving the CME volume using the graduated cylindrical shell (GCS) model (Thernisien et al., 2006,2009, see Figure 1). We show that, assuming self-similar expansion, one can derive the volume of the CME from two GCS parameters and that it furthermore can be expressed as a function of distance.

## **Magnetic Evolution of Mini-Coronal Mass Ejections**

L. **Honarbaksh**, N. Alipour, H. Safari

Solar Phys. Volume 291, **Issue 3**, pp 941-952 **2016**

The present study investigates the relationship between mini-coronal mass ejections (mini-CMEs) and the evolution of their magnetic fluxes. An automatic detection algorithm was used to detect mini-dimmings in 171 Å images taken with the Atmospheric Imaging Assembly (AIA) onboard the Solar Dynamics Observatory (SDO). Using the difference

images for the dimmings, 131 events that satisfied mini-CME signatures were selected. Changes in their magnetic structure using photospheric line-of-sight magnetograms taken with the Heliospheric and Magnetic Imager (HMI) on SDO were investigated. It was found that 27 % of the events had slight changes and 73 % showed considerable changes in magnetic flux. About 18 % of the magnetic structures evolved by cancellation and 38 % by complex flux changes.

### **Quasi-periodic microjets driven by granular advection as observed with high-resolution imaging at He I 10830 Å**

[Zhenxiang Hong](#), [Ya Wang](#), [Haisheng Ji](#)

ApJ *ApJ* **928** 2022

<https://arxiv.org/pdf/2201.12837.pdf>

<https://iopscience.iop.org/article/10.3847/1538-4357/ac590c/pdf>

With high-resolution narrowband He I 10830 Å filtergrams from GST, we give an extensive analysis for 4 granular sized microeruptions which appear as the gentle ejection of material in He I 10830 Å band. The analysis was aided with the EUV data from AIA and line-of-sight magnetograms from HMI on board SDO. The microeruptions are situated on magnetic polarity inversion lines (PILs), and their roots are accurately traced down to intergranular lanes. Their durations are different, two microeruptions are repetitive microjets, lasting ~ 50 and 27 minutes respectively, while the other two events are singular, lasting ~ 5 minutes. For the two microjets, they are continuous and recurrent in He I 10830 Å band, and the recurrence is quasi-periodic with the period of ~ 5 minutes. We found that only transient co-spatial EUV brightenings are observed for the longer duration microjets and EUV brightenings are absent for the two singular microeruptions. What is essential to the longer duration microjets is that granules with the concentration of positive magnetic field persistently transport the magnetic field to the PILs, canceling the opposite magnetic flux and making the base of the two microjets and the underlying granules migrate with the speed of ~ 0.25 and 1.0 km/s. The observations support the scenario of magnetic reconnection for the quasi-periodic microjets and further show that the reconnection continuously generates multi-temperature components, especially the cool component with chromospheric temperature. In addition, the ongoing reconnection is modulated by p-mode oscillations inside the Sun. **July 22, 2011**

### **Observation of a reversal of breakout reconnection preceding a jet: evidence of oscillatory magnetic reconnection?**

Junchao [Hong](#), [Jiayan Yang](#), [Huadong Chen](#), [Yi Bi](#), [Bo Yang](#), [Hechao Chen](#)

ApJ **874** 146 2019

<https://arxiv.org/pdf/1903.01201.pdf>

[sci-hub.se/10.3847/1538-4357/ab0c9d](https://sci-hub.se/10.3847/1538-4357/ab0c9d)

Recent studies have revealed that solar jets involving minifilament eruptions may be initiated under the well-known magnetic-breakout mechanism. Before or just at the onset of those jets, there should be a current sheet, where breakout magnetic reconnection takes place, between open fields and the outside of the jet-base arcade carrying minifilament in its core. In this paper we present a jet produced by eruption of two minifilaments lying at the jet base. A current sheet is directly detected near the jet base before the onset of the eruption, suggesting the magnetic-breakout mechanism. However, we further find that the current sheet undergoes a transition. The current sheet first shortens to zero in length, but then lengthens towards an orthogonal direction relative to its initial orientation. The change of the current sheet gives rise to a reversal of the breakout reconnection, as the inflow and outflow regions before the transition become the outflow and inflow regions after the transition, respectively. We therefore propose that this observation provides evidence for the so-called oscillatory reconnection which is defined by a series of reconnection reversals but not yet proved to exist in real plasma environment of the solar atmosphere. **2014 November 16**

### **MINIFILAMENT ERUPTION AS THE SOURCE OF A BLOWOUT JET, C-CLASS FLARE, AND TYPE-III RADIO BURST**

Junchao [Hong](#), Yunchun Jiang, Jiayan Yang, Haidong Li1, and Zhe Xu1

2017 ApJ 835 35

<http://sci-hub.cc/doi/10.3847/1538-4357/835/1/35>

We report a strong minifilament eruption associated with Geostationary Operational Environmental Satellite C1.6 flare and WIND type-III radio burst. The minifilament, which lies at the periphery of active region 12259, is detected by Ha images from the New Vacuum Solar Telescope. The minifilament undergoes a partial and then a full eruption. Simultaneously, two co-spatial jets are successively observed in extreme ultraviolet images from the Solar Dynamic Observatory. The first jet exhibits a typical fan-spine geometry, suggesting that the co-spatial minifilament is possibly embedded in magnetic fields with a fan-spine structure. However, the second jet displays blowout morphology when the entire minifilament erupts upward, leaving behind a hard X-ray emission source in the base. Differential emission measure analyses show that the eruptive region is heated up to about 4 MK during the fan-spine jet, while up to about 7 MK during the blowout jet. In particular, the blowout jet is accompanied by an interplanetary type-III radio burst observed by WIND/WAVES in the frequency range from above 10 to 0.1 MHz. Hence, the minifilament eruption is correlated with the interplanetary type-III radio burst for the first time. These results not only suggest that coronal jets can result from magnetic reconnection initiated by erupting minifilaments with open fields, but also shed light on the potential influence of minifilament eruption on interplanetary space. **2015 January 14,**

## **MINI-FILAMENT ERUPTION AS THE INITIATION OF A JET ALONG CORONAL LOOPS**

Junchao [Hong](#), Yunchun Jiang, Jiayan Yang, Bo Yang<sup>1</sup>, Zhe Xu<sup>1</sup>, and Yongyuan Xiang

2016 ApJ 830 60

Minifilament eruptions (MFEs) and coronal jets are different types of solar small-scale explosive events. We report an MFE observed at the New Vacuum Solar Telescope (NVST). As seen in the NVST H $\alpha$  images, during the rising phase, the minifilament erupts outward orthogonally to its length, accompanied with a flare-like brightening at the bottom. Afterward, dark materials are found to possibly extend along the axis of the expanded filament body. The MFE is analogous to large filament eruptions. However, a simultaneous observation of the Solar Dynamics Observatory shows that a jet is initiated and flows out along nearby coronal loops during the rising phase of the MFE. Meanwhile, small hot loops, which connect the original eruptive site of the minifilament to the footpoints of the coronal loops, are formed successively. A differential emission measure analysis demonstrates that, on the top of the new small loops, a hot cusp structure exists. We conjecture that the magnetic fields of the MFE interact with magnetic fields of the coronal loops. This interaction is interpreted as magnetic reconnection that produces the jet and the small hot loops.

## **Coronal Bright Points Associated with Minifilament Eruptions**

Junchao [Hong](#), Yunchun Jiang, Jiayan Yang, Yi Bi, Haidong Li, Bo Yang<sup>1</sup>, and Dan Yang

2014 ApJ 796 73

Coronal bright points (CBPs) are small-scale, long-lived coronal brightenings that always correspond to photospheric network magnetic features of opposite polarity. In this paper, we subjectively adopt 30 CBPs in a coronal hole to study their eruptive behavior using data from the Atmospheric Imaging Assembly (AIA) and the Helioseismic and Magnetic Imager (HMI) on board the Solar Dynamics Observatory. About one-quarter to one-third of the CBPs in the coronal hole go through one or more minifilament eruption(s) (MFE(s)) throughout their lifetimes. The MFEs occur in temporal association with the brightness maxima of CBPs and possibly result from the convergence and cancellation of underlying magnetic dipoles. Two examples of CBPs with MFEs are analyzed in detail, where minifilaments appear as dark features of a cool channel that divide the CBPs along the neutral lines of the dipoles beneath. The MFEs show the typical rising movements of filaments and mass ejections with brightenings at CBPs, similar to large-scale filament eruptions. Via differential emission measure analysis, it is found that CBPs are heated dramatically by their MFEs and the ejected plasmas in the MFEs have average temperatures close to the pre-eruption BP plasmas and electron densities typically near 10<sup>9</sup> cm<sup>-3</sup>. These new observational results indicate that CBPs are more complex in dynamical evolution and magnetic structure than previously thought.

## **A MICRO CORONAL MASS EJECTION ASSOCIATED BLOWOUT EXTREME-ULTRAVIOLET JET**

Junchao [Hong](#), Yunchun Jiang, Ruisheng Zheng, Jiayan Yang, Yi Bi and Bo Yang

2011 ApJ 738 L20, [File?](#)

The so-called mini coronal mass ejections (CMEs) were recently identified as small-scale eruptive events showing the same on-disk characteristics as large-scale CMEs, and Moore et al. further found that one-third of polar X-ray jets are the so-called blowout jets, in which the jet-base magnetic arch, often carrying a filament, undergoes a miniature version of the blowout eruptions that produce major CMEs. By means of the two viewpoint observations from the Solar Dynamics Observatory (SDO) and the Ahead of Solar Terrestrial Relations Observatory (STEREO A), in this Letter, we present the first observations that a blowout jet from the eruption of an EUV mini-filament channel in the quiet Sun was indeed associated with a real micro-CME. Captured by the on-disk SDO observations, the whole life of the mini-filament channel, from the formation to eruption, was associated with convergences and cancellations of opposite-polarity magnetic flux in the photosphere, and its eruption was accompanied by a small flare-like brightening, a small corona dimming, and posteruptive loops. The near-limb counterpart of the eruption observed by STEREO A, however, showed up as a small EUV jet followed by a white-light jet. These observations not only confirm the previous results that mini-filaments have characteristics common to large-scale ones, but also give clear evidences that blowout jets can result from the eruptions of mini-filaments and are associated with mini-CME.

## **Short, large-amplitude speed enhancements in the near-Sunfast solar wind**

[T S Horbury](#) [L Matteini](#) [D Stansby](#)

MNRoyal Astronomical Society, Volume 478, Issue 2, 1 August 2018, Pages 1980–1986

<https://doi.org/10.1093/mnras/sty953>

[sci-hub.tw/10.1093/mnras/sty953](http://sci-hub.tw/10.1093/mnras/sty953)

We report the presence of intermittent, short discrete enhancements in plasma speed in the near-Sun high-speed solar wind. Lasting tens of seconds to minutes in spacecraft measurements at 0.3 au, speeds inside these enhancements can reach 1000 km s<sup>-1</sup>, corresponding to a kinetic energy up to twice that of the bulk high-speed solar wind. These events, which occur around 5 per cent of the time, are Alfvénic in nature with large magnetic field deflections and are the same temperature as the surrounding plasma, in contrast to the bulk fast wind which has a well-established positive speed–temperature correlation. The origin of these speed enhancements is unclear but they may be signatures of discrete jets associated with transient events in the chromosphere or corona. Such large short velocity changes represent a measurement and analysis challenge for the upcoming Parker Solar Probe and Solar Orbiter missions.

UKSP Nuggets #94 September 2018 [www.uksolphys.org/?p=14829](http://www.uksolphys.org/?p=14829)

## **Generation of twist on magnetic flux tubes at the base of the solar convection zone**

H. [Hotta](#) and T. Yokoyama

A&A 548, A74 (2012)

Using two-dimensional magnetohydrodynamics calculations, we investigate a twist generation mechanism on a magnetic flux tube at the base of the solar convection zone based on the idea of Choudhuri (2003, Sol. Phys., 215, 31) in which a toroidal magnetic field is wrapped by a surrounding mean poloidal field. During generation of the twist, the flux tube follows four phases. (1) It quickly splits into two parts with vortex motions rolling up the poloidal magnetic field. (2) Owing to the physical mechanism similar to that of the magneto-rotational instability, the rolled-up poloidal field is bent and amplified. (3) The magnetic tension of the disturbed poloidal magnetic field reduces the vorticity, and the lifting force caused by vortical motion decreases. (4) The flux tube gets twisted and begins to rise again without splitting. Investigation of these processes is significant because it shows that a flux tube without any initial twist can rise to the surface in relatively weak poloidal fields.

## Numerous Bidirectionally Propagating Plasma Blobs near the Reconnection Site of a Solar Eruption

[Zhenyong Hou](#), [Hui Tian](#), [Maria S. Madjarska](#), [Hechao Chen](#), [Tanmoy Samanta](#), [Xianyong Bai](#), [Zhentong Li](#), [Yang Su](#), [Wei Chen](#), [Yuanyong Deng](#)

A&A 687, A190 2024

<https://arxiv.org/pdf/2404.18092>

<https://www.aanda.org/articles/aa/pdf/2024/07/aa49765-24.pdf>

Current sheet is a common structure involved in solar eruptions. However, it is observed in minority of the events and the physical properties of its fine structures during a solar eruption are rarely investigated. Here, we report an on-disk observation that displays 108 compact, circular or elliptic bright structures, presumably plasma blobs, propagating bidirectionally along a flare current sheet during a period of  $\sim 24$  minutes. From extreme ultraviolet images, we have investigated the temporal variation of the blob number around the flare peak time. The current sheet connects the flare loops and the erupting filament. The width, duration, projected velocity, temperature, and density of these blobs are  $\sim 1.7 \pm 0.5$  Mm,  $\sim 79 \pm 57$  s,  $\sim 191 \pm 81$  km/s,  $\sim 106.4 \pm 0.1$  K, and  $\sim 1010.1 \pm 0.3$  cm $^{-3}$ , respectively. The reconnection site rises with a velocity of  $\leq 69$  km/s. The observational results suggest that plasmoid instability plays an important role in the energy release process of solar eruptions. **November 19, 2022**

## Partial Eruption of Solar Filaments. I. Configuration and Formation of Double-decker Filaments

[Yijun Hou](#), [Chuan Li](#), [Ting Li](#), [Jiangtao Su](#), [Ye Qiu](#), [Shuhong Yang](#), [Liheng Yang](#), + + +

ApJ 959 69 2023 as part of the Focus Issue "Early results from the Chinese Ha Solar Explorer (CHASE)"

<https://arxiv.org/pdf/2311.00456.pdf>

<https://iopscience.iop.org/article/10.3847/1538-4357/ad08bd/pdf>

Partial eruptions of solar filaments are the typical representative of solar eruptive behavior diversity. Here we investigate a typical filament partial eruption event and present integrated evidence for configuration of the pre-eruption filament and its formation. The CHASE H $\alpha$  observations reveal structured Doppler velocity distribution within the pre-eruption filament, where distinct redshift only appeared in the east narrow part of the south filament region and then disappeared after the partial eruption while the north part dominated by blueshift remained. Combining the SDO, ASO-S observations, and NLFFF modeling results, we verify that there were two independent material flow systems within the pre-flare filament, whose magnetic topology is a special double-decker configuration consisting of two magnetic flux ropes (MFRs) with opposite magnetic twist. During the formation of this filament system, continuous magnetic flux cancellation and footpoint motion were observed around its north end. Therefore, we propose a new double-decker formation scenario that the two MFRs composing such double-decker configuration originated from two magnetic systems with different initial connections and opposite magnetic twist. Subsequent magnetic reconnection with surrounding newly-emerging fields resulted in the motion of footpoint of the upper MFR to the region around footpoint of the lower MFR, thus leading to eventual formation of the double-decker configuration consisting of two MFRs with similar footpoints but opposite signs of magnetic twist. These results provide a potential way to determine unambiguously the progenitor configuration of a partial-eruptive filament and reveal a special type of double-decker MFR configuration and a new double-decker formation scenario. **2022 December 30**

## A Type II Radio Burst Driven by a Blowout Jet on the Sun

[Zhenyong Hou](#), [Hui Tian](#), [Wei Su](#), [Maria S. Madjarska](#), [Hechao Chen](#), [Ruisheng Zheng](#), [Xianyong Bai](#), [Yuanyong Deng](#)

ApJ 2023

<https://arxiv.org/pdf/2306.16725.pdf>

Type II radio bursts are often associated with coronal shocks that are typically driven by coronal mass ejections (CMEs) from the Sun. Here, we conduct a case study of a type II radio burst that is associated with a C4.5 class flare and a blowout jet, but without the presence of a CME. The blowout jet is observed near the solar disk center in the extreme-ultraviolet (EUV) passbands with different characteristic temperatures. Its evolution involves an initial phase and an ejection phase with a velocity of 560 km/s. Ahead of the jet front, an EUV wave propagates at a projected velocity of 403 km/s in the initial stage. The moving velocity of the source region of the type II radio burst is estimated to be 641

km/s, which corresponds to the shock velocity against the coronal density gradient. The EUV wave and the type II radio burst are closely related to the ejection of the blowout jet, suggesting that both are likely the manifestation of a coronal shock driven by the ejection of the blowout jet. The type II radio burst likely starts lower than those associated with CMEs. The combination of the velocities of the radio burst and the EUV wave yields a modified shock velocity at 757 km/s. The Alfvén Mach number is in the range of 1.09-1.18, implying that the shock velocity is 10%-20% larger than the local Alfvén velocity. **12 Nov 2022**

### **Coronal microjets in quiet-Sun regions observed with the Extreme Ultraviolet Imager onboard Solar Orbiter**

[Zhenyong Hou](#), [Hui Tian](#), [David Berghmans](#), [Hechao Chen](#), [Luca Teriaca](#), [Udo Schuhle](#), [Yuhang Gao](#), [Yajie Chen](#), [Jiansen He](#), [Linghua Wang](#), [Xianyong Bai](#)

ApJ **2021**

<https://arxiv.org/pdf/2108.08718.pdf>

We report the smallest coronal jets ever observed in the quiet Sun with recent high resolution observations from the High Resolution Telescopes (HRI-EUV and HRI-Ly $\{\alpha\}$ ) of the Extreme Ultraviolet Imager (EUI) onboard Solar Orbiter. In the HRI-EUV (174 Å) images, these microjets usually appear as nearly collimated structures with brightenings at their footpoints. Their average lifetime, projected speed, width, and maximum length are 4.6 min, 62 km s<sup>-1</sup>, 1.0 Mm, and 7.7 Mm, respectively. Inverted-Y shaped structures and moving blobs can be identified in some events. A subset of these events also reveal signatures in the HRI-Ly $\{\alpha\}$  (H I Ly $\{\alpha\}$  at 1216 Å) images and the extreme ultraviolet images taken by the Atmospheric Imaging Assembly onboard the Solar Dynamics Observatory. Our differential emission measure analysis suggests a multi-thermal nature and an average density of  $\sim 1.4 \times 10^9$  cm<sup>-3</sup> for these microjets. Their thermal and kinetic energies were estimated to be  $\sim 3.9 \times 10^{24}$  erg and  $\sim 2.9 \times 10^{23}$  erg, respectively, which are of the same order of the released energy predicted by the nanoflare theory. Most events appear to be located at the edges of network lanes and magnetic flux concentrations, suggesting that these coronal microjets are likely generated by magnetic reconnection between small-scale magnetic loops and the adjacent network field. **2020-05-20-21, 2020-05-30, 2020-10-19, 2020-10-22, 2020-11-19**

### **External reconnection and resultant reconfiguration of overlying magnetic fields during sympathetic eruptions of two filaments**

[Y. J. Hou](#), [T. Li](#), [Z. P. Song](#), [J. Zhang](#)

A&A **2020**

<https://arxiv.org/pdf/2006.06191.pdf>

Sympathetic eruptions of two solar filaments have been studied for several decades, but the detailed physical process through which one erupting filament triggers another is still under debate. Here we investigate a sympathetic event involving successive eruptions of two filaments on **2015 November 15-16**, which presented abundant sympathetic characteristics. The two filaments (F1 and F2) were separated by a narrow region of negative polarity, and F1 firstly erupted, producing a two-ribbon flare. When the outward-spreading ribbon produced by F1 approached stable F2, a weak brightening was observed to the south of F2 and then spread northward, inward approaching F2. Behind this inward-spreading brightening, a dimming region characterized by a plasma density reduction of 30% was extending. NLFFF extrapolations with a time sequence reveal that fields above pre-eruption F1 and F2 constituted a quadrupolar magnetic system with a possible null point. Moreover, the null point kept moving towards F2 and descending within the following hours. We infer that the rising F1 pushed its overlying fields towards the fields above stable F2 and caused successive external reconnection between the overlying fields. From outside to inside (lower and lower in height), the fields above pre-eruption F2 were gradually involved in the reconnection, manifesting as the inward-spreading brightening and extending dimming on the south side of F2. Furthermore, the external reconnection could reconfigure the overlying fields of F2 by transporting magnetic flux from its west part to the east part, which is further verified by the subsequent partial eruption of F2. We propose an integrated evidence chain to demonstrate the critical roles of external magnetic reconnection and the resultant reconfiguration of overlying fields on the sympathetic eruptions of two filaments.

### **Eruption of a multi-flux-rope system in solar active region 12673 leading to the two largest flares in Solar Cycle 24**

[Y. J. Hou](#), [J. Zhang](#), [T. Li](#), [S. H. Yang](#), [X. H. Li](#)

A&A 619, A100 **2018**

<https://arxiv.org/pdf/1808.06795.pdf>

Solar active region (AR) 12673 in 2017 September produced two largest flares in Solar Cycle 24: the X9.3 flare on **September 06** and the X8.2 flare on **September 10**. We attempt to investigate the evolutions of the two great flares and their associated complex magnetic system in detail. Aided by the NLFFF modeling, we identify a double-decker flux rope configuration above the polarity inversion line (PIL) in the AR core region. The north ends of these two flux ropes were rooted in a negative-polarity magnetic patch, which began to move along the PIL and rotate anticlockwise before the X9.3 flare on September 06. The strong shearing motion and rotation contributed to the destabilization of the two magnetic flux ropes, of which the upper one subsequently erupted upward due to the kink-instability. Then another two sets of twisted loop bundles beside these ropes were disturbed and successively erupted within 5 minutes like a chain reaction. Similarly, multiple ejecta components were detected to consecutively erupt during the X8.2 flare occurring in

the same AR on September 10. We examine the evolution of the AR magnetic fields from **September 03 to 06** and find that five dipoles emerged successively at the east of the main sunspot. The interactions between these dipoles took place continuously, accompanied by magnetic flux cancellations and strong shearing motions. In AR 12673, significant flux emergence and successive interactions between the different emerging dipoles resulted in a complex magnetic system, accompanied by the formations of multiple flux ropes and twisted loop bundles. We propose that the eruptions of a multi-flux-rope system resulted in the two largest flares in Solar Cycle 24.

### **Flux rope proxies and fan-spine structures in active region NOAA 11897**

Y. J. **Hou**, T. Li, J. Zhang

A&A 592, A138 **2016**

<http://arxiv.org/pdf/1606.09322v1.pdf>

Employing the high-resolution observations from the Solar Dynamics Observatory (SDO) and the Interface Region Imaging Spectrograph (IRIS), we statistically investigate flux rope proxies in NOAA AR 11897 from **14-Nov-2013 to 19-Nov-2013** and display two fan-spine structures in this AR. For the first time, we detect flux rope proxies of NOAA 11897 for total 30 times in 4 different locations. These flux rope proxies were either tracked in both lower and higher temperature wavelengths or only detected in hot channels. Specially, none of these flux rope proxies was observed to erupt, but just faded away gradually. In addition to these flux rope proxies, we firstly detect a secondary fan-spine structure. It was covered by dome-shaped magnetic fields which belong to a larger fan-spine topology. These new observations imply that considerable amounts of flux ropes can exist in an AR and the complexity of AR magnetic configuration is far beyond our imagination.

### **Partially Erupted Prominence Material as a Diagnostic of Coronal Mass Ejection Trajectory**

**B. A. Hovis-Afflerbach**, **B. J. Thompson**, **E. I. Mason**

Space Weather **Volume 21, Issue 8** August **2023** e2022SW003256

<https://agupubs.onlinelibrary.wiley.com/doi/epdf/10.1029/2022SW003256>

Coronal mass ejections (CMEs) are energetic releases of large-scale magnetic structures from the Sun. CMEs can have impacts on spacecraft and at Earth. This trajectory is typically assumed to be radial, but often the CME moves outward with some spatial offset from the source region where the eruption initially occurred. A CME is frequently accompanied by a prominence eruption, a movement of cool, dense material up into the corona that can be ejected or fall back down. We investigate eruptions in which some portion of the prominence material falls back to the Sun along field lines which have reconfigured in the eruption, rather than draining back to the source or escaping with the CME. Using a method called persistence mapping, 304 Å images from the Solar Dynamics Observatory (SDO), and coronagraph images from the Solar and Heliospheric Observatory, we measure and compare the offsets in latitude of 20 CMEs and their respective prominences with respect to the source region. The 20 events were chosen to sample over the first 10 years of the SDO mission. We find that the offsets are correlated. We find no difference between eruptions offset toward the equator or the poles, suggesting that the offset is a result of local changes in the eruptive field, rather than of the Sun's global magnetic field structure. These findings help us contextualize individual eruptions and highlight changes in the local magnetic field associated with the prominence eruption. **2011-02-24, 2012-04-22, 2019-04-22**

**Table 2** Data for All 20 Eruptions, Including Eruptive Region Types and Measurements in Degrees

### **The Evolution of Our Understanding of Coronal Mass Ejections**

**Review**

Russell **Howard**, Angelos Vourlidas, and Guillermo Stenborg

Front. Astron. Space Sci. 10: 1264226. **2023**

doi: 10.3389/fspas.2023.1264226

<https://www.frontiersin.org/articles/10.3389/fspas.2023.1264226/full> **File**

The unexpected observation of a sudden expulsion of mass through the solar corona in 1971 opened up a new field of interest in solar and stellar physics. The discovery came from a white-light coronagraph, which creates an artificial eclipse of the Sun, enabling the viewing of the faint glow from the corona. This observation was followed by many more observations and new missions. In the five decades since that discovery, there have been five generations of coronagraphs, each with improved performance, enabling continued understanding of the phenomena, which became known as Coronal Mass Ejection (CME) events. The conceptualization of the CME structure evolved from the elementary 2-dimensional loop to basically two fundamental types: a 3-dimensional magnetic flux rope and a non-magnetic eruption from pseudo-streamers. The former persists to 1 AU and beyond, whereas the latter dissipates by 15 R<sub>☉</sub>. Historically, most of the studies have been devoted to understanding the CME large-scale structure and its associations, but this is changing. With the advent of the fourth and fifth coronagraph generations, more attention is being devoted to their internal structure and initiation mechanisms. In this review, we describe the evolution of CME observations and their associations with other solar and heliospheric phenomena, with one of the

more important correlations being its recognition as a driver of space-weather. We conclude with a brief overview of open questions and present some ideas for future observations.

### **Evolution of CME Mass in the Corona**

Russell A. [Howard](#), Angelos Vourlidas

[Solar Physics](#) April 2018, 293:55

<http://sci-hub.tw/http://link.springer.com/10.1007/s11207-018-1274-9>

The idea that coronal mass ejections (CMEs) pile up mass in their transport through the corona and heliosphere is widely accepted. However, it has not been shown that this is the case. We perform an initial study of the volume electron density of the fronts of 13 three-part CMEs with well-defined frontal boundaries observed with the Solar and Heliospheric Observatory/Large Angle and Spectrometric COronagraph (SOHO/LASCO) white-light coronagraphs. We find that, in all cases, the volume electron density decreases as the CMEs travel through the LASCO-C2 and -C3 fields of view, from  $2.6\text{--}30 R_{\odot}$  to  $2.6\text{--}30 R_{\odot}$ . The density decrease follows closely a power law with an exponent of  $-3$ , which is consistent with a simple radial expansion. This indicates that in this height regime there is no observed pile-up. **05 Oct. 1996, 18 Jan. 1997, 04 Feb. 1997, 09 Mar. 1997, 14 Dec. 1997, 17 May 1999, 30 May 1999, 09 Feb. 2000, 17 Jul. 2000, 23 Jul. 2000, 08 Jan. 2001, 13 Jan. 2001, 20 Feb. 2001**

### **Measuring the magnetic field of coronal mass ejections near the Sun using pulsars,**

[Howard](#), T.A., K. Stovall, Dowell, J., G. Taylor, and S. White,

*Astrophys. J.*, 831 208, 2016.

<http://sci-hub.cc/10.3847/0004-637X/831/2/208>

The utility of Faraday rotation to measure the magnetic field of the solar corona and large-scale transients within is a small, yet growing field in solar physics. This is largely because it has been recognized as a potentially valuable frontier in space weather studies, because the ability to measure the intrinsic magnetic field within coronal mass ejections (CMEs) when they are close to the Sun is of great interest for understanding a key element of space weather. Such measurements have been attempted over the last few decades using radio signals from artificial sources (i.e., spacecraft on the far side of the Sun), but studies involving natural radio sources are scarce in the literature. We report on a preliminary study involving an attempt to detect the Faraday rotation of a CME that passed in front of a pulsar (PSR B0950+08) in 2015 August. We combine radio measurements with those from a broadband visible light coronagraph, to estimate the upper limit of the magnetic field of the CME when it was in the corona. We find agreement between different approaches for obtaining its density, and values that are consistent with those predicted from prior studies of CME density close to the Sun. **2015-08-21**

### **Overview of the remote sensing observations from PSP solar encounter 10 with perihelion at 13.3 R<sub>sun</sub>**

[Russell A. Howard](#), [Guillermo Stenborg](#), [Angelos Vourlidas](#), [Brendan M. Gallagher](#), [Mark G. Linton](#), [Phillip Hess](#), [Nathan B. Rich](#), [Paulett C. Liewer](#)

*ApJ* 2022

<https://arxiv.org/pdf/2207.12175.pdf>

The closest perihelion pass of Parker Solar Probe (PSP), so far, occurred between **16 and 26 of November 2021** and reached  $\sim 13.29 R_{\text{sun}}$  from Sun center. This pass resulted in very unique observations of the solar corona by the Wide-field Instrument for Solar Probe (WISPR). WISPR observed at least ten CMEs, some of which were so close that the structures appear distorted. All of the CMEs appeared to have a magnetic flux rope (MFR) structure and most were oriented such that the view was along the axis orientation, revealing very complex interiors. Two CMEs had a small MFR develop in the interior, with a bright circular boundary surrounding a very dark interior. Trailing the larger CMEs were substantial outflows of small blobs and flux-rope like structures within striated ribbons, lasting for many hours. When the heliophysics plasma sheet (HPS) was inclined, as it was during the days around perihelion on November 21, 2021, the outflow was over a very wide latitude range. One CME was overtaken by a faster one, with a resultant compression of the rear of the leading CME and an unusual expansion in the trailing CME. The small Thomson Surface creates brightness variations of structures as they pass through the field of view. In addition to this dynamic activity, a brightness band from excess dust along the orbit of asteroid/comet 3200 Phaethon is also seen for several days. **16, 19, 20-21, 22-23, 24-26 Nov 2021**

### **CHALLENGING SOME CONTEMPORARY VIEWS OF CORONAL MASS EJECTIONS.**

#### **II. THE CASE FOR ABSENT FILAMENTS**

T. A. [Howard](#)<sup>1</sup>, C. E. DeForest<sup>1</sup>, U. G. Schneck<sup>2</sup>, and C. R. Alden

2017 *ApJ* 834 86 DOI 10.3847/1538-4357/834/1/86

<http://c.brightcove.com/article/10.3847/1538-4357/834/1/86/pdf>

<http://iopscience.iop.org/sci-hub.cc/0004-637X/834/1/86/> **File**

When a coronal mass ejection (CME) appears in a coronagraph it often exhibits three parts. This "classic" three-part configuration consists of a bright leading edge, a dark circular- or teardrop-shaped cavity, and a bright core within the cavity. It is generally accepted that these are manifestations of coronal plasma pileup, the driving magnetic flux rope, and the associated eruptive filament, respectively. The latter has become accepted by the community since coronagraph

CMEs have been commonly associated with eruptive filaments for over 40 years. In this second part of our series challenging views on CMEs, we present the case that the inner core of the three-part coronagraph CME may not be, and in the most common cases is not, a filament. We present our case in the form of four exhibits showing that most of the CMEs in a broad survey are not associated with an eruptive filament at the Sun, and that the cores of those CMEs that are filament-associated do not geometrically resemble or consist of material from the associated filament. We conclude with a discussion on the possible causes of the bright CME core and what happens to the filament material postlaunch. We discuss how the CME core could arise spontaneously from the eruption of a flux rope from the Sun, or could be the result of a mathematical caustic produced by the geometric projection of a twisted flux rope. **2010.12.14, 2011.05.01, 2011.10.25, 2011.11.02, 2012.01.27, 2012.01.31, 2012.03.24, 2012.04.14, 2012.04.28, 2012.06.27, 2012.07.26, 2012.08.20, 2012.10.22, 2012.11.18**

**Table 1 List of Selected CMEs for Our Study**

## **CHALLENGING SOME CONTEMPORARY VIEWS OF CORONAL MASS EJECTIONS.**

### **I. THE CASE FOR BLAST WAVES**

T. A. **Howard**<sup>1</sup> and V. J. Pizzo

**2016** ApJ 824 92

<http://sci-hub.cc/doi/10.3847/0004-637X/824/2/92> **File**

Since the closure of the "solar flare myth" debate in the mid-1990s, a specific narrative of the nature of coronal mass ejections (CMEs) has been widely accepted by the solar physics community. This narrative describes structured magnetic flux ropes at the CME core that drive the surrounding field plasma away from the Sun. This narrative replaced the "traditional" view that CMEs were blast waves driven by solar flares. While the flux rope CME narrative is supported by a vast quantity of measurements made over five decades, it does not adequately describe every observation of what have been termed CME-related phenomena. In this paper we present evidence that some large-scale coronal eruptions, particularly those associated with EIT waves, exhibit characteristics that are more consistent with a blast wave originating from a localized region (such as a flare site) rather than a large-scale structure driven by an intrinsic flux rope. We present detailed examples of CMEs that are suspected blast waves and flux ropes, and show that of our small sample of 22 EIT-wave-related CMEs, 91% involve a blast wave as at least part of the eruption, and 50% are probably blast waves exclusively. We conclude with a description of possible signatures to look for in determining the difference between the two types of CMEs and with a discussion on modeling efforts to explore this possibility.

**2003.10.28, 2010.05.04, 2010.08.01, 2011.02.13, 2011.07.11, 2011.08.02**

**Table 1 Our Selections of CMEs Associated with EIT Waves Derived from the Nitta et al. list.**

## **Regarding the detectability and measurement of coronal mass ejections Review**

Timothy A. **Howard**

J. Space Weather Space Clim., 5, A22 (2015) **File**

<http://www.swsc-journal.org/articles/swsc/pdf/2015/01/swsc140065.pdf>

In this review I discuss the problems associated with the detection and measurement of coronal mass ejections (CMEs). CMEs are important phenomena both scientifically, as they play a crucial role in the evolution of the solar corona, and technologically, as their impact with the Earth leads to severe space weather activity in the form of magnetic storms. I focus on the observation of CMEs using visible white light imagers (coronagraphs and heliospheric imagers), as they may be regarded as the binding agents between different datasets and different models that are used to reconstruct them. Our ability to accurately measure CMEs observed by these imagers is hampered by many factors, from instrumental to geometrical to physical. Following a brief review of the history of CME observation and measurement, I explore the impediments to our ability to measure them and describe possible means for which we may be able to mitigate those impediments. I conclude with a discussion of the claim that we have reached the limit of the information that we can extract from the current generation of white light imagers, and discuss possible ways forward regarding future instrument capabilities. **27 February 2000, 12 December 2008, 2013/05/03**

## **Measuring an Eruptive Prominence at Large Distances from the Sun. II. Approaching 1 AU**

T. A. **Howard**

**2015** ApJ 806 176

The physical properties of eruptive prominences are unknown at large distances from the Sun. They are rarely, if ever, measured by in situ spacecraft and until recently our ability to measure them beyond the fields of view of solar imagers has been severely limited. The data quality of heliospheric imaging has reached a point where some quantitative measurements of prominences are now possible. I present the first such measurements of a bright prominence continually out to distances of around 1 AU from the Sun. This work follows on from the preparatory work presented in an accompanying paper, which showed that the brightness of a prominence can be safely assumed to arise entirely from Thomson scattering in the STEREO/HI fields of view. Measurements of distance, speed, and mass are provided along with those from its accompanying coronal mass ejection (CME) to demonstrate their geometric, kinematic, and mass relationships. I find that the prominence travels with a slower speed than that of the CME, but its location relative to the CME structure does not conform to the expected location for basic geometric expansion. Further, the mass of the prominence was found to decrease by around an order of magnitude while that of the CME increased by an order of magnitude across the same distance.



## Measuring an Eruptive Prominence at Large Distances from the Sun. I. Ionization and Early Evolution

T. A. **Howard**

2015 ApJ 806 175

Measurements of H $\alpha$  emission within an eruptive solar prominence are presented, using white light polarization properties as a proxy for the presence of H $\alpha$  in the STEREO COR1 and COR2 coronagraphs. The transition from H $\alpha$  emission to Thomson scattering radiance serves as an indicator of the ionization of the prominence, and I discuss the physical implications regarding the behavior of the neutrals and ions, and also for the measurement of coronal mass ejection properties using the Thomson scattering assumption. I find that the prominence has a high concentration of neutrals at around two solar radii that gradually exhibit ionization characteristics as it moves away from the Sun. The prominence reaches complete ionization, or at least a state where the Thomson-scattered brightness dominates, by the time it reaches around seven solar radii. This is consistent with predictions inferred from direct H $\alpha$  measurements made from earlier studies in the 1980s and with the predicted ionization rate of neutral hydrogen near solar maximum. These results pave the way for an accompanying paper that reports on measurements of the prominence at large distances from the Sun using the assumptions verified here.

## The Formation and Launch of a Coronal Mass Ejection Flux Rope: A Narrative Based on Observations

T. A. **Howard** and C. E. DeForest

2014 ApJ 796 33, **File**

We present a data-driven narrative of the launch and early evolution of the magnetic structure that gave rise to the coronal mass ejection (CME) on **2008 December 12**. The structure formed on December 7 and launched early on December 12. We interpret this structure as a flux rope based on prelaunch morphology, postlaunch magnetic measurements, and the lack of large-scale magnetic reconnection signatures at launch. We ascribe three separate onset mechanisms to the complete disconnection of the flux rope from the Sun. It took 19 hr for the flux rope to be fully removed from the Sun, by which time the segment that first disconnected was around 40 R $\odot$  away. This implies that the original flux rope was stretched or broken; we provide evidence for a possible bisection. A transient dark arcade was observed on the Sun that was later obscured by a bright arcade, which we interpret as the strapping field stretching and magnetically reconnecting as it disconnected from the coronal field. We identify three separate structures in coronagraph images to be manifestations of the same original flux rope, and we describe the implications for CME interpretation. We cite the rotation in the central flux rope vector of the magnetic clouds observed in situ by ACE/Wind and STEREO-B as evidence of the kink instability of the eastern segment of the flux rope. Finally, we discuss possible alternative narratives, including multiple prelaunch magnetic structures and the nonflux rope scenario. Our results support the view that, in at least some CMEs, flux rope formation occurs before launch.

<http://www.boulder.swri.edu/~howard/index.html>

## Space Weather and Coronal Mass Ejections **Book**

Timothy A. **Howard**

Springer, 2013

[http://books.google.ru/books?id=ihO4BAAAQBAJ&pg=PA97&lpg=PA97&dq=DeForest,+C.+E.&source=bl&ots=XIvsgYLFfB&sig=525J\\_9PFZBGda9BsysLsvRRQh34&hl=ru&sa=X&ei=HxlfVOr7HoG6PdDNgegL&ved=0CC4Q6AEwBQ#v=onepage&q=DeForest%2C%20C.%20E.&f=false](http://books.google.ru/books?id=ihO4BAAAQBAJ&pg=PA97&lpg=PA97&dq=DeForest,+C.+E.&source=bl&ots=XIvsgYLFfB&sig=525J_9PFZBGda9BsysLsvRRQh34&hl=ru&sa=X&ei=HxlfVOr7HoG6PdDNgegL&ved=0CC4Q6AEwBQ#v=onepage&q=DeForest%2C%20C.%20E.&f=false)

25 March 2008, 12-17 Dec 2008, 2010-04-03,

## Stealth Coronal Mass Ejections: A Perspective

Timothy A. **Howard**, Richard A. Harrison

Solar Physics, July 2013, Volume 285, Issue 1-2, pp 269-280

“Stealth CME” has become a commonly used term in recent studies of solar activity. It refers to a coronal mass ejection (CME) with no apparent solar surface association, and therefore has no easily identifiable signature to locate the region on the Sun from which the CME erupted. We review the literature and express caution in categorising CMEs in this way. CMEs were discovered some 40 years ago and there have been numerous statistical studies of associations with phenomena in the solar atmosphere which clearly identify a range of associations, from bright flares and large prominence eruptions to small flares, and even a lack of flares or any identifiable surface activity at all. In this sense the stealth CME concept is not new. One major question relates to whether the range of associations reveal different CME classes, i.e. different CME launch processes, or are indicative of a spectrum of coronal responses to one common process. We favour the latter and stress that this spectrum must be considered in the description of the CME launch, meaning that the physics of a so-called stealth CME must not be fundamentally different from a CME associated with major surface events. On the other hand we also stress that the use of a stealth CME category implies that all surface activity could indeed be detected using modern instrumentation. We argue that this may not be the case, and that even in the SDO era of full-Sun, high resolution imaging, we are restricted by instrument sensitivity and bandwidth issues. Thus, having reviewed the case for stealth CMEs as a distinct category, we stress the need to keep the concept in perspective.

## WHITE-LIGHT OBSERVATIONS OF SOLAR WIND TRANSIENTS AND COMPARISON WITH AUXILIARY DATA SETS

T. A. [Howard](#)<sup>1</sup>, C. E. DeForest<sup>1</sup>, and A. A. Reinard

2012 ApJ 754 102

This paper presents results utilizing a new data processing pipeline for STEREO/SECCHI. The pipeline is used to identify and track 24 large- and small-scale solar wind transients from the Sun out to 1 AU. This comparison was performed during a few weeks around the minimum at the end of Solar Cycle 23 and the start of Cycle 24 (2008 December to 2009 January). We use coronagraph data to identify features near the Sun, track them through HI-2A, and identify their signatures with in situ data at the Earth and STEREO-B. We provide measurements and preliminary analysis of the in situ signatures of these features near 1 AU. Along with the demonstration of the utility of heliospheric imagers for tracking even small-scale structures, we identify and discuss an important limitation in using geometric triangulation for determining three-dimensional properties.

## INNER HELIOSPHERIC FLUX ROPE EVOLUTION VIA IMAGING OF CORONAL MASS EJECTIONS

T. A. [Howard](#) and C. E. DeForest

2012 ApJ 746 64, [File](#)

Understanding the evolution of flux ropes in coronal mass ejections (CMEs) is of importance both to the scientific and technological communities. Scientifically their presence is critical to models describing CME launch and they likely play a role in CME evolution. Technologically they are the major contributor to severe geomagnetic storms. Using a new processing technique on the STEREO/SECCHI heliospheric imaging data, we have tracked a magnetic flux rope observed by the Wind spacecraft in **December 2008** to its origins observed by coronagraphs. We thereby establish that the cavity in the classic three-part coronagraph CME is the feature that becomes the magnetic cloud. This implies that the bright material ahead of the cavity is piled-up coronal or solar wind material. We track the evolution of the cavity en-route and find that its structure transforms from concave inward (curving away from the Sun) to concave outward (toward the Sun) around 0.065 AU from the Sun. The pileup was tracked and its leading edge remained concave inward throughout its journey. Two other CMEs in **January 2009** are also inspected and a similar cavity is observed in each, suggesting that they too each contained a flux rope. The results presented here are the first direct observation, through continuous tracking, associating a particular flux rope observed in situ with the same flux rope before ejection from the corona. We speculate that detailed heliospheric imagery of CMEs may lead to a means by which flux ropes can be identified remotely in the heliosphere.

## "Coronal Mass Ejections: An Introduction", [Boook](#) [File](#)

T. [Howard](#).

Series: Astrophysics and Space Science Library, Vol. 376, 2011

The [book](#) brings the reader up to date on the status quo of CME study: the history of their observation; techniques for their detection; their space weather impact; and theories describing their onset, evolution and eventual fate. It also provides an exhaustive list of historical and topical references from experts in the field past and present.

[Read online:](#)

<http://www.springerlink.com/content/978-1-4419-8789-1#section=894524&page=13&locus=20>

## Application of a new phenomenological coronal mass ejection model to space weather forecasting,

[Howard](#), T. A., and S. J. Tappin

Space Weather, 8, S07004, doi:10.1029/2009SW000531 (2010).

Recent work by the authors has produced a new phenomenological model for coronal mass ejections (CMEs). This model, called the Tappin-Howard (TH) Model, takes advantage of the breakdown of geometrical linearity when CMEs are observed by white-light imagers at large distances from the Sun. The model extracts 3-D structure and kinematic information on the CME using heliospheric image data. This can estimate arrival times of the CME at 1 AU and impact likelihood with the Earth. Hence the model can be used for space weather forecasting. We present a preliminary evaluation of this potential with three mock trial forecasts performed using the TH Model. These are already-studied events from 2003, 2004 and 2007 but we performed the trials assuming that they were observed for the first time. The earliest prediction was made 17 hours before impact and predicted arrival times reached differences within one hour for at least one forecast for all three events. The most accurate predicted arrival time was 15 min from the actual, and all three events reach accuracies of the order of 30 min. Arrival speeds were predicted to be very similar to the bulk plasma speed within the CME near 1 AU for each event, with the largest difference around 300 km/s and the least 40 km/s. The

model showed great potential and we aspire to fully validate it for integration with existing tools for space weather forecasting.

### **Three-Dimensional Reconstruction of Two Solar Coronal Mass Ejections Using the STEREO Spacecraft**

Timothy A. Howard · S. James Tappin

Solar Phys, 252: 373–383, 2008, DOI 10.1007/s11207-008-9262-0, File

Previous attempts to produce three-dimensional (3-D) reconstructions of coronal mass ejections (CMEs) have required either modeling efforts or comparisons with secondary associated eruptions near the solar surface. This is because coronagraphs are only able to produce sky-plane-projected images of CMEs and it has hence been impossible to overcome projection effects by using coronagraphs alone. The SECCHI suite aboard the twin STEREO spacecraft allows us to provide the means for 3-D reconstruction of CMEs directly from coronagraph measurements alone for the first time. We present these measurements from two CMEs observed in November 2007. By identifying common features observed simultaneously with the LASCO coronagraphs aboard SOHO and the COR coronagraphs aboard STEREO we have triangulated the source region of both CMEs. We present the geometrical analysis required for this triangulation and identify the location of the CME in solar-meridional, ecliptic, and Carrington coordinates. None of the two events were associated with an easily detectable solar surface eruption, so this triangulation technique is the only means by which the source location of these CMEs could be identified. We present evidence that both CMEs originated from the same magnetic structure on the Sun, but from a different magnetic field configuration. Our results reveal some insight into the evolution of the high corona magnetic field, including its behavior over time scales of a few days and its reconfiguration after a major eruption.

### **Interplanetary coronal mass ejections that are undetected by solar coronagraphs, Howard, T. A., and G. M. Simnett**

J. Geophys. Res., 113, A08102, 2008

<http://dx.doi.org/10.1029/2007JA012920>

From February 2003 to September 2005 the Solar Mass Ejection Imager on the Coriolis spacecraft detected 207 interplanetary coronal mass ejections (ICME) in the inner heliosphere. We have examined the data from the Large Angle Spectroscopic Coronagraph (LASCO) on the SOHO spacecraft for evidence of coronal transient activity that might have been the solar progenitor of the Solar Mass Ejection Imager (SMEI) events, taking into account the projected speed of the SMEI event and its position angle in the plane of the sky. We found a significant number of SMEI events where there is either only a weak or unlikely coronal mass ejection (CME) detected by LASCO or no event at all. A discussion of the effects of projection across large distances on the ICME measurements is made, along with a new technique called the Cube-Fit procedure that was designed to model the ICME trajectory more accurately than simple linear fits to elongation-time plots. Of the 207 SMEI events, 189 occurred during periods of full LASCO data coverage. Of these, 32 or 17% were found to have a weak or unlikely LASCO counterpart, and 14 or 7% had no apparent LASCO transient association. Using solar X-ray, EUV and H $\alpha$  data we investigated three main physical possibilities for ICME occurrence with no LASCO counterpart: (1) Corotating interaction regions (CIRs), (2) erupting magnetic structures (EMS), and (3) flare blast waves. We find that only one event may possibly be a CIR and that flare blast waves can be ruled out. *The most likely phenomenon is investigated and discussed, that of EMS. Here, the transient erupts in the same manner as a typical CME, except that they do not have sufficient mass to be detected by LASCO. As the structure moves outward, it accumulates and concentrates solar wind material until it is bright enough to be detected by SMEI.*

### **Kinematic properties of solar coronal mass ejections: Correction for projection effects in spacecraft coronagraph measurements,**

Howard, T. A., D. Nandy, and A. C. Koepke,

J. Geophys. Res., 113, A01104, 2008, File

<http://solar.physics.montana.edu/~nandi/papers/nandy07c.pdf>

By identifying solar surface source regions of CMEs using X-ray and H $\alpha$  flare and disappearing filament data, and through considerations of CME trajectories in three-dimensional (3-D) geometry, we have devised a methodology to correct for the projection effect. We outline this method here.

We conclude that while using the plane-of-sky measurements may be suitable for studies of general trends in a large sample of events, correcting for projection effects is mandatory for those investigations which rely on a numerically precise determination of the properties of individual CMEs.

### **A Historical Perspective on Coronal Mass Ejections.**

R.A. Howard

In: (2006). Solar Eruptions and Energetic Particles. doi:10.1029/165gm03

[sci-hub.tw/10.1029/165GM03](http://sci-hub.tw/10.1029/165GM03)

The concept of mass leaving the Sun was thought possible over 100 years ago from the observations of prominence material that was seen to be moving outward at speeds in excess of the escape velocity. While the direct observation was elusive, the coupling between solar activity and geomagnetic storms became quite apparent. In the 1940's the concept of corpuscular radiation from the sun was proposed and then in the 1950's used to explain the discontinuity in a comet tail. Parker's theory in 1957 predicted a continuous outflow from the sun that was then observed by in-situ spacecraft less than 10 years later. The first optical observations of a transient event showing mass moving through the solar corona in 1971 were accompanied by excitement, fascination and speculation. Two questions at that time were: What causes the CME eruption? What is their significance? These questions and others are still with us. In this paper, the coronal mass ejection is viewed in its historical context.

### **Excitation of Quasiperiodic Fast-propagating Waves in the Early Stage of the Solar Eruption**

Jialiing Hu<sup>1,2,3</sup>, Jing Ye<sup>1,3,4</sup>, Yuhao Chen<sup>1,2,3</sup>, Zhixing Mei<sup>1,3</sup>, Zehao Tang<sup>1,2,3</sup>, and Jun Lin

2024 ApJ 962 42

<https://iopscience.iop.org/article/10.3847/1538-4357/ad1993/pdf>

We propose a mechanism for the excitation of large-scale quasiperiodic fast-propagating magnetoacoustic (QFP) waves observed on both sides of the coronal mass ejection. Through a series of numerical experiments, we successfully simulated the quasi-static evolution of the equilibrium locations of the magnetic flux rope in response to the change of the background magnetic field, as well as the consequent loss of the equilibrium that eventually gives rise to the eruption. During the eruption, we identified QFP waves propagating radially outward of the flux rope, and tracing their origin reveals that they result from the disturbance within the flux rope. Acting as an imperfect waveguide, the flux rope allows the internal disturbance to escape to the outside successively via its surface, invoking the observed QFP waves. Furthermore, we synthesized the images of QFP waves on the basis of the data given by our simulations and found consistency with observations. This indicates that the leakage of the disturbance outside the flux rope could be a reasonable mechanism for QFP waves. **2012 May 7**

### **Spectroscopic and Imaging Observations of Spatially Extended Magnetic Reconnection in the Splitting of a Solar Filament Structure**

Huidong Hu<sup>1</sup>, Ying D. Liu<sup>1,2</sup>, Lakshmi Pradeep Chitta<sup>3</sup>, Hardi Peter<sup>3</sup>, and Mingde Ding<sup>4,5</sup>

2022 ApJL 940 L12

<https://iopscience.iop.org/article/10.3847/2041-8213/ac9dfd/pdf>

<https://arxiv.org/pdf/2211.10216>

On the Sun, Doppler shifts of bidirectional outflows from the magnetic-reconnection site have been found only in confined regions through spectroscopic observations. Without spatially resolved spectroscopic observations across an extended region, the distribution of reconnection and its outflows in the solar atmosphere cannot be made clear. Magnetic reconnection is thought to cause the splitting of filament structures, but unambiguous evidence has been elusive. Here we report spectroscopic and imaging analysis of a magnetic-reconnection event on the Sun, using high-resolution data from the Interface Region Imaging Spectrograph and the Solar Dynamics Observatory. Our findings reveal that the reconnection region extends to an unprecedented length of no less than 14,000 km. The reconnection splits a filament structure into two branches, and the upper branch erupts eventually. Doppler shifts indicate clear bidirectional outflows of  $\sim 100 \text{ km s}^{-1}$ , which decelerate beyond the reconnection site. Differential-emission-measure analysis reveals that in the reconnection region the temperature reaches over 10 MK and the thermal energy is much larger than the kinetic energy. This Letter provides definite spectroscopic evidence for the splitting of a solar filament by magnetic reconnection in an extended region. **2017 July 13-14**

IRIS Nugget 9 Dec 2022

<https://iris.lmsal.com/nugget>

### **Validation and interpretation of three-dimensional configuration of a magnetic cloud flux rope**

Qiang Hu, Chunming Zhu, Wen He, Jiong Qiu, Lan K. Jian, Avijeet Prasad

ApJ 2022

<https://arxiv.org/pdf/2204.03457>

One "strong" magnetic cloud (MC) with the magnetic field magnitude reaching  $\sim 40 \text{ nT}$  at 1 au during **2012 June 16-17** is examined in association with a pre-existing magnetic flux rope (MFR) identified on the Sun. The MC is characterized by a quasi-three dimensional (3D) flux rope model based on in situ measurements from the Wind spacecraft. The magnetic flux contents and other parameters are quantified. In addition, a correlative study with the corresponding measurements of the same structure crossed by the Venus Express (VEX) spacecraft at a heliocentric distance 0.7 au and with an angular separation  $\sim 6^\circ$  in longitude is performed to validate the MC modeling results. The spatial variation between the Wind and VEX magnetic field measurements is attributed to the 3D configuration of the structure as featured by a knotted bundle of flux. The comparison of the magnetic flux contents between the MC and the source region on the Sun indicates that the 3D reconnection process accompanying an M1.9 flare may correspond to the magnetic reconnection between the field lines of the pre-existing MFR rooted in the opposite polarity footpoints. Such a process reduces the amount of the axial magnetic flux in the erupted flux rope, by approximately 50%, in this case.

## The Grad-Shafranov Reconstruction of Toroidal Magnetic Flux Ropes: First Applications

Qiang Hu, [M. G. Linton](#), [B. E. Wood](#), [P. Riley](#), [T. Nieves-Chinchilla](#)

Solar Phys. 2017

<https://arxiv.org/pdf/1707.09454.pdf>

This article completes and extends a recent study of the Grad-Shafranov (GS) reconstruction in toroidal geometry, as applied to a two and a half dimensional configurations in space plasmas with rotational symmetry. A further application to the benchmark study of an analytic solution to the toroidal GS equation with added noise shows deviations in the reconstructed geometry of the flux rope configuration, characterized by the orientation of the rotation axis, the major radius, and the impact parameter. On the other hand, the physical properties of the flux rope, including the axial field strength, and the toroidal and poloidal magnetic flux, agree between the numerical and exact GS solutions. We also present a real event study of a magnetic cloud flux rope from *in situ* spacecraft measurements. The devised procedures for toroidal GS reconstruction are successfully executed. Various geometrical and physical parameters are obtained with associated uncertainty estimates. The overall configuration of the flux rope from the GS reconstruction is compared with the corresponding morphological reconstruction based on white-light images. The results show overall consistency, but also discrepancy in that the inclination angle of the flux rope central axis with respect to the ecliptic plane differs by about 20-30 degrees in the plane of the sky. We also compare the results with the original straight-cylinder GS reconstruction and discuss our findings. **06-07-Jun-2008**

## Multi-spacecraft Observations of the Coronal and Interplanetary Evolution of a Solar Eruption Associated with Two Active Regions

Huidong Hu, Ying D. Liu, Rui Wang, Xiaowei Zhao, Bei Zhu, Zhongwei Yang

ApJ 840 76 2017

<https://arxiv.org/pdf/1704.05496.pdf>

<https://iopscience.iop.org/article/10.3847/1538-4357/aa6d54/pdf>

We investigate the coronal and interplanetary evolution of a coronal mass ejection (CME) launched on **2010 September 4** from a source region linking two active regions (ARs) 11101 and 11103, using extreme ultraviolet imaging, magnetogram, white-light and *in situ* observations from SDO, STEREO, SOHO, VEX and Wind. A potential-field source-surface model is employed to examine the configuration of the coronal magnetic field surrounding the source region. The graduated cylindrical shell model and a triangulation method are applied to determine the kinematics of the CME in the corona and interplanetary space. From the remote sensing and *in situ* observations we obtain some key results: (1) the CME was deflected in both the eastward and southward directions in the low corona by the magnetic pressure from the two ARs and possibly interacted with another ejection, which caused that the CME arrived at VEX that was longitudinally distant from the source region; (2) although VEX was closer to the Sun, the observed and derived CME arrival times at VEX are not earlier than those at Wind, which suggests the importance of determining both the frontal shape and propagation direction of the CME in interplanetary space; (3) the ICME was compressed in the radial direction while the longitudinal transverse size was extended.

## Sun-to-Earth Characteristics of the 2012 July 12 Coronal Mass Ejection and Associated Geo-effectiveness

Huidong Hu, Ying D. Liu, Rui Wang, [Christian Möstl](#), [Zhongwei Yang](#)

ApJ 829 97 2016

<http://arxiv.org/pdf/1607.06287v1.pdf> File

We analyze multi-spacecraft observations associated with the 2012 July 12 Coronal Mass Ejection (CME), covering the source region on the Sun from SDO, stereoscopic imaging observations from STEREO, magnetic field characteristics at MESSENGER, and type II radio burst and *in situ* measurements from Wind. A triangulation method based on STEREO stereoscopic observations is employed to determine the kinematics of the CME, and the outcome is compared with the result derived from the type II radio burst with a solar wind electron density model. A Grad-Shafranov technique is applied to Wind *in situ* data to reconstruct the flux-rope structure and compare it with the observation of the solar source region, which helps understand the geo-effectiveness associated with the CME structure. Conclusions are as follows: (1) the CME undergoes an impulsive acceleration, a rapid deceleration before reaching MESSENGER, and then a gradual deceleration out to 1 AU, which should be noticed in CME kinematics models; (2) the type II radio burst was probably produced from a high-density interaction region between the CME-driven shock and a nearby streamer or from the shock flank with lower heights, which implies uncertainties in the determination of CME kinematics using solely type II radio bursts; (3) the flux-rope orientation and chirality deduced from *in situ* reconstruction at Wind agree with those obtained from solar source observations; (4) the prolonged southward magnetic field near the Earth is mainly from the axial component of the largely southward inclined flux rope, which indicates the importance of predicting both the flux-rope orientation and magnetic field components in geomagnetic activity forecasting.

## Structures of Interplanetary Magnetic Flux Ropes and Comparison with Their Solar Sources

Qiang Hu, Jiong Qiu, B. Dasgupta, A. Khare, and G. M. Webb

ApJ 793 53, 2014; File

[https://dl.dropboxusercontent.com/u/96898685/ms\\_fr\\_v4.pdf](https://dl.dropboxusercontent.com/u/96898685/ms_fr_v4.pdf)  
<http://arxiv.org/pdf/1408.1470v1.pdf>

During the process of magnetic flux rope ejection, magnetic reconnection is essential to release the flux rope. The question remains: how does the magnetic reconnection change the flux rope structure? In this work, we continue with the original study by Qiu et al. (2007) by using a larger sample of flare-CME-ICME events to compare properties of ICME/MC flux ropes measured at 1 AU and properties of associated solar progenitors including flares, filaments, and CMEs. In particular, the magnetic field-line twist distribution within interplanetary magnetic flux ropes is systematically derived and examined. Our analysis shows that, similar to what was found before, for most of these events, the amount of twisted flux per AU in MCs is comparable with the total reconnection flux on the Sun, and the sign of the MC helicity is consistent with the sign of helicity of the solar source region judged from the geometry of postflare loops. Remarkably, we find that about one half of the 18 magnetic flux ropes, most of them being associated with erupting filaments, have a nearly uniform and relatively low twist distribution from the axis to the edge, and the majority of the other flux ropes exhibit very high twist near the axis, of up to  $\geq 5$  turns per AU, which decreases toward the edge. The flux ropes are therefore not linear force free. We also conduct detailed case studies showing the contrast of two events with distinct twist distribution in MCs as well as different flare and dimming characteristics in solar source regions, and discuss how reconnection geometry reflected in flare morphology may be related to the structure of the flux rope formed on the Sun. 03/08/2008, 05/28/2010, 08/04/2010, 03/30/2011, 06/05/2011, 08/05/2011, 09/09/2011, 09/17/2011, **2011 September 13-17**, 10/24/2011

### **Science Operation and Data Analysis Center of the Advanced Space-Based Solar Observatory (ASO-S) Mission.**

**Huang, Y.**, Li, Y., Liu, S. et al.

Sol Phys 299, 135 (2024).

<https://doi.org/10.1007/s11207-024-02368-x>

A reliable data analysis center plays a crucial role in the successful execution of a space mission. The Science Operation and Data analysis Center (SODC) of Advanced Space-based Solar Observatory (ASO-S) is a bridge between the science team of ASO-S and data users (Huang et al. 2019). ASO-S plays a crucial role in understanding the solar eruptions (such as flares and coronal mass ejections) and the magnetism behind them. In this article, we outline the current status of ASO-S, as well as its data products and analysis software. These resources aid in the enhanced understanding of solar magnetism and its associated energetic eruptions.

### **Formation and Dynamics in an Observed Preeruptive Filament**

Jing **Huang**<sup>1,2,3</sup>, Yin Zhang<sup>1,2</sup>, Baolin Tan<sup>1,2,3</sup>, Xianyong Bai<sup>1,2,3</sup>, Leping Li, + + +

**2023** ApJL 958 L13

<https://iopscience.iop.org/article/10.3847/2041-8213/ad083e/pdf>

The formation of filaments/prominences is still a debated topic. Many different processes have been proposed: levitation, injection of cool plasma, merging filaments, and cooling plasma in hot loops. We take the opportunity to make a multiwavelength analysis of the formation of an active-region filament, combining several UV and EUV observations including the new Ne VII 465 Å filtergrams provided by the Solar Upper Transition Region Imager on board the Space Advanced Technology satellite. The filament is mainly observed at the limb for 3 hr. It is progressively formed through a series of stages, including emergence and cooling of hot loops, reconnection between small filaments, material transfer in a large filament channel, and reconnection between filaments and emerged hot loops. From the observations at 465 Å, we find that the new-formed filaments show bright structures as in 304 Å, while the long-lived stable filaments display dark morphology as in 211 Å. This suggests that the plasma around 0.5 MK would be an essential component of new-formed filaments and the material temperature in filaments would be variable during their evolution. The filament formed by the recombination of two filaments and an emerged hot loop finally erupts. After reconnection, the final filament shows a highly twisted structure of both bright and dark strands, which is surrounded by several weak and dispersive looplike structures. This eruptive filament has a complex multichannel topology and covers a wide range of temperatures. **2022 September 23**

### **Statistical Study of Ejections in Coronal Hole Regions As Possible Sources of Solar Wind Switchbacks and Small-scale Magnetic Flux Ropes**

Nengyi **Huang**<sup>1,2</sup>, Sophia D'Anna<sup>1</sup>, and Haimin Wang<sup>1,2</sup>

**2023** ApJL 946 L17

<https://iopscience.iop.org/article/10.3847/2041-8213/acc0f1/pdf>

The omnipresence of transient fluctuations in the solar wind, such as switchbacks (SBs) and small-scale magnetic flux ropes (SMFRs), have been well observed by the in situ observation of Parker Solar Probe (PSP), yet their sources are not clear. Possible candidates fall into two categories: solar origin and in situ generation in the solar wind. Among the solar-origin scenarios, the small-scale activities (such as ejections and eruptions) in coronal hole (CH) regions, where solar wind originates, are suggested as candidates. Using full-disk extreme ultraviolet images from Atmospheric Imaging Assembly on board the Solar Dynamic Observatory, we identify small-scale ejections in CH regions during PSP Encounters 5, 7, and 8, and study their statistical properties. These ejections belong to two categories: standard jets and blowout jets. With 27,832 ejections identified in 24 days (about 2/3 of them are blowout jets), we updated the expected frequency for PSP to detect their counterparts in the heliospace. The ejections we identified are comparable to

the frequency of PSP-detected SMFRs, but they are insufficient to serve as the only producer of SBs or SB patches. Certain smaller events missed by this study, such as jetlets, may fill the gap. **2020-01-23, 2020-06-09-10, 2021-04-29**

## **The Kinematic Evolution of Erupting Structures in Confined Solar Flares**

Z. W. [Huang](#)<sup>1,2</sup>, X. Cheng<sup>1,2,3</sup>, and M. D. Ding<sup>1,2</sup>

**2020** ApJL 904 L2

<https://doi.org/10.3847/2041-8213/abc5b0>

In this Letter, we study the kinematic properties of ascending hot blobs associated with confined flares. Taking advantage of high-cadence extreme-ultraviolet images provided by the Atmospheric Imaging Assembly on board the Solar Dynamics Observatory, we find that for the 26 events selected here, the hot blobs are first impulsively accelerated outward, but then quickly slow down to motionlessness. Their velocity evolution is basically synchronous with the temporal variation of the Geostationary Operational Environmental Satellite soft X-ray flux of the associated flares, except that the velocity peak precedes the soft X-ray peak by minutes. Moreover, the duration of the acceleration phase of the erupting blobs is moderately correlated with that of the flare rise phase. For nine of the 26 cases, the erupting blobs even appear minutes prior to the onset of the associated flares. Our results show that a fraction of confined flares also involve the eruption of a magnetic flux rope, which sometimes is formed and heated prior to the flare onset. We suggest that the initiation and development of these confined flares are similar to that of eruptive ones, and the main difference may lie in the background field constraint, which is stronger for the former than for the latter.

## **Heating at the remote footpoints as a brake on jet flows along loops in the solar atmosphere**

[Zhenghua Huang](#), [Qingmin Zhang](#), [Lidong Xia](#), [Bo Li](#), [Zhao Wu](#), [Hui Fu](#)

ApJ **2020**

<https://arxiv.org/pdf/2007.04132.pdf>

<https://iopscience.iop.org/article/10.3847/1538-4357/ab96bd/pdf>

We report on observations of a solar jet propagating along coronal loops taken by the Solar Dynamics Observatory (SDO), the Interface Region Imaging Spectrograph (IRIS) and 1-m New Vacuum Solar Telescope (NVST). The ejecta of the jet consist of multi-thermal components and propagate with a speed greater than 100 km/s. Brightenings are found in the remote footpoints of the coronal loops having compact and round-shape in the H $\alpha$  images. The emission peak of the remote brightening in the Atmospheric Imaging Assembly (AIA) 94 Å passband lags 60 s behind that in the jet base. The brightenings in the remote footpoints are believed to be consequences of heating by nonthermal electrons, MHD waves and/or conduction front generated by the magnetic reconnection processes of the jet. The heating in the remote footpoints leads to extension of the brightening along the loops toward the jet base, which is believed to be the chromospheric evaporation. This apparently acts as a brake on the ejecta, leading to a deceleration in the range from 1.5 to 3 km s<sup>-2</sup> with an error of  $\sim 1.0$  km s<sup>-2</sup> when the chromospheric evaporation and the ejecta meet at locations near the loop apexes. The dynamics of this jet allows a unique opportunity to diagnose the chromospheric evaporation from the remote footpoints, from which we deduce a velocity in the range of 330–880 km/s. **4 May 2015**

## **Formation and Eruption of a Mini-sigmoid Originating in Coronal Hole**

Z. W. [Huang](#), [X. Cheng](#), [Y. N. Su](#), [T. Liu](#), [M. D. Ding](#)

**2020**

<https://arxiv.org/pdf/1912.10404.pdf>

In this paper, we study in detail the evolution of a mini-sigmoid originating in a cross-equatorial coronal hole, where the magnetic field is mostly open and seriously distinct from the closed background field above active-region sigmoids. The source region first appeared as a bipole, which subsequently experienced a rapid emergence followed by a long-term decay. Correspondingly, the coronal structure initially appeared as arc-like loops, then gradually sheared and transformed into continuously sigmoidal loops, mainly owing to flux cancellation near the polarity inversion line. The temperature of J-shaped and sigmoidal loops is estimated to be about  $2.0 \times 10^6$  K, greater than that of the background coronal hole. Using the flux-rope insertion method, we further reconstruct the nonlinear force-free fields that well reproduces the transformation of the potential field into a sigmoidal field. The fact that the sheared and sigmoidal loops are mainly concentrated at around the high-Q region implies that the reconnection most likely takes place there to form the sigmoidal field and heat the plasma. Moreover, the twist of sigmoidal field lines is estimated to be around 0.8, less than the values derived for the sigmoids from active regions. However, the sigmoidal flux may quickly enter an unstable regime at the very low corona ( $< 10$  Mm) due to the open background field. The results suggest that the mini-sigmoid, at least the one in our study, has the same formation and eruption process as the large-scale one, but is significantly influenced by the overlying flux. **2017 January 28-31**

## **Localized Microwave and EUV Bright Structures in an Eruptive Prominence**

Jing [Huang](#)<sup>1</sup>, Baolin Tan<sup>1</sup>, Satoshi Masuda<sup>2</sup>, Xin Cheng<sup>3</sup>, Susanta Kumar Bisoi<sup>1</sup>, and Victor Melnikov<sup>1</sup>

**2019** ApJ 874 176

<https://doi.org/10.3847/1538-4357/ab0e80>

We study a solar eruptive prominence with flare/coronal mass ejection (CME) event by microwave and extreme ultraviolet (EUV) observations. Its evolution can be divided into three phases: slow rise, fast expansion, and ejection. In the slow-rise phase, the prominence continuously twists for more than one hour with a patch of bright emission appearing around the top. When the north leg interacts with the local small-size loops, the fast expansion is initiated and the flare takes place there. The prominence grows rapidly, and a series of localized brightenings appear in the whole

prominence structure. Then the ejection occurs, followed by a CME. In microwave images, the brightness temperature ( $T_b$ ) at 17 and 34 GHz can be divided into three components. The strongest emission with  $T_b$  at 25,000–300,000 K is related to the bright flare region near the north foot. The medium  $T_b$  (10,000–20,000 K) outlines a series of small-scale bright enhancements scattering in the prominence, which are superposed on a weak background with  $T_b$  at 5000–10,000 K. These localized bright structures, first appearing at the top and then scattering in the entire prominence structure, are cospatial with EUV bright threads, fibers, or spots in both high- and low-temperature passbands. They display significant temporal variations on the scale of 3–5 s in the microwave observations. Thus, the plasma inside the prominence is spatially structured and changes with time in both density and temperature. This behavior could be interpreted in the frame of the small-scale and short-term process of energy releases in the twisted magnetic structure.

2015 May 9

### **Magnetic braids in eruptions of a spiral structure in the solar atmosphere**

Zhenghua [Huang](#), [Lidong Xia](#), [Chris J. Nelson](#), [Jiajia Liu](#), [Thomas Wiegelmann](#), [Hui Tian](#), [James A. Klimchuk](#), [Yao Chen](#), [Bo Li](#)

ApJ **854** 80 **2018**

<https://arxiv.org/pdf/1801.05967.pdf>

<http://sci-hub.tw/http://iopscience.iop.org/0004-637X/854/2/80/>

We report on high-resolution imaging and spectral observations of eruptions of a spiral structure in the transition region, which were taken with the Interface Region Imaging Spectrometer (IRIS), the Atmospheric Imaging Assembly (AIA) and the Helioseismic and Magnetic Imager (HMI). The eruption coincided with the appearance of two series of jets, with velocities comparable to the Alfvén speeds in their footpoints. Several pieces of evidence of magnetic braiding in the eruption are revealed, including localized bright knots, multiple well-separated jet threads, transition region explosive events and the fact that all these three are falling into the same locations within the eruptive structures.

Through analysis of the extrapolated three-dimensional magnetic field in the region, we found that the eruptive spiral structure corresponded well to locations of twisted magnetic flux tubes with varying curl values along their lengths. The eruption occurred where strong parallel currents, high squashing factors, and large twist numbers were obtained. The electron number density of the eruptive structure is found to be  $\sim 3 \times 10^{12} \text{ cm}^{-3}$ , indicating that significant amount of mass could be pumped into the corona by the jets. Following the eruption, the extrapolations revealed a set of seemingly relaxed loops, which were visible in the AIA 94 Å channel indicating temperatures of around 6.3 MK. With these observations, we suggest that magnetic braiding could be part of the mechanisms explaining the formation of solar eruption and the mass and energy supplement to the corona. **2014 June 11**

### **Explosive events on subarcsecond scale in IRIS observations: a case study**

Zhenghua [Huang](#), Maria S. Madjarska, Lidong Xia, J. G. Doyle, Klaus Galsgaard, Hui Fu

ApJ **797** 88 **2014**

<http://star.arm.ac.uk/preprints/2014/659.pdf>

We present study of a typical explosive event (EE) at subarcsecond scale witnessed by strong non-Gaussian profiles with blue- and red-shifted emission of up to 150 km/s seen in the transition-region Si iv 1402.8 Å, and the chromospheric Mg ii k 2796.4 Å and C ii 1334.5 Å observed by the Interface Region Imaging Spectrograph (IRIS) at unprecedented spatial and spectral resolution. For the first time an EE is found to be associated with very small-scale ( $\sim 120$  km wide) plasma ejection followed by retraction in the chromosphere. These small-scale jets originate from a compact bright-point-like structure of  $\sim 1.5''$  size as seen in the IRIS 1330 Å images. SDO/AIA and SDO/HMI co-observations show that the EE lies in the footpoint of a complex loop-like brightening system. The EE is detected in the higher temperature channels of AIA 171 Å, 193 Å, and 131 Å suggesting that it reaches a higher temperature of  $\log T = 5.36 \pm 0.06$  (K). Brightenings observed in the AIA channels with durations  $90 \sim 120$  s are probably caused by the plasma ejections seen in the chromosphere. The wings of the C ii line behave in a similar manner to the Si iv's, indicating close formation temperatures, while the Mg ii k wings show additional Doppler-shifted emission. Magnetic convergence or emergence followed by cancellation at a rate of  $5 \sim 10^{14} \text{ Mx/s}$  is associated with the EE region. The combined changes of the locations and the flux of different magnetic patches suggest that magnetic reconnection must have taken place. Our results challenge several theories put forward in the past to explain non-Gaussian line profiles, i.e., EEs. Our case study on its own, however, cannot reject these theories, thus further in-depth studies on the phenomena producing EEs are required. **2013 October 4**

### **H $\alpha$ spectroscopy and multi-wavelength imaging of a solar flare caused by filament eruption**

Z. [Huang](#), M. S. Madjarska, K. Koleva, J. G. Doyle, P. Duchlev, M. Dechev, and K. Reardon

E-print, May 2014; A&A

<http://star.arm.ac.uk/preprints/2014/652.pdf>

We study a sequence of eruptive events including filament eruption, a GOES C4.3 flare and a coronal mass ejection. We aim to identify the possible trigger(s) and precursor(s) of the filament destabilisation; investigate flare kernel characteristics; flare ribbons/kernels formation and evolution; study the interrelation of the filament-eruption/flare/coronal-mass-ejection phenomena as part of the integral active-region magnetic field configuration; determine H  $\alpha$  line profile evolution during the eruptive phenomena. Multi-instrument observations are analysed including H  $\alpha$  line profiles, speckle images at H  $\alpha$   $-0.8$  Å and H  $\alpha$   $+0.8$  Å from IBIS at DST/NSO, EUV images and magnetograms from the SDO, coronagraph images from STEREO and the X-ray flux observations from FERMI and GOES. We establish that the filament destabilisation and eruption are the main trigger for the flaring activity. A



surge-like event with a circular ribbon in one of the filament footpoints is determined as the possible trigger of the filament destabilisation. Plasma draining in this footpoint is identified as the precursor for the filament eruption. A magnetic flux emergence prior to the filament destabilisation followed by a high rate of flux cancellation of  $1.34 \times 10^{16} \text{ Mx s}^{-1}$  is found during the flare activity. The flare X-ray lightcurves reveal three phases that are found to be associated with three different ribbons occurring consecutively. A kernel from each ribbon is selected and analysed. The kernel lightcurves and  $H \alpha$  line profiles reveal that the emission increase in the line centre is stronger than that in the line wings. A delay of around 5-6 mins is found between the increase in the line centre and the occurrence of red asymmetry. Only red asymmetry is observed in the ribbons during the impulsive phases. Blue asymmetry is only associated with the dynamic filament. **11 Nov 2010**

## INITIATION AND EARLY DEVELOPMENT OF THE 2008 APRIL 26 CORONAL MASS EJECTION

J. [Huang](#)<sup>1,2</sup>, P. D´emoulin<sup>2</sup>, M. Pick<sup>2</sup>, F. Auch`ere<sup>3</sup>, Y. H. Yan<sup>1</sup>, and A. Bouteille<sup>2</sup>

*Astrophysical Journal*, 729:107 (10pp), **2011**, [File](#)

We present a detailed study of a coronal mass ejection (CME) with high temporal cadence observations in radio and extreme-ultraviolet (EUV). The radio observations combine imaging of the low corona with radio spectra in the outer corona and interplanetary space. The EUV observations combine the three points of view of the *STEREO* and *SOHO* spacecraft. The beginning of the CME initiation phase is characterized by emissions that are signatures of the reconnection of the outer part of the erupting configuration with surrounding magnetic fields. Later on, a main source of emission is located in the core of the active region. It is an indirect signature of the magnetic reconnection occurring behind the erupting flux rope. Energetic particles are also injected in the flux rope and the corresponding radio sources are detected. Other radio sources, located in front of the EUV bright front, trace the interaction of the flux rope with the surrounding fields. Hence, the observed radio sources enable us to detect the main physical steps of the CME launch. We find that imaging radio emissions in the metric range permits us to trace the extent and orientation of the flux rope which is later detected in interplanetary space. Moreover, combining the radio images at various frequencies with fast EUV imaging permits us to characterize in space and time the processes involved in the CME launch.

## Flare/CME Cartoons

Hugh [Hudson](#), Nicolina Chrysaphi, and Norman Gray

uksp\_nug #110 **2020** <http://www.uksolphys.org/uksp-nugget/110-flarecme-cartoons/>

## Chapter 9 - High-Energy Solar Physics

**Review**

H.S. [Hudson](#) and A.L. MacKinnon

In: *The Sun as a Guide to Stellar Physics* **Book**

Eds. Oddbjørn Engvold, Jean-Claude Vial, and Andrew Skumanich

Elsevier, November **2018**

<https://www.sciencedirect.com/book/9780128143346/the-sun-as-a-guide-to-stellar-physics>

This chapter deals generally with the high-energy astrophysics of the Sun, specifically with solar flares and coronal mass ejections (CMEs), but it also touches on the whole range of nonthermality or departures from Maxwellian distributions in solar plasmas. Radio, x-ray, and  $\gamma$ -ray observations provide primary remote-sensing observations of these departures, but such signatures can be hidden by brighter thermal emissions that may not be as fundamental in physics events. The solar paradigm for flare/CME development appears to match many of the new stellar observations of similar phenomena, but the limitations of observational sensitivity mean that we have few direct observations of the expected hard x-rays and none at all of the  $\gamma$ -rays that could confirm this.

## Momentum Distribution in Solar Flare Processes

H. S. [Hudson](#), L. Fletcher, G. H. Fisher, W. P. Abbett and A. Russell

*Solar Physics*, Volume 277, Number 1, 77-88, **2012**

We discuss the consequences of momentum conservation in processes related to solar flares and coronal mass ejections (CMEs), in particular describing the relative importance of vertical impulses that could contribute to the excitation of seismic waves (“sunquakes”). The initial impulse associated with the primary flare energy transport in the impulsive phase contains sufficient momentum, as do the impulses associated with the acceleration of the evaporation flow (the chromospheric shock) or the CME itself. We note that the deceleration of the evaporative flow, as coronal closed fields arrest it, will tend to produce an opposite impulse, reducing the energy coupling into the interior. The actual mechanism of the coupling remains unclear at present.

## CORONAL MASS EJECTIONS: OVERVIEW OF OBSERVATIONS

H. S. [HUDSON](#)<sup>1,\*</sup>, J.-L. BOUGERET<sup>2</sup> and J. BURKEPILE<sup>3</sup>

### Observing coronal mass ejections without coronagraphs.

Hudson, H.S., Cliver, E.W.,

2001. J. Geophys. Res. 106, 25199–25214.

### Multiwavelength Imaging and Spectral Analysis of Jet-like Phenomena in a Solar Active Region Using IRIS and AIA

Llŷr Dafydd **Humphries**<sup>1</sup>, Erwin Verwichte<sup>2</sup>, David Kuridz <sup>1</sup>, and Huw Morgan<sup>1</sup>

2020 ApJ 898 17

<https://doi.org/10.3847/1538-4357/ab974d>

<https://sci-hub.tw/https://iopscience.iop.org/article/10.3847/1538-4357/ab974d>

<https://arxiv.org/pdf/2010.04042.pdf>

High-resolution observations of dynamic phenomena give insight into properties and processes that govern the low solar atmosphere. We present the analysis of jet-like phenomena emanating from a penumbral foot-point in active region (AR) 12192 using imaging and spectral observations from the Interface Region Imaging Spectrograph (IRIS) and the Atmospheric Imaging Assembly (AIA) on board the Solar Dynamics Observatory. These jets are associated with line-of-sight (LoS) Doppler speeds of  $\pm 10$ –22 km s<sup>-1</sup> and bright fronts which seem to move across the Plane-of-Sky (PoS) at speeds of 23–130 km s<sup>-1</sup>. Such speeds are considerably higher than the expected sound speed in the chromosphere. The jets have signatures which are visible both in the cool and hot channels of IRIS and AIA. Each jet lasts on average 15 minutes and occur 5–7 times over a period of 2 hours. Possible mechanisms to explain this phenomenon are suggested, the most likely of which involve p-mode or Alfv n wave shock trains impinging on the transition region (TR) and corona as a result of steepening photospheric wavefronts or gravity waves. **Oct. 25, 2014**

### Automated Detection of Solar Eruptions

Neal **Hurlburt**

Journal of Space Weather and Space Climate, 5, A39 2015 **Open Access**

<http://arxiv.org/pdf/1504.03395v1.pdf>

Observation of the solar atmosphere reveals a wide range of motions, from small scale jets and spicules to global-scale coronal mass ejections. Identifying and characterizing these motions are essential to advancing our understanding the drivers of space weather. Both automated and visual identifications are currently used in identifying CMEs. To date, eruptions near the solar surface (which may be precursors to CMEs) have been identified primarily by visual inspection. Here we report on EruptionPatrol (EP): a software module that is designed to automatically identify eruptions from data collected by SDO/AIA. We describe the method underlying the module and compare its results to previous identifications found in the Heliophysics Event Knowledgebase. EP identifies eruptions events that are consistent with those found by human annotations, but in a significantly more consistent and quantitative manner. Eruptions are found to be distributed within 15Mm of the solar surface. They possess peak speeds ranging from 4 to 100 km/sec and display a power-law probability distribution over that range. These characteristics are consistent with previous observations of prominences. **2010-Aug-01**

### Cross-field Diffusion Effects on Particle Transport in a Solar Coronal Flux Rope

Edin **Husidic**<sup>1,2</sup>, Nicolas Wijsen<sup>1</sup>, Luis Linan<sup>1</sup>, Michaela Brchnelova<sup>1</sup>, Rami Vainio<sup>2</sup>, and Stefaan Poedts<sup>1,3</sup>

2024 ApJL 976 L31

<https://iopscience.iop.org/article/10.3847/2041-8213/ad8d56/pdf>

Solar energetic particles associated with solar flares and coronal mass ejections (CMEs) are key agents of space weather phenomena, posing severe threats to spacecraft and astronauts. Recent observations by Parker Solar Probe indicate that the magnetic flux ropes of a CME can trap energetic particles and act as barriers, preventing other particles from crossing. In this Letter, we introduce the novel COCONUT+PARADISE model to investigate the confinement of energetic particles within a flux rope and the effects of cross-field diffusion (CFD) on particle transport in the solar corona, particularly in the presence of a CME. Using the global magnetohydrodynamic coronal model COolfluid COroNal Unstructured (COCONUT), we generate background configurations containing a CME modeled as a Titov–D moulin flux rope (TDFR). We then utilize the particle transport code PArticle Radiation Asset Directed at Interplanetary Space Exploration (PARADISE) to inject monoenergetic 100 keV protons inside one of the TDFR legs near its footpoint and evolve the particles through the COCONUT backgrounds. To study CFD, we employ two different approaches regarding the perpendicular proton mean free path (MFP): a constant MFP and a Larmor radius-dependent MFP. We contrast these results with those obtained without CFD. While particles remain fully trapped within the TDFR without CFD, we find that even relatively small perpendicular MFP values allow particles on the outer layers to escape. In contrast, the initially interior trapped particles stay largely confined. Finally, we highlight how our model and this Letter's results are relevant for future research on particle acceleration and transport in an extended domain encompassing both the corona and inner heliosphere.

## **Automated detection of coronal mass ejections in three-dimensions using multi-viewpoint observations**

J. [Hutton](#) and H. Morgan

A&A 599, A68 (2017)

<http://www.aanda.org/articles/aa/pdf/2017/03/aa29516-16.pdf>

A new, automated method of detecting coronal mass ejections (CMEs) in three dimensions for the LASCO C2 and STEREO COR2 coronagraphs is presented. By triangulating isolated CME signal from the three coronagraphs over a sliding window of five hours, the most likely region through which CMEs pass at  $5 R_{\odot}$  is identified. The centre and size of the region gives the most likely direction of propagation and approximate angular extent. The Automated CME Triangulation (ACT) method is tested extensively using a series of synthetic CME images created using a wireframe flux rope density model, and on a sample of real coronagraph data; including halo CMEs. The accuracy of the angular difference ( $\sigma$ ) between the detection and true input of the synthetic CMEs is  $\sigma = 7.14^{\circ}$ , and remains acceptable for a broad range of CME positions relative to the observer, the relative separation of the three observers and even through the loss of one coronagraph. For real data, the method gives results that compare well with the distribution of low coronal sources and results from another instrument and technique made further from the Sun. The true three dimension (3D)-corrected kinematics and mass/density are discussed. The results of the new method will be incorporated into the CORIMP database in the near future, enabling improved space weather diagnostics and forecasting. **14th January, 2009, 27th January, 2012, 1st September, 2012, 2013-07-26, 26th October, 2013**

## **ERUPTING FILAMENTS WITH LARGE ENCLOSING FLUX TUBES AS SOURCES OF HIGH-MASS THREE-PART CMEs, AND ERUPTING FILAMENTS IN THE ABSENCE OF ENCLOSING FLUX TUBES AS SOURCES OF LOW-MASS UNSTRUCTURED CMEs**

Joe [Hutton](#) and Huw Morgan

2015 ApJ 813 35

The 3-part appearance of many coronal mass ejections (CMEs) arising from erupting filaments emerges from a large magnetic flux tube structure, consistent with the form of the erupting filament system. Other CMEs arising from erupting filaments lack a clear 3-part structure and reasons for this have not been researched in detail. This paper aims to further establish the link between CME structure and the structure of the erupting filament system and to investigate whether CMEs which lack a 3-part structure have different eruption characteristics. A survey is made of **221 near-limb filament eruptions observed from 2013 May 03 to 2014 June 30** by Extreme UltraViolet (EUV) imagers and coronagraphs. Ninety-two filament eruptions are associated with 3-part structured CMEs, 41 eruptions are associated with unstructured CMEs. The remaining 88 are categorized as failed eruptions. For 34% of the 3-part CMEs, processing applied to EUV images reveals the erupting front edge is a pre-existing loop structure surrounding the filament, which subsequently erupts with the filament to form the leading bright front edge of the CME. This connection is confirmed by a flux-rope density model. Furthermore, the unstructured CMEs have a narrower distribution of mass compared to structured CMEs, with total mass comparable to the mass of 3-part CME cores. This study supports the interpretation of 3-part CME leading fronts as the outer boundaries of a large pre-existing flux tube. Unstructured (non 3-part) CMEs are a different family to structured CMEs, arising from the eruption of filaments which are compact flux tubes in the absence of a large system of enclosing closed field.

## **Comparison Between Radio Loud and Radio Quiet Fast CMEs: A Reason for Radio Quietness**

[M. Syed Ibrahim](#), [E. Ebenezer](#) & [A. Shanmugaraju](#)

[Solar Physics](#) volume 298, Article number: 59 (2023)

<https://doi.org/10.1007/s11207-023-02151-4>

It is well known that fast CMEs are mostly associated with magnetohydrodynamic (MHD) shocks in the solar corona, forming type-II radio bursts. However, the absence of type-II radio bursts is not uncommon. Herein, we aim to analyze the differences between the radio loud (RL) and radio quiet (RQ) fast Coronal Mass Ejections (CMEs) (speed  $\geq 900 \text{ km s}^{-1}$ ) during Solar Cycle 24 (2008 – 2021). From the 309 fast CMEs, we could identify 143 events with a known source origin on the visible disk (Earth view). We identified the associated flares/CMEs for 143 events using running-difference images from (i) Solar Dynamic Observatory/Atmospheric Imaging Assembly (SDO/AIA) and (ii) Large Angle Spectrometric Coronagraph (LASCO) observations. Among these 143 events, RQ and RL groups have 70 and 73 events, respectively. CALLISTO and Wind/WAVES observations are used to identify these RL and RQ sets. We analyzed the possibilities of streamer-CME and CME-CME interaction. In this study, we report the important differences between RL and RQ CMEs and the underlying reasons for the radio quietness of fast CMEs. In the LASCO field of view, the majority of RL CMEs (almost 90%) interacted with streamers and/or pre-CMEs, whereas only 25% of RQ CMEs did the same, and there was no pre-CME interaction. The observational evidence led to the conclusion that substantial density perturbation/interaction increases the probability of production of type-II radio emissions by the shock of RL CMEs.

## **Investigation of two coronal mass ejections from circular ribbon source region: Origin, Sun-Earth propagation and Geo-effectiveness**

[Syed Ibrahim](#), [Wahab Uddin](#), [Bhuwan Joshi](#), [Ramesh Chandra](#), [Arun Kumar Awasthi](#)

Research in Astronomy and Astrophysics

2021

<https://arxiv.org/pdf/2110.06547.pdf>

In this article, we compare the properties of two coronal mass ejections (CMEs) that show similar source region characteristics but different evolutionary behavior in the later phases. We discuss the two events in terms of their near-Sun characteristics, interplanetary evolution, and geo-effectiveness. We carefully analyzed the initiation and propagation parameters of these events to establish the precise CME-ICME connection and their near-Earth consequences. The First event was associated with poor geo-magnetic storm disturbance index (Dst  $\approx$ -20 nT) while the second event is associated with intense geomagnetic storm of DST  $\approx$ -119 nT. The configuration of the sunspots in the active regions and their evolution are observed by Helioseismic and Magnetic Imager (HMI). For source region imaging, we rely on data obtained from Atmospheric Imaging Assembly (AIA) on board Solar Dynamics Observatory (SDO) and H $\alpha$  filtergrams from Solar Tower Telescope at Aryabhata Research Institute of Observational Sciences (ARIES). For both the CMEs, flux rope eruptions from the source region triggered flares of similar intensities ( $\approx$ M1). At the solar source region of the eruptions, we observed circular ribbon flare (CRF) for both the cases, suggesting fan-spine magnetic configuration in the active region corona. **2013 May 02, 2014 February 16**

## **Interplanetary Coronal Mass Ejections During Solar Cycles 23 and 24: Sun–Earth Propagation Characteristics and Consequences at the Near-Earth Region**

M. Syed **Ibrahim**, Bhuwan Joshi, K.-S. Cho, R.-S. Kim, Y.-J. Moon

[Solar Physics](#) May 2019, 294:54 **File**

[sci-hub.se/10.1007/s11207-019-1443-5](http://sci-hub.se/10.1007/s11207-019-1443-5)

In this article, we present a statistical study probing the relation between interplanetary coronal mass ejections (ICMEs) observed at 1 AU and their corresponding coronal mass ejections at the near-Sun region. The work encompasses the ICME activity that occurred during Solar Cycles 23 and 24 (1996 – 2017) while presenting an overall picture of ICME events during the complete Solar Cycle 24 for the first time. The importance of this study further lies in comparing two subsets of ICMEs, i.e. magnetic clouds (MCs) and ejecta (EJ), to explore how the observed structures of ICMEs at 1 AU could be associated with the properties of CMEs during their launch at the Sun. We find that, although Solar Cycle 24 saw a significant reduction in the number of ICME events compared to the previous cycle, the fraction of MCs was much higher during Cycle 24 than Cycle 23 (60% versus 41%). In general, the ICME transit-time decreases with the increase in the CME initial speed, although a broad range of transit times were observed for a given CME speed. We also find that the high-speed ICMEs ( $\geq$ 500 kms $^{-1}$ ) form a distinct group in terms of the deficit in their transit times when compared with low-speed events ( $\leq$ 500 kms $^{-1}$ ), which means that high-speed ICMEs acquire a much higher internal energy from the source active regions during the initiation process that effectively overcomes the aerodynamic drag force while they transit in the interplanetary medium. The CME propagation from the Sun to the near-Earth environment shows both an overall positive and negative acceleration (i.e. deceleration), although the acceleration is limited to only low-speed CMEs that are launched with a speed comparable with or less than the mean solar wind speed ( $\approx$ 400–450 kms $^{-1}$ ). Within a given cycle, the similarities of MC and EJ profiles with respect to the CME–ICME speed relation as well as interplanetary acceleration support the hypothesis that all CMEs have a flux rope structure and that the trajectory of the CMEs essentially determines the observed ICME structure at 1 AU. **13 December 2006, 22 June 2015**

## **Properties and relationship between solar eruptive flares and Coronal Mass Ejections during rising phase of Solar Cycles 23 and 24**

M.Syed **Ibrahim**, [A.Shanmugaraju](#), [Y.-J.Moon](#), [B.Vrsnak](#), [S.Umapathy](#)

[Advances in Space Research](#) Volume 61, Issue 1, 1 January 2018, Pages 540-551

[https://ac.els-cdn.com/S027311771730666X/1-s2.0-S027311771730666X-main.pdf?\\_tid=4faa2d64-de43-11e7-8054-00000aab0f01&acdnat=1512976814\\_f6b3fddde3a016b209ccb968996e7adf](https://ac.els-cdn.com/S027311771730666X/1-s2.0-S027311771730666X-main.pdf?_tid=4faa2d64-de43-11e7-8054-00000aab0f01&acdnat=1512976814_f6b3fddde3a016b209ccb968996e7adf)

Statistical relationship between major flares and the associated CMEs during rising phases of Solar Cycles 23 and 24 are studied. Totally more than 6000 and 10,000 CMEs were observed by SOHO/LASCO (Solar and Heliospheric Observatory/Large Angle Spectrometric Coronagraph) during 23rd [May 1996–June 2002] and 24th [December 2008–December 2014] solar cycles, respectively. In particular, we studied the relationship between properties of flares and CMEs using the limb events (longitude 70–85°) to avoid projection effects of CMEs and partial occultation of flares that occurred near 90°. After selecting a sample of limb flares, we used certain spatial and temporal constraints to find the flare-CME pairs. Using these constraints, we compiled 129 events in Solar Cycle 23 and 92 events in Solar Cycle 24. We compared the flare-CME relationship in the two solar cycles and no significant differences are found between the two cycles. We only found out that the CME mean width was slightly larger and the CME mean acceleration was slightly higher in cycle 24, and that there was somewhat a better relation between flare flux and CME deceleration in cycle 24 than in cycle 23.

## **Propagation of Coronal Mass Ejections Observed During the Rising Phase of Solar Cycle 24**

M. Syed **Ibrahim**, P. K. Manoharan, A. Shanmugaraju

[Solar Physics](#) September 2017, 292:133 **File**

In this study, we investigate the interplanetary consequences and travel time details of 58 coronal mass ejections (CMEs) in the Sun–Earth distance. The CMEs considered are halo and partial halo events of width  $>120^\circ$ . These CMEs occurred during 2009 – 2013, in the ascending phase of the Solar Cycle 24. Moreover, they are Earth-directed events that originated close to the centre of the solar disk (within about  $\pm 30^\circ$  from the Sun’s centre) and propagated approximately along the Sun–Earth line. For each CME, the onset time and the initial speed have been

estimated from the white-light images observed by the LASCO coronagraphs onboard the SOHO space mission. These CMEs cover an initial speed range of  $\sim 260\text{--}2700\text{ km s}^{-1}$ . For these CMEs, the associated interplanetary shocks (IP shocks) and interplanetary CMEs (ICMEs) at the near-Earth environment have been identified from *in-situ* solar wind measurements available at the OMNI data base. Most of these events have been associated with moderate to intense IP shocks. However, these events have caused only weak to moderate geomagnetic storms in the Earth's magnetosphere. The relationship of the travel time with the initial speed of the CME has been compared with the observations made in the previous Cycle 23, during 1996–2004. In the present study, for a given initial speed of the CME, the travel time and the speed at 1 AU suggest that the CME was most likely not much affected by the drag caused by the slow-speed dominated heliosphere. Additionally, the weak geomagnetic storms and moderate IP shocks associated with the current set of Earth-directed CMEs indicate magnetically weak CME events of Cycle 24. The magnetic energy that is available to propagate CME and cause geomagnetic storm could be significantly low. **15 March 2013.**

**Table 1** Observational parameters of 58 CME events (eight interacting CMEs are marked with asterisk symbols).

## A New Solar Imaging System for Observing High-Speed Eruptions: Solar Dynamics Doppler Imager (SDDI)

Kiyoshi [Ichimoto](#), Takako T. Ishii, Kenichi Otsuji, [Goichi Kimura](#)...

Sol Phys (2017) 292: 63. doi:10.1007/s11207-017-1082-7

A new solar imaging system was installed at Hida Observatory to observe the dynamics of flares and filament eruptions. The system (Solar Dynamics Doppler Imager; SDDI) takes full-disk solar images with a field of view of  $2520\text{ arcsec} \times 2520\text{ arcsec}$  at multiple wavelengths around the  $\text{H}\alpha$  line at  $6562\text{ \AA}$ . Regular operation was started in May 2016, in which images at 73 wavelength positions spanning from  $\text{H}\alpha - 9\text{ \AA}$  to  $\text{H}\alpha + 9\text{ \AA}$  are obtained every 15 seconds. The large dynamic range of the line-of-sight velocity measurements ( $\pm 400\text{ km s}^{-1}$ ) allows us to determine the real motions of erupting filaments in 3D space. It is expected that SDDI provides unprecedented datasets to study the relation between the kinematics of filament eruptions and coronal mass ejections (CME), and to contribute to the real-time prediction of the occurrence of CMEs that cause a significant impact on the space environment of the Earth.

## Analysis of a long-duration AR throughout five solar rotations: Magnetic properties and ejective events

Francisco A. [Iglesias](#), [Hebe Cremades](#), [Luciano A. Merenda](#), [Cristina H. Mandrini](#), [Fernando M. Lopez](#), [Marcelo C. Lopez Fuentes](#), [Ignacio Ugarte-Urra](#)

Advances in Space Research **2019**

<https://arxiv.org/pdf/1911.01265.pdf>

Coronal mass ejections (CMEs), which are among the most magnificent solar eruptions, are a major driver of space weather and can thus affect diverse human technologies. Different processes have been proposed to explain the initiation and release of CMEs from solar active regions (ARs), without reaching consensus on which is the predominant scenario, and thus rendering impossible to accurately predict when a CME is going to erupt from a given AR. To investigate AR magnetic properties that favor CMEs production, we employ multi-spacecraft data to analyze a long duration AR (NOAA 11089, 11100, 11106, 11112 and 11121) throughout its complete lifetime, spanning five Carrington rotations from **July to November 2010**. We use data from the Solar Dynamics Observatory to study the evolution of the AR magnetic properties during the five near-side passages, and a proxy to follow the magnetic flux changes when no magnetograms are available, i.e. during far-side transits. We characterized the angular widths, speeds and masses of 108 CMEs that we associated to the AR, when examining a 124-day period. Such an ejectivity tracking was possible thanks to the multiviewpoint images provided by the STEREO and SOHO in a quasi-quadrate configuration. We also inspected the X-ray flares registered by the GOES satellite and found 162 to be associated to the AR under study. Given the substantial number of ejections studied, we use a statistical approach instead of a single-event analysis. We found three well defined periods of very high CMEs activity and two periods with no mass ejections that are preceded or accompanied by characteristic changes in the AR magnetic flux, free magnetic energy and/or presence of electric currents. Our large sample of CMEs and long term study of a single AR, provide further evidence relating AR magnetic activity to CME and Flare production. **19-23 July 2010, 2-28 Aug 2010, 30 Aug-4 Sep 2010, 5-17 Sep 2010, 8-16 Oct 2010, 17-23 Oct 2010, 28 Oct-6 Nov 2010, 10-15 Nov 2010, 17 Nov 2010**

**Table 1:** Identification numbers (ID), dates (in dd/mm format) and times of 108 white-light ejective events (CMEs), originating from the AR under study.

## A Three-dimensional Magnetohydrodynamic Simulation of the Formation of Solar Chromospheric Jets with Twisted Magnetic Field Lines

H. [Iijima](#)<sup>1</sup> and T. Yokoyama

2017 ApJ 848 38

This paper presents a three-dimensional simulation of chromospheric jets with twisted magnetic field lines. Detailed treatments of the photospheric radiative transfer and the equations of state allow us to model realistic thermal convection near the solar surface, which excites various MHD waves and produces chromospheric jets in the simulation. A tall chromospheric jet with a maximum height of 10–11 Mm and lifetime of 8–10 minutes is formed

above a strong magnetic field concentration. The magnetic field lines are strongly entangled in the chromosphere, which helps the chromospheric jet to be driven by the Lorentz force. The jet exhibits oscillatory motion as a natural consequence of its generation mechanism. We also find that the produced chromospheric jet forms a cluster with a diameter of several Mm with finer strands. These results imply a close relationship between the simulated jet and solar spicules.

### **Effect of coronal temperature on the scale of solar chromospheric jets**

H. [Iijima](#), T. Yokoyama

ApJL 812 L30 2015

<http://arxiv.org/pdf/1509.06677v1.pdf>

We investigate the effect of coronal temperature on the formation process of solar chromospheric jets using two-dimensional magnetohydrodynamic simulations of the region from the upper convection zone to the lower corona. We develop a new radiative magnetohydrodynamic code for the dynamic modeling of the solar atmosphere, employing a LTE equation of state, optically thick radiative loss in the photosphere, optically thin radiative loss in the chromosphere and the corona, and thermal conduction along the magnetic field lines. Many chromospheric jets are produced in the simulations by shock waves passing through the transition region. We find that these jets are projected farther outward when the coronal temperature is lower (similar to that in coronal holes) and shorter when the coronal temperature is higher (similar to that in active regions). When the coronal temperature is high, the deceleration of the chromospheric jets is consistent with the model in which deceleration is determined by the periodic chromospheric shock waves. However, when the coronal temperature is low, the gravitational deceleration becomes more important and the chromospheric jets approach ballistic motion.

### **Simple Model for Temporal Variations of H $\alpha$ Spectrum by an Eruptive Filament from a Superflare on a Solar-type Star**

[Kai Ikuta](#), [Kazunari Shibata](#)

ApJ 2024

<https://arxiv.org/pdf/2401.04279.pdf>

Flares are intense explosions on the solar and stellar surfaces, and solar flares are sometimes accompanied by filament or prominence eruptions. Recently, a large filament eruption associated with a superflare on a solar-type star EK Dra was discovered for the first time. The absorption of the H $\alpha$  spectrum initially exhibited a blueshift with the velocity of 510 (km s<sup>-1</sup>), and decelerated in time probably due to gravity. Stellar coronal mass ejections (CMEs) were thought to occur, although the filament eruption did not exceed the escape velocity under the surface gravity. To investigate how such filament eruption occur and whether CMEs are associated with the filament eruption or not, we perform one-dimensional hydrodynamic simulation of the flow along an expanding magnetic loop emulating a filament eruption under adiabatic and unsteady conditions. The loop configuration and expanding velocity normal to the loop are specified in the configuration parameters, and we calculate the line-of-sight velocity of the filament eruption using the velocities along and normal to the loop. We found that (i) the temporal variations of the H $\alpha$  spectrum for EK Dra can be explained by falling filament eruption in the loop with longer time and larger spatial scales than that of the Sun, and (ii) the stellar CMEs are also thought to be associated with the filament eruption from the superflare on EK Dra, because the rarefied loop unobserved in the H $\alpha$  spectrum needs to expand faster than the escape velocity, whereas the observed filament eruption does not exceed the escape velocity.

### **Energy release from a stream of infalling prominence debris on 2011 September 7-8**

Andrew R. [Inglis](#), [Holly R. Gilbert](#), [Leon Ofman](#)

ApJ 2017

<https://arxiv.org/pdf/1708.01555.pdf>

In recent years high-resolution and high-cadence EUV imaging has revealed a new phenomenon, impacting prominence debris, where prominence material from failed or partial eruptions can impact the lower atmosphere and release energy. We report a clear example of energy release and EUV brightening due to infalling prominence debris that occurred on **2011 September 7-8**. The initial eruption of prominence material was associated with an X1.8-class flare from AR11283, occurring at 22:30 UT on 2011 September 7. Subsequently, a semi-continuous stream of this material was observed to return to the solar surface with a velocity  $v > 150$  km/s, impacting a region remote from the original active region between 00:20 - 00:40 UT on 2011 September 8. Using SDO/AIA, the differential emission measure of the plasma was estimated throughout this brightening event. We found that the radiated energy of the impacted plasma was  $L \sim 10^{27}$  ergs, while the thermal energy peaked at  $\sim 10^{28}$  ergs. From this we were able to determine the mass content of the debris to be in the range  $2 \times 10^{14} < m < 2 \times 10^{15}$  g. Given typical prominence masses, the likely debris mass is towards the lower end of this range. This clear example of a prominence debris event shows that significant energy release takes place during these events, and that such impacts may be used as a novel diagnostic tool for investigating prominence material properties.

### **Analysis of UV and EUV emission from impacts on the Sun after 2011 June 7 eruptive flare**

Davina [Innes](#), Philipp Heinrich, Bernd Inhester, Li-Jia Guo

A&A 2016

<http://arxiv.org/pdf/1603.06379v1.pdf>

On **2011 June 7** debris from a large filament eruption fell back to the Sun causing bright ultraviolet (UV) and extreme ultraviolet (EUV) splashes across the surface. These impacts may give clues on the process of stellar accretion. The aim is to investigate how the impact emission is influenced by structures in the falling ejecta and at the solar surface. We determine the UV and EUV light curves of a sample of impacts. The ballistic impact velocity is estimated from the ejection and landing times and, where possible, compared with the velocity derived by tracking the downflows in SDO/AIA and STEREO/EUVI images. Estimates of the column density before impact are made from the darkness of the falling plasma in the 193 Å channel. The impact velocities were between 230 and 450 km/s. All impacts produced bright EUV emission at the impact site but bright UV was only observed when the impacting fragments reached the chromosphere. There was no clear relation between EUV intensity and kinetic energy. Low UV to EUV intensity ratios ( $I\{UV\}/I\{EUV\}$ ) were seen (i) from impacts of low column-density fragments, (ii) when splashes, produced by some impacts, prevented subsequent fragments from reaching the chromosphere, and (iii) from an impact in an active region. The earliest impacts with the lowest velocity ( $\sim 250$  km/s) had the highest  $I\{UV\}/I\{EUV\}$ . The  $I\{UV\}/I\{EUV\}$  decreases with impact velocity, magnetic field at the impact site, and EUV ionising flux. Many of the infalling fragments dissipate above the chromosphere either due to ionisation and trapping in magnetic structures, or to them encountering a splash from an earlier impact. If the same happens in accreting stars then the reduced X-ray compared to optical emission that has been observed is more likely due to absorption by the trailing stream than locally at the impact site.

## **Observations of solar X-ray and EUV jets and their related phenomena** Review

Davina **Innes**, Radoslav Bucik, Li-Jia Guo, Nariaka Nitte

Astronomische Nachrichten **2016**

<http://arxiv.org/pdf/1603.03258v1.pdf>

Solar jets are fast-moving, elongated brightenings related to ejections seen in both images and spectra on all scales from barely visible chromospheric jets to coronal jets extending up to a few solar radii. The largest, most powerful jets are the source of type III radio bursts, energetic electrons and ions with greatly enhanced 3He and heavy element abundances. The frequent coronal jets from polar and equatorial coronal holes may contribute to the solar wind. The primary acceleration mechanism for all jets is believed to be release of magnetic stress via reconnection; however the energy buildup depends on the jets' source environment. In this review, we discuss how certain features of X-ray and EUV jets, such as their repetition rate and association with radio emission, depends on their underlying photospheric field configurations (active regions, polar and equatorial coronal holes, and quiet Sun). **3 Aug 2010, 2012 July 02, 2014 May 16**

## **Observations of Supra-arcade Fans: Instabilities at the Head of Reconnection Jets**

D. E. **Innes**<sup>1,2</sup>, L.-J. Guo<sup>1,2</sup>, A. Bhattacharjee<sup>2,3,4</sup>, Y.-M. Huang<sup>2,3,4</sup>, and D. Schmit

**2014 ApJ 796 27.**

Supra-arcade fans are bright, irregular regions of emission that develop during eruptive flares above flare arcades. The underlying flare arcades are thought to be a consequence of magnetic reconnection along a current sheet in the corona. At the same time, theory predicts plasma jets from the reconnection sites which are extremely difficult to observe directly because of their low densities. It has been suggested that the dark supra-arcade downflows (SADs) seen falling through supra-arcade fans may be low-density jet plasma. The head of a low-density jet directed toward higher-density plasma would be Rayleigh-Taylor unstable, and lead to the development of rapidly growing low- and high-density fingers along the interface. Using Solar Dynamics Observatory/Atmospheric Imaging Assembly 131 Å images, we show details of SADs seen from three different orientations with respect to the flare arcade and current sheet, and highlight features that have been previously unexplained, such as the splitting of SADs at their heads, but are a natural consequence of instabilities above the arcade. Comparison with three-dimensional magnetohydrodynamic simulations suggests that SADs are the result of secondary instabilities of the Rayleigh-Taylor type in the exhaust of reconnection jets.

## **Quiet Sun Explosive Events: Jets, Splashes, and Eruptions**

D. E. **Innes**, L. Teriaca

Solar Physics, February **2013**, Volume 282, Issue 2, pp 453-469

Explosive events appear as broad non-Gaussian wings in the line profiles of small transition-region phenomena. Images from the Solar Dynamics Observatory (SDO) give a first view of the plasma dynamics at the sites of explosive events seen simultaneously in O vi spectra of a region of quiet Sun, taken with the ultraviolet spectrometer Solar Ultraviolet Measurements of Emitted Radiation (SUMER) onboard the Solar and Heliospheric Observatory (SOHO). Distinct event bursts were seen either at the junction of supergranular network cells or near emerging flux. Three are described in the context of their surrounding transition region (304 Å) and coronal (171 Å) activity. One showed plasma ejections from an isolated pair of sites, with a time lag of 50 seconds between events. At the site where the later explosive event was seen, the extreme ultraviolet (EUV) images show a hot core surrounded by a small, expanding ring of chromospheric emission, which we interpret as a "splash." The second explosive-event burst was related to flux cancellation, inferred from Helioseismic and Magnetic Imager (HMI) magnetograms, and a coronal dimming surrounded by a ring of bright EUV emission with explosive events at positions where the spectrometer slit crossed the bright ring. The third series of events occurred at the base of a slow, small coronal mass ejection (**mini-CME**). All events studied here imply jet-like

flows probably triggered by magnetic reconnection at supergranular junctions. Events come from sites close to the footpoints of jets seen in Atmospheric Imaging Assembly (AIA) images, and possibly from the landing site of high-velocity flows. They are not caused by rapid rotation in spicules.

### **Break up of returning plasma after the 7 June 2011 filament eruption by Rayleigh-Taylor instabilities\***

D. E. [Innes](#)<sup>1</sup>, R. H. Cameron<sup>1</sup>, L. Fletcher<sup>2</sup>, B. Inhester<sup>1</sup> and S. K. Solanki<sup>1</sup>  
A&A 540, L10 (2012)

Context. A prominence eruption on **7 June 2011** produced spectacular curtains of plasma falling through the lower corona. At the solar surface they created an incredible display of extreme ultraviolet brightenings.

Aims. To identify and analyze some of the local instabilities which produce structure in the falling plasma.

Methods. The structures were investigated using SDO/AIA 171 Å and 193 Å images in which the falling plasma appeared dark against the bright coronal emission.

Results. Several instances of the Rayleigh-Taylor instability were investigated. In two cases the Alfvén velocity associated with the dense plasma could be estimated from the separation of the Rayleigh-Taylor fingers. A second type of feature, which has the appearance of self-similar branching horns was discussed.

### **Quiet Sun mini-coronal mass ejections activated by supergranular flows\_**

D. E. [Innes](#)<sup>1</sup>, A. Genetelli<sup>1,2</sup>, R. Attie<sup>1</sup>, and H. E. Potts<sup>3</sup>

A&A 495, 319–323 (2009); DOI: [10.1051/0004-6361:200811011](https://doi.org/10.1051/0004-6361/200811011); **File**

Context. The atmosphere of the quiet Sun is controlled by photospheric flows sweeping up concentrations of mixed polarity magnetic field. Along supergranule boundaries and junctions, there is a strong correlation between magnetic flux and bright chromospheric and transition region emission.

Aims. The aim is to investigate the relationship between photospheric flows and small flare-like brightenings seen in Extreme Ultraviolet images.

Methods. We describe observations of small eruptions seen in quiet Sun images taken with the Extreme UltraViolet Imager (EUVI) on STEREO. The photospheric flows during the eruption build-up phase are investigated by tracking granules in high resolution MDI continuum images.

Results. Eruptions with characteristics of small coronal mass ejections (CMEs) occur at the junctions of supergranular cells. The eruptions produce brightening at the onset site, dark cloud or small filament ejections, and faint waves moving with plane-of-sky speeds up to 100 km s<sup>-1</sup>. In the two examples studied, they appear to be activated by converging and rotating supergranular flows, twisting small concentrations of opposite polarity magnetic field. An estimate of the occurrence rate is about 1400 events per day over the whole Sun. One third of these events seem to be associated with waves. Typically, the waves last for about 30 min and travel a distance of 80 Mm, so at any one time they cover 1/50th of the lower corona.

### **Quiet Sun Mini-CMEs Observed in STEREO**

[Innes](#), D.1; Genetelli, A.2; Attie, R.1; Potts, H.

ESPM Freiburg 2008, **Presentation**

Mini-CMEs are eruptions of cool chromospheric material into the corona seen up to 50 Mm from the source. They are usually accompanied by flare-like brightenings at the onset site. The velocities are typically 20-30 km/s, but may be 5 times faster at onset.

STEREO 171 A observations of a region around a small equatorial coronal hole when it was crossing the disk center are studied over a period of 24 hours. Many events are seen. Events are generally characterized by dark clouds in the 171 images and strong brightening in the chromosphere. Selected events will be discussed with emphasis on the underlying photospheric magnetic field and photospheric flows.

### **Detection of a High-velocity Prominence Eruption Leading to a CME Associated with a Superflare on the RS CVn-type Star V1355 Orionis**

Shun [Inoue](#)<sup>1</sup>, Hiroyuki Maehara<sup>2</sup>, Yuta Notsu<sup>3,4,5</sup>, Kosuke Namekata<sup>6</sup>, Satoshi Honda<sup>7</sup>, Keiichi Namizaki<sup>8</sup>, Daisaku Nogami<sup>8,9</sup>, and Kazunari Shibata<sup>10,11</sup>

2023 ApJ 948 9

<https://iopscience.iop.org/article/10.3847/1538-4357/acb7e8/pdf>

Stellar coronal mass ejections (CMEs) have recently received much attention for their impacts on exoplanets and stellar evolution. Detecting prominence eruptions, the initial phase of CMEs, as the blueshifted excess component of Balmer lines is a technique to capture stellar CMEs. However, most of prominence eruptions identified thus far have been slow and less than the surface escape velocity. Therefore, whether these eruptions were developing into CMEs remained unknown. In this study, we conducted simultaneous optical photometric observations with Transiting Exoplanet Survey Satellite and optical spectroscopic observations with the 3.8 m Seimei Telescope for the RS CVn-type star V1355 Orionis that frequently produces large-scale superflares. We detected a superflare releasing  $7.0 \times 10^{35}$  erg. In the early stage of this flare, a blueshifted excess component of H $\alpha$  extending its velocity up to 760–1690 km s<sup>-1</sup> was observed and thought to originate from prominence eruptions. The velocity greatly exceeds the escape velocity (i.e.,  $\sim 350$  km s<sup>-1</sup>), which provides important evidence that stellar prominence eruptions can develop into CMEs. Furthermore, we found that the prominence is very massive ( $9.5 \times 10^{18}$  g < M <  $1.4 \times 10^{21}$  g). These data will clarify whether such



events follow existing theories and scaling laws on solar flares and CMEs even when the energy scale far exceeds solar cases.

## **An Evolution and Eruption of the Coronal Magnetic Field through a Data-Driven MHD Simulation**

[Satoshi Inoue](#), [Keiji Hayashi](#), [Takahiro Miyoshi](#)

ApJ 946 46 2023

<https://arxiv.org/pdf/2210.07492>

<https://iopscience.iop.org/article/10.3847/1538-4357/ac9eaa/pdf>

We present a newly developed data-driven magnetohydrodynamics (MHD) simulation code under a zero-beta approximation based on a method proposed by Hayashi et al. 2018 and 2019. Although many data-driven MHD simulations have been developed and conducted, there are not many studies on how accurately those simulations can reproduce the phenomena observed in the solar corona. In this study, we investigated the performance of our data-driven simulation quantitatively using ground-truth data. The ground-truth data was produced by an MHD simulation in which the magnetic field is twisted by the sunspot motions. A magnetic flux rope (MFR) is created by the cancellation of the magnetic flux at the polarity inversion line due to the converging flow on the sunspot, which eventually leads the eruption of the MFR. We attempted to reproduce these dynamics using the data-driven MHD simulation. The coronal magnetic fields are driven by the electric fields, which are obtained from a time-series of the photospheric magnetic field that is extracted from the ground-truth data, on the surface. As a result, the data-driven simulation could capture the subsequent MHD processes, the twisted coronal magnetic field and formation of the MFR, and also its eruption. We report these results and compare with the ground-truth data, and discuss how to improve the accuracy and optimize numerical method.

## **Onset mechanism of solar eruptions**

[Satoshi Inoue](#) [Yumi BambacKanya Kusanob](#)

[Journal of Atmospheric and Solar-Terrestrial Physics Volume 180](#), November 2018, Pages 3-8  
[sci-hub.tw/10.1016/j.jastp.2017.08.035](http://sci-hub.tw/10.1016/j.jastp.2017.08.035)

Solar eruptions are the most energetic phenomena observed in the [solar system](#) observed as flares, [coronal mass ejections](#)(CMEs) and filament/prominence eruption. The helically twisted flux tube is widely thought to be the source and driver of solar eruptions and to carry the plasma into the [interplanetary space](#). Those may eventually reach the [magnetosphere](#) and cause strong disturbances of the [geomagnetic field](#). Therefore, the understanding of the onset of solar eruptions is important not only in the framework of solar physics but also for the space weather forecast. In this paper, we report on new insight into the onset mechanism of solar eruptions recently obtained from our new studies. We perform the studies in terms of the observational approach with state-of-the-art solar physics satellites and the numerical one with the latest super computer system. We specified two types of small magnetic perturbations of the photospheric [magnetic field](#). These can enhance the magnetic reconnection in the pre-existing non-potential magnetic field, which produces a large flux tube and then drives the eruption. We further confirmed that this reconnection is a key process for the eruption in our latest data-constrained simulation. We report our latest results and our interpretation of the onset mechanism of solar eruptions. **2006 December 13, 2011 Feb 13-15**

## **Magnetohydrodynamic Modeling of a Solar Eruption Associated with X9.3 Flare Observed in Active Region 12673**

[Satoshi Inoue](#), [Daikou Shiota](#), [Yumi Bamba](#), [Sung-Hong Park](#)

ApJ 867 83 2018

<https://arxiv.org/pdf/1809.02309.pdf>

[sci-hub.tw/10.3847/1538-4357/aae079](http://sci-hub.tw/10.3847/1538-4357/aae079)

On **2017 September 6**, the solar active region 12673 produced an X9.3 flare, regarded to be the largest to have occurred in solar cycle 24. In this work we have performed a magnetohydrodynamic (MHD) simulation in order to reveal the three-dimensional (3D) dynamics of the magnetic fields associated with the X9.3 solar flare. We first performed an extrapolation of the 3D magnetic field based on the observed photospheric magnetic field prior to the flare and then used this as the initial condition for the MHD simulation, which revealed a dramatic eruption. In particular, we found that a large coherent flux rope composed of highly twisted magnetic field lines formed during the eruption. A series of small flux ropes were found to lie along a magnetic polarity inversion line prior to the flare. Reconnection occurring between each flux rope during the early stages of the eruption formed the large, highly twisted flux rope. Furthermore, we observed a writhing motion of the erupting flux rope. Understanding these dynamics is important in the drive to increase the accuracy of space weather forecasting. We report on the detailed dynamics of the 3D eruptive flux rope and discuss the possible mechanisms of the writhing motion.

## **Formation and dynamics of a solar eruptive flux tube**

[Satoshi Inoue](#), [Kanya Kusano](#), [Jörg Büchner](#) & [Jan Skála](#)

Nature Communications volume 9, Article number: 174(2018)

<https://www.nature.com/articles/s41467-017-02616-8.pdf>

Solar eruptions are well-known drivers of extreme space weather, which can greatly disturb the Earth's magnetosphere and ionosphere. The triggering process and initial dynamics of these eruptions are still an area of intense study. Here we perform a magnetohydrodynamic simulation taking into account the observed photospheric magnetic field to reveal the dynamics of a solar eruption in a real magnetic environment. In our simulation, we confirmed that tether-cutting reconnection occurring locally above the polarity inversion line creates a twisted flux tube, which is lifted into a toroidal unstable area where it loses equilibrium, destroying the force-free state, and driving the eruption. Consequently, a more highly twisted flux tube is built up during this initial phase, which can be further accelerated even when it returns to a stable area. We suggest that a nonlinear positive feedback process between the flux tube evolution and reconnection is the key to ensure this extra acceleration. **2011 February 13**

## **Magnetohydrodynamics modeling of coronal magnetic field and solar eruptions based on the photospheric magnetic field**

**Review**

Satoshi **Inoue**

Progress in Earth and Planetary Science **2016** 3:19

<http://progearthplanetsci.springeropen.com/articles/10.1186/s40645-016-0084-7>

E-print, 4 July **2016**

In this paper, we summarize current progress on using the observed magnetic fields for magnetohydrodynamics (MHD) modeling of the coronal magnetic field and of solar eruptions, including solar flares and coronal mass ejections (CMEs). Unfortunately, even with the existing state-of-the-art solar physics satellites, only the photospheric magnetic field can be measured. We first review the 3D extrapolation of the coronal magnetic fields from measurements of the photospheric field. Specifically, we focus on the nonlinear force-free field (NLFFF) approximation extrapolated from the three components of the photospheric magnetic field. On the other hand, because in the force-free approximation the NLFFF is reconstructed for equilibrium states, the onset and dynamics of solar flares and CMEs cannot be obtained from these calculations. Recently, MHD simulations using the NLFFF as an initial condition have been proposed for understanding these dynamics in a more realistic scenario. These results have begun to reveal complex dynamics, some of which have not been inferred from previous simulations of hypothetical situations, and they have also successfully reproduced some observed phenomena. Although MHD simulations play a vital role in explaining a number of observed phenomena, there still remains much to be understood. Herein, we review the results obtained by state-of-the-art MHD modeling combined with the NLFFF. **13 February 2011, 15 February 2011, 11 September 2011, 29 March 2014**

## **Magnetohydrodynamic Simulation of the X2.2 Solar Flare on 2011 February 15: II. Dynamics Connecting the Solar Flare and the Coronal Mass Ejection**

S. **Inoue**, K. Hayashi, [T. Magara](#), [G. S. Choe](#), [Y. D. Park](#)

ApJ **2015**

<http://arxiv.org/pdf/1501.07663v2.pdf>

We clarify a relationship of the dynamics of a solar flare and a growing Coronal Mass Ejection (CME) by investigating the dynamics of magnetic fields during the X2.2-class flare taking place in the solar active region 11158 on **2011 February 15**, based on simulation results obtained from Inoue et al. 2014. We found that the strongly twisted lines formed through the tether-cutting reconnection in the twisted lines of a nonlinear force-free field (NLFFF) can break the force balance within the magnetic field, resulting in their launch from the solar surface. We further discover that a large-scale flux tube is formed during the eruption as a result of the tether-cutting reconnection between the eruptive strongly twisted lines and these ambient weakly twisted lines. Then the newly formed large flux tube exceeds the critical height of the torus instability. The tether-cutting reconnection thus plays an important role in the triggering a CME. Furthermore, we found that the tangential fields at the solar surface illustrate different phases in the formation of the flux tube and its ascending phase over the threshold of the torus instability. We will discuss about these dynamics in detail.

## **FRiED: A NOVEL THREE-DIMENSIONAL MODEL OF CORONAL MASS EJECTIONS**

A. **Isavnin**

**2016** ApJ 833 267

<http://sci-hub.cc/10.3847/1538-4357/833/2/267>

<https://arxiv.org/pdf/1703.01659.pdf>

We present a novel three-dimensional (3D) model of coronal mass ejections (CMEs) that unifies all key evolutionary aspects of CMEs and encapsulates their 3D magnetic field configuration. This fully analytic model is capable of reproducing the global geometrical shape of a CME with all major deformations taken into account, i.e., deflection, rotation, expansion, "pancaking," front flattening, and rotational skew. Encapsulation of 3D magnetic structure allows the model to reproduce in-situ measurements of magnetic field for trajectories of spacecraft-CME encounters of any degree of complexity. As such, the model can be used single-handedly for the consistent analysis of both remote and in-situ observations of CMEs at any heliocentric distance. We demonstrate the latter by successfully applying the model for the analysis of two CMEs. **2010 December 12, 2011 October 1**

## **Three-Dimensional Evolution of Flux-Rope CMEs and Its Relation to the Local Orientation of the Heliospheric Current Sheet**

A. [Isavnin](#), A. Vourlidas, E. K. J. Kilpua

Solar Phys., **2014**, **File**

Flux ropes ejected from the Sun may change their geometrical orientation during their evolution, which directly affects their geoeffectiveness. Therefore, it is crucial to understand how solar flux ropes evolve in the heliosphere to improve our space-weather forecasting tools. We present a follow-up study of the concepts described by Isavnin, Vourlidas, and Kilpua (Solar Phys. 284, 203, 2013). We analyze 14 coronal mass ejections (CMEs), with clear flux-rope signatures, observed during the decay of Solar Cycle 23 and rise of Solar Cycle 24. First, we estimate initial orientations of the flux ropes at the origin using extreme-ultraviolet observations of post-eruption arcades and/or eruptive prominences. Then we reconstruct multi-viewpoint coronagraph observations of the CMEs from  $\approx 2$  to  $30 R_{\odot}$  with a three-dimensional geometric representation of a flux rope to determine their geometrical parameters. Finally, we propagate the flux ropes from  $\approx 30 R_{\odot}$  to 1 AU through MHD-simulated background solar wind while using in-situ measurements at 1 AU of the associated magnetic cloud as a constraint for the propagation technique. This methodology allows us to estimate the flux-rope orientation all the way from the Sun to 1 AU. We find that while the flux-rope deflection occurs predominantly below  $30 R_{\odot}$ , a significant amount of deflection and rotation happens between  $30 R_{\odot}$  and 1 AU. We compare the flux-rope orientation to the local orientation of the heliospheric current sheet (HCS). We find that slow flux ropes tend to align with the streams of slow solar wind in the inner heliosphere. During the solar-cycle minimum the slow solar-wind channel as well as the HCS usually occupy the area in the vicinity of the solar equatorial plane, which in the past led researchers to the hypothesis that flux ropes align with the HCS. Our results show that exceptions from this rule are explained by interaction with the Parker-spiraled background magnetic field, which dominates over the magnetic interaction with the HCS in the inner heliosphere at least during solar-minimum conditions.

## **Three-Dimensional Evolution of Erupted Flux Ropes from the Sun ( $2-20 R_{\odot}$ ) to 1 AU**

A. [Isavnin](#), A. Vourlidas, E. K. J. Kilpua

Solar Physics

May **2013**, ApJ, Volume 284, Issue 1, pp 203-215; **File**

Studying the evolution of magnetic clouds entrained in coronal mass ejections using in-situ data is a difficult task, since only a limited number of observational points is available at large heliocentric distances. Remote sensing observations can, however, provide important information for events close to the Sun. In this work we estimate the flux rope orientation first in the close vicinity of the Sun ( $2-20 R_{\odot}$ ) using forward modeling of STEREO/SECCHI and SOHO/LASCO coronagraph images of coronal mass ejections and then in situ using Grad-Shafranov reconstruction of the magnetic cloud. Thus, we are able to measure changes in the orientation of the erupted flux ropes as they propagate from the Sun to 1 AU. We present both techniques and use them to study 15 magnetic clouds observed during the minimum following Solar Cycle 23 and the rise of Solar Cycle 24. This is the first multievent study to compare the three-dimensional parameters of CMEs from imaging and in-situ reconstructions. The results of our analysis confirm earlier studies showing that the flux ropes tend to deflect towards the solar equatorial plane. We also find evidence of rotation on their travel from the Sun to 1 AU. In contrast to past studies, our method allows one to deduce the evolution of the three-dimensional orientation of individual flux ropes rather than on a statistical basis.

## **A THREE-DIMENSIONAL LINE-TIED MAGNETIC FIELD MODEL FOR SOLAR ERUPTIONS**

Philip A. [Isenberg](#) and Terry G. Forbes

The Astrophysical Journal, 670:1453Y1466, **2007**

We introduce a three-dimensional analytical model of a coronal flux rope with its ends embedded in the solar surface. The model allows the flux rope to move in the corona while maintaining line-tied conditions at the solar surface. These conditions ensure that the normal component of the coronal magnetic field at the surface remains fixed during an eruption and that no magnetic energy enters the corona through the surface to drive the eruption. The model is based on the magnetic configuration of Titov&De moulin, where a toroidal flux rope is held in equilibrium by an overlying magnetic arcade. We investigate the stability of this configuration to specific perturbations and show that it is subject to the torus instability when the flux rope length exceeds a critical value. A force analysis of the configuration shows that flux ropes are most likely to erupt in a localized region near the apex, while the regions near the surface remain relatively undisturbed. Thus, the flux rope will tend to form an aneurysm-like structure once it erupts. Our analysis also suggests how the flux rope rotation seen in some eruptions and simulations may be related to the observed orientation of the overlying arcade field. This model exhibits the potential for catastrophic loss of equilibrium as a possible trigger for eruptions, but further study is required to prove this property.

## **Suzaku detection of enigmatic geocoronal solar wind charge exchange event associated with coronal mass ejection**

[Daiki Ishi](#), [Kumi Ishikawa](#), [Masaki Numazawa](#), [Yoshizumi Miyoshi](#), [Naoki Terada](#), [Kazuhiisa Mitsuda](#), [Takaya Ohashi](#), [Yuichiro Ezoe](#)

PASJ

**2019**

<https://arxiv.org/pdf/1902.07652.pdf>

Suzaku detected an enhancement of soft X-ray background associated with solar eruptions on **2013 April 14-15**. The solar eruptions were accompanied by an M6.5 solar flare and a coronal mass ejection with magnetic flux ropes. The enhanced soft X-ray background showed a slight variation in half a day and then a clear one in a few hours. The former spectrum was composed of oxygen emission lines, while the later one was characterized by a series of emission lines from highly ionized carbon to silicon. The soft X-ray enhancement originated from geocoronal solar wind charge exchange. However, there appeared to be no significant time correlation with the solar wind proton flux measured by the ACE and WIND satellites. From other solar wind signatures, we considered that an interplanetary shock associated with the coronal mass ejection and a turbulent sheath immediately behind the shock compressed the ambient solar wind ions and then resulted in the soft X-ray enhancement. Furthermore, the enriched emission lines were presumed to be due to an unusual set of ion abundances and ionization states within the coronal mass ejection. We found a better time correlation with the solar wind alpha flux rather than the solar wind proton flux. Our results suggest that the solar wind proton flux is not always a good indicator of geocoronal solar wind charge exchange, especially associated with coronal mass ejections. Instead, the solar wind alpha flux should be investigated when such a soft X-ray enhancement is detected in astronomical observations.

### **Double arc instability in the solar corona**

N. **Ishiguro**, K. Kusano

ApJ **843** 101 **2017**

<https://arxiv.org/pdf/1706.06112.pdf>

<http://sci-hub.cc/10.3847/1538-4357/aa799b>

The stability of the magnetic field in the solar corona is important for understanding the causes of solar eruptions. Although various scenarios have been suggested to date, the tether-cutting reconnection scenario proposed by Moore et al.(2001) is one of the widely accepted models to explain the onset process of solar eruptions. Although the tether-cutting reconnection scenario proposed that sigmoidal field formed by the internal reconnection is the magnetic field in pre-eruptive state, the stability of the sigmoidal field has not yet been investigated quantitatively. In this paper, in order to elucidate the stability problem of pre-eruptive state, we developed a simple numerical analysis, in which the sigmoidal field is modeled by a double arc electric current loop and its stability is analyzed. As a result, we found that the double arc loop is more easily destabilized than the axisymmetric torus, and it becomes unstable even if the external field does not decay with altitude, which is in contrast to the axisymmetric torus instability. This suggests that the tether-cutting reconnection may well work as the onset mechanism of solar eruptions, and if so the critical condition for eruption under certain geometry may be determined by a new type of instability rather than the torus instability. Based on them, we propose a new type of instability called double arc instability (DAI). We discuss the critical conditions for DAI and derive a new parameter  $\kappa$  defined as the product of the magnetic twist and the normalized flux of tether-cutting reconnection.

### **Particle Acceleration and Heating in Regions of Magnetic Flux Emergence**

Heinz **Isliker**, [Vasilis Archontis](#), [Loukas Vlahos](#)

ApJ **2019**

<https://arxiv.org/pdf/1907.04296.pdf>

The interaction between emerging and pre-existing magnetic fields in the solar atmosphere can trigger several dynamic phenomena, such as eruptions and jets. A key element during this interaction is the formation of large scale current sheets and, eventually, their fragmentation that leads to the creation of a strongly turbulent environment. In this paper, we study the kinetic aspects of the interaction (reconnection) between emerging and ambient magnetic fields. We show that the statistical properties of the spontaneously fragmented and fractal electric fields are responsible for the efficient heating and acceleration of charged particles, which form a power law tail at high energies on sub-second time scales. A fraction of the energized particles escapes from the acceleration volume, with a super-hot component with temperature close to 150MK, and with a power law high energy tail with index between -2 and -3. We estimate the transport coefficients in energy space from the dynamics of the charged particles inside the fragmented and fractal electric fields, and the solution of a fractional transport equation, as appropriate for a strongly turbulent plasma, agrees with the test particle simulations. We also show that the acceleration mechanism is not related to Fermi acceleration, and the Fokker Planck equation is inconsistent and not adequate as a transport model. Finally, we address the problem of correlations between spatial transport and transport in energy space. Our results confirm the observations reported for high energy particles (hard X-rays, type III bursts and solar energetic particles) during the emission of solar jets.

### **Spectral and Polarization Properties of Photospheric Emission from Stratified Jets**

Hirota **Ito**<sup>1</sup>, Shigehiro Nagataki<sup>1</sup>, Jin Matsumoto<sup>1</sup>, Shiu-Hang Lee<sup>1</sup>, Alexey Tolstov<sup>1</sup>, Jirong Mao<sup>1</sup>, Maria Dainotti<sup>1</sup>, and Akira Mizuta

**2014** ApJ 789 159

We explore the spectral and polarization properties of photospheric emissions from stratified jets in which multiple components, separated by sharp velocity shear regions, are distributed in lateral directions. Propagation of thermal photons injected at a high optical depth region are calculated until they escape from the photosphere. It is found that the presence of the lateral structure within the jet leads to the nonthermal feature of the spectra and significant polarization signal in the resulting emission. The deviation from thermal spectra, as well as the polarization degree, tends to be enhanced as the velocity gradient in the shear region increases. In particular, we show that emissions from multicomponent jet can reproduce the typical observed spectra of gamma-ray bursts irrespective of the position of the

observer when a velocity shear region is closely spaced in various lateral ( $\theta$ ) positions. The degree of polarization associated with the emission is significant (>few percent) at a wide range of observer angles and can be higher than 30%.

## **SOLAR RADIO TYPE-I NOISE STORM MODULATED BY CORONAL MASS EJECTIONS**

K. [Iwai](#)<sup>1</sup>, Y. Miyoshi<sup>2</sup>, S. Masuda<sup>2</sup>, M. Shimojo<sup>3</sup>, D. Shiota<sup>4</sup>, S. Inoue<sup>5</sup>, F. Tsuchiya<sup>1</sup>, A. Morioka<sup>1</sup> and H. Misawa

**2012 ApJ 744 167, File**

The first coordinated observations of an active region using ground-based radio telescopes and the Solar Terrestrial Relations Observatory (STEREO) satellites from different heliocentric longitudes were performed to study solar radio type-I noise storms. A type-I noise storm was observed between 100 and 300 MHz during a period from **2010 February 6 to 7**. During this period the two STEREO satellites were located approximately  $65^\circ$  (ahead) and  $-70^\circ$  (behind) from the Sun-Earth line, which is well suited to observe the earthward propagating coronal mass ejections (CMEs). The radio flux of the type-I noise storm was enhanced after the preceding CME and began to decrease before the subsequent CME. This time variation of the type-I noise storm was directly related to the change of the particle acceleration processes around its source region. Potential-field source-surface extrapolation from the Solar and Heliospheric Observatory/Michelson Doppler Imager (SOHO/MDI) magnetograms suggested that there was a multipolar magnetic system around the active region from which the CMEs occurred around the magnetic neutral line of the system. From our observational results, we suggest that the type-I noise storm was activated at a side-lobe reconnection region that was formed after eruption of the preceding CME. This magnetic structure was deformed by a loop expansion that led to the subsequent CME, which then suppressed the radio burst emission.

## **Automatic analysis of double coronal mass ejections from coronagraph images**

Matthew [Jacobs](#), Lin-Ching Chang, Antti Pulkkinen,

Space Weather Volume 13, Issue 11 November **2015** Pages 761–777

Coronal mass ejections (CMEs) can have major impacts on man-made technology and humans, both in space and on Earth. These impacts have created a high interest in the study of CMEs in an effort to detect and track events and forecast the CME arrival time to provide time for proper mitigation. A robust automatic real-time CME processing pipeline is greatly desired to avoid laborious and subjective manual processing. Automatic methods have been proposed to segment CMEs from coronagraph images and estimate CME parameters such as their heliocentric location and velocity. However, existing methods suffered from several shortcomings such as the use of hard thresholding and an inability to handle two or more CMEs occurring within the same coronagraph image. Double-CME analysis is a necessity for forecasting the many CME events that occur within short time frames. Robust forecasts for all CME events are required to fully understand space weather impacts. This paper presents a new method to segment CME masses and pattern recognition approaches to differentiate two CMEs in a single coronagraph image. The proposed method is validated on a data set of 30 halo CMEs, with results showing comparable ability in transient arrival time prediction accuracy and the new ability to automatically predict the arrival time of a double-CME event. The proposed method is the first automatic method to successfully calculate CME parameters from double-CME events, making this automatic method applicable to a wider range of CME events. **1999-07-06, 2002-05-22, 2005-09-09, 2011-11-09**

Michelangelo Romano

## **A Numerical Study of the Response of the Coronal Magnetic Field to Flux Emergence**

C. [Jacobs](#), S. Poedts

Solar Physics, October **2012**, Volume 280, Issue 2, pp 389-405

Large-scale solar eruptions, known as coronal mass ejections (CMEs), are regarded as the main drivers of space weather. The exact trigger mechanism of these violent events is still not completely clear; however, the solar magnetic field indisputably plays a crucial role in the onset of CMEs. The strength and morphology of the solar magnetic field are expected to have a decisive effect on CME properties, such as size and speed. This study aims to investigate the evolution of a magnetic configuration when driven by the emergence of new magnetic flux in order to get a better insight into the onset of CMEs and their magnetic structure. The three-dimensional, time-dependent equations for ideal magnetohydrodynamics are numerically solved on a spherical mesh. New flux emergence in a bipolar active region causes destabilisation of the initial stationary structure, finally resulting in an eruption. The initial magnetic topology is suitable for the 'breakout' CME scenario to work. Although no magnetic flux rope structure is present in the initial condition, highly twisted magnetic field lines are formed during the evolution of the system as a result of internal reconnection due to the interaction of the active region magnetic field with the ambient field. The magnetic energy built up in the system and the final speed of the CME depend on the strength of the overlying magnetic field, the flux emergence rate, and the total amount of emerged flux. The interaction with the global coronal field makes the eruption a large-scale event, involving distant parts of the solar surface.

**See presentation at ESPM13**

## **Initiation and early evolution of coronal mass ejections: A numerical approach**

[Carla Jacobs](#), F.P. Zuccarello S. Poedts, I. Roussev N. Lugaz

presentation at ESPM13, **2011**

## Models for coronal mass ejections

Carla **Jacobs**, b and Stefaan Poedtsa

Journal of Atmospheric and Solar-Terrestrial Physics, Volume 73, Issue 10, **2011**, Pages 1148-1155, **File**  
Coronal mass ejections (CMEs) play a key role in space weather. The mathematical modelling of these violent solar phenomena can contribute to a better understanding of their origin and evolution and as such improve space weather predictions. We **review** the state-of-the-art in CME simulations, including a brief overview of current models for the background solar wind as it has been shown that the background solar wind affects the onset and initial evolution of CMEs quite substantially. We mainly focus on the attempt to retrieve the initiation and propagation of CMEs in the framework of computational magnetofluid dynamics (CMFD). Advanced numerical techniques and large computer resources are indispensable when attempting to reconstruct an event from Sun to Earth. Especially the simulations developed in dedicated event studies yield very realistic results, comparable with the observations. However, there are still a lot of free parameters in these models and ad hoc source terms are often added to the equations, mimicking the physics that is not really understood yet in detail.

Research highlights

► New insights in the origin and dynamics of coronal mass ejections. ► New developments in the numerical modelling of CMEs. ► State-of-the-art solar wind models. ► New pieces of the space weather puzzle.

## The Internal Structure of Coronal Mass Ejections: Are all Regular Magnetic Clouds Flux Ropes?

C. **Jacobs**, I. I. Roussev, N. Lugaz, and S. Poedts

ApJL, 695, L171-L175, **2009**; **File** doi: [10.1088/0004-637X/695/2/L171](https://doi.org/10.1088/0004-637X/695/2/L171)

In this Letter, we investigate the internal structure of a coronal mass ejection (CME) and its dynamics by invoking a realistic initiation mechanism in a quadrupolar magnetic setting. The study comprises a compressible three-dimensional magnetohydrodynamics simulation. We use an idealized model of the solar corona, into which we superimpose a quadrupolar magnetic source region. By applying shearing motions resembling flux emergence at the solar boundary, the initial equilibrium field is energized and it eventually erupts, yielding a fast CME. The simulated CME shows the typical characteristics of a magnetic cloud (MC) as it propagates away from the Sun and interacts with a bimodal solar wind. However, no distinct flux rope structure is present in the associated interplanetary ejection. In our model, a series of reconnection events between the eruptive magnetic field and the ambient field results in the creation of significant writhe in the CME's magnetic field, yielding the observed rotation of the magnetic field vector, characteristic of an MC. We demonstrate that the magnetic field lines of the CME may suffer discontinuous changes in their mapping on the solar surface, with footpoints subject to meandering over the course of the eruption due to magnetic reconnection. We argue that CMEs with internal magnetic structure such as that described here should also be considered while attempting to explain in situ observations of regular MCs at L1 and elsewhere in the heliosphere.

## Numerical Modeling of the Initiation of Coronal Mass Ejections

**Jacobs**, C.1; Lugaz, N.2; Poedts, S.1; Roussev, I.2

Freiburg ESP Meeting **2008**, **Poster 3.3-24** (<http://espm.kis.uni-freiburg.de/index.php?id=408>)

Coronal Mass Ejections (CMEs) are large expulsions of solar material that involve large disturbances in the structure of the solar corona and in the solar wind. There is general consensus that stressed magnetic field structures are present in the CME source region at the time of eruption. The different theoretical models with regard to CME initiation all have in common the existence of magnetic flux ropes, either present in the solar atmosphere before the CME lift-off, or created during the eruption. Some of the models, like the magnetic 'breakout', presume a specific magnetic topology of the preeruption coronal field. In this research, the initiation of CMEs is studied in the framework of computational ideal magnetohydrodynamics (MHD). A multipolar flux system is energized through photospheric motions of the magnetic foot points. We investigate the interplanetary propagation and magnetic field structure of CMEs originating from regions with different magnetic topology.

## Comparison between 2.5D and 3D simulations of coronal mass ejections:

C. **Jacobs**, B. van der Holst and S. Poedts

A&A 470 (2007) 359-365

<http://www.aanda.org/10.1051/0004-6361:20077305>

we conclude that the 2.5D simulations of the CME evolution are a good first approach and resemble well the 3D result, provided that the appropriate initiation parameters are chosen.

## Solar Mass Ejection Imager 3-D reconstruction of the 27–28 May 2003 coronal mass ejection sequence,

**Jackson**, B. V., M. M. Bisi, P. P. Hick, A. Buffington, J. M. Clover, and W. Sun, *J. Geophys. Res.*, 113, A00A15, doi:10.1029/2008JA013224, (2008).

<http://www.agu.org/pubs/crossref/2008/2008JA013224.shtml>

The Solar Mass Ejection Imager (SMEI) has recorded the inner-heliospheric response in white-light Thomson scattering for many hundreds of interplanetary coronal mass ejections (ICMEs). Some of these have been observed by the Solar and Heliospheric Observatory (SOHO) Large-Angle Spectroscopic Coronagraph (LASCO) instruments and also in situ by near-Earth spacecraft. This article presents a low-resolution three-dimensional (3-D) reconstruction of the 27–28 May 2003 halo CME event sequence observed by LASCO and later using SMEI observations; this sequence was also observed by all in situ monitors near Earth. The reconstruction derives its perspective views from outward flowing solar wind. Analysis results reveal the shape, extent, and mass of this ICME sequence as it reaches the vicinity of Earth. The extended shape has considerable detail that is compared with LASCO images and masses for this event. The 3-D reconstructed density, derived from the remote-sensed Thomson scattered brightness, is also compared with the Advanced Composition Explorer (ACE) and Wind spacecraft in situ plasma measurements. These agree well in peak and integrated total value for this ICME event sequence when an appropriately enhanced (~20%) electron number density is assumed to account for elements heavier than hydrogen in the ionized plasma.

## Estimating early coronal mass ejection propagation direction with DIRECD during the severe May 8 and follow-up June 8, 2024 events

**Shantanu Jain**, **Tatiana Podladchikova**, **Astrid M. Veronig**, **Galina Chikunova**, **Karin Dissauer**, **Mateja Dumbovic**, **Amaia Razquin**

*A&A* 692, A214 2024

<https://arxiv.org/pdf/2410.18549>

<https://www.aanda.org/articles/aa/pdf/2024/12/aa52324-24.pdf>

On **May 8, 2024**, solar active region 13664 produced an X-class flare, several M-class flares, and multiple Earth-directed Coronal Mass Ejections (CMEs). The initial CME caused coronal dimmings, characterized by localized reductions in extreme-ultraviolet (EUV) emissions, indicating mass loss and expansion during the eruption. After one solar rotation, on **June 8, 2024**, the same region produced another M-class flare followed by coronal dimmings observed by the SDO and STEREO spacecraft. We analyzed early CME evolution and direction from coronal dimming expansion at the end of the impulsive phase using the DIRECD (Dimming Inferred Estimation of CME Direction) method. To validate the 3D CME cone, we compared CME properties from the low corona with white-light coronagraph data. The May 8 CME expanded radially, with a 7.7 deg inclination, 70 deg angular width, and 0.81 R<sub>sun</sub> cone height, while the June 8 CME had a 15.7 deg inclination, 81 deg width, and 0.89 R<sub>sun</sub> height. Our study shows that tracking low coronal signatures, like coronal dimming expansion, can estimate CME direction early, providing crucial lead time for space weather forecasts.

## Coronal dimmings as indicators of early CME propagation direction

**Shantanu Jain**, **Tatiana Podladchikova**, **Galina Chikunova**, **Karin Dissauer**, **Astrid M. Veronig**

*A&A* 683, A15 2023

<https://arxiv.org/pdf/2311.13942.pdf>

<https://www.aanda.org/articles/aa/pdf/2024/03/aa47927-23.pdf>

*Context.* Coronal mass ejections (CMEs) are large-scale eruptions of plasma and magnetic field from the Sun that can cause severe disturbances in space weather. Earth-directed CMEs are responsible for the disruption of technological systems and damaging power grids. However, the early evolution of CMEs, especially Earth-directed ones, is poorly tracked using traditional coronagraphs along the Sun-Earth line.

*Aims.* The most distinct phenomena associated with CMEs in the low corona are coronal dimmings, which are localized regions of reduced emission in the extreme-ultraviolet (EUV) and soft X-rays formed due to mass loss and expansion during a CME. We present a new approach to estimating the early CME propagation direction based on the expansion of coronal dimmings.

*Methods.* We developed the Dimming Inferred Estimate of CME Direction (DIRECD) method. First, we performed simulations of CMEs in 3D using a geometric CME cone model and varying parameters such as width, height, source location, and deflection from the radial direction to study their influence on the CME projection onto the solar sphere. Second, we estimated the dominant direction of the dimming extent based on the evolution of the dimming area. Third, using the derived dominant direction of the dimming evolution on the solar sphere, we solved an inverse problem to reconstruct an ensemble of CME cones at different heights, widths, and deflections from the radial propagation. Finally, we searched for which CME parameter combinations the CME orthogonal projections onto the solar sphere would match the geometry of the dimming at the end of its impulsive phase best; we did so to derive the CME direction in 3D. We tested our approach on two case studies on 1 October, 2011 and 6 September, 2011. We also validated our results with 3D tie-pointing of the CME bubble in an EUV low corona and with 3D reconstructions by graduated cylindrical shell modeling (GCS) of white-light CMEs higher up in the corona.

*Results.* Using DIRECD, we found that the CME on **1 October, 2011** expanded dominantly toward the south-east, while the CME on **6 September, 2011** was inclined toward the north-west. This is in agreement with the CME direction estimates from previous studies using multi-viewpoint coronagraphic observations.

*Conclusions.* Our study demonstrates that coronal dimming information can be used to estimate the CME's direction early in its evolution. This allows us to provide information on the CME direction before it is observed in the coronagraph's field of view, which is of practical importance for space weather forecasting and the mitigation of potential adverse impacts on Earth.

## **Evolution of the critical torus instability height and CME likelihood in solar active regions**

[Alexander W. James](#), [David R. Williams](#), [Jennifer O'Kane](#)

A&A 665, A37 2022

<https://arxiv.org/pdf/2206.10639.pdf>

<https://www.aanda.org/articles/aa/pdf/2022/09/aa42910-21.pdf>

*Aims.* Working towards improved space weather predictions, we aim to quantify how the critical height at which the torus instability drives coronal mass ejections (CMEs) varies over time in a sample of solar active regions. *Methods.* We model the coronal magnetic fields of 42 active regions and quantify the critical height at their central polarity inversion lines throughout their observed lifetimes. We then compare these heights to the changing magnetic flux at the photospheric boundary and identify CMEs in these regions. *Results.* In our sample, the rates of CMEs per unit time are twice as high during phases when magnetic flux is increasing than when it is decreasing, and during those phases of increasing flux, the rate of CMEs is 63% higher when the critical height is rising than when it is falling. Furthermore, we support and extend the results of previous studies by demonstrating that the critical height in active regions is generally proportional to the separation of their magnetic polarities through time. When the separation of magnetic polarities in an active region increases, for example during the continuous emergence and expansion of a magnetic bipole, the critical height also tends to increase. Conversely, when the polarity separation decreases, for example due to the emergence of a new, compact bipole at the central inversion line of an existing active region or into a quiet Sun environment, the critical height tends to decrease. **2010-08-29**

Table 1. Table of events. 2010-2017

## **A new trigger mechanism for coronal mass ejections: the role of confined flares and photospheric motions in the formation of hot flux ropes**

[Alexander W James](#), [Lucie M Green](#), [Lidia van Driel-Gesztelyi](#), [Gherardo Valori](#)

A&A 644, A137 2020

<https://arxiv.org/pdf/2010.11204.pdf>

<https://doi.org/10.1051/0004-6361/202038781>

*Context:* Many previous studies have shown that the magnetic precursor of a coronal mass ejection (CME) takes the form of a magnetic flux rope, and a subset of them have become known as 'hot flux ropes' due to their emission signatures in  $\sim 10$  MK plasma. *Aims:* We seek to identify the processes by which these hot flux ropes form, with a view of developing our understanding of CMEs and thereby improving space weather forecasts. *Methods:* Extreme-ultraviolet observations were used to identify five pre-eruptive hot flux ropes in the solar corona and study how they evolved. Confined flares were observed in the hours and days before each flux rope erupted, and these were used as indicators of episodic bursts of magnetic reconnection by which each flux rope formed. The evolution of the photospheric magnetic field was observed during each formation period to identify the process(es) that enabled magnetic reconnection to occur in the  $\beta < 1$  corona and form the flux ropes. *Results:* The confined flares were found to be homologous events and suggest flux rope formation times that range from 18 hours to 5 days. Throughout these periods, fragments of photospheric magnetic flux were observed to orbit around each other in sunspots where the flux ropes had a footpoint. Active regions with right-handed (left-handed) twisted magnetic flux exhibited clockwise (anticlockwise) orbiting motions, and right-handed (left-handed) flux ropes formed. *Conclusions:* We infer that the orbital motions of photospheric magnetic flux fragments about each other bring magnetic flux tubes together in the corona, enabling component reconnection that forms a magnetic flux rope above a flaring arcade. This represents a novel trigger mechanism for solar eruptions and should be considered when predicting solar magnetic activity. **13 Mar 2012, 13 Jun 2012, 14 Jun 2012, 08 Oct 2012, 14 Jul 2017**

## **An Observationally-Constrained Model of a Flux Rope that Formed in the Solar Corona**

Alexander W. [James](#), [Gherardo Valori](#), [Lucie M. Green](#), [Yang Liu](#), [Mark C. M. Cheung](#), [Yang Guo](#), [Lidia van Driel-Gesztelyi](#)

ApJL 855 L16 2018

<https://arxiv.org/pdf/1802.07965.pdf>

<http://sci-hub.tw/http://iopscience.iop.org/2041-8205/855/2/L16/>

Coronal mass ejections (CMEs) are large-scale eruptions of plasma from the coronae of stars. Understanding the plasma processes involved in CME initiation has applications to space weather forecasting and laboratory plasma experiments. James et al. (Sol. Phys. 292, 71, 2017) used EUV observations to conclude that a magnetic flux rope formed in the solar corona above NOAA Active Region 11504 before it erupted on **14 June 2012** (SOL2012-06-14). In this work, we use data from the Solar Dynamics Observatory to model the coronal magnetic field of the active region one hour prior to eruption using a nonlinear force-free field extrapolation, and find a flux rope reaching a maximum height of 150 Mm



above the photosphere. Estimations of the average twist of the strongly asymmetric extrapolated flux rope are between 1.35 and 1.88 turns, depending on the choice of axis, although the erupting structure was not observed to kink. The decay index near the apex of the axis of the extrapolated flux rope is comparable to typical critical values required for the onset of the torus instability, so we suggest that the torus instability drove the eruption.

**UKSP Nugget:** #98 Jyne 2019

<http://www.uksolphys.org/uksp-nugget/98-observing-and-modelling-a-flux-rope-in-the-corona/>

### **On-disc Observations of Flux Rope Formation Prior to its Eruption**

A. W. **James**, L. M. Green, E. Palmerio, G. Valori, H. A. S. Reid, D. Baker, D. H. Brooks, L. van Driel-Gesztelyi, E. K. J. Kilpua

Solar Phys. 292:71 2017

<https://arxiv.org/pdf/1703.10837.pdf>

Coronal mass ejections (CMEs) are one of the primary manifestations of solar activity and can drive severe space weather effects. Therefore, it is vital to work towards being able to predict their occurrence. However, many aspects of CME formation and eruption remain unclear, including whether magnetic flux ropes are present before the onset of eruption and the key mechanisms that cause CMEs to occur. In this work, the pre-eruptive coronal configuration of an active region that produced an interplanetary CME with a clear magnetic flux rope structure at 1 AU is studied. A forward-S sigmoid appears in extreme-ultraviolet (EUV) data two hours before the onset of the eruption (SOL2012-06-14), which is interpreted as a signature of a right-handed flux rope that formed prior to the eruption. Flare ribbons and EUV dimmings are used to infer the locations of the flux rope footpoints. These locations, together with observations of the global magnetic flux distribution, indicate that an interaction between newly emerged magnetic flux and pre-existing sunspot field in the days prior to the eruption may have enabled the coronal flux rope to form via tether-cutting-like reconnection. Composition analysis suggests that the flux rope had a coronal plasma composition, supporting our interpretation that the flux rope formed via magnetic reconnection in the corona. Once formed, the flux rope remained stable for 2 hours before erupting as a CME.

### **Two Distinct Types of CME-flare Relationships Based on SOHO and STEREO Observations**

Soojoeng **Jang**<sup>1</sup>, Yong-Jae Moon<sup>1</sup>, Rok-Soon Kim<sup>2,3</sup>, Sujin Kim<sup>2,3</sup>, and Jae-Ok Lee<sup>2</sup>

2017 ApJ 845 169

<http://iopscience.iop.org/sci-hub.cc/0004-637X/845/2/169/>

In this paper, we present two distinct types of coronal mass ejection (CME)-flare relationships according to their observing time differences using 107 events from 2010 to 2013. The observing time difference,  $\Delta T$ , is defined as flare peak time minus CME first appearance time at Solar Terrestrial Relations Observatory (STEREO) COR1 field of view. There are 41 events for group A ( $\Delta T < 0$ ) and 66 events for group B ( $\Delta T \geq 0$ ). We compare CME 3D parameters (speed and kinetic energy) based on multi-spacecraft data (Solar and Heliospheric Observatory (SOHO) and STEREO A and B) and their associated flare properties (peak flux, fluence, and duration). Our main results are as follows. First, there are better relationships between CME and flare parameters for group B than that of group A. In particular, CME 3D kinetic energy for group B is well correlated with flare fluence with the correlation coefficient of 0.67, which is much stronger than that ( $cc = 0.31$ ) of group A. Second, the events belonging to group A have short flare durations of less than 1 hr (mean = 21 minutes), while the events for group B have longer durations up to 4 hr (mean = 81 minutes). Third, the mean value of height at peak speed for group B is 4.05 Rs, which is noticeably higher than that of group A (1.89 Rs). This is well correlated with the CME acceleration duration ( $cc = 0.75$ ). A higher height at peak speed and a longer acceleration duration of CME for group B could be explained by the fact that magnetic reconnections for group B continuously occur for a longer time than those for group A. **2011 September 7**

### **Coronal Dynamic Activities in the Declining Phase of a Solar Cycle**

Minhwan **Jang**, T. N. Woods, Sunhak Hong, G. S. Choe

2016

<https://arxiv.org/pdf/1610.02944v1.pdf>

It has been known that some solar activity indicators show a double-peak feature in their evolution through a solar cycle, which is not conspicuous in sunspot number. In this letter, we investigate the high solar dynamic activity in the declining phase of the sunspot cycle by examining the evolution of polar and low latitude coronal hole areas and the statistics of splitting and merging events of coronal holes and coronal mass ejections detected by SOHO/LASCO C3 in solar cycle 23. Although the total coronal hole area is at its maximum near the sunspot minimum, in which polar coronal holes prevail, it shows a comparable second maximum in the declining phase of the cycle, in which low latitude coronal holes are dominant. The events of coronal hole splitting or merging, which are attributed to surface motions of magnetic fluxes, are also mostly populated in the declining phase of the cycle. The far-reaching C3 coronal mass ejections are also over-populated in the declining phase of the cycle. From these results we suggest that solar dynamic activities due to the horizontal motions of magnetic fluxes extend far in the declining phase of the sunspot cycle.

**Хорошее Введение.**

### **COMPARISON BETWEEN 2D AND 3D PARAMETERS OF 306 FRONT-SIDE HALO CMEs FROM 2009 TO 2013**

Soojeong **Jang**<sup>1,2</sup>, Y.-J. Moon<sup>1</sup>, R.-S. Kim<sup>2,3</sup>, Harim Lee<sup>1</sup>, and K.-S. Cho

2016 ApJ 821 95 DOI: 10.3847/0004-637X/821/2/95

We investigate 306 LASCO front-side halo (partial and full) CMEs from 2009 to 2013, which are well-observed by both the Solar and Heliospheric Observatory (SOHO) and the Solar TERrestrial RELations Observatory (STEREO). These CMEs have two-dimensional (2D) parameters, such as speed, angular width, and propagation direction, from a single spacecraft (SOHO), as well as three-dimensional (3D) parameters from a multi-spacecraft (STEREO). These 2D CME parameters, which are based on plane-of-sky observations, are taken from the SOHO LASCO CME catalog and the NGDC flare catalog. We have determined their 3D CME parameters using the Stereoscopic CME analysis tool (StereoCAT) provided by the Community Coordinated Modeling Center at NASA. We compare 2D and 3D CME parameters, making this the most comprehensive statistical study on CME 3D parameters. As a result, we find that 2D speeds underestimate the 3D speed by about 20%. The 3D width ranges from  $30^\circ$  to  $158^\circ$ , values which are much smaller than the 2D widths with a mean value of  $225^\circ$ . We also find that the ratio between the 2D and 3D widths decreases with central meridian distance. The 3D propagation directions are similar to the flare locations, with a mean absolute difference of about  $13^\circ$ . The width-speed relationship in 3D is much stronger than that in 2D.

## **A multiple spacecraft detection of the 2 April 2022 M-class flare and filament eruption during the first close Solar Orbiter perihelion**

[M. Janvier](#), [S. Mzerguat](#), [P. R. Young](#), [É. Buchlin](#), <sup>+++</sup>

A&A 677, A130 2023

<https://arxiv.org/pdf/2307.02396.pdf>

<https://www.aanda.org/articles/aa/pdf/2023/09/aa46321-23.pdf>

Context. The Solar Orbiter mission completed its first remote-sensing observation windows in the spring of 2022. On 2 April 2022, an M-class flare followed by a filament eruption was seen both by the instruments on board the mission and from several observatories in Earth's orbit, providing an unprecedented view of a flaring region with a large range of observations.

Aims. We aim to understand the nature of the flaring and filament eruption events via the analysis of the available dataset. The complexity of the observed features is compared with the predictions given by the standard flare model in 3D.

Methods. In this paper, we use the observations from a multi-view dataset, which includes extreme ultraviolet (EUV) imaging to spectroscopy and magnetic field measurements. These data come from the Interface Region Imaging Spectrograph, the Solar Dynamics Observatory, Hinode, as well as several instruments on Solar Orbiter.

Results. The large temporal coverage of the region allows us to analyse the whole sequence of the filament eruption starting with its pre-eruptive state. Information given by spectropolarimetry from SDO/HMI and Solar Orbiter PHI/HRT shows that a parasitic polarity emerging underneath the filament is responsible for bringing the flux rope to an unstable state. As the flux rope erupts, Hinode EIS captures blue-shifted emission in the transition region and coronal lines in the northern leg of the flux rope prior to the flare peak. This may be revealing the unwinding of one of the flux rope legs. At the same time, Solar Orbiter SPICE captures the whole region, complementing the Doppler diagnostics of the filament eruption. Analyses of the formation and evolution of a complex set of flare ribbons and loops, of the hard and soft X-ray emissions with STIX, show that the parasitic emerging bipole plays an important role in the evolution of the flaring region.

Conclusions. The extensive dataset covering this M-class flare event demonstrates how important multiple viewpoints and varied observations are in order to understand the complexity of flaring regions. While the analysed data are overall consistent with the standard flare model, the present particular magnetic configuration shows that surrounding magnetic activity such as nearby emergence needs to be taken into account to fully understand the processes at work. This filament eruption is the first to be covered from different angles by spectroscopic instruments, and provides an unprecedented diagnostic of the multi-thermal structures present before and during the flare. This complete dataset of an eruptive event showcases the capabilities of coordinated observations with the Solar Orbiter mission.

## **From coronal observations to MHD simulations, the building blocks for 3D models of solar flares**

**Review**

Miho [Janvier](#), Guillaume Aulanier, Pascal Demoulin

Solar Phys. 2015, File

<http://arxiv.org/pdf/1505.05299v1.pdf>

Solar flares are energetic events taking place in the Sun's atmosphere, and their effects can greatly impact the environment of the surrounding planets. In particular, eruptive flares, as opposed to confined flares, launch coronal mass ejections into the interplanetary medium, and as such, are one of the main drivers of space weather. After briefly reviewing the main characteristics of solar flares, we summarize the processes that can account for the build up and release of energy during their evolution. In particular, we focus on the development of recent 3D numerical simulations that explain many of the observed flare features. These simulations can also provide predictions of the dynamical evolution of coronal and photospheric magnetic field. Here we present a few observational examples that, together with numerical modelling, point to the underlying physical mechanisms of the eruptions. **18 March 1999**, **27 Feb 2000**, **2 March 2000**, **19 October 2001**, **16/11/2002**, **17=07=2004**, **20 January 2005**, **12 February 2007**, **18 August 2010**, **15 February 2011**, **09/05/2011**, **e 22 October 2011**, **15/01/2012**, **14 October 2012**, **11/03/2014**

## **The 3D standard model for eruptive flares**

Miho **Janvier**

RHESSI Science Nuggets, No. 226, May, 2014

[http://sprg.ssl.berkeley.edu/~tohban/wiki/index.php/The\\_3D\\_standard\\_model\\_for\\_eruptive\\_flares](http://sprg.ssl.berkeley.edu/~tohban/wiki/index.php/The_3D_standard_model_for_eruptive_flares)

Eruptive solar flares, associated with coronal mass ejections (CMEs), are important energetic events taking place in the solar corona. The intense magnetic energy release originates from magnetic reconnection, which is also responsible for newly formed magnetic structures that are ejected as CMEs. Solar coronal observations reveal typical 3D magnetic structures during eruptive flares: flux ropes (twisted magnetic field lines structures), ultimately ejected in the interplanetary medium, and hot and dense flare loops. Magnetic reconnection takes place in regions of drastic changes in the magnetic connectivity: these are separatrices, defining different domains of connectivity, or quasi-separatrix layers (QSLs), which generalize in 3D the regions of strong connectivity gradients.

With an MHD numerical simulation recreating the evolution of a flux rope expansion during an eruptive flare [Ref. 1], we propose a 3D-extended, more complete version of the standard model for eruptive flares. We present below new understandings offered by this model.

Our 3D standard model, built from a 3D MHD simulation, extends our understanding of the observational characteristics, as well as the underlying physical mechanisms of eruptive flares. Its main characteristics are outlined in the cartoon of Figure 1. This model shows that both flare loops and flux rope are constructed by 3D reconnection, in the thin coronal current layer that maps as J-shaped current/flare ribbons onto the photosphere. Field lines entering this region reconnect successively, leading to a slipping motion, as recently seen in coronal observations. This change of connectivity allows shear transfer from dynamically evolving pre- to post-reconnected field lines, and is often observed as a strong-to-weak shear transfer in flare loops observations. The flux rope, on the other hand, is constantly growing as reconnected twisted field lines construct its outer shell. From its ejection in the interplanetary medium, a flux rope can be detected as a magnetic cloud by in situ instruments away from the Sun. **2011-05-09, 2011-02-15, 2012-12-07, See Aulanier, G.**

## Are There Different Populations of Flux Ropes in the Solar Wind?

M. **Janvier**, P. Demoulin, S. Dasso

E-print, Feb 2014

<http://arxiv.org/pdf/1401.6812v1.pdf>

Flux ropes are twisted magnetic structures, which can be detected by in situ measurements in the solar wind. However, different properties of detected flux ropes suggest different types of flux-rope population. As such, are there different populations of flux ropes? The answer is positive, and is the result of the analysis of four lists of flux ropes, including magnetic clouds (MCs), observed at 1 AU. The in situ data for the four lists have been fitted with the same cylindrical force-free field model, which provides an estimation of the local flux-rope parameters such as its radius and orientation. Since the flux-rope distributions have a large dynamic range, we go beyond a simple histogram analysis by developing a partition technique that uniformly distributes the statistical fluctuations over the radius range. By doing so, we find that small flux ropes with radius  $R < 0.1$  AU have a steep power-law distribution in contrast to the larger flux ropes (identified as MCs), which have a Gaussian-like distribution. Next, from four CME catalogs, we estimate the expected flux-rope frequency per year at 1 AU. We find that the predicted numbers are similar to the frequencies of MCs observed in situ. However, we also find that small flux ropes are at least ten times too abundant to correspond to CMEs, even to narrow ones. Investigating the different possible scenarios for the origin of those small flux ropes, we conclude that these twisted structures can be formed by blowout jets in the low corona or in coronal streamers.

## Slingshot prominences: coronal structure, mass loss and spin down

M. **Jardine**, [A. Collier Cameron](#), [J.-F. Donati](#), [G.A.J. Hussain](#)

MNRAS **2019**

<https://arxiv.org/pdf/1911.04339.pdf>

The structure of a star's coronal magnetic field is a fundamental property that governs the high-energy emission from the hot coronal gas and the loss of mass and angular momentum in the stellar wind. It is, however, extremely difficult to measure. We report a new method to trace this structure in rapidly-rotating young convective stars, using the cool gas trapped on coronal field lines as markers. This gas forms "slingshot prominences" which appear as transient absorption features in H- $\alpha$ . By using different methods of extrapolating this field from the surface measurements, we determine locations for prominence support and produce synthetic H- $\alpha$  stacked spectra. The absorption features produced with a potential field extrapolation match well those observed, while those from a non-potential field do not. In systems where the rotation and magnetic axes are well aligned, up to 50% of the prominence mass may transit the star and so produces an observable feature. This fraction may fall as low as 2% in very highly inclined systems. Ejected prominences carry away mass and angular momentum at rates that vary by two orders of magnitude, but which may approach those carried by the stellar wind.

## Stellar mass ejections

Moira **Jardine**, Jean-Francois Donati and Scott G. Gregory

Proceedings of the International Astronomical Union / Volume 4 / Symposium S257, pp 201 - 210

Published online: 16 Mar 2009

<http://journals.cambridge.org/action/displayIssue?iid=4866212>

**Review**

It has been known for some time now that rapidly-rotating solar-like stars possess the stellar equivalent of solar prominences. These may be three orders of magnitude more massive than their solar counterparts, and their ejection from the star may form a significant contribution to the loss of angular momentum and mass in the stellar wind. In addition, their number and distribution provide valuable clues as to the structure of the stellar corona and hence to the nature of magnetic activity in other stars.

## **Parametric study of the kinematic evolution of coronal mass ejection shock waves and their relation to flaring activity**

[Manon Jarry](#), [Alexis P. Rouillard](#), [Iliya Plotnikov](#), [Athanasios Kouloumvakos](#), [Alexander Warmuth](#)

A&A 672, A127 2023

<https://arxiv.org/pdf/2303.08663.pdf>

<https://www.aanda.org/articles/aa/pdf/2023/04/aa45480-22.pdf>

Coronal and interplanetary shock waves produced by coronal mass ejections (CMEs) are major drivers of space-weather phenomena, inducing major changes in the heliospheric radiation environment and directly perturbing the near-Earth environment, including its magnetosphere. A better understanding of how these shock waves evolve from the corona to the interplanetary medium can therefore contribute to improving nowcasting and forecasting of space weather. Early warnings from these shock waves can come from radio measurements as well as coronagraphic observations that can be exploited to characterise the dynamical evolution of these structures. Our aim is to analyse the geometrical and kinematic properties of 32 CME shock waves derived from multi-point white-light and ultraviolet imagery taken by the Solar Dynamics Observatory (SDO), Solar and Heliospheric Observatory (SoHO), and Solar-Terrestrial Relations Observatory (STEREO) to improve our understanding of how shock waves evolve in 3D during the eruption of a CME. We use our catalogue to search for relations between the shock wave's kinematic properties and the flaring activity associated with the underlying genesis of the CME piston. Past studies have shown that shock waves observed from multiple vantage points can be aptly reproduced geometrically by simple ellipsoids. The catalogue of reconstructed shock waves provides the time-dependent evolution of these ellipsoidal parameters. From these parameters, we deduced the lateral and radial expansion speeds of the shocks evolving over time. We compared these kinematic properties with those obtained from a single viewpoint by SoHO in order to evaluate projection effects. Finally, we examined the relationships between the shock wave and the associated flare when the latter was observed on the disc by considering the measurements of soft and hard X-rays. **23 July 2012**

**Table 2.** List of studied events. 2011-2017

## **Visibility of Prominences using the HeI D3 Line Filter on PROBA-3/ASPIICS Coronagraph**

[S. Jejić](#), [P. Heinzel](#), [N. Labrosse](#), [A. N. Zhukov](#), [A. Bemporad](#), [S. Fineschi](#), [S. Günár](#)

Solar Phys (2018) 293:33

<http://sci-hub.tw/10.1007/s11207-018-1251-3>

We determine an optimal width and shape of the narrow-band filter centered around the HeI D3 line for prominence and coronal mass ejection (CME) observations with the ASPIICS (Association of Spacecraft for Polarimetric and Imaging Investigation of the Corona of the Sun) coronagraph onboard the PROBA-3 (Project for On-board Autonomy) satellite, to be launched in 2020. We analyze HeI D3 line intensities for three representative non-LTE prominence models at temperatures 8, 30 and 100 kK computed by the radiative transfer code and the prominence visible-light (VL) emission due to Thomson scattering on the prominence electrons. We compute various useful relations at prominence line-of-sight (LOS) velocities of 0, 100, and 300 km s<sup>-1</sup> for 20-Å wide flat filter and three Gaussian filters with full width at half maximum (FWHM) equal to 5, 10, and 20 Å to show the relative brightness contribution of the HeI D3 line and the prominence VL to the visibility in a given narrow-band filter. We also discuss possible signal contamination by NaI D1 and D2 lines which otherwise may be useful to detect comets. Results mainly show: i) an optimal narrow-band filter should be flat or somewhere between flat and Gaussian with FWHM of 20 Å in order to detect fast moving prominence structures, ii) the maximum emission in the HeI D3 line is at 30 kK and the minimal at 100 kK, and iii) the ratio of emission in the HeI D3 line to the VL emission can provide a useful diagnostic for the temperature of prominence structures. This ratio is up to 10 for hot prominence structures, up to 100 for cool structures and up to 1000 for warm structures.

## **Hot prominence detected in the core of a coronal mass ejection**

### **II. Analysis of the C iii line detected by SOHO/UVCS**

[S. Jejić](#)<sup>1,2</sup>, [R. Susino](#)<sup>3</sup>, [P. Heinzel](#)<sup>1</sup>, [E. Džifčáková](#)<sup>1</sup>, [A. Bemporad](#)<sup>3</sup> and [U. Anzer](#)<sup>4</sup>

A&A 607, A80 (2017)

<https://www.aanda.org/articles/aa/pdf/2017/11/aa31364-17.pdf>

Context. We study the physics of erupting prominences in the core of coronal mass ejections (CMEs) and present a continuation of a previous analysis.

Aims. We determine the kinetic temperature and microturbulent velocity of an erupting prominence embedded in the core of a CME that occurred on **August 2, 2000** using the Ultraviolet Coronagraph and Spectrometer observations (UVCS) on board the Solar and Heliospheric Observatory (SOHO) simultaneously in the hydrogen L $\alpha$  and C iii lines. We develop the non-LTE (departures from the local thermodynamic equilibrium – LTE) spectral diagnostics based on L $\alpha$  and L $\beta$  measured integrated intensities to derive other physical quantities of the hot erupting prominence. Based on this, we synthesize the C iii line intensity to compare it with observations.

**Methods.** Our method is based on non-LTE modeling of eruptive prominences. We used a general non-LTE radiative-transfer code only for optically thin prominence points because optically thick points do not allow the direct determination of the kinetic temperature and microturbulence from the line profiles. The input parameters of the code were the kinetic temperature and microturbulent velocity derived from the  $L\alpha$  and C iii line widths, as well as the integrated intensity of the  $L\alpha$  and  $L\beta$  lines. The code runs in three loops to compute the radial flow velocity, electron density, and effective thickness as the best fit to the  $L\alpha$  and  $L\beta$  integrated intensities within the accuracy defined by the absolute radiometric calibration of UVCS data.

**Results.** We analyzed 39 observational points along the whole erupting prominence because for these points we found a solution for the kinetic temperature and microturbulent velocity. For these points we ran the non-LTE code to determine best-fit models. All models with  $\tau_0(L\alpha) \leq 0.3$  and  $\tau_0(\text{C iii}) \leq 0.3$  were analyzed further, for which we computed the integrated intensity of the C iii line using a two-level atom. The best agreement between computed and observed integrated intensity led to 30 optically thin points along the prominence. The results are presented as histograms of the kinetic temperature, microturbulent velocity, effective thickness, radial flow velocity, electron density, and gas pressure. We also show the relation between the microturbulence and kinetic temperature together with a scatter plot of computed versus observed C iii integrated intensities and the ratio of the computed to observed C iii integrated intensities versus kinetic temperature.

**Conclusions.** The erupting prominence embedded in the CME is relatively hot with a low electron density, a wide range of effective thicknesses, a rather narrow range of radial flow velocities, and a microturbulence of about 25 km s<sup>-1</sup>. This analysis shows a disagreement between observed and synthetic intensities of the C iii line, the reason for which most probably is that photoionization is neglected in calculations of the ionization equilibrium. Alternatively, the disagreement might be due to non-equilibrium processes.

## **Spectroscopic Observations and Modelling of Impulsive Alfvén Waves Along a Polar Coronal Jet**

P. [Jelínek](#), A.K. Srivastava, K. Murawski, P. Kayshap, B.N. Dwivedi

A&A 581, A131 2015

Using the Hinode/EIS 2" spectroscopic observations, we study the intensity, velocity, and FWHM variations of the strongest Fe XII 195.12 Å line along the jet to find the signature of Alfvén waves. We simulate numerically the impulsively generated Alfvén waves within the vertical Harris current-sheet, forming the jet plasma flows, and mimicking their observational signatures. Using the FLASH code and the atmospheric model with embedded weakly expanding magnetic field configuration within a vertical Harris current-sheet, we solve the two and half-dimensional (2.5-D) ideal magnetohydrodynamic (MHD) equations to study the evolution of Alfvén waves and vertical flows forming the plasma jet. At a height of ~5 Mm from the base of the jet, the red-shifted velocity component of Fe XII 195.12 Å line attains its maximum (5 km s<sup>-1</sup>) which converts into a blue-shifted one between the altitude of 5–10 Mm. The spectral intensity continuously increases up to 10 Mm, while FWHM still exhibits the low values with almost constant trend. This indicates that the reconnection point within the jet's magnetic field topology lies in the corona 5–10 Mm from its footpoint anchored in the Sun's surface. Beyond this height, FWHM shows a growing trend. This may be the signature of Alfvén waves that impulsively evolve due to reconnection and propagate along the jet. From our numerical data, we evaluate space- and time- averaged Alfvén waves velocity amplitudes at different heights in the jet's current-sheet, which contribute to the non-thermal motions and spectral line broadening. The synthetic width of Fe XII 195.12 Å line exhibits similar trend of increment as in the observational data, possibly proving the existence of impulsively generated (by reconnection) Alfvén waves which propagate along the jet. 22 April, 2009.

## **Modelling the Effect of Mass-Draining on Prominence Eruptions**

Jack M. [Jenkins](#), [Matthew Hopwood](#), [Pascal Démoulin](#), [Gherardo Valori](#), [Guillaume Aulanier](#), [David M. Long](#), [Lidia van Driel-Gesztelyi](#)

ApJ 873 49 2019

<https://arxiv.org/pdf/1901.10970.pdf>

<https://doi.org/10.3847/1538-4357/ab037a>

Quiescent solar prominences are observed to exist within the solar atmosphere for up to several solar rotations. Their eruption is commonly preceded by a slow increase in height that can last from hours to days. This increase in the prominence height is believed to be due to their host magnetic flux rope transitioning through a series of neighbouring quasi-equilibria before the main loss-of-equilibrium that drives the eruption. Recent work suggests that the removal of prominence mass from a stable, quiescent flux rope is one possible cause for this change in height. However, these conclusions are drawn from observations and are subject to interpretation. Here we present a simple model to quantify the effect of "mass-draining" during the pre-eruptive height-evolution of a solar flux rope. The flux rope is modeled as a line current suspended within a background potential magnetic field. We first show that the inclusion of mass, up to 10<sup>12</sup>-kg, can modify the height at which the line current experiences loss-of-equilibrium by up to 14%. Next, we show that the rapid removal of mass prior to the loss-of-equilibrium can allow the height of the flux rope to increase sharply and without upper bound as it approaches its loss-of-equilibrium point. This indicates that the critical height for the loss-of-equilibrium can occur at a range of heights depending explicitly on the amount and evolution of mass within

the flux rope. Finally, we demonstrate that for the same amount of drained mass, the effect on the height of the flux rope is up to two order of magnitude larger for quiescent than for active region prominences.

### **Understanding the Role of Mass-Unloading in Filament Eruptions**

Jack **Jenkins**, [David M Long](#), [Lidia van Driel-Gesztelyi](#), [Jack Carlyle](#)

Solar Phys. 2018, 293:7

<https://arxiv.org/pdf/1711.02565.pdf>

We describe a partial filament eruption on **11 December 2011** which demonstrates that the inclusion of mass is an important next step for understanding solar eruptions. Observations from the \textit{Solar Terrestrial Relations Observatory Behind} (STEREO-B) and the \textit{Solar Dynamics Observatory} (SDO) spacecraft were used to remove line-of-sight projection effects in filament motion and correlate the effect of plasma dynamics with the evolution of the filament height. Flux cancellation and nearby flux emergence are shown to have played a role in increasing the height of the filament prior to eruption. The two viewpoints allow the quantitative estimation of a large mass-unloading, the subsequent radial expansion, and the eruption of the filament to be investigated. A 1.8 to 4.1 lower-limit ratio between gravitational and magnetic tension forces was found. We therefore conclude that following the loss-of-equilibrium of the flux rope, the radial expansion of the flux rope was restrained by the filamentary material until 70% of the mass had evacuated the structure through mass-unloading.

### **Plasma Interactions with the Space Environment in the Acceleration Region: Indications of CME-trailing Reconnection Regions**

Elizabeth A. **Jensen**<sup>1,2</sup>, Carl Heiles<sup>3</sup>, David Wexler<sup>4</sup>, Amanda A. Kepley<sup>5</sup>, Thomas Kuiper<sup>6</sup>, Mario M. Bisi<sup>7</sup>, Deborah Domingue Lorin<sup>1</sup>, Elizabeth V. Kuiper<sup>8</sup>, and Faith Vilas<sup>1</sup>,

Astrophysical Journal, 861:118 (12pp), 2018 July 10

<http://sci-hub.tw/http://iopscience.iop.org/0004-637X/861/2/118/>

Coronal mass ejections (CMEs) are sources of major geomagnetic disturbances. On **2013 May 10**, a CME crossed the signal path between the MErcury Surface, Space ENvironment, GEochemistry, and Ranging (MESSENGER) spacecraft and Earth. Using the MESSENGER signal, characteristics of the density, velocity, and magnetic field properties of the crossing plasma were measured. An anomalously strong event occurred in the plasma trailing the CME's passage that correlated with a wave mode conversion, indicating a potential reconnection region. We determine that the plasma following CMEs should be considered when studying how CMEs evolve in interplanetary space and the severity of their geomagnetic impact.

### **Multi-fluid Model of a Sun-grazing Comet in the Rapidly Ionizing, Magnetized Low Corona**

Y.-D. **Jia**<sup>1</sup>, C. T. Russell<sup>1</sup>, W. Liu<sup>2</sup>, and Y. S. Shou

2014 ApJ 796 42

Two Sun-grazing comets were recently imaged in the low solar corona by space telescopes in unprecedented detail, revealing a wide range of new phenomena. This sparked growing interest in the interaction of comets with the coronal plasma and magnetic field and their diagnostic potential as solar probes. However, interpretation of such rich observational data requires profound understanding of relevant physical processes in an unexplored regime. Here advanced numerical modeling can provide critical clues. To this end, we present a prototype, multi-fluid, magnetohydrodynamic model of a steady-state comet in the low solar corona. These simulation results are compared with previously modeled comets in the solar wind environment. By inspecting their projection and column densities, we find a dominance of O<sup>6+</sup> ions in the cometary tail, which can explain the observed extreme ultraviolet emission. The tail is found to be comparable to recent EUV images of these comets. In addition, the comet tail appears wider when the observer's line of sight is perpendicular rather than parallel to the local magnetic field. This is opposite to the trend in the interplanetary space permeated in the solar wind, because the ratio between dynamic pressure and magnetic pressure is an order of magnitude smaller than at 1 AU. On the other hand, we find that iron ions in the comet head build up to a density comparable to that of oxygen ions, but are unlikely to form a visible tail because of the shorter mean free paths of the neutrals.

### **From fundamental theory to realistic modeling of the birth of solar eruptions.**

**Jiang, C.**

Sci. China Earth Sci. 67, 3765–3788 (2024).

<https://doi.org/10.1007/s11430-023-1402-3>

Solar eruptions, primarily manifested as solar flares, filament eruptions and coronal mass ejections, represent explosive releases of magnetic energy stored in the solar corona, with the potential to drive severe space weather. The initiation of solar eruptions remains an open question, leading to various theoretical models that are inferred from observations. However, these models are subjects of debate due to the absence of direct measurements of the three-dimensional (3D) magnetic fields in the corona. Numerical simulations, based on solving magnetohydrodynamics (MHD) equations that govern the macroscopic dynamics of solar corona, serve as a touchstone for testing these theoretical models. One early proposed model suggested that eruptions could be triggered by reconnection within a single sheared magnetic arcade, which is known as the tether-cutting reconnection model, but it was never confirmed through 3D MHD simulations until very recently. Consequently, two models have gained more popularity: one involving the eruption of a twisted magnetic flux rope (MFR) due to ideal instability (or loss of equilibrium), and the other known as the breakout eruption, which requires a quadrupolar configuration with a delicately located magnetic null point. Other mixed mechanisms,

involving both ideal instability and reconnection, are also proposed in association with localized magnetic flux emergence. Now with the validation of the tether-cutting model, the fundamental mechanisms are boiled down to two types of models, one primarily based on the ideal instability of a pre-existing MFR, and the other based on the reconnection of sheared field lines with or without an MFR. Recently, the modelling of the birth of solar eruption using observed data-based MHD simulations has advanced rapidly, becoming a crucial research tool in the study of the initiation mechanisms. These realistic modellings reveal a higher level of complexity compared to all currently available theories and idealized models.

## **Magnetic Reconnection as the Key Mechanism in Sunspot Rotation Leading to Solar Eruption**

[Chaowei Jiang](#), [Xueshang Feng](#), [Xinkai Bian](#), [Peng Zou](#), [Aiyong Duan](#), [Xiaoli Yan](#), [Qiang Hu](#), [Wen He](#), [Xinyi Wang](#), [Pingbing Zuo](#), [Yi Wang](#)

ApJ 2023

<https://arxiv.org/pdf/2308.09928.pdf>

The rotation of sunspots around their umbral center has long been considered as an important process in leading to solar eruptions, but the underlying mechanism remains unclear. A prevailing physical picture on how sunspot rotation leads to eruption is that, by twisting the coronal magnetic field lines from their footpoints, the rotation can build up a magnetic flux rope and drive it into some kinds of ideal magnetohydrodynamics (MHD) instabilities which initiate eruptions. Here with a data-inspired MHD simulation we studied the rotation of a large sunspot in solar active region NOAA 12158 leading to a major eruption, and found that it is distinct from prevailing theories based on ideal instabilities of twisted flux rope. The simulation suggests that, through successive rotation of the sunspot, the coronal magnetic field is sheared with a central current sheet created progressively within the sheared arcade before the eruption, but without forming a flux rope. Then the eruption is instantly triggered once fast reconnection sets in at the current sheet, while a highly twisted flux rope is created during the eruption. Furthermore, the simulation reveals an intermediate evolution stage between the quasi-static energy-storage phase and the impulsive eruption-acceleration phase. This stage may correspond to slow-rise phase in observation and it enhances building up of the current sheet.

## **Data-driven MHD simulation of a sunspot rotating active region leading to solar eruption**

[Chaowei Jiang](#), [Xueshang Feng](#), [Xinkai Bian](#), [Peng Zou](#), [Aiyong Duan](#), [Xiaoli Yan](#), [Qiang Hu](#), [Wen He](#), [Xinyi Wang](#), [Pingbing Zuo](#), [Yi Wang](#)

A&A 2023

<https://arxiv.org/pdf/2308.06977.pdf>

Solar eruptions are the leading driver of space weather, and it is vital for space weather forecast to understand in what conditions the solar eruptions can be produced and how they are initiated. The rotation of sunspots around their umbral center has long been considered as an important condition in causing solar eruptions. To unveil the underlying mechanisms, here we carried out a data-driven magnetohydrodynamics simulation for the event of a large sunspot with rotation for days in solar active region NOAA 12158 leading to a major eruption. The photospheric velocity as recovered from the time sequence of vector magnetograms are inputted directly at the bottom boundary of the numerical model as the driving flow. Our simulation successfully follows the long-term quasi-static evolution of the active region until the fast eruption, with magnetic field structure consistent with the observed coronal emission and onset time of simulated eruption matches rather well with the observations. Analysis of the process suggests that through the successive rotation of the sunspot the coronal magnetic field is sheared with a vertical current sheet created progressively, and once fast reconnection sets in at the current sheet, the eruption is instantly triggered, with a highly twisted flux rope originating from the eruption. This data-driven simulation stresses magnetic reconnection as the key mechanism in sunspot rotation leading to eruption. **6–11 September 2014**

## **A model of failed solar eruption initiated and destructed by magnetic reconnection**

[Chaowei Jiang](#), [Aiyong Duan](#), [Peng Zou](#), [Zhenjun Zhou](#), [Xinkai Bian](#), [Xueshang Feng](#), [Pingbing Zuo](#), [Yi Wang](#)

MNRAS Volume 525, Issue 4, November 2023, Pages 5857–5867,

<https://doi.org/10.1093/mnras/stad2658>

<https://arxiv.org/pdf/2307.15847.pdf>

Solar eruptions are explosive disruption of coronal magnetic fields, and often launch coronal mass ejections into the interplanetary space. Intriguingly, many solar eruptions fail to escape from the Sun, and the prevailing theory for such failed eruption is based on ideal MHD instabilities of magnetic flux rope (MFR); that is, a MFR runs into kink instability and erupts but cannot reach the height for torus instability. Here, based on numerical MHD simulation, we present a new model of failed eruption in which magnetic reconnection plays a leading role in the initiation and failure of the eruption. Initially, a core bipolar potential field is embedded in a background bipolar field, and by applying shearing and converging motions to the core field, a current sheet is formed within the core field. Then, tether-cutting reconnection is triggered at the current sheet, first slow for a while and becoming fast, driving an erupting MFR. Eventually, the rise of MFR is halted by the downward magnetic tension force of the overlying field, although the MFR apex has well exceeded the critical height of torus instability. More importantly, during the rise of the MFR, it experiences a significant rotation around the vertical axis (with a direction contrary to that predicted by kink instability), rendering the field direction at the rope apex almost inverse to the overlying field. As a result, a strong current sheet is

formed between the MFR and the overlying flux, and reconnection occurring in this current sheet ruins completely the MFR.

## **Data-driven modeling of solar coronal magnetic field evolution and eruptions**

Chaowei **Jiang**, Xueshang Feng, Yang Guo, Qiang Hu

The Innovation **2022**

[https://www.cell.com/the-innovation/fulltext/S2666-6758\(22\)00032-7](https://www.cell.com/the-innovation/fulltext/S2666-6758(22)00032-7)

<https://doi.org/10.1016/j.xinn.2022.100236>

Magnetic fields play a fundamental role in the structure and dynamics of the solar corona. As they are driven by their footpoint motions on the solar surface, which transport energy from the interior of the Sun into its atmosphere, the coronal magnetic fields are stressed continuously with buildup of magnetic nonpotentiality in the form of topology complexity (magnetic helicity) and local electric currents (magnetic free energy). The accumulated nonpotentiality is often released explosively by solar eruptions, manifested as solar flares and coronal mass ejections, during which magnetic energy is converted into mainly kinetic, thermal, and nonthermal energy of the plasma, which can cause adverse space weather. To reveal the physical mechanisms underlying solar eruptions, it is vital to know the three-dimensional (3D) structure and evolution of the coronal magnetic fields. Because of a lack of direct measurements, the 3D coronal magnetic fields are commonly studied using numerical modeling, whereas traditional models mostly aim for a static extrapolation of the coronal field from the observable photospheric magnetic field data. Over the last decade, dynamic models that are driven directly by observation magnetograms have been developed and applied successfully to study solar coronal magnetic field evolution as well as its eruption, which offers a novel avenue for understanding their underlying magnetic topology and mechanism. In this paper, we review the basic methodology of the data-driven coronal models, state-of-the-art developments, their typical applications, and new physics that have been derived using these models. Finally, we provide an outlook for future developments and applications of the data-driven models.

November 11, 2010, 15 Feb 2011, September 6, 2011

## **Formation of Magnetic Flux Rope during Solar Eruption.**

### **Evolution of Toroidal Flux and Reconnection Flux**

[Chaowei Jiang](#), [Jun Chen](#), [Aiyong Duan](#), [Xinkai Bian](#), [Xinyi Wang](#), [Jiaying Li](#), [Peng Zou](#), [Xueshang Feng](#)

Frontiers in Physics 9:746576 **2021**

<https://arxiv.org/pdf/2109.08422.pdf>

<https://www.frontiersin.org/articles/10.3389/fphy.2021.746576/full>

<https://doi.org/10.3389/fphy.2021.746576>

Magnetic flux ropes (MFRs) constitute the core structure of coronal mass ejections (CMEs), but hot debates remain on whether the MFR forms before or during solar eruptions. Furthermore, how flare reconnection shapes the erupting MFR is still elusive in three dimensions. Here we studied a new MHD simulation of CME initiation by tether-cutting magnetic reconnection in a single magnetic arcade. The simulation follows the whole life, including the birth and subsequent evolution, of an MFR during eruption. In the early phase, the MFR is partially separated from its ambient field by a magnetic quasi-separatrix layer (QSL) that has a double-J shaped footprint on the bottom surface. With the ongoing of the reconnection, the arms of the two J-shaped footprints continually separate from each other, and the hooks of the J shaped footprints expand and eventually become closed almost at the eruption peak time, and thereafter the MFR is fully separated from the un-reconnected field by the QSL. We further studied the evolution of the toroidal flux in the MFR and compared it with that of the reconnected flux. Our simulation reproduced an evolution pattern of increase-to-decrease of the toroidal flux, which is reported recently in observations of variations in flare ribbons and transient coronal dimming. The increase of toroidal flux is owing to the flare reconnection in the early phase that transforms the sheared arcade to twisted field lines, while its decrease is a result of reconnection between field lines in the interior of the MFR in the later phase.

## **A fundamental mechanism of solar eruption initiation**

[Chaowei Jiang](#), [Xueshang Feng](#), [Rui Liu](#), [XiaoLi Yan](#), [Qiang Hu](#), [Ronald L. Moore](#), [Aiyong Duan](#), [Jun Cui](#), [Pingbing Zuo](#), [Yi Wang](#) & [Fengsi Wei](#)

Nature Astronomy v. 5, issue 7 (2021) **File**

<https://arxiv.org/pdf/2107.08204.pdf>

<https://doi.org/10.1038/s41550-021-01414-z>

Solar eruptions are spectacular magnetic explosions in the Sun's corona, and how they are initiated remains unclear. Prevailing theories often rely on special magnetic topologies that may not generally exist in the pre-eruption source region of corona. Here, using fully three-dimensional magnetohydrodynamic simulations with high accuracy, we show that solar eruptions can be initiated in a single bipolar configuration with no additional special topology. Through photospheric shearing motion alone, an electric current sheet forms in the highly sheared core field of the magnetic arcade during its quasi-static evolution. Once magnetic reconnection sets in, the whole arcade is expelled impulsively, forming a fast-expanding twisted flux rope with a highly turbulent reconnecting region underneath. The simplicity and efficacy of this scenario argue strongly for its fundamental importance in the initiation of solar eruptions.



## Formation and Eruption of an Active Region Sigmoid. II. Magnetohydrodynamic Simulation of a Multistage Eruption

Chaowei [Jiang](#)<sup>1,2,3</sup>, Xueshang Feng<sup>1,2</sup>, and Qiang Hu<sup>3</sup>

2018 ApJ 866 96

[sci-hub.tw/10.3847/1538-4357/aadd08](http://sci-hub.tw/10.3847/1538-4357/aadd08)

[sci-hub.tw/10.3847/1538-4357/aadd08](http://sci-hub.tw/10.3847/1538-4357/aadd08)

Solar eruptions, mainly eruptive flares with coronal mass ejections, represent the most powerful drivers of space weather. Due to the low plasma- $\beta$  nature of the solar corona, solar eruption has its roots in the evolution of the coronal magnetic field. Although various theoretical models of the eruptive magnetic evolution have been proposed, they still oversimplify the realistic process in observation, which shows a much more complex process due to the invisible complex magnetic environment. In this paper, we continue our study of a complex sigmoid eruption in solar active region 11283, which is characterized by a multipolar configuration embedding a null-point topology and a sigmoidal magnetic flux rope. Based on extreme ultraviolet observations, it has been suggested that a three-stage magnetic reconnection scenario might explain the complex flare process. Here we reproduce the complex magnetic evolution during the eruption using a data-constrained high-resolution magnetohydrodynamic (MHD) simulation. The simulation clearly demonstrates three reconnection episodes, which occurred in sequence in different locations in the corona. Through these reconnections, the initial sigmoidal flux rope breaks one of its legs, and quickly gives birth to a new tornado-like magnetic structure that is highly twisted and has multiple connections to the Sun due to the complex magnetic topology. The simulated magnetic field configuration and evolution are found to be consistent with observations of the corona loops, filaments, and flare ribbons. Our study demonstrates that significant insight into a realistic, complex eruption event can be gained by a numerical MHD simulation that is constrained or driven by observed data. **2011 September 6**

## Data-driven magnetohydrodynamic modelling of a flux-emerging active region leading to solar eruption

Chaowei [Jiang](#), S. T. Wu, Xuesheng Feng, Qiang Hu

Nature Communications 7:11522 2016

<http://www.nature.com/ncomms/2016/160516/ncomms11522/pdf/ncomms11522.pdf>

Solar eruptions are well-recognized as major drivers of space weather but what causes them remains an open question. Here we show how an eruption is initiated in a non-potential magnetic flux-emerging region using magnetohydrodynamic modelling driven directly by solar magnetograms. Our model simulates the coronal magnetic field following a long-duration quasi-static evolution to its fast eruption. The field morphology resembles a set of extreme ultraviolet images for the whole process. Study of the magnetic field suggests that in this event, the key transition from the pre-eruptive to eruptive state is due to the establishment of a positive feedback between the upward expansion of internal stressed magnetic arcades of new emergence and an external magnetic reconnection which triggers the eruption. Such a nearly realistic simulation of a solar eruption from origin to onset can provide important insight into its cause, and also has the potential for improving space weather modelling. **6-8 September 2011**

See HMI Science Nuggets #54 May 2016 <http://hmi.stanford.edu/hminuggets/?p=1570>

## A Comparison Study of a Solar Active-Region Eruptive Filament and a Neighboring Non-Eruptive Filament

Chaowei [Jiang](#), S. T. Wu, [Xueshang Feng](#), [Qiang Hu](#)

RAA 2015

<http://arxiv.org/pdf/1508.05113v1.pdf>

Solar active region (AR) 11283 is a very magnetically complex region and it has produced many eruptions. However, there exists a non-eruptive filament in the plage region just next to an eruptive one in the AR, which gives us an opportunity to perform a comparison analysis of these two filaments. The coronal magnetic field extrapolated using a CESE-MHD-NLFFF code (Jiang & Feng 2013) reveals that two magnetic flux ropes (MFRs) exist in the same extrapolation box supporting these two filaments, respectively. Analysis of the magnetic field shows that the eruptive MFR contains a bald-patch separatrix surface (BPSS) co-spatial very well with a pre-eruptive EUV sigmoid, which is consistent with the BPSS model for coronal sigmoids. The magnetic dips of the non-eruptive MFRs match  $H\{\alpha\}$  observation of the non-eruptive filament strikingly well, which strongly supports the MFR-dip model for filaments. Compared with the non-eruptive MFR/filament (with a length of about 200 Mm), the eruptive MFR/filament is much smaller (with a length of about 20 Mm), but it contains most of the magnetic free energy in the extrapolation box and holds a much higher free energy density than the non-eruptive one. Both the MFRs are weakly twisted and cannot trigger kink instability. The AR eruptive MFR is unstable because its axis reaches above a critical height for torus instability, at which the overlying closed arcades can no longer confine the MFR stably. On the contrary, the quiescent MFR is very firmly held by its overlying field, as its axis apex is far below the torus-instability threshold height. Overall, this comparison investigation supports that MFR can exist prior to eruption and the ideal MHD instability can trigger MFR eruption. **September 6-7, 2011**

## Testing a Solar Coronal Magnetic Field Extrapolation Code with the Titov-Demoulin Magnetic Flux Rope Model

Chaowei **Jiang**, Xueshang Feng

RAA 2015

<http://arxiv.org/pdf/1507.01910v1.pdf>

In the solar corona, magnetic flux rope is believed to be a fundamental structure accounts for magnetic free energy storage and solar eruptions. Up to the present, the extrapolation of magnetic field from boundary data is the primary way to obtain fully three-dimensional magnetic information of the corona. As a result, the ability of reliable recovering coronal magnetic flux rope is important for coronal field extrapolation. In this paper, our coronal field extrapolation code (CESE-MHD-NLFFF, Jiang & Feng 2012) is examined with an analytical magnetic flux rope model proposed by Titov & Demoulin (1999), which consists of a bipolar magnetic configuration holding an semi-circular line-tied flux rope in force-free equilibrium. By using only the vector field in the bottom boundary as input, we test our code with the model in a representative range of parameter space and find that the model field is reconstructed with high accuracy. Especially, the magnetic topological interfaces formed between the flux rope and the surrounding arcade, i.e., the "hyperbolic flux tube" and "bald patch separatrix surface", are also reliably reproduced. By this test, we demonstrate that our CESE-MHD-NLFFF code can be applied to recovering magnetic flux rope in the solar corona as long as the vector magnetogram satisfies the force-free constraints.

## Interaction between an emerging flux region and a pre-existing fan-spine dome observed by IRIS and SDO

Fayu **Jiang**, Jun Zhang, Shuhong Yang

Publications of the Astronomical Society of Japan 2015

<http://arxiv.org/pdf/1503.04505v2.pdf>

We present multi-wavelength observations of a fan-spine dome in the active region NOAA 11996 with the Interface Region Imaging Spectrograph (IRIS) and the Atmospheric Imaging Assembly on board the Solar Dynamics Observatory (SDO) on **March 9, 2014**. The destruction of the fan-spine topology owing to the interaction between its magnetic fields and an nearby emerging flux region (EFR) is firstly observed. The line-of-sight magnetograms from the Helioseismic and Magnetic Imager on board the SDO reveal that the dome is located on the mixed magnetic fields, with its rim rooted in the redundant positive polarity surrounding the minority parasitic negative fields. The fan surface of the dome consists of a filament system and recurring jets are observed along its spine. The jet occurring around 13:54 UT is accompanied with a quasi-circular ribbon that brightens in the clockwise direction along the bottom rim of the dome, which may indicate an occurrence of slipping reconnection in the fan-spine topology. The EFR emerges continuously and meets with the magnetic fields of the dome. Magnetic cancellations take place between the emerging negative polarity and the outer positive polarity of the dome's fields, which lead to the rise of the loop connecting the EFR and brightenings related to the dome. A single Gaussian fit to the profiles of the IRIS SI IV 1394 Å line is used in the analysis. It appears that there are two rising components along the slit, except for the rise in the line-of-sight direction. The cancellation process repeats again and again. Eventually the fan-spine dome is destroyed and a new connectivity is formed. We suggest that magnetic reconnection between the EFR and the magnetic fields of the fan-spine dome in the process is responsible for the destruction of the dome.

## Interaction and Merging of two Sinistral Filaments

Yunchun **Jiang**<sup>1</sup>, Jiayan Yang<sup>1</sup>, Haimin Wang<sup>2</sup>, Haisheng Ji<sup>3</sup>, Yu Liu<sup>1</sup>, Haidong Li<sup>1</sup>, and Jianping Li  
2014 ApJ 793 14

In this paper, we report the interaction and subsequent merging of two sinistral filaments (F1 and F2) occurring at the boundary of AR 9720 on **2001 December 6**. The two filaments were close and nearly perpendicular to each other. The interaction occurred after F1 was erupted and the eruption was impeded by a more extended filament channel (FC) standing in the way, in which F2 was embedded. The erupted material ran into FC along its axis, causing F1 and F2 to merge into a single structure that subsequently underwent a large-amplitude to-and-fro motion. A significant plasma heating process was observed in the merging process, making the mixed material largely disappear from the H $\alpha$  passband, but appear in Extreme Ultraviolet Telescope 195?? images for a while. These observations can serve as strong evidence of merging reconnection between the two colliding magnetic structures. A new sinistral filament was formed along FC after the cooling of the merged and heated material. No coronal mass ejection was observed to be associated with the event; though, the eruption was accompanied by a two-ribbon flare with a separation motion, indicating that the eruption had failed. This event shows that, in addition to overlying magnetic fields, such an interaction is an effective restraint to make a filament eruption fail in this way.

## Formation and Eruption of an Active Region Sigmoid: I. Study by Nonlinear Force-Free Field Modeling

Chaowei **Jiang**, S. T. Wu, Xueshang Feng, Qiang Hu

E-print, Oct 2013, File; 2014 ApJ 780 55

<http://arxiv.org/abs/1310.8196>

We present a magnetic analysis of the formation and eruption of an active region (AR) sigmoid in AR 11283 from **2011 September 4 to 6**. To follow the quasi-static evolution of the coronal magnetic field, we reconstruct a time sequence of static fields using a recently developed nonlinear force-free field model constrained by the SDO/HMI vector magnetograms. A detailed analysis of the fields compared with the SDO/AIA observations suggests the following scenario for the evolution of the region. Initially, a new bipole emerges into the negative polarity of a pre-existing bipolar AR, forming a null point topology between the two flux systems. A weakly twisted flux rope (FR) is then built up slowly in the embedded core region, largely through flux-cancellation photospheric reconnections, forming a bald patch separatrix surface (BPSS) separating the FR from its ambient field. The FR grows gradually until its axis runs into a torus instability (TI) domain near the end of the third day, and the BPSS also develops a fully S-shape. Unlike in the case of standard TI, the FR does not erupt instantly since it is still attached at the photosphere along the bald patch (BP) portion of the polarity inversion line. The combined effects of the TI-driven expansion of the FR and the line-tying at the BP tear the FR into two parts with the upper portion freely expelled and the lower portion remaining behind the post-flare arcades. This process dynamically perturbs the BPSS and results in the transient enhanced brightening of the sigmoid. The accelerated expansion of the upper portion of the FR strongly pushes its envelope flux near the null point and triggers breakout reconnection at the null, as evidenced by a remarkable circular flare ribbon, which further facilitates the eruption. We discuss the important implications of these results for the formation and disruption of sigmoid region with an FR.

### **MHD Simulation of a Sigmoid Eruption of Active Region 11283**

Chaowei **Jiang**, Xueshang Feng, S. T. Wu, Qiang Hu

E-print, June **2013**, ApJ 771 L30

Current magnetohydrodynamic (MHD) simulations of the initiation of solar eruptions are still commonly carried out with idealized magnetic field models, whereas the realistic coronal field prior to eruptions can possibly be reconstructed from the observable photospheric field. Using a nonlinear force-free field extrapolation prior to a sigmoid eruption in AR 11283 as the initial condition in a MHD model, we successfully simulate the realistic initiation process of the eruption event, as is confirmed by a remarkable resemblance to the SDO/AIA observations. Analysis of the pre-eruption field reveals that the envelope flux of the sigmoidal core contains a coronal null and furthermore the flux rope is prone to a torus instability. Observations suggest that reconnection at the null cuts overlying tethers and likely triggers the torus instability of the flux rope, which results in the eruption. This kind of simulation demonstrates the capability of modeling the realistic solar eruptions to provide the initiation process. **2011 September 6**.

**Jiang**, Y., Yang, J., Hong, J., Bi, Y., & Zheng, R.

**2011**, ApJ, 738, 179

presented observations of three successive filament eruptions from different locations on **2003 November 19** and interpreted these sympathetic eruptions from coronal dimming investigations.

### **Evidence for a Magnetic Flux Rope in Observations of a Solar Prominence-Cavity System**

Patricia R. **Jibben**, Katharine K. Reeves, and Yingna Su

Front. Astron. Space Sci. 3:10. **2016**

<https://www.frontiersin.org/articles/10.3389/fspas.2016.00010/full>

<https://doi.org/10.3389/fspas.2016.00010>

Coronal cavities are regions of low coronal emission that usually sit above solar prominences. These systems can exist for days or months before erupting. The magnetic structure of the prominence-cavity system during the quiescent period is important to understanding the pre-eruption phase. We describe observations of a coronal cavity situated above a solar prominence observed on the western limb as part of an Interface Region Imaging Spectrograph (IRIS) and Hinode coordinated Observation Program (IHOP 264). During the observation run, an inflow of hot plasma observed by the Hinode X-Ray Telescope (XRT) envelopes the coronal cavity and triggers an eruption of chromospheric plasma near the base of the prominence. During and after the eruption, bright X-ray emission forms within the cavity and above the prominence. IRIS and the Hinode EUV Imaging Spectrometer (EIS) show strong blue shifts in both chromospheric and coronal lines during the eruption. The Hinode Solar Optical Telescope (SOT) Ca II H-line data show bright emission during the ejection with complex, turbulent, flows near the prominence and along the cavity wall. These observations suggest a cylindrical flux rope best represents the cavity structure with the ejected material flowing along magnetic field lines supporting the cavity. We also find evidence for heating of the plasma inside the cavity after the flows. A model of the magnetic structure of the cavity comprised of a weakly twisted flux rope can explain the observed loops in the X-ray and EUV data. Observations from the Coronal Multichannel Polarimeter (CoMP) are compared to predicted models and are inconclusive. We find that more sensitive measurements of the magnetic field strength along the line-of-sight are needed to verify this configuration.

### **Exploring the Dynamics of CME-Driven Shocks by Comparing Numerical Modeling and Observations**

Meng **Jin**, **Gang Li**, **Nariaki Nitta**, **Wei Liu**, **Vahe Petrosian**, **Ward Manchester**, **Christina Cohen**, **Frederic Effenberger**, **Zheyi Ding**, **Melissa Pesce-Rollins**, **Nicola Omodei**, **Nat Gopalswamy**

<https://arxiv.org/pdf/2409.18020>

Shocks driven by coronal mass ejections (CMEs) are primary drivers of gradual solar energetic particle (SEP) events, posing significant risks to space technology and astronauts. Concurrently, particles accelerated at these shocks may also propagate back to the Sun, potentially generating gamma-ray emissions through pion decay. We incorporated advanced modeling and multi-messenger observations to explore the role of CME-driven shocks in gamma-ray emissions and SEPs. Motivated by Fermi-LAT long-duration solar flares, we used the AWSoM MHD model to investigate the connection between the shocks and the properties of observed gamma-ray emissions. By coupling the AWSoM with iPATH model, we evaluate the impact of shock evolution complexity near the Sun on SEP intensity and spectra. Our result points to the importance of accurate background coronal and solar wind modeling, as well as detailed observations of CME source regions, in advancing our understanding of CME-driven shocks and the dynamics of associated energetic particles. **7 Mar 2012, 17 May 2012, 11 Apr 2013, 1 Sep 2014, 17 Jul 2021, 28 Oct 2021**

### Coronal Dimming as a Proxy for Stellar Coronal Mass Ejections

Meng **Jin**, [Mark C. M. Cheung](#), [Marc L. DeRosa](#), [Nariaki V. Nitta](#), [Carolus J. Schrijver](#), [Kevin France](#), [Adam Kowalski](#), [James P. Mason](#), [Rachel Osten](#)

Proceedings of IAU Symposium No. 354 - Solar and Stellar Magnetic Fields: Origins and Manifestations **2020**

<https://arxiv.org/pdf/2002.06249.pdf>

Solar coronal dimmings have been observed extensively in the past two decades and are believed to have close association with coronal mass ejections (CMEs). Recent study found that coronal dimming is the only signature that could differentiate powerful ares that have CMEs from those that do not. Therefore, dimming might be one of the best candidates to observe the stellar CMEs on distant Sun-like stars. In this study, we investigate the possibility of using coronal dimming as a proxy to diagnose stellar CMEs. By simulating a realistic solar CME event and corresponding coronal dimming using a global magnetohydrodynamics model (AWSoM: Alfvén-wave Solar Model), we first demonstrate the capability of the model to reproduce solar observations. We then extend the model for simulating stellar CMEs by modifying the input magnetic flux density as well as the initial magnetic energy of the CME flux rope. Our result suggests that with improved instrument sensitivity, it is possible to detect the coronal dimming signals induced by the stellar CMEs. **2011 February 15**

### Chromosphere to 1 AU Simulation of the 2011 March 7th Event: A Comprehensive Study of Coronal Mass Ejection Propagation

M. **Jin**, W. B. Manchester, B. van der Holst, I. Sokolov, G. Toth, A. Vourlidas, C. A. de Koning, T. I. Gombosi

ApJ **2016**

<https://arxiv.org/pdf/1611.08897v1.pdf>

[http://www.lmsal.com/~jinmeng/papers/mjin17a\\_apj.pdf](http://www.lmsal.com/~jinmeng/papers/mjin17a_apj.pdf)

We perform and analyze results of a global magnetohydrodynamic (MHD) simulation of the fast coronal mass ejection (CME) that occurred on **2011 March 7**. The simulation is made using the newly developed Alfvén Wave Solar Model (AWSoM), which describes the background solar wind starting from the upper chromosphere and extends to  $24 R_{\odot}$ . Coupling AWSoM to an inner heliosphere (IH) model with the Space Weather Modeling Framework (SWMF) extends the total domain beyond the orbit of Earth. Physical processes included in the model are multi-species thermodynamics, electron heat conduction (both collisional and collisionless formulations), optically thin radiative cooling, and Alfvén-wave turbulence that accelerates and heats the solar wind. The Alfvén-wave description is physically self-consistent, including non-Wentzel-Kramers-Brillouin (WKB) reflection and physics-based apportioning of turbulent dissipative heating to both electrons and protons. Within this model, we initiate the CME by using the Gibson-Low (GL) analytical flux rope model and follow its evolution for days, in which time it propagates beyond STEREO A. A detailed comparison study is performed using remote as well as *in situ* observations. Although the flux rope structure is not compared directly due to lack of relevant ejecta observation at 1 AU in this event, our results show that the new model can reproduce many of the observed features near the Sun (e.g., CME-driven extreme ultraviolet (EUV) waves, deflection of the flux rope from the coronal hole, "double-front" in the white light images) and in the heliosphere (e.g., shock propagation direction, shock properties at STEREO A).

### Data Constrained Coronal Mass Ejections in A Global Magnetohydrodynamics Model

M. **Jin**, W. B. Manchester, B. van der Holst, I. Sokolov, G. Toth, R. E. Mullinix, A. Taktakishvili, A. Chulaki, T. I. Gombosi

ApJ **834** 173 **2017**

<https://arxiv.org/pdf/1605.05360v1.pdf>

[http://www.lmsal.com/~jinmeng/papers/mjin17b\\_apj.pdf](http://www.lmsal.com/~jinmeng/papers/mjin17b_apj.pdf)

We present a first-principles-based coronal mass ejection (CME) model suitable for both scientific and operational purposes by combining a global magnetohydrodynamics (MHD) solar wind model with a flux rope-driven CME model. Realistic CME events are simulated self-consistently with high fidelity and forecasting capability by constraining initial flux rope parameters with observational data from GONG, SOHO/LASCO, and STEREO/COR. We automate this process so that minimum manual intervention is required in specifying the CME initial state. With the newly developed

data-driven Eruptive Event Generator Gibson-Low (EEGGL), we present a method to derive Gibson-Low (GL) flux rope parameters through a handful of observational quantities so that the modeled CMEs can propagate with the desired CME speeds near the Sun. A test result with CMEs launched with different Carrington rotation magnetograms are shown. Our study shows a promising result for using the first-principles-based MHD global model as a forecasting tool, which is capable of predicting the CME direction of propagation, arrival time, and ICME magnetic field at 1 AU (see companion paper by Jin et al. 2016b).

See [Introduction](#) about three different categories of the CME models

## **A Numerical Study of Long-Range Magnetic Impacts during Coronal Mass Ejections**

M. [Jin](#), C. J. Schrijver, M. C. M. Cheung, M. L. DeRosa, N. V. Nitta, A. M. Title

ApJ 820 16 2016 File

[http://www.lmsal.com/~schryver/Public/ms/LongRangeImpacts\\_ApJ.pdf](http://www.lmsal.com/~schryver/Public/ms/LongRangeImpacts_ApJ.pdf)

With the global view and high-cadence observations from SDO/AIA and STEREO, many spatially separated solar eruptive events appear to be coupled. However, the mechanisms for "sympathetic" events are still largely unknown. In this study, we investigate the impact of an erupting flux rope on surrounding solar structures through large-scale magnetic coupling. We build a realistic environment of the solar corona on **2011 February 15** using a global magnetohydrodynamics (MHD) model and initiate coronal mass ejections (CMEs) in active region (AR) 11158 by inserting Gibson-Low analytical flux ropes. We show that a CME's impact on the surrounding structures depends not only on the magnetic strength of these structures and their distance to the source region, but also on the interaction between the CME with the large-scale magnetic field. Within the CME expansion domain where the flux rope field directly interacts with the solar structures, expansion-induced reconnection often modifies the overlying field, thereby increasing the decay index. This effect may provide a primary coupling mechanism underlying the sympathetic eruptions. The magnitude of the impact is found to depend on the orientation of the erupting flux rope, with the largest impacts occurring when the flux rope is favorably oriented for reconnecting with the surrounding regions. Outside the CME expansion domain, the influence of the CME is mainly through field line compression or post-eruption relaxation. Based on our numerical experiments, we discuss a way to quantify the eruption impact, which could be useful for forecasting purposes.

## **NUMERICAL SIMULATIONS OF CORONAL MASS EJECTION ON 2011 MARCH 7: ONE-TEMPERATURE AND TWO-TEMPERATURE MODEL COMPARISON**

M. [Jin](#)<sup>1</sup>, W. B. Manchester<sup>1</sup>, B. van der Holst<sup>1</sup>, R. Oran<sup>1</sup>, I. Sokolov<sup>1</sup>, G. Toth<sup>1</sup>, Y. Liu<sup>2</sup>, X. D. Sun<sup>2</sup>, and T. I. Gombosi

2013 ApJ 773 50

During Carrington rotation (CR) 2107, a fast coronal mass ejection (CME;  $>2000 \text{ km s}^{-1}$ ) occurred in active region NOAA 11164. This event is also associated with a solar energetic particle event. In this study, we present simulations of this CME with one-temperature (1T) and two-temperature (2T: coupled thermodynamics of the electron and proton populations) models. Both the 1T and 2T models start from the chromosphere with heat conduction and radiative cooling. The background solar wind is driven by Alfvén-wave pressure and heated by Alfvén-wave dissipation in which we have incorporated the balanced turbulence at the top of the closed field lines. The magnetic field of the inner boundary is set up using a synoptic map from Solar Dynamics Observatory/Heliographic and Magnetic Imager. The Titov-Démoulin flux-rope model is used to initiate the CME event. We compare the propagation of fast CMEs and the thermodynamics of CME-driven shocks in both the 1T and 2T CME simulations. Also, the synthesized white light images are compared with the Solar and Heliospheric Observatory/Large Angle and Spectrometric Coronagraph observations. Because there is no distinction between electron and proton temperatures, heat conduction in the 1T model creates an unphysical temperature precursor in front of the CME-driven shock and makes the shock parameters (e.g., shock Mach number, compression ratio) incorrect. Our results demonstrate the importance of the electron heat conduction in conjunction with proton shock heating in order to produce the physically correct CME structures and CME-driven shocks.

## **Magnetic Eruption from a Three-ribbon Flare**

Ju [Jing](#)<sup>1</sup>, Jeongwoo Lee<sup>1</sup>, Mia Mancuso<sup>1</sup>, Qin Li<sup>1</sup>, Nian Liu<sup>1</sup>, Satoshi Inoue<sup>1</sup>, Yan Xu<sup>1</sup>, and Haimin Wang<sup>1</sup>

2024 ApJ 972 110

<https://iopscience.iop.org/article/10.3847/1538-4357/ad5ce3/pdf>

We present observations and analysis of an eruptive M1.5 flare (SOL2014-08-01T18:13) in NOAA active region (AR) 12127, characterized by three flare ribbons, a confined filament between ribbons, and rotating sunspot motions as observed by the Solar Dynamics Observatory. The potential field extrapolation model shows a magnetic topology involving two intersecting quasi-separatrix layers (QSLs) forming a hyperbolic flux tube (HFT), which constitutes the fishbone structure for the three-ribbon flare. Two of the three ribbons show separation from each other, and the third ribbon is rather stationary at the QSL footpoints. The nonlinear force-free field extrapolation model implies the presence of a magnetic flux rope (MFR) structure between the two separating ribbons, which was unclear in the

observation. This suggests that the standard reconnection scenario for eruptive flares applies to the two ribbons, and the QSL reconnection for the third ribbon. We find rotational flows around the sunspot, which may have caused the eruption by weakening the downward magnetic tension of the MFR. The confined filament is located in the region of relatively strong strapping field. The HFT topology and the accumulation of reconnected magnetic flux in the HFT may play a role in holding it from eruption. This eruption scenario differs from the one typically known for circular ribbon flares, which is mainly driven by a successful inside-out eruption of filaments. Our results demonstrate the diversity of solar magnetic eruption paths that arises from the complexity of the magnetic configuration.

### **Statistical Analysis of Torus and Kink Instabilities in Solar Eruptions**

Ju [Jing](#), [Chang Liu](#), [Jeongwoo Lee](#), [Hantao Ji](#), [Nian Liu](#), [Yan Xu](#), [Haimin Wang](#)

2018 *ApJ* **864** 138

<https://arxiv.org/pdf/1808.08924.pdf>

[sci-hub.tw/10.3847/1538-4357/aad6e4](https://sci-hub.tw/10.3847/1538-4357/aad6e4)

A recent laboratory experiment of ideal magnetohydrodynamic (MHD) instabilities reveals four distinct eruption regimes readily distinguished by the torus instability (TI) and helical kink instability (KI) parameters (Myers 2015). To establish its observational counterpart, we collect 38 solar flares (stronger than GOES class M5 in general) that took place within  $45^\circ$  of disk center during 2011–2017, 26 of which are associated with a halo or partial halo coronal mass ejection (CME) (i.e., ejective events), while the others are CMEless (i.e., confined events). This is a complete sample of solar events satisfying our selection criteria detailed in the paper. For each event, we calculate decay index  $n$  of the potential strapping field above the magnetic flux rope (MFR) in and around the flaring magnetic polarity inversion line (a TI parameter), and the unsigned twist number  $T_w$  of the non-linear force-free (NLFF) field lines forming the same MFR (a KI parameter). We then construct a  $n$ – $T_w$  diagram to investigate how the eruptiveness depends on these parameters. We find: (1)  $T_w$  appears to play little role in discriminating between confined and ejective events; (2) the events with  $n \geq 0.8$  are all ejective and all confined events have  $n \leq 0.8$ . However,  $n \geq 0.8$  is not a necessary condition for eruption, because some events with  $n \leq 0.8$  also erupted. In addition, we investigate the MFR's geometrical parameters, apex height and distance between footpoints, as a possible factor for the eruptiveness. We briefly discuss the difference of the present result for solar eruptions with that of the laboratory result in terms of the role played by magnetic reconnection. **2015-03-12**, **2015-06-22**

**Table 1.** Event List (2011-2017; **2017-09-04**, **2017-09-06**)

### **Comparison between the eruptive X2.2 flare on 2011 February 15 and confined X3.1 flare on 2014 October 24**

Ju [Jing](#), [Yan Xu](#), [Jeongwoo Lee](#), [Nariaki V. Nitta](#), [Chang Liu](#), [Sung-Hong Park](#), [Thomas Wiegelmann](#), [Haimin Wang](#)

Research in Astronomy and Astrophysics (RAA) Vol 15, No 9 1537-1546 **2015**

<http://www.raa-journal.org/raa/index.php/raa/article/view/2313>

We compare two contrasting X-class flares in terms of magnetic free energy, relative magnetic helicity and decay index of the active regions (ARs) in which they occurred. The events in question are the eruptive X2.2 flare from AR 11158 accompanied by a halo coronal mass ejection (CME) and the confined X3.1 flare from AR 12192 with no associated CME. These two flares exhibit similar behavior of free magnetic energy and helicity buildup for a few days preceding them. A major difference between the two flares is found to lie in the time-dependent change of magnetic helicity of the ARs that hosted them. AR 11158 shows a significant decrease in magnetic helicity starting  $\sim 4$  hours prior to the flare, but no apparent decrease in helicity is observed in AR 12192. By examining the magnetic helicity injection rates in terms of sign, we confirmed that the drastic decrease in magnetic helicity before the eruptive X2.2 flare was not caused by the injection of reversed helicity through the photosphere but rather the CME-related change in the coronal magnetic field. Another major difference we find is that AR 11158 had a significantly larger decay index and therefore weaker overlying field than AR 12192. These results suggest that the coronal magnetic helicity and the decay index of the overlying field can provide a clue about the occurrence of CMEs.

### **Evolution of a Magnetic Flux Rope and its Overlying Arcade Based on Nonlinear Force-free Field Extrapolations**

Ju [Jing](#), [Chang Liu](#), [Jeongwoo Lee](#), [Shuo Wang](#), [Thomas Wiegelmann](#), [Yan Xu](#), and [Haimin Wang](#)

*ApJ* **784** L13, **2014**

E-print, March **2014**;

Dynamic phenomena indicative of slipping reconnection and magnetic implosion were found in a time series of nonlinear force-free field (NLFFF) extrapolations for the active region 11515, which underwent significant changes in the photospheric fields and produced five C-class flares and one M-class flare over five hours on **2012 July 2**. NLFFF extrapolation was performed for the uninterrupted 5 hour period from the 12 minute cadence vector magnetograms of the Helioseismic and Magnetic Imager on board the Solar Dynamic Observatory. According to the time-dependent NLFFF model, there was an elongated, highly sheared magnetic flux rope structure that aligns well with an H $\alpha$  filament. This long filament splits sideways into two shorter segments, which further separate from each other over time at a speed of 1–4 km s $^{-1}$ , much faster than that of the footpoint motion of the magnetic field. During the separation, the magnetic arcade arching over the initial flux rope significantly decreases in height from  $\sim 4.5$  Mm to less than 0.5 Mm. We discuss the reality of this modeled magnetic restructuring by relating it to the observations of the magnetic

cancellation, flares, a filament eruption, a penumbra formation, and magnetic flows around the magnetic polarity inversion line.

## **Intense Flare-CME Event of the Year 2015: Propagation and Interaction Effects between Sun and Earth's Orbit**

Abhishek [Johri](#), P.K. Manoharan

Solar Phys. **2016**

<http://arxiv.org/pdf/1603.04555v1.pdf>

In this paper, We report the interplanetary effects of a fast coronal mass ejection (CME) associated with the intense X2.7 flare that occurred on **05 May 2015**. The near-Sun signatures of the CME at low-coronal heights  $<2 \{R_{\odot}\}$  are obtained from the EUV images at 171  $\{\text{\AA}\}$  and metric radio observations. The intensity and duration of the CME-driven radio bursts in the near-Sun and interplanetary medium indicate this CME event to be an energetic one. The interplanetary scintillation data, along with the low-frequency radio spectrum, played a crucial role in understanding the radial evolution of the speed and expansion of the CME in the inner heliosphere as well as its interaction with a preceding slow CME. The estimation of the speed of the CME at several points along the Sun to 1 AU shows that i) the CME went through a rapid acceleration as well as expansion up to a height of  $\approx 6 \{R_{\odot}\}$ , and ii) the CME continued to propagate at speed  $\geq 800 \text{ kms}^{-1}$  between the Sun and 1 AU. These results show that the CME likely overcame the drag exerted by the ambient/background solar-wind with the support of its internal magnetic energy. When the CME interacted with a slow preceding CME, the turbulence level associated with the CME-driven disturbance increased significantly.

## **The visual complexity of coronal mass ejections follows the solar cycle**

[S. R. Jones](#), [C. J. Scott](#), [L. A. Barnard](#), [R. Highfield](#), [C. J. Lintott](#), [E. Baeten](#)

Space Weather e2020SW002556 **Volume18, Issue10 2020**

<https://doi.org/10.1029/2020SW002556>

<https://agupubs.onlinelibrary.wiley.com/doi/epdf/10.1029/2020SW002556>

The Heliospheric Imagers on board NASA's twin STEREO spacecraft show that coronal mass ejections (CMEs) can be visually complex structures. To explore this complexity, we created a citizen science project with the UK Science Museum, in which participants were shown pairs of CME images and asked to decide which image in each pair appeared the most 'complicated'. A Bradley-Terry model was then applied to these data to rank the CMEs by their 'complicatedness', or 'visual complexity'. This complexity ranking revealed that the annual average visual complexity values follow the solar activity cycle, with a higher level of complexity being observed at the peak of the cycle. The average complexity of CMEs observed by STEREO-A was also found to be significantly higher than those observed by STEREO-B. Visual complexity was found to be associated with CME size and brightness, but our results suggest that complexity may be influenced by the scale-sizes of structure in the CMEs. **15 June 2011**

## **Tracking CMEs using data from the Solar Stormwatch project; observing deflections and other properties**

Shannon R. [Jones](#), Luke A. Barnard, Christopher J. Scott, Mathew J. Owens, Julia Wilkinson

Space Weather Volume 15, Issue 9 September **2017** Pages 1125–1140

<http://sci-hub.cc/10.1002/2017SW001640>

With increasing technological dependence, society is becoming ever more affected by changes in the near-Earth space environment caused by space weather. The primary driver of these hazards are coronal mass ejections (CMEs). Solar Stormwatch is a citizen science project in which volunteers participated in several activities which characterized CMEs in the remote sensing images from the Sun Earth Connection Coronal and Heliospheric Investigation (SECCHI) instrument package on the twin STEREO spacecraft. Here we analyze the results of the "Track-it-back" activity, in which CMEs were tracked back through the COR1, COR2, and EUVI images. Analysis of the COR1, COR2, and EUVI data together allows CMEs to be studied consistently throughout the whole field of view spanned by these instruments (out to 15 RS). A total of 4783 volunteers took part in this activity, creating a data set containing 23,801 estimates of CME timing, location, and size. We used these data to produce a catalogue of 41 CMEs, which is the first to consistently track CMEs through each of these instruments. We assess how the CME speeds, propagation directions, and widths vary as the CMEs propagate through the fields of view of the different imagers. In particular, we compare the observed CME deflections between the COR1 and COR2 fields of view to the separation between the CME source region and the heliospheric current sheet (HCS), demonstrating that in general, these CMEs appear to deflect toward the HCS, consistent with other modeling studies of CME propagation.

## **LOCALIZED PLASMA DENSITY ENHANCEMENTS OBSERVED IN STEREO COR1**

Shaella I. [Jones](#)<sup>1,2</sup> and Joseph M. Davila<sup>2</sup>

Astrophysical Journal, 701:1906–1910, **2009**

Measurements of solar wind speed in the solar corona, where it is primarily accelerated, have proven elusive. One of the more successful attempts has been the tracking of outward-moving density inhomogeneities in whitelight coronagraph images. These inhomogeneities, or "blobs," have been treated as passive tracers of the ambient

solar wind. Here we report on the extension of these observations to lower altitudes using the *STEREO* COR1 coronagraph, and discuss the implications of these measurements for theories about the origin of these features.

### **High-resolution observations of recurrent jets from an arch filament system**

[Reetika Joshi](#), [Luc Rouppe van der Voort](#), [Brigitte Schmieder](#), [Fernando Moreno-Insertis](#), [Avijeet Prasad](#), [Guillaume Aulanier](#), [Daniel Nóbrega-Siverio](#)

A&A 691, A198 2024

<https://arxiv.org/pdf/2408.17254>

<https://www.aanda.org/articles/aa/pdf/2024/11/aa49715-24.pdf>

Solar jets are collimated plasma ejections along magnetic field lines observed in hot (EUV jets) and cool (chromospheric surges) temperature diagnostics. Their trigger mechanisms and the relationship between hot and cool jets are still not completely understood. We aim to investigate the generation of a sequence of active region solar jets and their evolution from the photospheric to the coronal heights. Using the synergy of high spatial and temporal resolution observations by the SST, along with the SDO, we analyze a sequence of solar jets originating in a mixed polarity region between the leading and following sunspots of an active region. We use a NFFF extrapolation technique for deriving the magnetic field topology of the active region. A mixed polarity region is formed over a long period (24 hours) with persistent magnetic flux emergence. This region has been observed as an arch filament system (AFS) in chromospheric SST observations. In this region, negative polarities surrounded by positive polarities create a fan-surface with a null point at a height of 6 Mm detected in the NFFF extrapolation. SST observations in H-beta spectral line reveal a large flux rope over the AFS and moving from the North to South, causing successive EUV and cool jets to move in the East-West direction and later towards the South along the long open loops. The high resolution SST observations (0.038 arcsec per pixel) resolve the dark area observed at the jet base and reveal the existence of an AFS with an extended cool jet which may be the result of a peeling-like mechanism of the AFS. Based on the combined analysis of SST and AIA observations along with extrapolated magnetic topology, it is suggested that the magnetic reconnection site may move southward by approximately 20 Mm until it reaches a region where the open magnetic field lines are oriented North-South. **23-24 Jun 2022**

### **Generic low-atmosphere signatures of swirled-anemone jets**

[Joshi](#), Reetika ; [Aulanier](#), Guillaume ; [Radcliffe](#), Alice ; [Rouppe van der Voort](#), Luc ; [Pariat](#), Etienne ; [Nóbrega-Siverio](#), Daniel ; [Schmieder](#), Brigitte

A&A 687, A172 2024

<https://arxiv.org/pdf/2404.13171>

<https://doi.org/10.1051/0004-6361/202449553>

<https://www.aanda.org/articles/aa/pdf/2024/07/aa49553-24.pdf>Context. Solar jets are collimated plasma flows moving along magnetic field lines and accelerated at low altitude following magnetic reconnection. Several of them originate from anemone-shaped low-lying arcades and the most impulsive ones tend to be relatively wider and display untwisting motions. Aims. We aim to establish typical behaviours and observational signatures in the low atmosphere that can occur in response to the coronal development of such impulsive jets. Methods. We analysed an observed solar jet associated with a circular flare ribbon, using high-resolution observations from SST coordinated with IRIS and SDO. We related specifically-identified features with those developing in a generic 3D line-tied numerical simulation of reconnection-driven jets, performed with the ARMS code. Results. We identified three features in the SST observations: the formation of a hook along the circular ribbon, the gradual widening of the jet through the apparent displacement of its kinked edge towards –and not away– from the presumed reconnection site, and the falling back of some of the jet plasma towards a footpoint offset from that of the jet itself. The 3D numerical simulation naturally accounts for these features which were not imposed a priori. Our analyses allow to interpret them in the context of the 3D geometry of the asymmetric swirled anemone loops and their sequences of reconnection with ambient coronal loops. Conclusions. Given the relatively-simple conditions in which the observed jet occurred, together with the generic nature of the simulation that comprised minimum assumptions, we predict that the specific features that we identified and interpreted are probably typical of every impulsive jet. **June 11, 2014**

### **Interaction of solar jets with filaments: Triggering of large-amplitude filament oscillations**

[Reetika Joshi](#), [Manuel Luna](#), [Brigitte Schmieder](#), [Fernando Moreno-Insertis](#), [Ramesh Chandra](#)

A&A 672, A15 2023

<https://arxiv.org/pdf/2301.13103.pdf>

<https://www.aanda.org/articles/aa/pdf/2023/04/aa45647-22.pdf>

Large-amplitude oscillations (LAOs) are often detected in filaments. Using multiwavelength observations, their origin can be traced back to the interaction with eruptions and jets. We present two different case studies as observational evidence in support of 2.5D MHD numerical experiments that show that the LAOs in the filament channels can be initiated by solar jets. In the two studied events, we can identify a quadrupolar configuration with an X-point at the top of the parasitic region suggestive of a classical null-point. A reconnection flow emanates from this structure leading to a jet that propagates along the filament channel. In both cases we can identify the quiescent and eruptive phases of the jet. The triggered LAOs have periods of around 70-80 minutes and are damped after a few oscillations. The minimum magnetic field intensity inferred with seismology for the filament turns out to be around 30 Gauss. We conclude that the two case studies are consistent with the recent numerical model of Luna and Moreno-Insertis (2021), in which the LAOs are initiated by jets. The relationship between the onset of the jet and filament oscillations is straight-forward for



the first case and less for the second case. In the second event, although there is some evidence, we cannot rule out other possibilities such as activity unrelated to the null-point or changes in the magnetic structure of the filament. Both jets are associated with very weak flares which did not launch any EUV wave. Therefore the role of EUV waves for triggering the filament oscillations can be eliminated for these two case. **3 Feb 2015, 5 Feb 2015**

## Study of Solar Jets and Related Flares

Thesis

[Reetika Joshi](#)

Thesis 2022

<https://arxiv.org/pdf/2206.02478.pdf>

Solar jets are ubiquitous transient collimated mass outflows in the solar atmosphere over a wide range of sizes from small scale nanojets to a few solar radii, embedded in the solar chromosphere to solar corona. Jets are frequently accompanied by solar flares and these flares provide the force to propagate the plasma material upward and could be accompanied by coronal mass ejections. These jets could act as a source for transporting a significant mass and energy from the lower solar atmosphere to the upper coronal heights and consequently heating the solar corona and accelerating the solar wind. Magnetic reconnection is believed to be the triggering reason behind these jet activity. The thesis entitled: Study of Solar Jets and Related Flares, includes various case studies with different mechanisms to set off the jet initiation, associated large scale eruptions and mounts strong observational evidences to validate the numerical experiments for the magnetic flux emergence models. Such studies on solar jets along with their magnetic origin contribute to resolve the scandalous coronal heating problem and provide the evidences for the existing theoretical models and open a new window for the interplanetary science. **April 15-16, 2014, March 14-15, 2015, April 4, 2017, March 22, 2019**

## Analysis of the Evolution of a Multi-Ribbon Flare and Failed Filament Eruption

[Reetika Joshi](#), [Cristina H. Mandrini](#), [Ramesh Chandra](#), [Brigitte Schmieder](#), [Germán D. Cristiani](#), [Cecilia Mac Cormack](#), [Pascal Démoulin](#), [Hebe Cremades](#)

Solar Phys. **297**, Article number: 81 2022

<https://arxiv.org/pdf/2206.00531.pdf>

<https://link.springer.com/content/pdf/10.1007/s11207-022-02021-5.pdf>

How filaments form and erupt are topics about which solar researchers have wondered since more than a century and that are still open to debate. We present observations of a filament formation, its failed eruption, and the associated flare (SOL2019-05-09T05:51) that occurred in active region (AR) 12740 using data from SDO, STEREO-A, IRIS, and NSO/GONG. AR 12740 was a decaying region formed by a very disperse following polarity and a strong leading spot, surrounded by a highly dynamic zone where moving magnetic features (MMFs) were seen constantly diverging from the spot. Our analysis indicates that the filament was formed by the convergence of fibrils at a location where magnetic flux cancellation was observed. Furthermore, we conclude that its destabilization was also related to flux cancellation associated to the constant shuffling of the MMFs. A two-ribbon flare occurred associated to the filament eruption; however, because the large-scale magnetic configuration of the AR was quadrupolar, two additional flare ribbons developed far from the two main ones. We model the magnetic configuration of the AR using a force-free field approach at the AR scale size. This local model is complemented by a global potential-field source-surface one. Based on the local model, we propose a scenario in which the filament failed eruption and flare are due to two reconnection processes, one occurring below the erupting filament, leading to the two-ribbon flare, and another one above it between the filament flux-rope configuration and the large-scale closed loops. Our computation of the reconnected magnetic flux added to the erupting flux rope, compared to that of the large-scale field overlying it, lets us conclude that the latter was large enough to prevent the filament eruption. A similar conjecture can be drawn from the computation of the magnetic tension derived from the global field model.

## Multi thermal atmosphere of a mini solar flare during magnetic reconnection observed with IRIS

[Reetika Joshi](#), [Brigitte Schmieder](#), [Akiko Tei](#), [Guillaume Aulanier](#), [Juraj Lörinčík](#), [Ramesh Chandra](#), [Petr Heinzel](#)

A&A Volume 645, id.A80, 19 pages 2021

<https://arxiv.org/pdf/2010.15401.pdf>

<https://www.aanda.org/articles/aa/pdf/2021/01/aa39229-20.pdf>

The Interface Region Imaging Spectrograph (IRIS) with its high spatial and temporal resolution brings exceptional plasma diagnostics of solar chromospheric and coronal activity during magnetic reconnection. The aim of this work is to study the fine structure and dynamics of the plasma at a jet base forming a mini flare between two emerging magnetic fluxes (EMFs) observed with IRIS and the Solar Dynamics Observatory (SDO) instruments. We proceed to a spatio-temporal analysis of IRIS spectra observed in the spectral ranges of Mg II, C II, and Si IV ions. Doppler velocities from Mg II lines are computed by using a cloud model technique. Strong asymmetric Mg II and C II line profiles with extended blue wings observed at the reconnection site (jet base) are interpreted by the presence of two chromospheric temperature clouds, one explosive cloud with blueshifts at 290 km/s and one cloud with smaller Dopplershift (around 36 km/s). Simultaneously at the same location (jet base), strong emission of several transition region lines (e.g. O IV and Si IV), emission of the Mg II triplet lines of the Balmer-continuum and absorption of identified chromospheric lines in Si IV broad profiles have been observed and analysed. Such observations of IRIS line and continuum emissions

allow us to propose a stratification model for the white-light mini flare atmosphere with multiple layers of different temperatures along the line of sight, in a reconnection current sheet. It is the first time that we could quantify the fast speed (possibly Alfvénic flows) of cool clouds ejected perpendicularly to the jet direction by using the cloud model technique. We conjecture that the ejected clouds come from plasma which was trapped between the two EMFs before reconnection or be caused by chromospheric-temperature (cool) upflow material like in a surge, during reconnection. **March 22, 2019** Movies are available at <https://www.aanda.org>  
IRIS Nugget June 2021 <https://iris.lmsal.com/nugget>

## Sequential Lid Removal in a Triple-Decker Chain of CME-Producing Solar Eruptions

Navin Chandra [Joshi](#), Alphonse C. Sterling, Ronald L. Moore, Bhuwan Joshi

ApJ **901** 38 **2020**

<https://arxiv.org/abs/2008.04525>

<https://doi.org/10.3847/1538-4357/abacd0>

We investigate the onsets of three consecutive coronal mass ejection (CME) eruptions in 12 hours from a large bipolar active region (AR) observed by SDO, STEREO, RHESSI, and GOES. Evidently, the AR initially had a “triple-decker” configuration: three flux ropes in a vertical stack above the polarity inversion line (PIL). Upon being bumped by a confined eruption of the middle flux rope, the top flux rope erupts to make the first CME and its accompanying AR–spanning flare arcade rooted in a far-apart pair of flare ribbons. The second CME is made by eruption of the previously-arrested middle flux rope, which blows open the flare arcade of the first CME and produces a flare arcade rooted in a pair of flare ribbons closer to the PIL than those of the first CME. The third CME is made by blowout eruption of the bottom flux rope, which blows open the second flare arcade and makes its own flare arcade and pair of flare ribbons. Flux cancellation observed at the PIL likely triggers the initial confined eruption of the middle flux rope. That confined eruption evidently triggers the first CME eruption. The lid-removal mechanism instigated by the first CME eruption plausibly triggers the second CME eruption. Further lid removal by the second CME eruption plausibly triggers the final CME eruption. **2013 May 22**

## The role of small-scale surface motions in the transfer of twist to a solar jet from a remote stable flux rope★

Reetika [Joshi](#), [Brigitte Schmieder](#), [Guillaume Aulanier](#), [Véronique Bommier](#), [Ramesh Chandra](#)

A&A **642**, A169 **2020**

<https://arxiv.org/pdf/2008.06887.pdf>

<https://doi.org/10.1051/0004-6361/202038562>

<https://www.aanda.org/articles/aa/pdf/2020/10/aa38562-20.pdf>

Jets often have a helical structure containing both hot and cooler, denser than the corona, ejected plasma. Different mechanisms are proposed to trigger jets by magnetic reconnection between the emergence of magnetic flux and environment, or induced by twisted photospheric motions bringing the system to instability. Multi-wavelength observations of a twisted jet observed with SDO/AIA and IRIS was selected to understand how the twist was injected in the jet because fortunately, IRIS slit was just crossing the reconnection site. We follow the magnetic history of the active region based on the analysis of HMI vector magnetic field computed with the UNNOFIT code. This AR is the result of the collapse of two emerging magnetic fluxes (EMF) overlaid by AFS well-observed with AIA, IRIS, and NVST in H-alpha. In the magnetic field maps, we evidenced the pattern of a long sigmoidal flux rope (FR) along the polarity inversion line between the two EMFs which is the site of the reconnection. Before the jet, there was an extension of the FR, and a part of it was detached and formed a small bipole with a bald patch (BP) region which dynamically became an X-current sheet over the dome of one EMF where the reconnection took place. At the time of the reconnection, the Mg II spectra exhibited a strong extension of the blue wing which is decreasing over a distance of 10 Mm (from -300 km/s to a few km/s). This is the signature of the transfer of the twist to the jet. Comparison with numerical magnetohydrodynamics (MHD) simulations confirmed the existence of the long FR. We conjecture that there is a transfer of twist to the jet during the extension of the FR to the reconnection site without FR eruption. The reconnection would start in the low atmosphere in the BP reconnection region and extend at an X-point along the current sheet formed above. **March 21-22, 2019**

## Cause and Kinematics of a Jet-Like CME

[Reetika Joshi](#), [Yuming Wang](#), [Ramesh Chandra](#), [Quanhao Zhang](#), [Lijuan Liu](#), [Xiaolei Li](#)

ApJ **901** 94 **2020**

<https://arxiv.org/pdf/2008.05651.pdf> File

<https://doi.org/10.3847/1538-4357/abaf5a>

In this article, we present the multi-viewpoint and multi-wavelength analysis of an atypical solar jet based on the data from Solar Dynamics Observatory, SOlar, and Heliospheric Observatory, and Solar TERrestrial RELations Observatory. It is usually believed that the coronal mass ejections (CMEs) are developed from the large scale solar eruptions in the lower atmosphere. However, the kinematical and spatial evolution of the jet on **2013 April 28** guide us that the jet was clearly associated with a narrow CME having a width of approx 25 degrees with a speed of 450 km/s. To better understand the link between the jet and the CME, we did the coronal potential field extrapolation from the line of sight magnetogram of the AR. The extrapolations present that the jet eruption follows exactly the same path of the open

magnetic field lines from the source region which provides the route for the jet material to escape from the solar surface towards the outer corona.

### **A case-study of multi-temperature coronal jets for emerging flux MHD models**

[Reetika Joshi](#), [Ramesh Chandra](#), [Brigitte Schmieder](#), [Fernando Moreno-Insertis](#), [Guillaume Aulanier](#), [Daniel Nóbrega-Siverio](#), [Pooja Devi](#)

A&A 639, A22 2020

<https://arxiv.org/pdf/2005.06064.pdf>

<https://www.aanda.org/articles/aa/pdf/2020/07/aa37806-20.pdf>

Context: Hot coronal jets are a basic observed feature of the solar atmosphere whose physical origin is still being actively debated. Aims: We study six recurrent jets occurring in the active region NOAA 12644 on **April 04, 2017**. They are observed in all the hot filters of AIA as well as cool surges in IRIS slit-jaw high spatial and temporal resolution images. Methods: The AIA filters allow us to study the temperature and the emission measure of the jets using the filter ratio method. We study the pre-jet phases by analyzing the intensity oscillations at the base of the jets with the wavelet technique. Results: A fine co-alignment of the AIA and IRIS data shows that the jets are initiated at the top of a canopy-like, double-chambered structure with cool emission on one side and hot emission in the other. The hot jets are collimated in the hot temperature filters, have high velocities (around 250 km/s) and accompanied by the cool surges and ejected kernels both moving at about 45 km/s. In the pre-phase of the jets, at their base we find quasi-periodic intensity oscillations in phase with small ejections; they have a period between 2 and 6 minutes and are reminiscent of acoustic or MHD waves. Conclusions: This series of jets and surges provides a good case-study to test the 2D and 3D magnetohydrodynamic (MHD) models that result from magnetic flux emergence. The double-chambered structure found in the observations corresponds to the cold and hot loop regions found in the models beneath the current sheet that contains the reconnection site. The cool surge with kernels is comparable with the cool ejection and plasmoids that naturally appear in the models.

### **Generalisation of the Magnetic Field Configuration of typical and atypical Confined Flares**

Navin Chandra [Joshi](#), [Xiaoshuai Zhu](#), [Brigitte Schmieder](#), [Guillaume Aulanier](#), [Miho Janvier](#), [Bhuwan Joshi](#), [Tetsuya Magara](#), [Ramesh Chandra](#), [Satoshi Inoue](#)

ApJ 2018

<https://arxiv.org/pdf/1811.01228.pdf>

Atypical flares cannot be naturally explained with standard models. To predict such flares, we need to define their physical characteristics, in particular, their magnetic environment, and identify pairs of reconnected loops. Here, we present in detail a case-study of a confined flare preceded by flux cancellation that leads to the formation of a filament. The slow rise of the non-eruptive filament favours the growth and reconnection of overlying loops. The flare is only of C5.0 class but it is a long duration event. The reason is that it is comprised of three successive stages of reconnection. A non-linear force-free field extrapolation and a magnetic topology analysis allow us to identify the loops involved in the reconnection process and build a reliable scenario for this atypical confined flare. The main result is that a curved magnetic polarity inversion line in active regions is a key ingredient for producing such atypical flares. A comparison with previous extrapolations for typical and atypical confined flares leads us to propose a cartoon for generalizing the concept. **2014 May 15**

### **A Major Geoeffective CME from NOAA 12371: Initiation, CME–CME Interactions, and Interplanetary Consequences**

Bhuwan [Joshi](#), M. Syed Ibrahim, A. Shanmugaraju, D. Chakrabarty

[Solar Physics](#) July 2018, 293:107

<http://sci-hub.tw/http://link.springer.com/10.1007/s11207-018-1325-2>

In this article, we present a multi-wavelength and multi-instrument investigation of a halo coronal mass ejection (CME) from active region NOAA 12371 on **21 June 2015** that led to a major geomagnetic storm of minimum  $Dst = -204$  nT. The observations from the Atmospheric Imaging Assembly onboard the Solar Dynamics Observatory in the hot EUV channel of 94 Å confirm the CME to be associated with a coronal sigmoid that displayed an intense emission ( $T \sim 6$  MK) from its core before the onset of the eruption. Multi-wavelength observations of the source active region suggest tether-cutting reconnection to be the primary triggering mechanism of the flux rope eruption. Interestingly, the flux rope eruption exhibited a two-phase evolution during which the “standard” large-scale flare reconnection process originated two composite M-class flares. The eruption of the flux rope is followed by the coronagraphic observation of a fast, halo CME with linear projected speed of 1366 km s<sup>-1</sup>. The dynamic radio spectrum in the decameter-hectometer frequency range reveals multiple continuum-like enhancements in type II radio emission which imply the interaction of the CME with other preceding slow speed CMEs in the corona within  $\approx 10 \sim 90 R_{\odot}$ . The scenario of CME–CME interaction in the corona and interplanetary medium is further confirmed by the height–time plots of the CMEs occurring during 19–21 June. In situ measurements of solar wind magnetic field and plasma parameters at 1 AU exhibit two distinct magnetic clouds, separated by a magnetic hole. Synthesis of near-Sun observations, interplanetary radio emissions, and in situ measurements at 1 AU reveal complex processes of CME–CME interactions right from the source active region to the corona and interplanetary medium that have played a crucial role towards the large enhancement of the geoeffectiveness of the halo CME on 21 June 2015.

## Multiple Solar Jets from NOAA AR 12644

Reetika [Joshi](#), [Ramesh Chandra](#)

XXIXth IAU General Assembly Aug 2015? **2018**

<https://arxiv.org/pdf/1806.07063.pdf>

We present here the observations of solar jets observed on **April 04, 2017** from NOAA active region (AR) 12644 using high temporal and spatial resolution AIA instrument. We have observed around twelve recurring jets during the whole day. Magnetic flux emergence and cancellation have been observed at the jet location. The multi-band observations evidenced that these jets were triggered due to the magnetic reconnection at low coronal null-point.

## Flux Rope Breaking and Formation of a Rotating Blowout Jet

Navin Chandra [Joshi](#), [Naoto Nishizuka](#), [Boris Filippov](#), [Tetsuya Magara](#), [Andrey G. Tlatov](#)

MNRAS 476, Issue 1, p.1286-1298 **2018**

<https://arxiv.org/pdf/1802.01798.pdf>

We analyzed a small flux rope eruption converted into a helical blowout jet in a fan-spine configuration using multi-wavelength observations taken by SDO, which occurred near the limb on **2016 January 9**. In our study, first, we estimated the fan-spine magnetic configuration with the potential field calculation and found a sinistral small filament inside it. The filament along with the flux rope erupted upward and interacted with the surrounding fan-spine magnetic configuration, where the flux rope breaks in the middle section. We observed compact brightening, flare ribbons and post-flare loops underneath the erupting filament. The northern section of the flux rope reconnected with the surrounding positive polarity, while the southern section straightened. Next, we observed the untwisting motion of the southern leg, which was transformed into a rotating helical blowout jet. The sign of the helicity of the mini-filament matches the one of the rotating jet. This is consistent with the jet models presented by Adams et al. (2014) and Sterling et al. (2015). We focused on the fine thread structure of the rotating jet and traced three blobs with the speed of 60-120 km/s, while the radial speed of the jet is approx 400 km/s. The untwisting motion of the jet accelerated plasma upward along the collimated outer spine field lines, and it finally evolved into a narrow coronal mass ejection at the height of approx 9 R<sub>sun</sub>. On the basis of the detailed analysis, we discussed clear evidence of the scenario of the breaking of the flux rope and the formation of the helical blowout jet in the fan-spine magnetic configuration.

## Observational and model analysis of a two-ribbon flare possibly induced by a neighbouring blowout jet

Bhuvan [Joshi](#) (USO/PRL, India), [Julia K. Thalmann](#) (Univ. of Graz, Austria), [Prabir K. Mitra](#) (USO/PRL, India), [Ramesh Chandra](#) (Kumaun Univ., India), [Astrid M. Veronig](#) (Univ. of Graz, Austria)

ApJ **851** 29 **2017**

<https://arxiv.org/pdf/1710.08099.pdf>

In this paper, we present unique observations of a blowout coronal jet that possibly triggered a two-ribbon confined C1.2 flare in a bipolar solar active region NOAA 12615 on **2016 December 5**. The jet activity initiates at chromospheric/transition-region heights with a small brightening that eventually grows in a larger volume with well developed standard morphological jet features, viz., base and spire. The spire widens up with a collimated eruption of cool and hot plasma components, observed in the 304 and 94 Å channels of AIA, respectively. The speed of the plasma ejection, which forms the jet's spire, was higher for the hot component (~200 km/s) than the cooler one (~130 km/s). The NLFF model of coronal fields at pre- and post-jet phases successfully reveal opening of previously closed magnetic field lines with a rather inclined/low-lying jet structure. The peak phase of the jet emission is followed by the development of a two-ribbon flare that shows coronal loop emission in HXRs up to ~25 keV energy. The coronal magnetic fields rooted at the location of EUV flare ribbons, derived from the NLFF model, demonstrate the pre-flare phase to exhibit an "X-type" configuration while the magnetic fields at the post-flare phase are more or less parallel oriented. The comparisons of multi-wavelength measurements with the magnetic field extrapolations suggest that the jet activity likely triggered the two-ribbon flare by perturbing the field in the interior of the active region.

## Slippage of Jets Explained by the Magnetic Topology of NOAA Active Region 12035

R. [Joshi](#), [B. Schmieder](#), [R. Chandra](#), [G. Aulanier](#), [F.P. Zuccarello](#), [W. Uddin](#)

Solar Phys. 292:152 **2017**

<https://arxiv.org/pdf/1709.02791.pdf>

In this study, we present the investigation of eleven recurring solar jets originated from two different sites (site 1 and site 2) close to each other (~ 11 Mm) in the NOAA active region (AR) 12035 during **15--16 April 2014**. The jets were observed by the Atmospheric Imaging Assembly (AIA) telescope onboard the Solar Dynamics Observatory (SDO) satellite. Two jets were observed by the Aryabhata Research Institute of Observational Sciences (ARIES), Nainital, India telescope in H-alpha. On 15 April flux emergence is important in site 1 while on 16 April flux emergence and cancellation mechanisms are involved in both sites. The jets of both sites have parallel trajectories and move to the south with a speed between 100 and 360 km/s. We observed some connection between the two sites with some transfer of brightening. The jets of site 2 occurred during the second day and have a tendency to move towards the jets of site 1 and merge with them. We conjecture that the slippage of the jets could be explained by the complex topology of the

region with the presence of a few low-altitude null points and many quasi-separatrix layers (QSLs), which could intersect with one another.

### **Onset of a Large Ejective Solar Eruption from a Typical Coronal-Jet-Base Field Configuration**

Navin Chandra **Joshi**, Alphonse C. Sterling, Ronald L. Moore, [Tetsuya Magara](#), [Young-Jae Moon](#)

ApJ 845 26 2017

<https://arxiv.org/pdf/1706.09176.pdf>

<http://sci-hub.cc/10.3847/1538-4357/aa7c1b>

Utilizing multiwavelength observations and magnetic field data from SDO/AIA, SDO/HMI, GOES and RHESSI, we investigate a large-scale ejective solar eruption of **2014 December 18** from active region NOAA 12241. This event produced a distinctive three-ribbon flare, having two parallel ribbons corresponding to the ribbons of a standard two-ribbon flare, and a larger-scale third quasi-circular ribbon offset from the other two ribbons. There are two components to this eruptive event. First, a flux rope forms above a strong-field polarity-inversion line and erupts and grows as the parallel ribbons turn on, grow, and spread part from that polarity-inversion line; this evolution is consistent with the tether-cutting-reconnection mechanism for eruptions. Second, the eruption of the arcade that has the erupting flux rope in its core under goes magnetic reconnection at the null point of a fan dome that envelops the erupting arcade, resulting in formation of the quasi-circular ribbon; this is consistent with the breakout reconnection mechanism for eruptions. We find that the parallel ribbons begin well before (12 min) circular ribbon onset, indicating that tether-cutting reconnection (or a non-ideal MHD instability) initiated this event, rather than breakout reconnection. The overall setup for this large-scale (circular-ribbon diameter 100000 km) eruption is analogous to that of coronal jets (base size 10000 km), many of which, according to recent findings, result from eruptions of small-scale minifilaments. Thus these findings confirm that eruptions of sheared-core magnetic arcades seated in fan-spine null-point magnetic topology happen on a wide range of size scales on the Sun.

### **Formation and eruption of a flux rope from the sigmoid active region NOAA 11719 and associated M6.5 flare: A multi-wavelength study**

Bhuvan **Joshi** (USO/PRL, India), Upendra Kushwaha (USO/PRL, India), Astrid M. Veronig (Univ. of Graz, Austria), Sajal Kumar Dhara (USO/PRL, India), A. Shanmugaraju (Arul Anandhar College, India), Yong-Jae Moon (Kyung Hee Univ., South Korea)

ApJ 834 42 2017

<https://arxiv.org/pdf/1701.00967v1.pdf>

<http://sci-hub.cc/doi/10.3847/1538-4357/834/1/42>

We investigate the formation, activation and eruption of a flux rope from the sigmoid active region NOAA 11719 by analyzing E(UV), X-ray and radio measurements. During the pre-eruption period of ~7 hours, the AIA 94 Å images reveal the emergence of a coronal sigmoid through the interaction between two J-shaped bundles of loops which proceeds with multiple episodes of coronal loop brightenings and significant variations in the magnetic flux through the photosphere. These observations imply that repetitive magnetic reconnections likely play a key role in the formation of the sigmoidal flux rope in the corona and also contribute toward sustaining the temperature of the flux rope higher than the ambient coronal structures. Notably, the formation of the sigmoid is associated with the fast morphological evolution of an S-shaped filament channel in the chromosphere. The sigmoid activates toward eruption with the ascend of a large flux rope in the corona which is preceded by the decrease of photospheric magnetic flux through the core flaring region suggesting tether-cutting reconnection as a possible triggering mechanism. The flux rope eruption results in a two-ribbon M6.5 flare with a prolonged rise phase of ~21 min. The flare exhibits significant deviation from the standard flare model in the early rise phase during which a pair of J-shaped flare ribbons form and apparently exhibit converging motions parallel to the polarity inversion line which is further confirmed by the motions of HXR footpoint sources. In the later stages, the flare follows the standard flare model and the source region undergoes a complete sigmoid-to-arcade transformation. **11 Apr 2013**

### **PRE-ERUPTION OSCILLATIONS IN THIN AND LONG FEATURES IN A QUIESCENT FILAMENT**

Anand D. **Joshi**<sup>1,2</sup>, Yoichiro Hanaoka<sup>1</sup>, Yoshinori Suematsu<sup>1</sup>, Satoshi Morita<sup>1</sup>, Vasyl Yurchyshyn<sup>2,3</sup>, and Kyung-Suk Cho

2016 ApJ 833 243

<http://sci-hub.cc/doi/10.3847/1538-4357/833/2/243>

We investigate the eruption of a quiescent filament located close to an active region. Large-scale activation was observed in only half of the filament in the form of pre-eruption oscillations. Consequently only this half erupted nearly 30 hr after the oscillations commenced. Time-slice diagrams of 171 Å images from the Atmospheric Imaging Assembly were used to study the oscillations. These were observed in several thin and long features connecting the filament spine to the chromosphere below. This study traces the origin of such features and proposes their possible interpretation. Small-scale magnetic flux cancellation accompanied by a brightening was observed at the footpoint of the features shortly before their appearance, in images recorded by the Helioseismic and Magnetic Imager. A slow rise of the

filament was detected in addition to the oscillations, indicating a gradual loss of equilibrium. Our analysis indicates that a change in magnetic field connectivity between two neighbouring active regions and the quiescent filament resulted in a weakening of the overlying arcade of the filament, leading to its eruption. It is also suggested that the oscillating features are filament barbs, and the oscillations are a manifestation during the pre-eruption phase of the filaments. **2013 August 14**

### **Pre-flare coronal jet and evolutionary phases of a solar eruptive prominence associated with M1.8 flare: SDO and RHESSI observations**

Bhuwan **Joshi** (USO/PRL, India), Upendra Kushwaha (USO/PRL, India), Astrid Veronig (University of Graz, Austria), Kyung-Suk Cho (KASI, South Korea)

ApJ **832** 130 **2016**

<https://arxiv.org/pdf/1611.03629v1.pdf>

We investigate triggering, activation, and ejection of a solar eruptive prominence that occurred in a multi-polar flux system of active region NOAA 11548 on **2012 August 18** by analyzing data from AIA on board SDO, RHESSI, and EUVI/SECCHI on board STEREO. Prior to the prominence activation, we observed striking coronal activities in the form of a blowout jet which is associated with rapid eruption of a cool flux rope. Further, the jet-associated flux rope eruption underwent splitting and rotation during its outward expansion. These coronal activities are followed by the prominence activation during which it slowly rises with a speed of  $\sim 12$  km/s while the region below the prominence emits gradually varying EUV and thermal X-ray emissions. From these observations, we propose that the prominence eruption is a complex, multi-step phenomenon in which a combination of internal (tether-cutting reconnection) and external (i.e., pre-eruption coronal activities) processes are involved. The prominence underwent catastrophic loss of equilibrium with the onset of the impulsive phase of an M1.8 flare suggesting large-scale energy release by coronal magnetic reconnection. We obtained signatures of particle acceleration in the form of power law spectra with hard electron spectral index ( $\delta \sim 3$ ) and strong HXR footpoint sources. During the impulsive phase, a hot EUV plasmoid was observed below the apex of the erupting prominence that ejected in the direction of the prominence with a speed of  $\sim 177$  km/s. The temporal, spatial and kinematic correlations between the erupting prominence and the plasmoid imply that the magnetic reconnection supported the fast ejection of prominence in the lower corona.

### **Interaction of Two Filament Channels of Different Chiralities**

Navin Chandra **Joshi**, Boris Filippov, Brigitte Schmieder, [Tetsuya Magara](#), [Young-Jae Moon](#), [Wahab Uddin](#)

ApJ **825** 123 **2016**

<http://arxiv.org/pdf/1605.01812v1.pdf>

We present observations of interactions between the two filament channels of different chiralities and associated dynamics that occurred during **2014 April 18 -- 20**. While two flux ropes of different helicity with parallel axial magnetic fields can only undergo a bounce interaction when they are brought together, the observations at the first glance show that the heated plasma is moving from one filament channel to the other. The SDO/AIA 171 Å observations and the PFSS magnetic field extrapolation reveal the presence of fan-spine magnetic configuration over the filament channels with a null point located above them. Three different events of filament activations, partial eruptions, and associated filament channel interactions have been observed. The activation initiated in one filament channel seems to propagate along the neighbour filament channel. We believe that the activation and partial eruption of the filaments bring the field lines of flux ropes containing them closer to the null point and trigger the magnetic reconnection between them and the fan-spine magnetic configuration. As a result, the hot plasma moves along the outer spine line toward the remote point. Utilizing the present observations, for the first time we have discussed how two different-chirality filament channels can interact and show interrelation.

### **Chain Reconnections observed in Sympathetic Eruptions**

Navin Chandra **Joshi**, Brigitte Schmieder, Tetsuya Magara, Yang Guo, Guillaume Aulanier

ApJ **820** 126 **2016 File**

<http://arxiv.org/pdf/1602.07792v1.pdf>

The nature of various plausible causal links between sympathetic events is still a controversial issue. In this work, we present multi-wavelength observations of sympathetic eruptions, associated flares and coronal mass ejections (CMEs) occurring on **2013 November 17** in two close-by active regions. Two filaments i.e., F1 and F2 are observed in between the active regions. Successive magnetic reconnections, caused by different reasons (flux cancellation, shear and expansion) have been identified during the whole event. The first reconnection occurred during the first eruption via flux cancellation between the sheared arcades overlying filament F2, creating a flux rope and leading to the first double ribbon solar flare. During this phase we observed the eruption of overlying arcades and coronal loops, which leads to the first CME. The second reconnection is believed to occur between the expanding flux rope of F2 and the overlying arcades of the filament F1. We suggest that this reconnection destabilized the equilibrium of filament F1, which further facilitated its eruption. The third stage of reconnection occurred in the wake of the erupting filament F1 between the legs of overlying arcades. This may create a flux rope and the second double ribbon flare and a second CME. The fourth reconnection was between the expanding arcades of the erupting filament F1 and the nearby ambient field, which

produced the bi-directional plasma flows towards both upward and downward. Observations and a nonlinear force-free field extrapolation confirm the possibility of reconnection and the causal link between the magnetic systems.

**Хорошее Введение.**

### **Formation of Compound Flux Rope by The Merging of Two Filament Channels, Associated Dynamics and its Stability**

Navin Chandra **Joshi**, Tetsuya Magara, Satoshi Inoue

ApJ, 795 4 **2014**

<http://arxiv.org/pdf/1409.1359v1.pdf>

We present the observations of compound flux rope formation via merging of two nearby filament channels, associated dynamics and its stability that occurred on **2014 January 1** using multiwavelength data. We have also discussed the dynamics of cool and hot plasma moving along the newly formed compound flux rope. The merging started after the interaction between the southern leg of northward filament and the northern leg of the southward filament at around 01:21 UT and continue until a compound flux rope formed at around 01:33 UT. During the merging the cool filaments plasma heated up and started to move along the both side of the compound flux rope i.e., toward north (approx 265 km/s) and south (approx 118 km/s) from the point of merging. After travelling a distance of approx 150 Mm towards north the plasma become cool and started to returns back towards south ( approx 14 km/s) after 02:00 UT. The observations provide an clear example of compound flux rope formation via merging of two different flux ropes and occurrence of flare through tether cutting reconnection. However, the compound flux rope remained stable in the corona and made an confined eruption. The coronal magnetic field decay index measurements revealed that both the filaments and the compound flux rope axis lies within the stability domain (decay index less than 1.5), which may be the possible cause for their stability. The present study also deals with the relationship between the filaments chirality (sinistral) and the helicity (positive) of the surrounding flux rope.

### **Confined Partial Filament Eruption and its Reformation within a Stable Magnetic Flux Rope**

Navin Chandra **Joshi**, Abhishek K. Srivastava, Boris Filippov, Pradeep Kayshap, Wahab Uddin, Ramesh Chandra, Debi Prasad Choudhary, and B. N. Dwivedi

**2014** ApJ 787 11

We present observations of a confined partial eruption of a filament on **2012 August 4**, which restores its initial shape within 2 hr after eruption. From the Global Oscillation Network Group H $\alpha$  observations, we find that the filament plasma turns into dynamic motion at around 11:20 UT from the middle part of the filament toward the northwest direction with an average speed of 105 km s<sup>-1</sup>. A little brightening underneath the filament possibly shows the signature of low-altitude reconnection below the filament eruptive part. In Solar Dynamics Observatory/Atmospheric Imaging Assembly 171 Å images, we observe an activation of right-handed helically twisted magnetic flux rope that contains the filament material and confines it during its dynamical motion. The motion of cool filament plasma stops after traveling a distance of 215 Mm toward the northwest from the point of eruption. The plasma moves partly toward the right foot point of the flux rope, while most of the plasma returns after 12:20 UT toward the left foot point with an average speed of 60 km s<sup>-1</sup> to reform the filament within the same stable magnetic structure. On the basis of the filament internal fine structure and its position relative to the photospheric magnetic fields, we find filament chirality to be sinistral, while the activated enveloping flux rope shows a clear right-handed twist. Thus, this dynamic event is an apparent example of one-to-one correspondence between the filament chirality (sinistral) and the enveloping flux rope helicity (positive). From the coronal magnetic field decay index,  $n$ , calculation near the flux rope axis, it is evident that the whole filament axis lies within the domain of stability (i.e.,  $n < 1$ ), which provides the filament stability despite strong disturbances at its eastern foot point.

### **RHESSI AND TRACE OBSERVATIONS OF MULTIPLE FLARE ACTIVITY IN AR 10656 AND ASSOCIATED FILAMENT ERUPTION**

Bhuwan **Joshi**<sup>1</sup>, Upendra Kushwaha<sup>1</sup>, K.-S. Cho<sup>2</sup>, and Astrid M. Veronig

**2013** ApJ 771 1

We present Reuven Ramaty High Energy Solar Spectroscopic Imager (RHESSI) and Transition Region and Coronal Explorer (TRACE) observations of multiple flare activity that occurred in the NOAA active region 10656 over a period of 2 hr on **2004 August 18**. Out of four successive flares, three were class C events, and the final event was a major X1.8 solar eruptive flare. The activities during the pre-eruption phase, i.e., before the X1.8 flare, are characterized by three localized episodes of energy release occurring in the vicinity of a filament that produces intense heating along with non-thermal emission. A few minutes before the eruption, the filament undergoes an activation phase during which it slowly rises with a speed of  $\sim 12$  km s<sup>-1</sup>. The filament eruption is accompanied by an X1.8 flare, during which multiple hard X-ray (HXR) bursts are observed up to 100-300 keV energies. We observe a bright and elongated coronal structure simultaneously in E(UV) and 50-100 keV HXR images underneath the expanding filament during the period of HXR bursts, which provides strong evidence for ongoing magnetic reconnection. This phase is accompanied by very high plasma temperatures of  $\sim 31$  MK, followed by the detachment of the prominence from the solar source region. From the location, timing, strength, and spectrum of HXR emission, we conclude that the prominence eruption is driven by the distinct events of magnetic reconnection occurring in the current sheet below the erupting prominence. These multi-wavelength observations also suggest that the localized magnetic reconnections associated with different evolutionary stages of the filament in

the pre-eruption phase play an important role in destabilizing the active-region filament through the tether-cutting process, leading to large-scale eruption and X-class flare.

### **Study of Failed CME Core Associated with Asymmetric Filament Eruption**

**Joshi**, N. C.; Srivastava, A. K.; Filippov, B.; Uddin, W.; Kayshap, P.; Chandra, R.

E-print, April 2013, ApJ 771 65

<http://arxiv.org/abs/1304.6852>

We present the multi-wavelength observations of asymmetric filament eruption, associated CME and coronal downflows on **2012 June 17-18** during 20:00-05:00 UT. We use SDO/AIA, STEREO-B/SECCHI observations to understand the filament eruption scenario and its kinematics. While LASCO C2 observations have been analyzed to study the kinematics of the CME and associated downflows. SDO/AIA limb observations show that the filament exhibits whipping like asymmetric eruption. STEREO/EUVI disk observations reveal a two ribbon flare underneath the south-eastern part of the filament that is most probably occurred due to reconnection process in the coronal magnetic field in the wake of the filament eruption. The whipping like filament eruption later gives a slow CME in which the leading edge and the core propagate respectively with the average speed of approx 540 km s<sup>-1</sup> and approx 126 km s<sup>-1</sup> as observed in the LASCO C2 coronagraph. The CME core formed by the eruptive flux-rope shows the outer coronal downflows with the average speed of approx 56 km s<sup>-1</sup> after reaching up to approx 4.33 R<sub>sun</sub>. Initially, the core decelerates with approx 48 m s<sup>-2</sup>. The plasma first decelerates gradually up to the height of approx 4.33 R<sub>sun</sub> and then starts accelerating downward. We suggest a self-consistent model of a magnetic flux rope representing the magnetic structure of the CME core formed by eruptive filament that lost its previous stable equilibrium when reach at a critical height. With some reasonable parameters, and inherent physical conditions the model describes the non-radial ascending motion of the flux rope in the corona, its stopping at some height, and thereafter the downward motion, which are in good agreement with the observations.

### **ACCELERATION OF CORONAL MASS EJECTIONS FROM THREE-DIMENSIONAL RECONSTRUCTION OF STEREO IMAGES**

Anand D. **Joshi** and Nandita Srivastava

2011 ApJ 739 8, **File**

We employ a three-dimensional (3D) reconstruction technique for the first time to study the kinematics of six coronal mass ejections (CMEs), using images obtained from the COR1 and COR2 coronagraphs on board the twin STEREO spacecraft, and also the eruptive prominences (EPs) associated with three of them using images from the Extreme UltraViolet Imager. A feature in the EPs and leading edges (LEs) of all the CMEs was identified and tracked in images from the two spacecraft, and a stereoscopic reconstruction technique was used to determine the 3D coordinates of these features. True velocity and acceleration were determined from the temporal evolution of the true height of the CME features. Our study of the kinematics of the CMEs in 3D reveals that the CME LE undergoes maximum acceleration typically below 2 R<sub>sun</sub>. The acceleration profiles of CMEs associated with flares and prominences exhibit different behaviors. While the CMEs not associated with prominences show a bimodal acceleration profile, those associated with prominences do not. Two of the three associated prominences in the study show a high and increasing value of acceleration up to a distance of almost 4 R<sub>sun</sub>, but acceleration of the corresponding CME LE does not show the same behavior, suggesting that the two may not be always driven by the same mechanism. One of the CMEs, although associated with a C-class flare, showed unusually high acceleration of over 1500 m s<sup>-2</sup>. Our results therefore suggest that only the flare-associated CMEs undergo residual acceleration, which indicates that the flux injection theoretical model holds well for the flare-associated CMEs, but a different mechanism should be considered for EP-associated CMEs.

### **Multi-Wavelength Signatures of Magnetic Reconnection of a Flare-Associated Coronal Mass Ejection**

Bhuwan **Joshi**, P. K. Manoharan, Astrid M. Veronig, P. Pant, Kavita Pandey

Solar Phys., 242(1-2), Page: 143 – 158, 2007.

The study supports the standard CSHKP model of flares, which is consistent with nearly all eruptive flare models. More importantly, the results also contain evidence for breakout reconnection before the flare phase.

### **Measuring the magnetic origins of solar flares, CMEs and Space Weather**

[Philip Judge](#), [Matthias Rempel](#), [Rana Ezzedine](#), [Lucia Kleint](#), [Ricky Egeland](#), [Svetlana Berdyugina](#), [Thomas Berger](#), [Joan Burkepile](#), [Rebecca Centeno](#), [Giuliana de Toma](#), [Mausumi Dikpati](#), [Yuhong Fan](#), [Holly Gilbert](#), [Daniela Lacatus](#)

ApJ 917 27 2021

<https://arxiv.org/pdf/2106.07786.pdf>

<https://iopscience.iop.org/article/10.3847/1538-4357/ac081f/pdf>

<https://doi.org/10.3847/1538-4357/ac081f>

We take a broad look at the problem of identifying the magnetic solar causes of space weather. With the lackluster performance of extrapolations based upon magnetic field measurements in the photosphere, we identify a region in the



near UV part of the spectrum as optimal for studying the development of magnetic free energy over active regions. Using data from SORCE, Hubble Space Telescope, and SKYLAB, along with 1D computations of the near-UV (NUV) spectrum and numerical experiments based on the MURaM radiation-MHD and HanleRT radiative transfer codes, we address multiple challenges. These challenges are best met through a combination of near UV lines of bright  $\text{Mg II}$ , and lines of  $\text{Fe II}$  and  $\text{Fe I}$  (mostly within the 4s–4p transition array) which form in the chromosphere up to  $2 \times 10^4$  K. Both Hanle and Zeeman effects can in principle be used to derive vector magnetic fields. However, for any given spectral line the  $\tau=1$  surfaces are generally geometrically corrugated owing to fine structure such as fibrils and spicules. By using multiple spectral lines spanning different optical depths, magnetic fields across nearly-horizontal surfaces can be inferred in regions of low plasma  $\beta$ , from which free energies, magnetic topology and other quantities can be derived. Based upon the recently-reported successful suborbital space measurements of magnetic fields with the CLASP2 instrument, we argue that a modest space-borne telescope will be able to make significant advances in the attempts to predict solar eruptions. Difficulties associated with blended lines are shown to be minor in an Appendix.

## A Comparison of Solar X-Ray Flare Timescales and Peak Temperatures with Associated Coronal Mass Ejections

S. W. Kahler<sup>1</sup> and A. G. Ling<sup>2</sup>

2022 ApJ 934 175

<https://iopscience.iop.org/article/10.3847/1538-4357/ac7e56/pdf>

Recent work has shown that plots of solar flare X-ray peak temperatures,  $T_m$ , versus log peak fluxes,  $F_p$ , show statistically significant separations of lower  $T_m$  flares with fast ( $V_{cme} \geq 1000 \text{ km s}^{-1}$ ) and wide ( $W_{cme} = 360^\circ$ ) strong coronal mass ejections (CMEs) from higher  $T_m$  flares with no CMEs or slow ( $V_{cme} < 1000 \text{ km s}^{-1}$ ) or narrow ( $< 360^\circ$ ) weak CMEs. We extend that statistical separation to CME kinetic energies,  $E_{cme}$ . Flares with long-duration timescales also have well-known associations with fast CMEs and solar energetic ( $E > 10 \text{ MeV}$ ) particle events. Using a data set of  $585 \geq M3.0$  GOES X-ray flares, we ask whether longer flare timescales (rise times, TR; durations from onset to half-power decay, TD; decay times to half power, Td; and decay times to C2, TC2) also statistically discriminate among the three groups of CMEs for speeds, widths, and energies. All log–log plots of flare timescales versus  $F_p$  produce significant separations of the three groups of CMEs generally better than those of  $T_m$  versus log  $F_p$ . We use separations of CME distribution medians to sort the four flare timescales as effective discriminants among the three CME groups. Separations between the confined flares (no-CMEs) and weak CMEs are generally smaller than those between the weak CMEs and strong CMEs. A combination of  $T_m$  and TC2 provides optimum group separations, but  $T_m$  and log TD or log Td appears best for CME forecasting purposes. **2002 July 3, 2004 November 7, 2006 December 13, 2012 March 7** **Table 4** Appendix Table of 585 M3 Flares with Timescales and CME Associations (This table is available in its entirety in machine-readable form.)

## The Role of Peak Temperatures in Solar X-Ray Flare Associations with CME Speeds and Widths and in Flare Size Distributions

S. W. Kahler<sup>1</sup> and A. G. Ling<sup>2</sup>

2020 ApJ 901 63

<https://doi.org/10.3847/1538-4357/abae5e>

Recently, we reported that solar X-ray flares with relatively low peak (0.05–0.3 nm)/(0.1–0.8 nm) ratios  $R$ , a proxy for peak flare temperature  $T$ , were preferentially associated not only with solar energetic ( $E > 10 \text{ MeV}$ ) particle (SEP) events, but also with fast ( $V_{cme} \geq 1000 \text{ km s}^{-1}$ ) coronal mass ejections (CMEs) that produce the SEP events. Flares associated with a characteristic CME speed  $V_{cme}$  range from small and cool to large and hot, and cooler X-ray flares were preferentially associated with broader CME widths. Here we increase the list of analyzed Geostationary Operational Environmental Satellite flares from the previous 450 to 588 and validate the earlier results with flare peak X-ray temperatures  $T$  from the TEBBS (Temperature and Emission measure-based Background Subtraction) method catalog. Power-law size distributions of flare peak fluxes  $F_p$  are increasingly steeper for X-ray flares with (1) fast ( $V_{cme} \geq 1000 \text{ km s}^{-1}$ ); (2) slow ( $V_{cme} < 1000 \text{ km s}^{-1}$ ); and (3) no CMEs; in each case flares of larger  $F_p$  are characteristically hotter. The power-law size distribution of SEP event peak intensities  $I_p$  is flatter than any of the X-ray  $F_p$  distributions or a distribution formed from the product of the steep SEP  $I_p$  dependence on  $V_{cme}$  and the  $V_{cme}$  number distributions.

## Temperatures of Large Solar X-ray Events and Associated CME Speeds

S. Kahler,\* A. Ling

36th International Cosmic Ray Conference -ICRC2019- July 24th - August 1st, 2019 Madison, WI, U.S.A.

<https://pos.sissa.it/358/1089/pdf>

Recently we [1] repeated an earlier analysis by [2,3] showing that large ( $> M3$ ) solar X-ray flares associated with solar energetic particle (SEP) events have significantly lower peak X-ray flux ratios  $R$  of 0.04–0.5/0.1–0.8 nm, proxies for flare peak temperatures, than those without SEP events. Since we expect SEP events to be produced by shocks ahead of fast coronal mass ejections (CMEs), this would imply that an X-ray flare of a given peak flux is more likely to have a fast CME and associated SEP event when it has a relatively smaller  $R$ . We examine the role played by the ratios  $R$  in correlations between X-ray peak flare fluxes and CME speeds  $V_{cme}$ , and then compare CMEs widths  $W$ , speeds  $V_{cme}$ , X-ray flare durations  $\Delta T$ , and  $R$  with each other. We resolve the apparent conflict between a global scaling model of

eruptive events showing  $V_{cme}$  scaling with higher  $R$  and our confirmation that the [2,3] analysis implies faster CMEs are associated with flares of lower  $R$ .

### **Ratios of SEP/Suprathermal Intensities and Associated CME Speeds**

S. Kahler,\* A. Ling

36th International Cosmic Ray Conference -ICRC2019- July 24th - August 1st, 2019 Madison, WI, U.S.A.

<https://pos.sissa.it/358/1091/pdf>

Recently [1] have found correlations between peak intensities  $I_p$  of  $E > 10$  MeV SEP events and suprathermal H and He ion intensities observed in situ at 1 AU around the onsets of SEP events. The correlations depend on the solar source longitudes of the driver CMEs and the kind of solar wind (SW) (transient or normal) at the SEP event onset. How the 1 AU suprathermals are related to the solar coronal seed population of SEPs is not known. In a previous study [2] with a similar result, the ratio  $R$  of 20-MeV  $I_p$  to the 2-MeV H suprathermal backgrounds were plotted against CME speeds  $V_{cme}$ . In contrast to the usual strong correlations between  $I_p$  and  $V_{cme}$ , [2] found the dependence of  $R$  on  $V_{cme}$  to be very weak, suggesting that the primary factor determining  $I_p$  of SEP events may be the source seed population, rather than  $V_{cme}$ . We extend that work [1,2] by plotting both  $R$  and  $\log I_p$  against  $\log V_{cme}$  for various types of SW and different source longitudes to look for the dependences of  $R$  on  $V_{cme}$ . We confirm the lower correlations found for  $R$  and  $V_{cme}$ , but  $V_{cme}$  retains its role as an independent factor in SEP production. The better  $R$  correlation using 1.28-2.56 MeV H suggests a more significant role for lower energy 0.16-0.32 MeV H as shock seed particles. Conclusions of variations of  $R$  correlations among different SW types and solar longitudes are limited by the statistics of the SEP events.

### **Do Solar Coronal Holes Affect the Properties of Solar Energetic Particle Events?**

S. W. Kahler, C. N. Arge, S. Akiyama, N. Gopalswamy

Solar Physics, February 2014, Volume 289, Issue 2, pp 657-673; **File**

The intensities and timescales of gradual solar energetic particle (SEP) events at 1 AU may depend not only on the characteristics of shocks driven by coronal mass ejections (CMEs), but also on large-scale coronal and interplanetary structures. It has long been suspected that the presence of coronal holes (CHs) near the CMEs or near the 1-AU magnetic footpoints may be an important factor in SEP events. We used a group of 41  $E \approx 20$  MeV SEP events with origins near the solar central meridian to search for such effects. First we investigated whether the presence of a CH directly between the sources of the CME and of the magnetic connection at 1 AU is an important factor. Then we searched for variations of the SEP events among different solar wind (SW) stream types: slow, fast, and transient. Finally, we considered the separations between CME sources and CH footpoint connections from 1 AU determined from four-day forecast maps based on Mount Wilson Observatory and the National Solar Observatory synoptic magnetic-field maps and the Wang–Sheeley–Arge model of SW propagation. The observed in-situ magnetic-field polarities and SW speeds at SEP event onsets tested the forecast accuracies employed to select the best SEP/CH connection events for that analysis. Within our limited sample and the three analytical treatments, we found no statistical evidence for an effect of CHs on SEP event peak intensities, onset times, or rise times. The only exception is a possible enhancement of SEP peak intensities in magnetic clouds. **Table**

### **A COMPARISON OF THE INTENSITIES AND ENERGIES OF GRADUAL SOLAR ENERGETIC PARTICLE EVENTS WITH THE DYNAMICAL PROPERTIES OF ASSOCIATED CORONAL MASS EJECTIONS**

S. W. Kahler<sup>1</sup> and A. Vourlidas

2013 ApJ 769 143

Gradual solar energetic particle (SEP) events observed at 1 AU are produced by shocks driven by coronal mass ejections (CMEs). Characterizations of the remotely imaged CMEs and of their associated SEP events observed in situ can be used to increase our ability to forecast SEP events and to understand better the physical connections between the two phenomena. We carry out a statistical comparison of the peak intensities  $I_{p20}$ , of 120 western-hemisphere 20 MeV SEP events with those of their associated CMEs observed by the Solar and Heliospheric Observatory/Large Angle and Spectrometric Coronagraph over the past solar cycle. For a subset of 96 events observed with the EPACT instrument on the Wind spacecraft we also compare the SEP 2 MeV peak intensities  $I_{p2}$ , power-law energy spectral exponents  $\gamma$ , total SEP energies  $E_{sep}$ , and 2 MeV  $\text{nuc}^{-1}$  H/He ratios with CME properties. New analyses of white-light CME images enable us to improve calculations of the CME masses and potential energies and then to determine two values of their kinetic energies based on frontal  $V$  (fr) and center-of-mass  $V$  (cm) speeds. Despite considerable scatter in the SEP and CME data, the large dynamical ranges of both the SEP and CME parameters allow us to determine statistical trends in the comparisons of the logs of the parameters.  $I_{p2}$ ,  $I_{p20}$ , and  $E_{sep}$  are significantly correlated with CME kinetic energies, masses, and speeds, while  $\gamma$  trends lower (harder). Those correlations are higher with  $V$  (fr) than with  $V$  (cm) parameters, indicating a less significant role for the body of the CME than for the CME front in SEP production. The high ratios ( $\geq 10\%$ ) of  $E_{sep}$  to CME energies found by Mewaldt et al. are confirmed, and the fits are consistent with a linear relationship between the two energies. The 2 MeV  $\text{nuc}^{-1}$  H/He ratios decrease with increasing CME speeds, which may be an effect of shock geometry. We discuss several factors that limit the estimates of both the SEP and CME energies.

## A COMPARISON OF SOLAR ENERGETIC PARTICLE EVENT TIMESCALES WITH PROPERTIES OF ASSOCIATED CORONAL MASS EJECTIONS

S. W. [Kahler](#)

2013 ApJ 769 110

The dependence of solar energetic proton (SEP) event peak intensities  $I_p$  on properties of associated coronal mass ejections (CMEs) has been extensively examined, but the dependence of SEP event timescales is not well known. We define three timescales of 20 MeV SEP events and ask how they are related to speeds  $v$  CME or widths  $W$  of their associated CMEs observed by LASCO/SOHO. The timescales of the EPACT/Wind 20 MeV events are  $T_O$ , the onset time from CME launch to SEP onset;  $T_R$ , the rise time from onset to half the peak intensity ( $0.5I_p$ ); and  $T_D$ , the duration of the SEP intensity above  $0.5I_p$ . This is a statistical study based on 217 SEP-CME events observed during 1996-2008. The large number of SEP events allows us to examine the SEP-CME relationship in five solar-source longitude ranges. In general, we statistically find that  $T_O$  declines slightly with  $v$  CME, and  $T_R$  and  $T_D$  increase with both  $v$  CME and  $W$ .  $T_O$  is inversely correlated with  $\log I_p$ , as expected from a particle background effect. We discuss the implications of this result and find that a background-independent parameter  $T_O+T_R$  also increases with  $v$  CME and  $W$ . The correlations generally fall below the 98% significance level, but there is a significant correlation between  $v$  CME and  $W$  which renders interpretation of the timescale results uncertain. We suggest that faster (and wider) CMEs drive shocks and accelerate SEPs over longer times to produce the longer  $T_R$  and  $T_D$  SEP timescales.

## DEFLECTIONS OF FAST CORONAL MASS EJECTIONS AND THE PROPERTIES OF ASSOCIATED SOLAR ENERGETIC PARTICLE EVENTS

S. W. [Kahler](#)<sup>1</sup>, S. Akiyama<sup>2</sup>, and N. Gopalswamy

2012 ApJ 754 100, [File](#)

The onset times and peak intensities of solar energetic particle (SEP) events at Earth have long been thought to be influenced by the open magnetic fields of coronal holes (CHs). The original idea was that a CH lying between the solar SEP source region and the magnetic footpoint of the 1 AU observer would result in a delay in onset and/or a decrease in the peak intensity of that SEP event. Recently, Gopalswamy et al. showed that CHs near coronal mass ejection (CME) source regions can deflect fast CMEs from their expected trajectories in space, explaining the appearance of driverless shocks at 1 AU from CMEs ejected near solar central meridian (CM). This suggests that SEP events originating in CME-driven shocks may show variations attributable to CH deflections of the CME trajectories. Here, we use a CH magnetic force parameter to examine possible effects of CHs on the timing and intensities of 41 observed gradual E  $\sim$  20 MeV SEP events with CME source regions within  $20^\circ$  of CM. We find no systematic CH effects on SEP event intensity profiles. Furthermore, we find no correlation between the CME leading-edge measured position angles and SEP event properties, suggesting that the widths of CME-driven shock sources of the SEPs are much larger than the CMEs. Independently of the SEP event properties, we do find evidence for significant CME deflections by CH fields in these events.

## Observational Properties of Coronal Mass Ejections [Review](#)

[Kahler](#) S.W.

Solar Eruptions and Energetic Particles, ed. N. Gopalswamy, R. Mewaldt, and J. Torsti, Geophysical Monograph 165, p. 21-32, 2006.

<https://sci-hub.ru/10.1029/165GM05>

Coronal mass ejections (CMEs) have been known and observed for over 30 years. The total number of observed CMEs is now approaching 10,000, most of them detected with the LASCO coronagraph on the SOHO spacecraft. We review statistical work on CME widths, latitudes, accelerations, speeds, masses, and rates of occurrence. Solar-cycle variations of these parameters are presented. Recent work has focused on CME internal properties and compositions and on CME dynamics, particularly at low ( $< 3 R_o$ ) altitudes. The challenges to understand the magnetic topology of narrow ( $< 20$  deg width) CMEs, to determine the relationship of coronal holes to CMEs, and to observe magnetic reconnection that effects magnetic disconnections of CMEs from the Sun are discussed.

## Solar flares and coronal mass ejections. [\(Review\)](#)

[Kahler](#), S.W.,

1992. Ann Rev. Astron. Astrophys. 30, 113-141.

<http://sci-hub.ru/10.1146/annurev.aa.30.090192.000553>

<https://articles.adsabs.harvard.edu/pdf/1992ARA%26A..30..113K>

This review addresses two basic questions. First, how did we form such a fundamentally incorrect view of the effects of flares after so much observational and theoretical work? Second, what is the observational and theoretical evidence to support a primary role for CMEs, and what can we say about the relationship between flares and CMEs? In Section 2 we present flare and CME observations in a historical context to show the changing perspective between the two phenomena. In Section 3 we discuss the coronal phenomena that bear on the relationship between flares and CMEs. Interplanetary effects are discussed in Section 4.

## The Evolution of Quasi-Separatrix Layer in Two Solar Eruptive Events

Kang [Kai-Feng](#), Yan Xiao-li, Xu Zhi, Wu Ning, Lin Jun

[Chinese Astronomy and Astrophysics](#) Volume 42, Issue 3 Pages 386-420 2018

<https://www.sciencedirect.com/journal/chinese-astronomy-and-astrophysics/vol/42/issue/3>

Quasi-separatrix layer, also called as QSL, is a region where magnetic connectivity changes drastically, and mostly well coincides with the location of flare ribbons in observations. The research on the relations of this topological structure with the 3-dimensional magnetic reconnection, and solar flares has attracted more and more attention. In this paper, using the theory of QSL we investigate a C5.7 classical two-ribbon solar flare (event 1) which occurred at AR11384 on **2011 December 26**, and an M6.5 solar flare (event 2) which occurred at AR12371 on **2015 June 22**, respectively. Combining the multi-wavelength data of AIA (Atmospheric Imaging Assembly) and vector magnetograms of HMI (Helioseismic and Magnetic Imager) onboard SDO (Solar Dynamics Observatory), we extrapolate the coronal magnetic field using the PF (Potential Field) and NLFFF (Nonlinear Force Free Field) models, and calculate the evolution of the AR (Active Region) magnetic free energy. Then, we calculate the logarithmic distribution of Q-factors (magnetic squashing factor) at different heights above the solar photosphere with the results of the PF and NLFFF extrapolations, in order to determine the location of QSL. Afterward, we investigate the evolutionary relation between the QSLs at different heights above the solar photosphere and the flare ribbons observed at the corresponding heights. Finally, we study the multi-wavelength evolution features of the 2 flare events, and obtain by calculation the mean slip velocities of magnetic lines in the event 2 at 304 Å and 335 Å to be 4.6 km s<sup>-1</sup> and 6.3 km s<sup>-1</sup>, respectively. We find that the calculated location of QSL in the chromosphere and corona is in good agreement with the location of flare ribbons at the same height, and the QSLs at different heights have almost the same evolutionary behavior in time as the flare ribbons of the corresponding heights, which highlights the role of QSL in the research of 3D magnetic reconnection and solar flare, and we suggest that the energy release in the flare of event 2 may be triggered by the magnetic reconnection at the place of QSL. We also suggest that the QSL is very important for us to study the essential relation between the 3D and 2D magnetic reconnections.

## Kinematic study of radio-loud CMEs associated with solar flares and DH type II radio emissions during solar cycles 23 and 24

[P. Pappa Kalaivani](#), [O. Prakash](#), [A. Shanmugaraju](#), [G. Michalek](#), [G. Selvarani](#)

Solar Phys. 2022

<https://arxiv.org/pdf/2204.07968.pdf>

We have statistically analyzed 379 radio-loud (RL) CMEs and their associated flares during the period 1996 - 2019 covering both solar cycles (SC) 23 and 24. We classified them into two sets of populations based on the observation period: i) 235 events belong to SC 23 (August 1996 - December 2008) and ii) 144 events belong to SC 24 (January 2009 - December 2019). The average residual acceleration of RL CMEs in SC 24 ( $-17.39 \pm 43.51 \text{ m s}^{-2}$ ) is two times lower than that of the RL CMEs in SC 23 ( $-8.29 \pm 36.23 \text{ m s}^{-2}$ ), which means that deceleration of RL CMEs in SC 24 is twice as fast as in SC 23. RL CMEs of SC 23 ( $1443 \pm 504 \text{ km s}^{-1}$ ;  $13.82 \pm 7.40 \text{ \textcircled{R}}$ ) reach their peak speed at higher altitudes than RL CMEs of SC 24 ( $1920 \pm 649 \text{ km s}^{-1}$ ;  $12.51 \pm 7.41 \text{ \textcircled{R}}$ ). We also observed that the mean apparent widths of RL CMEs in SC 23 are less than in SC 24 which is statistically significant. SC 23 has a lower average CME nose height ( $3.85 \text{ \textcircled{R}}$ ) at the start time of DH type II bursts than that of SC 24 ( $3.46 \text{ \textcircled{R}}$ ). The starting frequencies of DH type II bursts associated with RL CMEs for SC 24 are significantly larger (formed at lower heights) than that of SC 23. We found that there is a good correlation between the drift rates and the mid-frequencies of DH type II radio bursts for both the solar cycles ( $\text{R} = 0.80$ ,  $\epsilon = 1.53$ ). Most of the RL CMEs kinematics and their associated solar flare properties are found similar for SC 23 and SC 24. We concluded that the reduced total pressure in the heliosphere for SC 24 enables RL CMEs to expand wider and decelerate faster, resulting in DH type II radio emissions at lower heights than SC 23.

## Analysis of type II and type III radio bursts associated with SEPs from non-interacting/interacting radio-loud CMEs

[P Pappa Kalaivani](#), [O Prakash](#), [A Shanmugaraju](#), [Li Feng](#), [Lei Lu](#), [Weiqun Gan](#), [G Michalek](#)

Astrophysics 2021

<https://arxiv.org/pdf/2107.09955.pdf>

We analyze radio bursts observed in events with interacting/non-interacting CMEs that produced major SEPs ( $I_p > 10 \text{ MeV}$ ) from April 1997 to December 2014. We compare properties of meter (m), deca-hectometer (DH) type II as well as DH type III bursts, and time lags for interacting-CME-associated (IC) events and non-interacting-CME-associated (NIC) events. About 70% of radio emissions were observed in events of both types from meters to kilometers. We found high correlations between the drift rates and mid-frequencies of type II radio bursts calculated as the mean geometric between their starting and ending frequencies for both NIC and IC-associated events (Correlation coefficient  $\text{R}^2 = 0.98$ , power-law index  $\epsilon = 1.68 \pm 0.16$  and  $\text{R}^2 = 0.93$ ,  $\epsilon = 1.64 \pm 0.19$  respectively). We also found a correlation between the frequency drift rates of DH type II bursts and space speeds of CMEs in NIC-associated events. The absence of such correlation for IC-associated events confirms that the shock speeds changed in CME-CME interactions. For the events with western source locations, the mean peak intensity of SEPs in IC-associated events is four times larger than that in NIC-associated SEP events. From the mean time lags between the start times of SEP events and the start of m, DH type II, and DH type III radio bursts, we inferred that particle enhancements in NIC-

associated SEP events occurred earlier than in IC-associated SEP events. The difference between NIC events and IC events in the mean values of parameters of type II and type III bursts is statistically insignificant. **18 Apr 2014**

### **Eruptive Solar Prominence at 37 GHz**

J. [Kallunki](#), M. Tornikoski

[Solar Physics](#) July 2017, 292:84

On **27 June 2012**, an eruptive solar prominence was observed in the extreme ultraviolet (EUV) and radio wavebands. At the Aalto University Metsähovi Radio Observatory (MRO) it was observed at 37 GHz. It was the first time that the MRO followed a radio prominence with dense sampling in the millimetre wavelengths. This prompted us to study the connection of the 37 GHz event with other wavelength domains. At 37 GHz, the prominence was tracked to a height of around  $1.6 R_{\odot}$ – $1.6 R_{\odot}$ , at which the loop structure collapsed. The average velocity of the radio prominence was  $55 \pm 6$  km s<sup>-1</sup>– $155 \pm 6$  km s<sup>-1</sup>. The brightness temperature of the prominence varied between  $800 \pm 100$  K and  $3200 \pm 100$  K. We compared our data with the Solar Dynamic Observatory (SDO)/Atmospheric Imaging Assembly (AIA) instrument's 304 Å EUV data, and found that the prominence behaves very similarly in both wavelengths. The EUV data also reveal flaring activity nearby the prominence. We present a scenario in which this flare works as a trigger that causes the prominence to move from a stable stage to an acceleration stage.

### **Gnevyshev Peaks in the CME Average Speeds in Cycle 23**

R. P. [Kane](#)

*Solar Phys.*, 261(1), Page: 209 – 213, **2010**, [File](#)

Sunspots have a major 11-year cycle, but the three to four years near the maximum may show two or more peaks called Gnevyshev peaks. Earlier, it was reported that in Solar Cycle 23, the double peak in sunspot numbers was reflected in the electromagnetic radiations and coronal mass ejection (CME) frequencies in the solar atmosphere, but with phase differences. In this article, it is shown that the average CME speeds also show Gnevyshev peaks but with phase differences.

### **Fluctuations of Solar Activity during the Declining Phase of the 11-Year Sunspot Cycle**

R.P. [Kane](#)

*Solar Phys* (2009) 255: 163–168, DOI 10.1007/s11207-008-9303-8

### **Gnevyshev Peaks and Gaps for Coronal Mass Ejections of Different Widths Originating in Different Solar Position Angles**

R.P. [Kane](#)

*Solar Phys* (2008) 249: 369–380

<http://springerlink.com/content/h528p165342m2716/fulltext.pdf>

The sunspot number series at the peak of sunspot activity often has two or three peaks (Gnevyshev peaks; Gnevyshev, *Solar Phys.* **1**, 107, 1967; *Solar Phys.* **51**, 175, 1977). The sunspot group number (SGN) data were examined for 1997 – 2003 (part of cycle 23) and compared with data for coronal mass ejection (CME) events. It was noticed that they exhibited mostly two Gnevyshev peaks in each of the four latitude belts 0° – 10°, 10° – 20°, 20° – 30°, and >30°, in both N (northern) and S (southern) solar hemispheres. The SGN were confined to within latitudes ±50° around the Equator, mostly around ±35°, and seemed to occur later in lower latitudes, indicating possible latitudinal migration as in the Maunder butterfly diagrams. In CMEs, less energetic CMEs (of widths <71°) showed prominent Gnevyshev peaks during sunspot maximum years in almost all latitude belts, including near the poles. The CME activity lasted longer than the SGN activity. However, the CME peaks did not match the SGN peaks and were almost simultaneous at different latitudes, indicating no latitudinal migration. In energetic CMEs including halo CMEs, the Gnevyshev peaks were obscure and ill-defined. The solar polar magnetic fields show polarity reversal during sunspot maximum years, first at the North Pole and, a few months later, at the South Pole. However, the CME peaks and gaps did not match with the magnetic field reversal times, preceding them by several months, rendering any cause – effect relationship doubtful.

### **Latitude Dependence of the Variations of Sunspot Group Numbers (SGN) and Coronal Mass Ejections (CMEs) in Cycle 23**

R.P. [Kane](#)

*Solar Phys* (2008) 249: 355–367

<http://springerlink.com/content/y811g024vg2826n5/fulltext.pdf>

The 12-month running means of the conventional sunspot number  $R_z$ , the sunspot group numbers (SGN) and the frequency of occurrence of Coronal Mass Ejections (CMEs) were examined for cycle 23 (1996 – 2006). For the whole disc, the SGN and  $R_z$  plots were almost identical. Hence, SGN could be used as a proxy for  $R_z$ , for which latitude data are not available. SGN values were used for 5° latitude belts 0° – 5°, 5° – 10°, 10° – 15°, 15° – 20°, 20° – 25°, 25° – 30° and >30°, separately in each hemisphere north and south. Roughly, from latitudes 25° – 30° N to 20° – 25° N, the peaks seem to have occurred *later* for lower latitudes, from latitudes 20° – 25° N to 15° – 20° N, the peaks are stagnant or occur slightly *earlier*, and then from latitudes 15° – 20° N to 0° – 5° N, the peaks seem to have occurred again *later* for lower latitudes. Thus, some latitudinal migration is suggested, clearly in the northern hemisphere, not very clearly in the southern hemisphere,

first to the equator in 1998, stagnant or slightly poleward in 1999, and then to the equator again from 2000 onwards, the latter reminiscent of the Maunder butterfly diagrams. Similar plots for CME occurrence frequency also showed multiple peaks (two or three) in almost all latitude belts, but the peaks were almost simultaneous at all latitudes, indicating no latitudinal migration. For similar latitude belts, SGN and CME plots were dissimilar in almost all latitude belts except  $10^\circ - 20^\circ$  S. The CME plots had in general more peaks than the SGN plots, and the peaks of SGN often did not match with those of CME. In the CME data, it was noticed that whereas the values declined from 2002 to 2003, there was no further decline during 2003 – 2006 as one would have expected to occur during the declining phase of sunspots, where 2007 is almost a year of sunspot minimum. An inquiry at GSFC-NASA revealed that the person who creates the preliminary list was changed in 2004 and the new person picks out more weak CMEs. Thus a subjectivity (overestimates after 2002) seems to be involved and hence, values obtained before and during 2002 are not directly comparable to values recorded after 2002, except for CMEs with widths exceeding  $60^\circ$ .

## **Similarities and Dissimilarities between the Variations of CME and Other Solar Parameters at Different Heliographic Latitudes and Time Scales**

R.P. Kane

Solar Phys (2008) 248: 177–190

From the LASCO CME (Coronal Mass Ejection) catalog, the occurrence frequencies of all CMEs (all strong and weak CMEs, irrespective of their widths) were calculated for 3-month intervals and their 12-month running means determined for cycle 23 (1996 – 2007) and were compared with those of other solar parameters. The annual values of all-CME frequency were very well correlated (+0.97) with sunspot numbers, but several other parameters also had similarly high correlations. Comparisons of 12-month running means indicated that the sunspot numbers were very well correlated with solar electromagnetic radiations (Lyman- $\alpha$ , 2800-MHz flux, coronal green line index, solar flare indices, and X-ray background); but for corpuscular radiations [proton fluxes, solar energetic particles (SEP), CMEs, interplanetary CMEs (ICMEs), and stream interaction regions (SIR)] and solar open magnetic fields, the correlations were lower. A notable feature was the appearance of two peaks during 2000 – 2002, and those double peaks in different parameters matched approximately except for proton fluxes and SEP and SIR frequencies. When hemispheric intensities were considered, north – south asymmetries appeared, more in some parameters than in others. When intensities in smaller latitude belts ( $10^\circ$ ) were compared, sunspot group numbers (SGN) were found to be confined mostly to latitudes within  $\pm 30^\circ$  of the solar equator, showing *two* peaks in all latitude belts, and during the course of the 11-year cycle, the double peaks shifted from middle to equatorial solar latitudes, just as seen in the Maunder butterfly diagrams. In contrast, CME frequency was comparable at all latitude belts (including high, near-polar latitudes), having more than two peaks in almost all latitude belts, and the peaks were almost simultaneous in all latitude belts. Thus, the matching of SGN peaks with those of CME peaks was poor. Incidentally, the CME frequency data for all events (all widths) after 2003 are not comparable to earlier data, owing to inclusion of very weak (narrow) CMEs in later years. The frequencies are comparable with earlier data only for widths exceeding about  $70^\circ$ .

The 12-month running means of the conventional sunspot number  $R_z$ , the sunspot group numbers (SGN) and the frequency of occurrence of Coronal Mass Ejections (CMEs) were examined for cycle 23 (1996 – 2006). For the whole disc, the SGN and  $R_z$  plots were almost identical. Hence, SGN could be used as a proxy for  $R_z$ , for which latitude data are not available. SGN values were used for  $5^\circ$  latitude belts  $0^\circ - 5^\circ$ ,  $5^\circ - 10^\circ$ ,  $10^\circ - 15^\circ$ ,  $15^\circ - 20^\circ$ ,  $20^\circ - 25^\circ$ ,  $25^\circ - 30^\circ$  and  $>30^\circ$ , separately in each hemisphere north and south. Roughly, from latitudes  $25^\circ - 30^\circ$  N to  $20^\circ - 25^\circ$  N, the peaks seem to have occurred *later* for lower latitudes, from latitudes  $20^\circ - 25^\circ$  N to  $15^\circ - 20^\circ$  N, the peaks are stagnant or occur slightly *earlier*, and then from latitudes  $15^\circ - 20^\circ$  N to  $0^\circ - 5^\circ$  N, the peaks seem to have occurred again *later* for lower latitudes. Thus, some latitudinal migration is suggested, clearly in the northern hemisphere, not very clearly in the southern hemisphere, first to the equator in 1998, stagnant or slightly poleward in 1999, and then to the equator again from 2000 onwards, the latter reminiscent of the Maunder butterfly diagrams. Similar plots for CME occurrence frequency also showed multiple peaks (two or three) in almost all latitude belts, but the peaks were almost simultaneous at all latitudes, indicating no latitudinal migration. For similar latitude belts, SGN and CME plots were dissimilar in almost all latitude belts except  $10^\circ - 20^\circ$  S. The CME plots had in general more peaks than the SGN plots, and the peaks of SGN often did not match with those of CME. In the CME data, it was noticed that whereas the values declined from 2002 to 2003, there was no further decline during 2003 – 2006 as one would have expected to occur during the declining phase of sunspots, where 2007 is almost a year of sunspot minimum. An inquiry at GSFC-NASA revealed that the person who creates the preliminary list was changed in 2004 and the new person picks out more weak CMEs. Thus a subjectivity (overestimates after 2002) seems to be involved and hence, values obtained before and during 2002 are not directly comparable to values recorded after 2002, except for CMEs with widths exceeding  $60^\circ$ .

## **COMPARISON OF THE VARIATIONS OF CMEs AND ICMEs WITH THOSE OF OTHER SOLAR AND INTERPLANETARY PARAMETERS DURING SOLAR CYCLE 23**

R. P. KANE

Solar Physics (2006) 233: 107–115

This paper examines the variations of coronal mass ejections (CMEs) and interplanetary CMEs (ICMEs) during solar cycle 23 and compares these with those of several other indices. During cycle 23, solar and interplanetary parameters had an increase from 1996 (sunspot minimum) to ~2000, but the interval 1998–2002 had short-term fluctuations. Sunspot numbers had peaks in 1998,

1999, 2000 (largest), 2001 (second largest), and 2002. Other solar indices had matching peaks, but the peak in 2000 was larger than the peak in 2001 only for a few indices, and smaller or equal for other solar indices. The solar open magnetic flux had very different characteristics for different solar latitudes. The high solar latitudes ( $45^\circ$ – $90^\circ$ ) in both N and S hemispheres had flux evolutions *anti-parallel* to sunspot activity. Fluxes in low solar latitudes ( $0^\circ$ – $45^\circ$ ) evolved roughly parallel to sunspot activity, but the finer structures (peaks etc. during sunspot maximum years) did not match with sunspot peaks. Also, the low latitude fluxes had considerable N–S asymmetry. For CMEs and ICMEs, there were increases similar to sunspots during 1996–2000, and during 2000–2002, there was good matching of peaks. But the peaks in 2000 and 2001 for CMEs and ICMEs had similar sizes, in contrast to the 2000 peak being greater than the 2001 peak for sunspots. Whereas ICMEs started decreasing from 2001 onwards, CMEs continued to remain high in 2002, probably due to extra contribution from high-latitude prominences, which had no equivalent interplanetary ICMEs or shocks. Cosmic ray intensity had features matching with those of sunspots during 2000–2001, with the 2000 peak (on a reverse scale, actually a cosmic ray decrease or trough) larger than the 2001 peak. However, cosmic ray decreases started with a delay and ended with a delay with respect to sunspot activity.

## Data-driven MHD simulation of successive solar plasma eruptions

[Takafumi Kaneko](#), [Sung-Hong Park](#), [Kanya Kusano](#)

ApJ **909** 155 2021

<https://arxiv.org/pdf/2101.12395.pdf>

<https://doi.org/10.3847/1538-4357/abe414>

Solar flares and plasma eruptions are sudden releases of magnetic energy stored in the plasma atmosphere. To understand the physical mechanisms governing their occurrences, three-dimensional magnetic fields from the photosphere up to the corona must be studied. The solar photospheric magnetic fields are observable, whereas the coronal magnetic fields cannot be measured. One method for inferring coronal magnetic fields is performing data-driven simulations, which involves time-series observational data of the photospheric magnetic fields with the bottom boundary of magnetohydrodynamic simulations. We developed a data-driven method in which temporal evolutions of the observational vector magnetic field can be reproduced at the bottom boundary in the simulation by introducing an inverted velocity field. This velocity field is obtained by inversely solving the induction equation and applying an appropriate gauge transformation. Using this method, we performed a data-driven simulation of successive small eruptions observed by the Solar Dynamics Observatory and the Solar Magnetic Activity Telescope in November 2017. The simulation well reproduced the converging motion between opposite-polarity magnetic patches, demonstrating successive formation and eruptions of helical flux ropes. **2017 November 4-5**

## Simulation Study of Solar Plasma Eruptions Caused by Interactions between Emerging Flux and Coronal Arcade Fields

T. [Kaneko](#), T. Yokoyama

2014 ApJ 796 44

<http://arxiv.org/pdf/1410.0189v1.pdf>

We investigate the triggering mechanisms of plasma eruptions in the solar atmosphere due to interactions between emerging flux and coronal arcade fields by using two-dimensional MHD simulations. We perform parameter surveys with respect to arcade field height, magnetic field strength, and emerging flux location. Our results show that two possible mechanisms exist, and which mechanism is dominant depends mostly on emerging flux location. One mechanism appears when the location of emerging flux is close to the polarity inversion line (PIL) of an arcade field. This mechanism requires reconnection between the emerging flux and the arcade field, as pointed out by previous studies. The other mechanism appears when the location of emerging flux is around the edge of an arcade field. This mechanism does not require reconnection between the emerging flux and the arcade field but does demand reconnection in the arcade field above the PIL. Furthermore, we found that the eruptive condition for this mechanism can be represented by a simple formula.

## Onset Mechanism of M6.5 Solar Flare Observed in Active Region 12371

Jihye [Kang](#), [Satoshi Inoue](#), [Kanya Kusano](#), [Sung-Hong Park](#), [Yong-Jae Moon](#)

ApJ **2019**

<https://arxiv.org/pdf/1911.05337.pdf>

We studied a flare onset process in terms of stability of a three-dimensional (3D) magnetic field in active region 12371 producing an eruptive M6.5 flare in **2015 June 22**. In order to reveal the 3D magnetic structure, we first extrapolated the 3D coronal magnetic fields based on time series of the photospheric vector magnetic fields under a nonlinear force-free field (NLFFF) approximation. The NLFFFs nicely reproduced the observed sigmoidal structure which is widely considered as pre-eruptive magnetic configuration. We, in particular, found that the sigmoid is composed of two branches of sheared arcade loops. On the basis of the NLFFFs, we investigated the sheared arcade loops to explore the onset process of the eruptive flare using three representative MHD instabilities: the kink, torus and double arc instabilities. The double arc instability, recently proposed by Ishiguro & Kusano, is a double arc loop can be more easily destabilized than a torus loop. Consequently, the NLFFFs are found to be quite stable against the kink and torus instabilities. However, the sheared arcade loops formed prior to the flare possibly becomes unstable against the double arc instability. As a possible scenario on the onset process of the M6.5 flare, we suggest three-step process: (1) double arc loop are formed by the sheared arcade loops through the tether-cutting reconnection during an early phase of the flare, (2) the double arc instability contributes to the expansion of destabilized double arc loops and (3) finally, the torus instability makes the full eruption.

## **Spectropolarimetric Radio Imaging of Faint Gyrosynchrotron Emission from a CME : A Possible Indication of the Insufficiency of Homogeneous Models**

[Devojyoti Kansabanik](#), [Surajit Mondal](#), [Divya Oberoi](#)

ApJ **968** 55 **2024**

<https://arxiv.org/pdf/2404.14714.pdf>

<https://iopscience.iop.org/article/10.3847/1538-4357/ad43e9/pdf>

The geo-effectiveness of coronal mass ejections (CMEs) is determined primarily by their magnetic fields. Modeling of Gyrosynchrotron (GS) emission is a promising remote sensing technique to measure the CME magnetic field at coronal heights. However, faint GS emission from CME flux ropes is hard to detect in the presence of bright solar emission from the solar corona. With high dynamic-range spectropolarimetric meter wavelength solar images provided by the Murchison Widefield Array, we have detected faint GS emission from a CME out to  $\sim 8.3 R_{\odot}$ , the largest heliocentric distance reported to date. High-fidelity polarimetric calibration also allowed us to robustly detect circularly polarized emission from GS emission. For the first time in literature, Stokes V detection has jointly been used with Stokes I spectra to constrain GS models. One expects that the inclusion of polarimetric measurement will provide tighter constraints on GS model parameters. Instead, we found that homogeneous GS models, which have been used in all prior works, are unable to model both the total intensity and circular polarized emission simultaneously. This strongly suggests the need for using inhomogeneous GS models to robustly estimate the CME magnetic field and plasma parameters. **3-4 May 2014**

## **A Double-decker Flux Rope Model for the Solar Eruption on 2012 March 10**

Nishu [Karna](#)<sup>1</sup>, Suman Dhaka<sup>2</sup>, Antonia Savcheva<sup>3</sup>, Jie Zhang<sup>2</sup>, and Bernhard Kliem<sup>4</sup>

**2024** ApJ 961 11

<https://iopscience.iop.org/article/10.3847/1538-4357/ad1187/pdf>

We present a magnetic configuration of a compound solar eruption observed on **2012 March 10**, from NOAA AR 11429 near the disk center, which displayed a soft X-ray sigmoid before the eruption. We constructed a series of magnetic field models, including double-decker flux rope configurations, using the flux rope insertion method. This produces three-dimensional coronal magnetic field models constrained by the photospheric magnetogram and observed EUV coronal structures. We used different combinations of flux rope paths. We found that two flux ropes sharing the same path at different heights quickly experience a partial merging in the initial iteration of the magnetofrictional relaxation process. Different paths with less than 30% overlap allowed us to construct stable double-decker structures. The high spatial and temporal resolution of the Solar Dynamics Observatory/Atmospheric Imaging Assembly facilitated the selection of a best-fit model that matches the observations best. Moreover, by varying fluxes in this validated nonlinear force-free field double-decker configuration, we successfully reproduce all three scenarios of eruptions of double-decker configurations: (i) eruption due to the instability of higher flux rope; (ii) eruption due to rising lower flux rope and merging with higher flux rope; and (iii) eruption due to the instability of both flux ropes. This demonstrates that magnetofrictional simulation can capture the large-scale magnetic structure of eruptions for a realistic field configuration at eruption onset.

## **Magnetofrictional Modeling of an Erupting Pseudostreamer**

Nishu [Karna](#)<sup>1</sup>, Antonia Savcheva<sup>1,2</sup>, Sarah Gibson<sup>3</sup>, Svetlin Tassev<sup>1</sup>, Katharine K. Reeves<sup>1</sup>, Edward E. DeLuca<sup>1</sup>, and Kévin Dalmasse<sup>4</sup>

**2021** ApJ 913 47

<https://doi.org/10.3847/1538-4357/abf2b8>

In this study, we present the magnetic configuration of an erupting pseudostreamer observed on **2015 April 19**, on the southwest limb of the Sun, with a prominence cavity embedded inside. The eruption resulted in a partial halo coronal mass ejection. The prominence eruption begins with a slow rise and then evolves to a fast-rise phase. We analyze this erupting pseudostreamer using the flux-rope insertion method and magnetofrictional relaxation to establish a sequence of plausible out-of-equilibrium magnetic configurations. This approach allows the direct incorporation of observations of structures seen in the corona (filament and cavity) to appropriately model the pseudostreamer based on SDO/HMI line-of-sight photospheric magnetograms. We also perform a topological analysis in order to determine the location of quasiseparatrix layers (QSLs) in the models, producing Q-maps to examine how the QSL locations progress in the higher iterations. We found that the axial flux in our best-fit unstable model was a factor of 20 times higher than we found in our marginally stable case. We computed the average magnetic field strength of the prominence and found that the unstable model exhibits twice the average field strength of the stable model. The eruption height from our modeling matches very well with the prominence eruption height measured from the AIA observation. The Q-maps derived from the model reproduce structures observed in LASCO/C2. Thus, the modeling and topological analysis results are fully consistent with the observed morphological features, implying that we have captured the large magnetic structure of the erupting filament in our magnetofrictional simulation.



## **Solar Eruptions in Nested Magnetic Flux Systems**

Judith T. **Karpen**<sup>1</sup>, Pankaj Kumar<sup>1,2</sup>, Peter F. Wyper<sup>3</sup>, C. Richard DeVore<sup>1</sup>, and Spiro K. Antiochos<sup>4</sup>  
2024 ApJ 966 27

<https://iopscience.iop.org/article/10.3847/1538-4357/ad2eaa/pdf>

The magnetic topology of erupting regions on the Sun is a key factor in the energy buildup and release, and the subsequent evolution of flares and coronal mass ejections (CMEs). The presence/absence of null points and separatrices dictates whether and where current sheets form and magnetic reconnection occurs. Numerical simulations show that energy buildup and release via reconnection in the simplest configuration with a null, the embedded bipole, is a universal mechanism for solar eruptions. Here we demonstrate that a magnetic topology with nested bipoles and two nulls can account for more complex dynamics, such as failed eruptions and CME–jet interactions. We investigate the stalled eruption of a nested configuration on **2013 July 13** in NOAA Active Region 11791, in which a small bipole is embedded within a large transequatorial pseudo-streamer containing a null. In the studied event, the inner active region erupted, ejecting a small flux rope behind a shock accompanied by a flare; the flux rope then reconnected with pseudo-streamer flux and, rather than escaping intact, mainly distorted the pseudo-streamer null into a current sheet. EUV and coronagraph images revealed a weak shock and a faint collimated outflow from the pseudo-streamer. We analyzed Solar Dynamics Observatory and Solar TERrestrial RELations Observatory observations and compared the inferred magnetic evolution and dynamics with three-dimensional magnetohydrodynamics simulations of a simplified representation of this nested fan-spine system. The results suggest that the difference between breakout reconnection at the inner null and at the outer null naturally accounts for the observed weak jet and stalled ejection. We discuss the general implications of our results for failed eruptions.

## **Reconnection-Driven Coronal-Hole Jets with Gravity and Solar Wind**

J. T. **Karpen**, C. R. DeVore, S. K. Antiochos, E. Pariat

2017 ApJ 834 62

<http://arxiv.org/pdf/1606.09201v1.pdf>

Coronal-hole jets occur ubiquitously in solar coronal holes, at EUV and X-ray bright points associated with intrusions of minority magnetic polarity. The embedded-bipole model for these jets posits that they are driven by explosive, fast reconnection between the stressed closed field of the embedded bipole and the open field of the surrounding coronal hole. Previous numerical studies in Cartesian geometry, assuming uniform ambient magnetic field and plasma while neglecting gravity and solar wind, demonstrated that the model is robust and can produce jet-like events in simple configurations. We have extended these investigations by including spherical geometry, gravity, and solar wind in a nonuniform, coronal hole-like ambient atmosphere. Our simulations confirm that the jet is initiated by the onset of a kink-like instability of the internal closed field, which induces a burst of reconnection between the closed and external open field, launching a helical jet. Our new results demonstrate that the jet propagation is sustained through the outer corona, in the form of a traveling nonlinear Alfvén wave front trailed by slower-moving plasma density enhancements that are compressed and accelerated by the wave. This finding agrees well with observations of white-light coronal-hole jets, and can explain microstreams and torsional Alfvén waves detected in situ in the solar wind. We also use our numerical results to deduce scaling relationships between properties of the coronal source region and the characteristics of the resulting jet, which can be tested against observations.

## **THE MECHANISMS FOR THE ONSET AND EXPLOSIVE ERUPTION OF CORONAL MASS EJECTIONS AND ERUPTIVE FLARES**

J. T. **Karpen**<sup>1</sup>, S. K. Antiochos<sup>1</sup>, and C. R. DeVore

2012 ApJ 760 81

We have investigated the onset and acceleration of coronal mass ejections (CMEs) and eruptive flares. To isolate the eruption physics, our study uses the breakout model, which is insensitive to the energy buildup process leading to the eruption. We performed 2.5D simulations with adaptive mesh refinement that achieved the highest overall spatial resolution to date in a CME/eruptive flare simulation. The ultra-high resolution allows us to separate clearly the timing of the various phases of the eruption. Using new computational tools, we have determined the number and evolution of all X- and O-type nulls in the system, thereby tracking both the progress and the products of reconnection throughout the computational domain. Our results show definitively that CME onset is due to the start of fast reconnection at the breakout current sheet. Once this reconnection begins, eruption is inevitable; if this is the only reconnection in the system, however, the eruption will be slow. The explosive CME acceleration is triggered by fast reconnection at the flare current sheet. Our results indicate that the explosive eruption is caused by a resistive instability, not an ideal process. Moreover, both breakout and flare reconnections begin first as a form of weak tearing characterized by slowly evolving plasmoids, but eventually transition to a fast form with well-defined Alfvénic reconnection jets and rapid flux transfer. This transition to fast reconnection is required for both CME onset and explosive acceleration. We discuss the key implications of our results for CME/flare observations and for theories of magnetic reconnection.

## **Early Evolution of Earth-Directed Coronal Mass Ejections in the Vicinity of Coronal Holes.**

**Karuppiah**, S., Dumbović, M., Martinić, K. et al.

Sol Phys 299, 87 (2024).

<https://doi.org/10.1007/s11207-024-02319-6>

We investigate the deflection and rotation behaviour of 49 Earth-directed coronal mass ejections (CMEs) spanning the period from 2010 to 2020 aiming to understand the potential influence of coronal holes (CHs) on their trajectories. Our analysis incorporates data from coronagraphic observations captured from multiple vantage points, as well as extreme ultraviolet (EUV) observations utilised to identify associated coronal signatures such as solar flares and filament eruptions. For each CME, we perform a 3D reconstruction using the Graduated Cylindrical Shell (GCS) model. We perform the GCS reconstruction in multiple time steps, from the time at which the CME enters the field of view (FOV) of the coronagraphs to the time it exits. We analyse the difference in the longitude, latitude, and inclination between the first and last GCS reconstructions as possible signatures of deflection/rotation. Furthermore, we examine the presence of nearby CHs at the time of eruption and employ the Collection of Analysis Tools for Coronal Holes (CATCH) to estimate relevant CH parameters, including magnetic-field strength, centre of mass, and area. To assess the potential influence of CHs on the deflection and rotation of CMEs, we calculate the Coronal Hole Influence Parameter (CHIP) for each event and analyse its relationship with their trajectories. A statistically significant difference is observed between CHIP force and the overall change in a CME's direction in the lower corona. The overall change in a CME's direction accounts cumulatively for the change in latitude, longitude, and rotation. This suggests that the CHIP force in the low corona has a significant influence on the overall change in the direction of Earth-directed CMEs. However, as the CME evolves outward, the CHIP force becomes less effective in causing deflection or rotation at greater distances. Additionally, we observe a negative correlation between the deflection rate of the CMEs and their velocity, suggesting that higher velocities are associated with lower deflection rates. Hence, the velocity of a CME, along with the magnetic field from CHs, appears to play a significant role in the deflection of CMEs. By conducting this comprehensive analysis, we aim to enhance our understanding of the complex interplay between CHs, CME trajectories, and relevant factors such as velocity and magnetic-field strength.

### **Statistical Relation between Solar Flares and Coronal Mass Ejections with Respect to Sigmoidal Structures in Active Regions**

Y. [Kawabata](#), Y. [Iida](#), T. [Doi](#), S. [Akiyama](#), S. [Yashiro](#), T. [Shimizu](#)

ApJ **869** 99 **2018** <https://doi.org/10.3847/1538-4357/aaebfc>

<https://arxiv.org/pdf/1810.10808.pdf>

[sci-hub.tw/10.3847/1538-4357/aaebfc](https://sci-hub.tw/10.3847/1538-4357/aaebfc)

Statistical dependencies among features of coronal mass ejections (CMEs), solar flares, and sigmoidal structures in soft-X-ray images were investigated. We applied analysis methods to all the features in the same way in order to investigate the reproducibility of the correlations among them, which may be found from the combination of previous statistical studies. The samples of 211 M-class and X-class flares, which were observed between 2006 and 2015 by Hinode/X-ray telescope, Solar and Heliospheric Observatory/Large Angle and Spectrometric Coronagraph, and GOES, were examined statistically. Five kinds of analysis were performed: Occurrence rate analysis, linear-correlation analysis, association analysis, the Kolmogorov--Smirnov test, and Anderson-Darling test. The analyses show three main results. First, the sigmoidal structure and long duration events (LDEs) has stronger dependency on the CME occurrence than large X-ray class events in on-disk events. Second, for the limb events, the significant dependency exists between LDEs and CME occurrence, and between X-ray class and CME occurrence. Third, there existed 32.4% of on-disk flare events, which had sigmoidal structure and were not accompanied by CMEs. However, the occurrence probability of CMEs without sigmoidal structures is very small, 8.8 %, in on-disk events. While the first and second results are consistent with previous studies, we newly provided the difference between the on-disk events and limb events. The third result that non-sigmoidal regions produce less eruptive events is also different from previous results. We suggest that sigmoidal structures in soft X-ray images will be a helpful feature for CME prediction regarding on-disk flare events.

**13 December 2006**

**PSTEP Science Nuggets #18 2019**

[http://www.pstep.jp/news\\_en/nuggets18en.html](http://www.pstep.jp/news_en/nuggets18en.html)

### **Velocity Structure and Temperature Dependence of Extreme-Ultraviolet Jet Observed by Hinode**

Toshiki [Kawai](#), [Natsuo Kanda](#), [Shinsuke Imada](#)

Solar Phys. **294**:74 **2019**

<https://arxiv.org/pdf/1904.10271.pdf>

[sci-hub.se/10.1007/s11207-019-1469-8](https://sci-hub.se/10.1007/s11207-019-1469-8)

The acceleration mechanism of EUV/X-ray jets is still unclear. For the most part, there are two candidates for the mechanism. One is magnetic reconnection, and the other is chromospheric evaporation. We observed a relatively compact X-ray jet that occurred between 10:50 - 11:10 UT on **February 18, 2011** by using the Solar Dynamics Observatory/Atmospheric Imaging Assembly, and the X-ray Telescope, Solar Optical Telescope, and EUV Imaging Spectrometer aboard Hinode. Our results are as follows: 1) The EUV and X-ray observations show the general characteristics of X-ray jets, such as an arch structure straddling a polarity inversion line, a jet bright point shown at one side of the arch leg, and a spire above the arch. 2) The multi-wavelength observations and Ca II H-band image show the existence of a low-temperature (~10 000K) plasma (i.e., filament) at the center of the jet. 3) In the magnetogram and Ca II H-band image, the filament exists over the polarity inversion line and arch structure is also straddling it. In addition, magnetic cancellation occurs around the jet a few hours before and after the jet is observed. 4) The temperature distribution of the accelerated plasma, which was estimated from Doppler velocity maps, the calculated differential emission measure, and synthetic spectra show that there is no clear dependence between the plasma velocity and its

temperature. For the third result above, observational results suggest that magnetic cancellation is probably related to the occurrence of the jet and filament formation. This result suggests that the trigger of the jet is magnetic cancellation rather than an emerging magnetic arch flux. The fourth result indicates that acceleration of the plasma accompanied by an X-ray jet seems to be caused by magnetic reconnection rather than chromospheric evaporation.

### Updating Measures of CME Arrival Time Errors

[C. Kay](#), [E. Palmerio](#), [P. Riley](#), [M. L. Mays](#), [T. Nieves-Chinchilla](#), [M. Romano](#), [Y. M. Collado-Vega](#), [C. Wiegand](#), [A. Chulaki](#)

Space Weather [Volume22, Issue7](#) e2024SW003951 2024

<https://doi.org/10.1029/2024SW003951>

<https://agupubs.onlinelibrary.wiley.com/doi/epdf/10.1029/2024SW003951>

Coronal mass ejections (CMEs) drive space weather effects at Earth and the heliosphere. Predicting their arrival is a major part of space weather forecasting. In 2013, the Community Coordinated Modeling Center started collecting predictions from the community, developing an Arrival Time Scoreboard (ATSB). Riley et al. (2018, <https://doi.org/10.1029/2018sw001962>) analyzed the first 5 years of the ATSB, finding a bias of a few hours and uncertainty of order 15 hr. These metrics have been routinely quoted since 2018, but have not been updated despite continued predictions. We revise analysis of the ATSB using a sample 3.5 times the size of that in the original study. We find generally the same overall metrics, a bias of  $-2.5$  hr, mean absolute error of 13.2 hr, and standard deviation of 17.4 hr, with only a slight improvement comparing between the previously-used and new sets. The most well-established, frequently-submitted model results tend to outperform those from seldomly-contributed models. These “best” models show a slight improvement over the 11 year span, with more scatter between the models during early times and a convergence toward the same error metrics in recent years. We find little evidence of any correlations between the arrival time errors and any other properties. The one noticeable exception is a tendency for late predictions for short transit times and vice versa. We propose that any model-driven systematic errors may be washed out by the uncertainties in CME reconstructions in characterization of the background solar wind, and suggest that improving these may be the key to better predictions.

### Collection, Collation, and Comparison of 3D Coronal CME Reconstructions

Catalogs

[C. Kay](#), [E. Palmerio](#)

Space Weather. [Volume22, Issue1](#) e2023SW003796 2024

<https://arxiv.org/pdf/2311.10712.pdf>

<https://agupubs.onlinelibrary.wiley.com/doi/epdf/10.1029/2023SW003796>

Predicting the impacts of coronal mass ejections (CMEs) is a major focus of current space weather forecasting efforts. Typically, CME properties are reconstructed from stereoscopic coronal images and then used to forward model a CME's interplanetary evolution. Knowing the uncertainty in the coronal reconstructions is then a critical factor in determining the uncertainty of any predictions. A growing number of catalogs of coronal CME reconstructions exist, but no extensive comparison between these catalogs has yet been performed. Here we develop a Living List of Attributes Measured in Any Coronal Reconstruction (LLAMACoRe), an online collection of individual catalogs, which we intend to continually update. In this first version, we use results from 24 different catalogs with 3D reconstructions using STEREO observations between 2007--2014. We have collated the individual catalogs, determining which reconstructions correspond to the same events. LLAMACoRe contains 2954 reconstructions for 1863 CMEs. Of these, 510 CMEs contain multiple reconstructions from different catalogs. Using the best-constrained values for each CME, we find that the combined catalog reproduces the generally known solar cycle trends. We determine the typical difference we would expect between two independent reconstructions of the same event and find values of 4.0 deg in the latitude, 8.0 deg in the longitude, 24.0 deg in the tilt, 9.5 deg in the angular width, 0.1 in the shape parameter  $\kappa$ , 115 km/s in the velocity, and  $2.5e15$  g in the mass. These remain the most probable values over the solar cycle, though we find more extreme outliers in the deviation toward solar maximum.

### OSPREDI: A Coupled Approach to Modeling CME-Driven Space Weather With Automatically Generated, User-Friendly Outputs

[C. Kay](#), [M. L. Mays](#), [Y. M. Collado-Vega](#)

Space Weather e2021SW002914 2022

<https://arxiv.org/pdf/2109.06960.pdf>

<https://agupubs.onlinelibrary.wiley.com/doi/epdf/10.1029/2021SW002914>

Coronal mass ejections (CMEs) drive space weather activity at Earth and throughout the solar system. Current CME-related space weather predictions rely on information reconstructed from coronagraphs, sometimes from only a single viewpoint, to drive a simple interplanetary propagation model, which only gives the arrival time or limited additional information. We present the coupling of three established models into OSPREDI (Open Solar Physics Rapid Ensemble Information), a new tool that describes Sun-to-Earth CME behavior, including the location, orientation, size, shape, speed, arrival time, and internal thermal and magnetic properties, on the timescale needed for forecasts. First, Forecasting a CME's Altered Trajectory (ForeCAT) describes the trajectory that a CME takes through the solar corona. Second, ANother Type of Ensemble Arrival Time Results simulates the propagation, including expansion and deformation, of a CME in interplanetary space and determines the evolution of internal properties via conservation laws. Finally, ForeCAT In situ Data Observer produces in situ profiles for a CME's interaction with a synthetic

spacecraft. OSPREI includes ensemble modeling by varying each input parameter to probe any uncertainty in their values, yielding probabilities for all outputs. Standardized visualizations are automatically generated, providing easily accessible, essential information for space weather forecasting. We show OSPREI results for a CMEs observed in the corona on **22 April and 09 May 2021**. We approach these CME as a forecasting proof-of-concept, using information analogous to what would be available in real time rather than fine-tuning input parameters to achieve a best fit for a detailed scientific study. The OSPREI “prediction” shows good agreement with the arrival time and in situ properties. **21 April 2021, 09 May 2021**

## Using the Coronal Evolution to Successfully Forward Model CMEs' In Situ Magnetic Profiles†

C. **Kay**, N. Gopalswamy

JGR 2017

Predicting the effects of a coronal mass ejection (CME) impact requires knowing if impact will occur, which part of the CME impacts, and its magnetic properties. We explore the relation between CME deflections and rotations, which change the position and orientation of a CME, and the resulting magnetic profiles at 1 AU. For 45 STEREO-era, Earth-impacting CMEs, we determine the solar source of each CME, reconstruct its coronal position and orientation, and perform a ForeCAT [Kay et al., 2015a] simulation of the coronal deflection and rotation. From the reconstructed and modeled CME deflections and rotations we determine the solar cycle variation and correlations with CME properties. We assume no evolution between the outer corona and 1 AU and use the ForeCAT results to drive the FIDO in situ magnetic field model [Kay et al., 2017a], allowing for comparisons with ACE and Wind observations. We do not attempt to reproduce the arrival time. On average FIDO reproduces the in situ magnetic field for each vector component with an error equivalent to 35% of the average total magnetic field strength when the total modeled magnetic field is scaled to match the average observed value. Random walk best fits distinguish between ForeCAT's ability to determine FIDO's input parameters and the limitations of the simple flux rope model. These best fits reduce the average error to 30%. The FIDO results are sensitive to changes of order a degree in the CME latitude, longitude, and tilt, suggesting that accurate space weather predictions require accurate measurements of a CME's position and orientation.

## Deflection and Rotation of CMEs from Active Region 11158

C. **Kay**, N. Gopalswamy, X. Hong, S. Yashiro

Solar Phys. 292:78 2017

<https://arxiv.org/pdf/1704.07694.pdf>

Between the **13 and 16 of February 2011** a series of coronal mass ejections (CMEs) erupted from multiple polarity inversion lines within active region 11158. For seven of these CMEs we use the Graduated Cylindrical Shell (GCS) flux rope model to determine the CME trajectory using both Solar Terrestrial Relations Observatory (STEREO) extreme ultraviolet (EUV) and coronagraph images. We then use the Forecasting a CME's Altered Trajectory (ForeCAT) model for nonradial CME dynamics driven by magnetic forces, to simulate the deflection and rotation of the seven CMEs. We find good agreement between the ForeCAT results and the reconstructed CME positions and orientations. The CME deflections range in magnitude between 10 degrees and 30 degrees. All CMEs deflect to the north but we find variations in the direction of the longitudinal deflection. The rotations range between 5°/mydeg and 50°/mydeg with both clockwise and counterclockwise rotations occurring. Three of the CMEs begin with initial positions within 2 degrees of one another. These three CMEs all deflect primarily northward, with some minor eastward deflection, and rotate counterclockwise. Their final positions and orientations, however, respectively differ by 20 degrees and 30 degrees. This variation in deflection and rotation results from differences in the CME expansion and radial propagation close to the Sun, as well as the CME mass. Ultimately, only one of these seven CMEs yielded discernible in situ signatures near Earth, despite the active region facing near Earth throughout the eruptions. We suggest that the differences in the deflection and rotation of the CMEs can explain whether each CME impacted or missed the Earth.

## Predicting the Magnetic Field of Earth-impacting CMEs

C. **Kay**<sup>1</sup>, N. Gopalswamy<sup>1</sup>, A. Reinard<sup>2</sup>, and M. Opher<sup>3</sup>

2017 ApJ 835 117 File

<http://sci-hub.cc/doi/10.3847/1538-4357/835/2/117>

Predicting the impact of coronal mass ejections (CMEs) and the southward component of their magnetic field is one of the key goals of space weather forecasting. We present a new model, the ForeCAT In situ Data Observer (FIDO), for predicting the in situ magnetic field of CMEs. We first simulate a CME using ForeCAT, a model for CME deflection and rotation resulting from the background solar magnetic forces. Using the CME position and orientation from ForeCAT, we then determine the passage of the CME over a simulated spacecraft. We model the CME's magnetic field using a force-free flux rope and we determine the in situ magnetic profile at the synthetic spacecraft. We show that FIDO can reproduce the general behavior of four observed CMEs. FIDO results are very sensitive to the CME's position and orientation, and we show that the uncertainty in a CME's position and orientation from coronagraph images corresponds to a wide range of in situ magnitudes and even polarities. This small range of positions and orientations also includes CMEs that entirely miss the satellite. We show that two derived parameters (the normalized angular distance between the CME nose and satellite position and the angular difference between the CME tilt and the position angle of the satellite with respect to the CME nose) can be used to reliably determine whether an impact or miss occurs.

We find that the same criteria separate the impacts and misses for cases representing all four observed CMEs. **2010 April 3, 2011 Feb 15, 2012 Jul 12, 2014 Sep 10**

### **Using the Coronal Evolution to Successfully Forward Model CMEs' In Situ Magnetic Profiles**

C. Kay, N. Gopalswamy

JGR Volume 122, Issue 12 December **2017** Pages 11,810–11,834

<http://sci->

<http://onlinelibrary.wiley.com/doi/10.1002/2017JA024541/abstract;jsessionid=2DF604EC239663BA90D09F3C3BE44317.f01t04>

Predicting the effects of a coronal mass ejection (CME) impact requires knowing if impact will occur, which part of the CME impacts, and its magnetic properties. We explore the relation between CME deflections and rotations, which change the position and orientation of a CME, and the resulting magnetic profiles at 1 AU. For 45 STEREO-era, Earth-impacting CMEs, we determine the solar source of each CME, reconstruct its coronal position and orientation, and perform a ForeCAT (Forecasting a CME's Altered Trajectory) simulation of the coronal deflection and rotation. From the reconstructed and modeled CME deflections and rotations, we determine the solar cycle variation and correlations with CME properties. We assume no evolution between the outer corona and 1 AU and use the ForeCAT results to drive the ForeCAT In situ Data Observer (FIDO) in situ magnetic field model, allowing for comparisons with ACE and Wind observations. We do not attempt to reproduce the arrival time. On average FIDO reproduces the in situ magnetic field for each vector component with an error equivalent to 35% of the average total magnetic field strength when the total modeled magnetic field is scaled to match the average observed value. Random walk best fits distinguish between ForeCAT's ability to determine FIDO's input parameters and the limitations of the simple flux rope model. These best fits reduce the average error to 30%. The FIDO results are sensitive to changes of order a degree in the CME latitude, longitude, and tilt, suggesting that accurate space weather predictions require accurate measurements of a CME's position and orientation. **24 May 2010.**

### **Using ForeCAT Deflections and Rotations to Constrain the Early Evolution of CMEs**

C. Kay, M. Opher, R. C. Colaninno, A. Vourlidas

ApJ 827 70 **2016**

<http://arxiv.org/pdf/1606.03460v1.pdf>

To accurately predict the space weather effects of coronal mass ejection (CME) impacts at Earth one must know if and when a CME will impact Earth, and the CME parameters upon impact. Kay et al. (2015b) presents Forecasting a CME's Altered Trajectory (ForeCAT), a model for CME deflections based on the magnetic forces from the background solar magnetic field. Knowing the deflection and rotation of a CME enables prediction of Earth impacts, and the CME orientation upon impact. We first reconstruct the positions of the **2008 April 10 and the 2012 July 12** CMEs from the observations. The first of these CMEs exhibits significant deflection and rotation (34 degrees deflection and 58 degrees rotation), while the second shows almost no deflection or rotation (<3 degrees each). Using ForeCAT, we explore a range of initial parameters, such as the CME location and size, and find parameters that can successfully reproduce the behavior for each CME. Additionally, since the deflection depends strongly on the behavior of a CME in the low corona (Kay et al. (2015a, 2015b)), we are able to constrain the expansion and propagation of these CMEs in the low corona.

### **The Heliocentric Distance Where the Deflections and Rotations of Solar Coronal Mass Ejections Occur**

C. Kay, M. Opher

ApJL 811 L36 **2015**

<http://arxiv.org/pdf/1509.04948v1.pdf> File

Understanding the trajectory of a coronal mass ejection (CME), including any deflection from a radial path, and the orientation of its magnetic field is essential for space weather predictions. Kay et al. (2015b) developed a model, **Forecasting a CME's Altered Trajectory (ForeCAT)**, of CME deflections and rotation due to magnetic forces, not including the effects of reconnection. ForeCAT is able to reproduce the deflection of observed CMEs (Kay et al. 2015a). The deflecting CMEs tend to show a rapid increase of their angular momentum close to the Sun, followed by little to no increase at farther distances. Here we quantify the distance at which the CME deflection is "determined," which we define as the distance after which the background solar wind has negligible influence on the total deflection. We consider a wide range in CME masses and radial speeds and determine that the deflection and rotation of these CMEs can be well-described by assuming they propagate with constant angular momentum beyond 10 Rs. The assumption of constant angular momentum beyond 10 Rs yields underestimates of the total deflection at 1 AU of only 1% to 5% and underestimates of the rotation of 10%. Since the deflection from magnetic forces is determined by 10 Rs, non-magnetic forces must be responsible for any observed interplanetary deflections or rotations where the CME has increasing angular momentum. **April-May 2005**

### **Global Trends of CME Deflections Based on CME and Solar Parameters**

C. Kay, M. Opher, R. M. Evans

ApJ, 805 168 **2015**

<http://arxiv.org/pdf/1410.4496v1.pdf>

Accurate space weather forecasting requires knowledge of the trajectory of coronal mass ejections (CMEs),

including any deflections close to the Sun or through interplanetary space. Kay et al. 2013 introduced ForeCAT, a model of CME deflection resulting from the background solar magnetic field. For a magnetic field solution corresponding to Carrington Rotation (CR) 2029 (declining phase, **April-May 2005**), the majority of the CMEs deflected to the Heliospheric Current Sheet (HCS), the minimum in magnetic pressure on global scales. Most of the deflection occurred below 4 Rs. Here we extend ForeCAT to include a three dimensional description of the deflecting CME. We attempt to answer the following questions: a) Do all CMEs deflect to the magnetic minimum? and b) Does most deflection occur within the first few solar radii (~4 Rs)? Results for solar minimum and declining phase CMEs show that not every CME deflects to the magnetic minimum and that typically about half of the deflection occurs below 10 Rs. Slow, narrow, low mass CMEs in declining phase solar backgrounds with strong magnetic field and magnetic gradients exhibit the largest deflections. Local gradients related to active regions tend to cause the largest deviations from the deflection predicted by global magnetic gradients, but variations can also be seen for CMEs in the quiet sun regions of the declining phase CR.

## **Constraining the Mass and the Non-Radial Drag Coefficient of a Solar Coronal Mass Ejection**

C. **Kay**, L. F. G. dos Santos, M. Opher

ApJ Letters **801** L21 **2015**

<http://arxiv.org/pdf/1503.00664v1.pdf>

Decades of observations show that CMEs can deflect from a purely radial trajectory yet no consensus exists as to the cause of these deflections. Many of theories attribute the CME deflection to magnetic forces. We developed ForeCAT (Kay et al. 2013, Kay et al. 2015), a model for CME deflections based solely on magnetic forces, neglecting any reconnection effects. Here we compare ForeCAT predictions to the observed deflection of the **2008 December 12** CME and find that ForeCAT can accurately reproduce the observations. Multiple observations show that this CME deflected nearly  $30^\circ$  in latitude (Byrne et al. 2010, Gui et al. 2011) and  $4.4^\circ$  in longitude (Gui et al. 2011). From the observations, we are able to constrain all of the ForeCAT input parameters (initial position, radial propagation speed, and expansion) except the CME mass and the drag coefficient that affects the CME motion. By minimizing the reduced chi-squared,  $\chi^2_{\nu}$ , between the ForeCAT results and the observations we determine an acceptable mass range between  $4.5 \times 10^{14}$  and  $1 \times 10^{15}$  g and the drag coefficient less than 1.4 with a best fit at  $7.5 \times 10^{14}$  g and 0 for the mass and drag coefficient. ForeCAT is sensitive to the magnetic background and we are also able to constrain the rate at which the quiet sun magnetic field falls to be similar or to or fall slightly slower than the Potential Field Source Surface model.

## **FORECASTING A CORONAL MASS EJECTION'S ALTERED TRAJECTORY: ForeCAT**

C. **Kay**<sup>1</sup>, M. Opher<sup>1</sup>, and R. M. Evans

**2013** ApJ **775** 5

To predict whether a coronal mass ejection (CME) will impact Earth, the effects of the background on the CME's trajectory must be taken into account. We develop a model, ForeCAT (Forecasting a CME's Altered Trajectory), of CME deflection due to magnetic forces. ForeCAT includes CME expansion, a three-part propagation model, and the effects of drag on the CME's deflection. Given the background solar wind conditions, the launch site of the CME, and the properties of the CME (mass, final propagation speed, initial radius, and initial magnetic strength), ForeCAT predicts the deflection of the CME. Two different magnetic backgrounds are considered: a scaled background based on type II radio burst profiles and a potential field source surface (PFSS) background. For a scaled background where the CME is launched from an active region located between a coronal hole and streamer region, the strong magnetic gradients cause a deflection of  $81^\circ$  in latitude and  $264^\circ$  in longitude for a  $10^{15}$  g CME propagating out to 1 AU. Using the PFSS background, which captures the variation of the streamer belt (SB) position with height, leads to a deflection of  $16^\circ$  in latitude and  $41^\circ$  in longitude for the control case. Varying the CME's input parameters within observed ranges leads to the majority of CMEs reaching the SB within the first few solar radii. For these specific backgrounds, the SB acts like a potential well that forces the CME into an equilibrium angular position.

## **Multiwavelength observations of a breakout jet at an active region periphery**

**Pradeep Kayshap**, **Judith T. Karpen**, **Pankaj Kumar**

Solar Phys. Volume 299, article number 88 **2024**

<https://arxiv.org/pdf/2405.04766>

<https://doi.org/10.1007/s11207-024-02315-w>

We analysed Interface-Region Imaging Spectrograph (IRIS) and the Solar Dynamics Observatory/Atmospheric Imaging Assembly (SDO/AIA) observations of a small coronal jet that occurred at the solar west limb on **2014 August 29**. The jet source region, a small bright point, was located at an active-region periphery and contains a fan-spine topology with a mini-filament. Our analysis has identified key features and timings that motivate the following interpretation of this event. As the stressed core flux rises, a current sheet forms beneath it; the ensuing reconnection forms a flux rope above a flare arcade. When the rising filament-carrying flux rope reaches the stressed null, it triggers a jet via explosive interchange (breakout) reconnection. During the flux-rope interaction with the external magnetic field, we observed brightening above the filament and within the dome, along with a growing flare arcade. EUV images reveal quasi-

periodic ejections throughout the jet duration with a dominant period of 4 minutes, similar to coronal jetlets and larger jets. We conclude that these observations are consistent with the magnetic breakout model for coronal jets.

## Diagnostic of Homologous Solar Surge Plasma as observed by IRIS and SDO

[Pradeep Kayshap](#), [Rajdeep Singh Payal](#), [Sharad C. Tripathi](#), [Harihara Padhy](#)

MNRAS Volume 505, Issue 4, August 2021, Pages 5311–5326,

<https://doi.org/10.1093/mnras/stab1663>

<https://arxiv.org/pdf/2106.06222.pdf>

Surges have regularly been observed mostly in H $\alpha$  6563-Å and Ca-{\sc ii} 8542-Å. However, surge's response to other prominent lines of the interface-region (Mg-{\sc ii} k 2796.35-Å & h 2803.52-Å, O-{\sc iv} 1401.15-Å, Si-{\sc iv} 1402.77-Å) is not well studied. Here, the evolution and kinematics of six homologous surges are analysed using IRIS and AIA observations. These surges were observed on **7th July 2014**, located very close to the limb. DEM analysis is performed on these surges where the co-existence of cool ( $\log T/K = 6.35$ ) and relatively hot ( $\log T/K = 6.95$ ) components have been found at the base. This demonstrates that the bases of surges undergo substantial heating. During the emission of these surges in the above mentioned interface-region lines, being reported here for the first time, two peaks have been observed in the initial phase of emission, where one peak is found to be constant while other one as varying, i.e., non-constant (observed red to blueshifts across the surge evolution) in nature. This suggests the rotational motion of surge plasma. The heated base and rotating plasma suggests the occurrence of magnetic reconnection, most likely, as the trigger for homologous surges. During the emission of these surges, it is found that despite being optically thick (i.e.,  $R_{kh} < 2.0$ ), central reversal was not observed for Mg-{\sc ii} k & h lines. Further,  $R_{kh}$  increases with surge emission in time and it is found to have positive correlation with Doppler Velocity while negative with Gaussian width.

**IRIS Nugget, Oct 2021** [https://iris.lmsal.com/nugget?fbclid=IwAR1o93o3UdY64WtXS464tWd-ryIEYovbHY-hEmdUVnUmm9Nk399WA6XL\\_8I](https://iris.lmsal.com/nugget?fbclid=IwAR1o93o3UdY64WtXS464tWd-ryIEYovbHY-hEmdUVnUmm9Nk399WA6XL_8I)

## Rotating Network Jets in the quiet Sun as Observed by IRIS

[P. Kayshap](#), [K. Murawski](#), [A.K. Srivastava](#), [B.N. Dwivedi](#)

A&A 616, A99 2018

<https://arxiv.org/pdf/1805.02517.pdf>

**Aims.** We perform a detailed observational analysis of network jets to understand their kinematics, rotational motion and underlying triggering mechanism(s). We have analyzed the quiet-Sun (QS) data.

**Methods.** IRIS high resolution imaging and spectral observations (SJI: Si iv 1400.0 \AA, Raster: Si iv 1393.75 \AA) are used to analyze the omnipresent rotating network jets in the transition-region (TR). In addition, we have also used Atmospheric Imaging Assembly (AIA) onboard Solar Dynamic Observation (SDO) observations.

**Results.** The statistical analysis of fifty-one network jets is performed to understand various their mean properties, e.g., apparent speed ( $140.16 \pm 39.41$  km/s), length ( $3.16 \pm 1.18$  Mm), lifetimes ( $105.49 \pm 51.75$  s). The Si iv 1393.75 \AA line has secondary component along with its main Gaussian, which is formed due to the high-speed plasma flows (i.e., network jets). The variation of Doppler velocity across these jets (i.e., blue shift on one edge and red shift on the other) signify the presence of inherited rotational motion. The statistical analysis predicts that the mean rotational velocity (i.e.,  $\Delta V$ ) is 49.56 km/s. The network jets have high angular velocity in comparison to the other class of solar jets.

**Conclusions.** The signature of network jets are inherited in TR spectral lines in terms of the secondary component of the Si iv 1393.75 \AA line. The rotational motion of network jets is omnipresent, which is reported firstly for this class of jet-like features. The magnetic reconnection seems to be the most favorable mechanism for the formation of these network jets. **14.12.2014**

## Origin of Macrospicule and Jet in Polar Corona by A Small-scale Kinked Flux-Tube

[Kayshap, P.](#); [Srivastava, A. K.](#); [Murawski, K.](#); [Tripathi, D.](#)

E-print, May 2013; ApJL 770 L3 2013

We report an observation of a small scale flux-tube that undergoes kinking and triggers the macrospicule and a jet on **November 11, 2010** in the north polar corona. The small-scale flux-tube emerged well before the triggering of macrospicule and as the time progresses the two opposite halves of this omega shaped flux-tube bent transversely and approached towards each other. After  $\sim 2$  minutes, the two approaching halves of the kinked flux-tube touch each-other and internal reconnection as well as energy release takes place at the adjoining location and a macrospicule was launched which goes upto a height of 12 Mm. Plasma starts moving horizontally as well as vertically upward along with the onset of macrospicule and thereafter converts into a large-scale jet which goes up to  $\sim 40$  Mm in the solar atmosphere with a projected speed of  $\sim 95$  km s $^{-1}$ . We perform 2-D numerical simulation by considering the VAL-C initial atmospheric conditions to understand the physical scenario of the observed macrospicule and associated jet. The simulation results show that reconnection generated velocity pulse in the lower solar atmosphere steepens into slow shock and the cool plasma is driven behind it in form of macrospicule. The horizontal surface waves also appeared with the shock fronts at different heights, which most likely drove and spread the large-scale jet associated with the macrospicule.

## THE KINEMATICS AND PLASMA PROPERTIES OF A SOLAR SURGE TRIGGERED BY CHROMOSPHERIC ACTIVITY IN AR11271

P. [Kayshap](#)<sup>1,2</sup>, Abhishek K. Srivastava<sup>1</sup>, and K. Murawski

2013 ApJ 763 24

We observe a solar surge in NOAA AR11271 using the Solar Dynamics Observatory (SDO) Atmospheric Imaging Assembly 304 Å image data on **2011 August 25**. The surge rises vertically from its origin up to a height of 65 Mm with a terminal velocity of 100 km s<sup>-1</sup>, and thereafter falls and fades gradually. The total lifetime of the surge was 20 minutes. We also measure the temperature and density distribution of the observed surge during its maximum rise and find an average temperature and a density of 2.0 MK and 4.1 × 10<sup>9</sup> cm<sup>-3</sup>, respectively. The temperature map shows the expansion and mixing of cool plasma lagging behind the hot coronal plasma along the surge. Because SDO/HMI temporal image data do not show any detectable evidence of significant photospheric magnetic field cancellation for the formation of the observed surge, we infer that it is probably driven by magnetic-reconnection-generated thermal energy in the lower chromosphere. The radiance (and thus the mass density) oscillations near the base of the surge are also evident, which may be the most likely signature of its formation by a reconnection-generated pulse. In support of the present observational baseline of the triggering of the surge due to chromospheric heating, we devise a numerical model with conceivable implementation of the VAL-C atmosphere and a thermal pulse as an initial trigger. We find that the pulse steepens into a slow shock at higher altitudes which triggers plasma perturbations exhibiting the observed features of the surge, e.g., terminal velocity, height, width, lifetime, and heated fine structures near its base.

## Invited **Review**: Short-term Variability with the Observations from the Helioseismic and Magnetic Imager (HMI) Onboard the Solar Dynamics Observatory (SDO): Insights into Flare Magnetism

[Maria D. Kazachenko](#), [Marcel F. Albelo-Corchado](#), [Cole A. Tamburri](#) & [Brian T. Welsch](#)

[Solar Physics](#) volume 297, Article number: 59 (2022)

<https://link.springer.com/content/pdf/10.1007/s11207-022-01987-6.pdf> **File**

Continuous vector magnetic-field measurements by the Helioseismic and Magnetic Imager (HMI) onboard the Solar Dynamics Observatory (SDO) allow us to study magnetic-field properties of many flares. Here, we review new observational aspects of flare magnetism described using SDO data, including statistical properties of magnetic-reconnection fluxes and their rates, magnetic fluxes of flare dimmings, and magnetic-field changes during flares. We summarize how these results, along with statistical studies of coronal mass ejections (CMEs), have improved our understanding of flares and the flare/CME feedback relationship. Finally, we highlight future directions to improve the current state of understanding of solar-flare magnetism using observations. **14 Sep 2011, 7 March 2012, Sep 2014**

2. Flare Ribbons: Footpoints of Reconnected Fields
3. Coronal Dimmings: Footpoints of Expanding Coronal Structures
4. Flare-Associated Magnetic-Field Changes (FAMCs)
5. Relating CMEs and ICMEs to Their Source Regions

## Ideal MHD instabilities for coronal mass ejections

**Review**

Rony [Keppens](#), [Yang Guo](#), [Kirit Makwana](#), [Zhixing Mei](#), [Bart Ripperda](#), [Chun Xia](#), [Xiaozhou Zhao](#)

Reviews of Modern Plasma Physics **2019**

<https://arxiv.org/pdf/1910.12659.pdf>

We review and discuss insights on ideal magnetohydrodynamic (MHD) instabilities that can play a role in destabilizing solar coronal flux rope structures. For single flux ropes, failed or actual eruptions may result from internal or external kink evolutions, or from torus unstable configurations. We highlight recent findings from 3D magnetic field reconstructions and simulations where kink and torus instabilities play a prominent role.

For interacting current systems, we critically discuss different routes to coronal dynamics and global eruptions, due to current channel coalescence or to tilt-kink scenarios. These scenarios involve the presence of two nearby current channels and are clearly distinct from the popular kink or torus instability. Since the solar corona is pervaded with myriads of magnetic loops -- creating interacting flux ropes typified by parallel or antiparallel current channels as exemplified in various recent observational studies -- coalescence or tilt-kink evolutions must be very common for destabilizing adjacent flux rope systems. Since they also evolve on ideal MHD timescales, they may well drive many sympathetic eruptions witnessed in the solar corona. Moreover, they necessarily lead to thin current sheets that are liable to reconnection. We review findings from 2D and 3D MHD simulations for tilt and coalescence evolutions, as well as on particle acceleration aspects derived from computed charged particle motions in tilt-kink disruptions and coalescing flux ropes. The latter were recently studied in two-way coupled kinetic-fluid models, where the complete phase-space information of reconnection is incorporated. **2002 May 27**

## A Transient Coronal Sigmoid in Active Region NOAA 11909: Build-up Phase, M-class Eruptive Flare, and Associated Fast Coronal Mass Ejection

[Hema Kharavat](#), [Bhuwan Joshi](#), [Prabir K. Mitra](#), [P. K. Manoharan](#) & [Christian Monstein](#)

[Solar Physics](#) volume 296, Article number: 99 (2021)

<https://link.springer.com/content/pdf/10.1007/s11207-021-01830-4.pdf>

<https://doi.org/10.1007/s11207-021-01830-4>



In this article, we investigate the formation and disruption of a coronal sigmoid from the active region (AR) NOAA 11909 on **07 December 2013**, by analyzing multi-wavelength and multi-instrument observations. Our analysis suggests that the formation of the sigmoid initiated  $\approx 1$  hour before its eruption through a coupling between two twisted coronal loop systems. This sigmoid can be well regarded as of ‘transient’ class due to its short lifetime as the eruptive activities started just after  $\approx 20$  min of its formation. A comparison between coronal and photospheric images suggests that the coronal sigmoid was formed over a simple  $\beta\beta$ -type AR which also possessed dispersed magnetic field structure in the photosphere. The line-of-sight photospheric magnetograms also reveal small-scale flux cancellation events near the polarity inversion line, and overall flux cancellation during the extended pre-eruption phase which suggest the role of tether-cutting reconnection toward the build-up of the flux rope. The disruption of the sigmoid proceeded with a two-ribbon eruptive M1.2 flare (SOL2013-12-07T07:29). In radio frequencies, we observe type III and type II bursts in meter wavelengths during the impulsive phase of the flare. The successful eruption of the flux rope leads to a fast coronal mass ejection (with a linear speed of  $\approx 1085$  km s $^{-1}$ ) in SOHO/LASCO field-of-view. During the evolution of the flare, we clearly observe typical “sigmoid-to-arcade” transformation. Prior to the onset of the impulsive phase of the flare, flux rope undergoes a slow rise ( $\approx 15$  km s $^{-1}$ ) which subsequently transitions into a fast eruption ( $\approx 110$  km s $^{-1}$ ). The two-phase evolution of the flux rope shows temporal associations with the soft X-ray precursor and impulsive phase emissions of the M-class flare, respectively, thus pointing toward a feedback relationship between magnetic reconnection and early CME dynamics.

### **Association of solar flares with coronal mass ejections accompanied by Deca-Hectometric type II radio burst for two solar cycles 23 and 24**

Hema [Kharayat](#), Lalan Prasad & Sumit Pant

[Astrophysics and Space Science](#) May 2018, 363:87

<http://sci-hub.tw/10.1007/s10509-018-3309-y>

The aim of present study is to find the association of solar flares with coronal mass ejections (CMEs) accompanied by Deca-Hectometric (DH) type II radio burst for the period 1997–2014 (solar cycle 23 and ascending phase of solar cycle 24). We have used a statistical analysis and found that 10–20° latitudinal belt of northern region and 80–90° longitudinal belts of western region of the sun are more effective for flare-CME accompanied by DH type II radio burst events. M-class flares (52%) are in good association with the CMEs accompanied by DH type II radio burst. Further, we have calculated the flare position and found that most frequent flare site is at the center of the CME span. However, the occurrence probability of all flares is maximum outside the CME span. X-class flare associated CMEs have maximum speed than that of M, C, and B-class flare associated CMEs. We have also found a good correlation between flare position and central position angle of CMEs accompanied by DH type II radio burst.

### **Deciphering the Evolution of Thermodynamic Properties and their Connection to the Global Kinematics of High-Speed Coronal Mass Ejections Using FRIS Model**

[Soumyaranjan Khuntia](#), [Wageesh Mishra](#), [Yuming Wang](#), [Sudheer K Mishra](#), [Teresa Nieves-Chinchilla](#), [Shaoyu Lyu](#)

MNRAS Volume 535, Issue 3, December 2024, Pages 2585–2597,

<https://doi.org/10.1093/mnras/stae2523>

<https://arxiv.org/pdf/2411.03639>

<https://watermark.silverchair.com/stae2523.pdf>

Most earlier studies have been limited to estimating the kinematic evolution of coronal mass ejections (CMEs), and only limited efforts have been made to investigate their thermodynamic evolution. We focus on the interplay of the thermal properties of CMEs with their observed global kinematics. We implement the Flux rope Internal State (FRIS) model to estimate variations in the polytropic index, heating rate per unit mass, temperature, pressure, and various internal forces. The model incorporates inputs of 3D kinematics obtained from the Graduated Cylindrical Shell (GCS) model. In our study, we chose nine fast-speed CMEs from 2010 to 2012. Our investigation elucidates that the selected fast-speed CMEs show a heat-release phase at the beginning, followed by a heat-absorption phase with a near-isothermal state in their later propagation phase. The thermal state transition, from heat release to heat absorption, occurs at around  $3(\pm 0.3)$  to  $7(\pm 0.7)$   $R_{\odot}$  for different CMEs. We found that the CMEs with higher expansion speeds experience a less pronounced sharp temperature decrease before gaining a near-isothermal state. The differential emission measurement (DEM) analysis findings, using multi-wavelength observation from SDO/AIA, also show a heat release state of CMEs at lower coronal heights. We also find the dominant internal forces influencing CME radial expansion at varying distances from the Sun. Our study shows the need to characterize the internal thermodynamic properties of CMEs better in both observational and modeling studies, offering insights for refining assumptions of a constant value of the polytropic index during the evolution of CMEs. **2010 Apr 03, 2011 Feb 15, 2011 Aug 04, 2011 Sep 24, 2011 Nov 26, 2012 Mar 07, 2012 Jun 14, 2012 Jul 12, 2012 Sep 28**

**Table 2.** The list of selected fast CMEs from 2010 to 2012.

### **Unraveling the Thermodynamic Enigma between Fast and Slow Coronal Mass Ejections**

[Soumyaranjan Khuntia](#), [Wageesh Mishra](#), [Sudheer K Mishra](#), [Yuming Wang](#), [Jie Zhang](#), [Shaoyu Lyu](#)

ApJ 958 92 2023

<https://arxiv.org/pdf/2310.06750.pdf>

<https://iopscience.iop.org/article/10.3847/1538-4357/ad00ba/pdf>

Coronal Mass Ejections (CMEs) are the most energetic expulsions of magnetized plasma from the Sun that play a crucial role in space weather dynamics. This study investigates the diverse kinematics and thermodynamic evolution of two CMEs (CME1: **2011 September 24** and CME2: **2018 August 20**) at coronal heights where thermodynamic measurements are limited. The peak 3D propagation speed of CME1 is high (1,885 km/s) with two-phase expansion (rapid and nearly constant), while the peak 3D propagation speed of CME2 is slow (420 km/s) with only a gradual expansion. We estimate the distance-dependent variations in the polytropic index, heating rate, temperature, and internal forces implementing the revised FRIS model, taking inputs of 3D kinematics estimated from the GCS model. We find CME1 exhibiting heat-release during its early-rapid acceleration decrease and jumps to the heat-absorption state during its constant acceleration phase. In contrast to CME1, CME2 shows a gradual transition from the near-adiabatic to the heat-absorption state during its gradually increasing acceleration. Our analysis reveals that although both CMEs show differential heating, they experience heat-absorption during their later propagation phases, approaching the isothermal state. The faster CME1 achieves an adiabatic state followed by an isothermal state at smaller distances from the Sun than the slower CME2. We also find that the expansion of CMEs is primarily influenced by centrifugal and thermal pressure forces, with the Lorentz force impeding expansion. Multi-wavelength observations of flux-ropes at source regions support the FRIS model-derived findings at initially observed lower coronal heights.

## Statistical Analysis of the Relation between Coronal Mass Ejections and Solar Energetic Particles

[Kosuke Kihara](#), [Yuwei Huang](#), [Nobuhiko Nishimura](#), [Nariaki V. Nitta](#), [Seiji Yashiro](#), [Kiyoshi Ichimoto](#), [Ayumi Asai](#)

ApJ 2020

<https://arxiv.org/pdf/2007.08062.pdf> File

To improve the forecasting capability of impactful solar energetic particle (SEP) events, the relation between coronal mass ejections (CMEs) and SEP events needs to be better understood. Here we present a statistical study of SEP occurrences and timescales with respect to the CME source locations and speeds, considering all 257 fast ( $v_{\text{CME}} \geq 900$  km/s) and wide (angular width  $\geq 60^\circ$ ) CMEs that occurred between December 2006 and October 2017. We associate them with SEP events at energies above 10 MeV. Examination of the source region of each CME reveals that CMEs more often accompany a SEP event if they originate from the longitude of E20-W100 relative to the observer. However, a SEP event could still be absent if the CME is  $< 2000$  km/s. For the associated CME-SEP pairs, we compute three timescales for each of the SEP events, following Kahler (2005, 2013); namely the timescale of the onset (TO), the rise time (TR), and the duration (TD). They are correlated with the longitude of the CME source region relative to the footpoint of the Parker spiral ( $\Delta\Phi$ ) and  $v_{\text{CME}}$ . The TO tends to be short for  $|\Delta\Phi| < 60^\circ$ . This trend is weaker for TR and TD. The SEP timescales are only weakly correlated with  $v_{\text{CME}}$ . Positive correlations of both TR and TD with  $v_{\text{CME}}$  are seen in poorly connected (large  $|\Delta\Phi|$ ) events. Additionally, TO appears to be negatively correlated with  $v_{\text{CME}}$  for events with small  $|\Delta\Phi|$ . **3 Sep 2013**

**Table 1.** Properties of Fast and Wide CMEs and Associated SEP Events (2006-2017)

**Table 2.** Timescales of SEP Events

## Temporal and Periodic Variation of the MCMESI for the Last Two Solar Cycles; Comparison with the Number of Different Class X-Ray Solar Flares

A. [Kilcik](#), [P. Chowdhury](#), [V. Sarp](#), [V. Yurchyshyn](#), [B. Donmez](#), [J.P. Rozelot](#), [A. Ozguc](#)

Solar Phys. 2020

<https://arxiv.org/ftp/arxiv/papers/2008/2008.11506.pdf>

In this study we compared the temporal and periodic variations of the Maximum CME Speed Index (MCMESI) and the number of different class (C, M, and X) solar X-Ray flares for the last two solar cycles (Cycle 23 and 24). To obtain the correlation between the MCMESI and solar flare numbers the cross correlation analysis was applied to monthly data sets. Also to investigate the periodic behavior of all data sets the Multi Taper Method (MTM) and the Morlet wavelet analysis method were performed with daily data from 2009 to 2018. To evaluate our wavelet analysis Cross Wavelet Transform (XWT) and Wavelet Transform Coherence (WTC) methods were performed. Causal relationships between datasets were further examined by Convergence Cross Mapping (CCM) method. In results of our analysis we found followings; 1) The C class X-Ray flare numbers increased about 16 % during the solar cycle 24 compared to cycle 23, while all other data sets decreased; the MCMESI decreased about 16 % and the number of M and X class flares decreased about 32 %. 2) All the X-Ray solar flare classes show remarkable positive correlation with the MCMESI. While the correlation between the MCMESI and C class flares comes from the general solar cycle trend, it mainly results from the fluctuations in the data in case of the X class flares. 3) In general, all class flare numbers and the MCMESI show similar periodic behavior. 4) The 546 days periodicity detected in the MCMESI may not be of solar origin or at least the solar flares are not the source of this periodicity. 5) C and M Class solar flares have a stronger causative effect on the MCMESI compared to X class solar flares. However the only bidirectional causal relationship is obtained between the MCMESI and C class flare numbers.

## Maximum CME speed as an indicator of solar and geomagnetic activities

A. [Kilcik](#)1, V.B. Yurchyshyn1, V. Abramenko1, P.R. Goode1, N. Gopalswamy2, A. Ozguc3, J.P. Rozelot4  
BBSO Preprint #1456, 2010; Ap. J. 727:44 (6pp), 2011 January, File

We investigate the relationship between the monthly averaged maximal speeds of coronal mass ejections (CMEs), international sunspot number (ISSN) and the geomagnetic Dst and Ap indices covering the 1996-2008 time interval (solar cycle 23). Our new findings are as follows. i) There is a noteworthy relationship between monthly averaged maximum CME speeds and sunspot numbers, Ap and Dst indices. Various peculiarities in the monthly Dst index are better correlated with the fine structures in the CME speed profile than that in the ISSN data. ii) Unlike the sunspot numbers, the CME speed index does not exhibit a double peak maximum. Instead, the CME speed profile peaks during the declining phase of solar cycle 23. Similar to the Ap index, both CME speed and the Dst indices lag behind the sunspot numbers by several months. iii) CME number shows a double peak similar to that seen in the sunspot numbers. The CME occurrence rate remained very high even near the minimum of the solar cycle 23, when both sunspot number and the CME average maximum speed were reaching their minimum values. iv) A well defined peak of the Ap index between May 2002 and August 2004 was co-temporal with the excess of the mid-latitude coronal holes during solar cycle 23. The above findings suggest that the CME speed index may be a useful indicator of both solar and geomagnetic activity. It may have advantages over the sunspot numbers, because it better reflects the intensity of Earth directed solar eruptions.

## **A Statistical Study of the Relationship Between the Sunspot Number, Maximum CME Speed and Geomagnetic Indices**

A [Kilcik](#), V.B. Yurchyshyn, V. Abramenko, P.R. Goode, N. Gopalswamy, A. Ozguc and J.P. Rozelot  
BBSO Preprint #1424, 2010; **File**

We investigated the relationship between the monthly averaged maximal speeds of coronal mass ejections (CMEs), sunspot number (SSN) and the geomagnetic Dst and Ap indices covering the 1996-2008 time interval. The study was carried out using frequency and correlation analyses. Frequency analysis of the maximum speed of CMEs (or CME speed index) shows a cyclic behavior similar to that found for SSN and the Ap index. Our new findings are as follows. 1) Unlike the SSN, the CME speed index does not exhibit a double peak maximum. 2) The CME speed index has a correlative relationship with SSN and Dst and Ap indices (correlation coefficients are 0.76, -0.53, 0.68 respectively). Various peculiarities in the monthly Dst index are better correlated with the fine structures in the CME speed profile than that in the SSN data. 3) Similar to the Ap index, both CME speed and the Dst indices lag behind the sunspot numbers by several months. We thus conclude that CME speed index may be a good parameter to describe the geoeffectiveness of solar activity.

## **Estimating the Magnetic Structure of an Erupting CME Flux Rope From AR12158 Using Data-Driven Modeling**

[Emilia K. J. Kilpua](#)<sup>\*</sup>, Jens Pomoell, [Daniel Price](#), [Ranadeep Sarkar](#) and [Eleanna Asvestari](#)

Front. Astron. Space Sci., 8:631582. March 2021 |

<https://www.frontiersin.org/articles/10.3389/fspas.2021.631582/full>

<https://doi.org/10.3389/fspas.2021.631582>

We investigate here the magnetic properties of a large-scale magnetic flux rope related to a coronal mass ejection (CME) that erupted from the Sun on **September 12, 2014** and produced a well-defined flux rope in interplanetary space on **September 14–15, 2014**. We apply a fully data-driven and time-dependent magnetofrictional method (TMFM) using Solar Dynamics Observatory (SDO) magnetograms as the lower boundary condition. The simulation self-consistently produces a coherent flux rope and its ejection from the simulation domain. This paper describes the identification of the flux rope from the simulation data and defining its key parameters (e.g., twist and magnetic flux). We define the axial magnetic flux of the flux rope and the magnetic field time series from at the apex and at different distances from the apex of the flux rope. Our analysis shows that TMFM yields axial magnetic flux values that are in agreement with several observational proxies. The extracted magnetic field time series do not match well with in-situ components in direct comparison presumably due to interplanetary evolution and northward propagation of the CME. The study emphasizes also that magnetic field time-series are strongly dependent on how the flux rope is intercepted which presents a challenge for space weather forecasting.

## **Forecasting the Structure and Orientation of Earthbound Coronal Mass Ejections**

E. K. J. [Kilpua](#) [N. Lugaz](#) [L. Mays](#) [M. Temmer](#)

Space Weather 17 **Issue 4** Pages 498-526 2019

Space Weather Quarterly 16, issue 1, 6 -30 2019

[sci-hub.tw/10.1029/2018SW001944](http://sci-hub.tw/10.1029/2018SW001944)

Coronal Mass Ejections (CMEs) are the key drivers of strong to extreme space weather storms at the Earth that can have drastic consequences for technological systems in space and on ground. The ability of a CME to drive geomagnetic disturbances depends crucially on the magnetic structure of the embedded flux rope, which is thus essential to predict. The current capabilities in forecasting in advance (at least half-a-day before) the geoeffectiveness of a given CME is however severely hampered by the lack of remote-sensing measurements of the magnetic field in the corona and adequate tools to predict how CMEs deform, rotate and deflect during their travel through the coronal and interplanetary space as they interact with the ambient solar wind and other CMEs. These problems can lead not only to over- or underestimation of the severity of a storm, but also to forecasting “misses” and “false alarms” that are particularly difficult for the end-users. In this paper, we discuss the current status and future challenges and prospects related to forecasting of the magnetic structure and orientation of CMEs. We focus both on observational and modeling

(first-principle and semi-empirical) based approaches, and discuss the space- and ground-based observations that would be the most optimal for making accurate space weather predictions. We also cover the gaps in our current understanding related to the formation and eruption of the CME flux rope and physical processes that govern its evolution in the variable ambient solar wind background that complicate the forecasting.

## **Solar Sources of Interplanetary Coronal Mass Ejections During the Solar Cycle 23/24 Minimum**

E. K. J. [Kilpua](#), M. Mierla, A. N. Zhukov, L. Rodriguez, A. Vourlidas, B. Wood  
Solar Phys., 2014

We examine solar sources for 20 interplanetary coronal mass ejections (ICMEs) observed in 2009 in the near-Earth solar wind. We performed a detailed analysis of coronagraph and extreme ultraviolet (EUV) observations from the Solar Terrestrial Relations Observatory (STEREO) and Solar and Heliospheric Observatory (SOHO). Our study shows that the coronagraph observations from viewpoints away from the Sun–Earth line are paramount to locate the solar sources of Earth-bound ICMEs during solar minimum. SOHO/LASCO detected only six CMEs in our sample, and only one of these CMEs was wider than  $120^\circ$ . This demonstrates that observing a full or partial halo CME is not necessary to observe the ICME arrival. Although the two STEREO spacecraft had the best possible configuration for observing Earth-bound CMEs in 2009, we failed to find the associated CME for four ICMEs, and identifying the correct CME was not straightforward even for some clear ICMEs. Ten out of 16 (63 %) of the associated CMEs in our study were “stealth” CMEs, i.e. no obvious EUV on-disk activity was associated with them. Most of our stealth CMEs also lacked on-limb EUV signatures. We found that stealth CMEs generally lack the leading bright front in coronagraph images. This is in accordance with previous studies that argued that stealth CMEs form more slowly and at higher coronal altitudes than non-stealth CMEs. We suggest that at solar minimum the slow-rising CMEs do not draw enough coronal plasma around them. These CMEs are hence difficult to discern in the coronagraphic data, even when viewed close to the plane of the sky. The weak ICMEs in our study were related to both intrinsically narrow CMEs and the non-central encounters of larger CMEs. We also demonstrate that narrow CMEs (angular widths  $\leq 20^\circ$ ) can arrive at Earth and that an unstructured CME may result in a flux rope-type ICME.

## **STEREO observations of interplanetary coronal mass ejections and prominence deflection during solar minimum period**

E. K. J. [Kilpua](#)<sup>1</sup>, J. Pomoell<sup>1</sup>, A. Vourlidas<sup>3</sup>, R. Vainio<sup>1</sup>, J. Luhmann<sup>2</sup>, Y. Li<sup>2</sup>, P. Schroeder<sup>2</sup>, A. B. Galvin<sup>4</sup>, and K. Simunac

Ann. Geophys., 27, 4491–4503, 2009, [File](#)

[www.ann-geophys.net/27/4491/2009/](http://www.ann-geophys.net/27/4491/2009/)

In this paper we study the occurrence rate and solar origin of interplanetary coronal mass ejections (ICMEs) using data from the two Solar TERrestrial Relation Observatory (STEREO) and the Wind spacecraft. We perform a statistical survey of ICMEs during the late declining phase of solar cycle 23. Observations by multiple, well-separated spacecraft show that even at the time of extremely weak solar activity a considerable number of ICMEs were present in the interplanetary medium. Soon after the beginning of the STEREO science mission in January 2007 the number of ICMEs declined to less than one ICME per month, but in late 2008 the ICME rate clearly increased at each spacecraft although no apparent increase in the number of coronal mass ejections (CMEs) occurred. We suggest that the near-ecliptic ICME rate can increase due to CMEs that have been guided towards the equator from their high-latitude source regions by the magnetic fields in the polar coronal holes.

We consider two case studies to highlight the effects of the polar magnetic fields and CME deflection taking advantage of STEREO observations when the two spacecraft were in the quadrature configuration (i.e. separated by about 90 degrees). We study in detail the solar and interplanetary consequences of two CMEs that both originated from high-latitude source regions on **2 November 2008**. The first CME was slow (radial speed 298 km/s) and associated with a huge polar crown prominence eruption. The CME was guided by polar coronal hole fields to the equator and it produced a clear flux rope ICME in the near-ecliptic solar wind. The second CME (radial speed 438 km/s) originated from an active region 11007 at latitude  $35^\circ$  N. This CME propagated clearly north of the first CME and no interplanetary consequences were identified. The two case studies suggest that slow and elongated CMEs have difficulties overcoming the straining effect of the overlying field and as a consequence they are guided by the polar coronal fields and cause in-situ effects close to the ecliptic plane. The 3-D propagation directions and CME widths obtained by using the forward modelling technique were consistent with the solar and in-situ observations.

**Table 1.** ICMEs identified from the solar wind measurements by STA (A), STB (B) and Wind (W).

## **Triggering Mechanism for Eruption of Two Filaments Observed by the Solar Dynamics Observatory, Nobeyama Radioheliograph, and RHESSI**

Sujin [Kim](#)<sup>1</sup> and Vasyi Yurchyshyn<sup>2</sup>

2022 ApJL 932 L18

<https://iopscience.iop.org/article/10.3847/2041-8213/ac7236/pdf>

We investigate the eruptive process of two filaments, which is associated with an M-class flare that occurred in **2011 August 4**. The filaments are partly overlapped, one in the active region and the other just beside it, and erupt together as

a halo coronal mass ejection. For this study, we used the Atmospheric Imaging Assembly and the Heliospheric Magnetic Imager on board the Solar Dynamics Observatory, the Nobeyama Radioheliograph 17 GHz, and the RHESSI Hard X-ray satellite. We found three distinct phases in the microwave flux profile and in the rising pattern of the filaments during the event. In the first phase, there was weak nonthermal emission at 17 GHz and hard X-rays. Those nonthermal sources appeared on one edge of the western filament (F2) in the active region. The F2 began to be bright and rose upward rapidly, while the eastern filament (F1), which was extended to the quiet region, started to brighten from the peak time of the 17 GHz flux. In the second phase, the nonthermal emission weakened and the F2 rose up slowly, while the F1 began to rise up. In the third phase, two filaments erupted together. Since the F1 was stable for a long time in the quiet region, breaking the equilibrium state of the F1 would be decisive for the successful eruption of two filaments and it seems clear that the evolution of the F2 provoked the unstable F1. We suggest that tether-cutting reconnection between two overlapped filaments triggers the eruption of the two filaments as a tangled identity.

## **Relation of CME Speed and Magnetic Helicity in CME Source Regions on the Sun during the Early Phase of Solar Cycles 23 and 24**

R.-S. **Kim** S.-H. Park S. Jang K.-S. Cho B. S. Lee

Sol Phys (2017) 292: 66. doi:10.1007/s11207-017-1079-2

To investigate the relations between coronal mass ejection (CME) speed and magnetic field properties measured in the photospheric surface of CME source regions, we selected 22 disk CMEs in the rising and early maximum phases of the current Solar Cycle 24. For the CME speed, we used two-dimensional (2D) projected speed observed by the Large Angle and Spectroscopic Coronagraph onboard the Solar and Heliospheric Observatory (SOHO/LASCO), as well as a 3D speed calculated from the triangulation method using multi-point observations. Two magnetic parameters of CME source regions were considered: the average of magnetic helicity injection rate and the total unsigned magnetic flux. We then classified the selected CMEs into two groups, showing: i) a monotonically increasing pattern with one sign of helicity (group A: 16 CMEs) and ii) a pattern of significant helicity injection followed by its sign reversal (group B: 6 CMEs). We found that: 1) 3D speed generally shows better correlations with the magnetic parameters than the 2D speed for 22 CME events in Solar Cycle 24; 2) 2D speed and the magnetic parameters of 22 CME events in this solar cycle have lower values than those of 47 CME events in Solar Cycle 23; 3) all events of group B in Solar Cycle 24 occur only after the beginning of the maximum phase, a trend well consistent with that shown in Solar Cycle 23; 4) the 2D speed and the helicity parameter of group B events continue to increase in the declining phase of Solar Cycle 23, while those of group A events abruptly decrease in the same period. Our results indicate that the two CME groups have a different tendency in the solar cycle variations of CME speed and the helicity parameters. Active regions that show a complex helicity evolution pattern tend to appear in the maximum and declining phases, while active regions with a relatively simple helicity evolution pattern appear throughout the whole solar cycle.

## **Vertical Kink Oscillation of a Magnetic Flux Rope Structure in the Solar Corona**

S. **Kim**<sup>1</sup>, V. M. Nakariakov<sup>2,3,4</sup>, and K.-S. Cho

2014 *ApJ* 797 L22

Vertical transverse oscillations of a coronal magnetic rope, observed simultaneously in the 171 Å and 304 Å bandpasses of the Atmospheric Imaging Assembly on board the *Solar Dynamics Observatory* (SDO), are detected. The oscillation period is about 700 s and the displacement amplitude is about 1 Mm. The oscillation amplitude remains constant during the observation. Simultaneous observation of the rope in the bandpasses corresponding to the coronal and chromospheric temperatures suggests that it has a multi-thermal structure. Oscillatory patterns in 171 Å and 304 Å are coherent, which indicates that the observed kink oscillation is collective, in which the rope moves as a single entity. We interpret the oscillation as a fundamental standing vertically polarized kink mode of the rope, while the interpretation in terms of a perpendicular fast wave could not be entirely ruled out. In addition, the arcade situated above the rope and seen in the 171 Å bandpass shows an oscillatory motion with the period of about 1000 s.

## **Propagation Characteristics of CMEs Associated with Magnetic Clouds and Ejecta**

R.-S. **Kim**, N. Gopalswamy, K.-S. Cho, Y.-J. Moon, S. Yashiro

Solar Phys., Volume 284, Issue 1, pp 77-88, 2013, **File online first**

We have investigated the characteristics of magnetic cloud (MC) and ejecta (EJ) associated coronal mass ejections (CMEs) based on the assumption that all CMEs have a flux rope structure. For this, we used 54 CMEs and their interplanetary counterparts (interplanetary CMEs: ICMEs) that constitute the list of events used by the NASA/LWS Coordinated Data Analysis Workshop (CDAW) on CME flux ropes. We considered the location, angular width, and speed as well as the direction parameter, *D*. The direction parameter quantifies the degree of asymmetry of the CME shape in coronagraph images, and shows how closely the CME propagation is directed to Earth. For the 54 CDAW events, we found the following properties of the CMEs: i) the average value of *D* for the 23 MCs (0.62) is larger than that for the 31 EJs (0.49), which indicates that the MC-associated CMEs propagate more directly toward the Earth than the EJ-associated CMEs; ii) comparison between the direction parameter and the source location shows that the majority of the MC-associated CMEs are ejected along the radial direction, while many of the EJ-associated CMEs are ejected non-radially; iii) the mean speed of MC-associated CMEs (946 km s<sup>-1</sup>) is faster than that of EJ-associated CMEs (771 km s<sup>-1</sup>). For seven very fast CMEs (≥ 1500 km s<sup>-1</sup>), all CMEs with large *D* (≥ 0.4) are associated with MCs and the CMEs with small *D* are associated with EJs. From the statistical analysis of CME parameters, we found

the superiority of the direction parameter. Based on these results, we suggest that the CME trajectory essentially determines the observed ICME structure.

**Table List of shock-driving ICMEs during Solar Cycle 23 ( $E15^\circ \leq l \leq W15^\circ$ ).**

## **MAGNETIC FIELD STRENGTH IN THE UPPER SOLAR CORONA USING WHITE-LIGHT SHOCK STRUCTURES SURROUNDING CORONAL MASS EJECTIONS**

R.-S. **Kim**<sup>1,3</sup>, N. Gopalswamy<sup>1,3</sup>, Y.-J. Moon<sup>2</sup>, K.-S. Cho<sup>1,3,4</sup> and S. Yashiro

2012 ApJ 746 118, **File**

To measure the magnetic field strength in the solar corona, we examined 10 fast ( $\geq 1000$  km s<sup>-1</sup>) limb coronal mass ejections (CMEs) that show clear shock structures in Solar and Heliospheric Observatory/Large Angle and Spectrometric Coronagraph images. By applying the piston-shock relationship to the observed CME's standoff distance and electron density compression ratio, we estimated the Mach number, Alfvén speed, and magnetic field strength in the height range 3-15 solar radii ( $R_s$ ). The main results from this study are as follows: (1) the standoff distance observed in the solar corona is consistent with those from a magnetohydrodynamic model and near-Earth observations; (2) the Mach number as a shock strength is in the range 1.49-3.43 from the standoff distance ratio, but when we use the density compression ratio, the Mach number is in the range 1.47-1.90, implying that the measured density compression ratio is likely to be underestimated owing to observational limits; (3) the Alfvén speed ranges from 259 to 982 km s<sup>-1</sup> and the magnetic field strength is in the range 6-105 mG when the standoff distance is used; (4) if we multiply the density compression ratio by a factor of two, the Alfvén speeds and the magnetic field strengths are consistent in both methods; and (5) the magnetic field strengths derived from the shock parameters are similar to those of empirical models and previous estimates

## **A STUDY OF FLARE-ASSOCIATED X-RAY PLASMA EJECTIONS.**

### **I. ASSOCIATION WITH CORONAL MASS EJECTIONS**

Yeon-Han **Kim**<sup>1</sup>, 2 Y.-J. Moon<sup>1</sup> K.-S. Cho<sup>1</sup> Kap-Sung Kim<sup>2</sup> and Y. D. Park

ApJ 622 :1240–1250, 2005 **File**

We have made a comprehensive statistical study of the relationship between flare-associated X-ray plasma ejections and coronal mass ejections (CMEs). For this we considered all flare-mode data in Yohkoh SXT observations from 1999 April to 2001 March and then selected 279 limb flares seen at longitudes greater than 60°. For these events, we identified whether there were associated X-ray plasma ejections or not. We found that about half (137=279) of the flares have X-ray plasma ejections, and we present a comprehensive list of these with their event times and speeds. We then determined whether there was an association between the flares with plasma ejections and CMEs detected by the Solar and Heliospheric Observatory LASCO instrument, on the basis of temporal and spatial proximity. It is found that about 69% (95=137) of the X-ray plasma ejections are associated with CMEs and that about 84% (119=142) of the events without plasma ejections do not have related CMEs. The associations are found to increase with flare strength and duration. We find that X-ray plasma ejections occur nearly simultaneously with the hard X-ray flare peak, supporting the idea that the X-ray plasma ejections are tightly associated with the flaring process. When the CMEs are extrapolated into the Yohkoh field of view for 43 selected, well-observed events, it is found that about 80% of the CMEs preceded X-ray plasma ejections, by approximately 20 minutes on average. Our results show that X-ray plasma ejections usually do not represent the early signature of a CME's leading edge but are closely associated with CMEs. **1999 May 7, 1999 July 25, 2000 October 26, 2001 March 21**  
**TABLE 1 Observation Summary: 137 X-Ray Plasma Ejections and Associated Phenomena**

## **Relationships Between Sequential Chromospheric Brightening and the Corona **Review****

Michael S. **Kirk**, K. S. Balasubramaniam, Jason Jackiewicz, Holly R. Gilbert

Proceedings IAU Symposium No. xxx, 2017

<https://arxiv.org/pdf/1704.03835.pdf>

The chromosphere is a complex region that acts as an intermediary between the magnetic flux emergence in the photosphere and the magnetic features seen in the corona. Large eruptions in the chromosphere of flares and filaments are often accompanied by ejections of coronal mass off the sun. Several studies have observed fast-moving progressive trains of compact bright points (called Sequential Chromospheric Brightenings or SCBs) streaming away from chromospheric flares that also produce a coronal mass ejection (CME). In this work, we review studies of SCBs and search for commonalities between them. We place these findings into a larger context with contemporary chromospheric and coronal observations. SCBs are fleeting indicators of the solar atmospheric environment as it existed before their associated eruption. Since they appear at the very outset of a flare eruption, SCBs are good early indication of a CME measured in the chromosphere. **2010-11-06,**

**Table 1. A summary of the events used to investigate the evolution of SCBs.**

## **The Origin of Sequential Chromospheric Brightenings**

Michael S. **Kirk**, K.S. Balasubramaniam, Jason Jackiewicz, Holly R. Gilbert

Solar Phys. 2017

<https://arxiv.org/pdf/1704.03828.pdf>

Sequential chromospheric brightenings (SCBs) are often observed in the immediate vicinity of erupting flares and are associated with coronal mass ejections. Since their initial discovery in 2005, there have been several subsequent investigations of SCBs. These studies have used differing detection and analysis techniques, making it difficult to compare results between studies. This work employs the automated detection algorithm of Kirk et al. (Solar Phys. 283, 97, 2013) to extract the physical characteristics of SCBs in 11 flares of varying size and intensity. We demonstrate that the magnetic substructure within the SCB appears to have a significantly smaller area than the corresponding H-alpha emission. We conclude that SCBs originate in the lower corona around 0.1 R\_sun above the photosphere, propagate away from the flare center at speeds of 35 - 85 km/s, and have peak photosphere magnetic intensities of 148 +/- 2.9 G. In light of these measurements, we infer SCBs to be distinctive chromospheric signatures of erupting coronal mass ejections. 19 December 2002, 6 November 2010

**Table 1.** The events used in this work to investigate the automated identification and tracking of SCBs and are ribbons.

## Combining STEREO SECCHI COR2 and HI1 images for automatic CME front edge tracking

Vladimir [Kirnosov](#)<sup>1\*</sup>, Lin-Ching Chang<sup>1</sup> and Antti Pulkkinen

J. Space Weather Space Clim., 6, A41 (2016)

<http://www.swsc-journal.org/articles/swsc/pdf/2016/01/swsc150079.pdf>

COR2 coronagraph images are the most commonly used data for coronal mass ejection (CME) analysis among the various types of data provided by the STEREO (Solar Terrestrial Relations Observatory) SECCHI (Sun-Earth Connection Coronal and Heliospheric Investigation) suite of instruments. The field of view (FOV) in COR2 images covers 2–15 solar radii (Rs) that allow for tracking the front edge of a CME in its initial stage to forecast the lead-time of a CME and its chances of reaching the Earth. However, estimating the lead-time of a CME using COR2 images gives a larger lead-time, which may be associated with greater uncertainty. To reduce this uncertainty, CME front edge tracking should be continued beyond the FOV of COR2 images. Therefore, heliospheric imager (HI1) data that covers 15–90 Rs FOV must be included. In this paper, we propose a novel automatic method that takes both COR2 and HI1 images into account and combine the results to track the front edges of a CME continuously. The method consists of two modules: pre-processing and tracking. The pre-processing module produces a set of segmented images, which contain the signature of a CME, for both COR2 and HI1 separately. In addition, the HI1 images are resized and padded, so that the center of the Sun is the central coordinate of the resized HI1 images. The resulting COR2 and HI1 image set is then fed into the tracking module to estimate the position angle (PA) and track the front edge of a CME. The detected front edge is then used to produce a height-time profile that is used to estimate the speed of a CME. The method was validated using 15 CME events observed in the period from January 1, 2008 to August 31, 2009. The results demonstrate that the proposed method is effective for CME front edge tracking in both COR2 and HI1 images. Using this method, the CME front edge can now be tracked automatically and continuously in a much larger range, i.e., from 2 to 90 Rs, for the first time. These improvements can greatly help in making the quantitative CME analysis more accurate and have the potential to assist in space weather forecasting. **2008.04.26-27**

**Table 1.** The selected CME events used for the validation. 2008.02 – 2009.08

## Automatic CME front edge detection from STEREO white-light coronagraph images

### Authors

Vladimir [Kirnosov](#), Lin-Ching Chang, Antti Pulkkinen

Space Weather Volume 13, Issue 8 August 2015 Pages 469–483

The coronagraph images captured by a Solar Terrestrial Relations Observatory (STEREO) Ahead/Behind (A/B) spacecraft allow tracking of a coronal mass ejection (CME) from two different viewpoints and reconstructing its propagation in three-dimensional space. The reconstruction can be done using a triangulation technique that requires a CME front edge location. There are currently no robust automatic CME front edge detection methods that can be integrated with the triangulation technique. In this paper, we propose a novel automatic method to detect the front edge of the CME using STEREO coronagraph 2 red-colored Red, Green, Blue color model images. Our method consists of two modules: preprocessing and classification. The preprocessing module decomposes each coronagraph image into its three channels and uses only the red channel image for CME segmentation. The output of the preprocessing module is a set of segmented running-difference binary images which is fed into the classification module. These images are then transformed into polar coordinates followed by CME front edge detection based on the distance that CME travels in the field of view. The proposed method was validated against a manual method using total 56 CME events, 28 from STEREO A and 28 from STEREO B, captured in the period from 1 January 2008 to 16 August 2009. The results show that the proposed method is effective for CME front edge detection. The proposed method is useful in quantitative CME processing and analysis and will be immediately applicable to assist automatic triangulation method for real-time space weather forecasting.

## Spectro-Polarimetric Properties of Small-Scale Plasma Eruptions Driven by Magnetic Vortex Tubes

Irina N. [Kitiashvili](#)

PASJ, 2014

<http://arxiv.org/pdf/1407.2295v1.pdf>

Highly turbulent nature of convection on the Sun causes strong multi-scale interaction of subsurface layers with the photosphere and chromosphere. According to realistic 3D radiative MHD numerical simulations ubiquitous small-scale vortex tubes are generated by turbulent flows below the visible surface and concentrated in the intergranular lanes. The vortex tubes can capture and amplify magnetic field, penetrate into chromospheric layers and initiate quasi-periodic flow eruptions that generates Alfvénic waves, transport mass and energy into the solar atmosphere. The simulations revealed high-speed flow patterns, and complicated thermodynamic and magnetic structures in the erupting vortex tubes. The spontaneous eruptions are initiated and driven by strong pressure gradients in the near-surface layers, and accelerated by the Lorentz force in the low chromosphere. In this paper, the simulation data are used to further investigate the dynamics of the eruptions, their spectro-polarimetric characteristics for the Fe I 6301.5 and 6302.5 Å spectral lines, and demonstrate expected signatures of the eruptions in the Hinode SP data. We found that the complex dynamical structure of vortex tubes (downflows in the vortex core and upflows on periphery) can be captured by the Stokes I profiles. During an eruption, the ratio of down and upflows can suddenly change, and this effect can be observed in the Stokes V profile. Also, during the eruption the linear polarization signal increases, and this also can be detected with Hinode SP.

#### **4π Models of CMEs and ICMEs** A Review

Jens [Kleimann](#)

E-print, 11 Apr 2012; Solar Phys., November 2012, Volume 281, Issue 1, pp 353-367; **File**

Coronal mass ejections (CMEs), which dynamically connect the solar surface to the far reaches of interplanetary space, represent a major manifestation of solar activity. They are not only of principal interest but also play a pivotal role in the context of space weather predictions. The steady improvement of both numerical methods and computational resources during recent years has allowed for the creation of increasingly realistic models of interplanetary CMEs (ICMEs), which can now be compared to high-quality observational data from various space-bound missions. This review discusses existing models of CMEs, characterizing them by scientific aim and scope, CME initiation method, and physical effects included, thereby stressing the importance of fully 3-D (‘4π’) spatial coverage.

#### **Non-thermal electrons in an eruptive solar event: Magnetic structure, confinement, and escape into the heliosphere**

Karl-Ludwig [Klein](#)<sup>1,2,\*</sup>, Carolina Salas Matamoros<sup>3,\*</sup>, Abdallah Hamini<sup>1,2</sup> and Alexander Kollhoff<sup>4,\*</sup>  
A&A, 690, A382 (2024)

<https://doi.org/10.1051/0004-6361/202450456>

<https://www.aanda.org/articles/aa/pdf/2024/10/aa50456-24.pdf>

Context. Filament eruptions and coronal mass ejections (CMEs) reveal large-scale instabilities of magnetic structures in the solar corona. Some of them are accompanied by radio emission, which at decimetric and longer wavelengths is a signature of electron acceleration that may be different from the acceleration in impulsive flares. The radio emission is part of the broadband continua at decimetre and metre wavelengths called type IV bursts.

Aims. In this article we investigate a particularly well-observed combination of a filament eruption seen in H $\alpha$  and at extreme ultraviolet (EUV) wavelengths and a moving type IV burst on **2021 August 24**. The aim is to shed light on the relationship between the large-scale erupting magnetic structure and the acceleration and transport of non-thermal electrons.

Methods. We used imaging observations of a moving radio source and associated burst groups with the refurbished Nançay Radioheliograph and whole-Sun radio spectrography from different ground-based and space-borne instruments, in combination with X-ray, radio, and in situ electron observations at tens of keV from Solar Orbiter and EUV imaging by SDO/AIA. The radio sources are located with respect to the erupting magnetic structure traced by the filament (EUV 30.4 nm), and the timing of the electrons detected in situ is compared with the timing of the different radio emissions.

Results. We find that the moving radio source is located at the top of the erupting magnetic structure outlined by the filament, which we interpret as a magnetic flux rope. The flux rope erupts in a strongly non-radial direction, guided by the overlying magnetic field of a coronal hole. The electrons detected at Solar Orbiter are found to be released mainly in two episodes, 10–40 minutes after the impulsive phase. The releases coincide with two groups of radio bursts, which originate respectively on the flank and near the top of the erupting flux rope.

Conclusions. The observation allows an unusually clear association between a moving type IV radio burst, an erupting magnetic flux rope as core structure of a CME, and particle releases into the heliosphere. Non-thermal electrons are confined in the flux rope. Electrons escape to the heliosphere mainly in two distinct episodes, which we relate to magnetic reconnection between the flux rope and ambient open field lines.

#### **Eruptive Activity Related to Solar Energetic Particle Events** Review

Karl-Ludwig [Klein](#)

In: O.E. Malandraki, N.B. Crosby (eds.), Solar Particle Radiation Storms Forecasting and Analysis Chapter 2, 2018

<https://link.springer.com/content/pdf/10.1007%2F978-3-319-60051-2.pdf>

**File** Malandraki\_Crosby\_SEPs\_Forecasting and Analysis\_Book.pdf



Solar energetic particle events are associated with solar activity, especially flares and coronal mass ejections (CMEs). In this chapter a basic introduction is presented to the nature of flares and CMEs. Since both are manifestations of evolving magnetic fields in the solar corona, the chapter starts with a qualitative description of the magnetic structuring and electrodynamic coupling of the solar atmosphere. Flares and the radiative manifestations of energetic particles, i.e. bremsstrahlung, gyrosynchrotron and collective plasma emission of electrons, and nuclear gamma-ray emission are briefly presented. Observational evidence on the particle acceleration region in flares is given, as well as a very elementary qualitative overview of acceleration processes. Then CMEs, their origin and their association with shock waves are discussed, and related particle acceleration processes are briefly described.

## **The High Energy Solar Corona: Waves, Eruptions, Particles**

**Book**

Karl-Ludwig **Klein**, Alexander L. MacKinnon (Eds.)

[Lecture Notes in Physics](#) (LNP), volume 725, 2007

<https://link.springer.com/book/10.1007%2F978-3-540-71570-2>

## **The fast filament eruption leading to the X-flare on March 29, 2014**

Lucia **Kleint**, Marina Battaglia, Kevin Reardon, Alberto Sainz Dalda, Peter R. Young, Säm Krucker

ApJ **806** 9 2015

<http://arxiv.org/pdf/1504.00515v1.pdf>

We investigate the sequence of events leading to the solar X1 flare SOL2014-03-29T17:48. Because of the unprecedented joint observations of an X-flare with the ground-based Dunn Solar Telescope and the spacecraft IRIS, Hinode, RHESSI, STEREO, and SDO, we can sample many solar layers from the photosphere to the corona. A filament eruption was observed above a region of previous flux emergence, which possibly led to a change in magnetic field configuration, causing the X-flare. This was concluded from the timing and location of the hard X-ray emission, which started to increase slightly less than a minute after the filament accelerated. The filament showed Doppler velocities of  $\sim 2\text{--}5\text{ km s}^{-1}$  at chromospheric temperatures for at least one hour before the flare occurred, mostly blueshifts, but also redshifts near its footpoints. 15 minutes before the flare, its chromospheric Doppler shifts increased to  $\sim 6\text{--}10\text{ km s}^{-1}$  and plasma heating could be observed, before it lifted off with at least  $600\text{ km s}^{-1}$ , as seen in IRIS data. Compared to previous studies, this acceleration ( $\sim 3\text{--}5\text{ km s}^{-2}$ ) is very fast, while the velocities are in the common range for coronal mass ejections. An interesting feature was a low-lying twisted second filament near the erupting filament, which did not seem to participate in the eruption. After the flare ribbons started on each of the second filament's sides, it seems to have untangled and vanished during the flare. These observations are some of the highest resolution data of an X-class flare to date and reveal some small-scale features yet to be explained.

## **Flux Ropes as Singularities of the Vector Potential**

M. **Kleman**

Solar Phys. Volume 290, [Issue 3](#), pp 707-725 2015

A flux rope is a domain where a twisted magnetic field  $[B]$  is concentrated; it can be described as the core of a singularity of the outer field or the outer vector potential  $[A]$  (Kleman and Robbins in Solar Phys. 289, 1173, 2014). This latter case, occurring when the outer field is vanishing, is mathematically analysed for a straight infinite rope. Concepts from condensed-matter physics defect theory are used: the flux  $[\Phi]$ , measured as  $\oint C A \cdot ds$  along any loop  $[C]$  surrounding the rope, is a topological constant of the theory. A flux rope with a small outer magnetic field can be treated as a perturbation of the above. This theoretical framework allows for the use of classical configurations inside the core, e.g. the linear force-free field (LFFF) Lundquist model or the nonlinear (NLFFF) Gold-Hoyle model, but restricts the number of stable solutions: they are quantised into strata of increasing energies (an infinite number of strata in the first case, only one stratum in the second case); each stratum is defined by a number  $2\pi\zeta = b/r_0$ , where  $b$  is the periodicity along the axis of the rope and  $r_0$  is its radius, and the rope is made of a continuous set of stable states. We also analyse the merging of identical flux ropes (belonging to the same stratum), with conservation of the relative magnetic helicity: they merge into a unique rope of the first stratum, with a considerable release of energy. These results might apply to ropes that nucleate in the convection zone and the photosphere, where the magnetic field outside the ropes is weak, and less accurately to the magnetic clouds (MCs) into which they evolve after coronal mass ejections (CMEs) are triggered. However, the lowest LFFF stratum and the unique NLFFF stratum, which numerically come close to each other in this analysis, match the spacecraft data remarkably well.

## **Helicity shedding by flux rope ejection**

[B. Kliem](#), [N. Seehafer](#)

A&A 659, A49 2021

<https://arxiv.org/pdf/2112.05833.pdf>

<https://www.aanda.org/articles/aa/pdf/2022/03/aa42422-21.pdf>

We quantitatively address the conjecture that magnetic helicity must be shed from the Sun by eruptions launching coronal mass ejections in order to limit its accumulation in each hemisphere. By varying the ratio of guide and strapping field and the flux rope twist in a parametric simulation study of flux rope ejection from approximately marginally stable force-free equilibria, different ratios of self- and mutual helicity are set and the onset of the torus or helical kink instability is obtained. The helicity shed is found to vary over a broad range from a minor to a major part of the initial

helicity, with self helicity being largely or completely shed and mutual helicity, which makes up the larger part of the initial helicity, being shed only partly. Torus-unstable configurations with subcritical twist and without a guide field shed up to about two-thirds of the initial helicity, while a highly twisted, kink-unstable configuration sheds only about one-quarter. The parametric study also yields stable force-free flux rope equilibria up to a total flux-normalized helicity of 0.25, with a ratio of self- to total helicity of 0.32 and a ratio of flux rope to external poloidal flux of 0.94. These results numerically demonstrate the conjecture of helicity shedding by coronal mass ejections and provide a first account of its parametric dependence. Both self- and mutual helicity are shed significantly; this reduces the total initial helicity by a fraction of  $\sim 0.4$ – $0.65$  for typical source region parameters.

## **Flux Rope Formation by a Confined Solar Flare Preceding a Coronal Mass Ejection**

Bernhard Kliem, Jeongwoo Lee, Stephen M. White, Chang Liu, Satoshi Masuda

ApJ 909 91 2021

<https://arxiv.org/pdf/2101.02181.pdf> File

<https://doi.org/10.3847/1538-4357/abda37>

We present evidence that a magnetic flux rope, observed as an extreme-ultraviolet (EUV) hot channel, was formed before a coronal mass ejection (CME) and its associated long-duration flare during a preceding confined flare in a compound event. EUV images, microwave maps, and the extrapolated field show that the first, impulsive flare, SOL2015-06-21T01:42, results from the eruption of highly sheared low-lying flux and remains confined. Nevertheless, it spawns a vertical current sheet, where magnetic reconnection creates flare ribbons and loops, a nonthermal microwave source, and a sigmoidal hot channel. Until the second flare, SOL2015-06-21T02:36, magnetic reconnection continues at a lower rate and the sigmoid's elbows expand, while its center remains stationary under the erupted, still confined flux. The reconnection during and after the confined flare acts like "tether-cutting reconnection", leading the region to instability. The subsequent full eruption is seen as an accelerated rise of the entire hot channel, a fast halo CME, and the second, long-duration flare. The hot channel can only be interpreted as a magnetic flux rope. This event provides one of the clearest cases so far showing the formation of a flux rope prior to the onset of a CME. It demonstrates that flux ropes are formed or enhanced by confined eruptions that trigger reconnection in a vertical (flare) current sheet. This implies that a flux rope exists prior to a large fraction of all CMEs, those that are preceded by such confined eruptions.

## **II. A Double Flux Rope Model**

Bernhard Kliem, Tibor Török, Viacheslav S. Titov, Roberto Lionello, Jon A. Linker, Rui Liu, Chang Liu, Haimin Wang

ApJ, 792 107 2014

<http://arxiv.org/pdf/1407.2272v1.pdf>

Force-free equilibria containing two vertically arranged magnetic flux ropes of like chirality and current direction are considered as a model for split filaments/prominences and filament-sigmoid systems. Such equilibria are constructed analytically through an extension of the methods developed in Titov & Démoulin (1999) and numerically through an evolutionary sequence including shear flows, flux emergence, and flux cancellation in the photospheric boundary. It is demonstrated that the analytical equilibria are stable if an external toroidal (shear) field component exceeding a threshold value is included. If this component decreases sufficiently, then both flux ropes turn unstable for conditions typical of solar active regions, with the lower rope typically being unstable first. Either both flux ropes erupt upward, or only the upper rope erupts while the lower rope reconnects with the ambient flux low in the corona and is destroyed. However, for shear field strengths staying somewhat above the threshold value, the configuration also admits evolutions which lead to partial eruptions with only the upper flux rope becoming unstable and the lower one remaining in place. This can be triggered by a transfer of flux and current from the lower to the upper rope, as suggested by the observations of a split filament in Paper-I (Liu et al. 2012). It can also result from tether-cutting reconnection with the ambient flux at the X-type structure between the flux ropes, which similarly influences their stability properties in opposite ways. This is demonstrated for the numerically constructed equilibrium.

## **Catastrophe versus instability for the eruption of a toroidal solar magnetic flux rope**

B. Kliem, J. Lin, T. G. Forbes, E. R. Priest, T. Török

ApJ, 789 46, 2014

<http://arxiv.org/pdf/1404.5922v1.pdf>

The onset of a solar eruption is formulated here as either a magnetic catastrophe or as an instability. Both start with the same equation of force balance governing the underlying equilibria. Using a toroidal flux rope in an external bipolar or quadrupolar field as a model for the current-carrying flux, we demonstrate the occurrence of a fold catastrophe by loss of equilibrium for several representative evolutionary sequences in the stable domain of parameter space. We verify that this catastrophe and the torus instability occur at the same point; they are thus equivalent descriptions for the onset condition of solar eruptions.

## **Magnetohydrodynamic Modeling of the Solar Eruption on 2010 April 8**

B. Kliem<sup>1,2,3,4</sup>, Y. N. Su<sup>5</sup>, A. A. van Ballegoijen<sup>5</sup>, and E. E. DeLuca

2013 ApJ 779 129

<http://arxiv.org/abs/1304.6981>

The structure of the coronal magnetic field prior to eruptive processes and the conditions for the onset of eruption are important issues that can be addressed through studying the magnetohydrodynamic (MHD) stability and evolution of nonlinear force-free field (NLFFF) models. This paper uses data-constrained NLFFF models of a solar active region (AR) that erupted on **2010 April 8** as initial conditions in MHD simulations. These models, constructed with the techniques of flux rope insertion and magnetofrictional relaxation (MFR), include a stable, an approximately marginally stable, and an unstable configuration. The simulations confirm previous related results of MFR runs, particularly that stable flux rope equilibria represent key features of the observed pre-eruption coronal structure very well, and that there is a limiting value of the axial flux in the rope for the existence of stable NLFFF equilibria. The specific limiting value is located within a tighter range, due to the sharper discrimination between stability and instability by the MHD description. The MHD treatment of the eruptive configuration yields a very good agreement with a number of observed features, like the strongly inclined initial rise path and the close temporal association between the coronal mass ejection and the onset of flare reconnection. Minor differences occur in the velocity of flare ribbon expansion and in the further evolution of the inclination; these can be eliminated through refined simulations. We suggest that the slingshot effect of horizontally bent flux in the source region of eruptions can contribute significantly to the inclination of the rise direction. Finally, we demonstrate that the onset criterion, formulated in terms of a threshold value for the axial flux in the rope, corresponds very well to the threshold of the torus instability in the considered AR.

### **A Parametric Study of Erupting Flux Rope Rotation**

B. Kliem, T. Török, W. T. Thompson

Solar Physics, November **2012**, Volume 281, Issue 1, pp 137-166

The rotation of erupting filaments in the solar corona is addressed through a parametric simulation study of unstable, rotating flux ropes in bipolar force-free initial equilibrium. The Lorentz force due to the external shear-field component and the relaxation of tension in the twisted field are the major contributors to the rotation in this model, while reconnection with the ambient field is of minor importance, due to the field's simple structure. In the low-beta corona, the rotation is not guided by the changing orientation of the vertical field component's polarity inversion line with height. The model yields strong initial rotations which saturate in the corona and differ qualitatively from the profile of rotation vs. height obtained in a recent simulation of an eruption without preexisting flux rope. Both major mechanisms writhe the flux rope axis, converting part of the initial twist helicity, and produce rotation profiles which, to a large part, are very similar within a range of shear-twist combinations. A difference lies in the tendency of twist-driven rotation to saturate at lower heights than shear-driven rotation. For parameters characteristic of the source regions of erupting filaments and coronal mass ejections, the shear field is found to be the dominant origin of rotations in the corona and to be required if the rotation reaches angles of order 90 degrees and higher; it dominates even if the twist exceeds the threshold of the helical kink instability. The contributions by shear and twist to the total rotation can be disentangled in the analysis of observations if the rotation and rise profiles are simultaneously compared with model calculations. The resulting twist estimate allows one to judge whether the helical kink instability occurred. This is demonstrated for the erupting prominence in the "Cartwheel CME" on **9 April 2008**, which has shown a rotation of  $\approx 115^\circ$  up to a height of  $1.5 R_\odot$  above the photosphere. Out of a range of initial equilibria which include strongly kink-unstable (twist  $\Phi=5\pi$ ), weakly kink-unstable ( $\Phi=3.5\pi$ ), and kink-stable ( $\Phi=2.5\pi$ ) configurations, only the evolution of the weakly kink-unstable flux rope matches the observations in their entirety.

### **Rapid Cavity Formation and Expansion in CMEs**

Bernhard Kliem, Terry G. Forbes, Spiros Patsourakos, Angelos Vourlidas

UKSP Nugget, Feb **2012**

<http://www.uksolphys.org/?p=4161>

EUV cavities in fast CMEs are due to an inverse pinch effect.

**2011-03-08**

### **Simulations of the CME-Flare Relationship**

Kliem, B.1; Török, T.2

Freiburg ESP Meeting **2008**, Presentation

Observations of coronal mass ejections (CMEs) and solar flares have revealed a high correlation between the acceleration of the ejecta and the plasma heating and particle acceleration signified by the soft and hard X-ray emissions of the associated flare. The latter are generally thought to result from magnetic reconnection. This finding has stimulated the discussion of the CME-flare relationship, but at the same time it has made it difficult to find a conclusive answer as to whether magnetic reconnection or an ideal MHD instability is the prime cause of the eruptions. Numerical simulations of unstable flux ropes will be presented that are in very satisfactory quantitative agreement with erupting filaments, both, confined to the corona and ejective (i.e., developing into a CME). Some of these simulations indeed show a high degree of synchronization between the initial exponential acceleration of the flux rope, due to the ideal MHD instability, and the development of reconnection flows. However, others show a very delayed onset of reconnection, even after the flux rope's acceleration peak. In addition, the reconnection flows generally lag behind the

motions driven by the ideal instability as the flux rope rise velocity nears the saturation phase. Both findings indicate that the ideal MHD process is the primary driver of the coupled CME-flare phenomenon. The strong differences in the degree of synchronization, which the simulated systems show in the main rise phase of the eruption, are related to the magnetic topology prior to the eruption. Given the observational result of a high correlation between CME and flare development (Zhang & Dere 2006), these simulations yield constraints on the topology and lead us to conclude that a seed for a reconnecting current sheet must typically be present already at the onset of the eruption.

## **The Rise and Emergence of Untwisted Toroidal Flux Ropes on the Sun**

K. J. [Knizhnik](#)<sup>1</sup>, J. E. Leake<sup>2</sup>, M. G. Linton<sup>1</sup>, and S. Dacie<sup>3</sup>

2021 ApJ 907 19

<https://doi.org/10.3847/1538-4357/abccc0>

Magnetic flux ropes (MFRs) rising buoyantly through the Sun's convection zone are thought to be subject to viscous forces preventing them from rising coherently. Numerous studies have suggested that MFRs require a minimum twist in order to remain coherent during their rise. Furthermore, even MFRs that get to the photosphere may be unable to successfully emerge into the corona unless they are at least moderately twisted, since the magnetic pressure gradient needs to overcome the weight of the photospheric plasma. To date, however, no lower limit has been placed on the critical minimum twist required for an MFR to rise coherently through the convection zone or emerge through the photosphere. In this paper, we simulate an untwisted toroidal MFR that is able to rise from the convection zone and emerge through the photosphere as an active region that resembles those observed on the Sun. We show that untwisted MFRs can remain coherent during their rise and then pile up near the photosphere, triggering undular instability, allowing the MFR to emerge through the photosphere. We propose that the toroidal geometry of our MFR is critical for its coherent rise. Upon emergence, a pair of lobes rises into the corona. The two lobes then interact and reconnect, resulting in a localized high speed jet. The resulting photospheric magnetogram displays the characteristic salt-and-pepper structure often seen in observations. Our major result is that MFRs need not be twisted to rise coherently through the convection zone and emerge through the photosphere.

## **The Mechanism for the Energy Buildup Driving Solar Eruptive Events**

Kalman J. [Knizhnik](#), [Spiro K. Antiochos](#), [C. Richard DeVore](#), [Peter F. Wyper](#)

ApJL 851 L17 2017

<https://arxiv.org/ftp/arxiv/papers/1711/1711.00166.pdf>

The underlying origin of solar eruptive events (SEEs), ranging from giant coronal mass ejections to small coronal-hole jets, is that the lowest-lying magnetic flux in the Sun's corona undergoes the continual buildup of stress and free energy. This magnetic stress has long been observed as the phenomenon of "filament channels:" strongly sheared magnetic field localized around photospheric polarity inversion lines. However, the mechanism for the stress buildup - the formation of filament channels - is still debated. We present magnetohydrodynamic simulations of a coronal volume that is driven by transient, cellular boundary flows designed to model the processes by which the photosphere drives the corona. The key feature of our simulations is that they accurately preserve magnetic helicity, the topological quantity that is conserved even in the presence of ubiquitous magnetic reconnection. Although small-scale random stress is injected everywhere at the photosphere, driving stochastic reconnection throughout the corona, the net result of the magnetic evolution is a coherent shearing of the lowest-lying field lines. This highly counter-intuitive result - magnetic stress builds up locally rather than spreading out to attain a minimum energy state - explains the formation of filament channels and is the fundamental mechanism underlying SEEs. Furthermore, this mechanism may be relevant to other astrophysical or laboratory plasmas.

## **Modeling UV and X-Ray Emission in a Post-CME Current Sheet**

Yuan-Kuen [Ko](#), John C. Raymond<sup>2</sup>, Bojan Vr̃snak<sup>3</sup>, Eugen Vujić

E-print, 12 Aug 2010, ApJ, 722:625–641, 2010, [File](#)

A post-coronal mass ejection (CME) current sheet (CS) is a common feature developed behind an erupting flux rope in CME models. Observationally, white light observations have recorded many occurrences of a thin ray appearing behind a CME eruption that closely resembles a post-CME CS in its spatial correspondence and morphology. UV and X-ray observations further strengthen this interpretation by the observations of high-temperature emission at locations consistent with model predictions. The next question then becomes whether the properties inside a post-CME CS predicted by a model agree with observed properties. In this work, we assume that the post-CME CS is a consequence of Petschek-like reconnection and that the observed ray-like structure is bounded by a pair of slow mode shocks developed from the reconnection site. We perform time-dependent ionization calculations and model the UV line emission. We find that such a model is consistent with *SOHO*/UVCS observations of the post-CME CS. The change of Fe xviii emission in one event implies an inflow speed of  $\sim 10$  km s<sup>-1</sup> and a corresponding reconnection rate of  $M_A \sim 0.01$ . We calculate the expected X-ray emission for comparison with X-ray observations by *Hinode*/XRT, as well as the ionic charge states as would be measured in situ at 1 AU. We find that the predicted

count rate for *Hinode*/XRT agrees with what was observed in a post-CME CS on **2008 April 9**, and the predicted ionic charge states are consistent with high ionization states commonly measured in the interplanetary CMEs. The model results depend strongly on the physical parameters in the ambient corona, namely the coronal magnetic field, the electron density, and temperature during the CME event. It is crucial to obtain these ambient coronal parameters and as many facets of the CS properties as possible by observational means so that the post-CME CS models can be scrutinized more effectively.

### **Dynamical and Physical Properties of a Post-Coronal Mass Ejection Current Sheet.**

**Ko**, Y.-K., Raymond, J. C., Lin, J., Lawrence, G., Li, J., and Fludra, A.  
(2003). *Astrophys. J.* 594, 1068–1084. doi:10.1086/376982

### **Tracking Filament Evolution in the Low Solar Corona using Remote-Sensing and In-situ Observations**

Manan **Kocher**, [Enrico Landi](#), [Susan T. Lepri](#)

*ApJS* 2017

<https://arxiv.org/ftp/arxiv/papers/1712/1712.04556.pdf>

In the present work, we analyze a filament eruption associated with an ICME that arrived at L1 on August 5th, 2011. In multi-wavelength SDO/AIA images, three plasma parcels within the filament were tracked at high-cadence along the solar corona. A novel absorption diagnostic technique was applied to the filament material travelling along the three chosen trajectories to compute the column density and temperature evolution in time. Kinematics of the filamentary material were estimated using STEREO/EUVI and STEREO/COR1 observations. The Michigan Ionization Code used inputs of these density, temperature, and speed profiles for the computation of ionization profiles of the filament plasma. Based on these measurements we conclude the core plasma was in near ionization equilibrium, and the ionization states were not frozen-in at the altitudes where they were visible in absorption in AIA images. Additionally, we report that the filament plasma was heterogeneous, and the filamentary material was continuously heated as it expanded in the low solar corona. **August 4th, 2011**

### **Multiwavelength Study of on-disk Coronal Hole Jets with IRIS and SDO observations**

[Koletti Myrto](#), [Gontikakis Costis](#), [Patsourakos Spiros](#), [Tsinganos Kanaris](#)

*A&A* 2024

<https://arxiv.org/pdf/2407.02291>

Solar jets are an important field of study, as they may contribute to the mass and energy transfer from the lower to the upper atmosphere. We use the Interface Region Imaging Spectrograph (IRIS) and Solar Dynamic Observatory (SDO) observations to study two small-scale jets originating in the same on-disk coronal hole observed in October 2013. We combine dopplergrams, intensity maps, and line width maps derived from IRIS Si IV 1393.755 Å spectra along with images from the Atmospheric Imaging Assembly (AIA) on SDO to describe the dynamics of the jets. Images from AIA, with the use of the emission measure loci technique and rectangular differential emission measure (DEM) distributions, provide estimations of the plasma temperatures. We used the O IV 1399.77 Å, 1401.16 Å spectral lines from IRIS to derive electron densities. For jet 1, the SDO images show a small mini-filament 2 minutes before the jet eruption, while jet 2 originates at a pre-existing coronal bright point. The analysis of asymmetric spectral profiles of the Si IV 1393.755 Å and 1402.770 Å lines reveals the existence of two spectral components with inversely dependent 1393.755 Å/1402.770 Å ratios at both regions. One of the components can be related to the background plasma emission originating outside the jet, while the secondary component represents higher-energy plasma flows associated with the jets. Both jets exhibit high densities of the order of 10<sup>11</sup> cm<sup>-3</sup> at their base and 10<sup>10</sup> cm<sup>-3</sup> at the spire, respectively, as well as similar average nonthermal velocities of ~ 50-60 km/s. However, the two jets show differences in their length, duration, and plane-of-sky velocity. Finally, the DEM analysis reveals that both jets exhibit multithermal distributions. **October 9, 2013**

### **Spatial Relationship between CMEs and Prominence Eruptions during SC 24 and SC 25**

Kostadinka **Koleva**<sup>1,2,3</sup>, Nat Gopalswamy<sup>1</sup>, Pooja Devi<sup>4</sup>, Seiji Yashiro<sup>1,2</sup>, and Grzegorz Michalek<sup>5</sup>  
2024 *ApJ* 966 22

<https://iopscience.iop.org/article/10.3847/1538-4357/ad2df3/pdf>

During their propagation, coronal mass ejections (CMEs) and prominences sometimes display a nonradial motion. During the years after the solar minimum, the CME central position angle tended to be offset closer to the equator compared to that of the associated prominence eruptions (PE). No such effect was observed during solar maximum. The purpose of this paper is to investigate the latitudinal offsets of CMEs with respect to their source regions. We study 256 events from SC 24 and SC 25, listed in the Coordinate Data Analysis Workshop Data Center. We analyzed the CMES radial offset from the associated PEs by comparing their latitudes in the plane of the sky. This work is an extension of the previous work by Gopalswamy et al., but with an independent data set. We have confirmed the systematic equatorward offset of CME from the solar source region for the rising phase of Solar Cycle 25. Our analysis of the relation between CME linear speed and PE-CME latitudinal offset indicated that the velocities of the deflected CMEs are mainly in the range of 200 and 800 km s<sup>-1</sup>. In this study, we compared the nonradial offsets for the rising and decay phases of SC 24 and our analysis has shown that during the decay phase more events deflected toward the pole can be

observed. The observed variation is attributed to the presence of a substantial number of low-latitude coronal holes during the decay phase and to the influence from nearby active regions. **2010 June 20, 2017 October 18.**

### **Sympathetic Quiet and Active Region Filament Eruptions**

[Kostadinka Koleva](#), [Pooja Devi](#), [Ramesh Chandra](#), [Reetika Joshi](#), [Peter Duchlev](#), [Momchil Dechev](#)

Solar Phys. **297**, Article number: 44 **2022**

<https://arxiv.org/pdf/2202.08157.pdf>

<https://link.springer.com/content/pdf/10.1007/s11207-022-01981-y.pdf>

We present the observations of three sympathetic filament eruptions occurring on **19 July 2015** namely F1, F2, and F3. The events were observed in UV/EUV wavelengths by Atmospheric Imaging Assembly onboard the Solar Dynamics Observatory and by Global Oscillation Network Group telescope in H $\{\alpha\}$  line. As filament F1 starts to erupt, a part of it falls close to the location of the F2 and F3 filaments. This causes the eruption of F2 and F3 during which the two filaments merge together and trigger a medium-class CME and a long-duration GOES C2.1 class flare. We discuss the dynamics and kinematics of these three filament eruptions and related phenomena.

### **Filament Eruptions Associated with Flares, Coronal Mass Ejections and Solar Energetic Particle Events**

K. [Koleva](#)<sup>1</sup>, P. [Duchlev](#)<sup>1</sup>, M. [Dechev](#)<sup>1</sup>, R. [Miteva](#)<sup>2</sup>, K. [Kozarev](#)<sup>1</sup>, A. [Veronig](#)<sup>3</sup>, M. [Temmer](#)<sup>3</sup>

Proceedings of Tenth Workshop “Solar Influences on the Magnetosphere, Ionosphere and Atmosphere”

Primorsko, Bulgaria, June 4÷8, **2018**

[http://ws-sozopol.stil.bas.bg/2018Primorsko/Kolevaetal\\_WS-10.pdf](http://ws-sozopol.stil.bas.bg/2018Primorsko/Kolevaetal_WS-10.pdf)

We present analysis of three cases of filament eruptions (FEs) that occurred on **04 Aug 2011, 09 Nov 2011 and 05 Apr 2012** and their associations with flares as sources of solar energetic particles (SEPs) and coronal mass ejections. The associated FEs and SEP-related solar flares were selected by simultaneous observations in X-ray, EUV and radio wavelengths.

### **Kinematics and helicity evolution of a loop-like eruptive prominence \***

K. [Koleva](#)<sup>1</sup>, M. S. [Madjarska](#)<sup>2</sup>, P. [Duchlev](#)<sup>1</sup>, C. J. [Schrijver](#)<sup>5</sup>, J.-C. [Vial](#)<sup>3,4</sup>, E. [Buchlin](#)<sup>3,4</sup> and M. [Dechev](#)

E-print, 14 Feb 2012; A&A 540, A127 (**2012**)

Aims. We aim at investigating the morphology as well as kinematic and helicity evolution of a loop-like prominence during its eruption.

Methods. We used multi-instrument observations from AIA/SDO, EUVI/STEREO and LASCO/SoHO. The kinematic, morphological, geometrical, and helicity evolution of a loop-like eruptive prominence were studied in the context of the magnetic flux rope model of solar prominences.

Results. The prominence eruption evolved as a height-expanding twisted loop with both legs anchored in the chromosphere of a plage area. The eruption process consisted of a prominence activation, acceleration, and a phase of constant velocity. The prominence body was composed of counter-clockwise twisted threads around the main prominence axis. The twist during the eruption was estimated at  $6\pi$  (3 turns). The prominence reached a maximum height of 526 Mm before contracting to its primary location and was partially reformed in the same place two days after the eruption. This ejection, however, triggered a coronal mass ejection (CME) observed in LASCO C2. The prominence was located in the northern periphery of the CME magnetic field configuration and, therefore, the background magnetic field was asymmetric with respect to the filament position. The physical conditions of the falling plasma blobs were analysed with respect to the prominence kinematics.

Conclusions. The same sign of the prominence body twist and writhe, as well as the amount of twisting above the critical value of  $2\pi$  after the activation phase indicate that possibly conditions for kink instability were present. No signature of magnetic reconnection was observed anywhere in the prominence body and its surroundings. The filament/prominence descent following the eruption and its partial reformation at the same place two days later suggest a confined type of eruption. The asymmetric background magnetic field possibly played an important role in the failed eruption. **between 17:30 UT and 19:30 UT on 2010 March 30**

### **Search for flares and associated CMEs on late-type main-sequence stars in optical SDSS spectra**

[Florian Koller](#), [Martin Leitzinger](#), [Manuela Temmer](#), [Petra Odert](#), [Paul G. Beck](#), [Astrid Veronig](#)

A&A **2020**

<https://arxiv.org/pdf/2012.00786.pdf>

This work aims to detect and classify stellar flares and potential stellar coronal mass ejection (CME) signatures in optical spectra provided by the Sloan Digital Sky Survey (SDSS) data release 14. The sample is constrained to all F, G, K, and M main-sequence type stars, resulting in more than 630,000 stars. This work makes use of the individual spectral exposures provided by the SDSS.

An automatic flare search was performed by detecting significant amplitude changes in the H $\alpha$  and H $\beta$  spectral lines after a Gaussian profile was fit to the line core. CMEs were searched for by identifying asymmetries in the Balmer lines caused by the Doppler effect of plasma motions in the line of sight.

We identified 281 flares on late-type stars (spectral types K3 to M9). We identified six possible CME candidates showing excess flux in Balmer line wings. Flare energies in H $\alpha$  were calculated and masses of the CME candidates were estimated. The derived H $\alpha$  flare energies range from  $3 \times 10^{28}$ – $2 \times 10^{33}$  erg. The H $\alpha$  flare energy increases with earlier types, while the fraction of flaring times increases with later types. Mass estimates for the CME candidates are in the range of  $6 \times 10^{16}$ – $6 \times 10^{18}$  g, and the highest projected velocities are  $\sim 300$ – $700$  km/s. The low detection rate of CMEs we obtained agrees with previous studies, suggesting that for late-type main-sequence stars the CME occurrence rate that can be detected with optical spectroscopy is low.

### **Nonlinear oscillations of coalescing magnetic flux ropes**

Dmitrii Y. [Kolotkov](#), Valery M. Nakariakov, and George Rowlands

Phys. Rev. E **2016**

<http://journals.aps.org/pre/accepted/6007fY62C3a1bd4f86428ce58d48609acbd7bf0e8>

An analytical model of highly nonlinear oscillations occurring during a coalescence of two magnetic flux ropes, based upon two-fluid hydrodynamics, is developed. The model accounts for the effect of electric charge separation, and describes perpendicular oscillations of the current sheet formed by the coalescence. The oscillation period is determined by the current sheet thickness, the plasma parameter beta, and the oscillation amplitude. The oscillation periods are typically greater than or about the ion plasma oscillation period. In the nonlinear regime, the oscillations of the ion and electron concentrations have a shape of a narrow symmetric spikes.

### **Splitting and eruption of an active region filament caused by magnetic reconnection**

[Defang Kong](#), [Jincheng Wang](#), [Genmei Pan](#)

ApJ **2024** 972 99

<https://arxiv.org/abs/2408.08569>

<https://iopscience.iop.org/article/10.3847/1538-4357/ad66bb/pdf>

To gain a deeper understanding of the intricate process of filament eruption, we present a case study of a filament splitting and eruption by using multi-wavelength data of the Solar Dynamics Observatory (SDO). It is found that the magnetic reconnection between the filament and the surrounding magnetic loops resulted in the formation of two new filaments, which erupted successively. The observational evidences of magnetic reconnection, such as the obvious brightening at the junction of two different magnetic structures, the appearance of a bidirectional jet, and subsequent filament splitting, were clearly observed. Even though the two newly formed filaments experienced failed eruptions, three obvious dimmings were observed at the footpoints of the filaments during their eruptions. Based on these observations, it is suggested that magnetic reconnection is the trigger mechanism for the splitting of the original filament and the subsequent eruption of the newly formed filaments. Furthermore, the process of filament splitting dominated by magnetic reconnection can shed light on the explanation of double-deck filament formation. **March 9, 2019**

### **High-resolution spectroscopy of an erupting minifilament and its impact on the nearby chromosphere**

I. [Kontogiannis](#), [E. Dineva](#), [A. Diercke](#), [M. Verma](#), [C. Kuckein](#), [H. Balthasar](#), [C. Denker](#)

ApJ **898** 144 **2020**

<https://arxiv.org/pdf/2007.01564.pdf>

<https://doi.org/10.3847/1538-4357/aba117>

We study the evolution of a mini-filament eruption in a quiet region at the center of the solar disk and its impact on the ambient atmosphere. We used high-spectral resolution imaging spectroscopy in H $\alpha$  acquired by the echelle spectrograph of the Vacuum Tower Telescope (VTT), Tenerife, Spain, photospheric magnetic field observations from the Helioseismic and Magnetic Imager (HMI), and UV/EUV imaging from the Atmospheric Imaging Assembly (AIA) of the Solar Dynamics Observatory (SDO). The H $\alpha$  line profiles were noise-stripped using Principal Component Analysis (PCA) and then inverted to produce physical and cloud model parameter maps. The minifilament formed between small-scale, opposite-polarity magnetic features through a series of small reconnection events and it erupted within an hour after its appearance in H $\alpha$ . Its development and eruption exhibited similarities with large-scale erupting filaments, indicating the action of common mechanisms. Its eruption took place in two phases, namely a slow rise and a fast expansion, and it produced a coronal dimming, before the minifilament disappeared. During its eruption we detected a complicated velocity pattern, indicative of a twisted, thread-like structure. Part of its material returned to the chromosphere producing observable effects on nearby low-lying magnetic structures. Cloud model analysis showed that the minifilament was initially similar to other chromospheric fine structures, in terms of optical depth, source function and Doppler width, but it resembled a large-scale filament on its course to eruption. High spectral resolution observations of the chromosphere can provide a wealth of information regarding the dynamics and properties of minifilaments and their interactions with the surrounding atmosphere. **May 26, 2019**

### **Which Photospheric Characteristics are Most Relevant to Active-Region Coronal Mass Ejections?**

Ioannis [Kontogiannis](#), [Manolis K. Georgoulis](#), [Jordan A. Guerra](#), [Sung-Hong Park](#), [D. Shaun Bloomfield](#)

Solar Phys. 294:130 2019

<https://arxiv.org/pdf/1909.06088.pdf>

<https://link.springer.com/content/pdf/10.1007%2Fs11207-019-1523-6.pdf>

We investigate the relation between characteristics of coronal mass ejections and parameterizations of the eruptive capability of solar active regions widely used in solar flare prediction schemes. These parameters, some of which are explored for the first time, are properties related to topological features, namely, magnetic polarity inversion lines (MPILs) that indicate large amounts of stored non-potential (i.e. free) magnetic energy. We utilize the Space Weather Database of Notifications, Knowledge, Information (DONKI) and the Large Angle and Spectrometric Coronagraph (LASCO) databases to find flare-associated coronal mass ejections and their kinematic characteristics while properties of MPILs are extracted from Helioseismic and Magnetic Imager (HMI) vector magnetic-field observations of active regions to extract the properties of source-region MPILs. The correlation between all properties and the characteristics of CMEs ranges from moderate to very strong. More significant correlations hold particularly for fast CMEs, which are most important in terms of adverse space-weather manifestations. Non-neutralized currents and the length of the main MPIL exhibit significantly stronger correlations than the rest of the properties. This finding supports a causal relationship between coronal mass ejections and non-neutralized electric currents in highly sheared, conspicuous MPILs. In addition, non-neutralized currents and MPIL length carry distinct, independent information as to the eruptive potential of active regions. The combined total amount of non-neutralized electric currents and the length of the main polarity inversion line, therefore, reflect more efficiently than other parameters the eruptive capacity of solar active regions and the CME kinematic characteristics stemming from these regions.

**Table 1.** Our eruptive flare sample and supporting information (see Section. 2) (2011-2016)

## VLA Measurements of Faraday Rotation Through a Coronal Mass Ejection Using Multiple Lines of Sight

[Jason E. Kooi](#), [Madison L. Ascione](#), [Lianis V. Reyes-Rosa](#), [Sophia K. Rier](#) & [Mohammad Ashas](#)

*Solar Physics* volume 296, Article number: 11 (2021)

<https://link.springer.com/content/pdf/10.1007/s11207-020-01755-4.pdf>

Coronal mass ejections (CMEs) are large eruptions of magnetized plasma from the Sun that play an important role in space weather. The key to understanding the fundamental physics of a CME is measurement of the plasma properties within heliocentric distances of  $<20 R_{\odot}$ . Faraday rotation, a radioastronomical propagation measurement, is an extremely valuable diagnostic for studying CMEs. Faraday rotation measurements [RM] contain information on the magnetic field in the medium causing the Faraday rotation. Recent observations of CME-induced Faraday rotation (e.g., Howard et al. in *Astrophys. J.* 831, 208, 2016; Kooi et al. in *Solar Phys.* 292, 56, 2017; Bisi et al. in EGU General Assembly Conference Abstracts, 13243, 2017) have all been restricted to a single line of sight (LOS) and, therefore, limited to providing estimates of the magnetic field strength. Modeling by Liu et al. (*Astrophys. J.* 665, 1439, 2007) and Jensen and Russell (*Geophys. Res. Lett.* 35, L02103, 2008) demonstrated that multiple LOS are necessary to recover the magnetic field strength and structure of the observed CME. We report the first successful observations of Faraday rotation through a CME using multiple lines of sight: 13 LOS across seven target radio fields. We made these radio observations using the Karl G. Jansky Very Large Array (VLA) at 1–2 GHz frequencies in the triggered operation mode on **31 July 2015**, using a constellation of cosmic radio sources through the solar corona at heliocentric distances of 8.2–19.5  $R_{\odot}$ . For LOS within 10  $R_{\odot}$ , the CME's contribution to the measured RM was  $\approx 0$  to  $-20$  rad  $m^{-2}$ , a significant enhancement over the coronal contribution. We assumed a force-free flux-rope structure for the CME's magnetic field and explored three separate models for the CME's plasma density: constant density, thin shell, and thick shell. The plasma densities and axial magnetic field strengths for the three models ranged over 5.4–6.4  $\times 10^3$   $cm^{-3}$  and 26–35 mG, respectively. Further, using all 13 LOS, we successfully determined the CME's orientation and helicity.

CESRA #2793 Feb 2021

<http://www.astro.gla.ac.uk/users/eduard/cesra/?p=2793>

## VLA Measurements of Faraday Rotation through Coronal Mass Ejections

Jason E. [Kooi](#), Patrick D. Fischer, Jacob J. Buffo, Steven R. Spangler

*Solar Physics* April 2017, 292:56

<http://link.springer.com/content/pdf/10.1007%2Fs11207-017-1074-7.pdf>

Coronal mass ejections (CMEs) are large-scale eruptions of plasma from the Sun, which play an important role in space weather. Faraday rotation is the rotation of the plane of polarization that results when a linearly polarized signal passes through a magnetized plasma such as a CME. Faraday rotation is proportional to the path integral through the plasma of the electron density and the line-of-sight component of the magnetic field. Faraday-rotation observations of a source near the Sun can provide information on the plasma structure of a CME shortly after launch. We report on simultaneous white-light and radio observations made of three CMEs in August 2012. We made sensitive Very Large Array (VLA) full-polarization observations using 1–2 GHz frequencies of a constellation of radio sources through the solar corona at heliocentric distances that ranged from 6– $(15 \sim \{R\}_{\odot})$ . Two sources (0842+1835 and 0900+1832) were occulted by a single CME, and one source (0843+1547) was occulted by two CMEs. In addition to our radioastronomical observations, which represent one of the first active hunts for CME Faraday rotation since Bird et al. (*Solar Phys.*, 98, 341, 1985) and the first active hunt using the VLA, we obtained white-light coronagraph images from the Large Angle and Spectrometric Coronagraph (LASCO) C3 instrument to determine the Thomson-scattering brightness [ $\{B\}_{\{T\}}$ ], providing a means to independently estimate the plasma density and determine its contribution to the observed Faraday rotation. A constant-density force-free flux rope embedded in the



background corona was used to model the effects of the CMEs on  $\mathbf{B}_T$  and Faraday rotation. The plasma densities ( $2.2 \times 10^3 \text{ cm}^{-3}$ ) and axial magnetic-field strengths (2–12 mG) inferred from our models are consistent with the modeling work of Liu et al. (Astrophys. J., 665, 1439, 2007) and Jensen and Russell (Geophys. Res. Lett., 35, L02103, 2008), as well as previous CME Faraday-rotation observations by Bird et al. (1985). **2 August 2012, 30 August 2012**  
**CESRA highlight: Nov 2017** <http://cesra.net/?p=1671>

### **On the evolution of pre-flare patterns of a 3-dimensional model of AR 11429**

M. B. [Korsos](#), [S. Poedts](#), [N. Gyenge](#), [M. K. Georgoulis](#), [S. Yu](#), [S. K. Bisoi](#), [Y. Yan](#), [M. S. Ruderman](#), [R. Erdelyi](#)  
**2018**

<https://arxiv.org/pdf/1801.00433.pdf>

We apply a novel pre-flare tracking of sunspot groups towards improving the estimation of flare onset time by focusing on the evolution of the 3D magnetic field construction of AR 11429. The 3D magnetic structure is based on potential field extrapolation encompassing a vertical range from the photosphere through the chromosphere and transition region into the low corona. The basis of our proxy measure of activity prediction is the so-called weighted horizontal gradient of magnetic field (WG\_M) defined between spots of opposite polarities close to the polarity inversion line of an active region. The temporal variation of the distance of the **barycenter** of the opposite polarities is also found to possess potentially important diagnostic information about the flare onset time estimation as function of height similar to its counterpart introduced initially in an application at the photosphere only in Korsos et al. (2015). We apply the photospheric pre-flare behavioural patterns of sunspot groups to the evolution of their associated 3D-constructed AR 11429 as function of height. We found that at a certain height in the lower solar atmosphere the onset time may be estimated much earlier than at the photosphere or at any other heights. Therefore, we present a tool and recipe that may potentially identify the optimum height for flare prognostic in the solar atmosphere allowing to improve our flare prediction capability and capacity. **2012.03.07-10**

### **An application of the weighted horizontal magnetic gradient to solar compact and eruptive events**

M. B. [Korsos](#), [Michael S. Ruderman](#), [R. Erdelyi](#)  
**2017**

<https://arxiv.org/pdf/1801.00281.pdf>

We propose to apply the weighted horizontal magnetic gradient (WGM), introduced in Korsos et al (2015), for analysing the pre-flare and pre-CME behaviour and evolution of Active Regions (ARs) using the SDO/HMI-Debrecen Data catalogue. To demonstrate the power of investigative capabilities of the WGM method, in terms of flare and CME eruptions, we studied two typical ARs, namely, AR 12158 and AR 12192. The choice of ARs represent canonical cases. AR 12158 produced an X1.6 flare with fast "halo" CME ( $v_{\text{linear}}=1267 \text{ km s}^{-1}$ ) while in AR 12192 there occurred a range of powerful X-class eruptions, i.e. X1.1, X1.6, X3.1, X1.0, X2.0 and X2.0-class energetic flares, interestingly, none with an accompanying CME. The value itself and temporal variation of WGM is found to possess potentially important diagnostic information about the intensity of the expected flare class. Furthermore, we have also estimated the flare onset time from the relationship of duration of converging and diverging motions of the area-weighted barycenters of two subgroups of opposite magnetic polarities. This test turns out not only to provide information about the intensity of the expected flare-class and the flare onset time but may also indicate whether a flare will occur with/without fast CME.

We have also found that, in the case when the negative polarity **barycenter** has moved around and the positive one "remained" at the same coordinates preceding eruption, the flare occurred with fast "halo" CME.

Otherwise, when both the negative and the positive polarity barycenters have moved around, the AR produced flares without CME. If these properties found for the movement of the barycenters are generic pre-cursors of CME eruption (or lack of it), identifying them may serve as an excellent pre-condition for refining the forecast of the lift-off of CMEs. **9 September 2014, 22 October 2014**

### **ON THE STATE OF A SOLAR ACTIVE REGION BEFORE FLARES AND CMEs**

M. B. [Korsós](#)<sup>1,2</sup> and R. Erdélyi  
**2016** ApJ 823 153

Several attempts have been made to find reliable diagnostic tools to determine the state prior to flares and related coronal mass ejections (CMEs) in solar active regions (ARs). Characterization of the level of mixed states is carried out using the Debrecen sunspot Data for 116 flaring ARs. Conditional flare probabilities (CFPs) are calculated for different flaring classes. The association with slow/fast CMEs is examined. Two precursor parameters are introduced: (i) the sum of the (daily averaged) horizontal magnetic gradient  $G_S$  ( $G_{DS}$ ) and (ii) the separation parameter  $\rho$ . We found that if for a flaring AR then the CFP of the expected highest-intensity flare being X-class is more than 70%. If the CFP is more than 45% for the highest-intensity flare(s) to be M-class, and if there is larger than 60% CFP that C-class flare(s) may have the strongest intensity within 48 hr. Next, from analyzing  $G_S$  for determining CFP we found: if  $\rho > 6.5$ , then it is very likely that C-class flare(s) may be the most intense; if  $\rho < 6.5$  then there is  $\sim 45\%$  CFP that M-class could have the highest intensity; finally, if  $\rho < 6.5$  then there is at least 70% chance that the strongest energy release will be X-class in the next 48 hr.

ARs are unlikely to produce X-class flare(s) if  $\log(G S) > 5.5$ . Finally, in terms of providing an estimate of an associated slow/fast CME, we found that, if  $0.4$  or  $6.5$ , there is no accompanying fast CME in the following 24 hr.

### **Analysis of a Limb Eruptive Event**

P. [Kotrč](#),<sup>1</sup> Yu. A. Kupryakov,<sup>1,2</sup> M. Barta,<sup>1</sup> L. K. Kashapova,<sup>3</sup> and W. Liu<sup>1</sup>

Ground-based Solar Observations in the Space Instrumentation Era

ASP Conference Series, Vol. 504, p. 51, 2016

<http://aspbooks.org/publications/504/051.pdf>

We present the analysis of an eruptive event that took place on the eastern limb on **April 21, 2015**, which was observed by the Ondřejov horizontal telescope and spectrograph. The eruption of the highly twisted prominence was followed by the onset of soft X-ray sources. We identified the structures observed in  $H\alpha$  spectra with the details on the  $H\alpha$  filtergrams and analyzed the evolution of Doppler component velocities. The timing and observed characteristics of the eruption were compared with the prediction of the model based on the twisting of the flux ropes and the kink/torus instability.

### **Modeling of $H\alpha$ Eruptive Events Observed at the Solar Limb**

P. [Kotrč](#), M. Bárta, P. Schwartz, Y. A. Kupryakov, L. K. Kashapova, M. Karlický

Solar Physics, June 2013, Volume 284, Issue 2, pp 447-466

We present spectra and slit-jaw images of limb and on-disk eruptive events observed with a high temporal resolution by the Ondřejov Observatory optical spectrograph. Analysis of the time series of full width at half-maximum (FWHM) in  $H\alpha$ ,  $H\beta$ , and radio and soft X-ray (SXR) fluxes indicates two phenomenologically distinct types of observations which differ significantly in the timing of FWHM and SXR/radio fluxes. We investigated one such unusual case of a limb eruptive event in more detail. Synthesis of all observed data supports the interpretation of the  $H\alpha$  broadening in the sense of regular macroscopic plasma motions, contrary to the traditional view (emission from warm dense plasma). The timing and observed characteristics indicate that we may have actually observed the initiation of a prominence eruption. We test this scenario via modeling of the initial phase of the flux rope eruption in a magnetohydrodynamic (MHD) simulation, calculating subsequently – under some simplifying assumptions – the modeled  $H\alpha$  emission and spectrum. The modeled and observed data correspond well. Nevertheless, the following question arises: To what extent is the resulting emission sensitive to the underlying model of plasma dynamics? To address this issue, we have computed a grid of kinematic models with various arbitrary plasma flow patterns and then calculated their resulting emission. Finally, we suggest a diagnostics based on the model and demonstrate that it can be used to estimate the Alfvén velocity and plasma beta in the prominence, which are otherwise hard to obtain.

### **CME Expansion as the Driver of Metric Type II Shock Emission as Revealed by Self-Consistent Analysis of High Cadence EUV Images and Radio Spectrograms**

[Kouloumvakos](#), A.; [Patsourakos](#), S.; [Hillaris](#), A.; [Vourlidis](#), A.; [Preka-Papadema](#), P.; [Moussas](#), X.; [Caroubalos](#), C.; [Tsitsipis](#), P.; [Kontogeorgos](#), A.

E-print, Dec 2013, **File**; Solar Phys. June 2014, Volume 289, Issue 6, pp 2123-2139

On **13 June 2010**, an eruptive event occurred near the solar limb. It included a small filament eruption and the onset of a relatively narrow coronal mass ejection (CME) surrounded by an extreme ultraviolet wave front recorded by the Solar Dynamics Observatory's (SDO) Atmospheric Imaging Assembly (AIA) at high cadence. The ejection was accompanied by a GOES M1.0 soft X-ray flare and a Type-II radio burst; high-resolution dynamic spectra of the latter were obtained by the ARTEMIS IV radio spectrograph. The combined observations enabled a study of the evolution of the ejecta and the EUV wavefront and its relationship with the coronal shock manifesting itself as metric Type-II burst. By introducing a novel technique, which deduces a proxy of the EUV compression ratio from AIA imaging data and compares it with the compression ratio deduced from the band-split of the Type-II metric radio burst, we are able to infer the potential source locations of the radio emission of the shock on that AIA images. Our results indicate that the expansion of the CME ejecta is the source for both EUV and radio shock emissions. Early in the CME expansion phase, the Type-II burst seems to originate in the sheath region between the EUV bubble and the EUV shock front in both radial and lateral directions. This suggests that both the nose and the flanks of the expanding bubble could have driven the shock.

### **Observation of galactic cosmic ray spallation events from the SoHO mission 20-Year operation of LASCO**

S. [Koutchmy](#), [E. Tavabi](#), [O. Urtado](#)

MNRAS 2018

<https://arxiv.org/ftp/arxiv/papers/1805/1805.04930.pdf>

A shower of secondary Cosmic Ray (CR) particles is produced at high altitudes in the Earth's atmosphere, so the primordial Galactic Cosmic Rays (GCRs) are never directly measured outside the Earth magnetosphere and atmosphere. They approach the Earth and other planets in the complex pattern of rigidity's dependence, generally excluded by the magnetosphere. GCRs revealed by images of single nuclear reactions also called spallation events are described here. Such an event was seen on **Nov. 29, 2015** using a unique LASCO C3 space coronagraph routine image taken during the

Solar and Heliospheric Observatory (SoHO) mission observing uninterruptedly at the Lagrangian L1 point. The spallation signature of a GCR identified well outside the Earth's magnetosphere is obtained for the 1st time. The resulting image includes different diverging linear "tracks" of varying intensity, leading to a single pixel, this frame identifies the site on the silicon CCD chip of the coronagraph camera. There was no solar flare reported at that time, nor Coronal Mass Ejection (CME) and no evidence of optical debris around the spacecraft. More examples of smaller CR events have been discovered through the 20 years of continuous observations from SoHO. This is the first spallation event from a CR, recorded outside the Earth's magnetosphere. We evaluate the probable energy of these events suggesting a plausible galactic source. **14th July 2000**

## **Analysis and interpretation of a fast limb CME with eruptive prominence, C-flare, and EUV dimming**

S. [Koutchmy](#)<sup>1</sup>, V. Slemzin<sup>2</sup>, B. Filippov<sup>3</sup>, J.-C. Noens<sup>4</sup>, D. Romeuf<sup>5</sup>, and L. Golub<sup>6</sup>  
A&A 483, 599-608 (2008)

DOI: 10.1051/0004-6361:20078311

*Aims.* Coronal mass ejections or CMEs are large dynamical solar-corona events. The mass balance and kinematics of a fast limb CME, including its prominence progenitor and the associated flare, will be compared with computed magnetic structures to look for their origin and effect.

*Methods.* Multi-wavelength ground-based and spaceborne observations are used to study a fast W-limb CME event of **December 2, 2003**, taking into account both on and off disk observations. Its erupting prominence is measured at high cadence with the Pic du Midi full H  $\alpha$  line-flux imaging coronagraph. EUV images from SOHO/EIT and CORONAS-F/SPIRIT space instruments are processed including difference imaging. SOHO/LASCO images are used to study the mass excess and motions. Computed coronal structures from extrapolated surface magnetic fields are compared to observations.

*Results.* A fast bright expanding coronal loop is identified in the region recorded slightly later by GOES as a C7.2 flare, followed by a brightening and an acceleration phase of the erupting material with both cool and hot components. The total coronal radiative flux dropped by ~7% in the 19.5 nm channel and by 4% in the 17.5 nm channel, revealing a large dimming effect at and above the limb over a 2 h interval. The typical 3-part structure observed 1 h later by the Lasco C2 and C3 coronagraphs shows a core shaped similarly to the eruptive filament/prominence. The total measured mass of the escaping CME (~1.5x10<sup>16</sup> g from C2 LASCO observations) definitely exceeds the estimated mass of the escaping cool prominence material although assumptions made to analyze the H  $\alpha$  erupting prominence, as well as the corresponding EUV darkening of the filament observed several days before, made this evaluation uncertain by a factor of 2. This mass budget suggests that the event is not confined to the eruption region alone. From the current free extrapolation we discuss the shape of the magnetic neutral surface and a possible scenario leading to an instability, including the small scale dynamics inside and around the filament.

## **Connecting the Properties of Coronal Shock Waves with those of Solar Energetic Particles**

[Kouloumvakos](#) A., A. P. Rouillard, Y. Wu, R. Vainio, A. Vourlidis, I. Plotnikov, A. Afanasiev, H. Önel  
**2019 ApJ 876 80**

[sci-hub.si/10.3847/1538-4357/ab15d7](https://sci-hub.si/10.3847/1538-4357/ab15d7)

<https://iopscience.iop.org/article/10.3847/1538-4357/ab15d7/pdf>

We develop and exploit a new catalog of coronal pressure waves modeled in 3D to study the potential role of these waves in accelerating solar energetic particles (SEPs) measured in situ. Our sample comprises modeled shocks and SEP events detected during solar cycle 24 observed over a broad range of longitudes. From the 3D reconstruction of shock waves using coronagraphic observations we derived the 3D velocity along the entire front as a function of time. Combining new reconstruction techniques with global models of the solar corona, we derive the 3D distribution of basic shock parameters such as Mach numbers, compression ratios, and shock geometry. We then model in a time-dependent manner how the shock wave connects magnetically with spacecraft making in situ measurements of SEPs. This allows us to compare modeled shock parameters deduced at the magnetically well-connected regions, with different key parameters of SEPs such as their maximum intensity. This approach accounts for projection effects associated with remote-sensing observations and constitutes the most extensive study to date of shock waves in the corona and their relation to SEPs. We find a high correlation between the maximum flux of SEPs and the strength of coronal shock waves quantified, for instance, by the Mach number. We discuss the implications of that work for understanding particle acceleration in the corona. **13 Dec 2006, 2012 July 23**

**Table 1** List of the SEP Events Analyzed in This Study (2011-2017)

## **Filament eruption deflection and associated CMEs**

[K. Koleva](#), [R. Chandra](#), [P. Duchlevy](#), [P. Devi](#)

Proceedings of IAUS 388 **2024**

<https://arxiv.org/pdf/2411.10110>

We present the observations of a quiescent filament eruption and its deflection from the radial direction. The event occurred in the southern solar hemisphere on **2021 May 9** and was observed by the Atmospheric Imaging Assembly (AIA) on board the Solar Dynamics Observatory (SDO), by the STEREO A Observatory and GONG. Part of the filament erupted in the west direction, while major part of the filament deviated towards east direction. LASCO

observed a very weak CME towards the west direction where it faded quickly. Moreover, the eruption was associated with CME observed by STEREO A COR1 and COR2. Our observations provide the evidence that the filament eruption was highly non-radial in nature

### **The Coronal Analysis of SHocks and Waves (CASHeW) Framework**

K. [Kozarev](#), [A. Davey](#), [A. Kendrick](#), [M. Hammer](#), [C. Keith](#)

Journal of Space Weather and Space Climate (SWSC) 7, A32 2017

<https://arxiv.org/pdf/1710.05302.pdf>

<https://www.swsc-journal.org/articles/swsc/pdf/2017/01/swsc170030.pdf>

Coronal Bright Fronts (CBF) are large-scale wavelike disturbances in the solar corona, related to solar eruptions. They are observed in extreme ultraviolet (EUV) light as transient bright fronts of finite width, propagating away from the eruption source. Recent studies of individual solar eruptive events have used EUV observations of CBFs and metric radio type II burst observations to show the intimate connection between low coronal waves and coronal mass ejection (CME)-driven shocks. EUV imaging with the Atmospheric Imaging Assembly (AIA) instrument on the Solar Dynamics Observatory (SDO) has proven particularly useful for detecting CBFs, which, combined with radio and in situ observations, holds great promise for early CME-driven shock characterization capability. This characterization can further be automated, and related to models of particle acceleration to produce estimates of particle fluxes in the corona and in the near Earth environment early in events. We present a framework for the Coronal Analysis of SHocks and Waves (CASHeW). It combines analysis of NASA Heliophysics System Observatory data products and relevant data-driven models, into an automated system for the characterization of off-limb coronal waves and shocks and the evaluation of their capability to accelerate solar energetic particles (SEPs). The system utilizes EUV observations and models written in the Interactive Data Language (IDL). In addition, it leverages analysis tools from the SolarSoft package of libraries, as well as third party libraries. We have tested the CASHeW framework on a representative list of coronal bright front events. Here we present its features, as well as initial results. With this framework, we hope to contribute to the overall understanding of coronal shock waves, their importance for energetic particle acceleration, as well as to the better ability to forecast SEP events fluxes.

2011-05-11, June 7, 2011, December 12, 2013

### **Presentation of the project "An investigation of the early stages of solar eruptions - from remote observations to energetic particles"**

[Kozarev](#), Kamen; [Veronig, Astrid](#); [Duchlev, Peter](#); [Koleva, Kostadinka](#); [Dechev, Momchil](#); [Miteva, Rositsa](#); [Temmer, Manuela](#); [Dissauer, Karin](#)

Space, Ecology, Safety - SES 2017, Thirteenth International Scientific conference "Space, Ecology, Safety - SES1027", held 2-4 November 2017 in Sofia, Bulgaria. Edited by G. Mardirossian, Ts. Srebrova and G. Jeleu. ISSN: 1313-3888, p. 63-67, 2017

[http://www.astro.bas.bg/SES2017/Kozarevetal\\_SES2017.pdf](http://www.astro.bas.bg/SES2017/Kozarevetal_SES2017.pdf)

Coronal mass ejections (CMEs), one of the most energetic manifestations of solar activity, are complex events, which combine multiple related phenomena occurring on the solar surface, in the extended solar atmosphere (corona), as well as in interplanetary space. We present here an outline of a new collaborative project between scientists from the Bulgarian Academy of Sciences (BAS), Bulgaria and the University of Graz, Austria. The goal of this research project is to answer the following questions: 1) What are the properties of erupting filaments, CMEs, and CME-driven shock waves near the Sun, and of associated solar energetic particle (SEP) fluxes in interplanetary space? 2) How are these properties related to the coronal acceleration of SEPs? To achieve the scientific goals of this project, we will use remote solar observations with high spatial and temporal resolution to characterize the early stages of coronal eruption events in a systematic way - studying the pre-eruptive behavior of filaments and flares during energy build-up, the kinematics and morphology of CMEs and compressive shock waves, and the signatures of high energy non-thermal particles in both remote and in situ observations.

### **Properties of a Coronal Shock Wave as A Driver of Early SEP Acceleration**

Kamen A. [Kozarev](#), John C. Raymond, Vasili V. Lobzin, Michael Hammer

ApJ 799 167 2015

<http://arxiv.org/pdf/1406.2363v1.pdf>

Coronal mass ejections (CMEs) are thought to drive collisionless shocks in the solar corona, which in turn have been shown capable of accelerating solar energetic particles (SEPs) in minutes. It has been notoriously difficult to extract information about energetic particle spectra in the corona, due to lack of in-situ measurements. It is possible, however, to combine remote observations with data-driven models in order to deduce coronal shock properties relevant to the local acceleration of SEPs and their heliospheric connectivity to near-Earth space. We present such novel analysis applied to the **May 11, 2011** CME event on the western solar limb, focusing on the evolution of the eruption-driven, dome-like shock wave observed by the Atmospheric Imaging Assembly (AIA) EUV telescopes on board the Solar Dynamics Observatory spacecraft. We analyze the shock evolution and estimate its strength using emission measure modeling. We apply a new method combining a geometric model of the shock front with a potential field source surface model to estimate time-dependent field-to-shock angles and heliospheric connectivity during shock passage in the low corona. We find that the shock was weak, with an initial speed of ~450 km/s. It was initially mostly quasi-parallel, but significant portion of it turned quasi-perpendicular later in the event. There was good magnetic connectivity to near-

Earth space towards the end of the event as observed by the AIA instrument. The methods used in this analysis hold a significant potential for early characterization of coronal shock waves and forecasting of SEP spectra based on remote observations.

### **Global Numerical Modeling of Energetic Proton Acceleration in a Coronal Mass Ejection Traveling through the Solar Corona**

Kamen A. [Kozarev](#)<sup>1,2</sup>, Rebekah M. Evans<sup>3</sup>, Nathan A. Schwadron<sup>4</sup>, Maher A. Dayeh<sup>5</sup>, Merav Opher<sup>1</sup>, Kelly E. Korreck<sup>2</sup>, and Bart van der Holst

2013 ApJ 778 43

<http://arxiv.org/pdf/1406.2377v1.pdf>

The acceleration of protons and electrons to high (sometimes GeV/nucleon) energies by solar phenomena is a key component of space weather. These solar energetic particle (SEP) events can damage spacecraft and communications, as well as present radiation hazards to humans. In-depth particle acceleration simulations have been performed for idealized magnetic fields for diffusive acceleration and particle propagation, and at the same time the quality of MHD simulations of coronal mass ejections (CMEs) has improved significantly. However, to date these two pieces of the same puzzle have remained largely decoupled. Such structures may contain not just a shock but also sizable sheath and pileup compression regions behind it, and may vary considerably with longitude and latitude based on the underlying coronal conditions. In this work, we have coupled results from a detailed global three-dimensional MHD time-dependent CME simulation to a global proton acceleration and transport model, in order to study time-dependent effects of SEP acceleration between 1.8 and 8 solar radii in the **2005 May 13** CME. We find that the source population is accelerated to at least 100 MeV, with distributions enhanced up to six orders of magnitude. Acceleration efficiency varies strongly along field lines probing different regions of the dynamically evolving CME, whose dynamics is influenced by the large-scale coronal magnetic field structure. We observe strong acceleration in sheath regions immediately behind the shock.

### **Flux-Rope Coronal Mass Ejection Geometry and Its Relation to Observed Morphology**

J. [Krall](#) and O. C. St. Cyr, *The Astrophysical Journal*, 652:1740-1746, 2006, file

### **Flux Rope Model of the 2003 October 28-30 Coronal Mass Ejection and Interplanetary Coronal Mass Ejection**

[Krall](#), J.; Yurchyshyn, V. B.; Slinker, S.; Skoug, R. M.; Chen, J.

*Astrophysical Journal*, 642:541–553, 2006

the erupting flux rope (EFR) model (Chen and Garren 1993; Chen 1996; Krall,

Chen, and Santoro 2000) was able to reproduce many details of the CME/ICME event on October 28-30, 2003.

### **Are All Coronal Mass Ejections Hollow Flux Ropes?**

J. [Krall](#)

*Astrophysical Journal*, Volume 657, Number 1, Page 559.

<http://www.journals.uchicago.edu/cgi-bin/resolve?ApJ70099>

### **On the influence of CMEs on the global 3-D coronal electron density**

M. [Kramar](#)<sup>1,2</sup>, J. Davila<sup>2</sup>, H. Xie<sup>1,2</sup>, and S. Antiochos

*Ann. Geophys.*, 29, 1019-1028, **2011**, File

In order to analyze the influence of a Coronal Mass Ejection (CME) on the coronal streamer belt, we made 3-D reconstructions of the electron density in the corona at heliospheric distances from 1.5 to 4 R<sub>☉</sub>; for periods before and after a CME occurred. The reconstructions were performed using a tomography technique. We studied two CME cases: (i) a slow CME on **1 June 2008**; (ii) two fast CMEs on **31 December 2007** and **2 January 2008**. For the first case of slow CME, it was found: (i) the potential magnetic field configuration in the CME initiation region before the CME does not agree with the coronal density structure while after the CME the agreement between the field and density is much better. This could be manifestation of that the field was non-potential before the CME and after the CME the field relaxes towards a more potential state. (ii) It was shown that the dimming caused by the slow CME is not due to rotation of the corona and a line-of-sight (LOS) effect but a streamer blow out effect took place

### **Are CMEs capable of producing Moreton waves? A case study: the 2006 December 6 event**

G. [Krause](#); [M. Cécere](#); [E. Zurbriggen](#); [A. Costa](#); [C. Francile](#) ...

*Monthly Notices of the Royal Astronomical Society*, Volume 474, Issue 1, 11 February **2018**, Pages 770–778, <https://doi.org/10.1093/mnras/stx2817>

<https://academic.oup.com/mnras/article/474/1/770/4688933>

Considering the chromosphere and a stratified corona, we examine, by performing 2D compressible magnetohydrodynamics simulations, the capability of a coronal mass ejection (CME) scenario to drive a Moreton wave. We find that given a typical flux rope (FR) magnetic configuration, in initial pseudo-equilibrium, the larger the magnetic field and the lighter (and hotter) the FR, the larger the amplitude and the speed of the chromospheric disturbance, which eventually becomes a Moreton wave. We present arguments to explain why Moreton waves are much rarer than CME occurrences. In the frame of the present model, we explicitly exclude the action of flares that could be associated with the CME. Analysing the Mach number, we find that only fast magnetosonic shock waves will be able to produce Moreton events. In these cases an overexpansion of the FR is always present and it is the main factor responsible for the Moreton generation. Finally, we show that this scenario can account for the Moreton wave of the **2006 December 6** event (Francile et al. 2013).

## **RHESSI Heliophysics Senior Review 2015**

### **High Energy Solar Spectroscopic Imager**

Samuel **Krucker**, Brian Dennis, Albert Shih, Manfred Bester

[http://hesperia.gsfc.nasa.gov/senior\\_review/2015/senior\\_review\\_proposal\\_2015.pdf](http://hesperia.gsfc.nasa.gov/senior_review/2015/senior_review_proposal_2015.pdf)

- Evolution of Solar Eruptive Events

- Flare-accelerated Electrons

- Flare-accelerated Ions

- Flare-heated Plasma

- Global Structure of the Photosphere

**3 Nov 2010, 2011-03-07, 6 Sept 2011, 3 March 2012, 2012 July 19, 13 May 2013, 2014-01-28, March 29, 2014, 2014-04-19, 24 Sept 2014, 24 Oct 2014, 14 Dec 2014**

## **ELECTRON ACCELERATION ASSOCIATED WITH SOLAR JETS**

Säm **Krucker**, E. P. Kontar, S. Christe, L. Glesener, and R. P. Lin

**2011**, ApJ, 742, 82

<https://iopscience.iop.org/article/10.1088/0004-637X/742/2/82/pdf>

This paper investigates the solar source region of supra-thermal (few keV up to the MeV range) electron beams observed near Earth by combining in situ measurements of the three-dimensional Plasma and Energetic Particles experiment on the WIND spacecraft with remote-sensing hard X-ray observations by the Reuven Ramaty High Energy Solar Spectroscopic Imager. The in situ observations are used to identify events, and the hard X-ray observations are then searched for signatures of supra-thermal electrons radiating bremsstrahlung emission in the solar atmosphere. Only prompt events detected above 50 keV with a close temporal correlation between the flare hard X-ray emission and the electrons seen near Earth are selected, limiting the number of events to 16. We show that for 7 of these 16 events, hard X-ray imaging shows three chromospheric sources: two at the footpoints of the post-flare loop and one related to an apparently open field line. The remaining events show two footpoints (seven events, four of which show elongated sources possibly hiding a third source) or are spatially unresolved (two events). Out of the 16 events, 6 have a solar source region within the field of view of the Transition Region and Corona Explorer (TRACE). All events with TRACE data show EUV jets that have the same onset as the hard X-ray emission (within the cadence of tens of seconds). After the hard X-ray burst ends, the jets decay. These results suggest that escaping prompt supra-thermal electron events observed near Earth are accelerated in flares associated with reconnection between open and closed magnetic field lines, the so-called interchange reconnection scenario.

**Table 1** Hard X-ray Flares Associated with Supra-thermal Electron Events Seen Near Earth 2002-2005

## **An analysis of interplanetary solar radio emissions associated with a coronal mass ejection**

Vratislav **Krupar**, Jonathan Eastwood, Oksana Kruparova, Ondrej Santolik, Jan Soucek, Jasmina Magdalenic, Angelos Vourlidas, Milan Maksimovic, Volker Bothmer, Niclas Mrotzek, Adam Pluta, David Barnes, Jackie Davies, Juan Carlos Martinez Oliveros, Stuart Bale

ApJ 823 L5 **2016**

<http://arxiv.org/pdf/1606.04301v1.pdf>

Coronal mass ejections (CMEs) are large-scale eruptions of magnetized plasma that may cause severe geomagnetic storms if Earth-directed. Here we report a rare instance with comprehensive in situ and remote sensing observations of a CME combining white-light, radio, and plasma measurements from four different vantage points. For the first time, we have successfully applied a radio direction-finding technique to an interplanetary type II burst detected by two identical widely separated radio receivers. The derived locations of the type II and type III bursts are in general agreement with the white light CME reconstruction. We find that the radio emission arises from the flanks of the CME, and are most likely associated with the CME-driven shock. Our work demonstrates the complementarity between radio triangulation and 3D reconstruction techniques for space weather applications. **2013 November 29**

## **Determining the dynamics and magnetic fields in He I 10830 Å during a solar filament eruption**

C. **Kuckein** (1), [S. J. González Manrique](#) (2, 3 and 4), [L. Kleint](#) (5), [A. Asensio Ramos](#)

A&A 640, A71 **2020**

<https://arxiv.org/pdf/2006.10473.pdf>

<https://www.aanda.org/articles/aa/pdf/2020/08/aa38408-20.pdf>

We investigate the dynamics and magnetic properties of the plasma, such as line-of-sight velocity (LOS), optical depth, vertical and horizontal magnetic fields, belonging to an erupted solar filament. The filament eruption was observed with the GREGOR Infrared Spectrograph (GRIS) at the 1.5-meter GREGOR telescope on **2016 July 3**. Three consecutive full-Stokes slit-spectropolarimetric scans in the He I 10830 Å spectral range were acquired. The Stokes I profiles were classified using the machine learning k-means algorithm and then inverted with different initial conditions using the HAZEL code. The erupting-filament material presents the following physical conditions: (1) ubiquitous upward motions with peak LOS velocities of ~73 km/s; (2) predominant large horizontal components of the magnetic field, on average, in the range of 173-254 G, whereas the vertical components of the fields are much lower, on average between 39-58 G; (3) optical depths in the range of 0.7-1.1. The average azimuth orientation of the field lines between two consecutive raster scans (<2.5 minutes) remained constant. The analyzed filament eruption belonged to the fast rising phase, with total velocities of about 124 km/s. The orientation of the magnetic field lines does not change from one raster scan to the other, indicating that the untwisting phase has not started yet. The untwisting seems to start about 15 min after the beginning of the filament eruption.

## **Direct Imaging of a Prolonged Plasma/Current Sheet and Quasiperiodic Magnetic Reconnection on the Sun**

[Pankaj Kumar](#), [Judith T. Karpen](#), [Vasyl Yurchyshyn](#), [C. Richard DeVore](#), [Spiro K. Antiochos](#)  
ApJ **2024**

<https://arxiv.org/pdf/2407.07687>

Magnetic reconnection is widely believed to be the fundamental process in the solar atmosphere that underlies magnetic energy release and particle acceleration. This process is responsible for the onset of solar flares, coronal mass ejections, and other explosive events (e.g., jets). Here, we report direct imaging of a prolonged plasma/current sheet along with quasiperiodic magnetic reconnection in the solar corona using ultra-high-resolution observations from the 1.6-meter Goode Solar Telescope (GST) at BBSO and Solar Dynamics Observatory/Atmospheric Imaging Assembly (SDO/AIA). The current sheet appeared near a null point in the fan-spine topology and persisted over an extended period (~20 hours). The length and apparent width of the current sheet were about 6 arcsec and 2 arcsec respectively, and the plasma temperature was ~10-20 MK. We observed quasiperiodic plasma inflows and outflows (bidirectional jets with plasmoids) at the reconnection site/current sheet. Furthermore, quasiperiodic reconnection at the long-lasting current sheet produced recurrent eruptions (small flares and jets) and contributed significantly to the recurrent impulsive heating of the active region. Direct imaging of a plasma/current sheet and recurrent null-point reconnection for such an extended period has not been reported previously. These unprecedented observations provide compelling evidence that supports the universal model for solar eruptions (i.e., the breakout model) and have implications for impulsive heating of active regions by recurrent reconnection near null points. The prolonged and sustained reconnection for about 20 hours at the breakout current sheet provides new insights into the dynamics and energy release processes in the solar corona. **August 22, 2022**

## **Magnetohydrodynamics simulation of magnetic flux rope formation in a quadrupolar magnetic field configuration**

[Sanjay Kumar](#), [Avijeet Prasad](#), [Sushree S. Nayak](#), [Satyam Agarwal](#), [R. Bhattacharyya](#)  
**2023**

<https://arxiv.org/pdf/2307.06025.pdf>

Magnetic flux ropes (MFRs) play an important role in high-energetic events like solar flares and coronal mass ejections in the solar atmosphere. Importantly, solar observations suggest an association of some flaring events with quadrupolar magnetic configurations. However, the formation and subsequent evolution of MFRs in such magnetic configurations still need to be fully understood. In this paper, we present idealized magnetohydrodynamics (MHD) simulations of MFR formation in a quadrupolar magnetic configuration. A suitable initial magnetic field having a quadrupolar configuration is constructed by modifying a three-dimensional (3D) linear force-free magnetic field. The initial magnetic field contains neutral lines, which consist of X-type null points. The simulated dynamics initially demonstrate the oppositely directed magnetic field lines located across the polarity inversion lines (PILs) moving towards each other, resulting in magnetic reconnections. Due to these reconnections, four highly twisted MFRs form over the PILs. With time, the foot points of the MFRs move towards the X-type neutral lines and reconnect, generating complex magnetic structures around the neutral lines, thus making the MFR topology more complex in the quadrupolar configuration than those formed in bipolar loop systems. Further evolution reveals the non-uniform rise of the MFRs. Importantly, the simulations indicate that the pre-existing X-type null points in magnetic configurations can be crucial to the evolution of the MFRs and may lead to the observed brightenings during the onset of some flaring events in the quadrupolar configurations.

## **Plasmoids, Flows, and Jets During Magnetic Reconnection in a Failed Solar Eruption**

[Pankaj Kumar](#), [Judith T. Karpen](#), [Spiro K. Antiochos](#), [C. Richard DeVore](#), [Peter F. Wyper](#), [Kyung-Suk Cho](#)  
ApJ **943** 156 **2023**

<https://arxiv.org/pdf/2212.11159.pdf>

<https://iopscience.iop.org/article/10.3847/1538-4357/acaea4/pdf>

We report a detailed analysis of a failed eruption and flare in active region 12018 on **2014 April 3** using multiwavelength observations from SDO/AIA, IRIS, STEREO, and Hinode/SOT. At least four jets were observed to

emanate from the cusp of this small active region (large bright point) with a null-point topology during the two hours prior to the slow rise of a filament. During the filament slow rise multiple plasma blobs were seen, most likely formed in a null-point current sheet near the cusp. The subsequent filament eruption, which was outside the IRIS field of view, was accompanied by a flare but remained confined. During the explosive flare reconnection phase, additional blobs appeared repetitively and moved bidirectionally within the flaring region below the erupting filament. The filament kinked, rotated, and underwent leg-leg reconnection as it rose, yet it failed to produce a coronal mass ejection. Tiny jet-like features in the fan loops were detected during the filament slow-rise/pre-flare phase. We interpret them as signatures of reconnection between the ambient magnetic field and the plasmoids leaving the null-point sheet and streaming along the fan loops. We contrast our interpretation of these tiny jets, which occur within the large-scale context of a failed filament eruption, with the local nanoflare-heating scenario proposed by Antolin et al. (2021).

### **Kink Oscillation of a Flux Rope During a Failed Solar Eruption**

[Pankaj Kumar](#), [Valery M. Nakariakov](#), [Judith T. Karpen](#), [C. Richard DeVore](#), [Kyung-Suk Cho](#)

ApJL **932** L9 **2022**

<https://arxiv.org/pdf/2205.03480.pdf>

<https://iopscience.iop.org/article/10.3847/2041-8213/ac6e3e/pdf>

We report a decaying kink oscillation of a flux rope during a confined eruptive flare, observed off the solar limb by SDO/AIA, that lacked a detectable white-light coronal mass ejection. The erupting flux rope underwent kinking, rotation, and apparent leg-leg interaction during the event. The oscillations were observed simultaneously in multiple AIA channels at 304, 171, and 193 Å, indicating that multithermal plasma was entrained in the rope. After reaching the overlying loops in the active region, the flux rope exhibited large-amplitude, decaying kink oscillations with an apparent initial amplitude of 30 Mm, period of about 16 min, and decay time of about 17 min. We interpret these oscillations as a fundamental standing kink mode of the flux rope. The oscillation polarization has a clear vertical component, while the departure of the detected waveform from a sinusoidal signal suggests that the oscillation could be circularly or elliptically polarized. The estimated kink speed is 1080 km/s, corresponding to an Alfvén speed of about 760 km/s. This speed, together with the estimated electron density in the rope from our DEM analysis,  $n_e \approx (1.5\text{--}2.0) \times 10^9 \text{ cm}^{-3}$ , yields a magnetic field strength of about 15 G. To the best of our knowledge, decaying kink oscillations of a flux rope with non-horizontal polarization during a confined eruptive flare have not been reported before. These oscillations provide unique opportunities for indirect measurements of the magnetic-field strength in low-coronal flux ropes during failed eruptions. **2014 April 3**

### **Quasiperiodic Energy Release and Jets at the Base of Solar Coronal Plumes**

[Pankaj Kumar](#), [Judith T. Karpen](#), [Vadim M. Uritsky](#), [Craig E. Deforest](#), [Nour E. Raouafi](#), [C. Richard DeVore](#)

ApJ **933** 21 **2022**

<https://arxiv.org/pdf/2204.13871.pdf>

<https://iopscience.iop.org/article/10.3847/1538-4357/ac6c24/pdf>

Coronal plumes are long, ray-like, open structures, which have been considered as possible sources for the solar wind. Their origin in the largely unipolar coronal holes has long been a mystery. Earlier spectroscopic and imaging observations revealed blue-shifted plasma and propagating disturbances (PDs) in plumes that are widely interpreted in terms of flows and/or propagating slow-mode waves, but these interpretations (flows vs waves) remain under debate. Recently we discovered an important clue about plume internal structure: dynamic filamentary features called plumelets, which account for most of the plume emission. Here we present high-resolution observations from the Solar Dynamics Observatory/Atmospheric Imaging Assembly (SDO/AIA) and the Interface Region Imaging Spectrograph (IRIS) that revealed numerous, quasiperiodic, tiny jets (so-called jetlets) associated with transient brightening, flows, and plasma heating at the chromospheric footpoints of the plumelets. By analogy to larger coronal jets, these jetlets are most likely produced within the plume base by magnetic reconnection between closed and open flux at stressed 3D null points. The jetlet-associated brightenings are in phase with plumelet-associated PDs, and vary with a period of about 3 to 5 minutes, which is remarkably consistent with the photospheric/chromospheric p-mode oscillation. This reconnection at the open-closed boundary in the chromosphere/transition region is likely modulated or driven by local manifestations of the global p-mode waves. The jetlets extend upward to become plumelets, contribute mass to the solar wind, and may be sources of the switchbacks recently detected by the Parker Solar Probe. **19 Mar 2016**

### **From Pseudostreamer Jets to CMEs: Observations of the Breakout Continuum**

[Pankaj Kumar](#), [Judith T. Karpen](#), [Spiro K. Antiochos](#), [Peter F. Wyper](#), [C. Richard DeVore](#), [Benjamin J. Lynch](#)

**2021 ApJ 907** 41

<https://arxiv.org/pdf/2011.07029.pdf> File

<https://iopscience.iop.org/article/10.3847/1538-4357/abca8b/pdf>

The magnetic breakout model, in which reconnection in the corona leads to destabilization of a filament channel, explains numerous features of eruptive solar events, from small-scale jets to global-scale coronal mass ejections (CMEs). The underlying multipolar topology, pre-eruption activities, and sequence of magnetic reconnection onsets (first breakout, then flare) of many observed fast CMEs/eruptive flares are fully consistent with the model. Recently, we have demonstrated that most observed coronal-hole jets in fan/spine topologies also are induced by breakout reconnection at the null point above a filament channel (with or without a filament). For these two types of eruptions



occurring in similar topologies, the key question is, why do some events generate jets while others form CMEs? We focused on the initiation of eruptions in large bright points/small active regions that were located in coronal holes and clearly exhibited null-point (fan/spine) topologies: such configurations are referred to as pseudostreamers. We analyzed and compared SDO/AIA, SOHO/LASCO, and RHESSI observations of three events. Our analysis of the events revealed two new observable signatures of breakout reconnection prior to the explosive jet/CME outflows and flare onset: coronal dimming and the opening-up of field lines above the breakout current sheet. Most key properties were similar among the selected erupting structures, thereby eliminating region size, photospheric field strength, magnetic configuration, and pre-eruptive evolution as discriminating factors between jets and CMEs. We consider the factors that contribute to the different types of dynamic behavior, and conclude that the main determining factor is the ratio of the magnetic free energy associated with the filament channel compared to the energy associated with the overlying flux inside and outside the pseudostreamer dome. **2015 Jan 12, 2015 April 20, 2015 April 21**

### **First Detection of Plasmoids from Breakout Reconnection on the Sun**

Pankaj [Kumar](#), [Judith T. Karpen](#), [Spiro K. Antiochos](#), [Peter F. Wyper](#), [C. Richard DeVore](#)

APJL **885** L15 **2019**

<https://arxiv.org/pdf/1909.06637.pdf>

[sci-hub.se/10.3847/2041-8213/ab45f9](https://sci-hub.se/10.3847/2041-8213/ab45f9)

Transient collimated plasma ejections (jets) occur frequently throughout the solar corona, in active regions, quiet Sun, and coronal holes. Although magnetic reconnection is generally agreed to be the mechanism of energy release in jets, the factors that dictate the location and rate of reconnection remain unclear. Our previous studies demonstrated that the magnetic breakout model explains the triggering and evolution of most jets over a wide range of scales, through detailed comparisons between our numerical simulations and high-resolution observations. An alternative explanation, the resistive-kink model, invokes breakout reconnection without forming and explosively expelling a flux rope. Here we report direct observations of breakout reconnection and plasmoid formation during two jets in the fan-spine topology of an embedded bipole. For the first time, we observed the formation and evolution of multiple small plasmoids with bidirectional flows associated with fast reconnection in 3D breakout current sheets in the solar corona. The first narrow jet was launched by reconnection at the breakout current sheet originating at the deformed 3D null, without significant flare reconnection or a filament eruption. In contrast, the second jet and release of cool filament plasma were triggered by explosive breakout reconnection when the leading edge of the rising flux rope formed by flare reconnection beneath the filament encountered the preexisting breakout current sheet. These observations solidly support both reconnection-driven jet models: the resistive kink for the first jet, and the breakout model for the second explosive jet with a filament eruption. **2014 May 1**

### **Multiwavelength Study of Equatorial Coronal-Hole Jets**

Pankaj [Kumar](#), [Judith T. Karpen](#), [Spiro K. Antiochos](#), [Peter F. Wyper](#), [C. Richard DeVore](#), [Craig E. DeForest](#)

ApJ **873** 93 **2019**

<https://arxiv.org/pdf/1902.00922.pdf>

[sci-hub.se/10.3847/1538-4357/ab04af](https://sci-hub.se/10.3847/1538-4357/ab04af)

Jets (transient/collimated plasma ejections) occur frequently throughout the solar corona and contribute mass/energy to the corona and solar wind. By combining numerical simulations and high-resolution observations, we have made substantial progress recently on determining the energy buildup and release processes in these jets. Here we describe a study of 27 equatorial coronal-hole jets using Solar Dynamics Observatory/AIA and HMI observations on **2013 June 27-28 and 2014 January 8-10**. Out of 27 jets, 18 (67%) are associated with mini-filament ejections; the other 9 (33%) do not show mini-filament eruptions but do exhibit mini-flare arcades and other eruptive signatures. This indicates that every jet in our sample involved a filament-channel eruption. From the complete set of events, 6 jets (22%) are apparently associated with tiny flux-cancellation events at the polarity inversion line, and 2 jets (7%) are associated with sympathetic eruptions of filaments from neighboring bright points. Potential-field extrapolations of the source-region photospheric magnetic fields reveal that all jets originated in the fan-spine topology of an embedded bipole associated with an extreme ultraviolet coronal bright point. Hence, all our jets are in agreement with the breakout model of solar eruptions. We present selected examples and discuss the implications for the jet energy build-up and initiation mechanisms.

### **Evidence For The Magnetic Breakout Model in an Equatorial Coronal-Hole Jet**

Pankaj [Kumar](#), [Judith T. Karpen](#), [Spiro K. Antiochos](#), [Peter F. Wyper](#), [C. Richard DeVore](#), [Craig E. DeForest](#)

ApJ **854** 155 **2018**

<https://arxiv.org/pdf/1801.08582.pdf>

<http://sci-hub.tw/http://iopscience.iop.org/0004-637X/854/2/155/>

Small, impulsive jets commonly occur throughout the solar corona, but are especially visible in coronal holes. Evidence is mounting that jets are part of a continuum of eruptions that extends to much larger coronal mass ejections and eruptive flares. Because coronal-hole jets originate in relatively simple magnetic structures, they offer an ideal testbed for theories of energy buildup and release in the full range of solar eruptions. We analyzed an equatorial coronal-hole jet observed by SDO/AIA on **09 January 2014**, in which the magnetic-field structure was consistent with the embedded-bipole topology that we identified and modeled previously as an origin of coronal jets. In addition, this event

contained a mini-filament, which led to important insights into the energy storage and release mechanisms. SDO/HMI magnetograms revealed footpoint motions in the primary minority-polarity region at the eruption site, but show negligible flux emergence or cancellation for at least 16 hours before the eruption. Therefore, the free energy powering this jet probably came from magnetic shear concentrated at the polarity inversion line within the embedded bipole. We find that the observed activity sequence and its interpretation closely match the predictions of the breakout jet model, strongly supporting the hypothesis that the breakout model can explain solar eruptions on a wide range of scales.

### **Characteristics of Radio-Loud CMEs**

Pankaj **Kumar**, P.K. Manoharan, K.S. Cho

2017

[https://www.researchgate.net/publication/315637846\\_Characteristics\\_of\\_radio-loud\\_CMEs](https://www.researchgate.net/publication/315637846_Characteristics_of_radio-loud_CMEs)

In this paper, we study the characteristics of 46 radio-loud (RL) Coronal Mass Ejections (CMEs), which occurred during 1997-2006. All these RL CMEs were associated with M- and X-class flares. We selected 46 RL CMEs, out of which 26 events (57%) were associated with Solar Energetic Particle (SEP) events detected at 1 AU. Furthermore, we study the link between the flare accelerated electrons in the low corona and protons at 1 AU and found a positive correlation (30%). It suggests the link between the injection sites for electrons and protons, which are most likely accelerated at the flare current sheet. We also study the relation between the CME speed and peak proton flux ( $>10$  MeV) at 1 AU and found a good correlation ( $\sim 60\%$ ), which suggests the proton acceleration by CME driven shocks. In addition, we found two branches (lower and upper) of SEP events with different characteristics. The lower branch SEP events are associated with impulsive rise along with more proton flux whereas the upper branch SEP events exhibit gradual rise and less proton flux. We suggest that flares (current sheet) and CMEs (shocks) both are involved in the particle acceleration for the lower branch, whereas in the upper branch mostly CME driven shocks play an important role in the particle acceleration. **2 May 1998, 29 March, 2001**

### **Multiwavelength Observations of a Flux Rope Formation by Series of Magnetic Reconnection in the Chromosphere**

Pankaj **Kumar**, Vasylyur Yurchyshyn, Kyung-Suk Cho, Haimin Wang

A&A 603, A36 2017

<https://arxiv.org/pdf/1703.09871.pdf>

Using high-resolution observations from the 1.6 m New Solar Telescope (NST) operating at the Big Bear Solar Observatory (BBSO), we report direct evidence of merging/reconnection of cool H $\alpha$  loops in the chromosphere during two homologous flares (B- and C-class) caused by a shear motion at the footpoint of two loops. The reconnection between these loops caused the formation of an unstable flux rope which showed counterclockwise rotation. The flux rope could not reach the height of torus instability and failed to form a coronal mass ejection. The HMI magnetograms revealed rotation of the negative/positive (N1/P2) polarity sunspots in the opposite directions, which increased the right and left-handed twist in the magnetic structures rooted at N1/P2. Rapid photospheric flux cancellation (duration  $\sim 20$ -30 min, rate  $\sim 3.44 \times 10^{20}$  Mx h $^{-1}$ ) was observed during and even after the first B6.0 flare and continued until the end of the second C2.3 flare. The RHESSI X-ray sources were located at the site of the loop's coalescence. To the best of our knowledge, such a clear interaction of chromospheric loops along with rapid flux cancellation has not been reported before. These high-resolution observations suggest the formation of a small flux rope by a series of magnetic reconnection within chromospheric loops associated with very rapid flux cancellation. **23 May 2015**

### **On the role of repetitive magnetic reconnections in evolution of magnetic flux-ropes in solar corona**

Sanjay **Kumar**, R. Bhattacharyya, Bhuwan Joshi, P. K. Smolarkiewicz

2016

<http://arxiv.org/pdf/1609.08260v1.pdf>

Parker's magnetostatic theorem extended to astrophysical magnetofluids with large magnetic Reynolds number supports *ceaseless regeneration of current sheets and hence, spontaneous magnetic reconnections recurring in time*.

Consequently, a scenario is possible where the repeated reconnections provide an autonomous mechanism governing emergence of coherent structures in astrophysical magnetofluids. In this work, such a scenario is explored by performing numerical computations commensurate with the magnetostatic theorem. In particular, the computations explore the evolution of a flux-rope governed by repeated reconnections in a magnetic geometry resembling bipolar loops of solar corona. The revealed morphology of the evolution process, including onset and ascent of the rope, reconnection locations and the associated topology of the magnetic field lines, agrees with observations, and thus substantiates physical realisability of the advocated mechanism.

### **ON THE ROLE OF REPETITIVE MAGNETIC RECONNECTIONS IN EVOLUTION OF MAGNETIC FLUX ROPES IN SOLAR CORONA**

Sanjay **Kumar**<sup>1</sup>, R. Bhattacharyya<sup>1</sup>, Bhuwan Joshi<sup>1</sup>, and P. K. Smolarkiewicz

2016 ApJ 830 80

Parker's magnetostatic theorem, extended to astrophysical magnetofluids with large magnetic Reynolds number, supports ceaseless regeneration of current sheets and, hence, spontaneous magnetic reconnections recurring in time. Consequently, a scenario is possible where the repeated reconnections provide an autonomous mechanism governing emergence of coherent structures in astrophysical magnetofluids. In this work, such a scenario is explored by performing numerical computations commensurate with the magnetostatic theorem. In particular, the computations explore the evolution of a flux rope governed by repeated reconnections in a magnetic geometry resembling bipolar loops of solar corona. The revealed morphology of the evolution process—including onset and ascent of the rope, reconnection locations, and the associated topology of the magnetic field lines—agrees with observations, and thus substantiates physical realizability of the advocated mechanism.

## **Formation and Eruption of a Small Flux Rope in the Chromosphere Observed by NST, IRIS, and SDO**

Pankaj **Kumar**, Vasyl Yurchyshyn, Haimin Wang, Kyung-Suk Cho

ApJ 809 83 2015

<http://arxiv.org/pdf/1507.01761v1.pdf>

Using high-resolution images from 1.6 m New Solar Telescope (NST) at Big Bear Solar Observatory (BBSO), we report the direct evidence of chromospheric reconnection at the polarity inversion line (PIL) between two small opposite polarity sunspots. Small jet-like structures (with velocities of  $\sim 20$ - $55$  km/s) were observed at the reconnection site before the onset of the first M1.0 flare. The slow rise of untwisting jets was followed by the onset of cool plasma inflow ( $\sim 10$  km/s) at the reconnection site, causing the onset of a two-ribbon flare. The reconnection between two sheared J-shaped cool H $\alpha$  loops causes the formation of a small twisted flux rope (S shaped) in the chromosphere. In addition, Helioseismic and Magnetic Imager (HMI) magnetograms show the flux cancellation (both positive and negative) during the first M1.0 flare. The emergence of negative flux and cancellation of positive flux (with shear flows) continue until the successful eruption of the flux rope. The newly formed chromospheric flux rope becomes unstable and rises slowly with the speed of  $\sim 108$  km/s during a second C8.5 flare that occurred after  $\sim 3$  hours of the first M1.0 flare. The flux rope was destroyed by repeated magnetic reconnection induced by its interaction with the ambient field (fan-spine topology) and looks like an untwisting surge ( $\sim 170$  km/s) in the coronal images recorded by Solar Dynamic Observatory/Atmospheric Imaging Assembly (SDO/AIA). These observations suggest the formation of a chromospheric flux rope (by magnetic reconnection associated with flux cancellation) during the first M1.0 flare and its subsequent eruption/disruption during the second C8.5 flare. **12 June 2014**

## **Multiwavelength observation of a large-scale flux rope eruption above kinked mini-filament**

Pankaj **Kumar**, Kyung-Suk Cho

A&A, 572, A83 2014

<http://.org/pdf/1409.7213v1.pdf>

We analyse multiwavelength observations of a western limb flare (C3.9) occurred in AR NOAA 111465 on **30 April 2012**. The high resolution images recorded by SDO/AIA 304, 1600 \AA and Hinode/SOT H $\alpha$  show the activation of a mini-filament (rising speed  $\sim 40$  km s $^{-1}$ ) associated with kink instability and the onset of a C-class flare near the southern leg of the filament. The first magnetic reconnection occurred at one of the footpoints of the filament causing the breaking of its southern leg. The filament shows unwinding motion of the northern leg and apex in the counterclockwise direction and failed to erupt. A flux-rope (visible only in hot channels, i.e., AIA 131 and 94 \AA channels and Hinode/SXT) structure was appeared along the neutral line during the second magnetic reconnection taking place above the kinked filament. Formation of the RHESSI hard X-ray source (12-25 keV) above the kinked filament and simultaneous appearance of the hot 131 \AA loops associated with photospheric brightenings (AIA 1700 \AA) suggest the particle acceleration along these loops from the top of the filament. In addition, EUV disturbances/waves observed above the filament in 171 \AA also show a close association with magnetic reconnection. The flux rope rises slowly ( $\sim 100$  km s $^{-1}$ ) producing a rather big twisted structure possibly by reconnection with the surrounding sheared magnetic fields within  $\sim 15$ - $20$  minutes, and showed an impulsive acceleration reaching a height of about 80--100 Mm. AIA 171 and SWAP 174 \AA images reveal a cool compression front (or CME frontal loop) surrounding the hot flux rope structure.

## **Simultaneous EUV and radio observations of bidirectional plasmoids ejection during magnetic reconnection\***

Pankaj **Kumar** and Kyung-Suk Cho

A&A 557, A115 (2013)

We present a multiwavelength study of the X-class flare, which occurred in active region (AR) NOAA 11339 on **3 November 2011**. The extreme ultraviolet (EUV) images recorded by SDO/AIA show the activation of a remote filament (located north of the AR) with footpoint brightenings about 50 min prior to the flare's occurrence. The kinked filament rises up slowly, and after reaching a projected height of  $\sim 49$  Mm, it bends and falls freely near the AR, where the X-class flare was triggered. Dynamic radio spectrum from the Green Bank Solar Radio Burst Spectrometer

(GBSRBS) shows simultaneous detection of both positive and negative drifting pulsating structures (DPSs) in the decimetric radio frequencies (500–1200 MHz) during the impulsive phase of the flare. The global negative DPSs in solar flares are generally interpreted as a signature of electron acceleration related to the upward-moving plasmoids in the solar corona. The EUV images from AIA 94 Å reveal the ejection of multiple plasmoids, which move simultaneously upward and downward in the corona during the magnetic reconnection. The estimated speeds of the upward- and downward-moving plasmoids are  $\sim 152$ – $362$  and  $\sim 83$ – $254$  km s<sup>-1</sup>, respectively. These observations strongly support the recent numerical simulations of the formation and interaction of multiple plasmoids due to tearing of the current-sheet structure. On the basis of our analysis, we suggest that the simultaneous detection of both the negative and positive DPSs is most likely generated by the interaction or coalescence of the multiple plasmoids moving upward and downward along the current-sheet structure during the magnetic reconnection process. Moreover, the differential emission measure (DEM) analysis of the active region reveals a hot flux-rope structure (visible in AIA 131 and 94 Å) prior to the flare initiation and ejection of the multitemperature plasmoids during the flare impulsive phase.

## **Multiwavelength Study of a Solar Eruption from AR NOAA 11112:**

### **II. Large-Scale Coronal Wave and Loop Oscillation**

Pankaj [Kumar](#)<sup>1</sup>, K.-S. Cho<sup>1, 2, 3</sup>, P. F. Chen<sup>4</sup>, S.-C. Bong<sup>1</sup> and Sung-Hong Park

Solar Physics, February **2013**, Volume 282, Issue 2, pp 523-541, [File](#)

We analyze multiwavelength observations of an M2.9/1N flare that occurred in AR NOAA 11112 on **16 October 2010**. AIA 211 Å EUV images reveal the presence of a faster coronal wave (decelerating from  $\approx 1390$  to  $\approx 830$  km s<sup>-1</sup>) propagating ahead of a slower wave (decelerating from  $\approx 416$  to  $\approx 166$  km s<sup>-1</sup>) towards the western limb. The dynamic radio spectrum from Sagamore Hill radio telescope shows the presence of a metric type II radio burst, which reveals the presence of a coronal shock wave (speed  $\approx 800$  km s<sup>-1</sup>). The speed of the faster coronal wave, derived from AIA 211 Å images, is found to be comparable to the coronal shock speed. AIA 171 Å high-cadence observations showed that a coronal loop, which was located at a distance of  $\approx 0.32R_{\odot}$  to the west of the flaring region, started to oscillate by the end of the impulsive phase of the flare. The results indicate that the faster coronal wave may be the first driver of the transversal oscillations of coronal loop. As the slower wave passed through the coronal loop, the oscillations became even stronger. There was a plasmoid eruption observed in EUV and a white-light CME was recorded, having velocity of  $\approx 340$ – $350$  km s<sup>-1</sup>. STEREO 195 Å images show an EIT wave, propagating in the same direction as the lower-speed coronal wave observed in AIA, but decelerating from  $\approx 320$  to  $\approx 254$  km s<sup>-1</sup>. These observations reveal the co-existence of both waves (i.e. coronal Moreton and EIT waves), and the type II radio burst seems to be associated with the coronal Moreton wave.

## **Multiwavelength Study of a Solar Eruption from AR NOAA 11112**

### **I. Flux Emergence, Sunspot Rotation and Triggering of a Solar Flare**

Pankaj [Kumar](#), Sung-Hong Park, K.-S. Cho, S.-C. Bong

Solar Physics, February **2013**, Volume 282, Issue 2, pp 503-521

We analyze the multiwavelength observations of an M2.9/1N flare that occurred in the active region (AR) NOAA 11112 in the vicinity of a huge filament system on **16 October 2010**. SDO/HMI magnetograms reveal the emergence of a bipole (within the existing AR) 50 hours prior to the flare event. During the emergence, both the positive and negative sunspots in the bipole show translational as well as rotational motion. The positive-polarity sunspot shows significant motion/rotation in the south-westward/clockwise direction, and we see continuously pushing/sliding of the surrounding opposite-polarity field region. On the other hand, the negative-polarity sunspot moves/rotates in the westward/anticlockwise direction. The positive-polarity sunspot rotates  $\approx 70^\circ$  within 30 hours, whereas the one with negative polarity rotates  $\approx 20^\circ$  within 10 hours. SDO/AIA 94 Å EUV images show the emergence of a flux tube in the corona, consistent with the emergence of the bipole in HMI. The footpoints of the flux tube were anchored in the emerging bipole. The initial brightening starts at one of the footpoints (western) of the emerging loop system, where the positive-polarity sunspot pushes/slides towards a nearby negative-polarity field region. A high speed plasmoid ejection (speed  $\approx 1197$  km s<sup>-1</sup>) was observed during the impulsive phase of the flare, which suggests magnetic reconnection of the emerging positive-polarity sunspot with the surrounding opposite-polarity field region. The entire AR shows positive-helicity injection before the flare event. Moreover, the newly emerging bipole reveals the signature of a negative (left-handed) helicity. These observations provide unique evidence of the emergence of twisted flux tubes from below the photosphere to coronal heights, triggering a flare mainly due to the interaction between the emerging positive-polarity sunspot and a nearby negative-polarity sunspot by the shearing motion of the emerging positive sunspot towards the negative one. Our observations also strongly support the idea that the rotation can most likely be attributed to the emergence of twisted magnetic fields, as proposed by recent models.

## **INITIATION OF CORONAL MASS EJECTION AND ASSOCIATED FLARE CAUSED BY HELICAL KINK INSTABILITY OBSERVED BY SDO/AIA**

Pankaj [Kumar](#), K.-S. Cho<sup>1,2,3</sup>, S.-C. Bong<sup>1</sup>, Sung-Hong Park<sup>1</sup> and Y. H. Kim

2012 ApJ 746 67, [File](#)

In this paper, we present multiwavelength observations of helical kink instability as a trigger of a coronal mass ejection (CME) which occurred in active region NOAA 11163 on **2011 February 24**. The CME was associated with an M3.5 limb flare. High-resolution observations from the Solar Dynamics Observatory/Atmospheric Imaging Assembly suggest the development of helical kink instability in the erupting prominence, which implies a flux rope structure of the magnetic field. A brightening starts below the apex of the prominence with its slow rising motion ( $\sim 100 \text{ km s}^{-1}$ ) during the activation phase. A bright structure, indicative of a helix with  $\sim 3$ -4 turns, was transiently formed at this position. The corresponding twist of  $\sim 6\pi$ - $8\pi$  is sufficient to generate the helical kink instability in a flux rope according to recently developed models. A slowly rising blob structure was subsequently formed at the apex of the prominence, and a flaring loop was observed near the footpoints. Within 2 minutes, a second blob was formed in the northern prominence leg. The second blob erupts (like a plasmoid ejection) with the detachment of the northern prominence leg, and flare intensity maximizes. The first blob at the prominence apex shows rotational motion in the counterclockwise direction in the plane of sky, interpreted as the unwinding motion of a helix, and it also erupts to give the CME. RHESSI hard X-ray (HXR) sources show the two footpoint sources and a loop-top source during the flare. We found RHESSI HXR flux, soft X-ray flux derivative, and CME acceleration in the low corona correlate well, which is in agreement with the standard flare model (CSHKP). We also discuss the possible role of ballooning as well as torus instabilities in driving the CME. We conclude that the CME and flare were triggered by the helical kink instability in a flux rope and accelerated mainly by the torus instability.

### **Multi-Wavelength Observations of a Flux Rope Failed in the Eruption and Associated M-Class Flare from NOAA AR 11045**

Pankaj [Kumar](#)<sup>1;2</sup> \_ A.K. Srivastava<sup>1;4</sup> \_ B. Filippov<sup>3</sup> \_ R. Erdelyi<sup>4</sup> \_ Wahab Uddin<sup>1</sup>  
E-print, July 2011, [File](#);

We present the multi-wavelength observations of a flux rope that was trying to erupt from NOAA AR 11045 and the associated M-class solar flare on **12 February 2010** using space and ground based observations from TRACE, STEREO, SOHO/MDI, Hinode/XRT and BBSO. While the flux rope was rising from the active region, an M1.1/2F class flare was triggered nearby one of its footpoints. We suggest that the flare triggering was due to the reconnection of a rising flux rope with the surrounding low-lying magnetic loops. The flux rope reached a projected height of  $\sim 0.15R_{\odot}$  with a speed of  $\sim 90 \text{ km s}^{-1}$  while the soft X-ray flux enhanced gradually during its rise. The flux rope was suppressed by an overlying field and the field plasma moved towards the negative polarity field to the west of its activation site. We find the first observational evidence of the initial suppression of a flux rope due to a remnant filament visible both at chromospheric and coronal temperatures that evolved couple of days before at the same location in the active region. SOHO/MDI magnetograms show the emergence of a bipole  $\sim 12$  h prior to the flare initiation. The emerged negative polarity moved towards the flux rope activation site, and flare triggering near the photospheric polarity inversion line (PIL) took place. The motion of the negative polarity region towards PIL helped in the build-up of magnetic energy at the flare and flux rope activation site. This study provides a unique observational

### **Effects of optimisation parameters on data-driven magnetofrictional modelling of active regions**

[A. Kumari](#), [D. J. Price](#), [F. Daei](#), [J. Pomoell](#), [E. K. J. Kilpua](#)

A&A 2023

<https://arxiv.org/pdf/2305.16080.pdf>

Data-driven time-dependent magnetofrictional modelling (TMFM) of active region magnetic fields has been proven to be a useful tool to study the corona. The input to the model is the photospheric electric field that is inverted from a time series of the photospheric magnetic field. Constraining the complete electric field, that is, including the non-inductive component, is critical for capturing the eruption dynamics. We present a detailed study of the effects of optimisation of the non-inductive electric field on the TMFM of AR12473. We aim to study the effects of varying the non-inductive electric field on the data-driven coronal simulations, for two alternative parametrisations. By varying parameters controlling the strength of the non-inductive electric field, we wish to explore the changes in flux rope formation and their early evolution and other parameters, for instance, axial flux and magnetic field magnitude. The non-inductive electric field component in the photosphere is critical for energising and introducing twist to the coronal magnetic field, thereby allowing unstable configurations to be formed. We estimated this component using an approach based on optimising the injection of magnetic energy. However, the flux rope formation, evolution and eruption time varies depending on the values of the optimisation parameters. The flux rope is formed and has overall similar evolution and properties with a large range of non-inductive electric fields needed to determine the non-inductive electric field component that is critical for energising and introducing twist to the coronal magnetic field. This study shows that irrespective of non-inductive electric field values, flux ropes are formed and erupted, which indicates that data-driven TMFM can be used to estimate flux rope properties early in their evolution without employing a lengthy optimisation process. **December 22, 2015 to January 02, 2016**

### **On the occurrence of type IV solar radio bursts in the solar cycle 24 and their association with coronal mass ejections**

[Anshu Kumari](#), [D. E. Morosan](#), [E. K. J. Kilpua](#)

2021 ApJ 906 79

<https://arxiv.org/pdf/2011.03509.pdf>  
<https://doi.org/10.3847/1538-4357/abc878>

Solar activity, in particular coronal mass ejections (CMEs), are often accompanied by bursts of radiation at metre wavelengths. Some of these bursts have a long duration and extend over a wide frequency band, namely, type IV radio bursts. However, the association of type IV bursts with coronal mass ejections is still not well understood. In this article, we perform the first statistical study of type IV solar radio bursts in the solar cycle 24. Our study includes a total of 446 type IV radio bursts that occurred during this cycle. Our results show that a clear majority, ~81% of type IV bursts, were accompanied by CMEs, based on a temporal association with white-light CME observations. However, we found that only ~2.2% of the CMEs are accompanied by type IV radio bursts. We categorised the type IV bursts as moving or stationary based on their spectral characteristics and found that only ~18% of the total type IV bursts in this study were moving type IV bursts. Our study suggests that type IV bursts can occur with both 'Fast' ( $\geq 500$  km/s) and 'Slow' ( $< 500$  km/s), and also both 'Wide' ( $\geq 60^\circ$ ) and 'Narrow' ( $< 60^\circ$ ) CMEs. However, the moving type IV bursts in our study were mostly associated with 'Fast' and 'Wide' CMEs (~52%), similar to type II radio bursts. Contrary to type II bursts, stationary type IV bursts have a more uniform association with all CME types. **October 03, 2011, October 18, 2017**

## Strength of the Solar Coronal Magnetic Field – A Comparison of Independent Estimates Using Contemporaneous Radio and White-Light Observations

Anshu [Kumari](#), R. Ramesh, C. Kathiravan, T. J. Wang

[Solar Physics](#) November 2017, 292:161

<https://arxiv.org/pdf/1711.02307.pdf>

We estimated the coronal magnetic field strength (BB) during the **23 July 2016** coronal mass ejection (CME) event using i) the flux rope structure of the CME in the white-light coronagraph images and ii) the band-splitting in the associated type II burst. No models were assumed for the coronal electron density ( $N(r)N(r)$ ) we used in the estimation. The results obtained with these two independent methods correspond to different heliocentric distances ( $r$ ) in the range  $\approx 2.5$ – $4.5 R_\odot$ – $\approx 2.5$ – $4.5 R_\odot$ , but they show excellent consistency and could be fit with a single power-law distribution of the type  $B(r)=5.7r^{-2.6}$  GB( $r)=5.7r^{-2.6}$  G, which is applicable in that distance range. The power-law index (i.e.  $-2.6$ ) is in good agreement with the results obtained in previous studies by different methods.

## New Evidence for a Coronal Mass Ejection-driven High Frequency Type II Burst near the Sun

Anshu [Kumari](#)<sup>1</sup>, R. Ramesh<sup>1</sup>, C. Kathiravan<sup>1</sup>, and N. Gopalswamy

**2017** ApJ 843 10

<http://sci-hub.cc/10.3847/1538-4357/aa72e7>

We report observations of the high frequency type II radio burst ( $\approx 430$ – $30$  MHz) that occurred in the solar corona on **2015 November 4**. The drift rate of the burst, estimated close to the start frequency of its fundamental component ( $\approx 215$  MHz), is unusually high ( $\approx 2$  MHz  $s^{-1}$ ). Our analysis shows that the estimated speed of the magnetohydrodynamic shock driver of the burst varies with time. The peak speed and acceleration are very large,  $\approx 2450$  km  $s^{-1}$  and  $\approx 17$  km  $s^{-2}$ , respectively. There is spatio-temporal correlation between the type II burst and the associated coronal mass ejection (CME) in the whitelight and extreme-ultraviolet images. The time profile of the shock speed and the light curve of the associated soft X-ray flare correlate well. These results indicate that in the present case, (i) the magnetohydrodynamic shock responsible for the high frequency coronal type II burst is driven by the CME and (ii) the time profile of the type II burst shock speed represents the near-Sun kinematics of the CME.

**CESRA highlight #1818, April 2018** <http://cesra.net/?p=1818>

## Coronal Mass Ejections

Series: [Space Sciences Series of ISSI](#), Vol. 21

[Kunow](#), H.; Crooker, N.U.; Linker, J.A.; Schwenn, R.; Von Steiger, R. (Eds.)

*Reprinted from Space Science Reviews Journal, Vol. 123/1-4*

**2007**, VI, 484 p., 162 illus., 46 in colour, Hardcover

ISBN: 978-0-387-45086-5

## Simulation of Spectral Observations of an Eruptive Prominence.

[Kupryakov](#), Y.A., Bychkov, K.V., Belova, O.M. et al.

Geomagn. Aeron. 64, 19–23 (**2024**).

<https://doi.org/10.1134/S0016793223600881>

The paper presents the results of an analysis of observations of an eruptive prominence on the MFS and HSFA2 spectrographs of the Ondřejov Observatory (Astronomical Institute, Czech Republic) in the hydrogen, helium, and calcium lines. After spectral processing, the integral radiation fluxes in the lines were determined and the physical parameters of the plasma were calculated theoretically using a model in the absence of local thermodynamic equilibrium. Comparison of the observed and calculated values showed that the observed radiation fluxes in the lines can be explained in a model of stationary gas radiation taking into account the opacity in the spectral lines. To calculate the theoretical fluxes, in some cases, it was necessary to introduce radiation from several layers with different

temperatures and heights. The calculated radiation fluxes agree with the observed ones to within 10%. As a result of the simulation, the main parameters of the plasma of the prominence were obtained: temperature, concentration, etc. The values of the radiation fluxes in the spectral lines are evidence of inhomogeneity of the emitting gas, and there may be regions next to each other with temperatures differing by an order of magnitude.

## **KELVIN–HELMHOLTZ INSTABILITY IN SOLAR CHROMOSPHERIC JETS: THEORY AND OBSERVATION**

D. Kuridze<sup>1,5</sup>, T. V. Zaqarashvili<sup>2,3,4</sup>, V. Henriques<sup>1</sup>, M. Mathioudakis<sup>1</sup>, F. P. Keenan<sup>1</sup>, and A. Hanslmeier<sup>2</sup>

2016 ApJ 830 133

Using data obtained by the high-resolution CRisp Imaging SpectroPolarimeter instrument on the Swedish 1 m Solar Telescope, we investigate the dynamics and stability of quiet-Sun chromospheric jets observed at the disk center. Small-scale features, such as rapid redshifted and blueshifted excursions, appearing as high-speed jets in the wings of the H $\alpha$  line, are characterized by short lifetimes and rapid fading without any descending behavior. To study the theoretical aspects of their stability without considering their formation mechanism, we model chromospheric jets as twisted magnetic flux tubes moving along their axis, and use the ideal linear incompressible magnetohydrodynamic approximation to derive the governing dispersion equation. Analytical solutions of the dispersion equation indicate that this type of jet is unstable to Kelvin–Helmholtz instability (KHI), with a very short (few seconds) instability growth time at high upflow speeds. The generated vortices and unresolved turbulent flows associated with the KHI could be observed as a broadening of chromospheric spectral lines. Analysis of the H $\alpha$  line profiles shows that the detected structures have enhanced line widths with respect to the background. We also investigate the stability of a larger-scale H $\alpha$  jet that was ejected along the line of sight. Vortex-like features, rapidly developing around the jet's boundary, are considered as evidence of the KHI. The analysis of the energy equation in the partially ionized plasma shows that ion–neutral collisions may lead to fast heating of the KH vortices over timescales comparable to the lifetime of chromospheric jets.

## **Failed filament eruption inside a coronal mass ejection in active region 11121\***

D. Kuridze<sup>1,4</sup>, M. Mathioudakis<sup>1</sup>, A. F. Kowalski<sup>2</sup>, P. H. Keys<sup>1</sup>, D. B. Jess<sup>1,5</sup>, K. S. Balasubramaniam<sup>3</sup> and F. P. Keenan

A&A 552, A55 (2013)

**Aims.** We study the formation and evolution of a failed filament eruption observed in NOAA active region 11121 near the southeast limb on **November 6, 2010**.

**Methods.** We used a time series of SDO/AIA 304, 171, 131, 193, 335, and 94 Å images, SDO/HMI magnetograms, as well as ROSA and ISOON H $\alpha$  images to study the erupting active region.

**Results.** We identify coronal loop arcades associated with a quadrupolar magnetic configuration, and show that the expansion and cancellation of the central loop arcade system over the filament is followed by the eruption of the filament. The erupting filament reveals a clear helical twist and develops the same sign of writhe in the form of inverse  $\gamma$ -shape.

**Conclusions.** The observations support the “magnetic breakout” process in which the eruption is triggered by quadrupolar reconnection in the corona. We propose that the formation mechanism of the inverse  $\gamma$ -shape flux rope is the magnetohydrodynamic helical kink instability. The eruption has failed because of the large-scale, closed, overlying magnetic loop arcade that encloses the active region.

## **MAGNETIC FIELD STRUCTURES TRIGGERING SOLAR FLARES AND CORONAL MASS EJECTIONS**

K. Kusano<sup>1,4</sup>, Y. Bamba<sup>1</sup>, T. T. Yamamoto<sup>1</sup>, Y. Iida<sup>2,5</sup>, S. Toriumi<sup>2,5</sup>, and A. Asai

2012 ApJ 760 31

Solar flares and coronal mass ejections, the most catastrophic eruptions in our solar system, have been known to affect terrestrial environments and infrastructure. However, because their triggering mechanism is still not sufficiently understood, our capacity to predict the occurrence of solar eruptions and to forecast space weather is substantially hindered. Even though various models have been proposed to determine the onset of solar eruptions, the types of magnetic structures capable of triggering these eruptions are still unclear. In this study, we solved this problem by systematically surveying the nonlinear dynamics caused by a wide variety of magnetic structures in terms of three-dimensional magnetohydrodynamic simulations. As a result, we determined that two different types of small magnetic structures favor the onset of solar eruptions. These structures, which should appear near the magnetic polarity inversion line (PIL), include magnetic fluxes reversed to the potential component or the nonpotential component of major field on the PIL. In addition, we analyzed two large flares, the X-class flare on **2006 December 13** and the M-class flare on **2011 February 13**, using imaging data provided by the Hinode satellite, and we demonstrated that they conform to the simulation predictions. These results suggest that forecasting of solar eruptions is possible with sophisticated observation of a solar magnetic field, although the lead time must be limited by the timescale of changes in the small magnetic structures.

## Development and Parameters of a Non-Self-Similar CME Caused by Eruption of a Quiescent Prominence

I.V. [Kuzmenko](#) (1), [V.V. Grechnev](#)

Solar Phys. 292:143 2017

<https://arxiv.org/pdf/1709.01226.pdf> File

<https://link.springer.com/content/pdf/10.1007%2Fs11207-017-1167-3.pdf>

The eruption of a large quiescent prominence on **17 August 2013** and associated coronal mass ejection (CME) were observed from different vantage points by Solar Dynamics Observatory (SDO), Solar-Terrestrial Relations Observatory (STEREO), and Solar and Heliospheric Observatory (SOHO). Screening of the quiet Sun by the prominence produced an isolated negative microwave burst. We estimated parameters of the erupting prominence from a model of radio absorption and measured from 304 Å images. Their variations obtained by both methods are similar and agree within a factor of two. The CME development was studied from the kinematics of the front and different components of the core and their structural changes. The results are verified using movies in which the CME expansion was compensated according to the measured kinematics. We found that the CME mass ( $3.6 \times 10^{15}$  g) was mainly supplied by the prominence ( $\approx 6 \times 10^{15}$  g), while a considerable part drained back. The mass of the coronal-temperature component did not exceed  $10^{15}$  g. The CME was initiated by the erupting prominence, which constituted its core and remained active. The structural and kinematical changes started in the core and propagated outward. The CME structures continued to form during expansion, which did not become self-similar up to  $25R_{\odot}$ . The aerodynamic drag was insignificant. The core formed until  $4R_{\odot}$ . Some of its components were observed to straighten and stretch forward, indicating the transformation of tangled structures of the core into a simpler flux rope, which grew and filled the cavity as the CME expanded.

## Synthetic radio views on simulated solar flux ropes

Alexey [Kuznetsov](#), Rony Keppens, Chun Xia

Solar Phys. 2016

<http://arxiv.org/pdf/1601.02370v1.pdf>

In this paper, we produce synthetic radio views on simulated flux ropes in the solar corona, where finite-beta magnetohydrodynamic (MHD) simulations serve to mimic the flux rope formation stages, as well as their stable endstates. These endstates represent twisted flux ropes where balancing Lorentz forces, gravity and pressure gradients determine the full thermodynamic variation throughout the flux rope. The obtained models are needed to quantify radiative transfer in radio bands, and allow us to contrast weak to strong magnetic field conditions. Field strengths of up to 100 G in the flux rope yield the radio views dominated by optically thin free-free emission. The forming flux rope shows clear morphological changes in its emission structure as it deforms from an arcade to a flux rope, both on disk and at the limb. For an active region filament channel with a field strength of up to 680 G in the flux rope, gyroresonance emission (from the third-fourth gyrolayers) can be detected and even dominates over free-free emission at the frequencies of up to 7 GHz. Finally, we also show synthetic views on a simulated filament embedded within a (weak-field) flux rope, resulting from an energetically consistent MHD simulation. For this filament, synthetic views at the limb show clear similarities with actual observations, and the transition from optically thick (below 10 GHz) to optically thin emission can be reproduced. On the disk, its dimension and temperature conditions are as yet not realistic enough to yield the observed radio brightness depressions.

## The density compression ratio of shock fronts associated with coronal mass ejections

Ryun-Young [Kwon](#), [Angelos Vourlidis](#)

Journal of Space Weather and Space Climate 8, A08 2018

<https://arxiv.org/pdf/1801.04355.pdf>

<https://www.swsc-journal.org/articles/swsc/pdf/2018/01/swsc170031.pdf>

We present a new method to extract the three-dimensional electron density profile and density compression ratio of shock fronts associated with Coronal Mass Ejections (CMEs) observed in white light coronagraph images. We demonstrate the method with two examples of fast halo CMEs ( $\sim 2000 \text{ km s}^{-1}$ ) observed on **2011 March 7** and **2014 February 25**. Our method uses the ellipsoid model to derive the three-dimensional (3D) geometry and kinematics of the fronts. The density profiles of the sheaths are modeled with double-Gaussian functions with four free parameters and the electrons are distributed within thin shells behind the front. The modeled densities are integrated along the lines of sight to be compared with the observed brightness in COR2-A, and a  $\chi^2$  approach is used to obtain the optimal parameters for the Gaussian profiles. The upstream densities are obtained from both the inversion of the brightness in a pre-event image and an empirical model. Then the density ratio and Alfvénic Mach number are derived. We find that the density compression peaks around the CME nose, and decreases at larger position angles. The behavior is consistent with a driven shock at the nose and a freely-propagating shock wave at the CME flanks. Interestingly, we find that the supercritical region extends over a large area of the shock and last longer (several tens of minutes) than past reports. *It follows that CME shocks are capable of accelerating energetic particles in the corona over extended spatial and temporal scales and are likely responsible for the wide longitudinal distribution of these particles in the inner heliosphere.* Our results also demonstrate the power of multi-viewpoint coronagraphic observations and forward modeling in remotely deriving key shock properties in an otherwise inaccessible regime.



## Investigating the Wave Nature of the Outer Envelope of Halo Coronal Mass Ejections

Ryun-Young [Kwon](#)<sup>1,3</sup> and Angelos Vourlidas<sup>2</sup>

2017 ApJ 836 246

<http://sci-hub.cc/doi/10.3847/1538-4357/aa5b92>

We investigate the nature of the outer envelope of halo coronal mass ejections (H-CMEs) using multi-viewpoint observations from the Solar Terrestrial Relations Observatory-A, -B, and Solar and Heliospheric Observatory coronagraphs. The 3D structure and kinematics of the halo envelopes and the driving CMEs are derived separately using a forward modeling method. We analyze three H-CMEs with peak speeds from 1355 to 2157 km s<sup>-1</sup>; sufficiently fast to drive shocks in the corona. We find that the angular widths of the halos range from 192° to 252°, while those of the flux ropes range between only 58° and 91°, indicating that the halos are waves propagating away from the CMEs. The halo widths are in agreement with widths of Extreme Ultraviolet (EUV) waves in the low corona further demonstrating the common origin of these structures. To further investigate the wave nature of the halos, we model their 3D kinematic properties with a linear fast magnetosonic wave model. The model is able to reproduce the position of the halo flanks with realistic coronal medium assumptions but fails closer to the CME nose. The CME halo envelope seems to arise from a driven wave (or shock) close to the CME nose, but it is gradually becoming a freely propagating fast magnetosonic wave at the flanks. This interpretation provides a simple unifying picture for CME halos, EUV waves, and the large longitudinal spread of solar energetic particles. **2011 March 7, 2013 April 11, and 2014 February 25**

## THREE-DIMENSIONAL GEOMETRY OF A CURRENT SHEET IN THE HIGH SOLAR CORONA: EVIDENCE FOR RECONNECTION IN THE LATE STAGE OF THE CORONAL MASS EJECTIONS

Ryun-Young [Kwon](#)<sup>1,2</sup>, Angelos Vourlidas<sup>2</sup>, and David Webb

2016 ApJ 826 94

Motivated by the standard flare model, ray-like structures in the wake of coronal mass ejections (CMEs) have been often interpreted as proxies of the reconnecting current sheet connecting the CME with the postflare arcade. We present the three-dimensional properties of a post-CME ray derived from white light images taken from three different viewing perspectives on **2013 September 21**. By using a forward modeling method, the direction, cross section, and electron density are determined within the heliocentric distance range of 5–9 R<sub>☉</sub>. The width and depth of the ray are  $0.42 \pm 0.08 R_{\odot}$  and  $1.24 \pm 0.35 R_{\odot}$ , respectively, and the electron density is  $(2.0 \pm 0.5) \times 10^4 \text{ cm}^{-3}$ , which seems to be constant with height. Successive blobs moving outward along the ray are observed around 13 hr after the parent CME onset. We model the three-dimensional geometry of the parent CME with the Gradual Cylindrical Shell model and find that the CME and ray are coaxial. We suggest that coaxial post-CME rays, seen in coronagraph images, with successive formation of blobs could be associated with current sheets undergoing magnetic reconnection in the late stage of CMEs.

## Are Halo-like Solar Coronal Mass Ejections Merely a Matter of Geometric Projection Effects?

Ryun-Young [Kwon](#), Jie Zhang, and Angelos Vourlidas

2015 ApJ 799 L29

[http://spaceweather.gmu.edu/public/rkwon/manuscript\\_halo\\_CMEs/manuscript.pdf](http://spaceweather.gmu.edu/public/rkwon/manuscript_halo_CMEs/manuscript.pdf)

We investigated the physical nature of halo coronal mass ejections (CMEs) based on the stereoscopic observations from the two STEREO spacecraft, Ahead and Behind (hereafter A and B), and the SOHO spacecraft. Sixty-two halo CMEs occurred as observed by SOHO LASCO C2 for the three-year period from 2010 to 2012 during which the separation angles between SOHO and STEREO were nearly 90°. In such quadrature configuration, the coronagraphs of STEREO, COR2-A and -B, showed the side view of those halo CMEs seen by C2. It has been widely believed that the halo appearance of a CME is caused by the geometric projection effect, i.e., a CME moves along the Sun-observer line. In other words, it would appear as a non-halo CME if viewed from the side. However, to our surprise, we found that 41 out of 62 events (66%) were observed as halo CMEs by all coronagraphs. This result suggests that a halo CME is not just a matter of the propagating direction. In addition, we show that a CME propagating normal to the line of sight can be observed as a halo CME due to the associated fast magnetosonic wave or shock front. We conclude that the apparent width of CMEs, especially halos or partial halos is driven by the existence and the extent of the associated waves or shocks and does not represent an accurate measure of the CME ejecta size. This effect needs to be taken into careful consideration in space weather predictions and modeling efforts. **2012 March 18**

## NEW INSIGHTS INTO THE PHYSICAL NATURE OF CORONAL MASS EJECTIONS AND ASSOCIATED WAVES/SOCKS WITHIN THE FRAMEWORK OF THREE-DIMENSIONAL STRUCTURE

Ryun-Young [Kwon](#), Jie Zhang, and Oscar Olmedo

ApJ, 794 148 **2014**

<http://spaceweather.gmu.edu/public/rkwon/> **File**

We present new insights into the physical nature of coronal mass ejections (CMEs) and associated shock waves within the framework of the three-dimensional (3D) structure. We have developed a compound model in order to determine the 3D structure of multiple fronts composing a CME, using data sets taken from STEREO, SDO, and SOHO. We applied the method to time series observations of a CME on **2012 March 7**. From the analyses, we revealed that a CME could

consist of two different fronts: one is represented well with the ellipsoid model, implying that CMEs are bubble-shaped structures and the other is reproduced well with the graduated cylindrical shell model, indicating that CMEs are flux rope-shaped structures. The bubble-shaped structure is seen as the outermost front of the CME, and the flux rope-shaped structure is seen as the bright frontal loop or three-part morphology. From our results, we conclude that (1) a CME could consist of two distinct structures, a bubble shaped structure and a flux rope-shaped structure, (2) the bubble-shaped structure is a fast magnetosonic shock wave while the flux rope-shaped structure is the mass carried outward by the underlying magnetic structure, (3) the driven shock front could be either a piston-shock type or a bow-shock type, (4) the observed EUV wave in the low corona is the footprint of the bubble-shaped wave, and (5) the halo CME is primarily the projection of the bubble-shaped shock wave but not the underlying flux rope.

## **Global Coronal Seismology in the Extended Solar Corona through Fast Magnetosonic Waves Observed by STEREO SECCHI COR1**

Ryun-Young [Kwon](#)<sup>1,2,3</sup>, Maxim Kramar<sup>1,2</sup>, Tongjiang Wang<sup>1,2</sup>, Leon Ofman<sup>1,2,4</sup>, Joseph M. Davila<sup>2</sup>, Jongchul Chae<sup>5</sup>, and Jie Zhang

2013 ApJ 776 55

We present global coronal seismology for the first time, which allows us to determine inhomogeneous magnetic field strength in the extended corona. From the measurements of the propagation speed of a fast magnetosonic wave associated with a **coronal mass ejection (CME)** and the coronal background density distribution derived from the polarized radiances observed by the STEREO SECCHI COR1, we determined the **magnetic field strengths** along the trajectories of the wave at different heliocentric distances. We found that the results have an uncertainty less than 40%, and are consistent with values determined with a potential field model and reported in previous works. The characteristics of the coronal medium we found are that (1) the density, magnetic field strength, and plasma  $\beta$  are lower in the **coronal hole** region than in streamers; (2) the magnetic field strength decreases slowly with height but the electron density decreases rapidly so that the local fast magnetosonic speed increases while plasma  $\beta$  falls off with height; and (3) the variations of the local fast magnetosonic speed and plasma  $\beta$  are dominated by variations in the electron density rather than the magnetic field strength. These results imply that **Moreton and EIT waves** are downward-reflected fast magnetosonic waves from the upper solar corona, rather than freely propagating fast magnetosonic waves in a certain atmospheric layer. In addition, the azimuthal components of CMEs and the driven waves may play an important role in various manifestations of shocks, such as **type II radio bursts and solar energetic particle events**.

## **Survey of Magnetic Helicity Injection in Regions Producing X-Class Flares**

[LaBonte](#), B. J., [Georgoulis](#), M. K., & [Rust](#), D. M.

E-print, Aug. 2007

we surveyed magnetic helicity injection into 48 X-flare producing active regions recorded by the MDI between 1996 July and 2005 July.

Most of the X-flare regions generated the helicity needed for a CME in a few days to a few hours.

## **The Evolution of Ion Charge States in Coronal Mass Ejections**

[J. Martin Laming](#), [Elena Provornikova](#), [Yuan-Kuen Ko](#)

ApJ 954 145 2023

<https://arxiv.org/pdf/2307.15762.pdf>

<https://iopscience.iop.org/article/10.3847/1538-4357/acebc2/pdf>

We model the observed charge states of the elements C, O, Mg, Si, and Fe in the coronal mass ejections (CMEs) ejecta. We concentrate on "halo" CMEs observed in situ by ACE/SWICS to measure ion charge states, and also remotely by STEREO when in near quadrature with Earth, so that the CME expansion can be accurately specified. Within this observed expansion, we integrate equations for the CME ejecta ionization balance, including electron heating parameterized as a fraction of the kinetic and gravitational energy gain of the CME. We also include the effects of non-Maxwellian electron distributions, characterized as a kappa function. Focusing first on the **2010 April 3** CME, we find a somewhat better match to observed charge states with kappa in the range 2-4, close to the theoretical minimum value of kappa = 3/2, implying a hard spectrum of non-thermal electrons. Similar, but more significant results come from the **2011 February 15** event, although it is quite different in terms of its evolution. We discuss the implications of these values, and of the heating required, in terms of the magnetic reconnection Lundquist number and anomalous resistivity associated with CME evolution close to the Sun.

## **Observing Solar Coronal Mass Ejections from Space**

[Philippe Lamy](#)

Proceedings of the IAU Symposium 388, 2024

<https://arxiv.org/pdf/2407.08354>

**Review**

In this contribution to the panel discussion of the IAU Symposium 388 "Solar and Stellar Coronal Mass Ejections", I concentrate on white-light observations of solar coronal mass ejections (CMEs) from space and specifically address the following aspects: i) history of observations, ii) available catalogs of CMEs, iii) achievements of space observations of CMEs, iv) future of CME observation, and v) challenges and future directions.

## **The State of the White-Light Corona over the Minimum and Ascending Phases of Solar Cycle 25 -- Comparison with Past Cycles**

Philippe **Lamy** (1), [Hugo Gilardy](#) (1)

Solar Phys. **297**, Article number: 140 **2022**

<https://arxiv.org/pdf/2205.06462.pdf>

<https://doi.org/10.1007/s11207-022-02057-7>

We report on the state of the corona over the minimum and ascending phases of Solar Cycle (SC) 25 on the basis of the temporal evolutions of its radiance and of the properties of coronal mass ejections (CMEs) as determined from white-light observations performed by the SOHO/LASCO-C2 coronagraph. These evolutions are further compared with those determined during the past two SC. The integrated radiance of the K-corona and the occurrence rate of CMEs closely track the indices/proxies of solar activity, prominently the total magnetic field for the radiance and the radio flux for the CMEs, all undergoing a steep increase during the ascending phase of SC 25. This increase is much steeper than anticipated on the basis of the predicted quasi similarity between SC 25 and 24, and is confirmed by the recent evolution of the sunspot number. The radiance reached the same base level during the minima of SC 24 and 25, but the latitudinal extent of the streamer belt differed, being flatter during the latter minimum and in fact more similar to that of the minimum of SC 23. Phasing the descending branches of SC 23 and 24 led to a duration of SC 24 of 11.0 years, similar to that given by the sunspot number. In contrast, the base level of the occurrence rate of CMEs during the minimum of SC 25 was significantly larger than during the two previous minima. The southern hemisphere is conspicuously more active than the northern one in agreement with several predictions and the current evolution of the hemispheric sunspot numbers. The mean apparent width of CMEs and the number of halo CMEs remains at relatively large, constant levels throughout the early phase of SC 25 implying the persistence of weak total pressure in the heliosphere. These results and the perspective of a corona more active than anticipated are extremely promising for the forthcoming observations by Solar Orbiter and Parker Solar Probe.

## **Coronal Mass Ejections over Solar Cycles 23 and 24**

**Review**

P. L. **Lamy**, [O. Floyd](#), [B. Boclet](#), [J. Wojak](#), [H. Gilardy](#)...

*Space Science Reviews* August **2019**, 215:39

<https://link.springer.com/content/pdf/10.1007%2Fs11214-019-0605-y.pdf>

We present a statistical analysis of solar coronal mass ejections (CMEs) based on 23 years of quasi-continuous observations with the LASCO coronagraph, thus covering two complete Solar Cycles (23 and 24). We make use of five catalogs, one manual (CDAW) and four automated (ARTEMIS, CACTus, SEEDS, and CORIMP), to characterize the temporal evolutions and distributions of their properties: occurrence and mass rates, waiting times, periodicities, angular width, latitude, speed, acceleration and kinetic energy. Our analysis points to inevitable discrepancies between catalogs due to the complex nature of CMEs and to the different techniques implemented to detect them, but also to large areas of convergence that are critically important to ascertain the reliability of the results. The temporal variations of these properties are compared to four indices/proxies of solar activity: the radio flux at 10.7 cm (F10.7), the international sunspot number (SSN), the sunspot area (SSA), and the total magnetic field (TMF), either globally or separately in the northern and southern hemispheres in the case of the last three. We investigate the association of CMEs with flares, erupting prominences, active regions and streamers. We find that the CME occurrence and mass rates globally track the indices/proxies of solar activity with no time lag, prominently the radio flux F10.7, but the linear relationships were different during the two solar cycles, implying that the CME rates were relatively larger during SC 24 than during SC 23. However, there exists a pronounced divergence of the CME rates in the northern hemisphere during SC 24 as these rates were substantially larger than predicted by the temporal variation of the sunspot number. The distribution of kinetic energy follows a log-normal law and that of angular width follows an exponential law implying that they are random and independent. The distribution of waiting time (WTD) has a long power-law tail extending from 3 to 100 hr with a power-law index which varies with the solar cycle, thus reflecting the temporal variability of the process of CME formation. There is very limited evidence for periodicities in the occurrence and mass rates of CMEs, a striking feature being the dichotomy between the two hemispheres. Rather weak correlations are present among the various CME parameters and particularly none between speed and acceleration. The association of CMEs with flares and erupting prominences involves only a few percents of the overall population of CMEs but the associated CMEs have distinctly larger mass, speed, kinetic energy and angular width. A more pronounced association is found with active regions but the overwhelming one is with streamers further confirmed by the similarity between the heliolatitudinal distribution of CMEs and that of the electron density reconstructed from time-dependent tomographic inversion. We find no evidence of bimodality in the distributions of physical parameters that would support the existence of two classes, particularly that based on speed and acceleration, the distributions thus favoring a continuum of properties. There exists an excess of narrow CMEs which however does not define a special class. These narrow CMEs are likely associated with the ubiquitous mini-filaments eruptions and with mini flux ropes originating from small magnetic bipoles, the disruption mechanisms being similar to those launching larger CMEs. This supports the concept that CMEs at large arise from closed-field coronal regions at both large and small scales.

## **Anomalous Surge of the White-Light Corona at the Onset of the Declining Phase of Solar Cycle 24**

P. Lamy, B. Boclet, J. Wojak, D. Vibert

Solar Physics April 2017, 292:60

<http://link.springer.com/content/pdf/10.1007%2Fs11207-017-1085-4.pdf>

In late 2014, when the current Solar Cycle 24 entered its declining phase, the white-light corona as observed by the LASCO-C2 coronagraph underwent an unexpected surge that increased its global radiance by 60%, reaching a peak value comparable to the peak values of the more active Solar Cycle 23. A comparison of the temporal variation of the white-light corona with the variations of several indices and proxies of solar activity indicate that it best matches the variation of the total magnetic field. The daily variations point to a localized enhancement or bulge in the electron density that persisted for several months. Carrington maps of the radiance and of the HMI photospheric field allow connecting this bulge to the emergence of the large sunspot complex AR 12192 in October 2014, the largest since AR 6368 observed in November 1990. The resulting unusually high increase of the magnetic field and the distortion of the neutral sheet in a characteristic inverse S-shape caused the coronal plasma to be trapped along a similar pattern. A 3D reconstruction of the electron density based on time-dependent solar rotational tomography supplemented by 2D inversion of the coronal radiance confirms the morphology of the bulge and reveals that its level was well above the standard models of a corona of the maximum type, by typically a factor of 3. A rather satisfactory agreement is found with the results of the thermodynamic MHD model produced by Predictive Sciences, although discrepancies are noted. The specific configuration of the magnetic field that led to the coronal surge resulted from the interplay of various factors prevailing at the onset of the declining phase of the solar cycles, which was particularly efficient in the case of Solar Cycle 24. **18-28 November 2014.**

## **Density Diagnostics of Coronal Mass Ejection Cores with the Solar Dynamics Observatory/Atmospheric Imaging Assembly**

E. Landi<sup>1</sup> and M. P. Miralles

2014 ApJ 780 L7

In this Letter, we investigate the application of the intensity ratio from pairs of narrow-band images from the Atmospheric Imaging Assembly (AIA) on the Solar Dynamics Observatory, the Extreme Ultraviolet (EUV) Imager (EUVI) on board the Sun Earth Connection Coronal and Heliospheric Investigation, and the EUV Imaging Telescope (EIT) on board the Solar and Heliospheric Observatory, to density diagnostics of optically thin plasmas. By inspecting the filtered spectra allowed by each instrument's effective area, we find that ratios between AIA images in the 171 Å and 193 Å channels can be used to determine the plasma electron density at transition region temperatures. This diagnostic potential is due to a pair of O V transitions which dominate the effective spectra of these two channels at temperatures around  $2.5\text{-}3.0 \times 10^5$  K. The temperature and electron density ranges where the 171/193 ratio is density sensitive are relevant for the cores of accelerating coronal mass ejections (CMEs) in the inner solar corona. We discuss how AIA series of images can be used for simultaneous temperature and density diagnostics of CME cores.

## **Hot Plasma Associated with a Coronal Mass Ejection**

E. Landi<sup>1</sup>, M. P. Miralles<sup>2</sup>, J. C. Raymond<sup>2</sup>, and H. Hara

2013 ApJ 778 29

We analyze coordinated observations from the EUV Imaging Spectrometer (EIS) and X-Ray Telescope (XRT) on board Hinode of an X-ray Plasma Ejection (XPE) that occurred during the coronal mass ejection (CME) event of **2008 April 9**. The XPE was trailing the CME core from behind, following the same trajectory, and could be identified both in EIS and XRT observations. Using the EIS spectrometer, we have determined the XPE plasma parameters, measuring the electron density, thermal distribution, and elemental composition. We have found that the XPE composition and electron density were very similar to those of the pre-event active region plasma. The XPE temperature was higher, and its thermal distribution peaked at around 3 MK; also, typical flare lines were absent from EIS spectra, indicating that any XPE component with temperatures in excess of 5 MK was likely either faint or absent. We used XRT data to investigate the presence of hotter plasma components in the XPE that could have gone undetected by EIS and found that—if at all present—these components have small emission measure values and their temperature is in the 8-12.5 MK range. The very hot plasma found in earlier XPE observations obtained by Yohkoh seems to be largely absent in this CME, although plasma ionization timescales may lead to non-equilibrium ionization effects that could make bright lines from ions formed in a 10 MK plasma not detectable by EIS. Our results supersede the XPE findings of Landi et al., who studied the same event with older response functions for the XRT Al-poly filter; the differences in the results stress the importance of using accurate filter response functions.

## **POST-CORONAL MASS EJECTION PLASMA OBSERVED BY HINODE**

E. Landi<sup>1</sup>, J. C. Raymond<sup>2</sup>, M. P. Miralles<sup>2</sup>, and H. Hara

2012 ApJ 751 21

In the present work we study the evolution of an active region after the eruption of a coronal mass ejection (CME) using observations from the EIS and XRT instruments on board Hinode. The field of view includes a post-eruption arcade, a current sheet, and a coronal dimming. The goal of this paper is to provide a comprehensive set of measurements for all these aspects of the CME phenomenon made on the same CME event. The main physical properties of the plasma along the line of sight—electron density, thermal structure, plasma composition, size, and, when possible, mass—are measured and monitored with time for the first three hours following the CME event of **2008 April 9**. We find that the loop arcade observed by EIS and XRT may not be related to the post-eruption arcade. Post-CME plasma is hotter than the surrounding corona, but its temperature never exceeds 3 MK. Both the electron density and thermal structure do not show significant evolution with time, while we found that the size of the loop arcade in the Hinode plane of the sky decreased with time. The plasma composition is the same in the current sheet, in the loop arcade, and in the ambient plasma, so all these plasmas are likely of coronal origin. No significant plasma flows were detected.

## PHYSICAL CONDITIONS IN A CORONAL MASS EJECTION FROM *HINODE*, *STEREO*, AND *SOHO* OBSERVATIONS

E. [Landi1](#), J. C. Raymond<sup>2</sup>, M. P. Miralles<sup>2</sup>, and H. Hara<sup>3</sup>

*Astrophysical Journal*, 711:75–98, **2010** March; **File**

In the present work, we analyze multiwavelength observations from *Hinode*, *Solar and Heliospheric Observatory (SOHO)*, and *STEREO* of the early phases of a coronal mass ejection (CME). We use *Hinode*/EIS and *SOHO*/UVCS high-resolution spectra to measure the physical properties of the CME ejecta as a function of time at 1.1 and 1.9 solar radii. *Hinode*/XRT images are used in combination with EIS spectra to constrain the high temperature plasma properties of the ejecta. SECCHI/EUVI, SECCHI/COR 1, *SOHO*/EIT, and *SOHO*/LASCO images are used to measure the CME trajectory, velocity, and acceleration. The combination of measurements of plane of the sky velocities from two different directions allows us to determine the total velocity of the CME plasma up to 5 solar radii. Plasma properties, dynamical status, thermal structure, and brightness distributions are used to constrain the energy content of the CME plasma and to determine the heating rate. We find that the heating is larger than the kinetic energy, and compare it to theoretical predictions from models of CME plasma heating and acceleration.

## Space, time and velocity association of successive coronal mass ejections

Alejandro [Lara](#). Nat Gopalswamy, [Tatiana Niembro](#), [Román Pérez-Enríquez](#), [Seiji Yashiro](#)

*A&A* 635, A112 **2020**

<https://arxiv.org/pdf/2002.03998.pdf>

<https://doi.org/10.1051/0004-6361/201936016>

Our aim is to investigate the possible physical association between consecutive coronal mass ejections (CMEs). Through a statistical study of the main characteristics of 27761 CMEs observed by SOHO/LASCO during the past 20 years. We found the waiting time (WT) or time elapsed between two consecutive CMEs is <5 hrs for 59% and <25 hrs for 97% of the events, and the CME WTs follow a Pareto Type IV statistical distribution. The difference of the position-angle of a considerable population of consecutive CME pairs is less than 30°, indicating the possibility that their source locations are in the same region. The difference between the speed of trailing and leading consecutive CMEs follows a generalized Student t-distribution. The fact that the WT and the speed difference have heavy-tailed distributions along with a detrended fluctuation analysis shows that the CME process has a long-range dependence. As a consequence of the long-range dependence, we found a small but significant difference between the speed of consecutive CMEs, with the speed of the trailing CME being higher than the speed of the leading CME. The difference is largest for WTs < 2 hrs and tends to be zero for WTs > 10 hrs, and it is more evident during the ascending and descending phases of the solar cycle. We suggest that this difference may be caused by a drag force acting over CMEs closely related in space and time.

## The Source Region of Coronal Mass Ejections

Alejandro [Lara](#)

*The Astrophysical Journal*, Vol. 688, No. 1: 647-655, **2008**.

<http://www.journals.uchicago.edu/doi/abs/10.1086/591725>

We use the large database of coronal mass ejections (CMEs) observed by SOHO LASCO during solar cycle 23 to statistically obtain information about the source regions of CMEs. By determining the functional form of the position angle (P.A.) distribution, we are able to construct a random set of CME direction vectors (DVCME) under the following conditions: (1) assume a radial movement of the CME center of mass and (2) propose a latitude and longitude ( $\lambda$ ,  $\phi$ ) photospheric position for the DVCME in such a way that (3) the distribution of the projected (on the plane of the sky) DVCME must be equal to the observed distribution of position angles. We iteratively adjust the proposed positions ( $\lambda$ ,  $\phi$ ) until both distributions are equal, based on the Kolmogorov-Smirnov statistics. In this way, we obtain a set of DVCME that we use to study the relation between the CME source region and the overall coronal and photospheric magnetic field structures. We found that the CME activity has a small “preference” for the northern hemisphere during the first part of solar cycle, and for the southern hemisphere during the second part. This P.A. asymmetry is related to the overall magnetic field north-south asymmetry. We found also that most CME source regions are situated between high magnetic field regions, and are not necessarily associated to any one such region. For instance, during the

minimum and ascending phase of the cycle, ~85% and ~60%, respectively, of the CME source regions are confined to the equatorial plane ( $\lambda = 0^\circ$ ), between the two active region belts ( $\lambda = \pm 40^\circ$ ). We conclude from this study that CME sources are in general high-altitude magnetic loops, or more precisely, transequatorial loops, occurring during the minimum and ascending phases of the cycle.

### **Short-Period Fluctuations in Coronal Mass Ejection Activity during Solar Cycle 23**

Alejandro [Lara](#) · Andrea Borgazzi · Odim Mendes Jr. · Reinaldo R. Rosa · Margarete Oliveira Domingues  
Solar Phys (2008) 248: 155–166

<http://www.springerlink.com/content/44k0w353n6445633/fulltext.pdf>

We have constructed a time series of the number of coronal mass ejections (CMEs) observed by SOHO/LASCO during solar cycle 23. Using spectral analysis techniques (the maximum entropy method and wavelet analysis) we found short-period (<one year) semiperiodic activity. Among others, we found interesting periodicities at 193, 36, 28, and 25 days. We discuss the implications of such short-period activity in terms of the emergence and escape of magnetic flux from the convection zone, through the low solar atmosphere (where these periodicities have been found for numerous activity parameters), toward interplanetary space. This analysis shows that CMEs remove the magnetic flux in a quasiperiodic process in a way similar to that of magnetic flux emergence and other solar eruptive activity.

### **Are halo coronal mass ejections special events?**

Alejandro [Lara](#),<sup>1</sup> Nat Gopalswamy,<sup>2</sup> Hong Xie,<sup>3</sup> Eduardo Mendoza-Torres,<sup>4</sup>  
Roma'n Pe' rez-Eri' quez,<sup>5</sup> and Gregory Michalek

JOURNAL OF GEOPHYSICAL RESEARCH, VOL. 111, A06107, doi:10.1029/2005JA011431, 2006, **File**

### **A statistical study of CMEs associated with metric type II bursts**

A. [Lara](#), N. Gopalswamy, S. Nunes, G. Muñ' oz, and S. Yashiro  
GEOPHYSICAL RESEARCH LETTERS, VOL. 30, NO. 12, 8016, 2003

[sci-hub.se/10.1029/2002GL016481](http://sci-hub.se/10.1029/2002GL016481)

We present a statistical study of the characteristics of CMEs which show temporal association with type II bursts in the metric domain but not in the decameter/hectometric (DH) domain. This study is based on a set of 80 metric (m) type II bursts associated with surface events in the solar western hemisphere. It was found that in general, the distribution of the widths and speeds of the CMEs associated with metric (but not DH) type II bursts are shifted towards higher values compared to those of all CMEs observed by LASCO in the 1996 – 2001 period. We also found that these distributions have lower values than the same distributions of the CMEs associated with DH type II bursts. In terms of energy, this means that the CMEs associated only with metric type II bursts are more energetic (wider and faster) than regular CMEs but less energetic than the CMEs associated with DH type II bursts.

### **Evolution of coronal mass ejections with and without sheaths from the inner to the outer heliosphere: Statistical investigation for 1975 to 2022**

C. [Larrodera](#)<sup>1,2</sup> and M. Temmer<sup>2</sup>

A&A, 685, A89 (2024)

<https://arxiv.org/pdf/2402.16653.pdf>

<https://www.aanda.org/articles/aa/pdf/2024/05/aa48641-23.pdf>

**Aims.** This study covers a thorough statistical investigation of the evolution of interplanetary coronal mass ejections (ICMEs) with and without sheaths through a broad heliocentric distance and temporal range. The analysis treats the sheath and magnetic obstacle (MO) separately in order to gain more insight on their physical properties. In detail, we aim to unravel different characteristics of these structures occurring over the inner and outer heliosphere.

**Methods.** The method is based on a large statistical sample of ICMEs probed over different distances in the heliosphere. For this, information about detection times for the sheath and MO from 13 individual ICME catalogs was collected and crosschecked. The time information was then combined into a main catalog that was used as the basis for the statistical investigation. The data analysis based on this catalog covers a large number of spacecraft missions, enabling in situ solar wind measurements from 1975 to 2022. This allowed us to study the differences between solar cycles.

**Results.** All the structures under study (sheath, MO with and without sheath) show the biggest increase in size together with the largest decrease in density at a distance of ~0.75 AU. At 1 AU, we found different sizes for MOs with and without a sheath, with the former being larger. Up to 1 AU, the upstream solar wind shows the strongest pileup close to the interface with the sheath. For larger distances, the pileup region seems to shift, and it recedes from that interface further into the upstream solar wind. This might refer to a change in the sheath formation mechanism (driven versus non-driven) with heliocentric distance, suggesting the relevance of the CME propagation and the expansion behavior in the outer heliosphere. A comparison to previous studies showed inconsistencies over the solar cycle, which makes more detailed studies necessary in order to fully understand the evolution of ICME structures.

**Appendix A: Description of catalogs** **Table A.1.** References of the individual catalogs used.

## Multiwavelength Stereoscopic Observation of the 2013 May 1 Solar Flare and CME

Erica [Lastufka](#)<sup>1,2</sup>, Säm Krucker<sup>1,3</sup>, Ivan Zimovets<sup>4</sup>, Bulat Nizamov<sup>5</sup>, Stephen White<sup>6</sup>, Satoshi Masuda<sup>7</sup>, Dmitriy Golovin<sup>4</sup>, Maxim Litvak<sup>4</sup>, Igor Mitrofanov<sup>4</sup>, and Anton Sanin<sup>4</sup>

2019 ApJ 886 9

[sci-hub.se/10.3847/1538-4357/ab4a0a](https://sci-hub.se/10.3847/1538-4357/ab4a0a)

A M-class behind-the-limb solar flare on **2013 May 1** (SOL2013-05-01T02:32), accompanied by a ( $\sim 400$  km s<sup>-1</sup>) coronal mass ejection (CME), was observed by several space-based observatories with different viewing angles. We investigated the RHESSI-observed occulted hard X-ray (HXR) emissions that originated at least  $0.1 R_s$  above the flare site. Emissions below  $\sim 10$  keV revealed a hot, extended (11 MK,  $>60''$ ) thermal source from the escaping CME core, with densities around  $10^9$  cm<sup>-3</sup>. In such a tenuous hot plasma, ionization times scales are several minutes, consistent with the nondetection of the hot CME core in SDO/AIA's 131 Å filter. The nonthermal RHESSI source originated from an even larger area ( $\sim 100''$ ) at lower densities ( $10^8$  cm<sup>-3</sup>) located above the hot core, but still behind the CME front. This indicates that the observed part of the nonthermal electrons are not responsible for heating the CME core. Possibly the hot core was heated by nonthermal electrons before it became visible from Earth, meaning that the unocculted part of the nonthermal emission likely originates from a more tenuous part of the CME core, where nonthermal electrons survive long enough to become visible from Earth. Simultaneous HXR spectra from the Mars Odyssey mission, which viewed the flare on disk, indicated that the number of nonthermal electrons  $>20$  keV within the high coronal source is  $\sim 0.1\% - 0.5\%$  compared with the number within the chromospheric flare ribbons. The detection of high coronal HXR sources in this moderate size event suggests that such sources are likely a common feature within solar eruptive events.

## Coronal Mass Ejections with and without DH Type II Radio Bursts

M. Benedict [Lawrance](#), A. Shanmugaraju, Bojan Vršnak

Solar Phys. Volume 290, [Issue 11](#), pp 3365-3377 2015

A statistical analysis of 135 out of 141 X-class flares observed during 1997 – 2012 with and without deca-hectometric (DH) type II radio bursts has been performed. It was found that 79 events (X-class flares and coronal mass ejections – Group I) were associated with DH type II radio bursts and 62 X-class flare events were not. Out of these 62 events without DH type IIs, 56 events (Group II) have location information, and they were selected for this study. Of these 56 events, only 32 were associated with CMEs. Most of the DH-associated X-class events ( $\sim 79\%$ ) were halo CMEs, in contrast to 14% in Group II. The average CME speed of the X-class flares associated with DH type IIs is 1555 km s<sup>-1</sup>, which is nearly twice that of the X-class flare-associated CMEs without DH event (744 km s<sup>-1</sup>). The X-class flares associated with DH radio bursts have a mean flare intensity ( $3.63 \times 10^{-4}$  W m<sup>-2</sup>) that is 38% greater than that of X-class flares without DH radio bursts ( $2.23 \times 10^{-4}$  W m<sup>-2</sup>). In addition to the greater intensity, it is also found that the duration and rise time of flares associated with DH radio emission (DH flares) is more than twice than that of the flares without DH radio emission. When the events were further divided into two categories with respect to their source locations in eastern and western regions, 65% of the events in the radio-loud category (with DH radio bursts) are from the western hemisphere and the remaining 35% are from the eastern hemisphere. On the other hand, in the radio-quiet category (without DH radio bursts), nearly 60% of the events are from the eastern hemisphere in contrast to those of the radio-loud category. It is found that 81% of the events from eastern regions have flare durations  $> 30$  min in the DH-flare category, in contrast to a nearly equal number from the western side for flare durations longer/shorter than 30 min. Similarly, the eastern events in the DH-flare category have a longer average rise-time of 34 min, while the western events have an average flare rise-time of 26 min. On the other hand, the CME speed and flare strength are found to be nearly equal among east and west side events, except that both these parameters are greater for events with DH type IIs.

## The Role of Reconnection in the Onset of Solar Eruptions

[James Leake](#), [Mark Linton](#), [Spiro Antiochos](#)

ApJ 934 10 2022

<https://arxiv.org/pdf/2205.12957.pdf>

<https://iopscience.iop.org/article/10.3847/1538-4357/ac74b7/pdf>

Solar eruptive events such as coronal mass ejections and eruptive flares are frequently associated with the emergence of magnetic flux from the convection zone into the corona. We use three dimensional magnetohydrodynamic numerical simulations to study the interaction of coronal magnetic fields with emerging flux and determine the conditions that lead to eruptive activity. A simple parameter study is performed, varying the relative angle between emerging magnetic flux and a pre-existing coronal dipole field. We find that in all cases, the emergence results in a sheared magnetic arcade that transitions to a twisted coronal flux rope via low-lying magnetic reconnection. This structure, however, is constrained by its own outer field, and so is non-eruptive in the absence of reconnection with the overlying coronal field. The amount of this overlying reconnection is determined by the relative angle between the emerged and pre-existing fields. The reconnection between emerging and pre-existing fields is necessary to generate sufficient expansion of the emerging structure so that flare-like reconnection below the coronal flux rope becomes strong enough to trigger its release. Our results imply that the relative angle is the key parameter in determining whether the resultant active regions exhibit eruptive behavior, and is thus a potentially useful candidate for predicting eruptions in newly emerging active regions. More generally, our results demonstrate that the detailed interaction between the convection zone/photosphere and the corona must be calculated self-consistently in order to model solar eruptions accurately.

## **Simulations of Emerging Magnetic Flux. II. The Formation of Unstable Coronal Flux Ropes and the Initiation of Coronal Mass Ejections**

James E. [Leake](#)<sup>1</sup>, Mark G. Linton<sup>2</sup>, and Spiro K. Antiochos

2014 ApJ 787 46

<http://arxiv.org/pdf/1402.2645v2.pdf>

We present results from three-dimensional magnetohydrodynamic simulations of the emergence of a twisted convection zone flux tube into a pre-existing coronal dipole field. As in previous simulations, following the partial emergence of the sub-surface flux into the corona, a combination of vortical motions and internal magnetic reconnection forms a coronal flux rope. Then, in the simulations presented here, external reconnection between the emerging field and the pre-existing dipole coronal field allows further expansion of the coronal flux rope into the corona. After sufficient expansion, internal reconnection occurs beneath the coronal flux rope axis, and the flux rope erupts up to the top boundary of the simulation domain (~36 Mm above the surface). We find that the presence of a pre-existing field, orientated in a direction to facilitate reconnection with the emerging field, is vital to the fast rise of the coronal flux rope. The simulations shown in this paper are able to self-consistently create many of the surface and coronal signatures used by coronal mass ejection (CME) models. These signatures include surface shearing and rotational motions, quadrupolar geometry above the surface, central sheared arcades reconnecting with oppositely orientated overlying dipole fields, the formation of coronal flux ropes underlying potential coronal field, and internal reconnection which resembles the classical flare reconnection scenario. This suggests that proposed mechanisms for the initiation of a CME, such as "magnetic breakout," are operating during the emergence of new active regions.

## **Simulations of Emerging Magnetic Flux. I. The Formation of Stable Coronal Flux Ropes**

James E. [Leake](#)<sup>1</sup>, Mark G. Linton<sup>2</sup>, and Tibor Török

2013 ApJ 778 99

<http://arxiv.org/pdf/1308.6204v1.pdf>

We present results from three-dimensional visco-resistive magnetohydrodynamic simulations of the emergence of a convection zone magnetic flux tube into a solar atmosphere containing a pre-existing dipole coronal field, which is orientated to minimize reconnection with the emerging field. We observe that the emergence process is capable of producing a coronal flux rope by the transfer of twist from the convection zone, as found in previous simulations. We find that this flux rope is stable, with no evidence of a fast rise, and that its ultimate height in the corona is determined by the strength of the pre-existing dipole field. We also find that although the electric currents in the initial convection zone flux tube are almost perfectly neutralized, the resultant coronal flux rope carries a significant net current. These results suggest that flux tube emergence is capable of creating non-current-neutralized stable flux ropes in the corona, tethered by overlying potential fields, a magnetic configuration that is believed to be the source of coronal mass ejections.

## **Tests of Dynamical Flux Emergence as a Mechanism for CME Initiation**

James E. [Leake](#), Mark G. Linton, Spiro K. Antiochos

E-print, 30 July 2010, ApJ, 722:550–565, 2010, [File](#)

Current coronal mass ejection (CME) models set their lower boundary to be in the lower corona. They do not calculate accurately the transfer of free magnetic energy from the convection zone to the magnetically dominated corona because they model the effects of flux emergence using kinematic boundary conditions or simply assume the appearance of flux at these heights. We test the importance of including dynamical flux emergence in CME modeling by simulating, in 2.5D, the emergence of sub-surface flux tubes into different coronal magnetic field configurations. We investigate how much free magnetic energy, in the form of shear magnetic field, is transported from the convection zone to the corona, and whether dynamical flux emergence can drive CMEs. We find that multiple coronal flux ropes can be formed during flux emergence, and although they carry some shear field into the corona, the majority of shear field is confined to the lower atmosphere. Less than 10% of the magnetic energy in the corona is in the shear field, and this, combined with the fact that the coronal flux ropes bring up significant dense material, means that they do not erupt. Our results have significant implications for all CME models which rely on the transfer of free magnetic energy from the lower atmosphere into the corona but which do not explicitly model this transfer. Such studies of flux emergence and CMEs are timely, as we have new capabilities to observe this with Hinode and SDO, and therefore to test the models against observations.

## **Modeling CME encounters at Parker Solar Probe with OSPREI: Dependence on photospheric and coronal conditions**

[Vincent E. Ledvina](#), [Erika Palmerio](#), [Christina Kay](#), [Nada Al-Haddad](#), [Pete Riley](#)



A&A 2023

<https://arxiv.org/pdf/2303.10793.pdf>

Context: Coronal mass ejections (CMEs) are eruptions of plasma from the Sun that travel through interplanetary space and may encounter Earth. CMEs often enclose a magnetic flux rope (MFR), the orientation of which largely determines the CME's geoeffectiveness. Current operational CME models do not model MFRs, but a number of research ones do, including the Open Solar Physics Rapid Ensemble Information (OSPREDI) model. Aims: We report the sensitivity of OSPREDI to a range of user-selected photospheric and coronal conditions. Methods: We model four separate CMEs observed in situ by Parker Solar Probe (PSP). We vary the input photospheric conditions using four input magnetograms (HMI Synchronic, HMI Synoptic, GONG Synoptic Zero-Point Corrected, and GONG ADAPT). To vary the coronal field reconstruction, we employ the Potential-Field Source-Surface (PFSS) model and we vary its source-surface height in the range 1.5--3.0  $R_{\odot}$  with 0.1  $R_{\odot}$  increments. Results: We find that both the input magnetogram and PFSS source surface often affect the evolution of the CME as it propagates through the Sun's corona into interplanetary space, and therefore the accuracy of the MFR prediction compared to in-situ data at PSP. There is no obvious best combination of input magnetogram and PFSS source surface height. Conclusions: The OSPREDI model is moderately sensitive to the input photospheric and coronal conditions. Based on where the source region of the CME is located on the Sun, there may be best practices when selecting an input magnetogram to use. **21 June 2020, 9 June 2021, 7 November 2021, 26 January 2022**

## Microwave Perspective on Magnetic Breakout Eruption

Jeongwoo Lee

Front. Astron. Space Sci., 9:855737. 2022

<https://www.frontiersin.org/articles/10.3389/fspas.2022.855737/full>

<https://www.frontiersin.org/articles/10.3389/fspas.2022.855737/pdf>

<https://doi.org/10.3389/fspas.2022.855737>

Microwave maps may provide critical information on the flux rope interaction and the breakout eruption if their polarization is measured with high precision. We demonstrate this diagnostic capability using the 17 GHz maps from the Nobeyama Radioheliograph (NoRH) of a circular ribbon flare SOL2014-12-17T04:51. The EUV images from SDO/AIA and the coronal magnetic field extrapolated from the HMI magnetogram are also used to support the interpretation of the microwave data. The most obvious evidence for the breakout eruption comes from the sign change of the microwave polarization over the AR at heliographic coordinates S20E09, indicating change of the overlying fields from a closed fan structure to a spine-like structure. Another important piece of evidence comes from the spatial and temporal variations of quasi-periodic pulsations (QPP) detected at the 17 GHz. The QPP was more obvious in one loop leg before the eruption and later moved to the spine field region on and after the flare. This indicates that the oscillatory power is transferred from an interacting flux rope to the outer spine, along which the reconnection launches torsional Alfvén waves, in good agreement with MHD model predictions for breakout eruption. In the practical viewpoint, these two diagnostics work because microwave observations are free of saturation even in strong flaring regions.

## Rapid Evolution of Bald Patches in a Major Solar Eruption

[Jonathan H. Lee](#), [Xudong Sun](#), [Maria D. Kazachenko](#)

ApJL 2021

<https://arxiv.org/pdf/2111.00336.pdf>

Bald patch (BP) is a magnetic topological feature where U-shaped field lines turn tangent to the photosphere. Field lines threading the BP trace a separatrix surface where reconnection preferentially occurs. Here we study the evolution of multiple, strong-field BPs in active region 12673 during the most intense, X9.3 flare of solar cycle 24. The central BP, located between the initial flare ribbons, largely "disintegrated" within 35 minutes. The more remote, southern BP survived. The disintegration manifested as a 9-degree rotation of the median shear angle; the perpendicular component of the horizontal field (with respect to the polarity inversion line) changed sign. The parallel component exhibited a step-wise, permanent increase of 1 kG, consistent with previous observations of the flare-related "magnetic imprint". The observations suggest that magnetic reconnection during a major eruption may involve entire BP separatrices, leading to a change of magnetic topology from BPs to sheared arcades. **6 Sep 2017**

[HMI Science Nuggets](#) #172 Feb 2022 <http://hmi.stanford.edu/hminuggets/?p=3791>

## Heating and Eruption of a Solar Circular-ribbon Flare

Jeongwoo Lee<sup>1,2,3</sup>, Judith T. Karpen<sup>4</sup>, Chang Liu<sup>1,2,3</sup>, and Haimin Wang<sup>1,2,3</sup>

2020 ApJ 893 158

<https://doi.org/10.3847/1538-4357/ab80c4>

We studied a circular-ribbon flare, SOL2014-12-17T04:51, with emphasis on its thermal evolution as determined by the differential emission measure (DEM) inversion analysis of the extreme ultraviolet (EUV) images of the Atmospheric Imaging Assembly instrument on board the Solar Dynamics Observatory. Both temperature and emission measure start to rise much earlier than the flare, along with an eruption and formation of a hot halo over the fan structure. In the main flare phase, another set of ribbons forms inside the circular ribbon, and expands as expected for ribbons at the footpoints of a postflare arcade. An additional heating event further extends the decay phase, which is also characteristic of some

eruptive flares. The basic magnetic configuration appears to be a fan–spine topology, rooted in a minority-polarity patch surrounded by majority-polarity flux. We suggest that reconnection at the null point begins well before the impulsive phase, when the null is distorted into a breakout current sheet, and that both flare and breakout reconnection are necessary in order to explain the subsequent local thermal evolution and the eruptive activities in this confined magnetic structure. Using local DEMs, we found a postflare temperature increase inside the fan surface, indicating that the so-called EUV late phase is due to continued heating in the flare loops.

### **Formation of Post-CME Blobs Observed by LASCO-C2 and K-Cor on 2017 September 10**

Jae-Ok Lee<sup>1</sup>, Kyung-Suk Cho<sup>1,2</sup>, Kyoung-Sun Lee<sup>3</sup>, Il-Hyun Cho<sup>4</sup>, Junggi Lee<sup>5</sup>, Yukinaga Miyashita<sup>1</sup>, Yeon-Han Kim<sup>1</sup>, Rok-Soon Kim<sup>1</sup>, and Soojeong Jang<sup>1</sup>  
2020 ApJ 892 129

<https://doi.org/10.3847/1538-4357/ab799a>

<https://doi.org/10.3847/1538-4357/ab799a>

Understanding the formation of post-CME blobs, we investigate 2 blobs in the outer corona observed by LASCO-C2 and 34 blobs in the inner corona by K-Cor on **2017 September 10** from 17:11 to 18:58 UT. By visual inspection of the structure of a post-CME current sheet (CS) and its associated blobs, we find that the CS is well identified in the K-Cor and its radial lengths are nine times longer than lateral widths, indicating the CS is unstable to the linear tearing mode. The inner corona blobs can be classified into two groups: 27 blobs generated in the middle of the CS (Group 1) and 7 blobs occurred above the tips of it (Group 2). Their lateral widths are  $\langle 0.02R_{\odot} \rangle$  and  $\langle 0.05R_{\odot} \rangle$ , which is smaller than, or similar to, those  $\langle 0.06R_{\odot} \rangle$  of the CS. They have elongated shapes: ratios of lateral to radial widths are  $\langle 0.53 \rangle$  and  $\langle 0.40 \rangle$ , respectively. In the first group, only three blobs propagate above the tip of the CS while the others are located in the CS. In the second group, only two blobs have associations with those of outer corona in their temporal and spatial relationship and their initial heights are 1.81 and 1.95  $R_{\odot}$ , measured from the center of the Sun. The others cannot be identified in the outer corona. Our results first demonstrate that LASCO-C2 blobs could be generated by the tearing mode instability near the tips of post-CME CSs, similar to the magnetic reconnection process in the tail CS of Earth's magnetosphere.

### **Non-equilibrium ionization effects on solar EUV and X-ray imaging observations**

Jin-Yi Lee, John C. Raymond, Katharine K. Reeves, Chengcai Shen, Yong-Jae Moon, Yeon-Han Kim  
ApJ 879 111 2019

<https://arxiv.org/pdf/1905.11632.pdf>

[sci-hub.se/10.3847/1538-4357/ab24bb](https://doi.org/10.3847/1538-4357/ab24bb)

During transient events such as major solar eruptions, the plasma can be far from the equilibrium ionization state because of rapid heating or cooling. Non-equilibrium ionization (NEI) is important in rapidly evolving systems where the thermodynamical timescale is shorter than the ionization or recombination time scales. We investigate the effects of NEI on EUV and X-ray observations by the Atmospheric Imaging Assembly (AIA) on board Solar Dynamic Observatory and X-ray Telescope (XRT) on board Hinode. Our model assumes that the plasma is initially in ionization equilibrium at low temperature, and it is heated rapidly by a shock or magnetic reconnection. We tabulate the responses of the AIA and XRT passbands as functions of temperature and a characteristic timescale,  $\tau$ . We find that most of the ions reach equilibrium at  $\tau \leq 1012 \text{ cm}^{-3}\text{s}$ . Comparing ratios of the responses between different passbands allows us to determine whether a combination of plasmas at temperatures in ionization equilibrium can account for a given AIA and XRT observation. It also expresses how far the observed plasma is from equilibrium ionization. We apply the ratios to a supra-arcade plasma sheet on **2012 January 27**. We find that the closer the plasma is to the arcade, the closer it is to a single-temperature plasma in ionization equilibrium. We also utilize the set of responses to estimate the temperature and density for shocked plasma associated with a coronal mass ejection on **2010 June 13**. The temperature and density ranges we obtain are in reasonable agreement with previous works.

### **Three-dimensional Oscillations of 21 Halo Coronal Mass Ejections Using Multi-spacecraft Data**

Harim Lee<sup>1</sup>, Y.-J. Moon<sup>1,2</sup>, V. M. Nakariakov<sup>1,3</sup>, Hyeonock Na<sup>1</sup>, Il-Hyun Cho<sup>2</sup>, and Eunsu Park  
2018 ApJ 868 18

[sci-hub.tw/10.3847/1538-4357/aae5f6](https://doi.org/10.3847/1538-4357/aae5f6)

We investigate the 3D structure of kinematic oscillations of full halo coronal mass ejections (FHCMEs) using multi-spacecraft coronagraph data from two non-parallel lines of sight. For this, we consider 21 FHCMEs which are simultaneously observed by the Solar and Heliospheric Observatory and the Solar Terrestrial Relations Observatory A or B, from *2010 June to 2012 August* when the spacecraft were roughly in quadrature. Using sequences of running difference images, we estimate the instantaneous projected speeds of the FHCMEs at 24 different azimuthal angles in the planes of the sky of those coronagraphs. We find that all these FHCMEs have experienced kinematic oscillations characterized by quasi-periodic variations of the instantaneous projected radial velocity with periods ranging from 24 to 48 min. The oscillations detected in the analyzed events are found to show distinct azimuthal wave modes. Thirteen events (about 62%) are found to oscillate with the azimuthal wave number  $m = 1$ . The oscillating directions of the nodes of the  $m = 1$  mode for these FHCMEs are consistent with those of their position angles (or the direction of eruption),

with a mean difference of about  $23^\circ$ . The oscillation amplitude is found to correlate well with the projected radial speed of the CME. An estimation of Lorentz accelerations shows that they are dominant over other forces, implying that the magnetic force is responsible for the kinematic oscillations of CMEs. However, we cannot rule out other possibilities: a global layer of enhanced current around the CMEs or the nonlinear nature of its driver, for example the effect of vortex shedding. **2011 September 22, 2011 September 24, 2012 January 27, 2012 March 10**

**Table 1** Oscillation Parameters of 21 HCMEs

## **MHD Simulation for Investigating the Dynamic State Transition Responsible for a Solar Eruption in Active Region 12158**

Hwanhee Lee<sup>1</sup> and Tetsuya Magara

2018 ApJ 859 132 DOI [10.3847/1538-4357/aabfe6](https://doi.org/10.3847/1538-4357/aabfe6)

We present a magnetohydrodynamic model of solar eruption based on the dynamic state transition from the quasi-static state to the eruptive state of an active region (AR) magnetic field. For the quasi-static state before an eruption, we consider the existence of a slow solar wind originating from an AR, which may continuously make the AR magnetic field deviate from mechanical equilibrium. In this model, we perform a three-dimensional magnetohydrodynamic simulation of AR 12158 producing a coronal mass ejection, where the initial magnetic structure of the simulation is given by a nonlinear force-free field derived from an observed photospheric vector magnetic field. We then apply a pressure-driven outflow to the upper part of the magnetic structure to achieve a quasi-static pre-eruptive state. The simulation shows that the eruptive process observed in this AR may be caused by the dynamic state transition of an AR magnetic field, which is essentially different from the destabilization of a static magnetic field. The dynamic state transition is determined from the shape evolution of the magnetic field line according to the [κH-mechanism](#). This work demonstrates how the mechanism works to produce a solar eruption in the dynamic solar corona governed by the gravitational field and the continuous outflows of solar wind.

## **Heating of an erupting prominence associated with a solar coronal mass ejection on 2012 January 27**

Jin-Yi Lee, John C. Raymond, Katharine K. Reeves, [Yong-Jae Moon](#), [Kap-Sung Kim](#)

ApJ 844 3 2017

<https://arxiv.org/pdf/1706.09116.pdf>

<http://sci-hub.cc/10.3847/1538-4357/aa79a4>

We investigate the heating of an erupting prominence and loops associated with a coronal mass ejection and X-class flare. The prominence is seen in absorption in EUV at the beginning of its eruption. Later the prominence changes to emission, which indicates heating of the erupting plasma. We find the densities of the erupting prominence using the absorption properties of hydrogen and helium in different passbands. We estimate the temperatures and densities of the erupting prominence and loops seen as emission features using the differential emission measure method, which uses both EUV and X-ray observations from the Atmospheric Imaging Assembly on board Solar Dynamics Observatory and the X-ray Telescope on board Hinode. We consider synthetic spectra using both photospheric and coronal abundances in these calculations. We verify the methods for the estimation of temperatures and densities for the erupting plasmas. Then we estimate the thermal, kinetic, radiative loss, thermal conduction, and heating energies of the erupting prominence and loops. We find that the heating of the erupting prominence and loop occurs strongly at early times in the eruption. This event shows a writhing motion of the erupting prominence, which may indicate a hot flux rope heated by thermal energy release during magnetic reconnection.

## **Which Bow Shock Theory, Gasdynamic or Magnetohydrodynamic, Better Explains CME Stand-off Distance Ratios from LASCO-C2 Observations ?**

Jae-Ok Lee<sup>1,2</sup>, Y.-J. Moon<sup>1</sup>, Jin-Yi Lee<sup>3</sup>, R.-S. Kim<sup>2</sup>, and K.-S. Cho<sup>2</sup>

2017 ApJ 838 70

<http://sci-hub.cc/10.3847/1538-4357/aa656f>

It is generally believed that fast coronal mass ejections (CMEs) can generate their associated shocks, which are characterized by faint structures ahead of CMEs in white-light coronagraph images. In this study, we examine whether the observational stand-off distance ratio, defined as the CME stand-off distance divided by its radius, can be explained by bow shock theories. Of 535 SOHO/LASCO CMEs (from 1996 to 2015) with speeds greater than  $1000 \text{ km s}^{-1}$  and angular widths wider than  $60^\circ$ , we select 18 limb CMEs with the following conditions: (1) their Alfvénic Mach numbers are greater than one under Mann's magnetic field and Saito's density distributions; and (2) the shock structures ahead of the CMEs are well identified. We determine observational CME stand-off distance ratios by using brightness profiles from LASCO-C2 observations. We compare our estimates with theoretical stand-off distance ratios from gasdynamic (GD) and magnetohydrodynamic (MHD) theories. The main results are as follows. Under the GD theory, 39% (7/18) of the CMEs are explained in the acceptable ranges of adiabatic gamma ( $\gamma$ ) and CME geometry. Under the MHD theory, all the events are well explained when we consider quasi-parallel MHD shocks with  $\gamma = 5/3$ . When we use polarized brightness (pB) measurements for coronal density distributions, we also find similar results: 8% (1/12) under GD theory and 100% (12/12) under MHD theory. Our results demonstrate that the bow shock relationships based on MHD theory are more suitable than those based on GD theory for analyzing CME-driven shock signatures. **1997 Nov 14, 1999 July 25, 1999 Nov 16, 2000 May 05, 2002 Jan 14,**

2002 Jun 26, 2003 Nov 04, 2005 Jul 17, 2005 Jul 27, 2005 Jul 30, 2011 Sep 22, 2012 Jan 27, 2012 Jul 19, 2013 May 13, 2013 May 22, 2013 Oct 25, 2014 Apr 02, 2015 Feb 10  
Table 1 Observational CME Parameters of 18 Events

## SOLAR ERUPTION AND LOCAL MAGNETIC PARAMETERS

Jeongwoo Lee<sup>1,2</sup>, Chang Liu<sup>3</sup>, Ju Jing<sup>3</sup>, and Jongchul Chae

2016 *ApJL* 831 L18 DOI 10.3847/2041-8205/831/2/L18

<http://sci-hub.cc/doi/10.3847/2041-8205/831/2/L18>

<https://arxiv.org/pdf/1708.04055.pdf>

It is now a common practice to use local magnetic parameters such as magnetic decay index for explaining solar eruptions from active regions, but there can be an alternative view that the global properties of the source region should be counted as a more important factor. We discuss this issue based on *Solar Dynamics Observatory* observations of the **three successive eruptions within 1.5 hr from the NOAA active region 11444** and the magnetic parameters calculated using the nonlinear force-free field model. Two violent eruptions occurred in the regions with relatively high magnetic twist number (0.5–1.5) and high decay index (0.9–1.1) at the nominal height of the filament (12") and otherwise a mild eruption occurred, which supports the local-parameter paradigm. Our main point is that the time sequence of the eruptions did not go with these parameters. It is argued that an additional factor, in the form of stabilizing force, should operate to determine the onset of the first eruption and temporal behaviors of subsequent eruptions. As supporting evidence, we report that the heating and fast plasma flow continuing for a timescale of an hour was the direct cause for the first eruption and that the unidirectional propagation of the disturbance determined the timing of subsequent eruptions. Both of these factors are associated with the overall magnetic structure rather than local magnetic properties of the active region. **2012 March 27**

## DEPENDENCE OF OCCURRENCE RATES OF SOLAR FLARES AND CORONAL MASS EJECTIONS ON THE SOLAR CYCLE PHASE AND THE IMPORTANCE OF LARGE-SCALE CONNECTIVITY

Kangjin Lee<sup>1</sup>, Y.-J. Moon<sup>1</sup>, and V. M. Nakariakov<sup>1,2</sup>

2016 *ApJ* 831 131 DOI 10.3847/0004-637X/831/2/131

We investigate the dependence of the occurrence rates of major solar flares (M- and X-class) and front-side halo coronal mass ejections (FHCMEs), observed from 1996 to 2013, on the solar cycle (SC) phase for six active McIntosh sunspot group classes: Fkc, Ekc, Dkc, Fki, Eki, and Dki. We classify SC phases as follows: (1) ascending phase of SC 23 (1996–1999), (2) maximum phase of SC 23 (2000–2002), (3) descending phase of SC 23 (2003–2008), and (4) ascending phase of SC 24 (2009–2013). We find that the occurrence rates of major flares and FHCMEs during the descending phase are noticeably higher than those during the other phases for most sunspot group classes. For the most active sunspot group class, Fkc, the occurrence rate of FHCMEs during the descending phase of SC 23 is three times as high as that during the ascending phase of SC 23. The potential of each McIntosh sunspot group class to produce major flares or FHCMEs is found to depend on the SC phase. The occurrence rates (R) of major flares and FHCMEs are strongly anti-correlated with the annual average latitude of the sunspot groups (L): for major flares and for FHCMEs. This finding indicates the possible role of large-scale coronal connectivity, e.g., trans-equatorial loops, in powerful energy releases. Interestingly, this relationship is very similar to that between the volumetric coronal heating rate and X-ray loop lengths, indicating common energy release mechanisms.

## SOLAR MULTIPLE ERUPTIONS FROM A CONFINED MAGNETIC STRUCTURE

Jeongwoo Lee<sup>1</sup>, Chang Liu<sup>2</sup>, Ju Jing<sup>2</sup>, and Jongchul Chae

2016 *ApJ* 829 L1 File

<https://arxiv.org/pdf/1708.04056.pdf>

How eruption can recur from a confined magnetic structure is discussed based on the Solar Dynamics Observatory observations of the NOAA active region 11444, which produced three eruptions within 1.5 hr on **2012 March 27**. The active region (AR) had the positive-polarity magnetic fields in the center surrounded by the negative-polarity fields around. Since such a distribution of magnetic polarity tends to form a dome-like magnetic fan structure confined over the AR, the multiple eruptions were puzzling. Our investigation reveals that this event exhibits several properties distinct from other eruptions associated with magnetic fan structures: (i) a long filament encircling the AR was present before the eruptions; (ii) expansion of the open–closed boundary (OCB) of the field lines after each eruption was suggestive of the growing fan-dome structure, and (iii) the ribbons inside the closed magnetic polarity inversion line evolved in response to the expanding OCB. It thus appears that in spite of multiple eruptions the fan-dome structure remained undamaged, and the closing back field lines after each eruption rather reinforced the fan-dome structure. We argue that the multiple eruptions could occur in this AR in spite of its confined magnetic structure because the filament encircling the AR was adequate for slipping through the magnetic separatrix to minimize the damage to its overlying fan-dome structure. The result of this study provides a new insight into the productivity of eruptions from a confined magnetic structure.

## Photospheric Abundances of Polar Jets on the Sun Observed by Hinode

Kyoung-Sun Lee<sup>1</sup>, David H. Brooks<sup>2</sup>, and Shinsuke Imada

2015 ApJ 809 114

Many jets are detected at X-ray wavelengths in the Sun's polar regions, and the ejected plasma along the jets has been suggested to contribute mass to the fast solar wind. From in situ measurements in the magnetosphere, it has been found that the fast solar wind has photospheric abundances while the slow solar wind has coronal abundances. Therefore, we investigated the abundances of polar jets to determine whether they are the same as that of the fast solar wind. For this study, we selected 22 jets in the polar region observed by Hinode/EUV Imaging Spectroscopy (EIS) and X-ray Telescope (XRT) simultaneously on **2007 November 1–3**. We calculated the First Ionization Potential (FIP) bias factor from the ratio of the intensity between high (S) and low (Si, Fe) FIP elements using the EIS spectra. The values of the FIP bias factors for the polar jets are around 0.7–1.9, and 75% of the values are in the range of 0.7–1.5, which indicates that they have photospheric abundances similar to the fast solar wind. The results are consistent with the reconnection jet model where photospheric plasma emerges and is rapidly ejected into the fast wind.

See EIS Nugget 2016

[http://solarb.mssl.ucl.ac.uk/SolarB/nuggets/nugget\\_2016jan.jsp](http://solarb.mssl.ucl.ac.uk/SolarB/nuggets/nugget_2016jan.jsp)

## Forecast of a Daily Halo CME Occurrence Probability Depending on Class and Area Change of the Associated Sunspot

Kangjin Lee, Yong-Jae Moon, Jin-Yi Lee

Solar Phys. Volume 290, Issue 6, pp 1661-1669 2015

We investigate the halo (partial and full) coronal mass ejection (CME) occurrence probability depending on class and area change of the associated sunspot using front-side halo CMEs from 1996 to 2011. We select the most halo CME-productive 14 sunspot classifications: Cao, Cko, Dai, Dao, Dko, Dki, Dkc, Eao, Eai, Eko, Eki, Ekc, Fki, and Fkc. For each class, we assign three subgroups according to sunspot class area change: “Decrease”, “Steady”, or “Increase”. As a result, in the case of asymmetric (k) and compact (c) groups, their CME occurrence probabilities increase. We also find that the halo-CME occurrence probabilities for the “Increase” subgroups are noticeably higher than those for the other subgroups. Our results demonstrate statistically that magnetic-flux emergence or cancellation enhances CME occurrence. We expect that this model can be routinely operated to forecast the halo-CME occurrence probability.

## Radial and Azimuthal Oscillations of Halo Coronal Mass Ejections in the Sun

Harim Lee<sup>1</sup>, Y.-J. Moon<sup>1</sup>, and V. M. Nakariakov

2015 ApJ 803 L7

[http://www2.warwick.ac.uk/fac/sci/physics/research/cfsa/people/valery/research/eprints/2041-8205\\_803\\_1\\_L7.pdf](http://www2.warwick.ac.uk/fac/sci/physics/research/cfsa/people/valery/research/eprints/2041-8205_803_1_L7.pdf)

We present the first observational detection of radial and azimuthal oscillations in full halo coronal mass ejections (HCMEs). We analyze nine HCMEs well-observed by the Large Angle and Spectrometric Coronagraph (LASCO) from 2011 February to June. Using the LASCO C3 running difference images, we estimated the instantaneous apparent speeds of the HCMEs in different radial directions from the solar disk center. We find that the development of all these HCMEs is accompanied by quasi-periodic variations of the instantaneous radial velocity with the periods ranging from 24 to 48 minutes. The amplitudes of the instant speed variations reach about a half of the projected speeds. The amplitudes are found to anti-correlate with the periods and correlate with the HCME speed, indicating the nonlinear nature of the process. The oscillations have a clear azimuthal structure in the heliocentric polar coordinate system. The oscillations in seven events are found to be associated with distinct azimuthal wave modes with the azimuthal wave number  $m = 1$  for six events and  $m = 2$  for one event. The polarization of the oscillations in these seven HCMEs is broadly consistent with those of their position angles with the mean difference of  $43^\circ$ . The oscillations may be connected with natural oscillations of the plasmoids around a dynamical equilibrium, or self-oscillatory processes, e.g., the periodic shedding of Alfvénic vortices. Our results indicate the need for an advanced theory of oscillatory processes in coronal mass ejections.

## Ensemble Modeling of Successive Halo CMEs: A Case Study

C. O. Lee, C. N. Arge, D. Odstrcil, G. Millward, V. Pizzo, N. Lugaz

Solar Phys., 2015

The Wang–Sheeley–Arge (WSA)–Enlil cone modeling system is used for making routine arrival-time forecasts of Earth-directed halo coronal mass ejections (CMEs), since they typically produce the most geoeffective events. A major objective of this work is to better understand the sensitivity of the WSA–Enlil modeling results to input model parameters and how these parameters contribute to the overall model uncertainty and performance. In this study, ensemble-modeling results for a succession of three halo CME events that occurred on **2–4 August 2011** are presented. We investigate the sensitivity of the modeled CME arrival times to small variations in the input-cone properties by creating ensemble sets of numerical simulations for each CME event, based on multiple sets of cone parameters. We find that the accuracy of the modeled CME arrival times not only depends on the small variations to the initial input geometry, but also on the reliable specification of the background solar wind, which is driven by the input maps of the photospheric magnetic field. The accuracy in the arrival-time predictions also depends on whether the cone parameters for all three CMEs are specified in a single WSA–Enlil simulation. The inclusion or exclusion of one or two of the preceding CMEs affects the solar-wind conditions through which the succeeding CME propagates. Although the accuracy of the modeled arrival times is sensitive to the input maps that are used to drive the background solar wind, the spread in the modeling ensemble remains mostly unchanged when different input maps are used.

## **Helical Blowout Jets in the Sun: Untwisting and Propagation of Waves**

E. J. Lee, V. Archontis, A. W. Hood

ApJL, **798** L10 **2015**

<http://arxiv.org/pdf/1412.4853v1.pdf>

We report on numerical experiment of the recurrent onset of helical "blowout" jets in an emerging flux region (EFR). We find that these jets are running with velocities of  $\sim 100\text{--}250\text{ km s}^{-1}$  and they transfer a vast amount of heavy plasma into the outer solar atmosphere. During their emission, they undergo an untwisting motion as a result of reconnection between the twisted emerging and the non-twisted pre-existing magnetic field in the solar atmosphere. For the first time in the context of blowout jets, we provide a direct evidence that their untwisting motion is associated with the propagation of torsional Alfvén waves in the corona.

## **Are 3-D coronal mass ejection parameters from single-view observations consistent with multiview ones?**

Harim Lee, Y.-J. Moon, Hyeonock Na, Soojeong Jang, Jae-Ok Lee

JGR Volume 120, Issue 12 December **2015** Pages 10,237–10,249

To prepare for when only single-view observations are available, we have made a test whether the 3-D parameters (radial velocity, angular width, and source location) of halo coronal mass ejections (HCMEs) from single-view observations are consistent with those from multiview observations. For this test, we select 44 HCMEs from December 2010 to June 2011 with the following conditions: partial and full HCMEs by SOHO and limb CMEs by twin STEREO spacecraft when they were approximately in quadrature. In this study, we compare the 3-D parameters of the HCMEs from three different methods: (1) a geometrical triangulation method, the STEREO CAT tool developed by NASA/CCMC, for multiview observations using STEREO/SECCHI and SOHO/LASCO data, (2) the graduated cylindrical shell (GCS) flux rope model for multiview observations using STEREO/SECCHI data, and (3) an ice cream cone model for single-view observations using SOHO/LASCO data. We find that the radial velocities and the source locations of the HCMEs from three methods are well consistent with one another with high correlation coefficients ( $\geq 0.9$ ). However, the angular widths by the ice cream cone model are noticeably underestimated for broad CMEs larger than  $100^\circ$  and several partial HCMEs. A comparison between the 3-D CME parameters directly measured from twin STEREO spacecraft and the above 3-D parameters shows that the parameters from multiview are more consistent with the STEREO measurements than those from single view.

## **Mass and energy of erupting solar plasma observed with the X-Ray Telescope on Hinode**

Jin-Yi Lee, John C. Raymond, Katharine K. Reeves, Yong-Jae Moon, and Kap-Sung Kim

ApJ, **798** 106 **2014**

<http://arxiv.org/pdf/1411.2229v1.pdf>

We investigate seven eruptive plasma observations by Hinode/XRT. Their corresponding EUV and/or white light CME features are visible in some events. Five events are observed in several passbands in X-rays, which allows the determination of the eruptive plasma temperature using a filter ratio method. We find that the isothermal temperatures vary from 1.6 to 10 MK. These temperatures are an average weighted toward higher temperature plasma. We determine the mass constraints of eruptive plasmas by assuming simplified geometrical structures of the plasma with isothermal plasma temperatures. This method provides an upper limit to the masses of the observed eruptive plasmas in X-ray passbands since any clumping causes the overestimation of the mass. For the other two events, we assume the temperatures are at the maximum temperature of the XRT temperature response function, which gives a lower limit of the masses. We find that the masses in XRT,  $\sim 3 \times 10^{13} - 5 \times 10^{14}$  g, are smaller in their upper limit than total masses obtained by LASCO,  $\sim 1 \times 10^{15}$  g. In addition, we estimate the radiative loss, thermal conduction, thermal, and kinetic energies of the eruptive plasma in X-rays. For four events, we find that the thermal conduction time scales are much shorter than the duration of eruption. This result implies that additional heating during the eruption may be required to explain the plasma observations in X-rays for the four events. **2007/05/23, 2008/04/09, 2008/12/30, 2009/01/11, 2009/12/13, 2010/01/22, 2010/01/30**

## **On Flux Rope Stability and Atmospheric Stratification in Models of Coronal Mass Ejections Triggered by Flux Emergence**

E. Lee, V.S. Lukin, M.G. Linton

A&A, 569, A94 **2014**

<http://arxiv.org/pdf/1403.0231v1.pdf>

Flux emergence is widely recognized to play an important role in the initiation of coronal mass ejections. The Chen-Shibata (2000) model, which addresses the connection between emerging flux and flux rope eruptions, can be implemented numerically to demonstrate how emerging flux through the photosphere can ultimately cause the eruption of a coronal flux rope. The model's sensitivity to the initial conditions is investigated with a parameter study. We aim to understand the stability of the coronal flux rope in the context of X-point collapse, and study the effect of boundary

driving on both unstratified and stratified atmospheres. A modified version of the model is implemented in a code with high numerical accuracy with different combinations of initial parameters governing the magnetic equilibrium and gravitational stratification of the atmosphere. In the absence of driving, we assess the behavior of waves in the vicinity of the X-point. With boundary driving applied, we study the effect of stratification on the eruption. We find that the Chen-Shibata equilibrium can be unstable to an X-point collapse even in the absence of driving due to wave accumulation at the X-point. Such a collapse can generate a coronal mass ejection, or produce a failed eruption. However, the equilibrium can be stabilized by reducing the compressibility of the plasma, which allows small-amplitude waves to pass through the X-point without accumulation. For stable initial configurations, simulations of the flux emergence via photospheric boundary driving demonstrate the impact of atmospheric stratification on the dynamics of resulting eruptions. In particular, in a stratified atmosphere, we identify a novel mechanism for producing quasi-periodic behavior at the reconnection site behind a coronal mass ejection as a possible explanation of similar phenomena previously observed in solar and stellar flares.

### **Dependence of Geomagnetic Storms on Their Associated Halo CME Parameters**

Jae-Ok Lee<sup>1</sup>, Y.-J. Moon<sup>1, 2</sup>, Kyoung-Sun Lee<sup>3</sup> and R.-S. Kim

Solar Phys, 2014, File

We compare the geoeffective parameters of halo coronal mass ejections (CMEs). We consider 50 front-side full-halo CMEs (FFH CMEs), which are from the list of Michalek, Gopalswamy, and Yashiro (Solar Phys. 246, 399, 2007), whose asymmetric-cone model parameters and earthward-direction parameter were available. For each CME we use its projected velocity [ $V_p$ ], radial velocity [ $V_r$ ], angle between cone axis and sky plane [ $\gamma$ ] from the cone model, earthward-direction parameter [D], source longitude [L], and magnetic-field orientation [M] of its CME source region. We make a simple linear-regression analysis to find out the relationship between CME parameters and Dst index. The main results are as follows: i) The combined parameters [ $(V_r D)^{1/2}$  and  $V_r \gamma$ ] have higher correlation coefficients [cc] with the Dst index than the other parameters [ $V_p$  and  $V_r$ ]: cc=0.76 for  $(V_r D)^{1/2}$ , cc=0.70 for  $V_r \gamma$ , cc=0.55 for  $V_r$ , and cc=0.17 for  $V_p$ . ii) Correlation coefficients between  $V_r \gamma$  and Dst index depend on L and M; cc=0.59 for 21 eastern events [E], cc=0.80 for 29 western events [W], cc=0.49 for 17 northward magnetic-field events [N], and cc=0.69 for 33 southward magnetic-field events [S]. iii) Super geomagnetic storms ( $Dst \leq -200$  nT) only appear in the western and southward magnetic-field events. The mean absolute Dst values of geomagnetic storms ( $Dst \leq -50$  nT) increase with an order of E+N, E+S, W+N, and W+S events; the mean absolute Dst value (169 nT) of W+S events is significantly larger than that (75 nT) of E+N events. Our results demonstrate that not only do the cone-model parameters together with the earthward-direction parameter improve the relationship between CME parameters and Dst index, but also the longitude and the magnetic-field orientation of a FFH CME source region play a significant role in predicting geomagnetic storms.

### **Are the Faint Structures Ahead of Solar Coronal Mass Ejections Real Signatures of Driven Shocks?**

Jae-Ok Lee<sup>1</sup>, Y.-J. Moon<sup>1,2</sup>, Jin-Yi Lee<sup>2</sup>, Kyoung-Sun Lee<sup>3</sup>, Sujin Kim<sup>4</sup>, and Kangjin Lee

2014 ApJ 796 L16

Recently, several studies have assumed that the faint structures ahead of coronal mass ejections (CMEs) are caused by CME-driven shocks. In this study, we have conducted a statistical investigation to determine whether or not the appearance of such faint structures depends on CME speeds. For this purpose, we use 127 Solar and Heliospheric Observatory/Large Angle Spectroscopic CORonagraph (LASCO) front-side halo (partial and full) CMEs near the limb from 1997 to 2011. We classify these CMEs into two groups by visual inspection of CMEs in the LASCO-C2 field of view: Group 1 has the faint structure ahead of a CME and Group 2 does not have such a structure. We find the following results. (1) Eighty-seven CMEs belong to Group 1 and 40 CMEs belong to Group 2. (2) Group 1 events have much higher speeds (average = 1230 km s<sup>-1</sup> and median = 1199 km s<sup>-1</sup>) than Group 2 events (average = 598 km s<sup>-1</sup> and median = 518 km s<sup>-1</sup>). (3) The fraction of CMEs with faint structures strongly depends on CME speeds (V): 0.93 (50/54) for fast CMEs with  $V \geq 1000$  km s<sup>-1</sup>, 0.65 (34/52) for intermediate CMEs with  $500 \text{ km s}^{-1} \leq V < 1000 \text{ km s}^{-1}$ , and 0.14 (3/21) for slow CMEs with  $V < 500 \text{ km s}^{-1}$ . We also find that the fraction of CMEs with deca-hecto metric type II radio bursts is consistent with the above tendency. Our results indicate that the observed faint structures ahead of fast CMEs are most likely an enhanced density manifestation of CME-driven shocks.

### **FAST EXTREME-ULTRAVIOLET DIMMING ASSOCIATED WITH A CORONAL JET SEEN IN MULTI-WAVELENGTH AND STEREOSCOPIC OBSERVATIONS**

K.-S. Lee<sup>1</sup>, D. E. Innes<sup>2</sup>, Y.-J. Moon<sup>1,3</sup>, K. Shibata<sup>4</sup>, Jin-Yi Lee<sup>1</sup>, and Y.-D. Park

2013 ApJ 766 1

We have investigated a coronal jet observed near the limb on **2010 June 27** by the Hinode/X-Ray Telescope (XRT), EUV Imaging Spectrograph (EIS), and Solar Optical Telescope (SOT), and by the Solar Dynamics Observatory (SDO)/Atmospheric Imaging Assembly (AIA), and on the disk by STEREO-A/EUVI. From EUV (AIA and EIS) and soft X-ray (XRT) images we have identified both cool and hot jets. There was a small loop eruption seen in Ca II images of the SOT before the jet eruption. We found that the hot jet preceded its associated cool jet by about 2 minutes. The cool jet showed helical-like structures during the rising period which was supported by the spectroscopic analysis of the jet's emission. The STEREO observation, which enabled us to observe the jet projected against the disk, showed dimming at 195 Å along a large loop connected to the jet. We measured a propagation speed of ~800 km s<sup>-1</sup> for the dimming front. This is comparable to the Alfvén speed in the loop computed from a magnetic field extrapolation of the

photospheric field measured five days earlier by the SDO/Helioseismic and Magnetic Imager, and the loop densities obtained from EIS Fe XIV  $\lambda 264.79/274.20$  line ratios. We interpret the dimming as indicating the presence of Alfvénic waves initiated by reconnection in the upper chromosphere.

### Ensemble Modeling of CME Propagation

C. O. Lee<sup>1</sup>, C. N. Arge<sup>1</sup>, D. Odstrčil<sup>2</sup>, G. Millward<sup>3</sup>, V. Pizzo<sup>3</sup>, J. M. Quinn<sup>1</sup> and C. J. Henney  
Solar Phys. **2012**, doi 10.1007/s11207-012-9980-1, **File**

The current progression toward solar maximum provides a unique opportunity to use multi-perspective spacecraft observations together with numerical models to better understand the evolution and propagation of coronal mass ejections (CMEs). Of interest to both the scientific and forecasting communities are the Earth-directed “halo” CMEs, since they typically produce the most geoeffective events. However, determining the actual initial geometries of halo CMEs is a challenge due to the plane-of-sky projection effects. Thus the recent **15 February 2011** halo CME event has been selected for this study. During this event the Solar TERrestrial RELations Observatory (STEREO) A and B spacecraft were fortuitously located  $\sim 90^\circ$  away from the Sun–Earth line such that the CME was viewed as a limb event from these two spacecraft, thereby providing a more reliable constraint on the initial CME geometry. These multi-perspective observations were utilized to provide a simple geometrical description that assumes a cone shape for a CME to calculate its angular width and central position. The event was simulated using the coupled Wang–Sheeley–Arge (WSA)-Enlil 3D numerical solar corona-solar wind model. Daily updated global photospheric magnetic field maps were used to drive the background solar wind. To improve our modeling techniques, the sensitivity of the modeled CME arrival times to the initial input CME geometry was assessed by creating an ensemble of numerical simulations based on multiple sets of cone parameters for this event. It was found that the accuracy of the modeled arrival times not only depends on the initial input CME geometry, but also on the accuracy of the modeled solar wind background, which is driven by the input maps of the photospheric field. To improve the modeling of the background solar wind, the recently developed data-assimilated magnetic field synoptic maps produced by the Air Force Data Assimilative Photospheric flux Transport (ADAPT) model were used. The ADAPT maps provide a more instantaneous snapshot of the global photospheric field distribution than that provided by traditional daily updated synoptic maps. Using ADAPT to drive the background solar wind, an ensemble set of eight different CME arrival times was generated, where the spread in the predictions was  $\sim 13$  hours and was nearly centered on the observed CME shock arrival time.

### Three Dimensional Structure and Energy Balance of a Coronal Mass Ejection

J.-Y. Lee, J. C. Raymond, Y.-K. Ko, and K.-S. Kim

E-print, Oct 2008; Astrophysical Journal, 692:1271–1286, **2009** February; **File**

<http://solar.physics.montana.edu/cgi-bin/eprint/index.pl?entry=8608>

The Ultraviolet Coronagraph Spectrometer (UVCS) observed Doppler shifted material of a partial Halo Coronal Mass Ejection (CME) on **December 13 2001**. The observed ratio of [O VI]/[O V] is a reliable density diagnostic important for assessing the state of the plasma. Earlier UVCS observations of CMEs found evidence that the ejected plasma is heated long after the eruption. We have investigated the heating rates, which represent a significant fraction of the CME energy budget. The parameterized heating and radiative and adiabatic cooling have been used to evaluate the temperature evolution of the CME material with a time dependent ionization state model. The functional form of a flux rope model for interplanetary magnetic clouds was also used to parameterize the heating. We find that continuous heating is required to match the UVCS observations. To match the O VI-bright knots, a higher heating rate is required such that the heating energy is greater than the kinetic energy. The temperatures for the knots bright in Ly $\alpha$  and C III emission indicate that smaller heating rates are required for those regions. In the context of the flux rope model, about 75% of the magnetic energy must go into heat in order to match the O VI observations. We derive tighter constraints on the heating than earlier analyses, and we show that thermal conduction with the Spitzer conductivity is not sufficient to account for the heating at large heights.

### Three-dimensional Structure of the 2002 April 21 Coronal Mass Ejection

J.-Y. Lee, J. C. Raymond, Y.-K. Ko, and K.-S. Kim

*The Astrophysical Journal*, 651:566–575, **2006**

The reconstructed [Fe xviii] emission allows two interpretations, as ejection of preexisting hot plasma or as a current sheet.

### Stellar Coronal Mass Ejections

[Martin Leitzinger](#), [Petra Odert](#)

Serb. Astron. J. } 200 (2020), 1 – 5

<https://arxiv.org/pdf/2212.09079.pdf>

Stellar coronal mass ejections (CMEs) are a growing research field, especially during the past decade. The large number of so far detected exoplanets raises the open question for the CME activity of stars, as CMEs may strongly affect exoplanetary atmospheres. In addition, as CMEs contribute to stellar mass- and angular momentum loss and are

**Review**



therefore relevant for stellar evolution, there is need for a better characterization of this phenomenon. In this article we review the different methodologies used up to now to attempt the detection of stellar CMEs. We discuss the limitations of the different methodologies and conclude with possible future perspectives of this research field.

### **A census of Coronal Mass Ejections on solar-like stars**

M. [Leitzinger](#), [P. Odert](#), [R. Greimel](#), [K. Vida](#), [L. Kriskovics](#), [E.W. Guenther](#), [H. Korhonen](#), [F. Koller](#), [A. Hanslmeier](#), [Zs. Kóvári](#), [H. Lammer](#)

MNRAS Volume 493, Issue 3, April 2020, Pages 4570–4589,

<https://doi.org/10.1093/mnras/staa504>

<https://arxiv.org/pdf/2002.04430.pdf>

Coronal Mass Ejections (CMEs) may have major importance for planetary and stellar evolution. Stellar CME parameters, such as mass and velocity, have yet not been determined statistically. So far only a handful of stellar CMEs has been detected mainly on dMe stars using spectroscopic observations. We therefore aim for a statistical determination of CMEs of solar-like stars by using spectroscopic data from the ESO phase 3 and Polarbase archives. To identify stellar CMEs we use the Doppler signal in optical spectral lines being a signature of erupting filaments which are closely correlated to CMEs. We investigate more than 3700 hours of on-source time of in total 425 dF-dK stars. We find no signatures of CMEs and only few flares. To explain this low level of activity we derive upper limits for the non-detections of CMEs and compare those with empirically modelled CME rates. To explain the low number of detected flares we adapt a flare power law derived from EUV data to the H $\{\alpha\}$  regime, yielding more realistic results for H $\{\alpha\}$  observations. In addition we examine the detectability of flares from the stars by extracting Sun-as-a-star H $\{\alpha\}$  light curves. The extrapolated maximum numbers of observable CMEs are below the observationally determined upper limits, which indicates that the on-source times were mostly too short to detect stellar CMEs in H $\{\alpha\}$ . We conclude that these non-detections are related to observational biases in conjunction with a low level of activity of the investigated dF-dK stars.

### **DIRECT OBSERVATIONAL EVIDENCE OF FILAMENT MATERIAL WITHIN INTERPLANETARY CORONAL MASS EJECTIONS**

S. T. [Lepri](#) and T. H. Zurbuchen

The Astrophysical Journal Letters, 723:L22–L27, 2010

Coronal mass ejections (CMEs) are explosive events that escape the Sun's corona carrying solar material and energy into the heliosphere. The classic picture of a CME observed in the corona presents a "three-part structure," including a bright front at the leading edge indicating dense plasma, a low-density cavity, the possible signature of an embedded magnetic flux rope, and the so-called core, a high-density region observed to be associated with an erupting filament. Although there are experimental analogs to the first two parts of the CME when observed in situ, there are only a handful of in situ observations of cold, filament-type plasma. This has been a source of major uncertainty and qualitative disagreement between remote and in situ observations of these ejecta. We present the first comprehensive and long-term survey of such low charge states observed by the *Advanced Composition Explorer* SolarWind Ion Composition Spectrometer, using a novel data analysis process developed to identify ions with low ionic charge states. Using a very stringent set of observational signatures, we find that more than 4% of detected interplanetary CMEs have significant contributions of ions with low charge states. These time periods of low-charge ions often occur concurrent with some of the hottest ions, previously interpreted to be affected by flare heating during the CME initiation.

### **Observations of Twist, Current Helicity, and Writhe in the Magnetic Knots of $\delta$ -sunspots Consistent with the Kink Instability of a Highly Twisted Flux Rope**

Peter J. [Levens](#)<sup>1</sup>, Aimee A. Norton<sup>1</sup>, Mark G. Linton<sup>2</sup>, Kalman J. Knizhnik<sup>2</sup>, and Yang Liu<sup>1</sup>

2023 ApJL 954 L20

<https://iopscience.iop.org/article/10.3847/2041-8213/acf0c6/pdf>

We measure current helicity (Hrc) as well as proxies for twist ( $\alpha$ ) and writhe (W) in the isolated magnetic knots of three  $\delta$ -sunspots and report that the observations are consistent with a kink instability acting on a highly twisted flux tube.  $\delta$ -spots are active regions (ARs) in which positive and negative umbrae share a penumbra. We identify and isolate "magnetic knots," i.e., opposite polarity umbrae that are in close proximity and forming the  $\delta$ -configuration, in ARs NOAA 11158, 11267, and 11476 as observed with data from the Solar Dynamic Observatory Helioseismic and Magnetic Imager. We find that Hrc,  $\alpha$ , and W have the same sign for each magnetic knot, as predicted in simulations of a kink instability acting on highly twisted flux tubes. The deformed flux tube causing the  $\delta$ -formation, the magnetic knot, is only a portion of the entire AR and demonstrates the potential for the kink instability to act on a smaller spatial scale within the AR. Each magnetic footpoint contains a single sign of the radial current,  $J_r$ , which suggests that we are observing the core of the flux rope without return currents. As a counterexample, we analyze one  $\beta$ -spot that shows Hrc and  $\alpha$  have the opposite signs of W. While our observations support the formation mechanism of the magnetic knots in  $\delta$ -spots being the kink instability, a much larger sample is needed to determine confidently the prevalence of the kink instability as the cause of flux tube deformation. 2011-02-14, 2011-08-07, 2012-05-07

## **Magnetic field in atypical prominence structures: Bubble, tornado and eruption**

P. J. [Levens](#), B. Schmieder, A. López Ariste, N. Labrosse, K. Dalmasse, B. Gelly

2016 *ApJ* 826 164

<http://arxiv.org/pdf/1605.05964v1.pdf>

Spectropolarimetric observations of prominences have been obtained with the THEMIS telescope during four years of coordinated campaigns. Our aim is now to understand the conditions of the cool plasma and magnetism in 'atypical' prominences, namely when the measured inclination of the magnetic field departs, to some extent, from the predominantly horizontal field found in 'typical' prominences. What is the role of the magnetic field in these prominence types? Are plasma dynamics more important in these cases than the magnetic support? We focus our study on three types of 'atypical' prominences (tornadoes, bubbles and jet-like prominence eruptions) that have all been observed by THEMIS in the He I D<sub>3</sub> line, from which the Stokes parameters can be derived. The magnetic field strength, inclination and azimuth in each pixel are obtained by using the Principal Component Analysis inversion method on a model of single scattering in the presence of the Hanle effect. The magnetic field in tornadoes is found to be more or less horizontal, whereas for the eruptive prominence it is mostly vertical. We estimate a tendency towards higher values of magnetic field strength inside the bubbles than outside in the surrounding prominence. In all of the models in our database, only one magnetic field orientation is considered for each pixel. While sufficient for most of the main prominence body, this assumption appears to be oversimplified in atypical prominence structures. We should consider these observations as the result of superposition of multiple magnetic fields, possibly even with a turbulent field component. **12 October, 2012, 15 October, 2012., May 7, 2014, May 23-24, 2014, 15 July 2014.**

## **Structure of prominence legs: Plasma and magnetic field**

P. J. [Levens](#), B. Schmieder, N. Labrosse, A. López Ariste

2016 *ApJ* 818 31

<http://arxiv.org/pdf/1512.04727v1.pdf>

We investigate the properties of a 'solar tornado' observed on **15 July 2014**, and aim to link the behaviour of the plasma to the internal magnetic field structure of the associated prominence. We made multi-wavelength observations with high spatial resolution and high cadence using SDO/AIA, the IRIS spectrograph and the Hinode/SOT instrument. Along with spectropolarimetry provided by the THEMIS telescope we have coverage of both optically thick emission lines and magnetic field information. AIA reveals that the two legs of the prominence are strongly absorbing structures which look like they are rotating, or oscillating in the plane of the sky. The two prominence legs, which are both very bright in Ca II (SOT), are not visible in the IRIS Mg II slit-jaw images. This is explained by the large optical thickness of the structures in Mg II which leads to reversed profiles, and hence to lower integrated intensities at these locations than in the surroundings. Using lines formed at temperatures lower than 1 MK, we measure relatively low Doppler shifts on the order of +/- 10 km/s in the tornado-like structure. Between the two legs we see loops in Mg II, with material flowing from one leg to the other, as well as counterstreaming. It is difficult to interpret our data as showing two rotating, vertical structures which are unrelated to the loops. This kind of 'tornado' scenario does not fit with our observations. The magnetic field in the two legs of the prominence is found to be preferentially horizontal.

## **Sympathetic solar eruption on 2024 February 9**

[Shu-Yue Li](#), [Qing-Min Zhang](#), [Bei-Li Ying](#), [Li Feng](#), [Ying-Na Su](#), [Mu-Sheng Lin](#), [Yan-Jie Zhang](#)

Research in Astron. Astrophys. 2024

<https://arxiv.org/pdf/2412.01123>

In this paper, we perform a follow-up investigation of the solar eruption originating from active region (AR) 13575 on **2024 February 9**. The primary eruption of a hot channel (HC) generates an X3.4 class flare, a full-halo coronal mass ejection (CME), and an extreme-ultraviolet (EUV) wave. Interaction between the wave and a quiescent prominence (QP) leads to a large-amplitude, transverse oscillation of QP. After the transverse oscillation, QP loses equilibrium and rises up. The ascending motion of the prominence is coherently detected and tracked up to 1.68 R by the Solar UltraViolet Imager (SUVI) onboard the GOES-16 spacecraft and up to 2.2 R by the Solar Corona Imager (SCI UV) of the Lyman-alpha Solar Telescope (LST) onboard the ASO-S spacecraft. The velocity increases linearly from 12.3 to 68.5 km s at 18:30 UT. The sympathetic eruption of QP drives the second CME with a typical three-part structure. The bright core comes from the eruptive prominence, which could be further observed up to 3.3 R by the Large Angle Spectroscopic Coronagraph (LASCO) onboard the SOHO mission. The leading edge of the second CME accelerates continuously from 120 to 277 kms. The EUV wave plays an important role in linking the primary eruption with the sympathetic eruption.

## **Failure of a solar filament eruption caused by magnetic reconnection with overlying coronal loops**

[Leping Li](#), [Hongqiang Song](#), [Yijun Hou](#), [Guiping Zhou](#), [Baolin Tan](#), [Kaifan Ji](#), [Yongyuan Xiang](#), [Zhenyong Hou](#), [Yang Guo](#), [Ye Qiu](#), [Yingna Su](#), [Haisheng Ji](#), [Qingmin Zhang](#), [Yudi Ou](#)

*ApJ* 2024

<https://arxiv.org/pdf/2412.01126>

Failure of a filament eruption caused by magnetic reconnection between the erupting filament and the overlying magnetic field has been previously proposed in numerical simulations. It is, however, rarely observed. In this study, we report the reconnection between an erupting filament and its overlying coronal loops, that results in the failure of the

filament eruption. On **2023 September 24**, a filament was located in active region 13445. It slowly rose, quickly erupted, rapidly decelerated, and finally stopped, with an untwisting motion. As a failed eruption, the event is associated with an M4.4 flare but no coronal mass ejection. During the eruption, the filament became bright, and the overlying loops appeared first in the high-temperature channels. They have average temperatures of  $\sim 12.8$  and  $\sim 9.6$  MK, respectively, indicating that both of them were heated. Two sets of new loops, separately connecting the filament endpoints and the overlying loop footpoints, then formed. Subsequently, the heated overlying loops were seen sequentially in the low-temperature channels, showing the cooling process, which is also supported by the light curves. Plasmoids formed, and propagated bidirectionally along the filament and the overlying loops, indicating the presence of plasmoid instability. These results suggest that reconnection occurs between the erupting filament and the overlying loops. The erupting filament eventually disappeared, with the appearance of more newly-formed loops. We propose that the reconnection between the erupting filament and the overlying loops ruins the filament completely, and hence results in the failed eruption.

## **Large Eruptive and Confined Flares in Relation to the Solar Active Region Evolution**

Fuyu Li<sup>1,2,3</sup>, Changhui Rao<sup>1,2,4</sup>, Huaning Wang<sup>2,5</sup>, Xinhua Zhao<sup>3</sup>, Nanbin Xiang<sup>6</sup>, Linhua Deng<sup>7</sup>, Haitang Li<sup>8</sup>, and Yu Liu<sup>8</sup>

2024 ApJL 976 L2

<https://iopscience.iop.org/article/10.3847/2041-8213/ad8c37/pdf>

Solar active regions (ARs) provide the required magnetic energy and the topology configuration for flares. Apart from conventional static magnetic parameters, the evolution of AR magnetic flux systems should have nonnegligible effects on magnetic energy store and the trigger mechanism of eruptions, which would promote the prediction for the flare using photospheric observations conveniently. Here we investigate 322 large (M- and X-class) flares from 2010 to 2019, almost the whole solar cycle 24. The flare occurrence rate is obviously higher in the developing phase, which should be due to the stronger shearing and complex configurations caused by affluent magnetic emergences. However, the probability of flare eruptions in decaying phases of ARs is obviously higher than that in the developing phase. The confined flares were in nearly equal counts to eruptive flares in developing phases, whereas the eruptive flares were half over confined flares in decaying phases. Yearly looking at flare eruption rates demonstrates the same conclusion. The relationship between sunspot group areas and confined/erupted flares also suggested that the strong field make constraints on the mass ejection, though it can contribute to flare productions. The flare indexes also show a similar trend. It is worth mentioning that all the X-class flares in the decaying phase were erupted, without the strong field constraint. The decaying of magnetic flux systems had facilitation effects on flare eruptions, which may be consequent on the splitting of magnetic flux systems.

## **Eruption of a million-Kelvin warm magnetic flux rope on the Sun**

[Leping Li](#), [Hongqiang Song](#), [Hardi Peter](#), [Lakshmi Pradeep Chitta](#), [Xin Cheng](#), [Zhentong Li](#), [Guiping Zhou](#)

ApJ 967 130 2024

<https://arxiv.org/pdf/2404.09514.pdf>

<https://iopscience.iop.org/article/10.3847/1538-4357/ad3fb3/pdf>

Solar magnetic flux rope (MFR) plays a central role in the physics of coronal mass ejections (CMEs). It mainly includes a cold filament at typical chromospheric temperatures (10000 K) and a hot channel at high coronal temperatures (10 MK). The warm MFR at quiescent coronal temperatures of a million Kelvin is, however, rarely reported. In this study, using multiwavelength images from Atmospheric Imaging Assembly (AIA) on board the Solar Dynamic Observatory (SDO) and Extreme Ultraviolet Imager (EUVI) on board the Solar Terrestrial Relations Observatory-A (STEREO-A), we present an eruption of a warm channel, that represents an MFR with quiescent coronal temperatures (0.6-2.5 MK). On **2022 May 8**, we observed the failed eruption of a hot channel, with the average temperature and emission measure (EM) of 10 MK and  $1.1 \times 10^{28} \text{ cm}^{-5}$ , using AIA high-temperature images in active region (AR) 13007. This failed eruption was associated with a C8.2 flare, with no CME. Subsequently, we observed a warm channel that appeared in AIA and EUVI low-temperature images, rather than AIA high-temperature images. It then erupted, and transformed toward a semi-circular shape. An associated C2.1 flare, along with the signatures of magnetic reconnection in AIA high-temperature images, were identified. Additionally, we observed a CME associated with this event. Compared with the hot channel, the warm channel is cooler and rarer with the average temperature and EM of 1.7 (1.6) MK and  $2.0 \times 10^{26}$  ( $2.3 \times 10^{26}$ )  $\text{cm}^{-5}$ . All the results suggest an unambiguous observation of the million-Kelvin warm MFR, that erupted as a CME, and fill a gap in the temperature domain of coronal MFRs. **2022 May 8**

## **Formation of a long filament through the connection of two filament segments observed by CHASE**

[H.T. Li](#), [X. Cheng](#), [Y.W. Ni](#), [C. Li](#), [S.H. Rao](#), [J.H. Guo](#), [M.D. Ding](#), [P.F. Chen](#)

ApJL 2023

<https://arxiv.org/pdf/2311.14531.pdf>

We present imaging and spectroscopic diagnostics of a long filament during its formation with the observations from the Chinese H $\alpha$  Solar Explorer and Solar Dynamics Observatory. The seed filament first appeared at about 05:00 UT on **2022 September 13**. Afterwards, it grew gradually and connected to another filament segment nearby, building up a long filament at about 20:00 UT on the same day. The CHASE H $\alpha$  spectra show an obvious centroid absorption with mild broadening at the main spine of the long filament, which is interpreted as the evidence of filament material accumulation. More interestingly, near the footpoints of the filament, persistent redshifts have been detected in the

H $\alpha$  spectra during the filament formation, indicating continuous drainage of filament materials. Furthermore, through inspecting the extreme ultraviolet images and magnetograms, it is found that EUV jets and brightenings appeared repeatedly at the junction of the two filament segments, where opposite magnetic polarities converged and canceled to each other continuously. These results suggest the occurrence of intermittent magnetic reconnection that not only connects magnetic structures of the two filament segments but also supplies cold materials for the filament channel likely by the condensation of injected hot plasma, even though a part of cold materials fall down to the filament footpoints at the same time.

### **Multi-thermal jet formation triggered by flux emergence**

[Xiaohong Li](#), [Rony Keppens](#), [Yuhao Zhou](#)

ApJL 2023

<https://arxiv.org/pdf/2304.01043.pdf>

Flux emergence is responsible for various solar eruptions. Combining observation and simulations, we investigate the influence of flux emergence at one footpoint of an arcade on coronal rain as well as induced eruptions. The emergence changes the pressure in the loops, and the internal coronal rain all moves to the other side. The emerging flux reconnects with the overlying magnetic field, forming a current sheet and magnetic islands. The plasma is ejected outwards and heated, forming a cool jet  $\sim 6000$  K and a hot X-ray jet  $\sim 4$  MK simultaneously. The jet dynamical properties agree very well between observation and simulation. In the simulation, the jet also displays transverse oscillations with a period of 8 minutes, a so-called whip-like motion. The movement of the jet and dense plasmoids changes the configuration of the local magnetic field, facilitating the occurrence of Kelvin-Helmholtz instability, and vortex-like structures form at the boundary of the jet. Our simulation clearly demonstrates the effect of emergence on coronal rain, the dynamical details of reconnecting plasmoid chains, the formation of multi-thermal jets, and the cycling of cool mass between the chromosphere and the corona. **2014 October 9**

### **Heating of quiescent coronal loops caused by nearby eruptions observed with the Solar Dynamics Observatory and the Solar Upper Transition Region Imager**

[Leping Li](#), [Hui Tian](#), [Huadong Chen](#), [Hongqiang Song](#), [Zhenyong Hou](#), [Xianyong Bai](#), [Kaifan Ji](#), [Yuanyong Deng](#)

ApJ 949 66 2023

<https://arxiv.org/pdf/2303.15758.pdf>

How structures, e.g., magnetic loops, in the upper atmosphere, i.e., the transition region and corona, are heated and sustained is one of the major unresolved issues in solar and stellar physics. Various theoretical and observational studies on the heating of coronal loops have been undertaken. The heating of quiescent loops caused by eruptions is, however, rarely observed. In this study, employing data from the Solar Dynamics Observatory (SDO) and Solar Upper Transition Region Imager (SUTRI), we report the heating of quiescent loops associated with nearby eruptions. In active regions (ARs) 13092 and 13093, a long filament and a short filament, and their overlying loops are observed on 2022 September 4. In AR 13093, a warm channel erupted toward the northeast, whose material moved along its axis toward the northwest under the long filament, turned to the west above the long filament, and divided into two branches falling to the solar surface. Subsequently, the short filament erupted toward the southeast. Associated with these two eruptions, the quiescent loops overlying the long filament appeared in SDO/Atmospheric Imaging Assembly (AIA) high-temperature images, indicating the heating of loops. During the heating, signature of magnetic reconnection between loops is identified, including the inflowing motions of loops, and the formation of X-type structures and newly reconnected loops. The heated loops then cooled down. They appeared sequentially in AIA and SUTRI lower-temperature images. All the results suggest that the quiescent loops are heated by reconnection between loops caused by the nearby warm channel and filament eruptions. **4 Sep 2022**

### **Evidence of external reconnection between an erupting mini-filament and ambient loops observed by Solar Orbiter/EUI**

[Z. F. Li](#), [X. Cheng](#), [M. D. Ding](#), [L. P. Chitta](#), [H. Peter](#), [D. Berghmans](#), [P. J. Smith](#), [F. Auchere](#), [S. Parenti](#), [K. Barczynski](#), [L. Harra](#), [U. Schuehle](#), [E. Buchlin](#), [C. Verbeeck](#), [R. Aznar Cuadrado](#), [A. N. Zhukov](#), [D. M. Long](#), [L. Teriaca](#), [L. Rodriguez](#)

A&A 673, A83 2023

<https://arxiv.org/pdf/2303.16046.pdf>

<https://www.aanda.org/articles/aa/pdf/2023/05/aa45814-22.pdf>

Mini-filament eruptions are one of the most common small-scale transients in the solar atmosphere. However, their eruption mechanisms are still not understood thoroughly. Here, with a combination of 174 Å images of high spatio-temporal resolution taken by the Extreme Ultraviolet Imager on board Solar Orbiter and images of the Atmospheric Imaging Assembly on board Solar Dynamics Observatory, we investigate in detail an erupting mini-filament over a weak magnetic field region on **2022 March 4**. Two bright ribbons clearly appeared underneath the erupting mini-filament as it quickly ascended, and subsequently, some dark materials blew out when the erupting mini-filament interacted with the outer ambient loops, thus forming a blowout jet characterized by a widening spire. At the same time, multiple small bright blobs of 1-2 Mm appeared at the interaction region and propagated along the post-eruption loops toward the footpoints of the erupting fluxes at a speed of  $\sim 100$  km/s. They also caused a semi-circular brightening structure. Based on these features, we suggest that the mini-filament eruption first experiences internal and then external

reconnection, the latter of which mainly transfers mass and magnetic flux of the erupting mini-filament to the ambient corona.

## Quasi-periodic Variations of Coronal Mass Ejections with Different Angular Widths

[Xia Li](#), [Hui Deng](#), [Feng Wang](#), [Linhua Deng](#), [Ying Mei](#)

ApJ **264** 51 **2023**

<https://arxiv.org/pdf/2301.07379>

<https://iopscience.iop.org/article/10.3847/1538-4365/acb431/pdf>

Coronal mass ejections (CMEs) are energetic expulsions of organized magnetic features from the Sun. The study of CME quasi-periodicity helps establish a possible relationship between CMEs, solar flares, and geomagnetic disturbances. We used the angular width of CMEs as a criterion for classifying the CMEs in the study. Based on 25 years of observational data, we systematically analyzed the quasi-periodic variations corresponding to the CME occurrence rate of different angular widths in the northern and southern hemispheres, using frequency and time-frequency analysis methods. There are various periods for CMEs of different angular widths: 9 months, 1.7 years, and 3.3-4.3 years. Compared with previous studies based on the occurrence rate of CMEs, we obtained the same periods of 1.2(+0.01) months, 3.1(+0.04) months, ~6.1(+0.4) months, 1.2(+0.1) years, and 2.4(+0.4) years. We also found additional periods of all CMEs that appear only in one hemisphere or during a specific solar cycle. For example, 7.1(+0.2) months and 4.1(+0.2) years in the northern hemisphere, 1(+0.004) months, 5.9(+0.2) months, 1(+0.1) years, 1.4(+0.1) years, and 2.4(+0.4) years in the southern hemisphere, 6.1(+0.4) months in solar cycle 23 (SC23) and 6.1(+0.4) months, 1.2(+0.1) years, and 3.7(+0.2) years in solar cycle 24 (SC24). The analysis shows that quasi-periodic variations of the CMEs are a link among oscillations in coronal magnetic activity, solar flare eruptions, and interplanetary space.

## Failed Solar Eruption of A Multi-thermal Flux Rope

[Leping Li](#), [Hongqiang Song](#), [Hardi Peter](#), [Lakshmi Pradeep Chitta](#)

ApJL **941** L1 **2022**

<https://arxiv.org/pdf/2211.11148.pdf>

<https://iopscience.iop.org/article/10.3847/2041-8213/aca47b/pdf>

A magnetic flux rope (FR), hosting hot plasma, is thought to be central to the physics of coronal mass ejection. Such FRs are widely observed with passbands of the Atmospheric Imaging Assembly (AIA) onboard the Solar Dynamics Observatory (SDO), that are sensitive to emission from the hot plasma around 10 MK. In contrast, observations of warmer (around 1 MK) counterparts of FRs are sparse. In this study, we report the failed eruption of a multi-thermal FR, hosting both hot and warm plasma. On **2015 May 1**, a hot channel appeared in the AIA high temperature passbands out of the southeastern solar limb to the south of a nearby flare, and then erupted outward. During the eruption, it rotated perpendicular to the erupting direction. The hot channel stopped erupting, and disappeared gradually, showing a failed eruption. During the hot channel eruption, a warm channel appeared sequentially in the AIA low temperature passbands. It underwent the similar evolution, including the failed eruption, rotation, and disappearance, to the hot channel. A bright compression front is formed in front of the warm channel eruption in AIA low temperature images. Under the hot and warm channel eruptions, a small flare occurred, upon which several current sheets, connecting the erupting channels and the underneath flare, formed in the AIA high temperature passbands. Investigating the spatial and temporal relation between the hot and warm channels, we suggest that both channels twist together, constituting the same multi-thermal FR that has plasma with the high and low temperatures.

## Flare Quasi-Periodic Pulsation Associated with Recurrent Jets

Dong [Li](#), Fanpeng Shi, Haisheng Zhao, Shaolin Xiong, Liming Song, Wenxi Peng, Xinqiao Li, Wei Chen, and Zongjun Ning

Front. Astron. Space Sci. **9**: 1032099. **2022**

doi: 10.3389/fspas.2022.1032099

<https://arxiv.org/pdf/2209.10952.pdf>

<https://www.frontiersin.org/articles/10.3389/fspas.2022.1032099/pdf>

Quasi-periodic pulsations (QPPs), which carry time features and plasma characteristics of flare emissions, are frequently observed in light curves of solar/stellar flares. In this study, we investigated non-stationary QPPs associated with recurrent jets during an M1.2 flare on **2022 July 14**. A quasi-period of  $\sim 45 \pm 10$  s, determined by the wavelet transform technique, is simultaneously identified at wavelengths of soft/hard X-ray and microwave emissions, which are recorded by the Gravitational Wave High-Energy Electromagnetic Counterpart All-sky Monitor, Fermi and the Nobeyama Radio Polarimeters, respectively. A group of recurrent jets with an intermittent cadence of about  $45 \pm 10$  s are found in the Atmospheric Imaging Assembly (AIA) image series at 304 Å, but they are 180 s earlier than the flare QPP. All observational facts suggest that the flare QPPs could be excited by recurrent jets, and they should be associated with non-thermal electrons that are periodically accelerated by a repeated energy release process, such as repetitive magnetic reconnection. Moreover, the same quasi-period is discovered at double footpoints connected by a hot flare loop in AIA 94 Å, and the phase speed is measured to be  $\sim 1,420$  km s<sup>-1</sup>. Based on the differential emission measure, the average temperatures, number densities, and magnetic field strengths at the loop top and footpoint are estimated to be  $\sim 7.7/6.7$  MK,  $\sim 7.5/3.6 \times 10^{10}$  cm<sup>-3</sup>, and  $\sim 143/99$  G, respectively. Our measurements indicate that the 45-s QPP is probably modulated by the kink-mode wave of the flare loop.

## Reconfiguration and eruption of a solar filament by magnetic reconnection with an emerging magnetic field

[Leping Li](#), [Hardi Peter](#), [Lakshmi Pradeep Chitta](#), [Hongqiang Song](#), [Zhe Xu](#), [Yongyuan Xiang](#)

ApJ **935** 85 2022

<https://arxiv.org/pdf/2207.04579.pdf>

<https://iopscience.iop.org/article/10.3847/1538-4357/ac7ffa/pdf>

Both observations and simulations suggest that the solar filament eruption is closely related to magnetic flux emergence. It is thought that the eruption is triggered by magnetic reconnection between the filament and the emerging flux. However, the details of such a reconnection are rarely presented. In this study, we report the detailed reconnection between a filament and its nearby emerging fields, that led to the reconfiguration and subsequent partial eruption of the filament located over the polarity inversion line of active region 12816. Before the reconnection, we observed repeated brightenings in the filament at a location that overlies a site of magnetic flux cancellation. Plasmoids form at this brightening region, and propagate bi-directionally along the filament. These indicate the tether-cutting reconnection that results in the formation and eruption of a flux rope. To the northwest of the filament, magnetic fields emerge, and reconnect with the context ones, resulting in repeated jets. Afterwards, another magnetic fields emerge near the northwestern filament endpoints, and reconnect with the filament, forming the newly reconnected filament and loops. Current sheet repeatedly occurs at the interface, with the mean temperature and emission measure of 1.7 MK and  $1.1 \times 10^{28} \text{ cm}^{-5}$ . Plasmoids form in the current sheet, and propagate along it and further along the newly reconnected filament and loops. The newly reconnected filament then erupts, while the unreconnected filament remains stable. We propose that besides the orientation of emerging fields, some other parameters, such as the position, distance, strength, and area, are also crucial for triggering the filament eruption. **2021 April 21-22**

## A New Magnetic Parameter of Active Regions Distinguishing Large Eruptive and Confined Solar Flares

Ting Li<sup>1,2</sup>, Xudong Sun<sup>3</sup>, Yijun Hou<sup>1,2</sup>, Anqin Chen<sup>4</sup>, Shuhong Yang<sup>1,2</sup>, and Jun Zhang<sup>5</sup>

2022 ApJL 926 L14

<https://iopscience.iop.org/article/10.3847/2041-8213/ac5251/pdf>

With the aim of investigating how the magnetic field in solar active regions (ARs) controls flare activity, i.e., whether a confined or eruptive flare occurs, we analyze 106 flares of Geostationary Operational Environmental Satellite class  $\geq M1.0$  during 2010–2019. We calculate mean characteristic twist parameters  $\alpha_{\text{FPIL}}$  within the "flaring polarity inversion line" region and  $\alpha_{\text{HFED}}$  within the area of high photospheric magnetic free energy density, which both provide measures of the nonpotentiality of the AR core region. Magnetic twist is thought to be related to the driving force of electric current-driven instabilities, such as the helical kink instability. We also calculate total unsigned magnetic flux ( $\Phi_{\text{AR}}$ ) of ARs producing the flare, which describes the strength of the background field confinement. By considering both the constraining effect of background magnetic fields and the magnetic nonpotentiality of ARs, we propose a new parameter  $\alpha/\Phi_{\text{AR}}$  to measure the probability for a large flare to be associated with a coronal mass ejection (CME). We find that in about 90% of eruptive flares,  $\alpha_{\text{FPIL}}/\Phi_{\text{AR}}$  and  $\alpha_{\text{HFED}}/\Phi_{\text{AR}}$  are beyond critical values ( $2.2 \times 10^{-24}$  and  $3.2 \times 10^{-24} \text{ Mm}^{-1} \text{ Mx}^{-1}$ ), whereas they are less than critical values in  $\sim 80\%$  of confined flares. This indicates that the new parameter  $\alpha/\Phi_{\text{AR}}$  is well able to distinguish eruptive flares from confined flares. Our investigation suggests that the relative measure of magnetic nonpotentiality within the AR core over the restriction of the background field largely controls the capability of ARs to produce eruptive flares. **2011-09-06, 2014-10-24, 2014-12-04, 2015-06-22**

## Magnetic Flux and Magnetic Non-potentiality of Active Regions in Eruptive and Confined Solar Flares

[Ting Li](#), [Anqin Chen](#), [Yijun Hou](#), [Astrid M. Veronig](#), [Shuhong Yang](#), [Jun Zhang](#)

ApJ Letters **917** L29 2021

<https://arxiv.org/pdf/2108.01299.pdf>

<https://doi.org/10.3847/2041-8213/ac1a15>

With the aim of understanding how the magnetic properties of active regions (ARs) control the eruptive character of solar flares, we analyze 719 flares of Geostationary Operational Environmental Satellite (GOES) class  $\geq C5.0$  during 2010–2019. We carry out the first statistical study that investigates the flare-coronal mass ejections (CMEs) association rate as function of the flare intensity and the AR characteristics that produces the flare, in terms of its total unsigned magnetic flux ( $\Phi_{\text{AR}}$ ). Our results show that the slope of the flare-CME association rate with flare intensity reveals a steep monotonic decrease with  $\Phi_{\text{AR}}$ . This means that flares of the same GOES class but originating from an AR of larger  $\Phi_{\text{AR}}$ , are much more likely confined. Based on an AR flux as high as  $1.0 \times 10^{24} \text{ Mx}$  for solar-type stars, we estimate that the CME association rate in X100-class "superflares" is no more than 50%. For a sample of 132 flares  $\geq M2.0$  class, we measure three non-potential parameters including the length of steep gradient polarity inversion line (LSGPIL), the total photospheric free magnetic energy ( $E_{\text{free}}$ ) and the area with large shear angle ( $A_{\Psi}$ ). We find that confined flares tend to have larger values of LSGPIL,  $E_{\text{free}}$  and  $A_{\Psi}$  compared to eruptive flares. Each non-potential parameter shows a moderate positive correlation with  $\Phi_{\text{AR}}$ . Our results imply that  $\Phi_{\text{AR}}$  is a decisive quantity describing the eruptive character of a flare, as it provides a global parameter relating to the strength of the background field confinement. **2011 February 15**

## On-disk solar coronal condensations facilitated by magnetic reconnection between open and closed magnetic structures

[Leping Li](#), [Hardi Peter](#), [Lakshmi Pradeep Chitta](#), [Hongqiang Song](#)

ApJ 910 82 2021

<https://arxiv.org/pdf/2102.04605.pdf>

<https://doi.org/10.3847/1538-4357/abe537>

Coronal condensation and rain are a crucial part of the mass cycle between the corona and chromosphere. In some cases, condensation and subsequent rain originate in the magnetic dips formed during magnetic reconnection. This provides a new and alternative formation mechanism for coronal rain. Until now, only off-limb, rather than on-disk, condensation events during reconnection have been reported. In this paper, employing extreme-ultraviolet (EUV) images of the Solar Terrestrial Relations Observatory (STEREO) and Solar Dynamics Observatory (SDO), we investigate the condensations facilitated by reconnection from **2011 July 14 to 15**, when STEREO was in quadrature with respect to the Sun-Earth line. Above the limb, in STEREO/EUV Imager (EUVI) 171 Å-images, higher-lying open structures move downward, reconnect with the lower-lying closed loops, and form dips. Two sets of newly reconnected structures then form. In the dips, bright condensations occur in EUVI 304 Å-images repeatedly which then flow downward to the surface. In the on-disk observations by SDO/Atmospheric Imaging Assembly (AIA) in the 171 Å-channel, these magnetic structures are difficult to identify. Dark condensations appear in AIA 304 Å-images, and then move to the surface as on-disk coronal rain. The cooling and condensation of coronal plasma is revealed by the EUV light curves. If only the on-disk observations would be available, the relation between the condensations and reconnection, shown clearly by the off-limb observations, would not be identified. Thus, we suggest that some on-disk condensation events seen in transition region and chromospheric lines may be facilitated by reconnection.

## Magnetic reconnection between loops accelerated by nearby filament eruption

[Leping Li](#), [Hardi Peter](#), [Lakshmi Pradeep Chitta](#), [Hongqiang Song](#), [Kaifan Ji](#), [Yongyuan Xiang](#)

ApJ 908 213 2021

<https://arxiv.org/pdf/2012.08710>

<https://doi.org/10.3847/1538-4357/abd47e>

Magnetic reconnection modulated by non-local disturbances in the solar atmosphere has been investigated theoretically, but rarely observed. In this study, employing Ha and extreme ultraviolet (EUV) images and line of sight magnetograms, we report acceleration of reconnection by adjacent filament eruption. In Ha images, four groups of chromospheric fibrils are observed to form a saddle-like structure. Among them, two groups of fibrils converge and reconnect. Two newly reconnected fibrils then form, and retract away from the reconnection region. In EUV images, similar structures and evolution of coronal loops are identified. Current sheet forms repeatedly at the interface of reconnecting loops, with width and length of 1-2 and 5.3-7.2 Mm, and reconnection rate of 0.18-0.3. It appears in the EUV low-temperature channels, with average differential emission measure (DEM) weighed temperature and EM of 2 MK and  $2.5 \times 10^{27} \text{ cm}^{-5}$ . Plasmoids appear in the current sheet and propagate along it, and then further along the reconnection loops. The filament, located at the southeast of reconnection region, erupts, and pushes away the loops covering the reconnection region. Thereafter, the current sheet has width and length of 2 and 3.5 Mm, and reconnection rate of 0.57. It becomes much brighter, and appears in the EUV high-temperature channels, with average DEM-weighted temperature and EM of 5.5 MK and  $1.7 \times 10^{28} \text{ cm}^{-5}$ . In the current sheet, more hotter plasmoids form. More thermal and kinetic energy is hence converted. These results suggest that the reconnection is significantly accelerated by the propagating disturbance caused by the nearby filament eruption. **2013 March 15**

## !!! Magnetic Flux of Active Regions Determining the Eruptive Character of Large Solar Flares

[Ting Li](#), [Yijun Hou](#), [Shuhong Yang](#), [Jun Zhang](#), [Lijuan Liu](#), [Astrid M. Veronig](#)

ApJ 900 128 2020

<https://arxiv.org/pdf/2007.08127.pdf>

<https://doi.org/10.3847/1538-4357/aba6ef>

<https://iopscience.iop.org/article/10.3847/1538-4357/aba6ef/pdf> File

We establish the largest eruptive/confined flare database to date and analyze 322 flares of  $\{GOES\}$  class M1.0 and larger that occurred during 2010–2019, i.e., almost spanning the entire solar cycle 24. We find that the total unsigned magnetic flux ( $\Phi_{AR}$ ) of active regions (ARs) is a key parameter in governing the eruptive character of large flares, with the proportion of eruptive flares exhibiting a strong anti-correlation with  $\Phi_{AR}$ . This means that an AR containing a large magnetic flux has a lower probability for the large flares it produces to be associated with a coronal mass ejection (CME). This finding is supported by the high positive correlation we obtained between the critical decay index height and  $\Phi_{AR}$ , implying that ARs with a larger  $\Phi_{AR}$  have a stronger magnetic confinement. Moreover, the confined flares originating from ARs larger than  $1.0 \times 10^{23} \text{ Mx}$  have several characteristics in common: stable filament, slipping magnetic reconnection and strongly sheared post-flare loops. Our findings reveal new relations between the magnetic flux of ARs and the occurrence of CMEs in association with large flares. These relations obtained here provide quantitative criteria for forecasting CMEs and adverse space weather, and have also important implications for

"superflares" on solar-type stars and stellar CMEs. **2011-10-02, 06 March 2012, 2012-07-10, 2014-10-22, 2014-10-24, 2014-12-19**

HMI Naggets # 162 **2021** <http://hmi.stanford.edu/hminuggets/?p=3624>

### **NVST observations of collision-induced apparent fan-shaped jets**

Ting [Li](#), [Yijun Hou](#), [Jun Zhang](#), [Yongyuan Xiang](#)

Volume 492, Issue 2, February **2020**, Pages 2510–2516,

<https://doi.org/10.1093/mnras/stz3630>

Using high-quality H  $\alpha$  observations from the New Vacuum Solar Telescope, we first report apparent fan-shaped jets (AFJs) generated during the interaction between primary fan-shaped jets (FJs) and nearby facula magnetic structure. The primary FJs were intermittently launched from a sunspot penumbra with negative-polarity magnetic fields in active region 12740 on **2019 May 6**, accompanied by impulsive brightenings at the base. While the propagating FJ encountered and collided with the negative-polarity magnetic structure of the west facula, the density of jet material was enhanced to the east of the facula. Meanwhile, the jet structures exhibited a deflection towards the north-west at the jet-facula collision location. Then the primary FJ evolved into two parts, with one part being reflected away from the facula and the other part forming an AFJ. Easily distinguished from the primary FJ, the ejecting AFJ was more ordered and had an apparent end at the facula. The AFJ was impulsively accelerated to speeds of 100 km s<sup>-1</sup>, and reached lengths of up to 40 Mm. The observed AFJ had a similar morphology to the fan-shaped quasi-separatrix layer (QSL) between the penumbra and facula magnetic systems, implying that the material of the AFJ was mainly guided by the fan plane of the QSL. We suggest that the collision does not cause a change in the field-line connectivity and only leads to the redistribution of jet material.

### **The Formation of CME from Coupling Fan-spine Magnetic System: A Difficult Journey**

Haidong [Li](#), Jiayan Yang, Junchao Hong, and Hechao Chen

**2019** ApJL 886 L34

[sci-hub.se/10.3847/2041-8213/ab564e](https://sci-hub.se/10.3847/2041-8213/ab564e)

We present the eruption of a mini-filament that caused a large-scale complicated coronal mass ejection (CME) on **2014 March 28**, using the high-resolution observations taken by the Solar Dynamic Observatory. Three-dimensional coronal magnetic field extrapolated from the nonlinear force-free field code reveals that the magnetic environment of the eruption source region was a large fan-spine magnetic system that hosted another small fan-spine system under its fan, and the mini-filament was located under the fan structure of the small fan-spine system. Our analysis results suggest that the eruption of the mini-filament underwent three reconnection processes before the formation of the CME. First, the erupting filament triggered the null point reconnection in the small fan-spine system. During this stage, the sudden expansion of the spine field lines also excited a large-scale extreme-ultraviolet wave. Second, the spine field lines of the small fan-spine system were pushed up by the erupting filament and therefore further triggered the null point reconnection in the large fan-spine magnetic system. Third, during the second stage, magnetic reconnection also occurred between the two legs of the stretched confining field lines of the mini-filament. The present study suggests that the formation of the observed CME from the coupling fan-spine magnetic system was more complicated than previously thought, needing to undergo multistage magnetic reconnection processes in the low corona.

### **Two Types of Solar Confined Flares**

Ting [Li](#), [Lijuan Liu](#), [Yijun Hou](#), [Jun Zhang](#)

ApJ **881** 151 **2019**

<https://arxiv.org/pdf/1907.04510.pdf> **File**

<https://iopscience.iop.org/article/10.3847/1538-4357/ab3121/pdf>

With the aim of understanding the physical mechanisms of confined flares, we selected 18 confined flares during 2011-2017, and classified the confined flares into two types based on their different dynamic properties and magnetic configurations. "Type I" of confined flares are characterized by slipping reconnection, strong shear, and stable filament. "Type II" flares have nearly no slipping reconnection, and have a configuration in potential state after the flare. Filament erupts but is confined by strong strapping field. "Type II" flares could be explained by 2D MHD models while "type I" flares need 3D MHD models. 7 flares of 18 (~39 %) belong to "type I" and 11 (~61 %) are "type II" confined flares. The post-flare loops (PFLs) of "type I" flares have a stronger non-potentiality, however, the PFLs in "type II" flares are weakly sheared. All the "type I" flares exhibit the ribbon elongations parallel to the polarity inversion line (PIL) at speeds of several tens of km s<sup>-1</sup>. For "type II" flares, only a small proportion shows the ribbon elongations along the PIL. We suggest that different magnetic topologies and reconnection scenarios dictate the distinct properties for the two types of flares. Slipping magnetic reconnections between multiple magnetic systems result in "type I" flares. For "type II" flares, magnetic reconnections occur in anti-parallel magnetic fields underlying the erupting filament. Our study shows that "type I" flares account for more than one third of the overall large confined flares, which should not be neglected in further studies. **2011 March 09, 2012 July 04, 2014 October 26,**

**Table 1:** Event list

### **Flow instabilities in solar jets in their upstream and downstream regimes**

Xiaohong [Li](#), [Jun Zhang](#), [Shuhong Yang](#), [Yijun Hou](#)



ApJ 875 52 2019  
<https://arxiv.org/pdf/1904.05120.pdf>  
[sci-hub.se/10.3847/1538-4357/ab0f39](https://sci-hub.se/10.3847/1538-4357/ab0f39)

Using the Atmospheric Imaging Assembly 304 A images obtained from the Solar Dynamics Observatory, we study two jets which occurred during the M5.8 class flare on **2017 April 3** and the M5.5 class flare on **2016 July 23**, respectively. During the M5.8 class flare, many vortex-like structures occurred in the upstream and downstream regimes of the associated jet. While the jet was ejected upwards to the corona, some dark material at its base flowed through a bright structure with a velocity of 110 km/s. The boundary between the material and the structure changed from smooth to uneven. Later, the jet material at the higher atmosphere started to fall down with velocities of over 200 km/s, and the left boundary of the jet developed into a sawtooth pattern. The vortex-like structures were formed, and the growth rates of two structures were presented. During the M5.5 class flare, we also observed many vortex-like structures in the downstream regime of the jet. At the late stage of the jet, some material at the south boundary of the jet fell back to the solar surface, and vortex-like structures at the boundary grew from ripple-like minima into vortices with diameters of 3.4-5.4 Mm. The growth rates of the vortex-like structures were calculated. We suggest that the vortex-like structures in the upstream regime are the manifestations of Kelvin-Helmholtz instability, and those in the downstream regime are simultaneously driven by Kelvin-Helmholtz instability and Rayleigh-Taylor instability.

### **A Fan Spine Jet: Nonradial Filament Eruption and the Plasmoid Formation**

Haidong Li<sup>1,2</sup> and Jiayan Yang

2019 ApJ 872 87

<https://doi.org/10.3847/1538-4357/aafb3a>

Using the data from SDO and NVST, we studied a circular filament eruption in association with the formation of jet under a nonaxisymmetric fan spine configuration. A nonradial motion of the filament toward a null point and the formation of a jet were presented in detail. This event contained a small circular filament, which was located above the polarity inversion line. The nonlinear force-free field extrapolation shows the presence of a nonaxisymmetric fan spine structure above the filament. Thus, the filament was confined by this magnetic field structure. Since the confining magnetic pressure decreases much faster toward the null point than anywhere else, the filament displayed a shift motion toward the null point that resulted in a collision, and a reconnection signature of bidirectional flows was observed. Due to the external magnetic reconnection, the topology of the filament field was reconfigured, accompanying by the scattered filament material spreading along nearby coronal loops, which resulted in a blowout jet. Particularly, some ejected plasma blobs were also observed in the vicinity of the interfaces between the filament and neighboring coronal loops. These blobs originating from the dissipation region may be plasmoids in association with tearing mode instability. We suggested that in pre-jet phase the nonaxisymmetric fan spine configuration can act on the erupting filament, laterally deflecting and channeling its motion toward the null point, which may facilitate the jet formation by magnetic reconnection.

### **Transition-region explosive events produced by plasmoid instability**

Dong Li

Research in Astronomy and Astrophysics 2018

<https://arxiv.org/pdf/1811.01559.pdf>

Magnetic reconnection is thought to be a key process in most of solar eruptions. Thanks to high-resolution observations and simulations, the studied scale of reconnection process has become smaller and smaller. Spectroscopic observations show that the reconnection site can be very small, which always exhibits a bright core and two extended wings with fast speeds, i.e., transition-region explosive events. In this paper, using the PLUTO code, we perform a 2-D magnetohydrodynamic simulation to investigate the small-scale reconnection in double current sheets. Based on our simulation results, such as the line-of-sight velocity, number density and plasma temperature, we can synthesize the line profile of Si IV 1402.77 Å which is a well known emission line to study the transition-region explosive events on the Sun. The synthetic line profile of Si IV 1402.77 Å is complex with a bright core and two broad wings which can extend to be nearly 200 km/s. Our simulation results suggest that the transition-region explosive events on the Sun are produced by plasmoid instability during the small-scale magnetic reconnection.

### **Solar jet-like features rooted on flare ribbons**

Xiaohong Li, Jun Zhang, Shuhong Yang, Yijun Hou

Publications of the Astronomical Society of Japan

2018

<https://arxiv.org/pdf/1811.00281.pdf>

Employing the high spatio-temporal Interface Region Imaging Spectrograph 1330 Å observations, we investigated the jet-like features that occurred during the X8.2 class flare in NOAA active region (AR) 12673 on **2017 September 10**. These jet-like features were rooted on the flare ribbons. We examined 15 features, and the mean values of the lifetimes, projected widths, lengths and velocities of these features were 87 s, 890 km, 2.7 Mm and 70 km s<sup>-1</sup>, respectively. We also observed many jet-like features which happened during the X1.0 class flare on **2014 October 25**. We studied the spectra at the base of a jet-like feature during its development. The Fe XXI 1354.08 Å line in the corona displays blueshift, while the Si IV 1402.77 Å line in the transition region exhibits redshift, which indicates the chromospheric evaporation. This is the first time that the jet-like features are reported to be rooted on the flare ribbons, and we suggest that these jet-like features were driven by the mechanism of chromospheric evaporation.

## Reconstructing solar wind inhomogeneous structures from stereoscopic observations in white-light: Small transients along the Sun-Earth line

Xiaolei [Li](#), [Yuming Wang](#), [Rui Liu](#), [Chenglong Shen](#), [Quanhao Zhang](#), [Bin Zhuang](#), [Jiajia Liu](#), [Yutian Chi](#)  
JGR 2018

<https://arxiv.org/ftp/arxiv/papers/1809/1809.03651.pdf>

The Heliospheric Imagers (HI) on board the two spacecraft of the Solar Terrestrial Relations Observatory (STEREO) provided white-light images of transients in the solar wind from dual perspectives from 2007 to 2014. In this paper, we develop a new method to identify and locate the transients automatically from simultaneous images from the two inner telescopes, known as HI-1, based on a correlation analysis. Correlation coefficient (cc) maps along the Sun-Earth line are constructed for the period from 1 Jan 2010 to 28 Feb 2011. From the maps, transients propagating along the Sun-Earth line are identified, and a 27-day periodic pattern is revealed, especially for small-scale transients. Such a periodicity in the transient pattern is consistent with the rotation of the Sun's global magnetic structure and the periodic crossing of the streamer structures and slow solar wind across the Sun-Earth line, and this substantiates the reliability of our method and the high degree of association between the small-scale transients of the slow solar wind and the coronal streamers. Besides, it is suggested by the cc map that small-scale transients along the Sun-Earth line are more frequent than large-scale transients by a factor of at least 2, and that they quickly diffused into background solar wind within about 40 Rs in terms of the signal-to-noise ratio of white-light emissions. The method provides a new tool to reconstruct inhomogeneous structures in the heliosphere from multiple perspectives.

## Spectroscopic and imaging observations of small-scale reconnection events

Dong [Li](#), [Leping Li](#), [Zongjun Ning](#)

MNRAS Volume 479, Issue 2, 11 September 2018, Pages 2382–2388

<https://arxiv.org/pdf/1806.10205.pdf>

<http://sci-hub.ru/10.1093/mnras/sty1712>

We present spectroscopic and imaging observations of small-scale reconnection events on the Sun. Using the Interface Region Imaging Spectrograph (IRIS) observations, one reconnection event is first detected as IRIS jets with fast bi-directional velocities in the chromosphere and transition region, which are identified as non-Gaussian broadenings with two extended wings in the line profiles of Si iv, C ii, and Mg ii k. The magnetograms under the IRIS jets from Helioseismic and Magnetic Images exhibit magnetic flux cancellation simultaneously, supporting that the IRIS jets are driven by magnetic reconnection. The Atmospheric Imaging Assembly images also show an extreme ultraviolet (EUV) brightening which is shortly after the underlying IRIS jets, i.e., in the 131 Å, 171 Å, 193 Å, 211 Å, and 94 Å channels, implying that the over-lying EUV brightening in the corona is caused by the IRIS jets in the chromosphere and transition region. We also find another three reconnection events which show the same features during this IRIS observation. Our observational results suggest that the small-scale reconnection events might contribute to the coronal heating. The new result is that the process of magnetic reconnection is detected from the photosphere through chromosphere and transition region to the corona. **2017 September 18**

## Observing Kelvin-Helmholtz instability in solar blowout jet

Xiaohong [Li](#), [Jun Zhang](#), [Shuhong Yang](#), [Yijun Hou](#), [Robert Erdelyi](#)  
Scientific Reports 2018

<https://www.nature.com/articles/s41598-018-26581-4.pdf>

Kelvin-Helmholtz instability (KHI) is a basic physical process in fluids and magnetized plasmas, with applications successfully modelling e.g. exponentially growing instabilities observed at magnetospheric and heliospheric boundaries, in the solar or Earth's atmosphere and within astrophysical jets. Here, we report the discovery of the KHI in solar blowout jets and analyse the detailed evolution by employing high-resolution data from the Interface Region Imaging Spectrograph (IRIS) satellite launched in 2013. The particular jet we focus on is rooted in the surrounding penumbra of the main negative polarity sunspot of Active Region 12365, where the main body of the jet is a super-penumbral structure. At its maximum, the jet has a length of 90 Mm, a width of 19.7 Mm, and its density is about 40 times higher than its surroundings. During the evolution of the jet, a cavity appears near the base of the jet, and bi-directional flows originated from the top and bottom of the cavity start to develop, indicating that magnetic reconnection takes place around the cavity. Two upward flows pass along the left boundary of the jet successively. Next, KHI develops due to a strong velocity shear ( $\sim 204 \text{ km s}^{-1}$ ) between these two flows, and subsequently the smooth left boundary exhibits a sawtooth pattern, evidencing the onset of the instability. **12 June 2015**

## The surge-like eruption of a miniature filament associated with circular flare ribbon

Haidong [Li](#), Jiayan Yang, Yunchun Jiang, Yi Bi, Zhining Qu, Hechao Chen

[Astrophysics and Space Science](#) February 2018, 363:26

<http://sci-hub.tw/10.1007/s10509-017-3244-3>

We present a study of a mini-filament erupting in association with a circular ribbon flare observed by NVST and SDO/AIA on **2014 March 17**. The filament was located at one footpoint region of a large loops. The potential field extrapolation shows that it was embedded under a magnetic null point configuration. First, we observed a brightening of

the filament at the corresponding EUV images, close to one end of the filament. With time evolution, a circular flare ribbon was observed around the filament at the onset of the eruption, which is regarded as a signature of reconnection at the null point. After the filament activation, its eruption took the form of a surge, which ejected along one end of a large-scale closed coronal loops with a curtain-like shape. We conjecture that the null point reconnection may facilitate the eruption of the filament.

### **High-resolution Observations of Sympathetic Filament Eruptions by NVST**

Shangwei Li<sup>1,2</sup>, Yingna Su<sup>1,5</sup>, Tuanhui Zhou<sup>1</sup>, Adriaan van Ballegoijen<sup>3</sup>, Xudong Sun<sup>4</sup>, and Haisheng Ji  
2017 ApJ 844 70

<https://arxiv.org/pdf/1803.06088.pdf>

<http://sci-hub.cc/10.3847/1538-4357/aa78f5>

We investigate two sympathetic filament eruptions observed by the New Vacuum Solar Telescope on **2015 October 15**. The full picture of the eruptions is obtained from the corresponding Solar Dynamics Observatory (SDO)/Atmospheric Imaging Assembly (AIA) observations. The two filaments start from active region NOAA 12434 in the north and end in one large quiescent filament channel in the south. The left filament erupts first, followed by the right filament eruption about 10 minutes later. Clear twist structure and rotating motion are observed in both filaments during the eruption. Both eruptions failed, since the filaments first rise up, then flow toward the south and merge into the southern large quiescent filament. We also observe repeated activations of mini filaments below the right filament after its eruption. Using magnetic field models constructed based on SDO/HMI magnetograms via the flux rope insertion method, we find that the left filament eruption is likely to be triggered by kink instability, while the weakening of overlying magnetic fields due to magnetic reconnection at an X-point between the two filament systems might play an important role in the onset of the right filament eruption.

### **Blowout Surge due to Interaction between a Solar Filament and Coronal Loops**

Haidong Li<sup>1,2,3</sup>, Yunchun Jiang<sup>1,2</sup>, Jiayan Yang<sup>1,2</sup>, Zhining Qu<sup>4</sup>, Bo Yang<sup>1,2</sup>, Zhe Xu<sup>1,2,3</sup>, Yi Bi<sup>1,2</sup>, Junchao Hong<sup>1,2</sup>, and Hechao Chen  
2017 ApJL 842 L20

<http://iopscience.iop.org/sci-hub.cc/2041-8205/842/2/L20/>

We present an observation of the interaction between a filament and the outer spine-like loops that produces a blowout surge within one footpoint of large-scale coronal loops on **2015 February 6**. Based on the observation of the AIA 304 and 94 Å, the activated filament is initially embedded below a dome of a fan-spine configuration. Due to the ascending motion, the erupting filament reconnects with the outer spine-like field. We note that the material in the filament blows out along the outer spine-like field to form the surge with a wider spire, and a two-ribbon flare appears at the site of the filament eruption. In this process, small bright blobs appear at the interaction region and stream up along the outer spine-like field and down along the eastern fan-like field. As a result, a leg of the filament becomes radial and the material in it erupts, while another leg forms the new closed loops. Our results confirm that the successive reconnection occurring between the erupting filament and the coronal loops may lead to a strong thermal/magnetic pressure imbalance, resulting in a blowout surge.

### **High-resolution Observation of Downflows at One End of a Pre-eruption Filament**

Qin Li, Na Deng, Ju Jing, Haimin Wang  
2017 ApJ 841 112

<https://arxiv.org/pdf/1705.08003.pdf>

<http://iopscience.iop.org/sci-hub.cc/0004-637X/841/2/112/>

Studying the dynamics of filaments at pre-eruption phase can shed light on the precursor of eruptive events. Such studies in high-resolution (in the order of 0.1") are highly desirable yet very rare so far. In this work, we present a detailed observation of a pre-eruption evolution of a filament obtained by the 1.6 m New Solar Telescope (NST) at Big Bear Solar Observatory (BBSO). One end of the filament is anchored at the sunspot in NOAA active region (AR) 11515, which is well observed by NST H $\alpha$  off-bands four hours before till one hour after the filament eruption. A M1.6 flare is associated with the eruption. We observed persistent downflowing materials along the H $\alpha$  multi-threaded component of the loop towards the AR end during the pre-eruption phase. We traced the trajectories of plasma blobs along the H $\alpha$  threads and obtained the plane-of-sky velocity of 45 km s<sup>-1</sup> on average. We further estimated the real velocities of the downflows and the altitude of the filament by matching the observed H $\alpha$  threads with magnetic field lines extrapolated from a nonlinear force-free field (NLFFF) model. Observation of chromospheric brightenings (BZs) at the footpoints of the falling plasma blobs is also presented in the paper. The lower limit of the kinetic energy per second of the downflows through the BZs is found to be  $\sim 1021$  erg. Larger FOV observations from BBSO full disk H $\alpha$  images show that the AR end of the filament started ascending four hours before the flare. We attribute the observed downflows at the AR end of the filament to the draining effect of the filament rising prior to its eruption. During the slow-rise phase, the downflows continuously drained away  $\sim 1015g$  mass from the filament over a few hours, which is believed to be essential for the instability at last, and could be an important precursor of eruptive events. **2012 July 5**

## Rotating Magnetic Structures Associated with a Quasi-circular Ribbon Flare

Haidong Li<sup>1,2</sup>, Yunchun Jiang<sup>1</sup>, Jiayan Yang<sup>1</sup>, Bo Yang<sup>1,2</sup>, Zhe Xu<sup>1,2</sup>, Junchao Hong<sup>1</sup>, and Yi Bi<sup>1</sup>  
2017 ApJ 836 235 10.3847/1538-4357/aa5eac

<http://sci-hub.cc/10.3847/1538-4357/aa5eac>

We present the detection of a small eruption and the associated quasi-circular ribbon flare during the emergence of a bipole occurring on **2015 February 3**. Under a fan dome, a sigmoid was rooted in a single magnetic bipole, which was encircled by negative polarity. The nonlinear force-free field extrapolation shows the presence of twisted field lines, which can represent a sigmoid structure. The rotation of the magnetic bipole may cause the twisting of magnetic field lines. An initial brightening appeared at one of the footpoints of the sigmoid, where the positive polarity slides toward a nearby negative polarity field region. The sigmoid displayed an ascending motion and then interacted intensively with the spine-like field. This type of null point reconnection in corona led to a violent blowout jet, and a quasi-circular flare ribbon was also produced. The magnetic emergence and rotational motion are the main contributors to the energy buildup for the flare, while the cancellation and collision might act as a trigger.

## Plasma Brightenings in a Failed Solar Filament Eruption

Y. Li, M. D. Ding

ApJ Volume 838, Number 1 v 838:15 2017

<https://arxiv.org/pdf/1702.05136.pdf>

<http://iopscience.iop.org/article/10.3847/1538-4357/aa6348/pdf>

Failed filament eruptions are solar eruptions that are not associated with coronal mass ejections. In a failed filament eruption, the filament materials usually show some ascending and falling motions as well as generate bright EUV emissions. Here we report a failed filament eruption that occurred in a quiet-Sun region observed by the Atmospheric Imaging Assembly on board the Solar Dynamics Observatory. In this event, the filament spreads out but gets confined by the surrounding magnetic field. When interacting with the ambient magnetic field, the filament material brightens up and flows along the magnetic field lines through the corona to the chromosphere. We find that some materials slide down along the lifting magnetic structure containing the filament and impact the chromosphere to cause two ribbon-like brightenings in a wide temperature range through kinetic energy dissipation. There is evidence suggesting that magnetic reconnection occurs between the filament magnetic structure and the surrounding magnetic fields where filament plasma is heated to coronal temperatures. In addition, thread-like brightenings show up on top of the erupting magnetic fields at low temperatures, which might be produced by an energy imbalance from a fast drop of radiative cooling due to plasma rarefaction. Thus, this single event of failed filament eruption shows existence of a variety of plasma brightenings that may be caused by completely different heating mechanisms. **2016 July 22**

## Imaging Observations of Magnetic Reconnection in a Solar Eruptive Flare

Y. Li, X. Sun, M. D. Ding, J. Qiu, E. R. Priest

ApJ 835 190 2017

<https://arxiv.org/pdf/1612.09417v1.pdf>

Solar flares are one of the most energetic events in the solar atmosphere. It is widely accepted that flares are powered by magnetic reconnection in the corona. An eruptive flare is usually accompanied by a coronal mass ejection, both of which are probably driven by the eruption of a magnetic flux rope (MFR). Here we report an eruptive flare on **2016 March 23** observed by the Atmospheric Imaging Assembly on board the Solar Dynamics Observatory. The extreme-ultraviolet imaging observations exhibit the clear rise and eruption of an MFR. In particular, the observations reveal solid evidence for magnetic reconnection from both the corona and chromosphere during the flare. Moreover, weak reconnection is observed before the start of the flare. We find that the preflare weak reconnection is of tether-cutting type and helps the MFR to rise slowly. Induced by a further rise of the MFR, strong reconnection occurs in the rise phases of the flare, which is temporally related to the MFR eruption. We also find that the magnetic reconnection is more of 3D-type in the early phase, as manifested in a strong-to-weak shear transition in flare loops, and becomes more 2D-like in the later phase, as shown by the apparent rising motion of an arcade of flare loops.

## RELATIONSHIP BETWEEN DISTRIBUTION OF MAGNETIC DECAY INDEX AND FILAMENT ERUPTIONS

H. Li<sup>1,2</sup>, Y. Liu<sup>1</sup>, A. Elmhamdi<sup>3</sup>, and A.-S. Kordi<sup>3</sup>

2016 ApJ 830 132

<http://sci-hub.cc/10.3847/0004-637X/830/2/132>

The decay index  $n$  of a horizontal magnetic field is considered to be an important parameter in judging the stability of a flux rope. However, the spatial distribution of this parameter has not been extensively explored so far. In this paper, we present a delineative study of the three-dimensional maps of  $n$  for two eruptive events, in which filaments underwent asymmetrical eruptions. The corresponding  $n$ -distributions are both found to show that the filaments tend to erupt at abnormal regions (dubbed ABN regions) of  $n$ . These ABN regions appear to be divided into two subregions, with larger and smaller  $n$ . Moreover, an analysis of the magnetic topological configuration of the ABN regions has been also performed. The results indicate that these ABN regions are associated with a kind of special quasi-separatrix layer across which the connectivity of magnetic field is discontinuous. The presented observations and analyses strongly suggest that the torus instability in ABN regions may play a crucial role for the triggering of an asymmetrical eruption.

Additionally, our investigation can provide a way of forecasting how a filament might erupt, and predicting the location for an asymmetrically eruptive filament to be split through analyzing the spatial structure of n.

2011 May 02, 2011 Jun 05

## **OSCILLATION OF CURRENT SHEETS IN THE WAKE OF A FLUX ROPE ERUPTION OBSERVED BY THE SOLAR DYNAMICS OBSERVATORY**

L. P. Li<sup>1</sup>, J. Zhang<sup>1</sup>, J. T. Su<sup>1</sup>, and Y. Liu

2016 ApJ 829 L33

An erupting flux rope (FR) draws its overlying coronal loops upward, causing a coronal mass ejection. The legs of the overlying loops with opposite polarities are driven together. Current sheets (CSs) form, and magnetic reconnection, producing underneath flare arcades, occurs in the CSs. Employing Solar Dynamic Observatory/Atmospheric Imaging Assembly images, we study a FR eruption on **2015 April 23**, and for the first time report the oscillation of CSs underneath the erupting FR. The FR is observed in all AIA extreme-ultraviolet passbands, indicating that it has both hot and warm components. Several bright CSs, connecting the erupting FR and the underneath flare arcades, are observed only in hotter AIA channels, e.g., 131 and 94 Å. Using the differential emission measure (EM) analysis, we find that both the temperature and the EM of CSs temporally increase rapidly, reach the peaks, and then decrease slowly. A significant delay between the increases of the temperature and the EM is detected. The temperature, EM, and density spatially decrease along the CSs with increasing heights. For a well-developed CS, the temperature (EM) decreases from 9.6 MK ( $8 \times 10^{28} \text{ cm}^{-5}$ ) to 6.2 MK ( $5 \times 10^{27} \text{ cm}^{-5}$ ) in 52 Mm. Along the CSs, dark supra-arcade downflows (SADs) are observed, and one of them separates a CS into two. While flowing sunward, the speeds of the SADs decrease. The CSs oscillate with a period of 11 minutes, an amplitude of 1.5 Mm, and a phase speed of  $200 \pm 30 \text{ km s}^{-1}$ . One of the oscillations lasts for more than 2 hr. These oscillations represent fast-propagating magnetoacoustic kink waves.

## **Slipping Magnetic Reconnection of Flux Rope Structures as a Precursor to an Eruptive X-class Solar Flare**

Ting Li, Kai Yang, Yijun Hou, Jun Zhang

ApJ 2016

<http://arxiv.org/pdf/1608.02057v1.pdf>

We present the quasi-periodic slipping motion of flux rope structures prior to the onset of an eruptive X-class flare on **2015 March 11**, obtained by the *Interface Region Imaging Spectrograph* (*IRIS*) and the *Solar Dynamics Observatory* (*SDO*). The slipping motion occurred at the north part of the flux rope and seemed to successively peel off the flux rope. The speed of the slippage was  $30\text{--}40 \text{ km s}^{-1}$ , with an average period of  $130 \pm 30 \text{ s}$ . The Si IV 1402.77 Å line showed a redshift of  $10\text{--}30 \text{ km s}^{-1}$  and a line width of  $50\text{--}120 \text{ km s}^{-1}$  at the west legs of slipping structures, indicative of reconnection downflow. The slipping motion lasted about 40 min and the flux rope started to rise up slowly at the late stage of the slippage. Then an X2.1 flare was initiated and the flux rope was impulsively accelerated. One of the flare ribbons swept across a negative-polarity sunspot and the penumbral segments of the sunspot decayed rapidly after the flare. We studied the magnetic topology at the flaring region and the results showed the existence of a twisted flux rope, together with quasi-separatrix layers (QSLs) structures binding the flux rope. Our observations imply that quasi-periodic slipping magnetic reconnection occurs along the flux-rope-related QSLs in the preflare stage, which drives the later eruption of the flux rope and the associated flare.

## **Magnetic reconnection between a solar filament and nearby coronal loops**

Leping Li, Jun Zhang, Hardi Peter, Eric Priest, Huadong Chen, Lijia Guo, Feng Chen, Duncan Mackay

*Nature Physics* 2016

<http://arxiv.org/pdf/1605.03320v1.pdf>

Magnetic reconnection, the rearrangement of magnetic field topology, is a fundamental physical process in magnetized plasma systems all over the universe<sup>1,2</sup>. Its process is difficult to be directly observed. Coronal structures, such as coronal loops and filament spines, often sketch the magnetic field geometry and its changes in the solar corona<sup>3</sup>. Here we show a highly suggestive observation of magnetic reconnection between an erupting solar filament and its nearby coronal loops, resulting in changes in connection of the filament. X-type structures form when the erupting filament encounters the loops. The filament becomes straight, and bright current sheets form at the interfaces with the loops. Many plasmoids appear in these current sheets and propagate bi-directionally. The filament disconnects from the current sheets, which gradually disperse and disappear, reconnects to the loops, and becomes redirected to the loop footpoints. This evolution of the filament and the loops suggests successive magnetic reconnection predicted by theories<sup>1</sup> but rarely detected with such clarity in observations. Our results on the formation, evolution, and disappearance of current sheets, confirm three-dimensional magnetic reconnection theory and have implications for the evolution of dissipation regions and the release of magnetic energy for reconnection in many magnetized plasma systems. **January 1, 2012**

## **Trigger of a blowout jet in a solar coronal mass ejection associated with a flare**

Xiaohong Li, Shuhong Yang, Huadong Chen, Ting Li, Jun Zhang

ApJL 814 L13 2015

<http://arxiv.org/pdf/1511.01603v1.pdf>

Using the multi-wavelength images and the photospheric magnetograms from the *Solar Dynamics Observatory*, we study the flare which was associated by the only one coronal mass ejection (CME) in active region (AR) 12192. The eruption of a filament caused a blowout jet, and then an M4.0 class flare occurred. This flare was located at the edge of AR instead of in the core region. The flare was close to the apparently "open" fields, appearing as extreme-ultraviolet structures that fan out rapidly. Due to the interaction between flare materials and "open" fields, the flare became an eruptive flare, leading to the CME. Then at the same site of the first eruption, another small filament erupted. With the high spatial and temporal resolution H $\alpha$  data from the New Vacuum Solar Telescope at the *Fuxian Solar Observatory*, we investigate the interaction between the second filament and the nearby "open" lines. The filament reconnected with the "open" lines, forming a new system. To our knowledge, the detailed process of this kind of interaction is reported for the first time. Then the new system rotated due to the untwisting motion of the filament, implying that the twist was transferred from the closed filament system to the "open" system. In addition, the twist seemed to propagate from the lower atmosphere to the upper layers, and was eventually spread by the CME to the interplanetary space. **2014 October 24**

### **The quasi-periodic behavior of recurrent jets caused by emerging magnetic flux**

H. D. Li, Y. C. Jiang, J. Y. Yang, Y. Bi,

*Astrophysics and Space Science* October **2015**, 359:44

A series of recurring jets occurred at the edge of an active region NOAA 11459 on **2012 April 20**, and they were observed simultaneously at EUV and soft X-ray wavelengths. They also were sometimes associated with a hard X-ray source at the base region. The jets might have resulted from magnetic reconnection between the newly emerging flux and the preexisting magnetic field that corresponded to the footpoint region of large-scale coronal loops. We obtained two periods of 171 Å intensity variations at the jet footpoint region, which were about 5 and 13 min. At the jet base, the short and long periodic brightenings might have originated from magneto-acoustic waves and magnetic reconnection. It is plausible that the p-modes might possibly trigger magnetic reconnection, and that reconnection might release stored magnetic energy to produce the jets.

### **High-resolution Observations of a Flux Rope with the Interface Region Imaging Spectrograph**

Ting Li, Jun Zhang

*Solar Phys.* Volume 290, Issue 10, pp 2857-2870 **2015**

<http://arxiv.org/pdf/1508.07409v1.pdf>

We report the observations of a flux rope at transition region temperatures with the Interface Region Imaging Spectrograph (IRIS) on **30 August 2014**. Initially, magnetic flux cancellation constantly took place and a filament was activated. Then the bright material from the filament moved southward and tracked out several fine structures. These fine structures were twisted and tangled with each other, and appeared as a small flux rope at 1330 Å, with a total twist of about  $4\pi$ . Afterwards, the flux rope underwent a counter-clockwise (viewed top-down) unwinding motion around its axis. Spectral observations of C II 1335.71 Å at the southern leg of the flux rope showed that Doppler redshifts of 6-24 km s<sup>-1</sup> appeared at the western side of the axis, which is consistent with the counter-clockwise rotation motion. We suggest that the magnetic flux cancellation initiates reconnection and some activation of the flux rope. The stored twist and magnetic helicity of the flux rope are transported into the upper atmosphere by the unwinding motion in the late stage. The small-scale flux rope (width of 8.3''') had a cylindrical shape with helical field lines, similar to the morphology of the large-scale CME core (width of 1.54 R $\odot$ ) on **2 June 1998**. This similarity shows the presence of flux ropes of different scales on the Sun.

### **Filament Activation in Response to Magnetic Flux Emergence and Cancellation in Filament Channels**

Ting Li, Jun Zhang, Haisheng Ji

*Solar Phys.* Volume 290, [Issue 6](#), pp 1687-1702 **2015**

<http://arxiv.org/pdf/1504.01109v1.pdf>

We make a comparative analysis for two filaments that showed quite different activation in response to the flux emergence within the filament channels. The observations from the Solar Dynamics Observatory (SDO) and Global Oscillation Network Group (GONG) are carried out to analyze the two filaments on **2013 August 17-20 and September 29**. The first event showed that the main body of the filament was separated into two parts when an active region (AR) emerged with a maximum magnetic flux of about  $6.4 \times 10^{21}$  Mx underlying the filament. The close neighborhood and common direction of the bright threads in the filament and the open AR fan loops suggest similar magnetic connectivity of these two flux systems. The equilibrium of the filament was not destroyed within 3 days after the start of the emergence of the AR. To our knowledge, similar observations have never been reported before. In the second event, the emerging flux occurred nearby a barb of the filament with a maximum magnetic flux of  $4.2 \times 10^{20}$  Mx, about one order of magnitude less than that of the first event. The emerging flux drove the convergence of two patches of parasitic polarity in the vicinity of the barb, and resulted in cancellation between the parasitic polarity and nearby network fields. About 20 hours after the onset of the emergence, the filament was entirely erupted. Our findings

imply that the location of emerging flux within the filament channel is probably crucial to filament evolution. If the flux emergence appears nearby the barbs, flux cancellation of emerging flux with the filament magnetic fields is prone to occur, which probably causes the filament eruption. The comparison of the two events shows that the emergence of an entire AR may still not be enough to disrupt the stability of a filament system and the actual eruption does occur only after the flux cancellation sets in.

## **Slipping Magnetic Reconnection Triggering a Solar Eruption of a Triangle-flag Flux Rope**

Ting Li & Jun Zhang

ApJL, 791 L13, 2014

[http://www.researchgate.net/publication/263928819\\_Slipping\\_Magnetic\\_Reconnection\\_Triggering\\_a\\_Solar\\_Eruption\\_of\\_a\\_Triangle-flag\\_Flux\\_Rope?ev=prf\\_pub](http://www.researchgate.net/publication/263928819_Slipping_Magnetic_Reconnection_Triggering_a_Solar_Eruption_of_a_Triangle-flag_Flux_Rope?ev=prf_pub)

<http://arxiv.org/pdf/1407.4180v1.pdf>

We firstly report the simultaneous activities of a slipping motion of flare loops and a slipping eruption of a flux rope in 131 Å and 94 Å channels on **2014 February 02**. The east hook-like flare ribbon propagated slippingly at a speed of about 50 km s<sup>-1</sup>, which lasted about 40 min and extended by more than 100 Mm, but the west flare ribbon moved in the opposite direction with a speed of 30 km s<sup>-1</sup>. At the later phase of the flare activity, a "bi-fan" system of flare loops was well developed. The east footpoints of the flux rope showed an apparent slipping motion along the hook of the ribbon, simultaneously the fine structures of the flux rope rose up rapidly at a speed of 130 km s<sup>-1</sup>, much faster the whole flux rope. We infer that the east footpoints of the flux rope are successively heated by a slipping magnetic reconnection during the flare, which results in the apparent slippage of the flux rope. The slipping motion delineates a "triangle-flag surface" of the flux rope, implying that the topology of a flux rope is more complex than anticipated.

## **Homologous Flux Ropes Observed by SDO/AIA**

Ting Li & Jun Zhang

E-print, Oct 2013; 2013 ApJ 778 L29

<http://arxiv.org/abs/1310.8041>

We firstly present the emph{Solar Dynamics Observatory} observations of four homologous flux ropes in active region (AR) 11745 on **2013 May 20-22**. The four flux ropes are all above the neutral line of the AR, with endpoints anchoring at the same region, and have the generally similar morphology. For the first three flux ropes, they rose up with a velocity of less than 30 km s<sup>-1</sup> after their appearances, and subsequently their intensities at 131 Å decreased and the flux ropes became obscure. The fourth flux rope erupted ultimately with a speed of about 130 km s<sup>-1</sup> and formed a coronal mass ejection. The associated filament showed an obvious anti-clockwise twist motion at the initial stage, and the twist was estimated at 4π. This indicates that kink instability possibly triggers the early rise of the fourth flux rope. The activated filament material was spatially within the flux rope and they showed consistent evolution in their early stages. Our findings provide new clues for understanding the characteristics of flux ropes. Firstly, there are multiple flux ropes that are successively formed at the same location during an AR evolution process. Secondly, a slow-rise flux rope does not necessarily result in a CME, and a fast-eruption flux rope results in a CME.

## **FINE-SCALE STRUCTURES OF FLUX ROPES TRACKED BY ERUPTING MATERIAL**

Ting Li and Jun Zhang

2013 ApJ 770 L25

We present Solar Dynamics Observatory observations of two flux ropes tracked out by material from a surge and a failed filament eruption on **2012 July 29 and August 4**, respectively. For the first event, the interaction between the erupting surge and a loop-shaped filament in the east seems to "peel off" the filament and add bright mass into the flux rope body. The second event is associated with a C-class flare that occurs several minutes before the filament activation. The two flux ropes are, respectively, composed of  $85 \pm 12$  and  $102 \pm 15$  fine-scale structures, with an average width of about 1.6". Our observations show that two extreme ends of the flux rope are rooted in opposite polarity fields and each end is composed of multiple footpoints (FPs) of fine-scale structures. The FPs of the fine-scale structures are located at network magnetic fields, with magnetic fluxes from  $5.6 \times 10^{18}$  Mx to  $8.6 \times 10^{19}$  Mx. Moreover, almost half of the FPs show converging motion of smaller magnetic structures over 10 hr before the appearance of the flux rope. By calculating the magnetic fields of the FPs, we deduce that the two flux ropes occupy at least  $4.3 \times 10^{20}$  Mx and  $7.6 \times 10^{20}$  Mx magnetic fluxes, respectively.

## **Eruptions of two flux ropes observed by SDO and STEREO**

Leping Li, and Jun Zhang

E-print, March 2013; A&A, Letter, 552, L11 (2013), File

Aims. We report for the first time the hot and cool components of two flux ropes simultaneously observed by SDO and STEREO, and the relationship between the flux rope eruptions and the coronal mass ejection (CME).

Methods. Employing SDO and STEREO A and B observations, we investigated the eruptive event of two flux ropes and their associated activities in active region (AR) 11402 on **January 23, 2012**.

Results. In SDO/AIA 94 Å (6.4 MK) and 131 Å (10 MK) images, a twisted flux rope appeared from 00:44 UT, which was located in AR 11402. Another longer saddle-shaped flux rope, with twisted fine structures, appeared 25 min later. This was located across the two ARs 11401 and 11402. These two flux ropes initially rose rapidly, then slowly, and finally were again accelerated fast. The two flux ropes are also identified in the STEREO A and B 195 Å (1.4 MK), 304 Å (0.06–0.08 MK), 284 Å (1.8 MK), and 171 Å (1.0 MK) observations. We suggest that the flux ropes may have both hot and cool components. Investigating the flux rope eruptions with their associated CME, we find that the erupting flux ropes are co-spatial with the CME bright core and the expanding overlying flux loops with the CME bright front.

### **A Twin-CME Scenario for Ground Level Enhancement Events**

G. Li · R. Moore · R.A. Mewaldt · L. Zhao · A.W. Labrador

Space Sci Rev, 171, Numbers 1–4, 141–160, 2012, File

Ground Level Enhancement (GLEs) events are extreme Solar Energetic Particle (SEP) events. Protons in these events often reach ~GeV/nucleon. Understanding the underlying particle acceleration mechanism in these events is a major goal for Space Weather studies. In Solar Cycle 23, a total of 16 GLEs have been identified. Most of them have preceding CMEs and in-situ energetic particle observations show some of them are enhanced in ICME or flare-like material. Motivated by this observation, we discuss here a scenario in which two CMEs erupt in sequence during a short period of time from the same Active Region (AR) with a pseudo-streamer-like pre-eruption magnetic field configuration. The first CME is narrower and slower and the second CME is wider and faster. We show that the magnetic field configuration in our proposed scenario can lead to magnetic reconnection between the open and closed field lines that drape and enclose the first CME and its driven shock. The combined effect of the presence of the first shock and the existence of the open close reconnection is that when the second CME erupts and drives a second shock, one finds both an excess of seed population and an enhanced turbulence level at the front of the second shock than the case of a single CME-driven shock. Therefore, a more efficient particle acceleration will occur. The implications of our proposed scenario are discussed.

### **Three-Dimensional Reconstruction of an Erupting Filament with SDO and STEREO Observations**

Ting Li, Jun Zhang, Yuzong Zhang, Shuhong Yang

E-print, July 2011, File;

On 2010 August 1, a global solar event was launched involving almost the entire Earth-facing side of the Sun. This event mainly consisted of a C3.2 flare, a polar crown filament eruption and two Earth-directed coronal mass ejections (CMEs). The observations from the Solar Dynamics Observatory (SDO) and the Solar Terrestrial Relations Observatory (STEREO) showed that all the activities were coupled together, suggesting a global character of the magnetic eruption. We reconstruct the three-dimensional geometry of the polar crown filament using observations from three different viewpoints (STEREO A, B and SDO) for the first time. The filament undergoes two eruption processes. Firstly, the main body of the filament rises up, while it also moves towards the low-latitude region with a change in inclination by ~48° and expands only in the altitudinal and latitudinal direction in the field of view of Atmospheric Imaging Assembly. We investigate the true velocities and accelerations of different locations along the filament, and find that the highest location always has the largest acceleration during this eruption process. During the late phase of the first eruption, part of the filament material separates from the eastern leg. This material displays a projectile motion and moves towards the west at a constant velocity of 141.8 km s<sup>-1</sup>. This may imply that the polar crown filament consists of at least two groups of magnetic systems.

### **Sequential Coronal Mass Ejections from AR8038 in May 1997**

Y. Li · B.J. Lynch · B.T. Welsch · G.A. Stenborg · J.G. Luhmann · G.H. Fisher · Y. Liu · R.W. Nightingale

Solar Phys (2010) 264: 149–164, File

Three homologous coronal mass ejections (CMEs) occurred on 5, 12 and 16 May 1997 from the single magnetic polarity inversion line (PIL) of AR8038. The three events together provide STEREO-like quadrature views of the 12 May 1997 CME and EIT double dimming. The recurrent CMEs with the nearly identical post-CME potential state and the ‘sigmoid to arcade to sigmoid’ transformations indicate a repeatable store – release – restore process of the free energy. How was the free magnetic energy re-introduced to the potential state corona after each release in this decaying active region? Making use of the known time interval bounded by the adjacent homologous CMEs, we made the following measures. The



unsigned magnetic flux of AR8038,  $\Phi_{AR}$ , decreased by approximately 18% during 66 h, while the unsigned flux,  $\Phi_{PIL}$ , in a Gaussian-weighted PIL-region containing the flare site increased by about 50% during 36 hrs prior to the C1.3 flare on 12 May 1997. The significant increase of  $\Phi_{PIL}$  demonstrates the magnetic gradient increase and the build-up of free energy in the PIL-region during the time leading to the eruption. Fourier local correlation tracking (FLCT) flow speed in AR8038 ranges from 0 to 292.8ms<sup>-1</sup> with a mean value of 63.2ms<sup>-1</sup>. The flow field contains a persistent converging flow towards the flaring PIL and an effective shear flow distributed in the AR. Minor angular motions were found. An integrated proxy Poynting flux  $S_h$  estimates the energy input to the corona to be on the order of 1.15  $\times 10^{32}$  erg during the 66 hrs before the C1.3 flare. It suggests that sufficient energy for a flare/CME can be introduced to the corona on the order of several days by the flows deduced from photospheric magnetic field motions in this small decaying active region.

## Cyclical Behavior of Coronal Mass Ejections

K.J. Li · P.X. Gao · Q.X. Li · J. Mu · T.W. Su

Solar Phys., 2009, 257(1), 149 – 154, DOI: 10.1007/s11207-009-9333-x, **File**

With the use of coronal mass ejections (CMEs) observed by the Large Angle and Spectrometric Coronagraph (LASCO) onboard the *Solar and Heliospheric Observatory* (SOHO) from January 1996 through December 2005, it is found that, for the cyclical activity of CMEs, there is surprisingly no equatorward drift at low latitudes (thus, no “butterfly diagram”) and no poleward drift at high latitudes, and no antiphase relationship between CME activity at low and high latitudes. The cyclical behaviors of CMEs differ in a significant way from that of the small-scale solar photospherical and chromospheric phenomena. Thus, our analysis leads to results that are inconsistent with a close, physical relationship with small-scale aspects of solar activity, and it is suggested that there is possibly a single so-called large-scale activity cycle in CMEs.

## The Solar Magnetic Field and Coronal Dynamics of the Eruption on 2007 May 19

Y. Li, B. J. Lynch, G. Stenborg, J. G. Luhmann, K. E. J. Huttunen, B. T.

Welsch, P. C. Liewer, and A. Vourlidas

The Astrophysical Journal Letters, Vol. 681, No. 1: L37-L40, 2008.

<http://www.journals.uchicago.edu/doi/pdf/10.1086/590340>

The solar eruption on 2007 May 19, from AR 10956 near solar disk center, consisted of a B9.5 flare (12:48 UT), a filament eruption, an EUV dimming, a coronal wave, and a multifront CME. The eruption was observed by the twin *STEREO* spacecraft at a separation angle of 8.5°. We report analysis of the source region photospheric magnetic field and its preeruption evolution using MDI magnetograms, the coronal magnetic field topology estimated via PFSS modeling, and the coronal dynamics of the eruption through *STEREO* EUVI wavelet-enhanced anaglyph movies. Despite its moderate magnitude and size, AR 10956 was a complex and highly nonpotential active region with a multipolar configuration, and hosted frequent flares, multiple filament eruptions, and CMEs.

In the 2 days prior to the May 19 eruption, the total unsigned magnetic flux of the region decreased by ~17%.

We interpret the photospheric magnetic field evolution, the coronal field topology, and the observed coronal dynamics in the context of current models of CME initiation and discuss the prospects for future MHD modeling inspired by these analyses.

## Results from the Study of an M7.6 Flare and its Associated CME --

Hui Li and Youping Li, E-print, Dec 2006

[Advances in Space Research, Volume 41, Issue 6, Pages 962-968, 2008](#)

An M7.6 flare was well observed on **October 24, 2003** in active region 10486 by a few instruments and satellites, including GOES, TRACE, SOHO, RHESSI and NoRH. Multi-wavelength study shows that this flare underwent two episodes. During the first episode, only a looptop source of <40 keV was observed in reconstructed RHESSI images, which showed shrinkage with a velocity of 12–14 km s<sup>-1</sup> in a period of about 12 min. During the second process, in addition to the looptop source, two footpoint sources were observed in energy channel of as high as ~200 keV. One of them showed fast propagation along one of the two TRACE 1600 Å flare ribbons and the 195 Å loop footpoints, which could be explained by successive magnetic reconnection. The associated CME showed a mass pickup process with decreasing center-of-mass velocity. The decrease of the CME kinetic energy and the increase of its potential energy lead to an almost constant total energy during the CME propagation. Our results reveal that the flare and its associated CME have comparable energy content, and the flare is of non-thermal property.

## Rotational flows in solar coronal flux rope cavities

Valeria Liakh, Rony Keppens

ApJL 953 L13 2023

<https://arxiv.org/pdf/2307.14934.pdf>

<https://iopscience.iop.org/article/10.3847/2041-8213/acea78/pdf>

We present a 2.5-dimensional magnetohydrodynamic simulation of a systematically rotating prominence inside its coronal cavity using the open-source \texttt{MPI-AMRVAC} code. Our simulation starts from a non-adiabatic, gravitationally stratified corona, permeated with a sheared arcade magnetic structure. The flux rope (FR) is formed through converging and shearing footpoints driving, simultaneously applying randomized heating at the bottom. The latter induces a left-right asymmetry of temperature and density distributions with respect to the polarity-inversion line. This asymmetry drives flows along the loops before the FR formation, which gets converted to net rotational motions upon reconnection of the field lines. As the thermal instability within the FR develops, angular momentum conservation about its axis leads to a systematic rotation of both hot coronal and cold condensed plasma. The initial rotational velocity exceeds  $60 \text{ km s}^{-1}$ . The synthesized images confirm the simultaneous rotations of the coronal plasma seen in 211 and 193 Å and condensations seen in 304 Å. Furthermore, the formation of the dark cavity is evident in 211 and 193 Å images. Our numerical experiment is inspired by observations of so-called giant solar prominence tornadoes, and reveals that asymmetric FR formation can be crucial in triggering rotational motions. We reproduce observed spinning motions inside the coronal cavity, augmenting our understanding of the complex dynamics of rotating prominences.

## **Multi-spacecraft Observations of the 2022 March 25 CME and EUV Wave: An Analysis of Their Propagation and Interrelation**

Alessandro **Liberatore**, Paulett C. Liewer, Angelos Vourlidas, Carlos R. Braga, Marco Velli, Olga Panasenco, Daniele Telloni, and Salvatore Mancuso

2023 ApJ 957 110

<https://iopscience.iop.org/article/10.3847/1538-4357/acf8bf/pdf>

This paper reports on a well-defined EUV wave associated with a coronal mass ejection (CME) observed on **2022 March 25**. The CME was observed by Solar Orbiter (SolO) during its first close perihelion (0.32 au) and by several other spacecraft from different viewpoints. The EUV wave was visible by the Extreme Ultraviolet Imager on board the Solar Terrestrial Relations Observatory (STEREO-A/STA) in near quadrature to SolO. We perform a detailed analysis of the early phase of this CME in relation to the evolution of the associated EUV wave. The kinematics of the EUV wave and CME are derived via visual identification of the fronts using both the STA and SolO data. The analysis of an associated metric type II radio burst provides information on the early phase of the CME and wave propagation. Finally, we compare the EUV speed to the local magnetic field and Alfvén speed using standard models of the corona. The analysis of the decoupling between the EUV wave and the CME driver via imaging, kinematic study, radio data analysis, and comparison with maps/models clearly indicates that the EUV front is consistent with a wave initially driven by the lateral expansion of the CME, which evolves into a fast-mode magnetosonic wave after decoupling from the CME.

## **Evolution of a Steamer-Blowout CME as Observed by Imagers on Parker Solar Probe and the Solar Terrestrial Relations Observatory**

[P. C. Liewer](#), [J. Qiu](#), [A. Vourlidas](#), [J. R. Hall](#), [P. Penteado](#)

A&A 2021

<https://arxiv.org/pdf/2012.05174.pdf>

<https://www.aanda.org/articles/aa/pdf/2021/06/aa39641-20.pdf>

<https://doi.org/10.1051/0004-6361/202039641>

Context: On **26-27 January 2020**, the wide-field imager WISPR on Parker Solar Probe (PSP) observed a coronal mass ejection (CME) from a distance of approximately 30 solar radii as it passed through the instrument's 95 degree field-of-view, providing an unprecedented view of the flux rope morphology of the CME's internal structure. The same CME was seen by STEREO, beginning on 25 January.

Aims: Our goal was to understand the origin and determine the trajectory of this CME.

Methods: We analyzed data from three well-placed spacecraft: Parker Solar Probe (PSP), Solar Terrestrial Relations Observatory-Ahead (STEREO-A), and Solar Dynamics Observatory (SDO). The CME trajectory was determined using the method described in Liewer et al. (2020) and verified using simultaneous images of the CME propagation from STEREO-A. The fortuitous alignment with STEREO-A also provided views of coronal activity leading up to the eruption. Observations from SDO, in conjunction with potential magnetic field models of the corona, were used to analyze the coronal magnetic evolution for the three days leading up to the flux rope ejection from the corona on 25 January.

Results: We found that the 25 January CME is likely the end result of a slow magnetic flux rope eruption that began on 23 January and was observed by STEREO-A/Extreme Ultraviolet Imager (EUVI). Analysis of these observations suggest that the flux rope was apparently constrained in the corona for more than a day before its final ejection on 25 January. STEREO-A/COR2 observations of swelling and brightening of the overlying streamer for several hours prior to eruption on January 25 led us to classify this as a streamer-blowout CME. The analysis of the SDO data suggests that restructuring of the coronal magnetic fields caused by an emerging active region led to the final ejection of the flux rope. **25-27 January 2020**

## **Trajectory Determination for Coronal Ejecta Observed by WISPR/Parker Solar Probe**

[P. C. Liewer](#), [J. Qiu](#), [P. Penteado](#), [J. R. Hall](#), [A. Vourlidas](#), [R. A. Howard](#)

Solar Phys. **295**, Article number: 140 2020

<https://arxiv.org/pdf/2009.09323.pdf>

<https://link.springer.com/content/pdf/10.1007/s11207-020-01715-y.pdf>

The *Wide-field Imager for Solar Probe* (WISPR) on the *Parker Solar Probe* (PSP), observing in white light, has a fixed angular field of view, extending from  $13.5^\circ$  to  $108^\circ$  from the Sun and approximately  $50^\circ$  in the transverse directions. Because of the highly elliptical orbit of PSP, the physical extent of the imaged coronal region varies directly as the distance from the Sun, requiring new techniques for analysis of the motions of observed density features. Here, we present a technique for determining the 3D trajectory of CMEs and other coronal ejecta moving radially at a constant velocity by first tracking the motion in a sequence of images and then applying a curve-fitting procedure to determine the trajectory parameters (distance vs. time, velocity, longitude and latitude). To validate the technique, we have determined the trajectory of two CMEs observed by WISPR that were also observed by another white-light imager, either LASCO/C3 or STEREO-A/H1I. The second viewpoint was used to verify the trajectory results from this new technique and help determine its uncertainty. **2018 November 1-2, 2019 April 2-3**

## Observations and Analysis of the Non-Radial Propagation of Coronal Mass Ejections Near the Sun

Paulett **Liewer**, Olga Panasenco, Angelos Vourlidas, Robin Colaninno

Solar Phys. Volume 290, [Issue 11](#), pp 3343-3364 **2015**

The trajectories of coronal mass ejection (CME) are often observed to deviate from radial propagation from the source while within the coronagraph field of view ( $R < 15\text{--}30 R_{\text{sun}}$ ). To better understand nonradial propagation within the corona, we first analyze the trajectories of **five CMEs** for which both the source and 3D trajectory (latitude, longitude, and velocity) can be well determined from solar imaging observations, primarily using observations from the twin *Solar Terrestrial Relations Observatory* (STEREO) spacecraft. Next we analyze the cause of any nonradial propagation using a potential field source surface (PFSS) model to determine the direction of the magnetic pressure forces exerted on the CME at various heights in the corona. In two cases, we find that the CME deviation from radial propagation primarily occurs before it reaches the coronagraph field of view (below 1.5 solar radii). Based on the observations and the magnetic pressure forces calculated from the PFSS model, we conclude that for these cases the deviation is the result of strong active-region fields causing an initial asymmetric expansion of the CME that gives rise to the apparent rapid deflection and nonradial propagation from the source. Within the limitations of the PFSS model, the magnetic fields for all five cases appear to guide the CMEs out of the corona through the weak-field region around the heliospheric current sheet even when the current sheet is inclined and warped.

## Stereoscopic Analysis of the 31 August 2007 Prominence Eruption and Coronal Mass Ejection

P. C. **Liewer**, O. Panasenco, J. R. Hall

Solar Physics, January **2013**, Volume 282, Issue 1, pp 201-220

The spectacular prominence eruption and CME of 31 August 2007 are analyzed stereoscopically using data from NASA's twin Solar Terrestrial Relations Observatory (STEREO) spacecraft. The technique of tie pointing and triangulation (T&T) is used to reconstruct the prominence (or filament when seen on the disk) before and during the eruption. For the first time, a filament barb is reconstructed in three-dimensions, confirming that the barb connects the filament spine to the solar surface. The chirality of the filament system is determined from the barb and magnetogram and confirmed by the skew of the loops of the post-eruptive arcade relative to the polarity reversal boundary below. The T&T analysis shows that the filament rotates as it erupts in the direction expected for a filament system of the given chirality. While the prominence begins to rotate in the slow-rise phase, most of the rotation occurs during the fast-rise phase, after formation of the CME begins. The stereoscopic analysis also allows us to analyze the spatial relationships among various features of the eruption including the pre-eruptive filament, the flare ribbons, the erupting prominence, and the cavity of the coronal mass ejection (CME). We find that erupting prominence strands and the CME have different (non-radial) trajectories; we relate the trajectories to the structure of the coronal magnetic fields. The possible cause of the eruption is also discussed.

## Stereoscopic Analysis of STEREO/SECCHI Data for CME Trajectory Determination

P. C. **Liewer**, J. R. Hall, R. A. Howard, E. M. De Jong, W. T. Thompson, A. Thernisien

E-print, 6 Oct **2010**, [File](#) ; JASTP, Volume 73, Issue 10, 20 June **2011**, Pages 1173-1186

The Sun Earth Connection Coronal and Heliospheric Investigation (SECCHI) coronagraphs on the twin Solar Terrestrial Relations Observatory (STEREO) spacecraft provide simultaneous views of the corona and coronal mass ejections from two view points. Here, we analyze simultaneous image pairs using the technique of tie-pointing and triangulation (T&T) to determine the three-dimensional trajectory of seven coronal mass ejections (CMEs). The bright leading edge of a CME seen in coronagraph images results from line-of-sight integration through the CME front; the two STEREO coronagraphs see different apparent leading edges, leading to a systematic error in its three-dimensional reconstruction. We analyze this systematic error using a simple geometric model of a CME front. We validate the technique and analysis by comparing T&T trajectory determinations for seven CMEs with trajectories determined by Thernisien, Vourlidas and Howard (2009) using a forward modeling technique not susceptible to this systematic effect. We find that, for the range of spacecraft separation studied ( $\leq 50^\circ$ ), T&T gives reliable trajectories (uncertainty  $< 10^\circ$  in direction and  $< 15\%$  velocity) for CME propagating within approximately  $70^\circ$  of perpendicular to Sun-Earth line. For CMEs close to the Sun-Earth or Sun-Spacecraft lines, T&T is subject to larger errors, especially in the velocity.

#### Research highlights

► The coronagraphs on the twin Solar TERrestrial RELations Observatory (STEREO) spacecraft allow stereoscopic viewing of coronal mass ejections (CMEs). ► The technique of tie-pointing and triangulation is used to determine the trajectories (velocity and propagation angle) of CMEs. ► CMEs are optically thin and the images from the two spacecraft show different apparent leading edges and the error cause by this is analyzed. ► The ranges where the technique is reliable and where it is not are discussed.

### **Observations of a Series of Flares and Associated Jet-like Eruptions Driven by the Emergence of Twisted Magnetic Fields**

Eun-Kyung [Lim](#), Vasyi Yurchyshyn, Sung-Hong Park, Sujin Kim, Kyung-Suk Cho, Pankaj Kumar, Jongchul Chae, Heesu Yang, Kyuhyoung Cho, Donguk Song, Yeon-Han Kim  
ApJ 817 39 2016

<http://arxiv.org/pdf/1512.01330v1.pdf>

We studied temporal changes of morphological and magnetic properties of a succession of four confined flares followed by an eruptive flare using the high-resolution New Solar Telescope (NST) operating at the Big Bear Solar Observatory (BBSO), Helioseismic and Magnetic Imager (HMI) magnetograms and Atmospheric Image Assembly (AIA) EUV images provided by Solar Dynamics Observatory (SDO). From the NST/H $\alpha$  and the SDO/AIA~304 Å observations we found that each flare developed a jet structure that evolved in a manner similar to evolution of the blowout jet : 1) an inverted-Y shape jet appeared and drifted away from its initial position; 2) jets formed a curtain-like structure that consisted of many fine threads accompanied with subsequent brightenings near the footpoints of the fine threads; and finally 3) the jet showed a twisted structure visible near the flare maximum. Analysis of the HMI data showed that both the negative magnetic flux and the magnetic helicity have been gradually increasing in the positive polarity region indicating the continuous injection of magnetic twist before and during the series of flares. Based on these results, we suggest that the continuous emergence of twisted magnetic flux played an important role in producing a successive flares and developing a series of blowout jets. **2012-07-02**

### **Drag Force on Coronal Mass Ejections (CMEs)**

Chia-Hsien [Lin](#), [James Chen](#)

JGR [Volume 127, Issue 6](#) 2022 e2020JA028744

<https://doi.org/10.1029/2020JA028744>

The drag force experienced by coronal mass ejections (CMEs) plays an important role in determining the dynamics of CMEs. Numerous empirical studies have attempted to estimate the drag coefficient ( $cd$ ) using the assumption that the observed deceleration of CMEs is primarily caused by drag alone. The observed CME motion, however, is determined by the net force—the sum of all the forces, and data contain no information to allow one to separately determine the individual forces. In the present work, we revisit the forces acting on CMEs using the erupting flux rope (EFR) model, making no assumptions on the magnitude of any force. Calculating the individual forces for four observed CME trajectories, it is shown that drag is generally not the dominant retarding force and that drag, magnetic tension, and pressure gradient can yield comparable deceleration. No force can be assumed negligible. It is further shown that the EFR equations can qualitatively replicate the observed deceleration with zero drag, contradicting the assertion that deceleration of CMEs necessarily implies the dominance of drag. A theoretical derivation of the drag coefficient  $cd$  for flux-rope CMEs is given for a range of idealized flows including the so-called “snow plow” effect. We show that  $cd \sim 0-1$  unless the snow-plow effect is significant or the solar wind flows are specularly reflected, in which case  $cd \sim 2-3$ . The values of  $cd$  predicted by the EFR model for the observed trajectories are  $cd \approx 1.1-1.2$  for three events and  $cd \approx 0.4$  for one.

### **The Temporal and Spatial Behaviors of CME Occurrence Rate at Different Latitudes**

[Jiaqi Lin](#), [Feng Wang](#), [Linhua Deng](#), [Hui Deng](#), [Ying Mei](#), [Yangfan Xie](#)

ApJ 932 62 2022

<https://arxiv.org/pdf/2205.05908>

<https://iopscience.iop.org/article/10.3847/1538-4357/ac6f54/pdf>

The statistical study of the Coronal Mass Ejections (CMEs) is a hot topic in solar physics. To further reveal the temporal and spatial behaviors of the CMEs at different latitudes and heights, we analyzed the correlation and phase relationships between the occurrence rate of CMEs, the Coronal Brightness Index (CBI), and the 10.7-cm solar radio flux (F10.7). We found that the occurrence rate of the CMEs correlates with CBI relatively stronger at high latitudes ( $>=60$ ) than at low latitudes ( $<=50$ ). At low latitudes, the occurrence rate of the CMEs correlates relatively weaker with CBI than F10.7. There is a relatively stronger correlation relationship between CMEs, F10.7, and CBI during Solar Cycle 24 (SC24) than Solar Cycle 23 (SC23). During SC23, the high-latitude CME occurrence rate lags behind F10.7 by three months, and during SC24, the low-latitude CME occurrence rate leads to the low-latitude CBI by one month. The correlation coefficient values turn out to be larger when the very faint CMEs are removed from the samples of the CDAW catalog. Based on our results, we may speculate that the source regions of the high/low-latitude CMEs may vary in height, and the process of magnetic energy accumulation and dissipation is from the lower to the upper atmosphere of the Sun. The temporal offsets between different indicators could help us better understand the physical processes responsible for the solar-terrestrial interactions.

## **Eruptivity in Solar Flares: The Challenges of Magnetic Flux Ropes**

Pei Hsuan [Lin](#)<sup>1</sup>, Kanya Kusano<sup>1</sup>, and K. D. Leka<sup>1,2</sup>

2021 ApJ 913 124

<https://doi.org/10.3847/1538-4357/abf3c1>

Two new schemes for identifying field lines involved in eruptions, the r-scheme and q-scheme, are proposed to analyze the eruptive and confined nature of solar flares, as extensions to the original rm scheme proposed in Lin et al. Motivated by three solar flares originating from NOAA Active Region 12192 that are misclassified by rm, we introduce refinements to the r-scheme employing the "magnetic twist flux" to approximate the force balance acting on a magnetic flux rope (MFR); in the q-scheme, the reconnected field is represented by those field lines that anchor in the flare ribbons. Based on data obtained by the Solar Dynamics Observatory/Helioseismic and Magnetic Imager, the coronal magnetic field for 51 flares larger than M5.0 class, from 29 distinct active regions, is constructed using a nonlinear force-free field extrapolation model. Statistical analysis based on linear discriminant function analysis is then performed, revealing that despite both schemes providing moderately successful classifications for the 51 flares, the coronal mass ejection-eruptivity classification for the three target events can only be improved with the q-scheme. We find that the highly twisted field lines and the flare-ribbon field lines have equal average force-free constant  $\alpha$ , but all of the flare-ribbon-related field lines are shorter than 150 Mm in length. The findings lead us to conclude that it is challenging to distinguish the MFR from the ambient magnetic field using any quantity based on common magnetic nonpotentiality measures.

## **A New Parameter of the Photospheric Magnetic Field to Distinguish Eruptive-flare Producing Solar Active Regions**

Pei Hsuan [Lin](#)<sup>1</sup>, Kanya Kusano<sup>1</sup>, Daikou Shiota<sup>2</sup>, Satoshi Inoue<sup>1</sup>, K. D. Leka<sup>1,3</sup>, and Yuta Mizuno<sup>1</sup>

2020 ApJ 894 20

[sci-hub.tw/10.3847/1538-4357/ab822c](http://sci-hub.tw/10.3847/1538-4357/ab822c)

Solar flares and coronal mass ejections (CMEs) are eruptive phenomena caused by coronal magnetic fields. In particular, large eruptive events originate in active regions (AR) with strong surface magnetic fields. However, it is still unclear what determines the capability of an AR to specifically produce eruptive flares and CMEs, and this hinders our knowledge of the initiation mechanism for the eruptive component of these phenomena. In this study, we propose a new parameter  $r_m$  to measure the possibility that a flare that occurs in an AR can be eruptive and produce a CME. The parameter  $r_m$  is defined by the ratio of the magnetic flux of twist higher than a threshold  $T_c$  to the surrounding—and specifically, the overlying—magnetic flux. The value of  $r_m$  for each AR can be estimated using nonlinear force-free field extrapolation models of the coronal magnetic field. Based on the data obtained by the Solar Dynamics Observatory/Helioseismic and Magnetic Imager, we calculated the values of  $r_m$  for 29 ARs at 51 times prior to flares larger than M5.0 class. We find that the footpoints of field lines with twist higher than 0.2 can represent the subsequent flare ribbons well, and field lines that overlie and "fence in" the highly twisted region will work to confine the eruption, generating confined flares. Discriminant function analysis is used to show that  $r_m$  is moderately well able to distinguish ARs that have the capability of producing eruptive flares. **13-15 February 2011, 2014-01-07**

Table 1 Event List for Analysis (2011-2015)

## **A comparison of coronal mass ejection models with observations for two large CMEs detected during the Whole Heliosphere Interval**

Chia-Hsien [Lin](#), James Chen

Terr. Atmos. Ocean. Sci., Vol. 26, No. 2, Part I, 121-134, April 2015

<http://arxiv.org/pdf/1512.07000v1.pdf>

Two major coronal mass ejections (CMEs) observed during the Whole Heliosphere Interval (WHI) are compared with the catastrophe (CA) and eruptive flux rope (EF) models. The objective is to test two distinct mechanisms for CMEs by modeling these well-observed CMEs and comparing predictions of the theories and observed data. The two CMEs selected for this study occurred on **25 March and 5 April 2008**, respectively. For the 25 March event, an M 1.7 class flare, a filament eruption, and hard X-ray (HXR) and soft X-ray (SXR) emissions were observed during the CME onset. The observed CME kinematics and SXR light curve of this event are found to be more consistent with the EF model than with the CA model. For the 5 April event, the SXR light curve shows multiple enhancements, some of which temporally coincide with successive side loop brightening and multiple foot points at the source region after the eruption. The physical connection between the side-loop multiple brightenings and the eruption cannot be determined from the data. Both models produced observationally consistent kinematics profiles, and the EF model correctly predicted the first emission enhancement. Neither model includes multiple brightenings in the formulation.

## **A statistical study of the subsurface structure and eruptivity of solar active regions**

Chia-Hsien [Lin](#)

ApJ 2015

<http://arxiv.org/pdf/1512.07007v1.pdf>

A statistical study of 77 solar active regions (ARs) is conducted to investigate the existence of identifiable correlations between the subsurface structural disturbances and the activity level of the active regions. The disturbances examined in this study are  $\langle |\delta\Gamma_1/\Gamma_1| \rangle$ ,  $\langle |\delta c_2/c_2| \rangle$ , and  $\langle |\delta c_2/c_2 - \delta\Gamma_1/\Gamma_1| \rangle$ . where  $\Gamma_1$  and  $c$  are the thermodynamic properties of first

adiabatic index and sound speed modified by magnetic field, respectively. The averages are over three depth layers:  $0.975\text{--}0.98R_{\odot}$ ,  $0.98\text{--}0.99R_{\odot}$  and  $0.99\text{--}0.995R_{\odot}$  to represent the structural disturbances in that layer. The level of the surface magnetic activity is measured by the Magnetic Activity Index (MAI) of active region and the relative and absolute MAI differences (rdMAI and dMAI) between the active and quiet regions. The eruptivity of each active region is quantified by its Flare Index, total number of coronal mass ejections (CMEs), and total kinetic energy of the CMEs. The existence and level of the correlations are evaluated by scatter plots and correlation coefficients. No definitive correlation can be claimed from the results. While a weak positive trend is visible between dMAI and  $\langle|\delta\Gamma_1/\Gamma_1|\rangle$  and  $\langle|\delta c_2/c_2|\rangle$  in the layer  $0.975\text{--}0.98R_{\odot}$ , their correlation levels, being approximately 0.6, are not sufficiently high to justify the correlation. Some subsurface disturbances are seen to increase with eruptivity indices among ARs with high eruptivity. The statistical significance of such trend, however, cannot be ascertained due to the small number of very eruptive ARs in our sample.

## **Review** on Current Sheets in CME Development: Theories and Observations

Jun **Lin**, Nicholas A. Murphy, Chengcai Shen, John C. Raymond, Katharine K. Reeves, Jiayong Zhong, Ning Wu, Yan Li

Space Science Reviews Volume 194, Issue 1, pp 237-302 Nov 2015 **File** **Open Access**

We introduce how the catastrophe model for solar eruptions predicted the formation and development of the long current sheet (CS) and how the observations were used to recognize the CS at the place where the CS is presumably located. Then, we discuss the direct measurement of the CS region thickness by studying the brightness distribution of the CS region at different wavelengths. The thickness ranges from 104 km to about 105 km at heights between  $0.27$  and  $1.16 R_{\odot}$  from the solar surface. But the traditional theory indicates that the CS is as thin as the proton Larmor radius, which is of order tens of meters in the corona. We look into the huge difference in the thickness between observations and theoretical expectations. The possible impacts that affect measurements and results are studied, and physical causes leading to a thick CS region in which reconnection can still occur at a reasonably fast rate are analyzed. Studies in both theories and observations suggest that the difference between the true value and the apparent value of the CS thickness is not significant as long as the CS could be recognised in observations. We review observations that show complex structures and flows inside the CS region and present recent numerical modelling results on some aspects of these structures. Both observations and numerical experiments indicate that the downward reconnection outflows are usually slower than the upward ones in the same eruptive event. Numerical simulations show that the complex structure inside CS and its temporal behavior as a result of turbulence and the Petschek-type slow-mode shock could probably account for the thick CS and fast reconnection. But whether the CS itself is that thick still remains unknown since, for the time being, we cannot measure the electric current directly in that region. We also review the most recent laboratory experiments of reconnection driven by energetic laser beams, and discuss some important topics for future works.

**Table 1** Dates of the events discussed in this work and the section(s) where they are mentioned

## Solar Eruptive Events (SEE) 2020 Mission Concept

**Review**

R. P. **Lin**, A. Caspi, S. Krucker, H. Hudson, G. Hurford, S. Bandler, S. Christe, J. Davila, B. Dennis, G. Holman, R. Milligan, A. Y. Shih, S. Kahler, E. Kontar, M. Wiedenbeck, J. Cirtain, G. Doschek, G. H. Share, A. Vourlidas, J. Raymond, D. M. Smith, M. McConnell, G. Emslie

White Paper submitted to the Heliophysics Decadal Survey

eprint arXiv:1311.5243, 2013

<http://arxiv.org/pdf/1311.5243v1.pdf>

Major solar eruptive events (SEEs), consisting of both a large flare and a near simultaneous large fast coronal mass ejection (CME), are the most powerful explosions and also the most powerful and energetic particle accelerators in the solar system, producing solar energetic particles (SEPs) up to tens of GeV for ions and hundreds of MeV for electrons. The intense fluxes of escaping SEPs are a major hazard for humans in space and for spacecraft. Furthermore, the solar plasma ejected at high speed in the fast CME completely restructures the interplanetary medium (IPM) - major SEEs therefore produce the most extreme space weather in geospace, the interplanetary medium, and at other planets. Thus, understanding the flare/CME energy release process(es) and the related particle acceleration processes are major goals in Heliophysics. To make the next major breakthroughs, we propose a new mission concept, SEE 2020, a single spacecraft with a complement of advanced new instruments that focus directly on the coronal energy release and particle acceleration sites, and provide the detailed diagnostics of the magnetic fields, plasmas, mass motions, and energetic particles required to understand the fundamental physical processes involved. **23 July 2002**,

## Exploring Possible Correlation Between the Eruptivity and the Subsurface Structure of Solar Active Regions

**Lin**, C.-H.

Proceedings of the NSO Workshop # 27, "Fifty Years of Seismology of the Sun and Stars"

Astronomical Society of the Pacific Conference Series, volume 478, p. 331, 2013

We investigate whether any correlation exists between the surface and coronal activity levels of active regions and their subsurface structural disturbances. The subsurface disturbances examined are  $\delta\Gamma_1/\Gamma_1$ ,  $\delta v_2/v_2$ , and  $\delta v_2/v_2 - \delta\Gamma_1/\Gamma_1$ , where  $\Gamma_1$  is adiabatic index and  $v$  is wave speed. The relative differences are between active and quiet region pairs at the same latitude. The activity level of each active region is quantified by four indices: difference in Magnetic Activity Index between the active-quiet region pairs (dMAI), Flare Index (FI), total number of associated coronal mass ejections

(Ncme), and total kinetic energy of the CMEs (KESum). A statistical study on seventy seven active regions is conducted. The existence and level of correlations are assessed by visual inspection of scatter plots and correlation coefficient. The results indicate positive correlations between the subsurface disturbances and dMAI and KESum. The level of correlation is stronger among the active regions with high productivity of flares and/or CMEs. FI is found to be positively correlated only with  $|\delta v^2/v^2|$  in the layer 0.98–0.99  $R_{\odot}$  among the CME productive active regions. Little correlation is found between Ncme and any of the subsurface disturbances.

### **Solar Eruptive Events (SEE) Mission for the Next Solar Maximum**

**Lin, Robert P.; Krucker, S.; Caspi, A.; Hurford, G.; Dennis, B.; Holman, G.; Christe, S.; Shih, A. Y.; Bandler, S.; Davila, J.; Milligan, R.; Kahler, S.; Weidenbeck, M.; Doschek, G.; Vourlidis, A.; Share, G.; Raymond, J.; McConnell, M.; Emslie, G.**

American Astronomical Society, SPD meeting #42, id.22.04; Bulletin of the American Astronomical Society, Vol. 43, 2011

[https://www.researchgate.net/publication/258764414\\_Solar\\_Eruptive\\_Events\\_SEE\\_2020\\_Mission\\_Concept](https://www.researchgate.net/publication/258764414_Solar_Eruptive_Events_SEE_2020_Mission_Concept)

Major solar eruptive events consisting of both a large flare and a near simultaneous large fast coronal mass ejection (CME), are the most powerful explosions and also the most powerful and energetic particle accelerators in the solar system, producing solar energetic particles (SEPs) up to tens of GeV for ions and 10s-100s of MeV for electrons. The intense fluxes of escaping SEPs are a major hazard for humans in space and for spacecraft. Furthermore, the solar plasma ejected at high speed in the fast CME completely restructures the interplanetary medium, producing the most extreme space weather in geospace, at other planets, and in the heliosphere. Thus, the understanding of the flare/CME energy release process and of the related particle acceleration processes in SEEs is a major goal in Heliophysics. Here we present a concept for a Solar Eruptive Events (SEE) mission, consisting of a comprehensive set of advanced new instruments on the single spacecraft in low Earth orbit, that focus directly on the coronal energy release and particle acceleration in flares and CMEs. SEE will provide new focussing hard X-ray imaging spectroscopy of energetic electrons in the flare acceleration region, new energetic neutral atom (ENA) imaging spectroscopy of SEPs being accelerated by the CME at altitudes above 2 solar radii, gamma-ray imaging spectroscopy of flare-accelerated energetic ions, plus detailed EUV/UV/Soft X-ray diagnostics of the plasmas density, temperature, and mass motions in the energy release and particle acceleration regions. Together with ground-based measurements of coronal magnetic fields from ATST, FASR, and COSMO, SEE will enable major breakthroughs in our understanding of the fundamental physical processes involved in major solar eruptive events.

### **Investigating the driving mechanisms of coronal mass ejections**

Chia-Hsien **Lin**, Peter T. Gallagher, and Claire L. Raftery

A&A 516, A44, 2010, **File**

**Aims.** The objective of this study was to examine the kinematics of coronal mass ejections (CMEs) using EUV and coronagraph images, and to make a quantitative comparison with a number of theoretical models. One particular aim was to investigate the acceleration profile of CMEs in the low corona.

**Methods.** We selected two CME events for this study, which occurred on **2006 December 17** (CME06) and **2007 December 31** (CME07). CME06 was observed using the EIT and LASCO instruments on-board SOHO, while CME07 was observed using the SECCHI imaging suite on STEREO. The first step of the analysis was to track the motion of each CME front and derive its velocity and acceleration. We then compared the observational kinematics, along with the information of the associated X-ray emissions from GOES and RHESSI, with the kinematics proposed by three CME models (catastrophe, breakout and toroidal instability).

**Results.** We found that CME06 lasted over eight hours while CME07 released its energy in less than three hours. After the eruption, both CMEs were briefly slowed down before being accelerated again. The peak accelerations during the re-acceleration phase coincided with the peak soft X-ray emissions for both CMEs. Their values were  $\sim 60 \text{ m s}^{-2}$  for CME06 and  $\sim 600 \text{ m s}^{-2}$  for CME07. CME07 reached a maximum speed of over  $1000 \text{ km s}^{-1}$  before being slowed down to propagate away at a constant, final speed of  $\sim 700 \text{ km s}^{-1}$ . CME06 did not reach a constant speed but was moving at a small acceleration by the end of the observation. Our comparison with the theories suggested that CME06 can be best described by a hybrid of the catastrophe model and breakout model while the characteristics of CME07 were most consistent with the breakout model. Based on the catastrophe model, we deduced that the reconnection rate in the current sheet for CME06 was intermediate, the onset of its eruption occurred at a height of  $\sim 200 \text{ Mm}$ , and the Alfvén speed and the magnetic field strength at this height were approximately  $130\text{--}250 \text{ km s}^{-1}$  and 7 Gauss, respectively.

### **INVESTIGATION OF THICKNESS AND ELECTRICAL RESISTIVITY OF THE CURRENT SHEETS IN SOLAR ERUPTIONS**

J. **Lin**<sup>1,2</sup>, J. Li<sup>3</sup>, Y.-K. Ko<sup>2</sup>, and J. C. Raymond<sup>2</sup>

Astrophysical Journal, 693:1666–1677, 2009 March 10

<http://www.iop.org/EJ/toc/-alert=43190/0004-637X/693/2>

A discussion of the thickness of current sheets in solar eruptions,  $d$ , led Lin et al. in 2007 to estimate very large values for the effective resistivity,  $\eta_e$ . Here, we address some questions raised by that paper. We apply the limb synoptic map technique and find  $d$  between  $5.0 \times 10^4$  and  $4.6 \times 10^5 \text{ km}$ , increasing with both time and altitude. The possibility that large apparent  $d$  and  $\eta_e$  result from projection effects is examined and rejected. We derive theoretical scaling laws relating  $d$  to other observables that corroborate this conclusion and thus help confine both  $d$  and  $\eta_e$  to a reasonable range. The possible impact of our results on the existing models of particle acceleration in reconnecting

current sheets is also briefly discussed.

### **Features and Properties of Coronal Mass Ejection/Flare Current Sheets**

J. [Lin](#), J. Li, T. G. Forbes, Y.-K. Ko, J. C. Raymond, and A. Vourlidas

The Astrophysical Journal Letters, Volume 658, Number 2, Page L123, 2007

<http://www.journals.uchicago.edu/cgi-bin/resolve?ApJL21199>

### **Self-consistent propagation of flux ropes in realistic coronal simulations**

L. [Linan](#)<sup>1</sup>, F. Regnault<sup>2</sup>, B. Perri<sup>3</sup>, M. Brchnelova<sup>1</sup>, B. Kuzma<sup>4</sup>, A. Lani<sup>5</sup>, S. Poedts<sup>1,6</sup> and B.

Schmieder<sup>1,7,8</sup>

A&A 675, A101 (2023)

<https://www.aanda.org/articles/aa/pdf/2023/07/aa46235-23.pdf>

Context. The text has been edited to adhere to American English based on the spelling style used in the text. In order to anticipate the geoeffectiveness of coronal mass ejections (CMEs), heliospheric simulations are used to propagate transient structures injected at 0.1 AU. Without direct measurements near the Sun, the properties of these injected CMEs must be derived from models coming from observations or numerical simulations, and thus they contain a lot of uncertainty.

Aims. The aim of this paper is to demonstrate the possible use of the new coronal model COCONUT to compute a detailed representation of a numerical CME at 0.1 AU after its injection at the solar surface and propagation in a realistic solar wind, as derived from observed magnetograms.

Methods. We present the implementation and propagation of modified Titov-Démoulin flux ropes in the COCONUT 3D magnetohydrodynamics coronal model. Background solar wind was reconstructed in order to model two opposite configurations representing a solar activity maximum and minimum, respectively. Both configurations were derived from magnetograms that were obtained by the Helioseismic and Magnetic Imager on board the Solar Dynamic Observatory satellite. We tracked the propagation of 24 flux ropes that differ only by their initial magnetic flux. In particular, we investigated the geometry of the flux ropes during the early stages of their propagation as well as the influence of their initial parameters and solar wind configuration on 1D profiles derived at 0.1 AU.

Results. At the beginning of the propagation, the shape of the flux ropes varied between simulations during low and high solar activity. We found dynamics that are consistent with the standard CME model, such as pinching of the CME legs and the appearance of post-flare loops. Despite the differences in geometry, the synthetic density and magnetic field time profiles at 0.1 AU are very similar in both solar wind configurations. These profiles are also similar to those observed further in the heliosphere and suggest the presence of a magnetic ejecta composed of the initially implemented flux rope and a sheath ahead of it. Finally, we uncovered relationships between the properties of the magnetic ejecta, such as relationships between density or speed and the initial magnetic flux of our flux ropes.

Conclusions. The implementation of the modified Titov-Démoulin flux rope in COCONUT enables us to retrieve the major properties of CMEs at 0.1 AU for any phase of the solar cycle. When combined with heliospheric simulations, COCONUT could lead to more realistic and self-consistent CME evolution models and thus more reliable predictions.

### **Energy and helicity fluxes in line-tied eruptive simulations**

Luis [Linan](#), [Étienne Pariat](#), [Guillaume Aulanier](#), [Kostas Moraitis](#), [Gherardo Valori](#)

A&A 636, A41 2020

<https://arxiv.org/pdf/2003.01698.pdf>

<https://www.aanda.org/articles/aa/pdf/2020/04/aa37548-20.pdf>

Based on a decomposition of the magnetic field into potential and nonpotential components, magnetic energy and relative helicity can both also be decomposed into two quantities: potential and free energies, and volume-threading and current-carrying helicities. In this study, we perform a coupled analysis of their behaviors in a set of parametric 3D magnetohydrodynamic (MHD) simulations of solar-like eruptions. We present the general formulations for the time-varying components of energy and helicity in resistive MHD. We calculated them numerically with a specific gauge, and compared their behaviors in the numerical simulations, which differ from one another by their imposed boundary-driving motions. Thus, we investigated the impact of different active regions surface flows on the development of the energy and helicity-related quantities. Despite general similarities in their overall behaviors, helicities and energies display different evolutions that cannot be explained in a unique framework. While the energy fluxes are similar in all simulations, the physical mechanisms that govern the evolution of the helicities are markedly distinct from one simulation to another: the evolution of volume-threading helicity can be governed by boundary fluxes or helicity transfer, depending on the simulation. The eruption takes place for the same value of the ratio of the current-carrying helicity to the total helicity in all simulations. However, our study highlights that this threshold can be reached in different ways, with different helicity-related processes dominating for different photospheric flows. This means that the details of the pre-eruptive dynamics do not influence the eruption-onset helicity-related threshold. Nevertheless, the helicity-flux dynamics may be more or less efficient in changing the time required to reach the onset of the eruption.

### **Time variations of the non-potential and volume-threading magnetic helicities**

Luis [Linan](#), [Étienne Pariat](#), [Kostas Moraitis](#), [Gherardo Valori](#), [James E. Leake](#)

ApJ 2018



<https://arxiv.org/pdf/1809.03765.pdf>

Relative magnetic helicity is a gauge invariant quantity suitable for the study of the magnetic helicity content of heliospheric plasmas. Relative magnetic helicity can be decomposed uniquely into two gauge invariant quantities, the magnetic helicity of the non-potential component of the field, and a complementary volume-threading helicity. Recent analysis of numerical experiments simulating the generation of solar eruptions have shown that the ratio of the non-potential helicity to the total relative helicity is a clear marker of the eruptivity of the magnetic system, and that the high value of that quantity could be a sufficient condition for the onset of the instability generating the eruptions. The present study introduces the first analytical examination of the time variations of these non-potential and volume-threading helicities. The validity of the analytical formulas derived are confirmed with analysis of three-dimensional (3D) magnetohydrodynamics (MHD) simulations of solar coronal dynamics. Both the analytical investigation, and the numerical application show that, unlike magnetic helicity, the non-potential and the volume-threading helicities are not conserved quantities, even in the ideal MHD regime. A term corresponding to the transformation between the non-potential and volume-threading helicities frequently dominates their dynamics. This finding has an important consequence for their estimation in the solar corona: unlike with relative helicity, their volume coronal evolution cannot be ascertained by the flux of these quantities through the volume's boundaries. Only techniques extrapolating the 3D coronal field will enable both the proper study of the non-potential and volume-threading helicities, and the observational analysis of helicity-based solar-eruptivity proxies.

## Peak Temperatures of Large Solar X-Ray Flares and Associated CME Speeds and Widths

A. G. [Ling](#) and S. W. Kahler

2020 ApJ 891 54

<https://iopscience.iop.org/article/10.3847/1538-4357/ab6f6c/pdf>

We recently repeated an earlier analysis by Garcia showing that large ( $\geq M3.0$ ) solar X-ray flares associated with solar energetic particle (SEP) events have significantly lower peak X-ray flux ratios  $R = (0.04-0.5 \text{ nm})/(0.1-0.8 \text{ nm})$ , proxies for flare peak temperatures, than those without SEP events. As we expect SEP events to be produced by shocks ahead of fast coronal mass ejections (CMEs), a smaller  $R$  for an X-ray flare of a given peak flux  $F_p$  should also be more likely to be accompanied by a fast ( $V_{cme} > 1000 \text{ km s}^{-1}$ ) CME. We confirm this expectation, examine the role played by the ratios  $R$  in correlations between  $F_p$  and CME speeds  $V_{cme}$ , and then compare CME widths  $W$ ,  $V_{cme}$ , and  $R$  with each other. We consider an apparent conflict between a global scaling model of eruptive events showing  $V_{cme}$  scaling with higher  $R$  and our confirmation that the Garcia analysis implies that faster CMEs are associated with flares of lower  $R$ . The  $R$  values are examined for 16 large flares of the well-studied AR 12192, for which nearly all flares had no associated CMEs. Those flares share the same high values of  $R$  as other active region (AR) flares with no CMEs. We also find that small ( $< M3.0$ ) flares of filament eruptions leading to SEP events share the lower  $R$  values of larger flares with fast CMEs.

**Table 2** X-ray Flares and CME Speeds of FE SEP Events

**Table 3** X-ray Flares  $> M3$  and Associated CMEs and SEP Events (This table is available in its entirety in machine-readable form.)

## Development of a Current Sheet in the Wake of a Fast CME

A.G. [Ling](#), D. F. Webb, J. T. Burkepile, E. W. Cliver

E-print, Jan 2014; 2014 ApJ 784 91

[http://www.pergamentum.com/eprint/2005CMErayPaper\\_accepted.pdf](http://www.pergamentum.com/eprint/2005CMErayPaper_accepted.pdf)

A bright ray that developed in the wake of a fast coronal mass ejection (CME) on **2005 September 7** presents a unique opportunity to study the early development and physical characteristics of a reconnecting current sheet. Polarization brightness images from the Mk4 K-Coronameter at the Mauna Loa Solar Observatory (MLSO) are used to determine the structure of the ray along its axis low in the corona as it progressed outward. Coverage of the early development of the ray out to  $\sim 1.3 R_{\odot}$  for a period of  $\sim 27$  hours after the start of the event enables for the first time in white light a measurement of a CME current sheet from the top of the arcade to the base of the flux rope. Measured widths of the ray are combined to obtain the kinematics of the upper and lower "Y" points described in reconnection flux-rope models such as Lin and Forbes (2000). The time dependence of these points are used to derive values for the speed and acceleration of the growth of the current sheet. We note the appearance of a large structure which increases in size as it expands outward in the early development of the ray, and an apparent oscillation with period of  $\sim 0.5$  hour in the position angle of the ray.

## CORHEL-CME: An Interactive Tool For Modeling Solar Eruptions

[Jon Linker](#), [Tibor Torok](#), [Cooper Downs](#), [Ronald Caplan](#), [Viacheslav Titov](#), [Andres Reyes](#), [Roberto Lionello](#), [Pete Riley](#)

Journal of Physics Conference Series

2023

<https://arxiv.org/pdf/2311.03596.pdf>

Coronal Mass Ejections (CMEs) are immense eruptions of velocities greater than 2000 km/s. They are responsible for some of the most severe space weather at Earth, including geomagnetic storms and solar energetic particle (SEP) events. We have developed CORHEL-CME, an interactive tool that allows non-expert users to routinely model multiple CMEs in a realistic coronal and heliospheric environment. The tool features a web-based user interface that allows the user to select a time period of interest, and employs RBSL flux ropes to create stable and unstable pre-eruptive configurations within a background global magnetic field. The properties of these configurations can first be explored in

a zero-beta magnetohydrodynamic (MHD) model, followed by complete CME simulations in thermodynamic MHD, with propagation out to 1 AU. We describe design features of the interface and computations, including the innovations required to efficiently compute results on practical timescales with moderate computational resources. CORHEL-CME is now implemented at NASA's Community Coordinated Modeling Center (CCMC) using NASA Amazon Web Services (AWS). It will be available to the public by the time this paper is published. **January 23, 2012**

## **Magnetic Helicity and Free Magnetic Energy as Tools to Probe Eruptions in two Differently Evolving Solar Active Regions**

**E. Liokati**, **A. Nindos**, **M. K. Georgoulis**

A&A 672, A38 2023

<https://arxiv.org/pdf/2301.08495.pdf>

<https://www.aanda.org/articles/aa/pdf/2023/04/aa45631-22.pdf>

Using vector magnetograms from the HMI/SDO and a magnetic connectivity-based method, we calculate the instantaneous relative magnetic helicity and free magnetic energy budgets for several days in two solar active regions (ARs), AR11890 and AR11618, both with complex photospheric magnetic field configurations. The ARs produced several major eruptive flares while their photospheric magnetic field exhibited primarily flux decay in AR11890 and primarily flux emergence in AR11618. Throughout much of their evolution both ARs featured substantial budgets of free magnetic energy and of both positive and negative helicity. In fact, the imbalance between the signed components of their helicity was as low as in the quiet Sun and their net helicity eventually changed sign 14-19 hours after their last major flare. Despite such incoherence, the eruptions occurred at times of net helicity peaks that were co-temporal with peaks in the free magnetic energy. The losses associated with the eruptive flares in the normalized free magnetic energy were in the range 10-60%. For the helicity, changes ranged from 25% to the removal of the entire excess helicity of the prevailing sign, leading a roughly zero net helicity, but with significant equal and opposite budgets of both helicity senses. The removal of the slowly varying background component of the free energy and helicity timeseries revealed that all eruption-related peaks of both quantities exceeded the  $2\sigma$  levels of their detrended timeseries. There was no eruption when only one or none of these quantities exceeded its  $2\sigma$  level. Our results indicate that differently evolving ARs may produce major eruptive flares even when, in addition to the accumulation of significant free magnetic energy budgets, they accumulate large amounts of both negative and positive helicity without a strong dominance of one handedness over the other. **18-25 Nov 2012, 5-11 Nov 2013**

**HMI Science Nuggets** #192 2023 <http://hmi.stanford.edu/hminuggets/?p=4115>

## **Magnetic helicity and energy of emerging solar active regions and their eruptivity**

**E. Liokati** (1), **A. Nindos** (1), **Y. Liu** (2)

A&A 662, A6 2022

<https://arxiv.org/pdf/2202.04353.pdf>

<https://www.aanda.org/articles/aa/pdf/2022/06/aa42868-21.pdf>

Aims. We investigate the role of the accumulation of both magnetic helicity and magnetic energy in the generation of coronal mass ejections (CMEs) from emerging solar active regions (ARs). Methods. Using vector magnetic field data obtained by the Helioseismic and Magnetic Imager on board the Solar Dynamics Observatory, we calculate the magnetic helicity and magnetic energy injection rates as well as the resulting accumulated budgets in 52 emerging ARs from the start time of magnetic flux emergence until they reach heliographic longitude of  $45^\circ$  West (W45). Results. Seven of the ARs produced CMEs while 45 did not. In a statistical sense, the eruptive ARs accumulate larger budgets of both magnetic helicity and energy than the noneruptive ones over intervals that start from flux emergence start time and end (i) at the end of flux emergence phase, and (ii) when the AR produces its first CME or crosses W45, whichever happens first. We found magnetic helicity and energy thresholds of  $9 \times 10^{41} \text{ Mx}^2$  and  $2 \times 10^{32} \text{ erg}$ , respectively, which, if crossed, ARs are likely to erupt. The segregation, in terms of accumulated magnetic helicity and energy budgets, of the eruptive ARs from the noneruptive ones is violated in one case when an AR erupts early in its emergence phase and in six cases with noneruptive ARs exhibiting large magnetic helicity and energy budgets. Decay index calculations may indicate that these ARs did not erupt because the overlying magnetic field provided stronger or more extended confinement than in eruptive ARs. Conclusions. Our results indicate that emerging ARs tend to produce CMEs when they accumulate significant budgets of both magnetic helicity and energy. Any study of their eruptive potential should place magnetic helicity on equal footing with magnetic energy. **6-9 Jan 2011, 19-24 Oct 2011, 18-22 Feb 2012, 19-25 Apr 2012**

**Table 1:** Properties of emerging active regions 2010-2012

**HMI Science Nuggets** #177 March 2022

<http://hmi.stanford.edu/hminuggets/?p=3879>

## **The Contribution of Coronal Jets To The Solar Wind**

**R. Lionello**, **T. Török**, **V. S. Titov**, **J. E. Leake**, **Z. Mikić**, **J. A. Linker**, **M. G. Linton**

2016 ApJL 831 L2

<https://arxiv.org/pdf/1610.03134v1.pdf>

Transient collimated plasma eruptions in the solar corona, commonly known as coronal (or X-ray) jets, are among the most interesting manifestations of solar activity. It has been suggested that these events contribute to the mass and energy content of the corona and solar wind, but the extent of these contributions remains uncertain. We have recently

modeled the formation and evolution of coronal jets using a three-dimensional (3D) magnetohydrodynamic (MHD) code with thermodynamics in a large spherical domain that includes the solar wind. Our model is coupled to 3D MHD flux-emergence simulations, i.e., we use boundary conditions provided by such simulations to drive a time-dependent coronal evolution. The model includes parametric coronal heating, radiative losses, and thermal conduction, which enables us to simulate the dynamics and plasma properties of coronal jets in a more realistic manner than done so far. Here we employ these simulations to calculate the amount of mass and energy transported by coronal jets into the outer corona and inner heliosphere. Based on observed jet-occurrence rates, we then estimate the total contribution of coronal jets to the mass and energy content of the solar wind to (0.4-3.0) % and (0.3-1.0) %, respectively. Our results are largely consistent with the few previous rough estimates obtained from observations, supporting the conjecture that coronal jets provide only a small amount of mass and energy to the solar wind. We emphasize, however, that more advanced observations and simulations are needed to substantiate this conjecture.

## **Solar Plasma Noise in TianQin Laser Propagation: An Extreme Case and Statistical Analysis**

Yanan [Liu](#) (刘亚南)<sup>1,2</sup>, Wei Su (苏威)<sup>1,2</sup>, Xuefeng Zhang (张雪峰)<sup>1</sup>, Jixiang Zhang (张吉祥)<sup>1</sup>, and Shenwei Zhou (周莘为)<sup>1</sup>

2024 ApJ 975 291

<https://iopscience.iop.org/article/10.3847/1538-4357/ad7bb7/pdf>

TianQin (TQ) proposes to detect gravitational-wave signals by using laser interferometry. However, the laser propagation effect introduces a potential noise factor for TQ. In this work, we used magnetohydrodynamic (MHD) simulations to obtain the space magnetic field and plasma distributions during an *extremely strong solar eruption*, and based on the MHD simulation result, we investigated laser propagation noise for TQ. For the extremely strong solar eruption event, we find that the laser propagation noise closely approaches 100% of TQ's displacement noise requirement for the Michelson combination, while the laser propagation noise is still about 30% of TQ's displacement noise requirement for time-delay interferometry (TDI)-X combination. In addition, we investigate the laser propagation noise for 12 cases with different solar wind conditions. Our finding reveals a linear correlation between the laser propagation noise and several space weather parameters, e.g., solar wind dynamic pressure, Sym-H, and Dst, where the correlation coefficients for solar wind dynamic pressure are strongest. Combining the cumulative distribution of solar wind dynamic pressure from 1999 to 2021 with the linear correlation between solar wind dynamic pressure and laser propagation noise, we have determined that the occurrence rate of the laser propagation noise to be greater than 30% of TQ's displacement noise requirement for the Michelson combination over the entire solar activity week is about 15%. In addition, we find that TDI can suppress the laser propagation noise, and reduce the occurrence rate of the laser propagation noise exceeding 30% of TQ's requirement to less than 1%.

## **Nonparametric Statistics on Magnetic Properties at the Footpoints of Erupting Magnetic Flux Ropes**

[Rui Liu](#), [Wensi Wang](#)

ApJ 973 50 2024

<https://arxiv.org/pdf/2407.15148>

<https://iopscience.iop.org/article/10.3847/1538-4357/ad66bd/pdf>

It is under debate whether the magnetic field in the solar atmosphere carries neutralized electric currents; particularly, whether a magnetic flux rope (MFR), which is considered the core structure of coronal mass ejections, carries neutralized electric currents. Recently Wang et al. (2023, ApJ, 943, 80) studied magnetic flux and electric current measured at the footpoints of 28 eruptive MFRs from 2010 to 2015. Because of the small sample size, no rigorous statistics has been done. Here, we include 9 more events from 2016 to 2023 and perform a series of nonparametric statistical tests at a significance level of 5%. The tests confirm that there exist no significant differences in magnetic properties between conjugated footpoints of the same MFR, which justifies the method of identifying the MFR footpoints through coronal dimming. The tests demonstrate that there exist no significant differences between MFRs with pre-eruption dimming and those with only post-eruption dimming. However, there is a medium level of association between MFRs carrying substantial net current and those produce pre-eruption dimming, which can be understood by the Lorentz-self force of the current channel. The tests also suggest that in estimating the magnetic twist of MFRs, it is necessary to take into account the spatially inhomogeneous distribution of electric current density and magnetic field.

2012-03-10, 2012-06-14

Table 1. Magnetic properties at the footpoints of 9 MFRs from 2016 to 2023

## **Improving the Automated Coronal Jet Identification with U-NET**

[Jiajia Liu](#), [Chunyu Ji](#), [Yimin Wang](#), [Szabolcs Soós](#), [Ye Jiang](#), [Robertus Erdélyi](#), [M. B. Korsós](#), [Yuming Wang](#)

ApJ 972 187 2024

<https://arxiv.org/pdf/2407.08119>

<https://iopscience.iop.org/article/10.3847/1538-4357/ad66be/pdf>

Coronal jets are one of the most common eruptive activities in the solar atmosphere. They are related to rich physics processes, including but not limited to magnetic reconnection, flaring, instabilities, and plasma heating. Automated identification of off-limb coronal jets has been difficult due to their abundant nature, complex appearance, and relatively small size compared to other features in the corona. In this paper, we present an automated coronal jet

identification algorithm (AJIA) that utilizes true and fake jets previously detected by a laborious semi-automated jet detection algorithm (SAJIA, Liu et al. 2023) as the input of an image segmentation neural network U-NET. It is found that AJIA could achieve a much higher (0.81) detecting precision than SAJIA (0.34), meanwhile giving the possibility of whether each pixel in an input image belongs to a jet. We demonstrate that with the aid of artificial neural networks, AJIA could enable fast, accurate, and real-time coronal jet identification from SDO/AIA 304 Å observations, which are essential in studying the collective and long-term behavior of coronal jets and their relation with the solar activity cycles.

### **Why are non-radial solar eruptions less frequent than radial ones?**

[Qingjun Liu](#), [Chaowei Jiang](#), [Xuesheng Feng](#), [Pingbing Zuo](#), [Yi Wang](#)

MNRAS Letters, Volume 533, Issue 1, September 2024, Pages L25–L30,

<https://doi.org/10.1093/mnrasl/slae057>

<https://arxiv.org/pdf/2406.16522>

<https://watermark.silverchair.com/slae057.pdf>

Coronal mass ejections from the Sun are not always initiated along a radial trajectory; such non-radial eruptions are well known to be caused by the asymmetry of the pre-eruption magnetic configuration, which is primarily determined by the uneven distribution of magnetic flux at the photosphere. Therefore, it is naturally expected that the non-radial eruptions should be rather common, at least as frequent as radial ones, given the typically asymmetrical nature of photospheric magnetic flux. However, statistical studies have shown that only a small fraction of eruptions display non-radial behavior. Here we aim to shed light on this counterintuitive fact, based on a series of numerical simulations of eruption initiation in bipolar fields with different asymmetric flux distributions. As the asymmetry of the flux distribution increases, the eruption direction tends to deviate further away from the radial path, accompanied by a decrease in eruption intensity. In case of too strong asymmetry, no eruption is triggered, indicating that excessively inclined eruptions cannot occur. Therefore, our simulations suggest that asymmetry plays a negative role in producing eruption, potentially explaining the lesser frequency of non-radial solar eruptions compared to radial ones. With increasing asymmetry, the degree of non-potentiality the field can attain is reduced. Consequently, the intensity of the pre-eruption current sheet decreases, and reconnection becomes less efficient, resulting in weaker eruptions.

### **Filament eruption by multiple reconnections**

[Y. Liu](#), [G. P. Ruan](#), [B. Schmieder](#), [J. H. Guo](#), [Y. Chen](#), [R. S. Zheng](#), [J. T. Su](#), [B. Wang](#)

A&A 687, A130 2024

<https://arxiv.org/pdf/2406.00769>

<https://www.aanda.org/articles/aa/pdf/2024/07/aa49774-24.pdf>

Context. Filament eruption is a common phenomenon in solar activity, but the triggering mechanism is not well understood. Aims. We focus our study on a filament eruption located in a complex nest of three active regions close to a coronal hole. Methods. The filament eruption is observed at multiple wavelengths: by the Global Oscillation Network Group (GONG), the Solar Terrestrial Relations Observatory (STEREO), the Solar Upper Transition Region Imager (SUTRI), and the Atmospheric Imaging Assembly (AIA) and Helioseismic and Magnetic Imager (HMI) on board the Solar Dynamic Observatory (SDO). Thanks to hightemporal-resolution observations, we were able to analyze the evolution of the fine structure of the filament in detail. The filament changes direction during the eruption, which is followed by a halo coronal mass ejection detected by the Large Angle Spectrometric Coronagraph (LASCO) on board the Solar and Heliospheric Observatory ((SOHO). A Type III radio burst was also registered at the time of the eruption. To investigate the process of the eruption, we analyzed the magnetic topology of the filament region adopting a nonlinear force-free-field (NLFFF) extrapolation method and the polytropic global magnetohydrodynamic (MHD) modeling. We modeled the filament by embedding a twisted flux rope with the regularized Biot-Savart Laws (RBSL) method in the ambient magnetic field. Results. The extrapolation results show that magnetic reconnection occurs in a fan-spine configuration resulting in a circular flare ribbon. The global modeling of the corona demonstrates that there was an interaction between the filament and open field lines, causing a deflection of the filament in the direction of the observed CME eruption and dimming area. Conclusions. The modeling supports the following scenario: magnetic reconnection not only occurs with the filament itself (the flux rope) but also with the background magnetic field lines and open field lines of the coronal hole located to the east of the flux rope. This multiwavelength analysis indicates that the filament undergoes multiple magnetic reconnections on small and large scales with a drifting of the flux rope. **4 October 2022**

### **A Model of Solar Magnetic Flux Rope Eruption Initiated Primarily by Magnetic Reconnection**

[Qingjun Liu](#), [Chaowei Jiang](#), [Xinkai Bian](#), [Xuesheng Feng](#), [Pingbing Zuo](#), [Yi Wang](#)

MNRAS Volume 529, Issue 1, Pages 761–771 2024

<https://arxiv.org/pdf/2402.11172.pdf>

<https://doi.org/10.1093/mnras/stae530>

<https://watermark.silverchair.com/stae530.pdf>

There is a heated debate regarding the specific roles played by ideal magnetohydrodynamic (MHD) instability and magnetic reconnection in the causes of solar eruptions. In the context with a pre-existing magnetic flux rope (MFR) before an eruption, it is widely believed that an ideal MHD instability, in particular, the torus instability, is responsible

for triggering and driving the eruption, while reconnection, as invoked in the wake of the erupting MFR, plays a secondary role. Here we present a new numerical MHD model in which the eruption of a pre-existing MFR is primarily triggered and driven by reconnection. In this model, a stable MFR embedded in a strapping field is set as the initial condition. A surface converging flow is then applied at the lower boundary, pushing magnetic flux towards to the main polarity inversion line. It drives a quasi-static evolution of the system, during which a current layer is built up below the MFR with decreasing thickness. Once reconnection starts in the current sheet, the eruption commences, which indicates that the reconnection plays a determining role in triggers the eruption. By further analyzing the works done by in the magnetic flux of the pre-existing MFR and the newly reconnected flux during the acceleration stage of the eruption, we find that the latter plays a major role in driving the eruption. Such a model may explain observed eruptions in which the pre-eruption MFR has not reached the conditions for ideal instability.

## Direct In Situ Measurements of a Fast Coronal Mass Ejection and Associated Structures in the Corona

Ying D. Liu, [Bei Zhu](#), [Hao Ran](#), [Huidong Hu](#), [Mingzhe Liu](#), [Xiaowei Zhao](#), [Rui Wang](#), [Michael L. Stevens](#), [Stuart D. Bale](#)

ApJ 2024

<https://arxiv.org/pdf/2401.06449.pdf>

We report on the first direct in situ measurements of a fast coronal mass ejection (CME) and shock in the corona, which occurred on **2022 September 5**. In situ measurements from the Parker Solar Probe (PSP) spacecraft near perihelion suggest two shocks with the second one decayed, which is consistent with more than one eruptions in coronagraph images. Despite a flank crossing, the measurements indicate unique features of the young ejecta: a plasma much hotter than the ambient medium suggestive of a hot solar source, and a large plasma  $\beta$  implying a highly non-force-free state and the importance of thermal pressure gradient for CME acceleration and expansion. Reconstruction of the global coronal magnetic fields shows a long-duration change in the heliospheric current sheet (HCS), and the observed field polarity reversals agree with a more warped HCS configuration. Reconnection signatures are observed inside an HCS crossing as deep as the sonic critical point. As the reconnection occurs in the sub-Alfvénic wind, the reconnected flux sunward of the reconnection site can close back to the Sun, which helps balance magnetic flux in the heliosphere. The nature of the sub-Alfvénic wind after the HCS crossing as a low Mach-number boundary layer (LMBL) leads to in situ measurements of the near subsonic plasma at a surprisingly large distance. Specifically, an LMBL may provide favorable conditions for the crossings of the sonic critical point in addition to the Alfvén surface.

## Non-Neutralized Electric Currents as a Proxy for Eruptive Activity in Solar Active Regions

Y. LIU<sup>1</sup>, T. TOROK<sup>2</sup>, V. S. TITOV<sup>2</sup>, J. E. LEAKE<sup>3</sup>, X. SUN (孙旭东)<sup>4</sup> AND M. JIN

ApJ 961 148 2024

[http://sun.stanford.edu/~yliu/papers/neutralization\\_finalVersion.pdf](http://sun.stanford.edu/~yliu/papers/neutralization_finalVersion.pdf)

<https://iopscience.iop.org/article/10.3847/1538-4357/ad11da/pdf>

It has been suggested that the ratio of photospheric direct to return current,  $|DC/RC|$ , may be a better proxy for assessing the ability of solar active regions to produce a coronal mass ejection (CME) than others such as the amount of shear along the polarity inversion line (PIL). To test this conjecture, we measure both quantities prior to eruptive and confined flares of varying magnitude. We find that eruptive-flare source regions have  $|DC/RC| > 1.63$  and PIL shear above  $45^\circ$  (average values of  $3.2$  and  $68^\circ$ , respectively), tending to be larger for stronger events, while both quantities are on average smaller for confined-flare source regions ( $2.2$  and  $68^\circ$ , respectively), albeit with substantial overlap. Many source regions, especially those of eruptive X-class flares, exhibit elongated direct currents (EDCs) bracketing the eruptive PIL segment, which typically coincide with areas of continuous PIL shear above  $45^\circ$ . However, a small subset of confined-flare source regions have  $|DC/RC|$  close to unity, very low PIL shear ( $< 38^\circ$ ), and no clear EDC signatures, rendering such regions less likely to produce a CME. A simple quantitative analysis reveals that  $|DC/RC|$  and PIL shear are almost equally good proxies for assessing CME-productivity, comparable to other proxies suggested in the literature. We also show that an inadequate selection of the current-integration area typically yields a substantial underestimation of  $|DC/RC|$ , discuss specific cases that require careful consideration for  $|DC/RC|$  calculation and interpretation of the results, and suggest to improve photospheric CME-productivity proxies by incorporating coronal measures such as the decay index. **7-9 March 2011, 10-12 July 2012, January 7, 2014, 2014-10-24, 7 November 2014, 19 December 2014, 6 Sep 2017, See APPENDIX Table 1.** Ratio of total direct to total return current,  $|DC/RC|$ , and magnetic shear along the PIL for strong flares (X and M class) with and without CMEs and for weak flares with CMEs

## Magnetic Field and Plasma Diagnostics for Solar Coronal Mass Ejections: A Case Study Using the Forward Modeling Approach

[X. Liu](#), [H. Tian](#), [T. Török](#), [S. Gibson](#), [Z. Yang](#), [W. Li](#) & [T. Samanta](#)

*Solar Physics* volume 298, Article number: 112 (2023)

<https://doi.org/10.1007/s11207-023-02207-5>

The proposed COroanal Solar Magnetism Observatory (COSMO) Large Coronagraph (LC) will provide unique observations to study coronal mass ejections (CMEs) with its ability to diagnose the magnetic field and plasma properties in the solar corona. In this article, we take a realistic magnetohydrodynamic CME model and synthesize the signals of several coronal emission lines (CELs) to perform a forward modeling of COSMO LC observations of a CME.

We use the Stokes parameters of the Fe XIII 10747 Å line to diagnose the magnetic field and plasma properties of the CME flux rope. The results show that COSMO LC can provide magnetic field measurements of CME progenitors with a high spatial resolution (pixel size = 2"). During a CME eruption, the COSMO LC observations may be used to qualitatively study the evolution of the magnetic field using a lower spatial resolution (pixel size = 6"). We then use the synthetic signals of several other CELs to diagnose the physical conditions in the CME leading front, including the shock. The COSMO LC observations of the Fe XIII 10798/10747 Å and Ni XV 8026/6703 Å line pairs could provide density diagnostics of the front. By observing several CELs with different formation temperatures, the COSMO LC could be used to diagnose the temperature and ionization states in the front. We suggest that the Fe XIII 10747 Å line should be given the highest priority when observing CMEs, while observations of the Fe XIII 10798 Å, Fe XIV 5303 Å, and Fe XV 7062 Å lines, and the Ni XV 8026/6703 Å line pair can also provide valuable information on CMEs.

## Field-aligned and Magnetic Reconnection Flows in a Magnetohydrodynamic Simulation of Prominence-cavity System

Tie Liu<sup>1,2</sup>, Yingna Su<sup>3,4</sup>, Yang Guo<sup>1,2</sup>, Jie Zhao<sup>3,4</sup>, and Haisheng Ji<sup>3,4</sup>

2023 ApJ 949 36

<https://iopscience.iop.org/article/10.3847/1538-4357/acca82/pdf>

Nested ring-shaped line-of-sight (LOS) oriented flows in coronal cavities have been observed in recent years but rarely explained. Using a magnetohydrodynamic simulation of a prominence-cavity system, we investigate the relationship between the simulated field-aligned flows, magnetic reconnection flows, and the LOS-oriented flows observed by the Coronal Multi-Channel Polarimeter. The field-aligned flows are along magnetic field lines toward the dips and driven by the hydrodynamic forces exerted by the prominence condensation. The reconnection flows are driven by the overlying reconnection and tether-cutting reconnection. The velocity of the reconnection flows increases from the quasi-static phase to the fast-rise phase, reaching several kilometers per second, which is similar to the speed of the field-aligned flows. We calculate the synthetic Doppler images by forward modeling and compare them with the observed LOS-oriented flows. The synthetic images show that the LOS-oriented flows of one ring with opposite internal flow driven by the field-aligned flows are identified in the simulation. And the synthetic images integrated along three different LOSs can resemble the observed direction reversal of the LOS-oriented flow in about 20 hr, when the included angle of two adjacent LOSs is about 10°. These results suggest that the observed LOS-oriented flows of one ring with an opposite internal flow may be explained by the LOS integration effect of field-aligned flows along different loops.

## Power-law Distribution of Solar-Cycle Modulated Coronal Jets

Jiajia Liu, Anchuan Song, David B. Jess, Jie Zhang, Michail Mathioudakis, Szabolcs Soós, Francis P. Keenan, Yuming Wang, Robert Erdélyi

ApJS 266 17 2023

<https://arxiv.org/pdf/2304.03466.pdf>

<https://iopscience.iop.org/article/10.3847/1538-4365/acc85a/pdf>

Power-law distributions have been studied as a significant characteristic of non-linear dissipative systems. Since discovering the power-law distribution of solar flares that was later extended to nano-flares and stellar flares, it has been widely accepted that different scales of flares share the same physical process. Here, we present the newly developed Semi-Automated Jet Identification Algorithm (SAJIA) and its application for detecting more than 1200 off-limb solar jets during Solar Cycle 24. Power-law distributions have been revealed between the intensity/energy and frequency of these events, with indices found to be analogous to those for flares and coronal mass ejections (CMEs). These jets are also found to be spatially and temporally modulated by the solar cycle forming a butterfly diagram in their latitudinal-temporal evolution, experiencing quasi-annual oscillations in their analysed properties, and very likely gathering in certain active longitudinal belts. Our results show that coronal jets display the same nonlinear behaviour as that observed in flares and CMEs, in solar and stellar atmospheres, strongly suggesting that they result from the same nonlinear statistics of scale-free processes as their counterparts in different scales of eruptive events. Although these jets, like flares and other large-scale dynamic phenomena, are found to be significantly modulated by the solar cycle, their corresponding power-law indices still remain similar. **2010 June 27**

**Table 1.** Visibility of 20 randomly chosen coronal jets 2011-2017

## The evolution of a spot-spot type solar active region which produced a major solar eruption

Lijuan Liu

Frontiers in Astronomy and Space Sciences 10: 1135256 2023

<https://arxiv.org/pdf/2303.03637.pdf>

doi: 10.3389/fspas.2023.1091777

<https://www.frontiersin.org/articles/10.3389/fspas.2023.1135256/pdf>

Solar active regions (ARs) are the main sources of large solar flares and coronal mass ejections. It is found that the ARs producing large eruptions usually show compact, highly-sheared polarity inversion lines (PILs). A scenario named as collisional-shearing is proposed to explain the formation of this type of PILs and the subsequent eruptions, which stresses the role of collision and shearing induced by relative motions of different bipoles in their emergence. However, in observations, if not considering the evolution stage of the ARs, about one third of the ARs that produce large solar eruptions govern a spot-spot type configuration. In this work, we studied the full evolution of an emerging AR, which owned a spot-spot type configuration when producing a major eruption, to explore the possible evolution gap between

collisional shearing process in flux emergence and the formation of the spot-spot type, eruption-producing AR. It was found that the AR was formed through three bipoles emerged sequentially. The bipoles were arranged in parallel on the photosphere, so that the AR exhibited an overall large bipole configuration. In the fast emergence phase of the AR, the shearing gradually occurred due to the proper motions of the polarities, but no significant collision occurred due to the parallel arrangement of the bipoles. Nor did the large eruption occur. After the fast emergence, one large positive polarity started decay. Its dispersion led to the collision to a negative polarity which belonged to another bipole. A huge hot channel was formed through precursor flarings around the collision region. The hot channel erupted later, accompanied by an M7.3-class flare. The results suggest that in the spot-spot type AR, along with the shearing induced by the proper motions of the polarities, a decay process may lead to the collision of the polarities, driving the subsequent eruptions. **12-18 Apr 2014**

## **Changes of Magnetic Energy and Helicity in Solar Active Regions from Major Flares**

[Yang Liu](#), [Brian T. Welsch](#), [Gherardo Valori](#), [Manolis K. Georgoulis](#), [Yang Guo](#), [Etienne Pariat](#), [Sung-Hong Park](#), [Julia K. Thalmann](#)

ApJ **2022**

<https://arxiv.org/pdf/2211.09990.pdf>

Magnetic free energy powers solar flares and coronal mass ejections (CMEs), and the buildup of magnetic helicity might play a role in the development of unstable structures that subsequently erupt. To better understand the roles of energy and helicity in large flares and eruptions, we have characterized the evolution of magnetic energy and helicity associated with **21 X-class flares from 2010 to 2017**. Our sample includes both confined and eruptive events, with 6 and 15 in each category, respectively. Using HMI vector magnetic field observations from several hours before to several hours after each event, we employ (a) the Differential Affine Velocity Estimator for Vector Magnetograms (DAVE4VM) to determine the photospheric fluxes of energy and helicity, and (b) non-linear force-free field (NLFFF) extrapolations to estimate the coronal content of energy and helicity in source-region fields. Using Superposed Epoch analysis (SPE), we find, on average: (1) decreases in both magnetic energy and helicity, in both photospheric fluxes and coronal content, that persist for a few hours after eruptions, but no clear changes, notably in relative helicity, for confined events; (2) significant increases in the twist of photospheric fields in eruptive events, with twist uncertainties too large in confined events to constrain twist changes (and lower overall twist in confined events); and (3) on longer time scales (event time +12 hours), replenishment of free magnetic energy and helicity content to near pre-event levels for eruptive events. For eruptive events, magnetic helicity and free energy in coronal models clearly decrease after flares, with the amounts of decrease proportional to each region's pre-flare content. **2011 February 13–17, July 12, 2012**

**Table 1.** List of X-class flares in 13 ARs in our sample, all of which are within  $50^\circ$  from the central meridian and occurred after May 2010.

## **Numerical Research on the Effect of the Initial Parameters of CME Flux-rope Model on Simulation Results. III. Different Initial Energy of CMEs**

Yousheng [Liu](#)<sup>1,2</sup>, Fang Shen<sup>1,2</sup>, Yi Yang<sup>1,2</sup>, and Mengxuan Ma<sup>1,2</sup>

2022 ApJ 940 11

<https://iopscience.iop.org/article/10.3847/1538-4357/ac9b16/pdf>

In numerical studies, the initial parameters of coronal mass ejections (CMEs) have great influence on the simulation results. In our previous work, it has been proved that when the initial velocity is constant, the initial total mass mainly determines the propagation of the CME. On this basis, we carry out further research from the perspective of CME initial energy. We introduced a graduated cylindrical shell model into a 3D interplanetary total variation diminishing magnetohydrodynamic model to study the effect of different parameters of CMEs on simulation results. In this paper, we simulate several CME cases with different initial parameters and study the simulation results with a different initial energy composition. Actually, in interplanetary space, the kinetic energy of the CME always plays a dominant role. In order to study the effect of the initial thermal energy and magnetic energy on the propagation process of the CME, in this simulation, we adjust the initial parameters to make the thermal energy and magnetic energy reach the same level as the kinetic energy or an even higher level. Our results show that the initial total energy of the CME basically determines its arrival time at Earth, which indicates that the kinetic energy, thermal energy, and magnetic energy have similar effects on the propagation of the CMEs. Moreover, when the total energy keeps constant, the decrease of initial density will lead to the enhancement of CME expansion, which may make the front of the CME reach Earth earlier.

## **Formation and Eruption of Hot Channels during an M6.5 Class Solar Flare**

[Yanjie Liu](#), [Yingna Su](#), [Rui Liu](#), [Jialin Chen](#), [Tie Liu](#), [Haisheng Ji](#)

ApJ **941** 83 **2022**

<https://arxiv.org/pdf/2211.06060.pdf>

<https://iopscience.iop.org/article/10.3847/1538-4357/aca08c/pdf>

We investigate the formation and eruption of hot channels associated with the M6.5 class flare (SOL2015-06-22T18:23) occurring in NOAA AR 12371 on **2015 June 22**. Two flare precursors are observed before the flare main phase.

Observations in 94 Å and 131 Å by SDO/AIA have revealed the early morphology of the first hot channel as a group of hot loops, which is termed as seed hot channel. A few seed hot channels are formed above the polarity inversion line (PIL) and the formation is associated with footpoint brightenings' parallel motion along the PIL, which proceeds into the early stage of the flare main phase. During this process, seed hot channels build up and rise slowly, being

accelerated at the peak of the second precursor. They merge in the process of acceleration forming a larger hot channel, which then forms an "inverted  $\gamma$ " shape kinking structure. Before the flare peak, the second kinking hot channel with negative crossing appears near the first kinking hot channel that has erupted. The eruption of these two hot channels produce two peaks on the main flare's GOES light curve. The footpoint brightenings' propagation along the PIL indicate that the first kinking hot channel may be formed due to zipper reconnection. The occurrence of merging between seed hot channels observed by AIA is supported by the extrapolated nonlinear force-free field models. The observed writhing motion of the first kinking hot channel may be driven by the Lorentz force. **June 22, 2015**

## **Data-constrained MHD simulation for the eruption of a filament-sigmoid system in solar active region 11520**

[Tie Liu](#), [Yuhong Fan](#), [Yingna Su](#), [Yang Guo](#), [Ya Wang](#), [Haisheng Ji](#)

ApJ **940** 62 **2022**

<https://arxiv.org/pdf/2211.02354.pdf>

<https://iopscience.iop.org/article/10.3847/1538-4357/ac961a/pdf>

The separation of a filament and sigmoid is observed during an X1.4 flare on **July 12, 2012** in solar active region 11520, but the corresponding magnetic field change is not clear. We construct a data-constrained magnetohydrodynamic simulation of the filament-sigmoid system with the flux rope insertion method and magnetic flux eruption code, which produces the magnetic field evolution that may explain the separation of the low-lying filament and high-lying hot channel (sigmoid). The initial state of the magnetic model contains a magnetic flux rope with a hyperbolic flux tube, a null point structure and overlying confining magnetic fields. We find that the magnetic reconnections at the null point make the right footpoint of the sigmoid move from one positive magnetic polarity (P1) to another (P3). The tether-cutting reconnection at the hyperbolic flux tube occurs and quickly cuts off the connection of the low-lying filament and high-lying sigmoid. In the end, the high-lying sigmoid erupts and grows into a coronal mass ejection, while the low-lying filament stays stable. The observed double J-shaped flare ribbons, semi-circular ribbon, and brightenings of several loops are reproduced in the simulation, where the eruption of the magnetic flux rope includes the impulsive acceleration and propagation phases.

## **Numerical Simulation of Solar Magnetic Flux Emergence Using the AMR--CESE--MHD Code**

[Zhipeng Liu](#), [Chaowei Jiang](#), [Xueshang Feng](#), [Pingbing Zuo](#), [Yi Wang](#)

**2022**

<https://arxiv.org/pdf/2210.12717.pdf>

Magnetic flux emergence from the solar interior to the atmosphere is believed to be a key process of formation of solar active regions and driving solar eruptions. Due to the limited capability of observation, the flux emergence process is commonly studied using numerical simulations. In this paper, we developed a numerical model to simulate the emergence of a twisted magnetic flux tube from the convection zone to the corona using the AMR--CESE--MHD code, which is based on the conservation-element solution-element method with adaptive mesh refinement. The result of our simulation agrees with that of many previous ones with similar initial conditions but using different numerical codes. In the early stage, the flux tube rises from the convection zone as driven by the magnetic buoyancy until it reaches close to the photosphere. The emergence is decelerated there and with piling-up of the magnetic flux, the magnetic buoyancy instability is triggered, which allows the magnetic field to partially enter into the atmosphere. Meanwhile, two gradually separated polarity concentration zones appear in the photospheric layer, transporting the magnetic field and energy into the atmosphere through their vortical and shearing motions. Correspondingly, the coronal magnetic field has also been reshaped to a sigmoid configuration containing a thin current layer, which resembles the typical pre-eruptive magnetic configuration of an active region. Such a numerical framework of magnetic flux emergence as established will be applied in future investigations of how solar eruptions are initiated in flux emergence active regions.

## **Fan-shaped jet close to a light bridge**

[Y. Liu](#), [G.P. Ruan](#), [B. Schmieder](#), [S. Masson](#), [Y. Chen](#), [J.T. Su](#), [B. Wang](#), [X.Y. Bai](#), [Y. Su](#), [Wenda Cao](#)

A&A **667**, A24 **2022**

<https://arxiv.org/pdf/2207.13246.pdf>

<https://www.aanda.org/articles/aa/pdf/2022/11/aa43292-22.pdf>

<https://doi.org/10.1051/0004-6361/202243292>

On the Sun, jets in light bridges are frequently observed with high-resolution instruments. The respective roles played by convection and the magnetic field in triggering such jets are not yet clear. We report a small fan-shaped jet along a LB observed by the 1.6m Goode Solar Telescope (GST) with the TiO Broadband Filter Imager (BFI), the Visible Imaging Spectrometer (VIS) in H $\alpha$ , and the Near-Infrared Imaging Spectropolarimeter (NIRIS), along with the Stokes parameters. The high spatial and temporal resolution of those instruments allowed us to analyze the features identified during the jet [this http URL](#). Constructing the H $\alpha$  Dopplergrams, we found that the plasma is first moving upward, whereas during the second phase of the jet, the plasma is flowing back. Working with time slice diagrams, we investigated the propagation-projected speed of the fan and its bright base. The fan-shaped jet developed within a few minutes, with diverging beams. At its base, a bright point was slipping along the LB and ultimately invaded the umbra of the sunspot. The H $\alpha$  profiles of the bright points enhanced the intensity in the wings, similarly to the case of Ellerman [this http URL](#). Temporally, the extreme ultraviolet brightenings developed at the front of the dark material jet



and moved at the same speed as the fan, leading us to propose that the fan-shaped jet material compressed and heated the ambient plasma at its extremities in the corona. Our multi-wavelength analysis indicates that the fan-shaped jet could result from magnetic reconnection across the highly diverging field low in the chromosphere, leading to an apparent slipping motion of the jet material along the LB. However, we did not find any opposite magnetic polarity at the jet base, as would typically be expected in such a configuration. We therefore discuss other plausible physical mechanisms, based on waves and convection, that may have triggered the event. **August 25 2016**

### **Cross-scale Dynamics Driven by Plasma Jet Braking in Space**

C. M. Liu<sup>1,2,3</sup>, A. Vaivads<sup>3</sup>, Y. V. Khotyaintsev<sup>2</sup>, H. S. Fu<sup>1</sup>, D. B. Graham<sup>2</sup>, K. Steinvall<sup>2,4</sup>, Y. Y. Liu<sup>1</sup>, and J. L. Burch<sup>5</sup>

2022 ApJ 926 198

<https://iopscience.iop.org/article/10.3847/1538-4357/ac4979/pdf>

Plasma jets are ubiquitous in space. In geospace, jets can be generated by magnetic reconnection. These reconnection jets, typically at fluid scale, brake in the near-Earth region, dissipate their energies, and drive plasma dynamics at kinetic scales, generating field-aligned currents that are crucial to magnetospheric dynamics. Understanding of the cross-scale dynamics is fundamentally important, but observation of coupling among phenomena at various scales is highly challenging. Here we report, using unprecedentedly high-cadence data from NASA's Magnetospheric Multiscale Mission, the first observation of cross-scale dynamics driven by jet braking in geospace. We find that jet braking causes MHD-scale distortion of magnetic field lines and development of an ion-scale jet front that hosts strong Hall electric fields. Parallel electric fields arising from the ion-scale Hall potential generate intense electron-scale field-aligned currents, which drive strong Debye-scale turbulence. Debye-scale waves conversely limit intensity of the field-aligned currents, thereby coupling back to the large-scale dynamics. Our study can help in understanding how energy deposited in large-scale structures is transferred into small-scale structures in space.

### **Investigation on the Spatiotemporal Structures of Supra-Arcade Spikes**

[Rui Liu, Yuming Wang](#)

A&A 2021

<https://arxiv.org/pdf/2106.04752.pdf>

The vertical current sheet (VCS) trailing coronal mass ejections (CMEs) is the key place where the flare energy release and the CME buildup take place through magnetic reconnection. It is often studied from the edge-on perspective for the morphological similarity with the two-dimensional "standard" picture, but its three dimensional structure can only be revealed when the flare arcade is observed side on. The structure and dynamics in the so-called supra-arcade region thus contain important clues to the physical processes in flares and CMEs. Here we focus on the supra-arcade spikes (SASs), interpreted as the VCS viewed side-on, to study their spatiotemporal structures. By identifying each individual spike during the decay phase of four selected flares, in which the associated CME is traversed by a near-Earth spacecraft, we found that the widths of spikes are log-normal distributed, while the Fourier power spectra of the overall supra-arcade EUV emission, including bright spikes and dark downflows as well as the diffuse background, are power-law distributed, in terms of either spatial frequency  $k$  or temporal frequency  $\nu$ , which reflects the fragmentation of the VCS. We demonstrate that coronal emission-line intensity observations dominated by Kolmogorov turbulence would exhibit a power spectrum of  $E(k) \sim k^{-13/3}$  or  $E(\nu) \sim \nu^{-7/2}$ , which is consistent with our observations. By comparing the number of SASs and the turns of field lines as derived from the ICMEs, we found a consistent axial length of  $\sim 3.5$  AU for three events with a CME speed of  $\sim 1000$  km/s in the inner heliosphere, but a much longer axial length ( $\sim 8$  AU) for the fourth event with an exceptionally fast CME speed of  $\sim 1500$  km/s, suggesting that this ICME is flattened and its "nose" has well passed the Earth when the spacecraft traversed its leg. **2011-Oct-22, 2013-Apr-11, 2013-Nov-07, 2014-Apr-02**

### **Tether-cutting and Overlying Magnetic Reconnections in an MHD Simulation of Prominence-cavity System**

[Tie Liu, Yingna Su](#)

ApJ 2021

<https://arxiv.org/ftp/arxiv/papers/2105/2105.06683.pdf>

We investigate the magnetic reconnection in an MHD simulation of a coronal magnetic flux rope (MFR) confined by a helmet streamer, where a prominence-cavity system forms. This system includes a hot cavity surrounding a prominence with prominence horns and a central hot core above the prominence. The evolution of the system from quasi-equilibrium to eruption can be divided into four phases: quasi-static, slow rise, fast rise, and propagation phases. The emerged MFR initially stays quasi-static and magnetic reconnection occurs at the overlying high-Q (squashing factor) apex region, which gradually evolves into a hyperbolic flux tube (HFT). The decrease of the integrated magnetic tension force (above the location of the overlying reconnection) is due to the removal of overlying confinement by the enhanced overlying reconnection between the MFR and the overlying fields at the apex HFT, thus engines the slow rise of the MFR with a nearly constant velocity. Once the MFR reaches the regime of torus instability, another HFT immediately forms at the dip region under the MFR, followed by the explosive flare reconnection. The integrated resultant force (above the location of the flare reconnection) exponentially increases, which drives the exponential fast rise of the MFR. The system enters the propagation phase, once its apex reaches the height of about one solar radius above the photosphere. The simulation reproduces the main processes of one group of prominence eruptions especially those occurring on the quiet Sun.

## The configuration and failed eruption of a complex magnetic flux rope above a $\delta$ sunspot region

[Lijuan Liu](#), [Jiajia Liu](#), [Jun Chen](#), [Yuming Wang](#), [Guoqiang Wang](#), [Zhenjun Zhou](#), [Jun Cui](#)

A&A 648, A106 2021

<https://arxiv.org/pdf/2102.06005.pdf>

<https://www.aanda.org/articles/aa/pdf/2021/04/aa40277-21.pdf>

<https://doi.org/10.1051/0004-6361/202140277>

**Aims.** We investigate the configuration of a complex flux rope above a  $\delta$  sunspot region in NOAA AR 11515, and its eruptive expansion during a confined M5.3-class flare.

**Methods.** We study the formation of the  $\delta$  sunspot using continuum intensity images and photospheric vector magnetograms provided by SDO/HMI. We use EUV and UV images provided by SDO/AIA, and hard X-ray emission recorded by RHESSI to investigate the eruptive details. The coronal magnetic field is extrapolated with a non-linear force free field (NLFFF) method, based on which the flux rope is identified by calculating the twist number  $T_w$  and squashing factor  $Q$ . We search the null point via a modified Powell hybrid method.

**Results.** The collision between two emerging spot groups form the  $\delta$  sunspot. A bald patch (BP) forms at the collision location, above which a complex flux rope is identified. The flux rope has multiple layers, with one compact end and one bifurcated end, having  $T_w$  decreasing from the core to the boundary. A null point is located above the flux rope. The eruptive process consists of precursor flaring at a 'v'-shaped coronal structure, rise of the filament, and flaring below the filament, corresponding well with the NLFFF topological structures, including the null point and the flux rope with BP and hyperbolic flux tube (HFT). Two sets of post-flare loops and three flare ribbons support the bifurcation configuration of the flux rope.

**Conclusions.** The precursor reconnection, which occurs at the null point, weakens the overlying confinement to allow the flux rope to rise, fitting the breakout model. The main phase reconnection, which may occur at the BP or HFT, facilitates the flux rope rising. The results suggest that the  $\delta$  spot configuration presents an environment prone to the formation of complex magnetic configurations which will work together to produce activities. **2012 July 04**

## The Source Locations of Major Flares and CMEs in the Emerging Active Regions

[Lijuan Liu](#), [Yuming Wang](#), [Zhenjun Zhou](#), [Jun Cui](#)

ApJ 909 142 2021

<https://arxiv.org/pdf/2101.07452.pdf>

<https://doi.org/10.3847/1538-4357/abde37>

<https://iopscience.iop.org/article/10.3847/1538-4357/abde37/pdf>

Major flares and coronal mass ejections (CMEs) tend to originate from the compact polarity inversion lines (PILs) in the solar active regions (ARs). Recently, a scenario named as "collisional shearing" is proposed by [Chintzoglou\\_2019](#) to explain the phenomenon, which suggests that the collision between different emerging bipoles is able to form the compact PIL, driving the shearing and flux cancellation that are responsible to the subsequent large activities. In this work, through tracking the evolution of 19 emerging ARs from their birth until they produce the first major flares or CMEs, we investigated the source PILs of the activities, i.e., the active PILs, to explore the generality of "collisional shearing". We find that none of the active PILs is the self PIL (sPIL) of a single bipole. We further find that 11 eruptions originate from the collisional PILs (cPILs) formed due to the collision between different bipoles, 6 from the conjoined systems of sPIL and cPIL, and 2 from the conjoined systems of sPIL and ePIL (external PIL between the AR and the nearby preexisting polarities). Collision accompanied by shearing and flux cancellation is found developing at all PILs prior to the eruptions, with 84% (16/19) cases having collisional length longer than 18~Mm. Moreover, we find that the magnitude of the flares is positively correlated with the collisional length of the active PILs, indicating that the intenser activities tend to originate from the PILs with severer collision. The results suggest that the "collisional shearing", i.e., bipole-bipole interaction during the flux emergence is a common process in driving the major activities in emerging ARs. **2010-06-11-12, 2011-02-17-18, 2012-02-18-19, 2012-03-21, 2013-06-18-19, 2013-10-13, 2013-10-13-16, 2013-11-05, 2013-11-08, 2014-06-10**

Table 2010-2014

## Editorial: Magnetic Flux Ropes: From the Sun to the Earth and Beyond

**Review**

Rui [Liu](#)<sup>1,2,3\*</sup>, Jie Zhang<sup>4</sup>, Yuming Wang<sup>1,2</sup> and Hongqiang Song<sup>5</sup>

Front. Astron. Space Sci., 7:605957. 2020 |

<https://doi.org/10.3389/fspas.2020.605957>

<https://www.frontiersin.org/articles/10.3389/fspas.2020.605957/full>

The purpose of this Frontiers Research Topic on magnetic flux ropes is to provide a forum to bring together multi-wavelength remote sensing and in-situ diagnostics, to integrate observation and numerical modeling, and to confront established models with new observations. The articles published in this Topic represent the most active fronts of research on a few important questions, namely, how flux ropes originate and evolve toward destabilization and beyond, how they are structured, and how they interact with each other and with surrounding magnetic fields and plasma. Below we briefly summarize the major results achieved by these articles.

## Magnetic Flux Ropes in the Solar Corona: Structure and Evolution toward Eruption

**Review**

[Rui Liu](#)

<https://arxiv.org/pdf/2007.11363.pdf>

Magnetic flux ropes are characterized by coherently twisted magnetic field lines, which are ubiquitous in magnetized plasmas. As the core structure of various eruptive phenomena in the solar atmosphere, flux ropes hold the key to understanding the physical mechanisms of solar eruptions, which impact the heliosphere and planetary atmospheres. Strongest disturbances in the Earth's space environments are often associated with large-scale flux ropes from the Sun colliding with the Earth's magnetosphere, leading to adverse, sometimes catastrophic, space-weather effects. However, it remains elusive as to how a flux rope forms and evolves toward eruption, and how it is structured and embedded in the ambient field. The present paper addresses these important questions by reviewing current understandings of coronal flux ropes from an observer's perspective, with emphasis on their structures and nascent evolution toward solar eruptions, as achieved by combining observations of both remote sensing and in-situ detection with modeling and simulation. It highlights an initiation mechanism for coronal mass ejections (CMEs) in which plasmoids in current sheets coalesce into a 'seed' flux rope whose subsequent evolution into a CME is consistent with the standard model, thereby bridging the gap between microscale and macroscale dynamics. 1998 Oct 18, 2002 May 27, 11-12 Feb 2007, 7 Aug 2010, 2012 Jan 03, 2013 May 13, 2013 Aug 11, 4 Nov 2015

### **Predicting Coronal Mass Ejections Using SDO/HMI Vector Magnetic Data Products and Recurrent Neural Networks**

Hao Liu<sup>1,2</sup>, Chang Liu<sup>1,3,4</sup>, Jason T. L. Wang<sup>1,2</sup>, and Haimin Wang<sup>1,3,4</sup>

2020 ApJ 890 12

<https://sci-hub.si/10.3847/1538-4357/ab6850>

<https://arxiv.org/pdf/2002.10953.pdf>

We present two recurrent neural networks (RNNs), one based on gated recurrent units and the other based on long short-term memory, for predicting whether an active region (AR) that produces an M- or X-class flare will also produce a coronal mass ejection (CME). We model data samples in an AR as time series and use the RNNs to capture temporal information on the data samples. Each data sample has 18 physical parameters, or features, derived from photospheric vector magnetic field data taken by the Helioseismic and Magnetic Imager on board the Solar Dynamics Observatory. We survey M- and X-class flares that occurred from 2010 to 2019 May using the Geostationary Operational Environmental Satellite's X-ray flare catalogs provided by the National Centers for Environmental Information (NCEI), and select those flares with identified ARs in the NCEI catalogs. In addition, we extract the associations of flares and CMEs from the Space Weather Database of Notifications, Knowledge, Information. We use the information gathered above to build the labels (positive versus negative) of the data samples at hand. Experimental results demonstrate the superiority of our RNNs over closely related machine learning methods in predicting the labels of the data samples. We also discuss an extension of our approach to predict a probabilistic estimate of how likely an M- or X-class flare is to initiate a CME, with good performance results. To our knowledge this is the first time that RNNs have been used for CME prediction.

### **Numerical Simulation on the Propagation and Deflection of Fast Coronal Mass Ejections (CMEs) Interacting with a Corotating Interaction Region in Interplanetary Space**

Yousheng Liu<sup>1,2</sup>, Fang Shen<sup>1,2,3</sup>, and Yi Yang<sup>1,2</sup>

2019 ApJ 887 150

<https://iopscience.iop.org/article/10.3847/1538-4357/ab543e/pdf>

Previous research has shown that the deflection of coronal mass ejections (CMEs) in interplanetary space, especially fast CMEs, is a common phenomenon. The deflection caused by the interaction with background solar wind is an important factor to determine whether CMEs could hit Earth or not. As the Sun rotates, there will be interactions between solar wind flows with different speeds. When faster solar wind runs into slower solar wind ahead, it will form a compressive area corotating with the Sun, which is called a corotating interaction region (CIR). These compression regions always have a higher density than the common background solar wind. When interacting with CME, will this make a difference in the deflection process of CME? In this research, first, a three-dimensional (3D) flux-rope CME initialization model is established based on the graduated cylindrical shell (GCS) model. Then this CME model is introduced into the background solar wind, which is obtained using a 3D IN (INterplanetary) -TVD-MHD model. The Carrington Rotation (CR) 2154 is selected as an example to simulate the propagation and deflection of fast CME when it interacts with background solar wind, especially with the CIR structure. The simulation results show that: (1) the fast CME will deflect eastward when it propagates into the background solar wind without the CIR; (2) when the fast CME hits the CIR on its west side, it will also deflect eastward, and the deflection angle will increase compared with the situation without CIR.

### **Formation of a Magnetic Flux Rope in the Early Emergence Phase of NOAA Active Region 12673**

Lijuan Liu (刘丽娟)<sup>1,2,3</sup>, Xin Cheng (程鑫)<sup>3,4</sup>, Yuming Wang (汪毓明)<sup>2,5</sup>, and Zhenjun Zhou

2019 ApJ 884 45

<https://doi.org/10.3847/1538-4357/ab3c6c>

<https://arxiv.org/pdf/1908.06360.pdf>

In this work, we investigate the formation of a magnetic flux rope (MFR) above the central polarity inversion line (PIL) of NOAA Active Region 12673 during its early emergence phase. Through analyzing the photospheric vector magnetic field, extreme ultraviolet (EUV) and ultraviolet (UV) images, extrapolated three-dimensional (3D) nonlinear force-free fields (NLFFFs), and the photospheric motions, we find that with the successive emergence of different bipoles in the central region, the conjugate polarities separate, resulting in collision between the nonconjugated opposite polarities. Nearly potential loops appear above the PIL at first, then get sheared and merge at the collision locations as evidenced by the appearance of a continuous EUV sigmoid on **2017 September 4**, which also indicates the formation of an MFR. The 3D NLFFFs further reveal the gradual buildup of the MFR, accompanied by the appearance of two elongated bald patches (BPs) at the collision locations and a very-low-lying hyperbolic flux tube configuration between the BPs. Finally, the MFR has relatively steady axial flux and average twist number of around  $2.1 \times 1020$  Mx and  $-1.5$ , respectively. Shearing motions are found developing near the BPs when the collision occurs, with flux cancellation and UV brightenings being observed simultaneously, indicating the development of a process named collisional shearing (first identified by Chintzoglou et al.). The results clearly show that the MFR is formed by collisional shearing, i.e., through shearing and flux cancellation driven by the collision between nonconjugated opposite polarities during their emergence.

## The Eruption of Outer Spine-like Loops Leading to a Double-stage Circular-ribbon Flare

Chang [Liu](#)<sup>1,2,3</sup>, Jeongwoo Lee<sup>1,3</sup>, and Haimin Wang<sup>1,2,3</sup>

2019 ApJ 883 47

<https://doi.org/10.3847/1538-4357/ab3923>

Circular-ribbon flares occur in a confined magnetic structure, but can also be associated with coronal mass ejections (CMEs) when a filament embedded under the fan erupts. Here we study an M8.7 circular-ribbon flare (SOL2014-12-17T04:51), which is accompanied by a CME yet without a clear indication of filament eruption. Using a nonlinear force-free field model, we find that the outer spine-like loops form a magnetic flux rope (FR1) rooted at the edge of the fan, and that there is another flux rope (FR2) at the main magnetic polarity inversion line (PIL) under a fan-like flux rope FR3. We divide the event evolution into two stages by combining modeling results with EUV observations. The onset stage is featured with bidirectional jets that occurred between a filament and FR1, immediately followed by an upward motion of the latter. During this first stage, the inner/outer spine-related ribbons and the circular ribbon begin to brighten up. After about 10 minutes, another ejection stems from the main PIL region. In this second stage, all ribbons are significantly enhanced, and the twist of FR2 footpoints is decreased. We discuss these results in favor of a scenario where the initial reconnection between the filament and FR1 activates the latter to reconnect with FR3 with opposite twist. This produces larger scale erupting loops and consequently causes a weakening of FR3, which induces another eruption of FR2 from below. This event thus represents a new type of eruptive circular-ribbon flare caused by unstable outer spine-like loops.

## How Many Twists Do Solar Coronal Jets Release?

Jiajia [Liu](#), [Yuming Wang](#), [Robertus Erdélyi](#)

Frontiers in Astronomy and Space Sciences 2019

<https://arxiv.org/pdf/1905.09576.pdf>

[https://www.frontiersin.org/articles/10.3389/fspas.2019.00044/full?utm\\_source=F-AAE&utm\\_medium=EMLF&utm\\_campaign=MRK\\_1056122\\_76\\_Astron\\_20190730\\_arts\\_A](https://www.frontiersin.org/articles/10.3389/fspas.2019.00044/full?utm_source=F-AAE&utm_medium=EMLF&utm_campaign=MRK_1056122_76_Astron_20190730_arts_A)  
<http://sci-hub.se/https://www.frontiersin.org/articles/10.3389/fspas.2019.00044/full>

Highly twisted magnetic flux ropes, with finite length, are subject to kink instabilities, and could lead to a number of eruptive phenomena in the solar atmosphere, including flares, coronal mass ejections (CMEs) and coronal jets. The kink instability threshold, which is the maximum twist a kink-stable magnetic flux rope could contain, has been widely studied in analytical models and numerical simulations, but still needs to be examined by observations. In this article, we will study twists released by 30 off-limb rotational solar coronal jets, and compare the observational findings with theoretical kink instability thresholds. We have found that: 1) the number of events with more twist release becomes less; 2) each of the studied jets has released a twist number of at least 1.3 turns (a twist angle of  $2.6\pi$ ); and 3) the size of a jet is highly related to its twist pitch instead of twist number. Our results suggest that the kink instability threshold in the solar atmosphere should not be a constant. The found lower limit of twist number of 1.3 turns should be merely a necessary but not a sufficient condition for a finite solar magnetic flux rope to become kink unstable. **27 June 2010**  
**Table 1:** Parameters of 30 solar coronal jets observed between 2010 and 2016

## A Comparative Study of 2017 July and 2012 July Complex Eruptions: Are Solar Superstorms "Perfect Storms" in Nature?

Ying D. [Liu](#), [Xiaowei Zhao](#), [Huidong Hu](#), [Angelos Vourlidis](#), [Bei Zhu](#)

ApJ Supl. 241 15 2019

<https://doi.org/10.3847/1538-4365/ab0649>

It is paramount from both scientific and societal perspectives to understand the generation of extreme space weather. We discuss the formation of solar superstorms based on a comparative study of the **2012 July 23** and **2017 July 23** eruptions. The first one is Carrington-class, and the second could rival the 1989 March event that caused the most intense geomagnetic storm of the space age. Observations of these events in the historically weak solar cycle 24 indicate that a solar superstorm can occur in any solar cycle and at any phase of the cycle. Recurrent patterns are identified in both cases, including the long-lived eruptive nature of the active region, a complex event composed of successive

eruptions from the same active region, and in-transit interaction between the successive eruptions resulting in exceptionally strong ejecta magnetic fields at 1 AU. Each case also shows unique characteristics. Preconditioning of the upstream solar wind leading to unusually high solar wind speeds at 1 AU is observed in the first case whereas not in the latter. This may suggest that the concept of "preconditioning" appears to be necessary for making a Carrington-class storm. We find a considerable deflection by nearby coronal holes in the second case but not in the first. On the basis of these results, we propose a hypothesis for further investigation that superstorms are "perfect storms" in nature, i.e., a combination of circumstances that results in an event of unusual magnitude. Historical records of some extreme events seem to support our hypothesis.

## **Geometry, Kinematics and Heliospheric Impact of a Large CME-driven Shock in 2017 September**

Ying D. [Liu](#), [Bei Zhu](#), [Xiaowei Zhao](#)

ApJ **871** 8 **2019**

<https://arxiv.org/pdf/1811.10162.pdf>

[sci-hub.tw/10.3847/1538-4357/aaf425](https://sci-hub.tw/10.3847/1538-4357/aaf425)

A powerful coronal mass ejection (CME) occurred on 2017 September 10 near the end of the declining phase of the historically weak solar cycle 24. We obtain new insights concerning the geometry and kinematics of CME-driven shocks in relation to their heliospheric impacts from the optimal, multi-spacecraft observations of the eruption. The shock, which together with the CME driver can be tracked from the early stage to the outer corona, shows a large oblate structure produced by the vast expansion of the ejecta. The expansion speeds of the shock along the radial and lateral directions are much larger than the translational speed of the shock center, all of which increase during the flare rise phase, peak slightly after the flare maximum and then decrease. The near simultaneous arrival of the CME-driven shock at the Earth and Mars, which are separated by  $156.6^\circ$  in longitude, is consistent with the dominance of expansion over translation observed near the Sun. The shock decayed and failed to reach STEREO A around the backward direction. Comparison between ENLIL MHD simulations and the multi-point in situ measurements indicates that the shock expansion near the Sun is crucial for determining the arrival or non-arrival and space weather impact at certain heliospheric locations. The large shock geometry and kinematics have to be taken into account and properly treated for accurate predictions of the arrival time and space weather impact of CMEs. **10 Sept 2017**

## **Impacts of EUV Wavefronts on Coronal Structures in Homologous Coronal Mass Ejections**

Rui [Liu](#), [Yuming Wang](#), [Jeongwoo Lee](#), [Chenglong Shen](#)

ApJ **2018**

<https://arxiv.org/pdf/1811.01326.pdf>

Large-scale propagating fronts are frequently observed during solar eruptions, yet it is open whether they are waves or not, partly because the propagation is modulated by coronal structures, whose magnetic field we still cannot measure. However, when a front impacts coronal structures, an opportunity arises for us to look into the magnetic properties of both interacting parties in the low- $\beta$  corona. Here we studied large-scale EUV fronts accompanying three coronal mass ejections (CMEs), each originating from a kinking rope-like structure in the NOAA active region (AR) 12371. These eruptions were homologous and the surrounding coronal structures remained stationary. Hence we treated the events as one observed from three different viewing angles, and found that the primary front directly associated with the CME consistently transmits through 1) a polar coronal hole, 2) the ends of a crescent-shaped equatorial coronal hole, leaving a stationary front outlining its AR-facing boundary, and 3) two quiescent filaments, producing slow and diffuse secondary fronts. The primary front also propagates along an arcade of coronal loops and slows down due to foreshortening at the far side, where local plasma heating is indicated by an enhancement in  $211 \text{ \AA}$  (Fe XIV) but a dimming in  $193 \text{ \AA}$  (Fe XII) and  $171 \text{ \AA}$  (Fe IX). The strength of coronal magnetic field is therefore estimated to be  $\sim 2 \text{ G}$  in the polar coronal hole and  $\sim 4 \text{ G}$  in the coronal arcade neighboring the active region. These observations substantiate the wave nature of the primary front and shed new light on slow fronts. **2015 June 21, 22 and 25**

## **Rapid buildup of a magnetic flux rope during a confined X2.2 class flare in NOAA AR 12673**

Lijuan [Liu](#), [Xin Cheng](#), [Yuming Wang](#), [Zhenjun Zhou](#), [Yang Guo](#), [Jun cui](#)

**2018 ApJL 867 L5**

<https://arxiv.org/pdf/1810.04424.pdf>

[sci-hub.tw/10.3847/2041-8213/aae826](https://sci-hub.tw/10.3847/2041-8213/aae826)

Magnetic flux ropes (MFRs) are believed to be the core structure in solar eruptions, nevertheless, their formation remains intensely debated. Here we report a rapid buildup process of an MFR-system during a confined X2.2 class flare occurred on **2017 September 6** in NOAA AR 12673, three hours after which the structure erupted to a major coronal mass ejection (CME) accompanied by an X9.3 class flare. For the X2.2 flare, we do not find EUV dimmings, separation of its flare ribbons, or clear CME signatures, suggesting a confined flare. For the X9.3 flare, large-scale dimmings, separation of its flare ribbons, and a CME show it to be eruptive. By performing a time sequence of nonlinear force-free fields (NLFFFs) extrapolations we find that: until the eruptive flare, an MFR-system was located in the AR. During the confined flare, the axial flux and the lower bound of the magnetic helicity for the MFR-system were dramatically enhanced by about 86% and 260%, respectively, although the mean twist number was almost unchanged. During the eruptive flare, the three parameters were all significantly reduced. The results evidence the buildup and release of the MFR-system during the confined and the eruptive flare, respectively. The former may be achieved by flare

reconnection. We also calculate the pre-flare distributions of the decay index above the main polarity inversion line (PIL) and find no significant difference. It indicates that the buildup of the magnetic flux and helicity of the MFR-system may play a role in facilitating its final eruption.

### **Magnetic Field Modeling of hot channels in Four Flare/CME Events**

Tie [Liu](#), [Yingna Su](#), [Xin Cheng](#), [Adriaan van Ballegooijen](#), [Haisheng Ji](#)

ApJ **2018**

<https://arxiv.org/pdf/1810.03795.pdf>

[sci-hub.tw/10.3847/1538-4357/aae692](https://sci-hub.tw/10.3847/1538-4357/aae692)

We investigate the formation and magnetic topology of four flare/CME events with filament-sigmoid systems, in which the sigmoidal hot channels are located above the filaments, and they appear in pairs prior to eruption. The formation of hot channels usually takes several to dozens of hours during which two J-shape sheared arcades gradually evolve into sigmoidal hot channels, then they keep stable for tens of minutes or hours and erupt. While the low-lying filaments show no significant change. We construct a series of magnetic field models and find that the best-fit preflare models contain magnetic flux ropes with hyperbolic flux tubes (HFTs). The field lines above the HFT correspond to the high-lying hot channel, while those below the HFT surround the underlying filaments. In particular, the continuous and long field lines representing the flux rope located above the HFT match the observed hot channels well in three events. While for **SOL2014-04-18** event, the flux bundle that mimics the observed hot channel is located above the flux rope. The flux rope axis lies in a height range of 19.8 Mm and 46 Mm above the photosphere for the four events, among which the flux rope axis in **SOL2012-07-12** event has a maximum height, which probably explains why it is often considered as a double-decker structure. Our modeling suggests that the high-lying hot channel may be formed by magnetic reconnections between sheared field lines occurring above the filament prior to eruption. **2013-04-11, 2014-04-18, 2014-09-10**

### **A comparative study between a failed and a successful eruption initiated from the same polarity inversion line in AR 11387**

[Lijuan Liu](#), [Yuming Wang](#), [Zhenjun Zhou](#), [Karin Dissauer](#), [Manuela Temmer](#), [Jun Cui](#)

ApJ **858** 121 **2018**

<https://arxiv.org/pdf/1804.00867.pdf>

<https://iopscience.iop.org/article/10.3847/1538-4357/aabba2/pdf>

In this paper, we analyzed a failed and a successful eruption that initiated from the same polarity inversion line within NOAA AR 11387 on **December 25, 2011**. They both started from a reconnection between sheared arcades, having distinct pre-eruption conditions and eruption details: before the failed one, the magnetic fields of the core region had a weaker non-potentiality; the external fields had a similar critical height for torus instability, a similar local torus-stable region, but a larger magnetic flux ratio (of low corona and near-surface region) as compared to the successful one. During the failed eruption, a smaller Lorentz force impulse was exerted on the outward ejecta; the ejecta had a much slower rising speed. Factors that might lead to the initiation of the failed eruption are identified: 1) a weaker non-potentiality of the core region, and a smaller Lorentz force impulse gave the ejecta a small momentum; 2) the large flux ratio, and the local torus-stable region in the corona provided strong confinements that made the erupting structure regain an equilibrium state.

[HMI Science Nuggets](#) #99 May **2018** <http://hmi.stanford.edu/hminuggets/?p=2481>

### **Multi-Spacecraft Observations of the Rotation and Non-Radial Motion of a CME Flux Rope causing an intense geomagnetic storm**

Yi A. [Liu](#), [Ying D. Liu](#), [Huidong Hu](#), [Rui Wang](#), [Xiaowei Zhao](#)

ApJ **2018**

We present an investigation of the rotation and non-radial motion of a coronal mass ejection (CME) from AR 12468 on **2015 December 16** using observations from SDO, SOHO, STEREO A and Wind. The EUV and HMI observations of the source region show that the associated magnetic flux rope (MFR) axis pointed to the east before the eruption. We use a nonlinear force-free field (NLFFF) extrapolation to determine the configuration of the coronal magnetic field and calculate the magnetic energy density distributions at different heights. The distribution of the magnetic energy density shows a strong gradient toward the northeast. The propagation direction of the CME from a Graduated Cylindrical Shell (GCS) modeling deviates from the radial direction of the source region by about 45 deg in longitude and about 30 deg in latitude, which is consistent with the gradient of the magnetic energy distribution around the AR. The MFR axis determined by the GCS modeling points southward, which has rotated counterclockwise by about 95 deg compared with the orientation of the MFR in the low corona. The MFR reconstructed by a Grad-Shafranov (GS) method at 1 AU has almost the same orientation as the MFR from the GCS modeling, which indicates that the MFR rotation occurred in the low corona. It is the rotation of the MFR that caused the intense geomagnetic storm with the minimum Dst of -155 nT. These results suggest that the coronal magnetic field surrounding the MFR plays a crucial role in the MFR rotation and propagation direction.

### **Untwisting Jets Related to Magnetic Flux Cancellation**

Jiajia [Liu](#)<sup>1</sup>, Robert Erdélyi<sup>1,2</sup>, Yuming Wang<sup>3,2</sup>, and Rui Liu<sup>3,2</sup>

**2018** ApJ **852** 10

<http://iopscience.iop.org/article/10.3847/1538-4357/aa992d/pdf>

The rotational motion of solar jets is believed to be a signature of the untwisting process resulting from magnetic reconnection, which takes place between twisted closed magnetic loops (i.e., magnetic flux ropes) and open magnetic field lines. The identification of the pre-existing flux rope, and the relationship between the twist contained in the rope and the number of turns the jet experiences, are then vital in understanding the jet-triggering mechanism. In this paper, we will perform a detailed analysis of imaging, spectral, and magnetic field observations of four homologous jets, among which the fourth one releases a twist angle of  $2.6\pi$ . Nonlinear force-free field extrapolation of the photospheric vector magnetic field before the jet eruption presents a magnetic configuration with a null point between twisted and open fields—a configuration highly in favor of the eruption of solar jets. The fact that the jet rotates in the opposite sense of handedness to the twist contained in the pre-eruption photospheric magnetic field confirms the unwinding of the twist by the jet's rotational motion. The temporal relationship between jets' occurrence and the total negative flux at their source region, together with the enhanced magnetic submergence term of the photospheric Poynting flux, shows that these jets are highly associated with local magnetic flux cancellation. **2015 July 10**

### **Disintegration of an Eruptive Filament via Interactions with Quasi-Separatrix Layers**

Rui [Liu](#), Jun [Chen](#), Yuming [Wang](#)

SCIENCE CHINA Physics, Mechanics & Astronomy **2017**

<https://arxiv.org/pdf/1712.02901.pdf>

The disintegration of solar filaments via mass drainage is a frequently observed phenomenon during a variety of filament activities. It is generally considered that the draining of dense filament material is directed by both gravity and magnetic field, yet the detailed process remains elusive. Here we report on a partial filament eruption during which filament material drains downward to the surface not only along the filament's legs, but to a remote flare ribbon through a fan-out curtain-like structure. It is found that the magnetic configuration is characterized by two conjoining dome-like quasi-separatrix layers (QSLs). The filament is located underneath one QSL dome, whose footprint apparently bounds the major flare ribbons resulting from the filament eruption, whereas the remote flare ribbon matches well with the other QSL dome's far-side footprint. We suggest that the interaction of the filament with the overlying QSLs results in the splitting and disintegration of the filament. **2013 December 31**

### **Untwisting Jets Related to Magnetic Flux Cancellation**

Jiajia [Liu](#), Robert [Erdélyi](#), Yuming [Wang](#), Rui [Liu](#)

ApJ **2017**

<https://arxiv.org/pdf/1711.06066.pdf>

The rotational motion of solar jets is believed to be a signature of the untwisting process resulting from magnetic reconnection, which takes place between twisted closed magnetic loops (i.e., magnetic flux ropes) and open magnetic field lines. The identification of the pre-existing flux rope, and the relationship between the twist contained in the rope and the number of turns the jet experiences, are then vital in understanding the jet-triggering mechanism. In this paper, we will perform a detailed analysis of imaging, spectral and magnetic field observations of four homologous jets, among which the fourth one releases a twist angle of  $2.6\pi$ . Non-linear force free field extrapolation of the photospheric vector magnetic field before the jet eruption presents a magnetic configuration with a null point between twisted and open fields - a configuration highly in favor of the eruption of solar jets. The fact that the jet rotates in the opposite sense of handedness to the twist contained in the pre-eruption photospheric magnetic field, confirms the unwinding of the twist by the jet's rotational motion. Temporal relationship between jets' occurrence and the total negative flux at their source region, together with the enhanced magnetic submergence term of the photospheric Poynting flux, shows that these jets are highly associated with local magnetic flux cancellation. **July 9 2015**

### **Propagation and Interaction Properties of Successive Coronal Mass Ejections in Relation to a Complex Type II Radio Burst**

Ying D. [Liu](#)<sup>1,2</sup>, Xiaowei Zhao<sup>1,2</sup>, and Bei Zhu

**2017** ApJ 849 112

<http://sci-hub.cc/10.3847/1538-4357/aa9075>

We examine the propagation and interaction properties of three successive coronal mass ejections (CMEs) from **2001 November 21–22**, with a focus on their connection with the behaviors of the associated long-duration complex type II radio burst. In combination with coronagraph and multi-point in situ observations, the long-duration type II burst provides key features for resolving the propagation and interaction complexities of the three CMEs. The two CMEs from November 22 interacted first and then overtook the November 21 CME at a distance of about 0.85 au from the Sun. The timescale for the shock originally driven by the last CME to propagate through the preceding two CMEs is estimated to be about 14 and 6 hr, respectively. We present a simple analytical model without any free parameters to characterize the whole Sun-to-Earth propagation of the shock, which shows a remarkable consistency with all the available data and MHD simulations even out to the distance of Ulysses (2.34 au). The coordination of in situ measurements at the Earth and Ulysses, which were separated by about  $71^\circ$  in latitude, gives important clues for the understanding of shock structure and the interpretation of in situ signatures. The results also indicate a means by which to increase geo-effectiveness with multiple CMEs, which can be considered as another manifestation of the "perfect storm" scenario proposed by Liu et al., although the current case is not "super" in the same sense as the 2012 July 23 event.

**CESRA highlight** #1693 Dec **2017** <http://www.astro.gla.ac.uk/users/eduard/cesra/?p=1693>

## Electric-Current Neutralization, Magnetic Shear, and Eruptive Activity in Solar Active Regions

Yang [Liu](#), [Xudong Sun](#), [Tibor Török](#), [Viacheslav S. Titov](#), [James E. Leake](#)

ApJ 846 L6 2017

<https://arxiv.org/pdf/1708.04411.pdf>

The physical conditions that determine whether or not solar active regions (ARs) produce strong flares and coronal mass ejections (CMEs) are not yet well understood. Here we investigate the association between electric-current neutralization, magnetic shear along polarity inversion lines (PILs), and eruptive activity in four ARs; two emerging and two well-developed ones. We find that the CME-producing ARs are characterized by a strongly non-neutralized total current, while the total current in the ARs that did not produce CMEs is almost perfectly neutralized. The difference in the PIL-shear between these two groups is much less pronounced, which suggests that the degree of current-neutralization may serve as a better proxy for assessing the ability of ARs to produce CMEs. **2010-05-23, 2011-02-15, 9 March 2012, 2014-10-23**

RHESSI Nugget No. 305, Aug 2017

[http://sprg.ssl.berkeley.edu/~tohban/wiki/index.php/Electric Current Neutralization and Solar Eruption in Active Regions](http://sprg.ssl.berkeley.edu/~tohban/wiki/index.php/Electric_Current_Neutralization_and_Solar_Eruption_in_Active_Regions)

## The causes of quasi-homologous CMEs

Lijuan [Liu](#), Yuming Wang, Rui Liu, Zhenjun Zhou, M. Temmer, J. K. Thalmann, Jiajia Liu, Kai Liu, Chenglong Shen, Quanhao Zhang, A. M. Veronig

2017 ApJ 844 141

<https://arxiv.org/pdf/1706.08878.pdf>

<http://iopscience.iop.org/sci-hub.cc/0004-637X/844/2/141/>

In this paper, we identified the magnetic source locations of 142 quasi-homologous (QH) coronal mass ejections (CMEs), of which 121 are from solar cycle (SC) 23 and 21 from SC 24. Among those CMEs, 63% originated from the same source location as their predecessor (defined as S-type), while 37% originated from a different location within the same active region as their predecessor (defined as D-type). Their distinctly different waiting time distribution, peaking around 7.5 and 1.5 hours for S- and D-type CMEs, suggests that they might involve different physical mechanisms with different characteristic time scales. Through detailed analysis based on non-linear force free (NLFF) coronal magnetic field modeling of two exemplary cases, we propose that the S-type QH CMEs might involve a recurring energy release process from the same source location (by magnetic free energy replenishment), whereas the D-type QH CMEs can happen when a flux tube system disturbed by a nearby CME. **2000-06-06, 2000-11-24, 2002-07-15, 2004-11-03, 2011-02-14, 2012-03-06/07**

## Structure, Propagation and Expansion of a CME-Driven Shock in the Heliosphere: A Revisit of the 2012 July 23 Extreme Storm

Ying D. [Liu](#), Huidong Hu, Bei Zhu, Janet G. Luhmann, Angelos Vourlidas

ApJ 2016

<https://arxiv.org/pdf/1611.04239v1.pdf>

We examine the structure, propagation and expansion of the shock associated with the **2012 July 23** extreme coronal mass ejection (CME). Characteristics of the shock determined from multi-point imaging observations are compared to in situ measurements at different locations and a complex radio type II burst, which according to our definition has multiple branches that may not all be fundamental-harmonic related. The white-light shock signature can be modeled reasonably well by a spherical structure and was expanding backward even on the opposite side of the Sun. The expansion of the shock, which was roughly self-similar after the first ~1.5 hours from launch, largely dominated over the translation of the shock center for the time period of interest. Our study also suggests a bow-shock morphology around the nose at later times due to the outward motion in combination with the expansion of the ejecta. The shock decayed and failed to reach Mercury in the backward direction and STEREO B and Venus in the lateral directions, as indicated by the imaging and in situ observations. The shock in the nose direction, however, may persist to the far outer heliosphere, with predicted impact on Dawn around 06 UT on July 25 and on Jupiter around 23:30 UT on July 27 by an MHD model. The type II burst shows properties generally consistent with the spatial/temporal variations of the shock deduced from imaging and in situ observations. In particular, the low-frequency bands agree well with the in situ measurements of a very low density ahead of the shock at STEREO A.

## On the Magnetic and Energy Characteristics of Recurrent Homologous Jets from An Emerging Flux

Jiajia [Liu](#), Yuming Wang, Robertus Erdélyi, [Rui Liu](#), [Scott W. McIntosh](#), [Tingyu Gou](#), [Jun Chen](#), [Kai Liu](#), [Lijuan Liu](#), [Zonghao Pan](#)

ApJ 833 150 2016

<http://arxiv.org/abs/1608.07705>

In this paper, we present the detailed analysis of recurrent homologous jets originating from an emerging negative magnetic flux at the edge of an Active Region. The observed jets show multi-thermal features. Their evolution shows high consistence with the characteristic parameters of the emerging flux, suggesting that with more free magnetic



energy, the eruptions tend to be more violent, frequent and blowout-like. The average temperature, average electron number density and axial speed are found to be similar for different jets, indicating that they should have been formed by plasmas from similar origins. Statistical analysis of the jets and their footpoint region conditions reveals a strong positive relationship between the footpoint-region total 131 Å intensity enhancement and jets' length/width. Stronger linearly positive relationships also exist between the total intensity enhancement/thermal energy of the footpoint regions and jets' mass/kinetic/thermal energy, with higher cross-correlation coefficients. All the above results, together, confirm the direct relationship between the magnetic reconnection and the jets, and validate the important role of magnetic reconnection in transporting large amount of free magnetic energy into jets. It is also suggested that there should be more free energy released during the magnetic reconnection of blowout than of standard jet events.

**July 9th 2015**

**Erratum 2018** ApJ 853 201 <http://iopscience.iop.org/article/10.3847/1538-4357/aaa75a/pdf>

## **On the Observation and Simulation of Solar Coronal Twin Jets**

Jijia [Liu](#), Fang Fang, Yuming Wang, [Scott W. McIntosh](#), [Yuhong Fan](#), [Quanhao Zhang](#)

**2016**

<http://arxiv.org/pdf/1608.07759v1.pdf>

We present the first observation, analysis and modeling of solar coronal twin jets, which occurred after a preceding jet. Detailed analysis on the kinetics of the preceding jet reveals its blowout-jet nature, which resembles the one studied in Liu et al. 2014. However the erupting process and kinetics of the twin jets appear to be different from the preceding one. In lack of the detailed information on the magnetic fields in the twin jet region, we instead use a numerical simulation using a three-dimensional (3D) MHD model as described in Fang et al. 2014, and find that in the simulation a pair of twin jets form due to reconnection between the ambient open fields and a highly twisted sigmoidal magnetic flux which is the outcome of the further evolution of the magnetic fields following the preceding blowout jet. Based on the similarity between the synthesized and observed emission we propose this mechanism as a possible explanation for the observed twin jets. Combining our observation and simulation, we suggest that with continuous energy transport from the subsurface convection zone into the corona, solar coronal twin jets could be generated in the same fashion addressed above. **10-11 Apr 2013**

## **Why is a flare-rich active region CME-poor?**

Lijuan [Liu](#), Yuming Wang, Jingxiu Wang, [Chenglong Shen](#), [Pinzhong Ye](#), [Rui Liu](#), [Jun Chen](#), [Quanhao Zhang](#), [S. Wang](#)

**2016** ApJ 826 119

<http://arxiv.org/pdf/1607.07531v1.pdf> **File**

Solar active regions (ARs) are the major sources of two kinds of the most violent solar eruptions, namely flares and coronal mass ejections (CMEs). The largest AR in the past 24 years, NOAA AR 12192, crossed the visible disk from **2014 October 17 to 30**, unusually produced more than one hundred flares, including 32 M-class and 6 X-class ones, but only one small CME. Flares and CMEs are believed to be two phenomena in the same eruptive process. Why is such a flare-rich AR so CME-poor? We compared this AR with other four ARs; two were productive in both and two were inert. The investigation of the photospheric parameters based on the SDO/HMI vector magnetogram reveals that the flare-rich AR 12192, as the other two productive ARs, has larger magnetic flux, current and free magnetic energy than the two inert ARs, but contrast to the two productive ARs, it has no strong, concentrated current helicity along both sides of the flaring neutral line, indicating the absence of a mature magnetic structure consisting of highly sheared or twisted field lines. Furthermore, the decay index above the AR 12192 is relatively low, showing strong constraint. These results suggest that productive ARs are always large and have enough current and free energy to power flares, but whether or not a flare is accompanied by a CME is seemingly related to (1) if there is mature sheared or twisted core field serving as the seed of the CME, (2) if the constraint of the overlying arcades is weak enough. **2011-02-15, 2012-03-07, 2014-10-24**

## **Structure, Stability, and Evolution of Magnetic Flux Ropes from the Perspective of Magnetic Twist**

Rui [Liu](#)<sup>1</sup>, Bernhard Kliem<sup>2</sup>, Viacheslav S. Titov<sup>3</sup>, Jun Chen<sup>1</sup>, Yuming Wang<sup>1</sup>, Haimin Wang<sup>4,5</sup>, Chang Liu<sup>4,5</sup>, Yan Xu<sup>4,5</sup>, & Thomas Wiegelmann

HMI Science Nuggets #49 April **2016**

<http://hmi.stanford.edu/hminuggets/?p=1397>

The MFR's peak  $|Tw|$  temporarily increases within half an hour before each flare while it decreases after the flare peak for both confined and eruptive flares (Fig. 1(b)). This pre-flare increase in  $|Tw|$  has little effect on the AR's free magnetic energy or any other parameters derived for the whole region, due to its moderate amount and the MFR's relatively small volume, while its decrease after flares is clearly associated with the stepwise decrease in the whole region's free magnetic energy due to the flare. Thus, we suggest that  $Tw$  may serve as a useful parameter in forewarning the onset of eruption. **2013 August 10–12**

## ON THE OBSERVATION AND SIMULATION OF SOLAR CORONAL TWIN JETS

Jiajia [Liu](#)<sup>1,2</sup>, Fang Fang<sup>3</sup>, Yuming Wang<sup>1,4</sup>, Scott W. McIntosh<sup>5</sup>, Yuhong Fan<sup>5</sup>, and Quanhao Zhang  
2016 ApJ 817 126

We present the first observation, analysis, and modeling of solar coronal twin jets, which occurred after a preceding jet. Detailed analysis on the kinetics of the preceding jet reveals its blowout-jet nature, which resembles the one studied in Liu et al. However, the erupting process and kinetics of the twin jets appear to be different from the preceding one. Lacking detailed information on the magnetic fields in the twin jet region, we instead use a numerical simulation using a three-dimensional (3D) MHD model as described in Fang et al., and find that in the simulation a pair of twin jets form due to reconnection between the ambient open fields and a highly twisted sigmoidal magnetic flux, which is the outcome of the further evolution of the magnetic fields following the preceding blowout jet. Based on the similarity between the synthesized and observed emission, we propose this mechanism as a possible explanation for the observed twin jets. Combining our observation and simulation, we suggest that with continuous energy transport from the subsurface convection zone into the corona, solar coronal twin jets could be generated in the same fashion addressed above.

## Quasi-periodic Fast-mode Magnetosonic Wave Trains Within Coronal Waveguides Associated with Flares and CMEs

Wei [Liu](#), Leon Ofman, Brittany Broder, Marian Karlicky, and Cooper Downs  
Proceedings of the 14th International Solar Wind Conference, 2015

[http://sun.stanford.edu/~weiliu/research/publications/2016/2016AIP\\_WeiLiu\\_QFPs\\_SolWind14.pdf](http://sun.stanford.edu/~weiliu/research/publications/2016/2016AIP_WeiLiu_QFPs_SolWind14.pdf)

Quasi-periodic, fast-mode, propagating wave trains (QFPs) are a new observational phenomenon recently discovered in the solar corona by the Solar Dynamics Observatory with extreme ultraviolet (EUV) imaging observations. They originate from flares and propagate at speeds up to  $\sim 2000$  km s<sup>-1</sup> within funnel-shaped waveguides in the wakes of coronal mass ejections (CMEs). QFPs can carry sufficient energy fluxes required for coronal heating during their occurrences. They can provide new diagnostics for the solar corona and their associated flares. We present recent observations of QFPs focusing on their spatio-temporal properties, temperature dependence, and statistical correlation with flares and CMEs. Of particular interest is the **2010-Aug-01** C3.2 flare with correlated QFPs and drifting zebra and fiber radio bursts, which might be different manifestations of the same fast-mode wave trains. We also discuss the potential roles of QFPs in accelerating and/or modulating the solar wind.

## Structure, Stability, and Evolution of Magnetic Flux Ropes from the Perspective of Magnetic Twist

Rui [Liu](#), Bernhard Kliem, Viacheslav S. Titov, [Jun Chen](#), [Yuming Wang](#), [Haimin Wang](#), [Chang Liu](#), [Yan Xu](#), [Thomas Wiegelmann](#)

ApJ 818 148 2016

<http://arxiv.org/pdf/1512.02338v1.pdf>

We investigate the evolution of NOAA Active Region 11817 during **2013 August 10--12**, when it developed a complex field configuration and produced four confined, followed by two eruptive, flares. These C-and-above flares are all associated with a magnetic flux rope (MFR) located along the major polarity inversion line, where shearing and converging photospheric flows are present. Aided by the nonlinear force-free field modeling, we identify the MFR through mapping magnetic connectivities and computing the twist number  $T_w$  for each individual field line. The MFR is moderately twisted ( $|T_w| < 2$ ) and has a well-defined boundary of high squashing factor  $Q$ . We found that the field line with the extremum  $|T_w|$  is a reliable proxy of the rope axis, and that the MFR's peak  $|T_w|$  temporarily increases within half an hour before each flare while it decreases after the flare peak for both confined and eruptive flares. This pre-flare increase in  $|T_w|$  has little effect on the active region's free magnetic energy or any other parameters derived for the whole region, due to its moderate amount and the MFR's relatively small volume, while its decrease after flares is clearly associated with the stepwise decrease in free magnetic energy due to the flare. We suggest that  $T_w$  may serve as a useful parameter in forewarning the onset of eruption, and therefore, the consequent space weather effects. The helical kink instability is identified as the prime candidate onset mechanism for the considered flares.

## A SOLAR CORONAL JET EVENT TRIGGERS A CORONAL MASS EJECTION

Jiajia [Liu](#), Yuming Wang, Chenglong Shen, Kai Liu, Zonghao Pan, and S. Wang  
2015 ApJ 813 115

<http://arxiv.org/pdf/1511.06110v1.pdf>

In this paper, we present multi-point, multi-wavelength observations and analysis of a solar coronal jet and coronal mass ejection (CME) event. Employing the GCS model, we obtained the real (three-dimensional) heliocentric distance and direction of the CME and found it to propagate at a high speed of over 1000 km s<sup>-1</sup>. The jet erupted before the CME and shared the same source region. The temporal and spacial relationship between these two events lead us to the possibility that the jet triggered the CME and became its core. This scenario hold the promise of enriching our understanding of the triggering mechanism of CMEs and their relations to coronal large-scale jets. On the other hand, the magnetic field configuration of the source region observed by the Solar Dynamics Observatory (SDO)/HMI

instrument along with the off-limb inverse Y-shaped configuration observed by SDO/AIA in the 171 Å passband provide the first detailed observation of the three-dimensional reconnection process of a large-scale jet as simulated in Pariat et al. The eruption process of the jet highlights the importance of filament-like material during the eruption of not only small-scale X-ray jets, but likely also of large-scale EUV jets. Based on our observations and analysis, we propose the most probable mechanism for the whole event, with a blob structure overlaying the three-dimensional structure of the jet, to describe the interaction between the jet and the CME. **January 15th 2013**

### **First High-resolution Spectroscopic Observations of an Erupting Prominence Within a Coronal Mass Ejection by the Interface Region Imaging Spectrograph (IRIS)**

Wei **Liu**, Bart De Pontieu, Jean-Claude Vial, Alan M. Title, Mats Carlsson, Han Uitenbroek, Takenori J. Okamoto, Thomas E. Berger, Patrick Antolin  
ApJ **803** 85 **2015**

<http://arxiv.org/pdf/1502.04738v1.pdf>

Spectroscopic observations of prominence eruptions associated with coronal mass ejections (CMEs), although relatively rare, can provide valuable plasma and 3D geometry diagnostics. We report the first observations by the Interface Region Imaging Spectrograph (IRIS) mission of a spectacular fast CME/prominence eruption associated with an equivalent X1.6 flare on **2014 May 9**. The maximum plane-of-sky and Doppler velocities of the eruption are 1200 and 460 km/s, respectively. There are two eruption components separated by ~200 km/s in Doppler velocity: a primary, bright component and a secondary, faint component, suggesting a hollow, rather than solid, cone-shaped distribution of material. The eruption involves a left-handed helical structure undergoing counter-clockwise (viewed top-down) unwinding motion. There is a temporal evolution from upward eruption to downward fallback with less-than-free-fall speeds and decreasing nonthermal line widths. We find a wide range of Mg II k/h line intensity ratios (less than ~2 expected for optically-thin thermal emission): the lowest ever-reported median value of 1.17 found in the fallback material and a comparably high value of 1.63 in nearby coronal rain and intermediate values of 1.53 and 1.41 in the two eruption components. The fallback material exhibits a strong ( $>5\sigma$ ) linear correlation between the k/h ratio and the Doppler velocity as well as the line intensity. We demonstrate that Doppler dimming of scattered chromospheric emission by the erupted material can potentially explain such characteristics.

### **Early Evolution of an Energetic Coronal Mass Ejection and Its Relation to EUV Waves**

Rui **Liu**, Yuming Wang, and Chenglong Shen

E-print, Oct **2014 File**; ApJ, 797 37 **2014**;

<http://arxiv.org/pdf/1410.1960v1.pdf>

We study a coronal mass ejection (CME) associated with an X-class flare, whose initiation is clearly observed in low corona with high-cadence, high-resolution EUV images, providing us a rare opportunity to witness the early evolution of an energetic CME in detail. The eruption starts with a slow expansion of cool overlying loops (~1 MK) following a jet-like event in the periphery of the active region. Underneath the expanding loop system a reverse S-shaped dimming is seen immediately above the brightening active region in hot EUV passbands. The dimming is associated with a rising diffuse arch (~6 MK), which we interpret as a preexistent, high-lying flux rope. This is followed by the arising of a double hot channel (~10 MK) from the core of the active region. The higher structures rise earlier and faster than lower ones, with the leading front undergoing extremely rapid acceleration up to 35 km s<sup>-2</sup>. This suggests that the torus instability is the major eruption mechanism and that it is the high-lying flux rope rather than the hot channels that drives the eruption. The compression of coronal plasmas skirting and overlying the expanding loop system, whose aspect ratio h/r increases with time as a result of the rapid upward acceleration, plays a significant role in driving an outward-propagating global EUV wave and a sunward-propagating local EUV wave, respectively. **2013 May 15**

### **Sun-to-Earth Characteristics of Two Coronal Mass Ejections Interacting near 1 AU: Formation of a Complex Ejecta and Generation of a Two-Step Geomagnetic Storm**

Ying D. **Liu**, Zhongwei Yang, Rui Wang, Janet G. Luhmann, John D. Richardson, Noé Lugaz  
ApJL, **2014**

<http://arxiv.org/pdf/1409.2954v1.pdf>

On **2012 September 30 - October 1** the Earth underwent a two-step geomagnetic storm. We examine the Sun-to-Earth characteristics of the coronal mass ejections (CMEs) responsible for the geomagnetic storm with combined heliospheric imaging and in situ observations. The first CME, which occurred on **2012 September 25**, is a slow event and shows an acceleration followed by a nearly invariant speed in the whole Sun-Earth space. The second event, launched from the Sun on **2012 September 27**, exhibits a quick acceleration, then a rapid deceleration and finally a nearly constant speed, a typical Sun-to-Earth propagation profile for fast CMEs [liu13]. These two CMEs interacted near 1 AU as predicted by the heliospheric imaging observations and formed a complex ejecta observed at Wind, with a shock inside that enhanced the pre-existing southward magnetic field. Reconstruction of the complex ejecta with the in situ data indicates an overall left-handed flux rope-like configuration, with an embedded concave-outward shock front, a maximum magnetic field strength deviating from the flux rope axis and convex-outward field lines ahead of the shock. While the reconstruction results are consistent with the picture of CME-CME interactions, a magnetic cloud-like structure without clear signs of CME interactions [lugaz14] is anticipated when the merging process is finished.

## When and how does a Prominence-like Jet Gain Kinetic Energy?

Jiajia [Liu](#), Yuming Wang<sup>1</sup>, Rui Liu, Quanhao Zhang, Kai Liu, Chenglong Shen, and S. Wang  
2014 ApJ 782 94

<http://arxiv.org/pdf/1401.0736v3.pdf>

A jet is a considerable amount of plasma being ejected from the chromosphere or lower corona into the higher corona and is a common phenomenon. Usually, a jet is triggered by a brightening or a flare, which provides the first driving force to push plasma upward. In this process, magnetic reconnection is thought to be the mechanism to convert magnetic energy into thermal, nonthermal, and kinetic energies. However, most jets could reach an unusual high altitude and end much later than the end of its associated flare. This fact implies that there is another way to continuously transfer magnetic energy into kinetic energy even after the reconnection. The picture described above is well known in the community, but how and how much magnetic energy is released through a way other than reconnection is still unclear. By studying a prominence-like jet observed by SDO/AIA and STEREO-A/EUVI, we find that *the continuous relaxation of the post-reconnection magnetic field structure is an important process for a jet to climb up higher than it could through only reconnection*. The kinetic energy of the jet gained through the relaxation is 1.6 times that gained from the reconnection. The resultant energy flux is hundreds of times larger than the flux required for the local coronal heating, suggesting that such jets are a possible source to keep the corona hot. Furthermore, rotational motions appear all the time during the jet. Our analysis suggests that torsional Alfvén waves induced during reconnection could not be the only mechanism to release magnetic energy and drive jets. **2012 July 8**

## EVIDENCE FOR SOLAR TETHER-CUTTING MAGNETIC RECONNECTION FROM CORONAL FIELD EXTRAPOLATIONS

CHANG [LIU](#)<sup>1</sup>, NA DENG<sup>1</sup>, JEONGWOO LEE<sup>1,2</sup>, THOMAS WIEGELMANN<sup>3</sup>, RONALD L. MOORE<sup>4</sup>, AND HAIMIN WANG<sup>1</sup>

E-print, Oct 2013, <http://arxiv.org/pdf/1310.5098v1.pdf>; 2013 ApJ 778 L36

Magnetic reconnection is one of the primary mechanisms for triggering solar eruptive events, but direct observation of its rapid process has been of challenge. In this Letter we present, using a nonlinear force-free field (NLFFF) extrapolation technique, a visualization of field line connectivity changes resulting from tether-cutting reconnection over about 30 minutes during the **2011 February 13** M6.6 flare in NOAA AR 11158. Evidence for the tether-cutting reconnection was first collected through multiwavelength observations and then by the analysis of the field lines traced from positions of four conspicuous flare 1700 Å footpoints observed at the event onset. Right before the flare, the four footpoints are located very close to the regions of local maxima of magnetic twist index. Especially, the field lines from the inner two footpoints form two strongly twisted flux bundles (up to  $\sim 1.2$  turns), which shear past each other and reach out close to the outer two footpoints, respectively. Immediately after the flare, the twist index of regions around the footpoints greatly diminish and the above field lines become low lying and less twisted ( $\sim 0.6$  turns), overarched by loops linking the later formed two flare ribbons. About 10% of the flux ( $\sim 3 \times 10^{19}$  Mx) from the inner footpoints has undergone a footpoint exchange. This portion of flux originates from the edge regions of the inner footpoints that are brightened first. These rapid changes of magnetic field connectivity inferred from the NLFFF extrapolation are consistent with the tether-cutting magnetic reconnection model.

## Dynamical Processes At the Vertical Current Sheet Behind an Erupting Flux Rope

Rui [Liu](#)

MNRAS Volume 434, Issue 2, 11 September 2013, Pages 1309–1320

<https://sci-hub.tw/10.1093/mnras/stt1090>

We report in this paper a solar eruptive event, in which a vertical current sheet (VCS) is observed in the wake of an erupting flux rope in the SDO/AIA 131-Å passband. The VCS is first detected following the impulsive acceleration of the erupting flux rope but prior to the onset of a nonthermal HXR/microwave burst, with plasma blobs moving upward at speeds up to 1400 km s<sup>-1</sup> along the sheet. The timing suggests that the VCS with plasma blobs might not be the primary accelerator for nonthermal electrons emitting HXRs/microwaves. The initial, slow acceleration of the erupting structure is associated with the slow elevation of a thermal looptop HXR source and the subsequent, impulsive acceleration is associated with the downward motion of the looptop source. We find that the plasma blobs moving downward within the VCS into the cusp region and the flare loops retracting from the cusp region make a continuous process, with the former apparently initiating the latter, which provides a 3D perspective on reconnections at the VCS. We also identify a dark void moving within the VCS toward the flare arcade, which suggests that dark voids in supra-arcade downflows are of the same origin as plasma blobs within the VCS. **19 July 2012**

## ON SUN-TO-EARTH PROPAGATION OF CORONAL MASS EJECTIONS

Ying D. [Liu](#)<sup>1,2</sup>, Janet G. Luhmann<sup>2</sup>, Noé Lugaz<sup>3</sup>, Christian Möstl<sup>2,4</sup>, Jackie A. Davies<sup>5</sup>, Stuart D. Bale<sup>2</sup>, and Robert P. Lin

2013 ApJ 769 45

[http://sprg.ssl.berkeley.edu/~liuxying/pubs/2013\\_apj\\_prop.pdf](http://sprg.ssl.berkeley.edu/~liuxying/pubs/2013_apj_prop.pdf)

We investigate how coronal mass ejections (CMEs) propagate through, and interact with, the inner heliosphere between the Sun and Earth, a key question in CME research and space weather forecasting. CME Sun-to-Earth kinematics are constrained by combining wide-angle heliospheric imaging observations, interplanetary radio type II bursts, and in situ measurements from multiple vantage points. We select three events for this study, the 2012 January 19, 23, and March 7 CMEs. Different from previous event studies, this work attempts to create a general picture for CME Sun-to-Earth propagation and compare different techniques for determining CME interplanetary kinematics. Key results are obtained concerning CME Sun-to-Earth propagation: (1) the Sun-to-Earth propagation of fast CMEs can be approximately formulated into three phases: an impulsive acceleration, then a rapid deceleration, and finally a nearly constant speed propagation (or gradual deceleration); (2) the CMEs studied here are still accelerating even after the flare maximum, so energy must be continuously fed into the CME even after the time of the maximum heating and radiation has elapsed in the corona; (3) the rapid deceleration, presumably due to interactions with the ambient medium, mainly occurs over a relatively short timescale following the acceleration phase; and (4) CME-CME interactions seem a common phenomenon close to solar maximum. Our comparison between different techniques (and data sets) has important implications for CME observations and their interpretations: (1) for the current cases, triangulation assuming a compact CME geometry is more reliable than triangulation assuming a spherical front attached to the Sun for distances below 50-70 solar radii from the Sun, but beyond about 100 solar radii we would trust the latter more; (2) a proper treatment of CME geometry must be performed in determining CME Sun-to-Earth kinematics, especially when the CME propagation direction is far away from the observer; and (3) our approach to comparing wide-angle heliospheric imaging observations with interplanetary radio type II bursts provides a novel tool in investigating CME propagation characteristics. Future CME observations and space weather forecasting are discussed based on these results.

### **CONTRACTING AND ERUPTING COMPONENTS OF SIGMOIDAL ACTIVE REGIONS**

Rui Liu<sup>1,2</sup>, Chang Liu<sup>2</sup>, Tibor Török<sup>3</sup>, Yuming Wang<sup>1</sup>, and Haimin Wang

2012 ApJ 757 150

It has recently been noted that solar eruptions can be associated with the contraction of coronal loops that are not involved in magnetic reconnection processes. In this paper, we investigate five coronal eruptions originating from four sigmoidal active regions, using high-cadence, high-resolution narrowband EUV images obtained by the Solar Dynamic Observatory (SDO). The magnitudes of the flares associated with the eruptions range from GOES class B to class X. Owing to the high-sensitivity and broad temperature coverage of the Atmospheric Imaging Assembly (AIA) on board SDO, we are able to identify both the contracting and erupting components of the eruptions: the former is observed in cold AIA channels as the contracting coronal loops overlying the elbows of the sigmoid, and the latter is preferentially observed in warm/hot AIA channels as an expanding bubble originating from the center of the sigmoid. The initiation of eruption always precedes the contraction, and in the energetically mild events (B- and C-flares), it also precedes the increase in GOES soft X-ray fluxes. In the more energetic events, the eruption is simultaneous with the impulsive phase of the nonthermal hard X-ray emission. These observations confirm that loop contraction is an integrated process in eruptions with partially opened arcades. The consequence of contraction is a new equilibrium with reduced magnetic energy, as the contracting loops never regain their original positions. The contracting process is a direct consequence of flare energy release, as evidenced by the strong correlation of the maximal contracting speed, and strong anti-correlation of the time delay of contraction relative to expansion, with the peak soft X-ray flux. This is also implied by the relationship between contraction and expansion, i.e., their timing and speed.

### **INTERACTIONS BETWEEN CORONAL MASS EJECTIONS VIEWED IN COORDINATED IMAGING AND IN SITU OBSERVATIONS**

Ying D. Liu<sup>1,2</sup>, Janet G. Luhmann<sup>1</sup>, Christian Möstl<sup>1,3,4</sup>, Juan C. Martinez-Oliveros<sup>1</sup>, Stuart D. Bale<sup>1</sup>, Robert P. Lin<sup>1,5</sup>, Richard A. Harrison<sup>6</sup>, Manuela Temmer<sup>3</sup>, David F. Webb<sup>7</sup> and Dusan Odstrcil

2012 ApJ 746 L15

The successive coronal mass ejections (CMEs) from **2010 July 30 to August 1** present us the first opportunity to study CME-CME interactions with unprecedented heliospheric imaging and in situ observations from multiple vantage points. We describe two cases of CME interactions: merging of two CMEs launched close in time and overtaking of a preceding CME by a shock wave. The first two CMEs on August 1 interact close to the Sun and form a merged front, which then overtakes the July 30 CME near 1 AU, as revealed by wide-angle imaging observations. Connections between imaging observations and in situ signatures at 1 AU suggest that the merged front is a shock wave, followed by two ejecta observed at Wind which seem to have already merged. In situ measurements show that the CME from July 30 is being overtaken by the shock at 1 AU and is significantly compressed, accelerated, and heated. The interaction between the preceding ejecta and shock also results in variations in the shock strength and structure on a global scale, as shown by widely separated in situ measurements from Wind and STEREO B. These results indicate important implications of CME-CME interactions for shock propagation, particle acceleration, and space weather forecasting.

### **SOLAR SOURCE AND HELIOSPHERIC CONSEQUENCES OF THE 2010 APRIL 3 CORONAL MASS EJECTION: A COMPREHENSIVE VIEW**

Ying [Liu](#)<sup>1</sup>, Janet G. Luhmann<sup>1</sup>, Stuart D. Bale<sup>1</sup> and Robert P. Lin

2011 ApJ 734 84, [File](#)

We study the solar source and heliospheric consequences of the 2010 April 3 coronal mass ejection (CME) in the frame of the Sun-Earth connection using observations from a fleet of spacecraft. The CME is accompanied by a B7.4 long-duration flare, dramatic coronal dimming, and EUV waves. It causes significant heliospheric consequences and space weather effects such as radio bursts, a prominent shock wave, the largest/fastest interplanetary CME at 1 AU since the 2006 December 13 CME, the first gradual solar energetic particle (SEP) events in solar cycle 24, and a prolonged geomagnetic storm resulting in a breakdown of the Galaxy 15 satellite. This event, together with several following periods of intense solar activities, indicates awakening of the Sun from a long minimum. The CME EUV loop begins to rise at least 10 minutes before the flare impulsive phase. The associated coronal wave forms an envelope around the CME, a large-scale three-dimensional structure that can only be explained by a pressure wave. The CME and its preceding shock are imaged by both STEREO A and B almost throughout the whole Sun-Earth space. CME kinematics in the ecliptic plane are obtained as a function of distance out to 0.75 AU by a geometric triangulation technique. The CME has a propagation direction near the Sun-Earth line and a speed that first increases to 1000-1100 km s<sup>-1</sup> and then decreases to about 800 km s<sup>-1</sup>. Both the predicted arrival time and speed at the Earth are well confirmed by the in situ measurements. The gradual SEP events observed by three widely separated spacecraft show time profiles much more complicated than suggested by the standard conceptual picture of SEP event heliolongitude distribution. Evolving shock properties, the realistic time-dependent connection between the observer and shock source, and a possible role of particle perpendicular diffusion may be needed to interpret this SEP event spatial distribution.

### **Downstream structure and evolution of a simulated CME-driven sheath in the solar corona**

Y. C.-M. [Liu](#), M. Opher, Y. Wang and T. I. Gombosi

A&A 527, A46 (2011), [File](#)

**Context.** The transition of the magnetic field from the ambient magnetic field to the ejecta in the sheath downstream of a coronal mass ejection (CME) driven shock is analyzed in detail. The field rotation in the sheath occurs in a two-layer structure. In the first layer, layer 1, the magnetic field rotates in the coplanarity plane (plane of shock normal and the upstream magnetic field), and in layer 2 rotates off this plane. We investigate the evolution of the two layers as the sheath evolves away from the Sun.

**Aims.** In situ observations have shown that the magnetic field in the sheath region in front of an interplanetary coronal mass ejection (ICME) form a planar magnetic structure, and the magnetic field lines drape around the flux tube. Our objective is to investigate the magnetic configuration of the CME near the sun.

**Methods.** We used the space weather modeling framework (SWMF), a 3D magnetohydrodynamics (MHD) simulation code, to simulate the propagation of CMEs and the shock driven by it.

**Results.** We find that close to the Sun, layer 2 dominates the width of the sheath, diminishing its importance as the sheath evolves away from the Sun, in agreement with observations at 1 AU.

### **Sigmoid-to-Flux-Rope Transition Leading to A Loop-Like Coronal Mass Ejection**

Rui [Liu](#)<sup>1</sup>, Chang Liu<sup>1</sup>, Shuo Wang<sup>1</sup>, Na Deng, and Haimin Wang

E-print, Nov 2010, ApJL, 725:L84-L90, 2010; [File](#)

Sigmoids are one of the most important precursor structures for solar eruptions. In this Letter, we study a sigmoid eruption on **2010 August 1** with EUV data obtained by the Atmospheric Imaging Assembly (AIA) on board the Solar Dynamic Observatory (SDO). In AIA 94 Å (Fe XVIII; 6 MK), topological reconfiguration due to tether-cutting reconnection is unambiguously observed for the first time, i.e., two opposite J-shaped loops reconnect to form a continuous S-shaped loop, whose central portion is dipped and aligned along the magnetic polarity inversion line (PIL), and a compact loop crossing the PIL. A causal relationship between photospheric flows and coronal tether-cutting reconnections is evidenced by the detection of persistent converging flows toward the PIL using line-of-sight magnetograms obtained by the Helioseismic and Magnetic Imager (HMI) on board SDO. The S-shaped loop remains in quasi-equilibrium in the lower corona for about 50 minutes, with the central dipped portion rising slowly at ~10 km s<sup>-1</sup>. The speed then increases to ~60 km s<sup>-1</sup> about 10 minutes prior to the onset of a GOES-class C3.2 flare, as the S-shaped loop speeds up its transformation into an arch-shaped loop, which eventually leads to a loop-like coronal mass ejection (CME). The AIA observations combined with H $\alpha$  filtergrams as well as hard X-ray (HXR) imaging and spectroscopy are consistent with most flare loops being formed by reconnection of the stretched legs of less-sheared J-shaped loops that envelopes the rising flux rope, in agreement with the standard tether-cutting scenario.

### **A Reconnecting Current Sheet Imaged in A Solar Flare**

Rui [Liu](#), Jeongwoo Lee, Tongjiang Wang, Guillermo Stenborg, Chang Liu, Haimin Wang

E-print, Sept 2010, [File](#) ; ApJL, 723, L28, 2010

Magnetic reconnection changes the magnetic field topology and powers explosive events in astrophysical, space and laboratory plasmas. For flares and coronal mass ejections (CMEs) in the solar atmosphere, the standard model predicts the presence of a reconnecting current sheet, which has been the subject of considerable theoretical and numerical modeling over the last fifty years, yet direct, unambiguous observational verification has been absent. In this Letter we

show a bright sheet structure of global length ( $>0.25 R_{\text{sun}}$ ) and macroscopic width  $((5 - 10) \times 10^3 \text{ km})$  distinctly above the cusp-shaped flaring loop, imaged during the flare rising phase in EUV. The sheet formed due to the stretch of a transequatorial loop system, and was accompanied by various reconnection signatures that have been dispersed in the literature. This unique event provides a comprehensive view of the reconnection geometry and dynamics in the solar corona. **2004 July 29, slow drifting radio continuum**

## **Gradual Inflation of Active-Region Coronal Arcades Building up to Coronal Mass Ejections**

Rui [Liu](#), Chang Liu, Sung-Hong Park and Haimin Wang

BBSO preprint #1433, *Astrophysical Journal*, 723:229–240, **2010**, [File](#)

The pre-CME structure is of great importance to understanding the origin of CMEs, which, however, has been largely unknown for CMEs originating from active regions. In this paper, selected for studying are 16 active-region coronal arcades whose gradual inflation lead up to CMEs. 12 of them clearly build upon post-eruptive arcades resulting from a preceding eruption. The observed inflation sustains for  $8.7 \pm 4.1 \text{ h}$ , with the arcade rising from  $1.15 \pm 0.06 R_{\odot}$  to  $1.36 \pm 0.07 R_{\odot}$  within the EIT field of view (FOV). The rising speed is less than  $5 \text{ km s}^{-1}$  for most of the time. Only at the end of this quasi-static stage, it increases to tens of kilometers per second over tens of minutes. The arcade then erupts out of the EIT FOV as a CME with similar morphology. This pre-CME structure is apparently unaffected by the flares occurring during its quasi-static inflation phase, but is closely coupled with the flare occurring during its acceleration phase. For four events that were observed on the disk, it is found that the gradual inflation of the arcade is accompanied by significant helicity injection from photosphere. In particular, a swirling structure, which is reminiscent of a magnetic flux rope, was observed in one of the arcades over 4 h prior to the subsequent CME, and the growth of the arcade is associated with the injection of helicity of opposite sense into the active region via flux emergence. We propose a four-phase evolution paradigm for the observed CMEs, i.e., a quasi-static inflation phase which corresponds to the buildup of magnetic free energy in the corona, followed by the frequently observed three-phase paradigm, including an initial phase, an acceleration phase and a gradual phase.

## **Successive Solar Flares and Coronal Mass Ejections on 2005 September 13 from NOAA AR 10808**

Chang [Liu](#), Jeongwoo Lee, Marian Karlicky, Debi Prasad Choudhary, Na Deng, and Haimin Wang  
E-print, Aug **2009**; *ApJ*, 703:757–768, **2009** September 20

We present a multiwavelength study of the **2005 September 13** eruption from NOAA 10808 that produced total four flares and two fast coronal mass ejections (CMEs) within 1.5 hours. Our primary attention is paid to the fact that these eruptions occurred in close succession in time, and that all of them were located along an S-shaped magnetic polarity inversion line (PIL) of the active region. In our analysis, (1) the disturbance created by the first flare propagated southward along the PIL to cause a major filament eruption that led to the first CME and the associated second flare underneath. (2) The first CME partially removed the overlying magnetic fields over the northern Delta spot to allow the third flare and the second CME. (3) The ribbon separation during the fourth flare would indicate reclosing of the overlying field lines opened by the second CME. It is thus concluded that this series of flares and CMEs are interrelated to each other via magnetic reconnections between the expanding magnetic structure and the nearby magnetic fields. These results complement previous works made on this event with the suggested causal relationship among the successive eruptions.

## **CORONAL MASS EJECTIONS AND GLOBAL CORONAL MAGNETIC FIELD RECONFIGURATION**

Ying [Liu](#)<sup>1</sup>, Janet G. Luhmann<sup>1</sup>, Robert P. Lin<sup>1</sup>, Stuart D. Bale<sup>1</sup>, Angelos Vourlidas<sup>2</sup>, and Gordon J. D. Petrie<sup>3</sup>

*Astrophysical Journal*, 698:L51–L55, **2009**, [File](#)

We investigate the role of coronal mass ejections (CMEs) in the global coronal magnetic field reconfiguration, a debate that has lasted for about two decades. Key evidence of the coronal field restructuring during the **2007 December 31** CME is provided by combining imaging observations from widely separated spacecraft with the potential-field source-surface (PFSS) model, thanks to the extraordinarily quiet Sun at the present solar minimum. The helmet streamer, previously disrupted by the CME, re-forms but is displaced southward permanently; the preexisting heliospheric plasma sheet (HPS) is also disrupted as evidenced by the concave-outward shape of the CME. The south polar coronal hole shrinks considerably. Plasma blobs moving outward along the newly formed HPS suggest the occurrence of magnetic reconnection between the fields blown open by the CME and the ambient adjacent open fields. A streamer-like structure is also observed in the wake of the CME and interpreted as a plasma sheet where the thin post-CME current sheet is embedded. These results are important for understanding the coronal field evolution over a solar cycle as well as the complete picture of CME initiation and propagation.

## **(CME) GLE Events and Magnetic Field in Source Regions**

Yang [Liu](#)

## **Presentation at “Ground Level Enhancement (GLE)”**

Comparative Data Analysis Workshop (CDAW), LMSAL, Jan 6-9, 2009

The purpose of this research is to study influence of background field for propagation of halo CMEs.

The background field was found to have two different configurations: current sheet and non-current sheet (see, e. g. Shultz 1973; Wilcox et al. 1980; Neugebauer et al. 2002, 2004).

Summary:

- Types 2 & 3 CMEs appear to be significantly faster than type 1. This effect is not biased by flare importance.
- It is shown that the background magnetic configuration associated with halo CMEs does play a role in deciding the speeds of the CMEs.
- A correlation was found between the speed of type 3 CMEs and the peak of X-ray flux of the associated flares.

## **RELATIONSHIP BETWEEN A CORONAL MASS EJECTION-DRIVEN SHOCK AND A CORONAL METRIC TYPE II BURST**

Y. Liu, J. G. Luhmann, S. D. Bale, and R. P. Lin

ApJL 691 L151-L155 2009; File

<http://www.iop.org/EJ/abstract/1538-4357/691/2/L151>

It has been an intense matter of debate whether coronal metric type II bursts are generated by coronal mass ejection (CME)-driven shocks or flare blast waves. Using unprecedented high-cadence observations from STEREO/SECCHI, we investigate the relationship between a metric type II event and a shock driven by the **2007 December 31 CME**. The existence of the CME-driven shock is indicated by the remote deflection of coronal structures, which is in good timing with the metric type II burst. The CME speed is about 600 km s<sup>-1</sup> when the metric type II burst occurs, much larger than the Alfvén speed of 419-489 km s<sup>-1</sup> determined from band splitting of the type II burst. A causal relationship is well established between the metric and decametric-hectometric type II bursts. The shock height-time curve determined from the type II bands is also consistent with the shock propagation obtained from the streamer deflection. These results provide unambiguous evidence that the metric type II burst is caused by the CME-driven shock.

## **A Comprehensive View of the 2006 December 13 CME: From the Sun to Interplanetary Space**

Y. Liu, J. G. Luhmann, R. Muller-Mellin, P. C. Schroeder, L. Wang, R. P. Lin, S. D. Bale, Y. Li, M. H. Acuna, and J.-A. Sauvaud

The Astrophysical Journal, Vol. 689, No. 1: 563-571, 2008.

<http://www.journals.uchicago.edu/doi/abs/10.1086/592031>

The biggest halo coronal mass ejection (CME) since the Halloween storm in 2003, which occurred on 2006 December 13, is studied in terms of its solar source and heliospheric consequences. The CME was accompanied by an X3.4 flare, EUV dimmings, and coronal waves. It generated significant space weather effects such as an interplanetary shock, radio bursts, major solar energetic particle (SEP) events, and a magnetic cloud (MC) that were detected by a fleet of spacecraft including STEREO, ACE, WIND, and Ulysses. Reconstruction of the MC with the Grad-Shafranov (GS) method yields an axis orientation oblique to the flare ribbons. Observations of the SEP intensities and anisotropies show that the particles can be trapped, deflected, and reaccelerated by the large-scale transient structures. The CME-driven shock was observed at both the Earth and Ulysses when they were separated by 74° in latitude and 117° in longitude, which is the largest shock extent ever detected. The ejecta seem to have been missed at Ulysses. The shock arrival time at Ulysses is well predicted by an MHD model that can propagate the 1 AU data outward. The CME/shock is tracked remarkably well from the Sun all the way to Ulysses by coronagraph images, type II frequency drift, in situ measurements, and the MHD model. These results reveal a technique that combines MHD propagation of the solar wind and type II emissions to predict the shock arrival time at the Earth, which is a significant advance for space weather forecasting, especially when in situ data become available from the Solar Orbiter and Solar Sentinels.

## **A Simulation of a Coronal Mass Ejection Propagation and Shock Evolution in the Lower Solar Corona**

Y. C.-M. Liu, M. Opher, O. Cohen, P. C. Liewer, and T. I. Gombosi

The Astrophysical Journal, Vol. 680, No. 1: 757-763, 2008.

<http://www.journals.uchicago.edu/doi/pdf/10.1086/587867>

We present a detailed simulation of the evolution of a moderately slow coronal mass ejection (CME; 800 km s<sup>-1</sup> at 5 R<sub>⊙</sub>, where R<sub>⊙</sub> is solar radii) in the lower solar corona (2Y5 R<sub>⊙</sub>). The configuration of the Sun's magnetic field is based on the MDI data for the solar surface during Carrington rotation 1922. The pre-CME background solar wind is generated using the Wang-Sheeley-Argé (WSA) model. To initiate a CME, we inserted a modified Titov-Demoulin flux rope in an active region near the solar equator using the SpaceWeather Modeling Framework (SWMF). After the initiation stage (within 2.5 R<sub>⊙</sub>), the CME evolves at a nearly constant and slow acceleration of the order of 100 ms<sup>-2</sup>, which corresponds to an intermediate-acceleration CME. Detailed analysis of the pressures shows that the thermal



pressure accounts for most of the acceleration of the CME. The magnetic pressure contributes to the acceleration early in the evolution and becomes negligible when the CME moves beyond  $\sim 3 R_{\odot}$ . We also present the evolution of the shock geometry near the nose of the CME, which shows that the shock is quasi parallel most of the time.

## **A Study of Surges: II. On the Relationship between Chromospheric Surges and Coronal Mass Ejections**

Yu **Liu**

Solar Phys (2008) 249: 75–84; **File**

<http://www.springerlink.com/content/ur823033873g4m50/fulltext.pdf>

Liu *et al.* (*Astrophys. J.* **628**, 1056, 2005a) described one surge – coronal mass ejection (CME) event showing a close relationship between solar chromospheric surge ejection and CME that had not been noted before. In this work, large H $\alpha$  surges ( $> 72$  Mm, or 100 arcsec) are studied. Eight of these were associated with CMEs. According to their distinct morphological features, H $\alpha$  surges can be classified into three types: jetlike, diffuse, and closed loop. It was found that all of the jetlike surges were associated with jetlike CMEs (with angular widths  $\leq 30$  degrees); the diffuse surges were all associated with wide-angle CMEs (*e.g.*, halo); the closed-loop surges were not associated with CMEs. The exclusive relation between H $\alpha$  surges and CMEs indicates difference in magnetic field configurations. The jetlike surges and related narrow CMEs propagate along coronal fields that are originally open. The unusual transverse mass motions in the diffuse surges are suggested to be due to magnetic reconnections in the corona that produce wide-angle CMEs. For the closed loop surges, their paths are just outlining stable closed loops close to the solar surface. Thus no CMEs are associated with them.

## **RECONSTRUCTION OF THE 2007 MAY 22 MAGNETIC CLOUD: HOW MUCH CAN WE TRUST THE FLUX-ROPE GEOMETRY OF CMES?**

Y. **Liu**, G. Luhmann,<sup>1</sup> K. E. J. Huttunen,<sup>1</sup> R. P. Lin,<sup>1</sup> S. D. Bale,<sup>1</sup> C. T. Russell,<sup>3</sup> and A. B. Galvin<sup>4</sup>  
The Astrophysical Journal, 677:L133–L136, 2008

<http://www.journals.uchicago.edu/doi/pdf/10.1086/587839>

Coronal mass ejections (CMEs) are often assumed to be magnetic flux ropes, but direct proof has been lacking. A key feature, resulting from the translational symmetry of a flux rope, is that the total transverse pressure as well as the axial magnetic field has the same functional form over the vector potential along any crossing of the flux rope. We test this feature (and hence the flux-rope structure) by reconstructing the **2007 May 22** magnetic cloud (MC) observed at *STEREO B*, *Wind/ACE*, and possibly *STEREO A* with the Grad-Shafranov (GS) method. The model output from reconstruction at *STEREO B* agrees fairly well with the magnetic field and thermal pressure observed at *ACE/Wind*; the separation between *STEREO B* and *ACE/Wind* is about 0.06 AU, almost half of the MC radial width. For the first time, we reproduce observations at one spacecraft with data from another well separated spacecraft, which provides compelling evidence for the flux-rope geometry and is of importance for understanding CME initiation and propagation. We also discuss the global configuration of the MC at different spacecraft on the basis of the reconstruction results.

## **DETERMINING THE MAGNETIC FIELD ORIENTATION OF CORONAL MASS EJECTIONS FROM FARADAY ROTATION**

Y. **Liu**,<sup>1,2</sup> W. B. Manchester IV,<sup>3</sup> J. C. Kasper,<sup>1</sup> J. D. Richardson,<sup>1,2</sup> and J. W. Belcher<sup>1</sup>  
The Astrophysical Journal, 665:1439–1447, 2007

<http://www.journals.uchicago.edu/doi/pdf/10.1086/520038>

We describe a method with which to measure the magnetic field orientation of coronal mass ejections (CMEs) using Faraday rotation (FR). Two basic FR profiles, Gaussian-shaped with a single polarity or N-shaped with polarity reversals, are produced by a radio source occulted by a moving flux rope, depending on its orientation. These curves are consistent with Helios observations, providing evidence for the flux rope geometry of CMEs. Many background radio sources can map CMEs in FR onto the sky. We demonstrate with a simple flux rope that the magnetic field orientation and helicity of the flux rope can be determined 2–3 days before it reaches the Earth, which is of crucial importance for space weather forecasting. An FR calculation based on global magnetohydrodynamic (MHD) simulations of CMEs in a background heliosphere shows that FR mapping can also resolve a CME geometry that curves back to the Sun. We discuss implementation of the method using data from the Mileura Widefield Array (MWA).

## **The speed of halo Coronal Mass Ejections and properties of associated active regions**

Adv. Space Res. 39(11), Pages 1767-1772, 2007, **File**

Yang **Liu**

In this study, we looked for any correlations between speed of active region-related halo Coronal Mass Ejections (CMEs) and the energy contained in active regions. Twenty one CMEs from the Coordinated Data Analysis Workshops

(CDAW) event list are chosen to carry out this research. The solar sources of the CMEs have been carefully determined by the CDAW source identification team using various methods. This study shows that (1) there is no correlation between potential energy of active regions and the associated CMEs' speed; (2) there is no correlation between net magnetic flux of active regions and the associated CMEs' speed. Based on a limited sample of eight events that could be adequately modeled for analysis of free energy of the active regions, this study further shows that there is a correlation between free energy density of active regions and speed of the associated CMEs.

### **The Eruption from a Sigmoidal Solar Active Region on 2005 May 13**

Chang [Liu](#), Jeongwoo Lee, Vasyl Yurchyshyn, Na Deng, Kyung-Suk Cho, Marian Karlicky, and Haimin Wang

E-print, July 2007

The most important finding is that the flare brightening starts in the core of the active region earlier than that of the rising motion of the flux rope. This timing clearly addresses one of the main issues in the magnetic eruption onset of sigmoid, namely, whether the eruption is initiated by an internal tether-cutting to allow the flux rope to rise upward or a flux rope rises due to a loss of equilibrium to later induce tether cutting below it. Our high time cadence SXI and Halpha data shows that the first scenario is relevant to this eruption. As other major findings, we have the RHESSI HXR images showing a change of the HXR source from a confined footpoint structure to an elongated ribbon-like structure after the flare maximum, which we relate to the sigmoid-to-arcade evolution. Radio dynamic spectrum shows a type II precursor that occurred at the time of expansion of the sigmoid and a drifting pulsating structure in the flare rising phase in HXR. Finally type II and III bursts are seen at the time of maximum HXR emission, simultaneous with the maximum reconnection rate derived from the flare ribbon motion in UV.

### **Coronal Mass Ejections in July 2005 and an Unusual Heliospheric Event**

M. A. [Livshitsa](#), A. V. Belova, A. I. Shakhovskaya, E. A. Eroshenko, A. R. Osokinc, and L. K. Kashapova

Cosmic Research, **2013**, Vol. 51, No. 5, pp. 326–334.

Kosmicheskie Issledovaniya, **2013**, Vol. 51, No. 5, pp. 363–371.

Using the events in **July 2005** as an example, the causes and peculiarities of Forbush effects produced by solar sources remote from the central zone are discussed. The event in question differs from other effects observed at the periphery of interplanetary disturbances by strong variations in cosmic rays on the background of weak disturbances in the solar wind and magnetic field of the Earth. The cloud of magnetized plasma ejected from the Sun was large and fast, but it passed to the west from the Sun-Earth line. According to performed estimates, the mass of the ejected substance was close to the upper boundary of mass for coronal mass ejections (CMEs). Anomalous parameters and high modulation capability of the formed solar wind disturbance are explained, in particular, by the fact that it combined several CMEs and that the last fast disturbance was prepared by a series of impulsive events in the active region of the Sun. Usually, such a great mass is ejected directly after the main energy release in strong solar flares. In the given case, a powerful MHD disturbance occurred approximately half an hour after a maximum of hard X-ray burst under the conditions when gas pressure in the flare loops became close to magnetic pressure, which was just a premise of the largescale ejection.

### **Physics of post-eruptive solar arcades: Interpretation of RATAN-600 and STEREO spacecraft observations**

M. A. [Livshits](#), A. M. Urnov, F. F. Goryaev, L. K. Kashapova, I. Yu. Grigor'eva & T. I. Kal'tman

*Astronomy Reports*, **2011**, Vol. 55, No. 10, pp. 918–927. [File](#)

*Astronomicheskii Zhurnal*, **2011**, Vol. 88, No. 10, pp. 997–1007.

Results of simultaneous measurements of radiation fluxes from post-eruption arcades on the Sun at 171, 195, 284, and 304 Å (from STEREO spacecraft data) and at radio wavelengths (from the RATAN-600 radio telescope) are presented. An original probabilistic approach developed earlier by Urnov was used to determine the differential emission measure. This method requires no regularization, and the obtained results do not depend on the choice of the temperature grid. This approach has yielded the differential measure of emission at temperatures approximately from 0.3 to 15 MK. The subsequent calculation of thermal magnetobremstrahlung in a multi-temperature model with the magnetic field decreasing with height produces a spectrum similar to that observed on RATAN-600. Thus, in many non-stationary events with modest powers, a thermal multi-temperature model is quite able to explain the emission of post-eruption arcade systems, and it is not necessary to invoke the emission of accelerated particles. The proposed model enables direct estimation of the ratio of the magnetic and gas pressures at the tops of post-eruption arcades, and determination of the conditions required for the origin of secondary nonstationary processes in the decay stage of the main flare. **January 25, 2007**

### **What is a Macrospicule?**

Ivan P. [Loboda](#), [Sergej A. Bogachev](#)

**2019** ApJ 871 230

<https://arxiv.org/pdf/1902.01380.pdf>

Macrospicules are typically described as solar jets that are larger and longer-lived than spicules, and visible mostly in transition-region spectral lines. They show a broad variation in properties, which pose substantial difficulties for their identification, modelling, and the understanding of their role in the mass and energy balance of the solar atmosphere. In this study, we focused on a sub-population of these jets that undergo parabolic trajectories when observed in the He II 304 Å line using high-cadence observations of the Atmospheric Imaging Assembly (AIA) on board the Solar Dynamics Observatory (SDO) to accumulate a statistically significant sample, which included 330 such events. We found these jets to be typically narrow (3-6 Mm), collimated flows of plasma, which reach heights of about 25 Mm, thus being among the smallest jets observed in the extreme ultraviolet (EUV). Combined with the rise velocities of 70-140 km/s and lifetimes of around 15 min, this makes them plausible candidates for the EUV counterpart of type II spicules. Moreover, we have found their dynamics to be inconsistent with a purely ballistic motion; instead, there is a strong correlation between the initial velocities and decelerations of the jets, which indicates that they may be driven by magneto-acoustic shocks with a dominant period of  $10 \pm 2$  min. This makes these EUV jets similar in their dynamics to the conventional, or type I spicules, thus justifying the name of macro-spicules in this case, while a substantial difference in the shock periods (1-2 min for the chromospheric jets) suggests a dissimilarity in the formation conditions.

### **Signatures of two distinct driving mechanisms in the evolution of coronal mass ejections in the lower corona**

[Loesch, C.](#); [Opher, M.](#); [Alves, M. V.](#); [Evans, R. M.](#); [Manchester, W. B.](#)

*J. Geophys. Res.*, Vol. 116, No. A4, A04106, 2011

We present a comparison between two simulations of coronal mass ejections (CMEs), in the lower corona, driven by different flux rope mechanisms presented in the literature. Both mechanisms represent different magnetic field configurations regarding the amount of twist of the magnetic field lines and different initial energies. They are used as a “proof of concept” to explore how different initialization mechanisms can be distinguished from each other in the lower corona. The simulations are performed using the Space Weather Modeling Framework (SWMF) during solar minimum conditions with a steady state solar wind obtained through an empirical approach to mimic the physical processes driving the solar wind. Although the two CMEs possess different initial energies (differing by an order of magnitude) and magnetic configurations, the main observables such as acceleration, shock speed, Mach number, and  $B_n$  (the angle between the shock normal and the upstream magnetic field) present very similar behavior between 2 and 6  $R_\odot$ . We believe that through the analysis of other quantities, such as sheath width and postshock compression (pileup and shock indentation compressions), the effect of different magnetic configurations and initializations can be distinguished. We discuss that coronal models that employ a reduced value of polytropic index ( $\gamma$ ) may significantly change the energetics of the CME and that the background solar wind plays an important role in the CMEs' shock and sheath evolution.

### **The eruption of a magnetic flux rope observed by *Solar Orbiter* and *Parker Solar Probe***

[David M. Long](#), [Lucie M. Green](#), [Francesco Pecora](#), [David H. Brooks](#), +

*ApJ* 955 152 2023

<https://arxiv.org/pdf/2308.14651.pdf>

<https://iopscience.iop.org/article/10.3847/1538-4357/acefd5/pdf>

Magnetic flux ropes are a key component of coronal mass ejections, forming the core of these eruptive phenomena. However, determining whether a flux rope is present prior to eruption onset and, if so, the rope's handedness and the number of turns that any helical field lines make is difficult without magnetic field modelling or in-situ detection of the flux rope. We present two distinct observations of plasma flows along a filament channel on **4 and 5 September 2022** made using the *Solar Orbiter* spacecraft. Each plasma flow exhibited helical motions in a right-handed sense as the plasma moved from the source active region across the solar disk to the quiet Sun, suggesting that the magnetic configuration of the filament channel contains a flux rope with positive chirality and at least one turn. The length and velocity of the plasma flow increased from the first to the second observation, suggesting evolution of the flux rope, with the flux rope subsequently erupting within  $\sim 5$ -hours of the second plasma flow. The erupting flux rope then passed over the *Parker Solar Probe* spacecraft during its Encounter 13, enabling in-situ diagnostics of the structure. Although complex and consistent with the flux rope erupting from underneath the heliospheric current sheet, the in-situ measurements support the inference of a right-handed flux rope from remote-sensing observations. These observations provide a unique insight into the eruption and evolution of a magnetic flux rope near the Sun.

### **Multi-stage reconnection powering a solar coronal jet**

[David M. Long](#), [Lakshmi Pradeep Chitta](#), [Deborah Baker](#), [Iain G. Hannah](#), [Nawin Ngampoopun](#), [David Berghmans](#), [Andrei N. Zhukov](#), [Luca Teriaca](#)

*ApJ* 944 19 2023

<https://arxiv.org/pdf/2301.02034.pdf>

<https://iopscience.iop.org/article/10.3847/1538-4357/acb0c9/pdf>

Coronal jets are short-lived eruptive features commonly observed in polar coronal holes and are thought to play a key role in the transfer of mass and energy into the solar corona. We describe unique contemporaneous observations of a coronal blowout jet seen by the Extreme Ultraviolet Imager onboard the *Solar Orbiter* spacecraft (SO/EUI) and the

Atmospheric Imaging Assembly onboard the Solar Dynamics Observatory (SDO/AIA). The coronal jet erupted from the south polar coronal hole, and was observed with high spatial and temporal resolution by both instruments. This enabled identification of the different stages of a breakout reconnection process producing the observed jet. We find bulk plasma flow kinematics of  $\sim 100$ - $200$  km/s across the lifetime of its observed propagation, with a distinct kink in the jet where it impacted and was subsequently guided by a nearby polar plume. We also identify a faint faster feature ahead of the bulk plasma motion propagating with a velocity of  $\sim 715$  km/s which we attribute to untwisting of newly reconnected field lines during the eruption. A Differential Emission Measure (DEM) analysis using the SDO/AIA observations revealed a very weak jet signal, indicating that the erupting material was likely much cooler than the coronal passbands used to derive the DEM. This is consistent with the very bright appearance of the jet in the Lyman- $\alpha$  passband observed by SO/EUI. The DEM was used to estimate the radiative thermal energy of the source region of the coronal jet, finding a value of  $\sim 2 \times 10^{24}$  ergs, comparable to the energy of a nanoflare. **2021-Sept-14**

### **Plasma evolution within an erupting coronal cavity**

David M. [Long](#), [Louise K. Harra](#), [Sarah A. Matthews](#), [Harry P. Warren](#), [Kyoung-Sun Lee](#), [George Doschek](#), [Hirohisa Hara](#), [Jack M. Jenkins](#)

ApJ 855 74 2018

<https://arxiv.org/pdf/1802.01391.pdf>

<http://iopscience.iop.org/article/10.3847/1538-4357/aaad68/pdf>

Coronal cavities have previously been observed associated with long-lived quiescent filaments and are thought to correspond to the associated magnetic flux rope. Although the standard flare model predicts a coronal cavity corresponding to the erupting flux rope, these have only been observed using broadband imaging data, restricting analysis to the plane-of-sky. We present a unique set of spectroscopic observations of an active region filament seen erupting at the solar limb in the extreme ultraviolet (EUV). The cavity erupted and expanded rapidly, with the change in rise phase contemporaneous with an increase in non-thermal electron energy flux of the associated flare. Hot and cool filamentary material was observed to rise with the erupting flux rope, disappearing suddenly as the cavity appeared. Although strongly blue-shifted plasma continued to be observed flowing from the apex of the erupting flux rope, this outflow soon ceased. These results indicate that the sudden injection of energy from the flare beneath forced the rapid eruption and expansion of the flux rope, driving strong plasma flows which resulted in the eruption of an under-dense filamentary flux rope. **2017-Sept-10**

Hinode/ EIS Nugget April 2018 [http://solarb.mssl.ucl.ac.uk/SolarB/nuggets/nugget\\_2018apr.jsp](http://solarb.mssl.ucl.ac.uk/SolarB/nuggets/nugget_2018apr.jsp)

### **The energetics of a global shock wave in the low solar corona**

David M. [Long](#), [Deborah Baker](#), [David R. Williams](#), [Eoin P. Carley](#), [Peter T. Gallagher](#), [Pietro Zucca](#)

ApJ 2015

<http://arxiv.org/pdf/1412.2964v1.pdf> File

As the most energetic eruptions in the solar system, coronal mass ejections (CMEs) can produce shock waves at both their front and flanks as they erupt from the Sun into the heliosphere. However, the amount of energy produced in these eruptions, and the proportion of their energy required to produce the waves, is not well characterised. Here we use observations of a solar eruption from **2014 February 25** to estimate the energy budget of an erupting CME and the globally-propagating "EIT wave" produced by the rapid expansion of the CME flanks in the low solar corona. The "EIT wave" is shown using a combination of radio spectra and extreme ultraviolet images to be a shock front with a Mach number greater than one. Its initial energy is then calculated using the Sedov-Taylor blast-wave approximation, which provides an approximation for a shock front propagating through a region of variable density. This approach provides an initial energy estimate of  $\approx 2.8 \times 10^{31}$  ergs to produce the "EIT wave", which is approximately 10% the kinetic energy of the associated CME (shown to be  $\approx 2.5 \times 10^{32}$  ergs). These results indicate that the energy of the "EIT wave" may be significant and must be considered when estimating the total energy budget of solar eruptions.

### **Breakout and Tether-Cutting Eruption Models Are Both Catastrophic (Sometimes)**

D. W. [Longcope](#), T. G. Forbes

Solar Physics, June 2014, Volume 289, Issue 6, pp 2091-2122

<http://arxiv.org/pdf/1312.4435v1.pdf>

We present a simplified analytic model of a quadrupolar magnetic field and flux rope to model coronal mass ejections. The model magnetic field is two-dimensional, force-free and has current only on the axis of the flux rope and within two current sheets. It is a generalization of previous models containing a single current sheet anchored to a bipolar flux distribution. Our new model can undergo quasi-static evolution either due to changes at the boundary or due to magnetic reconnection at either current sheet. We find that all three kinds of evolution can lead to a catastrophe, known as loss of equilibrium. Some equilibria can be driven to catastrophic instability either through reconnection at the lower current sheet, known as tether cutting, or through reconnection at the upper current sheet, known as breakout. Other equilibria can be destabilized through only one and not the other. Still others undergo no instability, but they evolve increasingly rapidly in response to slow steady driving (ideal or reconnective). One key feature of every case is a response to reconnection different from that found in simpler systems. In our two-current-sheet model a reconnection electric field in one current sheet causes the current in that sheet to increase rather than decrease. This suggests the possibility for the microscopic reconnection mechanism to run away.

## Modeling and Measuring the Flux Reconnected and Ejected by the Two-Ribbon Flare/CME Event on 7 November 2004

Dana [Longcope](#) · Colin Beveridge · Jiong Qiu · B. Ravindra · Graham Barnes · Sergio Dasso  
Solar Phys, DOI 10.1007/s11207-007-0330-7, 2007

## Estimating the mass of CMEs from the analysis of EUV dimmings

F. M. [López](#)<sup>1,2</sup>, H. Cremades<sup>3</sup>, L. A. Balmaceda<sup>4</sup>, F. A. Nuevo<sup>5</sup> and A. M. Vázquez<sup>5,6</sup>  
A&A 627, A8 (2019)

<https://doi.org/10.1051/0004-6361/201834163>

Context. Reliable estimates of the mass of coronal mass ejections (CMEs) are required to quantify their energy and predict how they affect space weather. When a CME propagates near the observer's line of sight, these tasks involve considerable errors, which motivated us to develop alternative means for estimating the CME mass.

Aims. We aim at further developing and testing a method that allows estimating the mass of CMEs that propagate approximately along the observer's line of sight.

Methods. We analyzed the temporal evolution of the mass of 32 white-light CMEs propagating across heliocentric heights of 2.5–15  $R_{\odot}$ , in combination with that of the mass evacuated from the associated low coronal dimming regions. The mass of the white-light CMEs was determined through existing methods, while the mass evacuated by each CME in the low corona was estimated using a recently developed technique that analyzes the dimming in extreme-UV (EUV) images. The combined white-light and EUV analyses allow the quantification of an empirical function that describes the evolution of CME mass with height.

## Mass Loss Evolution in the EUV Low Corona from SDO/AIA Data

Fernando M. [López](#), Hebe Cremades, Federico A. Nuevo, [Laura A. Balmaceda](#), [Alberto A. Vázquez](#)  
Solar Phys. January 2017, 292:6

<https://arxiv.org/pdf/1611.00849v1.pdf>

We carry out an analysis of the evacuated mass from three coronal dimming regions observed by the *Imaging Atmospheric Imaging Assembly* (AIA) on board the *Solar Dynamics Observatory*. The three events are unambiguously identified with white-light coronal mass ejections (CMEs) associated in turn with surface activity of diverse nature: an impulsive (M-class) flare, a weak (B-class) flare and a filament eruption without a flare. The use of three AIA coronal passbands allows applying a differential emission measure technique to define the dimming regions and identify their evacuated mass through the analysis of the electronic density depletion associated to the eruptions. The temporal evolution of the mass loss from the three dimmings can be approximated by an exponential equation followed by a linear fit. We determine the mass of the associated CMEs from COR2 data. The results show that the evacuated masses from the low corona represent a considerable amount of the mass of the CMEs. We also find that plasma is still being evacuated from the low corona at the time when the CMEs reach the COR2 field of view. The temporal evolution of the angular width of the CMEs, of the dimming regions in the low corona, and of the flux registered by GOES in soft X-rays are all in close relation with the behavior of mass evacuation from the low corona. We discuss the implications of our findings toward a better understanding of the temporal evolution of several parameters associated to the analyzed dimmings and CMEs. 23 May 2010, 7 August 2010, 30 November 2010

## Deprojected Trajectory of Blobs in the Inner Corona

C. [López-Portela](#), [O. Panasenco](#), [X. Blanco-Cano](#), [G. Stenborg](#)

Solar Phys (2018) 293:99

<https://link.springer.com/content/pdf/10.1007%2Fs11207-018-1315-4.pdf>

We have carried out a statistical analysis of the kinematical behavior of small white-light transients (blobs) as tracers of the slow solar wind. The characterization of these faint white-light structures gives us insight on the origin and acceleration of the slow solar wind. The vantage observing points provided by the SECCHI and LASCO instruments on board the STEREO and SOHO spacecraft, respectively, allow us to reconstruct the 3D trajectories of these blob-like features and hence calculate their deprojected kinematical parameters. We have studied 44 blobs revealed in LASCO C2/C3 and SECCHI COR2 data from 2007 to 2008, a period within the solar minimum between Solar Cycles 23 and 24. We found that the blobs propagate along approximately constant position angles with accelerations from 1.40 to 15.34  $\text{ms}^{-2}$  between 3.42  $R_{\odot}$  and 14.80  $R_{\odot}$ , their radial sizes ranging between 0.57  $R_{\odot}$  and 1.69  $R_{\odot}$ . We also studied the global corona magnetic field morphology for a subset of blobs using a potential field source surface model for cases where blob detachments persist for two to five days. The study of localized blob releases indicates that these plasma structures start their transit at a distance of  $\sim 3.40 R_{\odot}$  and their origin is connected either with the boundaries of weak coronal holes or with streamers at equatorial latitudes.

## Comprehensive Characterization of the Dynamics of Two Coronal Mass Ejections in the Outer Corona.

Di [Lorenzo](#), L., Balmaceda, L., Cremades, H. et al.  
Sol Phys 299, 43 (2024).

<https://doi.org/10.1007/s11207-024-02290-2>

Coronal mass ejections (CMEs) play a key role in determining space-weather conditions. Therefore, it is important to understand their evolution throughout the heliosphere. In this work, we carefully analyze the evolution of two kinematically different CMEs that erupted on **16 June 2010** and **14 June 2011**, in a range of heliospheric distances of approximately 4 – 18 solar radii. From nearly simultaneous coronagraph images from the Solar-Terrestrial Relations Observatory and Solar and Heliospheric Observatory, we estimate the three-dimensional speed and acceleration–time profiles. We use these profiles to calculate the dynamic and thermodynamic parameters of the CMEs, such as the contribution of the forces and the polytropic index by means of the Flux Rope Internal State (FRIS) model, which assumes a self-similar evolution. We further test the validity of this assumption by comparing with observed quantities near the Sun and at 1 AU. We find that the kinematic properties of the two events differ in their evolution, which has an impact on the relative importance of the internal forces and on the thermodynamic quantities. In addition, our analysis reveals that the assumption of self-similar evolution is valid for the behavior in the middle corona for both events. At larger distances, however, this only holds for the 16 June 2010 event, which is significantly slower than the other.

### **Imaging evidence for solar wind outflows originating from a CME footprint**

[Juraj Lörinčík](#), [Jaroslav Dudík](#), [Guillaume Aulanier](#), [Brigitte Schmieder](#), [Leon Golub](#)

2021 *ApJ* **906** 62

<https://arxiv.org/pdf/2010.04250.pdf>

<https://doi.org/10.3847/1538-4357/abc8f6>

We report on the Atmospheric Imaging Assembly (AIA) observations of plasma outflows originating in a coronal dimming during the **2015 April 28th** filament eruption. After the filament started to erupt, two flare ribbons formed, one of which had a well-visible hook enclosing a core (twin) dimming region. Along multiple funnels located in this dimming, a motion of plasma directed outwards started to be visible in the 171 Å and 193 Å filter channels of the instrument. In time-distance diagrams, this motion generated a strip-like pattern, which lasted for more than five hours and which characteristics did not change along the funnel. We therefore suggest the motion to be a signature of outflows corresponding to velocities ranging between  $\approx 70$  and  $140 \text{ km s}^{-1}$ . Interestingly, the pattern of the outflows as well as their velocities were found to be similar to those we observed in a neighboring ordinary coronal hole. Therefore, the outflows were most likely a signature of a CME-induced slow solar wind flowing along the open-field structures rooted in the dimming region. Further, the evolution of the hook encircling the dimming region was examined in the context of the latest predictions imposed for the three-dimensional magnetic reconnection. The observations indicate that the filament's footpoints were, during their transformation to the dimming region, reconnecting with surrounding canopies. To our knowledge, our observations present the first imaging evidence for outflows of plasma from a dimming region.

### **Manifestations of three dimensional magnetic reconnection in an eruption of a quiescent filament: Filament strands turning to flare loops**

[Juraj Lorincik](#), [Jaroslav Dudik](#), [Guillaume Aulanier](#)

*ApJ* **885** 83 **2019**

<https://arxiv.org/pdf/1909.03825.pdf>

We report on observations of conversion of bright filament strands into flare loops during **2012 August 31** filament eruption. Prior to the eruption, individual bright strands composing one of the legs of the filament were observed in the 171 Å filter channel data of the Atmospheric Imaging Assembly. After the onset of the eruption, one of the hooked ribbons started to propagate and contract, sweeping footpoints of the bright filament strands as well as coronal loops located close by. Later on, hot flare loops appeared in regions swept by the hook, where the filament strands were rooted. Timing and localization of these phenomena suggest that they are caused by reconnection of field lines composing the filament at the hook, which, to our knowledge, has not been observed before. This process is not included in the standard flare model (CSHKP), as it does not address footpoints of erupting flux ropes and ribbon hooks. It has, however, been predicted using the recent three-dimensional extensions to the standard flare model. There, the erupting flux rope can reconnect with surrounding coronal arcades as the hooked extensions of current ribbons sweep its footpoints. This process results in formation of flare loops rooted in previous footpoints of the flux rope. Our observations of sweeping of filament footpoints are well described by this scenario. In all observed cases, all of the footpoints of the erupting filament became footpoints of flare loops. This process was observed to last for about 150 minutes, throughout the whole eruption.

### **Triggering an eruptive flare by emerging flux in a solar active-region complex**

[Louis](#), [Rohan E.](#); [Kliem](#), [Bernhard](#); [Ravindra](#), [B.](#); [Chintzoglou](#), [Georgios](#)

*Solar Phys.* Volume 290, Issue 12, pp 3641-3662 **2015**

<http://arxiv.org/pdf/1506.08035v1.pdf>

A flare and fast coronal mass ejection originated between solar active regions NOAA 11514 and 11515 on **July 1, 2012** in response to flux emergence in front of the leading sunspot of the trailing region 11515. Analyzing the evolution of the photospheric magnetic flux and the coronal structure, we find that the flux emergence triggered the eruption by interaction with overlying flux in a non-standard way. The new flux neither had the opposite orientation nor a location near the polarity inversion line, which are favorable for strong reconnection with the arcade flux under which it emerged. Moreover, its flux content remained significantly smaller than that of the arcade (approximately 40 %).

However, a loop system rooted in the trailing active region ran in part under the arcade between the active regions, passing over the site of flux emergence. The reconnection with the emerging flux, leading to a series of jet emissions into the loop system, caused a strong but confined rise of the loop system. This lifted the arcade between the two active regions, weakening its downward tension force and thus destabilizing the considerably sheared flux under the arcade. The complex event was also associated with supporting precursor activity in an enhanced network near the active regions, acting on the large-scale overlying flux, and with two simultaneous confined flares within the active regions.

## **THE TOPOLOGICAL CHANGES OF SOLAR CORONAL MAGNETIC FIELDS. II. THE RECLOSING OF AN OPENED FIELD**

B. C. [Low](#)<sup>1</sup> and [Å. M. Janse](#)<sup>1,2</sup>

Astrophysical Journal, 696:821–840, 2009 May

<http://www.iop.org/EJ/toc/-alert=43190/0004-637X/696/1>

This is a study of the spontaneous formation of current sheets responding to the closing of an opened magnetic field by resistive reconnection in an electrically, highly conducting atmosphere outside a unit sphere. Pairs of initial–final equilibrium states are calculated explicitly, taking the field to be composed of three systems of untwisted flux in both states. In the initial state, two of the three flux systems are closed potential fields whereas the third system contains an equilibrium current sheet that keeps the potential fields on its two sides globally open. The final state is an everywhere potential field, with all three flux systems closed, produced by the resistive dissipation of the current sheet in the initial state. The unit sphere is taken to be a rigid, perfectly conducting wall during reconnection, so that the normal flux distribution is unchanged on the unit sphere. Field solutions subject to this unchanging boundary condition are obtained with and without the assumption of axisymmetry. The mathematical model has been designed to show that the topological changes produced by the current-sheet dissipation are simple under axisymmetry but radically different in the absence of axisymmetry, a fundamental point established in the first paper of this series. In the general case, the topological changes imply that other current sheets must have formed. Some of these current sheets form on the separatrix flux surfaces of the multipolar field. Others form throughout the closed-flux systems induced by volumetric changes. **The opening and reclosing of magnetic fields during a solar coronal mass ejection may produce a multitude of current sheets not previously anticipated in the current understanding of this phenomenon.** Basic to this study is a general topological property of magnetic flux tubes treated separately in the Appendix.

## **Magnetic Flux Rope Identification and Characterization from Observationally-Driven Solar Coronal Models**

Chris [Lowder](#), [Anthony Yeates](#)

ApJ 846 106 2017

<https://arxiv.org/pdf/1708.04522.pdf>

Formed through magnetic field shearing and reconnection in the solar corona, magnetic flux ropes are structures of twisted magnetic field, threaded along an axis. Their evolution and potential eruption are of great importance for space weather. Here we describe a new methodology for the automated detection of flux ropes in simulated magnetic fields, based on fieldline helicity. More robust than previous methods, it also allows the full volume extent of each flux rope structure to be determined. Our Flux Rope Detection and Organization (FRoDO) code is publicly available, and measures the magnetic flux and helicity content of pre-erupting flux ropes over time, as well as detecting eruptions. As a first demonstration the code is applied to the output from a time-dependent magnetofrictional model, spanning 1996 June 15 - 2014 February 10. Over this period, 1561 erupting and 2099 non-erupting magnetic flux ropes are detected, tracked, and characterized. For this particular model data, erupting flux ropes have a mean net helicity magnitude of  $(2.66 \pm 6.82) \times 10^{43} \text{ Mx}^2$ , while non-erupting flux ropes have a significantly lower mean of  $(4.04 \pm 9.25) \times 10^{42} \text{ Mx}^2$ , although there is overlap between the two distributions. Similarly, the mean unsigned magnetic flux for erupting flux ropes is  $(4.04 \pm 6.17) \times 10^{21} \text{ Mx}$ , significantly higher than the mean value of  $(7.05 \pm 16.8) \times 10^{20} \text{ Mx}$  for non-erupting ropes. These values for erupting flux ropes are within the broad range expected from observational and theoretical estimates, although the eruption rate in this particular model is lower than that of observed coronal mass ejections. In future the FRoDO code will prove a valuable tool for assessing the performance of different non-potential coronal simulations and comparing them with observations. **1998 December 2-4**

## **Constraining the Physical Properties of Stellar Coronal Mass Ejections with Coronal Dimming: Application to Far Ultraviolet Data of $\epsilon$ Eridani**

[R. O. Parke Loyd](#), [James Mason](#), [Meng Jin](#), [Evgenya L. Shkolnik](#), [Kevin France](#), [Allison Youngblood](#), [Jackie Villadsen](#), [Christian Schneider](#), [Adam C. Schneider](#), [Joseph Llana](#), [Tahina Ramiamananantsoa](#), [Tyler Richey-Yowell](#)

ApJ 2022

<https://arxiv.org/pdf/2207.05115.pdf>

Coronal mass ejections (CMEs) are a prominent contributor to solar system space weather and might have impacted the Sun's early angular momentum evolution. A signal diagnostic of CMEs on the Sun is coronal dimming: a drop in coronal emission, tied to the mass of the CME, that is the direct result of removing emitting plasma from the corona.

We present the results of a coronal dimming analysis of Fe XII 1349 Å and Fe XXI 1354 Å emission from  $\epsilon$  Eridani ( $\epsilon$  Eri), a young K2 dwarf, with archival far-ultraviolet observations by the Hubble Space Telescope's Cosmic Origins Spectrograph. Following a flare in February 2015,  $\epsilon$  Eri's Fe XXI emission declined by  $81 \pm 5\%$ . Although enticing, a scant 3.8 min of preflare observations allows for the possibility that the Fe XXI decline was the decay of an earlier, unseen flare. Dimming nondetections following each of three prominent flares constrain the possible mass of ejected Fe XII-emitting (1 MK) plasma to less than a few  $\times 10^{15}$  g. This implies that CMEs ejecting this much or more 1 MK plasma occur less than a few times per day on  $\epsilon$  Eri. On the Sun, 1015 g CMEs occur once every few days. For  $\epsilon$  Eri, the mass loss rate due to CME-ejected 1 MK plasma could be  $< 0.6 M'_{\odot}$ , well below the star's estimated  $30 M'_{\odot}$  mass loss rate (wind + CMEs). The order-of-magnitude formalism we developed for these mass estimates can be broadly applied to coronal dimming observations of any star.

## Full velocities and propagation directions of coronal mass ejections inferred from simultaneous full-disk imaging and Sun-as-a-star spectroscopic observations

[Hong-peng Lu](#), [Hui Tian](#), [He-chao Chen](#), [Yu Xu](#), [Zhen-yong Hou](#), [Xian-yong Bai](#), [Guang-yu Tan](#), [Zi-hao Yang](#), [Jie Ren](#)

ApJ **953** 68 2023

<https://arxiv.org/pdf/2305.08765.pdf>

<https://iopscience.iop.org/article/10.3847/1538-4357/acd6a1/pdf>

Coronal mass ejections (CMEs) are violent ejections of magnetized plasma from the Sun, which can trigger geomagnetic storms, endanger satellite operations and destroy electrical infrastructures on the Earth. After systematically searching Sun-as-a-star spectra observed by the Extreme-ultraviolet Variability Experiment (EVE) onboard the Solar Dynamics Observatory (SDO) from May 2010 to May 2022, we identified eight CMEs associated with flares and filament eruptions by analyzing the blue-wing asymmetry of the O III 52.58 nm line profiles. Combined with images simultaneously taken by the 30.4 nm channel of the Atmospheric Imaging Assembly onboard SDO, the full velocity and propagation direction for each of the eight CMEs are derived. We find a strong correlation between geomagnetic indices (Kp and Dst) and the angle between the CME propagation direction and the Sun-Earth line, suggesting that Sun-as-a-star spectroscopic observations at EUV wavelengths can potentially help to improve the prediction accuracy of the geoeffectiveness of CMEs. Moreover, an analysis of synthesized long-exposure Sun-as-a-star spectra implies that it is possible to detect CMEs from other stars through blue-wing asymmetries or blueshifts of spectral lines. **20110214, 20120702, 20141115, 20150311, 20150625, 20151104, 20170906, 20211028**

Table 1. Information of eight CMEs

## Spectroscopic and Stereoscopic Observations of the Solar Jets

[Lei Lu](#), [Li Feng](#), [Ying Li](#), [Dong Li](#), [Zongjun Ning](#), [Weiqun Gan](#)

2019 ApJ **887** 154

<https://arxiv.org/pdf/1910.13649.pdf>

<https://doi.org/10.3847/1538-4357/ab530c>

We present a comprehensive study of a series of recurrent jets that occurred at the periphery of the NOAA active region 12114 on **2014 July 7**. These jets were found to share the same source region and exhibited rotational motions as they propagated outward. The multi-wavelength imaging observations made by the AIA and *IRIS* telescopes reveal that some of the jets contain cool plasma only, while some others contain not only cool but also hot plasma. The Doppler velocities calculated from the *IRIS* spectra show a continuous evolution from blue to red shifts as the jet motions change from upward to downward. Additionally, some jets exhibit opposite Doppler shifts on their both sides, indicative of rotating motions along their axes. The inclination angle and three-dimensional velocity of the largest jet were inferred from the imaging and spectroscopic observations, which show a high consistence with those derived from the stereoscopic analysis using dual-perspective observations by *SDO*/AIA and *STEREO*-B/EUVI. By relating the jets to the local UV/EUV and full-disk *GOES* X-ray emission enhancements, we found that the previous five small-scale jets were triggered by five bright points while the last/largest one was triggered by a C1.6 solar flare. Together with a number of type III radio bursts generated during the jet eruptions as well as a weak CME that was observed in association with the last jet, our observations provide evidences in support of multi-scale magnetic reconnection processes being responsible for the production of jet events.

## A Statistical Study of the Magnetic Imprints of X-Class Flares using SDO/HMI Vector Magnetograms

[Zekun Lu](#), [Weiguang Cao](#), [Gaoxiang Jin](#), [Yining Zhang](#), [Mingde Ding](#), [Yang Guo](#)

ApJ **2018**

<https://arxiv.org/pdf/1803.08310.pdf>

Magnetic imprints, the rapid and irreversible evolution of photospheric magnetic fields as a feedback from flares in the corona, have been confirmed by many previous studies. These studies showed that the horizontal field will permanently increase near the polarity inversion line (PIL) after eruptions, indicating that a more horizontal topology of photospheric magnetic field will be reconstructed. In this study, we analyze 17 near-disk X-class flares in 13 active regions (ARs) with heliographic angle no greater than 45 degrees since the launch of the Solar Dynamics Observatory (SDO). We find that confined flares without or with very weak CMEs tend to show very weak magnetic imprints on the photosphere. The imprint regions of the horizontal field could locate not only near the PIL but also near sunspot umbrae with strong



vertical fields. Making use of the observed CME mass and speed, we find that the CMEs with larger momentums will bring into stronger magnetic imprints. Furthermore, a linear relationship, with a confidence coefficient 0.82, between the CME momentum and the change of Lorentz force is revealed. Based on that, we quantify the back reaction time to be 336 s, which could be further applied to independently estimate the CME mass. **2011.02.15, 2011.03.09, 2011.09.06, 2011.09.07, 2011.09.24, 2012.03.07, 2012.07.12, 2013.11.05, 2013.11.08, 2013.11.10, 2014.03.29, 2014.10.22, 2014.10.26, 2014.11.07, 2014 December 20, 2015.03.11**

**Table 1.** List of 17 flare events from 13 ARs with heliographic angle no greater than 45°.

## Measure the Propagation of a halo CME and Its Driven Shock with the Observations from a Single Perspective at Earth

Lei **Lu**, Bernd Inhester, Li Feng, [Siming Liu](#), [Xinhua Zhao](#)

ApJ 835 188 2017

<https://arxiv.org/pdf/1612.09360v1.pdf>

We present a detailed study of an earth-directed coronal mass ejection (Full halo CME) event happened on **2011 February 15** making use of white light observations by three coronagraphs and radio observations by Wind/WAVES. We applied three different methods to reconstruct the propagation direction and traveling distance of the CME and its driven shock. We measured the kinematics of the CME leading edge from white light images observed by STEREO A and B, tracked the CME-driven shock using the frequency drift observed by Wind/WAVES together with an interplanetary density model, and obtained the equivalent scattering centers of the CME by Polarization Ratio(PR) method. For the first time, we applied PR method to different features distinguished from LASCO/C2 polarimetric observations and calculated their projections onto white light images observed by STEREO A and B. By combining the graduated cylindrical shell (GCS) forward modeling with the PR method, we proposed a new GCS-PR method to derive 3D parameters of a CME observed from a single perspective at Earth. Comparisons between different methods show a good degree of consistence in the derived 3D results.

## The Width of Magnetic Ejecta Measured Near 1 au: Lessons from STEREO-A Measurements in 2021--2022

[Noé Lugaz](#), [Bin Zhuang](#), [Camilla Scolini](#), [Nada Al-Haddad](#), [Charles J. Farrugia](#), [Réka M. Winslow](#), [Florian Regnault](#), [Christian Möstl](#), [Emma E. Davies](#), [Antoinette B. Galvin](#)

ApJ 2023

<https://arxiv.org/pdf/2312.03942.pdf>

Coronal mass ejections (CMEs) are large-scale eruptions with a typical radial size at 1 au of 0.21 au but their angular width in interplanetary space is still mostly unknown, especially for the magnetic ejecta (ME) part of the CME. We take advantage of STEREO-A angular separation of 20°-60° from the Sun-Earth line from October 2020 to August 2022, and perform a two-part study to constrain the angular width of MEs in the ecliptic plane: a) we study all CMEs that are observed remotely to propagate between the Sun-STEREO-A and the Sun-Earth lines and determine how many impact one or both spacecraft in situ, and b) we investigate all in situ measurements at STEREO-A or at L1 of CMEs during the same time period to quantify how many are measured by the two spacecraft. A key finding is that, out of 21 CMEs propagating within 30° of either spacecraft, only four impacted both spacecraft and none provided clean magnetic cloud-like signatures at both spacecraft. Combining the two approaches, we conclude that the typical angular width of a ME at 1 au is ~ 20°-30°, or 2-3 times less than often assumed and consistent with a 2:1 elliptical cross-section of an ellipsoidal ME. We discuss the consequences of this finding for future multi-spacecraft mission designs and for the coherence of CMEs. **2021 May 22, 2021 August 26, 2021 October 28, 2021 November 2, 2022 January 29, 2022 March 25, 2022 August 15**

**Table 1.** Overview of the 21 Cat I CMEs studied here 2020-2022

## A Coronal Mass Ejection and Magnetic Ejecta Observed In Situ by STEREO-A and Wind at 55° Angular Separation

[Noé Lugaz](#), [Tarik M. Salman](#), [Charles J. Farrugia](#), [Wenyuan Yu](#), [Bin Zhuang](#), [Nada Al-Haddad](#), [Camilla Scolini](#), [Réka M. Winslow](#), [Christian Möstl](#), [Emma E. Davies](#), [Antoinette B. Galvin](#)

ApJ 2022

<https://arxiv.org/pdf/2203.16477>

<https://doi.org/10.3847/1538-4357/ac602f>

<https://iopscience.iop.org/article/10.3847/1538-4357/ac602f/pdf>

We present an analysis of *in situ* and remote-sensing measurements of a coronal mass ejection (CME) that erupted on **2021 February 20** and impacted both the Solar TERrestrial Relations Observatory (STEREO)-A and the *Wind* spacecraft, which were separated longitudinally by 55°. Measurements on **2021 February 24** at both spacecraft are consistent with the passage of a magnetic ejecta (ME), making this one of the widest reported multi-spacecraft ME detections. The CME is associated with a low-inclined and wide filament eruption from the Sun's southern hemisphere, which propagates between STEREO-A and *Wind* around E34. At STEREO-A, the measurements indicate the passage of a moderately fast (~425~km\,s<sup>-1</sup>) shock-driving ME, occurring 2--3 days after the end of a high speed stream (HSS). At *Wind*, the measurements show a faster (~490~km\,s<sup>-1</sup>) and much shorter ME, not preceded by a shock nor a sheath, and occurring inside the back portion of the HSS. The ME orientation measured at both spacecraft is

consistent with a passage close to the legs of a curved flux rope. The short duration of the ME observed at *Wind* and the difference in the suprathermal electron pitch-angle data between the two spacecraft are the only results that do not satisfy common expectations. We discuss the consequence of these measurements on our understanding of the CME shape and extent and the lack of clear signatures of the interaction between the CME and the HSS.

### **Inconsistencies Between Local and Global Measures of CME Radial Expansion as Revealed by Spacecraft Conjunctions**

Noé **Lugaz**, Tarik M. Salman, Réka M. Winslow, Nada Al-Haddad, Charles J. Farrugia, Bin Zhuang, and Antoinette B. Galvin

2020 ApJ 899 119

<https://doi.org/10.3847/1538-4357/aba26b>

The radial expansion of coronal mass ejections (CMEs) is known to occur from remote observations, from the variation of their properties with radial distance, and from local in situ plasma measurements showing a decreasing speed profile throughout the magnetic ejecta (ME). However, little is known on how local measurements compare to global measurements of expansion. Here, we present results from the analysis of 42 CMEs measured in the inner heliosphere by two spacecraft in radial conjunction. The magnetic-field decrease with distance provides a measure of their global expansion. Near 1 au, the decrease in their bulk speed provides a measure of their local expansion. We find that these two measures have little relation with each other. We also investigate the relation between characteristics of CME expansion and CME properties. We find that the expansion depends on the initial magnetic-field strength inside the ME, but not significantly on the magnetic field inside the ME measured near 1 au. This is indirect evidence that CME expansion in the innermost heliosphere is driven by the high magnetic pressure inside the ME, while by the time the MEs reach 1 au, they are expanding due to the decrease in the solar-wind dynamic pressure with distance. We also determine the evolution of the ME tangential and normal magnetic-field components with distance, revealing significant deviations as compared to the expectations from force-free field configurations as well as some evidence that the front half of MEs expand at a faster rate than the back half.

### **Importance of CME Radial Expansion on the Ability of Slow CMEs to Drive Shocks**

Noé **Lugaz**<sup>1,2</sup>, Charles J. Farrugia<sup>1,2</sup>, Reka M. Winslow<sup>1</sup>, Colin R. Small<sup>2</sup>, Thomas Manion<sup>2</sup>, and Neel P. Savani<sup>3</sup>

2017 ApJ 848 75

<http://sci-hub.cc/http://iopscience.iop.org/0004-637X/848/2/75/>

Coronal mass ejections (CMEs) may disturb the solar wind by overtaking it or expanding into it, or both. CMEs whose front moves faster in the solar wind frame than the fast magnetosonic speed drive shocks. Such shocks are important contributors to space weather, by triggering substorms, compressing the magnetosphere, and accelerating particles. In general, near 1 au, CMEs with speed greater than about 500 km s<sup>-1</sup> drive shocks, whereas slower CMEs do not. However, CMEs as slow as 350 km s<sup>-1</sup> may sometimes, although rarely, drive shocks. Here we study these slow CMEs with shocks and investigate the importance of CME expansion in contributing to their ability to drive shocks and in enhancing shock strength. Our focus is on CMEs with average speeds under 375 km s<sup>-1</sup>. From *Wind* measurements from 1996 to 2016, we find 22 cases of such shock-driving slow CMEs, and for about half of them (11 out of the 22), the existence of the shock appears to be strongly related to CME expansion. We also investigate the proportion of all CMEs with speeds under 500 km s<sup>-1</sup> with and without shocks in solar cycles 23 and 24, depending on their speed. We find no systematic difference, as might have been expected on the basis of the lower solar wind and Alfvén speeds reported for solar cycle 24 versus 23. The slower expansion speed of CMEs in solar cycle 24 might be an explanation for this lack of increased frequency of shocks, but further studies are required. **1997 July 15, 2001 April 21, 2001 October 31,**

**Table 1** List of 22 CMEs with Average Speed Less or Equal to 375 km s<sup>-1</sup> That Drove a Shock

### **The Interaction of Successive Coronal Mass Ejections: A **Review****

Noé **Lugaz** Manuela Temmer Yuming Wang Charles J. Farrugia

Sol Phys (2017) 292: 64. **File**

<http://sci-hub.cc/10.1007/s11207-017-1091-6>

We present a review of the different aspects associated with the interaction of successive coronal mass ejections (CMEs) in the corona and inner heliosphere, focusing on the initiation of series of CMEs, their interaction in the heliosphere, the particle acceleration associated with successive CMEs, and the effect of compound events on Earth's magnetosphere. The two main mechanisms resulting in the eruption of series of CMEs are sympathetic eruptions, when one eruption triggers another, and homologous eruptions, when a series of similar eruptions originates from one active region. CME – CME interaction may also be associated with two unrelated eruptions. The interaction of successive CMEs has been observed remotely in coronagraphs (with the Large Angle and Spectrometric Coronagraph Experiment – LASCO – since the early 2000s) and heliospheric imagers (since the late 2000s), and inferred from in situ measurements, starting with early measurements in the 1970s. The interaction of two or more CMEs is associated with complex phenomena, including magnetic reconnection, momentum exchange, the propagation of a fast magnetosonic shock through a magnetic ejecta, and changes in the CME expansion. The presence of a preceding CME a few hours before a fast eruption has been found to be connected with higher fluxes of solar energetic particles (SEPs),

while CME – CME interaction occurring in the corona is often associated with unusual radio bursts, indicating electron acceleration. Higher suprathermal population, enhanced turbulence and wave activity, stronger shocks, and shock – shock or shock – CME interaction have been proposed as potential physical mechanisms to explain the observed associated SEP events. When measured in situ, CME – CME interaction may be associated with relatively well organized multiple-magnetic cloud events, instances of shocks propagating through a previous magnetic ejecta or more complex ejecta, when the characteristics of the individual eruptions cannot be easily distinguished. CME – CME interaction is associated with some of the most intense recorded geomagnetic storms. The compression of a CME by another and the propagation of a shock inside a magnetic ejecta can lead to extreme values of the southward magnetic field component, sometimes associated with high values of the dynamic pressure. This can result in intense geomagnetic storms, but can also trigger substorms and large earthward motions of the magnetopause, potentially associated with changes in the outer radiation belts. Future in situ measurements in the inner heliosphere by Solar Probe+ and Solar Orbiter may shed light on the evolution of CMEs as they interact, by providing opportunities for conjunction and evolutionary studies. **2000-06-10, 25-26 Nov 2000, 19-20 March 2001, 26 Mar-26 Apr 2001, 1 Apr 2001, 31 March – 1 April 2001, 1 August 2010, 25 May 2010, e August 2010 events f, 2011-08-01, 10 November 2012, 2013-05-22, 2011-02-15, 19 Feb 2014**

### **3. Effects of Successive CMEs on Particle Acceleration**

#### **3.2. Radio Signatures of CME – CME Interaction**

### **The Interaction of Two Coronal Mass Ejections: Influence of Relative Orientation**

N. [Lugaz](#)<sup>1</sup>, C. J. Farrugia<sup>1</sup>, W. B. Manchester IV<sup>2</sup>, and N. Schwadron

**2013 ApJ 778 20**

<http://arxiv.org/pdf/1309.2210v1.pdf>

We report on a numerical investigation of two coronal mass ejections (CMEs) that interact as they propagate in the inner heliosphere. We focus on the effect of the orientation of the CMEs relative to each other by performing four different simulations with the axis of the second CME rotated by 90° from one simulation to the next. Each magnetohydrodynamic simulation is performed in three dimensions with the Space Weather Modeling Framework in an idealized setting reminiscent of solar minimum conditions. We extract synthetic satellite measurements during and after the interaction and compare the different cases. We also analyze the kinematics of the two CMEs, including the evolution of their widths and aspect ratios. We find that the first CME contracts radially as a result of the interaction in all cases, but the amount of subsequent radial expansion depends on the relative orientation of the two CMEs. Reconnection between the two ejecta and between the ejecta and the interplanetary magnetic field determines the type of structure resulting from the interaction. When a CME with a high inclination with respect to the ecliptic overtakes one with a low inclination, it is possible to create a compound event with a smooth rotation in the magnetic field vector over more than 180°. Due to reconnection, the second CME only appears as an extended "tail," and the event may be mistaken for a glancing encounter with an isolated CME. This configuration differs significantly from the one usually studied of a multiple-magnetic-cloud event, which we found to be associated with the interaction of two CMEs with the same orientation.

### **THE DEFLECTION OF THE TWO INTERACTING CORONAL MASS EJECTIONS OF 2010 MAY 23-24 AS REVEALED BY COMBINED IN SITU MEASUREMENTS AND HELIOSPHERIC IMAGING**

N. [Lugaz](#)<sup>1</sup>, C. J. Farrugia<sup>1</sup>, J. A. Davies<sup>2</sup>, C. Möstl<sup>3,4,5</sup>, C. J. Davis<sup>2,6</sup>, I. I. Roussev<sup>7,8</sup>, and M. Temmer

**2012 ApJ 759 68, File**

In **2010 May 23-24**, Solar Dynamics Observatory (SDO) observed the launch of two successive coronal mass ejections (CMEs), which were subsequently tracked by the SECCHI suite on board STEREO. Using the COR2 coronagraphs and the heliospheric imagers (HIs), the initial direction of both CMEs is determined to be slightly west of the Sun-Earth line. We derive the CME kinematics, including the evolution of the CME expansion until 0.4 AU. We find that, during the interaction, the second CME decelerates from a speed above 500 km s<sup>-1</sup> to 380 km s<sup>-1</sup>, the speed of the leading edge of the first CME. STEREO observes a complex structure composed of two different bright tracks in HI2-A but only one bright track in HI2-B. In situ measurements from Wind show an "isolated" interplanetary CME, with the geometry of a flux rope preceded by a shock. Measurements in the sheath are consistent with draping around the transient. By combining remote-sensing and in situ measurements, we determine that this event shows a clear instance of deflection of two CMEs after their collision, and we estimate the deflection of the first CME to be about 10° toward the Sun-Earth line. The arrival time, arrival speed, and radius at Earth of the first CME are best predicted from remote-sensing observations taken before the collision of the CMEs. Due to the over-expansion of the CME after the collision, there are few, if any, signs of interaction in in situ measurements. This study illustrates that complex interactions during the Sun-to-Earth propagation may not be revealed by in situ measurements alone.

### **Heliospheric Observations of STEREO-Directed Coronal Mass Ejections in 2008 – 2010: Lessons for Future Observations of Earth-Directed CMEs**

N. [Lugaz](#), P. Kintner, C. Möstl, L. K. Jian, C. J. Davis and C. J. Farrugia

Solar Physics, **2012**, DOI: 10.1007/s11207-012-0007-8

We present a study of coronal mass ejections (CMEs) which impacted one of the STEREO spacecraft between January 2008 and early 2010. We focus our study on 20 CMEs which were observed remotely by the Heliospheric Imagers (HIs) onboard the other STEREO spacecraft up to large heliocentric distances. We compare the predictions of the Fixed- $\Phi$  and Harmonic Mean (HM) fitting methods, which only differ by the assumed geometry of the CME. It is possible to use these techniques to determine from remote-sensing observations the CME direction of propagation, arrival time and final speed which are compared to in-situ measurements. We find evidence that for large viewing angles, the HM fitting method predicts the CME direction better. However, this may be due to the fact that only wide CMEs can be successfully observed when the CME propagates more than  $100^\circ$  from the observing spacecraft. Overall eight CMEs, originating from behind the limb as seen by one of the STEREO spacecraft can be tracked and their arrival time at the other STEREO spacecraft can be successfully predicted. This includes CMEs, such as the events **on 4 December 2009 and 9 April 2010**, which were viewed  $130^\circ$  away from their direction of propagation. Therefore, we predict that some Earth-directed CMEs will be observed by the HIs until early 2013, when the separation between Earth and one of the STEREO spacecraft will be similar to the separation of the two STEREO spacecraft in 2009 – 2010.

## **NUMERICAL INVESTIGATION OF A CORONAL MASS EJECTION FROM AN ANEMONE ACTIVE REGION: RECONNECTION AND DEFLECTION OF THE 2005 AUGUST 22 ERUPTION**

N. [Lugaz](#)<sup>1,2</sup>, C. Downs<sup>2</sup>, K. Shibata<sup>1</sup>, I. I. Roussev<sup>2</sup>, A. Asai<sup>3</sup> and T. I. Gombosi  
**2011 ApJ 738 127**

We present a numerical investigation of the coronal evolution of a coronal mass ejection (CME) on **2005 August 22** using a three-dimensional thermodynamic magnetohydrodynamic model, the space weather modeling framework. The source region of the eruption was anemone active region (AR) 10798, which emerged inside a coronal hole. We validate our modeled corona by producing synthetic extreme-ultraviolet (EUV) images, which we compare to EIT images. We initiate the CME with an out-of-equilibrium flux rope with an orientation and chirality chosen in agreement with observations of an H $\alpha$  filament. During the eruption, one footpoint of the flux rope reconnects with streamer magnetic field lines and with open field lines from the adjacent coronal hole. It yields an eruption which has a mix of closed and open twisted field lines due to interchange reconnection and only one footpoint line-tied to the source region. Even with the large-scale reconnection, we find no evidence of strong rotation of the CME as it propagates. We study the CME deflection and find that the effect of the Lorentz force is a deflection of the CME by about  $3^\circ R^{-1}$  toward the east during the first 30 minutes of the propagation. We also produce coronagraphic and EUV images of the CME, which we compare with real images, identifying a dimming region associated with the reconnection process. We discuss the implication of our results for the arrival at Earth of CMEs originating from the limb and for models to explain the presence of open field lines in magnetic clouds.

## **DETERMINING THE AZIMUTHAL PROPERTIES OF CORONAL MASS EJECTIONS FROM MULTI-SPACECRAFT REMOTE-SENSING OBSERVATIONS WITH STEREO SECCHI**

N. [Lugaz](#)<sup>1</sup>, J. N. Hernandez-Charpak<sup>2</sup>, I. I. Roussev<sup>1</sup>, C. J. Davis<sup>3</sup>, A. Vourlidas<sup>4</sup>, and J. A. Davies<sup>3</sup>  
Astrophysical Journal, 715:493–499, **2010 May**; **File**

We discuss how simultaneous observations by multiple heliospheric imagers (HIs) can provide some important information about the azimuthal properties of coronal mass ejections (CMEs) in the heliosphere. We propose two simple models of CME geometry that can be used to derive information about the azimuthal deflection and the azimuthal expansion of CMEs from SECCHI/Hi observations. We apply these two models to four CMEs well observed by both STEREO spacecraft during the year 2008. We find that in three cases, the joint STEREO-A and B observations are consistent with CMEs moving radially outward. In some cases, we are able to derive the azimuthal cross section of the CME fronts, and we are able to measure the deviation from self-similar evolution. The results from this analysis show the importance of having multiple satellites dedicated to space weather forecasting, for example, in orbits at the Lagrangian L4 and L5 points.

## **Deriving the radial distances of wide coronal mass ejections from elongation measurements in the heliosphere – application to CME-CME interaction**

N. [Lugaz](#)<sup>1</sup>, A. Vourlidas<sup>2</sup>, and I. I. Roussev<sup>1</sup>  
Ann. Geophys., 27, 3479–3488, **2009**, **File**  
[www.ann-geophys.net/27/3479/2009/](http://www.ann-geophys.net/27/3479/2009/)

We present general considerations regarding the derivation of the radial distances of coronal mass ejections (CMEs) from elongation angle measurements such as those provided by SECCHI and SMEI, focusing on measurements in the Heliospheric Imager 2 (HI-2) field of view (i.e. past 0.3 AU). This study is based on a three-dimensional (3-D) magneto-hydrodynamics (MHD) simulation of two CMEs observed by SECCHI on **24–27 January 2007**. Having a 3-D simulation with synthetic HI images, we are able to compare the two basic methods used to derive CME positions from elongation angles, the so-called "Point-P" and "Fixed- $\phi$ " approximations. We confirm, following similar works, that both methods, while valid in the most inner heliosphere, yield increasingly large errors in HI-2 field of view for fast and wide CMEs. Using a simple model of a CME as an expanding self-similar sphere, we derive an analytical relationship between elongation angles and radial distances for wide CMEs. This relationship is simply the harmonic

mean of the "Point-P" and "Fixed- $\phi$ " approximations and it is aimed at complementing 3-D fitting of CMEs by cone models or flux rope shapes. It proves better at getting the kinematics of the simulated CME right when we compare the results of our line-of-sights to the MHD simulation. Based on this approximation, we re-analyze the J-maps (time-elongation maps) in 26–27 January 2007 and present the first observational evidence that *the merging of CMEs is associated with a momentum exchange from the faster ejection to the slower one due to the propagation of the shock wave associated with the fast eruption through the slow eruption*. **STEREO**

### **Solar-Terrestrial Simulation in the STEREO Era: The January 24-25, 2007 Eruptions**

N. [Lugaz](#), A. Vourlidas, I. I. Roussev, H. Morgan

E-print, March 2009, [File](#); Solar Phys.

The SECCHI instruments aboard the recently launched STEREO spacecraft enable for the first time the continuous tracking of coronal mass ejections (CMEs) from the Sun to 1 AU. We analyze line-of-sight observations of the **January 24-25, 2007** CMEs and fill the 20-hour gap in SECCHI coverage in January 25 by performing a numerical simulation using a three-dimensional magneto-hydrodynamic (MHD) code, the Space Weather Modeling Framework (SWMF). We show how the observations reflect the interaction of the two successive CMEs with each other and with the structured solar wind. We make a detailed comparison between the observations and synthetic images from our model, including time-elongation maps for several position angles. Having numerical simulations to disentangle observational from physical effects, we are able to study the three-dimensional nature of the ejections and their evolution in the inner heliosphere. This study reflects the start of a new era where, on one hand, models of CME propagation and interaction can be fully tested by using heliospheric observations and, on the other hand, observations can be better interpreted by using global numerical models.

### **The August 24, 2002 Coronal Mass Ejection: When a Western Limb Event Connects to Earth**

N. [Lugaz](#)<sup>1</sup>, Ilia I. Roussev<sup>1</sup> and Igor V. Sokolov<sup>2</sup>

Universal Heliophysical Processes

Proceedings IAU Symposium No. IAU257, 2008; [File](#)

N. Gopalswamy, D. Webb & A. Nindos, eds.

Abstract. We discuss how some coronal mass ejections (CMEs) originating from the western limb of the Sun are associated with space weather effects such as solar energetic particles (SEPs), shock or geo-effective ejecta at Earth. We focus on the August 24, 2002 coronal mass ejection, a fast ( $\sim 2000 \text{ km s}^{-1}$ ) eruption originating from W81. Using a three-dimensional magneto-hydrodynamic simulation of this ejection with the Space Weather Modeling Framework (SWMF), we show how a realistic initiation mechanism enables us to study the deflection of the CME in the corona and the heliosphere. Reconnection of the erupting magnetic field with that of neighboring streamers and active regions modify the solar connectivity of the field lines connecting to Earth and can also partly explain the deflection of the eruption during the first tens of minutes. Comparing the results at 1 AU of our simulation with observations by the ACE spacecraft, we find that the simulated shock does not reach Earth, but has a maximum angular span of about  $120^\circ$ , and reaches  $35^\circ$  West of Earth in 58 hours. We find no significant deflection of the CME and its associated shock wave in the heliosphere, and we discuss the consequences for the shock angular span.

### **THE BRIGHTNESS OF DENSITY STRUCTURES AT LARGE SOLAR ELONGATION ANGLES: WHAT IS BEING OBSERVED BY *STEREO SECCHI*?**

N. [Lugaz](#),<sup>1</sup> A. Vourlidas,<sup>2</sup> I. I. Roussev,<sup>1</sup> C. Jacobs,<sup>3</sup> W. B. Manchester IV,<sup>4</sup> and O. Cohen<sup>4</sup>

Astrophysical Journal, 684: L111–L114, 2008 September

<http://www.journals.uchicago.edu/toc/apjl/2008/684/2>

We discuss features of coronal mass ejections (CMEs) that are specific to heliospheric observations at large elongation angles. Our analysis is focused on a series of two eruptions that occurred on **2007 January 24–25**, which were tracked by the Heliospheric Imagers (HIs) on board *STEREO*. Using a three-dimensional (3D) magnetohydrodynamic simulation of these ejections with the **Space Weather Modeling Framework (SWMF)**, we illustrate how the combination of the 3D nature of CMEs, solar rotation, and geometry associated with the Thomson sphere results in complex effects in the brightness observed by the HIs. Our results demonstrate that these effects make any in-depth analysis of CME observations without 3D simulations challenging. In particular, the association of bright features seen by the HIs with fronts of CME-driven shocks is far from trivial. In this Letter, we argue that, on 2007 January 26, the HIs observed not only two CMEs, but also a dense corotating stream compressed by the CME-driven shocks.

### **The Evolution of Coronal Mass Ejection Density Structures**

N. [Lugaz](#), W. B. Manchester IV, and T. I. Gombosi

[The Astrophysical Journal](#), 627:1019-1030, 2005

We present a discussion of the time evolution of the mass and energy of a model coronal mass ejection (CME), analyzing both synthetic coronagraph images and three-dimensional data of the numerical ideal magnetohydrodynamics (MHD) simulation. Our global steady state coronal model possesses high-latitude coronal holes and a helmet streamer structure with a current sheet near the equator, reminiscent of near solar minimum conditions.

### **Data-driven, time-dependent modeling of pre-eruptive coronal magnetic field configuration at the periphery of NOAA AR 11726\***

E. Lumme<sup>1</sup>, J. Pomoell<sup>1</sup>, D. J. Price<sup>1</sup>, E. K. J. Kilpua<sup>1</sup>, M. D. Kazachenko<sup>2</sup>, G. H. Fisher<sup>3</sup> and B. T. Welsch<sup>4</sup>

A&A 658, A200 (2022)

<https://doi.org/10.1051/0004-6361/202038744>

<https://www.aanda.org/articles/aa/pdf/2022/02/aa38744-20.pdf>

**Context.** Data-driven, time-dependent magnetofrictional modeling has proved to be an efficient tool for studying the pre-eruptive build-up of energy for solar eruptions, and sometimes even the ejection of coronal flux ropes during eruptions. However, previous modeling works have illustrated the sensitivity of the results on the data-driven boundary condition, as well as the difficulty in modeling the ejections with proper time scales.

**Aims.** We aim to study the pre- and post-eruptive evolution of a weak coronal mass ejection producing eruption at the periphery of isolated NOAA active region (AR) 11726 using a data-driven, time-dependent magnetofrictional simulation, and aim to illustrate the strengths and weaknesses of our simulation approach.

**Methods.** We used state-of-the-art data processing and electric field inversion methods to provide the data-driven boundary condition for the simulation. We analyzed the field-line evolution, magnetic connectivity, twist, as well as the energy and helicity budgets in the simulation to study the pre- and post-eruptive magnetic field evolution of the observed eruption from AR11726.

**Results.** We find the simulation to produce a pre-eruptive flux rope system consistent with several features in the extreme ultraviolet and X-ray observations of the eruption, but the simulation largely fails to reproduce the ejection of the flux rope. We find the flux rope formation to be likely driven by the photospheric vorticity at one of the footpoints, although reconnection at a coronal null-point may also feed poloidal flux to the flux rope. The accurate determination of the non-inductive (curl-free) component of the photospheric electric field boundary condition is found to be essential for producing the flux rope in the simulation.

**Conclusions.** Our results illustrate the applicability of the data-driven, time-dependent magnetofrictional simulations in modeling the pre-eruptive evolution and formation process of a flux rope system, but they indicate that the modeling output becomes problematic for the post-eruptive times. For the studied event, the flux rope also constituted only a small part of the related active region.

### **Probing the Effect of Cadence on the Estimates of Photospheric Energy and Helicity Injections in Eruptive Active Region NOAA AR 11158**

E. Lumme, M. D. Kazachenko, G. H. Fisher, B. T. Welsch, J. Pomoell, E. K. J. Kilpua

*Solar Physics* June 2019, 294:84

<https://link.springer.com/content/pdf/10.1007%2Fs11207-019-1475-x.pdf>

We study how the input-data cadence affects the photospheric energy and helicity injection estimates in eruptive NOAA Active Region 11158. We sample the novel 2.25-minute vector magnetogram and Dopplergram data from the Helioseismic and Magnetic Imager (HMI) instrument onboard the Solar Dynamics Observatory (SDO) spacecraft to create input datasets of variable cadences ranging from 2.25 minutes to 24 hours. We employ state-of-the-art data processing, velocity, and electric-field inversion methods for deriving estimates of the energy and helicity injections from these datasets. We find that the electric-field inversion methods that reproduce the observed magnetic-field evolution through the use of Faraday's law are more stable against variable cadence: the PDFI (PTD-Doppler-FLCT-Ideal, where PTD refers to Poloidal-Toroidal Decomposition, and FLCT to Fourier Local Correlation Tracking) electric-field inversion method produces consistent injection estimates for cadences from 2.25 minutes up to two hours, implying that the photospheric processes acting on time scales below two hours contribute little to the injections, or that they are below the sensitivity of the input data and the PDFI method. On other hand, the electric-field estimate derived from the output of DAVE4VM (Differential Affine Velocity Estimator for Vector Magnetograms), which does not fulfill Faraday's law exactly, produces significant variations in the energy and helicity injection estimates in the 2.25 minutes – two hours cadence range. We also present a third, novel DAVE4VM-based electric-field estimate, which corrects the poor inductivity of the raw DAVE4VM estimate. This method is less sensitive to the changes of cadence, but it still faces significant issues for the lowest of considered cadences ( $\geq$  two hours). We find several potential problems in both PDFI- and DAVE4VM-based injection estimates and conclude that the quality of both should be surveyed further in controlled environments. **11-17 Feb 2011**

### **Study of the excitation of large amplitude oscillations in a prominence by nearby flares**

[Manuel Luna](#), [Reetika Joshi](#), [Brigitte Schmieder](#), [Fernando Moreno-Insertis](#), [Valeriia Liakh](#), [Jaume Terradas](#)

A&A 2024

<https://arxiv.org/pdf/2410.10223>

Large amplitude oscillations commonly occur in solar prominences, triggered by energetic phenomena such as jets and flares. On **March 14-15, 2015**, a filament partially erupted in two stages, leading to oscillations in different parts. This

study explores longitudinal oscillations from the eruption, focusing on the mechanisms behind their initiation, with special attention to the large oscillation on March 15. The oscillations and jets are analyzed using the time-distance technique. For flares and their interaction with the filament, we analyze AIA channels and use the DEM technique. Initially, a jet fragments the filament, splitting it into two segments. One remains in place, while the other detaches and moves. This causes oscillations in both segments: (a) the position change causes the detached segment to oscillate with a period of  $69 \pm 3$  minutes; (b) the jet flows cause the remaining filament to oscillate with a period of  $62 \pm 2$  minutes. In the second phase, on March 15, another jet seemingly activates the detached filament eruption, followed by a flare. A large longitudinal oscillation occurs in the remnant segment with a period of  $72 \pm 2$  minutes and velocity amplitude  $73 \pm 1 \text{ km s}^{-1}$ . During the oscillation trigger, bright field lines connect the flare with the filament, appearing only in the AIA 131Å and 94Å channels, indicating the presence of hot plasma. DEM analysis confirms this, showing plasma around 10 MK pushing the prominence from its southeastern side, displacing it along the field lines and starting the oscillation. From this, the flare -- not the preceding jet--triggers the oscillation. The hot plasma flows into the filament channel. We explain how flares trigger large oscillations in filaments by proposing that post-flare loops reconnect with the filament channel's magnetic field.

### **Automatic detection technique for solar filament oscillations in GONG data**

M. Luna<sup>1,2</sup>, J. R. Mérou Mestrel<sup>1,2</sup> and F. Auchère<sup>3</sup>

A&A 666, A195 (2022)

<https://www.aanda.org/articles/aa/pdf/2022/10/aa44181-22.pdf>

Context. Solar filament oscillations have been known for decades. The new capabilities of the new telescopes have afforded routine observations of these periodic motions. Oscillations in filaments show key aspects of their structure. A systematic study of filament oscillations over the solar cycle can shed light on the evolution of the prominences.

Aims. This work is a proof of concept that aims to automatically detect and parametrise these oscillations using H $\alpha$  data from the GONG network of telescopes.

Methods. The proposed technique studies the periodic fluctuations of every pixel of the H $\alpha$  data cubes. Using the fast Fourier transform, we computed the power spectral density (PSD). We defined a criterion to consider whether it is a real oscillation or a spurious fluctuation. This consisted of considering that the peak in the PSD must be greater than several times the background noise with a confidence level of 95%. The background noise is well fitted to a combination of red and white noise. We applied the method to several observations that were reported in the literature to determine its reliability. We also applied the method to a test case, which was a data set in which the oscillations of the filaments were not known a priori.

Results. The method shows that the filaments contain areas in which the PSD is above the threshold value. The periodicities we obtained generally agree with the values that were obtained by other methods. In the test case, the method detects oscillations in several filaments.

Conclusions. We conclude that the proposed spectral technique is a powerful tool for automatically detecting oscillations in prominences using H $\alpha$  data. **January 1, 2014, February 9, 2014, February 13, 2014, June 16, 2014, March 15, 2015, February 9, 2022**

### **Large-amplitude prominence oscillations following the impact by a coronal jet**

[Manuel Luna](#), [Fernando Moreno-Insertis](#)

ApJ 912 75 2021

<https://arxiv.org/pdf/2103.02661.pdf>

<https://doi.org/10.3847/1538-4357/abec46>

Observational evidence shows that coronal jets can hit prominences and set them in motion. The impact leads to large-amplitude oscillations (LAOs) of the prominence. In this paper we attempt to understand this process via 2.5D MHD numerical experiments. In our model, the jets are generated in a sheared magnetic arcade above a parasitic bipolar region located in one of the footpoints of the filament channel (FC) supporting the prominence. The shear is imposed with velocities not far above observed photospheric values; it leads to a multiple reconnection process, as in previous jet models. Both a fast Alfvénic perturbation and a slower supersonic front preceding a plasma jet are issued from the reconnection site; in the later phase, a more violent (eruptive) jet is produced. The perturbation and jets run along the FC; they are partially reflected at the prominence and partially transmitted through it. There results a pattern of counter-streaming flows along the FC and oscillations of the prominence. The oscillations are LAOs (with amplitude above  $10 \text{ km s}^{-1}$ ) in parts of the prominence both in the longitudinal and transverse directions. In some field lines, the impact is so strong that the prominence mass is brought out of the dip and down to the chromosphere along the FC. Two cases are studied with different heights of the arcade above the parasitic bipolar region, leading to different heights for the region of the prominence perturbed by the jets. The obtained oscillation amplitudes and periods are in general agreement with the observations.

### **Large-Amplitude Longitudinal Oscillations Triggered by the Merging of Two Solar Filaments: Observations and Magnetic Field Analysis**

M. Luna, Y. Su, B. Schmieder, R. Chandra, T. A. Kucera

ApJ 850 143 2017

<https://arxiv.org/pdf/1711.01038.pdf>

We follow the eruption of two related intermediate filaments observed in  $H\alpha$  (from GONG) and in EUV (from SDO/AIA) and the resulting large-amplitude longitudinal oscillations of the plasma in the filament channels. The events occurred in and around the decayed active region AR12486 on **2016 January 26**. Our detailed study of the oscillation reveals that the periods of the oscillations are about one hour. In  $H\alpha$  the period decreases with time and exhibits strong damping. The analysis of 171- $\text{\AA}$  images shows that the oscillation has two phases, an initial long period phase and a subsequent oscillation with a shorter period. In this wavelength the damping appears weaker than in  $H\alpha$ . The velocity is the largest ever detected in a prominence oscillation, approximately  $100 \text{ km s}^{-1}$ . Using SDO/HMI magnetograms we reconstruct the magnetic field of the filaments modeled as flux ropes by using a flux-rope insertion method. Applying seismological techniques we determine that the radii of curvature of the field lines in which cool plasma is condensed are in the range 75-120 Mm, in agreement with the reconstructed field. In addition, we infer a field strength of  $\geq 7$  to 30 gauss, depending on the electron density assumed; that is also in agreement with the values from the reconstruction (8-20 gauss). The poloidal flux is zero and the axis flux is of the order of 1020 to 1021 Mx, confirming the high shear existing even in a non-active filament.

### **Where and how does a decay-index profile become saddle-like?**

[Runbin Luo](#), [Rui Liu](#)

ApJ **929** 2 **2022**

<https://arxiv.org/pdf/2203.03913>

<https://iopscience.iop.org/article/10.3847/1538-4357/ac5b06/pdf>

The decay index of solar magnetic fields is known as an important parameter in regulating solar eruptions from the standpoint of the torus instability. In particular, a saddle-like profile of decay index, which hosts a local torus-stable regime at higher altitudes than where the decay index first exceeds the instability threshold, is found to be associated with some confined or two-step eruptions. To understand the occurrence of such a profile, we employed dipoles to emulate different kinds of photospheric flux distributions. Corroborated by observations of representative active regions (ARs), our major results are: 1) in bipolar configurations the critical height increases away from the AR center along the polarity inversion line (PIL) and its average is roughly half of the centroid distance between opposite polarities; 2) in quadrupolar configurations saddle-like profiles appear above the PIL when the two dipoles oriented in the same direction are significantly more separated in this direction than in the perpendicular direction, and when the two dipoles are oriented differently or have unequal fluxes; 3) saddle-like profiles in quadrupolar configurations are associated with magnetic skeletons such as a null point or a hyperbolic flux tube, and the role of such profiles in eruptions is anticipated to be double-edged if magnetic reconnection is involved.

### **Connecting Solar and Stellar Flares/CMEs: Expanding Heliophysics to Encompass Exoplanetary Space Weather**

**Review**

[B. J. Lynch](#), [B. E. Wood](#), [M. Jin](#), [T. Török](#), [X. Sun](#), [E. Palmerio](#), [R. A. Osten](#), [A. A. Vidotto](#), [O. Cohen](#), [J. D. Alvarado-Gómez](#), [J. J. Drake](#), [V. S. Airapetian](#), [Y. Notsu](#), [A. Veronig](#), [K. Namekata](#), [R. M. Winslow](#), [L. K. Jian](#), [A. Vourlidis](#), [N. Lugaz](#), [N. Al-Haddad](#), [W. B. Manchester](#), [C. Scolini](#), [C. J. Farrugia](#), [E. E. Davies](#), [T. Nieves-Chinchilla](#), [F. Carcaboso](#), [C. O. Lee](#), [T. M. Salman](#)

White paper submitted to the Heliophysics 2024--2033 Decadal Survey **2022**

<https://arxiv.org/pdf/2210.06476.pdf>

The aim of this white paper is to briefly summarize some of the outstanding gaps in the observations and modeling of stellar flares, CMEs, and exoplanetary space weather, and to discuss how the theoretical and computational tools and methods that have been developed in heliophysics can play a critical role in meeting these challenges. The maturity of data-inspired and data-constrained modeling of the Sun-to-Earth space weather chain provides a natural starting point for the development of new, multidisciplinary research and applications to other stars and their exoplanetary systems. Here we present recommendations for future solar CME research to further advance stellar flare and CME studies. These recommendations will require institutional and funding agency support for both fundamental research (e.g. theoretical considerations and idealized eruptive flare/CME numerical modeling) and applied research (e.g. data inspired/constrained modeling and estimating exoplanetary space weather impacts). In short, we recommend continued and expanded support for: (1.) Theoretical and numerical studies of CME initiation and low coronal evolution, including confinement of "failed" eruptions; (2.) Systematic analyses of Sun-as-a-star observations to develop and improve stellar CME detection techniques and alternatives; (3.) Improvements in data-inspired and data-constrained MHD modeling of solar CMEs and their application to stellar systems; and (4.) Encouraging comprehensive solar--stellar research collaborations and conferences through new interdisciplinary and multi-agency/division funding mechanisms.

### **On the utility of flux rope models for CME magnetic structure below $30R_{\odot}$**

[Benjamin Lynch](#), [Nada Al-Haddad](#), [Wenyuan Yu](#), [Erika Palmerio](#), [Noé Lugaz](#)

Adv. Space Res **Volume 70**, Issue 6, Pages 1614-1640 **2022**

<https://arxiv.org/pdf/2205.02144.pdf>

<https://reader.elsevier.com/reader/sd/pii/S0273117722003659>

We present a comprehensive analysis of the three-dimensional magnetic flux rope structure generated during the Lynch et al. (2019) magnetohydrodynamic (MHD) simulation of a global-scale, 360 degree-wide streamer blowout coronal



mass ejection (CME) eruption. We create both fixed and moving synthetic spacecraft to generate time series of the MHD variables through different regions of the flux rope CME. Our moving spacecraft trajectories are derived from the spatial coordinates of Parker Solar Probe's past encounters 7 and 9 and future encounter 23. Each synthetic time series through the simulation flux rope ejecta is fit with three different in-situ flux rope models commonly used to characterize the large-scale, coherent magnetic field rotations observed in a significant fraction of interplanetary CMEs (ICMEs). We present each of the in-situ flux rope model fits to the simulation data and discuss the similarities and differences between the model fits and the MHD simulation's flux rope spatial orientations, field strengths and rotations, expansion profiles, and magnetic flux content. We compare in-situ model properties to those calculated with the MHD data for both classic bipolar and unipolar ICME flux rope configurations as well as more problematic profiles such as those with a significant radial component to the flux rope axis orientation or profiles obtained with large impact parameters. We find general agreement among the in-situ flux rope fitting results for the classic profiles and much more variation among results for the problematic profiles. We also examine the force-free assumption for a subset of the flux rope models and quantify properties of the Lorentz force within MHD ejecta intervals. We conclude that the in-situ flux rope models are generally a decent approximation to the field structure, but all the caveats associated with in-situ flux rope models will still apply...

## **Modeling a Coronal Mass Ejection from an Extended Filament Channel. I. Eruption and Early Evolution**

[Benjamin J. Lynch](#), [Erika Palmerio](#), [C. Richard DeVore](#), [Maria D. Kazachenko](#), [Joel T. Dahlin](#), [Jens Pomoell](#), [Emilia K. J. Kilpua](#)

ApJ **914** 39 **2021**

<https://arxiv.org/pdf/2104.08643.pdf>

<https://iopscience.iop.org/article/10.3847/1538-4357/abf9a9/pdf>

<https://doi.org/10.3847/1538-4357/abf9a9>

We present observations and modeling of the magnetic field configuration, morphology, and dynamics of a large-scale, high-latitude filament eruption observed by the Solar Dynamics Observatory. We analyze the **2015 July 9-10** filament eruption and the evolution of the resulting coronal mass ejection (CME) through the solar corona. The slow streamer-blowout CME leaves behind an elongated post-eruption arcade above the extended polarity inversion line that is only poorly visible in extreme ultraviolet (EUV) disk observations and does not resemble a typical bright flare-loop system. Magnetohydrodynamic (MHD) simulation results from our data-inspired modeling of this eruption compare favorably with the EUV and white-light coronagraph observations. We estimate the reconnection flux from the simulation's flare-arcade growth and examine the magnetic-field orientation and evolution of the erupting prominence, highlighting the transition from an erupting sheared-arcade filament channel into a streamer-blowout flux-rope CME. Our results represent the first numerical modeling of a global-scale filament eruption where multiple ambiguous and complex observational signatures in EUV and white light can be fully understood and explained with the MHD simulation. In this context, our findings also suggest that the so-called "stealth CME" classification, as a driver of unexpected or "problem" geomagnetic storms, belongs more to a continuum of observable/non-observable signatures than to separate or distinct eruption processes.

## **A Model for Coronal Inflows and In/Out Pairs**

[Benjamin J. Lynch](#)

**2020** ApJ **905** 139

<https://arxiv.org/pdf/2010.13959.pdf>

<https://doi.org/10.3847/1538-4357/abc5b3>

This report presents a three-dimensional (3D) numerical magnetohydrodynamics (MHD) model of the white-light coronagraph observational phenomena known as coronal inflows and in/out pairs. Coronal inflows in the LASCO/C2 field of view (approximately 2-6 Rs) were thought to arise from the dynamic and intermittent release of solar wind plasma associated with the helmet streamer belt as the counterpart to outward-propagating streamer blobs, formed by magnetic reconnection. This interpretation was essentially confirmed with the subsequent identification of in/out pairs and the multispacecraft observations of their 3D structure. The MHD simulation results show relatively narrow lanes of density depletion form high in the corona and propagate inwards with sinuous motion which has been characterized as 'tadpole-like' in coronagraph imagery. The height-time evolution and velocity profiles of the simulation inflows and in/out pairs are compared to their corresponding observations and a detailed analysis of the underlying magnetic field structure associated with the synthetic white-light and mass density evolution is presented. Understanding the physical origin of this structured component of the slow solar wind's intrinsic variability could make a significant contribution to solar wind modeling and the interpretation of remote and in-situ observations from Parker Solar Probe and Solar Orbiter. **2015 July 10**

## **Modeling a Carrington-scale Stellar Superflare and Coronal Mass Ejection from $\kappa$ 1Cet**

[Benjamin J. Lynch](#), [Vladimir S. Airapetian](#), [C. Richard DeVore](#), [Maria D. Kazachenko](#), [Teresa Lüftinger](#), [Oleg Kochukhov](#), [Lisa Rosén](#), [William P. Abbett](#)

ApJ **880** 97 **2019**

<https://arxiv.org/pdf/1906.03189.pdf>

<https://doi.org/10.3847/1538-4357/ab287e>

Observations from the Kepler mission have revealed frequent superflares on young and active solar-like stars. Superflares result from the large-scale restructuring of stellar magnetic fields, and are associated with the eruption of coronal material (a coronal mass ejection, or CME) and energy release that can be orders of magnitude greater than those observed in the largest solar flares. These catastrophic events, if frequent, can significantly impact the potential habitability of terrestrial exoplanets through atmospheric erosion or intense radiation exposure at the surface. We present results from numerical modeling designed to understand how an eruptive superflare from a young solar-type star,  $\kappa$ 1Cet, could occur and would impact its astrospheric environment. Our data-inspired, three-dimensional magnetohydrodynamic modeling shows that global-scale shear concentrated near the radial-field polarity inversion line can energize the closed-field stellar corona sufficiently to power a global, eruptive superflare that releases approximately the same energy as the extreme 1859 Carrington event from the Sun. We examine proxy measures of synthetic emission during the flare and estimate the observational signatures of our CME-driven shock, both of which could have extreme space-weather impacts on the habitability of any Earth-like exoplanets. We also speculate that the observed 1986 Robinson-Bopp superflare from  $\kappa$ 1Cet was perhaps as extreme for that star as the Carrington flare was for the Sun.

### **A model for stealth coronal mass ejections†**

B. J. **Lynch**, S. Masson, Y. Li, C. R. DeVore, J. G. Luhmann, S. K. Antiochos, G. H. Fisher  
JGR Vol: 121, Pages: 10,677–10,697 2016

<http://sci-hub.cc/doi/10.1002/2016JA023432>

<https://arxiv.org/pdf/1612.08323v1.pdf>

Stealth coronal mass ejections (CMEs) are events in which there are almost no observable signatures of the CME eruption in the low corona but often a well-resolved slow flux rope CME observed in the coronagraph data. We present results from a three-dimensional numerical magnetohydrodynamics (MHD) simulation of the **2008 June 1-2** slow streamer blowout CME that Robbrecht et al. [2009] called “the CME from nowhere.” We model the global coronal structure using a 1.4 MK isothermal solar wind and a low-order potential field source surface representation of the Carrington Rotation 2070 magnetogram synoptic map. The bipolar streamer belt arcade is energized by simple shearing flows applied in the vicinity of the helmet streamer’s polarity inversion line. The flows are large-scale and impart a shear typical of that expected from the differential rotation. The slow expansion of the energized helmet-streamer arcade results in the formation of a radial current sheet. The subsequent onset of expansion-induced flare reconnection initiates the stealth CME while gradually releasing the stored magnetic energy. We present favorable comparisons between our simulation results and the multi-viewpoint SOHO-LASCO and STEREO-SECCHI coronagraph observations of the pre-eruption streamer structure and the initiation and evolution of the stealth streamer blowout CME.

See <https://phys.org/news/2017-05-space-weather-simulates-solar-storms.html>

### **Reconnection Properties of Large-Scale Current Sheets During Coronal Mass Ejection Eruptions**

B. J. **Lynch**, J. K. Edmondson, M. D. Kazachenko, S. E. Guidoni  
2016 *ApJ* 826 43

2014 <http://arxiv.org/pdf/1410.1089v1.pdf>

We present a detailed analysis of the properties of magnetic reconnection at large-scale current sheets in a high cadence version of the Lynch and Edmondson (2013) 2.5D MHD simulation of sympathetic magnetic breakout eruptions from a pseudostreamer source region. We examine the resistive tearing and breakup of the three main current sheets into chains of X- and O-type null points and follow the dynamics of magnetic island growth, their merging, transit, and ejection with the reconnection exhaust. For each current sheet, we quantify the evolution of the length-to-width aspect ratio (up to  $\sim 100:1$ ), Lundquist number ( $\sim 104$ ), and reconnection rate (inflow-to-outflow ratios reaching  $\sim 0.15$ ). We examine the statistical and spectral properties of the fluctuations in the current sheets resulting from the plasmoid instability, including the distribution of magnetic island width, mass, and flux content. We show that the temporal evolution of the spectral index of the reconnection-generated magnetic energy density fluctuations appear to reflect global properties of the current sheet evolution. Our results are in excellent agreement with recent, high resolution reconnection-in-a-box simulations even though our current sheets’ formation, growth, and dynamics are intrinsically coupled to the global evolution of sequential sympathetic CME eruptions.

### **Interchange Reconnection Alfvén Wave Generation**

B. J. **Lynch**, J. K. Edmondson, Y. Li

Solar Physics, August 2014, Volume 289, Issue 8, pp 3043-3058

Given recent observational results of interchange reconnection processes in the solar corona and the theoretical development of the S-Web model for the slow solar wind, we extend the analysis of the 3D MHD simulation of interchange reconnection by Edmondson et al. (*Astrophys. J.* 707, 1427, 2009). Specifically, we analyze the consequences of the dynamic streamer-belt jump that corresponds to flux opening by interchange reconnection. Information about the magnetic field restructuring by interchange reconnection is carried throughout the system by Alfvén waves propagating away from the reconnection region, distributing the shear and twist imparted by the driving

flows, including shedding the injected stress-energy and accumulated magnetic helicity along newly open fieldlines. We quantify the properties of the reconnection-generated wave activity in the simulation. There is a localized high-frequency component associated with the current sheet/reconnection site and an extended low-frequency component associated with the large-scale torsional Alfvén wave generated from the interchange reconnection field restructuring. The characteristic wavelengths of the torsional Alfvén wave reflect the spatial size of the energized bipolar flux region. Lastly, we discuss avenues of future research by modeling these interchange reconnection-driven waves and investigating their observational signatures.

## **SYMPATHETIC MAGNETIC BREAKOUT CORONAL MASS EJECTIONS FROM PSEUDOSTREAMERS**

B. J. [Lynch](#)<sup>1</sup> and J. K. Edmondson

**2013** ApJ 764 87

We present high-resolution 2.5D MHD simulation results of magnetic breakout-initiated coronal mass ejections (CMEs) originating from a coronal pseudostreamer configuration. The coronal null point in the magnetic topology of pseudostreamers means that the initiation of consecutive sympathetic eruptions is a natural consequence of the system's evolution. A generic source region energization process—ideal footprint shearing parallel to the pseudostreamer arcade polarity inversion lines—is all that is necessary to store sufficient magnetic energy to power consecutive CME eruptions given that the pseudostreamer topology enables the breakout initiation mechanism. The second CME occurs because the eruptive flare reconnection of the first CME simultaneously acts as the overlying pre-eruption breakout reconnection for the sympathetic eruption. We examine the details of the magnetic and kinetic energy evolution and the signatures of the overlying null point distortion, current sheet formation, and magnetic breakout reconnection giving rise to the runaway expansion that drives the flare reconnection below the erupting sheared field core. The numerical simulation's spatial resolution and output cadence are sufficient to resolve the formation of magnetic islands during the reconnection process in both the breakout and eruptive flare current sheets. We quantify the flux transfer between the pseudostreamer arcades and show that the eruptive flare reconnection processes flux  $\sim 10$  times faster than the pre-eruption breakout reconnection. We show that the breakout reconnection jets cause bursty, intermittent upflows along the pseudostreamer stalk, as well as downflows in the adjacent pseudostreamer arcade, both of which may be observable as pre-eruption signatures. Finally, we examine the flux rope CME trajectories and show that the breakout current sheet provides a path of least resistance as an imbalance in the surrounding magnetic energy density and results in a non-radial CME deflection early in the eruption.

## **IONIC COMPOSITION STRUCTURE OF CORONAL MASS EJECTIONS IN AXISYMMETRIC MAGNETOHYDRODYNAMIC MODELS**

B. J. [Lynch](#)<sup>1</sup>, A. A. Reinard<sup>2</sup>, T. Mulligan<sup>3</sup>, K. K. Reeves<sup>4</sup>, C. E. Rakowski<sup>5</sup>, J. C. Allred<sup>6</sup>, Y. Li<sup>1</sup>, J. M. Laming<sup>5</sup>, P. J. MacNeice<sup>7</sup> and J. A. Linker

**2011** ApJ 740 112

We present the ionic charge state composition structure derived from axisymmetric MHD simulations of coronal mass ejections (CMEs), initiated via the flux-cancellation and magnetic breakout mechanisms. The flux-cancellation CME simulation is run on the Magnetohydrodynamics-on-A-Sphere code developed at Predictive Sciences, Inc., and the magnetic breakout CME simulation is run on ARC7 developed at NASA GSFC. Both MHD codes include field-aligned thermal conduction, radiative losses, and coronal heating terms which make the energy equations sufficient to calculate reasonable temperatures associated with the steady-state solar wind and model the eruptive flare heating during CME formation and eruption. We systematically track a grid of Lagrangian plasma parcels through the simulation data and calculate the coronal density and temperature history of the plasma in and around the CME magnetic flux ropes. The simulation data are then used to integrate the continuity equations for the ionic charge states of several heavy ion species under the assumption that they act as passive tracers in the MHD flow. We construct two-dimensional spatial distributions of commonly measured ionic charge state ratios in carbon, oxygen, silicon, and iron that are typically elevated in interplanetary coronal mass ejection (ICME) plasma. We find that the slower CME eruption has relatively enhanced ionic charge states and the faster CME eruption shows basically no enhancement in charge states—which is the opposite trend to what is seen in the in situ ICME observations. The primary cause of the difference in the ionic charge states in the two simulations is not due to the different CME initiation mechanisms per se. Rather, the difference lies in their respective implementation of the coronal heating which governs the steady-state solar wind, density and temperature profiles, the duration of the connectivity of the CME to the eruptive flare current sheet, and the contribution of the flare-heated plasma associated with the reconnection jet outflow into the ejecta. Despite the limitations inherent in the first attempt at this novel procedure, the simulation results provide strong evidence in support of the conclusion that enhanced heavy ion charge states within CMEs are a direct consequence of flare heating in the low corona. We also discuss future improvements through combining numerical CME modeling with quantitative ionic charge state calculations.

### **Sun to 1 AU propagation and evolution of a slow streamer-blowout coronal mass ejection**

[Lynch](#), B. J.; Li, Y.; Thernisien, A. F. R.; Robbrecht, E.; Fisher, G. H.; Luhmann, J. G.; Vourlidis, A. J. Geophys. Res., Vol. 115, No. A7, A07106, **2010**; **File**

<http://dx.doi.org/10.1029/2009JA015099>

We present a comprehensive analysis of the evolution of the classic, slow streamer-blowout CME of **1 June 2008** observed by the STEREO twin spacecraft to infer relevant properties of the pre-eruption source region which includes a substantial portion of the coronal helmet streamer belt. The CME was directed ~~E40th Base and the Sun~~ Heliospheric Imager observations are consistent with the CME propagating essentially radially to 1 AU. The elongation-time J-map constructed from the STEREO-A HI images tracks the arrival of two density peaks that bound the magnetic flux rope ICME seen at STEREO-B on 6 June 2008. From the STEREO-A elongation-time plots we measure the ICME flux rope radial size  $R_c(t)$  and find it well approximated by the constant expansion value  $V_{exp} = 24.5$  km/s obtained from the STEREO-B declining velocity profile within the magnetic cloud. The flux rope spatial orientation, determined by forward modeling fits to the STEREO COR2 and HI1 data, approaches the observed 1 AU flux rope orientation and suggests large-scale rotation during propagation, as predicted by recent numerical simulations. We compare the ICME flux content to the PFSS model coronal field for Carrington Rotation 2070 and find sufficient streamer belt flux to account for the observed ICME poloidal/twist flux if reconnection during CME initiation process is responsible for the conversion of overlying field into the flux rope twist component in the standard fashion. However, the PFSS model field cannot account for the ICME toroidal/axial flux component. We estimate the field strength of the pre-eruption sheared/axial component in the low corona and the timescales required to accumulate this energized pre-eruption configuration via differential rotation and flux cancelation by supergranular diffusion at the polarity inversion line. We show that both mechanisms are capable of generating the desired shear component over time periods of roughly 1–2 months. We discuss the implications for slow streamer-blowout CMEs arising as a natural consequence of the corona's re-adjustment to the long term evolutionary driving of the photospheric fields.

### **Rotation of Coronal Mass Ejections During Eruption**

B. J. **Lynch**, S. K. Antiochos, Y. Li, J. G. Luhmann, C. R. DeVore

E-print, March 2009; File; ApJ **697** 1918-1927 doi: [10.1088/0004-637X/697/2/1918](https://doi.org/10.1088/0004-637X/697/2/1918)

<http://www.iop.org/EJ/toc/-alert=43190/0004-637X/697/2>

Understanding the connection between coronal mass ejections (CMEs) and their interplanetary counterparts (ICMEs) is one of the most important problems in solar-terrestrial physics. We calculate the rotation of erupting field structures predicted by numerical simulations of CME initiation via the magnetic breakout model. In this model the initial potential magnetic field has a multipolar topology and the system is driven by imposing a shear flow at the photospheric boundary. Our results yield insight on how to connect solar observations of the orientation of the filament or polarity inversion line (PIL) in the CME source region, the orientation of the CME axis as inferred from coronagraph images, and the ICME flux rope orientation obtained from in-situ measurements. We present the results of two numerical simulations that differ only in the direction of the applied shearing motions (i.e., the handedness of the sheared arcade systems and their resulting CME fields). In both simulations, eruptive flare reconnection occurs underneath the rapidly expanding sheared fields transforming the ejecta fields into 3-dimensional flux rope structures. As the erupting flux ropes propagate through the low corona (from  $2-4 R_{\odot}$ ) the right-handed breakout flux rope rotates clockwise and the left-handed breakout flux rope rotates counterclockwise, in agreement with recent observations of the rotation of erupting filaments. We find that by  $3.5 R_{\odot}$  the average rotation angle between the flux rope axes and the active region PIL is approximately 50 degrees. We discuss the implications of these results for predicting, from the observed chirality of the pre-eruption filament and/or other properties of the CME source region, the direction and amount of rotation that magnetic flux rope structures will experience during eruption. We also discuss the implications of our results for CME initiation models.

### **TOPOLOGICAL EVOLUTION OF A FAST MAGNETIC BREAKOUT CME IN THREE DIMENSIONS**

B. J. **Lynch**,<sup>1</sup> S. K. Antiochos,<sup>2</sup> C. R. DeVore,<sup>3</sup> J. G. Luhmann,<sup>1</sup> and T. H. Zurbuchen<sup>4</sup>

Astrophysical Journal, 683:1192Y1206, 2008

<http://www.journals.uchicago.edu/toc/apj/2008/683/2>

We present the extension of the magnetic breakout model for CME initiation to a fully three-dimensional, spherical geometry. Given the increased complexity of the dynamic magnetic field interactions in three dimensions, we first present a summary of the well known axisymmetric breakout scenario in terms of the topological evolution associated with the various phases of the eruptive process. In this context, we discuss the analogous topological evolution during the magnetic breakout CME initiation process in the simplest three-dimensional multipolar system. We show that an extended bipolar active region embedded in an oppositely directed background dipole field has all the necessary topological features required for magnetic breakout, i.e., a fan separatrix surface between the two distinct flux systems, a pair of spine field lines, and a true three-dimensional coronal null point at their intersection. We then present the results of a numerical MHD simulation of this three-dimensional system where boundary shearing flows introduce free magnetic energy, eventually leading to a fast magnetic breakout CME. The eruptive flare reconnection facilitates the rapid conversion of this stored free magnetic energy into kinetic energy and the associated acceleration causes the erupting field and plasma structure to reach an asymptotic eruption velocity of  $k1100 \text{ km s}^{-1}$  over an  $\sim 15$  minute time period. The simulation results are discussed using the topological insight developed to interpret the various phases of the eruption and the complex, dynamic, and interacting magnetic field structures.

## Three-dimensional Reconstruction of Coronal Mass Ejections by CORAR Technique through Different Stereoscopic Angle of STEREO Twin Spacecraft

[Shaoyu Lyu](#), [Yuming Wang](#), [Xiaolei Li](#), [Jingnan Guo](#), [Chuanbing Wang](#), [Quanhao Zhang](#)

2021 *ApJ* **909** 182

<https://arxiv.org/ftp/arxiv/papers/2101/2101.03276.pdf>

<https://doi.org/10.3847/1538-4357/abd9c9>

Recently, we developed the Correlation-Aided Reconstruction (CORAR) method to reconstruct solar wind inhomogeneous structures, or transients, using dual-view white-light images (Li et al. 2020; Li et al. 2018). This method is proved to be useful for studying the morphological and dynamical properties of transients like blobs and coronal mass ejection (CME), but the accuracy of reconstruction may be affected by the separation angle between the two spacecraft (Lyu et al. 2020). Based on the dual-view CME events from the Heliospheric Imager CME Join Catalogue (HIJoinCAT) in the HELCATS (Heliospheric Cataloguing, Analysis and Techniques Service) project, we study the quality of the CME reconstruction by the CORAR method under different STEREO stereoscopic angles. We find that when the separation angle of spacecraft is around  $150^\circ$ , most CME events can be well reconstructed. If the collinear effect is considered, the optimal separation angle should locate between  $120^\circ$  and  $150^\circ$ . Compared with the CME direction given in the Heliospheric Imager Geometrical Catalogue (HIGeoCAT) from HELCATS, the CME parameters obtained by the CORAR method are reasonable. However, the CORAR-obtained directions have deviations towards the meridian plane in longitude, and towards the equatorial plane in latitude. An empirical formula is proposed to correct these deviations. This study provides the basis for the spacecraft configuration of our recently proposed Solar Ring mission concept (Wang et al. 2020b). **2009-08-26, 2009-12-22, 2010-04-06, 2010-08-18**

## Optimal stereoscopic angle for reconstructing solar wind inhomogeneous structures

[Lyu, S.](#), [Li, X.](#), & [Wang, Y.](#)

2020, *Advances in Space Research*, 66, 2251

<https://arxiv.org/pdf/2005.06838.pdf>

<https://doi.org/10.1016/j.asr.2020.07.045>

This paper is aimed at finding the best separation angle between spacecraft for the three-dimensional reconstruction of solar-wind inhomogeneous structures by the CORrelation-Aided Reconstruction (CORAR) method. The analysis is based on the dual-point heliospheric observations from the STEREO HI-1 cameras. We produced synthetic HI-1 white-light images containing artificial blob-like structures in different positions in the common field of view of the two HI-1 cameras and reconstruct the structures with CORAR method. The distributions of performance levels of the reconstruction for spacecraft separation of  $60^\circ$ ,  $90^\circ$ ,  $120^\circ$  and  $150^\circ$  are obtained. It is found that when the separation angle is  $120^\circ$ , the performance of the reconstruction is the best and the separation angle of  $90^\circ$  is the next. A brief discussion of the results are given as well. Based on this study, we suggest the optimal layout scheme of the recently proposed Solar Ring mission, which is designed to routinely observe the Sun and the inner heliosphere from multiple perspectives in the ecliptic plane.

## Coronal Mass Ejections as Expanding Force-Free Structures

[M. Lyutikov](#) and [K. N. Gourgouliatos](#)

*Solar Physics*, Volume 270, Number 2, 537-549, 2011

We model solar coronal mass ejections (CMEs) as expanding force-free magnetic structures and find the self-similar dynamics of configurations with spatially constant  $\alpha$ , where  $\mathbf{J}=\alpha \mathbf{B}$ , in spherical and cylindrical geometries, expanding spheromaks and Lundquist fields, respectively. The field structures remain force-free, under the conventional non-relativistic assumption that the dynamical effects of the inductive electric fields can be neglected. While keeping the internal magnetic field structure of the stationary solutions, expansion leads to complicated internal velocities and rotation, caused by inductive electric fields. The structure depends only on overall radius  $R(t)$  and rate of expansion  $\dot{R}(t)$  measured at a given moment, and thus is applicable to arbitrary expansion laws. In case of cylindrical Lundquist fields, magnetic flux conservation requires that both axial and radial expansion proceed with equal rates. In accordance with observations, the model predicts that the maximum magnetic field is reached before the spacecraft reaches the geometric center of a CME.

## Interplanetary Rotation of 2021 December 4 Coronal Mass Ejection on Its Journey to Mars

[Mengxuan Ma](#), [Liping Yang](#), [Fang Shen](#), [Chenglong Shen](#), [Yutian Chi](#), [Yuming Wang](#), [Yufen Zhou](#), [Man Zhang](#), [Daniel Heyner](#), [Uli Auster](#), [Ingo Richter](#), [Beatriz Sanchez-Cano](#)

*ApJ* **976** 183 2024

<https://arxiv.org/pdf/2410.20803>

<https://iopscience.iop.org/article/10.3847/1538-4357/ad8a5a/pdf>

The magnetic orientation of coronal mass ejections (CMEs) is of great importance to understand their space weather effects. Although many evidences suggest that CMEs can undergo significant rotation during the early phases of evolution in the solar corona, there are few reports that CMEs rotate in the interplanetary space. In this work, we use multi-spacecraft observations and a numerical simulation starting from the lower corona close to the solar surface to understand the CME event on **2021 December 4**, with an emphatic investigation of its rotation. This event is observed as a partial halo CME from the back side of the Sun by coronagraphs, and reaches the BepiColombo spacecraft and the MAVEN/Tianwen-1 as a magnetic flux rope-like structure. The simulation discloses that in the solar corona the CME is

approximately a translational motion, while the interplanetary propagation process evidences a gradual change of axis orientation of the CME's flux rope-like structure. It is also found that the downside and the right flank of the CME moves with the fast solar wind, and the upside does in the slow-speed stream. The different parts of the CME with different speeds generate the nonidentical displacements of its magnetic structure, resulting in the rotation of the CME in the interplanetary space. Furthermore, at the right flank of the CME exists a corotating interaction region (CIR), which makes the orientation of the CME alter, and also deviates from its route due to the CIR. These results provide new insight on interpreting CMEs' dynamics and structures during their travelling through the heliosphere.

## **Coronal Mass Ejection Data Clustering and Visualization of Decision Trees**

Ruizhe Ma<sup>1</sup>, Rafal A. Angryk<sup>1</sup>, Pete Riley<sup>2</sup>, and Soukaina Filali Boubrahimi

2018 ApJS 236 14

<http://sci-hub.tw/10.3847/1538-4365/aab76f>

Coronal mass ejections (CMEs) can be categorized as either "magnetic clouds" (MCs) or non-MCs. Features such as a large magnetic field, low plasma-beta, and low proton temperature suggest that a CME event is also an MC event; however, so far there is neither a definitive method nor an automatic process to distinguish the two. Human labeling is time-consuming, and results can fluctuate owing to the imprecise definition of such events. In this study, we approach the problem of MC and non-MC distinction from a time series data analysis perspective and show how clustering can shed some light on this problem. Although many algorithms exist for traditional data clustering in the Euclidean space, they are not well suited for time series data. Problems such as inadequate distance measure, inaccurate cluster center description, and lack of intuitive cluster representations need to be addressed for effective time series clustering. Our data analysis in this work is twofold: clustering and visualization. For clustering we compared the results from the popular hierarchical agglomerative clustering technique to a distance density clustering heuristic we developed previously for time series data clustering. In both cases, dynamic time warping will be used for similarity measure. For classification as well as visualization, we use decision trees to aggregate single-dimensional clustering results to form a multidimensional time series decision tree, with averaged time series to present each decision. In this study, we achieved modest accuracy and, more importantly, an intuitive interpretation of how different parameters contribute to an MC event.

## **STATISTICAL STUDY OF CORONAL MASS EJECTIONS WITH AND WITHOUT DISTINCT LOW CORONAL SIGNATURES**

S. Ma<sup>1,2,3</sup>, G. D. R. Attrill<sup>1</sup>, L. Golub<sup>1</sup>, and J. Lin<sup>2</sup>

Astrophysical Journal, 722:289–301, 2010, File

<https://iopscience.iop.org/article/10.1088/0004-637X/722/1/289/pdf>

Taking advantage of the two viewpoints of the *STEREO* spacecraft, we present a statistical study of coronal mass ejections (CMEs) with and without distinct low coronal signatures (LCSs) from 2009 January 1 to August 31. During this period, the lines of sight from *STEREO A* and *B* are almost perpendicular and nearly a quarter of the Sun was observed by both. We identified 34 CMEs that originated from around this area and find that (1) about 1 out of 3 CMEs that were studied during 8 months of solar minimum activity are stealth CMEs; a CME is stealth if no distinct LCS (such as coronal dimming, coronal wave, filament eruption, flare, post-eruptive arcade) can be found on the disk. (2) The speeds of the stealth CMEs without LCSs are typically below 300 km s<sup>-1</sup>. Comparing with the slow CMEs with LCSs, the stealth CMEs did not show any clear differences in their velocity and acceleration evolution. (3) The source regions of the stealth CMEs are usually located in the quiet Sun rather than active regions. Detailed study indicates that more than half of the stealth CMEs in this paper showed some faint change of the coronal structures (likely parts of flux ropes) when they could be observed over the solar limb before or during the CME evolution. Finally, we note that space weather detection systems based on LCSs totally independent of coronagraph data may fail to detect a significant proportion of CMEs.

## **MODELS OF THE LARGE-SCALE CORONA. II. MAGNETIC CONNECTIVITY AND OPEN FLUX VARIATION**

D. H. Mackay and A. A. van Ballegoijen

Astrophysical Journal, 642:1193–1204, 2006 May, File

In this paper the changing connectivity of the coronal magnetic field during the formation and ejection of magnetic flux ropes is considered. Using recent simulations of the coronal field, it is shown that reconnection may occur both above and below the flux ropes. Those occurring above slowly strip away coronal arcades overlying the flux ropes and allow the flux ropes to be ejected. In contrast, those below help to push the flux ropes out. It is found that the reconnection

occurring below each flux rope may result in significant skew being maintained within the coronal field above the PIL after the flux rope is ejected. In addition, after the eruption, as the coronal field closes down, the large-scale transport of open flux across the bipoles takes place through the process of "interchange reconnection." As a result, new photospheric domains of open flux are created within the centers of the bipoles, where field lines were previously closed. The net open flux in the simulation may be split into two distinct contributions. The first contribution is due to the nonpotential equilibrium coronal fields of the bipoles. The second contribution is a temporary enhancement to

this during the ejection of the flux ropes, where previously closed field lines become open. It is shown that the nonpotential equilibrium contribution to the open flux is significantly higher than that due to a potential field deduced from the same photospheric boundary conditions. These results suggest that the nonpotential nature of coronal magnetic fields may affect the variation of the Sun's open flux during periods of high solar activity and should be considered in future simulations.

### **The kinematics of solar inner coronal transients,**

**MacQueen**, R.M. and Fisher, R.R.,  
Sol. Phys., 89, 89, **1983**

### **The plasmoid instability in a confined solar flare**

David **MacTaggart**, [Lyndsay Fletcher](#)

MNRAS **2019**

<https://arxiv.org/pdf/1905.01201.pdf>

Eruptive flares (EFs) are associated with erupting filaments and, in some models, filament eruption drives flare reconnection. Recently, however, observations of a confined flare (CF) have revealed all the hallmarks of an EF (impulsive phase, flare ribbons, etc.) without the filament eruption itself. Therefore, if the filament is not primarily responsible for impulsive flare reconnection, what is? In this Letter, we argue, based on minimal requirements, that the plasmoid instability is a strong candidate for explaining the impulsive phase in the observed CF. We present magnetohydrodynamic simulation results of the nonlinear development of the plasmoid instability, in a model active region magnetic field geometry, to strengthen our claim. We also discuss how the ideas described in this Letter can be generalised to other situations, including EFs.

### **The magnetic structure of surges in small-scale emerging flux regions**

**MacTaggart**, D., Guglielmino, S.L., Haynes, A.L., Simitev, R., and Zuccarello, F.

A&A, **2015**

<http://eprints.gla.ac.uk/102318/1/102318.pdf>

<http://arxiv.org/pdf/1502.01842v1.pdf>

**Aims.** To investigate the relationship between surges and magnetic reconnection during the emergence of small-scale active regions. In particular, to examine how the large-scale geometry of the magnetic field, shaped by different phases of reconnection, guides the flowing of surges. **Methods.** We present three flux emergence models. The first model, and the simplest, consists of a region emerging into a horizontal ambient field that is initially parallel to the top of the emerging region. The second model is the same as the first but with an extra smaller emerging region which perturbs the main region. This is added to create a more complex magnetic topology and to test how this complicates the development of surges compared to the first model. The last model has a non-uniform ambient magnetic field to model the effects of emergence near a sunspot field and impose asymmetry on the system through the ambient magnetic field. At each stage, we trace the magnetic topology to identify the locations of reconnection. This allows for field lines to be plotted from different topological regions, highlighting how their geometry affects the development of surges. **Results.** In the first model, we identify distinct phases of reconnection. Each phase is associated with a particular geometry for the magnetic field and this determines the paths of the surges. The second model follows a similar pattern to the first but with a more complex magnetic topology and extra eruptions. The third model highlights how an asymmetric ambient field can result in preferred locations for reconnection, subsequently guiding the direction of surges. **Conclusions.** Each of the identified phases highlights the close connection between magnetic field geometry, reconnection and the flow of surges. These phases can now be detected observationally and may prove to be key signatures in determining whether or not an emerging region will produce a large-scale (CME-type) eruption.

### **On magnetic reconnection and flux rope topology in solar flux emergence**

D. **MacTaggart**, A.L. Haynes

E-print, Nov **2013**; MNRAS

We present an analysis of the formation of atmospheric flux ropes in a magnetohydro-dynamic (MHD) solar flux emergence simulation. The simulation domain ranges from the top of the solar interior to the low corona. A twisted magnetic flux tube emerges from the solar interior and into the atmosphere where it interacts with the ambient magnetic field. By studying the connectivity of the evolving magnetic field, we are able to better understand the process of flux rope formation in the solar atmosphere. In the simulation, two flux ropes are produced as a result of flux emergence. Each has a different evolution resulting in different topological structures. These are determined by plasma flows and magnetic reconnection. As the flux rope is the basic structure of the coronal mass ejection (CME), we discuss the implications of our findings for solar eruptions.

### **Can magnetic breakout be achieved from multiple flux emergence?**

**MacTaggart**, D., Hood, A.W.

E-print, May **2009**; A&A

We study the breakout model using multiple flux emergence to produce the magnetic configuration and the trigger. We do not impose any artificial motions on the boundaries. Once the original flux tube configuration is chosen the system is

left to evolve itself. We perform non-linear simulations in 2.5D by solving the compressible and resistive MHD equations using a Lagrangian remap, shock capturing code (Lare2D). To produce a quadrupolar configuration from flux emergence we build on previous work where the interaction of two flux tubes forms the required quadrupole. Instead of imposing a shearing flow, a third flux tube is then allowed to emerge up through the central arcade. Breakout is not achieved in any of the experiments. This is due to the interaction of the third tube with the quadrupole and the effect of the plasma beta being  $O(1)$  at the photosphere and  $\geq O(1)$  in the solar interior. When beta is of these orders, flows generated in the plasma can influence the magnetic field and so photospheric footpoints do not remain fixed.

### **Eruptions from coronal bright points: A spectroscopic view by IRIS of a mini-filament eruption, QSL reconnection, and reconnection-driven outflows**

[Maria S. Madjarska](#), [Duncan H. Mackay](#), [Klaus Galsgaard](#), [Thomas Wiegmann](#), [Haixia Xie](#)

A&A 2022

<https://arxiv.org/pdf/2202.00370.pdf>

The present study investigates a mini-filament eruption associated with cancelling magnetic fluxes. The eruption originates from a small-scale loop complex commonly known as a Coronal Bright Point (CBP). The event is uniquely recorded in both the imaging and spectroscopic data taken with IRIS. We analyse IRIS spectroscopic and slit-jaw imaging observations as well as images taken in the extreme-ultraviolet channels of AIA, and line-of-sight magnetic-field data from HMI onboard the SDO. We also employ an NLFFF relaxation approach based on the HMI magnetogram time series. We identify a strong small-scale brightening as a micro-flare in a CBP. The mini-eruption manifests with the ejection of hot (CBP loops) and cool (mini-filament) plasma recorded in both the imaging and spectroscopic data. The micro-flare is preceded by the appearance of an elongated bright feature in the IRIS slit-jaw 1400 Å images located above the polarity inversion line. The micro-flare starts with an IRIS pixel size brightening and propagates bi-directionally along the elongated feature. We detect in both the spectral and imaging IRIS data and AIA data, strong flows along and at the edges of the elongated feature which we believe represent reconnection outflows. Both edges of the elongated feature that wrap around the edges of the erupting MF evolve into a J-type shape creating a sigmoid appearance. A quasi-separatrix layer (QSL) is identified in the vicinity of the polarity inversion line by computing the squashing factor  $Q$  in different horizontal planes of the NLFFF model. The QSL reconnection site has the same spectral appearance as the so-called explosive events identified by strong blue- and red-shifted emission, thus answering a long outstanding question about the true nature of this spectral phenomenon. **2017 April 5**

### **Eruptions from coronal hole bright points: observations and non-potential modelling**

[Maria S. Madjarska](#), [Klaus Galsgaard](#), [Duncan H. Mackay](#), [Kostadinka Koleva](#), [Momchil Dechev](#)

A&A 2020

<https://arxiv.org/pdf/2009.04628.pdf>

A single case study of a CBP in an equatorial coronal hole with an exceptionally large size is investigated to extend our understanding of the formation of mini-filaments, their destabilisation and the origin of the eruption triggering the formation of jet-like features recorded in the extreme-ultraviolet (EUV) and X-ray emission. We aim to explore the nature of the so-called *micro-flares in CBPs associated with jets in coronal holes and mini coronal mass ejections* in the quiet Sun. Co-observations from the Atmospheric Imaging Assembly (AIA) and Helioseismic Magnetic Imager (HMI) on board the Solar Dynamics Observatory, and GONG H $\alpha$  images are used together with a Non-Linear Force Free Field (NLFFF) relaxation approach, where the latter is based on a time series of HMI line-of-sight magnetograms. A mini-filament (MF) that formed beneath the CBP arcade around 3–4 h before the eruption is seen in the H $\alpha$  and EUV AIA images to lift up and erupt triggering the formation of an X-ray jet. No significant photospheric magnetic flux concentration displacement (convergence) is observed and neither is magnetic flux cancellation between the two main magnetic polarities forming the CBP in the time period leading to the MF liftoff. The CBP micro-flare is associated with three flare kernels that formed shortly after the MF liftoff. No observational signature is found for reconnection beneath the erupting MF. The applied NLFFF modelling successfully reproduces both the CBP loop complex as well as the magnetic flux rope that hosts the MF during the build-up to the eruption. **2013 October 12**

### **A coronal wave and an asymmetric eruptive filament in SUMER, CDS, EIT, and TRACE co-observations**

[M.S. Madjarska](#), [J.G. Doyle](#), [J. Shetye](#)

A&A, 2015

<http://arxiv.org/pdf/1412.1984v1.pdf>

The objectives of the present study is to provide a better physical understanding of the complex inter-relation and evolution of several solar coronal features comprising a double-peak flare, a coronal dimming caused by a CME, a CME-driven compression, and a fast-mode wave. For the first time, the evolution of an asymmetric eruptive filament is analysed in simultaneous SUMER spectroscopic and TRACE and EIT imaging data. We use imaging observations from EIT and TRACE in the 195Å channel and spectroscopic observations from the CDS in a rastering and SUMER in a sit-and-stare observing mode. The SUMER spectra cover spectral lines with formation temperatures from  $\log T(K) \sim 4.0$  to 6.1. Although the event was already analysed in two previous studies, our analysis brings a wealth of new information on the dynamics and physical properties of the observed phenomena. We found that the dynamic event is related to a complex flare with two distinct impulsive peaks, one according to the GOES classification as C1.1 and the second - C1.9. The first energy release triggers a fast-mode wave and a CME with a clear CME driven compression ahead of it.



This activity is related to, or possibly caused, by an asymmetric filament eruption. The filament is observed to rise with its leading edge moving at a speed of  $\sim 300$  km/s detected both in the SUMER and CDS data. The rest of the filament body moves at only  $\sim 150$  km/s while untwisting. No signature is found of the fast-mode wave in the SUMER data, suggesting that the plasma disturbed by the wave had temperatures above 600 000 K. The erupting filament material is found to emit only in spectral lines at transition region temperatures. Earlier identification of a coronal response detected in the Mg X 609.79 Å line is found to be caused by a blend from the O IV 609.83 Å line. **1998 June 13**

## Evolution and Dynamics of a Solar Active Prominence

Tetsuya [Magara](#)

2015

<http://arxiv.org/pdf/1508.00672v1.pdf>

The life of a solar active prominence, one of the most remarkable objects on the Sun, is full of dynamics; after first appearing on the Sun the prominence continuously evolves with various internal motions and eventually produces a global eruption toward the interplanetary space. Here we report that the whole life of an active prominence is successfully reproduced by performing as long-term a magnetohydrodynamic simulation of a magnetized prominence plasma as was ever done. The simulation reveals underlying dynamic processes that give rise to observed properties of an active prominence: invisible subsurface flows self-consistently produce the cancellation of magnetic flux observed at the photosphere, while observed and somewhat counterintuitive strong upflows are driven against gravity by enhanced gas pressure gradient force along a magnetic field line locally standing vertical. The most highlighted dynamic event, transition into an eruptive phase, occurs as a natural consequence of the self-consistent evolution of a prominence plasma interacting with a magnetic field, which is obtained by seamlessly reproducing dynamic processes involved in the formation and eruption of an active prominence.

## ENERGY INJECTION VIA FLUX EMERGENCE ON THE SUN DEPENDING ON THE GEOMETRIC SHAPE OF MAGNETIC FIELD

T. [Magara](#)

2011 ApJ 731 122

Flux emergence is a complicated process involving flow and magnetic field, which provides a way of injecting magnetic energy into the solar atmosphere. We show that energy injection via this complicated process is characterized by a physical quantity called the emergence velocity, which is determined by the spatial relationship between the flow velocity and magnetic field vectors. By using this quantity, we demonstrate that the geometric shape of magnetic field might play an important role in the energy injection via flux emergence.

## Triangulation of the continuum-like radio emission in a CME-CME interaction event

Jasmina [Magdalenic](#)\*1, Manuela Temmer2, Vratislav Krupar3,4, Christophe Marque5, Astrid Veronig2, and Bojan Vrsnak

CESRA 2016 p.69

[http://cesra2016.sciencesconf.org/conference/cesra2016/pages/CESRA2016\\_prog\\_abs\\_book\\_v3.pdf](http://cesra2016.sciencesconf.org/conference/cesra2016/pages/CESRA2016_prog_abs_book_v3.pdf)

We present a study of the radio emission associated with the complex interaction of two coronal mass ejections (CMEs), successively launched from the same active region (NOAA AR 11158), on **February 14 and February 15, 2011**. Although this CME-CME interaction event was widely studied (e.g. Temmer et al., 2014, Maricic et al., 2014, Mishra & Srivastava, 2014) none of the analyses determined the origin of the associated continuum-like radio emission observed in the decameter-to-hectometer frequency range. The continuum-like emission patch has a particular morphology and might be considered either as a continuation of the decametric type II radio emission associated with the second CME, either as a continuation of the type III radio bursts associated with a flare from NOAA AR 11158. This ambiguity additionally complicates the question on the possible origin of the continuum-like emission. The association of this type of continuumlike radio emission and the CME-CME interaction was up to now established only by their temporal coincidence (Gopalswamy et al., 2001), which is not applicable in this event due to a complex and long-lasting interaction of the CMEs. The radio triangulation study (see also Magdalenic et al., 2014) provided us with the 3D source positions of the continuum-like emission and the associated type II burst, which were compared with the positions of the interacting CMEs. First results indicated that the continuum-like radio emission is not the continuation of the type III radio bursts, but it is also not the radio signature of the CME-CME interaction.

## Evolution of the Alfvén Mach number associated with coronal mass ejection shock

Ciara A. [Maguire](#), [Eoin P. Carley](#), [Joseph McCauley](#), [Peter T. Gallagher](#)

A&A 633, A56 (2020)

<https://arxiv.org/pdf/1912.01863.pdf>

<https://doi.org/10.1051/0004-6361/201936449>

The Sun regularly produces large-scale eruptive events, such as coronal mass ejections (CMEs) that can drive shock waves through the solar corona. Such shocks can result in electron acceleration and subsequent radio emission in the form of a type II radio burst. However, the early-phase evolution of shock properties and its relationship to type II burst evolution is still subject to investigation. Here we study the evolution of a CME-driven shock by comparing three

commonly used methods of calculating the Alfvén Mach number (MA), namely: shock geometry, a comparison of CME speed to a model of the coronal Alfvén speed, and the type II band-splitting method. We applied the three methods to the **2017 September 2** event, focusing on the shock wave observed in extreme ultraviolet (EUV) by the Solar Ultraviolet Imager (SUVI) on board GOES-16, in white-light by the Large Angle and Spectrometric Coronagraph (LASCO) on board SOHO, and the type II radio burst observed by the Irish Low Frequency Array (I-LOFAR). We show that the three different methods of estimating shock MA yield consistent results and provide a means of relating shock property evolution to the type II emission duration. The type II radio emission emerged from near the nose of the CME when MA was in the range 1.4-2.4 at a heliocentric distance of  $\sim 1.6 R_{\odot}$ . The emission ceased when the CME nose reached  $\sim 2.4 R_{\odot}$ , despite an increasing Alfvén Mach number (up to 4). We suggest the radio emission cessation is due to the lack of quasi-perpendicular geometry at this altitude, which inhibits efficient electron acceleration and subsequent radio emission.

## **Toroidal modified Miller-Turner CME model in EUHFORIA: II. Validation and comparison with flux rope and spheromak**

Anwasha [Maharana](#), [Luis Linan](#), [Stefaan Poedts](#), [Jasmina Magdalenic](#)

A&A 691, A146 2024

<https://arxiv.org/pdf/2408.03882>

<https://www.aanda.org/articles/aa/pdf/2024/11/aa50459-24.pdf>

<https://doi.org/10.1051/0004-6361/202450459>

*Context.* Rising concerns about the impact of space-weather-related disruptions demand modelling and reliable forecasting of coronal mass ejection (CME) impacts.

*Aims.* In this study, we demonstrate the application of the modified Miller-Turner (mMT) model implemented within European Heliospheric FORecasting Information Asset (EUHFORIA) in forecasting the geo-effectiveness of observed coronal mass ejection (CME) events in the heliosphere. Our goal is to develop a model that not only has a global geometry, in order to improve overall forecasting, but is also fast enough for operational space-weather forecasting.

*Methods.* We test the original full torus implementation and introduce a new three-fourths Torus version called the Horseshoe CME model. This new model has a more realistic CME geometry, and overcomes the inaccuracies of the full torus geometry. We constrain the torus geometrical and magnetic field parameters using observed signatures of the CMEs before, during, and after the eruption. We perform EUHFORIA simulations for two validation cases – the isolated CME event of **12 July 2012** and the CME–CME interaction event of **8–10 September 2014**. We performed an assessment of the model’s capability to predict the most important  $B_z$  component using the advanced dynamic time-warping (DTW) technique.

*Results.* The Horseshoe model predictions of CME arrival time and geo-effectiveness for both validation events compare well with the observations and are weighed against the results obtained with the spheromak and FRi3D models, which were already available in EUHFORIA.

*Conclusions.* The runtime of the Horseshoe model simulations is close to that of the spheromak model, which is suitable for operational space weather forecasting. However, the capability of the magnetic field prediction at 1 AU of the Horseshoe model is close to that of the FRi3D model. In addition, we demonstrate that the Horseshoe CME model can be used for simulating successive CMEs in EUHFORIA, overcoming a limitation of the FRi3D model.

**12-16 July 2012, 10-13 September 2014**

## **Rotation and interaction of the September 8 and 10, 2014 CMEs tested with EUHFORIA**

Anwasha [Maharana](#), [Camilla Scolini](#), [Brigitte Schmieder](#), [Stefaan Poedts](#)

A&A 675, A136 2023

<https://arxiv.org/pdf/2305.06881.pdf>

<https://www.aanda.org/articles/aa/pdf/2023/07/aa45902-23.pdf>

*Aim:* We aim to show how interactions undergone by a CME in the corona and heliosphere can play a significant role in altering its geoeffectiveness predicted at the time of its eruption. To do so, we consider a case study of two successive CMEs launched from the active region NOAA 12158 in early September 2014. The second CME was predicted to be extensively geoeffective based on the remote-sensing observations of the source region. However, in situ measurements at 1 au recorded only a short-lasting weak negative  $B_z$  component followed by a prolonged positive  $B_z$  component.

*Methods:* The European Heliosphere FORecasting Information Asset (EUHFORIA) is used to perform a selfconsistent 3D MHD data-driven simulation of the two CMEs in the heliosphere. First, the ambient solar wind is modelled, followed by the time-dependent injection of CME1 with the LFF spheromak and CME2 with the "Flux Rope in 3D" (FRi3D) model. The initial conditions of the CMEs are determined by combining observational insights near the Sun, fine-tuned to match the in situ observations near 1 au, and additional numerical experiments of each individual CME.

*Results:* By introducing CME1 before CME2 in the EUHFORIA simulation, we modelled the negative  $B_z$  component in the sheath region ahead of CME2 whose formation can be attributed to the interaction between CME1 and CME2. To reproduce the positive  $B_z$  component in the magnetic ejecta of CME2, we had to initialise CME2 with an orientation determined at 0.1 au and consistent with the orientation interpreted at 1 au, instead of the orientation observed during its eruption.

*Conclusions:* EUHFORIA simulations suggest the possibility of a significant rotation of CME2 in the low corona in order to explain the in situ observations at 1 au. Coherent magnetic field rotations with enhanced strength (potentially

geoeffective) can be formed in the sheath region as a result of interactions between two CMEs in the heliosphere even if the individual CMEs are not geoeffective. **8-10 Sep 2014, 10-11 Sep 2014**

### **Implementation and validation of the FRi3D flux rope model in EUHFORIA**

[Anwasha Maharana](#), [Alexey Isavnin](#), [Camilla Scolini](#), [Nicolas Wijsen](#), [Luciano Rodriguez](#), [Marilena Mierla](#), [Jasmina Magdalenic](#), [Stefaan Poedts](#)

Advances in Space Research (2022)

<https://arxiv.org/pdf/2207.06707.pdf>

The Flux Rope in 3D (FRi3D, Isavnin, 2016), a coronal mass ejection (CME) model with global three-dimensional (3D) geometry, has been implemented in the space weather forecasting tool EUHFORIA (Pomoell and Poedts, 2018). By incorporating this advanced flux rope model in EUHFORIA, we aim to improve the modelling of CME flank encounters and, most importantly, the magnetic field predictions at Earth. After using synthetic events to showcase FRi3D's capabilities of modelling CME flanks, we optimize the model to run robust simulations of real events and test its predictive capabilities. We perform observation-based modelling of the halo CME event that erupted on **12 July 2012**. The geometrical input parameters are constrained using the forward modelling tool included in FRi3D with additional flux rope geometry flexibilities as compared to the pre-existing models. The magnetic field input parameters are derived using the differential evolution algorithm to fit FRi3D parameters to the in situ data at 1 AU. An observation-based approach to constrain the density of CMEs is adopted, in order to achieve a better estimation of mass corresponding to the FRi3D geometry. The CME is evolved in EUHFORIA's heliospheric domain and a comparison of FRi3D's predictive performance with the previously implemented spheromak CME in EUHFORIA is presented. For this event, FRi3D improves the modelling of the total magnetic field magnitude and Bz at Earth by ~30% and ~70%, respectively. Moreover, we compute the expected geoeffectiveness of the storm at Earth using an empirical Dst model and find that the FRi3D model improves the predictions of minimum Dst by ~20% as compared to the spheromak CME model. Finally, we discuss the limitations of the current implementation of FRi3D in EUHFORIA and propose possible improvements.

### **Type II solar radio burst band-splitting: Measure of coronal magnetic field strength**

[AymanMahrous](#), [KhaledAlieldena](#), [BojanVršnakb](#), [MohamedYoussefa](#)

[Journal of Atmospheric and Solar-Terrestrial Physics Volume 172](#), July 2018, Pages 75-82

<http://sci-hub.tw/10.1016/j.jastp.2018.03.018>

Studies of the relationship between solar radio bursts and CMEs are essential for understanding of the nature of type II bursts. In this study, we examine the type II solar radio burst recorded on **16 March 2016** by the Learmonth radio [spectrograph](#) and compare its characteristics with the [kinematics](#) of the associated CMEs observed by STEREO and SOHO spacecraft. The burst showed a well-defined band-split, which was used to estimate the [magnetic field](#) strength in the [solar corona](#). The magnetic field decreases from  $\approx 4$  G at  $R \approx 2.6 R_{\odot}$  to 0.62 G at  $R \approx 3.77 R_{\odot}$  depending on the coronal [electron density](#) model employed. We found that two CMEs occurred successively in a 4-h interval. During this interval, a type II radio burst occurred, lasting for about 10 min. Tracking of the shock that produced type II burst and comparison with the CMEs heights as observed by STEREO and SOHO spacecraft help us to deduce the driver of the shock. According to the analysis, the type II burst occurrence was associated with the interaction of the shock driven by the second CME with a streamer located south of the first CME, since that the type II band-split significantly increased during the shock-streamer interaction. Our results show that the analysis of the type II burst band-split supplemented by the coronagraphic observations of the corona is an important tool for the understanding of the coronal eruptive processes.

### **CME–flare association during the 23rd solar cycle**

A. [Mahrous](#), M. Shaltout, M.M. Beheary, R. Mawad, and M. Youssef

[Advances in Space Research, Volume 43, Issue 7](#), 1 April 2009, Pages 1032-1035

The relation between coronal mass ejections (CMEs) and solar flares are statistically studied. More than 10,000 CME events observed by SOHO/LASCO during the period 1996–2005 have been analyzed. The soft X-ray flux measurements provided by the Geostationary Operational Environmental Satellite (GOES), recorded more than 20,000 flares in the same time period. The data is filtered under certain temporal and spatial conditions to select the CME–flare associated events. The results show that CME–flare associated events are triggered with a lift-off time within the range 0.4–1.0 h. We list a set of 41 CME–flare associated events satisfying the temporal and spatial conditions. The listed events show a good correlation between the CME energy and the X-ray flux of the CME–flare associated events with correlation coefficient of 0.76.

### **THE RADIO–CORONAL MASS EJECTION EVENT ON 2001 APRIL 15**

Dalmiro Jorge Filipe [Maia](#), Ricardo Gama, Claude Mercier, Monique Pick, Alain Kerdraon, and Marian Karlicky

Astrophysical Journal, 660:874–881, 2007

<http://www.journals.uchicago.edu/doi/pdf/10.1086/508011>

On 2001 April 15, the Nancy radioheliograph observed fast-moving, expanding loops in images taken in the wavelength range between 164 and 432 MHz. We were able to follow the progression of the radio loops, starting from a few tenths to more than  $1 R_{\odot}$  above the solar limb, with a time cadence of order seconds. The loops seen in radio agree very well with the features of the coronal mass ejection (CME) seen later, more than  $2.5 R_{\odot}$  above the limb, in white-

light images by the Large Angle Spectrometric Coronagraph (LASCO) experiment on board the Solar and Heliospheric Observatory (SOHO) spacecraft. The event is well associated with an energetic electron event seen by the Electron, Proton, and Alpha Monitor (EPAM) experiment on board the Advanced Composition Explorer (ACE) spacecraft. A detailed transport model for the electrons shows that, not only the inferred onset at the Sun, but also the duration of the particle release, are similar for the radio loop and the in situ electron event detected near the Earth.

### **Evolution of reconnection flux during eruption of magnetic flux ropes**

[Samriddhi Sankar Maity](#), [Piyali Chatterjee](#), [Ranadeep Sarkar](#), [Ijas S. Mytheen](#)

ApJ 2024

<https://arxiv.org/pdf/2407.18188>

Coronal mass ejections (CMEs) are powerful drivers of space weather, with magnetic flux ropes (MFRs) widely regarded as their primary precursors. However, the variation in reconnection flux during the evolution of MFR during CME eruptions remains poorly understood. In this paper, we develop a realistic 3D magneto-hydrodynamic model using which we explore the temporal evolution of reconnection flux during the MFR evolution using both numerical simulations and observational data. Our initial coronal configuration features an isothermal atmosphere and a potential arcade magnetic field beneath which an MFR emerges at the lower boundary. As the MFR rises, we observe significant stretching and compression of the overlying magnetic field beneath it. Magnetic reconnection begins with the gradual formation of a current sheet, eventually culminating with the impulsive expulsion of the flux rope. We analyze the temporal evolution of reconnection fluxes during two successive MFR eruptions while continuously emerging the twisted flux rope through the lower boundary. We also conduct a similar analysis using observational data from the Helioseismic and Magnetic Imager (HMI) and the Atmospheric Imaging Assembly (AIA) for an eruptive event. Comparing our MHD simulation with observational data, we find that reconnection flux play a crucial role in determination of CME speeds. From the onset to the eruption, the reconnection flux shows a strong linear correlation with the velocity. This nearly realistic simulation of a solar eruption provides important insights into the complex dynamics of CME initiation and progression. **2011 August 04**

### **Probing Velocity Dispersion inside CMEs in Inner Corona: New Insights on CME Initiation**

[Satabdwa Majumdar](#), [Elke D' Huys](#), [Marilena Mierla](#), [Nitin Vashishtha](#), [Dana-Camelia Talpeanu](#), [Dipankar Banerjee](#), [Martin A. Reiss](#)

ApJL 2024

<https://arxiv.org/pdf/2407.02244>

This work studies the kinematics of the leading edge and the core of 6 Coronal Mass Ejections (CMEs) in the combined field of view of Sun Watcher using Active Pixel System detector and Image Processing (SWAP) on-board PROject for On-Board Autonomy (PROBA-2) and the ground-based K-Cor coronagraph of the Mauna Loa Solar Observatory (MLSO). We report, for the first time, on the existence of a critical height  $h_c$ , which marks the onset of velocity dispersion inside the CME. This height for the studied events lies between 1.4-1.8  $R_{\odot}$ , in the inner corona. We find the critical heights to be relatively higher for gradual CMEs, as compared to impulsive ones, indicating that the early initiation of these two classes might be different physically. We find several interesting imprints of the velocity dispersion on CME kinematics. The critical height is strongly correlated with the flux-rope minor radius and the mass of the CME. Also, the magnitude of velocity dispersion shows a reasonable positive correlation with the above two parameters. We believe these results will advance our understanding of CME initiation mechanisms and will help provide improved constraints to CME initiation models. **2014 - 11 - 05, 2014 - 12 - 21, 2020 - 11 - 26, 2021 - 05 - 07, 2021 - 06 - 10, 2022 - 05 - 24**

**Table 1.** The table shows the summary of the studied events

### **A CME Source Region Catalogue and their Associated Properties**

[Satabdwa Majumdar](#), [Ritesh Patel](#), [Vaibhav Pant](#), [Dipankar Banerjee](#), [Aarushi Rawat](#), [Abhas Pradhan](#), [Paritosh Singh](#)

ApJS 268 38 2023

<https://arxiv.org/pdf/2307.13208.pdf>

See <https://allssc.aries.res.in/catalogs>

<https://iopscience.iop.org/article/10.3847/1538-4365/aceb62/pdf>

The primary objective of this study is to connect the coronal mass ejections (CMEs) to their source regions, primarily creating a CME source region (CSR) catalogue, and secondly probing into the influence the source regions have on different statistical properties of CMEs. We create a source region catalogue for 3327 CMEs **from 1998 to 2017**, thus capturing the different phases of cycle 23 and 24. The identified source regions are segregated into 3 classes, Active Regions (ARs), Prominence Eruptions (PEs) and Active Prominences (APs), while the CMEs are segregated into slow and fast based on their average projected speeds. We find the contribution of these three source region types to the occurrences of slow and fast CMEs to be different in the above period. A study of the distribution of average speeds reveals different power-laws for CMEs originating from different sources, and the power-law is different during the different phases of cycles 23 and 24. A study of statistical latitudinal deflections showed equator-ward deflections, while the magnitude of deflections again bears an imprint of the source regions. An East-West asymmetry is also noted, particularly in the rising phase of cycle 23, with the presence of active longitudes for the CMEs, with a preference towards the Western part of the Sun. Our results show that different aspects of CME kinematics bear a strong imprint of

the source regions they originate from, thus indicating the existence of different ejection and/or propagation mechanisms of these CMEs.

## **On the Variation of Volumetric Evolution of CMEs from Inner to Outer Corona**

[Satabdwa Majumdar](#), [Ritesh Patel](#), [Vaibhav Pant](#)

ApJ **929** 11 **2022**

<https://arxiv.org/pdf/2202.11924.pdf>

<https://iopscience.iop.org/article/10.3847/1538-4357/ac5909/pdf>

Some of the major challenges faced in understanding the early evolution of Coronal Mass Ejections (CMEs) are due to limited observations in the inner corona ( $<3 R_{\odot}$ ) and the plane of sky measurements. In this work, we have thus extended the application of the Graduated Cylindrical Shell (GCS) model to the inner coronal observations from the ground-based coronagraph K-Cor of the Mauna Loa Solar Observatory (MLSO) along with the pair of observations from COR-1 onboard the Solar Terrestrial Relations Observatory (STEREO). We study the rapid initial acceleration and width expansion phase of 5 CMEs in white-light in the lower heights. We also study the evolution of the modelled volume of these CMEs in inner corona and report for the first time, a power law dependence of the CME volume with distance from the Sun. We further find the volume of ellipsoidal leading front and the conical legs follow different power laws, thus indicating differential volume expansion through a CME. The study also reveals two distinct power laws for the total volume evolution of CMEs in the inner and outer corona, thus suggesting different expansion mechanisms at these different heights. These results besides aiding our current understanding on CME evolution, will also provide better constraints to CME initiation and propagation models. Also, since the loss of STEREO-B (and hence COR-1B data) from 2016, this modified GCS model presented here will still enable stereoscopy in the inner corona for the 3D study of CMEs in white-light. **2014 February 12, 2014 April 29, 2014 June 14, 2014 June 26, 2016 January 1**

## **An Insight into the Coupling of CME Kinematics in Inner and Outer Corona and the Imprint of Source Regions**

[Satabdwa Majumdar](#), [Ritesh Patel](#), [Vaibhav Pant](#), [Dipankar Banerjee](#)

ApJ **919** 115 **2021**

<https://arxiv.org/pdf/2107.08198.pdf>

<https://doi.org/10.3847/1538-4357/ac1592>

Despite studying Coronal Mass Ejections (CMEs) for several years, we are yet to have a complete understanding of their kinematics. In this regard, the change in kinematics of the CMEs, as they travel from the inner corona ( $<3 R_{\odot}$ ) to the higher heights is essential. We do a follow up statistical study of several 3D kinematic parameters of 59 CMEs studied by Majumdar et al. (2020). The source regions of these CMEs are identified and classified as Active Regions (ARs), Active Prominences (APs), and Prominence Eruptions (PEs). We study several statistical correlations between different kinematic parameters of the CMEs. We show that the average kinematic parameters change as they propagate from the inner to the outer corona, indicating the importance of the region where normally the common practice is to perform averaging. We also find that the parameters in the outer corona is highly influenced by those in the inner corona, thus indicating the importance of inner corona in the understanding of the kinematics. We further find that the source regions of the CMEs tend to have a distinct imprint on the statistical correlations between different kinematic parameters, and that an overall correlation tends to wash away this crucial information. The results of this work lends support towards possibly different dynamical classes for the CMEs from active regions and prominences which is manifested in their kinematics.

## **Connecting 3D evolution of Coronal Mass Ejections to their Source Regions**

[Satabdwa Majumdar](#), [Vaibhav Pant](#), [Ritesh Patel](#), [Dipankar Banerjee](#)

ApJ **899** 6 **2020**

<https://arxiv.org/pdf/2007.00923.pdf>

<https://doi.org/10.3847/1538-4357/aba1f2>

Since Coronal Mass Ejections (CMEs) are the major drivers of space weather, it is crucial to study their evolution starting from the inner corona. In this work we use Graduated Cylindrical Shell (GCS) model to study the 3D evolution of 59 CMEs in the inner ( $<3 R_{\odot}$ ) and outer ( $>3 R_{\odot}$ ) corona using observations from COR-1 and COR-2 on-board Solar Terrestrial Relations Observatory (STEREO) spacecraft. We identify the source regions of these CMEs and classify them as CMEs associated with Active Regions (ARs), Active Prominences (APs), and Prominence Eruptions (PEs). We find 27 % of CMEs show true expansion and 31 % show true deflections as they propagate outwards. Using 3D kinematic profiles of CMEs, we connect the evolution of true acceleration with the evolution of true width in the inner and outer corona. Thereby providing the observational evidence for the influence of the Lorentz force on the kinematics to lie in the height range of  $2.5-3 R_{\odot}$ . We find a broad range in the distribution of peak 3D speeds and accelerations ranging from  $396$  to  $2465 \text{ km s}^{-1}$  and  $176$  to  $10922 \text{ m s}^{-2}$  respectively with a long tail towards high values coming mainly from CMEs originating from ARs or APs. Further, we find the magnitude of true acceleration is be inversely correlated to its duration with a power law index of  $-1.19$ . We believe that these results will provide important inputs for the planning of upcoming space missions which will observe the inner corona and the models that study CME initiation and propagation. **2 Apr 2011, 30 May 2011, 12 Mar 2012, 30 Apr 2012, 2012 – 11 – 09**  
**Table 1.** The GCS model parameters of all the CMEs are tabulated below (2007-2014)

## Speed and Acceleration of CMEs Associated with Sustained Gamma-Ray Emission Events Observed by Fermi/LAT

P. Mäkelä, N. Gopalswamy, S. Akiyama, H. Xie, S. Yashiro

ApJ 2023

<https://arxiv.org/pdf/2307.05585.pdf> File

The sustained gamma-ray emission (SGRE) from the Sun is a prolonged enhancement of >100 MeV gamma-ray emission that extends beyond the flare impulsive phase. The origin of the >300 MeV protons resulting in SGRE is debated, both flares and shocks driven by coronal mass ejections (CMEs) being the suggested sites of proton acceleration. We compared the near-Sun acceleration and space speed of CMEs with 'Prompt' and 'Delayed' (SGRE) gamma-ray components (Ajello et al. 2021). We found that 'Delayed'-component-associated CMEs have higher initial acceleration and space speed than 'Prompt-only'-component-associated CMEs. We selected halo CMEs (HCMEs) associated with type II radio bursts (shock-driving HCMEs) and compared the average acceleration and space speed between HCME populations with or without SGRE events, major solar energetic particle (SEP) events, metric, or decameter-hectometric (DH) type II radio bursts. We found that the SGRE-producing HCMEs associated with a DH type II radio burst and/or a major SEP event have higher space speeds and especially initial accelerations than those without an SGRE event. We estimated the radial distance and speed of the CME-driven shocks at the end time of the 2012 January 23 and March 07 SGRE events using white-light images of STEREO Heliospheric Imagers and radio dynamic spectra of Wind WAVES. The shocks were at the radial distances of 0.6-0.8 au and their speeds were high enough (~975 km s<sup>-1</sup> and ~750 km s<sup>-1</sup>, respectively) for high-energy particle acceleration. Therefore, we conclude that our findings support the CME-driven shock as the source of >300 MeV protons. **2012: January 23 and March 07**

**Table A.** CME and X-ray flare data for Fermi/LAT solar flares 2010-2017  
**Table B.** Cycle 24 HCMEs with type II radio bursts 2010-2017

## Source Regions of the Type II Radio Burst Observed During a CME-CME Interaction on 2013 May 22

P. Mäkelä, N. Gopalswamy, M. J. Reiner, S. Akiyama, V. Krupar

ApJ 827 141 2016

<http://arxiv.org/pdf/1606.06989v1.pdf>

We report on our study of radio source regions during the type II radio burst on **2013 May 22** based on direction finding (DF) analysis of the Wind/WAVES and STEREO/WAVES (SWAVES) radio observations at decameter-hectometric (DH) wavelengths. The type II emission showed an enhancement that coincided with interaction of two coronal mass ejections (CMEs) launched in sequence along closely spaced trajectories. The triangulation of the SWAVES source directions posited the ecliptic projections of the radio sources near the line connecting the Sun and the STEREO-A spacecraft. The WAVES and SWAVES source directions revealed shifts in the latitude of the radio source indicating that the spatial location of the dominant source of the type II emission varies during the CME-CME interaction. The WAVES source directions close to 1 MHz frequencies matched the location of the leading edge of the primary CME seen in the images of the LASCO/C3 coronagraph. This correspondence of spatial locations at both wavelengths confirms that the CME-CME interaction region is the source of the type II enhancement. Comparison of radio and white-light observations also showed that at lower frequencies scattering significantly affects radio wave propagation. See CESRA highlights #1042 Dec 2016 <http://www.astro.gla.ac.uk/users/eduard/cesra/?p=1042>

## The radial speed-expansion speed relation for Earth-directed CMEs

P. Mäkelä, N. Gopalswamy, S. Yashiro

Space Weather Volume 14, Issue 5 May 2016 Pages 368–378 File

<http://cdaw.gsfc.nasa.gov/publications/makela/makela2016SpaceWeather.pdf>

Earth-directed coronal mass ejections (CMEs) are the main drivers of major geomagnetic storms. Therefore, a good estimate of the disturbance arrival time at Earth is required for space weather predictions. The STEREO and SOHO spacecraft were viewing the Sun in near quadrature during January 2010 to September 2012, providing a unique opportunity to study the radial speed ( $V_{rad}$ )-expansion speed ( $V_{exp}$ ) relationship of Earth-directed CMEs. This relationship is useful in estimating the  $V_{rad}$  of Earth-directed CMEs, when they are observed from Earth view only. We selected **19 Earth-directed CMEs** observed by the Large Angle and Spectrometric Coronagraph (LASCO)/C3 coronagraph on SOHO and the Sun Earth Connection Coronal and Heliospheric Investigation (SECCHI)/COR2 coronagraph on STEREO during January 2010 to September 2012. We found that of the three tested geometric CME models the full ice-cream cone model of the CME describes best the  $V_{rad}$ - $V_{exp}$  relationship, as suggested by earlier investigations. We also tested the prediction accuracy of the empirical shock arrival (ESA) model proposed by Gopalswamy et al. (2005a), while estimating the CME propagation speeds from the CME expansion speeds. If we use STEREO observations to estimate the CME width required to calculate the  $V_{rad}$  from the  $V_{exp}$  measurements, the mean absolute error (MAE) of the shock arrival times of the ESA model is 8.4 h. If the LASCO measurements are used to estimate the CME width, the MAE still remains below 17 h. Therefore, by using the simple  $V_{rad}$ - $V_{exp}$  relationship to estimate the  $V_{rad}$  of the Earth-directed CMEs, the ESA model is able to predict the shock arrival times with accuracy comparable to most other more complex models.

**Table 1.** List of 19 Earth-directed CMEs driving a shock (2010-2012).

## Estimating the Height of CMEs Associated with a Major SEP Event at the Onset of the Metric Type II Radio Burst during Solar Cycles 23 and 24

P. Mäkelä, N. Gopalswamy, S. Akiyama, H. Xie, and S. Yashiro

ApJ 2015

<http://cdaw.gsfc.nasa.gov/publications/makela/makela2015ApJ.pdf>

We studied the coronal mass ejection (CME) height at the onset of 59 metric type II radio bursts associated with major solar energetic particle (SEP) events, excluding ground level enhancements (GLEs), during solar cycles 23 and 24. We calculated CME heights using a simple flare-onset method used by Gopalswamy et al. (2012b) to estimate CME heights at the metric type II onset for cycle-23 GLEs. We found the mean CME height for non-GLE events ( $1.72 R_{\odot}$ ) to be  $\sim 12\%$  greater than that ( $1.53 R_{\odot}$ ) for cycle-23 GLEs. The difference could be caused by more impulsive acceleration of the GLE-associated CMEs. For cycle-24 non-GLE events, we compared the CME heights obtained using the flare-onset method and the 3-D spherical-shock fitting method and found the correlation to be good ( $CC=0.68$ ). We found the mean CME height for cycle 23 non-GLE events ( $1.79 R_{\odot}$ ) to be greater than for cycle 24 non-GLE events ( $1.58 R_{\odot}$ ), but statistical tests do not definitely reject the possibility of coincidence. We suggest that the lower formation height of the shocks during cycle 24 indicates a change in the Alfvén speed profile because solar magnetic fields are weaker and the plasma density levels are closer to the surface than usual during cycle 24. We also found that complex type III bursts showing diminution of type III emission in the 7-14 MHz frequency range are more likely associated with events with the CME height at the type II onset above  $2 R_{\odot}$ , supporting suggestions that the CME/shock structure causes the feature. **Table. Event Data**

## Coronal Hole Influence on the Observed Structure of Interplanetary CMEs

Pertti Mäkelä, Nat Gopalswamy, Hong Xie, Amaal A. Mohamed, Sachiko Akiyama, Seiji Yashiro

E-print, Jan 2013; Solar Phys. Volume 284, Issue 1, pp 59-75, 2013, File

<http://cdaw.gsfc.nasa.gov/publications/makela/makela2013SolPhys.pdf>

We report on the coronal hole (CH) influence on the **54 magnetic cloud (MC) and non-MC associated coronal mass ejections (CMEs)** selected for studies during the Coordinated Data Analysis Workshops (CDAWs) focusing on the question if all CMEs are flux ropes. All selected CMEs originated from source regions located between longitudes 15E-15W. Xie, Gopalswamy, and St. Cyr (2013, Solar Phys., doi:10.1007/s11207-012-0209-0) found that these MC and non-MC associated CMEs are on average deflected towards and away from the Sun-Earth line respectively. We used a CH influence parameter (CHIP) that depends on the CH area, average magnetic field strength, and distance from the CME source region to describe the influence of all on-disk CHs on the erupting CME. We found that for CHIP values larger than 2.6 G the MC and non-MC events separate into two distinct groups where MCs (non-MCs) are deflected towards (away) from the disk center. Division into two groups was also observed when the distance to the nearest CH was less than  $3.2 \times 10^5$  km. At CHIP values less than 2.6 G or at distances of the nearest CH larger than  $3.2 \times 10^5$  km the deflection distributions of the MC and non-MCs started to overlap, indicating diminishing CH influence. These results give support to the idea that all CMEs are flux ropes, but those observed to be non-MCs at 1 AU could be deflected away from the Sun-Earth line by nearby CHs, making their flux rope structure unobservable at 1 AU.

**Table; 18 October 1999, 6 December 1997, 9 April 2001, 12 May 1997, 13 April 1999, 17 February 2000, 25 July 2000 MC, 15 March 2002 MC**

## Convolutional Neural Networks for Predicting the Strength of the Near-Earth Magnetic Field Caused by Interplanetary Coronal Mass Ejections

Anna Malanushenko<sup>1\*</sup>, Natasha Flyer<sup>2</sup> and Sarah Gibson<sup>1</sup>

Front. Astron. Space Sci., 2020

<https://doi.org/10.3389/fspas.2020.00062>

<https://www.frontiersin.org/articles/10.3389/fspas.2020.00062/full>

In this paper, we explore the potential of neural networks for making space weather predictions based on near-Sun observations. Our second goal is to determine the extent to which coronal polarimetric observations of erupting structures near the Sun encode sufficient information to predict the impact these structures will have on Earth. In particular, we focus on predicting the maximal southward component of the magnetic field (“-Bz”) inside an interplanetary coronal mass ejection (ICME) as it impacts the Earth. We use Gibson & Low (G&L) self-similarly expanding flux rope model (Gibson and Low, 1998) as a first test for the project, which allows to consider CMEs with varying location, orientation, size, and morphology. We vary 5 parameters of the model to alter these CME properties, and generate a large database of synthetic CMEs (over 36k synthetic events). For each model CME, we synthesize near-Sun observations, as seen from an observer in quadrature (assuming the CME is directed earthwards), of either three components of the vector magnetic field, (Bx, By, Bz) (“Experiment 1”), or of synthetic Stokes images, (L/I, Az, V/I) (“Experiment 2”). We then allow the flux rope to expand and record max{-Bz} as the ICME passes 1AU. We further conduct two separate machine learning experiments and develop two different regression-based deep convolutional neural networks (CNNs) to predict max{-Bz} based on these two kinds of the near-Sun input data. Experiment 1 is a test which we do as a proof of concept, to see if a 3-channel CNN (hereafter CNN1), similar to those used in RGB image recognition, can reproduce the results of the self-similar (i.e., scale-invariant) expansion of the G&L model. Experiment 2 is less trivial, as Stokes vector is not linearly related to B, and the line-of-sight integration in the optically thin corona presents additional difficulties for interpreting the signal. This second CNN (hereafter CNN2), although

resembling CNN1 in Experiment 1, will have a different number of layers and set of hyperparameters due to a much more complicated mapping between the input and output data. We find that, given three components of  $B$ , CNN1 can predict  $\max\{-B_z\}$  with 97% accuracy, and for three components of the Stokes vector as input, CNN2 can predict  $\max\{-B_z\}$  with 95%, both measured in the relative root square error.

### **The SLED project and the dynamics of coronal flux ropes**

[Malherbe Jean-Marie](#), [Mein Pierre](#), [Sayede Frederic](#), [Rudawy Pawel](#), [Phillips Kenneth](#), [Keenan Francis](#), [Rybak Jan](#)

Adv. Space Res. 2021

<https://arxiv.org/pdf/2108.13507.pdf>

Investigations of the dynamics of the hot coronal plasma are crucial for understanding various space weather phenomena and making in-depth analyzes of the global heating of the solar corona. We present here numerical simulations of observations of siphon flows along loops (simple semi-circular flux ropes) to demonstrate the capabilities of the Solar Line Emission Dopplerometer (SLED), a new instrument under construction for imaging spectroscopy. It is based on the Multi-channel Subtractive Double Pass (MSDP) technique, which combines the advantages of filters and slit spectrographs. SLED will observe coronal structures in the forbidden lines of FeX 637.4 nm and FeXIV 530.3 nm, and will measure Doppler shifts up to 150 km/s at high precision (50 m/s) and cadence (1 Hz). It is optimized for studies of the dynamics of fast evolving events such as flares or Coronal Mass Ejections (CMEs), as well as for the detection of high-frequency waves. Observations will be performed with the coronagraph at Lomnický Stit Observatory (LSO), and will also occur during total solar eclipses as SLED is a portable instrument.

### **STEREO DIRECT IMAGING OF A CORONAL MASS EJECTION-DRIVEN SHOCK TO 0.5 AU**

Shane A. [Maloney](#) and Peter T. Gallagher

E-print, June 2011, **File** ; 2011 ApJ 736 L5

Fast coronal mass ejections (CMEs) generate standing or bow shocks as they propagate through the corona and solar wind. Although CME shocks have previously been detected indirectly via their emission at radio frequencies, direct imaging has remained elusive due to their low contrast at optical wavelengths. Here we report the first images of a CME-driven shock as it propagates through interplanetary space from 8  $R_{\odot}$  to 120  $R_{\odot}$  (0.5 AU), using observations from the STEREO Heliospheric Imager. The CME was measured to have a velocity of  $\sim 1000$  km s $^{-1}$  and a Mach number of  $4.1 \pm 1.2$ , while the shock front standoff distance ( $\Delta$ ) was found to increase linearly to  $\sim 20 R_{\odot}$  at 0.5 AU. The normalized standoff distance ( $\Delta/DO$ ) showed reasonable agreement with semi-empirical relations, where  $DO$  is the CME radius. However, when normalized using the radius of curvature,  $\Delta/RO$  did not agree well with theory, implying that  $RO$  was underestimated by a factor of 3-8. This is most likely due to the difficulty in estimating the larger radius of curvature along the CME axis from the observations, which provide

### **Reconstructing the 3-D Trajectories of CMEs in the Inner Heliosphere**

Shane A. [Maloney](#), Peter T. Gallagher and R. T. James McAteer<sup>1</sup>

E-print, May 2009, Solar Phys (2009) 256: 149–166; **File**

A method for the full three-dimensional (3-D) reconstruction of the trajectories of coronal mass ejections (CMEs) using Solar Terrestrial Relations Observatory (STEREO) data is presented. Four CMEs that were simultaneously observed by the inner and outer coronagraphs (COR1 and 2) of the Ahead and Behind STEREO satellites were analysed. These observations were used to derive CME trajectories in 3-D out to  $\sim 15 R_{\odot}$ . The reconstructions using COR1/2 data support a radial propagation model. Assuming pseudo-radial propagation at large distances from the Sun ( $15 - 240 R_{\odot}$ ), the CME positions were extrapolated into the Heliospheric Imager (HI) field-of-view. We estimated the CME velocities in the different fields-of-view. It was found that CMEs slower than the solar wind were accelerated, while CMEs faster than the solar wind were decelerated, with both tending to the solar wind velocity.

### **The Interaction of Coronal Mass Ejections with Alfvénic Turbulence**

Ward [Manchester](#) IV and Bart Van Der Holst

[Journal of Physics: Conference Series](#), Volume 900, Number 1 012015 2017

<http://iopscience.iop.org/article/10.1088/1742-6596/900/1/012015/pdf>

We provide a first attempt to understand the interaction between Alfvén wave turbulence, kinetic instabilities and temperature anisotropies in the environment of a fast coronal mass ejection (CME) near the Sun. The impact of a fast CME on the solar corona causes turbulent energy, thermal energy and dissipative heating to increase by orders of magnitude, and produces conditions suitable for a host of kinetic instabilities. We study these CME-induced effects with the recently developed Alfvén Wave Solar Model, with which we are able to self-consistently simulate the turbulent energy transport and dissipation as well as isotropic electron heating and anisotropic proton heating. Furthermore, the model also offers the capability to address the effects of fire hose, mirror mode, and cyclotron kinetic instabilities on proton energy partitioning all in a global-scale numerical simulation. We find amplified turbulent energy in the CME sheath, along with strong wave reflection at the shock combine to cause wave dissipation rates to increase by more than a factor of 100. In contrast, wave energy is greatly diminished by adiabatic expansion in the flux rope. Finally, we find proton temperature anisotropies are limited by kinetic instabilities to a level consistent with solar wind observations.



## The Physical Processes of CME/ICME Evolution

Review

Ward [Manchester IV](#), Emilia K. J. Kilpua, Ying D. Liu, Noé Lugaz, Pete Riley, Tibor Török, Bojan Vršnak

[Space Science Reviews](#)

2017

<https://link.springer.com/content/pdf/10.1007%2Fs11214-017-0394-0.pdf>

As observed in Thomson-scattered white light, coronal mass ejections (CMEs) are manifest as large-scale expulsions of plasma magnetically driven from the corona in the most energetic eruptions from the Sun. It remains a tantalizing mystery as to how these erupting magnetic fields evolve to form the complex structures we observe in the solar wind at Earth. Here, we strive to provide a fresh perspective on the post-eruption and interplanetary evolution of CMEs, focusing on the physical processes that define the many complex interactions of the ejected plasma with its surroundings as it departs the corona and propagates through the heliosphere. We summarize the ways CMEs and their interplanetary CMEs (ICMEs) are rotated, reconfigured, deformed, deflected, decelerated and disguised during their journey through the solar wind. This study then leads to consideration of how structures originating in coronal eruptions can be connected to their far removed interplanetary counterparts. Given that ICMEs are the drivers of most geomagnetic storms (and the sole driver of extreme storms), this work provides a guide to the processes that must be considered in making space weather forecasts from remote observations of the corona. **17-18 Apr 1999, 14 July 2000, 27 May 2002, 28 October 2003, 2 November 2008, 12 December 2008, 16 June 2010, 7 Mar 2012**

## THE COUPLED EVOLUTION OF ELECTRONS AND IONS IN CORONAL MASS EJECTION-DRIVEN SHOCKS

W. B. [Manchester IV](#), B. van der Holst, G. Tóth, and T. I. Gombosi

2012 ApJ 756 81

We present simulations of coronal mass ejections (CMEs) performed with a new two-temperature coronal model developed at the University of Michigan, which is able to address the coupled thermodynamics of the electron and proton populations in the context of a single fluid. This model employs heat conduction for electrons, constant adiabatic index ( $\gamma = 5/3$ ), and includes Alfvén wave pressure to accelerate the solar wind. The Wang-Sheeley-Arge empirical model is used to determine the Alfvén wave pressure necessary to produce the observed bimodal solar wind speed. The Alfvén waves are dissipated as they propagate from the Sun and heat protons on open magnetic field lines to temperatures above 2 MK. The model is driven by empirical boundary conditions that includes GONG magnetogram data to calculate the coronal field, and STEREO/EUVI observations to specify the density and temperature at the coronal boundary by the Differential Emission Measure Tomography method. With this model, we simulate the propagation of fast CMEs and study the thermodynamics of CME-driven shocks. Since the thermal speed of the electrons greatly exceeds the speed of the CME, only protons are directly heated by the shock. Coulomb collisions low in the corona couple the protons and electrons allowing heat exchange between the two species. However, the coupling is so brief that the electrons never achieve more than 10% of the maximum temperature of the protons. We find that heat is able to conduct on open magnetic field lines and rapidly propagates ahead of the CME to form a shock precursor of hot electrons.

## THREE-DIMENSIONAL MHD SIMULATION OF THE 2003 OCTOBER 28 CORONAL MASS EJECTION: COMPARISON WITH LASCO CORONAGRAPH OBSERVATIONS

Ward B. [Manchester IV](#),<sup>1</sup> Angelos Vourlidas,<sup>2</sup> Ga'bor To'th,<sup>1</sup> Noe' Lugaz,<sup>3</sup> Iliia I. Roussev,<sup>3</sup> Igor V. Sokolov,<sup>1</sup> Tamas I. Gombosi,<sup>1</sup> Darren L. De Zeeuw,<sup>1</sup> and Merav Opher<sup>4</sup>

Astrophysical Journal, 684:1448-1460, 2008 September; **File**

<http://www.journals.uchicago.edu/toc/apj/2008/684/2>

We numerically model the coronal mass ejection (CME) event of 2003 October 28 that erupted from AR 10486 and propagated to Earth in less than 20 hr, causing severe geomagnetic storms. The magnetohydrodynamic (MHD) model is formulated by first arriving at a steady state corona and solar wind employing synoptic magnetograms. We initiate two CMEs from the same active region, one approximately a day earlier that preconditions the solar wind for the much faster CME on the 28th. This second CME travels through the corona at a rate of over 2500 km s<sup>-1</sup>, driving a strong forward shock. We clearly identify this shock in an image produced by the Large Angle Spectrometric Coronagraph (LASCO) C3 and reproduce the shock and its appearance in synthetic white-light images from the simulation. We find excellent agreement with both the general morphology and the quantitative brightness of the model CME with LASCO observations. These results demonstrate that the CME shape is largely determined by its interaction with the ambient solarwind and may not be sensitive to the initiation process. We then show how the CME would appear as observed by wide-angle coronagraphs on board the Solar Terrestrial Relations Observatory (STEREO) spacecraft. We find complex time evolution of the white-light images as a result of the way in which the density structures pass through the Thomson sphere. **The simulation is performed with the SpaceWeatherModeling Framework (SWMF).**

## Three-dimensional reconstruction of CME-driven shock-streamer interaction from radio and EUV observations: a different take on the diagnostics of coronal magnetic fields

S. [Mancuso](#), [F. Frassati](#), [A. Bemporad](#), [D. Barghini](#)

Astronomy & Astrophysics, Letters 624, L2

2019

<https://arxiv.org/pdf/1903.06604.pdf>

<https://www.aanda.org/articles/aa/pdf/2019/04/aa35157-19.pdf>

On **2014 October 30**, a band-split type II radio burst associated with a coronal mass ejection (CME) observed by the Atmospheric Imaging Assembly (AIA) on board the Solar Dynamic Observatory (SDO) occurred over the southeast limb of the Sun. The fast expansion in all directions of the plasma front acted as a piston and drove a spherical fast shock ahead of it, whose outward progression was traced by simultaneous images obtained with the Nançay Radioheliograph (NRH). The geometry of the CME/shock event was recovered through 3D modeling, given the absence of concomitant stereoscopic observations, and assuming that the band-split type II burst was emitted at the intersection of the shock surface with two adjacent low-Alfvén speed coronal streamers. From the derived spatiotemporal evolution of the standoff distance between shock and CME leading edge, we were finally able to infer the magnetic field strength  $B_{in}$  in the inner corona. A simple radial profile of the form  $B(r)=(12.6\pm 2.5)r^{-4}$  nicely fits our results, together with previous estimates, in the range  $r=1.1-2.0$  solar radii.

## Combined Analysis of Ultraviolet and Radio Observations of the 7 May 2004 CME/Shock Event

Salvatore [Mancuso](#)

Solar Physics, Volume 273, Number 2, 511-523, 2011

We report results from the combined analysis of UV and radio observations of a CME-driven shock observed on **7 May 2004** above the southeast limb of the Sun at 1.86 R<sub>☉</sub>

the Solar and Heliospheric Observatory (SOHO). The coronal mass ejection (CME) was first detected in white-light by the SOHO's Large Angle and Spectrometric Coronagraph (LASCO) C2 telescope and shock-associated type II metric emission was recorded simultaneously by ground-based radio spectrographs. The shock speed ( $\approx 690$  km s<sup>-1</sup>), as deduced from the analysis of the type II emission drift in the radio spectra and the pre-shock local electron density estimated with the diagnostics provided by UVCS observations of the O vi  $\lambda\lambda$  1031.9, 1037.6 doublet line intensities, is just a factor  $\approx 0.1$  higher than the CME speed inferred by means of the white-light (and EUV) data in the middle corona. The local magnetosonic speed, computed from a standard magnetic field model, was estimated as high as  $\approx 600$  km s<sup>-1</sup>, implying that the CME speed was probably just sufficient to drive a weak fast-mode MHD shock ahead of the front. Simultaneously with the type II radio emission, significant changes in the O vi doublet line intensities and profiles were recorded in the UVCS spectra and found compatible with abrupt post-shock plasma acceleration and modest ion heating. This work provides further evidence for the CME-driven origin of the shocks observed in the middle corona.

## Interpretation of the SOHO/UVCS observations of two CME-driven shocks

Salvatore [Mancuso](#),  and Alessandro Bemporad

[Advances in Space Research](#), Volume 44, Issue 4, 17 August 2009, Pages 451-456

We report on the analysis of two fast CME-driven shocks observed with the UltraViolet Coronagraph Spectrometer (UVCS) on board the Solar and Heliospheric Observatory (SOHO). The first event, detected on **2002 March 22** at 4.1 R<sub>☉</sub> with the UVCS slit placed in correspondence with the flank of the expanding CME surface, represents the highest UV detection of a shock obtained so far with the UVCS instrument in the corona. The second one, detected on **2002 July 23** at 1.6 R<sub>☉</sub> with the UVCS slit placed in correspondence with the front of the expanding CME surface, shows an anomalous deficiency of ion heating with respect to what observed in previous CME/shocks observed by UVCS, possibly reflecting the effect of different coronal plasma conditions over the solar cycle. From the two different sets of observations we derived an estimate for the shock compression ratio  $X$ , which turns out to be  $X = 2.4 \pm 0.2$  and  $X = 2.2 \pm 0.1$ , respectively, for the first and second event. Comparison between the two events provides complementary perspectives on the dynamical evolution of CME-driven shocks.

## UV and Radio Observations of the Coronal Shock Associated with the 2002 July 23 Coronal Mass Ejection Event

S. [Mancuso](#) and D. Avetta

The Astrophysical Journal, Vol. 677, No. 1: 683-691, 2008.

<http://www.journals.uchicago.edu/doi/pdf/10.1086/528839>

We report on the analysis of a fast coronal mass ejection (CME)-driven shock observed on **2002 July 23** with the Ultraviolet Coronagraph Spectrometer (UVCS) on board the Solar and Heliospheric Observatory (SOHO). The CME was first detected in white light by the Large Angle and Spectrometric Coronagraph Experiment (LASCO), and shock-associated type II metric emission was recorded by several ground-based radio spectrographs. The evolution of the excess broadening of the O vi k1032 line profiles observed by UVCS at 1.63 R<sub>☉</sub> is consistent with the passage of a CME-driven shock surface enveloping a bubble-type, conically expanding CME, and its dynamics is found to be well associated with the complex, multiple type II radio emission detected in the metric band. Our results suggest that there might be a deficiency of ion heating in the present event with respect to what was observed in previous CME shocks detected by UVCS, and that this paucity might be attributed to different local plasma conditions, such as higher ambient coronal plasma  $\rho$ . We conclude that plasma  $\rho$  could be an important parameter in determining the effect of ion heating at collisionless shock fronts in the solar corona.

## **A highly dynamic small-scale jet in a polar coronal hole**

[Sudip Mandal](#), [Lakshmi Pradeep Chitta](#), [Hardi Peter](#), [Sami K. Solanki](#), [Regina Aznar Cuadrado](#), [Luca Teriaca](#), [Udo Schühle](#), [David Berghmans](#), [Frédéric Auchère](#)

A&A 664, A28 2022

<https://arxiv.org/pdf/2206.02236.pdf>

<https://www.aanda.org/articles/aa/pdf/2022/08/aa43765-22.pdf>

We present an observational study of the plasma dynamics at the base of a solar coronal jet, using high resolution extreme ultraviolet imaging data taken by the Extreme Ultraviolet Imager **on board Solar Orbiter**, and by the Atmospheric Imaging Assembly on board Solar Dynamics Observatory. We observed multiple plasma ejection events over a period of  $\sim 1$  hour from a dome-like base that is  $\text{ca.} \sim 4$  Mm wide and is embedded in a polar coronal hole. Within the dome below the jet spire, multiple plasma blobs with sizes around 1--2 Mm propagate upwards to dome apex with speeds of the order of the sound speed ( $\text{ca.} \sim 120 \text{ km s}^{-1}$ ). Upon reaching the apex, some of these blobs initiate flows with similar speeds towards the other footpoint of the dome. At the same time, high speed super-sonic outflows ( $\sim 230 \text{ km s}^{-1}$ ) are detected along the jet spire. These outflows as well as the intensity near the dome apex appear to be repetitive. Furthermore, during its evolution, the jet undergoes many complex morphological changes including transitions between the standard and blowout type eruption. These new observational results highlight the underlying complexity of the reconnection process that powers these jets and also provide insights into the plasma response when subjected to rapid energy injection. **2021-Sep-14**

## **Magnetic energy release: flares and coronal mass ejections**

Cristina H. [Mandrini](#)

Solar and Stellar Variability: Impact on Earth and Planets, Proceedings IAU Symposium No. 264, 2009, p. 257-266, A.G. Kosovichev, A.H. Andrei & J.-P. Rozelot, eds., **2010**, **File**

Free energy stored in the magnetic field is the source that powers solar and stellar activity at all temporal and spatial scales. The energy released during transient atmospheric events is contained in current-carrying magnetic fields that have emerged twisted and may be further stressed via motions in the lower atmospheric layers (i.e. loop-footpoint motions). Magnetic reconnection is thought to be the mechanism through which the stored magnetic energy is transformed into kinetic energy of accelerated particles and mass flows, and radiative energy along the whole electromagnetic spectrum. This mechanism works efficiently at scale lengths much below the spatial resolution of even the highest resolution solar instruments; however, it may imply a large-scale restructuring of the magnetic field inferred indirectly from the combined analysis of observations and models of the magnetic field topology. The aftermath of magnetic energy release includes events ranging from nanoflares, which are below our detection limit, to powerful flares, which may be accompanied by the ejection of large amounts of plasma and magnetic field (so called coronal mass ejections, CMEs), depending on the amount of total available free magnetic energy, the magnetic flux density distribution, the magnetic field configuration, etc. We describe key observational signatures of flares and CMEs on the Sun, their magnetic field topology, and discuss how the combined analysis of solar and interplanetary observations can be used to constrain the flare/CME ejection mechanism.

## **Interplanetary flux rope ejected from an X-ray bright point. The smallest magnetic cloud source-region ever observed**

[Mandrini](#), C. H.; [Pohjolainen](#), S.; [Dasso](#), S.; [Green](#), L. M.; [Démoulin](#), P.; [van Driel-Gesztelyi](#), L.; [Copperwheat](#), C.; [Foley](#), C.

Astronomy and Astrophysics, Volume 434, Issue 2, May **2005**, pp.725-740

<http://www.aanda.org/articles/aa/pdf/2005/17/aa1079.pdf>

Using multi-instrument and multi-wavelength observations (SOHO/MDI and EIT, TRACE and Yohkoh/SXT), as well as computing the coronal magnetic field of a tiny bipole combined with modelling of Wind in situ data, we provide evidences for the smallest event ever observed which links a sigmoid eruption to an interplanetary magnetic cloud (MC). The tiny bipole, which was observed very close to the solar disc centre, had a factor one hundred less flux than a classical active region (AR). In the corona it had a sigmoidal structure, observed mainly in EUV, and we found a very high level of non-potentiality in the modelled magnetic field, 10 times higher than we have ever found in any AR. From May 11, 1998, and until its disappearance, the sigmoid underwent three intense impulsive events. The largest of these events had extended EUV dimmings and a cusp. The Wind spacecraft detected 4.5 days later one of the smallest MC ever identified (about a factor one hundred times less magnetic flux in the axial component than that of an average MC). The link between this last eruption and the interplanetary magnetic cloud is supported by several pieces of evidence: good timing, same coronal loop and MC orientation, same magnetic field direction and magnetic helicity sign in the coronal loops and in the MC. We further quantify this link by estimating the magnetic flux (measured in the dimming regions and in the MC) and the magnetic helicity (pre- to post-event change in the solar corona and helicity content of the MC). Within the uncertainties, both magnetic fluxes and helicities are in reasonable agreement, which brings further evidences of their link. These observations show that the ejections of tiny magnetic flux ropes are indeed possible and put new constraints on CME models. **10-15 May 1998**

## Recent Research: Large-scale Disturbances, their Origin and Consequences

G. Mann and B. Vršnak;

Lect. Notes Phys. **725**, 203–218 (2007), File

DOI 10.1007/978-3-540-71570-2\_10

This article gives a flavour of recent research dedicated to the large-scale coronal disturbances and the related interplanetary phenomena. The discussions include the take-off and propagation of coronal mass ejections (CMEs); the CME-flare relationship; the origin and propagation of shocks; the role of flares, CMEs, and shocks in particle acceleration; radio signatures of CMEs and shocks; coronal and IP plasma diagnostics offered by the radio emission excited by these phenomena.

## Current State of Reduced Solar Activity: Intense Space Weather Events in the Inner Heliosphere

P.K. Manoharan, K. Mahalakshmi, A. Johri, B.V. Jackson, D. Ravikumar,

K. Kalyanasundaram, S.P. Subramanian, A. K. Mittal

SUN and GEOSPHERE Vol.13, No.2 – 2018, 135-144 File

[http://newserver.stil.bas.bg/SUNGEO/00SGArhiv/SG\\_v13\\_No2\\_2018-pp-135-143.pdf](http://newserver.stil.bas.bg/SUNGEO/00SGArhiv/SG_v13_No2_2018-pp-135-143.pdf)

We present a study of 21 geomagnetic storms, occurred during 2011–2017 in association with the propagation of coronal mass ejections (CMEs). These storms are selected with the minimum storm disturbance index (SYM-H) intensity of -100 nT or less and are distributed from the maximum to the minimum of the weak solar cycle 24. We identify and investigate these storm-driving CMEs (halo and partial halo CMEs) by combining EUV and white-light images in the nearSun region, interplanetary scintillation images in between the Sun and the Earth, and in-situ measurements at the nearEarth orbit. These CMEs cover a wide range of initial speeds, ~180 to 2680 km/s. For about 50% of the CMEs, the fast initial speed at the near-Sun region does not correlate with the final speed at the near-Earth orbit. The storm indexes range between -100 and -233 nT and they are associated with minimum Bz values in the range of -12 to -38 nT. The Forbush decrease (FD) levels associated with these storms vary in the range of about -2% to -10%. A comparison of travel times of CMEs to 1 AU with the observed initial/final speeds and estimated initial speed suggests that a large fraction of fast initial speeds could possibly be due to the sudden expansion of the CME into a relatively low pressure interplanetary medium. Most of the geomagnetic storms (i.e., 19 storms) have been caused by the strong intrinsic magnetic field of the CME and only 2 storms are produced by the sheath region between the arrival times of interplanetary shock and CME. The geomagnetic storm index is compared with the possible reconnection electric field component, BzVICME. It suggests an empirical relationship for the likely lower level of storm index,  $\text{SYM-H} = -70 - 0.003 \cdot \text{BzVICME}$  (nT), in which Bz and VICME are respectively given in units of nT and km/s. **21 June 2015**

## Coronal mass ejections—Propagation time and associated internal energy

P.K. Manoharan a., A. Mujiber Rahman

Journal of Atmospheric and Solar-Terrestrial Physics **73** (2011) 671–677, File

In this paper, we analyze 91 coronal mass ejection (CME) events studied by Manoharan et al. (2004) and Gopalswamy and Xie (2008). These earth-directed CMEs are large (width  $>160^\circ$ ) and cover a wide range of speeds ( $\sim 1202\text{--}2400$  km s<sup>-1</sup>) in the LASCO field of view. This set of events also includes interacting CMEs and some of them take longer time to reach 1 AU than the travel time inferred from their speeds at 1 AU. We study the link between the travel time of the CME to 1 AU (combined with its final speed at the Earth) and the effective acceleration in the Sun–Earth distance. Results indicate that (1) for almost all the events (85 out of 91 events), the speed of the CME at 1 AU is always less than or equal to its initial speed measured at the near-Sun region, (2) the distributions of initial speeds, CME-driven shock and CME speeds at 1 AU clearly show the effects of aero-dynamical drag between the CME and the solar wind and in consequence, the speed of the CME tends to equalize to that of the background solar wind, (3) for a large fraction of CMEs (for  $\sim 50\%$  of the events), the inferred effective acceleration along the Sun–Earth line dominates the above drag force. The net acceleration suggests an average dissipation of energy  $\sim 10^{31\text{--}32}$  ergs, which is likely provided by the Lorentz force associated with the internal magnetic energy carried by the CME.

## Relative Kinematics of the Leading Edge and the Prominence in Coronal Mass Ejections

Darije Maričić · Bojan Vršnak · Dragan Roša

Solar Phys (2009) 260: 177–189, File

We present a statistical analysis of the relationship between the kinematics of the leading edge and the eruptive prominence in coronal mass ejections (CMEs). We study the acceleration phase of **18** CMEs in which kinematics was measured from the pre-eruption stage up to the post-acceleration phase. In all CMEs, the three part structure (the leading edge, the cavity, and the prominence) was clearly recognizable from early stages of the eruption. The data show a distinct correlation between the duration of the leading edge (LE)

acceleration and eruptive prominence (EP) acceleration. In the majority of events (78%) the acceleration phase onset of the LE is very closely synchronized (within  $\pm 20$  min) with the acceleration of EP. However, in two events the LE acceleration started significantly earlier than the EP acceleration ( $>50$  min), and in two events the EP acceleration started earlier than the LE acceleration ( $>40$  min). The average peak acceleration of LEs ( $281 \text{ ms}^{-2}$ ) is about two times larger than the average peak acceleration of EPs ( $136 \text{ ms}^{-2}$ ). For the first time, our results quantitatively demonstrate the level of synchronization of the acceleration phase of LE and EP in a rather large sample of events, *i.e.*, we quantify how often the eruption develops in a “self-similar” manner.

## **Acceleration phase of coronal mass ejections: II. Synchronization of the energy release in the associated flare.**

**Marićić**, D., Vršnak, B., Stanger, A.L., Veronig, A.M., Temmer, M., Roša, D.: **2007**, *Solar Phys.* **241**, 99 – 112. doi:[10.1007/s11207-007-0291-x](https://doi.org/10.1007/s11207-007-0291-x).

## **Coronal Mass Ejection of 26 February 2000: Complete Analysis of the Three-part CME Structure**

D. **Marićić**<sup>1</sup>, B. Vršnak<sup>2</sup>, D. Roša<sup>1</sup>, D. Hržina  
Sun and Geosphere, **2012**; 7(2): 85-89

We analyze the kinematics and morphology of the limb coronal mass ejection (CME) of **26 February 2000**, utilizing observations from Mauna Loa Solar Observatory (MLSO), the Solar and Heliospheric Observatory (SOHO) and the Geostationary Operational Environmental Satellite (GOES). Also, we analyze the relation between dynamics of the CME and the energy release in the associated flare.

An intricate structure (prominence, prominence-like absorbing feature, cavity and bright overlying arcade) is clearly recognizable in the low corona during the pre-eruption phase of slow rise. This provided measurements of kinematics of various features from the very beginning of the eruption up to the post-acceleration phase which was followed up to 32 solar radii. Such events are observed only occasionally, and are of great importance for the comprehension of the nature of forces driving CMEs. The acceleration maximum was attained at the radial distance of 2.4 solar radii from the solar center and ceased beyond 12 solar radii. The time profiles of the acceleration of various features of CME are showing "self-similar" expansion and implying a common driver. The acceleration phase was synchronized to a certain degree with the impulsive phase of the associated two-ribbon flare. Observations provide clear evidence that CME eruption caused a global restructuring of the magnetic field in the outer and inner corona. Furthermore, kinematics and morphological properties of this CME show possibility that in some events the prominence can evolve into a structure which looks like three-part structure CME, *i.e.* where the frontal rim is just a part of helically twisted prominence.

## **Coronal mass ejection of 15 May 2001: I. Evolution of morphological features of the eruption.**

**Marićić**, D., Vršnak, B., Stanger, A.L., Veronig, A.: **2004**, *Solar Phys.* **225**, 337 – 353. doi:[10.1007/s11207-004-3748-1](https://doi.org/10.1007/s11207-004-3748-1).

## **Signatures of Secondary Collisionless Magnetic Reconnection Driven by Kink Instability of a Flux Rope**

S. **Markidis**, G. Lapenta, G.L. Delzanno, P. Henri, M.V. Goldman, D.L. Newman, T. Intrator, E. Laure **2014**

<http://arxiv.org/pdf/1408.1144v1.pdf>

The kinetic features of secondary magnetic reconnection in a single flux rope undergoing internal kink instability are studied by means of three-dimensional Particle-in-Cell simulations. Several signatures of secondary magnetic reconnection are identified in the plane perpendicular to the flux rope: a quadrupolar electron and ion density structure and a bipolar Hall magnetic field develop in proximity of the reconnection region. The most intense electric fields form perpendicularly to the local magnetic field, and a reconnection electric field is identified in the plane perpendicular to the flux rope. An electron current develops along the reconnection line in the opposite direction of the electron current supporting the flux rope magnetic field structure. Along the reconnection line, several bipolar structures of the electric field parallel to the magnetic field occur making the magnetic reconnection region turbulent. The reported signatures of secondary magnetic reconnection can help to localize magnetic reconnection events in space, astrophysical and fusion plasmas.

## **The Solar Corona: What Are The Remaining Fundamental Physical Questions?**

**(Invited Review)**

Petrus C. **Martens**

Proceedings of the International Symposium on Solar-Terrestrial Physics, November 2012, Pune, India  
Bull. Astron. Soc. India, **2013-2014**, in press.

<http://solar.physics.montana.edu/martens/papers/martens-draft3.pdf>; **File**

The two key unresolved physical questions in our knowledge of the solar corona are: (1) **How is the corona heated** to a temperature of several MK, and, directly related to that, why is the coronal emission structured in nearly constant cross-section loops? And, (2) **what is the mechanism that determines the onset of solar flares and eruptions**, and, again directly related, **can flares be predicted?** I will introduce these questions, discuss some proposed solutions that are not complete, and my view on getting to the full solutions.

### **The Build-up to Eruptive Solar Events Viewed as the Development of Chiral Systems**

Sara F. **Martin**, Olga Panasenco, Mitchell A. Berger, Oddbjorn Engvold, Yong Lin, Alexei A. Pevtsov, Nandita Srivastava

2nd ATST - EAST Workshop in Solar Physics: Magnetic Fields from the Photosphere to the Corona, ASP Conference Series, Vol. 463, p.157, **2012, File**

When we examine the chirality or observed handedness of the chromospheric and coronal structures involved in the long-term build-up to eruptive events, we find that they evolve in very specific ways to form two and only two sets of large-scale chiral systems. Each system contains spatially separated components with both signs of chirality, the upper portion having negative (positive) chirality and the lower part possessing positive (negative) chirality. The components within a system are a filament channel (represented partially by sets of chromospheric fibrils), a filament (if present), a filament cavity, sometimes a sigmoid, and always an overlying arcade of coronal loops. When we view these components as parts of large-scale chiral systems, we more clearly see that it is not the individual components of chiral systems that erupt but rather it is the approximate upper parts of an entire evolving chiral system that erupts. We illustrate the typical pattern of build-up to eruptive solar events first without and then including the chirality in each stage of the build-up. We argue that a complete chiral system has one sign of handedness above the filament spine and the opposite handedness in the barbs and filament channel below the filament spine. If the spine has handedness, the observations favor its having the handedness of the filament cavity and coronal loops above. As the separate components of a chiral system form, we show that the system appears to maintain a balance of right-handed and left-handed features, thus preserving an initial near-zero net helicity. Each individual chiral system may produce many successive eruptive events above a single filament channel.

**6 Jun, 2010, 17 Sept, 2010, 20 Sept 2010, 2010 Sep 28,30 Sept 2010**

### **Determination of CME orientation and consequences for their propagation**

[Karmen Martinic](#), [Mateja Dumbovic](#), [Manula Temmer](#), [Astrid Veronig](#), [Bojan Vršnak](#)

A&A 661, A155 **2022**

<https://arxiv.org/pdf/2204.10112.pdf>

<https://www.aanda.org/articles/aa/pdf/2022/05/aa43433-22.pdf>

The configuration of the interplanetary magnetic field and features of the related ambient solar wind in the ecliptic and meridional plane are different. Therefore, one can expect that the orientation of the flux-rope axis of a coronal mass ejection (CME) influences the propagation of the CME itself. However, the determination of the CME orientation, especially from image data, remains a challenging task to perform. This study aims to provide a reference to different CME orientation determination methods in the near-Sun environment. Also, it aims to investigate the non-radial flow in the sheath region of the interplanetary CME (ICME) in order to provide the first proxy to relate the ICME orientation with its propagation. We investigated 22 isolated CME-ICME events in the period 2008-2015. We determined the CME orientation in the near-Sun environment using the following: 1) a 3D reconstruction of the CME with the graduated cylindrical shell (GCS) model applied to coronagraphic images provided by the STEREO and SOHO missions and; 2) an ellipse fitting applied to single spacecraft data from SOHO/LASCO C2 and C3 coronagraphs. In the near-Earth environment, we obtained the orientation of the corresponding ICME using in situ plasma and field data and also investigated the non-radial flow (NRF) in its sheath region. The ability of GCS and ellipse fitting to determine the CME orientation is found to be limited to reliably distinguish only between the high or low inclination of the events. Most of the CME-ICME pairs under investigation were found to be characterized by a low inclination. For the majority of CME-ICME pairs, we obtain consistent estimations of the tilt from remote and in situ data. The observed NRFs in the sheath region show a greater y direction to z direction flow ratio for high-inclination events, indicating that the CME orientation could have an impact on the CME propagation. **3-5 April 2010**

Table 1. Results of the GCS modeling 2008-2016

### **Interplanetary Magnetic Flux Ropes as Agents Connecting Solar Eruptions and Geomagnetic Activities**

K. **Marubashi**, K.-S. Cho, H. Ishibashi

[Solar Physics](#) December **2017**, 292:189

<https://link.springer.com/content/pdf/10.1007%2Fs11207-017-1204-2.pdf>

We investigate the solar wind structure for 11 cases that were selected for the campaign study promoted by the International Study of Earth-affecting Solar Transients (ISEST) MiniMax24 Working Group 4. We can identify clear flux rope signatures in nine cases. The geometries of the nine interplanetary magnetic flux ropes (IFRs) are examined with a model-fitting analysis with cylindrical and toroidal force-free flux rope models. For seven cases in which magnetic fields in the solar source regions were observed, we compare the IFR geometries with magnetic structures in their solar source regions. As a result, we can confirm the coincidence between the IFR orientation and the orientation of the magnetic polarity inversion line (PIL) for six cases, as well as the so-called helicity rule as regards the

handedness of the magnetic chirality of the IFR, depending on which hemisphere of the Sun the IFR originated from, the northern or southern hemisphere; namely, the IFR has right-handed (left-handed) magnetic chirality when it is formed in the southern (northern) hemisphere of the Sun. The relationship between the orientation of IFRs and PILs can be taken as evidence that the flux rope structure created in the corona is in most cases carried through interplanetary space with its orientation maintained. In order to predict magnetic field variations on Earth from observations of solar eruptions, further studies are needed about the propagation of IFRs because magnetic fields observed at Earth significantly change depending on which part of the IFR hits the Earth. **7 – 9 March 2012, 12 – 14 July 2012, 23 – 24 July 2012, 4 – 8 October 2012, 15 – 17 March 2013, 1 June 2013, 10 – 13 September 2014, 15 – 17 March 2015, 22 – 24 June 2015**

## **An Observational Study of a "Rosetta-Stone" Solar Eruption**

[E I Mason](#), [Spiro Antiochos](#), [Angelos Vourlidas](#)

**2021** *ApJL* **914** L8

<https://arxiv.org/ftp/arxiv/papers/2105/2105.09164.pdf>

<https://doi.org/10.3847/2041-8213/ac0259>

This Letter reports observations of an event that connects all major classes of solar eruptions: those that erupt fully into the heliosphere versus those that fail and are confined to the Sun, and those that eject new flux into the heliosphere, in the form of a flux rope, versus those that eject only new plasma in the form of a jet. The event originated in a filament channel overlying a circular polarity inversion line (PIL) and occurred on 2013-03-20 during the extended decay phase of the active region designated NOAA 12488/12501. The event was especially well-observed by multiple spacecraft and exhibited the well-studied null-point topology. We analyze all aspects of the eruption using SDO AIA and HMI, STEREO-A EUVI, and SOHO LASCO imagery. One section of the filament undergoes a classic failed eruption with cool plasma subsequently draining onto the section that did not erupt, but a complex structured CME/jet is clearly observed by SOHO LASCO C2 shortly after the failed filament eruption. We describe in detail the slow buildup to eruption, the lack of an obvious trigger, and the immediate reappearance of the filament after the event. The unique mixture of major eruption properties observed during this event places severe constraints on the structure of the filament channel field and, consequently, on the possible eruption mechanism. **2016 MARCH 13**

## **SunCET: The Sun Coronal Ejection Tracker Concept**

**(SunCET: A compact EUV instrument to fill a critical observational gap)**

[James Paul Mason](#), [Phillip C. Chamberlin](#), [Daniel Seaton](#), [Joan Burkepile](#), [Robin Colaninno](#), [Karin Dissauer](#), [Francis G. Eparvier](#), [Yuhong Fan](#), [Sarah Gibson](#), [Andrew R. Jones](#), [Christina Kay](#), [Michael Kirk](#), [Richard Kohnert](#), [W. Dean Pesnell](#), [Barbara J. Thompson](#), [Astrid M. Veronig](#), [Matthew J. West](#), [David Windt](#), [Thomas N. Woods](#)

*Journal of Space Weather and Space Climate* **11**, 20 **2021**

<https://arxiv.org/pdf/2101.09215.pdf>

<https://doi.org/10.1051/swsc/2021004>

<https://www.swsc-journal.org/articles/swsc/pdf/2021/01/swsc200047.pdf>

The Sun Coronal Ejection Tracker (SunCET) is an extreme ultraviolet imager and spectrograph instrument concept for tracking coronal mass ejections through the region where they experience the majority of their acceleration: the difficult-to-observe middle corona. It contains a wide field of view ( $0-4\text{--}R_s$ ) imager and a  $1\text{--}\text{\AA}$  spectral-resolution-irradiance spectrograph spanning  $170\text{--}340\text{--}\text{\AA}$ . It leverages new detector technology to read out different areas of the detector with different integration times, resulting in what we call "simultaneous high dynamic range", as opposed to the traditional high dynamic range camera technique of subsequent full-frame images that are then combined in post-processing. This allows us to image the bright solar disk with short integration time, the middle corona with a long integration time, and the spectra with their own, independent integration time. Thus, SunCET does not require the use of an opaque or filtered occulter. SunCET is also compact --  $\sim 15 \times 15 \times 10\text{--cm}$  in volume -- making it an ideal instrument for a CubeSat or a small, complementary addition to a larger mission. Indeed, SunCET is presently in a NASA-funded, competitive Phase A as a CubeSat and has also been proposed to NASA as an instrument onboard a 184 kg Mission of Opportunity.

## **CME Acceleration as a Probe of the Coronal Magnetic Field**

**mini Review**

[James Paul Mason](#), [Phillip C. Chamberlin](#), [Thomas N. Woods](#), [Andrew Jones](#), [Astrid M. Veronig](#), [Karin Dissauer](#), [Michael Kirk](#), [SunCET Team](#)

Heliophysics 2050 Workshop **2020**

<https://arxiv.org/ftp/arxiv/papers/2009/2009.05625.pdf>

By 2050, we expect that CME models will accurately describe, and ideally predict, observed solar eruptions and the propagation of the CMEs through the corona. We describe some of the present known unknowns in observations and models that would need to be addressed in order to reach this goal. We also describe how we might prepare for some of the unknown unknowns that will surely become challenges.

## **Relationship of EUV Irradiance Coronal Dimming Slope and Depth to Coronal Mass Ejection Speed and Mass**

James Paul [Mason](#), Thomas N. Woods, David F. Webb, [Barbara J. Thompson](#), [Robin C. Colaninno](#), [Angelos Vourlidas](#)

ApJ 830 20 2016

<http://arxiv.org/pdf/1607.05284v1.pdf> File

Extreme ultraviolet (EUV) coronal dimmings are often observed in response to solar eruptive events. These phenomena can be generated via several different physical processes. For space weather, the most important of these is the temporary void left behind by a coronal mass ejection (CME). Massive, fast CMEs tend to leave behind a darker void that also usually corresponds to minimum irradiance for the cooler coronal emissions. If the dimming is associated with a solar flare, as is often the case, the flare component of the irradiance light curve in the cooler coronal emission can be isolated and removed using simultaneous measurements of warmer coronal lines. We apply this technique to 37 dimming events identified during two separate two-week periods in 2011, plus an event on 2010 August 7 analyzed in a previous paper, to parameterize dimming in terms of depth and slope. We provide statistics on which combination of wavelengths worked best for the flare-removal method, describe the fitting methods applied to the dimming light curves, and compare the dimming parameters with corresponding CME parameters of mass and speed. The best linear relationships found are  $v_{\text{CME}}[\text{kms}] \approx m_{\text{CME}}[\text{g}]^{\dots\dots\dots}$ . These relationships could be used for space weather operations of estimating CME mass and speed using near-realtime irradiance dimming measurements. **2010 Aug 7, February 10-24 and August 1-14 2011**

**Table 1.** Event list. Times and locations are approximate. Only 29 of the events have dimming and CME derived parameters to allow the study of the relationships between dimmings and CMEs.

### **Microwave radio emissions as a proxy for coronal mass ejection speed in arrival predictions of interplanetary coronal mass ejections at 1 AU**

Carolina Salas [Matamoros](#)<sup>1,2\*</sup>, Karl Ludwig Klein<sup>1</sup> and Gerard Trottet

J. Space Weather Space Clim., 7, A2 (2017)

<http://www.swsc-journal.org/articles/swsc/pdf/2017/01/swsc160027.pdf>

The propagation of a coronal mass ejection (CME) to the Earth takes between about 15 h and several days. We explore whether observations of non-thermal microwave bursts, produced by near-relativistic electrons via the gyrosynchrotron process, can be used to predict travel times of interplanetary coronal mass ejections (ICMEs) from the Sun to the Earth. In a first step, a relationship is established between the CME speed measured by the Solar and Heliospheric Observatory/Large Angle and Spectrometric Coronagraph (SoHO/LASCO) near the solar limb and the fluence of the microwave burst. This relationship is then employed to estimate speeds in the corona of earthward-propagating CMEs. These speeds are fed into a simple empirical interplanetary acceleration model to predict the speed and arrival time of the ICMEs at Earth. The predictions are compared with observed arrival times and with the predictions based on other proxies, including soft X-rays (SXR) and coronagraphic measurements. We found that CME speeds estimated from microwaves and SXR predict the ICME arrival at the Earth with absolute errors of  $11 \pm 7$  and  $9 \pm 7$  h, respectively. A trend to underestimate the interplanetary travel times of ICMEs was noted for both techniques. This is consistent with the fact that in most cases of our test sample, ICMEs are detected on their flanks. Although this preliminary validation was carried out on a rather small sample of events (11), we conclude that microwave proxies can provide early estimates of ICME arrivals and ICME speeds in the interplanetary space. This method is limited by the fact that not all CMEs are accompanied by non-thermal microwave bursts. But its usefulness is enhanced by the relatively simple observational setup and the observation from ground, which makes the instrumentation less vulnerable to space weather hazards. **11 Apr 1997, 2002 Aug 23, 2003 Oct 24, 2004 Jun 16, 2008 Mar 25, 28 Oct 2011, 9 Mar 2012**

**Table 1.** Table of events: event number (col. 1), date (col. 2), time of the first appearance of the CME in LASCO/C2 coronagraph (col. 3), CME speed in the plane of the sky reported in LASCO-CME (col. 4), SXR peak time (col. 5), times of onset (col. 6), end (col. 7), fluences at 3 GHz (col. 8), 9 GHz (col. 9), maximum (col. 10) of microwave bursts. Lower limits of the maximum fluence mean that the real maximum was outside the observed frequency range.

**Table 3.** Comparison between ICME arrival times measured at Wind spacecraft and predicted based on 9 GHz fluence: See CESRA highlight #1336 May 2017 <http://cesra.net/?p=1336>

### **Synthesis of infrared Stokes spectra in an evolving solar chromospheric jet**

[T Matsumoto](#), [Y Kawabata](#), [Y Katsukawa](#), [H Iijima](#), [C Quintero Noda](#)

MNRAS, Volume 523, Issue 1, July 2023, Pages 974–981,

<https://doi.org/10.1093/mnras/stad1509>

Chromospheric jets are plausible agents of energy and mass transport in the solar chromosphere, although their driving mechanisms have not yet been elucidated. Magnetic field measurements are key for distinguishing the driving mechanisms of chromospheric jets. We performed a full Stokes synthesis in the infrared range with a realistic radiative magnetohydrodynamics simulation that generated a chromospheric jet to predict spectropolarimetric observations from the Sunrise Chromospheric Infrared spectro-Polarimeter (SCIP) onboard the SUNRISE III balloon telescope. The jet was launched by the collision between the transition region and an upflow driven by the ascending motion of the twisted magnetic field at the envelope of the flux tube. This motion is consistent with upwardly propagating non-linear Alfvénic waves. The upflow could be detected as continuous Doppler signals in the Ca II 849.8 nm line at the envelope where the dark line core intensity and strong linear polarization coexist. The axis of the flux tube was bright in both Fe I 846.8 nm and Ca II 849.8 nm lines with downflowing plasma inside it. The structure, time evolution, and Stokes signals predicted in our study will improve the physical interpretation of future spectropolarimetric observations with SUNRISE III/SCIP.



## **Long-Term Cosmic Ray Variability and the CME-Index**

Helen [Mavromichalaki](#) and Evangelos Paouris

Advances in Astronomy, Volume 2012 (2012), Article ID 607172, 8 pages

<http://www.hindawi.com/journals/aa/2012/607172/>

The cosmic ray modulation in relation to solar activity indices and heliospheric parameters during the period January 1996–October 2011, covering the solar cycle 23 and the ascending phase of solar cycle 24, is studied. The new perspective of this contribution is that the CME-index, obtained from only the CMEs with angular width greater than 30 degrees, gives much better results than in previous works. The proposed model for the calculation of the modulated cosmic ray intensity obtained from the combination of solar indices and heliospheric parameters gives a very satisfactory value of the standard deviation. The best reproduction of the cosmic ray intensity is obtained by taking into account solar and interplanetary indices such as sunspot number, interplanetary magnetic field, CME-index, and heliospheric current sheet tilt. The standard deviation between the observed and calculated values is about 6.63% for the solar cycle 23 and 4.13% for the ascending part of solar cycle 24.

## **A statistical study of CME-Preflare associated events**

Ramy [Mawad](#), [M. Youssef](#) [Advances in Space Research](#)

Volume 62, Issue 2, 15 July 2018, Pages 417–425

<http://sci-hub.tw/http://linkinghub.elsevier.com/retrieve/pii/S0273117718303727>

We investigated the relationship of associated CME-Preflare during the solar period 1996–2010. We found 292 CME-Preflare associated events (~2%). Those associated events have 0–1 h interval time, popular events occur within half an hour before flare starting time. Post-flares–CME associated events are wider than CME-Preflare associated events. CME-Preflare associated events are ejected from the northern hemisphere during the [solar cycle](#) 23rd, while the non-associated CMEs are ejected from the [southern hemisphere](#). Polar CME-Preflare associated events are more energetic than the equatorial events. This means that post-flare–CME associated events are more decelerated than CME-Preflare associated events, CME-Flare associated simultaneously events and other CMEs. The CME-Preflare associated events are slower than the post-flare–CME associated events, and slightly faster than non-associated CME events. Post-flare–CME associated events are in average more massive than Preflare CME associated events and all other CMEs ejected from the Sun. CME-Preflare associated has a mean average speed which is equivalent to the mean average [solar wind](#) speed approximately.

## **Filaments disappearances in relation to solar flares during the solar cycle 23**

R. [Mawad](#), Mosalam Shaltout, M. Ewaida, M. Yousef, S. Yousef,

Advances in Space Research, Volume 55, Issue 2, 15 January 2015, Pages 696–704

<http://www.sciencedirect.com/science/article/pii/S0273117714006930>

We studied the association between the filament disappearances and solar flares during 1996–2010; we listed 639 associated filament disappearances with solar flares under temporal and spatial condition, those particular 639 filament disappearance were associated with 1676 solar flares during the period 1996–2010. The best angular distance between filament disappearances and associated solar flares ranged between 30° and 60°. The number of the associated events increased with increasing solar activity and decreased with quiet sun. The location of filament disappearances ranges between latitude  $\pm 50^\circ$  and longitude  $\pm 70^\circ$ . We found that longer filament disappearances have activity and ability of contemporary association with flares more than shorter filament disappearance, filament disappearance powers the associated flares more than non-associated flares events. The associated flares have higher solar flux, longer duration, and higher importance compared to non-associated flares with filament disappearance. In addition the associated filament disappearance with flares have two types depending on their duration, short-lived (<9 h), and long-lived (>9 h).

## **Filaments disappearance in relation to coronal mass ejections during the solar cycle 23**

R. [Mawad](#), Mosalam Shaltout, M. Yousef, S. Yousef, M. Ewaida

Advances in Space Research, Volume 55, Issue 2, 15 January 2015, Pages 688–695

<http://www.sciencedirect.com/science/article/pii/S0273117714006929>

We have studied the relationship between filament disappearances with CMEs during solar period 1996–2010. We used the observed disappearing filaments in H $\alpha$  data from Meudon given in NOAA, and coronal mass ejections data (CMEs) from SOHO/LASCO. We obtained 278 CME events (14%) contemporary filament disappearances and CME ejections (from a total of 2018 filament disappearance events and 15,874 CME events during 1996–2010). We found that the number of associated CME–filament disappearance events increased with the increase of the solar activity and significantly decreased with quiet sun. The longer filament disappearances have activity and ability to contemporary association with CMEs more than shorter filament disappearances. The filament disappearance powers the associated CMEs. CMEs which are associated with filament disappearance are ejected with higher speeds, massive, more energetic, and smaller angular width compared to non-associated CME events. In addition, the associated filament disappearance CMEs have two types depending on their duration; short-lived (<9 h), and long-lived (>9 h).

## **Simultaneous longitudinal and transverse oscillations in filament threads after a failed eruption**

Rakesh [Mazumder](#), [Vaibhav Pant](#), [Manuel Luna](#), [Dipankar Banerjee](#)

A&A 633, A12 2020

<https://arxiv.org/pdf/1910.11260.pdf>

<https://doi.org/10.1051/0004-6361/201936453>

Longitudinal and transverse oscillations are frequently observed in the solar prominences and/or filaments. These oscillations are excited by a large scale shock wave, impulsive flares at one leg of the filament threads, or due to any low coronal eruptions. We report simultaneous longitudinal and transverse oscillations in the filament threads of a quiescent region filament. We observe a big filament in the north-west of the solar disk on 6th July 2017. On **7th July 2017** it starts rising around 13:00 UT. Then we observe a failed eruption and subsequently, the filament threads start to oscillate around 16 UT. We observe both transverse and longitudinal oscillations in a filament thread. The oscillations damp down and filament threads almost disappear. We place horizontal and vertical artificial slits on the filament threads to capture the longitudinal and transverse oscillations of the threads. Data from Atmospheric Imaging Assembly (AIA) onboard Solar Dynamics Observatory (SDO) is used to detect the oscillations. We find the signatures of large amplitude longitudinal oscillations (LALOs). We also detect damping in LALOs. In one thread of the filament, we observe large amplitude transverse oscillations (LATOs). Using the pendulum model we estimate the lower limit of magnetic field strength and radius of curvature from the observed parameter of LALOs. We show the co-existence of two different wave modes in the same filament threads. We estimate magnetic field from LALOs and hence suggest a possible range of the length of the filament threads using LATOs.

### Propagation of the 7 January 2014 CME and Resulting Geomagnetic Non-Event

M. L. [Mays](#), B. J. Thompson, L. K. Jian, R. C. Colaninno, D. Odstrcil, C. Möstl, M. Temmer, N. P. Savani, A. Taktakishvili, P. J. MacNeice, Y. Zheng

2015

<http://arxiv.org/pdf/1509.06477v1.pdf>

On 7 January 2014 an X1.2 flare and CME with a radial speed  $\approx 2500$  km s<sup>-1</sup> was observed from near an active region close to disk center. This led many forecasters to estimate a rapid arrival at Earth ( $\approx 36$  hours) and predict a strong geomagnetic storm. However, only a glancing CME arrival was observed at Earth with a transit time of  $\approx 49$  hours and a KP geomagnetic index of only 3-. We study the interplanetary propagation of this CME using the ensemble Wang-Sheeley-Arge (WSA)-ENLIL+Cone model, that allows a sampling of CME parameter uncertainties. We explore a series of simulations to isolate the effects of the background solar wind solution, CME shape, tilt, location, size, and speed, and the results are compared with observed in-situ arrivals at Venus, Earth, and Mars. Our results show that a tilted ellipsoid CME shape improves the initial real-time prediction to better reflect the observed in-situ signatures and the geomagnetic storm strength. CME parameters from the Graduated Cylindrical Shell model used as input to WSA--ENLIL+Cone, along with a tilted ellipsoid cloud shape, improve the arrival-time error by 14.5, 18.7, 23.4 hours for Venus, Earth, and Mars respectively. These results highlight that CME orientation and directionality with respect to observatories play an important role in understanding the propagation of this CME, and for forecasting other glancing CME arrivals. This study also demonstrates the importance of three-dimensional CME fitting made possible by multiple viewpoint imaging.

### Ensemble Modeling of CMEs Using the WSA-ENLIL+Cone Model

M. L. [Mays](#), A. Taktakishvili, A. Pulkkinen, [P. J. MacNeice](#), [L. Rastätter](#), [D. Odstrcil](#), [L. K. Jian](#), [I. G. Richardson](#), [J. A. LaSota](#), [Y. Zheng](#), ...

Solar Phys. 2015

<http://arxiv.org/pdf/1504.04402v2.pdf>

Ensemble modeling of coronal mass ejections (CMEs) provides a probabilistic forecast of CME arrival time that includes an estimation of arrival-time uncertainty from the spread and distribution of predictions and forecast confidence in the likelihood of CME arrival. The real-time ensemble modeling of CME propagation uses the Wang-Sheeley-Arge (WSA)-ENLIL+Cone model installed at the Community Coordinated Modeling Center (CCMC) and executed in real-time at the CCMC/[Space Weather](#) Research Center. The current implementation of this ensemble-modeling method evaluates the sensitivity of WSA-ENLIL+Cone model simulations of CME propagation to initial CME parameters. We discuss the results of real-time ensemble simulations for a total of 35 CME events that occurred between January 2013 – July 2014. For the 17 events where the CME was predicted to arrive at Earth, the mean absolute arrival-time prediction error was 12.3 hours, which is comparable to the errors reported in other studies. For predictions of CME arrival at Earth, the correct-rejection rate is 62 %, the false-alarm rate is 38 %, the correct-alarm ratio is 77 %, and the false-alarm ratio is 23 %. The arrival time was within the range of the ensemble arrival predictions for 8 out of 17 events. The Brier Score for CME arrival-predictions is 0.15 (where a score of 0 on a range of 0 to 1 is a perfect forecast), which indicates that on average, the predicted probability, or likelihood, of CME arrival is fairly accurate. The reliability of ensemble CME-arrival predictions is heavily dependent on the initial distribution of CME input parameters (e.g. speed, direction, and width), particularly the median and spread. Preliminary analysis of the probabilistic forecasts suggests undervariability, indicating that these ensembles do not sample a wide-enough spread in CME input parameters. Prediction errors can also arise from ambient-model parameters, the accuracy of the solar-wind background derived from coronal maps, or other model limitations. Finally, predictions of the K P geomagnetic index differ from observed values by less than one for 11 out of 17 of the ensembles and K P prediction errors computed from the mean predicted K P show a mean absolute error of 1.3. **11 April 2013, 18 April 2014**

**Table 1.: Summary of the ensemble simulation results for 35 CME events (January 2013 - June 2014).**

## **Simultaneous longitudinal and transverse oscillations in filament threads after a failed eruption\***

Rakesh **Mazumder**<sup>1,2</sup>, Vaibhav Pant<sup>3</sup>, Manuel Luna<sup>4,5</sup> and Dipankar Banerjee  
A&A 633, A12 (2020)

<https://doi.org/10.1051/0004-6361/201936453>

<https://arxiv.org/pdf/1910.11260.pdf>

Context. Longitudinal and transverse oscillations are frequently observed in the solar prominences and/or filaments. These oscillations are excited by a large-scale shock wave, impulsive flares at one leg of the filament threads, or due to any low coronal eruptions. We report simultaneous longitudinal and transverse oscillations in the filament threads of a quiescent region filament. We observe a large filament in the northwest of the solar disk on July 6, 2017. On July 7, 2017, it starts rising around 13:00 UT. We then observe a failed eruption and subsequently the filament threads start to oscillate around 16:00 UT.

Aims. We analyse oscillations in the threads of a filament and utilize seismology techniques to estimate magnetic field strength and length of filament threads.

Methods. We placed horizontal and vertical artificial slits on the filament threads to capture the longitudinal and transverse oscillations of the threads. Data from Atmospheric Imaging Assembly onboard Solar Dynamics Observatory were used to detect the oscillations.

Results. We find signatures of large-amplitude longitudinal oscillations (LALOs). We also detect damping in LALOs. In one thread of the filament, we observe large-amplitude transverse oscillations (LATOs). Using the pendulum model, we estimate the lower limit of magnetic field strength and radius of curvature from the observed parameter of LALOs.

Conclusions. We show the co-existence of two different wave modes in the same filament threads. We estimate magnetic field from LALOs and suggest a possible range of the length of the filament threads using LATOs. **July 6-7 2017**

## **Quiet Region Jet by Eruption of Minifilament and Associated Change in Magnetic Flux**

Rakesh **Mazumder**

Astronomy Reports **2018**

<https://arxiv.org/pdf/1812.10090.pdf>

We observe a coronal jet around 22:08 UT on **23 rd March of 2017**, in a quiet region towards the north-east of the solar disk. A minifilament eruption leads to this jet. We analyze dynamics of the minifilament from its formation until its eruption. We observe that the minifilament starts forming around 15:50 UT. Then at a later time, it disappears but again appears and finally erupts as a blowout jet around 22:08 UT. We study the evolution of photospheric magnetic field beneath the minifilament. Initially, we observe subsequent increase and decrease of positive magnetic flux. Prior to the initiation of the eruption, positive magnetic flux shows a continuous decrease until the minifilament disappears. The positive magnetic flux increases and decreases due to new positive flux emergence and cancellation of positive magnetic flux with negative magnetic flux respectively.

## **Frozen-in Fractals All Around: Inferring the Large-Scale Effects of Small-Scale Magnetic Structure**

R. T. James **McAteer**

Solar Phys. **2015**

The large-scale structure of the magnetic field in the solar corona provides the energy to power large-scale solar eruptive events. Our physical understanding of this structure, and hence our ability to predict these events, is limited by the type of data currently available. It is shown that the multifractal spectrum is a powerful tool to study this structure, by providing a physical connection between the details of photospheric magnetic gradients and current density at all size scales. This uses concepts associated with geometric measure theory and the theory of weakly differentiable functions to compare Ampère's law to the wavelet-transform modulus maximum method. The Hölder exponent provides a direct measure of the rate of change of current density across spatial size scales. As this measure is independent of many features of the data (pixel resolution, data size, data type, presence of quiet-Sun data), it provides a unique approach to studying magnetic-field complexity and hence a potentially powerful tool for a statistical prediction of solar-flare activity. Three specific predictions are provided to test this theory: the multifractal spectra will not be dependent on the data type or quality; quiet-Sun gradients will not persist with time; structures with high current densities at large size scales will be the source of energy storage for solar eruptive events.

## **Radio Burst and Circular Polarization Studies of the Solar Corona at Low Frequencies**

Patrick I. **McCauley**

**Thesis** **2019**

<https://arxiv.org/pdf/1912.01747.pdf>

Low-frequency (80-240 MHz) radio observations of the solar corona are presented using the Murchison Widefield Array (MWA), and several discoveries are reported. The corona is reviewed, followed by chapters on Type III bursts and circularly-polarized quiescent emission. The second chapter details new Type III burst dynamics. One source component at higher frequencies splits into two at lower frequencies, where the two components rapidly diverge. This is

attributed to electron beams traversing a divergent magnetic field configuration, which is supported by extreme ultraviolet jet observations outlining a coronal null point. The third chapter uses Type III burst heights as density probes. Harmonic plasma emission implies  $\sim 4\times$  enhancements over background models. This can be explained by electron beams traveling along dense fibers or by propagation effects that elevate apparent source heights. The quiescent corona is compared to model predictions to conclude that propagation effects can largely but not entirely explain the apparent density enhancements. The fourth chapter surveys over 100 spectropolarimetric observing runs. Around 700 compact sources are detected with polarization fractions from less than 0.5% to nearly 100%. They are interpreted as plasma emission noise storm sources down to levels not previously observable. A "bullseye" structure is reported for coronal holes, where an outer ring surrounds an oppositely-polarized central component that does not match the sign expected of thermal bremsstrahlung. The large-scale polarization structure is shown to be well-correlated with that of a global magnetic field model. The last chapter summarizes results and outlines future work. *A preliminary comparison of polarization images to model predictions is shared, along with coronal mass ejection observations revealing a radio arc that is morphologically similar to the white-light structure.*

#### **Chapter 2 Type III Solar Radio Burst Source Region Splitting due to a Quasi-separatrix Layer**

Patrick I. McCauley, Iver H. Cairns, John Morgan, Sarah E. Gibson, James C. Harding, Colin Lonsdale, and Divya Oberoi Published in *The Astrophysical Journal*, 851:151 (2017)

#### **Chapter 3 Densities Probed by Coronal Type III Radio Burst Imaging**

Patrick I. McCauley, Iver H. Cairns, and John Morgan Published in *Solar Physics*, 293:132 (2018)

#### **Chapter 4 The Low-Frequency Solar Corona in Circular Polarization**

Patrick I. McCauley, Iver H. Cairns, Stephen M. White, Surajit Mondal, Emil Lenc, John Morgan, and Divya Oberoi Published in *Solar Physics*, 294:106 (2019)

### **Prominence and Filament Eruptions Observed by the Solar Dynamics Observatory: Statistical Properties, Kinematics, and Online Catalog**

Patrick I. **McCauley**, Yingna Su, Nicole Schanche, Kaitlin E. Evans, Chuan Su, Sean McKillop, Katharine K. Reeves

*Solar Phys.* Volume 290, [Issue 6](#), pp 1703-1740 2015, **File**

<http://arxiv.org/pdf/1505.02090v1.pdf>

We present a statistical study of prominence and filament eruptions observed by the Atmospheric Imaging Assembly (AIA) aboard the Solar Dynamics Observatory (SDO). Several properties are recorded for 904 events that were culled from the Heliophysics Event Knowledgebase (HEK) and incorporated into an online catalog for general use. These characteristics include the filament and eruption type, eruption symmetry and direction, apparent twisting and writhing motions, and the presence of vertical threads and coronal cavities. Associated flares and white-light coronal mass ejections (CME) are also recorded. Total rates are given for each property along with how they differ among filament types. We also examine the kinematics of 106 limb events to characterize the distinct slow- and fast-rise phases often exhibited by filament eruptions. The average fast-rise onset height, slow-rise duration, slow-rise velocity, maximum field-of-view (FOV) velocity, and maximum FOV acceleration are 83 Mm, 4.4 hours, 2.1 km/s, 106 km/s, and 111 m/s<sup>2</sup>, respectively. All parameters exhibit lognormal probability distributions similar to that of CME speeds. A positive correlation between latitude and fast-rise onset height is found, which we attribute to a corresponding negative correlation in the average vertical magnetic field gradient, or decay index, estimated from potential field source surface (PFSS) extrapolations. We also find the decay index at the fast-rise onset point to be 1.1 on average, consistent with the critical instability threshold theorized for straight current channels. Finally, we explore relationships between the derived kinematics properties and apparent twisting motions. We find that events with evident twist have significantly faster CME speeds and significantly lower fast-rise onset heights, suggesting relationships between these values and flux rope helicity.

### **Parker Solar Probe Encounters the Leg of a Coronal Mass Ejection at 14 Solar Radii**

D. J. **McComas**<sup>1</sup>, T. Sharma<sup>1</sup>, E. R. Christian<sup>2</sup>, C. M. S. Cohen<sup>3</sup>, M. I. Desai<sup>4,5</sup>, M. E. Hill<sup>6</sup>, L. Y. Khoo<sup>1</sup>, W. H. Matthaeus<sup>7</sup>, D. G. Mitchell<sup>6</sup>, F. Pecora<sup>7</sup>Show full author list

2023 *ApJ* 943 71

<https://iopscience.iop.org/article/10.3847/1538-4357/acab5e/pdf>

We use Parker Solar Probe (PSP) observations to report the first direct measurements of the particle and field environments while crossing the leg of a coronal mass ejection (CME) very close to the Sun ( $\sim 14 R_s$ ). An analysis that combines imaging from 1 au and PSP with a CME model, predicts an encounter time and duration that correspond to an unusual, complete dropout in low-energy solar energetic ions from H–Fe, observed by the Integrated Science Investigation of the Sun (IS $\odot$ IS). The surrounding regions are populated with low-intensity protons and heavy ions from 10s to 100 keV, typical of some quiet times close in to the Sun. In contrast, the magnetic field and solar wind plasma show no similarly abrupt changes at the boundaries of the dropout. Together, the IS $\odot$ IS energetic particle observations, combined with remote sensing of the CME and a dearth of other "typical" CME signatures, indicate that this CME leg is significantly different from the magnetic and plasma structure normally assumed for CMEs near the Sun and observed in interplanetary CMEs farther out in the solar wind. The dropout in low-energy energetic ions may be due to the cooling of suprathermal ions at the base of the CME leg flux tube, owing to the rapid outward expansion during the release of the CME. **20-21 Nov 2021**

## Observations of Switchback Chains in a Double Solar Proton Event

Emily McDougall, [Bala Poduval](#)

Solar Phys. 2024

<https://arxiv.org/abs/2407.01815>

Although recent research suggests a link in support of a model of switchback formation in the solar corona via interchange reconnection that is propagated outward with the solar wind and similarities in their ion composition to plasma instability produced plasmoids, these plasma instabilities have yet to be observationally linked to magnetic switchbacks. In this paper we aim to use the theoretical framework of a twin coronal mass ejection event which is known to include interchange reconnection processes and compare this model with experimental observations using Parker Solar Probe FIELDS and  $\text{is}$  instrumentation of an actual event containing two CMEs identified via the associated solar proton event in order to further test and refine the hypothesis of interchange reconnection as a possible physical origin for the magnetic switchback phenomenon. We also intend to introduce a plasma model for the formation of the switchbacks noted within the CME event. 2022 17-18 August

## Magnetic Flux Cancellation as the Trigger Mechanism of Solar Coronal Jets

Riley A. McGlasson, [Navdeep K. Panesar](#), [Alphonse C. Sterling](#), [Ronald Moore](#)

ApJ 882 16 2019

<https://arxiv.org/pdf/1906.06452.pdf>

Coronal jets are transient narrow features in the solar corona that originate from all regions of the solar disk: active regions, quiet sun, and coronal holes. Recent studies indicate that at least some coronal jets in quiet regions and coronal holes are driven by the eruption of a minifilament following flux cancellation at a magnetic neutral line. We have tested the veracity of that view by examining 60 random jets in quiet regions and coronal holes using multithermal (304 Å, 171 Å, 193 Å, and 211 Å) extreme ultraviolet (EUV) images from the Solar Dynamics Observatory (SDO)/Atmospheric Imaging Assembly (AIA) and line-of-sight magnetograms from the SDO/Helioseismic and Magnetic Imager (HMI). By examining the structure and changes in the magnetic field before, during, and after jet onset, we found that 85% of these jets resulted from a minifilament eruption triggered by flux cancellation at the neutral line. The 60 jets have a mean base diameter of  $8800 \pm 3100$  km and a mean duration of  $9 \pm 3.6$  minutes. These observations confirm that minifilament eruption is the driver and magnetic flux cancellation is the primary trigger mechanism for most coronal hole and quiet region coronal jets. 2016 November 25, 2017 January 2, 2017 March 22, 2017 April 10

Table 1. Measured Parameters of Coronal Jet Observations (2016-2017)

## The Impact of New EUV Diagnostics on CME-Related Kinematics

Scott W. McIntosh · Bart De Pontieu · Robert J. Leamon

Solar Phys (2010) 265: 5–17; File

We present the application of novel diagnostics to the spectroscopic observation of a Coronal Mass Ejection (CME) on disk by the Extreme Ultraviolet Imaging Spectrometer (EIS) on the *Hinode* spacecraft. We apply a recently developed line profile asymmetry analysis to the spectroscopic observation of NOAA AR 10930 on 14 – 15 December 2006 to three raster observations before and during the eruption of a  $1000 \text{ km s}^{-1}$  halo CME. We see the impact that the observer's line-of-sight and magnetic field geometry have on the diagnostics used. Further, and more importantly, we identify the on-disk signature of a high-speed outflow behind the CME in the dimming region arising as a result of the eruption. Supported by recent coronal observations of the STEREO spacecraft, we speculate about the momentum flux resulting from this outflow as a secondary momentum source to the CME. The results presented highlight the importance of spectroscopic measurements in relation to CME kinematics, and the need for full-disk synoptic spectroscopic observations of the coronal and chromospheric plasmas to capture the signature of such explosive energy release as a way of providing better constraints of CME propagation times to L1, or any other point of interest in the heliosphere.

Electronic Supplementary Material:

[http://springerlink.com/content/08576315n003w53u/11207\\_2010\\_Article\\_9538\\_ESM.html](http://springerlink.com/content/08576315n003w53u/11207_2010_Article_9538_ESM.html)

## Numerical Simulation on the Leading Edge of Coronal Mass Ejection in the Near-Sun Region

Zhixing Mei<sup>1,2</sup>, Jing Ye<sup>1,2,3</sup>, Yan Li<sup>1,2</sup>, Shanshan Xu<sup>1,4</sup>, Yuhao Chen<sup>1,4</sup>, and Jialiang Hu<sup>1,4</sup>

2023 ApJ 958 15

<https://iopscience.iop.org/article/10.3847/1538-4357/acf8c5/pdf>

The coronal mass ejections (CMEs) observed by white-light coronagraphs, such as the Large Angle and Spectrometric Coronagraph (LASCO) C2/C3, commonly exhibit the three-part structure, with the bright leading edge as the outermost part. In this work, we extend previous work on the leading edge by performing a large-scale 3D magnetohydrodynamic numerical simulation on the evolution of an eruptive magnetic flux rope (MFR) in a near-Sun region based on a radially stretched calculation grid in spherical coordination and the incorporation of solar wind. In the early stage, the new simulation almost repeats the previous results, i.e., the expanding eruptive MFR and associated CME bubble interact

with the ambient magnetic field, which leads to the appearance of the helical current ribbon/boundary (HCB) wrapping around the MFR. The HCB can be interpreted as a possible mechanism of the CME leading edge. Later, the CME bubble propagates self-consistently to a larger region beyond a few solar radii from the solar center, similar to the early stage of evolution. The continuous growth and propagation of the CME bubbles leading to the HCB can be traced across the entire near-Sun region. Furthermore, we can observe the HCB in the white-light synthetic images as a bright front feature in the large field of view of LASCO C2 and C3.

### **Velocity Distribution Associated With EUV Disturbances Caused by Eruptive MFR**

[Zhixing Mei](#) 1,2\*, [Qiangwei Cai](#) 3, [Jing Ye](#) 1,2, [Yan Li](#) 1,2 and [Bojing Zhu](#) 1,2,4

Front. Astron. Space Sci. 8:771882. 2021

<https://www.frontiersin.org/articles/10.3389/fspas.2021.771882/full>

<https://doi.org/10.3389/fspas.2021.771882>

Extreme ultraviolet (EUV) disturbances are ubiquitous during eruptive phenomena like solar flare and Coronal Mass Ejection (CME). In this work, we have performed a three-dimensional (3D) magnetohydrodynamic numerical simulation of CME with an analytic magnetic fluxrope (MFR) to study the complex velocity distribution associated with EUV disturbances. When the MFR erupts upward, a fast shock (FS) appears as a 3D dome, followed by outward moving plasma. In the center of the eruptive source region, an expanding CME bubble and a current sheet continuously grow, both of which are filled by inward moving plasma. At the flanks of the CME bubble, a complex velocity distribution forms because of the dynamical interaction between inward and outward plasma, leading to the formation of slow shock (SS) and velocity separatrix (VS). We note two types of vortices near the VS, not mentioned in the preceding EUV disturbance simulations. In first type of vortex, the plasma converges toward the vortex center, and in the second type, the plasma spreads out from the center. The forward modeling method has been used to create the synthetic SDO/AIA images, in which the eruptive MFR and the FS appear as bright structures. Furthermore, we also deduce the plasma velocity field by utilizing the Fourier local correlation tracking method on the synthetic images. However, we do not observe the VS, the SS, and the two types of vortices in this deduced velocity field.

### **The Triple-layered Leading Edge of Solar Coronal Mass Ejections**

Z. X. [Mei](#)1,2, R. Keppens3, Q. W. Cai4, J. Ye1,2, Y. Li1,2, X. Y. Xie1,2,5,6, and J. Lin1,2,5

ApJL 898 L21 2020

<https://doi.org/10.3847/2041-8213/aba2ce>

In a high-resolution, 3D resistive magnetohydrodynamic simulation of an eruptive magnetic flux rope (MFR), we revisit the detailed 3D magnetic structure of a coronal mass ejection (CME). Our results highlight that there exists a helical current ribbon/boundary (HCB) that wraps around the CME bubble. This HCB results from the interaction between the CME bubble and the ambient magnetic field, where it represents a tangential discontinuity in the magnetic topology. Its helical shape is ultimately caused by the kinking of the MFR that resides within the CME bubble. In synthetic Solar Dynamics Observatory/Atmospheric Imaging Assembly images, processed to logarithmic scale to enhance otherwise unobservable features, we show a clear triple-layered leading edge: a bright fast shock front, followed by a bright HCB, and within it a bright MFR. These are arranged in sequence and expand outward continuously. For kink unstable eruptions, we suggest that the HCB is a possible explanation for the bright leading edges seen near CME bubbles and also for the non-wave component of global EUV disturbances.

### **Parametric study on kink instabilities of twisted magnetic flux ropes in the solar atmosphere**

Z. X. [Mei](#)1,2, R. Keppens1, I. I. Roussev3,1 and J. Lin2

A&A 609, A2 (2017)

**Aims.** Twisted magnetic flux ropes (MFRs) in the solar atmosphere have been researched extensively because of their close connection to many solar eruptive phenomena, such as flares, filaments, and coronal mass ejections (CMEs). In this work, we performed a set of 3D isothermal magnetohydrodynamic (MHD) numerical simulations, which use analytical twisted MFR models and study dynamical processes parametrically inside and around current-carrying twisted loops. We aim to generalize earlier findings by applying finite plasma  $\beta$  conditions.

**Methods.** Inside the MFR, approximate internal equilibrium is obtained by pressure from gas and toroidal magnetic fields to maintain balance with the poloidal magnetic field. We selected parameter values to isolate best either internal or external kink instability before studying complex evolutions with mixed characteristics. We studied kink instabilities and magnetic reconnection in MFRs with low and high twists.

**Results.** The curvature of MFRs is responsible for a tire tube force due to its internal plasma pressure, which tends to expand the MFR. The curvature effect of toroidal field inside the MFR leads to a downward movement toward the photosphere. We obtain an approximate internal equilibrium using the opposing characteristics of these two forces. A typical external kink instability totally dominates the evolution of MFR with infinite twist turns. Because of line-tied conditions and the curvature, the central MFR region loses its external equilibrium and erupts outward. We emphasize the possible role of two different kink instabilities during the MFR evolution: internal and external kink. The external kink is due to the violation of the Kruskal-Shafranov condition, while the internal kink requires a safety factor  $q = 1$  surface inside the MFR. We show that in mixed scenarios, where both instabilities compete, complex evolutions occur owing to reconnections around and within the MFR. The S-shaped structures in current distributions appear naturally without invoking flux emergence. Magnetic reconfigurations common to eruptive MFRs and flare loop systems are found in our simulations.

## Current-driven flare and CME models†

Review

D. B. Melrose

JGR Volume 122, Issue 8 Pages 7963–7978 2017

<http://sci-hub.cc/10.1002/2017JA024035>

<https://arxiv.org/pdf/1708.04367.pdf>

Roles played by the currents in the impulsive phase of a solar flare and in a coronal mass ejection (CME) are reviewed. Solar flares are magnetic explosions: magnetic energy stored in unneutralized currents in coronal loops is released into energetic electrons in the impulsive phase and into mass motion in a CME. The energy release is due to a change in current configuration effectively reducing the net current path. A flare is driven by the electromotive force (EMF) due to the changing magnetic flux. The EMF drives a flare-associated current whose cross-field closure is achieved by redirection along field lines to the chromosphere and back. The essential roles that currents play are obscured in the “standard” model and are described incorrectly in circuit models. A semi-quantitative treatment of the energy and the EMF is provided by a multi-current model, in which the currents are constant and the change in the current paths is described by time-dependent inductances. There is no self-consistent model that includes the intrinsic time dependence, the EMF, the flare-associated current and the internal energy transport during a flare. The current, through magnetic helicity, plays an important role in a CME, with twist converted into writhe allowing the kink instability plus reconnection to lead to a new closed loop, and with the current-current force accelerating the CME through the torus instability.

## Trajectories of coronal mass ejection from solar-type stars

Fabian Menezes, Adriana Valio, Yuri Netto, Alexandre Araújo, Christina Kay, Merav Opher

Monthly Notices of the Royal Astronomical Society, Volume 522, Issue 3, 2023, Pages 4392–4403,

<https://doi.org/10.1093/mnras/stad1078>

The Sun and other solar-type stars have magnetic fields that permeate their interior and surface, extend through the interplanetary medium, and are the main drivers of stellar activity. Stellar magnetic activity affects the physical processes and conditions of the interplanetary medium and orbiting planets. Coronal mass ejections (CMEs) are the most impactful of these phenomena in near-Earth space weather and consist of plasma clouds with a magnetic field, ejected from the solar corona. Precisely predicting the trajectory of CMEs is crucial in determining whether a CME will hit a planet and impact its magnetosphere and atmosphere. Despite the rapid developments in the search for stellar CMEs, their detection is still very incipient. In this work, we aim to better understand the propagation of CMEs by analysing the influence of initial parameters on CME trajectories, such as position, velocities, and the stellar magnetic field's configuration. We reconstruct magnetograms for Kepler-63 (KIC 11554435) and Kepler-411 (KIC 11551692) from spot transit mapping, and use a CME deflection model, ForeCAT, to simulate trajectories of hypothetical CMEs launched into the interplanetary medium from Kepler-63 and Kepler-411. We apply the same methodology to the Sun, for comparison. Our results show that in general deflections and rotations of CMEs decrease with their radial velocity and increase with ejection latitude. Moreover, magnetic fields stronger than the Sun's, such as Kepler-63's, tend to cause greater CME deflections.

## Eruptions of Magnetic Ropes in Two Homologous Solar Events on 2002 June 1 and 2: a Key to Understanding of an Enigmatic Flare

N.S. Meshalkina, A.M. Uralov, V.V. Grechnev, A.T. Altyntsev, L.K. Kashapova

*Pub. Astron. Soc. Japan* 61, 791-, 2009. File

<http://arxiv.org/pdf/0908.0384v1.pdf>

The goal of this paper is to understand the drivers, configurations, and scenarios of two similar eruptive events, which occurred in the same solar active region 9973 on **2002 June 1 and 2**. The June 2 event was previously studied by Sui, Holman, and Dennis (2006, 2008), who concluded that it was challenging for popular flare models. Using multi-spectral data, we analyze a combination of the two events. Each of the events exhibited an evolving cusp-like feature. We have revealed that these apparent “cusps” were most likely mimicked by twisted magnetic flux ropes, but unlikely to be related to the inverted Y-like magnetic configuration in the standard flare model. The ropes originated inside a funnel-like magnetic domain whose base was bounded by an EUV ring structure, and the top was associated with a coronal null point. The ropes appear to be the major drivers for the events, but their rise was not triggered by reconnection in the coronal null point. We propose a scenario and a three-dimensional scheme for these events in which the filament eruptions and flares were caused by interaction of the ropes.

## Nonlinear Force-free Field Modeling of Solar Coronal Jets in Theoretical Configurations

K. A. Meyer<sup>1</sup>, A. S. Savcheva<sup>2</sup>, D. H. Mackay<sup>3</sup>, and E. E. DeLuca<sup>2</sup>

2019 *ApJ* 880 62

[sci-hub.se/10.3847/1538-4357/ab271a](https://sci-hub.se/10.3847/1538-4357/ab271a)

Coronal jets occur frequently on the Sun, and may contribute significantly to the solar wind. With the suite of instruments available now, we can observe these phenomena in greater detail than ever before. Modeling and simulations can assist further with understanding the dynamic processes involved, but previous studies tended to consider only one mechanism (e.g., emergence or rotation) for the origin of the jet. In this study we model a series of idealized archetypal jet configurations and follow the evolution of the coronal magnetic field. This is a step toward understanding these idealized situations before considering their observational counterparts. Several simple situations are set up for the evolution of the photospheric magnetic field: a single parasitic polarity rotating or moving in a circular

path; as well as opposite polarity pairs involved in flyby (shearing), cancellation or emergence; all in the presence of a uniform, open background magnetic field. The coronal magnetic field is evolved in time using a magnetofrictional relaxation method. While magnetofriction cannot accurately reproduce the dynamics of an eruptive phase, the structure of the coronal magnetic field, as well as the buildup of electric currents and free magnetic energy are instructive. Certain configurations and motions produce a flux rope and allow the significant buildup of free energy, reminiscent of the progenitors of so-called blowout jets, whereas other, simpler configurations are more comparable to the standard jet model. The next stage is a comparison with observed coronal jet structures and their corresponding photospheric evolution.

### **Association between tornadoes and hosting prominence instability**

Irakli [Mghebrishvili](#), [Teimuraz V. Zaqarashvili](#), [Vasil Kukhianidze](#), [David Kuridze](#), [David Tsiklauri](#), [Bidzina M. Shergelashvili](#), [Stefaan Poedts](#)

ApJ **861** 112 **2018**

<https://arxiv.org/pdf/1807.01345.pdf>

We studied the dynamics of all prominence tornadoes detected by the Solar Dynamics Observatory/Atmospheric Imaging Assembly from 2011 January 01 to December 31. In total, 361 events were identified during the whole year, but only 166 tornadoes were traced until the end of their lifetime. Out of 166 tornadoes, 80 (48%) triggered CMEs in hosting prominences, 83 (50%) caused failed coronal mass ejections (CMEs) or strong internal motion in the prominences, and only 3 (2%) finished their lifetimes without any observed activity. Therefore, almost all prominence tornadoes lead to the destabilization of their hosting prominences and half of them trigger CMEs. Consequently, prominence tornadoes may be used as precursors for CMEs and hence for space weather predictions. **2011 April 29, 2011-07-05, 2011.10.10-13**

**Table 2.** A catalog of prominence tornadoes during the year 2011

### **Dynamics of a solar prominence tornado observed by SDO/AIA on 2012 November 7-8**

I. [Mghebrishvili](#), T. V. [Zaqarashvili](#), [V. Kukhianidze](#), [G. Ramishvili](#), [B. Shergelashvili](#), [A. Veronig](#), [S. Poedts](#)

ApJ **810** 89 **2015**

<http://arxiv.org/pdf/1508.06788v1.pdf>

<http://sci-hub.tw/http://iopscience.iop.org/0004-637X/861/2/112/>

We study the detailed dynamics of a solar prominence tornado using time series of 171, 304, 193 and 211 {\AA} spectral lines obtained by Solar Dynamics Observatory/ Atmospheric Imaging Assembly during **2012 November 7-8**. The tornado first appeared at 08:00 UT, November 07, near the surface, gradually rose upwards with the mean speed of  $\sim 1.5 \text{ km s}^{-1}$  and persisted over 30 hr. Time-distance plots show two patterns of quasi-periodic transverse displacements of the tornado axis with periods of 40 and 50 minute at different phases of the tornado evolution. The first pattern occurred during the rising phase and can be explained by the upward motion of the twisted tornado. The second pattern occurred during the later stage of evolution when the tornado already stopped rising and could be caused either by MHD kink waves in the tornado or by the rotation of two tornado threads around a common axis. The later hypothesis is supported by the fact that the tornado sometimes showed a double structure during the quasi-periodic phase. 211 and 193 {\AA} spectral lines show a coronal cavity above the prominence/tornado, which started expansion at  $\sim 13:00$  UT and continuously rose above the solar limb. The tornado finally became unstable and erupted together with the corresponding prominence as coronal mass ejection (CME) at 15:00 UT, November 08. The final stage of the evolution of the cavity and the tornado-related prominence resembles the magnetic breakout model. On the other hand, the kink instability may destabilize the twisted tornado, and consequently prominence tornadoes can be used as precursors for CMEs.

### **Two Quasi-periodic Fast-propagating Magnetosonic Wave Events Observed In Active Region NOAA 11167**

Yuhu [Miao](#), [Yu Liu](#), [A. Elmhamdi](#), [A. S. Kordi](#), [Y. D. Shen](#), [Rehab Al-Shammari](#), [Khaled Al-Mosabeh](#), [Chaowei Jiang](#), [Ding Yuan](#)

ApJ **889** 139 **2020**

<https://arxiv.org/pdf/1912.11792.pdf>

<https://doi.org/10.3847/1538-4357/ab655f>

We report a detailed observational study of two quasi-periodic fast-propagating (QFP) magnetosonic wave events occurred on **2011 March 09 and 10**, respectively. Interestingly, both the two events have two wave trains (WTs): one main and strong (WT-1) whereas the second appears small and weak (WT-2). Peculiar and common characteristics of the two events are observed, namely: 1) the two QFP waves are accompanied with brightenings during the whole stage of the eruptions; 2) both the two main wave trains are nearly propagating along the same direction; 3) EUV waves are found to be associated with the two events. Investigating various aspects of the target events, we argue that: 1) the second event is accompanied with a flux rope eruption during the whole stage; 2) the second event eruption produces a new filament-like (FL) dark feature; 3) the ripples of the two WT-2 QFP waves seem to result from different triggering mechanisms. Based on the obtained observational results, we propose that the funnel-like coronal loop system is indeed playing an important role in the two WT-1 QFP waves. The development of the second WT-2 QFP wave can be



explained as due to the dispersion of the main EUV front. The co-existence of the two events offer thereby a significant opportunity to reveal what driving mechanisms and structures are tightly related to the waves.

### **A new small satellite sunspot triggering recurrent standard- and blowout-coronal jets**

Yuhu [Miao](#), [Y. Liu](#), [Y. D. Shen](#), [A. Elmhamdi](#), [A. S. Kordi](#), [H. B. Li](#), [Z. Z. Abidin](#), [Z. J. Tian](#)

ApJ **877** 61 **2019**

<https://arxiv.org/pdf/1904.05496.pdf>

[sci-hub.se/10.3847/1538-4357/ab1a42](https://sci-hub.se/10.3847/1538-4357/ab1a42)

In this paper, we report a detailed analysis of recurrent jets originated from a location with emerging, canceling and converging negative magnetic field at the east edge of NOAA active region AR11166 from **2011 March 09 to 10**. The event presented several interesting features. First, a satellite sunspot appeared and collided with a pre-existing opposite polarity magnetic field and caused a recurrent solar jet event. Second, the evolution of the jets showed blowout-like nature and standard characteristics. Third, the satellite sunspot exhibited a motion toward southeast of AR11166 and merged with the emerging flux near the opposite polarity sunspot penumbra, which afterward, due to flux convergence and cancellation episodes, caused recurrent jets. Fourth, three of the blowout jets associated with coronal mass ejections (CMEs), were observed from field of view of the Solar Terrestrial Relations Observatory. Fifth, almost all the blowout jet eruptions were accompanied with flares or with more intense brightening in the jet base region, while almost standard jets did not manifest such obvious feature during eruptions. The most important, the blowout jets were inclined to faster and larger scale than the standard jets. The standard jets instead were inclined to relative longer-lasting. The obvious shearing and twisting motions of the magnetic field may be interpreted as due to the shearing and twisting motions for a blowout jet eruption. From the statistical results, about 30% blowout jets directly developed into CMEs. It suggests that the blowout jets and CMEs should have a tight relationship.

### **A Blowout Jet Associated with One Obvious Extreme-ultraviolet Wave and One Complicated Coronal Mass Ejection Event**

Y. [Miao](#)<sup>1,2,3</sup>, Y. Liu<sup>1</sup>, H. B. Li<sup>1,3</sup>, Y. Shen<sup>1,4,5</sup>, S. Yang<sup>5</sup>, A. Elmhamdi<sup>6</sup>, A. S. Kordi<sup>6</sup>, and Z. Z. Abidin

**2018** ApJ 869 39 <https://doi.org/10.3847/1538-4357/aaeac1>

[sci-hub.tw/10.3847/1538-4357/aaeac1](https://sci-hub.tw/10.3847/1538-4357/aaeac1)

In this paper, we present a detailed analysis of a coronal blowout jet eruption that was associated with an obvious extreme-ultraviolet (EUV) wave and one complicated coronal mass ejection (CME) event based on the multiwavelength and multi-view-angle observations from the Solar Dynamics Observatory and the Solar Terrestrial Relations Observatory. It is found that the triggering of the blowout jet was due to the emergence and cancellation of magnetic fluxes on the photosphere. During the rising stage of the jet, the EUV wave appeared just ahead of the jet top, lasting about 4 minutes and at a speed of 458–762 km s<sup>-1</sup>. In addition, obvious dark material is observed along the EUV jet body, which confirms the observation of a mini-filament eruption at the jet base in the chromosphere. Interestingly, two distinct but overlapped CME structures can be observed in corona together with the eruption of the blowout jet. One is a narrow jet shape, while the other one is a bubble shape. The jet-shaped component was unambiguously related to the outwardly running jet itself, while the bubble-like one might either be produced due to the reconstruction of the high coronal fields or by the internal reconnection during the mini-filament ejection according to the double-CME blowout jet model first proposed by Shen et al., suggesting more observational evidence should be supplied to clear the current ambiguity based on large samples of blowout jets in future studies.

### **A coronal blowout jet associated with a jet-like CME and a bubble-like CME**

Y. [Miao](#), Y. Liu, Y. Shen, A. Elmhamdi, S. Kordi

**2017**

<https://arxiv.org/pdf/1703.10022.pdf>

Based on high-resolution *\sl* Big Bear Solar Observatory (*\sl* BBSO), *\sl* Solar Dynamics Observatory (*\sl* SDO) and *\sl* Solar Terrestrial Relations Observatory (*\sl* STEREO) data, a small H $\alpha$  filament eruption is observed during the blowout jet phase whose length is estimated to be larger than 400 Mm with an average velocity of about *\speed{270}* in the active region NOAA 11166 on **March 09, 2011**. An evident magnetic flux cancellation is observed on the photosphere during the double-CME blowout jet. We also find that the blowout jet had an unwinding motion during the eruption phase. Interestingly, a short time shock wave appeared at the beginning of the eruption, the shock wave was very difficult to be observed in jet eruption events. From *\sl* SDO 193  $\text{\AA}$ , can easily to distinguish the shock wave. From *\sl* SDO viewpoint, the bubble-like CME was formed by the front part of the jet, and the jet-like CME was formed by rectilinear part of the jet. But from *\sl* STEREO COR1 A and B viewpoints, the result shows an overlapping behavior of the jet-like and the bubble-like CMEs as highlighted by *\sl* STEREO observations. From the analysis of the high-cadence COR1 data, we propose that the observed overlapping of the two CMEs was due to the special magnetic field distribution on the photosphere that we depict in a simple sketch model. The studied event, blowout jet with two simultaneous CMEs, with its atypical structures indicates again that a variety of solar activities with different spatial scales might simultaneously take place and integrate into one solar eruption phenomenon.

### **A Statistical Analysis of Deflection of Coronal Mass Ejections in the Field of View of LASCO Coronagraphs**

Grzegorz [Michalek](#)<sup>1</sup>, Nat Gopalswamy<sup>2</sup>, Seiji Yashiro<sup>2,3</sup>, and Kostadinka Koleva<sup>2,3,4</sup>

2023 ApJ 956 59

<https://iopscience.iop.org/article/10.3847/1538-4357/acf28d/pdf>

Coronal mass ejections (CMEs) can generate the most severe geomagnetic disturbances. One of the most critical factors affecting a CME's geoeffectiveness is its trajectory. It is crucial to determine whether and when CME will hit Earth. It is commonly assumed that CMEs experience a deflection of propagation in the corona and in interplanetary space. In this study, we analyze more than 14,000 CMEs listed in the Coordinated Data Analysis Workshop (CDAW) catalog during 1996–2022 to estimate their deflection in the Large and Spectrometric Coronagraph field of view (LFOV). In our statistical analysis, the deflection was determined using the CME height–time measurements listed in the CDAW catalog. We have shown that, in the solar corona, CME deflection is a common phenomenon, heavily influenced by solar activity cycles as well as phases of these cycles. We have demonstrated that during periods of solar activity minima the deflection of CMEs is mostly toward the equator, and during periods of maxima it is mostly toward the poles. This general trend of deflection is further modified by the specific structure of the magnetic field generated during successive cycles of solar activity (e.g., the asymmetry between the hemispheres). A systematic increase in deflection with time was also recognized. We have also found that the deflection increases linearly with the distance from the Sun in the LFOV (the line slope is 0.5). **20010819, 20040519, 20100413**

### Study of the Mass-loss Rate from the Sun

Grzegorz **Michalek**<sup>1</sup>, Nat Gopalswamy<sup>2</sup>, and Seiji Yashiro<sup>2,3</sup>

The Astrophysical Journal, 930:74 (16pp), **2022** May 1

<https://iopscience.iop.org/article/10.3847/1538-4357/ac4fcb/pdf>

We investigate the temporal evolution of the yearly total mass-loss rate (YTMLR) from the Sun through coronal mass ejections (CMEs) over solar cycles 23 and 24. The mass determination of CMEs can be subject to significant uncertainty. To minimize this problem, we have used extensive statistical analysis. For this purpose, we employed data included in the Coordinated Data Analysis Workshop (CDAW) catalog. We estimated the contributions to mass loss from the Sun from different subsamples of CMEs (selected on the basis of their masses, angular widths, and position angles). The temporal variations of the YTMLR were compared to those of the sunspot number (SSN), X-ray flare flux, and the Disturbance Storm Time (Dst) index. We show that the CME mass included in the CDAW catalog reflects with high accuracy the actual mass-loss rate from the Sun through CMEs. Additionally, it is shown that the CME mass distribution in the log-lin representation reflects the Gaussian distribution very well. This means that the CMEs included in the CDAW catalog form one coherent population of ejections that have been correctly identified. Unlike the CME occurrence rate, it turns out that the YTMLR is a very good indicator of solar activity (e.g., SSN) and space weather (e.g., Dst index) consequences. These results are very important, since the YTMLR, unlike the mass loss through solar wind, significantly depends on solar cycles.

### Periodic Oscillations in LASCO Coronal Mass Ejection Speeds: Space Seismology

Grzegorz **Michalek**<sup>1</sup>, Nat Gopalswamy<sup>2</sup>, and Seiji Yashiro<sup>2,3</sup>

**2022** ApJL 927 L16

<https://iopscience.iop.org/article/10.3847/2041-8213/ac54b0/pdf>

Coronal mass ejections (CMEs) are energetic eruptions of organized magnetic structures from the Sun. Therefore, the reconnection of the magnetic field during ejection can excite periodic speed oscillations of CMEs. A previous study showed that speed oscillations are frequently associated with CME propagation. The Solar and Heliospheric Observatory mission's white-light coronagraphs have observed about 30,000 CMEs from 1996 January to the end of 2019 December. This period of time covers two solar cycles (23 and 24). In the present study, the basic attributes of speed oscillations during this period of time were analyzed. We showed that the oscillation parameters (period and amplitude) significantly depend not only on the phase of a given solar cycle but also on the intensity of individual cycles as well. This reveals that the basic attributes of speed oscillation are closely related to the physical conditions prevailing inside the CMEs as well as in the interplanetary medium in which they propagate. Using this approximation, we estimated that, on average, the CME internal magnetic field varies from 18 up to 25 mG between minimum and maximum solar activity. The obtained results show that a detailed analysis of speed oscillations can be a very efficient tool for studying not only the physical properties of the ejections themselves but also the condition of the interplanetary medium in which they expand. This creates completely new perspectives for studying the physical parameters of CMEs shortly after their eruption in the Sun's environment (space seismology). **2004 February 8, 2004 February 11**

### On the Coronal Mass Ejection Detection Rate during Solar Cycles 23 and 24

Grzegorz **Michalek**<sup>1</sup>, Nat Gopalswamy<sup>2</sup>, and Seiji Yashiro<sup>2,3</sup>

**2019** ApJ 880 51

[sci-hub.se/10.3847/1538-4357/ab26a7](https://iopscience.iop.org/article/10.3847/1538-4357/ab26a7)

The Solar and Heliospheric Observatory (SOHO) mission's white light coronagraphs have observed more than 25,000 coronal mass ejections (CMEs) from 1996 January to the end of 2015 July. This period of time covers almost two solar cycles (23 and 24). The basic attributes of CMEs, reported in the SOHO/Large Angle and Spectrometric Coronagraph (LASCO) catalog, during these solar cycles were statistically analyzed. The question of the CME detection rate and its connection to the solar cycles was considered in detail. Based on the properties and detection rate, CMEs can be divided into two categories: regular and specific events. The regular events are pronounced and follow the pattern of sunspot number. On the other hand, the special events are poorer and more correlated with the general conditions of heliosphere and corona. Nevertheless, both groups of CMEs are the result of the same physical phenomenon, viz. release of

magnetic energy from closed field regions. It was demonstrated that the enhanced CME rate, since the solar cycle 23 polar-field reversal, is due to a significant decrease of total (magnetic and plasma) heliospheric pressure as well as the changed magnetic pattern of solar corona. CMEs expel free magnetic energy and helicity from the Sun; therefore, they are related to complex solar magnetic field structure. It is also worth emphasizing that the CMEs listed in the SOHO/LASCO catalog are real ejections (not false identification). Their detection rate reflects the global evolution of the magnetic field on the Sun, and not only changes in the magnetic structures associated with sunspots.

### **Statistical Analysis of Periodic Oscillations in LASCO Coronal Mass Ejection Speeds**

G. [Michalek](#), A. Shanmugaraju, N. Gopalswamy, S. Yashiro, S. Akiyama

Solar Phys. Volume 291, Issue 12, pp 3751–3764 2016

<http://link.springer.com/article/10.1007/s11207-016-1000-4>

A large set of coronal mass ejections (CMEs, 3463) has been selected to study their periodic oscillations in speed in the Solar and Heliospheric Observatory (SOHO) mission's Large Angle and Spectrometric Coronagraph (LASCO) field of view. These events, reported in the SOHO/LASCO catalog in the period of time 1996–2004, were selected based on having at least 11 height–time measurements. This selection criterion allows us to construct at least ten-point speed–distance profiles and evaluate kinematic properties of CMEs with a reasonable accuracy. To identify quasi-periodic oscillations in the speed of the CMEs a sinusoidal function was fitted to speed–distance profiles and the speed–time profiles. Of the considered events 22 % revealed periodic velocity fluctuations. These speed oscillations have on average amplitude equal to  $(87 \sim \text{km}) \cdot \text{s}^{-1}$  and period  $(7.8 R_{\odot} / 241 \sim \text{min})$  (in distance/time). The study shows that speed oscillations are a common phenomenon associated with CME propagation implying that all the CMEs have a similar magnetic flux-rope structure. The nature of oscillations can be explained in terms of magnetohydrodynamic (MHD) waves excited during the eruption process. More accurate detection of these modes could, in the future, enable us to characterize magnetic structures in space (space seismology). 19/12/1996, 03/07/2000

### **CME Velocity and Acceleration Error Estimates Using the Bootstrap Method**

Grzegorz [Michalek](#), Nat Gopalswamy, Seiji Yashiro

[Solar Physics](#) August 2017, 292:114

The bootstrap method is used to determine errors of basic attributes of coronal mass ejections (CMEs) visually identified in images obtained by the Solar and Heliospheric Observatory (SOHO) mission's Large Angle and Spectrometric Coronagraph (LASCO) instruments. The basic parameters of CMEs are stored, among others, in a database known as the SOHO/LASCO CME catalog and are widely employed for many research studies. The basic attributes of CMEs (e.g. velocity and acceleration) are obtained from manually generated height-time plots. The subjective nature of manual measurements introduces random errors that are difficult to quantify. In many studies the impact of such measurement errors is overlooked. In this study we present a new possibility to estimate measurement errors in the basic attributes of CMEs. This approach is a computer-intensive method because it requires repeating the original data analysis procedure several times using replicate datasets. This is also commonly called the bootstrap method in the literature. We show that the bootstrap approach can be used to estimate the errors of the basic attributes of CMEs having moderately large numbers of height-time measurements. The velocity errors are in the vast majority small and depend mostly on the number of height-time points measured for a particular event. In the case of acceleration, the errors are significant, and for more than half of all CMEs, they are larger than the acceleration itself.

### **Dynamics of CMEs in the LASCO Field of View**

G. [Michalek](#), N. Gopalswamy, S. Yashiro, K. Bronarska

Solar Phys. Volume 290, [Issue 3](#), pp 903–917 2015

A large set (16 000) of coronal mass ejections (CMEs) observed during 1996–2011 was selected to study their dynamics in the LASCO field of view (LFOV). These events were selected based on the criterion that at least three height–time measurements were available for each CME. The height–time measurements included in the SOHO/LASCO catalog were used to determine velocities and accelerations of the respective CMEs at successive distances from the Sun. Next, these parameters were sorted into 30 subsamples depending on the distance from the Sun at which they were determined. The mean velocities and accelerations calculated for the successive distance-dependent subsamples of CMEs were used to study their dynamics. We demonstrate that CMEs in the LFOV manifest three distinct phases of propagation: (i) The propelling Lorentz force dominates the dynamics of CMEs in the inner (C2 LASCO) FOV, (ii) a stable propagation occurs as a result of the balance between the propelling and drag forces, (iii) the drag force dominates at the outer edge of the LFOV. When we considered different categories of CME separately, we found different acceleration–distance profiles for different categories.

### **CMEs and Active Regions on the Sun**

Grzegorz [Michalek](#) and Seiji Yashiro

Advanced Space Research, 52, Issue 3, 521–527, 2013

<http://cdaw.gsfc.nasa.gov/publications/michalek/michalek2013AdvSpRes.pdf>

The relationship between active regions (ARs) and coronal mass ejections (CMEs) is studied. For this purpose a statistical analysis of 694 CMEs associated with ARs was carried out. We considered the relationship between

properties of the CMEs and ARs characterized using the McIntosh classification. We demonstrated that CMEs are likely to be launched from ARs in the mature phase of their evolution when they have complex magnetic field. The fastest and halo CMEs can be ejected only from the most complex ARs (when an AR is a bipolar group of spots with large asymmetric penumbras around the main spot with many smaller spots in the group). We also showed that the wider events have a tendency to originate from uncomplicated magnetic structures. This tendency was used for estimation of the real angular widths of the halo CMEs. The probability of launching of fast CMEs increases together with increase of the complexity and size of ARs. The widest, but slow, CMEs originate from the simplest magnetic structure which are still able to produce CMEs. Our results could be useful for forecasting of space weather.

## **Dynamics of CMEs in the LASCO Field of View – Statistical Analysis**

G. Michalek

Solar Physics, Volume 276, Numbers 1-2, 277-291, 2012, **File**

A large set of CMEs (2207) has been selected to study their dynamics in the SOHO/LASCO field of view (LFOV). These selected events have at least seven height–time measurements and their acceleration can be determined separately in the C2 and C3 LFOVs. It was demonstrated that the balance between the aerodynamic drag and driving Lorentz forces may change during CME propagation in the LFOV. The drag force dominates the CME propagation close to the Sun (in the C2 LFOV), but farther from the Sun (in the C3 LFOV) the Lorentz force takes over the drag force. We also demonstrated that the acceleration of CMEs depends not only on their velocities but also on their masses and widths.

Less massive CMEs (mass <  $3 \times 10^{14}$  kg) are generally decelerated and more massive CMEs (mass >  $3 \times 10^{14}$  kg) are accelerated in the LFOV. Based on the acceleration behavior we are able to classify the observed events into four different types.

**Erratum** Solar Physics May 2016, Volume 291, Issue 5, pp 1577–1577

## **Is the Asymmetric Cone Model for Halo Coronal Mass Ejections Correct?**

G. Michalek

Solar Physics, Volume 261, Number 1, Page: 107 – 114, 2010, **FILE**

A set of 106 limb CMEs which are wide and could be possible halo events, when directed towards Earth, are used to check the accuracy of the asymmetric cone model. For this purpose characteristics of CMEs (widths and radial speeds) measured for the possible halo CMEs are compared with these obtained for halo CMEs using the asymmetric cone model (Michalek, *Solar Phys.* **237**, 101, 2006). It was shown that the width and speed distributions for both datasets are very similar and with a probability of  $p > 0.93$  (using the Kolmogorov–Smirnov test) were drawn from the same distribution of events. We also determined the accurate relationship between radial ( $V_{\text{rad}}$ ) and expansion ( $V_{\text{exp}}$ ) speeds of halo CMEs. This relation for the halo CMEs is simply  $V_{\text{rad}} = V_{\text{exp}}$  and could be very useful for space weather application.

## **Expansion Speed of Coronal Mass Ejections**

G. Michalek · N. Gopalswamy · S. Yashiro

Solar Phys (2009) 260: 401–406, **File**

A large set of limb coronal mass ejections (CMEs) are used to determine the accurate relationship between radial ( $V_{\text{rad}}$ ) and expansion ( $V_{\text{exp}}$ ) speeds of CMEs. It is demonstrated that this relation is exceptionally well described by the function  $f(w) = 1/2(1 + \cot w)$ , representing a full cone model for the CME with a half-width,  $w$ . We also demonstrate that for extremely fast CMEs ( $V_{\text{exp}} > 3000$  km s<sup>-1</sup>), it is better to use the approximation  $V_{\text{rad}} \approx V_{\text{LE}}$ . This implies that such CMEs expand spherically above the solar surface.

## **Two types of flare-associated coronal mass ejections:**

G. Michalek

A&A 494 (2009) 263-268

<http://www.aanda.org/10.1051/0004-6361:200810662>

*Aims.* Here, we study the relationship between flares and CMEs.

*Methods.* For this purpose a statistical analysis of 578 flare-associated CMEs is presented. We considered two types of flare-associated CMEs: CMEs that follow and precede flare onset.

*Results.* We shown that both samples have quite different characteristics. The first type of CMEs tends to be decelerated (median acceleration =  $-5.0$  m s<sup>-2</sup>), faster (median velocity =  $519$  km s<sup>-1</sup>), and physically related to flares (a correlation coefficient between the energy of the CME and the peak of the X-ray flare =  $0.80$ ). The CMEs preceding associated flares are mostly accelerated (median acceleration =  $5.4$  m s<sup>-2</sup>), slightly slower (median velocity =  $487$  km s<sup>-1</sup>), and poorly related to flares (a correlation coefficient between the energy of the CME and the peak of the X-ray flare =  $0.12$ ).

*Conclusions.* These two types of flare-associated CMEs demonstrate that magnetic reconnection, which influences the CME acceleration, could be significantly different in the two types of events.

## Space Weather Application Using Projected Velocity Asymmetry of Halo CMEs

G. Michalek · N. Gopalswamy · S. Yashiro

Solar Phys (2008) 248: 113–123, **File**

<http://www.springerlink.com/content/1576772m28w324t5/fulltext.pdf>

Halo coronal mass ejections (HCMEs) originating from regions close to the center of the Sun are likely to be responsible for severe geomagnetic storms. It is important to predict geoeffectiveness of HCMEs by using observations when they are still near the Sun. Unfortunately, coronagraphic observations do not provide true speeds of CMEs because of projection effects. In the present paper, we present a new technique to allow estimates of the space speed and approximate source location using projected speeds measured at different position angles for a given HCME (velocity asymmetry). We apply this technique to HCMEs observed during 2001 – 2002 and find that the improved speeds are better correlated with the travel times of HCMEs to Earth and with the magnitudes of ensuing geomagnetic storms. **Table**

### 4.2. Magnitudes of Geomagnetic Disturbances

Michalek, G.: 2006, Solar Phys., 237, 101.

Several methods for calculating radial velocities of CMEs have recently been proposed by, e.g., Leblanc et al. (2001), Michalek, Gopalswamy, and Yashiro (2003, symmetric cone model), Schwenn et al. (2005, lateral expansion speed), and Michalek (2006, asymmetric cone model).

## Prediction of SpaceWeather Using an Asymmetric Cone Model for Halo CMEs

G. Michalek · N. Gopalswamy · S. Yashiro

Solar Phys (2007) 246: 399–408, **File**

Halo coronal mass ejections (HCMEs) are responsible of the most severe geomagnetic storms. A prediction of their geoeffectiveness and travel time to Earth's vicinity is crucial to forecast space weather. Unfortunately, coronagraphic observations are subjected to projection effects and do not provide true characteristics of CMEs. Recently, Michalek (Solar Phys. 237, 101, 2006) developed an asymmetric cone model to obtain **the space speed, width, and source location of HCMEs**. We applied this technique to obtain the parameters of all front-sided HCMEs observed by the SOHO/LASCO experiment during a period from the beginning of 2001 until the end of 2002 (solar cycle 23). These parameters were applied for space weather forecasting. **Our study finds that the space speeds are strongly correlated with the travel times of HCMEs to Earth's vicinity and with the magnitudes related to geomagnetic disturbances.**

## Width of Radio-Loud and Radio-Quiet CMEs

G. Michalek · N. Gopalswamy · H. Xie

Solar Phys (2007) 246: 409–414

<http://www.springerlink.com/content/1748x1p6538v6243/fulltext.pdf>

In the present paper we report on the difference in angular sizes between radioloud and radio-quiet CMEs. For this purpose we compiled these two samples of events using *Wind*/WAVES and SOHO/LASCO observations obtained during 1996 – 2005. We show that the radio-loud CMEs are almost twice as wide as the radio-quiet CMEs (considering expanding parts of CMEs). Furthermore, we show that the radio-quiet CMEs have a narrow expanding bright part with a large extended diffusive structure. These results were obtained by measuring the CME widths in three different ways.

## Three Eruptions Observed by Remote Sensing Instruments Onboard Solar Orbiter

[Marilena Mierla](#), [Hebe Cremades](#), [Vincenzo Andretta](#), [Iulia Chifu](#), et al.

*Solar Physics* volume 298, Article number: 42 (2023)

<https://link.springer.com/article/10.1007/s11207-023-02137-2#Sec1>

<https://link.springer.com/content/pdf/10.1007/s11207-023-02137-2.pdf> **File**

On February 21 and March 21 – 22, 2021, the Extreme Ultraviolet Imager (EUI) onboard Solar Orbiter observed three prominence eruptions. The eruptions were associated with coronal mass ejections (CMEs) observed by Metis, Solar Orbiter's coronagraph. All three eruptions were also observed by instruments onboard the Solar–Terrestrial Relations Observatory (Ahead; STEREO-A), the Solar Dynamics Observatory (SDO), and the Solar and Heliospheric Observatory (SOHO). Here we present an analysis of these eruptions. We investigate their morphology, direction of propagation, and 3D properties. We demonstrate the success of applying two 3D reconstruction methods to three CMEs and their corresponding prominences observed from three perspectives and different distances from the Sun. This allows us to analyze the evolution of the events, from the erupting prominences low in the corona to the corresponding CMEs high in the corona. We also study the changes in the global magnetic field before and after the eruptions and the magnetic field configuration at the site of the eruptions using magnetic field extrapolation methods. This work highlights the importance of multi-perspective observations in studying the morphology of the erupting prominences, their source regions, and associated CMEs. The upcoming Solar Orbiter observations from higher latitudes will help to constrain this kind of study better. **21 Feb 2021, 21 Mar 2021**

## Prominence eruption observed in He II 304 Å up to >6 R<sub>⊙</sub> by EUI/FSI aboard Solar Orbiter★

M. Mierla<sup>1,2</sup>, A. N. Zhukov<sup>1,3</sup>, D. Berghmans<sup>1</sup>, S. Parenti<sup>4</sup>, F. Auchère<sup>4</sup>, et al.

A&A 662, L5 (2022)

<https://arxiv.org/pdf/2205.15214.pdf>

<https://www.aanda.org/articles/aa/pdf/2022/06/aa44020-22.pdf>

**Aims.** We report observations of a unique, large prominence eruption that was observed in the He II 304 Å passband of the Extreme Ultraviolet Imager/Full Sun Imager telescope aboard Solar Orbiter on **15–16 February 2022**.

**Methods.** Observations from several vantage points – Solar Orbiter, the Solar-Terrestrial Relations Observatory, the Solar and Heliospheric Observatory, and Earth-orbiting satellites – were used to measure the kinematics of the erupting prominence and the associated coronal mass ejection. Three-dimensional reconstruction was used to calculate the deprojected positions and speeds of different parts of the prominence. Observations in several passbands allowed us to analyse the radiative properties of the erupting prominence.

**Results.** The leading parts of the erupting prominence and the leading edge of the corresponding coronal mass ejection propagate at speeds of around 1700 km s<sup>-1</sup> and 2200 km s<sup>-1</sup>, respectively, while the trailing parts of the prominence are significantly slower (around 500 km s<sup>-1</sup>). Parts of the prominence are tracked up to heights of over 6 R<sub>⊙</sub>. The He II emission is probably produced via collisional excitation rather than scattering. Surprisingly, the brightness of a trailing feature increases with height.

**Conclusions.** The reported prominence is the first observed in He II 304 Å emission at such a great height (above 6 R<sub>⊙</sub>).

## Polarimetric Studies of a Fast Coronal Mass Ejection

[Marilena Mierla](#), [Bernd Inhester](#), [Andrei N. Zhukov](#), [Sergei V. Shestov](#), [Alessandro Bemporad](#), [Philippe Lamy](#), [Serge Koutchmy](#)

Solar Phys. 297, Article number: 78 2022

<https://arxiv.org/pdf/2206.04411.pdf>

<https://doi.org/10.1007/s11207-022-02018-0>

In this work we performed a polarimetric study of a fast and wide coronal mass ejection (CME) observed on **12 July 2012** by the COR1 and COR2 instruments onboard Solar TERrestrial RELations Observatory (STEREO) mission. The CME source region was an X1.4 flare located at approximately S15W01 on the solar disk as observed from the Earth's perspective. The position of the CME as derived from the 3D Graduated Cylindrical Shell (GCS) reconstruction method was at around S18W00 at 2.5 solar radii and S07W00 at 5.7 solar radii, meaning that the CME was deflected towards the Equator while propagating outward in the corona. The projected speed of the leading edge of the CME also evolved from around 200 km s<sup>-1</sup> in the lower corona to around 1000 km s<sup>-1</sup> in the COR2 field of view. The degree of polarisation of the CME is around 65 % but it can go as high as 80 % in some CME regions. The CME showed deviation of the polarisation angle from the tangential in the range of 10° - 15° (or more). Our analysis showed that this is mostly due to the fact that the sequence of three polarised images from where the polarised parameters are derived is not taken simultaneously, but at a difference of few seconds in time. In this interval of time, the CME is moving by at least two pixels in the FOV of the instruments and this displacement results in uncertainties in the polarisation parameters (degree of polarisation, polarisation angle, etc.). We propose some steps forward to improve the derivation of the polarisation. This study is important for analysing the future data from instruments with polarisation capabilities.

## Study of a Prominence Eruption using PROBA2/SWAP and STEREO/EUVI Data

M. Mierla, D. B. Seaton, D. Berghmans, I. Chifu, A. De Groof, B. Inhester, L. Rodriguez, G. Stenborg, A. N. Zhukov

Solar Physics, August 2013, Volume 286, Issue 1, pp 241-253

Observations of the early rise and propagation phases of solar eruptive prominences can provide clues about the forces acting on them through the behavior of their acceleration with height. We have analyzed such an event, observed on **13 April 2010** by SWAP on PROBA2 and EUVI on STEREO. A feature at the top of the erupting prominence was identified and tracked in images from the three spacecraft. The triangulation technique was used to derive the true direction of propagation of this feature. The reconstructed points were fitted with two mathematical models: i) a power-law polynomial function and ii) a cubic smoothing spline, in order to derive the accelerations. The first model is characterized by five degrees of freedom while the second one is characterized by ten degrees of freedom. The results show that the acceleration increases smoothly, and it is continuously increasing with height. We conclude that the prominence is not accelerated immediately by local reconnection, but rather is swept away as part of a large-scale relaxation of the coronal magnetic field.

## On 3D reconstruction of coronal mass ejections: II. Longitudinal and latitudinal width analysis of 31 August 2007 event

M. Mierla, b, c, , , B. Inhesterd, L. Rodriguezb, S. Gissotb, A. Zhukovb, e and N. Srivastavaf

Journal of Atmospheric and Solar-Terrestrial Physics, Volume 73, Issue 10, 2011, Pages 1166-1172, File

[sci-hub.tw/10.1016/j.jastp.2010.11.028](http://sci-hub.tw/10.1016/j.jastp.2010.11.028)

In an earlier work, Mierla et al. (2009) applied four different reconstruction techniques to three coronal mass ejections (CMEs) at a given time. This study is a follow up of the above work in which we apply a local correlation tracking and tie-point reconstruction technique (LCT-TP) to the CME observed on 31 August 2007 by the COR1 and COR2 coronagraphs onboard the STEREO spacecraft at different times. The results show considerable scatter in the direction parallel to the line of sight, which is a direct indication of the CME depth. We derive the longitudinal and latitudinal sizes of the CME as a function of time. We find that a reasonable lower estimate of the longitudinal size is  $18^{\circ}$ – $44^{\circ}$  with an absolute largest extent of  $78^{\circ}$ – $110^{\circ}$ . We also find that a reasonable lower estimate for the latitudinal size of the CME is  $18^{\circ}$ – $32^{\circ}$  with an absolute largest extent of  $44^{\circ}$ – $56^{\circ}$ . In general, the latitudinal size is smaller than the longitudinal size, indicating an elliptical cone like structure or a flux rope like structure with very little tilt relative to the ecliptic. Self-similar expansion is observed above a height of 6.9R. As our analysis is based on a statistical approach, large scatter is expected. In order for the method to be validated, more cases have to be studied.

Research Highlights

► Three-dimensional reconstruction of a structured coronal mass ejection is performed. ► Longitudinal and latitudinal extents of the ejection are derived. ► The results indicate an elliptical or a flux rope like structure. ► Self-similar expansion is observed above a height of 6.9 solar radii.

## Low polarised emission from the core of coronal mass ejections

M. Mierla<sup>1,2,3</sup>, I. Chifu<sup>4,5</sup>, B. Inhester<sup>4</sup>, L. Rodriguez<sup>1</sup> and A. Zhukov  
A&A 530, L1 (2011), [File](#)

Letters to the Editor

**Aims.** In white-light coronagraph images, cool prominence material is sometimes observed as bright patches in the core of coronal mass ejections (CMEs). If, as generally assumed, this emission is caused by Thomson-scattered light from the solar surface, it should be strongly polarised tangentially to the solar limb. However, the observations of a CME made with the SECCHI/STEREO coronagraphs on 31 August 2007 show that the emission from these bright core patches is exceptionally low polarised.

**Methods.** We used the polarisation ratio method of Moran & Davila (2004) to localise the barycentre of the CME cloud. By analysing the data from both STEREO spacecraft we could resolve the plane-of-the-sky ambiguity this method usually suffers from. Stereoscopic triangulation was used to independently localise the low-polarisation patch relative to the cloud.

**Results.** We demonstrated for the first time that the bright core material is located close to the centre of the CME cloud. We show that the major part of the CME core emission, more than 85% in our case, is H $\alpha$  radiation and only a small fraction is Thomson-scattered light. Recent calculations also imply that the plasma density in the patch is  $8 \times 10^8$  cm<sup>-3</sup> or more compared to  $2.6 \times 10^6$  cm<sup>-3</sup> for the Thomson-scattering CME environment surrounding the core material.

31 August 2007,

## On the 3-D reconstruction of Coronal Mass Ejections using coronagraph data,

Mierla, M., Inhester, B., Antunes, A., Boursier, Y., Byrne, J. P., Colaninno, R., Davila, J., de Koning, C. A., Gallagher, P. T., Gissot, S., Howard, R. A., Howard, T. A., Kramar, M., Lamy, P., Liewer, P. C., Maloney, S., Marqué, C., McAteer, R. T. J., Moran, T., Rodriguez, L., Srivastava, N., Cyr, O. C. St., Stenborg, G., Temmer, M., Thernisien, A., Vourlidas, A., West, M. J., Wood, B. E., and Zhukov, A. N.  
Ann. Geophys., 28, 203-215, 2010, [File](#)

Coronal Mass ejections (CMEs) are enormous eruptions of magnetized plasma expelled from the Sun into the interplanetary space, over the course of hours to days. They can create major disturbances in the interplanetary medium and trigger severe magnetic storms when they collide with the Earth's magnetosphere. It is important to know their real speed, propagation direction and 3-D configuration in order to accurately predict their arrival time at the Earth. Using data from the SECCHI coronagraphs onboard the STEREO mission, which was launched in October 2006, we can infer the propagation direction and the 3-D structure of such events. In this review, we first describe different techniques that were used to model the 3-D configuration of CMEs in the coronagraph field of view (up to 15  $R_{\odot}$ ). Then, we apply these techniques to different CMEs observed by various coronagraphs. A comparison of results obtained from the application of different reconstruction algorithms is presented and discussed.

## On 3D Reconstruction of Coronal Mass Ejections:

### I. Method Description and Application to SECCHI-COR Data

M. Mierla · B. Inhester · C. Marqué · L. Rodriguez · S. Gissot · A.N. Zhukov · D. Berghmans · J. Davila  
Solar Phys (2009) 259: 123–141, [File](#)

The data from SECCHI-COR1 and SECCHI-COR2 coronagraphs onboard the STEREO mission, which was launched in October 2006, provide us with the first-ever stereoscopic images of the Sun's corona. These observations were found to be useful in inferring the three-dimensional structure of coronal mass ejections (CMEs) and their propagation direction in space. We apply four methods for reconstructing CMEs: *i*) Forward modeling technique; *ii*) Local correlation tracking (to identify the same feature in COR Ahead and COR Behind images) plus tie-point reconstruction

technique; *iii*) Center of mass of the structures in a given epipolar plane plus tie-point reconstruction technique; *iv*) Polarization ratio technique. The four techniques are applied to three structured CMEs observed by COR1 and COR2 instruments, respectively, on **15 May 2007, 31 August 2007, and 25 March 2008**. A comparison of the results obtained from the application of the four reconstruction algorithms is presented and discussed.

### **A Quick Method for Estimating the Propagation Direction of Coronal Mass Ejections Using STEREO-COR1 Images**

M. **Mierla** · J. Davila · W. Thompson · B. Inhester · N. Srivastava · M. Kramar · O.C. St. Cyr · G. Stenborg · R.A. Howard

Solar Phys (2008) 252: 385–396, **File**

<http://www.springerlink.com/content/w680q280063r165q/fulltext.pdf>

We describe here a method to obtain the position of a coronal moving feature in a three-dimensional coordinate system based on height – time measurements applied to STEREO data. By using the height – time diagrams from the two SECCHI-COR1 coronagraphs onboard STEREO, one can easily determine the direction of propagation of a coronal mass ejection (*i.e.*, if the moving plasma is oriented toward or away from the Earth). This method may prove to be a useful tool for space weather forecasting by easily identifying the direction of propagation as well as the real speed of the coronal mass ejections.

### **AN INTRODUCTION TO THEORY AND MODELS OF CMES, SHOCKS, AND SOLAR ENERGETIC PARTICLES**

Z. **MIKIC**<sup>1,\*</sup> and M. A. LEE

Space Science Reviews (2006) 123: 57–80

### **An operational software tool for the analysis of coronagraph images: Determining CME parameters for input into the WSA-Enlil heliospheric model**

G. **Millward**<sup>1,2,\*</sup>, D. Biesecker, <sup>2</sup>, V. Pizzo, C. A. de Koning

Space Weather, Volume 11, Issue 2, pages 57–68, February 2013

Coronal mass ejections (CMEs)—massive explosions of dense plasma that originate in the lower solar atmosphere and propagate outward into the solar wind—are the leading cause of significant space weather effects within Earth's environment. Computational models of the heliosphere such as WSA-Enlil offer the possibility of predicting whether a given CME will become geo-effective and, if so, the likely time of arrival at Earth. To be meaningful, such a forecast model is dependent upon accurately characterizing key parameters for the CME, notably its speed and direction of propagation, and its angular width. Studies by Zhao et al. (2002) and Xie et al. (2004) suggest that these key CME parameters can be deduced from geometric analysis of the elliptical “halo” forms observed in coronagraph images on spacecraft such as the Solar and Heliospheric Observatory (SOHO) and which result from a CME whose propagation is roughly toward or away from the observer. Both studies assume that the CME presents a circular cross-section and maintains a constant angular width during its radial expansion, the so called “cone model.” Development work at the NOAA Space Weather Prediction Center (SWPC) has been concerned with building and testing software tools to allow forecasters to determine these CME parameters routinely within an operational context, a key aspect of transitioning the WSA-Enlil heliospheric model into operations at the National Weather Service. We find “single viewpoint” cone analysis, while a useful start, to be highly problematic in many real-world situations. In particular, it is extremely difficult to establish objectively the correct ellipse that should be applied to a given halo form and that small changes in the exact ellipse chosen can lead to large differences in the deduced CME parameters. The inaccuracies in the technique are particularly evident for analysis of the “nearly circular” elliptical forms which result from CMEs that are propagating directly toward the observer and are therefore the most likely to be geo-effective. In working to resolve this issue we have developed a new three-dimensional (3-D) graphics-based analysis system which seeks to reduce inaccuracies by analyzing a CME using coronagraph images taken concurrently by SOHO and also by the two Solar TERrestrial RELations Observatory (STEREO) spacecraft, which provide additional viewing locations well away from the Sun-Earth line. The resulting “three view” technique has led to the development of the CME Analysis Tool (CAT), an operational software system in routine use at the SWPC as the primary means to determine CME parameters for input into the WSA-Enlil model. Results from the operational WSA-Enlil system are presented: utilizing CAT to provide CME input parameters, we show that, during the first year of operations at SWPC, the WSA-Enlil model has forecasted the arrival of CMEs at Earth with an average error 7.5 h.

### **Coronal Mass Ejections, Magnetic Fields, and the Green Corona in Cycle 23**

M. **Minarovjech** · V. Rušin · M. Saniga

Solar Phys (2008) 248: 167–176

<http://www.springerlink.com/content/k6727801mt5r58x1/fulltext.pdf>



We study a time – latitudinal distribution of CMEs observed by the SOHO spacecraft, their projected speeds and associated magnetic fields, as well as the north – south (N – S) asymmetry of solar surface magnetic fields, and the coronal green line intensities. We have found that (a) there exists an intricate relation between the average projected velocity of CMEs and the mean value of large-scale magnetic fields; (b) there exists a pronounced N– S asymmetry in both the distribution and the number of CMEs; (c) this asymmetry is in favor of the northern hemisphere at the beginning of the cycle, and of the southern hemisphere from 2001 onward, being, in fact, (d) closely related with the N– S asymmetry in the distribution of large-scale magnetic fields and the coronal green line intensities.

### **Origin of Quasi-Periodic Pulsation at the Base of Kink Unstable Jet**

[Sudheer K. Mishra](#), [Kartika Sangal](#), [Pradeep Kayshap](#), [Petr Jelinek](#), [A.K. Srivastava](#), [S.P. Rajaguru](#)

ApJ **945** 113 **2023**

<https://arxiv.org/pdf/2301.01534.pdf>

<https://iopscience.iop.org/article/10.3847/1538-4357/acb058/pdf>

We study a blowout jet that occurs at the west limb of the Sun on **August 29th, 2014** using high-resolution imaging/spectroscopic observations provided by SDO/AIA and IRIS. An inverse  $\gamma$ -shape flux-rope appears before the jet's morphological indication of the onset of kink instability. The twisted field lines of kink-unstable flux-rope reconnect at its bright knot and launch the blowout jet at  $\approx 06:30:43$  UT with an average speed of  $234 \text{ km s}^{-1}$ . Just after the launch, the northern leg of the flux rope erupts completely. The time-distance diagrams show multiple spikes or bright dots, which is the result of periodic fluctuations, i.e., quasi-periodic fluctuations (QPPs). The wavelet analysis confirms that QPPs have a dominant period of  $\approx 03$  minutes. IRIS spectra ( $\text{Si IV}$ ,  $\text{C II}$ , and  $\text{Mg II}$ ) may also indicate the occurrence of magnetic reconnection through existence of broad & complex profiles and bi-directional flows in the jet. Further, we have found that line broadening is periodic with a period of  $\approx 03$  minutes, and plasma upflow is always occurs when the line width is high, i.e., multiple reconnection may produce periodic line broadening. The EM curves also show the same period of  $\approx 03$  minutes in different temperature bins. The images and EM show that this jets spire is mainly cool (chromospheric/transition region) rather than hot (coronal) material. Further, line broadening, intensity, and EM curves have a period of  $\approx 03$  minutes, which strongly supports that multiple magnetic reconnection triggers QPPs in the blowout jet.

### **Evolution of Kelvin–Helmholtz Instability in the Fan-spine Topology**

Sudheer K. [Mishra](#)<sup>1</sup>, Balveer Singh<sup>2</sup>, A. K. Srivastava<sup>2</sup>, Pradeep Kayshap<sup>3</sup>, and B. N. Dwivedi<sup>2</sup>

**2021** ApJ **923** 72

<https://doi.org/10.3847/1538-4357/ac2a43>

We use multiwavelength imaging observations from the Atmospheric Imaging Assembly (AIA) on board the Solar Dynamics Observatory to study the evolution of the Kelvin–Helmholtz (K–H) instability in a fan-spine magnetic field configuration. This magnetic topology exists near an active region **AR12297** and is rooted in a nearby sunspot. In this magnetic configuration, two layers of cool plasma flow in parallel and interact with each other inside an elongated spine. The slower plasma flow ( $5 \text{ km s}^{-1}$ ) is the reflected stream along the spine's field lines from the top, which interacts with the impulsive plasma upflows ( $114\text{--}144 \text{ km s}^{-1}$ ) from below. This process generates a shear motion and subsequent evolution of the K–H instability. The amplitude and characteristic wavelength of the K–H unstable vortices increase, satisfying the criterion of the fastest-growing mode of this instability. We also describe how the velocity difference between two layers and the velocity of K–H unstable vortices are greater than the Alfvén speed in the second denser layer, which also satisfies the criterion of the growth of the K–H instability. In the presence of the magnetic field and sheared counterstreaming plasma as observed in the fan-spine topology, we estimate the parametric constant  $\Lambda \geq 1$ , which confirms the dominance of velocity shear and the evolution of the linear phase of the K–H instability. This observation indicates that in the presence of complex magnetic field structuring and flows, the fan-spine configuration may evolve into rapid heating, while the connectivity changes due to the fragmentation via the K–H instability.

### **Large-Scale Vortex Motion and Multiple Plasmoid Ejection Due to Twisting Prominence Threads and Associated Reconnection**

[Sudheer K. Mishra](#), [Abhishek K. Srivastava](#), [P.F. Chen](#)

Solar Phys. **295**, Article number: 167 **2020**

<https://arxiv.org/pdf/2011.02950.pdf>

<https://link.springer.com/content/pdf/10.1007/s11207-020-01733-w.pdf>

We analyze the characteristics of a quiescent polar prominence using the Atmospheric Imaging Assembly (AIA) onboard the Solar Dynamics Observatory (SDO). Initially, small-scale barb-like structures are evident on the solar disk, which firstly grow vertically and thereafter move towards the south-west limb. Later, a spine connects these barbs and we observe apparent rotating motions in the upper part of the prominence. These apparent rotating motions might play an important role for the evolution and growth of the filament by transferring cool plasma and magnetic twist. The large-scale vortex motion is evident in the upper part of the prominence, and consists of a swirl-like structure within it. The slow motion of the footpoint twists the legs of the prominence due to magnetic shear, causing two different kinds of magnetic reconnection. The internal reconnection is initiated by a resistive tearing-mode instability, which leads to the formation of multiple plasmoids in the elongated current sheet. The estimated growth rate was found to be  $0.02\text{--}0.05$ . The magnetic reconnection heats the current sheet for a small duration. However, most of the energy release due to magnetic reconnection is absorbed by the surrounding cool and dense plasma and used to accelerate the plasmoid

ejection. The multiple plasmoid ejections destroy the current sheet. Therefore, the magnetic arcades collapse near the X-point. Oppositely directed magnetic arcades may reconnect with the southern segment of the prominence and an elongated thin current sheet is formed. This external reconnection drives prominence eruption. **9 – 14 June 2018.**

### **Probing the Thermodynamic State of a Coronal Mass Ejection (CME) Up to 1 AU**

Wageesh [Mishra](#), Yuming Wang, Luca Teriaca, Jie Zhang, and Yutian Chi

Front. Astron. Space Sci., 30 January 2020 | <https://doi.org/10.3389/fspas.2020.00001>

<https://www.frontiersin.org/articles/10.3389/fspas.2020.00001/pdf>

Several earlier studies have attempted to estimate some of the thermodynamic properties of Coronal Mass Ejections (CMEs) either very close to the Sun or at 1 AU. In the present study, we attempt to extrapolate the internal thermodynamic properties of **2010 April 3** flux rope CME from near the Sun to 1 AU. For this purpose, we use the flux rope internal state (FRIS) model which is constrained by the kinematics of the CME. The kinematics of the CME is estimated using the STEREO/COR and HI observations in combination with drag based model (DBM) of CME propagation. Using the FRIS model, we focus on estimating the polytropic index of the CME plasma, heating/cooling rate, entropy changing rate, Lorentz force and thermal pressure force acting inside the CME. Our study finds that the polytropic index of the selected CME ranges between 1.7 and 1.9. This implies that the CME is in the heat-releasing state (i.e., entropy loss) throughout its journey from the Sun to Earth. The hindering role of Lorentz force and contributing role of thermal pressure force in governing the expansion of the CME is also identified. On comparing the estimated properties of the CME flux rope from the FRIS model with the in situ observations of the CME taken at 1 AU, we find relevant discrepancies between the results predicted by the model and the observations. We outline the approximations made in our study of probing the internal state of the CME during its heliospheric evolution and discuss the possible causes of the observed discrepancies.

[THIS ARTICLE IS PART OF THE RESEARCH TOPIC](#)

[Magnetic Flux Ropes: From the Sun to the Earth and Beyond View all 9 Articles](#)

### **Linkage of Geoeffective Stealth CMEs Associated with the Eruption of Coronal Plasma channel and Jet-Like Structure**

Sudheer K. [Mishra](#), [A.K. Srivastava](#)

Solar Phys. **2019**

<https://arxiv.org/pdf/1911.07134.pdf>

We analyze the eruption of a coronal plasma channel (CPC) and an overlying flux rope using \textit{Atmospheric Imaging Assembly/Solar Dynamic Observatory} (AIA/SDO) and \textit{Solar TERrestrial RELations Observatory} (STEREO)-A spacecraft data. The CPC erupted first with its low and very faint coronal signature. Later, above the CPC, a diffuse and thin flux rope also developed and erupted. The spreading CPC further triggered a rotating jet-like structure from the coronal hole lying to its northward end. This jet-like eruption may have evolved due to the interaction between spreading CPC and the open field lines of the coronal hole lying towards its northward foot-point. The CPC connected two small trans-equatorial coronal holes lying respectively in the northern and southern hemisphere on either side of the Equator. These eruptions were collectively associated with the stealth-type CMEs and CME associated with a jet-like eruption. The source region of the stealth CMEs lay between two coronal holes connected by a coronal plasma channel. Another CME was also associated with a jet-like eruption that occurred from the coronal hole in the northern hemisphere. These CMEs evolved without any low coronal signature and yet were responsible for the third strongest geomagnetic storm of Solar cycle 24. These stealth CMEs further merged and collectively passed through the interplanetary space. The compound CME further produced an intense geomagnetic storm (GMS) with Dst index = -176 nT. The z-component of the interplanetary magnetic field [Bz] switched to negative (-18 nT) during this interaction, and simultaneous measurement of the disturbance in the Earth's magnetic field (Kp=7) indicates the onset of the geomagnetic storm. **20-28 Aug 2018**

### **The Evolution of Magnetic Rayleigh-Taylor Unstable Plumes and Hybrid KH-RT Instability into A Loop-like Eruptive Prominence**

Sudheer K. [Mishra](#), [A.K. Srivastava](#)

**2019** *ApJ* **874** 57

<https://arxiv.org/pdf/1902.05044.pdf>

<https://doi.org/10.3847/1538-4357/ab06f2>

MRT unstable plumes are observed in a loop-like eruptive prominence using SDO/AIA observations. The small-scale cavities are developed within the prominence, where perturbations trigger dark plumes (P1 & P2) propagating with the speed of 35-46 km s<sup>-1</sup>. The self-similar plume formation shows initially the growth of linear MRT unstable plume (P1), and thereafter the evolution of non-linear single mode MRT unstable second plume (P2). The Differential Emission Measure (DEM) analysis shows that plumes are less denser and hotter than the prominence. We have estimated the observational growth rate for both plumes as  $1.32 \pm 0.29 \times 10^{-3} \text{ s}^{-1}$  and  $1.48 \pm 0.29 \times 10^{-3} \text{ s}^{-1}$  respectively, which are comparable to the estimated theoretical growth rate ( $1.95 \times 10^{-3} \text{ s}^{-1}$ ). The nonlinear phase of an MRT unstable plume (P2) may collapse via Kelvin-Helmholtz vortex formation in the downfaling plasma. Later, a plasma thread has been evident in the rising segment of this prominence. It may be associated with the tangled field and Rayleigh-Taylor instability. The tangled field initiates shearing at the prominence-cavity boundary. Due to this shear motion, the plasma downfall has occurred at the right part of the prominence-cavity

boundary. It triggers the characteristic of KH unstable vortices and MRT unstable plasma bubbles propagating at different speeds and merging with each other. The shear motion and lateral plasma downfall may initiate hybrid KH-RT instability there. **18 November 2014**

### **Modeling the thermodynamic evolution of Coronal Mass Ejections (CMEs) using their kinematics**

Wageesh [Mishra](#), [Yuming Wang](#)

ApJ **865** 50 **2018**

<https://arxiv.org/pdf/1808.06794.pdf>

<https://doi.org/10.3847/1538-4357/aadb9b>

Earlier studies on Coronal Mass Ejections (CMEs), using remote sensing and in situ observations, have attempted to determine some of the internal properties of CMEs, which were limited to a certain position or a certain time. For understanding the evolution of the internal thermodynamic state of CMEs during their heliospheric propagation, we improve the self-similar flux rope internal state (FRIS) model, which is constrained by measured propagation and expansion speed profiles of a CME. We implement the model to a CME erupted on **2008 December 12** and probe the internal state of the CME. It is found that the polytropic index of the CME plasma decreased continuously from 1.8 to 1.35 as the CME moved away from the Sun, implying that the CME released heat before it reached adiabatic state and then absorbed heat. We further estimate the entropy changing and heating rate of the CME. We also find that the thermal force inside the CME is the internal driver of CME expansion while Lorentz force prevented the CME from expanding. It is noted that centrifugal force due to poloidal motion decreased with the fastest rate and Lorentz force decreased slightly faster than thermal pressure force as CME moved away from the Sun. We also discuss the limitations of the model and approximations made in the study.

### **Solar cycle variation of coronal mass ejections contribution to solar wind mass flux**

Wageesh [Mishra](#), [Nandita Srivastava](#), [Zavkiddin Mirtoshev](#), [Yuming Wang](#)

Proceedings IAU Symposium No. 340, **2018**

<https://arxiv.org/pdf/1805.07593.pdf>

Coronal Mass Ejections (CMEs) contributes to the perturbation of solar wind in the heliosphere. Thus, depending on the different phases of the solar cycle and the rate of CME occurrence, contribution of CMEs to solar wind parameters near the Earth changes. In the present study, we examine the long term occurrence rate of CMEs, their speeds, angular widths and masses. We attempt to find correlation between near sun parameters, determined using white light images from coronagraphs, with solar wind measurements near the Earth from in-situ instruments. Importantly, we attempt to find what fraction of the averaged solar wind mass near the Earth is provided by the CMEs during different phases of the solar cycles.

### **Evolution of Magnetic Rayleigh-Taylor Instability into the Outer Solar Corona and Low Inter Planetary Space**

Sudheer K. [Mishra](#), [Talwinder Singh](#), [P. Kayshap](#), [A.K. Srivastava](#)

ApJ **856** 86 **2018**

<https://arxiv.org/pdf/1802.02293.pdf>

We analyze the observations from Solar TERrestrial Relations Observatory (STEREO)-A\&B/COR-1 of an eruptive prominence in the intermediate corona on **7 June 2011** at 08:45 UT, which consists of magnetic Rayleigh-Taylor (MRT) unstable plasma segments. Its upper northward segment shows spatio-temporal evolution of MRT instability in form of finger structures upto the outer corona and low inter-planetary space. Using method of Dolei et al.(2014), It is estimated that the density in each bright finger is greater than corresponding dark region lying below of it in the surrounding intermediate corona. The instability is evolved due to wave perturbations that are parallel to the magnetic field at the density interface. We conjecture that the prominence plasma is supported by tension component of the magnetic field against gravity. Using linear stability theory, magnetic field is estimated as 21-40 mG to suppress growth of MRT in the observed finger structures. In the southward plasma segment, a horn-like structure is observed at 11:55 UT in the intermediate corona that also indicates MRT instability. Falling blobs are also observed in both the plasma segments. In the outer corona upto 6-13 solar radii, the mushroom-like plasma structures have been identified in the upper northward MRT unstable plasma segment using STEREO-A/COR-2. These structures most likely grew due to the breaking and twisting of fingers at large spatial scales in weaker magnetic fields. In the lower inter-planetary space upto 20 solar radii, these structures are fragmented into various small-scale localized plasma spikes most likely due to turbulent mixing.

### **Assessing the collision nature of coronal mass ejections in the inner heliosphere**

Wageesh [Mishra](#), [Yuming Wang](#), [Nandita Srivastava](#), [Chenglong Shen](#)

ApJ Supplement Series **232** 5 **2017**

<https://arxiv.org/pdf/1707.08299.pdf>

<http://sci-hub.cc/10.3847/1538-4365/aa8139>

<https://iopscience.iop.org/article/10.3847/1538-4365/aa8139/pdf>

There have been few attempts in the past to understand the collision of individual cases of interacting Coronal Mass Ejections (CMEs). We selected 8 cases of interacting CMEs and estimated their propagation and expansion speeds,

direction of impact and masses exploiting coronagraphic and heliospheric imaging observations. Using these estimates with ignoring the errors therein, we find that the nature of collision is perfectly inelastic for 2 cases (e.g., 2012 March and November), inelastic for 2 cases (e.g., 2012 June and 2011 August), elastic for 1 case (e.g., 2013 October) and super-elastic for 3 cases (e.g., 2011 February, 2010 May and 2012 September). Admitting large uncertainties in the estimated directions, angular widths and pre-collision speeds; the probability of perfectly inelastic collision for 2012 March and November cases diverge from 98%-60% and 100%-40%, respectively, reserving some probability for other nature of collision. Similarly, the probability of inelastic collision diverge from 95%-50% for 2012 June case, 85%-50% for 2011 August case, and 75%-15% for 2013 October case. We note that probability of super-elastic collision for 2011 February, 2010 May and 2012 September CMEs diverge from 90%-75%, 60%-45% and 90%-50%, respectively. Although the sample size is small, we find a good dependence of nature of collision on CMEs parameters. The crucial pre-collision parameters of the CMEs responsible for increasing the probability of super-elastic collision, in descending order of priority, are their lower approaching speed, higher expansion speed of the following CME over the preceding one, and longer duration of collision phase. **2010 May 23-24 , 2011 February 14-15, 2011 August 3-4 , 2012 March 4-5 , 2012 June 13-14, 2012 September 25-28 , 2012 November 9-10, 2013 October 25**  
**Table 1.** Selected CMEs Events

## **On Understanding the Nature of Collision of Coronal Mass Ejections Observed by STEREO**

Wageesh [Mishra](#), Yuming Wang, Nandita Srivastava  
ApJ **831** 99 **2016**

<http://arxiv.org/pdf/1607.07692v1.pdf> **File**

Our study attempts to understand the collision characteristics of two coronal mass ejections (CMEs) launched successively from the Sun on **2013 October 25**. The estimated kinematics, from three-dimensional (3D) reconstruction techniques applied to observations of CMEs by SECCHI/Coronagraphic (COR) and Heliospheric Imagers (HIs), reveal their collision around 37  $R_{\odot}$  from the Sun. In the analysis, we take into account the propagation and expansion speeds, impact direction, angular size as well as the masses of the CMEs. These parameters are derived from imaging observations, but may suffer from large uncertainties. Therefore, by adopting head-on as well as oblique collision scenarios, we have quantified the range of uncertainties involved in the calculation of the coefficient of restitution for expanding magnetized plasmoids. Our study shows that the comparatively large expansion speed of the following CME than that of the preceding CME, results in a higher probability of super-elastic collision. We also infer that a relative approaching speed of the CMEs lower than the sum of their expansion speeds increases the chance of super-elastic collision. The analysis under a reasonable errors in observed parameters of the CME, reveals the larger probability of occurrence of an inelastic collision for the selected CMEs. We suggest that the collision nature of two CMEs should be discussed in 3D, and the calculated value of the coefficient of restitution may suffer from a large uncertainty.

## **Kinematics of Interacting CMEs of September 25 and 28, 2012**

Wageesh [Mishra](#), Nandita Srivastava, Talwinder Singh

JGR Volume 120, Issue 12 Pages 10,221–10,236 **2015**

<http://arxiv.org/pdf/1511.06970v1.pdf>

We have studied two Coronal Mass Ejections (CMEs) that occurred on **September 25 and 28, 2012** and interacted near the Earth. By fitting the Graduated Cylindrical Shell (GCS) model on the SECCHI/COR2 images and applying the Stereoscopic Self-Similar Expansion (SSSE) method on the SECCHI/HI images, the initial direction of both the CMEs is estimated to be west of the Sun-Earth line. Further, the three-dimensional (3D) heliospheric kinematics of these CMEs have been estimated using Self-Similar Expansion (SSE) reconstruction method. We show that use of SSE method with different values of angular extent of the CMEs, leads to significantly different kinematics estimates for the CMEs propagating away from the observer. Using the estimated kinematics and true masses of the CMEs, we have derived the coefficient of restitution for the collision which is found to be close to elastic. The in situ measurements at 1 AU show two distinct structures of interplanetary CMEs, heating of the following CME, as well as ongoing interaction between the preceding and the following CME. We highlight the signatures of interaction in remote and in situ observations of these CMEs and the role of interaction in producing a major geomagnetic storm.

## **Evolution and Consequences of Coronal Mass Ejections in the Heliosphere**

[Wageesh Mishra](#)

The **thesis** was submitted in Mar **2015** to MLS university, Udaipur, for which the university granted the degree in Jan 2016

<https://arxiv.org/pdf/2204.09879.pdf>

Investigating the heliospheric evolution and consequences of Coronal mass ejections (CMEs) is critical to understanding the solar-terrestrial relationship. For the first time, Heliospheric Imagers (HIs) onboard STEREO, providing multiple views of CMEs in the heliosphere, observed the vast and crucial observational gap between the Sun and the Earth. Using J-maps constructed from coronagraphs (CORs) and HIs observations, we continuously tracked different density enhanced features of CMEs. We implemented several reconstruction methods to estimate the three-dimensional (3D) kinematics of CMEs during their evolution from the Sun to Earth. Our study provides evidence that the 3D speeds of CMEs near the Sun are not reasonably sufficient for understanding the propagation and accurate forecasting of the arrival time at the Earth of a majority of CMEs. This finding can be due to many factors that

significantly change the CME kinematics beyond the COR field of view, such as the interaction/collision of two or more CMEs or the interaction of CMEs with the ambient solar wind medium. We attempted to understand the evolution and consequences of the interacting/colliding CMEs in the heliosphere using STEREO/HI, WIND, and ACE observations. The study found a significant change in the dynamics of the CMEs after their collision and interaction. The in situ observations show the signatures of CME-CME interaction as heating and compression, formation of magnetic holes (MHs), and interaction region (IR). We also noticed that long-lasting IR, formed at the rear edge of preceding CME, is responsible for large geomagnetic perturbations. Our study highlights the significance of using HIs observations in studying heliospheric evolution of CMEs, CME-CME collision, identifying and associating the three-part structure of CMEs in their remote and in situ observations, and hence for improved space weather forecasting. **2008 December 12, 2010 February 7, 2010 February 12, 2010 March 14, 2010 April 3, 2010 April 6, 2010 April 8, 2010 October 6, 2010 October 10, 2010 October 26, 2011 February 13-15, 2012 November 9-10**

### **Configuration and the Cause of Failed Flux Rope Eruption**

[Prabir K. Mitra](#) (USO/PRL, India), [Bhuwan Joshi](#) (USO/PRL, India), [Astrid M. Veronig](#) (Univ. of Graz, Austria), [Thomas Wiegelmann](#) (MPIS, Germany)

ApJ **926** 143 **2022**

<https://arxiv.org/pdf/2112.14412.pdf>

<https://iopscience.iop.org/article/10.3847/1538-4357/ac4756/pdf>

In this paper, we present multiwavelength observations of the triggering of a failed-eruptive M-class flare from the active region NOAA 11302, and investigate the possible reasons for the associated failed eruption. Photospheric observations and Non-Linear Force Free Field extrapolated coronal magnetic field revealed that the flaring region had a complex quadrupolar configuration with a pre-existing coronal null point situated above the core field. Prior to the onset of the M-class flare, we observed multiple periods of small-scale flux enhancements in GOES and RHESSI soft X-ray observations, from the location of the null point. The pre-flare configuration and evolution reported here are similar to the ones presented in the breakout model but at much lower coronal heights. The core of the flaring region was characterized by the presence of two flux ropes in a double-decker configuration. During the impulsive phase of the flare, one of the two flux ropes initially started erupting but resulted in a failed eruption. Calculation of the magnetic decay index revealed a saddle-like profile where decay index initially increased to the torus unstable limits within the heights of the flux ropes but then decreased rapidly reaching to negative values, which was most likely responsible for the failed eruption of the initially torus unstable flux rope. **2011 September 26**

### **Identification of Pre-flare Processes and Their Possible Role in Driving a Large-scale Flux Rope Eruption with Complex M-class Flare in the Active Region NOAA 12371**

[Prabir K. Mitra](#), [Bhuwan Joshi](#), [Avijeet Prasad](#)

*Solar Physics* February **2020**, 295:29

<https://doi.org/10.1007/s11207-020-1596-2>

<https://arxiv.org/pdf/2002.05890.pdf>

In this article, we study the origin of precursor flare activity and investigate its role towards triggering the eruption of a flux rope which resulted into a dual-peak M-class flare (SOL2015-06-21T02:36) in the active region NOAA 12371. The flare evolved in two distinct phases with peak flux levels of M2.1 and M2.6 at an interval of  $\approx 54 \sim 54$  min. The active region exhibited striking moving magnetic features (MMFs) along with sunspot rotation. Nonlinear force-free field (NLFFF) modelling of the active region corona reveals a magnetic flux rope along the polarity inversion line in the trailing sunspot group which is observationally manifested by the co-spatial structures of an active region filament and a hot channel identified in the 304 and 94 Å images, respectively, from the Atmospheric Imaging Assembly (AIA). The active region underwent a prolonged phase of flux enhancement followed by a relatively shorter period of flux cancellation prior to the onset of the flare which led to the build up and activation of the flux rope. Extreme ultra-violet (EUV) images reveal localised and structured pre-flare emission, from the region of MMFs, adjacent to the location of the main flare. Our analysis reveals strong, localised regions of photospheric currents of opposite polarities at the precursor location, thereby making the region susceptible to small-scale magnetic reconnection. Precursor reconnection activity from this location most likely induced a slipping reconnection towards the northern leg of the hot channel which led to the destabilisation of the flux rope. The application of magnetic virial theorem suggests that there was an overall growth of magnetic free energy in the active region during the prolonged pre-flare phase which decayed rapidly after the hot channel eruption and its successful transformation into a halo coronal mass ejection (CME).

### **Pre-flare processes, flux rope activation, large-scale eruption and associated X-class flare from the active region NOAA 11875**

[Prabir K. Mitra](#) (USO/PRL), [Bhuwan Joshi](#) (USO/PRL)

ApJ **2019**

<https://arxiv.org/pdf/1908.04059.pdf>

We present a multi-wavelength analysis of the eruption of a hot coronal channel associated with an X1.0 flare (SOL2013-10-28T02:03) from the active region NOAA 11875 by combining observations from AIA/SDO, HMI/SDO, RHESSI, and HiRAS. EUV images at high coronal temperatures indicated the presence of a hot channel at the core of the active region from the early pre-flare phase evidencing the pre-existence of a quasi-stable magnetic flux rope. The hot channel underwent an activation phase after a localized and prolonged pre-flare event occurring adjacent to one of

its footpoints. Subsequently, the flux rope continued to rise slowly for  $\approx 16$  min during which soft X-ray flux gradually built-up characterizing a distinct precursor phase. The flux rope transitioned from the state of slow rise to the eruptive motion with the onset of the impulsive phase of the X1.0 flare. The eruptive expansion of the hot channel is accompanied by a series of type III radio bursts in association with impulsive rise of strong hard X-ray non-thermal emissions that included explicit hard X-ray sources of energies up to  $\approx 50$  keV from the coronal loops and  $\approx 100$  keV from their footpoint locations. Our study contains evidence that pre-flare activity occurring within the spatial extent of a stable flux rope can destabilize it toward eruption. Moreover, sudden transition of the flux rope from the state of slow rise to fast acceleration precisely bifurcated the precursor and the impulsive phases of the flare which points toward a feedback relationship between early CME dynamics and the strength of the large-scale magnetic reconnection.

### **Successive flux rope eruptions from $\delta$ -Sunspots region of NOAA 12673 and associated X-class eruptive flares on 2017 September 6**

Prabir K. [Mitra](#) (USO/PRL, India), [Bhuwan Joshi](#) (USO/PRL, India), [Avijeet Prasad](#) (USO/PRL, India), [Astrid M. Veronig](#) (Univ. of Graz, Austria), [R. Bhattacharyya](#) (USO/PRL, India)

ApJ 869 69 2018

<https://arxiv.org/pdf/1810.13146.pdf>

In this paper, we present a multi-wavelength analysis of two X-class solar eruptive flares of classes X2.2 and X9.3 that occurred in the sigmoidal active region NOAA 12673 on **2017 September 6**, by combining observations of Atmospheric Imaging Assembly and Helioseismic Magnetic Imager instruments on board the Solar Dynamics Observatory. On the day of the reported activity, the photospheric structure of the active region displayed a very complex network of  $\delta$ -sunspots that gave rise to the formation of a coronal sigmoid observed in the hot EUV channels. Both X-class flares initiated from the core of the sigmoid sequentially within an interval of  $\sim 3$  hours and progressed as a single "sigmoid-to-arcade" event. Differential emission measure analysis reveals strong heating of plasma at the core of the active region right from the pre-flare phase which further intensified and spatially expanded during each event. The identification of a pre-existing magnetic null by non-force-free-field modeling of the coronal magnetic fields at the location of early flare brightenings and remote faint ribbon-like structures during the pre-flare phase, which were magnetically connected with the core region, provide support for the breakout model of solar eruption. The magnetic extrapolations also reveal flux rope structures prior to both flares which are subsequently supported by the observations of the eruption of hot EUV channels. The second X-class flare diverged from the standard flare scenario in the evolution of two sets of flare ribbons, that are spatially well separated, providing firm evidence of magnetic reconnections at two coronal heights.

### **Initiation of CMEs: A review**

Nishant [Mittal](#), Udit Narain

Journal of Atmospheric and Solar-Terrestrial Physics 72(2010)643–652; **File**

Solar coronal mass ejections (CMEs) are a striking manifestation of solar activity seen in the solar corona, which bring out coronal plasma as well as magnetic flux into the interplanetary space and may cause strong interplanetary disturbances and geomagnetic storms. Understanding the initiation of CMEs and forecasting them are an important topic in both solar physics and geophysics. In this paper, we review recent progresses in research on the initiation of CMEs. Several initiation mechanisms and models are discussed. No single model/simulation is able to explain all the observations available to date, even for a single event.

### **On some properties of coronal mass ejections in solar cycle 23**

[Mittal](#), N., & Narain, U.

2009, New Astronomy, 14, 341

We have investigated some properties such as speed, apparent width, acceleration, latitude, mass and kinetic energy, etc. of all types of coronal mass ejections (CMEs) observed during the period 1996–2007 by SOHO/LASCO covering the solar cycle 23. The results are in satisfactory agreement with previous investigations.

### **The relation between coronal holes and coronal mass ejections during the rise, maximum, and declining phases of Solar Cycle 23**

[Mohamed](#), A. A.; [Gopalswamy](#), N.; [Yashiro](#), S.; [Akiyama](#), S.; [Млкелд](#), P.; [Xie](#), H.; [Jung](#), H.

J. Geophys. Res., Vol. 117, No. A1, A01103, 2012; **File**

<http://dx.doi.org/10.1029/2011JA016589>

We study the interaction between coronal holes (CHs) and coronal mass ejections (CMEs) using a resultant force exerted by all the coronal holes present on the disk and is defined as the coronal hole influence parameter (CHIP). The CHIP magnitude for each CH depends on the CH area, the distance between the CH centroid and the eruption region, and the average magnetic field within the CH at the photospheric level. The CHIP direction for each CH points from the CH centroid to the eruption region. We focus on Solar Cycle 23 CMEs originating from the disk center of the Sun (central meridian distance  $\leq 15^\circ$ ) and resulting in magnetic clouds (MCs) and non-MCs in the solar wind. The CHIP is found to be the smallest during the rise phase for MCs and non-MCs. The maximum phase has the largest CHIP value (2.9 G) for non-MCs. The CHIP is the largest (5.8 G) for driverless (DL) shocks, which are shocks at 1 AU with no discernible MC or non-MC. These results suggest that the behavior of non-MCs is similar to that of the DL shocks and

different from that of MCs. In other words, the CHs may deflect the CMEs away from the Sun-Earth line and force them to behave like limb CMEs with DL shocks. This finding supports the idea that all CMEs may be flux ropes if viewed from an appropriate vantage point.

### **Novel scaling laws to derive spatially resolved flare and CME parameters from sun-as-a-star observables**

Atul **Mohan**<sup>1,2\*</sup>, Natchimuthuk Gopalswamy<sup>1</sup>, Hemapriya Raju<sup>3,1</sup> and Sachiko Akiyama<sup>1,2</sup>  
A&A, 691, L8 (2024)

<https://www.aanda.org/articles/aa/pdf/2024/11/aa51072-24.pdf>

Coronal mass ejections (CMEs) are often associated with X-ray (SXR) flares powered by magnetic reconnection in the low corona, while the CME shocks in the upper corona and interplanetary (IP) space accelerate electrons often producing the type II radio bursts. The CME and the reconnection event are part of the same energy release process as highlighted by the correlation between reconnection flux ( $\phi_{\text{rec}}$ ) that quantifies the strength of the released magnetic free energy during the SXR flare, and the CME kinetic energy that drives the IP shocks leading to type II bursts. Unlike the Sun, these physical parameters cannot be directly inferred in stellar observations. Hence, scaling laws between unresolved sun-as-a-star observables, namely SXR luminosity (LX) and type II luminosity (LR), and the physical properties of the associated dynamical events are crucial. Such scaling laws also provide insights into the interconnections between the particle acceleration processes across low-corona to IP space during solar-stellar “flare-CME-type II” events. Using long-term solar data in the SXR to radio waveband, we derived a scaling law between two novel power metrics for the flare and CME-associated processes. The metrics of “flare power” ( $P_{\text{flare}} = \sqrt{LX\phi_{\text{rec}}}$ ) and “CME power” ( $PCME = \sqrt{LRVCME^2}$ ), where VCME is the CME speed, scale as  $P_{\text{flare}} \propto PCME^{0.76 \pm 0.04}$ . In addition, LX and  $\phi_{\text{rec}}$  show power-law trends with PCME with indices of  $1.12 \pm 0.05$  and  $0.61 \pm 0.05$ , respectively. These power laws help infer the spatially resolved physical parameters, VCME and  $\phi_{\text{rec}}$ , from disk-averaged observables, LX and LR during solar-stellar flare-CME-type II events.

### **CME-associated type-IV radio bursts: The solar paradigm and the unique case of AD Leo**

[Atul Mohan](#), [Nat Gopalswamy](#), [Surajit Mondal](#), [Anshu Kumari](#), [Sindhuja G](#)

Proceedings of IAUS 388 2024

<https://arxiv.org/abs/2410.00787>

The type-IV bursts, associated with coronal mass ejections (CMEs), occasionally extend to the decameter-hectrometric (DH) range. We present a comprehensive catalog of simultaneous multi-vantage point observations of DH type-IV bursts by Wind and STEREO spacecraft since 2006. 73% of the bursts are associated with fast ( $>900\text{kms}^{-1}$ ) and wide ( $>600$ ) CMEs, which are mostly geoeffective halo CMEs. Also, we find that the bursts are best observed by the spacecraft located within  $|600|$  line of sight (LOS), highlighting the importance of LOS towards active latitudes while choosing target stars for a type-IV search campaign. In young active M dwarfs, CME-associated bursts have remained elusive despite many monitoring campaigns. We present the first detection of long-duration type-III, type-IV, and type-V bursts during an active event in AD Leo (M3.5V;  $0.4M_{\odot}$ ). The observed burst characteristics support a multipole model over a solar-like active region magnetic field profile on the star. **2004.11.09**

**The full catalog of /CME\_list/radio/type4 1997-2023**

[https://cdaw.gsfc.nasa.gov/CME\\_list/radio/type4/](https://cdaw.gsfc.nasa.gov/CME_list/radio/type4/)

### **A catalog of multi-vantage point observations of type-II bursts: Statistics and correlations**

[Atul Mohan](#), [Nat Gopalswamy](#), [Hemapriya Raju](#), [Sachiko Akiyama](#)

Proceedings of IAUS 388 2024

<https://arxiv.org/pdf/2410.00814>

Coronal mass ejection (CME) often produces a soft X-ray (SXR) flare associated with the low-coronal reconnection and a type-II radio burst associated with an interplanetary (IP) CME-shock. SXR flares and type-II bursts outshine the background emission, making them sun-as-a-star observables. Though there exist SXR flare catalogs covering decades of observations, they do not provide the associated type-II luminosity. Besides, since radio burst emission could be beamed, the observed flux dynamic spectrum may vary with line of sight. Using long-term calibrated decameter-hectrometric dynamic spectra from the Wind and STEREO spacecraft, we build a catalog of multi-vantage point observations of type-II bursts. Cross-matching with existing catalogs we compile the properties of the associated flare, reconnection, and the CME. Cross-correlation analysis was done between various parameters. Two novel metrics of flare and CME power show a strong correlation revealing a link between particle acceleration strengths in the low-corona and IP space. **2013.12.28**

**Catalog of the multi-mission DH type-II events and associated CMEs 2006-2023**

[https://cdaw.gsfc.nasa.gov/CME\\_list/radio/multimission\\_type2/](https://cdaw.gsfc.nasa.gov/CME_list/radio/multimission_type2/)

### **Magnetic diagnostics of prominence eruptions through the Hanle effect of the He I 1083 nm line**

[Momchil Molnar](#), [Roberto Casini](#)

ApJ 977 97 2024

<https://arxiv.org/pdf/2410.23197>

<https://iopscience.iop.org/article/10.3847/1538-4357/ad8de4/pdf>

The magnetic field vector of the solar corona is not regularly and comprehensively being measured, because of the complexity and degeneracy inherently present in the types of observations currently available. To address some of the current limitations of coronal polarimetry, we present computations that demonstrate the possibility of magnetometry using the unsaturated Hanle effect of the He I 1083 nm line. The main purpose of this investigation is to show how the geometric properties of the linear polarization of this line can be used to routinely diagnose the orientation of the field in erupting prominences, thus providing an important constraint on the Bz determination at 1 AU. For this work, we adopted a simplified magnetic model of a flux rope, consisting of a toroidal helical structure embedded in a hydrostatically stratified corona. Our results demonstrate the possibility to discern different orientations of the magnetic field vector in such structures under rather general and practicable viewing conditions. In particular, observations from the Sun-Earth Lagrange points are found to provide excellent locations for the deployment of synoptic instruments aiming at the estimation of the magnetic field of Earth-directed Coronal Mass Ejections. We complete our demonstration by showing how a small (~5 cm) space-borne coronagraph can achieve sufficient signal-to-noise ratios to make the coronal magnetometry goal outlined above feasible.

## **Estimation of the physical parameters of a CME at high coronal heights using low frequency radio observations**

Surajit [Mondal](#), [Divya Oberoi](#), [Angelos Vourlidas](#)

ApJ **893** 28 **2020**

<https://arxiv.org/pdf/1909.12041.pdf>

<https://doi.org/10.3847/1538-4357/ab7fab>

Measuring the physical parameters of Coronal Mass Ejections (CMEs), particularly their entrained magnetic field, is crucial for understanding their physics and for assessing their geo-effectiveness. At the moment, only remote sensing techniques can probe these quantities in the corona, the region where CMEs form and acquire their defining characteristics. Radio observations offer the most direct means for estimating the magnetic field when gyrosynchrotron emission is detected. In this work we measure various CME plasma parameters, including its magnetic field, by modelling the gyrosynchrotron emission from a CME. The dense spectral coverage over a wide frequency range provided by the Murchison Widefield Array (MWA) affords a much better spectral sampling than possible before. The MWA images also provide much higher imaging dynamic range, enabling us to image these weak emissions. Hence we are able to detect radio emission from a CME at larger distances ( $4.73R_{\odot}$ ) than have been reported before. The flux densities reported here are amongst the lowest measured in similar works. Our ability to make extensive measurements on a slow and otherwise unremarkable CME suggest that with the availability of data from the new generation instruments like the MWA, it should now be possible to make routine direct detections of radio counterparts of CMEs. **November 4, 2015**

## **On the partial eruption of a bifurcated solar filament structure**

[Aabha Monga](#), [Rahul Sharma](#), [Jijia Liu](#), [Consuelo Cid](#), [Wahab Uddin](#), [Ramesh Chandra](#), [Robertus Erdelyi](#)

MNRAS Volume 500, Issue 1, Pages 684–695 **2020**

<https://arxiv.org/pdf/2009.08619.pdf>

<https://doi.org/10.1093/mnras/staa2902>

The partial eruption of a filament channel with bifurcated substructures is investigated using datasets obtained from both ground-based and space-borne facilities. Small-scale flux reconnection/cancellation events in the region triggered the pile-up of ambient magnetic field, observed as bright EUV loops in close proximity of the filament channel. This led to the formation of a V-shaped cusp structure at the site of interaction between the coalesced EUV loops and the filament channel, with the presence of distinct plasmoid structures and associated bidirectional flows. Analysis of imaging data from SDO/AIA further suggests the vertical split of the filament structure into two substructures. The perturbed upper branch of the filament structure rose up and erupted with the onset of an energetic GOES M1.4 flare at 04:30 UT on **January 28, 2015**. The estimated twist number and squashing factor obtained from nonlinear force-free field extrapolation of the magnetic field data support the vertical split in filament structure with high twist in upper substructure. The loss in equilibrium of the upper branch due to torus instability, implying this as a potential triggering mechanism of the observed partial eruption.

## **SYMPATHETIC CORONAL MASS EJECTIONS**

Y.-J. [Moon](#),<sup>1,2</sup> G. S. Choe,<sup>3</sup> Haimin Wang,<sup>1</sup> and Y. D. Park<sup>2</sup>

Astrophysical Journal, 588:1176–1182, **2003**

We address the question whether there exist sympathetic coronal mass ejections (CMEs), which take place almost simultaneously in different locations with a certain physical connection. For this study, the following three investigations are performed. First, we have examined the waiting-time distribution of the CMEs that were observed by the SOHO Large Angle and Spectrometric Coronagraph (LASCO) from 1999 February to 2001 December. The observed waiting-time distribution is found to be well approximated by a time-dependent Poisson distribution without any noticeable overabundance at short waiting times. Second, we have investigated the angular difference distribution of successive CME pairs to examine their spatial correlations.



A remarkable overabundance relative to background levels is found within  $10^\circ$  of the position angle difference, which supports the existence of quasi-homologous CMEs that occur sequentially in the same active region. Both of the above results indicate that sympathetic (interdependent) CMEs are far less frequent than independent CMEs. Third, we have examined the EUV Imaging Telescope running difference images and the LASCO images of quasi-simultaneous CME pairs and found a candidate sympathetic CME pair, of which the second CME may be initiated by the eruption of the first CME. Possible mechanisms of the sympathetic CME triggering are discussed.

## **Stealth Non-standard-model Confined Flare Eruptions: Sudden Reconnection Events in Ostensibly Inert Magnetic Arches from Sunspots**

Ronald L. Moore, Sanjiv K. Tiwari, Navdeep K. Panesar, V. Aparna, Alphonse C. Sterling

ApJ 2024

<https://arxiv.org/pdf/2408.09021> File

We report seven examples of a long-ignored type of confined solar flare eruption that does not fit the standard model for confined flare eruptions. Because they are confined eruptions, do not fit the standard model, and unexpectedly erupt in ostensibly inert magnetic arches, we have named them stealth non-standard-model confined flare eruptions. Each of our flaring magnetic arches stems from a big sunspot. We tracked each eruption in full-cadence UV and EUV images from the Atmospheric Imaging Assembly (AIA) of Solar Dynamics Observatory (SDO) in combination with magnetograms from SDO's Helioseismic and Magnetic Imager (HMI). We present the onset and evolution of two eruptions in detail: one of six that each make two side-by-side main flare loops, and one that makes two crossed main flare loops. For these two cases, we present cartoons of the proposed pre-eruption field configuration and how sudden reconnection makes the flare ribbons and flare loops. Each of the seven eruptions is consistent with being made by sudden reconnection at an interface between two internal field strands of the magnetic arch, where they cross at a small (10 - 20 degrees) angle. These stealth non-standard-model confined flare eruptions therefore plausibly support the idea of E. N. Parker for coronal heating in solar coronal magnetic loops by nanoflare bursts of reconnection at interfaces of internal field strands that cross at angles of 10 - 20 degrees. 2012 Jan 8, 2013 Jan 14, 2013 Jun 27, 2014 Jan 23, 2014 Nov 19, 2014 Nov 20

## **On Making Magnetic-flux-rope $\Omega$ Loops for Solar Bipolar Magnetic Regions of All Sizes by Convection Cells**

Ronald L. Moore<sup>1,2</sup>, Sanjiv K. Tiwari<sup>3,4</sup>, Navdeep K. Panesar<sup>3,4</sup>, and Alphonse C. Sterling<sup>2</sup>

2020 ApJL 902 L35

<https://doi.org/10.3847/2041-8213/abbade>

We propose that the flux-rope  $\Omega$  loop that emerges to become any bipolar magnetic region (BMR) is made by a convection cell of the  $\Omega$ -loop's size from initially horizontal magnetic field ingested through the cell's bottom. This idea is based on (1) observed characteristics of BMRs of all spans ( $\sim 1000$  to  $\sim 200,000$  km), (2) a well-known simulation of the production of a BMR by a supergranule-sized convection cell from horizontal field placed at cell bottom, and (3) a well-known convection-zone simulation. From the observations and simulations, we (1) infer that the strength of the field ingested by the biggest convection cells (giant cells) to make the biggest BMR  $\Omega$  loops is  $\sim 103$  G, (2) plausibly explain why the span and flux of the biggest observed BMRs are  $\sim 200,000$  km and  $\sim 1022$  Mx, (3) suggest how giant cells might also make "failed-BMR"  $\Omega$  loops that populate the upper convection zone with horizontal field, from which smaller convection cells make BMR  $\Omega$  loops of their size, (4) suggest why sunspots observed in a sunspot cycle's declining phase tend to violate the hemispheric helicity rule, and (5) support a previously proposed amended Babcock scenario for the sunspot cycle's dynamo process. Because the proposed convection-based heuristic model for making a sunspot-BMR  $\Omega$  loop avoids having  $\sim 105$  G field in the initial flux rope at the bottom of the convection zone, it is an appealing alternative to the present magnetic-buoyancy-based standard scenario and warrants testing by high-enough-resolution giant-cell magnetoconvection simulations.

## **Onset of the Magnetic Explosion in Solar Polar Coronal X-Ray Jets**

Ronald L. Moore<sup>1,2</sup>, Alphonse C. Sterling<sup>1</sup>, and Navdeep K. Panesar<sup>1</sup>

2018 ApJ 859 3

<http://sci-hub.tw/http://iopscience.iop.org/0004-637X/859/1/3/>

<https://arxiv.org/ftp/arxiv/papers/1805/1805.12182.pdf>

We follow up on the Sterling et al. discovery that nearly all polar coronal X-ray jets are made by an explosive eruption of a closed magnetic field carrying a miniature filament in its core. In the same X-ray and EUV movies used by Sterling et al., we examine the onset and growth of the driving magnetic explosion in 15 of the 20 jets that they studied. We find evidence that (1) in a large majority of polar X-ray jets, the runaway internal/tether-cutting reconnection under the erupting minifilament flux rope starts after both the minifilament's rise and the spire-producing external/breakout reconnection have started; and (2) in a large minority, (a) before the eruption starts, there is a current sheet between the explosive closed field and the ambient open field, and (b) the eruption starts with breakout reconnection at that current sheet. The variety of event sequences in the eruptions supports the idea that the magnetic explosions that make polar X-ray jets work the same way as the much larger magnetic explosions that make a flare and coronal mass ejection (CME). That idea and recent observations indicating that magnetic flux cancellation is the fundamental process that builds the field in and around the pre-jet minifilament and triggers that field's jet-driving explosion together suggest that flux

cancellation inside the magnetic arcade that explodes in a flare/CME eruption is usually the fundamental process that builds the explosive field in the core of the arcade and triggers that field's explosion.

Aug 28 2010, Sep 8 2010, Sep 17 2010,

Table 1 Our Polar X-Ray Jets with Times of Events Observed in Them by Hinode/XRT or SDO/AIA (2010)

### **THE COOL COMPONENT AND THE DICHOTOMY, LATERAL EXPANSION, AND AXIAL ROTATION OF SOLAR X-RAY JETS**

Ronald L. Moore<sup>1</sup>, Alphonse C. Sterling<sup>1,2,3</sup>, David A. Falconer<sup>1,2,3</sup>, and Dominic Robe

2013 ApJ 769 134

We present results from a study of 54 polar X-ray jets that were observed in coronal X-ray movies from the X-ray Telescope on Hinode and had simultaneous coverage in movies of the cooler transition region ( $T \sim 105$  K) taken in the He II 304 Å band of the Atmospheric Imaging Assembly (AIA) on Solar Dynamics Observatory. These dual observations verify the standard-jet/blowout-jet dichotomy of polar X-ray jets previously found primarily from XRT movies alone. In accord with models of blowout jets and standard jets, the AIA 304 Å movies show a cool ( $T \sim 105$  K) component in nearly all blowout X-ray jets and in a small minority of standard X-ray jets, obvious lateral expansion in blowout X-ray jets but none in standard X-ray jets, and obvious axial rotation in both blowout X-ray jets and standard X-ray jets. In our sample, the number of turns of axial rotation in the cool-component standard X-ray jets is typical of that in the blowout X-ray jets, suggesting that the closed bipolar magnetic field in the jet base has substantial twist not only in all blowout X-ray jets but also in many standard X-ray jets. We point out that our results for the dichotomy, lateral expansion, and axial rotation of X-ray jets add credence to published speculation that type-II spicules are miniature analogs of X-ray jets, are generated by granule-size emerging bipoles, and thereby carry enough energy to power the corona and solar wind.

### **THE LIMIT OF MAGNETIC-SHEAR ENERGY IN SOLAR ACTIVE REGIONS**

Ronald L. Moore<sup>1</sup>, David A. Falconer<sup>1,2,3</sup>, and Alphonse C. Sterling

2012 ApJ 750 24

It has been found previously, by measuring from active-region magnetograms a proxy of the free energy in the active region's magnetic field, (1) that there is a sharp upper limit to the free energy the field can hold that increases with the amount of magnetic field in the active region, the active region's magnetic flux content, and (2) that most active regions are near this limit when their field explodes in a coronal mass ejection/flare eruption. That is, explosive active regions are concentrated in a main-sequence path bordering the free-energy-limit line in (flux content, free-energy proxy) phase space. Here, we present evidence that specifies the underlying magnetic condition that gives rise to the free-energy limit and the accompanying main sequence of explosive active regions. Using a suitable free-energy proxy measured from vector magnetograms of 44 active regions, we find evidence that (1) in active regions at and near their free-energy limit, the ratio of magnetic-shear free energy to the non-free magnetic energy the potential field would have is of the order of one in the core field, the field rooted along the neutral line, and (2) this ratio is progressively less in active regions progressively farther below their free-energy limit. Evidently, most active regions in which this core-field energy ratio is much less than one cannot be triggered to explode; as this ratio approaches one, most active regions become capable of exploding; and when this ratio is one, most active regions are compelled to explode.

### **Observed Aspects of Reconnection in Solar Eruptions**

Ronald L. Moore · Alphonse C. Sterling · G. Allen Gary · Jonathan W. Cirtain · David A. Falconer

Space Sci Rev., 2011, File

The observed magnetic field configuration and signatures of reconnection in the large solar magnetic eruptions that make major flares and coronal mass ejections and in the much smaller magnetic eruptions that make X-ray jets are illustrated with cartoons and representative observed eruptions. The main reconnection signatures considered are the imaged bright emission from the heated plasma on reconnected field lines. In any of these eruptions, large or small, the magnetic field that drives the eruption and/or that drives the buildup to the eruption is initially a closed bipolar arcade. From the form and configuration of the magnetic field in and around the driving arcade and from the development of the reconnection signatures in coordination with the eruption, we infer that (1) at the onset of reconnection the reconnection current sheet is small compared to the driving arcade, and (2) the current sheet can grow to the size of the driving arcade only after reconnection starts and the unleashed erupting field dynamically forces the current sheet to grow much larger, building it up faster than the reconnection can tear it down. We conjecture that the fundamental reason the quasi-static pre-eruption field is prohibited from having a large current sheet is that the magnetic pressure is much greater than the plasma pressure in the chromosphere and low corona in eruptive solar magnetic fields.

### **THE WIDTH OF A SOLAR CORONAL MASS EJECTION AND THE SOURCE OF THE DRIVING MAGNETIC EXPLOSION: A TEST OF THE STANDARD SCENARIO FOR CME PRODUCTION**

Ronald L. Moore, Alphonse C. Sterling, and Steven T. Suess

The Astrophysical Journal, 668:1221Y1231, 2007, File

We show that the strength ( $B_{\text{Flare}}$ ) of the magnetic field in the area covered by the flare arcade following a CME producing ejective solar eruption can be estimated from the final angular width ( $\text{Final}_{\text{CME}}$ ) of the CME in the outer corona and the final angular width ( $\text{Final}_{\text{Flare}}$ ) of the flare arcade:  $B_{\text{Flare}} \approx 1.4 \text{ Final}_{\text{CME}} \rho_{\text{Flare}} S_{\text{Flare}} \text{ G}$ .

In this paper, we present a way to assess, from the width of the CME and the area and magnetic location of the flare, whether the CME exploded from the flare site.

## **THE CORONAL-DIMMING FOOTPRINT OF A STREAMER-PUFF CORONAL MASS EJECTION: CONFIRMATION OF THE MAGNETIC-ARCH-BLOWOUT SCENARIO**

Ronald L. **Moore** and Alphonse C. Sterling

The Astrophysical Journal, 661:543Y550, 2007

Streamer-puff CMEs are a subclass (one variety) of a broader class of “over-and-out” CMEs that are often much larger than streamer puffs but are similar to them in that they are produced by the blowout of a large quasi-potential magnetic arch by a magnetic explosion that erupts from one foot of the large arch, where it is marked by a filament eruption and/or an ejective flare.

## **Initiation of Coronal Mass Ejections (Review)**

Ronald L. **Moore** and Alphonse C. Sterling

AGU Geophysical Monograph 165, Solar Eruptions and Energetic Particles, ed. N. Gopalswamy, R. Mewaldt, & J. Torsti, p. 43, 2006; **File**

We describe three different mechanisms that singly or in combination can trigger the explosion: (1) runaway internal tether-cutting reconnection, (2) runaway external tether-cutting reconnection, and (3) ideal MHD instability or loss of equilibrium.

## **Onset of the Magnetic Explosion in Solar Flares and Coronal Mass Ejections**

Ronald L. **Moore**<sup>1</sup>, Alphonse C. Sterling<sup>1,4</sup>, Hugh S. Hudson<sup>2</sup>, and James R. Lemen<sup>3</sup>  
2001 ApJ 552 833

<https://iopscience.iop.org/article/10.1086/320559/pdf>

We present observations of the magnetic field configuration and its transformation in six solar eruptive events that show good agreement with the standard bipolar model for eruptive flares. The observations are X-ray images from the Yohkoh soft X-ray telescope (SXT) and magnetograms from Kitt Peak National Solar Observatory, interpreted together with the 1-8 Å X-ray flux observed by GOES. The observations yield the following interpretation. (1) Each event is a magnetic explosion that occurs in an initially closed single bipole in which the core field is sheared and twisted in the shape of a sigmoid, having an oppositely curved elbow on each end. The arms of the opposite elbows are sheared past each other so that they overlap and are crossed low above the neutral line in the middle of the bipole. The elbows and arms seen in the SXT images are illuminated strands of the sigmoidal core field, which is a continuum of sheared/twisted field that fills these strands as well as the space between and around them. (2) Although four of the explosions are ejective (appearing to blow open the bipole) and two are confined (appearing to be arrested within the closed bipole), all six begin the same way. In the SXT images, the explosion begins with brightening and expansion of the two elbows together with the appearance of short bright sheared loops low over the neutral line under the crossed arms and, rising up from the crossed arms, long strands connecting the far ends of the elbows. (3) All six events are single-bipole events in that during the onset and early development of the explosion they show no evidence for reconnection between the exploding bipole and any surrounding magnetic fields. We conclude that in each of our events the magnetic explosion was unleashed by runaway tether-cutting via implosive/explosive reconnection in the middle of the sigmoid, as in the standard model. The similarity of the onsets of the two confined explosions to the onsets of the four ejective explosions and their agreement with the model indicate that runaway reconnection inside a sheared core field can begin whether or not a separate system of overlying fields, or the structure of the bipole itself, allows the explosion to be ejective. Because this internal reconnection apparently begins at the very start of the sigmoid for the onset and growth of the magnetic explosion in eruptive flares and coronal mass ejections. **24-25 Feb 1992, 12 Jul 1992, 17-18 Dec 1993, 28 Feb 1994, 19-20 Oct 1994, 13 Nov 1994**

## **Energy and helicity evolution in a flux emergence simulation**

K. **Moraitis**<sup>1,✉</sup>, V. Archontis<sup>1</sup> and G. Chouliaras<sup>2</sup>

A&A, 690, A181 (2024)

<https://doi.org/10.1051/0004-6361/202450924>

<https://www.aanda.org/articles/aa/pdf/2024/10/aa50924-24.pdf>

**Aims.** The main aim of this work is to study the evolution of the recently introduced relative helicity of the magnetic polarity inversion line (PIL) in a magnetohydrodynamics simulation.

**Methods.** The simulation used is a typical flux emergence simulation in which there is additionally an oblique, pre-existing magnetic field. The interaction of the emerging and ambient fields produces intense coronal activity, with four jets standing out. The 3D magnetic field allows us to compute various energies and helicities, and to study their evolution during the simulation, especially around the identified jets. We examine the evolution of all quantities in three different regions: in the whole volume, in three separate subvolumes of the whole volume, and in a 2D region around the PIL on the photosphere.

**Results.** We find that the helicities are in general more responsive to the jets, followed by the free energy. The eruptivity index, the ratio of the current-carrying helicity to the relative helicity, does not show the typical behaviour it has in

other cases, as its variations do not follow the production of the jets. By considering the subvolumes we find that the magnetic field gets more potential and less helical with height. The PIL relative helicity confirms the recent results it showed in observed active regions, exhibiting stronger variations during the jets compared to the standard relative helicity. Moreover, the current-carrying helicity around the PIL has a similar behaviour to the PIL relative helicity, and so this quantity could be equally useful in solar eruptivity studies.

## Using relative field line helicity as an indicator for solar eruptivity

[K. Moraitis](#), [S. Patsourakos](#), [A. Nindos](#), [J.K. Thalmann](#), [É. Pariat](#)

A&A 683, A87 (2024)

<https://arxiv.org/pdf/2312.13950.pdf>

<https://www.aanda.org/articles/aa/pdf/2024/03/aa48275-23.pdf>

Context. Relative field line helicity (RFLH) is a recently developed quantity which can approximate the density of relative magnetic helicity.

Aims. This paper aims to determine whether RFLH can be used as an indicator of solar eruptivity. Methods. Starting from magnetographic observations from the Helioseismic and Magnetic Imager instrument onboard the Solar Dynamic Observatory of a sample of seven solar active regions (ARs), which comprises over 2000 individual snapshots, we reconstruct the AR's coronal magnetic field with a widely-used non-linear force-free method. This enables us to compute RFLH using two independent gauge conditions for the vector potentials. We focus our study around the times of strong flares in the ARs, above the M class, and in regions around the polarity inversion lines (PILs) of the magnetic field, and of RFLH.

Results. We find that the temporal profiles of the relative helicity that is contained in the magnetic PIL follow those of the relative helicity that is computed by the accurate volume method for the whole AR. Additionally, the PIL relative helicity can be used to define a parameter similar to the well-known parameter R (Schrijver 2007), whose high values are related with increased flaring probability. This helicity-based R-parameter correlates well with the original one, showing in some cases even higher values, and additionally, it experiences more pronounced decreases during flares. This means that there exists at least one parameter deduced from RFLH, that has important value as a solar eruptivity indicator. **12-16 February 2011, 3-4 August 2011, 12 July 2012, 18-25 November 2012, 5-13 November 2013, 20-25 October 2014, 6 September 2017**

## Magnetic helicity and eruptivity in active region 12673

[K. Moraitis](#), [X. Sun](#), [E. Pariat](#), [L. Linan](#)

A&A 2019

<https://arxiv.org/abs/1907.06365>

Context. In **September 2017** the largest X-class flare of Solar Cycle 24 occurred from the most active region (AR) of this cycle, AR 12673. The AR attracted much interest because of its unique morphological and evolution characteristics. Among the parameters examined in the AR was magnetic helicity, but either only approximately, and/or intermittently.

Aims. This work is interested in studying the evolution of the relative magnetic helicity and of the two components of its decomposition, the non-potential, and the volume-threading one, in the time interval around the highest activity of AR 12673. Special emphasis is given on the study of the ratio of the non-potential to total helicity, that was recently proposed as an indicator of ARs eruptivity. Methods. For these, we first approximate the coronal magnetic field of the AR with two different optimization-based extrapolation procedures, and choose the one that produces the most reliable helicity value at each instant. Moreover, in one of these methods, we weight the optimization by the uncertainty estimates derived from the Helioseismic and Magnetic Imager (HMI) instrument, for the first time. We then follow an accurate method to compute all quantities of interest. Results. The first observational determination of the evolution of the non-potential to total helicity ratio seems to confirm the quality it has in indicating eruptivity. This ratio increases before the major flares of AR 12673, and afterwards it relaxes to smaller values. Additionally, the evolution patterns of the various helicity, and energy budgets of AR 12673 are discussed and compared with other works. **6 Sept 2017**

## THREE-DIMENSIONAL POLARIMETRIC CORONAL MASS EJECTION LOCALIZATION TESTED THROUGH TRIANGULATION

Thomas G. [Moran](#)<sup>1,2</sup>, Joseph M. Davila<sup>3</sup>, and William T. Thompson<sup>4</sup>

*Astrophysical Journal*, 712:453–458, **2010** March, **File**

We have tested the validity of the coronal mass ejection (CME) polarimetric reconstruction technique for the first time using triangulation and demonstrated that it can provide the angle and distance of CMEs to the plane of the sky. In this study, we determined the three-dimensional orientation of the CMEs that occurred on 2007 August 21 and 2007 December 31 using polarimetric observations obtained simultaneously with the *Solar Terrestrial Relations Observatory*/Sun Earth Connection Coronal and Heliospheric Investigation spacecraft COR1-A and COR1-B coronagraphs. We obtained the CME orientations using both the triangulation and polarimetric techniques and found that angles to the sky plane yielded by the two methods agree to within  $\approx 5^\circ$ , validating the polarimetric reconstruction technique used to analyze CMEs observed with the *Solar and Heliospheric Observatory*/Large Angle Spectrometric Coronagraph. In addition, we located the CME source regions using EUV and magnetic field measurements and found that the corresponding mean angles to the sky plane of those regions agreed with those yielded by the geometric and polarimetric methods within uncertainties. Furthermore, we compared

the locations provided by polarimetric COR1 analysis with those determined from other analyses using COR2 observations combined with geometric techniques and forward modeling. We found good agreement with those studies relying on geometric techniques but obtained results contradictory to those provided by forward modeling.

## **Energy and helicity evolution in a flux emergence simulation**

[K. Moraitis](#), [V. Archontis](#), [G. Chouliaras](#)

A&A 2024

<https://arxiv.org/pdf/2409.02445>

**Aims.** The main aim of this work is to study the evolution of the recently introduced relative helicity of the magnetic polarity inversion line (PIL) in a magnetohydrodynamics simulation. **Methods.** The simulation used is a typical flux emergence simulation in which there is additionally an oblique, pre-existing magnetic field. The interaction of the emerging and ambient fields produces intense coronal activity, with four jets standing out. The 3D magnetic field allows us to compute various energies and helicities, and to study their evolution during the simulation, especially around the identified jets. We examine the evolution of all quantities in three different regions: in the whole volume, in three separate subvolumes of the whole volume, and in a 2D region around the PIL on the photosphere. **Results.** We find that the helicities are in general more responsive to the jets, followed by the free energy. The eruptivity index, the ratio of the current-carrying helicity to the relative helicity, does not show the typical behaviour it has in other cases, as its variations do not follow the production of the jets. By considering the subvolumes we find that the magnetic field gets more potential and less helical with height. The PIL relative helicity confirms the recent results it showed in observed active regions, exhibiting stronger variations during the jets compared to the standard relative helicity. Moreover, the current-carrying helicity around the PIL has a similar behaviour to the PIL relative helicity, and so this quantity could be equally useful in solar eruptivity studies.

## **Relative field line helicity of a large eruptive solar active region**

[K. Moraitis](#), [S. Patsourakos](#), [A. Nindos](#)

A&A 649, A107 2021

<https://arxiv.org/pdf/2103.03643.pdf>

<https://www.aanda.org/articles/aa/pdf/2021/05/aa40384-21.pdf>

<https://doi.org/10.1051/0004-6361/202140384>

**Context.** Magnetic helicity is a physical quantity of great importance in the study of astrophysical and natural plasmas. Although a density for helicity cannot be defined, a good proxy for it is field line helicity. The appropriate quantity for use in solar conditions is relative field line helicity (RFLH). **Aims.** This work aims to study in detail the behaviour of RFLH, for the first time, in a solar active region (AR). **Methods.** The target active region is the large, eruptive AR 11158. In order to compute RFLH and all other quantities of interest we use a non-linear force-free reconstruction of the AR coronal magnetic field of excellent quality. **Results.** We find that the photospheric morphology of RFLH is quite different than that of the magnetic field or of the electrical current, and this is not sensitive to the chosen gauge in the computation of RFLH. The value of helicity experiences a large decrease, 25% of its pre-flare value, during an X-class flare of the AR, a change that is also depicted in the photospheric morphology of RFLH. Moreover, the area of this change coincides with the area that encompasses the flux rope, the magnetic structure that later erupted. **Conclusions.** The use of RFLH can provide important information about the value and location of the magnetic helicity expelled from the solar atmosphere during eruptive events. **15 February 2011**

## **PLASMA JETS AND ERUPTIONS IN SOLAR CORONAL HOLES: A THREE-DIMENSIONAL FLUX EMERGENCE EXPERIMENT**

F. [Moreno-Insertis](#)<sup>1,2</sup> and K. Galsgaard

2013 ApJ 771 20

A three-dimensional (3D) numerical experiment of the launching of a hot and fast coronal jet followed by several violent eruptions is analyzed in detail. These events are initiated through the emergence of a magnetic flux rope from the solar interior into a coronal hole. We explore the evolution of the emerging magnetically dominated plasma dome surmounted by a current sheet and the ensuing pattern of reconnection. A hot and fast coronal jet with inverted-Y shape is produced that shows properties comparable to those frequently observed with EUV and X-ray detectors. We analyze its 3D shape, its inhomogeneous internal structure, and its rise and decay phases, lasting for some 15-20 minutes each. Particular attention is devoted to the field line connectivities and the reconnection pattern. We also study the cool and high-density volume that appears to encircle the emerged dome. The decay of the jet is followed by a violent phase with a total of five eruptions. The first of them seems to follow the general pattern of tether-cutting reconnection in a sheared arcade, although modified by the field topology created by the preceding reconnection evolution. The two following eruptions take place near and above the strong-field concentrations at the surface. They show a twisted,  $\Omega$ -loop-like rope expanding in height, with twist being turned into writhe, thus hinting at a kink instability (perhaps combined with a torus instability) as the cause of the eruption. The succession of a main jet ejection and a number of violent eruptions that resemble mini-CMEs and their physical properties suggest that this experiment may provide a model for the blowout jets recently proposed in the literature.

## **An atlas of coronal electron density at 5Rs I: Data processing and calibration**

Huw [Morgan](#)

<http://arxiv.org/pdf/1509.03113.pdf>

Astrophysical Journal Supplement Series, Volume 219, Issue 2, article id. 23, 21 pp. 2015

Tomography of the solar corona can provide crucial constraints for models of the low corona, unique information on changes in coronal structure and rotation rates, and a valuable boundary condition for models of the heliospheric solar wind. This is the first of a series of three papers which aim to create a set of maps of the coronal density over an extended period (1996-present). The papers will describe the data processing and calibration (this paper), the tomography method (paperii) and resulting atlas of coronal electron density at a height of  $5R_s$  between years 1996-2014 (paperiii). This first paper presents a detailed description of data processing and calibration for the Large-Angle and Spectrometric Coronagraph (LASCO) C2 instrument onboard the Solar and Heliospheric Observatory (SOHO) and the COR2 instruments of the Sun Earth Connection Coronal and Heliospheric Investigation (SECCHI) package aboard the Solar Terrestrial Relations Observatory (STEREO) A & B spacecraft. The methodology includes noise suppression, background subtraction, separation of large dynamic events, conversion of total brightness to K-coronal brightness and simple functions for crosscalibration between C2/LASCO and COR2/SECCHI. Comparison of the brightness of stars between LASCO C2 total and polarized brightness ( $pB$ ) observations provide in-flight calibration factors for the  $pB$  observations, resulting in considerable improved agreement between C2 and COR2 A, and elimination of curious artifacts in the C2  $pB$  images. The crosscalibration between LASCO C2 and the STEREO coronagraphs allows, for the first time, the potential use of multi-spacecraft coronagraph data for tomography and for CME analysis.

## **THE EXPANSION OF ACTIVE REGIONS INTO THE EXTENDED SOLAR CORONA**

Huw [Morgan](#)<sup>1,2,3</sup>, Lauren Jeska<sup>1</sup>, and Drew Leonard

2013 ApJS 206 19

Advanced image processing of Large Angle and Spectrometric Coronagraph Experiment (LASCO) C2 observations reveals the expansion of the active region closed field into the extended corona. The nested closed-loop systems are large, with an apparent latitudinal extent of  $50^\circ$ , and expanding to heights of at least  $12 R_\odot$ . The expansion speeds are  $\sim 10 \text{ km s}^{-1}$  in the AIA/SDO field of view, below  $\sim 20 \text{ km s}^{-1}$  at  $2.3 R_\odot$ , and accelerate linearly to  $\sim 60 \text{ km s}^{-1}$  at  $5 R_\odot$ . They appear with a frequency of one every  $\sim 3 \text{ hr}$  over a time period of around three days. They are not coronal mass ejections (CMEs) since their gradual expansion is continuous and steady. They are also faint, with an upper limit of 3% of the brightness of background streamers. Extreme ultraviolet images reveal continuous birth and expansion of hot, bright loops from a new active region at the base of the system. The LASCO images show that the loops span a radial fan-like system of streamers, suggesting that they are not propagating within the main coronal streamer structure. The expanding loops brighten at low heights a few hours prior to a CME eruption, and the expansion process is temporarily halted as the closed field system is swept away. Closed magnetic structures from some active regions are not isolated from the extended corona and solar wind, but can expand to large heights in the form of quiescent expanding loops.

## **AUTOMATICALLY DETECTING AND TRACKING CORONAL MASS EJECTIONS. I. SEPARATION OF DYNAMIC AND QUIESCENT COMPONENTS IN CORONAGRAPH IMAGES**

Huw [Morgan](#)<sup>1,2</sup>, Jason P. Byrne<sup>2</sup>, and Shadia Rifai Habba

2012 ApJ 752 144, [File](#)

Automated techniques for detecting and tracking coronal mass ejections (CMEs) in coronagraph data are of ever increasing importance for space weather monitoring and forecasting. They serve to remove the biases and tedium of human interpretation, and provide the robust analysis necessary for statistical studies across large numbers of observations. An important requirement in their operation is that they satisfactorily distinguish the CME structure from the background quiescent coronal structure (streamers, coronal holes). Many studies resort to some form of time differencing to achieve this, despite the errors inherent in such an approach—notably spatiotemporal crosstalk. This article describes a new deconvolution technique that separates coronagraph images into quiescent and dynamic components. A set of synthetic observations made from a sophisticated model corona and CME demonstrates the validity and effectiveness of the technique in isolating the CME signal. Applied to observations by the LASCO C2 and C3 coronagraphs, the structure of a faint CME is revealed in detail despite the presence of background streamers that are several times brighter than the CME. The technique is also demonstrated to work on SECCHI/COR2 data, and new possibilities for estimating the three-dimensional structure of CMEs using the multiple viewing angles are discussed. Although quiescent coronal structures and CMEs are intrinsically linked, and although their interaction is an unavoidable source of error in any separation process, we show in a companion paper that the deconvolution approach outlined here is a robust and accurate method for rigorous CME analysis. Such an approach is a prerequisite to the higher-level detection and classification of CME structure and kinematics.

## **A Method for Separating Coronal Mass Ejections from the Quiescent Corona**

Huw [Morgan](#) and Shadia Habbal

Astrophysical Journal, 711:631–640, **2010** March, **File**

A method for separating coronal mass ejections (CMEs) from the quiescent corona in white-light coronagraph images is presented. Such a separation allows the study of CME structure, as well as enabling a study of the quiescent coronal structure, without contamination by the CME. The fact that the large-scale quiescent corona is very close to radial, whilst CMEs are highly non-radial, enables the separation of the two components. The method is applied to Large Angle Spectrometric Coronagraph/*Solar and Heliospheric Observatory* C2 and C3 observations, and is successful in revealing CME signal, faint CMEs and blobs, and dark rarefactions within a CME. The success of the separation is tested at solar minimum, a time when streamers are in general most non-radial. The technique is also compared to other commonly used methods. The separation method enables (1) the study of extremely faint CME structure, down to almost the noise level of the coronagraphs, (2) paves the way for automated categorization of CME internal structure, and (3) provides a cleaner basis for tomography of the quiescent corona, without contamination from CMEs.

### **Moving solar radio bursts and their association with coronal mass ejections**

[D. E. Morosan](#), [A. Kumari](#), [E. K. J. Kilpua](#), [A. Hamini](#)

A&A 2021

<https://arxiv.org/pdf/2103.05942.pdf>

Context: Solar eruptions, such as coronal mass ejections (CMEs), are often accompanied by accelerated electrons that can in turn emit radiation at radio wavelengths. This radiation is observed as solar radio bursts. The main types of bursts associated with CMEs are type II and type IV bursts that can sometimes show movement in the direction of the CME expansion, either radially or laterally. However, the propagation of radio bursts with respect to CMEs has only been studied for individual events.

Aims: Here, we perform a statistical study of 64 moving bursts with the aim to determine how often CMEs are accompanied by moving radio bursts. This is done in order to ascertain the usefulness of using radio images in estimating the early CME expansion.

Methods: Using radio imaging from the Naçay Radioheliograph (NRH), we constructed a list of moving radio bursts, defined as bursts that move across the plane of sky at a single frequency. We define their association with CMEs and the properties of associated CMEs using white-light coronagraph observations. We also determine their connection to classical type II and type IV radio burst categorisation.

Results: We find that just over a quarter of type II and half of type IV bursts that occurred during the NRH observing windows in Solar Cycle 24 are accompanied by moving radio emission. All but one of the moving radio bursts are associated with white--light CMEs and the majority of moving bursts (90%) are associated with wide CMEs (>60 degrees in width). In particular, all but one of the moving bursts corresponding to type IIs are associated with wide CMEs; however, and unexpectedly, the majority of type II moving bursts are associated with slow white-light CMEs (<500 km/s). On the other hand, the majority of moving type IV bursts are associated with fast CMEs (>500 km/s). **14**

**June 2012**

### **Electron acceleration and radio emission following the early interaction of two coronal mass ejections**

[D. E. Morosan](#), [E. Palmerio](#)<sup>1</sup>, [J. E. Räsänen](#), [E. K. J. Kilpua](#), [J. Magdalenic](#), [B. J. Lynch](#), [A. Kumari](#), [J. Pomoell](#), [M. Palmroth](#)

A&A 642, A151 **2020**

<https://arxiv.org/pdf/2008.10245.pdf>

<https://doi.org/10.1051/0004-6361/202038801>

Context. Coronal mass ejections (CMEs) are large eruptions of magnetised plasma from the Sun that are often accompanied by solar radio bursts produced by accelerated electrons.

Aims. A powerful source for accelerating electron beams are CME-driven shocks, however, there are other mechanisms capable of accelerating electrons during a CME eruption. So far, studies have relied on the traditional classification of solar radio bursts into five groups (Type I-V) based mainly on their shapes and characteristics in dynamic spectra. Here, we aim to determine the origin of moving radio bursts associated with a CME that do not fit into the present classification of the solar radio emission.

Methods. By using radio imaging from the Naçay Radioheliograph, combined with observations from the Solar Dynamics Observatory, Solar and Heliospheric Observatory, and Solar Terrestrial Relations Observatory spacecraft, we investigate the moving radio bursts accompanying two subsequent CMEs on **22 May 2013**. We use three-dimensional reconstructions of the two associated CME eruptions to show the possible origin of the observed radio emission.

Results. We identified three moving radio bursts at unusually high altitudes in the corona that are located at the northern CME flank and move outwards synchronously with the CME. The radio bursts correspond to fine-structured emission in dynamic spectra with durations of ~1 s, and they may show forward or reverse frequency drifts. Since the CME expands closely following an earlier CME, a low coronal CME-CME interaction is likely responsible for the observed radio emission.

### **Three-dimensional reconstruction of multiple particle acceleration regions during a coronal mass ejection★**

D. E. [Morosan](#)<sup>1</sup>, [E. Palmerio](#)<sup>1,2</sup>, [J. Pomoell](#)<sup>1</sup>, [R. Vainio](#)<sup>3</sup>, [M. Palmroth](#)<sup>1,4</sup> and [E. K. J. Kilpua](#)<sup>1</sup>

A&A 635, A62 (2020)

<https://arxiv.org/pdf/2001.08473.pdf>

<https://doi.org/10.1051/0004-6361/201937133>

Context. Some of the most prominent sources for particle acceleration in our Solar System are large eruptions of magnetised plasma from the Sun called coronal mass ejections (CMEs). These accelerated particles can generate radio emission through various mechanisms.

Aims. CMEs are often accompanied by a variety of solar radio bursts with different shapes and characteristics in dynamic spectra. Radio bursts directly associated with CMEs often show movement in the direction of CME expansion. Here, we aim to determine the emission mechanism of multiple moving radio bursts that accompanied a flare and CME that took place on **14 June 2012**.

Methods. We used radio imaging from the Nançay Radioheliograph, combined with observations from the Solar Dynamics Observatory and Solar Terrestrial Relations Observatory spacecraft, to analyse these moving radio bursts in order to determine their emission mechanism and three-dimensional (3D) location with respect to the expanding CME. Results. In using a 3D representation of the particle acceleration locations in relation to the overlying coronal magnetic field and the CME propagation, for the first time, we provide evidence that these moving radio bursts originate near the CME flanks and that some are possible signatures of shock-accelerated electrons following the fast CME expansion in the low corona.

Conclusions. The moving radio bursts, as well as other stationary bursts observed during the eruption, occur simultaneously with a type IV continuum in dynamic spectra, which is not usually associated with emission at the CME flanks. Our results show that moving radio bursts that could traditionally be classified as moving type IVs can represent shock signatures associated with CME flanks or plasma emission inside the CME behind its flanks, which are closely related to the lateral expansion of the CME in the low corona. In addition, the acceleration of electrons generating this radio emission appears to be favoured at the CME flanks, where the CME encounters coronal streamers and open field regions.

Movies associated to Fig. 1 are available at <https://www.aanda.org>

## Multiple regions of shock-accelerated particles during a solar coronal mass ejection

**Morosan**, Diana E.; Carley, Eoin P.; Hayes, Laura A.; Murray, Sophie A.; Zucca, Pietro; Fallows, Richard A.; McCauley, Joe; Kilpua, Emilia K. J.; Mann, Gottfried; Vocks, Christian; Gallagher, Peter T.

Nature Astronomy Volume 3, p. 452-461 **2019**

[sci-hub.se/10.1038/s41550-019-0689-z](https://arxiv.org/abs/1810.08473)

<https://www.nature.com/articles/s41550-019-0689-z.pdf>

[https://www.researchgate.net/publication/331183002\\_Multiple\\_regions\\_of\\_shock-accelerated\\_particles\\_during\\_a\\_solar\\_coronal\\_mass\\_ejection](https://www.researchgate.net/publication/331183002_Multiple_regions_of_shock-accelerated_particles_during_a_solar_coronal_mass_ejection)

The Sun is an active star that can launch large eruptions of magnetized plasma into the heliosphere, known as coronal mass ejections (CMEs). These can drive shocks that accelerate particles to high energies, often resulting in radio emission at low frequencies (<200 MHz). So far, the relationship between the expansion of CMEs, shocks and particle acceleration is not well understood, partly due to the lack of radio imaging at low frequencies during the onset of shock-producing CMEs. Here, we report multi-instrument radio, white-light and ultraviolet imaging of the second largest flare in solar cycle 24 (2008–present) and its associated fast CME ( $3,038 \pm 288$  km s<sup>-1</sup>). We identify the location of a multitude of radio shock signatures, called herringbones, and find evidence for shock-accelerated electron beams at multiple locations along the expanding CME. These observations support theories of non-uniform, rippled shock fronts driven by an expanding CME in the solar corona. **10 September 2017**

**RHESSI Science Nuggets # 348 Apr 2019**

[http://sprg.ssl.berkeley.edu/~tohban/wiki/index.php/Multiple\\_Regions\\_of\\_Shock-accelerated\\_Particles\\_during\\_a\\_Solar\\_Coronal\\_Mass\\_Ejection](http://sprg.ssl.berkeley.edu/~tohban/wiki/index.php/Multiple_Regions_of_Shock-accelerated_Particles_during_a_Solar_Coronal_Mass_Ejection)

## The Association of a J-burst with a Solar Jet

D. E. **Morosan**, P. T. Gallagher, R. A. Fallows, [H. Reid](#), [G. Mann](#), [M. M. Bisi](#), [J. Magdalenic](#), .....

A&A 606, A81 **2017**

<https://arxiv.org/pdf/1707.03428.pdf>

The Sun is an active star that produces large-scale energetic events such as solar flares and coronal mass ejections and numerous smaller-scale events such as solar jets. These events are often associated with accelerated particles that can cause emission at radio wavelengths. The reconfiguration of the solar magnetic field in the corona is believed to be the cause of the majority of solar energetic events and accelerated particles. Here, we investigate a bright J-burst that was associated with a solar jet and the possible emission mechanism causing these two phenomena. Methods. We used data from the Solar Dynamics Observatory (SDO) to observe a solar jet, and radio data from the Low Frequency Array (LOFAR) and the Nançay Radioheliograph (NRH) to observe a J-burst over a broad frequency range (33–173 MHz) on **9 July 2013** at ~11:06 UT. The J-burst showed fundamental and harmonic components and it was associated with a solar jet observed at extreme ultraviolet wavelengths with SDO. The solar jet occurred at a time and location coincident with the radio burst with a velocity of 510 km s<sup>-1</sup>. The jet occurred in the northern hemisphere in the negative polarity region of an extended area of bipolar plage as opposed to a group of complex active regions in the southern hemisphere. Newly emerged positive flux in the negative magnetic polarity region of the bipolar plage appeared to be the trigger of



the jet. Radio imaging showed that the J-burst emitting electrons originated in a region above the newly emerged magnetic field of positive polarity and then followed long, closed magnetic field lines.

## The Impact of Geometry on Observations of CME Brightness and Propagation

J.S. [Morrill](#) · R.A. Howard · A. Vourlidas · D.F. Webb · V. Kunkel

Solar Phys (2009) 259: 179–197, [File](#)

Coronal mass ejections (CMEs) have a significant impact on space weather and geomagnetic storms and so have been the subject of numerous studies. Most CME observations have been made while these events are near the Sun (*e.g.*, SOHO/LASCO). Recent data from the *Coriolis*/SMEI and STEREO/SECCHI-HI instruments have imaged CMEs farther into the heliosphere. Analyses of CME observations near the Sun measure the properties of these events by assuming that the emission is in the plane of the sky and hence the speed and mass are lower limits to the true values. However, this assumption cannot be used to analyze optical observations of CMEs far from the Sun, such as observations from SMEI and SECCHI-HI, since the CME source is likely to be far from the limb. In this paper we consider the geometry of observations made by LASCO, SMEI, and SECCHI. We also present results that estimate both CME speed and trajectory by fitting the CME elongations observed by these instruments. Using a constant CME speed does not generally produce profiles that fit observations at both large and small elongation, simultaneously. We include the results of a simple empirical model that alters the CME speed to an estimated value of the solar wind speed to simulate the effect of drag on the propagating CME. This change in speed improves the fit between the model and observations over a broad range of elongations.

## Observations of quasi-periodic phenomena associated with a large blowout solar jet

R. J. [Morton](#), A. K. Srivastava, R. Erd'elyi

E-print, April 2012, [A&A](#)

A variety of periodic phenomena have been observed in conjunction with large solar jets. We aim to find further evidence for {(quasi-)}periodic behaviour in solar jets and determine what the periodic behaviour can tell us about the excitation mechanism and formation process of the large solar jet. Using the 304 {AA} (He-II), 171 {AA} (Fe IX), 193 {AA} (Fe XII/XXIV) and 131 {AA} (Fe VIII/XXI) filters on-board the Solar Dynamic Observatory (SDO) Atmospheric Imaging Assembly (AIA), we investigate the intensity oscillations associated with a solar jet. Evidence is provided for multiple magnetic reconnection events occurring between a pre-twisted, closed field and open field lines. Components of the jet are seen in multiple SDO/AIA filters covering a wide range of temperatures, suggesting the jet can be classified as a blowout jet. Two bright, elongated features are observed to be co-spatial with the large jet, appearing at the jet's footpoints. Investigation of these features reveal they are defined by multiple plasma ejections. The ejecta display (quasi-)periodic behaviour on timescales of 50 s and have rise velocities of 40-150 km,s-1 along the open field lines. Due to the suggestion that the large jet is reconnection-driven and the observed properties of the ejecta, we further propose that these ejecta events are similar to type-II spicules. The bright features also display (quasi-)periodic intensity perturbations on the timescale of 300 s. Possible explanations for the existence of the (quasi-)periodic perturbations in terms of jet dynamics and the response of the transition region are discussed.

20 January 2011

## The Stellar CME-flare relation: What do historic observations reveal? [Review](#)

Sofia-Paraskevi [Moschou](#), [Jeremy J. Drake](#), [Ofer Cohen](#), [Julián D. Alvarado-Gómez](#), [Cecilia Garraffo](#), [Federico Fraschetti](#)

ApJ 877 105 2019

<https://arxiv.org/pdf/1904.09598.pdf> [File](#)

[sci-hub.se/10.3847/1538-4357/ab1b37](https://sci-hub.se/10.3847/1538-4357/ab1b37)

Solar CMEs and flares have a statistically well defined relation, with more energetic X-ray flares corresponding to faster and more massive CMEs. How this relation extends to more magnetically active stars is a subject of open research. Here, we study the most probable stellar CME candidates associated with flares captured in the literature to date, all of which were observed on magnetically active stars. We use a simple CME model to derive masses and kinetic energies from observed quantities, and transform associated flare data to the GOES 1--8-Å band. Derived CME masses range from ~10<sup>15</sup> to 10<sup>22</sup> g. Associated flare X-ray energies range from 10<sup>31</sup> to 10<sup>37</sup> erg. Stellar CME masses as a function of associated flare energy generally lie along or below the extrapolated mean for solar events. In contrast, CME kinetic energies lie below the analogous solar extrapolation by roughly two orders of magnitude, indicating approximate parity between flare X-ray and CME kinetic energies. These results suggest that the CMEs associated with very energetic flares on active stars are more limited in terms of the ejecta velocity than the ejecta mass, possibly because of the restraining influence of strong overlying magnetic fields and stellar wind drag. Lower CME

kinetic energies and velocities present a more optimistic scenario for the effects of CME impacts on exoplanets in close proximity to active stellar hosts.

### **A Monster CME Obscuring A Demon Star Flare**

Sofia-Paraskevi [Moschou](#), [Jeremy J. Drake](#), [Ofar Cohen](#), [Julian D. Alvarado-Gomez](#), [Cecilia Garraffo](#)

ApJ **850** 191 **2017**

<https://arxiv.org/pdf/1710.07361.pdf>

We explore the scenario of a Coronal Mass Ejection (CME) being the cause of the observed continuous X-ray absorption of the August 30 1997 superflare on the eclipsing binary Algol (the Demon Star). The temporal decay of the absorption is consistent with absorption by a CME undergoing self-similar evolution with uniform expansion velocity. We investigate the kinematic and energetic properties of the CME using the ice-cream cone model for its three-dimensional structure in combination with the observed profile of the hydrogen column density decline with time. Different physically justified length scales were used that allowed us to estimate lower and upper limits of the possible CME characteristics. Further consideration of the maximum available magnetic energy in starspots leads us to quantify its mass as likely lying in the range  $2 \times 10^{21}$ – $2 \times 10^{22}$  g and kinetic energy in the range  $7 \times 10^{35}$ – $3 \times 10^{38}$  erg. The results are in reasonable agreement with extrapolated relations between flare X-ray fluence and CME mass and kinetic energy derived for solar CMEs.

### **SDO Observations of Solar Jets**

S. P. [Moschou](#), K. Tsinganos, A. Vourlidas, V. Archontis

Solar Physics, June **2013**, Volume 284, Issue 2, pp 427-438

We present an analysis of high cadence observations of solar jets observed in the Extreme Ultraviolet (EUV), at 304 Å, with the Atmospheric Imaging Assembly instrument aboard the Solar Dynamics Observatory (SDO). The jets in our sample lie very close to the solar limb to minimize projection effects. Two of the events show clear helical patterns during ejection. We also find that some of the jets are recurrent and that most of them cannot overcome solar gravity. We investigate the temporal evolution of the jets by measuring the height of their leading edge as a function of time. By fitting the resulting height–time diagrams, we derive the magnitude of their initial ejection speed and plasma acceleration by assuming ballistic motion. Moreover, we calculate the upward acceleration of the jets based on the dynamical velocity of the plasma, without assuming a ballistic motion. In both models, the acceleration profiles suggest the influence of forces other than gravity. In particular, we find indications of an upwards driving force which weakens the decelerating effect of the solar gravitational field along the motion of the jet. This force is larger in the dynamical model, which indicates that the ballistic approximation does not properly determine the rising motion of the plasma jets.

### **Predictions of solar coronal mass ejections with heliospheric imagers verified with the Heliophysics System Observatory**

C. [Möstl](#), A. Isavnin, P. D. Boakes, [E. K. J. Kilpua](#), [J. A. Davies](#), [R. A. Harrison](#), [D. Barnes](#), [V. Krupar](#), [J. P. Eastwood](#), [S. W. Good](#), [R. J. Forsyth](#), [V. Bothmer](#), [M. A. Reiss](#), [T. Amerstorfer](#), [R. M. Winslow](#), [B. J. Anderson](#), [L. C. Philpott](#), [L. Rodriguez](#), [A. P. Rouillard](#), [P. T. Gallagher](#), [T. L. Zhang](#)

Space Weather **2017**

<https://arxiv.org/ftp/arxiv/papers/1703/1703.00705.pdf>

We present a major step forward towards accurately predicting the arrivals of coronal mass ejections (CMEs) on the terrestrial planets, including the Earth. For the first time, we are able to assess a CME prediction model using data over almost a full solar cycle of observations with the Heliophysics System Observatory. We validate modeling results on 1337 CMEs observed with the Solar Terrestrial Relations Observatory (STEREO) heliospheric imagers (HI) with data from 8 years of observations by 5 spacecraft in situ in the solar wind, thereby gathering over 600 independent in situ CME detections. We use the self-similar expansion model for CME fronts assuming 60 degree longitudinal width, constant speed and constant propagation direction. Using these assumptions we find that 23%-35% of all CMEs that were predicted to hit a certain spacecraft lead to clear in situ signatures, so that for 1 correct prediction, 2 to 3 false alarms would have been issued. In addition, we find that the prediction accuracy of HI does not degrade with longitudinal separation from Earth. Arrival times are predicted on average within 2.6 +/- 16.6 hours difference to the in situ arrival time, similar to analytical and numerical modeling. We also discuss various factors that may improve the accuracy of space weather forecasting using wide-angle heliospheric imager observations. These results form a first order approximated baseline of the prediction accuracy that is possible with HI and other methods used for data by an operational space weather mission at the Sun-Earth L5 point.

**Catalogs:** **HIGeoCat:** [https://www.helcats-fp7.eu/catalogues/wp3\\_cat.html](https://www.helcats-fp7.eu/catalogues/wp3_cat.html) Manuscript submitted to Space Weather, 2 March 2017

**ARRCAT:** doi:10.6084/m9.figshare.4588324 <https://doi.org/10.6084/m9.figshare.4588324.v1>

**ICMECAT:** doi:10.6084/m9.figshare.4588315 <https://doi.org/10.6084/m9.figshare.4588315.v1>

**ICME lists:** **Wind ICME list:** T. Nieves-Chinchilla et al. <https://wind.nasa.gov/ICMEindex.php>

**STEREO ICME list:** Lan Jian, [http://www-ssc.igpp.ucla.edu/forms/stereo/stereo\\_level\\_3.html](http://www-ssc.igpp.ucla.edu/forms/stereo/stereo_level_3.html) updated by our study.

**VEX:** Good & Forsyth [2016], updated by our study.

**MESSENGER:** Winslow et al. [2015], Good and Forsyth [2016], updated by our study.

**In situ data: Wind:** <https://cdaweb.sci.gsfc.nasa.gov>

**STEREO:** [http://aten.igpp.ucla.edu/forms/stereo/level2\\_plasma\\_and\\_magnetic\\_field.html](http://aten.igpp.ucla.edu/forms/stereo/level2_plasma_and_magnetic_field.html)

**MESSENGER:** <http://ppi.pds.nasa.gov/search/?sc=Messenger&t=Mercury&i=MAG>

**VEX:** data obtained from magnetometer PI T.L. Zhang [Tielong.Zhang@oeaw.ac.at](mailto:Tielong.Zhang@oeaw.ac.at)

## **THE KELVIN-HELMHOLTZ INSTABILITY AT CORONAL MASS EJECTION BOUNDARIES IN THE SOLAR CORONA: OBSERVATIONS AND 2.5D MHD SIMULATIONS**

U. V. **Möstl**, M. Temmer, and A. M. Veronig

2013 ApJ 766 L12 <http://arxiv.org/pdf/1304.5884v1.pdf>

The Atmospheric Imaging Assembly on board the Solar Dynamics Observatory observed a coronal mass ejection with an embedded filament on **2011 February 24**, revealing quasi-periodic vortex-like structures at the northern side of the filament boundary with a wavelength of approximately 14.4 Mm and a propagation speed of about  $310 \pm 20$  km s<sup>-1</sup>. These structures could result from the Kelvin-Helmholtz instability occurring on the boundary. We perform 2.5D numerical simulations of the Kelvin-Helmholtz instability and compare the simulated characteristic properties of the instability with the observations, where we obtain qualitative as well as quantitative accordance. We study the absence of Kelvin-Helmholtz vortex-like structures on the southern side of the filament boundary and find that a magnetic field component parallel to the boundary with a strength of about 20% of the total magnetic field has stabilizing effects resulting in an asymmetric development of the instability.

## **Linking remote imagery of a coronal mass ejection to its in situ signatures at 1 AU**

Christian **Möstl**, Charles J. Farrugia, Manuela Temmer, Christiane Miklenic, Astrid M. Veronig, Antoinette B. Galvin, Martin Leitner, Helfried K. Biernat

E-print, Oct 2009

In a case study (**June 6-7, 2008**) we report on how the internal structure of a coronal mass ejection (CME) at 1 AU can be anticipated from remote observations of white-light images of the heliosphere. Favorable circumstances are the absence of fast equatorial solar wind streams and a low CME velocity which allow us to relate the imaging and in-situ data in a straightforward way. The STEREO-B spacecraft encountered typical signatures of a magnetic flux rope inside an interplanetary CME (ICME) whose axis was inclined at 45 degree to the solar equatorial plane. Various CME direction-finding techniques yield consistent results to within 15 degree. Further, remote images from STEREO-A show that (1) the CME is unambiguously connected to the ICME and can be tracked all the way to 1 AU, (2) the particular arc-like morphology of the CME points to an inclined axis, and (3) the three-part structure of the CME may be plausibly related to the in situ data. This is a first step in predicting both the direction of travel and the internal structure of CMEs from complete remote observations between the Sun and 1 AU, which is one of the main requirements for forecasting the geo-effectiveness of CMEs.

## **Eruptions from quiet Sun coronal bright points. I. Observations**

Chauzhou **Mou**, [Maria S. Madjarska](#), [Klaus Galsgaard](#), [Lidong Xia](#)

A&A 2018

<https://arxiv.org/pdf/1808.04541.pdf>

Observations of the full lifetime of CBPs in data taken with the AIA on board SDO in four passbands, He II 304 A, Fe IX/X 171 A, Fe XII 193 A, and Fe XVIII 94 A are investigated for the occurrence of plasma ejections, micro-flaring, mini-filament eruptions and mini coronal mass ejections (mini-CMEs). First and foremost, our study shows that the majority (76%) of quiet Sun CBPs (31 out of 42 CBPs) produce at least one eruption during their lifetime. From 21 eruptions in 11 CBPs, 18 occur in average ~17 hrs after the CBP formation for an average lifetime of the CBPs in AIA 193 A of ~21 hrs. This time delay in the eruption occurrence coincides in each BP with the convergence and cancellation phase of the CBP bipole evolution during which the CBPs become smaller until they fully disappear. The remaining three happen 4 - 6 hrs after the CBP formation. In sixteen out of 21 eruptions the magnetic convergence and cancellation involve the CBP main bipoles, while in three eruptions one of the BP magnetic fragments and a pre-existing fragment of opposite polarity converge and cancel. In one BP with two eruptions cancellation was not observed. The CBP eruptions involve in most cases the expulsion of chromospheric material either as elongated filamentary structure (mini-filament, MF) or a volume of cool material (cool plasma cloud, CPC), together with the CBP or higher overlying hot loops. Coronal waves were identified during three eruptions. A micro-flaring is observed beneath all erupting MFs/CPCs. It remains uncertain whether the destabilised MF causes the micro-flaring or the destabilisation and eruption of the MF is triggered by reconnection beneath the filament. In most eruptions, the cool erupting plasma obscures partially or fully the micro-flare until the erupting material moves away from the CBP. From 21 eruptions 11 are found to produce mini-CMEs. **2011 January 1-3**

**Table 1.** General information on the QS BPs associated with eruptions (Jan 2011).

## **Kink-and-Disconnection Failed Eruption in 3D.**

**Mrozek**, T., Li, Z., Karlický, M. et al.

Sol Phys 299, 81 (2024).

<https://doi.org/10.1007/s11207-024-02325-8>

<https://link.springer.com/content/pdf/10.1007/s11207-024-02325-8.pdf>

We present a case study of a failed eruption that accompanied an M1.5 GOES class solar flare. It was observed by STIX onboard Solar Orbiter, HXI onboard the Advanced Space-based Solar Observatory, AIA onboard Solar Dynamics Observatory, and WAVES onboard the STEREO-A. The important input is from stereoscopic hard X-ray (HXR) observations obtained by HXI and STIX, whose vantage points were separated by  $31.5^\circ$ , allowing us to unfold the 3D geometry of the event. The eruption was a two-phase event. First, it started with the rope helical kink and then was slowed down, but with the structure still unstable, it erupted two minutes later due to ongoing reconnection in the interacting legs of the kinked structure. A Type III burst was observed in association with the eruption, indicating the acceleration of semirelativistic electrons into the heliosphere. During the second phase, a hot cloud was disconnected and confined in the overlying magnetic field, where the overlying loops connected two adjacent active regions. The estimated and corrected for real geometry velocities are in the range of  $385 - 400 \text{ km s}^{-1}$ , whereas acceleration reached  $4.78 - 6.33 \text{ km s}^{-2}$ . These extreme values are much more demanding from a perspective of conditions that are needed to stop the eruption. Images obtained simultaneously by HXI and STIX located in different vantage points showed that flare-related sources are not lying along a normal to the solar surface. The understanding of the eruption analyzed here has been highly enriched thanks to the stereoscopic information about HXR source locations. **2023-02-08**

### **Catalog of Solar Failed Eruptions and Other Dynamic Features Registered by SDO/AIA**

Tomasz **Mrozek**<sup>1,2</sup>, Sylwester Kołomański<sup>1</sup>, Marek Stęślicki<sup>2</sup>, and Dominik Gronkiewicz<sup>3</sup>

**2020** ApJS 249 21

<https://iopscience.iop.org/article/10.3847/1538-4365/ab9e00/pdf>

In this paper we present our attempt to constrain the first catalog of solar failed eruptions. We used our automatic algorithm that is able to search for dynamic features in the Solar Dynamics Observatory (SDO)/Atmospheric Imaging Assembly (AIA) database. We ran the algorithm on the entire SDO/AIA 171 Å data set. For the time interval from 2010 May 20 to 2019 May 20 we found 12,192 dynamic events. The dynamic events were classified in three groups. Apart from failed eruptions (1214) we obtained a large group of successful eruptions (2064) and other dynamic events (8914). The automatic algorithm enabled us to collect several observational characteristics, which are provided in files that may be downloaded from the catalog web page. In this paper we present the methodology of catalog preparation and preliminary results of the statistical analysis of observational characteristics obtained by the automatic algorithm.

<http://eruptivesun.com>, <http://eruptivesun.com/help>

### **The Photospheric Footpoints of Solar Coronal Hole Jets**

K. **Muglach**<sup>1,2</sup>

**2021** ApJ 909 133

<https://doi.org/10.3847/1538-4357/abd5ad>

We study the photospheric footpoints of a set of 35 coronal jets in a coronal hole as observed by Hinode/EIS. We use SDO/AIA data to coalign the spectroscopic EIS data with SDO/HMI line-of-sight magnetograms and calculate the plane-of-sky flow field using local correlation tracking (LCT) on SDO/HMI white light images. The jets are put into categories according to the changes observed in the photospheric magnetic flux at the footpoints of the coronal bright point where the jets originate: flux cancellation, complex flux changes (flux appearance/emergence and cancellation), and no flux changes. We also present three jets in detail. Observed magnetic flux evolution, LCT flow field structure and location of the jet footpoints at supergranular boundaries do not support the flux emergence scenario used in most jet simulations and are also not consistent with a rotational photospheric driver. Detailed numerical jet simulations using our observed photospheric features, in particular converging flows and flux cancellation do not currently exist, although such models would provide a realistic eruptive event scenario.

### **Properties of flares and CMEs on EV Lac: Possible erupting filament**

[Priscilla Muheki](#), [Eike W Guenther](#), [Tom Mutabazi](#), [Edward Jurua](#)

Monthly Notices of the Royal Astronomical Society, Volume 499, Issue 4, December **2020**, Pages 5047–5058,

<https://doi.org/10.1093/mnras/staa3152>

<https://arxiv.org/pdf/2010.03336.pdf>

Flares and CMEs are very powerful events in which energetic radiation and particles are ejected within a short time. These events thus can strongly affect planets that orbit these stars. This is particularly relevant for planets of M-stars, because these stars stay active for a long time during their evolution and yet potentially habitable planets orbit at short distance. Unfortunately, not much is known about the relation between flares and CMEs in M-stars as only very few CMEs have so far been observed in M-stars. In order to learn more about flares and CMEs on M-stars we monitored the active M-star EV Lac spectroscopically at high resolution. We find 27 flares with energies between  $1.6E31$  and  $1.4E32$  erg in H $\alpha$  during 127 hours of spectroscopic monitoring and 49 flares with energies between  $6.3E31$  and  $1.1E33$  erg during the 457 hours of TESS observation. Statistical analysis shows that the ratio of the continuum flux in the TESS-band to the energy emitted in H $\alpha$  is  $10.408 \pm 0.026$ . Analysis of the spectra shows an increase in the flux of the He II 4686 Å line during the impulsive phase of some flares. In three large flares, we detect a continuum source with a temperature between 6 900 and 23 000 K. In none of the flares we find a clear CME event indicating that these must be very rare in active M-stars. However, in one relatively weak event, we found an asymmetry in the Balmer lines of  $\sim 220$  km/s which we interpret as a signature of an erupting filament.

## Formation and Thermodynamic Evolution of plasmoids in active region jets

Sargam M. [Mulay](#), [Durgesh Tripathi](#), [Helen Mason](#), [Giulio Del Zanna](#), [Vasilis Archontis](#)

MNRAS Volume 518, Issue 2, January 2023, Pages 2287–2299

<https://arxiv.org/ftp/arxiv/papers/2211/2211.01740.pdf>

<https://watermark.silverchair.com/stac3035.pdf>

We have carried out a comprehensive study of the temperature structure of plasmoids, which successively occurred in recurrent active region jets. The multithermal plasmoids were seen to be travelling along the multi-threaded spire as well as at the footpoint region in the EUV/UV images recorded by the Atmospheric Imaging Assembly (AIA). The Differential Emission Measure (DEM) analysis was performed using EUV AIA images, and the high-temperature part of the DEM was constrained by combining X-ray images from the X-ray telescope (XRT/Hinode). We observed a systematic rise and fall in brightness, electron number densities and the peak temperatures of the spire plasmoid during its propagation along the jet. The plasmoids at the footpoint (FPs) (1.0-2.5 MK) and plasmoids at the spire (SPs) (1.0-2.24 MK) were found to have similar peak temperatures, whereas the FPs have higher DEM weighted temperatures (2.2-5.7 MK) than the SPs (1.3-3.0 MK). A lower limit to the electron number densities of plasmoids - SPs (FPs) were obtained that ranged between  $3.4-6.1 \times 10^8$  ( $3.3-5.9 \times 10^8$ )  $\text{cm}^{-3}$  whereas for the spire, it ranged from  $2.6-3.2 \times 10^8 \text{ cm}^{-3}$ . Our analysis shows that the emission of these plasmoids starts close to the base of the jet(s), where we believe that a strong current interface is formed. This suggests that the blobs are plasmoids induced by a tearing-mode instability. **31 Oct 2011**

## Cool and hot emission in a recurring active region jet

Sargam M. [Mulay](#), Giulio Del Zanna, and Helen Mason

uksp\_nug #108 **2020**

<http://www.uksolphys.org/uksp-nugget/108-cool-and-hot-emission-in-a-recurring-active-region-jet/>

We have carried out a multi-instrument, multi-thermal analysis on an active region jet. A better constraint on the lower temperatures for the DEMs was obtained by including the IRIS spectra along with AIA images in the DEM analysis. A difference of three orders of magnitude between the total EM values indicate the presence of low-temperature plasma ( $\log T [\text{K}] < 5.4$ ) at the footpoint, while the SJI images and Fe XVIII emission maps of the footpoint of the jet showed the hot emission is co-spatially and co-temporally associated with cool emission within the resolution/cadence of the observations. **July 10, 2015**

## Study of the spatial association between an active region jet and a nonthermal type III radio burst★

Sargam M. [Mulay](#)<sup>1,2</sup>, Rohit Sharma<sup>3</sup>, Gherardo Valori<sup>4</sup>, Alberto M. Vásquez<sup>5</sup>, Giulio Del Zanna<sup>2</sup>, Helen Mason<sup>2</sup> and Divya Oberoi<sup>6</sup>

A&A 632, A108 (**2019**)

<https://doi.org/10.1051/0004-6361/201936369>

<https://sci-hub.st/10.1051/0004-6361/201936369>

**Aims.** We aim to investigate the spatial location of the source of an active region (AR) jet and its relation with associated nonthermal type III radio emission.

**Methods.** An emission measure (EM) method was used to study the thermodynamic nature of the AR jet. The nonthermal type III radio burst observed at meterwavelength was studied using the Murchison Widefield Array (MWA) radio imaging and spectroscopic data. The local configuration of the magnetic field and the connectivity of the source region of the jet with open magnetic field structures was studied using a nonlinear force-free field (NLFFF) extrapolation and potential field source surface (PFSS) extrapolation respectively.

**Results.** The plane-of-sky velocity of the AR jet was found to be  $\sim 136 \text{ km s}^{-1}$ . The EM analysis confirmed the presence of low temperature 2 MK plasma for the spire, whereas hot plasma, between 5 and 8 MK, was present at the footpoint region which also showed the presence of Fe XVIII emission. A lower limit on the electron number density was found to be  $1.4 \times 10^8 \text{ cm}^{-3}$  for the spire and  $2.2 \times 10^8 \text{ cm}^{-3}$  for the footpoint. A temporal and spatial correlation between the AR jet and nonthermal type III burst confirmed the presence of open magnetic fields. An NLFFF extrapolation showed that the photospheric footpoints of the null point were anchored at the location of the source brightening of the jet. The spatial location of the radio sources suggests an association with the extrapolated closed and open magnetic fields although strong propagation effects are also present.

**Conclusions.** The multi-scale analysis of the field at local, AR, and solar scales confirms the interlink between different flux bundles involved in the generation of the type III radio signal with flux transferred from a small coronal hole to the periphery of the sunspot via null point reconnection with an emerging structure. **September 2-3, 2013**

## Flare-related Recurring Active Region Jets: Evidence for Very Hot Plasma

Sargam M. [Mulay](#) Sarah Matthews Takahiro Hasegawa Giulio Del Zanna Helen Mason Toshifumi Shimizu

[Solar Physics](#) December **2018**, 293:160

[sci-hub.tw/10.1007/s11207-018-1376-4](https://sci-hub.tw/10.1007/s11207-018-1376-4)

We present a study of two active region jets (AR jets) that are associated with two C-class X-ray flares. The recurrent, homologous jets originated from the northern periphery of a sunspot. We confirm flare-like temperatures at the

footpoints of these jets using spectroscopic observations of Fe xxiii (263.76 Å) and Fe xxiv (255.11 Å) emission lines. The emission measure loci method was used to obtain an isothermal temperature, and the results show a decrease (17.7 to 13.6 MK) in the temperature during the decay phase of the C 3.0 flare. The electron number densities at the footpoints were found to range from  $1.7 \times 10^{10}$ – $1.7 \times 10^{10}$  to  $2.0 \times 10^{11}$ – $32.0 \times 10^{11}$  cm<sup>-3</sup> using the Fe xiv line pair ratio. Nonthermal velocities were found to range from 34 – 100 km/s for Fe xxiv and 51 – 89 km/s for Fe xxiii. The plane-of-sky velocities were calculated to be  $462 \pm 21$  and  $228 \pm 23$  km/s for the two jets using the Atmospheric Imaging Assembly (AIA) 171 Å channel. The AIA light curves of the jet footpoint regions confirmed the temporal and spatial correlation between the two X-ray flares and the jet footpoint emission. The Gamma-ray Burst Monitor (GBM) also confirmed superhot plasma of 27 (25) MK with a nonthermal energy of  $2.38 \times 10^{26}$ – $3.8 \times 10^{26}$  (2.87– $10.27$ ) ergs<sup>-1</sup> in the jet footpoint region during the rise (peak) phase of one of the flares. The temperatures of the jet footpoint regions obtained from EIS agree very well (within an uncertainty of 20%) with temperatures obtained from the Geostationary Environmental Operational Satellite (GOES) flux ratios. These results provide clear evidence for very hot plasma (>10 MK) at the footpoints of the flare-related jets, and they confirm the heating and cooling of the plasma during the flares.

### Cool and hot emission in a recurring active region jet★

Sargam M. **Mulay**, Giulio Del Zanna and Helen Mason  
A&A 606, A4 (2017)

<https://www.aanda.org/articles/aa/pdf/2017/10/aa30429-17.pdf>

**Aims.** We present a thorough investigation of the cool and hot temperature components in four recurring active region jets observed on **July 10, 2015** using the Atmospheric Imaging Assembly (AIA), X-ray Telescope (XRT), and Interface Region Imaging Spectrograph (IRIS) instruments.

**Methods.** A differential emission measure (DEM) analysis was performed on areas in the jet spire and footpoint regions by combining the IRIS spectra and the AIA observations. This procedure better constrains the low temperature DEM values by adding IRIS spectral lines. Plasma parameters, such as Doppler velocities, electron densities, nonthermal velocities and a filling factor were also derived from the IRIS spectra.

**Results.** In the DEM analysis, significant cool emission was found in the spire and the footpoint regions. The hot emission was peaked at  $\log T$  [K] = 5.6–5.9 and 6.5 respectively. The DEM curves show the presence of hot plasma ( $T = 3$  MK) in the footpoint region. We confirmed this result by estimating the Fe XVIII emission from the AIA 94 Å channel which was formed at an effective temperature of  $\log T$  [K] = 6.5. The average XRT temperatures were also found to be in agreement with  $\log T$  [K] = 6.5. The emission measure (EM) was found to be three orders of magnitude higher in the AIA-IRIS DEM compared with that obtained using only AIA. The O IV (1399/1401 Å) electron densities were found to be  $2.0 \times 10^{10}$  cm<sup>-3</sup> in the spire and  $7.6 \times 10^{10}$  cm<sup>-3</sup> in the footpoint. Different threads along the spire show different plane-of-sky velocities both in the lower corona and transition region. Doppler velocities of 32 km s<sup>-1</sup> (blueshifted) and 13 km s<sup>-1</sup> (redshifted) were obtained in the spire and footpoint, respectively from the Si IV 1402.77 Å spectral line. Nonthermal velocities of 69 and 53 km s<sup>-1</sup> were recorded in the spire and footpoint region, respectively. We obtained a filling factor of 0.1 in the spire at  $\log T$  [K] = 5.

**Conclusions.** The recurrent jet observations confirmed the presence of significant cool emission co-spatial with the coronal emission.

### Temperature and Density Structure of a Recurring Active Region Jet

Sargam M. **Mulay**, Giulio Del Zanna, Helen Mason  
A&A 598, A11 (2017)

<http://arxiv.org/pdf/1609.08472v1.pdf>

**Aims.** We present a study of a recurring jet observed on **October 31, 2011** by the Atmospheric Imaging Assembly (AIA) on board the Solar Dynamic Observatory, the X-ray Telescope (XRT) and EUV Imaging Spectrometer (EIS) on board Hinode. We discuss the physical parameters of the jet that are obtained using imaging and spectroscopic observations, such as density, differential emission measure, peak temperature, velocity, and filling factor.

**Methods.** A differential emission measure (DEM) analysis was performed at the region of the jet spire and the footpoint using EIS observations and also by combining AIA and XRT observations. The resulting EIS DEM curves were compared to those obtained with AIA-XRT. The DEM curves were used to create synthetic spectra with the CHIANTI atomic database. The predicted total count rates for each AIA channel were compared with the observed count rates. The effects of varying elemental abundances and the temperature range for the DEM inversion were investigated. Spectroscopic diagnostics were used to obtain an electron number density distribution for the jet spire and the jet footpoint.

**Results.** The plasma along the line of sight in the jet spire and jet footpoint was found to be peak at 2.0 MK ( $\log T$  [K] = 6.3). We calculated electron densities using the Fe XII (λ186/λ195) line ratio in the region of the spire ( $N_e = 7.6 \times 10^{10}$  cm<sup>-3</sup>) and the footpoint ( $1.1 \times 10^{11}$  cm<sup>-3</sup>). The plane-of-sky velocity of the jet is found to be 524 km s<sup>-1</sup>. The resulting EIS DEM values are in good agreement with those obtained from AIA-XRT. The synthetic spectra contributing to each AIA channel confirms the multi-thermal nature of the AIA channels in both regions. There is no indication of high temperatures, such as emission from Fe XVII (λ254.87) ( $\log T$  [K] = 6.75) seen in the jet spire. In the case of the jet footpoint, synthetic spectra predict weak contributions from Ca XVII (λ192.85) and Fe XVII (λ254.87). With further investigation, we confirmed emission from the Fe XVIII (93.932 Å) line in the AIA 94 Å channel in the region of the footpoint. We also found good agreement between the estimated and predicted Fe XVIII count rates. A study of the temporal evolution of the jet footpoint and the presence of high-temperature emission from the Fe XVIII

( $\lambda 93.932$ ) ( $\log T [K] = 6.85$ ) line leads us to conclude that the hot component in the jet footpoint was present initially and that the jet had cooled down by the time EIS observed it.

### **Multiwavelength study of 20 jets that emanate from the periphery of active regions**

Sargam M. **Mulay**, Durgesh Tripathi, Giulio Del Zanna, and Helen Mason

CESRA highlights #959, Nov. 2016

<http://www.astro.gla.ac.uk/users/eduard/cesra/?p=959>

We present a multiwavelength analysis of 20 EUV jets observed between August 2010 and June 2013. In this study, we included events which were observed on the solar disk within  $\pm 60^\circ$  latitude and occurred at the periphery of active regions close to sunspots. We discuss the physical parameters of the jets and their relation with other phenomena such as nonthermal type-III radio bursts and magnetic activity in the photosphere. **2010 August 02**

### **Multiwavelength study of twenty jets emanating from the periphery of active regions**

Sargam M. **Mulay**, Durgesh Tripathi, Giulio Del Zanna, Helen Mason

A&A 589, A79 2016

We present a multiwavelength analysis of 20 EUV jets which occurred at the periphery of active regions close to sunspots. We discuss the physical parameters of the jets and their relation with other phenomena such as H alpha surges, nonthermal type III radio bursts and hard X-ray emission. Using AIA wavelength channels sensitive to coronal temperatures, we studied the temperature distribution in the jets using the line-of-sight Differential Emission Measure technique. We also investigated the role of the photospheric magnetic field using the LOS magnetogram data from the HMI. The lifetime of jets range from 5 to 39 minutes with an average of 18 minutes and their velocities range from 87 to 532 km/s with an average of 271 km/s. Most of the jets are co-temporal with nonthermal type III radio bursts observed by the Wind/WAVES spacecraft. We confirm the source region of these bursts using the Potential Field Source Surface technique. 10 out of 20 events showed that the jets originated in a region of flux cancellation and 6 jets in a region of flux emergence. 4 events showed flux emergence and then cancellation during the jet evolution. DEM analyses showed that for most of the spires of the jets, the DEM peaked at around  $\log T [K] = 6.2/6.3$ . In addition, we derived an emission measure and a lower limit of electron density at the location of the spire and the footpoint. These results are in agreement with those obtained earlier by studying individual active region jets. The observation of flux cancellation, the association with HXR emission and emission of nonthermal type III radio bursts, suggest that the initiation and therefore, heating is taking place at the base of the jet. This is also supported by the high temperature plasma revealed by the DEM analysis in the jet footpoint. Our results provide substantial constraints for theoretical modeling of the jets and their thermodynamic nature. **2010 August 2, 17 September 2010, 14 February 2011, 16 February 2011, 1 March 2011, 7 March 2011, 17 October 2011, 11 December 2011, 5 March 2012, 10 October 2012, 2013 March 02, 28 April 2013, 4 May 2013, 25 May 2013, 17 Jun 2013, 18 Jun 2013**

**Table 1. Statistically measured physical parameters of 20 EUV active region jets**

### **Initiation of CME event observed on November 3, 2010: Multi-wavelength Perspective**

Sargam **Mulay**, Srividya Subramanian, Durgesh Tripathi, Hiroaki Isobe, Lindsay Glesener

ApJ, 794 78 2014

<http://arxiv.org/pdf/1407.5837v1.pdf>

One of the major unsolved problems in Solar Physics is that of CME initiation. In this paper, we have studied the initiation of a flare associated CME which occurred on **2010 November 03** using multi-wavelength observations recorded by Atmospheric Imaging Assembly (AIA) on board Solar Dynamics Observatory (SDO) and Reuven Ramaty High Energy Solar Spectroscopic Imager (RHESSI). We report an observation of an inflow structure initially in 304- $\text{\AA}$  and in 1600- $\text{\AA}$  images, a few seconds later. This inflow structure was detected as one of the legs of the CME. We also observed a non-thermal compact source concurrent and near co-spatial with the brightening and movement of the inflow structure. The appearance of this compact non-thermal source, brightening and movement of the inflow structure and the subsequent outward movement of the CME structure in the corona led us to conclude that the CME initiation was caused by magnetic reconnection.

### **Origin of Radio-quiet Coronal Mass Ejections in Flare Stars**

D. J. **Mullan** and R. R. Paudel

2019 ApJ 873 1

<https://doi.org/10.3847/1538-4357/ab041b>

Type II radio bursts are observed in the Sun in association with many coronal mass ejections (CMEs). In view of this association, there has been an expectation that, by scaling from solar flares to the flares that are observed on M dwarfs, radio emission analogous to solar type II bursts should be detectable in association with M dwarf flares. However, several surveys have revealed that this expectation does not seem to be fulfilled. Here we hypothesize that the presence of larger global field strengths in low-mass stars, suggested by recent magnetoconvective modeling, gives rise to such large Alfvén speeds in the corona that it becomes difficult to satisfy the conditions for the generation of type II radio bursts. As a result, CMEs propagating in the corona/wind of flare stars are expected to be "radio-quiet" as regards type II bursts. In view of this, we suggest that, in the context of type II bursts, scaling from solar to stellar flares is of limited effectiveness.

## **Analysis of the Coronal Mass Ejections through Axial Field Direction of Solar Filaments and IMF Bz**

Kashvi [Mundra](#), [V. Aparna](#), [Petrus C. H. Martens](#)

ApJ 2020

<https://arxiv.org/pdf/2011.02123.pdf>

In the past, there have been many studies claiming that the effects of geomagnetic storms strongly depend on the orientation of the magnetic-cloud part of the Coronal Mass Ejections (CMEs). Aparna & Martens (2020), using Halo-CME data from 2007-2017, have shown that the magnetic field orientation of filaments at the location where CMEs originate can be effectively used for predicting the onset of geo-magnetic storms. The purpose of this study is to extend their survey by analyzing the halo-CME data for 1996-2006. The correlation of filament axial direction and their corresponding Bz signatures are used to form a more extensive reasoning for the claims presented by Aparna & Martens before. This study utilizes SOHO EIT 195 Å, MDI magnetogram images, KSO and BBSO H $\alpha$  images for the time period, along with ACE data for inter-planetary magnetic field signatures. Correlating all these, we have found that the trend in Aparna & Martens' study of a high likelihood of the correlation between the axial field direction and Bz orientation, persists for the data between 1996-2006 as well. **September 16th, 2000, 02/09/2001, 2000-11-01**

## **Asymmetric Magnetic Reconnection in Coronal Mass Ejection Current Sheets**

[Murphy](#), N. A.; [Miralles](#), M. P.; [Pope](#), C. L.; [Raymond](#), J. C.; [Reeves](#), K. K.; [Seaton](#), D. B.; [Webb](#), D. F.

The Fifth Hinode Science Meeting. ASP Conference Series, Vol. 456, Proceedings of a conference held 10-14 October 2011 at Royal Sonesta Hotel, Cambridge, Massachusetts. Edited by Leon Golub, Ineke De Moortel and Toshifumi Shimizu. San Francisco: Astronomical Society of the Pacific, **2012.**, p.199

We present resistive MHD simulations of magnetic reconnection in the context of coronal mass ejection current sheets. We hypothesize that several commonly observed features of solar flares such as sub-Alfvénic downflows, candle flame shaped post-flare loops, and current sheet drifting are the result of asymmetry in the inflow and/or outflow directions during the reconnection process.

## **ASYMMETRIC MAGNETIC RECONNECTION IN SOLAR FLARE AND CORONAL MASS EJECTION CURRENT SHEETS**

N. A. [Murphy](#)<sup>1</sup>, M. P. [Miralles](#)<sup>1</sup>, C. L. [Pope](#)<sup>1,2</sup>, J. C. [Raymond](#)<sup>1</sup>, H. D. [Winter](#)<sup>1</sup>, K. K. [Reeves](#)<sup>1</sup>, D. B. [Seaton](#)<sup>3</sup>, A. A. [van Ballegoijen](#)<sup>1</sup>, and J. [Lin](#)

**2012** ApJ 751 56

We present two-dimensional resistive magnetohydrodynamic simulations of line-tied asymmetric magnetic reconnection in the context of solar flare and coronal mass ejection current sheets. The reconnection process is made asymmetric along the inflow direction by allowing the initial upstream magnetic field strengths and densities to differ, and along the outflow direction by placing the initial perturbation near a conducting wall boundary that represents the photosphere. When the upstream magnetic fields are asymmetric, the post-flare loop structure is distorted into a characteristic skewed candle flame shape. The simulations can thus be used to provide constraints on the reconnection asymmetry in post-flare loops. More hard X-ray emission is expected to occur at the footpoint on the weak magnetic field side because energetic particles are more likely to escape the magnetic mirror there than at the strong magnetic field footpoint. The footpoint on the weak magnetic field side is predicted to move more quickly because of the requirement in two dimensions that equal amounts of flux must be reconnected from each upstream region. The X-line drifts away from the conducting wall in all simulations with asymmetric outflow and into the strong magnetic field region during most of the simulations with asymmetric inflow. There is net plasma flow across the X-line for both the inflow and outflow directions. The reconnection exhaust directed away from the obstructing wall is significantly faster than the exhaust directed toward it. The asymmetric inflow condition allows net vorticity in the rising outflow plasmoid which would appear as rolling motions about the flux rope axis.

## **Connecting Coronal Mass Ejections to their Solar Active Region Sources: Combining Results from the HELCATS and FLARECAST Projects**

Sophie A. [Murray](#), [Jordan A. Guerra](#), [Pietro Zucca](#), [Sung-Hong Park](#), [Eoin P. Carley](#), [Peter T. Gallagher](#), [Nicole Vilmer](#), [Volker Bothmer](#)

Solar Phys. 293:60 **2018**

<https://arxiv.org/pdf/1803.06529.pdf> File

<https://link.springer.com/content/pdf/10.1007%2Fs11207-018-1287-4.pdf>

Coronal mass ejections (CMEs) and other solar eruptive phenomena can be physically linked by combining data from a multitude of ground-based and space-based instruments alongside models, however this can be challenging for automated operational systems. The EU Framework Package 7 HELCATS project provides catalogues of CME observations and properties from the Helio-spheric Imagers onboard the two NASA/STEREO spacecraft in order to track the evolution of CMEs in the inner heliosphere. From the main HICAT catalogue of over 2,000 CME detections, an automated algorithm has been developed to connect the CMEs observed by STEREO to any corresponding solar flares and active region (AR) sources on the solar surface. CME kinematic properties, such as speed and angular width, are compared with AR magnetic field properties, such as magnetic flux, area, and neutral line characteristics. The resulting LOWCAT catalogue is also compared to the extensive AR property database created by the EU Horizon 2020



FLARECAST project, which provides more complex magnetic field parameters derived from vector magnetograms. Initial statistical analysis has been undertaken on the new data to provide insight into the link between flare and CME events, and characteristics of eruptive ARs. Warning thresholds determined from analysis of the evolution of these parameters is shown to be a useful output for operational space weather purposes. Parameters of particular interest for further analysis include total unsigned flux, vertical current, and current helicity. The automated method developed to create the LOWCAT catalogue may also be useful for future efforts to develop operational CME forecasting. **21 June 2011, 2012-03-05**

## **Kink Instability of Flux Ropes in Partially Ionized Plasmas**

Giulia [Murtas](#), Andrew Hillier, and Ben Snow

2024 ApJ 977 108

<https://iopscience.iop.org/article/10.3847/1538-4357/ad79f6/pdf>

In the solar atmosphere, flux ropes are subject to current-driven instabilities that are crucial in driving plasma eruptions, ejections, and heating. A typical ideal magnetohydrodynamics instability developing in flux ropes is the helical kink, which twists the flux rope axis. The growth of this instability can trigger magnetic reconnection, which can explain the formation of chromospheric jets and spicules, but its development has never been investigated in a partially ionized plasma (PIP). Here, we study the kink instability in PIP to understand how it develops in the solar chromosphere, where it is affected by charge-neutral interactions. Partial ionization speeds up the onset of the nonlinear phase of the instability, as the plasma  $\beta$  of the isolated plasma is smaller than the total plasma  $\beta$  of the bulk. The distribution of the released magnetic energy changes in fully ionized plasma and PIP, with a larger increase in internal energy associated with the PIP cases. The temperature in PIP increases faster also due to heating terms from the two-fluid dynamics. PIP effects trigger kink instability on shorter time scales, which is reflected in more explosive chromospheric flux rope dynamics. These results are crucial to understanding the dynamics of small-scale chromospheric structures—minifilament eruptions—that thus far have been largely neglected but could significantly contribute to chromospheric heating and jet formation.

## **Solar Jet Hunter: A citizen science initiative to identify and characterize coronal jets at 304 Å**

[S. Musset](#), [P. Jol](#), [R. Sankar](#), [S. Alnahari](#), [C. Kapsiak](#), [E. Ostlund](#), [K. Lasko](#), [L. Glesener](#), [L. Fortson](#), [G. D. Fleishman](#), [N. K. Panesar](#), [Y. Zhang](#), [M. Jeunon](#), [N. Hurlburt](#)

A&A 688, A127 2024

<https://arxiv.org/pdf/2309.14871.pdf>

Context. Solar coronal jets seen in EUV are ubiquitous on the Sun, have been found in and at the edges of active regions, at the boundaries of coronal holes, and in the quiet Sun. Jets have various shapes, sizes, brightness, velocities and duration in time, which complicates their detection by automated algorithms. So far, solar jets reported in the Heliophysics Event Knowledgebase (HEK) have been mostly reported by humans looking for them in the data, with different levels of precision regarding their timing and positions.

Aims. We create a catalogue of solar jets observed in EUV at 304 Å containing precise and consistent information on the jet timing, position and extent.

Methods. We designed a citizen science project, "Solar Jet Hunter", on the Zooniverse platform, to analyze EUV observations at 304 Å from the Solar Dynamic Observatory/Atmospheric Imaging Assembly (SDO/AIA). We created movie strips for regions of the Sun in which jets have been reported in HEK and ask the volunteers to 1) confirm the presence of at least one jet in the data and 2) report the timing, position and extent of the jet. Results. We report here the design of the project and the results obtained after the analysis of data from 2011 to 2016. 365 "coronal jet" events from HEK served as input for the citizen science project, equivalent to more than 120,000 images distributed into 9,689 "movie strips". Classification by the citizen scientists resulted with only 21% of the data containing a jet, and 883 individual jets being identified.

Conclusions. We demonstrate how citizen science can enhance the analysis of solar data with the example of Solar Jet Hunter. The catalogue of jets thus created is publicly available and will enable statistical studies of jets and related phenomena. This catalogue will also be used as a training set for machines to learn to recognize jets in further data sets.

**25 Jul 2010, 20, 22 Jan 2015, 22 May 2016**

## **Energetic electrons and coronal jets**

## **Presentation**

Sophie [Musset](#)

Fleishman's Webinar 18 Dec 2020

[https://www.youtube.com/watch?v=4I57\\_w5IQ4&feature=youtu.be](https://www.youtube.com/watch?v=4I57_w5IQ4&feature=youtu.be)

## **Statistical study of hard X-ray emitting electrons associated with flare-related coronal jets**

Sophie [Musset](#), [Mariana Jeunon](#), [Lindsay Glesener](#)

2020 ApJ 889 183

<https://arxiv.org/pdf/1903.10414.pdf>

[sci-hub.si/10.3847/1538-4357/ab6222](https://sci-hub.si/10.3847/1538-4357/ab6222)

We present the statistical analysis of 33 flare-related coronal jets, and discuss the link between the jet and the flare properties in these events. We selected jets that were observed between 2010 and 2016 by the Atmospheric Imaging Assembly (AIA) on board the Solar Dynamic Observatory (SDO) and are temporally and spatially associated to flares

observed by the Reuven Ramaty High Energy Solar Spectrometric Imager (RHESSI). For each jet, we calculated the jet duration and projected velocity in the plane of sky. The jet duration distribution has a median of 18.8 minutes. The projected velocities are between 31 km/s and 456 km/s with a median at 210 km/s. For each associated flare, we performed X-ray imaging and spectroscopy and identify non-thermal emission. Non-thermal emission was detected in only 1/4 of the event considered. We did not find a clear correlation between the flare thermal energy or SXR peak flux and the jet velocity. A moderate anti-correlation was found between the jet duration and the flare SXR peak flux. There is no preferential time delay between the flare and the jet. **The X-ray emission is generally located at the base of the jet.** The analysis presented in this paper suggests that the flare and jet are part of the same explosive event, that the jet is driven by the propagation of an Alfvénic perturbation, and that the energy partition between flare and jets varies substantially from one event to another. **Aug 2 2010, 1 Apr 2011, 24 Apr 2013, 13 Nov 2014**  
**APPENDIX: LIST OF EUV JETS (2010-2016)**

### **A dynamic magnetic tension force as the cause of failed solar eruptions**

**Myers**, Clayton E.; Yamada, Masaaki; Ji, Hantao; Yoo, Jongsoo; Fox, William; Jara-Almonte, Jonathan; Savcheva, Antonia; Deluca, Edward E.  
Nature, Volume 528, Issue 7583, pp. 526-529 (2015).

Coronal mass ejections are solar eruptions driven by a sudden release of magnetic energy stored in the Sun's corona. In many cases, this magnetic energy is stored in long-lived, arched structures called magnetic flux ropes. When a flux rope destabilizes, it can either erupt and produce a coronal mass ejection or fail and collapse back towards the Sun. The prevailing belief is that the outcome of a given event is determined by a magnetohydrodynamic force imbalance called the torus instability. This belief is challenged, however, by observations indicating that torus-unstable flux ropes sometimes fail to erupt. This contradiction has not yet been resolved because of a lack of coronal magnetic field measurements and the limitations of idealized numerical modelling. Here we report the results of a laboratory experiment that reveal a previously unknown eruption criterion below which torus-unstable flux ropes fail to erupt. We find that such 'failed torus' events occur when the guide magnetic field (that is, the ambient field that runs toroidally along the flux rope) is strong enough to prevent the flux rope from kinking. Under these conditions, the guide field interacts with electric currents in the flux rope to produce a dynamic toroidal field tension force that halts the eruption. This magnetic tension force is missing from existing eruption models, which is why such models cannot explain or predict failed torus events.

### **Comparison of Kinematics of Solar Eruptive Prominences and Spatial Distribution of the Magnetic Decay Index**

Ivan **Myshyakov**<sup>1,3</sup> and Tsvetan Tsvetkov<sup>2</sup>

Astrophysical Journal, 889:28 2020

[sci-hub.si/10.3847/1538-4357/ab6334](https://doi.org/10.3847/1538-4357/ab6334)

Theoretical studies of electric current instability explaining solar prominence eruptions show that the loss of equilibrium may develop in a case when the surrounding magnetic field decreases sufficiently rapidly with height. The magnetic decay index, a parameter indicating whether the external magnetic field has a configuration that may lead to a certain type of electric current instability, is a useful instrument for predicting the behavior of prominences. In our study, we consider three eruptive prominences. We perform potential-field extrapolation to obtain the spatial distribution of the magnetic decay index in the coronal space identified with the prominences. Analysis of time-dependent height profiles of the prominences revealed that eruptions started at heights close to those, where the computed magnetic decay index exceeded a value equal to 1.5. This indicates that the torus instability is a possible mechanism of the considered eruptive events. **2011-Jan- 28, 2011 June 06, 2013 Feb 27**

### **A New Method to Estimate Halo CME Mass Using Synthetic CMEs Based on a Full Ice Cream Cone Model**

Hyeonock **Na**<sup>1</sup>, Yong-Jae Moon<sup>1,2</sup>, Jin-Yi Lee<sup>2</sup>, and Il-Hyun Cho<sup>2</sup>

2021 ApJ 906 46

<https://doi.org/10.3847/1538-4357/abc690>

In this study, we suggest a new method to estimate the mass of a halo coronal mass ejection (CME) using synthetic CMEs. For this, we generate synthetic CMEs based on two assumptions: (1) the CME structure is a full ice cream cone, and (2) the CME electron number density follows a power-law distribution ( $\rho_{\text{cme}} = \rho_0 r^{-n}$ ). The power-law exponent  $n$  is obtained by minimizing the rms error between the electron number density distributions of an observed CME and the corresponding synthetic CME at a position angle of the CME leading edge. By applying this methodology to 56 halo CMEs, we estimate two kinds of synthetic CME masses. One is a synthetic CME mass that considers only the observed CME region ( $M_{\text{cme1}}$ ), the other is a synthetic CME mass that includes both the observed CME region and the occulted area ( $M_{\text{cme2}}$ ). From these two cases, we derive conversion factors that are the ratio of a synthetic CME mass to an observed CME mass. The conversion factor for  $M_{\text{cme1}}$  ranges from 1.4 to 3.0 and its average is 2.0. For  $M_{\text{cme2}}$ , the factor ranges from 1.8 to 5.0 with an average of 3.0. These results imply that the observed halo CME mass can be underestimated by about 2 times when we consider the observed CME region, and about 3 times when we consider the region including the occulted area. Interestingly these conversion factors have a very strong negative correlation with angular widths of halo CMEs.

## Development of a Full Ice-cream Cone Model for Halo Coronal Mass Ejections

Hyeonock Na, Y.-J. Moon, and Harim Lee

2017 ApJ 839 82

<http://sci-hub.cc/10.3847/1538-4357/aa697c>

It is essential to determine three-dimensional parameters (e.g., radial speed, angular width, and source location) of coronal mass ejections (CMEs) for the space weather forecast. In this study, we investigate which cone type represents a halo CME morphology using 29 CMEs (12 Solar and Heliospheric Observatory (SOHO)/Large Angle and Spectrometric Coronagraph (LASCO) halo CMEs and 17 Solar Terrestrial Relations Observatory (STEREO)/Sun–Earth Connection Coronal and Heliospheric Investigation COR2 halo CMEs) from 2010 December to 2011 June. These CMEs are identified as halo CMEs by one spacecraft (SOHO or one of STEREO A and B) and limb ones by the other spacecraft (One of STEREO A and B or SOHO). From cone shape parameters of these CMEs, such as their front curvature, we find that the CME observational structures are much closer to a full ice-cream cone type than a shallow ice-cream cone type. Thus, we develop a full ice-cream cone model based on a new methodology that the full ice-cream cone consists of many flat cones with different heights and angular widths to estimate the three-dimensional parameters of the halo CMEs. This model is constructed by carrying out the following steps: (1) construct a cone for a given height and angular width, (2) project the cone onto the sky plane, (3) select points comprising the outer boundary, and (4) minimize the difference between the estimated projection speeds with the observed ones. By applying this model to 12 SOHO/LASCO halo CMEs, we find that 3D parameters from our method are similar to those from other stereoscopic methods (i.e., a triangulation method and a Graduated Cylindrical Shell model). **2011 February 15,**

**Table 1** Three-dimensional Parameters of 12 CMEs Based on the Full ice-cream cone Model and Two Stereoscopic Methods **2010 Dec 14 - 2011 Jun 21**

## Comparison of Cone Model Parameters for Halo Coronal Mass Ejections

Hyeonock Na, Y.-J. Moon, Soojeong Jang, Kyoung-Sun Lee, Hae-Yeon Kim

Solar Physics, November 2013, Volume 288, Issue 1, pp 313-329, **File**

Halo coronal mass ejections (HCMEs) are a major cause of geomagnetic storms, hence their three-dimensional structures are important for space weather. We compare three cone models: an elliptical-cone model, an ice-cream-cone model, and an asymmetric-cone model. These models allow us to determine three-dimensional parameters of HCMEs such as radial speed, angular width, and the angle  $[\gamma]$  between sky plane and cone axis. We compare these parameters obtained from three models using 62 HCMEs observed by SOHO/LASCO from 2001 to 2002. Then we obtain the root-mean-square (RMS) error between the highest measured projection speeds and their calculated projection speeds from the cone models. As a result, we find that the radial speeds obtained from the models are well correlated with one another ( $R > 0.8$ ). The correlation coefficients between angular widths range from 0.1 to 0.48 and those between  $\gamma$ -values range from  $-0.08$  to  $0.47$ , which is much smaller than expected. The reason may be the different assumptions and methods. The RMS errors between the highest measured projection speeds and the highest estimated projection speeds of the elliptical-cone model, the ice-cream-cone model, and the asymmetric-cone model are  $376 \text{ km s}^{-1}$ ,  $169 \text{ km s}^{-1}$ , and  $152 \text{ km s}^{-1}$ . We obtain the correlation coefficients between the location from the models and the flare location ( $R > 0.45$ ). Finally, we discuss strengths and weaknesses of these models in terms of space-weather application. **Table 2001 to 2002**

## X-ray flares and coronal mass ejections (CMEs) during very quiet solar activity conditions of 2009

Kamsali Nagaraja, Praveen Kumar Basuvaraj, S. C. Chakravarty

Indian Journal of Pure and Applied Physics, 2018

<https://arxiv.org/pdf/2008.11157.pdf>

Solar flares (SFs) are sudden brightening observed over the Sun surface which is associated with a large energy release. Flares with burst of X-ray emission are normally followed by a mass ejection of electrons and ions from the solar atmosphere called Coronal Mass Ejections (CMEs). There is an evidence that solar magnetic field can change its configuration through reconnection and release energy, accelerating solar plasma causing SFs and CMEs. This study examines the SFs and CMEs data from SOHO and GOES satellites during the very low solar activity year of 2009 and moderately high solar activity of 2002. The results indicate that certain modifications in the existing mechanisms of generating SFs and CMEs would be necessary for developing more realistic forecast models affecting the space weather conditions.

## Multi-wavelength Campaign Observations of a Young Solar-type Star, EK Draconis I. Discovery of Prominence Eruptions Associated with Superflares

Kosuke Namekata, Vladimir S. Airapetian, Pascal Petit, Hiroyuki Maehara, +++

2024 ApJ 961 23

<https://arxiv.org/pdf/2311.07380.pdf>

<https://iopscience.iop.org/article/10.3847/1538-4357/ad0b7c/pdf>

Young solar-type stars frequently produce superflares, serving as a unique window into the young Sun–Earth environments. Large solar flares are closely linked to coronal mass ejections (CMEs) associated with filament/prominence eruptions, but its observational evidence for stellar superflares remains scarce. Here, we present a

12-day multi-wavelength campaign observation of young solar-type star EK Draconis (G1.5V, 50-120 Myr age) utilizing TESS, NICER, and Seimei telescope. The star has previously exhibited blueshifted H $\alpha$  absorptions as evidence for a filament eruption associated with a superflare. Our simultaneous optical and X-ray observations identified three superflares of  $1.5 \times 10^{33}$  --  $1.2 \times 10^{34}$  erg. We report the first discovery of two prominence eruptions on a solar-type star, observed as blueshifted H $\alpha$  emissions at speed of 690 and 430 km s $^{-1}$  and masses of  $1.1 \times 10^{19}$  and  $3.2 \times 10^{17}$  g, respectively. The faster, massive event shows a candidate of post-flare X-ray dimming with the amplitude of up to  $\sim 10$  %. Several observational aspects consistently point to the occurrence of a fast CME associated with this event. The comparative analysis of the estimated length scales of flare loops, prominences, possible dimming region, and starspots provides the overall picture of the eruptive phenomena. Furthermore, the energy partition of the observed superflares in the optical and X-ray bands is consistent with flares from the Sun, M-dwarfs, and close binaries, yielding the unified empirical relations. These discoveries provide profound implications of impact of these eruptive events on the early Venus, Earth and Mars and young exoplanets.

### Hunting for stellar coronal mass ejections

[Kosuke Namekata](#), [Hiroyuki Maehara](#), [Satoshi Honda](#), [Yuta Notsu](#), [Daisaku Nogami](#), [Kazunari Shibata](#)  
Proceedings of IAUGA 2022 Focus Meeting 5 "Beyond the Goldilocks Zone: the Effect of Stellar Magnetic Activity on Exoplanet Habitability" 2022  
<https://arxiv.org/pdf/2211.05506.pdf>

Solar flares are often accompanied by filament/prominence eruptions, sometimes leading to coronal mass ejections (CMEs). By analogy, we expect that stellar flares are also associated with stellar CMEs whose properties are essential to know the impact on exoplanet habitability. Probable detections of stellar CMEs are still rare, but in this decade, there are several reports that (super-)flares on M/K-dwarfs and evolved stars sometimes show blue-shifted optical/UV/X-ray emissions lines, XUV/FUV dimming, and radio bursts. Some of them are interpreted as indirect evidence of stellar prominence eruptions/CMEs on cool stars. More recently, evidence of stellar filament eruption, probably leading to a CME, is reported even on a young solar-type star (G-dwarf) as a blue-shifted absorption of H $\alpha$  line associated with a superflare. Notably, the erupted masses for superflares are larger than those of the largest solar CMEs, indicating severe influence on exoplanet environments. The ratio of the kinetic energy of stellar CMEs to flare energy is significantly smaller than expected from the solar scaling relation and this discrepancy is still in debate. We will review the recent updates of stellar CME studies and discuss the future direction in this paper.

### Probable detection of an eruptive filament from a superflare on a solar-type star

[Kosuke Namekata](#), [Hiroyuki Maehara](#), [Satoshi Honda](#), +++  
Nature Astronomy (2021)  
<https://arxiv.org/pdf/2112.04808.pdf>  
<https://www.nature.com/articles/s41550-021-01532-8.pdf>  
<https://doi.org/10.1038/s41550-021-01532-8>

Solar flares are often accompanied by filament/prominence eruptions ( $\sim 104$  K and  $\sim 10^{10}$ – $11$  cm $^{-3}$ ), sometimes leading to coronal mass ejections (CMEs) that directly affect the Earth's environment. 'Superflares' are found on some active solar-type (G-type main-sequence) stars, but the association of filament eruptions/CMEs has not been established. Here we show that our optical spectroscopic observation of the young solar-type star EK Draconis reveals the evidence for a stellar filament eruption associated with a superflare. This superflare emitted a radiated energy of  $2.0 \times 10^{33}$  erg, and blue-shifted hydrogen absorption component with a large velocity of  $\sim 510$  km s $^{-1}$  was observed shortly after. The temporal changes in the spectra greatly resemble those of solar filament eruptions. Comparing this eruption with solar filament eruptions in terms of the length scale and velocity strongly suggests that a stellar CME occurred. The erupted filament mass of  $1.1 \times 10^{18}$  g is 10 times larger than those of the largest solar CMEs. The massive filament eruption and an associated CME provide the opportunity to evaluate how they affect the environment of young exoplanets/young Earth and stellar mass/angular-momentum evolution. **7 Jul 2016**

See [https://www.gazeta.ru/science/2021/12/10\\_a\\_14299729.shtml](https://www.gazeta.ru/science/2021/12/10_a_14299729.shtml)

### Twisted Solar Active Region Magnetic Fields as Drivers of Space Weather: Observational and Theoretical Investigations

Dibyendu [Nandy](#) a,†, Duncan H. Mackay b, Richard C. Canfield a and P.C.H. Martens  
Journal of Atmospheric and Solar-Terrestrial Physics  
Volume 70, Issues 2-4, February 2008, Pages 605-613, **File**.

The properties and dynamics of magnetic fields on the Sun's photosphere and outer layers { notably those within solar active regions { govern the eruptive activity of the Sun. These photospheric magnetic fields also act as the evolving lower boundary of the Sun-Earth coupled system. Quantifying the physical attributes of these magnetic fields and exploring the mechanisms underlying their influence on the near-Earth space environment are of vital importance for forecasting and mitigating adverse space weather effects. In this context, we discuss here a novel technique for measuring twist in the magnetic field lines of solar active regions that does not invoke the force-free field assumption. Twist in solar active regions can play an important role in driving activity and the initiation of CMEs via the kink instability

mechanism; we outline a procedure for determining this solar active region eruptive potential. We also discuss how twist in active region magnetic fields can be used as inputs in simulations of the coronal and heliospheric fields; specifically, we explore through simulations, the formation, evolution and ejection of magnetic flux ropes that originate in twisted magnetic structures. The results and ideas presented here are relevant for exploring the role of twisted solar active region magnetic fields and flux ropes as drivers of space weather in the Sun-Earth system.

## **Statistical Study of Network Jets Observed in the Solar Transition Region: a Comparison Between Coronal Holes and Quiet-Sun Regions**

Nancy [Narang](#), Rebecca T. Arbacher, Hui Tian, Dipankar Banerjee, Steven R. Cranmer, Ed E. DeLuca, Sean McKillop

Solar Phys. Volume 291, Issue 4, pp 1129-1142 2016

<http://arxiv.org/pdf/1604.06295v1.pdf>

Recent IRIS observations have revealed a prevalence of intermittent small-scale jets with apparent speeds of 80–250 km s<sup>-1</sup>, emanating from small-scale bright regions inside network boundaries of coronal holes. We find that these network jets appear not only in coronal holes but also in quiet-sun regions. Using IRIS 1330 Å (C II) slit-jaw images, we extracted several parameters of these network jets, e.g. apparent speed, length, lifetime, and increase in foot-point brightness. Using several observations, we find that some properties of the jets are very similar, but others are obviously different between the quiet Sun and coronal holes. For example, our study shows that the coronal-hole jets appear to be faster and longer than those in the quiet Sun. This can be directly attributed to a difference in the magnetic configuration of the two regions, with open magnetic field lines rooted in coronal holes and magnetic loops often present in the quiet Sun. We also detected compact bright loops that are most likely transition region loops and are mostly located in quiet-Sun regions. These small loop-like regions are generally devoid of network jets. In spite of different magnetic structures in the coronal hole and quiet Sun in the transition region, there appears to be no substantial difference for the increase in footpoint brightness of the jets, which suggests that the generation mechanism of these network jets is very likely the same in both regions. **2014-01-23-24, 2014-01-29, 2014-02-12**

## **Thermal conduction effects on formation of chromospheric solar tadpole-like jets**

[Anamaría Navarro](#), [F. D. Lora-Clavijo](#), [K. Murawski](#), [Stefaan Poedts](#)

MNRAS 2020

<https://arxiv.org/pdf/2011.02006.pdf>

We measure the effects of non-isotropic thermal conduction on generation of solar chromospheric jets through numerical simulations carried out with the use of one fluid MHD code MAGNUS. Following the work of Srivastava et al. (2018), we consider the atmospheric state with a realistic temperature model and generate the ejection of plasma through a gas pressure driver operating in the top chromosphere. We consider the magnetic field mimicking a flux tube and perform parametric studies by varying the magnetic field strength and the amplitude of the driver. We find that in the case of thermal conduction the triggered jets exhibit a considerably larger energy and mass fluxes and their shapes are more collimated and penetrate more the solar corona than for the ideal MHD equations. Low magnetic fields allow these jets to be more energetic, and larger magnetic fields decrease the enhancement of mass and energy due to the inclusion of the thermal conductivity.

## **Exploring the magnetic and thermal evolution of a coronal jet**

[Sushree S Nayak](#), [Samrat Sen](#), [Arpit Kumar Shrivastav](#), [R. Bhattacharyya](#), [P.S. Athiray](#)

ApJ 975 143 2024

<https://arxiv.org/pdf/2409.03484>

<https://iopscience.iop.org/article/10.3847/1538-4357/ad779c/pdf>

Coronal jets are the captivating eruptions which are often found in the solar atmosphere, and primarily formed due to magnetic reconnection. Despite their short-lived nature and lower energy compared to many other eruptive events, e.g. flares and coronal mass ejections, they play an important role in heating the corona and accelerating charged particles. However, their generation in the ambience of non-standard flare regime is not fully understood, and warrant a deeper investigation, in terms of their onset, growth, eruption processes, and thermodynamic evolution. Toward this goal, this paper reports the results of a data-constrained three-dimensional (3D) magnetohydrodynamics (MHD) simulation of an eruptive jet; initialized with a Non-Force-Free-Field (NFFF) extrapolation and carried out in the spirit of Implicit Large Eddy Simulation (ILES). The simulation focuses on the magnetic and dynamical properties of the jet during its onset, and eruption phases, that occurred on **February 5, 2015** in an active region NOAA AR12280, associated with a seemingly three-ribbon structure. In order to correlate its thermal evolution with computed energetics, the simulation results are compared with differential emission measurement (DEM) analysis in the vicinity of the jet. Importantly, this combined approach provides an insight to the onset of reconnection in transients in terms of emission and the corresponding electric current profiles from MHD evolutions. The presented study captures the intricate topological dynamics, finds a close correspondence between the magnetic and thermal evolution in and around the jet location. Overall, it enriches the understanding of the thermal evolution due to MHD processes, which is one of the broader aspects to reveal the coronal heating problem.

## A Data-constrained Magnetohydrodynamic Simulation of Successive Events of Blowout Jet and C-class Flare in NOAA AR 12615

Sushree S. [Nayak](#)<sup>1</sup>, R. Bhattacharyya<sup>1</sup>, A. Prasad<sup>2</sup>, Qiang Hu<sup>2</sup>, Sanjay Kumar<sup>3</sup>, and B. Joshi<sup>1</sup>

2019 ApJ 875 10

[sci-hub.se/10.3847/1538-4357/ab0a0b](https://doi.org/10.3847/1538-4357/ab0a0b)

Magnetohydrodynamic simulation is carried out for the NOAA AR 12615 in the time span  $t \in \{05:48, 06:18\}$  UT on **2016 December 5**; covering events of a blowout jet and a C1.2 flare. The events are selected based on the small interval between their occurrences, which provides us with an opportunity to explore two energetically different events of magnetic reconnection (MR) within the run time of a single magnetohydrodynamic (MHD) simulation. The simulation is initiated with magnetic field extrapolated from the vector magnetogram provided by the Helioseismic Magnetic Imager/Solar Dynamics Observatory, using a non-force-free approximation. The extrapolated Lorentz force is found to decay at a rate faster than the volume current density, making the higher corona to be effectively force-free while the Lorentz force affects only the lower corona and the photosphere—a desirable feature that agrees with the contemporary understanding. For the simulation, the plasma is idealized to be incompressible, thermally homogeneous and having perfect electrical conductivity. The results affirm MRs near a set of two three-dimensional (3D) magnetic nulls to be responsible for initiating the jet. Moreover, a flux rope located near the nulls contributes to the jet by changing its magnetic field lines from an anchored to an open topology. The scenario agrees with the standard mini-filament breakout model for blowout jets and provides its first demonstration from a 3D data-constrained MHD simulation where the computational output is reconciled with magnetogram(s) only once. The generation of flare ribbons is attributed to reconnections at a 3D null and a quasi-separatrix layer (QSL), highlighting the importance of topological complexity in flare initiation.

## Characterization of the Early Dynamics of Solar Coronal Bright Fronts

Mohamed [Nedal](#), [Kamen Kozarev](#), [Rositsa Miteva](#), [Oleg Stepanyuk](#), [Momchil Dechev](#)

Bulgarian Astronomical Journal 2024

<https://arxiv.org/pdf/2404.03396.pdf>

We present a comprehensive characterization of 26 CME-driven compressive waves known as Coronal Bright Fronts (CBFs) observed in the low solar corona between 2010 and 2017. These CBFs have been found to be associated with SEP events near Earth, indicating their importance in understanding space weather phenomena. The aim of this study is to analyze and describe the early dynamics of CBFs using a physics-based heliospheric SEP forecasting system known as the SPREAdFAST framework. This framework utilizes a chain of data-driven analytic and numerical models to predict SEP fluxes at multiple locations in the inner heliosphere by considering their acceleration at CMEs near the Sun and subsequent interplanetary transport. To estimate the time-dependent plasma and compression parameters of the CBFs, we utilized sequences of base-difference images obtained from the AIA instrument on board the SDO satellite, and measurements of the height-time profiles of the CMEs obtained from the LASCO instrument on board the SOHO satellite. We employed kinematic measurements and plasma model results to derive these parameters. The SPREAdFAST framework facilitated the analysis and correlation of these observations with SEP events near Earth. Our analysis yielded statistical relations and distributions for both the shocks and plasma parameters associated with the 26 CBFs investigated. By combining the observations from the AIA and LASCO instruments, as well as the data products from the SPREAdFAST framework, we obtained a comprehensive understanding of the early dynamics of CBFs, including their temporal evolution, plasma properties, and compressional characteristics. These findings contribute to the growing body of knowledge in the field and have implications for space weather forecasting and the study of SEP events. **2011-05-11**

**Table 1:** List of the CBF events with their associated flares and CMEs 2010-2017

## Investigating the Coronal Mass Ejections associated with DH type-II radio bursts and solar flares during the ascending phase of the solar cycle 24

Mohamed [Nedal](#), [M.Youssef AymanMahrous](#), [RababHelal](#)

[Advances in Space Research](#) Volume 63, Issue 5, 1 March 2019, Pages 1824-1836

[sci-hub.tw/10.1016/j.asr.2018.11.001](https://doi.org/10.1016/j.asr.2018.11.001)

We studied a set of 74 CMEs, with shedding the light on the halo-CMEs (HCMEs), that are associated with decametric – hectometric (DH) type-II radio bursts (1–16 MHz) and [solar flares](#) during the period 2008–2014. The events were classified into 3 groups (disk, intermediate, and limb events) based on their longitudinal distribution.

We found that the events are mostly distributed around  $15.32^\circ$  and  $15.97^\circ$  at the northern and southern solar hemispheres, respectively. We found that there is a clear dependence between the longitude and the CME's width, speed, acceleration, mass, and [kinetic energy](#). For the CMEs' widths, most of the events were HCMEs (~62%), while the partial HCMEs comprised ~35% and the rest of events were CMEs with widths less than  $120^\circ$ . For the CMEs' speeds, masses, and kinetic energies, the mean values showed a direct proportionality with the longitude, in which the limb events had the highest speeds, the largest masses, and the highest kinetic energies. The mean peak flux of the solar flares for different longitudes was comparable, but the disk flares were more energetic. The intermediate flares were considered as gradual flares since they tended to last longer, while the limb flares were considered as impulsive flares since they tended to last shorter.

A weak correlation ( $R = 0.32$ ) between the kinetic energy of the CMEs and the duration of the associated flares has been noticed, while there was a good correlation ( $R = 0.76$ ) between the kinetic energy of the CMEs and the peak flux of the

associated flares. We found a fair correlation ( $R = 0.58$ ) between the kinetic energy of the CMEs and the duration of the associated DH type-II radio bursts.

### **A multi-instrument study of ultraviolet bursts and associated surges in AR 12957**

[C. J. Nelson](#), [D. Calchetti](#), [A. Gandorfer](#), [J. Hirzberger](#), [J. Sinjan](#), [S. K. Solanki](#), [D. Berghmans](#), [H. Strecker](#), [J. Blanco](#)

A&A 691, A247 2024

<https://arxiv.org/pdf/2410.07770>

<https://www.aanda.org/articles/aa/pdf/2024/11/aa51925-24.pdf>

The relationship between UV Bursts and solar surges is complex, with these events sometimes being observed together and sometimes being observed independently. Why this sporadic association exists is unknown, however, it likely relates to the physical conditions at the site of the energy release that drives these events. Here, we aim to better understand the relationship between UV Bursts and solar surges through a multi-instrument analysis of several associated events that occurred around the trailing sunspot in AR 12957. We use data from Solar Orbiter, the Solar Dynamics Observatory (SDO), and the Interface Region Imaging Spectrograph (IRIS) to achieve our aims. These data were sampled on **3rd March 2022** between 09:30:30 UT and 11:00:00 UT, during which time a coordinated observing campaign associated with the Slow Solar Wind Connection Solar Orbiter Observing Plan took place. Numerous small-scale negative polarity magnetic features (MMFs) are observed to move quickly (potentially up to 3.3 km/s) away from a sunspot until they collide with a more stable positive polarity plage region around 7 Mm away. Several UV Bursts are identified in IRIS slit-jaw imager (SJI) 1400 Å data co-spatial to where these opposite polarity fields interact, with spatial scales (2 Mm<) and lifetimes (20< min) larger than typical values for such events. Two surges are also observed to occur at these locations, with one being short (5 Mm) and hot (bright in IRIS SJI images), whilst the other is a cooler (dark in coronal imaging channels), longer surge that appears to fill an active region loop. Magnetic reconnection between the negative polarity MMFs around the sunspot and the positive polarity plage region appears to be the driver of these events. Both the speed of the MMFs and the locally open magnetic topology of the plage region could possibly be important for forming the surges.

### **Spatially resolved signatures of bi-directional flows observed in inverted-Y shaped jets**

[C. J. Nelson](#), [N. Freij](#), [S. Bennett](#), [R. Erdélyi](#), [M. Mathioudakis](#)

ApJ 883 115 2019

<https://arxiv.org/pdf/1908.05132.pdf>

<https://iopscience.iop.org/article/10.3847/1538-4357/ab3a54/pdf>

Numerous apparent signatures of magnetic reconnection have been reported in the solar photosphere, including inverted-Y shaped jets. The reconnection at these sites is expected to cause localised bi-directional flows and extended shock waves; however, these signatures are rarely observed as extremely high spatial-resolution data are required. Here, we use H-alpha imaging data sampled by the Swedish Solar Telescope's CRisp Imaging SpectroPolarimeter to investigate whether bi-directional flows can be detected within inverted-Y shaped jets near the solar limb. These jets are apparent in the H-alpha line wings, while no signature of either jet is observed in the H-alpha line core, implying reconnection took place below the chromospheric canopy. Asymmetries in the H-alpha line profiles along the legs of the jets indicate the presence of bi-directional flows, consistent with cartoon models of reconnection in chromospheric anemone jets. These asymmetries are present for over two minutes, longer than the lifetimes of Rapid Blue Excursions, and beyond  $\sim 1 \text{ \AA}$  into the wings of the line indicating that flows within the inverted-Y shaped jets are responsible for the imbalance in the profiles, rather than motions in the foreground. Additionally, surges form following the occurrence of the inverted-Y shaped jets. This surge formation is consistent with models which suggest such events could be caused by the propagation of shock waves from reconnection sites in the photosphere to the upper atmosphere. Overall, our results provide evidence that magnetic reconnection in the photosphere can cause bi-directional flows within inverted-Y shaped jets and could be the driver of surges. **21st June 2012**

### **Power spectra of solar brightness variations at various inclinations A43**

N.-E. [Nèmec](#)<sup>1</sup>, A. I. Shapiro<sup>1</sup>, N. A. Krivova<sup>1</sup>, S. K. Solanki<sup>1,2</sup>, R. V. Tagirov<sup>1,3</sup>, R. H. Cameron<sup>1</sup>, and S. Dreizler<sup>4</sup>

A&A 636, A43 (2020)

<https://www.aanda.org/articles/aa/pdf/2020/04/aa37588-20.pdf>

Context. Magnetic features on the surfaces of cool stars lead to variations in their brightness. Such variations on the surface of the Sun have been studied extensively. Recent planet-hunting space telescopes have made it possible to measure brightness variations in hundred thousands of other stars. The new data may undermine the validity of setting the sun as a typical example of a variable star. Putting solar variability into the stellar context suffers, however, from a bias resulting from solar observations being carried out from its near-equatorial plane, whereas stars are generally observed at all possible inclinations.

Aims. We model solar brightness variations at timescales from days to years as they would be observed at different inclinations. In particular, we consider the effect of the inclination on the power spectrum of solar brightness variations. The variations are calculated in several passbands that are routinely used for stellar measurements.

Methods. We employ the surface flux transport model to simulate the time-dependent spatial distribution of magnetic features on both the near and far sides of the Sun. This distribution is then used to calculate solar brightness variations following the Spectral And Total Irradiance REconstruction approach.

Results. We have quantified the effect of the inclination on solar brightness variability at timescales down to a single day. Thus, our results allow for solar brightness records to be made directly comparable to those obtained by planet-hunting space telescopes. Furthermore, we decompose solar brightness variations into components originating from the solar rotation and from the evolution of magnetic features.

## **Relation of Microstreams in the Polar Solar Wind to Switchbacks and Coronal X-ray Jets**

Marcia Neugebauer, [Alphonse C. Sterling](#)

2021

<https://arxiv.org/ftp/arxiv/papers/2110/2110.00079.pdf>

Ulysses data obtained at high solar latitudes during periods of minimum solar activity in 1994 and 2007 are examined to determine the relation between velocity structures called microstreams and folds in the magnetic field called switchbacks. A high correlation is found. The possibility of velocity peaks in microstreams originating from coronal X-ray jets is re-examined; we now suggest that microstreams are the consequence of the alternation of patches of switchbacks and quiet periods, where the switchbacks could be generated by minifilament/flux rope eruptions that cause coronal jets. **3 Dec 2007, 19 Dec 2007**

## **The Merging of a Coronal Dimming and the Southern Polar Coronal Hole**

Nawin [Ngampoopun](#)<sup>1</sup>, David M. Long<sup>1,2</sup>, Deborah Baker<sup>1</sup>, Lucie M. Green<sup>1</sup>, Stephanie L.

Yardley<sup>1,3,4</sup>, Alexander W. James<sup>1,5</sup>, and Andy S. H. To

2023 ApJ 950 150

<https://arxiv.org/pdf/2305.06106.pdf>

<https://iopscience.iop.org/article/10.3847/1538-4357/acd44e/pdf>

We report on the merging between the southern polar coronal hole and an adjacent coronal dimming induced by a coronal mass ejection on **2022 March 18**, resulting in the merged region persisting for at least 72 hr. We use remote sensing data from multiple co-observing spacecraft to understand the physical processes during this merging event. The evolution of the merger is examined using Extreme-Ultraviolet (EUV) images obtained from the Atmospheric Imaging Assembly on board the Solar Dynamic Observatory and Extreme Ultraviolet Imager, which is on board the Solar Orbiter spacecraft. The plasma dynamics are quantified using spectroscopic data obtained from the EUV Imaging Spectrometer on board Hinode. The photospheric magnetograms from the Helioseismic and Magnetic Imager are used to derive the magnetic field properties. To our knowledge, this work is the first spectroscopical analysis of the merging of two open-field structures. We find that the coronal hole and the coronal dimming become indistinguishable after the merging. The upflow speeds inside the coronal dimming become more similar to that of a coronal hole, with a mixture of plasma upflows and downflows observable after the merging. The brightening of the bright points and the appearance of coronal jets inside the merged region further imply ongoing reconnection processes. We propose that component reconnection between the coronal hole and coronal dimming fields plays an important role during this merging event because the footpoint switching resulting from the reconnection allows the coronal dimming to intrude onto the boundary of the southern polar coronal hole.

## **Decayless longitudinal oscillations of a solar filament maintained by quasi-periodic jets**

[Y. W. Ni](#), [J. H. Guo](#), [Q. M. Zhang](#), [J. L. Chen](#), [C. Fang](#), [P. F. Chen](#)

A&A 663, A31 2022

<https://arxiv.org/pdf/2203.15660.pdf>

<https://www.aanda.org/articles/aa/pdf/2022/07/aa42979-21.pdf>

Context: As a ubiquitous phenomenon, large-amplitude longitudinal filament oscillations usually decay in 1--4 periods. Recently, we observed a decayless case of such oscillations in the corona. Aims: We try to understand the physical process that maintains the decayless oscillation of the filament. Methods: Multi-wavelength imaging observations and magnetograms are collected to study the dynamics of the filament oscillation and its associated phenomena. To explain the decayless oscillations, we also perform one-dimensional hydrodynamic numerical simulations using the MPI-AMRVAC code. Results: In observations, the filament oscillates decaylessly with a period of  $36.4 \pm 0.3$  min for almost 4 hours before eruption. During oscillations, four quasi-periodic jets emanate from a magnetic cancellation site near the filament. The time interval between neighboring jets is  $\sim 68.9 \pm 1.0$  min. Numerical simulations constrained by the observations reproduced the decayless longitudinal oscillations. However, it is surprising to find that the period of the decayless oscillations is not consistent with the pendulum model. Conclusions: We propose that the decayless longitudinal oscillations of the filament are maintained by quasi-periodic jets, which is verified by the hydrodynamic simulations. More importantly, it is found that, when driven by quasi-periodic jets, the period of the filament longitudinal oscillations depends also on the driving period of the jets, not simply the pendulum period. With a parameter survey in simulations, we derived a formula, by which one can derive the pendulum oscillation period using the observed period of decayless filament oscillations and the driving periods of jets. **2014 July 5**

## **Blob formation and ejection in coronal jets due to the plasmoid and Kelvin-Helmholtz instabilities**

Lei [Ni](#), Qing-Min Zhang, Nicholas A. Murphy, Jun Lin



2017 ApJ 841 27

<https://arxiv.org/pdf/1705.00180.pdf>

We perform two-dimensional resistive magnetohydrodynamic simulations of coronal jets driven by flux emergence along the lower boundary. The reconnection layers are susceptible to the formation of blobs that are ejected in the jet. Our simulation with low plasma  $\beta$  (Case I) shows that magnetic islands form easily and propagate upwards in the jet. These islands are multithermal and thus are predicted to show up in hot channels (335 \AA), and 211 \AA) and the cool channel (304 \AA) in observations by the Atmospheric Imaging Assembly (AIA) on the *Solar Dynamics Observatory*. The islands have maximum temperatures of 8 MK, lifetimes of 120 s, diameters of 6 Mm, and velocities of 200 km s<sup>-1</sup>. These parameters are similar to the properties of blobs observed in EUV jets by AIA. The Kelvin-Helmholtz instability develops in our simulation with moderately high plasma  $\beta$  (Case II), and leads to the formation of bright vortex-like blobs above the multiple high magneto-sonic Mach number regions that appear along the jet. These vortex-like blobs can also be identified in the AIA channels. However, they eventually move downward and disappear after the high magneto-sonic Mach number regions disappear. In the lower plasma  $\beta$  case, the lifetime for the jet is shorter, the jet and magnetic islands are formed with higher velocities and temperatures, the current sheet fragments are more chaotic, and more magnetic islands are generated. Our results show that the plasmoid instability and Kelvin-Helmholtz instability along the jet are both possible causes of the formation of blobs observed at extreme ultraviolet (EUV) wavelengths.

## Fast Magnetic Reconnection in the Solar Chromosphere Mediated by the Plasmoid Instability

Lei Ni<sup>1,2</sup>, Bernhard Kliem<sup>1,3</sup>, Jun Lin<sup>1</sup>, and Ning Wu

2015 ApJ 799 79

<http://arxiv.org/pdf/1509.06895v1.pdf>

Magnetic reconnection in the partially ionized solar chromosphere is studied in 2.5 dimensional magnetohydrodynamic simulations including radiative cooling and ambipolar diffusion. A Harris current sheet with and without a guide field is considered. Characteristic values of the parameters in the middle chromosphere imply a high magnetic Reynolds number of  $\sim 106$ - $107$  in the present simulations. Fast magnetic reconnection then develops as a consequence of the plasmoid instability without the need to invoke anomalous resistivity enhancements. Multiple levels of the instability are followed as it cascades to smaller scales, which approach the ion inertial length. The reconnection rate, normalized to the asymptotic values of magnetic field and Alfvén velocity in the inflow region, reaches values in the range  $\sim 0.01$ - $0.03$  throughout the cascading plasmoid formation and for zero as well as for strong guide field. The outflow velocity reaches  $\approx 40$  km s<sup>-1</sup>. Slow-mode shocks extend from the X-points, heating the plasmoids up to  $\sim 8 \times 10^4$  K. In the case of zero guide field, the inclusion of both ambipolar diffusion and radiative cooling causes a rapid thinning of the current sheet (down to  $\sim 30$  m) and early formation of secondary islands. Both of these processes have very little effect on the plasmoid instability for a strong guide field. The reconnection rates, temperature enhancements, and upward outflow velocities from the vertical current sheet correspond well to their characteristic values in chromospheric jets.

## IMPACT OF TEMPERATURE-DEPENDENT RESISTIVITY AND THERMAL CONDUCTION ON PLASMOID INSTABILITIES IN CURRENT SHEETS IN THE SOLAR CORONA

Lei Ni<sup>1,2</sup>, Ilia I. Roussev<sup>1,3</sup>, Jun Lin<sup>1</sup>, and Udo Ziegler

2012 ApJ 758 20

In this paper, we investigate, by means of two-dimensional magnetohydrodynamic simulations, the impact of temperature-dependent resistivity and thermal conduction on the development of plasmoid instabilities in reconnecting current sheets in the solar corona. We find that the plasma temperature in the current-sheet region increases with time and it becomes greater than that in the inflow region. As secondary magnetic islands appear, the highest temperature is not always found at the reconnection X-points, but also inside the secondary islands. One of the effects of anisotropic thermal conduction is to decrease the temperature of the reconnecting X-points and transfer the heat into the O-points, the plasmoids, where it gets trapped. In the cases with temperature-dependent magnetic diffusivity,  $\eta \sim T^{-3/2}$ , the decrease in plasma temperature at the X-points leads to (1) an increase in the magnetic diffusivity until the characteristic time for magnetic diffusion becomes comparable to that of thermal conduction, (2) an increase in the reconnection rate, and (3) more efficient conversion of magnetic energy into thermal energy and kinetic energy of bulk motions. These results provide further explanation of the rapid release of magnetic energy into heat and kinetic energy seen during flares and coronal mass ejections. In this work, we demonstrate that the consideration of anisotropic thermal conduction and Spitzer-type, temperature-dependent magnetic diffusivity, as in the real solar corona, are crucially important for explaining the occurrence of fast reconnection during solar eruptions.

## Classification of CMEs Based on Their Dynamics

J. Nicewicz, G. Michalek

Solar Phys. Volume 291, Issue 5, pp 1417–1432 2016 File

A large set of coronal mass ejections CMEs (6621) has been selected to study their dynamics seen with the Large Angle and Spectroscopic Coronagraph (LASCO) onboard the Solar and Heliospheric Observatory (SOHO) field of view

(LFOV). These events were selected based on having at least six height-time measurements so that their dynamic properties, in the LFOV, can be evaluated with reasonable accuracy. Height-time measurements (in the SOHO/LASCO catalog) were used to determine the velocities and accelerations of individual CMEs at successive distances from the Sun. Linear and quadratic functions were fitted to these data points. On the basis of the best fits to the velocity data points, we were able to classify CMEs into four groups. The types of CMEs do not only have different dynamic behaviors but also different masses, widths, velocities, and accelerations. We also show that these groups of events are initiated by different onset mechanisms. The results of our study allow us to present a consistent classification of CMEs based on their dynamics.

## Testing the Asymmetric Cone Model for Halo CMEs Using STEREO/SECCHI Coronagraphic Observations

Janusz **Nicewicz**, Grzegorz Michalek

Advances in Space Research, 2014

<http://www.sciencedirect.com/science/article/pii/S0273117714002646#>

Space weather is significantly controlled by halo coronal mass ejections (HCMEs) originating close to the central meridian and directing toward the Earth. Unfortunately, coronagraphic observations (especially for HCMEs) are subject to a projection effect which makes it impossible to determine the true radial velocity and width of CMEs. However, these parameters can be estimated by correcting for the projection effect using the asymmetric cone model (Michalek, Solar Phys. 237, 101, 2006). A set of 20 CMEs, observed as halo events in the LASCO field of view and simultaneously as limb events in the STEREO/SECCHI field of view, are used to check the accuracy of the asymmetric cone model. For this purpose, characteristics of the considered CMEs (angular widths and radial speeds) measured in STEREO/SECCHI images are compared with those obtained by the asymmetric cone model. We demonstrate that the widths and speeds determined by both methods are very similar. Correlation coefficients for speeds and angular widths are 0.99 and 0.96, respectively. We have also shown that the projection effect is unpredictable and could sometimes be very significant (up to 100% of the velocity measured in the LASCO field of view). On average, the SOHO/LASCO projected speeds for the HCMEs are 23% smaller than the radial velocities obtained from the STEREO/SECCHI images.

## Redefining Flux Ropes in Heliophysics

**Review**

Teresa **Nieves-Chinchilla**, Sanchita Pal, Tarik Salman, Fernando Carcaboso, et al.

Front. Astron. Space Sci. 10: 1114838 2023

<https://www.frontiersin.org/articles/10.3389/fspas.2023.1114838/full>

<https://www.frontiersin.org/articles/10.3389/fspas.2023.1114838/pdf>

Magnetic flux ropes manifest as twisted bundles of magnetic field lines. They carry significant amounts of solar mass in the heliosphere. This paper underlines the need to advance our understanding of the fundamental physics of heliospheric flux ropes and provides the motivation to significantly improve the status quo of flux rope research through novel and requisite approaches. It briefly discusses the current understanding of flux rope formation and evolution, and summarizes the strategies that have been undertaken to understand the dynamics of heliospheric structures. The challenges and recommendations put forward to address them are expected to broaden the in-depth knowledge of our nearest star, its dynamics, and its role in its region of influence, the heliosphere.

## Inner Heliospheric Evolution of a "Stealth" CME Derived from Multi-view Imaging and Multipoint in Situ observations. I. Propagation to 1 AU

T. **Nieves-Chinchilla**<sup>1,2</sup>, A. Vourlidas<sup>3</sup>, G. Stenborg<sup>4</sup>, N. P. Savani<sup>2,5</sup>, A. Koval<sup>2,6</sup>, A. Szabo<sup>2</sup>, and L. K. Jian

2013 ApJ 779 55

Coronal mass ejections (CMEs) are the main driver of space weather. Therefore, a precise forecasting of their likely geo-effectiveness relies on an accurate tracking of their morphological and kinematical evolution throughout the interplanetary medium. However, single viewpoint observations require many assumptions to model the development of the features of CMEs. The most common hypotheses were those of radial propagation and self-similar expansion. The use of different viewpoints shows that, at least for some cases, those assumptions are no longer valid. From radial propagation, typical attributes that can now be confirmed to exist are over-expansion and/or rotation along the propagation axis. Understanding the 3D development and evolution of the CME features will help to establish the connection between remote and in situ observations, and hence help forecast space weather. We present an analysis of the morphological and kinematical evolution of a STEREO-B-directed CME on **2009 August 25-27**. By means of a comprehensive analysis of remote imaging observations provided by the SOHO, STEREO, and SDO missions, and in situ measurements recorded by Wind, ACE, and MESSENGER, we prove in this paper that the event exhibits signatures of deflection, which are usually associated with changes in the direction of propagation and/or also with rotation. The interaction with other magnetic obstacles could act as a catalyst of deflection or rotation effects. We also propose a method to investigate the change of the CME tilt from the analysis of height-time direct measurements. If this method is validated in further work, it may have important implications for space weather studies because it will allow for inference of the interplanetary counterpart of the CME's orientation.

## Remote and in situ observations of an unusual Earth-directed coronal mass ejection from multiple viewpoints

[Nieves-Chinchilla, T.](#); [Colaninno, R.](#); [Vourlidas, A.](#); [Szabo, A.](#); [Lepping, R. P.](#); [Boardsen, S. A.](#); [Anderson, B. J.](#); [Korth, H.](#)

J. Geophys. Res., Vol. 117, No. A6, A06106, 2012

<http://dx.doi.org/10.1029/2011JA017243>

During **June 16–21, 2010**, an Earth-directed coronal mass ejection (CME) event was observed by instruments onboard STEREO, SOHO, MESSENGER and Wind. This event was the first direct detection of a rotating CME in the middle and outer corona. Here, we carry out a comprehensive analysis of the evolution of the CME in the interplanetary medium comparing in situ and remote observations, with analytical models and three-dimensional reconstructions. In particular, we investigate the parallel and perpendicular cross section expansion of the CME from the corona through the heliosphere up to 1 AU. We use height-time measurements and the Gradual Cylindrical Shell (GCS) technique to model the imaging observations, remove the projection effects, and derive the 3-dimensional extent of the event. Then, we compare the results with in situ analytical Magnetic Cloud (MC) models, and with geometrical predictions from past works. We find that the parallel (along the propagation plane) cross section expansion agrees well with the in situ model and with the Bothmer and Schwenn (1998) empirical relationship based on in situ observations between 0.3 and 1 AU. Our results effectively extend this empirical relationship to about 5 solar radii. The expansion of the perpendicular diameter agrees very well with the in situ results at MESSENGER (~0.5 AU) but not at 1 AU. We also find a slightly different, from Bothmer and Schwenn (1998), empirical relationship for the perpendicular expansion. More importantly, we find no evidence that the CME undergoes a significant latitudinal over-expansion as it is commonly assumed. Instead, we find evidence that effects due to CME rotation and expansion can be easily confused in the images leading to a severe overestimation of the proper 3D size of the event. Finally, we find that the reconstructions of the CME morphology from the in situ observations at 1 AU are in agreement with the remote sensing observations but they show a big discrepancy at MESSENGER. We attribute this discrepancy to the ambiguity of selecting the proper boundaries due to the lack of accompanying plasma measurements.

## Magnetic helicity and energy budgets of jet events from an emerging solar active region

[A. Nindos](#), [S. Patsourakos](#), [K. Moraitis](#), [V. Archontis](#), [E. Liokati](#), [M. K. Georgoulis](#), [A. A. Norton](#)

A&A 689, L11 2024

<https://arxiv.org/pdf/2409.00931>

<https://www.aanda.org/articles/aa/pdf/2024/09/aa51441-24.pdf>

Using photospheric vector magnetograms obtained by the Helioseismic and Magnetic Imager on board the Solar Dynamic Observatory and a magnetic connectivity-based method, we compute the magnetic helicity and free magnetic energy budgets of a simple bipolar solar active region (AR) during its magnetic flux emergence phase which lasted ~47 hrs. The AR did not produce any coronal mass ejections (CMEs) or flares with an X-ray class above C1.0 but it was the site of 60 jet events during its flux emergence phase. The helicity and free energy budgets of the AR were below established eruption-related thresholds throughout the interval we studied. However, in addition to their slowly-varying evolution, each of the time profiles of the helicity and free energy budgets showed discrete localized peaks, with eight pairs of them occurring at times of jets emanating from the AR. These jets featured larger base areas and longer durations than the other jets of the AR. We estimated, for the first time, the helicity and free magnetic energy changes associated with these eight jets which were in the ranges of  $0.5\text{--}7.1 \times 10^{40} \text{ Mx}^2$  and  $1.1\text{--}6.9 \times 10^{29} \text{ erg}$ , respectively. Although these values are one to two orders of magnitude smaller than those usually associated with CMEs, the relevant percentage changes were significant and ranged from 13% to 76% for the normalized helicity and from 9% to 57% for the normalized free magnetic energy. Our study indicates that occasionally jets may have a significant imprint in the evolution of helicity and free magnetic energy budgets of emerging active regions. **8 Aug 2010**

## When do solar erupting hot magnetic flux ropes form?

[A. Nindos](#), [S. Patsourakos](#), [A. Vourlidas](#), [X. Cheng](#), [J. Zhang](#)

A&A 642, A109 2020

<https://arxiv.org/pdf/2008.04380.pdf>

<https://doi.org/10.1051/0004-6361/202038832>

We investigate the formation times of eruptive magnetic flux ropes relative to the onset of solar eruptions, which is important for constraining models of coronal mass ejection (CME) initiation. We inspected uninterrupted sequences of 131 Å images that spanned more than eight hours and were obtained by the Atmospheric Imaging Assembly (AIA) on board the Solar Dynamics Observatory (SDO) to identify the formation times of hot flux ropes that erupted in CMEs from locations close to the limb. The appearance of the flux ropes as well as their evolution toward eruptions were determined using morphological criteria. Two-thirds (20/30) of the flux ropes were formed well before the onset of the eruption (from 51 minutes to more than eight hours), and their formation was associated with the occurrence of a confined flare. We also found four events with preexisting hot flux ropes whose formations occurred a matter of minutes (from three to 39) prior to the eruptions without any association with distinct confined flare activity. Six flux ropes were formed once the eruptions were underway. However, in three of them, prominence material could be seen in

131 Å images, which may indicate the presence of preexisting flux ropes that were not hot. The formation patterns of the last three groups of hot flux ropes did not show significant differences. For the whole population of events, the mean and median values of the time difference between the onset of the eruptive flare and the appearance of the hot flux rope were 151 and 98 minutes, respectively. Our results provide, on average, indirect support for CME models that involve preexisting flux ropes; on the other hand, for a third of the events, models in which the ejected flux rope is formed during the eruption appear more appropriate. **2011-02-24, 2011-09-22, 2012-07-27, 2012-11-07-08, 2013-05-03, 2013-05-16-17, 2013-05-20, 2013-06-07, 2013-10-22, 2013-10-26, 2014-01-07-08, 2014-02-24**  
**Table 1.** Timing of HFR eruptive events (2011-2014)

## **How Common are Hot Magnetic Flux Ropes in the Low Solar Corona? A Statistical Study of EUV Observations**

A. **Nindos**, S. Patsourakos, A. Vourlidas, C. Tagikas

ApJ **808** 117 **2015**

<http://arxiv.org/pdf/1507.03766v1.pdf>

We use data at 131, 171, and 304 Å from the Atmospheric Imaging Assembly (AIA) aboard the Solar Dynamics Observatory (SDO) to search for hot flux ropes in 141 M-class and X-class solar flares that occurred at solar longitudes equal to or larger than 50 degrees. Half of the flares were associated with coronal mass ejections (CMEs). The goal of our survey is to assess the frequency of hot flux ropes in large flares irrespective of their formation time relative to the onset of eruptions. The flux ropes were identified in 131 Å images using morphological criteria and their high temperatures were confirmed by their absence in the cooler 171 and 304 Å passbands. We found hot flux ropes in 45 of our events (32% of the flares); 11 of them were associated with confined flares while the remaining 34 were associated with eruptive flares. Therefore almost half (49%) of the eruptive events involved a hot flux rope configuration. The use of supplementary Hinode X-Ray Telescope (XRT) data indicates that these percentages should be considered as lower limits of the actual rates of occurrence of hot flux ropes in large flares.

**Table 1.** Catalog of events and their classification according to AIA data

**4.2. Confined Events with Hot Flux Ropes**

**4.3. Eruptive Events with Hot Flux Ropes**

## **ON THE ROLE OF THE BACKGROUND OVERLYING MAGNETIC FIELD IN SOLAR ERUPTIONS**

A. **Nindos**<sup>1</sup>, S. Patsourakos<sup>1</sup> and T. Wiegmann

**2012** ApJ **748** L6

The primary constraining force that inhibits global solar eruptions is provided by the overlying background magnetic field. Using magnetic field data from both the Helioseismic and Magnetic Imager aboard the Solar Dynamics Observatory and the spectropolarimeter of the Solar Optical Telescope aboard Hinode, we study the long-term evolution of the background field in active region AR1158 that produced three major coronal mass ejections (CMEs). The CME formation heights were determined using EUV data. We calculated the decay index  $-(z/B)(\partial B/\partial z)$  of the magnetic field  $B$  (i.e., how fast the field decreases with height,  $z$ ) related to each event from the time of the active region emergence until well after the CMEs. At the heights of CME formation, the decay indices were 1.1-2.1. Prior to two of the events, there were extended periods (of more than 23 hr) where the related decay indices at heights above the CME formation heights either decreased (up to -15%) or exhibited small changes. The decay index related to the third event increased (up to 118%) at heights above 20 Mm within an interval that started 64 hr prior to the CME. The magnetic free energy and the accumulated helicity into the corona contributed the most to the eruptions by their increase throughout the flux emergence phase (by factors of more than five and more than two orders of magnitude, respectively). Our results indicate that the initiation of eruptions does not depend critically on the temporal evolution of the variation of the background field with height.

## **On the relationship of shock waves to flares and coronal mass ejections**

A. **Nindos**<sup>1</sup>, C. E. Alissandrakis<sup>1</sup>, A. Hillaris<sup>2</sup>, and P. Preka-Papadema<sup>2</sup>

A&A **531**, A31 (**2011**), **File**

<http://arxiv.org/pdf/1105.1268v1.pdf>

Context. Metric type II bursts are the most direct diagnostic of shock waves in the solar corona.

Aims. There are two main competing views about the origin of coronal shocks: that they originate in either blast waves ignited by the pressure pulse of a flare or piston-driven shocks due to coronal mass ejections (CMEs). We studied three well-observed type II bursts in an attempt to place tighter constraints on their origins.

Methods. The type II bursts were observed by the ARTEMIS radio spectrograph and imaged by the Nançay Radioheliograph (NRH) at least at two frequencies. To take advantage of projection effects, we selected events that occurred away from disk center.

Results. In all events, both flares and CMEs were observed. In the first event, the speed of the shock was about 4200 km s<sup>-1</sup>, while the speed of the CME was about 850 km s<sup>-1</sup>. This discrepancy ruled out the CME as the primary shock driver. The CME may have played a role in the ignition of another shock that occurred just after the high speed one. A CME driver was excluded from the second event as well because the CMEs that appeared in the coronagraph data were

not synchronized with the type II burst. In the third event, the kinematics of the CME which was determined by combining EUV and white light data was broadly consistent with the kinematics of the type II burst, and, therefore, the shock was probably CME-driven.

Conclusions. Our study demonstrates the diversity of conditions that may lead to the generation of coronal shocks.

March 2, 2000, March 7, 2000, May 2, 2000

## Magnetic helicity of solar active regions

Review

A. Nindos

Proceedings of the International Astronomical Union / Volume 4 / Symposium S257, pp 133 – 143,

Published online: 16 Mar 2009, File

Magnetic helicity is a quantity that describes the linkage and twistedness/shear in the magnetic field. It has the unique feature that it is probably the only physical quantity which is approximately conserved even in resistive MHD. This makes magnetic helicity an ideal tool for the exploration of the physics of eruptive events. The concept of magnetic helicity can be used to monitor the whole history of a CME event from the emergence of twisted magnetic flux from the convective zone to the eruption and propagation of the CME into interplanetary space. In this article, I discuss the sources of the magnetic helicity injected into active regions and the role of magnetic helicity in the initiation of solar eruptions.

## Radio Emission of Flares and Coronal Mass Ejections

Invited Review

A. Nindos · H. Aurass · K.-L. Klein · G. Trottet

Solar Phys., 253: 3–41, 2008, DOI 10.1007/s11207-008-9258-9, File

We review recent progress on our understanding of radio emission from solar flares and coronal mass ejections (CMEs) with emphasis on those aspects of the subject that help us address questions about energy release and its properties, the configuration of flare – CME source regions, coronal shocks, particle acceleration and transport, and the origin of solar energetic particle (SEP) events. Radio emission from electron beams can provide information about the electron acceleration process, the location of injection of electrons in the corona, and the properties of the ambient coronal structures. Mildly relativistic electrons gyrating in the magnetic fields of flaring loops produce radio emission via the gyrosynchrotron mechanism, which provides constraints on the magnetic field and the properties of energetic electrons. CME detection at radio wavelengths tracks the eruption from its early phase and reveals the participation of a multitude of loops of widely differing scale. Both flares and CMEs can ignite shock waves and radio observations offer the most robust tool to study them. The incorporation of radio data into the study of SEP events reveals that a clear-cut distinction between flare-related and CME-related SEP events is difficult to establish.

## The Role of a Flux Rope Ejection in Three-dimensional Magnetohydrodynamic Simulation of a Solar Flare

Keisuke Nishida, Naoto Nishizuka and Kazunari Shibata

E-print, Aug 2013, 2013 ApJ 775 L39

We investigated the dynamic evolution of a 3-dimensional (3D) flux rope eruption and magnetic reconnection process in a solar flare, by simply extending 2-dimensional (2D) resistive magnetohydrodynamic simulation model of solar flares with low beta plasma to 3D model. We succeeded in reproducing a current sheet and bi-directional reconnection outflows just below the flux rope during the eruption in our 3D simulations. We calculated four cases of a strongly twisted flux rope and a weakly twisted flux rope in 2D and 3D simulations. The time evolution of a weakly twisted flux rope in 3D simulation shows similar behaviors to 2D simulation, while a strongly twisted flux rope in 3D simulation shows clearly different time evolution from 2D simulation except for the initial phase evolution. The ejection speeds of both strongly and weakly twisted flux ropes in 3D simulations are larger than 2D simulations, and the reconnection rates in 3D cases are also larger than 2D cases. This indicates a positive feedback between the ejection speed of a flux rope and the reconnection rate even in the 3D simulation, and we conclude that the plasmoid-induced reconnection model can be applied to 3D. We also found that small scale plasmoids are formed inside a current sheet and make it turbulent. These small scale plasmoid ejections has role in locally increasing reconnection rate intermittently as observed in solar flares, coupled with a global eruption of a flux rope.

## Multi-instrument observations of a failed flare eruption associated with MHD waves in a loop bundle

Giuseppe Nisticò, Vanessa Polito, Valery M. Nakariakov, Giulio del Zanna

A&A 600, A37 (2017)

<https://arxiv.org/pdf/1612.02077v1.pdf>

[http://www.astro.physik.uni-goettingen.de/~nistico/publications/paper\\_arXiv\\_6Dec.pdf](http://www.astro.physik.uni-goettingen.de/~nistico/publications/paper_arXiv_6Dec.pdf)

We present observations of a B7.9-class flare that occurred on the 24th January, 2015, using the Atmospheric Imaging Assembly (AIA) of the Solar Dynamics Observatory (SDO), the EUV Imaging Spectrometer (EIS) and the X-Ray Telescope of Hinode. The flare triggers the eruption of a dense cool plasma blob as seen in AIA 171\AA, which is unable to completely break out and remains confined within a local bundle of active region loops. During this process,

transverse oscillations of the threads are observed. The cool plasma is then observed to descend back to the chromosphere along each loop strand. At the same time, a larger diffuse co-spatial loop observed in the hot wavebands of SDO/AIA and Hinode/XRT is formed, exhibiting periodic intensity variations along its length. The formation and evolution of magnetohydrodynamic (MHD) waves depend upon the values of the local plasma parameters (e.g. density, temperature and magnetic field), which can hence be inferred by coronal seismology. In this study we aim to assess how the observed MHD modes are affected by the variation of density and temperature. We combined analysis of EUV/X-ray imaging and spectroscopy using SDO/AIA, Hinode/EIS and XRT. We show that the evolution of the detected waves is determined by the temporal variations of the local plasma parameters, caused by the flare heating and the consequent cooling. We apply coronal seismology to both waves obtaining estimations of the background plasma parameters. **24th January, 2015**

## **Solar Activities Associated with 3He-rich Solar Energetic Particle Events Observed by Solar Orbiter**

Nariaki **Nitta**, Radoslav Bučik, Radoslav Bučik, Glenn Mason, George Ho, Christina Cohen, Raul Gómez-Herrero, Linghua Wang, and Laura Balmaceda

Front. Astron. Space Sci. 10: 1148467. **2023**

doi: 10.3389/fspas.2023.1148467

<https://www.frontiersin.org/articles/10.3389/fspas.2023.1148467/full>

<https://www.frontiersin.org/articles/10.3389/fspas.2023.1148467/pdf>

A series of 3He-rich solar energetic particle (SEP) events was observed by Solar Orbiter in May 2021 at a radial distance of 0.95 AU. An isolated active region AR 12824 was likely the ultimate source of these SEP events. The period of the enhanced flux of 3He was also a period of frequent type III bursts in the decametric-hectometric range, confirming their close relationship. As in past studies, we try to find the solar activities possibly responsible for 3He-rich SEP events, using the type III bursts close to the particle injection times estimated from the velocity dispersion. But this exercise is not as straightforward as in many of the past studies since the region produced many more type III bursts and jet-like eruptions than the SEP injections. We may generalize the solar activities for the 3He-rich SEP events in question as coronal jets, but their appearances do not necessarily conform to classic jets that consist of a footpoint and a spire. Conversely, such jets often did not accompany type III bursts. The areas that produced jet-like eruptions changed within the active region from the first to the second set of 3He-rich SEP events, which may be related to the extended coronal mass ejection that launched stealthily. **21–24 May 2021**

## **Earth-Affecting Coronal Mass Ejections Without Obvious Low Coronal Signatures**

Nariaki V. **Nitta**, Tamitha Mulligan

*Solar Physics* September **2017**, 292:125 **File**

<https://link.springer.com/article/10.1007%2Fs11207-017-1147-7>

We present a study of the origin of coronal mass ejections (CMEs) that were not accompanied by obvious low coronal signatures (LCSs) and yet were responsible for appreciable disturbances at 1 AU. These CMEs characteristically start slowly. In several examples, extreme ultraviolet (EUV) images taken by the Atmospheric Imaging Assembly onboard the Solar Dynamics Observatory reveal coronal dimming and a post-eruption arcade when we make difference images with long enough temporal separations, which are commensurate with the slow initial development of the CME. Data from the EUV imager and COR coronagraphs of the Sun Earth Connection Coronal and Heliospheric Investigation onboard the Solar Terrestrial Relations Observatory, which provide limb views of Earth-bound CMEs, greatly help us limit the time interval in which the CME forms and undergoes initial acceleration. For other CMEs, we find similar dimming, although only with lower confidence as to its link to the CME. It is noted that even these unclear events result in unambiguous flux rope signatures in in situ data at 1 AU. There is a tendency that the CME source regions are located near coronal holes or open field regions. This may have implications for both the initiation of the stealthy CME in the corona and its outcome in the heliosphere. **16-20 June 2010, 23-28 Dec 2010, 19-24 Jan 2011, 30 Jan-4 Feb 2011, 3-6 March 2011, 25-29 March 2011, 25-28 May 2011, 4-5-8 October 2012, 27-31 May 2013, 2-6 June 2013, 23-27 June 2013, 30 June-5 July 2013, 3-7 Jan 2015, 8-12 Oct 2016**

**Table 1** Partial list of stealthy events (solar)

**Table 2** Partial list of stealthy events (1 AU)

## **Large-scale Coronal Propagating Fronts in Solar Eruptions as Observed by the Atmospheric Imaging Assembly on Board the Solar Dynamics Observatory - An Ensemble Study**

**Nitta**, N. V., Schrijver, C. J., Title, A. M., Liu, W.

E-print, Aug **2013**, **File**; ApJ

This paper presents a study of a large sample of global disturbances in the solar corona with characteristic propagating fronts as intensity enhancement, similar to the phenomena that have often been referred to as EIT waves or EUV waves. Now Extreme Ultraviolet (EUV) images obtained by the Atmospheric Imaging Assembly (AIA) on board the Solar Dynamics Observatory (SDO) provide a significantly improved view of these large-scale coronal propagating fronts (LCPFs). Between April 2010 and January 2013, a total of 171 LCPFs have been identified through visual inspection of AIA images in the 193 Å channel. Here we focus on the 138 LCPFs that are seen to propagate across the solar disk, first studying how they are associated with flares, coronal mass ejections (CMEs) and type II radio bursts. We measure the speed of the LCPF in various directions until it is clearly altered by active regions or coronal holes. The highest speed is

extracted for each LCPF. It is often considerably higher than EIT waves. We do not find a pattern where faster LCPFs decelerate and slow LCPFs accelerate. Furthermore, the speeds are not strongly correlated with the flare intensity or CME magnitude, nor do they show an association with type II bursts. We do not find a good correlation either between the speeds of LCPFs and CMEs in a subset of 86 LCPFs observed by one or both of the Solar and Terrestrial Relations Observatory (STEREO) spacecraft as limb events.

**2011 February 15;**

**Table 1. The 171 LCPFs; The catalog of LCPFs with all these movies are online at [http://aia.lmsal.com/AIA\\_Waves/index.html](http://aia.lmsal.com/AIA_Waves/index.html)**

## **The Association of Solar Flares with Coronal Mass Ejections During the Extended Solar Minimum**

**Nitta**, N. V., Aschwanden, A. M., Freeland, S. L., Lemen, J. R., Wuelser, J.-P., Zarro, D. M.

E-print, Aug **2013**, **File**; Solar Phys. April **2014**, Volume 289, Issue 4, pp 1257-1277

We study the association of solar flares with coronal mass ejections (CMEs) during the deep, extended solar minimum of 2007-2009, using extreme-ultraviolet (EUV) and white-light (coronagraph) images from the Solar Terrestrial Relations Observatory (STEREO). Although all of the fast ( $v > 900$  km s<sup>-1</sup>) and wide ( $\theta > 100$  deg) CMEs are associated with a flare that is at least identified in GOES soft X-ray light curves, a majority of flares with relatively high X-ray intensity for the deep solar minimum (e.g.  $\geq 10^{-6}$  W m<sup>-2</sup> or C1) are not associated with CMEs. Intense flares tend to occur in active regions with strong and complex photospheric magnetic field, but the active regions that produce CME-associated flares tend to be small, including those that have no sunspots and therefore no NOAA active-region numbers. Other factors on scales comparable to and larger than active regions seem to exist that contribute to the association of flares with CMEs. We find the possible low coronal signatures of CMEs, namely eruptions, dimmings, EUV waves, and Type III bursts, in 91%, 74%, 57%, and 74%, respectively, of the 35 flares that we associate with CMEs. None of these observables can fully replace direct observations of CMEs by coronagraphs.

14 May 2007. 3 June 2007, **2007-12-31, 2009-02-13**,

**Table 2. Coronal waves observed by EUVI during March 2007 –December 2009**

## **Observables Indicating Two Major Coronal Mass Ejections During the WHI**

N. V. **Nitta**

E-print, Aug **2013**

Solar Physics, Volume 274, Numbers 1-2, 219-232, **2011**

Two of the five fast ( $v \geq 900$  km s<sup>-1</sup>) coronal mass ejections (CMEs) between January 2007 and December 2009 were observed during the Whole Heliosphere Interval (WHI: 20 March–16 April **2008**). The main purpose of this article is to discuss possible observational signatures that could have been used to predict these CMEs. During the WHI, there were three active regions aligned almost East–West in a longitudinal span of about 60°. They were NOAA active region (AR) 10987, 10988, and 10989. In terms of the sunspot area, AR 10988 was the largest. However, the fast CMEs were launched from AR 10989 on **25 March** and from AR 10987 on **5 April**. One explanation for this may be that AR 10988, unlike the other two regions, emerged underneath a predominantly closed magnetic-field environment, as shown by global magnetic-field extrapolations. Around the times of these CMEs, however, magnetic-field observations of the source regions were essentially missing, because they were close to, or behind, the limb as viewed from Earth. Therefore, we explore an extended view in longitude of the regions from the Solar Terrestrial Relations Observatory (STEREO). The two STEREO spacecraft were located  $\approx 24^\circ$  East and West of the Sun–Earth line during the period of interest. We study the frequency of microflares in the three regions and changes in large-scale structures including streamers, but the CMEs do not seem to be correlated with either of them. Instead, activation of filaments or prominences may directly signal subsequent eruptions.

## **Solar surges related to UV bursts**

### ***Characterization through k-means, inversions, and density diagnostics\****

D. **Nóbrega-Siverio**<sup>1,2,3,4</sup>, S. L. Guglielmino<sup>5,6</sup> and A. Sainz Dalda

A&A 655, A28 (**2021**)

<https://www.aanda.org/articles/aa/pdf/2021/11/aa41472-21.pdf>

<https://doi.org/10.1051/0004-6361/202141472>

Context. Surges are cool and dense ejections typically observed in chromospheric lines and closely related to other solar phenomena such as UV bursts or coronal jets. Even though surges have been observed for decades now, questions regarding their fundamental physical properties such as temperature and density, as well as their impact on upper layers of the solar atmosphere remain open.

Aims. Our aim is to address the current lack of inverted models and diagnostics of surges, as well as to characterize the chromospheric and transition region plasma of these phenomena.

Methods. We have analyzed an episode of recurrent surges related to UV bursts observed with the Interface Region Imaging Spectrograph (IRIS) in April 2016. The mid- and low-chromosphere of the surges were unprecedentedly

examined by getting their representative Mg IIh&k line profiles through the k-means algorithm and performing inversions on them using the state-of-the-art STiC code. We have studied the far-UV spectra focusing on the O IV 1399.8 Å and 1401.2 Å lines, which were previously unexplored for surges, carrying out density diagnostics to determine the transition region properties of these ejections. We have also used numerical experiments performed with the Bifrost code for comparisons.

Results. Thanks to the k-means clustering, we reduced the number of Mg IIh&k profiles to invert by a factor 43.2. The inversions of the representative profiles show that the mid- and low-chromosphere of the surges are characterized, with a high degree of reliability, by temperatures mainly around  $T = 6$  kK at  $-6.0 \leq \log_{10}(\tau) \leq -3.2$ . For the electronic number density,  $n_e$ , and line-of-sight velocity, VLOS, the most reliable results from the inversions are within  $-6.0 \leq \log_{10}(\tau) \leq -4.8$ , with  $n_e$  ranging from  $\sim 1.6 \times 10^{11}$  cm $^{-3}$  up to  $10^{12}$  cm $^{-3}$ , and VLOS of a few km s $^{-1}$ . We find, for the first time, observational evidence of enhanced O IV emission within the surges, indicating that these phenomena have a considerable impact on the transition region even in the weakest far-UV lines. The O IV emitting layers of the surges have an electron number density ranging from  $2.5 \times 10^{10}$  cm $^{-3}$  to  $10^{12}$  cm $^{-3}$ . The numerical simulations provide theoretical support in terms of the topology and location of the O IV emission within the surges.

**IRIS Nugget 9 Dec 2021** <https://iris.lmsal.com/nugget?cmd=view-pod&pubDate=2021-12-09>

## **On the importance of the nonequilibrium ionization of Si IV and O IV and the line-of-sight in solar surges**

[D. Nóbrega-Siverio](#), [F. Moreno-Insertis](#), [J. Martínez-Sykora](#)

ApJ 2018

<https://arxiv.org/pdf/1803.10251.pdf>

Surges are ubiquitous cool ejections in the solar atmosphere that often appear associated with transient phenomena like UV bursts or coronal jets. Recent observations from the Interface Region Imaging Spectrograph (IRIS) show that surges, although traditionally related to chromospheric lines, can exhibit enhanced emission in Si IV with brighter spectral profiles than for the average transition region (TR). In this paper, we explain why surges are natural sites to show enhanced emissivity in TR lines. We performed 2.5D radiative-MHD numerical experiments using the Bifrost code including the nonequilibrium ionization of silicon and oxygen. A surge is obtained as a by-product of magnetic flux emergence; the TR enveloping the emerged domain is strongly affected by nonequilibrium effects: assuming statistical equilibrium would produce an absence of Si IV and O IV ions in most of the region. Studying the properties of the surge plasma emitting in the Si IV 1402.77 Å and O IV 1401.16 Å lines, we find that a) the timescales for the optically-thin losses and heat conduction are very short, leading to departures from statistical equilibrium, and b) the surge emits in Si IV more and has an emissivity ratio of Si IV to O IV larger than a standard TR. Using synthetic spectra, we conclude the importance of line-of-sight effects: given the involved geometry of the surge, the line-of-sight can cut the emitting layer at small angles and/or cross it multiple times, causing prominent, spatially intermittent brightenings both in Si IV and O IV.

## **Surges and Si IV bursts in the solar atmosphere. Understanding IRIS and SST observations through RMHD experiments**

[D. Nóbrega-Siverio](#), [J. Martínez-Sykora](#), [F. Moreno-Insertis](#), [L. Rouppe van der Voort](#)

ApJ 850 153 2017

<https://arxiv.org/pdf/1710.08928.pdf>

Surges often appear as a result of the emergence of magnetized plasma from the solar interior. Traditionally, they are observed in chromospheric lines such as H $\alpha$ 6563 Å and Ca II 8542 Å. However, whether there is a response to the surge appearance and evolution in the Si IV lines or, in fact, in many other transition region lines has not been studied. In this paper we analyze a simultaneous episode of an H $\alpha$  surge and a Si IV burst that occurred on **2016 September 03** in active region AR12585. To that end, we use coordinated observations from the Interface Region Imaging Spectrograph (IRIS) and the Swedish 1-m Solar Telescope (SST). For the first time, we report emission of Si IV within the surge, finding profiles that are brighter and broader than the average. Furthermore, the brightest Si IV patches within the domain of the surge are located mainly near its footpoints. To understand the relation between the surges and the emission in transition region lines like Si IV, we have carried out 2.5D radiative MHD (RMHD) experiments of magnetic flux emergence episodes using the Bifrost code and including the non-equilibrium ionization of silicon. Through spectral synthesis we explain several features of the observations. We show that the presence of Si IV emission patches within the surge, their location near the surge footpoints and various observed spectral features are a natural consequence of the emergence of magnetized plasma from the interior to the atmosphere and the ensuing reconnection processes.

## **The cool surge following flux emergence in a radiation-MHD experiment**

[D. Nóbrega-Siverio](#), [F. Moreno-Insertis](#), [J. Martínez-Sykora](#)

2016



<http://arxiv.org/pdf/1601.04074v1.pdf>

Cool and dense ejections, typically H $\alpha$  surges, often appear alongside EUV or X-Ray coronal jets as a result of the emergence of magnetized plasma from the solar interior. Idealized numerical experiments explain those ejections as being indirectly associated with the magnetic reconnection taking place between the emerging and preexisting systems. However, those experiments miss basic elements that can importantly affect the surge phenomenon. In this paper we study the cool surges using a realistic treatment of the radiation transfer and material plasma properties. To that end, the Bifrost code is used, which has advanced modules for the equation of state of the plasma, photospheric and chromospheric radiation transfer, heat conduction and optically thin radiative cooling. We carry out a 2.5D experiment of the emergence of magnetized plasma through (meso)granular convection cells and the low atmosphere to the corona. Through detailed Lagrange tracing, we study the formation and evolution of the cool ejection and, in particular, the role of the entropy sources: this allows us to discern families of evolutionary patterns for the plasma elements. In the launch phase many elements suffer accelerations well in excess of gravity; when nearing the apex of their individual trajectories, instead, the plasma elements follow quasi-parabolic trajectories with acceleration close to  $g_{\odot}$ . We show how the formation of the cool ejection is mediated by a wedge-like structure composed of two shocks, one of which leads to the detachment of the surge from the original emerged plasma dome.

### **Estimating the lateral speed of a fast shock driven by a coronal mass ejection at the location of solar radio emissions**

S. **Normo**<sup>1,2</sup>, D. E. Morosan<sup>1,2</sup>, E. K. J. Kilpua<sup>1</sup> and J. Pomoell<sup>1</sup>  
A&A, 686, A159 (2024)

<https://doi.org/10.1051/0004-6361/202449277>

<https://www.aanda.org/articles/aa/pdf/2024/06/aa49277-24.pdf>

**Context.** Fast coronal mass ejections (CMEs) can drive shock waves capable of accelerating electrons to high energies. These shock-accelerated electrons act as sources of electromagnetic radiation, often in the form of solar radio bursts. Recent findings suggest that radio imaging of solar radio bursts can provide a means to estimate the lateral expansion of CMEs and associated shocks in the low corona.

**Aims.** Our aim is to estimate the expansion speed of a CME-driven shock at the locations of radio emission using 3D reconstructions of the shock wave from multiple viewpoints.

**Methods.** In this study, we estimated the 3D location of radio emission using radio imaging from the Nançay Radioheliograph and the 3D location of a CME-driven shock. The 3D shock was reconstructed using white-light and extreme ultraviolet images of the CME from the Solar Terrestrial Relations Observatory, Solar Dynamics Observatory, and the Solar and Heliospheric Observatory. The lateral expansion speed of the CME-driven shock at the electron acceleration locations was then estimated using the approximate 3D locations of the radio emission on the surface of the shock.

**Results.** The radio bursts associated with the CME were found to reside at the flank of the expanding CME-driven shock. We identified two prominent radio sources at two different locations and found that the lateral speed of the shock was between 800 and 1000 km s<sup>-1</sup> at these locations. Such a high speed during the early stages of the eruption already indicates the presence of a fast shock in the low corona. We also found a larger ratio between the radial and lateral expansion speed compared to values obtained higher up in the corona.

**Conclusions.** We estimated for the first time the 3D expansion speed of a CME-driven shock at the location of the accompanying radio emission. The high shock speed obtained is indicative of a fast acceleration during the initial stage of the eruption. This acceleration leading to lateral speeds in the range of 800–1000 km s<sup>-1</sup> is most likely one of the key parameters contributing to the presence of metric radio emissions, such as type II radio bursts. **1 September 2014**

### **First magnetic seismology of the CME reconnection outflow layer in the low corona with 2.5-D MHD simulations of the Kelvin-Helmholtz instability**

**Nykyri**, K. and Foullon, C.

<http://onlinelibrary.wiley.com/doi/10.1002/grl.50807/pdf>

E-print, Sept 2013; Geophysical Research Letters Vol. 40 (16), pp. 4154–4159, 2013

For conditions observed in the low corona, we perform 2.5-D magnetohydrodynamic (MHD) simulations of the Kelvin-Helmholtz instability (KHI) at the surface of a coronal mass ejection (CME). We match the observed time development of the KHI with simulated growth from 110 MHD experiments representing a parametric range of realistic magnetic field strengths and orientations and two key values of the velocity shear,  $\Delta V$ , inferred from observations. The results are field strengths  $B_e \approx 8?9$  G and  $B_s \approx 10?11$  G in the CME reconnection outflow layer and the surrounding sheath, respectively, for  $\Delta V \approx 770$  km s<sup>-1</sup>; for nearly perpendicular orientation ( $1?$  tilt) of  $B_s$  with respect to the flow plane,  $B_e$  can be tilted between 3 and 10?; tilting  $B_s$  up to 15? would slow the growth of the KHI by too much. Our simulations also reveal hidden dynamics and structure of the CME ejecta layer such as plasma mixing via reconnection in the vortices.

### **Coronal Mass Ejections and the Index of Effective Solar Multipole**

V. N. **Obridko**, E. V. Ivanov, A. Özgüç, A. Kilcik and V. B. Yurchyshyn

Solar Physics, 2012, 281(2), 779–792, **File**

The paper considers the relationship between the cyclic variations in the velocity of coronal mass ejections (CME) and the large-scale magnetic field structure (LSMF) in cycles 21 – 23. To characterize a typical size of the LSMF structure,

we have used the index of the effective solar multipole (ESMI). The cyclic behavior of the CME occurrence rate and velocity proved to be similar to that of ESMI. The hysteresis observed in variations of the CME maximum velocity is interpreted as a manifestation of different contributions from the two field structures (local and global magnetic fields) in different phases of the 11-year activity cycle. It is suggested that cyclic variations in the maximum velocity of coronal mass ejections are due to different conditions for the formation of the complexes of active regions connected by coronal arch systems, which are the main source of high-velocity CMEs.

### **Spatial distribution of jets in solar active regions**

[Jonas Odermatt](#), [Krzysztof Barczynski](#), [Louise K. Harra](#), [Conrad Schwanitz](#), [Säm Krucker](#)

A&A 665, A29 2022

<https://arxiv.org/pdf/2207.09923.pdf>

<https://www.aanda.org/articles/aa/pdf/2022/09/aa43120-22.pdf>

Context. Solar active regions are known to have jets. These jets are associated with heating and the release of particles into the solar wind.

Aim. Our aim is to understand the spatial distribution of coronal jets within active regions to understand if there is a preferential location for them to occur.

Methods. We analysed five active regions using Solar Dynamics Observatory Atmospheric Imaging Assembly data over a period of 2-3.5 days when the active regions were close to disk centre. Each active region had a different age, magnetic field strength, and topology. We developed a methodology for determining the position and length of the jets.

Results. Jets are observed more frequently at the edges of the active regions and are more densely located around a strong leading sunspot. The number of coronal jets for our active regions is dependent on the age of the active region.

The older active regions produce more jets than younger ones. Jets were observed dominantly at the edges of the active regions, and not as frequently in the centre. The number of jets is independent of the average unsigned magnetic field and total flux density in the whole active region. The jets are located around the edges of the strong leading sunspot. **2-4 Apr 2019, 12-15 Apr 2019, 23-25 Feb 2021, 12-14 May 2021,**

### **Stellar coronal mass ejections II. Constraints from spectroscopic observations**

[P. Odert](#), [M. Leitzinger](#), [E. W. Guenther](#), [P. Heinzel](#)

MNRAS Volume 494, Issue 3, May 2020, Pages 3766–3783, 2020

<https://arxiv.org/pdf/2004.04063.pdf>

<https://doi.org/10.1093/mnras/staa1021>

Detections of stellar coronal mass ejections (CMEs) are still rare. Observations of strong Balmer line asymmetries during flare events have been interpreted as being caused by CMEs. Here, we aim to estimate the maximum possible Balmer line fluxes expected from CMEs to infer their detectability in spectroscopic observations. Moreover, we use these results together with a model of intrinsic CME rates to infer the potentially observable CME rates for stars of different spectral types under various observing conditions, as well as the minimum required observing time to detect stellar CMEs in Balmer lines. We find that generally CME detection is favored for mid- to late-type M dwarfs, as they require the lowest signal-to-noise ratio for CME detection, and the fraction of observable-to-intrinsic CMEs is largest. They may require, however, longer observing times than stars of earlier spectral types at the same activity level, as their predicted intrinsic CME rates are lower. CME detections are generally favored for stars close to the saturation regime, because they are expected to have the highest intrinsic rates; the predicted minimum observing time to detect CMEs on just moderately active stars is already >100 h. By comparison with spectroscopic data sets including detections as well as non-detections of CMEs, we find that our modeled maximum observable CME rates are generally consistent with these observations on adopting parameters within the ranges determined by observations of solar and stellar prominences.

### **Stellar Coronal Mass Ejections I. Estimating occurrence frequencies and mass-loss rates**

[P. Odert](#), [M. Leitzinger](#), [A. Hanslmeier](#), [H. Lammer](#)

MNRAS 472, Issue 1, p.876-890 2017

<https://arxiv.org/pdf/1707.02165.pdf>

Stellar coronal mass ejections (CMEs) may play an important role in mass- and angular momentum loss of young Sun-like stars. If occurring frequently, they may also have a strong effect on planetary evolution by increasing atmospheric erosion. So far it has not been possible to infer the occurrence frequency of stellar CMEs from observations. *Based on their close relation with flares on the Sun, we develop an empirical model combining solar flare-CME relationships* with stellar flare rates to estimate the CME activity of young Sun-like and late-type main-sequence stars. By comparison of the obtained CME mass-loss rates with observations of total mass-loss rates, we find that our modeled rates may exceed those from observations by orders of magnitude for the most active stars. This reveals a possible limit to the extrapolation of such models to the youngest stars. We find that the most uncertain component in the model is the flare-CME association rate adopted from the Sun, which does not properly account for the likely stronger coronal confinement in active stars. Simple estimates of this effect reveal a possible suppression of CME rates by several orders of magnitude for young stars, indicating that this issue should be addressed in more detail in the future.

### **SDO/AIA OBSERVATION OF KELVIN–HELMHOLTZ INSTABILITY IN THE SOLAR CORONA**

L. [Ofman](#)<sup>1,2,3</sup> and B. J. Thompson

2011 ApJ 734 L11,

We present observations of the formation, propagation, and decay of vortex-shaped features in coronal images from the Solar Dynamics Observatory associated with an eruption starting at about 2:30 UT on **2010 April 8**. The series of vortices were formed along the interface between an erupting (dimming) region and the surrounding corona. They ranged in size from several to 10 arcsec and traveled along the interface at 6-14 km s<sup>-1</sup>. The features were clearly visible in six out of the seven different EUV wave bands of the Atmospheric Imaging Assembly. Based on the structure, formation, propagation, and decay of these features, we identified the event as the first observation of the Kelvin-Helmholtz instability (KHI) in the corona in EUV. The interpretation is supported by linear analysis and by a nonlinear 2.5-dimensional magnetohydrodynamic model of KHI. We conclude that the instability is driven by the velocity shear between the erupting and closed magnetic field of the coronal mass ejection. The shear-flow-driven instability can play an important role in energy transfer processes in coronal plasma.

### **Exceptional Extended Field-of-view Observations by PROBA2/SWAP on 2017 April 1 and 3**

Jennifer P. **O'Hara**<sup>1</sup>, Marilena Mierla<sup>1,2</sup>, Olena Podladchikova<sup>1</sup>, Elke D'Huys<sup>1</sup>, and Matthew J. West<sup>1</sup>

2020 ApJ 883 59

<https://doi.org/10.3847/1538-4357/ab3b08>

<https://iopscience.iop.org/article/10.3847/1538-4357/ab3b08/pdf>

On **2017 April 1 and 3**, two large eruptions on the western solar limb, which were associated with M4.4- and M5.8-class flares, respectively, were observed with the Sun Watcher with Active Pixels and Image Processing (SWAP) Extreme Ultraviolet (EUV) solar telescope on board the Project for On Board Autonomy 2 (PROBA2) spacecraft. The large field-of-view (FOV) of SWAP, combined with an advantageous off-point, allows us to study the eruptions up to approximately 2 solar radii (R<sub>s</sub>), where space-based coronagraph observations begin. These measurements provide us with some of the highest EUV observations of an eruption, giving crucial additional data points to track the early evolution of Coronal Mass Ejections. In SWAP observations, we track the evolution of off-limb erupting features as well as associated on-disk EUV waves, and the kinematics of both are calculated. The first eruption shows a clear deceleration throughout the lower corona into coronagraph observations, whereas the second eruption, which had a lower initial velocity, shows no obvious acceleration or deceleration profile. This paper presents a unique set of observations, allowing features observed in EUV to be traced to greater heights in the solar atmosphere, helping to bridge the gap to the FOV of white-light coronagraphs. Even with these favorable data sets, it remains a challenging task to associate features observed in EUV with those observed in white light, highlighting our urgent need for single-instrument observations of the combined lower and middle corona.

### **Solar origins of a strong stealth CME detected by Solar Orbiter**

Jennifer **O'Kane**, [Lucie M. Green](#), [Emma E. Davies](#), [Christian Möstl](#), [Jürgen Hinterreiter](#), [Johan L. Freiherr von Forstner](#), [Andreas J. Weiss](#), [David M. Long](#), [Tanja Amerstorfer](#)

A&A 2021

<https://arxiv.org/pdf/2103.17225.pdf>

Aims. We aim to locate the origin of a stealth coronal mass ejection (CME) detected in situ by the MAG instrument on board Solar Orbiter, and make connections between the CME observed at the Sun, and the interplanetary CME (ICME) measured in situ. Methods. Remote sensing data are analysed using advanced image processing techniques to identify the source region of the stealth CME, and the global magnetic field at the time of the eruption is examined using Potential Field Source Surface (PFSS) models. The observations of the stealth CME at the Sun are compared with the magnetic field measured by the Solar Orbiter spacecraft, and plasma properties measured by the Wind spacecraft. Results. The source of the CME is found to be a quiet Sun cavity in the northern hemisphere. We find that the stealth CME has a strong magnetic field in situ, despite originating from a quiet Sun region with an extremely weak magnetic field. Conclusions. The interaction of the ICME with its surrounding environment is the likely cause of a higher magnetic field strength measured in situ. Stealth CMEs require multi-wavelength and multi-viewpoint observations in order to confidently locate the source region, however their elusive signatures still pose many problems for space weather forecasting. The findings have implications for Solar Orbiter observing sequences with instruments such as EU1 that are designed to capture stealth CMEs. **12-15 Apr 2020, 19-20 Apr 2020**

### **The Magnetic Environment of a Stealth Coronal Mass Ejection**

Jennifer **O'Kane**, [Cecilia Mac Cormack](#), [Cristina H. Mandrini](#), [Pascal Démoulin](#), [Lucie M. Green](#), [David M. Long](#), [Gherardo Valori](#)

ApJ 908 89 2021

<https://arxiv.org/pdf/2012.03757.pdf>

<https://doi.org/10.3847/1538-4357/abd2bf>

Interest in stealth coronal mass ejections (CMEs) is increasing due to their relatively high occurrence rate and space weather impact. However, typical CME signatures such as extreme-ultraviolet dimmings and post-eruptive arcades are hard to identify and require extensive image processing techniques. These weak observational signatures mean that little is currently understood about the physics of these events. We present an extensive study of the magnetic field configuration in which the stealth CME of **3 March 2011** occurred. Three distinct episodes of flare ribbon formation are observed in the stealth CME source active region (AR). Two occurred prior to the eruption and suggest the occurrence of magnetic reconnection that builds the structure which will become eruptive. The third occurs in a time

close to the eruption of a cavity that is observed in STEREO-B 171A data; this subsequently becomes part of the propagating CME observed in coronagraph data. We use both local (Cartesian) and global (spherical) models of the coronal magnetic field, which are complemented and verified by the observational analysis. We find evidence of a coronal null point, with field lines computed from its neighbourhood connecting the stealth CME source region to two ARs in the northern hemisphere. We conclude that reconnection at the null point aids the eruption of the stealth CME by removing field that acted to stabilise the pre-eruptive structure. This stealth CME, despite its weak signatures, has the main characteristics of other CMEs, and its eruption is driven by similar mechanisms.

### **Stealth Coronal Mass Ejections from Active Regions**

Jennifer **O'kane**, [Lucie Green](#), [David M. Long](#), [Hamish Reid](#)

ApJ Volume 882, Issue 2, article id. 85, **2019**

<https://arxiv.org/pdf/1907.12820.pdf>

<https://iopscience.iop.org/article/10.3847/1538-4357/ab371b/pdf>

Stealth coronal mass ejections (CMEs) are eruptions from the Sun that have no obvious low coronal signature. These CMEs are characteristically slower events, but can still be geoeffective and affect space weather at Earth. Therefore, understanding the science underpinning these eruptions will greatly improve our ability to detect and, eventually, forecast them. We present a study of two stealth CMEs analysed using advanced image processing techniques that reveal their faint signatures in observations from the extreme ultraviolet (EUV) imagers onboard the Solar and Heliospheric Observatory (SOHO), Solar Dynamics Observatory (SDO), and Solar Terrestrial Relations Observatory (STEREO) spacecraft. The different viewpoints given by these spacecraft provide the opportunity to study each eruption from above and the side contemporaneously. For each event, EUV and magnetogram observations were combined to reveal the coronal structure that erupted. For one event, the observations indicate the presence of a magnetic flux rope before the CME's fast rise phase. We found that both events originated in active regions and are likely to be sympathetic CMEs triggered by a nearby eruption. We discuss the physical processes that occurred in the time leading up to the onset of each stealth CME and conclude that these eruptions are part of the low-energy and velocity tail of a distribution of CME events, and are not a distinct phenomenon. **October 27th 2009, March 2 2011**  
**RHESSI Science Nugget #355 2019**

[http://sprg.ssl.berkeley.edu/~tohban/wiki/index.php/Stealth\\_Coronal\\_Mass\\_Ejections\\_from\\_Active\\_Regions](http://sprg.ssl.berkeley.edu/~tohban/wiki/index.php/Stealth_Coronal_Mass_Ejections_from_Active_Regions)

### **CHROMOSPHERIC AND CORONAL OBSERVATIONS OF SOLAR FLARES WITH THE HELIOSEISMIC AND MAGNETIC IMAGER**

Juan-Carlos Martínez **Oliveros**<sup>1</sup>, Säm Krucker<sup>1,2</sup>, Hugh S. Hudson<sup>1,3</sup>, Pascal Saint-Hilaire<sup>1</sup>, Hazel Bain<sup>1</sup>, Charles Lindsey<sup>4</sup>, Rick Bogart<sup>5</sup>, Sebastien Couvidat<sup>5</sup>, Phil Scherrer<sup>5</sup>, and Jesper Schou<sup>6</sup>  
**2014** ApJL 780 L28

<https://iopscience.iop.org/article/10.1088/2041-8205/780/2/L28/pdf>

<https://iopscience.iop.org/article/10.1088/2041-8205/780/2/L28>

We report observations of white-light ejecta in the low corona, for two X-class flares on **2013 May 13**, using data from the Helioseismic and Magnetic Imager (HMI) of the Solar Dynamics Observatory. At least two distinct kinds of sources appeared (chromospheric and coronal), in the early and later phases of flare development, in addition to the white-light footpoint sources commonly observed in the lower atmosphere. The gradual emissions have a clear identification with the classical loop-prominence system, but are brighter than expected and possibly seen here in the continuum rather than line emission. We find the HMI flux exceeds the radio/X-ray interpolation of the bremsstrahlung produced in the flare soft X-ray sources by at least one order of magnitude. This implies the participation of cooler sources that can produce free-bound continua and possibly line emission detectable by HMI. One of the early sources dynamically resembles "coronal rain", appearing at a maximum apparent height and moving toward the photosphere at an apparent constant projected speed of  $134 \pm 8 \text{ km s}^{-1}$ . Not much literature exists on the detection of optical continuum sources above the limb of the Sun by non-coronagraphic instruments and these observations have potential implications for our basic understanding of flare development, since visible observations can in principle provide high spatial and temporal resolution.

### **HMI as “Coronagraph”?**

Juan-Carlos Martínez **Oliveros**

HMI Science Nuggets #9, March **2014**

<http://hmi.stanford.edu/hminuggets/?p=560>

Reports of white-light ejecta above the limb of the Sun and imaged without the aid of a true coronagraph are exceedingly rare. Here we report the successful use of HMI to observe flare effects in the corona by the use of differencing as a substitute for an actual occulter. **2013 May 13**

### **THE 2010 AUGUST 1 TYPE II BURST: A CME-CME INTERACTION AND ITS RADIO AND WHITE-LIGHT MANIFESTATIONS**

Juan Carlos Martínez **Oliveros**<sup>1</sup>, Claire L. Raftery<sup>1</sup>, Hazel M. Bain<sup>1</sup>, Ying Liu<sup>1</sup>, Vratislav Krupar<sup>2,3</sup>, Stuart Bale<sup>1,4</sup> and Säm Krucker

**2012** ApJ 748 66, **File**

We present observational results of a type II burst associated with a CME-CME interaction observed in the radio and white-light (WL) wavelength range. We applied radio direction-finding techniques to observations from the STEREO and Wind spacecraft, the results of which were interpreted using WL coronagraphic measurements for context. The results of the multiple radio direction-finding techniques applied were found to be consistent both with each other and with those derived from the WL observations of coronal mass ejections (CMEs). The results suggest that the type II burst radio emission is causally related to the CMEs interaction.

### **LORENTZ SELF-FORCE OF AN ELLIPSE CURRENT LOOP MODEL**

Oscar [Olmedo](#)<sup>1,3</sup>, Jie Zhang<sup>2</sup>, and Valbona Kunkel

**2013** ApJ 771 125

In this work, the Lorentz self-force of an ellipse current loop model is derived. We are motivated by the fact that it has been reported in the literature that coronal mass ejection morphology can resemble an ellipse in the field of view of coronagraph images. Deriving the Lorentz self-force using an ellipse geometry has the advantage of being able to be solved analytically, as opposed to other more complex geometries. The derived ellipse model is compared with the local curvature approximation, where the Lorentz self-force at the ellipse major/minor axis is compared with the Lorentz self-force of a torus with curvature equal to the local curvature at the ellipses major/minor axis. It is found that the local curvature approximation is valid for moderate values of eccentricity.

### **PARTIAL TORUS INSTABILITY**

Oscar [Olmedo](#) and Jie Zhang

*Astrophysical Journal*, 718:433–440, **2010** July

Flux ropes are now generally accepted to be the magnetic configuration of coronal mass ejections (CMEs), which may be formed prior to or during solar eruptions. In this study, we model the flux rope as a current-carrying partial torus loop with its two footpoints anchored in the photosphere, and investigate its stability in the context of the torus instability (TI). Previous studies on TI have focused on the configuration of a circular torus and revealed the existence of a critical decay index of the overlying constraining magnetic field. Our study reveals that the critical index is a function of the fractional number of the partial torus, defined by the ratio between the arc length of the partial torus above the photosphere and the circumference of a circular torus of equal radius. We refer to this finding as the partial torus instability (PTI). It is found that a partial torus with a smaller fractional number has a smaller critical index, thus requiring a more gradually decreasing magnetic field to stabilize the flux rope. On the other hand, a partial torus with a larger fractional number has a larger critical index. In the limit of a circular torus when the fractional number approaches 1, the critical index goes to a maximum value. We demonstrate that the PTI helps us to understand the confinement, growth, and eventual eruption of a flux-rope CME.

### **Automatic Detection and Tracking of Coronal Mass Ejections in Coronagraph Time Series**

O. [Olmedo](#) · J. Zhang · H. Wechsler · A. Poland · K. Borne

*Solar Phys* (**2008**) 248: 485–499

<http://www.springerlink.com/content/9h27250051m874r0/fulltext.pdf>

We present the current capabilities of a software tool to automatically detect coronal mass ejections (CMEs) based on time series of coronagraph images: the solar eruptive event detection system (SEEDS). The software developed consists of several modules: preprocessing, detection, tracking, and event cataloging. The detection algorithm is based on a 2D to 1D projection method, where CMEs are assumed to be bright regions moving radially outward as observed in a running-difference time series. The height, velocity, and acceleration of the CME are automatically determined. A threshold-segmentation technique is applied to the individual detections to automatically extract an approximate shape of the CME leading edge. We have applied this method to a 12-month period of continuous coronagraph images sequence taken at a 20-minute cadence by the Large Angle and Spectrometric Coronagraph (LASCO) instrument (using the C2 instrument only) onboard the *Solar and Heliospheric Observatory* (SOHO) spacecraft. Our automated method, with a high computational efficiency, successfully detected about 75% of the CMEs listed in the CDAW CME catalog, which was created by using human visual inspection. Furthermore, the tool picked up about 100% more small-size or anomalous transient coronagraph events that were ignored by human visual inspection. The output of the software is made available online at <http://spaceweather.gmu.edu/seeds/>. The parameters of scientific importance extracted by the software package are the position angle, angular width, velocity, peak, and average brightness. Other parameters could easily be added if needed. The identification of CMEs is known to be somewhat subjective. As our system is further developed, we expect to make the process significantly more objective.

### **QUANTITATIVE MEASUREMENTS OF CORONAL MASS EJECTION-DRIVEN SHOCKS FROM LASCO OBSERVATIONS**

Veronica [Ontiveros](#)<sup>1,3</sup> and Angelos Vourlidas

*Astrophysical Journal*, 693:267–275, **2009** March 1; **File**

In this paper, we demonstrate that coronal mass ejection (CME)-driven shocks can be detected in white light coronagraph images and in which properties such as the density compression ratio and shock direction can be measured. Also, their propagation direction can be deduced via simple modeling. We focused on CMEs during

the ascending phase of solar cycle 23 when the large-scale morphology of the corona was simple. We selected events which were good candidates to drive a shock due to their high speeds ( $V > 1500 \text{ km s}^{-1}$ ). The final list includes 15 CMEs. For each event, we calibrated the LASCO data, constructed excess mass images, and searched for indications of faint and relatively sharp fronts ahead of the bright CME front. We found such signatures in 86% (13/15) of the events and measured the upstream/downstream densities to estimate the shock strength. Our values are in agreement with theoretical expectations and show good correlations with the CME kinetic energy and momentum. Finally, we used a simple forward modeling technique to estimate the three-dimensional shape and orientation of the white light shock features. We found excellent agreement with the observed density profiles and the locations of the CME source regions. Our results strongly suggest that the observed brightness enhancements result from density enhancements due to a bow-shock structure driven by the CME.

## **A Quiet Sun Transition Region Energetically Isolated Jet: Evidence to Cool Plasma Injections Into The Hot Corona**

N. Brice **Orange**, David L. Chesny, Hakeem M. Oluseyi

**2015**

<http://arxiv.org/pdf/1501.05211v1.pdf>

Increasing evidence for coronal heating contributions from cooler solar atmospheric layers challenges standard solar atmospheric descriptions of bright TR emission and pervasive lower TR plasma downflows. As such, questions related to the role of dynamic transients in contributing to the total coronal energy budget are elevated. Using AIA and HMI observations in conjunction with numerical models of 3D coronal magnetic field topologies, we investigate a jet that is: erupting from a footpoint shared by heated non-potential and potential loops, energetically isolated in the TR, and occurring adjacent to a small-scale coronal filament. A non-casual relationship is established between QSTR jet dynamics and magnetic flux emergence and cancellation events, witnessed in its underlying magnetic field environment. Non-potential and potential loop demise contribute to the jet via eruptive ejections driven from cooler atmospheric layers; however, in different fashions. Small-scale flaring events from potential loop reconnection with pre-existing fields, inject both hot and cool plasma blobs to coronal heights, i.e., the adjacent QSTR jet and coronal filament. Non-potential loop dynamics precludes a medium energy microflare deposit, just below the TR at the jet's origin, that heats the jet from a cool chromospheric ballistic plasma injection. Our results are evidence to energy redistribution via chromospheric to coronal mass cycling, driven by small-scale flaring. Our results confirm speculations that cool atmospheric microflare energy deposits lead to injections of cool dense plasma to coronal heights, which here visibly shine bright as a dynamic QS transient. Finally, this work elevates arguments of non-negligible coronal heating contributions from cool atmospheric layers, in QS conditions, and increases evidence for solar wind mass feeding in the presence of dynamic QS transients. 18 October 2011.

## **Connecting Flares and Transient Mass-loss Events in Magnetically Active Stars**

Rachel A. **Osten**<sup>1,3</sup> and Scott J. Wolk

**2015** ApJ 809 79

<http://arxiv.org/pdf/1506.04994v1.pdf>

We explore the ramifications of associating the energetics of extreme magnetic reconnection events with transient mass-loss in a stellar analogy with solar eruptive events. We establish energy partitions relative to the total bolometric radiated flare energy for different observed components of stellar flares and show that there is rough agreement for these values with solar flares. We apply an equipartition between the bolometric radiated flare energy and kinetic energy in an accompanying mass ejection, seen in solar eruptive events and expected from reconnection. This allows an integrated flare rate in a particular waveband to be used to estimate the amount of associated transient mass-loss. This approach is supported by a good correspondence between observational flare signatures on high flaring rate stars and the Sun, which suggests a common physical origin. If the frequent and extreme flares that young solar-like stars and low-mass stars experience are accompanied by transient mass-loss in the form of coronal mass ejections, then the cumulative effect of this mass-loss could be large. We find that for young solar-like stars and active M dwarfs, the total mass lost due to transient magnetic eruptions could have significant impacts on disk evolution, and thus planet formation, and also exoplanet habitability.

## **Sun-as-a-star Analyses of Various Solar Active Events Using H $\alpha$ Spectral Images Taken by SMART/SDDI**

[Takato Otsu](#), [Ayumi Asai](#), [Kiyoshi Ichimoto](#), [Takako T. Ishii](#), [Kosuke Namekata](#)

ApJ **939** 98 **2022**

<https://arxiv.org/pdf/2210.02819.pdf>

<https://iopscience.iop.org/article/10.3847/1538-4357/ac9730/pdf>

Sun-as-a-star analyses, in which observational data is spatially integrated, are useful for interpreting stellar data. For future applications to stellar observations, we performed Sun-as-a-star analyses of H $\alpha$  spectra for various active events on the Sun, not only for flares and filament eruptions/surges on the solar disk, but also for eruptions of off limb prominences using H $\alpha$  spectral images taken by the Solar Magnetic Activity Research Telescope / Solar Dynamics Doppler Imager (SMART/SDDI) at Hida Observatory, Kyoto University. All the analyzed events show emission relative to the pre-event state and the changes in their H $\alpha$  equivalent widths are all on the orders of 10–4 Å. Sun-as-a-star H $\alpha$  spectra exhibit different features depending on the causes of the emission: (i) Flares show emission at the H $\alpha$  line center, together with red asymmetry and line broadening, as reported in a previous study. (ii) Filament eruptions

with and without flares show emission near the H $\alpha$  line center, accompanied by blue-/red-shifted absorption. Notably, disappearance of dark filaments leads to the apparent enhancement of the H $\alpha$  line center emission. (iii) Eruptions of off limb prominences show blue-/red-shifted emission. These spectral features enable us to identify the active phenomena on Sun-like stars. We have also found that even the filament eruptions showing red-shifted absorptions in Sun-as-a-star H $\alpha$  spectra lead to coronal mass ejections (CMEs). This result suggests that even if the falling components of stellar filament eruptions are detected as red-shifted absorptions in H $\alpha$  spectra, such stellar filament eruptions may also develop into CMEs. **2016 November 5, 2017 February 19, 2017 April 2, 2017 April 23, 2017 June 19, 2017 September 8, 2021 April 19 – 20, 2021 May 5**

**Table 1.** List of events analyzed in this paper 2016-2021

### Photospheric signatures of CME onset

[Aslam Ottupara](#), [David MacTaggart](#), [Tom Williams](#), [Lyndsay Fletcher](#), [Paolo Romano](#)

MNRAS 534, 444–454 **2024**

<https://arxiv.org/pdf/2409.07261>

Coronal mass ejections (CMEs) are solar eruptions that involve large-scale changes to the magnetic topology of an active region. There exists a range of models for CME onset which are based on twisted or sheared magnetic field above a polarity inversion line (PIL). We present observational evidence that topological changes at PILs, in the photosphere, form a key part of CME onset, as implied by many models. In particular, we study the onset of 30 CMEs and investigate topological changes in the photosphere by calculating the magnetic winding flux, using the `\texttt{ARTop}` code. By matching the times and locations of winding signatures with CME observations produced by the `\texttt{ALMANAC}` code, we confirm that these signatures are indeed associated with CMEs. Therefore, as well as presenting evidence that changes in magnetic topology at the photosphere are a common signature of CME onset, our approach also allows for the finding of the source location of a CME within an active region. **2011 Feb 15, 2011 Jul 08, 2011 Oct 15, 2013 Jun 18**

**Table 1.** A table of 30 CME events with winding signatures related to CME onset. 2010-2015

### Initiation and Eruption of a Two-turn Helical Quiescent Filament on 2013 August 2

Yudi [Ou](#)<sup>1,2</sup>, Yingna [Su](#)<sup>1,2</sup>, Jialin [Chen](#)<sup>2,3</sup>, Yanjie [Liu](#)<sup>1,2</sup>, Jinhua [Shen](#)<sup>4</sup>, and Haisheng [Ji](#)<sup>1,2</sup>

**2024** ApJ 966 6

<https://iopscience.iop.org/article/10.3847/1538-4357/ad34b4/pdf>

We investigate a quiescent filament that erupted on **2013 August 2**; the eruption was observed in EUV and H $\alpha$  by the Solar Dynamics Observatory and GONG. After a B9.7 flare in the nearby active region, the dark filament materials near its eastern footpoint start to move in the direction of eruption, and are followed by a counterclockwise rotation identified as the motion of a combination of dark and bright filament materials. Then the entire filament rises up and keeps rotating in a clockwise direction during the eruption. More interestingly, the filament exhibits an unusual two-helix structure near its western footpoint during the eruption, which indicates the existence of a highly twisted flux rope. This hypothesis is confirmed by magnetic field modeling using the flux rope insertion method. In the best-fit unstable model, the lower limits of the estimated maximum and average twist numbers of the erupting flux rope reach  $7.5\pi$  and  $4\pi$ , which suggests that kink instability plays an important role in the eruption. During these magnetically coupled sympathetic eruptions, the highly twisted filament under the western lobe of a pseudo-streamer-like structure becomes unstable and erupts due to the removal of confinement by magnetic reconnection at the overlying hyperbolic flux tube, which is initiated by the B9.7 flare in the nearby active region. The initial filament motion occurs at the more unstable eastern footpoint, where the surrounding fields are weaker and decrease with height more rapidly.

### Mid-term Periodicity of Coronal Mass Ejections during the Time Interval 1996–2022

Zhuolang [Ouyang](#)<sup>1,2</sup>, Hui [Deng](#)<sup>1,2</sup>, Feng [Wang](#)<sup>1,2</sup>, LinHua [Deng](#)<sup>3,4</sup>, Ying [Mei](#)<sup>1,2</sup>, and XiaoJuan [Zhang](#)

**2024** ApJ 970 37

<https://iopscience.iop.org/article/10.3847/1538-4357/ad4d9f/pdf>

Coronal mass ejections (CMEs) exhibit a wide range of quasiperiodic variations and are crucial for our understanding of the cyclical evolution of large-scale magnetic fields. However, the mid-term periodicities of different types of CMEs associated with different processes at the source location need to be clearly understood. Based on the CDAW catalog released by the Large Angle and Spectroscopic Coronagraph mission on the Solar and Heliospheric Observatory, we investigated the period of CMEs based on the speeds and accelerations using the continuous wavelet transformation method. Our results revealed that the distribution of CMEs over time is quite distinctly different for different speeds, and there are Rieger-type periods and quasi-biennial oscillations of the CMEs. The two types of periodic signals show significant differences in solar cycles 23 and 24. Furthermore, the periodicity patterns for the northern hemisphere differ from those in the southern hemisphere. The potential mechanisms and explanations of the results are also discussed.

### Is flux rope a necessary condition for the progenitor of coronal mass ejections?

Y. [Ouyang](#), K. Yang, P. F. Chen

ApJ 815 72 **2015**

<http://arxiv.org/pdf/1511.01605v1.pdf>

A magnetic flux rope structure is believed to exist in most coronal mass ejections (CMEs). However, it has been long debated whether the flux rope exists before eruption or is formed during eruption via magnetic reconnection. The

controversy has been continuing because of our lack of routine measurements of the magnetic field in the pre-eruption structure, such as solar filaments. However, recently an indirect method was proposed to infer the magnetic field configuration based on the sign of helicity and the bearing direction of the filament barbs. In this paper, we apply this method to two erupting filament events, one on **2014 September 2** and the other on **2011 March 7**, and find that the first filament is supported by a magnetic flux rope and the second filament is supported by a sheared arcade, i.e., the first one is an inverse-polarity filament and the second one is a normal-polarity filament. With the identification of the magnetic configurations in these two filaments, we stress that a flux rope is not a necessary condition for the pre-CME structure.

## **Ion Charge States and Potential Geoeffectiveness: The Role of Coronal Spectroscopy for Space-Weather Forecasting**

M. J. [Owens](#) [M. Lockwood](#) [L. A. Barnard](#)

Space Weather Volume 16, Issue 6 June 2018 Pages 694-703

<http://sci-hub.tw/10.1029/2018SW001855>

Severe space weather is driven by interplanetary coronal mass ejections (ICMEs), episodic eruptions of solar plasma, and magnetic flux that travel out through the heliosphere and can perturb the Earth's magnetosphere and ionosphere. In order for space-weather forecasts to allow effective mitigating action, forecasts must be made as early as possible, necessitating identification of potentially "geoeffective" ICMEs close to the Sun. This presents two challenges. First, geoeffectiveness is primarily determined by the magnetic field intensity and orientation, both of which are difficult to measure close to the Sun. Second, the magnetic field evolves in transit between the Sun and the Earth, sometimes in a highly nonlinear way. Conversely, solar wind ion charge states, such as the ratio of O7+ to O6+, are fixed by the electron temperature at the coronal height where ion-electron collisions are last possible as the ICME erupts. After this point, they are said to be "frozen in" as they do not evolve further as the ICME propagates through the solar wind. In this study we show that ion charge states, while not geoeffective in and of themselves, act as strong markers for the geoeffectiveness of the ICME. The probability of severe space weather is around 7 times higher in "hot" ICMEs than "cold" ICMEs, as defined by O7+/O6+. We suggest that coronal spectroscopy of ICMEs could complement current forecasting techniques, providing valuable additional information about potential geoeffectiveness.

## **Propagation of information within coronal mass ejections**

Matthew [Owens](#) (Reading)

UK Solar Physics (UKSP) – Nuggets # 82 2017 [www.uksolphys.org/?p=13322](http://www.uksolphys.org/?p=13322)

Communication by Alfvén waves sets a basic limit to the coherence of propagating CMEs.

## **Coronal mass ejections are not coherent magnetohydrodynamic structures**

M. J. [Owens](#), [M. Lockwood](#) & [L. A. Barnard](#)

Scientific Reports 7, Article number: 4152(2017)

<https://www.nature.com/articles/s41598-017-04546-3.pdf>

Coronal mass ejections (CMEs) are episodic eruptions of solar plasma and magnetic flux that travel out through the solar system, driving extreme space weather. Interpretation of CME observations and their interaction with the solar wind typically assumes CMEs are coherent, almost solid-like objects. We show that supersonic radial propagation of CMEs away from the Sun results in geometric expansion of CME plasma parcels at a speed faster than the local wave speed. Thus information cannot propagate across the CME. Comparing our results with observed properties of over 400 CMEs, we show that CMEs cease to be coherent magnetohydrodynamic structures within 0.3 AU of the Sun. This suggests Earth-directed CMEs are less like billiard balls and more like dust clouds, with apparent coherence only due to similar initial conditions and quasi homogeneity of the medium through which they travel. The incoherence of CMEs suggests interpretation of CME observations requires accurate reconstruction of the ambient solar wind with which they interact, and that simple assumptions about the shape of the CMEs are likely to be invalid when significant spatial/temporal gradients in ambient solar wind conditions are present.

## **Effects of Hysteresis Between Maximum CME Speed Index and Typical Solar Activity Indicators During Cycle 23**

A. [Özgüç](#), A. Kilcik, J. P. Rozelot

Solar Physics, December 2012, Volume 281, Issue 2, pp 839-846

Using the smoothed time series of maximum CME speed index for solar cycle 23, it is found that this index, analyzed jointly with six other solar activity indicators, shows a hysteresis phenomenon. The total solar irradiance, coronal index, solar radio flux (10.7 cm), Mg ii core-to-wing ratio, sunspot area, and H $\alpha$  flare index follow different paths for the ascending and the descending phases of solar cycle 23, while a saturation effect exists at the maximum phase of the cycle. However, the separations between the paths are not the same for the different solar activity indicators used: the H $\alpha$  flare index and total solar irradiance depict broad loops, while the Mg ii core-to-wing ratio and sunspot area depict narrow hysteresis loops. The lag times of these indices with respect to the maximum CME speed index are discussed,



confirming that the hysteresis represents a clue in the search for physical processes responsible for changing solar emission.

### **Matching temporal signatures of solar features to their corresponding solar wind outflows** [Diego de Pablos](#), [David M. Long](#), [Christopher J. Owen](#), [Gherardo Valori](#), [Georgios Nicolaou](#), [Louise K. Harra](#)

Solar Phys. **296**, Article number: 68 2021

<https://arxiv.org/pdf/2103.09077.pdf>

<https://doi.org/10.1007/s11207-021-01813-5>

<https://link.springer.com/content/pdf/10.1007/s11207-021-01813-5.pdf>

The role of small-scale coronal eruptive phenomena in the generation and heating of the solar wind remains an open question. Here, we investigate the role played by coronal jets in forming the solar wind by testing whether temporal variations associated with jetting in EUV intensity can be identified in the outflowing solar wind plasma. This type of comparison is challenging due to inherent differences between remote-sensing observations of the source and in situ observations of the outflowing plasma, as well as travel time and evolution of the solar wind throughout the heliosphere. To overcome these, we propose a novel algorithm combining signal filtering, two-step solar wind ballistic backmapping, window shifting, and Empirical Mode Decomposition. We first validate the method using synthetic data, before applying it to measurements from the Solar Dynamics Observatory, and Wind spacecraft. The algorithm enables the direct comparison of remote sensing observations of eruptive phenomena in the corona to in situ measurements of solar wind parameters, among other potential uses. After application to these datasets, we find several time windows where signatures of dynamics found in the corona are embedded in the solar wind stream, at a time significantly earlier than expected from simple ballistic backmapping, with the best performing in situ parameter being the solar wind mass flux. **9-14 Nov 2016**

### **Corrugated Features in Coronal-mass-ejection-driven Shocks: A Discussion on the Predisposition to Particle Acceleration**

A. [Páez](#)<sup>1</sup>, V. Jatenco-Pereira<sup>1</sup>, D. Falceta-Gonçalves<sup>2</sup>, and M. Opher

2019 ApJ 879 122

<https://arxiv.org/pdf/1907.07884.pdf>

[sci-hub.se/10.3847/1538-4357/ab2460](https://sci-hub.se/10.3847/1538-4357/ab2460)

The study of the acceleration of particles is an essential element of research in heliospheric science. Here, we discuss the predisposition to the particle acceleration around shocks driven by coronal mass ejections (CMEs) with corrugated wave-like features. We adopt these attributes on shocks formed from disturbances due to the bimodal solar wind, CME deflection, irregular CME expansion, and the ubiquitous fluctuations in the solar corona. In order to understand the role of a wavy shock in particle acceleration, we define three initial smooth shock morphologies each associated with a fast CME. Using polar Gaussian profiles we model these shocks in the low corona. We establish the corrugated appearance on smooth shock by using combinations of wave-like functions that represent the disturbances from the medium and CME piston. For both shock types, smooth and corrugated, we calculate the shock normal angles between the shock normal and the radial upstream coronal magnetic field in order to classify the quasi-parallel and quasi-perpendicular regions. We consider that corrugated shocks are predisposed to different processes of particle acceleration due to irregular distributions of shock normal angles around the shock. We suggest that disturbances due to CME irregular expansion may be a decisive factor in origin of particle acceleration. Finally, we regard that accepting these features on shocks may be the starting point for investigating some questions regarding the sheath and shock, like downstream jets, instabilities, shock thermalization, shock stability, and injection particle processes.

### **Kelvin–Helmholtz Instability at the CME–Sheath and Sheath–Solar-wind Interfaces**

A. [Páez](#)<sup>1</sup>, V. Jatenco-Pereira<sup>1</sup>, D. Falceta-Gonçalves<sup>2</sup>, and M. Opher<sup>3</sup>

2017 ApJ 851 112

Wave-like features recently observed in some coronal mass ejections (CMEs) have been associated with the presence of Kelvin–Helmholtz instability (KHI) in the low corona. Previous works found observational evidence of KHI in a CME; this was followed by numerical simulations in order to determine the magnetic field strength allowing for its existence. Here, we present the first discussion of KHI formation in the outer corona at heliocentric distances from  $4 R_{\odot}$  to  $30 R_{\odot}$ . We study separately the CME–sheath and sheath–solar-wind (Sh–SW) interfaces of two CMEs that propagated in the slow and fast SWs. Mapping the velocities, densities, and magnetic field strengths of the CMEs, sheaths, and SWs in the CME's flanks, we solve the Chandrasekhar condition for KHI formation. Calculations show that KHI formation is more likely in a CME propagating in a slow SW (CME 1) than that propagating in a fast SW due to the large shear flow between the CME and the slow SW. Comparing the interfaces for both CME cases, we note that the Sh–SW interface of CME 1 is more conducive to the instability because of the similar strengths of the magnetic field necessary for KHI formation and of the SW magnetic field.

### **Modelling of asymmetric nanojets in coronal loops**

[Paolo Pagano](#), [Patrick Antolin](#), [Antonio Petralia](#)

A&A 2021

<https://arxiv.org/pdf/2109.04854.pdf>

Observations of reconnection jets in the solar corona are emerging as a possible diagnostic to study highly elusive coronal heating. Such nanojets can be observed in coronal loops and they have been linked to nanoflares. However, while models successfully describe the bilateral post-reconnection magnetic slingshot effect that leads to the jets, observations reveal that nanojets are unidirectional, or highly asymmetric, with only the jet travelling inward with respect to the coronal loop's curvature being clearly observed. The aim of this work is to address the role of the curvature of the coronal loop in asymmetric reconnection jets. In order to do so, we first use a simplified analytical model where we estimate the post-reconnection tension forces based on the local intersection angle between the pre-reconnection magnetic field lines and on their post-reconnection retracting length towards new equilibria. Second, we use a simplified numerical magnetohydrodynamic (MHD) model to study how two opposite propagating jets evolve in curved magnetic field lines. Our analytical model demonstrates that in the post-reconnection reorganised magnetic field, the inward directed magnetic tension is inherently stronger (up to 3 orders of magnitude) than the outward directed one and that, with a large enough retracting length, a regime exists where the outward directed tension disappears, leading to no outward jet at large, observable scales. Our MHD numerical model provides support for these results proving also that in the following time evolution the inward jets are consistently more energetic. The degree of asymmetry is also found to increase for small-angle reconnection and for more localised reconnection regions. This work shows that the curvature of the coronal loops plays a role in the asymmetry of the reconnection jets and inward directed jets are more likely to occur and more energetic.

## Hydrogen Non-Equilibrium Ionisation Effects in Coronal Mass Ejections

P. Pagano, A. Bemporad, D. H. Mackay

A&A 637, A49 2020

<https://arxiv.org/pdf/2003.12337.pdf>

<https://www.aanda.org/articles/aa/pdf/2020/05/aa37638-20.pdf>

A new generation of coronagraphs to study the solar wind and CMEs are being developed and launched. These coronagraphs will heavily rely on multi-channel observations where visible light (VL) and UV-EUV observations provide new plasma diagnostics. One of these instruments, Metis on board ESA-Solar Orbiter, will simultaneously observe VL and the UV Lyman- $\alpha$  line. The number of neutral Hydrogen atoms (a small fraction of coronal protons) is a key parameter for deriving plasma properties such as temperature from the observed Lyman- $\alpha$  line intensity. However, these measurements are significantly affected if non-equilibrium ionisation effects occur. The aim of this work is to determine if non-equilibrium ionisation effects are relevant in CMEs and in particular when and in which regions of the CME. We use a magneto-hydrodynamic simulation of a magnetic flux rope ejection to generate a CME. From this we then reconstruct the ionisation state of Hydrogen atoms in the CME by evaluating both the advection of neutral and ionised Hydrogen atoms and the ionisation and recombination rates in the MHD simulation. We find that the equilibrium ionisation assumption holds mostly in the core of the CME. In contrast non-equilibrium ionisation effects are significant at the CME front, where we find about 100 times more neutral Hydrogen atoms than prescribed by ionisation equilibrium conditions, even if this neutral Hydrogen excess might be difficult to identify due to projection effects. This work provides key information for the development of a new generation of diagnostic techniques that aim at combining visible light and Lyman- $\alpha$  line emissions. The results show that non-ionisation equilibrium effects need to be considered when we analyse CME fronts. To incorrectly assume equilibrium ionisation in these regions would lead to a systematic underestimate of plasma temperatures.

## A Prospective New Diagnostic Technique for Distinguishing Eruptive and Non-Eruptive Active Regions

P. Pagano, D.H. Mackay, S.L. Yardley

ApJ 883 112 2019

<https://arxiv.org/pdf/1908.09223.pdf>

<https://doi.org/10.3847/1538-4357/ab3e42>

Active regions are the source of the majority of magnetic flux rope ejections that become Coronal Mass Ejections (CMEs). To identify in advance which active regions will produce an ejection is key for both space weather prediction tools and future science missions such as Solar Orbiter. The aim of this study is to develop a new technique to identify which active regions are more likely to generate magnetic flux rope ejections. The new technique will aim to: (i) produce timely space weather warnings and (ii) open the way to a qualified selection of observational targets for space-borne instruments. We use a data-driven Non-linear Force-Free Field (NLFFF) model to describe the 3D evolution of the magnetic field of a set of active regions. We determine a metric to distinguish eruptive from non-eruptive active regions based on the Lorentz force. Furthermore, using a subset of the observed magnetograms, we run a series of simulations to test whether the time evolution of the metric can be predicted. The identified metric successfully differentiates active regions observed to produce eruptions from the non-eruptive ones in our data sample. A meaningful prediction of the metric can be made between 6 to 16 hours in advance. This initial study presents an interesting first step in the prediction of CME onset using only LOS magnetogram observations combined with NLFFF modelling. Future studies will address how to generalise the model such that it can be used in a more operational sense and for a variety of simulation approaches. **2012.08.29-09.02**

**Table 1.** Properties of the active regions analysed in this study (2012-2015)

## A New Space Weather Tool for Identifying Eruptive Active Regions

P. Pagano, D. H. Mackay, S. L. Yardley

ApJ 886 81 2019

<https://arxiv.org/pdf/1910.04226.pdf>

[sci-hub.se/10.3847/1538-4357/ab4cf1](https://sci-hub.se/10.3847/1538-4357/ab4cf1)

One of the main goals of solar physics is the timely identification of eruptive active regions. Space missions such as Solar Orbiter or future Space Weather forecasting missions would largely benefit from this achievement. Our aim is to produce a relatively simple technique that can provide real time indications or predictions that an active region will produce an eruption. We expand on the theoretical work of \cite{Pagano2019fp} that was able to distinguish eruptive from non-eruptive active regions. From this we introduce a new operational metric that uses a combination of observed line-of-sight magnetograms, 3D data-driven simulations and the projection of the 3D simulations forward in time. Results show that the new metric correctly distinguishes active regions as eruptive when observable signatures of eruption have been identified and as non-eruptive when there are no observable signatures of eruption. After successfully distinguishing eruptive from non-eruptive active regions we illustrate how this metric may be used in a "real-time" operational sense where three levels of warning are categorised. These categories are: high risk (red), medium risk (amber) and low risk (green) of eruption. Through considering individual cases we find that the separation into eruptive and non-eruptive active regions is more robust the longer the time series of observed magnetograms used to simulate the build up of magnetic stress and free magnetic energy within the active region. Finally, we conclude that this proof of concept study delivers promising results where the ability to categorise the risk of an eruption is a major achievement. 2011.08.02, 2012.03.20, 2012.05.09-14, 2012.06.14, 2012.09.01, 2013.03.03, 2013.08.06-12, 2015.11.13-18

Table 1. Active region properties, as in Pagano et al. (2019).

## A new technique for observationally derived boundary conditions for space weather

P. Pagano, D.H. Mackay, A.R. Yeates

Journal of Space Weather and Space Climate 8, A26 2018

<https://arxiv.org/pdf/1802.07516.pdf>

In recent years, space weather research has focused on developing modelling techniques to predict the arrival time and properties of coronal mass ejections (CMEs) at the Earth. The aim of this paper is to propose a new modelling technique suitable for the next generation of Space Weather predictive tools that is both efficient and accurate. The aim of the new approach is to provide interplanetary space weather forecasting models with accurate time dependent boundary conditions of erupting magnetic flux ropes in the upper solar corona. To produce boundary conditions, we couple two different modelling techniques, MHD simulations and a quasi-static non-potential evolution model. Both are applied on a spatial domain that covers the entire solar surface. The non-potential model uses a time series of observed synoptic magnetograms to drive the non-potential quasi-static evolution of the coronal magnetic field. This allows us to follow the formation and loss of equilibrium of magnetic flux ropes. Following this a MHD simulation captures the dynamic evolution of the erupting flux rope. The present paper focuses on the MHD simulations that follow the ejection of magnetic flux ropes to 4Rs. We first propose a technique for specifying the pre-eruptive plasma properties in the corona. Next, time dependent MHD simulations describe the ejection of two magnetic flux ropes, that produce time dependent boundary conditions for the magnetic field and plasma at 4Rs. In the present paper, we show that the dual use of quasi-static non-potential magnetic field simulations and full time dependent MHD simulations can produce realistic inhomogeneous boundary conditions for space weather forecasting tools. Before a fully operational model can be produced there are a number of technical and scientific challenges that still need to be addressed.

## Future capabilities of CME polarimetric 3D reconstructions with the METIS instrument: A numerical test

Paolo Pagano, Alessandro Bemporad, Duncan Mackay

A&A 582, A72 2015

<http://arxiv.org/pdf/1508.05276v1.pdf>

Understanding the 3D structure of coronal mass ejections (CMEs) is crucial for understanding the nature and origin of solar eruptions. To derive information on the 3D structure of CMEs from white-light (total and polarized brightness) images, the polarization ratio technique is widely used. The soon-to-be-launched METIS coronagraph on board Solar Orbiter will use this technique to produce new polarimetric images. We determine the accuracy at which the position of the centre of mass, direction and speed of propagation, and the column density of the CME can be determined along the line of sight. We perform a 3D MHD simulation of a flux rope ejection where a CME is produced. From the simulation we (i) synthesize the corresponding METIS white-light (total and polarized brightness) images and (ii) apply the polarization ratio technique to these synthesized images and compare the results with the known density distribution from the MHD simulation. We find that the polarization ratio technique reproduces with high accuracy the position of the centre of mass along the line of sight. However, some errors are inherently associated with this determination. The polarization ratio technique also allows information to be derived on the real 3D direction of propagation of the CME. In addition, we find that the column density derived from white-light images is accurate and we propose an improved technique where the combined use of the polarization ratio technique and white-light images minimizes the error in the estimation of column densities. Our method allows us to thoroughly test the performance of the polarization ratio technique and allows a determination of the errors associated with it, which means that it can be used to quantify the results from the analysis of the forthcoming METIS observations in white light (total and polarized brightness).

## Assessing the polarization ratio technique for 3D CME reconstructions

Paolo **Pagano**, Duncan Mackay, Alessandro Bemporad

UKSP Nugget #54, Jan 2015

<http://www.uksolphys.org/uksp-nugget/54-assessing-the-polarization-ratio-technique-for-3d-cme-reconstructions/>

Because of the solar corona is optically thin in white light, the true 3D structure of Coronal Mass Ejections (CMEs) is concealed by projection effects: we can only observe the integrated emission along the line of sight. However, a knowledge of the corona in 3D is crucial for understanding the nature and origin of solar eruptions. In particular, it would improve our comprehension of the coronal structures that generate CMEs, of the magnetic topology of the erupting region (and thus the coronal magnetic field) and finally it would allow us to predict the trajectory of CMEs in the interplanetary space, increasing the safety of manned operation in space and of satellites in Space Weather. The polarization ratio technique [1] is widely used to derive information on the 3D structure of CMEs from white light images, both total brightness and polarized brightness. Future coronagraphs, like METIS on board Solar Orbiter, will use this technique to produce new polarimetric images [2]. The polarization ratio technique utilises the fact that the polarized (pB) and unpolarized (uB) brightnesses from Thomson scattering have different dependences on the scattering angle, hence on the location  $z$  of the electrons along the Line of Sight (LOS). This different dependence on the angle allows the determination of the average plasma location along the LOS from the ratio pB/uB observed in single view-point images, with a well known  $\pm z$  ambiguity due to the symmetry of Thomson scattering about the plane of the sky ( $z = 0$ ).

The aim of our study is to provide a key to correctly interpret the results from the polarization ratio technique and to estimate quantitatively the uncertainties connected to its application.

## Simulating AIA observations of a flux rope ejection

Paolo **Pagano**, Duncan H. Mackay, Stefaan Poedts

A&A 568, A120 , 2014

<http://arxiv.org/pdf/1407.8397v1.pdf>

Extreme ultraviolet (EUV) images from the Atmospheric Imaging Assembly (AIA) on board the Solar Dynamic Observatory (SDO) are providing new insights into the early phase of CME evolution. Observations now show the ejection of magnetic flux ropes from the solar corona and how they evolve into CMEs. These observations are difficult to interpret in terms of basic physical mechanisms and quantities. To fully understand CMEs we need to compare equivalent quantities derived from both observations and theoretical models. To this end we aim to produce synthesised AIA observations from simulations of a flux rope ejection. To carry this out we include the role of thermal conduction and radiative losses, both of which are important for determining the temperature distribution of the solar corona during a CME. We perform a simulation where a flux rope is ejected from the solar corona. From the density and temperature of the plasma in the simulation we synthesise AIA observations. The emission is then integrated along the line of sight using the instrumental response function of AIA. We synthesise observations of AIA in the channels at 304 Å, 171 Å, 335 Å, and 94 Å. The synthesised observations show a number of features similar to actual observations and in particular reproduce the general development of CMEs in the low corona as observed by AIA. In particular we reproduce an erupting and expanding arcade in the 304 Å and 171 Å channels with a high density core. The ejection of a flux rope reproduces many of the features found in the AIA observations. This work is therefore a step forward in bridging the gap between observations and models, and can lead to more direct interpretations of EUV observations in terms of flux rope ejections. We plan to improve the model in future studies in order to perform a more quantitative comparison.

## Effect of gravitational stratification on the propagation of a CME★

P. **Pagano**<sup>1</sup>, D. H. Mackay<sup>1</sup> and S. Poedts<sup>2</sup>

A&A 560, A38 (2013)

Context. Coronal mass ejections (CMEs) are the most violent phenomenon found on the Sun. One model that explains their occurrence is the flux rope ejection model. A magnetic flux rope is ejected from the solar corona and reaches the interplanetary space where it interacts with the pre-existing magnetic fields and plasma. Both gravity and the stratification of the corona affect the early evolution of the flux rope.

Aims. Our aim is to study the role of gravitational stratification on the propagation of CMEs. In particular, we assess how it influences the speed and shape of CMEs and under what conditions the flux rope ejection becomes a CME or when it is quenched.

Methods. We ran a set of MHD simulations that adopt an eruptive initial magnetic configuration that has already been shown to be suitable for a flux rope ejection. We varied the temperature of the background corona and the intensity of the initial magnetic field to tune the gravitational stratification and the amount of ejected magnetic flux. We used an automatic technique to track the expansion and the propagation of the magnetic flux rope in the MHD simulations.

From the analysis of the parameter space, we evaluate the role of gravitational stratification on the CME speed and expansion.

**Results.** Our study shows that gravitational stratification plays a significant role in determining whether the flux rope ejection will turn into a full CME or whether the magnetic flux rope will stop in the corona. The CME speed is affected by the background corona where it travels faster when the corona is colder and when the initial magnetic field is more intense. The fastest CME we reproduce in our parameter space travels at  $\sim 850$  km s<sup>-1</sup>. Moreover, the background gravitational stratification plays a role in the side expansion of the CME, and we find that when the background temperature is higher, the resulting shape of the CME is flattened more.

**Conclusions.** Our study shows that although the initiation mechanisms of the CME are purely magnetic, the background coronal plasma plays a key role in the CME propagation, and full MHD models should be applied when one focuses especially on the production of a CME from a flux rope ejection.

## **Magnetohydrodynamic simulations of the ejection of a magnetic flux rope\***

P. [Pagano](#)<sup>1</sup>, D. H. Mackay<sup>1</sup> and S. Poedts<sup>2</sup>

A&A 554, A77 (2013)

**Context.** Coronal mass ejections (CME's) are one of the most violent phenomena found on the Sun. One model to explain their occurrence is the flux rope ejection model. In this model, magnetic flux ropes form slowly over time periods of days to weeks. They then lose equilibrium and are ejected from the solar corona over a few hours. The contrasting time scales of formation and ejection pose a serious problem for numerical simulations.

**Aims.** We simulate the whole life span of a flux rope from slow formation to rapid ejection and investigate whether magnetic flux ropes formed from a continuous magnetic field distribution, during a quasi-static evolution, can erupt to produce a CME.

**Methods.** To model the full life span of magnetic flux ropes we couple two models. The global non-linear force-free field (GNLFFF) evolution model is used to follow the quasi-static formation of a flux rope. The MHD code ARMVAC is used to simulate the production of a CME through the loss of equilibrium and ejection of this flux rope.

**Results.** We show that the two distinct models may be successfully coupled and that the flux rope is ejected out of our simulation box, where the outer boundary is placed at  $2.5 R_{\odot}$ . The plasma expelled during the flux rope ejection travels outward at a speed of 100 km s<sup>-1</sup>, which is consistent with the observed speed of CMEs in the low corona.

**Conclusions.** Our work shows that flux ropes formed in the GNLFFF can lead to the ejection of a mass loaded magnetic flux rope in full MHD simulations. Coupling the two distinct models opens up a new avenue of research to investigate phenomena where different phases of their evolution occur on drastically different time scales.

## **Modeling the life of a flux rope from formation to ejection**

Paolo [Pagano](#) and Duncan H. Mackay

UKSP nugget: 26, Aug 2012

Magnetic flux ropes – twisted bundles of magnetic field – are common structures in the solar corona which are responsible for many observed coronal features. For instance, flux rope ejections are the main progenitors of CMEs. The life of a magnetic flux rope normally undergoes two different phases. First is the formation of the flux rope in a coronal active region, a process that can last weeks. Second, the flux rope can be ejected into the outer atmosphere, in a period of a few hours. The slow formation phase can be approximated as quasi-static, in a regime dominated by magnetic forces, whereas the ejection phase is sudden and fast, the coronal plasma is compressed and heated, and the evolution is driven by both magnetic field and plasma. In this nugget we describe how we can model the full life span of a magnetic flux rope, from formation to ejection, by coupling our MHD ejection model with a magnetofrictional model for the slow formation phase.

## **Modeling magnetohydrodynamics and non-equilibrium SoHO/UVCS line emission of CME shocks**

P. [Pagano](#)<sup>1,2,3</sup>, J. C. Raymond<sup>2</sup>, F. Reale<sup>1,3</sup>, and S. Orlando<sup>3</sup>

A&A 481, 835-844 (2008)

DOI: 10.1051/0004-6361:20079088

## **MHD evolution of a fragment of a CME core in the outer solar corona:**

P. [Pagano](#), F. Reale, S. Orlando and G. Peres

A&A 464 (2007) 753-760

<http://www.aanda.org/10.1051/0004-6361:20065866>

## **Automated Processing of LASCO Coronal Images: Spurious Point-Source-Filtering and Missing-Blocks Correction**

E. **Pagot**, P. Lamy, A. Llebaria, B. Boclet

Solar Physics, April 2014, Volume 289, Issue 4, pp 1433-1453

We report on automated procedures for correcting the images of the LASCO coronagraph for i) spurious quasi-point-sources such as the impacts of cosmic rays, stars, and planets, and ii) the absence of signal due to transmission errors or dropouts, which results in blocks of missing information in the images. Correcting for these undesirable artifacts is mandatory for all quantitative works on the solar corona that require data inversion and/or long series of images, for instance. The nonlinear filtering of spike noise or point-like objects is based on mathematical morphology and implements the procedure opening by morphological reconstruction. However, a simple opening filter is applied whenever the fractional area of corrupted pixels exceeds 50 % of the original image. We describe different strategies for reconstructing the missing information blocks. In general, it is possible to implement the method of averaged neighbors using the two images obtained immediately before and after the corrupted image. For the other cases, and in particular when missing blocks overlapped in three images, we developed an original procedure of weighted interpolation along radial profiles from the center of the Sun that intercept the missing block(s). This procedure is also adequate for the saturated images of bright planets (such as Venus) that bleed along the neighboring pixels. Missing blocks in polarized images may generally be reconstructed using the associated unpolarized image of the same format. But in the case of overlapping missing blocks, we implemented our procedure of weighted interpolation. All tests performed on numerous LASCO-C2 images at various periods of solar activity (i.e. varying complexity of the structure of the corona) demonstrate the excellent performance of these new procedures, with results vastly superior to the methods implemented so far in the pipeline-processing of the LASCO images.

### **Eruption and Interplanetary Evolution of a Stealthy Streamer-Blowout CME Observed by PSP at ~0.5~AU**

**Sanchita Pal**, [Benjamin J. Lynch](#), [Simon W. Good](#), [Erika Palmerio](#), [Eleanna Asvestari](#), [Jens Pomoell](#), [Michael L. Stevens](#), [Emilia K. J. Kilpua](#)

**Front. Astron. Space Sci.** 9: 903676 2022

<https://arxiv.org/pdf/2205.07713.pdf>

<https://www.frontiersin.org/articles/10.3389/fspas.2022.903676/full>

<https://doi.org/10.3389/fspas.2022.903676>

Streamer-blowout coronal mass ejections (SBO-CMEs) are the dominant CME population during solar minimum. Although they are typically slow and lack clear low-coronal signatures, they can cause geomagnetic storms. With the aid of extrapolated coronal fields and remote observations of the off-limb low corona, we study the initiation of an SBO-CME preceded by consecutive CME eruptions consistent with a multi-stage sympathetic breakout scenario. From inner-heliospheric Parker Solar Probe (PSP) observations, it is evident that the SBO-CME is interacting with the heliospheric magnetic field and plasma sheet structures draped about the CME flux rope. We estimate that  $18 \pm 11\%$  of the CME's azimuthal magnetic flux has been eroded through magnetic reconnection and that this erosion began after a heliospheric distance of  $\sim 0.35$  AU from the Sun was reached. This observational study has important implications for understanding the initiation of SBO-CMEs and their interaction with the heliospheric surroundings. **22 June 2020**

### **Uncovering Erosion Effects on Magnetic Flux Rope Twist**

**Sanchita Pal**, [Emilia Kilpua](#), [Simon Good](#), [Jens Pomoell](#), [Daniel J. Price](#)

**A&A** 2021

<https://arxiv.org/pdf/2104.03569.pdf>

Magnetic clouds (MCs) are transient structures containing large-scale magnetic flux ropes from solar eruptions. The twist of magnetic field lines around the rope axis reveals information about flux rope formation processes and geoeffectivity. During propagation, MC flux ropes may erode via reconnection with the ambient solar wind. Any erosion reduces the magnetic flux and helicity of the ropes, and changes their cross-sectional twist profiles. This study relates twist profiles in MC flux ropes observed at 1 AU to the amount of erosion undergone by the MCs in interplanetary space. The twist profiles of two well-identified MC flux ropes associated with the clear appearance of post eruption arcades in the solar corona are analysed. To infer the amount of erosion, the magnetic flux content of the ropes in the solar atmosphere is estimated, and compared to estimates at 1 AU. The first MC shows a monotonically decreasing twist from the axis to periphery, while the second displays high twist at the axis, rising twist near the edges, and lower twist in between. The first MC displays a larger reduction in magnetic flux between the Sun and 1 AU, suggesting more erosion, than that seen in the second MC. In the second cloud, rising twist at the rope edges may have been due to an envelope of overlying coronal field lines with relatively high twist, formed by reconnection beneath the erupting flux rope in the low corona. This high-twist envelope remained almost intact from the Sun to 1 AU due to the low erosion levels. In contrast, the high-twist envelope of the first cloud may have been entirely peeled away via erosion by the time it reaches 1 AU. **April 3-5-6, 2010, July 9-13-14, 2013**

### **Dependence of Coronal Mass Ejection Properties on Their Solar Source Active Region Characteristics and Associated Flare Reconnection Flux**

**Sanchita Pal**<sup>1</sup>, **Dibyendu Nandy**<sup>1,2</sup>, **Nandita Srivastava**<sup>1,3</sup>, **Nat Gopalswamy**<sup>4</sup>, and **Suman Panda**

**2018 ApJ** 865 4

<https://arxiv.org/pdf/1808.04144.pdf> **File**

<http://sci-hub.tw/10.3847/1538-4357/aada10>

<https://iopscience.iop.org/article/10.3847/1538-4357/aada10/pdf>

The near-Sun kinematics of coronal mass ejections (CMEs) determine the severity and arrival time of associated geomagnetic storms. We investigate the relationship between the deprojected speed and kinetic energy of CMEs and magnetic measures of their solar sources, reconnection flux of associated eruptive events, and intrinsic flux-rope characteristics. Our data covers the period 2010–2014 in solar cycle 24. Using vector magnetograms of source active regions, we estimate the size and nonpotentiality. We compute the total magnetic reconnection flux at the source regions of CMEs using the post-eruption arcade method. By forward modeling the CMEs, we find their deprojected geometric parameters and constrain their kinematics and magnetic properties. Based on an analysis of this database, we report that the correlation between CME speed and their source active region size and global nonpotentiality is weak, but not negligible. We find the near-Sun velocity and kinetic energy of CMEs to be well correlated with the associated magnetic reconnection flux. We establish a statistically significant empirical relationship between the CME speed and reconnection flux that may be utilized for prediction purposes. Furthermore, we find CME kinematics to be related with the axial magnetic field intensity and relative magnetic helicity of their intrinsic flux ropes. The amount of coronal magnetic helicity shed by CMEs is found to be well correlated with their near-Sun speeds. The kinetic energy of CMEs is well correlated with their intrinsic magnetic energy density. Our results constrain processes related to the origin and propagation of CMEs and may lead to better empirical forecasting of their arrival and geoeffectiveness. **2012 June 14**  
**Table 1** Properties of Selected CMEs and Associated Source Region Information (2010-2014)

### **A Sun-to-Earth analysis of magnetic helicity of the 17-18 March 2013 interplanetary coronal mass ejection**

Sanchita **Pal**, [Nat Gopalswamy](#), [Dibyendu Nandy](#), [Sachiko Akiyama](#), [Seiji Yashiro](#), [Pertti Makela](#), [Hong Xie](#)  
**2017 ApJ** 851 123

<https://arxiv.org/pdf/1712.01114.pdf>

We compare the magnetic helicity in the 17-18 March 2013 interplanetary coronal mass ejection (ICME) flux-rope at 1 AU and in its solar counterpart. The progenitor coronal mass ejection (CME) erupted on **15 March 2013** from NOAA active region 11692 and associated with an M1.1 flare. We derive the source region reconnection flux using post-eruption arcade (PEA) method (Gopalswamy et al. 2017a) that uses the photospheric magnetogram and the area under the PEA. The geometrical properties of the near-Sun flux rope is obtained by forward-modeling of white-light CME observations. Combining the geometrical properties and the reconnection flux we extract the magnetic properties of the CME flux rope (Gopalswamy et al. 2017b). We derive the magnetic helicity of the flux rope using its magnetic and geometric properties obtained near the Sun and at 1 AU. We use a constant- $\alpha$  force-free cylindrical flux rope model fit to the in situ observations in order to derive the magnetic and geometric information of the 1-AU ICME. We find a good correspondence in both amplitude and sign of the helicity between the ICME and the CME assuming a semi-circular (half torus) ICME flux rope with a length of  $\pi$  AU. We find that about 83% of the total flux rope helicity at 1 AU is injected by the magnetic reconnection in the low corona. We discuss the effect of assuming flux rope length in the derived value of the magnetic helicity. This study connecting the helicity of magnetic flux ropes through the Sun-Earth system has important implications for the origin of helicity in the interplanetary medium and the topology of ICME flux ropes at 1 AU and hence their space weather consequences.

### **Flux emergence event underneath a filament**

J. **Palacios**, Y. Cerrato, C. Cid, A. Guerrero, E. Saiz

Proceedings of the International Astronomical Union, **2015**, Volume 305 'Polarimetry: From the Sun to Stars and Stellar Environments **2017**

<https://arxiv.org/pdf/1704.00681.pdf>

Flux emergence phenomena are relevant at different temporal and spatial scales. We have studied a flux emergence region underneath a filament. This filament elevated itself smoothly, and the associated CME reached Earth. In this study we investigate the size and amount of flux in the emergence event. The flux emergence site appeared just beneath a filament. The emergence acquired a size of 24 Mm in half a day. The unsigned magnetic flux density from LOS-magnetograms is around 1 kG at its maximum. The transverse field as well as the filament eruption were also analysed. **2013, 29 Sept**

### **Supergranular-scale magnetic flux emergence beneath an unstable filament**

J. **Palacios**, C. Cid, A. Guerrero, E. Saiz, Y. Cerrato

A&A 583, A47 **2015**

<http://arxiv.org/pdf/1509.05602v1.pdf>

Here we report evidence of a large solar filament eruption on 2013, September 29. This smooth eruption, which passed without any previous flare, formed after a two-ribbon flare and a coronal mass ejection towards Earth. The coronal mass ejection generated a moderate geomagnetic storm on 2013, October 2 with very serious localized effects. The whole event passed unnoticed to flare-warning systems.

We have conducted multi-wavelength analyses of the Solar Dynamics Observatory through Atmospheric Imaging Assembly (AIA) and Helioseismic and Magnetic Imager (HMI) data. The AIA data on 304, 193, 211, and 94 Å sample the transition region and the corona, respectively, while HMI provides photospheric magnetograms, continuum, and linear polarization data, in addition to the fully inverted data provided by HMI.

We have observed a supergranular-sized emergence close to a large filament in the boundary of the active region NOAA11850. Filament dynamics and magnetogram results suggest that the magnetic flux emergence takes place in the photospheric level below the filament. Reconnection occurs underneath the filament between the dipped lines that support the filament and the supergranular emergence. The very smooth ascent is probably caused by this emergence and torus instability may play a fundamental role, which is helped by the emergence.

### **Spatially Separated Electron and Proton Beams in a Simulated Solar Coronal Jet**

Ross **Pallister**<sup>1</sup>, Peter F. Wyper<sup>2</sup>, David I. Pontin<sup>1,3</sup>, C. Richard DeVore<sup>4</sup>, and Federica Chiti<sup>1</sup>

2021 ApJ 923 163

<https://iopscience.iop.org/article/10.3847/1538-4357/ac2e6d/pdf>

<https://doi.org/10.3847/1538-4357/ac2e6d>

Magnetic reconnection is widely accepted to be a major contributor to nonthermal particle acceleration in the solar atmosphere. In this paper we investigate particle acceleration during the impulsive phase of a coronal jet, which involves bursty reconnection at a magnetic null point. A test-particle approach is employed, using electromagnetic fields from a magnetohydrodynamic simulation of such a jet. Protons and electrons are found to be accelerated nonthermally both downwards toward the domain's lower boundary and the solar photosphere, and outwards along the axis of the coronal jet and into the heliosphere. A key finding is that a circular ribbon of particle deposition on the photosphere is predicted, with the protons and electrons concentrated in different parts of the ribbon. Furthermore, the outgoing protons and electrons form two spatially separated beams parallel to the axis of the jet, signatures that may be observable in in-situ observations of the heliosphere.

### **A coronal mass ejection encountered by four spacecraft within 1 au from the Sun: ensemble modelling of propagation and magnetic structure**

Erika **Palmerio**, Christina Kay, Nada Al-Haddad, Benjamin J Lynch, Domenico Trotta, Wenyuan Yu, Vincent E Ledvina, Beatriz Sánchez-Cano, Pete Riley, Daniel Heyner ++

MNRAS Volume 536, Issue 1, January 2025, Pages 203–222,

<https://arxiv.org/pdf/2411.12706>

<https://doi.org/10.1093/mnras/stae2606>

<https://watermark.silverchair.com/stae2606.pdf>

Understanding and predicting the structure and evolution of coronal mass ejections (CMEs) in the heliosphere remains one of the most sought-after goals in heliophysics and space weather research. A powerful tool for improving current knowledge and capabilities consists of multispacecraft observations of the same event, which take place when two or more spacecraft fortuitously find themselves in the path of a single CME. Multiprobe events can not only supply useful data to evaluate the large-scale of CMEs from 1D in situ trajectories, but also provide additional constraints and validation opportunities for CME propagation models. In this work, we analyse and simulate the coronal and heliospheric evolution of a slow, streamer-blowout CME that erupted on **2021 September 23** and was encountered in situ by four spacecraft approximately equally distributed in heliocentric distance between 0.4 and 1 au. We employ the Open Solar Physics Rapid Ensemble Information modelling suite in ensemble mode to predict the CME arrival and structure in a hindcast fashion and to compute the ‘best-fitting’ solutions at the different spacecraft individually and together. We find that the spread in the predicted quantities increases with heliocentric distance, suggesting that there may be a maximum (angular and radial) separation between an inner and an outer probe beyond which estimates of the in situ magnetic field orientation (parametrized by flux rope model geometry) increasingly diverge. We discuss the importance of these exceptional observations and the results of our investigation in the context of advancing our understanding of CME structure and evolution as well as improving space weather forecasts.

### **On the Mesoscale Structure of CMEs at Mercury's Orbit: BepiColombo and Parker Solar Probe Observations**

[Erika Palmerio](#), [Fernando Carcaboso](#), [Leng Ying Khoo](#), [Tarik M. Salman](#), +++

ApJ 2024

<https://arxiv.org/pdf/2401.01875.pdf>

On **2022 February 15**, an impressive filament eruption was observed off the solar eastern limb from three remote-sensing viewpoints, namely Earth, STEREO-A, and Solar Orbiter. In addition to representing the most-distant observed filament at extreme ultraviolet wavelengths -- captured by Solar Orbiter's field of view extending to above  $6 R_{\odot}$  -- this event was also associated with the release of a fast ( $\sim 2200 \text{ km}\cdot\text{s}^{-1}$ ) coronal mass ejection (CME) that was directed towards BepiColombo and Parker Solar Probe. These two probes were separated by  $2^{\circ}$  in latitude,  $4^{\circ}$  in longitude, and 0.03 au in radial distance around the time of the CME-driven shock arrival in situ. The relative proximity of the two probes to each other and to the Sun ( $\sim 0.35$  au) allows us to study the mesoscale structure of CMEs at Mercury's orbit for the first time. We analyse similarities and differences in the main CME-related structures measured at the two locations, namely the interplanetary shock, the sheath region, and the magnetic ejecta. We find that, despite the separation between the two spacecraft being well within the typical uncertainties associated with determination of CME geometric parameters from remote-sensing observations, the two sets of in-situ measurements display some profound differences that make understanding of the overall 3D CME structure particularly challenging. Finally, we discuss our findings within the context of space weather at Mercury's distances and in terms of the need to investigate solar



transients via spacecraft constellations with small separations, which has been gaining significant attention during recent years.

## **Modeling a Coronal Mass Ejection from an Extended Filament Channel. II. Interplanetary Propagation to 1 au**

[Erika Palmerio](#), [Anwasha Maharana](#), [Benjamin J. Lynch](#), [Camilla Scolini](#), [Simon W. Good](#), [Jens Pomoell](#), [Alexey Isavnin](#), [Emilia K. J. Kilpua](#)

ApJ 958 91 2023

<https://arxiv.org/pdf/2310.05846.pdf>

<https://iopscience.iop.org/article/10.3847/1538-4357/ad0229/pdf>

We present observations and modeling results of the propagation and impact at Earth of a high-latitude, extended filament channel eruption that commenced on **2015 July 9**. The coronal mass ejection (CME) that resulted from the filament eruption was associated with a moderate disturbance at Earth. This event could be classified as a so-called "problem storm" because it lacked the usual solar signatures that are characteristic of large, energetic, Earth-directed CMEs that often result in significant geoeffective impacts. We use solar observations to constrain the initial parameters and therefore to model the propagation of the **2015 July 9** eruption from the solar corona up to Earth using 3D magnetohydrodynamic heliospheric simulations with three different configurations of the modeled CME. We find the best match between observed and modeled arrival at Earth for the simulation run that features a toroidal flux rope structure of the CME ejecta, but caution that different approaches may be more or less useful depending on the CME-observer geometry when evaluating the space weather impact of eruptions that are extreme in terms of their large size and high degree of asymmetry. We discuss our results in the context of both advancing our understanding of the physics of CME evolution and future improvements to space weather forecasting.

## **New Observations Needed to Advance Our Understanding of Coronal Mass Ejections**

[Erika Palmerio](#), [Benjamin J. Lynch](#), [Christina O. Lee](#), [Lan K. Jian](#) +++

White Paper submitted to the Heliophysics 2024-2033 Decadal Survey 2023

<https://arxiv.org/pdf/2309.05480.pdf>

Coronal mass ejections (CMEs) are large eruptions from the Sun that propagate through the heliosphere after launch. Observational studies of these transient phenomena are usually based on 2D images of the Sun, corona, and heliosphere (remote-sensing data), as well as magnetic field, plasma, and particle samples along a 1D spacecraft trajectory (in-situ data). Given the large scales involved and the 3D nature of CMEs, such measurements are generally insufficient to build a comprehensive picture, especially in terms of local variations and overall geometry of the whole structure. This White Paper aims to address this issue by identifying the data sets and observational priorities that are needed to effectively advance our current understanding of the structure and evolution of CMEs, in both the remote-sensing and in-situ regimes. It also provides an outlook of possible missions and instruments that may yield significant improvements into the subject.

## **CMEs and SEPs During November-December 2020: A Challenge for Real-Time Space Weather Forecasting**

[Erika Palmerio](#), [Christina O. Lee](#), [M. Leila Mays](#), [Janet G. Luhmann](#),

Space Weather e2021SW002993 2022

<https://arxiv.org/pdf/2203.16433.pdf>

<https://agupubs.onlinelibrary.wiley.com/doi/epdf/10.1029/2021SW002993>

<https://doi.org/10.1029/2021SW002993>

Predictions of coronal mass ejections (CMEs) and solar energetic particles (SEPs) are a central issue in space weather forecasting. In recent years, interest in space weather predictions has expanded to include impacts at other planets beyond Earth as well as spacecraft scattered throughout the heliosphere. In this sense, the scope of space weather science now encompasses the whole heliospheric system, and multi-point measurements of solar transients can provide useful insights and validations for prediction models. In this work, we aim to analyse the whole inner heliospheric context between two eruptive flares that took place in late 2020, i.e. the M4.4 flare of **November 29** and the C7.4 flare of **December 7**. This period is especially interesting because the STEREO-A spacecraft was located  $\sim 60^\circ$  east of the Sun-Earth line, giving us the opportunity to test the capabilities of "predictions at 360°" using remote-sensing observations from the Lagrange L1 and L5 points as input. We simulate the CMEs that were ejected during our period of interest and the SEPs accelerated by their shocks using the WSA-Enlil-SEPMOD modelling chain and four sets of input parameters, forming a "mini-ensemble". We validate our results using in-situ observations at six locations, including Earth and Mars. We find that, despite some limitations arising from the models' architecture and assumptions, CMEs and shock-accelerated SEPs can be reasonably studied and forecast in real time at least out to several tens of degrees away from the eruption site using the prediction tools employed here.

## **Predicting the Magnetic Fields of a Stealth CME Detected by Parker Solar Probe at 0.5 AU**

[Erika Palmerio](#), [Christina Kay](#), [Nada Al-Haddad](#), [Benjamin J. Lynch](#), [Wenyuan Yu](#), [Michael L. Stevens](#), [Sanchita Pal](#), [Christina O. Lee](#)

ApJ **920** 65 **2021**

<https://arxiv.org/pdf/2109.04933.pdf>

<https://iopscience.iop.org/article/10.3847/1538-4357/ac25f4/pdf>

<https://doi.org/10.3847/1538-4357/ac25f4>

Stealth coronal mass ejection (CMEs) are eruptions from the Sun that are not associated with appreciable low-coronal signatures. Because they often cannot be linked to a well-defined source region on the Sun, analysis of their initial magnetic configuration and eruption dynamics is particularly problematic. In this manuscript, we address this issue by undertaking the first attempt at predicting the magnetic fields of a stealth CME that erupted in 2020 June from the Earth-facing Sun. We estimate its source region with the aid of off-limb observations from a secondary viewpoint and photospheric magnetic field extrapolations. We then employ the Open Solar Physics Rapid Ensemble Information (OSPREDI) modelling suite to evaluate its early evolution and forward-model its magnetic fields up to Parker Solar Probe, which detected the CME in situ at a heliocentric distance of 0.5 AU. We compare our hindcast prediction with in-situ measurements and a set of flux rope reconstructions, obtaining encouraging agreement on arrival time, spacecraft crossing location, and magnetic field profiles. This work represents a first step towards reliable understanding and forecasting of the magnetic configuration of stealth CMEs and slow, streamer-blowout events. **2020 June 21-26**

### **Investigating Remote-sensing Techniques to Reveal Stealth Coronal Mass Ejections**

[Erika Palmerio](#), [Nariaki V. Nitta](#), [Tamitha Mulligan](#), [Marilena Mierla](#), [Jennifer O'Kane](#), [Ian G.](#)

[Richardson](#), [Suvadip Sinha](#), [Nandita Srivastava](#), [Stephanie L. Yardley](#), [Andrei N. Zhukov](#)

Frontiers in Astronomy and Space Sciences **8**:695966 **2021**

<https://arxiv.org/pdf/2106.07571.pdf>

<https://www.frontiersin.org/articles/10.3389/fspas.2021.695966/full>

<https://doi.org/10.3389/fspas.2021.695966>

Eruptions of coronal mass ejections (CMEs) from the Sun are usually associated with a number of signatures that can be identified in solar disc imagery. However, there are cases in which a CME that is well observed in coronagraph data is missing a clear low-coronal counterpart. These events have received attention during recent years, mainly as a result of the increased availability of multi-point observations, and are now known as 'stealth CMEs'. In this work, we analyse examples of stealth CMEs featuring various levels of ambiguity. All the selected case studies produced a large-scale CME detected by coronagraphs and were observed from at least one secondary viewpoint, enabling a priori knowledge of their approximate source region. To each event, we apply several image processing and geometric techniques with the aim to evaluate whether such methods can provide additional information compared to the study of "normal" intensity images. We are able to identify at least weak eruptive signatures for all events upon careful investigation of remote-sensing data, noting that differently processed images may be needed to properly interpret and analyse elusive observations. We also find that the effectiveness of geometric techniques strongly depends on the CME propagation direction with respect to the observers and the relative spacecraft separation. Being able to observe and therefore forecast stealth CMEs is of great importance in the context of space weather, since such events are occasionally the solar counterparts of so-called 'problem geomagnetic storms'. **2008 June 1, 2011 March 3, 2012 February 4, 2016 October 9**

### **CME Magnetic Structure and IMF Preconditioning Affecting SEP Transport**

[Erika Palmerio](#), [Emilia K. J. Kilpua](#), [Olivier Witasse](#), [David Barnes](#), [Beatriz Sánchez-Cano](#), [Andreas J.](#)

[Weiss](#), [Teresa Nieves-Chinchilla](#), [Christian Möstl](#), [Lan K. Jian](#), [Marilena Mierla](#), [Andrei N. Zhukov](#), [Jingnan](#)

[Guo](#), [Luciano Rodriguez](#), [Patrick J. Lowrance](#), [Alexey Isavnin](#), [Lucile Turc](#), [Yoshifumi Futaana](#), [Mats](#)

[Holmström](#)

Space Weather **2021**

<https://arxiv.org/pdf/2102.05514.pdf>

Coronal mass ejections (CMEs) and solar energetic particles (SEPs) are two phenomena that can cause severe space weather effects throughout the heliosphere. The evolution of CMEs, especially in terms of their magnetic structure, and the configuration of the interplanetary magnetic field (IMF) that influences the transport of SEPs are currently areas of active research. These two aspects are not necessarily independent of each other, especially during solar maximum when multiple eruptive events can occur close in time. Accordingly, we present the analysis of a CME that erupted on **2012 May 11** (SOL2012-05-11) and an SEP event following an eruption that took place on **2012 May 17** (SOL2012-05-17). After observing the May 11 CME using remote-sensing data from three viewpoints, we evaluate its propagation through interplanetary space using several models. Then, we analyse in-situ measurements from five predicted impact locations (Venus, Earth, the Spitzer Space Telescope, the Mars Science Laboratory en route to Mars, and Mars) in order to search for CME signatures. We find that all in-situ locations detect signatures of an SEP event, which we trace back to the May 17 eruption. These findings suggest that the May 11 CME provided a direct magnetic connectivity for the efficient transport of SEPs. We discuss the space weather implications of CME evolution, regarding in particular its magnetic structure, and CME-driven IMF preconditioning that facilitates SEP transport. Finally, this work remarks the importance of using data from multiple spacecraft, even those that do not include space weather research as their primary objective. **2012 May 11-17**

### **Multipoint study of successive coronal mass ejections driving moderate disturbances at 1 AU**

Erika [Palmerio](#), [Camilla Scolini](#), [David Barnes](#), [Jasmina Magdalenic](#), [Matthew J. West](#), [Andrei N. Zhukov](#), [Luciano Rodriguez](#), [Marilena Mierla](#), [Simon W. Good](#), [Diana E. Morosan](#), [Emilia K. J. Kilpua](#), [Jens Pomoell](#), [Stefaan Poedts](#)

ApJ 2019

<https://arxiv.org/pdf/1906.01353.pdf>

We analyse in this work the propagation and geoeffectiveness of four successive coronal mass ejections (CMEs) that erupted from the Sun during **21--23 May 2013** and that were detected in interplanetary space by the Wind and/or STEREO-A spacecraft. All these CMEs featured critical aspects for understanding so-called "problem space weather storms" at Earth. In the first three events a limb CMEs resulted in moderately geoeffective in-situ structures at their target location in terms of the disturbance storm time (Dst) index (either measured or estimated). The fourth CME, which also caused a moderate geomagnetic response, erupted from close to the disc centre as seen from Earth, but it was not visible in coronagraph images from the spacecraft along the Sun--Earth line and appeared narrow and faint from off-angle viewpoints. Making the correct connection between CMEs at the Sun and their in-situ counterparts is often difficult for problem storms. We investigate these four CMEs using multiwavelength and multipoint remote-sensing observations (extreme ultraviolet, white light, and radio), aided by 3D heliospheric modelling, in order to follow their propagation in the corona and in interplanetary space and to assess their impact at 1 AU. Finally, we emphasise the difficulties in forecasting moderate space weather effects provoked by problematic and ambiguous events and the importance of multispacecraft data for observing and modelling problem storms.

### **Determining the Intrinsic CME Flux Rope Type Using Remote-sensing Solar Disk Observations**

E. [Palmerio](#), E. K. J. Kilpua, A. W. James, L. M. Green, J. Pomoell, A. Isavnin, G. Valori

Solar Physics February 2017, 292:39

A key aim in space weather research is to be able to use remote-sensing observations of the solar atmosphere to extend the lead time of predicting the geoeffectiveness of a coronal mass ejection (CME). In order to achieve this, the magnetic structure of the CME as it leaves the Sun must be known. In this article we address this issue by developing a method to determine the intrinsic flux rope type of a CME solely from solar disk observations. We use several well-known proxies for the magnetic helicity sign, the axis orientation, and the axial magnetic field direction to predict the magnetic structure of the interplanetary flux rope. We present two case studies: the **2 June 2011** and the **14 June 2012** CMEs. Both of these events erupted from an active region, and despite having clear in situ counterparts, their eruption characteristics were relatively complex. The first event was associated with an active region filament that erupted in two stages, while for the other event the eruption originated from a relatively high coronal altitude and the source region did not feature a filament. Our magnetic helicity sign proxies include the analysis of magnetic tongues, soft X-ray and/or extreme-ultraviolet sigmoids, coronal arcade skew, filament emission and absorption threads, and filament rotation. Since the inclination of the post-eruption arcades was not clear, we use the tilt of the polarity inversion line to determine the flux rope axis orientation and coronal dimmings to determine the flux rope footpoints, and therefore, the direction of the axial magnetic field. The comparison of the estimated intrinsic flux rope structure to in situ observations at the Lagrangian point L1 indicated a good agreement with the predictions. Our results highlight the flux rope type determination techniques that are particularly useful for active region eruptions, where most geoeffective CMEs originate.

### **Sigmoid Formation Through Slippage of A Single J-shaped Coronal Loop**

[Hanya Pan](#), [Tingyu Gou](#), [Rui Liu](#)

ApJ 937 77 2022

<https://arxiv.org/pdf/2208.14034.pdf>

<https://iopscience.iop.org/article/10.3847/1538-4357/ac8d64/pdf>

A well-known precursor of an imminent solar eruption is the appearance of a hot S-shaped loop, also known as sigmoid, in an active region (AR). Classically, the formation of such an S-shaped loop is envisaged to be implemented by magnetic reconnection of two oppositely oriented J-shaped loops. However, the details of reconnection are elusive due to weak emission and subtle evolution during the pre-eruptive phase. In this paper, we investigate how a single J-shaped loop transforms into an S-shaped one through the slippage of one of its footpoints in NOAA AR 11719 on **2013 April 11**. During an interval of about 16 min, the J-shaped loop slips through a low-corona region of strong electric current density in a bursty fashion, reaching a peak apparent speed as fast as over 1000 km s<sup>-1</sup>, at the slipping footpoint. The enhancement of electric current density, as suggested by non-linear force-free field modeling, indicates that the "non-idealness" of coronal plasma becomes locally important, which may facilitate magnetic reconnection. The loop segment undergoing slipping motions is heated; meanwhile, above the fixed footpoint coronal emission dims due to a combination effect of the lengthening and heating of the loop, the latter of which is manifested in the temporal variation of dimming slope and of emission measure. These features together support an asymmetric scenario of sigmoid formation through slipping reconnection of a single J-shaped loop, which differs from the standard tether-cutting scenario involving a double J-shaped loop system.

### **Pre-eruption Splitting of the Double-Decker Structure in a Solar Filament**

[Hanya Pan](#), [Rui Liu](#), [Tingyu Gou](#), [Bernhard Kliem](#), [Yingna Su](#), [Jun Chen](#), [Yuming Wang](#)

ApJ **909** 32 **2021**

<https://arxiv.org/pdf/2101.03296.pdf>

<https://doi.org/10.3847/1538-4357/abda4e>

Solar filaments often erupt partially. Although how they split remains elusive, the splitting process has the potential of revealing the filament structure and eruption mechanism. Here we investigate the pre-eruption splitting of an apparently single filament and its subsequent partial eruption on **2012 September 27**. The evolution is characterized by three stages with distinct dynamics. During the quasi-static stage, the splitting proceeds gradually for about 1.5 hrs, with the upper branch rising at a few kilometers per second and displaying swirling motions about its axis. During the precursor stage that lasts for about 10 min, the upper branch rises at tens of kilometers per second, with a pair of conjugated dimming regions starting to develop at its footpoints; with the swirling motions turning chaotic, the axis of the upper branch whips southward, which drives an arc-shaped EUV front propagating in the similar direction. During the eruption stage, the upper branch erupts with the onset of a C3.7-class two-ribbon flare, while the lower branch remains stable. Judging from the well separated footpoints of the upper branch from those of the lower one, we suggest that the pre-eruption filament processes a double-decker structure composed of two distinct flux bundles, whose formation is associated with gradual magnetic flux cancellations and converging photospheric flows around the polarity inversion line.

### **Apparent Solar Tornado-Like Prominences**

Olga [Panasenco](#), Sara F. Martin, Marco Velli

Solar Physics, February **2014**, Volume 289, Issue 2, pp 603-622

Recent high-resolution observations from the Solar Dynamics Observatory (SDO) have reawakened interest in the old and fascinating phenomenon of solar tornado-like prominences. This class of prominences was first introduced by Pettit (Astrophys. J. 76, 9, 1932), who studied them over many years. Observations of tornado prominences similar to the ones seen by SDO had already been documented by Secchi (Le Soleil, 1877). High-resolution and high-cadence multiwavelength data obtained by SDO reveal that the tornado-like appearance of these prominences is mainly an illusion due to projection effects. We discuss two different cases where prominences on the limb might appear to have a tornado-like behavior. One case of apparent vortical motions in prominence spines and barbs arises from the (mostly) 2D counterstreaming plasma motion along the prominence spine and barbs together with oscillations along individual threads. The other case of apparent rotational motion is observed in a prominence cavity and results from the 3D plasma motion along the writhed magnetic fields inside and along the prominence cavity as seen projected on the limb. Thus, the “tornado” impression results either from counterstreaming and oscillations or from the projection on the plane of the sky of plasma motion along magnetic-field lines, rather than from a true vortical motion around an (apparent) vertical or horizontal axis. We discuss the link between tornado-like prominences, filament barbs, and photospheric vortices at their base.

### **Origins of Rolling, Twisting and Non-Radial Propagation of Eruptive Solar Events**

Olga [Panasenco](#), Sara F. Martin, Marco Velli, Angelos Vourlidis

E-print, Dec **2012**; Solar Phys., **2013**, Volume 287, Issue 1-2, pp 391-413

We demonstrate that major asymmetries in erupting filaments and CMEs, namely major twists and non-radial motions are typically related to the larger-scale ambient environment around eruptive events. Our analysis of prominence eruptions observed by the STEREO, SDO and SOHO spacecraft shows that prominence spines retain, during the initial phases, the thin ribbon-like topology they had prior to the eruption. This topology allows bending, rolling, and twisting during the early phase of the eruption, but not before. The combined ascent and initial bending of the filament ribbon is non-radial in the same general direction as for the enveloping CME. However, the non-radial motion of the filament is greater than that of the CME. In considering the global magnetic environment around CMEs, as approximated by the Potential Field Source Surface (PFSS) model, we find that the non-radial propagation of both erupting filaments and associated CMEs is correlated with the presence of nearby coronal holes, which deflect the erupting plasma and embedded fields. In addition, CME and filament motions respectively are guided towards weaker field regions, namely null points existing at different heights in the overlying configuration. Due to the presence of the coronal hole, the large-scale forces acting on the CME may be asymmetric. We find that the CME propagates usually non-radially in the direction of least resistance, which is always away from the coronal hole. We demonstrate these results using both low and high latitude examples.

### **Solar Orbiter and SDO Observations, and Bifrost MHD Simulations of Small-scale Coronal Jets**

[Navdeep K. Panesar](#), [Viggo H. Hansteen](#), [Sanjiv K. Tiwari](#), [Mark C. M. Cheung](#), [David Berghmans](#), [Daniel Müller](#)

ApJ **2022**

<https://arxiv.org/pdf/2211.06529.pdf>

We report high-resolution, high-cadence observations of five small-scale coronal jets in an on-disk quiet Sun region observed with Solar Orbiter's EUVI in 174 Å. We combine the EUVI images with the EUV images of SDO/AIA and

investigate magnetic setting of the jets using co-aligned line-of-sight magnetograms from SDO/HMI. The jets are miniature versions of typical coronal jets as they show narrow collimated spires with a base brightening. Three out of five jets result from a detectable minifilament eruption following flux cancellation at the neutral line under the minifilament, analogous to coronal jets. To better understand the physics of jets, we also analyze five small-scale jets from a high-resolution Bifrost MHD simulation in synthetic FeIX/FeX emissions. The jets in the simulation reside above neutral lines and four out of five jets are triggered by magnetic flux cancellation. The temperature maps show the evidence of cool gas in the same four jets. Our simulation also shows the signatures of opposite Doppler shifts (of the order of  $\pm 10$ s of km/s) in the jet spire, which is evidence of untwisting motion of the magnetic field in the jet spire. The average jet duration, spire length, base width, and speed in our observations (and in synthetic FeIX/FeX images) are  $6.5 \pm 4.0$  min ( $9.0 \pm 4.0$  min),  $6050 \pm 2900$  km ( $6500 \pm 6500$  km),  $2200 \pm 850$  km, ( $3900 \pm 2100$  km), and  $60 \pm 8$  km/s ( $42 \pm 20$  km/s), respectively. Our observation and simulation results provide a unified picture of small-scale solar coronal jets driven by magnetic reconnection accompanying flux cancellation. This picture also aligns well with the most recent reports of the formation and eruption mechanisms of larger coronal jets. **20-May-2020**

## **Genesis and Coronal-jet-generating Eruption of a Solar Minifilament Captured by IRIS Slit-raster Spectra**

[Navdeep K. Panesar](#), [Sanjiv K. Tiwari](#), [Ronald L. Moore](#), [Alphonse C. Sterling](#), [Bart De Pontieu](#)

ApJ **939** 25 **2022**

<https://arxiv.org/pdf/2209.00059.pdf>

<https://iopscience.iop.org/article/10.3847/1538-4357/ac8d65/pdf>

We present the first IRIS Mg II slit-raster spectra that fully capture the genesis and coronal-jet-generating eruption of a central-disk solar minifilament. The minifilament arose in a negative-magnetic-polarity coronal hole. The Mg II spectroheliograms verify that the minifilament plasma temperature is chromospheric. The Mg II spectra show that the erupting minifilament's plasma has blueshifted upflow in the jet spire's onset and simultaneous redshifted downflow at the location of the compact jet bright point (JBP). From the Mg II spectra together with AIA EUV images and HMI magnetograms, we find: (i) the minifilament forms above a flux cancellation neutral line at an edge of a negative-polarity network flux clump; (ii) during the minifilament's fast-eruption onset and jet-spire onset, the JBP begins brightening over the flux-cancellation neutral line. From IRIS2 inversion of the Mg II spectra, the JBP's Mg II bright plasma has electron density, temperature, and downward (red-shift) Doppler speed of  $10^{12}$  cm<sup>-3</sup>, 6000 K, and 10 km/s, respectively, and the growing spire shows clockwise spin. We speculate: (i) during the slow rise of the erupting minifilament-carrying twisted flux rope, the top of the erupting flux-rope loop, by writhing, makes its field direction opposite that of encountered ambient far-reaching field; (ii) the erupting kink then can reconnect with the far-reaching field to make the spire and reconnect internally to make the JBP. We conclude that this coronal jet is normal in that magnetic flux cancellation builds a minifilament-carrying twisted flux rope and triggers the JBP-generating and jet-spire-generating eruption of the flux rope. **08-April-2020**

**IRIS Nugget 10 Jun 2023** <https://iris.lmsal.com/nugget>

## **Network Jets as the Driver of Counter-Streaming Flows in a Solar Filament/Filament Channel**

[Navdeep K. Panesar](#), [Sanjiv K. Tiwari](#), [Ronald L. Moore](#), [Alphonse C. Sterling](#)

ApJL **897** L2 **2020**

<https://arxiv.org/pdf/2006.04249.pdf>

<https://doi.org/10.3847/2041-8213/ab9ac1>

Counter-streaming flows in a small (100" -long) solar filament/filament channel are directly observed in high-resolution SDO/AIA EUV images of a region of enhanced magnetic network. We combine images from SDO/AIA, SDO/HMI and IRIS to investigate the driving mechanism of these flows. We find that: (i) counter-streaming flows are present along adjacent filament/filament channel threads for about 2 hours, (ii) both ends of the filament/filament channel are rooted at the edges of magnetic network flux lanes along which there are impinging fine-scale opposite-polarity flux patches, (iii) recurrent small-scale jets (known as network jets) occur at the edges of the magnetic network flux lanes at the ends of the filament/filament channel, (iv) the recurrent network jet eruptions clearly drive the counter-streaming flows along threads of the filament/filament channel, (v) some of the network jets appear to stem from sites of flux cancellation, between network flux and merging opposite-polarity flux, and (vi) some show brightening at their bases, analogous to the base brightening in coronal jets. The average speed of the counter-streaming flows along the filament/filament channel threads is 70 km/s. The average widths of the AIA filament/filament channel and the H $\alpha$  filament are 4" and 2.5", respectively, consistent with the earlier findings that filaments in EUV images are wider than in H $\alpha$  images. Thus, our observations show that the continually repeated counter-streaming flows come from network jets, and these driving network-jet eruptions are possibly prepared and triggered by magnetic flux cancellation. **8 Jan 2016**

## **Onset of the Magnetic Explosion in Solar Coronal Jets in Quiet Regions on the Central Disk**

[Navdeep K. Panesar](#), [Ronald L. Moore](#), [Alphonse C. Sterling](#)

ApJ **894** 104 **2020**

<https://arxiv.org/pdf/2006.04253.pdf>

<https://doi.org/10.3847/1538-4357/ab88ce>

We examine the initiation of 10 coronal jet eruptions in quiet regions on the central disk, thereby avoiding near-limb spicule-forest obscuration of the slow-rise onset of the minifilament eruption. From the SDO/AIA 171A 12-second-cadence movie of each eruption, we (1) find and compare the start times of the minifilament's slow rise, the jet-base bright point, the jet-base interior brightening, and the jet spire, and (2) measure the minifilament's speed at the start and end of its slow rise. From (a) these data, (b) prior observations showing that each eruption was triggered by magnetic flux cancelation under the minifilament, and (c) the breakout-reconnection current sheet observed in one eruption, we confirm that quiet-region jet-making minifilament eruptions are miniature versions of CME-making filament eruptions, and surmise that in most quiet region jets: (1) the eruption starts before runaway reconnection starts, (2) runaway reconnection does not start until the slow-rise speed is at least about 1 km/s, and (3) at and before eruption onset there is no current sheet of appreciable extent. We therefore expect: (i) many CME-making filament eruptions are triggered by flux cancelation under the filament, (ii) emerging bipoles seldom, if ever, directly drive jet production because the emergence is seldom, if ever, fast enough, and (iii) at a separatrix or quasi-separatrix in any astrophysical setting of magnetic field in low-beta plasma, a current sheet of appreciable extent can be built only dynamically by a magnetohydrodynamic convulsion of the field, not by quasi-static gradual converging of the field. **2012 Mar 22, 2012 Sep 21, 2012 Nov 13**

**Table 1.** Key Data for our 10 Central-Disk Quiet-Region Jet Eruption Onsets (2012)

### Hi-C 2.1 Observations of Jetlet-like Events at Edges of Solar Magnetic Network Lane

Navdeep K. [Panesar](#), [Alphonse C. Sterling](#), [Ronald L. Moore](#), [Amy R. Winebarger](#), [Sanjiv K. Tiwari](#), [Sabrina L. Savage](#), [Leon Golub](#), [Laurel A. Rachmeler](#), [Ken Kobayashi](#), [David H. Brooks](#), [Jonathan W. Cirtain](#), [Bart De Pontieu](#), [David E. McKenzie](#), [Richard J. Morton](#), [Hardi Peter](#), [Paola Testa](#), [Robert W. Walsh](#), [Harry P. Warren](#)

ApJL 2019

<https://arxiv.org/pdf/1911.02331.pdf>

We present high-resolution, high-cadence observations of six, fine-scale, on-disk jet-like events observed by the High-resolution Coronal Imager 2.1 (Hi-C 2.1) during its sounding-rocket flight. We combine the Hi-C 2.1 images with images from SDO/AIA, and IRIS, and investigate each event's magnetic setting with co-aligned line-of-sight magnetograms from SDO/HMI. We find that: (i) all six events are jetlet-like (having apparent properties of jetlets), (ii) all six are rooted at edges of magnetic network lanes, (iii) four of the jetlet-like events stem from sites of flux cancelation between majority-polarity network flux and merging minority-polarity flux, and (iv) four of the jetlet-like events show brightenings at their bases reminiscent of the base brightenings in coronal jets. The average spire length of the six jetlet-like events ( $9,000 \pm 3000$  km) is three times shorter than that for IRIS jetlets ( $27,000 \pm 8000$  km). While not ruling out other generation mechanisms, the observations suggest that at least four of these events may be miniature versions of both larger-scale coronal jets that are driven by minifilament eruptions and still-larger-scale solar eruptions that are driven by filament eruptions. Therefore, we propose that our Hi-C events are driven by the eruption of a tiny sheared-field flux rope, and that the flux-rope field is built and triggered to erupt by flux cancelation. **2018 May 29**

### IRIS and SDO Observations of Solar Jetlets Resulting from Network-Edge Flux Cancelation

Navdeep K. [Panesar](#), [Alphonse C. Sterling](#), [Ronald L. Moore](#), [Sanjiv K. Tiwari](#), [Bart De Pontieu](#), [Aimee A. Norton](#)

ApJL 868 L27 2018

<https://arxiv.org/pdf/1811.04314.pdf>

[sci-hub.tw/10.3847/2041-8213/aaef37](https://arxiv.org/pdf/1811.04314.pdf)

Recent observations show that the buildup and triggering of minifilament eruptions that drive coronal jets result from magnetic flux cancelation at the neutral line between merging majority- and minority-polarity magnetic flux patches. We investigate the magnetic setting of ten on-disk small-scale UV/EUV jets (jetlets), smaller than coronal X-ray jets but larger than chromospheric spicules) in a coronal hole by using IRIS UV images and SDOAIA EUV images and line-of-sight magnetograms from SDO/HMI. We observe recurring jetlets at the edges of magnetic network flux lanes in the coronal hole. From magnetograms co-aligned with the IRIS and AIA images, we find, clearly visible in nine cases, that the jetlets stem from sites of flux cancelation proceeding at an average rate of  $1.5 \times 10^{18} \text{ Mx hr}^{-1}$ , and show brightenings at their bases reminiscent of the base brightenings in larger-scale coronal jets. We find that jetlets happen at many locations along the edges of network lanes (not limited to the base of plumes) with average lifetimes of 3 min and speeds of 70 kms. The average jetlet-base width (4000 km) is three to four times smaller than for coronal jets (18,000 km). Based on these observations of ten obvious jetlets, and our previous observations of larger-scale coronal jets in quiet regions and coronal holes, we infer that flux cancelation is an essential process in the buildup and triggering of jetlets. Our observations suggest that network jetlet eruptions might be small-scale analogs of both larger-scale coronal jets and the still-larger-scale eruptions producing CMEs. **19-March-2016**

[HMI Science Nuggets](#) #117 2019 <http://hmi.stanford.edu/hminuggets/?p=2751>

### Magnetic Flux Cancelation as the Trigger of Solar Coronal-Hole Coronal Jets

Navdeep K. [Panesar](#), [Alphonse C. Sterling](#), [Ronald L. Moore](#)

ApJ 853 189 2018

<https://arxiv.org/pdf/1801.05344.pdf>

We investigate in detail the magnetic cause of minifilament eruptions that drive coronal-hole jets. We study 13 random on-disk coronal hole jet eruptions, using high resolution X-ray images from Hinode/XRT, EUV images from SDO/AIA, and magnetograms from SDO/HMI. For all 13 events, we track the evolution of the jet-base region and find that a minifilament of cool (transition-region-temperature) plasma is present prior to each jet eruption. HMI magnetograms show that the minifilaments reside along a magnetic neutral line between majority-polarity and minority-polarity magnetic flux patches. These patches converge and cancel with each other, with an average cancelation rate of  $\sim 0.6 \times 10^{18} \text{ Mx hr}^{-1}$  for all 13 jets. Persistent flux cancelation at the neutral line eventually destabilizes the minifilament field, which erupts outward and produces the jet spire. Thus, we find that all 13 coronal-hole-jet-driving minifilament eruptions are triggered by flux cancelation at the neutral line. These results are in agreement with our recent findings Panesar et al 2016b for quiet-region jets, where flux cancelation at the underlying neutral line triggers the minifilament eruption that drives each jet. Thus from that study of quiet-Sun jets and this study of coronal hole jets, we conclude that flux cancelation is the main candidate for triggering quiet region and coronal hole jets. **2012 July 02, 2017 Jan 03**  
**Table 1.** Timing and location for the observed coronal-hole jets

## Magnetic Flux Cancelation as the Origin of Solar Quiet Region Pre-Jet Minifilaments

Navdeep K. Panesar, Alphonse C. Sterling, Ronald L. Moore

ApJ 844 131 2017

<https://arxiv.org/pdf/1706.09079.pdf>

We investigate the origin of ten solar quiet region pre-jet minifilaments, using EUV images from SDO/AIA and magnetograms from SDO/HMI. We recently found panesar16b that quiet region coronal jets are driven by minifilament eruptions, where those eruptions result from flux cancelation at the magnetic neutral line under the minifilament. Here, we study the longer-term origin of the pre-jet minifilaments themselves. We find that they result from flux cancelation between minority-polarity and majority-polarity flux patches. In each of ten pre-jet regions, we find that opposite-polarity patches of magnetic flux converge and cancel, with a flux reduction of 10--40% from before to after the minifilament appears. For our ten events, the minifilaments exist for periods ranging from 1.5 hr to two days before erupting to make a jet. Apparently, the flux cancelation builds highly sheared field that runs above and traces the neutral line, and the cool-transition-region-plasma minifilament forms in this field and is suspended in it. We infer that the convergence of the opposite-polarity patches results in reconnection in the low corona that builds a magnetic arcade enveloping the minifilament in its core, and that the continuing flux cancelation at the neutral line finally destabilizes the minifilament field so that it erupts and drives the production of a coronal jet. Thus our observations strongly support that quiet region magnetic flux cancelation results in both the formation of the pre-jet minifilament and its jet-driving eruption. **1 July 2012, 4-5 Aug 2012, 19 Sep 2012**

**Table 1.** Measured parameters for the observed quiet region pre-jet minifilaments

## Magnetic Flux Cancellation as the Trigger of Solar Quiet-Region Coronal Jets

Navdeep K. Panesar, Alphonse C. Sterling, Ronald L. Moore, Prithi Chakrapani

ApJL 832 L7 2016

<https://arxiv.org/pdf/1610.08540v1.pdf> File

We report observations of ten random on-disk solar quiet region coronal jets found in high resolution Extreme Ultraviolet (EUV) images from the Solar Dynamics Observatory (SDO)/Atmospheric Imaging Assembly (AIA) and having good coverage in magnetograms from the SDO/Helioseismic and Magnetic Imager (HMI). Recent studies show that coronal jets are driven by the eruption of a small-scale filament (called a minifilament). However the trigger of these eruptions is still unknown. In the present study we address the question: what leads to the jet-driving minifilament eruptions? The EUV observations show that there is a cool-transition-region-plasma minifilament present prior to each jet event and the minifilament eruption drives the jet. By examining pre-jet evolutionary changes in the line-of-sight photospheric magnetic field we observe that each pre-jet minifilament resides over the neutral line between majority-polarity and minority-polarity patches of magnetic flux. In each of the ten cases, the opposite-polarity patches approach and merge with each other (flux reduction between 21 and 57%). After several hours, continuous flux cancelation at the neutral line apparently destabilizes the field holding the cool-plasma minifilament to erupt and undergo internal reconnection, and external reconnection with the surrounding-coronal field. The external reconnection opens the minifilament field allowing the minifilament material to escape outwards, forming part of the jet spire. Thus we found that each of the ten jets resulted from eruption of a minifilament following flux cancellation at the neutral line under the minifilament. These observations establish that magnetic flux cancellation is usually the trigger of quiet region coronal jet eruptions. **20-21-Sept-2012, 12-13-Nov-2012 See Introduction**

## HOMOLOGOUS JET-DRIVEN CORONAL MASS EJECTIONS FROM SOLAR ACTIVE REGION 12192

### A Series of Homologous Jets that Drove CMEs from The Giant Solar Active Region of 2014 October

Navdeep K. Panesar, Alphonse C. Sterling, Ronald L. Moore

ApJL 822 L23 2016

<http://arxiv.org/pdf/1604.05770v1.pdf>

We report observations of homologous coronal jets and their coronal mass ejections (CMEs) observed by instruments onboard the Solar Dynamics Observatory (SDO) and Solar and Heliospheric Observatory (SOHO) spacecraft. The homologous jets originated from a location with emerging and canceling magnetic field at the southeast edge of the giant active region (AR) of 2014 October, NOAA 12192. This AR produced in its interior many non-jet major flare eruptions (X and M class) that made no CME. During **20-27 October**, in contrast to the major-flare eruptions in the interior, six of the homologous jets from the edge resulted in CMEs. Each jet-driven CME (~200-300 kms) was slower-moving than most CMEs; had angular width (20-50 degree) comparable to that of the base of a coronal streamer straddling the AR; and was of the 'streamer-puff' variety, whereby the preexisting streamer was transiently inflated but not destroyed by the passage of the CME. Much of the transition-region-temperature plasma in the CME-producing jets escaped from the Sun, whereas relatively more of the transition-region plasma in non-CME-producing jets fell back to the solar surface. Also, the CME-producing jets tended to be faster and longer-lasting than the non-CME-producing jets. Our observations imply: each jet and CME resulted from reconnection opening of twisted field that erupted from the jet base; and the erupting field did not become a plasmoid as previously envisioned for streamer-puff CMEs, but instead the jet-guiding streamer-base loop was blown out by the loop's twist from the reconnection.

## **Destabilization of a Solar Prominence/Filament Field System by a Series of Eight Homologous Eruptive Flares**

Navdeep K. [Panesar](#), Alphonse C. Sterling, [Davina E. Innes](#), [Ronald L. Moore](#)

ApJ **811** 5 **2015**

<http://arxiv.org/pdf/1508.01952v1.pdf>

Homologous flares are flares that occur repetitively in the same active region, with similar structure and morphology. A series of at least eight homologous flares occurred in active region NOAA 11237 over **16 - 17 June 2011**. A nearby prominence/filament was rooted in the active region, and situated near the bottom of a coronal cavity. The active region was on the southeast solar limb as seen from SDO/AIA, and on the disk as viewed from STEREO/EUVI-B. The dual perspective allows us to study in detail behavior of the prominence/filament material entrained in the magnetic field of the repeatedly-erupting system. Each of the eruptions was mainly confined, but expelled hot material into the prominence/filament cavity system (PFCS). The field carrying and containing the ejected hot material interacted with the PFCS and caused it to inflate, resulting in a step-wise rise of the PFCS approximately in step with the homologous eruptions. The eighth eruption triggered the PFCS to move outward slowly, accompanied by a weak coronal dimming. As this slow PFCS eruption was underway, a final ejective flare occurred in the core of the active region, resulting in strong dimming in the EUVI-B images and expulsion of a coronal mass ejection (CME). A plausible scenario is that the repeated homologous flares could have gradually destabilized the PFCS, and its subsequent eruption removed field above the active region and in turn led to the ejective flare, strong dimming, and CME.

## **Investigating width distribution of slow and fast CMEs in solar cycles 23 and 24**

[V. Pant](#), [R. Majumdar](#), [R. Patel](#), [A. Chauhan](#), [D. Banerjee](#), [N. Gopalswamy](#)

Frontiers in Astronomy and Space Sciences Volume 8, id.73 8:634358 **2021**

<https://arxiv.org/pdf/2104.12850.pdf>

<https://www.frontiersin.org/articles/10.3389/fspas.2021.634358/full>

<https://doi.org/10.3389/fspas.2021.634358>

Coronal Mass Ejections (CMEs) are highly dynamic events originating in the solar atmosphere, that show a wide range of kinematic properties and are the major drivers of the space weather. The angular width of the CMEs is a crucial parameter in the study of their kinematics. The fact that whether slow and fast CMEs (as based on their relative speed to the average solar wind speed) are associated with different processes at the location of their ejection is still debatable. Thus, in this study, we investigate their angular width to understand the differences between the slow and fast CMEs. We study the width distribution of slow and fast CMEs and find that they follow different power law distributions, with a power law indices ( $\alpha$ ) of -1.1 and -3.7 for fast and slow CMEs respectively. To reduce the projection effects, we further restrict our analysis to only limb events as derived from manual catalog and we find similar results. We then associate the slow and fast CMEs to their source regions, and classified the sources as Active Regions (ARs) and Prominence Eruptions (PEs). We find that slow and fast CMEs coming from ARs and PEs, also follow different power laws in their width distributions. This clearly hints towards a possibility that different mechanisms might be involved in the width expansion of slow and fast CMEs coming from different sources. These results are also crucial from the space weather perspective since the width of the CME is an important factor in that aspect. **May 03, 2012**

## **Twisting/Swirling Motions During a Prominence Eruption as seen from SDO/AIA**

[V. Pant](#), [A. Datta](#), [D. Banerjee](#), [K. Chandrashekar](#), [S. Ray](#)

ApJ **860** 80 **2018**

<https://arxiv.org/pdf/1804.10767.pdf>

A quiescent prominence was observed at north-west limb of the Sun using different channels of Atmospheric Imaging Assembly (AIA) onboard Solar Dynamics Observatory (SDO). We report and analyse twisting/swirling motions during and after the prominence eruption. We segregate the observed rotational motions into small and large scale. Small scale rotational motions manifest in the barbs of the prominence while the large scale rotation manifests as the roll motion during the prominence eruption. We noticed that both footpoints of the prominence rotate in the counter-clockwise direction. We propose that similar sense of rotation in both footpoints leads to prominence eruption. The prominence erupted asymmetrically near the southern footpoint which may be due to uneven mass distribution and location of the



cavity near southern footpoint. Furthermore, we study the swirling motion of the plasma along different circular paths in the cavity of the prominence after the prominence eruption. The rotational velocities of the plasma moving along different circular paths are estimated to be  $\sim 9\text{--}40\text{ km s}^{-1}$ . These swirling motions can be explained in terms of twisted magnetic field lines in the prominence cavity. Finally, we observe the twist built up in the prominence, being carried away by the coronal mass ejection (CME) as seen in the Large Angle Spectrometric Coronagraph (LASCO) onboard Solar and Heliospheric Observatory (SOHO). **2012 November 26**

### **Automated Detection of Coronal Mass Ejections in STEREO Heliospheric Imager data**

V. **Pant**, S. Willems, L. Rodriguez, M. Mierla, D. Banerjee, J. A. Davies

ApJ 833 80 **2016**

<https://arxiv.org/pdf/1610.01904v1.pdf>

We have performed, for the first time, the successful automated detection of Coronal Mass Ejections (CMEs) in data from the inner heliospheric imager (HI-1) cameras on the STEREO A spacecraft. Detection of CMEs is done in time-height maps based on the application of the Hough transform, using a modified version of the CACTus software package, conventionally applied to coronagraph data. In this paper we describe the method of detection. We present the result of the application of the technique to a few CMEs that are well detected in the HI-1 imagery, and compare these results with those based on manual cataloging methodologies. We discuss in detail the advantages and disadvantages of this method. **2010-04-03**

### **Propagating Conditions and the Time of ICME Arrival: A Comparison of the Effective Acceleration Model with ENLIL and DBEM Models**

Evangelos **Paouris**, [Jaša Čalogović](#), [Mateja Dumbović](#), [M. Leila Mays](#), [Angelos Vourlidis](#), [Athanasios Papaioannou](#), [Anastasios Anastasiadis](#) & [Georgios Balasis](#)

[Solar Physics](#) volume 296, Article number: 12 (**2021**)

<https://link.springer.com/content/pdf/10.1007/s11207-020-01747-4.pdf>

The Effective Acceleration Model (EAM) predicts the Time-of-Arrival (ToA) of the Coronal Mass Ejection (CME) driven shock and the average speed within the sheath at 1 AU. The model is based on the assumption that the ambient solar wind interacts with the interplanetary CME (ICME) resulting in constant acceleration or deceleration. The upgraded version of the model (EAMv3), presented here, incorporates two basic improvements: (i) a new technique for the calculation of the acceleration (or deceleration) of the ICME from the Sun to 1 AU and (ii) a correction for the CME plane-of-sky speed. A validation of the upgraded EAM model is performed via comparisons to predictions from the ensemble version of the Drag-Based model (DBEM) and the WSA-ENLIL+Cone ensemble model. A common sample of 16 CMEs/ICMEs, in 2013–2014, is used for the comparison. Basic performance metrics such as the mean absolute error (MAE), mean error (ME) and root mean squared error (RMSE) between observed and predicted values of ToA are presented. MAE for EAM model was  $8.7 \pm 1.68$  hours while for DBEM and ENLIL was  $14.3 \pm 2.2$  and  $12.8 \pm 1.7$  hours, respectively. ME for EAM was  $-1.4 \pm 2.7$  hours in contrast with  $-9.7 \pm 3.4$  and  $-6.1 \pm 3.3$  hours from DBEM and ENLIL. We also study the hypothesis of stronger deceleration in the interplanetary (IP) space utilizing the EAMv3 and DBEM models. In particular, the DBEM model perform better when a greater value of drag parameter, of order of a factor of 3, is used in contrast to previous studies. EAMv3 model shows a deceleration of ICMEs at greater distances, with a mean value of 0.72 AU.

**Table 2** Details for the 16 common CMEs/ICMEs and the calculated metrics for ENLIL, DBEMv1 and EAMv3 models. (2013-2014)

### **Assessing the projection correction of Coronal Mass Ejection speeds on Time-of-Arrival prediction performance using the Effective Acceleration Model**

[Evangelos Paouris](#), [Angelos Vourlidis](#), [Athanasios Papaioannou](#), [Anastasios Anastasiadis](#)

Space Weather e2020SW002617 **2020**

<https://arxiv.org/ftp/arxiv/papers/2012/2012.04703.pdf>

<https://agupubs.onlinelibrary.wiley.com/doi/epdf/10.1029/2020SW002617>

White light images of Coronal Mass Ejections (CMEs) are projections on the plane-of-sky (POS). As a result, CME kinematics are subject to projection effects. The error in the true (deprojected) speed of CMEs is one of the main causes of uncertainty to Space Weather forecasts, since all estimates of the CME Time-of-Arrival (ToA) at a certain location within the heliosphere require, as input, the CME speed. We use single viewpoint observations for 1037 flare-CME events between 1996-2017 and propose a new approach for the correction of the CME speed assuming radial propagation from the flare site. Our method is uniquely capable to produce physically reasonable deprojected speeds across the full range of source longitudes. We bound the uncertainty in the deprojected speed estimates via limits in the true angular width of a CME based on multiview-point observations. Our corrections range up to 1.37-2.86 for CMEs originating from the center of the disk. On average, the deprojected speeds are 12.8% greater than their POS speeds. For slow CMEs (VPOS < 400 km/s) the full ice-cream cone model performs better while for fast and very fast CMEs (VPOS > 700 km/s) the shallow ice-cream model gives much better results. CMEs with 691-878 km/s POS speeds have a minimum ToA mean absolute error (MAE) of 11.6 hours. This method, is robust, easy to use, and has immediate applicability to Space Weather forecasting applications. Moreover, regarding the speed of CMEs, our work suggests that single viewpoint observations are generally reliable.

## Ineffectiveness of Narrow CMEs for Cosmic Ray Modulation

Forbush

Evangelos [Paouris](#)

Solar Physics, June 2013, Volume 284, Issue 2, pp 589-597

Monthly coronal mass ejection (CME) counts, – for all CMEs and CMEs with widths  $> 30^\circ$ , – and monthly averaged speeds for the events in these two groups were compared with both the monthly averaged cosmic ray intensity and the monthly sunspot number. The monthly P i-index, which is a linear combination of monthly CME count rate and average speed, was also compared with the cosmic ray intensity and sunspot number. The main finding is that narrow CMEs, which were numerous during 2007 – 2009, are ineffective for modulation. A cross-correlation analysis, calculating both the Pearson ( $r$ ) product–moment correlation coefficient and the Spearman ( $\rho$ ) rank correlation coefficient, has been used. Between all CMEs and cosmic ray intensity we found correlation coefficients  $r = -0.49$  and  $\rho = -0.46$ , while between CMEs with widths  $> 30^\circ$  and cosmic ray intensity we found  $r = -0.75$  and  $\rho = -0.77$ , which implies a significant increase. Finally, the best expression for the P i-index for the examined period was analyzed. The highly anticorrelated behavior among this CME index, the cosmic ray intensity ( $r = -0.84$  and  $\rho = -0.83$ ), and the sunspot number ( $r = +0.82$  and  $\rho = +0.89$ ) suggests that the first one is a very useful solar–heliospheric parameter for heliospheric and space weather models in general.

## Revisiting Empirical Solar Energetic Particle Scaling Relations II. Coronal Mass Ejections

Athanasios [Papaioannou](#), [Konstantin Herbst](#), [Tobias Ramm](#), [David Lario](#), [Astrid M. Veronig](#)

A&A 690, A60 2024

<https://arxiv.org/pdf/2407.16479>

<https://www.aanda.org/articles/aa/pdf/2024/10/aa50705-24.pdf>

Aims. The space radiation environment conditions and the maximum expected coronal mass ejection (CME) speed are being assessed through the investigation of scaling laws between the peak proton flux and fluence of Solar Energetic Particle (SEP) events with the speed of the CMEs. Methods. We utilize a complete catalog of SEP events, covering the last ~25 years of CME observations (i.e. 1997 to 2017). We calculate the peak proton fluxes and integrated event fluences for those events reaching an integral energy of up to  $E > 100$  MeV, covering the period of the last ~25 years of CME observations. For a sample of 38 strong SEP events, we first investigate the statistical relations between the recorded peak proton fluxes (IP) and fluences (FP) at a set of integral energies of  $E > 10$  MeV,  $E > 30$  MeV,  $E > 60$  MeV, and  $E > 100$  MeV versus the projected CME speed near the Sun (VCME) obtained by the Solar and Heliospheric Observatory/Large Angle and Spectrometric Coronagraph (SOHO/LASCO). Based on the inferred relations, we further calculate the integrated energy dependence of both IP and FP, assuming that they follow an inverse power-law with respect to energy. By making use of simple physical assumptions, we combine our derived scaling laws to estimate the upper limits for VCME, IP, and FP focusing on two cases of known extreme SEP events that occurred on February 23, 1956 (GLE05) and in AD774/775, respectively. Given physical constraints and assumptions, several options for the upper limit VCME, associated with these events, are investigated. Results. A scaling law relating IP and FP to the CME speed as  $V^{\{5\}}_{CME}$  for CMEs ranging between ~3400-5400 km/s is consistent with values of FP inferred for the cosmogenic nuclide event of AD774/775. At the same time, the upper CME speed that the current Sun can provide possibly falls within an upper limit of VCME  $\leq 5500$  km/s.

## Thermal and Non-Thermal Properties of Active Region Recurrent Coronal Jets

[Alin R. Paraschiv](#), [Alina C. Donea](#), [Philip G. Judge](#)

ApJ 935 172 2022

<https://arxiv.org/pdf/2207.12612.pdf>

<https://iopscience.iop.org/article/10.3847/1538-4357/ac80fb/pdf>

We present observations of recurrent active region coronal jets and derive their thermal and non-thermal properties, by studying the physical properties of the plasma simultaneously at the base footpoint, and along the outflow of jets. The sample of analyzed solar jets were observed by SDO-AIA in Extreme Ultraviolet and by RHESSI in the X-Ray domain. The main thermal plasma physical parameters: temperature, density, energy flux contributions, etc. are calculated using multiple inversion techniques to obtain the differential emission measure from extreme-ultraviolet filtergrams. The underlying models are assessed, and their limitations and applicability are scrutinized. Complementarily, we perform source reconstruction and spectral analysis of higher energy X-Ray observations to further assess the thermal structure and identify non-thermal plasma emission properties. We discuss a peculiar penumbral magnetic reconnection site, which we previously identified as a “Coronal Geyser”. Evidence supporting cool and hot thermal emission, and non-thermal emission, is presented for a subset of geyser jets. These active region jets are found to be energetically stronger than their polar counterparts, but we find their potential influence on heliospheric energetics and dynamics to be limited. We scrutinize whether the geyser does fit the non-thermal erupting microflare picture, finding that our observations at peak flaring times can only be explained by a combination of thermal and non-thermal emission models. This analysis of geysers provides new information and observational constraints applicable to theoretical modeling of solar jets.  
25.09.2011

## The Trigger Mechanism of Recurrent Solar Active Region Jets Revealed by the Magnetic Properties of a Coronal Geyser Site

Alin Razvan [Paraschiv](#), [Alina Donea](#), [K.D. Leka](#)

ApJ 891 149 2020

<https://arxiv.org/pdf/2002.11819.pdf>  
<https://doi.org/10.3847/1538-4357/ab7246>

Solar active region jets are small-scale collimated plasma eruptions that are triggered from magnetic sites embedded in sunspot penumbral regions. Multiple trigger mechanisms for recurrent jets are under debate. Vector magnetic field data from SDO-HMI observations are used to analyze a prolific photospheric configuration, identified in extreme ultraviolet observations as a 'Coronal Geyser', that triggered a set of at least 10 recurrent solar active region jets. We focus on interpreting the magnetic fields of small-scale flaring sites aiming to understand the processes that govern recurrent jet eruptions. We perform a custom reprocessing of the SDO-HMI products, including disambiguation and uncertainty estimation. We scrutinized the configuration and dynamics of the photospheric magnetic structures. The magnetic configuration is described via the analysis of the photospheric magnetic vertical fields, to identify the process is responsible for driving the jet eruptions. We report that the two widely debated magnetic trigger processes, namely magnetic flux cancellation and magnetic flux emergence, appear to be responsible on a case by case basis for generating each eruption in our set. We find that 4 of 10 jets were due to flux cancellation while the rest were clearly not, and were more likely due to flux emergence. **25 Sep 2011**

**HMI Science Nuggets** #136 March 2020 <http://hmi.stanford.edu/hminuggets/?p=3186>

## **On Solar Recurrent Coronal Jets: Coronal Geysers as Sources of Electron Beams and Interplanetary Type-III Radio Bursts**

Alin Razvan **Paraschiv** and Alina Donea

**2019 ApJ** 873 110

<https://doi.org/10.3847/1538-4357/ab04a6>  
<https://arxiv.org/pdf/1903.04682.pdf>

Coronal jets are transitory small-scale eruptions that are omnipresent in solar observations. Active regions jets produce significant perturbations on the ambient solar atmosphere and are believed to be generated by microflare reconnection. Multiple sets of recurrent jets are identified in extreme-ultraviolet filter imaging. In this work we analyze the long timescale recurrence of coronal jets originating from a unique footpoint structure observed in the lower corona. We report the detection of penumbral magnetic structures in the lower corona. These structures, which we call "coronal geysers," persist through multiple reconnection events that trigger recurrent jets in a quasi-periodical trend. Recurrent jet eruptions have been associated with Type-III radio bursts that are manifestations of traveling non-thermal electron beams. We examine the assumed link, as the coronal sources of interplanetary Type-III bursts are still open for debate. We scrutinized the hypothesized association by temporally correlating a statistically significant sample of six Geyser structures that released at least 50 recurrent jets, with correspondent Type-III radio bursts detected in the interplanetary medium. Data analysis of these phenomena provides new information on small-scale reconnection, non-thermal electron beam acceleration, and energy release. We find that the penumbral Geyser-like flaring structures produce recurring jets. They can be long-lived, quasi-stable, and act as coronal sources for Type-III bursts, and, implicitly, upward accelerated electron beams. **25 Sep. 2011, 2012-06-30, 2012-07-02, 2013-12-25, 2014-10-22, 2015-07-09**

## **Physical properties of solar polar jets: A statistical study with Hinode XRT data**

A. R. **Paraschiv**<sup>1,3\*</sup>, A. Bemporad<sup>1</sup> and A. C. Sterling

*A&A* 579, A96 (2015)

**Aims.** The target of this work is to investigate the physical nature of polar jets in the solar corona and their possible contribution to coronal heating and solar wind flow based on the analysis of X-ray images acquired by the Hinode XRT telescope. We estimate the different forms of energy associated with many of these small-scale eruptions, in particular the kinetic energy and enthalpy.

**Methods.** Two Hinode XRT campaign datasets focusing on the two polar coronal holes were selected to analyze the physical properties of coronal jets; the analyzed data were acquired using a series of three XRT filters. Typical kinematical properties (e.g., length, thickness, lifetime, ejection rate, and velocity) of 18 jets are evaluated from the observed sequences, thus providing information on their possible contribution to the fast solar wind flux escaping from coronal holes. Electron temperatures and densities of polar-jet plasmas are also estimated using ratios of the intensities observed in different filters.

**Results.** We find that the largest amount of energy eventually provided to the corona is thermal. The energy due to waves may also be significant, but its value is comparatively uncertain. The kinetic energy is lower than thermal energy, while other forms of energy are comparatively low. Lesser and fainter events seem to be hotter, thus the total contribution by polar jets to the coronal heating could have been underestimated so far. The kinetic energy flux is usually around three times smaller than the enthalpy counterpart, implying that this energy is converted into plasma heating more than in plasma acceleration. This result suggests that the majority of polar jets are most likely not escaping from the Sun and that only cooler ejections could possibly have enough kinetic energy to contribute to the total solar wind flow.

## **Linking the Sun to the Heliosphere Using Composition Data and Modelling. A Test Case with a Coronal Jet**

Susanna **Parenti**, [Julia Chifu](#), [Giulio Del Zanna](#), [Justin Edmondson](#), [Alessandra Giunta](#), [Viggo H. Hansteen](#), [Aleida Higginson](#), [J. Martin Laming](#), [Susan T. Lepri](#), [Benjamin J. Lynch](#), [Yeimy J. Rivera](#), [Rudolf von Steiger](#), [Thomas Wiegelmann](#), [Robert F. Wimmer-Schweingruber](#), [Natalia Zambrana Prado](#), [Gabriel Pelouze](#)

<https://arxiv.org/pdf/2110.06111.pdf><https://link.springer.com/content/pdf/10.1007/s11214-021-00856-1.pdf>

Our understanding of the formation and evolution of the corona and the heliosphere is linked to our capability of properly interpreting the data from remote sensing and in-situ observations. In this respect, being able to correctly connect in-situ observations with their source regions on the Sun is the key for solving this problem. In this work we aim at testing a diagnostics method for this connectivity. This paper makes use of a coronal jet observed on **2010 August 2nd** in active region 11092 as a test for our connectivity method. This combines solar EUV and in-situ data together with magnetic field extrapolation, large scale MHD modeling and FIP (First Ionization Potential) bias modeling to provide a global picture from the source region of the jet to its possible signatures at 1AU. Our data analysis reveals the presence of outflow areas near the jet which are within open magnetic flux regions and which present FIP bias consistent with the FIP model results. In our picture, one of these open areas is the candidate jet source. Using a back-mapping technique we identified the arrival time of this solar plasma at the ACE spacecraft. The in-situ data show signatures of changes in the plasma and magnetic field parameters, with FIP bias consistent with the possible passage of the jet material. Our results highlight the importance of remote sensing and in-situ coordinated observations as a key to solve the connectivity problem. We discuss our results in view of the recent Solar Orbiter launch which is currently providing such unique data. **2-5 Aug 2010**

## Solar Prominences: Observations

### Comparison of magnetic energy and helicity in coronal jet simulations

E. [Pariat](#), P. F. [Wyper](#), L. [Linan](#)

A&amp;A 669, A33 2022

<https://arxiv.org/pdf/2211.11265.pdf><https://www.aanda.org/articles/aa/pdf/2023/01/aa45142-22.pdf>

While free/non-potential magnetic energy is a necessary element of any active phenomenon in the solar corona, its role as a marker of the trigger of eruptive process remains elusive. Based on the unique decomposition of the magnetic field into potential and non-potential components, magnetic energy and helicity can also both be uniquely decomposed into two quantities. Using two 3D MHD parametric simulations of a configuration that can produce coronal jets, we compare the dynamics of the magnetic energies and of the relative magnetic helicities. Both simulations share the same initial set-up and line-tied bottom-boundary driving profile. However, they differ by the duration of the forcing. In one simulation the system is driven sufficiently so that an helical jet is induced. The generation of the jet is however markedly delayed: a relatively long phase of lower-intensity reconnection takes place before the jet is eventually induced. In the other reference simulation, the system is driven during a shorter time, and no jet is produced. As expected, we observe that the Jet producing simulation contains a higher value of non-potential energy and non-potential helicity. Focusing on the phase between the end of the driving-phase and the jet generation, we note that magnetic energies remain relatively constant, while magnetic helicities have a noticeable evolution. During this post-driving phase, the ratio of the non-potential to total magnetic energy very slightly decreases while the helicity eruptivity index significantly increases. The jet is generated when the system is at the highest value of this helicity eruptivity index. This proxy critically decreases during the jet generation phase. The free energy also decreases but does not present any peak when the jet is being generated.

### Relative magnetic helicity as a diagnostic of solar eruptivity

E. [Pariat](#), J. E. Leake, G. Valori, M. G. Linton, F. P. Zuccarello, K. Dalmasse

A&amp;A 601, A125 2017

<https://arxiv.org/pdf/1703.10562.pdf><https://www.aanda.org/articles/aa/pdf/2017/05/aa30043-16.pdf>

The discovery of clear criteria that can deterministically describe the eruptive state of a solar active region would lead to major improvements on space weather predictions. Using series of numerical simulations of the emergence of a magnetic flux rope in a magnetized coronal, leading either to eruptions or to stable configurations, we test several global scalar quantities for the ability to discriminate between the eruptive and the non-eruptive simulations. From the magnetic field generated by the three-dimensional magnetohydrodynamical simulations, we compute and analyse the evolution of the magnetic flux, of the magnetic energy and its decomposition into potential and free energies, and of the relative magnetic helicity and its decomposition. Unlike the magnetic flux and magnetic energies, magnetic helicities are able to markedly distinguish the eruptive from the non-eruptive simulations. We find that the ratio of the magnetic helicity of the current-carrying magnetic field to the total relative helicity presents the highest values for the eruptive simulations, in the pre-eruptive phase only. We observe that the eruptive simulations do not possess the highest value of total magnetic helicity. In the framework of our numerical study, the magnetic energies and the total relative helicity do not correspond to good eruptivity proxies. Our study highlights that the ratio of magnetic helicities diagnoses very clearly the eruptive potential of our parametric simulations. Our study shows that magnetic-helicity-based quantities may be very efficient for the prediction of solar eruptions.

## A model for straight and helical solar jets II. Parametric study of the plasma beta

E. [Pariat](#)<sup>1</sup>, K. Dalmasse<sup>2</sup>, C. R. DeVore<sup>3</sup>, S. K. Antiochos<sup>3</sup> and J. T. Karpen<sup>3</sup>

A&A 596, A36 (2016)

Context. Jets are dynamic, impulsive, well-collimated plasma events that develop at many different scales and in different layers of the solar atmosphere.

Aims. Jets are believed to be induced by magnetic reconnection, a process central to many astrophysical phenomena.

Within the solar atmosphere, jet-like events develop in many different environments, e.g., in the vicinity of active regions, as well as in coronal holes, and at various scales, from small photospheric spicules to large coronal jets. In all these events, signatures of helical structure and/or twisting/rotating motions are regularly observed. We aim to establish that a single model can generally reproduce the observed properties of these jet-like events.

Methods. Using our state-of-the-art numerical solver ARMS, we present a parametric study of a numerical tridimensional magnetohydrodynamic (MHD) model of solar jet-like events. Within the MHD paradigm, we study the impact of varying the atmospheric plasma  $\beta$  on the generation and properties of solar-like jets.

Results. The parametric study validates our model of jets for plasma  $\beta$  ranging from 10-3 to 1, typical of the different layers and magnetic environments of the solar atmosphere. Our model of jets can robustly explain the generation of helical solar jet-like events at various  $\beta \leq 1$ . We introduce the new result that the plasma  $\beta$  modifies the morphology of the helical jet, explaining the different observed shapes of jets at different scales and in different layers of the solar atmosphere.

Conclusions. Our results enable us to understand the energisation, triggering, and driving processes of jet-like events. Our model enables us to make predictions of the impulsiveness and energetics of jets as determined by the surrounding environment, as well as the morphological properties of the resulting jets.

## **A model for straight and helical solar jets: I. Parametric studies of the magnetic field geometry**

E. [Pariat](#), K. Dalmasse, C. R. DeVore, S. K. Antiochos, J. T. Karpen

A&A, 573, A130 (2015)

[http://lesia.obspm.fr/perso/etienne-pariat/Pariat\\_Jets\\_ParamGeo\\_final.pdf](http://lesia.obspm.fr/perso/etienne-pariat/Pariat_Jets_ParamGeo_final.pdf)

Jets are dynamic, impulsive, well collimated plasma events developing at many different scales and in different layers of the solar atmosphere. Jets are believed to be induced by magnetic reconnection, a process central to many astrophysical phenomena. Studying their dynamics can help us to better understand the processes acting in larger eruptive events (e.g., flares and coronal mass ejections) as well as mass, magnetic helicity and energy transfer at all scales in the solar atmosphere. The relative simplicity of their magnetic geometry and topology, compared with larger solar active events, makes jets ideal candidates for studying the fundamental role of reconnection in energetic events. In this study, using our state-of-the-art numerical solver ARMS, we present several parametric studies of a three-dimensional numerical magneto-hydrodynamic model of solar jet-like events. We study the impact of the magnetic field inclination and photospheric field distribution on the generation and properties of two morphologically different types of solar jets, straight and helical, which can account for the observed so-called "standard" and "blowout" jets. The present parametric studies validate our model of jets for different geometric properties of the magnetic configuration. We find that a helical jet is always triggered for the range of parameters that we tested. This demonstrates that the 3D magnetic null-point configuration is a very robust structure for the energy storage and impulsive release characteristic of helical jets. In certain regimes determined by the magnetic geometry, a straight jet precedes the onset of a helical jet. We show that the reconnection occurring during the straight jet phase influences the triggering of the helical jet. Our results allow us to better understand the energization, triggering, and driving processes of straight and helical jets. Our model predicts the impulsiveness and energetics of jets in terms of the surrounding magnetic field configuration. Finally, we discuss the interpretation of the observationally defined standard and blowout jets in the context of our model, and the physical factors that determine which type of jet will occur.

## **Study of Magnetic Helicity Injection in the Active Regions NOAA 9236 Producing Multiple Flare-associated CME Events**

Sung-Hong [Park](#), Kanya Kusano, Kyung-Suk Cho, Jongchul Chae, Su-Chan Bong, Pankaj Kumar, So-Young Park, Yeon-Han Kim, Young-Deuk Park

E-print, Aug 2013; 2013 ApJ 778 13

To better understand a preferred magnetic field configuration and its evolution during Coronal Mass Ejection events, we investigated the spatial and temporal evolution of photospheric magnetic fields in the active region NOAA 9236 that produced eight flare-associated CMEs during the time period of **2000 November 23-26**. The time variations of the total magnetic helicity injection rate and the total unsigned magnetic flux are determined and examined not only in the entire active region but also in some local regions such as the main sunspots and the CME-associated flaring regions using SOHO/MDI magnetogram data. As a result, we found that: (1) in the sunspots, a large amount of positive (right-handed) magnetic helicity was injected during most of the examined time period, (2) in the flare region, there was a continuous injection of negative (left-handed) magnetic helicity during the entire period, accompanied by a large increase of the

unsigned magnetic flux, and (3) the flaring regions were mainly composed of emerging bipoles of magnetic fragments in which magnetic field lines have substantially favorable conditions for making reconnection with large-scale, overlying, and oppositely directed magnetic field lines connecting the main sunspots. These observational findings can also be well explained by some MHD numerical simulations for CME initiation (e.g., reconnection-favored emerging flux models). We therefore conclude that reconnection-favored magnetic fields in the flaring emerging flux regions play a crucial role in producing the multiple flare-associated CMEs in NOAA 9236.

## **THE OCCURRENCE AND SPEED OF CMEs RELATED TO TWO CHARACTERISTIC EVOLUTION PATTERNS OF HELICITY INJECTION IN THEIR SOLAR SOURCE REGIONS**

Sung-Hong [Park](#)<sup>1</sup>, Kyung-Suk Cho<sup>1,2,3</sup>, Su-Chan Bong<sup>1</sup>, Pankaj Kumar<sup>1</sup>, Jongchul Chae<sup>4</sup>, Rui Liu<sup>5,6</sup>, and Haimin Wang

2012 ApJ 750 48, [File](#)

Long-term (a few days) variation of magnetic helicity injection was calculated for 28 solar active regions that produced 47 coronal mass ejections (CMEs) to find its relationship to the CME occurrence and speed using SOHO/MDI line-of-sight magnetograms. As a result, we found that the 47 CMEs can be categorized into two different groups by two characteristic evolution patterns of helicity injection in their source active regions, which appeared for ~0.5-4.5 days before their occurrence: (1) a monotonically increasing pattern with one sign of helicity (Group A; 30 CMEs in 23 active regions) and (2) a pattern of significant helicity injection followed by its sign reversal (Group B; 17 CMEs in 5 active regions). We also found that CME speed has a correlation with average helicity injection rate with linear correlation coefficients of 0.85 and 0.63 for Group A and Group B, respectively. In addition, these two CME groups show different characteristics as follows: (1) the average CME speed of Group B (1330 km s<sup>-1</sup>) is much faster than that of Group A (870 km s<sup>-1</sup>), (2) the CMEs in Group A tend to be single events whereas those in Group B mainly consist of successive events, and (3) flares related to the CMEs in Group B are relatively more energetic and impulsive than those in Group A. Our findings therefore suggest that the two CME groups have different pre-CME conditions in their source active regions and different CME characteristics.

## **STUDY OF MAGNETIC HELICITY IN SOLAR ACTIVE REGIONS AND ITS RELATIONSHIP WITH SOLAR ERUPTIONS**

Sung-Hong [Park](#)

Thesis, 2010, [File](#)

<http://solar.njit.edu/SolarPhDStudents.htm>

It is generally believed that eruptive phenomena in the solar atmosphere such as solar flares and coronal mass ejections (CMEs) occur in solar active regions with complex magnetic structures. The magnetic complexity is quantified in terms of twists, kinks, and interlinkages of magnetic field lines. Magnetic helicity has been recognized as a useful measure for these properties of a given magnetic field system. Magnetic helicity studies have been naturally directed to the energy buildup and instability leading to solar eruptions. However, in spite of many years of study, detailed aspects of initiation mechanisms of eruptive events are still not well understood. The objective of this dissertation is to understand a long-term (a few days) variation of magnetic helicity in active regions and its relationship with flares and CMEs.

## **Source Region and Launch Characteristics of Magnetic-arch-blowout Solar Coronal Mass Ejections Driven by Homologous Compact-flare Blowout Jets**

[Binal D. Patel](#), [Bhuwan Joshi](#), [Alphonse C. Sterling](#), [Ronald L. Moore](#)

ApJ 969 48 2024

<https://arxiv.org/pdf/2405.03292>

<https://iopscience.iop.org/article/10.3847/1538-4357/ad4995/pdf>

We study the formation of four coronal mass ejections (CMEs) originating from homologous blowout jets. All of the blowout jets originated from NOAA active region (AR) 11515 on 2012 July 2, within a time interval of  $\approx 14$  hr. All of the CMEs were wide (angular widths  $\approx 95$ – $150^\circ$ ), and propagated with speeds ranging between  $\approx 300$ – $500$  km s<sup>-1</sup> in LASCO coronagraph images. Observations at various EUV wavelengths in Solar Dynamics Observatory/Atmospheric Imaging Assembly images reveal that in all the cases, the source region of the jets lies at the boundary of the leading part of AR 11515 that hosts a small filament before each event. Coronal magnetic field modeling based on nonlinear force free extrapolations indicate that in each case the filament is contained inside of a magnetic flux rope that remains constrained by overlying compact loops. The southern footpoint of each filament is rooted in the negative polarity region where the eruption onsets occur. This negative-polarity region undergoes continuous flux changes, including emergence and cancellation with opposite polarity in the vicinity of the flux rope, and the EUV images reveal brightening episodes near the filament's southeastern footpoint before each eruption. Therefore, these flux changes are

likely the cause of the subsequent eruptions. These four homologous eruptions originate near adjacent feet of two large-scale loop systems connecting from that positive-polarity part of the AR to two remote negative-polarity regions, and result in large-scale consequences in the solar corona.

## **The Closest View of a Fast Coronal Mass Ejection: How Faulty Assumptions near Perihelion Lead to Unrealistic Interpretations of PSP/WISPR Observations**

[Ritesh Patel](#), [Matthew J. West](#), [Daniel B. Seaton](#), [Phillip Hess](#), [Tatiana Niembro](#), [Katharine K. Reeves](#)

ApJL **955** L1 **2023**

<https://arxiv.org/pdf/2308.11055.pdf>

<https://iopscience.iop.org/article/10.3847/2041-8213/acf2f0/pdf>

We report on the closest view of a coronal mass ejection observed by the Parker Solar Probe (PSP)/Wide-field Imager for {Parker} Solar PRobe (WISPR) instrument on **September 05, 2022**, when PSP was traversing from a distance of 15.3~to~13.5~ $R_{\odot}$  from the Sun. The CME leading edge and an arc-shaped {\emph{concave-up}} structure near the core} was tracked in WISPR~field of view using the polar coordinate system, for the first time. Using the impact distance on Thomson surface, we measured average speeds of CME leading edge and concave-up structure as  $\approx 2500 \pm 270$ , km, s<sup>-1</sup> and  $\approx 400 \pm 70$ , km, s<sup>-1</sup> with a deceleration of  $\approx 20$ ~m~s<sup>-2</sup> for the later. {The use of the plane-of-sky approach yielded an unrealistic speed of more than three times of this estimate.} We also used single viewpoint STEREO/COR-2A images to fit the Graduated Cylindrical Shell (GCS) model to the CME while incorporating the source region location from EU1 of Solar Orbiter and estimated a 3D speed of  $\approx 2700$ , km, s<sup>-1</sup>. We conclude that this CME exhibits the highest speed during the ascending phase of solar cycle 25. This places it in the category of extreme speed CMEs, which account for only 0.15% of all CMEs listed in the CDAW CME catalog.

## **A Simple Radial Gradient Filter for Batch-Processing of Coronagraph Images**

[Ritesh Patel](#), [Satabdwa Majumdar](#), [Vaibhav Pant](#), [Dipankar Banerjee](#)

Solar Phys. **2022**

<https://arxiv.org/pdf/2201.13043.pdf>

Images of the extended solar corona, as observed by white-light coronagraphs as observed by different white-light coronagraphs include the K- and F-corona and suffer from a radial variation in intensity. These images require separation of the two coronal components with some additional image-processing to reduce the intensity gradient and analyse the structures and processes occurring at different heights in the solar corona within the full field of view. To process these bulk coronagraph images with steep radial-intensity gradients, we have developed an algorithm: Simple Radial Gradient Filter (SiRGraF). This algorithm is based on subtracting a minimum background (F-corona) created using long-duration images and then dividing the resultant by a uniform intensity gradient image to enhance the K-corona. We demonstrate the utility of this algorithm to bring out the short time-scale transient structures of the corona. SiRGraF could be used to reveal and analyse such structures. It is not suitable for quantitative estimations based on intensity. We have successfully tested the algorithm on images of the LASCO-C2 onboard the Solar and Heliospheric Observatory (SOHO), and COR-2A onboard the STEREO with good signal to noise ratio (SNR) along with low-SNR images of STEREO/COR-1A and the KCoronagraph. We also compared the performance of SiRGraF with Normalising Radial Gradient Filter (NRGF). We found that when hundreds of images have to be processed, SiRGraF works faster than NRGF, providing similar brightness and contrast in the images and separating the transient features. Moreover, SiRGraF works better on low-SNR images of COR-1A than NRGF, providing better identification of dynamic coronal structures throughout the field of view. We discuss the advantages and limitations of the algorithm. **07 July 2001, 01 August 2010, 03 April 2014, 02 July 2015,**

## **DH Type II Radio Bursts During Solar Cycles 23 and 24: Frequency-dependent Classification and their Flare-CME Associations**

Binal D. [Patel](#) (USO/PRL), [Bhuwan Joshi](#) (USO/PRL), [Kyung-Suk Cho](#) (SSD/KASI), [Rok-Soon Kim](#) (DASS/UST)

Solar Phys. **2021**

<https://arxiv.org/pdf/2108.12990.pdf>

We present the characteristics of DH type II bursts for the Solar Cycles 23 and 24. The bursts are classified according to their end frequencies into three categories, i.e. Low Frequency Group (LFG;  $20 \text{ kHz} \leq f \leq 200 \text{ kHz}$ ), Medium Frequency Group (MFG;  $200 \text{ kHz} < f \leq 1 \text{ MHz}$ ), and High Frequency Group (HFG;  $1 \text{ MHz} < f \leq 16 \text{ MHz}$ ). We find that the sources for LFG, MFG, and HFG events are homogeneously distributed over the active region belt. Our analysis shows a drastic reduction of the DH type II events during Solar Cycle 24 which includes only 35% of the total events (i.e. 179 out of 514). Despite having smaller number of DH type II events in the Solar Cycle 24, it contains a significantly higher fraction of LFG events compared to the previous cycle (32% versus 24%). However, within the LFG group the cycle 23 exhibits significant dominance of type II bursts that extend below 50 kHz, suggesting rich population of powerful CMEs travelling beyond half of the Sun-Earth distance. The events of LFG group display strongest association with faster and wider (more than 82% events are halo) CMEs while at the source location they predominantly trigger large M/X class flares (in more than 83% cases). Our analysis also indicates that CME initial speed or flare energetics are partly related with the duration of type II burst and that survival of CME associated shock is determined by multiple factors/parameters related to CMEs, flares, and state of coronal and interplanetary medium. The profiles relating CME heights with respect to the end frequencies of DH type II bursts suggest that for HFG and

MFG categories, the location for majority of CMEs ( $\approx 65\%$ - $70\%$ ) is in well compliance with ten-fold Leblanc coronal density model, while for LFG events a lower value of density multiplier ( $\approx 3$ ) seems to be compatible. **2011 November 26, 2013 May 22**

### **Automated Detection of Accelerating Solar Eruptions using Parabolic Hough Transform**

[Ritesh Patel](#), [Vaibhav Pant](#), [Priyanka Iyer](#), [Dipankar Banerjee](#), [Marilena Mierla](#), [Matthew J. West](#)

Solar Phys. **296**, Article number: 31 **2021**

<https://arxiv.org/pdf/2010.14786.pdf>

<https://link.springer.com/content/pdf/10.1007/s11207-021-01770-z.pdf>

Solar eruptions such as Coronal Mass Ejections (CMEs) observed in the inner solar corona (up to  $4 R_{\odot}$ ) show acceleration profiles which appear as parabolic ridges in height-time plots. Inspired by the white-light automated detection algorithms, Computer Aided CME Tracking System (CACTus) and Solar Eruptive Events Detection System (SEEDS), we employ the parabolic Hough Transform for the first time to automatically detect off-disk solar eruptions {from height-time plots. Due to the limited availability of white-light observations in the inner corona, we use Extreme UltraViolet (EUV) images of the Sun. In this paper we present a new algorithm, CME Identification in Inner Solar Corona (CIISCO), which is based on Fourier motion filtering and the parabolic Hough transform, and demonstrate its implementation using EUV observations taken from {it Atmospheric Imaging Assembly} (AIA) on-board the Solar Dynamics Observatory (SDO), {it Extreme Ultra Violet Imager} (EUVI) on-board the STEREO-A and B satellites, and {it Sun Watcher using Active Pixel System detector and Image Processing} (SWAP) Imager on-board PROBA2. We show that CIISCO is able to identify any {off-disk} outward moving feature in EUV images. The use of automated detection algorithms, like CIISCO, can potentially be used to provide early warnings of CMEs if an EUV telescope is located at  $\pm 90^{\circ}$  from the Sun-Earth line, providing CME characteristics and kinematics close to the Sun. This paper also presents the limitations of this algorithm and the prospects for future improvement. **2011-12-24, 2012-04-08, 2012-08-31, 2013-05-01**

### **Statistical Study of Plasmoids associated with post-CME Current Sheet**

[Ritesh Patel](#), [Vaibhav Pant](#), [K. Chandrashekhar](#), [Dipankar Banerjee](#)

A&A **644**, A158 **2020**

<https://arxiv.org/pdf/2010.03326.pdf>

<https://doi.org/10.1051/0004-6361/202039000>

We investigate the properties of plasmoids observed in the current sheet formed after an X-8.3 flare followed by a fast CME eruption on **September 10, 2017** using Extreme Ultraviolet (EUV) and white-light coronagraph images. The main aim is to understand the evolution of plasmoids at different spatio-temporal scales using existing ground- and space-based instruments. We identified the plasmoids in current sheet observed in the successive images of {it Atmospheric Imaging Assembly} (AIA) and white-light coronagraphs, K-Cor and LASCO/C2. We found that the current sheet is accompanied by several plasmoids moving upwards and downwards. Our analysis showed that the downward and upward moving plasmoids have average width of 5.92 Mm and 5.65 Mm, respectively in the AIA field of view (FOV). However, upward moving plasmoids have average width of 64 Mm in the K-Cor which evolves to a mean width of 510 Mm in the LASCO/C2 FOV. Upon tracking the plasmoids in successive images, we observe that downward and upward moving plasmoids have average speeds of  $\sim 272$  km  $s^{-1}$  and  $\sim 191$  km  $s^{-1}$  respectively in the EUV passbands. We note that the plasmoids become super-Alfvénic when they reach at LASCO FOV. Furthermore, we estimate that the null-point of the current sheet at  $\approx 1.15 R_{\odot}$  where bidirectional plasmoid motion is observed. We study the width distribution of plasmoids formed and notice that it is governed by a power law with a power index of  $-1.12$ . Unlike previous studies there is no difference in trend for small and large scale plasmoids. The presence of accelerating plasmoids near the neutral point indicates a longer diffusion region as predicted by MHD models.

### **Onboard Automated CME Detection Algorithm for Visible Emission Line Coronagraph on ADITYA-L1**

[Ritesh Patel](#), [K Amareswari](#), [Vaibhav Pant](#), [Dipankar Banerjee](#), [Sankarasubramanian K](#), [Amit Kumar](#)

Solar Phys. **293**:103 **2018**

<https://arxiv.org/pdf/1806.07932.pdf>

ADITYA-L1 is India's first space mission to study the Sun from Lagrangian 1 position. { \textit{Visible Emission Line Coronagraph} } (VELC) is one of the seven payloads in ADITYA-L1 mission scheduled to be launched around 2020. One of the primary objectives of the VELC is to study the dynamics of coronal mass ejections (CMEs) in the inner corona. This will be accomplished by taking high resolution ( $\approx 2.51$  arcsec pixel $^{-1}$ ) images of corona from  $1.05 R_{\odot}$  --  $3 R_{\odot}$  at high cadence of 1 s in 10 \AA passband centered at 5000 \AA. Due to limited telemetry at Lagrangian 1 position we plan to implement an onboard automated CME detection algorithm. The detection algorithm is based on the intensity thresholding followed by the area thresholding in successive difference images spatially re-binned to improve signal to noise ratio. We present the results of the application of this algorithm on the data from existing space- and ground-based coronagraph. Since, no existing space-based coronagraph has FOV similar to VELC, we have created synthetic coronal images for VELC FOV after including photon noise and injected different type of CMEs. The performance of CME detection algorithm is tested on these images. We found that for VELC images, the telemetry can be reduced by a factor of 85% or more keeping CME detection rate of 70% or above at the same time. Finally, we discuss the advantages and disadvantages of this algorithm. The application of such onboard algorithm in future will



enable us to take higher resolution images with improved cadence from space and also reduce the load on limited telemetry at the same time. This will help in better understanding of CMEs by studying their characteristics with improved spatial and temporal resolutions. **2012-06-14** , **2013-10-28** , **2016-01-01**

### **Automated detection of Coronal Mass Ejections in Visible Emission Line Coronagraph (VELC) on-board ADITYA-L1**

[Ritesh Patel](#), [K. Amareswari](#), [Vaibhav Pant](#), [Dipankar Banerjee](#), [K. Sankarasubramanian](#)

Proceedings of IAU Symposium, No. 340,

**2018**

<https://arxiv.org/pdf/1805.05802.pdf>

An onboard automated coronal mass ejections (CMEs) detection algorithm has been developed for Visible Emission Line Coronagraph (VELC) onboard ADITYA-L1. The aim of this algorithm is to reduce the load on telemetry by sending the high spatial ( $\sim 2.51$  arcsec pixel $^{-1}$ ) and temporal (1 s) resolution images of corona from  $1.05 R_{\odot}$  to  $3 R_{\odot}$ , containing CMEs and rejecting others. It is based on intensity thresholding followed by an area thresholding in successive running difference images which are re-binned to lower resolution to improve signal to noise. Here we present the results of application of the algorithm on synthetic corona images generated for the VELC field of view (FOV).

### **Decoding the Pre-Eruptive Magnetic Field Configurations of Coronal Mass Ejections Review**

[S. Patsourakos](#), [A. Vourlidas](#), [T. Török](#), [B. Kliem](#), [S. K. Antiochos](#), [V. Archontis](#), [G. Aulanier](#), [X. Cheng](#), [G. Chintzoglou](#), [M.K. Georgoulis](#), [L.M. Green](#), [J. E. Leake](#), [R. Moore](#), [A. Nindos](#), [P. Syntelis](#), [S. L. Yardley](#), [V. Yurchyshyn](#), [J. Zhang](#)

Space Science Reviews **216**, Article number: 131 **2020**

<https://arxiv.org/pdf/2010.10186.pdf> **File**

<https://link.springer.com/content/pdf/10.1007/s11214-020-00757-9.pdf>

A clear understanding of the nature of the pre-eruptive magnetic field configurations of Coronal Mass Ejections (CMEs) is required for understanding and eventually predicting solar eruptions. Only two, but seemingly disparate, magnetic configurations are considered viable; namely, sheared magnetic arcades (SMA) and magnetic flux ropes (MFR). They can form via three physical mechanisms (flux emergence, flux cancellation, helicity condensation). Whether the CME culprit is an SMA or an MFR, however, has been strongly debated for thirty years. We formed an International Space Science Institute (ISSI) team to address and resolve this issue and report the outcome here. We review the status of the field across modeling and observations, identify the open and closed issues, compile lists of SMA and MFR observables to be tested against observations and outline research activities to close the gaps in our current understanding. We propose that the combination of multi-viewpoint multi-thermal coronal observations and multi-height vector magnetic field measurements is the optimal approach for resolving the issue conclusively. We demonstrate the approach using MHD simulations and synthetic coronal images.

Our key conclusion is that the differentiation of pre-eruptive configurations in terms of SMAs and MFRs seems artificial. Both observations and modeling can be made consistent if the pre-eruptive configuration exists in a hybrid state that is continuously evolving from an SMA to an MFR. Thus, the 'dominant' nature of a given configuration will largely depend on its evolutionary stage (SMA-like early-on, MFR-like near the eruption). **March 8, 2011**

### **A Helicity-Based Method to Infer the CME Magnetic Field Magnitude in Sun and Geospace: Generalization and Extension to Sun-Like and M-Dwarf Stars and Implications for Exoplanet Habitability**

S. [Patsourakos](#), M. K. Georgoulis

[Solar Physics](#) July **2017**, 292:89

<https://link.springer.com/content/pdf/10.1007%2Fs11207-017-1124-1.pdf>

Patsourakos et al. (*Astrophys. J.*817, 14, [2016](#)) and Patsourakos and Georgoulis (*Astron. Astrophys.*595, A121, [2016](#)) introduced a method to infer the axial magnetic field in flux-rope coronal mass ejections (CMEs) in the solar corona and farther away in the interplanetary medium. The method, based on the conservation principle of magnetic helicity, uses the relative magnetic helicity of the solar source region as input estimates, along with the radius and length of the corresponding CME flux rope. The method was initially applied to cylindrical force-free flux ropes, with encouraging results. We hereby extend our framework along two distinct lines. First, we generalize our formalism to several possible flux-rope configurations (linear and nonlinear force-free, non-force-free, spheromak, and torus) to investigate the dependence of the resulting CME axial magnetic field on input parameters and the employed flux-rope configuration. Second, we generalize our framework to both Sun-like and active M-dwarf stars hosting superflares. In a qualitative sense, we find that Earth may not experience severe atmosphere-eroding magnetospheric compression even for eruptive solar superflares with energies  $\approx 10^4 \sim 10^5$  times higher than those of the largest Geostationary Operational Environmental Satellite (GOES) X-class flares currently observed. In addition, the two recently discovered exoplanets with the highest Earth-similarity index, Kepler 438b and Proxima b, seem to lie in the prohibitive zone of atmospheric erosion due to interplanetary CMEs (ICMEs), except when they possess planetary magnetic fields that are much higher than that of Earth.

## Near-Sun and 1 AU magnetic field of coronal mass ejections: A parametric study

S. Patsourakos, M. K. Georgoulis

A&A 595, A121 2016

<http://arxiv.org/pdf/1609.00134v1.pdf>

<http://www.aanda.org/sci-hub/cc/articles/aa/pdf/2016/11/aa28277-16.pdf>

**Aims.** The magnetic field of coronal mass ejections (CMEs) determines their structure, evolution, and energetics, as well as their geoeffectiveness. However, we currently lack routine diagnostics of the near-Sun CME magnetic field, which is crucial for determining the subsequent evolution of CMEs.

**Methods.** We recently presented a method to infer the near-Sun magnetic field magnitude of CMEs and then extrapolate it to 1 AU. This method uses relatively easy to deduce observational estimates of the magnetic helicity in CME-source regions along with geometrical CME fits enabled by coronagraph observations. We hereby perform a parametric study of this method aiming to assess its robustness. We use statistics of active region (AR) helicities and CME geometrical parameters to determine a matrix of plausible near-Sun CME magnetic field magnitudes. In addition, we extrapolate this matrix to 1 AU and determine the anticipated range of CME magnetic fields at 1 AU representing the radial falloff of the magnetic field in the CME out to interplanetary (IP) space by a power law with index  $a_B$ .

**Results.** The resulting distribution of the near-Sun (at 10 Rs) CME magnetic fields varies in the range [0.004, 0.02] G, comparable to, or higher than, a few existing observational inferences of the magnetic field in the quiescent corona at the same distance. We also find that a theoretically and observationally motivated range exists around  $a_B = -1.6 \pm 0.2$ , thereby leading to a ballpark agreement between our estimates and observationally inferred field magnitudes of magnetic clouds (MCs) at L1.

**Conclusions.** In a statistical sense, our method provides results that are consistent with observations.

## THE MAJOR GEOEFFECTIVE SOLAR ERUPTIONS OF 2012 MARCH 7: COMPREHENSIVE SUN-TO-EARTH ANALYSIS

S. Patsourakos<sup>1</sup>, M. K. Georgoulis<sup>2</sup>, A. Vourlidas<sup>3</sup>, A. Nindos<sup>1</sup>, .....

2016 ApJ 817 14

During the interval **2012 March 7–11** the geospace experienced a barrage of intense space weather phenomena including the second largest geomagnetic storm of solar cycle 24 so far. Significant ultra-low-frequency wave enhancements and relativistic-electron dropouts in the radiation belts, as well as strong energetic-electron injection events in the magnetosphere were observed. These phenomena were ultimately associated with two ultra-fast ( $>2000$  km s<sup>-1</sup>) coronal mass ejections (CMEs), linked to two X-class flares launched on early 2012 March 7. Given that both powerful events originated from solar active region NOAA 11429 and their onsets were separated by less than an hour, the analysis of the two events and the determination of solar causes and geospace effects are rather challenging. Using satellite data from a flotilla of solar, heliospheric and magnetospheric missions a synergistic Sun-to-Earth study of diverse observational solar, interplanetary and magnetospheric data sets was performed. It was found that only the second CME was Earth-directed. Using a novel method, we estimated its near-Sun magnetic field at 13 R<sub>⊙</sub> to be in the range [0.01, 0.16] G. Steep radial fall-offs of the near-Sun CME magnetic field are required to match the magnetic fields of the corresponding interplanetary CME (ICME) at 1 AU. Perturbed upstream solar-wind conditions, as resulting from the shock associated with the Earth-directed CME, offer a decent description of its kinematics. The magnetospheric compression caused by the arrival at 1 AU of the shock associated with the ICME was a key factor for radiation-belt dynamics.

## DIRECT EVIDENCE FOR A FAST CORONAL MASS EJECTION DRIVEN BY THE PRIOR FORMATION AND SUBSEQUENT DESTABILIZATION OF A MAGNETIC FLUX ROPE

S. Patsourakos<sup>1</sup>, A. Vourlidas<sup>2</sup>, and G. Stenborg

2013 ApJ 764 125

Magnetic flux ropes play a central role in the physics of coronal mass ejections (CMEs). Although a flux-rope topology is inferred for the majority of coronagraphic observations of CMEs, a heated debate rages on whether the flux ropes pre-exist or whether they are formed on-the-fly during the eruption. Here, we present a detailed analysis of extreme-ultraviolet observations of the formation of a flux rope during a confined flare followed about 7 hr later by the ejection of the flux rope and an eruptive flare. The two flares occurred during **2012 July 18 and 19**. The second event unleashed a fast ( $>1000$  km s<sup>-1</sup>) CME. We present the first direct evidence of a fast CME driven by the prior formation and destabilization of a coronal magnetic flux rope formed during the confined flare on July 18.

## Evidence for a current sheet forming in the wake of a Coronal Mass Ejection from multi-viewpoint coronagraph observations

S. Patsourakos, A. Vourlidas

E-print, Oct 2010, File; A&A, 525, A27 (2011)

Ray-like features observed by coronagraphs in the wake of Coronal Mass Ejections (CMEs) are sometimes interpreted as the white light counterparts of current sheets (CSs) produced by the eruption. The 3D geometry of these ray-like features is largely unknown and its knowledge should clarify their association to the CS and place constraints on CME physics and coronal conditions. With this study we test these important implications for the first time. An example of

such a post-CME ray was observed by various coronagraphs, including these of the SECCHI instrument suite of the STEREO twin spacecraft and the Large Angle Spectrometric Coronagraph LASCO onboard the Solar and Heliospheric Observatory (SOHO). The ray was observed in the aftermath of a CME which occurred on **9 April 2008**. The twin STEREO spacecraft were separated by about degrees on that day. This significant separation combined with a third "eye" view supplied by LASCO allow for a truly multi-viewpoint observation of the ray and of the CME. We applied 3D forward geometrical modeling to the CME and to the ray as simultaneously viewed by SECCHI-A and B and by SECCHI-A and LASCO, respectively. We found that the ray can be approximated by a rectangular slab, nearly aligned with the CME axis, and much smaller than the CME in both terms of thickness and depth ( $\sim 0.05$  and  $0.15 R_{\text{sun}}$  respectively). We found that the ray and CME are significantly displaced from the associated post-CME flaring loops. The properties and location of the ray are fully consistent with the expectations of the standard CME theories for post-CME current sheets. Therefore, our multi-viewpoint observations supply strong evidence that the observed post-CME ray is indeed related to a post-CME current sheet.

## **The Genesis of an Impulsive Coronal Mass Ejection observed at Ultra-High Cadence by AIA on SDO**

S. [Patsourakos](#), A. Vourlidas, G. Stenborg

E-print Oct **2010**, ApJL, 724:L188–L193, **2010**, **File**

Movies available at [http://dl.dropbox.com/u/3971111/movies\\_aia\\_cme.tar.gz](http://dl.dropbox.com/u/3971111/movies_aia_cme.tar.gz).

The study of fast, eruptive events in the low solar corona is one of the science objectives of the Atmospheric Imaging Assembly (AIA) imagers on the recently launched Solar Dynamics Observatory (SDO), which take full disk images in ten wavelengths with arcsecond resolution and 12 sec cadence. We study with AIA the formation of an impulsive coronal mass ejection (CME) which occurred on **June 13, 2010** and was associated with an M1.0 class flare. Specifically, we analyze the formation of the CME EUV bubble and its initial dynamics and thermal evolution in the low corona using AIA images in three wavelengths (171, 193 and 211 Å). We derive the first ultra-high cadence measurements of the temporal evolution of the CME bubble aspect ratio (=bubble-height/bubble-radius). Our main result is that the CME formation undergoes three phases: it starts with a slow self-similar expansion followed by a fast but short-lived ( $\sim 70$  sec) period of strong lateral over-expansion which essentially creates the CME. Then the CME undergoes another phase of self-similar expansion until it exits the AIA field of view. During the studied interval, the CME height-time profile shows a strong, short-lived, acceleration followed by deceleration. The lateral overexpansion phase coincides with the deceleration phase. The impulsive flare heating and CME acceleration are closely coupled. However, the lateral overexpansion of the CME occurs during the declining phase and is therefore not linked to flare reconnection. In addition, the multi-thermal analysis of the bubble does not show significant evidence of temperature change.

## **Toward understanding the early stages of an impulsively accelerated coronal mass ejection SECCHI observations**

S. [Patsourakos](#), A. Vourlidas<sup>2</sup>, and B. Kliem<sup>3,4</sup>

E-print, 9 Aug **2010**, **File**, A&A, 522, A100, **2010**

**Context.** The expanding magnetic flux in coronal mass ejections (CMEs) often forms a cavity. Studies of CME cavities have so far been limited to the pre-event configuration or to evolved CMEs at large heights, and to two-dimensional imaging data.

**Aims.** Quantitative analysis of three-dimensional cavity evolution at CME onset can reveal information that is relevant to the genesis of the eruption.

**Methods.** A spherical model is simultaneously fit to Solar Terrestrial Relations Observatory (STEREO) Extreme Ultraviolet Imager (EUVI) and Inner Coronagraph (COR1) data of an impulsively accelerated CME on **25 March 2008**, which displays a well-defined extreme ultraviolet (EUV) and white-light cavity of nearly circular shape already at low heights  $h \approx 0.2R_{\odot}$ . The center height  $h(t)$  and radial expansion  $r(t)$  of the cavity are obtained in the whole height range of the main acceleration. We interpret them as the axis height and as a quantity proportional to the minor radius of a flux rope, respectively.

**Results.** The three-dimensional expansion of the CME exhibits two phases in the course of its main upward acceleration. From the first  $h$  and  $r$  data points, taken shortly after the onset of the main acceleration, the erupting flux shows an overexpansion compared to its rise, as expressed by the decrease of the aspect ratio from  $\alpha = h/r \approx 3$  to  $\alpha \approx (1.5-2)$ . This phase is approximately coincident with the impulsive rise of the acceleration and is followed by a phase of very gradual change of the aspect ratio (a nearly self-similar expansion) toward  $\alpha \sim 2.5$  at  $h \sim 10R_{\odot}$ . The initial overexpansion of the CME cavity can be caused by flux conservation around a rising flux rope of decreasing axial current and by the addition of flux to a growing, or even newly forming, flux rope by magnetic reconnection. Further analysis will be required to decide which of these contributions is dominant. The data also suggest that the horizontal component of the impulsive cavity expansion (parallel to the solar surface) triggers the associated EUV wave, which subsequently detaches from the CME volume.

## **Coronal Density Structures and CMEs: Superior Solar Conjunctions of Mars Express, Venus Express, and Rosetta: 2004, 2006, and 2008**

Martin [Pätzold](#), Matthias Hahn, Silvia Tellmann, Bernd Häusler, Michael K. Bird, G. Leonard Tyler, Sami W. Asmar and Bruce T. Tsurutani

Solar Physics, Volume 279, Number 1 (**2012**), 127-152

Coronal radio-sounding experiments were carried out using the S-band (2.3 GHz) and X-band (8.4 GHz) signals of the ESA Mars Express, Venus Express, and Rosetta spacecraft during five superior conjunctions occurring in 2004, 2006

(3×), and 2008/2009. Differential frequency and propagation delay (ranging) observations were recorded during these opportunities over the better part of a solar cycle, yielding information on the large-scale structure of the coronal electron-density distribution and its variations, including fluctuations on time scales from seconds to hours. These results concern primarily regions of slow solar wind because the radio propagation path is generally confined to the low heliolatitude regions by the conjunction. The mean frequency fluctuation and total electron content are determined as a function of heliocentric distance, and, with a few exceptions caused by streamers and CMEs, are found to be consistent with previous results from experiments on Ulysses. Dense coronal streamers and several coronal mass ejection (CME) events were identified in the radio-frequency data, some of which were observed in white light by the LASCO coronagraphs onboard SOHO. For those events with sufficient mutual coverage, good correlations are found between the electron-content fluctuations and structure imaged by the LASCO instrument.

## **Acceleration of Coronal Mass Ejection Plasma in the Low Corona as Measured by the Citizen CATE Experiment**

Matthew J Penn<sup>1,2</sup>, Robert Baer<sup>3</sup>, Donald Walter<sup>4</sup>, Michael Pierce<sup>5</sup>, Richard Gelderman<sup>6</sup>, Andrei Ursache<sup>7</sup>, David Elmore<sup>8</sup>, Adrianna Mitchell<sup>9</sup>, Sarah Kovac<sup>10</sup>, Honor Hare<sup>11</sup>Show full author list  
2020 PASP 132 014201

<https://iopscience.iop.org/article/10.1088/1538-3873/ab558c/pdf>

The citizen Continental-America Telescopic Eclipse (CATE) Experiment was a new type of citizen science experiment designed to capture a time sequence of white-light coronal observations during totality from 17:16 to 18:48 UT on **2017 August 21**. Using identical instruments the CATE group imaged the inner corona from 1 to 2.1 R<sub>Sun</sub> with 1<sup>1</sup>/<sub>43</sub> pixels at a cadence of 2.1 s. A slow coronal mass ejection (CME) started on the SW limb of the Sun before the total eclipse began. An analysis of CATE data from 17:22 to 17:39 UT maps the spatial distribution of coronal flow velocities from about 1.2 to 2.1 R<sub>Sun</sub>, and shows the CME material accelerates from about 0 to 200 km s<sup>-1</sup> across this part of the corona. This CME is observed by LASCO C2 at 3.1–13 R<sub>Sun</sub> with a constant speed of 254 km s<sup>-1</sup>. The CATE and LASCO observations are not fit by either constant acceleration nor spatially uniform velocity change, and so the CME acceleration mechanism must produce variable acceleration in this region of the corona.

## **An Unreported White-light Prominence**

Matt Penn and Hugh Hudson  
RHESSI Science Nuggets #270 March 2016  
1998-11-22 2005-09-07 (X17)

## **On the Construction of Phenomenological Coronal Mass Ejection Models**

**D. V. Peregoudov**

Space Weather e2020SW002659 **Volume19, Issue3** 2021

<https://doi.org/10.1029/2020SW002659>

<https://doi.org/10.1029/2020SW002659>

<https://agupubs.onlinelibrary.wiley.com/doi/epdf/10.1029/2020SW002659>

We consider recently developed 3DCORE coronal mass ejection model. We find that the magnetic field of 3DCORE violates both Maxwellian equations: the one for absence of magnetic monopoles and the one for Faraday induction ('frozen-in' condition). We recall basic heliospheric magnetohydrodynamical equations and show that they lead to a number of conservation laws. These conservation laws should be taken into account when developing a phenomenological coronal mass ejection model. We show that conservation laws take extremely simple form when written in Lagrange coordinates frozen into plasma. Thus these are easy to conform and practically there are no reasons not to conform them. We propose a modification of 3DCORE magnetic field that satisfies Maxwellian equations.

## **Bright hot impacts by erupted fragments falling back on the Sun: magnetic channelling**

A. Petralia, F. Reale, S. Orlando, P. Testa

2016 ApJ 832 2

<http://arxiv.org/pdf/1609.04634v1.pdf>

Dense plasma fragments were observed to fall back on the solar surface by the Solar Dynamics Observatory after an eruption on **7 June 2011**, producing strong EUV brightenings. Previous studies investigated impacts in regions of weak magnetic field. Here we model the ~ 300 km/s impact of fragments channelled by the magnetic field close to active regions. In the observations, the magnetic channel brightens before the fragment impact. We use a 3D-MHD model of spherical blobs downfalling in a magnetized atmosphere. The blob parameters are constrained from the observation. We run numerical simulations with different ambient density and magnetic field intensity. We compare the model emission in the 171Å channel of the Atmospheric Imaging Assembly with the observed one. We find that a model of downfall channelled in a ~ 1MK coronal loop confined by a magnetic field of ~ 10–20G, best explains qualitatively and quantitatively the observed evolution. The blobs are highly deformed, further fragmented, when the ram pressure becomes comparable to the local magnetic pressure and they are deviated to be channelled by the field, because of the differential stress applied by the perturbed magnetic field. Ahead of them, in the relatively dense coronal medium, shock fronts propagate, heat and brighten the channel between the cold falling plasma and the solar surface. This study shows a new mechanism which brightens downflows channelled by the magnetic field, such as in accreting young stars,

and also works as a probe of the ambient atmosphere, providing information about the local plasma density and magnetic field.

### **On the enhanced coronal mass ejection detection rate since the solar cycle 23 polar field reversal**

Gordon **Petrie**

ApJ 812 74    **2015**

<http://arxiv.org/pdf/1508.06729v1.pdf>

Coronal mass ejections (CMEs) with angular width  $>30^\circ$  have been observed to occur at a higher rate during solar cycle 24 compared to cycle 23, per sunspot number. This result is supported by data from three independent databases constructed using Large Angle and Spectrometric Coronagraph Experiment (LASCO) coronagraph images, two employing automated detection techniques and one compiled manually by human observers. According to the two databases that cover a larger field of view, the enhanced CME rate actually began shortly after the cycle 23 polar field reversal, in 2004, when the polar fields returned with a 40% reduction in strength and interplanetary radial magnetic field became  $\approx 30\%$  weaker. This result is consistent with the link between anomalous CME expansion and heliospheric total pressure decrease recently reported by Gopalswamy et al.

### **Coronal Mass Ejections from Magnetic Systems Encompassing Filament Channels Without Filaments**

Alexei A. **Pevtsov**, Olga Panasenco and Sara F. Martin

Solar Physics, Volume 277, Number 1, 185-201, **2012**, **File**

Well-developed filament channels may be present in the solar atmosphere even when there is no trace of filament material inside them. Such magnetic systems with filament channels without filaments can result in coronal mass ejections that might appear to have no corresponding solar surface source regions. In this case study, we analyze CMEs on **9 August 2001** and **3 March 2011** and trace their origins to magnetic systems with filament channels containing no obvious filament material on the days around the eruptions.

### **Coronal Mass Ejections, Associated Shocks and their Interactions with the Ambient Medium**

Monique **Pick**, G. Stenborg, P. Zucca, P. D´emoulin, A. Lecacheux, A. Kerdraon

CESRA **2016** p.70

[http://cesra2016.sciencesconf.org/conference/cesra2016/pages/CESRA2016\\_prog\\_abs\\_book\\_v3.pdf](http://cesra2016.sciencesconf.org/conference/cesra2016/pages/CESRA2016_prog_abs_book_v3.pdf)

This presentation is a contribution to the understanding of the role of the coronal environment in the development of CMEs and of the associated shocks. This study has benefited from multi-wavelength imaging observations and radio spectral data over a large frequency range. We selected events launched far from the local vertical direction and we followed step by step their progression from the low corona into higher altitudes, detected in white light. The availability of images from a combination of EUV imagers in quadrature combined with radio imaging observations allowed us to identify the successive complex interactions (e.g., compression, reconnection) between the CMEs and the ambient medium. For one event, the CME resulted from the interaction of an eruptive jet with the surrounding medium; the progression of this CME was closely associated with the occurrence of two successive type II bursts from distinct origins. Two other events originating from their source in the north hemisphere, underwent a large deflection in the low corona and finally emerged in the southern hemisphere following with a radial direction. We shall briefly discuss the potential implication of this results for space weather purposes.

### **Homologous solar events on **2011 January 27**: Build-up and propagation in a complex coronal environment**

M. **Pick**, G. Stenborg, P. Demoulin, P. Zucca, A. Lecacheux

ApJ                    **2016**

[http://www.lesia.obspm.fr/perso/pascal-demoulin/16/pick16\\_homologous\\_CMEs.pdf](http://www.lesia.obspm.fr/perso/pascal-demoulin/16/pick16_homologous_CMEs.pdf)    **File**

In spite of the wealth of imaging observations at extreme-ultraviolet, X-ray, and radio wavelengths, there are still a relatively small number of cases where the whole imagery becomes available to study the full development of a coronal mass ejection (CME) event and its associated shock. The aim of this study is to contribute to the understanding of the role of the coronal environment in the development of CMEs and formation of shocks, and on their propagation. We have analyzed the interactions of a couple of homologous CME events with the ambient coronal structures. Both events were launched in a direction far from the local vertical, and exhibited a radical change of their direction of propagation during their progression from the low corona into higher altitudes. Observations at extreme ultraviolet wavelengths from the Atmospheric Imaging Assembly instrument onboard the Solar Dynamic Observatory were used to track the events in the low corona. The development of the events at higher altitudes was followed with the white light coronagraphs onboard the Solar and Heliospheric Observatory. Radio emissions produced during the development of the events were well recorded by the Nancay solar instruments. By detecting accelerated electrons, the radio observations are an important complement to the extreme ultraviolet imaging. They allowed us to characterize the

development of the associated shocks, and helped unveil the physical processes behind the complex interactions between the CMEs and ambient medium (e.g., compression, reconnection).

## **CME development in the corona and interplanetary medium: A multi-wavelength approach**

M. [Pick](#), B. Kliem

EAS Publications Ser. 55, 299, **2012**, [File](#)

<http://arxiv.org/pdf/1407.2271v1.pdf>

This [review](#) focuses on the so called three-part CMEs which essentially represent the standard picture of a CME eruption. It is shown how the multi-wavelength observations obtained in the last decade, especially those with high cadence, have validated the early models and contributed to their evolution. These observations cover a broad spectral range including the EUV, white-light, and radio domains. **02 June 2002**, **29 January 2008**, **2008-06-03-05**, **2010 November 3**,

## **MULTI-WAVELENGTH OBSERVATIONS OF CMES AND ASSOCIATED PHENOMENA**

*Report of Working Group F*

M. [PICK](#)<sup>1,\*</sup>, T. G. FORBES<sup>2</sup>, G. MANN<sup>3</sup>, H. V. CANE<sup>4</sup>, J. CHEN<sup>5</sup>, A. CIARAVELLA<sup>6</sup>, H. CREMADES<sup>7</sup>, R. A. HOWARD<sup>8</sup>, H. S. HUDSON<sup>9</sup>, A. KLASSEN<sup>3</sup>, K. L. KLEIN<sup>1</sup>, M. A. LEE<sup>2</sup>, J. A. LINKER<sup>10</sup>, D. MAIA<sup>11</sup>, Z. MIKIC<sup>10</sup>, J. C. RAYMOND<sup>12</sup>, M. J. REINER<sup>13</sup>, G. M. SIMNETT<sup>14</sup>, N. SRIVASTAVA<sup>15</sup>, D. TRIPATHI<sup>7</sup>, R. VAINIO<sup>16</sup>, A. VOURLIDAS<sup>8</sup>, J. ZHANG<sup>17</sup>, T. H. ZURBUCHEN<sup>18</sup>, N. R. SHEELEY<sup>8</sup> and C. MARQUÉ

Space Science Reviews (2006) 123: 341–382

## **Physical properties of a fan-shaped jet backlit by an X9.3 flare**

[A.G.M. Pietrow](#), [M. Druett](#), [J. de la Cruz Rodriguez](#), [F. Calvo](#), [D. Kiselman](#)

A&A 659, A58 **2022**

<https://arxiv.org/pdf/2110.10541.pdf>

<https://doi.org/10.1051/0004-6361/202142346>

<https://www.aanda.org/articles/aa/pdf/2022/03/aa42346-21.pdf>

Fan-shaped jets can be observed above light bridges and are driven by reconnection of the vertical umbral field with the more horizontal field above the light bridges. Because these jets are not fully opaque in chromospheric lines, one cannot study their spectra without the highly complex considerations of radiative transfer in spectral lines from the atmosphere behind the fan. We get around this by taking advantage of a unique set of observations of the H $\alpha$  line along with the Ca II 8542 and Ca II K lines obtained with the Swedish 1-m Solar Telescope where a fan-shaped jet was backlit by an X9.3 flare. The H $\alpha$  flare ribbon emission profiles from behind the fan are highly broadened and flattened, allowing us to investigate the fan as if it were backlit by continuous emission. Using this model we derived the opacity and velocity of the material in the jet and what we believe to be the first observationally derived estimate of the mass and density of material in a fan-shaped jet. Using inversions of Ca II 8542 emission via STiC, we were also able to estimate the temperature in the jet. Finally, we use the masses and POS and LOS velocities as functions of time to investigate the downward supply of energy and momentum to the photosphere in the collapse of this jet, and evaluate it as a potential driver for a sunquake beneath. We found that the physical properties of the fan material are reasonably chromospheric in nature, with a temperature of  $7050 \pm 250$  K and a mean density of  $2 \pm 0.3 \times 10^{-11}$  g cm<sup>-3</sup>. The total mass observed in  $\alpha$  was found to be  $3.9 \pm 0.7 \times 10^{13}$ g and the kinetic energy delivered to the base of the fan in its collapse was nearly two orders of magnitude below typical sunquake energies. We therefore rule out this jet as the sunquake driver, but cannot completely rule out larger fan jets as potential drivers. **6 Sep 2017**

## **Theoretical basis for operational ensemble forecasting of coronal mass ejections**

V. J. [Pizzo](#), C. de Koning, M. Cash, G. Millward, D. A. Biesecker, L. Puga, M. Codrescu and D. Odstrcil  
Space Weather v.13, No. 10 (pages 676–697) **2015** DOI: 10.1002/2015SW001221

We lay out the theoretical underpinnings for the application of the Wang-Sheeley-Argé-Enlil modeling system to ensemble forecasting of coronal mass ejections (CMEs) in an operational environment. In such models, there is no magnetic cloud component, so our results pertain only to CME front properties, such as transit time to Earth. Within this framework, we find no evidence that the propagation is chaotic, and therefore, CME forecasting calls for different tactics than employed for terrestrial weather or hurricane forecasting. We explore a broad range of CME cone inputs and ambient states to flesh out differing CME evolutionary behavior in the various dynamical domains (e.g., large, fast CMEs launched into a slow ambient, and the converse; plus numerous permutations in between). CME propagation in both uniform and highly structured ambient flows is considered to assess how much the solar wind background affects the CME front properties at 1 AU. Graphical and analytic tools pertinent to an ensemble approach are developed to enable uncertainties in forecasting CME impact at Earth to be realistically estimated. We discuss how uncertainties in

CME pointing relative to the Sun-Earth line affects the reliability of a forecast and how glancing blows become an issue for CME off-points greater than about the half width of the estimated input CME. While the basic results appear consistent with established impressions of CME behavior, the next step is to use existing records of well-observed CMEs at both Sun and Earth to verify that real events appear to follow the systematic tendencies presented in this study.

## Combined geometrical modelling and white-light mass determination of coronal mass ejections

Adam **Pluta**<sup>1</sup>, Niclas Mrotzek<sup>1</sup>, Angelos Vourlidas<sup>2,3</sup>, Volker Bothmer<sup>1</sup> and Neel Savani<sup>4</sup>

A&A 623, A139 (2019)

<https://doi.org/10.1051/0004-6361/201833829>

[sci-hub.tw/10.1051/0004-6361/201833829](https://arxiv.org/abs/1905.08382)

**Context.** We use forward modelling on multi-viewpoint coronagraph observations to estimate the 3-dimensional morphology, initial speed and deprojected masses of Coronal Mass Ejections (CMEs). The CME structure is described via the Graduated Cylindrical Shell (GCS) model, which enables the measurement of CME parameters in a consistent and comparable manner.

**Aims.** This is the first large-scale use of the GCS model to estimate CME masses, so we discuss inherent peculiarities and implications for the mass determination with a special focus on CME events emerging from close to the observer's central meridian. Further, we analyse the CME characteristics best suited to estimate the CME mass in a timely manner to make it available to CME arrival predictions.

**Methods.** We apply the method to a set of 122 bright events observed simultaneously from two vantage points with the COR2 coronagraphs onboard of the twin NASA STEREO spacecraft. The events occurred between January 2007 and December 2013 and are compiled in an online catalogue within the EU FP7 project HELCATS. We statistically analyse the derived CME parameters, their mutual connection and their relation to the solar cycle.

**Results.** We show that the derived morphology of intense disk events is still systematically overestimated by up to a factor of 2 with stereoscopic modelling, which is the same order of magnitude as for observations from only one vantage point. The overestimation is very likely a combination of projection effects as well as the increased complexity of separating CME shocks and streamers from CME fronts for such events. We further show that CME mass determination of disk events can lead to overestimation of the mass by about a factor of 10 or more, in case of overlapping bright structures.

**Conclusions.** We conclude that for stereoscopic measurements of disk events, the measurement of the initial CME speed is the most reliable one. We further suggest that our presented CME speed-mass correlation is most suited to estimate the CME mass early from coronagraph observations.

## Three-part structure of a solar coronal mass ejection observed in low coronal signatures of Solar Orbiter

Tatiana **Podladchikova**<sup>1\*</sup>, Shantanu Jain<sup>1</sup>, Astrid M. Veronig<sup>2,3</sup>, Stefan Purkhart<sup>2</sup>, Galina Chikunova<sup>5,1</sup>, Karin Dissauer<sup>4</sup> and Mateja Dumbović<sup>5</sup>

A&A, 691, A344 (2024)

<https://www.aanda.org/articles/aa/pdf/2024/11/aa51777-24.pdf>

**Context.** Coronal mass ejections (CMEs) are large-scale eruptions of plasma and magnetic field from the Sun propagating through the heliosphere. Observations of the **March 28, 2022**, event provide unique images of a three-part solar CME in the low corona in active region 12975: a bright core or filament, a dark cavity, and a bright front edge.

**Aims.** We investigated the relationship between coronal dimming, filament eruption, and early CME propagation in this rarely seen case. We employed 3D filament and CME shock reconstructions along with estimations of early CME evolution inferred from the associated expansion of the coronal dimming.

**Methods.** We performed 3D reconstructions using data from Solar Orbiter, Solar TERrestrial RELations Observatory (STEREO-A), and Solar Dynamics Observatory (SDO) to analyse the path, height, and kinematics of the erupting filament. We developed the ATLAS-3D (Advanced Technique for single Line-of-sight Acquisition of Structures in 3D) method and validated it by comparing it to traditional approaches to reconstructing filament loops and the CME shock structure. ATLAS-3D uses Solar Orbiter data exclusively and integrates existing 3D filament reconstructions from the early stages of the event to establish spatial relationships between the filament and the CME frontal edge. Additionally, we employed the DIRECD method to estimate the characteristics of early CME propagation based on its coronal dimming evolution.

**Results.** The filament height increased from 28 to 616 Mm (0.04 to 0.89 R<sub>sun</sub>) over 30 minutes, from 11:05 to 11:35 UT, with a peak velocity of  $648 \pm 51 \text{ km s}^{-1}$  and a peak acceleration of  $1624 \pm 332 \text{ m s}^{-2}$ . At 11:45 UT, the filament deflected by about  $12^\circ$ , reaching a height of 841 Mm (1.21 R<sub>sun</sub>). Simultaneously, the quasi-spherical CME shock expanded from 383 to 837 Mm (0.55 to 1.2 R<sub>sun</sub>) between 11:25 and 11:35 UT. Over 10 minutes, the distance between the filament apex and the CME leading edge more than doubled, from approximately 93 to 212 Mm (0.13 to 0.3 R<sub>sun</sub>), demonstrating significant growth and increasing separation between them. Key parameters estimated from DIRECD and the 3D filament reconstructions include the CME direction (inclined by  $6^\circ$  from radial expansion), a half-width of  $21^\circ$ , and a cone height of 1.12 R<sub>sun</sub>, which was derived at the end of the dimming's impulsive phase. The reconstructed 3D CME cone, which represents the inner part of the CME, closely matches the observed filament shape at 11:45 UT in terms of both height and angular width. Validation with white-light coronagraph data confirmed the accuracy of the 3D cone, particularly in terms of filament and CME characteristics, including projections to STEREO-A COR2 times.

Conclusions. The eruptive event on March 28, 2022, showed rapid filament development and its subsequent deflection from the primary propagation direction. This confirms that connections between dimming and CME expansion can be established by the end of the dimming's impulsive phase, preceding the filament's deflection at 11:45 UT, illustrating further self-similar CME evolution. Our approach links the expanding dimming with the early CME development, highlighting dimmings as indicators and the DIRECD method's utility in correlating the 2D dimming with 3D CME structure. These findings provide valuable insights into early CME evolution and demonstrate the importance of using multi-viewpoint observations and novel reconstruction methods in space weather forecasting.

### **Three-part structure of solar coronal mass ejection observed in low coronal signatures of Solar Orbiter**

[Tatiana Podladchikova](#), [Shantanu Jain](#), [Astrid M. Veronig](#), [Stefan Purkhart](#), [Galina Chikunova](#), [Karin Dissauer](#), [Mateja Dumbovic](#)

Publication in Astronomy and Astrophysics **2024**  
?A&A 2024

<https://arxiv.org/pdf/2410.20603>

This study examines the relationship between early solar coronal mass ejection (CME) propagation, the associated filament eruption, and coronal dimming in the rare event observed on **March 28, 2022**, which featured a three-part CME in the low corona of active region AR 12975, including a bright core/filament, dark cavity, and bright front edge. We employ 3D filament and CME shock reconstructions using data from SoLO, STEREO-A, and SDO to track the filament's path, height, and kinematics. Our analysis across three viewpoints shows the outer front in SoLO/EUI 304 Å aligns with shock structures in STEREO-A/EUVI 195 Å, showing a full 3D EUV wave dome, later matching the outer CME front in STEREO-A COR2. We introduce the method ATLAS-3D (Advanced Technique for single Line-of-sight Acquisition of Structures in 3D) and validate it against traditional approaches to reconstruct CME shock using SOLO data exclusively. Additionally, we estimate early CME propagation characteristics based on coronal dimming evolution with the DIRECD method. Results indicate that the filament height increased from 28 to 616 Mm (0.04 to 0.89 Rs) within 30 minutes (11:05 to 11:35 UT), reaching peak velocity of around 648 km/s and acceleration of around 1624 m/s<sup>2</sup>. At 11:45 UT, the filament deflected by 12° to a height of 841 Mm (1.21 Rs), while the CME shock expanded from 383 to 837 Mm (0.55 to 1.2 Rs) over 10 minutes. Key parameters include a CME direction inclined by 6°, a 21° half-width, and a 1.12 Rs cone height at the dimming's impulsive phase end. This event demonstrates that expanding dimming correlates with early CME development, with the DIRECD method linking 2D dimming to 3D CME evolution. These insights underscore the value of multi-viewpoint observations and advanced reconstructions for improving space weather forecasting.

### **EXTREME ULTRAVIOLET OBSERVATIONS AND ANALYSIS OF MICRO-ERUPTIONS AND THEIR ASSOCIATED CORONAL WAVES**

O. [Podladchikova](#)<sup>1</sup>, A. Vourlidas<sup>2</sup>, R. A. M. Van der Linden<sup>1</sup>, J.-P. Wulser<sup>3</sup>, and S. Patsourakos<sup>2</sup>  
Astrophysical Journal, 709:369–376, **2010** January, **File**

The Solar Terrestrial Relations Observatory EUV telescopes have uncovered small-scale eruptive events, tentatively referred to as “mini-CMEs” because they exhibit morphologies similar to large-scale coronal mass ejections (CMEs). Coronal waves and widespread diffuse dimmings followed by the expansion of the coronal waves are the most brightly manifestations of large-scale CMEs. The high temporal and spatial resolution of the EUV data allows us to detect and analyze these eruptive events, to resolve their fine structure, and to show that the observed “mini-waves” have a strong similarity to the large-scale “EIT” waves. Here, we analyze a micro-event observed on **2007 October 17** by the Sun Earth Connection Coronal and Heliospheric Investigation EUV Imager (EUVI) in 171 Å (Fe ix) with a 2.5 minute cadence. The mini-CME differs from its large-scale counterparts by having smaller geometrical size, a shorter lifetime, and reduced intensity of coronal wave and dimmings. The small-scale coronal wave develops from micro-flaring sites and propagate up to a distance of 40,000 km in a wide angular sector of the quiet Sun over 20 minutes. The area of the small-scale dimming is two orders of magnitude smaller than for large-scale events. The average speed of the small-scale coronal wave studied is 14 km s<sup>-1</sup>. Our observations give strong indications that small-scale EUV coronal waves associated with the micro-eruptions propagate in the form of slow mode waves almost perpendicular to the background magnetic field.

### **Separating the effects of earthside and far side solar events. A case study**

Silja [Pohjolainen](#), Nasrin Talebpour Sheshvan, Christian Monstein

[Advances in Space Research](#) **2023**

<https://pdf.sciencedirectassets.com/271642/AIP/1-s2.0-S0273117723007317/main.pdf>

On **8 November 2013** a halo-type coronal mass ejection (CME) was observed, together with flares and type II radio bursts, but the association between the flares, radio bursts, and the CME was not clear. Our aim is to identify the origin of the CME and its direction of propagation, and to exclude features that were not connected to it. On the Earth-facing side, a GOES C5.7 class flare occurred close to the estimated CME launch time, followed by an X1.1 class flare. The latter flare was associated with an EUV wave and metric type II bursts. On the far side of the Sun, a filament eruption, EUV dimmings, and ejected CME loops were observed by imaging instruments onboard the Solar TERrestrial RELations Observatory (STEREO) spacecraft that were viewing the backside of the Sun. The STEREO radio instruments observed an interplanetary (IP) type II radio burst at decameter-hectometric wavelengths, which was not observed by the radio



instrument onboard the Wind spacecraft located at L1 near Earth. We show that the halo CME originated from the eruption on the far side of the Sun, and that the IP type II burst was created by a shock wave ahead of the halo CME. The radio burst remained unobserved from the earthside, even at heliocentric source heights larger than 9 solar radii. During the CME propagation, the X-class flare eruption caused a small plasmoid ejection earthward, the material of which was superposed on the earlier CME structures observed in projection. The estimated heights of the metric type II burst match well with the EUV wave launched by the X-class flare. As this radio emission did not continue to lower frequencies, we conclude that the shock wave did not propagate any further. Either the shock driver died out, as a blast wave, or the driver speed no longer exceeded the local Alfvén speed.

## **Propagation of Solar Energetic Particles during Multiple Coronal Mass Ejection Events**

Silja [Pohjolainen](#), Firas Al-Hamadani, Eino Valtonen

Solar Physics, 2015

<http://arxiv.org/pdf/1512.04881v1.pdf>

We study solar energetic particle (SEP) events during multiple solar eruptions. The analysed sequences, on **24-26 November 2000, 9-13 April 2001, and 22-25 August 2005**, consisted of halo-type coronal mass ejections (CMEs) that originated from the same active region and were associated with intense flares, EUV waves, and interplanetary (IP) radio type II and type III bursts. The first two solar events in each of these sequences showed SEP enhancements near Earth, but the third in the row did not. We observed that in these latter events the type III radio bursts were stopped at much higher frequencies than in the earlier events, indicating that the bursts did not reach the typical plasma density levels near Earth. To explain the missing third SEP event in each sequence, we suggest that the earlier-launched CMEs and the CME-driven shocks either reduced the seed particle population and thus led to inefficient particle acceleration, or that the earlier-launched CMEs and shocks changed the propagation paths or prevented the propagation of both the electron beams and SEPs, so that they did not get detected near Earth even when the shock arrivals were recorded.

**Table 5.** Close-by events that show a flare, a CME, and a decametric-hectometric (DH) type II burst, found from the list of Wind/WAVES type II bursts and CMEs at [http://cdaw.gsfc.nasa.gov/CME\\_list/radio/waves\\_type2.html](http://cdaw.gsfc.nasa.gov/CME_list/radio/waves_type2.html).

## **CMEs, Shocks and their Radio Signatures**

Silja [Pohjolainen](#)

ESPM Freiburg 2008, Presentation

Coronal mass ejections (CMEs) are large-scale transients that can be observed at a multitude of wavelengths. The dynamics of CMEs are not known in detail. In the low corona, this is partly due to the lack of imaging data and partly because other processes can mask the CME initiation and liftoff phase. Flares, filament eruptions, waves, and wave-like features often occur simultaneously with CMEs. For example, a debate exists on coronal shock waves, whether they are CME-driven or due to flares, or both. With radio emission we can trace propagating shocks, electron beams, and rising structures, and the emission source locations can reveal their origin. With radio emission we can also follow CMEs to large distances in the interplanetary space and thus obtain their full kinematics.

This [overview](#) describes some of the most recent findings from the radio signatures during CME liftoff and propagation, and discusses how well the current models on CME and shock formation agree with the observations.

## **CME Propagation Characteristics from Radio Observations**

S. [Pohjolainen](#), L. van Driel-Gesztelyi, J.L. Culhane, P.K. Manoharan, H.A. Elliott

E-print, July 2007; Solar Phys (2007) 244: 167–188

Solar Physics Topical Issue (Sun–Earth Connection), accepted July 2007

We explore the relationship among three coronal mass ejections (CMEs), observed on 28 October 2003, 7 November 2004, and 20 January 2005, the type II burst-associated shock waves in the corona and solar wind, as well as the arrival of their related shock waves and magnetic clouds at 1 AU. Using six different coronal/interplanetary density models, we calculate the speeds of shocks from the frequency drifts observed in metric and decametric radio wave data. We compare these speeds with the velocity of the CMEs as observed in the plane-of-the-sky white-light observations and calculated with a cone model for the 7 November 2004 event. We then follow the propagation of the ejecta using Interplanetary Scintillation (IPS) measurements, which were available for the 7 November 2004 and 20 January 2005 events. Finally, we calculate the travel time of the interplanetary (IP) shocks between the Sun and Earth and discuss the velocities obtained from the different data. This study highlights the difficulties in making velocity estimates that cover the full CME propagation time

## **Two successive partial mini-filament confined ejections**

M. [Poisson](#), [C. Bustos](#), [M. López Fuentes](#), [C. H. Mandrini](#), [G.D. Cristiani](#)

2019 Advances in Space Research

<https://arxiv.org/pdf/1911.00901.pdf>

Active region (AR) NOAA 11476 produced a series of confined plasma ejections, mostly accompanied by flares of X-ray class M, from **08 to 10 May 2012**. The structure and evolution of the confined ejections resemble that of EUV

surges; however, their origin is associated to the destabilization and eruption of a mini-filament, which lay along the photospheric inversion line (PIL) of a large rotating bipole. Our analysis indicate that the bipole rotation and flux cancellation along the PIL have a main role in destabilizing the structure and triggering the ejections. The observed bipole emerged within the main following AR polarity. Previous studies have analyzed and discussed in detail two events of this series in which the mini-filament erupted as a whole, one at 12:23 UT on 09 May and the other at 04:18 UT on 10 May. In this article we present the observations of the confined eruption and M4.1 flare on 09 May 2012 at 21:01 UT (SOL2012-05-09T21:01:00) and the previous activity in which the mini-filament was involved. For the analysis we use data in multiple wavelengths (UV, EUV, X-rays, and magnetograms) from space instruments. In this particular case, the mini-filament is seen to erupt in two different sections. The northern section erupted accompanied by a C1.6 flare and the southern section did it in association with the M4.1 flare. The global structure and direction of both confined ejections and the location of a far flare kernel, to where the plasma is seen to flow, suggest that both ejections and flares follow a similar underlying mechanism.

## **INFLUENCE OF SOLAR WIND HEATING FORMULATIONS ON THE PROPERTIES OF SHOCKS IN THE CORONA**

Jens [Pomoell](#), Rami Vainio

2012 ApJ 745 151

One of the challenges in constructing global magnetohydrodynamic (MHD) models of the inner heliosphere for, e.g., space weather forecasting purposes, is to correctly capture the acceleration and expansion of the solar wind. In current models, various ad hoc heating prescriptions are introduced in order to obtain a realistic steady-state solar wind solution. In this work, we demonstrate, by performing MHD simulations of erupting coronal mass ejections (CMEs) on identical solar wind solutions employing different heating formulations, that the dynamics and properties of the CME-driven shocks are significantly altered depending on the applied heating prescription. Furthermore, we show how two popular heating formulations can be altered so as to yield shock properties consistent with theory and available coronal shock observations.

## **Simulations of shock structures of a flare/CME event in the low corona**

Jens [Pomoell](#), Rami Vainio and Silja Pohjolainen

Proceedings of the International Astronomical Union / Volume 4 / Symposium S257, pp 493 – 495,

Published online: 16 Mar 2009

<http://journals.cambridge.org/action/displayIssue?iid=4866212>

We study the MHD processes related to a flare/CME event in the lower solar corona using numerical simulations. Our initial state is an isothermal gravitationally stratified corona with an embedded flux rope magnetic field structure. The eruption is driven by applying an artificial force to the flux rope. The results show that as the flux rope rises, a shock structure is formed, reaching from ahead of the flux rope all the way to the solar surface. The speed of the shock quickly exceeds that of the driving flux rope, and the shock escapes from the driver. Thus, the shock exhibits characteristics both of the driven and blast wave type. In addition, the temperature distribution behind the shock is loop-like, implying that erupting loop-like structures observed in soft X-ray images might be shocks. Finally, we note that care must be taken when performing correlation analysis of the speed and location of type II bursts and ejecta.

## **MHD modeling of coronal large-amplitude waves related to CME lift-off,**

[Pomoell](#), J., Vainio, R., and Kissmann, R.:

E-print, March 2008, **File**; Solar Phys., submitted, 2008.

We have employed a two-dimensional magnetohydrodynamic simulation code to study mass motions and large-amplitude coronal waves related to the lift-off of a coronal mass ejection (CME). The eruption of the filament is achieved by an artificial force acting on the plasma inside the flux rope. By varying the magnitude of this force, the reaction of the ambient corona to CMEs with different acceleration profiles can be studied. Our model of the ambient corona is gravitationally stratified with a quadrupolar magnetic field, resulting in an ambient Alfvén speed that increases as a function of height, as typically deduced for the low corona. The results of the simulations show that the erupting flux rope is surrounded by a shock front, which is strongest near the leading edge of the erupting mass, but also shows compression near the solar surface. For rapidly accelerating filaments, the shock front forms already in the low corona. Although the speed of the driver is less than the Alfvén speed near the top of the atmosphere, the shock survives in this region as well, but as a freely propagating wave. The leading edge of the shock becomes strong early enough to drive a metric type II burst in the corona. The speed of the weaker part of the shock front near the surface is lower corresponding to the magnetosonic speed there. We analyze the (line-of-sight) emission measure of the corona during the simulation and recognize a wave receding from the eruption site, which strongly resembles EIT waves in the low corona. Behind the EIT wave, we clearly recognize a coronal dimming, also observed during CME lift-off. We point out that the morphology of the hot downstream region of the shock would be that of a hot erupting loop, so care has to be taken not to misinterpret soft X-ray imaging observations in this respect. Finally, the geometry of the magnetic field around the erupting mass is analyzed in terms of precipitation of particles accelerated in the eruption complex. Field lines connected to the shock are further away from the photospheric neutral line below the filament than the field lines connected to the current sheet below the flux rope. Thus, if the DC fields in the current sheet accelerate predominantly electrons and the shock accelerates ions, the

geometry is consistent with recent observations of gamma rays being emitted further out from the neutral line than hard X-rays.

## **DETERMINATION OF THE HELIOSPHERIC RADIAL MAGNETIC FIELD FROM THE STANDOFF DISTANCE OF A CME-DRIVEN SHOCK OBSERVED BY THE STEREO SPACECRAFT**

Watanachak [Poomvises](#)<sup>1,2</sup>, Nat Gopalswamy<sup>1</sup>, Seiji Yashiro<sup>1,2</sup>, Ryun-Young Kwon<sup>1,2</sup>, and Oscar Olmedo **2012** ApJ 758 118, [File](#)

We report on the determination of radial magnetic field strength in the heliocentric distance range from 6 to 120 solar radii ( $R_{\odot}$ ) using data from Coronagraph 2 (COR2) and Heliospheric Imager I (HI1) instruments on board the Solar Terrestrial Relations Observatory spacecraft following the standoff-distance method of Gopalswamy & Yashiro. We measured the shock standoff distance of the **2008 April 5** coronal mass ejection (CME) and determined the flux-rope curvature by fitting the three-dimensional shape of the CME using the Graduated Cylindrical Shell model. The radial magnetic field strength is computed from the Alfvén speed and the density of the ambient medium. We also compare the derived magnetic field strength with in situ measurements made by the Helios spacecraft, which measured the magnetic field at the heliocentric distance range from 60 to 215  $R_{\odot}$ . We found that the radial magnetic field strength decreases from 28 mG at 6  $R_{\odot}$  to 0.17 mG at 120  $R_{\odot}$ . In addition, we found that the radial profile can be described by a power law.

## **CORONAL MASS EJECTION PROPAGATION AND EXPANSION IN THREE-DIMENSIONAL SPACE IN THE HELIOSPHERE BASED ON STEREO/SECCHI OBSERVATIONS**

[Poomvises](#), W., Zhang, J., & Olmedo, O.

**2010**, ApJ, 717, L159, [File](#)

We report on several new findings regarding the kinematic and morphological evolution of coronal mass ejections (CMEs) in the inner heliosphere using the unprecedented STEREO/SECCHI observations. The CME tracking is based on the three-dimensional Raytrace model, which is free of the projection effect, resulting in true CME velocities. We also measure the cross section size of the CME and hence its expansion velocity. For the four major CME events investigated, we find that their leading edge (LE) velocity converges from an initial range between 400 km s<sup>-1</sup> and 1500 km s<sup>-1</sup> at 5-10  $R_{\odot}$  to a narrow range between 500 km s<sup>-1</sup> and 750 km s<sup>-1</sup> at 50  $R_{\odot}$ . The expansion velocity is also found to converge into a narrow range between 75 km s<sup>-1</sup> and 175 km s<sup>-1</sup>. Both LE and expansion velocities are nearly constant after 50  $R_{\odot}$ . We further find that the acceleration of CMEs in the inner heliosphere from ~10 to 90  $R_{\odot}$  can be described by an exponential function, with an initial value as large as ~-80 m s<sup>-2</sup> but exponentially decreasing to almost zero (more precisely, less than  $\pm 5$  m s<sup>-2</sup> considering the uncertainty of measurements). These results provide important observational constraints on understanding CME dynamics in interplanetary space

## **How Negative Energy and Kelvin–Helmholtz Instabilities Grow by Longitudinal Waves in Solar Atmospheric Jets**

H. [Pourjavadi](#)<sup>1</sup>, S. Vasheghani Farahani<sup>2</sup>, and Z. Fazell

**2021** ApJ 918 77

<https://doi.org/10.3847/1538-4357/ac0e8f>

We model the propagation of slow magnetoacoustic body waves in solar jets in the course of negative energy wave excitation in the context of magnetohydrodynamic theory. Explicit approximate expressions are provided for the dispersion relation of slow body waves, providing insight into the influence of the steady flow speed, radiative cooling, and plasma- $\beta$  at a glance. Analytic expressions are provided regarding critical speeds in the presence of backward waves, negative energy wave speeds, and instabilities. The buildup of the Kelvin–Helmholtz instability above the negative energy wave instability is expressed through analytic expressions that provide insight into the interplay of equilibrium conditions and dispersive effects as they affect the instability growth rate of slow body waves at various altitudes. As slow magnetoacoustic waves propagate with the same speed in the long-wavelength limit, slow body kink waves experience stronger dispersion than sausage waves. Backward waves are also probable at lower steady flow speeds for medium wavelengths when the jet hosts slow body kink waves that provide greater domains for dissipative processes. Slow body sausage waves grow faster while nearing the long-wavelength limit, while the internal plasma- $\beta$  decreases the instability growth rate. The seismological aspect is that energy transfer to the external medium is observed on various timescales. The observational aspect is that slow body kink waves may exist at higher altitudes as energy has already been extracted to the external medium due to negative energy unstable slow body sausage waves in earlier stages contributing toward coronal heating.

## **Kinematics and Flare Properties of Radio-Loud CMEs**

O. [Prakash](#), S. Umapathy, A. Shanmugaraju and V. Vasanth

Solar Physics, **2012**, , 281(2), 765-777.

<https://link.springer.com/content/pdf/10.1007/s11207-012-0111-9.pdf>

A detailed analysis of the characteristics of coronal mass ejections (CMEs) and flares associated with decameter-hectometer wavelength type-II radio bursts (hereafter DH-type-II radio bursts, DH-CMEs or radio-loud CMEs) observed in the period 1997 – 2008 is presented. A sample of 61 limb events is divided into two populations based on

the residual acceleration: accelerating CMEs ( $a_r > 0$ ) and decelerating CMEs ( $a_r < 0$ ). We found that average speed (residual acceleration) of all limb DH-CMEs (called radio-loud CMEs) is nearly three (two) times greater than the average speed of the general population CMEs (radio-quiet CMEs). While the initial acceleration ( $a_i$ ) of the accelerating DH-CMEs is smaller than that of decelerating DH-CMEs (0.79 and 1.62 km s<sup>-2</sup>, respectively), the average speed and magnitude of residual acceleration of the accelerating and decelerating DH-CMEs are similar ( $\langle V_{CME} \rangle$ : 1254 km s<sup>-1</sup> and 1303 km s<sup>-1</sup>;  $\langle a_r \rangle$ : 0.026 km s<sup>-2</sup> and 0.028 km s<sup>-2</sup>, respectively). The accelerating DH-CMEs attain their peak speed at larger heights than decelerating DH-CMEs. A good positive and negative linear correlation for accelerating and decelerating DH-CMEs ( $R_a = 0.74$  and  $R_d = -0.77$ , respectively) is found. The flares associated with accelerating DH-CME events have longer rise times and decay times than flares of decelerating DH-CME. The accelerating and decelerating DH-CMEs events associated with DH-type-II bursts have similar ending frequencies. The analysis of time lags between DH-type-II start and the flare onset shows that the delays are longer in accelerating DH-CMEs than decelerating DH-CMEs ( $P \sim 7\%$ ). However, the time lags between the DH-type-II start and the CMEs onset are similar.

## Characteristics of DH type II bursts, CMEs and flares with respect to the acceleration of CMEs

[O. Prakash](#), [S. Umapathy](#), [A. Shanmugaraju](#), [P. Pappa kalaivani](#) & [Bojan Vršnak](#)  
[Astrophysics and Space Science](#) volume 337, pages47–64(2012)  
<https://link.springer.com/content/pdf/10.1007/s10509-011-0817-4.pdf>

A detailed investigation on DH-type-II radio bursts recorded in Deca-Hectometer (hereinafter DH-type-II) wavelength range and their associated CMEs observed during the year 1997–2008 is presented. The sample of 212 DH-type-II associated with CMEs are classified into three populations: (i) Group I (43 events): DH-type-II associated CMEs are accelerating in the LASCO field view ( $a > 15$  m s<sup>-2</sup>); (ii) Group II (99 events): approximately constant velocity CMEs ( $-15 < a < 15$  m s<sup>-2</sup>) and (iii) Group III (70 events): represents decelerating CMEs ( $a < -15$  m s<sup>-2</sup>). Our study consists of three steps: (i) statistical properties of DH-type-II bursts of Group I, II and III events; (ii) analysis of time lags between onsets of flares and CMEs associated with DH-type-II bursts and (iii) statistical properties of flares and CMEs of Group I, II and III events. We found statistically significant differences between the properties of DH-type-II bursts of Group I, II and III events. The significance ( $P_a$ ) is found using the one-way ANOVA-test to examine the differences between means of groups. For example, there is significant difference in the duration ( $P_a = 5\%$ ), ending frequency ( $P_a = 4\%$ ) and bandwidth ( $P_a = 4\%$ ). The accelerating and decelerating CMEs have more kinetic energy than the constant speed CMEs. There is a significant difference between the nose height of CMEs at the end time of DH-type-II ( $P_a \ll 1\%$ ). From the time delay analysis, we found: (i) there is no significant difference in the delay (flare start—DH-type-II start and flare peak—DH-type-II start); (ii) small differences in the time delay between the CME onset and DH-type-II start, delay between the flare start and CME onset times. However, there are high significant differences in: flare duration ( $P_a = 1\%$ ), flare rise time ( $P_a = 0.5\%$ ), flare decay time ( $P_a = 5\%$ ) and CMEs speed ( $P_a \ll 1\%$ ) of Group I, II and III events. The general LASCO CMEs have lower width and speeds when compared to the DH CMEs. It seems there is a strong relation between the kinetic energy of CMEs and DH-type-II properties.

## Formation of an observed eruptive flux rope above the torus instability threshold through tether-cutting magnetic reconnection

[Avijeet Prasad](#), [Sanjay Kumar](#), [Alphonse C. Sterling](#), [Ronald L. Moore](#), [Guillaume Aulanier](#), [R. Bhattacharyya](#), [Qiang Hu](#)  
A&A 677, A43 2023

<https://arxiv.org/pdf/2307.06572.pdf>  
<https://www.aanda.org/articles/aa/pdf/2023/09/aa46267-23.pdf>

Erupting magnetic flux ropes (MFRs) play a crucial role in producing solar flares. However, the formation of erupting MFRs in complex coronal magnetic configurations and their subsequent evolution in the flaring events are not fully understood. We performed an MHD simulation of active region NOAA 12241 to understand the formation of a rising MFR during the onset of an M6.9 flare on **2014 December 18**, around 21:41 UT. The MHD simulation was initialised with an extrapolated non-force-free magnetic field generated from the photospheric vector magnetogram of the active region taken a few minutes before the flare. The initial magnetic field topology displays a pre-existing sheared arcade enveloping the polarity inversion line. The simulated dynamics exhibit the movement of the oppositely directed legs of the sheared arcade field lines towards each other due to the converging Lorentz force, resulting in the onset of tether-cutting magnetic reconnection that produces an underlying flare arcade and flare ribbons. Concurrently, an MFR above the flare arcade develops inside the sheared arcade and shows a rising motion. The MFR is found to be formed in a torus-unstable region, thereby explaining its eruptive nature. Interestingly, the location and rise of the rope are in good agreement with the corresponding observations seen in EUV channels. Furthermore, the foot points of the simulation's flare arcade match well with the location of the observed parallel ribbons of the flare. The presented simulation supports the development of the MFR by the tether-cutting magnetic reconnection inside the sheared coronal arcade during flare onset. The MFR is then found to extend along the polarity inversion line (PIL) through slip-running reconnection. The MFR's eruptive nature is ascribed both to its formation in the torus-unstable region and also to the runaway tether-cutting reconnection.

## The winding number of coronal flux ropes

### I. Data-driven time-dependent magnetofrictional modelling

D. J. **Price**, J. Pomoell and E. K. J. Kilpua

A&A, 686, A197 (2024)

<https://www.aanda.org/articles/aa/pdf/2024/06/aa48409-23.pdf>

Context. Magnetic flux ropes are key structures in solar and solar-terrestrial research. Their magnetic twist is an important quantity for understanding their eruptivity, their evolution in interplanetary space, and their consequences for planetary space environments. The magnetic twist is expressed in terms of a winding number that describes how many times a field line winds about the axis of the flux rope (FR). Due to the complexity of calculating the winding number, current methods rely largely on its approximation.

Aims. We use a data-driven simulated FR to investigate the winding number  $T_g$  in comparison to the commonly used twist proxy  $T_w$ , which describes a winding of two infinitesimally close field lines. We also estimate the magnetic flux enclosed in the resultant FR(s).

Methods. We use the magnetic field analysis tools (MAFIAT) software to compute  $T_g$  and  $T_w$  for data-driven time-dependent magnetofrictional modelling of AR12473.

Results. We find that the FR boundaries can significantly differ depending on whether they are defined using the twist approximation  $T_w$  or the winding number  $T_g$ . This also significantly affects the FR structure and the estimates of the enclosed magnetic flux. For the event analysed here,  $T_g$  also reveals that the twisted flux system consists of two separate intertwined FRs.

Conclusions. The results of this study suggest that the computation of the winding number ( $T_g$ ) is important for investigations of solar FRs. **30 December, 2015**

## Predicting the Geoeffectiveness of CMEs Using Machine Learning

[Andreea-Clara Pricopi](#), [Alin Razvan Paraschiv](#), [Diana Besliu-Ionescu](#), [Anca-Nicoleta Marginean](#)

ApJ 934 176 2022

<https://arxiv.org/pdf/2206.11472.pdf>

<https://iopscience.iop.org/article/10.3847/1538-4357/ac7962/pdf>

Coronal mass ejections (CMEs) are the most geoeffective space weather phenomena, being associated with large geomagnetic storms, having the potential to cause disturbances to telecommunication, satellite network disruptions, power grid damages and failures. Thus, considering these storms' potential effects on human activities, accurate forecasts of the geoeffectiveness of CMEs are paramount. This work focuses on experimenting with different machine learning methods trained on white-light coronagraph datasets of close to sun CMEs, to estimate whether such a newly erupting ejection has the potential to induce geomagnetic activity. We developed binary classification models using logistic regression, K-Nearest Neighbors, Support Vector Machines, feed forward artificial neural networks, as well as ensemble models. At this time, we limited our forecast to exclusively use solar onset parameters, to ensure extended warning times. We discuss the main challenges of this task, namely the extreme imbalance between the number of geoeffective and ineffective events in our dataset, along with their numerous similarities and the limited number of available variables. We show that even in such conditions, adequate hit rates can be achieved with these models. **1997-01-20, 2006-07-09, 2010-12-21, 2012-05-21, 2014-04-01**

Table 1. A sample of the aggregated dataset used for this work

Table 8. Example false negatives predicted by the ensemble model on the test set

## Chromospheric and coronal heating and jet acceleration due to reconnection driven by flux cancellation. I. At a three-dimensional current sheet

[E. R. Priest](#), [P. Syntelis](#)

A&A 2021

<https://arxiv.org/pdf/2101.04600.pdf>

Context. The recent discovery of much greater magnetic flux cancellation taking place at the photosphere than previously realised has led us in our previous works to suggest magnetic reconnection driven by flux cancellation as the cause of a wide range of dynamic phenomena, including jets of various kinds and solar atmospheric heating. Aims.

Previously, the theory considered energy release at a two-dimensional current sheet. Here we develop the theory further by extending it to an axisymmetric current sheet in three dimensions without resorting to complex variable theory.

Methods. We analytically study reconnection and treat the current sheet as a three-dimensional structure. We apply the theory to the cancellation of two fragments of equal but opposite flux that approach each other and are located in an overlying horizontal magnetic field. Results. The energy release occurs in two phases. During Phase 1, a separator is formed and reconnection is driven at it as it rises to a maximum height and then moves back down to the photosphere, heating the plasma and accelerating a plasma jet as it does so. During Phase 2 the fluxes cancel in the photosphere and accelerate a mixture of cool and hot plasma upwards.

## The Creation of Twist by Reconnection of Flux Tubes

E. R. **Priest** & [D. W. Longcope](#)

*Solar Physics* volume 295, Article number: 48 (2020)

<https://link.springer.com/content/pdf/10.1007/s11207-020-01608-0.pdf>

[sci-hub.si/10.1007/s11207-020-01608-0](https://sci-hub.si/10.1007/s11207-020-01608-0)

A fundamental process in a plasma is the magnetic reconnection of one pair of flux tubes (such as solar coronal loops) to produce a new pair. During this process magnetic helicity is conserved, but mutual helicity can be transformed to self-helicity, so that the new tubes acquire twist. However, until recently, when Wright (Astrophys. J. 878, 102, 2019) supplied a solution, the partition of self-helicity between the two tubes was an outstanding puzzle. Here we examine Wright's result in detail and apply it to a variety of cases. The simplest case, which Wright himself used to illustrate the result, is that of thin ribbons or flux sheets. We first explicitly apply his method to the usually expected standard case (when the tubes approach one another without twisting before reconnection) and confirm his result is valid for flux sheaths and tubes as well as sheets.

For the reconnection of sheets, it is shown that the orientation of the sheets needs to be chosen carefully. For flux sheaths and tubes, Wright's results are demonstrated to hold for the standard case. There is both a local and a global aspect to the effect of reconnection. The local effect of reconnection is to produce an equipartition of the added self-helicity (and therefore of twist), but the extra global effect of the location and orientation of the feet of the sheet, shell or tube in general adds different amounts of magnetic helicity to the two structures.

It is important, as Wright realized, to account for any twist or writhe already existing in the fluxes prior to reconnection. Here we show explicitly that, if a section of a flux sheet is twisted by a multiple of  $\pi$  with its ends held fixed and is then reconnected with another sheet, then the effect of the reconnection is to add that multiple of  $\pi$  to one sheet and subtract it from the other, while conserving the total helicity. If, on the other hand, the central part of a flux sheath is twisted before reconnection by any angle, then the effect of reconnection is to add that amount of twist to one sheath and subtract it from the other, while conserving the total helicity. Thus, for the local part of the process in both sheets and sheaths, there is no longer helicity equipartition

## **Flux-Rope Twist in Eruptive Flares and CMEs: due to Zipper and Main-Phase Reconnection**

Eric **Priest**, Dana Longcope

Solar Phys. 292:25 2017

<https://arxiv.org/pdf/1701.00147v1.pdf>

The nature of three-dimensional reconnection when a twisted flux tube erupts during an eruptive flare or coronal mass ejection is considered. The reconnection has two phases: first of all, 3D "zipper reconnection" propagates along the initial coronal arcade, parallel to the polarity inversion line (PIL), then subsequent quasi-2D "main phase reconnection" in the low corona around a flux rope during its eruption produces coronal loops and chromospheric ribbons that propagate away from the PIL in a direction normal to it.

One scenario starts with a sheared arcade: the zipper reconnection creates a twisted flux rope of roughly one turn ( $2\pi$  radians of twist), and then main phase reconnection builds up the bulk of the erupting flux rope with a relatively uniform twist of a few turns. A second scenario starts with a pre-existing flux rope under the arcade. Here the zipper phase can create a core with many turns that depend on the ratio of the magnetic fluxes in the newly formed flare ribbons and the new flux rope. Main phase reconnection then adds a layer of roughly uniform twist to the twisted central core. Both phases and scenarios are modeled in a simple way that assumes the initial magnetic flux is fragmented along the PIL. The model uses conservation of magnetic helicity and flux, together with equipartition of magnetic helicity, to deduce the twist of the erupting flux rope in terms the geometry of the initial configuration. Interplanetary observations show some flux ropes have a fairly uniform twist, which could be produced when the zipper phase and any pre-existing flux rope possess small or moderate twist (up to one or two turns). Other interplanetary flux ropes have highly twisted cores (up to five turns), which could be produced when there is a pre-existing flux rope and an active zipper phase that creates substantial extra twist.

## **Evolution of Magnetic Helicity During Eruptive Flares and Coronal Mass Ejections**

Eric **Priest**, Dana Longcope, Miho Janvier

Solar Phys. Volume 291, **Issue 7**, pp 2017–2036 2016

<http://arxiv.org/pdf/1607.03874v1.pdf>

During eruptive solar flares and coronal mass ejections, a non-potential magnetic arcade with much excess magnetic energy goes unstable and reconnects. It produces a twisted erupting flux rope and leaves behind a sheared arcade of hot coronal loops. We suggest that: the twist of the erupting flux rope can be determined from conservation of magnetic flux and magnetic helicity and equipartition of magnetic helicity. It depends on the geometry of the initial pre-eruptive structure.

Two cases are considered, in the first of which a flux rope is not present initially but is created during the eruption by the reconnection. In the second case, a flux rope is present under the arcade in the pre-eruptive state, and the effect of the eruption and reconnection is to add an amount of magnetic helicity that depends on the fluxes of the rope and arcade and the geometry.

## **Twisted versus braided magnetic flux ropes in coronal geometry**

### **II. Comparative behaviour**

C. **Prior** and A. R. Yeates

A&A 591, A16 (2016)

<http://www.aanda.org/articles/aa/pdf/2016/07/aa28053-15.pdf>

**Aims.** Sigmoidal structures in the solar corona are commonly associated with magnetic flux ropes whose magnetic field lines are twisted about a mutual axis. Their dynamical evolution is well studied, with sufficient twisting leading to large-scale rotation (writhing) and vertical expansion, possibly leading to ejection. Here, we investigate the behaviour of flux ropes whose field lines have more complex entangled/braided configurations. Our hypothesis is that this internal structure will inhibit the large-scale morphological changes. Additionally, we investigate the influence of the background field within which the rope is embedded.

**Methods.** A technique for generating tubular magnetic fields with arbitrary axial geometry and internal structure, introduced in part I of this study, provides the initial conditions for resistive-MHD simulations. The tubular fields are embedded in a linear force-free background, and we consider various internal structures for the tubular field, including both twisted and braided topologies. These embedded flux ropes are then evolved using a 3D MHD code.

**Results.** Firstly, in a background where twisted flux ropes evolve through the expected non-linear writhing and vertical expansion, we find that flux ropes with sufficiently braided/entangled interiors show no such large-scale changes. Secondly, embedding a twisted flux rope in a background field with a sigmoidal inversion line leads to eventual reversal of the large-scale rotation. Thirdly, in some cases a braided flux rope splits due to reconnection into two twisted flux ropes of opposing chirality – a phenomenon previously observed in cylindrical configurations.

**Conclusions.** Sufficiently complex entanglement of the magnetic field lines within a flux rope can suppress large-scale morphological changes of its axis, with magnetic energy reduced instead through reconnection and expansion. The structure of the background magnetic field can significantly affect the changing morphology of a flux rope.

## **Twisted versus braided magnetic flux ropes in coronal geometry**

### **I. Construction and relaxation**

C. **Prior** and A. R. Yeates

A&A 587, A125 (2016)

We introduce a technique for generating tubular magnetic fields with arbitrary axial geometry and internal topology. As an initial application, this technique is used to construct two magnetic flux ropes that have the same sigmoidal tubular shape, but have different internal structures. One is twisted, the other has a more complex braided magnetic field. The flux ropes are embedded above the photospheric neutral line in a quadrupolar linear force-free background. Using resistive-magnetohydrodynamic simulations, we show that both fields can relax to stable force-free equilibria whilst maintaining their tubular structure. Both end states are nonlinear force-free; the twisted field contains a single sign of alpha (the force-free parameter), indicating a twisted flux rope of a single dominant chirality, the braided field contains both signs of alpha, indicating a flux rope whose internal twisting has both positive and negative chirality. The electric current structures in these final states differ significantly between the braided field, which has a diffuse structure, and the twisted field, which displays a clear sigmoid. This difference might be observable.

## **Exploring the coronal evolution of AR 12473 using time-dependent, data-driven magnetofrictional modelling\***

D. J. **Price**, J. Pomoell and E. K. J. Kilpua

A&A 644, A28 (2020)

<https://doi.org/10.1051/0004-6361/202038925>

<https://www.aanda.org/articles/aa/pdf/2020/12/aa38925-20.pdf>

**Aims.** We present a detailed examination of the magnetic evolution of AR 12473 using time-dependent, data-driven magnetofrictional modelling.

**Methods.** We used maps of the photospheric electric field inverted from vector magnetogram observations, obtained by the Helioseismic and Magnetic Imager onboard the Solar Dynamics Observatory (SDO), to drive our fully time-dependent, data-driven magnetofrictional model. Our modelled field was directly compared to extreme ultraviolet observations from the Atmospheric Imaging Assembly, also onboard SDO. Metrics were also computed to provide a quantitative analysis of the evolution of the magnetic field.

**Results.** The flux rope associated with the eruption on **28 December 2015** from AR 12473 was reproduced by the simulation and found to have erupted due to a torus instability.

**Erratum:** A&A 653, C1 (2021) <https://www.aanda.org/articles/aa/pdf/2021/09/aa38925e-20.pdf>

## **Chromospheric and coronal heating and jet acceleration due to reconnection driven by flux cancellation. I. At a three-dimensional current sheet**

**E. R. Priest**, **P. Syntelis**

A&A 647, A31 2021

<https://arxiv.org/pdf/2101.04600.pdf>

<https://doi.org/10.1051/0004-6361/202038917>

**Context.** The recent discovery of much greater magnetic flux cancellation taking place at the photosphere than previously realised has led us in our previous works to suggest magnetic reconnection driven by flux cancellation as the cause of a wide range of dynamic phenomena, including jets of various kinds and solar atmospheric heating. **Aims.**

Previously, the theory considered energy release at a two-dimensional current sheet. Here we develop the theory further by extending it to an axisymmetric current sheet in three dimensions without resorting to complex variable theory.

**Methods.** We analytically study reconnection and treat the current sheet as a three-dimensional structure. We apply the

theory to the cancellation of two fragments of equal but opposite flux that approach each other and are located in an overlying horizontal magnetic field. Results. The energy release occurs in two phases. During Phase 1, a separator is formed and reconnection is driven at it as it rises to a maximum height and then moves back down to the photosphere, heating the plasma and accelerating a plasma jet as it does so. During Phase 2 the fluxes cancel in the photosphere and accelerate a mixture of cool and hot plasma upwards.

### **An Investigation of the CME of 3 November 2011 and Its Associated Widespread Solar Energetic Particle Event**

A. J. **Prise**, L. K. Harra, S. A. Matthews, D. M. Long, A. D. Aylward  
Solar Physics, May 2014, Volume 289, Issue 5, pp 1731-1744

<http://arxiv.org/pdf/1312.2965v1.pdf>

<http://www.jodrellbank.manchester.ac.uk/meetings/nam2012/archive/SPI/Prise.pdf>

Multi-spacecraft observations are used to study the in-situ effects of a large coronal mass ejection (CME) erupting from the farside of the Sun on 3 November 2011, with particular emphasis on the associated solar energetic particle (SEP) event. At that time both Solar Terrestrial Relations Observatory (STEREO) spacecraft were located more than 90 degrees from Earth and could observe the CME eruption directly, with the CME visible on-disk from STEREO-B and off the limb from STEREO-A. Signatures of pressure variations in the corona such as deflected streamers were seen, indicating the presence of a coronal shock associated with this CME eruption. The evolution of the CME and an associated extreme-ultraviolet (EUV) wave were studied using EUV and coronagraph images. It was found that the lateral expansion of the CME low in the corona closely tracked the propagation of the **EUV wave**, with measured velocities of  $240 \pm 19 \text{ km s}^{-1}$  and  $221 \pm 15 \text{ km s}^{-1}$  for the CME and wave, respectively. Solar energetic particles were observed to arrive first at STEREO-A, followed by electrons at the Wind spacecraft at L1, then STEREO-B, and finally protons arrived simultaneously at Wind and STEREO-B. By carrying out a velocity-dispersion analysis on the particles arriving at each location, it was found that energetic particles arriving at STEREO-A were released first and that the release of particles arriving at STEREO-B was delayed by about 50 minutes. Analysis of the expansion of the CME to a wider longitude range indicates that this delay is a result of the time taken for the CME edge to reach the footpoints of the magnetic-field lines connected to STEREO-B. The CME expansion is not seen to reach the magnetic footpoint of Wind at the time of solar-particle release for the particles detected here, suggesting that these particles may not be associated with this CME.

### **Data processing of Visible Emission Line Coronagraph Onboard ADITYA L1**

**Muthu Priyal**, **Jagdev Singh**, **B. Raghavendra Prasad**, **Chavali Sumana**, **Varun Kumar**, +++

Advances in Space Research (2023)

<https://arxiv.org/pdf/2307.03173.pdf>

ADITYA-L1 is India's first dedicated mission to observe the sun and its atmosphere from a halo orbit around L1 point. Visible emission line coronagraph (VELC) is the prime payload on board at Aditya-L1 to observe the sun's corona. VELC is designed as an internally occulted reflective coronagraph to meet the observational requirements of wide wavelength band and close to the solar limb (1.05 Ro). Images of the solar corona in continuum and spectra in three emission lines 5303Å [Fe xiv], 7892Å [Fe xi] and 10747 [Fe xiii] obtained with high cadence to be analyzed using software algorithms automatically. A reasonable part of observations will be made in synoptic mode, those, need to be analyzed and results made available for public use. The procedure involves the calibration of instrument and detectors, converting the images into fits format, correcting the images and spectra for the instrumental effects, align the images etc. Then, develop image processing algorithms to detect the occurrence of energetic events using continuum images. Also derive physical parameters, such as temperature and velocity structure of solar corona using emission line observations. Here, we describe the calibration of detectors and the development of software algorithms to detect the occurrence of CMEs and analyze the spectroscopic data.

### **Automatic Determination of the Conic Coronal Mass Ejection Model Parameters**

A. **Pulkkinen**, T. Oates & A. Taktakishvili

Solar Physics, Volume 261, Number 1, Page: 115 – 126, 2010, **FILE**

Characterization of the three-dimensional structure of solar transients using incomplete plane of sky data is a difficult problem whose solutions have potential for societal benefit in terms of space weather applications. In this paper transients are characterized in three dimensions by means of conic coronal mass ejection (CME) approximation. A novel method for the automatic determination of cone model parameters from observed halo CMEs is introduced. The method uses both standard image processing techniques to extract the CME mass from white-light coronagraph images and a novel inversion routine providing the final cone parameters. A bootstrap technique is used to provide model parameter distributions. When combined with heliospheric modeling, the cone model parameter distributions will provide direct means for ensemble predictions of transient propagation in the heliosphere.

An initial validation of the automatic method is carried by comparison to manually determined cone model parameters. It is shown using 14 halo CME events that there is reasonable agreement, especially between the heliocentric locations of the cones derived with the two methods. It is argued that both the heliocentric locations and the opening half-angles of the automatically determined cones may be more realistic than those obtained from the manual analysis.



## Multipoint study of the rapid filament evolution during a confined C2 flare on 28 March 2022, leading to eruption

[Stefan Purkhart](#), [Astrid M. Veronig](#), [Bernhard Kliem](#), [Robert Jarolim](#), [Karin Dissauer](#), [Ewan C. M. Dickson](#), [Tatiana Podladchikova](#), [Säm Krucker](#)

A&A 689, A259 2024

<https://arxiv.org/pdf/2407.07777>

<https://www.aanda.org/articles/aa/pdf/2024/09/aa50092-24.pdf>

We studied the rapid filament evolution in AR 12975 during a confined C2 flare on 28 March 2022, which led to an eruptive M4 flare 1.5 h later. It is characterized by the breakup of the filament, the disappearance of its southern half, and the flow of the remaining plasma into a longer channel with a topology similar to an EUV hot channel during the flare. Our multipoint study takes advantage of Solar Orbiter's position at 0.33 AU and 83.5° west of the Sun-Earth line. STIX and EUVI onboard Solar Orbiter observed the event at the limb. AIA and HMI onboard SDO provided on-disk observations from which we derived DEM maps and NLFF magnetic field extrapolations. We find that both filament channels likely existed in close proximity before the flare. Based on field structures associated with AIA 1600 Å flare ribbons and kernels, we propose a loop-loop reconnection scenario between field lines that surround and pass beneath the shorter filament channel, and field lines following a portion of the longer channel. Reconnection occurs in an essentially vertical current sheet at a PIL below the breakup region, leading to the formation of the flare loop arcade and the EUV hot channel. The scenario is supported by concentrated currents and free magnetic energy built up by antiparallel flows along the PIL before the flare. The reconnection probably propagated to involve the original filament itself, leading to its breakup and reformation. The reconnection geometry provides a general mechanism for the formation of the long filament channel and realizes the concept of tether cutting, which was active throughout the filament's rise phase, lasting from at least 30 min before the C2 flare until the eruption. The C2 flare represents a period of fast reconnection during this otherwise more steady process, during which most of the original filament was reconnected and joined the longer channel.

## Automated Prediction of CMEs Using Machine Learning of CME– Flare Associations

R. [Qahwaji](#) · T. Colak · M. Al-Omari · S. Ipson

Solar Phys (2008) 248: 471–483

<http://www.springerlink.com/content/t457311218p25315/fulltext.pdf>

Machine-learning algorithms are applied to explore the relation between significant flares and their associated CMEs. The NGDC flares catalogue and the SOHO/LASCO CME catalogue are processed to associate X and M-class flares with CMEs based on timing information. Automated systems are created to process and associate years of flare and CME data, which are later arranged in numerical-training vectors and fed to machine-learning algorithms to extract the embedded knowledge and provide learning rules that can be used for the automated prediction of CMEs. Properties representing the intensity, flare duration, and duration of decline and duration of growth are extracted from all the associated (A) and not-associated (NA) flares and converted to a numerical format that is suitable for machine-learning use. The machine-learning algorithms Cascade Correlation Neural Networks (CCNN) and Support Vector Machines (SVM) are used and compared in our work. The machine-learning systems predict, from the input of a flare's properties, if the flare is likely to initiate a CME. Intensive experiments using Jack-knife techniques are carried out and the relationships between flare properties and CMEs are investigated using the results. The predictive performance of SVM and CCNN is analysed and recommendations for enhancing the performance are provided.

## Statistical properties of H $\alpha$ jets in the polar coronal hole and their implications in coronal activities

[Youqian Qi](#), [Zhenghua Huang](#), [Lidong Xia](#), [Hui Fu](#), [Mingzhe Guo](#), [Zhenyong Hou](#), [Weixin Liu](#), [Mingzhe Sun](#), [Dayang Liu](#)

A&A 657, A118 2022

<https://arxiv.org/pdf/2110.15543>

<https://doi.org/10.1051/0004-6361/202141401>

<https://www.aanda.org/articles/aa/pdf/2022/01/aa41401-21.pdf>

Dynamic features, such as chromospheric jets, transition region network jets, coronal plumes and coronal jets, are abundant in the network regions of the solar polar coronal holes. We investigate the relationship between chromospheric jets and coronal activities (e.g., coronal plumes and jets). We analyze observations of a polar coronal hole including the filtergrams that were taken by the New Vacuum Solar Telescope (NVST) at the H $\alpha$ -0.6 Å to study the H $\alpha$  jets, and the Atmospheric Imaging Assembly (AIA) 171 Å images to follow the evolution of coronal activities. H $\alpha$  jets are persistent in the network regions, only some regions (denoted as R1-R5) are rooted with discernible coronal plumes. With an automated method, we identify and track 1320 H $\alpha$  jets in the network regions. We find that the average lifetime, height and ascending speed of the H $\alpha$  jets are 75.38 s, 2.67 Mm, 65.60 km s $^{-1}$ , respectively. The H $\alpha$  jets rooted in R1-R5 are higher and faster than those in the others. We also find that propagating disturbances (PDs) in coronal plumes have a close connection with the H $\alpha$  jets. The speeds of 28 out of 29 H $\alpha$  jets associated with PDs are about 50 km s $^{-1}$ . In a case of coronal jet, we find that the speeds of both the coronal jet and the H $\alpha$  jet are over 150 km s $^{-1}$ , suggesting that both cool and hot jets can be coupled together. Based on our analyses, it is evident that more dynamic H $\alpha$  jets could release the energies to the corona,

which might be the results of the development of Kelvin-Helmholtz instability (KHi) or small-scaled magnetic activities. We suggest that chromospheric jets, transition region network jets and ray-like features in the corona are coherent phenomena, and they are important tunnels for cycling energy and mass in the solar atmosphere.

### **Tracing Field Lines That Are Reconnecting or Expanding or Both**

[Jiong Qiu](#)

Frontiers in Astronomy and Space Sciences, vol. 11, id. 1401846,  
2024

<https://doi.org/10.3389/fspas.2024.1401846>

<https://arxiv.org/pdf/2409.04573>

Explosive energy release in the solar atmosphere is driven magnetically, but mechanisms triggering the onset of the eruption remain in debate. In the case of flares and CMEs, ideal or non-ideal instabilities usually occur in the corona, but direct observations and diagnostics there are difficult to obtain. To overcome this difficulty, we analyze observational signatures in the upper chromosphere or transition region, in particular, brightenings and dimmings at the feet of coronal magnetic structures. In this paper, we examine the time evolution of spatially resolved light curves in two eruptive flares, and identify a variety of tempo-spatial sequences of brightenings and dimmings, such as dimming followed by brightening, and dimming preceded by brightening. These brightening-dimming sequences are indicative of the configuration of energy release in the form of plasma heating or bulk motion. We demonstrate the potential of using these analyses to diagnose properties of magnetic reconnection and plasma expansion in the corona during the early stage of the eruption. **2011 June 21, 2012-07-12**

### **Three-dimensional velocity fields of the solar filament eruptions detected by CHASE**

[Ye Qiu](#), [Chuan Li](#), [Yang Guo](#), [Zhen Li](#), [Mingde Ding](#), [Linggao Kong](#)

ApJ **2024**

<https://arxiv.org/pdf/2401.16730.pdf>

The eruption of solar filaments, also known as prominences appearing off-limb, is a common phenomenon in the solar atmosphere. It ejects massive plasma and high-energy particles into interplanetary space, disturbing the solar-terrestrial environment. It is vital to obtain the three-dimensional velocity fields of erupting filaments for space-weather predictions. We derive the three-dimensional kinematics of an off-limb prominence and an on-disk filament, respectively, using the full-disk spectral and imaging data detected by the Chinese H $\alpha$  Solar Explorer (CHASE). It is found that both the prominence and the filament experience a fast semicircle-shaped expansion at first. The prominence keeps propagating outward with an increasing velocity until escaping successfully, whereas the south leg of the prominence finally moves back to the Sun in a swirling manner. For the filament, the internal plasma falls back to the Sun associated with an anticlockwise rotation in the late ejection, matching the failed eruption without a coronal mass ejection. During the eruptions, both the prominence and the filament show material splitting along the line-of-sight direction, revealed by the bimodal H $\alpha$  spectral profiles. For the prominence, the splitting begins at the top and gradually spreads to almost the whole prominence with a fast blue-shift component and a slow red-shift component. The material splitting in the filament is more fragmental. As shown by the present results, the CHASE full-disk spectroscopic observations make it possible to systematically study the three-dimensional kinematics of solar filament eruptions. **2022 August 17, 2023 May 8**

### **The Magnetic Topology and Eruption Mechanism of a Multiple-ribbon Flare**

[Ye Qiu](#), [Yang Guo](#), [M. D. Ding](#), [Ze Zhong](#)

ApJ **901** 13 **2020**

<https://arxiv.org/pdf/2008.08866.pdf>

<https://doi.org/10.3847/1538-4357/abae5b>

Multiple-ribbon flares are usually complex in their magnetic topologies and eruption mechanisms. In this paper, we investigate an X2.1 flare (SOL2015-03-11T16:22) that occurred in active region 12297 near the center of the solar disk by both potential and nonlinear force-free field models extrapolated with the data observed by the Helioseismic and Magnetic Imager (HMI) on board Solar Dynamics Observatory (SDO). We calculate the three-dimensional squashing degree distribution. The results reveal that there are two flux ropes in this active region, covered by a large scale hyperbolic flux tube (HFT), which is the intersection of quasi-separatrix layers with a null point embedded in it. When the background magnetic field diminishes due to the separation of the northwest dipole and the flux cancellation, the central flux rope rises up forming the two brightest central ribbons. It then squeezes the upper lying HFT structure to generate further brightenings. This very energetic flare with a complex shape is accompanied by a coronal mass ejection (CME). We adopt the simplified line-tied force-balance equation of the current ring model and assign the observed value of the decay index to the equation to simulate the acceleration profile of the CME in the early stage. It is found that the path with an inclination of 45° from radial best fits the profile of the actual acceleration.

### **Gradual Solar Coronal Dimming and Evolution of Coronal Mass Ejection in the Early Phase**

[Jiong Qiu](#)<sup>1</sup> and [Jianxia Cheng](#)

2017 ApJL 838 L6

<http://sci-hub.cc/10.3847/2041-8213/aa6798>

<https://arxiv.org/pdf/1707.02480.pdf>

Weak gradual dimming persists for more than half an hour before the onset of the two-ribbon flare and the fast rise of the CME. It is followed by abrupt rapid dimming. The two-stage dimming occurs in a pair of conjugate dimming regions adjacent to the two flare ribbons, and the flare onset marks the transition between the two stages of dimming. At the onset of the two-ribbon flare, transient brightenings are also observed inside the dimming regions, before rapid dimming occurs at the same places. These observations suggest that the CME structure, most probably anchored at the twin dimming regions, undergoes a slow rise before the flare onset, and its kinematic evolution has significantly changed at the onset of flare reconnection. We explore diagnostics of the CME evolution in the early phase with analysis of the gradual dimming signatures prior to the CME eruption. **2011 December 26**

## **ON THE MAGNETIC FLUX BUDGET IN LOW-CORONA MAGNETIC RECONNECTION AND INTERPLANETARY CORONAL MASS EJECTIONS**

Jiong **Qiu**,<sup>1</sup> Qiang Hu,<sup>2</sup> Timothy A. Howard,<sup>1</sup> and Vasyli B. Yurchyshyn<sup>3</sup>  
The Astrophysical Journal, 659:758Y772, 2007

We present the first quantitative comparison between the total magnetic reconnection flux in the low corona in the wake of coronal mass ejections (CMEs) and the magnetic flux in magnetic clouds (MCs) that reach 1 AU 2Y3 days after CME onset. The total reconnection flux is measured from flare ribbons, and the MC flux is computed using in situ observations at 1 AU, all ranging from  $10^{20}$  to  $10^{22}$  Mx. It is found that for the nine studied events in which the association between flares, CMEs, and MCs is identified, the MC flux is correlated with the total reconnection flux  $\Phi_r$ . Further, the poloidal (azimuthal) MC flux  $\Phi_p$  is comparable with the reconnection flux  $\Phi_r$ , and the toroidal (axial) MC flux  $\Phi_t$  is a fraction of  $\Phi_r$ . Events associated with filament eruption do not exhibit a different  $\Phi_t, \Phi_p - \Phi_r$  relation from events not accompanied by erupting filaments. The relations revealed between these independently measured physical quantities suggest that for the studied samples, the magnetic flux and twist of interplanetary magnetic flux ropes, reflected by MCs, are highly relevant to low-corona magnetic reconnection during the eruption. We discuss the implications of this result for the formation mechanism of twisted magnetic flux ropes, namely, whether the helical structure of the magnetic flux rope is largely pre-existing or formed in situ by low-corona magnetic reconnection. **We also measure magnetic flux encompassed in coronal dimming regions ( $\Phi_d$ ) and discuss its relation to the reconnection flux inferred from flare ribbons and MC flux.**

## **Magnetic Reconnection Flux and Coronal Mass Ejection Velocity,**

**Qiu, J.**, and Yurchyshyn, V. B. (2005),  
*Astrophys. J.*, 634, L121–L124. **File**

a strong correlation between CME speeds and the reconnected magnetic flux in two-ribbon flares  
We explore the relationship between the total reconnection flux  $\Phi_{rec}$  estimated from flare observations and the velocity  $V_{CME}$  of coronal mass ejections (CMEs) observed with the Large Angle and Spectrometric Coronagraph (LASCO) Experiment. Our study includes 13 events with varying magnetic configurations in source regions. It is shown that  $V_{CME}$  is proportional to  $\Phi_{rec}$ , with a linear cross-correlation of 89% and confidence level greater than 99.5%. This result confirms the importance of magnetic flux transferred by magnetic reconnection in the early stage of fast CMEs. On the other hand, the CME velocity and kinematic energy are probably independent of magnetic configurations of source regions.

## **Observations of a Fast-mode Magnetosonic Wave Propagating along a Curving Coronal Loop on 2011 November 11**

Z. N. **Qu**<sup>1,2</sup>, L. Q. Jiang<sup>1</sup>, and S. L. Chen  
2017 ApJ 851 41

<http://iopscience.iop.org/article/10.3847/1538-4357/aa9beb/pdf>

The detailed analysis of an interesting quasi-periodic fast-propagating (QFP) magnetosonic wave is presented using high-resolution observations taken by the Solar Dynamic Observatory. The QFP wave occurred over the west solar limb during the fast eruption phase of a nearby prominence. It propagated along a group of curving coronal loop and manifested two types of wave trains that showed different morphologies and propagation characteristics. The wavefronts of the first type wave trains are relatively broad, and they changed their propagation direction when they pass through the turning part of the guiding loop. On the contrary, the wavefronts of the other type wave trains are narrow, and their propagation did not affected by geometric changes of the guiding loop. Measurements indicate that the average speeds of the broad (narrow) wave trains is  $305(343) \text{ km s}^{-1}$ , and the period of the wave trains ranges from 54 to 458 s. We propose that the narrow wave trains may manifest the leakage of the wave trains from the guiding coronal loop, or were guided by another group of invisible coronal loop. In addition, the projection effect and weak magnetic field strength of the guiding coronal loop are proposed to explain the slow wave speed.

## **Polarimetric Properties of Flux Ropes and Sheared Arcades in Coronal Prominence Cavities**

L.A. **Rachmeler** · S.E. Gibson · J.B. Dove · C.R. DeVore · Y. Fan  
Solar Phys., 2013

The coronal magnetic field is the primary driver of solar dynamic events. Linear and circular polarization signals of certain infrared coronal emission lines contain information about the magnetic field, and to access this information either a forward or an inversion method must be used. We study three coronal magnetic configurations that are applicable to polar-crown filament cavities by doing forward calculations to produce synthetic polarization data. We analyze these forward data to determine the distinguishing characteristics of each model. We conclude that it is possible to distinguish between cylindrical flux ropes, **spheromak flux ropes**, and sheared arcades using coronal polarization measurements. If one of these models is found to be consistent with observational measurements, it will mean positive identification of the magnetic morphology that surrounds certain quiescent filaments, which will lead to a better understanding of how they form and why they erupt.

## **RECONNECTIONLESS CME ERUPTION: PUTTING THE ALY–STURROCK CONJECTURE TO REST**

L. A. **Rachmeler**, C. E. DeForest<sup>2</sup>, and C. C. Kankelborg<sup>3</sup>

Astrophysical Journal, 693:1431–1436, 2009 March

<http://www.iop.org/EJ/toc/-alert=43190/0004-637X/693/2>

We demonstrate that magnetic reconnection is not necessary to initiate fast Coronal mass ejections (CMEs). The Aly–Sturrock conjecture states that the magnetic energy of a given force-free boundary field is maximized when the field is open. This is problematic for CME initiation because it leaves little or no magnetic energy to drive the eruption, unless reconnection is present to allow some of the flux to escape without opening. Thus, it has been thought that reconnection must be present to initiate CMEs. This theory has not been subject to rigorous numerical testing because conventional magnetohydrodynamics (MHD) numerical models contain numerical diffusion, which introduces uncontrolled numerical reconnection. We use a quasi-Lagrangian simulation technique to run the first controlled experiments of CME initiation in the complete lack of reconnection. We find that a flux rope confined by an arcade, when twisted beyond a critical amount, can escape to an open state, allowing some of the surrounding arcade to shrink, and releasing magnetic energy from the global field. This mechanism includes a true ideal MHD instability. We conclude that reconnection is not a necessary trigger for fast CME eruptions.

## **Evidence for internal tether-cutting in a flare/CME observed by MESSENGER, RHESSI and STEREO**

Claire L. **Raftery**, Peter T. Gallagher, R. T. James McAteer, Chia-Hsien Lin, Gareth Delahunt

E-print, July 27, 2010 ApJ 721 1579, **File**

The relationship between eruptive flares and coronal mass ejections (CME) is a topic of ongoing debate, especially regarding the possibility of a common initiation mechanism. We studied the kinematic and hydrodynamic properties of a well-observed event that occurred on **2007 December 31** using data from MESSENGER, RHESSI and STEREO, in order to gain new physical insight into the evolution of the flare and CME. The initiation mechanism was determined by comparing observations to the internal tether-cutting, breakout and ideal MHD models. Evidence of pre-eruption reconnection immediately eliminated the ideal MHD model. The timing and location of the soft and hard X-ray sources led to the conclusion that the event was initiated by the internal tether-cutting mechanism. In addition, a thermal source was observed to move in a downward direction during the impulsive phase of the event, followed by upwards motion during the decay phase, providing evidence for X- to Y-type magnetic reconnection

## **The energy exchange mechanism in large-scale magnetic plasmoids collision**

Anil **Raghav**, [Ankita Kule](#)

2017

<https://arxiv.org/pdf/1710.05755.pdf>

Recently, a super-elastic collision of large-scale plasmoids i.e. solar coronal mass ejections (CMEs) has been observed and further supported by numerical simulations. However, the energy gain by the system in the collision process is not clear. In-fact during plasmoids collision process, the energy exchange mechanism is still a chronic issue. Here, we present conclusive in situ evidence of sunward torsional Alfvén waves in the magnetic cloud after the super-elastic collision of the largest plasmoids in the heliosphere. We conclude that magnetic reconnection and Alfvén waves are the possible energy exchange mechanism during plasmoids interaction.

## **Conditions for Chromospheric Plasma Acceleration or Trigger of Chromospheric Mass Ejections by Magnetic-field-aligned Electric Fields**

B. R. **Ragot**

2020 ApJ 897 76

<https://doi.org/10.3847/1538-4357/ab910a>

Backward-propagating or reverse fluctuations in Alfvénic turbulence were recently found to produce magnetic-field-aligned (MFA) electric fields that can easily transfer their energy to the plasma, either in the form of heat (or electron beams that quickly dissipate their energy as heat) if electrons absorb most of the MFA energy, or in the form of translational motion of the plasma if the ions absorb most of the MFA energy. Conditions for the direct proton acceleration (jet formation) in the quiet chromosphere included a temperature  $\leq 10^4$  K and a magnetic field between

about 10 and 100 G, conditions very similar to those under which chromospheric plasma jets or dynamic jet-like spicules are observed with the Interface Region Imaging Spectrograph. Here the conditions for direct ion acceleration by MFA electric fields are determined for a much broader range of electron densities and plasma temperatures, to include both quiet and flaring conditions of the chromospheric plasma. For the higher chromospheric electron densities of solar flaring conditions, direct ion and therefore plasma acceleration by MFA electric fields is found to be possible in the much stronger (kG) magnetic fields of active regions, provided the plasma temperature remains less than about 105 K. Under flaring conditions, the MFA electric fields may cause the acceleration or at least trigger the upward motion of dense ( $>10^{12}$ – $10^{13}$  cm $^{-3}$ ) chromospheric plasma. It is also suggested that chromospheric nonresonant MFA acceleration, by producing local electron beams, may eliminate the need for electron beams to propagate from the flaring corona down to the denser chromosphere.

## **An investigation of the causal relationship between sunspot groups and coronal mass ejections by determining source active regions**

[Abd-ur Raheem](#), [Huseyin Cavus](#), [Gani Caglar Coban](#), [Ahmet Cumhuri Kinaci](#), [Haimin Wang](#), [Jason T L Wang](#)

Monthly Notices of the Royal Astronomical Society, Volume 506, Issue 2, **2021**, Pages 1916–1926,

<https://doi.org/10.1093/mnras/stab1816>

<https://doi.org/10.1093/mnras/stab1717>

Although the source active regions of some coronal mass ejections (CMEs) were identified in CME catalogues, vast majority of CMEs do not have an identified source active region. We propose a method that uses a filtration process and machine learning to identify the sunspot groups associated with a large fraction of CMEs and compare the physical parameters of these identified sunspot groups with properties of their corresponding CMEs to find mechanisms behind the initiation of CMEs. These CMEs were taken from the Coordinated Data Analysis Workshops (CDAW) data base hosted at NASA's website. The Helioseismic and Magnetic Imager (HMI) Active Region Patches (HARPs) were taken from the Stanford University's Joint Science Operations Center (JSOC) data base. The source active regions of the CMEs were identified by the help of a custom filtration procedure and then by training a long short-term memory network (LSTM) to identify the patterns in the physical magnetic parameters derived from vector and line-of-sight magnetograms. The neural network simultaneously considers the time series data of these magnetic parameters at once and learns the patterns at the onset of CMEs. This neural network was then used to identify the source HARPs for the CMEs recorded from 2011 till 2020. The neural network was able to reliably identify source HARPs for 4895 CMEs out of 14 604 listed in the CDAW data base during the aforementioned period.

## **Solar and interplanetary parameters of CMEs with and without type II radio bursts**

A. Mujiber [Rahman](#) a,<sup>†</sup>, S. Umamathy a,1, A. Shanmugaraju b,2, Y.-J. Moon

[Advances in Space Research](#) 50 (2012) 516–525; [File](#)

We have analyzed 101 CMEs, and their associated ICMEs and interplanetary (IP) shocks observed during the period 1997–2005. The main aim of the present work is to study the interplanetary characteristics of metric and DH type II associated CMEs such as, shock strength, IP shock speed, ICME speed, stand off distance and transit time. Among these 101 CMEs, 38 events show both metric and DH type II bursts characteristics. There are no metric and DH type II association for 52 events. While DH type II alone is found in 7 cases, metric type II alone is found in 4 events. It is found that the mean speeds of CMEs increase progressively from CMEs without type II events to CMEs associated with metric and DH type IIs as suggested by [Gopalswamy et al. \(2005\)](#). In addition, we found that the speeds of ICMEs and IP shocks progressively increase in the following order: events without metric and DH type IIs, events with metric alone, events with DH alone and events with both metric and DH type IIs. Similarly the Mach number is found to increase in the same order. While there is not much change in the stand-off distance among these cases, it is minimum ( $\sim 18 R_{\odot}$ ) for CMEs with speed greater than 2200 km/s. The above results confirm that more energetic CMEs can produce both metric and DH type IIs for which the interplanetary parameters such as mean values of ICME speed and IP shock speed and Mach number are found to be higher.

**Table 1a:** List of CMEs associated with X-ray flares, metric and DH type II bursts ((i) Events without metric and DH type II bursts).

**Table 1b:** List of CMEs associated with X-ray flares, metric and DH type II bursts.

## **Interpretable ML-Based Forecasting of CMEs Associated with Flares**

[Hemapriya Raju](#) & [Saurabh Das](#)

[Solar Physics](#) volume 298, Article number: 96 (2023)

<https://doi.org/10.1007/s11207-023-02187-6>

Coronal mass ejections (CMEs) that cause geomagnetic disturbances on the Earth can be found in conjunction with flares, filament eruptions, or independently. Though flares and CMEs are understood as triggered by the common physical process of magnetic reconnection, the degree of association is challenging to predict. From the vector magnetic field data captured by the Helioseismic and Magnetic Imager (HMI) onboard the Solar Dynamics Observatory (SDO), active regions are identified and tracked in what is known as Space Weather HMI Active Region Patches (SHARPs). Eighteen magnetic field features are derived from the SHARP data and fed as input for the machine-learning models to classify whether a flare will be accompanied by a CME (positive class) or not (negative class). Since the frequency of flare accompanied by CME occurrence is less than flare alone events, to address the class imbalance, we have explored the approaches such as undersampling the majority class, oversampling the minority class, and synthetic minority

oversampling technique (SMOTE) on the training data. We compare the performance of eight machine-learning models, among which the Support Vector Machine (SVM) and Linear Discriminant Analysis (LDA) model perform best with True Skill Score (TSS) around  $0.78 \pm 0.09$  and  $0.8 \pm 0.05$ , respectively. To improve the predictions, we attempt to incorporate the temporal information as an additional input parameter, resulting in LDA achieving an improved TSS of  $0.92 \pm 0.04$ . We utilize the wrapper technique and permutation-based model interpretation methods to study the significant SHARP parameters responsible for the predictions made by SVM and LDA models. This study will help develop a real-time prediction of CME events and better understand the underlying physical processes behind the occurrence.

## **An Estimate of the Magnetic Field Strength Associated with a Solar Coronal Mass Ejection from Low Frequency Radio Observations**

K. Sasikumar [Raja](#)<sup>1</sup>, R. Ramesh<sup>1</sup>, K. Hariharan<sup>1</sup>, C. Kathiravan<sup>1</sup>, and T. J. Wang

2014 ApJ 796 56S

<https://arxiv.org/pdf/1611.05249v1.pdf>

We report ground based, low frequency heliograph (80 MHz), spectral (85-35 MHz), and polarimeter (80 and 40 MHz) observations of drifting, non-thermal radio continuum associated with the "halo" coronal mass ejection that occurred in the solar atmosphere on **2013 March 15**. The magnetic field strengths (B) near the radio source were estimated to be  $B = 2.2 \pm 0.4$  G at 80 MHz and  $B = 1.4 \pm 0.2$  G at 40 MHz. The corresponding radial distances (r) are  $r = 1.9 R_{\odot}$  (80 MHz) and  $r = 2.2 R_{\odot}$  (40 MHz).

## **IN SITU HEATING OF THE 2007 MAY 19 CME EJECTA DETECTED BY STEREO/PLASTIC AND ACE**

Cara E. [Rakowski](#)<sup>1</sup>, J. Martin Laming<sup>2</sup> and Maxim Lyutikov<sup>3</sup>

2011 ApJ 730 30, [File](#)

In situ measurements of ion charge states can provide unique insight into the heating and evolution of coronal mass ejections (CMEs) when tested against realistic non-equilibrium ionization modeling. In this work, **we investigate the representation of the CME magnetic field as an expanding spheromak configuration**, where the plasma heating is prescribed by the choice of anomalous resistivity and the spheromak dynamics. We chose as a test case the 2007 May 19 CME observed by STEREO and ACE. The spheromak is an appealing physical model, because the location and degree of heating are fixed by the choice of anomalous resistivity and the spheromak expansion rate which we constrain with observations. This model can provide the heating required between  $1.1R_{\oplus}$  and Earth's orbit to produce charge states observed in the CME flux rope. However, this source of heating in the spheromak alone has difficulty accounting for the rapid heating to Fe8-Fe11+ at lower heights, as observed in STEREO EUVI due to the rapid radiative cooling that occurs at the high densities involved. Episodes of heating and cooling clearly unrelated to spheromak expansion are observed prior to the eruption, and presumably still play a role during the eruption itself. Spheromak heating is also not capable of reproducing the high Fe charge states (Fe16+ and higher) seen in situ exterior to the flux rope in this CME. Thus, while the spheromak configuration may be a valid model for the magnetic topology, other means of energization are still required to provide much of the rapid heating observed.

## **ION CHARGE STATES IN HALO CORONAL MASS EJECTIONS: WHAT CAN WE LEARN ABOUT THE EXPLOSION?**

Cara E. [Rakowski](#)<sup>1</sup>, J. Martin Laming<sup>2</sup> and Susan T. Leprie<sup>3</sup>

The Astrophysical Journal, 667:602Y609, 2007

We find that plasma in the CME "core" typically requires further heating following filament eruption, with thermal energy input similar to the kinetic energy input. This extra heating is presumably the result of post-eruptive reconnection.

## **New Results on the Onset of a Coronal Mass Ejection from 5303 Å Emission Line Observations with VELC/ADITYA-L1**

R. [Ramesh](#)<sup>1</sup>, V. Muthu Priyal<sup>1</sup>, Jagdev Singh<sup>1</sup>, K. Sasikumar Raja<sup>1</sup>, P. Savarimuthu<sup>1</sup>, and Priya Gavshinde<sup>1</sup>

2024 ApJL 976 L6

<https://iopscience.iop.org/article/10.3847/2041-8213/ad8c45/pdf>

We report on the onset of a coronal mass ejection (CME) using spectroscopic observations in the 5303 Å coronal emission line with the Visible Emission Line Coronagraph (VELC) onboard ADITYA-L1, the recently launched first Indian space solar mission. The CME was observed on **2024 July 16** in association with an X1.9 class soft X-ray flare from heliographic location S05W85. The VELC observations were near the west limb of the Sun during the CME. The results obtained helped to constrain the onset time of the CME. In addition, they indicate a  $\approx 50\%$  decrease in the coronal intensity near the source region of the CME due to mass depletion, a  $\approx 15\%$  enhancement in the emission line width, and a redshifted Doppler velocity of about  $\approx 10$  km s<sup>-1</sup>. The nonthermal velocity associated with the line broadening is  $\approx 24.87$  km s<sup>-1</sup>.

## **New results on the direct observations of thermal radio emission from a solar coronal mass ejection**

[R. Ramesh](#), [A. Kumari](#), [C. Kathiravan](#), [D. Ketaki](#), [T. J. Wang](#)

Geophysical Research Letters v. 48, **Issue8**, e2020GL091048 **2021**

<https://arxiv.org/pdf/2103.04148.pdf>

<https://doi.org/10.1029/2020GL091048>

We report observations of thermal emission from the frontal structure of a coronal mass ejection (CME) using data obtained with the Gauribidanur Radioheliograph (GRAPH) simultaneously at 80 MHz and 53 MHz on **2016 May 1**. The CME was due to activity on the far-side of the Sun, but near its limb. No non-thermal radio burst activity were noticed. This provided an opportunity to observe the faint thermal radio emission from the CME, and hence directly estimate the electron density, mass, and magnetic field strength of the plasma entrained in the CME. Considering that CMEs are mostly observed only in whitelight and reports on their plasma characteristics are also limited, the rare direct radio observations of thermal emission from a CME and independent diagnosis of its plasma parameters are important measurements in the field of CME physics.

CESRA #3008 Aug **2021**

<http://www.astro.gla.ac.uk/users/eduard/cesra/?p=3008>

## **HIGH ANGULAR RESOLUTION RADIO OBSERVATIONS OF A CORONAL MASS EJECTION SOURCE REGION AT LOW FREQUENCIES DURING A SOLAR ECLIPSE**

R. [Ramesh](#), C. Kathiravan, Indrajit V. Barve and M. Rajalingam

**2012 ApJ 744 165**

We carried out radio observations of the solar corona in the frequency range 109-50 MHz during the annular eclipse of **2010 January 15** from the Gauribidanur Observatory, located about 100 km north of Bangalore in India. The radio emission in the above frequency range originates typically in the radial distance range  $1.2-1.5 R_{\odot}$  in the "undisturbed" solar atmosphere. Our analysis indicates that (1) the angular size of the smallest observable radio source (associated with a coronal mass ejection in the present case) is  $1' \pm 0.3$ , (2) the source size does not vary with radial distance, (3) the peak brightness temperature of the source corresponding to the above size at a typical frequency like 77 MHz is  $3 \times 10^9$  K, and (4) the coronal magnetic field near the source region is 70 mG.

## **CORONAL MASS EJECTIONS AND SUNSPOTS—SOLAR CYCLE PERSPECTIVE**

K. B. [Ramesh](#)

Astrophysical Journal Letters, 712:L77–L80, **2010 March, File**

Recent studies have indicated that the occurrence of the maxima of coronal mass ejection (CME) rate and sunspot number (SSN) were nearly two years apart. We find that the two-year lag of CME rate manifests only when the SSN index is considered and the lag is minimal (two–three months) when the sunspot area is considered. CMEs with speeds greater than the average speed follow the sunspot cycle much better than the entire population of CMEs. Analysis of the linear speeds of CMEs further indicates that during the descending phase of the solar cycle the loss of magnetic flux is through more frequent and less energetic CMEs. We emphasize that the magnetic field attaining the nonpotentiality that represents the free energy content, rather than the flux content as measured by the area of the active region, plays an important role in producing CMEs.

## **RADIOHELIOGRAPH OBSERVATIONS OF METRIC TYPE II BURSTS AND THE KINEMATICS OF CORONAL MASS EJECTIONS**

R. [Ramesh](#)<sup>1</sup>, C. Kathiravan<sup>1</sup>, Sreeja S. Kartha<sup>1</sup>, and N. Gopalswamy<sup>2</sup>

Astrophysical Journal, 712:188–193, **2010 March, File**

Assuming that metric type II radio bursts from the Sun are due to magnetohydrodynamic shocks driven by coronal mass ejections (CMEs), we estimate the average CME acceleration from its source region up to the position of the type II burst. The acceleration values are in the range  $\approx 600-1240 \text{ m s}^{-2}$ , which are consistent with values obtained using non-radio methods. We also find that (1) CMEs with comparatively larger acceleration in the low corona are associated with soft X-ray flares of higher energy; the typical acceleration of a CME associated with X1.0 class soft X-ray flare being  $\approx 1020 \text{ m s}^{-2}$ , and (2) CMEs with comparatively higher speed in the low corona slow down quickly at large distances from the Sun—the deceleration of a CME with a typical speed of  $1000 \text{ km s}^{-1}$  being  $\approx -15 \text{ m s}^{-2}$  in the distance range of  $\approx 3-32 R_{\odot}$ .

## **[Parker Solar Probe: Insights into the Physics of the Near-Solar Environment](#)**

Nour E. Raouafi

**ApJ collection 2023**

<https://iopscience.iop.org/collections/apj-230531-01>

**5 Sep 2022**

## **Magnetic Reconnection as the Driver of the Solar Wind**

Nour E. **Raouafi**<sup>1</sup>, G. Stenborg<sup>1</sup>, D. B. Seaton<sup>2</sup>, H. Wang<sup>3,4,5</sup>, J. Wang<sup>3,4,5</sup>, C. E. DeForest<sup>2</sup>, S. D. Bale<sup>6,7</sup>, J. F. Drake<sup>8</sup>, V. M. Uritsky<sup>9,10</sup>, J. T. Karpen<sup>10</sup> Show full author list  
**2023** ApJ 945 28

<https://iopscience.iop.org/article/10.3847/1538-4357/acaf6c/pdf>

<https://arxiv.org/pdf/2301.00903.pdf>

We present EUV solar observations showing evidence for omnipresent jetting activity driven by small-scale magnetic reconnection at the base of the solar corona. We argue that the physical mechanism that heats and drives the solar wind at its source is ubiquitous magnetic reconnection in the form of small-scale jetting activity (a.k.a. jetlets). This jetting activity, like the solar wind and the heating of the coronal plasma, is ubiquitous regardless of the solar cycle phase. Each event arises from small-scale reconnection of opposite-polarity magnetic fields producing a short-lived jet of hot plasma and Alfvén waves into the corona. The discrete nature of these jetlet events leads to intermittent outflows from the corona, which homogenize as they propagate away from the Sun and form the solar wind. This discovery establishes the importance of small-scale magnetic reconnection in solar and stellar atmospheres in understanding ubiquitous phenomena such as coronal heating and solar wind acceleration. Based on previous analyses linking the switchbacks to the magnetic network, we also argue that these new observations might provide the link between the magnetic activity at the base of the corona and the switchback solar wind phenomenon. These new observations need to be put in the bigger picture of the role of magnetic reconnection and the diverse form of jetting in the solar atmosphere. **2019-07-29, 2021-04-28**

### **Solar Coronal Jets: Observations, Theory, and Modeling**

**Review**

N.E. **Raouafi**, S. Patsourakos, E. Pariat, P.R. Young, A.C. Sterling, A. Savcheva, M. Shimojo, F. Moreno-Inertis, C.R. DeVore, V. Archontis, T. Török, H. Mason, W. Curdt, K. Meyer, K. Dalmasse, Y. Matsui  
Space Science Reviews **2016** 201: [Issue 1](#), pp 1–53 **File**

<http://arxiv.org/pdf/1607.02108v1.pdf>

Coronal jets represent important manifestations of ubiquitous solar transients, which may be the source of significant mass and energy input to the upper solar atmosphere and the solar wind. While the energy involved in a jet-like event is smaller than that of "nominal" solar flares and coronal mass ejections (CMEs), jets share many common properties with these phenomena, in particular, the explosive magnetically driven dynamics. Studies of jets could, therefore, provide critical insight for understanding the larger, more complex drivers of the solar activity. On the other side of the size-spectrum, the study of jets could also supply important clues on the physics of transients close or at the limit of the current spatial resolution such as spicules. Furthermore, jet phenomena may hint to basic process for heating the corona and accelerating the solar wind; consequently their study gives us the opportunity to attack a broad range of solar-heliospheric problems.

### **FIELD LINES TWISTING IN A NOISY CORONA: IMPLICATIONS FOR ENERGY STORAGE AND RELEASE, AND INITIATION OF SOLAR ERUPTIONS**

A.F. **Rappazzo**<sup>1</sup>, M. Velli<sup>2</sup>, and G. Einaudi

**2013** ApJ 771 76

We present simulations modeling closed regions of the solar corona threaded by a strong magnetic field where localized photospheric vortical motions twist the coronal field lines. The linear and nonlinear dynamics are investigated in the reduced magnetohydrodynamic regime in Cartesian geometry. Initially the magnetic field lines get twisted and the system becomes unstable to the internal kink mode, confirming and extending previous results. As typical in this kind of investigations, where initial conditions implement smooth fields and flux-tubes, we have neglected fluctuations and the fields are laminar until the instability sets in. However, previous investigations indicate that fluctuations, excited by photospheric motions and coronal dynamics, are naturally present at all scales in the coronal fields. Thus, in order to understand the effect of a photospheric vortex on a more realistic corona, we continue the simulations after kink instability sets in, when turbulent fluctuations have already developed in the corona. In the nonlinear stage the system never returns to the simple initial state with ordered twisted field lines, and kink instability does not occur again. Nevertheless, field lines get twisted, although in a disordered way, and energy accumulates at large scales through an inverse cascade. This energy can subsequently be released in micro-flares or larger flares, when interaction with neighboring structures occurs or via other mechanisms. The impact on coronal dynamics and coronal mass ejections initiation is discussed.

### **Kinematics of coronal mass ejections in the LASCO field of view**

Anitha **Ravishankar**<sup>1</sup>, Grzegorz Michałek<sup>1</sup> and Seiji Yashiro<sup>2</sup>

A&A 639, A68 (2020)

<https://www.aanda.org/articles/aa/pdf/2020/07/aa37834-20.pdf>

In this paper we present a statistical study of the kinematics of 28894 coronal mass ejections (CMEs) recorded by the Large Angle and Spectrometric Coronagraph (LASCO) on board the Solar and Heliospheric Observatory spacecraft from 1996 until mid-2017. The initial acceleration phase is characterized by a rapid increase in CME velocity just after eruption in the inner corona. This phase is followed by a non-significant residual acceleration (deceleration) characterized by an almost constant speed of CMEs. We demonstrate that the initial acceleration is in the range 0.24–2616 m s<sup>-2</sup> with median (average) value of 57 m s<sup>-2</sup> (34 m s<sup>-2</sup>) and it takes place up to a distance of about



28 RSUN with median (average) value of 7.8 RSUN (6 RSUN). Additionally, the initial acceleration is significant in the case of fast CMEs ( $V > 900 \text{ km s}^{-1}$ ), where the median (average) values are about  $295 \text{ m s}^{-2}$  ( $251 \text{ m s}^{-2}$ ), respectively, and much weaker in the case of slow CMEs ( $V < 250 \text{ km s}^{-1}$ ), where the median (average) values are about  $18 \text{ m s}^{-2}$  ( $17 \text{ m s}^{-2}$ ), respectively. We note that the significant driving force (Lorentz force) can operate up to a distance of 6 RSUN from the Sun during the first 2 hours of propagation. We found a significant anti-correlation between the initial acceleration magnitude and the acceleration duration, whereas the residual acceleration covers a range from  $-1224$  to  $0 \text{ m s}^{-2}$  with a median (average) value of  $-34 \text{ m s}^{-2}$  ( $-17 \text{ m s}^{-2}$ ). One intriguing finding is that the residual acceleration is much smaller during the 24th cycle in comparison to the 23rd cycle of solar activity. Our study has also revealed that the considered parameters, initial acceleration (ACCINI), residual acceleration (ACCRES), maximum velocity (VMAX), and time at maximum velocity (TimeMAX) mostly follow solar cycles and the intensities of the individual cycle.

## **Non-interacting coronal mass ejections and solar energetic particles near the quadrature configuration of Solar TERrestrial RELations Observatory**

Anitha [Ravishankar](#) and Grzegorz Michalek

A&A 638, A42 (2020) **File**

<https://www.aanda.org/articles/aa/pdf/2020/06/aa37528-20.pdf>

<https://arxiv.org/pdf/2010.01443>

We present our results on the correlation of non-interacting coronal mass ejections (CMEs) and solar energetic particles (SEPs). A statistical analysis was conducted on 25 SEP events and the associated CME and flare during the ascending phase of solar cycle 24, i.e., 2009–2013, which marks the quadrature configuration of Solar TERrestrial RELations Observatory (STEREO). The complete kinematics of CMEs is well studied near this configuration of STEREO. In addition, we have made comparison studies of STEREO and Solar and Heliospheric Observatory results. It is well known that the CME speeds and SEP intensities are closely correlated. We further examine this correlation by employing instantaneous speeds (maximum speed and the CME speed and Mach number at SEP peak flux) to check whether they are a better indicator of SEP fluxes than the average speed. Our preliminary results show a better correlation by this approach. In addition, the correlations show that the fluxes of protons in energy channel  $>10 \text{ MeV}$  are accelerated by shock waves generated by fast CMEs, whereas the particles of  $>50 \text{ MeV}$  and  $>100 \text{ MeV}$  energy bands are mostly accelerated by the same shock waves but partly by the associated flares. In contrast, the X-ray flux of solar flares and SEP peak flux show a poor correlation. **2012-07-12**

Table A.1. Observational parameters of 25 CMEs and the associated SEPs and Flares during the period 2009–2013.

## **Estimation of Arrival Time of Coronal Mass Ejections in the Vicinity of the Earth Using Solar and Heliospheric Observatory and Solar TERrestrial RELations Observatory Observations**

Anitha [Ravishankar](#), Grzegorz Michalek

[Solar Physics](#) September 2019, 294:125

<https://link.springer.com/content/pdf/10.1007%2Fs11207-019-1470-2.pdf>

<https://doi.org/10.1007/s11207-019-1470-2>

The arrival time of coronal mass ejections (CMEs) in the vicinity of the Earth is one of the most important parameters in determining space weather. We have used a new approach to predicting this parameter. First, in our study, we have introduced a new definition of the speed of ejection. It can be considered as the maximum speed that the CME achieves during the expansion into the interplanetary medium. Additionally, in our research we have used not only observations from the Solar and Heliospheric Observatory (SOHO) spacecraft but also from Solar TERrestrial RELations Observatory (STEREO) spacecrafts. We focus on halo and partial-halo CMEs during the ascending phase of Solar Cycle 24. During this period the STEREO spacecraft were in quadrature position in relation to the Earth. We demonstrated that these conditions of the STEREO observations can be crucial for an accurate determination of the transit times (TTs) of CMEs to the Earth. In our research we defined a new initial velocity of the CME, the maximum velocity determined from the velocity profiles obtained from a moving linear fit to five consecutive height–time points. This new approach can be important from the point of view of space weather as the new parameter is highly correlated with the final velocity of ICMEs. It allows one to predict the TTs with the same accuracy as previous models. However, what is more important is the fact that the new approach has radically reduced the maximum TT estimation errors to 29 hours. Previous studies determined the TT with a maximum error equal to 50 hours.

**Table 1** Observational parameters of 51 ICMEs in the period 2009 – 2013.

## **Comparison of energies between eruptive phenomena and magnetic field in AR 10930,**

[Ravindra](#), B., and T.A. Howard,

Bull. Astron. Soc. India, 38, 147-163, 2010.

[http://www.boulder.swri.edu/~howard/Papers/2010\\_Ravindra.pdf](http://www.boulder.swri.edu/~howard/Papers/2010_Ravindra.pdf) -File

We present a study comparing the energy carried away by a coronal mass ejection (CME) and the radiative energy loss in associated flare plasma, with the decrease in magnetic free energy during a release in active region NOAA 10930 on December 13, 2006 during the declining phase of the solar cycle 23. The ejected

CME was fast and directed towards the Earth with a projected speed of  $\approx 1780 \text{ km s}^{-1}$  and a de-projected speed of  $\approx 3060 \text{ km s}^{-1}$ . We regard these as lower and upper limits for our calculations. It was accompanied by an X3.4 class flare in the active region. The CME carried  $(1.2\text{--}4.5) \times 10^{32} \text{ erg}$  (projected-deprojected) of kinetic and gravitational potential energy. The estimated radiative energy loss during the flare was found to be  $9.04 \times 10^{30} \text{ erg}$ . The sum of these energies was compared with the decrease in measured free magnetic energy during the flare/CME. The free energy is that above the minimum energy configuration and was estimated using the magnetic virial theorem. The estimated decrease in magnetic free energy is large,  $3.11 \times 10^{32} \text{ erg}$  after the flare/CME compared to the pre-flare energy. Given the range of possible energies we estimate that 50–100% of the CME energy arose from the active region. The rest of the free magnetic energy was distributed among the radiative energy loss, particle acceleration, plasma and magnetic field reorientation.

### **Modeling and measuring the flux reconnected and ejected by the two-ribbon flare on 2004-11-07 -- D. Longcope, C. Beveridge, J.**

Qiu, B. **Ravindra**, G. Barnes and S. Dasso, E-print, Nov 2006

<http://solar.physics.montana.edu/cgi-bin/eprint/index.pl?entry=2065>

This work is an attempt to combine observations of two-ribbon flare and a magnetic cloud into a coherent scenario of three-dimensional reconnection. Measurements of the magnetic fluxes in the AR, swept up by the flare ribbons, and in the MC can be compared to elucidate the inter-relation of these features.

Two Ribbon Flares. The CSHKP model. Coronal Mass Ejections.

Three Dimensional Reconnection

### **Relationship between solar energetic particle intensities and coronal mass ejection kinematics using STEREO/SECCHI field of view**

Anitha **Ravishankar** and Grzegorz Michalek

A&A 646, A142 (2021)

<https://www.aanda.org/articles/aa/pdf/2021/02/aa39537-20.pdf>

<https://doi.org/10.1051/0004-6361/202039537>

<https://arxiv.org/pdf/2102.12640.pdf>

Solar energetic particles (SEPs) accelerated from shocks driven by coronal mass ejections (CMEs) are one of the major causes of geomagnetic storms on Earth. Therefore, it is necessary to predict the occurrence and intensity of such disturbances. For this purpose we analyzed in detail 38 non-interacting halo and partial halo CMEs, as seen by the Solar and Heliospheric Observatory/Large Angle and Spectrometric Coronagraph, generating SEPs (in  $> 10 \text{ MeV}$ ,  $> 50 \text{ MeV}$ , and  $> 100 \text{ MeV}$  energy channels) during the quadrature configuration of the Solar TERrestrial RELations Observatory (STEREO) twin spacecrafts with respect to the Earth, which marks the ascending phase of solar cycle 24 (i.e., 2009–2013). The main criteria for this selection period is to obtain height–time measurements of the CMEs without significant projection effects and in a very large field of view. Using the data from STEREO/Sun Earth Connection Coronal and Heliospheric Investigation (STEREO/SECCHI) images we determined several kinematic parameters and instantaneous speeds of the CMEs. First, we compare instantaneous CME speed and Mach number versus SEP fluxes for events originating at the western and eastern limb; we observe high correlation for the western events and anticorrelation for the eastern events. Of the two parameters, the Mach number offers higher correlation. Next we investigated instantaneous CME kinematic parameters such as maximum speed, maximum Mach number, and the CME speed and Mach number at SEP peak flux versus SEP peak fluxes. Highly positive correlation is observed for Mach number at SEP peak flux for all events. The obtained instantaneous Mach number parameters from the empirical models was verified with the start and end time of type II radio bursts, which are signatures of CME-driven shock in the interplanetary medium. Furthermore, we conducted estimates of delay in time and distance between CME, SEP, and shock parameters. We observe an increase in the delay in time and distance when SEPs reach peak flux with respect to CME onset as we move from the western to the eastern limb. Western limb events (longitude  $60^\circ$ ) have the best connectivity and this decreases as we move towards the eastern limb. This variation is due to the magnetic connectivity from the Sun to the Earth, called the Parker spiral interplanetary magnetic field. Comparative studies of the considered energy channels of the SEPs also throw light on the reacceleration of suprathermal seed ions by CME-driven shocks that are pre-accelerated in the magnetic reconnection. **22 September 2011, 13 March 2012, 12 July 2012**

**See Comment on “Non-interacting coronal mass ejections and solar energetic particles near the quadrature configuration of solar terrestrial relations observatory”: CME shocks are fast magnetosonic shocks and not intermediate Alfvén shocks**

B. T. **Tsurutani**<sup>1</sup>, L. Shan<sup>2</sup>, G. S. Lakhina<sup>3</sup>, C. Mazelle<sup>4</sup>, X. Meng<sup>1</sup>, A. Du<sup>2</sup> and Z. Liu<sup>2</sup>

A&A 656, A152 (2021)

<https://www.aanda.org/articles/aa/pdf/2021/12/aa41029-21.pdf>  
<https://doi.org/10.1051/0004-6361/202141029>

## **Non-interacting coronal mass ejections and solar energetic particles near the quadrature configuration of Solar TERrestrial Relations Observatory**

Anitha **Ravishankar** and Grzegorz Michalek

A&A 638, A42 (2020) **File**

<https://www.aanda.org/articles/aa/pdf/2020/06/aa37528-20.pdf>

<https://arxiv.org/pdf/2010.01443>

<https://doi.org/10.1051/0004-6361/202037528>

We present our results on the correlation of non-interacting coronal mass ejections (CMEs) and solar energetic particles (SEPs). A statistical analysis was conducted on 25 SEP events and the associated CME and flare during the ascending phase of solar cycle 24, i.e., 2009–2013, which marks the quadrature configuration of Solar TERrestrial Relations Observatory (STEREO). The complete kinematics of CMEs is well studied near this configuration of STEREO. In addition, we have made comparison studies of STEREO and SOLar and Heliospheric Observatory results. It is well known that the CME speeds and SEP intensities are closely correlated. We further examine this correlation by employing instantaneous speeds (maximum speed and the CME speed and Mach number at SEP peak flux) to check whether they are a better indicator of SEP fluxes than the average speed. Our preliminary results show a better correlation by this approach. In addition, the correlations show that the fluxes of protons in energy channel  $>10$  MeV are accelerated by shock waves generated by fast CMEs, whereas the particles of  $>50$  MeV and  $>100$  MeV energy bands are mostly accelerated by the same shock waves but partly by the associated flares. In contrast, the X-ray flux of solar flares and SEP peak flux show a poor correlation. **2012-07-12**

Table A.1. Observational parameters of 25 CMEs and the associated SEPs and Flares during the period 2009–2013.

**See Comment on “Non-interacting coronal mass ejections and solar energetic particles near the quadrature configuration of solar terrestrial relations observatory”: CME shocks are fast magnetosonic shocks and not intermediate Alfvén shocks**

B. T. **Tsurutani**<sup>1</sup>, L. Shan<sup>2</sup>, G. S. Lakhina<sup>3</sup>, C. Mazelle<sup>4</sup>, X. Meng<sup>1</sup>, A. Du<sup>2</sup> and Z. Liu<sup>2</sup>

A&A 656, A152 (2021)

<https://www.aanda.org/articles/aa/pdf/2021/12/aa41029-21.pdf>

<https://doi.org/10.1051/0004-6361/202141029>

## **Kinematics of coronal mass ejections in the LASCO field of view**

Anitha **Ravishankar**, [Grzegorz Michalek](#), [Seiji Yashiro](#)

Astronomy & Astrophysics, Volume 639, id.A68, 12 pp, July 2020

<https://arxiv.org/pdf/2010.02682.pdf>

In this paper we present a statistical study of the kinematics of 28894 coronal mass ejections (CMEs) recorded by the Large Angle and Spectrometric Coronagraph (LASCO) on board the Solar and Heliospheric Observatory spacecraft from 1996 until mid-2017. The initial acceleration phase is characterized by a rapid increase in CME velocity just after eruption in the inner corona. This phase is followed by a non-significant residual acceleration (deceleration) characterized by an almost constant speed of CMEs. We demonstrate that the initial acceleration is in the range  $0.24$ - $2616$   $\text{ms}^{-2}$  with median (average) value of  $57$   $\text{ms}^{-2}$  ( $34$   $\text{ms}^{-2}$ ) and it takes place up to a distance of about 28 solar radius with median (average) value of 7.8 solar radius (6 solar radius). Additionally, the initial acceleration is significant in the case of fast CMEs ( $V > 900$   $\text{kms}^{-1}$ ), where the median (average) values are about  $295$   $\text{ms}^{-2}$  ( $251$   $\text{ms}^{-2}$ ), respectively, and much weaker in the case of slow CMEs ( $V < 250$   $\text{kms}^{-1}$ ), where the median (average) values are about  $18$   $\text{ms}^{-2}$  ( $17$   $\text{ms}^{-2}$ ), respectively. We note that the significant driving force (Lorentz force) can operate up to a distance of 6 solar radius from the Sun during the first 2 hours of propagation. We found a significant anti-correlation between the initial acceleration magnitude and the acceleration duration, whereas the residual acceleration covers a range from  $-1224$  to  $0$   $\text{ms}^{-2}$  with a median (average) value of  $-34$   $\text{ms}^{-2}$  ( $-17$   $\text{ms}^{-2}$ ). One intriguing finding is that the residual acceleration is much smaller during the 24th cycle in comparison to the 23rd cycle of solar activity. Our study has also revealed that the considered parameters, initial acceleration (ACC INI), residual acceleration (ACC RES), maximum velocity (V MAX), and time at maximum velocity (Time MAX) mostly follow solar cycles and the intensities of the individual cycle.

## **Spatial Offsets in Flare-CME Current Sheets**

John C. **Raymond**<sup>1</sup>, Silvio Giordano<sup>2</sup>, and Angela Ciaravella<sup>3</sup>

2017 ApJ 843 121

<http://sci-hub.cc/10.3847/1538-4357/aa7848>

Magnetic reconnection plays an integral part in nearly all models of solar flares and coronal mass ejections (CMEs). The reconnection heats and accelerates the plasma, produces energetic electrons and ions, and changes the magnetic topology to form magnetic flux ropes and to allow CMEs to escape. Structures that appear between flare loops and CME cores in optical, UV, EUV, and X-ray observations have been identified as current sheets and have been interpreted in terms of the nature of the reconnection process and the energetics of the events. Many of these studies have used UV spectral observations of high temperature emission features in the [Fe xviii] and Si xii lines. In this paper,

we discuss several surprising cases in which the [Fe xviii] and Si xii emission peaks are spatially offset from each other. We discuss interpretations based on asymmetric reconnection, on a thin reconnection region within a broader streamer-like structure, and on projection effects. Some events seem to be easily interpreted as the projection of a sheet that is extended along the line of sight that is viewed an angle, but a physical interpretation in terms of asymmetric reconnection is also plausible. Other events favor an interpretation as a thin current sheet embedded in a streamer-like structure. **1997 May 5, 2002 January 10, 2003 January 3, 2003 June 13, 2003 November 4**  
**Table 1** UVCS Current Sheet Observations Selected for this Study (1997-2003)

## **Bright hot impacts by erupted fragments falling back on the Sun: UV redshifts in stellar accretion**

F. [Reale](#), S. Orlando, P. Testa, E. Landi, C. J. Schrijver

ApJL, 797 L5 **2014**

<http://arxiv.org/pdf/1410.7193v1.pdf>

A solar eruption after a flare on **7 Jun 2011** produced EUV-bright impacts of fallbacks far from the eruption site, observed with the Solar Dynamics Observatory. These impacts can be taken as a template for the impact of stellar accretion flows. Broad red-shifted UV lines have been commonly observed in young accreting stars. Here we study the emission from the impacts in the Atmospheric Imaging Assembly's UV channels and compare the inferred velocity distribution to stellar observations. We model the impacts with 2D hydrodynamic simulations. We find that the localised UV 1600Å emission and its timing with respect to the EUV emission can be explained by the impact of a cloud of fragments. The first impacts produce strong initial upflows. The following fragments are hit and shocked by these upflows. The UV emission comes mostly from the shocked front shell of the fragments while they are still falling, and is therefore redshifted when observed from above. The EUV emission instead continues from the hot surface layer that is fed by the impacts. Fragmented accretion can therefore explain broad redshifted UV lines (e.g. C IV 1550Å) to speeds around 400 km/s observed in accreting young stellar objects.

## **2D and 3D Analysis of a Torus-unstable Quiet-Sun Prominence Eruption**

T. [Rees-Crockford](#)<sup>1</sup>, D. S. Bloomfield<sup>1</sup>, E. Scullion<sup>1</sup>, and S.-H. Park<sup>2</sup>

**2020** ApJ 897 35

<https://iopscience.iop.org/article/10.3847/1538-4357/ab92a0/pdf>

The role of ideal-MHD instabilities in a prominence eruption is explored through 2D and 3D kinematic analysis of an event observed with the Solar Dynamics Observatory and the Solar Terrestrial Relations Observatory between 22:06 UT on **2013 February 26** and 04:06 UT on **2013 February 27**. A series of 3D radial slits are used to extract height–time profiles ranging from the midpoint of the prominence leading edge to the southeastern footpoint. These height–time profiles are fit with a kinematic model combining linear and nonlinear rise phases, returning the nonlinear onset time ( $t_{nl}$ ) as a free parameter. A range (1.5–4.0) of temporal power indices (i.e.,  $\beta$  in the nonlinear term) are considered to prevent prescribing any particular form of nonlinear kinematics. The decay index experienced by the leading edge is explored using a radial profile of the transverse magnetic field from a PFSS extrapolation above the prominence region. Critical decay indices are extracted for each slit at their own specific values of height at the nonlinear phase onset ( $h(t_{nl})$ ) and filtered to focus on instances resulting from kinematic fits with  $\beta$  (restricting  $\beta$  to 1.9–3.9). Based on this measure of the critical decay index along the prominence structure, we find strong evidence that the torus instability is the mechanism driving this prominence eruption. Defining any single decay index as being "critical" is not that critical because there is no single canonical or critical value of decay index through which all eruptions must succeed.

## **Exploring Plasma Heating in the Current Sheet Region in a Three-Dimensional Coronal Mass Ejection Simulation**

Katharine K. [Reeves](#), [Tibor Török](#), [Zoran Mikić](#), [Jon Linker](#), [Nicholas A. Murphy](#)

ApJ **887** 103 **2019**

<https://arxiv.org/pdf/1910.05386.pdf>  
[sci-hub.se/10.3847/1538-4357/ab4ce8](https://arxiv.org/pdf/1910.05386.pdf)

We simulate a coronal mass ejection (CME) using a three-dimensional magnetohydrodynamic (MHD) code that includes coronal heating, thermal conduction, and radiative cooling in the energy equation. The magnetic flux distribution at 1 Rs is produced by a localized subsurface dipole superimposed on a global dipole field, mimicking the presence of an active region within the global corona. Transverse electric fields are applied near the polarity inversion line to introduce a transverse magnetic field, followed by the imposition of a converging flow to form and destabilize a flux rope, producing an eruption. We examine the quantities responsible for plasma heating and cooling during the eruption, including thermal conduction, radiation, adiabatic effects, coronal heating, and ohmic heating. We find that ohmic heating is an important contributor to hot temperatures in the current sheet region early in the eruption, but in the late phase adiabatic compression plays an important role in heating the plasma there. Thermal conduction also plays an important role in the transport of thermal energy away from the current sheet region throughout the reconnection process, producing a "thermal halo" and widening the region of high temperatures. We simulate emission from solar telescopes for this eruption and find that there is evidence for emission from heated plasma above the flare loops late in the eruption, when the adiabatic heating is the dominant heating term. These results provide an explanation for hot

supra-arcade plasma sheets that are often observed in X-rays and extreme ultraviolet wavelengths during the decay phase of large flares.

## **An exploration of heating mechanisms in a supra-arcade plasma sheet formed after a coronal mass ejection**

Katharine K. [Reeves](#), Michael S. Freed, David E. McKenzie, Sabrina L. Savage

ApJ 836 55 2017

<https://arxiv.org/pdf/1701.03497v1.pdf>

<https://drive.google.com/file/d/0Bw0HCnNdNiTeQ0NoQ2ZHm1FwUEE/view>

We perform a detailed analysis of the thermal structure of the region above the post-eruption arcade for a flare that occurred on **2011 October 22**. During this event, a sheet of hot plasma is visible above the flare loops in the 131 Å bandpass of the Atmospheric Imaging Assembly (AIA) on the Solar Dynamics Observatory (SDO). Supra-arcade downflows (SADs) are observed traveling sunward through the post-eruption plasma sheet. We calculate differential emission measures using the AIA data and derive an emission measure weighted average temperature in the supra-arcade region. In areas where many SADs occur, the temperature of the supra-arcade plasma tends to increase, while in areas where no SADs are observed, the temperature tends to decrease. We calculate the plane-of-sky velocities in the supra-arcade plasma and use them to calculate the potential heating due to adiabatic compression and viscous heating. Ten of the 13 SADs studied have noticeable signatures in both the adiabatic and the viscous terms. The adiabatic heating due to compression of plasma in front of the SADs is on the order of 0.1 - 0.2 MK/s, which is similar in magnitude to the estimated conductive cooling rate. This result supports the notion that SADs contribute locally to the heating of plasma in the supra-arcade region. We also find that in the region without SADs, the plasma cools at a rate slower than the estimated conductive cooling, indicating additional heating mechanisms may act globally to keep the plasma temperature high.

## **Direct Observations of Magnetic Reconnection Outflow and CME Triggering in a Small Erupting Solar Prominence**

Katharine K. [Reeves](#), Patrick I. McCauley and Hui Tian

ApJL 807 7 2015

We examine a small prominence eruption that occurred on **2014 May 1** at 01:35 UT and was observed by the Interface Region Imaging Spectrometer (IRIS) and the Atmospheric Imaging Assembly (AIA) on the Solar Dynamics Observatory (SDO). Pre- and post-eruption images were taken by the X-Ray Telescope (XRT) on Hinode. Pre-eruption, a dome-like structure exists above the prominence, as demarcated by coronal rain. As the eruption progresses, we find evidence for reconnection between the prominence magnetic field and the overlying field. Fast flows are seen in AIA and IRIS, indicating reconnection outflows. Plane-of-sky flows of  $\sim 300$  km s<sup>-1</sup> are observed in the AIA 171 Å channel along a potentially reconnected field line. IRIS detects intermittent fast line-of-sight flows of  $\sim 200$  km s<sup>-1</sup> coincident with the AIA flows. Differential emission measure calculations show heating at the origin of the fast flows. Post-eruption XRT images show hot loops probably due to reconfiguration of magnetic fields during the eruption and subsequent heating of plasma in these loops. Although there is evidence for reconnection above the prominence during the eruption, high spatial resolution images from IRIS reveal potential reconnection sites below the prominence. A height-time analysis of the erupting prominence shows a slow initial rise with a velocity of  $\sim 0.4$  km s<sup>-1</sup> followed by a rapid acceleration with a final velocity of  $\sim 250$  km s<sup>-1</sup>. Brightenings in IRIS during the transition between these two phases indicate the eruption trigger for the fast part of the eruption is likely a tether-cutting mechanism rather than a break-out mechanism.

## **CURRENT SHEET ENERGETICS, FLARE EMISSIONS, AND ENERGY PARTITION IN A SIMULATED SOLAR ERUPTION**

Katharine K. [Reeves](#)<sup>1</sup>, Jon A. Linker<sup>2</sup>, Zoran Mikić<sup>2</sup> and Terry G. Forbes

2010 ApJ 721 1547

We investigate coronal energy flow during a simulated coronal mass ejection (CME). We model the CME in the context of the global corona using a 2.5D numerical MHD code in spherical coordinates that includes coronal heating, thermal conduction, and radiative cooling in the energy equation. The simulation domain extends from 1 to 20 R<sub>s</sub>. To our knowledge, this is the first attempt to apply detailed energy diagnostics in a flare/CME simulation when these important terms are considered in the context of the MHD equations. We find that the energy conservation properties of the code are quite good, conserving energy to within 4% for the entire simulation (more than 6 days of real time). We examine the energy release in the current sheet as the eruption takes place, and find, as expected, that the Poynting flux is the dominant carrier of energy into the current sheet. However, there is a significant flow of energy out of the sides of the current sheet into the upstream region due to thermal conduction along field lines and viscous drag. This energy outflow is spatially partitioned into three separate components, namely, the energy flux flowing out the sides of the current sheet, the energy flowing out the lower tip of the current sheet, and the energy flowing out the upper tip of the current sheet. The energy flow through the lower tip of the current sheet is the energy available for heating of the flare loops. We examine the simulated flare emissions and energetics due to the modeled CME and find reasonable agreement with

flare loop morphologies and energy partitioning in observed solar eruptions. The simulation also provides an explanation for coronal dimming during eruptions and predicts that the structures surrounding the current sheet are visible in X-ray observations.

## **RELATING CORONAL MASS EJECTION KINEMATICS AND THERMAL ENERGY RELEASE TO FLARE EMISSIONS USING A MODEL OF SOLAR ERUPTIONS**

Katharine K. [Reeves](#)<sup>1</sup> and Stephanie J. Moats<sup>1,2</sup>

*Astrophysical Journal*, 712:429–434, 2010 March, [File](#)

We use a model of solar eruptions that combines a loss-of-equilibrium coronal mass ejection (CME) model with a multi-threaded flare loop model in order to understand the relationship between the CME kinematics, thermal energy release, and soft X-ray emissions in solar eruptions. We examine the correlation between CME acceleration and the peak soft X-ray flux in many modeled cases with different parameters, and find that the two quantities are well correlated. We also examine the timing of the peak acceleration and the light curve derivative, and find that these quantities tend to peak at similar times for cases where the magnetic field is high and the inflow Alfvén Mach number is fast. Finally, we study the relationship between the total thermal energy released in the model and the calculated peak soft X-ray flux of the resulting flare. We find that there is a power-law relationship between these two quantities, with  $F_{\text{peak}} \sim E\alpha$ , where  $\alpha$  is between 2.54 and 1.54, depending on the reconnection rate. This finding has repercussions for the assumptions underlying the Neupert effect, in which the peak soft X-ray flux is assumed to be proportional to the thermal energy release.

## **Post-Eruptive Phenomena in CMEs and Substorms – Indicators of A Universal Process?**

K. K. [Reeves](#),<sup>1</sup> T. B. Guild,<sup>2</sup> W. J. Hughes,<sup>3</sup> K. E. Korreck,<sup>1</sup> J. Lin,<sup>1</sup> J. Raymond,<sup>1</sup> S. Savage,<sup>4</sup> N. A. Schwadron,<sup>3</sup> H. E. Spence,<sup>3</sup> D. F. Webb<sup>5</sup> and M. Wiltberger<sup>6</sup>

E-print, April 2008; *JGR*, VOL. 113, A00B02, doi:10.1029/2008JA013049, 2008  
[http://hea-www.harvard.edu/trace/SSXG/kreeves/2008ja013049\\_preprint.pdf](http://hea-www.harvard.edu/trace/SSXG/kreeves/2008ja013049_preprint.pdf)

Abstract. We examine phenomena associated with eruptions in the two different regimes of the solar corona and the terrestrial magnetosphere. We find striking similarities between the speeds of shrinking magnetic field lines in the corona and dipolarization fronts traversing the magnetosphere. We also examine the similarities between supra-arcade downflows observed during solar flares and bursty bulk flows seen in the magnetotail, and find that these phenomena have remarkably similar speeds, velocity profiles and size scales. Thus we show manifest similarities in the magnetic reconfiguration in response to the ejection of coronal mass ejections in the corona and the ejection of plasmoids in the magnetotail. The subsequent return of loops to a quasi-potential state in the corona and field dipolarization in the magnetotail are physical analogs and trigger similar phenomena such as downflows, which provides key insights into the underlying drivers of the plasma dynamics.

## **Evaluating Uncertainties in Coronal Electron Temperature and Radial Speed Measurements Using a Simulation of the Bastille Day Eruption**

Nelson [Reginald](#), Orville St. Cyr, Joseph Davila, Lutz Rastaetter, Tibor Török

*Solar Physics* May 2018, 293:82

<https://link.springer.com/article/10.1007/s11207-018-1301-x>

Obtaining reliable measurements of plasma parameters in the Sun's corona remains an important challenge for solar physics. We previously presented a method for producing maps of electron temperature and speed of the solar corona using K-corona brightness measurements made through four color filters in visible light, which were tested for their accuracies using models of a structured, yet steady corona. In this article we test the same technique using a coronal model of the Bastille Day (14 July 2000) coronal mass ejection, which also contains quiet areas and streamers. We use the coronal electron density, temperature, and flow speed contained in the model to determine two K-coronal brightness ratios at (410.3, 390.0 nm) and (423.3, 398.7 nm) along more than 4000 lines of sight. Now assuming that for real observations, the only information we have for each line of sight are these two K-coronal brightness ratios, we use a spherically symmetric model of the corona that contains no structures to interpret these two ratios for electron temperature and speed. We then compare the interpreted (or measured) values for each line of sight with the true values from the model at the plane of the sky for that same line of sight to determine the magnitude of the errors. We show that the measured values closely match the true values in quiet areas. However, in locations of coronal structures, the measured values are predictably underestimated or overestimated compared to the true values, but can nevertheless be used to determine the positions of the structures with respect to the plane of the sky, in front or behind. Based on our results, we propose that future white-light coronagraphs be equipped to image the corona using four color filters in order to routinely create coronal maps of electron density, temperature, and flow speed.

## Exploring the Impact of the Aging Effect on Inferred Properties of Solar Coronal Mass Ejections

F. [Regnault](#)<sup>1</sup>, N. Al-Haddad<sup>1</sup>, N. Lugaz<sup>1</sup>, C. J. Farrugia<sup>1</sup>, B. Zhuang<sup>1</sup>, W. Yu<sup>1</sup>, and A. Strugarek<sup>2</sup>  
2024 ApJL 966 L17

<https://iopscience.iop.org/article/10.3847/2041-8213/ad3806/pdf>

In situ measurements of coronal mass ejections (CMEs) when they pass over an interplanetary probe are one of the main ways we directly measure their properties. However, such in situ profiles are subject to several observational constraints that are still poorly understood. This work aims at quantifying one of them, namely, the aging effect, using a CME simulated with a three-dimensional magnetohydrodynamical code. The synthetic in situ profile and the instantaneous profile of the magnetic field strength differ more from each other when taken close to the Sun than far from it. Moreover, out of three properties we compute in this study (i.e., size, distortion parameter, and expansion speed), only the expansion speed shows a dependence of the aging as a function of distance. It is also the property that is the most impacted by the aging effect as it can amount to more than  $100 \text{ km s}^{-1}$  for CMEs observed closer than 0.15 au. This work calls for caution when deducing the expansion speed from CME profiles when they still are that close to the Sun since the aging effect can significantly impact the derived properties.

## Eruption and propagation of twisted flux ropes from the base of the solar corona to 1 au

F. [Regnault](#), [A. Strugarek](#), [M. Janvier](#), [F. Auchère](#), [N. Lugaz](#), [N. Al-Haddad](#)

A&A 670, A14 2023

<https://arxiv.org/pdf/2211.02569.pdf>

<https://www.aanda.org/articles/aa/pdf/2023/02/aa44483-22.pdf>

Interplanetary Coronal Mass Ejections (ICMEs) originate from the eruption of complex magnetic structures occurring in our star's atmosphere. Determining the general properties of ICMEs and the physical processes at the heart of their interactions with the solar wind is a hard task, in particular using only unidimensional in situ profiles. Thus, these phenomena are still not well understood. In this study we simulate the propagation of a set of flux ropes in order to understand some of the physical processes occurring during the propagation of an ICME such as their growth or their rotation. We present simulations of the propagation of a set of flux ropes in a simplified solar wind. We consider different magnetic field strengths and sizes at the initiation of the eruption, and characterize their influence on the properties of the flux ropes during their propagation. We use the 3D MHD module of the PLUTO code on an Adaptive Mesh Refinement grid. The evolution of the magnetic field of the flux rope during the propagation matches evolution law deduced from in situ observations. We also simulate in situ profiles that spacecraft would have measured at the Earth, and we compare with the results of statistical studies. We find a good match between simulated in situ profiles and typical profiles obtained in these studies. During their propagation, flux ropes interact with the magnetic field of the wind but still show realistic signatures of ICMEs when analyzed with synthetic satellite crossings. We also show that flux ropes with different shapes and orientations can lead to similar unidimensional crossings. This warrants some care when extracting magnetic topology of ICMEs using unidimensional crossings.

## A new look at a polar crown cavity as observed by SDO/AIA Structure and dynamics ★

S. [Régnier](#), R. W. Walsh and C. E. Alexander

A&A 533, L1 (2011), [File](#)

Context. The Solar Dynamics Observatory (SDO) was launched in February 2010 and is now providing an unprecedented view of the solar activity at high spatial resolution and high cadence covering a broad range of temperature layers of the atmosphere.

Aims. We aim at defining the structure of a polar crown cavity and describing its evolution during the erupting process.

Methods. We use the high-cadence time series of SDO/AIA observations at  $304 \text{ \AA}$  (50000 K) and  $171 \text{ \AA}$  (0.6 MK) to determine the structure of the polar crown cavity and its associated plasma, as well as the evolution of the cavity during the different phases of the eruption. We report on the observations recorded on **13 June 2010** located on the north-west limb.

Results. We observe coronal plasma shaped by magnetic field lines with a negative curvature (U-shape) sitting at the bottom of a cavity. The cavity is located just above the polar crown filament material. We thus observe the inner part of the cavity above the filament as depicted in the classical three part coronal mass ejection (CME) model composed of a filament, a cavity, and a CME front. The filament (in this case a polar crown filament) is part of the cavity, and it makes a continuous structuring from the filament to the CME front depicted by concentric ellipses (in a 2D cartoon).

Conclusions. We propose to define a polar crown cavity as a density depletion sitting above denser polar crown filament plasma drained down the cavity by gravity. As part of the polar crown filament, plasma at different temperatures (ranging from 50000 K to 0.6 MK) is observed at the same location on the cavity dips and sustained by a competition between the gravity and the curvature of magnetic field lines. The eruption of the polar crown cavity as a solid body can be decomposed into two phases: a slow rise at a speed of  $0.6 \text{ km s}^{-1}$  and an acceleration phase at a mean speed of  $25 \text{ km s}^{-1}$ .

## **Penumbral Waves driving Solar chromospheric fan-shaped jets**

A. [Reid](#), [V. M. J. Henriques](#), [M. Mathioudakis](#), [T. Samanta](#)

ApJL 2018

<https://arxiv.org/pdf/1802.07537.pdf>

We use H $\alpha$  imaging spectroscopy taken via the Swedish 1-m Solar Telescope (SST) to investigate the occurrence of fan-shaped jets at the solar limb. We show evidence for near-simultaneous photospheric reconnection at a sunspot edge leading to the jets appearance, with upward velocities of 30 km/s, and extensions up to 8 Mm. The brightening at the base of the jets appears recurrent, with a periodicity matching that of the nearby sunspot penumbra, implying running penumbral waves could be the driver of the jets. The jets' constant extension velocity implies that a driver counteracting solar gravity exists, possibly as a result of the recurrent reconnection erupting material into the chromosphere. These jets also show signatures in higher temperature lines captured from the Solar Dynamics Observatory (SDO), indicating a very hot jet front, leaving behind optically thick cool plasma in its wake. **2014 August 02**

**UKSP Nugget: #86** Dec 2017 <http://www.uksolphys.org/uksp-nugget/86-evidence-of-recurrent-reconnection-driving-fan-shaped-jets/>

## **Ellerman Bombs with Jets: Cause and Effect**

A. [Reid](#)<sup>1,2</sup>, [M. Mathioudakis](#)<sup>1</sup>, [E. Scullion](#)<sup>3</sup>, [J. G. Doyle](#)<sup>2</sup>, [S. Shelyag](#)<sup>4</sup>, and [P. Gallagher](#)

2015 ApJ 805 64

Ellerman Bombs (EBs) are thought to arise as a result of photospheric magnetic reconnection. We use data from the Swedish 1 m Solar Telescope to study EB events on the solar disk and at the limb. Both data sets show that EBs are connected to the foot points of forming chromospheric jets. The limb observations show that a bright structure in the H $\alpha$  blue wing connects to the EB initially fueling it, leading to the ejection of material upwards. The material moves along a loop structure where a newly formed jet is subsequently observed in the red wing of H $\alpha$ . In the disk data set, an EB initiates a jet which propagates away from the apparent reconnection site within the EB flame. The EB then splits into two, with associated brightenings in the inter-granular lanes. Micro-jets are then observed, extending to 500 km with a lifetime of a few minutes. Observed velocities of the micro-jets are approximately 5–10 km s<sup>-1</sup>, while their chromospheric counterparts range from 50 to 80 km s<sup>-1</sup>. MURaM simulations of quiet Sun reconnection show that micro-jets with properties similar to those of the observations follow the line of reconnection in the photosphere, with associated H $\alpha$  brightening at the location of increased temperature.

## **THE RELATIONSHIP BETWEEN CORONAL DIMMING AND CORONAL MASS EJECTION PROPERTIES**

A. A. [Reinard](#)<sup>1,3</sup> and D. A. [Biesecker](#)<sup>2</sup>

Astrophysical Journal, 705:914–919, 2009, File

Coronal dimmings are closely related to the footpoints of coronal mass ejections (CMEs) and, as such, offer information about CME origins and evolution. In this paper, we investigate the relationship between CME and dimming properties. In particular, we compare CME quantities for events with and without associated dimmings. We find that dimming-associated CMEs, on average, have much higher speeds than non-dimming-associated events. In fact, CMEs without an associated dimming do not appear to travel faster than 800 km s<sup>-1</sup>, i.e., the fast solar wind speed. Dimming-associated events are also more likely to be associated with flares, and those flares tend to have the highest magnitudes. We propose that each of these phenomena is affected by the energy available in the source region. Highly energetic source regions produce fast CMEs that are accompanied by larger flares and visible dimmings, while less energetic source regions produce slow CMEs that are accompanied by smaller flares and may or may not have dimmings. The production of dimmings in the latter case may depend on a number of factors including initiation height of the CME, source region magnetic configuration, and observational effects. These results have important implications for understanding and predicting CME initiations.

## **CORONAL MASS EJECTION-ASSOCIATED CORONAL DIMMINGS**

A. A. [Reinard](#), D. A. [Biesecker](#),

The Astrophysical Journal, 674:576-585, 2008, File

We report on a statistical analysis of 96 CME-associated EUV coronal dimmings between 1998 and 2000. We investigate the size and location of the events and characterize how these events evolve with time. The durations typically range from 3 to 12 hr. The dimmings appear most frequently within the belt of active regions (20–50° latitude). Dimming events are generally symmetric in latitude and longitude with some tendency to be broader in latitude. The temporal profiles of most events are characterized by a sharp rise and a gradual recovery. Although the majority of cases are well fit by a single recovery slope, a large minority of events have a two-part decay with an initial decaying slope that is similar in magnitude to the rising slope and a secondary, flatter, decay lasting several hours.

## **Coronal mass ejection kinematics deduced from white light (Solar Mass Ejection Imager) and radio (Wind/WAVES) observations**

[M. J. Reiner](#), [B. V. Jackson](#), [D. F. Webb](#), [D. R. Mizuno](#), [M. L. Kaiser](#), [J.-L. Bougeret](#)



JGR [Volume 110, Issue A9](#) A09S14 2005

<https://agupubs.onlinelibrary.wiley.com/doi/epdf/10.1029/2004JA010943>

<https://doi.org/10.1029/2004JA010943>

White-light and radio observations are combined to deduce the coronal and interplanetary kinematics of a fast coronal mass ejection (CME) that was ejected from the Sun at about 1700 UT on **2 November 2003**. The CME, which was associated with an X8.3 solar flare from W56°, was observed by the Mauna Loa and Solar and Heliospheric Observatory (SOHO) Large-Angle Spectrometric Coronagraph (LASCO) coronagraphs to 14 R<sub>⊙</sub>. The measured plane-of-sky speed of the LASCO CME was 2600 km s<sup>-1</sup>. To deduce the kinematics of this CME, we use the plane-of-sky white light observations from both the Solar Mass Ejection Imager (SMEI) all-sky camera on board the Coriolis spacecraft and the SOHO/LASCO coronagraph, as well as the frequency drift rate of the low-frequency radio data and the results of the radio direction-finding analysis from the WAVES experiment on the Wind spacecraft. In agreement with the in situ observations for this event, we find that both the white light and radio observations indicate that the CME must have decelerated significantly beginning near the Sun and continuing well into the interplanetary medium. More specifically, by requiring self-consistency of all the available remote and in situ data, together with a simple, but not unreasonable, assumption about the general characteristic of the CME deceleration, we were able to deduce the radial speed and distance time profiles for this CME as it propagated from the Sun to 1 AU. The technique presented here, which is applicable to mutual SMEI/WAVES CME events, is expected to provide a more complete description and better quantitative understanding of how CMEs propagate through interplanetary space, as well as how the radio emissions, generated by propagating CME/shocks, relate to the shock and CME. This understanding can potentially lead to more accurate predictions for the onset times of space weather events, such as those that were observed during this unique period of intense solar activity.

### **CONSTRAINTS ON CORONAL MASS EJECTION DYNAMICS FROM SIMULTANEOUS RADIO AND WHITE-LIGHT OBSERVATIONS**

M. J. [Reiner](#), A. Vourlidas, O. C. St. Cyr, J. T. Burkepile, R. A. Howard, M. L. Kaiser, N. P. Prestage, and J.-L. Bougeret

*Astrophysical Journal*, 590:533–546, **2003**; **File**

Simultaneous radio and white-light observations are used to deduce information on the dynamics of two coronal mass ejection (CME) events that occurred about 2 hr apart on 2001 January 20 and that were associated with eruptions from the same active region on the Sun. The analysis combines both space-based and ground-based data. The radio data were obtained from the WAVES experiment on the Wind spacecraft and from the Culgoora radiospectrograph in Australia. The white-light data were from the LASCO experiment on SOHO and from the Mk4 coronameter at the Mauna Loa Solar Observatory. For these CME events we demonstrate that the frequency drift rate of the type II radio emissions, generated by the shocks driven by the white-light CMEs, are consistent with the plane-of-sky height-time measurements, provided that the propagation direction of the CMEs and their associated radio sources was along a radial line from the Sun at a solar longitude of E50°. These results imply that the “true” CME speeds were estimated to be 1.4 times higher than the measured plane-of-sky speeds and that the CMEs originated from solar eruptions centered near E50°. This CME origin is consistent with the known active region and flare site associated with these two CME events. Furthermore, we argue that the type II radio emissions generated by these CMEs must have originated in enhanced density regions of the corona. We investigate whether the type II radiation could have originated in one or more dense coronal streamers, whose densities were estimated from the polarization brightness measurements made by LASCO at that time. Finally, we use these radio and white-light observations to speculate about the dynamics and scales involved in the interaction between these two CMEs.

### **Towards data-driven modeling and real-time prediction of solar flares and coronal mass ejections**

[M. Rempel](#), [Y. Fan](#), [M. Dikpati](#), [A. Malanushenko](#) (HAO/NCAR), [M. D. Kazachenko](#) (CU/NSO), [M. C. M. Cheung](#), [G. Chintzoglou](#) (LMSAL), [X. Sun](#) (U. of Hawaii), [G. H. Fisher](#) (U. of Berkeley), [T. Y. Chen](#) (Columbia)

Heliophysics 2050 White Paper **2023**

<https://arxiv.org/ftp/arxiv/papers/2212/2212.14384.pdf>

Modeling of transient events in the solar atmosphere requires the confluence of 3 critical elements: (1) model sophistication, (2) data availability, and (3) data assimilation. This white paper describes required advances that will enable statistical flare and CME forecasting (e.g. eruption probability and timing, estimation of strength, and CME details, such as speed and magnetic field orientation) similar to weather prediction on Earth.

### **CME-Flare Association and the Role of Reconnection in CME Acceleration.**

[Reva](#), A., [Loboda](#), I., [Bogachev](#), S. & [Alexey Kirichenko](#)

*Sol Phys* 299, 55 (**2024**).

<https://doi.org/10.1007/s11207-024-02302-1>

The association of coronal mass ejections (CMEs) with flares is related to the question of whether reconnection is necessary for the CME eruption. Indeed, if reconnection happens during a CME eruption, the plasma is heated, which can be observed as a flare. In this work, we study the CME-flare association using data obtained with the Mg XII spectroheliograph on board the *Complex Orbital Observations Near-Earth of Activity on the Sun* (CORONAS-F) satellite. This instrument is sensitive only to the emission of plasma with a temperature greater than 4 MK, which makes it a convenient tool for detection of flaring activity. During our analysis, we first searched for CMEs detected during the Mg XII observations by the *Large Angle and Spectroscopic Coronagraph* (LASCO). Then, we visually checked the Mg XII images for flaring activity. We found that during the Mg XII observations (2001–2003), 198 CMEs were detected by LASCO. One hundred sixty of them (81%) are associated with flares seen in the Mg XII images. The strength of flares associated with *narrow CMEs – jet-like ejecta* – is uniformly distributed in the A–C GOES class range. The speed of narrow CMEs does not depend on the flare strength. For normal CMEs (motion of both magnetic field and plasma), the flare strength varies from A to X class with a peak of the distribution at the C level. The median speed and the kinetic energy of normal CMEs weakly depend on flare strength for weak flares (below C) and strongly for strong ones (M and X). Our results suggest that at solar maximum reconnection occurs during most CMEs. For strong flares (M and X), the reconnection is a dominant acceleration mechanism. For weak flares (C and below), other mechanisms start to play a bigger role.

### Plasma Heating During Coronal Mass Ejections Observed in X-Rays

[Anton Reva](#), [Sergey Bogachev](#), [Ivan Loboda](#), [Alexey Kirichenko](#) & [Artem Ulyanov](#)

[Solar Physics](#) volume 298, Article number: 61 (2023)

<https://doi.org/10.1007/s11207-023-02154-1>

<https://link.springer.com/content/pdf/10.1007/s11207-023-02154-1.pdf>

In this work, we study where heating takes place during coronal mass ejections (CMEs). For this purpose, we have used the data of the Mg XII spectroheliograph on board the Complex Orbital Observations Near-Earth of Activity on the Sun (CORONAS)-F satellite. This instrument obtained images of the solar corona in the Mg XII 8.42 Å line, which emits only at temperatures higher than 4 MK. After analyzing the Mg XII data archive from 2001 to 2003, we found ten high-temperature eruptive events. Each of them was associated with a CME and nine were associated with a flare. The eruptive structures had temperatures higher than 4 MK and a characteristic size of 100–200 Mm. The events were observed by the Mg XII spectroheliograph for 10 min to 3 h. In the Mg XII images, the peak intensity of the eruptive structures was 0.2–14.4% of the peak intensity of the flaring active regions below them. Based on the shape of the events, we divided them into three groups: loop-like, sheet-like, and cloud-like. We interpreted loop-like events as hot flux ropes and sheet-like ones as hot plasma surrounding current sheets. Based on the available data, we cannot determine the nature of the cloud-like events. Their appearance could be caused by projection effects, a postflare reconnection, a shock wave, or a small-scale reconnection in the CME volume. Our estimates suggest that, in solar maxima, plasma should be heated above 4 MK during approximately one out of six CMEs. 2001 Dec 11, 26 Feb 2002, 27 Feb 2002, 26 May 2002, 29 May 2002, 30 May 2002, 23 Aug 2002, 24 Aug 2002, 15 Feb 2003, 16 Feb 2003,

### Observations of the Coronal Mass Ejection with a Complex Acceleration Profile

[A.A. Reva](#), [A.S. Kirichenko](#), [A.S. Ulyanov](#), [S.V. Kuzin](#)

2017 ApJ 851 108

<https://arxiv.org/pdf/1712.06430.pdf>

We study the coronal mass ejection (CME) with a complex acceleration profile. The event occurred on **April 23, 2009**. It had an impulsive acceleration phase, an impulsive deceleration phase, and a second impulsive acceleration phase. During its evolution, the CME showed signatures of different acceleration mechanisms: kink instability, prominence drainage, flare reconnection, and a CME-CME collision. The special feature of the observations is the usage of the TESIS EUV telescope. The instrument could image the solar corona in the Fe 171 Å line up to a distance of  $2 R_{\odot}$  from the center of the Sun. This allows us to trace the CME up to the LASCO/C2 field of view without losing the CME from sight. The onset of the CME was caused by kink instability. The mass drainage occurred after the kink instability. The mass drainage played only an auxiliary role: it decreased the CME mass, which helped to accelerate the CME. The first impulsive acceleration phase was caused by the flare reconnection. We observed the two ribbon flare and an increase of the soft X-ray flux during the first impulsive acceleration phase. The impulsive deceleration and the second impulsive acceleration phases were caused by the CME-CME collision. The studied event shows that CMEs are complex phenomena that cannot be explained with only one acceleration mechanism. We should seek a combination of different mechanisms that accelerate CMEs at different stages of their evolution.

### CURRENT SHEET STRUCTURES OBSERVED BY THE TESIS EUV TELESCOPE DURING A FLUX ROPE ERUPTION ON THE SUN

[A. A. Reva](#), [A. S. Ulyanov](#), and [S. V. Kuzin](#)

2016 ApJ 832 16

<https://arxiv.org/pdf/1611.04346v1.pdf>

We use the TESIS EUV telescope to study the current sheet signatures observed during flux rope eruption. The special feature of the TESIS telescope was its ability to image the solar corona up to a distance of  $2 R_{\odot}$  from the Sun's center in

the Fe 171 Å line. The Fe 171 Å line emission illuminates the magnetic field lines, and the TESIS images reveal the coronal magnetic structure at high altitudes. The analyzed coronal mass ejection (CME) had a core with a spiral—flux rope—structure. The spiral shape indicates that the flux rope radius varied along its length. The flux rope had a complex temperature structure: cold legs (70,000 K, observed in He 304 Å line) and a hotter core (0.7 MK, observed in Fe 171 Å line). Such a structure contradicts the common assumption that the CME core is a cold prominence. When the CME impulsively accelerated, a dark double Y-structure appeared below the flux rope. The Y-structure timing, location, and morphology agree with the previously performed MHD simulations of the current sheet. We interpreted the Y-structure as a hot envelope of the current sheet and hot reconnection outflows. The Y-structure had a thickness of 6.0 Mm. Its length increased over time from 79 Mm to more than 411 Mm.

## **BREAKOUT RECONNECTION OBSERVED BY THE TESIS EUV TELESCOPE**

A. A. [Reva](#), A. S. Ulyanov, S. V. Shestov, and S. V. Kuzin

2016 ApJ 816 90

<http://arxiv.org/pdf/1601.04511v1.pdf>

We present experimental evidence of the coronal mass ejection (CME) breakout reconnection, observed by the TESIS EUV telescope. The telescope could observe solar corona up to  $2 R_{\odot}$  from the Sun center in the Fe 171 Å line. Starting from **2009 April 8**, TESIS observed an active region (AR) that had a quadrupolar structure with an X-point  $0.5 R_{\odot}$  above photosphere. A magnetic field reconstructed from the Michelson Doppler Imager data also has a multipolar structure with an X-point above the AR. At 21:45 UT on April 9, the loops near the X-point started to move away from each other with a velocity of  $\approx 7 \text{ km s}^{-1}$ . At 01:15 UT on April 10, a bright stripe appeared between the loops, and the flux in the GOES 0.5–4 Å channel increased. We interpret the loops' sideways motion and the bright stripe as evidence of the breakout reconnection. At 01:45 UT, the loops below the X-point started to slowly move up. At 15:10 UT, the CME started to accelerate impulsively, while at the same time a flare arcade formed below the CME. After 15:50 UT, the CME moved with constant velocity. The CME evolution precisely followed the breakout model scenario.

**April 17, 2009**

## **Initiation and Early Evolution of the Coronal Mass Ejection on 2009 May 13 from Extreme-ultraviolet and White-light Observations**

A. A. [Reva](#), A. S. Ulyanov, S. A. Bogachev, and S. V. Kuzin

2014 ApJ 793 140

<http://arxiv.org/pdf/1509.07713v1.pdf>

We present the results of the observations of a coronal mass ejection (CME) that occurred on **2009 May 13**. The most important feature of these observations is that the CME was observed from the very early stage (the solar surface) up to a distance of 15 solar radii ( $R_{\odot}$ ). Below  $2 R_{\odot}$ , we used the data from the TESIS extreme-ultraviolet telescopes obtained in the Fe 171 Å and He 304 Å lines, and above  $2 R_{\odot}$ , we used the observations of the LASCO C2 and C3 coronagraphs. The CME was formed at a distance of  $0.2\text{--}0.5 R_{\odot}$  from the Sun's surface as a U-shaped structure, which was observed both in the 171 Å images and in the white light. Observations in the He 304 Å line showed that the CME was associated with an erupting prominence, which was not located above—as the standard model predicts—but rather in the lowest part of the U-shaped structure close to the magnetic X point. The prominence location can be explained with the CME breakout model. Estimates showed that CME mass increased with time. The CME trajectory was curved—its heliolatitude decreased with time. The CME started at a latitude of  $50^{\circ}$  and reached the ecliptic plane at distances of  $2.5 R_{\odot}$ . The CME kinematics can be divided into three phases: initial acceleration, main acceleration, and propagation with constant velocity. After the CME, onset GOES registered a sub-A-class flare.

## **Eruptivity Criteria for Solar Coronal Flux Ropes in Magnetohydrodynamic and Magnetofrictional Models**

[Oliver E.K. Rice](#), [Anthony R. Yeates](#)

ApJ 955 114 2023

<https://arxiv.org/pdf/2308.13807.pdf>

<https://iopscience.iop.org/article/10.3847/1538-4357/acefc1/pdf>

We investigate which scalar quantity or quantities can best predict the loss of equilibrium and subsequent eruption of magnetic flux ropes in the solar corona. Our models are initialized with a potential magnetic arcade, which is then evolved by means of two effects on the lower boundary: firstly a gradual shearing of the arcade, modelling differential rotation on the solar surface, and secondly supergranular diffusion. These result in flux cancellation at the polarity inversion line and the formation of a twisted flux rope. We use three model setups: full magnetohydrodynamics (MHD) in cartesian coordinates, and the magnetofrictional model in both cartesian and polar coordinates. The flux ropes are translationally-invariant, allowing for very fast computational times and thus a comprehensive parameter study, comprising hundreds of simulations and thousands of eruptions. Similar flux rope behavior is observed using either magnetofriction or MHD, and there are several scalar criteria that could be used as proxies for eruptivity. The most consistent predictor of eruptions in either model is the squared current in the axial direction of the rope, normalised by the relative helicity, although a variation on the previously proposed 'eruptivity index' is also found to perform well in both the magnetofrictional and MHD simulations.

## Eruptivity Criteria for Two-dimensional Magnetic Flux Ropes in the Solar Corona

[Oliver E.K. Rice](#), [Anthony R. Yeates](#)

Frontiers in Astronomy and Space Sciences 9:849135 2022

<https://arxiv.org/pdf/2203.07951.pdf>

<https://doi.org/10.3389/fspas.2022.849135>

We apply the magneto-frictional approach to investigate which quantity or quantities can best predict the loss of equilibrium of a translationally-invariant magnetic flux rope. The flux rope is produced self-consistently by flux cancellation combined with gradual footpoint shearing of a coronal arcade which is open at the outer boundary. This models the magnetic field in decaying active regions on the Sun. Such a model permits two types of eruption: episodic small events caused by shearing and relaxation of the overlying arcade, and major eruptions of the main low-lying coronal flux rope. Through a parameter study, we find that the major eruptions are best predicted not by individual quantities but by thresholds in the ratios of squared rope current to either magnetic energy or relative magnetic helicity. We show how to appropriately define the latter quantity for translationally-invariant magnetic fields, along with a related eruptivity index that has recently been introduced for three-dimensional magnetic fields. In contrast to previous configurations studied, we find that the eruptivity index has only a weak predictive skill, and in fact is lower prior to eruption, rather than higher. This is because the overlying background magnetic field has the same direction as the arcade itself. Thus we propose that there are a whole class of solar eruptions that cannot be predicted by a high eruptivity index.

## CME observations using LOFAR: Latest results from interplanetary scintillation and Faraday rotation

Fallows [Richard](#)\*1, Mario Bisi<sup>2</sup>, Elizabeth Jensen<sup>3</sup>, Charlotte Sobey<sup>4</sup>, Bernie Jackson<sup>5</sup>, and Tarraneh Eftekhari

CESRA 2016 abstracts p.31

[http://cesra2016.sciencesconf.org/conference/cesra2016/pages/CESRA2016\\_prog\\_abs\\_book\\_v1.pdf](http://cesra2016.sciencesconf.org/conference/cesra2016/pages/CESRA2016_prog_abs_book_v1.pdf)

Several observations using the Low Frequency Array (LOFAR - a radio telescope centred on the Netherlands with stations across Europe) have been undertaken to observe the passage of CMEs through interplanetary space. By measuring the interplanetary scintillation (IPS) of compact radio sources as a CME passes across the lines of sight, the velocity and relative density of the various components from nose to prominence material can be assessed. Observations of Faraday rotation (FR) in signals from polarised sources such as pulsars can be used as a remote-sensing method of determining magnetic fields: If the contributions from the interstellar medium and Earth's ionosphere can be accurately assessed and subtracted, this can act as a remote probe of the heliospheric magnetic field, representing one of the only methods by which global measurements of this parameter could be made. Here, we summarise the initial results of dedicated LOFAR observations designed to observe the full passage of several CMEs using measurements of IPS and present the first tentative results from attempts to determine heliospheric magnetic field parameters during the passage of a CME.

## Solar Energetic Particle-Associated Coronal Mass Ejections Observed by the Mauna Loa Solar Observatory Mk3 and Mk4 Coronameters

I. G. [Richardson](#), [O. C. St Cyr](#), [J. T. Burkepile](#), [H. Xie](#), [B. J. Thompson](#)

Solar Phys. 298, Article number: 105 2023

<https://arxiv.org/pdf/2308.10826.pdf>

<https://link.springer.com/content/pdf/10.1007/s11207-023-02192-9.pdf>

We report on the first comprehensive study of the coronal mass ejections (CMEs) associated with ~25 MeV solar energetic proton (SEP) events in 1980-2013 observed in the low/inner corona by the Mauna Loa Solar Observatory (MLSO) Mk3 and Mk4 coronameters. Where possible, these observations are combined with spacebased observations from the Solar Maximum Mission C/P, P78-1 SOLWIND or SOHO/LASCO coronagraphs. The aim of the study is to understand directly-measured (rather than inferred from proxies) CME motions in the low to middle corona and their association with SEP acceleration, and hence attempt to identify early signatures that are characteristic of SEP acceleration in ground-based CME observations that may be used to warn of impending SEP events. Although we find that SEP events are associated with CMEs that are on average faster and wider than typical CMEs observed by MLSO, a major challenge turns out to be determining reliable estimates of the CME dynamics in the low corona from the 3-minute cadence Mk3/4 observations since different analysis techniques can produce inconsistent results. This complicates the assessment of what early information on a possible SEP event is available from these low coronal observations. **25 Mar 1981, 7 Nov 1987, 2-3 Nov 2003, June 16, 2005, September 7, 2005, 11 Jun-30 Jul 2012, June 13, 2022**

**Table 1.** MLSO Mk3 Coronameter CMEs Associated With ~ 25 MeV Solar Proton Events. 1980-1998

**Table 2.** MLSO Mk4 Coronameter CMEs Associated With ~ 25 MeV Solar Proton Events 1999-2013

## CORONAL MASS EJECTION DYNAMICS REGARDING RADIAL AND EXPANSION SPEEDS

Nivaor R. [Rigozo](#)<sup>1</sup>, Alisson Dal Lago<sup>2</sup> and D. J. R. Nordeman

2011 ApJ 738 107, [File](#)

A new technique for the detection of coronal mass ejection (CME) speeds using image processing was applied. This technique permits us to determine the CME dynamics: radial and expansion distances, velocities, and accelerations. The CME dynamics is determined by the selection of a radial direction in a given Large Angle and Spectroscopic Coronagraph image, which starts just before the occulter (close to the center) and extends to the extremity of the image. By taking a series of images and extracting the same radial direction, it is possible to have a time history of any moving feature along this direction. This technique allows us to choose the number of directions that is used in the CME detection to determine its dynamics. This paper presents the results for the dynamical features (radial and expansion) of five CME events observed on **1999 February 5, 2001 February 2, 2002 March 1, 2003 December 2, and 2007 December 31.**

## **Properties of the Fast Forward Shock Driven by the [July 23 2012](#) Extreme Coronal Mass Ejection**

[Riley](#), Pete; Giacalone, Joe; Liu, Ying

IAU General Assembly, Meeting #29, id.2255759 **2015**

Late on July 23, 2012, the STEREO-A spacecraft encountered a fast forward shock driven by a coronal mass ejection launched earlier that same day. The estimated travel time of the disturbance, together with the massive magnetic field strengths measured within the ejecta, made it one of the most extreme events observed during the space era. In this study, we examine the properties of the shock wave. Because an instrument malfunction limited the available plasma measurements during the interval surrounding the CME, our approach has been modified to capitalize on the available measurements and suitable proxies, where possible. We were able to infer the following properties. First, the shock normal,  $n$ , was pointing predominantly in the radial direction (0.97,-0.09,-0.23). Second, the angle between  $n$  and the upstream magnetic field,  $\theta_{Bn}$ , was estimated to be  $\sim 34$  Deg., making the shock "quasi-parallel," and consistent with there being an earlier "preconditioning" ICME. Third, the shock speed was estimated to be between  $\sim 2700$  and  $\sim 3300$  km/s, depending on the technique employed. Finally, in contrast to an earlier study, we found no evidence that the properties of the shock were modified by energetic particles: The change in ram pressure upstream of the shock was  $\sim 5$  times larger than the pressure from the energetic particles.

## **"Bursty" Reconnection Following Solar Eruptions: MHD Simulations and Comparison with Observations**

Pete [Riley](#), Roberto Lionello, Zoran Mikic, Jon Linker, Eric Clark, Jun Lin, and Yuan-Kuen Ko

The Astrophysical Journal, 655:591–597, **2007**, **File**.

2003 Nov 18, E-limb. Post-eruptive arcades are frequently seen in the aftermath of coronal mass ejections (CMEs). The formation of these loops at successively higher altitudes, coupled with the classic "two-ribbon" flare seen in  $H_{\alpha}$ , are interpreted as reconnection of the coronal magnetic field that has been dragged outward by the CME. White-light observations of "rays," which have been interpreted as being coincident with the current sheet at the reconnection site underneath the erupting CME, also provide evidence for its occurrence. "Blobs" occasionally seen within these rays suggest an even richer level of structure. In this report, we present numerical simulations that reproduce both the observed rays and the formation and evolution of the blobs.

## **ON THE RATES OF CORONAL MASS EJECTIONS: REMOTE SOLAR AND IN SITU OBSERVATIONS**

P. [Riley](#), C. Schatzman, H. V. Cane, I. G. Richardson, and N. Gopalswamy

The Astrophysical Journal, 647:648Y653, **2006**, **File**

## **3D MHD Time-dependent Charge State Ionization and Recombination Modeling of the Bastille Day Coronal Mass Ejection**

Yeimy J. [Rivera](#)<sup>1</sup>, John C. Raymond<sup>1</sup>, Katharine K. Reeves<sup>1</sup>, Susan T. Lepri<sup>2</sup>, Roberto Lionello<sup>3</sup>, Cooper Downs<sup>3</sup>, Maurice L. Wilson<sup>4</sup>, and Nicolas Trueba<sup>1</sup>

2023 *ApJ* **955** 65

<https://iopscience.iop.org/article/10.3847/1538-4357/aceef8/pdf>

Heavy ion signatures of coronal mass ejections (CMEs) indicate that rapid and strong heating takes place during the eruption and early stages of propagation. However, the nature of the heating that produces the highly ionized charge states often observed in situ is not fully constrained. An MHD simulation of the Bastille Day CME serves as a test bed to examine the origin and conditions of the formation of heavy ions evolving within the CME in connection with those observed during its passage at L1. In particular, we investigate the bimodal nature of the Fe charge state distribution, which is a quintessential heavy ion signature of CME substructure, as well as the source of the highly ionized plasma. We find that the main heating experienced by the tracked plasma structures linked to the ion signatures examined is due to field-aligned thermal conduction via shocked plasma at the CME front. Moreover, the bimodal Fe distributions can be generated through significant heating and rapid cooling of prominence material. However, although significant heating was achieved, the highest ionization stages of Fe ions observed in situ were not reproduced. In addition, the carbon and oxygen charge state distributions were not well replicated owing to anomalous heavy ion dropouts observed throughout the ejecta. Overall, the results indicate that additional ionization is needed to match observation. An important driver of ionization could come from suprathermal electrons, such as those produced via Fermi acceleration

during reconnection, suggesting that the process is critical to the development and extended heating of extreme CME eruptions, like the Bastille Day CME. **14 Jul 2000**

## **Identifying Spectral Lines to Study Coronal Mass Ejection Evolution in the Lower Corona**

Yeimy J. **Rivera**, Enrico Landi, and Susan T. Lepri

**2019** ApJS 243 34

[sci-hub.se/10.3847/1538-4365/ab2bfe](https://doi.org/10.3847/1538-4365/ab2bfe)

As prominences propagate away from the Sun via a coronal mass ejection (CME), they expand, accelerate, and are strongly heated. The heating is substantial enough to continuously ionize the prominence plasma, making it difficult to follow its dynamic evolution with a single extreme ultraviolet (EUV) narrow-band channel or a white light instrument. In this work, we identify useful spectral lines that can be utilized to study the prominence during the early stages of propagation. We generate nonequilibrium ion fractions from a previously studied multi-thermal component CME using the Michigan Ionization Code to compute synthetic intensities along the CME path. We test several emission lines produced by the multi-thermal evolution of the CME that span the EUV to the visible and infrared wavelength range, 100–14400 Å, and equilibrium formation temperatures between  $\log(T_e) = 4.3\text{--}6.7$ . We assess the visibility and diagnostic potential up to 2 solar radii of many lines in a wavelength range encompassing the EUV to the near-infrared, including those observed by many existing and past instruments, as well as upcoming observatories, such as the Daniel K. Inouye Solar Telescope, Upgraded Coronal Multi-channel Polarimeter, and Solar Orbiter/Spectral Imaging of the Coronal Environment.

## **Empirical Modeling of CME Evolution Constrained to ACE/SWICS Charge State Distributions**

Yeimy J. **Rivera**, Enrico Landi, Susan T. Lepri, and Jason A. Gilbert

**2019** ApJ 874 164

[sci-hub.se/10.3847/1538-4357/ab0e11](https://doi.org/10.3847/1538-4357/ab0e11)

It is generally accepted that coronal mass ejections (CMEs) undergo rapid heating as they are released from the Sun. However, to date, the heating mechanism remains an open question. To gain insight into the plasma heating, we derive the density, temperature, and velocity evolution of the **2005 January 9** interplanetary CME event from launch to ion freeze-in distance by examining ion distributions collected within the ejecta near the Earth. We use the Michigan Ionization Code to simulate the ion evolution and determine thermodynamic properties through an extensive iterative search that finds agreement between simulated and observed ion populations. The final results show that the ion distributions can be effectively reconstructed using a combination of ions generated within four distinct plasma structures traveling together. Three of the modeled plasma components derived originate from the prominence and the prominence–corona transition region (PCTR) structures, while a fourth plasma shares features common to the ambient corona. The absolute abundances computed for each plasma reveal that the prominence material contains photospheric composition, while the remaining PCTR and warmer plasma have coronal abundances. Furthermore, we computed an energy release rate for each plasma structure that includes the kinetic, potential, and thermal energy rates, along with the radiative cooling, thermal conduction, and adiabatic cooling rates. We found the prominence material's energy release rate to be consistently larger compared to the other components. In future work, the energy results will be used to investigate the feasibility of a proposed heating mechanism in an effort to gain a more comprehensive understanding of the eruption process.

## **NO TRACE LEFT BEHIND:**

## **STEREO OBSERVATION OF A CORONAL MASS EJECTION WITHOUT LOW CORONAL SIGNATURES**

**Stealth**

Eva **Robbrecht**<sup>1</sup>, Spiros Patsourakos<sup>1</sup> and Angelos Vourlidas<sup>2</sup>

ApJ, **701** 283-291 doi: [10.1088/0004-637X/701/1/283](https://doi.org/10.1088/0004-637X/701/1/283) **2009**, **File**;

The availability of high quality synoptic observations of the EUV and visible corona during the SOHO mission has advanced our understanding of the low corona manifestations of CMEs. The EUV imager/white light coronagraph connection has been proven so powerful, it is routinely assumed that if no EUV signatures are present when a CME is observed by a coronagraph, then the event must originate behind the visible limb. This assumption carries strong implications for space weather forecasting but has not been put to the test. This paper presents the first detailed analysis of a frontside, large-scale CME that has no obvious counterparts in the low corona as observed in EUV and H<sub>α</sub> wavelengths. The event was observed by the SECCHI instruments onboard the STEREO mission. The COR2A coronagraph observed a slow flux-rope type CME, while an extremely faint partial halo was observed in COR2B. The event evolved very slowly and is typical of the streamerblowout CME class. EUVI A 171 Å images show a concave feature above the east limb, relatively stable for about two days before the eruption, when it rises into the coronagraphic fields and develops into the core of the CME. None of the typical low corona signatures of a CME (flaring, EUV dimming, filament eruption, waves) were observed in the EUVI-B images, which we attribute to the unusually large height from which the flux-rope lifted off. This interpretation is supported by the CME mass measurements and estimates of the expected EUV dimming intensity. Only thanks to the availability of the two viewpoints we were able to identify the likely source region. The event originated along a neutral line over the quiet sun. No active regions were present anywhere on the visible (from STEREO B) face of the disk. Leaving no trace behind on the solar disk, this observation shows unambiguously that a CME eruption does not need to have clear on-disk signatures. Also it sheds

light on the question of ‘mystery’ geomagnetic storms, storms without clear solar origin (formerly called problem storms). We discuss the implications for space weather monitoring. Preliminary inspection of STEREO data indicates that events like this are not uncommon, particularly during the ongoing period of deep solar minimum. **June 2, 2008.**

## **AUTOMATED LASCO CME CATALOG FOR SOLAR CYCLE 23: ARE CMEs SCALE INVARIANT?**

E. [Robbrecht](#) et al **2009** ApJ 691 1222-1234

In this paper, we present the first automatically constructed LASCO coronal mass ejection (CME) catalog, a result of the application of the Computer Aided CME Tracking software (CACTus) on the LASCO archive during the interval 1997 September-2007 January. We have studied the CME characteristics and have compared them with similar results obtained by manual detection (CDAW CME catalog). On average, CACTus detects less than two events per day during solar minimum, up to eight events during maximum, nearly half of them being narrow ( $<20^\circ$ ). Assuming a correction factor, we find that the CACTus CME rate is surprisingly consistent with CME rates found during the past 30 years. The CACTus statistics show that small-scale outflow is ubiquitously observed in the outer corona. The majority of CACTus-only events are narrow transients related to previous CME activity or to intensity variations in the slow solar wind, reflecting its turbulent nature. A significant fraction (about 15%) of CACTus-only events were identified as independent events, thus not related to other CME activity. **The CACTus CME width distribution is essentially scale invariant in angular span over a range of scales from  $20^\circ$  to  $120^\circ$  while previous catalogs present a broad maximum around  $30^\circ$ .** The possibility that the size of coronal mass outflows follow a power-law distribution could indicate that no typical CME size exists, i.e., that the narrow transients are not different from the larger well defined CMEs.

## **Simulated Encounters of Parker Solar Probe with A Coronal-Hole Jet**

Merrill A [Roberts](#), [Vadim M Uritsky](#), [C Richard DeVore](#), [Judith T Karpen](#)

**2018** ApJ 866 14

<https://arxiv.org/pdf/1710.10323.pdf>

[sci-hub.tw/10.3847/1538-4357/aadb41](http://sci-hub.tw/10.3847/1538-4357/aadb41)

Solar coronal jets are small, transient features typically observed in coronal holes (CH). The upcoming Parker Solar Probe (PSP) mission provides the first opportunity to encounter CH jets in situ and clarify their internal structure and dynamics, necessitating a detailed grasp of a CH jet's defining characteristics. We present simulated PSP encounters with a CH jet, using projected PSP orbital parameters and a fully three-dimensional MHD model of a CH jet. We find that the three internal jet regions featuring different wave modes and levels of compressibility have distinct identifying signatures which could be detected by PSP. The leading wavefront of the jet and the plasma immediately behind it are characterized by a low density, trans-Alfvénic plasma flow, accompanied by the sudden onset of large-amplitude transverse velocity and magnetic field oscillations which are highly correlated in space and time. This region is shown to be purely Alfvénic, with the jet front itself showing characteristics of a fast switch-on type MHD shock. The lowest jet region appears as a compressible, non-Alfvénic region carrying most of the jet's mass. The region between the initial front and the dense region is mixed, sharing characteristics of the other two regions. We further examine a co-rotational encounter, holding the simulated spacecraft over the jet-producing region, to simulate PSP's co-rotational orbital phases, providing a comparison of all three jet regions. **2000 September 23**

## **The chromosphere above a $\delta$ -sunspot in the presence of fan-shaped jets**

Carolina [Robustini](#), [Jorrit Leenaarts](#), [Jaime de la Cruz Rodríguez](#)

A&A 609, A14 **2017**

<https://arxiv.org/pdf/1709.03864.pdf>

$\delta$ -sunspots are known to be favourable locations for fast and energetic events like flares and CMEs. The photosphere of this type of sunspots has been thoroughly investigated in the past three decades. The atmospheric conditions in the chromosphere are not so well known, however. This study is focused on the chromosphere of a  $\delta$ -sunspot that harbours a series of fan-shaped jets in its penumbra. The aim of this study is to establish the magnetic field topology and the temperature distribution in the presence of jets in the photosphere and the chromosphere. We use data from the Swedish 1-m Solar Telescope (SST) and the Solar Dynamics Observatory. We invert the spectropolarimetric FeI 6302-Å and CaII 8542-Å data from the SST using the non-LTE inversion code NICOLE to estimate the magnetic field configuration, temperature and velocity structure in the chromosphere. A loop-like magnetic structure is observed to emerge in the penumbra of the sunspot. The jets are launched from the loop-like structure. Magnetic reconnection between this emerging field and the pre-existing vertical field is suggested by hot plasma patches on the interface between the two fields. The height at which the reconnection takes place is located between  $\log \tau_{500} = -2$  and  $\log \tau_{500} = -3$ . The magnetic field vector and the atmospheric temperature maps show a stationary configuration during the whole observation. **2013 July 15**

## **Fan-shaped jets above the light bridge of a sunspot driven by reconnection★**

Carolina [Robustini](#)<sup>1</sup>, [Jorrit Leenaarts](#)<sup>1</sup>, [Jaime de la Cruz Rodríguez](#)<sup>1</sup> and [Luc Rouppe van der Voort](#)  
A&A 590, A57 (2016)

<http://www.aanda.org/articles/aa/pdf/2016/06/aa28022-15.pdf>

We report on a fan-shaped set of high-speed jets above a strongly magnetized light bridge (LB) of a sunspot observed in the H $\alpha$  line. We study the origin, dynamics, and thermal properties of the jets using high-resolution imaging spectroscopy in H $\alpha$  from the Swedish 1m Solar Telescope and data from the Solar Dynamics Observatory and Hinode. The H $\alpha$  jets have lengths of 7–38 Mm, are impulsively accelerated to a speed of  $\sim 100$  km s $^{-1}$  close to photospheric footpoints in the LB, and exhibit a constant deceleration consistent with solar effective gravity. They are predominantly launched from one edge of the light bridge, and their footpoints appear bright in the H $\alpha$  wings. Atmospheric Imaging Assembly data indicates elongated brightenings that are nearly co-spatial with the H $\alpha$  jets. We interpret them as jets of transition region temperatures. The magnetic field in the light bridge has a strength of 0.8–2 kG and it is nearly horizontal. All jet properties are consistent with magnetic reconnection as the driver. **2013 July 5**

### **Peacock jets above the light bridge of a sunspot driven by reconnection**

Carolina **Robustini**, Jorrit Leenaarts, Jaime de la Cruz Rodriguez, Luc Rouppe van der Voort

ApJL **2015**

<http://arxiv.org/pdf/1508.07927v1.pdf>

We report on a fan-shaped set of high-speed jets above the light bridge (LB) of a sunspot observed in the H-alpha line. We study the origin, dynamics and thermal properties of the jets using high-resolution imaging spectroscopy in H-alpha from the Swedish 1-m Solar Telescope and data from the Atmospheric Imaging Assembly (AIA) at the Solar Dynamics Observatory. The H-alpha jets have lengths of 14-38 Mm, are impulsively accelerated to a speed of  $\sim 100$  km/s close to photospheric footpoints in the LB, and exhibit a constant deceleration consistent with solar effective gravity. They are launched from one edge of the light bridge, and their footpoints appear bright in the H-alpha wings. AIA data indicates elongated brightenings that are nearly co-spatial with the H-alpha jets. We interpret them as jets of at least transition region temperatures. The photospheric line-of-sight magnetic field in the light bridge is weaker than, and has opposite polarity compared to, the umbra. All measured jet properties are consistent with the emergence of bipolar magnetic field in the LB that reconnects with the pre-existing vertical field of the sunspot umbra. **2013 July 5**

### **3D Reconstruction and Interplanetary Expansion of the 2010 April 3rd CME**

Martina **Rodari**, [Mateja Dumbović](#), [Manuela Temmer](#), [Lukas M. Holzkecht](#), [Astrid Veronig](#)

Central European Astrophysical Bulletin **2019**

<https://arxiv.org/pdf/1904.05611.pdf>

We analyse the **2010 April 3rd** CME using spacecraft coronagraphic images at different vantage points (SOHO, STEREO-A and STEREO-B). We perform a 3D reconstruction of both the flux rope and shock using the Graduated Cylindrical Shell (GCS) model to calculate CME kinematic and morphologic parameters (e.g. velocity, acceleration, radius). The obtained results are fitted with empirical models describing the expansion of the CME radius in the heliosphere and compared with in situ measurements from Wind spacecraft: the CME is found to expand linearly towards Earth. Finally, we relate the event with decreases in the Galactic Cosmic Ray (GCR) Flux, known as Forbush decreases (FD), detected by EPHIN instrument onboard SOHO spacecraft. We use the analytical diffusion-expansion model (ForbMod) to calculate the magnetic field power law index, obtaining a value of approximately 1.6, thus estimating a starting magnetic field of around 0.01 G and an axial magnetic flux of around  $5 \times 10^{20}$  Mx at 15.6 R $_{\text{sun}}$ .

### **First Spectral Analysis of a Solar Plasma Eruption Using ALMA**

Andrew S. **Rodger**<sup>1</sup>, Nicolas Labrosse<sup>1</sup>, Sven Wedemeyer<sup>2,3</sup>, Mikolaj Szydlarski<sup>2,3</sup>, Paulo J. A.

Simões<sup>1,4,5</sup>, and Lyndsay Fletcher<sup>1</sup>

**2019** ApJ 875 163

<https://iopscience.iop.org/article/10.3847/1538-4357/aafdfb/pdf>

The aim of this study is to demonstrate how the logarithmic millimeter continuum gradient observed using the Atacama Large Millimeter/submillimeter Array (ALMA) may be used to estimate optical thickness in the solar atmosphere. We discuss how using multiwavelength millimeter measurements can refine plasma analysis through knowledge of the absorption mechanisms. Here we use subband observations from the publicly available science verification (SV) data, while our methodology will also be applicable to regular ALMA data. The spectral resolving capacity of ALMA SV data is tested using the enhancement coincident with an X-ray bright point and from a plasmoid ejection event near active region NOAA12470 observed in Band 3 (84–116 GHz) on **2015 December 17**. We compute the interferometric brightness temperature light curve for both features at each of the four constituent subbands to find the logarithmic millimeter spectrum. We compared the observed logarithmic spectral gradient with the derived relationship with optical thickness for an isothermal plasma to estimate the structures' optical thicknesses. We conclude, within 90% confidence, that the stationary enhancement has an optical thickness between  $0.02 \leq \tau \leq 2.78$ , and that the moving enhancement has  $0.11 \leq \tau \leq 2.78$ , thus both lie near to the transition between optically thin and thick plasma at 100 GHz. From these estimates, isothermal plasmas with typical Band 3 background brightness temperatures would be expected to have electron temperatures of  $\sim 7370$ – $15300$  K for the stationary enhancement and between  $\sim 7440$  and  $9560$  K for the moving enhancement, thus demonstrating the benefit of subband ALMA spectral analysis.

### **Origin and Ion Charge State Evolution of Solar Wind Transients during 4–7 August 2011**

D. **Rodkin**, F. Goryaev, P. Pagano, G. Gibb, V. Slemzin, Y. Shugay, I. Veselovsky, D. H. Mackay

[Solar Physics](#) July **2017**, 292:90



We present a study of the complex event consisting of several solar wind transients detected by the Advanced Composition Explorer (ACE) on 4–7 August 2011, which caused a geomagnetic storm with  $Dst = -110$  nT. The supposed coronal sources, three flares and coronal mass ejections (CMEs), occurred on **2–4 August 2011** in active region (AR) 11261. To investigate the solar origin and formation of these transients, we study the kinematic and thermodynamic properties of the expanding coronal structures using the Solar Dynamics Observatory/Atmospheric Imaging Assembly (SDO/AIA) EUV images and differential emission measure (DEM) diagnostics. The Helioseismic and Magnetic Imager (HMI) magnetic field maps were used as the input data for the 3D magnetohydrodynamic (MHD) model to describe the flux rope ejection (Pagano, Mackay, and Poedts, [2013b](#)). We characterize the early phase of the flux rope ejection in the corona, where the usual three-component CME structure formed. The flux rope was ejected with a speed of about 200 km s<sup>-1</sup> to the height of 0.25 R<sub>⊙</sub>. The kinematics of the modeled CME front agrees well with the Solar Terrestrial Relations Observatory (STEREO) EUV measurements. Using the results of the plasma diagnostics and MHD modeling, we calculate the ion charge ratios of carbon and oxygen as well as the mean charge state of iron ions of the 2 August 2011 CME, taking into account the processes of heating, cooling, expansion, ionization, and recombination of the moving plasma in the corona up to the frozen-in region. We estimate a probable heating rate of the CME plasma in the low corona by matching the calculated ion composition parameters of the CME with those measured in situ for the solar wind transients. We also consider the similarities and discrepancies between the results of the MHD simulation and the observations.

### **The Eruption of 22 April 2021 as Observed by Solar Orbiter: Continuous Magnetic Reconnection and Heating After the Impulsive Phase**

[L. Rodriguez](#), [A. Warmuth](#), [V. Andretta](#), [M. Mierla](#), [A. N. Zhukov](#), + + +

[Solar Physics](#) volume 298, Article number: 1 (2023)

<https://doi.org/10.1007/s11207-022-02090-6>

We report on one of the first solar-eruptive events that was simultaneously observed by three of the remote-sensing instruments onboard Solar Orbiter during the cruise phase. The Extreme Ultraviolet Imager (EUI) observed an eruption on **22 April 2021**. The corresponding CME was recorded by the coronagraph Metis. Finally, the Spectrometer/Telescope for Imaging X-rays (STIX) sampled the associated X-ray flare, which was partially occulted. From the Earth, the eruption-source region was observed close to disk center.

We provide an analysis of the eruption as observed by these various instruments. In particular, we show that in this eruption, *continuous magnetic reconnection and heating have to be present even well after the impulsive phase*. The need for this is derived from multiple independent lines of evidence – using both flare and CME observations – that have not been reported before for a single event. The combination of data from Solar Orbiter, as well as other space-based assets, clearly showcases the scientific potential for the science phase of Solar Orbiter, and the unique observations available.

### **Comparing the Heliospheric Cataloging, Analysis, and Techniques Service (HELCASTS) Manual and Automatic Catalogues of Coronal Mass Ejections Using Solar Terrestrial Relations Observatory/Heliospheric Imager (STEREO/HI) Data**

[L. Rodriguez](#), [D. Barnes](#), . . . . . [S. Poedts](#)

[Solar Physics](#) volume 297, Article number: 23 (2022)

<https://link.springer.com/content/pdf/10.1007/s11207-022-01959-w.pdf>

We present the results of a comparative study between automatic and manually compiled coronal mass ejection (CME) catalogues based on observations from the Heliospheric Imagers (HIs) onboard NASA's Solar Terrestrial Relations Observatory (STEREO) spacecraft. Using the Computer Aided CME Tracking software (CACTus), CMEs are identified in HI data using an automatic feature-detection algorithm, while the Heliospheric Imagers Catalogue (HICAT) includes CMEs that are detected by visual inspection of HI images. Both catalogues were compiled as part of the EU FP7 Heliospheric Cataloguing, Analysis and Techniques Service (HELCASTS) project ([www.helcats-fp7.eu](http://www.helcats-fp7.eu)). We compare observational parameters of the CMEs from CACTus to those listed in HICAT, such as CME frequency, position angle (PA), and PA-width. We also compare CACTus-derived speeds to speeds derived from applying geometric modelling to the majority of the HICAT CMEs, the results of which are listed in the HELCASTS Heliospheric Imagers Geometric Catalogue (HIGeoCAT). We find that

both CACTus and HICAT catalogues contain a similar number of events when we exclude events narrower than 20°, which are not included in the HICAT catalogue but are found to be identified by CACTus. PA-distributions are strongly peaked around 90° and 270°, with a slightly larger CME frequency northwards of the equatorial plane (particularly for the STEREO-A versions of both catalogues). The CME PA-widths in both HICAT and CACTus catalogues peak at approximately 60°. Manually derived speeds from HIGeoCAT and automatically derived speeds by CACTus correlate well for values lower than 1000 km s<sup>-1</sup>, in particular when CMEs are propagating close to the plane of the sky. **25**

**February 2010**

### **Three frontside full halo coronal mass ejections with a nontypical geomagnetic response**

[Rodriguez](#), [L.](#); [Zhukov](#), [A. N.](#); [Cid](#), [C.](#); [Cerrato](#), [Y.](#); [Saiz](#), [E.](#); [Cremades](#), [H.](#); [Dasso](#), [S.](#); [Menvielle](#), [M.](#); [Aran](#), [A.](#); [Mandrini](#), [C.](#); [Poedts](#), [S.](#); [Schmieder](#), [B.](#)

Space Weather, Vol. 7, No. 6, S06003, 2009

<http://dx.doi.org/10.1029/2008SW000453>

Forecasting potential geoeffectiveness of solar disturbances (in particular, of frontside full halo coronal mass ejections) is important for various practical purposes, e.g., for satellite operations, radio communications, global positioning system applications, power grid, and pipeline maintenance. We analyze **three frontside full halo coronal mass ejections (CMEs) that occurred in the year 2000** (close to the activity maximum of solar cycle 23), together with associated solar and heliospheric phenomena as well as their impact on the Earth's magnetosphere. Even though all three were fast full halos (with plane of the sky speeds higher than 1100 km/s), the geomagnetic response was very different for each case. After analyzing the source regions of these halo CMEs, it was found that the halo associated with the strongest geomagnetic disturbance was the one that initiated farther away from disk center (source region at **W66**); while the other two CMEs originated closer to the central meridian but had weaker geomagnetic responses. Therefore, these three events do not fit into the general statistical trends that relate the location of the solar source and the corresponding geoeffectivity. We investigate possible causes of such a behavior. Nonradial direction of eruption, passage of the Earth through a leg of an interplanetary flux rope, and strong compression at the eastern flank of a propagating interplanetary CME during its interaction with the ambient solar wind are found to be important factors that have a direct influence on the resulting north-south interplanetary magnetic field (IMF) component and thus on the CME geoeffectiveness. We also find indications that interaction of two CMEs could help in producing a long-lasting southward IMF component. Finally, we are able to explain successfully the geomagnetic response using plasma and magnetic field in situ measurements at the L1 point. We discuss the implications of our results for operational space weather forecasting and stress the difficulties of making accurate predictions with the current knowledge and tools at hand.

### **Evidence of a complex structure within the 2013 August 19 coronal mass ejection Radial and longitudinal evolution in the inner heliosphere★**

L. **Rodríguez-García**<sup>1</sup>, T. Nieves-Chinchilla<sup>2</sup>, R. Gómez-Herrero<sup>1</sup>, I. Zouganelis<sup>3</sup>, A. Vourlidas<sup>4</sup>, L. A. Balmaceda<sup>2,5</sup>, M. Dumbović<sup>6</sup>, L. K. Jian<sup>2</sup>, L. Mays<sup>2</sup>, F. Carcaboso<sup>1,2,7</sup>, L. F. G. dos Santos<sup>8</sup> and J.

Rodríguez-Pacheco<sup>1</sup>

A&A 662, A45 (2022)

<https://arxiv.org/pdf/2203.02713.pdf>

<https://www.aanda.org/articles/aa/pdf/2022/06/aa42966-21.pdf>

Context. Late on **2013 August 19**, a coronal mass ejection (CME) erupted from an active region located near the far-side central meridian from Earth's perspective. The event and its accompanying shock were remotely observed by the STEREO-A, STEREO-B, and SOHO spacecraft. The interplanetary counterpart (ICME) was intercepted by MESSENGER near 0.3 au and by both STEREO-A and STEREO-B near 1 au, which were separated from each other by 78° in heliolongitude.

Aims. The main objective of this study is to follow the radial and longitudinal evolution of the ICME throughout the inner heliosphere and to examine possible scenarios for the different magnetic flux-rope configuration observed on the solar disk and measured in situ at the locations of MESSENGER and STEREO-A, separated by 15° in heliolongitude, and at STEREO-B, which detected the ICME flank.

Methods. Solar disk observations are used to estimate the “magnetic flux-rope type”, namely, the magnetic helicity, axis orientation, and axial magnetic field direction of the flux rope. The graduated cylindrical shell model is used to reconstruct the CME in the corona. The analysis of in situ data, specifically the plasma and magnetic field, is used to estimate the global interplanetary shock geometry and to derive the magnetic flux-rope type at different in situ locations, which is compared to the type estimated from solar disk observations. The elliptical cylindrical analytical model is used for the in situ magnetic flux-rope reconstruction.

Results. Based on the CME geometry and on the spacecraft configuration, we find that the magnetic flux-rope structure detected at STEREO-B belongs to the same ICME detected at MESSENGER and STEREO-A. The opposite helicity deduced at STEREO-B might be due to that fact that it intercepted one of the legs of the structure far from the flux-rope axis, in contrast to STEREO-A and MESSENGER, which were crossing through the core of the magnetic flux rope. The different flux-rope orientations measured at MESSENGER and STEREO-A probably arise because the two spacecraft measure a curved, highly distorted, and rather complex magnetic flux-rope topology. The ICME may have suffered additional distortion in its evolution in the inner heliosphere, such as the west flank propagating faster than the east flank when arriving near 1 au.

Conclusions. This work illustrates how a wide, curved, highly distorted, and rather complex CME showed different orientations as observed on the solar disk and measured in situ at 0.3 au and near 1 au. Furthermore, the work shows how the ambient conditions can significantly affect the expansion and propagation of the CME and ICME, introducing additional irregularities to the already asymmetric eruption. The study also manifests how these complex structures cannot be directly reconstructed with the currently available models and that multi-point analysis is of the utmost importance in such complex events.

### **Combined Multipoint Remote and in situ Observations of the Asymmetric Evolution of a Fast Solar Coronal Mass Ejection**

T. **Rollett**<sup>1,2</sup>, C. Möstl<sup>1,2</sup>, M. Temmer<sup>1</sup>, R. A. Frahm<sup>3</sup>, J. A. Davies<sup>4</sup>, A. M. Veronig<sup>1</sup>, B. Vršnak<sup>5</sup>, U. V. Amerstorfer<sup>1</sup>, C. J. Farrugia<sup>6</sup>, T. Žic<sup>5</sup>, and T. L. Zhang

2014 ApJ 790 L6

<http://arxiv.org/pdf/1407.4687v1.pdf>

We present an analysis of the fast coronal mass ejection (CME) of **2012 March 7**, which was imaged by both STEREO spacecraft and observed in situ by MESSENGER, Venus Express, Wind, and Mars Express. Based on detected arrivals at four different positions in interplanetary space, it was possible to strongly constrain the kinematics and the shape of the ejection. Using the white-light heliospheric imagery from STEREO-A and B, we derived two different kinematical profiles for the CME by applying the novel constrained self-similar expansion method. In addition, we used a drag-based model to investigate the influence of the ambient solar wind on the CME's propagation. We found that two preceding CMEs heading in different directions disturbed the overall shape of the CME and influenced its propagation behavior. While the Venus-directed segment underwent a gradual deceleration (from  $\sim 2700 \text{ km s}^{-1}$  at  $15 R_{\odot}$  to  $\sim 1500 \text{ km s}^{-1}$  at  $154 R_{\odot}$ ), the Earth-directed part showed an abrupt retardation below  $35 R_{\odot}$  (from  $\sim 1700$  to  $\sim 900 \text{ km s}^{-1}$ ). After that, it was propagating with a quasi-constant speed in the wake of a preceding event. Our results highlight the importance of studies concerning the unequal evolution of CMEs. Forecasting can only be improved if conditions in the solar wind are properly taken into account and if attention is also paid to large events preceding the one being studied.

## **Constraining the Kinematics of Coronal Mass Ejections in the Inner Heliosphere with In-Situ Signatures**

T. [Rollett](#), C. Möstl, M. Temmer, A. M. Veronig, C. J. Farrugia and H. K. Biernat

Solar Physics, Volume 276, Numbers 1-2, 293-314, **2012**, [File](#)

We present a new approach to combine remote observations and in-situ data by STEREO/HI and Wind, respectively, to derive the kinematics and propagation directions of interplanetary coronal mass ejections (ICMEs). We use two methods, Fixed- $\varphi$  ( $F\varphi$ ) and Harmonic Mean (HM), to convert ICME elongations into distance, and constrain the ICME direction such that the ICME distance–time and velocity–time profiles are most consistent with in-situ measurements of the arrival time and velocity. The derived velocity–time functions from the Sun to 1 AU for the three events under study (**1–6 June 2008**, **13–18 February 2009**, **3–5 April 2010**) do not show strong differences for the two extreme geometrical assumptions of a wide ICME with a circular front (HM) or an ICME of small spatial extent in the ecliptic ( $F\varphi$ ). Due to the geometrical assumptions, HM delivers the propagation direction further away from the observing spacecraft with a mean difference of  $\approx 25^\circ$ .

## **Evolution of the Magnetic Helicity Flux during the Formation and Eruption of Flux Ropes**

P. [Romano](#)<sup>1</sup>, F. P. Zuccarello<sup>2,3,4</sup>, S. L. Guglielmino<sup>5</sup>, and F. Zuccarello

**2014** ApJ 794 118

We describe the evolution and the magnetic helicity flux for two active regions (ARs) since their appearance on the solar disk: NOAA **11318** and NOAA **11675**. Both ARs hosted the formation and destabilization of magnetic flux ropes. In the former AR, the formation of the flux rope culminated in a flare of C2.3 GOES class and a coronal mass ejection (CME) observed by Large Angle and Spectrometric Coronagraph Experiment. In the latter AR, the region hosting the flux rope was involved in several flares, but only a partial eruption with signatures of a minor plasma outflow was observed. We found a different behavior in the accumulation of the magnetic helicity flux in the corona, depending on the magnetic configuration and on the location of the flux ropes in the ARs. Our results suggest that the complexity and strength of the photospheric magnetic field is only a partial indicator of the real likelihood of an AR producing the eruption of a flux rope and a subsequent CME.

## **On the possible reason for the formation of impulsive coronal mass ejections**

D.V. [Romanov](#), K.V. Romanov, V.A. Romanov, N.V. Kuchеров, V.G. Eselevich, , M.V. Eselevich

Advances in Space Research, Volume 55, Issue 3, 1 February **2015**, Pages 949–957

<http://www.sciencedirect.com/science/article/pii/S027311771400581X>

The stability of a thin magnetic tube located at different depths of the convective zone has been studied numerically and analytically. Three spectral regions are shown to be responsible for different processes related to solar activity. Numerical simulation shows that Parker instability in the high frequency domain (wave number  $m > 20$ ) may accelerate magnetic fibrils to emerge into the solar atmosphere at supersonic speed. Such a physical process may be responsible for impulsive CME generation. **11.02.2011, 05 January 2013**

## **Horizontal photospheric flows trigger a filament eruption**

T. [Roudier](#), [B. Schmieder](#), [B. Filippov](#), [R. Chandra](#), [J.M. Malherbe](#)

A&A 618, A43 **2018**

<https://arxiv.org/pdf/1808.02272.pdf>

A large filament composed principally of two sections erupted sequentially in the southern hemisphere on **January 26 2016**. The central, thick part of the northern section was first lifted up and led to the eruption of the full filament. This event was observed in H-alpha with GONG and CLIMSO, and in ultraviolet (UV) with the AIA/SDO imager. The aim of the paper is to relate the photospheric motions below the filament and its environment to the eruption of the filament. An analysis of the photospheric motions using SDO/HMI continuum images with the coherent structure tracking (CST)

algorithm developed to track granules, as well as large-scale photospheric flows, has been performed. The supergranule pattern is clearly visible outside the filament channel but difficult to detect inside because the modulus of the vector velocity is reduced in the filament channel, mainly in the magnetized areas. The horizontal photospheric flows are strong on the west side of the filament channel and oriented towards the filament. The ends of the filament sections are found in areas of concentration of corks. Whirled flows are found locally around the feet. The strong horizontal flows with an opposite direction to the differential rotation create strong shear and convergence along the magnetic polarity inversion line (PIL) in the filament channel. The filament has been destabilized by the converging flows, which initiate an ascent of the middle section of the filament until the filament reaches the critical height of the torus instability inducing, consequently, the eruption. The "n" decay index indicated an altitude of 60 Mm for the critical height. It is conjectured that the convergence along the PIL is due to the large-scale size cells of convection that transport the magnetic field to their borders.

## **Modeling the Early Evolution of a Slow Coronal Mass Ejection Imaged by the Parker Solar Probe**

Alexis P. [Rouillard](#), [Nicolas Poirier](#), [Michael Lavarra](#), [Antony Bourdelle](#), [Kévin Dalmasse](#), [Athanasios Kouloumvakos](#), [Angelos Vourlidas](#), [Valbona Kunkel](#), [Phillip Hess](#), [Russ A. Howard](#), [Guillermo Stenborg](#), [Nour E. Raouafi](#)

ApJS 2020

<https://arxiv.org/pdf/2002.08756.pdf>

During its first solar encounter, the Parker Solar Probe (PSP) acquired unprecedented up-close imaging of a small Coronal Mass Ejection (CME) propagating in the forming slow solar wind. The CME originated as a cavity imaged in extreme ultraviolet that moved very slowly ( $<50$  km/s) to the 3-5 solar radii ( $R_{\odot}$ ) where it then accelerated to supersonic speeds. We present a new model of an erupting Flux Rope (FR) that computes the forces acting on its expansion with a computation of its internal magnetic field in three dimensions. The latter is accomplished by solving the Grad-Shafranov equation inside two-dimensional cross sections of the FR. We use this model to interpret the kinematic evolution and morphology of the CME imaged by PSP. We investigate the relative role of toroidal forces, momentum coupling, and buoyancy for different assumptions on the initial properties of the CME. The best agreement between the dynamic evolution of the observed and simulated FR is obtained by modeling the two-phase eruption process as the result of two episodes of poloidal flux injection. Each episode, possibly induced by magnetic reconnection, boosted the toroidal forces accelerating the FR out of the corona. We also find that the drag induced by the accelerating solar wind could account for about half of the acceleration experienced by the FR. We use the model to interpret the presence of a small dark cavity, clearly imaged by PSP deep inside the CME, as a low-density region dominated by its strong axial magnetic fields. **2018 November 1-3**

## **Deriving the properties of coronal pressure fronts in 3-D: application to the 17 May 2012 ground level enhancement**

Alexis P. [Rouillard](#), Illya Plotnikov, Rui F. Pinto, Margot Tirole, Michael Lavarra, Pietro Zucca, Rami Vainio, Allan J. Tylka, Angelos Vourlidas, Marc De Rosa, Jon Linker, Alexander Warmuth, Gottfried Mann, Christina M. Cohen, Robert A. Mewaldt

2016

<http://arxiv.org/pdf/1605.05208v1.pdf>

We study the link between an expanding coronal shock and the energetic particles measured near Earth during the Ground Level Enhancement (GLE) of 17 May 2012. We developed a new technique based on multipoint imaging to triangulate the 3-D expansion of the shock forming in the corona. It uses images from three vantage points by mapping the outermost extent of the coronal region perturbed by the pressure front. We derive for the first time the 3-D velocity vector and the distribution of Mach numbers,  $M_{FM}$ , of the entire front as a function of time. Our approach uses magnetic field reconstructions of the coronal field, full magneto-hydrodynamic simulations and imaging inversion techniques. We find that the highest  $M_{FM}$  values appear along the coronal neutral line within a few minutes of the CME eruption; this neutral line is usually associated with the source of the heliospheric and plasma sheet. We can also estimate the time evolution of the shock speed, shock geometry and Mach number along different modeled magnetic field lines. Despite the level of uncertainty in deriving the shock Mach numbers, all employed reconstruction techniques show that the release time of GeV particles occurs when the coronal shock becomes super-critical ( $M_{FM} > 3$ ) near the tip of helmet streamers. Combining in-situ measurements with heliospheric imagery, we also demonstrate that magnetic connectivity between the accelerator (the coronal shock of 17 May 2012) and the near-Earth environment is established via a magnetic cloud that erupted from the same active region roughly five days earlier. This analysis also shows that the derivation of magnetic connectivity between the coronal shock and a probe must result from a full analysis of the interplanetary medium extending back in time by at least five days before the event of interest.

**Table B1.** Characteristics of WL CMEs and in situ measurements during GLE events

## **Relating white light and in situ observations of coronal mass ejections: [A review](#)**

A.P. [Rouillard](#)

Journal of Atmospheric and Solar-Terrestrial Physics, Volume 73, Issue 10, **2011**, Pages 1201-1213, **File**  
This paper provides a short review of some of the basic concepts related to the observations of coronal mass ejections (CMEs) in white light images and at large distances from the Sun. We review the various ideas which have been put forward to explain the dramatic changes in CME appearance in white light images from the Sun to 1 AU, focusing on

results obtained by comparing white light observations of CMEs to the in situ measurements of Interplanetary CMEs (or ICMEs). We start with a list of definitions for the various in situ structures that form an ICME. A few representative examples of the formation of sheath regions and other interaction regions as well as the expansion of magnetic flux ropes are used to illustrate the basic phenomena which induce significant brightness variations during a CME's propagation to 1 AU and beyond. The white light signatures of a number of CMEs observed by the coronagraphs have been successfully simulated numerically by assuming that most of the coronal plasma observed in white light images is located on the surface of a croissant-shaped structure reminiscent of a magnetic flux rope. At large distances from the Sun, white light imagers show that the appearance of CMEs changes dramatically due to the changing position of the CME relative to the Thomson sphere, the expansion of the ejecta and the interaction of the ejecta with the ambient solar wind.

Research Highlights

► Review of white light observations made by STEREO. ► Direct links between white light observations of CMEs and in situ measurements of magnetic flux ropes near 1 AU. ► Discussion of the various types of ejecta observed simultaneously in white light and in situ.

## **Eruptive events in the solar atmosphere: new insights from theory and 3-D numerical modelling**

Iliia I. [Roussev](#)

2008, *J. Contemp. Phys.*, 49, 237

Ejections of magnetised plasma from the Sun, commonly known as coronal mass ejections (CMEs), are one of the most stunning manifestations of solar activity. These ejections play a leading role in the Sun-Earth connection, because of their large-scale, energetics and direct impact on the space environment near the Earth. As CMEs evolve in the solar corona and interplanetary space they drive shock waves, which act as powerful accelerators of charged particles in the inner solar system. Some of these particles, known as solar energetic particles (SEPs), can strike our planet, and in doing so they can disrupt satellites and knock out power systems on the ground, among other effects. These particles, along with the intensive X-ray radiation from solar flares, also endanger human life in outer space. That is why it is important for space scientists to understand and predict the ever changing environmental conditions in outer space due to solar eruptive events - the so-called space weather. To enable the development of accurate space weather forecast, in the past three decades solar scientists have been challenged to provide an improved understanding of the physical causes of the CME phenomenon and its numerous effects. **This paper summarises the most recent advances from theory and modelling in understanding the origin and evolution of solar eruptive events and related phenomena.**

## **Recent Advances from Theory and 3-D Numerical Modeling in Understanding the Origin and Evolution of CMEs and Related SEP Events**

[Roussev](#), I.1; [Sokolov](#), I.2; [Lugaz](#), N.3

Freiburg ESP Meeting 2008, **Presentation**

To date, it is well established that Coronal Mass Ejections (CMEs) play a leading role in the Sun-Earth connection, because of their large-scale, energetics and direct impact on the space environment near the Earth. As CMEs evolve in the solar corona and interplanetary space they drive shock waves, which act as powerful accelerators of charged particles in the heliosphere by means of Fermi acceleration processes. Some of these so-called Solar Energetic Particles (SEPs) can strike our planet, and in doing so they can disrupt satellites and knock out power systems on the ground, among other effects. The SEPs, along with the intensive X-ray radiation from solar flares, also endanger human life in outer space. That is why it is important for solar scientists to understand and predict the ever changing environmental conditions in outer space due to solar eruptive events -- the space weather. To enable the development of accurate space weather forecast, in the past 35 years solar scientists have been challenged to provide an improved understanding of the physical causes of CMEs and related phenomena, such as the production of SEPs. **This talk summarizes** the most recent advances from theory and 3-D numerical modeling in understanding the origin and evolution of CMEs and related SEP events.

## **NEW PHYSICAL INSIGHT ON THE CHANGES IN MAGNETIC TOPOLOGY DURING CORONAL MASS EJECTIONS:**

### **CASE STUDIES FOR THE 2002 APRIL 21 AND AUGUST 24 EVENTS**

Iliia I. [Roussev](#),<sup>1</sup> Noe´ [Lugaz](#),<sup>1</sup> and Igor V. [Sokolov](#)<sup>2</sup>

The Astrophysical Journal, 668: L87–L90, 2007

<http://www.journals.uchicago.edu/doi/pdf/10.1086/522588>

In order to investigate the dynamics of the coronal mass ejections on **2002 April 21 and August 24**, we

performed a series of numerical simulations with an ad hoc driver for the eruptions. The resulting evolution of the solar corona for each event was followed by means of three-dimensional MHD simulations. We used *SOHO* MDI data to set realistic boundary conditions for the ambient magnetic field of the Sun. In our model, the loss of equilibrium of the coronal magnetic field and subsequent eruption were achieved by stretching the opposite polarity feet of a newly emerged magnetic dipole. The stressed magnetic field reconnects through null points and, in the case of the August 24 event, also through a quasi-separator. As a result, magnetic flux and helicity are transferred from the expanding flux system containing the evolving dipole to the nearby flux systems. Another result is the jumplike change in the location of one footprint of the erupting magnetic field. This Letter emphasizes the importance of studying CMEs on a case-by-case basis if we are to understand their dynamics, energetics, and interplanetary consequences.

### **Bidirectional Reconnection Outflows in an Active Region**

Guiping **Ruan**<sup>1,2,3</sup>, Brigitte Schmieder<sup>2</sup>, Sophie Masson<sup>2</sup>, Pierre Mein<sup>2</sup>, Nicole Mein<sup>2</sup>, Guillaume Aulanier<sup>2</sup>, and Yao Chen<sup>1</sup>

2019 ApJ 883 52

<https://doi.org/10.3847/1538-4357/ab3657>

We report on bidirectional coronal reconnection outflows reaching  $\pm 200$  km s<sup>-1</sup> as observed in an active region with the Si iv and C ii spectra of the Interface Region Imaging Spectrograph (IRIS). The evolution of the active region with an emerging flux, a failed filament eruption, and a jet is followed in Solar Dynamical Observatory (SDO)/Atmospheric Imaging Assembly (AIA) filters from 304 to 94 Å, IRIS slit jaw images, and SDO/Helioseismic and Magnetic Imager movies. The bidirectional outflow reconnection is located at a bright point visible in multiwavelength AIA filters above an arch filament system. This suggests that the reconnection occurs between rising loops above the emergence of magnetic bipoles and the longer, twisted magnetic field lines remnant of the failed filament eruption one hour before. The reconnection occurs continuously in the corona between quasi-parallel magnetic field lines, which is possible in a 3D configuration. The reconnection also triggers a jet with transverse velocities around 60 km s<sup>-1</sup>. Blueshifts and redshifts along its axis confirm the existence of a twist along the jet, which could have been transferred from the filament flux rope. The jet finally blows up the material of the filament before coming back during the second phase. In the H $\alpha$  Dopplergrams provided by the MSDP spectrograph, we see more redshift than blueshift, indicating the return of the jet and filament plasma.

### **A Solar Eruption Driven by Rapid Sunspot Rotation**

Guiping **Ruan**, Yao Chen, Shuo Wang, Hongqi Zhang, Gang Li, Ju Jing, Jiangtao Su, Xing Li, Haiqing Xu, Guohui Du, and Haimin Wang

2014 ApJ 784 165

<http://arxiv.org/pdf/1402.6043v1.pdf>

We present the observation of a major solar eruption that is associated with fast sunspot rotation. The event includes a sigmoidal filament eruption, a coronal mass ejection, and a GOES X2.1 flare from NOAA active region 11283. The filament and some overlying arcades were partially rooted in a sunspot. The sunspot rotated at  $\sim 10^\circ$  hr<sup>-1</sup> during a period of 6 hr prior to the eruption. In this period, the filament was found to rise gradually along with the sunspot rotation. Based on the Helioseismic and Magnetic Imager observation, for an area along the polarity inversion line underneath the filament, we found gradual pre-eruption decreases of both the mean strength of the photospheric horizontal field ( $B_h$ ) and the mean inclination angle between the vector magnetic field and the local radial (or vertical) direction. These observations are consistent with the pre-eruption gradual rising of the filament-associated magnetic structure. In addition, according to the nonlinear force-free field reconstruction of the coronal magnetic field, a pre-eruption magnetic flux rope structure is found to be in alignment with the filament, and a considerable amount of magnetic energy was transported to the corona during the period of sunspot rotation. Our study provides evidence that in this event sunspot rotation plays an important role in twisting, energizing, and destabilizing the coronal filament-flux rope system, and led to the eruption. We also propose that the pre-event evolution of  $B_h$  may be used to discern the driving mechanism of eruptions. **6 Sept 2011.**

### **Rayleigh-Taylor instability of a magnetic tangential discontinuity in the presence of flow**

M. S. **Ruderman**

A&A 580, A37 (2015)

We studied the magnetic Rayleigh-Taylor (MRT) instability of a magnetohydrodynamic tangential discontinuity in an infinitely conducting incompressible plasma in the presence of flow. We assumed that the flow magnitude is small enough to guarantee that there is no Kelvin-Helmholtz (KH) instability. In addition, we assumed that there is the magnetic shear, that is, the magnetic field has different directions at the two side of the discontinuity. In this case, only perturbations whose wavelength is greater than the critical one are unstable. As a consequence, the perturbation growth rate is bounded, and the initial-value problem describing their evolution is well posed. We also studied the absolute and convective nature of the MRT instability using the Briggs method. We obtained the necessary and sufficient condition for a perturbation propagating in a given direction to be only convectively unstable but absolutely stable. We also obtained the condition for perturbations propagating in any direction to be only convectively unstable, but absolutely stable. *The results of the general analysis were applied to the MRT instability of prominence threads and the heliopause. Similar to previous research, we assumed that the thread disappearance is related to the MRT instability and the thread lifetime is equal to the inverse instability increment. Using this assumption we estimated the angle*

between the magnetic field inside the thread and in the surrounding plasma and studied how this estimate depends on the magnitude of the flow inside the thread. We found that this dependence is very weak. To apply this to the heliopause stability, we carried out the local analysis and restricted it to the near flanks of the heliopause only where the plasma flow can be considered incompressible. We showed that, for values of the magnetic field magnitude observed by Voyager 1, there is no KH instability. We then studied the MRT instability that can occur when the heliosheath is accelerated in the antisolar direction due to the increase in the solar wind dynamic pressure. We showed that, for typical values of the plasma flow and magnetic field parameters, there are directions such that perturbations propagating in this directions are absolutely unstable.

## **Eruptive events with exceptionally bright emission in HI Ly-alpha observed by the Metis coronagraph**

[G. Russano](#), [V. Andretta](#), [Y. De Leo](#), [L. Teriaca](#), [M. Uslenghi](#), [S. Giordano](#), [D. Telloni](#), [P. Heinzel](#), + + +  
A&A 683, A191 (2024)

<https://arxiv.org/pdf/2312.01899.pdf>

<https://www.aanda.org/articles/aa/pdf/2024/03/aa47741-23.pdf>

Context. Ultraviolet (UV) emission from coronal mass ejections can provide information on the evolution of plasma dynamics, temperature, and elemental composition, as demonstrated by the UV Coronagraph Spectrometer (UVCS) on board the Solar and Heliospheric Observatory (SOHO). Metis, the coronagraph on board Solar Orbiter, provides for the first time coronagraphic imaging in the UV HI Ly- $\alpha$  line and, simultaneously, in polarized visible light, thus providing a host of information on the properties of coronal mass ejections and solar eruptions such as their overall dynamics, time evolution, mass content, and outflow propagation velocity in the expanding corona.

Aims. For this work, we analyzed six coronal mass ejections observed by Metis between April and October 2021, which are characterized by a very strong HI Ly- $\alpha$  emission. We studied in particular the morphology, kinematics, and the temporal and radial evolution of the emission of such events, focusing on the brightest UV features.

Methods. The kinematics of the eruptive events under consideration were studied by determining the height-time profiles of the brightest parts on the Metis plane of the sky. Furthermore, the 3D positions in the heliosphere of the coronal mass ejections were determined by employing co-temporal images, when available, from two other coronagraphs: LASCO/C2 on board SOHO, and COR2 on board STEREO-A. In three cases, the most likely source region on the solar surface could be identified. Finally, the radiometrically calibrated Metis images of the bright UV features were analyzed to provide estimates of their volume and density. From the kinematics and radiometric analysis, we obtained indications of the temperatures of the bright UV cores of these events. These results were then compared with previous studies with the UVCS spectrocoronagraph.

Results. The analysis of these strong UV-emitting features associated with coronal mass ejections demonstrates the capabilities of the current constellation of space coronagraphs, Metis, LASCO/C2, and COR2, in providing a complete characterization of the structure and dynamics of eruptive events in their propagation phase from their inception up to several solar radii. Furthermore, we show how the unique capabilities of the Metis instrument to observe these events in both the HI Ly- $\alpha$  line and polarized VL radiation allow plasma diagnostics on the thermal state of these events.

April 25-26 2021, 11 Sep. 2021, 2 Oct. 2021, 25 Oct. 2021, 28 Oct. 2021

## **Distribution and clustering of fast coronal mass ejections**

A. [Ruzmaikin](#),<sup>1</sup> J. Feynman,<sup>1</sup> and S. A. Stoev<sup>2</sup>

JGR, VOL. 116, A04220, doi:10.1029/2010JA016247, 2011, File

The purpose of this paper is to investigate the statistical properties of high - speed coronal mass ejections (fast CMEs), which play a major role in Space Weather. We study the cumulative distribution of the initial CME speeds applying a new, advanced statistical method based on the scaling properties of averages of maximal speeds selected in time intervals of fixed sizes. This method allows us for the first time to obtain a systematic statistical description of the fast CME speeds. Using this method, we identify a self - similar (power law) high - speed portion of the spectrum of the speed maxima in the range of speeds from about 700 km/s to 2000 km/s. This self - similar range of the speed distribution provides a meaningful definition of “the fast” CMEs and indicates that these CMEs are produced by a process that is the same across the range of scales. The investigation of the temporal behavior of the fast CME events indicates that the time intervals between fast CMEs are not independent, i.e., fast CMEs arrive in clusters. We characterize the fast CMEs clustering by the exponent  $\alpha$  called the extremal index, which is the inverse of the averaged number of CMEs per cluster. An independent correlation analysis of the tail of the CME distribution confirms and further quantifies the temporal dependence among the fast CME events. To illustrate the predictive capabilities of the method, we identify clusters in the time series of CMEs with speeds greater than 1000 km/s and calculate their statistical characteristics such as the size and duration of the clusters. The method used in this paper can be applied to many other extreme geophysical events.

## **Plasmoids and Resulting Blobs due to the Interaction of Magnetoacoustic Waves with a 2.5D Magnetic Null Point**

S. [Sabri](#)<sup>1</sup>, H. Ebadi<sup>1,3</sup>, and S. Poedts<sup>2,3</sup>

2020 ApJ 902 11

<https://doi.org/10.3847/1538-4357/abb081>

We performed a numerical study for interpreting observations of plasma blobs occurring in the solar corona. Considering all of the previous studies and the presence of magnetic null points together with propagating magnetohydrodynamic waves in the solar corona, we guessed that the interaction of fast magnetoacoustic waves with null points could give rise to blobs under coronal conditions. The outcome of these interactions contributes to coronal jets and flares that directly affects us on Earth. The propagation of magnetoacoustic waves in the vicinity of a magnetic null point contributes to the high current density accumulation at the small scale around the magnetic null point, which has significant magnetic gradients. When nonlinearity becomes dominant, the variation of current density could result in instabilities and thus anomalous resistivity. Moreover, it is demonstrated that plasmoids with eruption events take place in the solar corona without considering the transition region. In our numerical simulation results, it is interesting that plasma blobs manifest themselves in many parameters, including current density, temperature, plasma density, flows, and magnetic fields, simultaneously and consistent with the generation of plasmoids. In this work, it is found that plasmoid instability is the reason for the plasma blobs and tiny blobs are produced by the tearing instability occurring in thin current sheets.

## **Dynamics of solar Coronal Mass Ejections: forces that impact their propagation**

Nishtha [Sachdeva](#)

Ph.D. [Thesis](#) 2019

<https://arxiv.org/pdf/1907.12673.pdf>

We investigate the Sun-Earth dynamics of a set of 38 well-observed Coronal Mass Ejections (CMEs) using data from the STEREO, SOHO missions and WIND instrument. We seek to quantify the relative contributions of Lorentz force and aerodynamic drag on their propagation. The CMEs are 3D reconstructed using the Graduated Cylindrical Shell (GCS) model to derive observed CME parameters. Using a microphysical prescription of the drag coefficient, we find that solar wind aerodynamic drag adequately accounts for the dynamics of the fastest CMEs from as low as 3.5 Rs. For relatively slower CMEs, however, we find that when the drag-based model is initiated below the distances ranging from 12 to 50 Rs, the observed CME trajectories cannot be accounted for. This suggests that aerodynamic drag force dominates the dynamics of slower CMEs only above these [this http URL](#) investigate CME dynamics below the heights where aerodynamic drag dominates, we consider the Torus Instability model for the driving Lorentz force. We find that for fast CMEs, Lorentz forces become negligible in comparison to aerodynamic drag as early as 3.5-4 Rs. For slow CMEs, however, they become negligible only by 12-50 Rs. This justifies the success of the drag-only model for fast CMEs. In case of slow CMEs, the Lorentz force is only slightly smaller than the drag force even beyond 12-50 Rs. For these slow events, our results suggest that some of the magnetic flux carried by CMEs might be expended in expansion or heating. These dissipation effects might be important in describing the propagation of slower CMEs. To the best of our knowledge, this is the first systematic study in this regard using a diverse CME sample. A physical understanding of the forces that affect CME propagation and how they compare with each other at various heliocentric distances is an important ingredient in building tools for describing and predicting CME trajectories. **February 27, 2000, March 19, 2010, April 03, 2010, April 08, 2010, June 16, 2010, September 11, 2010, October 26, 2010, December 23, 2010, January 24, 2011, February 15, 2011, March 03, 2011, March 25, 2011, April 09, 2011, June 14, 2011, June 21, 2011, July 09, 2011, August 4, 2011, September 14, 2011, October 22, 2011, October 26, 2011, October 27, 2011, November 19, 2011, January 23, 2012, January 27, 2012, February 27, 2012, March 13, 2012, April 19, 2012, June 14, 2012, July 12, 2012, September 28, 2012, October 05, 2012, October 27, 2012, November 09, 2012, November 23, 2012, March 15, 2013, April 11, 2013, June 28, 2013, September 29, 2013, November 07, 2013,**

**Table 2.1:** Details of observed characteristics of the CMEs in the sample set. (2010-2013)

## **CME dynamics using STEREO & LASCO observations: the relative importance of Lorentz forces and solar wind drag**

Nishtha [Sachdeva](#), Prasad Subramanian, Angelos Vourlidas, Volker Bothmer

Solar Phys. 292:118 2017

<https://arxiv.org/pdf/1705.04871.pdf>

We seek to quantify the relative contributions of Lorentz forces and aerodynamic drag on the propagation of solar coronal mass ejections (CMEs). We use Graduated Cylindrical Shell (GCS) model fits to a representative set of 38 CMEs observed with the SOHO and STEREO spacecraft. We find that the Lorentz forces generally peak between 1.65 and 2.45 Rsun for all CMEs. For fast CMEs, Lorentz forces become negligible in comparison to aerodynamic drag as early as 3.5--4 Rsun. For slow CMEs, however, they become negligible only by 12--50 Rsun. For these slow events, our results suggest that some of the magnetic flux might be expended in CME expansion or heating. In other words, not all of it contributes to directed propagation. Our results are expected to be important in building a physical model for understanding the Sun-Earth dynamics of CMEs.

**Table 1.** Details of all the CMEs in the sample set.

**Table 2.** Parameters for the solar wind drag and Lorentz force analysis are shown here.

## **CME propagation: Where does the solar wind drag take over?**

Nishtha [Sachdeva](#), Prasad Subramanian, Robin Colaninno, Angelos Vourlidas

ApJ 809 158 2015

<http://arxiv.org/pdf/1507.05199v1.pdf>



We investigate the Sun-Earth dynamics of a set of eight well observed solar coronal mass ejections (CMEs) using data from the STEREO spacecraft. We seek to quantify the extent to which momentum coupling between these CMEs and the ambient solar wind (i.e., the aerodynamic drag) influences their dynamics. To this end, we use results from a 3D flux rope model fit to the CME data. We find that solar wind aerodynamic drag adequately accounts for the dynamics of the fastest CME in our sample. For the relatively slower CMEs, we find that drag-based models initiated below heliocentric distances ranging from 15 to 50  $R_{\odot}$  cannot account for the observed CME trajectories. This is at variance with the general perception that the dynamics of slow CMEs are influenced primarily by solar wind drag from a few  $R_{\odot}$  onwards. Several slow CMEs propagate at roughly constant speeds above 15--50  $R_{\odot}$ . Drag-based models initiated above these heights therefore require negligible aerodynamic drag to explain their observed trajectories. **2010 Mar 19-23, 2010 Apr 03 -05, 2010 Apr 08-11, 2010 Jun 16-20, 2010 Sep 11-14, 2010 Oct 26-31, 2011 Feb 15-18, 2011 Mar 25-29**

## **Analysis of solar eruptions deflecting in the low corona: influence of the magnetic environment**

[A. Sahade](#), [A. Vourlidas](#), [C. Mac Cormack](#)

ApJ **2024**

<https://arxiv.org/pdf/2411.11599>

Coronal mass ejections (CMEs) can exhibit non-radial evolution. The background magnetic field is considered the main driver for the trajectory deviation relative to the source region. The influence of the magnetic environment has been largely attributed to the gradient of the magnetic pressure. In this work, we propose a new approach to investigate the role of topology on CME deflection and to quantify and compare the action between the magnetic field gradient ('gradient' path) and the topology ('topological' path).

We investigate 8 events simultaneously observed from Solar Orbiter, STEREO-A and SDO; and, with a new tracking technique, we reconstruct the 3D evolution of the eruptions. Then, we compare their propagation with the predictions from the two magnetic drivers. We find that the 'topological' path describes the CME actual trajectory much better than the more traditional 'gradient path'.

Our results strongly indicate that the ambient topology may be the dominant driver for deflections in the low corona, and that presents a promising method to estimate the direction of propagation of CMEs early in their evolution. **2021-02-22, 2021-03-21, 2021-04-26, 2021-12-26, 2021-12-31, 2022-03-19, 2022-03-20, 2022-03-28**

Table 1. Event list and coordinates

## **Understanding the deflection of the 'Cartwheel CME': data analysis and modeling**

[Abril Sahade](#), [Angelos Vourlidas](#), [Laura Balmaceda](#), [Mariana Cecere](#)

ApJ **953** 150 **2023**

<https://arxiv.org/pdf/2303.15998.pdf>

<https://iopscience.iop.org/article/10.3847/1538-4357/ace420/pdf>

We study the low corona evolution of the 'Cartwheel' coronal mass ejection (CME; **2008-04-09**) by reconstructing its 3D path and modeling it with magneto-hydrodynamic simulations. This event exhibits a double-deflection that has been reported and analyzed in previous works but whose underlying cause remained unclear. The 'Cartwheel CME' travels toward a coronal hole (CH) and against the magnetic gradients. Using a high-cadence, full trajectory reconstruction, we accurately determine the location of the magnetic flux rope (MFR) and, consequently, the magnetic environment in which it is immersed. We find a pseudostreamer (PS) structure whose null point may be responsible for the complex evolution of the MFR at the initial phase. From the pre-eruptive magnetic field reconstruction, we estimate the dynamic forces acting on the MFR and provide a new physical insight on the motion exhibited by the **2008-04-09** event. By setting up a similar magnetic configuration in a 2.5D numerical simulation we are able to reproduce the observed behavior, confirming the importance of the PS null point. We find that the magnetic forces directed toward the null point cause the first deflection, directing the MFR towards the CH. Later, the magnetic pressure gradient of the CH produces the reversal motion of the MFR.

## **Pseudostreamer influence on flux rope evolution**

[A. Sahade](#), [M. Cécere](#), [M.V. Sieyra](#), [G. Krause](#), [H. Cremades](#), [A. Costa](#)

A&A Volume 662, id.A113, **2022**

<https://arxiv.org/pdf/2205.07936.pdf>

[https://ui.adsabs.harvard.edu/link\\_gateway/2022A%26A...662A.113S/PUB\\_PDF](https://ui.adsabs.harvard.edu/link_gateway/2022A%26A...662A.113S/PUB_PDF)

A critical aspect of solar activity is the coupling between eruptions and the surrounding coronal magnetic field, which determines the trajectory and morphology of the eruptive event. Pseudostreamers (PSs) are coronal magnetic structures formed by arcs of twin loops capped by magnetic field lines from coronal holes of the same polarity that meet at a central spine. They contain a single magnetic null point in the spine, potentially influencing the evolution of nearby flux ropes (FRs). To understand the net effect of the PS on FR eruptions is first necessary to study diverse and isolated FR-PS scenarios, which are not influenced by other magnetic structures. We performed numerical simulations in which a FR structure is in the vicinity of a PS magnetic configuration. The combined magnetic field of the PS and the FR results in the formation of two magnetic null points. We evolve this scenario by numerically solving the magnetohydrodynamic equations in 2.5D. The simulations consider a fully ionised compressible ideal plasma in the presence of a gravitational field and a stratified atmosphere. We find that the dynamic behaviour of the FR can be categorised into three different classes based on the FR trajectories and whether it is eruptive or confined. Our analysis indicates that the magnetic null

points are decisive in the direction and intensity of the FR deflection and their hierarchy depends on the topological arrangement of the scenario. Moreover, the PS lobe acts as a magnetic cage enclosing the FR. We report that the total unsigned magnetic flux of the cage is a key parameter defining whether the FR is ejected or not.

### **Polarity relevance in flux rope deflections triggered by coronal holes**

[Abril Sahade](#), [Mariana Cécere](#), [Andrea Costa](#), [Hebe Cremades](#)

A&A 652, A111 2021

<https://arxiv.org/pdf/2104.07127.pdf>

<https://www.aanda.org/articles/aa/pdf/2021/08/aa41085-21.pdf>

<https://doi.org/10.1051/0004-6361/202141085>

Many observations show that coronal holes (CHs) deviate coronal mass ejections (CMEs) away from them. However, there are some peculiar events reported where the opposite occurs. To contribute to a space weather forecast efforts, in relation to the prediction of CME trajectories, we study the interaction between flux ropes (FRs) and CHs through numerical simulations. We perform 2.5D numerical simulations where FRs and CHs interact with different relative polarity configurations. We also reconstruct the trajectory and magnetic environment of a peculiar event occurred on **30 April 2012**. The numerical simulations indicate that at low coronal levels, depending on the relative magnetic field polarity between the FR and the CH, the deflection will be attractive, i.e. the FR moves towards the CH (for anti-aligned polarities) or repulsive, i.e. the FR moves away to the CH (for aligned polarities). This is likely due to the formation of vanishing magnetic field regions or null points, located between the FR and the CH or, at the other side of the FR, respectively. The analysed observational event shows a double-deflection, first departing from the radial direction by approaching the CH and then moving away from it suggesting that the trajectory could result from a magnetic configuration with an anti-aligned polarity. We numerically reproduce the double deflection of the observed event, providing support to this conjecture.

### **Influence of coronal holes on CME deflections: numerical study**

[Abril Sahade](#), [Mariana Cécere](#), [Gustavo Krause](#)

ApJ 896 53 2020

<https://arxiv.org/pdf/2004.10834.pdf>

<https://doi.org/10.3847/1538-4357/ab8f25>

The understanding of the causes that produce the deflection of coronal mass ejections (CMEs) is essential for the space weather forecast. In this article, we study the effects on CMEs trajectories produced by the different properties of a coronal hole close to the ejection area. For this analysis, we perform numerical simulations of the ideal magnetohydrodynamics equations that emulate the early rising of the CME in presence of a coronal hole. We find that, the stronger the magnetic field and the wider the coronal hole area, the larger the CME deflection. This effect is reduced when the coronal hole moves away from the ejection region. To characterize this behavior, we propose a dimensionless parameter that depends on the coronal hole properties and properly quantifies the deflection. Also, we show that the presence of the coronal hole near a CME magnetic structure produces a minimum magnetic energy region which is responsible for the deflection. Thus, we find a relationship between the coronal hole properties, the location of this region and the CME deflection.

### **Homologous compact major blowout-eruption solar flares and their production of broad CMEs**

[Suraj Sahu](#), [Bhuvan Joshi](#), [Alphonse C. Sterling](#), [Prabir K. Mitra](#), [Ronald L. Moore](#)

ApJ 930 41 2022

<https://arxiv.org/pdf/2203.03954>

<https://iopscience.iop.org/article/10.3847/1538-4357/ac5cc1/pdf>

We analyze the formation mechanism of three homologous broad coronal mass ejections (CMEs) resulting from a series of solar blowout-eruption flares with successively increasing intensities (M2.0, M2.6, and X1.0). The flares originated from active region NOAA 12017 during **2014 March 28-29** within an interval of approximately 24 hr. Coronal magnetic field modeling based on nonlinear-force-free-field extrapolation helps to identify low-lying closed bipolar loops within the flaring region enclosing magnetic flux ropes. We obtain a double flux rope system under closed bipolar fields for the all the events. The sequential eruption of the flux ropes led to homologous flares, each followed by a CME. Each of the three CMEs formed from the eruptions gradually attain a large angular width, after expanding from the compact eruption-source site. We find these eruptions and CMEs to be consistent with the 'magnetic-arch-blowout' scenario: each compact-flare blowout eruption was seated in one foot of a far-reaching magnetic arch, exploded up the encasing leg of the arch, and blew out the arch to make a broad CME.

### **OBSERVATIONS OF LINEAR POLARIZATION IN A SOLAR CORONAL LOOP PROMINENCE SYSTEM OBSERVED NEAR 6173 Å**

Pascal [Saint-Hilaire](#)<sup>1</sup>, Jesper Schou<sup>2</sup>, Juan-Carlos Martínez Oliveros<sup>1</sup>, Hugh S. Hudson<sup>1,3</sup>, Säm Krucker<sup>1,4</sup>, Hazel Bain<sup>1</sup>, and Sébastien Couvidat<sup>5</sup>

2014 ApJL 786 L19

<https://iopscience.iop.org/article/10.1088/2041-8205/786/2/L19/pdf>

White-light observations by the Solar Dynamics Observatory's Helioseismic and Magnetic Imager of a loop-prominence system occurring in the aftermath of an X-class flare on **2013 May 13** near the eastern solar limb show a linearly polarized component, reaching up to ~20% at an altitude of ~33 Mm, about the maximum amount expected if the emission were due solely to Thomson scattering of photospheric light by the coronal material. The mass associated with the polarized component was  $8.2 \times 10^{14}$  g. At 15 Mm altitude, the brightest part of the loop was  $3(\pm 0.5)\%$  linearly polarized, only about 20% of that expected from pure Thomson scattering, indicating the presence of an additional unpolarized component at wavelengths near Fe I (617.33 nm). We estimate the free electron density of the white-light loop system to possibly be as high as  $1.8 \times 10^{12}$  cm<sup>-3</sup>.

## **X-RAY EMISSION FROM THE BASE OF A CURRENT SHEET IN THE WAKE OF A CORONAL MASS EJECTION**

P. [Saint-Hilaire](#), S. Krucker, and R.P. Lin

*Astrophysical Journal*, 699:245–253, **2009**, **File**

Following a coronal mass ejection (CME) which started on **2002 November 26**, *RHESSI* observed for 12 hr an X-ray source above the solar limb, at altitudes between 0.1 and 0.3 *R*<sub>s</sub> above the photosphere. The *Geostationary Operational Environmental Satellite* baseline was remarkably high throughout this event. The X-ray source's temperature peaked around 10–11 MK, and its emission measure increased throughout this time interval. Higher up, at 0.7 *R*<sub>s</sub>, hot (initially >8 MK) plasma has been observed by Ultraviolet Coronagraph Spectrometer on *Solar and Heliospheric Observatory* for 2.3 days. This hot plasma was interpreted as the signature of a current sheet (CS) trailing the CME. The thermal energy content of the X-ray source is more than an order of magnitude larger than in the CS. Hence, it could be the source of the hot plasma in the CS, although CS heating by magnetic reconnection within it cannot be discounted. To better characterize the X-ray spectrum, we have used novel techniques (back-projection-based and visibility-based) for long integration (several hours) imaging spectroscopy. There is no observed nonthermal hard X-ray bremsstrahlung emission, leading to the conclusion that there is either very little particle acceleration occurring in the vicinity of this postflare X-ray source, or that either the photon spectral index would have had to be uncharacteristically (in flare parlance) high ( $\gamma \sim 8$ ) and/or the low-energy cutoff very low ( $E_c \sim 6$  keV).

## **Observational Study on the Fine Structure and Dynamics of a Solar Jet. II. Energy Release Process Revealed by Spectral Analysis**

Takahito [Sakaue](#), [Akiko Tei](#), [Ayumi Asai](#), [Satoru Ueno](#), [Kiyoshi Ichimoto](#), [Kazunari Shibata](#)  
PASJ Volume 70, Issue 6, 1 December **2018**

<https://arxiv.org/pdf/1710.08441.pdf>

We report a solar jet phenomenon associated with the C5.4 class flare on **2014 November 11 (10)**. The data of jet was provided by Solar Dynamics Observatory (SDO), X-Ray Telescope (XRT) aboard Hinode, Interface Region Imaging Spectrograph (IRIS) and Domeless Solar Telescope (DST) at Hida Observatory, Kyoto University. These plentiful data enabled us to present this series of papers to discuss the entire processes of the observed phenomena including the energy storage, event trigger, and energy release. In this paper, we focus on the energy release process of the observed jet, and mainly describe our spectral analysis on the H-alpha data of DST to investigate the internal structure of the H-alpha jet and its temporal evolution. This analysis reveals that in the physical quantity distributions of the H-alpha jet, such as line-of-sight velocity and optical thickness, there is a significant gradient in the direction crossing the jet. We interpret this internal structure as the consequence of the migration of energy release site, based on the idea of ubiquitous reconnection. Moreover, by measuring the horizontal flow of the fine structures in jet, we succeeded in deriving the three-dimensional velocity field and the line-of-sight acceleration field of the H-alpha jet. The analysis result indicates a part of ejecta in the H-alpha jet experienced the additional acceleration after it had been ejected from the lower atmosphere. This secondary acceleration was specified to occur in the vicinity of the intersection between the trajectories of the H-alpha jet and X-ray jet observed by Hinode/XRT. We propose that a fundamental cause of this phenomenon is the magnetic reconnection involving the plasmoid in the observed jet.

## **Observational Study on the Fine Structure and Dynamics of a Solar Jet. I. Energy Build-Up Process around a Satellite Spot**

Takahito [Sakaue](#), [Akiko Tei](#), [Ayumi Asai](#), [Satoru Ueno](#), [Kiyoshi Ichimoto](#), [Kazunari Shibata](#)  
PASJ Volume 69, Issue 5, 1 October **2017**, 80, **2017**

<https://arxiv.org/pdf/1707.01262.pdf>

We report a solar jet phenomenon associated with successive flares on **November 10th 2014**. These explosive events were involved with the satellite spots' emergence around a delta-type sunspot in the decaying active region NOAA 12205. The data of this jet was provided by Solar Dynamic Observatory (SDO), X-Ray Telescope (XRT) aboard Hinode, Interface Region Imaging Spectrograph (IRIS) and Domeless Solar Telescope (DST) at Hida Observatory, Kyoto University. These plentiful data enabled us to present this series of papers to discuss the entire processes of the observed phenomena including the energy storage, event trigger, and energy release. In this paper, we focus on the energy build-up and trigger phases, by analyzing the photospheric horizontal flow field around the active region with an optical flow method. The analysis reveals the following three. (i) The observed explosive phenomena involved three satellite spots, the magnetic fluxes of which successively reconnected with their pre-existing ambient fields. (ii) All of these satellite spots emerged in the moat region of a pivotal delta-type sunspot, especially near its convergent boundary with the neighboring supergranules or moat regions of adjacent sunspots. (iii) Around the jet ejection site, the positive

polarities of satellite spot and adjacent emerging flux encountered the global magnetic field with negative polarity in the moat region of the pivotal delta-type sunspot, and thus the polarity inversion line was formed along the convergent boundary of the photospheric horizontal flow channels.

### **Coronal mass ejection-related particle acceleration regions during a simple eruptive event**

Carolina [Salas-Matamoros](#)<sup>1,5</sup>, Karl-Ludwig Klein<sup>1,2</sup> and Alexis P. Rouillard<sup>3</sup>

A&A 590, A135 (2016) **File**

<http://www.aanda.org/articles/aa/pdf/2016/06/aa28015-15.pdf>

An intriguing feature of many solar energetic particle (SEP) events is the detection of particles over a very extended range of longitudes in the heliosphere. This may be due to peculiarities of the magnetic field in the corona, to a broad accelerator, to cross-field transport of the particles, or to a combination of these processes. The eruptive flare on **26 April 2008** provided an opportunity to study relevant processes under particularly favourable conditions since it occurred in a very quiet solar and interplanetary environment. This enabled us to investigate the physical link between a single well-identified coronal mass ejection (CME), electron acceleration as traced by radio emission, and the production of SEPs. We conduct a detailed analysis, which combines radio observations (Nançay Radio Heliograph and Nançay Decametre Array, Wind/Waves spectrograph) with remote-sensing observations of the corona in extreme ultraviolet (EUV) and white light, as well as in situ measurements of energetic particles near 1 AU (SoHO and STEREO spacecraft). By combining images taken from multiple vantage points, we were able to derive the time-dependent evolution of the 3D pressure front that was developing around the erupting CME. Magnetic reconnection in the post-CME current sheet accelerated electrons, which remained confined in closed magnetic fields in the corona, while the acceleration of escaping particles can be attributed to the pressure front ahead of the expanding CME. The CME accelerated electrons remotely from the parent active region, owing to the interaction of its laterally expanding flank, which was traced by an EUV wave, with the ambient corona. SEPs detected at one STEREO spacecraft and SoHO were accelerated later, when the frontal shock of the CME intercepted the spacecraft-connected interplanetary magnetic field line. The injection regions into the heliosphere inferred from the radio and SEP observations are separated in longitude by about 140°. The observations for this event show that it is misleading to interpret multi-spacecraft SEP measurements in terms of one acceleration region in the corona. The different acceleration regions are linked to different vantage points in the interplanetary space.

### **On the Statistical Relationship between CME Speed and Soft X-ray Flux and Fluence of the Associated Flare**

C. [Salas-Matamoros](#), K.-L. Klein

Solar Phys. May 2015, Volume 290, [Issue 5](#), pp 1337-1353 **2015**

<https://sci-hub.ru/10.1007/s11207-015-0677-0>

<http://arxiv.org/pdf/1503.08613v1.pdf>

<https://link.springer.com/content/pdf/10.1007/s11207-015-0677-0.pdf>

Both observation and theory reveal a close relationship between the kinematics of coronal mass ejections (CMEs) and the thermal energy release traced by the related soft X-ray (SXR) emission. The major problem of empirical studies of this relationship is the distortion of the CME speed by the projection effect in the coronagraphic measurements. We present a re-assessment of the statistical relationship between CME velocities and SXR parameters, using the SOHO/LASCO catalog and GOES whole Sun observations during the period 1996 to 2008. 49 events were identified where CMEs originated near the limb, at central meridian distances between 70° and 85°, and had a reliably identified SXR burst, the parameters of which - peak flux and fluence - could be determined with some confidence. We find similar correlations between the logarithms of CME speed and of SXR peak flux and fluence as several earlier studies, with correlation coefficients of 0.48 and 0.58, respectively. Correlations are slightly improved over an unrestricted CME sample when only limb events are used. However, a broad scatter persists. We derive the parameters of the CME-SXR relationship and use them to predict ICME arrival times at Earth. *We show that the CME speed inferred from SXR fluence measurements tends to perform better than SoHO/LASCO measurements in the prediction of ICME arrival times near 1 AU. The estimation of the CME speed from SXR observations can therefore make a valuable contribution to space weather predictions.*

Table 1. Table of events:

Table 2.: Comparison of travel time of CMEs

### **The temporal and spatial scales of density structures released in the slow solar wind during solar activity maximum**

Eduardo [Sanchez-Diaz](#), [Alexis P. Rouillard](#), [Jackie A. Davies](#), [Benoit Lavraud](#), [Rui F. Pinto](#), [Emilia Kilpua](#)

ApJ **2017**

<https://arxiv.org/ftp/arxiv/papers/1711/1711.02486.pdf>

In a recent study, we took advantage of a highly tilted coronal neutral sheet to show that density structures, extending radially over several solar radii (Rs), are released in the forming slow solar wind approximately 4-5 Rs above the solar surface (Sanchez-Diaz et al. 2017). We related the signatures of this formation process to intermittent magnetic

reconnection occurring continuously above helmet streamers. We now exploit the heliospheric imagery from the Solar Terrestrial Relation Observatory (STEREO) to map the spatial and temporal distribution of the ejected structures. We demonstrate that streamers experience quasi-periodic bursts of activity with the simultaneous outpouring of small transients over a large range of latitudes in the corona. This cyclic activity leads to the emergence of well-defined and broad structures. Derivation of the trajectories and kinematic properties of the individual small transients that make up these large-scale structures confirms their association with the forming Slow Solar Wind (SSW). We find that these transients are released, on average, every 19.5 hours, simultaneously at all latitudes with a typical radial size of 12 Rs. Their spatial distribution, release rate and three-dimensional extent are used to estimate the contribution of this cyclic activity to the mass flux carried outward by the SSW. Our results suggest that, in interplanetary space, the global structure of the heliospheric current sheet is dominated by a succession of blobs and associated flux ropes. We demonstrated this with an example event using STEREO-A in-situ measurements. **2013 May 28 to June 06, 2013 July 08-10**

## **Observational evidence for the associated formation of blobs and raining inflows in the solar Corona**

Eduardo [Sanchez-Diaz](#), Alexis P. Rouillard, Jackie A. Davies, Benoit Lavraud, Neil R. Sheeley, Rui F. Pinto, Emilia Kilpua, Illya Plotnikov, Vincent Genot  
**2017 ApJL 835 L7**

<https://arxiv.org/pdf/1612.05487v1.pdf>

The origin of the slow solar wind is still a topic of much debate. The continual emergence of small transient structures from helmet streamers is thought to constitute one of the main sources of the slow wind. Determining the height at which these transients are released is an important factor in determining the conditions under which the slow solar wind forms. To this end, we have carried out a multipoint analysis of small transient structures released from a north-south tilted helmet streamer into the slow solar wind over a broad range of position angles during Carrington Rotation 2137. Combining the remote-sensing observations taken by the Solar-Terrestrial Relations Observatory (STEREO) mission with coronagraphic observations from the Solar and Heliospheric Observatory (SoHO) spacecraft, we show that the release of such small transient structures (often called blobs), which subsequently move away from the Sun, is associated with the concomitant formation of transient structures collapsing back towards the Sun; the latter have been referred to by previous authors as raining inflows. This is the first direct association between outflowing blobs and raining inflows, which locates the formation of blobs above the helmet streamers and gives strong support that the blobs are released by magnetic reconnection. **2013 May 28 to June 06**

## **Multi-point study of the energy release and impulsive CME dynamics in an eruptive C7 flare**

[J. Saqri](#), [A. M. Veronig](#), [E. C. M. Dickson](#), [T. Podladchikova](#), [A. Warmuth](#), [H. Xiao](#), [D. E. Gary](#), [A. F. Battaglia](#), [S. Krucker](#)

**A&A 672, A23 2023**

<https://arxiv.org/pdf/2302.11232.pdf>

<https://www.aanda.org/articles/aa/pdf/2023/04/aa45079-22.pdf>

Context. The energy release in eruptive flares and the kinematics of the associated coronal mass ejections (CMEs) are interlinked and require favorable observing positions as both on-disk and off-limb signatures are necessary to characterize these events. Aims. We combine observations from different vantage points to perform a detailed study of a long duration eruptive C7 class flare that occurred on **17 April 2021** and was partially occulted from Earth view. The dynamics and thermal properties of the flare-related plasma flows, the flaring arcade, and the energy releases and particle acceleration are studied together with the kinematic evolution of the associated CME in order to place this long duration event in context of previous eruptive flare studies. Methods. We use data from the Spectrometer-Telescope for Imaging X-rays (STIX) onboard the Solar Orbiter to analyze the spectral characteristics, timing, and spatial distribution of the flare X-ray emission. Data from the Extreme Ultraviolet Imager (EUVI) onboard the Solar Terrestrial Relations Observatory-Ahead (STEREO-A) spacecraft are used for context images as well as to track the ejected plasma close to the Sun. With Atmospheric Imaging Assembly extreme ultraviolet (EUV) images from the Solar Dynamics Observatory, the flare is observed off-limb and differential emission measure maps are reconstructed. The coronagraphs onboard STEREO-A are used to track the CME out to around 8 R.

Results. The flare showed hard X-ray (HXR) bursts over the duration of an hour in two phases lasting from 16:04 UT to 17:05 UT. During the first phase, a strong increase in emission from hot plasma and impulsive acceleration of the CME was observed. The CME acceleration profile shows a three-part evolution of slow rise, acceleration, and propagation in line with the first STIX HXR burst phase, which is triggered by a rising hot (14 MK) plasmoid. During the CME acceleration phase, we find signatures of ongoing magnetic reconnection behind the erupting structure, in agreement with the standard eruptive flare scenario. The subsequent HXR bursts that occur about 30 minutes after the primary CME acceleration show a spectral hardening (from  $\delta \approx 7$  to  $\delta \approx 4$ ) but do not correspond to further CME acceleration and chromospheric evaporation. *Therefore, the CME-flare feedback relationship may only be of significance within the first 25 minutes of the event under study, as thereafter the flare and the CME eruption evolve independently of each other.*

## **Evolution of Coronal Cavity from Quiescent to Eruptive Phase in Association with Coronal Mass Ejection**

Ranadeep [Sarkar](#), [Nandita Srivastava](#), [Marilena Mierla](#), [Matthew J West](#), [Elke D'Huys](#)

ApJ **875** 101 **2019**  
<https://arxiv.org/pdf/1904.00899.pdf>  
<https://sci-hub.se/10.3847/1538-4357/ab11c5>

We present the evolution of a coronal cavity encompassing its quiescent and eruptive phases in the lower corona. Using the multi-vantage point observations from the SDO/AIA, STEREO SECCHI/EUVI and PROBA2/SWAP EUV imagers, we capture the sequence of quasi-static equilibria of the quiescent cavity which exhibited a slow rise and expansion phase during its passage on the solar disc from 2010 May 30 to 2010 June 13. By comparing the decay-index profiles of the cavity system during the different stages of its quiescent and pre-eruptive phases we find that the decay-index value at the cavity centroid height can be used as a good indicator to predict the cavity eruption in the context of torus instability. Combining the observations of SWAP and LASCO C2/C3 we show the evolution of the EUV cavity into the white-light cavity as a three-part structure of the associated CME observed to erupt on **2010 June 13**. By applying successive geometrical fits to the cavity morphology we find that the cavity exhibited non self-similar expansion in the lower corona, below  $2.2 \pm 0.2 R_s$ , which points to the spatial scale for the radius of source surface where the coronal magnetic field lines are believed to become radial. Furthermore, the kinematic study of the erupting cavity captures both the "impulsive" and "residual" phases of acceleration along with a strong deflection of the cavity at  $1.3 R_s$ . We also discuss the role of driving forces behind the dynamics of the morphological and kinematic evolution of the cavity.

**2010-05-30, 2010/06/04-07, 2010/06/13**

### **A Comparative Study of the Eruptive and Non-Eruptive Flares Produced by the Largest Active Region of Solar Cycle 24**

Ranadeep [Sarkar](#), [Nandita Srivastava](#)

Solar Phys. **293**:16 **2018**

<https://arxiv.org/pdf/1801.00473.pdf>  
<https://link.springer.com/content/pdf/10.1007%2Fs11207-017-1235-8.pdf>

We investigate the morphological and magnetic characteristics of solar active region (AR) NOAA 12192. AR 12192 was the largest region of Solar Cycle 24; it underwent noticeable growth and produced 6 X-class flares, 22 M-class flares, and 53 C-class flares in the course of its disc passage. However, the most peculiar fact of this AR is that it was associated with only one CME in spite of producing several X-class flares. In this work, we carry out a comparative study between the eruptive and non-eruptive flares produced by AR 12192. We find that the magnitude of abrupt and permanent changes in the horizontal magnetic field and Lorentz force are significantly smaller in the case of the confined flares compared to the eruptive one. We present the areal evolution of AR 12192 during its disc passage. We find the flare-related morphological changes to be weaker during the confined flares, whereas the eruptive flare exhibits a rapid and permanent disappearance of penumbral area away from the magnetic neutral line after the flare.

Furthermore, from the extrapolated nonlinear force-free magnetic field, we examine the overlying coronal magnetic environment over the eruptive and non-eruptive zones of the AR. We find that the critical decay index for the onset of torus instability was achieved at a lower height over the eruptive flaring region, than for the non-eruptive core area. These results suggest that the decay rate of the gradient of overlying magnetic field strength may play a decisive role to determine the CME productivity of the AR. In addition, the magnitude of changes in the flare-related magnetic characteristics are found to be well correlated with the nature of solar eruptions. **2014.10.22-25**

**HMI Science Nuggets, #90** March **2018** <http://hmi.stanford.edu/hminuggets/?p=2333>

### **Transverse oscillations in a coronal loop triggered by a jet**

S. [Sarkar](#), V. Pant, A. K. Srivastava, D. Banerjee

Solar Phys. **2016**

<https://arxiv.org/pdf/1611.04063v1.pdf>

We detect and analyse transverse oscillations in a coronal loop, lying at the south east limb of the Sun as seen from the Atmospheric Imaging Assembly (AIA) onboard the Solar Dynamics Observatory (SDO). The jet is believed to trigger transverse oscillations in the coronal loop. The jet originates from a region close to the coronal loop on **19 th September 2014** at 02:01:35 UT. The length of the loop is estimated to be between 377-539-Mm. Only one complete oscillation is detected with an average period of about  $32 \pm 5$ -min. Using MHD seismologic inversion techniques, we estimate the magnetic field inside the coronal loop to be between 2.68-4.5-G. The velocity of the hot and cool components of the jet is estimated to be 168-km-s<sup>-1</sup> and 43-km-s<sup>-1</sup>, respectively. The energy density of the jet is found to be greater than the energy density of the oscillating coronal loop. Therefore, we conclude that the jet triggered transverse oscillations in the coronal loop. To our knowledge, this is the first coronal loop seismology study using the properties of a jet propagation triggered oscillations.

### **RECONNECTION OUTFLOWS AND CURRENT SHEET OBSERVED WITH HINODE/XRT IN THE 2008 APRIL 9 "CARTWHEEL CME" FLARE**

Sabrina L. [Savage](#)<sup>1</sup>, David E. McKenzie<sup>1</sup>, Katharine K. Reeves<sup>2</sup>, Terry G. Forbes<sup>3</sup>, and Dana W. Longcope<sup>1</sup>

Astrophysical Journal, 722:329-342, **2010**, File

Supra-arcade downflows (SADs) have been observed with *Yohkoh*/SXT (soft X-rays (SXR)), *TRACE* (extreme ultraviolet (EUV)), *SOHO*/LASCO (white light), *SOHO*/SUMER (EUV spectra), and *Hinode*/XRT (SXR).

Characteristics such as low emissivity and trajectories, which slow as they reach the top of the arcade, are consistent with post-reconnection magnetic flux tubes retracting from a reconnection site high in the corona until they reach a lower-energy magnetic configuration. Viewed from a perpendicular angle, SADs should appear as shrinking loops rather than downflowing voids. We present X-ray Telescope (XRT) observations of supra-arcade downflowing loops (SADs) following a coronal mass ejection (CME) on 2008 April 9 and show that their speeds and decelerations are consistent with those determined for SADs. We also present evidence for a possible current sheet observed during this flare that extends between the flare arcade and the CME. Additionally, we show a correlation between reconnection outflows observed with XRT and outgoing flows observed with LASCO.

## **Predicting the magnetic vectors within coronal mass ejections arriving at Earth:**

### **2. Geomagnetic response: BZ VALIDATION**

N. P. [Savani](#)<sup>1, 2</sup> A. Vourlidis,<sup>3</sup> I. G. Richardson,<sup>4, 2</sup> A. Szabo,<sup>2</sup> B. J. Thompson,<sup>2</sup> A. Pulkkinen,<sup>2</sup> M. L. Mays,<sup>5, 2</sup> T. Nieves-Chinchilla,<sup>5, 2</sup> V. Bothmer<sup>6</sup>

Space Weather **2016**

This is a companion to [Savani et al., 2015] that discussed how a first-order prediction of the internal magnetic field of a coronal mass ejection (CME) may be made from observations of its initial state at the Sun for space weather forecasting purposes (BSS model). For eight CME events, we investigate how uncertainties in their predicted magnetic structure influence predictions of the geomagnetic activity. We use an empirical relationship between the solar wind plasma drivers and Kp index together with the inferred magnetic vectors, to make a prediction of the time variation of Kp (Kp(BSS)). We find a 2\_ uncertainty range on the magnetic field magnitude ( $jB_j$ ) provides a practical and convenient solution for predicting the uncertainty in geomagnetic storm strength. We also find the estimated CME velocity is a major source of error in the predicted maximum Kp. The time variation of Kp(BSS) is important for predicting periods of enhanced and maximum geomagnetic activity, driven by southerly-directed magnetic fields, and periods of lower activity driven by northerly directed magnetic field. We compare the skill score of our model to a number of other forecasting models, including the NOAA/SWPC and CCMC/SWRC estimates. The BSS model was the most unbiased prediction model while the other models predominately tended to significantly over-forecast. The True skill score of the BSS prediction model (TSS = 0:43 \_ 0:06) exceeds the results of 2 baseline models and the NOAA/SWPC forecast. The BSS model prediction performed equally with CCMC/SWRC predictions while demonstrating a lower uncertainty. . 3 Apr 2010, 25 Mar 2011, 10 Mar 2012, 14 Jun 2012, 12 Jul 2012, 27 Sep 2012, 7 Jan 2014, 10 Sep 2014

## **Predicting the magnetic vectors within coronal mass ejections arriving at Earth**

### **1. Initial architecture**

[Savani](#), N. P.; Vourlidis, A.; Szabo, A.; Mays, M. L.; Thompson, B. J.; Richardson, I. G.; Evans, R.; Pulkkinen, A.; Nieves-Chinchilla, T.

Space Weather , Volume 13, Issue 6 June 2015 Pages 374–385,

<http://arxiv.org/pdf/1502.02067v1.pdf> **File**

<http://onlinelibrary.wiley.com/doi/10.1002/2015SW001171/full>

The process by which the Sun affects the terrestrial environment on short timescales is predominately driven by the amount of magnetic reconnection between the solar wind and Earth's magnetosphere. Reconnection occurs most efficiently when the solar wind magnetic field has a southward component. The most severe impacts are during the arrival of a coronal mass ejection (CME) when the magnetosphere is both compressed and magnetically connected to the heliospheric environment. Unfortunately, forecasting magnetic vectors within coronal mass ejections remain elusive. Here we report how, by combining a statistically robust helicity rule for a CME's solar origin with a simplified flux rope topology, the magnetic vectors within the Earth-directed segment of a CME can be predicted. In order to test the validity of this proof-of-concept architecture for estimating the magnetic vectors within CMEs, a total of eight CME events (between 2010 and 2014) have been investigated. With a focus on the large false alarm of **January 2014**, this work highlights the importance of including the early evolutionary effects of a CME for forecasting purposes. The angular rotation in the predicted magnetic field closely follows the broad rotational structure seen within the in situ data. This time-varying field estimate is implemented into a process to quantitatively predict a time-varying Kp index that is described in detail in paper II. Future statistical work, quantifying the uncertainties in this process, may improve the more heuristic approach used by early forecasting systems.

## **OBSERVATIONAL EVIDENCE OF A CORONAL MASS EJECTION DISTORTION DIRECTLY ATTRIBUTABLE TO A STRUCTURED SOLAR WIND**

N. P. [Savani](#)<sup>1,5</sup>, M. J. Owens<sup>1,5</sup>, A. P. Rouillard<sup>2,3</sup>, R. J. Forsyth<sup>1</sup>, and J. A. Davies<sup>4</sup>

Astrophysical Journal Letters, 714:L128–L132, 2010 May; **File**

We present the first observational evidence of the near-Sun distortion of the leading edge of a coronal mass ejection (CME) by the ambient solar wind into a concave structure. On **2007 November 14**, a CME was observed by coronagraphs onboard the *STEREO-B* spacecraft, possessing a circular cross section. Subsequently the CME passed through the field of view of the *STEREO-B* Heliospheric Imagers where the leading edge was observed to distort into an increasingly concave structure. The CME observations are compared to an analytical flux rope model constrained by a magnetohydrodynamic solar wind solution. The resultant bimodal speed profile is used to kinematically

distort a circular structure that replicates the initial shape of the CME. The CME morphology is found to change rapidly over a relatively short distance. This indicates an approximate radial distance in the heliosphere where the solar wind forces begin to dominate over the magnetic forces of the CME influencing the shape of the CME.

## **The Relation between Solar Eruption Topologies and Observed Flare Features II: Dynamical Evolution**

A. [Savcheva](#), E. Pariat, S. McKillop, P. McCauley, E. Hanson, Y. Su, & E. DeLuca  
2016 ApJ 817 43

[http://www.pergamentum.com/eprint/savcheva\\_et\\_al\\_ribbonsA\\_II.pdf](http://www.pergamentum.com/eprint/savcheva_et_al_ribbonsA_II.pdf)

A long established goal of solar physics is to build understanding of solar eruptions and develop flare and CME forecasting models. In this paper, we continue our investigation of non-linear forces free field (NLFFF) models by comparing topological properties of the solutions to the evolution of the flare ribbons. In particular, we show that data constrained NLFFF models of three erupting sigmoid regions (**SOL2010-04-08**, **SOL2010-08-07**, and **SOL2012-05-12**) built to reproduce the active region magnetic field in the pre-flare state can be rendered unstable and the subsequent sequence of unstable solutions produce quasi-separatrix layers (QSLs) that match the flare ribbon evolution as observed by SDO/AIA. We begin with a best-fit equilibrium model for the pre-flare active region; we then add axial flux to the flux rope in the model to move it across the stability boundary; at this point the magnetofrictional code no longer converges to an equilibrium solution, the flux rope rises as the solutions are iterated. We interpret the sequence of magnetofrictional steps as an evolution of the active region as the flare/CME begins. The magnetic field solutions at different steps are compared with the flare ribbons. The results are fully consistent with the 3D extension of the standard flare/CME model. Our ability to capture essential topological features of flaring active regions with a non-dynamic magneto-frictional code strongly suggests that the pre-flare, large scale topological structures are preserved as the flux rope becomes unstable and lifts off.

## **A New Sigmoid Catalog from Hinode and the Solar Dynamics Observatory: Statistical Properties and Evolutionary Histories**

A. S. [Savcheva](#), S. C. McKillop, P. I. McCauley, E. M. Hanson, E. E. DeLuca  
Solar Physics, Volume 289, Issue 9, pp 3297-3311, 2014; **File**

We present a new sigmoid catalog covering the duration of the Hinode mission and the Solar Dynamics Observatory (SDO) until the end of 2012. The catalog consists of 72 mostly long-lasting sigmoids. We collect and make available all X-ray and EUV data from Hinode, SDO, and the Solar TERrestrial Relations Observatory (STEREO), and we determine the sigmoid lifetimes, sizes, and aspect ratios. We also collect the line-of-sight magnetograms from the Helioseismic and Magnetic Imager (HMI) for SDO or the Michelson Doppler Imager (MDI) on the Solar and Heliospheric Observatory (SOHO) to measure flux versus time for the lifetime of each region. We determine that the development of a sigmoidal shape and eruptive activity is more strongly correlated with flux cancellation than with emergence. We find that **the eruptive properties of the regions correlate well with the maximum flux**, largest change, and net change in flux in the regions. These results have implications for constraining future flux-rope models of ARs and gaining insight into their evolutionary properties.

## **SIGMOIDAL ACTIVE REGION ON THE SUN: COMPARISON OF A MAGNETOHYDRODYNAMICAL SIMULATION AND A NONLINEAR FORCE-FREE FIELD MODEL**

A. [Savcheva](#)<sup>1,2</sup>, E. Pariat<sup>3</sup>, A. van Ballegoijen<sup>1</sup>, G. Aulanier<sup>3</sup>, and E. DeLuca  
2012 ApJ 750 15

[http://www.pergamentum.com/eprint/Savcheva\\_et\\_al\\_MHD\\_NLFFF.pdf](http://www.pergamentum.com/eprint/Savcheva_et_al_MHD_NLFFF.pdf)

In this paper we show that when accurate nonlinear force-free field (NLFFF) models are analyzed together with high-resolution magnetohydrodynamic (MHD) simulations, we can determine the physical causes for the coronal mass ejection (CME) eruption on **2007 February 12**. We compare the geometrical and topological properties of the three-dimensional magnetic fields given by both methods in their pre-eruptive phases. We arrive at a consistent picture for the evolution and eruption of the sigmoid. Both the MHD simulation and the observed magnetic field evolution show that flux cancellation plays an important role in building the flux rope. We compute the squashing factor,  $Q$ , in different horizontal maps in the domains. The main shape of the quasi-separatrix layers (QSLs) is very similar between the NLFFF and MHD models. The main QSLs lie on the edge of the flux rope. While the QSLs in the NLFFF model are more complex due to the intrinsic large complexity in the field, the QSLs in the MHD model are smooth and possess lower maximum value of  $Q$ . In addition, we demonstrate the existence of hyperbolic flux tubes (HFTs) in both models in vertical cross sections of  $Q$ . The main HFT, located under the twisted flux rope in both models, is identified as the most probable site for reconnection. We also show that there are electric current concentrations coinciding with the main QSLs. Finally, we perform torus instability analysis and show that a combination between reconnection at the HFT and the resulting expansion of the flux rope into the torus instability domain is the cause of the CME in both models.

## **Propagation of Torsional Alfvén Pulses in Zero-beta Flux Tubes**



Joseph **Scalisi**<sup>1</sup>, William Oxley<sup>1</sup>, Michael S. Ruderman<sup>1,2,5</sup>, and Robertus Erdélyi<sup>1,3,4</sup>

2021 ApJ 911 39

<https://doi.org/10.3847/1538-4357/abe8db>

In this study, we investigate analytically the generation of mass flux due to a torsional Alfvén pulse. We derive that the presence of torsional Alfvén waves, which have been observed in, e.g., photospheric magnetic bright points (MBPs), can result in vertical plasma motions. The formation of this mass flux may even be a viable contribution to the generation of chromospheric mass transport, playing potential roles in the form of localized lower solar atmospheric jets. This relationship is studied using a flux tube model, with the waves introduced at the lower boundary of the tube as a magnetic shear perturbation. Due to the nature of MBPs we simplify the model by using the zero-beta approximation for the plasma inside the tube. The analytical results are demonstrated by an example of the type of Alfvén wave perturbation that one might expect to observe, and comparison is made with properties of spicules known from observations. We find that field-aligned plasma flux is formed nonlinearly as a result of the Lorentz force generated by the perturbations, and could be consistent with jet formation, although the current model is not intended to determine the entire evolution of a jet. Critical discussion of the model follows, including suggestions for improvements and for high-resolution proposed observations in order to constrain the driving magnetic and velocity shear.

### **THE BLOB CONNECTION: SEARCHING FOR LOW CORONAL SIGNATURES OF SOLAR POST-CME BLOBS**

Nicole E **Schanche**<sup>1</sup>, Katharine K Reeves<sup>1</sup>, and David F. Webb<sup>2</sup>

2016 ApJ 831 47

Bright linear structures, thought to be indicators of a current sheet (CS), are often seen in Large Angle and Spectrometric Coronagraph (LASCO) on the Solar and Heliospheric Observatory (SOHO) white-light data in the wake of coronal mass ejections (CMEs). In a subset of these post-CME structures, relatively bright blobs are seen moving outward along the rays. These blobs have been interpreted as consequences of the plasmoid instability in the CS, and can help us to understand the dynamics of the reconnection. We examine several instances, taken largely from the SOHO/LASCO CME-rays Catalog, where these blobs are clearly visible in white-light data. Using radially filtered, difference, wavelet enhanced, and multiscale Gaussian normalized images to visually inspect Solar Dynamics Observatory/Atmospheric Imaging Assembly (AIA) data in multiple wavelengths, we look for signatures of material that correspond both temporally and spatially to the later appearance of the blobs in LASCO/C2. Constraints from measurements of the blobs allow us to predict the expected count rates in DN pixel<sup>-1</sup> s<sup>-1</sup> for each AIA channel. The resulting values would make the blobs bright enough to be detectable at 1.2 R<sub>☉</sub>. However, we do not see conclusive evidence for corresponding blobs in the AIA data in any of the events. We do the same calculation for the "cartwheel CME," an event in which blobs were seen in X-rays, and find that our estimated count rates are close to those observed. We suggest several possibilities for the absence of the EUV blobs including the formation of the blob higher than the AIA field of view, blob coalescence, and overestimation of blob densities.

### **CMEs from AR 10365: Morphology and Physical Parameters of the Ejections and of the Associated Current Sheet**

G. **Schettino**, G. Poletto, and M. Romoli

2010 ApJ 708 1135-1144, **FILE**

We study the evolution and physical parameters of three consecutive coronal mass ejections (CMEs) that occurred at the west limb of the Sun on **2003 June 2** at 00:30, 08:54, 16:08 UT, respectively. The Large Angle and Spectrometric Coronagraph Experiment (LASCO) CME catalog shows that the CMEs entered the C2 field of view with position angles within a 5deg interval. This suggests a common origin for the ejections, to be identified with the magnetic system associated with the active region that lies below the CMEs. The close proximity in time and source location of the events prompted us to analyze LASCO white light data and Ultraviolet Coronagraph Spectrometer (UVCS) spectra with the aim of identifying similarities and differences among the three CMEs. It turns out that two of them display the typical three-part structure, while no conclusion can be drawn about the morphology of the third ejection. The CMEs plasma is "cool," i.e., electron temperatures in the CMEs front are of the order of 2 x 10<sup>5</sup> K, with no significant variation between different events. However, ejection speeds vary by a factor of [?]1.5 between consecutive events and electron densities (more precisely emission measures) by a factor of [?]6 between the first CME and the second and third CMEs. In the aftermath of all events, we found evidence of current sheets (CSs) both in LASCO and UVCS. We give here the CS physical parameters (electron temperature, density, and kinetic temperature) and follow, in one of the events, their temporal evolution over a 6 hr time interval. A discussion of our results, in the framework of previous findings, concludes the paper.

### **UV TRANSIENT BRIGHTENINGS ASSOCIATED WITH A CORONAL MASS EJECTION**



Full text

[PDF \(295 KB\)](#) | [HTML](#) | [References](#)

[G. Schettino](#)<sup>1</sup>, [G. Poletto](#)<sup>2</sup> and [M. Romoli](#)<sup>1</sup>

2009 ApJ 697 L72-L76 doi: [10.1088/0004-637X/697/1/L72](https://doi.org/10.1088/0004-637X/697/1/L72)

In this paper, we analyze transient UV brightenings in spectra acquired by SOHO/UltraViolet Coronagraph Spectrometer (UVCS) on **2003 June 2** in association with a coronal mass ejection (CME) that occurred at the West limb of the Sun at 08:54 UT. Brightenings have been observed in lines from cool (C III, O VI), intermediate (Si VIII, Si XII), and high ([Fe XVIII]) temperature ions over about 7 hr from the CME. Brightenings in cool lines are interpreted in terms of mini-ejections that appear at the time of, and after, the passage of the CME front through the UVCS slit. We give here their temperature and density and we point out that, assuming a spherical shape, a few of these mini-CMEs can provide a mass comparable to that quoted for typical CMEs. Hot lines, like the [Fe XVIII] line at 974.9 Å which shows up in the CME associated current sheet (CS), undergo transient brightness as well, but hot lines brightenings are more difficult to interpret. We propose here a scenario where they are signatures of the passage through the UVCS slit of plasmoids similar to those observed in the filamentary CS of the magnetotail that form as a consequence of the tearing-mode instability or of a time-dependent Petschek-type reconnection.

### Low geo-effectiveness of fast halo CMEs related to the 12 X-class flares in 2002

[B. Schmieder](#), [R.S. Kim](#), [B. Grison](#), [K. Bocchialini](#), [R.Y. Kwon](#), [S. Poedts](#), [P. Démoulin](#)  
2020

<https://arxiv.org/pdf/2003.10777.pdf>

It is generally accepted that extreme space weather events tend to be related to strong flares and fast halo coronal mass ejections CMEs. In the present paper, we carefully identify the chain of events from the Sun to the Earth induced by all 12 X-class flares that occurred in 2002. In this small sample, we find an unusual high rate (58%) of solar sources with a longitude larger than 74 degrees. Yet, all 12 X-class flares are associated with at least one CME. The fast halo CMEs (50%) are related to interplanetary CMEs (ICMEs) at L1 and weak Dst minimum values ( $>-51$  nT); while 5 (41%) of the 12 X-class flares are related to solar proton events (SPE). We conclude that: (i) All twelve analyzed solar events, even those associated with fast halo CMEs originating from the central disk region, and those ICMEs and SPEs were not very geo-effective. This unexpected result demonstrates that the suggested events in the chain (fast halo CME, X-class flares, central disk region, ICME, SPE) are not infallible proxies for geo-effectiveness. (ii) The low value of integrated and normalized southward component of the IMF ( $B^*z$ ) may explain the low geo-effectiveness for this small sample. In fact,  $B^*z$  is well correlated to the weak Dst and low auroral electrojet (AE) activity. Hence, the only space weather impact at Earth in 2002 we can explain is based on  $B^*z$  at L1. **2002: Apr-21, May-20, Jul-03, Jul-15, Jul-18, Jul-20, Jul-23, Aug-03, Aug-21, Aug-24, Aug-30, Oct-31**

Table 1. Properties of the 12 X-class ares in 2002 and their related phenomena.

### Solar Active Region Electric Currents Before and During Eruptive Flares

**Review**

Brigitte [Schmieder](#), [Guillaume Aulanier](#)

AGU book , A&A **2019**

<https://arxiv.org/pdf/1903.04050.pdf>

The chapter "Solar Active Region Electric Currents Before and During Eruptive Flares" is a discussion on electric currents in the pre-eruption state and in the course of eruptions of solar magnetic structures, using information from solar observations, nonlinear force-free field extrapolations relying on these observations, and three-dimensional magnetohydrodynamic (MHD) models. The discussion addresses the issue of neutralized vs. non-neutralized currents in active regions and concludes that MHD models are able to explain non-neutralized currents in active regions by the existence of strong magnetic shear along the polarity inversion lines, thus confirming previous observations that already contained this result. The models have also captured the essence of the behavior of electric currents in active regions during solar eruptions, predicting current-density increases and decreases inside flare ribbons and in the interior of expanding flux ropes respectively. The observed photospheric current density maps, inferred from vector magnetic field observations, exhibit similar whirling ribbon patterns to the MHD model results, that are interpreted as the signatures of flux ropes and of quasi-separatrix layers (QSLs) between the magnetic systems in active regions. Enhancement of the total current in these QSLs during the eruptions and decreasing current densities at the footpoint of erupting flux ropes, has been confirmed in the observations. **February 15, 2011 , September 10, 2014**

### CME flux rope and shock identifications and locations: Comparison of white light data, graduated cylindrical shell (GCS) model, and MHD simulations†

J. M. [Schmidt](#), Iver H. Cairns, Hong Xie, O. C. St. Cyr, N. Gopalswamy

JGR Volume 121, Issue 3 Pages 1886–1906 **2016**

Coronal mass ejections (CMEs) are major transient phenomena in the solar corona that are observed with groundbased and spacecraft based coronagraphs in white light or with in situ measurements by spacecraft. CMEs transport mass and momentum and often drive shocks. In order to derive the CME and shock trajectories with high precision, we apply the graduated cylindrical shell (GCS) model to fit a flux rope to the CME directed towards STEREO A after about 19:00 UT on **29 November 2013**, and check the quality of the heliocentric distance - time evaluations by carrying out a three-dimensional magnetohydrodynamic (MHD) simulation of the same CME with the BATS-R-US code. Heliocentric distances of the CME and shock leading edges are determined from the simulated white light images and magnetic field strength data. We find very good agreement between the predicted and observed heliocentric distances, showing that the

GCS model and the BATS-R-US simulation approach work very well and are consistent. In order to assess the validity of CME and shock identification criteria in coronagraph images, we also compute synthetic white light images of the CME and shock. We find that the outer edge of a cloud-like illuminated area in the observed and predicted images in fact coincides with the leading edge of the CME flux rope, and that the outer edge of a faint illuminated band in front of the CME leading edge coincides with the CME-driven shock front.

## **Type II solar radio bursts predicted by 3D MHD CME and kinetic radio emission simulations†**

J. M. [Schmidt\\*](#), Iver H. Cairns

JGR, Volume 119, Issue 1, pages 69–87, January 2014

Impending space weather events at Earth are often signalled by type II solar radio bursts. These bursts are generated upstream of shock waves driven by coronal mass ejections (CMEs) that move away from the Sun. We combine elaborate three-dimensional (3D) magnetohydrodynamic (MHD) predictions of realistic CMEs near the Sun with a recent analytic kinetic radiation theory in order to simulate two type II bursts. Magnetograms of the Sun are used to reconstruct initial solar magnetic and active region fields for the modeling. STEREO spacecraft data are used to dimension the flux rope of the initial CME, launched into an empirical data driven corona and solar wind. We demonstrate impressive accuracy in time, frequency, and intensity for the two type II bursts observed by the WIND spacecraft on **15 February 2011 and 7 March 2012**. Propagation of the simulated CME-driven shocks through coronal plasmas containing pre-existing density and magnetic field structures that stem from the coronal setup and CME initiation closely reproduce the isolated islands of type II emission observed. These islands form because of a competition between the growth of the radio source due to spherical expansion, and a fragmentation of the radio source due to increasingly radial fields in the nose region of the shock and interactions with streamers in the flank regions of the shock. Our study provides strong support for this theory for type II bursts and implies that the physical processes involved are understood. It also supports a near-term capability to predict and track these events for space weather predictions.

## **PREDICTION OF TYPE II SOLAR RADIO BURSTS BY THREE-DIMENSIONAL MHD CORONAL MASS EJECTION AND KINETIC RADIO EMISSION SIMULATIONS**

J. M. [Schmidt](#)<sup>1</sup>, Iver H. Cairns<sup>1</sup>, and D. S. Hillan

2013 ApJ 773 L30

Type II solar radio bursts are the primary radio emissions generated by shocks and they are linked with impending space weather events at Earth. We simulate type II bursts by combining elaborate three-dimensional MHD simulations of realistic coronal mass ejections (CMEs) at the Sun with an analytic kinetic radiation theory developed recently. The modeling includes initialization with solar magnetic and active region fields reconstructed from magnetograms of the Sun, a flux rope of the initial CME dimensioned with STEREO spacecraft observations, and a solar wind driven with averaged empirical data. We demonstrate impressive accuracy in time, frequency, and intensity for the CME and type II burst observed on **2011 February 15**. This implies real understanding of the physical processes involved regarding the radio emission excitation by shocks and supports the near-term development of a capability to predict and track these events for space weather prediction.

## **SLOW MAGNETOACOUSTIC WAVE OSCILLATION OF AN EXPANDING CORONAL LOOP**

J. M. [Schmidt](#)<sup>1,2</sup> and L. Ofman

2011 ApJ 739 75

We simulated an expanding loop or slow coronal mass ejection (CME) in the solar corona dimensioned with size parameters taken from real coronal expanding loops observed with the STEREO spacecraft. We find that the loop expands to Sun's size within about one hour, consistent with slow CME observations. At the top of the loop, plasma is being blown off the loop, enabled with the reconnection between the loop's flux rope magnetic field and the radial magnetic field of the Sun, thus yielding feeding material for the formation of the slow solar wind. This mechanism is in accordance with the observed blob formation of the slow solar wind. We find wave packets traveling with local sound speed downward toward the footpoints of the loop, already seen in coronal seismology observations and simulations of stationary coronal loops. Here, we generalize these results for an expanding medium. We also find a reflection of the wave packets, identified as slow magnetoacoustic waves, at the footpoints of the loop. This confirms the formation of standing waves within the coronal loop. In particular, the reflected waves can partly escape the loop top and contribute to the heating of the solar wind. The present study improves our understanding on how loop material can emerge to form blobs, major ingredients of slow CMEs, and how the release of the wave energy stored in slow magnetoacoustic waves, and transported away from the Sun within expanding loops, contributes to the acceleration and formation of the slow solar wind.

## **Synthetic radio maps of CME-driven shocks below 4 solar radii heliocentric distance,**

**Schmidt, J. M., and N. Gopalswamy**

J. Geophys. Res., 113, A08104, **2008**

<http://dx.doi.org/10.1029/2007JA013002>

We present 2 1/2 D numerical MagnetoHydroDynamic (MHD) simulations of coronal mass ejections (CMEs) in conjunction with plasma simulations of radio emission from the CME-driven shocks. The CME-driven shock extends to an almost spherical shape during the temporal evolution of the CME. Our plasma simulations can reproduce the dynamic spectra of coronal type II radio bursts, with the frequency drift rates corresponding to the shock speeds. We find further, that the CME-driven shock is an effective radio emitter at metric wavelengths, when the CME has reached a heliocentric distance of about two solar radii ( $R_{\odot}$ ). We apply our simulation results to explain the radio images of type II bursts obtained by radio heliographs, in particular to the banana-shaped images of radio sources associated with fast CMEs.

## **Recent advances in solar data-driven MHD simulations of the formation and evolution of CME flux ropes**

**Review**

**Brigitte Schmieder, Jinhan Guo, Stefaan Poedts**

Reviews of Modern Plasma Physics **2024**

<https://arxiv.org/pdf/2408.06595>

Filament eruptions and coronal mass ejections are physical phenomena related to magnetic flux ropes carrying electric current. A magnetic flux rope is a key structure for solar eruptions, and when it carries a southward magnetic field component when propagating to the Earth. It is the primary driver of strong geomagnetic storms. As a result, developing a numerical model capable of capturing the entire progression of a flux rope, from its inception to its eruptive phase, is crucial for forecasting adverse space weather. The existence of such flux ropes is revealed by the presence of sigmoids in active regions or hot channels by observations from space and ground instruments. After proposing cartoons in 2D, potential, linear, non-linear-force-free-field (NLFFF) and non-force-free-field (NFFF) magnetic extrapolations, 3D numerical magnetohydrodynamic (MHD) simulation models were developed, first in a static configuration and later dynamic data-driven MHD models using high resolution observed vector magnetograms. This paper reviews a few recent developments in data-driven mode, such as the time-dependent magneto-frictional (TMF) and thermodynamic magnetohydrodynamic (MHD) models. Hereafter, to demonstrate the capacity of these models to reveal the physics of observations, we present the results for three events explored in our group: 1. the eruptive X1.0 flare on **28 October 2021**; 2. the filament eruption on **18 August 2022**; and 3. the confined X2.2 flare on **6 September 2017**. These case studies validate the ability of data-driven models to retrieve observations, including the formation and eruption of flux ropes, 3D magnetic reconnection, CME three-part structures and the failed eruption. Based on these results, we provide some arguments for the formation mechanisms of flux ropes, the physical nature of the CME leading front, and the constraints of failed eruptions.

## **Solar jets: SDO and IRIS observations in the perspective of new MHD simulations**

**Review**

**Brigitte Schmieder**

Frontiers 9:820183. **2022**

doi: 10.3389/fspas.2022.820183

<https://arxiv.org/pdf/2201.11541.pdf>

<https://www.frontiersin.org/articles/10.3389/fspas.2022.820183/full>

They have been observed in Halpha and optical lines for more than 50 years and called surges. The term "jet" comes from X-ray observations after the launch of the Yohkoh satellite in 1991. They are the means of transporting energy through the heliosphere and participate to the corona heating and the acceleration of solar wind. Several characteristics have been derived about their velocities, their rates of occurrence, and their relationship with CMEs. However, the initiation mechanism of jets, e.g. emerging flux, flux cancellation, or twist, is still debated. In the last decade coordinated observations of the Interface Region Imaging Spectrograph (IRIS) with the instruments on board the Solar Dynamic Observatory (SDO) allow to make a step forward for understanding the trigger of jets and the relationship between hot jets and cool surges. We observe at the same time the development of 2D and 3D MHD numerical simulations to interpret the results. This paper summarizes recent studies of jets showing the loci of magnetic reconnection in null points or in bald patch regions forming a current sheet. In the pre-jet phase a twist is frequently detected by the existence of a mini filament close to the dome of emerging flux. The twist can also be transferred to the jet from a flux rope in the vicinity of the reconnection by slippage of the polarities. Bidirectional flows are detected at the reconnection sites. We show the role of magnetic currents detected in the footprints of flux rope and quasi-separatrix layers for initiating the jets.

We select a few studies and show that with the same observations, different interpretations are possible based on different approaches e.g. non linear force free field extrapolation or 3D MHD simulation. **11 November 1980, 23 Apr 1992, 9 Feb 1993, 17 Sep 2010, 16 Apr 2014, 30 Mar 2017, 4 Apr 2017**

## **Solar jets observed with the Interface Region Imaging Spectrograph (IRIS)**

**Brigitte Schmieder, Reetika Joshi, Ramesh Chandra**

Advances in Space Research **2021**

<https://arxiv.org/pdf/2111.09002.pdf>

Solar jets are impulsive, collimated plasma ejections that are triggered by magnetic reconnection. They are observed for many decades in various temperatures and wavelengths, therefore their kinematic characteristics, such as velocity and recurrence, have been extensively studied. Nevertheless, the high spatial resolution of the Interface Region Imaging Spectrograph (IRIS) launched in 2013 allowed us to make a step forward in the understanding of the relationship between surges and hot jets. In this paper we report on several results of recent studies of jets observed by IRIS. Cool and hot plasma have been detected with ejections of cool blobs having a speed reaching 300 km/s during the impulsive phase of jet formation and slow velocity surges surrounding hot jets after the reconnection phase. Plasma characteristics of solar jets, such as the emission measure, temperature, and density have been quantified. A multi-layer atmosphere at the reconnection site based on observed IRIS spectra has been proposed. IRIS evidenced bidirectional flows at reconnection sites, and tilt along the spectra which were interpreted as the signature of twist in jets. The search of possible sites for reconnection could be achieved by the analysis of magnetic topology. Combining Solar Dynamics Observatory/Helioseismic Magnetic Imager (SDO/HMI) vector magnetograms and IRIS observations, it was found that reconnection site could be located at null points in the corona as well as in bald patch regions low in the photosphere. In one case study a magnetic sketch could explain the initiation of a jet starting in a bald patch transformed to a current sheet in a dynamical way, and the transfer of twist from a flux rope to the jet during the magnetic reconnection process. **July 10 2015, March 30 2017, April 4 2017, March 22 2019**

### **Extreme solar storms based on solar magnetic field**

**Review**

Brigitte **Schmieder**

Journal of Atmospheric and Solar-Terrestrial Physics Volume 180, Pages 46-51, November 2018  
Varsiti Conference in Varna June 2016

<https://arxiv.org/pdf/1708.01790.pdf>  
[sci-hub.tw/10.1016/j.jastp.2017.07.018](http://sci-hub.tw/10.1016/j.jastp.2017.07.018)

**File (2017)**

Many questions have to be answered before understanding the relationship between the emerging magnetic flux through the solar surface and the extreme geoeffective events. Which threshold determines the onset of the eruption? What is the upper limit in energy for a flare? Is the size of sunspot the only criteria to get extreme solar events?

Based on observations of previous solar cycles, and theory, the main ingredients for getting X ray class flares and large Interplanetary Corona Mass Ejections e.g. the built up of the electric current in the corona, are presented such as the existence of magnetic free energy, magnetic helicity, twist and stress in active regions. The upper limit of solar flare energy in space research era and the possible chances to get super-flares and extreme solar events can be predicted using MHD simulation of coronal mass ejections. **September 1, 1859, July 25 1946, April 4-5, 1947, August 1972, October 28 2003, October 28, October 29 and November 4, November 17 2003, October 2014.**

### **Halpna Doppler shifts in a tornado in the solar corona**

B.**Schmieder**, P.Mein, N.Mein, P.J.Levens, N.Labrosse, L.Ofman

A&A 597, A109 2017

<https://arxiv.org/pdf/1612.02232v1.pdf>  
<http://www.aanda.org/articles/aa/pdf/2017/01/aa28771-16.pdf>

Context. High resolution movies in 193 Å from the Atmospheric Imaging Assembly (AIA) on the Solar Dynamic Observatory SDO show apparent rotation in the leg of a prominence observed during a coordinated campaign. Such structures are commonly referred to as tornadoes. Time-distance intensity diagrams of the AIA data show the existence of oscillations suggesting that the structure is rotating.

Aims. The aim of this paper is to understand if the cool plasma at chromospheric temperatures inside the tornado is rotating around its central axis. The tornado was also observed in Halpna with a cadence of 30 seconds by the MSDP spectrograph, operating at the Solar Tower in Meudon. The MSDP provides sequences of simultaneous spectra in a 2D field of view from which a cube of Doppler velocity maps is retrieved.

Results. The Halpna Doppler maps show a pattern with alternatively blueshifted and redshifted areas of 5 to 10 arcsec wide. Over time the blueshifted areas become redshifted and vice versa, with a quasi-periodicity of 40 to 60 minutes. Weaker amplitude oscillations with periods of 4 to 6 minutes are superimposed onto these large period oscillations.

Conclusions. The Doppler pattern observed in Halpna cannot be interpreted as rotation of the cool plasma inside the tornado. The H $\alpha$  velocity observations give strong constraints on the possible interpretations of the AIA tornado.

**September 24, 2013**

### **Flare-CME models: an observational perspective**

**Review**

**Schmieder** B., Aulanier G., Vrsnak B.

Solar Phys. *Solar and Stellar Flares: Observations, Simulations, and Synergies* Volume 290, Issue 12, pp 3457-3486 2015 **File**

[http://www.lesia.obspm.fr/perso/guillaume-aulanier/73\\_2015.FlareCmeObs.pdf](http://www.lesia.obspm.fr/perso/guillaume-aulanier/73_2015.FlareCmeObs.pdf)

Eruptions, flares, and coronal mass ejection (CMEs) are due to physical phenomena mainly driven by an initially force-free current-carrying magnetic field. We review some key observations relevant to the current theoretical trigger mechanisms of the eruption and to the energy release via reconnection. Sigmoids observed in X-rays and UV, as well as the pattern (double J-shaped) of electric currents in the photosphere show clear evidence of the existence of currents

parallel to the magnetic field and can be the signature of a flux rope that is detectable in CMEs. The magnetic helicity of filaments and active regions is an interesting indirectly measurable parameter because it can quantify the twist of the flux rope. On the other hand, the magnetic helicity of the solar structures allows us to associate solar eruptions and magnetic clouds in the heliosphere. The magnetic topology analysis based on the 3D magnetic field extrapolated from vector magnetograms is a good tool for identifying the reconnection locations (null points and/or the 3D large volumes ? hyperbolic flux tube, HFT). Flares are associated more with quasi-separatrix layers (QSLs) and HFTs than with a single null point, which is a relatively rare case. We review various mechanisms that have been proposed to trigger CMEs and their observable signatures: by "breaking" the field lines overlying the flux rope or by reconnection below the flux rope to reduce the magnetic tension, or by letting the flux rope to expand until it reaches a minimum threshold height (loss of equilibrium or torus instability). Additional mechanisms are commonly operating in the solar atmosphere. Examples of observations are presented throughout the article and are discussed in this framework.

**15 May 2001, 12 September 2005, 14 September 2005, November 2010 forming AR 11123, 15 February 2011, 6 September 2011**

### **Twisting Solar Coronal Jet launched at the boundary of an active region**

B. [Schmieder](#)<sup>1</sup>, Y. Guo<sup>2</sup>, F. Moreno-Insertis<sup>3;4</sup>, G. Aulanier<sup>1</sup>, L. Yelles Chaouche<sup>3;4</sup>, N. Nishizuka<sup>5;6</sup>, L. K. Harra<sup>6</sup>, J. K. Thalmann<sup>7</sup>, S. Vargas Dominguez<sup>8</sup>, and Y. Liu<sup>9</sup>  
E-print, Sept **2013**; A&A 559, A1 (**2013**)

**Aims.** A broad jet was observed in a weak magnetic field area at the edge of active region NOAA 11106 that also produced other nearby recurring and narrow jets. The peculiar shape and magnetic environment of the broad jet raised the question of whether it was created by the same physical processes of previously studied jets with reconnection occurring high in the corona.

**Methods.** We carried out a multi-wavelength analysis using the EUV images from the Atmospheric Imaging Assembly (AIA) and magnetic fields from the Helioseismic and Magnetic Imager (HMI) both on-board the SDO satellite, which we coupled to a high-resolution, nonlinear force-free field extrapolation. Local correlation tracking was used to identify the photospheric motions that triggered the jet, and time-slices were extracted along and across the jet to unveil its complex nature. A topological analysis of the extrapolated field was performed and was related to the observed features.

**Results.** The jet consisted of many different threads that expanded in around 10 minutes to about 100 Mm in length, with the bright features in later threads moving faster than in the early ones, reaching a maximum speed of about 200 km s<sup>-1</sup>. Time-slice analysis revealed a striped pattern of dark and bright strands propagating along the jet, along with apparent damped oscillations across the jet. This is suggestive of a (un)twisting motion in the jet, possibly an Alfvén wave. Bald patches in field lines, low-altitude flux ropes, diverging flow patterns, and a null point were identified at the basis of the jet.

**Conclusions.** Unlike classical  $\alpha$  or Eitel-tower shaped jets that appear to be caused by reconnection in current sheets containing null points, reconnection in regions containing bald patches seems to be crucial in triggering the present jet. There is no observational evidence that the flux ropes detected in the topological analysis were actually being ejected themselves, as occurs in the violent phase of blowout jets; instead, the jet itself may have gained the twist of the flux rope(s) through reconnection. This event may represent a class of jets different from the classical quiescent or blowout jets, but to reach that conclusion, more observational and theoretical work is necessary.

### **Solar filament eruptions and their physical role in triggering Coronal Mass Ejections**

[Schmieder](#) B., Demoulin P., Aulanier G.

**Review**

E-print, Dec **2012**; Advances in Space Research, v. 51, No. 11, p. 1967-1980, **2013**, File

<http://www.sciencedirect.com/science/article/pii/S027311771300032X>

Solar filament eruptions play a crucial role in triggering coronal mass ejections (CMEs). More than 80 % of eruptions lead to a CME. This correlation has been studied extensively during the past solar cycles and the last long solar minimum. The statistics made on events occurring during the rising phase of the new solar cycle 24 is in agreement with this finding. Both filaments and CMEs have been related to twisted magnetic fields. Therefore, nearly all the MHD CME models include a twisted flux tube, called a flux rope. Either the flux rope is present long before the eruption, or it is built up by reconnection of a sheared arcade from the beginning of the eruption. In order to initiate eruptions, different mechanisms have been proposed: new emergence of flux, and/or dispersion of the external magnetic field, and/or reconnection of field lines below or above the flux rope. These mechanisms reduce the downward magnetic tension and favor the rise of the flux rope. Another mechanism is the kink instability when the configuration is twisted too much. In this paper we open a forum of discussions revisiting observational and theoretical papers to understand which mechanisms trigger the eruption. We conclude that all the above quoted mechanisms could bring the flux rope to an unstable state. However, the most efficient mechanism for CMEs is the loss-of-equilibrium or torus instability, when the flux rope has reached an unstable threshold determined by a decay index of the external magnetic field.

**27 May 2005, 4-7 Dec 2007, 17 September 2010, 3 November 2010, 23 January 2012,**

See <http://inspirehep.net/record/1207540/plots>

### **What are the physical mechanisms of eruptions and CMEs?**

Brigitte [Schmieder](#), , Guillaume Aulanier

Advances in Space Research, Volume 49, Issue 11, 1 June **2012**, Pages 1598–1606; File

CMEs are due to physical phenomena that drive both, eruptions and flares in active regions. Eruptions/CMEs must be driven from initially force-free current-carrying magnetic field. Twisted flux ropes, sigmoids, current lanes and pattern in photospheric current maps show a clear evidence of currents parallel to the magnetic field. Eruptions occur starting from equilibria which have reached some instability threshold. Revisiting several data sets of CME observations we identified different mechanisms leading to this unstable state from a force free field. Boundary motions related to magnetic flux emergence and shearing favor the increase of coronal currents leading to the large flares of November 2003. On the other hand, we demonstrated by numerical simulations that magnetic flux emergence is not a sufficient condition for eruptions. Filament eruptions are interpreted either by a torus instability for an event occurring during the minimum of solar activity either by the diffusion of the magnetic flux reducing the tension of the restraining arcade. We concluded that CME models (tether cutting, break out, loss of equilibrium models) are based on these basic mechanisms for the onset of CMEs.

## Using an Ellipsoid Model to Track and Predict the Evolution and Propagation of Coronal Mass Ejections

S. [Schreiner](#)<sup>1</sup>, C. Cattell<sup>1</sup>, K. Kersten<sup>1</sup> and A. Hupach

Solar Phys., **2013**, Volume 288, Issue 1, pp 291-309

We present a method for tracking and predicting the propagation and evolution of coronal mass ejections (CMEs) using the imagers on the STEREO and SOHO satellites. By empirically modeling the material between the inner core and leading edge of a CME as an expanding, outward propagating ellipsoid, we track its evolution in three-dimensional space. Though more complex empirical CME models have been developed, we examine the accuracy of this relatively simple geometric model, which incorporates relatively few physical assumptions, including i) a constant propagation angle and ii) an azimuthally symmetric structure. Testing our ellipsoid model developed herein on three separate CMEs, we find that it is an effective tool for predicting the arrival of density enhancements and the duration of each event near 1 AU. For each CME studied, the trends in the trajectory, as well as the radial and transverse expansion are studied from 0 to ~0.3 AU to create predictions at 1 AU with an average accuracy of 2.9 hours.

Erratum: Solar Physics, November 2013, Volume 288, Issue 1, p 311

## A Statistical Study of Distant Consequences of Large Solar Energetic Events

Carolus J. [Schrijver](#), Paul A. Higgins

Solar Phys. Volume 290, Issue 10, pp 2943-2950 **2015**

<http://arxiv.org/pdf/1509.05680v1.pdf> **File**

Large solar flares and eruptions may influence remote regions through perturbations in the outer-atmospheric magnetic field, leading to causally related events outside of the primary or triggering eruptions that are referred to as "sympathetic events." We quantify the occurrence of sympathetic events using the full-disk observations by the Atmospheric Imaging Assembly onboard the Solar Dynamics Observatory associated with all flares of GOES class M5 or larger from 01 May 2010 through 31 December 2014. Using a superposed-epoch analysis, we find an increase in the rate of flares, filament eruptions, and substantial sprays and surges more than 20 degrees away from the primary flares within the first four hours at a significance of 1.8 standard deviations. We also find that the rate of distant events drops by two standard deviations, or a factor of 1.2, when comparing intervals between 4 hours and 24 hours before and after the start times of the primary large flares. We discuss the evidence for the concluding hypothesis that the gradual evolution leading to the large flare and the impulsive release of the energy in that flare both contribute to the destabilization of magnetic configurations in distant active regions and quiet-Sun areas. These effects appear to leave distant regions, in an ensemble sense, in a more stable state, so that fewer energetic events happen for at least a day following large energetic events. **2011-09-07**

**Table 1. 18 flares with no distant events within 24 hours; 13 flares with one distant event within 24 hours; 16 flares with two or more distant events within 24 hours:**

## Pathways of large-scale magnetic couplings between coronal events

C.J. [Schrijver](#), A.M. Title, A.R. Yeates and M.L. DeRosa

E-print, May **2013**, **File**; **2013** ApJ 773 93

The high-cadence, comprehensive view of the solar corona by SDO/AIA shows many events that are widely separated in space while occurring close together in time. In some cases, sets of coronal events are evidently causally related, while in many other instances indirect evidence can be found. We present case studies to highlight a variety of coupling processes involved in coronal events. We find that physical linkages between events do occur, but concur with earlier studies that these couplings appear to be crucial to understanding the initiation of major eruptive or explosive phenomena relatively infrequently. We note that the post-eruption reconfiguration time scale of the large-scale corona, estimated from the EUV afterglow, is on average longer than the mean time between CMEs, so that many CMEs originate from a corona that is still adjusting from a previous event. We argue that the coronal field is intrinsically global: current systems build up over days to months, the relaxation after eruptions continues over many hours, and evolving connections easily span much of a hemisphere. This needs to be reflected in our modeling of the connections from the solar surface into the heliosphere to properly model the solar wind, its perturbations, and the generation and propagation of solar energetic particles. However, the large-scale field cannot be constructed reliably by currently available observational resources. We assess the potential of high-quality observations from beyond Earth's perspective

and advanced global modeling to understand the couplings between coronal events in the context of CMEs and solar energetic particle events. **2010/08/01, 2011/02/14-15, 2011/09/25-26, 2011/11/09, 2011/11/22, 2011/11/30, 2011/12/11, 2011/12/25, 2012/02/09**

## **THE 2011 FEBRUARY 15 X2 FLARE, RIBBONS, CORONAL FRONT, AND MASS EJECTION: INTERPRETING THE THREE-DIMENSIONAL VIEWS FROM THE SOLAR DYNAMICS OBSERVATORY AND STEREO GUIDED BY MAGNETOHYDRODYNAMIC FLUX-ROPE MODELING**

Carolus J. [Schrijver](#)<sup>1</sup>, Guillaume Aulanier<sup>2</sup>, Alan M. Title<sup>1</sup>, Etienne Pariat<sup>2</sup> and Cecile Delannée  
E-print, June **2011**, **File**; **2011** ApJ 738 167, **File**?

The **2011 February 15** X2.2 flare and associated Earth-directed halo coronal mass ejection were observed in unprecedented detail with high resolution in spatial, temporal, and thermal dimensions by the Atmospheric Imaging Assembly (AIA) on the Solar Dynamics Observatory, as well as by instruments on the two STEREO spacecraft, then at near-quadrature relative to the Sun-Earth line. These observations enable us to see expanding loops from a flux-rope-like structure over the shearing polarity-inversion line between the central  $\delta$ -spot groups of AR 11158, developing a propagating coronal front ("EIT wave"), and eventually forming the coronal mass ejection moving into the inner heliosphere. The observations support the interpretation that all of these features, including the "EIT wave," are signatures of an expanding volume traced by loops (much larger than the flux rope only), surrounded by a moving front rather than predominantly wave-like perturbations; this interpretation is supported by previously published MHD models for active-region and global scales. The lateral expansion of the eruption is limited to the local helmet-streamer structure and halts at the edges of a large-scale domain of connectivity (in the process exciting loop oscillations at the edge of the southern polar coronal hole). The AIA observations reveal that plasma warming occurs within the expansion front as it propagates over quiet Sun areas. This warming causes dimming in the 171 Å (Fe IX and Fe X) channel and brightening in the 193 and 211 Å (Fe XII-XIV) channels along the entire front, while there is weak 131 Å (Fe VIII and Fe XXI) emission in some directions. An analysis of the AIA response functions shows that sections of the front running over the quiet Sun are consistent with adiabatic warming; other sections may require additional heating which MHD modeling suggests could be caused by Joule dissipation. Although for the events studied here the effects of volumetric expansion are much more obvious than true wave phenomena, we discuss how different magnetic environments within and around the erupting region can lead to the signatures of either or both of these aspects.

## **Long-range magnetic couplings between solar flares and coronal mass ejections observed by SDO and STEREO**

C.J. [Schrijver](#) and A.M. Title

E-print, 18 Jan **2011**, **File**; JGR, 116, A04108, doi:10.1029/2010JA016224, **2011**

The combination of SDO and STEREO observations enable us to view much of the solar surface and atmosphere simultaneously and continuously. These near-global observations often show near-synchronous long-distance interactions between magnetic domains that exhibit flares, eruptions, and frequent minor forms of activity. Here, we analyze a series of flares, filament eruptions, coronal mass ejections, and related events which occurred on **2010/08/01-02**. These events extend over a full hemisphere of the Sun, only two-thirds of which is visible from the Earth's perspective. The combination of coronal observations and global field modeling reveals the many connections between these events by magnetic field lines, particularly those at topological divides. We find that all events of substantial coronal activity, including those where flares and eruptions initiate, are connected by a system of separatrices, separators, and quasi-separatrix layers, with little activity within the deep interiors of domains of connectivity. We conclude that for this sequence of events the evolution of field on the hemisphere invisible from Earth's perspective is essential to the evolution, and possibly even to the initiation, of the flares and eruptions over an area that spans at least 180 degrees in longitude. Our findings emphasize that the search for the factors that play a role in the initiation and evolution of eruptive and explosive phenomena, sought after for improved space-weather forecasting, requires knowledge of much, if not all, of the solar surface field.

## **ERUPTIONS FROM SOLAR EPHEMERAL REGIONS AS AN EXTENSION OF THE SIZE DISTRIBUTION OF CORONAL MASS EJECTIONS**

Carolus J. [Schrijver](#)

ApJ 710 1480-1485, **2010**

Observations of the quiet solar corona in the 171 Å (~1 MK) passband of the *Transition Region and Coronal Explorer* (*TRACE*) often show disruptions of the coronal part of small-scale ephemeral bipolar regions that resemble the phenomena associated with coronal mass ejections (CMEs) on much larger scales: ephemeral regions exhibit flare-like brightenings, rapidly rising filaments carrying absorbing material at chromospheric temperatures, or the temporary dimming of the surrounding corona. I analyze all available *TRACE* observing sequences between **1998 April 1 and 2009 September 30** with full-resolution 171 Å image sequences spanning a day or more within 500 arcsec of disk center, observing essentially the quiet Sun with good exposures and relatively low background. Ten such data sets are identified between 2000 and 2008, spanning 570 hr of observing with a total of 17,133 exposures. Eighty small-scale coronal eruptions are identified. Their size distribution forms a smooth extension of the distribution of angular widths of CMEs, suggesting that the eruption frequency for bipolar magnetic regions is essentially scale free over at least 2 orders



of magnitude, from eruptions near the arcsecond resolution limit of *TRACE* to the largest CMEs observed in the inner heliosphere. This scale range may be associated with the properties of the nested set of ranges of connectivity in the magnetic field in which increasingly large and energetic events can reach higher and higher into the corona until the heliosphere is reached.

## **Driving Major Solar Flares and Eruptions: A Review**

Carolus J. [Schrijver](#)

**Advances in Space Research**

[Volume 43, Issue 5](#), 2 March 2009, Pages 739-755; [File](#)

This review focuses on the processes that energize and trigger M- and X-class solar flares and associated flux-rope destabilizations. Numerical modeling of specific solar regions is hampered by uncertain coronal-field reconstructions and by poorly understood magnetic reconnection; these limitations result in uncertain estimates of field topology, energy, and helicity. The primary advances in understanding field destabilizations therefore come from the combination of generic numerical experiments with interpretation of sets of observations. These suggest a critical role for the emergence of twisted flux ropes into pre-existing strong field for many, if not all, of the active regions that produce M- or X-class flares. The flux and internal twist of the emerging ropes appear to play as important a role in determining whether an eruption will develop predominantly as flare, confined eruption, or CME, as do the properties of the embedding field. Based on reviewed literature, I outline a scenario for major flares and eruptions that combines flux-rope emergence, mass draining, near-surface reconnection, and the interaction with the surrounding field. Whether deterministic forecasting is in principle possible remains to be seen: to date no reliable such forecasts can be made. Large-sample studies based on long-duration, comprehensive observations of active regions from their emergence through their flaring phase are needed to help us better understand these complex phenomena.

## **Nonlinear Force-free Field Modeling of a Solar Active Region around the Time of a Major Flare and Coronal Mass Ejection**

C. J. [Schrijver](#), M. L. DeRosa, T. Metcalf, G. Barnes, B. Lites, T. Tarbell, J. McTiernan, G. Valori, T. Wiegmann, M. S. Wheatland, T. Amari, G. Aulanier, P. Demoulin, M. Fuhrmann, K. Kusano, S. Regnier, and J. K. Thalmann

The Astrophysical Journal, Vol. 675, No. 2: 1637-1644, 2008.

<http://www.journals.uchicago.edu/doi/pdf/10.1086/527413>

Solar flares and coronal mass ejections are associated with rapid changes in field connectivity and are powered by the partial dissipation of electrical currents in the solar atmosphere. A critical unanswered question is whether the currents involved are induced by the motion of preexisting atmospheric magnetic flux subject to surface plasma flows or whether these currents are associated with the emergence of flux from within the solar convective zone. We address this problem by applying state-of-the-art nonlinear force-free field (NLFFF) modeling to the highest resolution and quality vector-magnetographic data observed by the recently launched **Hinode** satellite on NOAA AR 10930 around the time of a powerful X3.4 flare (2006 December 10 through the second half of **2006 December 14**). We compute 14 NLFFF models with four different codes and a variety of boundary conditions. We find that the model fields differ markedly in geometry, energy content, and force-freeness. We discuss the relative merits of these models in a general critique of present abilities to model the coronal magnetic field based on surface vector field measurements. For our application in particular, we find a fair agreement of the best-fit model field with the observed coronal configuration, and argue (1) that strong electrical currents emerge together with magnetic flux preceding the flare, (2) that these currents are carried in an ensemble of thin strands, (3) that the global pattern of these currents and of field lines are compatible with a large-scale twisted flux rope topology, and (4) that the  $\sim 10^{32}$  erg change in energy associated with the coronal electrical currents suffices to power the flare and its associated coronal mass ejection.

## **THE PHOTOSPHERIC ENERGY AND HELICITY BUDGETS OF THE FLUX-INJECTION HYPOTHESIS**

P. W. [Schuck](#)

Astrophysical Journal, 714:68–88, 2010 May

The flux-injection hypothesis for driving coronal mass ejections (CMEs) requires the transport of substantial magnetic energy and helicity flux through the photosphere concomitant with the eruption. Under the magnetohydrodynamics approximation, these fluxes are produced by twisting magnetic field and/or flux emergence in the photosphere. A CME trajectory, observed **2000 September 12** and fitted with a flux-rope model, constrains energy and helicity budgets for testing the flux-injection hypothesis. Optimal velocity profiles for several driving scenarios are estimated by minimizing the photospheric plasma velocities for a cylindrically symmetric flux-rope magnetic field subject to the flux budgets required by the flux-rope model. Ideal flux injection, involving only flux emergence, requires hypersonic upflows in excess of the solar escape velocity

617 km s<sup>-1</sup> over an area of  $6 \times 10^8$  km<sup>2</sup> to satisfy the energy and helicity budgets of the flux-rope model.

These estimates are compared with magnetic field and Doppler measurements from *Solar and Heliospheric Observatory*/Michelson Doppler Imager on 2000 September 12 at the footpoints of the CME. The observed

Doppler signatures are insufficient to account for the required energy and helicity budgets of the flux-injection hypothesis.

## Magnetic flux balance in the heliosphere

**Schwadron**, N. A., D. E. Connick, and C. W. Smith

(2010), *Astrophys. J.*, , 722, L132–L136.

<http://iopscience.iop.org/2041-8205/722/2/L132/fulltext/>

Understanding the evolution of magnetic flux in the heliosphere remains an unresolved issue. The current solar minimum between cycles 23 and 24 is anomalously long, which gives rare insight into the long-term evolution of heliospheric magnetic flux when the coronal mass ejection (CME) rate and the flux emergence rate from CMEs were very low. The precipitous drop of heliospheric magnetic flux to levels lower than have ever been observed directly shows that there may be a persistent loss of open magnetic flux through disconnection, the reconnection between opposite polarity heliospheric magnetic field lines relatively near the Sun (beneath the Alfvén point). Here, we develop a model for the levels of magnetic flux in the inner heliosphere balancing new flux injected by CMEs, flux lost through disconnection, and closed flux lost through interchange reconnection near the Sun. This magnetic flux balance is a fundamental property that regulates the plasma and radiation environment of our solar system.

## CORONAL OBSERVATIONS OF CMEs

## Review

*Report of Working Group A*

R. **SCHWENN**<sup>1,\*</sup>, J. C. RAYMOND<sup>2</sup>, D. ALEXANDER<sup>3</sup>, A. CIARAVELLA<sup>1,4</sup>,

N. GOPALSWAMY<sup>5</sup>, R. HOWARD<sup>6</sup>, H. HUDSON<sup>7</sup>, P. KAUFMANN<sup>8,9</sup>,

A. KLASSEN<sup>10</sup>, D. MAIA<sup>11</sup>, G. MUNOZ-MARTINEZ<sup>12</sup>, M. PICK<sup>13</sup>, M. REINER<sup>5</sup>,

N. SRIVASTAVA<sup>14</sup>, D. TRIPATHI<sup>1</sup>, A. VOURLIDAS<sup>6</sup>, Y.-M. WANG<sup>6</sup> and J. ZHANG

*Space Science Reviews* (2006) 123: 127–176; **File**

CMEs have been observed for over 30 years with a wide variety of instruments. It is now possible to derive detailed and quantitative information on CME morphology, velocity, acceleration and mass. Flares associated with CMEs are observed in X-rays, and several different radio signatures are also seen. Optical and UV spectra of CMEs both on the disk and at the limb provide velocities along the line of sight and diagnostics for temperature, density and composition. From the vast quantity of data we attempt to synthesize the current state of knowledge of the properties of CMEs, along with some specific observed characteristics that illuminate the physical processes occurring during CME eruption. These include the common three-part structures of CMEs, which is generally attributed to compressed material at the leading edge, a low-density magnetic bubble and dense prominence gas. Signatures of shock waves are seen, but the location of these shocks relative to the other structures and the occurrence rate at the heights where Solar Energetic Particles are produced remains controversial. The relationships among CMEs, Moreton waves, EIT waves, and EUV dimming are also cloudy. The close connection between CMEs and flares suggests that magnetic reconnection plays an important role in CME eruption and evolution. We discuss the evidence for reconnection in current sheets from white-light, X-ray, radio and UV observations. Finally, we summarize the requirements for future instrumentation that might answer the outstanding questions and the opportunities that new space-based and ground-based observatories will provide in the future.

## The association of coronal mass ejections with their effects near the Earth

R. **Schwenn**<sup>1</sup>, A. Dal Lago<sup>2</sup>, E. Huttunen<sup>3</sup>, and W. D. Gonzalez

*Ann. Geophys.*, 23, 1033-1059, 2005, **File**

[www.ann-geophys.net/23/1033/2005/](http://www.ann-geophys.net/23/1033/2005/)

To this day, the prediction of space weather effects near the Earth suffers from a fundamental problem: The radial propagation speed of "halo" CMEs (i.e. CMEs pointed along the Sun-Earth-line that are known to be the main drivers of space weather disturbances) towards the Earth cannot be measured directly because of the unfavorable geometry. From inspecting many limb CMEs observed by the LASCO coronagraphs on SOHO we found that there is usually a good correlation between the radial speed and the lateral expansion speed  $V_{\text{exp}}$  of CME clouds. This latter quantity can also be determined for earthward-pointed halo CMEs. Thus,  $V_{\text{exp}}$  may serve as a proxy for the otherwise inaccessible radial speed of halo CMEs. We studied this connection using data from both ends: solar data and interplanetary data obtained near the Earth, for a period from January 1997 to 15 April 2001. The data were primarily provided by the LASCO coronagraphs, plus additional information from the EIT instrument on SOHO. Solar wind data from the plasma instruments on the SOHO, ACE and Wind spacecraft were used to identify the arrivals of ICME signatures. Here, we use "ICME" as a generic term for all CME effects in interplanetary space, thus comprising not only ejecta themselves but also shocks as well. Among 181 front side or limb full or partial halo CMEs recorded by LASCO, on the one hand, and 187 ICME events registered near the Earth, on the other hand, we found 91 cases where CMEs were uniquely associated with ICME signatures in front of the Earth. Eighty ICMEs were associated with a shock, and for 75 of them both the halo expansion speed  $V_{\text{exp}}$  and the travel time  $T_{\text{tr}}$  of the shock could be determined. The function  $T_{\text{tr}}=203-20.77*\ln(V_{\text{exp}})$  fits the data best. This empirical formula can be used for predicting further ICME arrivals, with a 95% error margin of about one day. Note, though, that in 15% of comparable cases, a full or partial halo CME does not cause any ICME signature at Earth at all; every fourth partial halo CME and every sixth limb halo CME does not hit the Earth (false alarms). Furthermore, every fifth transient shock or ICME or isolated geomagnetic storm is not caused by an identifiable partial or full halo CME on the front side (missing alarms)

Several methods for calculating radial velocities of CMEs have recently been proposed by, e.g., Leblanc et al. (2001), Michałek, Gopalswamy, and Yashiro (2003, symmetric cone model), Schwenn et al. (2005, lateral expansion speed), and Michalek (2006, asymmetric cone model).

## **Observation-based modelling of magnetised Coronal Mass Ejections with EUHFORIA**

Camilla [Scolini](#), [Luciano Rodriguez](#), [Marilena Mierla](#), [Jens Pomoell](#), [Stefaan Poedts](#)

A&A

2019

<https://arxiv.org/pdf/1904.07059.pdf>

Coronal Mass Ejections (CMEs) are the primary source of strong space weather disturbances at Earth. Their geoeffectiveness is largely determined by their dynamic pressure and internal magnetic fields, for which reliable predictions at Earth are not possible with traditional cone CME models. We study two Earth-directed CMEs using the European Heliospheric FORecasting Information Asset (EUHFORIA) model, testing the predictive capabilities of a linear force-free spheromak CME model initialised using parameters derived from remote-sensing observations. Using observation-based CME input parameters, we perform MHD simulations of the events with the cone and spheromak CME models. Results show that spheromak CMEs propagate faster than cone CMEs when initialised with the same kinematic parameters. We interpret these differences as due to different Lorentz forces acting within cone and spheromak CMEs, leading to different CME expansions. Such discrepancies can be mitigated by initialising spheromak CMEs with a reduced speed corresponding to the radial speed only. Results at Earth evidence that the spheromak model improves the predictions of  $B_z$  up to 12-60(22-40) percentage points compared to a cone model. Considering virtual spacecraft located around Earth,  $B_z$  predictions reach 45-70%(58-78%) of the observed peak values. The spheromak model predicts inaccurate magnetic field parameters at Earth for CMEs propagating away from the Sun-Earth line, while it successfully predicts the CME properties and arrival time in the case of strictly Earth-directed events. Modelling CMEs propagating away from the Sun-Earth line requires extra care due to limitations related to the assumed spherical shape. The spatial variability of modelling results and the typical uncertainties in the reconstructed CME direction advocate the need to consider predictions at Earth and at virtual spacecraft around it. **14 June 2012, 12 July 2012**

## **Effect of the Initial Shape of Coronal Mass Ejections on 3-D MHD Simulations and Geoeffectiveness Predictions**

C. [Scolini](#) C. [Verbeke](#) S. [Poedts](#) E. [Chané](#) J. [Pomoell](#) F. P. [Zuccarello](#)

Space Weather Volume 16, Issue 6 June 2018 Pages 754-771

<http://sci-hub.tw/https://onlinelibrary.wiley.com/doi/abs/10.1029/2018SW001806>

Coronal mass ejections (CMEs) are the major space weather drivers, and an accurate modeling of their onset and propagation up to 1 AU represents a key issue for more reliable space weather forecasts. In this paper we use the newly developed European Heliospheric FORecasting Information Asset (EUHFORIA) heliospheric model to test the effect of different CME shapes on simulation outputs. In particular, we investigate the notion of “spherical” CME shape, with the aim of bringing to the attention of the space weather community the great implications of the CME shape implementation details for simulation results and geoeffectiveness predictions. We take as case study an artificial Earth-directed CME launched on **6 June 2008**, corresponding to a period of quiet solar wind conditions near Earth. We discuss the implementation of the cone model used to inject the CME into the modeled ambient solar wind, running several simulations of the event and investigating the outputs in interplanetary space and at different spacecraft and planetary locations. We apply empirical relations to simulation outputs at L1 to estimate the expected CME geoeffectiveness in terms of the magnetopause stand-off distance and the induced  $K_p$  index. Our analysis shows that talking about spherical CMEs is ambiguous unless one has detailed information on the implementation of the CME shape in the model. All the parameters specifying the CME shape in the model significantly affect simulation results at 1 AU as well as the predicted CME geoeffectiveness, confirming the pivotal role played by the shape implementation details in space weather forecasts.

## **Halo Coronal Mass Ejections during Solar Cycle 24: reconstruction of the global scenario and geoeffectiveness**

Camilla [Scolini](#), [Mauro Messerotti](#), [Stefaan Poedts](#), [Luciano Rodriguez](#)

Journal of Space Weather and Space Climate 2018, 8, A09

<https://arxiv.org/pdf/1712.05847.pdf>

<https://www.swsc-journal.org/articles/swsc/pdf/2018/01/swsc170032.pdf> **File**

Coronal mass ejections (CMEs), in particular Earth-directed ones, are regarded as the main drivers of geomagnetic activity. In this study, we present a statistical analysis of a set of 53 fast ( $V \geq 1000 \text{ km s}^{-1}$ ) Earth-directed halo CMEs observed by the SOHO/LASCO instrument during the period Jan. 2009–Sep. 2015, and we then use this CME sample to test the forecasting capabilities of a new Sun-to-Earth prediction scheme for the geoeffectiveness of Earth-directed halo CMEs. First, we investigate the CME association with other solar activity features such as solar flares, active regions, and others, by means of multi-instrument observations of the solar magnetic and plasma properties, with the final aim of identifying recurrent peculiar features that can be used as precursors of CME-driven geomagnetic storms. Second, using coronagraphic images to derive the CME kinematical properties at 0.1 AU, we propagate the events to 1 AU by means of 3D global MHD simulations. In particular, we use the WSA-ENLIL+Cone model to reconstruct the propagation and global evolution of each event up to their arrival at Earth, where simulation results are compared with

interplanetary CME (ICME) in-situ signatures. We then use simulation outputs upstream of Earth to predict their impact on geospace. By applying the pressure balance condition at the magnetopause and the coupling function proposed by Newell et al. [J Geophys Res: Space Phys 113 (2008)] to link upstream solar wind properties to the global Kp index, we estimate the expected magnetospheric compression and geomagnetic activity level, and compare our predictions with global data records. The analysis indicates that 82% of the fast Earth-directed halo CMEs arrived at Earth within the next 4 days. Almost the totality of them compressed the magnetopause below geosynchronous orbits and triggered a minor or major geomagnetic storm afterwards. Among them, complex sunspot-rich active regions associated with X- and M-class flares are the most favourable configurations from which geoeffective CMEs originate. The analysis of related Solar Energetic Particle (SEP) events shows that 74% of the CMEs associated with major SEPs were geoeffective, i.e. they triggered a minor to intense geomagnetic storm ( $K_p \geq 5$ ). Moreover, the SEP production is enhanced in the case of fast and interacting CMEs. In this work we present a first attempt at applying a Sun-to-Earth geoeffectiveness prediction scheme – based on 3D simulations and solar wind-geomagnetic activity coupling functions – to a statistical set of fast Earth-directed, potentially geoeffective halo CMEs. The results of the prediction scheme are promising and in good agreement with the actual data records for geomagnetic activity. However, we point out the need for future studies performing a fine-tuning of the prediction scheme, in particular in terms of the evaluation of the CME input parameters and the modelling of their internal magnetic structure. **5-13 March 2012, 18-27 June 2015,**

**Table 1.** Complete list of the selected CME events.

### **Peristaltic Pumping near Post-CME Supra-Arcade Current Sheets**

Roger B. [Scott](#), Dana W. Longcope, David E. McKenzie

E-print, Aug **2013**; ApJ **2013** 776 54

<http://arxiv.org/pdf/1308.5026v1.pdf>

Measurements of temperature and density near supra-arcade current sheets suggest that plasma on unreconnected field lines may experience some degree of ‘pre-heating’ and ‘pre-densification’ prior to their reconnection. Models of patchy reconnection allow for heating and acceleration of plasma along reconnected field lines but do not offer a mechanism for transport of thermal energy across field lines. Here we present a model in which a reconnected flux tube retracts, deforming the surrounding layer of unreconnected field. The deformation creates constrictions that act as peristaltic pumps, driving plasma flow along affected field lines. Under certain circumstances these flows lead to shocks that can extend far out into the unreconnected field, altering the plasma properties in the affected region. These findings have direct implications for observations in the solar corona, particularly in regard to such phenomena as high temperatures near current sheets in eruptive solar flares and wakes seen in the form of descending regions of density depletion or supra-arcade downflows.

### **Observations of an Eruptive Solar Flare in the Extended EUV Solar Corona**

Daniel B. [Seaton](#), [Jonathan M. Darnel](#)

**2018** ApJL 852 L9

<https://arxiv.org/pdf/1712.06003.pdf>

<http://iopscience.iop.org/sci-hub.tw/2041-8205/852/1/L9/>

We present observations of a powerful solar eruption, accompanied by an X8.2 solar flare, from NOAA Active Region 12673 on **2017 September 10** by the Solar Ultraviolet Imager (SUVI) on the GOES-16 spacecraft. SUVI is noteworthy for its relatively large field of view, which allows it to image solar phenomena to heights approaching 2 solar radii. These observations include the detection of an apparent current sheet associated with magnetic reconnection in the wake of the eruption and evidence of an extreme-ultraviolet wave at some of the largest heights ever reported. We discuss the acceleration of the nascent coronal mass ejection to approximately 2000 km/s at about 1.5 solar radii. We also note that the onset of the event as seen by SUVI is suggestive of the magnetic breakout model of solar eruptions. We compare these observations with models of eruptions and eruption-related phenomena. We also describe the SUVI data and discuss how the scientific community can access SUVI observations of the event.

### **Observations of the Formation, Development, and Structure of a Current Sheet in an Eruptive Solar Flare**

Daniel B. [Seaton](#), Allison E. Bartz, Jonathan M. Darnel

**2017** ApJ 835 139

<https://arxiv.org/pdf/1610.06905v1.pdf>

We present AIA observations of a structure we interpret as a current sheet associated with an X4.9 flare and coronal mass ejection that occurred on **2014-February~25** in NOAA Active Region 11990. We characterize the properties of the current sheet, finding that the sheet remains on the order of a few thousand km thick for much of the duration of the event and that its temperature generally ranged between 8–10MK. We also note the presence of other phenomena believed to be associated with magnetic reconnection in current sheets, including supra-arcade downflows and shrinking loops. We estimate that the rate of reconnection during the event was  $MA \approx 0.004-0.007$ , a value consistent with model predictions. We conclude with a discussion of the implications of this event for reconnection-based eruption models.

### **SWAP–SECCHI OBSERVATIONS OF A MASS-LOADING TYPE SOLAR ERUPTION**

Daniel B. [Seaton](#)<sup>1</sup>, Marilena Mierla<sup>1,2,3</sup>, David Berghmans<sup>1</sup>, Andrei N. Zhukov<sup>1,4</sup>, and Laurent Dolla<sup>1</sup>

Astrophysical Journal Letters, 727:L10 (5pp), 2011 January; **File**

We present a three-dimensional reconstruction of an eruption that occurred on **2010 April 3** using observations from SWAP on board *PROBA2* and SECCHI on board *STEREO*. The event unfolded in two parts: an initial flow of cooler material confined to a height low in the corona, followed by a flux rope eruption higher in the corona. We conclude that mass off-loading from the first part triggered a rise and, subsequently, catastrophic loss of equilibrium of the flux rope.

For a much more complete overview readers may wish to consult [Lin et al. \(2015, File\)](#)

## **Small-scale Turbulent Motion of the Plasma in a Solar Filament as the Precursor of Eruption**

[Daikichi Seki](#), [Kenichi Otsuji](#), [Hiroaki Isobe](#), [Giulio Del Zanna](#), [Takako T. Ishii](#), [Takahito Sakaue](#), [Kiyoshi Ichimoto](#), [Kazunari Shibata](#)

ApJ **918** 38 **2021**

<https://arxiv.org/pdf/2106.11875.pdf>

<https://doi.org/10.3847/1538-4357/ac0d51>

A filament, a dense cool plasma supported by the magnetic fields in the solar corona, often becomes unstable and erupts. It is empirically known that the filament often demonstrates some activations such as a turbulent motion prior to eruption. In our previous study (Seki et al. 2017), we analysed the Doppler velocity of an H $\alpha$  filament and found that the standard deviation of the line-of-sight-velocity (LOS $v$ ) distribution in a filament, which indicates the increasing amplitude of the small-scale motions, increased prior to the onset of the eruption. Here, we present a further analysis on this filament eruption, which initiated approximately at 03:40UT on **2016 November 5** in the vicinity of NOAA AR 12605. It includes a coronal line observation and the extrapolation of the surrounding magnetic fields. We found that both the spatially averaged micro-turbulence inside the filament and the nearby coronal line emission increased 6 and 10 hours prior to eruption, respectively. In this event, we did not find any significant changes in the global potential-field configuration preceding the eruption for the past 2 days, which indicates that there is a case in which it is difficult to predict the eruption only by tracking the extrapolated global magnetic fields. In terms of space weather prediction, our result on the turbulent motions in a filament could be used as the useful precursor of a filament eruption.

## **Relationship between three-dimensional velocity of filament eruptions and CME association**

[Daikichi Seki](#), [Kenichi Otsuji](#), [Takako T. Ishii](#), [Ayumi Asai](#), [Kiyoshi Ichimoto](#)

Earth, Planets and Space **2021**

<https://arxiv.org/pdf/2102.04578.pdf>

It is widely recognised that filament disappearances or eruptions are frequently associated with Coronal Mass Ejections (CMEs). Since CMEs are a major source of disturbances of the space environment surrounding the Earth, it is important to investigate these associations in detail for the better prediction of CME occurrence. However, the proportion of filament disappearances associated with CMEs is under debate. The estimates range from  $\sim 10\%$  to  $\sim 90\%$  and could be affected by the manners to select the events. In this study, we aim to reveal what parameters control the association between filament eruptions and CMEs. We analysed the relationships between CME associations and the physical parameters of filaments including their length, maximum ascending velocity, and direction of eruptions using 28 events of filament eruptions observed in H $\alpha$ . We found that the product of the maximum radial velocity and the filament length is well correlated with the CME occurrence. If the product is larger than  $8.0 \times 10^6 \text{ km}^2 \text{ s}^{-1}$ , the filament will become a CME with a probability of 93%, and if the product is smaller than this value, it will not become a CME with a probability of 100%. We suggest a kinetic-energy threshold above which filament eruptions are associated with CMEs. Our findings also suggest the importance of measuring the velocity vector of filament eruption in three-dimensional space for the better prediction of CME occurrence.

**Table 2** Filament eruptions used in this study. Data are taken from the SMART/SDDI Filament Disappearance **Catalogue** [24]. (2016-2019)

## **SMART/SDDI Filament Disappearance Catalogue** (2016–2019)

[Daikichi Seki](#), [Kenichi Otsuji](#), [Takako T. Ishii](#), [Kumi Hirose](#), [Tomoya Iju](#), [Satoru UeNo](#), [Denis P. Cabezas](#), [Ayumi Asai](#), [Hiroaki Isobe](#), [Kiyoshi Ichimoto](#), [Kazunari Shibata](#)

Sun and Geosphere **Vol.14, No. 2, p.95-104** **2019**

<https://arxiv.org/ftp/arxiv/papers/2003/2003.03454.pdf>

[http://newserver.stil.bas.bg/SUNGEO//00SGArhiv/SG\\_v14\\_No2\\_2019-pp95-103.pdf](http://newserver.stil.bas.bg/SUNGEO//00SGArhiv/SG_v14_No2_2019-pp95-103.pdf)

This paper describes a new SMART/SDDI Filament Disappearance Catalogue, in which we listed almost all the filament disappearance events that the Solar Dynamics Doppler Imager (SDDI) has observed since its installation on the Solar Magnetic Activity Research Telescope (SMART) in May 2016. Our aim is to build a database that can help predict the occurrence and severity of coronal mass ejections (CMEs). The catalogue contains miscellaneous information associated with filament disappearance such as flare, CME, active region, three-dimensional trajectory of erupting filaments, detection in Interplanetary Scintillation (IPS), occurrence of interplanetary CME (ICME) and Dst index. We also provide statistical information on the catalogue data. The catalogue is available from the following website: [this https URL. https://www.kwasan.kyoto-u.ac.jp/observation/event/sddi-catalogue/](https://www.kwasan.kyoto-u.ac.jp/observation/event/sddi-catalogue/) (2016–2019) **2016-11-**

**05**

## **Small-scale motions in solar filaments as the precursors of eruptions**

Daikichi [Seki](#), [Kenichi Otsuji](#), [Hiroaki Isobe](#), [Takako T. Ishii](#), [Kiyoshi Ichimoto](#), [Kazunari Shibata](#)  
PASJ Volume 71, Issue 3, , 56, 2019  
<https://arxiv.org/ftp/arxiv/papers/1902/1902.08718.pdf>  
[sci-hub.se/10.1093/pasj/psz031](http://sci-hub.se/10.1093/pasj/psz031)

Filaments, the dense cooler plasma floating in the solar corona supported by magnetic fields, generally exhibit certain activations before they erupt. In our previous study (Seki et al. 2017), we observed that the standard deviation of the line-of-sight (LOS) velocities of the small-scale motions in a filament increased prior to its eruption. However, because that study only analyzed one event, it is unclear whether such an increase in the standard deviation of LOS velocities is common in filament eruptions. In this study, 12 filaments that vanished in H $\alpha$  line center images were analyzed in a manner similar to the one in our previous work; these included two quiescent filaments, four active region filaments, and six intermediate filaments. We verified that in all the 12 events, the standard deviation of the LOS velocities increased before the filaments vanished. Moreover, we observed that the quiescent filaments had approximately 10 times longer duration of an increase in the standard deviation than the other types of filaments. We concluded that the standard deviation of the LOS velocities of the small-scale motions in a filament can potentially be used as the precursor of a filament eruption. **May 4, 2016, 7 July 2016, 04/09/2016, 09/09/2016, 2016 November 5, 19/02/2017, April 23, 2017, 24/04/2017, 29 Apr 2017**

**Table** Filament disappearance events observed by SDDI (May 2016 - May 2017)

**PSTEP Science Nuggets #22 2019** [http://www.pstep.jp/news\\_en/nuggets22en.html](http://www.pstep.jp/news_en/nuggets22en.html)

### **Increase in the amplitude of line-of-sight velocities of the small-scale motions in a solar filament before eruption**

Daikichi [Seki](#), [Kenichi Otsuji](#), [Hiroaki Isobe](#), [Takako T. Ishii](#), [Takahito Sakaue](#), [Kumi Hirose](#)  
ApJL 843 L24 2017

<https://arxiv.org/pdf/1705.09041.pdf>

We present a study on the evolution of the small scale velocity field in a solar filament as it approaches to the eruption. The observation was carried out by the Solar Dynamics Doppler Imager (SDDI) that was newly installed on the Solar Magnetic Activity Research Telescope (SMART) at Hida Observatory. The SDDI obtains a narrow-band full disk image of the sun at 73 channels from H $\alpha$  - 9.0 \AA to H $\alpha$  + 9.0 \AA, allowing us to study the line-of-sight (LOS) velocity of the filament before and during the eruption. The observed filament is a quiescent filament that erupted on **2016 November 5**. We derived the LOS velocity at each pixel in the filament using the Becker's cloud model, and made the histograms of the LOS velocity at each time. The standard deviation of the LOS velocity distribution can be regarded as a measure for the amplitude of the small scale motion in the filament. We found that the standard deviation on the previous day of the eruption was mostly constant around 2-3 km s<sup>-1</sup>, and it slightly increased to 3-4 km s<sup>-1</sup> on the day of the eruption. It shows further increase with a rate of 1.1 m s<sup>-2</sup> about three hours before eruption and again with a rate of 2.8 m s<sup>-2</sup> about an hour before eruption. From this result we suggest the increase in the amplitude of the small scale motions in a filament can be regarded as a precursor of the eruption.

### **On the reduced geoeffectiveness of solar cycle 24: a moderate storm perspective**

R. [Selvakumaran](#), B. Veenadhari, S. Akiyama, Megha Pandya, N. Gopalswamy, S. Yashiro, Sandeep Kumar, P. Mäkelä, H. Xie

JGR 2016 DOI: 10.1002/2016JA022885

The moderate and intense geomagnetic storms are identified for the first 77 months of solar cycle 23 and 24. The solar sources responsible for the moderate geomagnetic storms are identified during the same epoch for both the cycles. Solar cycle 24 has shown nearly 80 % reduction in the occurrence of intense storms where as it is only 40 % in case of moderate storms when compared to previous cycle. The solar and interplanetary characteristics of the moderate storms driven by CME are compared for solar cycle 23 and 24 in order to see reduction in geoeffectiveness has anything to do with the occurrence of moderate storm. Though there is reduction in the occurrence of moderate storms, the Dst distribution does not show much difference. Similarly the solar source parameters like CME speed, mass and width did not show any significant variation in the average values as well as the distribution. The correlation between VBz and Dst is determined and it is found to be moderate with value of 0.68 for cycle 23 and 0.61 for cycle 24. The magnetospheric energy flux parameter epsilon ( $\epsilon$ ) is estimated during the main phase of all moderate storms during solar cycles 23 and 24. The energy transfer decreased in solar cycle 24 when compared to cycle 23. These results are significantly different when all geomagnetic storms are taken in to consideration for both the solar cycles.

### **Multiwavelength Analysis of the Kinematics of a Long Duration Flare-CME Event on 27 January 2012**

[G. Selvarani](#), [S. Prasanna Subramanian](#), [A. Shanmugaraju](#) & [K. Suresh](#)

*Solar Physics* volume 295, Article number: 121 (2020)

<https://link.springer.com/content/pdf/10.1007/s11207-020-01693-1.pdf>

We present a detailed analysis of a long-duration flare associated with a coronal mass ejection (CME) event that occurred on 27 January 2012 in the active region (AR) 11402. We analyze the kinematics of the CME and the close relationship between the flare, radio burst, and CME. We used STEREO (Solar Terrestrial Relations Observatory)/EUVI A (Extreme Ultraviolet Imager) and white light data from STEREO (COR1 A and COR2 A) and LASCO (Large Angle and Spectrometric COronagraph) (C2/C3) coronagraphs, and X-ray data from the GOES

(Geostationary Operational Environmental Satellite) spacecraft. The height of the CME is measured using the Graduated Cylindrical Shell (GCS) model. Our results show that: i) the speed of the CME (1460 km/s at 2.54 R<sub>☉</sub>) is comparable to the speed of the type II radio burst (1581 km/s), ii) the height of the type II radio burst is lower than that of the CME leading edge, iii) the CME acceleration phase is found to be related to the rise time of the flare and its propagation phase is related to the decay phase of the flare, iv) the type II radio burst origin is likely to be near the CME region where a CME-streamer interaction takes place around 1.6 R<sub>☉</sub>, and v) the sequence of events and the CME kinematics show a close association between the CME and type II radio emissions.

## Investigation on M-class Flare-Associated Coronal Mass Ejections with and Without DH Type II Radio Bursts

G. **Selvarani**, A. Shanmugaraju, Bojan Vrsnak, M. Benedict Lawrance

Sol Phys (2017) 292: 74. doi:10.1007/s11207-017-1097-0

<http://link.springer.com/article/10.1007/s11207-017-1097-0>

We perform a statistical analysis on 157 M-class soft X-ray flares observed during 1997–2014 with and without decahmetric (DH) type II radio bursts aiming at the reasons for the non-occurrence of DH type II bursts in certain events. All the selected events are associated with halo Coronal Mass Ejections (CMEs) detected by the Solar and Heliospheric Observatory (SOHO) / Large Angle Spectrometric and COronograph (LASCO). Out of 157 events, 96 (61%; “Group I”) events are associated with a DH type II burst observed by the Radio and Plasma Wave (WAVES) experiment onboard the Wind spacecraft and 61 (39%; “Group II”) events occur without a DH type II burst. The mean CME speed of Group I is  $(1022 \pm 100) \text{ km/s}$  and that of Group II is  $(647 \pm 100) \text{ km/s}$ . It is also found that the properties of the selected M-class flares such as flare intensity, rise time, duration and decay time are greater for the DH associated flares than the non-DH flares. Group I has a slightly larger number (56%) of western events than eastern events (44%), whereas Group II has a larger number of eastern events (62%) than western events (38%). We also compare this analysis with the previous study by Lawrance, Shanmugaraju, and Vrsnak (Solar Phys. 290, 3365L, 2015) concerning X-class flares and confirm that high-intensity flares (X-class and M-class) have the same trend in the CME and flare properties. Additionally we consider aspects like acceleration and the possibility of CME-streamer interaction. The average deceleration of CMEs with DH type II bursts is weaker ( $a = -4.39 \text{ m/s}^2$ ) than that of CMEs without a type II burst ( $a = -12.21 \text{ m/s}^2$ ). We analyze the CME-streamer interactions for Group I events using the model proposed by Mancuso and Raymond (Astron. Astrophys. 413, 363, 2004) and find that the interaction regions are the most probable source regions for DH type II radio bursts. **2002 March 15**

**Table 2** M-class flares and their associated CMEs and DH type IIs (eastern events).

**Table 3** M-class flares and their associated CMEs and DH type IIs (western events).

**Table 5** Comparison of LASCO C2 height with CME-streamer interaction height calculated using the Mancuso and Raymond (2004) model.

## From eruption to post-flare rain: A 2.5D MHD model★

Samrat **Sen**<sup>1,2,3</sup>, Avijeet Prasad<sup>4,5</sup>, Valeriia Liakh<sup>3</sup> and Rony Keppens<sup>3</sup>

A&A, 688, A64 (2024)

<https://arxiv.org/pdf/2405.10688>

<https://www.aanda.org/articles/aa/pdf/2024/08/aa49767-24.pdf>

Context. Erupting magnetic flux ropes play an important role in producing solar flares, whereas fine-scale condensed coronal rain is often found in post-flare loops. However, the formation of the MFRs in the pre-flare stage and how this leads to coronal rain in a post-eruption magnetic loop is not fully understood.

Aims. We explore the formation and eruption of MFRs, followed by the appearance of coronal rain in the post-flare loops to understand the magnetic and thermodynamic properties of eruptive events and their multi-thermal aspects in the solar atmosphere.

Methods. We performed a resistive-magnetohydrodynamic simulation with the open-source code MPI-AMRVAC to explore the evolution of sheared magnetic arcades that can lead to flux rope eruptions. The system was in mechanical imbalance at the initial state and evolved self-consistently in a nonadiabatic atmosphere under the influence of radiative losses, thermal conduction, and background heating. We used an additional level of adaptive mesh refinement to achieve the smallest cell size of  $\approx 32.7$  km in each direction to reveal the fine structures in the system.

Results. The system achieves a semi-equilibrium state after a short transient evolution from its initial mechanically imbalanced condition. A series of erupting MFRs is formed due to spontaneous magnetic reconnection across current sheets that are created underneath the erupting flux ropes. A gradual development of thermal imbalance is noted at a loop top in the post-eruption phase, which leads to catastrophic cooling and to the formation of condensations. We obtain plasma blobs that fall down along the magnetic loop in the form of coronal rain. The dynamical and thermodynamic properties of these cool condensations agree well with observations of post-flare coronal rain. Conclusions. Our simulation supports the development and eruption of multiple MFRs and the formation of coronal rain in post-flare loops. This is one of the key aspects required to reveal the mystery of coronal heating in the solar atmosphere.

## Pseudostreamer influence on flux rope evolution★

A. **Sahade**<sup>1,2,3</sup>, M. Céceré<sup>1,3</sup>, M. V. Sieyra<sup>4</sup>, G. Krause<sup>5,6</sup>, H. Cremades<sup>7</sup> and A. Costa<sup>1</sup>

A&A 662, A113 (2022)

<https://www.aanda.org/articles/aa/pdf/2022/06/aa43618-22.pdf>

Context. A highly important aspect of solar activity is the coupling between eruptions and the surrounding coronal magnetic field topology, which determines the trajectory and morphology of the ejected plasma. Pseudostreamers (PSs) are coronal magnetic structures formed by arcs of twin loops capped by magnetic field lines from coronal holes of the same polarity that meet at a central spine. PSs contain a single magnetic null point in the spine, immediately above the closed field lines, which potentially influences the evolution of nearby flux ropes (FRs).

Aims. Because of the impact of magnetic FR eruptions on space weather, we aim to improve current understanding of the deflection of coronal mass ejections (CMEs). To understand the net effect of PSs on FR eruptions, it is first necessary to study diverse and isolated FR–PS scenarios that are not influenced by other magnetic structures.

Methods. We performed numerical simulations in which a FR structure is in the vicinity of a PS magnetic configuration. The combined magnetic field of the PS and the FR results in the formation of two magnetic null points. We evolve this scenario by numerically solving the magnetohydrodynamic equations in 2.5D. The simulations consider a fully ionised compressible ideal plasma in the presence of a gravitational field and a stratified atmosphere.

Results. We find that the dynamic behaviour of the FR can be categorised into three different classes based on the FR trajectories and whether it is eruptive or confined. Our analysis indicates that the magnetic null points are decisive in the direction and intensity of the FR deflection and their hierarchy depends on the topological arrangement of the scenario. Moreover, the PS lobe acts as a magnetic cage enclosing the FR. We report that the total unsigned magnetic flux of the cage is a key parameter defining whether or not the FR is ejected.

### **Evolution of magnetic fields and energy release processes during homologous eruptive flares**

Suraj **Sahu** (USO/PRL), [Bhuwan Joshi](#) (USO/PRL), [Avijeet Prasad](#) (University of Oslo), [Kyung-Suk Cho](#) (SSD/KASI)

ApJ **943** 70 **2023**

<https://arxiv.org/pdf/2212.04150.pdf>

<https://iopscience.iop.org/article/10.3847/1538-4357/acac2d/pdf>

We explore the processes of repetitive build-up and explosive release of magnetic energy together with the formation of magnetic flux ropes that eventually resulted into three homologous eruptive flares of successively increasing intensities (i.e., M2.0, M2.6, and X1.0). The flares originated from NOAA active region 12017 during **2014 March 28-29**. EUV observations and magnetogram measurements together with coronal magnetic field modeling suggest that the flares were triggered by the eruption of flux ropes embedded by a densely packed system of loops within a small part of the active region. In X-rays, the first and second events show similar evolution with single, compact sources, while the third event exhibits multiple emission centroids with a set of strong non-thermal conjugate sources at 50-100 keV during the HXR peak. The photospheric magnetic field over an interval of approximately 44 hr encompassing the three flares undergoes important phases of emergence and cancellation processes together with significant changes near the polarity inversion lines within the flaring region. Our observations point toward the tether-cutting mechanism as the plausible triggering process of the eruptions. Between the second and third event, we observe a prominent phase of flux emergence which temporally correlates with the build-up phase of free magnetic energy in the active region corona. In conclusion, our analysis reveals an efficient coupling between the rapidly evolving photospheric and coronal magnetic fields in the active region that led to a continued phase of the build-up of free energy, resulting into the homologous flares of successively increasing intensities. **Spikes**

### **CMEchaser, Detecting Line-of-Sight Occultations Due to Coronal Mass Ejections**

Golam **Shaifullah**, [Caterina Tiburzi](#) & [Pietro Zucca](#)

[Solar Physics](#) volume 295, Article number: 136 (2020)

<https://arxiv.org/pdf/2008.12153.pdf>

<https://link.springer.com/content/pdf/10.1007/s11207-020-01705-0.pdf>

We present a python-based tool to detect the occultation of back-ground sources by foreground solar coronal mass ejections. The tool takes as input standard celestial coordinates of the source and translates those to the helioprojective plane, and is thus well suited for use with a wide variety of background astronomical sources. This tool provides an easy means to search through a large archival dataset for such crossings and relies on the well-tested AstroPy and SunPy modules. **August 15, 2012, April 20, 2014, August 13 to 28, 2015**

### **A Study on the Nested Rings CME Structure Observed by the WISPR Imager Onboard Parker Solar Probe**

[Shaheda Begum Shaik](#), [Mark G. Linton](#), [Sarah E. Gibson](#), [Phillip Hess](#), [Robin C. Colaninno](#), [Guillermo Stenborg](#), [Carlos R. Braga](#), [Erika Palmerio](#)

ApJ **2024**

<https://arxiv.org/pdf/2410.09601>

Despite the significance of coronal mass ejections (CMEs) in space weather, a comprehensive understanding of their interior morphology remains a scientific challenge, particularly with the advent of many state-of-the-art solar missions such as Parker Solar Probe (Parker) and Solar Orbiter (SO). In this study, we present an analysis of a complex CME as observed by the Wide-Field Imager for Solar PRobe (WISPR) heliospheric imager during Parker's seventh solar encounter. The CME morphology does not fully conform with the general three-part density structure, exhibiting a front and core not significantly bright, with a highly structured overall configuration. In particular, its morphology reveals



non-concentric nested rings, which we argue are a signature of the embedded helical magnetic flux rope (MFR) of the CME. For that, we analyze the morphological and kinematical properties of the nested density structures and demonstrate that they outline the projection of the three-dimensional structure of the flux rope as it crosses the lines of sight of the WISPR imager, thereby revealing the magnetic field geometry. Comparison of observations from various viewpoints suggests that the CME substructures can be discerned owing to the ideal viewing perspective, close proximity, and spatial resolution of the observing instrument. **20–21 January 2021**

### **A statistical study of CME-associated flare during the solar cycle 24**

AMK [Shaltout](#); Eid A Amin; M.M. Beheary; R. H. Hamid

Advances in Space Research [Volume 63, Issue 7](#), 1 April 2019, Pages 2300-2311

[https://www.sciencedirect.com/science/article/pii/S0273117718309359?dgcid=raven\\_sd\\_via\\_email](https://www.sciencedirect.com/science/article/pii/S0273117718309359?dgcid=raven_sd_via_email)

We investigate on the relationship between flares and coronal mass ejections (CMEs) in which a flare started before and after the CME events which differ in their physical properties, indicating potentially different initiation mechanisms. The physical properties of two types flare-correlated CME remain an interesting and important question in space weather. We study the relationship between flares and CMEs using a different approach requiring both temporal and spatial constraints during the period from December 1, 2008 to April 30, 2017 in which the CMEs data were acquired by SOHO/LASCO (Solar and Heliospheric Observatory/Large Angle Spectrometric Coronagraph) over the solar cycle 24. The soft X-ray flare flux data, such as flare class, location, onset time and integrated flux, are collected from Geostationary Environmental satellite (GOES) \textbf{and XRT Flare catalogs}. We selected 301 CMEs-flares pairs applying simultaneously temporal and spatial constraints in all events for the distinguish between two associated CME-flare types. We study the correlated properties of coincident flares and CMEs during this period, specifically separating the sample into two types: flares that precede a CME and flares that follow a CME. We found an opposite correlation relationship between the acceleration and velocity of CMEs in the After- and Before-CMEs events. We found a log-log relation between the width and mass of CMEs in the two associated types. The CMEs and flares properties show that there were significant differences in all physical parameters such as (mass, angular width, kinetic energy, speed and acceleration) between two flare-associated CME types.

### **CAMEL. II. A 3D Coronal Mass Ejection [Catalog](#) Based on Coronal Mass Ejection Automatic Detection with Deep Learning**

Jiahui [Shan](#)<sup>1,2</sup>, Huapeng Zhang<sup>3,4</sup>, Lei Lu<sup>1,2</sup>, Yan Zhang<sup>3,4</sup>, Li Feng<sup>1,2</sup>, Yunyi Ge<sup>1</sup>, Jianchao Xue<sup>1,2</sup>, and Shuting Li<sup>1,2</sup>

**2024** ApJS 272 18

<https://iopscience.iop.org/article/10.3847/1538-4365/ad37bc/pdf>

<https://arxiv.org/pdf/2406.02946>

The catalog websites written at <http://github.com/hlastro/CAMEL-II>

Coronal mass ejections (CMEs) are major drivers of geomagnetic storms, which may cause severe space weather effects. Automating the detection, tracking, and three-dimensional (3D) reconstruction of CMEs is important for operational predictions of CME arrivals. The COR1 coronagraphs on board the Solar Terrestrial Relations Observatory spacecraft have facilitated extensive polarization observations, which are very suitable for the establishment of a 3D CME system. We have developed such a 3D system comprising four modules: classification, segmentation, tracking, and 3D reconstructions. We generalize our previously pretrained classification model to classify COR1 coronagraph images. Subsequently, as there are no publicly available CME segmentation data sets, we manually annotate the structural regions of CMEs using Large Angle and Spectrometric Coronagraph C2 observations. Leveraging transformer-based models, we achieve state-of-the-art results in CME segmentation. Furthermore, we improve the tracking algorithm to solve the difficult separation task of multiple CMEs. In the final module, tracking results, combined with the polarization ratio technique, are used to develop the first single-view 3D CME catalog without requiring manual mask annotation. Our method provides higher precision in automatic 2D CME catalog and more reliable physical parameters of CMEs, including 3D propagation direction and speed. The aforementioned 3D CME system can be applied to any coronagraph data with the capability of polarization measurements. **2007-05-15, 2007-08-31, 2008-03-25, 2012-01-19, 2012-03-07**

### **Temporal and Spatial Association Between a Solar Flare, CME, and Radio Burst on 19 November 2013**

[A. Shanmugaraju](#), [M. Syed Ibrahim](#), [K. Suresh](#), [P. Vijayalakshmi](#) & [Sajal Kumar Dhara](#)

[Solar Physics](#) volume 296, Article number: 77 (2021)

<https://link.springer.com/content/pdf/10.1007/s11207-021-01823-3.pdf>

<https://doi.org/10.1007/s11207-021-01823-3>

We present multi-wavelength and multi-instrument observations and analysis of a major X 1.0 class flare, radio burst, halo coronal mass ejection (CME), and loop eruption from the solar active region NOAA 11893 on **19 November 2013** (SOL2013-11-19T10:26). The aim of this work is twofold: The first aim to study the evolution of the loop eruption and the second is to find the link between this eruption and radio emissions. Initial signatures of eruption from the solar source region are confirmed using observations from the Atmospheric Imaging Assembly onboard the Solar Dynamics Observatory in the hot channel at 94 Å wavelength. These observations confirm that the source of the CME was associated with a magnetic-loop eruption, which was visible before the flare initiation. The photospheric magnetic configuration displayed a complex network of  $\beta\delta$  sunspots. After the eruption, a CME was observed by the Solar and

Heliospheric Observatory/Large Angle and Spectrometric Coronagraph with linear speed and acceleration of 740 kms<sup>-1</sup> and -2 ms<sup>-2</sup>, respectively. Dynamic radio-spectrum observation from the Learmonth Observatory in the metric frequency range shows Type-III and Type-II radio emissions that reveal the field-line opening and coronal-shock formation closely associated with the CME. From the metric Type-II radio observation and assuming Newkirk's density model, we estimate the shock formation height range of 1.14--1.54 R<sub>⊙</sub> with the corresponding shock speed (≈650 kms<sup>-1</sup>). With the heliographic observations from the Nançay heliograph at different frequencies we could disentangle Type-II bursts from Type-III bursts. Likely, the Type-III burst would correspond to the loop eruption while the Type-II comes from the northern flank of the CME.

## Occurrence Rate of Radio-Loud and Halo CMEs in Solar Cycle 25: Prediction Using their Correlation with the Sunspot Number

A. Shanmugaraju, P. Pappa Kalaivani, Y.-J. Moon & O. Prakash

*Solar Physics* volume 296, Article number: 75 (2021)

<https://arxiv.org/pdf/2103.13699.pdf>

<https://link.springer.com/content/pdf/10.1007/s11207-021-01818-0.pdf>

<https://doi.org/10.1007/s11207-021-01818-0>

Solar coronal mass ejections (CMEs) are known for their space-weather and geomagnetic consequences. Among all CMEs, the so-called radio-loud (RL) and halo CMEs are considered the most energetic in the sense that they are usually faster and wider than the general population of CMEs. Hence the study of RL and halo CMEs has become important and the prediction of their occurrence rate in a future cycle will help their forecasting. In this article we predict the occurrence rates of RL and halo CMEs in Solar Cycle (SC) 25, obtaining good correlations between the numbers of RL and halo CMEs in each year and the yearly mean sunspot number in the previous two cycles. The values of the sunspot number predicted by NOAA/NASA for SC 25 are considered to be representative and the corresponding numbers of RL and halo CMEs are determined using linear relations. Our results show that the maximum number of RL and halo CMEs will be around 39±3 and 45±4, respectively. Removing backside events, a set of front-side events is also considered separately and front-side events in SC 25 are also predicted. The peak values of front-side RL and halo events have been estimated to be around 31±3 and 29±3, respectively. These results are discussed in comparison with the predicted sunspot number values by different authors.

## Heights of Coronal Mass Ejections and Shocks Inferred from Metric and DH Type II Radio Bursts

A. Shanmugaraju, M. Benedict Lawrance, Y. J. Moon, Jae-Ok Lee, K. Suresh

*Solar Physics* September 2017, 292:136

A set of 27 continuous events that showed extension of metric Type-II radio bursts (m-Type IIs) into the deca-hectometric (DH) domain is considered. The coronal mass ejections (CMEs) associated with this type of continuous event supply more energy to produce space-weather effects than the CMEs that produce Type-II bursts in any one region. Since the heights of shock formation at the start of m-Type IIs were not available from observations, they were estimated using kinematic modeling in previous studies. In the present study, the heights of shock formation during metric and DH Type-II bursts are determined using two methods: i) the CME leading-edge method and ii) a method employing known electron-density models and start/end frequencies. In the first method, assuming that the shocks are generated by the associated CMEs at the leading edge, the height of the CME leading edge (LE) is calculated at the onset and end of m-Type IIs using the kinematic equation with constant acceleration or constant speed. The LE heights of CMEs that are assumed to be the heights of shock formation/end of nearly 79% of m-Type IIs are found to be within the acceptable range of 1--3 R<sub>⊙</sub>1--3 R<sub>⊙</sub>. For other events, the heights are beyond this range, for which the shocks might either have been generated at the CME flanks/flare-blast waves, or the initial CME height might have been different. The CME/shock height at the onset and end of 17 DH Type IIs are found to be in the range of 2--6 R<sub>⊙</sub>2--6 R<sub>⊙</sub> and within 30 R<sub>⊙</sub>30 R<sub>⊙</sub>, respectively. In addition, the CME LE heights from observations at the onset and end of metric/DH Type IIs are compared with the heights corresponding to the observed frequency that is determined using the known electron-density models, and they are in agreement with the model results. The heights are also estimated using the space speed available for 15 halo CMEs, and it is found that the difference is smaller at the m-Type II start/end (0.02 to 0.66 R<sub>⊙</sub>0.66 R<sub>⊙</sub>) and slightly greater at the DH Type II end (0.19 to 1.94 R<sub>⊙</sub>1.94 R<sub>⊙</sub>). Finally, the possibility of CME-streamer interactions at the start of DH Type IIs is checked, and it is found that many of the events with streamers have lower start frequencies. In addition, these results are discussed in comparison with the values reported in the literature. This study will be useful to find the source region of metric and DH Type IIs and to understand the CME-shock propagation.

**Table 1** 27 continuous events and the estimated shock-formation heights (2001-2005)

**Table 3** Halo events (height estimated using LASCO speed and space speed).

**Table 4** Streamer associated (Group A\*) and unassociated DH-Type-II events (Group B).

## Halo Coronal Mass Ejections and Their Relation to DH Type-II Radio Bursts

A. Shanmugaraju, M. Benedict Lawrance

*Solar Physics*, Volume 290, Issue 10, pp 2963-2973 2015

A set of 88 halo CMEs observed by the Solar and Heliospheric Observatory/Large Angle Solar Coronagraph (SOHO/LASCO) during the period 2005 to 2010 is considered to study the relationship of these halo CMEs with Type-

II radio bursts in the deca–hectametric (DH) wavelength range observed by Wind/(Plasma and Radio Waves: WAVES). Among the 88 events, 39 halo CMEs are found to be associated with DH Type-II radio bursts and their characteristics are analyzed with the following results: i) The heights of the CME leading edge at the time of the starting frequencies of many of the selected DH Type-II events (74 %) are in the range (2–10  $R_{\odot}$ ) where the shocks are formed. ii) The mean speed of DH-associated halo CMEs (1610  $\text{km s}^{-1}$ ) is nearly twice the mean speed (853  $\text{km s}^{-1}$ ) of halo CMEs without DH Type-II radio bursts, implying that the peak of the Alfvén speed profile in the outer corona where DH Type-II radio bursts start might be around 800  $\text{km s}^{-1}$ . iii) The shock speed of DH Type-II radio bursts calculated using the heights of shock signatures of the corresponding CME events is found to be slightly higher than the CME speed. iv) The CME speed plays a major role in the determination of the ending frequency of DH Type-II radio bursts but not the starting frequency. v) The relationship between the characteristics of DH Type-II radio bursts and CMEs is explained in the context of the universal drift-rate spectrum.

### **Empirical Relationship Between CME Parameters and Geo-effectiveness of Halo CMEs in the Rising Phase of Solar Cycle 24 (2011 – 2013)**

A. [Shanmugaraju](#), M. Syed Ibrahim, Y.-J. Moon, A. Mujiber Rahman, S. Umapathy  
Solar Phys. Volume 290, Issue 5, pp.1417-1427 2015

We analyzed the physical characteristics of 40 halo coronal mass ejections (CMEs) and their geo-effective parameters observed during the period 2011 to 2013 in the rising phase of [Solar Cycle 24](#). Out of all halo CMEs observed by [SOHO/LASCO](#), we selected 40 halo CMEs and investigated their geomagnetic effects. In particular, we estimated the CME direction parameter (DP) from coronagraph observations, and we obtained the geomagnetic storm disturbance index (Dst) value corresponding to each event by following certain criteria. We studied the correlation between near-Sun parameters of CMEs such as speed and DP with Dst. For this new set of events in the current solar cycle, the relations are found to be consistent with those of previous studies. When the direction parameter increases, the Dst value also increases for symmetrical halo CME ejections. If  $DP > 0.6$ , these events produce high Dst values. In addition, the intensity of geomagnetic storm calculated using an empirical model with the near-Sun parameters is nearly equal to the observed values. More importantly, we find that the geo-effectiveness in the rising phase of [Solar Cycle 24](#) is much weaker than that in Cycle 23.

### **Interaction Between Two CMEs During 14–15 February 2011 and Their Unusual Radio Signature**

A. [Shanmugaraju](#), S. Prasanna Subramanian, Bojan Vrsnak, M. Syed Ibrahim  
Solar Physics, Volume 289, Issue 12, pp.4621-4632 2014

We report a detailed analysis of an interaction between two coronal mass ejections (CMEs) that were observed on 14–15 February 2011 and the corresponding radio enhancement, which was similar to the “CME cannibalism” reported by Gopalswamy et al. (Astrophys. J. 548, L91, 2001). A primary CME, with a mean field-of-view velocity of 669  $\text{km s}^{-1}$  in the Solar and Heliospheric Observatory (SOHO)/Large Angle Spectrometric Coronagraph (LASCO), was more than as twice as fast as the slow CME preceding it (326  $\text{km s}^{-1}$ ), which indicates that the two CMEs interacted. A radio-enhancement signature (in the frequency range 1 MHz–400 kHz) due to the CME interaction was analyzed and interpreted using the CME data from LASCO and from the Solar Terrestrial Relations Observatory (STEREO) HI-1, radio data from Wind/Radio and Plasma Wave Experiment (WAVES), and employing known electron-density models and kinematic modeling. The following results are obtained: i) The CME interaction occurred around 05:00–10:00 UT in a height range 20–25  $R_{\odot}$ . An unusual radio signature is observed during the time of interaction in the Wind/WAVES dynamic radio spectrum. ii) The enhancement duration shows that the interaction segment might be wider than 5  $R_{\odot}$ . iii) The shock height estimated using density models for the radio enhancement region is 10–30  $R_{\odot}$ . iv) Using kinematic modeling and assuming a completely inelastic collision, the decrease of kinetic energy based on speeds from LASCO data is determined to be  $0.77 \times 10^{23}$  J, and  $3.67 \times 10^{23}$  J if speeds from STEREO data are considered. vi) The acceleration, momentum, and force are found to be  $a = -168 \text{ m s}^{-2}$ ,  $I = 6.1 \times 10^{18} \text{ kg m s}^{-1}$ , and  $F = 1.7 \times 10^{15} \text{ N}$ , respectively, using STEREO data.

### **Interacting CMEs and their associated flare and SEP activities**

A. [Shanmugaraju](#), S. Prasanna Subramanian  
2014 Astrophysics and Space Science, Volume 352, Issue 2, pp.385-393  
<http://arxiv.org/pdf/1405.6316v1.pdf>

We have analyzed a set of 25 interacting events which are associated with the DH type II bursts. These events are selected from the Coronal Mass Ejections observed during the period 1997-2010 in SOHO/LASCO and DH type IIs in Wind/WAVES. Their pre and primary CMEs from nearby active regions are identified using LASCO and EIT images and their height-time diagrams. Their interacting time and height are obtained, and their associated activities, such as, flares and solar energetic particles ( $>10\text{pfu}$ ) are also investigated. Results from the analysis are: primary CMEs are much faster than the pre-CMEs, their X-ray flares are also stronger (X and M class) compared to the flares (C and M class) of pre-CMEs. Most of the events occurred during the period 2000-2006. From the observed width and speed of pre and primary CMEs, the pre-CMEs are found to be less energetic than the primary CMEs. While the primary CMEs are tracked up to the end of LASCO field of view, most of the pre-CMEs are tracked up to  $< 26R_s$ . The SEP intensity is

found to be related with the integrated flux of the X-ray flares associated with the primary CMEs for nine events originating from the western region.

**Table 1: Data corresponding to all the pre and primary CMEs observed during the period 1997 – 2010**  
1997 Nov 06, 2000 July 22, 2001 Jan 20, 2001 Apr 02, 2002 Apr 14, 2003 Mar 18, 2003 Nov 18, 2003 Dec 2, 2004 July 23, 2004 July 25, 2004 Nov 06, 2004 Nov 07, 2004 Dec 29, 2004 Dec 30, 2005 Jan 17, 2005 Jan 20, 2005 June 03, 2005 July 07, 2005 July 13, 2005 July 14, 2005 July 30, 2005 Sep 13, 2007 June 03, 2010 Aug 18

## **Determination of coronal magnetic fields from 10 to 26 R $\odot$ using the density compression ratios of CME-driven shocks**

**Shanmugaraju**, A.; Suresh, K.; Moon, Y.-J.

Astrophysics and Space Science, Volume 351, Issue 1, pp.67-73, **2014**; **File**

Recently, the estimation of coronal magnetic field using new methods, such as standoff distance method or density compression ratio method has been reported. In the present work, we utilized the density compression ratio of CME-driven shocks for 10 events at 29 different locations in the upper solar corona (10-26 R  $\odot$ ) and determined the coronal magnetic field for two different adiabatic indices ( $\gamma=4/3$  and  $5/3$ ). In addition, radial dependence of shock parameters in the corona is studied. It is found that the magnetic field estimated in the above range agree with the general trend. In addition, we obtained a radial profile of magnetic field [ $B(R)=623 R^{-1.4}$ ] in the entire upper corona (3-30 R  $\odot$ ) by combining the magnetic field estimated by Kim et al. (Astrophys. J. 746:118, 2012) in the range 3-15 R  $\odot$  and that estimated in the present study in the range (10-26 R  $\odot$ ). The power-law indices are nearly in agreement with recent results of CME-driven shocks reported in the literature. The results are discussed with the comparison of newly reported coronal magnetic field values obtained by different techniques and found that the power-law relation closely follow the literature values.

## **Correlation between CME and Flare Parameters (with and without Type II Bursts)**

A. **Shanmugaraju**, Y.-J. Moon and Bojan Vršnak

Solar Physics, Volume 270, Number 1, 273-284, **2011**, **File**

CMEs and flares are the two energetic phenomena on the Sun responsible for generating shocks. Our main aim is to study the relation between the physical properties of CMEs and flares associated with and without type II radio bursts. We considered a set of 290 SOHO/LASCO CMEs associated with GOES X-ray flares observed during the period from January 1997 to December 2000. The relationship between the flares and CMEs is examined for the two sets i) with metric-type IIs and ii) without metric-type IIs. Physical properties such as rise time, duration, and strength of the flares and width, speed, and acceleration of CMEs are considered. We examined the energy relationship and temporal relationship between the CMEs and flares. First, all the events in each group were considered, and then the limb events in each group were considered separately. While there is a relationship between the temporal characteristics of flares and CME properties in the case of with-type IIs, it is absent in the case of all without-type IIs. Among all the relations studied, the correlation between flare duration and CME properties is found to be highly significant compared to the other relations. Also, the relationship between flare strength and CME speed found in the with-type II events is absent in the case of all without-type II events. However, when the limb without-type II events (with reduced time window between flare and CME) are studied separately, we found the energy relationship and the temporal relationship.

## **QUASI-PERIODIC OSCILLATIONS IN LASCO CORONAL MASS EJECTION SPEEDS**

A. **Shanmugaraju**<sup>1</sup>, Y.-J. Moon<sup>2</sup>, K.-S. Cho<sup>3</sup>, S. C. Bong<sup>3</sup>, N. Gopalswamy<sup>4</sup>, S. Akiyama<sup>4</sup>, S. Yashiro<sup>4</sup>, S. Umapathy<sup>5</sup>, and B. Vrsnak<sup>6</sup>

Astrophysical Journal, 708:450–455, **2010** January

Quasi-periodic oscillations in the speed profile of coronal mass ejections (CMEs) in the radial distance range 2–30 solar radii are studied. We considered the height–time data of the 307 CMEs recorded by the Large Angle and Spectrometric Coronagraph (LASCO) during 2005 January–March. In order to study the speed–distance profile of the CMEs, we have used only 116 events for which there are at least 10 height–time measurements made in the LASCO field of view. The instantaneous CME speed is estimated using a pair of height–time data points, providing the speed–distance profile. We found quasi-periodic patterns in at least 15 speed–distance profiles, where the speed amplitudes are larger than the speed errors. For these events we have determined the speed amplitude and period of oscillations. The periods of quasi-periodic oscillations are found in the range 48–240 minutes, tending to increase with height. The oscillations have similar properties as those reported by Krall et al., who interpreted them in terms of the flux-rope model. The nature of forces responsible for the motion of CMEs and their oscillations are discussed.

## **Radial Evolution of Well-Observed Slow CMEs in the Distance Range 2 – 30 R<sub>⊙</sub>**

A. **Shanmugaraju** · Y.-J. Moon · Bojan Vrsnak · Dijana Vrbanec

Solar Phys (2009) 257: 351–361; **File**

We performed a detailed analysis of 27 slow coronal mass ejections (CMEs) whose heights were measured in at least 30 coronagraphic images and were characterized by a high quality index ( $\geq 4$ ). Our primary aim was to study the radial evolution of these CMEs and their properties in the range 2 – 30 solar radii. The instantaneous speeds of CMEs were calculated by using

successive height – time data pairs. The obtained speed – distance profiles  $[v(R)]$  are fitted by a power law  $v = a(R - b)^c$ . The power-law indices are found to be in the ranges  $a = 30 - 386$ ,  $b = 1.95 - 3.92$ , and  $c = 0.03 - 0.79$ . The power-law exponent  $c$  is found to be larger for slower and narrower CMEs. With the exception of two events that had approximately constant velocity, all events were accelerating. The majority of accelerating events shows a  $v(R)$  profile very similar to the solar-wind profile deduced by Sheeley *et al.* (*Astrophys. J.* **484**, 472, 1997). This indicates that the dynamics of most slow CMEs are dominated by the solar wind drag.

### Investigation of CME dynamics in the LASCO field of view:

A. **Shanmugaraju**, Y.-J. Moon, K.-S. Cho, N. Gopalswamy and S. Umapathy

A&A 484 (2008) 511-516

<http://www.aanda.org/10.1051/0004-6361:20078978>

<http://www.aanda.org/articles/aa/pdf/2008/23/aa8978-07.pdf>

*Context.* The speed-distance profile of CMEs is important for understanding the propagation of CMEs.

*Aims.* Our main aim is to study the initial speed of CMEs in the LASCO field of view and its role in subsequent CME propagation using the acceleration-speed profile. The secondary aim is to obtain the speed growth rate.

*Methods.* We considered the height-time data of 307 CMEs observed by SOHO/LASCO during January-March 2005.

To study the CME speed profile, we used only 116 events for which there were at least 10 height-time measurements in the LASCO field of view. Using this data, we obtained their initial speed, extrapolated initial speed, and growth rate.

*Results.* The following results were found from this analysis. (i) The initial speed obtained from the first two data points is in the range 24-1208 km s<sup>-1</sup>, which is nearly similar to the range of linear speed (67-920 km s<sup>-1</sup>) obtained from a least squares fit through the entire h-t data set for each CME. (ii) However, the initial speed or extrapolated initial speed is much better correlated with acceleration and growth rate than the linear speed. (iii) Nearly two thirds of the events (74/116) are found to be accelerating. (iv) The speed growth rate is within the range -0.058 to 0.061x10<sup>3</sup> s<sup>-1</sup>, and it decreases with the distance. (v) The final observed distance in the LASCO field of view depends very weakly upon the initial speed, or extrapolated initial speed whereas it depends strongly on the linear speed. The above results demonstrate the role played by the initial speed of the CMEs.

### Origin of coronal shocks without mass ejections

**Shanmugaraju**, A. Moon, Y.-J. Cho, K.-S. Dryer, M. Umapathy, S.

Solar Phys. Volume 233, Issue 1, pp.117-127 **2006**

We present an analysis of all the events (around 400) of coronal shocks for which the shock-associated metric type IIs were observed by many spectrographs during the period April 1997 December 2000. The main objective of this analysis is to give evidence for the type IIs related to only flare-blast waves, and thus to find out whether there are any type II-associated coronal shocks without mass ejections. By carefully analyzing the data from multi-wavelength observations (Radio, GOES X-ray, H $\alpha$ , SOHO/LASCO and SOHO/EIT-EUV data), we have identified only 30 events for which there were actually no reports of CMEs. Then from the analysis of the LASCO and EIT running difference images, we found that there are some shocks (nearly 40%, 12/30) which might be associated with weak and narrow mass ejections. These weak and narrow ejections were not reported earlier. For the remaining 60% events (18/30), there are no mass ejections seen in SOHO/LASCO. But all of them are associated with flares and EIT brightenings. Pre-assuming that these type IIs are related to the flares, and from those flare locations of these 18 cases, 16 events are found to occur within the central region of the solar disk (longitude  $\leq 45^\circ$ ). In this case, the weak CMEs originating from this region are unlikely to be detected by SOHO/LASCO due to low scattering. The remaining two events occurred beyond this longitudinal limit for which any mass ejections would have been detected if they were present. For both these events, though there are weak eruption features (EIT dimming and loop displacement) in the EIT images, no mass ejection was seen in LASCO for one event, and a CME appeared very late for the other event. While these two cases may imply that the coronal shocks can be produced without any mass ejections, we cannot deny the strong relationship between type IIs and CMEs.

### CONSISTENT SELF-SIMILAR MAGNETOHYDRODYNAMICS EVOLUTION OF CORONAL TRANSIENTS

David **Shapakhidze**<sup>1</sup>, Arnold Debosscher<sup>2</sup>, Andria Rogava<sup>1,2,3</sup>, and Stefaan Poedts<sup>2</sup>

Astrophysical Journal, 712:565–573, **2010** March

The self-similar model of coronal transients by B.C. Lewis reconsidered. Due to a modification of the basic set of the initial assumptions of the model, a new class of more consistent solutions is found. The main advantage of these new solutions is that they do *not* contain areas with a physically inconsistent negative pressure. Instead, the novel solutions are derived on the basis of a special prescription for the thermal pressure of the transients that guarantees, by design, its positiveness throughout the whole evolution domain. The possible importance of these solutions for understanding the physics of the transient interplanetary coronal mass ejections (ICMEs; originating from the Sun), and magnetic clouds as a subclass of these, is discussed. A practical example is cited illustrating the application of our analytic results to describe some properties of real ICMEs. Some directions and scopes for further research are outlined.

## Characteristics of Sustained >100 $\gamma$ -ray Emission Associated with Solar Flares

G. H. [Share](#), R. J. Murphy, A. K. Tolbert, B. R. Dennis, S. M. White, R. A. Schwartz, and A. J. Tylka  
ApJ Supplement 2017

[http://www.astro.umd.edu/~share/publications/share\\_2017.pdf](http://www.astro.umd.edu/~share/publications/share_2017.pdf) File

We characterize and provide a catalog of thirty >100 MeV sustained  $\gamma$ -ray emission (SGRE) events observed by Fermi LAT. These events are temporally and spectrally distinct from the associated solar flares. Their spectra are consistent with decay of pions produced by >300 MeV protons and are not consistent with electron bremsstrahlung. SGRE start times range from CME onset to two hours later. Their durations range from about four minutes to twenty hours and appear to be correlated with durations of >100 MeV SEP proton events. The >300 MeV protons producing SGRE have spectra that can be fit with power laws with a mean index of  $\sim 4$  and RMS spread of 1.8.  $\gamma$ -ray line measurements indicate that SGRE proton spectra are steeper above 300 MeV than they are below 300 MeV. The number of SGRE protons >500 MeV is on average about ten times more than the number in the associated flare and about fifty to one hundred times less than the number in the accompanying SEP. SGRE can extend tens of degrees from the flare site. Sustained bremsstrahlung from MeV electrons was observed in one SGRE event. Flare >100 keV X-ray emission appears to be associated with SGRE and with intense SEPs. From this observation, we provide arguments that lead us to propose that sub-MeV to MeV protons escaping from the flare contribute to the seed population that is accelerated by shocks onto open field lines to produce SEPs and onto field lines returning to the Sun to produce SGRE. **3 June 1983?, 2011-02-24, 2011 March 7, 2011-05-29, 2011-06-02, 2011-06-07, 2011-08-04, 2011-08-09, 2011-09-06, 2011-09-07, 2011-09-24, 22-Jan-12, 2012-01-23, 2012-01-27, 2012-03-04, 2012-03-05, 06-Mar-12, 2012 March 7, 2012-03-09, 2012-03-10, 2012-03-13, 2012-05-17, 2012-06-03, 2012-07-06, 2012-10-23, 2012-11-27, 2013-04-11, 2013-05-13, 2013-05-14, 2013-05-15, 2013-10-11, 2013-10-25, 2013-10-28, 2014 February 25, 2014-09-01, 2015-06-21**

**Table 1.** LAT Sustained >100 MeV Emission (SGRE) Events from June 2008 to December 2016

**Table 4.** Onset Times of CMEs, Type II Radio, and SGREs

**Table A1.** Solar Eruptive Events from June 2008 to May 2012

**Table C2.** Spectral Characteristics of Sustained-Emission Events

**Table E3.** Radio Bursts from LAT Sustained >100 MeV Events

## On the Bright Loop Top Emission in Post Eruption Arcades

Rohit [Sharma](#), Durgesh Tripathi, Hiroaki Isobe, Avyarthana Ghosh  
ApJ 823 47 2016

<http://arxiv.org/pdf/1603.04959v1.pdf>

The observations of post eruption arcades (PEAs) in X-rays and EUV reveal strong localised brightenings at the loop top regions. The origin of these brightenings and their dynamics is not well understood to date. Here, we study the dynamics of PEAs using one-dimensional hydrodynamic modelling with the focus on the the understanding of the formation of localised brightening. Our findings suggest that these brightenings are the result of collisions between the counter-streaming chromospheric evaporation from both the foot points. We further perform forward modelling of the emission observed in simulated results in various spectral lines observed by the Extreme-Ultraviolet Imaging Telescope aboard Hinode. The forward modelled intensities in various spectral lines are in close agreement with a flare observed in **December 17, 2006** by EIS.

## On properties of radio-rich coronal mass ejections

Joginder [Sharma](#) · Nishant Mittal · Vivek Tomar · Udit Narain

Astrophys Space Sci (2008) 317: 261–265, DOI 10.1007/s10509-008-9886-4

We have studied properties of the radio-rich coronal mass ejections (CMEs) (observed during 1997–2006) which produce type II (1–14 MHz) i.e. decametric–hectometric or DH radio burst. These DH CMEs are relatively faster and wider than the normal CMEs. The average speed and apparent width of these CMEs is 1048 km/s and  $98^\circ$ , respectively. Majority (about 54%) of DH CMEs decelerate, but about 21% show positive acceleration. The remaining 25% move with little acceleration. These special characteristics of radio-rich CMEs could be used to identify the population of geoeffective CMEs, which are quite relevant to space weather.

## Coronal Inflows during the Interval 1996-2014

N. R. [Sheeley](#), Jr. and Y.-M. Wang

2014 ApJ 797 10

We extend our previous counts of coronal inflows from the 5?yr interval 1996-2001 to the 18?yr interval 1996-2014. By comparing stackplots of these counts with similar stackplots of the source-surface magnetic field and its longitudinal gradient, we find that the inflows occur in long-lived streams with counting rates in excess of 18 inflows per day at sector boundaries where the gradient exceeds  $0.22 \text{ G rad}^{-1}$ . These streams are responsible for the high (86%) correlation between the inflow rate and the longitudinal field gradient. The overall inflow rate was several times larger in sunspot cycle 23 than it has been so far in cycle 24, reflecting the relatively weak source-surface fields during this cycle. By comparison, in cycles 21-22, the source-surface field and its gradient had bursts of great strength, as if large numbers of inflows occurred during those cycles. We find no obvious relation between inflows and coronal mass ejections (CMEs) on timescales of days to weeks, regardless of the speeds of the CMEs, and only a 60% correlation on

timescales of months, provided the CMEs are fast ( $V > 600 \text{ km/s}$ ). We conclude that most of the flux carried out by CMEs is returned to the Sun via field line reconnection well below the  $2.0 R_{\odot}$  inner limit of the LASCO field of view, and that the remainder accumulates in the outer corona for an eventual return at sector boundaries.

## **TRACKING STREAMER BLOBS INTO THE HELIOSPHERE**

N. R. [Sheeley](#), Jr. and A. P. Rouillard<sup>1</sup>

*Astrophysical Journal*, 715:300–309, 2010 May

In this paper, we use coronal and heliospheric images from the *Solar Terrestrial Relations Observatory (STEREO)* spacecraft to track streamer blobs into the heliosphere and to observe them being swept up and compressed by the fast wind from low-latitude coronal holes. From an analysis of their elongation/time tracks, we discover a “locus of enhanced visibility” where neighboring blobs pass each other along the line of sight and their corotating spiral is seen edge-on. The detailed shape of this locus accounts for a variety of east–west asymmetries and allows us to recognize the spiral of blobs by its signatures in the *STEREO* images: in the eastern view from *STEREO-A*, the leading edge of the spiral is visible as a moving wavefront where foreground ejections overtake background ejections against the sky and then fade. In the western view from *STEREO-B*, the leading edge is only visible close to the Sun–spacecraft line where the radial path of ejections nearly coincides with the line of sight. In this case, we can track large-scale waves continuously back to the lower corona and see that they originate as face-on blobs.

## **THE STRUCTURE OF STREAMER BLOBS**

N. R. [Sheeley](#), Jr., D. D.-H. Lee<sup>1</sup>, K. P. Casto<sup>2</sup>, Y.-M. Wang, and N. B. Rich<sup>3</sup>

*Astrophysical Journal*, 694:1471–1480, 2009 April; **File**

We have used Sun–Earth Connection Coronal and Heliospheric Investigation observations obtained from the *STEREO A* and *B* spacecraft to study complementary face-on and edge-on views of coronal streamers. The face-on views are analogous to what one might see looking down on a flat equatorial streamer belt at sunspot minimum, and show streamer blobs as diffuse arches gradually expanding outward from the Sun. With the passage of time, the legs of the arches fade, and the ejections appear as a series of azimuthal structures like ripples on a pond. The arched topology is similar to that obtained in face-on views of streamer disconnection events (including in/out pairs and streamer blowout mass ejections), and suggests that streamer blobs have the helical structure of magnetic flux ropes.

## **In/Out Pairs and the Detachment of Coronal Streamers**

N. R. [Sheeley](#), Jr. and Y.-M. Wang

*The Astrophysical Journal*, 655:1142Y1156, 2007, **File**

The simultaneous ejection of material inward toward the Sun and outward away from it.

We conclude that in/out pairs belong to a broad class of streamer detachments, which include “streamer blowout” coronal mass ejections, and we suppose that all of these events occur when rising magnetic loops reconnect to produce an outgoing helical flux rope and an ingoing arcade of collapsing loops.

## **Detection of coronal mass ejection associated shock waves in the outer corona.**

[Sheeley](#), N.R., Hakala, W.N., Wang, Y.,

2000. *J. Geophys. Res.* 105, 5081–5092.

## **Continuous tracking of coronal outflows: Two kinds of coronal mass ejections**

N. R. [Sheeley](#) Jr., J. H. Walters, • Y.-M. Wang, and R. A. Howard

*JGR*, VOL. 104, NO. All, PAGES 24,739-24,767, NOVEMBER 1, 1999; **File**

We have developed a new technique for tracking white-light coronal intensity features and have used this technique to construct continuous height/time maps of coronal ejecta as they move outward through the 2-30  $R_{\odot}$  field of view of the Large-Angle Spectrometric Coronagraph (LASCO) on the Solar and Heliospheric Observatory (SOHO) spacecraft. Displayed as gray-scale images, these height/time maps provide continuous histories of the motions along selected radial paths in the corona and reveal a variety of accelerating and decelerating features, including two principal types of coronal mass ejections (CMEs): (1) Gradual CMEs, apparently formed when prominences and their cavities rise up from below coronal streamers: When seen broadside, these events acquire balloon-like shapes containing central cores, and their leading edges accelerate gradually to speeds in the range 400-600 km/s before leaving the 2-30  $R_{\odot}$  field of view. The cores fall behind with speeds in the range 300-400 km/s. Seen along the line of sight, these events appear as smooth halos around the occulting disk, consistent with head-on views of optically thin bubbles stretched out from the Sun. At the relatively larger radial distances seen from this “head-on” perspective, gradually accelerating CMEs fade out sooner and seem to reach a constant speed more quickly than when seen broadside. Some suitably directed gradual CMEs are associated with interplanetary shocks and geomagnetic

storms. (2) Impulsive CMEs, often associated with flares and Moreton waves on the visible disk: When seen broadside, these CMEs move uniformly across the 2-30 R s field of view with speeds typically in excess of 750 km/s. At the relatively larger radial distances seen from a head-on perspective, impulsive events tend to have a more ragged structure than the gradual CMEs and show clear evidence of deceleration, sometimes reducing their speeds from 1000 to 500 km/s in 1 hour. Such decelerations are too large to represent ballistic motions in the Sun's gravitational field but might be caused by shock waves, sweeping up material far from the Sun.

### **SOLWIND observations of coronal mass ejections during 1979-1985**

[Sheeley](#), N. R., Jr.; [Howard](#), R. A.; [Koomen](#), M. J.; [Michels](#), D. J.

In NASA. Marshall Space Flight Center Solar Flares and Coronal Physics Using P/OF as a Research Tool p 241-256 (SEE N86-24614 14-92) **1986**

Coronal observations have been processed for parts of each year during the interval 1979-1985. Around sunspot maximum, coronal mass ejections (CMEs) occurred at the rate of approximately 2 per day, and had a wide range of physical and morphological properties. During the recent years of relatively low sunspot number, CMEs occurred at the rate of only 0.2 per day, and were dominated by the class of so-called streamer blowout. These special CMEs maintained a nearly constant occurrence rate of roughly 0.1 per day during the entire interval.

### **Atmospheric Response to of an Active Region to new Small Flux Emergence**

D.L. [Shelton](#), L.K. Harra, L.M. Green

Solar Phys. **2015**

<http://arxiv.org/pdf/1412.5623v1.pdf>

We investigate the atmospheric response to a small emerging flux region (EFR) that occurred in the positive polarity of Active Region 11236 on **23-24 June 2011**. Data from the \textit{Solar Dynamics Observatory's Atmospheric Imaging Assembly} (AIA), the \textit{Helioseismic and Magnetic Imager} (HMI) and Hinode's \textit{EUV imaging spectrometer} (EIS) are used to determine the atmospheric response to new flux emerging into a pre-existing active region.

Brightenings are seen forming in the upper photosphere, chromosphere, and corona over the EFR's location whilst flux cancellation is observed in the photosphere. The impact of the flux emergence is far reaching, with new large-scale coronal loops forming up to 43 Mm from the EFR and coronal upflow enhancements of approximately 10 km s<sup>-1</sup> on the north side of the EFR. Jets are seen forming in the chromosphere and the corona over the emerging serpentine field. This is the first time that coronal jets have been seen over the serpentine field.

### **Double-decker Pair of Flux Ropes Formed by Two Successive Tether-cutting Eruptions**

[Yuangeng Shen](#), [Dongxu Liu](#), [Surui Yao](#), [Chengrui Zhou](#), [Zehao Tang](#), [Zhining Qu](#), [Xinping Zhou](#), [Yadan Duan](#), [Song Tan](#), [Ahmed Ahmed Ibrahim](#)

ApJ **964** 125 **2024**

<https://arxiv.org/pdf/2401.11080.pdf>

<https://iopscience.iop.org/article/10.3847/1538-4357/ad2349/pdf>

Double-decker filaments and their eruptions have been widely observed in recent years, but their physical formation mechanism is still unclear. Using high spatiotemporal resolution, multi-wavelength observations taken by the New Vacuum Solar Telescope and the Solar Dynamics Observatory, we show the formation of a double-decker pair of flux rope system by two successive tether-cutting eruptions in a bipolar active region. Due to the combined effect of photospheric shearing and convergence motions around the active region's polarity inversion line (PIL), the arms of two overlapping inverse-S-shaped short filaments reconnected at their intersection, which created a simultaneous upward-moving magnetic flux rope (MFR) and a downward-moving post-flare-loop (PFL) system striding the PIL. Meanwhile, four bright flare ribbons appeared at the footpoints of the newly formed MFR and the PFL. As the MFR rose, two elongated flare ribbons connected by a relatively larger PFL appeared on either side of the PIL. After a few minutes, another MFR formed in the same way at the same location and then erupted in the same direction as the first one. Detailed observational results suggest that the eruption of the first MFR might experienced a short pause before its successful eruption, while the second MFR was a failed eruption. This implies that the two newly formed MFRs might reach a new equilibrium at relatively higher heights for a while, which can be regarded as a transient double-decker flux rope system. The observations can well be explained by the tether-cutting model, and we propose that two successive confined tether-cutting eruptions can naturally produce a double-decker flux rope system, especially when the background coronal magnetic field has a saddle-like distribution of magnetic decay index profile in height. **2022 March 20**

### **Non-equilibrium Ionization Modeling of Petschek-type Shocks in Reconnecting Current Sheets in Solar Eruptions**

[Chengcai Shen](#), [John C. Raymond](#), [Nicholas A. Murphy](#)

ApJ **943** 111 **2023**

<https://arxiv.org/pdf/2211.01188.pdf>



<https://iopscience.iop.org/article/10.3847/1538-4357/aca6e7/pdf>

Non-equilibrium ionization (NEI) is essentially required for astrophysical plasma diagnostics once the plasma status departs from ionization equilibrium assumptions. In this work, we perform fast NEI calculations combined with magnetohydrodynamic (MHD) simulations and analyze the ionization properties of a Petschek-type magnetic reconnection current sheet during solar eruptions. Our simulation reveals Petschek-type slow-mode shocks in the classical Spitzer thermal conduction models and conduction flux-limitation situations. The results show that under-ionized features can be commonly found in shocked reconnection outflows and thermal halo regions outside the shocks. The departure from equilibrium ionization strongly depends on plasma density. In addition, this departure is sensitive to the observable target temperature: the high-temperature iron ions are strongly affected by NEI effects. The under-ionization also affects the synthetic SDO/AIA intensities, which indicates that the reconstructed hot reconnection current sheet structure may be significantly under-estimated either for temperature or apparent width. We also perform the MHD-NEI analysis on the reconnection current sheet in the classical solar flare geometry. Finally, we show the potential reversal between the under-ionized and over-ionized state at the lower tip of reconnection current sheets where the downward outflow collides with closed magnetic loops, which can strongly affect multiple SDO/AIA band ratios along the reconnection current sheet.

### **White-light QFP Wave Train and the Associated Failed Breakout Eruption**

Yuangeng **Shen**<sup>1,2,3,5</sup>, Surui Yao<sup>1</sup>, Zehao Tang<sup>1,3</sup>, Xinping Zhou<sup>1,3</sup>, Zhining Qu<sup>4</sup>, Yadan Duan<sup>1,3</sup>, Chengrui Zhou<sup>1,3</sup> and Song Tan<sup>1,3</sup>

A&A 665, A51 (2022)

<https://arxiv.org/pdf/2207.08110.pdf>

<https://www.aanda.org/articles/aa/pdf/2022/09/aa43924-22.pdf>

Quasi-periodic fast-propagating (QFP) magnetosonic wave trains are commonly observed in the low corona at extreme ultraviolet wavelength bands. Here, we report the first white-light imaging observation of a QFP wave train propagating outwardly in the outer corona ranging from 2 to 4  $R_{\odot}$ . The wave train was recorded by the Large Angle Spectroscopic Coronagraph on board the Solar and Heliospheric Observatory (SOHO), and was associated with a GOES M1.5 flare in NOAA active region AR12172 at the southwest limb of the solar disk. Measurements show that the speed and period of the wave train were about 218 km s<sup>-1</sup> and 26 min, respectively. The extreme ultraviolet imaging observations taken by the Atmospheric Imaging Assembly on board the Solar Dynamic Observatory reveal that in the low corona the QFP wave train was associated with the failed eruption of a breakout magnetic system consisting of three low-lying closed loop systems enclosed by a high-lying large-scale one. Data analysis results show that the failed eruption of the breakout magnetic system was mainly because of the magnetic reconnection that occurred between the two lateral low-lying closed-loop systems. This reconnection enhances the confinement capacity of the magnetic breakout system because the upward-moving reconnected loops continuously feed new magnetic fluxes to the high-lying large-scale loop system. For the generation of the QFP wave train, we propose that it could be excited by the intermittent energy pulses released by the quasi-periodic generation, rapid stretching, and expansion of the upward-moving, strongly bent reconnected loops. **2014 October 2**

### **Numerical Research on the Effect of the Initial Parameters of a CME Flux-rope Model on Simulation Results. II. Different Locations of Observers**

Fang **Shen**<sup>3,1,2</sup>, Yousheng Liu<sup>1,2</sup>, and Yi Yang<sup>1,2</sup>

2021 ApJ 915 30

<https://iopscience.iop.org/article/10.3847/1538-4357/ac004e/pdf>

<https://doi.org/10.3847/1538-4357/ac004e>

In numerical studies of the initiation and propagation of coronal mass ejections (CMEs), it has been proven that the shape, size, and plasma parameters of CMEs could significantly affect simulation results and subsequent space weather predictions. In our previous research, we proposed a new way to initiate a CME based on the graduated cylindrical shell model, and studied the effect of different initial parameters of CMEs on the simulation results when the observer is aligned with the initial propagation direction of the CME. In this paper, we investigate the influence of the different initial parameters of CMEs on simulation results at the observational points with different longitudes and latitudes. Our results indicate that as long as the initial mass of the CME remains unchanged, the initial geometric thickness will have a different influence in the latitudinal and longitudinal directions. The deflection of the CMEs always occurs in both latitudinal and longitudinal directions, when the CMEs interact with the background solar wind structures, such as the corotating interaction region, in the heliosphere.

### **Numerical Research on the Effect of the Initial Parameters of a CME Flux-rope Model on Simulation Results**

Fang **Shen**<sup>4,1,2,3</sup>, Yousheng Liu<sup>1,2</sup>, and Yi Yang<sup>1,2</sup>

2021 ApJS 253 12

<https://doi.org/10.3847/1538-4365/abd4d2>

<https://iopscience.iop.org/article/10.3847/1538-4365/abd4d2/pdf>

Coronal mass ejections (CMEs) are the major drivers of space weather, and an accurate modeling of their initialization and propagation up to 1 au and beyond is an important issue for space weather research and forecasts. In this research, we use the newly developed three-dimensional (3D) flux-rope CME initialization model and 3D IN (interplanetary)-TVD MHD model to study the effect of different CME initial parameters on simulation outputs. The initial CME flux

model is established based on the graduated cylindrical shell model. In order to test the influence of the CME initial parameters on the simulation results, we try to run several simulations with different CME initial parameters, then investigate the outputs in interplanetary space. Here, we focus only on cases in which observers are located in the same initial direction of propagation of the CME. Our analysis shows that the parameters specifying the CME initialization in the model, including the initial density, the thickness of CME flux tube, initial mass, and initial magnetic field, have different effects on the simulation results for observers near the Earth and Mars, and on the process of propagation of the CME in interplanetary space. This confirms the important role played by details of the initial implementation of geometric and physical parameters on space weather research and forecasts.

## Observation and Modeling of Solar Jets

**Review**

[Yuandeng Shen](#)

Proceedings of the Royal Society A 2021

<https://arxiv.org/pdf/2101.04846.pdf>

The solar atmosphere is full of complicated transients manifesting the reconfiguration of solar magnetic field and plasma. Solar jets represent collimated, beam-like plasma ejections; they are ubiquitous in the solar atmosphere and important for the understanding of solar activities at different scales, magnetic reconnection process, particle acceleration, coronal heating, solar wind acceleration, as well as other related phenomena. Recent high spatiotemporal resolution, wide-temperature coverage, spectroscopic, and stereoscopic observations taken by ground-based and space-borne solar telescopes have revealed many valuable new clues to restrict the development of theoretical models. This review aims at providing the reader with the main observational characteristics of solar jets, physical interpretations and models, as well as unsolved outstanding questions in future studies. **2000 Sep 23, 2013 June 02**

## Stereoscopic Observations of an Erupting Mini-filament Driven Two-Sided-Loop Jet and the Applications for Diagnosing Filament Magnetic field

[Yuandeng Shen](#), [Zhining Qu](#), [Ding Yuan](#), [Heading Chen](#), [Yadan Duan](#), [Chengrui Zhou](#), [Zehao Tang](#), [Jin Huang](#), [Yu Liu](#)

ApJ 883 104 2019

<https://arxiv.org/pdf/1908.03660.pdf>

<https://doi.org/10.3847/1538-4357/ab3a4d>

The ubiquitous solar jets or jet-like activities are generally regarded as an important source of energy and mass input to the upper solar atmosphere and the solar wind. However, questions about their triggering and driving mechanisms are not completely understood. By taking advantage of high temporal and high spatial resolution stereoscopic observations taken by the Solar Dynamic Observatory (SDO) and the Solar Terrestrial Relations Observatory (STEREO), we report an intriguing two-sided-loop jet occurred on **2013 June 02**, which was dynamically associated with the eruption of a mini-filament below an overlying large filament, and two distinct reconnection processes are identified during the formation stage. The SDO observations reveals that the two-sided-loop jet showed a concave shape with a projection speed of about 80 - 136. From the other view angle, the STEREO ahead observations clearly showed that the trajectory of the two arms of the two-sided-loop were along the cavity magnetic field lines hosting the large filament. Contrary to the well-accepted theoretical model, the present observation sheds new light on our understanding of the formation mechanism of two-sided-loop jets. Moreover, the eruption of the two-sided-loop jet not only supplied mass to the overlying large filament, but also provided a rare opportunity to diagnose the magnetic structure of the overlying large filament via the method of three-dimensional reconstruction.

## Coronal EUV, QFP, and kink waves simultaneously launched during the course of jet-loop interaction

[Yuandeng Shen](#), [Zehao Tang](#), [Hongbo Li](#), [Yu Liu](#)

MNRAS Letters 2018

<https://arxiv.org/pdf/1807.09533.pdf>

We present the observations of an extreme ultraviolet (EUV) wave, a quasi-periodic fast-propagating (QFP) magnetosonic wave, and a kink wave that were simultaneously associated with the impingement of a coronal jet upon a group of coronal loops. After the interaction, the coronal loop showed obvious kink oscillation that had a period of about 428 seconds. In the meantime, a large-scale EUV wave and a QFP wave are observed on the west of the interaction position. It is interesting that the QFP wave showed refraction effect during its passing through two strong magnetic regions. The angular extent, speed, and lifetime of the EUV (QFP) wave were about 140 (40) degree, 423 (322) km/s, and 6 (26) minutes, respectively. It is measured that the period of the QFP wave was about 390 +/- 100 second. Based on the observational analysis results, we propose that the kink wave was probably excited by the interaction of the jet; the EUV was probably launched by the sudden expansion of the loop system due to the impingement of the coronal jet; and the QFP wave was possibly formed through the dispersive evolution of the disturbance caused by the jet-loop interaction. **2011 February 14**

## Homologous Large-amplitude Nonlinear Fast-mode Magnetosonic Waves Driven by Recurrent Coronal Jets

[Yuandeng Shen](#)<sup>1,2,3,4</sup>, [Yu Liu](#)<sup>1,4</sup>, [Ying D. Liu](#)<sup>2,5</sup>, [Jiangtao Su](#)<sup>3,5</sup>, [Zehao Tang](#)<sup>1,5</sup>, and [Yuhu Miao](#)<sup>1</sup>,  
The Astrophysical Journal, 861:105 (13pp), **2018 July 10**

<http://iopscience.iop.org/article/10.3847/1538-4357/aac9be/pdf>  
<https://arxiv.org/pdf/1805.12303.pdf>

The detailed observational analysis of a homologous extreme-ultraviolet (EUV) wave event is presented to study the driving mechanism and the physical property of the EUV waves, combining high-resolution data taken by the Solar Dynamics Observatory and the Solar TERrestrial RELations Observatory. It is observed that four homologous EUV waves originated from the same active region AR11476 within about one hour, and the time separations between consecutive waves were of 8–20 minutes. The waves showed narrow arc-shaped wavefronts and propagated in the same direction along a large-scale transequatorial loop system at a speed of 648–712 km s<sup>-1</sup> and a deceleration of 0.985–1.219 km s<sup>-2</sup>. The EUV waves were accompanied by weak flares, coronal jets, and radio type III bursts, in which the EUV waves were delayed with respect to the start times of the radio type III bursts and coronal jets about 2–13 and 4–9 minutes, respectively. Unlike in previous studies of homologous EUV waves, no coronal mass ejections were found in the present event. Based on the observational results and the close temporal and spatial relationships between the EUV waves and the coronal jets, for the first time, we propose that the observed homologous EUV waves were large-amplitude nonlinear fast-mode magnetosonic waves or shocks driven by the associated recurrent coronal jets and that they resemble the generation mechanism of a piston shock in a tube. In addition, it is found that the recurrent jets were tightly associated with the alternating flux cancellation and emergence in the eruption source region and radio type III bursts. **2010-04-28, 2010-11-11, 2012 May 14**

### **Dispersively formed quasi-periodic fast magnetosonic wavefronts due to the eruption of a nearby mini-filament**

Yuandeng [Shen](#); [Tengfei Song](#); [Yu Liu](#)

Monthly Notices of the Royal Astronomical Society: Letters, Volume 477, Issue 1, 11 June **2018**, Pages L6–L10

<https://doi.org/10.1093/mnrasl/sly044>

Observational analysis is performed to study the excitation mechanism and propagation properties of a quasi-periodic fast-propagating (QFP) magnetosonic wave. The QFP wave was associated with the eruption of a nearby mini-filament and a small B4 Geostationary Operational Environmental Satellite (GOES) flare, which may indicate that the generation of a QFP wave does not require much flare energy. The propagation of the QFP wave was along a bundle of funnel-shaped open loops with a speed of about  $1100 \pm 78$  km s<sup>-1</sup> and an acceleration of  $-2.2 \pm 1.1$  km s<sup>-2</sup>. Periodicity analysis indicates that the periods of the QFP wave are  $43 \pm 6$  and  $79 \pm 18$  s. For the first time, we find that the periods of the QFP wave and the accompanying flare are inconsistent, which is different from the findings reported in previous studies. We propose that the present QFP wave was possibly caused by the mechanism of dispersive evolution of the initially broad-band disturbance resulting from the nearby mini-filament eruption.

### **A quasi-periodic fast-propagating magnetosonic wave associated with the eruption of a magnetic flux rope**

Yuandeng [Shen](#), [Yu Liu](#), [Tengfei Song](#), [Zhanjun Tian](#)

**2018 ApJ 853 1**

<https://arxiv.org/pdf/1712.09045.pdf>

<http://sci-hub.tw/http://iopscience.iop.org/0004-637X/853/1/1/>

Using high temporal and high spatial resolution observations taken by the Atmospheric Imaging Assembly onboard the Solar Dynamics Observatory, we present the detailed observational analysis of a high quality quasi-periodic fast-propagating (QFP) magnetosonic wave that was associated with the eruption of a magnetic flux rope and a GOES C5.0 flare. For the first time, we find that the QFP wave lasted during the entire flare lifetime rather than only the rising phase of the accompanying flare as reported in previous studies. In addition, the propagation of the different parts of the wave train showed different kinematics and morphologies. For the southern (northern) part, the speed, duration, intensity variation are about  $875 \pm 29$  ( $1485 \pm 233$ ) km/s, 45 (60) minutes, and 4% (2%), and the pronounced periods of them are  $106 \pm 12$  and  $160 \pm 18$  ( $75 \pm 10$  and  $120 \pm 16$ ) seconds, respectively. It is interesting that the northern part of the wave train showed obvious refraction effect when they pass through a region of strong magnetic field. Periodicity analysis result indicates that all the periods of the QFP wave can be found in the period spectrum of the accompanying flare, suggesting their common physical origin. We propose that the quasi-periodic nonlinear magnetohydrodynamics process in the magnetic reconnection that produces the accompanying flare should be important for exciting of QFP wave, and the different magnetic distribution along different paths can account for the different speeds and morphology evolution of the wave fronts. **2014 March 23**

### **On a small-scale EUV wave: the driving mechanism and the associated oscillating filament**

Yuandeng [Shen](#), [Yu Liu](#), [Zhanjun Tian](#), [Zhining Qu](#)

ApJ **2017**

<https://arxiv.org/pdf/1711.04905.pdf>

We present observations of a small-scale Extreme-ultraviolet (EUV) wave that was associated with a mini-filament eruption and a GOES B1.9 micro-flare in the quiet Sun region. The initiation of the event was due to the photospheric magnetic emergence and cancellation in the eruption source region, which first caused the ejection of a small plasma ejecta, then the ejecta impacted on a nearby mini-filament and thereby led to the filament's eruption and the associated flare. During the filament eruption, an EUV wave at a speed of  $182 \pm 317$  km/s was formed ahead of an expanding

coronal loop, which propagated faster than the expanding loop and showed obvious deceleration and reflection during the propagation. In addition, the EUV wave further resulted in the transverse oscillation of a remote filament whose period and damping time are 15 and 60 minutes, respectively. Based on the observational results, we propose that the small-scale EUV wave should be a fast-mode magnetosonic wave that was driven by the expanding coronal loop. Moreover, with the application of filament seismology, it is estimated that the radial magnetic field strength is about 7 Gauss. The observations also suggest that small-scale EUV waves associated with miniature solar eruptions share similar driving mechanism and observational characteristics with their large-scale counterparts. **March 21, 2016**

### **On a solar blowout jet: driven mechanism and the formation of cool and hot components**

Yuangeng [Shen](#), [Ying D. Liu](#), [Jiangtao Su](#), [Zhining Qu](#), [Zhanjun Tian](#)

ApJ **851** 67 **2017**

<https://arxiv.org/pdf/1711.02270.pdf>

<http://iopscience.iop.org/sci-hub.tw/0004-637X/851/1/67/>

We present the observations of a blowout jet that experienced two distinct ejection stages. The first stage started from the emergence of a small positive magnetic polarity, which cancelled with the nearby negative magnetic field and caused the rising of a mini-filament and its confining loops. This further resulted in a small jet due to the magnetic reconnection between the rising confining loops and the overlying open field. The second ejection stage was mainly due to the successive removal of the confining field by the reconnection. Thus that the filament erupted and the erupting cool filament material directly combined with the hot jet originated from the reconnection region and therefore formed the cool and hot components of the blowout jet. During the two ejection stages, cool  $H\{\alpha\}$  jets are also observed cospatial with their coronal counterparts, but their appearance times are earlier than the hot coronal jets a few minutes. Therefore, the hot coronal jets are possibly caused by the heating of the cool  $H\{\alpha\}$  jets, or the rising of the reconnection height from chromosphere to the corona. The scenario that magnetic reconnection occurred between the confining loops and the overlying open loops are supported by many observational facts, including the bright patches on the both sides of the mini-filament, hot plasma blobs along the jet body, and periodic metric radio type III bursts at the very beginnings of the two stages. The evolution and characteristics of these features manifest the detailed non-linear process in the magnetic reconnection. **April 16, 2014**

### **On the Collision Nature of Two Coronal Mass Ejections: A Review**

Fang [Shen](#), Yuming Wang, Chenglong Shen, Xueshang Feng

[Solar Physics](#) August **2017**, 292:104

<https://link.springer.com/content/pdf/10.1007%2Fs11207-017-1129-9.pdf>

Observational and numerical studies have shown that the kinematic characteristics of two or more coronal mass ejections (CMEs) may change significantly after a CME collision. The collision of CMEs can have a different nature, i.e. inelastic, elastic, and superelastic processes, depending on their initial kinematic characteristics. In this article, we first review the existing definitions of collision types including Newton's classical definition, the energy definition, Poisson's definition, and Stronge's definition, of which the first two were used in the studies of CME-CME collisions. Then, we review the recent research progresses on the nature of CME-CME collisions with the focus on which CME kinematic properties affect the collision nature. It is shown that observational analysis and numerical simulations can both yield an inelastic, perfectly inelastic, merging-like collision, or a high possibility of a superelastic collision. Meanwhile, previous studies based on a 3D collision picture suggested that a low approaching speed of two CMEs is favorable for a superelastic nature. Since CMEs are an expanding magnetized plasma structure, the CME collision process is quite complex, and we discuss this complexity. Moreover, the models used in both observational and numerical studies contain many limitations. All of the previous studies on collisions have not shown the separation of two colliding CMEs after a collision. Therefore the collision between CMEs cannot be considered as an ideal process in the context of a classical Newtonian definition. In addition, many factors are not considered in either observational analysis or numerical studies, e.g. CME-driven shocks and magnetic reconnections. Owing to the complexity of the CME collision process, a more detailed and in-depth observational analysis and simulation work are needed to fully understand the CME collision process.

**Table 1 Summary of the previous studies on the nature of CME-CME collisions.**

### **Evolution of the 2012 July 12 CME from the Sun to the Earth: Data-Constrained Three-Dimensional MHD Simulations<sup>†</sup>**

Fang [Shen](#)<sup>1,\*</sup>, Chenglong Shen<sup>2</sup>, Jie Zhang<sup>3</sup>, Phillip Hess<sup>3</sup>, Yuming Wang<sup>2</sup>, Xueshang Feng<sup>1</sup>, Hongze Cheng<sup>2</sup> and Yi Yang

JGR, **2015**

<http://arxiv.org/ftp/arxiv/papers/1501/1501.01704.pdf>

The dynamic process of coronal mass ejections (CMEs) in the heliosphere provides us the key information for evaluating CMEs' geo-effectiveness and improving the accurate prediction of CME-induced Shock Arrival Time (SAT) at the Earth. We present a data-constrained three-dimensional (3D) magnetohydrodynamic (MHD) simulation of the evolution of the CME in a realistic ambient solar wind for the **July 12-16, 2012** event by using the 3D COIN-TVD MHD code. A detailed comparison of the kinematic evolution of the CME between the observations and the simulation is carried out, including the usage of the time-elongation maps from the perspectives of both Stereo A and Stereo B. In this case study, we find that our 3D COIN-TVD MHD model, with the magnetized plasma blob as the driver, is able to

re-produce relatively well the real 3D nature of the CME in morphology and their evolution from the Sun to Earth. The simulation also provides a relatively satisfactory comparison with the in-situ plasma data from the Wind spacecraft.

### **Full Halo Coronal Mass Ejections: Arrival at the Earth**

Chenglong **Shen**, Yuming Wang, Zonghao Pan, Bin Miao, Pinzhong Ye, S. Wang

JGR, Volume 119, Issue 7, pages 5107–5116, 2014

<http://arxiv.org/pdf/1406.4589v1.pdf>

A geomagnetic storm is mainly caused by a front-side coronal mass ejection (CME) hitting the Earth and then interacting with the magnetosphere. However, not all front-side CMEs can hit the Earth. Thus, which CMEs hit the Earth and when they do so are important issues in the study and forecasting of space weather. In our previous work (Shen et al., 2013), the de-projected parameters of the full-halo coronal mass ejections (FHCMEs) that occurred from 2007 March 1 to 2012 May 31 were estimated, and there are 39 front-side events could be fitted by the Graduated Cylindrical Shell (GCS) model. In this work, we continue to study whether and when these front-side FHCMEs (FFHCMEs) hit the Earth. It is found that 59% of these FFHCMEs hit the Earth, and for central events, whose deviation angles  $\epsilon$ , which are the angles between the propagation direction and the Sun-Earth line, are smaller than 45 degrees, the fraction increases to 75%. After checking the deprojected angular widths of the CMEs, we found that all of the Earth-encountered CMEs satisfy a simple criterion that the angular width ( $\omega$ ) is larger than twice the deviation angle ( $\epsilon$ ). This result suggests that some simple criteria can be used to forecast whether a CME could hit the Earth.

Furthermore, for Earth-encountered CMEs, the transit time is found to be roughly anti-correlated with the de-projected velocity, but some events significantly deviate from the linearity. For CMEs with similar velocities, the differences of their transit times can be up to several days. Such deviation is further demonstrated to be mainly caused by the CME geometry and propagation direction, which are essential in the forecasting of CME arrival. **2010 April 7-9**

**Table 1: The GCS model's parameters and the times of the associated ICMEs of the FFHCMEs occurred from 2007 to 2012 May 31**

### **Full halo coronal mass ejections: Do we need to correct the projection effect in terms of velocity?†**

Chenglong **Shen**\*, Yuming Wang, Zonghao Pan, Min Zhang, Pinzhong Ye, S. Wang

Journal of Geophysical Research: v. 118, Issue 11, pages 6858–6865, 2013, File

The projection effect is one of the biggest obstacles in learning the real properties of coronal mass ejections (CMEs) and forecasting their geoeffectiveness. To evaluate the projection effect, 86 full halo CMEs (FHCMEs) listed in the CDAW CME catalog from 2007 March 1 to 2012 May 31 are investigated. By applying the Graduated Cylindrical Shell (GCS) model, we obtain the de-projected values of the propagation velocity, direction and angular width of these FHCMEs, and compare them with the projected values measured in the plane-of-sky. Although these CMEs look full halo in the view angle of SOHO, it is found that their propagation directions and angular widths could vary in a large range, implying projection effect is a major reason causing a CME being halo, but not the only one. Furthermore, the comparison of the de-projected and projected velocities reveals that most FHCMEs originating within 45° of the Sun-Earth line with a projected speed slower than 900 km s<sup>-1</sup> suffer from large projection effect, while the FHCMEs originating far from the vicinity of solar disk center or moving faster than 900 km s<sup>-1</sup> have small projection effect. Thus, for the latter class of FHCMEs, it is not necessary to correct the measured velocities. 2011-02-15, 2007-07-30, 2010-08-31

### **NON-EQUILIBRIUM IONIZATION MODELING OF THE CURRENT SHEET IN A SIMULATED SOLAR ERUPTION**

Chengcai **Shen**<sup>1,2,3</sup>, Katharine K. Reeves<sup>1</sup>, John C. Raymond<sup>1</sup>, Nicholas A. Murphy<sup>1</sup>, Yuan-Kuen Ko<sup>4</sup>, Jun Lin<sup>2</sup>, Zoran Mikić<sup>5</sup>, and Jon A. Linker

2013 ApJ 773 110

The current sheet that extends from the top of flare loops and connects to an associated flux rope is a common structure in models of coronal mass ejections (CMEs). To understand the observational properties of CME current sheets, we generated predictions from a flare/CME model to be compared with observations. We use a simulation of a large-scale CME current sheet previously reported by Reeves et al. This simulation includes ohmic and coronal heating, thermal conduction, and radiative cooling in the energy equation. Using the results of this simulation, we perform time-dependent ionization calculations of the flow in a CME current sheet and construct two-dimensional spatial distributions of ionic charge states for multiple chemical elements. We use the filter responses from the Atmospheric Imaging Assembly (AIA) on the Solar Dynamics Observatory and the predicted intensities of emission lines to compute the count rates for each of the AIA bands. The results show differences in the emission line intensities between equilibrium and non-equilibrium ionization. The current sheet plasma is underionized at low heights and overionized at large heights. At low heights in the current sheet, the intensities of the AIA 94 Å and 131 Å channels are lower for non-equilibrium ionization than for equilibrium ionization. At large heights, these intensities are higher for non-equilibrium ionization than for equilibrium ionization inside the current sheet. The assumption of ionization equilibrium would lead to a significant underestimate of the temperature low in the current sheet and overestimate at larger heights. We also

calculate the intensities of ultraviolet lines and predict emission features to be compared with events from the Ultraviolet Coronagraph Spectrometer on the Solar and Heliospheric Observatory, including a low-intensity region around the current sheet corresponding to this model.

### **Could the collision of CMEs in the heliosphere be super-elastic? Validation through three-dimensional simulations**

Fang **Shen**, Chenglong Shen, Yuming Wang, Xueshang Feng and Changqing Xiang  
Geophysical Research Letters, Volume 40, Issue 8, 28 April 2013, Pages: 1457–1461, **File**  
<http://arxiv.org/pdf/1303.4059v2.pdf>

Though coronal mass ejections (CMEs) are magnetized fully ionized gases, a recent observational study of a CME collision event in **2008 November** has suggested that their behavior in the heliosphere is like elastic balls, and their collision is probably superelastic [C. Shen et al., 2012]. If this is true, this finding has an obvious impact on the space weather forecasting because the direction and velocity of CMEs may change. To verify it, we numerically study the event through three-dimensional MHD simulations. The nature of CMEs' collision is examined by comparing two cases. In one case, the two CMEs collide as observed, but in the other, they do not. Results show that the collision leads to extra kinetic energy gain by 3–4% of the initial kinetic energy of the two CMEs. It firmly proves that the collision of CMEs could be superelastic.

### **Kinematics and Fine Structure of an Unwinding Polar Jet Observed by the SDO/AIA**

**Shen**, Yuandeng; Liu, Yu; Su, Jiangtao; Ibrahim, Ahmed  
E-print, July 2013; ApJL, 2011 ApJ 735 L43

We present an observational study of the kinematics and fine structure of an unwinding polar jet, with high temporal and spatial observations taken by the Atmospheric Imaging Assembly on board the Solar Dynamic Observatory and the Solar Magnetic Activity Research Telescope. During the rising period, the shape of the jet resembled a cylinder with helical structures on the surface, while the mass of the jet was mainly distributed on the cylinder's shell. In the radial direction, the jet expanded successively at its western side and underwent three distinct phases: the gradually expanding phase, the fast expanding phase, and the steady phase. Each phase lasted for about 12 minutes. The angular speed of the unwinding motion of the jet and the twist transferred into the outer corona during the eruption are estimated to be  $11.1 \pm 10^{-3}$  rad s<sup>-1</sup> (period = 564 s) and 1.17–2.55 turns (or  $2.34\text{--}5.1\pi$ ), respectively. On the other hand, by calculating the azimuthal component of the magnetic field in the jet and comparing the free energy stored in the non-potential magnetic field with the jet's total energy, we find that the non-potential magnetic field in the jet is enough to supply the energy for the ejection. These new observational results strongly support the scenario that the jets are driven by the magnetic twist, which is stored in the twisted closed field of a small bipole, and released through magnetic reconnection between the bipole and its ambient open field. **2010 August 21**

### **A time series of filament eruptions observed by three eyes from space: from failed to successful eruptions**

Yuandeng **Shen**, Yu Liu, and Rui Liu

E-print, July 2013; Research in Astronomy and Astrophysics Volume 11 Number 5, 2011

We present stereoscopic observations of six sequential eruptions of a filament in the active region NOAA 11045 on **2010 Feb 8**, with the advantage of the STEREO twin viewpoints in combination with Earth's viewpoint from SOHO instruments and ground-based telescopes. The last one of the six eruptions is a coronal mass ejection, but the others are not. The flare in this successful one is more intense than in the others. Moreover, the velocity of filament material in the successful one is also the largest among them. Interestingly, all the filament velocities are found to be proportional to the power of their flares. We calculate magnetic field intensity at low altitude, the decay indexes of the external field above the filament, and the asymmetry properties of the overlying fields before and after the failed eruptions and find little difference between them, indicating the same coronal confinement exists for both the failed and successful eruptions. The results suggest that, besides the confinement of the coronal magnetic field, the energy released in the low corona should be another crucial element affecting a failed or successful filament eruption. That is, a coronal mass ejection can only be launched if the energy released exceeds some critical value, given the same initial coronal conditions.

### **COMPOUND TWIN CORONAL MASS EJECTIONS IN THE 2012 MAY 17 GLE EVENT**

C. **Shen**<sup>1,2</sup>, G. Li<sup>3</sup>, X. Kong<sup>3,4</sup>, J. Hu<sup>3</sup>, X. D. Sun<sup>2</sup>, L. Ding<sup>5</sup>, Y. Chen<sup>4</sup>, Yuming Wang<sup>1</sup>, and L. Xia  
**2013 ApJ 763 114, File**

We report a multiple spacecraft observation of the **2012 May 17** GLE event. Using the coronagraph observations by SOHO/LASCO, STEREO-A/COR1, and STEREO-B/COR1, we identify two eruptions resulting in two coronal mass ejections (CMEs) that occurred in the same active region and close in time (~2 minutes) in the 2012 May 17 GLE event. Both CMEs were fast. Complicated radio emissions, with multiple type II episodes, were observed from ground-based stations: Learmonth and BIRS, as well as the WAVES instrument on board the Wind spacecraft. High time-resolution SDO/AIA imaging data and SDO/HMI vector magnetic field data were also examined. A complicated pre-eruption

magnetic field configuration, consisting of twisted flux-tube structure, is reconstructed. Solar energetic particles (SEPs) up to several hundred MeV nucleon<sup>-1</sup> were detected in this event. Although the eruption source region was near the west limb, the event led to ground-level enhancement. The existence of two fast CMEs and the observation of high-energy particles with ground-level enhancement agrees well with a recently proposed "twin CME" scenario.

### **Sympathetic Partial and Full Filament Eruptions Observed in One Solar Breakout Event**

Yuandeng Shen, Yu Liu, Jiangtao Su

ApJ, 2012, 750, 12

We report two sympathetic solar eruptions including a partial and a full flux rope eruption in a quadrupolar magnetic region where a large and a small filament resided above the middle and the east neutral lines, respectively. The large filament first rose slowly at a speed of 8 km/s for 23 minutes; it then accelerated to 102 km/s. Finally, this filament erupted successfully and caused a coronal mass ejection. During the slow rising phase, various evidence for breakout-like external reconnection has been identified at high and low temperature lines. The eruption of the small filament started around the end of the large filament's slow rising. This filament erupted partially, and no associated coronal mass ejection could be detected. Based on a potential field extrapolation, we find that the topology of the three-dimensional coronal field above the source region is composed of three low-lying lobes and a large overlying flux system, and a null point located between the middle lobe and the overlying antiparallel flux system. We propose a possible mechanism within the framework of the magnetic breakout model to interpret the sympathetic filament eruptions, in which the magnetic implosion mechanism is thought to be a possible link between the sympathetic eruptions, and the external reconnection at the null point transfers field lines from the middle lobe to the lateral lobes and thereby leads to the full (partial) eruption of the observed large (small) filament. Other possible mechanisms are also discussed briefly. We conclude that the structural properties of coronal fields are important for producing sympathetic eruptions. 2011 May 12

### **ON A CORONAL BLOWOUT JET: THE FIRST OBSERVATION OF A SIMULTANEOUSLY PRODUCED BUBBLE-LIKE CME AND A JET-LIKE CME IN A SOLAR EVENT**

Yuandeng Shen<sup>1,2,3</sup>, Yu Liu<sup>1,3</sup>, Jiangtao Su<sup>3,4</sup> and Yuanyong Deng<sup>3</sup>

2012 ApJ 745, 164

The coronal blowout jet is a peculiar category among various jet phenomena, in which the sheared base arch, often carrying a small filament, experiences a miniature version of blowout eruption that produces large-scale coronal mass ejection (CME). In this paper, we report such a coronal blowout jet with high-resolution multi-wavelength and multi-angle observations taken from Solar Dynamics Observatory, Solar Terrestrial Relations Observatory, and Big Bear Solar Observatory. For the first time, we find that simultaneous bubble-like and jet-like CMEs were dynamically related to the blowout jet that showed cool and hot components next to each other. Our observational results indicate that (1) the cool component resulted from the eruption of the filament contained within the jet's base arch, and it further caused the bubble-like CME; (2) the jet-like CME was associated with the hot component, which was the outward moving heated plasma generated by the reconnection of the base arch and its ambient open field lines. On the other hand, bifurcation of the jet's cool component was also observed, which resulted from the uncoupling of the erupting filament's two legs that were highly twisted at the very beginning. Based on these results, we propose a model to interpret the coronal blowout jet, in which the external reconnection not only produces the jet-like CME, but also leads to the rising of the filament. Subsequently, internal reconnection starts underneath the rising filament and thereby causes the bubble-like CME.

### **Three-dimensional MHD simulation of the evolution of the April 2000 CME event and its induced shocks using a magnetized plasma blob model**

Shen, F.; Feng, X. S.; Wu, S. T.; Xiang, C. Q.; Song, W. B.

J. Geophys. Res., Vol. 116, No. A4, A04102, 2011

A three-dimensional (3-D) time-dependent, numerical magnetohydrodynamic (MHD) model with asynchronous and parallel time-marching method is used to investigate the propagation of coronal mass ejections (CMEs) in the nonhomogenous background solar wind flow. The background solar wind is constructed based on the self-consistent source surface with observed line-of-sight of magnetic field and density from the source surface of 2.5 Rs to the Earth's orbit (215 Rs) and beyond. The CMEs are simulated by means of a very simple flux rope model: a high-density, high-velocity, and high-temperature magnetized plasma blob is superimposed on a steady state background solar wind with an initial launch direction. The dynamical interaction of a CME with the background solar wind flow between 2.5 and 220 Rs is investigated. The evolution of the physical parameters at the cobpoint, which is located at the shock front region magnetically connected to ACE spacecraft, is also investigated. We have chosen the well-defined halo-CME event of 4–6 April 2000 as a test case. In this validation study we find that this 3-D MHD model, with the asynchronous and parallel time-marching method, the self-consistent source surface as initial boundary conditions, and the simple flux rope as CME model, provide a relatively satisfactory comparison with the ACE spacecraft observations at the L1 point.

## **Kinematic Evolution of a Slow CME in Corona Viewed by STEREO-B on 8 October 2007**<<<

Chenglong [Shen](#), Yuming Wang, Bin Gui, Pinzhong Ye & S. Wang  
Solar Phys (2011) 269: 389–400; **File**

We studied the kinematic evolution of the **8 October 2007** CME in the corona based on observations from Sun – Earth Connection Coronal and Heliospheric Investigation (SECCHI) onboard satellite B of Solar TERrestrial RELations Observatory (STEREO). The observational results show that this CME obviously deflected to a lower latitude region of about  $30^\circ$  at the beginning. After this, the CME propagated radially. We also analyze the influence of the background magnetic field on the deflection of this CME. We find that the deflection of this CME at an early stage may be caused by a nonuniform distribution of the background magnetic-field energy density and that the CME tended to propagate to the region with lower magnetic-energy density. In addition, we found that the velocity profile of this gradual CME shows multiphased evolution during its propagation in the COR1-B FOV. The CME velocity first remained constant:  $23.1 \text{ km s}^{-1}$ . Then it accelerated continuously with a positive acceleration of  $\approx 7.6 \text{ m s}^{-2}$ .

## **Evolution of the Thermodynamic Properties of a Coronal Mass Ejection in the Inner Corona**

[Jyoti Sheoran](#), [Vaibhav Pant](#), [Ritesh Patel](#), [Dipankar Banerjee](#)

Frontiers in Astronomy and Space Sciences, 10: 1092881 2023

<https://arxiv.org/pdf/2301.13184.pdf>

doi: 10.3389/fspas.2023.1092881

<https://www.frontiersin.org/articles/10.3389/fspas.2023.1092881/pdf>

The thermodynamic evolution of Coronal Mass Ejections (CMEs) in the inner corona ( $< 1.5 R_{\text{sun}}$ ) is not yet completely understood. In this work, we study the evolution of thermodynamic properties of a CME core observed in the inner corona on **July 20, 2017**, by combining the MLSO/K-Cor white-light and the MLSO/CoMP Fe XIII 10747 Å line spectroscopic data. We also estimate the emission measure weighted temperature (TEM) of the CME core by applying the Differential Emission Measure (DEM) inversion technique on the SDO/AIA six EUV channels data and compare it with the effective temperature ( $T_{\text{eff}}$ ) obtained using Fe XIII line width measurements. We find that the  $T_{\text{eff}}$  and TEM of the CME core show similar variation and remain almost constant as the CME propagates from  $\sim 1.05$  to  $1.35 R_{\text{sun}}$ . The temperature of the CME core is of the order of million-degree kelvin, indicating that it is not associated with a prominence. Further, we estimate the electron density of this CME core using K-Cor polarized brightness (pB) data and found it decreasing by a factor of  $\sim 3.6$  as the core evolves. An interesting finding is that the temperature of the CME core remains almost constant despite expected adiabatic cooling due to the expansion of the CME core, which suggests that the CME core plasma must be heated as it propagates. We conclude that the expansion of this CME core behaves more like an isothermal than an adiabatic process.

## **Influence of misalignments on the performance of externally occulted solar coronagraphs.**

### **Application to PROBA-3/ASPIICS**

S. V. [Shestov](#), A. N. Zhukov

A&A

2018

<https://www.aanda.org/articles/aa/pdf/forth/aa32386-17.pdf>

**Context:** The ASPIICS instrument is a novel externally occulted coronagraph that will be launched on board the PROBA-3 mission of the European Space Agency. The external occulter will be placed on one satellite  $\sim 150 \text{ m}$  ahead of the second satellite that will carry an optical instrument. During 6 hours out of 19.38 hours of orbit, the satellites will fly in a precise (accuracy around a few millimeters) formation, constituting a giant externally occulted coronagraph. The large distance between the external occulter and the primary objective will allow observations of the white-light solar corona starting from extremely low heights  $\sim 1.1R$ .

**Aims:** We intend to analyze influence of shifts of the satellites and misalignments of optical elements on the ASPIICS performance in terms of diffracted light. Based on the quantitative influence of misalignments on diffracted light, we provide a recipe for choosing the size of the internal occulter (IO) to achieve a trade-off between the minimal height of observations and sustainability to possible misalignments. **Methods:** We considered different types of misalignments and analyzed their influence from optical and computational points of view. We implemented a numerical model of the diffracted light and its propagation through the optical system and computed intensities of diffracted light throughout the instrument. Our numerical approach is based on the axisymmetrical Fourier-based model of the coronagraph, published recently. Here we extend the model to include nonsymmetrical cases and possible misalignments.

**Results:** The numerical computations fully confirm the main properties of the diffracted light that we obtained from semi-analytical consideration. We obtain that relative influences of various misalignments are significantly different. We show that the internal occulter with  $R_{\text{IO}} = 1.694 \text{ mm} = 1.1R$  is large enough to compensate possible misalignments expected to occur in PROBA-3/ASPIICS. Besides that we show that apodizing the edge of the internal occulter leads to additional suppression of the diffracted light. **Conclusions:** We conclude that the most important misalignment is the tilt of the telescope with respect to the line connecting the center of the external occulter and the entrance aperture. Special care should be taken to co-align the external occulter and the coronagraph, which means co-aligning the diffraction fringe from the external occulter and the internal occulter. We suggest that the best orientation strategy is to point the coronagraph to the center of the external occulter.

## **Energy estimation of small-scale jets from the quiet-Sun region**★



Fanpeng **Shi** (史帆鹏)<sup>1,2</sup>, Dong Li (李东)<sup>1,2</sup>, Zongjun Ning (宁宗军)<sup>1,2</sup>, Jun Xu (徐俊)<sup>1,2</sup>, Yuxiang Song (宋宇祥)<sup>1,2</sup> and Yuzhi Yang (杨宇知)<sup>1,2</sup>

A&A, 686, A279 (2024)

<https://www.aanda.org/articles/aa/pdf/2024/06/aa49377-24.pdf>

Context. Solar jets play a role in coronal heating and the supply of solar wind.

Aims. In this study, we calculate the energies of 23 small-scale jets emerging from a quiet-Sun region in order to investigate their contributions to coronal heating.

Methods. We used data from the High-Resolution Imager (HRI) of the Extreme Ultraviolet Imager (EUI) on board the Solar Orbiter. Small-scale jets were observed by the HRI/EUV 174 Å passband in the high cadence of 6 s. These events were identified by the time–distance stacks along the trajectories of jets. Using the simultaneous observation from the Atmospheric Imaging Assembly (AIA) on board the Solar Dynamics Observatory (SDO), we also performed a differential emission measure (DEM) analysis on these small-scale jets to obtain the physical parameters of plasma, which enabled us to estimate the kinetic and thermal energies of the jets.

Results. We find that most of the jets exhibit common unidirectional or bidirectional motions, while some show more complex behaviors; namely, a mixture of unidirection and bidirection. A majority of jets also present repeated eruption blobs (plasmoids), which may be signatures of the quasi-periodic magnetic reconnection that has been observed in solar flares. The inverted Y-shaped structure can be recognized in several jets. These small-scale jets typically have a width of  $\sim 0.3$  Mm, a temperature of  $\sim 1.7$  MK, an electron number density of  $\geq 10^9$  cm<sup>-3</sup>, with speeds in a wide range from  $\sim 20$ – $170$  km s<sup>-1</sup>. Most of these jets have an energy of  $10^{23}$ – $10^{24}$  erg, which is marginally smaller than the energy of typical nanoflares. The thermal energy fluxes of 23 jets are estimated to be  $(0.74$ – $2.96) \times 10^5$  erg cm<sup>-2</sup> s<sup>-1</sup>, which is almost on the same order of magnitude as the energy flow required to heat the quiet-Sun corona, although the kinetic energy fluxes vary over a wide range because of their strong dependence on velocity. Furthermore, the frequency distribution of thermal energy and kinetic energy both follow the power-law distribution  $N(E) \propto E^{-\alpha}$ .

Conclusions. Our observations suggest that although these jets cannot provide sufficient energy to heat the whole quiet-Sun coronal region, they are likely to account for a significant portion of the energy demand in the local regions where the jets occur. **March 30 2023**

## Time-Dependent Two-Fluid Magnetohydrodynamic Model and Simulation of the Chromosphere

Qusai Al **Shidi**, [Ofer Cohen](#), [Paul Song](#), [Jiannan Tu](#)

Solar Phys. **2019**

<https://arxiv.org/pdf/1904.01572.pdf>

The sun's chromosphere is a highly dynamic, partially-ionized region where spicules (hot jets of plasma) form. Here we present a two-fluid MHD model to study the chromosphere, which includes ion-neutral interaction and frictional heating. Our simulation recovers a magnetic canopy shape that forms quickly, but is also quickly disrupted by the formation of a jet. Our simulation produces a shock self-consistently, where the jet is driven by the frictional heating, which is much greater than the ohmic heating. Thus, our simulation demonstrates that the jet could be driven purely by thermal effects due to ion-neutral collisions and not by magnetic reconnection. We plan to improve the model to include photo-chemical effects, neutral radiation and new observations from the Parker Solar Probe mission in the model.

## Self-similar expansion model of cylindrical flux ropes combined with Alfvén wave current system

Hironori **Shimazu**

Solar Phys. 294:104 **2019**

<https://arxiv.org/pdf/1902.04791.pdf>

[sci-hub.se/10.1007/s11207-019-1497-4](https://doi.org/10.1007/s11207-019-1497-4)

Magnetic flux ropes in space are generally connected to some regions electromagnetically. We consider the whole closed current system of the expanding flux ropes including the electric current associated with them. By combining the theories regarding the self-similar expansion of cylindrical flux ropes and the Alfvén wave current system, we examine conditions under which the electric current matches. These matching conditions are satisfied when the time dependence of the current flowing in the closed circuit agrees with that which maintains the expanding flux rope. In consequence, we encountered three possible forms of expansion. The two-step eruption of solar filaments may be interpreted as a transition from one form of expansion to another. If this process works, increasing the diffusion outside of the flux rope is necessary to trigger the transition.

## First ALMA Observation of a Plasmoid Ejection from an X-ray Bright Point

M. **Shimojo**, H. S. Hudson, S. M. White, T. S. Bastian, K. Iwai

ApJL **2017**

<https://arxiv.org/pdf/1704.04881.pdf>

Eruptive phenomena such as plasmoid ejections or jets are an important feature of solar activity with the potential for improving our understanding of the dynamics of the solar atmosphere. Such ejections are often thought to be signatures of the outflows expected in regions of fast magnetic reconnection. The 304 Å EUV line of Helium, formed at around  $10^5$  K, is found to be a reliable tracer of such phenomena, but the determination of physical parameters from such observations is not straightforward. We have observed a plasmoid ejection from an X-ray bright point simultaneously at

millimeter wavelengths with ALMA, at EUV wavelengths with AIA, in soft X-rays with Hinode/XRT. This paper reports the physical parameters of the plasmoid obtained by combining the radio, EUV and X-ray data. As a result, we conclude that the plasmoid can consist either of (approximately) isothermal  $10^5$  K plasma that is optically thin at 100 GHz, or else a  $10^4$  K core with a hot envelope. The analysis demonstrates the value of the additional temperature and density constraints that ALMA provides, and future science observations with ALMA will be able to match the spatial resolution of space-borne and other high-resolution telescopes. **2015-12-17**

### **Magnetohydrodynamic Modeling for a Formation Process of Coronal Mass Ejections: Interaction Between an Ejecting Flux Rope and an Ambient Field**

Daikou [Shiota](#), Kanya Kusano, Takahiro Miyoshi, and Kazunari Shibata

**2010** ApJ 718 1305-1314

We performed a magnetohydrodynamic simulation of a formation process of coronal mass ejections (CMEs), focusing on the interaction (reconnection) between an ejecting flux rope and its ambient field. We examined three cases with different ambient fields: one had no ambient field, while the other two had dipole fields with opposite directions, parallel and anti-parallel to that of the flux rope surface. We found that while the flux rope disappears in the anti-parallel case, in the other cases the flux ropes can evolve to CMEs and show different amounts of flux rope rotation. The results imply that the interaction between an ejecting flux rope and its ambient field is an important process for determining CME formation and CME orientation, and also show that the amount and direction of the magnetic flux within the flux rope and the ambient field are key parameters for CME formation. The interaction (reconnection) plays a significant role in the rotation of the flux rope especially with a process similar to "tilting instability" in a spheromak-type experiment of laboratory plasma.

### **MAGNETOHYDRODYNAMIC MODELING FOR A FORMATION PROCESS OF CORONAL MASS EJECTIONS: INTERACTION BETWEEN AN EJECTING FLUX ROPE AND AN AMBIENT FIELD**

Daikou [Shiota](#)<sup>1</sup>, Kanya Kusano<sup>2,3</sup>, Takahiro Miyoshi<sup>4</sup>, and Kazunari Shibata<sup>5</sup>

Astrophysical Journal, 718:1305–1314, **2010**, File

We performed a magnetohydrodynamic simulation of a formation process of coronal mass ejections (CMEs), focusing on the interaction (reconnection) between an ejecting flux rope and its ambient field. We examined three cases with different ambient fields: one had no ambient field, while the other two had dipole fields with opposite directions, parallel and anti-parallel to that of the flux rope surface. We found that while the flux rope disappears in the anti-parallel case, in the other cases the flux ropes can evolve to CMEs and show different amounts of flux rope rotation. The results imply that the interaction between an ejecting flux rope and its ambient field is an important process for determining CME formation and CME orientation, and also show that the amount and direction of the magnetic flux within the flux rope and the ambient field are key parameters for CME formation. The interaction (reconnection) plays a significant role in the rotation of the flux rope especially with a process similar to "tilting instability" in a spheromak-type experiment of laboratory plasma.

### **A quantitative MHD study of the relation among arcade shearing, flux rope formation, and eruption due to the tearing instability,**

[Shiota](#), D., K. Kusano, T. Miyoshi, N. Nishikawa, and K. Shibata

J. Geophys. Res., 113, A03S05, (**2008**),

The quantitative relationship between the magnetohydrodynamic (MHD) activity of solar coronal arcade and the magnetic helicity injection, which is caused by shearing motion, has been investigated, using azimuthally symmetric model of MHD simulation. We have calculated several cases in which the width of the shearing region is varied and examined the relationship between the magnetic arcade dynamics and magnetic helicity evolution. As a result, it is found that as the shearing motion is imposed on narrower regions along each side of the magnetic inversion line, the magnetic arcade can be easily destabilized by the resistive tearing mode. However, in this case, even though reconnection driven by the tearing mode produces plasmoids, the plasmoid elevation is almost in proportion to the total amount of magnetic helicity contained in the arcade, and it is too slow to explain the trigger process of coronal mass ejections (CMEs). On the other hand, in the case where the shearing motion is imposed on the entire region, much larger magnetic helicity injection is required to injected arcade in order to destabilize the system, compared to practical helicity injection measured in the solar corona. The results suggest that it may be difficult to trigger a CME just by the axisymmetric shearing motion and that some other mechanisms should be involved in the triggering process of a CME. The results also imply that the relation between the magnetic helicity and the overlying magnetic flux can be a key parameter for the CME occurrence.

### **Longitudinal Distribution of Solar Flares and Their Association with Coronal Mass Ejections and Forbush Decreases<<<<**

Pankaj K. [Shrivastava](#), Mukesh K. Jothe & Mahendra Singh

Solar Physics, Volume 269, Number 2, 401-410, 2011, File

Major H $\alpha$  solar-flare events of high optical importance have been employed to study their heliographic distribution in longitude around the Sun for the period of 2001 to 2006. A statistical analysis was performed to obtain their relationship with halo/partial-halo CMEs and Forbush decreases (Fds) of cosmic-ray intensity. Our analysis indicates that 63% of the solar flares associated with halo CMEs and Fds occur in the western hemisphere and of 37% of such flares occur in the eastern hemisphere. Similarly, we found that nearly 60% of the solar flares associated with partial-halo CMEs and Fds occur in the western hemisphere and the rest (40%) occur in the eastern hemisphere. Finally, we conclude that the flares in association with CMEs and located in the western hemisphere of the solar disk are more effective in producing Fds. The magnitudes of Fds are observed to be higher when in association of halo CMEs. A slight excess in the eastern hemisphere is found for both the halo and partial-halo CMEs.

## Analysis of large deflections of prominence-CME events during the rising phase of solar cycle 24

[M.V. Sieyra](#), [M. Cécere](#), [H. Cremades](#), [F.A. Iglesias](#), [A. Sahade](#), [M. Mierla](#), [G. Stenborg](#), [A. Costa](#), [M. West](#), [E. D'Huys](#)

2020 *Solar Physics* volume 295, Article number: 126

<https://arxiv.org/pdf/2007.14317.pdf>

<https://link.springer.com/content/pdf/10.1007/s11207-020-01694-0.pdf>

The analysis of the deflection of coronal mass ejection (CME) events plays an important role in the improvement of the forecasting of their geo-effectiveness. Motivated by the scarcity of comprehensive studies of CME events with focus on the governing conditions that drive deflections during their early stages, we performed an extensive analysis of 13 CME events that exhibited large deflections during their early development in the low corona. The study was carried out by exploiting solar corona imaging observations at different heights and wavelengths from instruments onboard several space and ground solar observatories, namely the Project for Onboard Autonomy 2 (PROBA2), Solar Dynamics Observatory (SDO), Solar TERrestrial RELations Observatory (STEREO), Solar and Heliospheric Observatory (SOHO) spacecraft, and from National Solar Observatory (NSO). The selected events were observed between October 2010 and September 2011, to take advantage of the location in near quadrature of the STEREO spacecraft and Earth in this time period. In particular, we determined the 3D trajectory of the front envelope of the CMEs and their associated prominences with respect to their solar sources by means of a forward modeling and tie-pointing tool, respectively. By using a potential field source surface model, we estimated the coronal magnetic fields of the ambient medium through which the events propagate to investigate the role of the magnetic energy distribution in the non-radial propagation of both structures (front envelope and prominence) and in their kinematic properties. The ambient magnetic environment during the eruption and early stages of the events is found to be crucial in determining the trajectory of the CME events, in agreement with previous reports. **2011-01-30, 2011-03-27, 29 March 2011, 2011-05-13, 2011-08-11**

**Table 1:** The 13 selected events that satisfy  $|\Delta CPA| < 20^\circ$  and  $\Delta \Psi < 20^\circ$  between October 2010 and September 2011.

## The search for a causal link between CMEs and large flares

G. M. [Simnett](#)

ILWS WORKSHOP 2006, GOA, FEBRUARY 19-24, 2006

We discuss here a model whereby non-thermal energetic particles provide both the link between CMEs and flares, and a significant part of the flare energy.

## Modeling a Coronal Mass Ejection as a Magnetized Structure with EUHFORIA

G. [Sindhuja](#)<sup>1</sup>, Jagdev Singh<sup>1</sup>, E. Asvestari<sup>2</sup>, and B. Raghavendra Prasad<sup>1</sup>

2022 ApJ 925 25

<https://iopscience.iop.org/article/10.3847/1538-4357/ac3bd2/pdf>

We studied an Earth-directed coronal mass ejection (CME) that erupted on **2015 March 15**. Our aim was to model the CME flux rope as a magnetized structure using the European Heliospheric Forecasting Information Asset (EUHFORIA). The flux rope from eruption data (FRED) output was applied to the EUHFORIA spheromak CME model. In addition to the geometrical properties of the CME flux rope, we needed to input the parameters that determine the CME internal magnetic field like the helicity, tilt angle, and toroidal flux of the CME flux rope. According to the FRED technique geometrical properties of the CME flux rope are obtained by applying a graduated cylindrical shell fitting of the CME flux rope on the coronagraph images. The poloidal field magnetic properties can be estimated from the reconnection flux in the source region utilizing the post-eruption arcade method, which uses the Heliospheric Magnetic Imager magnetogram together with the Atmospheric Imaging Assembly (AIA) 193 Å images. We set up two EUHFORIA runs with RUN-1 using the toroidal flux obtained from the FRED technique and RUN-2 using the toroidal flux that was measured from the core dimming regions identified from the AIA 211 Å images. We found that the EUHFORIA simulation outputs from RUN-1 and RUN-2 are comparable to each other. Overall using the EUHFORIA spheromak model, we successfully obtained the magnetic field rotation of the flux rope, while the arrival time near Earth and the strength of the interplanetary CME magnetic field at Earth are not as accurately modeled.

## A Study of the Observational Properties of Coronal Mass Ejection Flux Ropes near the Sun\*

G. [Sindhuja](#)<sup>1</sup> and N. Gopalswamy<sup>2</sup>

2020 ApJ 889 104

<https://doi.org/10.3847/1538-4357/ab620f>

We present the observational properties of coronal mass ejection (CME) flux ropes (FRs) near the Sun based on a set of 35 events from solar cycle 24 (2010–2017). We derived the CME FR properties using the Flux Rope from Eruption Data technique. According to this technique, the geometrical properties are obtained from a flux-rope fit to CMEs and the magnetic properties from the reconnected flux in the source region. In addition, we use the magnetic flux in the dimming region at the eruption site. Geometric properties like radius of the FR and the aspect ratio are derived from the FR fitting. The reconnected flux exhibits a positive correlation with flare fluence in soft X-rays (SXR), peak flare intensity in SXRs, CME speed, and kinetic energy, with correlation coefficients (cc) 0.78, 0.6, 0.48, and 0.55, respectively. We found a moderate positive correlation between magnetic flux in the core dimming regions and the toroidal flux obtained from the Lundquist solution for a force-free FR (cc = 0.43). Furthermore, we correlate the core dimming flux and CME mass (cc = 0.34). The area of the core dimming region shows a moderate correlation with the radius of the FR (cc = 0.4). Thus, we infer that greater magnetic content (poloidal and toroidal fluxes) indicates a more energetic eruption in terms of flare size, CME speed, kinetic energy, mass, and radius of the FR, suggesting important implications for space weather predictions.

## An observational study on CME flux ropes near the Sun

G. [Sindhuja](#)

VarSITI Newsletter Vol. 21 p. 6-7 2019

[http://newsserver.stil.bas.bg/varsiti/newsL/VarSITI\\_Newsletter\\_Vol21.pdf](http://newsserver.stil.bas.bg/varsiti/newsL/VarSITI_Newsletter_Vol21.pdf)

2011 December 26

## Calcium Bright Knots and the Formation of Chromospheric Anemone Jets on the Sun

Kunwar Alkendra Pratap [Singh](#)<sup>1,2</sup>, Keisuke Nishida<sup>2</sup>, and Kazunari Shibata<sup>2,3</sup>

2024 ApJL 962 L35

<https://iopscience.iop.org/article/10.3847/2041-8213/ad24e7/pdf>

Space-based observations show that the solar atmosphere from the solar chromosphere to the solar corona is filled with small-scale jets and is linked with small-scale explosions. These jets may be produced by mechanisms similar to those of large-scale flares and such jets may be related to the heating of the corona and chromosphere as well as the acceleration of solar wind. The chromospheric anemone jets on the Sun remain puzzling because their footpoints (or bright knots) have not been well resolved and the formation process of such enigmatic small-scale jets remains unclear. We propose a new model for chromospheric jets using the 3D magnetohydrodynamic simulations, which show that the continuous, upward rising of small-scale twisted magnetic flux ropes in a magnetized solar chromosphere drives small-scale magnetic reconnection and the launching of several small-scale jets during the evolution of the chromospheric anemone jets. Our new, self-consistent, 3D computer modeling of small-scale, but ever-changing flux rope emergence in the magnetized solar atmosphere is fully consistent with observations and provides a universal mechanism for nanoflare and jet formation.

## Ensemble simulations of the 12 July 2012 Coronal Mass Ejection with the Constant Turn Flux Rope Model

[Talwinder Singh](#), [Tae K. Kim](#), [Nikolai V. Pogorelov](#), [Charles N. Arge](#)

2022 ApJ 933 123

<https://arxiv.org/pdf/2205.13009.pdf>

<https://iopscience.iop.org/article/10.3847/1538-4357/ac73f3/pdf>

Flux-rope-based magnetohydrodynamic modeling of coronal mass ejections (CMEs) is a promising tool for the prediction of the CME arrival time and magnetic field at Earth. In this work, we introduce a constant-turn flux rope model and use it to simulate the **12-July-2012** 16:48 CME in the inner heliosphere. We constrain the initial parameters of this CME using the graduated cylindrical shell (GCS) model and the reconnected flux in post-eruption arcades. We correctly reproduce all the magnetic field components of the CME at Earth, with an arrival time error of approximately 1 hour. We further estimate the average subjective uncertainties in the GCS fittings, by comparing the GCS parameters of 56 CMEs reported in multiple studies and catalogs. We determined that the GCS estimates of the CME latitude, longitude, tilt, and speed have average uncertainties of 5.74 degrees, 11.23 degrees, 24.71 degrees, and 11.4% respectively. Using these, we have created 77 ensemble members for the 12-July-2012 CME. We found that 55% of our ensemble members correctly reproduce the sign of the magnetic field components at Earth. We also determined that the uncertainties in GCS fitting can widen the CME arrival time prediction window to about 12 hours for the 12-July-2012 CME. On investigating the forecast accuracy introduced by the uncertainties in individual GCS parameters, we conclude that the half-angle and aspect ratio have little impact on the predicted magnetic field of the 12-July-2012 CME, whereas the uncertainties in longitude and tilt can introduce a relatively large spread in the magnetic field predicted at Earth.

## Quasi-periodic spicule-like cool jets driven by Alfvén pulses

[B. Singh](#), [A.K. Srivastava](#), [K. Sharma](#), [S.K. Mishra](#), [B.N. Dwivedi](#)

MNRAS 2022

<https://arxiv.org/pdf/2202.00501.pdf>

We perform a 2.5 dimensional magnetohydrodynamic (MHD) simulation to understand a comprehensive view of the formation of spicule-like cool jets due to initial transverse velocity pulses akin to Alfvén pulses in the solar chromosphere. We invoke multiple velocity ( $V_z$ ) pulses between 1.5 and 2.0 Mm in the solar atmosphere, which create the initial transverse velocity perturbations. These pulses transfer energy non-linearly to the field aligned perturbations due to the ponderomotive force. This physical process further creates the magnetoacoustic shocks followed by quasi-periodic plasma motions in the solar atmosphere. The field aligned magnetoacoustic shocks move upward which subsequently cause quasi-periodic rise and fall of the chromospheric plasma into the overlying corona as a thin and cool spicule-like jets. The magnitude of the initial applied transverse velocity pulses are taken in the range of 50-90 km s<sup>-1</sup>. These pulses are found to be strong enough to generate the spicule-like jets. We analyze the evolution, kinematics and energetics of these spicule-like jets. We find that the transported mass flux and kinetic energy density are substantial in the localized solar-corona. These mass motions generate in situ quasi-periodic oscillations on the scale of  $\approx 4.0$  min above the transition region.

## **Application of a Modified Spheromak Model to Simulations of Coronal Mass Ejection in the Inner Heliosphere**

Talwinder [Singh](#) , [Tae K. Kim](#) , [Nikolai V. Pogorelov](#) , [Charles N. Arge](#)

Space Weather **2020** e2019SW002405

<https://doi.org/10.1029/2019SW002405>

The magnetic fields of interplanetary coronal mass ejections (ICMEs), which originate close to the Sun in the form of a flux rope, determine their geoeffectiveness. Therefore, robust flux rope-based models of CMEs are required to perform magnetohydrodynamic (MHD) simulations aimed at space weather predictions. We propose a modified spheromak model and demonstrate its applicability to CME simulations. In this model, such properties of a simulated CME as the poloidal and toroidal magnetic fluxes, and the helicity sign can be controlled with a set of input parameters. We propose a robust technique for introducing CMEs with an appropriate speed into a background, MHD solution describing the solar wind in the inner heliosphere. Through a parametric study, we find that the speed of a CME is much more dependent on its poloidal flux than on the toroidal flux. We also show that the CME speed increases with its total energy, giving us control over its initial speed. We further demonstrate the applicability of this model to simulations of CME-CME collisions. Finally, we use this model to simulate the **12 July 2012** CME and compare the plasma properties at 1 AU with observations. The predicted CME properties agree reasonably with observational data.

## **A Modified Spheromak Model Suitable for Coronal Mass Ejection Simulations**

Talwinder [Singh](#), [Mehmet S. Yalim](#), [Nikolai V. Pogorelov](#), [Nat Gopalswamy](#)

**2020** *ApJ* **894** 49

<https://arxiv.org/pdf/2002.10409.pdf> **File**

<https://doi.org/10.3847/1538-4357/ab845f>

Coronal Mass Ejections (CMEs) are one of the primary drivers of extreme space weather. They are large eruptions of mass and magnetic field from the solar corona and can travel the distance between Sun and Earth in half a day to a few days. Predictions of CMEs at 1 Astronomical Unit (AU), in terms of both its arrival time and magnetic field configuration, are very important for predicting space weather. Magnetohydrodynamic (MHD) modeling of CMEs, using flux-rope-based models is a promising tool for achieving this goal. In this study, we present one such model for CME simulations, based on spheromak magnetic field configuration. We have modified the spheromak solution to allow for independent input of poloidal and toroidal fluxes. The motivation for this is a possibility to estimate these fluxes from solar magnetograms and extreme ultraviolet (EUV) data from a number of different approaches. **We estimate the poloidal flux of CME using post eruption arcades (PEAs) and toroidal flux from the coronal dimming.** In this modified spheromak, we also have an option to control the helicity sign of flux ropes, which can be derived from the solar disk magnetograms using the magnetic tongue approach. We demonstrate the applicability of this model by simulating the **12 July 2012** CME in the solar corona.

## **On modelling the kinematics and evolutionary properties of pressure pulse driven impulsive solar jets**

Balveer [Singh](#), [Kushagra Sharma](#), [Abhishek K. Srivastava](#)

Annales Geophysicae **2019**

<https://arxiv.org/pdf/1908.11560.pdf>

In this paper, we describe the kinematical and evolutionary properties of the impulsive cool jets in the solar atmosphere using numerical simulation by Godunov-type PLUTO code at two different strength of the quiet-Sun magnetic field ( $B=56, 112$  Gauss). These types of chromospheric jets are originated by the pressure pulse, which mimics after effects of the localized heating in the lower solar atmosphere. These jets may be responsible for the transport of mass and energy in the localized upper atmosphere (i.e., corona). The detection of the height-time profiles for the jets, originated by imposing the different pressure pulses, exhibit the asymmetric near parabolic behaviour. This infers that the upward motion of the jet occurs under the influence of pressure perturbation. However, its downward motion is not only governed by the gravitational free fall, but also due to the complex plasma motions near its base under the effect of counter propagating pulses. Maximum height and life-time of the jets w.r.t. the strength of the pressure pulse show a

linear increasing trend. This suggests that if the extent of the heating and thus pressure perturbations will be longer then more longer chromospheric jets can be triggered from the same location in the chromosphere. For the certain amplitude of pressure pulse, the strong magnetic field configuration ( $B=112$  Gauss) leads more longer jet compared to the weaker field ( $B=56$  Gauss). This suggests that the strong magnetic field guides the pressure pulse driven jets more efficiency towards the higher corona. In conclusion, our model mimics the properties and evolution of variety of the cool impulsive jets in the chromosphere (e.g., macrospicules, network jets, isolated repeated cool jets, confined & small surges etc).

## **Simulating Solar Coronal Mass Ejections constrained by Observations of their Speed and Poloidal flux**

Talwinder [Singh](#), [Mehmet Sarp Yalim](#), [Nikolai Pogorelov](#), [Nat Gopalswamy](#)

2019 ApJL 875 L17

<https://arxiv.org/pdf/1904.00140.pdf>

[sci-hub.se/10.3847/2041-8213/ab14e9](https://sci-hub.se/10.3847/2041-8213/ab14e9)

We demonstrate how the parameters of a Gibson-Low flux-rope-based coronal mass ejection (CME) can be constrained using remote observations. Our Multi Scale Fluid-Kinetic Simulation Suite (MS-FLUKSS) has been used to simulate the propagation of a CME in a data driven solar corona background computed using the photospheric magnetogram data. We constrain the CME model parameters using the observations of such key CME properties as its speed, orientation, and poloidal flux. The speed and orientation are estimated using multi-viewpoint white-light coronagraph images. The reconnected magnetic flux in the area covered by the post eruption arcade is used to estimate the poloidal flux in the CME flux rope. We simulate the partial halo CME on **7 March 2011** to demonstrate the efficiency of our approach. This CME erupted with the speed of 812 km/s and its poloidal flux, as estimated from source active region data, was  $4.9e21$  Mx. Using our approach, we were able to simulate this CME with the speed 840 km/s and the poloidal flux of  $5.1e21$  Mx, in remarkable agreement with the observations.

## **A Data-constrained Model for Coronal Mass Ejections Using the Graduated Cylindrical Shell Method**

T. [Singh](#)<sup>1</sup>, M. S. Yalim<sup>2</sup>, and N. V. Pogorelov<sup>1,2</sup>

2018 ApJ 864 18

<http://sci-hub.tw/http://iopscience.iop.org/article/10.3847/1538-4357/aad3b4/meta>

Coronal mass ejections (CMEs) are major drivers of extreme space weather conditions, as this is a matter of serious concern for our modern technologically dependent society. The development of numerical approaches that would simulate CME generation and propagation through the interplanetary space is an important step toward our capability to predict CME arrival times at Earth and their geoeffectiveness. In this paper, we utilize a data-constrained Gibson-Low (GL) flux rope model to generate CMEs. We derive the geometry of the initial GL flux rope using the graduated cylindrical shell method. This method uses multiple viewpoints from STEREO A and B Cor1/Cor2, and Solar and Heliospheric Observatory (SOHO)/LASCO C2/C3 coronagraphs to determine the size and orientation of a CME flux rope as it starts to erupt from the Sun. A flux rope generated in this way is inserted into a quasi-steady global magnetohydrodynamics (MHD) background solar wind flow driven by Solar Dynamics Observatory/HelioSeismic and Magnetic Imager line-of-sight magnetogram data, and erupts immediately. Numerical results obtained with the Multi-Scale Fluid-Kinetic Simulation Suite (MS-FLUKSS) code are compared with STEREO and SOHO/LASCO coronagraph observations, in particular in terms of the CME speed, acceleration, and magnetic field structure.

## **SYSTEMATIC MOTION OF FINE-SCALE JETS AND SUCCESSIVE RECONNECTION IN SOLAR CHROMOSPHERIC ANEMONE JET OBSERVED WITH THE SOLAR OPTICAL TELESCOPE/HINODE**

K. A. P. [Singh](#)<sup>1</sup>, H. Isobe<sup>2</sup>, K. Nishida<sup>1</sup>, and K. Shibata

2012 ApJ 760 28

The Solar Optical Telescope (SOT) on board Hinode allows observations with high spatiotemporal resolution and stable image quality. A  $\lambda$ -shaped chromospheric anemone jet was observed in high resolution with SOT/Hinode. We found that several fine-scale jets were launched from one end of the footpoint to the other. These fine-scale jets ( $\sim 1.5$ - $2.5$  Mm) gradually move from one end of the footpoint to the other and finally merge into a single jet. This process occurs recurrently, and as time progresses the jet activity becomes more and more violent. The time evolution of the region below the jet in Ca II H filtergram images taken with SOT shows that various parts (or knots) appear at different positions. These bright knots gradually merge into each other during the maximum phase. The systematic motion of the fine-scale jets is observed when different knots merge into each other. Such morphology would arise due to the emergence of a three-dimensional twisted flux rope in which the axial component (or the guide field) appears in the later stages of the flux rope emergence. The partial appearance of the knots could be due to the azimuthal magnetic field that appears during the early stage of the flux rope emergence. If the guide field is strong and reconnection occurs between the emerging flux rope and an ambient magnetic field, this could explain the typical feature of systematic motion in chromospheric anemone jets.

## **Solar Filament Eruptions as Precursors to Flare-CME Events: Establishing the Temporal Connection**

Suvadip [Sinha](#)<sup>1</sup>, Nandita Srivastava<sup>1,2</sup>, and Dibyendu Nandy<sup>1,3</sup>

2019 ApJ 880 84

[sci-hub.se/10.3847/1538-4357/ab2239](https://doi.org/10.3847/1538-4357/ab2239)

Elongated structures on the Sun's surface known as filaments are known to have a connection with energetic events of space weather consequence (flares and coronal mass ejections (CMEs)). In this work, we explore the connection between the eruptive dynamics of filaments and the initiation of solar flares and CMEs. We estimate the filament eruption start time by tracking the filament throughout its eruption phase. We define the filament eruption start time as the time from which the filament area starts to decrease as observed in H $\alpha$  images. A total of 33 eruptive filament events are reported in this study, out of which 73% are CME associated and 76% are related to solar flares. We find a good correlation between area decay rate of the quiescent filaments and the speed of the associated CMEs with a correlation coefficient of 0.75. By analyzing the time delay of the extreme ultraviolet brightening of solar flares relative to the start time of associated filament eruption, we show that in 83% of cases, filament eruption precedes the flare brightening, which indicates that eruptive filaments can be considered as one of the precursors for the occurrence of a solar flare. Finally, we study the time delay of the CME onset from the time of initiation of the filament eruption process and show that for most of the cases, CMEs occur within 2 hr from the start time of the filament eruptions. This study would be useful for space weather assessment and characterization based on automated trackers of solar filament dynamics. **2012 August 31, 2013 August 20**

**Table 1** List of Eruptive Filament Events (2012-2016)

## INITIAL-CONDITION INFLUENCES ON CME EXPANSION AND PROPAGATION

G.L. [SISCOE](#), N.U. CROOKER and H.A. ELLIOTT

Solar Physics (2006) 239: 293–316

## Modelling the interaction of Alfvénic fluctuations with coronal mass ejections in the low solar corona

[Chaitanya Prasad Sishtla](#), [Jens Pomoell](#), [Rami Vainio](#), [Emilia Kilpua](#), [Simon Good](#)

Astronomy & Astrophysics 679, A54 2023

<https://arxiv.org/pdf/2309.06266.pdf>

<https://www.aanda.org/articles/aa/pdf/2023/11/aa47250-23.pdf>

Alfvénic fluctuations of various scales are ubiquitous in the corona, with their non-linear interactions and eventual turbulent cascade resulting in an important heating mechanism that accelerates the solar wind. These fluctuations may be processed by large-scale, transient and coherent heliospheric structures such as coronal mass ejections (CMEs). In this study we investigate the interactions between Alfvénic solar wind fluctuations and CMEs using MHD simulations. We study the transmission of upstream solar wind fluctuations into the CME leading to the formation of CME sheath fluctuations. Additionally, we investigate the influence of the fluctuation frequencies on the extent of the CME sheath. We use an ideal magnetohydrodynamic (MHD) model with an adiabatic equation of state. An Alfvén pump wave is injected into the quiet solar wind by perturbing the transverse magnetic field and velocity components, and a CME is injected by inserting a flux-rope modelled as a magnetic island into the quasi-steady solar wind. The upstream Alfvén waves experience a decrease in wavelength and change in the wave vector direction due to the non-radial topology of the CME shock front. The CME sheath inhibits the transmission of high wavelength fluctuations due to the presence of non-radial flows in this region. The frequency of the solar wind fluctuations also affects the steepening of MHD fast waves causing the CME shock propagation speed to vary with the solar wind fluctuation frequencies.

## Solar surges related to UV bursts: Characterization through k-means, inversions and density diagnostics

[D. Nóbrega Siverio](#), [S.L. Guglielmino](#), [A. Sainz Dalda](#)

A&A 2021

<https://arxiv.org/pdf/2108.13960.pdf>

Surges are cool and dense ejections typically observed in chromospheric lines and closely related to other solar phenomena like UV bursts or coronal jets. Our aim is to address the current lack of inverted models and diagnostics of surges as well as characterizing their plasma properties. We have analyzed different surges related to UV bursts observed with the Interface Region Imaging Spectrograph (IRIS) on 2016 April. The mid- and low-chromosphere of the surges are examined by getting their representative Mg II h&k line profiles through the k-means algorithm and performing inversions on them using the STiC code. We have studied the far-UV spectra focusing on the O IV 1399.8 and 1401.2 Å lines, carrying out density diagnostics to determine the transition region properties of these ejections. We have also used experiments performed with the Bifrost code for comparisons. Thanks to k-means, we reduce the number of Mg II h&k profiles to invert by a factor 43.2. The inversions of the representative profiles show that the mid- and low-chromosphere of the surges have temperatures mainly around  $T = 6$  kK at  $-6.0 \leq \log_{10}(\tau) \leq -3.2$ . For the electronic number density,  $n_e$ , and line-of-sight velocity, VLOS, the most reliable results from the inversions are within  $-6.0 \leq \log_{10}(\tau) \leq -4.8$ , with  $n_e$  ranging from  $\sim 1.6 \times 10^{11}$  up to  $10^{12}$  cm $^{-3}$ , and VLOS of a few km s $^{-1}$ . We find, for the first time, observational evidence of enhanced O IV emission within the surges, indicating that these phenomena have a considerable impact on the transition region even in the weakest far-UV lines. The O IV emitting layers show electron number densities from  $2.5 \times 10^{10}$  to  $10^{12}$  cm $^{-3}$ . The simulations provide theoretical support in terms of the topology and of the location of the O IV emission of the surges. **13-14 Apr 2016**

## Small-scale solar jet formation and their associated waves and instabilities

Review

[Samuel Skirvin](#), [Gary Verth](#), [José Juan González-Avilés](#), [Sergiy Shelyag](#), [Rahul Sharma](#), [Francisco Guzmán](#), [Istvan Ballai](#), [Eamon Scullion](#), [Suzana S. A. Silva](#), [Viktor Fedun](#)

Adv. In Space Res. Volume 71, Issue 4, Pages 1866-1892 2023

<https://arxiv.org/pdf/2205.09598.pdf>

Studies on small-scale jets' formation, propagation, evolution, and role, such as type I and II spicules, mottles, and fibrils in the lower solar atmosphere's energetic balance, have progressed tremendously thanks to the combination of detailed observations and sophisticated mathematical modelling. This review provides a survey of the current understanding of jets, their formation in the solar lower atmosphere, and their evolution from observational, numerical, and theoretical perspectives. First, we review some results to describe the jet properties, acquired numerically, analytically and through high-spatial and temporal resolution observations. Further on, we discuss the role of hydrodynamic and magnetohydrodynamic instabilities, namely Rayleigh-Taylor and Kelvin-Helmholtz instabilities, in jet evolution and their role in the energy transport through the solar atmosphere in fully and partially ionised plasmas. Finally, we discuss several mechanisms of magnetohydrodynamic wave generation, propagation, and energy transport in the context of small-scale solar jets in detail. This review identifies several gaps in the understanding of small-scale solar jets and some misalignments between the observational studies and knowledge acquired through theoretical studies and numerical modelling. It is to be expected that these gaps will be closed with the advent of high-resolution observational instruments, such as Daniel K. Inouye Solar Telescope, Solar Orbiter, Parker Solar Probe, and Solar CubeSats for Linked Imaging Spectropolarimetry, combined with further theoretical and computational developments.

## Formation of Coronal Mass Ejection and Post-eruption Flow of Solar Wind on 2010 August 18 event

Vladimir [Slemzin](#), [Farid Goryaev](#), [Denis Rodkin](#)

ApJ 929 146 2022

<https://arxiv.org/pdf/2203.06976.pdf>

<https://iopscience.iop.org/article/10.3847/1538-4357/ac5901/pdf>

The state of the space environment plays a significant role for forecasting of geomagnetic storms produced by disturbances of the solar wind (SW). Coronal mass ejections (CMEs) passing through the heliosphere often have a prolonged (up to several days) trail with declining speed, which affects propagation of the subsequent SW streams. We studied the CME and the post-eruption plasma flows behind the CME rear in the event on **2010 August 18** observed in quadrature by several space-based instruments. Observations of the eruption in the corona with EUV telescopes and coronagraphs revealed several discrete outflows followed by a continuous structureless post-eruption stream. The interplanetary coronal mass ejection (ICME), associated with this CME, was registered by PLASMA and SupraThermal Ion Composition (PLASTIC) instrument aboard the Solar TERrestrial RELations Observatory (STEREO-A) between **August 20, 16:14 UT and August 21, 13:14 UT**, after which the SW disturbance was present over 3 days. Kinematic consideration with the use of the gravitational and Drag-Based models has shown that the discrete plasma flows can be associated with the ICME, whereas the post-eruption outflow was arrived in the declining part of the SW transient. We simulated the Fe-ion charge distributions of the ICME and post-CME parts of SW using the plasma temperature and density in the ejection region derived from the Differential Emission Measure analysis. The results demonstrate that in the studied event the post-ICME trailing region was associated with the post-eruption flow from the corona, rather than with the ambient SW entrained by the CME.

## Numerical Simulations of Solar Spicule Jets at a Magnetic Null-Point

V. [Smirnova](#), P. M. Konkol, A. A. Solov'ev, K. Murawski

Solar Phys. 2016

Two-dimensional numerical simulations of jet-like structures in the solar atmosphere are performed. These structures result from a pressure pulse that is launched at the null point of a potential magnetic arcade. The plasma jet exhibits a double structure with two components: (a) dense, cool, and short vertical stream and (b) a less dense, hot and tall part of the jet. The upper part of the hot and tall jet may represent a direct response of the system to the pressure pulse launched at the null point, and the second, slower cool and dense part of the jet is formed later through the stretching up of the stream as a result of plasma evacuation from the top of the magnetic arcade. Numerical results show that jet-like structures mimic some properties of both type I and type II spicules, according to the classification provided by De Pontieu et al. (Publ. Astron. Soc. Japan59, S655, 2007).

## Trend of photospheric magnetic helicity flux in active regions generating halo coronal mass ejections

A. [Smyrli](#)<sup>1,2</sup>, F. Zuccarello<sup>1</sup>, P. Romano<sup>3</sup>, F. P. Zuccarello<sup>4</sup>, S. L. Guglielmino<sup>1</sup>, D. Spadaro<sup>3</sup>, A. W. Hood<sup>2</sup>, and D. Mackay<sup>2</sup>

A&A 521, A56 (2010), File

Context. Coronal mass ejections (CMEs) are very energetic events ( $\sim 10^{32}$  erg) initiated in the solar atmosphere, resulting in the expulsion of magnetized plasma clouds that propagate into interplanetary space. It has been proposed that CMEs can play an important role in shedding magnetic helicity, avoiding its endless accumulation in the corona.



**Aims.** The aim of this work is to investigate the behavior of magnetic helicity accumulation in sites where the initiation of CMEs occurred to determine whether and how changes in magnetic helicity accumulation are temporally correlated with CME occurrence. **Methods.** We used MDI/SOHO line-of-sight magnetograms to calculate magnetic flux evolution and magnetic helicity injection in 10 active regions that gave rise to halo CMEs observed during the period 2000 February to 2003 June. **Results.** The magnetic helicity injection does not have a unique trend in the events analyzed: in 40% of the cases it shows a large sudden and abrupt change that is temporally correlated with a CME occurrence, while in the other cases it shows a steady monotonic trend, with a slight change in magnetic helicity at CME occurrence. **Conclusions.** The results obtained from the sample of events that we have analyzed indicate that major changes in magnetic helicity flux are observed in active regions characterized by emergence of new magnetic flux and/or generating halo CMEs associated with X-class flares or filament eruptions. In some of the analyzed cases the changes in magnetic helicity flux follow the CME events and can be attributed to a process of restoring a torque balance between the subphotospheric and the coronal domain of the flux tubes.

## **Predictions of DKIST/DL-NIRSP observations for an off-limb kink-unstable coronal loop**

B. [Snow](#), [G. J.J. Botha](#), [E. Scullion](#), [J. A. McLaughlin](#), [P.R. Young](#), [S. A. Jaeggli](#)

ApJ **2018**

<https://arxiv.org/pdf/1807.04972.pdf>

Synthetic intensity maps are generated from a 3D kink-unstable flux rope simulation using several DKIST/DL-NIRSP spectral lines to make a prediction of the observational signatures of energy transport and release. The reconstructed large field-of-view intensity mosaics and single tile sit-and-stare high-cadence image sequences show detailed, fine-scale structure and exhibit signatures of wave propagation, redistribution of heat, flows and fine-scale bursts. These fine-scale bursts are present in the synthetic Doppler velocity maps and can be interpreted as evidence for small-scale magnetic reconnection at the loop boundary. The spectral lines reveal the different thermodynamic structures of the loop, with the hotter lines showing the loop interior and braiding, and the cooler lines showing the radial edges of the loop. The synthetic observations of DL-NIRSP are found to preserve the radial expansion and hence the loop radius can be measured accurately. The electron number density can be estimated using the intensity ratio of the Fe- $\lambda$ 10747 and 10798- $\lambda$  lines at 10747 and 10798- $\lambda$ . The estimated density from this ratio is correct to within  $\pm 10\%$  during the later phases of the evolution, however it is less accurate initially when line-of-sight density inhomogeneities contribute to the Fe- $\lambda$ 10747 intensity, resulting in an overprediction of the density by  $\approx 30\%$ . The identified signatures are all above a conservative estimate for instrument noise and therefore will be detectable. In summary, we have used forward modelling to demonstrate that the coronal off-limb mode of DKIST/DL-NIRSP will be able to detect multiple independent signatures of a kink-unstable loop and observe small-scale transient features including loop braiding/twisting and small-scale reconnection events occurring at the radial edge of the loop.

## **Observational signatures of a kink-unstable coronal flux rope using Hinode/EIS**

Ben [Snow](#), Gert J. J. Botha, Stephane Regnier, Richard J. Morton, Erwin Verwichte, Peter R Young

2017 ApJ 842 16

<https://arxiv.org/pdf/1705.05114.pdf>

<http://sci-hub.cc/10.3847/1538-4357/aa6d0e>

The signatures of energy release and energy transport for a kink-unstable coronal flux rope are investigated via forward modelling. Synthetic intensity and Doppler maps are generated from a 3D numerical simulation. The CHIANTI database is used to compute intensities for three Hinode/EIS emission lines that cover the thermal range of the loop. The intensities and Doppler velocities at simulation resolution are spatially degraded to the Hinode/EIS pixel size ( $1\text{ arcsec}$ ), convolved using a Gaussian point-spread function ( $3\text{ arcsec}$ ), and exposed for a characteristic time of 50 seconds. The synthetic images generated for rasters (moving slit) and sit-and-stare (stationary slit) are analysed to find the signatures of the twisted flux and the associated instability. We find that there are several qualities of a kink-unstable coronal flux rope that can be detected observationally using Hinode/EIS, namely the growth of the loop radius, the increase in intensity towards the radial edge of the loop, and the Doppler velocity following an internal twisted magnetic field line. However, EIS cannot resolve the small, transient features present in the simulation, such as sites of small-scale reconnection (e.g. nanoflares)

## **The role of lateral magnetic reconnection in solar eruptive events**

A. [Soenen](#)<sup>1,2</sup>, A. [Bemporad](#)<sup>3</sup>, C. [Jacobs](#)<sup>1,2</sup>, and S. [Poedts](#)

Ann. Geophys., 27, 3941-3948, 2009, [File](#)

On 10–11 December 2005 a slow CME occurred in between two coronal streamers in the Western Hemisphere. SOHO/MDI magnetograms show a multipolar magnetic configuration at the photosphere consisting of a complex of active regions located at the CME source and two bipoles at the base of the lateral coronal streamers. White light observations reveal that the expanding CME affects both of the lateral streamers and induces the release of plasma within or close to them. These transient phenomena are possibly due to magnetic reconnections induced by the CME expansion that occurs either inside the streamer current sheet or between the CME flanks and the streamer. Our observations show that CMEs can be associated to not only a single reconnection process at a single location in the corona, but also to many reconnection processes occurring at different times and locations around the flux rope. Numerical simulations are used to demonstrate that the observed lateral reconnections can be reproduced. The observed secondary reconnections associated to CMEs may facilitate the CME release by globally decreasing the magnetic tension of the corona. Future CME models should therefore take into account the lateral reconnection effect.

## **A Titov–Démoulin Type Eruptive Event Generator for $\beta > 0$ Plasmas**

Igor V. [Sokolov](#)<sup>1</sup> and Tamas I Gombosi<sup>1</sup>

2023 ApJ 955 126

<https://iopscience.iop.org/article/10.3847/1538-4357/aceef5/pdf>

We provide exact analytical solutions for the magnetic field produced by prescribed current distributions located inside a toroidal filament of finite thickness. The solutions are expressed in terms of toroidal functions, which are modifications of the Legendre functions. In application to the MHD equilibrium of a twisted toroidal current loop in the solar corona, the Grad–Shafranov equation is decomposed into an analytic solution describing an equilibrium configuration against the pinch-effect from its own current and an approximate solution for an external strapping field to balance the hoop force. Our solutions can be employed in numerical simulations of coronal mass ejections (CMEs). When superimposed on the background solar coronal magnetic field, the excess magnetic energy of the twisted current loop configuration can be made unstable by applying flux cancellation to reduce the strapping field. Such loss of stability accompanied by the formation of an expanding flux rope is typical for the Titov & Démoulin eruptive event generator. The main new features of the proposed model are as follows: the filament is filled with finite  $\beta$  plasma with finite mass and energy, the model describes an equilibrium solution that will spontaneously erupt due to magnetic reconnection of the strapping magnetic field arcade, and there are analytic expressions connecting the model parameters to the asymptotic velocity and total mass of the resulting CME, providing a way to connect the simulated CME properties to multipoint coronagraph observations.

## **Twin CME Launched by a Blowout Jet Originated from the Eruption of a Quiet-Sun Mini-filament**

Ritika [Solanki](#), [Abhishek K. Srivastava](#), [Yamini K. Rao](#), [Bhola N. Dwivedi](#)

Solar Phys. 294:68 2019

<https://arxiv.org/pdf/1905.02475.pdf>

<https://link.springer.com/content/pdf/10.1007%2Fs11207-019-1453-3.pdf>

We study a quiet-Sun blowout jet which is observed on **2014 May 16** by the instruments on board Solar Dynamics Observatory (SDO). We find the twin CME as jet-like and bubble-like CME simultaneously as observed by LASCO C2 on board Solar and Heliospheric Observatory (SoHO), Solar Terrestrial Relation Observatory (STEREO A and STEREO B/COR2). They are respectively associated with the eruption of the northern and southern sections of the filament. A circular filament is rooted at the internetwork region at the base of the blowout jet. The collective magnetic cancellation is observed by SDO/HMI line of sight (LOS) magnetograms at the northern end of the filament, which makes this filament unstable and further makes it to erupt in two different stages. In the first stage, northern section of the filament is ejected, and causes an evolution of the northern part of the blowout jet. This part of the blowout jet is further extended as a collimated plasma beam to form a jet-like CME. We also observe the plasma blobs at the northern edge of the blowout jet resulting from Kelvin-Helmholtz (K-H) instability in its twisted magneto-plasma spire. In the second stage, southern section of the filament erupts in form of deformed/twisted magnetic flux rope which forms the southern part of the blowout jet. This eruption is most likely caused by the eruption of the northern section of filament, which removes the confined magnetic field of the southern section of the filament. Alternative scenarios may be a magnetic implosion between these magnetic structures confined in a much larger magnetic domain. This eruption of southern section of the filament further results in the bubble-like CME in the outer corona.

## **CME Productive and Non-productive Recurring Jets Near an Active Region AR11176**

Ritika [Solanki](#), [Abhishek K. Srivastava](#), [Bhola N. Dwivedi](#)

Solar Phys. 295:27 2020

<https://arxiv.org/pdf/2001.11702.pdf>

<https://doi.org/10.1007/s11207-020-1594-4>

We study the recurring jets near AR11176 during the period **2011 March 31 17:00 UT to April 1 05:00 UT** using observations from the Atmospheric Imaging Assembly (AIA) on board Solar Dynamics Observatory (SDO). Mini-filaments (mini-filament1 & 2) are found at the base of these recurring jets where mini-filament1 shows the partial signature of eruption in case of Jet1-3. However, the mini-filament2 shows a complete eruption driving a full blow-out jet (Jet4). The eruption of mini-filament2 triggers C-class flare and Jet4 eruption. The eruption of Jet4 triggers a coronal mass ejection (CME). The plane-of-sky velocity of recurring jets (Jet1-4) results in 160 km/s, 106 km/s, 151 km/s and 369 km/s. The estimated velocity of CME is 636 km/s. The continuous magnetic flux cancellation is observed at the base of the jet productive region which could be the cause of the eruption of mini-filaments and recurring jets. In the former case, the mini-filament1 shows partial eruption and first three jets (Jet1-3) are produced, but the rate of cancellation was rather low. However, in the latter case, mini-filament2 fully erupts (perhaps because of a higher cancellation rate), and this triggers a C-class flare and a CME-productive jet. At the base of first three jets (Jet1-3), the mini-filament1 causes to push the overlying dynamic complex thin loops resulting in the reconnection and drives the jet (Jet1-3) eruptions. The formation of the plasma blobs are observed during the eruption of the first jet (Jet1).

## **C-1.4 Class Flare and An Associated Peculiar Coronal Jet**

[Ritika Solanki](#), [A.K. Srivastava](#), [B.N. Dwivedi](#)

<https://arxiv.org/pdf/1805.05948.pdf>

Using HINODE/XRT, GOES, SDO/AIA observations, we study a compact C-1.4 class flare outside a major sunspot of AR 12178 on **4 October 2014**. This flare is associated with a peculiar coronal jet, which is erupted in two stages in the overlying corona above the compact flaring region. At the time of flare maximum, the first stage of the jet eruption occurs above the flare energy release site, and thereafter in the second stage its magneto-plasma system interacts with the overlying distinct magnetic field domain in its vicinity to build further the typical jet plasma column.

### **Force-free magnetic flux ropes: inner structure and basic properties**

[A A Solov'ev](#), [E A Kirichek](#)

MNRAS, Volume 505, Issue 3, August **2021**, Pages 4406–4416,

<https://doi.org/10.1093/mnras/stab1565>

There are two main properties of a shielded magnetic flux rope. The first is the net electric current through its cross-section should be zero, i.e.  $I=0$ . The second is the existence of a non-zero pressure of external magnetic field  $B_{ex}/8\pi B_{ex}^2/B_{ex}^2 2\pi 8\pi$  in order to keep in balance the magnetic rope with the strong force-free inner structure in a rarefied solar atmosphere. The first condition requires the existence of a special cylindrical surface within the magnetic flux rope on which the current density  $j$  changes sign, so that the direction of the current at the rope's periphery (return current) is opposite to the current at its axis (direct current). Numerical calculations have shown that, when the pressure  $B_{ex}/8\pi B_{ex}^2/B_{ex}^2 2\pi 8\pi$  drops to a certain limit, an indefinite increase in the electric current density  $j$  and the force-free parameter  $\alpha$  takes place in the vicinity of this special surface resulting in a dissipative collapse of the system. Such a drop in  $B_{ex}/8\pi B_{ex}^2/B_{ex}^2 2\pi 8\pi$  may happen due to a multitude of reasons with the most obvious reason being the uprise of a magnetic flux rope into rarefied layers of the chromosphere or corona. Due to the dissipative collapse a violent energy release begins in a thin azimuthal shell at the periphery of the twisted magnetic flux tube. On the basis of these properties of the force-free magnetic flux rope, the problems of plasma instabilities excitation and coronal heating are discussed.

### **Observation of a large-scale filament eruption initiated by two small-scale erupting filaments pushing out from below**

[Yongliang Song](#), [Jiangtao Su](#), [Qingmin Zhang](#), [Mei Zhang](#), [Yuanyong Deng](#), [Xianyong Bai](#), [Suo Liu](#), [Xiao Yang](#), [Jie Chen](#), [Haiqing Xu](#), [Kaifan Ji](#), [Ziyao Hu](#)

Solar Phys. **299**, 85 **2024**

<https://arxiv.org/pdf/2405.13311>

<https://doi.org/10.1007/s11207-024-02327-6>

Filament eruptions often result in flares and coronal mass ejections (CMEs). Most studies attribute the filament eruptions to their instabilities or magnetic reconnection. In this study, we report a unique observation of a filament eruption whose initiation process has not been reported before. This large-scale filament, with a length of about 360 Mm crossing an active region, is forced to erupt by two small-scale erupting filaments pushing out from below. This process of multi-filament eruption results in an M6.4 flare in the active region NOAA 13229 on **25th February 2023**. The whole process can be divided into three stages: the eruptions of two active-region filaments F1 and F2; the interactions between the erupting F1, F2, and the large-scale filament F3; and the eruption of F3. Though this multi-filament eruption occurs near the northwest limb of the solar disk, it produces a strong halo CME that causes a significant geomagnetic disturbance. Our observations present a new filament eruption mechanism, in which the initial kinetic energy of the eruption is obtained from and transported to by other erupting structures. This event provides us a unique insight into the dynamics of multi-filament eruptions and their corresponding effects on the interplanetary space.

### **The Structure of Coronal Mass Ejections Recorded by the K-Coronagraph at Mauna Loa Solar Observatory**

[Hongqiang Song](#), [Leping Li](#), [Zhenjun Zhou](#), [Lidong Xia](#), [Xin Cheng](#), [Yao Chen](#)

ApJL **952** L22 **2023**

<https://arxiv.org/pdf/2307.01398.pdf>

<https://iopscience.iop.org/article/10.3847/2041-8213/ace422/pdf>

Previous survey studies reported that coronal mass ejections (CMEs) can exhibit various structures in white-light coronagraphs, and  $\sim 30\%$  of them have the typical three-part feature in the high corona (e.g., 2--6  $R_{\odot}$ ), which has been taken as the prototypical structure of CMEs. It is widely accepted that CMEs result from eruption of magnetic flux ropes (MFRs), and the three-part structure can be understood easily by means of the MFR eruption. It is interesting and significant to answer why only  $\sim 30\%$  of CMEs have the three-part feature in previous studies. Here we conduct a synthesis of the CME structure in the field of view (FOV) of K-Coronagraph (1.05--3  $R_{\odot}$ ). In total, 369 CMEs are observed from 2013 September to 2022 November. After inspecting the CMEs one by one through joint observations of the AIA, K-Coronagraph and LASCO/C2, we find 71 events according to the criteria: 1) limb event; 2) normal CME, i.e., angular width  $\geq 30^\circ$ ; 3) K-Coronagraph caught the early eruption stage. All (or more than 90% considering several ambiguous events) of the 71 CMEs exhibit the three-part feature in the FOV of K-Coronagraph, while only 30--40% have the feature in the C2 FOV (2--6  $R_{\odot}$ ). For the first time, our studies show that 90--100% and 30--40% of normal CMEs possess the three-part structure in the low and high corona, respectively, which demonstrates that many CMEs

can lose the three-part feature during their early evolutions, and strongly supports that most (if not all) CMEs have the MFR structures. **2014 October 14, 2016 January 1, 2021 May 7, 2021 October 10**

**Table 1.** The information of 71 limb CMEs in the K-COR and LASCO/C2 observations. 2014-2022

## On the Nature of the Three-part Structure of Solar Coronal Mass Ejections

[Hongqiang Song](#), [Jie Zhang](#), [Leping Li](#), [Zihao Yang](#), [Lidong Xia](#), [Ruisheng Zheng](#), [Yao Chen](#)

ApJ **942** 19 **2023**

<https://arxiv.org/pdf/2212.04013.pdf>

<https://iopscience.iop.org/article/10.3847/1538-4357/aca6e0/pdf>

Coronal mass ejections (CMEs) result from eruptions of magnetic flux ropes (MFRs) and can possess a three-part structure in white-light coronagraphs, including a bright front, dark cavity and bright core. In the traditional opinion, the bright front forms due to the plasma pileup along the MFR border, the cavity represents the cross section of the MFR, and the bright core corresponds to the erupted prominence. However, this explanation on the nature of the three-part structure is being challenged. In this paper, we report an intriguing event occurred on **2014 June 14** that was recorded by multiple space- and ground-based instruments seamlessly, clearly showing that the CME front originates from the plasma pileup along the magnetic arcades overlying the MFR, and the core corresponds to a hot-channel MFR. Thus the dark cavity is not an MFR, instead it is a low-density zone between the CME front and a trailing MFR. These observations are consistent with a new explanation on the CME structure. If the new explanation is correct, most (if not all) CMEs should exhibit the three-part appearance in their early eruption stage. To examine this prediction, we make a survey study of all CMEs in 2011 and find that all limb events have the three-part feature in the low corona, regardless of their appearances in the high corona. Our studies suggest that the three-part structure is the intrinsic structure of CMEs, which has fundamental importance for understanding CMEs. **2011 March 27**

**Table 1.** The information of 28 limb CMEs without typical three-part structure in the C2 images but with the three-part feature in the EUV images

## Toward a Unified Explanation for the Three-part Structure of Solar Coronal Mass Ejections

[Hongqiang Song](#), [Leping Li](#), [Yao Chen](#)

ApJ **933** 68 **2022**

<https://arxiv.org/pdf/2205.11682.pdf>

<https://iopscience.iop.org/article/10.3847/1538-4357/ac7239/pdf>

Coronal mass ejections (CMEs) are associated with the eruption of magnetic flux ropes (MFRs), which usually appear as hot channels in active regions and coronal cavities in quiet-Sun regions. CMEs often exhibit the classical three-part structure in the lower corona when imaged with white-light coronagraphs, including the bright front, dark cavity, and bright core. The bright core and dark cavity have been regarded as the erupted prominence and MFR, respectively, for several decades. However, recent studies clearly demonstrated that both the prominence and hot-channel MFR can be observed as the CME core. The current research presents a three-part CME resulted from the eruption of a coronal prominence cavity on **2010 October 7** with observations from two vantage perspectives, i.e., edge-on from the Earth and face-on from the Solar Terrestrial Relations Observatory (STEREO). Our observations illustrates two important results: (1) For the first time, the erupting coronal cavity is recorded as a channel-like structure in the extreme-ultraviolet passband, analogous to the hot-channel morphology, and is dubbed as warm channel; (2) Both the prominence and warm-channel MFR (coronal cavity) in the extreme-ultraviolet passbands evolve into the CME core in the white-light coronagraphs of STEREO-A. The results support that we are walking toward a unified explanation for the three-part structure of CMEs, in which both prominences and MFRs (hot or warm channels) are responsible for the bright core.

## Multi-wavelength and Dual-perspective Observations of Eruption and Untwisting of Two Homologous Magnetic Flux Ropes

De-Chao [Song](#), [Y. Li](#), [Y. Su](#), [M. D. Ding](#), [W.Q. Gan](#)

ApJ **922** 238 **2021**

<https://arxiv.org/pdf/2109.11187.pdf>

<https://iopscience.iop.org/article/10.3847/1538-4357/ac294a/pdf>

<https://doi.org/10.3847/1538-4357/ac294a>

In this paper, we present a detailed morphological, kinematic, and thermal analysis of two homologous magnetic flux ropes (MFRs) from NOAA 11515 on **2012 July 8--9**. The study is based on multi-wavelength and dual-perspective imaging observations from the Solar Dynamics Observatory and the Solar Terrestrial Relations Observatory Ahead spacecraft, which can well reveal the structure and evolution of the two MFRs. We find that both of the MFRs show up in multiple passbands and their emissions mainly consist of a cold component peaking at a temperature of  $\sim 0.4$ -- $0.6$  MK and a hot component peaking at  $\sim 7$ -- $8$  MK. The two MFRs exhibit erupting, expanding, and untwisting motions that manifest distinctive features from two different viewpoints. Their evolution can be divided into two stages, a fast-eruption stage with speeds of about  $105$ -- $125$  km s $^{-1}$  for MFR-1 and  $50$ -- $65$  km s $^{-1}$  for MFR-2 and a slow-expansion (or untwisting) stage with speeds of about  $10$ -- $35$  km s $^{-1}$  for MFR-1 and  $10$ -- $30$  km s $^{-1}$  for MFR-2 in the plane of sky. We also find that during the two-stage evolution, the high temperature features mainly appear in the interface region between MFRs and ambient magnetic structures and also in the center of MFRs, which suggests that some heating processes take place in such places like magnetic reconnection and plasma compression. These observational results

indicate that the eruption and untwisting processes of MFRs are coupled with the heating process, among which an energy conversion exists.

## **Characteristics and applications of interplanetary coronal mass ejection composition** **Review**

[Hongqiang Song](#), [Shuo Yao](#)

SCIENCE CHINA Technological Sciences      2020

<https://arxiv.org/pdf/2006.11473.pdf>

In situ measurements of interplanetary coronal mass ejection (ICME) composition, including elemental abundances and charge states of heavy ions, open a new avenue to study coronal mass ejections (CMEs) besides remote-sensing observations. The ratios between different elemental abundances can diagnose the plasma origin of CMEs (e.g., from the corona or chromosphere/photosphere) due to the first ionization potential (FIP) effect, which means elements with different FIP get fractionated between the photosphere and corona. The ratios between different charge states of a specific element can provide the electron temperature of CMEs in the corona due to the freeze-in effect, which can be used to investigate their eruption process. In this review, we first give an overview of the ICME composition and then demonstrate their applications in investigating some important subjects related to CMEs, such as the origin of filament plasma and the eruption process of magnetic flux ropes. Finally, we point out several important questions that should be addressed further for better utilizing the ICME composition to study CMEs. **01-May-98**

## **Sympathetic eruptions of two filaments with an identifiable causal link observed by the Solar Dynamics Observatory**

Zhiping [Song](#), [Yijun Hou](#), [Jun Zhang](#), [Peng Wang](#)

ApJ **892** 79    2020

<https://arxiv.org/pdf/2002.07979.pdf>

<https://iopscience.iop.org/article/10.3847/1538-4357/ab77b3/pdf>

Filament eruptions occurring at different places within a relatively short time interval, but with a certain physical causal connection are usually known as sympathetic eruption. Studies on sympathetic eruptions are not uncommon. However, in the existed reports, the causal links between sympathetic eruptions remain rather speculative. In this work, we present detailed observations of a sympathetic filament eruption event, where an identifiable causal link between two eruptive filaments is observed. On **2015 November 15**, two filaments (F1 in the north and F2 in the south) were located at the southwestern quadrant of solar disk. The main axes of them were almost parallel to each other. Around 22:20 UT, F1 began to erupt, forming two flare ribbons. The southwestern ribbon apparently moved to southwest and intruded southeast part of F2. This continuous intrusion caused F2's eventual eruption. Accompanying the eruption of F2, flare ribbons and post-flare loops appeared in northwest region of F2. Meanwhile, neither flare ribbons nor post-flare loops could be observed in southeastern area of F2. In addition, the nonlinear force-free field (NLFFF) extrapolations show that the magnetic fields above F2 in the southeast region are much weaker than that in the northwest region. These results imply that the overlying magnetic fields of F2 were not uniform. So we propose that the southwest ribbon formed by eruptive F1 invaded F2 from its southeast region with relatively weaker overlying magnetic fields in comparison with its northwest region, disturbing F2 and leading F2 to erupt eventually.

## **The Structure of Solar Coronal Mass Ejections in the Extreme-Ultraviolet Passbands**

H. Q. [Song](#), [J. Zhang](#), [L. P. Li](#), [Y. D. Liu](#), [B. Zhu](#), [B. Wang](#), [R. S. Zheng](#), [Y. Chen](#)

ApJ      **887** 124      2019

<https://arxiv.org/pdf/1910.09735.pdf>

<https://iopscience.iop.org/article/10.3847/1538-4357/ab50b6/pdf>

So far most studies on the structure of coronal mass ejections (CMEs) are conducted through white-light coronagraphs, which demonstrate about one third of CMEs exhibit the typical three-part structure in the high corona (e.g., beyond 2 Rs), i.e., the bright front, the dark cavity and the bright core. In this paper, we address the CME structure in the low corona (e.g., below 1.3 Rs) through extreme-ultraviolet (EUV) passbands and find that the three-part CMEs in the white-light images can possess a similar three-part appearance in the EUV images, i.e., a leading edge, a low-density zone, and a filament or hot channel. The analyses identify that the leading edge and the filament or hot channel in the EUV passbands evolve into the front and the core later within several solar radii in the white-light passbands, respectively. What's more, we find that the CMEs without obvious cavity in the white-light images can also exhibit the clear three-part appearance in the EUV images, which means that the low-density zone in the EUV images (observed as the cavity in white-light images) can be compressed and/or transformed gradually by the expansion of the bright core and/or the reconnection of magnetic field surrounding the core during the CME propagation outward. Our study suggests that more CMEs can possess the clear three-part structure in their early eruption stage. The nature of the low-density zone between the leading edge and the filament or hot channel is discussed. **2013 September 24, 2014 January 06, 2015 February 9, 2017 September 10**

## **On the Nature of the Bright Core of Solar Coronal Mass Ejections**

H. Q. [Song](#)<sup>1</sup>, [J. Zhang](#)<sup>2</sup>, [X. Cheng](#)<sup>3</sup>, [L. P. Li](#)<sup>4</sup>, [Y. Z. Tang](#)<sup>1</sup>, [B. Wang](#)<sup>1</sup>, [R. S. Zheng](#)<sup>1</sup>, and [Y. Chen](#)<sup>1</sup>

2019 ApJ **883** 43

<https://iopscience.iop.org/article/10.3847/1538-4357/ab304c/pdf>    File

Coronal mass ejections (CMEs) often exhibit the classic three-part structure in a coronagraph, i.e., the bright front, dark cavity, and bright core, which are traditionally considered as the manifestations of coronal plasma pileup, magnetic flux rope (MFR), and filament, respectively. However, a recent survey based on 42 CMEs all possessing the three-part structure found that a large majority (69%) do not contain an eruptive filament at the Sun. Therefore, a challenging opinion is proposed and claims that the bright core can also correspond to the MFR, which is supported by the CME simulation. Then what is the nature of the CME core? In this paper, we address this issue through a CME associated with the eruption of a filament-hosting MFR on **2013 September 29**. This CME exhibits the three-part morphology in multiple white-light coronagraphs from different perspectives. The new finding is that the bright core contains both a sharp and a fuzzy component. Through tracking the filament motion continuously from its source region to the outer corona, we conclude that the sharp component corresponds to the filament. The fuzzy component is suggested to result from the MFR that supports the filament against the gravity in the corona. Our study can shed more light on the nature of CME cores, and explain the core whether or not the filament is involved with a uniform scenario. The nature of the CME cavity is also discussed.

### **The Reversal of a Solar Prominence Rotation about Its Ascending Direction during a Failed Eruption**

H. Q. [Song](#)<sup>1</sup>, Z. J. Zhou<sup>2</sup>, L. P. Li<sup>3</sup>, X. Cheng<sup>4</sup>, J. Zhang<sup>5</sup>, Y. Chen<sup>1</sup>, C. X. Chen<sup>1</sup>, X. W. Ma<sup>1</sup>, B. Wang<sup>1</sup>, and R. S. Zheng<sup>1</sup>

**2018** ApJL 864 L37

<http://sci-hub.tw/http://iopscience.iop.org/article/10.3847/2041-8213/aade49/meta>

The magnetic orientation of solar coronal mass ejections (CMEs) near the Earth's magnetosphere is one major parameter that influences the geoeffectiveness of CMEs. The orientation often varies during the eruption and propagation from the Sun to the Earth due to the deflection and/or rotation of CMEs. It is common to observe the counterclockwise (CCW) or clockwise (CW) rotation (viewed from above) of solar prominences in the corona, which can be used to predict the space weather effect of associated CMEs. In this Letter, we report an intriguing failed prominence eruption that occurred on **2010 December 10**, exhibiting the CCW and CW rotations sequentially in the corona. The eruption is recorded by both the Atmospheric Imaging Assembly on board the Solar Dynamics Observatory and the Extreme Ultraviolet Imager on board the Solar Terrestrial Relations Observatory. This stereoscopic combination allows us to reconstruct the three-dimensional structure and identify the rotation reversal without ambiguity. The prominence first rotates CCW about its ascending direction by  $\sim 135^\circ$  in  $\sim 26$  minutes and then reverses to the CW rotation by  $\sim 45^\circ$  in  $\sim 15$  minutes; i.e., the average CCW and CW rotation speeds are  $\sim 5.2$  and  $\sim 3.0$  deg minute<sup>-1</sup>, respectively. The possible mechanisms leading to the rotation and reversal are discussed. The kinematics of the prominence is also analyzed, which indicates that an upward force acts on the prominence during the entire process.

### **The Acceleration Process of a Solar Quiescent Filament in the Inner Corona**

H. Q. [Song](#), Y. Chen, J. Qiu, C. X. Chen, J. Zhang, X. Cheng, Y. D. Shen, and R. S. Zheng

**2018** ApJL 857 L21

<http://iopscience.iop.org/article/10.3847/2041-8213/aabcc3/pdf>

Coronal mass ejections (CMEs) are frequently associated with filament eruptions. Theoretical studies propose that both magnetic reconnection and ideal magnetohydrodynamic instability of magnetic flux ropes can convert coronal magnetic energy into the filament/CME kinetic energy. Numerical simulations and analytical considerations demonstrate that both mechanisms can have significant contributions to the filament/CME acceleration. Many observational studies support that reconnection plays an important role during the acceleration, while it remains open how to resolve observationally the contribution of the ideal instability to the acceleration. On the other hand, it is difficult to separate and compare their contributions through observations as both mechanisms often work in a close time sequence. In this Letter, the above issues are addressed by analyzing the eruption process of a quiescent filament. The filament started to rise from  $\sim 00:00$  UT on **2011 December 25**, 20 minutes earlier than the starting time of the flare impulsive phase ( $\sim 00:20$  UT), and reached the maximum velocity at the flare peak time ( $\sim 00:50$  UT). We divide the acceleration process into two stages, corresponding to the pre-flare and flare impulsive phases, respectively. The analysis indicates that an ideal flux-rope instability is dominant in the first stage, while reconnection below the flux rope becomes important during the second stage, and both mechanisms may have comparable contributions to the net acceleration of the filament.

### **The Three-part Structure of a Filament-unrelated Solar Coronal Mass Ejection**

H. Q. [Song](#)<sup>1,2</sup>, X. Cheng<sup>3</sup>, Y. Chen<sup>1</sup>, J. Zhang<sup>4</sup>, B. Wang<sup>1</sup>, L. P. Li<sup>2</sup>, B. Li<sup>1</sup>, Q. Hu<sup>5</sup>, and G. Li<sup>5</sup>

**2017** ApJ 848 21

<http://iopscience.iop.org/article/10.3847/1538-4357/aa8d1a/pdf>

[sci-hub.tw/10.3847/1538-4357/aa8d1a](http://sci-hub.tw/10.3847/1538-4357/aa8d1a)

Coronal mass ejections (CMEs) often exhibit the typical three-part structure in the corona when observed with white-light coronagraphs, i.e., the bright leading front, dark cavity, and bright core, corresponding to a high-low-high density sequence. As CMEs result from eruptions of magnetic flux ropes (MFRs), which can possess either lower (e.g., coronal-cavity MFRs) or higher (e.g., hot-channel MFRs) density compared to their surroundings in the corona, the traditional opinion regards the three-part structure as the manifestations of coronal plasma pileup (high density), coronal-cavity MFR (low density), and filament (high density) contained in the trailing part of MFR, respectively. In this paper, we

demonstrate that filament-unrelated CMEs can also exhibit the classical three-part structure. The observations were made from different perspectives through an event that occurred on **2011 October 4**. The CME cavity corresponds to the low-density zone between the leading front and the high-density core, and it is obvious in the low corona and gradually becomes fuzzy when propagating outward. The bright core corresponds to a high-density structure that is suggested to be an erupting MFR. The MFR is recorded from both edge-on and face-on perspectives, exhibiting different morphologies that are due to projection effects. We stress that the zone (MFR) with lower (higher) density in comparison to the surroundings can appear as the dark cavity (bright core) when observed through white-light coronagraphs, which is not necessarily the coronal-cavity MFR (erupted filament).

### **Evidence of the Solar EUV hot channel as a magnetic flux rope from remote-sensing and in-situ observations**

Hongqiang [Song](#), [Yao Chen](#), [Jie Zhang](#), [Xin Cheng](#), [Bing Wang](#), [Qiang Hu](#), [Gang Li](#), [Yuming Wang](#)  
ApJL **808** L15 **2015**

<http://arxiv.org/pdf/1507.00078v1.pdf>

Hot channels (HCs), high temperature erupting structures in the lower corona of the Sun, have been proposed as a proxy of magnetic flux ropes (MFRs) since their initial discovery. However, it is difficult to make definitive proof given the fact that there is no direct measurement of magnetic field in the corona. An alternative way is to use the magnetic field measurement in the solar wind from in-situ instruments. On **2012 July 12**, an HC was observed prior to and during a coronal mass ejection (CME) by the AIA high-temperature images. The HC is invisible in the EUVI low-temperature images, which only show the cooler leading front (LF). However, both the LF and an ejecta can be observed in the coronagraphic images. These are consistent with the high temperature and high density of the HC and support that the ejecta is the erupted HC. In the meanwhile, the associated CME shock was identified ahead of the ejecta and the sheath through the COR2 images, and the corresponding ICME was detected by `\textit{ACE}`, showing the shock, sheath and magnetic cloud (MC) sequentially, which agrees with the coronagraphic observations. Further, the MC contained a low-ionization-state center and a high-ionization-state shell, consistent with the pre-existing HC observation and its growth through magnetic reconnection. All of these observations support that the MC detected near the Earth is the counterpart of the erupted HC in the corona for this event. Therefore, our study provides strong observational evidence of the HC as an MFR.

### **First Taste of Hot Channel in Interplanetary Space**

H. Q. [Song](#)<sup>1</sup>, J. Zhang<sup>2</sup>, Y. Chen<sup>1</sup>, X. Cheng<sup>3</sup>, G. Li<sup>4</sup>, and Y. M. Wang  
**2015** ApJ **803** 96

<http://arxiv.org/pdf/1502.04408v1.pdf>

A hot channel (HC) is a high temperature ( $\sim 10$  MK) structure in the inner corona first revealed by the Atmospheric Imaging Assembly on board the Solar Dynamics Observatory. Eruptions of HCs are often associated with flares and coronal mass ejections (CMEs). Results of previous studies have suggested that an HC is a good proxy for a magnetic flux rope (MFR) in the inner corona as well as another well known MFR candidate, the prominence-cavity structure, which has a normal coronal temperature ( $\sim 1-2$  MK). In this paper, we report a high temperature structure (HTS,  $\sim 1.5$  MK) contained in an interplanetary CME induced by an HC eruption. According to the observations of bidirectional electrons, high temperature and density, strong magnetic field, and its association with the shock, sheath, and plasma pile-up region, we suggest that the HTS is the interplanetary counterpart of the HC. The scale of the measured HTS is around  $14 R_{\odot}$ , and it maintained a much higher temperature than the background solar wind even at 1 AU. It is significantly different from the typical magnetic clouds, which usually have a much lower temperature. Our study suggests that the existence of a corotating interaction region ahead of the HC formed a magnetic container to inhibit expansion of the HC and cool it down to a low temperature. **2012 January 27**,

### **Acceleration phases of a solar filament during its eruption**

Hongqiang [Song](#), Yao Chen, Jie Zhang, Xin Cheng, Hui Fu, Gang Li  
ApJL **804** L38 **2015**

<http://arxiv.org/pdf/1504.06062v1.pdf>

Filament eruptions often lead to coronal mass ejections (CMEs), which can affect critical technological systems in space and on the ground when they interact with the geo-magnetosphere in high speeds. Therefore, it is an important issue to investigate the acceleration mechanisms of CMEs in solar/space physics. Based on observations and simulations, the resistive magnetic reconnection and the ideal instability of magnetic flux rope have been proposed to accelerate CMEs. However, it remains elusive whether both of them play a comparable role during a particular eruption. It has been extremely difficult to separate their contributions as they often work in a close time sequence during one fast acceleration phase. Here we report an intriguing filament eruption event, which shows two apparently separated fast acceleration phases and provides us an excellent opportunity to address the issue. Through analyzing the correlations between velocity (acceleration) and soft (hard) X-ray profiles, we suggest that the instability and magnetic

reconnection make a major contribution during the first and second fast acceleration phases, respectively. Further, we find that both processes have a comparable contribution to accelerate the filament in this event. **2014 August 24**

### **Direct observations of magnetic flux rope formation during a solar coronal mass ejection**

Hongqiang **Song**, Jie Zhang, Yao Chen, Xin Cheng

ApJL, 792 L40, **2014**

<http://arxiv.org/pdf/1408.2000v1.pdf>

Coronal mass ejections (CMEs) are the most spectacular eruptive phenomena in the solar atmosphere. It is generally accepted that CMEs are results of eruptions of magnetic flux ropes (MFRs). However, a heated debate is on whether MFRs pre-exist before the eruptions or they are formed during the eruptions. Several coronal signatures, \textit{e.g.}, filaments, coronal cavities, sigmoid structures and hot channels (or hot blobs), are proposed as MFRs and observed before the eruption, which support the pre-existing MFR scenario. There is almost no reported observation about MFR formation during the eruption. In this letter, we present an intriguing observation of a solar eruptive event occurred on **2013 November 21** with the Atmospheric Imaging Assembly on board the \textit{Solar Dynamic Observatory}, which shows a detailed formation process of the MFR during the eruption. The process started with the expansion of a low-lying coronal arcade, possibly caused by the flare magnetic reconnection underneath. The newly-formed ascending loops from below further pushed the arcade upward, stretching the surrounding magnetic field. The arcade and stretched magnetic field lines then curved-in just below the arcade vertex, forming an X-point. The field lines near the X-point continued to approach each other and a second magnetic reconnection was induced. It is this high-lying magnetic reconnection that led to the formation and eruption of a hot blob ( $\sim 10$  MK), presumably a MFR, producing a CME. We suggest that two spatially-separated magnetic reconnections occurred in this event, responsible for producing the flare and the hot blob (CME), respectively.

### **Temperature Evolution of a Magnetic Flux Rope in a Failed Solar Eruption**

H. Q. **Song**, J. Zhang, X. Cheng, Y. Chen, R. Liu, Y. M. Wang, and B. Li

**2014** ApJ 784 48

In this paper, we report for the first time the detailed temperature evolution process of the magnetic flux rope in a failed solar eruption. Occurring on **2013 January 05**, the flux rope was impulsively accelerated to a speed of  $\sim 400$  km s $^{-1}$  in the first minute, then decelerated and came to a complete stop in two minutes. The failed eruption resulted in a large-size high-lying ( $\sim 100$  Mm above the surface), high-temperature "fire ball" sitting in the corona for more than two hours. The time evolution of the thermal structure of the flux rope was revealed through the differential emission measure analysis technique, which produced temperature maps using observations of the Atmospheric Imaging Assembly on board the Solar Dynamic Observatory. The average temperature of the flux rope steadily increased from  $\sim 5$  MK to  $\sim 10$  MK during the first nine minutes of the evolution, which was much longer than the rise time (about three minutes) of the associated soft X-ray flare. We suggest that the flux rope is heated by the energy release of the continuing magnetic reconnection, different from the heating of the low-lying flare loops, which is mainly produced by the chromospheric plasma evaporation. The loop arcade overlying the flux rope was pushed up by  $\sim 10$  Mm during the attempted eruption. The pattern of the velocity variation of the loop arcade strongly suggests that the failure of the eruption was caused by the strapping effect of the overlying loop arcade.

### **A STUDY OF FAST FLARELESS CORONAL MASS EJECTIONS**

H. Q. **Song**<sup>1,2</sup>, Y. Chen<sup>1</sup>, D. D. Ye<sup>1</sup>, G. Q. Han<sup>1</sup>, G. H. Du<sup>1</sup>, G. Li<sup>1,3</sup>, J. Zhang<sup>2</sup>, and Q. Hu

**2013** ApJ 773 129, **File**

Two major processes have been proposed to convert coronal magnetic energy into the kinetic energy of a coronal mass ejection (CME): resistive magnetic reconnection and the ideal macroscopic magnetohydrodynamic instability of a magnetic flux rope. However, it remains elusive whether both processes play a comparable role or one of them prevails during a particular eruption. To shed light on this issue, we carefully studied energetic but flareless CMEs, i.e., fast CMEs not accompanied by any flares. Through searching the Coordinated Data Analysis Workshops database of CMEs observed in Solar Cycle 23, we found 13 such events with speeds larger than 1000 km s $^{-1}$ . Other common observational features of these events are: (1) none of them originated in active regions, they were associated with eruptions of well-developed long filaments in quiet-Sun regions; (2) no apparent enhancement of flare emissions was present in soft X-ray, EUV, and microwave data. Further studies of two events reveal that (1) the reconnection electric fields, as inferred from the product of the separation speed of post-eruption ribbons and the photospheric magnetic field measurement, were generally weak; (2) the period with a measurable reconnection electric field is considerably shorter than the total filament-CME acceleration time. These observations indicate that for these fast CMEs, the magnetic energy was released mainly via the ideal flux-rope instability through the work done by the large-scale Lorentz force acting on the rope currents rather than via magnetic reconnections. We also suggest that reconnections play a less important role in accelerating CMEs in quiet-Sun regions of weak magnetic field than those in active regions of strong magnetic field. **98/01/03, 98/06/05, 99/09/16, 99/09/23, 00/07/24, 02/03/02, 02/05/11, 02/07/13, 02/08/06, 02/12/21, 02/12/26, 03/01/05, 05/01/04**



## **A Statistical Study on the Morphology of Rays and Dynamics of Blobs in the Wake of Coronal Mass Ejections**

H. Q. **Song**, X. L. Kong, Y. Chen, B. Li, G. Li, S. W. Feng and L. D. Xia

Solar Physics, Volume 276, Numbers 1-2, 261-276, **2012**, **File**

In this paper, with a survey through the Large Angle and Spectrometric Coronagraph (LASCO) data from 1996 to 2009, we present 11 events with plasma blobs flowing outwards sequentially along a bright coronal ray in the wake of a coronal mass ejection. The ray is believed to be associated with the current-sheet structure that formed as a result of solar eruption, and the blobs are products of magnetic reconnection occurring along the current sheet. The ray morphology and blob dynamics are investigated statistically. It is found that the apparent angular widths of the rays at a fixed time vary in a range of  $2.1-6.6^\circ$  ( $2.0-4.4^\circ$ )

observed durations of the events vary from 12 h to a few days with an average of 27 h. It is also found, based on the analysis of blob motions, that 58% (26) of the blobs were accelerated, 20% (9) were decelerated, and 22% (10) moved with a nearly constant speed. Comparing the dynamics of our blobs and those that are observed above the tip of a helmet streamer, we find that the speeds and accelerations of the blobs in these two cases differ significantly. It is suggested that these differences of the blob dynamics stem from the associated magnetic reconnection involving different magnetic field configurations and triggering processes.

## **Evolution of Coronal Jets during Solar Cycle 24**

Sz. **Soós**<sup>1,2</sup>, J. Liu (刘佳佳)<sup>3,4</sup>, M. B. Korsós<sup>1,2,5</sup>, and R. Erdélyi<sup>1,2,6</sup>

**2024** ApJ 965 43

<https://iopscience.iop.org/article/10.3847/1538-4357/ad29f8/pdf>

The focus of this study is on the spatial and temporal distributions of 2704 solar jets throughout Solar Cycle 24, from beginning to end. This work is a follow-up paper by Liu et al. With this extended data set, we have further confirmed the two distinct distributions of coronal jets: one located in polar regions and another at lower latitudes. Further analysis of the series of coronal jets revealed kink oscillations of the global solar magnetic field. Additionally, studying the northern and southern hemispheres separately showed an antiphase correlation that can be interpreted as a global sausage oscillatory pattern of the loci of the coronal jets. We also investigated how the variability of the solar cycle may impact the power law index of coronal jets by dividing the data set into the rising and declining phases of Solar Cycle 24. However, there is no compelling evidence to suggest that the power law index changes after the maximum. It is worth noting that based on this vast database of solar jets, the degradation of the 304 Å channel of the Atmospheric Imaging Assembly instrument on board the Solar Dynamics Observatory can also be identified and confirmed. Finally, we searched for compelling signatures of the presence of active longitude in the coronal jet database. There was no obvious evidence with a high probability of an active longitude; therefore, this question remains yet to be addressed further.

## **Turbulent Cascade and Energy Transfer Rate in a Solar Coronal Mass Ejection**

Luca **Sorriso-Valvo**<sup>1,2</sup>, Emiliya Yordanova<sup>1</sup>, Andrew P. Dimmock<sup>1</sup>, and Daniele Telloni<sup>3</sup>

**2021** ApJL 919 L30

<https://arxiv.org/pdf/2110.02664.pdf>

<https://doi.org/10.3847/2041-8213/ac26c5>

Turbulence properties are examined before, during, and after a coronal mass ejection (CME) detected by the Wind spacecraft in 2012 July. The power-law scaling of the structure functions, providing information on the power spectral density and flatness of the velocity, magnetic field, and density fluctuations, were examined. The third-order moment scaling law for incompressible, isotropic magnetohydrodynamic turbulence was observed in the preceding and trailing solar wind, as well as in the CME sheath and magnetic cloud. This suggests that the turbulence could develop sufficiently after the shock, or that turbulence in the sheath and cloud regions was robustly preserved even during the mixing with the solar wind plasma. The turbulent energy transfer rate was thus evaluated in each of the regions. The CME sheath shows an increase of energy transfer rate, as expected from the lower level of Alfvénic fluctuations and suggesting the role of the shock-wind interaction as an additional source of energy for the turbulent cascade. **12-15 Jul 2012**

## **Radio remote sensing of the corona and the solar wind**

Steven R. **Spangler** and Catherine A. Whiting

Proceedings of the International Astronomical Union / Volume 4 / Symposium S257, pp 529 – 541,

Published online: 16 Mar 2009

<http://journals.cambridge.org/action/displayIssue?iid=4866212>

Modern radio telescopes are extremely sensitive to plasma on the line of sight from a radio source to the antenna. Plasmas in the corona and solar wind produce measurable changes in the radio wave amplitude and phase, and the phase difference between wave fields of opposite circular polarization. Such measurements can be made of radio waves from spacecraft transmitters and extragalactic radio sources, using radio telescopes and spacecraft tracking antennas. Data have been taken at frequencies from about 80 MHz to 8000 MHz. Lower frequencies probe plasma at greater heliocentric distances. Analysis of these data yields information on the plasma density, density fluctuations, and plasma flow speeds in the corona and solar wind, and on the magnetic field in the solar corona. This paper will concentrate on

the information that can be obtained from measurements of Faraday rotation through the corona and inner solar wind. The magnitude of Faraday rotation is proportional to the line of sight integral of the plasma density and the line-of-sight component of the magnetic field. Faraday rotation provides an almost unique means of estimating the magnetic field in this part of space. This technique has contributed to measurement of the large scale coronal magnetic field, the properties of electromagnetic turbulence in the corona, possible detection of electrical currents in the corona, and probing of the internal structure of coronal mass ejections (CMEs). This paper concentrates on the search for small-scale coronal turbulence and remote sensing of the structure of CMEs. Future investigations with the Expanded Very Large Array (EVLA) or Murchison Widefield Array (MWA) could provide unique observational input on the astrophysics of CMEs.

## **A CRITICAL EXAMINATION OF THE FUNDAMENTAL ASSUMPTIONS OF SOLAR FLARE AND CORONAL MASS EJECTION MODELS**

D. S. [Spicer](#)<sup>1</sup>, R. Bingham<sup>2,3</sup>, and R. Harrison

2013 ApJ 768 8

The fundamental assumptions of conventional solar flare and coronal mass ejection (CME) theory are re-examined. In particular, the common theoretical assumption that magnetic energy that drives flares and CMEs can be stored in situ in the corona with sufficient energy density is found wanting. In addition, the observational constraint that flares and CMEs produce non-thermal electrons with fluxes of order  $10^{34}$ - $10^{36}$  electrons  $s^{-1}$ , with energies of order 10-20 keV, must also be explained. This constraint when imposed on the "standard model" for flares and CMEs is found to miss the mark by many orders of magnitude. We suggest, in conclusion, there are really only two possible ways to explain the requirements of observations and theory: flares and CMEs are caused by mass-loaded prominences or driven directly by emerging magnetized flux.

## **Numerical Simulations of the Decaying Transverse Oscillations in the Cool Jet**

[Abhishek K. Srivastava](#), [Balveer Singh](#)

"Physics", 2023

<https://arxiv.org/pdf/2306.13322.pdf>

We describe a 2.5D MHD simulation describing the evolution of cool jets triggered by initial vertical velocity perturbations in the solar chromosphere. We implement random velocity pulses of amplitude 20-50 km/s between 1 Mm and 1.5 Mm, along with various switch-off periods between 50 s and 300 s. The applied vertical velocity pulses create a series of magnetoacoustic shocks steepening above TR. These shocks interact with each other in the inner corona, leading to complex localized velocity fields. The upward propagation of such perturbations creates low-pressure regions behind them, which propel a variety of cool jets and plasma flows. We study the transverse oscillations of a representative cool jet J1, which moves up to the height of 6.2 Mm above the TR from its origin point. During its evolution, the plasma flows make the spine of jet J1 radially inhomogeneous, which is visible in the density and Alfvén speed smoothly varying across the jet. The highly dense J1 supports the propagating transverse wave of period of approximately 195 s with a phase speed of about 125 km/s. In the distance-time map of density, it is manifested as a transverse kink wave. However, the careful investigation of the distance-time maps of the x- and z-components of velocity reveals that these transverse waves are actually the mixed Alfvénic modes. The transverse wave shows evidence of damping in the jet. We conclude that the cross-field structuring of the density and characteristic Alfvén speed within J1 causes the onset of the resonant conversion and leakage of the wave energy outward to dissipate these transverse oscillations via resonant absorption. The wave energy flux is estimated as approximately of  $1.0 \times 10^6$  ergs  $cm^{-2} s^{-1}$ . This energy, if it dissipates through the resonant absorption into the corona where the jet is propagated, is sufficient energy for the localized coronal heating.

## **The prominence driven forced reconnection in the solar corona and associated plasma dynamics**

[A.K. Srivastava](#), [Sudheer K. Mishra](#), [P. Jelínek](#)

ApJ 920 18 2021

<https://arxiv.org/pdf/2107.06940.pdf>

<https://doi.org/10.3847/1538-4357/ac1519>

Using the multi-temperature observations from SDO/AIA on **30th December 2019**, we provide a signature of prominence driven forced magnetic reconnection in the corona and associated plasma dynamics during 09:20 UT to 10:38 UT. A hot prominence segment erupts with a speed of 21 km/s and destabilises the entire prominence system. Thereafter, it rose upward in the north during 09:28 UT to 09:48 UT with a speed of 24 km/s. The eruptive prominence stretches overlying field lines upward with the speed of 27-28 km/s, which further undergo into the forced reconnection. The coronal plasma also flows in southward direction with the speed of 7 km/s, and both these inflows trigger the reconnection at 09:48 UT. Thereafter, the east and westward magnetic channels are developed and separated. The east-west reorganization of the magnetic fields starts creating bi-directional plasma outflows towards the limb with their respective speed of 28 km/s and 37 km/s. Their upper ends are diffused in the overlying corona, transporting another set of upflows with the speed of 22 km/s and 19 km/s. The multi-temperature plasma ( $T_e=6.0$ - $7.2$ ) evolves and elongated upto a length of  $\sim 10^5$  km on the reorganized fields. The hot plasma and remaining prominence threads move from reconnection region towards another segment of prominence in the eastward direction. The prominence-

prominence/loop interaction and associated reconnection generate jet-like eruptions with the speed of 178-183 km/s. After the formation of jet, the overlying magnetic channel is disappeared in the corona.

### **Interplanetary and Geomagnetic Consequences of Interacting CMEs of 13-14 June 2012**

Nandita [Srivastava](#), [Wageesh Mishra](#), [D. Chakrabarty](#)

Solar Phys. **2017**

<https://arxiv.org/pdf/1712.08408.pdf>

We report on the kinematics of two interacting CMEs observed on **13 and 14 June 2012**. Both CMEs originated from the same active region NOAA 11504. After their launches which were separated by several hours, they were observed to interact at a distance of 100 Rs from the Sun. The interaction led to a moderate geomagnetic storm at the Earth with Dst index of approximately, -86 nT. The kinematics of the two CMEs is estimated using data from the Sun Earth Connection Coronal and Heliospheric Investigation (SECCHI) onboard the Solar Terrestrial Relations Observatory (STEREO). Assuming a head-on collision scenario, we find that the collision is inelastic in nature. Further, the signatures of their interaction are examined using the in situ observations obtained by Wind and the Advance Composition Explorer (ACE) spacecraft. It is also found that this interaction event led to the strongest sudden storm commencement (SSC) (approximately 150 nT) of the present Solar Cycle 24. The SSC was of long duration, approximately 20 hours. The role of interacting CMEs in enhancing the geoeffectiveness is examined.

### **On Thermal-Pulse-Driven Plasma Flows in Coronal Funnel as Observed by the Hinode/EUV Imaging Spectrometer (EIS)**

A. K. [Srivastava](#), P. Konkol, K. Murawski, B. N. Dwivedi, A. Mohan

Solar Phys., **2014**

Using one-arcsecond-slit-scan observations from the Hinode/EUV Imaging Spectrometer (EIS) on **5 February 2007**, we find the plasma outflows in the open and expanding coronal funnels at the eastern boundary of AR 10940. The Doppler-velocity map of Fe xii 195.120 Å shows the diffuse closed-loop system to be mostly red-shifted. The open arches (funnels) at the eastern boundary of AR exhibit blue-shifts with a maximum speed of about 10–15 km s<sup>-1</sup>. This implies outflowing plasma through these magnetic structures. In support of these observations, we perform a 2D numerical simulation of the expanding coronal funnels by solving the set of ideal MHD equations in appropriate VAL-III C initial temperature conditions using the FLASH code. We implement a rarefied and hotter region at the footpoint of the model funnel, which results in the evolution of slow plasma perturbations propagating outward in the form of plasma flows. We conclude that the heating, which may result from magnetic reconnection, can trigger the observed plasma outflows in such coronal funnels. This can transport mass into the higher corona, giving rise to the formation of the nascent solar wind.

### **Observations of intensity oscillations in a prominence-like cool loop system as observed by SDO/AIA: evidence of multiple harmonics of fast magnetoacoustic waves**

[Srivastava](#), A. K.; Dwivedi, B. N.; Kumar, Mukul

Astrophysics and Space Science, Volume 345, Issue 1, pp.25-32, **2013**

Using SDO/AIA 304 Å channel, we study the evolution of weak intensity oscillations in a prominence like cool loop system observed at North-West limb on **7 March 2011**. We use the standard wavelet tool to produce statistically significant power spectra of AIA 304 Å normalized fluxes derived respectively near the apex and footpoint of the fluxtube. We find periodicities of ≈667 s and ≈305 s respectively near apex and above footpoint with significance level >98 %. Observed statistically significant periodicities in the tube of projected length ≈170 Mm and width ≈10 Mm, are interpreted as most likely signature of evolution of various harmonics of tubular fast magnetoacoustic waves. Sausage modes are unlikely though they are compressive as they need bulky and highly denser loop system for their evolution for sustaining such large periods. We interpret the observed periodicities as multiple harmonics (fundamental and first) of fast magnetoacoustic kink waves that can generate some weak density perturbations (thus intensity oscillations) in the tube and can be observed pertaining to periodic variation in plasma column depth as tube is oblique in projection with respect to line-of-sight. The period ratio  $P_1/P_2=2.18$  is observed in the fluxtube, which is the signature of the magnetic field divergence of the cool loop system. We estimate tube expansion factor as 1.27 which is typical of EUV bipolar loops in the solar atmosphere. We estimate the lower bound average magnetic fields ranging from ≈9 to 90 Gauss depending upon typical densities as 10<sup>9</sup>-10<sup>11</sup> cm<sup>-3</sup> in the observed prominence-like cool loop system. We also observe the first signature of lowering fundamental mode period by a factor 0.85 due to cooling of this loop system.

### **Discovery of the Sausage-Pinch Instability in Solar Corona**

Abhi K. [Srivastava](#)<sup>1</sup>, R. Erdélyi<sup>2</sup>, V. Fedun<sup>2</sup>, P. Kayshap<sup>1</sup>, N.C. Joshi<sup>1</sup>, D. Tripathi

UKSP nugget 34, **2013**. <http://www.uksolphys.org/?p=6158>

A wide range of MHD instabilities have been observed in recent years in association with various solar dynamical processes. An instability known as the sausage instability ( $m = 0$ ) mode, which is theoretically investigated in astrophysical plasma [7,9,10], has – to the best of our knowledge – not yet been observed in the solar atmosphere

(although it is worth mentioning that sausage oscillations of the stable flux-tubes are well-observed [11,12,13]). In this nugget, we outline in brief the discovery of the sausage-pinch instability in the solar corona, in an activated partial filament eruption observed by SDO/AIA.

These types of magnetic instabilities can act as canonical plasma processes to trigger large-scale solar eruptions.

**12 September 2011**

## **OBSERVATIONAL EVIDENCE OF SAUSAGE-PINCH INSTABILITY IN SOLAR CORONA BY SDO/AIA**

A. K. [Srivastava](#)<sup>1</sup>, R. Erdélyi<sup>2</sup>, Durgesh Tripathi<sup>3</sup>, V. Fedun<sup>2,4</sup>, N. C. Joshi<sup>1</sup>, and P. Kayshap

**2013 ApJ 765 L42**

We present the first observational evidence of the evolution of sausage-pinch instability in active region 11295 during a prominence eruption using data recorded on **2011 September 12** by the Atmospheric Imaging Assembly (AIA) onboard the Solar Dynamics Observatory (SDO). We have identified a magnetic flux tube visible in AIA 304 Å that shows curvatures on its surface with variable cross-sections as well as enhanced brightness. These curvatures evolved and thereafter smoothed out within a timescale of a minute. The curved locations on the flux tube exhibit a radial outward enhancement of the surface of about 1-2 Mm (a factor of two larger than the original thickness of the flux tube) from the equilibrium position. AIA 193 Å snapshots also show the formation of bright knots and narrow regions in-between at the four locations as that of 304 Å along the flux tube where plasma emission is larger compared to the background. The formation of bright knots over an entire flux tube as well as the narrow regions in <60 s may be the morphological signature of the sausage instability. We also find the flows of confined plasma (propagation of brightness) in these bright knots along the field lines, which indicates the dynamicity of the flux tube that probably causes the dominance of the longitudinal field component over short temporal scales. The observed longitudinal motion of the plasma frozen in the magnetic field lines further vanishes the formed curvatures and plasma confinements as well as growth of instability to stabilize the flux tube.

## **Multiwavelength Observations of Supersonic Plasma Blob Triggered by Reconnection-Generated Velocity Pulse in AR10808**

A.K. [Srivastava](#), R. Erdélyi, K. Murawski, Pankaj Kumar

*Solar Phys.*, 281(2), 729-747, **2012**

Using multi-wavelength observations of Solar and Heliospheric Observatory (SoHO)/Michelson Doppler Imager (MDI), Transition Region and Coronal Explorer (TRACE, 171 Å), and H $\alpha$  from Culgoora Solar Observatory at Narrabri, Australia, we present a unique observational signature of a propagating supersonic plasma blob before an M6.2-class solar flare in active region 10808 on **9 September 2005**. The blob was observed between 05:27 UT and 05:32 UT with almost a constant shape for the first 2–3 min, and thereafter it quickly vanished in the corona. The observed lower-bound speed of the blob is estimated as  $\approx 215 \text{ km s}^{-1}$  in its dynamical phase. The evidence of the blob with almost similar shape and velocity concurrent in H $\alpha$  and TRACE 171 Å images supports its formation by a multi-temperature plasma. The energy release by a recurrent three-dimensional reconnection process via the separator dome below the magnetic null point, between the emerging flux and pre-existing field lines in the lower solar atmosphere, is found to be the driver of a radial velocity pulse outwards that accelerates this plasma blob in the solar atmosphere. In support of identification of the possible driver of the observed eruption, we solve the two-dimensional ideal magnetohydrodynamic equations numerically to simulate the observed supersonic plasma blob. The numerical modelling closely match the observed velocity, evolution of multi-temperature plasma, and quick vanishing of the blob found in the observations. Under typical coronal conditions, such blobs may also carry an energy flux of  $7.0 \times 10^6 \text{ erg cm}^{-2} \text{ s}^{-1}$  to balance the coronal losses above active regions.

## **On three-dimensional aspects of CMEs, their source regions and interplanetary manifestations: [Introduction to special issue](#) [Review](#)**

Nandita [Srivastava](#), , Marilena Mierlab, c, d and Luciano Rodriguez

*Journal of Atmospheric and Solar-Terrestrial Physics*, Volume 73, Issue 10, 20 June **2011**, Pages 1077-1081

Article Outline

1. Introduction

1.1. CMEs source regions: 3D observations and models

1.2. CMEs: 3D observations and models

1.3. Interplanetary CMEs: 3D observations and models

## **3D Reconstruction of the Leading Edge of the 20 May 2007 Partial Halo CME**

N. [Srivastava](#) · B. Inhester · M. Mierla · B. Podlipnik

*Solar Phys.* (2009) 259: 213–225; **File**

We have reconstructed the leading edge of a coronal mass ejection (CME) observed on 20 May 2007 by COR1 and COR2 of the SECCHI suite onboard the twin

STEREO spacecraft. The reconstruction of the leading edge of this CME was achieved using the tie-pointing method based on epipolar geometry. The true speeds derived from the reconstruction of the leading edge were estimated. These estimated true speeds were compared with the projected plane-of-sky speeds of the leading edge of the CME derived from LASCO aboard SoHO as well as from STEREO A and B images individually. The results show that a better estimation of the true speed of the CME in the Sun – Earth direction is achieved from the 3D reconstruction and therefore has an important bearing on space weather prediction.

### **Source region of the 18 November 2003 coronal mass ejection that led to the strongest magnetic storm of cycle 23**

**Srivastava**, Nandita; Mathew, Shibu K.; Louis, Rohan E.; Wiegmann, Thomas  
J. Geophys. Res., Vol. 114, No. A3, A03107, **2009**; **File**

<http://dx.doi.org/10.1029/2008JA013845>

[sci-hub.se/10.1029/2008JA013845](http://sci-hub.se/10.1029/2008JA013845)

The superstorm of **20 November 2003** was associated with a high-speed coronal mass ejection (CME) which originated in the NOAA AR 10501 on 18 November. This coronal mass ejection had severe terrestrial consequences leading to a geomagnetic storm with *Dst* index of  $-472$  nT, the strongest of the current solar cycle. In this paper, we attempt to understand the factors that led to the coronal mass ejection on 18 November. We have also studied the evolution of the photospheric magnetic field of NOAA AR 10501, the source region of this coronal mass ejection. For this purpose, the Michelson Doppler Imager line-of-sight magnetograms and vector magnetograms from Solar Flare Telescope, Mitaka, obtained during 17–19 November 2003 were analyzed. In particular, quantitative estimates of the temporal variation in magnetic flux, energy, and magnetic field gradient were estimated for the source active region. The evolution of these quantities was studied for the 3-day period with an objective to understand the preflare configuration leading up to the moderate flare which was associated with the geoeffective coronal mass ejection. We also examined the chromospheric images recorded in  $H_{\alpha}$  from Udaipur Solar Observatory to compare the flare location with regions of different magnetic field and energy. Our observations provide evidence that the flare associated with the CME occurred at a location marked by high magnetic field gradient which led to release of free energy stored in the active region.

### **Active region contributions to the solar wind over multiple solar cycles**

**D. Stansby**, [L. M. Green](#), [L. van Driel-Gesztelyi](#), [T. S. Horbury](#)

Solar Phys. **2021**

<https://arxiv.org/pdf/2104.04417.pdf>

Both coronal holes and active regions are source regions of the solar wind. The distribution of these coronal structures across both space and time is well known, but it is unclear how much each source contributes to the solar wind. In this study we use photospheric magnetic field maps observed over the past four solar cycles to estimate what fraction of magnetic open solar flux is rooted in active regions, a proxy for the fraction of all solar wind originating in active regions. We find that the fractional contribution of active regions to the solar wind varies between 30% to 80% at any one time during solar maximum and is negligible at solar minimum, showing a strong correlation with sunspot number. While active regions are typically confined to latitudes  $\pm 30^{\circ}$  in the corona, the solar wind they produce can reach latitudes up to  $\pm 60^{\circ}$ . Their fractional contribution to the solar wind also correlates with coronal mass ejection rate, and is highly variable, changing by  $\pm 20\%$  on monthly timescales within individual solar maxima. We speculate that these variations are primarily driven by coronal mass ejections causing global reconfigurations of the coronal magnetic field on sub-monthly timescales.

### **Magnetohydrodynamic models of coronal transients in the meridional plane.**

**Steinolfson**, R.S., Wu, S.T., Dryer, M., Tandberg-Hanssen, E., **1978**.

I- The effect of the magnetic field. *Astrophys. J.* 225, 259–274.

### **Investigating Coronal Holes and CMEs as Sources of Brightness Depletion Detected in PSP/WISPR Images**

Guillermo **Stenborg**<sup>1</sup>, Evangelos Paouris<sup>1,2</sup>, Russell A. Howard<sup>1</sup>, Angelos Vourlidas<sup>1</sup>, and Phillip Hess<sup>3</sup>  
**2023** *ApJ* 949 61

<https://iopscience.iop.org/article/10.3847/1538-4357/acd2cf/pdf>

The Parker Solar Probe (PSP) mission provides a unique opportunity to observe the solar corona from distances below  $20 R_{\odot}$ . In this work, we utilize white light images from the Wide-field Imager for Solar PRobe aboard the PSP from solar encounters 10 through 13 to examine the causes of brightness depletions of the corona during the rapid transit of PSP through the perihelia of its orbit. We analyze the effect of (1) coronal holes (CHs) and (2) energetic coronal mass ejection (CME) events on the observed brightness of the images. We speculate on the causes of the brightness depletions, ascribing them to the evacuation of (1) free electrons (reduced K-corona) and (2) interplanetary dust (reduced F-corona). In particular, we show that (1) the presence of CHs in all of the orbits is directly correlated with the depletion of the global white light emission recorded, and (2) a huge CME event in encounter 13 caused a very deep

depletion in its wake that removed the electron content as well as some of the interplanetary dust. **14-18 Nov 2021; 21 Nov 2021; 18, 24, 25, 27 Feb 2022; 13, 17 May 2022; 1, 2 Jun 2022; 27 Aug 2022; 5, 6, 14 Sep 2022**

## **Multi-instrument observations and tracking of a coronal mass ejection front from low to middle corona**

Oleg **Stepanyuk\*** and Kamen Kozarev

J. Space Weather Space Clim. **2024**, 14, 2

<https://www.swsc-journal.org/articles/swsc/pdf/2024/01/swsc230003.pdf>

The shape and dynamics of coronal mass ejections (CMEs) vary significantly based on the instrument and wavelength used. This has led to significant debate about the proper definitions of CME/shock fronts, pile-up/compression regions, and core observations in projection in optically thin vs. optically thick emission. Here we present an observational analysis of the evolving shape and kinematics of a large-scale CME that occurred on **May 7, 2021** on the eastern limb of the Sun as seen from 1 AU. The eruption was observed continuously, consecutively by the Atmospheric Imaging Assembly (AIA) telescope suite on the Solar Dynamics Observatory (SDO), the ground-based COronal Solar Magnetism Observatory (COSMO) K-coronagraph (K-Cor) on Mauna Loa, and the C2 and C3 telescopes of the Large Angle Solar Coronagraph (LASCO) on the Solar and Heliospheric Observatory (SoHO). We apply the updated multi-instrument version of the recently developed Wavetrack Python suite for automated detection and tracking of coronal eruptive features to evaluate and compare the evolving shape of the CME front as it propagated from the solar surface out to 20 solar radii. Our tool allows tracking features beyond just the leading edge and is an important step towards semi-automatic manufacturing of training sets for training data-driven image segmentation models for solar imaging. Our findings confirm the expected strong connection between EUV waves and CMEs. Our novel, detailed analysis sheds observational light on the details of EUV wave-shock-CME relations that lacking for the gap region between the low and middle corona.

## **Multi-Scale Image Preprocessing and Feature Tracking for Remote CME Characterization**

[Oleg Stepanyuk](#), [Kamen Kozarev](#), [Mohamed Nedal](#)

Journal of Space Weather and Space Climate **12**, 20 **2022**

<https://arxiv.org/pdf/2205.15088.pdf>

<https://www.swsc-journal.org/articles/swsc/pdf/2022/01/swsc210084.pdf>

Coronal Mass Ejections (CMEs) influence the interplanetary environment over vast distances in the solar system by injecting huge clouds of fast solar plasma and energetic particles (SEPs). A number of fundamental questions remain about how SEPs are produced, but current understanding points to CME-driven shocks and compressions in the solar corona. At the same time, unprecedented remote and in situ (Parker Solar Probe, Solar Orbiter) solar observations are becoming available to constrain existing theories. Here we present a general method for recognition and tracking on solar images of objects such as CME shock waves and filaments. The calculation scheme is based on a multi-scale data representation concept a trous wavelet transform, and a set of image filtering techniques. We showcase its performance on a small set of CME-related phenomena observed with the SDO/AIA telescope. With the data represented hierarchically on different decomposition and intensity levels, our method allows to extract certain objects and their masks from the imaging observations, in order to track their evolution in time. The method presented here is general and applicable to detecting and tracking various solar and heliospheric phenomena in imaging observations. It holds potential to prepare large training data sets for deep learning. We have implemented this method into a freely available Python library. **May 11, 2011; June 07, 2011; September 29, 2013, December 12, 2013,**

## **On the Onset Mechanism for Solar Coronal Jets, and Implications for the Onset Mechanism for CME-Producing Eruptions**

[Alphonse C. Sterling](#), [Ronald L. Moore](#), [Navdeep K. Panesar](#)

Proceedings of the IAU Symposium No. 388, **2024**

<https://arxiv.org/pdf/2410.01123>

Large-scale solar eruptions often include ejection of a filament, a solar flare, and expulsion of a coronal mass ejection (CME). Unravelling the magnetic processes that build up the free energy for these eruptions and trigger that energy's release in the eruption is a continuing challenge in solar physics. Such large-scale eruptions are comparatively infrequent, with the moderate level ones (say, GOES M-class events) occurring perhaps once every few days on average during active-activity times, and much less frequently during quieter times. In contrast, solar coronal jets, which are long (~50,000 km), narrow (less than about 10,000 km), transient (~10--20 min) plasma spires with bright bases and that are seen in soft X-rays and EUV, occur much more frequently, likely several hundred times per day independent of large-scale solar activity level. Recent studies indicate that coronal jets are small-scale versions of large-scale eruptions, often produced by eruption of a small-scale "miniflament," that results in a "miniflare" analogous to a larger typical solar flare, and that sometimes produces a CME analogue (a "narrow CME" or "white-light jet"). Under the assumption that jets are small-scale eruptions, their higher occurrence frequency and faster build-up evolution reveals perhaps fundamental aspects of all eruptions that are not as easy to discern in the more-complex magnetic environment and the slower build up to the larger eruptions. Therefore, the study of coronal jets can provide insights into the onset mechanism of CME-producing large-scale eruptions. **22 Jul 2011**

## How Small-scale Jet-like Solar Events from Miniature Flux Rope Eruptions Might Produce the Solar Wind

[Alphonse C. Sterling](#), [Navdeep K. Panesar](#), [Ronald L. Moore](#)

ApJ 963 4 2024

<https://arxiv.org/pdf/2401.09560.pdf>

<https://iopscience.iop.org/article/10.3847/1538-4357/ad1d5f/pdf>

We consider small-scale jet-like events that might make the solar wind, as has been suggested in recent studies. We show that the events referred to as "coronal jets" and as "jetlets" both fall on a power-law distribution that also includes large-scale eruptions and spicule-sized features; all of the jet-like events could contribute to the solar wind. Based on imaging and magnetic field data, it is plausible that many or most of these events might form by the same mechanism: Magnetic flux cancellation produces small-scale flux ropes, often containing a cool-material minifilament. This minifilament/flux rope erupts and reconnects with adjacent open coronal field, along which "plasma jets" flow and contribute to the solar wind. The erupting flux ropes can contain twist that is transferred to the open field, and these become Alfvénic pulses that form magnetic switchbacks, providing an intrinsic connection between switchbacks and the production of the solar wind. **20 May 2020**

## Solar Active Region Coronal Jets. III. Hidden-Onset Jets

[Alphonse C. Sterling](#), [Ronald L. Moore](#), [Navdeep K. Panesar](#)

ApJ 2023

<https://arxiv.org/pdf/2310.14109.pdf>

Solar quiet- and coronal-hole region coronal jets frequently clearly originate from erupting minifilaments, but active-region jets often lack an obvious erupting-minifilament source. We observe a coronal-jet-productive active region (AR), AR 12824, over **2021 May 22 0 -- 8 UT**, primarily using Solar Dynamics Observatory (SDO) Atmospheric Imaging Array (AIA) EUV images and SDO/Helioseismic and Magnetic Imager (HMI) magnetograms. Jets were concentrated in two locations in the AR: on the south side and on the northwest side of the AR's lone large sunspot. The south-location jets are oriented so that we have a clear view of the jets' origin low in the atmosphere: their source is clearly minifilaments erupting from locations showing magnetic flux changes/cancellations. After erupting a projected distance  $\sim 5''$  away from their origin site, the minifilaments erupt outward onto far-reaching field as part of the jet's spire, quickly losing their minifilament character. In contrast, the northwest-location jets show no clear erupting minifilament, but the source site of those jets are obscured along our line-of-sight by absorbing chromospheric material. EUV and magnetic data indicate that the likely source sites were  $\sim 15''$  from where we first see the jet spire; thus an erupting minifilament would likely lose its minifilament character before we first see the spire. We conclude that such AR jets could work like non-AR jets, but the erupting-minifilament jet source is often hidden by obscuring material. Another factor is that magnetic eruptions making some AR jets carry only a harder-to-detect comparatively thin ( $\sim 1-2''$ ) minifilament "strand."

## Future High-Resolution and High-Cadence Observations for Unraveling Small-Scale Explosive Solar Features

[Alphonse C. Sterling](#), [Ronald L. Moore](#), [Navdeep K. Panesar](#), [Tanmoy Samanta](#), [Sanjiv K. Tiwari](#), [Sabrina L. Savage](#)

Frontiers Astron. Space Sci. 10: 1117870. **2023** doi: 10.3389/fspas.2023.1117870

<https://arxiv.org/pdf/2302.13179.pdf>

<https://www.frontiersin.org/articles/10.3389/fspas.2023.1117870/full>

<https://www.frontiersin.org/articles/10.3389/fspas.2023.1117870/pdf>

Solar coronal jets are frequently occurring collimated ejections of solar plasma, originating from magnetically mixed polarity locations on the Sun of size scale comparable to that of a supergranule. Many, if not most, coronal jets are produced by eruptions of small-scale filaments, or minifilaments, whose magnetic field reconnects both with itself and also with surrounding coronal field. There is evidence that minifilament eruptions are a scaled-down version of typical filament eruptions that produce solar flares and coronal mass ejections (CMEs). Moreover, the magnetic processes building up to and triggering minifilament eruptions, which is often flux cancellation, might similarly build up and trigger the larger filaments to erupt. Thus, detailed study of coronal jets will inform us of the physics leading to, triggering, and driving the larger eruptions. Additionally, such studies potentially can inform us of smaller-scale coronal-jet-like features, such as jetlets and perhaps some spicules, that might work the same way as coronal jets. We propose a high-resolution ( $\sim 0.1$  pixels), high-cadence ( $\sim 5$  seconds) EUV-solar-imaging mission for the upcoming decades, that would be dedicated to observations of features of the coronal-jet size scale, and smaller-scale solar features produced by similar physics. Such a mission could provide invaluable insight into the operation of larger features such as CMEs that produce significant Space Weather disturbances, and also smaller-scale features that could be important for coronal heating, solar wind acceleration, and heliospheric features such as the magnetic switchbacks that are frequently observed in the solar wind. **2012 November 13, 2013 October 18-20, 2017 March 6, 3 Apr 2018**

## Inconspicuous Solar Polar Coronal X-ray Jets as the Source of Conspicuous Hinode/EUV Imaging Spectrometer (EIS) Doppler Outflows

[Alphonse C. Sterling](#), [Conrad Schwanitz](#), [Louise K. Harra](#), [Nour E. Raouafi](#), [Navdeep K. Panesar](#), [Ronald L. Moore](#)

ApJ **940** 85 **2022**

<https://arxiv.org/pdf/2210.09233.pdf>

<https://iopscience.iop.org/article/10.3847/1538-4357/ac9960/pdf>

We examine in greater detail five events previously identified as being sources of strong transient coronal outflows in a solar polar region in Hinode/EUV Imaging Spectrometer (EIS) Doppler data. Although relatively compact or faint and inconspicuous in Hinode/Soft X-ray Telescope (XRT) soft-X-ray (SXR) images and in Solar Dynamics Observatory (SDO)/Atmospheric Imaging Assembly (AIA) EUV images, we find that all of these events are consistent with being faint coronal X-ray jets. The evidence for this is that the events result from eruption of minifilaments of projected sizes spanning 5000 -- 14,000 km and with erupting velocities spanning 19 -- 46 km/s, which are in the range of values observed in cases of confirmed X-ray polar coronal hole jets. In SXR images, and in some EUV images, all five events show base brightenings, and faint indications of a jet spire that (in four of five cases where determinable) moves away from the brightest base brightening; these properties are common to more obvious X-ray jets. For a comparatively low-latitude event, the minifilament erupts from near (<~few arcsec) a location of near-eruption-time opposite-polarity magnetic-flux-patch convergence, which again is consistent with many observed coronal jets. Thus, although too faint to be identified as jets a priori, otherwise all five events are identical to typical coronal jets. This suggests that jets may be more numerous than recognized in previous studies, and might contribute substantially to solar wind outflow, and to the population of magnetic switchbacks observed in Parker Solar Probe (PSP) data. **7 Mar 2020**

### **Another Look at Erupting Minifilaments at the Base of Solar X-Ray Polar Coronal "Standard" and "Blowout" Jets**

[Alphonse C. Sterling](#), [Ronald L. Moore](#), [Navdeep K. Panesar](#)

ApJ **2022**

<https://arxiv.org/pdf/2201.12314.pdf>

We examine 21 solar polar coronal jets that we identify in soft X-ray images obtained from the Hinode/X-ray telescope (XRT). We identify 11 of these jets as blowout jets and four as standard jets (with six uncertain), based on their X-ray-spire widths being respectively wide or narrow (compared to the jet's base) in the XRT images. From corresponding Extreme Ultraviolet (EUV) images from the Solar Dynamics Observatory's (SDO) Atmospheric Imaging Assembly (AIA), essentially all (at least 20 of 21) of the jets are made by minifilament eruptions, consistent with other recent studies. Here, we examine the detailed nature of the erupting minifilaments (EMFs) in the jet bases. Wide-spire ("blowout") jets often have ejective EMFs, but sometimes they instead have an EMF that is mostly confined to the jet's base rather than ejected. We also demonstrate that narrow-spire ("standard") jets can have either a confined EMF, or a partially confined EMF where some of the cool minifilament leaks into the jet's spire. Regarding EMF visibility: we find that in some cases the minifilament is apparent in as few as one of the four EUV channels we examined, being essentially invisible in the other channels; thus it is necessary to examine images from multiple EUV channels before concluding that a jet does not have an EMF at its base. The size of the EMFs, measured projected against the sky and early in their eruption, is  $14'' \pm 7''$ , which is within a factor of two of other measured sizes of coronal-jet EMFs. **13 Jan 2017, 6 Mar 2017, 4 Jul 2017, 3 Apr 2018**

Table 1. Examined Coronal Jets 2017-2018

### **Possible Evolution of Minifilament-Eruption-Produced Solar Coronal Jets, Jetlets, and Spicules, into Magnetic-Twist-Wave "Switchbacks" Observed by the Parker Solar Probe (PSP)**

[Alphonse C. Sterling](#), [Ronald L. Moore](#), [Navdeep K. Panesar](#), [Tanmoy Samanta](#)

**2020**

<https://arxiv.org/pdf/2010.12991.pdf>

Many solar coronal jets result from erupting miniature-filament ("minifilament") magnetic flux ropes that reconnect with encountered surrounding far-reaching field. Many of those minifilament flux ropes are apparently built and triggered to erupt by magnetic flux cancelation. If that cancelation (or some other process) results in the flux rope's field having twist, then the reconnection with the far-reaching field transfers much of that twist to that reconnected far-reaching field. In cases where that surrounding field is open, the twist can propagate to far distances from the Sun as a magnetic-twist Alfvénic pulse. We argue that such pulses from jets could be the kinked-magnetic-field structures known as "switchbacks," detected in the solar wind during perihelion passages of the Parker Solar Probe (PSP). For typical coronal-jet-generated Alfvénic pulses, we expect that the switchbacks would flow past PSP with a duration of several tens of minutes; larger coronal jets might produce switchbacks with passage durations ~1hr. Smaller-scale jet-like features on the Sun known as "jetlets" may be small-scale versions of coronal jets, produced in a similar manner as the coronal jets. We estimate that switchbacks from jetlets would flow past PSP with a duration of a few minutes. Chromospheric spicules are jet-like features that are even smaller than jetlets. If some portion of their population are indeed very-small-scale versions of coronal jets, then we speculate that the same processes could result in switchbacks that pass PSP with durations ranging from about ~2 min down to tens of seconds.



## Coronal-Jet-Producing Minifilament Eruptions as a Possible Source of Parker Solar Probe (PSP) Switchbacks

Alphonse C. [Sterling](#), [Ronald L. Moore](#)

ApJ **896** L18 **2020**

<https://arxiv.org/pdf/2006.04990.pdf>

<https://doi.org/10.3847/2041-8213/ab96be>

The Parker Solar Probe (PSP) has observed copious rapid magnetic field direction changes in the near-Sun solar wind. These features have been called "switchbacks," and their origin is a mystery. But their widespread nature suggests that they may be generated by a frequently occurring process in the Sun's atmosphere. We examine the possibility that the switchbacks originate from coronal jets. Recent work suggests that many coronal jets result when photospheric magnetic flux cancels, and forms a small-scale "minifilament" flux rope that erupts and reconnects with coronal field. We argue that the reconnected erupting minifilament flux rope can manifest as an outward propagating Alfvénic fluctuation that steepens into an increasingly compact disturbance as it moves through the solar wind. Using previous observed properties of coronal jets that connect to coronagraph-observed white-light jets (a.k.a. "narrow CMEs"), along with typical solar wind speed values, we expect the coronal-jet-produced disturbances to traverse near-perihelion PSP in  $\sim 25$  min, with a velocity of  $\sim 400$  km/s. To consider further the plausibility of this idea, we show that a previously studied series of equatorial latitude coronal jets, originating from the periphery of an active region, generate white-light jets in the outer corona (seen in STEREO/COR2 coronagraph images; 2.5---15  $R_{\text{sun}}$ ), and into the inner heliosphere (seen in STEREO/Hi1 heliospheric imager images; 15---84  $R_{\text{sun}}$ ). Thus it is tenable that disturbances put onto open coronal magnetic field lines by coronal-jet-producing erupting minifilament flux ropes can propagate out to PSP space and appear as switchbacks. **30 June 2012**

## Possible Production of Solar Spicules by Microfilament Eruptions

Alphonse C. [Sterling](#), [Ronald L. Moore](#), [Tanmoy Samanta](#), [Vasyl Yurchyshyn](#)

ApJL **893** L45 **2020**

<https://arxiv.org/pdf/2004.04187.pdf>

<https://doi.org/10.3847/2041-8213/ab86a5>

We examine Big Bear Solar Observatory (BBSO) Goode Solar Telescope (GST) high-spatial resolution ( $0''.06$ ), high-cadence (3.45 s), H-alpha-0.8 Angstrom images of central-disk solar spicules, using data of Samanta et al. (2019). We compare with coronal-jet chromospheric-component observations of Sterling et al. (2010a). Morphologically, bursts of spicules, referred to as "enhanced spicular activities" by Samanta et al. (2019), appear as scaled-down versions of the jet's chromospheric component. Both the jet and the enhanced spicular activities appear as chromospheric-material strands, undergoing twisting-type motions of  $\sim 20$ ---50 km/s in the jet and  $\sim 20$ ---30 km/s in the enhanced spicular activities. Presumably, the jet resulted from a minifilament-carrying magnetic eruption. For two enhanced spicular activities that we examine in detail, we find tentative candidates for corresponding erupting microfilaments, but not expected corresponding base brightenings. Nonetheless, the enhanced-spicular-activities' interacting mixed-polarity base fields, frequent-apparent-twisting motions, and morphological similarities to the coronal jet's chromospheric-temperature component, suggest that erupting microfilaments might drive the enhanced spicular activities but be hard to detect, perhaps due to H-alpha opacity. Degrading the BBSO/GST-image resolution with a  $1''.0$ -FWHM smoothing function yields enhanced spicular activities resembling the "classical spicules" described by, e.g., Beckers (1968). Thus, a microfilament eruption might be the fundamental driver of many spicules, just as a minifilament eruption is the fundamental driver of many coronal jets. Similarly, a  $0''.5$ -FWHM smoothing renders some enhanced spicular activities to resemble previously-reported "twinned" spicules, while the full-resolution features might account for spicules sometimes appearing as 2D-sheet-like structures. **2007 April 1, 2017 June 19**

## Hi-C 2.1 Observations of Small-Scale Miniature-Filament-Eruption-Like Cool Ejections in Active Region Plage

Alphonse C. [Sterling](#), [Ronald L. Moore](#), [Navdeep K. Panesar](#), [Kevin P. Reardon](#), [Momchil Molnar](#), [Laurel A. Rachmeler](#), [Sabrina L. Savage](#), [Amy R. Winebarger](#)

ApJ **889** 187 **2020**

<https://arxiv.org/pdf/1912.02319.pdf>

<https://doi.org/10.3847/1538-4357/ab5dcc>

We examine 172 Ang ultra-high-resolution images of a solar plage region from the Hi-C 2.1 ("Hi-C") rocket flight of **2018 May 29**. Over its five-minute flight, Hi-C resolves a plethora of small-scale dynamic features that appear near noise level in concurrent Solar Dynamics Observatory (SDO) Atmospheric Imaging Assembly (AIA) 171 Ang images. For ten selected events, comparisons with AIA images at other wavelengths and with the Interface Region Imaging Spectrograph (IRIS) images indicate that these features are cool (compared to the corona) ejections. Combining Hi-C 172 Ang, AIA 171 Ang, IRIS 1400 Ang, and H $\alpha$ , we see that these ten cool ejections are similar to the H $\alpha$  "dynamic fibrils" and Ca ii "anemone jets" found in earlier studies. The front of some of our cool ejections are likely heated, showing emission in IRIS 1400 Ang. On average, these cool ejections have approximate widths:  $3''.2 \pm 2''.1$ , (projected) maximum heights and velocities:  $4''.3 \pm 2''.5$  and  $23 \pm 6$  km/s, and lifetimes:  $6.5 \pm 2.4$  min. We consider whether these Hi-C features might result from eruptions of sub-minifilaments (smaller than the minifilaments that erupt to produce coronal jets). Comparisons with SDO's Helioseismic and Magnetic Imager (HMI) magnetograms do not show magnetic mixed-polarity neutral lines at these events' bases, as would be expected for true scaled-down versions of solar filaments/minifilaments. But the features' bases are all close to single-polarity strong-flux-edge locations, suggesting

possible local opposite-polarity flux unresolved by HMI. Or, it may be that our Hi-C ejections instead operate via the shock-wave mechanism that is suggested to drive dynamic fibrils and the so-called type I spicules.

## **A Two-Sided-Loop X-Ray Solar Coronal Jet Driven by a Minifilament Eruption**

Alphonse C. [Sterling](#), [Louise K. Harra](#), [Ronald L. Moore](#), [David A. Falconer](#)

ApJ **871** 220 **2019**

<https://arxiv.org/pdf/1811.05557.pdf>

<https://doi.org/10.3847/1538-4357/aaf1d3>

Most of the commonly discussed solar coronal jets are of the type consisting of a single spire extending approximately vertically from near the solar surface into the corona. Recent research supports that eruption of a miniature filament (minifilament) drives many such single-spire jets, and concurrently generates a miniflare at the eruption site. A different type of coronal jet, identified in X-ray images during the Yohkoh era, are two-sided-loop jets, which extend from a central excitation location in opposite directions, along low-lying coronal loops more-or-less horizontal to the surface. We observe such a two-sided-loop jet from the edge of active region (AR) 12473, using data from Hinode XRT and EIS, and SDO AIA and HMI. Similar to single-spire jets, this two-sided-loop jet results from eruption of a minifilament, which accelerates to over 140 km/s before abruptly stopping after striking overlying nearly-horizontal loop field at about 30,000 km altitude and producing the two-sided-loop jet. Analysis of EIS raster scans show that a hot brightening, consistent with a small flare, develops in the aftermath of the eruption, and that Doppler motions (approx 40 km/s) occur near the jet-formation region. As with many single-spire jets, the magnetic trigger here is apparently flux cancelation, which occurs at a rate of approx  $4 \times 10^{18}$  Mx/hr, comparable to the rate observed in some single-spire AR jets. An apparent increase in the (line-of-sight) flux occurs within minutes of onset of the minifilament eruption, consistent with the apparent increase being due to a rapid reconfiguration of low-lying field during and soon after minifilament-eruption onset. **2015 December 30**

## **Coronal Jets, and the Jet-CME Connection**

**mini Review**

Alphonse C. [Sterling](#)

Journal of Physics: Conference Series, Volume 1100, Issue 1, article id. 012024 (2018)

<https://arxiv.org/pdf/1912.02808.pdf>

Solar coronal jets have been observed in detail since the early 1990s. While it is clear that these jets are magnetically driven, the details of the driving process has recently been updated. Previously it was suspected that the jets were a consequence of magnetic flux emergence interacting with ambient coronal field. New evidence however indicates that often the direct driver of the jets is erupting field, often carrying cool material (a "minifilament"), that undergoes interchange magnetic reconnection with preexisting field ([1]). More recent work indicates that the trigger for eruption of the minifilament is frequently cancelation of photospheric magnetic fields at the base of the minifilament. These erupting minifilaments are analogous to the better-known larger-scale filament eruptions that produce solar flares and, frequently, coronal mass ejections (CMEs). A subset of coronal jets drive narrow "white-light jets," which are very narrow CME-like features, and apparently a few jets can drive wider, although relatively weak, "streamer-puff" CMEs. Here we summarize these recent findings.

## **Magnetic Flux Cancelation as the Buildup and Trigger Mechanism for CME-Producing Eruptions in two Small Active Regions**

Alphonse C. [Sterling](#), [Ronald L. Moore](#), [Navdeep K. Panesar](#)

ApJ **864** 68 **2018**

<https://arxiv.org/pdf/1807.03237.pdf>

<http://sci-hub.tw/http://iopscience.iop.org/article/10.3847/1538-4357/aad550/meta>

We follow two small, magnetically isolated CME-producing solar active regions (ARs) from the time of their emergence until several days later, when their core regions erupt to produce the CMEs. In both cases, magnetograms show: (a) following an initial period where the poles of the emerging regions separate from each other, the poles then reverse direction and start to retract inward; (b) during the retraction period, flux cancelation occurs along the main neutral line of the regions; (c) this cancelation builds the sheared core field/flux rope that eventually erupts to make the CME. In the two cases, respectively 30% and 50% of the maximum flux of the region cancels prior to the eruption. Recent studies indicate that solar coronal jets frequently result from small-scale filaments eruptions, with those "minifilament" eruptions also being built up and triggered by cancelation of magnetic flux. Together, the small-AR eruptions here and the coronal jet results suggest that isolated bipolar regions tend to erupt when some threshold fraction, perhaps in the range of 50%, of the region's maximum flux has canceled. Our observed erupting filaments/flux ropes form at sites of flux cancelation, in agreement with previous observations. Thus, the recent finding that minifilaments that erupt to form jets also form via flux cancelation is further evidence that minifilaments are small-scale versions of the long-studied full-sized filaments. **2010 July 16 , 2013 October 20**

[HMI Science Nuggets](#) #113 Sept 2018 <http://hmi.stanford.edu/hminuggets/?p=2694>

## **Solar Active Region Coronal Jets II: Triggering and Evolution of Violent Jets**

Alphonse C. [Sterling](#), [Ronald L. Moore](#), [David A. Falconer](#), [Navdeep K. Panesar](#), [Francisco Martinez](#)

Astrophysical Journal, 844:28 (20pp), **2017**

<https://arxiv.org/pdf/1705.03040.pdf>

<https://iopscience.iop.org/article/10.3847/1538-4357/aa7945/pdf>

We study a series of X-ray-bright, rapidly-evolving active-region coronal jets outside the leading sunspot of AR 12259, using Hinode/XRT, SDO/AIA and HMI, and IRIS data. The detailed evolution of such rapidly evolving "violent" jets remained a mystery after our previous investigation of active region jets (Sterling et al. 2016, Paper 1). The jets we investigate here erupt from three localized subregions, each containing a rapidly evolving (positive) minority-polarity magnetic-flux patch bathed in a (majority) negative-polarity magnetic-flux background. At least several of the jets begin with eruptions of what appear to be thin (thickness  $\sim 2''$ ) miniature-filament (minifilament) "strands" from a magnetic neutral line where magnetic flux cancelation is ongoing, consistent with the magnetic configuration presented for coronal-hole jets in Sterling et al. (2015). Some jets strands are difficult/impossible to detect, perhaps due to, e.g. their thinness, obscuration by surrounding bright or dark features, or the absence of erupting cool-material minifilaments in those jets. Tracing in detail the flux evolution in one of the subregions, we find bursts of strong jetting occurring only during times of strong flux cancelation. Averaged over seven jetting episodes, the cancelation rate was  $\sim 1.5 \times 10^{19}$  Mx/hr. An average flux of  $\sim 5 \times 10^{18}$  Mx canceled prior to each episode, arguably building up  $\sim 10^{28}$  -  $10^{29}$  ergs of free magnetic energy per jet. From these and previous observations, we infer that flux cancelation is the fundamental process responsible for the pre-eruption buildup and triggering of at least many jets in active regions, quiet regions, and coronal holes. **2015 January 14**

### **A MICROFILAMENT-ERUPTION MECHANISM FOR SOLAR SPICULES**

Alphonse C. [Sterling](#)<sup>1</sup> and Ronald L. Moore<sup>1,2</sup>

**2016** ApJ 828 L9 DOI 10.3847/2041-8205/828/1/L9

<https://arxiv.org/pdf/1612.00430v1.pdf>

Recent investigations indicate that solar coronal jets result from eruptions of small-scale chromospheric filaments, called minifilaments; that is, the jets are produced by scaled-down versions of typical-sized filament eruptions. We consider whether solar spicules might in turn be scaled-down versions of coronal jets, being driven by eruptions of microfilaments. Assuming a microfilament's size is about a spicule's width ( $\sim 300$  km), the estimated occurrence number plotted against the estimated size of erupting filaments, minifilaments, and microfilaments approximately follows a power-law distribution (based on counts of coronal mass ejections, coronal jets, and spicules), suggesting that many or most spicules could result from microfilament eruptions. Observed spicule-base Ca II brightenings plausibly result from such microfilament eruptions. By analogy with coronal jets, microfilament eruptions might produce spicules with many of their observed characteristics, including smooth rise profiles, twisting motions, and EUV counterparts. The postulated microfilament eruptions are presumably eruptions of twisted-core micro-magnetic bipoles that are  $\sim 10$  wide. These explosive bipoles might be built and destabilized by merging and cancelation of approximately a few to 100 G magnetic-flux elements of size  $\dots$ . If, however, spicules are relatively more numerous than indicated by our extrapolated distribution, then only a fraction of spicules might result from this proposed mechanism. **15-Sep-2011**

### **MINIFILAMENT ERUPTIONS THAT DRIVE CORONAL JETS IN A SOLAR ACTIVE REGION**

Alphonse C. [Sterling](#)<sup>1</sup>, Ronald L. Moore<sup>1,2</sup>, David A. Falconer<sup>1,2</sup>, Navdeep K. Panesar<sup>1,2</sup>, Sachiko Akiyama<sup>3,4</sup>, Seiji Yashiro<sup>3,4</sup>, and Nat Gopalswamy

**2016** ApJ 821 100

<https://iopscience.iop.org/article/10.3847/0004-637X/821/2/100/pdf>

We present observations of eruptive events in an active region adjacent to an on-disk coronal hole on **2012 June 30**, primarily using data from the Solar Dynamics Observatory (SDO)/Atmospheric Imaging Assembly (AIA), SDO/Heliographic and Magnetic Imager (HMI), and STEREO-B. One eruption is of a large-scale ( $\sim 100''$ ) filament that is typical of other eruptions, showing slow-rise onset followed by a faster-rise motion starting as flare emissions begin. It also shows an "EUV crinkle" emission pattern, resulting from magnetic reconnections between the exploding filament-carrying field and surrounding field. Many EUV jets, some of which are surges, sprays and/or X-ray jets, also occur in localized areas of the active region. We examine in detail two relatively energetic ones, accompanied by GOES M1 and C1 flares, and a weaker one without a GOES signature. All three jets resulted from small-scale ( $\sim 20''$ ) filament eruptions consistent with a slow rise followed by a fast rise occurring with flare-like jet-bright-point brightenings. The two more-energetic jets showed crinkle patterns, but the third jet did not, perhaps due to its weakness. Thus all three jets were consistent with formation via erupting minifilaments, analogous to large-scale filament eruptions and to X-ray jets in polar coronal holes. Several other energetic jets occurred in a nearby portion of the active region; while their behavior was also consistent with their source being minifilament eruptions, we could not confirm this because their onsets were hidden from our view. Magnetic flux cancelation and emergence are candidates for having triggered the minifilament eruptions.

### **Small-scale filament eruptions as the driver of solar coronal hole X-ray jets**

Alphonse C. [Sterling](#), Ronald L. Moore, David A. Falconer, Mitzi Adams

**2015**, Nature, 523, 437-440

<https://arxiv.org/pdf/1705.03373.pdf>

Solar X-ray jets are evidently made by a burst of reconnection of closed magnetic field in a jet's base with ambient "open" field (1,2). In the widely-accepted version of the "emerging-flux" model, that reconnection occurs at a current sheet between the open field and emerging closed field and also makes a compact hot brightening that is usually

observed at the edge of the jet's base (1,3). Here we report on high-resolution X-ray and EUV observations of 20 randomly-selected X-ray jets in polar coronal holes. In each jet, contrary to the emerging-flux model, a miniature version of the filament eruptions that initiate coronal mass ejections (CMEs) (4-7) drives the jet-producing reconnection, and the compact hot brightening is made by internal reconnection of the legs of the minifilament-carrying erupting closed field, analogous to solar flares of larger-scale eruptions. Previous observations have found that some jets are driven by base-field eruptions (8-10,12), but only one such study, of only one jet, provisionally questioned the emerging-flux model (13). Our observations support the view that solar filament eruptions are made by a fundamental explosive magnetic process that occurs on a vast range of scales, from the biggest CME/flare eruptions down to X-ray jets, and perhaps down to even smaller jets that are candidates for powering coronal heating (10,14,15). A picture similar to that suggested by our observations was drawn before, inferred from different observations and based on a different origin of the erupting minifilament flux rope (11) (see Methods). **28 Aug 2010, 9 Sept 2010, 17 Sept 2010**  
Extended Data **Table 1: X-Ray Jets of This Study**

See [http://www.nature.com/nature/journal/v523/n7561/fig\\_tab/nature14556\\_SF3.html](http://www.nature.com/nature/journal/v523/n7561/fig_tab/nature14556_SF3.html)

### **New Aspects of a Lid-removal Mechanism in the Onset of an Eruption Sequence that Produced a Large Solar Energetic Particle (SEP) Event**

Alphonse C. [Sterling](#)<sup>1,2,3</sup>, Ronald L. Moore<sup>1,2</sup>, David A. Falconer<sup>1,2,3</sup>, and Javon M. Knox

**2014 ApJ 788 L20; File**

We examine a sequence of two ejective eruptions from a single active region on **2012 January 23**, using magnetograms and EUV images from the Solar Dynamics Observatory's (SDO) Helioseismic and Magnetic Imager (HMI) and Atmospheric and Imaging Assembly (AIA), and EUV images from STEREO/EUVI. This sequence produced two coronal mass ejections (CMEs) and a strong solar energetic particle event (SEP); here we focus on the magnetic onset of this important space weather episode. Cheng et al. showed that the first eruption's ("Eruption 1") flux rope was apparent only in "hotter" AIA channels, and that it removed overlying field that allowed the second eruption ("Eruption 2") to begin via ideal MHD instability; here we say that Eruption 2 began via a "lid removal" mechanism. We show that during Eruption 1's onset, its flux rope underwent a "tether weakening" (TW) reconnection with field that arched from the eruption-source active region to an adjacent active region. Standard flare loops from Eruption 1 developed over Eruption 2's flux rope and enclosed filament, but these overarching new loops were unable to confine that flux rope/filament. Eruption 1's flare loops, from both TW reconnection and standard-flare-model internal reconnection, were much cooler than Eruption 2's flare loops (GOES thermal temperatures of ~7.5 MK and 9 MK, compared to ~14 MK). The corresponding three sequential GOES flares were, respectively, due to TW reconnection plus earlier phase Eruption 1 tether-cutting reconnection, Eruption 1 later-phase tether-cutting reconnection, and Eruption 2 tether-cutting reconnection.

### **OBSERVATIONS FROM SDO, HINODE, AND STEREO OF A TWISTING AND WRITHING START TO A SOLAR-FILAMENT-ERUPTION CASCADE**

Alphonse C. [Sterling](#)<sup>1,3</sup>, Ronald L. Moore<sup>1</sup>, and Hirohisa Hara

**2012 ApJ 761 69; File**

We analyze data from SDO (AIA, HMI), Hinode (SOT, XRT, EIS), and STEREO (EUVI) of a solar eruption sequence of **2011 June 1** near 16:00 UT, with an emphasis on the early evolution toward eruption. Ultimately, the sequence consisted of three emission bursts and two filament ejections. SDO/AIA 304 Å images show absorbing-material strands initially in close proximity which over ~20 minutes form a twisted structure, presumably a flux rope with ~1029 erg of free energy that triggers the resulting evolution. A jump in the filament/flux rope's displacement (average velocity ~20 km s<sup>-1</sup>) and the first burst of emission accompanies the flux-rope formation. After ~20 more minutes, the flux rope/filament kinks and writhes, followed by a semi-steady state where the flux rope/filament rises at (~5 km s<sup>-1</sup>) for ~10 minutes. Then the writhed flux rope/filament again becomes MHD unstable and violently erupts, along with rapid (50 km s<sup>-1</sup>) ejection of the filament and the second burst of emission. That ejection removed a field that had been restraining a second filament, which subsequently erupts as the second filament ejection accompanied by the third (final) burst of emission. Magnetograms from SDO/HMI and Hinode/SOT, and other data, reveal several possible causes for initiating the flux-rope-building reconnection, but we are not able to say which is dominant. Our observations are consistent with magnetic reconnection initiating the first burst and the flux-rope formation, with MHD processes initiating the further dynamics. Both filament ejections are consistent with the standard model for solar eruptions.

### **LATERAL OFFSET OF THE CORONAL MASS EJECTIONS FROM THE X-FLARE OF 2006 DECEMBER 13 AND ITS TWO PRECURSOR ERUPTIONS**

Alphonse C. [Sterling](#)<sup>1,3</sup>, Ronald L. Moore<sup>1</sup> and Louise K. Harra

**2011 ApJ 743 63**

Two GOES sub-C-class precursor eruptions occurred within ~10 hr prior to and from the same active region as the **2006 December 13** X4.3-class flare. Each eruption generated a coronal mass ejection (CME) with center laterally far offset (45°) from the co-produced bright flare. Explaining such CME-to-flare lateral offsets in terms of the standard model for

solar eruptions has been controversial. Using Hinode/X-Ray Telescope (XRT) and EUV Imaging Spectrometer (EIS) data, and Solar and Heliospheric Observatory (SOHO)/Large Angle and Spectrometric Coronagraph (LASCO) and Michelson Doppler Imager (MDI) data, we find or infer the following. (1) The first precursor was a "magnetic-arch-blowout" event, where an initial standard-model eruption of the active region's core field blew out a lobe on one side of the active region's field. (2) The second precursor began similarly, but the core-field eruption stalled in the side-lobe field, with the side-lobe field erupting ~1 hr later to make the CME either by finally being blown out or by destabilizing and undergoing a standard-model eruption. (3) The third eruption, the X-flare event, blew out side lobes on both sides of the active region and clearly displayed characteristics of the standard model. (4) The two precursors were offset due in part to the CME originating from a side-lobe coronal arcade that was offset from the active region's core. The main eruption (and to some extent probably the precursor eruptions) was offset primarily because it pushed against the field of the large sunspot as it escaped outward. (5) All three CMEs were plausibly produced by a suitable version of the standard model.

## **INSIGHTS INTO FILAMENT ERUPTION ONSET FROM SOLAR DYNAMICS OBSERVATORY OBSERVATIONS**

Alphonse C. [Sterling](#)<sup>1,3</sup>, Ronald L. Moore<sup>1</sup> and Samuel L. Freeland

**2011 ApJ 731 L3; File**

We examine the buildup to and onset of an active region filament confined eruption of **2010 May 12**, using EUV imaging data from the Solar Dynamics Observatory (SDO) Atmospheric Imaging Array and line-of-sight magnetic data from the SDO Helioseismic and Magnetic Imager. Over the hour preceding eruption the filament undergoes a slow rise averaging ~3 km s<sup>-1</sup>, with a step-like trajectory. Accompanying a final rise step ~20 minutes prior to eruption is a transient preflare brightening, occurring on loops rooted near the site where magnetic field had canceled over the previous 20 hr. Flow-type motions of the filament are relatively smooth with speeds ~50 km s<sup>-1</sup> prior to the preflare brightening and appear more helical, with speeds ~50-100 km s<sup>-1</sup>, after that brightening. After a final plateau in the filament's rise, its rapid eruption begins, and concurrently an outer shell "cocoon" of the filament material increases in emission in hot EUV lines, consistent with heating in a newly formed magnetic flux rope. The main flare brightenings start ~5 minutes after eruption onset. The main flare arcade begins between the legs of an envelope-arcade loop that is nearly orthogonal to the filament, suggesting that the flare results from reconnection among the legs of that loop. This progress of events is broadly consistent with flux cancellation leading to formation of a helical flux rope that subsequently erupts due to onset of a magnetic instability and/or runaway tether cutting.

## **Evidence for magnetic flux cancelation leading to an ejective solar eruption observed by Hinode, TRACE, STEREO, and SoHO/MDI\***

A. C. [Sterling](#), C. Chifor<sup>2</sup>, H. E. Mason<sup>2</sup>, R. L. Moore<sup>1</sup> and P. R. Young

**A&A 521, A49 (2010), File**

**Aims.** We study the onset of a solar eruption involving a filament ejection on **2007 May 20**.

**Methods.** We observe the filament in H $\alpha$  images from Hinode/SOT and in EUV with TRACE and STEREO/SECCHI/EUVI. Hinode/XRT images are used to study the eruption in soft X-rays. From spectroscopic data taken with Hinode/EIS we obtain bulk-flow velocities, line profiles, and plasma densities in the onset region. The magnetic field evolution was observed in SoHO/MDI magnetograms.

**Results.** We observed a converging motion between two opposite polarity sunspots that form the primary magnetic polarity inversion line (PIL), along which resides filament material before eruption. Positive-flux magnetic elements, perhaps moving magnetic features (MMFs) flowing from the spot region, appear north of the spots, and the eruption onset occurs where these features cancel repeatedly in a negative-polarity region north of the sunspots. An ejection of material observed in H $\alpha$  and EUV marks the start of the filament eruption (its "fast-rise"). The start of the ejection is accompanied by a sudden brightening across the PIL at the jet's base, observed in both broad-band images and in EIS. Small-scale transient brightenings covering a wide temperature range (Log Te = 4.8-6.3) are also observed in the onset region prior to eruption. The preflare transient brightenings are characterized by sudden, localized density enhancements (to above Log ne [ cm<sup>-3</sup> ] = 9.75, in ) that appear along the PIL during a time when pre-flare brightenings were occurring. The measured densities in the eruption onset region outside the times of those enhancements decrease with temperature. Persistent downflows (red-shifts) and line-broadening ( ) are present along the PIL.

**Conclusions.** The array of observations is consistent with the pre-eruption sheared-core magnetic field being gradually destabilized by evolutionary tether-cutting flux cancelation that was driven by converging photospheric flows, and the main filament ejection being triggered by flux cancelation between the positive flux elements and the surrounding negative field. A definitive statement however on the eruption's ultimate cause would require comparison with simulations, or additional detailed observations of other eruptions occurring in similar magnetic circumstances.

**Хорошее Введение**

## **Sigmoid CME source regions at the Sun: some recent results**

**Review**

[Sterling, A. C.](#)

Journal of Atmospheric and Solar-Terrestrial Physics, Volume 62, Issue 16, p. 1427-1435. **2000**

[https://solarscience.msfc.nasa.gov/papers/Sterling/sigmoids\\_review.pdf](https://solarscience.msfc.nasa.gov/papers/Sterling/sigmoids_review.pdf)

Identifying coronal mass ejection (CME) precursors in the solar corona would be an important step in space weather forecasting, as well as a vital key to understanding the physics of CMEs. Twisted magnetic field structures are suspected of being the source of at least some CMEs. These features can appear sigmoid (S or inverse-S) shaped in soft X-ray (SXR) images. We review recent observations of these structures and their relation to CMEs, using SXR data from the Soft X-ray Telescope (SXT) on the Yohkoh satellite, and EUV data from the EUV Imaging Telescope (EIT) on the SOHO satellite. These observations indicate that the pre-eruption sigmoid patterns are more prominent in SXR than in EUV, and that sigmoid precursors are present in over 50% of CMEs. These findings are important for CME research, and may potentially be a major component to space weather forecasting. So far, however, the studies have been subject to restrictions that will have to be relaxed before sigmoid morphology can be used as a reliable predictive tool. Moreover, some CMEs do not display a SXR sigmoid structure prior to eruption, and some others show no prominent SXR signature of any kind before or during eruption. **19 Dec 1996, 7 Apr 1997**

## **Y OHKOH SXT AND SOHO EIT OBSERVATIONS OF SIGMOID-TO-ARCADE EVOLUTION OF STRUCTURES ASSOCIATED WITH HALO CORONAL MASS EJECTIONS**

ALPHONSE C. [STERLING](#), HUGH S. HUDSON, BARBARA J. THOMPSON, AND DOMINIC M. ZARRO  
ASTROPHYSICAL JOURNAL, 532:628–647, **2000, File**

A subset of the solar-disk counterparts to halo coronal mass ejections (CMEs) displays an evolution in soft X-rays (SXR) that is characterized by a pre-eruptive S-shaped structure, dubbed a "pre-eruptive sigmoid," which evolves into a post-eruptive cusp or arcade. We examine the morphological properties of the evolution of sigmoids into cusps and arcades for four such regions associated with SXR flares, using the Soft X-Ray Telescope (SXT) on the Yohkoh satellite and the EUV Imaging Telescope (EIT) on the Solar and Heliospheric Observatory (SOHO) satellite. Most of our EIT observations are with the 1.5 MK 195 Fe XII A. channel. At most, there is only a weak counterpart to the SXR sigmoid in the pre-eruptive 195 EUV A. images, indicating that the pre-eruptive sigmoid has a temperature greater than 1.5 MK. While more identifiable than in the 195 channel, a clear pre-eruptive sigmoid is also not observed in the 2.0 MK EIT 284 A. A. Fe XV channel. During the time of the flare, however, an EUV sigmoid brightens near the location of the SXR pre-eruptive sigmoid. Initially the SXR sigmoid lies along a magnetic neutral line. As the SXR flare progresses, new field lines appear with orientation normal to the neutral line and with footpoints rooted in regions of opposite polarity; these footpoints are different from those of the pre-eruptive sigmoid. The cusp structures in SXRs develop from these newly ignited field lines. In EIT images, the EUV sigmoid broadens as the flare progresses, forming an arcade beneath the SXR cusp. Our findings are consistent with a standard picture in which the origin of the flare and CME is caused by the eruption of a filament-like feature, with the stretching of field lines producing a cusp. We infer that the cusp-producing fields may be overlying the sigmoid fields in the pre-eruptive phase, but we do not directly observe such pre-eruptive overlying fields.

## **Oscillatory reconnection and waves driven by merging magnetic flux ropes in solar flares**

[J. Stewart](#), [P.K. Browning](#), [M. Gordovskyy](#)

MNRAS **2022**

<https://arxiv.org/pdf/2205.03106.pdf>

Oscillatory reconnection is a process that has been suggested to underlie several solar and stellar phenomena, and is likely to play an important role in transient events such as flares. Quasi-periodic pulsations (QPPs) in flare emissions may be a manifestation of oscillatory reconnection, but the underlying mechanisms remain uncertain. In this paper, we present 2D magnetohydrodynamic (MHD) simulations of two current-carrying magnetic flux ropes with an out-of-plane magnetic field undergoing oscillatory reconnection in which the two flux ropes merge into a single flux rope. We find that oscillatory reconnection can occur intrinsically without an external oscillatory driver during flux rope coalescence, which may occur both during large-scale coronal loop interactions and the merging of plasmoids in fragmented current sheets. Furthermore, we demonstrate that radially propagating non-linear waves are produced in the aftermath of flux rope coalescence, due to the post-reconnection oscillations of the merged flux rope. The behaviour of these waves is found to be almost independent of the initial out-of-plane magnetic field. It is estimated that the waves emitted through merging coronal loops and merging plasmoids in loop-top current sheets would have a typical phase speed of 90 km/s and 900 km/s respectively. It is possible that the properties of the waves emitted during flux rope coalescence could be used as a diagnostic tool to determine physical parameters within a coalescing region.

## **Magnetic Structure and Dynamics of the Erupting Solar Polar Crown Prominence on **2012 March 12****

Yingna [Su](#), Adriaan van Ballegooijen, Patrick I. McCauley, Haisheng Ji, Katharine K. Reeves, Edward E. DeLuca

ApJ **807** 144 **2015**

<http://arxiv.org/pdf/1505.06826v1.pdf>

We present an investigation of the polar crown prominence that erupted on 2012 March 12. This prominence is observed at the southeast limb by SDO/AIA (end-on view) and displays a quasi-vertical-thread structure. Bright U-shape/horn-like structure is observed surrounding the upper portion of the prominence at 171 angstrom before the eruption and becomes more prominent during the eruption. The disk view of STEREO-B shows that this long prominence is composed of a series of vertical threads and displays a half loop-like structure during the eruption. We

focus on the magnetic support of the prominence vertical threads by studying the structure and dynamics of the prominence before and during the eruption using observations from SDO and STEREO-B. We also construct a series of magnetic field models (sheared arcade model, twisted flux rope model, and unstable model with hyperbolic flux tube (HFT)). Various observational characteristics appear to be in favor of the twisted flux rope model. We find that the flux rope supporting the prominence enters the regime of torus instability at the onset of the fast rise phase, and signatures of reconnection (post-eruption arcade, new U-shape structure, rising blobs) appear about one hour later. During the eruption, AIA observes dark ribbons seen in absorption at 171 angstrom corresponding to the bright ribbons shown at 304 angstrom, which might be caused by the erupting filament material falling back along the newly reconfigured magnetic fields. Brightenings at the inner edge of the erupting prominence arcade are also observed in all AIA EUV channels, which might be caused by the heating due to energy released from reconnection below the rising prominence.

### **OBSERVATIONS OF A TWO-STAGE SOLAR ERUPTIVE EVENT (SEE): EVIDENCE FOR SECONDARY HEATING**

Yang [Su](#)<sup>1,2,3</sup>, Brian R. Dennis<sup>1</sup>, Gordon D. Holman<sup>1</sup>, Tongjiang Wang<sup>1,2</sup>, Phillip C. Chamberlin<sup>1</sup>, Sabrina Savage<sup>1</sup> and Astrid Veronig

**2012 ApJ 746 L5**

We present RHESSI, SDO/AIA, SOHO/LASCO, STEREO, and GOES observations of a partially occulted solar eruptive event that occurred at the southwest limb on **2011 March 8**. The GOES X-ray light curve shows two peaks separated by almost 2 hr that we interpret as two stages of a single event associated with the delayed eruption of a coronal mass ejection (CME). A hot flux rope formed during the first stage and continued expanding and rising throughout the event. The speed of the flux rope decreased from  $\sim 120$  to  $14 \text{ km s}^{-1}$  during the decay phase of the first stage and increased again during the second stage to become the CME with a speed of  $\sim 516 \text{ km s}^{-1}$ . RHESSI and GOES data analyses show that the plasma temperature reached over 20 MK in the first stage, then decreased to  $\sim 10$  MK and increased to 15 MK in the second stage. This event provides clear evidence for a secondary heating phase. The enhanced EUV and X-ray emission came from the high corona ( $\sim 60$  arcsec above the limb) in the second stage,  $\sim 40$  arcsec higher than the site of the initial flare emission. STEREO-A on-disk observations indicate that the post-flare loops during this stage were of larger scale sizes and spatially distinct from those in the first stage.

### **Observations and Magnetic Field Modeling of the Flare/CME event on 2010/04/08**

[Su](#), Y. N., Surges, V., van Ballegooijen, A. A., DeLuca, E., Golub, L.

E-print, April **2011**, [File](#); [ApJ](#)

We present a study of the flare/CME event that occurred in Active Region 11060 on **2010 April 8**. This event also involves a filament eruption, EIT wave, and coronal dimming. Prior to the flare onset and filament eruption, both SDO/AIA and STEREO/EUVI observe a nearly horizontal filament ejection along the internal polarity inversion line, where flux cancellations frequently occur as observed by SDO/HMI. Using the flux-rope insertion method developed by van Ballegooijen (2004), we construct a grid of magnetic field models using two magneto-frictional relaxation methods. We find that the poloidal flux is significantly reduced during the relaxation process, though one relaxation method preserves the poloidal flux better than the other. The best-fit pre-flare NLFFF model is constrained by matching the coronal loops observed by SDO/AIA and Hinode/XRT. We find that the axial flux in this model is very close to the threshold of instability. For the model that becomes unstable due to an increase of axial flux, the reconnected field lines below the X-point closely match the observed highly sheared flare loops at the event onset. The footpoints of the erupting flux rope are located around the coronal dimming regions. Both observational and modeling results support the premise that this event may be initiated by catastrophic loss-of-equilibrium caused by an increase of axial flux in the flux rope, which is driven by flux cancellations.

**Video 1&2 see** <http://hea-www.harvard.edu/trace/SSXG/ymsu/manuscript/2011ApJ/2011ApJ.html>

### **What Determines the Intensity of Solar Flare/CME Events?**

[Su](#), Y., Van Ballegooijen, A., McCaughey, J., DeLuca, E., Reeves, K. K., and Golub, L. (2007), *Astrophys. J.*, 665, 1448–1459

combined magnetic flux and shear to improve correlations with flare magnitudes and CME speeds,

### **OBSERVATIONS AND MAGNETIC FIELD MODELING OF THE FLARE/CORONAL MASS EJECTION EVENT ON 2010 APRIL 8**

Yingna [Su](#)<sup>1</sup>, Vincent Surges<sup>1,2</sup>, Adriaan van Ballegooijen<sup>1</sup>, Edward DeLuca<sup>1</sup> and Leon Golub

**2011 ApJ 734 53**, [File](#)

We present a study of the flare/coronal mass ejection event that occurred in Active Region 11060 on **2010 April 8**. This event also involves a filament eruption, EIT wave, and coronal dimming. Prior to the flare onset and filament eruption, both SDO/AIA and STEREO/EUVI observe a nearly horizontal filament ejection along the internal polarity inversion line, where flux cancellations frequently occur as observed by SDO/HMI. Using the flux-rope insertion method developed by van Ballegooijen, we construct a grid of magnetic field models using two magneto-frictional relaxation methods. We find that the poloidal flux is significantly reduced during the relaxation process, though one relaxation method preserves the poloidal flux better than the other. The best-fit pre-flare NLFFF model is constrained by matching

the coronal loops observed by SDO/AIA and Hinode/XRT. We find that the axial flux in this model is very close to the threshold of instability. For the model that becomes unstable due to an increase of the axial flux, the reconnected field lines below the X-point closely match the observed highly sheared flare loops at the event onset. The footpoints of the erupting flux rope are located around the coronal dimming regions. Both observational and modeling results support the premise that this event may be initiated by catastrophic loss of equilibrium caused by an increase of the axial flux in the flux rope, which is driven by flux cancellations.

### **Self-similar expansion of solar coronal mass ejections: implications for Lorentz self-force driving**

Prasad [Subramanian](#), K. P. Arunbabu, Angelos Vourlidas, Adwiteey Mauriya  
ApJ, 790 125, 2014

<http://arxiv.org/pdf/1406.0286v1.pdf>

We examine the propagation of several CMEs with well-observed flux rope signatures in the field of view of the SECCHI coronagraphs aboard the STEREO satellites using the GCS fitting method of Thernisien, Vourlidas & Howard (2009). We find that the manner in which they propagate is approximately self-similar; i.e., the ratio ( $\kappa$ ) of the flux rope minor radius to its major radius remains approximately constant with time. We use this observation of self-similarity to draw conclusions regarding the local pitch angle ( $\gamma$ ) of the flux rope magnetic field and the misalignment angle ( $\chi$ ) between the current density  $J$  and the magnetic field  $B$ . Our results suggest that the magnetic field and current configurations inside flux ropes deviate substantially from a force-free state in typical coronagraph fields of view, validating the idea of CMEs being driven by Lorentz self-forces. **21 June 2010, 01/02/2010, 14/02/2010, 12/06/2010, 20/06/2010, 01/03/2010, 26/03/2010, 13/04/2010, 29/01/2008,**

### **DRIVING CURRENTS FOR FLUX ROPE CORONAL MASS EJECTIONS**

Prasad [Subramanian](#)<sup>1</sup>, Angelos Vourlidas

E-print, Oct 2008; Astrophysical Journal, 693:1219–1222, 2009 March; **File**

<http://www.iop.org/EJ/toc/-alert=43190/0004-637X/693/2>

We present a method for measuring electrical currents enclosed by flux rope structures that are ejected within solar coronal mass ejections (CMEs). Such currents are responsible for providing the Lorentz self-force that propels CMEs. Our estimates for the driving current are based on measurements of the propelling force obtained using data from the LASCO coronagraphs aboard the SOHO satellite. We find that upper limits on the currents enclosed by CMEs are typically around  $10^{10}$  Amperes. We estimate that the magnetic flux enclosed by the CMEs in the LASCO field of view is a few  $\times 10^{21}$  Mx.

### **Energetics of Solar Coronal Mass Ejections –**

Prasad [Subramanian](#), Angelos Vourlidas

A&A 467, 685-693 (2007)

E-print Jan 2007; A&A, 2007, **File**

We examine the energetics of 39 flux-rope like coronal mass ejections (CMEs). This comprises a complete sample of the best examples of flux-rope CMEs observed by LASCO in 1996-2001. **Table.**

CME internal magnetic energy is a viable source of the required driving power.

### **Observations of Instability-driven Nanojets in Coronal Loops**

A. Ramada C. [Sukarmadji](#)<sup>1</sup>, Patrick Antolin<sup>1</sup>, and James A. McLaughlin<sup>1</sup>

2022 ApJ 934 190

<https://iopscience.iop.org/article/10.3847/1538-4357/ac7870/pdf>

The recent discovery of nanojets by Antolin et al. represents magnetic reconnection in a braided field, thus clearly identifying reconnection-driven nanoflares. Due to their small scale (500 km in width, 1500 km in length) and short timescales ( $<15$  s), it is unclear how pervasive nanojets are in the solar corona. In this paper, we present Interface Region Imaging Spectrograph and Solar Dynamics Observatory observations of nanojets found in multiple coronal structures, namely, in a coronal loop powered by a blowout jet, and in two other coronal loops with coronal rain. In agreement with previous findings, we observe that nanojets are accompanied by small nanoflare-like intensity bursts in the (E)UV, have velocities of  $150\text{--}250$  km s<sup>-1</sup> and occur transversely to the field line of origin, which is sometimes observed to split. However, we find a variety of nanojet directions in the plane transverse to the loop axis. These nanojets are found to have kinetic and thermal energies within the nanoflare range, and often occur in clusters. In the blowout jet case study, the Kelvin–Helmholtz instability (KHI) is directly identified as the reconnection driver. For the other two loops, we find that both, KHI and Rayleigh–Taylor instability (RTI) are likely to be the drivers. However, we find that KHI and RTI are each more likely in one of the other two cases. These observations of nanojets in a variety of structures and environments support nanojets being a general result of reconnection that are driven here by dynamic instabilities. **2014 May 3, 2014 July 1, 2015 June 12,**

### **Fast Downflows Observed during a Polar Crown Filament Eruption**



[Zheng Sun](#), [Hui Tian](#), [Ting Li](#), [Rui Liu](#), [Yadan Duan](#)

ApJ **974** 205 **2024**

<https://arxiv.org/pdf/2408.15892>

<https://iopscience.iop.org/article/10.3847/1538-4357/ad738d/pdf>

Solar filaments can undergo eruptions and result in the formation of coronal mass ejections (CMEs), which could significantly impact planetary space environments. Observations of eruptions involving polar crown filaments, situated in the polar regions of the Sun, are limited. In this study, we report a polar crown filament eruption (SOL2023-06-12), characterized by fast downflows below the filament. The downflows appear instantly after the onset of the filament eruption and persist for approximately 2 hours, exhibiting plane-of-sky (POS) velocities ranging between 92 and 144 km s<sup>-1</sup>. They originate from the leading edge of the filament and no clear acceleration is observed. Intriguingly, these downflows appear at two distinct sites, symmetrically positioned at the opposite ends of the conjugate flare ribbons. Based on the observations, we propose that the filament might be supported by a magnetic flux rope (MFR), and these downflows possibly occur along the legs of the MFR. The downflows likely result from continuous reconnections between the MFR and the overlying magnetic field structures, and could either be reconnection outflows or redirected filament materials. We also observed horizontal drifting of the locations of downflows, which might correspond to the MFR's footprint drifting. This type of downflows can potentially be utilized to track the footprints of MFRs during eruptions.

### **The Solar Origin of an Intense Geomagnetic Storm on 2023 December 1st: Successive Slipping and Eruption of Multiple Magnetic Flux Ropes**

[Zheng Sun](#), [Ting Li](#), [Yijun Hou](#), [Hui Tian](#), [Ziqi Wu](#), [Ke Li](#), [Yining Zhang](#), [Zhentong Li](#), [Xianyong Bai](#), [Li Feng](#), [Chuan Li](#), [Zhenyong Hou](#), [Qiao Song](#), [Jingsong Wang](#), [Guiping Zhou](#)

Solar Phys. **2024**

<https://arxiv.org/pdf/2405.14983>

The solar eruption that occurred on **2023 November 28** (SOL2023-11-28) triggered an intense geomagnetic storm on Earth on **2023 December 1**. The associated Earth's auroras manifested at the most southern latitudes in the northern hemisphere observed in the past two decades. In order to explore the profound geoeffectiveness of this event, we conducted a comprehensive analysis of its solar origin to offer potential factors contributing to its impact. Magnetic flux ropes (MFRs) are twisted magnetic structures recognized as significant contributors to coronal mass ejections (CMEs), thereby impacting space weather greatly. In this event, we identified multiple MFRs in the solar active region and observed distinct slipping processes of the three MFRs: MFR1, MFR2, and MFR3. All three MFRs exhibit slipping motions at a speed of 40--137 km s<sup>-1</sup>, extending beyond their original locations. Notably, the slipping of MFR2 extends to ~30 Mm and initiate the eruption of MFR3. Ultimately, MFR1's eruption results in an M3.4-class flare and a CME, while MFR2 and MFR3 collectively produce an M9.8-class flare and another halo CME. This study shows the slipping process in a multi-MFR system, showing how one MFR's slipping can trigger the eruption of another MFR. We propose that the CME--CME interactions caused by multiple MFR eruptions may contribute to the significant geoeffectiveness.

### **Observation of two splitting processes in a partial filament eruption on the sun: the role of breakout reconnection**

[Zheng Sun](#), [Ting Li](#), [Hui Tian](#), [Yinjun Hou](#), [Zhenyong Hou](#), [Hechao Chen](#), [Xianyong Bai](#), [Yuanyong Deng](#)

ApJ **953** 148 **2023**

<https://arxiv.org/pdf/2307.06895.pdf>

<https://iopscience.iop.org/article/10.3847/1538-4357/ace5b1/pdf>

Partial filament eruptions have often been observed, however, the physical mechanisms that lead to filament splitting are not yet fully understood. In this study, we present a unique event of a partial filament eruption that undergoes two distinct splitting processes. The first process involves vertical splitting and is accompanied by brightenings inside the filament, which may result from internal magnetic reconnection within the filament. Following the first splitting process, the filament is separated into an upper part and a lower part. Subsequently, the upper part undergoes a second splitting, which is accompanied by a coronal blowout jet. An extrapolation of the coronal magnetic field reveals a hyperbolic flux tube structure above the filament, indicating the occurrence of breakout reconnection that reduces the constraining field above. Consequently, the filament is lifted up, but at a nonuniform speed. The high-speed part reaches the breakout current sheet to generate the blowout jet, while the low-speed part falls back to the solar surface, resulting in the second splitting. In addition, continuous brightenings are observed along the flare ribbons, suggesting the occurrence of slipping reconnection process. This study presents, for the first time, the unambiguous observation of a two-stage filament splitting process, advancing our understanding of the complex dynamics of solar eruptions. **2022 September 20**

### **Interpreting LSTM Prediction on Solar Flare Eruption with Time-series Clustering**

Hu [Sun](#) (1), [Ward Manchester](#) (2), [Zhenbang Jiao](#) (1), [Xiantong Wang](#) (2), [Yang Chen](#)

ApJ **2020**

<https://arxiv.org/pdf/1912.12360.pdf>

We conduct a post hoc analysis of solar flare predictions made by a Long Short Term Memory (LSTM) model employing data in the form of Space-weather HMI Active Region Patches (SHARP) parameters. These data are

distinguished in that the parameters are calculated from data in proximity to the magnetic polarity inversion line where the flares originate. We train the the LSTM model for binary classification to provide a prediction score for the probability of M/X class flares to occur in next hour. We then develop a dimension-reduction technique to reduce the dimensions of SHARP parameter (LSTM inputs) and demonstrate the different patterns of SHARP parameters corresponding to the transition from low to high prediction score. Our work shows that a subset of SHARP parameters contain the key signals that strong solar flare eruptions are imminent. The dynamics of these parameters have a highly uniform trajectory for many events whose LSTM prediction scores for M/X class flares transition from very low to very high. The results suggest that there exist a few threshold values of a subset of SHARP parameters when surpassed could indicate a high probability of strong flare eruption. Our method has distilled the knowledge of solar flare eruption learnt by deep learning model and provides a more interpretable approximation where more physics related insights could be derived.

**Appendix A Summary of Sudden Transition Cases (2011-2017)**

## **Investigating the Magnetic Imprints of Major Solar Eruptions with SDO/HMI High-Cadence Vector Magnetograms**

Xudong [Sun](#), J. Todd Hoeksema, Yang Liu, [Maria Kazachenko](#), [Ruizhu Chen](#)

ApJ 839 67 2017

<https://arxiv.org/pdf/1702.07338.pdf>

<http://c.brightcove.com/article/10.3847/1538-4357/aa69c1/pdf>

The solar active region photospheric magnetic field evolves rapidly during major eruptive events, suggesting appreciable feedback from the corona. The new high-cadence (90 s or 135 s) vector magnetogram dataset from the Helioseismic and Magnetic Imager (HMI) is suited for investigating these "magnetic imprints". Observations of an archetypical event, SOL2011-02-15T01:56, show the following trends. Firstly, the horizontal magnetic field component (B<sub>h</sub>) exhibits permanent, step-like changes with a time scale of several minutes, whereas the radial component (B<sub>r</sub>) varies less. Secondly, B<sub>h</sub> near the main polarity inversion line increases significantly during the earlier phase of the associated flare, whereas B<sub>h</sub> in the periphery decreases at later times with smaller magnitudes. Thirdly, transient artifacts coincide with enhanced flare emission, where the Stokes profiles are no longer adequately modeled under standard settings, and the inferred magnetic field becomes unreliable. Our results corroborate previous findings, remove certain ambiguities that arise from line-of-sight only or lower-cadence vector observations, and provide insights on the momentum processes during solar eruption. The dataset may also be useful to the study of sunquakes and data-driven modeling of the solar corona.

**See HMI Science Nuggets –#67 Feb 2017**

<http://hmi.stanford.edu/hminuggets/?p=1820>

## **Observation of Magnetic reconnection at a 3D null point associated with a solar eruption**

J. Q. [Sun](#), J. Zhang, K. Yang, X. Cheng, M. D. Ding

ApJL 830 L4 2016

<http://arxiv.org/pdf/1609.06787v1.pdf>

Magnetic null has long been recognized as a special structure serving as a preferential site for magnetic reconnection (MR). However, the direct observational study of MR at null-points is largely lacking. Here, we show the observations of MR around a magnetic null associated with an eruption that resulted in an M1.7 flare and a coronal mass ejection. The GOES X-ray profile of the flare exhibited two peaks at 02:23 UT and 02:40 UT on **2012 November 8**, respectively. Based on the imaging observations, we find that the first and also primary X-ray peak was originated from MR in the current sheet underneath the erupting magnetic flux rope (MFR). On the other hand, the second and also weaker X-ray peak was caused by MR around a null-point located above the pre-eruption MFR. The interaction of the null-point and the erupting MFR can be described as a two-step process. During the first step, the erupting and fast expanding MFR passed through the null-point, resulting in a significant displacement of the magnetic field surrounding the null. During the second step, the displaced magnetic field started to move back, resulting in a converging inflow and subsequently the MR around the null. The null-point reconnection is a different process from the current sheet reconnection in this flare; the latter is the cause of the main peak of the flare, while the former is the cause of the secondary peak of the flare and the conspicuous high-lying cusp structure.

## **Extreme Ultraviolet Imaging of Three-dimensional Magnetic Reconnection in a Solar Eruption**

J. Q. [Sun](#), X. Cheng, M. D. Ding, [Y. Guo](#), [E. R. Priest](#), [C. E. Parnell](#), [S. J. Edwards](#), [J. Zhang](#), [P. F. Chen](#), [C. Fang](#)

Nature Communications 6, Article number: 7598, 2015

<http://arxiv.org/pdf/1506.08255v1.pdf>

Magnetic reconnection, a change of magnetic field connectivity, is a fundamental physical process in which magnetic energy is released explosively. It is responsible for various eruptive phenomena in the universe. However, this process is difficult to observe directly. Here, the magnetic topology associated with a solar reconnection event is studied in three dimensions (3D) using the combined perspectives of two spacecraft. The sequence of extreme ultraviolet (EUV) images

clearly shows that two groups of oppositely directed and non-coplanar magnetic loops gradually approach each other, forming a separator or quasi-separator and then reconnecting. The plasma near the reconnection site is subsequently heated from  $\sim 1$  to  $\geq 5$  MK. Shortly afterwards, warm flare loops ( $\sim 3$  MK) appear underneath the hot plasma. Other observational signatures of reconnection, including plasma inflows and downflows, are unambiguously revealed and quantitatively measured. These observations provide direct evidence of magnetic reconnection in a 3D configuration and reveal its origin. **2012 January 27**

### **Why Is the Great Solar Active Region 12192 CME-Poor?**

Xudong Sun, Monica G. Bobra, J. Todd Hoeksema, Yang Liu, Yan Li, Chenglong Shen, Sebastien Couvidat, Aimee A. Norton, George H. Fisher  
ApJL **804** L28 **2015**

<http://arxiv.org/pdf/1502.06950v1.pdf> **File**

Solar active region (AR) **12192 of October 2014** hosts the largest sunspot group in 24 years. It is the most prolific flaring site of Cycle 24, but surprisingly produced no coronal mass ejection (CME) from the core region during its disk passage. Here, we study the magnetic conditions that prevented eruption and the consequences that ensued. We find AR 12192 to be "big but mild"; its core region exhibits weaker non-potentiality, stronger overlying field, and smaller flare-related field changes compared to two other major flare-CME-productive ARs (11429 and 11158). These differences are present in the intensive-type indices (e.g., means) but generally not the extensive ones (e.g., totals). AR 12192's large amount of magnetic free energy does not translate into CME productivity. The unexpected behavior suggests that AR eruptiveness is limited by some relative measure of magnetic non-potentiality over the restriction of background field, and that confined flares may leave weaker photospheric and coronal imprints compared to their eruptive counterparts. **18-28 Oct 2014, 2012-03-07, 2011-02-15**

**Хорошее Введение про confined and eruptive flares.**

**See also HMI Science Nuggets, No. 37, April 2015**

<http://hmi.stanford.edu/hminuggets/?p=1153>

**Erratum:** ApJL, 850:L43 (1pp), **2017 December 1**

### **Dynamic Evolution of an X-shaped Structure above a Trans-equatorial Quadrupole Solar Active Region Group**

J. Q. Sun<sup>1,2</sup>, X. Cheng<sup>1,2</sup>, Y. Guo<sup>1,2</sup>, M. D. Ding<sup>1,2</sup>, and Y. Li  
**2014 ApJ 787 L27**

In the solar corona, magnetic reconnection usually takes place at the singular configuration of the magnetic field, in particular near a magnetic null, owing to its high susceptibility to perturbations. In this Letter, we report a rare X-shaped structure, encompassing a magnetic null, above a trans-equatorial quadrupole active region group that is well observed by the Atmospheric Imaging Assembly (AIA). The observations show that this X-shaped structure is visible in all AIA EUV passbands and stably exists for days. However, possibly induced by flare activities at the northern part of the quadrupole active region group, the X-shaped structure starts to destabilize while a jet erupts near its center at  $\sim 15:05$  UT on **2013 October 7**. Through nonlinear force-free field modeling, we identify a magnetic null that is above the quadrupole polarities and well corresponds to the X-shaped structure. After the jet eruption, the temperature and emission measure of the plasma near the X-shaped structure rise from  $\sim 2.3$  MK and  $\sim 1.2 \times 10^{27} \text{ cm}^{-5}$  at 15:01 UT to  $\sim 5.4$  MK and  $\sim 3.7 \times 10^{27} \text{ cm}^{-5}$  at 15:36 UT, respectively, revealed by the differential emission measure analysis, indicating that magnetic reconnection most likely takes place there to heat the plasma. Moreover, the height of the null increases  $\sim 10$  Mm, which is most likely due to the partial opening of the field lines near the fan surface that makes the null underneath rise to seek a new equilibrium.

### **A NON-RADIAL ERUPTION IN A QUADRUPOLAR MAGNETIC CONFIGURATION WITH A CORONAL NULL**

Xudong Sun, J. Todd Hoeksema, Yang Liu, Qingrong Chen, and Keiji Hayashi  
**2012 ApJ 757 149**

We report one of the several homologous non-radial eruptions from NOAA active region (AR) 11158 that are strongly modulated by the local magnetic field as observed with the Solar Dynamic Observatory. A small bipole emerged in the sunspot complex and subsequently created a quadrupolar flux system. Nonlinear force-free field extrapolation from vector magnetograms reveals its energetic nature: the fast-shearing bipole accumulated  $\sim 2 \times 10^{31}$  erg free energy (10% of AR total) over just one day despite its relatively small magnetic flux (5% of AR total). During the eruption, the ejected plasma followed a highly inclined trajectory, over  $60^\circ$  with respect to the radial direction, forming a jet-like, inverted-Y-shaped structure in its wake. Field extrapolation suggests complicated magnetic connectivity with a coronal null point, which is favorable of reconnection between different flux components in the quadrupolar system. Indeed, multiple pairs of flare ribbons brightened simultaneously, and coronal reconnection signatures appeared near the inferred null. Part of the magnetic setting resembles that of a blowout-type jet; the observed inverted-Y structure likely outlines the open field lines along the separatrix surface. Owing to the asymmetrical photospheric flux distribution, the confining magnetic pressure decreases much faster horizontally than upward. This special field geometry likely guided the non-radial eruption during its initial stage.

## A COMPARISON OF THE INITIAL SPEED OF CORONAL MASS EJECTIONS WITH THE MAGNETIC FLUX AND MAGNETIC HELICITY OF MAGNETIC CLOUDS

S.-K. [Sung](#)<sup>1,2,3</sup>, K. Marubashi<sup>1</sup>, K.-S. Cho<sup>1</sup>, Y.-H. Kim<sup>1</sup>, K.-H. Kim<sup>1,3</sup>, J. Chae<sup>2</sup>, Y.-J. Moon<sup>3</sup>, and I.-H. Kim<sup>3</sup>

Astrophysical Journal, 699:298–304, 2009, **File**

To investigate the relationship between the speed of a coronal mass ejection (CME) and the magnetic energy released during its eruption, we have compared the initial speed of CMEs ( $V_{CME}$ ) and the two parameters of their associated magnetic clouds (MC), magnetic flux ( $FMC$ ), and magnetic helicity per unit length ( $|HMC|/L$ ), for 34 pairs of CMEs and MCs. The values of these parameters in each MC have been determined by fitting the magnetic data of the MC to the linear force-free cylindrical model. As a result, we found that there are positive correlations between  $V_{CME}$  and  $FMC$ , and between  $V_{CME}$  and  $|HMC|/L$ . It is also found that the kinetic energy of CMEs ( $ECME$ ) is correlated with  $FMC$  and  $|HMC|/L$  of the associated MC. In contrast, we found no significant correlation between  $V_{CME}$  and  $FMC$ , nor between  $V_{CME}$  and  $|HMC|/L$ . Our results support the notion that the eruption of a CME is related to the magnetic helicity of the source active region.

## Evaluation of standoff distance method to determine the coronal magnetic field using CME-driven shocks

K. [Suresh](#), A. Shanmugaraju, M. Syed Ibrahim

Astrophysics and Space Science November 2016, 361:360

[http://link.springer.com/article/10.1007/s10509-016-2944-4?wt\\_mc=alerts.TOCjournals](http://link.springer.com/article/10.1007/s10509-016-2944-4?wt_mc=alerts.TOCjournals)

We have analyzed the propagation characteristics of four limb coronal mass ejections (CMEs) with their shocks. These CMEs were observed in 18 frames up to 18 solar radii using LASCO white light images. Gopalswamy and Yashiro (Astrophys. J. 736:L17, 2011) introduced the standoff distance method (SOD) to find the magnetic field in the corona using CME-driven shock. In this paper, we have used this technique to determine the magnetic field strength and to study the propagation/shock formation condition of these CMEs at 18 different locations. Since the thickness of shock sheath (standoff distance or SOD) is not constant around CME, we estimate the shock parameters and their variation in large and small SOD regions of the shock. The Mach number ranges from 1.7 to 2.8 and Alfvén speed varies from  $(197 \text{ to } 857 \text{ km s}^{-1})$ . Finally, we estimate the magnetic field variation in the corona. The magnetic field strength ranges from 4.9 to 26.2 mG from 8.3 to 17.5 solar radii. The estimated magnetic field strength in this study is consistent with the literature value (7.6 to 45.8 mG from Gopalswamy and Yashiro (Astrophys. J. 736:L17, 2011), and 6 to 105 mG from Kim et al. (Astrophys. J. 746:118, 2012)) and it smoothly follows the general coronal magnetic field profile. **Mar 25, 2008, Aug 18, 2010, Apr 9, 2012, Apr 15, 2012, Oct 22, 2012**

## Investigation on Radio-Quiet and Radio-Loud Fast CMEs and Their Associated Flares During Solar Cycles 23 and 24

K. [Suresh](#), A. Shanmugaraju

Solar Phys. Volume 290, [Issue 3](#), pp 875-889 **2015**

We present the results of a detailed analysis on the differences between radio-loud (RL) and radio-quiet (RQ) fast coronal mass ejections (CMEs) ( $V \geq 900 \text{ km s}^{-1}$ ) observed during the period 1996–2012. The analysis consists of three different steps in which we examined the properties of (i) RL and RQ CMEs, (ii) accelerating (class-A) and decelerating (class-D) CMEs among RL and RQ CMEs, and (iii) associated flares. The last two steps and events from a longer period are the extensions of the earlier work on RL and RQ CMEs that mainly aimed to determine the reason for the radio-quietness of some fast CMEs. During this period, we found that 38 % of fast CMEs are RL and 62 % of fast CMEs are RQ. Moreover, fewer RQ CMEs occur around the disc centre. The average speeds of RL and RQ CMEs are  $1358 \text{ km s}^{-1}$  and  $1092 \text{ km s}^{-1}$ . Around 10 % of the RQ events are halo CMEs, but  $\approx 66$  % of RL events are halo CMEs. The mean acceleration or deceleration value of RL-CMEs is slightly greater than that of RQ-CMEs. When we divide these events based on their acceleration behaviour into class A and class D, there are no considerable differences between classes A and D of RL-CMEs or between classes A and D of RQ CMEs, except for their initial acceleration values. But there are significant differences among their associated flare properties. According to our study here, the RQ CMEs are less energetic than RL CMEs, and they are not associated with flares as strong as those associated with RL CMEs. This confirms the previous results that RQ CMEs do not often exceed the critical Alfvén speed of  $1000 \text{ km s}^{-1}$  in the outer corona that is needed to produce type II radio bursts.

## Correlations between the CME acceleration, other CME parameters and flare energy

G.S. [Suryanarayana](#)

[Journal of Atmospheric and Solar-Terrestrial Physics](#) Volume 185, April 2019, Pages 1-6

<https://reader.elsevier.com/reader/sd/pii/S1364682618303936?token=CB263260630F0BB5166EA1A495BF4EA0DB39552277C6C7C0722457BB500255FA3C2D97018F71DF80EB4E1FEEB8B05F00sci-hub.tw/10.1016/j.jastp.2019.01.014>

While the [Coronal Mass Ejections](#) (CMEs) without associated flares are known to accelerate and decelerate being moderated by the [Lorentz force](#), gravity and the drag force due to [solar wind](#), the flare association is known to prolong

the acceleration. However, with or without the flare association, a significant proportion of slow CMEs decelerate and a similar proportion of fast CMEs accelerate. In the case of accelerating CMEs, various parameters of CMEs such as the mass, angular width etc. show good correlation and this improves with flare association. When the flares and CMEs are associated, there is apparently a division of energy between the flares and the CMEs. It is also known that the [magnetic flux](#) spanned by the flare arcade and ribbons after flare maximum, roughly equals the magnetic flux content of the CME and their ratio could be between one and two. The magnetic flux content of the CME can be estimated from the final angular width of the CME. Hence, we suggest that the CMEs experience net acceleration when the different parameters of CMEs such as angular width, mass etc. are correlated and when the CME parameters are correlated with flare duration and peak flux. The absence of the same may lead to CMEs experience net [deceleration](#).

### **CME productivity associated with Solar Flare peak X-ray emission flux**

[G.S.Suryanarayana](#) [K.M.Balakrishna](#)

[Advances in Space Research](#) Volume 61, Issue 9, 1 May 2018, Pages 2482-2489

<http://sci-hub.tw/http://linkinghub.elsevier.com/retrieve/pii/S0273117718301236>

It is often noticed that the occurrence rate of [Coronal Mass Ejections](#) (CMEs) increases with increase in flare duration where peak flux too increase. However, there is no complete association between the duration and peak flux. Distinct characteristics have been reported for active regions (ARs) where flares and CMEs occur in contrast to ARs where flares alone occur. It is observed that peak flux of flares is higher when associated with CMEs compared to peak flux of flares with which CMEs are not associated. In other words, it is likely that flare duration and peak flux are independently affected by distinct active region dynamics. Hence, we examine the relative ability of flare duration and peak flux in enhancing the CME productivity. We report that CME productivity is distinctly higher in association with the enhancement of flare peak flux in comparison to corresponding enhancement of flare duration.

### **Hot prominence detected in the core of a Coronal Mass Ejection:**

#### **III. Plasma filling factor from UVCS Lyman- $\alpha$ and Lyman- $\beta$ observations**

R. [Susino](#), [A. Bemporad](#), [S. Ječič](#), [P. Heinzel](#)

A&A 617, A21 2018

<https://arxiv.org/pdf/1805.12465.pdf>

This work deals with the study of an erupting prominence embedded in the core of a CME and focuses on the derivation of the prominence plasma filling factor. We explore two methods to measure the prominence plasma filling factor that are based on the combination of visible-light and ultraviolet spectroscopic observations. Theoretical relationships for resonant scattering and collisional excitation are used to evaluate the intensity of the H I Lyman- $\alpha$  and Lyman- $\beta$  lines, in two prominence points where simultaneous and cospatial LASCO-C2 and UVCS data were available. Thermodynamic and geometrical parameters assumed for the calculation are provided by both observations and the results of a detailed 1D non-LTE radiative-transfer model of the prominence, developed in our previous work (Heinzel 2016). The filling factor is derived from the comparison between the calculated and the measured intensities of the two lines. The results are then checked against the non-LTE model in order to verify the reliability of the methods. The resulting filling factors are consistent with the model in both the prominence points when the separation of the radiative and collisional components of the total intensity, required to estimate the filling factor, is performed using both the line intensities. An exploration of the parameter space shows that the results are weakly sensitive to the plasma velocity, but they depend more strongly on the assumed kinetic temperatures. The combination of visible-light and ultraviolet Lyman- $\alpha$  and Lyman- $\beta$  data can be used to approximately estimate the geometrical filling factor in erupting prominences, but the proposed techniques are reliable only for emission that is optically thin in the lines considered, condition that is not in general representative of prominence plasma. **August 2, 2000**

### **Determination of Coronal Mass Ejection physical parameters from combination of polarized visible light and UV Lyman- $\alpha$ observations**

R. [Susino](#), [A. Bemporad](#)

2016 ApJ 830 58

<http://arxiv.org/pdf/1609.01420v1.pdf>

Visible-light observations of Coronal Mass Ejections (CMEs) performed with coronagraphs and heliospheric imagers (in primis on board the SOHO and STEREO missions) have offered so far the best way to study the kinematics and geometrical structure of these fundamental events. Nevertheless, it has been widely demonstrated that only combination of multi-wavelength data (including X-ray spectra, EUV images, EUV-UV spectra, and radio dynamic spectra) can provide complete information on the plasma temperature and density distributions, non-thermal motions, magnetic fields, and other physical parameters, for both CMEs and CME-related phenomena. In this work, we analyze three CMEs by combining simultaneous data acquired in the polarized visible light by the LASCO-C2 coronagraph and in the UV H I Lyman- $\alpha$  line (1216 Å) by the UVCS spectrometer, in order to estimate the CME plasma electron density (using the polarization-ratio technique to infer the 3D structure of the CME) and temperature (from the comparison between the expected and measured Lyman- $\alpha$  intensities) along the UVCS field of view. This analysis is primarily aimed at testing the diagnostic methods that will be applied to coronagraphic observations of CMEs delivered by the Metis instrument on board the next ESA-Solar Orbiter mission. We find that CME cores are usually associated with cooler plasma ( $T \sim 10^6$  K), and that a significant increase of the electron temperatures is observed from the core to the

front of the CME (where  $T > 106.3$  K), which seems to be correlated, in all cases, with the morphological structure of the CME as derived from visible-light images. **2000 November 8, 2000 December 25, 2003 May 2-3**

### **PHYSICAL CONDITIONS OF CORONAL PLASMA AT THE TRANSIT OF A SHOCK DRIVEN BY A CORONAL MASS EJECTION**

R. **Susino**, A. Bemporad, and S. Mancuso

**2015** ApJ 812 119

We report here on the determination of plasma physical parameters across a shock driven by a coronal mass ejection using white light (WL) coronagraphic images and radio dynamic spectra (RDS). The event analyzed here is the spectacular eruption that occurred on **2011 June 7**, a fast CME followed by the ejection of columns of chromospheric plasma, part of them falling back to the solar surface, associated with a M2.5 flare and a type-II radio burst. Images acquired by the Solar and Heliospheric Observatory/LASCO coronagraphs (C2 and C3) were employed to track the CME-driven shock in the corona between 2–12  $R_{\odot}$  in an angular interval of about  $110^{\circ}$ . In this interval we derived two-dimensional (2D) maps of electron density, shock velocity, and shock compression ratio, and we measured the shock inclination angle with respect to the radial direction. Under plausible assumptions, these quantities were used to infer 2D maps of shock Mach number MA and strength of coronal magnetic fields at the shock's heights. We found that in the early phases (2–4  $R_{\odot}$ ) the whole shock surface is super-Alfvénic, while later on (i.e., higher up) it becomes super-Alfvénic only at the nose. This is in agreement with the location for the source of the observed type-II burst, as inferred from RDS combined with the shock kinematic and coronal densities derived from WL. For the first time, a coronal shock is used to derive a 2D map of the coronal magnetic field strength over intervals of 10  $R_{\odot}$  altitude and  $\sim 110^{\circ}$  latitude.

### **3D stereoscopic analysis of a Coronal Mass Ejection and comparison with UV spectroscopic data**

Roberto **Susino**, Alessandro Bemporad, Sergio Dolei

**2014**, ApJ 790 25

<http://arxiv.org/pdf/1406.3210v1.pdf>

A three-dimensional (3D) reconstruction of the **2007, May 20** partial-halo Coronal Mass Ejection (CME) has been made using STEREO/EUVI and STEREO/COR1 coronagraphic images. The trajectory and kinematics of the erupting filament have been derived from EUVI image pairs with the "tie-pointing" triangulation technique, while the polarization ratio technique has been applied to COR1 data to determine the average position and depth of the CME front along the line of sight. These 3D geometrical information have been combined for the first time with spectroscopic measurements of the OVI  $\lambda\lambda 1031.91, 1037.61$  \AA line profiles made with the Ultraviolet Coronagraph Spectrometer (UVCS) on board SOHO. Comparison between the prominence trajectory extrapolated at the altitude of UVCS observations and the core transit time measured from UVCS data made possible a firm identification of the CME core observed in white light and UV with the prominence plasma expelled during the CME. Results on the 3D structure of the CME front have been used to calculate synthetic spectral profiles of the OVI  $\lambda\lambda 1031.91$  \AA line expected along the UVCS slit, in an attempt to reproduce the measured line widths. Observed line widths can be reproduced within the uncertainties only in the peripheral part of the CME front; at the front center, where the distance of the emitting plasma from the plane of the sky is greater, synthetic widths turn out to be  $\sim 25\%$  lower than the measured ones. This provides strong evidence of line broadening due to plasma heating mechanisms in addition to bulk expansion of the emitting volume.

### **Plasma Heating in a Post Eruption Current Sheet: A Case Study Based on Ultraviolet, Soft, and Hard X-Ray Data**

R. **Susino**<sup>1,3</sup>, A. Bemporad<sup>1</sup>, and Säm Krucker

**2013** ApJ 777 93

Off-limb observations of the solar corona after coronal mass ejections (CMEs) often show strong, compact, and persistent UV sources behind the eruption. They are primarily observed by the SOHO/UVCS instrument in the "hot" [Fe XVIII]  $\lambda 974$  line and are usually interpreted as a signature of plasma heating due to magnetic reconnection in the post-CME current sheet (CS). Nevertheless, the physical process itself and the altitude of the main energy release are currently not fully understood. In this work, we study the evolution of plasma heating after the CME of **2004 July 28** by comparing UV spectra acquired by UVCS with soft and hard X-ray (SXR, HXR) images of the post-flare loops taken by GOES/SXI and RHESSI. The X-ray data show a long-lasting extended source that is rising upward, toward the high-temperature source detected by UVCS. UVCS data show the presence of significant non-thermal broadening in the CS (a signature of turbulent motions) and a strong density gradient across the CS region. The thermal energy released in the HXR source is on the order of  $\sim 10^{32}$  erg, a factor  $\sim 2$ -5 larger than the energy required to explain the high-temperature plasma sampled by UVCS. Nevertheless, the very different time evolutions of SXR and HXR sources compared with the UV emission suggest that reconnection occurring above the post-eruption arcades is not directly responsible for the

high-temperature plasma sampled higher up by UVCS. We conclude that an additional plasma heating mechanism (such as turbulent reconnection) in the CS is likely required.

## **ARE DECAYING MAGNETIC FIELDS ABOVE ACTIVE REGIONS RELATED TO CORONAL MASS EJECTION ONSET?**

J. [Suzuki](#)<sup>1</sup>, B. T. Welsch<sup>2</sup>, and Y. Li

2012 ApJ 758 22

Coronal mass ejections (CMEs) are powered by magnetic energy stored in non-potential (current-carrying) coronal magnetic fields, with the pre-CME field in balance between outward magnetic pressure of the proto-ejecta and inward magnetic tension from overlying fields that confine the proto-ejecta. In studies of global potential (current-free) models of coronal magnetic fields—Potential Field Source Surface (PFSS) models—it has been reported that model field strengths above flare sites tend to be weaker when CMEs occur than when eruptions fail to occur. This suggests that potential field models might be useful to quantify magnetic confinement. One straightforward implication of this idea is that a decrease in model field strength overlying a possible eruption site should correspond to diminished confinement, implying an eruption is more likely. We have searched for such an effect by post facto investigation of the time evolution of model field strengths above a sample of 10 eruption sites. To check if the strengths of overlying fields were relevant only in relatively slow CMEs, we included both slow and fast CMEs in our sample. In most events we study, we find no statistically significant evolution in either (1) the rate of magnetic field decay with height, (2) the strength of overlying magnetic fields near 50 Mm, or (3) the ratio of fluxes at low and high altitudes (below  $1.1 R_{\odot}$ , and between  $1.1$  and  $1.5 R_{\odot}$ , respectively). We did observe a tendency for overlying field strengths and overlying flux to increase slightly, and their rates of decay with height to become slightly more gradual, consistent with increased confinement. The fact that CMEs occur regardless of whether the parameters we use to quantify confinement are increasing or decreasing suggests that either (1) the parameters that we derive from PFSS models do not accurately characterize the actual large-scale field in CME source regions, (2) systematic evolution in the large-scale magnetic environment of CME source regions is not, by itself, a necessary condition for CMEs to occur, or both.

## **Varieties of Coronal Mass Ejections and Their Relation to Flares**

**Review**

[Svestka Z.](#)

Space Science Reviews, v. 95, Issue 1/2, p. 135-146 (2001), [File](#)

Most coronal mass ejections (CMEs) start as coronal storms which are caused by an opening of channels of closed field lines along the zero line of the longitudinal magnetic field. This can happen along any zero line on the Sun where the configuration is destabilized. If the opening includes a zero line inside an active region, one observes a chromospheric flare. If this does not happen, no flare is associated with the CME in the chromosphere, but the process, as well as the response in the corona (a Long Decay Event in X-rays) remains the same. The only difference between flare-associated and non-flare-associated CMEs is the strength of the magnetic field in the region of the field line opening. This can explain essentially all differences which have been observed between these two kinds of CMEs. However, there are obviously also other sources of CMEs, different from coronal storms: sprays (giving rise to narrow, pointed ejections), erupting interconnecting loops (often destabilized by flares), and growing coronal holes. This paper tries to summarize and interpret observations which support this general picture, and demonstrates that both CMEs and flares must be properly discussed in any study of solar-terrestrial relations.

## **Kelvin-Helmholtz instability and Alfvénic vortex shedding in solar eruptions**

P. [Syntelis](#), [P. Antolin](#)

ApJL **884** L4 **2019**

<https://arxiv.org/pdf/1909.05716.pdf>

<https://doi.org/10.3847/2041-8213/ab44ab>

We report on a three-dimensional MHD numerical experiment of a small scale coronal mass ejection (CME) -like eruption propagating through a non-magnetized solar atmosphere. We find that the Kelvin-Helmholtz instability (KHI) develops at various but specific locations at the boundary layer between the erupting field and the background atmosphere, depending on the relative angle between the velocity and magnetic field. KHI develops at the front and at two of the four sides of the eruption. KHI is suppressed at the other two sides of the eruption. We also find the development of Alfvénic vortex shedding flows at the wake of the developing CME due to the 3D geometry of the field. Forward modeling reveals that the observational detectability of the KHI in solar eruptions is confined to a narrow  $\approx 10^\circ$  range when observing off-limb, and therefore its occurrence could be underestimated due to projection effects. The new findings can have significant implications for observations, for heating and for particle acceleration by turbulence from flow-driven instabilities associated with solar eruptions of all scales.

## **Eruptions and Flaring Activity in Emerging Quadrupolar Regions**

P. [Syntelis](#), [E. J. Lee](#), [C. W. Fairbairn](#), [V. Archontis](#), [A. W. Hood](#)

A&A **630**, A134 **2019**

<https://arxiv.org/pdf/1909.01446.pdf>

Context. Some of the most dynamic active regions are associated with complex photospheric magnetic configurations such as quadrupolar regions, and especially ones with a  $\delta$ -spot configuration and a strong Polarity Inversion Line (PIL). Aims. We study the formation and eruption of magnetic flux ropes in quadrupolar regions. Methods. 3D MHD simulations of the partial emergence of a highly twisted flux tube from the solar interior into a non-magnetized stratified atmosphere. Results. We emerge two  $\Omega$ -shaped loops forming a quadrupolar region. The emerging flux forms two initially separated bipoles, that later come in contact creating a  $\delta$ -spot central region. Above the two bipoles, two magnetic lobes expand and interact through a series of current sheets at the interface between them. Two recurrent confined eruptions are produced. In both cases, reconnection between sheared low-lying field lines forms a flux rope. Reconnection between the two lobes high in the atmosphere forms retracting field lines that push against the flux rope, creating a current sheet between them. It also forms a third magnetic lobe between the two emerged ones, that later acts as a strapping field. The flux rope eruptions are triggered when the reconnection between the flux ropes and the field above them becomes efficient enough to remove the tension of the overlying field. These reconnection events occur internally in the system. The first erupting flux rope almost fully reconnects with the overlying field. The second eruption is confined by the overlying field. During the confined eruption, the flux rope is enhanced in size, flux and twist, similar to confined-flare-to-flux-rope observations. Proxies of the emission reveal the two erupting filaments channels. A flare arcade is formed only in the second eruption due to the longer-lasting and more efficient reconnection below the flux rope.

## **On the nature of recurrent 3D CME-like eruptions. II. Scaling of energy and collision of successive eruptions**

P. Syntelis, V. Archontis, K. Tsinganos

2019 *ApJ* 876 61

<https://arxiv.org/pdf/1904.03923.pdf>  
<https://sci-hub.se/10.3847/1538-4357/ab16d2>

We present results of three-dimensional MHD simulations of recurrent eruptions in emerging flux regions. The initial numerical setup is the same with the work by Syntelis et al. 2017 (hereafter, Paper I). Here, we perform a parametric study on the magnetic field strength ( $B_0$ ) of the emerging field. The kinetic energy of the produced ejective eruptions in the emerging flux region ranges from 1026–1028 erg, reaching up to the energies of small Coronal Mass Ejections (CMEs). The kinetic and magnetic energies of the eruptions scale linearly in a logarithmic plot. We find that the eruptions are triggered earlier for higher  $B_0$  and that  $B_0$  is not directly correlated to the frequency of occurrence of the eruptions. Using large numerical domains, we show the initial stage of the partial merging of two colliding erupting fields. The partial merging occurs partly by the reconnection between the field lines of the following and the leading eruption at the interface between them. We also find that tether-cutting reconnection of the field lines of the leading eruption underneath the following eruption magnetically links the two eruptions. Shocks develop inside the leading eruption during the collision.

UKSP Nugget: #103 July 2019 <http://www.uksolphys.org/uksp-nugget/103-modelling-multi-scale-solar-eruptions/>

## **Recurrent CME-like Eruptions in Emerging Flux Regions. I. On the Mechanism of Eruptions**

P. Syntelis<sup>1</sup>, V. Archontis<sup>1</sup>, and K. Tsinganos

2017 *ApJ* 850 95

<https://arxiv.org/pdf/1711.10249.pdf>

We report on three-dimensional (3D) magnetohydrodynamic (MHD) simulations of recurrent eruptions in emerging flux regions. We find that reconnection of sheared field lines, along the polarity inversion line of an emerging bipolar region, leads to the formation of a new magnetic structure, which adopts the shape of a magnetic flux rope (FR) during its rising motion. Initially, the FR undergoes a slow-rise phase and, eventually, it experiences a fast-rise phase and ejective eruption toward the outer solar atmosphere. In total, four eruptions occur during the evolution of the system. For the first eruption, our analysis indicates that the torus instability initiates the eruption and that tether-cutting reconnection of the field lines, which envelop the FR, triggers the rapid acceleration of the eruptive field. For the following eruptions, we conjecture that it is the interplay between tether-cutting reconnection and torus instability that causes the onset of the various phases. We show the 3D shape of the erupting fields, focusing more on how magnetic field lines reconnect during the eruptions. We find that when the envelope field lines reconnect mainly with themselves, hot and dense plasma is transferred closer to the core of the erupting FR. The same area appears to be cooler and less dense when the envelope field lines reconnect with neighboring sheared field lines. The plasma density and temperature distribution, together with the rising speeds, energies, and size of the erupting fields, indicate that they may account for small-scale (mini) coronal mass ejections.

## **The spectroscopic imprint of the pre-eruptive configuration resulting into two major coronal mass ejections**

Petros Syntelis, Costis Gontikakis, Spiros Patsourakos, Kanaris Tsinganos

*A&A* 588, A16 2016

<http://arxiv.org/pdf/1602.03680v1.pdf>

We present a spectroscopic analysis of the pre-eruptive configuration of active region NOAA 11429, prior to two very fast coronal mass ejections (CMEs) on **March 7, 2012** that are associated with this active region. We study the thermal components and the dynamics associated with the ejected flux ropes. Using differential emission measure (DEM) analysis of Hinode/EIS and SDO/AIA observations, we identify the emission components of both the flux rope and the



host active region. We then follow the time evolution of the flux rope emission components by using AIA observations. The plasma density and the Doppler and non-thermal velocities associated with the flux ropes are also calculated from the EIS data. The eastern and western parts of the active region, in which the two different fast CMEs originated during two X-class flares, were studied separately. In both regions we identified an emission component in the temperature range of  $\log T = 6.8 - 7.1$  associated with the presence of flux ropes. The time evolution of the eastern region showed an increase in the mean DEM in this temperature range by an order of magnitude, 5 hours prior to the first CME. This was associated with a gradual rise and heating of the flux rope as manifested by blue-shifts and increased non-thermal velocities in  $\lambda_{\text{Ca}}\{XV\} \sim 200.97 \text{ \AA}$ , respectively. An overall upward motion of the flux ropes was measured (relative blue-shifts of  $\sim 12 \text{ km/s}$ ). The measured electron density was found to be  $4 \times 10^9 - 2 \times 10^{10} \text{ cm}^{-3}$  (using the ratio of  $\lambda_{\text{Ca}}\{XV\} \sim 181.90 \text{ \AA}$  over  $\lambda_{\text{Ca}}\{XV\} \sim 200.97 \text{ \AA}$ ). We compare our findings with other works on the same AR to provide a unified picture of its evolution.

See **Plasma Diagnostics Prior to CMEs**

Hinode/EIS Nugget , Nov **2016**

Petros [Syntelis et al.](#)

[http://solarb.mssl.ucl.ac.uk/SolarB/nuggets/nugget\\_2016nov.jsp](http://solarb.mssl.ucl.ac.uk/SolarB/nuggets/nugget_2016nov.jsp)

## **CORONAL JETS SIMULATED WITH THE GLOBAL ALFVÉN WAVE SOLAR MODEL**

J. [Szente](#)<sup>1</sup>, G. Toth<sup>1</sup>, W. B. Manchester IV<sup>1</sup>, B. van der Holst<sup>1</sup>, E. Landi<sup>1</sup>, T. I. Gombosi<sup>1</sup>, C. R. DeVore<sup>2</sup>, and S. K. Antiochos<sup>2</sup>

**2017** ApJ 834 123

This paper describes a numerical modeling study of coronal jets to understand their effects on the global corona and their contribution to the solar wind. We implement jets into a well-established three-dimensional, two-temperature magnetohydrodynamic (MHD) solar corona model employing Alfvén-wave dissipation to produce a realistic solar-wind background. The jets are produced by positioning a compact magnetic dipole under the solar surface and rotating the boundary plasma around the dipole's magnetic axis. The moving plasma drags the magnetic field lines along with it, ultimately leading to a reconnection-driven jet similar to that described by [Pariat et al.](#) We compare line-of-sight synthetic images to multiple jet observations at EUV and X-ray bands, and find very close matches in terms of physical structure, dynamics, and emission. Key contributors to this agreement are the greatly enhanced plasma density and temperature in our jets compared to previous models. These enhancements arise from the comprehensive thermodynamic model that we use and, also, our inclusion of a dense chromosphere at the base of our jet-generating regions. We further find that the large-scale corona is affected significantly by the outwardly propagating torsional Alfvén waves generated by our polar jet, across  $40^\circ$  in latitude and out to  $24 R_\odot$ . We estimate that polar jets contribute only a few percent to the steady-state solar-wind energy outflow.

## **Quasi-periodic oscillations in flares and coronal mass ejections associated with magnetic reconnection**

Takuya [Takahashi](#), [Jiong Qiu](#), [Kazunari Shibata](#)

ApJ **848** 102 **2017**

<https://arxiv.org/pdf/1709.05234.pdf>

We propose a mechanism for quasi-periodic oscillations of both coronal mass ejections (CMEs) and flare loops as related to magnetic reconnection in eruptive solar flares. We perform two-dimensional numerical MHD simulations of magnetic flux rope eruption, with three different values of the global Lundquist number. In the low Lundquist number run, no oscillatory behavior is found. In the moderate Lundquist number run, on the other hand, quasi-periodic oscillations are excited both at the bottom of the flux rope and at the flare loop-top. In the high Lundquist number run, quasi-periodic oscillations are also excited; in the meanwhile, the dynamics become turbulent due to the formation of multiple plasmoids in the reconnection current sheet. In high and moderate Lundquist number runs, thin reconnection jet collide with the flux rope bottom or flare loop-top and dig them deeply. Steep oblique shocks are formed as termination shocks where reconnection jet is bent (rather than decelerated) in horizontal direction, resulting in supersonic back-flows. The structure becomes unstable, and quasi-periodic oscillation of supersonic back-flows appear at locally confined high-beta region at both the flux rope bottom and flare loop-top. We compare the observational characteristics of quasi-periodic oscillations in erupting flux ropes, post-CME current sheets, flare ribbons and light curves, with corresponding dynamical structures found in our simulation. **2014 April 18**

## **Scaling Relations in Coronal Mass Ejections and Energetic Proton Events associated with Solar Superflares**

Takuya [Takahashi](#), Yoshiyuki Mizuno, Kazunari Shibata

ApJL **833** L8 **2016**

<https://arxiv.org/pdf/1611.06015v1.pdf>

<https://iopscience.iop.org/article/10.3847/2041-8205/833/1/L8/pdf>

In order to discuss the potential impact of solar 'superflares' on space weather, we investigated statistical relations among energetic proton peak flux with energy higher than 10 MeV ( $F_p$ ), CME speed near the Sun ( $VCME$ ) obtained by  $\text{\textit{SOHO}}/LASC$ O coronagraph and flare soft X-ray peak flux in 1-8  $\text{\AA}$  band ( $FSXR$ ) during 110 major solar proton events (SPEs) recorded from 1996 to 2014. The linear regression fit results in the scaling relations  $VCME \propto F_p^{\alpha} SXR$ ,

$F_p \propto F^{\beta} \text{SXR}$  and  $F_p \propto V^{\gamma} \text{CME}$  with  $\alpha=0.30 \pm 0.04$ ,  $\beta=1.19 \pm 0.08$  and  $\gamma=4.35 \pm 0.50$ , respectively. On the basis of simple physical assumptions, on the other hand, we derive scaling relations expressing CME mass (MCME), CME speed and energetic proton flux in terms of total flare energy (Eflare) as,  $\text{MCME} \propto E^{2/3} \text{ flare}$ ,  $\text{VCME} \propto E^{1/6} \text{ flare}$  and  $F_p \propto E^{5/6} \text{ flare} \propto V \text{CME}$ , respectively. We then combine the derived scaling relations with observation, and estimated the upper limit of VCME and  $F_p$  to be associated with possible solar superflares.

See Major SEP Events [http://cdaw.gsfc.nasa.gov/CME\\_list/sepe/](http://cdaw.gsfc.nasa.gov/CME_list/sepe/)

## Prominence Activation by Coronal Fast Mode Shock

Takuya **Takahashi**, Ayumi Asai, Kazunari Shibata

2015 *ApJ* **801** 37

<http://arxiv.org/pdf/1501.01592v1.pdf>

An X5.4 class flare occurred in active region (AR) NOAA11429 on **2012 March 7**. The flare was associated with very fast coronal mass ejection (CME) with its velocity of over 2500 km/s. In the images taken with STEREO-B/COR1, a dome-like disturbance was seen to detach from expanding CME bubble and propagated further. A Type-II radio burst was also observed at the same time. On the other hand, in EUV images obtained by SDO/AIA, expanding dome-like structure and its foot print propagating to the north were observed. The foot print propagated with its average speed of about 670 km/s and hit a prominence located at the north pole and activated it. While the activation, the prominence was strongly brightened. On the basis of some observational evidence, we concluded that the foot print in AIA images and the ones in COR1 images are the same, that is MHD fast mode shock front. With the help of a linear theory, the fast mode mach number of the coronal shock is estimated to be between 1.11 and 1.29 using the initial velocity of the activated prominence. Also, the plasma compression ratio of the shock is enhanced to be between 1.18 and 2.11 in the prominence material, which we consider to be the reason of the strong brightening of the activated prominence. The applicability of linear theory to the shock problem is tested with nonlinear MHD simulation.

## Numerical simulations of shear-induced consecutive coronal mass ejections\*

D.-C. **Talpeanu**<sup>1,2</sup>, E. Chané<sup>1</sup>, S. Poedts<sup>1,3</sup>, E. D’Huys<sup>2</sup>, M. Mierla<sup>2,4</sup>, I. Roussev<sup>5,1</sup> and S. Hostenau<sup>1</sup>  
*A&A* **637**, A77 (2020)

<https://www.aanda.org/articles/aa/pdf/2020/05/aa37477-20.pdf>

Context. It is widely accepted that photospheric shearing motions play an important role in triggering the initiation of coronal mass ejections (CMEs). Even so, there are events for which the source signatures are difficult to locate, while the CMEs can be clearly observed in coronagraph data. These events are therefore called ‘stealth’ CMEs. They are of particular interest to space weather forecasters, since eruptions are usually discarded from arrival predictions if they appear to be backside, which means not presenting any clear low-coronal signatures on the visible solar disc. Such assumptions are not valid for stealth CMEs since they can originate from the front side of the Sun and be Earth-directed, but they remain undetected and can therefore trigger unpredicted geomagnetic storms.

Aims. We numerically model and investigate the effects of shearing motion variations onto the resulting eruptions and we focus in particular on obtaining a stealth CME in the trailing current sheet of a previous ejection.

Methods. We used the 2.5D magnetohydrodynamics package of the code MPI-AMRVAC to numerically simulate consecutive CMEs by imposing shearing motions onto the inner boundary, which represents, in our case, the low corona. The initial magnetic configuration consists of a triple arcade structure embedded into a bimodal solar wind, and the sheared polarity inversion line is found in the southern loop system. The mesh was continuously adapted through a refinement method that applies to current carrying structures, allowing us to easily track the CMEs in high resolution, without resolving the grid in the entire domain. We also compared the obtained eruptions with the observed directions of propagation, determined using a forward modelling reconstruction technique based on a graduated cylindrical shell geometry, of an initial multiple coronal mass ejection (MCME) event that occurred in September 2009. We further analysed the simulated ejections by tracking the centre of their flux ropes in latitude and their total speed. Radial Poynting flux computation was employed as well to follow the evolution of electromagnetic energy introduced into the system.

Results. Changes within 1% in the shearing speed result in three different scenarios for the second CME, although the preceding eruption seems insusceptible to such small variations. Depending on the applied shearing speed, we thus obtain a failed eruption, a stealth, or a CME driven by the imposed shear, as the second ejection. The dynamics of all eruptions are compared with the observed directions of propagation of an MCME event and a good correlation is achieved. The Poynting flux analysis reveals the temporal variation of the important steps of eruptions.

Conclusions. For the first time, a stealth CME is simulated in the aftermath of a first eruption, originating from an asymmetric streamer configuration, through changes in the applied shearing speed, indicating it is not necessary for a closed streamer to exist high in the corona for such an event to occur. We also emphasise the high sensitivity of the corona to small changes in motions at the photosphere, or in our simulations, at the low corona. **21 and 22 Sep 2009**

## Statistical Investigation of the Widths of Supra-arcade Downflows Observed During a Solar Flare

**Guangyu Tan**, **Yijun Hou**, **Hui Tian**

*MNRAS* **2023**

<https://arxiv.org/pdf/2304.11307.pdf>

Supra-arcade downflows (SADs) are dark voids descending towards the post-reconnection flare loops and exhibit obvious variation in properties like width. However, due to the lack of further statistical studies, the mechanism behind

such variations hitherto remains elusive. Here we statistically investigated widths of 81 SADs observed in one flare by the Solar Dynamics Observatory (SDO). For each of SADs, six moments were selected with equal time intervals to measure their widths at different stages of their evolution. It is found that most SADs show a roughly monotonous width decrease during their descents, while some SADs with small initial widths can have complex evolutions. 3D reconstruction results based on SDO and Solar Terrestrial Relations Observatory Ahead (STEREO-A) images and thermal properties analysis reveal that differences in magnetic and plasma environments may result in that SADs in the north are overall wider than those in the south. Additionally, correlation analysis between the width and other parameters of SADs was further conducted and revealed that: (1) SADs with different initial widths show no significant differences in their temperature and density evolution characteristics; (2) SADs with small initial widths usually appear in lower heights, where more frequent collisions between SADs could lead to their intermittent acceleration, width increment, and curved trajectories. These results indicate that SADs with different initial widths are produced the same way while different environments (magnetic field or plasma) could affect their subsequent width evolutions. **22 May 2013**

### **Stereoscopic Observation of Simultaneous Longitudinal and Transverse Oscillations in a Single Filament Driven by Two-sided-loop Jet**

[Song Tan](#), [Yuandeng Shen](#), [Xinping Zhou](#), [Zehao Tang](#), [Chengrui Zhou](#), [Yadan Duan](#), [Surui Yao](#)

MNRAS Volume 520, Issue 2 Pages 3080–3088, **2023**

<https://arxiv.org/pdf/2301.07989.pdf>

<https://doi.org/10.1093/mnras/stad295>

We report the first observations of simultaneous large-amplitude longitudinal and transverse oscillations of a quiescent filament triggered by a two-sided-loop jet formed by the magnetic reconnection between the filament and an emerging loop in the filament channel, recorded by the Solar Dynamics Observatory and the Solar TERrestrial RELations Observatory. The north arm of the jet firstly pushed the filament mass moving northwardly along the magnetic field lines consisting of the coronal cavity, then some elevated filament mass fell back and started to oscillate longitudinally at the bottom of the cavity (i.e., the magnetic dip). The northernmost part of the filament also showed transverse oscillation simultaneously. The amplitude and period of the longitudinal (transverse) oscillation are 12.96 (2.99) Mm and 1.18 (0.33) hours, respectively. By using the method of filament seismology, the radius of curvature of the magnetic dip is about 151 Mm, consistent with that obtained by the 3D reconstruction (166 Mm). Using different physical parameters of the observed longitudinal and transverse oscillations, the magnetic field strength of the filament is estimated to be about 23 and 21 Gauss, respectively. By calculating the energy of the moving filament mass, the minimum energy of the jet is estimated to be about  $1.96 \times 10^{28}$  erg. We conclude that the newly formed jet can not only trigger simultaneous longitudinal and transverse oscillations in a single filament, but also can be used as a seismology tool for diagnosing filament information, such as the magnetic structure, magnetic field strength, and magnetic twists. **29 November 2011**

### **Stereoscopic diagnosing of a filament-cavity flux rope system by tracing the path of a two-sided-loop jet**

[Song Tan](#), [Yuandeng Shen](#), [Xinping Zhou](#), [Yadan Duan](#), [Zehao Tang](#), [Chengrui Zhou](#), [Surui Yao](#)

MNRAS Letters **2022**

<https://arxiv.org/pdf/2206.13827.pdf>

The fine magnetic structure is vitally important to understanding the formation, stabilization and eruption of solar filaments, but so far, it is still an open question yet to be resolved. Using stereoscopic observations taken by the Solar Dynamics Observatory and Solar TERrestrial RELations Obsevatory, we studied the generation mechanism of a two-sided-loop jet (TJ) and the ejection process of the jet plasma into the overlying filament-cavity system. We find that the generation of the two-sided-loop jet was due to the magnetic reconnection between an emerging flux loop and the overlying filament. The jet's two arms ejected along the filament axis during the initial stage. Then, the north arm bifurcated into two parts at about 50 Mm from the reconnection site. After the bifurcation, the two bifurcated parts were along the filament axis and the cavity which hosted the filament, respectively. By tracing the ejecting plasma flows of the TJ inside the filament, we not only measured that the magnetic twist stored in the filament was at least  $5\pi$  but also found that the fine magnetic structure of the filament-cavity flux rope system is in well agreement with the theoretical results of Magnetic flux rope models. **29 November 2011**

### **Magnetic Gradient: A Natural Driver of Solar Eruptions**

Baolin [Tan](#), [Yan Yan](#), [Ting Li](#), [Yin Zhang](#), [Xingyao Chen](#)

Research in Astron. & Astrophys. **2020**

<https://arxiv.org/pdf/2001.04043.pdf>

It is well-known that there is a gradient, there will drive a flow inevitably. For example, a density-gradient may drive a diffusion flow, an electrical potential-gradient may drive an electric current in plasmas, etc. Then, what will be driven when a magnetic-gradient occurs in solar atmospheric plasmas? Considering the ubiquitous distribution of magnetic-gradient in solar plasma loops, this work demonstrates that magnetic-gradient pumping (MGP) mechanism is valid even in the partial ionized solar photosphere, chromosphere as well as in the corona. It drives energetic particle flows which carry and convey kinetic energy from the underlying atmosphere to move upwards, accumulate around the looptop and increase there temperature and pressure, and finally lead to eruptions around the looptop by triggering ballooning

instabilities. This mechanism may explain the formation of the observing hot cusp-structures above flaring loops in most preflare phases, therefore, the magnetic-gradient should be a natural driver of solar eruptions. Furthermore, we may also apply to understand many other astrophysical phenomena, such as the temperature distribution above sunspots, the formation of solar plasma jets, type-II spicule, and fast solar wind above coronal holes, as well as the fast plasma jets related to white dwarfs, neutron stars and black holes. **19-Jul-2012**

### **Sympathetic Standard and Blowout Coronal Jets Observed in a Polar Coronal Hole**

[Zehao Tang](#), [Yuandeng Shen](#), [Xinping Zhou](#), [Yadan Duan](#), [Chengrui Zhou](#), [Song Tan](#), [Elmhamdi Abouazza](#)

ApJL **2021**

<https://arxiv.org/pdf/2104.04309.pdf>

We present the sympathetic eruption of a standard and a blowout coronal jets originating from two adjacent coronal bright points (CBP1 and CBP2) in a polar coronal hole, using soft X-ray and extreme ultraviolet observations respectively taken by the Hinode and the Solar Dynamic Observatory. In the event, a collimated jet with obvious westward lateral motion firstly launched from CBP1, during which a small bright point appeared around CBP1's east end, and magnetic flux cancellation was observed within the eruption source region. Based on these characteristics, we interpret the observed jet as a standard jet associated with photospheric magnetic flux cancellation. About 15 minutes later, the westward moving jet spire interacted with CBP2 and resulted in magnetic reconnection between them, which caused the formation of the second jet above CBP2 and the appearance of a bright loop system in-between the two CBPs. In addition, we observed the writhing, kinking, and violent eruption of a small kink structure close to CBP2's west end but inside the jet-base, which made the second jet brighter and broader than the first one. These features suggest that the second jet should be a blowout jet triggered by the magnetic reconnection between CBP2 and the spire of the first jet. We conclude that the two successive jets were physically connected to each other rather than a temporal coincidence, and this observation also suggests that coronal jets can be triggered by external eruptions or disturbances, besides internal magnetic activities or magnetohydrodynamic instabilities. **2019 March 31**

### **Polar Coronal Plumes as Tornado-like Jets**

E. [Tavabi](#)<sup>1,2</sup>, S. Koutchmy<sup>3</sup>, and L. Golub

**2018** ApJ 866 35

[sci-hub.tw/10.3847/1538-4357/aadc64](http://sci-hub.tw/10.3847/1538-4357/aadc64)

We examine the dynamical behavior of white-light polar-plume structures in the inner corona that are observed from the ground during total solar eclipses, based on their extreme ultraviolet (EUV) hot and cool emission line counterparts observed from space. EUV observations from Solar Dynamics Observatory/Atmospheric Imaging Assembly (SDO/AIA) of a sequence of rapidly varying coronal hole structures are analyzed. Evidence of events showing acceleration in the 1.25 Mk line of Fe xii at 193 Å is given. The structures along the plume show an outward velocity of about 140 km s<sup>-1</sup> that can be interpreted as an upward propagating wave in the 304 Å and 171 Å lines; higher speeds are seen in 193 Å (up to 1000 km s<sup>-1</sup>). The ejection of the cold He ii plasma is delayed by about 4 minutes in the lowest layer and is delayed more than 12 minutes in the highest level compared to the hot 193 Å behavior. A study of the dynamics using time-slice diagrams reveals that a large amount of fast ejected material originates from below the plume, at the footpoints. The release of plasma material appears to come from a cylinder with quasi-parallel edge-enhanced walls. After the initial phase of a longitudinal acceleration, the speed substantially reduces, and the ejecta disperse into the environment. Finally, the detailed temporal and spatial relationships between the cool and hot components were studied with simultaneous multiwavelength observations, using more AIA data. The outward-propagating perturbation of the presumably magnetic walls of polar plumes supports the suggestion that Alfvén waves propagate outwardly along these radially extended walls. **2010 July 10-11**

### **Analysis of a Failed Eclipse Plasma Ejection Using EUV Observations**

E. [Tavabi](#), [S. Koutchmy](#), [C. Bazin](#)

Solar Phys. **293**:42 **2018**

<https://arxiv.org/ftp/arxiv/papers/1801/1801.09222.pdf>

The photometry of eclipse white-light (W-L) images showing a moving blob is interpreted for the first time together with observations from space with the PROject for On Board Autonomy (PROBA-2) mission (ESA). An off-limb event seen with great details in W-L was analyzed with the SWAP imager (Sun Watcher using Active pixel system detector and image Processing) working in the EUV near 174 Å. It is an elongated plasma blob structure of 25 Mm diameter moving above the E-limb with coronal loops under. Summed and co-aligned SWAP images are evaluated using a 20 hours sequence, in addition to the **July 11, 2010** eclipse W-L images taken from several sites. The Atmospheric Imaging Assembly (AIA) instruments on board the Solar Dynamical Observatory (SDO) recorded the event suggesting a magnetic reconnection near a high neutral point; accordingly, we also call it a magnetic plasmoid. The measured proper motion of the blob shows a velocity up to 12 km s<sup>-1</sup>. Electron densities of the isolated condensation (cloud or blob or plasmoid) is photometrically evaluated. The typical value is 10<sup>8</sup> cm<sup>-3</sup> at r=1.7 R, superposed on a background corona of 10<sup>7</sup> cm<sup>-3</sup> density. The mass of the cloud near its maximum brightness is found to be 1.6x10<sup>13</sup> gr which is typically 0.6x10<sup>-4</sup> of the overall mass of the corona. From the extrapolated magnetic field the cloud evolves inside a rather broad open region but decelerates, after reaching its maximum brightness. The influence of such small events for supplying material to the ubiquitous slow wind is noticed. A precise evaluation of the EUV photometric data after accurately removing the stray light, suggests an interpretation of the weak 174 Å radiation of the cloud as due to resonance scattering in the Fe IX/X lines.

## **Polar Coronal Plumes as Tornado-Like Jets**

E. [Tavabi](#), [S. Koutchmy](#), [L. Golub](#)

ApJ **2018**

<https://arxiv.org/ftp/arxiv/papers/1808/1808.07322.pdf>

We examine the dynamical behavior of white light polar plume structures in the inner corona that are observed from the ground during total solar eclipses, based on their EUV hot and cool emission line counterparts observed from space. EUV observations from SDO/AIA of a sequence of rapidly varying coronal hole structures are analyzed. Evidence of events showing acceleration in the 1.25 Mk line of Fe XII at 193 Å is given. The structures along the plume show an outward velocity of about 140 km/s that can be interpreted as an upwards propagating wave in the 304 Å and 171 Å lines; higher speeds are seen in 193 Å (up to 1000 km/s). The ejection of the cold He II plasma is delayed by about 4 min in the lowest layer and more than 12 min in the highest level compared to the hot 193 Å behavior. A study of the dynamics using time-slice diagrams reveals that a large amount of fast ejected material originates from below the plume, at the footpoints. The release of plasma material appears to come from a cylinder with quasi-parallel edge-enhanced walls. After the initial phase of a longitudinal acceleration, the speed substantially reduces and the ejecta disperse into the environment. Finally, the detailed temporal and spatial relationships between the cool and hot components were studied with simultaneous multi-wavelength observations, using more AIA data. The outward-propagating perturbation of the presumably magnetic walls of polar plumes supports the suggestion that Alfvén waves propagate outwardly along these radially extended walls. **10 July 2010**

## **Limb Event Brightenings (LEBs) with fast ejection using IRIS mission Observations**

E. [Tavabi](#), [S. Koutchmy](#), [L. Golub](#)

Solar Phys. Volume 290, Issue 10, pp 2871-2887 **2015**

<http://arxiv.org/ftp/arxiv/papers/1507/1507.06794.pdf>

The Interface Region Imaging Spectrograph (IRIS) of the recently commissioned NASA Small Explorer mission provides significantly more complete and higher resolution spectral coverage of the dynamical conditions inside the chromosphere and Transition Region (TR) than has heretofore been available. Near the solar limb high temporal, spatial ( $0''3$ ) and spectral resolution observations from ultraviolet IRIS spectra reveal high-energy limb event brightenings (LEBs) at low chromospheric height, near 1 Mm height above the limb. They can be characterized as explosive events producing jets. We selected 2 events showing spectra of a confined eruption just off or near the quiet Sun limb, the jet part showing obvious moving material with short duration large Doppler shifts in three directions identified as macrospicules on slit-jaw (SJ) images in SiIV and HeII 304. The events are analyzed from a sequence of very close rasters taken near the central meridian and the South Pole limb. The processed SJ images and the simultaneously observed fast spectral sequences with large Doppler shifts, with a pair of red shifted elements together with a faster blue shifted element from almost the same position, are analyzed. Shifts correspond to velocities up to 100 km/s in projection on the plane of the limb. The occurrence of erupting spicules and macrospicules from these regions is noticed from images taken before and after the spectra. The cool low-FIP element simultaneous line emissions of the MgII h & k resonance lines do not clearly show a similar signature due to optical thickness effects but SiIV broad band SJ images do. The bidirectional plasma jets ejected from a small reconnection site are interpreted as the result of coronal loop-loop interactions leading to reconnection in nearby sites. **Oct. 10, 2013**

## **Stochasticity and Persistence of Solar Coronal Mass Ejections**

D. [Telloni](#)<sup>1</sup>, V. Carbone<sup>2,3</sup>, F. Lepreti<sup>2</sup>, and E. Antonucci

**2014** ApJ 781 L1

The study of the statistical properties of coronal mass ejections (CMEs) reveals that their properties depend on the period of solar activity. In particular, when investigating the origin of the waiting time distribution between CMEs, a significant departure from a Poisson process during periods of high solar activity has been found, thus suggesting the existence of at least two physical processes underlying the origin of CMEs. One acts continuously, perhaps related to randomly occurring magnetic reconfigurations of the solar corona at large scales. The other plays a role only during the solar maximum, probably due to the photospheric emergence of magnetic flux as a statistically persistent mechanism, which generates long correlation times among CME events strong enough not to be destroyed by the former random process.

## **Space weather: the solar perspective -- an update to Schwenn (2006)**

**Review**

[Manuela Temmer](#)

Living Reviews in Solar Physics **2021**

<https://arxiv.org/pdf/2104.04261.pdf>

<https://link.springer.com/content/pdf/10.1007/s41116-021-00030-3.pdf>

The Sun, as an active star, is the driver of energetic phenomena that structure interplanetary space and affect planetary atmospheres. The effects of Space Weather on Earth and the solar system is of increasing importance as human spaceflight is preparing for lunar and Mars missions. This review is focusing on the solar perspective of the Space Weather relevant phenomena, coronal mass ejections (CMEs), flares, solar energetic particles (SEPs), and solar wind stream interaction regions (SIR). With the advent of the STEREO mission (launched in 2006), literally, new

perspectives were provided that enabled for the first time to study coronal structures and the evolution of activity phenomena in three dimensions. New imaging capabilities, covering the entire Sun-Earth distance range, allowed to seamlessly connect CMEs and their interplanetary counterparts measured in-situ (so called ICMEs). This vastly increased our knowledge and understanding of the dynamics of interplanetary space due to solar activity and fostered the development of Space Weather forecasting models. Moreover, we are facing challenging times gathering new data from two extraordinary missions, NASA's Parker Solar Probe (launched in 2018) and ESA's Solar Orbiter (launched in 2020), that will in the near future provide more detailed insight into the solar wind evolution and image CMEs from view points never approached before. The current review builds upon the Living Reviews paper by Schwenn from 2006, updating on the Space Weather relevant CME-flare-SEP phenomena from the solar perspective, as observed from multiple viewpoints and their concomitant solar surface signatures. **5-8 Dec 1981, 13-16 Aug 1982, 12 July 2007, December 12, 2008, December 22, 2009, 10 Jun 2010, June 12-13, 2010, 28 Oct 2003, November 18, 2003, 6-8 Aug 2007, March 7, 2011, August 9, 2011, March 7-11, 2012: May 17, 2012, June 30, 2012, 2-4 Dec 2012, June 14, 2012, February 25, 2014, August 24, 2014, January 1, 2016, September 6, 2017, 6-12 Sep 2017,**

### **Deriving CME Density From Remote Sensing Data and Comparison to In-Situ Measurements**

[M. Temmer](#) , [L. Holzkecht](#), [M. Dumbović](#) , [B. Vršnak](#) , [N. Sachdeva](#) , [S. G. Heinemann](#) , [K. Dissauer](#) , [C. Scolini](#) , [E. Asvestari](#) , [A. M. Veronig](#) , [S. J. Hofmeister](#)

JGR [Volume 126, Issue 1](#) January 2021 e2020JA028380

<https://doi.org/10.1029/2020JA028380>

<https://agupubs.onlinelibrary.wiley.com/doi/epdf/10.1029/2020JA028380>

We determine the three-dimensional geometry and deprojected mass of 29 well-observed coronal mass ejections (CMEs) and their interplanetary counterparts (ICMEs) using combined Solar Terrestrial Relations Observatory - Solar and Heliospheric Observatory white-light data. From the geometry parameters, we calculate the volume of the CME for the magnetic ejecta (flux-rope type geometry) and sheath structure (shell-like geometry resembling the (I)CME frontal rim). Working under the assumption that the CME mass is roughly equally distributed within a specific volume, we expand the CME self-similarly and calculate the CME density for distances close to the Sun (15–30 Rs) and at 1 AU. Specific trends are derived comparing calculated and in-situ measured proton densities at 1 AU, though large uncertainties are revealed due to the unknown mass and geometry evolution: (1) a moderate correlation for the magnetic structure having a mass that stays rather constant ( $cc \approx 0.56 - 0.59$ ), and (2) a weak correlation for the sheath density ( $cc \approx 0.26$ ) by assuming the sheath region is an extra mass—as expected for a mass pile-up process—that is in its amount comparable to the initial CME deprojected mass. High correlations are derived between in-situ measured sheath density and the solar wind density ( $cc \approx -0.73$ ) and solar wind speed ( $cc \approx 0.56$ ) as measured 24 h ahead of the arrival of the disturbance. This gives additional confirmation that the sheath-plasma indeed stems from piled-up solar wind material. While the CME interplanetary propagation speed is not related to the sheath density, the size of the CME may play some role in how much material could be piled up. **4 aug 2011, 15-16 Mar 2012**

**Table A1** Parameters of 29CMEs/ICMEs under study (2008-2014)

### **Deriving CME density from remote sensing data and comparison to in-situ measurements**

[M. Temmer](#), [L. Holzkecht](#), [M. Dumbovic](#), [B. Vrsnak](#), [N. Sachdeva](#), [S.G. Heinemann](#), [K. Dissauer](#), [C. Scolini](#), [E. Asvestari](#), [A. M. Veronig](#), [S. J. Hofmeister](#)

2020

<https://arxiv.org/abs/2011.06880>

We determine the 3D geometry and deprojected mass of 29 well-observed coronal mass ejections (CMEs) and their interplanetary counterparts (ICMEs) using combined STEREO-SOHO white-light data. From the geometry parameters we calculate the volume of the CME for the magnetic ejecta (flux-rope type geometry) and sheath structure (shell-like geometry resembling the (I)CME frontal rim). Working under the assumption that the CME mass is roughly equally distributed within a specific volume, we expand the CME self-similarly and calculate the CME density for distances close to the Sun (15-30 Rs) and at 1AU. Specific trends are derived comparing calculated and in-situ measured proton densities at 1AU, though large uncertainties are revealed due to the unknown mass and geometry evolution: i) a moderate correlation for the magnetic structure having a mass that stays rather constant ( $\sim 0.56-0.59$ ), and ii) a weak correlation for the sheath density ( $\sim 0.26$ ) by assuming the sheath region is an extra mass - as expected for a mass pile-up process - that is in its amount comparable to the initial CME deprojected mass. High correlations are derived between in-situ measured sheath density and the solar wind density ( $\sim -0.73$ ) and solar wind speed ( $\sim 0.56$ ) as measured 24 hours ahead of the arrival of the disturbance. This gives additional confirmation that the sheath-plasma indeed stems from piled-up solar wind material. While the CME interplanetary propagation speed is not related to the sheath density, the size of the CME may play some role in how much material could be piled up. **August 4, 2011, 15 Mar 2012**

### **On flare-CME characteristics from Sun to Earth combining remote-sensing image data with in-situ measurements supported by modeling**

M. [Temmer](#), J.K. Thalmann, K. Dissauer, [A.M. Veronig](#), [J. Tschernitz](#), [J. Hinterreiter](#), [L. Rodriguez](#)

Solar Phys. Volume 292, Issue 7, article id.93, 2017

<https://arxiv.org/pdf/1703.00694.pdf>

<https://link.springer.com/content/pdf/10.1007/s11207-017-1112-5.pdf>

We analyze the well observed flare-CME event from **October 1, 2011** (SOL2011-10-01T09:18) covering the complete chain of action - from Sun to Earth - for a better understanding of the dynamic evolution of the CME and its embedded magnetic field. We study the solar surface and atmosphere associated with the flare-CME from SDO and ground-based instruments, and also track the CME signature off-limb from combined EUV and white-light data with STEREO. By applying 3D reconstruction techniques (GCS, total mass) to stereoscopic STEREO-SoHO coronagraph data, we track the temporal and spatial evolution of the CME in interplanetary space and derive its geometry and 3D-mass. We combine the GCS and Lundquist model results to derive the axial flux and helicity of the MC from in-situ measurements (Wind). This is compared to nonlinear force-free (NLFF) model results as well as to the reconnected magnetic flux derived from the flare ribbons (flare reconnection flux) and the magnetic flux encompassed by the associated dimming (dimming flux). We find that magnetic reconnection processes were already ongoing before the start of the impulsive flare phase, adding magnetic flux to the flux rope before its final eruption. The dimming flux increases by more than 25% after the end of the flare, indicating that magnetic flux is still added to the flux rope after eruption. Hence, the derived flare reconnection flux is most probably a lower limit for estimating the magnetic flux within the flux rope. We find that the magnetic helicity and axial magnetic flux are reduced in interplanetary space by ~50% and 75%, respectively, possibly indicating to an erosion process. A mass increase of 10% for the CME is observed over the distance range from ~4-20 Rs. The temporal evolution of the CME associated core dimming regions supports the scenario that fast outflows might supply additional mass to the rear part of the CME.

## **Kinematical properties of coronal mass ejections**

**Review**

Manuela **Temmer**

Astronomische Nachrichten **2016 File**

<http://arxiv.org/pdf/1603.01398v1.pdf>

Coronal mass ejections (CMEs) are the most dynamic phenomena in our solar system. They abruptly disrupt the continuous outflow of solar wind by expelling huge clouds of magnetized plasma into interplanetary space with velocities enabling to cross the Sun-Earth distance within a few days. Earth-directed CMEs may cause severe geomagnetic storms when their embedded magnetic fields and the shocks ahead compress and reconnect with the Earth's magnetic field. The transit times and impacts in detail depend on the initial CME velocity, size, and mass, as well as on the conditions and coupling processes with the ambient solar wind flow in interplanetary space. The observed CME parameters may be severely affected by projection effects and the constant changing environmental conditions are hard to derive. This makes it difficult to fully understand the physics behind CME evolution, preventing to do a reliable forecast of Earth-directed events. This short review focusing on observational data, shows recent methods which were developed to derive the CME kinematical profile for the entire Sun-Earth distance range as well as studies which were performed to shed light on the physical processes that CMEs encounter when propagating from Sun to Earth.

**23 July 2012**

## **Asymmetry in the CME-CME interaction process for the events from 2011 February 14-15**

M. **Temmer**, A. M. Veronig, V. Peinhart, B. Vršnak

ApJ, **2014** ApJ 785 85

<http://arxiv.org/pdf/1402.6891v1.pdf>

We present a detailed study of the interaction process of two coronal mass ejections (CMEs) successively launched on 2011 February 14 (CME1) and 2011 February 15 (CME2). Reconstructing the 3D shape and evolution of the flux ropes we verify that the two CMEs interact. The frontal structure of both CMEs measured along different position angles (PA) over the entire latitudinal extent, reveals differences in the kinematics for the interacting flanks and the apexes. The interaction process is strongly PA-dependent in terms of timing as well as kinematical evolution. The central interaction occurs along PA-100{\deg}, which shows the strongest changes in kinematics. During interaction, CME1 accelerates from ~400 km/s to ~700 km/s and CME2 decelerates from ~1300 km/s to ~600 km/s. Our results indicate that a simplified scenario like inelastic collision may not be sufficient to describe the CME-CME interaction. Magnetic field structures of the intertwining flux ropes as well as momentum transfer due to shocks play an important role in the interaction process.

## **CHARACTERISTICS OF KINEMATICS OF A CORONAL MASS EJECTION DURING THE 2010 AUGUST 1 CME-CME INTERACTION EVENT**

Manuela **Temmer**<sup>1</sup>, Bojan Vršnak<sup>2</sup>, Tanja Rollett<sup>1</sup>, Bianca Bein<sup>1</sup>, Curt A. de Koning<sup>3</sup>, Ying Liu<sup>4,5</sup>, Eckhard Bosman<sup>6</sup>, Jackie A. Davies<sup>7</sup>, Christian Möstl<sup>1,4,6</sup>, Tomislav Žic<sup>2</sup>, Astrid M. Veronig<sup>1</sup>, Volker Bothmer<sup>7</sup>, Richard Harrison<sup>8</sup>, Nariaki Nitta<sup>9</sup>, Mario Bisi<sup>10,11</sup>, Olga Flor<sup>1</sup>, Jonathan Eastwood<sup>12</sup>, Dusan Odstrcil<sup>13</sup> and Robert Forsyth

**2012** ApJ 749 57, **File**

<http://arxiv.org/pdf/1202.0629v1.pdf>

We study the interaction of two successive coronal mass ejections (CMEs) during the **2010 August 1** events using STEREO/SECCHI COR and heliospheric imager (HI) data. We obtain the direction of motion for both CMEs by applying several independent reconstruction methods and find that the CMEs head in similar directions. This provides evidence that a full interaction takes place between the two CMEs that can be observed in the HI1 field of view. The

full de-projected kinematics of the faster CME from Sun to Earth is derived by combining remote observations with in situ measurements of the CME at 1 AU. The speed profile of the faster CME (CME2;  $\sim 1200 \text{ km s}^{-1}$ ) shows a strong deceleration over the distance range at which it reaches the slower, preceding CME (CME1;  $\sim 700 \text{ km s}^{-1}$ ). By applying a drag-based model we are able to reproduce the kinematical profile of CME2, suggesting that CME1 represents a magnetohydrodynamic obstacle for CME2 and that, after the interaction, the merged entity propagates as a single structure in an ambient flow of speed and density typical for quiet solar wind conditions. Observational facts show that magnetic forces may contribute to the enhanced deceleration of CME2. We speculate that the increase in magnetic tension and pressure, when CME2 bends and compresses the magnetic field lines of CME1, increases the efficiency of drag.

## **Coronal mass ejections and radio related aspects**

M. [Temmer](#)

### **CESRA\_2010, Presentation File**

Coronal mass ejections (CMEs) are the most violent activity signatures from our Sun. Discovered in the 70's, extensive studies were carried out particularly in the SOHO era, but still, our understanding of the physical characteristics of CMEs is limited. The present paper reviews recent results derived from studies of CMEs and associated flares, together with their radio related aspects. In particular we pay attention to recent STEREO results on the 3D propagation characteristics of CMEs in the interplanetary space which can be now tracked seamlessly from Sun to Earth. CME driven shocks indicated from interplanetary radio type II bursts are of special interest since, if Earth directed, are influencing the near Earth space environment and disturb our so called space weather.

## **Combined STEREO/RHESSI study of CME acceleration and particle acceleration in solar flares**

M. [Temmer](#), A.M. Veronig, E.P. Kontar, S. Krucker, B. Vrsnak

E-print, Feb. 2010, **File**, Ap. J. 712, Issue 2, pp. 1410-1420

<http://solar.physics.montana.edu/cgi-bin/eprint/index.pl?entry=13178>

Using the potential of two unprecedented missions, STEREO and RHESSI, we study three well observed fast CMEs that occurred close to the limb together with their associated high energy flare emissions in terms of RHESSI HXR spectra and flux evolution. From STEREO/EUVI and STEREO/COR1 data the full CME kinematics of the impulsive acceleration phase up to 4 Rs is measured with a high time cadence of less equal 2.5 min. For deriving CME velocity and acceleration we apply and test a new algorithm based on regularization methods. The CME maximum acceleration is achieved at heights  $h < 0.4 \text{ Rs}$ , the peak velocity at  $h < 2.1 \text{ Rs}$  (in one case as small as 0.5 Rs). We find that the CME acceleration profile and the flare energy release as evidenced in the RHESSI hard X-ray flux evolve in a synchronized manner. These results support the standard flare/CME model which is characterized by a feed-back relationship between the large-scale CME acceleration process and the energy release in the associated flare.

## **CME Projection Effects Studied with STEREO/COR and SOHO/LASCO**

M. [Temmer](#) · S. Preiss · A.M. Veronig

Solar Phys (2009) 256: 183–199, DOI 10.1007/s11207-009-9336-7, 2009, **File**

### **STEREO SCIENCE RESULTS AT SOLAR MINIMUM**

Based on a set of 11 CME events we study the impact of projection effects by tracking CME leading edge features in the plane of sky (traditional CME tracking) from combined STEREO-SECCHI and SOHO-LASCO observations up to  $20R_{\odot}$ . By using CME observations from two vantage points and applying triangulation techniques, the source region location of the CME on the solar surface was determined (heliospheric longitude and latitude) to correct for projection effects. With this information, the directivity and “true” speed of a CME can be estimated in a simple way. The comparison of the results obtained from the spacecraft pairs SOHO-LASCO/STEREO-A and SOHO-LASCO/STEREO-B allows us to study the reliability of the method. The determined CME source region is generally coincident within  $\sim 10^{\circ}$ .

## **Relation between CME Acceleration Profile and Flare Energy Release derived from Combined STEREO and RHESSI Observations**

[Temmer](#), M.1; Veronig, A.M.1; Vrsnak, B.2

### **Fraiburg ESP Meeting 2008, Presentation**

In the standard flare/CME picture magnetic reconnection occurs in a current sheet formed behind the CME, which may provide a feedback relationship between both phenomena. To study the relationship of the large-scale CME acceleration and the energy release in the associated flare we analyze three well observed events. The observations cover the early (low corona) evolution of the CMEs with the EUVI instruments aboard the twin STEREO spacecraft and the RHESSI hard X-ray emission of the associated flare. Since the flare hard X-rays are due to fast electrons, they provide the most



direct indicator of the evolution of the flare energy release in the flare. The results are compared to case studies for halo-CMEs where a close synchronization between the CME acceleration and the flare energy release was found (Temmer et al., ApJ, 2008, 673, L95).

### **ACCELERATION IN FAST HALO CMEs AND SYNCHRONIZED FLARE HXR BURSTS**

M. Temmer, A. M. Veronig, B. Vršnak, J. Rybačik, P. Gomořny, S. Stoiser, and D. Marić  
The Astrophysical Journal, 673: L95–L98, 2008, File

We study two well-observed, fast halo CMEs (2005.01.17; 2006.07.06), covering the full CME kinematics including the initiation and impulsive acceleration phase, and their associated flares. We find a close synchronization between the CME acceleration profile and the flare energy release as indicated by the *RHESSI* hard X-ray flux onsets, as well as peaks occur simultaneously within 5 minutes. These findings indicate a close physical connection between both phenomena and are interpreted in terms of a feedback relationship between the CME dynamics and the reconnection process in the current sheet beneath the CME.

### **High-Resolution Observation and Magnetic Modeling of a Solar Minifilament: the Formation, Eruption and Failing Mechanisms**

Weilin Teng, Yingna Su, Rui Liu, Jialin Chen, Yanjie Liu, Jun Dai, Wenda Cao, Jinhua Shen, Haisheng Ji  
ApJ 970 100 2024

<https://arxiv.org/pdf/2405.17303>

<https://iopscience.iop.org/article/10.3847/1538-4357/ad50d0/pdf>

Minifilaments are widespread small-scale structures in the solar atmosphere. To better understand their formation and eruption mechanisms, we investigate the entire life of a sigmoidal minifilament located below a large quiescent filament observed by BBSO/GST on 2015 August 3. The H $\alpha$  structure initially appears as a group of arched threads, then transforms into two J-shaped arcades, and finally forms a sigmoidal shape. SDO/AIA observations in 171 Å show that two coronal jets occur around the southern footpoint of the minifilament before the minifilament eruption. The minifilament eruption starts from the southern footpoint, then interacts with the overlying filament and fails. The aforementioned observational changes correspond to three episodes of flux cancellations observed by SDO/HMI. Unlike previous studies, the flux cancellation occurs between the polarity where southern footpoint of the minifilament is rooted in and an external polarity. We construct two magnetic field models before the eruption using the flux rope insertion method, and find an hyperbolic flux tube (HFT) above the flux cancellation site. The observation and modeling results suggest that the eruption is triggered by the external magnetic reconnection between the core field of the minifilament and the external fields due to flux cancellations. This study reveals a new triggering mechanism for minifilament eruptions and a new relationship between minifilament eruptions and coronal jets.

### **Tracking magnetic flux and helicity from Sun to Earth -- Multi-spacecraft analysis of a magnetic cloud and its solar source**

J. K. Thalmann, M. Dumbovic, K. Dissauer, T. Podladchikova, G. Chikunova, M. Temmer, E. Dickson, A. M. Veronig

A&A 2022

<https://arxiv.org/pdf/2210.02228.pdf>

We analyze the complete chain of effects caused by a solar eruptive event in order to better understand the dynamic evolution of magnetic-field related quantities in interplanetary space, in particular that of magnetic flux and helicity. We study a series of connected events (a confined C4.5 flare, a flare-less filament eruption and a double-peak M-class flare) that originated in NOAA active region (AR) 12891 on 2021 November 1 and November 2. We deduce the magnetic structure of AR 12891 using stereoscopy and nonlinear force-free (NLFF) magnetic field modeling, allowing us to identify a coronal flux rope and to estimate its axial flux and helicity. Additionally, we compute reconnection fluxes based on flare ribbon and coronal dimming signatures from remote sensing imagery. Comparison to corresponding quantities of the associated magnetic cloud (MC), deduced from in-situ measurements from Solar Orbiter and near-Earth spacecraft, allows us to draw conclusions on the evolution of the associated interplanetary coronal mass ejection (ICME). The latter are aided through the application of geometric fitting techniques (graduated cylindrical shell modeling; GCS) and interplanetary propagation models (drag based ensemble modeling; DBEM) to the ICME. NLFF modeling suggests the host AR's magnetic structure in the form of a left-handed (negative-helicity) sheared arcade/flux rope reaching to altitudes of 8-10 Mm above photospheric levels, in close agreement with the corresponding stereoscopic estimate. Revealed from GCS and DBEM modeling, the ejected flux rope propagated in a self-similar expanding manner through interplanetary space. Comparison of magnetic fluxes and helicities processed by magnetic reconnection in the solar source region and the respective budgets of the MC indicate a considerable contribution from the eruptive process, though the pre-eruptive budgets appear of relevance too.

### **Exceptions to the rule: the X-flares of AR 2192 Lacking Coronal Mass Ejections**

Thalmann, J. K.; Su, Y.; Temmer, M.; Veronig, A. M.

Ground-based Solar Observations in the Space Instrumentation Era

ASP Conference Series, Vol. 504, p. 203, 2016

<http://aspbooks.org/publications/504/203.pdf>

NOAA Active region (AR) 2192, that was present on the Sun in October 2014, was the largest region which occurred since November 1990 (see Figure 1). The huge size accompanied by a very high activity level, was quite unexpected as it appeared during the unusually weak solar cycle 24. Nevertheless, the AR turned out to be one of the most prolific flaring ARs of cycle 24. It produced in total 6 X, 29 M, 79 C flares during its disk passage from October 18-29, 2014 (see Figure 2). Surprisingly, all flares greater than GOES class M5 and X were confined, i.e. had no coronal mass ejections (CME) associated. All the flare events had some obvious similarity in morphology, as they were located in the core of the AR and revealed only minor separation motion away from the neutral line but a large initial separation of the conjugate flare ribbons. In the paper by Thalmann et al. (2015) we describe the series of flares and give details about the confined X1.6 flare event from October 22, 2014 as well as the single eruptive M4.0 flare event from October 24, 2014. The study of the X1.6 flare revealed a large initial separation of flare ribbons together with recurrent flare brightenings, which were related to two episodes of enhanced hard X-ray emission as derived from RHESSI observations. This suggests that magnetic field structures connected to specific regions were repeatedly involved in the process of reconnection and energy release. Opposite to the central location of the sequence of confined events within the AR, a single eruptive (M4.0) event occurred on the outskirts of the AR in the vicinity of open magnetic fields. Our investigations revealed a predominantly north-south oriented magnetic system of arcade fields overlying the AR that could have preserved the magnetic arcade to erupt, and consequently kept the energy release trapped in a localized volume of magnetic field high up in the corona (as supported by the absence of a lateral motion of the flare ribbons and the recurrent brightenings within them). We conclude that the background magnetic field configuration is an essential parameter for deriving the “eruptiveness” of flare events. Sun et al. (2015) supports this conclusion and derived for this AR a quite slow decay of the strength of the overlying magnetic field (decay index; see Török & Kliem 2005). Interestingly, our magnetic field modellings revealed no flux rope inherent to the AR, indicating that further investigations are needed. In a recent paper by Veronig & Polanec (2015), who investigated in more detail the X-flares using also ground-based observations in H $\alpha$  from Kanzelhöhe Observatory (Pötzi et al. 2015), it was shown that such confined events could be explained by the emerging-flux model, where newly emerging small flux tubes reconnect with pre-existing large coronal loops. **October 22, 2014, October 24, 2014**

### **The Impact of a Stealth CME on the Martian Topside Ionosphere**

Smitha V. [Thampi](#), [C. Krishnaprasad](#), [Govind G. Nampoothiri](#), [Tarun K. Pant](#)  
MNRAS **2021**

<https://arxiv.org/pdf/2102.09304.pdf>

Solar cycle 24 is one of the weakest solar cycles recorded, but surprisingly the declining phase of it had a slow CME which evolved without any low coronal signature and is classified as a stealth CME which was responsible for an intense geomagnetic storm at Earth (Dst = -176 nT). The impact of this space weather event on the terrestrial ionosphere has been reported. However, the propagation of this CME beyond 1 au and the impact of this CME on other planetary environments have not been studied so far. In this paper, we analyse the data from Sun-Earth L1 point as well as from the Martian orbit (near 1.5 au) to understand the characteristics of the stealth CME as observed beyond 1 au. The observations near Earth are using data from the Solar Dynamics Observatory (SDO) and the Advanced Composition Explorer (ACE) satellite located at L1 point whereas those near Mars are from the instruments for plasma and magnetic field measurements on board Mars Atmosphere and Volatile Evolution (MAVEN) mission. The observations show that the stealth CME has reached 1.5 au after 7 days of its initial observations at the Sun and caused depletion in the nightside topside ionosphere of Mars, as observed during the inbound phase measurements of the Langmuir Probe and Waves (LPW) instrument on board MAVEN. These observations have implications on the ion escape rates from the Martian upper atmosphere. **2018-08-20-28**

### **IMPLEMENTATION OF THE GRADUATED CYLINDRICAL SHELL MODEL FOR THE THREE-DIMENSIONAL RECONSTRUCTION OF CORONAL MASS EJECTIONS**

A. [Thernisien](#)

Astrophysical Journal Supplement Series, 194:33-38 (6pp), **2011**, **File**

<http://sci-hub.ru/10.1088/0067-0049/194/2/33>

<https://iopscience.iop.org/article/10.1088/0067-0049/194/2/33/pdf>

The graduated cylindrical shell (GCS) model developed by Thernisien et al. has been used with the goal of studying the three-dimensional morphology, position, and kinematics of coronal mass ejections observed by coronagraphs. These studies focused more on the results rather than the details of the model itself. As more researchers begin to use the model, it becomes necessary to provide a deeper discussion on how it is derived, which is the purpose of this paper. The model is built using the following features and constraints: (1) the legs are conical, (2) the front is pseudo-circular, (3) the cross section is circular, and (4) it expands in a self-similar way. We derive the equation of the model from these constraints. We also show that the ice-cream cone model is a limit of the GCS when the two legs overlap completely. Finally, we provide formulae for the calculation of various geometrical dimensions, such as angular width and aspect ratio, as well as the pseudo-code that is used for its computer implementation.

### **CME reconstruction: Pre-STEREO and STEREO era**

A. **Thernisien**<sup>a</sup>, A. Vourlidas<sup>b</sup>, and R.A. Howard<sup>b</sup>

Journal of Atmospheric and Solar-Terrestrial Physics, Volume 73, Issue 10, **2011**, Pages 1156-1165

<https://sci-hub.ru/10.1016/j.jastp.2010.10.019>

Since the first observations of coronal mass ejections (CMEs) in 1970s, their three-dimensional (3D) morphology has been a key ingredient for understanding their origin and evolution. The determination of their 3D structure using a single viewpoint, however posed a challenge because only their 2D projection on the sky plane is observed. The operation of the STEREO mission with its unique capability of imaging the inner heliosphere from two viewpoints has greatly improved this situation. It is therefore timely to review the pre-STEREO efforts in 3D CME reconstruction and compare them with the first STEREO results in this area. Our paper focuses on the techniques relevant to the CME morphology: forward modeling, polarimetric, spectroscopic, direct inversion. We also discuss the limitations and considerations involved in each technique. **9 September 1997, 1999-07-25, 2001-08-21, 2001-12-20, 2002-01-04, 2008 April 26**

Research Highlights

- **Review** of CME reconstruction techniques: forward modeling, polarization, spectroscopic and tomographic.
- STEREO data confirmed that most of the CMEs could be modeled using hollow croissant type morphology.
- Reconstruction of the fine details of the CME morphology are not yet achieved. ► Future study should strive to combine different techniques and merge data from different sensors.

## Forward Modeling of Coronal Mass Ejections Using STEREO/SECCHI Data

A. **Thernisien** · A. Vourlidas · R.A. Howard

Solar Phys (2009) 256: 111–130, DOI 10.1007/s11207-009-9346-5, **2009, File**

STEREO SCIENCE RESULTS AT SOLAR MINIMUM

We describe a forward modeling method developed to study the coronal mass ejections observed with STEREO/SECCHI. We present a survey of 26 CMEs modeled with this method. We selected most of the bright events observed since November 2007 to August 2008, after when the separation was greater than 40° degrees, thus showing noticeable differences between the two views. From these stereoscopic observations and using a geometric model of a flux rope, we are able to determine the three-dimensional direction of propagation, the three-dimensional velocity and acceleration of the CME front, and in most of the cases the flux rope orientation and length. We define a merit function that allows us to partially automate the fit, as well as perform a sensitivity analysis on the model parameters. We find a precision on the longitude and latitude to be of a maximum of  $\pm 17^\circ$  and  $\pm 4^\circ$ , respectively, for a 10% decrease of the merit function but a precision on the flux rope orientation and length to be almost one order of magnitude larger, showing that these parameters are more difficult to estimate using only coronagraph data. Finally, comparison with independent measurements shows a good agreement with the direction and speed we estimated.

## Modeling of Flux Rope Coronal Mass Ejections

A. F. R. **Thernisien**, R. A. Howard, and A. Vourlidas

The Astrophysical Journal, 652:763-773, **2006 (File)**

We present a forward-modeling technique for flux rope-like CMEs using an empirically defined model of a flux rope, the graduated cylindrical shell (GCS). To compare it with white-light coronagraph observations, we assume an electron distribution through the GCS and derive synthetic images in total and polarized brightness for various projections of the model using a Thomson scattering ray-tracing program. We test our forward modeling technique on 34 LASCO CMEs analyzed by Cremades&Bothmer. We are able to reproduce the CME morphology and derive the electron density (at the CME front) of these events using multi-instrument observations (MDI, H<sub>α</sub>, EIT, LASCO) under the assumption of self-similar expansion. This study suggests that a flux rope-like structure is a good description for these events. We also find that we need to invoke a deflection and/or rotation of the structure relative to the position and orientation of the source region in most cases. Finally, we demonstrate an original technique to fit the electron density of the CME leading edge. We find that, on average, the peak of the density at the CME front is 7.5 times that in the equatorial model of Saito et al., and can reach  $\sim 22$  times the model in some cases.

## The Mean Temperatures of CME-Related Dimming Masses

Emily **Thomson**, Hugh Hudson

Solar Phys. 298, Article number: 130 (**2023**)

<https://link.springer.com/content/pdf/10.1007/s11207-023-02222-6.pdf>

Sun-as-a-star EUV spectroscopy from EVE (the Extreme-ultraviolet Variability Experiment, on board SDO, the Solar Dynamics Observatory) frequently shows striking irradiance reductions following major solar flares. These coincide with dimming events as seen in EUV and X-ray images, involving the evacuation of large volumes of the corona by the associated coronal mass ejections. The EVE view of the dimming process is precise and quantitative, whereas difference imaging in the EUV reveals the structures to be full of complicated detail due most likely to unrelated activity. We have studied a sample of **11 events, mostly GOES X-class flares**, all of which were associated with coronal mass ejections. For a set of nine lines of Fe ions at stages VIII – XIII, corresponding to nominal peak formation temperatures below  $\log_{10}(T/K)=6.3$ , we have compared the emission-measure-weighted temperature of the preflare

global corona and that of the dimming mass, defined by the deficit at the time of greatest dimming. We find similar temperatures by this measure, but with a distinctly narrower variation in the preflare samples. For higher ionization states, weak emission commonly appears during the dimming intervals, consistent with residual late-phase flare development. The dimming depths do not appear to correlate with the preflare state of the global corona. **2012-03-07, 2013-11-05**

**Table 2** List of dimming events and their properties. 2010-2013

## Sensitivity Monitoring of the SECCHI COR1 Telescopes on STEREO

William T. **Thompson**

*Solar Physics* March **2018**, 293:49

<https://link.springer.com/content/pdf/10.1007%2Fs11207-018-1268-7.pdf>

Measurements of bright stars passing through the fields of view of the inner coronagraphs (COR1) on board the Solar Terrestrial Relations Observatory (STEREO) are used to monitor changes in the radiometric calibration over the course of the mission. Annual decline rates are found to be  $0.648 \pm 0.0660.648 \pm 0.066\%$ /year for COR1-A on STEREO Ahead and  $0.258 \pm 0.0600.258 \pm 0.060\%$ /year for COR1-B on STEREO Behind. These rates are consistent with decline rates found for other space-based coronagraphs in similar radiation environments. The theorized cause for the decline in sensitivity is darkening of the lenses and other optical elements due to exposure to high-energy solar particles and photons, although other causes are also possible. The total decline in the COR-B sensitivity when contact with Behind was lost on 1 October 2014 was 1.7%, while COR1-A was down by 4.4%. As of 1 November 2017, the COR1-A decline is estimated to be 6.4%. The SECCHI calibration routines will be updated to take these COR1 decline rates into account.

## Automatic Near-Real-Time Detection of CMEs in Mauna Loa K-Cor Coronagraph Images

W. T. **Thompson**, O. C. St. Cyr, J. T. Burkepile, A. Posner

*Space Weather* Volume 15, Issue 10 October **2017** Pages 1288–1299

<http://sci-hub.cc/10.1002/2017SW001694>

A simple algorithm has been developed to detect the onset of coronal mass ejections (CMEs), together with speed estimates, in near-real time using linearly polarized white-light solar coronal images from the Mauna Loa Solar Observatory K-Cor telescope. Ground observations in the low corona can warn of CMEs well before they appear in space coronagraphs. The algorithm used is a variation on the Solar Eruptive Event Detection System developed at George Mason University. It was tested against K-Cor data taken between 29 April 2014 and 20 February 2017, on days identified as containing CMEs. This resulted in testing of 139 days' worth of data containing 171 CMEs. The detection rate varied from close to 80% when solar activity was high down to as low as 20–30% when activity was low. The difference in effectiveness with solar cycle is attributed to the relative prevalence of strong CMEs between active and quiet periods. There were also 12 false detections, leading to an average false detection rate of 8.6%. The K-Cor data were also compared with major solar energetic particle (SEP) storms during this time period. There were three SEP events detected either at Earth or at one of the two STEREO spacecraft when K-Cor was observing during the relevant time period. The algorithm successfully generated alerts for two of these events, with lead times of 1–3 h before the SEP onset at 1 AU. The third event was not detected by the automatic algorithm because of the unusually broad width in position angle. **24-September 2014, 14 October 2014, 2 January 2016,**

## Alternating Twist Along an Erupting Prominence

W. T. **Thompson**

*Solar Physics*, April **2013**, Volume 283, Issue 2, pp 489-504

Triangulation measurements using observations from the two Solar Terrestrial Relations Observatory (STEREO) spacecraft, combined with observations from the Solar Dynamics Observatory (SDO), are used to characterize the behavior of a prominence involved in two successive coronal mass ejections **6–7 December 2010**. The STEREO separation at the time was  $171.6^\circ$ , which was functionally equivalent to a separation of  $8.4^\circ$ , and thus very favorable for feature co-identification above the limb. The first eruption at  $\approx 14:16$  UT on 6 December of the middle branch of the prominence starts off a series of magnetic reconfigurations in the right branch, which itself erupts at  $\approx 2:06$  UT the next day, about 12 hours after the first eruption. The cool prominence material seen at  $304 \text{ \AA}$  drains back down to the surface, but a flux-rope-like magnetic structure is seen to erupt in both  $195 \text{ \AA}$  by the STEREO/Extreme Ultraviolet Imager (EUVI), and in white light by the STEREO/COR1 inner coronagraph. In between the two eruptions, two different signs of helicity are seen in the measured twist of the right branch. This is interpreted to be caused by the overall prominence channel being composed of different segments with alternating helicity signs. The erupting parts on 6 and 7 December both show positive twist, but negative twist is seen in between these positive sections. Negative twist is consistent with the dextral chirality signs seen in the He II line at  $304 \text{ \AA}$  prior to both eruptions. However, during the period between the eruptions, a region of positive twist grows and replaces the region of negative twist, and finally erupts. We interpret these observations in the light of models that predict that helicity cancellation can be an important factor in the triggering of flares and coronal mass ejections.

## 3D Reconstruction of a Rotating Erupting Prominence

W. T. **Thompson**, B. Kliem and T. Török

*Solar Physics*, Volume 276, Numbers 1-2, 241-259, **2012**, File

A bright prominence associated with a coronal mass ejection (CME) was seen erupting from the Sun on **9 April 2008**. This prominence was tracked by both the Solar Terrestrial Relations Observatory (STEREO) EUVI and COR1 telescopes, and was seen to rotate about the line of sight as it erupted; therefore, the event has been nicknamed the “Cartwheel CME.” The threads of the prominence in the core of the CME quite clearly indicate the structure of a weakly to moderately twisted flux rope throughout the field of view, up to heliocentric heights of 4 solar radii. Although the STEREO separation was 48°, it was possible to match some sharp features in the later part of the eruption as seen in the 304 Å line in EUVI and in the H $\alpha$ -sensitive bandpass of COR1 by both STEREO Ahead and Behind. These features could then be traced out in three-dimensional space, and reprojected into a view in which the eruption is directed toward the observer. The reconstructed view shows that the alignment of the prominence to the vertical axis rotates as it rises up to a leading-edge height of  $\approx 2.5$  solar radii, and then remains approximately constant. The alignment at 2.5 solar radii differs by about 115° from the original filament orientation inferred from H $\alpha$  and EUV data, and the height profile of the rotation, obtained here for the first time, shows that two thirds of the total rotation are reached within  $\approx 0.5$  solar radii above the photosphere. These features are well reproduced by numerical simulations of an unstable moderately twisted flux rope embedded in external flux with a relatively strong shear field component.

### **STEREO SECCHI COR1-A/B Intercalibration at 180° Separation**

W. T. [Thompson](#), J. M. Davila, O. C. St. Cyr and N. L. Reginald

Solar Physics, Volume 272, Number 1, 215-225, **2011**

The twin Solar Terrestrial Relations Observatory (STEREO) spacecraft reached a separation angle of 180° on 6 February 2011. This provided a unique opportunity to test the intercalibration between the Sun–Earth Connection Coronal and Heliospheric Investigation (SECCHI) telescopes on both spacecraft for areas above the limb. So long as the corona is optically thin, at 180° separation each spacecraft sees the same corona from opposite directions. Thus, the data should appear as mirror images of each other. We report here on the results of the comparison of the images taken by the inner coronagraph (COR1) on the STEREO-Ahead and -Behind spacecraft in the hours when the separation was close to 180°. We find that the intensity values seen by the two telescopes agree with each other to a high degree of accuracy. This validates both the radiometric intercalibration between the COR1 telescopes, and the method used to remove instrumental background from the images. The relative error between COR1-A and COR1-B is found to be less than 10<sup>−9</sup> B/B $\odot$  over most of the field-of-view, growing to a few  $\times 10^{-9}$  B/B $\odot$  for the brighter pixels near the edge of the occulter. The primary source of error is the background determination. We also report on the analysis of star observations which show that the absolute radiometric calibration of either COR1 telescope has not changed significantly since launch.

### **Background Subtraction for the SECCHI/COR1 Telescope Aboard STEREO**

W.T. [Thompson](#) · K. Wei · J.T. Burkepile · J.M. Davila · O.C. St. Cyr

Solar Phys (2010) 262: 213–231

COR1 is an internally occulted Lyot coronagraph, part of the Sun Earth Connection Coronal and Heliospheric Investigation (SECCHI) instrument suite aboard the twin *Solar Terrestrial Relations Observatory* (STEREO) spacecraft. Because the front objective lens is subjected to a full solar flux, the images are dominated by instrumental scattered light which has to be removed to uncover the underlying K corona data. We describe a procedure for removing the instrumental background from COR1 images. F coronal emission is subtracted at the same time. The resulting images are compared with simultaneous data from the Mauna Loa Solar Observatory Mk4 coronagraph. We find that the background subtraction technique is successful in coronal streamers, while the baseline emission in coronal holes (*i.e.* between plumes) is suppressed. This is an expected behavior of the background subtraction technique. The COR1 radiometric calibration is found to be either 10 – 15% lower, or 5 – 10% higher than that of the Mk4, depending on what value is used for the Mk4 plate scale, while an earlier study found the COR1 radiometric response to be  $\sim 20\%$  higher than that of the Large Angle Spectroscopic Coronagraph (LASCO) C2 telescope. Thus, the COR1 calibration is solidly within the range of other operating coronagraphs. The background levels in both COR1 telescopes have been quite steady in time, with the exception of a single contamination event on 30 January 2009. Barring too many additional events of this kind, there is every reason to believe that both COR1 telescopes will maintain usable levels of scattered light for the remainder of the STEREO mission.

### **Use of the FITS World Coordinate System by STEREO/SECCHI**

W. T. [Thompson](#) & K. Wei

Solar Phys., 261(1), Page: 215 – 222, **2010**

The World Coordinate System (WCS) is a standard for embedding coordinate information in a Flexible Image Transport System (FITS) header. Its first extensive use within solar physics is by the *Sun Earth Connections Coronal and Heliospheric Investigation* (SECCHI) telescope suite onboard the *Solar Terrestrial Relations Observatory*

(STEREO). The WCS formalism assists in SECCHI data analysis in several ways: First of all, the spherical effects associated with the extremely wide fields-of-view of the *Heliospheric Imager* (HI) telescopes can be handled in a completely unambiguous and standard fashion. Of particular importance is that WCS positional keywords allow spacecraft-ephemeris information to be embedded within the FITS header without depending on mission-specific keywords. Ephemeris data is critical to the three-dimensional analysis that the STEREO mission is designed for. We also show how the WCS software in *SolarSoft* can be used to relate STEREO data to other missions such as the *Solar and Heliospheric Observatory* (SOHO). The ability of WCS to support a parallel celestial right ascension (R.A.)/declination (Dec) coordinate system and the use of WCS for COR1 synoptic maps are also discussed. The advantages that STEREO derived from WCS can equally be applied to other solar missions, in particular *Solar Orbiter*, and should be adopted by all future missions.

## The Radiometric and Pointing Calibration of SECCHI COR1 on STEREO

W.T. [Thompson](#) · N.L. Reginald

Solar Phys (2008) 250: 443–454

<http://springerlink.metapress.com/content/u040662v341354u5/fulltext.pdf>

COR1 is the innermost coronagraph of the Sun Earth Connection Coronal and Heliospheric Investigation (SECCHI) instrument suite aboard the twin *Solar Terrestrial Relations Observatory* (STEREO) spacecraft. The paired COR1 telescopes observe the white light K-corona from 1.4 to 4 solar radii in a waveband 22.5 nm wide centered on the H $\alpha$  line at 656 nm. An internal polarizer allows the measurement of both total and polarized brightness. The co-alignment of the two COR1 telescopes is derived from the star  $\lambda$  Aquarii for the Ahead spacecraft, and from an occultation of the Sun by the Moon for Behind. Observations of the planet Jupiter are used to establish absolute photometric calibrations for each telescope. The intercalibration of the two COR1 telescopes are compared using coronal mass ejection observations made early in the mission, when the spacecraft were close together. Comparisons are also made with the Solar and Heliospheric Observatory (SOHO) Large Angle and Spectrometric Coronagraph (LASCO) C2 and Mauna Loa Solar Observatory Mk4 coronagraphs.

## SOHO/EIT observations of an Earth-directed coronal mass ejection on May 12, 1997.

[Thompson](#), B.J., [Plunkett](#), S.P., [Gurman](#), J.B., [Newmark](#), J.S., [St. Cyr](#), O.C., [Michels](#), D.J., [Delaboudinière](#), J.P.,

1998. Geophys. Res. Lett. 25, 2461–2464.

<http://onlinelibrary.wiley.com/doi/10.1029/98GL50429/epdf>

An earth-directed coronal mass ejection (CME) was observed on May 12, 1997 by the SOHO Extreme ultraviolet Imaging Telescope (EIT). The CME, originating north of the central solar meridian, was later observed by the Large Angle Spectrometric Coronagraph (LASCO) as a “halo” CME: a bright expanding ring centered about the occulting disk. Beginning at about 04:35 UT, EIT recorded several CME signatures, including dimming regions close to the eruption, post-eruption arcade formation, and a bright wavefront propagating quasi-radially from the source region. Each of these phenomena appear to be associated with the same eruption, and the onset time of these features corresponds with the estimated onset time observed in LASCO. We discuss the correspondence of these features as observed by EIT with the structure of the CME in the LASCO data.

## How Is Helicity (and Twist) Partitioned in Magnetohydrodynamic Simulations of Reconnecting Magnetic Flux Tubes?

James [Threlfall](#), Andrew N. Wright, and Alan W. Hood

2020 ApJ 898 1

<https://doi.org/10.3847/1538-4357/ab9c2a>

<https://sci-hub.tw/https://iopscience.iop.org/article/10.3847/1538-4357/ab9c2a>

Magnetic helicity conservation provides a convenient way to analyze specific properties (namely, the linkage and twist) of reconnecting flux tubes and yield additional insight into the pre- and post-reconnection states of magnetic structures in the solar atmosphere. A previous study considered two flux tubes with footpoints anchored in two parallel planes. They showed that reconnection would add self-helicity equivalent to a half turn of twist to each flux tube. We address a related and fundamental question here: if two flux tubes anchored in a single plane reconnect, what are the resulting twists imparted to each of the reconnected tubes? Are they equal and do they have a simple exact value independent of footpoint location? To do this, we employ a new (computationally efficient) method which subdivides each flux tube into distinct elements and calculates the mutual helicity of many elemental pairs, the sum of which determines the self-helicity of the overall flux tube. Having tested the method using a simple analytical model, we apply the technique to a magnetohydrodynamic simulation where initially untwisted magnetic flux tubes are sheared and allowed to reconnect (based on a previous reconnection model). We recover values of self-helicity and twist in the final end state of the simulations which show excellent agreement with theoretical predictions.

## Flux Rope Formation Due to Shearing and Zipper Reconnection

J. [Threlfall](#), [A. W. Hood](#), [E. R. Priest](#)

Solar Phys. 293:98 2018

<https://arxiv.org/pdf/1806.06760.pdf>

Zipper reconnection has been proposed as a mechanism for creating most of the twist in the flux tubes that are present {prior to} eruptive flares and coronal mass ejections. We have conducted a first numerical experiment on this new regime of reconnection, where two initially untwisted parallel flux tubes are sheared and reconnected to form a large flux rope. We describe the properties of this experiment, including the linkage of magnetic flux between concentrated flux sources at the base of the simulation, the twist of the newly formed flux rope and the conversion of mutual magnetic helicity in the sheared pre-reconnection state into the self-helicity of the newly formed flux rope.

### **Formation and Eruption of a Double-decker Filament Triggered by Micro-bursts and Recurrent Jets in the Filament Channel**

Zhanjun [Tian](#), [Yuandeng Shen](#), [Yu Liu](#)

New Astronomy **2018**

<https://arxiv.org/pdf/1805.12314.pdf>

We present the observations of a double-decker filament to study its formation, triggering, and eruption physics. It is observed that the double-decker filament was formed by splitting of an original single filament. During the splitting process, intermittent bright point bursts are observed in the filament channel, which resulted in the generation of the upper filament branch. The eruption of the newly formed double-decker filament was possibly triggered by two recurrent two-sided loop jets in the filament channel and the continuous mass unloading from the upper filament body. The interaction between the first jet and the filament directly resulted in the unstable of the lower branch and the fast rising phase of the upper branch. The second jet occurred at the same site about three hours after the first one, which further disturbed and accelerated the rising of the lower filament branch. It is interesting that the rising lower branch overtook the upper one, and then the two branches probably merged into one filament. Finally, the whole filament erupted violently and caused a large-scale coronal mass ejection, leaving behind a pair of flare ribbons and two dimming regions on the both sides of the filament channel. We think that the intermittent bursts may directly result in the rearrangement of the filament magnetic field and therefore the formation of the double-decker filament, then the recurrent jets further caused the fully eruption of the entire filament system. The study provides convincing evidence for supporting the scenario that a double-decker filament can be formed by splitting a single filament into two branches.

**2017 November 16**

### **Frequently Occurring Reconnection Jets from Sunspot Light Bridges**

Hui [Tian](#), [Vasyl Yurchyshyn](#), [Hardi Peter](#), [Sami K. Solanki](#), [Peter R. Young](#), [Lei Ni](#), [Wenda Cao](#), [Kaifan Ji](#), [Yingjie Zhu](#), [Jingwen Zhang](#), [Tanmoy Samanta](#), [Yongliang Song](#), [Jiansen He](#), [Linghua Wang](#), [Yajie Chen](#)

ApJ **2018**

<https://arxiv.org/pdf/1801.06802.pdf>

Solid evidence of magnetic reconnection is rarely reported within sunspots, the darkest regions with the strongest magnetic fields and lowest temperatures in the solar atmosphere. Using the world's largest solar telescope, the 1.6-meter Goode Solar Telescope, we detect prevalent reconnection through frequently occurring fine-scale jets in the H $\alpha$  line wings at light bridges, the bright lanes that may divide the dark sunspot core into multiple parts. Many jets have an inverted Y-shape, shown by models to be typical of reconnection in a unipolar field environment. Simultaneous spectral imaging data from the Interface Region Imaging Spectrograph show that the reconnection drives bidirectional flows up to 200-km-s<sup>-1</sup>, and that the weakly ionized plasma is heated by at least an order of magnitude up to ~80,000 K. Such highly dynamic reconnection jets and efficient heating should be properly accounted for in future modeling efforts of sunspots. Our observations also reveal that the surge-like activity previously reported above light bridges in some chromospheric passbands such as the H $\alpha$  core has two components: the ever-present short surges likely to be related to the upward leakage of magnetoacoustic waves from the photosphere, and the occasionally occurring long and fast surges that are obviously caused by the intermittent reconnection jets. **2014 Oct 29**

### **Successive Two-sided loop Jets Caused by Magnetic Reconnection between Two adjacent Filamentary Threads**

Zhanjun [Tian](#), [Yu Liu](#), [Yuandeng Shen](#), [Abouazza Elmhamdi](#), [Jiangtao Su](#), [Ying D. Liu](#), [Ayman. S. Kordi](#)

ApJ **2017**

<https://arxiv.org/pdf/1707.04421.pdf>

We present observational analysis of two successive two-sided loop jets observed by the ground-based New Vacuum Solar Telescope (NVST) and the space-borne Solar Dynamics Observatory (SDO). The two successive two-sided loop jets manifested similar evolution process and both were associated with the interaction of two small-scale adjacent filamentary threads, magnetic emerging and cancellation processes at the jet's source region. High temporal and high spatial resolution observations reveal that the two adjacent ends of the two filamentary threads are rooted in opposite magnetic polarities within the source region. The two threads approached to each other, and then an obvious brightening patch is observed at the interaction position. Subsequently, a pair of hot plasma ejections are observed heading to opposite directions along the paths of the two filamentary threads, and with a typical speed of two-sided loop jets of the order 150 km/s. Close to the end of the second jet, we report the formation of a bright hot loop structure at the source region, which suggests the formation of new loops during the interaction. Based on the observational results, we propose that the observed two-sided loop jets are caused by the magnetic reconnection between the two adjacent filamentary threads, largely different from the previous scenario that a two-sided loop jet is generated by magnetic reconnection between an emerging bipole and the overlying horizontal magnetic fields. **April 16, 2014**

## Successive Two-sided Loop Jets Caused by Magnetic Reconnection between Two Adjacent Filamentary Threads

Zhanjun [Tian](#)<sup>1,2,3</sup>, Yu Liu<sup>1,4,5</sup>, Yuandeng Shen<sup>1,2,4,5,6</sup>, Abouazza Elmhamdi<sup>7</sup>, Jiangtao Su<sup>3,4,6</sup>, Ying D. Liu<sup>2,3</sup>, and Ayman. S. Kordi<sup>7</sup>

2017 ApJ 845 94

We present observational analysis of two successive two-sided loop jets observed by the ground-based New Vacuum Solar Telescope and the space-borne Solar Dynamics Observatory. The two successive two-sided loop jets manifested similar evolution processes and both were associated with the interaction of two small-scale adjacent filamentary threads, magnetic emerging, and cancellation processes at the jet's source region. High temporal and high spatial resolution observations reveal that the two adjacent ends of the two filamentary threads are rooted in opposite magnetic polarities within the source region. The two threads approached each other, and then an obvious brightening patch is observed at the interaction position. Subsequently, a pair of hot plasma ejections are observed heading in opposite directions along the paths of the two filamentary threads at a typical speed for two-sided loop jets of the order  $150 \text{ km s}^{-1}$ . Close to the end of the second jet, we report the formation of a bright hot loop structure at the source region, which suggests the formation of new loops during the interaction. Based on the observational results, we propose that the observed two-sided loop jets are caused by magnetic reconnection between the two adjacent filamentary threads, largely different from the previous scenario that a two-sided loop jet is generated by magnetic reconnection between an emerging bipole and the overlying horizontal magnetic fields.

## Observations of Coronal Mass Ejections with the Coronal Multichannel Polarimeter

H. [Tian](#), S. Tomczyk, S. W. McIntosh, C. Bethge, G. de Toma, S. Gibson

E-print, March 2013, **File**; Sol. Phys. (2013) 288:637–650

CoMP measures not only the polarization of coronal emission, but also the full radiance profiles of coronal emission lines. For the first time, CoMP observations provide high-cadence image sequences of the coronal line intensity, Doppler shift and line width simultaneously in a large field of view. By studying the Doppler shift and line width we may explore more of the physical processes of CME initiation and propagation. Here we identify a list of CMEs observed by CoMP and present the first results of these observations. Our preliminary analysis shows that CMEs are usually associated with greatly increased Doppler shift and enhanced line width. These new observations provide not only valuable information to constrain CME models and probe various processes during the initial propagation of CMEs in the low corona, but also offer a possible cheap and low-risk means of space weather monitoring.

**Table**; 2011 Dec 7, 2011 Dec 30, 2012 March 27, 2012 May 26

## EIS Observations of Solar Mass Eruptions

Hui [Tian](#)

EIS Science Nugget, Jan 2013

[http://msslxr.mssl.ucl.ac.uk:8080/SolarB/nuggets/nugget\\_2013jan.jsp](http://msslxr.mssl.ucl.ac.uk:8080/SolarB/nuggets/nugget_2013jan.jsp)

Plasma properties and dynamics of the CME ejecta and EUV jets:

Plasma properties and dynamics of coronal dimmings:

14-15 Dec, 2006

## What can we learn about solar coronal mass ejections, coronal dimmings, and Extreme-Ultraviolet jets through spectroscopic observations?

Hui [Tian](#), Scott W. McIntosh, Lidong Xia, Jiansen He, Xin Wang

E-print, Jan 2012; 2012 ApJ 748 106, **File**

Solar eruptions, particularly coronal mass ejections (CMEs) and extreme-ultraviolet (EUV) jets, have rarely been investigated with spectroscopic observations. We analyze several data sets obtained by the EUV Imaging Spectrometer onboard Hinode and find various types of flows during CMEs and jet eruptions. CME-induced dimming regions are found to be characterized by significant blueshift and enhanced line width by using a single Gaussian fit. While a red-blue (RB) asymmetry analysis and a RB-guided double Gaussian fit of the coronal line profiles indicate that these are likely caused by the superposition of a strong background emission component and a relatively weak ( $\sim 10\%$ ) high-speed ( $\sim 100 \text{ km s}^{-1}$ ) upflow component. This finding suggests that the outflow velocity in the dimming region is probably of the order of  $100 \text{ km s}^{-1}$ , not  $\sim 20 \text{ km s}^{-1}$  as reported previously. Density and temperature diagnostics of the dimming region suggest that dimming is primarily an effect of density decrease rather than temperature change. The mass losses in dimming regions as estimated from different methods are roughly consistent with each other and they are 20%-60% of the masses of the associated CMEs. With the guide of RB asymmetry analysis, we also find several temperature-dependent outflows (speed increases with temperature) immediately outside the (deepest) dimming region. These outflows may be evaporation flows which are caused by the enhanced thermal conduction or nonthermal electron beams along reconnecting field lines, or induced by the interaction between the opened field lines in the dimming region and the closed loops in the surrounding plage region. In an erupted CME loop and an EUV jet, profiles of emission lines formed at coronal and transition region temperatures are found to exhibit two well-separated components, an almost stationary component accounting for the background emission and a highly blueshifted ( $\sim 200$



km s<sup>-1</sup>) component representing emission from the erupting material. The two components can easily be decomposed through a double Gaussian fit and we can diagnose the electron density, temperature and mass of the ejecta. Combining the speed of the blueshifted component and the projected speed of the erupting material derived from simultaneous imaging observations, we can calculate the real speed of the ejecta.

## **A Magnetogram-matching Method for Energizing Magnetic Flux Ropes Toward Eruption**

Viacheslav S. [Titov](#) (1), [Cooper Downs](#) (1), [Tibor Török](#) (1), [Jon A. Linker](#) (1)

ApJ *ApJ* **936** 2022

<https://arxiv.org/pdf/2205.03982.pdf>

We propose a new "helicity-pumping" method for energizing coronal equilibria that contain a magnetic flux rope (MFR) toward an eruption. We achieve this in a sequence of MHD relaxations of small line-tied pulses of magnetic helicity, each of which is simulated by a suitable rescaling of the current-carrying part of the field. The whole procedure is "magnetogram-matching" because it involves no changes to the normal component of the field at the photospheric boundary. The method is illustrated by applying it to an observed force-free configuration whose MFR is modeled with our regularized Biot-Savart law method. We find that, in spite of the bipolar character of the external field, the MFR eruption is sustained by two reconnection processes. The first, which we refer to as breakthrough reconnection, is analogous to breakout reconnection in quadrupolar configurations. It occurs at a quasi-separator inside a current layer that wraps around the erupting MFR and is caused by the photospheric line-tying effect. The second process is the classical tether-cutting reconnection, which develops at the second quasi-separator inside a vertical current layer that is formed below the erupting MFR. Both reconnection processes work in tandem with the magnetic forces of the unstable MFR to propel it through the overlying ambient field, and their interplay may also be relevant for the thermal processes occurring in the plasma of solar flares. The considered example suggests that our method will be beneficial for both the modeling of observed eruptive events and theoretical studies of eruptions in idealized magnetic configurations.

## **Optimization of Magnetic Flux Ropes Modeled with the RBSL method**

[V. S. Titov](#), [C. Downs](#), [T. Török](#), [J. A. Linker](#), [R. M. Caplan](#), [R. Lionello](#)

ApJS **255** 9 2021

<https://arxiv.org/pdf/2106.02789.pdf>

<https://doi.org/10.3847/1538-4365/abfe0f>

The so-called regularized Biot-Savart laws (RBSLs) provide an efficient and flexible method for modeling pre-eruptive magnetic configurations of coronal mass ejections (CMEs) whose characteristics are constrained by observational images and magnetic-field data. This method allows one to calculate the field of magnetic flux ropes (MFRs) with small circular cross-sections and an arbitrary axis shape. The field of the whole configuration is constructed as a superposition of (1) such a flux-rope field and (2) an ambient potential field derived, for example, from an observed magnetogram. The RBSL kernels are determined from the requirement that the MFR field for a straight cylinder must be exactly force-free. For a curved MFR, however, the magnetic forces are generally unbalanced over the whole path of the MFR. To minimize these forces, we apply a modified Gauss-Newton method to find optimal MFR parameters. This is done by iteratively adjusting the MFR axis path and axial current. We then try to relax the resulting optimized configuration in a subsequent line-tied zero-beta magnetohydrodynamic simulation toward a force-free equilibrium. By considering two models of the sigmoidal pre-eruption configuration for the **2009 February 13** CME, we demonstrate how this approach works and what it is capable of. We show, in particular, that the building blocks of the core magnetic structure described by these models match to morphological features typically observed in such type of configurations. Our method will be useful for both the modeling of particular eruptive events and theoretical studies of idealized pre-eruptive MFR configurations.

## **Regularized Biot-Savart Laws for Modeling Magnetic Flux Ropes**

Viacheslav S. [Titov](#), [Cooper Downs](#), [Zoran Mikić](#), [Tibor Török](#), [Jon A. Linker](#), [Ronald M. Caplan](#)

**2018** ApJL **852** L21

<https://arxiv.org/pdf/1712.06708.pdf>

<http://iopscience.iop.org/sci-hub.tw/2041-8205/852/2/L21/>

Many existing models assume that magnetic flux ropes play a key role in solar flares and coronal mass ejections (CMEs). It is therefore important to develop efficient methods for constructing fluxrope configurations constrained by observed magnetic data and the morphology of the pre-eruptive source region. For this purpose, we have derived and implemented a compact analytical form that represents the magnetic field of a thin flux rope with an axis of arbitrary shape and circular crosssections. This form implies that the flux rope carries axial current  $I$  and axial flux  $F$ , so that the respective magnetic field is the curl of the sum of axial and azimuthal vector potentials proportional to  $I$  and  $F$ , respectively. We expressed the vector potentials in terms of modified Biot-Savart laws whose kernels are regularized at the axis in such a way that, when the axis is straight, these laws define a cylindrical force-free flux rope with a parabolic profile for the axial current density. For the cases we have studied so far, we determined the shape of the rope axis by following the polarity inversion line of the eruptions' source region, using observed magnetograms. The height variation along the axis and other flux-rope parameters are estimated by means of potential field extrapolations. Using this heuristic approach, we were able to construct pre-eruption configurations for the **2009 February 13** and **2011 October 1** CME events. These applications demonstrate the flexibility and efficiency of our new method for energizing pre-eruptive configurations in simulations of CMEs.

## 2010 August 1-2 sympathetic eruptions: II. Magnetic topology of the MHD background field

Viacheslav S. [Titov](#), [Zoran Mikic](#), [Tibor Torok](#), [Jon A. Linker](#), [Olga Panasenco](#)

ApJ **845** 141 **2017**

<https://arxiv.org/pdf/1707.07773.pdf>

Using a potential field source surface (PFSS) model, we recently analyzed the global topology of the background coronal magnetic field for a sequence of coronal mass ejections (CMEs) that occurred on 2010 August 1-2. Here we repeat this analysis for the background field reproduced by a magnetohydrodynamic (MHD) model that incorporates plasma thermodynamics. As for the PFSS model, we find that all three CME source regions contain a coronal hole that is separated from neighboring coronal holes by topologically very similar pseudo-streamer structures. However, the two models yield very different results for the size, shape, and flux of the coronal holes. We find that the helmet-streamer cusp line, which corresponds to a source-surface null line in the PFSS model, is structurally unstable and does not form in the MHD model. Our analysis indicates that generally, in MHD configurations, this line rather consists of a multiple-null separator passing along the edge of disconnected flux regions. Some of these regions are transient and may be the origin of so-called streamer blobs. We show that the core topological structure of such blobs is a three-dimensional "plasmoid", consisting of two conjoined flux ropes of opposite handedness, which connect at a spiral null point of the magnetic field. Our analysis reveals that such plasmoids appear also in pseudo-streamers on much smaller scales. These new insights into the coronal magnetic topology provide some intriguing implications for solar energetic particle events and for the properties of the slow solar wind.

## A Method for Embedding Circular Force-free Flux Ropes in Potential Magnetic Fields

V. S. [Titov](#), T. [Török](#), Z. [Mikic](#), and J. A. [Linker](#)

2014 ApJ 790 163.

We propose a method for constructing approximate force-free equilibria in pre-eruptive configurations in which a thin force-free flux rope is embedded into a locally bipolar-type potential magnetic field. The flux rope is assumed to have a circular-arc axis, a circular cross-section, and electric current that is either concentrated in a thin layer at the boundary of the rope or smoothly distributed across it with a maximum of the current density at the center. The entire solution is described in terms of the magnetic vector potential in order to facilitate the implementation of the method in numerical magnetohydrodynamic (MHD) codes that evolve the vector potential rather than the magnetic field itself. The parameters of the flux rope can be chosen so that its subsequent MHD relaxation under photospheric line-tied boundary conditions leads to nearly exact numerical equilibria. To show the capabilities of our method, we apply it to several cases with different ambient magnetic fields and internal flux-rope structures. These examples demonstrate that the proposed method is a useful tool for initializing data-driven simulations of solar eruptions.

## 2010 AUGUST 1-2 SYMPATHETIC ERUPTIONS. I. MAGNETIC TOPOLOGY OF THE SOURCE-SURFACE BACKGROUND FIELD

V. S. [Titov](#)<sup>1</sup>, Z. [Mikic](#)<sup>1</sup>, T. [Török](#)<sup>1</sup>, J. A. [Linker](#)<sup>1</sup>, and O. [Panasenco](#)

2012 ApJ 759 70

A sequence of apparently coupled eruptions was observed on **2010 August 1-2** by Solar Dynamics Observatory and STEREO. The eruptions were closely synchronized with one another, even though some of them occurred at widely separated locations. In an attempt to identify a plausible reason for such synchronization, we study the large-scale structure of the background magnetic configuration. The coronal field was computed from the photospheric magnetic field observed at the appropriate time period by using the potential field source-surface model. We investigate the resulting field structure by analyzing the so-called squashing factor calculated at the photospheric and source-surface boundaries, as well as at different coronal cross-sections. Using this information as a guide, we determine the underlying structural skeleton of the configuration, including separatrix and quasi-separatrix surfaces. Our analysis reveals, in particular, several pseudo-streamers in the regions where the eruptions occurred. Of special interest to us are the magnetic null points and separators associated with the pseudo-streamers. We propose that magnetic reconnection triggered along these separators by the first eruption likely played a key role in establishing the assumed link between the sequential eruptions. The present work substantiates our recent simplified magnetohydrodynamic model of sympathetic eruptions and provides a guide for further deeper study of these phenomena. Several important implications of our results for the S-web model of the slow solar wind are also addressed.

## 2010 AUGUST 1-2 SYMPATHETIC ERUPTIONS. I. MAGNETIC TOPOLOGY OF THE SOURCE-SURFACE BACKGROUND FIELD

V. S. [Titov](#)<sup>1</sup>, Z. [Mikic](#)<sup>1</sup>, T. [Török](#)<sup>1</sup>, J. A. [Linker](#)<sup>1</sup>, and O. [Panasenco](#)

2012 ApJ 759 70 **File**

A sequence of apparently coupled eruptions was observed on **2010 August 1-2** by Solar Dynamics Observatory and STEREO. The eruptions were closely synchronized with one another, even though some of them occurred at widely separated locations. In an attempt to identify a plausible reason for such synchronization, we study the large-scale structure of the background magnetic configuration. The coronal field was computed from the photospheric magnetic field observed at the appropriate time period by using the potential field source-surface model. We investigate the resulting field structure by analyzing the so-called squashing factor calculated at the photospheric and source-surface

boundaries, as well as at different coronal cross-sections. Using this information as a guide, we determine the underlying structural skeleton of the configuration, including separatrix and quasi-separatrix surfaces. Our analysis reveals, in particular, several pseudo-streamers in the regions where the eruptions occurred. Of special interest to us are the magnetic null points and separators associated with the pseudo-streamers. We propose that magnetic reconnection triggered along these separators by the first eruption likely played a key role in establishing the assumed link between the sequential eruptions. The present work substantiates our recent simplified magnetohydrodynamic model of sympathetic eruptions and provides a guide for further deeper study of these phenomena. Several important implications of our results for the S-web model of the slow solar wind are also addressed.

### **Evidence of Twisting and Mixed-polarity Solar Photospheric Magnetic Field in Large Penumbra Jets: IRIS and Hinode Observations**

Sanjiv K. [Tiwari](#), [Ronald L. Moore](#), [Bart De Pontieu](#), [Theodore D. Tarbell](#), [Navdeep K. Panesar](#), [Amy R. Winebarger](#), [Alphonse C. Sterling](#)

ApJ 2018

<https://arxiv.org/pdf/1811.09554.pdf>

A recent study using *Hinode* (SOT/FG) data of a sunspot revealed some unusually large penumbral jets that often repeatedly occurred at the same locations in the penumbra, namely at the tail of a penumbral filament or where the tails of multiple penumbral filaments converged. These locations had obvious photospheric mixed-polarity magnetic flux in  $\text{NaI}$  5896 Stokes-V images obtained with SOT/FG. Several other recent investigations have found that extreme ultraviolet (EUV)/X-ray coronal jets in quiet Sun regions (QRs), coronal holes (CHs) and near active regions (ARs) have obvious mixed-polarity fluxes at their base, and that magnetic flux cancellation prepares and triggers a minifilament flux-rope eruption that drives the jet. Typical QR, CH, and AR coronal jets are up to a hundred times bigger than large penumbral jets, and in EUV/X-ray images show clear twisting motion in their spires. Here, using IRIS  $\text{MgII}$  k 2796 Å SJ images and spectra in the penumbrae of two sunspots we characterize large penumbral jets. We find redshift and blueshift next to each other across several large penumbral jets, and interpret these as untwisting of the magnetic field in the jet spire. Using *Hinode*/SOT (FG and SP) data, we also find mixed-polarity magnetic flux at the base of these jets. Because large penumbral jets have mixed-polarity field at their base and have twisting motion in their spires, they might be driven the same way as QR, CH and AR coronal jets. **5-Aug-2015, 15-16 Sept 2017**

### **Transition-Region/Coronal Signatures and Magnetic Setting of Sunspot Penumbral Jets: *Hinode* (SOT/FG), Hi-C and *SDO*/AIA Observations**

Sanjiv K. [Tiwari](#), [Ronald L. Moore](#), [Amy R. Winebarger](#), [Shane E. Alpert](#)

ApJ 816 92 2016

<http://arxiv.org/pdf/1511.07900v1.pdf>

Penumbral microjets (PJs) are transient narrow bright features in the chromosphere of sunspot penumbrae, first characterized by Katsukawa et al (2007) using the  $\text{CaII}$  H-line filter on *Hinode*'s Solar Optical Telescope (SOT). It was proposed that the PJs form as a result of reconnection between two magnetic components of penumbra (spines and interspines), and that they could contribute to the transition region (TR) and coronal heating above sunspot penumbrae. We propose a modified picture of formation of PJs based on recent results on internal structure of sunspot penumbral filaments. Using data of a sunspot from *Hinode*/SOT, High Resolution Coronal Imager, and different passbands of the Atmospheric Imaging Assembly (AIA) onboard the *Solar Dynamics Observatory*, we examine whether PJs have signatures in the TR and corona. We find hardly any discernible signature of normal PJs in any AIA passbands, except a few of them showing up in the 1600 Å images. However, we discovered exceptionally stronger jets with similar lifetimes but bigger sizes (up to 600 km wide) occurring repeatedly in a few locations in the penumbra, where evidence of patches of opposite polarity fields at the tails of some penumbral filaments is seen in Stokes-V images. These large tail PJs do display signatures in the TR. Whether they have any coronal-temperature plasma is ambiguous. We infer that none of the PJs, including the large tail PJs, directly heat the corona in ARs significantly, but any penumbral jet might drive some coronal heating indirectly via generation of Alfvén waves and/or braiding of the coronal field. **11 July 2012**

### **Near-Sun Speed of CMEs and the Magnetic Non-potentiality of their Source Active Regions**

Sanjiv K. [Tiwari](#), [David A. Falconer](#), [Ronald L. Moore](#), [P. Venkatakrishnan](#), [Amy R. Winebarger](#), [Igor G. Khazanov](#)

GRL Volume 42, Issue 14, pp. 5702-5710 2015

<http://arxiv.org/ftp/arxiv/papers/1508/1508.01532.pdf>

We show that the speed of the fastest coronal mass ejections (CMEs) that an active region (AR) can produce can be predicted from a vector magnetogram of the AR. This is shown by logarithmic plots of CME speed (from the SOHO LASCO CME catalog) versus each of ten AR-integrated magnetic parameters (AR magnetic flux, three different AR magnetic-twist parameters, and six AR free-magnetic-energy proxies) measured from the vertical and horizontal field components of vector magnetograms (from the *Solar Dynamics Observatory*'s Helioseismic and Magnetic Imager) of the source ARs of 189 CMEs. These plots show: (1) the speed of the fastest CMEs that an AR can produce increases with each of these whole-AR magnetic parameters, and (2) that one of the AR magnetic-twist parameters and the

corresponding free-magnetic-energy proxy each determine the CME-speed upper-limit line somewhat better than any of the other eight whole-AR magnetic parameters. 2012-07-12

See HMI Science Nuggets, #42, 2015, <http://hmi.stanford.edu/hminuggets/?p=1270>

## Turbulent convection as a significant hidden provider of magnetic helicity in solar eruptions

[Shin Toriumi](#), [Hideyuki Hotta](#), [Kanya Kusano](#)

Scientific Reports 2023

<https://arxiv.org/pdf/2305.19323.pdf>

Solar flares and coronal mass ejections, the primary space weather disturbances affecting the entire heliosphere and near-Earth environment, mainly emanate from sunspot regions harbouring high degrees of magnetic twist. However, it is not clear how magnetic helicity, the quantity for measuring the magnetic twist, is supplied to the upper solar atmosphere via the emergence of magnetic flux from the turbulent convection zone. Here, we report state-of-the-art numerical simulations of magnetic flux emergence from the deep convection zone. By controlling the twist of emerging flux, we find that with the support of convective upflow, the untwisted emerging flux can reach the solar surface without collapsing, in contrast to previous theoretical predictions, and eventually create sunspots. Because of the turbulent twisting of magnetic flux, the produced sunspots exhibit rotation and inject magnetic helicity into the upper atmosphere, amounting to a substantial fraction of injected helicity in the twisted cases that is sufficient to produce flare eruptions. This result indicates that the turbulent convection is responsible for supplying a non-negligible amount of magnetic helicity and potentially contributes to solar flares.

## Magnetic Properties of Solar Active Regions that Govern Large Solar Flares and Eruptions

[Shin Toriumi](#), [Carolus J. Schrijver](#), [Louise K. Harra](#), [Hugh Hudson](#), [Kaori Nagashima](#)

ApJ 2017 834 56

<https://arxiv.org/pdf/1611.05047v1.pdf>

Solar flares and coronal mass ejections (CMEs), especially the larger ones, emanate from active regions (ARs). With the aim to understand the magnetic properties that govern such flares and eruptions, we systematically survey all flare events with GOES levels of  $\geq M5.0$  within 45 deg from disk center between May 2010 and April 2016. These criteria lead to a total of **51 flares from 29 ARs**, for which we analyze the observational data obtained by the Solar Dynamics Observatory. More than 80% of the 29 ARs are found to exhibit delta-sunspots and at least three ARs violate Hale's polarity rule. The flare durations are approximately proportional to the distance between the two flare ribbons, to the total magnetic flux inside the ribbons, and to the ribbon area. From our study, one of the parameters that clearly determine whether a given flare event is CME-eruptive or not is the ribbon area normalized by the sunspot area, which may indicate that the structural relationship between the flaring region and the entire AR controls CME productivity. AR characterization show that even X-class events do not require delta-sunspots or strong-field, high-gradient polarity inversion lines. An investigation of historical observational data suggests the possibility that **the largest solar ARs, with magnetic flux of  $2 \times 10^{23}$  Mx, might be able to produce "superflares" with energies of order of  $10^{34}$  erg**. The proportionality between the flare durations and magnetic energies is consistent with stellar flare observations, suggesting a common physical background for solar and stellar flares.

**Table 1. Properties of Flare Events**      **Table A1. Measured Parameters of Flare Events**

1946-07-25, 2011-02-13, 2011-02-15, 2011-03-09, 2011-07-30, 2011-08-03, 2011-08-04, 2012-01-23, 2012-03-07, 2012-03-09, 2012-03-10, 2012-05-10, 2012-07-02, 2012-07-04, 2012-07-05, 2012-07-12, 2013-04-11, 2013-10-24, 2013-11-01, 2013-11-03, 2013-11-05, 2013-11-08, 2013-11-10, 2013-12-31, 2014-01-07, 2014-02-04, 2014-03-29, 2014-04-18, 2014-09-10, 2014-09-28, 2014-10-22, 2014-10-24, 2014-10-25, 2014-10-26, 2014-10-27, 2014-11-07, 2014-12-04, 2014-12-17, 2014-12-18, 2014-12-20, 2015-03-10, 2015-03-11, 2015-06-22, 2015-06-25, 2015-08-24, 2015-09-28,

## Solar Eruptions Triggered by Flux Emergence Below or Near a Coronal Flux Rope

[T. Török](#), [M. G. Linton](#), [J. E. Leake](#), [Z. Mikić](#), [R. Lionello](#), [V. S. Titov](#), [C. Downs](#)

ApJ 962 149 2024

<https://arxiv.org/pdf/2312.14092.pdf>

<https://iopscience.iop.org/article/10.3847/1538-4357/ad1826/pdf>

Observations have shown a clear association of filament/prominence eruptions with the emergence of magnetic flux in or near filament channels. Magnetohydrodynamic (MHD) simulations have been employed to systematically study the conditions under which such eruptions occur. These simulations to date have modeled filament channels as two-dimensional (2D) flux ropes or 3D uniformly sheared arcades. Here we present MHD simulations of flux emergence into a more realistic configuration consisting of a bipolar active region containing a line-tied 3D flux rope. We use the coronal flux-rope model of Titov et al. (2014) as the initial condition and drive our simulations by imposing boundary conditions extracted from a flux-emergence simulation by Leake et al. (2013). We identify three mechanisms that determine the evolution of the system: (i) reconnection displacing foot points of field lines overlying the coronal flux rope, (ii) changes of the ambient field due to the intrusion of new flux at the boundary, and (iii) interaction of the (axial) electric currents in the pre-existing and newly emerging flux systems. The relative contributions and effects of these mechanisms depend on the properties of the pre-existing and emerging flux systems. Here we focus on the location and orientation of the emerging flux relative to the coronal flux rope. Varying these parameters, we investigate under which conditions an eruption of the latter is triggered.

## Sun-to-Earth MHD Simulation of the 14 July 2000 "Bastille Day" Eruption

Tibor [Török](#), [Cooper Downs](#), [Jon A. Linker](#), [Roberto Lionello](#), [Viacheslav S. Titov](#), [Zoran Mikić](#), [Pete Riley](#), [Ron M. Caplan](#), [Janvier Wijaya](#)

ApJ **856** 75 **2018**

<https://arxiv.org/pdf/1801.05903.pdf>

<http://sci-hub.tw/http://iopscience.iop.org/0004-637X/856/1/75/>

Solar eruptions are the main driver of space-weather disturbances at the Earth. Extreme events are of particular interest, not only because of the scientific challenges they pose, but also because of their possible societal consequences. Here we present a magnetohydrodynamic (MHD) simulation of the **14 July 2000** Bastille Day eruption, which produced a very strong geomagnetic storm. After constructing a thermodynamic MHD model of the corona and solar wind, we insert a magnetically stable flux rope along the polarity inversion line of the eruption's source region and initiate the eruption by boundary flows. More than  $10^{33}$  ergs of magnetic energy are released in the eruption within a few minutes, driving a flare, an EUV wave, and a coronal mass ejection (CME) that travels in the outer corona at about 1500 km/s, close to the observed speed. We then propagate the CME to Earth, using a heliospheric MHD code. Our simulation thus provides the opportunity to test how well in situ observations of extreme events are matched if the eruption is initiated from a stable magnetic-equilibrium state. We find that the flux-rope center is very similar in character to the observed magnetic cloud, but arrives about 8.5 hours later and about 15 degrees too far to the North, with field strengths that are too weak by a factor of about 1.6. The front of the flux rope is highly distorted, exhibiting localized magnetic-field concentrations as it passes 1 AU. We discuss these properties with regard to the development of space-weather predictions based on MHD simulations of solar eruptions.

## Modeling Jets in the Corona and Solar Wind

T. [Torok](#), R. Lionello, V.S. Titov, J.E. Leake, Z. Mikic, J.A. Linker, M.G. Linton

Ground-based Solar Observations in the Space Instrumentation Era

ASP Conference Series, Vol. 504, p. 185, **2016**

<http://arxiv.org/pdf/1511.09350v1.pdf>

<http://aspbooks.org/publications/504/185.pdf>

Coronal jets are transient, collimated eruptions that occur in regions of predominantly open magnetic field in the solar corona. Our understanding of these events has greatly evolved in recent years but several open questions, such as the contribution of coronal jets to the solar wind, remain. Here we present an overview of the observations and numerical modeling of coronal jets, followed by a brief description of "next-generation" simulations that include an advanced description of the energy transfer in the corona ("thermodynamic MHD"), large spherical computational domains, and the solar wind. These new models will allow us to address some of the open questions.

## The Evolution of Writhe in Kink-Unstable Flux Ropes and Erupting Filaments

Tibor [Torok](#), Bernhard Kliem, Mitchell A. Berger, Mark G. Linton, Pascal Demoulin, Lidia van Driel-Gesztelyi

**2014**

<http://arxiv.org/pdf/1403.1565v1.pdf>

The helical kink instability of a twisted magnetic flux tube has been suggested as a trigger mechanism for solar filament eruptions and coronal mass ejections (CMEs). In order to investigate if estimations of the pre-eruptive twist can be obtained from observations of writhe in such events, we quantitatively analyze the conversion of twist into writhe in the course of the instability, using numerical simulations. We consider the line tied, cylindrically symmetric Gold-Hoyle flux rope model and measure the writhe using the formulae by Berger and Prior which express the quantity as a single integral in space. We find that the amount of twist converted into writhe does not simply scale with the initial flux rope twist, but depends mainly on the growth rates of the instability eigenmodes of higher longitudinal order than the basic mode. The saturation levels of the writhe, as well as the shapes of the kinked flux ropes, are very similar for considerable ranges of initial flux rope twists, which essentially precludes estimations of pre-eruptive twist from measurements of writhe. However, our simulations suggest an upper twist limit of  $\sim 6\pi$  for the majority of filaments prior to their eruption.

## Initiation of Coronal Mass Ejections by Sunspot Rotation

[Torok](#), T., Temmer, M., Valori, G., Veronig, A. M., van Driel-Gesztelyi, L., Vrsnak, B.

E-print, Feb **2013**, **File**; Solar Phys. September 2013, Volume 286, Issue 2, pp 453-477

<http://arxiv.org/pdf/1401.2922v1.pdf>

We study a filament eruption, two-ribbon flare, and coronal mass ejection (CME) that occurred in active region NOAA 10898 on **6 July 2006**. The filament was located south of a strong sunspot that dominated the region. In the evolution leading up to the eruption, and for some time after it, a counter-clockwise rotation of the sunspot of about 30 degrees was observed. We suggest that the rotation triggered the eruption by progressively expanding the magnetic field above the filament. To test this scenario, we study the effect of twisting the initially potential field overlying a pre-existing flux rope, using three-dimensional zero-beta MHD simulations. We first consider a relatively simple and symmetric

system, and then study a more complex and asymmetric magnetic configuration, whose photospheric flux distribution and coronal structure are guided by the observations and a potential field extrapolation. In both cases, we find that the twisting leads to the expansion of the overlying field. As a consequence of the progressively reduced magnetic tension, the flux rope quasi-statically adapts to the changed environmental field, rising slowly. Once the tension is sufficiently reduced, a distinct second phase of evolution occurs where the flux rope enters an unstable regime characterized by a strong acceleration. Our simulations thus suggest a new mechanism for the triggering of eruptions in the vicinity of rotating sunspots.

### **A MODEL FOR MAGNETICALLY COUPLED SYMPATHETIC ERUPTIONS**

T. **Török**<sup>1</sup>, O. Panasenco<sup>2</sup>, V. S. Titov<sup>1</sup>, Z. Mikić<sup>1</sup>, K. K. Reeves<sup>3</sup>, M. Velli<sup>4</sup>, J. A. Linker<sup>1</sup> and G. De Toma

**2011 ApJ 739 L63, File**

Sympathetic eruptions on the Sun have been observed for several decades, but the mechanisms by which one eruption can trigger another remain poorly understood. We present a three-dimensional MHD simulation that suggests two possible magnetic trigger mechanisms for sympathetic eruptions. We consider a configuration that contains two coronal flux ropes located within a pseudo-streamer and one rope located next to it. A sequence of eruptions is initiated by triggering the eruption of the flux rope next to the streamer. The expansion of the rope leads to two consecutive reconnection events, each of which triggers the eruption of a flux rope by removing a sufficient amount of overlying flux. The simulation qualitatively reproduces important aspects of the global sympathetic event on **2010 August 1** and provides a scenario for the so-called twin filament eruptions. The suggested mechanisms are also applicable for sympathetic eruptions occurring in other magnetic configurations.

### **FILAMENT INTERACTION MODELED BY FLUX ROPE RECONNECTION**

T. **Török**<sup>1,2</sup>, R. Chandra<sup>1,3</sup>, E. Pariat<sup>1</sup>, P. D’emoulin<sup>1</sup>, B. Schmieder<sup>1</sup>, G. Aulanier<sup>1</sup>, M. G. Linton<sup>4</sup>, and C. H. Mandrini<sup>5</sup>

*Astrophysical Journal*, 728:65 (6pp), **2011; File**

H $\alpha$  observations of solar active region NOAA 10501 on **2003 November 20** revealed a very uncommon dynamic process: during the development of a nearby flare, two adjacent elongated filaments approached each other, merged at their middle sections, and separated again, thereby forming stable configurations with new footpoint connections. The observed dynamic pattern is indicative of “slingshot” reconnection between two magnetic flux ropes. We test this scenario by means of a three-dimensional zero  $\beta$  magnetohydrodynamic simulation, using a modified version of the coronal flux rope model by Titov and D’emoulin as the initial condition for the magnetic field. To this end, a configuration is constructed that contains two flux ropes which are oriented side-by-side and are embedded in an ambient potential field. The choice of the magnetic orientation of the flux ropes and of the topology of the potential field is guided by the observations. Quasi-static boundary flows are then imposed to bring the middle sections of the flux ropes into contact. After sufficient driving, the ropes reconnect and two new flux ropes are formed, which now connect the former adjacent flux rope footpoints of opposite polarity. The corresponding evolution of filament material is modeled by calculating the positions of field line dips at all times. The dips follow the morphological evolution of the flux ropes, in qualitative agreement with the observed filaments.

### **The writhe of helical structures in the solar corona**

T. **Török**<sup>1,2</sup>, M. A. Berger<sup>2,3</sup>, and B. Kliem<sup>2,4,5</sup>

*A&A* 516, A49 (**2010**), **File**

**Context.** Helicity is a fundamental property of magnetic fields, conserved in ideal MHD. In flux rope geometry, it consists of twist and writhe helicity. Despite the common occurrence of helical structures in the solar atmosphere, little is known about how their shape relates to the writhe, which fraction of helicity is contained in writhe, and how much helicity is exchanged between twist and writhe when they erupt.

**Aims.** Here we perform a quantitative investigation of these questions relevant for coronal flux ropes.

**Methods.** The decomposition of the writhe of a curve into local and nonlocal components greatly facilitates its computation. We use it to study the relation between writhe and projected S shape of helical curves and to measure writhe and twist in numerical simulations of flux rope instabilities. The results are discussed with regard to filament eruptions and coronal mass ejections (CMEs).

**Results.** (1) We demonstrate that the relation between writhe and projected S shape is *not* unique in principle, but that the ambiguity does not affect low-lying structures, thus supporting the established empirical rule which associates stable forward (reverse) S shaped structures low in the corona with positive (negative) helicity. (2) Kink-unstable erupting flux ropes are found to transform a far smaller fraction of their twist helicity into writhe helicity than often assumed. (3) Confined flux rope eruptions tend to show stronger writhe at low heights than ejective eruptions (CMEs). This argues against suggestions that the writhing facilitates the rise of the rope through the overlying field. (4) Erupting filaments which are S shaped already before the eruption and keep the sign of their axis writhe (which is expected if field of one chirality dominates the source volume of the eruption), must reverse their S shape in the course of the rise. Implications for the occurrence of the helical kink instability in such events are discussed. (5) The writhe of rising loops can easily be estimated from the angle of rotation about the direction of ascent, once the apex height exceeds the footpoint separation significantly.

Conclusions. Writhe can straightforwardly be computed for numerical data and can often be estimated from observations. It is useful in interpreting S shaped coronal structures and in constraining models of eruptions.

## Modelling CMEs Close to the Sun

[Török, T.](#)

Freiburg ESP Meeting 2008, Presentation

It is now widely accepted that large-scale solar eruptive phenomena like flares, eruptive prominences or filaments, and coronal mass ejections (CMEs) are magnetically driven. They are different observational manifestations of a more general process, namely a large-scale disruption of the coronal magnetic field ("solar eruption" in the following). It is also widely accepted that the energy necessary to drive solar eruptions is stored in the low corona, in form of sheared and twisted magnetic fields which are held in equilibrium prior to eruption by the ambient coronal field. An eruption occurs if this equilibrium is driven or perturbed such that it becomes unstable. In spite of this general understanding, the detailed processes which initiate and drive solar eruptions are not yet well understood. Several mechanisms have been proposed in the last decades. In recent years, the availability of 3D MHD simulations has helped to test the models and has greatly increased our understanding of these processes. In this talk, I will **review** current theoretical models and corresponding numerical simulations of solar eruptions. I will outline their differences and similarities and briefly discuss how current and future observations can help us to constrain the models. The simulation results indicate a flux rope instability or loss of equilibrium to be the canonical driving mechanism of solar eruptions in their fast acceleration phase close to the Sun, and they point towards a relatively large variety of possible mechanisms that initiate that phase. As an example for such an initiation mechanism, I will present new simulations which show how the eruption of a pre-existing 3D coronal flux rope can be triggered by magnetic flux emergence.

## Numerical Simulations of Fast and Slow Coronal Mass Ejections,

[Török, T.](#), and [Kliem, B.](#)

*Astron. Nachr.*, 328(8), 743–746. (2007)

increased magnetic complexity, reflected on steep magnetic gradients in the source ARs' corona, tends to produce faster CMEs.

## Propagation of untwisting solar jets from the low-beta corona into the super-Alfvénic wind: Testing a solar origin scenario for switchbacks

[Jade Touresse](#), [Etienne Pariat](#), [Clara Froment](#), [Valentin Aslanyan](#), [Peter F. Wyper](#), [Louis Seyfritz](#)

A&A 2024

<https://arxiv.org/pdf/2412.15930>

Parker Solar Probe's (PSP) discovery of the prevalence of switchbacks (SBs), localised magnetic deflections in the nascent solar wind, has sparked interest in uncovering their origins. A prominent theory suggests these SBs originate in the lower corona through magnetic reconnection processes, closely linked to solar jet phenomena. Jets are impulsive events, observed across scales and solar atmosphere layers, associated with the release of magnetic twist and helicity. This study examines whether self-consistent jets can form and propagate into the super-Alfvénic wind, assesses the impact of distinct Parker solar wind profiles on jet dynamics, and determines if jet-induced magnetic untwisting waves display signatures typical of SBs. We employed parametric 3D numerical MHD simulations using the ARMS code to model the self-consistent generation of solar jets. Our study focuses on the propagation of solar jets in distinct atmospheric plasma  $\beta$  and Alfvén velocity profiles, including a Parker solar wind. Our findings show that self-consistent coronal jets can form and propagate into the super-Alfvénic wind. Notable structures such as the leading Alfvénic wave and trailing dense-jet region were consistently observed across diverse plasma  $\beta$  atmospheres. The jet propagation dynamics are significantly influenced by atmospheric variations, with changes in Alfvén velocity profiles affecting the group velocity and propagation ratio of the leading and trailing structures. U-loops, prevalent at jet onset, do not persist in the low- $\beta$  corona, but magnetic untwisting waves associated with jets show SB-like signatures. However, full-reversal SBs were not observed. These findings may explain the absence of full reversal SBs in the sub-Alfvénic wind and illustrate the propagation of magnetic deflections through jet-like events, shedding light on possible SB formation processes.

## Transient Formation of Loops in the Core of an Active Region

[Durgesh Tripathi](#)

ApJ 2021

<https://arxiv.org/pdf/2101.06622.pdf>

We study the formation of transient loops in the core of the AR 11890. For this purpose, we have used the observations recorded by the Atmospheric Imaging Assembly (AIA) and the Interface Region Imaging Spectrograph (IRIS). For photospheric field configuration, we have used the line-of-sight (LOS) magnetograms obtained from the Helioseismic and Magnetic Imager (HMI). The transient is simultaneously observed in all the UV and EUV channels of AIA and the three slit-jaw images from IRIS. The co-existence of the transient in all AIA and IRIS SJI channels suggests the

transient's multi-thermal nature. The transient consists of short loops located at the base of the transient as well as long loops. A differential emission measure (DEM) analysis shows that the transient has a clumpy structure. The highest emission observed at the base is within the temperature bin of  $\log T=6.65-6.95$ . We observe the longer loops at a similar temperature, albeit very feeble. Using LOS magnetograms, we conclude that the magnetic reconnection may have caused the transient. Our observations further suggest that the physics of the formation of such transients may be similar to those of typical coronal jets, albeit in different topological configurations. Such multi-wavelength observations shed light on the formation of hot plasma in the solar corona and provide further essential constraints on modeling the thermodynamics of such transients. **8 Nov 2013**

*We note that the transient loop system studied here resembles the structure similar to those described by Hanaoka (1997) using the observations recorded by the Soft X-ray Telescope (SXT; Tsuneta et al. 1991) onboard Yohkoh. These were referred to as "double loop configuration of solar flares".*

### **SDO/AIA Observations of a Partially Erupting Prominence**

Durgesh [Tripathi](#)<sup>1</sup>, Katharine K. Reeves<sup>2</sup>, Sarah E. Gibson<sup>3</sup>, Abhishek Srivastava<sup>4</sup>, and Navin C. Joshi  
**2013 ApJ 778 142**

We report an observation of a partially erupting prominence and its associated dynamical plasma processes based on observations recorded by the Atmospheric Imaging Assembly (AIA) on board the Solar Dynamics Observatory. The prominence first went through a slow rise (SR) phase followed by a fast rise (FR) phase. The SR phase began after a couple of small brightenings were seen toward the footpoints. When the prominence had transitioned from SR to FR, it had already become kinked. The prominence shows strong brightening at the central kink location during the start of FR. We interpret this as an internal magnetic reconnection occurring at a vertical current sheet forming between the two legs of the erupting prominence (flux rope). The brightening at the central kink location is seen in all EUV channels of AIA. The contributions of differential emission at higher temperatures are larger compared to that for typical coronal temperatures supporting a reconnection scenario at the central kink location. The plasma above the brightening location is ejected as a hot plasmoid-like structure embedded in a coronal mass ejection, and those below the brightening move down in the form of blobs moving toward the Sun's surface. The unique time resolution of the AIA has allowed these eruptive aspects, including SR-to-FR, kinking, central current sheet formation, plasmoid-like eruption, and filament "splitting," to be observed in a single event, providing strong and comprehensive evidence in favor of the model of partially erupting flux ropes.

### **Dynamics of an Erupting Arched Magnetic Flux Rope in a Laboratory Plasma Experiment**

S.K.P. [Tripathi](#) · W. Gekelman  
*Solar Phys* (2013) 286:479–492

A laboratory plasma experiment has been built to study the eruption of arched magnetic flux ropes (AMFRs) in the presence of a large magnetized plasma. This experiment simulates the eruption of solar AMFRs in two essential steps: i) it produces an AMFR ( $n = 6.0 \times 10^{12} \text{ cm}^{-3}$ ,  $T_e = 14 \text{ eV}$ ,  $B \approx 1 \text{ kilo-gauss}$ ,  $L = 0.51 \text{ m}$ ) with a persistent appearance that lasts several Alfvén transit times using a lanthanum hexaboride (LaB6) plasma source, and ii) it generates controlled plasma flows from the footpoints of the AMFR using laser beams. An additional LaB6 plasma source generates a large magnetized plasma in the background. The laser-generated flows trigger the eruption by injecting dense plasma and magnetic flux into the AMFR. The experiment is highly reproducible and runs continuously with a 0.5 Hz repetition rate; hence, several thousand identical loop eruptions are routinely generated and their spatio-temporal evolution is recorded in three-dimensions using computer-controlled movable probes. Measurements demonstrate striking similarities between the erupting laboratory and solar arched magnetic flux ropes.

### **Laboratory Simulation of Arched Magnetic Flux Rope Eruptions in the Solar Atmosphere**

S. K. P. [Tripathi](#) and W. Gekelman  
E-print, Aug 2010

Dramatic eruption of an arched magnetic flux rope in a large ambient plasma has been studied in a laboratory experiment that simulates coronal loops. The eruption is initiated by laser generated plasma flows from the footpoints of the rope that significantly modify the magnetic-field topology and link the magnetic-field lines of the rope with the ambient plasma. Following this event, the flux rope erupts by releasing its plasma into the background. The resulting impulse excites intense magnetosonic waves that transfer energy to the ambient plasma and subsequently decay

### **A bright coronal downflow seen in multi-wavelength observations: evidence of a bifurcating flux-rope?**

D. [Tripathi](#), S.K. Solanki, H.E. Mason, D.F. Webb

E-print, July 2007; *Astronomy and Astrophysics*, Volume 472, Issue 2, September III 2007, pp.633-642  
Aims. To study the origin and characteristics of a bright coronal downflow seen after a coronal mass ejection associated with erupting prominences on **5 March 2000**.

Methods. This study extends that of Tripathi et al. (2006b) based on the Extreme-ultraviolet Imaging Telescope (EIT), the Soft X-ray Telescope (SXT) and the Large Angle Spectrometric Coronagraph (LASCO) observations. We combined those results with an analysis of the observations taken by the H<sub>α</sub> and the Mk4 coronagraphs at the Mauna Loa Solar



Observatory (MLSO). The combined data-set spans a broad range of temperature as well as continuous observations from the solar surface out to  $30 R_{\odot}$ .

Results. The downflow started at around  $1.6R_{\odot}$  and contained both hot and cold gas. The downflow was observed in the H $_{\alpha}$  and the Mk4 coronagraphs as well as the EIT and the SXT and was approximately co-spatial and co-temporal providing evidence of multi-thermal plasma. The H $_{\alpha}$  and Mk4 images show cusp-shaped structures close to the location where the downflow started. Mk4 observations reveal that the speed of the downflow in the early phase was substantially higher than the free-fall speed, implying a strong downward acceleration near the height at which the downflow started.

Conclusions. The origin of the downflow was likely to have been magnetic reconnection taking place inside the erupting flux rope that led to its bifurcation.

### **Observation of a bright coronal downflow by SOHO/EIT**

D. **Tripathi**, S. K. Solanki<sup>1</sup>, R. Schwenn<sup>1</sup>, V. Bothmer<sup>2</sup>, M. Mierla<sup>1</sup>, G. Stenborg<sup>3</sup>

Astronomy and Astrophysics, Volume 449, Issue 1, April I **2006**, pp.369-378, **File**

A distinct coronal downflow has been discovered in the course of a prominence eruption associated coronal mass ejection (CME) on 05-Mar-2000.

### **The basic characteristics of EUV post-eruptive arcades and their role as tracers of coronal mass ejection source regions**

D. **Tripathi**, V. Bothmer, and H. Cremades

A&A 422, 337–349 (**2004**)

<https://www.aanda.org/articles/aa/pdf/2004/28/aa0815.pdf>

DOI: 10.1051/0004-6361:20035815

The Extreme ultraviolet Imaging Telescope (EIT) on board the Solar and Heliospheric Observatory (SOHO) spacecraft provides unique observations of dynamic processes in the low corona. The EIT 195 Å data taken from 1997 to the end of 2002 were investigated to study the basic physical properties of post-eruptive arcades (PEAs) and their relationship with coronal mass ejections (CMEs) as detected by SOHO/LASCO (Large Angle Spectrometric Coronagraph). Over the investigated time period, 236 PEA events have been identified in total. For each PEA, its EUV lifetime as derived from the emission time at 195 Å, its heliographic position and length, and its corresponding photospheric source region inferred from SOHO/MDI (Michelson Doppler Imager) data has been studied, as well as the variation of these parameters over the investigated phase of solar cycle 23. An almost one to one correspondence is found between EUV PEAs and white-light CMEs. Based on this finding, PEAs can be considered as reliable tracers of CME events even without simultaneous coronagraph observations. A detailed comparison of the white-light, soft X-ray and EUV observation for some of the events shows, that PEAs form in the aftermath of CMEs likely in the course of the magnetic restructurings taking place at the coronal source sites. The average EUV emission life-time for the selected events ranged from 2 to 20 h, with an average of 7 h. The heliographic length of the PEAs was in the range of 2 to 40 degrees, with an average of 15 degrees. The length increased by a factor of 3 to 4 in the latitude range of 20 to 40 degrees in the northern and southern hemispheres, with longer PEAs being observed preferentially at higher latitudes. The PEAs were located mainly in the activity belts in both hemispheres, with the southern hemispheric ones being shifted by about 15 degree in latitude further away from the solar equator during 1997–2002. The decrease in latitude of the PEA positions was 10 to 15 degrees in the northern and southern hemispheres over this period. The axes of the PEAs were overlying magnetic polarity inversion lines when traced back to the MDI synoptic charts of the photospheric field. The magnetic polarities on both sides of the inversion lines agreed with the dominant magnetic pattern expected in cycle 23, i.e. being preferentially positive to the West of the PEA axes in the North and negative in the South. One third (31%) of the PEA events showed reversed polarities. The origin of PEAs is found not just in single bipolar regions (BPRs), but also in between pairs of neighboring BPRs.

### **On the Stabilization of a Twisted Magnetic Flux Tube**

Yuriy **Tsap**<sup>1,5</sup>, Viktor Fedun<sup>2</sup>, Oleg Cheremnykh<sup>3</sup>, Alexander Stepanov<sup>4</sup>, Alexandr Kryshnal<sup>3</sup>, and Yulia Kopylova<sup>4</sup>

**2020** ApJ 901 99

<https://iopscience.iop.org/article/10.3847/1538-4357/abaf01/pdf>

The linear magnetohydrodynamic stability of a shielding magnetic flux rope with a surface current under coronal solar conditions is analyzed in the framework of an energy principle. The equation describing the potential energy change induced by disturbances of the equilibrium was derived. It has been shown that the surface reverse current shielding the azimuthal component of the magnetic field lines outside a flux rope stabilizes the development of kink- and flute-type instabilities in the long-wavelength limit independently of the cross-sectional radial profile of current density. Kink modes are the most unstable ones as their generation requires less energy than other modes. Based on the obtained dispersion relation for kink oscillations, we proposed a new expression for the determination of magnetic field components of the twisted loop.

### **Eruptive Instability of the Magnetic-Flux Rope: Gravitational Force and Mass-Unloading**

Y. T. **Tsap**, B. P. Filippov, Y. G. Kopylova

[Solar Physics](#) February **2019**, 294:35

[sci-hub.tw/10.1007/s11207-019-1423-9](https://sci-hub.tw/10.1007/s11207-019-1423-9)

Based on the Kuperus–Raadu filament model, we analyze the vertical stability of a magnetic-flux rope as a whole, taking into account the gravitational force and mass-unloading. We use the small-perturbation method to determine conditions of the eruptive instability caused by vertical displacements. It has been shown that the upper limit of the magnetic-field decay index describing the flux-rope stability increases with an increase of its mass. The decrease of the flux-rope mass leads to activation and subsequent eruption of the filament. Possible mechanisms of the solar-filament destabilization are discussed.

## Reconnection fluxes in eruptive and confined flares and implications for superflares on the Sun

Johannes [Tschernitz](#), [Astrid M. Veronig](#), [Julia K. Thalmann](#), [Jürgen Hinterreiter](#), [Werner Pötzi](#)

2018 ApJ 853 41

<https://arxiv.org/pdf/1712.04701.pdf>

We study the energy release process of a set of 51 flares (32 confined, 19 eruptive) ranging from GOES class B3 to X17. We use H $\alpha$  filtergrams from Kanzelhöhe Observatory together with SDO HMI and SOHO MDI magnetograms to derive magnetic reconnection fluxes and rates. The flare reconnection flux is strongly correlated with the peak of the GOES 1–8 Å soft X-ray flux ( $c=0.92$ , in log-log space), both for confined and eruptive flares. Confined flares of a certain GOES class exhibit smaller ribbon areas but larger magnetic flux densities in the flare ribbons (by a factor of 2). In the largest events, up to  $\approx 50\%$  of the magnetic flux of the active region (AR) causing the flare is involved in the flare magnetic reconnection. These findings allow us to extrapolate toward the largest solar flares possible. A complex solar AR hosting a magnetic flux of  $2 \cdot 10^{23}$  Mx, which is in line with the largest AR fluxes directly measured, is capable of producing an X80 flare, which corresponds to a bolometric energy of about  $7 \cdot 10^{32}$  ergs. Using a magnetic flux estimate of  $6 \cdot 10^{23}$  Mx for the largest solar AR observed, we find that flares of GOES class  $\approx X500$  could be produced ( $E_{\text{bol}} \approx 3 \cdot 10^{33}$  ergs). These estimates suggest that the present day's Sun is capable of producing flares and related space weather events that may be more than an order of magnitude stronger than have been observed to date. **2011**

November 9, 2014 May 10

Table 2. List of events. (2000–2015)

Table 3. Flare reconnection fluxes  $\Phi$ , reconnection rates  $\dot{\Phi}$  and peak of GOES 1–8 Å SXR flux derivative  $F'_{\text{SXR}}$ .

## Comment on “Non-interacting coronal mass ejections and solar energetic particles near the quadrature configuration of solar terrestrial relations observatory”: CME shocks are fast magnetosonic shocks and not intermediate Alfvén shocks

B. T. [Tsurutani](#)<sup>1</sup>, L. Shan<sup>2</sup>, G. S. Lakhina<sup>3</sup>, C. Mazelle<sup>4</sup>, X. Meng<sup>1</sup>, A. Du<sup>2</sup> and Z. Liu<sup>2</sup>

A&A 656, A152 (2021)

<https://www.aanda.org/articles/aa/pdf/2021/12/aa41029-21.pdf>

<https://doi.org/10.1051/0004-6361/202141029>

Aims. The expression for the shock Mach number used by [Ravishankar and Michalek \(2020, A&A, 638, A42\)](#) is incorrect. We wish to provide a correct expression so they can redo their analyses.

Methods. Coronal mass ejection (CME) shocks are fast magnetosonic shocks and not intermediate Alfvén shocks. We give the steps for calculating the shock normal, shock velocity, and, thus, the shock Mach number. We also mention that the shock properties, such as being quasi-perpendicular or quasi-parallel, are another important parameter for the shock acceleration of energetic particles.

Results. We have corrected the errors existing in the Astronomy and Astrophysics literature concerning the mathematical expression for the Mach number for a CME shock. Hopefully, future authors will use the now-correct expression for the Mach number.

Conclusions. The correct shock Mach number expression has been given to [Ravishankar and Michalek](#). It is hoped that they will redo their calculations (including using other shock properties) to see if their 2020 conclusions still hold true or not.

## Quasiperiodic Velocity Fluctuations in Eruptive Prominences Observed by AIA/SDO

Tsvetan [Tsvetkov](#) and Nikola Petrov

2020 ApJ 893 40

[sci-hub.si/10.3847/1538-4357/ab7db6](https://sci-hub.si/10.3847/1538-4357/ab7db6)

The current study presents an investigation of the behavior of prominences during eruptions. Variations in the distribution of their velocities are detected at altitudes  $< 0.6 R_{\odot}$ . Detailed analyses are carried out for 304 Å Solar Dynamics Observatory/Atmospheric Imaging Assembly (SDO/AIA) observations. To track the behavior of prominences during eruptions, 41 events in the period 2010–2017 are studied. To follow the rise of a filament on higher altitudes (up to  $32 R_{\odot}$ ), Solar and Heliospheric Observatory/Large Angle and Spectrometric Coronagraph (SOHO/LASCO) data are also inspected. They are used to obtain kinematic profiles of eruptions. Obtained height–time and speed–time plots of the eruptions show velocity fluctuations in 83% of the explored cases, detected only in the SDO/AIA field of view, and not in any of the prominences observed at higher altitudes by SOHO/LASCO. Time intervals between fluctuations and heights at which they are detected are estimated. Strong periodicity cannot be determined. **2010 August 7**,

Table 2 List of EPs that Allow Measurements of the Time and Height Intervals between Two Consecutive Fluctuations

## Three case studies of height-time profiles of prominence eruptions observed by AIA and LASCO

Ts [Tsvetkov N.Petrov](#)

[Journal of Atmospheric and Solar-Terrestrial Physics](#)

Volume 177, October 2018, Pages 29-37

<http://sci-hub.se/10.1016/j.jastp.2018.05.013>

The motions of three solar eruptive prominences are studied. The behaviour of the rising prominence body during the eruption is tracked. Height-time profiles of the eruption up to  $6 R_{\odot}$  (based on observations by Solar Dynamics Observatory/Atmospheric Imaging Assembly (HeII 304 Å) and Large Angle and Spectrometric Coronagraph Experiment (LASCO) C2/Solar and Heliospheric Observatory (SOHO)) and possible changes of the velocity of the prominence material are presented. The mechanisms that generate the variations in the material movement are discussed. 2011 June 6 2012 July 28/29 2013 February 27

## DERIVATION OF THE MAGNETIC FIELD IN A CORONAL MASS EJECTION CORE VIA MULTI-FREQUENCY RADIO IMAGING

Samuel D. [Tun](#)<sup>1,3</sup> and A. Vourlidas<sup>2</sup>

ApJ 766:130, 2013

<https://iopscience.iop.org/article/10.1088/0004-637X/766/2/130/pdf>

The magnetic field within the core of a coronal mass ejection (CME) on 2010 August 14 is derived from analysis of multi-wavelength radio imaging data. This CME's core was found to be the source of a moving type IV radio burst, whose emission is here determined to arise from the gyrosynchrotron process. The CME core's true trajectory, electron density, and line-of-sight depth are derived from stereoscopic observations, constraining these parameters in the radio emission models. We find that the CME carries a substantial amount of mildly relativistic electrons ( $E < 100$  keV) in a strong magnetic field ( $B < 15$  G), and that the spectra at lower heights are preferentially suppressed at lower frequencies through absorption from thermal electrons. We discuss the results in light of previous moving type IV burst studies, and outline a plan for the eventual use of radio methods for CME magnetic field diagnostics.

## Validation of the magnetic energy vs. helicity scaling in solar magnetic structures

K. [Tziotziou](#), K. Moraitis, M.K. Georgoulis, V. Archontis

A&A, 2014

We assess the validity of the free magnetic energy - relative magnetic helicity diagram for solar magnetic structures. We used two different methods of calculating the free magnetic energy and the relative magnetic helicity budgets: a classical, volume-calculation nonlinear force-free (NLFF) method applied to finite coronal magnetic structures and a surface-calculation NLFF derivation that relies on a single photospheric or chromospheric vector magnetogram. Both methods were applied to two different data sets, namely synthetic active-region cases obtained by three-dimensional magneto-hydrodynamic (MHD) simulations and observed active-region cases, which include both eruptive and noneruptive magnetic structures. The derived energy-helicity diagram shows a consistent monotonic scaling between relative helicity and free energy with a scaling index  $0.84 \pm 0.05$  for both data sets and calculation methods. It also confirms the segregation between noneruptive and eruptive active regions and the existence of thresholds in both free energy and relative helicity for active regions to enter eruptive territory. We consider the previously reported energy-helicity diagram of solar magnetic structures as adequately validated and envision a significant role of the uncovered scaling in future studies of solar magnetism.

## Magnetic Energy and Helicity Budgets in NOAA AR 11158

Kostas [Tziotziou](#), Manolis K. Georgoulis, Yang Liu

E-print, June 2013; ApJ 772 115 2013

In previous works we introduced a nonlinear force-free method that self-consistently calculates the instantaneous budgets of free magnetic energy and relative magnetic helicity in solar active regions (ARs). Calculation is expedient and practical, using only a single vector magnetogram per computation. We apply this method to a timeseries of 600 high-cadence vector magnetograms of the eruptive NOAA AR 11158 acquired by the Helioseismic and Magnetic Imager onboard the Solar Dynamics Observatory over a five-day observing interval. Besides testing our method extensively, we use it to interpret the dynamical evolution in the AR, including eruptions. We find that the AR builds large budgets of both free magnetic energy and relative magnetic helicity, sufficient to power many more eruptions than the ones it gave within the interval of interest. For each of these major eruptions, we find eruption-related decreases and subsequent free-energy and helicity budgets that are consistent with the observed eruption (flare and coronal-mass-ejection [CME]) sizes. In addition, we find that (1) evolution in the AR is consistent with the recently proposed (free) energy - (relative) helicity diagram of solar ARs, (2) eruption-related decreases occur  $\{it\}$  before  $\{it\}$  the flare and the projected CME-launch times, suggesting that CME progenitors precede flares, and (3) self-terms of free energy and relative helicity most likely originate from respective mutual-terms, following a progressive mutual-to-self conversion pattern that most likely stems from magnetic reconnection. This results in the non-ideal formation of increasingly helical pre-eruption structures and instigates further research on the triggering of solar eruptions with magnetic helicity firmly placed in the eruption cadre.

## The Magnetic Topology of Coronal Mass Ejection sources

I. [Ugarte-Urra](#), H.P. Warren, A.R. Winebarger  
E-print, March 2007, Ap. J.

## Properties of High-Frequency Type II Radio Bursts and Their Relation to the Associated Coronal Mass Ejections

[A. C. Umuhire](#), [N. Gopalswamy](#), [J. Uvamahoro](#), [S. Akiyama](#), [S. Yashiro](#) & [P. Mäkelä](#)

[Solar Physics](#) volume 296, Article number: 27 (2021) **File**

<https://link.springer.com/content/pdf/10.1007/s11207-020-01743-8.pdf>

Solar radio bursts are often early indicators of space weather events such as coronal mass ejections (CMEs). In this study, we determined the properties of a sample of 40 high-starting-frequency ( $\geq 150$  MHz) type II radio bursts and the characteristics of the associated CMEs such as width, location and speed during 2010–2016. The high starting frequency implies shock formation closer to the solar surface, which has important ramifications for the analysis of particle acceleration near the Sun. We found the CME heliocentric distances at the onset time of metric type II bursts range from 1.16 to 1.90 solar radii ( $R_s$ ). The study was also extended to 128 metric type II bursts to include lower-starting-frequency events for further analysis. The projected CME heights range from 1.15 to 2.85  $R_s$ . The lower starting frequency correspond to shocks forming at larger heights. A weak correlation was found between the type-II starting frequency and CME heights, which is consistent with the density decline in the inner corona. The analysis confirmed a good correlation between the drift rate and the starting frequency of type II bursts (correlation coefficient  $\sim 0.8$ ). Taking into account the radial variation of CMEs speeds from the inner corona to the interplanetary medium, we observed the deviations from the universal drift-rate spectrum of type II bursts and confirmed the previous results relating type II bursts to CMEs. **13 Feb 2011**

**Table** 128 type II bursts 2010-2015

**CESRA #3067 Oct 2021** <https://www.astro.gla.ac.uk/users/eduard/cesra/?p=3067>

## Solar sources of interplanetary magnetic clouds leading to helicity prediction

Roger K. [Ulrich](#), [Pete Riley](#), [T. Tran](#)

Space Weather **Volume16, Issue11** Pages 1668-1685 **2018**

<https://arxiv.org/ftp/arxiv/papers/1811/1811.03560.pdf>

<http://sci-hub.tw/10.1029/2018SW001912>

<https://agupubs.onlinelibrary.wiley.com/doi/epdf/10.1029/2018SW001912>

This study identifies the solar origins of magnetic clouds that are observed at 1 AU and predicts the helical handedness of these clouds from the solar surface magnetic fields. We started with the magnetic clouds listed by the Magnetic Field Investigation (MFI) team supporting NASA's WIND spacecraft in what is known as the MFI table and worked backwards in time to identify solar events that produced these clouds. Our methods utilize magnetograms from the Helioseismic and Magnetic Imager (HMI) instrument on the Solar Dynamics Observatory (SDO) spacecraft so that we could only analyze MFI entries after the beginning of 2011. This start date and the end date of the MFI table gave us 37 cases to study. Of these we were able to associate only eight surface events with clouds detected by WIND at 1 AU. We developed a simple algorithm for predicting the cloud helicity which gave the correct handedness in all eight cases. The algorithm is based on the conceptual model that an ejected flux tube has two magnetic origination points at the positions of the strongest radial magnetic field regions of opposite polarity near the places where the ejected arches end at the solar surface. We were unable to find events for the remaining 29 cases: lack of a halo or partial halo CME in an appropriate time window, lack of magnetic and/or filament activity in the proper part of the solar disk, or the event was too far from disk center. The occurrence of a flare was not a requirement for making the identification but in fact flares, often weak, did occur for seven of the eight cases. **2011.02.15, 2011.06.01, 2011.06.02, 2011.09.13, 2012.06.06, 2012.06.14, 2012.09.02, 2012.11.10**

## Plasma Heating in an Erupting Prominence Detected from Microwave Observations with the Siberian Radioheliograph

[A. M. Uralov](#), [V. V. Grechnev](#), [S. V. Lesovoi](#) & [M. V. Globa](#)

[Solar Physics](#) volume 298, Article number: 117 (2023)

<https://doi.org/10.1007/s11207-023-02210-w>

A major eruptive flare occurred on **12 January 2022** in the northeast not far behind the solar limb (N32 E116). The eruption produced a fast coronal mass ejection (CME). The rising ejecta was observed by the telescopes in the extreme ultraviolet and by the multi-frequency Siberian Radioheliograph (SRH) in the 5.8 – 11.8 GHz range. We show how the slope of the decrease in the brightness temperature of the rising ejecta, measured from the microwave SRH images, is related to the heat inflow or outflow in its body during rapid expansion with high acceleration and under the assumption that the plasma ionization state changes insignificantly within the measurement interval. We found that the low-temperature plasma component in the erupting prominence underwent heating. Most likely, this was due to the predominance of ohmic heating because i) the polytropic index of expanding plasma expected in this case was closest to the experimentally measured one, and ii) the ohmic dissipation due to electron-proton collisions loses its efficiency during expansion much slower than the other mechanisms of heating or cooling.

## Self-similar Piston-Shock and CME

A. M. [Uralov](#), [V. V. Grechnev](#), [L. A. Ivanukin](#)

[Solar Physics](#) September 2019, 294:113

<https://link.springer.com/content/pdf/10.1007%2Fs11207-019-1506-7.pdf>

Based on a dimensional analysis, we discuss the existence conditions for one-dimensional self-similar solutions to the problem of a piston extending into an inhomogeneous plasma with magnetic field. In these solutions, the Mach number of a shock wave ahead of the piston is constant. As an application, we consider the **SOL2010-06-13** solar eruptive event, where this property was found for a coronal wave at the formation stage of a coronal mass ejection (CME). Using a known wave trajectory in the distance–time plane, it is possible to follow the trajectory of an effective (virtual) piston that is a driver of the wave. The trajectory of the virtual piston originates in an eruptive filament during its impulsive acceleration and terminates at a rim bounding an apparent CME bubble in extreme-ultraviolet images, when the rim appears. The velocity of the rim at that time is approximately equal to the fast-mode speed at this place before the expansion onset, and the shock-front has a speed corresponding to a Mach number of about 1.5. We also discuss an analogy between the shock-wave propagation caused by the eruption of a solar magnetic flux-rope and the inverse-pinch effect as known from laboratory plasma physics.

## Remote Sensing of Coronal Forces During a Solar Prominence Eruption

[V. M. Uritsky](#), [B. J. Thompson](#), [C. R. DeVore](#)

ApJ 2022

<https://arxiv.org/pdf/2205.02344.pdf>

We present a new methodology -- the Keplerian Optical Dynamics Analysis (KODA) -- for analyzing the dynamics of dense, cool material in the solar corona. The technique involves adaptive spatiotemporal tracking of propagating intensity gradients and their characterization in terms of time-evolving Keplerian areas swept out by the position vectors of moving plasma blobs. Whereas gravity induces purely ballistic motions consistent with Kepler's second law, non-central forces such as the Lorentz force introduce non-zero torques resulting in more complex motions. KODA algorithms enable direct evaluation of the line-of-sight component of the net torque density from the image-plane projection of the areal acceleration. The method is applied to the prominence eruption of **2011 June 7**, observed by the Solar Dynamics Observatory's Atmospheric Imaging Assembly. Results obtained include quantitative estimates of the magnetic forces, field intensities, and blob masses and energies across a vast region impacted by the post-reconnection redistribution of the prominence material. The magnetic pressure and energy are strongly dominant during the early, rising phase of the eruption, while the dynamic pressure and kinetic energy become significant contributors during the subsequent falling phases. Measured intensive properties of the prominence blobs are consistent with those of typical active-region prominences; measured extensive properties are compared with those of the whole pre-eruption prominence and the post-eruption coronal mass ejection of 2011 June 7, all derived by other investigators and techniques. We argue that KODA provides valuable information on characteristics of erupting prominences that are not readily available via alternative means, thereby shedding new light on their environment and evolution.

## Reconnection-Driven Magnetohydrodynamic Turbulence in a Simulated Coronal-Hole Jet

Vadim M. [Uritsky](#), [Merrill A. Roberts](#), [C. Richard DeVore](#), [Judith T. Karpen](#)

2017 ApJ 837 123

<http://arxiv.org/pdf/1607.03843v1.pdf>

Extreme-ultraviolet and X-ray jets occur frequently in magnetically open coronal holes on the Sun, especially at high solar latitudes. Some of these jets are observed by white-light coronagraphs as they propagate through the outer corona toward the inner heliosphere, and it has been proposed that they give rise to microstreams and torsional Alfvén waves detected in situ in the solar wind. To predict and understand the signatures of coronal-hole jets, we have performed a detailed statistical analysis of such a jet simulated with an adaptively refined magnetohydrodynamics model. The results confirm the generation and persistence of three-dimensional, reconnection-driven magnetic turbulence in the simulation. We calculate the spatial correlations of magnetic fluctuations within the jet and find that they agree best with the  $M_{\text{u}}^{\text{Biskamp}}$  - Biskamp scaling model including intermittent current sheets of various sizes coupled via hydrodynamic turbulent cascade. The anisotropy of the magnetic fluctuations and the spatial orientation of the current sheets are consistent with an ensemble of nonlinear Alfvén waves. These properties also reflect the overall collimated jet structure imposed by the geometry of the reconnecting magnetic field. A comparison with Ulysses observations shows that turbulence in the jet wake is in quantitative agreement with that in the fast solar wind.

## Extreme Solar Events: Setting up a Paradigm

[Usoskin](#), I., [Miyake](#), F., [Baroni](#), M. et al.

Space Sci Rev 219, 73 (2023).

<https://doi.org/10.1007/s11214-023-01018-1>

<https://link.springer.com/content/pdf/10.1007/s11214-023-01018-1.pdf> File

The Sun is magnetically active and often produces eruptive events on different energetic and temporal scales. Until recently, the upper limit of such events was unknown and believed to be roughly represented by direct instrumental observations. However, two types of extreme events were discovered recently: extreme solar energetic particle events on the multi-millennial time scale and super-flares on sun-like stars. Both discoveries imply that the Sun might rarely produce events, called extreme solar events (ESE), whose energy could be orders of magnitude greater than anything

**Review**

we have observed during recent decades. During the years following these discoveries, great progress has been achieved in collecting observational evidence, uncovering new events, making statistical analyses, and developing theoretical modelling. The ESE paradigm lives and is being developed. On the other hand, many outstanding questions still remain open and new ones emerge. Here we present an overview of the current state of the art and the forming paradigm of ESE from different points of view: solar physics, stellar–solar projections, cosmogenic-isotope data, modelling, historical data, as well as terrestrial, technological and societal effects of ESEs. Special focus is paid to open questions and further developments. This review is based on the joint work of the International Space Science Institute (ISSI) team #510 (2020–2022). 7176 BCE and 5259 BCE, **5410 BCE, 1279 CE, 1052 CE, 1859, 4-6 Dec 2006, 13 Dec 2006**

## **Modelling non-radially propagating coronal mass ejections and forecasting the time of their arrival at Earth**

[Angelos Valentino](#), [Jasmina Magdalenic](#)

A&A **2024**

<https://arxiv.org/pdf/2407.17295>

We present the study of two solar eruptive events observed on **December 7 2020 and October 28 2021**. Both events were associated with full halo CMEs and flares. These events were chosen because they show a strong non-radial direction of propagation in the low corona and their main propagation direction is not fully aligned with the Sun–Earth line. This characteristic makes them suitable for our study, which aims to inspect how the non-radial direction of propagation in the low corona affects the time of CMEs' arrival at Earth. We reconstructed the CMEs using coronagraph observations and modelled them with EUHFORIA and the cone model for [this http URL](#) compare the accuracy of forecasting the CME arrival time at Earth obtained from different methods, we also used so-called typeII bursts, radio signatures of associated shocks, to find the velocities of the CME-driven shocks and forecast the time of their arrival at Earth. We also estimated the CME arrival time using the 2D CME velocity. Our results show that the lowest accuracy of estimated CME Earth arrival times is found when the 2D CME velocity is used. The velocity of the typeII radio bursts provides better, but still not very accurate, results. Employing, as an input to EUHFORIA, the CME parameters obtained from the GCS fittings at consequently increasing heights, results in a strongly improved accuracy of the modelled CME and shock arrival time  $\Delta t$  changes from 14h to 10min for the first event, and from 12h to 30min for the second one. This improvement shows that when we increased the heights of the GCS reconstruction we accounted for the change in the propagation direction of the studied CMEs, which allowed us to accurately model the CME flank encounter at Earth. Our results show the great importance of the change in the direction of propagation of the CME in the low corona when modelling CMEs and estimating the time of their arrival at Earth.

## **Time Evolution of Force-Free Parameter and Free Magnetic Energy in Active Region NOAA 10365**

G. [Valori](#), P. Romano, A. Malanushenko, I. Ermolli, F. Giorgi, K. Steed, L. van Driel-Gesztelyi, F.

Zuccarello, J.-M. Malherbe

Solar Phys., **2014**

We describe the variation of the accumulated coronal helicity derived from the magnetic helicity flux through the photosphere in active region (AR) NOAA 10365, where several large flares and coronal mass ejections (CMEs) occurred. We used SOHO/MDI full-disk line-of-sight magnetograms to measure the helicity flux, and the integral of GOES X-ray flux as a proxy of the coronal energy variations due to flares or CMEs. Using the linear force-free field model, we transformed the accumulated helicity flux into a time sequence of the force-free parameter  $\alpha$  accounting for flares or CMEs via the proxy derived from GOES observations. This method can be used to derive the value of  $\alpha$  at different times during the AR evolution, and is a partial alternative to the commonly used match of field lines with EUV loops. By combining the accumulated helicity obtained from the observations with the linear force-free theory, we describe the main phases of the emergence process of the AR, and relate them temporally with the occurrence of flares or CMEs. Additionally, a comparison with the loop-matching method of fixing alpha at each time independently shows that the proposed method may be helpful in avoiding unrealistic or undetermined values of alpha that may originate from an insufficient quality of the image used to identify coronal loops at a given time. For the relative intensity of the considered events, the linear force-free field theory implies that there is a direct correlation between the released energy on the one hand and the product of the coronal helicity with the variation of  $\alpha$  due to the event on the other. Therefore, the higher the value of the accumulated coronal helicity, the smaller the force-free parameter variation required to produce the same decrease in the free energy during the CMEs.

## **BREAKOUT CORONAL MASS EJECTION OR STREAMER BLOWOUT: THE BUGLE EFFECT**

B. [van der Holst](#), W. Manchester IV, I.V. Sokolov, G. Tóth, T.I. Gombosi, D. DeZeeuw, and O. Cohen

Astrophysical Journal, 693:1178–1187, **2009**

<http://www.iop.org/EJ/toc/-alert=43190/0004-637X/693/2>

We present three-dimensional numerical magnetohydrodynamic (MHD) simulations of coronal mass ejections (CMEs) initiated by the breakout mechanism. The initial steady state consists of a bipolar active region embedded in the solar wind. The field orientation of the active region is opposite to that of the overarching helmet streamer, so that this pre-eruptive region consists of three arcades with a magnetic null line on the leading edge of the

central arcade. By applying footpoint motion near the polarity inversion line of the central arcade, the breakout reconnection is turned on. During the eruption, the plasma in front of the breakout arcade gets swept up. The latter effect causes a pre-event swelling of the streamer. The width of the helmet streamer increases in time and follows a “bugle” pattern. In this paper, we will demonstrate that if this pre-event streamer swelling is insufficient, reconnection on the sides of the erupting breakout arcade/flux rope sets in. This will ultimately disconnect the helmet top, resulting in a streamer blowout CME. On the other hand, if this pre-event swelling is effective enough, the breakout reconnection will continue all the way to the top of the helmet streamer. The breakout mechanisms will then succeed in creating a breakout CME.

### **Coronal Magnetic Reconnection Driven by CME Expansion—the 2011 June 7 Event**

L. van Driel-Gesztelyi<sup>1,2,3</sup>, D. Baker<sup>1</sup>, T. Török<sup>4</sup>, E. Pariat<sup>2</sup>, L. M. Green<sup>1</sup>, D. R. Williams<sup>1</sup>, J. Carlyle<sup>1,5</sup>, G. Valori<sup>2</sup>, P. Démoulin<sup>2</sup>, B. Kliem<sup>1,6,7</sup>, D. M. Long<sup>1</sup>, S. A. Matthews<sup>1</sup>, and J.-M. Malherb  
2014 ApJ 788 85

<http://arxiv.org/pdf/1406.3153v1.pdf>

Coronal mass ejections (CMEs) erupt and expand in a magnetically structured solar corona. Various indirect observational pieces of evidence have shown that the magnetic field of CMEs reconnects with surrounding magnetic fields, forming, e.g., dimming regions distant from the CME source regions. Analyzing Solar Dynamics Observatory (SDO) observations of the eruption from AR 11226 on **2011 June 7**, we present the first direct evidence of coronal magnetic reconnection between the fields of two adjacent active regions during a CME. The observations are presented jointly with a data-constrained numerical simulation, demonstrating the formation/intensification of current sheets along a hyperbolic flux tube at the interface between the CME and the neighboring AR 11227. Reconnection resulted in the formation of new magnetic connections between the erupting magnetic structure from AR 11226 and the neighboring active region AR 11227 about 200 Mm from the eruption site. The onset of reconnection first becomes apparent in the SDO/AIA images when filament plasma, originally contained within the erupting flux rope, is redirected toward remote areas in AR 11227, tracing the change of large-scale magnetic connectivity. The location of the coronal reconnection region becomes bright and directly observable at SDO/AIA wavelengths, owing to the presence of down-flowing cool, dense ( $10^{10} \text{ cm}^{-3}$ ) filament plasma in its vicinity. The high-density plasma around the reconnection region is heated to coronal temperatures, presumably by slow-mode shocks and Coulomb collisions. **These results provide the first direct observational evidence that CMEs reconnect with surrounding magnetic structures, leading to a large-scale reconfiguration of the coronal magnetic field.**

### **Magnetic Flux Emergence, Activity, Eruptions and Magnetic Clouds: Following Magnetic Field from the Sun to the Heliosphere** A review

L. van Driel-Gesztelyi · J.L. Culhane  
Space Sci Rev (2009) 144: 351–381, **File**

We present an [overview](#) of how the principal physical properties of magnetic flux which emerges from the toroidal fields in the tachocline through the turbulent convection zone to the solar surface are linked to solar activity events, emphasizing the effects of magnetic field evolution and interaction with other magnetic structures on the latter. We compare the results of different approaches using various magnetic observables to evaluate the probability of flare and coronal mass ejection (CME) activity and forecast eruptive activity on the short term (i.e. days). Then, after a brief overview of the observed properties of CMEs and their theoretical models, we discuss the ejecta properties and describe some typical magnetic and composition characteristics of magnetic clouds (MCs) and interplanetary CMEs (ICMEs). We review some individual examples to clarify the link between eruptions from the Sun and the properties of the resulting ejecta. The importance of a synthetic approach to solar and interplanetary magnetic fields and activity is emphasized.

### **Multi-scale reconnections in a complex CME**

Adv. Space Res. 42(5), *Pages 858-865*, 2008

L. van Driel-Gesztelyi, C.P. Goff, P. Démoulin, J.L. Culhane, S.A. Matthews, L.K. Harra, C.H. Mandrini, K.-L. Klein and H. Kurokawa

A series of three flares of GOES class M, M and C, and a CME were observed on **20 January 2004** occurring in close succession in NOAA 10540. Types II, III, and N radio bursts were associated. We use the combined observations from TRACE, EIT,  $H\alpha$  images from Kwasan Observatory, MDI magnetograms, GOES, and radio observations from Culgoora and Wind/ WAVES to understand the complex development of this event. We reach three main conclusions. First, we link the first two impulsive flares to tether-cutting reconnections and the launch of the CME. This complex observation shows that impulsive quadrupolar flares can be eruptive. Second, we relate the last of the flares, an LDE, to the relaxation phase following forced reconnections between the erupting flux rope and neighbouring magnetic field lines, when reconnection reverses and restores some of the pre-eruption magnetic connectivities. Finally, we show that reconnection with the magnetic structure of a previous CME launched about 8 h earlier injects electrons into open field lines having a local dip and apex (located at about six solar radii height). This is observed as an N-burst at decametre radio wavelengths. The dipped shape of these field lines is due to large-scale magnetic reconnection between expanding

magnetic loops and open field lines of a neighbouring streamer. This particular situation explains why this is the first N-burst ever observed at long radio wavelengths.

### **Why are CMEs large-scale coronal events: nature or nurture?**

L. [van Driel-Gesztelyi](#), G. D. R. Attrill, P. D'émoulin, C. H. Mandrini<sup>4</sup>, and L. K. Harra  
E-print, March 2008, [File](#) ; Annales. Geophys.

The apparent contradiction between small-scale source regions of, and large-scale coronal response to, coronal mass ejections (CMEs) has been a long-standing puzzle. For some, CMEs are considered to be inherently large-scale events - eruptions in which a number of flux systems participate in an unspecified manner, while others consider magnetic reconnection in special global topologies to be responsible for the large-scale response of the lower corona to CME events. Some of these ideas may indeed be correct in specific cases. However, what is the key element which makes CMEs large-scale? Observations show that the extent of the coronal disturbance matches the angular width of the CME – an important clue, which does not feature strongly in any of the above suggestions. We review observational evidence for the large-scale *nature* of CME source regions and find them lacking. Then we compare different ideas regarding how CMEs *evolve* to become large-scale. The large-scale magnetic topology plays an important role in this process. There is amounting evidence, however, that the key process is *magnetic reconnection* between the CME and other magnetic structures. We outline a CME evolution model, which is able to account for all the key observational signatures of large-scale CMEs and presents a clear picture *how* large portions, of the Sun become constituents of the CME. In this model reconnection is *driven* by the expansion of the CME core resulting from an over-pressure relative to the pressure in the CME's surroundings. This implies that the extent of the lower coronal signatures match the final angular width of the CME.

### **Toroidal Flux Ropes with Elliptical Cross Sections and Their Magnetic Helicity**

M. [Vandas](#), E. Romashets

[Solar Physics](#) September 2017, 292:129

Axially symmetric constant-alpha force-free magnetic fields in toroidal flux ropes with elliptical cross sections are constructed in order to investigate how their alphas and magnetic helicities depend on parameters of the flux ropes. Magnetic configurations are found numerically using a general solution of a constant-alpha force-free field with an axial symmetry in cylindrical coordinates for a wide range of oblatenesses and aspect ratios. Resulting alphas and magnetic helicities are approximated by polynomial expansions in parameters related to oblateness and aspect ratio. These approximations hold for toroidal as well as cylindrical flux ropes with an accuracy better than or of about 1%. Using these formulae, we calculate relative helicities per unit length of two (probably very oblate) magnetic clouds and show that they are very sensitive to the assumed magnetic cloud shapes (circular versus elliptical cross sections).

### **Source Imaging of a Moving Type-IV Solar Radio Burst and its Role in Tracking Coronal Mass Ejection From the Inner to the Outer Corona**

V. [Vasanth](#), [Yao Chen](#), [Maoshui Lv](#), [Hao Ning](#), [Chuangyang Li](#), [Shiwei Feng](#), [Zhao Wu](#), [Guohui Du](#)  
ApJ 2018

<https://arxiv.org/pdf/1810.11815.pdf>

Source imaging of solar radio bursts can be used to track energetic electrons and associated magnetic structures. Here we present a combined analysis of data at different wavelengths for an eruption associated with a moving type-IV (t-IVm) radio burst. In the inner corona, the sources are correlated with a hot and twisted eruptive EUV structure, while in the outer corona the sources are associated with the top front of the bright core of a white light coronal mass ejection (CME). This reveals the potential of using t-IVm imaging data to continuously track the CME by lighting up the specific component containing radio-emitting electrons. It is found that the t-IVm burst presents a clear spatial dispersion with observing frequencies. The burst manifests broken power-law like spectra in brightness temperature, which is as high as 107-109 K while the polarization level is in-general weak. In addition, the t-IVm burst starts during the declining phase of the flare with a duration as long as 2.5 hours. From the differential emission measure analysis of AIA data, the density of the T-IVm source is found to be at the level of a few to several  $10^8 \text{ cm}^{-3}$  at the start of the burst, and the temperature reaches up to 5-8 MK. These observations do not favor gyro-synchrotron to be the radiation mechanism, yet in line with a coherent plasma emission excited by energetic electrons trapped within the source. Further studies are demanded to elucidate the emission mechanism and explore the full diagnostic potential of t-IVm bursts. 2014 June 15

### **An Eruptive Hot-Channel Structure Observed at Metric Wavelength as a Moving Type-IV Solar Radio Burst**

V. [Vasanth](#), Yao Chen, Shiwei Feng, [Suli Ma](#), [Guohui Du](#), [Hongqiang Song](#), [Xiangliang Kong](#), [Bing Wang](#)  
ApJL 2016

<http://arxiv.org/pdf/1609.06546v1.pdf>

Hot channel (HC) structure, observed in the high-temperature passbands of the AIA/SDO, is regarded as one candidate of coronal flux rope which is an essential element of solar eruptions. Here we present the first radio imaging study of an HC structure in the metric wavelength. The associated radio emission manifests as a moving type-IV (t-IVm) burst. We show that the radio sources co-move outwards with the HC, indicating that the t-IV emitting energetic electrons are efficiently trapped within the structure. The t-IV sources at different frequencies present no considerable spatial



dispersion during the early stage of the event, while the sources spread gradually along the eruptive HC structure at later stage with significant spatial dispersion. The t-IV bursts are characterized by a relatively-high brightness temperature ( $\sim 107 - 109$  K), a moderate polarization, and a spectral shape that evolves considerably with time. This study demonstrates the possibility of imaging the eruptive HC structure at the metric wavelength and provides strong constraints on the t-IV emission mechanism, which, if understood, can be used to diagnose the essential parameters of the eruptive structure. **2012 March 4.**

## **A Statistical Study on CMEs Associated with DH-Type-II Radio Bursts Based on Their Source Location (Limb and Disk Events)**

V. **Vasanth**, S. Umapathy

Solar Physics, January **2013**, Volume 282, Issue 1, pp 239-247

We have statistically studied the 344 Coronal Mass Ejections (CMEs) associated with flares and DH-type-II radio bursts (1 – 14 MHz) during 1997 – 2008. We found that only 3 % of the total CMEs (344) compared to the general population CMEs (13208) drives DH-type-II radio bursts (Gopalswamy in Solar Eruptions and Energetic Particles, AGU Geophys. Monogr. 165, 207, 2006). Out of 344 events we have selected 236 events for further analysis. We divided the events into two groups: i) disk events (within  $45^\circ$  from the disk center) and ii) limb events (beyond  $45^\circ$  but within  $90^\circ$  from the disk center). We find that the average CME speed of the limb events ( $1370 \text{ km s}^{-1}$ ) is three times, while for the disk events ( $1055 \text{ km s}^{-1}$ ) it is two times the average speed of the general population CMEs ( $433 \text{ km s}^{-1}$ ). The average widths of the limb events ( $129^\circ$ ) and disk events ( $116^\circ$ ) are two times greater than the average width of the general population CMEs ( $58^\circ$ ). We found a better correlation between the CME speed and width (correlation coefficient  $R=0.56$ ) for the limb events than that of the disk events ( $R=0.47$ ). The shock speed of the CMEs associated with DH-type-II radio bursts is found by applying Leblanc, Dulk, and Bougeret's (Solar Phys. 183, 165, 1998) electron density model; the disk events are found to have an average speed of  $1190 \text{ km s}^{-1}$  and that of the limb events is  $1275 \text{ km s}^{-1}$ . From this study we compare the CME properties between limb and disk events. The properties like CME speed, width, shock speed, and correlation between CME speed and width are found to be higher for limb events than disk events. The results in disk events are subject to projection effects, and this study stresses the importance of these effects.

## **Magnetic Imprints of Eruptive and Noneruptive Solar Flares as Observed by Solar Dynamics Observatory**

N. **Vasantharaju**<sup>1,2</sup>, P. Vemareddy<sup>1</sup>, B. Ravindra<sup>1</sup>, and V. H. Doddamani<sup>3</sup>

**2022** ApJ 927 86

<https://iopscience.iop.org/article/10.3847/1538-4357/ac4d8c/pdf>

<https://arxiv.org/pdf/2201.06550.pdf>

The abrupt and permanent changes of photospheric magnetic field in the localized regions of active regions during solar flares called magnetic imprints (MIs), have been observed for the past nearly three decades. The well known "coronal implosion" model is assumed to explain such flare associated changes but the complete physical understanding is still missing and debatable. In this study, we made a systematic analysis of flare-related changes of photospheric magnetic field during 21 flares (14 eruptive and 7 non-eruptive) using the high-cadence ( $\sim 135$  s) vector-magnetogram data obtained from Helioseismic and Magnetic Imager. The MI regions for eruptive flares are found to be strongly localised, whereas the majority of non-eruptive events ( $>70\%$ ) have scattered imprint regions. To quantify the strength of the MIs, we derived the integrated change of horizontal field and total change of Lorentz force over an area. These quantities correlate well with the flare strength, irrespective of whether flares being eruptive or not, short or long duration. Further, the free-energy (FE), determined from virial-theorem estimates, exhibits statistically significant downward trend which starts around the flare time is observed in majority of flares. The change of FE during flares do not depend on eruptivity but have a strong positive correlation ( $\approx 0.8$ ) with the Lorentz force change, indicating that the part of FE released would penetrate into the photosphere. While these results strongly favor the idea of significant feedback from corona on the photospheric magnetic field, the characteristics of MIs are quite indistinguishable for flares being eruptive or not. **15-Feb-11, 20110309, 20110730, 20120307, 11-Apr-13, 28-Oct-13, 20131108, 02-Feb-14, 20141024, 20150523, 22-Jun-15**

**Table 1.** List of 21 flare events from 17 ARs and their associated magnetic properties 2011-2015

## **Finding the critical decay index in solar prominence eruptions**

N. **Vasantharaju**, **P. Vemareddy**, **B. Ravindra**, **V. H. Doddamani**

ApJ **885** 89 **2019**

<https://arxiv.org/pdf/1909.10442.pdf>

<https://doi.org/10.3847/1538-4357/ab4793>

<https://iopscience.iop.org/article/10.3847/1538-4357/ab4793/pdf>

The background field is assumed to play prime role in the erupting structures like prominences. In the flux rope models, the critical decay index ( $n_c$ ) is a measure of the rate at which background field intensity decreases with height over the flux rope or erupting structure. In the real observations, the critical height of the background field is unknown, so a typical value of  $n_c=1.5$  is adopted from the numerical studies. In this study, we determined the  $n_c$  of 10 prominence eruptions (PEs). The prominence height in 3D is derived from two-perspective observations of Solar Dynamics Observatory and Solar TERrestrial RELations Observatory. Synoptic maps of photospheric radial magnetic field are used to construct the background field in the corona. During the eruption, the height-time curve of the sample events

exhibits the slow and fast-rise phases and is fitted with the linear-cum-exponential model. From this model, the onset height of fast-rise motion is determined and is considered as the critical height for the onset of the torus-instability because the erupting structure is allowed to expand exponentially provided there is no strapping background field. Corresponding to the critical height, the  $nc$  values of our sample events are varied to be in the range of 0.8-1.3. Additionally, the kinematic analysis suggests that the acceleration of PEs associated with flares are significantly enhanced compared to flare-less PEs. We found that the flare magnetic reconnection is the dominant contributor than the torus-instability to the acceleration process during the fast-rise phase of flare-associated PEs in low corona ( $<1.3R_{\odot}$ ). **20110307, 20110511, 20110612, 20111109, 20111224, 20121226, 20130211, 20130316, 20140708, 20150509**

[HMI Science Nuggets](#) #144 Oct 2020

<http://hmi.stanford.edu/hminuggets/?p=3358>

### **Formation and eruption of sigmoidal structure from a weak field region of NOAA 11942**

N. [Vasantharaju](#), [P. Vemareddy](#), [B. Ravindra](#), [V. H. Doddamani](#)

ApJ **874** 182 **2019**

<https://arxiv.org/pdf/1902.08105.pdf>

[https://ui.adsabs.harvard.edu/link\\_gateway/2019ApJ...874..182V/PUB\\_PDF](https://ui.adsabs.harvard.edu/link_gateway/2019ApJ...874..182V/PUB_PDF)

<https://iopscience.iop.org/article/10.3847/1538-4357/ab0a06/pdf>

Using observations from Solar Dynamics Observatory, we studied an interesting example of a sigmoid formation and eruption from small-scale flux canceling regions of active region (AR) 11942. Analysis of HMI and AIA observations infer that initially the AR is compact and bipolar in nature, evolved to sheared configuration consisting of inverse J-shaped loops hosting a filament channel over a couple of days. By tracking the photospheric magnetic features, shearing and converging motions are observed to play a prime role in the development of S-shaped loops and further flux cancellation leads to tether-cutting reconnection of J-loops. This phase is co-temporal with the filament rise motion followed by sigmoid eruption at 21:32 UT on January 6. The flux rope rises in phases of slow ( $v_{avg} = 26 \text{ km}\cdot\text{s}^{-1}$ ) and fast ( $a_{avg} = 55 \text{ ms}^{-2}$ ) rise motion categorizing the CME as slow with an associated weak C1.0 class X-ray flare. The flare ribbon separation velocity peaks at around peak time of the flare at which maximum reconnection rate ( $2.14 \text{ Vcm}^{-1}$ ) occurs. Further, the EUV light-curves of 131, 171Å~have delayed peaks of 130 minutes compared to 94Å~and is explained by differential emission measure. Our analysis suggests that the energy release is proceeded in a much long time duration, manifesting the onset of filament rise and eventual eruption driven by converging and canceling flux in the photosphere. Unlike strong eruption events, the observed slow CME and weak flare are indications of slow runaway tether-cutting reconnection where most of the sheared arcade is relaxed during the extended post phase of the eruption. **January 6, 2014**

### **Prominence instability and CMEs triggered by massive coronal rain in the solar atmosphere**

Z. [Vashalomidze](#) (1, 2 and 3), [T. V. Zaqarashvili](#) (1, 2 and 3), [V. Kukhianidze](#) (2 and 3), [G. Ramishvili](#) (2 and 3), [A. Hanslmeier](#) (1), [P. Gomory](#) (4)

A&A **658**, A18 **2022**

<https://arxiv.org/pdf/2110.01287.pdf>

<https://doi.org/10.1051/0004-6361/202040233>

<https://www.aanda.org/articles/aa/pdf/2022/02/aa40233-20.pdf>

Triggering process for prominence instability and consequent CMEs is not fully understood. Prominences are maintained by the Lorentz force against the gravity, therefore reduction of the prominence mass due to the coronal rain may cause the change of the force balance and hence destabilisation of the structures. We aim to study the observational evidence of the influence of coronal rain on the stability of prominence and subsequent eruption of CMEs. We used the simultaneous observations from AIA/SDO and SECCHI/STEREO spacecrafts from different angles to follow the dynamics of prominence/filaments and to study the role of coronal rain in their destabilisation. Three different prominences/filaments observed during years 2011-2012 were analysed using observations acquired by SDO and STEREO. In all three cases massive coronal rain from the prominence body led to the destabilisation of prominence and subsequently to the eruption of CMEs. The upward rising of prominences consisted in the slow and the fast rise phases. The coronal rain triggered the initial slow rise of prominences, which led to the final instability (the fast rise phase) after 18-28 hours in all cases. The estimated mass flux carried by coronal rain blobs showed that the prominences became unstable after 40% of mass loss. We suggest that the initial slow rise phase was triggered by the mass loss of prominence due to massive coronal rain, while the fast rise phase, i.e. the consequent instability of prominences, was caused by the torus instability and/or magnetic reconnection with overlying coronal field. Therefore, the coronal rain triggered the instability of prominences and consequent CMEs. If this is the case, then the coronal rain can be used to predict the CMEs and hence to improve the space weather predictions. **16-18 May, 2011, December 22-24, 2011, August 07-08, 2012**

### **Eruption of prominence triggered by coronal rain in the solar atmosphere observed by SDO/AIA and Stereo/EUVI**

Z. M. [Vashalomidze](#) (1), [T. V. Zaqarashvili](#) (1,2 and 3), [V. D. Kukhianidze](#) (1), [G. T. Ramishvili](#) (1)

Astrophysics, Vol. 62, No. 4, December, **2019**

DOI 10.1007/s10511-019-09602-6

<https://arxiv.org/ftp/arxiv/papers/2110/2110.01309.pdf>

The triggering process for coronal mass ejections (CME) in the solar atmosphere is not fully understood. We use observations from different spacecraft at several wavelengths to detect an instability process for a prominence/filament with a subsequent eruption of CME. Time series of spectral lines at 304, 171, 193, and 211 Å have been obtained with the SDO spacecraft, and at 304, 171, 195, and 284 Å with the STEREO spacecraft. A prominence/filament system was observed during **November 8-23, 2011**, at different angles by SDO, STEREO\_A, and STEREO\_B. The observations show that a giant tornado began to develop near the base of the prominence at 20:00 UT on **November 20**, which later caused the appearance of droplets of coronal rain (at 16:00 UT, November 21) which fell downward from the main mass of the prominence. The coronal rain continued until 20:20 UT, November 22, and caused instability of the prominence, after which a CME took place at 22:30 UT on **November 22**. We assume that the loss of mass owing to coronal rain may lead to instability of prominences and their subsequent eruption. Observations of coronal rain falling from the main part of the mass of prominences could be used for predicting space weather.

### **Formation and evolution of coronal rain observed by SDO/AIA on February 22, 2012**

Z. [Vashalomidze](#), V. [Kukhianidze](#), T.V. [Zaqarashvili](#), R. [Oliver](#), B. [Shergelashvili](#), G. [Ramishvili](#), S. [Poedts](#), P. [De Causmaecker](#)

A&A 577, A136 2015

<http://arxiv.org/pdf/1504.03471v1.pdf>

The formation and dynamics of coronal rain are currently not fully understood. Coronal rain is the fall of cool and dense blobs formed by thermal instability in the solar corona towards the solar surface with acceleration smaller than gravitational free fall. We aim to study the observational evidence of the formation of coronal rain and to trace the detailed dynamics of individual blobs. We used time series of the 171 Å, and 304 Å, spectral lines obtained by the Atmospheric Imaging Assembly (AIA) on board the Solar Dynamic Observatory (SDO) above active region AR 11420 on **February 22, 2012**. Observations show that a coronal loop disappeared in the 171 Å channel and appeared in the 304 Å line more than one hour later, which indicates a rapid cooling of the coronal loop from 1 MK to 0.05 MK. An energy estimation shows that the radiation is higher than the heat input, which indicates so-called catastrophic cooling. The cooling was accompanied by the formation of coronal rain in the form of falling cold plasma. We studied two different sequences of falling blobs. The first sequence includes three different blobs. The mean velocities of the blobs were estimated to be 50 km s<sup>-1</sup>, 60 km s<sup>-1</sup> and 40 km s<sup>-1</sup>. A polynomial fit shows the different values of the acceleration for different blobs, which are lower than free-fall in the solar corona. The first and second blob move along the same path, but with and without acceleration, respectively. We performed simple numerical simulations for two consecutive blobs, which show that the second blob moves in a medium that is modified by the passage of the first blob. Therefore, the second blob has a relatively high speed and no acceleration, as is shown by observations. The second sequence includes two different blobs with mean velocities of 100 km s<sup>-1</sup> and 90 km s<sup>-1</sup>, respectively.

### **Exploring the Impact of Imaging Cadence on Inferring CME Kinematics**

[Nitin Vashishtha](#), [Satabdwa Majumdar](#), [Ritesh Patel](#), [Vaibhav Pant](#), [Dipankar Banerjee](#)

Frontiers in Astronomy and Space Sciences 10: 1232197 2023

<https://arxiv.org/pdf/2308.11944.pdf>

<https://www.frontiersin.org/articles/10.3389/fspas.2023.1232197/pdf>

The kinematics of coronal mass ejections (CMEs) are essential for understanding their initiation mechanisms and predicting their planetary impact. Most acceleration and deceleration occur below 4 R<sub>☉</sub>, which is crucial for initiation understanding. Furthermore, the kinematics of CMEs in the inner corona (< 3 R<sub>☉</sub>) are closely related to their propagation in the outer corona and their eventual impact on Earth. Since the CME kinematics are mainly probed using coronagraph data, it is crucial to investigate how imaging cadence affects the precision of data analysis and conclusions drawn and also for determining the flexibility of designing observational campaigns with upcoming coronagraphs. We study ten CMEs observed by the K-Coronagraph of the MLSO. We manually track the CMEs using high cadence (15 s) white-light observations of K-Cor and vary the cadence as 30 s, 1 min, 2 min, and 5 min to study the impact of cadence on the kinematics. We also employed the bootstrapping method to estimate the fitting parameters. Our results indicate that the average velocity of the CMEs does not have a high dependence on the imaging cadence, while the average acceleration shows significant dependence on the same, with the confidence interval showing significant shifts for the average acceleration for different cadences. The decrease in cadence also influences the determination of acceleration onset time. We further find that it is difficult to find an optimum cadence to study all CMEs, as it is also influenced by the pixel resolution of the instrument and the speed of the CME. However, except for very slow CMEs (speeds less than 300 Kms<sup>-1</sup>), our results indicate a cadence of 1 min to be reasonable for the study of their kinematics. The results of this work will be important in the planning of observational campaigns for the existing and upcoming missions that will observe the inner corona. **07/05/2021, June 10, 2021, 10/10/2021**

**Table 1.** Bootstrapped velocity and its 95% confidence interval obtained from linear fitting to height-time plot for different CMEs corresponding to different cadences. 2014-2022

### **Magnetic evolution of active regions: formation and eruption of magnetic flux ropes Review**

[P. Vemareddy](#)

IAU 388 proc. 2024

<https://arxiv.org/pdf/2410.02670>

Magnetic flux ropes (FRs) are twisted structures appearing on the sun, predominantly in the magnetically concentrated regions. These structures appear as coronal features known as filaments or prominences in H $\alpha$  observations, and as

sigmoids in X-ray, EUV observations. Using the continuous vector magnetic field observations from \textit{Helioseismic and Magnetic Imager} onboard \textit{Solar Dynamics Observatory}, we study the evolution of the magnetic fields in the active regions (ARs) to understand the conditions of twisted flux formation. While ARs emerge and evolve further, flux motions such as shearing and rotation are efficient mechanisms to form twisted flux ropes. Magnetic helicity quantifies the twisted magnetic fields and helicity injection through photosphere leads to its accumulation in the corona. Therefore, coronal helicity accumulation leads to twisted FR formation and its eruption. The magnetic helicity injection is seen to evolve distinctly in the regions of flux rope formation and eruption. The ARs that are associated with eruptive activity are observed with helicity injection predominantly with one sign over a period of a few days. The ARs that inject helicity with a changing sign are unlikely to form twisted FRs because coronal helicity during the period of one sign of injected helicity gets cancelled by the opposite sign of injection in the later period. As a result, the coronal field reconfigures from sheared to potential structure. For a given AR, the upper limit of helicity that could cause a CME eruption is not yet understood, which can be the subject of future studies of ARs. Magnetic reconnection plays a crucial role in both the initiation and driving of FR eruptions after their formation. Data-driven simulations of the AR evolution provide more insights on the flux rope formation and its onset of eruption. **13-14 Feb 2011, 30 Aug 2012, 19 Apr 2013, 7-10 Jan 2015, 19-25 Jun 2015**

## **Simulating the formation and eruption of flux rope by magneto-friction model driven by time-dependent electric fields**

[P. Vemareddy](#)

ApJ **975** 251 **2024**

<https://arxiv.org/pdf/2409.14045>

<https://iopscience.iop.org/article/10.3847/1538-4357/ad8089/pdf>

Aiming to capture the formation and eruption of flux ropes (FRs) in the source active regions (ARs), we simulate the coronal magnetic field evolution of the AR 11429 employing the time-dependent magneto-friction model (TMF). The initial field is driven by electric fields that are derived from time-sequence photospheric vector magnetic field observations by invoking ad-hoc assumptions. The simulated magnetic structure evolves from potential to twisted fields over the course of two days, followed by rise motion in the later evolution, depicting the formation of FR and its slow eruption later. The magnetic configuration resembles an inverse S-sigmoidal structure, composed of a potential field enveloping the inverse J-shaped fields that are shared past one another and a low lying twisted field along the major PIL. To compare with observations, proxy emission maps based on averaged current density along the field lines are generated from the simulated field. These emission maps exhibit a remarkable one-to-one correspondence with the spatial characteristics in coronal EUV images, especially the filament-trace supported by the twisted magnetic field in the south-west subregion. Further, the topological analysis of the simulated field reveals the co-spatial flare ribbons with the quasi-separatrix layers, which is consistent with the standard flare models; therefore, the extent of the twist and orientation of the erupting FR is indicated to be the real scenario in this case. The TMF model simulates the coronal field evolution, correctly capturing the formation of the FR in the observed time scale and the twisted field generated from these simulations serve as the initial condition for the full MHD simulations. **7-9 Mar 2012**

## **Eruption of prominence initiated by loss of equilibrium: multipoint observations**

P [Vemareddy](#), M Syed Ibrahim

MNRAS, Volume 527, Issue 2, January **2024**, Pages 1774–1783,

<https://doi.org/10.1093/mnras/stad3323>

<https://academic.oup.com/mnras/article-pdf/527/2/1774/53252392/stad3323.pdf>

Using the SDO/AIA, SOHO/LASCO, STEREO/SECCHI, and ground-based H  $\alpha$ , radio observations, we studied a prominence eruption (PE) from the western limb that occurred on **2013 December 4**. PE is associated with a moderate coronal mass ejection (CME) and GOES class C4.7 flare. Before a couple of days, the prominence pre-existed as an inverse-S shaped filament lying above fragmented opposite polarities between two active regions. Initially, the prominence appears as kinked or writhed as observed from different vantage points. From a careful study of magnetic field observations, we infer that the flux emergence at one leg of the prominence causes the loss of equilibrium which then initiates the slow upward motion of the prominence followed by onset of the eruption at a projected height of 35 Mm. The fast rise motion is also in synchronization with the flare impulsive phase but the average acceleration is quite small ( $150 \text{ ms}^{-2}$ ) compared to strong flare cases. In the LASCO field of view (FOV), the CME continues to accelerate at  $3 \text{ ms}^{-2}$  attaining a speed of  $450 \text{ km s}^{-1}$  at  $16 R_{\odot}$ . In the extended STEREO-A FOV upto  $38 R_{\odot}$ , the CME decelerates  $0.82 \text{ m s}^{-2}$ . The PE launched type III bursts delayed by 14 min with respect to the flare peak time (04:58 UT). Since the prominence is lying in the fragmented polarities, it is likely that the sheared arcade has little contribution to the poloidal flux of the rising magnetic flux rope and subsequently weak flare is recorded. This study of PE emphasizes the influence of the magnetic reconnection on the CME speed, launch of type II, III burst, and the CME propagation distance farther away from the Sun.

## **Filament eruption from active region 13283 leading to fast halo-CME and intense geomagnetic storm on 23 April 2023**

[P. Vemareddy](#)

ApJ **961** 199 **2024**

<https://arxiv.org/pdf/2312.08790.pdf>

<https://iopscience.iop.org/article/10.3847/1538-4357/ad1662/pdf>

Using multi-instrument and multi-wavelength observations, we studied a CME eruption that led to intense geomagnetic storm on **23 April 2023**. The eruption occurred on **April 21** in solar active region 13283 near the disk-center. The AR was in its decay stage, with fragmented polarities and a pre-existing long filament channel, a few days before the eruption. The study of magnetic field evolution suggests that the flux-rope (filament) has been built up by monotonous helicity accumulation over several days, and further converging and canceling fluxes lead to helicity injection change, resulting in the unstable nature of the magnetic flux-rope (MFR) and its further eruption. Importantly, the CME morphology revealed that the MFR apex underwent a rotation of upto  $56^\circ$  in clockwise-direction owing to its positive helicity. The CME decelerates in the LASCO-FOV and has a plane-of-sky velocity of 1226 km/s at  $20 R_\odot$ . In the Heliospheric Imager FOV, the CME lateral expansion is tracked more than the earthward motion. This implies that the arrival time estimation is difficult to assess. The in-situ arrival of ICME shock was at 07:30 UT on April 23, and a geomagnetic storm commenced at 08:30 UT. The flux rope fitting to the in-situ magnetic field observations reveals that the MC flux rope orientation is consistent with its near Sun orientation, which has a strong negative  $B_z$ -component. The analysis of this study indicates that the near-Sun rotation of the filament during its eruption to the CME is the key to the negative  $B_z$ -component and consequently the intense geomagnetic storm.

## Nature of helicity injection in non-erupting solar active regions

[P Vemareddy](#)

*MNRAS*, Volume 516, Issue 1, **2022**, Pages 158–166,

<https://doi.org/10.1093/mnras/stac2253>

Using time-sequence vector magnetic field and coronal observations from Solar Dynamics Observatory, we report the observations of the magnetic field evolution and coronal activity in four emerging active regions (ARs). The ARs emerge with leading polarity being the same as for the majority of ARs in a hemisphere of solar cycle 24. After emergence, the magnetic polarities separate each other without building a sheared polarity inversion line. In all four ARs, the magnetic fields are driven by foot point motions such that the sign of the helicity injection ( $dH/dt$ ) in the first half of the evolution is changed to the opposite sign in the later part of the observation time. This successive injection of opposite helicity is also consistent with the sign of mean force-free twist parameter ( $\alpha_{av}$ ). Further, the EUV light curves off the ARs in 94 Å and GOES X-ray flux reveal flaring activity below C-class magnitude. Importantly, the white-light coronagraph images in conjunction with the AR images in Atmospheric Imaging Assembly (AIA) 94 Å delineate the absence of associated Coronal Mass ejections (CMEs) with the studied ARs. These observations imply that the ARs with successive injection of opposite sign magnetic helicity are not favourable to twisted flux rope formation with excess coronal helicity, and therefore are unable to launch CMEs, according to recent reports. This study provides the characteristics of helicity flux evolution in the ARs referring to the conservative property of magnetic helicity and more such studies would help to quantify the eruptive capability of a given AR.

## Eruption of EUV Hot-Channel near Solar Limb and Associated Moving Type-IV Radio Burst

[P. Vemareddy](#), [P. Démoulin](#), [K. Sasikumar Raja](#), [J. Zhang](#), [N. Gopalswamy](#), [N. Vasantharaju](#)

ApJ **927** 108 **2022**

<https://arxiv.org/pdf/2201.06899.pdf>

<https://iopscience.iop.org/article/10.3847/1538-4357/ac4dfe/pdf>

Using the observations from Solar Dynamics Observatory, we study an eruption of a hot-channel flux rope (FR) near the solar-limb on **February 9, 2015**. The pre-eruptive structure is visible mainly in EUV 131 Å images with two highly-sheared loop structures. They undergo slow rise motion and then reconnect to form an eruptive hot-channel as in the tether-cutting reconnection model. The J-shaped flare-ribbons trace the footpoint of the FR which is identified as the hot-channel. Initially, the hot channel is observed to rise slowly at 40 km s<sup>-1</sup>, followed by an exponential rise from 22:55 UT at a coronal height of  $87 \pm 2$  Mm. Following the onset of the eruption at 23:00 UT, the flare-reconnection adds to the acceleration process of the CME within 3  $R_\odot$ . Later on, the CME continues to accelerate at 8 m s<sup>-2</sup> during its propagation period. Further, the eruption launched type-II followed by III, IVm radio bursts. The start and end times of type-IVm correspond to the CME core height of 1.5 and 6.1  $R_\odot$ , respectively. Also the spectral index is negative suggesting the non-thermal electrons trapped in the closed loop structure. Accompanied with type-IVm, this event is unique in the sense that the flare ribbons are very clearly observed along with the erupting hot channel, which strongly supports that the hooked-part of J-shaped flare ribbons outlines the boundary of the erupting FR.

## Successive Injection of Opposite Magnetic Helicity: Evidence for Active Regions without Coronal Mass Ejections

[P. Vemareddy](#)

*MNRAS* Volume 507, Issue 4, Pages 6037–6044, **2021**

<https://arxiv.org/pdf/2108.07741.pdf>

<https://doi.org/10.1093/mnras/stab2401>

[https://ui.adsabs.harvard.edu/link\\_gateway/2021MNRAS.507.6037V/PUB\\_PDF](https://ui.adsabs.harvard.edu/link_gateway/2021MNRAS.507.6037V/PUB_PDF)

Magnetic helicity (MH) is a measure of twist and shear of magnetic field. MH is injected in the active region (AR) corona through photospheric footpoint motions causing twisted and sheared magnetic fields. From the conservation property of the helicity, it was conjectured that an already twisted flux rope (FR) with continuous injection of MH inevitably erupts to remove the excess accumulated coronal helicity. Therefore, understanding the nature and evolution of the photospheric helicity flux transfer is crucial to reveal the intensity of the flare/CME activity. Using the time-sequence vector-magnetograms of {Helioseismic Magnetic Imager}, we study the evolution of MH injection in

emerging AR 12257. The photospheric flux motions in this AR inject positive helicity in the first 2.5 days followed by negative helicity later. This successive injection of opposite helicity is consistent with the sign of mean force-free twist parameter ( $\alpha_{av}$ ), orientation of magnetic-tongues. Also, the extrapolated AR magnetic structure exhibits transformation of global-shear without a twisted FR in the core of the AR. No CMEs are launched from this AR but C-class flaring activity is observed predominantly in the second half of the evolution period. The ARs with sign reversal of the MH injection are not favorable to twisted FR formation with excess coronal helicity and therefore are important to identify CME-less ARs readily. A possible scenario in these ARs is that when one sign of helicity flux is replaced by opposite sign, the magnetic field of different connectivity with opposite shear undergoes reconnection at different scales giving rise to both intermittent flares and enhanced coronal heating. **2015 01 07-10**

## **Relation of Non-neutralized electric currents and the activity in active regions**

P. [Vemareddy](#)

RHESSI Science Nuggets #386 Oct 2020

[https://sprg.ssl.berkeley.edu/~tohban/wiki/index.php/Relation\\_of\\_Non-](https://sprg.ssl.berkeley.edu/~tohban/wiki/index.php/Relation_of_Non-neutralized_electric_currents_and_the_activity_in_active_regions)

[neutralized electric currents and the activity in active regions](https://sprg.ssl.berkeley.edu/~tohban/wiki/index.php/Relation_of_Non-neutralized_electric_currents_and_the_activity_in_active_regions) March 7, 2012

## **Degree of electric current neutralization and the activity in solar Active Regions**

P. [Vemareddy](#)

MNRAS 2019

<https://arxiv.org/pdf/1904.02648.pdf>

Using time-sequence vector magnetic field observation from \textit{Helioseismic and Magnetic Imager}, we examined the connection of non-neutralized currents and the observed activity in 20 solar active-regions (ARs). The net current in a given magnetic polarity is algebraic sum of direct-current (DC) and return-current (RC) and the ratio  $|DC/RC|$  is a measure of degree of net-current-neutralization (NCN). In the emerging ARs, the non-neutrality of these currents builds with the onset of flux emergence, following the relaxation to neutrality during the separation motion of bipolar regions. Accordingly, some emerging ARs are source regions of CMEs occurring at the time of higher level non-neutrality. ARs in the post-emergence phase can be CME productive provided they have interacting bipolar regions with converging and shearing motions. In these cases, the net current evolves with higher level ( $>1.3$ ) of non-neutrality. Differently, the  $|DC/RC|$  in flaring and quiet ARs vary near unity. In all the AR samples, the  $|DC/RC|$  is higher for chiral current density than that for vertical current density. Owing to the fact that the non-neutralized currents arise in the vicinity of sheared polarity-inversion-lines (SPILs), the profiles of the total length of SPIL segments and the degree of NCN follow each other with a positive correlation. We find that the SPIL is localized as small segments in flaring-ARs whereas it is long continuous in CME-producing ARs. These observations demonstrate the dividing line between the CMEs and flares with the difference being in global or local nature of magnetic shear in the AR that reflected in non-neutralized currents. **2010-05-23, 2012-09-02, 2013-04-21**

## **Very fast helicity injection leading to critically stable state and large eruptive activity in solar active region NOAA 12673**

P. [Vemareddy](#)

ApJ 872 182 2019

<https://arxiv.org/abs/1901.09358>

<https://iopscience.iop.org/article/10.3847/1538-4357/ab0200/pdf>

<https://doi.org/10.3847/1538-4357/ab0200>

Using the photospheric magnetic and coronal observations of Solar Dynamics Observatory, we studied the build-up and eruption of coronal non-potential magnetic structure in emerging active region (AR) 12673. The velocity field derived from tracked vector-magnetograms indicates persistent shear and converging motions of flux regions about the polarity inversion line (PIL). A major helicity injection occurs during rapid flux emergence consistent with the very fast flux emergence phase. While this helicity flux builds-up the sigmoid by September 4, the helicity injection by the continued shear and converging motions in the later evolution contributes to sigmoid sustenance and its core field twist as a manifestation of the flux rope which erupts after exceeding critical value of twist. Moreover, the total length of sheared PIL segments correlates with the non-neutralized current and maintains a higher value in both the polarity regions as a signature of eruptive capability of the AR according to the flux rope models. The modelled magnetic field qualitatively reproduces the sigmoidal structure capturing major features like twisted core flux as flux rope, and hook-shaped parts connecting at the middle of the PIL. Study of quasi-separatrix-layers reveals that the sheared arcade, enclosing the flux rope, is stressed to a critically stable state and its coronal height becomes doubled from September 4-6. While demonstrating the fast injection of helicity per unit flux as the crucial factor for severe space-weather events, this study explains the formation of the flux rope and recurrent eruptive nature of the AR by the critically stable state of sheared arcade early on September 6. **4-6 Sept 2017**

HMI Science Nuggets #123 Apr 2019 <http://hmi.stanford.edu/hminuggets/?p=2868>

## **Study of Three-Dimensional Magnetic Structure and the Successive Eruptive Nature of Active Region 12371**

P. [Vemareddy](#), [P. Demóulin](#)

ApJ 857 90 2018

<https://arxiv.org/pdf/1803.04728.pdf>

<https://iopscience.iop.org/article/10.3847/1538-4357/aab6b7/pdf>

We study the magnetic structure of successively erupting sigmoid in active region 12371 by modeling the quasi-static coronal field evolution with non-linear force-free field (NLFFF) equilibria. HMI/SDO vector magnetograms are used as input to the NLFFF model. In all eruption events, the modeled structure resembles the observed pre-eruptive coronal sigmoid and the NLFFF core-field is a combination of double inverse J-shaped and inverse-S field-lines with dips touching the photosphere. Such field-lines are formed by flux-cancellation reconnection of opposite-J field-lines at bald-patch locations. It implies the formation of a weakly twisted flux-rope from large scale sheared arcade field lines. Later on, this flux-rope undergo coronal tether-cutting reconnection until a CME is triggered. The modeled structure captured these major features of sigmoid-to-arcade-to-sigmoid transformation, that is being recurrent under continuous photospheric flux motions. Calculations of the field-line twist reveal a fractional increase followed by a decrease of the number of pixels having a range of twist. This traces the buildup process of a twisted core-field by slow photospheric motions and the relaxation after eruption, respectively. Our study infers that the large eruptivity of this AR is due to a steep decrease of the background coronal field meeting the torus instability criteria at low height ( $\approx 40$  Mm) in contrast to non-eruptive ARs. **18-25 June, 2015**

RHESSI Science Nuggets №318 March 2018

[http://sprg.ssl.berkeley.edu/~tohban/wiki/index.php/Homologous\\_CME/flares\\_from\\_AR\\_12371](http://sprg.ssl.berkeley.edu/~tohban/wiki/index.php/Homologous_CME/flares_from_AR_12371)

### **Prominence eruption initiated by helical kink-instability of an embedded flux rope**

P. Vemareddy, N. Gopalswamy, B. Ravindra

ApJ 850 38 2017

<https://arxiv.org/pdf/1709.10035.pdf>

<https://iopscience.iop.org/article/10.3847/1538-4357/aa9020/pdf>

We study the triggering mechanism of a limb-prominence eruption and the associated coronal mass ejection near AR 12342 using SDO and LASCO/SOHO observations. The prominence is seen with an embedded flux thread (FT) at one end and bifurcates from the middle to a different footpoint location. The morphological evolution of the FT is similar to an unstable flux rope (FR), which we regard as prominence embedded FR. The FR twist exceeds the critical value. In addition, the morphology of the prominence plasma in 304Å-images marks the helical nature of the magnetic skeleton with a total of 2.96 turns along arc length. The potential field extrapolation model indicates that the critical height of the background magnetic field gradient falls within the inner corona (105Mm) consistent with the extent of coronal plasma loops. These results suggest that the helical kink instability in the embedded FR caused the slow rise of the prominence to a height of the torus instability domain. Moreover, the differential emission measure analysis unveils heating of the prominence plasma to coronal temperatures during eruption, suggesting a reconnection-related heating underneath the upward rising embedded FR. The prominence starts with a slow rise motion of 10km/s, followed by fast and slow acceleration phases having an average acceleration of 28.9m/s<sup>2</sup>, 2.4m/s<sup>2</sup> in C2, C3 field of view respectively. As predicted by previous numerical simulations, the observed synchronous kinematic profiles of the CME leading edge and the core supports the involved FR instability in the prominence initiation. **May 9, 2015**

### **Successive Homologous Coronal Mass Ejections Driven by Shearing and Converging Motions in Solar Active Region NOAA 12371**

P. Vemareddy

2017 ApJ 845 59

<https://arxiv.org/pdf/1709.09870.pdf>

<http://sci-hub.cc/10.3847/1538-4357/aa7ff4>

We study the magnetic field evolution in AR 12371, related to its successive eruptive nature. During the disk transit of seven days, the active region (AR) launched four sequential fast coronal mass ejections (CMEs), which are associated with long duration M-class flares. Morphological study delineates a pre-eruptive coronal sigmoid structure above the polarity inversion line (PIL) similar to Moore et al.'s study. The velocity field derived from tracked magnetograms indicates persistent shear and converging motions of polarity regions about the PIL. While these shear motions continue, the crossed arms of two sigmoid elbows are being brought to interaction by converging motions at the middle of the PIL, initiating the tether-cutting reconnection of field lines and the onset of the CME explosion. The successive CMEs are explained by a cyclic process of magnetic energy storage and release referred to as "sigmoid-to-arcade-to-sigmoid" transformation driven by photospheric flux motions. Furthermore, the continued shear motions inject helicity flux with a dominant negative sign, which contributes to core field twist and its energy by building a twisted flux rope (FR). After a limiting value, the excess coronal helicity is expelled by bodily ejection of the FR, which is initiated by some instability as realized by intermittent CMEs. This AR is in contrast with the confined AR 12192 with a predominant negative sign and larger helicity flux, but much weaker ( $-0.02$  turns) normalized coronal helicity content. While predominant signed helicity flux is a requirement for CME eruption, our study suggests that the magnetic flux normalized helicity flux is a necessary condition accommodating the role of background flux and appeals to a further study of a large sample of ARs. **2014 October 17–30, 2015 Jun 18-25, 2015 Jul 01**

### **Successive Injection of Opposite Magnetic Helicity in Solar Active Region NOAA 11928**

P. **Vemareddy**, P. Démoulin

A&A **2016**

<https://arxiv.org/pdf/1611.00699v1.pdf>

Understanding the nature and evolution of the photospheric helicity flux transfer is a key to reveal the role of magnetic helicity in coronal dynamics of solar active regions. Using SDO/HMI photospheric vector magnetograms and the derived flow velocity field, we computed boundary driven helicity flux with a 12 minute cadence during the emergence of AR 11928. Accounting the foot point connectivity defined by non-linear force-free magnetic extrapolations, we derived and analyzed the corrected distribution of helicity flux maps. The photospheric helicity flux injection is found to changes sign during the steady emergence of the AR. This reversal is confirmed with the evolution of the photospheric electric currents and with the coronal connectivity as observed in EUV wavelengths with SDO/AIA. During about the three first days of emergence, the AR coronal helicity is positive while later on the field configuration is close to a potential field. As theoretically expected, the magnetic helicity cancelation is associated to enhanced coronal activity. The study suggests a boundary driven transformation of the chirality in the global AR magnetic structure. This may be the result of the emergence of a flux rope with positive twist around its apex while it has negative twist in its legs. The origin of such mixed helicity flux rope in the convective zone is challenging for models.

**2013.12.17-20**

### **Sunspot Rotation as a Driver of Major Solar Eruptions in NOAA Active Region 12158**

P. **Vemareddy**, X. Cheng, B. Ravindra

ApJ **829** 24 **2016**

<http://arxiv.org/pdf/1607.03806v1.pdf>

We studied the developing conditions of sigmoid structure under the influence of magnetic non-potential characteristics of a rotating sunspot in the active region (AR) 12158. Vector magnetic field measurements from Helioseismic Magnetic Imager and coronal EUV observations from Atmospheric Imaging Assembly reveal that the erupting inverse-S sigmoid had roots in the location of the rotating sunspot. Sunspot rotates at a rate of 0-5deg/h with increasing trend in the first half followed by a decrease. Time evolution of many non-potential parameters had a well correspondence with the sunspot rotation. The evolution of the AR magnetic structure is approximated by a time series of force free equilibria. The NLFFF magnetic structure around the sunspot manifests the observed sigmoid structure. Field lines from the sunspot periphery constitute the body of the sigmoid and those from interior overly the sigmoid similar to a fluxrope structure. While the sunspot is being rotating, two major CME eruptions occurred in the AR. During the first (second) event, the coronal current concentrations enhanced (degraded) consistent with the photospheric net vertical current, however the magnetic energy is released during both the cases. The analysis results suggest that the magnetic connections of the sigmoid are driven by slow motion of sunspot rotation, which transforms to a highly twisted flux rope structure in a dynamical scenario. An exceeding critical twist in the flux rope probably leads to the loss of equilibrium and thus triggering the onset of two eruptions. **September 8, 2014, September 10, 2014**

### **A FULL STUDY ON THE SUN-EARTH CONNECTION OF AN EARTH-DIRECTED CME MAGNETIC FLUX ROPE**

Panditi **Vemareddy**<sup>1</sup> and Wageesh Mishra<sup>2</sup>

**2015** ApJ 814 59

<https://iopscience.iop.org/article/10.1088/0004-637X/814/1/59/pdf>

<https://doi.org/10.1088/0004-637X/814/1/59>

We present an investigation of an eruption event of a coronal mass ejection (CME) magnetic flux rope (MFR) from the source active region (AR) NOAA 11719 on **2013 April 11** utilizing observations from the Solar Dynamic Observatory, the Solar Terrestrial Relations Observatory, the Solar and Heliospheric Observatory, and the WIND spacecraft. The source AR consists of a pre-existing sigmoidal structure stacked over a filament channel which is regarded as an MFR system. EUV observations of low corona suggest further development of this MFR system by added axial flux through tether-cutting reconnection of loops at the middle of the sigmoid under the influence of continuous slow flux motions for two days. Our study implies that the MFR system in the AR is initiated to upward motion by kink instability and further driven by torus instability. The CME morphology, captured in simultaneous three-point coronagraph observations, is fitted with a Graduated Cylindrical Shell (GCS) model and discerns an MFR topology with its orientation aligning with a magnetic neutral line in the source AR. This MFR expands self-similarly and is found to have source AR twist signatures in the associated near-Earth magnetic cloud (MC). We further derived the kinematics of this CME propagation by employing a plethora of stereoscopic as well as single-spacecraft reconstruction techniques. While stereoscopic methods perform relatively poorly compared to other methods, fitting methods worked best in estimating the arrival time of the CME compared to in situ measurements. Supplied with the values of constrained solar wind velocity, drag parameter, and three-dimensional kinematics from the GCS fit, we construct CME kinematics from the drag-based model consistent with in situ MC arrival.

### **Flux emergence in the solar active region NOAA 11158: the evolution of net current**

Panditi **Vemareddy**, Parameswaran Venkatakrishnan, Solipuram Karthikreddy

Research in Astronomy and Astrophysics (RAA) Vol 15, No 9 1547-1558 (**2015**)

<http://arxiv.org/pdf/1502.05458v1.pdf>



We present a detailed investigation of the evolution of observed net vertical current using a time series of vector magnetograms of the active region (AR) NOAA 11158 obtained from the Helioseismic and Magnetic Imager. We also discuss the relation of net current to the observed eruptive events. The AR evolved from the  $\beta\gamma$  to  $\beta\gamma\delta$  configuration over a period of six days. The AR had two sub-regions of activity with opposite chirality: one dominated by sunspot rotation producing a strong CME, and the other showing large shear motions producing a strong flare. The net current in each polarity over the CME producing sub-region increased to a maximum and then decreased when the sunspots were separated. The time profile of net current in this sub-region followed the time profile of the rotation rate of the south-polarity sunspot in the same sub-region. The net current in the flaring sub-region showed a sudden increase at the time of the strong flare and remained unchanged until the end of the observation, while the sunspots maintained their close proximity. The systematic evolution of the observed net current is seen to follow the time evolution of total length of strongly sheared polarity inversion lines in both of the sub-regions. The observed photospheric net current could be explained as an inevitable product of the emergence of a twisted flux rope, from a higher pressure confinement below the photosphere into the lower pressure environment of the photosphere. **February 13-16, 2011**

## **Initiation and Eruption Process of Magnetic Flux Rope from Solar Active Region NOAA 11719 to Earth Directed-CME**

P. **Vemareddy**, J. Zhang

ApJ, **797** 80 **2014**

<http://arxiv.org/pdf/1410.2158v1.pdf>

An eruption event launched from solar active region (AR) NOAA 11719 is investigated based on coronal EUV observations and photospheric magnetic field measurements obtained from Solar Dynamic Observatory. The AR consists of a filament channel originating from major sunspot and its south section is associated with inverse-S sigmoidal system as observed in AIA passbands. We regard the sigmoid as the main body of the flux rope (FR). There also exists a twisted flux bundle crossing over this FR. This overlying flux bundle transforms in shape similar to kink-rise evolution which has correspondence with rise motion of the FR. The emission measure and temperature along the FR exhibits increasing trend with its rising motion, indicating reconnection in the thinning current sheet underneath the FR. Net magnetic flux of the AR evaluated at north and south polarities showed decreasing behavior whereas the net current in these fluxes exhibits increasing trend. As the negative (positive) flux is having dominant positive (negative) current, the chirality of AR flux system is likely negative (left handed) to be consistent with the chirality of inverse-S sigmoidal FR. This analysis of magnetic fields of source AR suggest that the cancelling fluxes are prime factors to the monotonous twisting of the FR system reaching to a critical state to trigger kink instability and the rise motion. This rise motion possibly led to onset of torus instability resulting in Earth-directed CME and the progressive reconnection in thinning current sheet underneath the rising FR leads to M6.5 flare. **April 11, 2013**

## **ON THE INJECTION OF HELICITY BY THE SHEARING MOTION OF FLUXES IN RELATION TO FLARES AND CORONAL MASS EJECTIONS**

P. **Vemareddy**<sup>1</sup>, A. Ambastha<sup>1</sup>, R. A. Maurya<sup>2</sup>, and J. Chae

**2012** ApJ **761** 86

An investigation of helicity injection by photospheric shear motions is carried out for two active regions (ARs), NOAA 11158 and 11166, using line-of-sight magnetic field observations obtained from the Helioseismic and Magnetic Imager on board the Solar Dynamics Observatory. We derived the horizontal velocities in the ARs from the differential affine velocity estimator (DAVE) technique. Persistent strong shear motions at maximum velocities in the range of 0.6-0.9 km s<sup>-1</sup> along the magnetic polarity inversion line and outward flows from the peripheral regions of the sunspots were observed in the two ARs. The helicities injected in NOAA 11158 and 11166 during their six-day evolution period were estimated as  $14.16 \times 10^{42}$  Mx<sup>2</sup> and  $9.5 \times 10^{42}$  Mx<sup>2</sup>, respectively. The estimated injection rates decreased up to 13% by increasing the time interval between the magnetograms from 12 minutes to 36 minutes, and increased up to 9% by decreasing the DAVE window size from  $21 \times 18$  to  $9 \times 6$  pixel<sup>2</sup>, resulting in 10% variation in the accumulated helicity. In both ARs, the flare-prone regions (R2) had inhomogeneous helicity flux distribution with mixed helicities of both signs and coronal mass ejection (CME) prone regions had almost homogeneous distribution of helicity flux dominated by a single sign. The temporal profiles of helicity injection showed impulsive variations during some flares/CMEs due to negative helicity injection into the dominant region of positive helicity flux. A quantitative analysis reveals a marginally significant association of helicity flux with CMEs but not flares in AR 11158, while for the AR 11166, we find a marginally significant association of helicity flux with flares but not CMEs, providing evidence of the role of helicity injection at localized sites of the events. These short-term variations of helicity flux are further discussed in view of possible flare-related effects. This study suggests that flux motions and spatial distribution of helicity injection are important to understanding the complex nature of the magnetic flux system of the AR, and how it can lead to conditions favorable for eruptive events.

## **Filament Eruption in NOAA 11093 Leading to a Two-Ribbon M1.0 Class Flare and CME**

P. [Vemareddy](#), R. A. Maurya and A. Ambastha

Solar Physics, Volume 277, Number 2, 337-354, **2012**, **File**

We present a multi-wavelength analysis of an eruption event that occurred in active region NOAA 11093 on **7 August 2010**, using data obtained from SDO, STEREO, RHESSI, and the GONG H $\alpha$  network telescope. From these observations, we inferred that an upward slow rising motion of an inverse S-shaped filament lying along the polarity inversion line resulted in a CME subsequent to a two-ribbon flare. Interaction of overlying field lines across the filament with the side-lobe field lines, associated EUV brightening, and flux emergence/cancellation around the filament were the observational signatures of the processes leading to its destabilization and the onset of eruption. Moreover, the time profile of the rising motion of the filament/flux rope corresponded well with flare characteristics, viz., the reconnection rate and hard X-ray emission profiles. The flux rope was accelerated to the maximum velocity as a CME at the peak phase of the flare, followed by deceleration to an average velocity of 590 km s<sup>-1</sup>. We suggest that the observed emergence/cancellation of magnetic fluxes near the filament caused it to rise, resulting in the tethers to cut and reconnection to take place beneath the filament; in agreement with the tether-cutting model. The corresponding increase/decrease in positive/negative photospheric fluxes found in the post-peak phase of the eruption provides unambiguous evidence of reconnection as a consequence of tether cutting.

## **Quantifying errors in 3D CME parameters derived from synthetic data using white-light reconstruction techniques**

[Christine Verbeke](#), [M. Leila Mays](#), [Christina Kay](#), [Pete Riley](#), [Erika Palmerio](#), [Mateja Dumbović](#), [Marilena Mierla](#), [Camilla Scolini](#), [Manuela Temmer](#), [Evangelos Paouris](#), [Laura A. Balmaceda](#), [Hebe Cremades](#), [Jürgen Hinterreiter](#)

Adv. in Space Res. **2023**

doi: [10.1016/j.asr.2022.08.056](https://doi.org/10.1016/j.asr.2022.08.056)

<https://arxiv.org/pdf/2302.00531.pdf>

<https://pdf.sciencedirectassets.com/271642/AIP/1-s2.0-S027311772200792X/main.pdf>

(Shortened version) Current efforts in space weather forecasting of CMEs have been focused on predicting their arrival time and magnetic structure. To make predictions, methods have been developed to derive the true CME speed, size and position, among others. Difficulties in determining input parameters for CME forecasting arise from the lack of direct measurements of the coronal magnetic fields and uncertainties in estimating the CME 3D geometric and kinematic parameters. White-light coronagraph images are usually employed by a variety of CME reconstruction techniques. We explore how subjectivity affects the 3D CME parameters that are obtained from the GCS reconstruction technique. We have designed two different synthetic scenarios where the "true" geometric parameters are known in order to quantify such uncertainties for the first time. We explore this as follows: 1) Using the ray-tracing option from the GCS model software, and 2) Using 3D MHD simulation data from the MAS code. Our experiment includes different viewing configurations using single and multiple viewpoints. CME reconstructions using a single viewpoint had the largest errors and error ranges for both synthetic GCS and simulated MHD white-light data. Increasing the number of viewpoints to two, the errors decreased by about 4° in latitude, 22° in longitude, 14° in tilt, and 10° in half-angle, pointing towards a need for at least two viewpoints. We found the following CME parameter error bars as a starting point for quantifying the minimum error in CME parameters from white-light reconstructions:  $\Delta\theta$  (latitude)=6°,  $\Delta\phi$  (longitude)=11°,  $\Delta\gamma$  (tilt)=25°,  $\Delta\alpha$  (half-angle)=10°,  $\Delta h$  (height)=0.6R $\odot$ , and  $\Delta\kappa$  (ratio)=0.1.

## **Over-expansion of coronal mass ejections modelled using 3D MHD EUHFORIA simulations**

[C. Verbeke](#), [B. Schmieder](#), [P. Démoulin](#), [S. Dasso](#), [B. Grison](#), [E. Samara](#), [C. Scolini](#), [S. Poedts](#)

Advances in Space Research **2022**

<https://arxiv.org/pdf/2207.03168.pdf>

Coronal mass ejections (CMEs) are large scale eruptions observed close to the Sun. They are travelling through the heliosphere and possibly interacting with the Earth environment creating interruptions or even damaging new technology instruments. Most of the time their physical conditions (velocity, density, pressure) are only measured in situ at one point in space, with no possibility to have information on the variation of these parameters during their journey from Sun to Earth. Our aim is to understand the evolution of internal physical parameters of a set of three particular fast halo CMEs. These CMEs were launched between 15 and 18 July 2002. Surprisingly, the related interplanetary CMEs (ICMEs), observed near Earth, have a low, and in one case even very low, plasma density. We use the European Heliosphere FORecasting Information Asset (EUHFORIA) model to simulate the propagation of the CMEs in the background solar wind by placing virtual spacecraft along the Sun--Earth line. We set up the initial conditions at 0.1 au, first with a cone model and then with a linear force free spheromak model. A relatively good agreement between simulation results and observations concerning the speed, density and arrival times of the ICMEs is obtained by adapting the initial CME parameters. In particular, this is achieved by increasing the initial magnetic pressure so that a fast expansion is induced in the inner heliosphere. This implied the develop First, we show that a magnetic configuration with an out of force balance close to the Sun mitigates the EUHFORIA assumptions related to an initial uniform velocity. Second, the over-expansion of the ejected magnetic

configuration in the inner heliosphere is one plausible origin for the low density observed in some ICMEs at 1 au. The in situ observed very low density has a possible coronal origin of fast expansion for two of the three ICMEs. **15 and 18 July 2002**

### **High-resolution spectroscopy of a surge in an emerging flux region**

M. [Verma](#), C. [Denker](#), A. [Diercke](#), C. [Kuckein](#), H. [Balthasar](#), E. [Dineva](#), I. [Kontogiannis](#), P. S. [Pal](#), M. [Sobotka](#)

A&A 639, A19 2020

<https://arxiv.org/pdf/2005.03966.pdf>

<https://www.aanda.org/articles/aa/pdf/2020/07/aa36762-19.pdf>

High-spectral resolution observations using the VTT echelle spectrograph in the chromospheric H $\alpha$  line were obtained in the early growth phase of active region NOAA 12722. Noise-stripped H $\alpha$  line profiles yield maps of line-core and bisector velocities, which were contrasted with velocities inferred from Cloud Model inversions. The SDO provided additional continuum images, line-of-sight (LOS) magnetograms, and UV/EUV images, which link the different solar atmospheric layers. The active region started as a bipolar region with continuous flux emergence when a new flux system emerged in the leading part during the VTT observations, resulting in two homologous surges. While flux cancellation at the base of the surges provided the energy for ejecting the cool plasma, strong proper motions of the leading pores changed the magnetic field topology making the region susceptible for surging. Despite the surge activity in the leading part, an arch filament system in the trailing part of the old flux remained stable. Thus, stable and violently expelled mass-loaded ascending magnetic structures can co-exist in close proximity. Investigating the height dependence of LOS velocities revealed the existence of neighboring strong up- and downflows. However, downflows occur with a time lag. The opacity of the ejected cool plasma decreases with distance from the base of the surge while the speed of the ejecta increases. The location at which the surge becomes invisible in H $\alpha$  corresponds to the interface where the surge brightens in He II 304. Broad-shoulders and dual-lobed H $\alpha$  profiles suggest accelerated/decelerated and highly structured LOS plasma flows. Significantly broadened H $\alpha$  profiles imply significant heating at the base of the surges, which is also supported by bright kernels in UV/EUV images uncovered by swaying motions of dark fibrils at the base of the surges. **~13 Sep 2018**

## **ON THE ORIGIN OF SOLAR HALO CORONAL MASS EJECTIONS**

**VERMA V.K.1, MITTAL NISHANT**

ПАЖ Том: 45 Номер: [3](#) Год: **2019** Страницы: 210

We present an investigation of halo coronal mass ejections (HCMEs) to understand the origin of HCMEs which is very important because HCMEs are regarded as main causes of heliospheric and geomagnetic disturbances. In this study, we have investigated 313 HCMEs observed during 1996–2012 by LASCO, coronal holes (CHs) and solar flares phenomena. On investigation of 313 HCMEs and related solar flares and coronal holes data, we find that all 313 HCMEs were observed when there were CHs and solar flares within  $10^{\circ}$  to  $60^{\circ}$ . We also find that the 128 (40.8%) and 88 (23.6%) HCMEs events were observed when there were CHs and solar flares within  $10^{\circ}$  and  $20^{\circ}$ , respectively. The speed of HCMEs does not increase with the increase of the area of CHs while the solar winds speed increases with increase of CHs area. We are of the view that the HCMEs may have been produced by some mechanism, in which the mass ejected by solar flares or active prominences, gets connected with the open magnetic lines of CHs (source of high speed solar wind streams) and moves along them to appear as a HCMEs, earlier suggested by Verma and Pande (1989) and Verma (1998, 2002). The various results obtained in the present analysis are discussed in the light of existing scenario of heliospheric physics.

### **Indications of stellar coronal mass ejections through coronal dimmings**

Astrid M. [Veronig](#), Petra Odert, Martin Leitzinger, Karin Dissauer, Nikolaus C. Fleck, Hugh S. Hudson  
Nature Astronomy Volume 5, p. 697-706 **2021**

<https://www.nature.com/articles/s41550-021-01345-9.epdf>

<https://doi.org/10.1038/s41550-021-01345-9>

<https://arxiv.org/ftp/arxiv/papers/2110/2110.12029.pdf>

Coronal mass ejections (CMEs) are huge expulsions of magnetized matter from the Sun and stars, traversing space with speeds of millions of kilometres per hour. Solar CMEs can cause severe space weather disturbances and consumer power outages on Earth, whereas stellar CMEs may even pose a hazard to the habitability of exoplanets. Although CMEs ejected by our Sun can be directly imaged by white-light coronagraphs, for stars this is not possible. So far, only a few candidates for stellar CME detections have been reported. Here we demonstrate a different approach that is based on sudden dimmings in the extreme ultraviolet and X-ray emission caused by the CME mass loss. We report dimming detections associated with flares on cool stars, indicative of stellar CMEs, and which are benchmarked by Sun-as-a-star extreme ultraviolet measurements. This study paves the way for comprehensive detections and characterizations of CMEs on stars, which are important factors in planetary habitability and stellar evolution. **9 Aug 2011, 2012 March 7, 10 Mar 2012, 28 Oct 2013, 1-3 Nov 2013, 5 Nov 2013, 19 Nov 2013**

**Supplementary Table 1:** Solar dimming parameters and related flares (2011-2015).

## Genesis and impulsive evolution of the 2017 September 10 coronal mass ejection

Astrid M. [Veronig](#), [Tatiana Podladchikova](#), [Karin Dissauer](#), [Manuela Temmer](#), [Daniel B. Seaton](#), [David Long](#), [Jingnan Guo](#), [Bojan Vrsnak](#), [Louise Harra](#), [Bernhard Kliem](#)

ApJ 868 107 2018

<https://arxiv.org/pdf/1810.09320.pdf>

<http://iopscience.iop.org/article/10.3847/1538-4357/aaeac5/pdf>

The X8.2 event of 10 September 2017 provides unique observations to study the genesis, magnetic morphology and impulsive dynamics of a very fast CME. Combining GOES-16/SUVI and SDO/AIA EUV imagery, we identify a hot ( $T \approx 10\text{--}15$  MK) bright rim around a quickly expanding cavity, embedded inside a much larger CME shell ( $T \approx 1\text{--}2$  MK). The CME shell develops from a dense set of large AR loops ( $\geq 0.5$  Rs), and seamlessly evolves into the CME front observed in LASCO C2. The strong lateral overexpansion of the CME shell acts as a piston initiating the fast EUV wave. The hot cavity rim is demonstrated to be a manifestation of the dominantly poloidal flux and frozen-in plasma added to the rising flux rope by magnetic reconnection in the current sheet beneath. The same structure is later observed as the core of the white light CME, challenging the traditional interpretation of the CME three-part morphology. The large amount of added magnetic flux suggested by these observations explains the extreme accelerations of the radial and lateral expansion of the CME shell and cavity, all reaching values of  $5\text{--}10$  km s $^{-2}$ . The acceleration peaks occur simultaneously with the first RHESSI 100–300 keV hard X-ray burst of the associated flare, further underlining the importance of the reconnection process for the impulsive CME evolution. Finally, the much higher radial propagation speed of the flux rope in relation to the CME shell causes a distinct deformation of the white light CME front and shock.

## SMESE: A Small Explorer for Solar Eruptions

J.-C. [Vial](#), F. Auchère<sup>a</sup>, J. Chang<sup>b</sup>, C. Fang<sup>c</sup>, W.Q. Gan<sup>b</sup>, K.-L. Klein<sup>d</sup>, J.-Y. Prado<sup>e</sup>, G. Trotter<sup>d</sup>, C. Wang<sup>f</sup> and Y.H. Yan<sup>g</sup>

[Advances in Space Research](#)

[Volume 40, Issue 12, 2007](#), Pages 1787-1801

The Small Explorer for Solar Eruptions (SMESE) mission is a microsatellite proposed by France and China. The payload of SMESE consists of three packages: LYOT (a Lyman  $\alpha$  imager and a Lyman  $\alpha$  coronagraph), DESIR (an Infra-Red Telescope working at 35–80 and 100–250  $\mu\text{m}$ ), and HEBS (a High-Energy Burst Spectrometer working in X- and  $\gamma$ -rays). a launch around 2012–2013

## Stellar flares, superflares and coronal mass ejections -- entering the Big data era **Review**

[Krisztián Vida](#), [Zsolt Kővári](#), [Martin Leitzinger](#), [Petra Odert](#), [Katalin Oláh](#), [Bálint Seli](#), [Levente Kriskovics](#), [Robert Greimel](#), [Anna Görgei](#)

Universe 2024

<https://arxiv.org/pdf/2407.16446>

Flares, sometimes accompanied by coronal mass ejections (CMEs), are the result of sudden changes in the magnetic field of stars with high energy release through magnetic reconnection, which can be observed across a wide range of the electromagnetic spectrum from radio waves to the optical range to X-rays. In our observational review, we attempt to collect some fundamental new results, which can largely be linked to the Big data era that has arrived due to the expansion of space photometric observations of the last two decades. We list the different types of stars showing flare activity, their observation strategies, and discuss how their main stellar properties relate to the characteristics of the flares (or even CMEs) they emit. Our goal is to focus, without claiming to be complete, on those results that may in one way or another challenge the "standard" flare model based on the solar paradigm. 2024 May 10

## Detecting coronal mass ejections with machine learning methods

[K. Vida](#), [B. Seli](#), [T. Szklenár](#), [L. Kriskovics](#), [A. Görgei](#), [Zs. Kővári](#)

Proceeding of IAU Symposium 365 2024

<https://arxiv.org/pdf/2401.07588.pdf>

Flares on the Sun are often associated with ejected plasma: these events are known as coronal mass ejections (CMEs). These events, although are studied in detail on the Sun, have only a few dozen known examples on other stars, mainly detected using the Doppler-shifted absorption/emission features in Balmer lines and tedious manual analysis. We present a possibility to find stellar CMEs with the help of high-resolution solar spectra.

## The quest for stellar coronal mass ejections in late-type stars: I. Investigating Balmer-line asymmetries of single stars in Virtual Observatory data

[Krisztián Vida](#), [Martin Leitzinger](#), [Levente Kriskovics](#), [Bálint Seli](#), [Petra Odert](#), [Orsolya Eszter Kovács](#), [Heidi Korhonen](#), [Lidia van Driel-Gesztelyi](#)

A&A 2019

<https://arxiv.org/pdf/1901.04229.pdf>

Flares and CMEs can have deleterious effects on their surroundings: they can erode atmospheres of orbiting planets over time and also have high importance in stellar evolution. Most of the CME detections in the literature are single events found serendipitously sparse for statistical investigation. We aimed to gather a large amount of spectral data of

M-dwarfs to drastically increase the number of known events to make statistical analysis possible in order to study the properties of potential stellar CMEs. Using archive data we investigated asymmetric features of Balmer-lines, that could indicate the Doppler-signature of ejected material. Of more than 5500 spectra we found 478 with line asymmetries--including nine larger events--on 25 objects, with 1.2-19.6 events/day on objects with line asymmetries. Most events are connected with enhanced Balmer-line peaks, suggesting these are connected to flares similar to solar events. Detected speeds mostly do not reach surface escape velocity: the typical observed maximum velocities are in the order of 100-300km/s, while the typical masses of the ejecta were in the order of 10<sup>15</sup>-10<sup>18</sup>g. Statistical analysis suggests that events are more frequent on cooler stars with stronger chromospheric activity. Detected maximum velocities are lower than those observed on the Sun, while event rates were somewhat lower than we could expect from the solar case. These findings may support the idea that most of the CMEs could be suppressed by strong magnetic field. Alternatively, it is possible that we can observe only an early low-coronal phase before CMEs are accelerated at higher altitudes. Our findings could indicate that later-type, active dwarfs could be a safer environment for exoplanetary systems CME-wise than previously thought, and atmosphere loss due to radiation effects would play a stronger role in exoplanetary atmosphere evolution than CMEs.

See also <http://articles.adsabs.harvard.edu/full/2017CEAB...41...67H>

## Unraveling the Origins of an Extreme Solar Eruptive Event with Hard X-Ray Imaging Spectroscopy

Juliana T. **Vievering**<sup>1</sup>, Angelos Vourlidis<sup>1</sup>, and Säm Krucker<sup>2,3</sup>

2024 ApJ 972 48

<https://iopscience.iop.org/article/10.3847/1538-4357/ad57b7/pdf>

Hard X-ray (HXR) observations are crucial for understanding the initiation and evolution of solar eruptive events, as they provide a key signature of flare-accelerated electrons and heated plasma. The potential of high-cadence HXR imaging for deciphering the erupting structure, however, has not received adequate attention in an era of extreme ultraviolet (EUV) imaging abundance. An extreme solar eruptive event on **2022 September 5** observed on the solar far side by both Parker Solar Probe and Solar Orbiter provides the opportunity to showcase the power of HXR imaging in the absence of high-cadence EUV imaging. We investigate the evolution of flare energy release through HXR timing, imaging, and spectral analyses using data from the Spectrometer/Telescope for Imaging X-rays (STIX) on board Solar Orbiter. STIX provides the highest cadence imaging of the energy release sites for this far-side event and offers crucial insight into the nature of energy release, timing of flare particle acceleration, and evolution of the acceleration efficiency. We find that this is a two-phase eruptive event, rather than two distinct eruptions, as has been previously suggested. The eruption begins with an initial peak in flare emission on one side of the active region (AR), marking the rise/destabilization of a loop system followed by notable episodes of energy release across the AR and an eruptive phase associated with a very fast coronal mass ejection, type III radio bursts, and solar energetic particles. We demonstrate that high-cadence HXR imaging spectroscopy is indispensable for understanding the formation of powerful, space-weather relevant eruptions.

## Evolution of Solar Eruptive Events: Investigating the Relationships among Magnetic Reconnection, Flare Energy Release, and Coronal Mass Ejections

Juliana T. **Vievering**<sup>1</sup>, Angelos Vourlidis<sup>1</sup>, Chunming Zhu<sup>2</sup>, Jiong Qiu<sup>2</sup>, and Lindsay Glesener<sup>3</sup>

2023 ApJ 946 81

<https://iopscience.iop.org/article/10.3847/1538-4357/acbe3d/pdf>

We study the evolution of solar eruptive events by investigating the temporal relationships among magnetic reconnection, flare energy release, and the acceleration of coronal mass ejections (CMEs). Leveraging the optimal viewing geometry of the Solar TERrestrial Relations Observatory (STEREO) relative to the Solar Dynamics Observatory (SDO) and the Reuven Ramaty High-Energy Solar Spectroscopic Imager (RHESSI) during 2010-2013, we identify 12 events with sufficient spatial and temporal coverage for a detailed examination. STEREO and SDO data are used to measure the CME kinematics and the reconnection rate, respectively, and hard X-ray (HXR) measurements from RHESSI provide a signature of the flare energy release. This analysis expands upon previous solar eruptive event timing studies by examining the fast-varying features, or "bursts," in the HXR and reconnection rate profiles, which represent episodes of energy release. Through a time lag correlation analysis, we find that HXR bursts occur throughout the main CME acceleration phase for most events, with the HXR bursts lagging the acceleration by  $2 \pm 9$  minutes for fast CMEs. Additionally, we identify a nearly one-to-one correspondence between bursts in the HXR and reconnection rate profiles, with HXRs lagging the reconnection rate by  $1.4 \pm 2.8$  minutes. The studied events fall into two categories: events with a single dominant HXR burst and events with a train of multiple HXR bursts. Events with multiple HXR bursts, indicative of intermittent reconnection and/or particle acceleration, are found to correspond with faster CMEs.

2010 August 1, 2011-06-21, 2011-11-09, 2012-08-31

Table 1 Event List 2010-2013

## Magnetic Properties of Source Regions of CMEs and DH Type II Radio Bursts

[P. Vijayalakshmi](#), [A. Shanmugaraju](#) & [S. Aswin Amirtha Raj](#)

Solar Phys. volume 298, Article number: 144 (2023)

<https://doi.org/10.1007/s11207-023-02234-2>

The Sun is a dynamic star that exhibits various phenomena, including solar flares, coronal mass ejections (CMEs), and Type II radio bursts. CMEs are large-scale eruptions of plasma and magnetic field from the Sun that can disrupt the interplanetary medium and the Earth's magnetic field. Type II radio bursts are radio emissions associated with shocks generated by the CMEs. Only a few CMEs are associated with Type II radio bursts and the reasons for the absence of these bursts are still under debate. The magnetic properties of source active regions (ARs) from where CMEs with and without decameter-hectometer (DH) Type II radio bursts originate are investigated. Relations between the speed of CMEs and the source region properties are also obtained for these two groups of events (with and without radio bursts). The data from the Solar Dynamics Observatory (SDO) and the Radio and Plasma Wave (WAVES) Experiment on board the Wind spacecraft and the CMEs observed by the Solar and Heliospheric Observatory (SOHO) mission for the period of 2010–2014 in Solar Cycle 24 are utilized for this study. The statistical properties (like range, mean, median, and standard deviation) of source AR magnetic properties and the speed of the CMEs associated with DH Type II radio bursts (first group called radio loud) are found to be higher than those of CMEs without DH Type II radio bursts (second group called radio quiet). In addition, we found a positive correlation between the magnetic properties of the source AR and the speed of the CMEs with DH Type II radio bursts, but it is absent for events without DH Type II bursts. We also found that the probability of CME-streamer interaction is higher for the first group than for the second group, which shows a strong relation between the CME-streamer interaction and Type II bursts. These results reveal distinct magnetic characteristics in the source region for radio loud and radio quiet CMEs.

### **Analysis of Front Side Halo CMEs and Their Solar Source Active Region and Flare Ribbon Properties**

P. Vijayalakshmi, A. Shanmugaraju, M. Bendict Lawrance, Y.-J. Moon, Hyeonock Na & E. Ebenezer  
[Solar Physics](#) volume 298, Article number: 19 (2023)  
<https://doi.org/10.1007/s11207-023-02113-w>

Halo coronal mass ejections (CMEs) from the Sun are the subset of CMEs, which are more energetic than the normal CMEs. Only the more energetic CMEs are observable in white-light coronagraphs when they are traveling along the line of sight (LOS) and a CME is better observed when it is traveling perpendicularly to the LOS. We investigated the flare associated front side halo CMEs, their active regions (ARs) and flare ribbon properties observed during the period of 2010–2016 in Solar Cycle 24. The aim of this study is to investigate the statistical relationship between the kinematic properties of CMEs and their source active region and flare ribbon properties. The properties of the solar source region (sunspot classification according to Hale and McIntosh, sunspot area, and the number of spots) and flare ribbons (total unsigned magnetic flux, total unsigned reconnection flux, active region area, and ribbon area) are obtained for the selected events and analyzed to find the dependence of the halo CME properties (linear speed, kinetic energy, space speed, and mass) on the source region characteristics. From the preliminary analysis, 13% of halo CMEs are found to be associated with X-class flares, 52% with M-class flares, and 35% with C-class flares. It is found that many events (45/60) were produced by  $\beta\gamma\delta\beta\gamma\delta$  and  $\beta\gamma\beta\gamma$  Hale-type sunspot groups and Ekc/Dkc/Fkc McIntosh sunspot classes, which implies a degree of complexity of the involved sunspots. We found moderate correlations between the active region properties and CME properties, but strong correlation between the flare ribbons and CME properties. This result indicates that the kinematics of CMEs are determined by the role of magnetic reconnection and the flux related to it. We estimated the synthetic CME mass (using a synthetic CME generated based on a full ice-cream cone structure proposed recently by Na et al., *Astrophys. J.* 906, 46, [2021](#)). It is demonstrated that the estimated mass of halo CMEs is 1.44 times (without occulted area) and 2 times (with occulted area) that of the observed CME mass. Further, the relations between the halo CME synthetic mass with the active region and flare ribbon properties have been obtained.

### **An Application of the Stereoscopic Self-Similar-Expansion Model to the Determination of CME-Driven Shock Parameters**

L. Volpes, V. Bothmer  
*Solar Phys.* Volume 290, Issue 10, pp 3005-3022 2015  
<http://arxiv.org/pdf/1509.03181v1.pdf>

We present an application of the stereoscopic self-similar-expansion model (SSSEM) to Solar Terrestrial Relations Observatory (STEREO)/Sun-Earth Connection Coronal and Heliospheric Investigation (SECCHI) observations of the **03 April 2010** CME and its associated shock. The aim is to verify whether CME-driven shock parameters can be inferred from the analysis of j-maps. For this purpose we use the SSSEM to derive the CME and the shock kinematics. Arrival times and speeds, inferred assuming either propagation at constant speed or with uniform deceleration, show good agreement with Advanced Composition Explorer (ACE) measurements. The shock standoff distance [ $\Delta$ ], the density compression [ $\rho_{\text{dpu}}$ ] and the Mach number [ $M$ ] are calculated combining the results obtained for the CME and shock kinematics with models for the shock location. Their values are extrapolated to L1 and compared to in-situ data. The in-situ standoff distance is obtained from ACE solar-wind measurements, and the Mach number and compression ratio are provided by the Harvard-Smithsonian Center for Astrophysics interplanetary shock database. They are  $\rho_{\text{dpu}}=2.84$  and  $M=2.2$ . The best fit to observations is obtained when the SSSEM half width  $\lambda=40\text{deg}$  and the CME and shock propagate with uniform deceleration. In this case we find  $\Delta=23R_{\odot}$ ,  $\rho_{\text{dpu}}=2.61$ , and  $M=2.93$ . The study shows that CME-driven shock parameters can be estimated from the analysis of time-elongation plots and can be used to predict their in-situ values.

### **The Critical Coronal Transition Region: A Physics-framed Strategy to Uncover the Genesis of the Solar Wind and Solar Eruptions**

[Angelos Vourlidas](#), [Amir Caspi](#), [Yuan-Kuen Ko](#), [J. Martin Laming](#), [James P. Mason](#), [Mari Paz Miralles](#), [Nour-Eddine Raouafi](#), [John C. Raymond](#), [Daniel B. Seaton](#), [Leonard Strachan](#), [Nicholeen Viall](#), [Juliana Vievering](#), [Matthew J. West](#)

White paper submitted to the Decadal Survey for Solar and Space Physics (Heliophysics) 2024-2033 **2023**

<https://arxiv.org/ftp/arxiv/papers/2307/2307.13595.pdf>

Our current theoretical and observational understanding suggests that critical properties of the solar wind and Coronal Mass Ejections (CMEs) are imparted within 10 Rs, particularly below 4 Rs. This seemingly narrow spatial region encompasses the transition of coronal plasma processes through the entire range of physical regimes from fluid to kinetic, and from primarily closed to open magnetic field structures. From a physics perspective, therefore, it is more appropriate to refer to this region as the Critical Coronal Transition Region (CCTR) to emphasize its physical, rather than spatial, importance to key Heliophysics science.

This white paper argues that the comprehensive exploration of the CCTR will answer two of the most central Heliophysics questions, "How and where does the solar wind form?" and "How do eruptions form?", by unifying hardware/software/modeling development and seemingly disparate research communities and frameworks. We describe the outlines of decadal-scale plan to achieve that by 2050.

### **Exploring the critical coronal transition region: the key to uncovering the genesis of the solar wind and solar eruptions.** **Review**

[Vourlidas](#), A., [Viall](#), N., [Laming](#), M., [Cranmer](#), S., [Arge](#), C., [DeForest](#), C., et al.

Earth Space Sci. Open Arch. **2020-2021**

**Meeting Name:** Heliophysics 2050 Workshop **Meeting Date:** 03-05 May 2021

<https://www.essoar.org/pdfjs/10.1002/essoar.10504451.1>

<https://doi.org/10.1002/essoar.10504451.1>

All current understanding (theoretical and observational) suggests that the development of the solar wind and CMEs takes place within 10 Rs, particularly below 4 Rs. This seemingly narrow spatial region encompasses the transition of coronal plasma processes through the entire range of physical regimes from fluid to kinetic, and from primarily closed magnetic field structures to primarily open. For these reasons, we refer to it as the Critical Coronal Transition Region (CCTR). Its comprehensive exploration will answer two of the most central Heliophysics questions with repercussions across NASA and society. Here, we outline a path to answer these questions in the next 30 years.

### **The Coronal Mass Ejection Visibility Function of Modern Coronagraphs**

[Angelos Vourlidas](#), [L. A. Balmaceda](#), [H. Xie](#), [O. C. St. Cyr](#)

ApJ **900** 161 **2020**

<https://arxiv.org/ftp/arxiv/papers/2008/2008.03348.pdf>

<https://iopscience.iop.org/article/10.3847/1538-4357/abada5/pdf>

We analyze the detection capability of Coronal Mass Ejections (CMEs) for all currently operating coronagraphs in space. We define as CMEs events that propagate beyond 10 solar radii with morphologies broadly consistent with a magnetic flux rope presence. We take advantage of multi-viewpoint observations over five month-long intervals, corresponding to special orbital configurations of the coronagraphs aboard the STEREO and SOHO missions. This allows us to sort out CMEs from other outward-propagating features (e.g. waves or outflows), and thus to identify the total number of unique CMEs ejected during those periods. We determine the CME visibility functions of the STEREO COR2-A/B and LASCO C2/C3 coronagraphs directly as the ratio of observed to unique CMEs. The visibility functions range from 0.71 to 0.92 for a 95% confidence interval. By comparing detections between coronagraphs on the same spacecraft and from multiple spacecraft, we assess the influence of field of view, instrument performance, and projection effects on the CME detection ability without resorting to proxies, such as flares or radio bursts. We find that no major CMEs are missed by any of the coronagraphs, that a few slow halo-like events may be missed in synoptic cadence movies and, that narrow field of view coronagraphs have difficulties discriminating between CMEs and other ejections leading to false detection rates. We conclude that CME detection can only be validated with multi-viewpoint imaging-- two visibility functions to observed CME rates resulting in upward corrections of 40%. **2009-04-11, 2011-05-20**

### **Radio Observations of Coronal Mass Ejections: Space Weather Aspects** **Review**

[Angelos Vourlidas](#), [Eoin P Carley](#) and [Nicole Vilmer](#)

Front. Astron. Space Sci. **7**:43 **2020**

<https://www.frontiersin.org/articles/10.3389/fspas.2020.00043/full>

<https://sci-hub.st/10.3389/fspas.2020.00043> **File**

We review the current state-of-affairs in radio observations of Coronal Mass Ejections (CMEs) from a Space Weather perspective. In particular, we examine the role of radio observations in predicting or presaging an eruption, in capturing the formation stages of the CME, and in following the CME evolution in the corona and heliosphere. We then look to the future and identify capabilities and research areas where radio observations---particularly, spectropolarimetric imaging---offer unique advantages for Space Weather research on CMEs. We close with a discussion of open issues and possible strategies for enhancing the relevance and importance of radio astronomy for Space Weather science. **2003 June 17, 2003 November 1, 2010 January 15, Aug. 2, 2012**

## Streamer Blowout Coronal Mass Ejections: Their Properties and Relation to the Coronal Magnetic Field Structure

Angelos [Vourlidas](#), [David F. Webb](#)

ApJ **861** 103 **2018**

<https://arxiv.org/ftp/arxiv/papers/1806/1806.00644.pdf>

<http://sci-hub.tw/http://iopscience.iop.org/0004-637X/861/2/103/>

We present a comprehensive analysis of a particular class of coronal mass ejection (CME) event, called streamer-blowout CME (SBOs). The events are characterized by a gradual swelling of the overlying streamer, lasting hours to days, followed by a slow, wide CME, generally exhibiting a 3-part structure, which leaves the streamer significantly depleted in its wake. We identify 909 SBO events in the LASCO/C2 observations between 1996 and 2015. The average blowout lasts for 40.5 hours but the evacuation can take days for some events. SBO-CMEs are wider and more massive than the average CME. Their properties generally vary during and between solar cycles. Their minimum (maximum) monthly occurrence rate of one (six) events in cycle 23 has doubled in cycle 24---a probable manifestation of the weaker global fields in the current cycle. The locations of SBOs follow the tilt of the global dipole (but not from 2014 onwards), do not correlate with sunspot numbers and exhibit flux rope morphology at a much higher rate (61%) than regular CMEs (40%). We propose that these characteristics are consistent with SBOs arising from extended polarity inversion lines outside active regions (e.g. quiet sun and polar crown filaments) through the release, via reconnection, of magnetic energy, likely accumulated via differential rotation. **March 22-25, 2000, 2003/10/30, 2008/11/27**

## Multi-viewpoint Coronal Mass Ejection Catalog Based on STEREO COR2 Observations

Angelos [Vourlidas](#)<sup>1,4</sup>, Laura A. Balmaceda<sup>2,5,6</sup>, Guillermo Stenborg<sup>3</sup>, and Alisson Dal Lago<sup>2</sup>

**2017** ApJ **838** 141 **File**

<http://sci-hub.cc/10.3847/1538-4357/aa67f0>

We present the first multi-viewpoint coronal mass ejection (CME) catalog. The events are identified visually in simultaneous total brightness observations from the twin SECCHI/COR2 coronagraphs on board the Solar Terrestrial Relations Observatory mission. The Multi-View CME Catalog differs from past catalogs in three key aspects: (1) all events between the two viewpoints are cross-linked, (2) each event is assigned a physics-motivated morphological classification (e.g., jet, wave, and flux rope), and (3) kinematic and geometric information is extracted semi-automatically via a supervised image segmentation algorithm. The database extends from the beginning of the COR2 synoptic program (2007 March) to the end of dual-viewpoint observations (2014 September). It contains 4473 unique events with 3358 events identified in both COR2s. Kinematic properties exist currently for 1747 events (26% of COR2-A events and 17% of COR2-B events). We examine several issues, made possible by this cross-linked CME database, including the role of projection on the perceived morphology of events, the missing CME rate, the existence of cool material in CMEs, the solar cycle dependence on CME rate, speeds and width, and the existence of flux rope within CMEs. We discuss the implications for past single-viewpoint studies and for Space Weather research. The database is publicly available on the web including all available measurements. We hope that it will become a useful resource for the community. **2009-01-18, 2009-01-22, 2010-04-03, 2011-02-26, 2012-01-26, 2012-10-14, 2013-05-12, 2013-06-08, 2013-10-11, 2013-10-23**

See <http://solar.jhuapl.edu/Data-Products/COR-CME-Catalog.php>

## Hurricane Season in the Inner Heliosphere: Observations of Coronal Mass Ejections during Solar Maximum Review

A. [Vourlidas](#)

The 11th Hellenic Astronomical Conference, 8-12 September **2013**, Athens; **Presentation**

**7-3-2012, 23-7-2012**

## How Many CMEs Have Flux Ropes? Deciphering the Signatures of Shocks, Flux Ropes, and Prominences in Coronagraph Observations of CMEs Review

A. [Vourlidas](#), B.J. Lynch, R.A. Howard, Y. Li

E-print, July **2012**; Solar Phys. **2013**, Volume 284, Issue 1, pp 179-201, **File**

We intend to provide a comprehensive answer to the question on whether all Coronal Mass Ejections (CMEs) have flux rope structure. To achieve this, we present a synthesis of the LASCO CME observations over the last sixteen years, assisted by 3D MHD simulations of the breakout model, EUV and coronagraphic observations from extsl{STEREO} and extsl{SDO}, and statistics from a revised LASCO CME database. We argue that the bright loop often seen as the CME leading edge is the result of pileup at the boundary of the erupting flux rope irrespective of whether a cavity or, more generally, a 3-part CME can be identified. Based on our previous work on white light shock detection and supported by the MHD simulations, we identify a new type of morphology, the 'two-front' morphology. It consists of a faint front followed by diffuse emission and the bright loop-like CME leading edge. We show that the faint front is caused by density compression at a wave (or possibly shock) front driven by the CME. We also present high-detailed multi-wavelength EUV observations that clarify the relative positioning of the prominence at the bottom of a coronal cavity with clear flux rope structure. Finally, we visually check the full LASCO CME database for flux rope structures. In the process, we classify the events into two clear flux rope classes ('3-part', 'Loop'), jets and outflows (no clear



structure). We find that at least 40% of the observed CMEs have clear flux rope structures and that 29% of the database entries are either misidentifications or inadequately measured and should be discarded from statistical analyses. We propose a new definition for flux rope CMEs (FR-CMEs) as a coherent magnetic, twist-carrying coronal structure with angular width of at least 40° and able to reach beyond 10 Rodot which erupts on a time scale of a few minutes to several hours. We conclude that flux ropes are a common occurrence in CMEs and pose a challenge for future studies to identify CMEs that are clearly extl{not/} FR-CMEs.

## **Uncovering the Birth of a Coronal Mass Ejection from Two-Viewpoint SECCHI Observations**

A. [Vourlidas](#)<sup>1</sup> \_ P. Syntelis<sup>2,4</sup> \_ K. Tsinganos

Solar Phys., October 2012, Volume 280, Issue 2, pp 509-523, **2012, File**

We investigate the initiation and formation of Coronal Mass Ejections (CMEs) via detailed two-viewpoint analysis of low corona observations of a relatively fast CME acquired by the SECCHI instruments aboard the STEREO mission. The event which occurred on **January 2, 2008**, was chosen because of several unique characteristics. It shows upward motions for at least four hours before the are peak. Its speed and acceleration profiles exhibit a number of inceptions which seem to have a direct counterpart in the GOES light curves. We detect and measure, in 3D, loops that collapse toward the erupting channel while the CME is increasing in size and accelerates. We suggest that these collapsing loops are our first evidence of magnetic evacuation behind the forming CME flux rope. We report the detection of a hot structure which becomes the core of the white light CME. We observe and measure unidirectional ows along the erupting filament channel which may be associated with the eruption process. Finally, we compare these observations to the predictions from the standard are-CME model and find a very satisfactory agreement. We conclude that the standard are-CME concept is a reliable representation of the initial stages of CMEs and that multi-viewpoint, high cadence EUV observations can be extremely useful in understanding the formation of CMEs.

## **Full-Sun Observations from STEREO: Recent Results and Future Science Opportunities**

A. [Vourlidas](#)

Presentation at ESPM-13, **2011**

[http://astro.academyofathens.gr/espm13/talks/Monday\\_Sep12/s1/A\\_Vourlidas.pdf](http://astro.academyofathens.gr/espm13/talks/Monday_Sep12/s1/A_Vourlidas.pdf)

## **THE FIRST OBSERVATION OF A RAPIDLY ROTATING CORONAL MASS EJECTION IN THE MIDDLE CORONA**

A. [Vourlidas](#)<sup>1</sup>, R. Colaninno<sup>1</sup>, T. Nieves-Chinchilla<sup>2</sup> and G. Stenborg

**2011 ApJ 733 L23, File**

In this Letter, we present the first direct detection of a rotating coronal mass ejection (CME) in the middle corona (5-15 R ). The CME rotation rate is 60° day<sup>-1</sup>, which is the highest rate reported yet. The Earth-directed event was observed by the STEREO/SECCHI and SOHO/LASCO instruments. We are able to derive the three-dimensional morphology and orientation of the CME flux rope by applying a forward-fitting model to simultaneous observations from three vantage points (SECCHI-A, -B, LASCO). Surprisingly, we find that even such rapidly rotating CME does not result in significant projection effects (variable angular width) in any single coronagraph view. This finding may explain the prevalent view of constant angular width for CMEs above 5 R and the lack of detections of rotating CMEs in the past. Finally, the CME is a "stealth" CME with very weak low corona signatures as viewed from Earth. It originated from a quiet-Sun neutral line. We tentatively attribute the fast rotation to a possible disconnection of one of the CME footpoints early in the eruption. We discuss the implications of such rotations to space weather prediction.

**2010 June 16.**

## **ERRATUM: "COMPREHENSIVE ANALYSIS OF CORONAL MASS EJECTION MASS AND ENERGY PROPERTIES OVER A FULL SOLAR CYCLE" (2010, ApJ, 722, 1522)**

A. [Vourlidas](#)<sup>1</sup>, R. A. Howard<sup>1</sup>, E. Esfandiari<sup>2</sup>, S. Patsourakos<sup>3</sup>, S. Yashiro<sup>4</sup> and G. Michalek<sup>5</sup>

**2011 ApJ 730 59**

In our recent paper (Vourlidas et al. 2010, Paper I hereafter), we reported various statistics regarding the masses and energies of coronal mass ejections (CMEs) including the detection of a 6 month CME mass variability. Since then, we have uncovered a processing error in the routines that create the mass images. They failed to take into account the image rotation during the 180° rolls of the *SOHO* spacecraft (see [http://soho.nascom.nasa.gov/hotshots/2004\\_01\\_04](http://soho.nascom.nasa.gov/hotshots/2004_01_04) for more information). Therefore, the mass and energy measurements for those periods did not correspond to the actual CME location. This error affected about half of the events since 2003 June when the spacecraft began rolling for 3 months at a time. We corrected the software error, reprocessed all images and measurements since 2003, and redid the analysis exactly as it was reported in Paper I. The final sample includes slightly more events (7820 CMEs) compared to the 7668 events used in Paper I. We found that the correction affected mostly our discussion on the solar cycle effects (Section 3.5 in Paper I). We describe these changes in detail below and provide updated figures where necessary.

## COMPREHENSIVE ANALYSIS OF CORONAL MASS EJECTION MASS AND ENERGY PROPERTIES OVER A FULL SOLAR CYCLE

A. [Vourlidas](#)<sup>1</sup>, R. A. Howard<sup>1</sup>, E. Esfandiari<sup>2</sup>, S. Patsourakos<sup>3</sup>, S. Yashiro<sup>4</sup>, and G. Michalek<sup>5</sup>  
*Astrophysical Journal*, 722:1522–1538, 2010, [File](#)

See [ERRATUM](#), 2011

The LASCO coronagraphs, in continuous operation since 1995, have observed the evolution of the solar corona and coronal mass ejections (CMEs) over a full solar cycle with high-quality images and regular cadence. This is the first time that such a data set becomes available and constitutes a unique resource for the study of CMEs. In this paper, we present a comprehensive investigation of the solar cycle dependence on the CME mass and energy over a full solar cycle (1996–2009) including the first in-depth discussion of the mass and energy analysis methods and their associated errors. Our analysis provides several results worthy of further studies. It demonstrates the possible existence of two event classes: “normal” CMEs reaching constant mass for  $>10 R_{\odot}$  and “pseudo”-CMEs which disappear in the C3 field of view. It shows that the mass and energy properties of CME reach constant levels and therefore should be measured only above  $\sim 10 R_{\odot}$ . The mass density ( $g/R_{\odot}^2$ ) of CMEs varies relatively little ( $<$ order of magnitude) suggesting that the majority of the mass originates from a small range in coronal heights. We find a sudden reduction in the CME mass in mid-2003 which may be related to a change in the electron content of the large-scale corona and we uncover the presence of a 6 month periodicity in the ejected mass from 2003 onward.

## A [Review](#) of Coronagraphic Observations of Shocks Driven by Coronal Mass Ejections

Angelos [Vourlidas](#)<sub>†</sub> and Veronica Ontiveros<sub>†</sub>,

AIP Conference Proceedings, Volume 1183, pp. 139-146 (2009), [File](#)

The existence of shocks driven by Coronal Mass Ejections (CMEs) has always been assumed based on the supersonic speeds for some of these events and on indirect evidence such as radio bursts and distant streamer deflections. However, the direct signature of the plasma enhancement at the shock front has escaped detection until recently. Since 2003, work on LASCO observations has shown that CME-driven shocks can be detected by white light coronagraph observations from a few solar radii to at least 20  $R_{\odot}$ . Shock properties, such as the density compression ratio and their direction can be extracted from the data. We review this work here and demonstrate how to recognize the various shock morphologies in the images. We also discuss how the two-viewpoint coronagraph observations from the STEREO mission allow the reconstruction of the 3D envelope of the shock revealing some interesting properties of the shocks (e.g., anisotropic expansion)

## FIRST DIRECT OBSERVATION OF THE INTERACTION BETWEEN A COMET AND A CORONAL MASS EJECTION LEADING TO A COMPLETE PLASMA TAIL DISCONNECTION

Angelos [Vourlidas](#), Chris J. Davis, Chris J. Eyles,<sup>1,2</sup> Steve R. Crothers, and Richard A. Harrison, Russell A. Howard, J. Daniel Moses, and Dennis G. Socker

*Astrophysical Journal*, 668: L79–L82, 2007

This a discovery report of the first direct imaging of the interaction a comet with a coronal mass ejection (CME) in the inner heliosphere with high temporal and spatial resolution. The observations were obtained by the Sun-Earth Connection Coronal and Heliospheric Investigation (SECCHI) Heliospheric Imager-1 (HI-1) aboard the *STEREO* mission. They reveal the extent of the plasma tail of comet 2P/Encke to unprecedented lengths and allow us to examine the mechanism behind a spectacular tail disconnection event. Our preliminary analysis suggests that the disconnection is driven by magnetic reconnection between the magnetic field entrained in the CME and the interplanetary field draped around the comet and not by pressure effects. Further analysis is required before we can conclude whether the reconnection occurs on the day side or on the tail side of the comet. However, the observations offer strong support to the idea that large-scale tail disconnections are magnetic in origin. The online movie reveals a wealth of interactions between solar wind structures and the plasma tail beyond the collision with the CME. Future analyses of this data set should provide critical insights on the structure of the inner heliosphere.

## The Proper Treatment of Coronal Mass Ejection Brightness:

### A New Methodology and Implications for Observations,

[Vourlidas](#), A., and R. A. Howard,

*Astrophysical Journal*, 642, 1216-1221 (2006), [File](#).

With the complement of coronagraphs and imagers in the SECCHI suite, we will follow a coronal mass ejection (CME) continuously from the Sun to Earth for the first time. The comparison, however, of the CME emission among the various instruments is not as easy as one might think. This is because the telescopes record the Thomson-scattered emission from the CME plasma, which has a rather sensitive dependence on the geometry between the observer and the scattering material. Here we describe the proper treatment of the Thomson-scattered emission, compare the CME brightness over a large range of elongation angles, and discuss the implications for existing and future white-light coronagraph observations.

## Direct Detection of a Coronal Mass Ejection-Associated Shock in Large Angle and Spectrometric Coronagraph Experiment White-Light Images

Vourlidas, A., et al.

*Astrophysical Journal*, 598, 1392-1402, (2003), File.

The Large Angle and Spectrometric Coronagraph Experiment (LASCO) C2 and C3 coronagraphs recorded a unique coronal mass ejection (CME) on **1999 April 2**. The event did not have the typical three-part CME structure and involved a small-filament eruption without any visible overlying streamer ejecta. The event exhibited an unusually clear signature of a wave propagating at the CME flanks. The speed and density of the CME front and flanks were consistent with the existence of a shock. To better establish the nature of the white-light wave signature, we employed a simple MHD simulation using the LASCO measurements as constraints. Both the measurements and the simulation strongly suggest that the white-light feature is the density enhancement from a fast-mode MHD shock. In addition, the LASCO images clearly show streamers being deflected when the shock impinges on them. It is the first direct imaging of this interaction.

## Analytical and empirical modelling of the origin and heliospheric propagation of coronal mass ejections, and space weather applications Review

Bojan Vršnak\*

J. Space Weather Space Clim. **2021**, 11, 34

<https://www.swsc-journal.org/articles/swsc/pdf/2021/01/swsc200091.pdf>

<https://doi.org/10.1051/swsc/2021012>

The focus is on the physical background and comprehension of the origin and the heliospheric propagation of interplanetary coronal mass ejections (ICMEs), which can cause most severe geomagnetic disturbances. The paper considers mainly the analytical modelling, providing useful insight into the nature of ICMEs, complementary to that provided by numerical MHD models. It is concentrated on physical processes related to the origin of CMEs at the Sun, their heliospheric propagation, up to the effects causing geomagnetic perturbations. Finally, several analytical and statistical forecasting tools for space weather applications are described. **November 3, 1997**

## Gradual pre-eruptive phase of solar coronal eruptions

B. Vršnak

Front. Astron. Space Sci. **2019** | doi: 10.3389/fspas.2019.00028

<https://www.frontiersin.org/articles/10.3389/fspas.2019.00028/full>

<https://sci-hub.se/10.3389/fspas.2019.00028>

Physical background of the evolution of a coronal magnetic flux rope embedded in the magnetic arcade during the gradual-rise pre-eruptive stage is studied.

It is assumed that this stage represents an externally-driven evolution of the preeruptive structure through a series of quasi-equilibrium states, until a point when system losses equilibrium and erupts. In particular, three driving processes are considered: twisting motions of the flux-rope footpoints, emergence of new magnetic flux beneath the flux rope, and the mass leakage down the flux-rope legs.

For that purpose, an analytical flux-rope model is employed, to inspect how fast the equilibrium height of the structure rises due to the increase of the poloidal-to-axial field ratio, the increase of axial electric current, and the decrease of mass. It is shown that the flux-rope twisting itself is not sufficient to reproduce the rising speeds observed during the pre-eruptive stage. Yet, it is essential for the loss-of-equilibrium process. On the other hand, the considered emerging flux and the mass loss processes reproduce well the rate at which the pre-eruptive structure rises before the main acceleration stage of the eruption sets in.

## Solar eruptions: The CME-flare relationship

B. Vršnak

Astronomische Nachrichten, Vol.337, Issue 10, p.1002-1009, **2016**

[sci-hub.ru/10.1002/asna.201612424](https://sci-hub.ru/10.1002/asna.201612424)

<https://onlinelibrary.wiley.com/doi/abs/10.1002/asna.201612424>

Coronal mass ejections (CMEs), caused by large-scale eruptions of the coronal magnetic field, often are accompanied by a more localized energy release in the form of flares, as a result of dissipative magnetic-field reconfiguration. Morphology and evolution of such flares, also denoted as dynamical flares are often explained as a consequence of reconnection of the arcade magnetic field, taking place below the erupting magnetic flux rope. A close relationship of the CME acceleration and the flare energy release is evidenced by various statistical correlations between parameters describing CMEs and flares, as well as by the synchronization of the CME acceleration phase with the impulsive phase of the associated flare. Such behavior implies that there must be a feedback relation between the dynamics of the CME and the flare-associated reconnection process. From the theoretical standpoint, magnetic reconnection affects the CME dynamics in several ways. First, it reduces the tension of the overlying arcade magnetic field and increases the magnetic

pressure below the flux rope, and in this way enhances the CME acceleration. Furthermore, it supplies the poloidal magnetic flux to the flux rope, which helps sustaining the electric current in the rope and prolonging the action of the driving Lorentz force to large distances. The role of these processes, directly relating solar flares and CMEs, is illustrated by employing a simple model, where the erupting structure is represented by a curved flux rope anchored at both sides in the dense/inert photosphere, being subject to the kink and torus instability. It is shown that in most strongly accelerated ejections, where values on the order of  $10 \text{ km s}^{-2}$  are attained, the poloidal flux supplied to the erupting rope has to be several times larger than was the initial flux.

### **Formation of Coronal Large-Amplitude Waves and the Chromospheric Response**

B. Vršnak<sup>1</sup>, T. Žic, S. Lulić, M. Temmer, A. M. Veronig

Solar Phys. Volume 291, Issue 1, pp.89-115 2016

An in-depth analysis of numerical simulations is performed to obtain a deeper insight into the nature of various phenomena occurring in the solar atmosphere as a consequence of the eruption of unstable coronal structures. Although the simulations take into account only the most basic characteristics of a flux-rope eruption, the simulation analysis reveals important information on various eruption-related effects. It quantifies the relation between the eruption dynamics and the evolution of the large-amplitude coronal magnetohydrodynamic wave and the associated chromospheric downward-propagating perturbation. We show that the downward propagation of the chromospheric Moreton-wave disturbance can be approximated by a constant-amplitude switch-on shock that moves through a medium of rapidly decreasing Alfvén velocity. The presented analysis reveals the nature of secondary effects that are observed as coronal upflows, secondary shocks, various forms of wave-trains, delayed large-amplitude slow disturbances, transient coronal depletions, etc. We also show that the eruption can cause an observable Moreton wave and a secondary coronal front only if it is powerful enough and is preferably characterized by significant lateral expansion. In weaker eruptions, only the coronal and transition-region signatures of primary waves are expected to be observed. In powerful events, the primary wave moves at an Alfvén Mach number significantly larger than 1 and steepens into a shock that is due to the nonlinear evolution of the wavefront. After the eruption-driven phase, the perturbation evolves as a freely propagating simple wave, characterized by a significant deceleration, amplitude decrease, and wave-profile broadening. In weak events the coronal wave does not develop into a shock and propagates at a speed close to the ambient magnetosonic speed.

### **The role of aerodynamic drag in propagation of interplanetary coronal mass ejections**

B. Vršnak<sup>1</sup>, T. Žic<sup>1</sup>, T. V. Falkenberg<sup>2</sup>, C. Möstl<sup>3,4</sup>, S. Vennerstrom<sup>2</sup>, and D. Vrbanec<sup>1</sup>

A&A 512, A43 (2010); File

Context. The propagation of interplanetary coronal mass ejections (ICMEs) and the forecast of their arrival on Earth is one of the central issues of space weather studies.

Aims. We investigate to which degree various ICME parameters (mass, size, take-off speed) and the ambient solar-wind parameters (density and velocity) affect the ICME Sun-Earth transit time.

Methods. We study solutions of a drag-based equation of motion by systematically varying the input parameters. The analysis is focused on ICME transit times and 1 AU velocities.

Results. The model results reveal that wide ICMEs of low masses adjust to the solar-wind speed already close to the sun, so the transit time is determined primarily by the solar-wind speed. The shortest transit times and accordingly the highest 1 AU velocities are related to narrow and massive ICMEs (i.e. high-density eruptions) propagating in high-speed solar wind streams. We apply the model to the Sun-Earth event associated with the CME of **25 July 2004** and compare the results with the outcome of the numerical MHD modeling.

**Хорошая сводка литературы.**

### **Morphology and density structure of post-CME current sheets**

B. Vršnak<sup>1</sup>, G. Poletto<sup>2</sup>, E. Vujić<sup>3</sup>, A. Vourlidas<sup>4</sup>, Y.-K. Ko<sup>4</sup>, J. C. Raymond<sup>5</sup>, A., Ciaravella<sup>6</sup>, T. Žic<sup>1</sup>, D. F. Webb<sup>7</sup>, A. Bemporad<sup>8</sup>, F. Landini<sup>9</sup>, G. Schettino<sup>9</sup>, C., Jacobs<sup>10</sup>, and S. T. Suess<sup>11</sup>

E-print, Feb 2009, File; A&A, 499 (2009) 905-916

<http://www.aanda.org/10.1051/0004-6361/200810844>

Context. Eruption of a coronal mass ejection (CME) drags and “opens” the coronal magnetic field, presumably leading to the formation of a large-scale current sheet and the field relaxation by magnetic reconnection.

Aims. We analyze physical characteristics of ray-like coronal features formed in the aftermath of CMEs, to check if the interpretation of this phenomenon in terms of reconnecting current sheet is consistent with the observations.

Methods. The study is focused on measurements of the ray width, density excess, and coronal velocity field as a function of the radial distance.

Results. The morphology of rays indicates that they occur as a consequence of Petschek-like reconnection in the large scale current sheet formed in the wake of CME. The hypothesis is supported by the flow pattern, often showing outflows along the ray, and sometimes also inflows into the ray. The inferred inflow velocities range from 3 to 30  $\text{kms}^{-1}$ , consistent with the narrow opening-angle of rays, adding up to a few degrees. The density of rays is an order of magnitude larger than in the ambient corona. The density-excess measurements are compared with the results of the analytical model in which the Petschek-like reconnection geometry is applied to the vertical current sheet, taking into account the decrease of the external coronal density and magnetic field with height.

Conclusions. The model results are consistent with the observations, revealing that the main cause of the density excess in rays is a transport of the dense plasma from lower to larger heights by the reconnection outflow.

## Processes and mechanisms governing the initiation and propagation of CMEs Review

B. Vršnak

Ann. Geophys., 26, 3089–3101, 2008

<https://sci-hub.tw/10.5194/angeo-26-3089-2008>

The most important observational characteristics of coronal mass ejections (CMEs) are summarized, emphasizing those aspects which are relevant for testing physical concepts employed to explain the CME take-off and propagation. In particular, the kinematics, scalings, and the CME-flare relationship are stressed. Special attention is paid to 3-dimensional (3-D) topology of the magnetic field structures, particularly to aspects related to the concept of semi-toroidal flux-rope anchored at both ends in the dense photosphere and embedded in the coronal magnetic arcade. Observations are compared with physical principles and concepts employed in explaining the CME phenomenon, and implications are discussed. A simple flux-rope model is used to explain various stages of the eruption. The model is able to reproduce all basic observational requirements: stable equilibrium and possible oscillations around equilibrium, metastable state and possible destabilization by an external disturbance, pre-eruptive gradual-rise until loss of equilibrium, possibility of fallback events and failed eruptions, relationship between impulsiveness of the CME acceleration and the source-region size, etc. However, it is shown that the purely ideal MHD process cannot account for highest observed accelerations which can attain values up to  $10 \text{ km s}^{-2}$ . Such accelerations can be achieved if the process of reconnection beneath the erupting flux-rope is included into the model. Essentially, the role of reconnection is in changing the magnetic flux associated with the flux-rope current and supplying "fresh" poloidal magnetic flux to the rope. These effects help sustain the electric current flowing along the flux-rope, and consequently, reinforce and prolong the CME acceleration. **The model straightforwardly explains the observed synchronization of the flare impulsive phase and the CME main-acceleration stage, as well as the correlations between various CME and flare parameters.**

## Origin of Coronal Shock Waves

Invited Review

Bojan Vršnak · Edward W. Cliver

Solar Phys, 253: 215–235, 2008, DOI 10.1007/s11207-008-9241-5; **File**

The basic idea of the paper is to present transparently and confront two different views on the origin of large-scale coronal shock waves, one favoring coronal mass ejections (CMEs), and the other one preferring flares. For this purpose, we first review the empirical aspects of the relationship between CMEs, flares, and shocks (as manifested by radio type II bursts and Moreton waves). Then, various physical mechanisms capable of launching MHD shocks are presented. In particular, we describe the shock wave formation caused by a three-dimensional piston, driven either by the CME expansion or by a flare-associated pressure pulse. Bearing in mind this theoretical framework, the observational characteristics of CMEs and flares are revisited to specify advantages and drawbacks of the two shock formation scenarios. Finally, we emphasize the need to document clear examples of flare-ignited large-scale waves to give insight on the relative importance of flare and CME generation mechanisms for type II bursts/Moreton waves.

## Dynamics of coronal mass ejections

### *The mass-scaling of the aerodynamic drag*

B. Vršnak, D. Vrbanec, and J. Čalogović

A&A 490, 811–815 (2008), DOI: 10.1051/0004-6361:200810215; **File**

<http://www.aanda.org/10.1051/0004-6361:200810215>

*Context.* Coronal and interplanetary propagation of coronal mass ejections (CMEs) is strongly affected by aerodynamic drag.

*Aims.* The dependence of the drag acceleration on the mass of the CMEs is investigated to establish a quantitative empirical relationship, which might be important in semi-empirical space-weather forecasting.

*Methods.* We employ a large sample of CMEs observed in the radial distance range of 2–30 solar radii by the Large Angle and Spectrometric Coronagraph on board the SoHO mission to statistically analyze the acceleration-velocity relationship in subsamples of various classes of CME masses.

*Results.* It is demonstrated that the slope and the  $v$ -axis intercept of the anti-correlation of the CME acceleration  $a$  and velocity  $v$  depend on the mean mass of CMEs included in the sample. The slope  $k$  of the correlation is less steep for subsamples of higher masses, revealing that massive CMEs are less affected by the aerodynamic drag. Furthermore, it is found that the  $v$ -axis intercept is shifted to higher velocities for subsamples of higher masses. This indicates that, on average, the driving force is greater in more massive CMEs.

*Conclusions.* The empirically established dependence of the  $a(v)$  slope on the CME mass is very close to the dependence  $k \propto m^{-1/3}$  which follows from the physical characteristics of the aerodynamic drag.

## Acceleration Phase of Coronal Mass Ejections:

### I. Temporal and Spatial Scale

## II. Synchronization of the Energy Release in the Associated Flare. File

Bojan [Vršnak](#), Darije Marić, Andrew L. Stanger, Astrid M. Veronig, Manuela Temmer, Dragan Rožić  
Solar Phys., 241 (1), Page: 85 – 98, 99 – 112, 2007

### Projection effects in coronal mass ejections:

B. [Vršnak](#), D. Sudar, D. Rudjak and T. Ić

A&A 469 (2007) 339–346

<http://www.aanda.org/10.1051/0004-6361:20077175>

### The CME-flare relationship: Are there really two types of CMEs?

B. [Vršnak](#), D. Sudar, and D. Ruždjak

A&A 435, 1149–1157 (2005), DOI: 10.1051/0004-6361:20042166

**Abstract.** We present a statistical analysis of 545 flare-associated CMEs and 104 non-flare CMEs observed in the heliocentric distance range 2–30 solar radii. We found that both data sets show quite similar characteristics, contradicting the concept of two distinct (flare/non-flare) types of CMEs. In both samples there is a significant fraction of CMEs showing a considerable acceleration or deceleration and both samples include a comparable ratio of fast and slow CMEs. We present kinematical curves of several fast non-flare CMEs moving at a constant speed or decelerating, i.e., behaving as expected for flare-associated CMEs. Analogously, we identified several slow flare-CMEs showing the acceleration peak beyond a height of 3 solar radii. On the other hand, it is true that CMEs associated with major flares are on average faster and broader than non-flare CMEs and small-flare CMEs. There is a well-defined correlation between the CME speed and the importance of the associated flare. In this respect, the non-flare CMEs show characteristics similar to CMEs associated with flares of soft X-ray class B and C, which is indicative of a “continuum” of events rather than supporting the existence of two distinct CME classes. Furthermore, we inferred that CMEs whose source region cannot be identified with either flares or eruptive prominences are on average slowest. The results indicate that the magnetic reconnection taking place in the current sheet beneath the CME significantly influences the CME dynamics.

### The effect of data-driving and relaxation model on magnetic flux rope evolution and stability

[Andreas Wagner](#), [Daniel J. Price](#), [Slava Bourgeois](#), [Farhad Daei](#), [Jens Pomoell](#), [Stefaan Poedts](#), [Anshu Kumari](#), [Teresa Barata](#), [Robertus Erdélyi](#), [Emilia K. J. Kilpua](#)

A&A 692, A74 2024

<https://arxiv.org/pdf/2410.18672>

<https://www.aanda.org/articles/aa/pdf/2024/12/aa50577-24.pdf>

We investigate the effect of data-driving on flux rope eruptivity in magnetic field simulations by analysing fully data-driven modelling results of active region (AR) 12473 and AR11176, as well as performing relaxation runs for AR12473 (found to be eruptive). Here, the driving is switched off systematically at different time steps. We analyse the behaviour of fundamental quantities, essential for understanding the eruptivity of magnetic flux ropes (MFRs). The data-driven simulations are carried out with the time-dependent magnetofrictional model (TMFM) for AR12473 and AR11176. For the relaxation runs, we employ the magnetofrictional method (MFM) and a zero-beta magnetohydrodynamic (MHD) model to investigate how significant the differences between the two relaxation procedures are when started from the same initial conditions. To determine the eruptivity of the MFRs, we calculate characteristic geometric properties, such as the cross-section, MFR height along with stability parameters, such as MFR twist and the decay index. For eruptive cases, we investigate the effect of sustained driving beyond the point of eruptivity on the MFR properties. We find that the fully-driven AR12473 MFR is eruptive while the AR11176 MFR is not. For the relaxation runs, we find that the MFM MFRs are eruptive when the driving is stopped around the flare time or later, while the MHD MFRs show eruptive behaviour even if the driving is switched off one and a half days before the flare occurs. We find that characteristic MFR properties can vary greatly even for the eruptive cases of different relaxation simulations. The results suggest that data driving can significantly influence the evolution of the eruption, with differences appearing even when the relaxation time is set to later stages of the simulation when the MFRs have already entered an eruptive phase. 27-29 Dec 2015

### Solar magnetic flux rope identification with GUITAR: GUI for Tracking and Analysing flux Ropes.

[Wagner A](#), [Price DJ](#), [Bourgeois S](#), [Pomoell J](#), [Poedts S](#) and [Kilpua EKJ](#)

(2024) Front. Astron. Space Sci. 11:1383072.

doi: 10.3389/fspas.2024.1383072

<https://www.frontiersin.org/articles/10.3389/fspas.2024.1383072/pdf>

Modelling the early evolution of magnetic flux ropes (MFRs) in the solar atmosphere is crucial for understanding their destabilization and eruption mechanism. Identifying the relevant magnetic field lines in simulation data, however, is not straightforward. In previous work an extraction and tracking method was developed to facilitate this task. Here, we present the corresponding graphical user interface (GUI), called GUITAR (GUI for Tracking and Analysing flux Ropes), with the aim to offer a variety of tools to the community for identifying and tracking MFRs. The starting point is a map of a selected proxy parameter for MFRs, e.g., a map of the twist-parameter  $T_w$ , current density, etc. We showcase how the GUITAR tools can be used to disentangle a multi-MFR system and facilitate in-depth analysis of their properties and evolution by applying them on a time-dependent data-driven magnetofrictional model (TMFM)

simulation of solar active region AR12473. We show the MFR extraction using Tw maps, together with targeted use of mathematical morphology algorithms and discuss the evolution of the system.

## **The Automatic Identification and Tracking of Coronal Flux Ropes -- Part II: New Mathematical Morphology-based Flux Rope Extraction Method and Deflection Analysis**

[Andreas Wagner](#), [Slava Bourgeois](#), [Emilia K. J. Kilpua](#), [Ranadeep Sarkar](#), [Daniel J. Price](#), [Anshu Kumari](#), [Jens Pomoell](#), [Stefaan Poedts](#), [Teresa Barata](#), [Robertus Erdélyi](#), [Orlando Oliveira](#), [Ricardo Gafeira](#)  
A&A 683, A39 2023

<https://arxiv.org/pdf/2312.00673.pdf>

<https://www.aanda.org/articles/aa/pdf/2024/03/aa48113-23.pdf>

We present a magnetic flux rope (FR) extraction tool for solar coronal magnetic field modelling data, which builds upon the methodology from Wagner et al. (2023). The newly developed method is then compared against its previous iteration. Furthermore, we apply the scheme to magnetic field simulations of active regions AR12473 (similar to our previous study) and AR11176. We compare the method to its predecessor and study the 3D movement of the newly extracted FRs up to heights of 200 and 300 Mm, respectively. **Methods.** The extraction method is based on the twist parameter Tw and a variety of mathematical morphology (MM) algorithms, including the opening transform and the morphological gradient. We highlight the differences between the methods by investigating the circularity of the FRs in the plane we extract from. The simulations for the active regions are carried out with a time-dependent data-driven magnetofrictional model (TMFM; Pomoell et al. (2019)). We investigate the FR trajectories by tracking their apex throughout the full simulation time span. **Results.** Comparing the newly developed method to the extraction scheme in Wagner et al. (2023), we demonstrate that this upgrade provides the user with more tools and less a-priori assumptions about the FR shape that, in turn, leads to a more accurate set of field lines. Despite some differences, both the newly extracted FR of AR12473 as well as the FR derived with the old iteration of the method show a similar general appearance, confirming that both methods indeed extract the same structure. The methods differ the most in their emergence/formation stages, where the newly extracted FR deviates significantly from a perfectly circular cross-section (that was the basic assumption of the initial method). The propagation analysis yields that the erupting FR from AR12473 showcases indeed stronger dynamics than the AR11176 FR and a significant deflection during its ascent through the domain. The modelling results are also verified with observations, with AR12473 being indeed dynamic and eruptive, while AR11176 only features an eruption outside of our simulation time window. **Conclusions.** We implemented a FR extraction method, incorporating mathematical morphology algorithms for 3D solar magnetic field simulations of active region FRs. This scheme was applied to AR12473 and AR11176. We find that the clearly eruptive FR of AR12473 experiences significant deflection during its rise. The AR11176 FR appears more stable, though there still is a notable deflection. This confirms that at these low coronal heights, FRs do undergo significant changes in the direction of their propagation even for less dynamic cases. **27-28 Mar 2011, 28 Dec 2015**

## **The Automatic Identification and Tracking of Coronal Flux Ropes -- Part I: Footpoints and Fluxes**

[Andreas Wagner](#), [Emilia K. J. Kilpua](#), [Ranadeep Sarkar](#), [Daniel J. Price](#), [Anshu Kumari](#), [Farhad Daei](#), [Jens Pomoell](#), [Stefaan Poedts](#)

A&A 677, A81 2023

<https://arxiv.org/pdf/2306.15019.pdf>

<https://www.aanda.org/articles/aa/pdf/2023/09/aa46260-23.pdf>

Investigating the early-stage evolution of an erupting flux rope from the Sun is important to understand the mechanisms of how it loses its stability and its space weather impacts. Our aim is to develop an efficient scheme for tracking the early dynamics of erupting solar flux ropes and use the algorithm to analyse its early-stage properties. The algorithm is tested on a data-driven simulation of an eruption that took place in active region AR12473. We investigate the modelled flux rope's footpoint movement and magnetic flux evolution and compare with observational data from the Solar Dynamics Observatory's Atmospheric Imaging Assembly in the 211 Å and 1600 Å channels. To carry out our analysis, we use the time-dependent data-driven magnetofrictional model (TMFM). We also perform another modelling run, where we stop the driving of the TMFM midway through the flux rope's rise through the simulation domain and evolve it instead with a zero-beta magnetohydrodynamic (MHD) approach. The developed algorithm successfully extracts a flux rope and its ascend through the simulation domain. We find that the movement of the modelled flux rope footpoints showcases similar trends in both TMFM and relaxation MHD run: they recede from their respective central location as the eruption progresses and the positive polarity footpoint region exhibits a more dynamic behaviour. The ultraviolet brightenings and extreme ultraviolet dimmings agree well with the models in terms of their dynamics. According to our modelling results, the toroidal magnetic flux in the flux rope first rises and then decreases. In our observational analysis, we capture the descending phase of toroidal flux. In conclusion, the extraction algorithm enables us to effectively study the flux rope's early dynamics and derive some of its key properties such as footpoint movement and toroidal magnetic flux. **28 Dec 2015**

## **Solar Eruptive Phenomena Associated with Solar Energetic Electron Spectral Types**

Wen [Wang](#)<sup>1,2</sup>, Linghua Wang<sup>2</sup>, Wenyan Li<sup>2</sup>, Säm Krucker<sup>3,4</sup>, Robert F. Wimmer-Schweingruber<sup>5</sup>, and Zheng Sheng<sup>1</sup>

2024 ApJ 969 164

<https://iopscience.iop.org/article/10.3847/1538-4357/ad47be/pdf>

The energy spectral shape of solar energetic electron events carries important information on the energetic electron source/acceleration at the Sun. We investigate the association of six newly identified solar energetic electron spectral types with solar eruptive phenomena, including the downward double-power-law (DDPL) spectrum with break energy EB above 20 keV ( $DDPLEB \geq 20\text{keV}$ ), DDPL with EB below 20 keV ( $DDPLEB < 20\text{keV}$ ), upward double-power law (UDPL), single-power-law (SPL), Ellison–Ramaty–like (ER), and logarithmic-parabola (LP). We find that the SPL type shows (the other five types show) an association with hard X-ray flares of  $\sim 38\%$  ( $\sim 55\%–82\%$ ) and an association with west-limb coronal mass ejections (CMEs) of  $\sim 76\%$  ( $\sim 85\%–93\%$ ). Among the other five types, the  $DDPLEB < 20\text{keV}$  and ER (LP and  $DDPLEB \geq 20\text{keV}$ ) types only have an association with type II radio bursts of  $\sim 7\%–8\%$  ( $\sim 16\%–20\%$ ) and an association with halo CMEs of  $\sim 5\%–9\%$  ( $\sim 11\%–21\%$ ); however, the UDPL type exhibits a significant ( $\sim 47\%$  and  $\sim 50\%$ ) association with type II bursts and halo CMEs, with a significantly faster median CME speed of  $1000–120+550\text{ km s}^{-1}$ . For  $DDPLEB \geq 20\text{keV}$  ( $DDPLEB < 20\text{keV}$ ) with a positive (no) correlation between spectral indexes and no (a positive) correlation between the spectral index and break energy, the spectrum appears to be flatter as the associated CME (flare) becomes faster (stronger). These results suggest that the SPL type can result from the initial acceleration process that likely occurs high in the corona, and then provide seed populations for further acceleration processes to form the other five types: the  $DDPLEB < 20\text{keV}$  and ER types via flare-related processes, the LP and  $DDPLEB \geq 20\text{keV}$  types via CME-related processes, and the UDPL type via CME-driven shocks. **2002-12-19**

### Negative-energy waves in the vertical threads of a solar prominence

[Jincheng Wang](#), [Dong Li](#), [Chuan Li](#), [Yijun Hou](#), [Zhike Xue](#), [Zhe Xu](#), [Liheng Yang](#), [Qiaoling Li](#)

ApJL **2024**

<https://arxiv.org/pdf/2404.03199.pdf>

Solar prominences, intricate structures on the Sun's limb, have been a subject of fascination due to their thread-like features and dynamic behaviors. Utilizing data from the New Vacuum Solar Telescope (NVST), Chinese H<sub>α</sub> Solar Explorer (CHASE), and Solar Dynamics Observatory (SDO), this study investigates the transverse swaying motions observed in the vertical threads of a solar prominence during its eruption onset on **May 11, 2023**. The transverse swaying motions were observed to propagate upward, accompanied by upflowing materials at an inclination of 31 degrees relative to the plane of the sky. These motions displayed small-amplitude oscillations with corrected velocities of around 3–4 km/s and periods of 13–17 minutes. Over time, the oscillations of swaying motion exhibited an increasing pattern in displacement amplitudes, oscillatory periods, and projected velocity amplitudes. Their phase velocities are estimated to be about 26–34 km/s. An important finding is that these oscillations' phase velocities are comparable to the upward flow velocities, measured to be around 30–34 km/s. We propose that this phenomenon is associated with negative-energy wave instabilities, which require comparable velocities of the waves and flows, as indicated by our findings. This phenomenon may contribute to the instability and observed disruption of the prominence. By using prominence seismology, the Alfvén speed and magnetic field strength of the vertical threads have been estimated to be approximately 21.5 km/s and 2 Gauss, respectively. This study reveals the dynamics and magnetic properties of solar prominences, contributing to our understanding of their behavior in the solar atmosphere.

### Lateral Confinement and the Remarkably Self-similar Nature

Y.-M. [Wang](#)<sup>1</sup> and P. Hess<sup>1</sup>

**2023** ApJ 952 85

<https://iopscience.iop.org/article/10.3847/1538-4357/acd638/pdf>

Coronal mass ejections (CMEs) that originate from pseudostreamers, which separate coronal holes of the same magnetic polarity, are characterized by a narrow ( $\sim 5^\circ–30^\circ$ ), fan-shaped appearance in white-light coronagraph images. Despite this striking morphological similarity, a wide variety of underlying eruptions are observed, including not only coronal jets, but also larger-scale filament eruptions, footpoint flares, and even extreme-ultraviolet (EUV) waves that reflect off the coronal hole boundaries. Using EUV images recorded by the Solar Dynamics Observatory during the early rising phase of cycle 25 (2020–2022), we describe examples of the different kinds of underlying eruptions and identify the corresponding fan-like ejections in Large Angle and Spectrometric Coronagraph images. We attribute the narrowness of the white-light CMEs to lateral confinement by the like-polarity open flux surrounding the pseudostreamer and point out that, although the multipolar topology facilitates the "breakout" of material through the cusp region, it also tends to inhibit the eruption of the pseudostreamer as a whole. We also note that the self-similar "continuum" formed by the pseudostreamer mass ejections does not include the larger, more space-weather-effective CMEs associated with helmet streamers, which are surrounded by open flux of opposite polarity and undergo much greater lateral expansion. **2020 April 25, 2020 October 30, 2021 February 11, 2021 February 16, 2021 September 24–26, 2021 September 25, 2021 September 26–28, 2021 December 23, 2022 January 14, 2022 March 12, 2022 May 16, 2022 May 22, 2022 July 2, 2022 July 17, 2022 July 26–28**

### The Formation and Early Evolution of a Coronal Mass Ejection and its Associated Shock Wave on **2014 January 8**

Linfeng [Wan](#), Xin Cheng, Tong Shi, Wei Su, M. D. Ding

ApJ **826** 174 **2016** File

<http://arxiv.org/pdf/1605.01132v1.pdf>

In this paper, we study the formation and early evolution of a limb coronal mass ejection (CME) and its associated shock wave that occurred on 2014 January 8. The extreme ultraviolet (EUV) images provided by the Atmospheric



Imaging Assembly (AIA) on board \textit{Solar Dynamics Observatory} disclose that the CME first appears as a bubble-like structure. Subsequently, its expansion forms the CME and causes a quasi-circular EUV wave. Interestingly, both the CME and the wave front are clearly visible at all of the AIA EUV passbands. Through a detailed kinematical analysis, it is found that the expansion of the CME undergoes two phases: a first phase with a strong but transient lateral over-expansion followed by a second phase with a self-similar expansion. The temporal evolution of the expansion velocity coincides very well with the variation of the 25--50 keV hard X-ray flux of the associated flare, which indicates that magnetic reconnection most likely plays an important role in driving the expansion. Moreover, we find that, when the velocity of the CME reaches  $\sim 600 \text{ km s}^{-1}$ , the EUV wave starts to evolve into a shock wave, which is evidenced by the appearance of a type II radio burst. The shock's formation height is estimated to be  $\sim 0.2 R_{\text{sun}}$ , which is much lower than the height derived previously. Finally, we also study the thermal properties of the CME and the EUV wave. We find that the plasma in the CME leading front and the wave front has a temperature of  $\sim 2 \text{ MK}$ , while that in the CME core region and the flare region has a much higher temperature of  $\geq 8 \text{ MK}$ .

## Unveiling key factors in solar eruptions leading to the solar superstorm in 2024 May

Rui Wang<sup>1,2,3\*</sup>, Ying D. Liu<sup>1,2,3</sup>, Xiaowei Zhao<sup>4,5</sup> and Huidong Hu<sup>1,2</sup>

A&A 692, A112 (2024)

<https://arxiv.org/pdf/2410.00891> File

<https://doi.org/10.1051/0004-6361/202452008>

<https://www.aanda.org/articles/aa/pdf/2024/12/aa52008-24.pdf>

NOAA active region (AR) 13664/8 produced the most intense geomagnetic effects since the Halloween event of 2003. The resulting extreme solar storm is thought to be the consequence of multiple interacting coronal mass ejections (CMEs). Notably, this AR exhibits exceptionally rapid magnetic flux emergence. The eruptions on which we focus all occurred along collisional polarity inversion lines (PILs) through collisional shearing during a three-day period of extraordinarily high flux emergence ( $\sim 1021 \text{ Mx h}^{-1}$ ). Our key findings reveal how photospheric magnetic configurations in eruption sources influence solar superstorm formation and geomagnetic responses, and link exceptionally strong flux emergence to sequential homologous eruptions: (1) We identified the source regions of seven halo CMEs that were distributed primarily along two distinct PILs. This distribution suggests two groups of homologous CMEs. (2) The variations in the magnetic flux emergence rates in the source regions are correlated with the CME intensities. This might explain the two contrasting cases of complex ejecta that are observed at Earth. (3) Our calculations of the magnetic field gradients around the CME source regions show strong correlations with eruptions. This provides crucial insights into solar eruption mechanisms and enhances our prediction capabilities for future events. **May 2024: 4-12, 8, 9, 10,11**

## SIP-IFVM: An efficient time-accurate implicit MHD model of corona and CME with strong magnetic field

[H. P. Wang](#), [J. H. Guo](#), [L. P. Yang](#), [S. Poedts](#), [F. Zhang](#), [A. Lani](#), [T. Baratashvili](#), [L. Linan](#), [R. Lin](#), [Y. Guo](#)

A&A 2024

<https://arxiv.org/pdf/2409.02022>

CMEs are one of the main drivers of space weather. However, robust and efficient numerical modeling of the initial stages of CME propagation and evolution process in the sub-Alfvénic corona is still lacking. Based on the highly efficient quasi-steady-state implicit MHD coronal model (Feng et al. 2021; Wang et al. 2022a), we further develop an efficient and time-accurate coronal model and employ it to simulate the CME's evolution and propagation. A pseudo-time marching method, where a pseudo time,  $\tau$ , is introduced at each physical time step to update the solution by solving a steady-state problem on  $\tau$ , is devised to improve the temporal accuracy. Moreover, an RBSL flux rope whose axis can be designed in an arbitrary shape is inserted into the background corona to trigger the CME event. We call it the SIP-IFVM coronal model and utilize it to simulate a CME evolution process from the solar surface to  $20 R_{\text{s}}$  in the background corona of CR 2219. It can finish the CME simulation covering 6 hours of physical time by less than 0.5 hours (192 CPU cores, 1 M cells) without much loss in temporal accuracy. Besides, an ad hoc simulation with initial magnetic fields artificially increased shows that this model can effectively deal with time-dependent low-beta problems ( $\beta < 0.0005$ ). Additionally, an Orszag-Tang MHD vortex flow simulation demonstrates that the pseudo-time-marching method adopted in this coronal model is also capable of simulating small-scale unsteady-state flows. The simulation results show that this MHD coronal model is very efficient and numerically stable and is promising to timely and accurately simulate time-varying events in solar corona with low plasma beta. **June 30, 2019**

## High Resolution Imaging Spectroscopy of a Tiny Sigmoidal Mini-filament Eruption

[Jiasheng Wang](#), [Jeongwoo Lee](#), [Jongchul Chae](#), [Yan Xu](#), [Wenda Cao](#), [Haimin Wang](#)

ApJ 2024

<https://arxiv.org/pdf/2402.08483.pdf>

Minifilament (MF) eruption producing small jets and micro-flares is regarded as an important source for coronal heating and the solar wind transients through studies mostly based on coronal observations in the extreme ultraviolet (EUV) and X-ray wavelengths. In this study, we focus on the chromospheric plasma diagnostics of a tiny minifilament in quiet Sun located at  $[71'', 450'']$  on **2021--08--07** at 19:11 UT observed as part of the ninth encounter of the PSP campaign. Main data obtained are the high cadence, high resolution spectroscopy from the Fast Imaging Solar Spectrograph (FISS) and high-resolution magnetograms from the Near InfraRed Imaging Spectropolarimeter (NIRIS)

on the 1.6-m Goode Solar Telescope (GST) at Big Bear Solar Observatory (BBSO). The mini-filament with size  $\sim 1'' \times 5''$  and a micro-flare are detected in both the  $H\alpha$  line center and SDO/AIA 193, 304-Å images. On the NIRIS magnetogram, we found that the cancellation of a magnetic bipole in the footpoints of the minifilament triggered its eruption in a sigmoidal shape. By inversion of the  $H\alpha$  and Ca II spectra under the embedded cloud model, we found a temperature increase of 3,800 K in the brightening region, associated with rising speed average of MF increased by  $18 \text{ km s}^{-1}$ . This cool plasma is also found in the EUV images. We estimate the kinetic energy change of the rising filament as  $1.5 \times 10^{25}$ -ergs, and thermal energy accumulation in the MF,  $1.4 \times 10^{25}$ -ergs. From the photospheric magnetograms, we find the magnetic energy change is  $1.6 \times 10^{26}$ -ergs across the PIL of converging opposite magnetic elements, which amounts to the energy release in the chromosphere in this smallest two-ribbon flare ever observed. **2021 August 7,**

## **Onset mechanism of an inverted U-shaped solar filament eruption revealed by NVST, SDO, and STEREO-A observations**

[Jincheng Wang](#), [Xiaoli Yan](#), [Qiangwei Cai](#), [Zhike Xue](#), [Liheng Yang](#), [Qiaoling Li](#), [Zhe Xu](#), [Yunfang Cai](#), [Liping Yang](#), [Yang Peng](#), [Xia Sun](#), [Xinsheng Zhang](#), [Yian Zhou](#)

A&A 684, A14 2024

<https://arxiv.org/pdf/2401.00185.pdf>

<https://www.aanda.org/articles/aa/pdf/2024/04/aa47962-23.pdf>

Context. Solar filaments, also called solar prominences when appearing on the solar limb, consist of dense, cool plasma suspended in the hot and tenuous corona, which are the main potential sources of solar storms.

Aims. To understand the onset mechanism of solar filaments, we investigate the eruption process of an inverted U-shaped solar filament and two precursory jet-like activities.

Methods. Utilizing observations from the New Vacuum Solar Telescope (NVST), Solar Dynamics Observatory (SDO), and Solar Terrestrial Relations Observatory-Ahead (STEREO-A), we investigate the event from two distinct observational perspectives: on the solar disk using NVST and SDO, and on the solar limb using STEREO-A. We employ both a non-linear force-free field model and a potential field model to reconstruct the coronal magnetic field, aiming to understand its magnetic properties.

Results. Two precursor jet-like activities were observed before the eruption, displaying an untwisted rotation. The second activity released an estimated twist of over two turns. During these two jet-like activities, “Y”-shaped brightenings, newly emerging magnetic flux accompanied by magnetic cancellation, and the formation of newly moving fibrils were identified. Combining these observational features, it can be inferred that these two precursor jet-like activities released the magnetic field constraining the filament and were caused by newly emerging magnetic flux. Before the filament eruption, it was observed that some moving flows had been ejected from the site as the onset of two jet-like activities, indicating the same physical process as two jet-like activities. Extrapolations revealed that the filament laid under the height of the decay index of 1.0 and had strong magnetic field (540 Gauss) and a high twist number (2.4 turns) before the eruption. An apparent rotational motion was observed during the filament eruption.

Conclusions. We deduce that the solar filament, exhibiting an inverted U-shape, is a significantly twisted flux rope. The eruption of the filament was initiated by the release of constraining magnetic fields through continuous magnetic reconnection. This reconnection process was caused by the emergence of newly magnetic flux. **September 12, 2017**

## **The Impulsive Acceleration of a Solar Filament Eruption Associated with a B-class Flare**

Xinyue [Wang](#)<sup>1</sup>, Hongqiang Song<sup>1</sup>, Yao Chen<sup>1,2</sup>, Leping Li<sup>3</sup>, Zhenyong Hou<sup>4</sup>, and Ruisheng Zheng<sup>1</sup>  
**2023 ApJ 957 58**

<https://iopscience.iop.org/article/10.3847/1538-4357/acff5d/pdf>

The eruption of magnetic flux ropes (MFRs), often taking filaments together, leads to coronal mass ejections (CMEs). Theoretical studies propose that both the resistive magnetic reconnection and the ideal instability of an MFR system can release magnetic-free energy and accelerate CMEs (i.e., MFRs or filaments) during eruptions. Observations find that the full kinematic evolution of CMEs usually undergoes three phases: the initiation phase, impulsive acceleration phase, and propagation phase. The impulsive acceleration phase often starts and ceases simultaneously with the flare onset time and peak time, respectively. This synchronization can be explained by the positive feedback relationship between the acceleration of CMEs and flare magnetic reconnection, and suggests that the reconnection has the dominant contribution to the acceleration of CMEs. It is rare to see strong evidence that supports the dominant contribution of ideal instability to the acceleration. In this paper, we report an intriguing filament eruption that occurred on **2011 May 11**. Its complete acceleration is well recorded by the Atmospheric Imaging Assembly on board the Solar Dynamics Observatory. The kinematic analysis shows that the impulsive acceleration phase starts and ceases obviously earlier than the flare onset time and peak time, respectively, which means a complete asynchronization between the impulsive acceleration phase and flare rise phase, and strongly supports that the ideal instability plays a dominant role in this impulsive acceleration. Furthermore, the accompanied flare is a B-class one, also implying that the contribution of reconnection is negligible in the energy release process.

**Erratum:** The Astrophysical Journal, 969:71 **2024** <https://iopscience.iop.org/article/10.3847/1538-4357/ad583a/pdf>

## **Radiative Magnetohydrodynamic Simulation of the Confined Eruption of a Magnetic Flux Rope: Unveiling the Driving and Constraining Forces**

Can **Wang**<sup>1,2</sup>, Feng Chen<sup>1,2</sup>, Mingde Ding<sup>1,2</sup>, and Zekun Lu<sup>1,2</sup>

2023 ApJ 956 106

<https://iopscience.iop.org/article/10.3847/1538-4357/acedfe/pdf>

We analyze the forces that control the dynamic evolution of a flux rope eruption in a three-dimensional radiative magnetohydrodynamic simulation. The confined eruption of the flux rope gives rise to a C8.5 flare. The flux rope rises slowly with an almost constant velocity of a few kilometers per second in the early stage when the gravity and Lorentz force are nearly counterbalanced. After the flux rope rises to the height at which the decay index of the external poloidal field satisfies the torus instability criterion, the significantly enhanced Lorentz force breaks the force balance and drives the rapid acceleration of the flux rope. Fast magnetic reconnection is immediately induced within the current sheet under the erupting flux rope, which provides strong positive feedback to the eruption. The eruption is eventually confined due to the tension force from the strong external toroidal field. Our results suggest that the gravity of plasma plays an important role in sustaining the quasi-static evolution of the pre-eruptive flux rope. The Lorentz force, which is contributed from both the ideal magnetohydrodynamic instability and magnetic reconnection, dominates the dynamic evolution during the eruption process.

## **Towards a live homogeneous database of solar active regions based on SOHO/MDI and SDO/HMI synoptic magnetograms. I. Automatic detection and calibration**

[Ruihui Wang](#), [Jie Jiang](#), [Yukun Luo](#)

Astrophysical Journal Supplement Series 2023

<https://arxiv.org/pdf/2308.06914.pdf> File

Recent studies indicate that a small number of rogue solar active regions (ARs) may have a significant impact on the end-of-cycle polar field and the long-term behavior of solar activity. The impact of individual ARs can be qualified based on their magnetic field distribution. This motivates us to build a live homogeneous AR database in a series of papers. As the first of the series, we develop a method to automatically detect ARs from 1996 onwards based on SOHO/MDI and SDO/HMI synoptic magnetograms. The method shows its advantages in excluding decayed ARs and unipolar regions and being compatible with any available synoptic magnetograms. The identified AR flux and area are calibrated based on the co-temporal SDO/HMI and SOHO/MDI data. The homogeneity and reliability of the database are further verified by comparing it with other relevant databases. We find that ARs with weaker flux have a weaker cycle dependence. Stronger ARs show the weaker cycle 24 compared with cycle 23. Several basic parameters, namely, location, area, and flux of negative and positive polarities of identified ARs are provided in the paper. This paves the way for AR's new parameters quantifying the impact on the long-term behavior of solar activity to be presented in the subsequent paper of the series. The constantly updated database covering more than two full solar cycles will be beneficial for the understanding and prediction of the solar cycle. The database and the detection codes are accessible online.

## **Observations of Mini Coronal Dimmings Caused by Small-scale Eruptions in the Quiet Sun**

[Rui Wang](#), [Ying D. Liu](#), [Xiaowei Zhao](#), [Huidong Hu](#)

ApJL 2023

<https://arxiv.org/pdf/2307.11406.pdf>

Small-scale eruptions could play an important role in coronal heating, generation of solar energetic particles (SEPs), and mass source of the solar wind. However, they are poorly observed, and their characteristics, distributions, and origins remain unclear. Here a mini coronal dimming was captured by the recently launched Solar Orbiter spacecraft. The observations indicate that a minifilament eruption results in the dimming and takes away approximately  $(1.65 \pm 0.54) \times 10^{13}$  g of mass, which also exhibits similar features as the sources of SEP events. The released magnetic free energy is of the order of  $\sim 10^{27}$  erg. Our results suggest that weak constraining force makes the flux rope associated with the minifilament easily enter a torus-unstable domain. We discuss that weak magnetic constraints from low-altitude background fields may be a general condition for the quiet-Sun eruptions, which provide a possible mechanism for the transport of coronal material and energy from the lower to the middle or even higher corona. 2020 May 20-21

## **The 2013 November 12 Solar Energetic Electron Event Associated with Solar Jets**

Wen **Wang**<sup>1,2</sup>, Andrea Francesco Battaglia<sup>2,3</sup>, Säm Krucker<sup>2,4</sup>, and Linghua Wang<sup>1</sup>

2023 ApJ 950 118

<https://iopscience.iop.org/article/10.3847/1538-4357/accc86/pdf>

We investigate the hard X-ray (HXR) flare-associated "prompt" solar energetic electron (SEE) 2013 November 12 event with joint EUV jet observations from Solar Dynamics Observatory/Atmospheric Imaging Assembly and STEREO-A/EUVI. The SEE energy spectrum observed by Wind/3D Plasma and Energetic Particle shows a triple-power-law shape with a low-energy break of  $10.0 \pm 1.7$  keV and a high-energy break of  $56.6 \pm 8.9$  keV, which has never been reported before for jet-related SEE events. Associated HXR emissions observed by RHESSI and FGST/Gamma-ray Burst Monitor show three distinctive peaks with different spectral indices  $\beta_{\text{HPE}}$  of HXR-producing electrons (HPEs) derived by means of thick-target bremsstrahlung model. The high-energy spectral index  $\beta_3 = 4.63 \pm 0.65$  of SEE is consistent with the HPE spectral index  $\beta_{\text{HPE}}$  derived in HXR peak 1 but different from  $\beta_{\text{HPE}}$  of HXR peak 2 and peak 3. The main stream of EUV jets reaches a speed of  $370 \pm 25$  km s<sup>-1</sup> after an acceleration of up to  $2.9 \pm 0.4$  km s<sup>-2</sup> in a timescale of  $\sim 2$  minutes, and the acceleration time coincides with the decay phase of HXR peak 1.

EUV observations from two different viewing directions help to reconstruct the jet magnetic configurations. After the investigation on HXR emissions and jet configurations, the interchange-reconnection model triggered by the emerging flux could be a satisfactory explanation for this jet event.

### **Efficient Electron Acceleration Driven by Flux Rope Evolution during Turbulent Reconnection**

Z. Wang<sup>1,2</sup>, A. Vaivads<sup>2</sup>, H. S. Fu<sup>1,3</sup>, J. B. Cao<sup>1,3</sup>, and Y. Y. Liu<sup>1,3</sup>

2023 ApJ 946 39

<https://iopscience.iop.org/article/10.3847/1538-4357/acbd3e/pdf>

Magnetic flux ropes or magnetic islands are important structures responsible for electron acceleration and energy conversion during turbulent reconnection. However, the evolution of flux ropes and the corresponding electron acceleration process still remain open questions. In this paper, we present a comparative study of flux ropes observed by the Magnetospheric Multiscale mission in the outflow region during an example of turbulent reconnection in Earth's magnetotail. Interestingly, we find the farther the flux rope is away from the X-line, the bigger the size of the flux rope and the slower it moves. We estimate the power density converted at the observed flux ropes via the three fundamental electron acceleration mechanisms: Fermi, betatron, and parallel electric field. The dominant acceleration mechanism at all three flux ropes is the betatron mechanism. The flux rope that is closest to the X-line, having the smallest size and the fastest moving velocity, is the most efficient in accelerating electrons. Significant energy also returns from particles to fields around the flux ropes, which may facilitate the turbulence in the reconnection outflow region. **2020 August 3**

### **High-resolution He I 10830 Å narrowband imaging for precursors of chromospheric jets and their quasi-periodic properties**

[Ya Wang](#), [Qingmin Zhang](#), [Zhenxiang Hong](#), [Jinhua Shen](#), [Haisheng Ji](#), [Wenda Cao](#)

A&A 672, A173 2023

<https://arxiv.org/pdf/2303.07049.pdf>

<https://www.aanda.org/articles/aa/pdf/2023/04/aa44607-22.pdf>

Solar jets are well-collimated plasma ejections in the solar atmosphere. They are prevalent in active regions, the quiet Sun, and even coronal holes. They display a range of temperatures, yet the nature of the cool components has not been fully investigated. In this paper, we show the existence of the precursors and quasi-periodic properties for two chromospheric jets, mainly utilizing the He I 10830 Å narrowband filtergrams taken by the Goode Solar Telescope (GST). The extreme ultraviolet (EUV) counterparts present during the eruption correspond to a blowout jet (jet 1) and a standard jet (jet 2), as observed by the Atmospheric Imaging Assembly (AIA) on board the Solar Dynamic Observatory (SDO). The high-resolution He I 10830 Å observation captures a long-lasting precursor for jet 1, signified by a series of cool ejections. They are recurrent jet-like features with a quasi-period of about five minutes. On the other hand, the cool components of jet 2, recurrently accompanied by EUV emissions, present a quasi-periodic behavior with a period of about five minutes. Both the EUV brightening and He I 10830 Å absorption show that there was a precursor for jet 2 that occurred about five minutes before its onset. We propose that the precursor of jet 1 may be the consequence of chromospheric shock waves, since the five-minute oscillation from the photosphere can leak into the chromosphere and develop into shocks. Then, we find that the quasi-periodic behavior of the cool components of jet 2 may be related to magnetic reconnections modulated by the oscillation in the photosphere. **22 Jul 2011**

### **MHD simulation of Solar Eruption from Active Region 11429 Driven by Photospheric Velocity Field**

[Xinyi Wang](#), [Chaowei Jiang](#), [Xueshang Feng](#)

ApJ 942 L41 2023

<https://arxiv.org/pdf/2301.00144.pdf>

<https://iopscience.iop.org/article/10.3847/2041-8213/acaec3/pdf>

Data-driven simulation is becoming an important approach for realistically characterizing the configuration and evolution of solar active regions, revealing the onset mechanism of solar eruption events and hopefully achieving the goal of accurate space weather forecast, which is beyond the scope of any existing theoretical modelling. Here we performed a full 3D MHD simulation using the data-driven approach and followed the whole evolution process from quasi-static phase to eruption successfully for solar active region NOAA 11429. The MHD system was driven at the bottom boundary by photospheric velocity field, which is derived by the DAVE4VM method from the observed vector magnetograms. The simulation shows that a magnetic flux rope was generated by persistent photospheric flow before the flare onset and then triggered to erupt by torus instability. Our simulation demonstrates a high degree of consistency with observations in the pre-eruption magnetic structure, the time scale of quasi-static stage, the pattern of flare ribbons as well as the time evolution of magnetic energy injection and total unsigned magnetic flux. We further found that an eruption can also be initiated in the simulation as driven by only the horizontal components of photospheric flow, but a comparison of the different simulations indicates that the vertical flow at the bottom boundary is necessary in reproducing more realistically these observed features, emphasizing the importance of flux emergence during the development of this AR. **2012 March 5-10**

## Investigating pre-eruptive magnetic properties at the footprints of erupting magnetic flux ropes

[Wensi Wang](#), [Jiong Qiu](#), [Rui Liu](#), [Chunming Zhu](#), [Kai E Yang](#), [Qiang Hu](#), [Yuming Wang](#)

ApJ 943 80 2022

<https://arxiv.org/pdf/2211.15909.pdf>

<https://iopscience.iop.org/article/10.3847/1538-4357/aca6e1/pdf>

It is well established that solar eruptions are powered by free magnetic energy stored in current-carrying magnetic field in the corona. It has also been generally accepted that magnetic flux ropes (MFRs) are a critical component of many coronal mass ejections (CMEs). What remains controversial is whether MFRs are present well before the eruption. Our aim is to identify progenitors of MFRs, and investigate pre-eruptive magnetic properties associated with these progenitors. Here we analyze 28 MFRs erupting within 45 deg from the disk center from 2010 to 2015. All MFRs' feet are well identified by conjugate coronal dimmings. We then calculate magnetic properties at the feet of the MFRs, prior to their eruptions, using Helioseismic and Magnetic Imager (HMI) vector magnetograms. Our results show that only 8 erupting MFRs are associated with significant non-neutralized electric currents, 4 of which also exhibit pre-eruptive dimmings at the foot-prints. Twist and current distributions are asymmetric at the two feet of these MFRs. The presence of pre-eruption dimmings associated with non-neutralized currents suggests the pre-existing MFRs. Furthermore, evolution of conjugate dimmings and electric currents within the foot-prints can provide clues about the internal structure of MFRs and their formation mechanism. 7 Mar 2011, 21 Jun 2011, 2 Aug 2011, 30 Sep 2011, 10 Mar 2012, 14 Jun 2012, 12 Aug 2013, 30 Aug 2013, 12 Oct 2013, 21 Sep 2014,

Table 1. Overview of Eruptions 2010-2015

## Overexpansion-dominated Coronal Mass Ejection Formation and Induced Radio Bursts

[B. T. Wang](#), [X. Cheng](#), [H. Q. Song](#), [M. D. Ding](#)

A&A 666, A166 2022

<https://arxiv.org/pdf/2209.06508.pdf>

<https://www.aanda.org/articles/aa/pdf/2022/10/aa44275-22.pdf>

Aims. Coronal Mass Ejections (CMEs) are the most fascinating explosion in the solar system; however, their formation is still not fully understood. Methods. Here, we investigate a well-observed CME on 2021 May 07 that showed a typical three-component structure and was continuously observed from 0 to 3 R<sub>sun</sub> by a combination of SDO/AIA (0--1.3 R<sub>sun</sub>), PROBA2/SWAP (0--1.7 R<sub>sun</sub>) and MLSO/K-Cor (1.05--3 R<sub>sun</sub>). Furthermore, we compare the morphological discrepancy between the CME white-light bright core and EUV blob. In the end, we explore the origin of various radio bursts closely related to the interaction of the CME overexpansion with nearby streamer. Results. An interesting finding is that the height increases of both the CME leading front and bright core are dominated by the overexpansion during the CME formation. The aspect ratios of the CME bubble and bright core, quantifying the overexpansion, are found to decrease as the SO/STIX 4--10 keV and GOES 1--8 A soft X-ray flux of the associated flare increases near the peaks, indicating an important role of the flare reconnection in the first overexpansion. The CME bubble even takes place a second overexpansion although relatively weak, which is closely related to the compression with a nearby streamer and likely arises from an ideal MHD process. Moreover, the CME EUV blob is found to be relatively lower and wider than the CME white-light bright core, may correspond to the bottom part of the growing CME flux rope. The interaction between the CME and the streamer leads to two type II radio bursts, one normally drifting and one stationary, which are speculated to be induced at two different sources of the CME-driven shock front. The bidirectional electrons evidenced by series of "C-shaped" type III bursts suggest that the interchange reconnection be also involved during the interaction of the CME and streamer.

## Two Homologous Quasi-periodic Fast-mode Propagating Wave Trains Induced by Two Small-scale Filament Eruptions

Jincheng Wang<sup>1,2,3</sup>, Xiaoli Yan<sup>1,2,3</sup>, Zhike Xue<sup>1,2</sup>, Liheng Yang<sup>1,2</sup>, Qiaoling Li<sup>4</sup>, Zhe Xu<sup>1,3</sup>, Liping Yang<sup>1,5</sup>, and Yang Peng<sup>1,5</sup>

2022 ApJL 936 L12

<https://iopscience.iop.org/article/10.3847/2041-8213/ac8b79/pdf>

We present two homologous quasi-periodic fast-mode propagating (QFP) wave trains excited by two small-scale filament eruptions nearby a sunspot on 2017 September 12. By using observations from several ground-based and space-based instruments, it is found that the eruptions of two small-scale filaments resulted in some accompanying solar phenomena/activities (such as radio bursts, GOES C-class flares, coronal bright fronts, and QFP wave trains). The QFP wave trains run behind the main coronal bright fronts with a constant propagating speed of about 800 km s<sup>-1</sup>, while two main coronal bright fronts traveled away from the flare kernel obeying the power-law functions

of  $S(t) = 894.9 * (t - 7.43)^{0.60} + 76.8$  and  $S(t) = 705.3 * (t - 19.12)^{0.47} + 57.5$ , respectively. The period of the first QFP wave train was estimated to be about 59 s, while the second QFP wave train has two periods of about 70 and 37 s. On the other hand, the intensity peaks of 94 and 335 Å passbands in the flare kernel exhibit some perturbations during the occurrences of the QFP wave trains. With the wavelet analysis and their synchronization, these perturbations and the QFP wave trains are tightly related phenomena, which suggests that they have a common exciting mechanism. Furthermore, we find that the emissions of the intensity peak mainly originate from the one footpoint of flare loops during the occurrence of the QFP wave trains. According to the above features, we conclude that the QFP wave trains

are excited in the energy release process associated with magnetic reconnection and are closely related to the outflow of the magnetic reconnection.

## **MHD Simulation of Homologous Eruptions from Solar Active Region 10930 Caused by Sunspot Rotation**

[Xinyi Wang](#), [Chaowei Jiang](#), [Xueshang Feng](#), [Aiying Duan](#), [Xinkai Bian](#)

ApJ **938** 61 **2022**

<https://arxiv.org/pdf/2208.08957.pdf>

<https://iopscience.iop.org/article/10.3847/1538-4357/ac8d0e/pdf>

The relationship between solar eruption and sunspot rotation has been widely reported, and the underlying mechanism requires to be studied. Here we performed a full 3D MHD simulation of data-constrained approach to study the mechanism of flare eruptions in active region (AR) NOAA 10930, which is characterized by continuous sunspot rotation and homologous eruptions. We reconstructed the potential magnetic field from the magnetogram of Hinode/SOT as the initial condition and drove the MHD system by applying continuous sunspot rotation at the bottom boundary. The key magnetic structure before the major eruptions and the pre-formed current sheet were derived, which is responsible for the complex MHD evolution with multiple stages. The major eruptions were triggered directly by fast reconnection in the pre-formed current sheet above the main polarity inversion line between the two major magnetic polarities of the AR. Furthermore, our simulation shows the homologous eruption successfully. It has reasonable consistence with observations in relative strength, energy release, X-ray and  $H\{\alpha\}$  features and time interval of eruptions. In addition, the rotation angle of the sunspot before the first eruption in the simulation is also close to the observed value. Our simulation offers a scenario different from many previous studies based on ideal instabilities of twisted magnetic flux rope, and shows the importance of sunspot rotation and magnetic reconnection in efficiently producing homologous eruptions by continuous energy injection and impulsive energy release in a recurrent way. **6, 13, 14 Dec 2006**

## **Radiative Magnetohydrodynamic Simulation of the Confined Eruption of a Magnetic Flux Rope: Magnetic Structure and Plasma Thermodynamics**

[Can Wang](#), [Feng Chen](#), [Mingde Ding](#), [Zekun Lu](#)

ApJL **933** L29 **2022**

<https://arxiv.org/pdf/2206.14188.pdf>

<https://iopscience.iop.org/article/10.3847/2041-8213/ac7c6f/pdf>

It is widely believed that magnetic flux ropes are the key structure of solar eruptions; however, their observable counterparts are not clear yet. We study a flare associated with flux rope eruption in a comprehensive radiative magnetohydrodynamic simulation of flare-productive active regions, especially focusing on the thermodynamic properties of the plasma involved in the eruption and their relation to the magnetic flux rope. The pre-existing flux rope, which carries cold and dense plasma, rises quasi-statically before the eruption onsets. During this stage, the flux rope does not show obvious signatures in extreme ultraviolet (EUV) emission. After the flare onset, a thin 'current shell' is generated around the erupting flux rope. Moreover, a current sheet is formed under the flux rope, where two groups of magnetic arcades reconnect and create a group of post-flare loops. The plasma within the 'current shell', current sheet, and post-flare loops are heated to more than 10 MK. The post-flare loops give rise to abundant soft X-ray emission. Meanwhile a majority of the plasma hosted in the flux rope is heated to around 1 MK, and the main body of the flux rope is manifested as a bright arch in cooler EUV passbands such as AIA 171 Å-channel.

## **Avalanches of magnetic flux rope in the state of self-organized criticality**

[W B Wang](#), [C Li](#), [Z L Tu](#), [J H Guo](#), [P F Chen](#), [F Y Wang](#)

Monthly Notices of the Royal Astronomical Society, Volume 512, Issue 2, May **2022**, Pages 1567–1573,

<https://doi.org/10.1093/mnras/stac633>

The self-organized criticality (SOC) is a universal theory to explain the ubiquitous power-law size distributions of astrophysical instabilities such as solar eruptions. One way to understand the dynamical processes of an SOC system is through cellular automaton (CA) simulations. Here, we develop a three-dimensional solar CA model that assumes a twisted magnetic flux rope (MFR), in which the avalanche takes place when a local magnetic vector potential exceeds a Gaussian distributed instability criterion, triggered by a global and space-dependent energy driving mechanism. To avoid non-physical released energies, an energy screening mechanism is applied to calculate the avalanche energies of each time-step. Our results show that the statistics of the CA simulated flaring events are comparable to the frequency distributions of observed solar flares originating from an individual active region. Due to the fact of the universality of MFRs, the CA model can be applied to many other astrophysical SOC systems.

## **Buildup of the Magnetic Flux Ropes in Homologous Solar Eruptions**

[Rui Wang](#), [Ying D. Liu](#), [Shangbin Yang](#), [Huidong Hu](#)

ApJ **925** 202 **2022**

<https://arxiv.org/pdf/2201.06817.pdf>

<https://iopscience.iop.org/article/10.3847/1538-4357/ac3f35/pdf>

Homologous coronal mass ejections (CMEs) are an interesting phenomenon, and it is possible to investigate the formation of CMEs by comparing multi-CMEs under a homologous physical condition. AR 11283 had been present on

the solar surface for several days when a bipole emerged on 2011 September 4. Its positive polarity collided with the pre-existing negative polarity belonging to a different bipole, producing recurrent solar activities along the polarity inversion line (PIL) between the colliding polarities, namely the so-called collisional PIL (cPIL). Our results show that a large amount of energy and helicity were built up in the form of magnetic flux ropes (MFRs), with recurrent release and accumulation processes. These MFRs were built up along the cPIL. A flux deficit method is adopted and shows that magnetic cancellation happens along the cPIL due to the collisional shearing scenario proposed by Chintzoglou et al. The total amount of canceled flux was  $\sim 0.7 \times 10^{21}$  Mx with an uncertainty of  $\sim 13.2\%$  within the confidence region of the  $30^\circ$  sun-center distance. The canceled flux amounts to 24% of the total unsigned flux of the bipolar magnetic region. The results show that the magnetic fields beside the cPIL are very sheared, and the average shear angle is above  $70^\circ$  after the collision. The fast expansion of the twist kernels of the MFRs and the continuous eruptive activities are both driven by the collisional shearing process. These results are important for better understanding the buildup process of the MFRs associated with homologous solar eruptions. **4-8 Sep 2011**

**HMI Science Nuggets** #173 Feb 2022 <http://hmi.stanford.edu/hminuggets/?p=3823>

## **Cosmic Ray Variation Lags behind Sunspot Number due to the Late Opening of Solar Magnetic Field**

Yuming Wang, [Jingnan Guo](#), [Gang Li](#), [Elias Roussos](#), [Junwei Zhao](#)

ApJ 2022

<https://arxiv.org/pdf/2201.01908.pdf>

Galactic cosmic rays (GCRs), the highly energetic particles that may raise critical health issues of astronauts in space, are modulated by solar activity with their intensity lagging behind the sunspot number (SSN) variation by about one year. Previously, this lag has been attributed to result of outward convecting solar wind and inward propagating GCRs. However, the lag's amplitude and its solar-cycle dependence are still not fully understood (e.g., Ross & Chaplin 2019). By investigating the solar surface magnetic field, we find that the source of heliospheric magnetic field, i.e., the open magnetic flux on the Sun, already lags behind SSN before it convects into heliosphere along with the solar wind, and the delay during odd cycles is longer than that during sequential even cycles. Thus, we propose that the GCR lag is primarily due to the greatly late opening of the solar magnetic field with respect to SSN, though solar wind convection and particle transport in the heliosphere also matters. We further investigate the origin of the open flux from different latitudes of the Sun and found that the total open flux is significantly contributed by that from low latitudes where coronal mass ejections frequently occur and also show an odd-even cyclic pattern. Our findings challenge existing theories, and may serve as the physical basis of long-term forecasts radiation dose estimates for manned deep-space exploration missions.

**Figure 6. The solar cycle variations of the CME numbers**

## **Velocities of an Erupting Filament**

[Shuo Wang](#), [Jack M. Jenkins](#), [Karin Muglach](#), [Valentin Martinez Pillet](#), [Christian Beck](#), [David M. Long](#), [Debi Prasad Choudhary](#), [James McAteer](#)

ApJ 926 18 2022

<https://arxiv.org/pdf/2111.07830.pdf>

<https://iopscience.iop.org/article/10.3847/1538-4357/ac3a04/pdf>

Solar filaments exist as stable structures for extended periods of time before many of them form the core of a CME. We examine the properties of an erupting filament on **2017 May 29--30** with high-resolution He I 10830 Å and H $\alpha$  spectra from the Dunn Solar Telescope, full-disk Dopplergrams of He I 10830 Å from the Chromospheric Telescope, and EUV and coronagraph data from SDO and STEREO. Pre-eruption line-of-sight velocities from an inversion of He I with the HAZEL code exhibit coherent patches of 5 Mm extent that indicate counter-streaming and/or buoyant behavior. During the eruption, individual, aligned threads appear in the He I velocity maps. The distribution of velocities evolves from Gaussian to strongly asymmetric. The maximal optical depth of He I 10830 Å decreased from  $\tau = 1.75$  to 0.25, the temperature increased by 13 kK, and the average speed and width of the filament increased from 0 to 25 km s $^{-1}$  and 10 to 20 Mm, respectively. All data sources agree that the filament rose with an exponential acceleration reaching 7.4 m s $^{-2}$  that increased to a final velocity of 430 km s $^{-1}$  at 22:24 UT; a CME was associated with this filament eruption. The properties during the eruption favor a kink/torus instability, which requires the existence of a flux rope. We conclude that full-disk chromospheric Dopplergrams can be used to trace the initial phase of on-disk filament eruptions in real-time, which might potentially be useful for modelling the source of any subsequent CMEs.

## **Detection of Flare-associated CME Candidates on Two M-dwarfs by GWAC and Fast, Time-resolved Spectroscopic Follow-ups**

J. Wang<sup>1,2</sup>, L. P. Xin<sup>2</sup>, H. L. Li<sup>2</sup>, G. W. Li<sup>2</sup>, S. S. Sun<sup>1,2,3</sup>, C. Gao<sup>1,2,3</sup>, X. H. Han<sup>2</sup>, Z. G. Dai<sup>4</sup>, E. W. Liang<sup>1</sup>, X. Y. Wang<sup>4</sup>Show full author list

2021 ApJ 916 92

<https://doi.org/10.3847/1538-4357/ac096f>

The flare-associated stellar coronal mass ejections (CMEs) of solar-like and late-type stars profoundly impact the habitability of any exoplanets in the systems. In this paper, we report the detection of flare-associated CMEs for two M-dwarfs, thanks to a high-cadence survey carried out by the Ground Wide-angle Camera system and fast photometric and

spectroscopic follow-ups. The flare energies in the R band are determined to be  $1.6 \times 10^{35}$  erg and  $8.1 \times 10^{33}$  erg based on modeling of their light curves. The time-resolved spectroscopic observations start at about 20 and 40 minutes after the trigger in both cases. The large projected maximum velocity of  $\sim 500\text{--}700$  km s<sup>-1</sup> suggests that the high-velocity wings of their H $\alpha$  emission lines most likely result from CME events in both stars, after excluding the possibility of chromospheric evaporation and coronal rain. The masses of the CMEs are estimated to be  $1.5\text{--}4.5 \times 10^{19}$  g and  $7.1 \times 10^{18}$  g.

### **High-resolution He I 10830 Å Narrowband Imaging for a Small-scale Chromospheric Jet**

Ya Wang<sup>1,2</sup>, Qingmin Zhang<sup>1,3</sup>, and Haisheng Ji<sup>1,3</sup>

2021 ApJ 913 59

<https://doi.org/10.3847/1538-4357/abf2b9>

Solar jets are ubiquitous phenomena in the solar atmosphere. They are important in mass and energy transport to the upper atmosphere and interplanetary space. Here, we report a detailed analysis of a small-scale chromospheric jet with high-resolution He I 10830 Å and TiO 7057 Å images observed by the 1.6 m aperture Goode Solar Telescope at the Big Bear Solar Observatory. The observation reveals the finest dark threads inside the jet are rooted in the intergranular lanes. Their width is equal to the telescope's diffraction limit at 10830 Å ( $\sim 100$  km). The jet is recurrent and its association with the emergence and convergence of magnetic flux is observed. Together with other important features like photospheric flow toward the magnetic polarity inversion line, a bald-patch magnetic configuration, and earlier excitation of helium atoms, we propose that the jet might be initiated by magnetic reconnection in a U-shaped loop configuration. The plasmoid configuration results from the possible buoyancy of the magnetic reconnection, which reoccurs in a second step with an overlying magnetic field line. Notably, the second-step magnetic reconnection produces not only bidirectional cool or hot flows but also a new U-shaped loop configuration. The feature may be used to explain the recurrent behavior of the jet, since the new U-shaped loop can be driven to reconnect again.

### **The Causes of Peripheral Coronal Loop Contraction and Disappearance Revealed in a Magnetohydrodynamic Simulation of Solar Eruption**

Juntao Wang, Chaowei Jiang, Ding Yuan, Peng Zou

ApJ 911 2 2021

<https://arxiv.org/pdf/2102.06877.pdf>

<https://doi.org/10.3847/1538-4357/abe637>

The phenomenon of peripheral coronal loop contraction during solar flares and eruptions, recently discovered in observations, gradually intrigues solar physicists. However, its underlying physical mechanism is still uncertain. One is Hudson (2000)'s implosion conjecture which attributes it to magnetic pressure reduction in the magnetic energy liberation core, while other researchers proposed alternative explanations. In previous observational studies we also note the disappearance of peripheral shrinking loops in the late phase, of which there is a lack of investigation and interpretation. In this paper, we exploit a full MHD simulation of solar eruption to study the causes of the two phenomena. It is found that the loop motion in the periphery is well correlated with magnetic energy accumulation and dissipation in the core, and the loop shrinkage is caused by a more significant reduction in magnetic pressure gradient force than in magnetic tension force, consistent with the implosion conjecture. The peripheral contracting loops in the late phase act as inflow to reconnect with central erupting structures, which destroys their identities and naturally explains their disappearance. We also propose a positive feedback between the peripheral magnetic reconnection and the central eruption.

### **Erupting Magnetic Flux Rope Affects Running Penumbra Waves**

Wensi Wang, Rui Liu

A&A 2021

<https://arxiv.org/pdf/2101.04915.pdf>

Context. It is well known that solar flares have broad impacts on the low atmosphere, but it is largely unknown how they affect sunspot waves and oscillations. It is also under debate as to whether the flare-induced photospheric changes are due to the momentum conservation with coronal mass ejections or due to magnetic reconnection. Aims. To shed light on the so-called "back reaction" of solar eruptions, we investigated how running penumbra waves (RPWs) at one foot of an erupting magnetic flux rope (MFR) responds to the rope buildup and subsequent erosion. Results. During the rope-buildup stage, the western foot of the rope, which is completely enclosed by a hooked ribbon, expands rapidly and consequently overlaps a sunspot penumbra. This converts the original penumbral field into the rope field, which is associated with a transient increase in electric currents flowing through the ribbon-swept penumbral region. During the rope-erosion stage, the rope foot shrinks as the eastern section of the hooked ribbon slowly sweeps the same penumbral region, where the rope field is converted into flare loops. This conversion induces mixed effects on the photospheric field inclination but heats up the low atmosphere at the footpoints of these flare loops to transition-region temperatures, therefore resulting in the post-eruption RPWs with an enhanced contrast in the 1600Å passband and an extended bandwidth to low frequencies at 3-5 mHz, compared with the pre-eruption RPWs that peak at 6 mHz. Conclusions. This observation clearly demonstrates that it is the magnetic reconnection in the corona that impacts the low atmosphere and leads to the changing behaviors of RPWs, which, in turn, offer a new window to diagnose flare reconnections. **2015**

November 4

See Paper I Wang, W., Liu, R., Wang, Y., et al. 2017, Nature communications, 8, 1330



## **A small-scale filament eruption inducing Moreton Wave, EUV Wave and Coronal Mass Ejection**

Jincheng [Wang](#), [Xiaoli Yan](#), [Defang Kong](#), [Zhike Xue](#), [Liheng Yang](#), [Qiaoling Li](#)

ApJ **2020**

<https://arxiv.org/pdf/2004.07488.pdf>

With the launch of SDO, many EUV waves were observed during solar eruptions. However, the joint observations of Moreton and EUV waves are still relatively rare. We present an event that a small-scale filament eruption simultaneously results in a Moreton wave, an EUV wave and a Coronal Mass Ejection in active region NOAA 12740. Firstly, we find that some dark elongate lanes or filamentary structures in the photosphere existed under the small-scale filament and drifted downward, which manifests that the small-scale filament was emerging and lifting from subsurface. Secondly, combining the simultaneous observations in different Extreme UltraViolet (EUV) and H $\alpha$  passbands, we study the kinematic characteristics of the Moreton and EUV waves. The comparable propagating velocities and the similar morphology of Moreton and different passbands EUV wavefronts were obtained. We deduce that Moreton and different passbands EUV waves were the perturbations in different temperature-associated layers induced by the coronal magneto-hydrodynamic shock wave. We also find the refracted, reflected and diffracted phenomena during the propagation of the EUV wave. By using power-law fittings, the kinematic characteristics of unaffected, refracted and diffracted waves were obtained. The extrapolation field derived by the potential field source surface (PFSS) model manifests that the existence of an interface of different magnetic system (magnetic separatrix) result in refraction, reflection and deviation of the EUV wave. **2019 May 06**

## **Magnetic Structure of an Erupting Filament**

Shuo [Wang](#), [Jack M. Jenkins](#), [Valentin Martinez Pillet](#), [Christian Beck](#), [David M. Long](#), [Debi Prasad Choudhary](#), [Karin Muglach](#), [James McAteer](#)

ApJ **892 75 2020**

<https://arxiv.org/pdf/2002.02104.pdf>

<https://doi.org/10.3847/1538-4357/ab7380>

The full 3-D vector magnetic field of a solar filament prior to eruption is presented. The filament was observed with the Facility Infrared Spectropolarimeter at the Dunn Solar Telescope in the chromospheric He i line at 10830 Å on **May 29 and 30, 2017**. We inverted the spectropolarimetric observations with the HANle and ZEeman Light (HAZEL) code to obtain the chromospheric magnetic field. A bimodal distribution of field strength was found in or near the filament. The average field strength was 24 Gauss, but prior to the eruption we find the 90th percentile of field strength was 435 Gauss for the observations on May 29. The field inclination was about 67 degree from the solar vertical. The field azimuth made an angle of about 47 to 65 degree to the spine axis. The results suggest an inverse configuration indicative of a flux rope topology. He i intensity threads were found to be co-aligned with the magnetic field direction. The filament had a sinistral configuration as expected for the southern hemisphere. The filament was stable on May 29, 2017 and started to rise during two observations on May 30, before erupting and causing a minor coronal mass ejection. There was no obvious change of the magnetic topology during the eruption process. Such information on the magnetic topology of erupting filaments could improve the prediction of the geoeffectiveness of solar storms.

## **On Deflection of Solar Coronal Mass Ejections by the Ambient Coronal Magnetic Field Configuration**

Jingjing [Wang](#), [J. Todd Hoeksema](#), [Siqing Liu](#)

JGR [Volume125, Issue8](#) August **2020** e2019JA027530

<https://arxiv.org/pdf/1909.06410.pdf>

<https://doi.org/10.1029/2019JA027530>

<https://agupubs.onlinelibrary.wiley.com/doi/epdf/10.1029/2019JA027530>

Solar Coronal Mass Ejections (CMEs) are sometimes deflected during their propagation. This deflection may be the consequence of interaction between a CME and a coronal hole or the solar wind. We analyze 44 halo-CMEs whose deflection angle exceeds 90 degrees. The coronal magnetic field configuration is computed from daily synoptic maps of magnetic field from SOHO/MDI and SDO/HMI using a Potential Field Source Surface (PFSS) model. By comparing the ambient magnetic field configuration and the measured position angles (MPA) of the CMEs, we conclude that the deflection of 80% of the CMEs (35 of 44) are consistent with the ambient magnetic field configuration, agreeing with previous studies. Of these 35, 71% are deflected toward the heliospheric current sheet (HCS), and 29 degrees toward a pseudo-streamer (PS), the boundary between the same-polarity magnetic field regions. This implies that the ambient coronal magnetic field configuration plays an important and major role in the deflection of CMEs, and that the HCS configuration is more important than PS. If we exclude 13 CMEs having much higher uncertainty from the sample, the agreement between the deflection of CMEs and the ambient field configuration increases substantially, reaching 94% in the new sample of 31 CMEs.

**Table 1.** Information table of 44 CMEs from the CDAW halo-CMEs list. (1998-2015)

## **Concept of the Solar Ring mission: Preliminary design and mission profile**

[YaMin Wang](#), [Xin Chen](#), [PengCheng Wang](#), [ChengBo Qiu](#), [YuMing Wang](#) & [YongHe Zhang](#)

[Science China Technological Sciences \(2020\)](#) , 63, 1699

<https://link.springer.com/content/pdf/10.1007/s11431-020-1612-y.pdf>

The Solar Ring mission, a concept to monitor the Sun and inner heliosphere from multiple perspectives, has been funded for pre-phase study by the Strategic Priority Program of Chinese Academy of Sciences in space sciences. The Solar Ring is comprised of 6 spacecraft, grouped in three pairs, moving around the Sun in an elliptical orbit in the ecliptic plane. The mission costs, including launch fee, deep-space maneuvers, and deployment time of the ring, are highly relevant to the working orbit, deep-space transfer, and phase angle within a group. The preliminary mission profile is analyzed and designed in this paper. The launch way, two spacecraft with one rocket, is adopted. The deployment time, phasing maneuvers, and C3 of launch energy are evaluated for the elliptical orbits with the perihelion between 0.7 and 0.9 AU using the rockets of Long March (LM) 3A and 3B. Numerical simulations show two candidate trajectories: fast deployment within 4 years by LM-3B, medium deployment more than 6 years by cheaper rocket of LM-3A. In order to obtain both fast deployment and low launch cost, another orbit profile is proposed by shortening the phase angle within a group. The suggested working orbits and the corresponding costs of launch, deployment time, and phasing maneuvers will strongly support the science objectives.

### **Formation and material supply of an active-region filament associated with newly emerging flux**

Jincheng [Wang](#), [Xiaoli Yan](#), [Qiaoling Guo](#), [Defang Kong](#), [Zhike Xue](#), [Liheng Yang](#), [Qiaoling Li](#)

MNRAS 488, Issue 3, September 2019, Pages 3794–3803

[sci-hub.se/10.1093/mnras/stz1935](http://sci-hub.se/10.1093/mnras/stz1935)

With the observations of Solar Dynamics Observatory(SDO)/Atmospheric Imaging Assembly (AIA) 304 Å and New Vacuum Solar Telescope (NVST) H $\alpha$  bands, we present the formation of an active-region filament in active region NOAA 11903 during the period from 02:00 to 10:00 UT on **2013 November 25**. A series of jets occurring in the vicinity of the south-western footpoint of the filament directly ejected cool and hot plasmas to filament height and supplied material for the filament. Some newly emerging flux is found in the vicinity of the south-western footpoint of the filament during these jets. In this paper, we mainly focus on the material supply for the formation of the filament. The plasma mass uploaded by the jets and the mass of the filament are estimated, which manifest the fact that the mass carried by the jets can supply sufficient material for the formation of the filament. We found two types of jets; one is H $\alpha$  jet, and the other is EUV jet. The significant finding is that some cool jets seen in the H $\alpha$  band but not in the SDO/AIA bands could also eject the cool material for the filament. These results suggest that cool plasma in the low atmosphere can be directly injected into the upper atmosphere and become the filament material by two types of jets. Moreover, the newly emerging flux with the non-potential field plays an important role in the appearance of the jets and the magnetic structure of the filament.

### **A New Automatic Tool for CME Detection and Tracking with Machine Learning Techniques**

Pengyu [Wang](#), [Yan Zhang](#), [Li Feng](#), [Hanqing Yuan](#), [Yuan Gan](#), [Shuting Li](#), [Lei Lu](#), [Beili Ying](#), [Weiqun Gan](#), [Hui Li](#)

ApJS 244 9 2019

<https://arxiv.org/pdf/1907.08798.pdf>

<https://doi.org/10.3847/1538-4365/ab340c>

With the accumulation of big data of CME observations by coronagraphs, automatic detection and tracking of CMEs has proven to be crucial. The excellent performance of convolutional neural network in image classification, object detection and other computer vision tasks motivates us to apply it to CME detection and tracking as well. We have developed a new tool for CME Automatic detection and tracking with Machine Learning (CAMEL) techniques. The system is a three-module pipeline. It is first a supervised image classification problem. We solve it by training a neural network LeNet with training labels obtained from an existing CME catalog. Those images containing CME structures are flagged as CME images. Next, to identify the CME region in each CME-flagged image, we use deep descriptor transforming to localize the common object in an image set. A following step is to apply the graph cut technique to finely tune the detected CME region. To track the CME in an image sequence, the binary images with detected CME pixels are converted from cartesian to polar coordinate. A CME event is labeled if it can move in at least two frames and reach the edge of coronagraph field of view. For each event, a few fundamental parameters are derived. The results of four representative CMEs with various characteristics are presented and compared with those from four existing automatic and manual catalogs. We find that CAMEL can detect more complete and weaker structures, and has better performance to catch a CME as early as possible. **22 Nov. 2011** , **01 Jan. 2012**, **18 Jan. 2012**, **21 Mar. 2012**

### **Possible Cool Prominence Materials Detected within Interplanetary Small Magnetic Flux Ropes**

J. M. [Wang](#)<sup>1,2</sup>, H. Q. Feng<sup>1</sup>, H. B. Li<sup>1</sup>, A. K. Zhao<sup>1</sup>, Z. J. Tian<sup>1</sup>, G. Q. Zhao<sup>1</sup>, Y. Zhao<sup>1</sup>, and Q. Liu<sup>1</sup>  
2019 ApJ 876 57

[sci-hub.se/10.3847/1538-4357/ab148b](http://sci-hub.se/10.3847/1538-4357/ab148b)

Previous studies indicate that interplanetary small magnetic flux ropes (SMFRs) are manifestations of microflare-associated small coronal mass ejections (CMEs), and the hot material with high-charge states heated by related microflares are found in SMFRs. Ordinary CMEs are frequently associated with prominence eruptions, and cool

prominence materials are found within some magnetic clouds (MCs). Therefore, the predicted small CMEs may also be frequently associated with small prominence eruptions. In this work, we aim to search for cool prominence materials within SMFRs. We examined all the O5+ and Fe6+ fraction data obtained by the Advanced Composition Explorer (ACE) spacecraft during 1998–2008 and found that 13 SMFRs might exhibit low-charge-state signatures of unusual O5+ and/or Fe6+ abundances. One of the 13 SMFRs also exhibited signatures of high ionic charge states. We also reported a SMFR with high Fe6+ fraction, but the values of Fe6+ is a little lower than the threshold defining unusual Fe6+. However, the Solar Dynamics Observatory/ Atmospheric Imaging Assembly observations confirmed that the progenitor CME of this SMFR is associated with a small eruptive prominence, and the observations also supported the prominence materials were embedded in the CME. These observations are at the edge of the capabilities of ACE/Solar Wind Ion Composition Spectrometer and it cannot be ruled out that they are solely caused by instrumental effects. If these observations are real, they provide new evidence for the conjecture that SMFRs are small-scale MCs but also imply that the connected small CMEs could be associated with flares and prominence eruptions.

**2002 July 19, 2006 September 21, 2011 May 28**

Table 1 The Cold Materials within Small Magnetic Flux Ropes (1998-2008)

## Signatures of Magnetic Flux Ropes in the Low Solar Atmosphere Observed in High Resolution Review

Haimin **Wang** and Chang Liu

Front. Astron. Space Sci., 04 April 2019

[sci-hub.se/10.3389/fspas.2019.00018](https://sci-hub.se/10.3389/fspas.2019.00018)

<https://www.frontiersin.org/articles/10.3389/fspas.2019.00018/full>

Magnetic flux ropes (MFRs) are important physical features closely related to solar eruptive activities with potential space weather consequences. Studying MFRs in the low solar atmosphere can shed light on their origin and subsequent magnetic structural evolution. In recent years, observations of solar photosphere and chromosphere reached a spatial resolution of 0.1 to 0.2 arcsec with the operation of meter class ground-based telescopes, such as the 1.6 m Goode Solar Telescope at Big Bear Solar Observatory and the 1 m New Vacuum Solar Telescope at Yunnan Observatory. The obtained chromospheric H $\alpha$  filtergrams with the highest resolution thus far have revealed detailed properties of MFRs before and during eruptions, and the observed pre-eruption structures of MFRs are well consistent with those demonstrated by non-linear force-free field extrapolations. There is also evidence that MFRs may exist in the photosphere. The magnetic channel structure, with multiple polarity inversions and only discernible in high-resolution magnetograph observations, may be a signature of photospheric MFRs. These MFRs are likely formed below the surface due to motions in the convection zone and appear in the photosphere through flux emergence. Triggering of some solar eruptions is associated with an enhancing twist in the low-atmospheric MFRs. **2013 August 11, 2014 February 2, 2014 June 12, 2015 June 22, 2015 August 24, 2015 October 15, 2017 September 6**

## Evolution of A Magnetic Flux Rope toward Eruption

Wensi **Wang**, **Chunming Zhu**, **Jiong Qiu**, **Rui Liu**, **Kai E. Yang**, **Qiang Hu**

ApJ **871** 25 **2018**

<https://arxiv.org/pdf/1812.03437.pdf>

[sci-hub.tw/10.3847/1538-4357/aaf3ba](https://sci-hub.tw/10.3847/1538-4357/aaf3ba)

It is well accepted that a magnetic flux rope (MFR) is a critical component of many coronal mass ejections (CMEs), yet how it evolves toward eruption remains unclear. Here we investigate the continuous evolution of a pre-existing MFR, which is rooted in strong photospheric magnetic fields and electric currents. The evolution of the MFR is observed by the Solar Terrestrial Relations Observatory (STEREO) and the Solar Dynamics Observatory (SDO) from multiple viewpoints. From STEREO's perspective, the MFR starts to rise slowly above the limb five hours before it erupts as a halo CME on **2012 June 14**. In SDO observations, conjugate dimmings develop on the disk, simultaneously with the gradual expansion of the MFR, suggesting that the dimmings map the MFR's feet. The evolution comprises a two-stage gradual expansion followed by another stage of rapid acceleration/eruption. Quantitative measurements indicate that magnetic twist of the MFR increases from 1.0  $\pm$  0.5 to 2.0  $\pm$  0.5 turns during the five-hour expansion, and further increases to about 4.0 turns per AU when detected as a magnetic cloud at 1 AU two day later. In addition, each stage is preceded by flare(s), implying reconnection is actively involved in the evolution and eruption of the MFR. The implications of these measurements on the CME initiation mechanisms are discussed.

## Helicity Removal and Coronal Fe xii Stalks: Evidence That the Axial Field Is Not Ejected but Resubmerged

Y.-M. **Wang**<sup>1</sup> and M. A. Berger<sup>2</sup>

**2018** ApJ **868** 66

[sci-hub.tw/10.3847/1538-4357/aae845](https://sci-hub.tw/10.3847/1538-4357/aae845)

The magnetic/current helicity of the coronal field is closely associated with the presence of a nonpotential axial component directed along the photospheric polarity inversion line (PIL), which is also the source of the axial/toroidal field in flux ropes and coronal mass ejections (CMEs). To better understand the role of this axial component in the evolution of coronal helicity, we use Fe xii 19.3 nm images and longitudinal magnetograms from the Solar Dynamics Observatory to track active regions (ARs) and their filament channels as they decay due to flux transport processes. We find that the Fe xii loop legs or "stalks," initially oriented almost perpendicular to the PIL, become closely aligned with

it after ~1–4 rotations; this alignment is attributed to the progressive cancellation of the transverse field component at the PIL. As the AR flux continues to decay, the PIL becomes ever more distorted and the directions of the stalks are increasingly randomized. These observations suggest that most of the original axial field in ARs is not expelled in CMEs, but instead pinches off after the eruptions and becomes concentrated at the PIL. Because the twist of the field decreases, however, the helicity itself decreases, with CMEs removing a significant fraction of it in the form of disconnected flux ropes. Like most of the AR flux, the bulk of the axial field is eventually canceled/resubmerged, brought to the equator by the subsurface meridional flow, and annihilated (along with the remaining helicity) by merging with its opposite-handed counterpart from the other hemisphere.

### **Unraveling the Links among Sympathetic Eruptions**

Dong [Wang](#), [Rui Liu](#), [Yuming Wang](#), [Tingyu Gou](#), [Quanhao Zhang](#), [Zhenjun Zhou](#), [Min Zhang](#)

2018 *ApJ* **869** 177

<https://arxiv.org/pdf/1811.01148.pdf>

Solar eruptions occurring at different places within a relatively short time interval are considered to be sympathetic. However, it is difficult to determine whether there exists a cause and effect between them. Here we study a failed and a successful filament eruption following an X1.8-class flare on **2014 December 20**, in which slipping-like magnetic reconnections serve as a key causal link among the eruptions. Reconnection signatures and effects are: at both sides of the filament experiencing the failed eruption, serpentine ribbons extend along chromospheric network to move away from the filament, while a hot loop apparently grows above it; at the filament undergoing the successful eruption, overlying cold loops contract, while coronal dimming appears at both sides even before the filament eruption. These effects are understood by reconnections continually transforming magnetic fluxes overlying one filament to the other, which adjusts how the magnetic field decays with increasing height above the filaments in opposite trends, therefore either strengthening or weakening the magnetic confinement of each filament.

### **Roles of photospheric motions and flux emergence in the major solar eruption on 2017**

**September 6**

Rui [Wang](#), [Ying D. Liu](#), [J. Todd Hoeksema](#), [I.V. Zimovets](#), [Yang Liu](#)

*ApJ* **869** 90 **2018**

<https://arxiv.org/pdf/1810.13092.pdf>

[sci-hub.tw/10.3847/1538-4357/aaed48](http://sci-hub.tw/10.3847/1538-4357/aaed48)

We study the magnetic field evolution in the active region (AR) 12673 that produced the largest solar flare in the past decade on **2017 September 6**. Fast flux emergence is one of the most prominent features of this AR. We calculate the magnetic helicity from photospheric tangential flows that shear and braid field lines (shear-helicity), and from normal flows that advect twisted magnetic flux into the corona (emergence-helicity), respectively. Our results show that the emergence-helicity accumulated in the corona is  $-1.6 \times 10^{43} \text{ Mx}^2$  before the major eruption, while the shear-helicity accumulated in the corona is  $-6 \times 10^{43} \text{ Mx}^2$ , which contributes about 79% of the total helicity. The shear-helicity flux is dominant throughout the overall investigated emergence phase. Our results imply that the emerged fields initially contain relatively low helicity. Much more helicity is built up by shearing and converging flows acting on preexisted and emerging flux. Shearing motions are getting stronger with the flux emergence, and especially on both sides of the polarity inversion line of the core field region. The evolution of the vertical currents shows that most of the intense currents do not appear initially with the emergence of the flux, which implies that most of the emerging flux is probably not strongly current-carrying. The helical magnetic fields (flux rope) in the core field region are probably formed by long-term photospheric motions. The shearing and converging motions are continuously generated driven by the flux emergence. AR 12673 is a representative as photospheric motions contribute most of the nonpotentiality in the AR with vigorous flux emergence.

[HMI Science Nuggets](#) #119 **2019** [hmi.stanford.edu/hminuggets/?p=2821](http://hmi.stanford.edu/hminuggets/?p=2821)

### **A Solar Eruption with Relatively Strong Geo-effectiveness Originating from Active Region Peripheral Diffusive Polarities**

Rui [Wang](#), [Ying D. Liu](#), [Huidong Hu](#), [Xiaowei Zhao](#)

2018 *ApJ* **863** 81

<https://arxiv.org/pdf/1807.03047.pdf>

<http://sci-hub.tw/http://iopscience.iop.org/article/10.3847/1538-4357/aad22d/meta>

We report the observations of a moderate but relatively intense geo-effective solar eruption on **2015 November 4** from the peripheral diffusive polarities of active region 12443. We use space-borne Solar Dynamics Observatory and ACE observations. EUV images identified helical pattern along a filament channel and we regard this channel as flux-rope structure. Flow velocity derived from tracked magnetograms infers converging motion along the polarity inversion line beneath the filament channel. An associated magnetic cancellation process was detected in the converging region. Further, the pre-eruptive EUV brightening was observed in the converging region, the most intense part of which appeared in the magnetic cancellation region. These observations imply that the converging and cancelling flux probably contributed to the formation of the helical magnetic fields associated with the flux rope. A filament-height estimation method suggests that the middle part of the filament probably lies at a low altitude and was consistent with the initial place of the eruption. A thick current channel associated with the flux rope is also determined. For an expanding thick current channel, the critical height of the decay index for torus instability lies in the range of 37 - 47

Mm. Southward magnetic fields in the sheath and the ejecta induced a geomagnetic storm with a Dst global minimum of  $\sim 90$  nT.

### **Formation of an active region filament driven by a series of jets**

Jincheng [Wang](#), [Xiaoli Yan](#), [ZhongQuan Qu](#), [Satoru UeNo](#), [Kiyoshi Ichimoto](#), [Linhua Deng](#), [Wenda Cao](#), [Zhong Liu](#)

ApJ 863:180 2018

<https://arxiv.org/pdf/1807.00992.pdf>

<http://iopscience.iop.org/article/10.3847/1538-4357/aad187/pdf>

We present a formation process of a filament in active region NOAA 12574 during the period from **2016 August 11 to 12**. Combining the observations of GONG H $\alpha$ , Hida spectrum and SDO/AIA 304 A, the formation process of the filament is studied. It is found that cool material ( $T \sim 104$  K) is ejected by a series of jets originating from the western foot-point of the filament. Simultaneously, the magnetic flux emerged from the photosphere in the vicinity of the western foot-point of the filament. These observations suggest that cool material in the low atmosphere can be directly injected into the upper atmosphere and the jets are triggered by the magnetic reconnection between pre-existing magnetic fields and new emerging magnetic fields. Detailed study of a jet at 18:02 UT on August 11 with GST/BBSO TiO observations reveals that some dark threads appeared in the vicinity of the western foot-point after the jet and the projection velocity of plasma along the filament axis was about  $162.6 \pm 5.4$  km/s. Using with DST/Hida observations, we find that the injected plasma by a jet at 00:42 UT on August 12 was rotating. Therefore, we conclude that the jets not only supplied the material for the filament, but also injected the helicity into the filament simultaneously. Comparing the quantity of mass injection by the jets with the mass of the filament, we conclude that the estimated mass loading by the jets is sufficient to account for the mass in the filament.

### **Gradual Streamer Expansions and the Relationship between Blobs and Inflows**

Y.-M. [Wang](#) and P. Hess

2018 ApJ 859 135 [10.3847/1538-4357/aabfd5](https://arxiv.org/abs/10.3847/1538-4357/aabfd5)

Coronal helmet streamers show a continual tendency to expand outward and pinch off, giving rise to flux ropes that are observed in white light as "blobs" propagating outward along the heliospheric current/plasma sheet. The blobs form within the  $r \sim 2-6 R_{\odot}$  heliocentric range of the Large Angle and Spectrometric Coronagraph (LASCO) C2 instrument, but the expected inward-moving counterparts are often not detected. Here we show that the height of blob formation varies as a function of the underlying photospheric field, with the helmet streamer loops expanding to greater heights when active regions (ARs) emerge underneath them. When the pinch-offs occur at  $r \sim 3-4 R_{\odot}$ , diverging inward/outward tracks sometimes appear in height-time maps constructed from LASCO C2 running-difference images. When the underlying photospheric field is weak, the blobs form closer to the inner edge of the C2 field of view and only the outward tracks are clearly visible. Conversely, when the emergence of large ARs leads to a strengthening of the outer coronal field and an increase in the total white-light radiance (as during late 2014), the expanding helmet-streamer loops pinch off beyond  $r \sim 4 R_{\odot}$ , triggering strong inflow streams whose outgoing counterparts are usually very faint. We deduce that the visibility of the blobs and inflows depends on the amount of material that the diverging components sweep up within the  $2-6 R_{\odot}$  field of view. We also note that the rate of blob production tends to increase when a helmet streamer is "activated" by underlying flux emergence.

### **Unambiguous Evidence of Coronal Implosions During Solar Eruptions and Flares**

[Juntao Wang](#), [P. J. A. Simoes](#), [L. Fletcher](#)

ApJ 2018

<https://arxiv.org/pdf/1804.02354.pdf>

In the implosion conjecture, coronal loops contract as the result of magnetic energy release in solar eruptions and flares. However, after almost two decades, observations of this phenomenon are still rare, and most of previous reports are plagued by projection effects so that loop contraction could be either true implosion or just a change in loop inclination. In this paper, to demonstrate the reality of loop contractions in the global coronal dynamics, we present four events with the continuously contracting loops in an almost edge-on geometry from the perspective of SDO/AIA, which are free from the ambiguity caused by the projection effects, also supplemented by contemporary observations from STEREO for examination. In the wider context of observations, simulations and theories, we argue that the implosion conjecture is valid in interpreting these events. Furthermore, distinct properties of the events allow us to identify two physical categories of implosion. One type demonstrates a rapid contraction at the beginning of the flare impulsive phase, as magnetic free energy is removed rapidly by a filament eruption. The other type, which has no visible eruption, shows a continuous loop shrinkage during the entire flare impulsive phase which we suggest manifests the ongoing conversion of magnetic free energy in a coronal volume. Corresponding scenarios are described, which can provide reasonable explanations for the observations. We also point out that implosions may be suppressed in cases when a heavily-mass-loaded filament is involved, possibly serving as an alternative account for their observational rarity. **2011-09-14, 2014-02-17, 2016-04-08, 2016-11-22**

### **"Twisting" Motions in Erupting Coronal Pseudostreamers as Evidence for Interchange Reconnection**

Y.-M. [Wang](#) and P. Hess

2018 ApJ 853 103

Using white-light observations from the COR1 coronagraph during 2008–2013, we have identified ~50 eruptive events in which a narrow streamer structure appears to rotate about its radial axis as it rises into the field of view beyond  $r \sim 1.4 R_{\odot}$ . Extreme-ultraviolet images and potential-field extrapolations suggest that most of these eruptions involve one arcade of a double-lobed pseudostreamer, which is surrounded by open flux of a single polarity. The "twisting" is manifested by the cavity of the erupting lobe, which evolves from a circular to a narrowing oval structure as it is ejected nonradially in the direction of the original X-point. At the same time, the loop legs on the trailing side of the rising cavity/flux rope expand and straighten out, starting at the outer edge of the lobe and progressing inward; this asymmetric opening-up contributes to the impression of a three-dimensional structure twisting away from the observer. On the leading side of the lobe, collapsing cusps are sometimes detected, suggesting the presence of a current sheet where the cavity loops reconnect with the oppositely directed open flux from the adjacent coronal hole. In some events, the inner loops of the cavity/flux rope may continue to expand outward without undergoing interchange reconnection. The transfer of material to open field lines, as well as the lateral confinement of the pseudostreamer by the surrounding coronal holes, acts to produce a relatively narrow, fan-like ejection that differs fundamentally from the large, bubble-shaped ejections associated with helmet streamers.

### Existing an Upper Limit in the Magnetic Energy of a Stable Magnetic Flux Rope?

Yuming Wang and Rui Liu

2017 Res. Notes AAS 1 10

<http://iopscience.iop.org/article/10.3847/2515-5172/aa9852>

### Buildup of a highly twisted magnetic flux rope during a solar eruption

Wang, W., Liu, R., Wang, Y., et al.

2017, Nature Communications, 8, 1330

<https://www.nature.com/articles/s41467-017-01207-x.pdf>

The magnetic flux rope is among the most fundamental magnetic configurations in plasma. Although its presence after solar eruptions has been verified by spacecraft measurements near Earth, its formation on the Sun remains elusive, yet is critical to understanding a broad spectrum of phenomena. Here we study the dynamic formation of a magnetic flux rope during a classic two-ribbon flare. Its feet are identified unambiguously with conjugate coronal dimmings completely enclosed by irregular bright rings, which originate and expand outward from the far ends of flare ribbons. The expansion is associated with the rapid ribbon separation during the flare main phase. Counting magnetic flux through the feet and the ribbon-swept area reveals that the rope's core is more twisted than its average of four turns. It propagates to the Earth as a typical magnetic cloud possessing a similar twist profile obtained by the Grad-Shafranov reconstruction of its three dimensional structure. **4 November 2015**

### Formation and Eruption Process of a Filament in Active Region NOAA 12241

Jincheng Wang<sup>1,2,3</sup>, Xiaoli Yan<sup>1,3</sup>, Zhongquan Qu<sup>1,2,3</sup>, Zhike Xue<sup>1,3</sup>, and Liheng Yang<sup>1,3</sup>

2017 ApJ 839 128

<http://iopscience.iop.org/article/10.3847/1538-4357/aa6bf3/pdf>

In order to better understand active-region filaments, we present an intensive study on the formation and eruption of a filament in active region NOAA 12241 during the period from **2014 December 18 to 19**. Using observations from the Helioseismic and Magnetic Imager (HMI) vector magnetograms, we investigate the helicity injection rate, Lorentz force, and vertical electric current in the entire region associated with the filament. The helicity injection rate before eruption is found to be larger than that after eruption, while the vertical electric current undergoes an increase at first and then a gradual decrease, similar to what the magnetic flux undergoes. Meanwhile, we find that the right part of the filament is formed by magnetic reconnection between two bundles of magnetic field lines while the left part originated from shearing motion. The interaction of the two parts causes the eruption of this filament. The mean horizontal magnetic fields in the vicinity of the magnetic polarity inversion line (PIL) enhance rapidly during the eruption. Another striking phenomenon, where the vertical electric currents close to the magnetic PIL suddenly expand toward two sides during the eruption, is found. We propose that this fascinating feature is associated with the release of energy during the eruption.

### Tornado-Like Evolution of A Kink-Unstable Solar Prominence

Wensi Wang, Rui Liu, Yuming Wang

ApJ 834 38 2016

<https://arxiv.org/pdf/1611.04667v1.pdf>

We report on the tornado-like evolution of a quiescent prominence on **2014 November 1**. The eastern section of the prominence first rose slowly transforming into an arch-shaped structure as high as ~150 Mm above the limb; the arch then writhed moderately in a left-handed sense, while the originally dark prominence material became in emission in the Fe IX 171-Å passband, and a braided structure appeared at the eastern edge of the warped arch. The unraveling of the braided structure was associated with a transient brightening in EUV and apparently contributed to the formation of a curtain-like structure (CLS). The CLS consisted of myriads of thread-like loops rotating counterclockwise about the vertical if viewed from above. Heated prominence material was observed to slide along these loops and land outside the filament channel. The tornado was eventually disintegrated and the remaining material flew along a left-handed helical

path of approximately a full turn, as corroborated through stereoscopic reconstruction, into the cavity of the stable, western section of the prominence. We suggest that the tornado-like evolution of the prominence was governed by the helical kink instability, and that the CLS formed through magnetic reconnections between the prominence field and the overlying coronal field.

### **Arcade Implosion Caused by a Filament Eruption in a Flare**

Juntao [Wang](#), P. J. A. Simoes, L. Fletcher, J. K. Thalmann, H. S. Hudson, I. G. Hannah  
ApJ **2016**

<https://arxiv.org/pdf/1610.05931v1.pdf> **File**

Coronal implosions - the convergence motion of plasmas and entrained magnetic field in the corona due to a reduction in magnetic pressure - can help to locate and track sites of magnetic energy release or redistribution during solar flares and eruptions. We report here on the analysis of a well-observed implosion in the form of an arcade contraction associated with a filament eruption, during the C3.5 flare SOL2013-06-19T07:29. A sequence of events including magnetic flux-rope instability and distortion, followed by filament eruption and arcade implosion, lead us to conclude that the implosion arises from the transfer of magnetic energy from beneath the arcade as part of the global magnetic instability, rather than due to local magnetic energy dissipation in the flare. The observed net contraction of the imploding loops, which is found also in nonlinear force-free field extrapolations, reflects a permanent reduction of magnetic energy underneath the arcade. This event shows that, in addition to resulting in expansion or eruption of overlying field, flux-rope instability can also simultaneously implode unopened field due to magnetic energy transfer. It demonstrates the "partial opening of the field" scenario, which is one of the ways in 3D to produce a magnetic eruption without violating the Aly-Sturrock hypothesis. In the framework of this observation we also propose a unification of three main concepts for active region magnetic evolution, namely the metastable eruption model, the implosion conjecture, and the standard "CSHKP" flare model.

### **On the twists of interplanetary magnetic flux ropes observed at 1 AU**

Yuming [Wang](#), Bin Zhuang, Qiang Hu, [Rui Liu](#), [Chenglong Shen](#), [Yutian Chi](#)  
JGR **2016**

<http://arxiv.org/pdf/1608.05607v1.pdf>

Magnetic flux ropes (MFRs) are one kind of fundamental structures in the solar physics, and involved in various eruption phenomena. Twist, characterizing how the magnetic field lines wind around a main axis, is an intrinsic property of MFRs, closely related to the magnetic free energy and stableness. So far it is unclear how much amount of twist is carried by MFRs in the solar atmosphere and in heliosphere and what role the twist played in the eruptions of MFRs. Contrasting to the solar MFRs, there are lots of in-situ measurements of magnetic clouds (MCs), the large-scale MFRs in interplanetary space, providing some important information of the twist of MFRs. Thus, starting from MCs, we investigate the twist of interplanetary MFRs with the aid of a velocity-modified uniform-twist force-free flux rope model. It is found that most of MCs can be roughly fitted by the model and nearly half of them can be fitted fairly well though the derived twist is probably over-estimated by a factor of 2.5. By applying the model to 115 MCs observed at 1 AU, we find that (1) the twist angles of interplanetary MFRs generally follow a trend of about  $0.61R$  radians, where  $R$  is the aspect ratio of a MFR, with a cutoff at about  $12\pi$  radians  $AU^{-1}$ , (2) most of them are significantly larger than  $2.5\pi$  radians but well bounded by  $21R$  radians, (3) strongly twisted magnetic field lines probably limit the expansion and size of MFRs, and (4) the magnetic field lines in the legs wind more tightly than those in the leading part of MFRs. These results not only advance our understanding of the properties and behavior of interplanetary MFRs, but also shed light on the formation and eruption of MFRs in the solar atmosphere. A discussion about the twist and stableness of solar MFRs are therefore given.

### **Sympathetic Solar Filament Eruptions**

Rui [Wang](#), Ying D. Liu, Ivan Zimovets, Huidong Hu, Xinghua Dai, Zhongwei Yang  
**2016** *ApJ* **827** L12

<http://arxiv.org/pdf/1608.01067v1.pdf>

The **2015 March 15** coronal mass ejection as one of the two that together drove the largest geomagnetic storm of solar cycle 24 so far was associated with sympathetic filament eruptions. We investigate the relations between the different filaments involved in the eruption. A surge-like small-scale filament motion is confirmed as the trigger that initiated the erupting filament with multi-wavelength observations and using a forced magnetic field extrapolation method. When the erupting filament moved to an open magnetic field region, it experienced an obvious acceleration process and was accompanied by a C-class flare and the rise of another larger filament that eventually failed to erupt. We measure the decay index of the background magnetic field, which presents a critical height of 118 Mm. Combining with a potential field source surface extrapolation method, we analyze the distributions of the large-scale magnetic field, which indicates that the open magnetic field region may provide a favorable condition for F2 rapid acceleration and have some relation with the largest solar storm. The comparison between the successful and failed filament eruptions suggests that the confining magnetic field plays an important role in the preconditions for an eruption.

### **On the Propagation of a Geoeffective Coronal Mass Ejection during [March 15 -- 17, 2015](#)**

Yuming [Wang](#), Quanhao Zhang, Jiajia Liu, [Chenglong Shen](#), [Fang Shen](#), [Zicai Yang](#), [T. Zic](#), [B. Vrsnak](#), [D. F. Webb](#), [Rui Liu](#), [S. Wang](#), [Jie Zhang](#), [Qiang Hu](#), [Bin Zhuang](#)  
JGR Volume 121, Issue 8 August 2016 Pages 7423–7434  
<http://arxiv.org/pdf/1607.07750v1.pdf> **File**

The largest geomagnetic storm so far in the solar cycle 24 was produced by a fast coronal mass ejection (CME) originating on 2015 March 15. It was an initially west-oriented CME and expected to only cause a weak geomagnetic disturbance. Why did this CME finally cause such a large geomagnetic storm? We try to find some clues by investigating its propagation from the Sun to 1 AU. First, we reconstruct the CME's kinematic properties in the corona from the SOHO and SDO imaging data with the aid of the graduated cylindrical shell (GCS) model. It is suggested that the CME propagated to the west  $\sim 33^\circ \pm 10^\circ$  away from the Sun-Earth line with a speed of about  $817 \text{ km s}^{-1}$  before leaving the field of view of the SOHO/LASCO C3 camera. A magnetic cloud (MC) corresponding to this CME was measured in-situ by the Wind spacecraft two days later. By applying two MC reconstruction methods, we infer the configuration of the MC as well as some kinematic information, which implies that the CME possibly experienced an eastward deflection on its way to 1 AU. However, due to the lack of observations from the STEREO spacecraft, the CME's kinematic evolution in interplanetary space is not clear. In order to fill this gap, we utilize numerical MHD simulation, drag-based CME propagation model (DBM) and the model for CME deflection in interplanetary space (DIPS) to recover the propagation process, especially the trajectory, of the CME from 30RS to 1 AU. It is suggested that the trajectory of the CME was deflected toward the Earth by about  $12^\circ$ , consistent with the implication from the MC reconstruction at 1 AU. This eastward deflection probably contributed to the CME's unexpected geoeffectiveness by pushing the center of the initially west-oriented CME closer to the Earth.

### **Relationship Between Sunspot Rotation and a Major Solar Eruption on 12 July 2012**

Rui [Wang](#), Ying D. Liu, Thomas Wiegelmann, Xin Cheng, Huidong Hu, Zhongwei Yang  
Solar Phys. Volume 291, Issue 4, pp 1159-1171 2016  
<http://sci-hub.io/doi/10.1007/s11207-016-0881-6>

We present an analysis of Solar Dynamics Observatory (SDO) observations of an X1.4 class flare on 12 July 2012 (SOL2012-07-12T15:37L082C105), which was associated with a pronounced sunspot rotation in the associated active region. Based on the magnetograms taken with the Helioseismic and Magnetic Imager (HMI) on the SDO, we measured the rotational speed of the sunspot. We also used a technique, called the differential affine velocity estimator for vector magnetograms (DAVE4VM), to determine the horizontal velocities and the magnetic helicity flux transport. The helicity flux rate due to shearing motion changed sign after the onset of the eruption. A high correlation between the sunspot rotation speed and the change in the total accumulated helicity was found. We also calculated the net fluxes of the respective magnetic polarities and the net vertical currents. The net current in the region of interest showed a synchronous change with the sunspot rotation rate. The magnetic configurations of the sigmoid filament in the active region and the associated possible interaction between different structures were further investigated by means of a nonlinear force-free field extrapolation. We identified a possible magnetic reconnection region from the three-dimensional magnetic fields and its association with EUV structures. These results suggest that the major eruption of this active region was connected with the sunspot rotation.

### **Toward an Understanding of Earth-Affecting Solar Eruptions**

Yuming [Wang](#)  
EOS 1 Apr 2016

Coronal mass ejection forecasting improves with technological developments and increasing availability of data.

### **THE EVOLUTION OF THE ELECTRIC CURRENT DURING THE FORMATION AND ERUPTION OF ACTIVE-REGION FILAMENTS**

Jincheng [Wang](#)<sup>1,2</sup>, Xiaoli Yan<sup>1,3</sup>, Zhongquan Qu<sup>1</sup>, Zhike Xue<sup>1</sup>, Yongyuan Xiang<sup>1</sup>, and Hao Li<sup>1</sup>  
2016 ApJ 817 156

We present a comprehensive study of the electric current related to the formation and eruption of active region filaments in NOAA AR 11884. The vertical current on the solar surface was investigated by using vector magnetograms (VMs) observed by HMI on board the Solar Dynamics Observatory. To obtain the electric current along the filament's axis, we reconstructed the magnetic fields above the photosphere by using nonlinear force-free field extrapolation based on photospheric VMs. Spatio-temporal evolutions of the vertical current on the photospheric surface and the horizontal current along the filament's axis were studied during the long-term evolution and eruption-related period, respectively. The results show that the vertical currents of the entire active region behaved with a decreasing trend and the magnetic fields also kept decreasing during the long-term evolution. For the eruption-related evolution, the mean transverse field strengths decreased before two eruptions and increased sharply after two eruptions in the vicinity of the polarity inversion lines underneath the filament. The related vertical current showed different behaviors in two of the eruptions. On the other hand, a very interesting feature was found: opposite horizontal currents with respect to the current of the filament's axis appeared and increased under the filament before the eruptions and



disappeared after the eruptions. We suggest that these opposite currents were carried by the new flux emerging from the photosphere bottom and might be the trigger mechanism for these filament eruptions.

### **Cluster of solar active regions and onset of coronal mass ejections.**

**Wang** J X, Zhang Y Z, He H, et al.

SCIENCE CHINA Physics, Mechanics & Astronomy (Sci China-Phys Mech Astron), **2015**, 58(9): 599601

**File**

<http://link.springer.com/journal/11433/58/9/page/1>

<http://phys.scichina.com:8083/sciGe/EN/article/showFieldArticle.do?fieldId=81>

Round-the-clock solar observations with full-disk coverage of vector magnetograms and multi-wavelength images demonstrate that solar active regions (ARs) are ultimately connected with magnetic field. Often two or more ARs are clustered, creating a favorable magnetic environment for the onset of coronal mass ejections (CMEs). In this work, we describe a new type of magnetic complex: cluster of solar ARs. An AR cluster is referred to as the close connection of two or more ARs which are located in nearly the same latitude and a narrow span of longitude. We illustrate three examples of AR clusters, each of which has two ARs connected and formed a common dome of magnetic flux system. They are clusters of NOAA (i.e., National Oceanic and Atmospheric Administration) ARs 11226 & 11227, 11429 & 11430, and 11525 & 11524. In these AR clusters, CME initiations were often tied to the instability of the magnetic structures connecting two partner ARs, in the form of inter-connecting loops and/or channeling filaments between the two ARs. We show the evidence that, at least, some of the flare/CMEs in an AR cluster are not a phenomenon of a single AR, but the result of magnetic interaction in the whole AR cluster. The observations shed new light on understanding the mechanism(s) of solar activity. Instead of the simple bipolar topology as suggested by the so-called standard flare model, a multi-bipolar magnetic topology is more common to host the violent solar activity in solar atmosphere. **2 June 2011, 6 March 2012, 1 July 2012**

### **The role of active region coronal magnetic field in determining coronal mass ejection propagation direction**

Rui **Wang**, Ying D. Liu, Xinghua Dai, Zhongwei Yang, Chong Huang, Huidong Hu

ApJ **814** 80 **2015**

<http://arxiv.org/pdf/1510.06177v1.pdf>

We study the role of the coronal magnetic field configuration of an active region in determining the propagation direction of a coronal mass ejection (CME). The CME occurred in the active region 11944 (S09W01) near the disk center on **2014 January 7** and was associated with an X1.2 flare. A new CME reconstruction procedure based on a polarimetric technique is adopted, which shows that the CME changed its propagation direction by around  $28^\circ$  in latitude within  $2.5 R_\odot$  and  $43^\circ$  in longitude within  $6.5 R_\odot$  with respect to the CME source region. This significant non-radial motion is consistent with the finding of Mo $\ddot{u}$ stl et al. (2015). We use nonlinear force-free field (NLFFF) and potential field source surface (PFSS) extrapolation methods to determine the configurations of the coronal magnetic field. We also calculate the magnetic energy density distributions at different heights based on the extrapolations. Our results show that the active region coronal magnetic field has a strong influence on the CME propagation direction. This is consistent with the "channelling" by the active region coronal magnetic field itself, rather than deflection by nearby structures. These results indicate that the active region coronal magnetic field configuration has to be taken into account in order to determine CME propagation direction correctly.

### **Coronal Mass Ejections and the Solar Cycle Variation of the Sun's Open Flux**

Y.-M. **Wang** and N. R. Sheeley, Jr.

**2015** ApJ 809 L24

<https://arxiv.org/ftp/arxiv/papers/2104/2104.07238.pdf>

The strength of the radial component of the interplanetary magnetic field (IMF), which is a measure of the Sun's total open flux, is observed to vary by roughly a factor of two over the 11 year solar cycle. Several recent studies have proposed that the Sun's open flux consists of a constant or "floor" component that dominates at sunspot minimum, and a time-varying component due to coronal mass ejections (CMEs). Here, we point out that CMEs cannot account for the large peaks in the IMF strength which occurred in 2003 and late 2014, and which coincided with peaks in the Sun's equatorial dipole moment. We also show that near-Earth interplanetary CMEs, as identified in the catalog of Richardson and Cane, contribute at most  $\sim 30\%$  of the average radial IMF strength even during sunspot maximum. We conclude that the long-term variation of the radial IMF strength is determined mainly by the Sun's total dipole moment, with the quadrupole moment and CMEs providing an additional boost near sunspot maximum. Most of the open flux is rooted in coronal holes, whose solar cycle evolution in turn reflects that of the Sun's lowest-order multipoles.

### **Witnessing magnetic twist with high-resolution observation from the 1.6-m New Solar Telescope**

Haimin **Wang**, Wenda Cao, Chang Liu, Yan Xu, Rui Liu, Zhicheng Zeng, Jongchul Chae and Haisheng Ji  
Nature Communications, 6, 7008, **2015**

<http://www.nature.com/ncomms/2015/150428/ncomms8008/pdf/ncomms8008.pdf>

Magnetic flux ropes are highly twisted, current-carrying magnetic fields. They are crucial for the instability of plasma involved in solar eruptions, which may lead to adverse space weather effects. Here we present observations of a flaring using the highest resolution chromospheric images from the 1.6-m New Solar Telescope at Big Bear Solar Observatory, supplemented by a magnetic field extrapolation model. A set of loops initially appear to peel off from an overall inverse S-shaped flux bundle, and then develop into a multi-stranded twisted flux rope, producing a two-ribbon flare. We show evidence that the flux rope is embedded in sheared arcades and becomes unstable following the enhancement of its twists. The subsequent motion of the flux rope is confined due to the strong strapping effect of the overlying field. These results provide a first opportunity to witness the detailed structure and evolution of flux ropes in the low solar atmosphere. **11 August 2013**

### **Correlation Between CME Occurrence Rate and Current Helicity in the Global Magnetic Field of Solar Cycle 23**

Chuanyu **Wang**, Mei Zhang

Solar Phys. Volume 290, [Issue 3](#), pp 811-818 **2015**

We investigate the correlation between the occurrence rate of the monthly coronal mass ejection (CME) and the magnitude of the current helicity in global magnetic field on the photosphere of solar cycle 23. We used the technique introduced by Pevtsov and Latushko (Astrophys. J. 528, 999,2000) to retrieve the vector magnetic field from longitudinal full-disk magnetograms, but applied a different method to calculate the current helicity and focused on the evolution of the magnitude of current helicity over a full solar cycle. We found that there is a close relationship between the variation of the current helicity in the global magnetic field and that of the monthly CME occurrence rate. This provides further evidence to support that helicity is an important ingredient for solar eruptions.

### **Pseudostreamers as the source of a separate class of solar coronal mass ejections,**

**Wang**, Y-M.

(**2015**), Astrophys. J. Lett., 803. L12.

<http://iopscience.iop.org/article/10.1088/2041-8205/803/1/L12/pdf>

Using white-light and extreme-ultraviolet imaging observations, we confirm that pseudostreamers (streamers that separate coronal holes of the same polarity) give rise to a different type of coronal mass ejection (CME) from that associated with helmet streamers (defined as separating coronal holes of opposite polarity). Whereas helmet streamers are the source of the familiar bubble-shaped CMEs characterized by gradual acceleration and a three-part structure, pseudostreamers produce narrower, fanlike ejections with roughly constant speeds. These ejections, which are typically triggered by underlying filament eruptions or small, flaring active regions, are confined laterally and channeled outward by the like-polarity open flux that converges onto the pseudostreamer plasma sheet from both sides. In contrast, helmet streamer CMEs are centered on the relatively weak field around the heliospheric current sheet and thus undergo greater lateral expansion. Pseudostreamer ejections have a morphological resemblance to white-light jets from coronal holes; however, unlike the latter, they are not primarily driven by interchange reconnection, and tend to have larger widths ( $\sim 20^\circ$ – $30^\circ$ ), lower speeds ( $\sim 250$ – $700$  km s $^{-1}$ ), and more complex internal structure. **2007 June 23, 2007 December 15, 2008 January 27, 2008 November 29, 2009 February 6, 2010 May 8, 2010 October 10, 2010 October 26, 2010 November 24**

### **Structure and Evolution of Magnetic Fields Associated with Solar Eruptions (Invited **Review**)**

Haimin **Wang**, Chang Liu

Research in Astronomy and Astrophysics, **2015**

<http://arxiv.org/pdf/1412.8676v1.pdf> **File**

This paper reviews the studies of solar photospheric magnetic field evolution in active regions and its relationship to solar flares. It is divided into two topics, the magnetic structure and evolution leading to solar eruptions and the rapid changes of photospheric magnetic field associated with eruptions. For the first topic, we describe the magnetic complexity, new flux emergence, flux cancellation, shear motions, sunspot rotation, and magnetic helicity injection, which may all contribute to the storage and buildup of energy and triggering of solar eruptions. For the second topic, we concentrate on the observations of rapid and irreversible changes of photospheric magnetic field associated with flares, and the implication on the restructuring of three-dimensional magnetic field. In particular, we emphasize the recent advances in observations of photospheric magnetic field, as state-of-the-art observing facilities (such as Hinode and Solar Dynamic Observatory) become available. The linkage between observations and theories and future prospectives in this research area are also discussed. **1989 March 10, 6 June 2000, 9 Apr 2001, 2001 September 24, 24-26 Oct 2001, 28 and 29 Oct 2003, 2003 November 2., 2003 November 29, 5-8 Nov 2004, 2006 December 6, 2006 December 13, 12-16 Feb 2011, 2011 February 13., 2011 February 15, 2011 July 2, 2012 March 7**

## **Magnetic Field Restructuring Associated with Two Successive Solar Eruptions**

Rui **Wang**, Ying D. Liu, Zhongwei Yang, Huidong Hu

2014, ApJ 791 84

<http://arxiv.org/pdf/1407.4004v1.pdf>

We examine two successive flare eruptions (X5.4 and X1.3) on **2012 March 7** in the NOAA active region 11429 and investigate the magnetic field reconfiguration associated with the two eruptions. Using an advanced non-linear force-free field (NLFFF) extrapolation method based on the SDO/HMI vector magnetograms, we obtain a stepwise decrease in the magnetic free energy during the eruptions, which is roughly 20%-30% of the energy of the pre-flare phase. We also calculate the magnetic helicity, and suggest that the changes of the sign of the helicity injection rate might be associated with the eruptions. Through the investigation of the magnetic field evolution, we find that the appearance of the "implosion" phenomenon has a strong relationship with the occurrence of the first X-class flare. Meanwhile, the magnetic field changes of the successive eruptions with implosion and without implosion were well observed.

## **Evolution of the Coronal Magnetic Configurations Including a Current-Carrying Flux Rope in Response to the Change in the Background Field**

Hong-Juan **Wang**, Si-Qing Liu, Jian-Cun Gong, Jun Lin

Research in Astronomy and Astrophysics, 2014

<http://arxiv.org/pdf/1406.6112v1.pdf>

We investigate equilibrium height of the flux rope, and its internal equilibrium in a realistic plasma environment by carrying out numerical simulations of the evolution of systems including a current-carrying flux rope. We find that the equilibrium height of the flux rope is approximately a power-law function of the relative strength of the background field. Our simulations indicate that the flux rope can escape more easily from a weaker background field. This further confirms the catastrophe in the magnetic configuration of interest can be triggered by decrease of strength of the background field. Our results show that it takes some time to reach internal equilibrium depending on the initial state of the flux rope. The plasma flow inside the flux rope due to the adjustment for the internal equilibrium of the flux rope remains small and does not last very long when the initial state of the flux rope commences from the stable branch of the theoretical equilibrium curve. This work also confirms the influence of the initial radius of flux rope on its evolution, the results indicate that the flux rope with larger initial radius erupts more easily. In addition, by using the realistic plasma environment and much higher resolution in our simulations, we notice some different characters compared to previous studies in Forbes (1990).

## **Deflected propagation of a coronal mass ejection from the corona to interplanetary space**

Yuming **Wang**, Boyi Wang, Chenglong Shen, Fang Shen, Noe Lugaz

JGR, 2014

<http://arxiv.org/pdf/1406.4684v1.pdf>

Among various factors affecting the space weather effects of a coronal mass ejection (CME), its propagation trajectory in the interplanetary space is an important one determining whether and when the CME will hit the Earth. Many direct observations have revealed that a CME may not propagate along a straight trajectory in the corona, but whether or not a CME also experiences a deflected propagation in the interplanetary space is a question, which has never been fully answered. Here by investigating the propagation process of an isolated CME from the corona to interplanetary space during **2008 September 12 -- 19**, we present solid evidence that the CME was deflected not only in the corona but also in the interplanetary space. The deflection angle in the interplanetary space is more than 20 degrees toward the west, resulting a significant change in the probability the CME encounters the Earth. A further modeling and simulation-based analysis suggest that the cause of the deflection in the interplanetary space is the interaction between the CME and the solar wind, which is different from that happening in the corona.

## **Is Solar Cycle 24 Producing More Coronal Mass Ejections Than Cycle 23?**

Y.-M. **Wang** and R. Colaninno

2014 ApJ 784 L27

Although sunspot numbers are roughly a factor of two lower in the current cycle than in cycle 23, the rate of coronal mass ejections (CMEs) appears to be at least as high in 2011-2013 as during the corresponding phase of the previous cycle, according to three catalogs that list events observed with the Large Angle and Spectrometric Coronagraph (LASCO). However, the number of CMEs detected is sensitive to such factors as the image cadence and the tendency (especially by human observers) to under-/overcount small or faint ejections during periods of high/low activity. In contrast to the total number, the total mass of CMEs is determined mainly by larger events. Using the mass measurements of 11,000 CMEs given in the manual CDAW catalog, we find that the mass loss rate remains well correlated with the sunspot number during cycle 24. In the case of the automated CACTus and SEEDS catalogs, the large increase in the number of CMEs during cycle 24 is almost certainly an artifact caused by the near-doubling of the LASCO image cadence after mid-2010. We confirm that fast CMEs undergo a much stronger solar-cycle variation than slow ones, and that the relative frequency of slow and less massive CMEs increases with decreasing sunspot number. We conclude that cycle 24 is not only producing fewer CMEs than cycle 23, but that these ejections also tend to be slower and less massive than those observed one cycle earlier.

## **Study of Rapid Formation of a Delta Sunspot Associated with the 2012 July 2 C7.4 Flare Using High-resolution Observations of New Solar Telescope**

Haimin **Wang**, Chang Liu, Shuo Wang, Na Deng, Yan Xu, Ju Jing and Wenda Cao

E-print, Aug 2013, ApJL

Rapid, irreversible changes of magnetic topology and sunspot structure associated with flares have been systematically observed in recent years. The most striking features include the increase of horizontal field at the polarity inversion line (PIL) and the co-spatial penumbral darkening. A likely explanation of the above phenomenon is the back reaction to the coronal restructuring after eruptions: a coronal mass ejection carries the upward momentum while the downward momentum compresses the field lines near the PIL. Previous studies could only use low resolution (above 1") magnetograms and white-light images. Therefore, the changes are mostly observed for X-class flares. Taking advantage of the 0.1" spatial resolution and 15s temporal cadence of the New Solar Telescope at Big Bear Solar Observatory, we report in detail the rapid formation of sunspot penumbra at the PIL associated with the C7.4 flare on 2012 July 2. It is unambiguously shown that the solar granulation pattern evolves to alternating dark and bright fibril structure, the typical pattern of penumbra. Interestingly, the appearance of such a penumbra creates a new delta sunspot. The penumbral formation is also accompanied by the enhancement of horizontal field observed using vector magnetograms from the Helioseismic and Magnetic Imager. We explain our observations as due to the eruption of a flux rope following magnetic cancellation at the PIL. Subsequently the re-closed arcade fields are pushed down towards the surface to form the new penumbra. NLFFF extrapolation clearly shows both the flux rope close to the surface and the overlying fields.

## **WAITING TIMES OF QUASI-HOMOLOGOUS CORONAL MASS EJECTIONS FROM SUPER ACTIVE REGIONS**

Yuming **Wang**, Lijuan Liu, Chenglong Shen, Rui Liu, Pinzhong Ye, and S. Wang

2013 ApJ 763 L43

Why and how do some active regions (ARs) frequently produce coronal mass ejections (CMEs)? These are key questions for deepening our understanding of the mechanisms and processes of energy accumulation and sudden release in ARs and for improving our space weather prediction capability. Although some case studies have been performed, these questions are still far from fully answered. These issues are now being addressed statistically through an investigation of the waiting times of quasi-homologous CMEs from super ARs in solar cycle 23. It is found that the waiting times of quasi-homologous CMEs have a two-component distribution with a separation at about 18 hr. The first component is a Gaussian-like distribution with a peak at about 7 hr, which indicates a tight physical connection between these quasi-homologous CMEs. The likelihood of two or more occurrences of CMEs faster than 1200 km s<sup>-1</sup> from the same AR within 18 hr is about 20%. Furthermore, the correlation analysis among CME waiting times, CME speeds, and CME occurrence rates reveals that these quantities are independent of each other, suggesting that the perturbation by preceding CMEs rather than free energy input is the direct cause of quasi-homologous CMEs. The peak waiting time of 7 hr probably characterizes the timescale of the growth of the instabilities triggered by preceding CMEs. This study uncovers some clues from a statistical perspective for us to understand quasi-homologous CMEs as well as CME-rich ARs.

## **THE RELATIONSHIP BETWEEN THE SUDDEN CHANGE OF THE LORENTZ FORCE AND THE MAGNITUDE OF ASSOCIATED FLARES**

Shuo **Wang**, Chang Liu, and Haimin Wang

2012 ApJ 757 L5

The rapid and irreversible change of photospheric magnetic fields associated with flares has been confirmed by many recent studies. These studies showed that the photospheric magnetic fields respond to coronal field restructuring and turn to a more horizontal state near the magnetic polarity inversion line (PIL) after eruptions. Recent theoretical work has shown that the change in the Lorentz force associated with a magnetic eruption will lead to such a field configuration at the photosphere. The Helioseismic Magnetic Imager has been providing unprecedented full-disk vector magnetograms covering the rising phase of the solar cycle 24. In this study, we analyze 18 flares in four active regions, with GOES X-ray class ranging from C4.7 to X5.4. We find that there are permanent and rapid changes of magnetic field around the flaring PIL, the most notable of which is the increase of the transverse magnetic field. The changes of fields integrated over the area and the derived change of Lorentz force both show a strong correlation with flare magnitude. It is the first time that such magnetic field changes have been observed even for C-class flares. Furthermore, for seven events with associated coronal mass ejections (CMEs), we use an estimate of the impulse provided by the Lorentz force, plus the observed CME velocity, to estimate the CME mass. We find that if the timescale of the back reaction is short, i.e., in the order of 10 s, the derived values of CME mass (~10<sup>15</sup> g) generally agree with those reported in literature.

## **Statistical study of coronal mass ejection source locations: Understanding CMEs viewed in coronagraphs**

**Wang**, Yuming; Chen, Caixia; Gui, Bin; Shen, Chenglong; Ye, Pinzhong; Wang, S.

J. Geophys. Res., Vol. 116, No. A4, A04104. **2011, File**

How to properly understand coronal mass ejections (CMEs) viewed in white light coronagraphs is crucial to many relative researches in solar and space physics. The issue is now particularly addressed in this paper through studying the source locations of all the 1078 Large Angle and Spectrometric Coronagraph (LASCO) CMEs listed in Coordinated Data Analysis Workshop (CDAW) CME catalog during 1997–1998 and their correlation with CMEs' apparent parameters. By manually checking LASCO and Extreme Ultraviolet Imaging Telescope (EIT) movies of these CMEs, we find that, except 231 CMEs whose source locations cannot be identified due to poor data, there are 288 CMEs with location identified on the frontside solar disk, 234 CMEs appearing above solar limb, and 325 CMEs without evident eruptive signatures in the field of view of EIT. On the basis of the statistical results of CMEs' source locations, there are four physical issues: (1) the missing rate of CMEs by SOHO LASCO and EIT, (2) the mass of CMEs, (3) the causes of halo CMEs, and (4) the deflections of CMEs in the corona, are exhaustively analyzed. It is found that (1) about 32% frontside CMEs cannot be recognized by SOHO, (2) the brightness of a CME at any heliocentric distance is roughly positively correlated with its speed, and the CME mass derived from the brightness is probably overestimated, (3) both projection effect and violent eruption are the major causes of halo CMEs, and especially for limb halo CMEs the latter is the primary one, and (4) most CMEs deflected toward equator near the solar minimum; these deflections can be classified into three types: the asymmetrical expansion, the nonradial ejection, and the deflected propagation.

### **OBSERVATIONAL EVIDENCE OF BACK REACTION ON THE SOLAR SURFACE ASSOCIATED WITH CORONAL MAGNETIC RESTRUCTURING IN SOLAR ERUPTIONS**

Haimin **Wang** and Chang Liu

Astrophysical Journal Letters, 716:L195–L199, **2010 June**

Most models of solar eruptions assume that coronal field lines are anchored in the dense photosphere and thus the photospheric magnetic fields would not have rapid, irreversible changes associated with eruptions resulted from the coronal magnetic reconnection. Motivated by the recent work of Hudson et al. on quantitatively evaluating the back reaction due to energy release from the coronal fields, in this Letter we synthesize our previous studies and present analysis of new events about flare-related changes of photospheric magnetic fields. For the 11 X-class flares where vector magnetograms are available, we always find an increase of transverse field at the polarity inversion line (PIL) although only four events had measurements with 1 minute temporal resolution. We also discuss 18 events with 1 minute cadence line-of-sight magnetogram observation, which all show prominent changes of magnetic flux contained in the flaring  $\delta$  spot region. Except in one case, the observed limbward flux increases while diskward flux decreases rapidly and irreversibly after flares. This observational evidence provides support, either directly or indirectly, for the theory and prediction of Hudson et al. that the photospheric magnetic fields must respond to coronal field restructuring and turn to a more horizontal state near the PIL after eruptions.

### **Is there more global solar activity on the Sun?**

J. X. **Wang**<sup>1</sup>, Y.Z. Zhang<sup>1</sup>, G.P. Zhou<sup>1</sup>, Y.Y. Wen<sup>1</sup> and J. Jiang<sup>2</sup>

Solar and Stellar Variability: Impact on Earth and Planets, Proceedings IAU Symposium No. 264, **2009**, p. 251-256, A.G. Kosovichev, A.H. Andrei & J.-P. Rozelot, eds.; **File**

**Y:\obridko\otchet09**

There appear indications of more global activity on the Sun which is larger, much beyond the scale of solar active regions (ARs). These indications include formation, flaring and eruption of the trans-equatorial loops seen in EUV and X-rays, formation and eruption of transequatorial filaments, global magnetic connectivity in EUV dimming associated with halo-coronal mass ejections, wide spread of radio burst sources in meter wavelength in the solar corona, and quasi-simultaneous magnetic flux emergence in both hemispheres seen during some major solar events. With examples of a few major events in the last solar cycle we discuss the possibility that there is large or global-scale activity on the Sun. Its spatial scale is many times larger than that of AR and temporal scale is over 10 hours. The exemplified trans-equatorial loops are anchored in ARs and their activity is temporally associated with flares in ARs too. In some sense the flares in ARs appear either as a part of or a precursor of the more global activity. It is likely that the combination of the flares in ARs and the associated global activity is responsible to the major solar-terrestrial events. More efforts in understanding the global activity are undertaken.

### **An analytical model probing the internal state of coronal mass ejections based on observations of their expansions and propagations**

**Wang**, Yuming; Zhang, Jie; Shen, Chenglong

J. Geophys. Res., Vol. 114, No. A10, A10104, **2009**

In this paper, a generic self-similar flux rope model is proposed to probe the internal state of CMEs in order to understand the thermodynamic process and expansion of CMEs in interplanetary space. Using this model, three physical parameters and their variations with heliocentric distance can be inferred based on coronagraph observations of CMEs' propagation and expansion. One is the polytropic index  $\Gamma$  of the CME plasma, and the other two are the average

Lorentz force and the thermal pressure force inside CMEs. By applying the model to the **8 October 2007** CME observed by STEREO/SECCHI, we find that (1) the polytropic index of the CME plasma increased from initially 1.24 to more than 1.35 quickly and then slowly decreased to about 1.34; it suggests that there be continuously heat injected/converted into the CME plasma and the value of  $\Gamma$  tends to be  $\frac{4}{3}$ , a critical value inferred from the model for a force-free flux rope; (2) the Lorentz force directed inward while the thermal pressure force outward, and both of them decreased rapidly as the CME moved out; the direction of the two forces reveals that the thermal pressure force is the internal driver of the CME expansion, whereas the Lorentz force prevented the CME from expanding. Some limitations of the model and approximations are discussed meanwhile.

## **A STATISTICAL STUDY OF SOLAR ACTIVE REGIONS THAT PRODUCE EXTREMELY FAST CORONAL MASS EJECTIONS**

Yuming **Wang**<sup>1, 2</sup> and Jie Zhang

The Astrophysical Journal, 680:1516-1522, 2008

<http://www.journals.uchicago.edu/doi/pdf/10.1086/587619>

We present statistical results on the properties of the solar source regions that produced the 57 fastest ( $\sim 1500$  km s<sup>-1</sup>) front-side coronal mass ejections (CMEs) from 1996 June to 2007 January. The properties of these fast-CMEY producing regions, 35 in total, are compared with those of all 1143 active regions (ARs) in the period studied. An automated method, based on SOHO MDI magnetic synoptic charts, is used to select and characterize the ARs. For each, a set of parameters is derived that includes the areas (positive, negative, and total, denoted  $A_P$ ,  $A_N$ , and  $A_T$ , respectively), the magnetic fluxes (positive, negative, and total,  $F_P$ ,  $F_N$ , and  $F_T$ ), the average magnetic field strength ( $B_{avg}$ ), a quasi elongation ( $e$ ) characterizing the overall shape of the AR, the number and length of polarity inversion lines (PILs, or neutral lines,  $N_{PIL}$  and  $L_{PIL}$ , respectively), and the average and maximum magnetic gradient on the PILs ( $G_{PIL,avg}$  and  $G_{PIL,max}$ ). Our statistical analysis shows a general trend between the scales of an AR and the likelihood of its producing a fast CME; that is, the larger the geometric size ( $A_T$ ), the larger the magnetic flux ( $F_T$ ), the stronger the magnetic field ( $B_{avg}$ ), and the more complex the magnetic configuration ( $N_{PIL}$  and  $L_{PIL}$ ), the greater the possibility of producing a fast CME. When all the ARs are sorted into three evenly sized groups with low, intermediate, and high values of these parameters, we find that for all the parameters, more than 60% of extremely fast CMEs are from the high-value group. The two PIL parameters are the best indicators of fast-CME production, with more than 80% coming from the high-value group.

## **A Comparative Study between Eruptive X-Class Flares Associated with Coronal Mass Ejections and Confined X-Class Flares**

Yuming **Wang**<sup>1,2</sup> and Jie Zhang<sup>1</sup>

2007 ApJ 665 1428

<https://iopscience.iop.org/article/10.1086/519765/pdf>

We examine the two kinds of major energetic phenomena that occur in the solar atmosphere: eruptive and confined events. The former describes flares with associated coronal mass ejections (CMEs), while the latter denotes flares without associated CMEs. We find that about 90% of X-class flares are eruptive, but the remaining 10% are confined. To probe why the largest energy releases could be either eruptive or confined, we investigate four X-class events from each of the two types. Both sets of events are selected to have very similar intensities (X1.0 to X3.6) and duration (rise time under 13 minutes and decay time over 9 minutes) in soft X-ray observations, to reduce any bias due to flare size on CME occurrence. We find that the occurrence of eruption (or confinement) is sensitive to the displacement of the location of the energy release, defined as the distance between the flare site and the flux-weighted magnetic center of the source active region. The displacement is 6-17 Mm for confined events but as large as 22-37 Mm for eruptive events. This means that confined events occur closer to the magnetic center, while the eruptive events tend to occur close to the edge of active regions. We use the potential field source-surface model to infer the coronal magnetic field above the source active regions and calculate the flux ratio of low ( $<1.1 R_\odot$ ) to high ( $\geq 1.1 R_\odot$ ) corona. We find that the confined events have a lower ratio ( $<5.7$ ) than the eruptive events ( $>7.1$ ). These results imply that a stronger overlying arcade field may prevent energy releases in the low corona from being eruptive, resulting in flares, but without CMEs. **1998 May 2, 2000 Mar 2, 2000 Jun 6, 2000 Sep 30, 2000 Nov 24, 2001 Apr 2, 2001 Jun 23, 2003 Jun 9, 2004 Feb 26, 2004 Jul 15, 2004 Jul 16, 2004 Jul 17, 2004 Oct 30**

**TABLE 1** Confined X-Class Flares from 1996 to 2004 and Selected Eruptive Flares

## **Kuafu and the studies of CME initiation**

Jingxiu **Wang** and Jun Zhang

[Advances in Space Research](#)

[Volume 40, Issue 12, 2007, Pages 1770-1779](#)

We first briefly review the current trend in the studies of coronal mass ejections (CMEs), then summarize some recent efforts in understanding the CME initiation. Emphasis has been put on the studies of Earth-directed CMEs whose associated surface activity and large scale magnetic source have been well identified.

key development in the low corona in the height of  $1-3 R_\odot$

The **Kuafu Mission** will meet the basic requirement for the new observations in CME initiation studies and serve as a monitor of space weather of the Sun-Earth system.

## **Transequatorial Filament Eruption and Its Link to a Coronal Mass Ejection \***

Jing-Xiu **Wang**<sup>1,2</sup>, Gui-Ping Zhou<sup>1</sup>, Ya-Yuan Wen<sup>1</sup>, Yu-Zong Zhang<sup>1</sup>, Hua-Ning Wang<sup>1</sup>, Yuan-Yong Deng<sup>1</sup>, Jun Zhang<sup>1</sup> and Louise K. Harra<sup>2,1</sup>

Chin. J. Astron. Astrophys. Vol. 6 (2006), No. 2, 247–259, **File**

[http://ourstar.bao.ac.cn/wangjx/paper/jw\\_tf\\_06.pdf](http://ourstar.bao.ac.cn/wangjx/paper/jw_tf_06.pdf)

We revisit the Bastille Day flare/CME Event of **2000 July 14**, and demonstrate that this flare/CME event is not related to only one single active region (AR). Activation and eruption of a huge transequatorial filament are seen to precede the simultaneous filament eruption and flare in the source active region, NOAA AR9077, and the full halo-CME in the high corona. Evidence of reconfiguration of large-scale magnetic structures related to the event is illustrated by SOHO EIT and Yohkoh SXT observations, as well as, the reconstructed 3D magnetic lines of force based on the force-free assumption. We suggest that the AR filament in AR9077 was connected to the transequatorial filament. The large-scale magnetic composition related to the transequatorial filament and its sheared magnetic arcade appears to be an essential part of the CME parent magnetic structure. Estimations show that the filament-arcade system has enough magnetic helicity to account for the helicity carried by the related CMEs. In addition, rather global magnetic connectivity, covering almost all the visible range in longitude and a huge span in latitude on the Sun, is implied by the Nançay Radioheliograph (NRH) observations. The analysis of the Bastille Day event suggests that although the triggering of a global CME might take place in an AR, a much larger scale magnetic composition seems to be the source of the ejected magnetic flux, helicity and plasma. The Bastille Day event is the first described example in the literature, in which a transequatorial filament activity appears to play a key role in a global CME. Many tens of halo-CME are found to be associated with transequatorial filaments and their magnetic environment.

## **Magnetohydrodynamic analysis of the January 20, 2001, CME-CME interaction effect.**

A. **Wang**, S.T. Wu, N. Gopalswamy,

Geophys. Monogr. **156**, 185 (2005)

## **A statistical study on the geoeffectiveness of Earth-directed coronal mass ejections from March 1997 to December 2000,**

**Wang**, Y. M., P. Z. Yee, S. Wang, G. P. Zhou, and J. Wang,

J. Geophys. Res., 107(A11), 1340, **2002**, **File**

We have identified 132 Earth-directed coronal mass ejections (CMEs) based on the observations of the Large Angle Spectroscopic Coronagraph (LASCO) and Extreme Ultraviolet Imaging Telescope (EIT) on board of Solar and Heliospheric Observatory (SOHO) from March 1997 to December 2000 and carried out a statistical study on their geoeffectiveness. The following results are obtained: (1) Only 45% of the total 132 Earth-directed halo CMEs caused geomagnetic storms with  $K_p \geq 5$ ; (2) The initial sites of these geoeffective halo CMEs are rather symmetrically distributed in the heliographic latitude of the visible solar disc, while asymmetrical in longitude with the majority located in the west side of the central meridian; (3) The frontside halo CMEs accompanied with solar flares (identified from GOES-8 satellite observations) seem to be more geoeffective; (4) Only a weak correlation between the CME projected speed and the transit time is revealed. However, for the severe geomagnetic storms (with  $K_p \geq 7$ ), a significant correlation at the confidence level of 99% is found.

## **COMPARISON OF THE 1998 APRIL 29 M6.8 AND 1998 NOVEMBER 5 M8.4 FLARES**

HAIMIN **WANG**, PHILIP R. GOODE, CARSTEN DENKER, GUO YANG, VASYL YURCHISHIN, NARIAKI NITTA, JOSEPH B. GURMAN, CHRIS ST. CYR, AND ALEXANDER G. KOSOVICHEV  
ASTROPHYSICAL JOURNAL, 536:971-981, **2000**, **File**

We combined, and analyzed in detail, the Ha and magnetograph data from Big Bear Solar Observatory (BBSO), full-disk magnetograms from the Michelson Doppler Imager (MDI) on board Solar and Heliospheric Observatory (SOHO), coronagraph data from the Large Angle Spectrometric Coronagraph (LASCO) of SOHO, Fe XII 195 data from the Extreme ultraviolet Imaging Telescope (EIT) of SOHO, A<sub>1</sub> and Yohkoh soft X-ray telescope (SXT) data of the M6.8 Care of 1998 April 29 in National Oceanic and Atmospheric Administration (NOAA) region 8375 and the M8.4 Care of 1998 November 5 in NOAA region 8384. These two Cares have remarkable similarities :

1. Partial halo coronal mass ejections (CMEs) were observed for both events. For the 1998 April 29 event, even though the Care occurred in the southeast of the disk center, the ejected material moved predominantly across the equator, and the central part of the CME occurred in the northeast limb. The direction in which the cusp points in the post-Care SXT images determines the dominant direction of the CMEs.

2. Coronal dimming was clearly observed in EIT Fe XII 195 for both but was not observed in A<sub>1</sub> Yohkoh SXT for either event. Dimming started 2 hr before the onset of the Cares, indicating large-scale coronal restructuring before both Cares.

3. No global or local photospheric magnetic field change was detected from either event ; in particular, no magnetic field change was found in the dimming areas.
4. Both events lasted several hours and, thus, could be classified as long duration events (LDEs). However, they are different in the following important aspects. For the 1998 April 29 event, the flare and the CME are associated with an erupting filament in which the two initial ribbons were well connected and then gradually separated. SXT pre-CARE images show the classical S-shape sheared configuration (sigmoid structure). For the 1998 November 5 event, two initial ribbons were well separated, and the SXT pre-CARE image shows the interaction of at least two loops. In addition, no filament eruption was observed. We conclude that even though these two events resulted in similar coronal consequences, they are due to two distinct physical processes : eruption of sheared loops and interaction of two loops.

**Wang, H., Chae, J., Yurchyshyn, V., Yang, G., Steinegger, M., & Goode, P. 2001, ApJ, 559, 1171**

two sympathetic M-class solar flares and associated CMEs that occurred on **2000 February 17** from two different active regions.

### **Dynamo-driven plasmoid ejections above a spherical surface \***

J. **Warnecke**<sup>1,2</sup>, A. Brandenburg<sup>1,2</sup> and D. Mitra

A&A 534, A11 (2011), E-print, Apr 2012

**Aims.** We extend earlier models of turbulent dynamos with an upper, nearly force-free exterior to spherical geometry, and study how flux emerges from lower layers to the upper ones without being driven by magnetic buoyancy. We also study how this affects the possibility of plasmoid ejection.

**Methods.** A spherical wedge is used that includes northern and southern hemispheres up to mid-latitudes and a certain range in longitude of the Sun. In radius, we cover both the region that corresponds to the convection zone in the Sun and the immediate exterior up to twice the radius of the Sun. Turbulence is driven with a helical forcing function in the interior, where the sign changes at the equator between the two hemispheres.

**Results.** An oscillatory large-scale dynamo with equatorward migration is found to operate in the turbulence zone. Plasmoid ejections occur in regular intervals, similar to what is seen in earlier Cartesian models. These plasmoid ejections are tentatively associated with coronal mass ejections (CMEs). The magnetic helicity is found to change sign outside the turbulence zone, which is in agreement with recent findings for the solar wind.

### **Observation of a Flare and Filament Eruption in Lyman- $\alpha$ on 8 September 2011 by the PROject for OnBoard Autonomy/Large Yield Radiometer (PROBA2/LYRA)**

**L. Wauters, M. Dominique, R. Milligan, I. E. Dammasch, M. Kretzschmar & J. Machol**

*Solar Physics* volume 297, Article number: 36 (2022)

<https://link.springer.com/content/pdf/10.1007/s11207-022-01963-0.pdf>

The Large Yield Radiometer (LYRA) instrument onboard the PROject for OnBoard Autonomy (PROBA2) observes the solar irradiance in four channels in the UV–EUV. One of these channels is centered around the hydrogen line at 121.6 nm. The solar Lyman- $\alpha$  emission line is an optically thick line mostly formed in the chromosphere. Although it is one of the strongest lines of the solar spectrum, only a limited number of instruments provided observations of solar flares in Lyman- $\alpha$ , and those observations differ significantly in shape, durations, and amplitude. We focus on an event that happened on **8 September 2011** (SOL2011-09-08T15:46). This event, an M6.7 flare, was associated with a filament eruption that happened during the decaying phase of the flare. Most of the irradiance fluctuations observed in the Lyman- $\alpha$  time series are synchronized with nonthermal emission fluctuations, as is predicted by flare models. However, there is a late-phase peak in Lyman- $\alpha$  observations that rather correlates with the timing of the filament eruption. We demonstrate that the eruption of the filament is at the origin of this peak.

**Correction:** *Solar Physics* volume 297, Article number: **39** (2022)

### **Is There a CME Rate Floor? CME and Magnetic Flux Values for the Last Four Solar Cycle Minima**

D. F. **Webb**<sup>1</sup>, R. A. Howard<sup>2</sup>, O. C. St. Cyr<sup>3</sup>, and A. Vourlidas<sup>4</sup>

2017 ApJ 851 142

<http://sci-hub.tw/10.3847/1538-4357/aa9b81>

The recent prolonged activity minimum has led to the question of whether there is a base level of the solar magnetic field evolution that yields a "floor" in activity levels and also in the solar wind magnetic field strength. Recently, a flux transport model coupled with magneto-frictional simulations has been used to simulate the continuous magnetic field evolution in the global solar corona for over 15 years, from 1996 to 2012. Flux rope eruptions in the simulations are estimated (Yeates), and the results are in remarkable agreement with the shape of the Solar Heliospheric Observatory/Large Angle and Spectrometric Coronagraph Experiment coronal mass ejection (CME) rate distribution. The eruption rates at the two recent minima approximate the observed-corrected CME rates, supporting the idea of a base level of solar magnetic activity. In this paper, we address this issue by comparing annual averages of the CME occurrence rates during the last four solar cycle minima with several tracers of the global solar magnetic field. We



conclude that CME activity never ceases during a cycle, but maintains a base level of 1 CME every 1.5 to ~3 days during minima. We discuss the sources of these CMEs. **1996 May-July, 2008 December - 2009 February**

## **Understanding Problem Forecasts of ISEST Campaign Flare-CME Events**

David [Webb](#), Nariaki Nitta

[Solar Physics](#) October 2017, 292:142 **File**

The goal of the International Study of Earth-affecting Solar Transients (ISEST) project as part of the Variability of the Sun and Its Terrestrial Impact (VarSITI) program is to understand the origin, evolution, and propagation of solar transients through the space between the Sun and Earth, and to improve our prediction capability for space weather. A goal of ISEST Working Group 4 (Campaign Events) is to study a set of well-observed Sun-to-Earth events to develop an understanding of why some events are successfully forecast (textbook cases), whereas others become problem or failed forecasts. In this article we study six cases during the rise of Solar Cycle 24 that highlight forecasting problems. Likely source coronal mass ejections (CMEs) were identified in all six cases, but the related solar surface activity ranged from uncertain or weak to X-class flares. The geoeffects ranged from none to severe as in the two Sun-Earth events in 2015 that caused severe storms. These events were chosen to illustrate some key problems in understanding the chain from cause to geoeffect. **6 Jan. 2012, 7 – 9 Mar. 2012, 12 – 14 July 2012, 23 – 24 July 2012, 4 – 8 Oct. 2012, 15 – 17 Mar. 2013, 1 June 2013, 7 – 9 Jan. 2014, 10 – 13 Sep. 2014, 15 – 17 Mar. 2015, 21 – 24 June 2015**

## **LASCO White-Light Observations of Eruptive Current Sheets Trailing CMEs**

David F. [Webb](#), Angelos Vourlidas

*Solar Phys.* Volume 291, Issue 12, pp 3725–3749 **2016 File**

<https://link.springer.com/content/pdf/10.1007/s11207-016-0988-9.pdf>

Many models of eruptive flares or coronal mass ejections (CMEs) involve formation of a current sheet connecting the ejecting CME flux rope with a magnetic loop arcade. However, there is very limited observational information on the properties and evolution of these structures, hindering progress in understanding eruptive activity from the Sun. In white-light images, narrow coaxial rays trailing the outward-moving CME have been interpreted as current sheets. Here, we undertake the most comprehensive statistical study of CME-rays to date. We use SOHO/LASCO data, which have a higher cadence, larger field of view, and better sensitivity than any previous coronagraph. We compare our results to a previous study of Solar Maximum Mission (SMM) CMEs, in 1984 – 1989, having candidate magnetic disconnection features at the CME base, about half of which were followed by coaxial bright rays. We examine all LASCO CMEs during two periods of minimum and maximum activity in Solar Cycle 23, resulting in many more events, ~130 CME-rays, than during SMM. Important results include: The occurrence rate of the rays is ~11 % of all CMEs during solar minimum, but decreases to ~7 %~7 % at solar maximum; this is most likely related to the more complex coronal background. The rays appear on average 3 – 4 hours after the CME core, and are typically visible for three-fourths of a day. The mean observed current sheet length over the ray lifetime is ~12  $R_{\odot}$ , with the longest current sheet of 18.5  $R_{\odot}$ . The mean CS growth rates are 188  $\text{kms}^{-1}$  at minimum and 324  $\text{kms}^{-1}$  at maximum. Outward-moving blobs within several rays, which are indicative of reconnection outflows, have average velocities of ~350  $\text{kms}^{-1}$  with small positive accelerations. A pre-existing streamer is blown out in most of the CME-ray events, but half of these are observed to reform within ~1. The long lifetime and long lengths of the CME-rays challenge our current understanding of the evolution of the magnetic field in the aftermath of CMEs. **9 – 10 August 2001**

## **Eruptive Prominences and Their Association with Coronal Mass Ejections**

David F. [Webb](#)

*Solar Prominences*

*Astrophysics and Space Science Library* Volume 415, **2015**, pp 411-432

[http://link.springer.com/chapter/10.1007/978-3-319-10416-4\\_16](http://link.springer.com/chapter/10.1007/978-3-319-10416-4_16)

We discuss the origins and characteristics of solar eruptive phenomena focusing on coronal mass ejections (CMEs) and their associated phenomena, particularly erupting prominences (EPs). Statistically, CMEs are most frequently associated with EPs and X-ray long-duration events. In a few large events the masses of the EP and CME have been separately measured, with the EP mass comprising a large fraction of the total CME mass. EP and CME near-surface precursors include the development of sigmoids, the darkening and broadening of filaments, and their slow rise and Doppler shifts, and the cancellation of magnetic flux near filament channels. Prominences exist within coronal cavities which themselves are embedded in helmet streamers extending to high heights. This entire structure can erupt bodily to become a CME; indeed the most massive and energetic CMEs appear to be of this type. CMEs carry into the heliosphere large quantities of coronal magnetic fields and plasma which are detected by remote sensing and measured in-situ at spacecraft. The most important in-situ CME signature is a magnetic cloud, considered to be the flux rope embedded in most if not all CMEs. Although most CMEs are frequently associated with EPs near the Sun, it is still not known why the prominence material is only rarely identified in-situ. In the last decade, however, we have had heliospheric imaging observations that are helping to distinguish prominence material from the rest of a CME.

## **An Ensemble Study of a January 2010 Coronal Mass Ejection (CME): Connecting a Non-obvious Solar Source with Its ICME/Magnetic Cloud**

D. F. [Webb](#), M. M. Bisi, C. A. de Koning, C. J. Farrugia, B. V. Jackson, L. K. Jian, N. Lugaz, K. Marubashi, C. Möstl, E. P. Romashets, ... show all 12  
Solar Phys., Volume 289, Issue 11, pp 4173-4208 **2014**

A distinct magnetic cloud (MC) was observed in-situ at the Solar TERrestrial RELations Observatory (STEREO)-B on **20–21 January 2010**. About three days earlier, on **17 January**, a bright flare and coronal mass ejection (CME) were clearly observed by STEREO-B, which suggests that this was the progenitor of the MC. However, the in-situ speed of the event, several earlier weaker events, heliospheric imaging, and a longitude mismatch with the STEREO-B spacecraft made this interpretation unlikely. We searched for other possible solar eruptions that could have caused the MC and found a faint filament eruption and the associated CME on **14–15 January** as the likely solar source event. We were able to confirm this source by using coronal imaging from the Sun Earth Connection Coronal and Heliospheric Investigation (SECCHI)/EUVI and COR and Solar and Heliospheric Observatory (SOHO)/Large Angle and Spectrometric Coronagraph (LASCO) telescopes and heliospheric imaging from the Solar Mass Ejection Imager (SMEI) and the STEREO/Heliospheric Imager instruments. We use several empirical models to understand the three-dimensional geometry and propagation of the CME, analyze the in-situ characteristics of the associated ICME, and investigate the characteristics of the MC by comparing four independent flux-rope model fits with the launch observations and magnetic-field orientations. The geometry and orientations of the CME from the heliospheric-density reconstructions and the in-situ modeling are remarkably consistent. Lastly, this event demonstrates that a careful analysis of all aspects of the development and evolution of a CME is necessary to correctly identify the solar counterpart of an ICME/MC.

## Coronal Mass Ejections: Observations

**A Review**

David F. [Webb](#) and Timothy A. Howard  
Living Rev. Solar Phys., 9, (2012), 3, **File**  
<http://www.livingreviews.org/lrsp-2012-3>

Solar eruptive phenomena embrace a variety of eruptions, including flares, solar energetic particles, and radio bursts. Since the vast majority of these are associated with the eruption, development, and evolution of coronal mass ejections (CMEs), we focus on CME observations in this review. CMEs are a key aspect of coronal and interplanetary dynamics. They inject large quantities of mass and magnetic flux into the heliosphere, causing major transient disturbances. CMEs can drive interplanetary shocks, a key source of solar energetic particles and are known to be the major contributor to severe space weather at the Earth. Studies over the past decade using the data sets from (among others) the SOHO, TRACE, Wind, ACE, STEREO, and SDO spacecraft, along with ground-based instruments, have improved our knowledge of the origins and development of CMEs at the Sun and how they contribute to space weather at Earth. SOHO, launched in 1995, has provided us with almost continuous coverage of the solar corona over more than a complete solar cycle, and the heliospheric imagers SMEI (2003–2011) and the HIs (operating since early 2007) have provided us with the capability to image and track CMEs continually across the inner heliosphere. We review some key coronal properties of CMEs, their source regions and their propagation through the solar wind. The LASCO coronagraphs routinely observe CMEs launched along the Sun-Earth line as halo-like brightenings. STEREO also permits observing Earth-directed CMEs from three different viewpoints of increasing azimuthal separation, thereby enabling the estimation of their three-dimensional properties. These are important not only for space weather prediction purposes, but also for understanding the development and internal structure of CMEs since we view their source regions on the solar disk and can measure their in-situ characteristics along their axes. Included in our discussion of the recent developments in CME-related phenomena are the latest developments from the STEREO and LASCO coronagraphs and the SMEI and HI heliospheric imagers.

## Solar Eruptive Phenomena

**Review**

David F. [Webb](#) and Timothy A. Howard  
Submitted to Living Reviews in Solar Physics, **2011**, **File**, <http://solarphysics.livingreviews.org>

## Coronal Mass Ejections: Observations

[Living Reviews in Solar Physics](#) December **2012**, 9:3  
<https://link.springer.com/content/pdf/10.12942%2Flrsp-2012-3.pdf>

Solar eruptive phenomena embrace a variety of solar eruptions, including solar flares, solar energetic particles, and radio bursts. Since the vast majority of solar eruptions are associated with the eruption, development and evolution of coronal mass ejections (CMEs), we focus on CME observations in this review. CMEs are a key aspect of coronal and interplanetary dynamics. They inject large amounts of mass and magnetic flux into the heliosphere, causing major transient disturbances. CMEs can drive interplanetary shocks, a key source of solar energetic particles and are known to be the major contributor to severe space weather at the Earth. Studies over the past decade using the data sets from (among others) the SOHO, TRACE, Wind, ACE, and STEREO spacecraft, along with ground-based instruments, have improved our knowledge of the origins and development of CMEs at the Sun and how they contribute to space weather at Earth. SOHO, launched in 1995, has provided us with almost continuous coverage of the solar corona over more than a complete solar cycle, and the heliospheric imagers SMEI (operating since early 2003) and the HIs (since early 2007) have provided us with the capability to image and track CMEs the inner heliosphere. We review some key coronal properties of CMEs, their source regions and their propagation through the solar wind. The LASCO coronagraphs now

routinely observe CMEs launched along the Sun-Earth line as halo-like brightening. STEREO also permits observing Earth-directed CMEs from three different viewpoints of increasing azimuthal separation, thereby enabling the estimation of their three-dimensional properties. These are important not only for space weather prediction purposes, but also for understanding the development and internal structure of CMEs since we view their source regions on the solar disk and can measure their in-situ characteristics along their axes. Included in our discussion of the recent developments in CME-related phenomena are the latest developments from the STEREO and LASCO coronagraphs and the SMEI and HI heliospheric imagers.

## **Coronal mass ejections and space weather**

D. F. [Webb](#) and N. Gopalswamy

in "Solar Influence on the Heliosphere and Earth's Environment: Recent Progress and Prospects", ed. N. Gopalswamy and A. Battacharyya, Quest Publications, Mumbai, p. 71, **2006**. **File**

Coronal mass ejections (CMEs) are a key feature of coronal and interplanetary (IP) dynamics. Major CMEs inject large amounts of mass and magnetic fields into the heliosphere and, when aimed Earthward, can cause major geomagnetic storms and drive IP shocks, a key source of solar energetic particles. Studies over this solar cycle using the excellent data sets from the SOHO, TRACE, Yohkoh, Wind, ACE and other spacecraft and ground-based instruments have improved our knowledge of the origins and early development of CMEs at the Sun and how they affect space weather at Earth. A new heliospheric experiment, the Solar Mass Ejection Imager, has completed 3 years in orbit and has obtained results on the propagation of CMEs through the inner heliosphere and their geoeffectiveness. We review key coronal properties of CMEs, their source regions, their manifestations in the solar wind, and their geoeffectiveness. Halo-like CMEs are of special interest for space weather because they suggest the launch of a geoeffective disturbance toward Earth. However, not all halo CMEs are equally geoeffective and this relationship varies over the solar cycle. Although CMEs are involved with the largest storms at all phases of the cycle, recurrent features such as interaction regions and high speed wind streams can also be geoeffective.

[Webb](#), D.F., Burkepile, J., Forbes, T.G., Riley, P.: **2003, Observational evidence of new current sheets trailing coronal mass ejections**. *J. Geophys. Res. (Space Phys.)* 108, 1440. DOI. ADS

## **On the plasma flow inside magnetic tornadoes on the Sun**

Sven [Wedemeyer](#), Oskar Steiner

PASJ, **2014**

<http://arxiv.org/pdf/1406.7270v1.pdf>

High-resolution observations with the Swedish 1-m Solar Telescope (SST) and the Solar Dynamics Observatory (SDO) reveal rotating magnetic field structures that extend from the solar surface into the chromosphere and the corona. These so-called magnetic tornadoes are primarily detected as rings or spirals of rotating plasma in the Ca II 854.2 nm line core (also known as chromospheric swirls). Detailed numerical simulations show that the observed chromospheric plasma motion is caused by the rotation of magnetic field structures, which again are driven by photospheric vortex flows at their footpoints. Under the right conditions, two vortex flow systems are stacked on top of each other. We refer to the lower vortex, which extends from the low photosphere into the convection zone, as intergranular vortex flow (IVF). Once a magnetic field structure is co-located with an IVF, the rotation is mediated into the upper atmospheric layers and an atmospheric vortex flow (AVF, or magnetic tornado) is generated. In contrast to the recent work by Shelyag et al., we demonstrate that particle trajectories in a simulated magnetic tornado indeed follow spirals and argue that the properties of the trajectories decisively depend on the location in the atmosphere and the strength of the magnetic field.

## **ARE GIANT TORNADOES THE LEGS OF SOLAR PROMINENCES?**

Sven [Wedemeyer](#)<sup>1</sup>, Eamon Scullion<sup>1</sup>, Luc Rouppe van der Voort<sup>1</sup>, Antonija Bosnjak<sup>1</sup>, and Patrick Antolin **2013** ApJ 774 123

<http://arxiv.org/abs/1306.2661>

Observations in the 171 Å channel of the Atmospheric Imaging Assembly of the space-borne Solar Dynamics Observatory show tornado-like features in the atmosphere of the Sun. These giant tornadoes appear as dark, elongated, and apparently rotating structures in front of a brighter background. This phenomenon is thought to be produced by rotating magnetic field structures that extend throughout the atmosphere. We characterize giant tornadoes through a statistical analysis of properties such as spatial distribution, lifetimes, and sizes. A total number of **201 giant tornadoes** are detected in a period of 25 days, suggesting that, on average, about 30 events are present across the whole Sun at a time close to solar maximum. Most tornadoes appear in groups and seem to form the legs of prominences, thus serving as plasma sources/sinks. Additional H $\alpha$  observations with the Swedish 1 m Solar Telescope imply that giant tornadoes rotate as a structure, although they clearly exhibit a thread-like structure. We observe tornado groups that grow prior to the eruption of the connected prominence. The rotation of the tornadoes may progressively twist the magnetic structure of the prominence until it becomes unstable and erupts. Finally, we investigate the potential relation of giant tornadoes to other phenomena, which may also be produced by rotating magnetic field structures. A comparison to cyclones,

magnetic tornadoes, and spicules implies that such events are more abundant and short-lived the smaller they are. This comparison might help to construct a power law for the effective atmospheric heating contribution as a function of spatial scale. **May 27th, 2012 to June 21st, 2012**

### **Rising of Two Crossing Prominences and the Resulting Oscillations.**

**Wei, H., Huang, Z., Zhang, Q. et al.**

Sol Phys 299, 64 (2024).

<https://doi.org/10.1007/s11207-024-02306-x>

Prominences are important features in the solar atmosphere. Their activities often develop into solar eruptions, such as flares and/or coronal mass ejections. We report here on observations of activities of two crossing prominences and the resulting oscillations observed with the Advanced Space-based Solar Observatory (ASO-S) and the Solar Dynamics Observatory. We observed the two crossing prominences rising simultaneously with a speed of about  $100 \text{ km s}^{-1}$ . The lower-lying prominence consists of threads that show increase of writhe during the rising process. We find evidence that the writhe of the lower-lying prominence is transferred into the overlying one. This transfer of writhe leads to a failure of the eruption of the lower-lying prominence and a shearing motion of the legs of the overlying prominence. The failed eruption of the lower-lying prominence also triggers kink oscillations of its threads, which show periods of about 300 s and amplitudes of less than 10 Mm. Such oscillations are considered to be intrinsic mode and can help to probe the magnetic field of the prominence. Our observations support the idea that the transfer and release of writhe play an important role in confining eruptions of a prominence, and interactions among prominences/filaments might be a crucial aspect of a solar eruption.

### **An EUV jet driven by a series of transition region micro-jets**

**Hengyuan Wei, Zhenghua Huang, Hui Fu, Ming Xiong, Lidong Xia, Chao Zhang, Kaiwen Deng, Haiyi Li**

ApJ 936 51 2022

<https://arxiv.org/pdf/2208.00112.pdf>

<https://iopscience.iop.org/article/10.3847/1538-4357/ac85bf/pdf>

Jets are one of the most common eruptive events in the solar atmosphere, and they are believed to be important in the context of coronal heating and solar wind acceleration. We present an observational study on a sequence of jets with the data acquired with the Solar Dynamics Observatory (SDO) and the Interface Region Imaging Spectrograph (IRIS). This sequence is peculiar in that an EUV jet,  $\sim 29^\circ$  long and with a dome-like base, appears to be a consequence of a series of transition region (TR) micro-jets that are a few arcsecs in length. We find that the occurrence of any TR micro-jets is always associated with the change of geometry of micro-loops at the footpoints of the microjets. A bundle of TR flux ropes is seen to link a TR micro-jet to the dome-like structure at the base of the EUV jet. This bundle rises as a response to the TR micro-jets, with the rising motion eventually triggering the EUV jet. We propose a scenario involving a set of magnetic reconnections, in which the series of TR micro-jets are associated with the processes to remove the constraints to the TR flux ropes and thus allow them to rise and trigger the EUV jet. Our study demonstrates that small-scale dynamics in the lower solar atmosphere are crucial in understanding the energy and mass connection between the corona and the solar lower atmosphere, even though many of them might not pump mass and energy to the corona directly. **2016 June 2**

### **Coronal Magnetic Field Measurements along a Partially Erupting Filament in a Solar Flare**

**Yuqian Wei, Bin Chen, Sijie Yu, Haimin Wang, Ju Jing, Dale E. Gary**

ApJ 923 213 2021

<https://arxiv.org/pdf/2110.06414.pdf>

<https://iopscience.iop.org/article/10.3847/1538-4357/ac2f99/pdf>

<https://doi.org/10.3847/1538-4357/ac2f99>

Magnetic flux ropes are the centerpiece of solar eruptions. Direct measurements for the magnetic field of flux ropes are crucial for understanding the triggering and energy release processes, yet they remain heretofore elusive. Here we report microwave imaging spectroscopy

Owens Valley Solar Array. This flare event is associated with a partial eruption of a twisted filament observed in  $H\{\alpha\}$  by the Goode Solar Telescope at the Big Bear Solar Observatory. The extreme ultraviolet (EUV) and X-ray signatures of the event are generally consistent with the standard scenario of eruptive flares, with the presence of double flare ribbons connected by a bright flare arcade. Intriguingly, this partial eruption event features a microwave counterpart, whose spatial and temporal evolution closely follow the filament seen in  $H\{\alpha\}$  and EUV. The spectral properties of the microwave source are consistent with nonthermal gyrosynchrotron radiation. Using spatially resolved microwave spectral analysis, we derive the magnetic field strength along the filament spine, which ranges from 600-1400 Gauss from its apex to the legs. The results agree well with the non-linear force-free magnetic model extrapolated from the pre-flare photospheric magnetogram. We conclude that the microwave counterpart of the erupting filament is likely due to flare-accelerated electrons injected into the filament-hosting magnetic flux rope cavity following the newly reconnected magnetic field lines. **6 Sep 2017, M1.4,19:26**

### **How eruptions of a small filament feed materials to a nearby larger-scaled filament**

[Hengyuan Wei](#), [Zhenghua Huang](#), [Zhenyong Hou](#), [Youqian Qi](#), [Hui Fu](#), [Bo Li](#), [Lidong Xia](#)

MNRAS:Letter Volume 498, Issue 1, October 2020, Pages L104–L108, **2020**

<https://arxiv.org/pdf/2007.12301.pdf>

<https://doi.org/10.1093/mnrasl/slaa134>

<https://sci-hub.st/https://academic.oup.com/mnrasl/article-abstract/498/1/L104/5899698?redirectedFrom=fulltext>

As one of the most common features in the solar atmosphere, filaments are significant not only in the solar physics but also in the stellar and laboratory plasma physics. With the New Vacuum Solar Telescope and the Solar Dynamics Observatory, here we report on multi-wavelength observations of eruptions of a small (30\arcsec) filament (SF) and its consequences while interacting with the ambient magnetic features including a large (300\arcsec) filament (LF). The eruptions of the SF drive a two-side-loop jet that is a result of magnetic reconnection between the SF threads and an over-lying magnetic channel. As a consequence of the eruption, the heating in the footpoints of the SF destabilises the barbs of the LF rooted nearby. Supersonic chromospheric plasma flows along the barbs of the LF are then observed in the  $\alpha$  passband and they apparently feed materials to the LF. We suggest they are shock-driven plasma flows or chromospheric evaporations, which both can be the consequences of the heating in the chromosphere by nonthermal particles generated in the magnetic reconnection associated with the two-side-loop jet. Our observations demonstrate that the destabilisation in the vicinity of the footpoints of a barb can drive chromospheric plasma feeding to the filament. **March 14 2013**

## **Distorted Magnetic Flux Ropes within Interplanetary Coronal Mass Ejections**

[Andreas J. Weiss](#), [Teresa Nieves-Chinchilla](#), [Christian Möstl](#)

ApJ **2024**

<https://arxiv.org/pdf/2406.13022>

Magnetic flux ropes within interplanetary coronal mass ejections are often characterized as simplistic cylindrical or toroidal tubes with field lines that twist around the cylinder or torus axis. Recent multi-point observations suggest that the overall geometry of these large-scale structures may be significantly more complex, so that the contemporary modeling approaches would be, in some cases, insufficient to properly understand the global structure of any interplanetary coronal mass ejection. In an attempt to partially rectify this issue, we have developed a novel magnetic flux rope model that allows for the description of arbitrary distortions of the cross-section or deformation of the magnetic axis. The distorted magnetic flux rope model is a fully analytic flux rope model, that can be used to describe significantly more complex geometries and is numerically efficient enough to be used for large ensemble simulations. To demonstrate the usefulness of our model, we focus on a specific implementation of our model and apply it to an ICME event that was observed *in situ* on **2023 April 23** at the L1 point by the Wind spacecraft and also by the STEREO-A spacecraft that was 10.2° further east and 0.9° south in heliographic coordinates. We demonstrate that our model can accurately reconstruct each observation individual and also gives a fair reconstruction of both events simultaneously using a multi-point reconstruction approach, which results in a geometry that is not fully consistent with a cylindrical or toroidal approximation.

## **Analysis of coronal mass ejection flux rope signatures using 3DCORE and approximate Bayesian Computation**

[Andreas J. Weiss](#), [Christian Möstl](#), [Tanja Amerstorfer](#), [Rachel L. Bailey](#), [Martin A. Reiss](#), [Jürgen Hinterreiter](#), [Ute A. Amerstorfer](#), [Maïke Bauer](#)

**2021 ApJS 252 9**

<https://arxiv.org/pdf/2009.00327.pdf>

<https://iopscience.iop.org/article/10.3847/1538-4365/abc9bd/pdf>

<https://doi.org/10.3847/1538-4365/abc9bd>

We present a major update to the 3D coronal rope ejection (3DCORE) technique for modeling coronal mass ejection flux ropes in conjunction with an Approximate Bayesian Computation (ABC) algorithm that is used for fitting the model to *in situ* magnetic field measurements. The model assumes an empirically motivated torus-like flux rope structure that expands self-similarly within the heliosphere, is influenced by a simplified interaction with the solar wind environment and carries along an embedded analytical magnetic field. The improved 3DCORE implementation allows us to generate extremely large ensemble simulations which we then use to find global best-fit model parameters using an ABC sequential Monte Carlo (SMC) algorithm. The usage of this algorithm, under some basic assumptions on the uncertainty of the magnetic field measurements, allows us to furthermore generate estimates on the uncertainty of model parameters using only a single *in situ* observation. We apply our model to synthetically generated measurements in order to prove the validity of our implementation for the fitting procedure. We also present a brief analysis of an event captured by Parker Solar Probe (PSP), within the scope of our model, shortly after its first fly-by of the Sun on **2018 November 12** at 0.25 AU. The presented tool set is easily extendable to the analysis of events captured by multiple spacecraft which will facilitate the study of such events. **12 Nov 2018**

## **Flux Accretion and Coronal Mass Ejection Dynamics**

Brian T. [Welsch](#)

Solar Phys. 293:113 **2018**

<https://arxiv.org/pdf/1701.09082v1.pdf>

<http://sci-hub.tw/https://link.springer.com/article/10.1007/s11207-018-1329-y>

Coronal mass ejections (CMEs) are the primary drivers of severe space weather disturbances in the heliosphere. Many CME models invoke ideal magnetohydrodynamics (MHD) to explain the onset and subsequent acceleration of ejections. Both observations and numerical modeling, however, suggest that magnetic reconnection likely plays a major role in most, if not all, fast CMEs. Here, we theoretically investigate the accretion of magnetic flux onto a rising ejection by reconnection involving the ejection's background field. This reconnection alters the magnetic structure of the ejection and its environment, thereby modifying the eruption's dynamics, generically leading to faster acceleration of the CME. Our analysis implies that CME models that neglect the effects of reconnection cannot accurately describe observed CME dynamics. Our ultimate aim is to characterize changes in CME acceleration in terms of observable properties of magnetic reconnection, such as the amount of reconnected flux, deduced from observations of flare ribbons and photospheric magnetic fields.

### **Coronal mass ejections acceleration problem**

Adv. Space. Sci. 42(5), Pages 852-857, 2008

Yayuan [Wen](#), Jingxiu Wang, Hui Zhao and Dalmiro Jorge Filipe Maia

A statistical study of acceleration and its error of coronal mass ejections (CMEs) observed by the Large Angle Spectrometric Coronagraph (LASCO) is performed. A total of 5594 CMEs events have been analyzed by using a least-square method and using the error in the height measures. We verify that slower CMEs (velocities in the interval from 200 to 500 km s<sup>-1</sup>) tend to have a positive acceleration (about 1 m s<sup>-2</sup>) at heights above 5 solar radii, while less than 10% CMEs show an average negative acceleration (about -2.2 m s<sup>-2</sup>) as they propagate from 5 to 30 solar radii. For most individual CMEs one can not say if they are accelerated or decelerated, only for 8% of all observed CMEs events one can extract the sign of the acceleration in the 5–30 solar radii.

### **The CME Acceleration Problem: Error Estimates in LASCO Coronal Mass Ejection Measurements**

Yayuan [Wen](#), Dalmiro Jorge Filipe Maia, and Jingxiu Wang

The Astrophysical Journal, Volume 657, Number 2, Page 1117, 2007

[ <http://www.journals.uchicago.edu/cgi-bin/resolve?ApJ64247> ]

We show in this paper how to obtain error estimates for the height measurements given in the catalog of CMEs observed by LASCO. We find that the error in CME leading-edge position measurements grows rather quickly in the first few solar radii, roughly with the square of the distance from Sun center, but becomes reasonably flat above 5 R<sub>☉</sub>, varying approximately as the square root of the distance. Above 5 R<sub>☉</sub> the typical errors in acceleration are of the same order or larger than the accelerations computed from catalog data. Kinematic quantities computed above 5 R<sub>☉</sub> for individual events will mostly reflect the distribution of the errors in the acceleration, and not the true acceleration experienced by the events.

### **SWAP Observations of Post-flare Giant Arches in the Long-Duration 14 October 2014 Solar Eruption**

Matthew J. [West](#) and Daniel B. Seaton

ApJL 801 L6 2015

<http://arxiv.org/pdf/1502.00801v1.pdf>

On 14 October 2014 the Sun Watcher with Active Pixels and Image Processing (SWAP) EUV solar telescope on-board the Project for On-Board Autonomy 2 (PROBA2) spacecraft observed an eruption that led to the formation of perhaps the largest post-eruptive loop system seen in the solar corona in solar cycle 24. The initial eruption occurred at about 18:30 UT on 14 October, behind the East Solar limb, and was observed as a coronal mass ejection and an M2.2 solar flare. In the 48 hours following the eruption, the associated post-eruptive loops grew to a height of approximately 400000 km (>0.5 solar-radii) at rates between 2-6 km/s. We conclude from our observations of this event that ordinary post-eruptive loops and so-called post-flare giant arches are fundamentally the same and are formed by the same magnetic reconnection mechanism.

### **Incorporation of Heliospheric Imagery into the CME Analysis Tool for improvement of CME Forecasting**

S. J. [Wharton](#), [G. H. Millward](#), [S. Bingham](#), [E. M. Henley](#), [S. Gonzi](#), [D. R. Jackson](#)

Space Weather 2019 File

[sci-hub.se/10.1029/2019SW002166](https://sci-hub.se/10.1029/2019SW002166)

Coronal Mass Ejections (CMEs) cause the largest geomagnetic disturbances at Earth which impact satellites, wired communication systems and power grids. The CME Analysis Tool (CAT) is used to determine a CME's initial longitude, latitude, angular width and radial speed from coronagraph images. These are the initial conditions for the Wang-Sheeley-Argge (WSA) Enlil solar wind model, along with the ambient solar wind properties derived from magnetograms. However, the coronagraph imagery is limited by field of view. We have incorporated heliospheric imagery (HI) from the Solar Terrestrial Relations Observatory (STEREO) into CAT to create the CME Analysis Tool with Heliospheric Imagery (CAT-HI). These HI images have a larger field of view, allowing tracking of CMEs to greater distances from the Sun. We have compared the performances of CAT and CAT-HI by examining the expected arrival times of CMEs at the L1 Lagrange point and found them to be consistent. However, CAT-HI is advantageous

because it could be used to prune ensemble forecasts and issue routine updates for CME arrival time forecasts. Finally, we discuss CAT-HI in the context of an operational mission at the L4 or L5 Lagrange points.

**Table 1.** Initial parameters for CMEs analysed in this study. (2016-2017)

**Table 2.** Results of statistical test for acceleration/deceleration. For each CME,

## Implementing Turbulence Transport in the CRONOS Framework and Application to the Propagation of CMEs

T. **Wiengarten**<sup>1</sup>, H. Fichtner<sup>1</sup>, J. Kleimann<sup>1</sup>, and R. Kissmann

2015 ApJ 805 155

<http://arxiv.org/pdf/1504.01858v1.pdf>

We present the implementation of turbulence transport equations in addition to the Reynolds-averaged magnetohydrodynamic equations within the Cronos framework. The model is validated by comparisons with earlier findings before it is extended to be applicable to regions in the solar wind that are not highly super-Alfvénic. We find that the respective additional terms result in absolute normalized cross-helicity to decline more slowly, while a proper implementation of the mixing terms can even lead to increased cross-helicities in the inner heliosphere. The model extension allows us to place the inner boundary of the simulations closer to the Sun, where we choose its location at 0.1 AU for future application to the Wang–Sheeley–Arge model. Here, we concentrate on effects on the turbulence evolution for transient events by injecting a coronal mass ejection (CME). We find that the steep gradients and shocks associated with these structures result in enhanced turbulence levels and reduced cross-helicity. Our results can now be used straightforwardly for studying the transport of charged energetic particles, where the elements of the diffusion tensor can now benefit from the self-consistently computed solar wind turbulence. Furthermore, we find that there is no strong back-reaction of the turbulence on the large-scale flow so that CME studies concentrating on the latter need not be extended to include turbulence transport effects.

## Automated detection of coronal Mass ejecta origins for space weather Applications (ALMANAC)

**Thomas Williams**, **Huw Morgan**

Space Weather e2022SW003253 **Volume20, Issue11 2022**

<https://arxiv.org/pdf/2211.04405.pdf>

<https://agupubs.onlinelibrary.wiley.com/doi/epdf/10.1029/2022SW003253>

Alerts of potentially hazardous coronal mass ejections (CME) are based on the detection of rapid changes in remote observations of the solar atmosphere. This paper presents a method that detects and estimates the central coordinates of CME eruptions in Extreme Ultraviolet (EUV) data, with the dual aim of providing an early alert, and giving an initial estimate of the CME direction of propagation to a CME geometrical model. In particular, we plan to link the ALMANAC method to the CME detection and characterisation module of the Space Weather Empirical Ensemble Package (SWEEP), which is a fully automated modular software package for operational space weather capability currently being developed for the UK Meteorological Office. In this work, ALMANAC is applied to observations by the Atmospheric Imaging Assembly (AIA) aboard the Solar Dynamics Observatory (SDO). As well as presenting the method, a proof of concept test is made on a limited set of data associated with twenty halo CMEs recorded by the Coordinated Data Analysis Workshop (CDAW) catalogue near the activity maximum of solar cycle 24. SDO/AIA data for each event is processed at 6 minute cadence to identify the on-disk location and time of each CME. The absolute mean deviance between the ALMANAC and CDAW source event coordinates are within 37.05 +/- 29.71 minutes and 11.01 +/- 10.39 degrees. These promising results give a solid foundation for future work, and will provide initial constraints to an automated CME alert and forecasting system. **2010-08-14, 2011-09-06, 2012-04-07, 2013-07-09, 2013-08-20, 2014-04-01**

**Table 1.** The results of CME source location obtained with ALMANAC for twenty example halo - CMEs identified from CDAW. 2010-2014

## Formation of a Dense Flux Rope by a Siphon Flow

Thomas **Williams** and Youra Taroyan

2018 ApJ 852 77

<http://iopscience.iop.org/article/10.3847/1538-4357/aa9d95/pdf>

The interaction of siphon flow with an initially linear Alfvén wave within an isolated chromospheric loop is investigated. The loop is modeled using 1.5D magnetohydrodynamics (MHD). The siphon flow undergoes a hydrodynamic (HD) shock, which allows the Alfvén instability to amplify the propagating waves as they interact with the shock and loop footpoints. The amplification leads to nonlinear processes strongly altering the loop equilibrium. Azimuthal twists of  $50 \text{ km s}^{-1}$  are generated and the loop becomes globally twisted with an azimuthal magnetic field of  $B_\theta \approx 5 \times B_z$ . The flow is accelerated to  $\approx 70 \text{ km s}^{-1}$  due to the propagating shock waves that form. Near the end of the simulation, where the nonlinear processes are strongest, flow reversal is seen within the descending leg of the loop, generating upflows up to  $28 \text{ km s}^{-1}$ . This flow reversal leads to photospheric material being "pulled" into the loop and spreading along its entirety. Within about 2.5 hr, the density increases by a factor of about 30 its original value.

## THE NONLINEAR EVOLUTION OF A TWIST IN A MAGNETIC SHOCKTUBE

Thomas **Williams**, Youra Taroyan, Viktor Fedun

2016 ApJ 817 92

The interaction between a small twist and a horizontal chromospheric shocktube is investigated. The magnetic flux tube is modeled using 1.5-D magnetohydrodynamics. The presence of a supersonic yet sub-Alfvénic flow along the flux tube allows the Alfvénic pulse driven at the photospheric boundary to become trapped and amplified between the stationary shock front and photosphere. The amplification of the twist leads to the formation of slow and fast shocks. The pre-existing stationary shock is destabilized and pushed forward as it merges with the slow shock. The propagating fast shock extracts the kinetic energy of the flow and launches rapid twists of  $10^{15}$  km s<sup>-1</sup> upon each reflection. A cavity is formed between the slow and fast shocks where the flux tube becomes globally twisted within less than an hour. The resultant highly twisted magnetic flux tube is similar to those prone to kink instabilities, which may be responsible for solar eruptions. The generated torsional flux is calculated.

### MASS ESTIMATES OF RAPIDLY MOVING PROMINENCE MATERIAL FROM HIGH-CADENCE EUV IMAGES

David R. [Williams](#), Deborah Baker, and Lidia van Driel-Gesztelyi

2013 ApJ 764 165

We present a new method for determining the column density of erupting filament material using state-of-the-art multi-wavelength imaging data. Much of the prior work on filament/prominence structure can be divided between studies that use a polychromatic approach with targeted campaign observations and those that use synoptic observations, frequently in only one or two wavelengths. The superior time resolution, sensitivity, and near-synchronicity of data from the Solar Dynamics Observatory's Advanced Imaging Assembly allow us to combine these two techniques using photoionization continuum opacity to determine the spatial distribution of hydrogen in filament material. We apply the combined techniques to SDO/AIA observations of a filament that erupted during the spectacular coronal mass ejection on **2011 June 7**. The resulting "polychromatic opacity imaging" method offers a powerful way to track partially ionized gas as it erupts through the solar atmosphere on a regular basis, without the need for coordinated observations, thereby readily offering regular, realistic mass-distribution estimates for models of these erupting structures.

### Solar CME Plasma Diagnostics Expressed as Potential Stellar CME Signatures

Maurice L. [Wilson](#) (1), [John C. Raymond](#) (1)

ApJ 2022

<https://arxiv.org/pdf/2205.12985.pdf>

Solar coronal mass ejections (CMEs) have a strong association with solar flares that is not fully understood. This characteristic of our Sun's magnetic activity may also occur on other stars, but the lack of successfully detected stellar CMEs makes it difficult to perform statistical studies that might show a similar association between CMEs and flares. Because of the potentially strong association, the search for stellar CMEs often starts with a successful search for superflares on magnetically active stars. Regardless of the flare's presence, we emphasize the utility of searching for CME-specific spectroscopic signatures when attempting to find and confirm stellar CME candidates. We use solar CMEs as examples of why a multitude of ultraviolet emission lines, when detected simultaneously, can substantially improve the credibility of spectroscopically discovered stellar CME candidates. We make predictions on how bright CME-related emission lines can be if they derived from distant stars. We recommend the use of three emission lines in particular (C IV 1550 Angstroms, O VI 1032 Angstroms, and C III 977 Angstroms) due to their potentially bright signal and convenient diagnostic capabilities that can be used to confirm if an observational signature truly derives from a stellar CME.

### Constraining the CME Core Heating and Energy Budget with SOHO/UVCS

Maurice L. [Wilson](#) (1), [John C. Raymond](#) (1), [Susan T. Lepri](#) (2), [Roberto Lionello](#) (1 and 3), [Nicholas A. Murphy](#) (1), [Katharine K. Reeves](#) (1), [Chengcai Shen](#) (1)

ApJ 927 27 2021

<https://arxiv.org/pdf/2111.03178.pdf>

<https://iopscience.iop.org/article/10.3847/1538-4357/ac4d35/pdf>

We describe the energy budget of a coronal mass ejection (CME) observed on **1999 May 17** with the Ultraviolet Coronagraph Spectrometer (UVCS). We constrain the physical properties of the CME's core material as a function of height along the corona by using the spectra taken by the single-slit coronagraph spectrometer at heliocentric distances of 2.6 and 3.1 solar radii. We use plasma diagnostics from intensity ratios, such as the O VI doublet lines, to determine the velocity, density, temperature, and non-equilibrium ionization states. We find that the CME core's velocity is approximately 250 km/s, and its cumulative heating energy is comparable to its kinetic energy for all of the plasma heating parameterizations that we investigated. Therefore, the CME's unknown heating mechanisms have the energy to significantly affect the CME's eruption and evolution. To understand which parameters might influence the unknown heating mechanism, we constrain our model heating rates with the observed data and compare them to the rate of heating generated within a similar CME that was constructed by the MAS code's 3D MHD simulation. The rate of heating from the simulated CME agrees with our observationally constrained heating rates when we assume a quadratic power law to describe a self-similar CME expansion. Furthermore, the heating rates agree when we apply a heating parameterization that accounts for the CME flux rope's magnetic energy being converted directly into thermal energy. This UVCS analysis serves as a case study for the importance of multi-slit coronagraph spectrometers for CME studies.



## **On the Contribution of Coronal Mass Ejections to the Heliospheric Magnetic Flux Budget on Different Time Scales**

Réka M. [Winslow](#)<sup>1,1</sup>, Camilla Scolini<sup>1,2</sup>, Noé Lugaz<sup>1</sup>, Nathan A. Schwadron<sup>1,3</sup>, and Antoinette B. Galvin<sup>1</sup>  
**2023 ApJ 958 41**

<https://iopscience.iop.org/article/10.3847/1538-4357/ad02f2/pdf>

Coronal mass ejections (CMEs) contribute closed magnetic flux to the heliosphere while they are connected at both ends to the Sun and play a key role in adding magnetic flux to the heliosphere. Here, we discuss how the type of magnetic reconnection that opens CME field lines in the inner heliosphere, i.e., interchange (IC) and/or interplanetary (IP) reconnection, determines the length of time CMEs contribute to the heliospheric flux budget. This distinction has not been taken into account in past studies that estimate the CME flux opening timescale. We outline key criteria to aid in distinguishing IC reconnection from IP reconnection based on in situ spacecraft data and highlight these through two example events. Studying the manner in which CMEs reconnect and open in the inner heliosphere yields important insights not only into CMEs' role in the heliospheric flux budget but also the evolution of CME complexity, connectivity, and topology. **2011 March 16-20, 2012 January 2-6**

## **Comparing SSN Index to X-ray Flare and Coronal Mass Ejection Rates from Solar Cycles 22-24**

Lisa M. [Winter](#), Rick Pernak, K.S. Balasubramaniam  
**Solar Phys. 2016**

<http://arxiv.org/pdf/1605.00503v1.pdf>

The newly revised sunspot number series allows for placing historical geoeffective storms in the context of several hundred years of solar activity. Using statistical analyses of the Geostationary Operational Environmental Satellites (GOES) X-ray observations from the past ~30 years and the Solar and Heliospheric Observatory (SOHO) Large Angle and Spectrometric Coronagraph (LASCO) Coronal Mass Ejection (CME) catalog (1996-present), we present sunspot-number-dependent flare and CME rates. In particular, we present X-ray flare rates as a function of sunspot number for the past three cycles. We also show that the 1-8 AA X-ray background flux is strongly correlated with sunspot number across solar cycles. Similarly, we show that the CME properties (e.g., proxies related to the CME linear speed and width) are also correlated with sunspot number for SC 23 and 24. These updated rates will enable future predictions for geoeffective events and place historical storms in the context of present solar activity.

## **MAXIMIZING MAGNETIC ENERGY STORAGE IN THE SOLAR CORONA**

Richard [Wolfson](#), Christina Drake, and Max Kennedy  
**2012 ApJ 750 25**

The energy that drives solar eruptive events such as coronal mass ejections (CMEs) almost certainly originates in coronal magnetic fields. Such energy may build up gradually on timescales of days or longer before its sudden release in an eruptive event, and the presence of free magnetic energy capable of rapid release requires nonpotential magnetic fields and associated electric currents. For magnetic energy to power a CME, that energy must be sufficient to open the magnetic field to interplanetary space, to lift the ejecta against solar gravity, and to accelerate the material to speeds of typically several hundred km s<sup>-1</sup>. Although CMEs are large-scale structures, many originate from relatively compact active regions on the solar surface—suggesting that magnetic energy storage may be enhanced when it takes place in smaller magnetic structures. This paper builds on our earlier work exploring energy storage in large-scale dipolar and related bipolar magnetic fields. Here we consider two additional cases: quadrupolar fields and concentrated magnetic bipoles intended to simulate active regions. Our models yield stored energies whose excess over that of the corresponding open field state can be greater than 100% of the associated potential field energy; this contrasts with maximum excess energies of only about 20% for dipolar and symmetric bipolar configurations. As in our previous work, energy storage is enhanced when we surround a nonpotential field with a strong overlying potential field that acts to "hold down" the nonpotential flux as its magnetic energy increases.

## **Evolution of photospheric flows under an erupting filament in the quiet-Sun region**

Jiří [Wollmann](#) (1), [Michal Švanda](#) (1 and 2), [David Korda](#) (1), [Thierry Roudier](#)  
**A&A 636, A102 2020**

<https://arxiv.org/pdf/2003.12515.pdf>

<https://www.aanda.org/articles/aa/pdf/2020/04/aa37525-20.pdf>

We studied the dynamics of the solar atmosphere in the region of a large quiet-Sun filament, which erupted on **21 October 2010**. The filament eruption started at its northern end and disappeared from the H $\alpha$  line-core filtergrams line within a few hours. The very fast motions of the northern leg were recorded in ultraviolet light by AIA. We aim to study a wide range of available datasets describing the dynamics of the solar atmosphere for five days around the filament eruption. This interval covers three days of the filament evolution, one day before the filament growth and one day after the eruption. We search for possible triggers that lead to the eruption of the filament. The surface velocity field in the region of the filament were measured by means of time-distance helioseismology and coherent structure tracking. The apparent velocities in the higher atmosphere were estimated by tracking the features in the 30.4 nm AIA observations. To capture the evolution of the magnetic field, we extrapolated the photospheric line-of-sight magnetograms and also computed the decay index of the magnetic field.

We found that photospheric velocity fields showed some peculiarities. Before the filament activation, we observed a temporal increase of the converging flows towards the filament's spine. In addition, the mean squared velocity increased temporarily before the activation and peaked just before it, followed by a steep decrease. We further see an increase in the average shear of the zonal flow component in the filament's region, followed by a steep decrease. The photospheric l.o.s. magnetic field shows a persistent increase of induction eastward from the filament spine. The decay index of the magnetic field at heights around 10 Mm shows a value larger than critical at the connecting point of the northern filament end.

## **Sequential Small Coronal Mass Ejections Observed In-situ and in White-Light Images by Parker Solar Probe**

[Brian E. Wood](#), [Phillip Hess](#), [Yu Chen](#), [Qiang Hu](#)

ApJ **953** 123 **2023**

<https://arxiv.org/pdf/2308.01372.pdf>

<https://iopscience.iop.org/article/10.3847/1538-4357/ace259/pdf>

We reconstruct the morphology and kinematics of a series of small transients that erupt from the Sun on **2021 April 24** using observations primarily from Parker Solar Probe (PSP). These sequential small coronal mass ejections (CMEs) may be the product of continuous reconnection at a current sheet, a macroscopic example of the more microscopic reconnection activity that has been proposed to accelerate the solar wind more generally. These particular CMEs are of interest because they are the first CMEs to hit PSP and be simultaneously imaged by it, using the Wide-field Imager for Solar Probe (WISPR) instrument. Based on imaging from WISPR and STEREO-A, we identify and model six discrete transients, and determine that it is the second of them (CME2) that first hits PSP, although PSP later more obliquely encounters the third transient as well. Signatures of these encounters are seen in the PSP in situ data. Within these data, we identify six candidate magnetic flux ropes (MFRs), all but one of which are associated with the second transient. The five CME2 MFRs have orientations roughly consistent with PSP encountering the right sides of roughly E-W oriented MFRs, which are sloping back towards the Sun.

## **Internal Structure of the 2019 April 2 CME**

[Brian E. Wood](#), [Carlos R. Braga](#), [Angelos Vourlidis](#)

ApJ **922** 234 **2021**

<https://arxiv.org/pdf/2110.14083.pdf>

<https://doi.org/10.3847/1538-4357/ac2aab>

We present the first analysis of internal coronal mass ejection (CME) structure observed very close to the Sun by the Wide-field Imager for Solar PRobe (WISPR) instrument on board Parker Solar Probe (PSP). The transient studied here is a CME observed during PSP's second perihelion passage on **2019 April 2**, when PSP was only 40  $R_{\text{sun}}$  from the Sun. The CME was also well observed from 1 au by the STEREO-A spacecraft, which tracks the event all the way from the Sun to 1 au. However, PSP/WISPR observes internal structure not apparent in the images from 1 au. In particular, two linear features are observed, one bright and one dark. We model these features as two loops within the CME flux rope channel. The loops can be interpreted as bundles of field lines, with the brightness of the bright loop indicative of lots of mass being loaded into those field lines, and with the dark loop being devoid of such mass loading. It is possible that these loops are actually representative of two independent flux rope structures within the overall CME outline.

## **Serial Flaring in an Active Region: Exploring Why Only One Flare Is Eruptive**

Magnus M. [Woods](#)<sup>1,2,3,4</sup>, Satoshi Inoue<sup>2</sup>, Louise K. Harra<sup>1</sup>, Sarah A. Matthews<sup>1</sup>, and Kanya Kusano<sup>2</sup>  
**2020 ApJ 890 84**

<https://iopscience.iop.org/article/10.3847/1538-4357/ab6bc8/pdf>

Over a four hour period between **2014 June 12–13** a series of three flares were observed within AR 12087. This sequence of flares started with a non-eruptive M-class flare, followed by a non-eruptive C-class flare, and finally ended with a second C-class flare that had an associated filament eruption. In this paper we combine spectroscopic analysis of Interface Region Imaging Spectrometer observations of the Si iv line during the three flares along with a series of nonlinear force-free field (NLFFF) extrapolations in order to investigate the conditions that lead the final flare to be eruptive. From this analysis it is found to be unlikely that the eruption was triggered by either kink instability or by tether-cutting reconnection, allowing the flux rope to rise into a region where it would be susceptible to the torus instability. The NLFFF modeling does, however, suggest that the overlying magnetic field has a fan-spine topology, raising the possibility that breakout reconnection occurring during the first two flares weakened the overlying field, allowing the flux rope to erupt in the subsequent third flare.

[HMI Science Nuggets](#) #135 March 2020 <http://hmi.stanford.edu/hminuggets/?p=3155>

## **A STEREO Survey of Magnetic Cloud Coronal Mass Ejections Observed at Earth in 2008--2012**

Brian E. [Wood](#), Chin-Chun Wu, Ronald P. Lepping, [Teresa Nieves-Chinchilla](#), [Russell A. Howard](#), [Mark G. Linton](#), [Dennis G. Socker](#)

Astrophysical Journal Supplement

**2017**

<https://arxiv.org/pdf/1701.01682v1.pdf>

We identify coronal mass ejections (CMEs) associated with magnetic clouds (MCs) observed near Earth by the Wind spacecraft from 2008 to mid-2012, a time period when the two STEREO spacecraft were well positioned to study Earth-directed CMEs. We find 31 out of 48 Wind MCs during this period can be clearly connected with a CME that is trackable in STEREO imagery all the way from the Sun to near 1 AU. For these events, we perform full 3-D reconstructions of the CME structure and kinematics, assuming a flux rope morphology for the CME shape, considering the full complement of STEREO and SOHO imaging constraints. We find that the flux rope orientations and sizes inferred from imaging are not well correlated with MC orientations and sizes inferred from the Wind data. However, velocities within the MC region are reproduced reasonably well by the image-based reconstruction. Our kinematic measurements are used to provide simple prescriptions for predicting CME arrival times at Earth, provided for a range of distances from the Sun where CME velocity measurements might be made. Finally, we discuss the differences in the morphology and kinematics of CME flux ropes associated with different surface phenomena (flares, filament eruptions, or no surface activity).

**Table 1. CMEs Associated with Wind MCs**

**Table 2. CME Measurements**

**Table 3. Relating CME Velocity to 1 AU Travel Time**

## **Imaging Prominence Eruptions Out to 1 AU**

Brian E. **Wood**, Russell A. Howard, Mark G. Linton

2016 *ApJ* 816 67

<http://arxiv.org/pdf/1512.06748v1.pdf>

Views of two bright prominence eruptions trackable all the way to 1AU are here presented, using the heliospheric imagers on the Solar TERrestrial RELations Observatory (STEREO) spacecraft. The two events first erupted from the Sun on **2011 June 7** and **2012 August 31**, respectively. Only these two examples of clear prominence eruptions observable this far from the Sun could be found in the STEREO image database, emphasizing the rarity of prominence eruptions this persistently bright. For the 2011 June event, a time-dependent 3-D reconstruction of the prominence structure is made using point-by-point triangulation. This is not possible for the August event due to a poor viewing geometry. Unlike the coronal mass ejection (CME) that accompanies it, the 2011 June prominence exhibits little deceleration from the Sun to 1 AU, as a consequence moving upwards within the CME. This demonstrates that prominences are not necessarily tied to the CME's magnetic structure far from the Sun. A mathematical framework is developed for describing the degree of self-similarity for the prominence's expansion away from the Sun. This analysis suggests only modest deviations from self-similar expansion, but close to the Sun the prominence expands radially somewhat more rapidly than self-similarity would predict.

## **Connecting Coronal Mass Ejections and Magnetic Clouds: A Case Study Using an Event from 22 June 2009**

B. E. **Wood**, A. P. Rouillard, C. Möstl, K. Battams, N. P. Savani, K. Marubashi, R. A. Howard, D. G. Socker  
*Solar Physics*, November 2012, Volume 281, Issue 1, pp 369-389

On 27 June 2009 the Wind and Advanced Composition Explorer (ACE) spacecraft near Earth detected a magnetic cloud (MC). The MC can be traced back to a slow coronal mass ejection (CME) launched from the Sun on **22 June 2009** but this connection relies entirely on heliospheric imaging of the Sun–Earth line from the two STEREO spacecraft, illustrating the value of such imaging. The STEREO and SOHO/LASCO views of this event collectively suggest strongly that the CME has the shape of a magnetic flux rope. The arrival times of two density peaks at ACE are consistent with the expected arrival times of the front and back of the flux rope observed in the images, and the velocity of the CME seen by ACE is also consistent with the STEREO measurements. However, the complex nature of the MC signature of this event complicates attempts to compare the flux rope orientations inferred from the imaging and in situ data. Various analyses of the in situ data, performed using both force-free and Grad–Shafranov approaches to MC modeling, yield a wide range of flux rope orientations depending on the type of analysis and on the exact time interval used. The best reproduction of the image-inferred orientation occurs when the first third of the MC time interval is ignored.

## **A CORONAL HOLE'S EFFECTS ON CORONAL MASS EJECTION SHOCK MORPHOLOGY IN THE INNER HELIOSPHERE**

B. E. **Wood**<sup>1</sup>, C.-C. Wu<sup>1</sup>, A. P. Rouillard<sup>2,3</sup>, R. A. Howard<sup>1</sup>, and D. G. Socker

2012 *ApJ* 755 43, **File**

We use STEREO imagery to study the morphology of a shock driven by a fast coronal mass ejection (CME) launched from the Sun on **2011 March 7**. The source region of the CME is located just to the east of a coronal hole. The CME ejecta is deflected away from the hole, in contrast with the shock, which readily expands into the fast outflow from the coronal hole. The result is a CME with ejecta not well centered within the shock surrounding it. The shock shape inferred from the imaging is compared with in situ data at 1 AU, where the shock is observed near Earth by the Wind spacecraft, and at STEREO-A. Shock normals computed from the in situ data are consistent with the shock morphology inferred from imaging.

## Reconstructing the 3D Morphology of the 17 May 2008 CME

B.E. Wood · R.A. Howard · A. Thernisien · S.P. Plunkett · D.G. Socker

Solar Phys (2009) 259: 163–178, **File**

We model the kinematics and three-dimensional distribution of mass in a coronal mass ejection (CME) observed on 17 May 2008, using a comprehensive analysis of STEREO images of the CME. The CME is a surprisingly fast one for solar minimum, reaching velocities of up to 1120 km s<sup>-1</sup>. It can be followed continuously from inception all the way out to 1 AU. We find that the appearance of the CME can be modeled reasonably well as a combination of two distinct fronts that expand outward in a self-similar fashion. The model implies that STEREO-B is struck by the weaker of these two fronts on 19 May, and the *in situ* instruments on STEREO-B do see a weak density and magnetic field enhancement at the expected time.

## AN EMPIRICAL RECONSTRUCTION OF THE 2008 APRIL 26 CORONAL MASS EJECTION

B. E. Wood and R. A. Howard

Astrophysical Journal, 702:901–910, 2009 September

We present a three-dimensional model of the density distribution of a coronal mass ejection (CME) from 2008 April 26. This CME was observed by the two spacecraft composing the Solar Terrestrial Relations Observatory (STEREO), which tracked the CME from near the Sun, into the interplanetary medium (IPM), and all the way to 1 AU. The CME was directed toward STEREO-B and hit that spacecraft on 2008 April 29. The STEREO images of the CME show an internal structure that can be interpreted as having a flux rope shape. The two different perspectives on the event provided by the two STEREO spacecraft allow us to make a particularly strong argument for the flux rope interpretation, and the STEREO data also allow us to study the evolution of the flux rope in the IPM. The flux rope is oriented close to the ecliptic plane, but with the western leg tilted northwards by about 20°. This implies an orientation roughly perpendicular to the neutral line of the active region at the event's point of origin, apparently an unusual geometry given that previous analyses have found that CME flux ropes are usually, but not always, oriented *parallel* to the neutral lines of their source regions. The CME model also consists of a front out ahead of the flux rope, possibly a shock launched by the flux rope driver. The model density distribution is reasonably successful at reproducing the CME appearance both close to the Sun in coronagraphic images, and far from the Sun in images of the IPM from STEREO's heliospheric imagers. This suggests that self-similar expansion is a reasonable first-order approximation for this particular CME, and also indicates that the flux rope's orientation does not change much during its journey through the IPM.

## Comprehensive Observations of a Solar Minimum Coronal Mass Ejection with the Solar Terrestrial Relations Observatory

B. E. Wood, R. A. Howard, S. P. Plunkett, and D. G. Socker

Astrophysical Journal, 694:707–717, 2009; **File**

We perform the first kinematic analysis of a coronal mass ejection (CME) observed by both imaging and *in situ* instruments on board the Solar Terrestrial Relations Observatory (STEREO). Launched on 2008 February 4, the CME is tracked continuously from initiation to 1 AU using the imagers on both STEREO spacecraft, and is then detected by the particle and field detectors on board STEREO-B on February 7. The CME is also detected *in situ* by the Advanced Composition Explorer and Solar and Heliospheric Observatory at Earth's L1 Lagrangian point. This event provides a good example of just how different the same event can look when viewed from different perspectives. We also demonstrate many ways in which the comprehensive and continuous coverage of this CME by STEREO improves confidence in our assessment of its kinematic behavior, with potential ramifications for space weather forecasting. The observations provide several lines of evidence in favor of the observable part of the CME being narrow in angular extent, a determination crucial for deciding how best to convert observed CME elongation angles from Sun-center to actual Sun-center distances.

## Serial Flaring in an Active Region: Exploring Why Only One Flare Is Eruptive

Magnus M. Woods<sup>1,2,3,4</sup>, Satoshi Inoue<sup>2</sup>, Louise K. Harra<sup>1</sup>, Sarah A. Matthews<sup>1</sup>, and Kanya Kusano<sup>2</sup>  
2020 ApJ 890 84

<https://iopscience.iop.org/article/10.3847/1538-4357/ab6bc8/pdf>

Over a four hour period between 2014 June 12–13 a series of three flares were observed within AR 12087. This sequence of flares started with a non-eruptive M-class flare, followed by a non-eruptive C-class flare, and finally ended with a second C-class flare that had an associated filament eruption. In this paper we combine spectroscopic analysis of Interface Region Imaging Spectrometer observations of the Si iv line during the three flares along with a series of nonlinear force-free field (NLFFF) extrapolations in order to investigate the conditions that lead the final flare to be eruptive. From this analysis it is found to be unlikely that the eruption was triggered by either kink instability or by tether-cutting reconnection, allowing the flux rope to rise into a region where it would be susceptible to the torus instability. The NLFFF modeling does, however, suggest that the overlying magnetic field has a fan-spine topology, raising the possibility that breakout reconnection occurring during the first two flares weakened the overlying field, allowing the flux rope to erupt in the subsequent third flare.

## The Triggering of the 29-March-2014 Filament Eruption

[Magnus M. Woods](#), [Satoshi Inoue](#), [Louise K. Harra](#), [Sarah A. Matthews](#), [Kanya Kusano](#), [Nadine M. E. Kalmoni](#)

2018 ApJ, 860:163

<https://arxiv.org/pdf/1805.05976.pdf>

<http://iopscience.iop.org/article/10.3847/1538-4357/aac5e1/pdf>

The X1 flare and associated filament eruption occurring in NOAA Active Region 12017 on SOL2014-03-29 has been the source of intense study. In this work, we analyse the results of a series of non linear force free field extrapolations of the pre and post flare period of the flare. In combination with observational data provided by the IRIS, Hinode and SDO missions, we have confirmed the existence of two flux ropes present within the active region prior to flaring. Of these two flux ropes, we find that intriguingly only one erupts during the X1 flare. We propose that the reason for this is due to tether cutting reconnection allowing one of the flux ropes to rise to a torus unstable region prior to flaring, thus allowing it to erupt during the subsequent flare.

## Time-dependent Hinode/EIS Atlas of a Coronal Mass Ejection Containing Cool Material

E. M. [Wraback](#)<sup>1</sup>, E. Landi<sup>1</sup>, and W. B. Manchester<sup>1</sup>

2024 ApJ 970 182

<https://iopscience.iop.org/article/10.3847/1538-4357/ad625f/pdf>

We report the first time-dependent spectral atlas of a coronal mass ejection (CME) observed by the Hinode/Extreme Ultraviolet Imaging Spectrometer (EIS). EIS observed the Cartwheel CME on **2008 April 9** at 09:30–10:00 UT in its full wavelength range and captured the bright core containing prominence material as it passed across the slit field of view. The measurement of the differential emission measure (DEM) showed that the observation captured two plasma components, a coronal component at  $\text{Log } T \approx 6.05$  K and a cold component at  $\text{Log } T \approx 5.30$  K, which we interpret as the prominence material in the CME core. We used this DEM to develop a spectral atlas for the four EIS spectra containing the CME material and the pre- and postevent spectra. These observations provide the basis for studying CME plasma evolution in the low solar corona, as well as guide observations from the current and upcoming spectrometers, including Solar Orbiter/SPICE, Solar-C/EUVST, and MUSE, which will advance our understanding of CME plasma evolution.

## Catalogue of solar filament disappearances 1964- 1980,

[Wright](#), C.S.

Report UAG-100, Nat. Geophys. Dat. Ctr, **1991**.

<https://repository.library.noaa.gov/view/noaa/1365>

## A Data-Constrained Three-Dimensional Magnetohydrodynamic Simulation Model for a Coronal Mass Ejection (CME) Initiation†

S. T. [Wu](#), Yufen Zhou, Chaowei Jiang, Xueshang Feng, Chin-Chun Wu, Qiang Hu

JGR Volume 121, Issue 2 Pages 1009–1023 **2016**

In this study, we present a three-dimensional magnetohydrodynamic model based on an observed eruptive twisted flux-rope (Sigmoid) deduced from solar vector magnetograms. This model is a combination of our two very well tested MHD models: (i) data-driven 3D Magnetohydrodynamic (MHD) active region evolution (MHD-DARE) model for the reconstruction of the observed flux rope and (ii) 3D MHD global coronal-heliosphere evolution (MHD-GCHE) model to track the propagation of the observed flux rope. The **2011 Sept 6**, AR11283, event is used to test this model. First, the formation of the flux rope (sigmoid) from AR11283 is reproduced by the MHD-DARE model with input from the measured vector magnetograms given by SDO/HMI. Second, these results are used as the initial-boundary condition for our MHD-GCHE model for the initiation of a CME as observed. The model output indicates that the flux-rope resulting from MHD-DARE produces the physical properties of a CME and the morphology resembles the observations made by STEREO/COR-1.

## Initial condition influence on coronal mass ejection propagation,

[Wu](#), P., N. A. Schwadron, G. L. Siscoe, and P. Riley

J. Geophys. Res., 113, A00B05, **2008**

<http://dx.doi.org/10.1029/2008JA013082>

In the melon-seed-overpressure-expansion (MSOE) model described by Siscoe et al. (2006) for the acceleration of coronal mass ejections (CMEs), magnetic repulsion force plays a central role. MSOE is a combination of Pneuman's (1984) melon seed concept with an overpressure expansion analytically formulated by Siscoe et al. (2006). The MSOE model creates a reduced formalism to describe CME acceleration and is highly advantageous for comparative studies. As originally presented, the MSOE model has the drawback of being able to produce only fast CMEs. For the work presented in this paper, we compare the acceleration of a 2.5-D magnetohydrodynamics (MHD)-modeled CME with

that of a version of the MSOE model. On the basis of the results of the MHD simulations, we divide the acceleration of a CME into two phases: (1) a tethered phase before detachment (when the CME is tethered by external closed loops) and (2) a repulsion phase after detachment (when the tethering force that binds the CME is much smaller than outward magnetic repulsion force). We find that during the repulsion phase, the acceleration can be described well by the standard MSOE model. However, during the tethered phase, the CME acceleration is much slower than MSOE predictions. We therefore refine the MSOE model to include tethering and can account for both fast and slow CMEs with the final CME speed controlled by the CME detachment height.

## THE ROLE OF MAGNETIC RECONNECTION IN CME ACCELERATION

S. T. WU, T. X. ZHANG, M. DRYER, X. S. FENG and ARJUN TAN  
Space Science Reviews (2005) 121: 33–47

## A Model for Flux Rope Formation and Disconnection in Pseudostreamer Coronal Mass Ejections

[P. F. Wyper](#), [B. J. Lynch](#), [C. R. DeVore](#), [P. Kumar](#), [S. K. Antiochos](#), [L. K. S. Daldorff](#)

ApJ 975 168 2024

<https://arxiv.org/pdf/2409.08126>

<https://iopscience.iop.org/article/10.3847/1538-4357/ad7941/pdf>

Coronal mass ejections (CMEs) from pseudostreamers represent a significant fraction of large-scale eruptions from the Sun. In some cases, these CMEs take a narrow jet-like form reminiscent of coronal jets; in others, they have a much broader fan-shaped morphology like CMEs from helmet streamers. We present results from a magnetohydrodynamic simulation of a broad pseudostreamer CME. The early evolution of the eruption is initiated through a combination of breakout interchange reconnection at the overlying null point and ideal instability of the flux rope that forms within the pseudostreamer. This stage is characterised by a rolling motion and deflection of the flux rope toward the breakout current layer. The stretching out of the strapping field forms a flare current sheet below the flux rope; reconnection onset there forms low-lying flare arcade loops and the two-ribbon flare footprint. Once the CME flux rope breaches the rising breakout current layer, interchange reconnection with the external open field disconnects one leg from the Sun. This induces a whip-like rotation of the flux rope, generating the unstructured fan shape characteristic of pseudostreamer CMEs. Interchange reconnection behind the CME releases torsional Alfvén waves and bursty dense outflows into the solar wind. Our results demonstrate that pseudostreamer CMEs follow the same overall magnetic evolution as coronal jets, although they present different morphologies of their ejecta. We conclude that pseudostreamer CMEs should be considered a class of eruptions that are distinct from helmet-streamer CMEs, in agreement with previous observational studies. **19-21 Apr 2015**

## Editorial: Flux rope interaction with the ambient corona: From jets to CMEs. **Review**

[Wyper P](#), [Kumar P](#) and [Lynch B](#)

Front. Astron. Space Sci. 9:980183. (2022)

<https://www.frontiersin.org/articles/10.3389/fspas.2022.980183/pdf>

Eruptive events within the Sun's corona occur across a broad range of scales, from abundant small-scale jets to highly energetic coronal mass ejections (CMEs) (e.g., [Webb and Howard, 2012](#); [Raouafi et al., 2016](#); [Kumar et al., 2021](#)). Flux ropes have been understood to be a fundamental constituent of CMEs for many years, but it has only been more recently that their role in smaller eruptive events has become more appreciated (e.g., [Sterling et al., 2015](#); [Wyper et al., 2017](#)). The key to understanding the differing morphology and nature of eruptions on these vastly differing scales is to understand the nature of the interaction between the flux ropes involved and the magnetic field of the surrounding corona. This Research Topic invited perspectives on (and examples of) flux rope eruptions across this broad range of scales, from formation to ejection, with the aim of highlighting commonalities and differences to aid in ultimately building a common framework for their understanding.

## A Model for the Coupled Eruption of a Pseudostreamer and Helmet Streamer

[P. F. Wyper](#), [S. K. Antiochos](#), [C. R. DeVore](#), [B. J. Lynch](#), [J. T. Karpen](#), [P. Kumar](#)

ApJ 909 54 2021

<https://arxiv.org/pdf/2101.01962.pdf>

<https://doi.org/10.3847/1538-4357/abd9ca>

A highly important aspect of solar activity is the coupling between eruptions and the surrounding coronal magnetic-field topology, which determines the trajectory and morphology of the event and can even lead to sympathetic eruptions from multiple sources. In this paper, we report on a numerical simulation of a new type of coupled eruption, in which a coronal jet initiated by a large pseudostreamer filament eruption triggers a streamer-blowout coronal mass ejection (CME) from the neighboring helmet streamer. Our configuration has a large opposite-polarity region positioned between the polar coronal hole and a small equatorial coronal hole, forming a pseudostreamer flanked by the coronal holes and the helmet streamer. Further out, the pseudostreamer stalk takes the shape of an extended arc in the heliosphere. We energize the system by applying photospheric shear along a section of the polarity inversion line within the pseudostreamer. The resulting sheared-arcade filament channel develops a flux rope that eventually erupts as a classic coronal-hole-type jet. However, the enhanced breakout reconnection above the channel as the jet is launched

progresses into the neighboring helmet streamer, partially launching the jet along closed helmet streamer field lines and blowing out the streamer top to produce a classic bubble-like CME. This CME is strongly deflected from the jet's initial trajectory and contains a mixture of open and closed magnetic field lines. We present the detailed dynamics of this new type of coupled eruption, its underlying mechanisms and the implications of this work for the interpretation of in-situ and remote-sensing observations. **2014-07-24**

### **Numerical Simulation of Helical Jets at Active Region Peripheries**

Peter F. [Wyper](#), [C. Richard DeVore](#), [Spiro K. Antiochos](#)

MNRAS Volume 490, Issue 3, December 2019, Pages 3679–3690

<https://arxiv.org/pdf/1909.09423.pdf>

[sci-hub.se/10.1093/mnras/stz2674](https://sci-hub.se/10.1093/mnras/stz2674)

Coronal jets are observed above minority polarity intrusions throughout the solar corona. Some of the most energetic occur on the periphery of active regions where the magnetic field is strongly inclined. These jets exhibit a non-radial propagation in the low corona as they follow the inclined field, and often have a broad, helical shape. We present a three-dimensional magnetohydrodynamic simulation of such an active-region-periphery helical jet. We consider an initially potential field with a bipolar flux distribution embedded in a highly inclined magnetic field, representative of the field nearby an active region. The flux of the minority polarity sits below a bald-patch separatrix initially. Surface motions are used to inject free energy into the closed field beneath the separatrix, forming a sigmoidal flux rope which eventually erupts producing a helical jet. We find that a null point replaces the bald patch early in the evolution and that the eruption results from a combination of magnetic breakout and an ideal kinking of the erupting flux rope. We discuss how the two mechanisms are coupled, and compare our results with previous simulations of coronal-hole jets. This comparison supports the hypothesis that the generic mechanism for all coronal jets is a coupling between breakout reconnection and an ideal instability. We further show that our results are in good qualitative and quantitative agreement with observations of active-region periphery jets.

**RHESSI Science Nuggets #361 Oct 2019 23 Oct 2013**

[http://sprg.ssl.berkeley.edu/~tohban/wiki/index.php/Non-radial\\_jets\\_on\\_the\\_edges\\_of\\_active\\_regions](http://sprg.ssl.berkeley.edu/~tohban/wiki/index.php/Non-radial_jets_on_the_edges_of_active_regions)

### **When are Coronal Jets miniature CMEs?**

P. F. [Wyper](#), [C. R. DeVore](#), [S. K. Antiochos](#)

UKSP Nugget: **89, June 2018**

<http://www.uksolphys.org/uksp-nugget/89-when-are-coronal-jets-miniature-cmes/>

Coronal jets are deceptively simple events that we are only now getting a clear understanding of. It is now apparent that in the cases where a mini-filament is involved they share similarities with large-scale filament eruptions. Such jets can therefore be thought of as mini-CMEs. We have introduced a model for jets driven by mini-filament eruptions that explains the link between these large-scale and small-scale events. Our work suggests that eruptions across vastly different scales in the corona can be understood within the same framework. The three realisations of the model we studied also help explain the differences between individual mini-filament jets. With further space missions on the horizon, particularly the improved views of the poles with Solar Orbiter, the future looks bright for further unpicking the secrets of these small but mighty events.

### **A Model for Coronal Hole Bright Points and Jets due to Moving Magnetic Elements**

Peter F. [Wyper](#), [C. Richard DeVore](#), [Judy T. Karpen](#), [Spiro K. Antiochos](#), [Anthony R. Yeates](#)

ApJ **2018**

<https://arxiv.org/pdf/1808.03688.pdf>

Coronal jets and bright points occur prolifically in predominantly unipolar magnetic regions, such as coronal holes, where they appear above minority-polarity intrusions. Intermittent low-level reconnection and explosive, high-energy-release reconnection above these intrusions are thought to generate bright points and jets, respectively. The magnetic field above the intrusions possesses a spine-fan topology with a coronal null point. The movement of magnetic flux by surface convection adds free energy to this field, forming current sheets and inducing reconnection. We conducted three-dimensional magnetohydrodynamic simulations of moving magnetic elements as a model for coronal jets and bright points. A single minority-polarity concentration was subjected to three different experiments: a large-scale surface flow that sheared part of the separatrix surface only, a large-scale surface flow that also sheared part of the polarity inversion line surrounding the minority flux, and the latter flow setup plus a "fly-by" of a majority-polarity concentration past the moving minority-polarity element. We found that different bright-point morphologies, from simple loops to sigmoids, were created. When only the field near the separatrix was sheared, steady interchange reconnection modulated by quasi-periodic, low-intensity bursts of reconnection occurred, suggestive of a bright point with periodically varying intensity. When the field near the PIL was strongly sheared, on the other hand, filament channels repeatedly formed and erupted via the breakout mechanism, explosively increasing the interchange reconnection and generating non-helical jets. The fly-by produced even more energetic and explosive jets. Our results explain several key aspects of coronal-hole bright points and jets, and the relationships between them.

### **A universal model for solar eruptions.**

[Wyper](#) PF, [Antiochos](#) SK, [DeVore](#) CR.

2017 Nature 544, 452–455. (doi:10.1038/nature22050)

[sci-hub.se/10.1038/nature22050](https://sci-hub.se/10.1038/nature22050)

Magnetically driven eruptions on the Sun, from stellar-scale coronal mass ejections<sup>1</sup> to small-scale coronal X-ray and extreme-ultraviolet jets<sup>2,3,4</sup>, have frequently been observed to involve the ejection of the highly stressed magnetic flux of a filament<sup>5,6,7,8,9</sup>. Theoretically, these two phenomena have been thought to arise through very different mechanisms: coronal mass ejections from an ideal (non-dissipative) process, whereby the energy release does not require a change in the magnetic topology, as in the kink or torus instability<sup>10,11</sup>; and coronal jets from a resistive process<sup>2,12</sup> involving magnetic reconnection. However, it was recently concluded from new observations that all coronal jets are driven by filament ejection, just like large mass ejections<sup>13</sup>. This suggests that the two phenomena have physically identical origin and hence that a single mechanism may be responsible, that is, either mass ejections arise from reconnection, or jets arise from an ideal instability. Here we report simulations of a coronal jet driven by filament ejection, whereby a region of highly sheared magnetic field near the solar surface becomes unstable and erupts. The results show that magnetic reconnection causes the energy release via ‘magnetic breakout’—a positive-feedback mechanism between filament ejection and reconnection. We conclude that if coronal mass ejections and jets are indeed of physically identical origin (although on different spatial scales) then magnetic reconnection (rather than an ideal process) must also underlie mass ejections, and that magnetic breakout is a universal model for solar eruptions.

### **A Breakout Model for Solar Coronal Jets with Filaments**

P. F. **Wyper**, C. R. DeVore, S. K. Antiochos

ApJ 2017

<https://arxiv.org/pdf/1712.00134.pdf>

Recent observations have revealed that many solar coronal jets involve the eruption of miniature versions of large-scale filaments. Such "mini-filaments" are observed to form along the polarity inversion lines of strong, magnetically bipolar regions embedded in open (or distantly closing) unipolar field. During the generation of the jet, the filament becomes unstable and erupts. Recently we described a model for these mini-filament jets, in which the well-known magnetic-breakout mechanism for large-scale coronal mass ejections is extended to these smaller events. In this work we use three-dimensional magnetohydrodynamic simulations to study in detail three realisations of the model. We show that the breakout-jet generation mechanism is robust and that different realisations of the model can explain different observational features. The results are discussed in relation to recent observations and previous jet models.

### **Three-Dimensional Simulations of Tearing and Intermittency in Coronal Jets**

P. F. **Wyper**, C. R. DeVore, J. T. Karpen, B. J. Lynch

ApJ 2016

<http://arxiv.org/pdf/1607.00692v1.pdf>

Observations of coronal jets increasingly suggest that local fragmentation and intermittency play an important role in the dynamics of these events. In this work we investigate this fragmentation in high-resolution simulations of jets in the closed-field corona. We study two realizations of the embedded-bipole model, whereby impulsive helical outflows are driven by reconnection between twisted and untwisted field across the domed fan plane of a magnetic null. We find that the reconnection region fragments following the onset of a tearing-like instability, producing multiple magnetic null points and flux-rope structures within the current layer. The flux ropes formed within the weak-field region in the center of the current layer are associated with "blobs" of density enhancement that become filamentary threads as the flux ropes are ejected from the layer, whereupon new flux ropes form behind them. This repeated formation and ejection of flux ropes provides a natural explanation for the intermittent outflows, bright blobs of emission, and filamentary structure observed in some jets. Additional observational signatures of this process are discussed. Essentially all jet models invoke reconnection between regions of locally closed and locally open field as the jet-generation mechanism. Therefore, we suggest that this repeated tearing process should occur at the separatrix surface between the two flux systems in all jets. A schematic picture of tearing-mediated jet reconnection in three dimensions is outlined. **2012 November 13**

### **Simulations of Solar Jets Confined by Coronal Loops**

P. F. **Wyper**, C. R. DeVore

ApJ 820 77 2015

<http://arxiv.org/pdf/1509.07901v1.pdf>

Coronal jets are collimated, dynamic events that occur over a broad range of spatial scales in the solar corona. In the open magnetic field of coronal holes, jets form quasi-radial spires that can extend far out into the heliosphere, while in closed-field regions the jet outflows are confined to the corona. We explore the application of the embedded-bipole model to jets occurring in closed coronal loops. In this model, magnetic free energy is injected slowly by footpoint motions that introduce twist within the closed dome of the jet source region, and is released rapidly by the onset of an ideal kink-like instability. Two length scales characterize the system: the width ( $N$ ) of the jet source region and the footpoint separation ( $L$ ) of the coronal loop that envelops the jet source. We find that the jet characteristics are highly sensitive to the ratio  $L/N$ , in both the conditions for initiation and the subsequent dynamics. The longest-lasting and most energetic jets occur along long coronal loops with large  $L/N$  ratios, and share many features of open-field jets, while smaller  $L/N$  ratios produce shorter-duration, less energetic jets that are affected by reflections from the far-loop footpoint. We quantify the transition between these behaviours and show that our model replicates key qualitative and quantitative aspects of both quiet-Sun and active-region loop jets. We also find that the reconnection between the closed



dome and surrounding coronal loop is very extensive: the cumulative reconnected flux at least matches the total flux beneath the dome for small  $L/N$ , and is more than double that value for large  $L/N$ .

## **Dynamic Topology and Flux Rope Evolution During Non-linear Tearing of 3D Null Point Current Sheets**

P. F. [Wyper](#), D. I Pontin

Physics of Plasmas, 2014

<http://arxiv.org/pdf/1406.6120v1.pdf>

In this work the dynamic magnetic field within a tearing-unstable three-dimensional (3D) current sheet about a magnetic null point is described in detail. We focus on the evolution of the magnetic null points and flux ropes that are formed during the tearing process. Generally, we find that both magnetic structures are created prolifically within the layer and are non-trivially related. We examine how nulls are created and annihilated during bifurcation processes, and describe how they evolve within the current layer. The type of null bifurcation first observed is associated with the formation of pairs of flux ropes within the current layer. We also find that new nulls form within these flux ropes, both following internal reconnection and as adjacent flux ropes interact. The flux ropes exhibit a complex evolution, driven by a combination of ideal kinking and their interaction with the outflow jets from the main layer. The finite size of the unstable layer also allows us to consider the wider effects of flux rope generation. We find that the unstable current layer acts as a source of torsional MHD waves and dynamic braiding of magnetic fields. The implications of these results to several areas of heliophysics are discussed.

## **PARTICLE ACCELERATION AND TRANSPORT DURING 3D CME ERUPTIONS**

Qian [Xia](#),<sup>1</sup> Joel T. Dahlin,<sup>2</sup> , \* Valentina Zharkova,<sup>1</sup> and Spiro K. Antiochos<sup>3</sup>

ApJ 894 89 2020

[https://solargsm.com/wp-content/uploads/2020/04/xia\\_etal\\_ArmTP\\_apj2020.pdf](https://solargsm.com/wp-content/uploads/2020/04/xia_etal_ArmTP_apj2020.pdf) File

<https://doi.org/10.3847/1538-4357/ab846d>

We calculate particle acceleration during corona mass ejection (CME) eruptions using combined magnetohydrodynamic (MHD) and test-particle models. The 2.5D/3D CMEs are generated via the breakout mechanism. In this scenario a reconnection at the “breakout” current sheet (CS) above the flux rope initiates the CME eruption by destabilizing a quasi-static force balance. Reconnection at the flare CS below the erupting flux rope drives the fast acceleration of the CME, which forms flare loops below and produces the energetic particles observed in flares. For test-particle simulations, two times are selected during the impulsive and decay phases of the eruption. Particles are revealed to be accelerated more efficiently in the flare CS rather than in the breakout CS even in the presence of large magnetic islands. Particles are first accelerated in the CSs (with or without magnetic islands) by the reconnection electric field mainly through particle curvature drift. We find, as expected, that accelerated particles precipitate into the chromosphere, or become trapped in the loop top by magnetic mirrors, or escape to interplanetary space along open field lines. Some trapped particles are reaccelerated, either via reinjection to the flare CS or through a local Betatron-type acceleration associated with compression of the magnetic field. The energetic particles produce relatively hard energy spectra during the impulsive phase. During the gradual phase, the relaxation of magnetic field shear reduces the guiding field in the flare CS, which leads to a decrease in particle energization efficiency. Important implications of our results for observations of particle acceleration in the solar coronal jets are also discussed.

## **Three-dimensional Prominence-hosting Magnetic Configurations: Creating a Helical Magnetic Flux Rope**

C. [Xia](#)<sup>1</sup>, R. Keppens<sup>1</sup>, and Y. Guo

2014 ApJ 780 130

The magnetic configuration hosting prominences and their surrounding coronal structure is a key research topic in solar physics. Recent theoretical and observational studies strongly suggest that a helical magnetic flux rope is an essential ingredient to fulfill most of the theoretical and observational requirements for hosting prominences. To understand flux rope formation details and obtain magnetic configurations suitable for future prominence formation studies, we here report on three-dimensional isothermal magnetohydrodynamic simulations including finite gas pressure and gravity. Starting from a magnetohydrostatic corona with a linear force-free bipolar magnetic field, we follow its evolution when introducing vortex flows around the main polarities and converging flows toward the polarity inversion line near the bottom of the corona. The converging flows bring the feet of different loops together at the polarity inversion line, where magnetic reconnection and flux cancellation happen. Inflow and outflow signatures of the magnetic reconnection process are identified, and thereby the newly formed helical loops wind around preexisting ones so that a complete flux rope grows and ascends. When a macroscopic flux rope is formed, we switch off the driving flows and find that the system relaxes to a stable state containing a helical magnetic flux rope embedded in an overlying arcade structure. A major part of the formed flux rope is threaded by dipped field lines that can stably support prominence matter, while the total mass of the flux rope is in the order of  $4\text{-}5 \times 10^{14}$  g.

## **Dark Ribbons Propagating and Sweeping across Extreme Ultraviolet Structures after Filament Eruptions**

Junmin [Xiao](#), Jun Zhang, Ting Li, and Shuhong Yang

2015 ApJ 805 25

With observations from the Atmospheric Imaging Assembly on board the Solar Dynamics Observatory, we first report that dark ribbons (DRs) moved apart from the filament channel and swept across EUV structures after filament eruptions on **2013 June 23** and **2012 February 10 and 24**, respectively. In the first event, the DR with a length of 168 Mm appeared at 100 Mm to the northwest of the filament channel, where the filament erupted 15 hr previously. The DR moved toward the northwest with the different sections having different velocities, ranging from 0.3 to 1.6 km s<sup>-1</sup>. When the DR's middle part swept across a strong EUV structure, the motion of this part was blocked, appearing to deflect the DR. With the DR propagation, the connection of the surrounding EUV structures gradually changed. After one day passed, the DR eventually disappeared. In the other two events, the dynamic evolution of the DRs was similar to that in the first event. Based on the observations, we speculate that the reconnection during the filament eruption changes the configuration of the surrounding magnetic fields systematically. During the reconnection process, magnetic fields are deflecting and the former arbitrarily distributed magnetic fields are rearranged along specific directions. The deflection of magnetic fields results in an instantaneous void region where the magnetic strength is smaller and the plasma density is lower. Consequently, the void region is observed as a DR and propagates outward with the reconnection developing.

### Numerical experiments on dynamic evolution of a CME-flare current sheet

[Xiaoyan Xie](#), [Zhixing Mei](#), [Chengcai Shen](#), [Qiangwei Cai](#), [Jing Ye](#), [Katharine K Reeves](#), [Ilya I Roussey](#), [Jun Lin](#)

MNRAS Volume 509, Issue 1, January 2022, Pages 406–420,

<https://doi.org/10.1093/mnras/stab2954>

In this paper, we performed magnetohydrodynamics numerical experiments to look into the dynamic behaviour of the current sheet (CS) between the coronal mass ejection (CME) and the associated solar flare, especially the CS oscillation and plasmoid motions in coronal conditions. During the evolution, the disrupting magnetic configuration becomes asymmetric first in the buffer region at the bottom of the CME bubble. The Rayleigh–Taylor instability in the buffer region and the deflected motion of the plasma driven by the termination shock at the bottom of the CME bubble cause the buffer region to oscillate around the y-axis. The local oscillation propagates downwards through the CS, prompting an overall CS oscillation. As the buffer region grows, the oscillation period becomes longer, increasing from about 30 s to about 16 min. Meanwhile, there is another separated oscillation with a period between 0.25 and 1.5 min in the cusp region of the flare generated by velocity shearing. The tearing mode instability yields formations of plasmoids inside the CS. The motions of all the plasmoids observed in the experiment accelerate, which implies that the large-scale CME/flare CS itself in the true eruptive event is filled with the diffusion region according to the standard theory of magnetic reconnection.

### Near-Sun Flux-Rope Structure of CMEs

H. [Xie](#), N. Gopalswamy, O. C. St. Cyr

Solar Physics, May 2013, Volume 284, Issue 1, pp 47-58; [File](#)

We have used the Krall flux-rope model (Krall and St. Cyr, *Astrophys. J.* 2006, 657, 1740) (KFR) to fit 23 magnetic cloud (MC)-CMEs and 30 non-cloud ejecta (EJ)-CMEs in the Living With a Star (LWS) Coordinated Data Analysis Workshop (CDAW) 2011 list. The KFR-fit results show that the CMEs associated with MCs (EJs) have been deflected closer to (away from) the solar disk center (DC), likely by both the intrinsic magnetic structures inside an active region (AR) and ambient magnetic structures (e.g. nearby ARs, coronal holes, and streamers, etc.). The mean absolute propagation latitudes and longitudes of the EJ-CMEs (18°, 11°) were larger than those of the MC-CMEs (11°, 6°) by 7° and 5°, respectively. Furthermore, the KFR-fit widths showed that the MC-CMEs are wider than the EJ-CMEs. The mean fitting face-on width and edge-on width of the MC-CMEs (EJ-CMEs) were 87 (85)° and 70 (63)°, respectively. The deflection away from DC and narrower angular widths of the EJ-CMEs have caused the observing spacecraft to pass over only their flanks and miss the central flux-rope structures. The results of this work support the idea that all CMEs have a flux-rope structure.

### Understanding shock dynamics in the inner heliosphere with modeling and Type II radio data: The 2010-04-03 event

[Xie](#), H.; [Odstroil](#), D.; [Mays](#), L.; [St. Cyr](#), O. C.; [Gopalswamy](#), N.; [Cremades](#), H.

*J. Geophys. Res.*, Vol. 117, No. A4, A04105, 2012, [preprint File](#)

<http://dx.doi.org/10.1029/2011JA017304>

The **2010 April 03** solar event was studied using observations from STEREO SECCHI, SOHO LASCO, and Wind kilometric Type II data (kmTII) combined with WSA-Cone-ENLIL model simulations performed at the Community Coordinated Modeling Center (CCMC). In particular, we identified the origin of the coronal mass ejection (CME) using STEREO EUVI and SOHO EIT images. A flux-rope model was fit to the SECCHI A and B, and LASCO images to determine the CME's direction, size, and actual speed. J-maps from STEREO COR2/HI-1/HI-2 and simulations from CCMC were used to study the formation and evolution of the shock in the inner heliosphere. In addition, we also studied the time-distance profile of the shock propagation from kmTII radio burst observations. The J-maps together

with in-situ data from the Wind spacecraft provided an opportunity to validate the simulation results and the kmTII prediction. Here we report on a comparison of two methods of predicting interplanetary shock arrival time: the ENLIL model and the kmTII method; and investigate whether or not using the ENLIL model density improves the kmTII prediction. We found that the ENLIL model predicted the kinematics of shock evolution well. The shock arrival times (SAT) and linear-fit shock velocities in the ENLIL model agreed well with those measurements in the J-maps along both the CME leading edge and the Sun-Earth line. The ENLIL model also reproduced most of the large scale structures of the shock propagation and gave the SAT prediction at Earth with an error of  $\sim 1 \pm 7$  hours. The kmTII method predicted the SAT at Earth with an error of  $\sim 15$  hours when using  $n_0 = 4.16 \text{ cm}^{-3}$ , the ENLIL model plasma density near Earth; but it improved to  $\sim 2$  hours when using  $n_0 = 6.64 \text{ cm}^{-3}$ , the model density near the CME leading edge at 1 AU.

## On the Origin, 3D Structure and Dynamic Evolution of CMEs Near Solar Minimum

H. Xie · O.C. St. Cyr · N. Gopalswamy · S. Yashiro · J. Krall · M. Kramar · J. Davila

Solar Phys (2009) 259: 143–161, [File](#)

We have conducted a statistical study 27 coronal mass ejections (CMEs) from January 2007 – June 2008, using the stereoscopic views of STEREO SECCHI A and B combined with SOHO LASCO observations. A flux-rope model, in conjunction with 3D triangulations, has been used to reconstruct the 3D structures and determine the actual speeds of CMEs. The origin and the dynamic evolution of the CMEs are investigated using COR1, COR2 and EUVI images. We have identified four types of solar surface activities associated with CMEs: *i*) total eruptive prominence (totEP), *ii*) partially eruptive prominence (PEP), *iii*) X-ray flare, and *iv*) X-type magnetic structure (X-line). Among the 27 CMEs, 18.5% (5 of 27) are associated with totEPs, 29.6% (8 of 27) are associated with PEPs, 26% (7 of 27) are flare related, and 26% (7 of 27) are associated with X-line structures, and 43% (3 of 7) are associated with both X-line structures and PEPs. Three (11%) could not be associated with any detectable activity. The mean actual speeds for totEP-CMEs, PEP-CMEs, flare-CMEs, and X-line-CMEs are  $404 \text{ km s}^{-1}$ ,  $247 \text{ km s}^{-1}$ ,  $909 \text{ km s}^{-1}$ , and  $276 \text{ km s}^{-1}$ , respectively; the average mean values of edge-on and broadside widths for the 27 CMEs are 52 and 85 degrees, respectively. We found that slow CMEs ( $V \leq 400 \text{ km s}^{-1}$ ) tend to deflect towards and propagate along the streamer belts due to the deflections by the strong polar magnetic fields of corona holes, while some faster CMEs show opposite deflections away from the streamer belts.

## Cone model for halo cmes: application to space weather forecasting

Xie, H., L. Ofman and G. Lawrence, ,  
Journal Geophys. Res., 109, A03109,  
[doi:10.1029/2003ja010226](https://doi.org/10.1029/2003ja010226), 2004.

## An explanation for the slow-rise phase of solar eruptions

Yaoyu Xing, Aiyang Duan, Chaowei Jiang  
MNRAS, Volume 534, Issue 1, October 2024, Pages 107–116,  
<https://doi.org/10.1093/mnras/stae2088>  
<https://watermark.silverchair.com/stae2088.pdf>

Solar eruptions are sudden release of the magnetic free energy accumulated within a quasi-static evolutionary process of the corona. Interestingly, many solar eruptions are preceded by a short-term slow-rise phase, during which the pre-eruption structure rises at a speed significantly larger than that of the quasi-static evolution. Here we suggest an explanation for the slow-rise phase based on a recent high-accuracy magnetohydrodynamic simulation for initiation of solar eruption. The simulation shows that by continuously shearing a bipolar magnetic arcade, an internal current sheet forms gradually, and an eruption begins once magnetic reconnection is triggered at the current sheet. We find in the simulation that the overlying field presents a slow-rise phase before the reconnection sets in. In addition, the rising speed is significantly larger than that of the core field during this phase. This slow rise is a manifestation of the growing expansion of the arcade in the process of approaching a fully open field state, which is inherent to the formation of a current sheet before the eruption. We also show three flare events with slow-rise phases that are highly consistent with these key characteristics in the simulation: an expansion of the overlying coronal loops with speeds much larger than the quasi-static evolution speed, and for those events with filament eruption, the slow rise of filament is much smaller than that of the overlying loops. In this type of events, the eruption might be initiated through the mechanism as shown in the simulation, and the expansion of overlying coronal loops is a better indicator of the slow-rise phase. 2016.03.23, 2021.10.28, 2022.10.02

## Unveiling the Initiation Route of Coronal Mass Ejections through their Slow Rise Phase

Chen Xing, Guillaume Aulanier, Xin Cheng, Chun Xia, Mingde Ding  
ApJ 966 70 2024  
<https://arxiv.org/pdf/2402.16679.pdf>

<https://iopscience.iop.org/article/10.3847/1538-4357/ad2ea9/pdf>

Understanding the early evolution of coronal mass ejections (CMEs), in particular their initiation, is the key to forecasting solar eruptions and induced disastrous space weather. Although many initiation mechanisms have been proposed, a full understanding of CME initiation, which is identified as a slow rise of CME progenitors in kinematics before the impulsive acceleration, remains elusive. Here, with a state-of-the-art thermal-magnetohydrodynamics simulation, we determine a complete CME initiation route in which multiple mainstream mechanisms occur in sequence yet are tightly coupled. The slow rise is first triggered and driven by the developing hyperbolic flux tube (HFT) reconnection. Subsequently, the slow rise continues as driven by the coupling of the HFT reconnection and the early development of torus instability. The end of the slow rise, i.e., the onset of the impulsive acceleration, is induced by the start of the fast magnetic reconnection coupled with the torus instability. These results unveil that the CME initiation is a complicated process involving multiple physical mechanisms, thus being hardly resolved by a single initiation mechanism.

## Identifying Footpoints of Pre-eruptive and Coronal Mass Ejection Flux Ropes with Sunspot Scars

[Chen Xing](#), [Guillaume Aulanier](#), [Brigitte Schmieder](#), [Xin Cheng](#), [Mingde Ding](#)

A&A 682, A3 2024

<https://arxiv.org/pdf/2310.13532.pdf>

<https://www.aanda.org/articles/aa/pdf/2024/02/aa47053-23.pdf>

**Context.** The properties of pre-eruptive structures and coronal mass ejections (CMEs) are characterized by those of their footpoints, the latter of which attract a great deal of interest. However, the matter of how to identify the footpoints of pre-eruptive structures and how to do so with the use of ground-based instruments still remains elusive.

**Aims.** In this work, we study an arc-shaped structure intruding in the sunspot umbra. It is located close to the (pre-)eruptive flux rope footpoint and it is expected to help identify the footpoint.

**Methods.** We analyzed this arc-shaped structure, which we call a “sunspot scar”, in a CME event on **July 12, 2012**, and in two CME events from observationally inspired magnetohydrodynamic simulations performed by OHM and MPI-AMRVAC.

**Results.** The sunspot scar displays a more inclined magnetic field with a weaker vertical component and a stronger horizontal component relative to that in the surrounding umbra and is manifested as a light bridge in the white light passband. The hot field lines anchored in the sunspot scar are spatially at the transition between the flux rope and the background coronal loops and temporally in the process of the slipping reconnection which builds up the flux rope.

**Conclusions.** The sunspot scar and its related light bridge mark the edge of the CME flux rope footpoint and particularly indicate the edge of the pre-eruptive flux rope footpoint in the framework of “pre-eruptive structures being flux ropes”.

Therefore, they provide a new perspective for the identification of pre-eruptive and CME flux rope footpoints, as well as new methods for studying the properties and evolution of pre-eruptive structures and CMEs with photospheric observations only.

## Evolution of the Toroidal Flux of CME Flux Ropes during Eruption

[C. Xing](#), [X. Cheng](#), [M. D. Ding](#)

The Innovation 2020

<https://arxiv.org/pdf/2011.10750.pdf>

[https://www.cell.com/the-innovation/fulltext/S2666-6758\(20\)30062-X](https://www.cell.com/the-innovation/fulltext/S2666-6758(20)30062-X)

<https://doi.org/10.1016/j.xinn.2020.100059>

Coronal mass ejections (CMEs) are large-scale explosions of the coronal magnetic field. It is believed that magnetic reconnection significantly builds up the core structure of CMEs, a magnetic flux rope, during the eruption. However, the quantitative evolution of the flux rope, particularly its toroidal flux, is still unclear. In this paper, we study the evolution of the toroidal flux of the CME flux rope for four events. The toroidal flux is estimated as the magnetic flux in the footpoint region of the flux rope, which is identified by a method that simultaneously takes the coronal dimming and the hook of the flare ribbon into account. We find that the toroidal flux of the CME flux rope for all four events shows a two-phase evolution: a rapid increasing phase followed by a decreasing phase. We further compare the evolution of the toroidal flux with that of the Geostationary Operational Environmental Satellites soft X-ray flux and find that they are basically synchronous in time, except that the peak of the former is somewhat delayed. The results suggest that the toroidal flux of the CME flux rope may be first quickly built up by the reconnection mainly taking place in the sheared overlying field and then reduced by the reconnection among the twisted field lines within the flux rope, as enlightened by a recent 3D magnetohydrodynamic simulation of CMEs. **2012/3/5, 2012/3/27, August 21, 2015, 2015/11/4**

## Quantifying the Toroidal Flux of Pre-existing Flux Ropes of CMEs

[C. Xing](#), [X. Cheng](#), [Jiong Qiu](#), [Qiang Hu](#), [E. R. Priest](#), [M. D. Ding](#)

ApJ 889 125 2020

<https://arxiv.org/pdf/1912.10623.pdf>

<https://iopscience.iop.org/article/10.3847/1538-4357/ab6321/pdf>

In past decades, much progress has been achieved on the origin and evolution of coronal mass ejections (CMEs). In-situ observations of the counterparts of CMEs, especially magnetic clouds (MCs) near the Earth, have provided measurements of the structure and total flux of CME flux ropes. However, it has been difficult to measure these

properties in the erupting CME flux rope, in particular in the pre-existing flux rope. In this work, we propose a model to estimate the toroidal flux of the pre-existing flux rope by subtracting the flux contributed by magnetic reconnection during the eruption from the flux measured in the MC. The flux by the reconnection is derived from geometric properties of two-ribbon flares based on a quasi-2D reconnection model. We then apply the model to four CME/flare events and find that the ratio of toroidal flux in the pre-existing flux rope to that of the associated MC lies in the range of 0.40--0.88. It indicates that the toroidal flux of the pre-existing flux rope has an important contribution to that of the CME flux rope and is usually at least as large as the flux arising from the eruption process for the selected events. **2003/10/28, 2003/11/18, 2010/5/23, 2011/10/2**

## Two Types of Long-duration Quasi-static Evolution of Solar Filaments

Chen [Xing](#), [Haochuan Li](#), [Bei Jiang](#), [Xin Cheng](#), [M. D. Ding](#)

ApJL 2018

<https://arxiv.org/pdf/1804.01232.pdf>

In this Letter, we investigate the long-duration quasi-static evolution of 12 pre-eruptive filaments (4 active region and 8 quiescent filaments), mainly focusing on the evolution of the filament height in three dimension (3D) and the decay index of the background magnetic field. The filament height in 3D is derived through two-perspective observations of \textit{Solar Dynamics Observatory} and \textit{Solar TERrestrial RELations Observatory}. The coronal magnetic field is reconstructed using the potential field source surface model. A new finding is that the filaments we studied show two types of long-duration evolution: one type is comprised of a long-duration static phase and a short slow rise phase with a duration of less than 12 hours and a speed of 0.1--0.7 km s<sup>-1</sup>, while the other one only presents a slow rise phase but with an extremely long duration of more than 60 hours and a smaller speed of 0.01--0.2 km s<sup>-1</sup>. At the moment approaching the eruption, the decay index of the background magnetic field at the filament height is similar for both active region and quiescent filaments. The average value and upper limit are ~0.9 and ~1.4, close to the critical index of torus instability. Moreover, the filament height and background magnetic field strength are also found to be linearly and exponentially related with the filament length, respectively. **14 Aug 2010, 3 Sept 2010, 19 Dec 2010, 7 Jun 2011**  
**TABLE 1** Parameters of filaments at the near-eruption stage (2010-2011)

## Sun-as-a-star observations of obscuration dimmings caused by filament eruptions

Yu [Xu](#), [Hui Tian](#), [Astrid M. Veronig](#), [Karin Dissauer](#)

ApJ 2024

<https://arxiv.org/pdf/2405.13671>

Filament eruptions often lead to coronal mass ejections (CMEs) on the Sun and are one of the most energetic eruptive phenomena in the atmospheres of other late-type stars. However, the detection of filament eruptions and CMEs on stars beyond the solar system is challenging. Here we present six filament eruption cases on the Sun and show that filament material obscuring part of the solar disk can cause detectable dimming signatures in sun-as-a-star flux curves of He II 304 Å. Those filament eruptions have similar morphological features, originating from small filaments inside active regions and subsequently strongly expanding to obscure large areas of the solar disk or the bright flare regions. We have tracked the detailed evolution of six obscuration dimmings and estimated the dimming properties, such as dimming depths, dimming areas, and duration. The largest dimming depth among the six events under study is 6.2% accompanied by the largest dimming area of 5.6% of the solar disk area. Other events have maximum dimming depths in a range of around 1% to 3% with maximum areas varying between about 3% to 4% of the solar disk area. The duration of the dimming spans from around 0.4 hours to 7.0 hours for the six events under study. A positive correlation was found between the dimming depth and area, which may help to set constraint on the filament sizes in stellar observations. **2011.08.04, 2012.01.11, 2013.02.05, 2014.04.15, 2022.04.11, 2023.07.14**

**Table 1.** Six cases of obscuration dimmings and their flare/CME information

## Imaging and spectroscopic observations of a confined solar filament eruption with two-stage evolution

[Zhe Xu](#), [Xiaoli Yan](#), [Liheng Yang](#), [Zhike Xue](#), [Jincheng Wang](#), [Yian Zhou](#)

MNRAS Volume 530, Issue 1, Pages 473–481 2024

<https://arxiv.org/pdf/2403.12639.pdf>

<https://doi.org/10.1093/mnras/stae822>

<https://academic.oup.com/mnras/article-pdf/530/1/473/57192015/stae822.pdf>

Solar filament eruptions are often characterized by stepwise evolution due to the involvement of multiple mechanisms, such as magnetohydrodynamic instabilities and magnetic reconnection. In this article, we investigated a confined filament eruption with a distinct two-stage evolution by using the imaging and spectroscopic observations from the Interface Region Imaging Spectrograph (IRIS) and the Solar Dynamics Observatory (SDO). The eruption originated from a kinked filament thread that separated from an active region filament. In the first stage, the filament thread rose slowly and was obstructed due to flux pile-up in its front. This obstruction brought the filament thread into reconnection with a nearby loop-like structure, which enlarged the flux rope and changed its connectivity through the foot-point migration. The newly formed flux rope became more kink unstable and drove the rapid eruption in the second stage. It ascended into the upper atmosphere and initiated the reconnection with the overlying field. Finally, the flux rope was totally disintegrated, producing several solar jets along the overlying field. These observations demonstrate that the

external reconnection between the flux rope and overlying field can destroy the flux rope, thus playing a crucial role in confining the solar eruptions. **2021-12-24**

## **Sun-as-a-star spectroscopic observations of the line-of-sight velocity of a solar eruption on October 28, 2021**

[Yu Xu](#), [Hui Tian](#), [Zhenyong Hou](#), [Zihao Yang](#), [Yuhang Gao](#), [Xianyong Bai](#)

ApJ Volume 931, Issue 2, id.76, **2022**

<https://arxiv.org/pdf/2204.11722.pdf>

<https://iopscience.iop.org/article/10.3847/1538-4357/ac69d5/pdf>

The propagation direction and true velocity of a solar coronal mass ejection, which are among the most decisive factors for its geo-effectiveness, are difficult to determine through single-perspective imaging observations. Here we show that Sun-as-a-star spectroscopic observations, together with imaging observations, could allow us to solve this problem. Using observations of the Extreme-ultraviolet Variability Experiment onboard the Solar Dynamics Observatory, we found clear blue-shifted secondary emission components in extreme ultraviolet spectral lines during a solar eruption on **October 28, 2021**. From simultaneous imaging observations, we found that the secondary components are caused by a mass ejection from the flare site. We estimated the line-of-sight (LOS) velocity of the ejecta from both the double Gaussian fitting method and the red-blue asymmetry analysis. The results of both methods agree well with each other, giving an average LOS velocity of the plasma of  $\sim 423 \text{ km s}^{-1}$ . From the 304 Å image series taken by the Extreme Ultraviolet Imager onboard the Solar Terrestrial Relation Observatory-A (STEREO-A) spacecraft, we estimated the plane-of-sky (POS) velocity from the STEREO-A viewpoint {to be around  $587 \text{ km s}^{-1}$ }. The full velocity of the bulk motion of the ejecta was then computed by combining the imaging and spectroscopic observations, which turns out to be around  $596 \text{ km s}^{-1}$  with an angle of  $42.4^\circ$  to the west of the Sun-Earth line and  $16.0^\circ$  south to the ecliptic plane.

**RHESSI Science Nuggets №430 May 2022** [https://sprg.ssl.berkeley.edu/~tohban/wiki/index.php/Sun-as-a-star\\_spectroscopic\\_observations\\_of\\_the\\_line-of-sight\\_velocity\\_of\\_a\\_solar\\_eruption\\_on\\_October\\_28,\\_2021](https://sprg.ssl.berkeley.edu/~tohban/wiki/index.php/Sun-as-a-star_spectroscopic_observations_of_the_line-of-sight_velocity_of_a_solar_eruption_on_October_28,_2021)

## **Multi-wavelength Observation of a Failed Eruption from a Helical Kink-unstable Prominence**

Haiqing [Xu](#), [Jiangtao Su](#), [Jie Chen](#), [Guiping Ruan](#), [Arun Kumar Awasthi](#), [Hongqi Zhang](#), [Mei Zhang](#), [Kaifan Ji](#), [Yuzong Zhang](#), [Jiajia Liu](#)

ApJ **901** 121 **2020**

<https://arxiv.org/pdf/2008.08299.pdf>

<https://doi.org/10.3847/1538-4357/abb01d>

Multi-wavelength observations of prominence eruptions provide an opportunity to uncover the physical mechanism of the triggering and the evolution process of the eruption. In this paper, we investigated an erupting prominence on **October 14, 2012**, recorded in H $\alpha$ , EUV, and X-ray wavelengths. The process of the eruption gives evidences on the existence of a helical magnetic structure and showing the twist being converting to writhe. The estimated twist is  $\sim 6\pi$  (3 turns), exceeding the threshold of the kink instability. The rising plasma then reached a high speed, estimated at  $228 \text{ km s}^{-1}$ , followed by a sudden rapid acceleration at  $2715 \text{ m s}^{-2}$ , and synchronous with a solar arc. Co-spatial cusp shaped structures were observed in both AIA 131Å and 94Å images, signifying the location of the magnetic reconnection. The erupted flux rope finally undergone a deceleration with a maximum value of  $391 \text{ m s}^{-2}$ , which is even larger than the free-fall acceleration on the Sun ( $273 \text{ m s}^{-2}$ ), suggesting that the eruption finally failed, possibly due to an inward magnetic tension force.

## **Homologous Circular-ribbon Flares Driven by Twisted Flux Emergence**

Z. [Xu](#)<sup>1</sup>, K. Yang<sup>2</sup>, Y. Guo<sup>2</sup>, J. Zhao<sup>3</sup>, Z. J. Zhao<sup>1</sup>, and L. Kashapova

**2017** ApJ **851** 30

In this paper, we report two homologous circular-ribbon flares associated with two filament eruptions. They were well observed by the New Vacuum Solar Telescope and the Solar Dynamics Observatory on **2014 March 5**. Prior to the flare, two small-scale filaments enclosed by a circular pre-flare brightening lie along the circular polarity inversion line around the parasitic polarity, which has shown a continuous rotation since its first appearance. Two filaments eventually erupt in sequence associated with two homologous circular-ribbon flares and display an apparent writhing signature. Supplemented by the nonlinear force-free field extrapolation and the magnetic field squashing factor investigation, the following are revealed. (1) This event involves the emergence of magnetic flux ropes into a pre-existing polarity area, which yields the formation of a 3D null-point topology in the corona. (2) Continuous input of the free energy in the form of a flux rope from beneath the photosphere may drive a breakout-type reconnection occurring high in the corona, supported by the pre-flare brightening. (3) This initiation reconnection could release the constraint on the flux rope and trigger the MHD instability to first make filament F1 lose equilibrium. The subsequent more violent magnetic reconnection with the overlying flux is driven during the filament rising. In return, the eruption of filament F2 is further facilitated by the reduction of the magnetic tension force above. These two processes form a positive feedback to each other to cause the energetic mass eruption and flare.

## **ON THE RELATIONSHIP BETWEEN THE CORONAL MAGNETIC DECAY INDEX AND CORONAL MASS EJECTION SPEED**

Yan [Xu](#), Chang Liu, Ju Jing, and Haimin Wang

2012 ApJ 761 52

Numerical simulations suggest that kink and torus instabilities are two potential contributors to the initiation and prorogation of eruptive events. A magnetic parameter called the decay index (i.e., the coronal magnetic gradient of the overlying fields above the eruptive flux ropes) could play an important role in controlling the kinematics of eruptions. Previous studies have identified a threshold range of the decay index that distinguishes between eruptive and confined configurations. Here we advance the study by investigating if there is a clear correlation between the decay index and coronal mass ejection (CME) speed. Thirty-eight CMEs associated with filament eruptions and/or two-ribbon flares are selected using the H $\alpha$  data from the Global H $\alpha$  Network. The filaments and flare ribbons observed in H $\alpha$  associated with the CMEs help to locate the magnetic polarity inversion line, along which the decay index is calculated based on the potential field extrapolation using Michelson Doppler Imager magnetograms as boundary conditions. The speeds of CMEs are obtained from the LASCO C2 CME catalog available online. We find that the mean decay index increases with CME speed for those CMEs with a speed below 1000 km s<sup>-1</sup> and stays flat around 2.2 for the CMEs with higher speeds. In addition, we present a case study of a partial filament eruption, in which the decay indices show different values above the erupted/non-erupted part.

Table 2000-2010

### Association between a Failed Prominence Eruption and the Drainage of Mass from Another Prominence

Jianchao Xue, Li Feng, Hui Li, Ping Zhang, Jun Chen, +++

Solar Phys. 299, 89 (2024).

<https://doi.org/10.1007/s11207-024-02336-5>

<https://arxiv.org/pdf/2406.11602>

Sympathetic eruptions of solar prominences have been studied for decades, however, it is usually difficult to identify their causal links. Here we present two failed prominence eruptions on **26 October 2022** and explore their connections. Using stereoscopic observations, the south prominence (PRO-S) erupts with untwisting motions, flare ribbons occur underneath, and new connections are formed during the eruption. The north prominence (PRO-N) rises up along with PRO-S, and its upper part disappears due to catastrophic mass draining along an elongated structure after PRO-S failed eruption. We suggest that the eruption of PRO-S initiates due to a kink instability, further rises up, and fails to erupt due to reconnection with surrounding fields. The elongated structure connecting PRO-N overlies PRO-S, which causes the rising up of PRO-N along with PRO-S and mass drainage after PRO-S eruption. This study suggests that a prominence may end its life through mass drainage forced by an eruption underneath.

**Correction:** *Sol Phys* 299, 96 (2024). <https://doi.org/10.1007/s11207-024-02345-4>

<https://link.springer.com/content/pdf/10.1007/s11207-024-02345-4.pdf>

### Spectral evolution of an eruptive polar crown prominence with IRIS observations

Jianchao Xue, Hui Li, Yang Su

Frontiers in Physics 9:750097 2021

<https://arxiv.org/pdf/2109.02908.pdf>

<https://www.frontiersin.org/articles/10.3389/fphy.2021.750097/full>

<https://doi.org/10.3389/fphy.2021.750097>

Prominence eruption is closely related to coronal mass ejections and is an important topic in solar physics. Spectroscopic observation is an effective way to explore the plasma properties, but the spectral observations of eruptive prominences are rare. In this paper we will introduce an eruptive polar crown prominence with spectral observations from the Interface Region Imaging Spectrograph (IRIS), and try to explain some phenomena that are rarely reported in previous works. The eruptive prominence experiences a slow-rise and fast-rise phase, while the line-of-sight motions of the prominence plasma could be divided into three periods: two hours before the fast-rise phase, opposite Doppler shifts are found at the two sides of the prominence axis; then, red shifts dominate the prominence gradually; in the fast-rise phase, the prominence gets to be blue-shifted. During the second period, a faint component appears in Mg II k window with a narrow line width and a large red shift. A faint region is also found in AIA 304-angstrom images along the prominence spine, and the faint region gets darker during the expansion of the spine. We propose that the opposite Doppler shifts in the first period is a feature of the polar crown prominence that we studied. The red shifts in the second period is possibly due to mass drainage during the elevation of the prominence spine, which could accelerate the eruption in return. The blue shifts in the third period is due to that the prominence erupts toward the observer. We suggest that the faint component appears due to the decreasing of the plasma density, and the latter results from the expansion of the prominence spine. **2015 April 28**

### A Small-scale Oscillatory Reconnection and the Associated Formation and Disappearance of a Solar Flux Rope

Zhike Xue<sup>1,2,3</sup>, Xiaoli Yan<sup>1,3</sup>, Chunlan Jin<sup>2</sup>, Liheng Yang<sup>1,3</sup>, Jincheng Wang<sup>1,3</sup>, Qiaoling Li<sup>1,3,4</sup>, and Li Zhao

2019 ApJL 874 L27

[sci-hub.se/10.3847/2041-8213/ab1135](https://sci-hub.se/10.3847/2041-8213/ab1135)

We present the observations of a small-scale oscillatory reconnection for the first time and its resulting in formation and disappearance of a flux rope with the high-resolution data obtained by the New Vacuum Solar Telescope and the Solar

Dynamics Observatory on **2013 July 24 and 25**. This oscillatory reconnection consists of four relatively independent magnetic reconnections which last for about 48, 158, 275, and 340 minutes, respectively. The durations of the four magnetic reconnections increase with time. Four current sheets along two nearly perpendicular directions are formed alternately. The oscillatory reconnection experiences two cycles, and the periods of the two oscillations are 206 and 615 minutes, which are much longer than the previous results. The period of the first oscillation is shorter than that of the second oscillation. Furthermore, a flux rope forms during the second magnetic reconnection. Its twist increases with the reconnection and transfers from the reconnection site to one leg, and this leads the flux rope to become more slender. Then, the flux rope disappears in the early stage of the third magnetic reconnection. We conclude that the formation and disappearance of the flux rope are caused by the oscillatory reconnection.

### **Observing Formation of Flux Rope by Tether-cutting Reconnection in the Sun**

Zhike [Xue](#)<sup>1,2,3</sup>, Xiaoli Yan<sup>1,2,3</sup>, Liheng Yang<sup>1,3</sup>, Jincheng Wang<sup>1,3,4</sup>, and Li Zhao<sup>1,3</sup>  
2017 ApJL 840 L23

<http://sci-hub.cc/10.3847/2041-8213/aa7066>

Tether-cutting reconnection is considered as one mechanism for the formation of a flux rope. It has been proposed for more than 30 years; however, so far, direct observations of it are very rare. In this Letter, we present observations of the formation of a flux rope via tether-cutting reconnection in NOAA AR 11967 on **2014 February 2** by combining observations with the New Vacuum Solar Telescope and the Solar Dynamic Observatory. The tether-cutting reconnection occurs between two sets of highly sheared magnetic arcades. Comprehensive observational evidence of the reconnection is as follows: changes of the connections between the arcades, brightenings at the reconnection site, hot outflows, formation of a flux rope, slow-rise motion of the flux rope, and flux cancellation. The outflows are along three directions from the reconnection site to the footpoints with the velocities from  $24 \pm 1 \text{ km s}^{-1}$  to  $69 \pm 5 \text{ km s}^{-1}$ . Additionally, it is found that the newly formed flux rope connects far footpoints and has a left-handed twisted structure with many fine threads and a concave-up-shape structure in the middle. All the observations are in agreement with the tether-cutting model and provide evidence that tether-cutting reconnection leads to the formation of the flux rope associated with flux shear flow and cancellation.

### **Observing the release of twist by magnetic reconnection in a solar filament eruption**

Zhike [Xue](#), Xiaoli Yan, Xin Cheng, Liheng Yang, Yingna Su, Bernhard Kliem, Jun Zhang, Zhong Liu, Yi Bi, Yongyuan Xiang, Kai Yang & Li Zhao  
Nature Communications **2016 File**

<http://www.nature.com/ncomms/2016/160616/ncomms11837/pdf/ncomms11837.pdf>

Magnetic reconnection is a fundamental process of topology change and energy release, taking place in plasmas on the Sun, in space, in astrophysical objects and in the laboratory. However, observational evidence has been relatively rare and typically only partial. Here we present evidence of fast reconnection in a solar filament eruption using high-resolution H-alpha images from the New Vacuum Solar Telescope, supplemented by extreme ultraviolet observations. The reconnection is seen to occur between a set of ambient chromospheric fibrils and the filament itself. This allows for the relaxation of magnetic tension in the filament by an untwisting motion, demonstrating a flux rope structure. The topology change and untwisting are also found through nonlinear force-free field modelling of the active region in combination with magnetohydrodynamic simulation. These results demonstrate a new role for reconnection in solar eruptions: the release of magnetic twist. **3 October 2014**

### **Eruptions of Two Coupled Filaments Observed by SDO, GONG and STEREO**

Z. K. [Xue](#), X. L. Yan, Z. Q. Qu, C. L. Xu, L. Zhao

Astrophysics and Space Science, Volume 353, Issue 2, pp 357-366, **2014**

<http://arxiv.org/pdf/1407.3908v1.pdf>

On **2012 July 11**, two solar filaments were observed in the northeast of the solar disk and their eruptions due to the interaction between them are studied by using the data from the Solar Dynamics Observatory (SDO), Solar TERrestrial RELations Observatory (STEREO) and Global Oscillation Network Group (GONG). The eastern filament (F1) first erupted toward the northeast. During the eruption of F1, some plasma from F1 fell down and was injected to the North-East part of another filament (F2), and some plasma of F1 fell down to the northern region close to F2 and caused the plasma to brighten. Meanwhile, the North-East part of F2 first started to be active and rise, but did not erupt finally. Then the South-West part of F2 erupted successfully. Therefore, the F2's eruption is a partial filament eruption. Two associated CMEs related to the eruptions were observed by STEREO/COR1. We find two possible reasons that lead to the instability and the eruption of F2. One main reason is that the magnetic loops overlying the two filaments were partially opened by the eruptive F1 and resulted in the instability of F2. The other is that the downflows from F1 might break the stability of F2.

### **A Data-constrained Magnetohydrodynamic Simulation of the X1.0 Solar Flare of **2021 October 28****

[Daiki Yamasaki](#), [Satoshi Inoue](#), [Yumi Bamba](#), [Jeongwoo Lee](#), [Haimin Wang](#)

ApJ **940** 119 **2022**

<https://arxiv.org/pdf/2210.14563> **File**



<https://iopscience.iop.org/article/10.3847/1538-4357/ac9df4/pdf>

The solar active region NOAA 12887 produced a strong X1.0 flare on **2021 October 28**, which exhibits X-shaped flare ribbons and a circle-shaped erupting filament. To understand the eruption process with these characteristics, we conducted a data-constrained magnetohydrodynamics simulation using a nonlinear force-free field of the active region about an hour before the flare as the initial condition. Our simulation reproduces the filament eruption observed in the H $\alpha$  images of GONG and the 304 angstrom images of SDO/AIA and suggests that two mechanisms can possibly contribute to the magnetic eruption. One is the torus instability of the pre-existing magnetic flux rope (MFR), and the other is upward pushing by magnetic loops newly formed below the MFR via continuous magnetic reconnection between two sheared magnetic arcades. The presence of this reconnection is evidenced by the SDO/AIA observations of the 1600 angstrom brightening in the footpoints of the sheared arcades at the flare onset. To clarify which process is more essential for the eruption, we performed an experimental simulation in which the reconnection between the sheared field lines is suppressed. In this case too, the MFR could erupt, but at a much reduced rising speed. We interpret this result as indicating that the eruption is not only driven by the torus instability, but additionally accelerated by newly formed and rising magnetic loops under continuous reconnection.

## **The Formation Process of the First Halo Coronal Mass Ejection in Solar Cycle 25: Magnetic Cancellation, Bidirectional Jet, and Hot Channel**

Xiaoli Yan<sup>1,2</sup>, Jincheng Wang<sup>1</sup>, Qiaoling Guo<sup>3</sup>, Zhike Xue<sup>1</sup>, Liheng Yang<sup>1</sup>, and Baolin Tan<sup>2</sup>  
2021 ApJ 919 34

<https://doi.org/10.3847/1538-4357/ac116d>

To better understand the trigger mechanism of a coronal mass ejection (CME), we present the evolution of a CME source region (active region NOAA 12790) and the formation of a hot channel before the occurrence of the first halo CME in solar cycle 25. Through analyzing the evolution of Solar Dynamics Observatory/Heliioseismic and Magnetic Imager line-of-sight magnetograms, it is found that continuous magnetic cancellation occurs at the polarity inversion line (PIL) in this active region. With ongoing magnetic cancellation, several bidirectional jets and unidirectional jets occur along the large-scale arched magnetic loops. A hot channel forms during the first bidirectional jet. After the occurrence of the fourth bidirectional jet, the hot channel immediately erupts and produces a C-class flare, a cusp structure, and a halo CME. It is worth pointing out that the cusp structure only appears in the 131 Å and 94 Å observations (temperature about 10 MK). The obvious contraction of the newly formed loops is observed at the top of the cusp structure. The observations reveal a clear physics process: magnetic cancellation of a bipolar magnetic field at the PIL results in the occurrence of the bidirectional/unidirectional jets and the formation of the hot channel. The axial magnetic flux feeding for the hot channel through the continued magnetic cancellation leads to the hot channel eruption, which results in the formation of the hot cusp structure and the occurrence of the C-class flare and the halo CME.

## **Dynamics evolution of a solar active-region filament from quasi-static state to eruption: rolling motion, untwisting motion, material transfer, and chirality**

[X.L. Yan](#), [Q.L. Li](#), [G.R. Chen](#), [Z.K. Xue](#), [L. Feng](#), [J.C. Wang](#), [L.H. Yang](#), [Y. Zhang](#)

ApJ **904** 15 2020

<https://arxiv.org/pdf/2009.10345.pdf>

<https://doi.org/10.3847/1538-4357/abba81>

To better understand magnetic structure and eruptive process of solar filaments, a solar active-region filament (labeled F2) eruption associated with a B-class flare was investigated by using high-resolution H $\alpha$  data from the 1 m New Vacuum Solar Telescope (NVST), combined with EUV observations of the Solar Dynamical Observatory (SDO). The filament F2 was disturbed by another filament (labeled F1) eruption that experienced a whip-like motion. Before the filament F2 eruption, the Dopplergrams show that the southern and the northern parts of the filament F2 body exhibit blueshift and redshift along the filament spine, simultaneously. It implies that the filament F2 was rolling from one side to the other. During the filament F2 eruption, the Doppler velocity shifts of the filament body are opposite to that before its eruption. It demonstrates that the filament body exhibits an untwisting motion, which can be also identified by tracing the movement of the eruptive filament threads. Moreover, it is found that the material of the filament F2 was transferred to the surrounding magnetic field loops, which is caused by magnetic reconnection between the filament F2 and the surrounding magnetic loops. According to the right-bearing threads of the filament F2 before its eruption, it can be deduced that the filament F2 is initially supported by a sheared arcade. The following observations reveal that the twisted magnetic structure of the filament F2 formed in the eruption phase. **May 7, 2019**

## **Triggering mechanism and material transfer of a failed solar filament eruption**

[X.L. Yan](#), [Z.K. Xue](#), [X. Cheng](#), [J. Zhang](#), [J.C. Wang](#), [D.F. Kong](#), [L.H. Yang](#), [G.R. Chen](#), [X.S. Feng](#)

ApJ **889** 106 2019

<https://arxiv.org/pdf/1912.07173.pdf>

Solar filament eruptions are often associated with solar flares and coronal mass ejections (CMEs), which are the major impacts on space weather. However, the fine structures and the trigger mechanisms of solar filaments are still unclear. To address these issues, we studied a failed solar active-region filament eruption associated with a C-class flare by using high-resolution H $\alpha$  images from the New Vacuum Solar Telescope (NVST), supplemented by EUV observations of the Solar Dynamical Observatory (SDO). Before the filament eruption, a small bi-pole magnetic field emerged below the filament. And then magnetic reconnection between the filament and the emerging bi-pole magnetic field triggered

the filament eruption. During the filament eruption, the untwisting motion of the filament can be clearly traced by the eruptive threads. Moreover, the foot-points of the eruptive threads are determined by tracing the descending filament materials. Note that the filament twisted structure and the right part of the eruptive filament threads cannot be seen before the filament eruption. These eruptive threads at the right part of the filament are found to be rooting in the weak negative polarities near the main negative sunspot. Moreover, a new filament formed in the filament channel due to material injection from the eruptive filament. The above observations and the potential field extrapolations are inclined to support that the filament materials were transferred into the overlying magnetic loops and the nearby filament channel by magnetic reconnection. These observations shed light on better understanding on the complexity of filament eruptions. **May 9, 2019**

## **Research progress based on observations of the New Vacuum Solar Telescope** **Review**

Xiaoli Yan, [Zhong Liu](#), [Jun Zhang](#), [Zhi Xu](#)

SCIENCE CHINA Technological Sciences

**2019**

<https://arxiv.org/pdf/1910.09127.pdf>

The purpose of this paper is to introduce the main scientific results made by the one-meter New Vacuum Solar Telescope (NVST), which was put into commission on 2010. NVST is one of the large aperture solar telescopes in the world, located on the shore of Fuxian lake of Yunnan province in China, aiming at serving solar physicists by providing them with high resolution photospheric and chromospheric observational data. Based on the data from NVST and complementary observations from space (e.g., Hinode, SDO and IRIS, etc), dozens of scientific papers have been published with a wide range of topics concentrating mainly on dynamics and activities of fine-scale magnetic structures and their roles in the eruptions of active-region filaments and flares. The achievements include dynamic characteristics of photospheric bright points, umbral dots, penumbral waves, and sunspot/light bridge oscillation, observational evidence of small-scale magnetic reconnection, and fine-scale dynamic structure of prominences. All these new results will shed light on the better understanding of solar eruptive activities. Data release, observation proposals, and future research subjects are introduced and discussed.

*Bright points. Umbral dot, penumbral wave. Sunspot light bridge. Formation, fine-scale structures, and eruption mechanism of solar filaments. Fine structure of solar prominences. Filament formation. Magnetic structures of active-region filaments. Filament eruption. Small-scale magnetic reconnection in the solar eruptions. Release of twist in a filament by magnetic reconnection. Interchange magnetic reconnection between a filament and nearby open fields. Magnetic reconnection between a twisted arch filament system and coronal loops. Magnetic reconnection between two active-region filaments. Oscillatory magnetic reconnection. Small-scale eruptive activities. Mini-filaments and jets. Formation and trigger mechanism of solar flares*

## **Simultaneous observation of a flux rope eruption and magnetic reconnection during an X-class solar flare**

X.L. Yan, [L.H. Yang](#), [Z.K. Xue](#), [Z.X. Mei](#), [D.F. Kong](#), [J.C. Wang](#), [Q.L. Li](#)

ApJL **853** L18 **2018**

<https://arxiv.org/pdf/1801.02738.pdf>

<http://sci-hub.tw/http://iopscience.iop.org/2041-8205/853/1/L18/>

In this letter, we present a spectacular eruptive flare (X8.2) associated with a coronal mass ejection (CME) on **2017 September 10** at the west limb of the Sun. A flux rope eruption is followed by the inflow, the formation of a current sheet and a cusp structure, which were simultaneously observed during the occurrence of this flare. The hierarchical layers of the cusp-shaped structure are well observed in 131 \AA observation. The scenario that can be created from these observations is very consistent with the predictions of some eruptive models. Except for the characteristics mentioned above in the process of the flare predicted by classical eruption models, the current sheet separating into several small current sheets is also observed at the final stage of the flux rope eruption. The quantitative calculation of the velocities and accelerations of the inflow, hot cusp structure, and post-flare loops is presented. The width of the current sheet is estimated to be about  $3 \times 10^3$  km. These observations are very useful to understand the process of solar eruptions.

## **Successive X-class flares and coronal mass ejections driven by shearing motion and sunspot rotation in active region NOAA 12673**

X.L. Yan, [J.C. Wang](#), [G.M. Pan](#), [D.F. Kong](#), [Z.K. Xue](#), [L.H. Yang](#), [Q.L. Li](#)

**2018** *ApJ* 856 79

<https://arxiv.org/pdf/1801.02290.pdf>

<http://sci-hub.tw/http://iopscience.iop.org/0004-637X/856/1/79/>

We present a clear case study on the occurrence of two successive X-class flares including a decade-class flare (X9.3) and two coronal mass ejections (CMEs) triggered by shearing motion and sunspot rotation in active region NOAA 12673 on 2017 September 6. A shearing motion between the main sunspots with opposite polarities started on September 5 and even lasted after the second X-class flare on September 6. Moreover, the main sunspot with negative polarity rotated around its umbral center and another main sunspot with positive polarity also exhibited a slow rotation. The sunspot with negative polarity at the northwest of active region also began to rotate counter-clockwise before the onset of the first X-class flare. The successive formation and eruption of two S-shaped structures were closely related to the counter-clockwise rotation of three sunspots. It is also found that the rotation of sunspots is faster during four hours

prior to the onset of the flares than the period before. The existence of a flux rope is found prior to the onset of two flares by using non-linear force free field extrapolation based on the vector magnetograms observed by SDO/HMI. These results suggest that shearing motion and sunspot rotation play an important role in the buildup of the free energy and the formation of flux ropes in the corona which produces solar flares and CMEs.

### **The eruption of a small-scale emerging flux rope as the driver of an M-class flare and a coronal mass ejection**

X.L. **Yan**, C.W. Jiang, Z.K. Xue, [J.C. Wang](#), [E.R. Priest](#), [L.H. Yang](#), [D.F. Kong](#), [W.D. Cao](#), [H.S. Ji](#)

ApJ **845** 18 **2017**

<https://arxiv.org/pdf/1707.00073.pdf>

<http://sci-hub.cc/10.3847/1538-4357/aa7e29>

Solar flares and coronal mass ejections (CMEs) are the most powerful explosions in the Sun. They are major sources of potentially destructive space weather conditions. However, the possible causes of their initiation remain controversial. By using high resolution data observed by NST of BBSO, supplemented by Solar Dynamics Observatory (SDO) observations, we present unusual observations of a small-scale emerging flux rope near a large sunspot, whose eruption produced an M-class flare and a coronal mass ejection. The presence of the small-scale flux rope was indicated by static nonlinear force free field (NLFFF) extrapolation as well as data-driven MHD modeling of the dynamic evolution of the coronal 3D magnetic field. During the emergence of the flux rope, rotation of satellite sunspots at the footpoints of the flux rope was observed. Meanwhile, the Lorentz force, magnetic energy, vertical current, and transverse fields were increasing during this phase. The free energy from the magnetic flux emergence and twisting magnetic fields is sufficient to power the M-class flare. These observations for the first time present the complete process from the emergence of the small-scale flux rope to the production of solar eruptions. **2015 August 24**

### **The formation of an inverse S-shaped active-region filament driven by sunspot motion and magnetic reconnection**

X.L. **Yan**, E.R. Priest, Q.L. Guo, Z.K. Xue, J.C. Wang, L.H. Yang

ApJ **832** 23 **2016**

<http://arxiv.org/pdf/1609.04871v1.pdf>

We present a detailed study of the formation of an inverse S-shaped filament prior to its eruption in active region NOAA 11884 from **October 31 to November 2, 2013**. In the initial stage, clockwise rotation of a small positive sunspot around the main negative trailing sunspot formed a curved filament. Then the small sunspot cancelled with negative magnetic flux to create a longer active-region filament with an inverse S-shape. At the cancellation site a brightening was observed in UV and EUV images and bright material was transferred to the filament. Later the filament erupted after cancellation of two opposite polarities under the upper part of the filament. Nonlinear force-free field (NLFFF) extrapolation of vector photospheric fields suggests that the filament may have a twisted structure, but this cannot be confirmed from the current observations.

### **The Formation and Magnetic Structures of Active-region Filaments Observed by NVST, SDO, and Hinode**

X.L. **Yan**, Z.K. Xue, G.M. Pan, J.C. Wang, Y.Y. Xiang, D.F. Kong, and L.H. Yang

Astrophysical Journal Supplement Series (*ApJS*) **219** 17 **2015**

To better understand the properties of solar active-region filaments, we present a detailed study on the formation and magnetic structures of two active-region filaments in active region NOAA **11884** during a period of four days. It is found that the shearing motion of the opposite magnetic polarities and the rotation of the small sunspots with negative polarity play an important role in the formation of two active-region filaments. During the formation of these two active-region filaments, one foot of the filaments was rooted in a small sunspot with negative polarity. The small sunspot rotated not only around another small sunspot with negative polarity, but also around the center of its umbra. By analyzing the nonlinear force-free field extrapolation using the vector magnetic fields in the photosphere, twisted structures were found in the two active-region filaments prior to their eruptions. These results imply that the magnetic fields were dragged by the shearing motion between opposite magnetic polarities and became more horizontal. The sunspot rotation twisted the horizontal magnetic fields and finally formed the twisted active-region filaments. **1-4 Nov 2013**

### **Unwinding motion of a twisted active-region filament**

X.L. **Yan**, Z.K. Xue, J.H. Liu, D.F. Kong, C.L. Xu

ApJ, **797** 52 **2014**

<http://arxiv.org/pdf/1410.1984v1.pdf>

To better understand the structures of active-region filaments and the eruption process, we study an active-region filament eruption in active region NOAA 11082 in detail on **June 22, 2010**. Before the filament eruption, the opposite unidirectional material flows appeared in succession along the spine of the filament. The rising of the filament triggered two B-class flares at the upper part of the filament. As the bright material was injected into the filament from the sites of the flares, the filament exhibited a rapid uplift accompanying the counterclockwise rotation of the filament body. From

the expansion of the filament, we can see that the filament is consisted of twisted magnetic field lines. The total twist of the filament is at least  $5\pi$  obtained by using time slice method. According to the morphology change during the filament eruption, it is found that the active-region filament was a twisted flux rope and its unwinding motion was like a solar tornado. We also find that there was a continuous magnetic helicity injection before and during the filament eruption. It is confirmed that magnetic helicity can be transferred from the photosphere to the filament. Using the extrapolated potential fields, the average decay index of the background magnetic fields over the filament is 0.91. Consequently, these findings imply that the mechanism of solar filament eruption could be due to the kink instability and magnetic helicity accumulation.

### **Case study of a complex active-region filament eruption**

X. L. Yan<sup>1,2</sup>, Z. Q. Qu<sup>1</sup>, D. F. Kong<sup>1,3</sup>, L. H. Deng<sup>1,3</sup> and Z. K. Xue  
A&A 557, A108 (2013)

Context. We investigated a solar active-region filament eruption associated with a C6.6 class flare and a coronal mass ejection (CME) in NOAA active region 08858 on **2000 February 9**.

Aims. We aim to better understand the relationship between filament eruptions and the associated flares and CMEs.

Methods. Using BBSO, SOHO/EIT, and TRACE observational data, we analyzed the process of the active-region filament eruption in the chromosphere and the corona. Using the SOHO/MDI magnetograms, we investigated the change of the magnetic fields in the photosphere. Using the GOES soft X-ray flux and the SOHO/LASCO images, we identified the flare and CME, which were associated with this active-region filament eruption.

Results. The brightenings in the chromosphere are a precursor of the filament expansion. The eruption itself can be divided into four phases: In the initial phase, the intertwined bright and dark strands of the filament expand. Then, the bright strands are divided into three parts with different expansion velocity. Next, the erupting filament-carrying flux rope expands rapidly and combines with the lower part of the expanding bright strands. Finally, the filament erupts accompanied by other dark strands overlying the filament. The overlying magnetic loops and the expansion of the filament strands can change the direction of the eruption.

Conclusions. The time delay between the velocity peaks of the filament and that of the two parts of the bright strands clearly demonstrates that the breakup of the bright loops tying on the filament into individual strands is important for its eruption. The eruption is a collection of multiple processes that are physically coupled rather than a single process.

### **SUNSPOT ROTATION, SIGMOIDAL FILAMENT, FLARE, AND CORONAL MASS EJECTION: THE EVENT ON 2000 FEBRUARY 10**

X. L. Yan<sup>1,2</sup>, Z. Q. Qu<sup>1</sup>, D. F. Kong<sup>1,2</sup>, and C. L. Xu  
2012 ApJ 754 16

We find that a sunspot with positive polarity had an obvious counterclockwise rotation and resulted in the formation and eruption of an inverse S-shaped filament in NOAA Active Region 08858 from **2000 February 9 to 10**. The sunspot had two umbrae which rotated around each other by  $195^\circ$  within about 24 hr. The average rotation rate was nearly  $8^\circ \text{ hr}^{-1}$ . The fastest rotation in the photosphere took place during 14:00 UT to 22:01 UT on February 9, with a rotation rate of nearly  $16^\circ \text{ hr}^{-1}$ . The fastest rotation in the chromosphere and the corona took place during 15:28 UT to 19:00 UT on February 9, with a rotation rate of nearly  $20^\circ \text{ hr}^{-1}$ . Interestingly, the rapid increase of the positive magnetic flux occurred only during the fastest rotation of the rotating sunspot, the bright loop-shaped structure, and the filament. During the sunspot rotation, the inverse S-shaped filament gradually formed in the EUV filament channel. The filament experienced two eruptions. In the first eruption, the filament rose quickly and then the filament loops carrying the cool and the hot material were seen to spiral counterclockwise into the sunspot. About 10 minutes later, the filament became active and finally erupted. The filament eruption was accompanied with a C-class flare and a halo coronal mass ejection. These results provide evidence that sunspot rotation plays an important role in the formation and eruption of the sigmoidal active-region filament.

### **A radio burst and its associated CME on 17 March 2002 --**

Y. Yan, M. Pick, M. Wang, S. Krucker, A. Vourlidas

Solar Physics (2006) 239: 277–292

the type III electron beams propagate in the interface highly compressed region between the ascending CME and the neighboring open field lines.

### **Two Intermittent Eruptions of a Minifilament Triggered by a Two-step Magnetic Reconnection Within a Fan-spine Configuration**

Liping Yang<sup>1,2</sup>, Zhike Xue<sup>1,3</sup>, Jincheng Wang<sup>1,3</sup>, Liheng Yang<sup>1,3</sup>, Qiaoling Li<sup>4,5</sup>, Yian Zhou<sup>1,3</sup>, Yang Peng<sup>1,2</sup>, and Xinsheng Zhang<sup>1,2</sup>

2024 ApJ 976 135

<https://iopscience.iop.org/article/10.3847/1538-4357/ad84f9/pdf>

Although numerous works have concentrated on minifilament eruption in complex configurations, the detailed triggering mechanism is still an open question. Using the observational data from the New Vacuum Solar Telescope and Solar Dynamics Observatory, we studied a two-step magnetic reconnection process that triggered a minifilament that erupted intermittently within a fan-spine structure in the active region NOAA 13272. The first-step reconnection occurred between a set of low-lying small-scale magnetic loops and their nearby inner spine, resulting in the appearance of a brightening at the reconnection site and the reconfiguration of the inner spine. As the reconfigured inner spine approached the outer spine, reconnection occurred between them at the null point and led to the minifilament erupting partially. Subsequently, this two-step reconnection scenario occurred again and triggered the minifilament to erupt completely. The null point reconnection was supported by the changes in the topological structure of the inner spine and the outer spine, circular ribbon flares, remote brightenings, and the brightening of the outer spine. The null point reconnection related to the second eruption was also confirmed by some plasmoids expelled from the reconnection site. Further, the results of the magnetic field extrapolation reveal the existence of a fan-spine structure involving a three-dimensional null point. We suggest that the two-step reconnection triggers the two eruptions, in which the null point reconnection plays a direct role, but the dynamical evolution of the inner spine and the outer spine driven by the first-step reconnection might be a precursor of the subsequent null point reconnection. **2023 April 7-8**

### **Why could a new-born active region produce coronal mass ejections?**

[Hanzhao Yang](#), [Lijuan Liu](#)

ApJ **973** 164 **2024**

<https://arxiv.org/pdf/2407.19710>

<https://iopscience.iop.org/article/10.3847/1538-4357/ad6900/pdf>

Solar active regions (ARs) are the main sources of flares and coronal mass ejections (CMEs). NOAA AR 12089, which emerged on **2014 June 10**, produced two C-class flares accompanied by CMEs within five hours after its emergence. When producing the two eruptive flares, the total unsigned magnetic flux ( $\Phi_{AR}$ ) and magnetic free energy ( $E_f$ ) of the AR are much smaller than the common CME-producing ARs. Why can this extremely small AR produce eruptive flares so early? We compare the AR magnetic environment for the eruptive flares to that for the largest confined flare from the AR. Besides the  $\Phi_{AR}$  and  $E_f$ , we calculate the ratio between the mean characteristic twist parameter ( $\alpha_{FPIL}$ ) within the flaring polarity inversion line (FPIL) region and  $\Phi_{AR}$ , a parameter considering both background magnetic field constraint and non-potentiality of the core region, for the three flares. We find higher  $\alpha_{FPIL}/\Phi_{AR}$  values during the eruptive flares than during the confined flare. Furthermore, we compute the decay index along the polarity inversion line, revealing values of 1.69, 3.45, and 0.98 before the two eruptive and the confined flares, respectively. Finally, nonlinear force-free field extrapolation indicates that a flux rope was repeatedly formed along the FPIL before eruptive flares, which ejected out and produced CMEs. No flux rope was found before the confined flare. Our research suggests that even a newly emerged, extremely small AR can produce eruptive flares if it has sufficiently weak background field constraint and strong non-potentiality in the core region. **10-12 Jun 2014**

### **Is it possible to detect coronal mass ejections on solar-type stars through extreme-ultraviolet spectral observations?**

[Zihao Yang](#), [Hui Tian](#), [Yingjie Zhu](#), [Yu Xu](#), [Linyi Chen](#), [Zheng Sun](#)

ApJ **966** 24 **2024**

<https://arxiv.org/pdf/2402.12297.pdf>

<https://iopscience.iop.org/article/10.3847/1538-4357/ad2a44/pdf>

Stellar coronal mass ejections (CMEs) from host stars are an important factor that affects the habitability of exoplanets. Although their solar counterparts have been well observed for decades, it is still very difficult to find solid evidence of stellar CMEs. Using the spectral line profile asymmetry caused by the Doppler shift of erupting plasma, several stellar CME candidates have been identified from spectral lines formed at chromospheric or transition region temperatures of the stars. However, a successful detection of stellar CME signals based on the profile asymmetries of coronal lines is still lacking. It is unclear whether we can detect such signals. Here we construct an analytical model for CMEs on solar-type stars, and derive an expression of stellar extreme-ultraviolet (EUV) line profiles during CME eruptions. For different instrumental parameters, exposure times, CME propagation directions and stellar activity levels, we synthesized the corresponding line profiles of Fe IX 171.07 Å and Fe XV 284.16 Å. Further investigations provide constraints on the instrumental requirements for successful detection and characterization of stellar CMEs. Our results show that it is possible to detect stellar CME signals and infer their velocities based on spectral profile asymmetries using an EUV spectrometer with a moderate spectral resolution and signal-to-noise ratio. Our work provides important references for the design of future EUV spectrometers for stellar CME detection and the development of observation strategies.

### **Two-sided Loop Solar Jet Driven by the Eruption of a Small Filament in a Big Filament Channel**

[Jiayan Yang](#), [Hechao Chen](#), [Junchao Hong](#), [Bo Yang](#), [Yi Bi](#)

ApJ **964** 7 **2024**

<https://arxiv.org/pdf/2402.10539.pdf>

<https://iopscience.iop.org/article/10.3847/1538-4357/ad23e5/pdf>

Similar to the cases of anemone jets, two-sided loop solar jets could also be produced by either flux emergence from the solar interior or small scale filament eruptions. Using the high-quality data from the Solar Dynamic Observatory (SDO), we analyzed a two-sided loop solar jet triggered by the eruption of a small filament in this paper. The jet was occurred in a pre-existing big filament channel. The detailed processes involved in the small filament eruption, the interaction between the erupted filament and the big filament channel, and the launch of the two-sided loop jet are presented. The observations further revealed notable asymmetry between the two branches of the jet spire, with the northeastern branch is narrow and short, while the southern branch is wide and long and accompanied by discernible untwisting motions. We explored the unique appearance of the jet by employing the local potential field extrapolation to calculate the coronal magnetic field configuration around the jet. The photospheric magnetic flux below the small filament underwent cancellation for approximately 7 hours before the filament eruption, and the negative flux near the southern foot-point of the filament decreased by about 56 percent during this interval. Therefore, we proposed that the primary photospheric driver of the filament eruption and the associated two-sided loop jet in this event is flux cancellation rather than flux emergence. **March 22, 2012**

### **Simultaneous observations of a breakout current sheet and a flare current sheet in a coronal jet event**

[Liheng Yang](#), [Xiaoli Yan](#), [Zhike Xue](#), [Zhe Xu](#), [Qingmin Zhang](#), [Yijun Hou](#), [Jincheng Wang](#), [Huadong Chen](#)  
MNRAS **2024**

<https://arxiv.org/pdf/2401.02123.pdf>

Previous studies have revealed that solar coronal jets triggered by the eruption of mini-filaments (MFs) conform to the famous magnetic-breakout mechanism. In such scenario, a breakout current sheet (BCS) and a flare current sheet (FCS) should be observed during the jets. With high spatial and temporal resolution data from the SDO, the NVST, the RHESSI, the Wind, and the GOES, we present observational evidence of a BCS and a FCS formation during coronal jets driven by a MF eruption occurring in the active region NOAA 11726 on **2013 April 21**. Magnetic field extrapolation show that the MF was enclosed by a fan-spine magnetic structure. The MF was activated by flux cancellation under it, and then slowly rose. A BCS formed when the magnetic fields wrapping the MF squeezed to antidiagonal external open fields. Simultaneously, one thin bright jet and two bidirectional jet-like structures were observed. As the MF erupted as a blowout jet, a FCS was formed when the two distended legs inside the MF field came together. One end of the FCS connected the post-flare loops. The peak temperature of BCS was calculated to be 2.5 MK. The length, width and peak temperature of FCS was calculated to be 4.35-4.93 Mm, 1.31-1.45 Mm, and 2.5 MK, respectively. The magnetic reconnection rate associated with the FCS was estimated to be from 0.266 to 0.333. This event also related to a type III radio burst, indicating its influence on interplanetary space. These observations support the scenario of the breakout model as the trigger mechanism of coronal jets, and flux cancellation was the driver of this event.

### **Sympathetic Partial Filament Eruptions Caused by the Interaction between Two Nearby Filaments**

Liping [Yang](#)<sup>1,2</sup>, Xiaoli Yan<sup>1,3</sup>, Zhike Xue<sup>1,3</sup>, Jincheng Wang<sup>1,3</sup>, Liheng Yang<sup>1,3</sup>, Qiaoling Li<sup>4,5</sup>, Zhe Xu<sup>1,3</sup>, Yang Peng<sup>1,2</sup>, Xia Sun<sup>6</sup>, and Xincheng Zhang<sup>1,2</sup>

**2023 ApJ 943 62**

<https://iopscience.iop.org/article/10.3847/1538-4357/aca9d2/pdf>

To better understand the physical connections in sympathetic solar eruptions, we investigated the interaction between two nearby filaments and their successive partial eruptions in the active region (AR) NOAA 12866 on **2021 September 9** by using data from the Solar Dynamics Observatory and the New Vacuum Solar Telescope. Based on H $\alpha$  and extreme ultraviolet observations, we found that the right part of one filament (F1) became active first and experienced an obvious rolling motion. Then the whole body of the filament became wider and expanded toward another filament (F2). They collided with each other, and the interaction between them was accompanied by the brightening and bidirectional flows that appeared between them. This implies that magnetic reconnection occurred between the threads of two filaments. The interaction resulted in a rightward motion of F2 at first, and then its activation, and finally part of it erupted. Furthermore, when the erupted F2 deflected rapidly toward the middle part of F1, the left part of F1 erupted with its overlying magnetic fields pushed by F2. These observational results imply that these successive eruptions within a short time are physically linked, and this was caused by the interaction of the filaments. Nonlinear force-free field extrapolation reveals that the magnetic structure of the filament F1 was composed of several magnetic flux ropes with different twists. These results further advance our understanding of partial filament eruptions and sympathetic solar eruptions.

### **Observational Study of Recurrent Jets Confined by Active Region Loops**

Liheng [Yang](#)<sup>1,2,3</sup>, Xiaoli Yan<sup>1,3</sup>, Zhike Xue<sup>1,3</sup>, Huadong Chen<sup>2</sup>, Jincheng Wang<sup>1,3</sup>, Zhe Xu<sup>1,3</sup>, and Qiaoling Li<sup>4</sup>

**2023 ApJ 945 96**

<https://iopscience.iop.org/article/10.3847/1538-4357/acb6f6/pdf>

With high spatial and temporal resolution data from the Solar Dynamics Observatory and the New Vacuum Solar Telescope (NVST), we present observations of recurrent jets confined by coronal loops that occurred in the active region NOAA 11726 from 02:00 to 12:00 UT on **2013 April 21**. Three jets are clearly observed by the NVST in

H $\alpha$  line. These recurrent jets originate from the emerging bipolar magnetic region at the north of the active region. Half of them are related to the magnetic flux emergence, and the others are associated with the magnetic flux cancellation. Their velocities range from  $80.6 \pm 1.3 \text{ km s}^{-1}$  to  $433.6 \pm 20.1 \text{ km s}^{-1}$ . Though they eject from the same source region, their shapes, sizes, and eruptive trajectories are not exactly the same. Most of them consist of cool (dark) and hot (bright) components. The differential emission measure distributions of the recurrent jets suggest that they are multithermal structures. The rotation directions of the recurrent jets are not consistent. Eight of them have a counterclockwise rotation, and the others have a clockwise rotation. The 12 recurrent jets are classified as blowout (accounting for 33%) and standard (accounting for 67%) jets. The velocity and density range of the blowout jets are slightly wider than those of the standard jets. The blowout jets have lower temperatures than the standard jets. These observational results suggest that the recurrent jets are probably triggered by recurrent magnetic reconnection between the emerging bipolar magnetic region and its overlying large-scale active region loops.

## **Weak Bidirectional Outflows and Flare Current Sheet in a Solar Coronal Jet Driven by the Eruption of a Minifilament**

Jiayan [Yang](#)<sup>1</sup>, Junchao Hong<sup>1</sup>, Bo Yang<sup>1</sup>, Yi Bi<sup>1</sup>, and Zhe Xu<sup>1</sup>

2023 ApJ 942 86

<https://iopscience.iop.org/article/10.3847/1538-4357/aca66f/pdf>

Different from the classical emerging-flux model for solar jets, recent studies proposed that the great majority of solar coronal jets are triggered by minifilament eruptions and two magnetic reconnection processes should take place during the course, named as external reconnection (breakout reconnection) and internal reconnection (flare reconnection). With the excellent data of the Solar Dynamics Observatory, we present the observational signatures of these two magnetic reconnection processes during a solar coronal jet that occurred in a huge coronal hole of northern hemisphere. The jet was triggered by the eruption of a minifilament that located at a coronal bright point in the coronal hole. Weak bidirectional outflows were observed when the erupting minifilament approached the ambient open field, ejecting along the triggered jet spire and the jet base simultaneously. In addition, a flare current sheet occurred after the eruption of the minifilament, connecting the jet spire and the jet bright point (or flare). We suggest the occurrence of the weak bidirectional outflows and the flare current sheet correspond to the external and the internal reconnections, respectively. Prior to the eruption of the minifilament and the jet, photospheric magnetic flux cancellation maintained for more than 7 hr in the source region, and the positive flux decreased for about 28.6% during this period. So, consistent with the recent observations, the trigger mechanism of the minifilament eruption and the following jet in this event may be flux cancellation rather than flux emergence. **2011 May 29**

## **Global Morphology Distortion of the 2021 October 9 Coronal Mass Ejection from an Ellipsoid to a Concave Shape**

Liping [Yang](#)<sup>1</sup>, Chuanpeng Hou<sup>2</sup>, Xueshang Feng<sup>1,3</sup>, Jiansen He<sup>2</sup>, Ming Xiong<sup>1,4</sup>, Man Zhang<sup>1</sup>, Yufen Zhou<sup>1</sup>, Fang Shen<sup>1,4</sup>, Xinhua Zhao<sup>1</sup>, Huichao Li<sup>3</sup>,<sup>1</sup>Show full author list

2023 ApJ 942 65

<https://iopscience.iop.org/article/10.3847/1538-4357/aca52d/pdf>

This paper presents a study of a **2021 October 9** coronal mass ejection (CME) with multipoint imaging and in situ observations. We also simulate this CME from the Sun to Earth with a passive tracer to tag the CME's motion. The coronagraphic images show that the CME is observed as a full halo by SOHO and as a partial halo by STEREO-A. The heliospheric images reveal that the propagation speed of the CME approaches about  $1^\circ \text{ hr}^{-1}$ , suggesting a slow CME. With simulated results matching these observation results, the simulation discloses that as the CME ejects from the Sun out to interplanetary space, its global morphology is distorted from an ellipsoid to a concave shape owing to interactions with the bimodal solar wind. The cross section of the CME's flux rope structure transforms from a circular shape into a flat one. As a result of the deflection, the propagation direction of the CME is far away from the Sun-Earth line. This means that the CME flank (or the ICME leg) likely arrives at both Solar Orbiter and the L1 point. From the CME's eruption to 1 au, its volume and mass increase by about two orders and one order of magnitude, respectively. Its kinetic energy is about 100 times larger than its magnetic energy at 1 au. These results have important implications for our understanding of CMEs' morphology, as well as their space weather impacts.

## **Can we detect coronal mass ejections through asymmetries of Sun-as-a-star extreme-ultraviolet spectral line profiles?**

[Zihao Yang](#), [Hui Tian](#), [Xianyong Bai](#), [Yajie Chen](#), [Yang Guo](#), [Yingjie Zhu](#), [Xin Cheng](#), [Yuhang Gao](#), [Yu Xu](#), [Hechao Chen](#), [Jiale Zhang](#)

ApJS **2022**

<https://arxiv.org/pdf/2204.03683.pdf>

Coronal mass ejections (CMEs) are the largest-scale eruptive phenomena in the solar system. Associated with enormous plasma ejections and energy release, CMEs have an important impact on the solar-terrestrial environment. Accurate predictions of the arrival times of CMEs at the Earth depend on the precise measurements on their three-dimensional velocities, which can be achieved using simultaneous line-of-sight (LOS) and plane-of-sky (POS) observations. Besides the POS information from routine coronagraph and extreme ultraviolet (EUV) imaging observations, spectroscopic observations could unveil the physical properties of CMEs including their LOS velocities. We propose that spectral line asymmetries measured by Sun-as-a-star spectrographs can be used for routine detections of CMEs and estimations of

their LOS velocities during their early propagation phases. Such observations can also provide important clues for the detection of CMEs on other solar-like stars. However, few studies have concentrated on whether we can detect CME signals and accurately diagnose CME properties through Sun-as-a-star spectral observations. In this work, we constructed a geometric CME model and derived the analytical expressions for full-disk integrated EUV line profiles during CMEs. For different CME properties and instrumental configurations, full disk-integrated line profiles were synthesized. We further evaluated the detectability and diagnostic potential of CMEs from the synthetic line profiles. Our investigations provide important constraints on the future design of Sun-as-a-star spectrographs for CME detections through EUV line asymmetries.

## **Numerical MHD Simulations of the 3D Morphology and Kinematics of the 2017 September 10 CME-driven Shock from the Sun to Earth**

Liping **Yang**<sup>1</sup>, Haopeng Wang<sup>1,2</sup>, Xueshang Feng<sup>1,3</sup>, Ming Xiong<sup>1,2</sup>, Man Zhang<sup>1</sup>, Bei Zhu<sup>4</sup>, Huichao Li<sup>3,1</sup>, Yufen Zhou<sup>1</sup>, Fang Shen<sup>1,2</sup>, Xinhua Zhao<sup>1</sup>Show full author list

**2021** ApJ 918 31

<https://doi.org/10.3847/1538-4357/ac0ef7>

A global, three-dimensional (3D) numerical simulation model has been employed to study the 3D morphology and kinematics of the large shock driven by the **2017 September 10** coronal mass ejection (CME). Based on actual solar observations, which include the photospheric magnetic field and the CME's speed and source location, the simulation result is delicately tuned by matching with coronal polarized brightness observations and in situ solar-wind measurements at 1 au. The simulation reproduces well the shock's shape and position in coronagraphic images. The shock's physical parameters at 1 au are similar to those constrained from the observations, with the simulated transit time being nearly the same as the observed one. The simulation reveals that the shock around the backward direction keeps propagating away from the Sun, and despite its large extent, the shock cannot be seen as a spherical structure forming a 360° envelope around the Sun. Identified as a fast forward shock, the shock has a sharp velocity jump and a large density compression with a Mach number larger than one from the nose toward the lateral parts, consistent with a driven shock all across the front. Compared to the nose, the right flank of the shock has a weak compression ratio, but probably yields enhanced energetic particles for observers aligned with it. It follows that large CME-driven shocks have the potential to accelerate energetic particles over a wide longitudinal separation and are likely responsible for the production of these particles in the inner heliosphere.

## **Two Episodes of a Filament Eruption from a Fan-spine Magnetic Configuration**

Jiayan **Yang**<sup>1,2</sup>, Junchao Hong<sup>1,2</sup>, Haidong Li<sup>1,2</sup>, and Yunchun Jiang<sup>1,2</sup>

**2020** ApJ 900 158

<https://doi.org/10.3847/1538-4357/aba7c0>

In this paper, we present detailed observations of a filament eruption associated with a B6.0 flare, a jet-like coronal mass ejection (CME), and a type-III radio burst on **2013 March 2**. The filament, which is located at the northwest edge of active region (AR) 11183, experienced a partial and then a full eruption. Each episode of the filament eruption produced a circular flare ribbon and a blowout jet, which is a mixture of hot and cool plasma that can be observed by the Solar Dynamics Observatory. Extrapolated coronal magnetic configuration using both the potential field source surface and the nonlinear force-free magnetic field models shows that the filament is embedded in a fan-spine magnetic topology. Considering the photospheric magnetic evolution, we suggest that the first episode of the filament eruption (partial eruption) is caused by the continuous photospheric magnetic flux cancellation below its western segment, while the eruption that follows results from the reduction of magnetic constraint above the filament in the aftermath of the first eruption episode and reconnection. Combining the observations with the extrapolated coronal magnetic configuration, we find that the event is an example that fits the null-point reconnection scenario. Our event is a result of null-point reconnection (interchange reconnection) between a closed filament magnetic field and the ambient open field at the edge of an AR, thus it has implications for the source of the slow speed solar wind and the source of the cold and dense plasma detected within.

## **Transfer of Twists from a Mini-filament to Large-scale Loops by Magnetic Reconnection**

Liheng **Yang**<sup>1,2,3</sup>, Xiaoli Yan<sup>1,2,4</sup>, Zhike Xue<sup>1,2,4</sup>, Ting Li<sup>4</sup>, Jincheng Wang<sup>1,2</sup>, Qiaoling Li<sup>1,2</sup>, and Xin Cheng<sup>3</sup>

**2019** ApJ 887 239

<https://doi.org/10.3847/1538-4357/ab55d7>

With high spatial and temporal resolution, H $\alpha$  data from the New Vacuum Solar Telescope, X-ray images from the X-ray telescope on board Hinode and simultaneous observations from the Solar Dynamics Observatory, we present multiwavelength observations of the interaction between a mini-filament (MF) and its overlying large-scale active-region loops (ARLs) that occurred in AR 12497 on **2016 February 13**. The MF was activated by the convergence and cancellation of the magnetic flux under it. Brightenings first appeared at the junction of the MF and its overlying large-scale ARLs. A blowout jet with some plasma blobs was observed to move along the newly formed large-scale ARLs, and caused the oscillations of these loops. The blowout jet exhibited a counterclockwise rotation due to the untwisting motion of the MF, suggesting that the twist is transferred from the MF to the ARLs. The transferred twist was measured to be about 0.34–0.52 turn. During the interaction progress, a group of hot loops formed in the high-temperature wavelength (94 Å). These hot loops connected the west footpoints of the original ARLs and the east footpoints of the



MF. The differential emission measure analysis demonstrated that these hot loops contained a high-temperature component ( $\sim 8$  MK). Meanwhile the footpoints of the ARLs were finally shifted to the west footpoint of the MF. These observations suggest that magnetic reconnection takes place between the MF and its overlying large-scale ARLs and results in a confined untwisting blowout jet.

### **Recurrent Two-Sided Loop Jets Caused by Magnetic Reconnection between Erupting Minifilaments and Nearby Large Filament**

Bo [Yang](#), [Jiayan Yang](#), [Yi Bi](#), [Zhe Xu](#), [Junchao Hong](#), [Haidong Li](#), [Hechao Chen](#)

ApJ **887** 220 **2019**

<https://arxiv.org/pdf/1911.02251.pdf>

<https://doi.org/10.3847/1538-4357/ab557e>

Using high spatial and temporal data from the New Vacuum Solar Telescope (NVST) and the Solar Dynamics Observatory (SDO), we present unambiguous observations of recurrent two-sided loop jets caused by magnetic reconnection between erupting minifilaments and nearby large filament. The observations demonstrate that three two-sided loop jets, which ejected along the large filament in opposite directions, had similar appearance and originated from the same region. We find that a minifilament erupted and drove the first jet. It reformed at the same neutral line later, and then underwent partial and total eruptions, drove the second and third jets, respectively. In the course of the jets, cool plasma was injected into the large filament. Furthermore, persistent magnetic flux cancellation occurred at the neutral line under the minifilament before its eruption and continued until the end of the observation. We infer that magnetic flux cancellation may account for building and then triggering the minifilament to erupt to produce the two-sided loop jets. This observation not only indicates that two-sided loop jets can be driven by minifilament eruptions, but also sheds new light on our understanding of the recurrent mechanism of two-sided loop jets. **2013 March 14**

### **Two-step evolution of a rising flux rope resulting in a confined solar flare**

Shuhong [Yang](#), [Jun Zhang](#), [Qiao Song](#), [Yi Bi](#), [Ting Li](#)

ApJ **2019**

<https://arxiv.org/pdf/1905.00808.pdf>

Combining the Solar Dynamics Observatory and the New Vacuum Solar Telescope observations, we study a confined flare triggered by a rising flux rope within the trailing sunspots of active region 12733. The flux rope lying above the sheared polarity inversion line can be constructed through magnetic extrapolation but could not be detected in multi-wavelength images at the pre-flare stage. The conspicuous shearing motions between the opposite-polarity fields in the photosphere are considered to be responsible for the flux rope formation. The maximum twist of the flux rope is as high as  $-1.76$ , and then the flux rope rises due to the kink instability. Only when the flare starts can the flux rope be observed in high-temperature wavelengths. The differential emission measure results confirm that this flux rope is a high-temperature structure. Associated with the rising flux rope, there appear many post-flare loops and a pair of flare ribbons. When the rising flux rope meets and reconnects with the large-scale overlying field lines, a set of large-scale twisted loops are formed, and two flare ribbons propagating in opposite directions appear on the outskirts of the former ribbons, indicating that the twist of the flux rope is transferred to a much larger system. These results imply that the external reconnection between the rising flux rope and the large-scale overlying loops plays an important role in the confined flare formation. **26 January 2019**

### **Filament Eruption and Its Reformation Caused by Emerging Magnetic Flux**

Bo [Yang](#), [Huadong Chen](#)

ApJ **874** 96 **2019**

<https://arxiv.org/pdf/1903.01235.pdf>

[sci-hub.se/10.3847/1538-4357/ab0c9e](https://doi.org/10.3847/1538-4357/ab0c9e)

We present observations of the eruption and then reformation of a filament caused by its nearby emerging magnetic flux. Driven by the emerging magnetic flux, the emerged positive fluxes moved toward and cancelled with its nearby negative fluxes, where the negative ends of a filament channel beneath the filament and a bundle of left-skewed coronal loops overlying the filament were anchored. Complemented by the nonlinear force-free field extrapolation, we find that the coronal magnetic field lines associated with the filament channel and the emerging magnetic fields consist of sheared field lines. Prior to the filament eruption, unambiguous observational evidence indicates that multiple interactions occurred between the emerging magnetic fields and the left-skewed coronal loops, implying a tether-weakening reconnection. Specifically, during the final episode of the tether-weakening reconnection, a remarkable sigmoid structure was formed and lifted up together with the filament. Accordingly, we speculate that the tether-weakening reconnection probably destabilized the filament system and triggered its rise. Subsequently, the filament and the sigmoid structure erupted together and produced a CME. After the eruption, the emerging magnetic fields continued to reconnect with the remaining filament channel, leading to the reformation of the filament. This observation strongly supports the idea that emerging magnetic flux plays an important role in triggering the filament to erupt, and the filament is reformed by magnetic reconnection between the emerging magnetic fields and its nearby filament channel. **2013 July 15**

### **Filament Eruption with a Deflection of Nearly 90 Degrees**

Jiayan [Yang](#)<sup>1</sup>, Jun Dai<sup>1,2</sup>, Hechao Chen<sup>1,2</sup>, Haidong Li<sup>1</sup>, and Yunchun Jiang

2018 ApJ 862 86

<http://sci-hub.tw/10.3847/1538-4357/aaccfd>

Using the data from the Solar Dynamics Observatory, the Ahead of Solar Terrestrial Relations Observatory, the Global Oscillation Network Group (GONG), and the Large Angle and Spectrometric Coronagraphs, the nearly  $90^\circ$  deflected eruption of a filament and the following coronal mass ejection (CME) occurring on the northern edge of AR 11123 on **2010 November 15** were presented in this paper. The filament was very small with the projected length of about  $2.6 \times 10^4$  km and centered at about  $S23^\circ W 38^\circ$ . The potential-field source-surface model identified that the filament was located near the northern flank of a helmet streamer. The filament initially erupted northward to the nearby open fields with speeds from 151 to 336 km s<sup>-1</sup>, resulting in a B7.6 subflare and some signatures of interchange reconnection. This suggested that the erupting filament interacted with the open fields at first. Then, guided by the highly-inclined open fields, it deflected about  $90^\circ$  southward on the plane of the sky to the magnetic minimum in the streamer configuration. In addition, the CME with the width of  $64^\circ$  and the central position angle of  $221^\circ$  was also deflected obviously in the inner corona to attain its final direction. Because the eruption failed to penetrate the open fields, these results corroborate the idea that open magnetic flux can act as a magnetic wall while a streamer belt can act as a potential well for coronal eruptions in the Sun.

### **Observational Evidence of Magnetic Reconnection Associated with Magnetic Flux Cancellation**

[Bo Yang](#), [Jiayan Yang](#), [Yi Bi](#), [Junchao Hong](#), [Haidong Li](#), [Zhe Xu](#), [Hechao Chen](#)

2018

<https://arxiv.org/pdf/1806.04857.pdf>

Using high spatial and temporal data from the *Solar Dynamics Observatory* (*SDO*) and the *Interface Region Imaging Spectrograph* (*IRIS*), several observational signatures of magnetic reconnection in the course of magnetic flux cancellation are presented, including two loop-loop interaction processes, multiple plasma blob ejections, and a sheet-like structure that appeared above the flux cancellation sites with a Y-shaped and an inverted Y-shaped ends. The *IRIS* 1400 Å observations show that the plasma blobs were ejected from the tip of the Y-shaped ends of the sheet-like structure. Obvious photospheric magnetic flux cancellation occurred after the first loop-loop interaction and continued until the end of the observation. Complemented by the nonlinear force-free field extrapolation, we found that two sets of magnetic field lines, which reveal an X-shaped configuration, align well with the interacted coronal loops. Moreover, a magnetic null point is found to be situated at about 0.9 Mm height right above the flux cancellation sites and located between the two sets of magnetic field lines. These results suggest that the flux cancellation might be a result of submergence of magnetic field lines following magnetic reconnection that occurs in the lower atmosphere of the Sun, and the ejected plasma blobs should be plasmoids created in the sheet-like structure due to the tearing-mode instability. This observation reveals detailed magnetic field structure and dynamic process above the flux cancellation sites and will help us to understand magnetic reconnection in the lower atmosphere of the Sun. **2015 January 9**

### **Mini-filament Eruptions Triggering Confined Solar Flares Observed by ONSET and SDO**

[Shuhong Yang](#), [Jun Zhang](#)

ApJL **860** L25 **2018**

<https://arxiv.org/pdf/1806.01763.pdf>

Using the observations from the Optical and Near-infrared Solar Eruption Tracer and the Solar Dynamics Observatory, we study an M5.7 flare in AR 11476 on **2012 May 10** and a micro-flare in the quiet Sun on **2017 March 23**. Before the onset of each flare, there is a reverse S-shaped filament above the polarity inversion line. Then the filaments become unstable and begin to rise. The rising filaments gain the upper hand over the tension force of the dome-like overlying loops and thus successfully erupt outward. The footpoints of the reconnecting overlying loops successively brighten and are observed as two flare ribbons, while the newly formed low-lying loops appear as the post-flare loops. These eruptions are similar to the classical model of successful filament eruptions associated with coronal mass ejections. However, the erupting filaments in this study move along large-scale lines and eventually reach the remote solar surface, i.e., no filament material is ejected into the interplanetary space. Thus both the flares are confined ones. These results reveal that some successful filament eruptions can trigger confined flares. Our observations also imply that this kind of filament eruptions may be ubiquitous on the Sun, from active regions with large flares to the quiet Sun with micro-flares.

### **Observation of the Kelvin–Helmholtz Instability in a Solar Prominence**

Heesu [Yang](#)<sup>1</sup>, Zhi Xu<sup>2</sup>, Eun-Kyung Lim<sup>1</sup>, Sujin Kim<sup>1,3</sup>, Kyung-Suk Cho<sup>1,3</sup>, Yeon-Han Kim<sup>1,3</sup>, Jongchul Chae<sup>4</sup>, Kyuhyoun Cho<sup>4</sup>, and Kaifan Ji<sup>2</sup>

2018 ApJ 857 115

<http://sci-hub.tw/http://iopscience.iop.org/0004-637X/857/2/115/>

Many solar prominences end their lives in eruptions or abrupt disappearances that are associated with dynamical or thermal instabilities. Such instabilities are important because they may be responsible for energy transport and conversion. We present a clear observation of a streaming kink-mode Kelvin–Helmholtz Instability (KHI) taking place in a solar prominence using the H $\alpha$ Lyot filter installed at the New Vacuum Solar Telescope, Fuxian-lake Solar Observatory in Yunnan, China. On one side of the prominence, a series of plasma blobs floated up from the

chromosphere and streamed parallel to the limb. The plasma stream was accelerated to about 20–60 km s<sup>-1</sup> and then undulated. We found that 2"- and 5"-size vortices formed, floated along the stream, and then broke up. After the 5"-size vortex, a plasma ejection out of the stream was detected in the Solar Dynamics Observatory/Atmospheric Imaging Assembly images. Just before the formation of the 5"-size vortex, the stream displayed an oscillatory transverse motion with a period of 255 s with the amplitude growing at the rate of 0.001 s<sup>-1</sup>. We attribute this oscillation of the stream and the subsequent formation of the vortex to the KHI triggered by velocity shear between the stream, guided by the magnetic field and the surrounding media. The plasma ejection suggests the transport of prominence material into the upper layer by the KHI in its nonlinear stage. **2016 June 4**

### **Formation of Cool and Warm Jets by Magnetic Flux Emerging from the Solar Chromosphere to Transition Region**

Liping [Yang](#)<sup>1,2,3</sup>, Hardi Peter<sup>4</sup>, Jiansen He<sup>2,3</sup>, Chuanyi Tu<sup>2</sup>, Linghua Wang<sup>2</sup>, Lei Zhang<sup>1</sup>, and Limei Yan<sup>2</sup>  
**2018 ApJ 852 16**

In the solar atmosphere, jets are ubiquitous at various spatial-temporal scales. They are important for understanding the energy and mass transports in the solar atmosphere. According to recent observational studies, the high-speed network jets are likely to be intermittent but continual sources of mass and energy for the solar wind. Here, we conduct a 2D magnetohydrodynamics simulation to investigate the mechanism of these network jets. A combination of magnetic flux emergence and horizontal advection is used to drive the magnetic reconnection in the transition region between a strong magnetic loop and a background open flux. The simulation results show that not only a fast warm jet, much similar to the network jets, is found, but also an adjacent slow cool jet, mostly like classical spicules, is launched. Differing from the fast warm jet driven by magnetic reconnection, the slow cool jet is mainly accelerated by gradients of both thermal pressure and magnetic pressure near the outer border of the mass-concentrated region compressed by the emerging loop. These results provide a different perspective on our understanding of the formation of both the slow cool jets from the solar chromosphere and the fast warm jets from the solar transition region.

### **Two Solar Tornadoes Observed with the Interface Region Imaging Spectrograph: Rotating Motion of Prominence Materials**

Zihao [Yang](#), [Hui Tian](#), [Hardi Peter](#), [Yang Su](#), [Tanmoy Samanta](#), [Jingwen Zhang](#), [Yajie Chen](#)  
**2018 ApJ 852 79**

<https://arxiv.org/pdf/1711.08968.pdf>

The barbs or legs of some prominences show an apparent motion of rotation, which are often termed solar tornadoes. It is under debate whether the apparent motion is a real rotating motion, or caused by oscillations or counter-streaming flows. We present analysis results from spectroscopic observations of two tornadoes by the Interface Region Imaging Spectrograph. Each tornado was observed for more than 2.5 hours. Doppler velocities are derived through a single Gaussian fit to the Mg<sup>ii</sup> 2796 Å and Si<sup>iv</sup> 1393 Å line profiles. We find coherent and stable red and blue shifts adjacent to each other across the tornado axes, favoring the interpretation of these tornadoes as rotating cool plasmas with temperatures of 10<sup>4</sup> K–10<sup>5</sup> K. This interpretation is further supported by simultaneous observations of the Atmospheric Imaging Assembly on board the Solar Dynamics Observatory, which reveal periodic motions of dark structures in the tornadoes. Our results demonstrate that spectroscopic observations can provide key information to disentangle different physical processes in solar prominences. **2014 April 9, 2017 March 12.**

### **Multi-label Learning for Detection of CME-Associated Phenomena**

Y. H. [Yang](#), H. M. Tian, B. Peng, T. R. Li, Z. X. Xie

[Solar Physics](#) September **2017**, 292:131

<https://link.springer.com/content/pdf/10.1007%2F11207-017-1136-x.pdf>

Coronal mass ejections (CMEs) are considered as one of the driving sources of space weather. They are usually associated with many physical phenomena, e.g. flares, coronal dimmings, and sigmoids. To detect these phenomena, traditional supervised-learning methods assumed that at most one event occurred in a CME; therefore each CME instance is associated with a single label and the phenomenon is processed in isolation. This simplifying assumption does not fit well, as CMEs might have multiple events simultaneously. We propose to detect multiple CME-associated events by multi-label learning methods. With the data available from the Atmospheric Imaging Assembly (AIA) and the Large Angle and Spectrometric Coronagraph (LASCO), texture features representing the events are extracted from all of the associated and not-associated CMEs and converted into feature vectors for multi-label learning use. Then a function is learned to predict the proper label sets for CMEs, such that eight events, i.e. coronal dimming, coronal hole, coronal jet, coronal wave, filament, filament eruption, flare, and sigmoid, are detected explicitly. To test the proposed detection algorithm, we adopt the four-fold cross-validation strategy on a set of 551 labeled CMEs from AIA. Experimental results demonstrate the good performance of the multi-label classification methods in terms of test error. **6 June 2012**

### **Interaction of Two Active Region Filaments Observed by NVST and SDO**

Liheng [Yang](#), Xiaoli Yan, Ting Li, [Zhike Xue](#), [Yongyuan Xiang](#)

[ApJ](#) **2017**

<https://arxiv.org/pdf/1703.01712.pdf>

Using high spatial and temporal resolution H $\alpha$  data from the New Vacuum Solar Telescope (NVST) and simultaneous observations from the Solar Dynamics Observatory (SDO), we present a rare event on the interaction between two filaments (F1 and F2) in AR 11967 on **2014 January 31**. The adjacent two filaments were almost perpendicular to each other. Their interaction was driven by the movement of F1 and started when the two filaments collided with each other. During the interaction, the threads of F1 continuously slipped from the northeast to the southwest, accompanied by the brightenings at the junction of two filaments and the northeast footpoint of F2. Part of F1 and the main body of F2 became invisible in H $\alpha$  wavelength due to the heating and the motion of F2. At the same time, bright material initiated from the junction of two filaments were observed to move along F1. The magnetic connectivities of F1 were found to be changed after their interaction. These observations suggest that magnetic reconnection was involved in the interaction of two filaments and resulted in the eruption of one filament.

## **Quantifying the Topology and Evolution of a Magnetic Flux Rope Associated with Multi-flare Activities**

Kai **Yang**, Yang Guo, M. D. Ding

ApJ **824** 148 **2016**

<http://arxiv.org/pdf/1604.07502v1.pdf>

Magnetic flux rope (MFR) plays an important role in solar activities. A quantitative assessment of the topology of an MFR and its evolution is crucial for a better understanding of the relationship between the MFR and the associated activities. In this paper, we investigate the magnetic field of active region 12017 from **2014 March 28 to 29**, where 12 flares were triggered by the intermittent eruptions of a filament (either successful or confined). Using the vector magnetic field data from the Helioseismic and Magnetic Imager on board the \textit{Solar Dynamics Observatory}, we calculate the magnetic energy and helicity injection in the active region, and extrapolate the 3D magnetic field with a nonlinear force-free field model. From the extrapolations, we find an MFR that is cospatial with the filament. We further determine the configuration of this MFR by a closed quasi-separatrix layer (QSL) around it. Then, we calculate the twist number and the magnetic helicity for the field lines composing the MFR. The results show that the closed QSL structure surrounding the MFR gets smaller as a consequence of the flare occurrence. We also find that the flares in our sample are mainly triggered by kink instability. Moreover, the twist number varies more sensitively than other parameters to the occurrence of flares.

## **Origin of Both the Fast Hot Jet and the Slow Cool Jet from Magnetic Flux Emergence and Advection in the Solar Transition Region**

Liping **Yang**, Hardi Peter, Jiansen He, Chuanyi Tu, Linghua Wang, Lei Zhang, Xueshang Feng

**2015**

<http://arxiv.org/pdf/1512.01869v1.pdf>

In the solar atmosphere, the jets are ubiquitous and found to be at various spatio-temporal scales. They are significant to understand energy and mass transport in the solar atmosphere. Recently, the high-speed transition region jets are reported from the observation. Here we conduct a numerical simulation to investigate the mechanism in their formation. Driven by the supergranular convection motion, the magnetic reconnection between the magnetic loop and the background open flux occurring in the transition region is simulated with a two-dimensional magnetohydrodynamics model. The simulation results show that not only a fast hot jet, much resemble the found transition region jets, but also an adjacent slow cool jet, mostly like classical spicules, is launched. The force analysis shows that the fast hot jet is continually driven by the Lorentz force around the reconnection region, while the slow cool jet is induced by an initial kick through the Lorentz force associated with the emerging magnetic flux. Also, the features of the driven jets change with the amount of the emerging magnetic flux, giving the varieties of both jets. These results will inspire our understanding of the formation of the prevalence of both the fast hot jet and slow cool jet from the solar transition region and chromosphere.

## **The Formation and Eruption of a Small Circular Filament Driven by Rotating Magnetic Structures in the Quiet Sun**

Bo **Yang**<sup>1,2,3</sup>, Yunchun Jiang<sup>1</sup>, Jiayan Yang<sup>1</sup>, Junchao Hong<sup>1</sup>, and Zhe Xu

**2015** ApJ 803 86

We present the first observation of the formation and eruption of a small circular filament driven by a rotating network magnetic field (RNF) in the quiet Sun. In the negative footpoint region of an inverse J-shaped dextral filament, the RNF was formed by the convergence to supergranular junctions of several magnetic flux patches of the same polarity, and it then rotated counterclockwise (CCW) for approximately 11 hr and showed up as a CCW rotating EUV cyclone, during which time the filament gradually evolved into a circular filament that surrounded the cyclone. When the calculated convergence and vortex flows appeared around the RNF during its formation and rotation phases, the injected magnetic helicity calculation also showed negative helicity accumulation during the RNF rotation that was consistent with the dextral chirality of the filament. Finally, the RNF rotation stopped and the cyclone disappeared, and, probably due to an emerging bipole and its forced cancellation with the RNF, the closure filament underwent an eruption along its axis in the (clockwise) direction opposite to the rotation directions of the RNF and cyclone. These observations suggest that the RNFs might play an important role in the formation of nearby small-scale circular filaments as they transport and inject

magnetic energy and helicity, and the formation of the EUV cyclones may be a further manifestation of the helicity injected into the corona by the rotation of the RNFs in the photosphere. In addition, the new emerging bipole observed before the filament eruption might be responsible for destabilizing the system and triggering the magnetic reconnection which proves useful for the filament eruption.

### **Interchange Reconnection Forced by the Filament Eruption Inside a Pseudo-streamer**

Jiayan **Yang**<sup>1</sup>, Yunchun Jiang<sup>1</sup>, Zhe Xu<sup>1,2</sup>, Yi Bi<sup>1</sup>, and Junchao Hon

2015 ApJ 803 68

We present rare observational signatures of interchange reconnection (IR) forced by the filament eruption inside a pseudo-streamer (PS). The PS was centered above a positive-polarity region bounded by two negative-polarity coronal holes (CHs), and thus its base contained two polarity inversion lines and a pair of loop arcades where two filaments were harbored. In white-light coronagraph data from two different views, it showed up as a fan-shaped structure consisting of fine rays and a coronal streamer. Followed by a two-ribbon flare and a coronal mass ejection, one of the filaments and its overlying arcade erupted away from the nearby CH and flew over the other arcade to interact with the PS's remote CH. As a result, distinct ribbon-like remote brightenings formed along the remote CH boundary and were connected to the positive-polarity flare ribbon by a loop system, but the nearby open-field region largely remained unchanged except that compact brightenings and a following small coronal dimming appeared close to one end of the erupted filament. In combination with the coronal magnetic configuration that derived from the potential-field source-surface model, these observations can be interpreted as follows: the erupting field was first deflected and guided by the nearby CH's open field and then reconnected with the oppositely oriented open field of the remote CH, during which both the closed field bridging the erupted filament and the remoter CH's open field were transported in the opposite direction. The observations thus supported the idea that PSs provide favorable environments for IR to take place and remote brightenings along their CH boundaries represent a credible IR signature on the solar surface.

### **Eruption of the magnetic flux rope in a quick decaying active region**

Shangbin **Yang**, Wenbin Xie, Jihong Liu

Advances in Space Research Volume 55, Issue 6, 15 March 2015, Pages 1553–1562

<http://www.sciencedirect.com/science/article/pii/S0273117715000228>

An isolated and quickly decaying active region (NOAA 9729) was observed as it passed across the solar disk. There was only one CME associated with the active region, which provides a good opportunity to investigate the whole process of the CME. A filament in this active region was observed to rise rapidly before stalling and disintegrating into flare loops. The rising filament seen in EIT images separates into two parts just before eruption. A new filament reforms several hours later after the CME; the axis of this new filament is rotated clockwise approximately  $22^\circ$  compared with that of the first filament, due to a changed orientation of the polarity inversion line. We also observed a bright transient slightly S-shaped X-ray sigmoid, which appears immediately after the filament eruption. The X-ray sigmoid quickly develops into a soft X-ray cusp and rises before dropping back down. Two magnetic cancellation regions were observed clearly just before filament eruption. The eruption process of the sigmoid structure in this quick decaying active region could be explained by using the 3D Tether-Cutting model. The magnetic flux rope erupted as the magnetic helicity approached its maximum and the normalized helicity was  $-0.036$  when the magnetic flux rope erupted, which is an order of magnitude smaller than the simulation results of the kink and torus instability, but is close to the predicted value of Zhang et al. (2008) based on the theoretical non-linear force-free model. **December 07, 2001**

### **New Vacuum Solar Telescope Observations of a Flux Rope Tracked by a Filament Activation**

Shuhong **Yang**<sup>1</sup>, Jun Zhang<sup>1</sup>, Zhong Liu<sup>2</sup>, and Yongyuan Xiang

2014 ApJ 784 L36

One main goal of the New Vacuum Solar Telescope (NVST) which is located at the Fuxian Solar Observatory is to image the Sun at high resolution. Based on the high spatial and temporal resolution NVST  $H\alpha$  data and combined with the simultaneous observations from the Solar Dynamics Observatory for the first time, we investigate a flux rope tracked by filament activation. The filament material is initially located at one end of the flux rope and fills in a section of the rope; the filament is then activated by magnetic field cancellation. The activated filament rises and flows along helical threads, tracking the twisted flux rope structure. The length of the flux rope is about 75 Mm, the average width of its individual threads is 1.11 Mm, and the estimated twist is  $1\pi$ . The flux rope appears as a dark structure in  $H\alpha$  images, a partial dark and partial bright structure in  $304 \text{ \AA}$ , and as a bright structure in  $171 \text{ \AA}$  and  $131 \text{ \AA}$  images. During this process, the overlying coronal loops are quite steady since the filament is confined within the flux rope and does not erupt successfully. It seems that, for the event in this study, the filament is located and confined within the flux rope threads, instead of being suspended in the dips of twisted magnetic flux.

### **NUMERICAL SIMULATIONS OF CHROMOSPHERIC ANEMONE JETS ASSOCIATED WITH MOVING MAGNETIC FEATURES**

Liping **Yang**<sup>1,2</sup>, Jiansen He<sup>1</sup>, Hardi Peter<sup>3</sup>, Chuanyi Tu<sup>1</sup>, Lei Zhang<sup>1</sup>, Xueshang Feng<sup>2</sup>, and Shaohua Zhang

2013 ApJ 777 16

Observations with the space-based solar observatory Hinode show that small-scale magnetic structures in the photosphere are found to be associated with a particular class of jets of plasma in the chromosphere called anemone jets. The goal of our study is to conduct a numerical experiment of such chromospheric anemone jets related to the moving magnetic features (MMFs). We construct a 2.5 dimensional numerical MHD model to describe the process of magnetic reconnection between the MMFs and the pre-existing ambient magnetic field, which is driven by the horizontal motion of the magnetic structure in the photosphere. We include thermal conduction parallel to the magnetic field and optically thin radiative losses in the corona to account for a self-consistent description of the evaporation process during the heating of the plasma due to the reconnection process. The motion of the MMFs leads to the expected jet and our numerical results can reproduce many observed characteristics of chromospheric anemone jets, topologically and quantitatively. As a result of the tearing instability, plasmoids are generated in the reconnection process that are consistent with the observed bright moving blobs in the anemone jets. An increase in the thermal pressure at the base of the jet is also driven by the reconnection, which induces a train of slow-mode shocks propagating upward. These shocks are a secondary effect, and only modulate the outflow of the anemone jet. The jet itself is driven by the energy input due to the reconnection of the MMFs and the ambient magnetic field.

### **AN OVER-AND-OUT HALO CORONAL MASS EJECTION DRIVEN BY THE FULL ERUPTION OF A KINKED FILAMENT**

Jiayan [Yang](#)<sup>1,2</sup>, Yunchun Jiang<sup>1</sup>, Yi Bi<sup>1</sup>, Haidong Li<sup>1</sup>, Junchao Hong<sup>1,3</sup>, Dan Yang<sup>1,3</sup>, Ruisheng Zheng<sup>1,3</sup> and Bo Yang

2012 ApJ 749 12, [File](#)

Over-and-out coronal mass ejections (CMEs) represent a broad class of CMEs that come from flare-producing magnetic explosions of various sizes but are laterally far offset from the flare, and their productions can be depicted by the magnetic-arch-blowout scenario. In this paper, we present observations of an over-and-out halo CME from the full eruption of a small kinking filament in an emerging active region (AR). In combination with the results of a derived coronal magnetic configuration, our observations showed that the CME was associated with a coronal helmet streamer, and the filament was located in the northern outskirts of the streamer base. Formed along a neutral line where flux cancellation was forced by the emerging AR with the surrounding opposite-polarity magnetic field, the filament underwent a full, non-radial eruption along the northern leg of the streamer arcade, accompanied by a clockwise deflection of the eruption direction. As a characteristic property of kink instability, the eruption displayed a clear inverse  $\gamma$  shape, indicative of a writhing motion of the filament apex. Coronal dimmings, including a remote one, formed in opposite-polarity footprint regions of the streamer arcade during the eruption, and the consequent CME was laterally offset from the AR. These observations suggest that the kink instability is likely to be the driver in the eruption. The event can be well explained by putting this driver into the magnetic-arch-blowout model, in which the eruption-direction deflection and the full-eruption nature of the kinking filament are caused by the guiding action of the streamer arcade and the external reconnection between them.

### **SYMPATHETIC FILAMENT ERUPTIONS FROM A BIPOLAR HELMET STREAMER IN THE SUN**

[Yang](#), J., Jiang, Y., Zheng, R., Bi, Y., Hong, J., & Yang, B.

2012, ApJ, 745, 9

<https://iopscience.iop.org/article/10.1088/0004-637X/745/1/9/pdf>

presented detailed observations of two filament eruptions on **2005 August 5** in a bipolar helmet streamer type configuration and interpreted these eruptions as sympathetic.

### **The magnetic field environment of active region 12673 that produced the energetic particle events of September 2017**

Stephanie L. [Yardley](#), [Lucie M. Green](#), [Alexander W. James](#), [David Stansby](#), [Teodora Mihalescu](#)

ApJ 2022

<https://arxiv.org/pdf/2208.12774.pdf> [File](#)

Forecasting solar energetic particles (SEPs), and identifying flare/CMEs from active regions (ARs) that will produce SEP events in advance is extremely challenging. We investigate the magnetic field environment of AR 12673, including the AR's magnetic configuration, the surrounding field configuration in the vicinity of the AR, the decay index profile, and the footpoints of Earth-connected magnetic field, around the time of four eruptive events. Two of the eruptive events are SEP-productive (**2017 September 4** at 20:00~UT and **September 6** at 11:56~UT), while two are not (**September 4** at 18:05~UT and **September 7** at 14:33~UT). We analysed a range of EUV and white-light coronagraph observations along with potential field extrapolations and find that the CMEs associated with the SEP-productive events either trigger null point reconnection that redirects flare-accelerated particles from the flare site to the Earth-connected field and/or have a significant expansion (and shock formation) into the open Earth-connected field. The rate of change of the decay index with height indicates that the region could produce a fast CME ( $v > 1500 \text{ km s}^{-1}$ ), which it did during events two and three. The AR's magnetic field environment, including sites of open magnetic field and null points along with the magnetic field connectivity and propagation direction of the CMEs play an important role in the escape and arrival of SEPs at Earth. Other SEP-productive ARs should be investigated to determine whether their magnetic field environment and CME propagation direction are significant in the escape and arrival of SEPs at Earth.

## Determining the source and eruption dynamics of a stealth CME using NLFFF modelling and MHD simulations

[Stephanie L. Yardley](#), [Paolo Pagano](#), [Duncan H. Mackay](#), [Lisa A. Upton](#)

A&A 652, A160 2021

<https://arxiv.org/pdf/2106.14800.pdf>

<https://www.aanda.org/articles/aa/pdf/2021/08/aa41142-21.pdf>

<https://doi.org/10.1051/0004-6361/202141142>

Coronal mass ejections (CMEs) that exhibit weak or no eruption signatures in the low corona, known as stealth CMEs, are problematic as upon arrival at Earth they can lead to geomagnetic disturbances that were not predicted by space weather forecasters. We investigate the origin and eruption of a stealth event that occurred on **2015 January 3** that was responsible for a strong geomagnetic storm upon its arrival at Earth. To simulate the coronal magnetic field and plasma parameters of the eruption we use a coupled approach. This approach combines an evolutionary nonlinear force-free field model of the global corona with a MHD simulation. The combined simulation approach accurately reproduces the stealth event and suggests that sympathetic eruptions occur. In the combined simulation we found that three flux ropes form and then erupt. The first two flux ropes, which are connected to a large AR complex behind the east limb, erupt first producing two near-simultaneous CMEs. These CMEs are closely followed by a third, weaker flux rope eruption in the simulation that originated between the periphery of AR 12252 and the southern polar coronal hole. The third eruption coincides with a faint coronal dimming, which appears in the SDO/AIA 211 Å observations, that is attributed as the source responsible for the stealth event and later the geomagnetic disturbance at 1 AU. The incorrect interpretation of the stealth event being linked to the occurrence of a single partial halo CME observed by LASCO/C2 is mainly due to the lack of STEREO observations being available at the time of the CMEs. The simulation also shows that the LASCO CME is not a single event but rather two near-simultaneous CMEs. These results show the significance of the coupled data-driven simulation approach in interpreting the eruption and that an operational L5 mission is crucial for space weather forecasting.

## Simulating the Coronal Evolution of Bipolar Active Regions to Investigate the Formation of Flux Ropes

[Stephanie L. Yardley](#), [Duncan H. Mackay](#), [Lucie M. Green](#)

Solar Phys. 296, Article number: 10 2021

<https://arxiv.org/pdf/2012.07708.pdf>

<https://link.springer.com/content/pdf/10.1007/s11207-020-01749-2.pdf>

The coronal magnetic field evolution of 20 bipolar active regions (ARs) is simulated from their emergence to decay using the time-dependent nonlinear force-free field method of Mackay et al. A time sequence of cleaned photospheric line-of-sight magnetograms, that covers the entire evolution of each AR, is used to drive the simulation. A comparison of the simulated coronal magnetic field with the 171 and 193 Å observations obtained by the Solar Dynamics Observatory (SDO)/ Atmospheric Imaging Assembly (AIA), is made for each AR by manual inspection. The results show that it is possible to reproduce the evolution of the main coronal features such as small- and large-scale coronal loops, filaments and sheared structures for 80% of the ARs. Varying the boundary and initial conditions, along with the addition of physical effects such as Ohmic diffusion, hyperdiffusion and a horizontal magnetic field injection at the photosphere, improves the match between the observations and simulated coronal evolution by 20%. The simulations were able to reproduce the build-up to eruption for 50% of the observed eruptions associated with the ARs. The mean unsigned time difference between the eruptions occurring in the observations compared to the time of eruption onset in the simulations was found to be ~5 hrs. The simulations were particularly successful in capturing the build-up to eruption for all four eruptions that originated from the internal polarity inversion line of the ARs. The technique was less successful in reproducing the onset of eruptions that originated from the periphery of ARs and large-scale coronal structures. For these cases global, rather than local, nonlinear force-free field models must be used. While the technique has shown some success, eruptions that occur in quick succession are difficult to reproduce by this method and future iterations of the model need to address this. **17-20 Mar 2012, 24 Mar 2012, 25 Feb 2013, 6-9 Dec 2014, 14-17 Nov 2015**

**Table 1.:** The 20 bipolar ARs simulated in this study (2012-2015).

## The role of flux cancellation in eruptions from bipolar active regions

S. L. [Yardley](#), [L. M. Green](#), [L. Van Driel-Gesztelyi](#), [D. R. Williams](#), [D. H. Mackay](#)

ApJ 866 8 2018

<https://arxiv.org/pdf/1808.10635.pdf>

[sci-hub.tw/10.3847/1538-4357/aade4a](https://sci-hub.tw/10.3847/1538-4357/aade4a)

The physical processes or trigger mechanisms that lead to the eruption of coronal mass ejections (CMEs), the largest eruptive phenomenon in the heliosphere, are still undetermined. Low-altitude magnetic reconnection associated with flux cancellation appears to play an important role in CME occurrence as it can form an eruptive configuration and reduce the magnetic flux that contributes to the overlying, stabilising field. We conduct the first comprehensive study of 20 small bipolar active regions in order to probe the role of flux cancellation as an eruption trigger mechanism. We categorise eruptions from the bipolar regions into three types related to location and find that the type of eruption produced depends on the evolutionary stage of the active region. In addition we find that active regions that form

eruptive structures by flux cancellation (low-altitude reconnection) had, on average, lower flux cancellation rates than the active region sample as a whole. Therefore, while flux cancellation plays a key role, by itself it is insufficient for the production of an eruption. The results support that although flux cancellation in a sheared arcade may be able to build an eruptive configuration, a successful eruption depends upon the removal of sufficient overlying and stabilising field. Convergence of the bipole polarities also appears to be present in regions that produce an eruption. These findings have important implications for understanding the physical processes that occur on our Sun in relation to CMEs and for space weather forecasting. **2012/03/17, 2012/03/20**

**Table** (2012-2015)

## **Simulating the Coronal Evolution of AR 11437 using SDO/HMI Magnetograms**

Stephanie L. [Yardley](#), [Duncan H. Mackay](#), [Lucie M. Green](#)

**2018** *ApJ* **852** 82

<https://arxiv.org/pdf/1712.00396.pdf>

The coronal magnetic field evolution of AR 11437 is simulated by applying the magnetofrictional relaxation technique of Mackay et al. (2011). A sequence of photospheric line-of-sight magnetograms produced by SDO/HMI are used to drive the simulation and continuously evolve the coronal magnetic field of the active region through a series of non-linear force-free equilibria. The simulation is started during the first stages of the active region emergence so that its full evolution from emergence to decay can be simulated. A comparison of the simulation results with SDO/AIA observations show that many aspects of the active region's observed coronal evolution are reproduced. In particular, it shows the presence of a flux rope, which forms at the same location as sheared coronal loops in the observations. The observations show that eruptions occur on **2012 March 17** at 05:09 UT and 10:45 UT and on **2012 March 20** at 14:31 UT. The simulation reproduces the first and third eruption, with the simulated flux rope erupting roughly 1 and 10 hours before the observed ejections, respectively. A parameter study is conducted where the boundary and initial conditions are varied along with the physical effects of Ohmic diffusion, hyperdiffusion and an additional injection of helicity. When comparing the simulations, the evolution of the magnetic field, free magnetic energy, relative helicity and flux rope eruption timings do not change significantly. This indicates that the key element in reproducing the coronal evolution of AR 11437 is the use of line-of-sight magnetograms to drive the evolution of the coronal magnetic field.

## **Flux cancellation and the evolution of the eruptive filament of 2011 June 7**

S. L. [Yardley](#), L. M. Green, D. R. Williams, L. van Driel-Gesztelyi, G. Valori, S. Dacie

*ApJ* **827** 151 **2016**

<http://arxiv.org/pdf/1606.08264v1.pdf>

We investigate whether flux cancellation is responsible for the formation of a very massive filament resulting in the spectacular 2011 June 7 eruption. We analyse and quantify the amount of flux cancellation that occurs in NOAA AR 11226 and its two neighbouring ARs (11227 & 11233) using line-of-sight magnetograms from the Heliospheric Magnetic Imager. During a 3.6-day period building up to the filament eruption,  $1.7 \times 10^{21}$  Mx, 21% of AR 11226's maximum magnetic flux, was cancelled along the polarity inversion line (PIL) where the filament formed. If the flux cancellation continued at the same rate up until the eruption then up to  $2.8 \times 10^{21}$  Mx (34% of the AR flux) may have been built into the magnetic configuration that contains the filament plasma. The large flux cancellation rate is due to an unusual motion of the positive polarity sunspot, which splits, with the largest section moving rapidly towards the PIL. This motion compresses the negative polarity and leads to the formation of an orphan penumbra where one end of the filament is rooted. Dense plasma threads above the orphan penumbra build into the filament, extending its length, and presumably injecting material into it. We conclude that the exceptionally strong flux cancellation in AR 11226 played a significant role in the formation of its unusually massive filament. In addition, the presence and coherent evolution of bald patches in the vector magnetic field along the PIL suggests that the magnetic field configuration supporting the filament material is that of a flux rope.

## **A Catalog of Prominence Eruptions Detected Automatically in the SDO/AIA 304 Å Images**

[S. Yashiro](#) (1 and 2), [N. Gopalswamy](#) (2), [S. Akiyama](#) (1 and 2), [P.A. Mäkelä](#)

**2020**

See [https://cdaw.gsfc.nasa.gov/CME\\_list/autope/](https://cdaw.gsfc.nasa.gov/CME_list/autope/)

<https://arxiv.org/ftp/arxiv/papers/2005/2005.11363.pdf>

We report on a statistical study of prominence eruptions (PEs) using a catalog of these events routinely imaged by the Atmospheric Imaging Assembly (AIA) on board the Solar Dynamics Observatory (SDO) in the 304 Å pass band. Using an algorithm developed as part of an LWS project, we have detected PEs in 304 Å synoptic images with 2-min cadence since May 2010. **A catalog of these PEs is made available online ([this https URL](#))**. The 304 Å images are polar-transformed and divided by a background map (pixels with minimum intensity during one day) to get the ratio maps above the limb. The prominence regions are defined as pixels with a ratio  $\geq 2$ . Two prominence regions with more than 50% of pixels overlapping are considered the same prominence. If the height of a prominence increases monotonically in 5 successive images, it is considered eruptive. All the PEs seen above the limb are detected by the routine, but only PEs with width  $\geq 15^\circ$  are included in the catalog to eliminate polar jets and other small-scale mass motions. The identifications are also cross-checked with the PEs identified in Nobeyama Radioheliograph images



([this http URL](#)). The catalog gives the date, time, central position angle, latitude, and width of the eruptive prominence. The catalog also provides links to JavaScript movies that combine SDO/AIA images with GOES soft X-ray data to identify the associated flares, and with SOHO/LASCO C2 images to identify the associated coronal mass ejections. We examined the statistical properties of the PEs and found that the high-latitude PE speed decreased with the decreasing of the average polar magnetic field strength of the previous cycle. **2011.05.30**

### **Automatic Detection of Prominence Eruptions from SDO/AIA Images at 304 Å...**

**Yashiro, S.**, Gopalswamy, N., and Akiyama, S.

(2017), JASTP, to be submitted.

See **A Catalog of Prominence Eruptions Detected Automatically in the SDO/AIA 304 Å Images\***

[https://cdaw.gsfc.nasa.gov/CME\\_list/autope/](https://cdaw.gsfc.nasa.gov/CME_list/autope/)

### **A Comparative Study of Confined and Eruptive Solar Flares using Microwave Observations**

**Yashiro, S.**; Akiyama, S.; Masuda, S.; Shimojo, M.; Asai, A.; Imada, S.; Gopalswamy, N.

American Geophysical Union, Fall Meeting **2015**, abstract #SH43B-2447

It is well known that about 10% X-class solar flares are not associated with coronal mass ejections (CMEs). These flares are referred to as confined flares, which are not associated with mass or energetic particles leaving the Sun. However, electrons are accelerated to MeV energies as indicated by the presence of microwave emission with a turnover frequency of ~15 GHz (Gopalswamy et al. 2009, IAU Symposium 257, p. 283). In this paper, we extend the study of confined flares to lower soft X-ray flare sizes (M and above) that occurred in the time window of the Nobeyama Radioheliograph (NoRH). We also make use of the microwave spectral information from the Nobeyama Radio Polarimeters (NoRP). During 1996 - 2014, NoRH and NoRP observed 663 flares with size M1.0 or larger. Using the CME observations made by SOHO/LASCO and STEREO/SECCHI, we found 215 flares with definite CME association (eruptive flares) and 202 flares that definitely lacked CMEs (confined flares). The remaining 146 flares whose CME association is unclear are excluded from the analysis. We examined the peak brightness temperature and the spatial size obtained by NoRH. Although there is a large overlap between the two populations in these properties, we found that microwave sources with the largest spatial extent and highest brightness temperature are associated with eruptive flares. Spectral analysis using NoRP data showed a tendency that more confined flares had higher turnover frequency ( $\geq 17$  GHz). We also compare the NoRH images with the photospheric magnetograms to understand the difference in the magnetic structure of the two types of flare sources.

### **Homologous flare–CME events and their metric type II radio burst association**

S. **Yashiro**, b, , , N. Gopalswamy, P. Mäkelä, b, S. Akiyama, b, W. Uddinc, A.K. Srivastava, N.C. Joshij, R. Chandrar, P.K. Manoharan, K. Mahalakshmi, V.C. Dwivedi, R. Jain, A.K. Awasthi, g, N.V. Nittah, M.J. Aschwanden, D.P. Choudhary

Advances in Space Research, Volume 54, Issue 9, 1 November **2014**, Pages 1941–1948

<http://www.sciencedirect.com/science/article/pii/S0273117714004268>

Active region NOAA 11158 produced many flares during its disk passage. At least two of these flares can be considered as homologous: the C6.6 flare at 06:51 UT and C9.4 flare at 12:41 UT on **February 14, 2011**. Both flares occurred at the same location (eastern edge of the active region) and have a similar decay of the GOES soft X-ray light curve. The associated coronal mass ejections (CMEs) were slow (334 and 337 km/s) and of similar apparent widths (43° and 44°), but they had different radio signatures. The second event was associated with a metric type II burst while the first one was not. The COR1 coronagraphs on board the STEREO spacecraft clearly show that the second CME propagated into the preceding CME that occurred 50 min before. These observations suggest that CME–CME interaction might be a key process in exciting the type II radio emission by slow CMEs.

### **Post-Eruption Arcades and Interplanetary Coronal Mass Ejections**

S. **Yashiro** · N. Gopalswamy · P. Makela · S. Akiyama

Solar Phys., Volume 284, Issue 1, pp 5-15, **2013**, File

<https://link.springer.com/content/pdf/10.1007/s11207-013-0248-1.pdf>

<https://doi.org/10.1007/s11207-013-0248-1>

We compare the temporal and spatial properties of posteruption arcades (PEAs) associated with coronal mass ejections (CMEs) at the Sun that end up as magnetic cloud (MC) and non-MC events in the solar wind. We investigate the length, width, area, tilt angle, and formation time of the PEAs associated with 22 MC and 29 non-MC events and we find no difference between the two populations. According to current ideas on the relation between flares and CMEs, the PEA is formed together with the CME flux-rope structure by magnetic reconnection. Our results indicate that at the Sun flux ropes form during CMEs in association with both MC and non-MC events; however, for non-MC events the fluxrope structure is not observed in the interplanetary space because of the geometry of the observation, *i.e.* the location of the spacecraft when the structure passes through it.

**Table: 59 events. 2000-07-14, 2000-07-25, 2000-10-02, 2000-11-24, 2004-01-20, 2005-05-17**

### **Statistical Relationship between Solar Flares and Coronal Mass Ejections**

Seiji [Yashiro](#)<sup>1,2,3</sup> and Nat Gopalswamy<sup>2</sup>

*Universal Heliophysical Processes Proceedings IAU Symposium No. 257, 2008 N. Gopalswamy & D. Webb, eds., pp 233 – 243, 2009, File*

We report on the statistical relationships between solar flares and coronal mass ejections (CMEs) observed during 1996-2007 inclusively. We used soft X-ray flares observed by the Geostationary Operational Environmental Satellite (GOES) and CMEs observed by the Large Angle and Spectrometric Coronagraph (LASCO) on board the Solar and Heliospheric Observatory (SOHO) mission. Main results are (1) the CME association rate increases with flare's peak flux, fluence, and duration, (2) the difference between flare and CME onsets shows a Gaussian distribution with the standard deviation  $\frac{3}{4} = 17$  min ( $\frac{3}{4} = 15$  min) for the first (second) order extrapolated CME onset, (3) the most frequent flare site is under the center of the CME span, not near one leg (outer edge) of the CMEs, (4) a good correlation was found between the flare fluence versus the CME kinetic energy. Implications for flare-CME models are discussed.

### **A comparison of coronal mass ejections identified by manual and automatic methods**

S. [Yashiro](#), G. Michalek, and N. Gopalswamy

*Annales Geophysicae, 2008*

A preprint of this paper can be downloaded as a [pdf file](#).

Coronal mass ejections (CMEs) are related to many phenomena (e.g. flares, solar energetic particles, geomagnetic storms), thus compiling of event catalogs is important for a global understanding these phenomena. CMEs have been identified manually for a long time, but in the SOHO era, automatic identification methods are being developed. In order to clarify the advantage and disadvantage of the manual and automatic CME catalogs, we examined the distributions of CME properties listed in the CDAW (manual) and CACTus (automatic) catalogs. Both catalogs have a good agreement on the wide CMEs (width > 120 deg) in their properties, while there is a significant discrepancy on the narrow CMEs (width < 30 deg): CACTus has a larger number of narrow CMEs than CDAW. We carried out an event-by-event examination of a sample of events and found that the CDAW catalog have missed many narrow CMEs during the solar maximum. Another significant discrepancy was found on the fast CMEs (speed > 1000 km/s): the majority of the fast CDAW CMEs are wide and originate from low latitudes, while the fast CACTus CMEs are narrow and originate from all latitudes. Event-by-event examination of a sample of events suggests that CACTus has a problem on the detection of the fast CMEs.

### **SPATIAL RELATIONSHIP BETWEEN SOLAR FLARES AND CORONAL MASS EJECTIONS**

S. [Yashiro](#),<sup>1,2</sup> G. Michalek,<sup>1,2,3</sup> S. Akiyama,<sup>1,2</sup> N. Gopalswamy,<sup>2</sup> and R. A. Howard<sup>4</sup>

*The Astrophysical Journal, Vol. 673, No. 2: 1174-1180. 2008, File*

We report on the spatial relationship between solar flares and coronal mass ejections (CMEs) observed during 1996-2005 inclusive. We identified 496 flare-CME pairs considering limb flares (distance from central meridian  $\sim 45^\circ$ ) with soft X-ray flare size  $\geq$  C3 level. The CMEs were detected by the Large Angle and Spectrometric Coronagraph (LASCO) on board the Solar and Heliospheric Observatory (SOHO). We investigated the flare positions with respect to the CME span for the events with X-class, M-class, and C-class flares separately. It is found that the most frequent flare site is at the center of the CME span for all the three classes, but that frequency is different for the different classes. Many X-class flares often lie at the center of the associated CME, while C-class flares widely spread to the outside of the CME span. The former is different from previous studies, which concluded that no preferred flare site exists. We compared our result with the previous studies and conclude that the long-term LASCO observation enabled us to obtain the detailed spatial relation between flares and CMEs. Our finding calls for a closer flare-CME relationship and supports eruption models typified by the CSHKP magnetic reconnection model.

### **Different Power-Law Indices in the Frequency Distributions of Flares with and without Coronal Mass Ejections**

S. [Yashiro](#), S. Akiyama, N. Gopalswamy, and R. A. Howard

*The Astrophysical Journal, 650:L143-L146, 2006*

<https://iopscience.iop.org/article/10.1086/508876/pdf>

<http://www.journals.uchicago.edu/cgi-bin/resolve?ApJL21070>

We investigated the frequency distributions of flares with and without coronal mass ejections (CMEs) as a function of flare parameters (peak flux, fluence, and duration of soft X-ray flares). We used CMEs observed by the Large Angle and Spectrometric Coronagraph (LASCO) on board the *Solar and Heliospheric Observatory (SOHO)* mission and soft X-ray flares (C3.2 and above) observed by the *Geostationary Operational Environmental*

*Satellite (GOES)* during 1996–2005. We found that the distributions obey a power law of the form  $dN/dX \propto X^{-\alpha}$ , where  $X$  is a flare parameter and  $dN$  is the number of events recorded within the interval  $[X, X + dX]$ . For the peak flux,  $\alpha$  for the fluence, and  $\alpha$  for the duration. The power-law indices for flares without CMEs are steeper than those for flares with CMEs. The larger power-law index for flares without CMEs supports the possibility that nanoflares contribute to coronal heating.

### **A Catalog of White Light Coronal Mass Ejections Observed by the SOHO Spacecraft**

S. Yashiro, N. Gopalswamy, G. Michalek, O. C. St. Cyr, S. P. Plunkett, N. B. Rich, and R. A. Howard  
[Journal of Geophysical Research](#), 109, A07105, doi:10.1029/2003JA010282, (2004)

The Solar and Heliospheric Observatory (SOHO) mission's white light coronagraphs have observed nearly 7000 coronal mass ejections (CMEs) between 1996 and 2002. We have documented the measured properties of all these CMEs in an online catalog. We describe this catalog and present a summary of the statistical properties of the CMEs. The primary measurements made on each CME are the apparent central position angle, the angular width in the sky plane, and the height (heliocentric distance) as a function of time. The height-time measurements are then fitted to first and second order polynomials to derive the average apparent speed and acceleration of the CMEs. The statistical properties of CMEs are: (1) the average width of normal CMEs ( $20 < \text{width} < 120$ ) increased from 47 deg (1996; solar minimum) to 61 deg (1999; early phase of solar maximum) and then decreased to 53 deg (2002; late phase of solar maximum), (2) CMEs were detected around the equatorial region during solar minimum, while during solar maximum CMEs appear at all latitudes, (3) the average apparent speed of CMEs increases from 300 km/s (solar minimum) to 500 km/s (solar maximum), (4) the average apparent speed of halo CMEs (957 km/s) is twice of that of normal CMEs (428 km/s), and (5) most of the slow CMEs ( $V < 250$  km/s) show acceleration while most of the fast CMEs ( $V > 900$  km/s) show deceleration. Solar cycle variation and statistical properties of CMEs are revealed with greater clarity in this study as compared to previous studies. Implications of our findings for CME models are discussed.

### **Three-dimensional simulation of thermodynamics on confined turbulence in a large-scale CME-flare current sheet**

Jing Ye, John C. Raymond, Zhixing Mei, Qiangwei Cai, Yuhao Chen, Yan Li, Jun Lin

ApJ 955 88 2023

<https://arxiv.org/pdf/2308.09496.pdf>

<https://iopscience.iop.org/article/10.3847/1538-4357/acf129/pdf>

Turbulence plays a key role for forming the complex geometry of the large-scale current sheet (CS) and fast energy release in a solar eruption. In this paper, we present full 3D high-resolution simulations for the process of a moderate Coronal Mass Ejection (CME) and the thermodynamical evolution of the highly confined CS. Copious elongated blobs are generated due to tearing and plasmoid instabilities giving rise to a higher reconnection rate and undergo the splitting, merging and kinking processes in a more complex way in 3D. A detailed thermodynamical analysis shows that the CS is mainly heated by adiabatic and numerical viscous terms, and thermal conduction is the dominant factor that balances the energy inside the CS. Accordingly, the temperature of the CS reaches to a maximum of about 20 MK and the range of temperatures is relatively narrow. From the face-on view in the synthetic Atmospheric Imaging Assembly 131 Å, the downflowing structures with similar morphology to supra-arcade downflows are mainly located between the post-flare loops and loop-top, while moving blobs can extend spikes higher above the loop-top. The downward-moving plasmoids can keep the twisted magnetic field configuration until the annihilation at the flare loop-top, indicating that plasmoid reconnection dominates in the lower CS. Meanwhile, the upward-moving ones turn into turbulent structures before arriving at the bottom of the CME, implying that turbulent reconnection dominates in the upper CS. The spatial distributions of the turbulent energy and anisotropy are addressed, which show a significant variation in the spectra with height.

### **Coronal Wave Trains and Plasma Heating Triggered by Turbulence in the Wake of a CME**

Jing Ye<sup>1,2</sup>, Qiangwei Cai<sup>3</sup>, Chengcai Shen<sup>4</sup>, John C. Raymond<sup>4</sup>, Zhixing Mei<sup>1,2</sup>, Yan Li<sup>1,2</sup>, and Jun Lin<sup>1,2,5</sup>

2021 ApJ 909 45

<https://doi.org/10.3847/1538-4357/abdeb5>

Magnetohydrodynamic (MHD) turbulence plays an important role for the fast energy release and wave structures related to coronal mass ejections (CMEs). The CME plasma has been observed to be strongly heated during solar eruptions, but the heating mechanism is not understood. In this paper, we focus on the hot, dense region at the bottom of the CME and the generation of coronal wave trains therein using a high-resolution 2.5D MHD simulation. Our results show that the interaction between the tearing current sheet and the turbulence, including the termination shocks (TSs) at the bottom of the CME, can make a significant contribution to heating the CME, and the heating rate in this region is found to be greater than the kinetic energy transfer rate. Also, the turbulence can be somewhat amplified by the TSs. The compression ratio of the TS under the CME can exceed 4 due to thermal conduction, but such a strong TS is hardly detectable in all Solar Dynamics Observatory/Atmospheric Imaging Assembly bands. And turbulence is an indispensable source for the periodic generation of coronal wave trains around the CME.

## The Role of Turbulence for Heating Plasmas in Eruptive Solar Flares

Jing Ye<sup>1,2</sup>, Qiangwei Cai<sup>1,2,3</sup>, Chengcai Shen<sup>4</sup>, John C. Raymond<sup>4</sup>, Jun Lin<sup>1,2,3</sup>, Ilia. I. Roussev<sup>1,5</sup>, and Zhixing Mei<sup>1,2</sup>

2020 ApJ 897 64

<https://doi.org/10.3847/1538-4357/ab93b5>

Magnetohydrodynamic turbulence is ubiquitous in the process of solar eruptions, and it is crucial for the fast release of energy and the formation of complex thermal structures that have been found in observations. In this paper, we focus on the turbulence in two specific regions: inside the current sheet (CS) and above the flare loops, considering the standard flare model. The gravitationally stratified solar atmosphere is used in MHD simulations, which include the Lundquist number of  $S = 106$ , thermal conduction, and radiative cooling. The numerical results are generally consistent with previous simulation work, especially the thermal structures and reconnection rate in flare phases. We can observe the formation of multiple termination shocks (TSs) as well as plasmoid collisions, which make the region above the loop-top more turbulent and heat plasmas to the higher temperature. The spectrum studies show that the property of the MHD turbulence inside the CS is anisotropic, while it is quasi-isotropic above the loop-top. The magnetic spectrum becomes softer when the plasmoids interact with the multiple TSs. Meanwhile, synthetic images and light curves of the Solar Dynamics Observatory/Atmospheric Imaging Assembly 94, 131, 171, 304, and 193 Å channels show intermittent radiation enhancement by turbulence above the loop-top. The spectrum study of the radiation intensity in these five wavelengths gives quite different power indices at the same time. In particular, quasiperiodic pulsations (QPPs) in the turbulent region above the loop-top are investigated, and we also confirm that the heating for plasmas via turbulence is an important contributor to the source of QPPs.

## How Good Is the Bipolar Approximation of Active Regions for Surface Flux Transport?

Anthony R. Yeates

*Solar Physics* volume 295, Article number: 119 (2020)

<https://link.springer.com/content/pdf/10.1007/s11207-020-01688-y.pdf>

We investigate how representing active regions with bipolar magnetic regions (BMRs) affects the end-of-cycle polar field predicted by the surface flux transport model. Our study is based on a new database of BMRs derived from the SDO/HMI active region patch data between 2010 and 2020. An automated code is developed for fitting each active region patch with a BMR, matching both the magnetic flux and axial dipole moment of the region and removing repeat observations of the same region. By comparing the predicted evolution of each of the 1090 BMRs with the predicted evolution of their original active region patches, we show that the bipolar approximation leads to a 24% overestimate of the net axial dipole moment, given the same flow parameters. This is caused by neglecting the more complex multipolar and/or asymmetric magnetic structures of many of the real active regions, and may explain why previous flux transport models had to reduce BMR tilt angles to obtain realistic polar fields. Our BMR database and the Python code to extract it are freely available. **30 September 2017**

## Source of a Prominent Poleward Surge During Solar Cycle 24

A. R. Yeates, D. Baker, L. van Driel-Gesztelyi

*Solar Phys.* 2015

<http://arxiv.org/pdf/1502.04854v1.pdf>

As an observational case study, we consider the origin of a prominent poleward surge of leading polarity, visible in the magnetic butterfly diagram during *Solar Cycle* 24. A new technique is developed for assimilating individual regions of strong magnetic flux into a surface-flux transport model. By isolating the contribution of each of these regions, the model shows the surge to originate primarily in a single high-latitude activity group consisting of a bipolar active region present in Carrington Rotations 2104–05 (November 2010–January 2011) and a multipolar active region in Rotations 2107–08 (February–April 2011). This group had a strong axial dipole moment opposed to Joy's law. On the other hand, the modelling suggests that the transient influence of this group on the butterfly diagram will not be matched by a large long-term contribution to the polar field because it is located at high latitude. This is in accordance with previous flux-transport models.

## COMPARISON OF A GLOBAL MAGNETIC EVOLUTION MODEL WITH OBSERVATIONS OF CORONAL MASS EJECTIONS

A. R. Yeates<sup>1,5</sup>, G. D. R. Attrill<sup>1</sup>, Dibyendu Nandy<sup>2</sup>, D. H. Mackay<sup>3</sup>, P. C. H. Martens<sup>4</sup> and A. A. van Ballegoijen<sup>4</sup>

ApJ 709 1238-1248, 2010, FILE

The relative importance of different initiation mechanisms for coronal mass ejections (CMEs) on the Sun is uncertain. One possible mechanism is the loss of equilibrium of coronal magnetic flux ropes formed gradually by large-scale surface motions. In this paper, the locations of flux rope ejections in a recently developed quasi-static global evolution model are compared with observed CME source locations over a 4.5 month period in 1999. Using extreme ultraviolet data, the low-coronal source locations are determined unambiguously for 98 out of 330 CMEs. An alternative method of determining the source locations using recorded H $\alpha$  events was found to be too inaccurate. Despite the incomplete observations, positive correlation (with coefficient up to 0.49) is found between the distributions of observed and

simulated ejections, but only when binned into periods of 1 month or longer. This binning timescale corresponds to the time interval at which magnetogram data are assimilated into the coronal simulations, and the correlation arises primarily from the large-scale surface magnetic field distribution; only a weak dependence is found on the magnetic helicity imparted to the emerging active regions. The simulations are limited in two main ways: they produce fewer ejections, and they do not reproduce the strong clustering of observed CME sources into active regions. Due to this clustering, the horizontal gradient of radial photospheric magnetic field is better correlated with the observed CME source distribution (coefficient 0.67). Our results suggest that while the gradual formation of magnetic flux ropes over weeks can account for many observed CMEs, especially at higher latitudes, there exists a second class of CMEs (at least half) for which dynamic active region flux emergence on shorter timescales must be the dominant factor. Improving our understanding of CME initiation in future will require both more comprehensive observations of CME source regions and more detailed magnetic field simulations.

## **Solar Cycle Variation of Magnetic Flux Ropes in a Quasi-Static Coronal Evolution Model**

A.R. [Yeates](#) · J.A. Constable · P.C.H. Martens

Solar Phys (2010) 263: 121–134; [File](#)

The structure of electric current and magnetic helicity in the solar corona is closely linked to solar activity over the 11-year cycle, yet is poorly understood. As an alternative to traditional current-free “potential-field” extrapolations, we investigate a model for the global coronal magnetic field which is non-potential and time-dependent, following the build-up and transport of magnetic helicity due to flux emergence and large-scale photospheric motions. This helicity concentrates into twisted magnetic flux ropes, which may lose equilibrium and be ejected. Here, we consider how the magnetic structure predicted by this model – in particular the flux ropes – varies over the solar activity cycle, based on photospheric input data from six periods of cycle 23. The number of flux ropes doubles from minimum to maximum, following the total length of photospheric polarity inversion lines. However, the number of flux rope ejections increases by a factor of eight, following the emergence rate of active regions. This is broadly consistent with the observed cycle modulation of coronal mass ejections, although the actual rate of ejections in the simulation is about a fifth of the rate of observed events. The model predicts that, even at minimum, differential rotation will produce sheared, non-potential, magnetic structure at all latitudes.

## **INITIATION OF CORONAL MASS EJECTIONS IN A GLOBAL EVOLUTION MODEL**

A. R. [Yeates](#)<sup>1</sup>, D. H. Mackay

E-print, April 2009, [File](#); ApJ, 699:1024–1037, 2009 July

Loss of equilibrium of magnetic flux ropes is a leading candidate for the origin of solar coronal mass ejections (CMEs). The aim of this paper is to explore to what extent this mechanism can account for the initiation of CMEs in the global context. A simplified MHD model for the global coronal magnetic field evolution in response to flux emergence and shearing by large-scale surface motions is described and motivated. Using automated algorithms for detecting flux ropes and ejections in the global magnetic model, the effects of key simulation parameters on the formation of flux ropes and the number of ejections are considered, over a 177-day period in 1999. These key parameters include the magnitude and sign of magnetic helicity emerging in active regions, and coronal diffusion. The number of flux ropes found in the simulation at any one time fluctuates between about 28 and 48, sustained by the emergence of new bipolar regions, but with no systematic dependence on the helicity of these regions. However, the emerging helicity does affect the rate of flux rope ejections, which doubles from 0.67 per day if the bipoles emerge untwisted to 1.28 per day in the run with greatest emerging twist. The number of ejections in the simulation is also increased by 20%-30% by choosing the majority sign of emerging bipole helicity in each hemisphere, or by halving the turbulent diffusivity in the corona. For reasonable parameter choices, the model produces approximately 50% of the observed CME rate. This indicates that the formation and loss of equilibrium of flux ropes may be a key element in explaining a significant fraction of observed CMEs.

## **KINETIC PROPERTIES OF CMEs CORRECTED FOR THE PROJECTION EFFECT**

CHIN-TEH [YEH](#), M. D. DING, and P. F. CHEN

Solar Physics (2005) 229: 313–322, 2005, [File](#)

## **Parameter effects on the total intensity of H I Ly $\alpha$ line for a modelled coronal mass ejection and its driven shock**

[Beili Ying](#), [Guanglu Shi](#), [Li Feng](#), [Lei Lu](#), [Jianchao Xue](#), [Shuting Li](#), [Weiqun Gan](#), [Hui Li](#)

Solar Phys. 299, 92 2024

<https://arxiv.org/pdf/2406.11297>

<https://doi.org/10.1007/s11207-024-02330-x>

The combination of the H I Ly $\alpha$  (121.6 nm) line formation mechanism with ultraviolet (UV) Ly $\alpha$  and white-light (WL) observations provides an effective method for determining the electron temperature of coronal mass ejections (CMEs). A key to ensuring the accuracy of this diagnostic technique is the precise calculation of theoretical Ly $\alpha$  intensities. This study performs a modelled CME and its driven shock via the 3D MHD simulation. We generate synthetic UV and WL images of the CME and shock to quantify the impact of different assumptions on theoretical Ly $\alpha$  intensities, such as the incident intensity of the Ly $\alpha$  line ( $I_{\text{disk}}$ ), the geometric scattering function ( $p(\theta)$ ), and the kinetic temperature ( $T_n$ ) assumed to be equal to the proton ( $T_p$ ) or electron ( $T_e$ ) temperatures. By comparing differences of the Ly $\alpha$  intensities under these assumptions, we find that: (1) Using the uniform or Carrington maps of the disk Ly $\alpha$  emission underestimates the corona Ly $\alpha$  intensity ( $< 10\%$ ) compared to the synchronic map, except for a slight overestimate ( $< 4\%$ ) in the partial CME core. The Carrington map yields lower uncertainties than the uniform disk. (2) The geometric scattering process has a minor impact on the Ly $\alpha$  intensity, with a maximum relative uncertainty of  $< 5\%$ . The Ly $\alpha$  intensity is underestimated for the most part but overestimated in the CME core. (3) Compared to the assumption  $T_n = T_p$ , using  $T_n = T_e$  leads to more complex relative uncertainties in CME Ly $\alpha$  intensity. The CME core and void are both overestimated, with the maximum uncertainty in the core exceeding 50% and the void remaining below 35%. In the CME front, both over- and under-estimates exist with relative uncertainties of  $< 35\%$ . The electron temperature assumption has a smaller impact on the shock, with an underestimated relative uncertainty of less than 20%.

### Is There a Dynamic Difference between Stealthy and Standard Coronal Mass Ejections?

Beili Ying<sup>1</sup>, Alessandro Bemporad<sup>2,1</sup>, Li Feng<sup>1,3</sup>, Nariaki V. Nitta<sup>4</sup>, and Weiqun Gan<sup>1,3</sup>

2023 ApJ 942 3, id.3,

<https://iopscience.iop.org/article/10.3847/1538-4357/aca52c/pdf>

<https://arxiv.org/pdf/2211.12825.pdf>

[https://ui.adsabs.harvard.edu/link\\_gateway/2023ApJ...942....3Y/PUB\\_PDF](https://ui.adsabs.harvard.edu/link_gateway/2023ApJ...942....3Y/PUB_PDF)

Stealthy coronal mass ejections (CMEs), lacking low coronal signatures, may result in significant geomagnetic storms. However, the mechanism of stealthy CMEs is still highly debated. In this work, we investigate whether there are differences between stealthy and standard CMEs in terms of their dynamic behaviors. Seven stealthy and eight standard CMEs with low speeds are selected. We calculate two-dimensional speed distributions of CMEs based on the cross-correlation method, rather than the unidimensional speed, and further obtain more accurate distributions and evolution of CME mechanical energies. Then we derive the CME driving powers and correlate them with CME parameters (total mass, average speed, and acceleration) for standard and stealthy CMEs. Besides, we study the forces that drive CMEs, namely, the Lorentz force, gravitational force, and drag force due to the ambient solar wind near the Sun. The results reveal that both standard and stealthy CMEs are propelled by the combined action of those forces in the inner corona. The drag force and gravitational force are comparable with the Lorentz force. However, the impact of the drag and Lorentz forces on the global evolution of stealthy CMEs is significantly weaker than that on standard CMEs. **2009 Jun 13, 2009 Jun 16, 2010 Dec 22, 2011 Jan 19, 2011 Mar 2, 2011 Mar 24, 2011 Aug 4, 2011 Sep 13, 2011 Sep 29, 2011 Oct 28, 2012 Jan 3, 2012 Mar 21, 2012 Oct 4, 2013 Jun 29**

Table 1 List of CME Events

### Three-dimensional analyses of an aspherical coronal mass ejection and its driven shock

Beili Ying, Li Feng, Bernd Inhester, Marilena Mierla, Weiqun Gan, Lei Lu, Shuting Li

A&A 660, A23 2022

<https://arxiv.org/pdf/2201.08019.pdf>

<https://doi.org/10.1051/0004-6361/202142797>

<https://www.aanda.org/articles/aa/pdf/2022/04/aa42797-21.pdf>

Context. Observations reveal that shocks can be driven by fast coronal mass ejections (CMEs) and play essential roles in particle accelerations. A critical ratio,  $\delta$ , derived from a shock standoff distance normalized by the radius of curvature (ROC) of a CME, allows us to estimate shock and ambient coronal parameters. However, true ROCs of CMEs are difficult to measure due to observed projection effects.

Aims. We investigate the formation mechanism of a shock driven by an aspherical CME without evident lateral expansion. Through three-dimensional (3D) reconstructions without a priori assumptions of the object morphology, we estimate two principal ROCs of the CME surface and demonstrate how the difference between two principal ROCs of the CME affects the estimate of the coronal physical parameters.

Methods. The CME was observed by the Sun Earth Connection Coronal and Heliospheric Investigation (SECCHI) instruments and the Large Angle and Spectrometric Coronagraph (LASCO). We used the mask-fitting method to obtain the irregular 3D shape of the CME and reconstructed the shock surface using the bow-shock model. Through smoothings with fifth-order polynomial functions and Monte Carlo simulations, we calculated the ROCs at the CME nose.

Results. We find that (1) the maximal ROC is 2-4 times the minimal ROC of the CME. A significant difference between the CME ROCs implies that the assumption of one ROC of an aspherical CME could cause over-/under-estimations of the shock and coronal parameters. (2) The shock nose obeys the bow-shock formation mechanism, considering the constant standoff distance and the similar speed between the shock and CME around the nose. (3) With a more precise  $\delta$  calculated via 3D ROCs in space, we derive corona parameters at high latitudes of about  $-50^\circ$ , including the Alfvén speed and the coronal magnetic field strength. **31 Aug 2010**

## **Extensive Study of a Coronal Mass Ejection with UV and WL coronagraphs: the need for multi-wavelength observations**

Beili [Ying](#), [Alessandro Bemporad](#), [Li Feng](#), [Lei Lu](#), [Weiqun Gan](#), [Hui Li](#)

ApJ 899 12 2020

<https://arxiv.org/pdf/2007.04575.pdf>

<https://doi.org/10.3847/1538-4357/aba431>

Coronal Mass Ejections (CMEs) often show different features in different band-passes. By combining data in white-light (WL) and ultraviolet (UV) bands, we have applied different techniques to derive plasma temperatures, electron density, internal radial speed, etc, within a fast CME. They serve as extensive tests of the diagnostic capabilities, developed for the observations provided by future multi-channel coronagraphs (such as Solar Orbiter/Metis, ASO-S/LST, PROBA-3/ASPIICS). The involved data include WL images acquired by SOHO/LASCO coronagraphs, and intensities measured by SOHO/UVCS at 2.45  $R_{\odot}$  in the UV (H I Ly $\alpha$  and O VI 1032 {AA} lines) and WL channels. Data from the UVCS WL channel have been employed for the first time to measure the CME position angle with polarization-ratio technique. Plasma electron and effective temperatures of the CME core and void are estimated by combining UV and WL data. Due to the CME expansion and the possible existence of prominence segments, the transit of the CME core results in decreases of the electron temperature down to 105 K. The front is observed as a significant dimming in the Ly $\alpha$  intensity, associated with a line broadening due to plasma heating and flows along the line-of-sight. The 2D distribution of plasma speeds within the CME body is reconstructed from LASCO images and employed to constrain the Doppler dimming of Ly $\alpha$  line, and simulate future CME observations by Metis and LST. **2002.04.30-05.01**

## **First Determination of 2D Speed Distribution within the Bodies of Coronal Mass Ejections**

Beili [Ying](#), [Alessandro Bemporad](#), [Silvio Giordano](#), [Paolo Pagano](#), [Li Feng](#), [Lei Lu](#), [Hui Li](#), [Weiqun Gan](#)

2019 ApJ 880 41

<https://arxiv.org/pdf/1905.11772.pdf>

[sci-hub.se/10.3847/1538-4357/ab2713](https://sci-hub.se/10.3847/1538-4357/ab2713)

The determination of the speed of Coronal Mass Ejections (CMEs) is usually done by tracking brighter features (such as the CME front and core) in visible light coronagraphic images and by deriving unidimensional profiles of the CME speed as a function of altitude or time. Nevertheless, CMEs are usually characterized by the presence of significant density inhomogeneities propagating outward with different radial and latitudinal projected speeds, resulting in a complex evolution eventually forming the Interplanetary CME. In this work, we demonstrate for the first time how coronagraphic image sequences can be analyzed to derive 2D maps of the almost instantaneous plasma speed distribution within the body of CMEs. The technique is first tested with the analysis of synthetic data, and then applied to real observations. Results from this work allow to characterize the distribution and time evolution of kinetic energy inside CMEs, as well as the mechanical energy (combined with the kinetic and potential energy) partition between the core and front of the CME. In the future, CMEs will be observed by two channels (VL and UV Ly- $\alpha$ ) coronagraphs, such as Metis on-board ESA Solar Orbiter mission as well as Ly- $\alpha$  Solar Telescope (LST) on-board Chinese Advanced Space-based Solar Observatory (ASO-S) mission. Our results will help the analysis of these future observations, helping in particular to take into account the 2D distribution of Ly- $\alpha$  Doppler dimming effect. **2010 October 28**

## **Properties of a Small-scale Short-duration Solar Eruption with a Driven Shock**

Beili [Ying](#), [Li Feng](#), [Lei Lu](#), [Jie Zhang](#), [Jasmina Magdalenic](#), [Yingna Su](#), [Yang Su](#), [Weiqun Gan](#)

2018 ApJ 856 24

<https://arxiv.org/pdf/1803.00333.pdf>

<http://sci-hub.tw/http://iopscience.iop.org/0004-637X/856/1/24/>

Large-scale solar eruptions have been extensively explored over many years. However, the properties of small-scale events with associated shocks have been rarely investigated. We present the analyses of a small-scale short-duration event originating from a small region. The impulsive phase of the M1.9-class flare lasted only for four minutes. The kinematic evolution of the CME hot channel reveals some exceptional characteristics including a very short duration of the main acceleration phase ( $< 2$  minutes), a rather high maximal acceleration rate ( $\sim 50$  km s $^{-2}$ ) and peak velocity ( $\sim 1800$  km s $^{-1}$ ). The fast and impulsive kinematics subsequently results in a piston-driven shock related to a metric type II radio burst with a high starting frequency of  $\sim 320$  MHz of the fundamental band. The type II source is formed at a low height of below 1.1  $R_{\odot}$  less than  $\sim 2$  minutes after the onset of the main acceleration phase. Through the band split of the type II burst, the shock compression ratio decreases from 2.2 to 1.3, and the magnetic field strength of the shock upstream region decreases from 13 to 0.5 Gauss at heights of 1.1 to 2.3  $R_{\odot}$ . We find that the CME ( $\sim 4 \times 10^{30}$  erg) and flare ( $\sim 1.6 \times 10^{30}$  erg) consume similar amount of magnetic energy. The same conclusion for large-scale eruptions implies that small- and large-scale events possibly share the similar relationship between CMEs and flares. The kinematic particularities of this event are possibly related to the small footprint-separation distance of the associated magnetic flux rope, as predicted by the Erupting Flux Rope model. **04–Nov–15**

## **ALMA Observations of the Solar Chromosphere on the Polar Limb**

Takaaki [Yokoyama](#), [Masumi Shimojo](#), [Takenori J. Okamoto](#), [Haruhisa Iijima](#)

ApJ 2018

<https://arxiv.org/pdf/1807.01411.pdf>

We report the results of the Atacama Large Millimeter/sub-millimeter Array (ALMA) observations of the solar chromosphere on the southern polar limb. Coordinated observations with the Interface Region Imaging Spectrograph (IRIS) are also conducted. ALMA provided unprecedented high spatial resolution in the millimeter band ( $\approx 2.0$  arcsec) at 100 GHz frequency with a moderate cadence (20 s). The results are as follows: (1) The ALMA 100 GHz images show saw-tooth patterns on the limb, and a comparison with SDO/AIA 171\AA images shows a good correspondence of the limbs with each other. (2) The ALMA 100 GHz movie shows a dynamic thorn-like structure elongating from the saw-tooth patterns on the limb, with lengths reaching at least 8 arcsec, thus suggesting jet-like activity in the ALMA microwave range. These **ALMA jets** are in good correspondence with IRIS jet clusters. (3) A blob ejection event is observed. By comparing with the IRIS Mg II slit-jaw images, the trajectory of the blob is located along the spicular patterns. **2017 April 29**

## A Spectroscopic Measurement of High Velocity Spray Plasma from an M-class Flare and Coronal Mass Ejection

Peter R. Young

Special issue "Progress in Solar Physics" of Adv. Sp. Research 2022

<https://arxiv.org/pdf/2204.09542.pdf>

Coronal mass ejection spray plasma associated with the M1.5-class flare of **16 February 2011** is found to exhibit a Doppler blue-shift of 850 km/s - the largest value yet reported from ultraviolet (UV) or extreme ultraviolet (EUV) spectroscopy of the solar disk and inner corona. The observation is unusual in that the emission line (Fe XII 193.51 Å) is not observed directly, but the Doppler shift is so large that the blue-shifted component appears in a wavelength window at 192.82 Å, intended to observe lines of O V, Fe XI and Ca XVII. The Fe XII 195.12 Å emission line is used as a proxy for the rest component of 193.51 Å. The observation highlights the risks of using narrow wavelength windows for spectrometer observations when observing highly-dynamic solar phenomena. The consequences of large Doppler shifts for ultraviolet solar spectrometers, including the upcoming Multi-slit Solar Explorer (MUSE) mission, are discussed.

## Dark jets in solar coronal holes

Peter R. Young

ApJ 2015

<http://arxiv.org/pdf/1501.02751v1.pdf>

A new solar feature termed a dark jet is identified from observations of an extended solar coronal hole that was continuously monitored for over 44 hours by the EUV Imaging Spectrometer on board the Hinode spacecraft in **2011 February 8-10**. Line-of-sight velocity maps derived from the coronal Fe XII  $\lambda$ 195.12 emission line, formed at 1.5 MK, revealed a number of large-scale, jet-like structures that showed significant blueshifts. The structures had either weak or no intensity signal in 193 Å filter images from the Atmospheric Imaging Assembly on board the Solar Dynamics Observatory, suggesting that the jets are essentially invisible to imaging instruments. The dark jets are rooted in bright points and occur both within the coronal hole and at the quiet Sun-coronal hole boundary. They exhibit a wide range of shapes, from narrow columns to fan-shaped structures, and sometimes multiple jets are seen close together. A detailed study of one dark jet showed line-of-sight speeds increasing along the jet axis from 52 to 107 km s<sup>-1</sup> and a temperature of 1.2-1.3 MK. The low intensity of the jet was due either to a small filling factor of 2% or to a curtain-like morphology. From the HOP 177 sample, dark jets are as common as regular coronal hole jets, but their low intensity suggests a mass flux around two orders of magnitude lower.

## Solar Dynamics Observatory and Hinode Observations of a Blowout Jet in a Coronal Hole

P. R. Young, K. Muglach

Solar Phys., 2014

A blowout jet occurred within the south coronal hole on **9 February 2011** at 09:00 UT and was observed by the Atmospheric Imaging Assembly (AIA) and Helioseismic and Magnetic Imager (HMI) onboard the Solar Dynamics Observatory, and by the EUV Imaging Spectrometer (EIS) and X-Ray Telescope (XRT) onboard the Hinode spacecraft during coronal-hole monitoring performed as part of Hinode Operations Program No. 177. Images from AIA show expanding hot and cold loops from a small bright point with plasma ejected in a curtain up to 30 Mm wide. The initial intensity front of the jet had a projected velocity of 200 km s<sup>-1</sup>, and the line-of-sight (LOS) velocities measured by EIS are between 100 and 250 km s<sup>-1</sup>. The LOS velocities increased along the jet, implying that an acceleration mechanism operates within the body of the jet. The jet plasma had a density of  $2.7 \times 10^8$  cm<sup>-3</sup> and a temperature of 1.4 MK. During the event a number of bright kernels were seen at the base of the bright point. The kernels have sizes of  $\approx 1000$  km, are variable in brightness, and have lifetimes of 1 – 15 minutes. An XRT filter ratio yields temperatures of 1.5 – 3.0 MK for the kernels. The bright point existed for at least ten hours, but disappeared within two hours after the jet, which lasted for 30 minutes. HMI data reveal converging photospheric flows at the location of the bright point, and the mixed-polarity magnetic flux canceled over a period of four hours on either side of the jet.



## **A statistical study of post-flare-associated CME events**

M. **Youssef**, , R. Mawad, , Mosalam Shaltout

Advances in Space Research, Volume 51, Issue 7, 1 April **2013**, Pages 1221–1229

We present a statistical study of post-flare-associated CMEs (PFA-CMEs) during the period from 1996 to 2010. By investigating all CMEs and X-ray flares, respectively, in the LASCO and GOES archives, we found 15875 CMEs of which masses are well measured and 25112 X-ray flares of which positions are determined from their optical counterparts. Under certain temporal and spatial criteria of these CMEs and solar flare events, 291 PFA-CMEs events have been selected. Linking the flare fluxes with CME speeds of these paired events, we found that there is a reasonable positive linear relation between the CME linear speed and associated flare flux. The results show also the CME width increases as the flux of its associated solar flare increases. Besides we found that there is a fine positive linear relation between the CME mass and its width. Matching the flare fluxes with CME masses of these paired events, we find the CME mass increases as the flux of its associated solar flare increases. Finally we find the PFA-CME events are in regular more decelerated than the other CMEs.

## **A 17 June 2011 Polar Jet and its Presence in the Background Solar Wind**

H.-S. **Yu**, B.V. Jackson, Y.-H. Yang, N.-H. Chen, A. Buffington, P.P. Hick

JGR Volume 121, Issue 6, pp. 4985-4997 **2016**

High-speed jet responses in the polar solar wind are enigmatic. Here, we measure a jet response that emanates from the southern polar coronal hole on **17 June 2011** at the extreme speed of over 1200 km/s. This response was recorded from the Sun-Earth line in SDO/AIA and LASCO/C2 and both STEREO EUVI and COR2 coronagraphs when the three spacecraft were situated  $\sim 90^\circ$  from one another. These certify the coronal 3D location of the response that is associated with an existing solar plume structure, and show its high speed to distances of over 14 Rs. This jetting is associated with magnetic flux changes in the polar region as measured by the SDO/HMI instrumentation over a period of several hours. The fastest coronal response observed can be tracked to a time near the period of greatest flux changes, and to the onset of the brightest flaring in AIA. This high-speed response can be tracked directly as a small patch of outward-moving brightness in coronal images as in Yu et al. [2014] where three slower events were followed from the perspective of Earth. This accumulated jet response has the largest mass and energy we have yet seen in 3D reconstructions from Solar Mass Ejection Imager (SMEI) observations, and its outward motion is certified for the first time using interplanetary scintillation (IPS) observations. This jet response is surrounded by similar high-speed patches but these are smoothed out in Ulysses polar measurements, we speculate about how these dynamic activities relate to solar wind acceleration.

## **The Three-dimensional Analysis of Hinode Polar Jets using Images from LASCO C2, the Stereo COR2 Coronagraphs, and SMEI**

H.-S. **Yu**<sup>1</sup>, B. V. Jackson<sup>1</sup>, A. Buffington<sup>1</sup>, P. P. Hick<sup>1</sup>, M. Shimojo<sup>2</sup>, and N. Sako

**2014** ApJ 784 166

Images recorded by the X-ray Telescope on board the Hinode spacecraft are used to provide high-cadence observations of solar jetting activity. A selection of the brightest of these polar jets shows a positive correlation with high-speed responses traced into the interplanetary medium. LASCO C2 and STEREO COR2 coronagraph images measure the coronal response to some of the largest jets, and also the nearby background solar wind velocity, thereby giving a determination of their speeds that we compare with Hinode observations. When using the full Solar Mass Ejection Imager (SMEI) data set, we track these same high-speed solar jet responses into the inner heliosphere and from these analyses determine their mass, flow energies, and the extent to which they retain their identity at large solar distances.

## **The analysis of polar jet responses using images from the LASCO C2 and STEREO COR 2 coronagraphs**

H.-S. **Yu**, B. V. Jackson, J. M. Clover, and A. Buffington

AIP Conf. Proc. 1539, 90 (**2013**); doi: 10.1063/1.4810997

[http://smei.ucsd.edu/new\\_smei/PDFs/publications/pdf\\_public/2013\\_AIPC\\_1539\\_90\\_Yu.pdf](http://smei.ucsd.edu/new_smei/PDFs/publications/pdf_public/2013_AIPC_1539_90_Yu.pdf)

High cadence images taken by the X-Ray Telescope (XRT) onboard *Hinode* and the Solar Dynamics Observatory Atmospheric Imaging Assembly (AIA) instrument provide an opportunity to observe solar jetting activity. The brightest several of these polar jets show a positive correlation with high-speed responses traced into the interplanetary medium, and have been reported in the full SMEI (Solar Mass Ejection Imager) data set images at large solar distances in the heliosphere where they retain a semblance of their original identity. LASCO C2 and STEREO COR 2 coronagraph images allow measurements of the coronal response to some of these jets, and the nearby background solar wind velocity, giving a determination of their speeds and energies that we can compare with *Hinode* and AIA observations. In this preliminary study we document two of these solar jet traversals into the inner heliosphere in the region intermediate to this region and the XRT and AIA observations. 14 September 2007, 17 June 2011,

## **ON THE CAUSES OF PLASMOID ACCELERATION AND CHANGES IN MAGNETIC FLUX IN A RESISTIVE MAGNETOHYDRODYNAMIC PLASMA**

H. S. **Yu**<sup>1</sup>, L. H. Lyu<sup>1</sup>, and S. T. Wu<sup>2</sup>

Astrophysical Journal, 726:79 (12pp), **2011**

Observationally, the change of acceleration of coronal mass ejections is commonly attributed to the change of the

reconnection rate. In this study, we use a two-dimensional magnetohydrodynamic simulation with finite resistivity to study: (1) the forces that lead to the acceleration of the plasma and plasmoid and (2) the time evolution of the topological change of the magnetic flux across the current sheet. Our results show that the fast flows are not limited to the direction perpendicular to the local magnetic field. The fast parallel flows are accelerated by the parallel component of the pressure gradient force. The net force perpendicular to the magnetic field can accelerate the plasma and the plasmoid along the current sheet. The acceleration of the plasmoid is also controlled by the mass contained in the plasmoid. We find that the fast ejection of the plasmoid can stretch the current sheet and consequently reduce the magnetic reconnection/reconfiguration rate temporally before a new plasmoid is formed. We show that the topological change of the magnetic flux is due to the non-uniform magnetic annihilation rate along the current sheet. Therefore, the reconnection/reconfiguration site does not necessarily stay at the neutral point. It can move with the Y-line next to the bifurcated current sheets.

## **Magnetic field re-configuration associated with a slow rise eruptive X1.2 flare in NOAA active region 11944**

Vasyl **Yurchyshyn**, Xu Yang, Gelu Nita, Gregory Fleishman, Valentina Abramenko, Satoshi Inoue, Eun-Kyung Lim, and Wenda Cao

Front. Astron. Space Sci. 9:816523 2022

<https://www.frontiersin.org/articles/10.3389/fspas.2022.816523/full>

<https://doi.org/10.3389/fspas.2022.816523>

Using multi-wavelength observations, we analysed magnetic field variations associated with a gradual X1.2 flare that erupted on **January 7, 2014** in active region (AR) NOAA 11944 located near the disk center. A fast coronal mass ejection (CME) was observed following the flare, which was noticeably deflected in the south-west direction. A chromospheric filament was observed at the eruption site prior to and after the flare. We used SDO/HMI data to perform non-linear force-free field extrapolation of coronal magnetic fields above the AR and to study the evolution of AR magnetic fields prior to the eruption. The extrapolated data allowed us to detect signatures of several magnetic flux ropes present at the eruption site several hours before the event. The eruption site was located under slanted sunspot fields with a varying decay index of 1.0-1.5. That might have caused the erupting fields to slide along this slanted magnetic boundary rather than vertically erupt, thus explaining the slow rise of the flare as well as the observed direction of the resulting CME. We employed sign-singularity tools to quantify the evolutionary changes in the model twist and observed current helicity data, and found rapid and coordinated variations of current systems in both data sets prior to the event as well as their rapid exhaustion after the event onset.

## **Multiwavelength Observations of a Slow Raise, Multi-Step X1.6 Flare and the Associated Eruption**

**Yurchyshyn**, V., Kumar, P., Cho, K.S., Lim, E.K., & Abramenko, V.

ApJ 812 17 2015

<http://www.bbo.njit.edu/~vayur/x1.6flare.pdf>

Using multi-wavelength observations we studied a slow rise, multi-step X1.6 flare that began on **November 7, 2014** as a localized eruption of core fields inside a  $\delta$ -sunspot and later engulfed the entire active region. This flare event was associated with formation of two systems of post eruption arcades and several J-shaped flare ribbons showing extremely fine details, irreversible changes in the photospheric magnetic fields, and it was accompanied by a fast and wide coronal mass ejection. Data from the Solar Dynamics Observatory, IRIS spacecraft along with the ground based data from the New Solar Telescope (NST) present evidence that i) the flare and the eruption were directly triggered by a flux emergence that occurred inside a  $\delta$ -sunspot at the boundary between two umbrae; ii) this event represented an example of the formation of an unstable flux rope observed only in hot AIA channels (131 and 94 Å) and LASCO C2 coronagraph images; iii) the global post eruption arcade spanned the entire AR and was due to global scale reconnection occurring at heights of about one solar radii, indicating on the global spatial and temporal scale of the eruption.

## **ROTATION OF WHITE LIGHT CME STRUCTURES AS INFERRED FROM LASCO CORONAGRAPH**

Vasyl **Yurchyshyn**, Valentyna Abramenko, Durgesh Tripathi

BBSO Preprint #1404, 2009; ApJ, 705:426–435, 2009, File

Understanding the connection between the magnetic configurations of a coronal mass ejection (CME) and their counterpart in the interplanetary medium is very important in terms of space weather predictions. Our previous findings indicate that the orientation of a halo CME elongation may correspond to the orientation of the underlying flux rope. Here we further explore these preliminary results by comparing orientation angles of elongated LASCO CMEs, both full and partial halos, to the EIT post eruption arcades (PEAs). By analyzing a sample of 100 events, we found that overwhelming majority of CMEs are elongated in the direction of the axial field of PEAs. During their evolution, CMEs appear to rotate by about 10 degree for most of the events (70%) with about 30-50 degrees for some events and the corresponding time profiles display regular and gradual changes. It seems that there is a slight preference for the CMEs to rotate toward the solar equator and heliospheric current sheet (59% of cases). We suggest that the rotation of the

ejecta may be due to the presence of heliospheric magnetic field, and it could shed light on the problems related to connecting solar surface phenomena to their interplanetary counterparts.

## **RELATIONSHIP BETWEEN EARTH - DIRECTED SOLAR ERUPTIONS AND MAGNETIC CLOUDS AT 1AU: A BRIEF REVIEW**

V. **YURCHYSHYN**, DURGESH TRIPATHI

E-print, May **2009**, File; Advances in Geosciences

We review relationships between coronal mass ejections (CMEs), EIT post eruption arcades, and the coronal neutral line associated with global magnetic field and magnetic clouds near the Earth. Our previous findings indicate that the orientation of a halo CME elongation may correspond to the orientation of the underlying flux rope. Here we revisit these preliminary reports by comparing orientation angles of elongated LASCO CMEs, both full and partial halos, to the post eruption arcades. Based on 100 analysed events, it was found that the overwhelming majority of halo CMEs are elongated in the direction of the axial field of the post eruption arcades. Moreover, this conclusion also holds for partial halo CMEs as well as for events that originate further from the disk center. This suggests that the projection effect does not drastically change the appearance of full and partial halos and their images still bear reliable information about the underlying magnetic fields. We also compared orientations of the erupted fields near the Sun and in the interplanetary space and found that the local tilt of the coronal neutral line at 2.5 solar radii is well correlated with the magnetic cloud axis measured near the Earth. We suggest that the heliospheric magnetic fields significantly affect the propagating ejecta. Sometimes, the ejecta may even rotate so that its axis locally aligns itself with the heliospheric current sheet.

## **The May 13, 2005 Eruption: Observations, Data Analysis and Interpretation –**

V. **Yurchyshyn**, C. Liu, V. Abramenko, J. Krall

Solar Physics (2006) 239: 317–335

persisting converging and shearing motions near the main neutral line could lead to the formation of twisted core fields and eventually their eruption via reconnection

## **STATISTICAL DISTRIBUTIONS OF SPEEDS OF CORONAL MASS EJECTIONS**

V. **Yurchyshyn**,<sup>1</sup> S. Yashiro,<sup>2</sup> V. Abramenko,<sup>1,3</sup> H. Wang,<sup>4</sup> and N. Gopalswamy<sup>5</sup>

Astrophysical Journal, 619:599–603, **2005**, File

<http://www.journals.uchicago.edu/doi/pdf/10.1086/426129>

We studied the distribution of plane-of-sky speeds determined for 4315 coronal mass ejections (CMEs) detected by the Large Angle and Spectrometric Coronagraph Experiment on board the Solar and Heliospheric Observatory (SOHO LASCO). We found that the speed distributions for accelerating and decelerating events are nearly identical and to a good approximation they can be fitted with a single lognormal distribution. This finding implies that, statistically, there is no physical distinction between the accelerating and the decelerating events. The lognormal distribution of the CME speeds suggests that the same driving mechanism of a nonlinear nature is acting in both slow and fast dynamical types of CMEs.

## **The Influence of Eruptive Processes in Active Regions on Oscillations of the Magnetic Field Parameters in Sunspot Umbrae.**

**Zagainova**, Y.S., Fainshtein, V.G.

Geomagn. Aeron. 63, 899–909 (**2023**).

<https://doi.org/10.1134/S0016793223070290>

For three events, the effect of eruptive processes in active regions on the characteristic of magnetic field oscillations in sunspot umbrae has been studied. Eruptive processes include solar flares and coronal mass ejections. The power spectra of oscillations of each analyzed parameter of the magnetic field in each sunspot of the studied active region (AR) are constructed, and, in general, for the entire AR. It was found that at certain stages the eruptive process has a noticeable effect on the power spectrum of oscillations of the magnetic field parameters in sunspot umbrae. It is shown that the power of the eruptive process, which is characterized by the X-ray flare, affects the features of the magnetic field oscillations in sunspot umbrae. The results obtained for ARs with eruptive processes are compared with the results for ARs without eruptive processes. The analysis of the influence of eruptive processes on the magnetic field oscillations in sunspot umbrae was carried out for the AR as a whole, and for some sunspots with the strongest response. For different events, the oscillation power spectrum was compared with the intensity maximum  $A_{max}$ , frequency  $f_m$ , which accounts for the maximum  $A_{max}$ , and the frequency power spectrum width  $\Delta f$ .

## **Effects in extreme ultraviolet and in magnetic field observed during stealth CME formation, geomagnetic responses to its impact on the magnetosphere**

Iu.S. **Zagainova** <sup>1</sup>, V.G. Fainshtein <sup>2</sup>, L.I. Gromova <sup>1</sup>, S.V. Gromov

Sun and Geosphere, **2019**; 14/1: 25 -30

[http://newserver.stil.bas.bg/SUNGEO//00SGArhiv/SG\\_v14\\_No1\\_2019-pp-25-30.pdf](http://newserver.stil.bas.bg/SUNGEO//00SGArhiv/SG_v14_No1_2019-pp-25-30.pdf)

By example of the **16 June 2010** event, stealth coronal mass ejection (Stealth-CME) emergence is shown to be probably accompanying by various manifestations of small-scale activity in the solar atmosphere and some features of variations in the magnetic field parameters. We also discuss the response of the geomagnetic field to the effect of this CME on the Earth magnetosphere.

### **Stealth coronal mass ejections: identification of source regions and geophysical effects.**

**Zagainova** Iu.S., Fainshtein V.G., Gromova L.I., Gromov S.V.

Proceedings of Tenth Workshop “Solar Influences on the Magnetosphere, Ionosphere and Atmosphere” Primorsko, Bulgaria, June 4–8, **2018**, p.13-18.

Впервые фронтальная структура (ФС) стелс-КВМ была обнаружена для события, зарегистрированного **16 июня 2010**.

### **How do fast impulse CMEs related to powerful flares but unrelated to eruptive filaments appear and move?**

Iu.S. **Zagainova**, V.G. Fainshtein

Advances in Space Research, Volume 55, Issue 3, 1 February **2015**, Pages 822–834

<http://www.sciencedirect.com/science/article/pii/S0273117714003391>

GOES-12/SXI and SDO/AIA data were used to examine the formation and initial stage of movement for several fast pulse ‘halo’-type coronal mass ejections (HCMEs) that were related to GOES M and X class flares but unrelated to solar filament eruptions. According to their formation, the HCMEs under study can be subdivided into three groups: (i) Most of the HCMEs studied resulted from broken equilibrium – presumably, due to an emerging new magnetic flux – of solitary wide loop-like emission structures identified with the future ejection observable in the 195 Å channel a few hours before the mass ejection starts moving or before the relevant flare onset; (ii) a CME can form from several individual loop-like structures or, possibly, a loop arcade; (iii) for some HCMEs, their formation starts with a group of coronal loops moving upwards as first observed in the ‘hot’ 131 Å channel. A few minutes later, loops start to move observable in images taken with the ‘colder’ 211 Å channel, still later in the 193 Å channel, and finally, in 171 Å channel images. The moving loop-like structures affect the overlying coronal areas in such a way that a frontal HCME structure forms, its brightness increasing from the ‘hottest’ to the ‘coldest’ line. Moreover, loops are observed moving sunwards, towards the CME origin, resulting in an area of lower brightness forming behind the frontal structure. All the coronal mass ejections we studied started to move before the related solar flares appeared. The kinematics of the HCME’s under examination has been studied along, generally, curvilinear trajectories in the plane-of-sky. It has been concluded that two types of coronal mass ejections exist differing in their time speed profile determined by the area and magnetic configuration of the active area where the mass ejection originated. Homologous HCMEs – i.e. appearing in the same active area at different times – have the same speed profile. **17 January 2005, 23 August 2005, 29 October 2003, 7 March 2012, 9 March 2012**

### **Kink instability of triangular jets in the solar atmosphere\***

T. V. **Zaqarashvili**<sup>1,4,5</sup>, S. Lomineishvili<sup>2,5</sup>, P. Leitner<sup>1</sup>, A. Hanslmeier<sup>1</sup>, P. Gömöry<sup>2</sup> and M. Roth<sup>3</sup>  
A&A 649, A179 (**2021**)

<https://www.aanda.org/articles/aa/pdf/2021/05/aa39381-20.pdf>

<https://doi.org/10.1051/0004-6361/202039381>

Context. It is known that hydrodynamic triangular jets (i.e. the jet with maximal velocity at its axis, which linearly decreases at both sides) are unstable to anti-symmetric kink perturbations. The inclusion of the magnetic field may lead to the stabilisation of the jets. Jets and complex magnetic fields are ubiquitous in the solar atmosphere, which suggests the possibility of the kink instability in certain cases.

Aims. The aim of the paper is to study the kink instability of triangular jets sandwiched between magnetic tubes (or slabs) and its possible connection to observed properties of the jets in the solar atmosphere.

Methods. A dispersion equation governing the kink perturbations is obtained through matching of analytical solutions at the jet boundaries. The equation is solved analytically and numerically for different parameters of jets and surrounding plasma. The analytical solution is accompanied by a numerical simulation of fully non-linear magnetohydrodynamic (MHD) equations for a particular situation of solar type II spicules.

Results. Magnetohydrodynamic triangular jets are unstable to the dynamic kink instability depending on the Alfvén Mach number (the ratio of flow to Alfvén speeds) and the ratio of internal and external densities. When the jet has the same density as the surrounding plasma, only super-Alfvénic flows are unstable. However, denser jets are also unstable in a sub-Alfvénic regime. Jets with an angle to the ambient magnetic field have much lower thresholds of instability than field-aligned flows. Growth times of the kink instability are estimated to be 6–15 min for type I spicules and 5–60 s for type II spicules matching with their observed lifetimes. The numerical simulation of full non-linear equations shows that the transverse kink pulse locally destroys the jet in less than a minute in type II spicule conditions.

Conclusions. Dynamic kink instability may lead to the full breakdown of MHD flows and consequently to an observed disappearance of spicules.

### **Stability of rotating magnetized jets in the solar atmosphere. I. Kelvin-Helmholtz instability**

T. V. **Zaqarashvili**, I. Zhelyazkov, L. Ofman

ApJ 813 123 2015

<http://arxiv.org/pdf/1510.01108v1.pdf>

Observations show various jets in the solar atmosphere with significant rotational motions, which may undergo instabilities leading to heat ambient plasma. We study the Kelvin-Helmholtz (KH) instability of twisted and rotating jets caused by the velocity jumps near the jet surface. We derive a dispersion equation with appropriate boundary condition for total pressure (including centrifugal force of tube rotation), which governs the dynamics of incompressible jets. Then, we obtain analytical instability criteria of Kelvin-Helmholtz instability in various cases, which were verified by numerical solutions to the dispersion equation. We find that twisted and rotating jets are unstable to KH instability when the kinetic energy of rotation is more than the magnetic energy of the twist. Our analysis shows that the azimuthal magnetic field of 1-5 G can stabilize observed rotations in spicule/macrosopicules and X-ray/EUV jets. On the other hand, non-twisted jets are always unstable to KH instability. In this case, the instability growth time is several seconds for spicule/macrosopicules and few minutes (or less) for EUV/X-ray jets. We also find that standing kink and torsional Alfvén waves are always unstable near the antinodes due to the jump of azimuthal velocity at the surface, while the propagating waves are generally stable. KH vortices may lead to enhanced turbulence development and heating of surrounding plasma, therefore rotating jets may provide energy for chromospheric and coronal heating.

### Observations of a Footpoint Drift of an Erupting Flux Rope

Alena [Zemanova](#), [Jaroslav Dudik](#), [Guillaume Aulanier](#), [Julia K. Thalmann](#), [Peter Gomory](#)

ApJ 883 96 2019

<https://arxiv.org/pdf/1908.02082.pdf>

<https://doi.org/10.3847/1538-4357/ab3926>

We analyze the imaging observations of an M-class eruptive flare of **2015 November, 4**. The pre-eruptive H alpha filament was modelled by the non-linear force free field model, which showed that it consisted of two helical systems. Tether-cutting reconnection involving these two systems led to the formation of a hot sigmoidal loop structure rooted in a small hook that formed at the end of the flare ribbon. Subsequently, the hot loops started to slip away from the small hook until it disappeared. The loops continued slipping and the ribbon elongated itself by several tens of arc seconds. A new and larger hook then appeared at the end of elongated ribbon with hot and twisted loops rooted there. After the eruption of these hot loops, the ribbon hook expanded and later contracted. We interpret these observations in the framework of the recent three dimensional (3D) extensions to the standard solar flare model, which predict the drift of the flux rope footpoints. The hot sigmoidal loop is interpreted as the flux rope, whose footpoints drift during the eruption. While the deformation and drift of the new hook can be described by the model, the displacement of the flux rope footpoint from the filament to that of the erupting flux rope indicate that the hook evolution can be more complex than those captured by the model.

### Resolving the Fan-Spine Reconnection Geometry of a Small-Scale Chromospheric Jet Event with the New Solar Telescope

Zhicheng [Zeng](#), Bin Chen, [Haisheng Ji](#), [Philip R. Goode](#), [Wenda Cao](#)

ApJL, 819, L3 2016

<http://arxiv.org/pdf/1602.04237v1.pdf>

Jets present ubiquitously in both quiet and active regions on the Sun. They are widely believed to be driven by magnetic reconnection. A fan-spine structure has been frequently reported in some coronal jets and flares, regarded as a signature of ongoing magnetic reconnection in a topology consisting of a magnetic null connected by a fan-like separatrix surface and a spine. However, for small-scale chromospheric jets, clear evidence of such structures is rather rare, although they are implied in earlier works that show an inverted-Y-shaped feature. Here we report high-resolution (0".16) observations of a small-scale chromospheric jet obtained by the New Solar Telescope (NST) using 10830-Å filtergrams. Bi-directional flows were observed across the separatrix regions in the 10830-Å images, suggesting that the jet was produced due to magnetic reconnection. At the base of the jet, a fan-spine structure was clearly resolved by the NST, including the spine and the fan-like surface, as well as the loops before and after the reconnection. A major part of this fan-spine structure, with the exception of its bright footpoints and part of the base arc, was invisible in the extreme ultraviolet and soft X-ray images (observed by the Atmosphere Imaging Assembly and the X-Ray Telescope, respectively), indicating that the reconnection occurred in the upper chromosphere. Our observations suggest that the evolution of this chromospheric jet is consistent with a two-step reconnection scenario proposed by [Torok2009](#)

**2012 July 8**

### Charge States, Helium Abundance, and FIP Bias of the Interplanetary CMEs Classified by Flares and Hot Channels

Huitong [Zhai](#)<sup>1</sup>, Hui Fu<sup>1</sup>, Zhenghua Huang<sup>1</sup>, and Lidong Xia<sup>1</sup>

2022 ApJ 928 136

<https://iopscience.iop.org/article/10.3847/1538-4357/ac56e4/pdf>

Identifying the material source of coronal mass ejections (CMEs) is crucial for understanding the generation mechanisms of CMEs. The composition parameters of interplanetary coronal mass ejections (ICMEs) associated with different activities on the Sun may be diverse, as the materials come from distinct regions or are generated by different processes. We classified ICMEs into three types by associated activities on the Sun, with (T1) and without (T3) flares

and hot channels, and only associated with flares (T2). The composition parameters of each type of ICMEs were analyzed. We found that all CMEs with hot channels are accompanied by flares, and strong flares are all associated with hot channels in our database. The average length of the filaments in T1 cases are much shorter than those in T3 cases. The average charge states of iron (QFe) and helium abundance (AHe) for T3 ICMEs are less than 12% and 7%, respectively. The QFe and AHe for T1 ICMEs present clear bimodal distributions with the minimum between two peaks at 12% and 7%, respectively. Nearly two-thirds of the hot plasma (with higher QFe) inside ICMEs is associated with higher AHe. The QFe and AHe are both positively correlated with the flare intensities. The AHe and filament scales are not explicitly linked to each other. The statistical results demonstrate that the material contribution of the filaments to ICMEs is low and more than half of the hot materials inside ICMEs originate from the chromosphere in our database. We suggest that they are heated by the chromospheric evaporation process at the hot channel (flux rope) footpoint regions before and/or during the flaring process.

**Table 1** The In Situ Parameters of CMEs and Associated Phenomenon on the Sun 2011-2012

## **Tracking an eruptive prominence using multiwavelength and multiview observations on 2023 March 7**

[Qingmin Zhang](#), [Yudi Ou](#), [Zhenghua Huang](#), [Yongliang Song](#), [Suli Ma](#)

ApJ 977 4 2024

<https://arxiv.org/pdf/2410.22724>

<https://iopscience.iop.org/article/10.3847/1538-4357/ad8bad/pdf>

In this paper, we carry out multiwavelength and multiview observations of the prominence eruption, which generates a C2.3 class flare and a coronal mass ejection (CME) on **2023 March 7**. For the first time, we apply the revised cone model to three-dimension reconstruction and tracking of the eruptive prominence for ~4 hrs. The prominence propagates non-radially and makes a detour around the large-scale coronal loops in active region NOAA 13243. The northward deflection angle increases from ~36 degrees to ~47 degrees before returning to ~36 degrees and keeping up. There is no longitudinal deflection throughout the propagation. The angular width of the cone increases from ~30 degrees and reaches a plateau at ~37 degrees. The heliocentric distance of the prominence rises from ~1.1 to ~10.0 solar radii, and the prominence experiences continuous acceleration (~51 m/s<sup>2</sup>) over two hours, which is probably related to the magnetic reconnection during the C-class flare. The true speed of CME front is estimated to be ~829 km/s, which is ~1.2 times larger than that of CME core (prominence). It is concluded that both acceleration and deflection of eruptive prominences in their early lives could be reproduced with the revised cone model.

## **Hemispheric Distribution of Halo Coronal Mass Ejection Source Locations**

XiaoJuan [Zhang](#)<sup>1,2,3</sup>, LinHua Deng<sup>4,5</sup>, Hui Deng<sup>2,3</sup>, Ying Mei<sup>2,3</sup>, and Feng Wang<sup>2,3</sup>

2024 ApJ 962 172

<https://iopscience.iop.org/article/10.3847/1538-4357/ad18af/pdf>

The hemispheric asymmetry of solar activity is one of the essential physical consequences of the interior dynamo process. However, the hemispheric distribution of halo coronal mass ejection (HCME) source locations has not been investigated in detail. Based on the HCME catalog identified from the Large Angle and Spectrometric Coronagraph Experiment on board the Solar and Heliospheric Observatory, we perform a hemispheric distribution analysis of the HCME source locations from 1996 April to 2022 June. The main results are as follows. (1) The HCME source locations are confined to the active region belt, and there is no "rush to the poles" phenomenon that is unique to large-scale magnetic activity. (2) The HCME source locations exhibit a general hemispheric asymmetry, and autoregressive moving-average model results show that the asymmetry of HCME source locations is significantly different from that of sunspot activity. (3) The hemispheric distribution of cycle 24 is different from that of cycle 23, potentially as a result of the heliospheric dynamic pressure having noticeably decreased after the polarity reversal of cycle 23. Our results contribute to a more comprehensive understanding of the hemispheric asymmetry of energetic magnetic structures and give a new perspective on understanding the geoeffectiveness of HCMEs.

## **Rotation and Confined Eruption of a Double Flux-Rope System**

[Xiaomeng Zhang](#), [Jinhan Guo](#), [Yang Guo](#), [Mingde Ding](#), [Rony Keppens](#)

ApJ 961 145 2024

<https://arxiv.org/pdf/2312.07406.pdf>

<https://iopscience.iop.org/article/10.3847/1538-4357/ad1521/pdf>

We perform a data-constrained simulation with the zero- $\beta$  assumption to study the mechanisms of strong rotation and failed eruption of a filament in active region 11474 on **2012 May 5** observed by Solar Dynamics Observatory and Solar Terrestrial Relations Observatory. The initial magnetic field is provided by nonlinear force-free field extrapolation, which is reconstructed by the regularized Biot-Savart laws and magnetofrictional method. Our simulation reproduces most observational features very well, e.g., the filament large-angle rotation of about 130°, the confined eruption and the flare ribbons, allowing us to analyze the underlying physical processes behind observations. We discover two flux ropes in the sigmoid system, an upper flux rope (MFR1) and a lower flux rope (MFR2), which correspond to the filament and hot channel in observations, respectively. Both flux ropes undergo confined eruptions. MFR2 grows by tether-cutting reconnection during the eruption. The rotation of MFR1 is related to the shear-field component along the axis. The toroidal field tension force and the non-axisymmetry forces confine the eruption of MFR1. We also suggest that the mutual interaction between MFR1 and MFR2 contributes to the large-angle rotation and the eruption failure. In

addition, we calculate the temporal evolution of the twist and writhe of MFR1, which is a hint of probable reversal rotation.

### **Energetics of a solar flare and a coronal mass ejection generated by a hot channel eruption**

[Qingmin Zhang](#), [Weilin Teng](#), [Dong Li](#), [Jun Dai](#), [Yanjie Zhang](#)

ApJ 2023

<https://arxiv.org/pdf/2310.14010.pdf>

Hot channels (HCs) are prevalent in the solar corona and play a critical role in driving flares and CMEs. In this paper, we estimate the energy contents of an X1.4 eruptive flare with a fast CME generated by a HC eruption on **2011 September 22**. Originating from NOAA AR11302, the HC is the most dramatic feature in 131 and 94 Å images observed by SDO/AIA. The flare is simultaneously observed by SDO/AIA, RHESSI, and STEREO-B/EUVI. The CME is simultaneously detected by the white-light coronagraphs of SOHO/LASCO and STEREO-B/COR1. Using multiwavelength and multiview observations of the eruption, various energy components of the HC, flare, and CME are calculated. The thermal and kinetic energies of the HC are  $(1.77 \pm 0.61) \times 10^{30}$  erg and  $(2.90 \pm 0.79) \times 10^{30}$  erg, respectively. The peak thermal energy of the flare and total radiative loss of SXR-emitting plasma are  $(1.63 \pm 0.04) \times 10^{31}$  erg and  $(1.03 - 1.31) \times 10^{31}$  erg, respectively. The ratio between the thermal energies of HC and flare is  $0.11 \pm 0.03$ , suggesting that thermal energy of the HC is not negligible. The kinetic and potential energies of the CME are  $(3.43 \pm 0.94) \times 10^{31}$  erg and  $(2.66 \pm 0.49) \times 10^{30}$  erg, yielding a total energy of  $(3.69 \pm 0.98) \times 10^{31}$  erg for the CME. Continuous heating of the HC is required to balance the rapid cooling by heat conduction, which probably originate from intermittent magnetic reconnection at the flare current sheet. Our investigation may provide insight into the buildup, release, and conversion of energies in large-scale solar eruptions.

### **A revised graduated cylindrical shell model and its application to a prominence eruption**

[Qing-Min Zhang](#), [Zhen-Yong Hou](#), [Xian-Yong Bai](#)

Research in Astron. Astrophys 2023

<https://arxiv.org/pdf/2307.00943.pdf>

In this paper, the well-known graduated cylindrical shell (GCS) model is slightly revised by introducing longitudinal and latitudinal deflections of prominences originating from active regions (ARs). Subsequently, it is applied to the three-dimensional (3D) reconstruction of an eruptive prominence in AR 13110, which produced an M1.7 class flare and a fast coronal mass ejection (CME) on **2022 September 23**. It is revealed that the prominence undergoes acceleration from  $\sim 246$  to  $\sim 708$  km s<sup>-1</sup>. Meanwhile, the prominence experiences southward deflection by  $15^\circ$  without longitudinal deflection, suggesting that the prominence erupts non-radially. Southward deflections of the prominence and associated CME are consistent, validating the results of fitting using the revised GCS model. Besides, the true speed of the CME is calculated to be  $1637 \pm 15$  km s<sup>-1</sup>, which is  $\sim 2.3$  times higher than that of prominence. This is indicative of continuing acceleration of the prominence during which flare magnetic reconnection reaches maximum beneath the erupting prominence. Hence, the reconstruction using the revised GCS model could successfully track a prominence in its early phase of evolution, including acceleration and deflection.

### **Transverse vertical oscillations during the contraction and expansion of coronal loops**

[Qingmin Zhang](#), [Yuhao Zhou](#), [Chuan Li](#), [Qiao Li](#), [Fanxiaoyu Xia](#), [Ye Qiu](#), [Jun Dai](#), [Yanjie Zhang](#)

ApJ 2023

<https://arxiv.org/pdf/2305.08338.pdf>

In this paper, we carry out a detailed analysis of the M1.6 class eruptive flare occurring in NOAA active region 13078 on **2022 August 19**. The flare is associated with a fast coronal mass ejection (CME) propagating in the southwest direction with an apparent speed of  $\sim 926$  km s<sup>-1</sup>. Meanwhile, a shock wave is driven by the CME at the flank. The eruption of CME generates an extreme-ultraviolet (EUV) wave expanding outward from the flare site with an apparent speed of  $\geq 200$  km s<sup>-1</sup>. As the EUV wave propagates eastward, it encounters and interacts with the low-lying adjacent coronal loops (ACLs), which are composed of two loops. The compression of EUV wave results in contraction, expansion, and transverse vertical oscillations of ACLs. The commencements of contraction are sequential from western to eastern footpoints and the contraction lasts for  $\sim 15$  minutes. The speeds of contraction lie in the range of 13–40 km s<sup>-1</sup> in 171 Å and 8–54 km s<sup>-1</sup> in 193 Å. A long, gradual expansion follows the contraction at lower speeds. Concurrent vertical oscillations are superposed on contraction and expansion of ACLs. The oscillations last for 2–9 cycles and the amplitudes are  $\leq 4$  Mm. The periods are between 3 to 12 minutes with an average value of 6.7 minutes. The results show rich dynamics of coronal loops.

### **Hemispheric distribution of coronal mass ejections from 1996 to 2020**

[X J Zhang](#), [L H Deng](#), [Z P Qiang](#), [Y Fei](#), [X A Tian](#), [C Li](#)

MNRAS Volume 520, Issue 3, April 2023, Pages 3923–3936,

<https://doi.org/10.1093/mnras/stad323>

Solar magnetic structures are known to be asymmetrically distributed between the two hemispheres. To date, the hemispheric variations of the coronal mass ejections (CMEs) at different latitudes, in different cycles, and for different types (regular and specific events) are still unclear. From the list of white-light CMEs in the Coordinated Data Analysis Web catalogue, we investigate the hemispheric asymmetry of high-latitude and low-latitude CMEs in the time interval

from 1996 January to 2020 December. The main results are shown for the following: (1) in each hemisphere, regular CMEs are significantly correlated with solar activity, particularly for low latitudes. However, specific CMEs are not correlated with solar activity; (2) the main reason for the hemispheric asymmetry of the CMEs is attributable to specific CMEs, not regular CMEs. The hemispheric asymmetry of high-latitude CMEs appears to have little connection to that of low-latitude CMEs; (3) for the total and specific CMEs, the relationship between the absolute asymmetry index at high and low latitudes has a positive correlation prior to the cycle maximum, but a negative correlation after the cycle maximum; and (4) the dominant hemisphere, the cumulative trend, and the amplitude of the total, specific, and regular CMEs in cycle 23 differ from those in cycle 24. Our analysis results could be useful for understanding the cyclical variation of the magnetic free energy during different solar cycles, and could also provide insight into more physical processes responsible for the solar–terrestrial relationship.

## **Influence of magnetic reconnection on the eruptive catastrophes of coronal magnetic flux ropes**

[Quanhao Zhang](#), [Xin Cheng](#), [Rui Liu](#), [Anchuan Song](#), [Xiaolei Li](#), [Yuming Wang](#)

Frontiers in Astronomy and Space Sciences **2023**

<https://arxiv.org/pdf/2212.14602.pdf>

Large-scale solar eruptive activities have a close relationship with coronal magnetic flux ropes. Previous numerical studies have found that the equilibrium of a coronal flux rope system could be disrupted if the axial magnetic flux of the rope exceeds a critical value, so that the catastrophe occurs, initiating the flux rope to erupt. Further studies discovered that the catastrophe does not necessarily exist: the flux rope system with certain photospheric flux distributions could be non-catastrophic. It is noteworthy that most previous numerical studies are under the ideal magnetohydrodynamic (MHD) condition, so that it is still elusive whether there is the catastrophe associated with the critical axial flux if magnetic reconnection is included in the flux rope system. In this paper, we carried out numerical simulations to investigate the evolutions of coronal magnetic rope systems under the ideal MHD and the resistive condition. Under the ideal MHD condition, our simulation results demonstrate that the flux rope systems with either too compact or too weak photospheric magnetic source regions are non-catastrophic versus varying axial flux of the rope, and thus no eruption could be initiated; if there is magnetic reconnection in the rope system, however, those flux rope systems could change to be capable of erupting via the catastrophe associated with increasing axial flux. Therefore, magnetic reconnection could significantly influence the catastrophic behaviors of flux rope system. It should be both the magnetic topology and the local physical parameters related to magnetic reconnection that determine whether the increasing axial flux is able to cause flux rope eruptions.

## **Observations of magnetic reconnection and particle acceleration locations in solar coronal jets**

[Yixian Zhang](#), [Sophie Musset](#), [Lindsay Glesener](#), [Navdeep Panesar](#), [Gregory Fleishman](#)

ApJ **943** 180 **2023**

<https://arxiv.org/pdf/2207.05668.pdf>

<https://iopscience.iop.org/article/10.3847/1538-4357/aca654/pdf>

We present a multi-wavelength analysis of two flare-related jets on **November 13, 2014**, using data from SDO/AIA, RHESSI, Hinode/XRT, and IRIS. Unlike most coronal jets where hard X-ray (HXR) emissions are usually observed near the jet base, in these events HXR emissions are found at several locations, including in the corona. We carry out the first differential emission measure (DEM) analysis that combines both AIA (and XRT when available) bandpass filter data and RHESSI HXR measurements for coronal jets, and obtain self-consistent results across a wide temperature range and into non-thermal energies. In both events, hot plasma first appeared at the jet base, but as the base plasma gradually cooled, hot plasma also appeared near the jet top. Moreover, non-thermal electrons, while only mildly energetic, are found in multiple HXR locations and contain a large amount of total energy. Particularly, the energetic electrons that produced the HXR sources at the jet top were accelerated near the top location, rather than traveling from a reconnection site at the jet base. This means that there was more than one particle acceleration site in each event. Jet velocities are consistent with previous studies, including upward and downward velocities around  $\sim 200$  km/s and  $\sim 100$  km/s respectively, and fast outflows of 400–700 km/s. We also examine the energy partition in the later event, and find that the non-thermal energy in accelerated electrons is most significant compared to other energy forms considered. We discuss the interpretations and provide constraints on mechanisms for coronal jet formation.

**RHESSI Science Nuggets #445** Mar **2023**

[https://sprg.ssl.berkeley.edu/~tohban/wiki/index.php/Particle\\_Acceleration\\_in\\_Two\\_Coronal\\_Jets](https://sprg.ssl.berkeley.edu/~tohban/wiki/index.php/Particle_Acceleration_in_Two_Coronal_Jets)

## **Dynamic Evolution of Magnetic Flux Ropes in Active Region 11429. I. EUV Observations**

Yin [Zhang](#)<sup>5,1</sup>, Jihong Liu<sup>2</sup>, Baolin Tan<sup>1,3</sup>, Xiaoshuai Zhu<sup>4</sup>, and Yihua Yan<sup>3,4</sup>

**2022** ApJ 940 125

<https://iopscience.iop.org/article/10.3847/1538-4357/ac9b52/pdf>

Studying the formation and dynamic evolution of the magnetic flux rope (MFR) is key to understanding the physics of most solar eruptions. In the present study, we investigate the dynamic evolution of four MFRs, which involve in a major eruption. The MFR1, which represents as filament (F1), first appears about 31 hr before the major eruption. The MFR2 appears as a hot-channel with a small filament (F2) in its east part. The hot-channel becomes intermittently visible about 2 hr before the major eruption. The MFR3 is formed by the reconnection between MFR1 and MFR2. The annular



components of MFR3 along the MFR2 part appear as a hollow helical structure from the background with the temperature of several MK after the reconnection. Coronal material then flows along the hollow structure from MFR1 part to MFR2 part to form a new filament (F3), which is hosted by MFR3 and acts as the axial component of MFR3 in the following evolution. The MFR4 appears during MFR3's eruption phase as conjugated extreme ultraviolet (EUV) brightenings. Both brightenings extend outward into irregular ribbons with conjugate EUV dimmings inside. Meanwhile, an erupted hot-channel, which roots in the conjugated brightening, is identified. The morphology of the MFRs are also profiled by four associated flare ribbon pairs. The on-disk observations shed light on our understanding of the topology of the MFRs and their formation and eruption. Further work should lay emphasis on the magnetic environment for the MFR formation and evolution. **2012 March 10**

## **Multiwavelength observations of a partial filament eruption on 13 June 2011**

[Yanjie Zhang](#), [Qingmin Zhang](#), [Jun Dai](#), [Dong Li](#), [Haisheng Ji](#)

Solar Phys. **297**, Article number: 138 **2022**

<https://arxiv.org/pdf/2210.05919.pdf>

<https://doi.org/10.1007/s11207-022-02072-8>

In this paper, we report the multiwavelength observations of the partial filament eruption associated with a C1.2 class flare in NOAA active region 11236 on **13 June 2011**. The event occurred at the eastern limb in the field of view (FOV) of Atmospheric Imaging Assembly (AIA) on board the Solar Dynamics Observatory (SDO) spacecraft and was close to the disk center in the FOV of Extreme-UltraViolet Imager (EUVI) on board the behind Solar Terrestrial Relations Observatory (STEREO) spacecraft. During eruption, the filament splits into two parts: the major part and runaway part. The major part flows along closed loops and experiences bifurcation at the loop top. Some of the materials move forward and reach the remote footpoint, while others return back to the original footpoint. The runaway part flows along open field lines, which is evidenced by a flare-related type III radio burst. The runaway part also undergoes bifurcation. The upper branch escapes the corona and evolves into a jet-like narrow coronal mass ejection (CME) at a speed of 324 km s<sup>-1</sup>, while the lower branch falls back to the solar surface. A schematic cartoon is proposed to explain the event and provides a new mechanism of partial filament eruptions

## **First detection of transverse vertical oscillation during the expansion of coronal loops**

[Qingmin Zhang](#), [Chuan Li](#), [Dong Li](#), [Ye Qiu](#), [Yanjie Zhang](#), [Yiwei Ni](#)

ApJL **937** L21 **2022**

<https://arxiv.org/pdf/2209.00194.pdf>

<https://iopscience.iop.org/article/10.3847/2041-8213/ac8e01/pdf>

In this Letter, we perform a detailed analysis of the M5.5-class eruptive flare occurring in active region 12929 on **2022 January 20**. The eruption of a hot channel generates a fast coronal mass ejection (CME) and a dome-shaped extreme-ultraviolet (EUV) wave at speeds of 740–860 km s<sup>-1</sup>. The CME is associated with a type II radio burst, implying that the EUV wave is a fast-mode shock wave. During the impulsive phase, the flare shows quasi-periodic pulsations (QPPs) in EUV, hard X-ray, and radio wavelengths. The periods of QPPs range from 18 s to 113 s, indicating that flare energy is released and nonthermal electrons are accelerated intermittently with multiple time scales. The interaction between the EUV wave and low-lying adjacent coronal loops (ACLs) results in contraction, expansion, and transverse vertical oscillation of ACLs. The speed of contraction in 171, 193, and 211 Å is higher than that in 304 Å. The periods of oscillation are 253 s and 275 s in 304 Å and 171 Å, respectively. A new scenario is proposed to explain the interaction. The equation that interprets the contraction and oscillation of the overlying coronal loops above a flare core can also interpret the expansion and oscillation of ACLs, suggesting that the two phenomena are the same in essence.

## **Birth places of extreme ultraviolet waves driven by impingement of solar jets upon coronal loops**

Liang [Zhang](#), [Ruisheng Zheng](#), [Huadong Chen](#), [Yao Chen](#)

ApJ **2022**

<https://arxiv.org/pdf/2204.00522.pdf>

Solar extreme ultraviolet (EUV) waves are large-scale propagating disturbances in the corona. It is generally believed that the vital key for the formation of EUV waves is the rapid expansion of the loops that overlie erupting cores in solar eruptions, such as coronal mass ejections (CMEs) and solar jets. However, the details of the interaction between the erupting cores and overlying loops are not clear, because that the overlying loops are always instantly opened after the energetic eruptions. Here, we present three typical jet-driven EUV waves without CME to study the interaction between the jets and the overlying loops that remained closed during the events. All three jets emanated from magnetic flux cancelation sites in source regions. Interestingly, after the interactions between jets and overlying loops, three EUV waves respectively formed ahead of the top, the near end (close to the jet source), and the far (another) end of the overlying loops. According to the magnetic field distribution of the loops extrapolated from Potential Field Source Surface method, it is confirmed that the birth places of three jet-driven EUV waves were around the weakest magnetic field strength part of the overlying loops. We suggest that the jet-driven EUV waves preferentially occur at the weakest part of the overlying loops, and the location can be subject to the magnetic field intensity around the ends of the loops. **2016 February 10, 2017 April 01, 2017 August 16**

## Tracking the 3D evolution of a halo coronal mass ejection using the revised cone model

[Q. M. Zhang](#)

A&A 660, A144 2022

<https://arxiv.org/pdf/2202.10676.pdf>

<https://www.aanda.org/articles/aa/pdf/2022/04/aa42942-21.pdf>

This paper aims to track the 3D evolution of a full halo CME on **2011 June 21**. The CME results from a non-radial eruption of a filament-carrying flux rope in NOAA active region 11236. The eruption is observed in EUV wavelengths by the EUVI on board the ahead and behind STEREO spacecrafts and the AIA on board SDO. The CME is observed by the COR1 coronagraph on board STEREO and the C2 coronagraph on board SOHO/LASCO. The revised cone model is slightly modified, with the top of the cone becoming a sphere, which is internally tangent to the legs. Using the multi-point observations, the cone model is applied to derive the morphological and kinematic properties of the CME. The cone shape fits nicely with the CME observed by EUVI and COR1 on board STEREO twin spacecraft and LASCO/C2 coronagraph. The cone angle increases sharply from  $54^\circ$  to  $130^\circ$  in the initial phase, indicating a rapid expansion. A relation between the cone angle and heliocentric distance of CME leading front is derived,  $\omega = 130^\circ - 480d^{-5}$ , where  $d$  is in unit of  $R_\odot$ . The inclination angle decreases gradually from  $\sim 51^\circ$  to  $\sim 18^\circ$ , suggesting a trend of radial propagation. The heliocentric distance increases gradually in the initial phase and quickly in the later phase up to  $\sim 11 R_\odot$ . The true speed of CME reaches  $\sim 1140 \text{ km s}^{-1}$ , which is  $\sim 1.6$  times higher than the apparent speed in the LASCO/C2 field of view. The revised model is promising in tracking the complete evolution of CMEs.

## Transverse Coronal-Loop Oscillations Induced by the Non-radial Eruption of a Magnetic Flux Rope

[Q. M. Zhang](#), [J. L. Chen](#), [S. T. Li](#), [L. Lu](#), [D. Li](#)

Solar Phys. 297, Article number: 18 2022

<https://arxiv.org/pdf/2201.07389.pdf>

<https://link.springer.com/content/pdf/10.1007/s11207-022-01952-3.pdf>

We investigate the transverse coronal-loop oscillations induced by the eruption of a prominence-carrying flux rope on **7 December 2012**. The flux rope originating from NOAA Active Region (AR) 11621 was observed in EUV wavelengths by the SDO/AIA and in  $H\alpha$  line center by the ground-based telescope at the BBSO. The early evolution of the flux rope is divided into two steps: a slow rise phase at a speed of  $\approx 230 \text{ km s}^{-1}$  and a fast rise phase at a speed of  $\approx 706 \text{ km s}^{-1}$ . The eruption generates a C5.8 flare and the onset of the fast rise is consistent with the HXR peak time of the flare. The embedded prominence has a lower speed of  $\approx 452 \text{ km s}^{-1}$ . During the early eruption of the flux rope, the nearby coronal loops are disturbed and experience independent kink-mode oscillations in the horizontal and vertical directions. The oscillation in the horizontal direction has an initial amplitude of  $\approx 3.1 \text{ Mm}$ , a period of  $\approx 294 \text{ seconds}$ , and a damping time of  $\approx 645 \text{ seconds}$ . It is most striking in  $171 \text{ \AA}$  and lasts for three to four cycles. The oscillations in the vertical directions are observed mainly in  $171$ ,  $193$ , and  $211 \text{ \AA}$ . The initial amplitudes lie in the range of  $3.4$ – $5.2 \text{ Mm}$ , with an average value of  $4.5 \text{ Mm}$ . The periods are between  $407 \text{ seconds}$  and  $441 \text{ seconds}$ , with an average value of  $423 \text{ seconds}$ . The oscillations are damping and last for nearly four cycles. The damping times lie in the range of  $570$ – $1012 \text{ seconds}$ , with an average value of  $741 \text{ seconds}$ . Assuming a semi-circular shape of the vertically oscillating loops, we calculate the loop lengths according to their heights. Using the observed periods, we carry out coronal seismology and estimate the internal Alfvén speeds ( $988$ – $1145 \text{ km s}^{-1}$ ) and the magnetic-field strengths ( $12$ – $43 \text{ G}$ ) of the oscillating loops.

## Numerical Study of Two Injection Methods for the 2007 November 15 Coronal Mass Ejection in the Inner Heliosphere

Man [Zhang](#)<sup>1</sup>, Xueshang Feng<sup>1,2</sup>, Fang Shen<sup>1,2</sup>, and Liping Yang<sup>1,2</sup>

2021 ApJ 918 35

<https://doi.org/10.3847/1538-4357/ac0b3f>

In this paper, we use two injection methods, i.e., coronal mass ejection (CME) with and without radial compression, to investigate the propagation of the **2007 November 15** CME in the inner heliosphere with a three-dimensional, time-dependent, numerical magnetohydrodynamic model. In order to reproduce the large-scale interplanetary magnetic field associated with the CME, the spheromak model is used to provide the intrinsic magnetic field structure of the CME. The modeled results also suggest that the CME without radial compression propagates in interplanetary space with a lower velocity and arrives at 1 au later. We interpret these differences as a result of different Lorentz forces acting on the two injection methods, which lead to different CME expansions in the heliosphere. Additionally, the model of a CME without radial compression tends to overestimate the radial extension at 1 au due to an overestimation of the CME radial size in the simulation and the modeled magnetic fields at 1 au are lower compared to the model of a CME with radial compression. The above results are all useful in understanding the dynamic process occurring between the CME and the solar wind.

## A revised cone model and its application to non-radial prominence eruptions

[Q. M. Zhang](#)

A&A Letter 653, L2 2021

<https://arxiv.org/pdf/2108.11831.pdf>

<https://www.aanda.org/articles/aa/pdf/2021/09/aa41982-21.pdf>

<https://doi.org/10.1051/0004-6361/202141982>

The traditional cone models achieve great success in studying the geometrical and kinematic properties of halo coronal mass ejections (CMEs). In this paper, a revised cone model is proposed to investigate the properties of CMEs as a result of non-radial prominence eruptions. The cone apex is located at the source region of an eruption instead of the Sun center. The cone axis deviates from the local vertical by an inclination angle of  $\theta_1$  and an angle of  $\phi_1$ . The length and angular width of the cone are  $r$  and  $\omega$ , respectively. The model is successfully applied to two CMEs originating from the western limb on **2011 August 11 and 2012 December 7**. By comparing the projections of the cones with the CME fronts simultaneously observed by the Atmospheric Imaging Assembly (AIA) on board the Solar Dynamics Observatory (SDO) and the Extreme-Ultraviolet Imager (EUVI) on board the ahead Solar TERrestrial RELations Observatory (STEREO), the properties of the CMEs are derived, including the distance, angular width, inclination angle, deviation from the plane of the sky, and true speed in space. This revised cone model provides a new and complementary approach in exploring the whole evolutions of CMEs.

## **Confined and eruptive catastrophes of solar magnetic flux ropes caused by mass loading and unloading**

[Quanhao Zhang](#), [Rui Liu](#), [Yuming Wang](#), [Xiaolei Li](#), [Shaoyu Lyu](#)

ApJ **921** 172 **2021**

<https://arxiv.org/pdf/2108.09401.pdf>

<https://doi.org/10.3847/1538-4357/ac1fef>

It is widely accepted that coronal magnetic flux ropes are the core structures of large-scale solar eruptive activities, which inflict dramatic impacts on the solar-terrestrial system. Previous studies have demonstrated that varying magnetic properties of a coronal flux rope system could result in a catastrophe of the rope, which may trigger solar eruptive activities. Since the total mass of a flux rope also plays an important role in stabilizing the rope, we use 2.5-dimensional magnetohydrodynamic (MHD) numerical simulations in this letter to investigate how a flux rope evolves as its total mass varies. It is found that an unloading process that decreases the total mass of the rope could result in an upward (eruptive) catastrophe in the flux rope system, during which the rope jumps upward and the magnetic energy is released. This indicates that mass unloading processes could initiate the eruption of the flux rope. Moreover, when the system is not too diffusive, there is also a downward (confined) catastrophe that could be caused by mass loading processes, via which the total mass accumulates. The magnetic energy, however, is increased during the downward catastrophe, indicating that mass loading processes could cause confined activities that may contribute to the storage of energy before the onset of coronal eruptions.

## **Recurrent coronal jets observed by SDO/AIA**

[Yan-Jie Zhang](#), [Qing-Min Zhang](#), [Jun Dai](#), [Zhe Xu](#), [Hai-Sheng Ji](#)

**2021**

<https://arxiv.org/pdf/2107.07194.pdf>

In this paper, we carry out multiwavelength observations of three recurring jets on **2014 November 7**. The jets originated from the same region at the edge of AR 12205 and propagated along the same coronal loop. The eruptions were generated by magnetic reconnection, which is evidenced by continuous magnetic cancellation at the jet base. The projected initial velocity of the jet2 is 402 km s. The accelerations in the ascending and descending phases of jet2 are not consistent, the former is considerably larger than the value of solar gravitational acceleration at the solar surface, while the latter is lower than solar gravitational acceleration. There are two possible candidates of extra forces acting on jet2 during its propagation. One is the downward gas pressure from jet1 when it falls back and meets with jet2. The other is the viscous drag from the surrounding plasma during the fast propagation of jet2. As a contrast, the accelerations of jet3 in the rising and falling phases are constant, implying that the propagation of jet3 is not significantly influenced by extra forces.

## **Multiwavelength Observations of the Formation and Eruption of a Complex Filament**

Y. [Zhang](#)<sup>1,2</sup>, T. S. Bastian<sup>2</sup>, J. H. Liu<sup>3</sup>, S. J. Yu<sup>4</sup>, S. Feng<sup>5</sup>, J. Chen<sup>1</sup>, and Y. H. Yan<sup>1,6</sup>

**2021** ApJ 910 40

<https://doi.org/10.3847/1538-4357/abded6>

<https://iopscience.iop.org/article/10.3847/1538-4357/abded6/pdf>

We present an analysis of the formation and eruption of a filament and fast coronal mass ejection associated with a flare that occurred in active region 11429 using observations in the ultraviolet, extreme ultraviolet, X-ray, and radio wavelength bands. Precursor activity began as an interaction between two filaments, F1 and F2, that are identified as having twisted magnetic flux ropes (MFRs). Transient brightenings in all wavelengths are observed as a result of this interaction, likely the result of magnetic reconnection between the two filaments. This interaction results in a reconfiguration of the two filaments into a long overlying filament and a shorter low-lying filament. The upper filament subsequently undergoes a partial confined eruption. Plasma flows originating near the east footpoint of F1 lead to an extension of the upper filament into the filament channel to the west, resulting in a new active region filament (ARF). This new filament begins a slow rise and expansion. During its slowly rising phase, the MFR in which the filament is embedded becomes visible, with both the filament and flux rope rising and expanding simultaneously. The twist of the magnetic rope is determined as four turns. The erupting configuration changes from a twisted arch shape to a

reversed  $\gamma$  shape within  $\sim 75$  s at the beginning of the fast-rise phase, representing a transformation from twist to writhe. The observations provide a clear example of filament formation via the tether-cutting reconnection of two nearby filaments. A helical kink instability may be the trigger of the ARF eruption. **2012 March 10**

### **How flux feeding causes eruptions of solar magnetic flux ropes with the hyperbolic flux tube configuration?**

[Quan hao Zhang](#), [Rui Liu](#), [Yuming Wang](#), [Zhenjun Zhou](#), [Bin Zhuang](#), [Xiaolei Li](#)

A&A 647, A171 2021

<https://arxiv.org/pdf/2101.12454.pdf>

<https://doi.org/10.1051/0004-6361/202039944>

<https://www.aanda.org/articles/aa/pdf/2021/03/aa39944-20.pdf>

Coronal magnetic flux ropes are generally considered to be the core structure of large-scale solar eruptions. Recent observations found that solar eruptions could be initiated by a sequence of "flux feeding," during which chromospheric fibrils rise upward from below, and merge with a pre-existing prominence. Further theoretical study has confirmed that the flux feeding mechanism is efficient in causing the eruption of flux ropes that are wrapped by bald patch separatrix surfaces. But it is unclear how flux feeding influences coronal flux ropes that are wrapped by hyperbolic flux tubes (HFT), and whether it is able to cause the flux-rope eruption. In this paper, we use a 2.5-dimensional magnetohydrodynamic model to simulate the flux feeding processes in HFT configurations. It is found that flux feeding injects axial magnetic flux into the flux rope, whereas the poloidal flux of the rope is reduced after flux feeding. Flux feeding is able to cause the flux rope to erupt, provided that the injected axial flux is large enough so that the critical axial flux of the rope is reached. Otherwise, the flux rope system evolves to a stable equilibrium state after flux feeding, which might be even farther away from the onset of the eruption, indicating that flux feeding could stabilize the rope system with the HFT configuration in this circumstance.

### **Spectroscopic observations of a flare-related coronal jet**

[O. M. Zhang](#), [Z. H. Huang](#), [Y. J. Hou](#), [D. Li](#), [Z. J. Ning](#), [Z. Wu](#)

A&A 647, A113 2021

<https://arxiv.org/pdf/2101.06629.pdf>

<https://doi.org/10.1051/0004-6361/202038924>

<https://www.aanda.org/articles/aa/pdf/2021/03/aa38924-20.pdf>

Coronal jets are ubiquitous in active regions (ARs) and coronal holes. In this paper, we study a coronal jet related to a C3.4 circular-ribbon flare in active region 12434 on **2015 October 16**. Two minifilaments were located under a 3D fan-spine structure before flare. The flare was generated by the eruption of one filament. The kinetic evolution of the jet was divided into two phases: a slow rise phase at a speed of  $\sim 131$  km s $^{-1}$  and a fast rise phase at a speed of  $\sim 363$  km s $^{-1}$  in the plane-of-sky. The slow rise phase may correspond to the impulsive reconnection at the breakout current sheet. The fast rise phase may correspond to magnetic reconnection at the flare current sheet. The transition between the two phases occurred at  $\sim 09:00:40$  UT. The blueshifted Doppler velocities of the jet in the Si  $\{\text{sc iv}\}$  1402.80 Å line range from  $-34$  to  $-120$  km s $^{-1}$ . The accelerated high-energy electrons are composed of three groups. Those propagating upward along open field generate type  $\{\text{III}\}$  radio bursts, while those propagating downward produce HXR emissions and drive chromospheric condensation observed in the Si  $\{\text{sc iv}\}$  line. The electrons trapped in the rising filament generate a microwave burst lasting for  $\leq 40$  s. Bidirectional outflows at the base of jet are manifested by significant line broadenings of the Si  $\{\text{sc iv}\}$  line. The blueshifted Doppler velocities of outflows range from  $-13$  to  $-101$  km s $^{-1}$ . The redshifted Doppler velocities of outflows range from  $\sim 17$  to  $\sim 170$  km s $^{-1}$ . Our multiwavelength observations of the flare-related jet are in favor of the breakout jet model and are important for understanding the acceleration and transport of nonthermal electrons.

### **Earth-affecting Solar Transients: A Review of Progresses in Solar Cycle 24**

Jie [Zhang](#), [Manuela Temmer](#), [Nat Gopalswamy](#), [Olga Malandraki](#), [Nariaki V. Nitta](#), [Spiros Patsourakos](#), [Fang Shen](#), [Bojan Vršnak](#), [Yuming Wang](#), [David Webb](#), [Mihir I. Desai](#), [Karin Dissauer](#), [Nina Dresing](#), [Mateja Dumbović](#), [Xueshang Feng](#), [Stephan G. Heinemann](#), [Monica Laurenza](#), [Noé Lugaz](#), [Bin Zhuang](#)

Progress in Earth and Planetary Science, Volume 8, Issue 1, article id.56, 2021 File

<https://progearthplanetsci.springeropen.com/counter/pdf/10.1186/s40645-021-00426-7.pdf>

<https://arxiv.org/ftp/arxiv/papers/2012/2012.06116.pdf> 2021

**2020** <https://arxiv.org/abs/2012.06116>

<https://arxiv.org/ftp/arxiv/papers/2012/2012.06116.pdf>

<https://doi.org/10.1186/s40645-021-00426-7>

This review article summarizes the advancement in the studies of Earth-affecting solar transients in the last decade that encompasses most of solar cycle 24. The Sun Earth is an integrated physical system in which the space environment of the Earth sustains continuous influence from mass, magnetic field and radiation energy output of the Sun in varying time scales from minutes to millennium. This article addresses short time scale events, from minutes to days that directly cause transient disturbances in the Earth space environment and generate intense adverse effects on advanced technological systems of human society. Such transient events largely fall into the following four types: (1) solar flares, (2) coronal mass ejections (CMEs) including their interplanetary counterparts ICMEs, (3) solar energetic particle (SEP) events, and (4) stream interaction regions (SIRs) including corotating interaction regions (CIRs). In the last decade, the

unprecedented multi viewpoint observations of the Sun from space, enabled by STEREO Ahead/Behind spacecraft in combination with a suite of observatories along the Sun-Earth lines, have provided much more accurate and global measurements of the size, speed, propagation direction and morphology of CMEs in both 3-D and over a large volume in the heliosphere. Several advanced MHD models have been developed to simulate realistic CME events from the initiation on the Sun until their arrival at 1 AU. Much progress has been made on detailed kinematic and dynamic behaviors of CMEs, including non-radial motion, rotation and deformation of CMEs, CME-CME interaction, and stealth CMEs and problematic ICMEs. The knowledge about SEPs has also been significantly improved. **2008-11-03, 7 March 2011, June 30, 2012, 12-14 July 2012, 2012.10.04-05, 8-10 October 2012, 29 May 2013, 2014-06-24**

### **Eruption of Solar Magnetic Flux Ropes Caused by Flux Feeding**

[Quanhao Zhang](#), [Yuming Wang](#), [Rui Liu](#), [Jie Zhang](#), [Youqiu Hu](#), [Wensi Wang](#), [Bin Zhuang](#), [Xiaolei Li](#)

ApJL **898** L12 **2020**

<https://arxiv.org/pdf/2007.01278.pdf>

<https://doi.org/10.3847/2041-8213/aba1f3>

Large-scale solar eruptions are believed to have a magnetic flux rope as the core structure. However, it remains elusive as to how the flux rope builds up and what triggers its eruption. Recent observations found that a prominence erupted following multiple episodes of "flux feeding". During each episode, a chromospheric fibril rose and merged with the prominence lying above. In this letter, we carried out 2.5-dimensional magnetohydrodynamic (MHD) numerical simulations to investigate whether the flux-feeding mechanism can explain such an eruption. The simulations demonstrate that the discrete emergence of small flux ropes can initiate eruptions by feeding axial flux into the preexistent flux rope until its total axial flux reaches a critical value. The onset of the eruption is dominated by an ideal MHD process. Our simulation results corroborate that the flux feeding is a viable mechanism to cause the eruption of solar magnetic flux ropes. **2012-10-20**

### **Longitudinal filament oscillations enhanced by two C-class flares**

Q. M. [Zhang](#), [J. H. Guo](#), [K. V. Tam](#), [A. A. Xu](#)

A&A **2020**

<https://arxiv.org/pdf/2001.01250.pdf>

In this paper, we report the multiwavelength observations of a very long filament in active region (AR) 11112 on **2010 October 18**. The filament was composed of two parts, the eastern part (EP) and western part (WP). We focus on longitudinal oscillations of the EP, which were enhanced by two homologous C-class flares in the same AR. The C1.3 flare was confined without a CME. Both EP and WP of the filament were slightly disturbed and survived the flare. After 5 hrs, eruption of the WP generated a C2.6 flare and a narrow, jet-like CME. Three oscillating threads (thda, thdb, thdc) are obviously identified in the EP and their oscillations are naturally divided into three phases by the two flares. The initial amplitude ranges from 1.6 to 30 Mm with a mean value of  $\sim 14$  Mm. The period ranges from 34 to 73 minutes with a mean value of  $\sim 53$  minutes. The curvature radii of the magnetic dips are estimated to be 29 to 133 Mm with a mean value of  $\sim 74$  Mm. The damping times ranges from  $\sim 62$  to  $\sim 96$  minutes with a mean value of  $\sim 82$  minutes. The value of  $\tau/P$  is between 1.2 and 1.8. For thda in the EP, the amplitudes were enhanced by the two flares from 6.1 Mm to 6.8 Mm after the C1.3 flare and further to 21.4 Mm after the C2.6 flare. The period variation as a result of perturbation from the flares was within 20%. The attenuation became faster after the C2.6 flare. To the best of our knowledge, this is the first report of large-amplitude, longitudinal filament oscillations enhanced by flares. Numerical simulations reproduce the oscillations of thda very well. The simulated amplitudes and periods are close to the observed values, while the damping time in the last phase is longer, implying additional mechanisms should be taken into account apart from radiative loss.

### **Three-dimensional MHD simulation of the 2008 December 12 coronal mass ejection: from the Sun to Interplanetary space A33**

Man [Zhang](#), Xue Shang Feng and Li Ping Yang

J. Space Weather Space Clim. **2019**, 9, A33

<https://www.swsc-journal.org/articles/swsc/pdf/2019/01/swsc180068.pdf>

– A three-dimensional time-dependent, numerical magnetohydrodynamic simulation is performed to investigate the propagation of a coronal mass ejection that occurred on 12 December 2008. The background solar wind is obtained by using a splitting finite-volume scheme based on a six-component grid system in spherical coordinate, with Parker's one-dimensional solar wind solution and measured photospheric magnetic fields as the initial values. A spherical plasmoid is superposed on the realistic ambient solar wind to study the 12 December 2008 coronal mass ejection event. The plasmoid is assumed to have a spheromak magnetic structure with a high-density, high-velocity, and high-pressure near the Sun. The dynamical interaction between the coronal mass ejection and the background solar wind flow is then investigated. We compared the model results with observations, and the model provide a relatively satisfactory comparison with the Wind spacecraft observations at 1 AU. We also investigated the numerical results assuming different parameters of the CME, we find that initial magnetic fields in the CME have a larger influence on the solar wind parameters at the Earth.

## Launch of a CME-associated eruptive prominence as observed with IRIS and ancillary instruments★

P. Zhang, É. Buchlin and J.-C. Vial

A&A 624, A72 (2019)

<https://www.aanda.org/articles/aa/pdf/2019/04/aa34259-18.pdf>  
[sci-hub.se/10.1051/0004-6361/201834259](https://doi.org/10.1051/0004-6361/201834259)

**Aims.** In this paper we focus on the possible observational signatures of the processes which have been put forward for explaining eruptive prominences. We also try to understand the variations in the physical conditions of eruptive prominences and estimate the masses leaving the Sun versus the masses returning to the Sun during eruptive prominences.

**Methods.** As far as velocities are concerned, we combined an optical flow method on the Atmospheric Imaging Assembly (AIA) 304 Å and Interface Region Imaging Spectrograph (IRIS). Mg II h&k observations in order to derive the plane-of-sky velocities in the prominence, and a Doppler technique on the IRIS Mg II h&k profiles to compute the line-of-sight velocities. As far as densities are concerned, we compared the absolute observed intensities with values derived from non-local thermodynamic equilibrium radiative transfer computations to derive the total (hydrogen) density and consequently compute the mass flows.

**Results.** The derived electron densities range from  $1.3 \times 10^9$  to  $6.0 \times 10^{10} \text{ cm}^{-3}$  and the derived total hydrogen densities range from  $1.5 \times 10^9$  to  $2.4 \times 10^{11} \text{ cm}^{-3}$  in different regions of the prominence. The mean temperature is around  $1.1 \times 10^4 \text{ K}$ , which is higher than in quiescent prominences. The ionization degree is in the range of 0.1–10. The total (hydrogen) mass is in the range of  $1.3 \times 10^{14}$ – $3.2 \times 10^{14} \text{ g}$ . The total mass drainage from the prominence to the solar surface during the whole observation time of IRIS is about one order of magnitude smaller than the total mass of the prominence. **2014 May 28**

## Subarcsecond blobs in flare-related coronal jets

Q. M. Zhang, L. Ni

ApJ 870 113 2019

<https://arxiv.org/pdf/1811.08570.pdf>  
<http://iopscience.iop.org/article/10.3847/1538-4357/aaf391/pdf>

In this paper, we report our multiwavelength observations of subarcsecond blobs in coronal jets. In AR 12149, a C5.5 circular-ribbon flare occurred on **2014 August 24**. Two jets (jet1 and jet2) were related to the flare. Jet1 appeared first. Jet2 appeared 6 minutes later. During its initial phase, a big plasmoid was ejected out of jet2. After the flare peak time, multiple bright and compact blobs appeared in the lower part of jet2, which were observed by IRIS/SJI. The blobs observed by SJI in 1330 Å have sizes of  $0.45$ – $1.35$  arcsec, nearly 84% of which are subarcsecond ( $<1$  arcsec). The mean value and standard deviation of the sizes are  $0.78$  and  $0.19$  arcsec, respectively. The velocities of the blobs range from 10 to more than  $220 \text{ km s}^{-1}$ . Three of the blobs had their counterparts in EUV wavelengths observed by SDO/AIA. The velocities are almost identical in UV and EUV wavelengths. We propose that the blobs observed in 1330 Å are the cool component ( $\sim 0.025 \text{ MK}$ ), while the blobs observed in EUV are the hot component of several MK. In jet1, only one blob was present. We conclude that the blobs are created by the tearing-mode instability of the current sheet at the base or inside the coronal jets. Our results have important implication for uncovering the fine structures of coronal jets and understanding the relationship between the blobs observed in UV and EUV wavelengths.

## Detection of Coronal Mass Ejections Using Multiple Features and Space–Time Continuity

Ling Zhang, Jian-qin Yin, Jia-ben Lin, Zhi-quan Feng, Jin Zhou

[Solar Physics](#) July 2017, 292:91

Coronal Mass Ejections (CMEs) release tremendous amounts of energy in the solar system, which has an impact on satellites, power facilities and wireless transmission. To effectively detect a CME in Large Angle Spectrometric Coronagraph (LASCO) C2 images, we propose a novel algorithm to locate the suspected CME regions, using the Extreme Learning Machine (ELM) method and taking into account the features of the grayscale and the texture. Furthermore, space–time continuity is used in the detection algorithm to exclude the false CME regions. The algorithm includes three steps: i) define the feature vector which contains textural and grayscale features of a running difference image; ii) design the detection algorithm based on the ELM method according to the feature vector; iii) improve the detection accuracy rate by using the decision rule of the space–time continuum. Experimental results show the efficiency and the superiority of the proposed algorithm in the detection of CMEs compared with other traditional methods. In addition, our algorithm is insensitive to most noise.

## Upward and downward catastrophes of coronal magnetic flux ropes in quadrupolar magnetic fields

Quanhao Zhang, Yuming Wang, Youqiu Hu, Rui Liu, Kai Liu, Jiajia Liu

2017 ApJ 851 96

<https://arxiv.org/pdf/1711.07870.pdf>

Coronal magnetic flux ropes are closely related to large-scale solar activities. Using a 2.5-dimensional time-dependent ideal magnetohydrodynamic (MHD) model in Cartesian coordinates, we carry out numerical simulations to investigate the evolution of a magnetic system consisting of a flux rope embedded in a fully-closed quadrupolar magnetic field with

different photospheric flux distributions. It is found that, when the photospheric flux is not concentrated too much towards the polarity inversion line (PIL) and the constraint exerted by the background field is not too weak, the equilibrium states of the system are divided into two branches: the rope sticks to the photosphere for the lower branch and levitates in the corona for the upper branch. These two branches are connected by an upward catastrophe (from the lower branch to the upper) and a downward catastrophe (from the upper branch to the lower). Our simulations reveal that there exist both upward and downward catastrophes in quadrupolar fields, which may be either force-free or non-force-free. The existence and the properties of these two catastrophes are influenced by the photospheric flux distribution, and a downward catastrophe is always paired with an upward catastrophe. Comparing the decay indices in catastrophic and non-catastrophic cases, we infer that torus unstable might be a necessary but not sufficient condition for a catastrophic system.

### **Influence of photospheric magnetic conditions on the catastrophic behaviors of flux ropes in active regions**

Quanhao [Zhang](#), Yuming Wang, Youqiu Hu, [Rui Liu](#), [Jiajia Liu](#)

ApJ 835 211 2017

<https://arxiv.org/pdf/1701.01622v1.pdf>

Since only the magnetic conditions at the photosphere can be routinely observed in current observations, it is of great significance to find out the influences of photospheric magnetic conditions on solar eruptive activities. Previous studies about catastrophe indicated that the magnetic system consisting of a flux rope in a partially open bipolar field is subject to catastrophe, but not if the bipolar field is completely closed under the same specified photospheric conditions. In order to investigate the influence of the photospheric magnetic conditions on the catastrophic behavior of this system, we expand upon the 2.5 dimensional ideal magnetohydrodynamic (MHD) model in Cartesian coordinates to simulate the evolution of the equilibrium states of the system under different photospheric flux distributions. Our simulation results reveal that a catastrophe occurs only when the photospheric flux is not concentrated too much toward the polarity inversion line and the source regions of the bipolar field are not too weak; otherwise no catastrophe occurs. As a result, under certain photospheric conditions, a catastrophe could take place in a completely closed configuration whereas it ceases to exist in a partially open configuration. This indicates that whether the background field is completely closed or partially open is not the only necessary condition for the existence of catastrophe, and that the photospheric conditions also play a crucial role in the catastrophic behavior of the flux rope system.

### **CUSP-SHAPED STRUCTURE OF A JET OBSERVED BY IRIS AND SDO**

Yuzong [Zhang](#) and Jun Zhang

ApJ 834 79 2017

<http://iopscience.iop.org/article/10.3847/1538-4357/834/1/79/pdf>

<https://arxiv.org/pdf/1611.05033v1.pdf>

On **2014 August 29**, the trigger and evolution of a cusp-shaped jet were captured in detail at 1330 Å by the Interface Region Imaging Spectrograph. At first, two neighboring mini-prominences arose in turn from the low solar atmosphere and collided with a loop-like system over them. The collisions between the loop-like system and the mini-prominences lead to the blowout, and then a cusp-shaped jet formed with a spire and an arch-base. In the spire, many brightening blobs originating from the junction between the spire and the arch-base moved upward in a rotating manner and then in a straight line in the late phase of the jet. In the arch-base, dark and bright material simultaneously tracked in a fan-like structure, and the majority of the material moved along the fan's threads. At the later phase of the jet's evolution, bidirectional flows emptied the arch-base, while downflows emptied the spire, thus making the jet entirely vanish. The extremely detailed observations in this study shed new light on how magnetic reconnection alters the inner topological structure of a jet and provides a beneficial complement for understanding current jet models.

### **DOWNWARD CATASTROPHE OF SOLAR MAGNETIC FLUX ROPES**

Quanhao [Zhang](#)<sup>1,2</sup>, Yuming Wang<sup>1,3</sup>, Youqiu Hu<sup>1</sup>, and Rui Liu<sup>1,4</sup>

2016 ApJ 825 109

<http://arxiv.org/pdf/1607.02213v1.pdf>

2.5-dimensional time-dependent ideal magnetohydrodynamic (MHD) models in Cartesian coordinates were used in previous studies to seek MHD equilibria involving a magnetic flux rope embedded in a bipolar, partially open background field. As demonstrated by these studies, the equilibrium solutions of the system are separated into two branches: the flux rope sticks to the photosphere for solutions at the lower branch but is suspended in the corona for those at the upper branch. Moreover, a solution originally at the lower branch jumps to the upper, as the related control parameter increases and reaches a critical value, and the associated jump is here referred to as an upward catastrophe. The present paper advances these studies in three aspects. First, the magnetic field is changed to be force-free; the system still experiences an upward catastrophe with an increase in each control parameter. Second, under the force-free approximation, there also exists a downward catastrophe, characterized by the jump of a solution from the upper branch to the lower. Both catastrophes are irreversible processes connecting the two branches of equilibrium solutions so as to form a cycle. Finally, the magnetic energy in the numerical domain is calculated. It is found that there exists a magnetic energy release for both catastrophes. The Ampère's force, which vanishes everywhere for force-free fields, appears only

during the catastrophes and does positive work, which serves as a major mechanism for the energy release. The implications of the downward catastrophe and its relevance to solar activities are briefly discussed.

### **Observations of multiple blobs in homologous solar coronal jets in closed loops**

Q. M. **Zhang**, H. S. Ji, Y. N. Su

Solar Phys. Volume 291, **Issue 3**, pp 859-876 **2016**

<http://arxiv.org/pdf/1601.04390v1.pdf>

Coronal bright points (CBPs) and jets are ubiquitous small-scale brightenings that are often associated with each other. In this paper, we report our multiwavelength observations of two groups of homologous jets. The first group was observed by the EUVI aboard the behind STEREO spacecraft in 171 Å and 304 Å on **2014 September 10**, from a location where data from the SDO could not observe. The jets (J1–J6) recurred for six times with intervals of 5–15 minutes. They originated from the same primary CBP (BP1) and propagated in the northeast direction along large-scale, closed coronal loops. Two of the jets (J3 and J6) produced sympathetic CBPs (BP2 and BP3) after reaching the remote footpoints of the loops. The time delays between the peak times of BP1 and BP2 (BP3) are  $240 \pm 75$  s ( $300 \pm 75$  s). The jets were not coherent. Instead, they were composed of bright and compact blobs. The sizes and apparent velocities of the blobs are 4.5–9 Mm and 140–380 km/s, respectively. The arrival times of the multiple blobs in the jets at the far-end of the loops indicate that the sympathetic CBPs are caused by jet flows rather than thermal conduction fronts. The second group was observed by the AIA aboard SDO in various wavelengths on **2010 August 3**. Similar to the first group, the jets originated from a short-lived bright point (BP) at the boundary of AR 11092 and propagated along a small-scale, closed loop before flowing into the active region. Several tiny blobs with sizes of  $\sim 1.7$  Mm and apparent velocity of  $\sim 238$  km/s were identified in the jets. We carried out the DEM inversions to investigate the temperatures of the blobs, finding that the blobs were multithermal with average temperature of 1.8–3.1 MK.

### **Flux rope proxies during 2013 detected by the Solar Dynamics Observatory\***

J. **Zhang**, S. H. Yang and T. Li

A&A 580, A2 (**2015**)

Context. The relationship between flux ropes and coronal mass ejections (CMEs) is of great importance for understanding the CME initiation, but we do not know how many flux ropes in the atmosphere can be detected.

Aims. We aim to determine the number of flux rope proxies and understand the distribution of the proxies over the visible solar disk.

Methods. By employing the observations from the Atmospheric Imaging Assembly onboard the Solar Dynamics Observatory, we counted the number of the flux rope proxies from 2013 January to 2013 December.

Results. We detected 1354 (3.7 every day) rope proxies during this period and classified them into three types according to their temperature properties and particular (sigmoid) structures. The first type is that the rope proxies are detected in both lower and higher temperature lines. The second is that the rope proxies can only be detected in higher temperature lines, and the third is that the proxies display sigmoid structures in extreme ultraviolet channels. Six hundred and fifty-eight proxies of the 1354 that belong to the first type are tracked by active or eruptive material of filaments or prominences. Four hundred and eighty-seven proxies appear to be rising from the lower atmosphere or brightening in the corona, and belong to the second type. The remaining 209 display sigmoid structures, and they are attributed to the third type. We detected 497 rope proxies, which is 37% of the total, in the northern hemisphere.

Conclusions. Our findings imply a significantly asymmetric distribution of the rope proxies over the visible solar disk.

### **Multiwavelength observations of a partially eruptive filament on 2011 September 8**

Q. M. **Zhang**, Z. J. Ning, Y. Guo, T. H. Zhou, X. Cheng, H. S. Ji, L. Feng, T. Wiegelmann

ApJ **805** 4 **2015**

<http://arxiv.org/pdf/1503.02933v1.pdf>

In this paper, we report our multiwavelength observations of a partial filament eruption event in NOAA active region 11283 on **2011 September 8**. A magnetic null point and the corresponding spine and separatrix surface are found in the active region. Beneath the null point, a sheared arcade supports the filament along the highly complex and fragmented polarity inversion line. After being activated, the sigmoidal filament erupted and split into two parts. The major part rose at the speeds of 90–150 km s<sup>-1</sup> before reaching the maximum apparent height of  $\sim 115$  Mm. Afterwards, it returned to the solar surface in a bumpy way at the speeds of 20–80 km s<sup>-1</sup>. The rising and falling motions were clearly observed in the extreme-ultraviolet (EUV), UV, and H $\alpha$  wavelengths. The failed eruption of the main part was associated with an M6.7 flare with a single hard X-ray source. The runaway part of the filament, however, separated from and rotated around the major part for  $\sim 1$  turn at the eastern leg before escaping from the corona, probably along large-scale open magnetic field lines. The ejection of the runaway part resulted in a very faint coronal mass ejection (CME) that propagated at an apparent speed of 214 km s<sup>-1</sup> in the outer corona. The filament eruption also triggered transverse kink-mode oscillation of the adjacent coronal loops in the same AR. The amplitude and period of the oscillation were 1.6



Mm and 225 s. Our results are important for understanding the mechanisms of partial filament eruptions and provide new constraints to theoretical models. The multiwavelength observations also shed light on space weather prediction.

### **A Prominence Eruption Driven by Flux Feeding from Chromospheric Fibrils**

Quanhao **Zhang**, Rui Liu, Yuming Wang, Chenglong Shen, Kai Liu, Jiajia Liu, and S. Wang

E-print, May 2014; ApJ, 789 133, 2014

<http://arxiv.org/pdf/1405.6833v1.pdf>

We present multi-wavelength observations of a prominence eruption originating from a quadrupolar field configuration, in which the prominence was embedded in a side-arcade. Within the two-day period prior to its eruption on **2012 October 22**, the prominence was perturbed three times by chromospheric fibrils underneath, which rose upward, became brightened, and merged into the prominence, resulting in horizontal flows along the prominence axis, suggesting that the fluxes carried by the fibrils were incorporated into the magnetic field of the prominence. These perturbations caused the prominence to oscillate and to rise faster than before. The absence of intense heating within the first two hours after the onset of the prominence eruption, which followed an exponential increase in height, indicates that ideal instability played a crucial role. The eruption involved interactions with the other side-arcade, leading up to a twin coronal mass ejection, which was accompanied by transient surface brightenings in the central arcade, followed by transient dimmings and brightenings in the two side-arcades. We suggest that flux feeding from chromospheric fibrils might be an important mechanism to trigger coronal eruptions.

### **Blobs in recurring EUV jets**

Q. M. **Zhang** and H. S. Ji

E-print, May 2014; A&A, 567, A11, 2014

<http://arxiv.org/pdf/1405.5132v1.pdf>

Coronal jets are one type of ubiquitous small-scale activities caused by magnetic reconnection in the solar corona. They are often associated with cool surges in the chromosphere. In this paper, we report our discovery of blobs in the recurrent and homologous jets that occurred at the western edge of NOAA active region 11259 on **2011 July 22**. The jets were observed in the seven extreme-ultraviolet (EUV) filters of the Atmospheric Imaging Assembly (AIA) instrument aboard the Solar Dynamics Observatory (SDO). Using the base-difference images of the six filters (94, 131, 171, 211, 193, and 335 Å), we carried out the differential emission measure (DEM) analyses to explore the thermodynamic evolutions of the jets. The jets were accompanied by cool surges observed in the H $\alpha$  line center of the ground-based telescope in the Big Bear Solar Observatory. The jets that had lifetimes of 20-30 min recurred at the same place for three times with interval of 40-45 min. Interestingly, each of the jets intermittently experienced several upward eruptions at the speed of 120-450 km s<sup>-1</sup>. After reaching the maximum heights, they returned back to the solar surface, showing near-parabolic trajectories. The falling phases were more evident in the low-T filters than in the high-T filters, indicating that the jets experienced cooling after the onset of eruptions. We identified bright and compact blobs in the jets during their rising phases. The simultaneous presences of blobs in all the EUV filters were consistent with the broad ranges of the DEM profiles of the blobs ( $5.5 \leq \log T \leq 7.5$ ), indicating their multi-thermal nature. The median temperatures of the blobs were  $\sim 2.3$  MK. The blobs that were  $\sim 3$  Mm in diameter had lifetimes of 24-60 s. To our knowledge, this is the first report of blobs in coronal jets. We propose that these blobs are plasmoids created by the magnetic reconnection as a result of tearing-mode instability and ejected out along the jets.

### **Simulated (STEREO) Views of the Solar Wind Disturbances Following the Coronal Mass Ejections of 1 August 2010**

Y. **Zhang** · A.M. Du · X.S. Feng · W. Sun · Y.D. Liu · C.D. Fry · C.S. Deehr · M. Dryer · B. Zieger · Y.Q. Xie

Solar Phys (2014) 289:319–338

[http://sprg.ssl.berkeley.edu/~liuxying/pubs/2014\\_sp\\_zhang.pdf](http://sprg.ssl.berkeley.edu/~liuxying/pubs/2014_sp_zhang.pdf)

Images observed by the twin spacecraft *Solar TERrestrial RELations Observatory* (STEREO) A and B appear as complex structures for two coronal mass ejections (CMEs) on **1 August 2010**. Therefore, a series of sky maps of Thomson-scattered white light by interplanetary coronal mass ejections (ICMEs) on 1 August 2010 are simulated using the Hakamada–Akasofu–Fry (HAF) three-dimensional solar-wind model. A comparison between the simulated images and observations of STEREO-A and -B clarifies the structure and evolution of ICMEs (including shocks) in the observed images. The results demonstrate that the simulated images from the HAF model are very useful in the interpretation of the observed images when the ICMEs overlap within the fields of view of the instruments onboard STEREO-A and -B.

### **The Formation and Eruption of Solar Quiescent Prominences**

Y. Z. **Zhang**

2013 ApJ 777 52

Following the two-stage catastrophic flux rope model presented by Zhang et al., we investigate how magnetic flux emergence affects the formation and evolution of solar quiescent prominences. The magnetic properties of the flux rope

are described with its toroidal magnetic flux per radian  $\Phi_p$  and poloidal flux  $\Phi$ , and  $\Phi_p$  is defined as the emerging strength (ES) of the magnetic flux. After the first catastrophe, the quiescent prominences are supported by the vertical current sheet and located in cavities below the curved transverse current sheet in the inner corona, for which both ES and  $\Phi$  are in the certain ranges. We calculate the strength range as  $0.25 < ES < 0.50$  for the quadrupolar field, and obtain the equation  $\Phi_p \Phi = \text{const.}$ , that is, the relationship between  $\Phi_p$  and  $\Phi$  of the emerging flux for which the quiescent prominences are formed in the inner corona. After the second catastrophe, the quiescent prominences would either fall down onto the solar surface or erupt as an important part of coronal mass ejections. During the eruption of the quiescent prominences, most of the magnetic energy in the flux rope is lost, and less than half of the energy loss of the rope is released in the form of Alfvén waves. We argue that there would be two important conditions required for the formation and eruption of solar quiescent prominences, a complicated source region and emerging toroidal magnetic flux that exceeds a critical strength.

## **A Comparative Study of Coronal Mass Ejections with and Without Magnetic Cloud Structure near the Earth: Are All Interplanetary CMEs Flux Ropes?**

J. Zhang, P. Hess, W. Poomvises

Solar Physics, May 2013, Volume 284, Issue 1, pp 89-104; **File**

An outstanding question concerning interplanetary coronal mass ejections (ICMEs) is whether all ICMEs have a magnetic flux rope structure. We test this question by studying two different ICMEs, one having a magnetic cloud (MC) showing smooth rotation of magnetic field lines and the other not. The two ICMEs are chosen in such a way that their progenitor CMEs are very similar in remote sensing observations. Both CMEs originated from close to the central meridian directly facing the Earth. Both CMEs were associated with a long-lasting post-eruption loop arcade and appeared as an elliptical halo in coronagraph images, indicating a flux rope origin. We conclude that the difference in the in-situ observation is caused by the geometric selection effect, contributed by the deflection of flux ropes in the inner corona and interplanetary space. The first event had its nose pass through the observing spacecraft; thus, the intrinsic flux rope structure of the CME appeared as a magnetic cloud. On the other hand, the second event had the flank of the flux rope intercept the spacecraft, and it thus did not appear as a magnetic cloud. We further argue that a conspicuous long period of weak magnetic field, low plasma temperature, and density in the second event should correspond to the extended leg portion of the embedded magnetic flux rope, thus validating the scenario of the flank-passing. These observations support the idea that all CMEs arriving at the Earth include flux rope drivers.

## **Observation of An Evolving Magnetic Flux Rope Prior To and During A Solar Eruption**

J. Zhang, X. Cheng, and M. D. Ding

E-print, March 2012, Nature Communications [www.nature.com/naturecommunications](http://www.nature.com/naturecommunications)  
[http://spaceweather.gmu.edu/xcheng/paper/Zhang\\_Cheng\\_Ding\\_2012.pdf](http://spaceweather.gmu.edu/xcheng/paper/Zhang_Cheng_Ding_2012.pdf) , File

Explosive energy release is a common phenomenon occurring in magnetized plasma systems ranging from laboratories, Earth's magnetosphere, the solar corona and astrophysical environments. Its physical explanation is usually attributed to magnetic reconnection in a thin current sheet. Here we report the important role of magnetic flux rope structure, a volumetric current channel, in producing explosive events. The flux rope is observed as a hot channel prior to and during a solar eruption from the Atmospheric Imaging Assembly (AIA) telescope on board the Solar Dynamic Observatory (SDO). It initially appears as a twisted and writhed sigmoidal structure with a temperature as high as 10 MK and then transforms toward a semi-circular shape during a slow rise phase, which is followed by fast acceleration and onset of a flare. The observations suggest that the instability of the magnetic flux rope trigger the eruption, thus making a major addition to the traditional magnetic-reconnection paradigm. **8 March 2011**

## **EFFECTS OF PHYSICAL FEATURES IN THE SOLAR ATMOSPHERE ON THE CORONAL MASS EJECTION EVOLUTION**

Y. Z. Zhang, X. S. Feng, and W. B. Song

Astrophysical Journal, 728:21 (5pp), 2011 February; **File**

Based on time-dependent MHD simulation, we investigate how physical features in the solar atmosphere affect the evolution of coronal mass ejections (CMEs). It is found that temperature and density play a crucial role in CME initiation. We argue that lower temperature facilitates the catastrophe's occurrence, and that the CMEs which initiate in low density could gain lower velocity. In our numerical experiment, by employing different values of  $\beta$ , the resulting eruptions of either slow or fast events may be obtained.

## **Why Are Halo Coronal Mass Ejections Faster?**

Q. M. Zhang<sup>1</sup>, Y. Guo<sup>1</sup>, P. F. Chen, M. D. Ding, and C. Fang

E-print, Feb. 2010, **File**, Research in Astron. & Astrophys.

Halo coronal mass ejections (CMEs) were found to be significantly faster than normal CMEs, which was a long-standing puzzle. In order to solve the puzzle, we first investigate the observed properties of 31 limb CMEs that display clearly loop-shaped frontal loops. The observational results show a strong tendency that slower CMEs are weaker in the white-light intensity. Then, we perform a Monte Carlo simulation of 20000 artificial limb CMEs that have average velocity of  $\sim 523$  km/s. The Thomson scattering of these events is calculated when they are assumed to be observed as

limb and halo events, respectively. It is found that the white-light intensity of many slow CMEs becomes remarkably reduced as they turn from being viewed as a limb event to as a halo event. When the intensity is below the background solar wind fluctuation, it is assumed that they would be missed by coronagraphs. The average velocity of "detectable" halo CMEs is ~922 km/s, very close to the observed value. It also indicates that wider events are more likely to be recorded. The results soundly suggest that the higher average velocity of halo CMEs is due to that a majority of slow events and a part of narrow fast events carrying less material are so faint that they are blended with the solar wind fluctuations, and therefore are not observed.

## **Magnetohydrodynamic simulation of non-flux rope coronal mass ejections**

Zhang, T. X.; Wu, S. T.

J. Geophys. Res., Vol. 114, No. A5, A05107, 2009,

<http://dx.doi.org/10.1029/2008JA013860>

Observations at 1 AU indicate that only 1/3 of coronal mass ejections (CMEs) have a flux rope structure, while the other 2/3 of CMEs have a complex disordered magnetic field. The initiation of the flux rope CMEs has been extensively simulated with various magnetohydrodynamic (MHD) models. However, the initiation of the non-flux rope CMEs is rarely done in numerical modeling. In this paper, we numerically simulate the physical origin and characteristics of the non-flux rope CMEs by using a three-dimensional, axisymmetric, time-dependent, self-consistent MHD model. The results show that the emergence of a counterclockwise flux rope from the lower coronal boundary at the open magnetic field region, near the closed magnetic field lines, can initiate a magnetic configuration, which causes the magnetic reconnection at the coronal base. Physically, the magnetic field of the emerged counterclockwise flux rope has antipolarity with the background open field, and the location of the magnetic flux emergence is at the edge of a coronal hole. This magnetic reconnection between closed and open field lines at the coronal base generates an Alfvénic jet-like plasma outflow. It could further develop into a non-flux rope CME if enough magnetic energy is deposited. Solar energetic particle (SEP) events in association with the non-flux rope CMEs are usually impulsive because the magnetic topology obtained from this simulation of non-flux rope CMEs corresponds to that proposed by Reames (2002) to lead impulsive SEP events.

## **On the Relationship between Flux Emergence and CME Initiation**

Yin Zhang · Mei Zhang · Hongqi Zhang

Solar Phys (2008) 250: 75–88

<http://www.springerlink.com/content/yn4p186g376x3805/fulltext.pdf>

We present in this paper a statistical study aimed at understanding the possible relationship between surface magnetic field variation and CME initiation. The three samples studied comprise 189 CME-source regions, 46 active regions, and 15 newly emerging active regions. Both large-scale and small-scale variations of longitudinal magnetic fields of these regions are studied. To quantitatively study these variations, three physical quantities are calculated: the average total magnetic flux (ATF), the flux variation rate (FVR), and the normalized flux variation rate (NFVR). Our results show that 60% of the CME-source regions are found to have magnetic flux increases during 12 hours before CME eruptions and 40% are found to have magnetic flux decreases. The NFVR of CME-source regions are found to be statistically identical to those of active regions, averaged over 111 hours, and significantly smaller than those of newly emerging active regions. In addition 91% of the CME-source regions are found to have small-scale flux emergence, whereas small-scale flux emergences are also easily identified in active regions during periods with no solar surface activity.

**Our study suggests that the relationship between flux emergence and CME eruption is complex and the appearance of flux emergence alone is not unique for the initiation of CME eruption.**

## **The dependence of the helicity bound of force-free magnetic fields on boundary conditions**

Mei Zhang and Natasha Flyer

E-print, May 2008; ApJ

This paper follows up on a previous study showing that in an open atmosphere such as the solar corona the total magnetic helicity of a force-free field must be bounded and the accumulation of magnetic helicity in excess of its upper bound would initiate a non-equilibrium situation resulting in an expulsion such as a coronal mass ejection (CME). In the current paper, we investigate the dependence of the helicity bound on the boundary condition for several families of nonlinear force-free fields. Our calculation shows that the magnitude of the helicity upper bound of force-free fields is non-trivially dependent on the boundary condition. Fields with a multipolar boundary condition can have a helicity upper bound ten times smaller than those with a dipolar boundary condition when helicity values are normalized by the square of their respective surface poloidal fluxes. This suggests that a coronal magnetic field may erupt into a CME when the applicable helicity bound falls below the already accumulated helicity as the result of a slowly changing boundary condition. Our calculation also shows that a monotonic accumulation of magnetic helicity can lead to the formation of a magnetic flux rope applicable to kink instability. This suggests that CME initiations by exceeding helicity bound and by kink instability can both be the consequences of helicity accumulation in the corona. Our study gives insights into the observed associations of CMEs with the magnetic features at their solar surface origins.

## **A statistical study on the relationship between surface field variation and CME initiation**

Adv. Space Res. 39(11), Pages 1762-1766, 2007.

Y. **Zhang**, M. Zhang and H.Q. Zhang

We find that 58% of CMEs are associated with magnetic flux increases during the short-term of 12 h before CME eruption and 42% are associated with magnetic flux decreases.

Our study suggests that the relationship between small-scale flux emergence and CME eruption is complex and that the appearance of flux emergence alone is not sufficient for the initiation of CME eruption.

## **A Statistical Study of Main and Residual Accelerations of Coronal Mass Ejections**

J. **Zhang** and K. P. Dere

The Astrophysical Journal, 649:1100-1109, 2006, File

## **A study of the kinematic evolution of coronal mass ejections.**

**Zhang**, J., Dere, K.P., Howard, R.A., Vourlidas, A.:

2004, Astrophys. J. 604, 420 – 432.

## **On the Temporal Relationship between Coronal Mass Ejections and Flares.**

**Zhang**, J., Dere, K.P., Howard, R.A., Kundu, M.R., White, S.M.,

2001. Astrophys. J. 559, 452–462.

## **A Survey and Statistical Study of Off-Limb Events Observed in SDO/HMI Continuum Intensity.**

**Zhao**, J.S., Liu, Y.

Sol Phys 298, 148 (2023).

<https://doi.org/10.1007/s11207-023-02240-4>

Several strong eruptive events that occurred near the solar limb were reported generating off-limb features detectable in the SDO/HMI's continuum intensity. These observations offer new insights into the emission mechanisms of off-limb flaring loops, magnetic strength in the loops, and electron density distributions, among others. However, only a limited number of such events were reported, and it is unclear whether off-limb white-light features are popular or only associated with specific eruptions. In this study, we surveyed all the flaring events that occurred between May 2010 and August 2023 with a magnitude stronger than M2.0 and a heliographic longitude larger than 65°. We found that among the 189 flares that met our selection criteria, 78 (41.3%) had off-limb features associated with them. Further statistical analysis showed, unsurprisingly, that the stronger the flare, the more likely it has an off-limb white-light feature, and the closer the flare is to the limb, the more likely an off-limb feature is detectable. We then categorized these off-limb white-light events into four types, closed-loop eruptions, open-loop eruptions, fast ejection, and flare arcades, and identified the events with visible flare ribbons. Coupling two examples of the white-light observations with simultaneous UV/EUV observations, we demonstrate the usefulness of the former in studying the flare dynamics and emission mechanisms. Our catalogue provides a rather complete list of the off-limb white-light events, which will benefit the community interested in studying such events.

## **Synthetic Lyman- $\alpha$ emissions for the coronagraph aboard the ASO-S mission**

### ***I. An eruptive prominence-cavity system***

J. **Zhao**<sup>1</sup>, P. Zhang<sup>1</sup>, S. E. Gibson<sup>2</sup>, Y. Fan<sup>2</sup>, L. Feng<sup>1</sup>, F. Yu<sup>1</sup>, H. Li<sup>1</sup> and W. Q. Gan<sup>1</sup>

A&A 665, A39 (2022)

<https://www.aanda.org/articles/aa/pdf/2022/09/aa43029-22.pdf>

Context. Strong ultraviolet (UV) emission from the sun will be observed by the Lyman- $\alpha$  Solar Telescope (LST) on board the Advanced Space-based Solar Observatory (ASO-S), scheduled for launch in 2022. It will provide continuous observations from the solar disk to the corona below a 2.5 solar radius with high resolution. To configure the appropriate observing modes and also to better understand its upcoming observations, a series of simulations and syntheses of different structures and processes need to be done in advance.

Aims. As prominence eruptions are the main drivers of space weather, the need to monitor such phenomena has been set as a priority among the objectives of ASO-S mission. In this work, we synthesize the evolution of a modeled prominence-cavity system before and during its eruption in the field of view (FOV) of LST.

Methods. We adopted the input magnetohydrodynamic (MHD) model of a prominence-cavity system, which is readily comparable to the Atmospheric Imaging Assembly (AIA) observations. The Lyman- $\alpha$  emission of the prominence and its eruptive counterparts are synthesized through the PRODOP code, which considers non-local thermodynamic equilibrium (NLTE) radiative transfer processes, while the other coronal part such as the cavity and surrounding streamer, are synthesized with the FORWARD package, which deals with optically thin structures.

Results. We present a discussion of the evolution of the eruptive prominence-cavity system, analyzing the synthetic emissions both on the disk near the limb and above the limb as viewed by the coronagraph, as well as the three-dimensional (3D) data of the MHD simulation.

Conclusions. The evolution of the prominence-cavity system exhibits the condensation of cavity mass onto the prominence and the evaporation of prominence plasma into the central cavity. The synthetic emission in Lyman- $\alpha$  shows a similar pattern as in the AIA extreme ultraviolet (EUV) wavelengths before eruption, namely, the appearance of a “horn” substructure as a precursor to the eruption. The emission of prominence with an optically thick assumption is one to two orders of magnitude lower than the optically thin one. Here, the dimming effect in Lyman- $\alpha$  is analyzed, for the first time, for the eruptive prominence-cavity system. Accompanying the prominence plasma motion during the eruption, the apparent dimming shows a preferred location evolving from the top and bottom of the bright core to the whole body above the bottom part, while the collisional component progressively dominates the total emission of the flux rope bright core at these locations. By analyzing the signal-to-noise ratio (S/N) with a consideration of LST’s optical design, we conclude that the substructures in the cavity and the bright core of the CME can be observed with sufficient S/N at different stages in the FOV of LST.

## **Chromospheric recurrent jets in a sunspot group and their inter-granular origin**

[Jie Zhao](#), [Jiangtao Su](#), [Xu Yang](#), [Hui Li](#), [Brigitte Schmieder](#), [Kwangsu Ahn](#), [Wenda Cao](#)

ApJ 932 95 2022

<https://arxiv.org/pdf/2205.06981.pdf>

<https://iopscience.iop.org/article/10.3847/1538-4357/ac6e3b/pdf>

We report on high resolution observations of recurrent fan-like jets by the Goode Solar telescope (GST) in multi-wavelengths inside a sunspot group. The dynamics behaviour of the jets is derived from the Ha line profiles. Quantitative values for one well-identified event have been obtained showing a maximum projected velocity of 42 km s<sup>-1</sup> and a Doppler shift of the order of 20 km s<sup>-1</sup>. The footpoints/roots of the jets have a lifted center on the Ha line profile compared to the quiet sun suggesting a long lasting heating at these locations. The magnetic field between the small sunspots in the group shows a very high resolution pattern with parasitic polarities along the inter-granular lanes accompanied by high velocity converging flows (4 km s<sup>-1</sup>) in the photosphere. Magnetic cancellations between the opposite polarities are observed in the vicinity of the footpoints of the jets. Along the inter-granular lanes horizontal magnetic field around 1000 Gauss is generated impulsively. Overall, all the kinetic features at the different layers through photosphere and chromosphere favor a convection-driven reconnection scenario for the recurrent fan-like jets, and evidence a site of reconnection between the photosphere and chromosphere corresponding to the inter-granular lanes. **2016 September 7**

## **Plasmoid-fed prominence formation (PF2) during flux rope eruption**

[Xiaozhou Zhao](#), [Rony Keppens](#)

ApJ 2022

<https://arxiv.org/pdf/2202.08367.pdf>

We report a new, plasmoid-fed scenario for the formation of an eruptive prominence (PF2), involving reconnection and condensation. We use grid-adaptive resistive two-and-a-half-dimensional magnetohydrodynamic (MHD) simulations in a chromosphere-to-corona setup to resolve this plasmoid-fed scenario. We study a pre-existing flux rope (FR) in the low corona that suddenly erupts due to catastrophe, which also drives a fast shock above the erupting FR. A current sheet (CS) forms underneath the erupting FR, with chromospheric matter squeezed into it. The plasmoid instability occurs and multiple magnetic islands appear in the CS once the Lundquist number reaches  $\sim 3.5 \times 10^4$ . The remnant chromospheric matter in the CS is then transferred to the FR by these newly formed magnetic islands. The dense and cool mass transported by the islands accumulates in the bottom of the FR, thereby forming a prominence during the eruption phase. More coronal plasma continuously condenses into the prominence due to the thermal instability as the FR rises. Due to the fine structure brought in by the PF2 process, the model naturally forms filament threads, aligned above the polarity inversion line. Synthetic views at our resolution of 15km show many details that may be verified in future high-resolution observations.

## **Mesoscale Phenomena during a Macroscopic Solar Eruption**

Xiaozhou [Zhao](#) (赵小舟) and Rony Keppens

2020 ApJ 898 90

<https://doi.org/10.3847/1538-4357/ab9a31>

Our previous magnetohydrodynamic simulation of a macroscopic solar eruption discussed in Zhao et al. (2019) showed that the current sheet (CS) evolution during eruption went through four stages: the CS growth stage, the dynamic growth stage, the hot CS stage, and the dynamic hot CS stage. We now focus on various mesoscale phenomena associated with the ongoing reconnection. In the dynamic growth stage, the remnant chromospheric matter in the CS is quasi-periodically pushed into the prominence, inducing fast shocks propagating at a speed of 210 km s<sup>-1</sup>. In the hot CS phase, various shock features relevant for particle acceleration are identified throughout the flare loop. Finally, during both dynamic stages, we quantify the properties of magnetic islands. A typical island is accelerated to Alfvénic speed by the Lorentz force and cools down by radiative cooling and thermal conduction. It also tends to expand in size before colliding with another island, with the FR or with the flare arcade. Islands in the dynamic growth stage have a higher density and lower temperature, and vice versa in the dynamic hot CS stage. Islands tend to move upward in the dynamic growth stage, while almost equal fractions of downward-moving and upward-moving islands in the dynamic hot CS stage. Translating the island trajectories to phase space, we find that the function  $\dot{y} = (ay^2 + by + c)\exp(\lambda y)$  fits the trajectory well, and its two fixed points represent the creation and the annihilation of the island.

## Quantifying the Propagation of Fast Coronal Mass Ejections from the Sun to Interplanetary Space Combining Remote Sensing and Multi-Point in-situ Observations

Xiaowei **Zhao**, Ying D. Liu, Huidong Hu, Rui Wang

ApJ 882 122 2019

<https://arxiv.org/pdf/1908.04450.pdf>

[sci-hub.se/10.3847/1538-4357/ab379b](https://sci-hub.se/10.3847/1538-4357/ab379b)

In order to have a comprehensive view of the propagation and evolution of coronal mass ejections (CMEs) from the Sun to deep interplanetary space beyond 1 au, we carry out a kinematic analysis of 7 CMEs in solar cycle 23. The events are required to have coordinated coronagraph observations, interplanetary type II radio bursts, and multi-point in-situ measurements at the Earth and Ulysses. A graduated cylindrical shell model, an analytical model without free parameters and a magnetohydrodynamic model are used to derive CME kinematics near the Sun, to quantify the CME/shock propagation in the Sun-Earth space, and to connect in-situ signatures at the Earth and Ulysses, respectively. We find that each of the 7 CME-driven shocks experienced a major deceleration before reaching 1 au and thereafter propagated with a gradual deceleration from the Earth to larger distances. The resulting CME/shock propagation profile for each case is roughly consistent with all the data, which verifies the usefulness of the simple analytical model for CME/shock propagation in the heliosphere. The statistical analysis of CME kinematics indicates a tendency that the faster the CME, the larger the deceleration, and the shorter the deceleration time period within 1 au. For several of these events, the associated geomagnetic storms were mainly caused by the southward magnetic fields in the sheath region. In particular, the interaction between a CME-driven shock and a preceding ejecta significantly enhanced the preexisting southward magnetic fields and gave rise to a severe complex geomagnetic storm. **1997 November 4, 2000 June 6, 2001 April 2, 2001 November 4, 2001 November 22, 2005 May 13, 2006 December 13**

Table 1. Solar source information, CME propagation direction, shock arrival time and Ulysses position relative to the Earth for the 7 CMEs.

## Forward Modeling of SDO/AIA and X-Ray Emission from a Simulated Flux Rope Ejection

Xiaozhou **Zhao**, Chun Xia<sup>4</sup>, Tom Van Doorselaere<sup>2</sup>, Rony Keppens<sup>2,4</sup>, and Weiqun Gan<sup>1</sup>

2019 ApJ 872 190

[sci-hub.se/10.3847/1538-4357/ab0284](https://sci-hub.se/10.3847/1538-4357/ab0284)

<https://arxiv.org/pdf/1904.09965.pdf>

We conduct forward-modeling analysis based on our 2.5 dimensional magnetohydrodynamics (MHD) simulation of magnetic flux rope (MFR) formation and eruption driven by photospheric converging motion. The current sheet (CS) evolution during the MFR formation and eruption process in our MHD simulation can be divided into four stages. The first stage shows the CS forming and gradually lengthening. Resistive instabilities that disrupt the CS mark the beginning of the second stage. Magnetic islands disappear in the third stage and reappear in the fourth stage. Synthetic images and light curves of the seven Solar Dynamics Observatory (SDO)/Atmospheric Imaging Assembly (AIA) channels, i.e., 94 Å, 131 Å, 171 Å, 193 Å, 211 Å, 304 Å, and 335 Å, and the 3–25 keV thermal X-ray are obtained with forward-modeling analysis. The loop-top source and the coronal sources of the soft X-ray are reproduced in forward modeling. The light curves of the seven SDO/AIA channels start to rise once resistive instabilities develop. The light curve of the 3–25 keV thermal X-ray starts to go up when the reconnection rate reaches one of its peaks. Quasiperiodic pulsations (QPPs) appear twice in the SDO/AIA 171 Å, 211 Å, and 304 Å channels, corresponding to the period of chaotic (re)appearance and CS-guided displacements of the magnetic islands. QPPs appear once in the SDO/AIA 94 Å and 335 Å channels after the disruption of the CS by resistive instabilities and in the 193 Å channel when the chaotic motion of the magnetic islands reappears.

## Numerical Studies of the Kelvin-Helmholtz Instability in the Coronal Jet

Tianle **Zhao**, [Lei Ni](#), [Jun Lin](#), [Udo Ziegler](#)

Research in Astron. Astrophys.

2018

<https://arxiv.org/pdf/1801.09511.pdf>

The Kelvin-Helmholtz (K-H) instability in the corona EUV jet is studied via 2.5 MHD numerical simulations. The jet results from magnetic reconnection due to the interaction of the new emerging magnetic field and the pre-existing magnetic field in the corona. Our results show that the Alfvén Mach number along the jet is about 5-14 just before the instability occurs, and it is even higher than 14 at some local areas. During the K-H instability process, several vortex-like plasma blobs of high temperature and high density appear along the jet, and magnetic fields have also been rolled up and the magnetic configuration including anti-parallel magnetic fields forms, which leads to magnetic reconnection at many X-points and current sheet fragments inside the vortex-like blob. After magnetic islands appear inside the main current sheet, the total kinetic energy of the reconnection outflows decreases, and cannot support the formation of the vortex-like blob along the jet any longer, then the K-H instability eventually disappears. We also present the results about how the guide field and the flux emerging speed affect the K-H instability. We find that the strong guide field inhibits the shock formation in the reconnection upward outflow regions but helps secondary magnetic islands appear earlier in the main current sheet, and then apparently suppresses the K-H instability. As the speed of the emerging magnetic field decreases, the K-H instability appears later, the highest temperature inside the vortex blob gets lower and the vortex structure gets smaller.

## Correlation between Angular Widths of CMEs and Characteristics of Their Source Regions

X. H. **Zhao**<sup>1,2</sup>, X. S. Feng<sup>1,2</sup>, H. Q. Feng<sup>3</sup>, and Z. Li<sup>4</sup>

2017 ApJ 849 79

<http://sci-hub.cc/http://iopscience.iop.org/0004-637X/849/2/79/>

The angular width of a coronal mass ejection (CME) is an important factor in determining whether the corresponding interplanetary CME (ICME) and its preceding shock will reach Earth. However, there have been very few studies of the decisive factors of the CME's angular width. In this study, we use the three-dimensional (3D) angular width of CMEs obtained from the Graduated Cylindrical Shell model based on observations of Solar Terrestrial Relations Observatory (STEREO) to study the relations between the CME's 3D width and characteristics of the CME's source region. We find that for the CMEs produced by active regions (ARs), the CME width has some correlations with the AR's area and flux, but these correlations are not strong. The magnetic flux contained in the CME seems to come from only part of the AR's total flux. For the CMEs produced by flare regions, the correlations between the CME angular width and the flare region's area and flux are strong. The magnetic flux within those CMEs seems to come from the whole flare region or even from a larger region than the flare. Our findings show that the CME's 3D angular width can be generally estimated based on observations of Solar Dynamics Observatory for the CME's source region instead of the observations from coronagraphs on board the Solar and Heliospheric Observatory and STEREO if the two foot points of the CME stay in the same places with no expansion of the CME in the transverse direction until reaching Earth. **2011-09-06**

**Table 1** Twenty-three CMEs Produced by Active Regions (ARs)

**Table 2** Ten CMEs Produced by Flare Regions during 2011.05–2011.09

## Formation and Initiation of Erupting Flux Rope and Embedded Filament Driven by Photospheric Converging Motion

Xiaozhou **Zhao** (赵小舟)<sup>1,2,3</sup>, Chun Xia<sup>2</sup>, Rony Keppens<sup>2</sup>, and Weiquan Gan

2017 ApJ 841 106

<http://sci-hub.cc/10.3847/1538-4357/aa7142>

In this paper, we study how a flux rope (FR) is formed and evolves into the corresponding structure of a coronal mass ejection (CME) numerically driven by photospheric converging motion. A two-and-a-half-dimensional magnetohydrodynamics simulation is conducted in a chromosphere-transition-corona setup. The initial arcade-like linear force-free magnetic field is driven by an imposed slow motion converging toward the magnetic inversion line at the bottom boundary. The convergence brings opposite-polarity magnetic flux to the polarity inversion, giving rise to the formation of an FR by magnetic reconnection and eventually to the eruption of a CME. During the FR formation, an embedded prominence gets formed by the levitation of chromospheric material. We confirm that the converging flow is a potential mechanism for the formation of FRs and a possible triggering mechanism for CMEs. We investigate the thermal, dynamical, and magnetic properties of the FR and its embedded prominence by tracking their thermal evolution, analyzing their force balance, and measuring their kinematic quantities. The phase transition from the initiation phase to the acceleration phase of the kinematic evolution of the FR was observed in our simulation. The FR undergoes a series of quasi-static equilibrium states in the initiation phase; while in the acceleration phase the FR is driven by Lorentz force and the impulsive acceleration occurs. The underlying physical reason for the phase transition is the change of the reconnection mechanism from the Sweet–Parker to the unsteady bursty regime of reconnection in the evolving current sheet underneath the FR.

## Propagation Characteristics of Two Coronal Mass Ejections From the Sun Far into Interplanetary Space

Xiaowei **Zhao**, Ying D.Liu, Huidong Hu, Rui Wang

ApJ 837 4 2017

<https://arxiv.org/pdf/1702.04122.pdf>

Propagation of coronal mass ejections (CMEs) from the Sun far into interplanetary space is not well understood due to limited observations. In this study we examine the propagation characteristics of two geo-effective CMEs, which occurred on **2005 May 6 and 13**, respectively. Significant heliospheric consequences associated with the two CMEs are observed, including interplanetary CMEs (ICMEs) at the Earth and Ulysses, interplanetary shocks, a long-duration type II radio burst, and intense geomagnetic storms. We use coronagraph observations from SOHO/LASCO, frequency drift of the long-duration type II burst, in situ measurements at the Earth and Ulysses, and magnetohydrodynamic (MHD) propagation of the observed solar wind disturbances at 1 AU to track the CMEs from the Sun far into interplanetary space. We find that both of the two CMEs underwent a major deceleration within 1 AU and thereafter a gradual deceleration when they propagated from the Earth to deep interplanetary space due to interactions with the ambient solar wind. The results also reveal that the two CMEs interacted with each other in the distant interplanetary space even though their launch times on the Sun were well separated. The intense geomagnetic storm for each case was caused by the southward magnetic fields ahead of the CME, stressing the critical role of the sheath region in geomagnetic storm generation, although for the first case there is a corotating interaction region involved.

## MULTI-SPACECRAFT OBSERVATIONS OF THE 2008 JANUARY 2 CME IN THE INNER HELIOSPHERE

X. H. [Zhao](#)<sup>1</sup>, X. S. Feng<sup>1</sup>, C. Q. Xiang<sup>1</sup>, Y. Liu<sup>2</sup>, Z. Li<sup>1,3</sup>, Y. Zhang<sup>4</sup>, and S. T. Wu<sup>5</sup>

*Astrophysical Journal*, 714:1133–1141, 2010 May, [File](#)

We perform a detailed analysis of a coronal mass ejection (CME) on **2008 January 2**. The combination of the *Solar and Heliospheric Observatory* and the twin *STEREO* spacecraft provides three-point observations of this CME. We track the CME in imaging observations and compare its morphology and kinematics viewed from different vantage points. The shape, angular width, distance, velocity, and acceleration of the CME front are different in the observations of these spacecraft. We also compare the efficiency of several methods, which convert the elongation angles of the CME front in images to radial distances. The results of our kinematic analysis demonstrate that this CME experiences a rapid acceleration at the early stage, which corresponds to the flash phase of the associated solar flare in time. Then, at a height of about 3.7 solar radius, the CME reaches a velocity of 790 km s<sup>-1</sup> and propagates outward without an obvious deceleration. Because of its propagation direction away from the observers, the CME is not detected in situ by either *ACE* or *STEREO*.

## Inversion Solutions of the Elliptic Cone Model for Disk Frontside Full Halo Coronal Mass Ejections

Xuepu [Zhao](#)

E-print, Aug. 2007; JGR, VOL. 113, A02101, doi:10.1029/2007JA012582, 2008

Three-dimensional configuration and evolution of coronal mass ejections,

A new algorithm is developed for inverting 6 unknown elliptic cone model parameters from 5 observed CME halo parameters. It is shown that the halo parameter  $\alpha$  includes the information on the CME propagation direction denoted by two model parameters. Based on the given halo parameter  $\alpha$ , two approaches are presented to find out the CME propagation direction. The two-point approach uses two values of  $\alpha$  observed simultaneously by COR1 and COR2 onboard STEREO A and B. The one-point approach combines the value of  $\alpha$  with such simultaneous observation as the location of CME-associated flare, which includes the information associated with CME propagation direction. Model validation experiments show that the CME propagation direction can be accurately determined using the two-point approach, and the other four model parameters can also be well inverted, especially when the projection angle is greater than  $60^\circ$ . The propagation direction and other four model parameters obtained using the one-point approach for six disk frontside full halo CMEs appear to be acceptable, though the final conclusion on its validation should be made after STEREO data are available.

[Zhao](#), X. P., **Determination of geometrical and kinematical properties of frontside halo coronal mass ejections**, in Proc. IAL symp. 226 on Coronal and Stellar Mass Ejections, eds. K. P. Dere, J. Wang, and Y. Yan, 42, 2005.

[Zhao](#), X. P., **Ice cream cone models for halo coronal mass ejections**, in preparation, 2007.

## How Rotating Solar Atmospheric Jets Become Kelvin--Helmholtz Unstable

Ivan [Zhelyazkov](#), [Ramesh Chandra](#), [Reetika Joshi](#)

Frontiers (in *Astronomy and Space Sciences*) 2019

<https://arxiv.org/pdf/1905.10789.pdf>

<https://sci-hub.se/10.3389/fspas.2019.00033>

Recent observations support the propagation of a number of magnetohydrodynamic (MHD) modes which, under some conditions, can become unstable and the developing instability is the Kelvin--Helmholtz instability (KHI). In its nonlinear stage the KHI can trigger the occurrence of wave turbulence which is considered as a candidate mechanism for coronal heating. We review the modeling of tornado-like phenomena in the solar chromosphere and corona as moving weakly twisted and spinning cylindrical flux tubes, showing that the KHI rises at the excitation of high-mode MHD waves. The instability occurs within a wavenumber range whose width depends on the MHD mode number  $m$ , the plasma density contrast between the rotating jet and its environment, and also on the twists of the internal magnetic field and the jet velocity. We have studied KHI in two twisted spinning solar polar coronal hole jets, in a twisted rotating jet emerging from a filament eruption, and in a rotating macrospicule. The theoretically calculated KHI development times of a few minutes for wavelengths comparable to the half-widths of the jets are in good agreement with the observationally determined growth times only for high order ( $10 \leq m \leq 65$ ) MHD modes. Therefore, we expect that the observed KHI in these cases is due to unstable high-order MHD modes. **1997 March 8, 2010 August 21, 2011 February 8, 2013 April 10–11**

## High mode magnetohydrodynamic waves propagation in a twisted rotating jet emerging from a filament eruption

[Ivan Zhelyazkov](#), [Ramesh Chandra](#)

MNRAS Volume 478, Issue 4, 21 August 2018, Pages 5505–5513 2018

<https://arxiv.org/pdf/1805.07536.pdf>



We study the conditions under which high mode magnetohydrodynamic (MHD) waves propagating on a rotating jet emerging from the filament eruption on **2013 April 10--11** can become unstable against the Kelvin--Helmholtz instability (KHI). The evolution of jet indicates the blob like structure at its boundary which could be one of the observable features of the KHI development. We model the jet as a twisted rotating axially moving magnetic flux tube and explore the propagation characteristics of the running MHD modes on the basis of dispersion relations derived in the framework of the ideal magnetohydrodynamics. It is established that unstable MHD waves with wavelengths in the range of 12--15~Mm and instability developing times from 1.5 to 2.6~min can be detected at the excitation of high mode MHD waves. The magnitude of the azimuthal mode number  $m$  crucially depends upon the twist of the internal magnetic field. It is found that at slightly twisted magnetic flux tube the appropriate azimuthal mode number is  $m=16$  while in the case of a moderately twisted flux tube it is equal to 18.

## **Kelvin--Helmholtz Instability in a Cool Solar Jet in the Framework of Hall Magnetohydrodynamics: A Case Study**

I. Zhelyazkov, Z. Dimitrov

*Solar Physics* January 2018, 293:11

<https://link.springer.com/content/pdf/10.1007%2Fs11207-017-1230-0.pdf>

We investigate the conditions under which the magnetohydrodynamic (MHD) modes in a cylindrical magnetic flux tube moving along its axis become unstable against the Kelvin--Helmholtz (KH) instability. We use the dispersion relations of MHD modes obtained from the linearized Hall MHD equations for cool (zero beta) plasma by assuming real wave numbers and complex angular wave frequencies/complex wave phase velocities. The dispersion equations are solved numerically at fixed input parameters and varying values of the ratio  $I_{\text{Hall}}/aI_{\text{Hall},a}$ , where  $I_{\text{Hall}}=c/\omega\pi I_{\text{Hall}}=c/\omega\pi$  ( $c$  being the speed of light, and  $\omega\pi$  the ion plasma frequency) and  $a$  is the flux tube radius. It is shown that the stability of the MHD modes depends upon four parameters: the density contrast between the flux tube and its environment, the ratio of external and internal magnetic fields, the ratio  $I_{\text{Hall}}/aI_{\text{Hall},a}$ , and the value of the Alfvén Mach number defined as the ratio of the tube axial velocity to Alfvén speed inside the flux tube. It is found that at high density contrasts, for small values of  $I_{\text{Hall}}/aI_{\text{Hall},a}$ , the kink ( $m=1$ ) mode can become unstable against KH instability at some critical Alfvén Mach number (or equivalently at critical flow speed), but a threshold  $I_{\text{Hall}}/aI_{\text{Hall},a}$  can suppress the onset of the KH instability. At small density contrasts, however, the magnitude of  $I_{\text{Hall}}/aI_{\text{Hall},a}$  does not affect noticeably the condition for instability occurrence – even though it can reduce the critical Alfvén Mach number. It is established that the sausage mode ( $m=0$ ) is not subject to the KH instability.

## **Kelvin--Helmholtz instability in a twisting solar polar coronal hole jet observed by SDO/AIA**

I. Zhelyazkov, T. V. Zaqarashvili, L. Ofman, R. Chandra

*Advances in Space Research* Volume 61, Issue 2, 15 January 2018, Pages 628-638

<https://arxiv.org/pdf/1706.03703.pdf>

We investigate the conditions under which the fluting ( $m=2$ ),  $m=3$ , and  $m=12$  magnetohydrodynamic (MHD) modes in a uniformly twisted flux tube moving along its axis become unstable in order to model the Kelvin--Helmholtz (KH) instability in a twisting solar coronal hole jet near the northern pole of the Sun. Using a twisting jet of **2010 August 21** by SDO/AIA and other observations of coronal jets we set the parameters of our theoretical model and have obtained that in a twisted magnetic flux tube of radius of 9.8~Mm, at a density contrast of 0.474 and fixed Alfvén Mach number of  $\approx 0.76$ , for three MHD modes there exist instability windows whose width crucially depends upon the internal magnetic field twist. It is found that for the considered modes an azimuthal magnetic field of 1.3--1.4~G (computed at the tube boundary) makes the width of the instability windows equal to zero, that is, it suppresses the KH instability onset. On the other hand, the times for developing KH instability of the  $m=12$  MHD mode at instability wavelengths between 15 and 12~Mm turn out to be in the range of 1.9 to 4.7~minutes that is in agreement with the growth rates estimated from the temporal evolution of the observed unstable jet's blobs in their initial stage.

## **Kelvin--Helmholtz instability in an active region jet observed with Hinode**

I. Zhelyazkov, R. Chandra, A. K. Srivastava

*Astrophys. Space Sci.* 2015

<http://arxiv.org/pdf/1512.07811v1.pdf>

Over past ten years a variety of jet-like phenomena were detected in the solar atmosphere, including plasma ejections over a range of coronal temperatures being observed as extreme ultraviolet (EUV) and X-ray jets. We study the possibility for the development of Kelvin--Helmholtz (KH) instability of transverse magnetohydrodynamic (MHD) waves traveling along an EUV jet situated on the west side of NOAA AR 10938 and observed by three instruments on board Hinode on **2007 January 15/16** (Chifor et al., *Astron. Astrophys.* 481, L57 (2008)). The jet was observed around  $\log T_e = 6.2$  with up-flow velocities exceeded 150 km/s. Using Fe XII  $\lambda 186$  and  $\lambda 195$  line ratios, the measured densities were found to be above  $\log N_e = 11$ . We have modeled that EUV jet as a vertically moving magnetic flux tube (untwisted and weakly twisted) and have studied the propagation characteristics of the kink ( $m=1$ ) mode and the higher  $m$  modes with azimuthal mode numbers  $m=2,3,4$ . It turns out that all these MHD waves can become unstable at flow velocities in the range of 112--114.8 km/s. The lowest critical jet velocity of 112 km/s is obtained when modeling the jet as compressible plasma contained in an untwisted magnetic flux tube. We have compared two analytically found criteria for predicting the threshold Alfvén Mach number for the onset of KH

instability and have concluded that one of them yields reliable values for the critical Alfvén Mach number. Our study of the nature of stable and unstable MHD modes propagating on the jet shows that in a stable regime all the modes are pure surface waves, while the unstable kink ( $m=1$ ) mode in untwisted compressible plasma flux tube becomes a leaky wave. In the limit of incompressible media (for the jet and its environment) all unstable modes are non-leaky surface waves.

### **Kelvin--Helmholtz instability in solar H-alpha surges**

I. Zhelyazkov, T. V. Zaqarashviki, R. Chandra, A. K. Srivastava, T. Mishonov

2015

<http://arxiv.org/pdf/1501.00867v1.pdf>

We study the evolutionary conditions for Kelvin--Helmholtz (KH) instability in a H-alpha solar surge observed in NOAA AR 8227 on **1998 May 30**. The jet with speeds in the range of 45--50 km/s, width of 7 Mm, and electron number density of  $3.83 \times 10^{10} \text{ cm}^{-3}$  is assumed to be confined in a twisted magnetic flux tube embedded in a magnetic field of 7 G. The temperature of the plasma flow is of the order of  $10^5$  K while that of its environment is taken to be  $2 \times 10^6$  K. The electron number density of surrounding magnetized plasma has a typical for the TR/lower corona region value of  $2 \times 10^9 \text{ cm}^{-3}$ . Under these conditions, the Alfvén speed inside the jet is equal to 78.3 km/s. We model the surge as a moving magnetic flux tube for two magnetic field configurations: (i) a twisted tube surrounded by plasma with homogeneous background magnetic field, and (ii) a twisted tube which environment is plasma with also twisted magnetic field. The magnetic field twist in given region is characterized by the ratio of azimuthal to the axial magnetic field components evaluated at the flux tube radius. The numerical studies of appropriate dispersion relations of MHD modes supported by the plasma flow in both magnetic field configurations show that unstable against Kelvin--Helmholtz instability can only be the MHD waves with high negative mode numbers and the instability occurs at sub-Alfvénic critical flow velocities in the range of 25--50 km/s.

### **Kelvin--Helmholtz instability of magnetohydrodynamic waves propagating on solar surges**

I. Zhelyazkov, R. Chandra, A. K. Srivastava, T. Mishonov

[Astrophysics and Space Science](#), April 2015, Volume 356, [Issue 2](#), pp 231-240

In the present paper, we study the evolutionary conditions for Kelvin--Helmholtz (KH) instability in a high-temperature solar surge observed in NOAA AR 11271 using the Solar Dynamics Observatory data on **2011 August 25**. The jet with speed of  $\approx 100 \text{ km s}^{-1}$ , width of 7 Mm, and electron number density of  $4.17 \times 10^9 \text{ cm}^{-3}$  is assumed to be confined in an untwisted/twisted magnetic flux tube with magnetic field of 10 G. The temperature of the plasma flow is  $2 \times 10^6$  K while that of its environment, according to the observational data, is of the order of 106 K. The electron number density of surrounding magnetized plasma is evaluated to be equal to  $1.15 \times 10^9 \text{ cm}^{-3}$ . Under these conditions, the Alfvén speed inside the flux tube is  $337.6 \text{ km s}^{-1}$ , the sound speed is around  $166 \text{ km s}^{-1}$ , while these characteristic speeds of the environment are  $\approx 719 \text{ km s}^{-1}$  and  $\approx 117 \text{ km s}^{-1}$ , respectively. We study the propagation of normal MHD modes in the flux tube considering the two cases, notably of untwisted magnetic flux tube and the twisted one. The numerical solution to the dispersion relation shows that the kink ( $m=1$ ) wave traveling in an untwisted flux tube becomes unstable if the jet speed exceeds  $1060 \text{ km s}^{-1}$ —a speed which is inaccessible for solar surges. A weak twist (the ratio of azimuthal to longitudinal magnetic field component) of the internal magnetic field in the range of 0.025–0.2 does not change substantially the critical flow velocity. Thus, one implies that, in general, the kink mode is stable against the KH instability. It turns out, however, that the  $m=-2$  and  $m=-3$  MHD modes can become unstable when the twist parameter has values between 0.2 and 0.4. Therefore, the corresponding critical jet speed for instability onset lies in the range of 93.5–99.3  $\text{km s}^{-1}$ . The instability wave growth rate, depending on the value of the wavelength, is of the order of several dozen inverse milliseconds. It remains to be seen whether these predictions will be observationally validated in future in the coronal jet-like structures in abundant measure.

### **Kelvin--Helmholtz instability in an active region jet observed with Hinode**

I. Zhelyazkov, R. Chandra & A. K. Srivastava

[Astrophysics and Space Science](#) February 2016, 361:51

<http://arxiv.org/pdf/1512.07811v1.pdf>

Over past ten years a variety of jet-like phenomena were detected in the solar atmosphere, including plasma ejections over a range of coronal temperatures being observed as extreme ultraviolet (EUV) and X-ray jets. We study the possibility for the development of Kelvin--Helmholtz (KH) instability of transverse magnetohydrodynamic (MHD) waves traveling along an EUV jet situated on the west side of NOAA AR 10938 and observed by three instruments on board Hinode on **2007 January 15/16** (Chifor et al. in *Astron. Astrophys.* 481:L57, 2008b). The jet was observed around  $\text{LogTe}=6.2$  with up-flow velocities exceeded  $150 \text{ km s}^{-1}$ . Using Fe xii  $\lambda 186$  and  $\lambda 195$  line ratios, the measured densities were found to be above  $\text{LogNe}=11$ . We have modeled that EUV jet as a vertically moving magnetic flux tube (untwisted and weakly twisted) and have studied the propagation characteristics of the kink ( $m=1$ ) mode and the higher  $m$  modes with azimuthal mode numbers  $m=2,3,4$ . It turns out that all these MHD waves can become unstable at flow velocities in the range of 112--114.8  $\text{km s}^{-1}$ . The lowest critical jet velocity of 112  $\text{km s}^{-1}$  is obtained when modeling the jet as compressible plasma contained in an untwisted magnetic flux tube. When the jet and its environments are treated as incompressible media, the critical jet velocity becomes higher, namely 114.8  $\text{km s}^{-1}$ . A weak twist of the equilibrium magnetic field in the same approximation of incompressible plasmas slightly decreases the threshold Alfvén Mach number,  $M_{\text{crA}}$ , and consequently the corresponding critical velocities, notably to 114.4  $\text{km s}^{-1}$  for the kink mode and to 112.4  $\text{km s}^{-1}$  for the higher  $m$  modes. We have also compared two analytically found

criteria for predicting the threshold Alfvén Mach number for the onset of KH instability and have concluded that one of them yields reliable values for  $M_{crA}$ . Our study of the nature of stable and unstable MHD modes propagating on the jet shows that in a stable regime all the modes are pure surface waves, while the unstable kink ( $m=1$ ) mode in untwisted compressible plasma flux tube becomes a leaky wave. In the limit of incompressible media (for the jet and its environment) all unstable modes are non-leaky surface waves.

### **Kelvin-Helmholtz instability on coronal mass ejecta in the lower corona**

I. Zhelyazkov, T. V. Zaqarashvili, R. Chandra

A&A 574, A55 2015

<http://arxiv.org/pdf/1411.6621v1.pdf>

We model an imaged Kelvin-Helmholtz (KH) instability on a coronal mass ejecta (CME) in the lower corona by investigating conditions under which kink ( $m=1$ ) and  $m=-3$  magnetohydrodynamic (MHD) modes in an uniformly twisted flux tube moving along its axis become unstable. We employ the dispersion relations of MHD modes derived from the linearised magnetohydrodynamic equations. We assume real wave numbers and complex angular wave frequencies, namely complex wave phase velocities. The dispersion relations are solved numerically at fixed input parameters (taken from observational data) and various mass flow velocities. It is shown that the stability of the modes depends upon four parameters, the density contrast between the flux tube and its environment, the ratio of the background magnetic fields in the two media, the twist of the magnetic field lines inside the tube, and the value of the Alfvén Mach number (the ratio of the tube velocity to Alfvén speed inside the flux tube). For a twisted magnetic flux tube at a density contrast of 0.88, background magnetic field ratio of 1.58, and a normalised magnetic field twist of 0.2, the critical speed for the kink ( $m=-3$ ) mode (where  $m$  is the azimuthal mode number) is  $678 \text{ km s}^{-1}$  just as it is observed. The growth rate for this harmonic at KH wavelength of 18.5 Mm and ejecta width of 4.1 Mm is equal to  $0.037 \text{ s}^{-1}$ , in agreement with observations. KH instability of the  $m=-3$  mode may also explain why the KH vortices are seen only at the one side of arising CME. The good agreement between observational and computational data shows that the imaged KH instability on CME can be explained in terms of emerging KH instability of the  $m=-3$  MHD mode in twisted magnetic flux tube moving along its axis. **03-Nov-10**

### **The deformation of an erupting magnetic flux rope in a confined solar flare**

[Ruisheng Zheng](#), [Yihan Liu](#), [Liang Zhang](#), [Yang Liu](#), [Changhui Rao](#), [Qing Lin](#), [Zhimao Du](#), [Libo Zhong](#), [Huadong Chen](#), [Yao Chen](#)

2023 *ApJL* 942 L16

<https://arxiv.org/pdf/2212.14498.pdf>

<https://iopscience.iop.org/article/10.3847/2041-8213/acabc9/pdf>

Magnetic flux ropes (MFRs), sets of coherently twisted magnetic field lines, are believed as core structures of various solar eruptions. Their evolution plays an important role to understand the physical mechanisms of solar eruptions, and can shed light on adverse space weather near the Earth. However, the erupting MFRs are occasionally prevented by strong overlying magnetic fields, and the MFR evolution during the descending phase in the confined cases is lack of attention. Here, we present the deformation of an erupting MFR accompanied by a confined double-peaked solar flare. The first peak corresponded to the MFR eruption in a standard flare model, and the second peak was closely associated with the flashings of an underlying sheared arcade (SA), the reversal slipping motion of the L-shaped flare ribbon, the falling of the MFR, and the shifting of top of filament threads. All results suggest that the confined MFR eruption involved in two-step magnetic reconnection presenting two distinct episodes of energy release in the flare impulsive phase, and the latter magnetic reconnection between the confined MFR and the underlying SA caused the deformation of MFR. **2021 August 29**

### **Compound eruptions of twin flux ropes in a solar active region**

[Ruisheng Zheng](#), [Liang Zhang](#), [Bing Wang](#), [Xiangliang Kong](#), [Hongqiang Song](#), [Zhao Wu](#), [Shiwei Feng](#), [Huadong Chen](#), [Yao Chen](#)

*ApJL* 921 L39 2021

<https://arxiv.org/pdf/2111.00713.pdf> File

<https://iopscience.iop.org/article/10.3847/2041-8213/ac33ae/pdf>

<https://doi.org/10.3847/2041-8213/ac33ae>

Compound eruptions represent that multiple closely spaced magnetic structures erupt consecutively within a short interval, and then lead to a single flare and a single CME. However, it is still subtle for the links between multiple eruptions and the associated single flare or/and single CME. In this Letter, we report the compound eruptions of twin close flux ropes (FR1 and FR2) within a few minutes that resulted in a flare with a single soft X-ray peak and a CME with two cores. The successive groups of expanding loops and double peaks of intensity flux in AIA cool wavelengths indicate two episodes of internal magnetic reconnections during the compound eruptions. Following the eruption of FR2, the erupting FR1 was accelerated, and then the expanding loops overlying FR2 were deflected. Moreover, the eruption of FR2 likely involved the external magnetic reconnection between the bottom of the overlying stretching field lines and the rebounding loops that were previously pushed by the eruption of FR1, which was evidenced by a pair of groups of newly-formed loops. All results suggest that the compound eruptions involved both internal and external magnetic reconnections, and two erupting structures of twin FRs interacted at the initial stage. We propose that two episodes of internal magnetic reconnections were likely united within a few minutes to form the continuous impulsive

phase of the single peaked flare, and two separated cores of the CME was possibly because that the latter core was too slow to merge with the former one. **2015 Dec 23**

### **Formation of a tiny flux rope in the center of an active region driven by magnetic flux emergence, convergence, and cancellation**

[Ruisheng Zheng](#), [Yao Chen](#), [Bing Wang](#), [Hongqiang Song](#), [Wenda Cao](#)

A&A 642, A199 2020

<https://arxiv.org/pdf/2009.04082.pdf>

<https://doi.org/10.1051/0004-6361/202037475>

<https://sci-hub.st/https://www.aanda.org/articles/aa/abs/2020/10/aa37475-20/aa37475-20.html>

Flux ropes are generally believed to be core structures of solar eruptions that are significant for the space weather, but their formation mechanism remains intensely debated. We report on the formation of a tiny flux rope beneath clusters of active region loops on **2018 August 24**. Combining the high-quality multiwavelength observations from multiple instruments, we studied the event in detail in the photosphere, chromosphere, and corona. In the source region, the continual emergence of two positive polarities (P1 and P2) that appeared as two pores (A and B) is unambiguous. Interestingly, P2 and Pore B slowly approached P1 and Pore A, implying a magnetic flux convergence. During the emergence and convergence, P1 and P2 successively interacted with a minor negative polarity (N3) that emerged, which led to a continuous magnetic flux cancellation. As a result, the overlying loops became much sheared and finally evolved into a tiny twisted flux rope that was evidenced by a transient inverse S-shaped sigmoid, the twisted filament threads with blueshift and redshift signatures, and a hot channel. All the results show that the formation of the tiny flux rope in the center of the active region was closely associated with the continuous magnetic flux emergence, convergence, and cancellation in the photosphere. Hence, we suggest that the magnetic flux emergence, convergence, and cancellation are crucial for the formation of the tiny flux rope.

### **The initiation of a solar streamer blowout coronal mass ejection arising from the streamer flank**

[Ruisheng Zheng](#), [Yao Chen](#), [Bing Wang](#)

ApJL 897 L21 2020

<https://arxiv.org/pdf/2007.00896.pdf>

<https://doi.org/10.3847/2041-8213/ab9ebd>

Streamer blowout (SBO) coronal mass ejections (CMEs) represent a particular class of CMEs that are characterized by a gradual swelling of the overlying streamer and a slow CME containing a flux-rope structure. SBO CMEs arising from the streamer flank fall into a special category of SBO CMEs involving three lower arches under the higher streamer arcade. However, the initiation mechanism for this special category of SBO CMEs remains elusive, due to the observational limitations. Here we report critical observations of a SBO CME associated with the eruption of a polar crown filament that originated from the streamer flank. The filament slowly rose toward the solar equator with the writhing motion, and underwent a sudden acceleration before its eruption. Interestingly, during the rising, the filament fields experienced gradual external reconnections, which is evidenced by the dip-shaped bottom of the enveloping flux-rope structure changing from a smooth concave, the slow inflows ( $\sim 1.8 \text{ km s}^{-1}$ ) from both the filament fields and the coronal loops beneath, and the persistent brightenings around the interface between the filament fields and the coronal loops beneath. The newly formed lower loops at the filament source and the Y-shaped structure in the stretched tail fields indicate the internal reconnections for the filament eruption. The clear signatures of the external and internal reconnections shed light on the initiation mechanisms of SBO CMEs. **2019 August 12-13**

### **An Extreme Ultraviolet Wave Associated with A Solar Filament Activation**

[Ruisheng Zheng](#), [Yao Chen](#), [Bing Wang](#), [Hongqiang Song](#)

ApJ 894 139 2020

<https://arxiv.org/pdf/2004.04904.pdf>

<https://doi.org/10.3847/1538-4357/ab863c>

Extreme ultraviolet (EUV) waves are impressive coronal propagating disturbances. They are closely associated with various eruptions, and can be used for the global coronal seismology and the acceleration of solar energetic particles. Hence, the study of EUV waves plays an important role in solar eruptions and Space Weather. Here we present an EUV wave associated with a filament activation that did not evolve into any eruption. Due to the continuous magnetic flux emergence and cancellation around its one end, the filament rose with untwisting motion, and the filament mass flowed towards another end along the rising fields. Intriguingly, following the filament activation, an EUV wave formed with a fast constant speed ( $\sim 500 \text{ km s}^{-1}$ ) ahead of the mass flow, and the overlying coronal loops expanded both in lateral and radial directions. Excluding the possibility of a remote flare and an absent coronal mass ejection, we suggest that the EUV wave was only closely associated with the filament activation. Furthermore, their intimate spatial and temporal relationship indicates that the EUV wave was likely directly triggered by the lateral expansion of overlying loops. We propose that the EUV wave can be interpreted as linear fast-mode wave, and the most vital key for the successful generation of the EUV wave is the impulsive early-phase lateral expansion of overlying loops that was driven by the activated filament mass flow without any eruption. **2015 May 7**

## **A Confined Partial Eruption of Double-decker Filaments**

Ruisheng [Zheng](#)<sup>1,8</sup>, Shuhong Yang<sup>2,3</sup>, Changhui Rao<sup>4,5,8</sup>, Yangyi Liu<sup>4,5</sup>, Libo Zhong<sup>4,5</sup>, Bing Wang<sup>1</sup>, Hongqiang Song<sup>1</sup>, Zhen Li<sup>6,7</sup>, and Yao Chen<sup>1</sup>

2019 ApJ 875 71

[sci-hub.se/10.3847/1538-4357/ab0f3f](https://doi.org/10.3847/1538-4357/ab0f3f)

Filament eruptions, one of the most energetic explosions on the Sun, release large quantities of magnetized plasma into the interplanetary space. Hence, the understanding of the initiation and evolution of filament eruptions can provide broader implications for space weather and geospace climate. Here, we present a confined partial eruption of double-decker structure that consisted of two vertically separated filaments on **2016 April 16**. Only the upper filament erupted, and the eruption was closely associated with an episode of flux cancellation, surrounding transient brightenings, and unambiguous tether-cutting reconnections of the overlying sheared loops. However, the lower filament was nearly intact through the eruption. Interestingly, the erupting material moved along large-scale external loops and eventually arrived at remote sites, indicating a confined partial eruption. All the results show that the partial eruption involved two magnetic reconnections at least, and the bottom magnetic cancellation and internal tether-cutting reconnections between filaments both play critical roles in triggering the eruption. We conjecture that the newly formed low-lying loops due to tether-cutting reconnections and the flare loops resulting from the partial eruption likely contribute to maintaining the equilibrium of the lower filament. It is also suggested that the restriction of some large-scale external magnetic structures is crucial to turn the successful partial eruption into a confined event.

## **The initial morphologies of the wavefronts of extreme ultraviolet waves**

Ruisheng [Zheng](#), [Zhike Xue](#), [Yao Chen](#), [Bing Wang](#), [Hongqiang Song](#)

ApJL 2018

<https://arxiv.org/pdf/1812.08371.pdf>

The morphologies of the wavefronts of extreme ultraviolet (EUV) waves can shed light on their physical nature and driving mechanism that are still strongly debated. In reality, the wavefronts always deform after interacting with ambient coronal structures during their propagation. Here, we focus on the initial wavefront morphologies of four selected EUV waves that are closely associated with jets or flux rope eruptions, using the high spatio-temporal resolution observations and different perspectives from the Solar Dynamics Observatory and the Solar-Terrestrial Relations Observatory. For the jet-driven waves, the jets originated from one end of the overlying closed loops, and the arc-shaped wavefront formed around the other far end of the expanding loops. The extrapolated field lines of the Potential Field Source Surface model show the close relationships between the jets, the wavefronts, and the overlying closed loops. For the flux-rope-driven waves, the flux ropes (sigmoids) lifted off beneath the overlying loops, and the circular wavefronts had an intimate spatio-temporal relation with the expanding loops. All the results suggest that the configuration of the overlying loops and their locations relative to the erupting cores are very important for the formation and morphology of the wavefronts, and both two jet-driven waves and two flux-rope-driven waves are likely triggered by the sudden expansion of the overlying closed loops. We also propose that the wavefront of EUV wave is possibly integrated by a chain of wave components triggered by a series of separated expanding loops. **2011 January 27, 2012 March 26, 2014 March 28, 2018 February 24**

## **Two-sided-loop jets associated with magnetic reconnection between emerging loops and twisted filament threads**

Ruisheng [Zheng](#), [Yao Chen](#), [Zhenghua Huang](#), [Bing Wang](#), [Hongqiang Song](#)

ApJ 861 108 2018

<https://arxiv.org/pdf/1806.00957.pdf>

<http://sci-hub.tw/http://iopscience.iop.org/0004-637X/861/2/108/>

Coronal jets are always produced by magnetic reconnection between emerging flux and pre-existing overlying magnetic fields. When the overlying field is vertical/oblique or horizontal, the coronal jet will appear as anemone type or two-sided-loop type. Most of observational jets are of the anemone type, and only a few of two-sided-loop jets have been reported. Using the high-quality data from New Vacuum Solar Telescope, Interface Region Imaging Spectrograph, and Solar Dynamics Observatory, we present an example of two-sided-loop jets simultaneously observed in the chromosphere, transition region, and corona. The continuous emergence of magnetic flux brought in successively emerging of coronal loops and the slowly rising of an overlying horizontal filament threads. Sequentially, there appeared the deformation of the loops, the plasmoids ejection from the loop top, and pairs of loop brightenings and jet moving along the untwisting filament threads. All the observational results indicate there exist magnetic reconnection between the emerging loops and overlying horizontal filament threads, and it is the first example of two-sided-loop jets associated with ejected plasmoids and twisted overlying fields. **2017 September 23**

## **An extreme ultraviolet wave generating upward secondary waves in a streamer-like solar structure**

Ruisheng [Zheng](#), [Yao Chen](#), [Shiwei Feng](#), [Bing Wang](#), [Hongqiang Song](#)

ApJL 2018

<https://arxiv.org/pdf/1804.06997.pdf>

Extreme ultraviolet (EUV) waves, spectacular horizontally propagating disturbances in the low solar corona, always trigger horizontal secondary waves (SWs) when they encounter ambient coronal structure. We present a first example of

upward SWs in a streamer-like structure after the passing of an EUV wave. The event occurred on **2017 June 1**. The EUV wave happened during a typical solar eruption including a filament eruption, a CME, a C6.6 flare. The EUV wave was associated with quasi-periodic fast propagating (QFP) wave trains and a type II radio burst that represented the existence of a coronal shock. The EUV wave had a fast initial velocity of  $\sim 1000 \text{ km s}^{-1}$ , comparable to high speeds of the shock and the QFP wave trains. Intriguingly, upward SWs rose slowly ( $\sim 80 \text{ km s}^{-1}$ ) in the streamer-like structure after the sweeping of the EUV wave. The upward SWs seemed to originate from limb brightenings that were caused by the EUV wave. All the results show the EUV wave is a fast-mode magnetohydrodynamic shock wave, likely triggered by the flare impulses. We suggest that part of the EUV wave was probably trapped in the closed magnetic fields of streamer-like structure, and upward SWs possibly resulted from the release of trapped waves in the form of slow-mode. It is believed that an interplay of the strong compression of the coronal shock and the configuration of the streamer-like structure is crucial for the formation of upward SWs.

### **Interchange reconnection associated with a confined filament eruption: Implications for the source of transient cold-dense plasma in solar winds**

Ruisheng **Zheng**, Yao Chen, Bing Wang, Gang Li

ApJ 840 3 2017

<https://arxiv.org/pdf/1703.09384.pdf>

The cold-dense plasma is occasionally detected in the solar wind with in situ data, but the source of the cold-dense plasma remains illusive. Interchange reconnections (IRs) between closed fields and nearby open fields are well known to contribute to the formation of solar winds. We present a confined filament eruption associated with a puff-like coronal mass ejection (CME) on **2014 December 24**. The filament underwent successive activations and finally erupted, due to continuous magnetic flux cancellations and emergences. The confined erupting filament showed a clear untwist motion, and most of the filament material fell back. During the eruption, some tiny blobs escaped from the confined filament body, along newly-formed open field lines rooted around the south end of the filament, and some bright plasma flowed from the north end of the filament to remote sites at nearby open fields. The newly-formed open field lines shifted southward with multiple branches. The puff-like CME also showed multiple bright fronts and a clear southward shift. All the results indicate an intermittent IR existed between closed fields of the confined erupting filament and nearby open fields, which released a portion of filament material (blobs) to form the puff-like CME. We suggest that the IR provides a possible source of cold-dense plasma in the solar wind.

### **Interaction of two filaments in a long filament channel associated with twin coronal mass ejections**

Ruisheng **Zheng**, Qingmin Zhang, Yao Chen, Bing Wang, Guohui Du, Chuanyang Li, Kai Yang

ApJ 836 160 2017

<https://arxiv.org/pdf/1701.05122v1.pdf>

Using the high-quality observations of the Solar Dynamics Observatory, we present the interaction of two filaments (F1 and F2) in a long filament channel associated with twin coronal mass ejections (CMEs) on **2016 January 26**. Before the eruption, a sequence of rapid cancellation and emergence of the magnetic flux has been observed, which likely triggered the ascending of the west filament (F1). The east footpoints of rising F1 moved toward the east far end of the filament channel, accompanying with post-eruption loops and flare ribbons. It likely indicated a large-scale eruption involving the long filament channel, resulted from the interaction between F1 and the east filament (F2). Some bright plasma flew over F2, and F2 stayed at rest during the eruption, likely due to the confinement of its overlying lower magnetic field. Interestingly, the impulsive F1 pushed its overlying magnetic arcades to form the first CME, and F1 finally evolved into the second CME after the collision with the nearby coronal hole. We suggest that the interaction of F1 and the overlying magnetic field of F2 led to the merging reconnection that form a longer eruptive filament loop. Our results also provide a possible picture of the origin of twin CMEs, and show the large-scale magnetic topology of the coronal hole is important for the eventual propagation direction of CMEs.

### **Solar jet-coronal hole collision and a related coronal mass ejection**

Ruisheng **Zheng**, Yao Chen, Guohui Du, Chuanyang Li

ApJL 819 L18 2016

<http://arxiv.org/pdf/1602.06493v1.pdf>

Jets are defined as impulsive, well-collimated upflows, occurring in different layers of the solar atmosphere with different scales. Their relationship with coronal mass ejections (CMEs), another type of solar impulsive events, remains elusive. Using the high-quality imaging data of AIA/SDO, here we show a well-observed coronal jet event, in which part of the jets, with the embedding coronal loops, runs into a nearby coronal hole (CH) and gets bounced towards the opposite direction. This is evidenced by the flat-shape of the jet front during its interaction with the CH and the V-shaped feature in the time-slice plot of the interaction region. About a half-hour later, a CME initially with a narrow and jet-like front is observed by the LASCO C2 coronagraph, propagating along the direction of the post-collision jet. We also observe some 304 Å dark material flowing from the jet-CH interaction region towards the CME. We thus suggest that the jet and the CME are physically connected, with the jet-CH collision and the large-scale magnetic topology of the CH being important to define the eventual propagating direction of this particular jet-CME eruption.

25 August 2015

## **Semicircular-like Secondary Flare Ribbons Associated with a Failed Eruption**

R. **Zheng**<sup>1</sup>, M. B. Korsós<sup>1,2</sup>, and R. Erdélyi

2015 ApJ 809 45

Flare ribbons (FRs) are one of the most apparent signatures of solar flares and have been treated as an indicator of magnetic reconnection. Drawing upon the observations from the Solar Dynamics Observatory, we present semicircular-like secondary FRs (SFRs) of a C2.3 flare on **2013 June 19**. Before the flare eruption, two bipoles in this core region subsequently emerged. Due to the interaction between the two bipoles, a tether-cutting eruption took place in the core region. The SFRs, surrounding the core region nearly simultaneously with the flare onset, were much weaker than the two normal FRs. Two ends of the SFRs experienced a separation and extension movement, but the middle part of the SFRs hardly expanded outward. We find SFRs are closely associated with the footpoint brightenings of some small loops around the core region. The eruption was confined by transequatorial loops (TLs), which resulted in the plasma material falling in the north end of the TLs and remote brightenings showing up in the south end of the TLs. The disappearance of the faint (filament) material during the emergence of the SFRs could indicate another eruption. We conclude that two or more magnetic reconnections are involved in this event and propose that SFRs consisting of a small part of true FRs resulted from the second magnetic reconnection and bright footpoints of loop clusters likely heated by the main flare.

## **Improving CME Forecasting Capability: An Urgent Need**

Yihua **Zheng**

Space Weather, Volume 11, Issue 11, pages 641–642, November 2013

<http://www.readcube.com/articles/10.1002/2013SW001004?>

## **Forecasting propagation and evolution of CMEs in an operational setting: What has been learned**

Yihua **Zheng**, Peter Macneice, Dusan Odstrcil, M. L. Mays, Lutz Rastaetter, Antti Pulkkinen, Aleksandre Taktakishvili, Michael Hesse, M. Masha Kuznetsova, Hyesook Lee and Anna Chulaki

Space Weather, Volume 11, Issue 10, pages 557–574, October 2013

One of the major types of solar eruption, coronal mass ejections (CMEs) not only impact space weather, but also can have significant societal consequences. CMEs cause intense geomagnetic storms and drive fast mode shocks that accelerate charged particles, potentially resulting in enhanced radiation levels both in ions and electrons. Human and technological assets in space can be endangered as a result. CMEs are also the major contributor to generating large amplitude Geomagnetically Induced Currents (GICs), which are a source of concern for power grid safety. Due to their space weather significance, forecasting the evolution and impacts of CMEs has become a much desired capability for space weather operations worldwide. Based on our operational experience at Space Weather Research Center at NASA Goddard Space Flight Center (<http://swrc.gsfc.nasa.gov>), we present here some of the insights gained about accurately predicting CME impacts, particularly in relation to space weather operations. These include: 1. The need to maximize information to get an accurate handle of three-dimensional (3-D) CME kinetic parameters and therefore improve CME forecast; 2. The potential use of CME simulation results for qualitative prediction of regions of space where solar energetic particles (SEPs) may be found; 3. The need to include all CMEs occurring within a ~24 h period for a better representation of the CME interactions; 4. Various other important parameters in forecasting CME evolution in interplanetary space, with special emphasis on the CME propagation direction. It is noted that a future direction for our CME forecasting is to employ the ensemble modeling approach.

## **A POSSIBLE DETECTION OF A FAST-MODE EXTREME ULTRAVIOLET WAVE ASSOCIATED WITH A MINI CORONAL MASS EJECTION OBSERVED BY THE SOLAR DYNAMICS OBSERVATORY**

Ruisheng **Zheng**, Yunchun Jiang, Junchao Hong, Jiayan Yang, Yi Bi, Liheng Yang and Dan Yang  
2011 ApJ 739 L39, File

"Extreme ultraviolet (EUV) waves" are large-scale wavelike transients often associated with coronal mass ejections (CMEs). In this Letter, we present a possible detection of a fast-mode EUV wave associated with a mini-CME observed by the Solar Dynamics Observatory. On **2010 December 1**, a small-scale EUV wave erupted near the disk center associated with a mini-CME, which showed all the low corona manifestations of a typical CME. The CME was triggered by the eruption of a mini-filament, with a typical length of about 30". Although the eruption was tiny, the wave had the appearance of an almost semicircular front and propagated at a uniform velocity of 220-250 km s<sup>-1</sup> with very little angular dependence. The CME lateral expansion was asymmetric with an inclination toward north, and the

southern footprints of the CME loops hardly shifted. The lateral expansion resulted in deep long-duration dimmings, showing the CME extent. Comparing the onset and the initial speed of the CME, the wave was likely triggered by the rapid expansion of the CME loops. Our analysis confirms that the small-scale EUV wave is a true wave, interpreted as a fast-mode wave.

### **MHD numerical study of the latitudinal deflection of coronal mass ejection†**

Y. F. [Zho](#), X. S. Feng

JGR, 2013

In this paper, we analyze and quantitatively study the deflection of CME in the latitudinal direction during its propagation from the Corona to interplanetary (IP) space using a three-dimensional (3D) numerical magnetohydrodynamics (MHD) simulation. To this end, **12 May 1997** CME event during the Carrington rotation 1922 is selected. Firstly, we try to reproduce the physical properties for this halo CME event observed by the WIND spacecraft. Then, we study the deflection of CME, and quantify the effect of the background magnetic field and the initiation parameters (such as the initial magnetic polarity and the parameters of the CME model) on the latitudinal deflection of CMEs. The simulations show that the initial magnetic polarity substantially affects the evolution of CMEs. The “parallel” CMEs (with the CME’s initial magnetic field parallel to that of the ambient field) originating from high latitude show a clear Equator-ward deflection at the beginning, and then propagate almost parallel to heliospheric current sheet (HCS), and the “anti-parallel” CMEs (with the CME’s initial magnetic field opposite to that of the ambient field) deflect toward the pole. Our results demonstrate that the latitudinal deflection extent of the “parallel” CMEs is not only mainly controlled by the background magnetic field strength, but also by the initial magnetic field strength of the CMEs. There is an anti-correlation between the latitudinal deflection extent and the CME average transit speed and the energy ratio  $E_{cme}/E_{sw}$ .

### **Unveiling the mechanism for the rapid acceleration phase in a solar eruption**

[Ze Zhong](#), [Yang Guo](#), [Thomas Wiegelmann](#), [Mingde Ding](#), [Yao Chen](#)

ApJL 947 L2 2023

<https://arxiv.org/pdf/2303.14050.pdf>

<https://iopscience.iop.org/article/10.3847/2041-8213/acc6ce/pdf>

Two major mechanisms have been proposed to drive the solar eruptions: the ideal magnetohydrodynamic instability and the resistive magnetic reconnection. Due to the close coupling and synchronicity of the two mechanisms, it is difficult to identify their respective contribution to solar eruptions, especially to the critical rapid acceleration phase. Here, to shed light on this problem, we conduct a data-driven numerical simulation for the flux rope eruption on **2011 August 4**, and quantify the contributions of the upward exhaust of the magnetic reconnection along the flaring current sheet and the work done by the large-scale Lorentz force acting on the flux rope. Major simulation results of the eruption, such as the macroscopic morphology, early kinematics of the flux rope and flare ribbons, match well with the observations. We estimate the energy converted from the magnetic slingshot above the current sheet and the large-scale Lorentz force exerting on the flux rope during the rapid acceleration phase, and find that (1) the work done by the large-scale Lorentz force is about 4.6 times higher than the former, and (2) decreased strapping force generated by the overlying field facilitates the eruption. These results indicate that the large-scale Lorentz force plays a dominant role in the rapid acceleration phase for this eruption.

### **On the Origin of a Broad Quasiperiodic Fast-propagating Wave Train: Unwinding Jet as the Driver**

Xinping [Zhou](#)<sup>1,2</sup>, Zehao Tang<sup>3</sup>, Zhining Qu<sup>1</sup>, Ke Yu<sup>1</sup>, Chengrui Zhou<sup>3</sup>, Yuqi Xiang<sup>1</sup>, Ahmed Ahmed Ibrahim<sup>4</sup>, and Yuandeng Shen

2024 ApJL 974 L3

<https://iopscience.iop.org/article/10.3847/2041-8213/ad7a68/pdf>

Large-scale extreme-ultraviolet waves commonly exhibit as single wave front and are believed to be caused by coronal mass ejections. Utilizing high spatiotemporal resolution imaging observations from the Solar Dynamics Observatory, we present two sequentially generated wave trains originating from the same active region: a narrow quasiperiodic fast-propagating (QFP) wave train that propagates along the coronal loop system above the jet and a broad QFP wave train that travels along the solar surface beneath the jet. The measurements indicate that the narrow QFP wave train and the accompanying flare’s quasiperiodic pulsations (QPPs) have nearly identical onsets and periods. This result suggests that the accompanying flare process excites the observed narrow QFP wave train. However, the broad QFP wave train starts approximately 2 minutes before the QPPs of the flare, but it is consistent with the interaction between the unwinding jet and the solar surface. Moreover, we find that the period of the broad QFP wave train, approximately 130 s, closely matches that of the unwinding jet. This period is significantly longer than the 30 s period of the accompanying flare’s QPPs. Based on these findings, we propose that the intermittent energy release of the accompanying flare excited the narrow QFP wave train confined propagating in the coronal loop system. The unwinding jet, rather than the intermittent energy release in the accompanying flare, triggered the broad QFP wave train propagating along the solar surface. **2011 January 27**,



## **Broad and Bi-directional narrow quasi-periodic fast-propagating wave trains associated with a filament-driven halo CME on 2023 April 21**

[Xinping Zhou](#), [Yuandeng Shen](#), [Yihua Yan](#), [Ke Yu](#), [Zhining Qu](#), [Ahmed Ahmed Ibrahim](#), [Zehao Tang](#), [Chengrui Zhou](#), [Song Tan](#), [Ye Qiu](#), [Hongfei Liang](#)

ApJ **968** 85 **2024**

<https://arxiv.org/pdf/2404.18391>

<https://iopscience.iop.org/article/10.3847/1538-4357/ad4456/pdf>

This paper presents three distinct wave trains that occurred on **2023 April 21**: a broad quasi-periodic fast-propagating (QFP) wave train and a bi-directional narrow QFP wave train. The broad QFP wave train expands outward in a circular wavefront, while bi-directional narrow QFP wave trains propagate in the northward and southward directions, respectively. The concurrent presence of the wave trains offers a remarkable opportunity to investigate their respective triggering mechanisms. Measurement shows that the broad QFP wave train's speed is 300- 1100 km/s in different propagating directions. There is a significant difference in the speed of the bi-directional narrow QFP wave trains: the southward propagation achieves 1400 km/s, while the northward propagation only reaches about 550 km/s accompanied by a deceleration of about 1- 2 kms<sup>-2</sup>. Using the wavelet analysis, we find that the periodicity of the propagating wave trains in the southward and northward directions closely matches the quasi-periodic pulsations (QPPs) exhibited by the flares. Based on these results, the narrow QFP wave trains were most likely excited by the intermittent energy release in the accompanying flare. In contrast, the broad QFP wave train had a tight relationship with the erupting filament, probably attributed to the unwinding motion of the erupting filament or the leakage of the fast sausage wave train inside the filament body.

## **Rapid Rotation of an Erupting Prominence and the Associated Coronal Mass Ejection on 13 May 2013**

[Yuhao Zhou](#), [Haisheng Ji](#) & [Qingmin Zhang](#)

*Solar Physics* volume 298, Article number: 35 (2023)

<https://arxiv.org/pdf/2302.00212.pdf>

<https://doi.org/10.1007/s11207-023-02126-5>

In this paper, we report the multiwavelength observations of an erupting prominence and the associated coronal mass ejection (CME) on 13 May 2013. The event occurs behind the western limb in the field of view of the Atmospheric Imaging Assembly (AIA) on board the Solar Dynamics Observatory (SDO) spacecraft. The prominence is supported by a highly twisted magnetic flux rope and shows rapid rotation in the counterclockwise direction during the rising motion. The rotation of the prominence lasts for  $\sim 47$  minutes. The average period, angular speed, and linear speed are  $\sim 806$  sec,  $\sim 0.46$  rad min<sup>-1</sup>, and  $\sim 355$  km s<sup>-1</sup>, respectively. The total twist angle reaches  $\sim 7\pi$ , which is considerably larger than the threshold for kink instability. Writhing motion during 17:42 – 17:46 UT is clearly observed by SWAP in 174 Å and Extreme-Ultraviolet Imager (EUVI) on board the behind Solar Terrestrial Relations Observatory (STEREO) spacecraft in 304 Å after reaching an apparent height of  $\sim 405$  Mm. Therefore, the prominence eruption is most probably triggered by kink instability. A pair of conjugate flare ribbons and post-flare loops are created and observed by STA/EUVI. The onset time of writhing motion is consistent with the commencement of the impulsive phase of the related flare. The 3D morphology and positions of the associated CME are derived using the graduated cylindrical shell (GCS) modeling. The kinetic evolution of the reconstructed CME is divided into a slow-rise phase ( $\sim 330$  km s<sup>-1</sup>) and a fast-rise phase ( $\sim 1005$  km s<sup>-1</sup>) by the writhing motion. The edge-on angular width of the CME is a constant (60°), while the face-on angular width increases from 96° to 114°, indicating a lateral expansion. The latitude of the CME source region decreases slightly from  $\sim 18^\circ$  to  $\sim 13^\circ$ , implying an equatorward deflection during propagation.

## **The mechanism of magnetic flux rope rotation during solar eruption.**

[Zhou Z](#), [Jiang C](#), [Yu X](#), [Wang Y](#), [Hao Y](#) and [Cui J](#)

(2023) *Front. Phys.* 11: 1119637. doi: 10.3389/fphy.2023.1119637

<https://www.frontiersin.org/articles/10.3389/fphy.2023.1119637/pdf>

<https://www.frontiersin.org/articles/10.3389/fphy.2023.1119637/full#main-content>

Solar eruptions often show the rotation of filaments, which is a manifestation of the rotation of erupting magnetic flux rope (MFR). Such a rotation of MFR can be induced by either the torque exerted by a background shear-field component (which is an external cause) or the relaxation of the magnetic twist of the MFR (an internal cause). For a given chirality of the erupting field, both the external and internal drivers cause the same rotation direction. Therefore, it remains elusive from direct observations which mechanism yields the dominant contribution to the rotation. In this paper, we exploit a full MHD simulation of solar eruption by tether-cutting magnetic reconnection to study the mechanism of MFR rotation. In the simulation, the MFR's height-rotation profile suggests that the force by the external shear-field component is a dominant contributor to the rotation. Furthermore, the torque analysis confirms that it is also the only factor in driving the counterclockwise rotation. On the contrary, the Lorentz torque inside the MFR makes a negative effect on this counterclockwise rotation.

## **The role of non-axisymmetry of magnetic flux rope in constraining solar eruptions**

[Ze Zhong](#), [Yang Guo](#), [Mingde Ding](#)

*Nature Communications* volume 12, Article number: 2734 (2021)

<https://arxiv.org/pdf/2105.07339.pdf>

<https://www.nature.com/articles/s41467-021-23037-8.pdf>

Whether a solar eruption is successful or failed depends on the competition between different components of the Lorentz force exerting on the flux rope that drives the eruption. The present models only consider the strapping force generated by the background magnetic field perpendicular to the flux rope and the tension force generated by the field along the flux rope. Using the observed magnetic field on the photosphere as a time-matching bottom boundary, we perform a data-driven magnetohydrodynamic simulation for the **30 January 2015** confined eruption and successfully reproduce the observed solar flare without a coronal mass ejection. Here we show a Lorentz force component, resulting from the radial magnetic field or the non-axisymmetry of the flux rope, which can essentially constrain the eruption. Our finding contributes to the solar eruption model and presents the necessity of considering the topological structure of a flux rope when studying its eruption behaviour.

## **Quantification of the Writhe Number of the Evolution of Solar Filament Axes**

Zhenjun **Zhou** (周振军)<sup>1,2,3,4</sup>, Chaowei Jiang<sup>5</sup>, Hongqiang Song<sup>6</sup>, Yuming Wang<sup>3</sup>, Yongqiang Hao<sup>1</sup>, and Jun Cui<sup>1</sup>

**2023** ApJ 944 175

<https://iopscience.iop.org/article/10.3847/1538-4357/acb6f8/pdf>

<https://arxiv.org/pdf/2302.11733>

Solar filament eruptions often show complex and dramatic geometric deformation that is highly relevant to the underlying physical mechanism triggering the eruptions. It is well known that the writhe of filament axes is a key parameter characterizing its global geometric deformation, but a quantitative investigation of the development of writhe during its eruption is still lacking. Here we introduce the Writhe Application Toolkit, which can be used to characterize accurately the topology of filament axes. This characterization is achieved based on the reconstruction and writhe number computation of three-dimensional paths of the filament axes from dual-perspective observations. We apply this toolkit to four dextral filaments located in the northern hemisphere with a counterclockwise (CCW) rotation during their eruptions. Initially, all these filaments possess a small writhe number ( $\leq 0.20$ ) indicating a weak helical deformation of the axes. As the CCW rotation kicks in, their writhe numbers begin to decrease and reach large negative values. Combined with the extended Călugăreanu theorem, the absolute value of twist is deduced to decrease during the rotation. Such a quantitative analysis strongly indicates a consequence of the conversion of twist into writhe for the studied events. **10 Dec 2010, 25 Dec 2011, 5 May 2012, 25 Oct 2012**

## **The Mechanism of Magnetic Flux Rope Rotation During Solar Eruption**

[Zhenjun Zhou](#), [Chaowei Jiang](#), [Xiaoyu Yu](#), [Yuming Wang](#), [Yongqiang Hao](#), [Jun Cui](#)

Frontiers **2023**

<https://arxiv.org/pdf/2302.11103.pdf>

Solar eruptions often show the rotation of filaments, which is a manifestation of the rotation of erupting magnetic flux rope (MFR). Such a rotation of MFR can be induced by either the torque exerted by a background shear-field component (which is an external cause) or the relaxation of the magnetic twist of the MFR (an internal cause). For a given chirality of the erupting field, both the external and internal drivers cause the same rotation direction. Therefore, it remains elusive from direct observations which mechanism yields the dominant contribution to the rotation. In this paper, we exploit a full MHD simulation of solar eruption by tether-cutting magnetic reconnection to study the mechanism of MFR rotation. In the simulation, the MFR's height-rotation profile suggests that the force by the external shear-field component is a dominant contributor to the rotation. Furthermore, the torque analysis confirms that it is also the only factor in driving the counterclockwise rotation. On the contrary, the Lorentz torque inside the MFR makes a negative effect on this counterclockwise rotation.

## **Rapid Rotation of an Erupting Prominence and the Associated Coronal Mass Ejection on 13 May 2013**

[Yuhao Zhou](#), [Haisheng Ji](#), [Qingmin Zhang](#)

Solar Phys. **2023**

<https://arxiv.org/pdf/2302.00212.pdf>

In this paper, we report the multiwavelength observations of an erupting prominence and the associated CME on **13 May 2013**. The event occurs behind the western limb in the field of view of SDO/AIA. The prominence is supported by a highly twisted magnetic flux rope and shows rapid rotation in the counterclockwise direction during the rising motion. The rotation of the prominence lasts for  $\sim 47$  minutes. The average period, angular speed, and linear speed are  $\sim 806$  s,  $\sim 0.46$  rad  $\text{min}^{-1}$ , and  $\sim 355$  km  $\text{s}^{-1}$ , respectively. The total twist angle reaches  $\sim 7\pi$ , which is considerably larger than the threshold for kink instability. Writhing motion during 17:42–17:46 UT is clearly observed by SWAP in  $174 \text{ \AA}$  and EUVI on board the behind STEREO spacecraft in  $304 \text{ \AA}$  after reaching an apparent height of  $\sim 405 \text{ Mm}$ . Therefore, the prominence eruption is most probably triggered by kink instability. A pair of conjugate flare ribbons and post-flare loops are created and observed by STA/EUVI. The onset time of writhing motion is consistent with the commencement of the impulsive phase of the related flare. The 3D morphology and positions of the associated CME are derived using the graduated cylindrical shell (GCS) modeling. The kinetic evolution of the reconstructed CME is divided into a slow-rise phase ( $\sim 330$  km  $\text{s}^{-1}$ ) and a fast-rise phase ( $\sim 1005$  km  $\text{s}^{-1}$ ) by the writhing motion. The edge-on angular width of the CME is a constant ( $60^\circ$ ), while the face-on angular width increases from  $96^\circ$  to  $114^\circ$ , indicating

a lateral expansion. The latitude of the CME source region decreases slightly from  $\sim 18^\circ$  to  $\sim 13^\circ$ , implying an equatorward deflection during propagation.

### **The Rotation of Magnetic Flux Rope Formed during Solar Eruption**

[Zhenjun Zhou](#), [Chaowei Jiang](#), [Rui Liu](#), [Yuming Wang](#), [Lijuan Liu](#), [Jun Cui](#)

ApJ **927** L14 **2022**

<https://arxiv.org/pdf/2202.09073.pdf>

<https://iopscience.iop.org/article/10.3847/2041-8213/ac5740/pdf>

The eruptions of solar filaments often show rotational motion about their rising direction, but it remains elusive what mechanism governs such rotation and how the rotation is related to the initial morphology of the pre-eruptive filament (and co-spatial sigmoid), filament chirality, and magnetic helicity. The conventional view regarding the rotation as a result of a magnetic flux rope (MFR) under-going the ideal kink instability still has confusion in explaining these relationships. Here we proposed an alternative explanation for the rotation during eruptions, by analyzing a magnetohydrodynamic simulation in which magnetic reconnection initiates an eruption from a sheared arcade configuration and an MFR is formed during eruption through the reconnection. The simulation reproduces a reverse S-shaped MFR with dextral chirality, and the axis of this MFR rotates counterclockwise while rising, which compares favorably with a typical filament eruption observed from dual viewing angles. By calculating the twist and writhe numbers of the modeled MFR during its eruption, we found that accompanied with the rotation, the nonlocal writhe of the MFR's axis decreases while the twist of its surrounding field lines increases, and this is distinct from the kink instability, which converts magnetic twist into writhe of the MFR axis. **10 May 2012**

### **CME-Driven and Flare-Ignited Fast Magnetosonic Waves Successively Detected in a Solar Eruption**

[Xinping Zhou](#), [Yuandeng Shen](#), [Jiangtao Su](#), [Zehao Tang](#), [Chengrui Zhou](#), [Yadan Duan](#), [Song Tan](#)

Sola Phys. volume 296, Article number: 169 **2021**

<https://arxiv.org/pdf/2109.02847.pdf>

<https://link.springer.com/content/pdf/10.1007/s11207-021-01913-2.pdf>

<https://doi.org/10.1007/s11207-021-01913-2>

We present SDO/AIA observation of three types of fast-mode propagating magnetosonic waves in a GOES C3.0 flare on **2013 April 23**, which was accompanied by a prominence eruption and a broad coronal mass ejection (CME). During the fast rising phase of the prominence, a large-scale dome-shaped extreme ultraviolet (EUV) wave firstly formed ahead of the CME bubble and propagated at a speed of about 430 km/s in the CME's lateral direction. One can identify the separation process of the EUV wave from the CME bubble. The reflection effect of the on-disk counterpart of this EUV wave was also observed when it interacted with a remote active region. Six minutes after the first appearance of the EUV wave, a large-scale quasi-periodic EUV train with a period of about 120 seconds appeared inside the CME bubble, which emanated from the flare epicenter and propagated outward at an average speed up to 1100 km/s. In addition, another narrow quasi-periodic EUV wave train was observed along a closed-loop system connecting two adjacent active regions, which also emanated from the flare epicenter, propagated at a speed of about 475 km/s and with a period of about 110 seconds. We propose that all the observed waves are fast-mode magnetosonic waves, in which the large-scale dome-shaped EUV wave ahead of the CME bubble was driven by the expansion of the CME bubble, while the large-scale quasi-periodic EUV train within the CME bubble and the narrow quasi-periodic EUV wave train along the closed-loop system were excited by the intermittent energy-releasing process in the flare. Coronal seismology application and energy carried by the waves are also estimated based on the measured wave parameters.

### **Sympathetic Filament Eruptions within a Fan-spine Magnetic System**

[Chengrui Zhou](#), [Yuandeng Shen](#), [Xinping Zhou](#), [Zehao Tang](#), [Yadan Duan](#), [Song Tan](#)

ApJ **923** 45 **2021**

<https://arxiv.org/pdf/2109.09285.pdf>

<https://doi.org/10.3847/1538-4357/ac28a0>

It is unclear whether successive filament eruptions at different sites within a short time interval are physically connected or not. Here, we present the observations of the successive eruptions of a small and a large filament in a tripolar magnetic field region whose coronal magnetic field showed as a fan-spine magnetic system. By analyzing the multi-wavelength observations taken by the Solar Dynamic Observatory (SDO) and the extrapolated three-dimensional coronal magnetic field, we find that the two filaments resided respectively in the two lobes that make up the inner fan structure of the fan-spine magnetic system. In addition, a small fan-spine system was also revealed by the squashing factor  $Q$  map, which located in the east lobe of the fan structure of the large fan-spine system. The eruption of the small filament was a failed filament eruption, which did not cause any coronal mass ejection (CME) except for three flare ribbons and two post-flare-loop systems connecting the three magnetic polarities. The eruption of the large filament not only caused similar post-flare-loop systems and flare ribbons as observed in the small filament eruption, but also a large-scale CME. Based on our analysis results, we conclude that the two successive filament eruptions were physically connected, in which the topology change caused by the small filament eruption is thought to be the physical linkage. In addition, the eruption of the small fan-spine structure further accelerated the instability and violent eruption of the large filament. **2013 October 20**

### **Magnetic Reconnection Invoked by Sweeping of the CME-Driven Fast-Mode Shock**

Guiping [Zhou](#), [Guannan Gao](#), [Jingxiu Wang](#), [Jun Lin](#), [Yingna Su](#), [Chunlan Jin](#), [Yuzong Zhang](#)

ApJ **905** 150 **2020**

<https://arxiv.org/pdf/2010.12957.pdf>

<https://doi.org/10.3847/1538-4357/abc5b2>

Coronal waves exist ubiquitously in the solar atmosphere. They are important not only in their own rich physics but also essential candidates of triggering magnetic eruptions in the remote. However, the later mechanism has never been directly confirmed. By revisiting the successive eruptions on **2012 March 7**, fast-mode shocks are identified to account for the X5.4 flare-related EUV wave with a velocity of 550 km/s, and appeared faster than  $2060 \pm 270$  km/s at the front of the corresponding coronal mass ejection in the slow-rising phase. They not only propagated much faster than the local Alfvén speed of about 260 km/s, but also simultaneously accompanied by type II radio burst, i.e., a typical feature of shock wave. The observations show that the shock wave disturbs the coronal loops C1 connecting active regions (ARs) 11429 and 11430, which is neighboring a null point region. Following a 40-min-oscillation, an external magnetic reconnection (EMR) occurred in the null point region. About 10 min later, a large-scale magnetic flux rope (MFR) overlaid by the C1 became unstable and erupted quickly. It is thought that the fast-mode shock triggered EMR in the null point region and caused the subsequent eruptions. This scenario is observed directly for the first time, and provides new hint for understanding the physics of solar activities and eruptions.

### **The Relationship between Chirality, Sense of Rotation, and Hemispheric Preference of Solar Eruptive Filaments**

Zhenjun [Zhou](#), [Rui Liu](#), [Xing Cheng](#), [Chaowei Jiang](#), [Yuming Wang](#), [Lijuan Liu](#), [Jun Cui](#)

ApJ **2020**

<https://arxiv.org/pdf/2002.05007.pdf>

The orientation, chirality, and dynamics of solar eruptive filaments is a key to understanding the magnetic field of coronal mass ejections (CMEs) and therefore to predicting the geoeffectiveness of CMEs arriving at Earth. However, confusion and contention remain over the relationship between the filament chirality, magnetic helicity, and sense of rotation during eruption. To resolve the ambiguity in observations, in this paper, we used stereoscopic observations to determine the rotation direction of filament apex and the method proposed by Chen et al. (2014) to determine the filament chirality. Our sample of 12 eruptive active-region filaments establishes a strong one-to-one relationship, i.e., during the eruption, sinistral/dextral filaments (located in the southern/northern hemisphere) rotate clockwise/counterclockwise when viewed from above, and corroborates a weak hemispheric preference, i.e., a filament and related sigmoid both exhibit a forward (reverse) S shape in the southern (northern) hemisphere, which suggests that the sigmoidal filament is associated with a low-lying magnetic flux rope with its axis dipped in the middle. As a result of rotation, the projected S shape of a filament is anticipated to be reversed during eruption.

**Table 1.** Characteristics of 12 selected active-region filaments.

### **Why torus-unstable solar filaments experience failed eruption?**

Zhenjun [Zhou](#), [Xin Cheng](#), [Jie Zhang](#), [Yuming Wang](#), [Dong Wang](#), [Lijuan Liu](#), [Bin Zhuang](#), [Jun Cui](#)

**2019** *ApJL* **877** L28

<https://arxiv.org/pdf/1905.00224.pdf>

<https://iopscience.iop.org/article/10.3847/2041-8213/ab21cb/pdf>

To investigate the factors that control the success and/or failure of solar eruptions, we study the magnetic field and 3-Dimensional (3D) configuration of 16 filament eruptions during 2010 July - 2013 February. All these events, i.e., erupted but failed to be ejected to become a coronal mass ejection (CME), are failed eruptions with the filament maximum height exceeding 100Mm. The magnetic field of filament source regions is approximated by a potential field extrapolation method. The filament 3D configuration is reconstructed from three vantage points by the observations of STEREO Ahead/Behind and SDO spacecraft. We calculate the decay index at the apex of these failed filaments and find that in 7 cases, their apex decay indexes exceed the theoretical threshold ( $n_{crit}=1.5$ ) of the torus instability. We further determine the orientation change or rotation angle of each filament top during the eruption. Finally, the distribution of these events in the parameter space of rotation angle versus decay index is established. Four distinct regimes in the parameter space are empirically identified. We find that, all the torus-unstable cases (decay index  $n > 1.5$ ), have a large rotation angles ranging from  $50^\circ$ – $130^\circ$ . The possible mechanisms leading to the rotation and failed eruption are discussed. These results imply that, besides the torus instability, the rotation motion during the eruption may also play a significant role in solar eruptions.

**Table 1.** Filament list, Sixteen [failed filament eruptions](#) (2010-2013)

### **Multiple Magnetic Reconnections Driven by a Large-scale Magnetic Flux Rope**

G. P. [Zhou](#)<sup>1</sup>, C. M. Tan<sup>1</sup>, Y. N. Su<sup>2,3</sup>, C. L. Shen<sup>4</sup>, B. L. Tan<sup>1</sup>, C. L. Jin<sup>1</sup>, and J. X. Wang

**2019** ApJ **873** 23

<https://doi.org/10.3847/1538-4357/ab01cf>

Magnetic flux ropes (MFRs), as the most probable core structure of solar eruptive activity, remain mysterious on their origination, magnetic environment, and erupting mechanisms. Here, we newly identify a large-scale hot channel MFR, named "MFR3", that connects an anti-Hale active region (AR) 11429 and a normal AR 11430 on **2012 March 7** based on multi-wavelength observations. An oscillation is first detected at the top of MFR3 during 00:10–00:30 UT as triggered by an X5.4 flare-related eruption of an MFR (named "MFR1" here) in AR 11429. Then, after a quiet period of ~20 minutes at around 00:52 UT, external magnetic reconnection (EMR) occurred above MFR3 manifested by not only

bidirectional outflow in extreme ultraviolet images, but also microwave quasi-periodic pulsation in broadband radio spectral observations for the first time. With the occurrence of EMR, the large-scale MFR3 quickly erupted at 01:01 UT and triggered an X1.3 flare, which is related to the eruption of the other MFR (named "MFR2" here) in AR 11429 at 01:05 UT. The erupting MFR3 and MFR2 appeared successively in the same associated halo coronal mass ejection (CME) as two different core structures. The identification of the large-scale MFR3 between two separated ARs and its complex activity may shed new light on our understanding of the initiation mechanism of a CME. Further work should lay emphasis on how a large-scale MFR3 forms in the solar atmosphere.

## **Toward Understanding the 3D Structure and Evolution of Magnetic Flux Ropes in an Extremely Long Duration Eruptive Flare**

Zhenjun **Zhou** , Jie Zhang<sup>4</sup>, Yuming Wang<sup>1,3</sup>, Rui Liu<sup>1,5</sup>, and Georgios Chintzoglou

2017 ApJ 851 133      **File**

<http://iopscience.iop.org/sci-hub.tw/0004-637X/851/2/133/>

In this work, we analyze the initial eruptive process of an extremely long duration C7.7-class flare that occurred on **2011 June 21**. The flare had a 2 hr long rise time in soft X-ray emission, which is much longer than the rise time of most solar flares, including both impulsive and gradual ones. Combining the facts that the flare occurred near the disk center as seen by the Solar Dynamic Observatory (SDO) but near the limb as seen by two Solar Terrestrial Relations Observatory (STEREO) spacecraft, we are able to track the evolution of the eruption in 3D in a rare slow-motion manner. The time sequence of the observed large-scale EUV hot channel structure in the Atmospheric Imaging Assembly (AIA) high-temperature passbands of 94 and 131 Å clearly shows the process of how the sigmoid structure prior to the eruption was transformed into a near-potential post-eruption loop arcade. We believe that the observed sigmoid represents the structure of a twisted magnetic flux rope (MFR), which has reached a height of about 60 Mm at the onset of the eruption. We argue that the onset of the flare precursor phase is likely triggered by the loss of the magnetohydrodynamic equilibrium of a preexisting MFR, which leads to the slow rise of the flux rope. The rising motion of the flux rope leads to the formation of a vertical current sheet underneath, triggering the fast magnetic reconnection that in turn leads to the main phase of the flare and fast acceleration of the flux rope.

## **A Study of External Magnetic Reconnection that Triggers a Solar Eruption**

G. P. **Zhou**<sup>1</sup>, J. Zhang<sup>2</sup>, J. X. Wang<sup>1</sup>, and M. S. Wheatland

2017 ApJL 851 L1

<http://iopscience.iop.org/article/10.3847/2041-8213/aa9c40/pdf>

External magnetic reconnection (EMR) is suggested to play an essential role in triggering a solar eruption, but is rarely directly observed. Here, we report on a filament eruption on **2014 October 3** that apparently involves the process of an early EMR. A total of  $1.7 \times 10^{20}$  Mx flux was first canceled along the filament-related polarity inversion line over 12 hr, and then the filament axis started to brighten in extreme ultraviolet (EUV). An impulsive EUV brightening began 30 minutes later, and we attribute this to EMR, as it is located at the center of a bidirectional outflow with a velocity of 60–75 km s<sup>-1</sup> along large-scale magnetic loops from active regions NOAA 12178 and 12179, respectively, and over the filament mentioned above. Following the EMR, the filament was activated; then, partial eruption occurred 6 minutes later in the west, in which the decay index above the magnetic flux rope (MFR) reached the critical value of 1.5. The observations are interpreted in terms of underlying magnetic flux cancelation leading to the buildup and eventual formation of the MFR with a filament embedded in it, and the MFR is elevated later. The activated MFR rises and pushes the overlying sheared field and forms a current sheet causing the EMR. The EMR in turn weakens the constraining effect of the overlying field, leading to the arising of the MFR, and subsequently erupting due to torus instability.

## **OBSERVATIONS OF MAGNETIC FLUX-ROPE OSCILLATION DURING THE PRECURSOR PHASE OF A SOLAR ERUPTION**

G. P. **Zhou**<sup>1,2,4</sup>, J. Zhang<sup>3</sup>, and J. X. Wang

2016 ApJ 823 L19

Based on combined observations from the Interface Region Imaging Spectrograph (IRIS) spectrometer with the coronal emission line of Fe xxi at 1354.08 Å and SDO/AIA images in multiple passbands, we report the finding of the precursor activity manifested as the transverse oscillation of a sigmoid, which is likely a pre-existing magnetic flux rope (MFR), that led to the onset of an X class flare and a fast halo coronal mass ejection (CME) on **2014 September 10**. The IRIS slit is situated at a fixed position that is almost vertical to the main axis of the sigmoid structure that has a length of about  $1.8 \times 10^5$  km. This precursor oscillation lasts for about 13 minutes in the MFR and has velocities in the range of [-9, 11] km s<sup>-1</sup> and a period of ~280 s. Our analysis, which is based on the temperature, density, length, and magnetic field strength of the observed sigmoid, indicates that the nature of the oscillation is a standing wave of fast magnetoacoustic kink mode. We further find that the precursor oscillation is excited by the energy released through an external magnetic reconnection between the unstable MFR and the ambient magnetic field. It is proposed that this precursor activity leads to the dynamic formation of a current sheet underneath the MFR that subsequently reconnects to trigger the onset of the main phase of the flare and the CME.

## **Using a 3-D MHD simulation to interpret propagation and evolution of a coronal mass ejection observed by multiple spacecraft: **The 3 April 2010 event****

Yufen **Zhou**<sup>1,2</sup>, Xueshang Feng<sup>1,\*</sup> and Xinhua Zhao  
Volume 119, Issue 12, pages 9321–9333, December 2014  
<http://onlinelibrary.wiley.com/doi/10.1002/2014JA020347/pdf>

The coronal mass ejection (CME) event on 3 April 2010 is the first fast CME observed by STEREO Sun Earth Connection Coronal and Heliospheric Investigation/Heliospheric Imager for the full Sun-Earth line. Such an event provides us a good opportunity to study the propagation and evolution of CME from the Sun up to 1 AU. In this paper, we study the time-dependent evolution and propagation of this event from the Sun to Earth using the 3-D SIP-CESE (Solar-InterPlanetary Conservation Element and Solution Element) MHD model. The CME is initiated by a simple spherical plasmoid model: a spheromak magnetic structure with high-speed, high-pressure, and high-plasma density plasmoid. The simulation performs a comprehensive study on the CME by comparing the simulation results with STEREO and Wind observations. It is confirmed from the comparison with observations that the MHD model successfully reproduces many features of both the fine solar coronal structure and the typical large-scale structure of the shock propagation and gives the shock arrival time at Earth with an error of ~2 h. Then we analyze in detail the several factors affecting the CME's geo-effectiveness: the CME's propagation trajectory, span angle, and velocity.

### **A current sheet traced from the Sun to interplanetary space**

G. P. **Zhou**<sup>1</sup>, C. J. Xiao<sup>2</sup>, J. X. Wang<sup>1</sup>, M. S. Wheatland<sup>3</sup> and H. Zhao<sup>4</sup>  
A&A 525, A156 (2011), **File**

Context. Magnetic reconnection is a central concept for understanding solar activity, including filament eruptions, flares, and coronal mass ejections (CMEs). The existence of transverse and vertical current sheets, sites where reconnection takes place in the solar atmosphere, is frequently proposed as a precondition for flare/CME models, but is rarely identified in observations.

Aims. We aim at identifying a transverse current sheet that existed in the pre-CME structure and persisted from the CME solar source to interplanetary space.

Methods. STEREO A/B provide us a unique opportunity to calculate the interplanetary current sheets for the magnetic cloud. We analyze such a structure related to the fast halo CME of **2006 December 13** with assembled observations. A current sheet at the front of the magnetic cloud is analyzed to its origin in a transverse current sheet in the CME solar source, which can be revealed in the magnetic field extrapolations, XRT, and LASCO observations.

Results. An interplanetary current sheet is identified as coming from the CME solar source by carefully mapping and examining multiple observations from the Sun to interplanetary space, along with nonlinear force-free magnetic field extrapolations of the active region NOAA 10930.

Conclusions. The structure identified in the pre-flare state is a global transverse current sheet, which plays a role in the CME initiation, and propagates from the corona to interplanetary space.

### **Large-Scale Source Regions of Earth-Directed Coronal Mass Ejections**

Guiping **Zhou**, Jingxiu Wang and Jun Zhang  
A&A, 445, No. 3, 1133-1141, **2006**, **File**

**Table**

### **TWO SUCCESSIVE CORONAL MASS EJECTIONS DRIVEN BY THE KINK AND DRAINAGE INSTABILITIES OF AN ERUPTIVE PROMINENCE**

G. P. **Zhou**, J. X. Wang, J. Zhang, P. F. Chen, H. S. Ji, K. Dere

The Astrophysical Journal, 651:1238-1244, **2006**, **File**

[http://ourstar.bao.ac.cn/wangjx/paper/zgp\\_06b.pdf](http://ourstar.bao.ac.cn/wangjx/paper/zgp_06b.pdf)

We describe a clear case of the initiation of a propagating bright arc and a CME on **2002 December 28**, which were associated with an eruptive prominence. In EIT 304 and 195 8 images, a very long filament showed evidence of severe twisting in one of its fragments, which appeared as a prominence on December 26; then, the prominence showed the conversion of its twist into writhe. Two days later, the prominence displayed a slow rising motion for hours. Internal twisting and mass motion took place before the rapid acceleration and final eruption. The propagating bright arc and the following CME corresponded to the early rising and the subsequently eruptive phases of the prominence, respectively. Signatures of magnetic reconnection, i.e., a cusp structure and postflare loops in EUV wave bands and hard X-ray sources in the corona, were observed after the prominence eruption. It appears that the kink instability and the mass drainage in the prominence played key roles in triggering the initiation of the CME. However, the rather impulsive acceleration of the CME resulted from magnetic reconnection beneath the filament.

### **Large-scale Coronal Dimming Foreshadowing a Solar Eruption on 2011 October 1**

Chunming **Zhu**<sup>1</sup>, C. Richard DeVore<sup>2</sup>, Joel T. Dahlin<sup>2,3</sup>, Jiong Qiu<sup>1</sup>, Maria D. Kazachenko<sup>4,5</sup>, Vadim M. Uritsky<sup>2,6</sup>, and Jackson S. Vandervelde<sup>2,7</sup>

**2024** ApJ 961 218

<https://iopscience.iop.org/article/10.3847/1538-4357/ad1603/pdf>

Understanding large-scale solar eruptions requires detailed investigation of the entire system's evolution, including the magnetic environment enveloping the source region and searches for precursor activity prior to event onset. We combine stereoscopic observations from the Solar Dynamics Observatory (SDO) and STEREO-B spacecraft for several hours before a filament ejection, M1.2-class eruptive flare, and coronal mass ejection (CME) originating in NOAA

active region (AR) 11305 on **2011 October 1**. Two episodes of significant preeruption coronal dimming that occurred well to the southeast of the ejected filament are identified. The CME subsequently took off with a substantial component of velocity toward the dimming, which became very pronounced during eruption. We used SDO/Helioseismic and Magnetic Imager (HMI) data to reconstruct the magnetic environment of the system and found that it contains a null point near the dimming region. AR 11305 had quite complex connections to nearby ARs 11302 and 11306, as well as to other regions of decayed AR flux. The intensifying and spatially expanding precursor dimming was accompanied by southeastward rising motions of loops toward the null point and northeastward and southwestward motions of loops retracting away. These motions and the dimming are consistent with persistent magnetic reconnection occurring at the null point as it moved upward and southeastward, thereby removing a strapping magnetic field high above AR 11305. Eventually, the filament was ejected explosively toward the null point. We conclude that the breakout model for solar eruptions provides a compelling account of this event. Furthermore, we conjecture that preeruption dimmings may be much more frequent than currently recognized.

## **Simulation of a Solar Jet Formed from an Untwisting Flux Rope Interacting with a Null Point**

[Jiahao Zhu](#), [Yang Guo](#), [Mingde Ding](#), [Brigitte Schmieder](#)

ApJ **949** 2 **2023**

<https://arxiv.org/pdf/2303.18098.pdf>

<https://iopscience.iop.org/article/10.3847/1538-4357/acc9a7/pdf>

Coronal jets are eruptions identified by a collimated, sometimes twisted spire. They are small-scale energetic events compared with flares. Using multi-wavelength observations from the Solar Dynamics Observatory/Atmospheric Imaging Assembly (SDO/AIA) and a magnetogram from Hinode/Spectro-Polarimeter (Hinode/SP), we study the formation and evolution of a jet occurring on 2019 March 22 in the active region NOAA 12736. A zero- $\beta$  magnetohydrodynamic (MHD) simulation is conducted to probe the initiation mechanisms and appearance of helical motion during this jet event. As the simulation reveals, there are two pairs of field lines at the jet base, indicating two distinct magnetic structures. One structure outlines a flux rope lying low above the photosphere in the north of a bald patch region and the other structure shows a null point high in the corona in the south. The untwisting motions of the observed flux rope was recovered by adding an anomalous (artificial) resistivity in the simulation. A reconnection occurs at the bald patch in the flux rope structure, which is moving upwards and simultaneously encounters the field lines of the null point structure. The interaction of the two structures results in the jet while the twist of the flux rope is transferred to the jet by the reconnected field lines. The rotational motion of the flux rope is proposed to be an underlying trigger of this process and responsible for helical motions in the jet spire. **2019 March 22**

## **How Does Magnetic Reconnection Drive the Early Stage Evolution of Coronal Mass Ejections?**

Chunming [Zhu](#), [Jiong Qiu](#), [Paulett Liewer](#), [Angelos Vourlidas](#), [Michael Spiegel](#), [Qiang Hu](#)

ApJ **893** 141 **2020**

<https://arxiv.org/pdf/2003.11134.pdf>

<https://doi.org/10.3847/1538-4357/ab838a>

Theoretically, CME kinematics are related to magnetic reconnection processes in the solar corona. However, the current quantitative understanding of this relationship is based on the analysis of only a handful of events. Here we report a statistical study of 60 CME-flare events from August 2010 to December 2013. We investigate kinematic properties of CMEs and magnetic reconnection in the low corona during the early phase of the eruptions, by combining limb observations from STEREO with simultaneous on-disk views from SDO. For a subset of 42 events with reconnection rate evaluated by the magnetic fluxes swept by the flare ribbons on the solar disk observed from SDO, we find a strong correlation between the peak CME acceleration and the peak reconnection rate. Also, the maximum velocities of relatively fast CMEs ( $> 600$  km/s) are positively correlated with the reconnection flux, but no such correlation is found for slow CMEs. A time-lagged correlation analysis suggests that the distribution of the time lag of CME acceleration relative to reconnection rate exhibits three peaks, approximately 10 minutes apart, and on average, acceleration-lead events have smaller reconnection rates. We further compare the CME total mechanical energy with the estimated energy in the current sheet. The comparison suggests that, for small-flare events, reconnection in the current sheet alone is insufficient to fuel CMEs. Results from this study suggest that flare reconnection may dominate the acceleration of fast CMEs, but for events of slow CMEs and weak reconnection, other mechanisms may be more important. **2012/07/12**  
**Table 1.** List of 60 CME-flare events observed by STEREO and SDO.

## **Complex Flare Dynamics Initiated by a Filament-Filament Interaction**

Chunming [Zhu](#), Rui Liu, David Alexander, Xudong Sun, James McAteer

2015 ApJ 813 60

<http://arxiv.org/pdf/1507.05889v1.pdf>

We report on an eruption involving a relatively rare filament-filament interaction on **2013 June 21**, observed by SDO and STEREO-B. The two filaments were separated in height within AR 11777. The onset of the eruption of the lower filament was accompanied simultaneously by the apparent descent of the upper filament resulting in a convergence and direct interaction of the two filaments. The interaction was accompanied by the heating of plasmas surrounding the upper filament and the subsequent coalescence of the filaments into a magnetically complex structure, whose eruption was associated with an M2.9 class solar flare. Magnetic loop shrinkage and descending dark voids were observed at

different locations as part of the large flare energy release giving us a unique insight into these dynamic flare phenomena.

## **A blow out jet caused by the eruption of a magnetic flux rope revealed by forced field extrapolation**

### **A Solar Blowout Jet Caused by the Eruption of a Magnetic Flux Rope**

Xiaoshuai **Zhu**, Huaning Wang, Xin Cheng, Chong Huang

ApJL 844 L20 2017

<https://arxiv.org/pdf/1703.08992.pdf>

We investigate three-dimensional (3D) magnetic structure of a blow out jet originated in the west edge of NOAA Active Region (AR) 11513 on **2012 July 02** through recently developed forced field extrapolation model. The results show that the blow out jet can be interpreted as the eruption of the magnetic flux rope (MFR) consisting of twisted and closed field lines. We further calculate the twist number  $T_w$  and squashing factor  $Q$  of the reconstructed magnetic field and find that the MFR corresponds well with the high  $T_w$  region as seen at 2D cutting plane perpendicular to the axis of the MFR. The outer boundary is also found to have very high  $Q$  values, thus may represent the bright structure at the base of the jet. The twist number of the MFR is estimated to be  $T_w = -1.54 \pm 0.67$ . The kink instability is thus considered as the initiation mechanism of the blow jet due to closing or even exceeding its theoretical threshold. Our results also show that the bright point at the decaying phase is actually comprised of some small loops that are heated by the reconnection occurred above. In summary, the blowout jet is mostly consistent with the scenario proposed by \cite{mcs10} except that the kink instability is found to be its possible trigger.

## **The Role of Interchange Reconnection in Facilitating a Filament Eruption**

C. **Zhu**, D. Alexander, X. Sun, A. Daou

Solar Phys., 2014

We study the interaction between an erupting solar filament and a nearby coronal hole, based on multi-viewpoint observations from the Solar Dynamics Observatory and STEREO. During the early evolution of the filament eruption, it exhibits a clockwise rotation that brings its easternmost leg in contact with the oppositely aligned field at the coronal hole boundary. The interaction between the two magnetic-field systems is manifested as the development of a narrow contact layer in which we see enhanced EUV brightening and bi-directional flows, suggesting that the contact layer is a region of strong and ongoing magnetic reconnection. The coronal mass ejection (CME) resulting from this eruption is highly asymmetric, with its southern portion opening up to the upper corona, while the northern portion remains closed and connected to the Sun. We suggest that the erupting flux rope that made up the filament reconnected with both the open and closed fields at the coronal hole boundary via interchange reconnection and closed-field disconnection, respectively, which led to the observed CME configuration.

## **Combining STEREO heliospheric imagers and Solar Orbiter to investigate the evolution of the 2022 March 10 CME**

B. **Zhuang**<sup>1</sup>, N. Lugaz<sup>1</sup>, N. Al-Haddad<sup>1</sup>, C. Scolini<sup>1</sup>, C. J. Farrugia<sup>1</sup>, F. Regnault<sup>1</sup>, E. E. Davies<sup>2</sup>, W. Yu<sup>1</sup>, R. M. Winslow<sup>1</sup> and A. B. Galvin<sup>1</sup>

A&A 682, A107 (2024)

<https://www.aanda.org/articles/aa/pdf/2024/02/aa47561-23.pdf>

Context. Coronal mass ejections (CMEs) are large-scale structures of magnetized plasma that erupt from the corona into interplanetary space. The launch of Solar Orbiter (SoLO) in 2020 enables in situ measurements of CMEs in the innermost heliosphere, at such distances where CMEs can be observed remotely within the inner field of view of heliospheric imagers (HIs). It thus provides the opportunity for investigations into the correspondence of the CME substructures measured in situ and observed remotely. We studied a CME that started on **2022 March 10** and was measured in situ by SoLO at  $\sim 0.44$  au.

Aims. Combining remote observations of CMEs from wide-angle imagers and in situ measurements in the innermost heliosphere allows us to compare CME properties derived through both techniques, validate the estimates, and better understand CME evolution, specifically the size and radial expansion, within 0.5 au.

Methods. We compared the evolution of different CME substructures observed in images from the HIs on board the Ahead Solar Terrestrial Relations Observatory (STEREO-A) and the CME signatures measured in situ by SoLO. The CME is found to possess a density enhancement at its rear edge in both remote and in situ observations, which validates the use of the signature of density enhancement following the CMEs to accurately identify the CME rear edge. We also estimated and compared the radial size and radial expansion speed of different substructures in both observations.

Results. The evolution of the CME front and rear edges in remote images is consistent with the in situ CME measurements. The radial expansion (i.e., radial size and radial expansion speed) of the whole CME structure consisting of the magnetic ejecta and the sheath is consistent with the in situ estimates obtained at the same time from SoLO. However, we do not find such consistencies for the magnetic ejecta region inside the CME because it is difficult to identify the magnetic ejecta edges in the remote images.

## **Evolution of the Radial Size and Expansion of Coronal Mass Ejections Investigated by Combining Remote and In Situ Observations**



Bin **Zhuang**<sup>1</sup>, Noé Lugaz<sup>1</sup>, Nada Al-Haddad<sup>1</sup>, Réka M. Winslow<sup>1</sup>, Camilla Scolini<sup>1</sup>, Charles J. Farrugia<sup>1</sup>, and Antoinette B. Galvin<sup>1</sup>

2023 ApJ 952 7

<https://iopscience.iop.org/article/10.3847/1538-4357/acd847/pdf>

<https://arxiv.org/pdf/2305.14339.pdf>

A fundamental property of coronal mass ejections (CMEs) is their radial expansion, which determines the increase in the CME radial size and the decrease in the CME magnetic field strength as the CME propagates. CME radial expansion can be investigated either by using remote observations or by in situ measurements based on multiple spacecraft in radial conjunction. However, there have been only few case studies combining both remote and in situ observations. It is therefore unknown if the radial expansion in the corona estimated remotely is consistent with that estimated locally in the heliosphere. To address this question, we first select 22 CME events between the years 2010 and 2013, which were well observed by coronagraphs and by two or three spacecraft in radial conjunction. We use the graduated cylindrical shell model to estimate the radial size, radial expansion speed, and a measure of the dimensionless expansion parameter of CMEs in the corona. The same parameters and two additional measures of the radial-size increase and magnetic-field-strength decrease with heliocentric distance of CMEs based on in situ measurements are also calculated. For most of the events, the CME radial size estimated by remote observations is inconsistent with the in situ estimates. We further statistically analyze the correlations of these expansion parameters estimated using remote and in situ observations, and discuss the potential reasons for the inconsistencies and their implications for the CME space weather forecasting. **17 Apr 2011, 2 Jan 2012, 13-15 Jun 2013, , 9 Jul 2013, 11-12 Jul 2013**

**Table 1** CME Events Observed by the Radially Aligned Spacecraft at Different Heliocentric Distances 2010-2013

## Acceleration and Expansion of a Coronal Mass Ejection in the High Corona: Role of Magnetic Reconnection

[Bin Zhuang](#), [Noé Lugaz](#), [Manuela Temmer](#), [Tingyu Gou](#), [Nada Al-Haddad](#)

ApJ 933 169 2022

<https://arxiv.org/pdf/2206.02090.pdf>

<https://iopscience.iop.org/article/10.3847/1538-4357/ac75d4/pdf>

The important role played by magnetic reconnection in the early acceleration of coronal mass ejections (CMEs) has been widely discussed. However, as CMEs may have expansion speeds comparable to their propagation speeds in the corona, it is not clear whether and how reconnection contributes to the true acceleration and expansion separately. To address this question, we analyze the dynamics of a moderately fast CME on **2013 February 27**, associated with a continuous acceleration of its front into the high corona, even though its speed had reached  $\sim 700\text{-km-s}^{-1}$  and larger than the solar wind speed. The apparent CME acceleration is found to be due to the CME expansion in the radial direction. The CME true acceleration, i.e., the acceleration of its center, is then estimated by taking into account the expected deceleration caused by the solar wind drag force acting on a fast CME. It is found that the true acceleration and the radial expansion have similar magnitudes. We find that magnetic reconnection occurs after the CME eruption and continues during the CME propagation in the high corona, which contributes to the CME dynamic evolution. Comparison between the apparent acceleration related to the expansion and the true acceleration that compensates the drag shows that, for this case, magnetic reconnection contributes almost equally to the CME expansion and to the CME acceleration. The consequences of these measurements for the evolution of CMEs as they transit from the corona to the heliosphere are discussed.

## Successive Coronal Mass Ejections Associated with Weak Solar Energetic Particle Events

[Bin Zhuang](#), [Noé Lugaz](#), [Tingyu Gou](#), [Liuguan Ding](#)

ApJ 2021

<https://arxiv.org/pdf/2109.02225.pdf>

The scenario of twin coronal mass ejections (CMEs), i.e., a fast and wide primary CME (priCME) preceded by previous CMEs (preCMEs), has been found to be favorable to a more efficient particle acceleration in large solar energetic particle (SEP) events. Here, we study 19 events during 2007--2014 associated with twin-CME eruptions but without large SEP observations at L1 point. We combine remote-sensing and in situ observations from multiple spacecraft to investigate the role of magnetic connectivity in SEP detection and the CME information in 3-dimensional (3D) space. We study one-on-one correlations of the priCME 3D speed, flare intensity, suprathermal backgrounds, and height of CME-CME interaction with the SEP intensity. Among these, the priCME speed is found to correlate with the SEP peak intensity at the highest level. We use the projection correlation method to analyze the correlations between combinations of these multiple independent factors and the SEP peak intensity. We find that the only combination of two or more parameters that has higher correlation with the SEP peak intensity than the CME speed is the CME speed combined with the propagation direction. This further supports the dominant role of the priCME in controlling the SEP enhancements, and emphasizes the consideration of the latitudinal effect. Overall, the magnetic connectivity in longitude as well as latitude and the relatively lower priCME speed may explain the existence of the twin-CME SEP-poor events. The role of the barrier effect of preCME(s) is discussed for an event on **2013 October 28**.

**Table 1:** Twin-CME (L1-point) SEP-poor events during 2007– 2014

**Table 2:** Twin-CME (L1-point) large SEP events in solar cycle 24

## Coronal Flux Rope Catastrophe Associated With Internal Energy Release

[Bin Zhuang](#), [Youqiu Hu](#), [Yuming Wang](#), [Quanhao Zhang](#), [Rui Liu](#), [Tingyu Gou](#), [Chenglong Shen](#)

JGR Volume123, Issue4 Pages 2513-2519 2018

<http://sci-hub.tw/https://onlinelibrary.wiley.com/doi/abs/10.1002/2018JA025283>

Magnetic energy during the catastrophe was predominantly studied by the previous catastrophe works since it is believed to be the main energy supplier for the solar eruptions. However, the contribution of other types of energies during the catastrophe cannot be neglected. This paper studies the catastrophe of the coronal flux rope system in the solar wind background, with emphasis on the transformation of different types of energies during the catastrophe. The coronal flux rope is characterized by its axial and poloidal magnetic fluxes and total mass. It is shown that a catastrophe can be triggered by not only an increase but also a decrease of the axial magnetic flux. Moreover, the internal energy of the rope is found to be released during the catastrophe so as to provide energy for the upward eruption of the flux rope. As far as the magnetic energy is concerned, it provides only part of the energy release, or even increases during the catastrophe, so the internal energy may act as the dominant or even the unique energy supplier during the catastrophe.

## The Significance of the Influence of the CME Deflection in Interplanetary Space on the CME Arrival at Earth

Bin [Zhuang](#)<sup>1,2</sup>, Yuming Wang<sup>1,3</sup>, Chenglong Shen<sup>1,3,4</sup>, Siqing Liu<sup>5,6</sup>, Jingjing Wang<sup>5,6</sup>, Zonghao Pan<sup>1,4</sup>, Huimin Li<sup>7</sup>, and Rui Liu

2017 ApJ 845 117 DOI [10.3847/1538-4357/aa7fc0](https://doi.org/10.3847/1538-4357/aa7fc0)

<http://iopscience.iop.org/sci-hub.cc/0004-637X/845/2/117/>

As one of the most violent astrophysical phenomena, coronal mass ejections (CMEs) have strong potential space weather effects. However, not all Earth-directed CMEs encounter the Earth and produce geo-effects. One reason is the deflected propagation of CMEs in interplanetary space. Although there have been several case studies clearly showing such deflections, it has not yet been statistically assessed how significantly the deflected propagation would influence the CME's arrival at Earth. We develop an integrated CME-arrival forecasting (iCAF) system, assembling the modules of CME detection, three-dimensional (3D) parameter derivation, and trajectory reconstruction to predict whether or not a CME arrives at Earth, and we assess the deflection influence on the CME-arrival forecasting. The performance of iCAF is tested by comparing the two-dimensional (2D) parameters with those in the Coordinated Data Analysis Workshop (CDAW) Data Center catalog, comparing the 3D parameters with those of the gradual cylindrical shell model, and estimating the success rate of the CME Earth-arrival predictions. It is found that the 2D parameters provided by iCAF and the CDAW catalog are consistent with each other, and the 3D parameters derived by the ice cream cone model based on single-view observations are acceptable. The success rate of the CME-arrival predictions by iCAF with deflection considered is about 82%, which is 19% higher than that without deflection, indicating the importance of the CME deflection for providing a reliable forecasting. Furthermore, iCAF is a worthwhile project since it is a completely automatic system with deflection taken into account. **3 Aug 2011**

**Table 1** 38 Selected Frontside Halo CMEs

## GLOBAL CORONAL MASS EJECTIONS

Andrei N. [Zhukov](#)

### CESRA\_2010, Presentation File

- Global CMEs are rare events characterized by a **very large extent of coronal dimmings**. They belong to the tail of the continuous distribution of dimming true angular widths.
- During such extreme events a **huge amount of the free energy is released** in the form of both kinetic (CME) and radiative (flare) energy.
- Global CMEs correspond to the **ejection of plasma from multiple interconnected large-scale coronal magnetic flux systems**.
- Dimmings may be considered **an important nonlocal manifestation of the CME initiation process** and need to be described in a realistic CME model.
- A major observational limitation is a low cadence (12 minutes) of SOHO/EIT – we **need high-cadence EUV imaging** from KuaFu!

## Using CME Observations for Geomagnetic Storm Forecasting

A.N. [Zhukov](#)

Space Weather, J. Liliensten (ed.), Astrophysics and Space Science Library 344, 5--13 (2007). **File**.

## Global Coronal Mass Ejections

A.N. [Zhukov](#) and I.S. Veselovsky

Astrophysical Journal, 664: L131–L134, 2007, **File** .

We characterize a CME by the apparent angular extent of associ-

ated dimmings above the solar limb, and define a global CME as a CME with the total apparent extent of limb dimmings of more than  $180^\circ$ . Several examples of global CMEs are discussed. All the global CMEs identified up to now are fast full halo CMEs associated with X-class flares (if they originate on the front side of the Sun). We demonstrate that global CMEs involve an eruption of several magnetic flux systems distributed on a large spatial scale comparable to a half of the solar disc (true angular width around  $180^\circ$ ). We discuss possible interpretations of the global CME phenomenon and challenges it presents to CME modeling. Our results suggest a non-local nature of the CME eruption mechanism.

## **A high-latitude coronal mass ejection observed by a constellation of coronagraphs: Solar Orbiter/Metis, STEREO-A/COR2, and SOHO/LASCO**

G. **Zimbardo**<sup>1,\*</sup>, B. Ying<sup>2</sup>, G. Nisticò<sup>1</sup>, L. Feng<sup>2</sup>, L. Rodríguez-García<sup>3</sup>, +++  
A&A 676, A48 (2023)

<https://www.aanda.org/articles/aa/pdf/2023/08/aa46011-23.pdf>

Context. A few days before the first perihelion of the Solar Orbiter nominal mission, which occurred on 2022 March 26, the Metis coronagraph on board Solar Orbiter detected a coronal mass ejection (CME) that was moving away from the far side of the Sun (with respect to Solar Orbiter) at high northern latitudes. The eruption was also seen by other spacecraft, in particular, by STEREO-A, which was in quadrature configuration with Solar Orbiter.

Aims. We analyse the different views of the CME by a constellation of spacecraft with the purpose to determine the speed and acceleration of the CME, and to identify the source region of the CME.

Methods. Considering the positions of various spacecraft on **2022 March 22**, this CME happened to be within the field of view of STEREO-A/SECCHI, and it was visible over the limb from SOHO/LASCO. We present the results of the 3D reconstruction of the CME based on the graduated cylindrical shell model and of the identification of the possible origin of the CME using extreme-ultraviolet (EUV) observations by Solar Orbiter/EUI, STEREO-A/EUVI, and SDO/AIA. The observations in EUV are compared with the coronal magnetic structure obtained by the potential field source surface method.

Results. The 3D reconstruction of the CME derives a central latitude of  $29^\circ$  N, a Stonyhurst longitude of  $-125^\circ$ , and an average radial speed at the apex of  $322 \pm 33$  km s<sup>-1</sup> between 4 and 13 R<sub>☉</sub>, which is probably not high enough to generate a shock wave. The estimated average acceleration of the CME is  $16 \pm 11$  m s<sup>-2</sup> in the same range of distances from the Sun. This CME may be associated with the disappearance of a coronal cloud prominence, which is seen in the EUV by STEREO-A/EUVI and SDO/AIA, and is also associated with rapidly evolving emerging magnetic flux.

## **Coronal and Chromospheric Signatures of Large-Scale Disturbances Associated with a Major Solar Eruption**

Weiguo **Zong**, Yu Dai

ApJ 809 151 2015

<http://arxiv.org/pdf/1507.05369v1.pdf>

We present both coronal and chromospheric observations of large-scale disturbances associated with a major solar eruption on **2005 September 7**. In GOES/SXI, arclike coronal brightenings are recorded propagating in the southern hemisphere. The SXI front shows an initially constant speed of 730 km s<sup>-1</sup> and decelerates later on, and its center is near the central position angle of the associated coronal mass ejection (CME) but away from flare site. Chromospheric signatures of the disturbances are observed in both MLSO/PICS H $\alpha$  and MLSO/CHIP He I 10830 Å, and can be divided into two parts. The southern signatures occur in regions where the SXI front sweeps over, with the H $\alpha$  bright front coincident with the SXI front while the He I dark front lagging the SXI front but showing a similar kinematics. Ahead of the path of the southern signatures, oscillations of a filament are observed. The northern signatures occur near the equator, with the H $\alpha$  and He I fronts coincident with each other. They first propagate westward, and then deflect to the north at the boundary of an equatorial coronal hole (CH). Based on these observational facts, we suggest that the global disturbances are associated with the CME lift-off, and show a hybrid nature: a mainly non-wave CME flank nature for the SXI signatures and the corresponding southern chromospheric signatures, and a shocked fast-mode coronal magnetohydrodynamics (MHD) wave nature for the northern chromospheric signatures.

## **Mechanism of the Failed Eruption of an Intermediate Solar Filament**

**Zou** Peng<sup>1</sup>, Jiang Chaowei<sup>1</sup>, Wang Juntao<sup>1</sup>, and Bian Xinkai<sup>1</sup>

2022 ApJ 928 160

<https://iopscience.iop.org/article/10.3847/1538-4357/ac581f/pdf>

Solar filament eruptions can generate coronal mass ejections (CMEs), which are huge threats to space weather. Thus, we need to understand their underlying mechanisms. Although many authors have studied the mechanisms for several decades, we still do not fully understand in what conditions a filament can erupt to become a CME or not. Previous studies have discussed extensively why a highly twisted and already erupted filament will be interrupted and considered that a strong overlying constraint field seems to be the key factor. However, few of them study filaments in the weak field, namely, quiescent filaments, as it is too hard to reconstruct the magnetic configuration there. Here we show a case study, in which we can fully reconstruct the configuration of an intermediate filament with the MHD-relaxation extrapolation model and discuss its initial eruption and eventual failure. By analyzing the magnetic configuration, we

suggest that the reconnection between the erupting magnetic flux rope (MFR) and the overlying field are the key factors that constrained the eruption of the filament. There is observational evidence that MFRs will reconnect with peripheral field lines. Usually, the reconnection between an MFR and peripheral fields will weaken the overlying constraint and promote further eruption, but in some cases in which the magnetic configuration of an MFR is far different from peripheral fields, the reconnection will play a negative role in MFR eruption. **2015 March 15**

## **A Statistical Study of Solar Filament Eruptions That Forms High-Speed Coronal Mass Ejections**

Peng [Zou](#), [Chaowei Jiang](#), [Fengsi Wei](#), [Pingbing Zuo](#), [Yi Wang](#)

ApJ **884** 157 **2019**

<https://arxiv.org/pdf/1908.08650.pdf>

<https://doi.org/10.3847/1538-4357/ab4355>

Coronal mass ejections (CMEs) play a decisive role in driving space weather, especially, the fast ones (e.g., with speeds above  $800\text{ km s}^{-1}$ ). Understanding the trigger mechanisms of fast CMEs can help us gaining important information in forecasting them. The filament eruptions accompanied with CMEs provide a good tracer in studying the early evolution of CMEs. Here we surveyed 66 filament-accompanied fast CMEs to analyse the correlation between the trigger mechanisms, namely either magnetic reconnection or ideal MHD process, associated flares, and CME speeds. Based on the data gathering from SDO, GONG and STEREO, we find that: (1) Active region (AR) filament and intermediate filaments (IFs) eruptions show a higher probability for producing fast CMEs than quiet Sun (QS) filaments, while the probability of polar crown (PC) filament eruptions is zero in our statistic; (2) AR filament eruptions that produce fast CMEs are more likely triggered by magnetic reconnection, while QS and IFs are more likely triggered by ideal MHD process; (3) For AR filaments and IFs, it seems that the specific trigger mechanism does not have a significant influence on the resulted CME speeds, while for the QS filaments, the ideal MHD mechanism can more likely generate a faster CME; (4) Comparing with previous statistic study, the onset heights of filament eruptions and the decay indexes of the overlying field show some differences: for AR filaments and IFs, the decay indexes are larger and much closer to the theoretical threshold, while for QS filaments, the onset heights are higher than those obtained in previous results. **2011-06-07, 2011-08-04, 2011-08-11, 2011-11-09, 2012-01-01, 2015-08-07**

**Table 1.** The list of all events of filament eruptions (2011-2017)

## **Can Injection Model Replenish the Filaments in Weak Magnetic Environment?**

Peng [Zou](#), [Chaowei Jiang](#), [Fengsi Wei](#), [Wenda Cao](#)

Research in Astronomy and Astrophysics **Vol 19, No 6**, 84 **2019**

<https://arxiv.org/pdf/1901.00659.pdf>

We observed an H $\alpha$  surge occurred in the active region NOAA 12401 on **2015 August 17**, and discuss its trigger mechanism, kinematic and thermal properties. It is suggested that this surge is caused by a chromospheric reconnection which ejects cool and dense material with the transverse velocity about  $21\text{--}28\text{ km s}^{-1}$  and the initial doppler velocity of  $12\text{ km s}^{-1}$ . This surge is similar to the injection of newly formed filament materials from their footpoints, except that the surge here occurred in a relatively weak magnetic environment of  $\sim 100\text{ G}$ . Thus we discuss the possibility of filament material replenishment via the erupting mass in such a weak magnetic field, which is often associated with quiescent filaments. It is found that the local plasma can be heated up to about 1.3 times of original temperature, which results in an acceleration about  $-0.017\text{ km s}^{-2}$ . It can lift the dense material up to  $10\text{ Mm}$  and higher with a inclination angle smaller than  $50^\circ$ , namely typical height of active region filaments. But it can hardly inject the material up to those filaments higher than  $25\text{ Mm}$ , namely some quiescent filaments. Thus we think injection model does not work well in the formation of quiescent filaments.

## **Shock location and CME 3D reconstruction of a solar type II radio burst with LOFAR**

[P. Zucca](#), [D. E. Morosan](#), [A. P. Rouillard](#), [R. Fallows](#), [P. T. Gallagher](#), [J. Magdalenic](#), [K-L. Klein](#), [G. Mann](#),

.....

A&A **2018**

<https://arxiv.org/pdf/1804.01025.pdf> **File**

Type II radio bursts are evidence of shocks in the solar atmosphere and inner heliosphere that emit radio waves ranging from sub-meter to kilometer lengths. These shocks may be associated with CMEs and reach speeds higher than the local magnetosonic speed. Radio imaging of decameter wavelengths ( $20\text{--}90\text{ MHz}$ ) is now possible with LOFAR, opening a new radio window in which to study coronal shocks that leave the inner solar corona and enter the interplanetary medium and to understand their association with CMEs. To this end, we study a coronal shock associated with a CME and type II radio burst to determine the locations at which the radio emission is generated, and we investigate the origin of the band-splitting phenomenon. **2013 October 26**

## **Understanding CME and associated shock in the solar corona by merging multi wavelengths observation**

Pietro [Zucca](#), Monique Pick, Pascal Demoulin, Alain Kerdraon, Alain Lecacheux, Peter T. Gallagher  
**2014** ApJ 795 68

<http://arxiv.org/pdf/1409.3691v1.pdf> ; **File**

Using multi-wavelength imaging observations, in EUV, white light and radio, and radio spectral data over a large frequency range, we analyzed the triggering and development of a complex eruptive event. This one includes two components, an eruptive jet and a CME which interact during more than 30 min, and can be considered as physically linked. This was an unusual event. The jet is generated above a typical complex magnetic configuration which has been investigated in many former studies related to the build-up of eruptive jets; this configuration includes fan-field lines originating from a corona null point above a parasitic polarity, which is embedded in one polarity region of large Active Region (AR). The initiation and development of the CME, observed first in EUV, does not show usual signatures. In this case, the eruptive jet is the main actor of this event. The CME appears first as a simple loop system which becomes destabilized by magnetic reconnection between the outer part of the jet and the ambient medium. The progression of the CME is closely associated with the occurrence of two successive types II bursts from distinct origin. An important part of this study is the first radio type II burst for which the joint spectral and imaging observations allowed: i) to follow, step by step, the evolution of the spectrum and of the trajectory of the radio burst, in relationship with the CME evolution; ii) to obtain, without introducing an electronic density model, the B-field and the Alfvén speed.

**2013 November 06**

### **Comparative case study of two methods to assess the eruptive potential of selected active regions**

[Francesca Zuccarello](#)<sup>1</sup>, [Iliaria Ermolli](#), [Marianna B. Korsos](#), [Fabrizio Giorgi](#), [Salvo L. Guglielmino](#), [Robertus Erdelyi](#), [Paolo Romano](#)

Research in Astronomy and Astrophysics **2021**

<https://arxiv.org/pdf/2110.01272.pdf>

Solar eruptive events, like flares and coronal mass ejections, are characterized by the rapid release of energy that can give rise to emission of radiation across the entire electromagnetic spectrum and to an abrupt significant increase in the kinetic energy of particles. These energetic phenomena can have important effects on the Space Weather conditions and therefore it is necessary to understand their origin, in particular, what is the eruptive potential of an active region (AR). In these case studies, we compare two distinct methods that were used in previous works to investigate the variations of some characteristic physical parameters during the pre-flare states of flaring ARs. These methods consider: i) the magnetic flux evolution and the magnetic helicity accumulation, and ii) the fractal and multi-fractal properties of flux concentrations in ARs. Our comparative analysis is based on time series of photospheric data obtained by the Solar Dynamics Observatory between March 2011 and June 2013. We selected two distinct samples of ARs: one is distinguished by the occurrence of more energetic M- and X-class flare events, that may have a rapid effect on not just the near-Earth space, but also on the terrestrial environment; the second is characterized by no-flares or having just few C- and B-class flares. We found that the two tested methods complement each other in their ability to assess the eruptive potentials of ARs and could be employed to identify ARs prone to flaring activity. Based on the presented case study, we suggest that using a combination of different methods may aid to identify more reliably the eruptive potentials of ARs and help to better understand the pre-flare states. **Mar 6-10, 2011, Sep 3-7, 2011, Mar 6-10, 2012, Jul 1-5, 2012, Jul 10-14, 2012**

### **Threshold of non-potential magnetic helicity ratios at the onset of solar eruptions**

Francesco P. [Zuccarello](#), [Etienne Pariat](#), [Gherardo Valori](#), [Luis Linan](#)

ApJ **863** 41 **2018**

<https://arxiv.org/pdf/1807.00532.pdf>

[https://sites.lesia.obspm.fr/helisol/files/2018/07/Zuccarello\\_helicity\\_ratios\\_Final.pdf](https://sites.lesia.obspm.fr/helisol/files/2018/07/Zuccarello_helicity_ratios_Final.pdf)

<http://sci-hub.tw/http://iopscience.iop.org/article/10.3847/1538-4357/aacdfc/meta>

The relative magnetic helicity is a quantity that is often used to describe the level of entanglement of non-isolated magnetic fields, such as the magnetic field of solar active regions. The aim of this paper is to investigate how different kinds of photospheric boundary flows accumulate relative magnetic helicity in the corona and if and how well magnetic helicity related quantities identify the onset of an eruption. We use a series of three-dimensional, parametric magnetohydrodynamic simulations of the formation and eruption of magnetic flux ropes. All the simulations are performed on the same grid, using the same parameters, but they are characterized by different driving photospheric flows, i.e., shearing, convergence, stretching, peripheral- and central- dispersion flows. For each of the simulations, the instant of the onset of the eruption is carefully identified by using a series of relaxation runs. We find that magnetic energy and total relative helicity are mostly injected when shearing flows are applied at the boundary, while the magnetic energy and helicity associated with the coronal electric currents increase regardless of the kind of photospheric flows. We also find that, at the onset of the eruptions, the ratio between the non-potential magnetic helicity and the total relative magnetic helicity has the same value for all the simulations, suggesting the existence of a threshold in this quantity. Such threshold is not observed for other quantities as, for example, those related to the magnetic energy.

### **Vortex and Sink Flows in Eruptive Flares as a Model for Coronal Implosions**

F. P. [Zuccarello](#)<sup>1,2,5</sup>, G. Aulanier<sup>2</sup>, J. Dudík<sup>3</sup>, P. Démoulin<sup>2</sup>, B. Schmieder<sup>2</sup>, and S. A. Gilchrist<sup>4</sup>

**2017** ApJ **837** 115

<http://iopscience.iop.org/sci-hub.cc/0004-637X/837/2/115/>

Eruptive flares are sudden releases of magnetic energy that involve many phenomena, several of which can be explained by the standard 2D flare model and its realizations in 3D. We analyze a 3D magnetohydrodynamics simulation, in the framework of this model, that naturally explains the contraction of coronal loops in the proximity of the flare sites, as well as the inflow toward the region above the cusp-shaped loops. We find that two vorticity arcs located along the flanks of the erupting magnetic flux rope are generated as soon as the eruption begins. The magnetic arcades above the flux rope legs are then subjected to expansion, rotation, or contraction depending on which part of the vortex flow advects them. In addition to the vortices, an inward-directed magnetic pressure gradient exists in the current sheet below the magnetic flux rope. It results in the formation of a sink that is maintained by reconnection. We conclude that coronal loop apparent implosions observed during eruptive flares are the result of hydromagnetic effects related to the generation of vortex and sink flows when a flux rope moves in a magnetized environment.

## **THE APPARENT CRITICAL DECAY INDEX AT THE ONSET OF SOLAR PROMINENCE ERUPTIONS**

F. P. **Zuccarello**, G. Aulanier, and S. A. Gilchrist

2016 ApJ 821 L23 DOI: [10.3847/2041-8205/821/2/L23](https://doi.org/10.3847/2041-8205/821/2/L23)

A magnetic flux rope (MFR) embedded in a line-tied external magnetic field that decreases with height as  $z^{-n}$  is unstable to perturbations if the decay index of the field  $n$  is larger than a critical value. The onset of this instability, called torus instability, is one of the main mechanisms that can initiate coronal mass ejections. Since flux ropes often possess magnetic dips that can support prominence plasma, this is also a valuable mechanism to trigger prominence eruptions. Magnetohydrodynamic (MHD) simulations of the formation and/or emergence of MFRs suggest a critical value for the onset of the instability in the range [1.4–2]. However, detailed observations of prominences suggest a value in the range [0.9–1.1]. In this Letter, by using a set of MHD simulations, we show why the large discrepancy between models and observations is only apparent. Our simulations indeed show that the critical decay index at the onset of the eruption is  $n = 1.4 \pm 0.1$  when computed at the apex of the flux rope axis, while it is  $n = 1.1 \pm 0.1$  when it is computed at the altitude of the topmost part of the distribution of magnetic dips. The discrepancy only arises because weakly twisted curved flux ropes do not have dips up to the altitude of their axis.

## **Critical decay index at the onset of solar eruptions**

F.P. **Zuccarello**, G. Aulanier, S.A. Gilchrist

ApJ 814 126 2015

<http://arxiv.org/pdf/1510.03713v1.pdf>

Magnetic flux ropes are topological structures consisting of twisted magnetic field lines that globally wrap around an axis. The torus instability model predicts that a magnetic flux rope of major radius  $R$  undergoes an eruption when its axis reaches a location where the decay index  $-d(\ln B_{\text{ex}})/d(\ln R)$  of the ambient magnetic field  $B_{\text{ex}}$  is larger than a critical value. In the current-wire model, the critical value depends on the thickness and time-evolution of the current channel. We use magneto-hydrodynamic (MHD) simulations to investigate if the critical value of the decay index at the onset of the eruption is affected by the magnetic flux rope's internal current profile and/or by the particular pre-eruptive photospheric dynamics. The evolution of an asymmetric, bipolar active region is driven by applying different classes of photospheric motions. We find that the critical value of the decay index at the onset of the eruption is not significantly affected by either the pre-eruptive photospheric evolution of the active region or by the resulting different magnetic flux ropes. As in the case of the current-wire model, we find that there is a 'critical range' [1.3–1.5], rather than a 'critical value' for the onset of the torus instability. This range is in good agreement with the predictions of the current-wire model, despite the inclusion of line-tying effects and the occurrence of tether-cutting magnetic reconnection.

## **Observational Evidence of Torus Instability as Trigger Mechanism for Coronal Mass Ejections: The 2011 August 4 Filament Eruption**

F. P. **Zuccarello**, D. B. Seaton, M. Mierla, S. Poedts, L. A. Rachmeler, P. Romano, and F. Zuccarello

2014 ApJ 785 88

<http://arxiv.org/pdf/1401.5936v1.pdf>

Solar filaments are magnetic structures often observed in the solar atmosphere and consist of plasma that is cooler and denser than their surroundings. They are visible for days -- and even weeks -- which suggests that they are often in equilibrium with their environment before disappearing or erupting. Several eruption models have been proposed that aim to reveal what mechanism causes (or triggers) these solar eruptions. Validating these models through observations represents a fundamental step in our understanding of solar eruptions. We present an analysis of the observation of a filament eruption that agrees with the torus instability model. This model predicts that a magnetic flux rope embedded in an ambient field undergoes an eruption when the axis of the flux rope reaches a critical height that depends on the topology of the ambient field. We use the two vantage points of SDO and STEREO to reconstruct the three-dimensional shape of the filament, to follow its morphological evolution and to determine its height just before eruption. The magnetograms acquired by SDO/HMI are used to infer the topology of the ambient field and to derive the critical height for the onset of the torus instability. Our analysis shows that the torus instability is the trigger of the eruption. We also find that some pre-eruptive processes, such as magnetic reconnection during the observed flares and flux cancellation at

the neutral line, facilitated the eruption by bringing the filament to a region where the magnetic field was more vulnerable to the torus instability.

**ERRATUM: 2014 ApJ 795 175**

### **Shearing motions and torus instability in the 2010 April 3 filament eruption**

**Zuccarello**, F. P.; Romano, P.; Zuccarello, F.; Poedts, S.

Nature of Prominences and their role in Space Weather, Proceedings of the International Astronomical Union, IAU Symposium, Volume 300, pp. 475-476, **2014**

The magnetic field evolution of active region NOAA 11059 is studied in order to determine the possible causes and mechanisms that led to the initiation of the 2010 April 3 coronal mass ejection (CME).

We find (1) that the magnetic configuration of the active region is unstable to the torus instability and (2) that persistent shearing motions characterized the negative polarity, resulting in a southward, almost parallel to the meridians, drift motion of the negative magnetic field concentrations.

We conclude that these shearing motions increased the axial field of the filament eventually bringing the flux rope axis to a height where the onset condition for the torus instability was satisfied.

### **Solar activity and its evolution across the corona: recent advances** **Review**

Francesca **Zuccarello**, Laura Balmaceda, Gael Cessateur, Hebe Cremades, Salvatore L. Guglielmino, Jean Lilensten, Thierry Dudok de Wit, Matthieu Kretzschmar, Fernando M. Lopez, Marilena Mierla, et al. (8 more)

**J. Space Weather Space Clim.** 3 (2013) A18, **File**

Solar magnetism is responsible for the several active phenomena that occur in the solar atmosphere. The consequences of these phenomena on the solar-terrestrial environment and on Space Weather are nowadays clearly recognized, even if not yet fully understood. In order to shed light on the mechanisms that are at the basis of the Space Weather, it is necessary to investigate the sequence of phenomena starting in the solar atmosphere and developing across the outer layers of the Sun and along the path from the Sun to the Earth. This goal can be reached by a combined multi-disciplinary, multi-instrument, multi-wavelength study of these phenomena, starting with the very first manifestation of solar active region formation and evolution, followed by explosive phenomena (i.e., flares, erupting prominences, coronal mass ejections), and ending with the interaction of plasma magnetized clouds expelled from the Sun with the interplanetary magnetic field and medium. This wide field of research constitutes one of the main aims of COST Action ES0803: Developing Space Weather products and services in Europe. In particular, one of the tasks of this COST Action was to investigate the Progress in Scientific Understanding of Space Weather. In this paper we review the state of the art of our comprehension of some phenomena that, in the scenario outlined above, might have a role on Space Weather, focusing on the researches, thematic reviews, and main results obtained during the COST Action ES0803.

### **NUMERICAL MODELING OF THE INITIATION OF CORONAL MASS EJECTIONS IN ACTIVE REGION NOAA 9415**

F. P. **Zuccarello**<sup>1,2,3</sup>, Z. Meliani<sup>4</sup>, and S. Poedts

**2012 ApJ 758 117**

Coronal mass ejections (CMEs) and solar flares are the main drivers of weather in space. Understanding how these events occur and what conditions might lead to eruptive events is of crucial importance for up to date and reliable space weather forecasting. The aim of this paper is to present a numerical magnetohydrodynamic (MHD) data-inspired model suitable for the simulation of the CME initiation and their early evolution. Starting from a potential magnetic field extrapolation of the active region (AR) NOAA 9415, we solve the full set of ideal MHD equations in a non-zero plasma- $\beta$  environment. As a consequence of the applied twisting motions, a force-free-magnetic field configuration is obtained, which has the same chirality as the investigated AR. We investigate the response of the solar corona when photospheric motions resembling the ones observed for AR 9415 are applied at the inner boundary. As a response to the converging shearing motions, a flux rope is formed that quickly propagates outward, carrying away the plasma confined inside the flux rope against the gravitational attraction by the Sun. Moreover, a compressed leading edge propagating at a speed of about 550 km s<sup>-1</sup> and preceding the CME is formed. The presented simulation shows that both the initial magnetic field configuration and the plasma-magnetic-field interaction are relevant for a more comprehensive understanding of the CME initiation and early evolution phenomenon.

### **The role of photospheric shearing motions in a filament eruption related to the 2010 April 3 coronal mass ejection** A28

F. P. **Zuccarello**, P. Romano, F. Zuccarello and S. Poedts

**A&A 537, A28 (2012)**

Context. Coronal mass ejections (CMEs) are huge expulsion of solar plasma and magnetic field in the interplanetary medium. Understanding the physics that lies beyond the CME initiation is one of the most fascinating research

questions. Several models have been proposed to explain the initiation of CMEs. However, which model better explains the different aspects of the initiation process and the early evolution of the CMEs is a subject of ongoing discussion. Aims. We investigate the magnetic field evolution of NOAA 11059 in order to provide a further contribution to our understanding of the possible causes and mechanisms that lead to the initiation of the geoeffective CME that occurred on **2010 April 3**.

Methods. Using KSO H $\alpha$  images we determine the chirality of the active region and some properties of the filament that eventually erupted. Using SOHO/MDI line-of-sight magnetograms we investigate the magnetic configuration of NOAA 11059 by means of both linear force free and potential field extrapolations. We also determine the photospheric velocity maps using the Differential Affine Velocity Estimator (DAVE).

Results. We find that the magnetic configuration of the active region is unstable to the torus instability. Moreover, we find that persistent shearing motions characterized the negative polarity, resulting in a southward, almost parallel to the meridians, drift motion of the negative magnetic field concentrations.

Conclusions. We conclude that persistent and coherent shearing motions played a significant role in facilitating the eruption. These shearing motions increased the axial field of the filament eventually bringing the fluxrope axis to a height where the onset condition for the torus instability was satisfied. Our observations show that both the magnetic configuration of the system and the photospheric dynamics that preceded the event, were favourable for the eruption to occur.

## **THE ROLE OF STREAMERS IN THE DEFLECTION OF CORONAL MASS EJECTIONS: COMPARISON BETWEEN STEREO THREE-DIMENSIONAL RECONSTRUCTIONS AND NUMERICAL SIMULATIONS**

F. P. [Zuccarello](#)<sup>1,2</sup>, A. Bemporad<sup>3</sup>, C. Jacobs<sup>1</sup>, M. Mierla<sup>4,5,6</sup>, S. Poedts<sup>1</sup> and F. Zuccarello

**2012 ApJ 744 66, File**

On **2009 September 21**, a filament eruption and the associated coronal mass ejection (CME) were observed by the Solar Terrestrial Relations Observatory (STEREO) spacecraft. The CME originated from the southern hemisphere and showed a deflection of about 15° toward the heliospheric current sheet (HCS) during the propagation in the COR1 field of view. The CME source region was near the central meridian, but no on-disk CME signatures could be seen from the Earth. The aim of this paper is to provide a physical explanation for the strong deflection of the CME observed on 2009 September 21. The two-sided view of the STEREO spacecraft allows us to reconstruct the three-dimensional travel path of the CME and the evolution of the CME source region. The observations are combined with a magnetohydrodynamic simulation, starting from a magnetic field configuration closely resembling the extrapolated potential field for that date. By applying localized shearing motions, a CME is initiated in the simulation, showing a similar non-radial evolution, structure, and velocity as the observed event. The CME gets deflected toward the current sheet of the larger northern helmet streamer due to an imbalance in the magnetic pressure and tension forces and finally gets into the streamer. This study shows that during solar minima, even CMEs originating from high latitude can be easily deflected toward the HCS, eventually resulting in geoeffective events. How rapidly they undergo this latitudinal migration depends on the strength of both the large-scale coronal magnetic field and the magnetic flux of the erupting filament.

## **Magnetic helicity balance during a filament eruption that occurred in active region NOAA 9682**

F. P. [Zuccarello](#)<sup>1,2</sup>, P. Romano<sup>2</sup>, F. Zuccarello<sup>3</sup> and S. Poedts

**A&A 530, A36 (2011), File**

Context. Photospheric shear plasma flows in active regions may be responsible for the magnetic helicity injection in the solar corona not only during the energy storage process before a solar eruption, but also during and after the release of the free magnetic energy caused by the eruption. Indeed, after a filament eruption or expansion the magnetic torque imbalance can induce shear flows that can be responsible for yet another injection of magnetic helicity into the corona.

Aims. We investigated the magnetic helicity balance in an active region where a confined solar eruption occurred. This was done to verify a possible relationship between the filament expansion and the helicity transport at its footpoints. We aimed to verify if this variation in the helicity transport rate could be interpreted as a consequence of the magnetic torque imbalance caused by the tube expansion, as proposed by Chae et al. (2003, J. Kor. Astron. Soc., 36, 33).

Methods. We used 171 Å TRACE data to measure some geometrical parameters of the new magnetic system produced by a filament eruption that occurred on **2001 November 1** in active region NOAA 9682. We used MDI full disk line-of-sight magnetogram data to measure the accumulation of magnetic helicity in the corona before and after the event.

Results. From the measured expansion factor in the magnetic arcade, visible at 171 Å during the eruption, we estimated that the resulting torque imbalance at the photosphere ought to lead to the injection of negative helicity following the eruption. We compared this with measurements of the helicity injection using photospheric velocity and magnetogram data.

Conclusions. In contradiction to the expectations from the Chae et al. model, the helicity injection after the eruption was positive. We offer the alternative interpretation that the helicity injection resulted from torque of the opposite sign, generated as the filament lost its negative helicity through magnetic reconnection with its surroundings.



## Modelling the initiation of coronal mass ejections: magnetic flux emergence versus shearing motions:

F. P. **Zuccarello**, C. Jacobs, A. Soenen, S. Poedts, B. van der Holst and F. Zuccarello  
A&A 507 (2009) 441-452

*Context.* Coronal mass ejections (CMEs) are enormous expulsions of magnetic flux and plasma from the solar corona into the interplanetary space. These phenomena release a huge amount of energy. It is generally accepted that both photospheric motions and the emergence of new magnetic flux from below the photosphere can put stress on the system and eventually cause a loss of equilibrium resulting in an eruption.

*Aims.* By means of numerical simulations we investigate both emergence of magnetic flux and shearing motions along the magnetic inversion line as possible driver mechanisms for CMEs. The pre-eruptive region consists of three arcades with alternating magnetic flux polarity, favouring the breakout mechanism.

*Methods.* The equations of ideal magnetohydrodynamics (MHD) were advanced in time by using a finite volume approach and solved in spherical geometry. The simulation domain covers a meridional plane and reaches from the

lower solar corona up to  $30 R_{\odot}$ . When we applied time-dependent boundary conditions at the inner boundary, the central arcade of the multiframe system expands, leading to the eventual eruption of the top of the helmet streamer. We compare the topological and dynamical evolution of the system when driven by the different boundary conditions. The available free magnetic energy and the possible role of magnetic helicity in the onset of the CME are investigated.

*Results.* In our simulation setup, both driving mechanisms result in a slow CME. Independent of the driving mechanism, the overall evolution of the system is the same: the actual CME is the detached helmet streamer. However, the evolution of the central arcade is different in the two cases. The central arcade eventually becomes a flux rope in the shearing case, whereas in the flux emergence case there is no formation of a flux rope. Furthermore, we conclude that magnetic helicity is not crucial to a solar eruption.

## INITIATION OF CORONAL MASS EJECTIONS BY MAGNETIC FLUX EMERGENCE IN THE FRAMEWORK OF THE BREAKOUT MODEL

F. P. **Zuccarello**,<sup>1,2</sup> A. Soenen,<sup>2</sup> S. Poedts,<sup>2</sup> F. Zuccarello,<sup>1</sup> and C. Jacobs<sup>2</sup>  
Astrophysical Journal, 689: L157–L160, 2008

The possible role of magnetic flux emergence in the initiation of coronal mass ejections (CMEs) is investigated in the framework of the breakout model. The ideal MHD equations are solved numerically on a spherical, axisymmetric (2.5-dimensional) domain. An initial multiframe system in steady equilibrium containing a pre-eruptive region consisting of three arcades with alternating magnetic flux polarity is kept in place by the magnetic tension of the overlying closed magnetic field of a helmet streamer. The emergence of new magnetic flux in the central arcade is simulated by means of a time-dependent boundary condition on the vector potential applied at the solar base. Height-time plots of the ejected material, as well as time evolution of the magnetic, kinetic and internal energy in the entire domain as functions of flux emergence rate, are produced. The results show that the emergence of new magnetic flux in the central arcade triggers a CME. The obtained eruption corresponds to a slow CME, and conversion of magnetic energy into kinetic energy is observed.

## COMPOSITION OF CORONAL MASS EJECTIONS

T. H. **Zurbuchen**<sup>1</sup>, M. Weberg<sup>1</sup>, R. von Steiger<sup>2,3</sup>, R. A. Mewaldt<sup>4</sup>, S. T. Lepri<sup>1</sup>, and S. K. Antiochos<sup>5</sup>  
2016 ApJ 826 10 DOI 10.3847/0004-637X/826/1/10

We analyze the physical origin of plasmas that are ejected from the solar corona. To address this issue, we perform a comprehensive analysis of the elemental composition of interplanetary coronal mass ejections (ICMEs) using recently released elemental composition data for Fe, Mg, Si, S, C, N, Ne, and He as compared to O and H. We find that ICMEs exhibit a systematic abundance increase of elements with first ionization potential (FIP) < 10 eV, as well as a significant increase of Ne as compared to quasi-stationary solar wind. ICME plasmas have a stronger FIP effect than slow wind, which indicates either that an FIP process is active during the ICME ejection or that a different type of solar plasma is injected into ICMEs. The observed FIP fractionation is largest during times when the Fe ionic charge states are elevated above  $Q_{\text{Fe}} > 12.0$ . For ICMEs with elevated charge states, the FIP effect is enhanced by 70% over that of the slow wind. We argue that the compositionally hot parts of ICMEs are active region loops that do not normally have access to the heliosphere through the processes that give rise to solar wind. *We also discuss the implications of this result for solar energetic particles accelerated during solar eruptions and for the origin of the slow wind itself.*

## Диагностика плазменных струй в короне Солнца

**Анфиногентов** С.А., Кальтман Т.И., Ступишин А.Г., Накаряков В.М., Лукичева М.А.

Солнечная-земная физика. 2021. Т. 7, No 2. С. 3–11.

<https://naukaru.ru/ru/storage/viewWindow/72935>

DOI: 10.12737/szf-72202101

В статье рассматривается диагностика плазменных струй в короне Солнца по данным современных космических и наземных телескопов, наблюдающих Солнце в крайнем ультрафиолетовом (КУФ) и микроволновом диапазонах. Обсуждаются наблюдательные параметры КУФ- и радиоизлучения в событиях, связанных с плазменными струями, в зависимости от механизма образования, условий излучения и эволюции

струй. Показаны возможности изучения солнечной короны, предоставляемые исследованием плазменных струй по наблюдениям одновременно в различных диапазонах. Для ряда струй измерены их первичные параметры и приведены предварительные результаты статистической обработки полученных данных. Подробно рассмотрены микроволновые наблюдения нескольких отдельных событий, выполненные с помощью наземных инструментов РАТАН-600, СРГ и радиогелиографа Нобеяма. Показаны диагностические возможности указанных инструментов при исследовании корональных струй. Для анализа трехмерной структуры коронального магнитного поля использованы данные SDO/HMI, по которым выполнена реконструкция поля в нижней короне. Полученная информация сопоставляется с результатами диагностики магнитного поля в основании короны по данным РАТАН-600. Целью разрабатываемых методов является определение физических механизмов, ответственных за генерацию, коллимацию и динамику плазменных струй в атмосфере Солнца. 2016-04-28, 2017-09-04, 2017-09-13, 2018-04-03, 2018-09-14, 2018-10-13

### ПРОСТРАНСТВЕННЫЕ И ВРЕМЕННЫЕ ОСОБЕННОСТИ ПОВЕДЕНИЯ МИКРОВОЛНОВОГО И УЛЬТРАФИОЛЕТОВОГО ИЗЛУЧЕНИЯ В ЭРУПТИВНЫХ СОБЫТИЯХ

БАКУНИНА И.А.<sup>1</sup>, МЕЛЬНИКОВ В.Ф.<sup>2</sup>, ШАИН А.В.<sup>2</sup>, АБРАМОВ-МАКСИМОВ В.Е.<sup>2</sup>, ОРГАЧЕВ А.С.<sup>3</sup>

Изв. Крао Том: 118 Номер: 1 Год: 2022 Страницы: 65-74

[https://www.elibrary.ru/download/elibrary\\_48073416\\_76156594.pdf](https://www.elibrary.ru/download/elibrary_48073416_76156594.pdf)

На сегодняшний день не вполне ясны наблюдательные признаки, определяющие способность активной области вызывать выброс вещества в высокие слои солнечной короны (coronal mass ejection – CME). Это затрудняет понимание физического механизма триггера CME. Данная работа посвящена поиску наблюдательных признаков, которые могут указывать на возникновение эруптивного процесса. Для этого мы провели сравнительный анализ условий до вспышки и во время вспышки для вспышечных событий, как сопровождаемых, так и не сопровождаемых CME. Мы изучили особенности пространственной и временной динамики микроволнового и ультрафиолетового излучений (данные радиогелиографа Нобеяма, SDO/AIA), а также магнитных полей (SDO/HMI) для 16 активных областей (АО). На этой выборке установлено, что вспышки, сопровождающиеся CME, чаще всего возникают в открытых магнитных конфигурациях, в областях со скрученными магнитными жгутами и со всплывающими потоками. CME также наблюдаются чаще всего во вспышках большей длительности и в тех АО, которые имеют более протяженные по площади источники в микроволновом излучении. 2012-03-09, 2013-11-03, 2014-09-28

Бакунина И.А., Мельников В.Ф., Абрамов-Максимов В.Е. Особенности корональных магнитных структур в бессиловом приближении для активных областей со вспышками рентгеновского класса M, сопровождающимися и не сопровождающимися корональными выбросами масс

Сборник трудов XXVI Всероссийской ежегодной конференции по физике Солнца «Солнце и солнечно-земная физика – 2022» ГАО РАН. С. 17-20

<http://www.gaoran.ru/russian/solphys/2022/book/conf2022.pdf>

### ИССЛЕДОВАНИЕ СТАТИСТИЧЕСКОЙ СВЯЗИ КОРОНАЛЬНЫХ ВЫБРОСОВ МАССЫ С СОЛНЕЧНЫМИ ВСПЫШКАМИ

БАРХАТОВ Н.А.\*<sup>1</sup>, ВОРОБЬЕВ В.Г.<sup>2</sup>, РЕВУНОВ С.Е.<sup>1</sup>, РЕВУНОВА Е.А.<sup>3</sup>

Известия РАН Том: 85 Номер: 3 Год: 2021 Страницы: 326-330

В исследовании на основе анализа статистической связи корональных выбросов массы с солнечными вспышками устанавливается последовательность этих событий. Определены временные задержки в появлении корональных выбросов массы относительно ассоциированного с ним вспышечного проявления солнечной активности. Обнаружено, что приоритетными являются ситуации, когда вспышки опережают корональные выбросы на несколько часов.

О возможном различии в формировании корональных выбросов массы двух типов.

Еселевич В.Г., Еселевич М.В., Зимовец И.В.

СОЛНЕЧНО-ЗЕМНАЯ ФИЗИКА Том 8. 2022. № 2 С. 12–22.

DOI : 10.12737/szf-82202202

<https://naukaru.ru/ru/storage/viewWindow/94294>

Анализ семи околосолнечных корональных выбросов массы (КВМ) показал, что на расстояниях  $R < 1.4R_{\odot}$  от центра Солнца по характеру формирования КВМ можно разделить на два типа. В случае КВМ типа 1 формирование фронтальной структуры (FS) происходит за счет процессов, протекающих внутри самой FS, представляющей собой внешнюю оболочку магнитного жгута. В случае КВМ типа 2 происходит эрупция внутренних арочных структур, которые взрывообразно расширяются, захватывают и ускоряют окружающие более удаленные арочные структуры, в результате слияния которых и формируется фронтальная структура КВМ типа 2. 27.01.2012, 19.07.2012, 24.08.2014,

## ОСОБЕННОСТИ НАЧАЛЬНОЙ СТАДИИ ФОРМИРОВАНИЯ БЫСТРОГО КРОНАЛЬНОГО ВЫБРОСА МАССЫ 25 ФЕВРАЛЯ 2014 Г

[ЕСЕЛЕВИЧ В.Г.](#)<sup>1</sup>, [ЕСЕЛЕВИЧ М.В.](#)<sup>1</sup>

[СОЛНЕЧНО-ЗЕМНАЯ ФИЗИКА](#) Том: 6Номер: 3 Год: 2020 Страницы: 3-17

Проведен анализ быстрого коронального выброса массы (КВМ) 25 февраля 2014 г. по изображениям в УФ-каналах 131, 211, 304 и 1700 Å инструмента SDO/AIA и по данным наблюдений в линии H $\alpha$  (6562.8 Å) на телескопах обсерваторий Teide и Big Bear. Формирование КВМ 25.02.2014 связано с выбросом и последующим взрывообразным расширением магнитного жгута, возникшего вблизи поверхности Солнца, предположительно, вследствие процесса tether-cutting магнитного пересоединения. Возникший в результате такого «взрыва» импульс полного давления (теплого плюс магнитного) воздействует на вышележащие корональные арочные структуры, приводя к их слиянию и формированию ускоренно движущейся фронтальной структуры КВМ. Этот же импульс давления является причиной возникновения взрывной столкновительной ударной волны перед КВМ, скорость которой быстро уменьшается с расстоянием. На больших расстояниях  $R > 7 R_{\odot}$  ( $R_{\odot}$  - радиус Солнца) от центра Солнца перед КВМ регистрируется ударная волна другого типа - поршневая столкновительная ударная волна, скорость которой мало меняется с расстоянием. На  $R \geq 15 R_{\odot}$  происходит переход от столкновительной ударной волны к бесстолкновительной.

## ОСОБЕННОСТИ ДИНАМИКИ УДАРНОЙ ВОЛНЫ, ВОЗБУЖДАЕМОЙ БЫСТРЫМ КРОНАЛЬНЫМ ВЫБРОСОМ МАССЫ

[ЕСЕЛЕВИЧ В.Г.](#)<sup>\*1</sup>, [ЕСЕЛЕВИЧ М.В.](#)<sup>1</sup>

Космические исследования Том: 57Номер: 3 Год: 2019 Страницы: 163-176

На примере события 27.1.2012 исследованы особенности динамики формирования ударной волны, возбуждаемой быстрым корональным выбросом массы (КВМ) со скоростью более 2000 км/с. Использовались данные: а) изображения Солнца в УФ канале 13.1 нм с инструмента AIA на расстояниях 1.0–1.4 радиусов Солнца от центра Солнца, б) изображения белой короны с коронографов LASCO C2 и C3 на  $R \approx 2.1$ –3.0 радиусов Солнца. Исследования показали справедливость закономерностей, установленных ранее для случаев сравнительно медленных КВМ (со скоростями  $< 1500$  км/с): 1) Формирование ударного фронта происходит, когда скорость лидирующей части КВМ относительно невозмущенного солнечного ветра становится больше локальной альвеновской скорости, что соответствует явлению “перехода через скорость звука” для замагниченной плазмы. 2) Изменение ширины ударного фронта и, соответственно, механизма диссипации энергии происходит в нем от “столкновительного” на расстояниях от центра Солнца менее десяти радиусов Солнца, к “бесстолкновительному” – на расстояниях более десяти радиусов Солнца. В событии 27.1.2012 удалось более детально исследовать процесс перехода от столкновительного к бесстолкновительному ударному фронту. Было обнаружено, что долготная протяженность ударного фронта, возбуждаемого быстрым КВМ, на расстояниях менее 6 радиусов Солнца увеличена почти в 10 раз по сравнению с более медленным КВМ. Одной из главных причин этого увеличения, кроме большой скорости, является тот факт, что движение КВМ происходило в плоскости пояса корональных стримеров. Сделан вывод о том, что на расстояниях менее 6 радиусов Солнца структура ударного фронта перед КВМ является “параллельного” типа, т.е. угол между вектором невозмущенного магнитного поля и нормалью к фронту близок к 0°.

## ВОЗМОЖНОСТЬ ГЕНЕРАЦИИ УДАРНОЙ ВОЛНЫ В КРОНЕ СОЛНЦА ПРИ ОТСУТСТВИИ КРОНАЛЬНОГО ВЫБРОСА МАССЫ

[ЕСЕЛЕВИЧ В.Г.](#)<sup>✉1</sup>, [ЕСЕЛЕВИЧ М.В.](#)<sup>1</sup>, [ЗИМОВЕЦ И.В.](#)<sup>2,3,4</sup>, [ШАРЫКИН И.Н.](#)

АЖ Том: 94Номер: 9 Год: 2017 Страницы: 793-807

Исследовано солнечное событие SOL2012-10-23T03:13, связанное со вспышкой балла X1.8, в котором отсутствовал корональный выброс массы (КВМ), но наблюдался радиовсплеск II типа. Использовался метод построения профилей разностной яркости в УФ и ЭУФ каналах инструмента AIA/SDO в пространстве и во времени одновременно с анализом всплеска радиоизлучения II типа. Показано, что в данном событии происходят формирование и распространение области сжатия, впереди которой на расстояниях  $R < 1.3 R_{\odot}$  от центра Солнца ( $R_{\odot}$  - радиус Солнца) регистрируется столкновительная ударная волна. На основе сравнения с результатами анализа подобного типа события SOL2011-02-28T07:34, полученными в статье [1], был сделан следующий вывод. Предполагаемой причиной возбуждения области сжатия и ударной волны является кратковременное (импульсное) воздействие на окружающую плазму эруптивного высокотемпературного магнитного жгута. Его начальная неустойчивость и эрупция могут быть инициированы всплывающим магнитным потоком, а нагрев может быть следствием магнитного пересоединения. Остановка эрупции жгута может быть связана с его взаимодействием с окружающими магнитными структурами (корональными петлями).

## ИССЛЕДОВАНИЕ НАЧАЛЬНОЙ СТАДИИ ФОРМИРОВАНИЯ “ИМПУЛЬСНОГО” КРОНАЛЬНОГО ВЫБРОСА МАССЫ

[Еселевич В.](#), [Еселевич М.](#), [Зимовец И.](#), [Руденко Г.](#)

АЖ Т. 93 №11, 990- 2016 File

Astronomy Reports November 2016, Volume 60, Issue 11, pp 1016–1027 File

Проведен анализ “импульсного” коронального выброса массы (КВМ) 24 августа 2014 г. по УФ изображениям в каналах 193, 304, 1600 и 1700 А инструмента SDO/AIA и по данным наблюдений в линии H (6562.8 А) телескопов обсерваторий El Teide и Big Bear. Показано, что формирование “импульсного” КВМ связано с появлением магнитной трубки (жгута), движущейся со скоростью км/с и содержащей плазму более холодную, чем плазма фотосферы. При движении в короне магнитная трубка сталкивается с корональным квазистационарным магнитным жгутом, два основания которого укоренены на фотосфере, и ускоряет его (приводит в движение). В результате такого взаимодействия происходит формирование КВМ, фронтальной структурой которого является поверхность коронального магнитного жгута. На стадии формирования в окрестности оснований КВМ по данным SDO/HMI не было зарегистрировано возрастания или изменения потока магнитного поля. Это может свидетельствовать в пользу того, что магнитная трубка начала свое движение из слоев, располагающихся в окрестности температурного минимума.

## О ВОЗМОЖНОЙ ПРИЧИНЕ ЧАСТОТНОГО РАСЩЕПЛЕНИЯ ГАРМОНИК СОЛНЕЧНОГО РАДИОВСПЛЕСКА ВТОРОГО ТИПА

В. Г. Еселевич, М. В. Еселевич, И. В. Зимовец

АЖ т92, №12, стр. 977-1008, 2015 File

На основе анализа данных инструмента AIA/SDO (канал 193 А°) впереди коронального выброса массы в лимбовом событии на Солнце 13 июня 2010 г. удалось одновременно зарегистрировать и измерить фронты двух различных ударных волн. Угловой размер каждого из этих фронтов относительно центра коронального выброса массы составил около 20°, а их направления распространения отличались на ≈25° (по позиционному углу на ≈4°). Более быстрый фронт, названный взрывной ударной волной, опережал фронт другой волны, названной поршневой, на  $R \approx (0.02-0.03) (R_{\odot} - \text{радиус Солнца})$  и имел максимальную начальную скорость  $VB \approx 850 \text{ км с}^{-1}$  (у поршневой  $VP \approx 700 \text{ км с}^{-1}$ ). Появление и движение этих ударных волн сопровождалось всплеском радиоизлучения II типа на фундаментальной частоте  $F$  и второй гармонике  $H$ . Каждая из частот была расщеплена на две близкие частоты  $f_1$  и  $f_2$ , различающиеся на величину  $\Delta f = f_2 - f_1 \sim F, H$ . На основе проведенного анализа был сделан вывод о том, что наблюдаемое частотное расщепление  $\Delta f$  частот  $F$  и  $H$  радиоизлучения II типа может быть результатом одновременного распространения поршневой и взрывной ударных волн с различными скоростями в нескольких разных направлениях, которые отличаются значениями концентрации корональной плазмы.

## Физические отличия в начальной фазе формирования двух типов корональных выбросов массы

В. Г. Еселевич, М. В. Еселевич

Астрономический журнал, 2014, С. 320-331

Исследованы физические отличия в формировании “постепенных” и “импульсных” корональных выбросов массы (СМЕ) на высотах ( $r$  - высота относительно поверхности Солнца,  $R_{\odot}$  - радиус Солнца) непосредственно перед и в течение начальной фазы их движения по данным ультрафиолетовых линий инструмента AIA/SDO. Показано, что основой структуры “постепенного” СМЕ является магнитный жгут, расположенный в короне. В течение часа и более перед начальной фазой в магнитном жгуте происходят следующие процессы: усиливается яркость и увеличивается поперечный размер - сначала низко лежащих внутренних структур жгута, а затем структур его внешней оболочки, наиболее удаленной от Солнца. При этом жгут остается неподвижным. Начальная фаза “постепенного” СМЕ начинается с движения внешней оболочки магнитного жгута, которая становится затем основой фронтальной структуры СМЕ. При этом внутренние низко лежащие структуры жгута остаются на этом этапе практически неподвижными. Начальная фаза “импульсного” СМЕ начинается с появлением вблизи фотосферы движущейся от Солнца полости, динамика которой предположительно отражает всплытие из-под фотосферы магнитной трубки с холодной плазмой. Встречая на своем пути арочные структуры, магнитная трубка сталкивается с ними и увлекает их за собой. Эти структуры участвуют в формировании СМЕ, основу которого составляет сама магнитная трубка.

## Физические отличия в начальной фазе формирования двух типов корональных выбросов массы

М.В.Еселевич

ИКИ-2014, Сессия: Солнце

<http://plasma2014.cosmos.ru/presentations>

See Eselevich

## РОЛЬ ВСПЛЫВАЮЩИХ МАГНИТНЫХ ТРУБОК ПРИ ФОРМИРОВАНИИ “ИМПУЛЬСНЫХ” КОРОНАЛЬНЫХ ВЫБРОСОВ МАССЫ

ЕСЕЛЕВИЧ В. Г.1, ЕСЕЛЕВИЧ М. В

АЖ, Том: 90, Номер: 11 Год: 2013 Страницы: 936

По данным солнечного инструмента AIA/SDO проведен анализ двух лимбовых “импульсных” корональных выбросов массы на Солнце, один из которых сопровождался активным протуберанцем, другой - вспышкой. Сделан вывод о том, что причиной формирования коронального выброса массы в обоих случаях является всплывающая с большой скоростью из-под фотосферы магнитная трубка. На пути движения магнитной трубки могут располагаться одна или несколько арочных структур, с которыми она взаимодействует и увлекает за собой. Эти структуры участвуют в формировании будущего коронального выброса массы, основу которого составляет магнитная трубка. **13 ИЮНЯ 2010, 27 АПРЕЛЯ 2011**

## **Природа возникновения корональных выбросов массы: современное состояние исследований и последние результаты**

**В. Г. Еселевич**

Презентация на ИКИ-13, **2013, Файл**

- 1) В настоящее время является общепризнанным, что солнечные вспышки, эруптивные протуберанцы и корональные выбросы массы (английская аббревиатура CME) не независимые явления, а результат различных проявлений внезапной и мощной дестабилизации коронального магнитного поля.
- 2) Предполагается, что эта дестабилизация связана с усилением коронального магнитного поля за счет: а) фотосферных движений или б) всплывающего из-под фотосферы нового магнитного потока (магнитной трубки). Причем, по-видимому, именно, всплывающая магнитная трубка, является наиболее распространенной причиной дестабилизации.
- 3) Для части событий всплывающая магнитная трубка является только триггером начала процесса формирования CME [Feynman & Martin, 1995; William et al., 2005], а для другой части – магнитная трубка может стать основой самого CME [Demoulin et al., 2002; Nindos et al., 2003]. Возможно, именно в этом суть отличий разных типов CME. Как это все происходит и какова физика этих процессов до сих пор не известно. В этом направлении развиваются различные модели и эксперимент, который должен дать окончательный ответ на этот вопрос.

## **РЕГИСТРАЦИЯ ВЗРЫВНОЙ И ПОРШНЕВОЙ УДАРНЫХ ВОЛН, СВЯЗАННЫХ С ВОЗНИКНОВЕНИЕМ И РАСПРОСТРАНЕНИЕМ КОРОНАЛЬНОГО ВЫБРОСА МАССЫ**

**В. Г. Еселевич**, М. В. Еселевич<sup>1</sup>, И. В. Зи мовец<sup>2</sup>

*АСТРОНОМИЧЕСКИЙ ЖУРНАЛ*, **2013**, том 90, №2, с. 166–176, **Файл**

По данным инструмента AIA космической обсерватории SDO (изображения в каналах 193 и 211 Å) и изображениям белой короны, полученным на коронографах LA SCO C2 и C3 космической обсерватории SOHO, проведен анализ коронального выброса массы на Солнце, произошедшего 3 ноября 2010 г. В данном событии удалось одновременно зарегистрировать и измерить фронты поршневой и взрывной ударных волн, вызванных формированием и распространением коронального выброса массы. Показано, что каждому из этих типов ударных волн может соответствовать распространяющийся впереди фронта источник радиовсплеска II типа.

## **СОЛНЕЧНЫЕ ВСПЫШЕЧНЫЕ ЭРУПЦИИ С ДЛИТЕЛЬНОЙ ЭКРАНИРОВКОЙ ИЗЛУЧЕНИЯ В ЛИНИИ HeII 304 Å И В МИКРОВОЛНОВОМ ДИАПАЗОНЕ**

**В. В. Гречнев**<sup>1</sup>, И. В. Кузьменко<sup>2</sup>, И. М. Черток<sup>3</sup>, А. М. Уралов<sup>1</sup>

*АСТРОНОМИЧЕСКИЙ ЖУРНАЛ*, **2011**, том 88, №7, с. 692–703

Извергнутая при солнечных эрупциях плазма с температурами, близкими к хромосферным, может экранировать часть излучения как компактных источников в активных областях, так и областей спокойного Солнца. Явления поглощения могут наблюдаться в микроволновом диапазоне в виде так называемых “отрицательных всплесков”, а также в линии HeII 304 Å. Рассмотрены три эруптивных события, связанных с довольно мощными вспышками. По записям потока “отрицательного всплеска” на нескольких радиочастотах для одного из рассмотренных событий оценены параметры поглощавшего излучения вещества выброса. В единичных событиях обнаружено “разрушение” эруптивного волокна и его распыление в виде облака по огромной поверхности, наблюдаемое в виде грандиозных депрессий излучения в линии HeII 304 Å. Одно из трех известных нам таких событий рассматривается в данной статье, еще одно из рассмотренных — возможный кандидат.

## **НАЧАЛЬНЫЕ СКОРОСТИ КОРОНАЛЬНЫХ ВЫБРОСОВ МАСС И ОСОБЕННОСТИ СОПРОВОЖДАЕМЫХ ВСПЫШЕК**

**Дивлекеев М.И.**

Пулково «Солнечная и солнечно-земная физика – 2015» с.115

In this paper we discuss three events: **July 30, 2005, May 5, 2012, and February 24**

**2015**. The trigger mechanisms of coronal mass ejections and the characteristics of the corresponding flares are studied. The average linear velocities of CME are estimated using the time of their expanding beyond the coronagraph’s occulting disk.

## **КИНЕМАТИЧЕСКИЕ ХАРАКТЕРИСТИКИ КВМ ТИПА STEALTH В ТРЕХМЕРНОМ ПРОСТРАНСТВЕ**

**Егоров Я.И., Файнштейн В.Г.**

**СОЛНЕЧНО-ЗЕМНАЯ ФИЗИКА** Том: 8 Номер: 3 Год: 2022 Страницы: 14-23

[https://elibrary.ru/download/elibrary\\_49522161\\_21032693.pdf](https://elibrary.ru/download/elibrary_49522161_21032693.pdf)

Для периода 2008-2014 гг. исследованы и сопоставлены кинематические характеристики движения корональных выбросов массы (КВМ) в трехмерном (3D) пространстве для трех групп КВМ: 1) КВМ типа stealth (далее - stealth-КВМ); 2) КВМ, возникшие на видимой стороне Солнца (для наблюдателя на Земле) и связанные с рентгеновскими вспышками и с эрупцией волокон; 3) все КВМ, зарегистрированные в указанный период. К stealth-КВМ мы отнесли КВМ, возникшие на видимой стороне Солнца и не связанные с рентгеновскими вспышками, а также с эрупцией волокон. Кинематические и некоторые физические характеристики этих КВМ были сопоставлены с аналогичными характеристиками выбросов массы, которые были отнесены к stealth-КВМ в работе [D'Neys et al., 2014]. После сравнения характеристик трех групп КВМ был сделан вывод, что в среднем stealth-КВМ имеют наименьшую скорость, кинетическую энергию, массу и угловой размер, центральный позиционный угол, а также угол  $\phi$  между направлением движения КВМ в плоскости эклиптики и линией Солнце-Земля и угол  $\lambda$  между направлением движения КВМ в 3D-пространстве и плоскостью эклиптики. Обсуждаются также распределения КВМ разных типов по кинематическим характеристикам.

**Таблица** Stealth-КВМ 2008–2012

## **СРАВНЕНИЕ ОСОБЕННОСТЕЙ ФОРМИРОВАНИЯ КОРОНАЛЬНЫХ ВЫБРОСОВ МАССЫ, ИМЕЮЩИХ РАЗНУЮ СКОРОСТЬ В ПОЛЕ ЗРЕНИЯ КОРОНГРАФОВ LASCO**

**Загайнова Ю.С.1, Файнштейн В.Г.2, Мышьяков И.И.2**

**Астрономия-2018** Том 2 Солнечно-земная физика – современное состояние и перспективы Стр. 82

<http://www.izmiran.ru/library/eaas2018/eaas-2018-2.pdf>

**22.10.2013, 07.01.2014**

## **СРАВНЕНИЕ ОСОБЕННОСТЕЙ ГЕНЕРАЦИИ КВМ, ДВИЖУЩИХСЯ В ПОЛЕ ЗРЕНИЯ КОРОНОГРАФОВ LASCO С РАЗЛИЧНОЙ СКОРОСТЬЮ**

**Загайнова Ю.С., Файнштейн В.Г.**

**КОСМИЧЕСКИЕ ИССЛЕДОВАНИЯ** Том: 57 Номер: 6 Год: 2019 Страницы: 430-439

Настоящая работа направлена на получение ответа на следующий вопрос: существуют ли принципиальные различия в генерации регистрируемых в поле зрения коронографов LASCO корональных выбросов массы (КВМ) с различными скоростями, прежде всего с маленькими и большими? К быстрым КВМ условно были отнесены выбросы массы, линейная проекционная скорость которых в поле зрения LASCO составляет  $> 1500$  км/с, к медленным –  $\leq 600$  км/с. КВМ с от 600 до 1500 км/с мы отнесли к выбросам массы с промежуточными скоростями. Результаты анализа приводим на примере трех событий КВМ типа гало (быстрого, медленного и движущегося с промежуточной скоростью) с источниками в пятенных группах, удаленных от центра солнечного диска не более чем на  $45^\circ$ . Для анализа использовали данные телескопов SDO/AIA и инструмента SDO/HMI, а также коронографов LASCO C2 и C3. Сопоставлены свойства активных областей, в которых возникли КВМ с разными скоростями. Сопоставлены морфологические особенности формирования отобранных выбросов массы по наблюдениям в линиях крайнего ультрафиолета и особенности их кинематики. С использованием данных векторных измерений фотосферного магнитного поля инструментом SDO/HMI над областями формирования КВМ в нелинейном бессиловом приближении рассчитаны распределения магнитного поля с высотой. Анализ этих распределений показал, что до начала связанной с КВМ вспышки быстрота изменения поля с высотой над местом генерации КВМ заметно отличается для всех отобранных событий.

## **ИССЛЕДОВАНИЕ ПАРАМЕТРОВ ДВИЖЕНИЯ КОРОНАЛЬНЫХ ВЫБРОСОВ МАССЫ ТИПА «ГАЛО» НА СТАДИИ ИХ ИНИЦИАЦИИ ПО ДАННЫМ GOES-12/SXI**

**Загайнова Ю.С., Файнштейн В.Г.**

**2012, File**

По данным GOES-12/SXI исследована начальная стадия движения шести быстрых (скорость больше 1500 км/с) корональных выбросов массы типа «гало» (ГКВМ) и прослежено движение этих ГКВМ в поле зрения SOHO/LASCO C2 и C3. Для этих ГКВМ найдены в зависимости от времени положение, скорость и ускорение их фронта, а также изменение со временем траектории их движения и отношение продольного размера КВМ к поперечному. Все изученные ГКВМ либо с самого начала их регистрации, либо спустя несколько минут, представляют собой петлеобразные структуры. Все рассмотренные ГКВМ начинают свое поступательное движение до начала связанной рентгеновской вспышки. Время основного ускорения (время достижения максимальной скорости в поле зрения коронографа LASCO/C2) близко ко времени нарастания интенсивности рентгеновского излучения связанной с ГКВМ вспышки. Подтверждены результаты работы Zhang&Dere (2006) о существовании обратной корреляции между амплитудой и длительностью ускорения, а также о равенстве измеренной длительности основного ускорения ГКВМ и времени нарастания интенсивности мягкого рентгеновского излучения из области связанной с ГКВМ вспышки. Установлены закономерности изменения со временем углового размера, траектории, ширины фронта и отношения продольного размера к поперечному размеру ГКВМ. **29.10.2003, 17.01.2005, 23.08.2005**

## СУЩЕСТВУЕТ ЛИ ПРЕДЕЛ ЭНЕРГИИ КОРОНАЛЬНЫХ ВЫБРОСОВ МАССЫ НА СОЛНЦЕ?

**Иванов Е.В.**

Пулково «Солнечная и солнечно-земная физика – 2015», с.165

The relationship between variations in the maximum velocity of coronal mass ejections (CME) and the typical dimension of structural elements of the large-scale solar magnetic field (LSMF) is investigated for the period 1996–2014. It is shown that the maximum velocity and, hence, the maximum energy of CME correspond to the values of the LSMF effective solar multipole index  $n \sim 4.0-4.4$ . These values determine the maximum size of the activity complexes, which together with observed maximum values of the magnetic field intensity in the complexes limits the possible maximum CME energy.

## ОБ ИЗМЕНЕНИИ ХАРАКТЕРА СВЯЗИ КОРОНАЛЬНЫХ ВЫБРОСОВ МАССЫ С СООТВЕТСТВУЮЩИМИ РЕНТГЕНОВСКИМИ ВСПЫШКАМИ В ТЕЧЕНИЕ 11-ЛЕТНЕГО СОЛНЕЧНОГО ЦИКЛА

**Е.В.Иванов**

ИКИ-2014, Сессия: Солнце

<http://plasma2014.cosmos.ru/presentations>

### ЭРУПЦИИ СПОКОЙНЫХ ВОЛОКОН И КОРОНАЛЬНЫЕ ДЖЕТЫ КАК ПРИЧИНЫ ДЕПРЕССИЙ МИКРОВОЛНОВОГО РАДИОИЗЛУЧЕНИЯ

**КУЗЬМЕНКО И. В.**

АЖ Том: 98 Номер: 12 Год: 2021 Страницы: 1019-1029

По данным различных спектральных диапазонов проведено исследование нескольких солнечных событий с отрицательными всплесками разного типа в микроволновом диапазоне. Использовались данные интегрального потока радиоизлучения, полученные в Уссурийской обсерватории, обсерватории Нобейма, данные Сети солнечных радиотелескопов BBC США (RSTN), спектрополяриметра ИСЗФ СО РАН. Анализ изображений проводился по данным космической обсерватории SDO/AIA в канале 304 Å и радиогелиографа Нобейма на частоте 17 ГГц. Показано, что причиной "изолированных" депрессий радиоизлучения являлось поглощение излучения радиоисточников и/или обширных областей спокойного Солнца низкотемпературным веществом крупного эруптивного волокна в отсутствие вспышек, что подтвердило выводы, сделанные в предыдущих исследованиях. Выявлено, что причиной отрицательных всплесков типа "депрессия перед всплеском" было затенение околомимбового радиоисточника веществом корональных джетов. В случае слабой вспышки, сопутствующей джету, отрицательный всплеск также мог иметь тип "изолированный". Рассмотрен случай возникновения более глубокой депрессии радиоизлучения на высоких частотах по сравнению с низкими, о чем ранее не сообщалось. Показано, что отрицательные всплески являются не такими редкими явлениями, как считалось ранее.

## Ударная волна в солнечном событии, связанном с эрупцией крупного протуберанца

**Кузьменко И.В.1, Гречнев В.В.2**

Тезисы XXV всероссийская ежегодная конференция

«Солнечная и солнечно-земная физика-2021», Пулково, 2021

<http://www.gaoran.ru/russian/solphys/2021/gao2021.pdf>

Эрупция крупного протуберанца, произошедшая 29 сентября 2013 г. вне активных областей, вызвала быстрый корональный выброс массы. Его высокая скорость предполагает наличие перед ним ударной волны, что подтверждается наблюдениями радиовсплеска II типа и окружающего выброс гало. Установлено, что ударная волна была импульсно возбуждена эруптивным протуберанцем и трансформировалась в головную позже на значительном расстоянии от Солнца. Расчётные положения фронта волны соответствуют её проявлениям на изображениях. Радиоизлучение II типа от 30 МГц до 70 кГц было вызвано распространением одной и той же ударной волны. Характер возбуждения и эволюции ударной волны в этом событии оказался таким же, как и в исследованных ранее вспыхивающих событиях.

## СПЕКТРАЛЬНЫЕ НАБЛЮДЕНИЯ ЭРУПЦИИ ВОЛОКНА

**МАШНИЧ Г. П.1, КИСЕЛЕВ А. В.**

АЖ Том: 96 Номер: 7 Год: 2019 Страницы: 607-616

Представлены результаты исследования движений в волокне во время медленного подъема и эрупции по спектральным наблюдениям, полученным в Саянской Солнечной Обсерватории, использованы SDO/HMI данные о продольном магнитном поле, а также EUV изображения SDO/AIA. Короткопериодические вертикальные колебания (~5 мин) волокна как целого обнаружены на фазе его подъема. Ускорение подъема волокна сопровождалось разрывом ортогональной петли над волокном, которая до события длительного время наблюдалась по EUV изображениям в канале 193 Å инструмента SDO/AIA. За 2 ч до частичной эрупции волокна по данным SDO/HMI в основаниях петли было зарегистрировано увеличение магнитного потока на  $2 \times 10^{19}$  максвелл. Из точки разрыва петли эмиссии распространялись к востоку и западу в направлении нейтральной

линии, на границах волоконного канала наблюдались поярчания... Эмиссионные петли были видны во всех каналах инструмента SDO/AIA, что свидетельствует о сильном нагреве плазмы волокна. Во время быстрой фазы эрупции волокно двигалось с ускорением  $\sim 21 \text{ м/с}^2$ . В период эрупции по Ндизображениям наблюдалось расщепление волокна на фрагменты, параллельные его оси. Наши результаты исследования эрупции волокна согласуются с известными в литературе результатами и дополнены новыми наблюдательными фактами. Перед фазой подъема обнаружены вертикальные колебания ( $\sim 5$  мин) волокна как целого. В период подъема наблюдалось взаимодействие волокна с лежащей выше корональной петлей.

## ДВИЖЕНИЯ И КОЛЕБАНИЯ В ВОЛОКНЕ ПЕРЕД ЭРУПЦИЕЙ

**МАШНИЧ** Г.П.1, **БАШКИРЦЕВ** В.С.

АЖ Том: 93Номер: 2 Год: 2016 Страницы: 247

В работе исследованы доплеровские движения в волокне и в фотосфере под волокном за несколько дней перед эрупцией. Большое волокно в северном полушарии с 31 августа по 2 сентября 2014 г. располагалось вблизи центрального меридиана и эруптировало **02.09.2014**. В результате эрупции волокно потеряло основную часть массы, а через сутки начался процесс его восстановления. На Горизонтальном солнечном телескопе Саянской солнечной обсерватории (ССО) в течение трех дней 31.08

□2.09.2014 вы спектральной области, которая включает линии  $\text{H}\beta$   $\lambda$  486.1 нм (хромосфера) и  $\text{Fe I}$   $\lambda$  485.9 нм (фотосфера). Из анализа доплеровских скоростей в волокне и в фотосфере под волокном получены следующие результаты. Сильные вращательные движения присутствуют в волокне длительное время (весь период наблюдений - 3 дня). В моменты дестабилизации из-за всплытия новых магнитных потоков согласованность стационарных движений между фотосферой и волокном нарушается. За несколько часов перед эрупцией в волокне время от времени возникает цуговой характер фотосферных короткопериодических колебаний (около 5 минут). На начальной фазе подъема волокна большие сегменты совершают почти вертикальные колебания.

Ожередов В.А., Струминский А.Б. Статистическая модель ускорения КВМ

**Сборник трудов XXVI Всероссийской ежегодной конференции по физике Солнца «Солнце и солнечно-земная физика – 2022» ГАО РАН.**

<http://www.gaoran.ru/russian/solphys/2022/book/conf2022.pdf> 7 марта 2011

## НАБЛЮДЕНИЯ КОРОНАЛЬНОГО ВЫБРОСА МАСС С ПОМОЩЬЮ ВУФ ТЕЛЕСКОПОВ ТЕСИС

А.А. **Рева**, А.С. Ульянов, С.А. Богачев, С.В. Кузин

ИКИ-2014, Сессия: Солнце

<http://plasma2014.cosmos.ru/presentations>

## ПОИСК СОЛНЕЧНЫХ ИСТОЧНИКОВ МЕЖПЛАНЕТНЫХ КОРОНАЛЬНЫХ ВЫБРОСОВ МАССЫ С ПОМОЩЬЮ ОБРАТНОЙ МОДЕЛИ МАГНИТОДИНАМИЧЕСКОГО ВЗАИМОДЕЙСТВИЯ СОЛНЕЧНОГО ВЕТРА В ГЕЛИОСФЕРЕ

**РОДЬКИН Д. Г.**\*, **СЛЕМЗИН В. А.**<sup>1</sup>, **ШУГАЙ Ю. С.**<sup>2</sup>

АЖ Том: 100Номер: 3 Год: 2023 Страницы: 289-296

При разработке и тестировании методов прогнозирования межпланетных корональных выбросов массы (МКВМ) большое значение имеет установление их связи с источниками на Солнце – корональными выбросами массы (КВМ), наблюдаемыми коронографами. Часто применяемый обратный баллистический расчет времени старта КВМ не учитывает изменения их скорости при движении в гелиосфере и может давать неопределенность вплоть до суток. С хорошей точностью (порядка  $\pm 10$  ч) движение КВМ в гелиосфере от Солнца до Земли описывается моделью магнитодинамического взаимодействия КВМ с фоновым солнечным ветром (drag-based model, DBM). В данной работе для поиска возможных корональных источников МКВМ, наблюдаемых у Земли, предлагается использование обратной модели магнитодинамического взаимодействия (reverse DBM, RDBM), с помощью которой по измеренным параметрам МКВМ в обратном ходе восстанавливается вероятное движение КВМ в гелиосфере и определяются их параметры на выходе из солнечной короны. В модели используются данные о скорости фонового солнечного ветра, рассчитываемые по площади корональных дыр в центральной части Солнца, представленные на сайте Центра анализа космической погоды НИИЯФ МГУ, с корректирующими коэффициентами.

## О СВОЙСТВАХ КОРОНАЛЬНЫХ ВЫБРОСОВ МАССЫ У ЗВЕЗД ПОЗДНИХ СПЕКТРАЛЬНЫХ КЛАССОВ

**САВАНОВ** И. С.

ПАЖ Том: 46Номер: 12 Год: 2020 Страницы: 888-893

DOI: [10.31857/S0320010820120049](https://doi.org/10.31857/S0320010820120049)



Методика оценок корональных выбросов массы (СМЕ) по энергии вспышек звезд применена к данным о вспышечной активности звезд поздних спектральных классов. В исследовании использованы данные каталогов о вспышках звезд, полученные по результатам наблюдений телескопа Кеплер, и представлены зависимости величин масс СМЕ от эффективной температуры объектов из этих каталогов. Установлено, что в этом случае диапазон изменений масс СМЕ составляет примерно 1019–1022 г, при этом по мере перехода к более горячим (более массивным) звездам наблюдается рост массы СМЕ. Рассмотрены данные для нескольких активных хорошо изученных звезд, которые характеризуют возможный диапазон изменений свойств СМЕ для холодных карликов. Полученные результаты сопоставлены с данными, найденными независимым методом оценок характеристик СМЕ по спектральным наблюдениям. Оценки масс СМЕ, установленные по эмпирическим зависимостям для энергий вспышек, превосходят по величине данные о массах СМЕ, найденные по асимметрии профилей Бальмеровских линий водорода.

## **Образование и распространение плазменных потоков корональных выбросов массы в солнечной короне и гелиосфере** Review

В. А. Слемзин<sup>1</sup>, Ф. Ф. Горяев<sup>1</sup>, Д. Г. Родькин<sup>1</sup>, Ю. С. Шугай<sup>2</sup>, С. В. Кузин<sup>1</sup>  
2018 File

Настоящий обзор посвящен вопросам формирования в солнечной короне и распространения в гелиосфере плазменных потоков корональных выбросов массы и производных от них транзитных потоков межпланетных корональных выбросов массы в солнечном ветре. Рассматриваются основные параметры корональных выбросов массы, их отличия от других типов потоков солнечного ветра, корреляция частоты выбросов со вспышками и состоянием солнечной активности. Особое внимание уделяется формированию и моделированию ионного состава плазмы корональных выбросов массы и транзитов солнечного ветра, который является одним из ключевых факторов идентификации типов потоков и их источников, особенно в сложных комплексных структурах, образующихся в гелиосфере при взаимодействии потоков. Рассматриваются современные модели прогнозирования параметров потоков солнечного ветра по данным наблюдений. Обзор содержит перечни источников данных о корональных выбросах и баз данных о параметрах потоков солнечного ветра, а также многочисленные ссылки на работы по исследованиям рассматриваемых явлений.

**Струминский А.Б., Садовский А.М., Григорьева И.Ю. Магнитная детонация и ускорение КВМ во вспышке X3.4 13 декабря 2006**

**Сборник трудов XXVI Всероссийской ежегодной конференции по физике Солнца «Солнце и солнечно-земная физика – 2022» ГАО РАН.**

<http://www.gaoran.ru/russian/solphys/2022/book/conf2022.pdf>

### **СВЯЗЬ МЕЖДУ ДЛИТЕЛЬНОСТЬЮ И ВЕЛИЧИНОЙ УСКОРЕНИЯ КОРОНАЛЬНЫХ ВЫБРОСОВ МАССЫ**

*Струминский А. Б., Григорьева И. Ю., Логачев Ю. И., Садовский А. М.*

**ГЕОМАГНЕТИЗМ И АЭРОНОМИЯ** Том: 61 Номер: 6 Год: 2021 Страницы: 683-693

DOI: 10.31857/S001679402105014X

Исследуется вопрос о том, какая последовательность процессов на Солнце приводит к положительной обратной связи между движением и нагревом плазмы, ускорением электронов, а в итоге, к формированию корональных выбросов массы, ударных волн и ускорению протонов. Для этого проведен анализ солнечных событий, связанных с тремя импульсными вспышками: M2.9 6 июля 2012 г., X2.2 и X9.3 6 сентября 2017 г. и одной длительной вспышкой M3.7 7 марта 2011 г. Электроны ускорялись до релятивистских энергий во всех четырех вспышках, но две последние сопровождалась корональными выбросами массы, ударными волнами и ускорением протонов с энергией >300 МэВ. Найдено два отличия вспышек без корональных выбросов массы. Первое отличие – были ограничены высотой, которая характерна для радиоизлучения 1415 МГц (верхняя хромосфера). Второе отличие – максимум меры эмиссии в них запаздывал относительно максимума температуры на время менее 2 мин. Если считать, что вспышка и корональные выбросы массы черпают энергию из одного резервуара, то время запаздывания можно рассматривать как характерное время ускорения корональных выбросов массы – существование дополнительного оттока энергии. Из теоретических оценок максимальной величины ускорения корональных выбросов массы, значений их минимальной и максимальной скорости следует возможный разброс времени ускорения корональных выбросов массы. Сравнения оценок и наблюдений показывает, что необходимая длительность ускорения для реализации межпланетного корональных выбросов массы была достигнута в событиях M3.7 7 марта 2011 г. и X9.3 6 сентября 2017 г.

### **РАДИАЛЬНЫЕ РАСПРЕДЕЛЕНИЯ ВЕЛИЧИНЫ МАГНИТНОГО ПОЛЯ В СОЛНЕЧНОЙ КОРОНЕ, ПОЛУЧЕННЫЕ С ИСПОЛЬЗОВАНИЕМ СВЕДЕНИЙ О БЫСТРЫХ ГАЛО-КВМ**

**ФАЙНШТЕЙН В.Г.1, ЕГОРОВ Я.И.**

Том: 4 Номер: 1 Год: 2018 Страницы: 3-13 File

(See <https://arxiv.org/pdf/1712.09046.pdf>)

В последние годы для измерения магнитного поля в солнечной короне используют сведения о расстоянии между телом быстрого коронального выброса массы (КВМ) и связанной с ним ударной волны. Во всех случаях этот подход применялся для нахождения радиальных распределений поля  $B(R)$  для направлений, почти перпендикулярных лучу зрения. Мы модифицировали этот метод для получения распределений  $B(R)$  поля вдоль направлений, близких к оси Солнце-Земля. Для этого с использованием модели ice-cream cone для КВМ по данным коронографов LASCO находились трехмерные характеристики быстрых КВМ типа гало и связанных

с ними ударных волн, движущихся почти вдоль оси Солнце-Земля. С помощью этих данных удалось получить распределения  $B(R)$  QUOTE до расстояния от центра Солнца  $\approx 43$  радиуса Солнца, что примерно в два раза дальше, чем в предыдущих работах, в которых использовались данные LASCO. Полученные результаты оказались в хорошем согласии с результатами предшествующих работ для расстояний до 20 радиусов Солнца. Сделан вывод о том, что для повышения точности такого метода нахождения поля в короне необходимо разработать способ выделения участков КВМ, движущихся в медленном и в быстром солнечном ветре. Предложен способ отбора КВМ, центральная (приосевая) часть которых действительно движется в медленном ветре. **18.11.03, 06.04.04, 03.11.04, 07.11.04, 15.01.05, 17.01.05, 30.07.05, 05.09.05, 13.09.05**

## **КИНЕМАТИКА КВМ И СВЯЗАННЫХ УДАРНЫХ ВОЛН ПО ДАННЫМ LASCO: СРАВНИТЕЛЬНЫЙ АНАЛИЗ**

**Файнштейн В.Г.** 1, Пичуев В.А. 1, Егоров Я.И. 1, Загайнова Ю.С.

Пулково «Солнечная и солнечно-земная физика – 2015», с.359

A fast coronal mass ejection (CME) can be divided into a CME body and associated shock wave (SW), as well as shocked plasma between them. This paper compares kinematic characteristics (position and velocity) of fast CME bodies and associated shock waves by SOHO/LASCO-C2, C3 coronagraphs for two coronal mass ejection types: limb CME and halo CME. The former case reflects a forward motion of the coronal mass ejection, as well as its expansion. The latter case shows that the CME kinematic characteristics are primarily determined by its expansion. Using «Ice cream cone model» for CME, we also compare kinematic characteristics of the halo CME body and associated shock wave in 3D space. For all the three CME groups, we have shown that on average the distance between the CME body and SW increases, and difference of their velocities decreases as the CME moves away from the Sun. The latter means that SW velocity decreases with distance (time) more rapidly than the velocity of a CME body.

## **ВАРИАЦИИ МАГНИТНОГО ПОЛЯ, СОПРОВОЖДАЮЩИЕ ВОЗНИКНОВЕНИЕ КВМ, СВЯЗАННОГО С ЭРУПЦИЕЙ ВОЛОКНА**

**Файнштейн В.Г.**, Егоров Я.И., Руденко Г.В., Анфиногентов С.А.

Пулково «Солнечная и солнечно-земная физика – 2015», с.359

Vector photospheric magnetic field measurements by SDO/HMI are used to study variations in the solar magnetic field in an active region accompanying emergence of the **June 7, 2011** CME associated with filament eruption and solar flare. We analyze variations in the modulus of the magnetic induction vector  $B$ , radial field component  $B_r$ , as well as in an angle  $\alpha$  between the magnetic field direction and radial direction from the solar center. We consider variations in the magnetic field in four areas of the active region where the modulus of the magnetic induction vector drastically changed before and after concurrent flare and main acceleration of eruptive filament and in two areas where magnetic induction did not change with time. The areas are situated close to the feet of eruptive filament, in the vicinity of a filament channel, at the flare center. We establish that the event was preceded with surfacing of a new magnetic flux in several areas. In one area, the polarity of a surfacing flux is favorable to magnetic field line reconnection with the ambient field. At the center of the flare, there appeared a sharp increase in the transverse field component after the beginning of the event. We reveal that the angle  $\alpha$  decreases with different rate several hours before the beginning of the event in all the areas examined, except for the flare region.

## **КАК ВОЗНИКАЮТ И ДВИЖУТСЯ БЫСТРЫЕ ИМПУЛЬСНЫЕ КВМ, СВЯЗАННЫЕ С МОЩНЫМИ ВСПЫШКАМИ И НЕ СВЯЗАННЫЕ С ЭРУПТИВНЫМИ ВОЛОКНАМИ?**

**Файнштейн В.Г.**, Загайнова Ю.С.

ИКИ-2014, Сессия: Солнце

<http://plasma2014.cosmos.ru/presentations>

## **ВЛИЯНИЕ ГЕОМЕТРИЧЕСКОЙ ФОРМЫ ПРОТУБЕРАНЦА И СТРУКТУРЫ КОРОНАЛЬНОГО МАГНИТНОГО ПОЛЯ НА ВЕРОЯТНОСТЬ ЭРУПЦИИ, РАЗВИТИЯ ВСПЫШКИ И КОРОНАЛЬНОГО ВЫБРОСА**

**Филиппов Б.П.**

ГИА Том: 64Номер: 1 Год: 2024 Страницы: 13-22

Условия равновесия магнитного жгута, в котором содержится протуберанец, зависят от свойств окружающего магнитного поля короны и геометрии самого жгута. Эрупция протуберанца обычно связывается с потерей устойчивости во внешнем поле при достижении высоты, выше которой индекс убывания поля превышает критическое значение развития эруптивной неустойчивости. Для жгутов с осью в виде прямой линии или окружности критическое значение индекса убывания поля лежит в пределах 1.0-1.5. На основании экстраполяции магнитного поля в короне по данным измерений поля в фотосфере можно было бы строить прогноз вероятности эрупции конкретного протуберанца. Однако учет того, что концы магнитного жгута укоренены в фотосфере и остаются зафиксированными вследствие вмороженности в фотосферную плазму, существенно влияет на критическое значение индекса и усложняет задачу прогноза. Если

магнитный жгут сохраняет форму сегмента тора в процессе эволюции, то критическое значение индекса убывания поля для его вершины зависит от того, какую часть тора он составляет, будучи минимальным для примерно половины тора и имея значение при этом, существенно меньшее единицы. Как будет развиваться эрупция жгута после потери равновесия, тоже зависит от того, какую часть полного тора он составляет в момент начала эрупции. Более короткие жгуты ускоряются очень энергично, но кратковременно, генерируя более сильные электрические индукционные поля, инициирующие вспышечные процессы. Однако конечная скорость, которую может набрать короткий жгут в процессе ускорения, меньше, чем у более длинных жгутов, ускоряющихся менее интенсивно, но более длительно. Индукционные эффекты у последних менее выражены, так что они способны произвести только слабые вспышечноподобные проявления. Таким образом, эрупция короткого протуберанца, который набрал сравнительно небольшую скорость, может быть остановлена на некоторой высоте в короне, не породив корональный выброс. Но такая "несостоявшаяся эрупция" способствует развитию вспышечных явлений. Напротив, эрупции длинных протуберанцев чаще ведут к образованию корональных выбросов и слабым вспышечным проявлениям.

### **ПРОЯВЛЕНИЕ МАГНИТНЫХ ЖГУТОВ В СТРУКТУРЕ СОЛНЕЧНЫХ ПРОТУБЕРАНЦЕВ**

*Филиппов Б.П.*

*Ги А* Том: 63Номер: 2 Год: 2023 Страницы: 174-180

Вид спокойных солнечных протуберанцев чаще всего напоминает широкий занавес или изгородь из вертикального частокола. Трудно вообразить, что такая структура может быть связана или даже образована магнитным жгутом, пучком закрученных в цилиндрическую спираль силовых линий, который иногда наглядно проявляется в волокнах активных областей. Однако при сравнительно небольшой активизации протуберанцев, когда составляющая их плазма начинает двигаться вдоль силовых линий поля, структура магнитного жгута может быть различима. Показан пример спокойного протуберанца, в котором наблюдается вращательное движение вдоль спиральных траекторий, обрисовывающих жгут. Вращение хорошо видно на временной диаграмме, составленной из узких полосок изображений протуберанца вдоль траектории движения.

### **ЗАВИСИМОСТЬ ВОЗНИКНОВЕНИЯ КОРОНАЛЬНОГО ВЫБРОСА ОТ ИСХОДНОЙ ДЛИНЫ ЭРУПТИВНОГО ПРОТУБЕРАНЦА**

*Филиппов Б.П.*

*Ги А* Том: 62Номер: 3 Год: 2022 Страницы: 275-282

Анализируется модель эрупции магнитного жгута, концы которого жестко закреплены в фотосфере. Длинные и короткие жгуты демонстрируют различные сценарии эрупции при прочих равных условиях. Короткие жгуты ускоряются быстро, но кратковременно, и довольно легко могут быть остановлены на сравнительно небольшой высоте, приводя к так называемым несостоявшимся эрупциям. Эрупция длинного жгута вероятнее приведет к его подъему на большую высоту и формированию коронального выброса. Такая тенденция прослеживается в реальных наблюдениях эруптивных явлений на Солнце.

### **НИЗКИЕ ЗНАЧЕНИЯ КРИТИЧЕСКОГО ИНДЕКСА УБЫВАНИЯ МАГНИТНОГО ПОЛЯ В ЭРУПЦИЯХ ПРОТУБЕРАНЦЕВ**

*Филиппов Б.П.*

*ГиА* Том: 62Номер: 1 Год: 2022 Страницы: 19-27

Предпринята попытка с максимально возможной точностью оценить критическое значение индекса убывания коронального магнитного поля  $n_c$  при эрупциях волокон/протуберанцев. Рассмотрен ряд событий в тот период, когда космические аппараты STEREO (Solar Terrestrial Relations Observatory) находились на угловом удалении около  $90^\circ$  от линии Солнце–Земля (2010–2011 гг.). Из девяти эрупций волокон, происходивших вблизи центрального меридиана Солнца, для земного наблюдателя в двух случаях индекс равен единице, а в остальных – меньше, с минимальным значением  $n_c = 0.2$ . Такие низкие значения почти не приводятся в литературе. Вместе с тем, они характерны для развития неустойчивости магнитного жгута с закрепленными концами.

### **“НЕСОСТОЯВШИЕСЯ” ЭРУПЦИИ СОЛНЕЧНЫХ ВОЛОКОН**

**ФИЛИППОВ Б. П.**

*АЖ* Том: 97Номер: 3 Год: 2020 Страницы: 256-264

Солнечные волокна (протуберанцы), которые внезапно начинают быстро подниматься, т.е. становятся эруптивными, иногда замедляются и останавливаются на относительно небольшой высоте. Причины, по которым эрупции оказываются “несостоявшимися”, во многом неясны. В работе анализируются два эруптивных явления с очень схожими исходной геометрией и конфигурацией внешнего магнитного поля, одно из которых развивается в корональный выброс, а второе прерывается вскоре после начала. Силой, останавливающей эрупцию, вероятно, чаще всего выступает натяжение изогнутых магнитных силовых линий. Решающим фактором представляется присутствие значительного компонента внешнего магнитного поля вдоль оси жгута в области несостоявшейся эрупции. Такой эффект был обнаружен в лабораторных экспериментах по изучению динамики плазменных жгутов и, вероятно, играет важную роль в эруптивных явлениях на Солнце.

### **Выбросы вещества из солнечной атмосферы**

**Review**

**Б.П. Филиппов**

УФН 189 905–924 (2019)

[https://ufn.ru/ufn2019/ufn2019\\_9/Russian/r199a.pdf](https://ufn.ru/ufn2019/ufn2019_9/Russian/r199a.pdf) File

Корональные выбросы являются самым крупномасштабным эруптивным явлением в солнечной системе. Их радикальное воздействие на космическую погоду объясняет большой интерес к наблюдениям, моделированию, прогнозированию этого явления. Описываются основные свойства выбросов вещества из солнечной атмосферы в межпланетное пространство, их физические параметры, частота событий и её зависимость от фазы цикла солнечной активности. Рассмотрены возможные источники выбросов в солнечной атмосфере, конфигурации магнитного поля, в которых может запасаться энергия, необходимая для внезапного взрывного ускорения

большой массы вещества. Анализируются основные неустойчивости корональных структур, ведущие к инициации и развитию эруптивных процессов. Показаны связь корональных выбросов с другими проявлениями солнечной активности и единство эруптивного процесса, наблюдаемого разными методами в различных слоях солнечной атмосферы и межпланетном пространстве. Обсуждаются признаки приближения преэруптивных областей на Солнце к катастрофе и возможности использования их для прогнозирования эрупций и возмущений космической погоды.

## **НАЧАЛЬНЫЕ ТРАЕКТОРИИ ЭРУПТИВНЫХ ПРОТУБЕРАНЦЕВ НА СОЛНЦЕ**

**ФИЛИППОВ** Б.П.

АЖ Том: 93Номер: 3 Год: 2016 Страницы: 321

Траектории эруптивных протуберанцев сопоставлены с формой нейтральных поверхностей в короне, рассчитанных в потенциальном приближении по данным фотосферных измерений. Наблюдения с разных углов зрения, полученные при помощи космических обсерваторий SDO и STEREO, позволяют определить точное положение протуберанца в различные моменты времени во время эрупции. Показано, что эруптивные протуберанцы на начальных участках траектории движутся вдоль нейтральных поверхностей ( ) потенциального магнитного поля короны. Это позволяет определить направление движения последующего коронального выброса и оценить его геоэффективность.

## **Воздействие корональных выбросов на удаленные корональные лучи**

Б. П. **Филиппов**<sup>1</sup>, П. Кайшап<sup>2</sup>, А. К. Сривастава<sup>2</sup>, О. В. Марценюк

АЖ, т.91, №8, С. 668-676, 2014

Проанализировано воздействие крупного коронального выброса на Солнце на корональный стример, расположенный на угловом удалении около 90 от главного направления распространения коронального выброса на основе наблюдений коронографа SOHO/LASCO 2 января 2012 г. Радиальные корональные лучи (стримеры) изгибаются, когда корональные выбросы проходят через корону даже на большом угловом удалении от положения лучей. Картина похожа на бегущую вдоль луча изгибающую волну. Некоторые авторы интерпретируют это явление как проявление распространяющихся ударных волн, генерируемые быстрыми корональными выбросами в короне, а другие считают это свидетельством возбуждения волнового процесса внутри лучевой структуры после внешнего толчка. В результате проведенного анализа не найдено убедительных аргументов в пользу обеих этих возможностей. Сделан вывод, что наблюдаемое поведение лучей является результатом воздействия магнитного поля движущегося в короне магнитного жгута, связанного с корональным выбросом. Движение крупномасштабного магнитного жгута, удаляющегося от Солнца, создает изменения в структуре окружающих силовых линий в короне, которые похожи на полупериод волны, бегущий вдоль коронального луча.

## **О КРИТИЧЕСКОМ ЗНАЧЕНИИ ИНДЕКСА УБЫВАНИЯ МАГНИТНОГО ПОЛЯ В ЭРУПТИВНЫХ ЯВЛЕНИЯХ НА СОЛНЦЕ**

**ФИЛИППОВ** Б.П.<sup>1</sup>, **МАРЦЕНЮК** О.В.<sup>1</sup>, **ДЕН** О.Е.<sup>1</sup>, **ПЛАТОВ** Ю.В

АЖ Том: 91Номер: 12 Год: 2014 Страницы: 1042

Рассчитано распределение индекса убывания потенциального коронального магнитного поля в активных областях на Солнце, в которых произошла эрупция волокон. Индекс убывания магнитного поля является удобным безразмерным параметром, характеризующим величину вертикальной компоненты градиента магнитного поля, от которой зависит устойчивость равновесия магнитных жгутов. Критическое значение индекса в рассмотренных событиях близко к единице, что соответствует теоретическому порогу неустойчивости прямого жгута. Данный критерий может быть использован для оценки вероятности эруптивных явлений.

## **ВЫСОТА СОЛНЕЧНОГО ВОЛОКНА ПЕРЕД ЭРУПЦИЕЙ**

Б. П. **Филиппов**

АЖ, 2013, текст

Анализируется соотношение высоты солнечного волокна над фотосферой перед эрупцией 21 октября 2010 г. с критической высотой устойчивого равновесия магнитного жгута в корональном магнитном поле. Наблюдения космических обсерваторий SDO (Solar Dynamic Observatory), SOHO (Solar and Heliospheric Observatory) и STEREO (Solar Terrestrial Relations Observatory) с различных точек зрения в пространстве дают возможность измерить эти параметры с высокой точностью. Показано, что высота волокна медленно возрастала в течение нескольких дней и эрупция наступила, когда она достигла критического значения 80 Мм.

## **КРУПНОМАСШТАБНЫЕ ЯВЛЕНИЯ НА СОЛНЦЕ, СВЯЗАННЫЕ С ЭРУПЦИЕЙ ВОЛОКОН ВНЕ АКТИВНЫХ ОБЛАСТЕЙ: СОБЫТИЕ 12.09.1999**

И. М. **Черток**<sup>1</sup>, В. В. Гречнев<sup>2</sup>, А.М.Уралов<sup>2</sup>

*АСТРОНОМИЧЕСКИЙ ЖУРНАЛ*, 2009, том 86, №4, с. 392–405

На примере события **12.09.1999** проанализированы крупномасштабные возмущения, связанные с корональными выбросами массы при эрупции волокон вне активных областей. Анализ основан на  $H\alpha$ -фильмограммах, изображениях крайнего УФ- и мягкого рентгеновского диапазонов, и данных коронографов. Эрупция волокна происходила в относительно слабых магнитных полях, но сопровождалась более масштабными явлениями, чем вспышечные события. После эрупции в течение нескольких часов развивалась крупномасштабная аркада, основаниями которой были расходящиеся ленты, подобные вспышечным. Объем события был ограничен “волной EIT”, квазистационарной на солнечной поверхности и расширяющейся над лимбом. Событие не имело импульсной компоненты, поэтому “волна EIT” над лимбом — магнитная структура, идентифицированная как фронтальная структура коронального выброса массы, в силу их совпадения по форме, структурным деталям и кинематике. В ареале события наблюдалось три типа диммингов, обусловленных (а) эвакуацией плазмы, (б) нагревом плазмы и ее последующей эвакуацией, (в) поглощением излучения в системе волокон, активизированных эрупцией. Факт возникновения димминга из-за нагрева плазмы был выявлен по данным мягкого рентгеновского диапазона, но он не обнаруживается по четырем каналам EIT. Это ставит вопрос о корректности некоторых выводов, сделанных ранее только по данным EIT. Обусловленные эрупцией трансформации магнитных полей имели место также в стационарной корональной дыре, примыкавшей к ареалу события. Расширение коронального выброса массы является автотельным и характеризуется быстро уменьшающимся ускорением, что не учитывается широко используемой полиномиальной аппроксимацией.

## КРУПНОМАСШТАБНАЯ АКТИВНОСТЬ В СОЛНЕЧНЫХ МОЩНЫХ ЭРУПТИВНЫХ СОБЫТИЯХ НОЯБРЯ 2004 г. ПО ДАННЫМ SOHO

И. М. Черток

*АСТРОНОМИЧЕСКИЙ ЖУРНАЛ, 2006, том 83, №1, с. 76–87*

По данным УФ-телескопа SOHO/EIT и коронографа LASCO проанализированы крупномасштабные солнечные возмущения, связанные с серией мощных вспышек и корональных выбросов массы, которые произошли **3–10 ноября 2004 г.**, на поздней фазе спада 23-го цикла и вызвали сильные геомагнитные бури. С использованием деротированных фиксированных разностных гелиограмм в корональном канале  $195^\circ\text{A}$  с 12-мин интервалом, а также в разнотемпературных каналах 171, 195, 284 и  $304^\circ\text{A}$  с 6-ч интервалом показано, что эти возмущения имели глобальный характер и были гомологичными, т.е. обладали аналогичными характеристиками и затрагивали одни и те же структуры. Практически во всех 9 событиях данной серии наблюдались две повторяющиеся системы крупномасштабных диммингов (областей пониженной яркости с временем жизни порядка 10–15 ч): (а) трансэкваториальные димминги, соединяющие северный приэкваториальный центр эрупции с южной активной областью; (б) северные димминги, охватывающие значительный сектор между двумя корональными дырами. В этом же северном секторе перед расширяющимися диммингами наблюдались корональные волны — уярчения, распространявшиеся от центра эрупции со скоростью сотни км/с. В каждом событии наиболее яркая центральная часть коронального выброса массы типа гало соответствовала северной системе диммингов. На основе полученных результатов обсуждаются свойства диммингов и корональных волн, а также связь между ними, и показано, что в процесс эрупции крупных корональных выбросов массы оказываются вовлеченными структуры глобальной солнечной магнитосферы с пространственным масштабом, намного превосходящим размеры активных областей и обычных комплексов активности.

## РАДИОПРЕДВЕСТНИКИ КОРОНАЛЬНЫХ ВЫБРОСОВ МАССЫ, ЗАРЕГИСТРИРОВАННЫХ В ФЕВРАЛЕ - МАРТЕ 2023 ГОДА

ШЕЙНЕР О.А.<sup>1</sup>, ФРИДМАН В.М.<sup>1</sup>

[КОСМИЧЕСКИЕ ИССЛЕДОВАНИЯ](#) Том: 62 Номер: 2 Год: 2024 Страницы: 157-167

На основе анализа данных за февраль - март 2023 г. рассмотрены результаты исследований связи между возникновением спорадического микроволнового излучения, предшествующего явлениям корональных выбросов массы, и этими явлениями с целью разработки методов краткосрочного прогнозирования корональных выбросов массы по радиоданным.

## К ВОПРОСУ О ЛОКАЛИЗАЦИИ МЕСТ РОЖДЕНИЯ КВМ НА СОЛНЦЕ

ЯЗЕВ С.А.\*<sup>1,2</sup>, ТОМОЗОВ В.М.<sup>2</sup>

*АСТРОНОМИЧЕСКИЙ ЖУРНАЛ* Том: 100 Номер: 11 Год: 2023 Страницы: 1069-1080

DOI: 10.31857/S0004629923100080

Исследована локализация зон возникновения КВМ на Солнце в период с ноября 2006 по февраль 2007 г. по каталогу SOHO. Описан метод сопоставления таких зон с активными областями (АО) как на видимом, так и на невидимом полушариях Солнца. Показано, что простое линейное продолжение проекций траектории движения КВМ на Солнце во многих случаях проходит мимо АО. 63.5% КВМ удалось привязать к АО, 19% – не удалось, а для 17.5% должен быть сделан выбор между АО и факельными площадками, где пятна наблюдались на 1–3 оборота Солнца раньше. Обсуждается гипотеза, что смещение начала

траектории движения КВМ от центроида АО связано с несимметричностью расположения магнитного жгута, на основе которого формируется КВМ, относительно АО: одно основание жгута находится вблизи сильных магнитных полей пятен, второе – в области слабых полей на периферии или за пределами АО.